Q
1
33
N/C

Science Abstracts

Physics Abstracts

Science Abstracts Series A
January–June 1973

Subject Index part A

U. of ILL. LIBRARY
OCT 25 1973
CHICAGO CIRCLE

inspec
The Institution of Electrical Engineers

CONTENTS

Title page i
Subject index S 1

SIX-MONTHLY INDEXES TO SCIENCE ABSTRACTS

Cumulative indexes to Science Abstracts are published twice a year covering the period January-June and July-December. They comprise author and subject indexes and some specialised or 'small' indexes. For Physics Abstracts and Electrical & Electronics Abstracts the Author Index and Subject Index are published as separate volumes. In this case the Small Indexes are included in the Author Index volume.

Author index

This lists in alphabetical order all authors of papers abstracted in the abstracts journal during the six months covered by the index, together with the title of the paper. Where there are co-authors of a paper the title of the paper is given only under the name of the first author. The serial number of the paper in the abstracts journal is in the form 3–12345, ie 1973—abstract no. 12345.

'Small' indexes

These are specialised indexes which allow the user to find quickly particular types of information which might be difficult to find using the subject or author indexes.

Bibliography index

In this index reference is made to articles which contain a significant list of references or biliography on the subjects listed.

Book index

This gives details of books received and abstracted by the abstracts journal.

Patent and Report indexes

These give details of those reports or patents which have been abstracted in the abstracts journal during the past six months.

Conference index

This index lists conferences for which published proceedings have been received and abstracted. Reference is given to the individual papers and their serial numbers in the abstracts journal.

Subject index

The Subject index provides an alphabetical subject key to the articles included in the abstracts journal. Some general guidance on its use is given below:

1. Look in the index for the name of the specific subject in which you are interested. In most cases this name will be a heading in the index and you will find relevant articles listed under it.

2. Occasionally you will be directed from the subject heading chosen to a different heading under which the relevant or additional articles are listed.

3. If you do not find the subject heading you first choose, try a more general heading.

4. Each entry under the heading relates to an article appearing in the abstracts journal and gives the serial number of that article in the journal preceded by the last digit of the current year, eg 3—12345: ie Abstract number 12345 in the abstracts journal for 1973.

Physics Abstracts

Volume 76, part 1 January–June 1973

Subject Index part A

The Institution of Electrical Engineers

Physics Abstracts is published every two weeks by the Institution of Electrical Engineers in association with the American Institute of Physics. Twice-yearly subject and author indexes covering the period January–June and July–December are included in the subscription. Printed by Unwin Brothers Limited, Old Woking, Surrey, England. Second class postage paid in New York, NY 10001, USA.

© 1973: THE INSTITUTION OF ELECTRICAL ENGINEERS

Subject Index

4π counters *see counters*
A centres *see colour centres*
A/D conversion *see analogue-digital conversion*
abacs *see nomograms*
aberrations
see also lenses; optical instrument testing; particle optics
acoustic lenses for u.s. imaging 3—79
astigmatism correction, for x-squared y-squared surface 3—703
astigmatism detection by scanning methods 3—365
astronomical telescopes, three-mirror objectives, analysis *(Russian)* 3—22134
asymmetrized quadrupole lenses, paraxial chromatic aberration 3—13782
centred spherical surfaces, sagittal curvature correction, recursion formulas for *(Russian)* 3—6451
charged particle analysers, optimum transport 3—3867
chromatic, elimination in underwater photographic recording 3—9980
chromatic, in pulse ranging systems 3—4075
chromatic of an electrostatic lens for monochromatic electron beams production 3—35723
clock paradox, explanation using light aberration 3—32422
converging beam holography, focusing properties *(Russian)* 3—698
double focusing mass spectrometer with parallel beams *(Rumanian)* 3—10094
double focussing mass spectrometer, influence of fringing fields on image aberrations 3—13454
double magnetic prism-e.s. mirror system, optimal characteristics, exptal. determ. *(French)* 3—13452
double plane symmetric systems, aberration coeffs. 3—35679
electron lenses, round and cylindrical with field free object space, theory *(German)* 3—26256
electron microscope image resolution and contrast for elastic scatt. and incoherent illumination 3—16924
electron microscope image resolution and contrast for elastic scatt. and incoherent illumination 3—16925
electron microscope objective lens, astigmatism measurement from spatial frequency spectrum of image *(Russian)* 3—6115
electron microscopy, contrast transfer theory, isoplanatism 3—376
electron optical transfer function rel. to astigmatism and field curvature 3—32614
electron optical transfer functions rel. to coma 3—32613
electrostatic prism spectrometer with quadrupole-octupole lenses, geometric aberrations 3—35488
electrostatic two-electrode cylindrical mirrors, numerical design 3—35725
eye, spherical aberration, crystalline lens contribution 3—31870
far u.v. stellar spectrograph for 200 to 900Å region, design and aberrations 3—31840
field curvature correction using single second order aspheric surface *(Russian)* 3—154
field emission illum. systems, performance estimates, design criteria, aberrations, defocus, stability 3—803
focusing lenses with one aspherical surface used in lasers, analysis and calc. 3—22321
holographic, incorrectly repositioned hologram in system with lenses having aberrations 3—37643
holographic image quality, wavefront aberration evaluation using ray-tracing 3—10453
illuminators, one-glass, radial temperature distribution effects *(Russian)* 3—5884
inchoherent object detection and resolution by aberrated system in presence of background noise 3—22862
ion orbits, Nth order aberrations in static magnetic fields 3—808
large astronomical telescopes, correcting system *(Italian)* 3—25525
laser beam in defocusing media, aberrations and extreme divergences *(Russian)* 3—6512
lens design, maximum depth of focus 3—173
lenses, surfaces of best focus 3—37940
optical radar data processing 3—6452
optical system design, introduction of higher order equalising coefficients for known aberration magnitudes *(Russian)* 3—32056
pulse-scanning imaging systems, range azimuth coupling aberrations 3—28518
rotating and deflecting a line focus, electron optical props. 3—37991
ruling defects in diffraction grating, effects on spectral lines *(Japanese)* 3—5889
Selfoc fibres, imaging, focusing props., spherical 3—13715
slit aperture, high numerical system with spherical aberration and defocusing, diffr. 3—26202
solid liquid compound hydroacoustic lens, low aberrations 3—35324
space photographic images effects, detection and correction 3—3822
spectroscopic mirrors, off-axis concave spherical, astigmatism reduction 3—28544
spherical, correction by use of composite light *(Czech)* 3—16814
spherical, of electron lens, theory of thin probe formation 3—13774
telescope, three mirror, closed form soln., spherical aberration, coma, astigmatism, field curvature 3—13111
thin double-plane-symmetric lenses, third order aberrations 3—32524
aberrations continued
turbulence degraded light, far field diffraction by circular apertures 3—5513
abrasion
see also hardness; wear
antireflection coatings, ghost imagery intensity, abrasion resistance, glass and plastic lenses 3—37639
austenitic alloys, resistance to abrasive wear 3—18669
diamond, synthetic, regional abrasion resist. 3—20702
glass-ceramic thin foil prep. technique for transmission electron microscopy 3—34645
groove profile shapes of abraded surfaces from contact area meas. 3—14930
optical surface loose abrasive grinding, working parameters 3—5897
silicate glasses, effects on static fatigue properties 3—9001
steel, abrasional dispersion of polymers on near-surface layers *(Russian)* 3—12373
steel, dependence of abrasive-wear resistance on structure 3—24930
steel, forged, 110G13, wear resist., effect of alloying elements 3—21674
Si, surface prep., optically flat, damage-free surfaces, effect of type of abrasive 3—39263
abrasive wear *see abrasion*
absolute gravity *see gravity*
absolute pressure measurement *see pressure measurement*
absolute temperature *see temperature*
absorption
see also individual particle absorption, e.g. electron absorption
see also acoustic wave absorption
beams and plates, flexural mode absorbers, synthesis and investigation 3—26097
bone and muscle energy absorption coeffs. of 3—5674
gas in liquid film falling on sphere, gas absorption 3—4535
gas-liquid dispersions with mass transfer meas. of liquid solute concentrations 3—32275
gravitational radiation, by dissipative fluid, eikonal approximation 3—35612
Loschmidt diffusion experiment, interferometric method 3—32077
Loschmidt diffusion experiment, perturbation analysis 3—33186
metal embrittlement due to absorption 3—12412
non-Newtonian falling liquid films, gas absorption 3—36108
sands, specific resistivity, rel. to grain size, absorption hypothesis *(German)* 3—5533
spectral coeff., temp. dependent, radiative flux, nonisothermal H shock layer 3—1327
CO_2 by rapid laminar fan-shaped water sheet 3—4536
n-CdSb, anisotropy factor rel. to surface states, absorpt. effects *(Russian)* 3—8246
Mo, of Ar ion in glow discharge 3—15072
Ta, of O electron microprobe detection, concentrations 3—35536
abundance ratio *see element relative abundance; isotope relative abundance*
acceleration
see also acceleration measurement; accelerometers
Fermi, auroral particle precipitation 3—12777
human tolerance, effects of elevated body temp. 3—28362
plasma, rotating, inertial e.m.f. due to thermal convection, Coriolis acceleration 3—29945
plasma acceleration in crossed electric and magnetic fields 3—29947
plasma electrodynamic acceleration in a coaxial accelerator 3—23914
rheological material with internal parameters, accel. waves anal. 3—6261
solar flare cosmic ray electron accel. by plasma waves in current sheet 3—28144
solar flare particle accel., electric current mechanism 3—28145
spark discharges, transition fro m streamers to continuous electron acceleration 3—30036
spatial linkages, matrix method of acceleration analysis 3—22601
acceleration measurement
boiling drop-form liquid, flow out of a Laval nozzle 3—36142
mass-spring accelerometer, optimum damping for minimum phase distortion 3—62
triaxial accelerometer, cavity type, capacitive sensing 3—61
accelerators (particle) *see particle accelerators*
accelerometers
see also acceleration measurement
Block-Moore quartz accelerometer, teleseismic and Earth noise monitoring data 3—28074
electrocapillary, electric equivalent circuit *(Polish)* 3—19155
high sensitivity, 10^{-8} m/s^2 threshold, aerospace applic. *(French)* 3—25663
mass-spring, optimum damping for minimum phase distortion 3—62
nuclear fuel element assembly, external meas. of mechanical integrity 3—11072
pendant, electronically damped, for inertial navigation, comparison with mechanical accelerometers 3—13218
quartz torions accelerometer data on tidal, Earth normal modes and seismic freq., review 3—27953

accelerometers continued
triaxial, cavity type, capacitive sensing 3−61
wide band, quartz torsion, operational improvements 3−5758
accidents
see also electric shocks; explosions; safety
BWR emergency core cooling system for loss of coolant accident 3−4337
core spray cooling after loss of coolant, numerical soln. of Yamanouchi model 3−11074
loss-of-coolant in nucl. reactor, stress anal. of containment vessel 3−11073
nuclear reactor core meltdown, hypothetical, fast reactor fuel interactions with floor material 3−17292
accommodation coefficient *see gases; kinetic theory of gases; surface phenomena*
acidity *see pH*
acids, organic *see organic compounds*
acoustic analysis
cochlear harmonics, effects of d.c. polarization 3−25635
computer-aided, applic. to speech pathology 3−9654
envelope/frequency connection 3−25620
passive localization, using Doppler shifted signal information 3−3653
acoustic applications
see also ultrasonic applications
acoustic emission technique for prediction of material failure *(Japanese)* 3−27843
conference, Boston, Mass., USA (1972) 3−16334
deep water tracking systems 3−3249
elastic spherical shell in ideal compressible liquid, determ. of thickness and radius by echo signals *(Russian)* 3−22197
emission detection of flaws in steel, test 3−27824
flow monitoring by emission, end closure welds on Fast Flux Test Facility reactor fuel pin 3−27834
image detection and recording 3−35362
materials testing, nondestructive, survey of the frontiers 3−18764
meteorology, acoustic radar facility for sounding in planetary boundary layer 3−37256
microscopy, review of progress 3−70
molecule, electrical neutrality testing method 3−33070
navigation system, satellite simulation, laboratory model expt. 3−31995
nuclear reactor operation and development, application of acoustic diagnostics 3−6983
polytetrafluoroethylene, relaxation processes investigation 3−27074
sediment core props. using acoustic vel. profilometer 3−3260
B_2O_3 glass, static and dynamic PVT obs. using acoustic densitometer 3−1774
acoustic delay lines
see also ultrasonic delay lines
thin-film optical waveguide, Bragg interaction of surface acoustic waves and optical waves, experiments for optimising interaction efficiency and bandwidth 3−28415
acoustic detectors *see acoustic transducers*
acoustic devices
see also acoustic delay lines; acoustic generators; acoustic radiators; acoustic receivers; acoustic resonators; acoustic surface wave devices; acoustic transducers; bells; ultrasonic devices
accumulator for high frequency ripple absorption in hydraulic system 3−16575
acoustic Doppler radar scattering equation, in turbulent atmosphere 3−9272
artificial ears, driving point impedance obs. 3−98
attenuators for brass wind instruments 3−5696
audiometer, hearing reference threshold, comparison with free field threshold *(German)* 3−31855
conference, Boston, Mass., USA (1972) 3−16334
curvilinear array, synthesis for large wave dimensions 3−28424
deep water tracking systems 3−3249
digital beamformer, output autocorrelation fn., quantizer fns. 3−37569
digital beamformers, influence of input quantizer step sizes on processing gain 3−86
end-fire line arrays, near field effects 3−35323
homing system for unmanned Arctic research submersible 3−2961
oceanfloor navigation systems, temperature fluctuations, transponder installation 3−3739
optimal adaptive beamformers, small signal suppression 3−3724
parametric receiving array, beam patterns, signal levels 3−9773
radar for atmosphere study 3−9406
reverberation chamber complexes, errors in acoustic reduction meas. *(Russian)* 3−3765
sound level meter 3−48
acoustic dispersion
see also ultrasonic dispersion
freon 12, sound scatter near critical pt. 3−4514
growth and decay of sonic waves in a thermally conducting radiative gas 3−17530
jellium, impure, small frequency and wavevector, longitudinal sound damping 3−20989
liquid crystals, nematic, acoustic wave dispersion and absorption 3−24216
meas. of vibrational relaxation in CO_2 gas with H_2O impurity *(Russian)* 3−4515
Mediterranean, Western, dispersion of axial SOFAR propagation 3−31966
inplasma, frequency-independent contrib. 3−23842
superluminosity, sound propagation and causality 3−19495
triehtyl amine-water solns., velocity of sound. initial separation point 3−30212
velocity dispersion in solid at low temp. in mag. field 3−28479
CO_2, sound scatter near critical pt. 3−4514
$LiNbO_3$ coated with CdSe, CdS, InSb, Rayleigh surface waves, calc. 3−11794
acoustic echoes *see echo*
acoustic emission
see also acoustic waves
ceramic, mechanically stressed 3−27832
acoustic emission continued
end closure welds on Fast Flux Test Facility reactor fuel pin, flow monitoring 3−27834
fatigue crack growth 3−25040
fracture mechanics applic. 3−34679
material failure prediction technique *(Japanese)* 3−27843
nondestructive testing and eval. survey 3−18764
nuclear acoustic hypersuperradiance phenomena 3−2453
nuclear reactor pressure vessels, in-service inspection applications 3−5791
nuclear reactor pressure vessels, nondestructive testing technique 3−5790
steel, Cr-Mn, crack tip plasticity characteriz. 3−34679
steel, low-C alloy, duplex microstruct. rel. to fracture behaviour 3−21646
steel, reactor pressure vessel, deform. and fracture behaviour 3−34680
stress corrosion cracking applic. 3−31216
Zircaloys, during stress corrosion cracking, correl. with fractography of cracking 3−31045
Cu, single crystal, dislocation attenuation and acoustic emission during deformation 3−11629
Cu-Al-Ni, acoustic emission in thermoelastic martensite transform. 3−5318
acoustic equipment
see also acoustic wave interferometers; ultrasonic equipment
baffles, suppression of transducer sidelobes 3−94
complex waveform generation using device with D/A convertor followed by low pass filter 3−28482
data buoy with hydro-acoustic data transmission channel 3−31474
for field visualization 3−32039
noise reduction ear enclosures 3−3467
nonlinear ear protectors, evaluation using constant temporary threshold shift technique 3−3466
relay transponder, for precise positioning of near-bottom equipment 3−28089
acoustic field
anisotropic, spatial cross-correlation 3−19124
asymptotic representation of point source field for coastal divergent channel 3−5736
caustics formation, interaction of sound with shells 3−28414
circular enclosure, characteristic freqs., numerical determination *(French)* 3−9768
circular piston source, pressure field of radiations created by nonlinear interaction of monochromatic carriers 3−9766
correlation functions meas. of nonstationary sound field 3−3764
high frequency fields, ray pattern description by use of virtual sources *(Russian)* 3−5737
hot jet, acoustic far field computation from turbulence parameters, crossed beam technique 3−3636
in-ear monitoring of noise exposure 3−3525
infinite circular cylindrical transducer, partially coated with compliant layer 3−28412
jets, turbulent, nearfield pressure 3−5716
migration of gas filled cavities in inhomogeneous sound field 3−4602
musical instruments, STL ionophone transducer for obs. 3−96
near and farfield radiation of annular ring, det. using impulse response and fast Fourier techniques 3−5724
plate vibrations and sound radiation, evaluation of acoustic properties 3−3665
pressure field in fluid layer between two parallel elastic plates 3−5701
pressure fields in finite container, mixed boundary value problem 3−1425
radiation patterns of multipole sources in motion 3−5722
reverberant, place dependence of timbre of complex tones 3−19118
reverberant chamber for sound power meas. in air or water 3−99
rigid duct containing dissipative silencer, attenuation characteristics 3−95
scattered field attainment, principal methods survey 3−32517
space time structure in a compressor intake duct 3−5787
stationary random sound signal, energy spectra of scattered field, in ocean 3−27994
transmission loss obs., effect of room size 3−3702
u.s., chemical reaction rates, effect of temp. and static pressure 3−27871
u.s., liquid H_2 bubble chamber, vapour bubble behaviour 3−25904
visualisation of time average pressure distribution in rectangular resonant cavity 3−9755
visualisation with photographic device *(Russian)* 3−3766
effects on vortex shedding in air flow, shear layer behind circular cylinder 3−29859
acoustic generators
see also earphones; loudspeakers
airbag-system, pressure-time curves *(German)* 3−16333
FLEXICHOC, oceanographic applications 3−9408
Rijke tube oscillations, double gauze system *(Russian)* 3−5712
sphere, expanding, pressure-time curves *(German)* 3−16333
standing wave acoustic parametric source for underwater sound, mathematical model 3−3733
submarine volcanic eruptions, spectral banding in hydroacoustic signals 3−9163
acoustic holography
capacitor-transducer array for real-time data recording 3−209
elastic waves, holographic imaging 3−37570
Fabry-Perot acoustic surface vibr. detector 3−32083
flaw detection in pressure vessel sections 3−27818
h.f., display using liquid crystals 3−19165
liquid surface, history and current status 3−210
nondestructive testing 3−25042
nondestructive testing technique 3−27819
nuclear reactor pressure vessel inspection technique, evaluation 3−6447
phase (binary) acoustic holograms 3−31975
progress and future development 3−211
synthetic aperture interferometry 3−9957
thick metal sections testing, imaging flaws by acoustic holographic scanning 3−21788

acoustic holography continued
u.s., for nondestructive testing 3−13225
u.s., non-destructive materials testing 3−18764
u.s., nuclear industry applications, remote sensing 3−17311
u.s. holography and nondestructive testing 3−27817
acoustic imaging
Bragg-diffraction imaging, application to nondestructive testing 3−21786
capacitor-transducer array for real-time holographic data recording 3−209
detection and recording using liquid crystal birefringence or ultrasonic effect on suspension 3−35362
liquid crystal display device 3−77
liquid surface acoustic holography, history and current status 3−210
liquid surface holographic u.s. imaging unit for soft tissue structures 3−10162
microscopy, review of progress 3−70
for nondestructive testing, imaging techniques, conference, Los Angeles, USA (1972) 3−19349
real-time u.s., by Bragg diffraction 3−71
scattering from randomly rough surface, numerical image model 3−37549
seismic holography, patent 3−12634
thick metal sections testing, imaging flaws by acoustic holographic scanning 3−21788
u.s., for underwater viewing 3−78
u.s., for weld inspection 3−2788
u.s., lens design 3−79
u.s., medical appls. 3−425
u.s. image convertor allowing diver to see in turbid water 3−80
acoustic impedance
see also acoustic wave velocity
absorption coefficients for various incidence angles 3−103
air cushion buffer *(German)* 3−16332
annular ring in planar baffle, and impulse response 3−5725
artificial ears, driving point impedance obs. 3−98
discs, coplanar unbaffled, self and mutual radiation impedances 3−19108
hole in wall duct *(German)* 3−31953
impedance tube method rel. to reverberation room measurement, for obs. of incident absorption of carpets 3−105
nonlocally reacting noise control materials, for air conditioning, theory 3−3704
plasterboard walls transmission loss, effect of studs 3−3701
polymer, compound vibrator method for determ. of complex deform. characts. 3−28471
self and mutual, of two coplanar unbaffled disks 3−3669
spherical standard sound source, internal impedance *(Japanese)* 3−28481
standing wave tube meas., quality criterion *(French)* 3−22269
transient measurement, data analysis and instrumentation 3−9840
u.s. impediography, biomedical application 3−93
in water, meas. by pressure chamber method *(German)* 3−22268
He solid-liquid boundary, phonon transmission, microscopic theory 3−1763
^{4}He-solid interface, Kaptiza resistance reduction through surface dislocation scattering 3−1764
W-vinyl powder composites, for acoustic dissipation 3−19106
acoustic intensity
see also acoustic noise
parameterless intensity contours for unbounded inhomogeneous media 3−3683
radiation force on solid elastic sphere, method of determination 3−88
ray acoustic intensity calc. due to point source in horizontally uniform media 3−9754
along single ray, calculations 3−37548
acoustic intensity measurement
impulse sound level meters *(German)* 3−13234
radiation pressure technique 3−84
sound level estimation in industrial environments 3−5788
acoustic magnetic resonance
see also acoustic paramagnetic resonance; ferroacoustic resonance
ferrite, magnetoelastic coupling *(Russian)* 3−12062
Cu, open-orbit antiresonances, obs. and mechanism 3−27207
$FeBO_3$, light-induced anisotropy obs. 3−18335
acoustic measurements *see acoustic variables measurement*
acoustic mode of crystals *see lattice dynamics*
acoustic noise
see also noise measurement
aerodynamic, VTOL jets, near field environments 3−3651
aerodynamic noise generation, unified theory 3−17521
aerodynamically generated, testing in conventional wind tunnels 3−3674
air conditioning systems 3−25625
aircraft noise, scaling perception 3−35341
amplitude modulated, detection 3−3656
Artic ice-water boundary, ambient noise generation in 100 to 1000 Hz. range 3−2950
audiometric effects of continuous and impulse noises 3−3514
band limited noise, detection of detection and insertion of tones 3−3534
from boundary layer turbulence 3−33208
broad-band, containing pure tones, subjective rating 3−3672
causes of objectionable noise and control 3−22206
control valves, pollution problem 3−25638
displacement pump noise level testing stand *(Polish)* 3−19164
distant shipping noise, statistic model 3−35333
equivalent constant sound level meter, using voltage to frequency conversion and pulse counting *(German)* 3−35367
flow noise, response of transducer with radially varying sensitivity 3−36090
flow noise, transition boundary layer, wall pressure field measurement 3−1397
flow noise rel. to fluid dilatations, 3−1378
geothermal ground-noise surveys in 0.5 to 5 Hz range rel. to geothermal reservoirs 3−25124
GSM2 noise meter, 16 to 20 kHz range *(German)* 3−5786
hearing, permanent loss due to excess noise *(Dutch)* 3−28348
hearing damage effect evaluation *(German)* 3−16311
acoustic noise continued
helicopter rotor tips, synthesis of shape for noise suppression 3−33210
h.f. spectrum in turbulent stream *(Russian)* 3−11399
histological effects of continuous and impulse noise interaction 3−3515
homophasic and antiphasic tonal signal detection and frequency discrimination 3−3537
impact aspects of environmental impact statements 3−3671
in-ear monitoring of noise exposure 3−3525
indoor booms, behavioural awakening and subjective reactions 3−16338
in industry, damaging levels, code of practice, in UK 3−9657
interference of sleep 3−3524
jet flow, direct correlation 3−7355
jets, moving source problem 3−9746
laser, ring, contraction of capture zone by external noise *(Russian)* 3−26240
level, by Stevens Mark VII method 3−35334
machines, measurement and standardisation 3−28421
masking with ripple noise and spatial frequency anal. 3−3539
measurement, long-range planning *(Swedish)* 3−22194
monaural and binaural free-field speech reception 3−3501
motor vehicle survey 3−9741
narrow band, pitch shift and masking 3−3538
NHK concert hall design *(Japanese)* 3−28418
noise dose meter, standards and recommendations 3−5777
oceanographic, extended range pressure sensitive hydrophone 3−9409
optimal and preferred listening levels in aircraft acoustical environments 3−3488
partition wall sound insulation efficiency auditory assessment *(Japanese)* 3−5734
perceived noise computational algorithm 3−5695
power spectrum of axisymmetric choked jet, noise spectrum in jet segments *(Russian)* 3−4566
process plant noise reduction and control by equipment design 3−28420
protuberance noise environments, review 3−5706
quiet threshold shift 3−37526
reduction between spaces, field measurement 3−102
reverberation limited, underwater signal detection 3−3735
rotating shock waves in turbofan engines, combination tone noise, spectral content prediction 3−11396
shallow water ambient noise in Cabot Strait, effect of floe ice coverage 3−2952
signal masking, critical time interval 3−25632
small aerofoils in flow, sound directivity pattern 3−33209
source in closed circuit subson. wind tunnels 3−5735
sources and theories, book 3−13175
steady state and impulse, temporary threshold shift in hearing 3−5646
subsonic air jet, for noise field 3−3652
subsonic jet, excess noise field 3−14452
supersonic jets, noise generating disturbances, holographic study 3−5705
surface-generated, surface dipole strength by cross-correlation method 3−35336
time varying sources, noise combination 3−37567
traffic, depressed roads, diffraction by wedges of finite impedance 3−25622
transportation noise pollution model study 3−28406
under Arctic ice, environmental factors 3−2962
underwater sound, book 3−22202
units of quantity perceived noisiness and perceived noise level 3−13191
wall structures of enclosures containing noise source, noise reduction 3−16335
water, sonoluminescence dependence on acoustic pressure of u.s. field meas. 3−26825
wave breaking on beach, simulator *(Spanish)* 3−25636
wind-generated noise, model rel. to sonar response applications 3−3666
acoustic paramagnetic resonance
coupled spin-lattice system, dynamical behaviour eqns. of motion 3−5129
hypersonic reentrant cavity coupling system 3−22272
ions, (3d)^4 at high magnetic fields 3−2346
liquid, narrow lines due to rot. mol. diffusion 3−2342
metals, Alpher-Rubin mechanism 3−34185
metals with impurities dynamics of u.s. propagation 3−18365
microwave ultrasonics in solid-state physics, book 3−20819
nonlinear elastic effects, model approach 3−2371
ruby, cross-relax. processes, Fe^{2+} conc. 3−2373
spin-phonon interactions in paramagnetic crystal 3−1753
Al_2O_3:Cr^{2+}(Mn^{3+}), elec. field effect on spectra, line shape analysis 3−8428
Al_2O_3:Cr^{2+}(Mn^{3+}), spectra obs. 3−8427
Al_2O_3:V^{4+} 3−2347
MgO:Fe ultrasonic spin echo obs. 3−15407
acoustic radiators
see also acoustic generators; Doppler effect
air bubbles in water, emission of harmonic and combination freq. waves 3−26830
annular ring near and farfield radiation, det. using impulse response and fast Fourier techniques 3−5724
baffled piston, nearfield pressure variations, exact soln. 3−35340
circular piston source, pressure field of radiations created by nonlinear interaction of monochromatic carriers 3−9766
corregated cylinder, waveguide and end fire radiator, for underwater acoustics 3−9774
disc or cone, radiating from two faces, acoustic press. calc. *(French)* 3−39827
distortion, nonlinear, due to elastic wave excitation in elastic medium by oscillator *(Russian)* 3−31969
laser-excited broadside acoustic array at modulation frequency 3−9751
marine propeller in nonuniform ship wake, lifting surface theory 3−3686

acoustic radiators continued
- piston, baffled circular, impulse response and time dependent force 3−35326
- point-excited infinite elastic plate 3−5699
- separate nonplanar monochromatic sources, nonlinear interaction 3−31957
- small aerofoils in flow, sound directivity pattern 3−33209
- sphere, impulse response and time dependent force 3−35326
- transient radiation from point excited infinite elastic plate 3−5700
- two layered elastic plate, pressure radiations 3−35318
- vibration of semiinfinite fluid loaded membrane 3−5702
- zoning of radiation mode of finite plate on wavenumber diagram 3−9743

acoustic reactance *see acoustic impedance*

acoustic receivers
- *see also microphones*
- parametric array, beam patterns, signal levels 3−9773
- STL ionophone transducer, sound field of musical instruments obs. 3−96

acoustic resistance *see acoustic impedance*

acoustic resonators
- Helmholtz, generalized theory, jet flow model 3−31972
- Helmholtz, nonlinear damping by acoustic liners *(Italian)* 3−22203
- polymer, compound vibrator method for determ. of complex deform. characts. 3−28471
- standing wave acoustić parametric source for underwater sound, mathematical model 3−3733
- u.s., characteristic vibration shapes 3−28907
- visualisation of time average pressure distribution in rectangular resonant cavity 3−9755

acoustic streaming
- natural convection in a sound field giving large streaming Reynolds numbers, boundary layer theory 3−38358
- scattering of sound by sound, plane wave approximation 3−28413

acoustic surface wave devices
- equivalent networks and transmission lines, microwave network formalism 3−9762
- piezoelec. transducers, energy considerations on wave propag. and generation 3−1871
- piezosemiconductor materials, 2nd order signal generation resulting from nonlinear interaction 3−33728
- planar interfaces, acoustic equivalent networks 3−9763
- propagation loss measurement, laser beam applic. 3−5778
- sea-surface waves, waveheight meas. system using transducer as echo-sounder 3−3226
- signal processing, appl. Rayleigh surface waves 3−3987
- transducers, acoustoelectric effect applic. *(German)* 3−15227
- u.s., detection by optical interferometry 3−35363
- CdSe-$LiNbO_3$ monolithic composite structures, acoustoelectric amplification 3−11934
- $SrTiO_3$ substrate, surface acoustic wave generation using electrostrictive effect 3−4908
- Te O_2 temperature dependence calculation 3−18016

acoustic transducers
- *see also electroacoustic transducers; ultrasonic transducers*
- at air-water surface, radiation resistance, effect of spherical scatterers 3−37566
- capacitor-transducer array for real-time acoustic holographic data recording 3−209
- ceramics, ferroelectric nonlinearities 3−18686
- class V flextensional underwater transducer, dynamic response for guided spherical shell 3−3728
- conferences, Boston, Mass., USA (1972) 3−16334
- cylindrical, in piezoeleec. medium of hexagonal symmetry, diffr. 3−28410
- echo ranging, self-reciprocity calibration 3−92
- electret-key, operation anal. 3−97
- emission, frequency response characteristics calibration 3−25671
- infinite circular cylindrical, partially coated with compliant layer 3−28412
- ionophone, STL. characteristics and appls. 3−96
- nearfield calibration arrays, theoretical design 3−31468
- piezosemiconductor, hexagonal, acoustic wave amplification and generation in elec. field 3−21121
- piezosemiconductors, acousto-plasmic transformations *(Russian)* 3−20922
- sea-surface waves, waveheight meas. system using transducer as echo-sounder 3−3226
- sidelobe suppression by use of acoustic baffles 3−94
- spherical, dipole mode vibration, underwater application 3−3225
- spherical focusing, with Gaussian surface velocity distrib. 3−22270
- underwater sound, book 3−22202

acoustic variables control
- cats anesthetized, middle ear muscle contractions rel. to bone conduction 3−31856

acoustic variables measurement
- *see also acoustic intensity measurement; acoustic wave velocity measurement; ultrasonic measurements*
- absorption coefficient meas. using electrical cancellation method *(Japanese)* 3−9760
- acoustic pulse trains of infinite duration, reflections and diffractions in anechoic rooms, obs. of transmission coefficient of architectural panels 3−104
- acoustic reduction meas., ultimate and systematic errors *(Russian)* 3−3765
- amplitude, low duty cycle acoustic signals 3−106
- attenuation, solid specimen, pulse-echo AB method without reverberations 3−32038
- circular metal plate, nodal circles radii determination 3−32366
- correlation functions meas. of nonstationary sound field 3−3764
- cryostat for u.s. attenuation study of solids down to 0.32 K 3−28502
- crystal rotatory power, optical probing 3−28477
- electroacoustic transducers, nearfield meas. 3−89
- Fabry-Perot acoustic surface vibr. detector, application to acoustic holography 3−32083
- hearing aid, electroacoustic, conical coupler for measurements *(German)* 3−37594
- impedance for various angles of incidence, absorption coefficients 3−103

acoustic variables measurement continued
- impedance in water, by pressure chamber method *(German)* 3−22268
- incident absorption, reverberation room method rel. to impedance tube method for carpets, diffraction effects, absorption coefficients 3−105
- intensity meas. by radiation force on solid elastic sphere 3−88
- l.f. attenuation in Indian Ocean 3−74
- modal content of sound in annular and circular ducts, Fourier analysis 3−35368
- noise, long-range planning *(Swedish)* 3−22194
- noise reduction between spaces, field measurement 3−102
- oceanographic meas. of coherence of signal, noise and reverberation 3−3224
- parameter determ. using combined Fourier and correlation techniques 3−3698
- piping systems, steam, noise minimisation, techniques 3−20321
- power, radiation pressure technique 3−84
- power meas. at milliwatt levels, differential microcalorimeter 3−129
- reverberant chamber for sound power meas. in air or water 3−99
- reverberant water tank 3−100
- reverberation time, architectural acoustic quality, techniques and equipment, rangefinding *(German)* 3−28417
- reverberation time characteristics meas. of domestic rooms 3−5731
- reverberation time measurements employing new protractor 3−32035
- speech transmission, distinctness as test of system quality *(Norwegian)* 3−3763
- transmission loss, room size effect 3−3702
- transmission loss meas., under-ice and in open water in Baffin Bay 3−76
- units of quantity perceived noisiness and perceived noise level 3−13191
- v.l.f. attenuation in deep ocean sound channel 3−75
- v.l.f. propagation meas. in South Pacific, project KIWI ONE 3−73

acoustic velocity *see acoustic wave velocity*

acoustic wave absorption
- *see also ultrasonic absorption*
- absorbents, use in industrial noise control 3−9750
- absorption coefficient meas. using electrical cancellation method *(Japanese)* 3−9760
- attenuation, in open-plan office 3−35329
- attenuation in rectangular and circular ducts with varying cross section 3−5718
- attenuation props. of resonant type dissipative silencer 3−95
- critical binary liquid mixture near critical point, attenuation 3−1698
- cryostat for u.s. attenuation study of solids down to 0.32 K 3−28502
- disordered solids, at low temp., thermal phonon scattering 3−20815
- double resonance, acoustic-Mossbauer, review 3−30678
- duct, circular and annular, attenuation of spiral modes 3−16342
- duct, lined rectangular with wall shear layers, convergence of numerical procedure 3−39832
- ear protectors, dBA attenuation 3−35257
- enclosures, radiated power insertion loss 3−3703
- ferroelectrics, piezoelectricity in paraelectric phase, temp. depend. 3−36846
- flexural wave propagation in a plate with periodic obstructions *(Russian)* 3−5711
- incident absorption, reverberation room method rel. to impedance tube method for carpets, diffraction effects, absorption coefficients 3−105
- lake Tanganyika, underwater attenuation, comparison with seawater 3−9779
- l.f. attenuation in Indian Ocean 3−74
- liquid crystals, nematic, acoustic wave dispersion and absorption 3−24216
- liquids, attenuation due to thermal relax., determ. from eqn. of state 3−1773
- liquids, resonator-decay technique, critique 3−37593
- metal, singularities of sound attenuation on Fermi surface topology change *(Russian)* 3−1700
- monoatomic rarefied gases, study of sound propagation using modified Navier-Stokes eqn. 3−29822
- polyatomic gases, Greenspan rule for many internal degrees of freedom 3−7304
- porous materials, acoustic properties 3−39828
- relativistic gas, dissipative, kinetic theory approach 3−33184
- resonance, paraelectric, quadrupole transitions, noncentral impurity ions 3−38624
- resonator type mufflers, influence of air flow on attenuation characteristics 3−22195
- reverberation room obs., traversing microphone spectra for diffuseness obs. 3−3681
- rock, sound wave attenuation const. meas. by free vibr. method *(Japanese)* 3−19109
- rocks, uniaxially compressed *(Russian)* 3−5439
- seawater, relaxational absorption below 1 kHz 3−2953
- semiconductor, attenuation in strong fields 3−5036
- semiconductor, nondegenerate, crossed field acoustic amplification in strong mag. fields 3−11937
- shallow water, mode attenuation coefficients 3−37563
- soils, velocity and absorption coefficients of sound propagation 3−5464
- solid in magnetic field at low temperature, attenuation 3−28479
- solid specimen, attenuation, pulse echo AB method, without reverberations 3−32038
- sound absorption by sound, case of collinear primary waves 3−5728
- standing wave tube meas., quality criterion *(French)* 3−22269
- surface wave propagation loss measurement, laser beam applic. 3−5778
- transient pressure attenuation by nonlinear resilient cylindrical scatterers 3−5704
- transmission loss meas., under-ice and in open water in Baffin Bay 3−76
- underwater, surface duct propagation, loss measurement 3−3717
- u.s. meas., method using excitation of electrostrictive vibrations 3−5779
- v.l.f. attenuation in deep ocean sound channel 3−75
- water saturated stainless steel Feltmetal 3−7856

acoustic wave absorption continued
- wave propagation through conservative random media, appl. to sound absorpt. by inhomogeneous flexible plate 3−13178
- windows, double, effect of edge conditions on sound insulation 3−19126
- Ag_3SbS_3 and Ag_3AsS_3, supersound absorption in perfect crystal 3−26980
- CO_2/O_2 mixtures, vibrational relaxation 3−1323
- Cu dislocatons, vibrating string model, damping and modulus effects 3−17935
- ^4He, superfluid, first sound absorp. coeff. near $T=0$ *(Russian)* 3−1853
- MgO, hypersonic attenuation, impurity and defects effect 3−1701
- O_2, vibrational relaxation times, at high pressures 3−5781
- O_2, vibrational relaxation times and sound velocities in the pressure range 10-110 atm. 3−20199
- W-vinyl powder composites, for acoustic dissipation 3−19106

acoustic wave amplification
- *see also acoustoelectric effects*
- caustics formation, interaction of sound with shells 3−28414
- growth and decay of sonic waves in a thermally conducting radiative gas 3−17530
- piezoelectric semiconductor, effective elastic constant theory 3−8230
- in positive column 3−29985
- semiconductor, in strong elec. field 3−5036
- semiconductor, nondegenerate, crossed field amplification in strong mag. fields 3−11937
- semiconductor, u.s. amplification, theory *(Russian)* 3−7891
- during solid rocket propellant combustion 3−35344
- surface waves, effects of inhomogeneities in electron density, drift velocity 3−1868
- travelling wave amplification in a nonhomogeneous elastic medium 3−37545
- CdS, curent fluctuations under sound amplification conditions *(Russian)* 3−2144
- CdS, Mandelstam-Brillouin scatt. obs. of parametric interaction of sound signals 3−36640
- CdS, nonlinear interaction of Bleustein-Gulyaev waves 3−8004
- CdS, subharmonic generation of surface and bulk acoustic waves at high pump amplitudes 3−1869
- CdSe-$LiNbO_3$ monolithic composite structures, surface wave amplification, acoustoelectric effect 3−11934
- $LiNbO_3$ coated with CdSe, CdS, InSb, Rayleigh surface waves, calc. 3−11794
- Te, u.s. amplification coeff., carrier conc. depend. 3−33959
- ZnO, wavelength depend. of photoenhancement of nonlinear surface wave convolution 3−38707

acoustic wave attenuation *see acoustic wave absorption; ultrasonic absorption*

acoustic wave diffraction
- *see also ultrasonic diffraction*
- infinite duration pulse trains, determ. of transmission coefficients of architectural panels 3−104
- light diffraction on sound for advanced laboratory 3−22222
- from periodic corrugated surface, semiinfinite alternately filled plates 3−37546
- plane pulse incident on three-dimensional corner, conical solutions 3−3677
- radiation of plane wave from active grating for given near field amplitude behind grating 3−5710
- spherical, diffraction on a sphere in a viscous medium *(Russian)* 3−35315
- thin-film optical waveguide, Bragg interaction of surface acoustic waves and optical waves, experiments for optimising interaction efficiency and bandwidth 3−28415
- transducer cylindrical, in piezoelec. medium of hexagonal symmetry, diffr. 3−28410
- turbulent boundary layer flow off sharp edge 3−5715
- wave field diffracted at boundary of shadow zone 3−3707
- by wedge *(French)* 3−16340
- by wedge and cone, study of unsteady boundary layer, determ. of stress tensor *(Russian)* 3−22199
- by wedges of finite impedance, traffic noise in depressed roads 3−25622

acoustic wave diffusion
- *see also acoustic wave scattering*
- underwater, vibrating surface *(French)* 3−9772

acoustic wave effects
- *see also ultrasonic effects*
- bubble growth by diffusion, in 11 kHz sound field 3−7401
- chromospheric heating of very hot stars by radiation driven sound waves 3−25435
- coherent sound vibration, effects on γ-γ ang. correl. 3−34269
- discharge, low frequency, a.c., sonic irradiation effect on discharge characteristics 3−30027
- human brainstem electrical responses to acoustic signals 3−3411
- Kapitza resistance, heat transfer calc. between solids 3−18255
- laser, single mode, dielectric modulation by acoustic waves 3−4080
- light diffraction and interference, partially coherent, two superposed acoustic waves, Huygen's principle, general formula 3−37935
- liquid crystal, nematic, orienting action of sound 3−7620
- plasma ion heating by ion acoustic turbulence model 3−14562
- point defect equil. distrib. around dislocations in acoustic wave field *(Russian)* 3−30124
- pseudosonic and electroacoustic waves, effect on e.m. propagation from plasma coated spherical antenna 3−1493
- rock fatigue damage 3−2913
- shear layer transition and excitation by sound excitation, turbulent breakdown 3−14453
- solar spectra, progressive wave effects on line profiles 3−39605
- Sun, empirical models, effect of mechanical waves rel. to heating 3−31553
- water waves, acoustically driven, in reson. tube 3−23762
- Al alloy, stresses during vibr. of plates under acoustic loads 3−31236
- CdS thin film, acoustoresistance, surface acoustic wave 3−38872
- He-Ne laser, single freq., freq. fluctuations rel. to sound press. and freq., external vibrs. 3−4083

acoustic wave interference
- *see also acoustic wave interferometers; acoustic wave interferometry*
- finite amplitude interaction of multiple tone signals 3−5703
- Florida straits, time-varying multipath interference of broad-band signals 3−31965
- multiple interference smoothing in hydrophone calibration 3−5782
- teaching demonstration of Doppler effect, interference and radiation resistance using a 'Sonalert' 3−32014

acoustic wave interferometers
- *see also acoustic wave interferometry*
- u.s., for elastic constants of solids 3−35366

acoustic wave interferometry
- *see also acoustic wave interferometers*
- gas constant determ. from velocity of sound meas. using acoustic interferometry 3−13215
- holographic synthetic aperture interferometry 3−9957

acoustic wave propagation
- *see also acoustic dispersion; Doppler effect; liquid helium sound propagation; shock waves; ultrasonic propagation*
- acceleration waves, in binary nonreacting mixture 3−35319
- acoustic dampers, energy dissipation mechanism 3−31958
- baffles and enclosures, effects *(Japanese)* 3−9761
- birefringent sheets, stress wave propag. obs. by dynamic polariscope 3−32054
- bubble filled liquids, press. wave propag., closed form. soln. 3−17551
- caustics formation, interaction of sound with shells 3−28414
- cholesteric glass, acoustic rotatory power *(French)* 3−7854
- chromospheric heating of very hot stars by radiation driven sound waves 3−25435
- coincidence and resonance principles 3−9756
- in combustion can, axial temp. and density gradients 3−9758
- conducting nonpiezoelectric crystal, conditions for shear acoustic surface wave propag. 3−4914
- conference, Boston, Mass., USA (1972) 3−16334
- conformal mapping, generation of parameterless examples of ray acoustics 3−3682
- critical binary liquid mixture near critical point, attenuation 3−1698
- crystals, cubic and trigonal, generation of harmonics of transverse elastic waves 3−33962
- in curved ducts, wave patterns of higher modes 3−5717
- cylindrical shells, empty and fluid filled, dispersion spectra 3−19105
- cylindrical wave focusing in ducts 3−10430
- disc or cone, radiating from two faces, acoustic press. calc. *(French)* 3−39827
- discs, coplanar unbaffled, self and mutual radiation impedances 3−19108
- dislocation, uniformly moving, generating acoustic signal, lattice normal mode expansion 3−36304
- distant shipping noise, statistic model 3−35333
- distribution of random wave field in randomly inhomogeneous media *(Russian)* 3−5713
- duct, acoustically treated rectangular with boundary layer, transmission of sound 3−16341
- in ducts with varying cross section, attenuation 3−5718
- dynamic acoustic fluid-elastic solid interactions, integral eqn. formulation 3−35322
- in elastic liquid, 'memory waves', exact solutions *(Russian)* 3−10294
- end-fire line arrays, near field effects 3−35323
- fluid layer bound by two solids, propagation characteristics, mode existence criteria, distribution of elastic energy 3−30333
- flux density in discrete index media and gradient index media 3−3679
- in geostrophic flow, environmental acoustics model 3−37192
- gravity waves, atmospheric propagation using a geometrical acoustics approximation 3−15963
- Green's function of right parallelepiped, perfectly reflecting walls, Laplace transforms, boundary conditions and acoustic potential 3−3687
- growth and decay of sonic waves in a thermally conducting radiative gas 3−17530
- infinite circular cylindrical transducer, partially coated with compliant layer 3−28412
- intensity determ., statistical averages 3−3680
- interstellar gas, cosmic ray effects on sound vibrations in presence of mag. field *(Russian)* 3−37478
- isotropic media, microwave network formalism 3−9762
- Lamb and torsional waves in plates and tubes 3−28925
- layer−half-space system characteristic equation *(Russian)* 3−5714
- line-of-sight signals, spectra of short term fluctuations 3−37552
- linear array beamforming, sensitivity to anisotropic noise and correlated sources 3−2959
- liquid, semi-infinite overlying a viscoelastic halfspace, acoustic field expressed as a Green's function 3−3689
- liquid crystal, nematic, orienting action of sound 3−7620
- liquid layer, acoustic response using a Green's function formation 3−3690
- liquids, viscous compressible in elastic tubes, propag. modes 3−23767
- long waves, propagation in curved ducts 3−9753
- matching of medium with real refractive index with interface with complex input impedance by inhomogeneous layer 3−5709
- Mediterranean, Western, dispersion of axial SOFAR propagation 3−31966
- middle ear transfer characts., tympanic muscle effects 3−3445
- modes in a compressed intake duct, determ. of acoustic field 3−5787
- monoatomic rarefied gases, study of sound propagation using modified Navier-Stokes eqn. 3−29822
- through moving fluids, interactions 3−5708
- N-waves, spherical and cylindrical 3−36122
- nematic crystals, implications of Parodi's relation 3−17743
- noise in open atm. 3−3025
- noise over open terrain from source near ground 3−3026
- nonlinear in elastic-plastic semi-space, due to moving and variable loading along boundary 3−37829
- ocean surface duct, acoustic transmission 3−37561
- along oilfield streamer cables 3−9740

acoustic wave propagation continued
open ended duct, matched asymptotic expansion methods 3−9752
parameterless intensity contours for unbounded inhomogeneous media 3−3683
perforated tube transmitting harmonic wave, sound radiation through holes 3−31959
phonon radiation from heated NaF crystal face into liquid ^{4}He, meas. of angular distrib. 3−1855
piezoelec. media, energy considerations for acoustic surface wave 3−1871
piezoelectric plate, propag. of transverse electroacoustic waves 3−1870
pipe tone, in continuous flow, excitation of subharmonics 3−39825
planar interfaces, acoustic equivalent networks 3−9763
plasma, multiple soliton production, Korteweg-de Vries equation 3−7529
plasma acoustic and e.m. mode coupling in microwave cavity partially filled with warm plasma 3−20468
plasma ion acoustic radiation generated by pseudowave 3−7518
plasma or matter and antimatter 3−17561
plasma time varying medium, wave power density compression 3−11475
plasmasphere magnetoacoustic channel under dome *(Russian)* 3−3121
polymer, compound vibrator method for determ. of complex deform. characts. 3−28471
polymers, stress relaxation fns. determ. 3−21736
pressure field in fluid layer between two parallel elastic plates 3−5701
pulses radiated in air by creeping waves on rigid spheres and cylinders 3−5726
rectangular reverberation chamber, acoustic power of point dipole source 3−9771
resonance, in two-dimensional cascade 3−25623
rigid duct containing dissipative silencer, attenuation characteristics 3−95
room, linear system approach 3−3697
Rytov's method, extension to large fluctuations case 3−31956
semiconductor, piezoelectric, nonlinear effects in high-intensity surface acoustic wave propag. 3−4913
separate nonplanar monochromatic sources, nonlinear interaction 3−31957
signals of arbitrary waveform, algorithm for propagation prediction 3−9764
solar atmosphere, chromospheric heating and pulse energy meas. 3−16121
solid in magnetic field at low temperature 3−28479
solid liquid compound hydroacoustic lens, low aberrations 3−35324
solid rod into liquid medium, pressure-radiation patterns 3−31954
'soliphons', solitary waves in liquids and crystals *(Russian)* 3−13179
spherical standard sound source, internal impedance *(Japanese)* 3−28481
spherically diverging sound waves, finite amplitude losses rel. to underwater acoustics 3−9765
statistical analysis, from airport noise modelling 3−28426
superluminosity, sound propagation and causality 3−19495
three-dimensional ray tracing, using Hamiltons equations in inhomogeneous anisotropic atmosphere 3−31365
transient radiation from point excited infinite elastic plate 3−5700
transmission loss meas., under-ice and in open water in Baffin Bay 3−76
transonic wave propagation in slender nozzles *(German)* 3−4583
velocity fluctuation effects 3−3688
v.l.f. meas. in South Pacific, project KIWI ONE 3−73
vortex filaments, line, exhausting from two dimens. semi-infinite duct, radiation emission 3−36093
water layers, having linear gradients of sound speed, normal mode propagation 3−37564
in waveguides, with sinusoidal walls 3−35320
weak discontinuity wave in finitely deformed elastic material 3−37828
CdSe layers on Y-Z-LiNbO$_3$ substrate, piezoelec. coupling of Rayleigh acoustic surface waves 3−30761
Cu, cubic, slowness diagrams for resonant wave interactions 3−32391
In superconducting film, transverse acoustic wave generation in electromag. field 3−15305
W-vinyl power composites, specific acoustic impedance 3−19106
Zn, hexagonal, slowness diagrams for resonant wave interactions 3−32391

acoustic wave reflection
see also echo; reverberation
acoustically rigid stationary spheres in ideal compressible liquid, structure of echo signal *(Russian)* 3−35316
bottom reflection for linear sediment layers, ray and wave solutions 3−3708
critical angle of reflection at water-quartz interface, experimental determination 3−4918
critical angle of reflection at water-quartz interface, general definition 3−4917
crystal of class 6v, normal incidence Bleustein-Gulyaev surface waves 3−38706
curved surface, ray acoustic consideration 3−3678
duct waveguide modes by jet-like exhaust flow, determ. in low-frequency limit 3−33244
echo signal from elastic spherical shell in ideal liq., approx. calc. *(Russian)* 3−19110
echo signal struct. from rigid sphere in liquid *(Russian)* 3−19111
fibre-reinforced materials 3−16670
frequency of least reflection rel. to energy redistribution for liquid-solid interface 3−4915
Green's function of right parallelepiped, perfectly reflecting walls, Laplace transforms, boundary conditions and acoustic potential 3−3687
guided sound transmission, through simply supported plate, exact soln. 3−39826
infinite duration pulse trains, determ. of transmission coefficients of architectural panels 3−104
liquid-absorbing solid interface, singular features 3−31961

acoustic wave reflection continued
oceanic thermocline with stepped structure, internal reflection of acoustic waves 3−3711
rough surfaces, sound refl. coeff. determ. by Brillouin scatt. *(Russian)* 3−39151
shockless large amplitude pulses at interfaces, reflection and transmission theory 3−14470
soft parabolic cylinder reflector, two dimensional model 3−37550
under-ice reverberation modelling using multiple regression techniques 3−2844
WKB solutions, extension to any high order of accuracy 3−26189

acoustic wave refraction
see also acoustic dispersion; ultrasonic refraction
atmospheric soundings, refraction by wind and temp. inhomogeneities 3−9273
duct waveguide modes by jet-like exhaust flow, Weiner-Hopf problem 3−33244
shock waves from underwater explosion 3−2960

acoustic wave scattering
see also ultrasonic scattering
acoustic Doppler radar scattering equation, in turbulent atmosphere 3−9272
by aerofoil of finite span, in compressible stream 3−9759
axially backscattered field of prolate spheroid 3−5720
backscattering from finite rigid cylinder 3−5721
capacitive wavestaff for water surface wave measurements, low power circuits 3−2966
by cylinder in a semi-infinite space 3−35314
first order nonlinear scattering of two plane sound waves, case of collinear primary waves 3−5728
fluctuations in turbulent upper ocean 3−3712
h.f. scattering methods, error bounds and domains of validity 3−5719
k-space formulation 3−5723
l.f., for acoustically hard and soft bodies 3−37547
line source in presence of sphere 3−37551
moving rough sphere, frequency spectrum 3−25621
multiple scattering, by periodic line of obstacles 3−31955
oceanic deep scattering layers, volume reverberation signals characterizing using level crossing information 3−3727
from periodic corrugated surface, semiinfinite alternately filled plates 3−37546
phonon bunching in scattering of sound by sound 3−1742
plane wave, by infinite semicylindrical bosses on plane surface 3−35317
for randomly rough surface, numerical image model 3−37549
from rough surface, forward and specular scattering 3−35325
rough surfaces at 100, 200, 500 kHz 3−9767
sea surface, forward scattering, evaluation of Helmholtz integral with model surfaces 3−3685
seawater deep-scattering-layer observations off New Zealand, volume scattering and column strengths 3−3731
by sound, plane wave approximation 3−28413
stationary random sound signal, energy spectra of scattered field, in ocean 3−27994
statistically uneven surfaces, Kirchhoff's method, perturbation method and multiple scattering 3−29023
thermal motion coupling of atoms in crystal from acoustic spectrum of thermal diffuse scatt. 3−11695
thin-film optical waveguides, scattering of light by acoustic waves colinear acousto-optic interaction 3−28416
by time varying obstacles 3−9757
transducer at air-water surface, radiation resistance, effect of spherical scatterers 3−37566
transient acoustic scattering by nonlinear resilient cylindrical scatterers 3−5704
ultrasonic probe for oceanic microstructure studies 3−3252
underwater, from rough surface, acoustic backscattering, at low grazing angles 3−37562
underwater, generalization of Rayleigh's theory *(German)* 3−39836
underwater, surface duct, with rough surface 3−3718
underwater fields, probability models 3−3734
underwater from lake surfaces, covariance functions and mean intensities 3−9776
underwater from lake surfaces 3−9775
upper ocean, study of sound fluctuations using turbulent scaling 3−3713
SF$_6$, spontaneous Brillouin scattering, hypersound speeds 3−5780

acoustic wave transmission
see also ultrasonic transmission
airborne sound insulation between rooms 3−5732
circular plate, transmission of acoustic wave through, internal damping and vibrations *(Japanese)* 3−5694
duct, effects of wall admittance changes, radiation of sound 3−39831
enclosures, radiated power insertion loss, sabine absorption 3−3703
field sound transmission loss measurements, room size effects 3−3702
gas, collisionless, effect of gas-surface interaction 3−4516
guided sound transmission, through simply supported plate, exact soln. 3−39826
loss, plasterboard walls, studs and cavity absorption effects 3−3701
loss characteristics, double panel constructions, interpanel connections, absorption material, mechanical properties 3−3700
ocean, principles involved in choosing explosive source and processing filter for loss obs. 3−3725
in ocean surface duct 3−37561
panel resonance, cavity-backed 3−39833
plate, cavity-backed 3−39834
radiation from two concentric cylindrical shells 3−39829
reverberation room obs., traversing microphone spectra for diffuseness obs. 3−3681
sheared flow problem, 1/N power law boundary layer 3−5707
shockless large amplitude pulses at interfaces, reflection and transmission theory 3−14470
solid in magnetic field at low temperature 3−28479
solid interface, acoustic wave transmission coeff., thermal contact resist. *(French)* 3−38709
sonic boom signals, transmission into rooms through open windows 3−25628
speech transmission laboratory, resume of work *(Japanese)* 3−9747

acoustic wave transmission continued
- Straits of Florida, underwater, fluctuations 3−3715
- submerged finite cylindrical shells 3−5727
- under Arctic ice, environmental factors 3−2962
- under-ice transmission loss rel. to ice roughness and seawater-ice interface 3−2843
- underwater moving media, BIFI range, open channel models 3−3716

acoustic wave velocity
- *see also acoustic dispersion; liquid helium sound propagation; shock waves; ultrasonic velocity*
- deuterised compounds, sound velocity at 20°C with increasing mol. wt. *(German)* 3−11689
- dicalcium strontium propionate, temp. depend. 3−1699
- dichlorodifluoromethane, law of corresponding states 3−11711
- dispersion in solid at low temp. in mag. field 3−28479
- fluctuations, influence on sound level fluctuations 3−3688
- fluorocarbon liquids, rel. to structure Rao and Schaaffs theories 3−1697
- gases, compressed, calc. using virial series 3−26765
- general relativistic formalism for propagation in high-pressure elastic solid 3−37883
- hadronic matter excitation, calc. of sound velocity, H-quantum 3−32642
- kinetic equation for hard sphere correlation functions, transport coefficients, sound velocity calc. 3−26148
- liquefied gas solns., sound speed meas. 3−27072
- liquid chemical systems, adiabatic compressibility expressions for complex sound vel. derivation 3−17892
- liquid metals, new meas. technique using e.m. detection 3−11688
- lithium halides, zero press., rel. to isotherm. calc. 3−27067
- organic liquids, Rayleigh line fine struct., hypersound vel. and absorpt. coeff. determ. 3−23562
- paraffin, liquid, nonlinear dependence of Landau-Platchek relation on temp. from 20°C to boiling point *(Russian)* 3−12138
- perturbations, underwater, internal tides near Eleuthera Island 3−3721
- polyatomic gases, calc. of second virial coefficient from acoustic data *(Russian)* 3−26762
- polymer, deform., internal energy rel. to speed of sound 3−30188
- pure water, sound speed eqn. 3−7855
- PVC, plasticized and antiplasticized, viscoelastic behaviour *(Russian)* 3−20250
- relativistic gas, dissipative, kinetic theory approach 3−33184
- rocks, uniaxially compressed *(Russian)* 3−5439
- seawater, calc. of equation of state 3−2954
- sodium halides, zero press., rel. to isotherm. calc. 3−27067
- solid, rel. to anal. of unsteady waves 3−17933
- sound velocity ratio effect in the theory of thermal conductivity 3−1721
- superluminosity, sound propagation and causality 3−19495
- triethyl amine-water solns., dispersion, initial separation point 3−30212
- water, calc. of equation of state 3−2954
- water and steam, on saturation line 3−31960
- water layers, having linear gradients of sound speed, normal mode propagation 3−37564
- water saturated stainless steel Feltmetal 3−7856
- CO_2, pressure range 1-40 kg/cm², frequency range 450-3470 Hz, temps. to 150C 3−4513
- $CsMnF_3$, antiferromag., magnetoelastic coupling and sound velocity 3−15400
- Cu, liquid, new meas. technique using e.m. detection 3−11688
- in F_2, liquid, meas. at 110 and 130 K, press. to 21 MN/m² 3−27071
- ^3He, liquid below 3mK, collisionless sound propag., vel. and attenuation meas. 3−38694
- O_2, vibrational relaxation times and sound velocities in the pressure range 10-110 atm. 3−20199
- SiO_2 colloidal suspensions, sound velocity 3−34658
- Sn, liquid, new meas. technique using e.m. detection 3−11688

acoustic wave velocity measurement
- *see also ultrasonic velocity measurement*
- gas constant determ. from velocity of sound meas. using acoustic interferometry 3−13215
- pulse superposition technique, for dichlorodifluoromethane 3−11711
- pure water, temperature dependence, anomalies 3−32037
- teaching method using metal rod 3−32016
- inSF_6, hypersound, by spontaneous Brillouin scattering 3−5780

acoustic waves
- *see also acoustic emission; shock waves; ultrasonic waves*
- bibliography on infrasonic waves, supplement 3−13176
- complex sound signals, loudness conversion model *(Russian)* 3−13132
- duct transmission, effects of wall admittance changes 3−39831
- envelope/frequency connection 3−25620
- flexural waves propagating in plates *(Russian)* 3−5711
- gas dynamics, Chaplygin operator and differential operator conjugation *(Russian)* 3−17529
- generation, passage of shock wave through heated turbulent fluid 3−36119
- metal surface, transform. of e.m. energy into sound, kinetic theory 3−27167
- nonharmonic wave excitation in elastic medium by oscillator *(Russian)* 3−31969
- radiation, by spheres undergoing elastic collision 3−39830
- radiation by edge dislocation emerging at crystal surface 3−4912
- radiation pressure, Larmor and adiabatic theorems 3−37906
- ray acoustic intensity calc. 3−9754
- Rijke tube, generation of harmonics by single heating element 3−39840
- subsonic stream under acoustic radiation, instability of vortex sheet 3−7387
- sunspots, running penumbral waves 3−18928
- vibration detection, angular γ-γ correlation *(Russian)* 3−34273
- GaAs, acoustic parametric processes discontinuities due to electron-phonon scattering near the Fermi surface 3−1750
- Ge, energy flow direction of acoustic surface wave 3−8005
- $PbMoO_4$ harmonic generation *(French)* 3−33612
- quartz, energy flow direction of acoustic surface wave 3−8005

acoustical laboratories
- *see also anechoic chambers*
- parameter determ. using combined Fourier and correlation techniques 3−3698
- reverberant room acoustic test facility 3−3695
- small anechoic room, construction and performance 3−28419

acoustics
- *see also acoustic applications; acoustic devices; acoustic equipment; acoustic noise; anechoic chambers; architectural acoustics; atmospheric acoustics; audio acoustics; hearing; musical acoustics; sound reproduction; ultrasonics; underwater sound; vibrations*
- circular pistons in infinite liq. medium, mutual impedance 3−28411
- cochlea, new boundary conditions for Peterson-Bogert model 3−25558
- electroacoustic analogies for acoustic systems described by undirect. wave eqns. 3−22196
- engineering, architectural and underwater, conference, Miami Beach, Fla., USA (1972) 3−3637
- radiation, by stimulated emission 3−35327
- vespa orientalis, acoustical communication 3−35338

acousto-optical devices
- *see also acousto-optical effects*
- Bragg cell for wavelength tuning of a dye laser, angular dispersion 3−22378
- consistency of conventions with those of optics 3−16787
- filter, tuning of dye laser, computer simulation 3−4098
- gas microanalyzers, sensitivity as function of gas pressure, characteristics *(Russian)* 3−6156
- holographic recording Bragg acousto-optic imaging system, noise reduction 3−22366
- laser beam modulator *(Russian)* 3−9963
- laser optical isolator, acousto-optic light deflector 3−32093
- laser raster scanner at TV rate 3−28587
- light beam deflector, eikonal function changes by temp. effect *(German)* 3−28516
- modulator for beam deflection from interior of laser resonator 3−22383
- page composer, Bragg imaging applic. 3−4132
- $CaMoO_4$, for tunable filter appl., Czochralski growth 3−12300
- $PbMoO_4$ light deflector 3−27609
- $PbMoO_4$ standing u.s. Bragg cell, appl. to multiplexing and demultiplexing 3−16408
- TeO_2, paratellurite, light deflector 3−5176
- TeO_2 laser raster scanner at TV rate 3−28588

acousto-optical effects
- *see also acousto-optical devices*
- acoustic radiation field visualisation with photographic device *(Russian)* 3−3766
- acoustic rotatory power of crystal, optical probing 3−28477
- Bragg diffraction for real-time u.s. imaging 3−71
- direct acoustically induced optical harmonic generation coefficient calc. 3−16911
- dye laser, rapid transverse tuning using an acoustooptic technique 3−6478
- interband absorption, in field of intense acoustic flux, theory *(Russian)* 3−27488
- laser, mode locked, cavity dumping, amplitude modulation 3−16886
- laser, single mode, dielectric modulation by acoustic waves 3−4080
- methyl chloride, dispersion of resonant optico-acoustical effect in gas 3−38339
- microwave ultrasonics in solid-state physics, book 3−20819
- piezoelectric semicond., light diffraction by acoustic and electron waves 3−39117
- piezosemiconducting crystals, new mechanism of acousto-optical interaction 3−39116
- Raman-Nath and Bragg diffr. by acoustic waves, expt. for advanced student lab. 3−22222
- steel in water, laser effect on u.s. reflection and transmission 3−22198
- thin-film optical waveguide, Bragg interaction of surface acoustic waves and optical waves, experiments for optimising interaction efficiency and bandwidth 3−28415
- thin-film optical waveguides, scattering of light by acoustic waves colinear acousto-optic interaction 3−28416
- u.s. field mapping by conventinal light diffraction 3−87
- As_2Se_3, vitreous, refractive index determ. 3−37621
- BCl_3, dispersion of resonant optico-acoustical effect in gas 3−38339
- CdS, Mandelstam-Brillouin scatt. obs. of parametric interaction of sound signals 3−36640
- $LiNbO_3$, elastic waves collinear interaction with light waves 3−21384
- NaF, light scatt. by second sound, thermo-optic and elastooptic parameters 3−34323
- $PbGeO_3$ single crystals in PbO-GeO_2 binary system, obs. 3−18549
- $PbMoO_4$, for acoustooptic light deflector 3−27609
- $PbMoO_4$ dispersion of refractive index, measurement, i.r. goniometer, Sellmeier coefficients 3−22317
- $5PbO.3GeO_2$ single crystals in PbO-GeO_2 binary system, obs. 3−18549
- SF_6, dispersion of resonant optico-acoustical effect in gas 3−38339
- TeO_2 dispersion of refractive index, measurement, i.r. goniometer, Sellmeier coefficients 3−22317
- ZnO, wavelength depend. of photoenhancement of nonlinear surface wave convolution 3−38707

acoustoelasticity *see elasticity*

acoustoelectric effects
- amplifying phonon system, Boltzman eqn. for phonon distrib. 3−33628
- automatic electric field measuring equipment 3−35441
- conducting nonpiezoelectric crystal, conditions for shear acoustic surface wave propag. 3−4914
- conductors, rel. to nonlinear Landau damping of u.s. waves 3−24220
- coupled acoustoelectric and thermoelectric instability, theory and expt. *(Russian)* 3−2099
- coupled electoacoustic wave propagation in inhomogeneous compressible magnetoplasma, wave equations 3−7511
- cubic and trigonal crystals, generation of harmonics of transverse elastic waves 3−33962

acoustoelectric effects continued
cylindrical compressible argon gas plasma wave guide, excitation experimental studies of electroacoustic waves 3—23826
domains, rel. to interband absorpt. in field of intense acoustic flux *(Russian)* 3—27488
electroacoustic analogies for acoustic systems described by undirect. wave eqns. 3—22196
fundamentals and applications, surface wave theory *(German)* 3—15227
lattice vibration generation, dynamical X-ray diffr. analysis 3—27088
liquid metal, meas. of acoustic wave velocity using e.m. detection technique 3—11688
metal films, interaction of u.s. surface waves with conduction electrons 3—11793
microwave ultrasonics in solid-state physics, book 3—20819
piezoelec. plate, propag. of transverse electroacoustic waves 3—1870
piezoelectric crystal, influence of piezoresist. 3—5039
piezoelectric semiconductor, degenerately doped, acoustoelec. gain const., calc. 3—18194
piezoelectric semiconductor, transverse wave interact., effective elastic constant theory 3—8230
piezoelectric semiconductors, parametric amplification of u.s. in strong mag. fields 3—21120
piezoelectric/semiconductor layered struct., longit. and transverse effect 3—36641
piezosemiconductor, hexagonal, acoustic wave amplification and generation in elec. field 3—21121
piezosemiconductor, transverse effect and anisotropy of phonon radiation pattern 3—33965
piezosemiconductor materials, 2nd order signal generation resulting from nonlinear interaction 3—33728
piezosemiconductors, acousto-plasmic transformations *(Russian)* 3—20922
plane-parallel plate, refl., transmission and transform. coeffs. of associated waves *(Russian)* 3—30332
semiconductor, acoustic wave attenuation and amplification in strong fields 3—5036
semiconductor. domains, piezoelec. potential and carrier distrib., microwave absorpt. and Brillouin scatt. 3—5040
semiconductor, nonpiezoelec., acoustic wave generation by moving domains *(Russian)* 3—2145
semiconductor, piezoelec., microwave absorpt. by bunched carriers in acoustoelec. domains 3—30896
semiconductor, piezoelectric, hexagonal, phonon generation and acoustoelec. e.m.f. 3—17951
semiconductor, sound amplification, kinetic theory 3—21119
semiconductor, surface mobility meas. using surface waves on adjacent piezoelec. 3—38828
semiconductors, measurement of electron-photon-phonon interactions for hypersonic phonons 3—7871
stimulated phonon-electron-photon scatt. theory 3—1738
u.s. amplification in solids, effects of nonuniform electric field 3—18193
CdS, acoustoelec. gain and lattice attenuation, Brillouin scatt. obs. 3—33961
CdS, acoustoelec. multi-peak domain propag., Brillouin scatt. study 3—24481
CdS, angular dispersion effects in acoustoelectric interaction 3—30522
CdS, Brillouin scatt. by propag. acoustoelec. domains 3—33960
CdS, Brillouin scatt. from acoustoelectrically amplified flux domains, dispersion spectrum 3—34352
CdS, Brillouin scattering, study *(German)* 3—30521
CdS, curent fluctuations under sound amplification conditions *(Russian)* 3—2144
n- CdS, deviations from Ohm's law at 77 K 3—30485
CdS, homogeneous crystals with trapping centres 3—24482
CdS, Mandelstam-Brillouin scatt. obs. of parametric interaction of sound signals 3—36640
CdS, nonlinear interaction of Bleustein-Gulyaev waves 3—8004
CdS, photocond., acoustoelectric aftercurrent obs. 3—2129
CdS, photoconductive, harmonic conversion of acoustoelectrically amplified phonons 3—2141
CdS, photocurrent, saturation and acoustoelectric oscillations *(Russian)* 3—11930
CdS, subharmonic generation of surface and bulk acoustic waves at high pump amplitudes 3—1869
CdS, u.s. absorpt. and velocity, transport theory *(Russian)* 3—1704
CdS coating on $LiNbO_3$ piezoelec. crystal, Rayleigh acoustic surface wave amplification and dispersion, calc. 3—11794
CdS platelet oscillators, current saturation rel. to illum. 3—11936
CdS platelets 3—33727
CdS thermal, acoustoelectrically interacting and built-up phonon studies by laser Brillouin scattering 3—1749
CdS thin films, acoustoresistance, surface-acoustic wave 3—38872
CdSe, photocurrent, saturation and acoustoelectric oscillations *(Russian)* 3—11930
CdSe coating on $LiNbO_3$ piezoelec. crystal, Rayleigh acoustic surface wave amplification and dispersion, calc. 3—11794
CdSe film, cause of current saturation *(German)* 3—15228
CdSe-$LiNbO_3$ monolithic composite structures, surface wave amplification 3—11934
GaAs, acoustoelectric domains, on and off axis, observation by stroboscopic illumination 3—5037
n-GaAs, acoustoelectric gain and lattice attenuation meas. 3—11935
n-GaAs, epitaxial, acoustoelec. instability, transverse mag. field effect 3—18195
GaAs, epitaxial films, domain investigation 3—24483
n-InSb, acoustic gain optimum freq. depend. on carrier density 3—8231
InSb, degenerate, u.s. attenuation, mag. field influence *(French)* 3—5041
n-InSb, highly doped, u.s. propag., longitudinal mag. field effects 3—38626
n-InSb, lattice absorpt. of sound, 77K, freq. depend. 0.5-3.0 GHz 3—33963
n-InSb, round-trip amplification of u.s. waves, under transverse mag. field 3—5038
InSb coating on $LiNbO_3$ piezoelec. crystal, Rayleigh acoustic surface wave amplification and dispersion, calc. 3—11794

acoustoelectric effects continued
InSb u.s. wave amplification in Hall and Corbino configs., 77K, 1 GHz *(French)* 3—21118
$LiIO_3$, u.s. absorpt., temp. depend. 3—33964
$LiNbO_3$/Si layered struct., longit. and transverse effect 3—36641
p-Si, in piezodielectric-semicond. layered struct., alternating e.m.f. on illumination *(Russian)* 3—2142
Te, acoustoelec. non-ohmic conduction, carrier conc. depend. 3—33959
Te, electron domain propag., interaction between holes and phonons 3—18156
Te, enhancement of capture rate of excess carriers due to acoustoelec. amplification 3—2143
ZnO, angular dispersion effects in acoustoelectric interaction 3—30522
ZnO films, inclined texture axis, rel. to use as u.s. transducers 3—33757

acoustooptics *see acousto-optical effects*

actinide alloys
see also actinide compounds
actinide-Pt metal-C systems, occurrence of ordered phases of Cu_3Au struct. type 3—2710
alloy chemistry 3—2709
Am alloys, Laves phases 3—4731
$Gd_xTh_{1-x}PdIn$, mag. props., 4.2-300 K, evidence for RKKY-type interaction 3—27364
La-Pu alloy, mag. susceptibility, obs. of mag. decoupling at Pu 3—2255
Mg-Th and Mg-Th-Zr systems, precip. sequences 3—21583
Np alloys, Laves phases 3—4731
Pr-Tb alloy, exchange field at Pr ion rel. to comp. 3—2267
$PrNi_5$, heat capacity 1.7-300K, Schottky type thermal anomalies 3—2280
Pu-Cr-N system, phase behaviour 3—1776
Pu-Ga, plastic deformation, mechanical props. influence of homogeneity *(French)* 3—34589
Pu-Ga (1 wt.%) cold rolled, annealing 3—12384
β-Pu-Np alloy, elec. resist., $T<4.2K$, self irrad. damage effects 3—2050
Pu-U alloy, supercond. transition temp. rel. to press. 3—2214
Pu_3Pd_4, cryst. struct., X-ray determ. 3—26989
Sc-Pu alloy, mag. susceptibility, obs. of mag. decoupling at Pu 3—2255
Th-C, nitride layer growth, 1400-2400°C 3—8770
Th-Ce, dil., thermopower, 2-300 K, impurity scatt., contrib. 3—30459
Th-Cu system, intermediate phase formation in liq. Na, struct., 200-700°C 3—2690
Th-Fe, Curie temp. pressure depend. 3—36720
Th-Ni intermetallic, struct., disordered substitutions 3—1603
Th-Y(La) alloys, sp. ht. and superconductivity 3—21168
$ThCu_{3.6}$, crystal structure obs., comparison with $GdAg_{3.6}$ structure 3—17763
Th_2Ni_{17}, cryst. struct. 3—17760
$ThSi_2$-Am(1 at.%) oscillating behaviour of supercond. transition 3—30564
U-7.5 wt pct Nb-2.5 wt pct Zr, low strain tensile behaviour 3—18649
U-Ga phase diagrams, magnetic properties 3—33654
γ-U-Mo solid solns., excess thermodynamic props. 3—32947
U-Ni-N ternary system, phase relationships 3—12332
U-Pu alloy, supercond. transition temp. rel. to press. 3—2214
U-Rh-C system, phase equilib. and thermodynamic props. *(German)* 3—12333
UFe_2-UAl_2 alloy, chem. ordering, electronic struct., ^{57}Fe Mossbauer obs. 3—1987
UFe_2-UGa_2 alloy, chem. ordering, electronic struct., ^{57}Fe Mossbauer obs. 3—1987
Y-Np alloy, mag. susceptibility, obs. of mag. decoupling at Np 3—2255

actinide compounds
see also compounds of individual actinides, e.g. uranium compounds
see also actinide alloys
actinide complexes, π sandwich type, struct. 3—14338
magnetic compounds, spin-lattice relax. 3—2397
monochalcogenides, band struct. calcs. 3—2006
monopictides, band struct. calcs. 3—2006
NaCl-type, hyperfine fields, crystal field and relativistic effects, angular wave function 3—2233

actinide metal compounds *see actinide compounds*

actinide metals *see actinides*

actinides
see also individual actinides, e.g. uranium
electronic struct. 3—1988
hybridized 6d-5f virtual bound states theory model 3—1986
magnetic hyperfine fields, relativistic effects 3—2228
magnetic props., review 3—2259
rare earths and actinides, conference, Durham, England, July (1971) 3—2223
transport props., comparison across series 3—2049

actinium
No entries

actinium compounds
No entries

actinometry *see photometry*

activation analysis *see chemical analysis by nuclear reactions and scattering*

active circuits *see active networks*

active filters
autodyne n.m.r. signal pickup with controllable high selectivity 3—19242

active networks
see also active filters
voltage waves, current waves and power waves concept 3—5745

active nitrogen *see nitrogen*

active oxygen *see oxygen*

active thin film circuits *see thin film circuits*

actuators
  see also electric actuators
  fluid for control and safety of pressure tube reactors 3—26494
adaptive control
  see also adaptive systems
  Mossbauer spectrometer, electronic block for controlling moving system 3—28700
adaptive systems
  see also adaptive control; learning systems; pattern recognition
  optical tracking telescope, combined open/closed loop and adaptive compensation 3—39760
  seismic data autocorrelation functions, adaptive estimation 3—5535
adders
  introduction of signal voltages, to potentiostats and galvanostats, use with function generator 3—6151
adherence *see adhesion*
adhesion
  n-alkane cryst. growth on graphite and C fibre surfaces 3—20703
  atactic polystyrene, solvent nature influence 3—27774
  biological cell membrane, physical forces for adhesion 3—9640
  butadiene/styrene radial teleblock copolymers, structural effects on adhesive props. 3—5354
  contact mechanism, review 3—27775
  continuum mechanics rel. to adhesive fracture 3—7840
  debonding at interface flow of elastic solids under transient wave influence 3—13589
  dispersed materials, unit for det. mutual adhesion *(Russian)* 3—12462
  Dow Corning dimethyl silicone adhesives, for solar cells, effect of u.v. and charged particle irradiation 3—5924
  elastomer, theories, review 3—14926
  epoxy adhesive, glass transition temp. relation to adhesive strength 3—5353
  epoxy adhesive, mech. props. at low temp. *(Japanese)* 3—12446
  fibre reinforced plastic bonded struct., strength *(Japanese)* 3—18712
  film, scratch test apparatus *(Japanese)* 3—20959
  heating surfaces, fully developed nucleate boiling, heat transfer, microgeometry 3—1787
  hot adhesive joining of heterogeneous materials, device for stress determ. *(Russian)* 3—12482
  mechanical testing, between glass fibres and resins *(German)* 3—21730
  metallic thin film, on insulating substrates, electrostatic contribution 3—8070
  metals, contact areas, intermetallic diffusion obs. 3—4800
  metals to ceramics, solid-state bonding, mechanism 3—8966
  metals to glasses, solid-state bonding, mechanism 3—8966
  microgeometry, heating surfaces, adhesion, fully developed nucleate boiling, heat transfer 3—1787
  osseous attachment of non-porous metals by composite bonding 3—2794
  plasticity, perfect, decohesion phenomenon 3—13583
  plasticity effects in adhesive fracture 3—3973
  polyethylene composites, filler surface state effect on props. 3—27759
  polymer compositions based on silicone adhesives, antifriction and mech. props. 3—25012
  polymer substrates, principles of bonding 3—12456
  polymer/filler glass sphere resin composite, hydrolytic stability, thermomechanical props. *(Russian)* 3—31152
  polymers, device for adhesion strength determ. by tangential shear method 3—18762
  printing ink, adhesion to steel and tin plate, effect of film formation 3—39405
  shock wave application *(Polish)* 3—24217
  stability of axially symmetrically loaded shallow closed conical shell, nonlin. problem *(Russian)* 3—28885
  steel ball, normal adhesion mechanism, contact zones, with Pb and In 3—4798
  testing, u.s. pulse-echo technique, 'slackness' and weak bonds 3—35365
  thin films, on glass substrates, meas. by direct pull method *(Russian)* 3—31238
  Ag film, scratch test apparatus obs. *(Japanese)* 3—20959
  Al_2O_3, sapphire whiskers, Ni coated, stability 3—30377
  Au powder particle adhesion, charge contribution 3—5049
  Cu film, scratch test apparatus obs. *(Japanese)* 3—20959
  MgF_2 film, scratch test apparatus obs. *(Japanese)* 3—20959
  Ta, sputtered film, 6-20 μ, on stainless steel, prep., mech. props. and corrosion resist. 3—27677
adiabatic compression, plasma *see plasma heating*
adiabatic demagnetisation *see demagnetisation*
adion *see adsorption*
administrative data processing
  power reactor Cs-134/137 mixtures, program for feasibility and prospects for private separation and marketing 3—19996
admittance
  SiO_2-Si m.o.s. structures, weakly inverted frequency dependence 3—8269
ADP *see administrative data processing*
ADP (ammonium dihydrogen phosphate) *see ammonium compounds*
adsorbed layers
  active sites in periodic adlayers, heterogeneous catalysis at line defects 3—9095
  adatom conc. profiler, Auger plasmon satellite intensities vs. depth 3—30904
  alkali metal overlayers on W(100), quantitative AES and LEED study 3—38704
  atoms, on metal, interaction with cond. electrons, rel. to transverse magnetoresist. 3—15186
  bubble shape theory applied to air transfer through adsorbed films 3—8015
  cationic cyanine dyes molecules on glass, ionisation energies 3—27901
  copper phthalocyanine pigments, α and β forms, adsorption props., optical props., effect of heating 3—38713

adsorbed layers continued
  dipolar molecules on metals, semiconductors or insulators, surface diffusion 3—27183
  dispersion interaction of two atoms on plane continuum dielec. substrate 3—24337
  ethane, condensed, behaviour as fn. of H coverage, cryopumping 3—8022
  on f.c.c. crystal, vib. props. 3—24340
  gas on solid, structure from LEED and Auger emission spectroscopy 3—24341
  gases, with elec. dipole moment, spontaneous polarization during condensation 3—20942
  graphite, plane wave method for study of He atom adsorption *(Italian)* 3—30531
  heterogenous, at line defects, simple boundary-controlled reactions anal. 3—9096
  hydrocarbons and haloganted cpds. adsorbed on silica gel, positron annihilation and hot reactions 3—27915
  indirect interaction between adatoms on tight binding solid, calc. 3—36481
  liquid, dynamic nucl. polarization by solid effect and thermal mixing 3—2427
  localised surface phonons due to adsorbed atoms monolayers, resonant states 3—33729
  metal aggregates on C substrate, catalytic props. 3—37142
  metal films, ultra thin, pseudomorphism, nucleation 3—30374
  methane on activated charcoal, mobile adsorption obs. by cold neutron scattering 3—27178
  nitrided surface layer on W, formation by ion bombardment 3—4922
  organic dyes on ZnO powder, mechanism for photoconduction sensitisation 3—11929
  phase transitions, liquid-solid type 3—36474
  polyarylate F-1, adsorption on macroporous silica gel, chromatographic adsorbents 3—38714
  solvation sheaths, on colloid particles, van der Waals attraction between particles 3—39413
  solvation sheaths, on colloid particles, Van der Waals attraction between particles 3—39414
  starch, n.m.r. of binding of adsorbed H_2O 3—30354
  water, rot. correl. motion from i.r. spectral study 3—17730
  water on AgI, ice structure, i.r. studies 3—39468
  water vapour flow through parallel plate channels, surface flow of multilayer adsorbed films 3—29924
  Ag, adsorption complexes formed from N_2O and O_2 3—8020
  Ag on Cu, Fick's eqn., soln. *(French)* 3—11804
  Ar, condensed, behaviour as fn. of H coverage, cryopumping 3—8022
  Ar on exfoliated graphite, adsorption isotherms 3—36480
  Ba films on W and Mo, (011) face, structure, work function, heat of adsorption 3—8018
  Ba on W, conduction electron interaction obs. by static skin effect method 3—20937
  C, contaminant on W, effect on secondary emission characts. *(Russian)* 3—8693
  CO, on (110) Ni surfaces, interaction 3—38716
  CO, on H-Y zeolite, ioniz., CO^+ radical studies 3—21809
  CO, on Ni(110) surface, decomp. 3—30346
  CO, on W(100) photoemission energy distrib. curves 3—39213
  CO, spontaneous polarization during condensation 3—20942
  CO_2, detection using attenuated total reflection 3—25714
  CO_2 condensed, behaviour as fn. of H coverage, cryopumping 3—8022
  C on clean and S, Na, Cs or O_2-covered f.c.c. Ni, vib. properties 3—24340
  Cs, on Si single crystal surface, heat of evaporation and ionization coeff. of atoms and ions 3—15069
  Cu, chemisorpt. of Bi on (100) surface LEED obs. of layer struct. 3—30355
  Cu, chemisorption of Bi on (111), LEED obs. of layer struct. 3—30356
  Cu on W, conduction electron interaction obs. by static skin effect method 3—20937
  D_2O motions at soap-water interface, deuteron relax. obs. 3—27173
  Ge monolayers, mobile limit, low-temp. sp. ht. 3—33682
  H atoms on W(100), through-bond interaction calcs. 3—30343
  H_2, on Ni thin film, elastic scattering of conduction electrons 3—27301
  H_2 on Ti film, surface potential 3—33984
  H_2O on MgO powder, effect on lattice parameter and strain 3—33509
  He films near monolayer densities, structure 3—20910
  He on graphite, calc. of ground state energy for superlattice states 3—38723
  ^3He, on zeolite, n.m.r., spin-lattice and spin-spin relax. obs. 3—30344
  ^3He degenerate films, pulsed nucl. reson. obs. of susceptibility and mag. interaction 3—4901
  ^4He film on graphite, melting anomalies rel. to short range order 3—36458
  ^4He on exfoliated graphite, adsorption isotherms 3—36480
  Hg on Au, surface sensitivity of ESCA for sub-monolayer quantities 3—24334
  K, on Si single crystal surface, heat of evaporation and ionization coeff. of atoms and ions 3—15069
  N_2, on W, λ-state 3—8019
  N_2 on exfoliated graphite, adsorption isotherms 3—36480
  NH_3 condensed, behaviour as fn. of H coverage, cryopumping 3—8022
  NO, preadsorbed on graphite, effect on gas adsorption 3—38720
  Na, on Si single crystal surface, heat of evaporation and ionization coeff. of atoms and ions 3—15069
  Ni(100) surface, influence of H_2, CO and O_2 adsorption on electron energy loss spectra *(German)* 3—36653
  O, on Fe, correl. of proton-excited X-ray and Auger spectroscopy anal. 3—1879
  O, on W(100) photoemission energy distrib. curves 3—39213
  O_2 adsorbed, paramagnetic relaxation of H and D atoms on silica gel 3—37144
  O_2 on metal oxides, rel. to electron trapping 3—30929
  O_2^- paramag. centres on TiO_2 and SnO_2, metastability 3—21811

adsorbed layers continued
  $^{17}O_2^-$ paramag. centres on MgO and ZnO, nonequivalency of oxygen nuclei 3−21810
  S on Pt, obs. by LEED and Auger spectroscopy *(French)* 3−36483
  W(100), of Ag, obs. of two phases 3−36482
  Xe, on Cu and Ag at 77K, struct., LEED obs. 3−30345

adsorption
  see also heat of adsorption
  adatom interacting pair, phonon contrib. to free energy 3−38724
  adsubble processes, foam and bubble fractionation 3−12464
  alkali halide cleavage plane, of Au, adatom diffusion and cluster migration 3−1888
  aqueous inorganic salt solution surfaces, negative adsorption of salts 3−12555
  aromatic amines, by metallic supports in gas-liquid chromatography 3−22542
  atom-surface interactions 3−5417
  BET method for measurement of specific surface *(French)* 3−15795
  blood coagulation factor, electrochem. behaviour, obs. on fibrinogen 3−39764
  blood coagulation factor, electrochem. behaviour, obs. on prothrombin and thrombin 3−39763
  chlorinated Cu phthalocyanine film, orientational adsorption rel. to epitaxial growth 3−15086
  crystal dissolution morphology, computer simulation 3−4847
  diatomic, on one-dimensional lattice spaces, Langmuir type isotherm 3−4923
  diffusion theory adsorption and desorption rate constants with experimental lifetimes, comparison 3−33736
  dispersion interaction of two atoms on plane continuum dielec. substrate 3−24337
  Dubinin Polanyi eqns. for predicting adsorption space at equilib. 3−33735
  E-glass, of water vapour, thermodynamic nature of adsorbate adsorbent interface 3−8016
  electric double-layer force between unlike spheres, calc. 3−31200
  electrochemical electrode processes and adsorption study, special techniques, review 3−12533
  electrode-solution interface, elec. double layer, ion and neutral mol. adsorption, review 3−3127[illegible]
  electron interaction obs. by static skin effect method 3−20937
  field emission current fluctuation rel. to adsorpt. on surface 3−15597
  field emission/field ion microscopy, review 3−27159
  fluid, application of eqns. for statistical mechanical distrib. functions of molecular fluid-solid interactions 3−4024
  fluidised beds matter transfer, theoretical soln. of penetration curve *(French)* 3−7463
  fourth order interaction, nature 3−18020
  gas atoms at solid surface, diffusion theory 3−24336
  gas mixtures, surface potential theory of multilayer adsorption 3−33733
  gas-solid energies and props. of isolated adsorbed atoms 3−36484
  Gibbs, effect of oscillatory influence of Gibbs adsorption 3−11435
  glass, cationic cyanine dye molecules, ionisation energies 3−27901
  glass surface properties, review 3−25017
  graphite, of Ar and Xe, surface microstruct. 3−38712
  graphite, of benzol and CCl_4, effects on friction *(Russian)* 3−11682
  graphite, of NO, isotherms, 77.5 and 90.2 K 3−38720
  graphite, with preadsorbed NO, of N_2, Ar, CO, Kr and O_2, isotherms, 77.5 K 3−38720
  interface between solid and soln., high-precision meas. apparatus 3−32029
  ionic double layer study and adsorption phenomena at electrodes 3−12530
  isotherm meas., fully automatic apparatus *(German)* 3−16531
  jets, vibrating, adsorption and diffusion limited surface aging 3−29923
  liquid crystal, lyotropic, deuteron relax. obs. of D_2O motions at soap-water interface 3−27173
  low energy gas-solid, resume of theory *(French)* 3−15065
  macromolecular adsorption kinetics 3−36486
  many body interactions 3−36479
  metal, adsorption effect in drawing with organic lubricants, oxide film form. 3−33604
  metal, smooth, study by radiochem. method 3−21838
  metal film, replacement of chemisorbed gases, elec. cond. and mass spectrometry obs. *(Japanese)* 3−20928
  metal thin films, of vapour and gas, effect on resist. 3−15276
  metal/electrolyte interface, of hydrogen *(French)* 3−2820
  minerals, of N or Ar by BET method *(French)* 3−15065
  mist droplets, passivation of condensation growth, cetyl alcohol vapour adsorption 3−39399
  mixed beds, properties of isotherms *(French)* 3−27180
  model protein compound, poly-L-alanine of water 3−1884
  monomer-dimer mixtures, boundary effects evaluation for simple cubic lattice by lattice constants method 3−38711
  multilayer, on heterogeneous surfaces 3−11802
  in packed bed, three simultaneous resistances *(French)* 3−4624
  partially mobile, of gases on homogeneous solid surfaces, statistical mechanics 3−30342
  patchwise heterogeneous surfaces, relative energy distrib., function calc. 3−33734
  photographic image form. with gas adsorption at semicond.-active gas interface 3−15841
  physical, semiconducting surfaces 3−1881
  polymer chain, on surface, lattice model 3−29779
  polymer solutions, adsorbed entangled layer in drag reduction 3−29864
  porous glass, of water vapour, hygroscopicity and no dimming phenomena *(Japanese)* 3−20935
  porous solids, heats of immersion 3−31209
  positronium atoms, adsorbed state on pore surface 3−38726
  powder surfaces, of ^{85}Kr, differential standard entropies and isotherm shape *(French)* 3−27175
  Pyrex, of Ar, anomalous Dubinin-Radushkevich plots 3−27177
  quantum chemical treatment of adsorbed species, on electrochemical electrodes, review 3−25102

adsorption continued
  silica, of water, effect of surface nature, temp. and coverage on spin-spin relaxation 3−38727
  spherical adsorbent grains, internal kinetics for nonlinear isotherms *(Russian)* 3−8012
  spread on surface, in zero gravity *(Russian)* 3−11799
  steel, activated adsorption of hydrogen, effect of mech. strength *(French)* 3−8905
  stress corrosion, adsorption-electrochemical hypothesis *(Russian)* 3−27670
  surface area and porosity of electrochemical electrodes meas., adsorption methods, review 3−12532
  surface texture, Auger electron spectroscopy, slow electron diffraction, field ion microscopy 3−1864
  surface-vacuum interface, conference, Enschede, Netherlands, June (1972) 3−30316
  tobermorite, synthetic, pore struct., adsorpt. study 3−39421
  transient molecular flow, influence of adsorption time *(German)* 3−26824
  water condensates, cryotrapping of air, N_2, O_2, Ar, press. depend. 3−15071
  Zircaloy-2, in methanol-I_2 solutions, stress-corrosion cracking, dissolution activation energy due to I_2 adsorption 3−24886
  Ag, on W(100) surface, epitaxial growth 3−1887
  Ag, sticking coeff. on liq. substrate 3−4924
  Ag film, detection of N atoms by resistivity changes 3−4925
  Ag tip, clean and contaminated, field emission study of impurity adsorption 3−30927
  Ag-Pd alloys, CO adsorption energy and ordered structure form. 3−1885
  AgI surface, water adsorption and ice nucleation 3−24335
  Ag(111), of I, site determ. by l.e.e.d. 3−11803
  Al powder, of hydrogen and moisture 3−1889
  γ-Al_2O_3 powder, of hydrogen and moisture 3−1889
  ^{241}Am source, preparation by surface adsorption on backings 3−285
  Au, of H_2O and Hg change in work function measurements by retarding potential method 3−38725
  Au on Ge field emitters, metal-semiconductor boundary growth 3−15251
  AuHg alloy, of H_2O and Hg change in work function measurements by retarding potential method 3−38725
  Au(111), (100), (110), faces, LEED and Auger obs. of S adsorption *(French)* 3−20940
  BPO_4, adsorption isotherm meas. for A gas 3−8014
  BeO, exoelectron emission, effect of O adsorption centres 3−24776
  Bi thin films, gravimetric investigation of growth kinetics 3−36269
  BiI_3, O_2 adsorption effect on trapping and recombination processes 3−27271
  CO on Ni films, desorption spectra, elec. resist. obs., adsorption states *(German)* 3−27184
  Cu, negative secondary ionic emission, adsorpt. and oxidation effects 3−30913
  Cu, of SF_6, stepwise adsorption isotherms, application to study of surface phases *(French)* 3−27176
  Cu alloys, adsorption-induced loss of strength during selective transfer in boundary friction 3−21706
  Cu film, of CO, effect on elec. conductivity 3−8144
  Fe, inhibiting action on hydrogen adsorption in sulphuric acid solns. *(French)* 3−1911
  GaAs, of Cs on (110) surface, 77-450 K 3−20941
  Ge, adsorbed C(N)(O)(P)(S)(Cl), Auger electron yield 3−2611
  p-Ge, autoemission volt ampere characts. with O_2 adsorption rel. to elec. breakdown 3−8709
  Ge, in gas media *(Russian)* 3−24338
  Ge, of Au, disperse struct. growth *(Russian)* 3−20943
  Ge, of Cd, initial stages of film deposition 3−18036
  Ge, of H and D cooperative, (111) faces, pulsed time of flight mass spectrometry, exchange reactions, kinetics 3−36485
  Ge, reflectivity spectra, 1.8-3.0 eV, Al absorpt. effects 3−39162
  Ge (100), of O_2 and H_2 *(Russian)* 3−15068
  Ge (110) surface, adsorption and nucleation of Zn 3−11806
  H on condensed gases, cryopumping 3−9917
  H_2 isoteric adsorption enthalpy of Pd and Pt atomically disposed thin film on C substrate *(German)* 3−27921
  He II film, accommodation coeff., 1.15-4K, on surface of levitated Nb superconducting sphere 3−27155
  He-Ne mixture, field adsorption and field ion microscopy 3−22514
  ^3He-^4He mixtures, dilute, superfluid film form., surface separation 3−4902
  KCl, condensation coeff. rel. to sub- and supersaturation, mol. beam method obs. 325-425°C *(German)* 3−1792
  KCl, relax. effects of (100) face during condensation *(German)* 3−1793
  Mo, of CO on (100) surface 3−30348
  N_2 adsorption measurements for the determination of pore size 3−37097
  Ni, of H on (100) surface, flash desorpt. obs. 3−30349
  Ni, of O_2, ESCA obs. 3−8017
  Ni, of T on (111) surface, superficial migration coeff. 3−30351
  Ni, polycryst., of CO, sticking probability and desorption spectrum obs. *(Japanese)* 3−20931
  Ni evaporated film, N_2 adsorption 3−38715
  Ni film, of N_2 and CO, effect on elec. conductivity 3−8144
  Ni polycrystalline surfaces, H_2 adsorption states at different temps. 3−11801
  Ni thin film, elastic scattering of conduction electrons by adsorbed H_2 3−27301
  Ni(100), of CO, orbital energy spectra 3−39206
  Ni(100), of Hg, orbital energy spectra 3−39206
  P_2 on Si(111) surface, adsorption kinetics, LEED and AES obs. 3−1883
  ^{233}Pa on Vycor glass, separation from $Th(NO_3)_4$ soln. *(German, English)* 3−6995
  Pd film, of CO, electrical resistance obs. *(Japanese)* 3−20929
  Pt, field emission tip, crystal face specificity for N_2 adsorption 3−24342
  Pt, of H_2, crystal field surface orbital−bond energy bond order model 3−4926
  Pt (100) crystal face, scattering of diatomic and polyatomic molecules 3−8001

adsorption continued
Pt film, of CO, electrical resistance obs. *(Japanese)* 3—20929
Pt(111) surface, adsorption and decomposition of CO 3—38722
PuO$_2$, of water vapour, isotherms, 30, 50 and 85°C 3—38719
Ru, of CO 3—20936
Si, adsorbed C(N)(O)(P)(S)(Cl), Auger electron yield 3—2611
Si, of Cs and O, rel. to surface negative electron affinity 3—30536
Si, of H and D cooperative, (111) faces, pulsed time of flight mass spectrometry, exchange reactions, kinetics 3—36485
Si, of O$_2$, electron beam-adsorbate interactions 3—30317
Si, surfaces, H and H$_2$O adsorption, desorption spectrometric results 3—11805
Si surface, electron beam-adsorbate interactions 3—20939
Si:Li, and segregation of dissolved Li to surface, photoemission meas. 3—24297
Si/Cs/O, negative electron affinity, struct. and electronic models 3—24339
SiO$_2$, of NO, isotherms, 77.5 and 90.2 K 3—38720
SiO$_2$/electrolyte interface, mobile ion transfer from contaminating aqueous solutions 3—39241
SnO$_2$, e.p.r. of adsorbed O$_2^-$ ions, lineshape analysis *(French)* 3—8423
SnO$_2$, of oxygen, e.p.r. centre form. *(French)* 3—8013
Ta, of O$_2$, thermodesorption effects *(Russian)* 3—15070
Ti, of Cl, segregation of Cl and S impurities from bulk 3—1882
Ti and alloys, of hydrogen during corrosion and cathodic polarization 3—1910
Ti film, of CO, electrical resistance obs. *(Japanese)* 3—20929
Ti film, of CO$_2$, binding state detn., mass spectrometry and elec. resistivity obs. *(Japanese)* 3—20930
TiO$_2$, e.p.r. of adsorbed O$_2^-$ ions, lineshape analysis *(French)* 3—8423
TiO$_2$, of oxygen, e.p.r. centre form. *(French)* 3—8013
TiO$_2$ anatase surfaces, model, interpretation of some interface processes 3—5414
^{235m}U isomeric nucleus, as probe for surface adsorption and desorption studies 3—28714
W, adsorbed O$_2$, kinetics and electron stimulated desorption 3—1886
W, coadsorption of CO and O, consecutive interactions 3—30347
W, hot filament, interaction with O$_2$, isotopic mixing obs. *(Japanese)* 3—20932
W, of CO, and reduction by hydrogen, field emission microscope obs. *(Japanese)* 3—20934
W, of K, field emission flicker noise, spectral density functions 3—15598
W, of N$_2$, and desorption, λ-state of N$_2$ 3—8019
W, of O, effect on work function, meas. using diode in space charge region *(French)* 3—36648
W, surface diffusion and clustering, interpretation of ion microscopy data 3—36475
W, surface diffusion and clustering, interpretation of field ion microscopy data 3—36476
W, surface diffusion of Sb, adsorpt. of Cs, work function changes 3—15067
W, trapping of K, 0.5-8 eV, 1100-1300 K 3—30350
W surface, nitrided layer formation by ion bombardment 3—4922
W surface, of CO, field emission microscope obs. *(Japanese)* 3—20933
W tips, displacements of individual adatoms by elec. field *(French)* 3—24343
W(100), adsorbed CO, photoemission energy distrib. curves 3—39213
W(100), interaction between two adsorbed H atoms 3—30343
W(100) surface, O$_2$ and C_s adsorption and co-adsorption, effect on work function *(French)* 3—27300
W(110), adsorbed O, photoemission energy distrib. curves 3—39213
W(112), of Li, contact pot. difference and LEED meas. 3—20938
ZnO, of NO molecule, reduction, doping depend., i.r. adsorption obs. *(German)* 3—39463
aerials *see antennas*
aerodromes *see airports*
aerodynamics
see also flow of gases; jets; shock waves; supersonic flow; turbulence; wind tunnels
aeroelastic optimisation os semi-infinite flat panel 3—11422
aircraft trailing vortices, growth of finite amplitude waves 3—7359
airfoils, press. distrib. prediction for inviscid. pot. and real fluid flow 3—7386
axisymmetric annular profile, potential flow calc. *(German)* 3—33246
axisymmetric flow, with heat addition to simulate base burning 3—33245
blunt conical nosetip, turbulent and transitional heat transfer rates 3—11416
caret wings with attached bow shock, first order perturbation flow determ. 3—7381
Chaplygin operator and differential operator conjugation *(Russian)* 3—17529
circular aerofoils with asymptotic critical Mach number, numerical results in relation to transonic similarity rule 3—17533
circular cones with variable incidence, transonic flow obs. *(Italian)* 3—33240
clamped rectangular plates in uniform subsonic flow, stability 3—38376
combustible jets, turbulent diffusion flame, aerodynamic and thermodynamic analysis 3—23799
drag, minimum total drag bodies, determ. using Newton-Busemann pressure coeff. law 3—11419
drag, updraft shape effects in convective storms 3—28022
dynamic wind-tunnel testing, aerodynamic support interference 3—6163
dynamical behaviour of T section determ. of whether vibrations occur under aerodynamic action of wind 3—16678
elliptically nosed cylinders, surface pressure meas. and schlieren photographs 3—7382
entropy layers in supersonic flow, numerical calc. 3—33242
explosions gasdynamics, detonation, shock-wave, blast-wave studies, review 3—33253
flat plate boundary layer, transitional flow characteristic, model *(Italian)* 3—36105

aerodynamics continued
flow-resistance gas heater 3—19173
flows in planar nozzles, expt. study 3—1335
fluidic amplifier, wall attachment type, flow pattern and switching mechanism 3—20348
forces, unsteady, in subsonic flow, resonance method meas. 3—23749
freq. response of a two-dimensional rigid airfoil *(German)* 3—6295
gravitational ideal incompressible fluid about fine profile limited to free line *(French)* 3—29830
gravitational ideal incompressible fluid about fine profile limited to free line *(French)* 3—29831
high subsonic flow, parabolic substitution in Euler eqns. 3—23751
homogeneous isotropic turbulence, turbulent transfer coeff., expt. determ. 3—26795
hypersonic nonlinear aerodynamic loading effect on panel flutter 3—33239
induced drag on rolling wing 3—4584
jet flow rel. to noise, direct correlation 3—7355
jet of radiating gas, optically thin, analysis by quasi-one-dimensional flow method, radiative effects 3—23811
jet-flapped airfoil problem, two-dimensional, numerical solution 3—11378
of jets discharged into fluidized beds 3—4627
Kelvin-Helmholtz wave growth on thin liquid sheets 3—29892
lateral vibrations of cylinders in wind, influence of antennae 3—23742
Laval nozzles in shock tube, aerodynamic characteristics 3—7394
mass and stiffness matrices, automated generation and condensation for finite element analysis *(German)* 3—19411
mixing chamber for opposing isothermal annular flows, construction and operation *(Russian)* 3—23750
molecular gas dynamics, boundary conditions, surface shocks, continuum flows, review 3—33261
near field acoustic environment, VTOL jets 3—3651
noise abatement, upper surface blowing lift augmentation system 3—3649
noise generation, unified theory 3—17521
noise reduction, jet interaction with lift augmenting flaps 3—3648
non-conical delta wings, flow over, applic. of shock expansion theory 3—11418
numerical methods for soln. of gas dynamic problems 3—1416
oscillating airfoils in low supersonic flow, wind tunnel interference 3—38383
out-of-plane force on circular cylinder from cross flow model 3—26816
plain intake as flow meas. device in pipelines 3—22576
over plate, noise abatement, flow of fluid over plate, STOL aircraft 3—3650
potential flow about rotation-symmetric fuselages, air intakes and propellor inlets, calc. *(German)* 3—23753
pressure distribution meas. at surface of aerodynamic body using special interrogator 3—32270
pressure on flat and anhedral delta wings with attached shock waves 3—7380
rocket payload design for D-region sampling, Monte Carlo simulation 3—12859
rolling up characteristics of trailing vortex sheet in transport aircraft 3—26817
rotating blades in forward flight, boundary layer separation 3—38373
rotor wakes, three dimensional anal. using a constant temp. hot wire anemometer 3—7313
satellites, artificial, factors theoretical analysis, spatial impulsive interaction model, results *(Italian)* 3—20342
secondary flows, turbomachinery aerodynamics, review 3—33221
shear flow with const. vortex, of heavy fluid around thin profile *(French)* 3—20343
shock waves, real gas equilibrium state calc. 3—7392
shock waves diffracted by sphere or cylinder, subsonic, transonic or supersonic flow *(Russian)* 3—14469
space vehicle bodies, in Mach number range Ma$_\infty$=3 to 10 *(German)* 3—38386
stability of rectangular plates in supersonic air flow, calc. using modified finite element method *(Russian)* 3—11425
stagnation point heat transfer, first Damkohler similarity parameter 3—26821
stagnation point skin friction parameter, var. with altitude for curved surface 3—1393
supercavitating airfoil cascade calc. 3—33270
supersonic detached flow between two bodies, turbulent jet theory application 3—33316
supersonic flight, optimum configurations for bangless sonic booms 3—4594
three-dimensional flow over a wing, Kutta-Joukowski condition *(French)* 3—7388
thrust nozzle optimisation, including boundary-layer effects, using numerical relaxation scheme 3—1333
transient flow in converging-diverging nozzles, Schlieren method 3—7393
transonic airfoils, transonic flow, computational methods, review 3—33247
turbine stage cooling by air injection into flow path 3—1379
turbulent boundary layer flow off sharp edge, acoustic wave diffraction 3—5715
turbulent boundary layer with suction 3—4578
two dimensional supersonic sails in high-Mach number airstreams, centred compressions 3—20345
two dimensional waverider configurations 3—1400
two-dimensional flow of incompressible fluid past arbitrarily shaped highly cambered bodies 3—4571
two-dimensional Neumann problem, higher order numerical solution of integral equation 3—20344
two-dimensional transonic airfoil sections, inverse design method 3—36114
viscous flow over a cone at moderate incidence, hypersonic tip region, numerical calc. 3—33243
vortex by modified Newton-Raphson methods 3—7391
vortex core jet near pt. of generation, vel. field analysis 3—1415

aerodynamics continued
- vortex wake transport and stability, atmospheric environment influence 3−1414
- wake flow of a cascade of oscillating airfoils 3−38411
- wings with blunt trailing edges, lift and drag meas. *(German)* 3−23754

aeronomy *see meteorology; terrestrial atmosphere; upper atmosphere*

aerosols
- *see also foams*
- atm., particle size distrib. formula, comparison with Γ-distrib. *(Russian)* 3−21942
- atmosphere, light polarization by mist haze, distinction from haze *(Russian)* 3−3008
- atmospheric, content as function of relative humidity, lidar obs. 3−3017
- atmospheric, due to human activities since Industrial Revolution *(French)* 3−21956
- atmospheric, humidity effects on aerosol transformation *(Russian)* 3−28015
- atmospheric, isotopes, cosmic ray spallation products, applications to the study of tracers and pollutants *(German)* 3−12862
- atmospheric, meas. from optical radar total scatt.-backscatt. ratio 3−9263
- atmospheric, optical props. and chemical comp. of stratospheric and tropospheric aerosols *(Russian)* 3−39525
- atmospheric, transformation of spectral thickness at high transparency *(Russian)* 3−39529
- atmospheric aerosol residence time determ. using ^{210}Pb, ^{210}Bi and ^{210}Po tracers 3−15975
- atmospheric aerosols, optical absorpt. 3−37197
- atmospheric charged particles, collision and coagulation efficiencies determ. *(Russian)* 3−39527
- atmospheric ferromagnetic particles, conc. and size distrib. meas. technique 3−37260
- atmospheric particles, extinction coeff. to mass ratio, humidity depend. 3−17493
- atmospheric surface, effect on atm. elec. parameters 3−28042
- atmospheric surface layer, statistical characts. of microstructure *(Russian)* 3−28016
- average spectral statistical dependences of the aerosol attenuation coeff. in the region 0.59-10 μm *(Russian)* 3−9267
- beta active hot particles, intrinsic sedimentation velocity effect on their steady-state electrical charge in the presence of an impurity of a contaminant aerosol *(Russian)* 3−2771
- beta-active hot aerosol particles, kinetics of unipolar charging 3−20264
- cascade impactor adapted to collect 0.6-2.5 μm particulate matter from town air 3−25331
- cations, Na concs. in Hawaiian atmosphere 3−12752
- charged clouds, confinement and transportation via electric curtain *(Japanese)* 3−35654
- condensation, coagulation and size distribution 3−31201
- conductive fluid droplet, image interaction with air ion *(Russian)* 3−34893
- counting and sizing photoelectric counter calibration, meteorological use *(Russian)* 3−3185
- cyclone, reverse-flow, steady-state model 3−17523
- deposition in polystyrene chamber 3−39415
- diffusionphoresis of volatile aerosol particles in slip conditions 3−34663
- dusty gas, weak shock wave propagation, perturbation study 3−11428
- electrostatic atomisation of liquids by discharge from capillary in electric field 3−4606
- flames, radiative propag., theory 3−27873
- flow indicator generation with polydisperse liquid aerosol, DOP 3−14506
- flow through glass fibre filters, probabilistic theory 3−17553
- gravitational force effect on aerosol motion in curvilinear gas flow 3−23793
- Greenland tropospheric aerosol measurements 3−34894
- holographic technique for sampling particles in moving aerosol 3−16445
- ionic ratio var. between reference seawater and marine aerosols 3−12683
- large nonvolatile aerosol particles, calc. of diffusophoresis velocity *(Russian)* 3−7466
- lidar observations of tropospheric aerosols, comments and critique 3−5495
- light scatt. props. rel. to Mie scatt. theory 3−13696
- liquid, collimated beam, prod. by harmonic elec. spraying 3−12465
- marine, physico-chemistry in undisturbed marine environment 3−12749
- marine aerosols, interaction with polluted continental air, S. California 3−12747
- mesosphere and stratosphere, satellite horizon scanning 3−39530
- metal-ion concentrations in marine atmospheric aerosol samples in Hawaii 3−12680
- microstructure determ. by optical method *(Russian)* 3−39411
- Mie scatt. props. of aerosols., size distribs., Los Angeles Basin 3−2967
- migration theory of aerosol particle settling from turbulent flow onto tube walls 3−33302
- monodisperse, spherical, in containment with natural convection, stability 3−11453
- oceanic, chemical comp. for determ. of wind transport to ocean 3−12753
- oceanic aerosol composition above Atlantic, sea-salt particles *(German)* 3−25243
- particle eddy diffusivities and turbulent deposition velocities for isothermal flow and smooth surfaces 3−33298
- particle motion, in unsteady temp. gradient 3−38408
- particle size parameters from imperfect frequency distribution curve *(Japanese)* 3−12463
- polydispersion coeff. of scattering for a power law of size distribution, an analytical representation *(Russian)* 3−12719
- polystyrene monodisperse aerosols production with a spinning disc 3−28800
- Saharan dust, vertical and areal distribution over western equatorial North Atlantic ocean 3−12751

aerosols continued
- sea salt particle transport, flame photometric analysis 3−12682
- single drops containing solids, drying characteristics rel. to sprays 3−2764
- size meas. by laser Doppler spectroscopy, operational limits, polydispersity effects and appl. 3−16429
- size meas. by laser Doppler spectroscopy, theory and expt. techniques 3−16428
- sizing, by holography 3−22259
- spectrochemical analysis 3−19365
- spectrum of atmospheric aerosol at 0.7 microns from meas. of clear sky during daytime *(Russian)* 3−39521
- spray drying apparatus, boundary temps. and evaporation zone dimensions 3−4558
- stellar extinction due to aerosol light scatt., blue moon phenomena 3−18850
- stratosphere, bistatic optical probing, conc., layer struct., optical thickness 3−25205
- stratosphere, observation of submicron particles 3−12729
- stratospheric Aitken nuclei counts, measurement errors due to a 'volatile' fraction 3−15971
- trace element concentrations in aerosols from San Francisco Bay Area 3−25214
- troposphere, size distribution models 3−12741
- tropospheric aerosol lifetimes, simulation study using numerical models *(French)* 3−28049
- tropospheric aerosol particle removal time by precipitation scavenging 3−28050
- turbulent flow of two-phase solids-in-air system 3−1433
- u.s. atomisation, disintegration mechanisms, photographic study 3−31202
- visibility reduction, simulation 3−37235
- AgI particles, freezing action on water drops in aerosol *(Bulgarian)* 3−9303
- Ni, aerosol particles in paraffin, mag. props. from 4.2 to 300 K 3−39006
- TiO_2, reflective layers on glass, aerosol spray deposition technique 3−22339

aerospace
- *see also aerospace applications of computers; aerospace control; aerospace instrumentation; aerospace propulsion; aerospace simulation; aerospace test facilities; aircraft; ground support systems; space research; space vehicles; terrestrial atmosphere*
- Aerosat programme *(French)* 3−28083
- hydrodynamic flow visualization, applications, review 3−32282
- hypersonic flight problems rel. to design of space shuttles 3−1408
- powder coating technology, aircraft materials applications 3−2772
- transonic airfoils, transonic flow, computational methods airfoil design, review 3−33247
- C ablation layers, radiative transfer, Jupiter and Earth entry 3−33336

aerospace applications of computers
- *see also aerospace control*
- astronomical position determination, Minsk 22 computer, geodetic stars *(Russian)* 3−3394
- celestial mechanics, special satellite orbit points prediction, analytical iterative algorithm, Brouwer theory 3−39583
- graphite billets for reentry nose tips, computer aided u.s. test system 3−37099
- guided missile cell-like structures, static magnetic fields in, computer-aided analysis 3−32491
- intergalactic filaments, formation, tidal forces, simulation 3−3370
- lunar surface position, computational method using the Cracovian association *(Japanese)* 3−18990
- NASA-MPE Ba ion cloud experiment, cylindrical shell computer model 3−34920
- Poisson Series Processor, appl. to celestial mechanics 3−39595
- precession and nutation in rectangular equatorial coordinates *(Russian)* 3−16094
- pulse signal propagation in ionospheric plasma 3−14532
- stellar clusters, dynamical evolution 3−3325
- topside sounder system of ionosphere sounding satellite, computer simulation 3−39566

aerospace control
- *see also attitude control*
- automatic flight control systems for civil aircraft, reliability characteristics 3−32116
- geostationary artificial satellite system METEOSAT, ground control system *(German)* 3−3166
- Mariner 9 mission objectives, communications and control systems *(Spanish)* 3−35214
- navigation system, satellite simulation, laboratory model expt. 3−31995
- planetary satellite transfer from hyperbolic to nearly circular orbit using aerodynamic braking 3−25378
- position control, orientation in rotating coordinate system *(Russian)* 3−19403
- satellite gravitational stabilization by flywheel, system parameters optimization 3−25374
- satellite nutational oscillations, damping with internal flywheel 3−25375
- spacecraft descending into Martian atmosphere, optimal control of final velocity 3−25373
- spacecraft oscillations with two-position attitude-control system 3−25376
- spacecraft reorientation, optimal control 3−6188
- transfer of spacecraft from hyperbolic to closed orbit round planet by atmospheric drag 3−25377

aerospace instrumentation
- *see also aircraft instrumentation; Langmuir probes*
- accelerometer, with 10^{-8} m/s^2 thresholds *(French)* 3−25663
- electric field detector, saw-tooth and ramp generator circuits, testing *(Spanish)* 3−28606
- gravity gradiometers in orbit for geodetic appl. 3−34780
- heading indicator systems, structure, operating precision 3−32116
- ice and water contents in clouds meas. from Raman scattering 3−9399
- Large Space Telescope, 3m aperture, configuration and mission objectives 3−25538
- nuclear science, conference, Miami USA, (1972) 3−28622

aerospace instrumentation continued
radiation effects, conference, seattle, Wasph., USA (1972) 3—17864
Radio Astronomy Explorer B antenna aspect data processor 3—35218
satellite altimeter for rapid global geoid mapping 3—34969
scintillation counting systems, automatic gain control 3—35478
self deployable light attenuators light shade for spaceborne astronomical sensors 3—31824
spacecraft electronic design, geophysical applications 3—5530
star sensor/mapper for Small Astronomy Satellites 3—31823
temperature measurement using liquid crystals for crack detection 3—31222
γ-ray monitor on OSO-7 spacecraft, response function for solar rays 3—37504
CdTe nucleonic system, for fuel gauging 3—32143

aerospace propulsion
colloid core reactor, experiment flow studies 3—7361
convergent conical nozzles, compressible flow investigation, propulsive performance 3—23808
electric propulsion, orbital low thrust parameters, synchronous satellites, analytic partial derivatives, elliptic orbits 3—3283
ion engine, discharge characts. 3—29995
Kaufman ion thruster, electrostatic dual-grid beam deflection system 3—11512
open-cycle gas core reactor, hydrogen effect in prototype 3—19925
optimum propulsion energy management, high speed spacecraft ejection from Solar System 3—9448
PHOEBUS-2 reactor, thermal balance and stress stationary limit conditions, calc. *(Italian)* 3—35927
photon-sail system using impinging laser beam 3—22966
quasistationary MPD thruster performance, theory and expt. *(Italian)* 3—36205
^{244}Cm radioisotopic power fuel development 3—19960
PuO_2 fuel for space vehicles, thermophysical and thermomechanical properties 3—19958
PuO_2 fuel heat source in spacecraft operation, radiation fields 3—19991
PuO_2 spherical fuel form development for use in space flight, hot pressing technique 3—19955
^{238}Pu isotopic fuels, large-scale production processes for heat source applications 3—19956

aerospace simulation
see also aerospace test facilities
high speed flows, three dimensional heat transfer and ablation distances 3—38354
out-of-plane force on circular cylinder from cross flow model 3—26816
rolling up characteristics of trailing vortex sheet in transport aircraft 3—26817
spacecraft re-entry plasma, mass spectroscopic determ. of dissoc. and ionisation 3—23928
vacuum and cryotechniques in space simulation chambers 3—3782

aerospace test facilities
see also wind tunnels
conical arc driver for high energy test facilities 3—38506
rolling up characteristics of trailing vortex sheet in transport aircraft 3—26817

afterglows
see also discharges (electric)
atmospheric species, cross sections for electron elastic and inelastic scattering 3—29738
collisions of metastable Xe and He atoms in afterglow of plasma discharge, excitation of Xe^+ 3—17380
flowing, primary ion radial variation eqn. eigenvalues, calc. method 3—33408
inert gases, electron and positive ion current collection by cylindrical Langmuir probe 3—14584
kinetic recomb. rate constants and absolute concs. of atoms in a gas flow system *(French)* 3—11517
nonlinear electroacoustic resonances *(French)* 3—17703
plasma, diffusion coeff. across mag. field, Langmuir probe curves 3—17566
Ar, disappearance of 2p state *(French)* 3—17358
Ar-N_2 mixtures, pulse radiolysis, energy transfer induced postluminesc. 3—23629
Ar + H_2O steady-state hollow cathode discharges, rate consts. determ. 3—15829
$CO_2H^+ + CH_4 \rightarrow CH_5^+ + CO_2$ proton transfer in flowing afterglows 3—39438
Cd excited atoms in discharge effective slow electron collision cross sections 3—17699
Cd-Ne plasma, Cd(5^3P_1) and Cd(5^1P_1) atom density decay due to e-Cd collisions 3—4687
$H_3^+ + N_2 \rightarrow N_2H^+ + H_2$ proton transfer in flowing afterglows 3—39438
$H_3O^+.(H_2O)_n$-series ions, electron recomb. meas. 3—14395
He, ambipolar-to-free diffusion, electron and ion temporal behaviour 3—20434
He, elastic electron-neutral atom interaction meas. of ultralow energies 3—29525
He, high pressure discharge, spectroscopic and plasma characteristics, afterglow and arc periods 3—30029
He afterglow, decay of 2^3S_1 state 3—14620
He flowing afterglow, pumped, excitation transfer, quenching reaction rate coeffs. 3—9056
He flowing afterglow, pumped, excitation transfer, rate coeff. for rot. relax. of He_2 3—9057
He plasma, electronic recomb., He_3^+ ions contrib. 3—20435
He plasma, low temp., atomic and mol. afterglow 3—23915
He-Xe discharge, pulsed laser action mechanism, radiation mechanism of afterglow 3—33412
He_2^+ electronic recombination, afterglow analysis technique 3—17704
N, Lewis-Rayleigh afterglow, vac. u.v. emission mechanism 3—7576
N_2, vibr. excited, quenching by CO_2 and N_2O, photoioniz. 3—4483
N_2^+, dissociative recomb. at elevated temps. 3—11293
Ne, electron-diffusion supercooling, expt. verification 3—36219
Ne_2^+ plasma, electron temp. dependence of recombination coefficient, microwave meas. 3—33389

afterglows continued
O_2, excitation of Herzberg bands, night airglow 3—12789
O_2^+, dissociative recomb. at elevated temps. 3—11292
S_2O, in afterglow, vibrational analysis of 2500-3400 Å bands 3—26908

AGC *see automatic gain control*

age (earth) *see earth age*

age determination, radioactive *see radioactive dating*

ageing *see aging*

aging
alloy, f.c.c. substitutional, crit. strain associated with dynamic strain ageing 3—39373
alloys, kinetics of ordering and antiphase domain growth vs. the kinetics of spinodal decomposition and coarsening 3—18609
borosilicate films, sintered, Vickers microhardness characterisation 3—39377
dislocation ageing, thermal and volumetric effects *(Russian)* 3—39332
drosophila melanogaster, radiation-induced life-span shortening and age-related structural alterations 3—28366
duralumin, quenched, solute dislocation interaction in dynamic strain aging 3—37058
Elinvar, effect on Young's modulus temp. depend. *(Russian)* 3—31055
ferrite spinels, mixed, nonstoichiometry of aging of mag. props. 3—21222
haemopoietic stem cells of mouse, age-dependent radiation effects 3—28377
high-temp., of Al alloy D16, effect on hardness *(Bulgarian)* 3—15655
insulating materials, physical properties, at cryotemperatures 3—9996
kinetics, electroluminescent diodes and injection lasers 3—29104
materials failure properties effect 3—21778
Nimonic, age-hardening, temp. depend. of strengthening characts. *(Russian)* 3—8839
plastic films, deterioration on accelerated aging in u.v. light *(Japanese)* 3—7279
polyethylene in fabricated parts, mech. props. temp. depend. 3—25003
polymethylmethacrylate, tensile strength during thermophoto-aging, effect of alcohols *(Russian)* 3—27768
polypropylene, quenched, aging study 3—27772
steel:carbon, dynamical deform. and aging, obs. of fracture *(Russian)* 3—24899
steel, austenite, shape of $M_{23}C_6$ particles after ageing 3—15689
steel, austenitic, Cr-Ni-Mn, ageing and creep rupture behaviour 3—8927
steel, austenitic, type 304L, hydrogen embrittlement effects 3—2745
steel, austenitic stainless, Nb-stabilized, creep strain effect on stacking fault precip. 3—8924
steel, cold-worked, dislocation struct. stability during high-temp. ageing *(Russian)* 3—8838
steel, high-strength, crack vel. and fractography, heat treatment effect, stress intensity 3—5332
steel, hydrogen embrittlement rel. to hydrogen/dislocation interaction 3—2744
steel, low alloy, containing vanadium carbide, microstruct. effects on creep props. 3—8935
steel, low-alloy, struct. and phase comp. changes 3—21687
steel, low-C, internal friction during strain aging, Snoek peak magnitude *(Russian)* 3—18614
steel, low-density 9G28Yu9MVB type, phase comp. and props. 3—21662
steel, maraging, Cr-Ni-Co-Mo, strengthening and precip. phenomena *(Russian)* 3—31060
steel, maraging, effect on change in dimensions 3—21666
steel, maraging, fractographic lines and fracture toughness 3—34573
steel, maraging, influence on impact strength of forgings 3—24926
steel, maraging, Mo alloying addition effects on aging kinetics 3—27646
steel, maraging, reverted austenite effect on mech. props. and toughness 3—34583
steel, maraging N18K9M5T, carbon effect on mech. props. 3—21664
steel, N14Kh5M3TYu, effect on mech. props. 3—21665
steel, quenched, strain aging of martensite *(Russian)* 3—24872
steel, St 35, work hardening and aging behaviour *(German)* 3—27683
steel, stainless, high-Cr-low-Ni-two-phase, strain aging, tensile strength *(Japanese)* 3—31068
steel, tool, fatigue limit in compression 3—21690
steel for dies, ageing effect 3—18672
ternary eutectic composites, mechanical props. and thermal stability *(Japanese)* 3—15701
Viton B fluorocarbon elastomer, chemorheology, long term aging 3—31185
Al alloys, thermomech. processing, improved fracture resist. 3—31048
Al/Si evaporated films, diffusion-limited Si precipitation 3—39237
Al-Ag alloys, quenched from liquid state, preprecipitation, small angle X-ray diffraction obs. 3—15667
Al-Cu alloys, heat treatment effect on strain ageing 3—31080
Al-Cu and Al-Cu-Mg directionally solidified eutectics, ageing response 3—34581
Al-Cu-Li alloys, resist. obs. of Al_2CuLi precip. 3—21660
Al-Mg alloy, Portevin-Le Chatelier phenomena *(French)* 3—31092
Al-Mg alloy, rel. to effect of Bi on stress-corrosion cracking *(Japanese)* 3—18634
Al-Mg commercial alloys, stress corrosion cracking and its prevention *(Japanese)* 3—18635
Al-Mg-Si, alloy, quench-aged, step-wise yielding and unlocking serrations 3—31093
Al-Mg-Si alloy, plastic deformation on the precipitation *(Japanese)* 3—15699
Al-Mg-Si:Cu, aging, effects of Mg loss, elec. resistance meas. 3—39361
Al-Si alloys, liq. quenching effect on age-hardening 3—39371

aging continued
Al-Zn (ZN 15 at.%) alloy, microhardness and structure transformations in ageing at elevated temp. 3−2714
Al-Zn alloys, decomposition, effect of high temp. aging 3−37015
Al-Zn-Mg alloys, mech. props. and fine struct. changes 3−21671
Al-Zn-Mg-Cu alloy, thermomech. treatment processed, age hardening mechanisms 3−24897
Be, resist. to microplastic deform. during aging 3−21672
Be single crystals, microhardness 3−24932
CaF$_2$, in gaseous ambients, hardening due to O contamination 3−4806
Co-Fe-Be alloy, age hardening, hardness-controlling additions *(German)* 3−8901
Cu-1.9 wt pct Co, age hardened, Hg embrittlement effect, slip mode and precip. morphology correl. 3−18647
Cu-3.6 wt pct Ti, age hardened, Hg embrittlement effect, slip mode and precip. morphology correl. 3−18647
Cu-Cr alloys, aging phenomena, electrical resistivity meas. *(Japanese)* 3−31067
Cu-Cr base alloys, precip. growth and nucleation, resist. study 3−24865
Cu-Fe alloys, ageing characts., mech. props. 3−37075
Cu-Ni-Be-Si alloy, mech. props. and precipitation *(Japanese)* 3−12352
Cu-Ni-Zn microduplex nickel silver, effect on tensile props. 3−34571
Cu-Si(5.09 at wt.%) alloy, aged, internal friction meas. 3−18678
Cu-Ti (4 at wt.%) alloy, X-ray small angle scattering study during early stages of spinodal decomposition *(Japanese)* 3−30995
Cu-Ti (4 at wt.%) alloy, X-ray small angle scattering study on later stages of aging after spinodal decomposition *(Japanese)* 3−30996
Cu-Ti(4 wt.%), side-bands, X-ray obs. *(Japanese)* 3−30999
Cu-Ti(4 wt.%) alloy, early stage side-bands, model *(Japanese)* 3−31000
Fe, hydrogen embrittelemtn rel. to hdyrogen/dislocation interaction 3−2744
Fe alloy, E1437B, ageing/deformation treatments influence on struct. and mech. props. *(Russian)* 3−24873
Fe alloy D16, aging effect on mech. props. 3−21677
Fe-Cr-Co-Mo alloy, precipitation on aging, structural and kinetic features 3−8787
Fe-Cr-Ni embrittled alloys, aging effect, Mossbauer obs. *(Japanese)* 3−27634
Fe-Cu(1.7 wt.%) alloy, Cu precipitation from α-Fe in pre-peak and peak hardness range of ageing 3−8797
Fe-Mn-Co alloys, effect on mag. props. *(Japanese)* 3−31077
Fe-N alloys, rapid strain aging, Snoek ordering, conc. depend. 3−24868
Fe-Ni-Al alloy, fracture and microstructure, aging 480-550°C *(Japanese)* 3−15672
Fe-Ni-Ti alloy, martensitic transforms. *(Russian)* 3−15684
Fe-Ni-Ti-Al-Nb alloys, in two-phase $(\alpha+\gamma)$ states, effects on props. and struct. *(Russian)* 3−12363
α-Fe-Sn solid solns., interaction between precip. reactions *(German)* 3−24838
Fe-Ta alloys, Laves phase precip. phenomena 3−37049
FeS$_x$ colloid 3−2770
Mg-Al spinel crystal, age strengthening kinetics 3−30930
Nb-Ti-Zr supercond. sheets, rel. to applied mag. field vs. crit. current density characts. *(Japanese)* 3−18257
Nb-Ti-Zr(Ge) supercond. sheets, effects on crit. current density anisotropy in applied mag. field *(Japanese)* 3−8298
Ni-base superalloy, Udimet 700 shock wave aging effect on tensile and stress-rupture properties 3−27682
Ni-Be alloy, age hardening, hardness-controlling additions *(German)* 3−8901
Ni-Mo-W corrosion resistant hard alloy development 3−21667
Ni-Ti (Ni rich) alloy, precipitation and its hardening effect *(Japanese)* 3−30992
Ni-Ti modulated structure growth on aging rel. to yield strength *(Japanese)* 3−12350
Ni-Ti-Al steel containing martensite, erosion resistance 3−34552
Pd film, artificial ageing effect on elec. and galvanomag. props. 3−8159
Si-Ge:P alloy, electron micro. exam. after annealing *(Russian)* 3−12346
Si-SiO$_2$ interface, stress ageing, surface state formation 3−21156
SrSO$_4$, precipitation from dilute solutions, recrystallisation and aging *(German)* 3−15818
SrSO$_4$, precipitation from concentrated solutions, recrystallisation and aging *(German)* 3−15819
Ti alloys, low-cycle fatigue strength 3−21693
α-Ti single crysts., thermal activation parameters of plastic deform. *(Russian)* 3−24184
Ti:Si, alloys dynamic strain ageing, 300-900 K, strain rate sensitivity, stress relaxation 3−34555
Ti-Mo-Zr-Sn, B-III titanium, thermomech. treated, struct. and props. 3−34582
Ti-Mo-Zr-Sn, βIII alloy, combined high and low temp. deform. processing effects 3−34578
Ti-Mo(15 wt.%) alloys, effect of preceding working and solution treatment on precipitation site of alpha during ageing *(Japanese)* 3−18588
Ti-Si(1 wt%) alloy, Mo effect on quenched and aged struct. 3−31064
V-C supersaturated solid soln., carbon precip. obs. 3−37036
WC/Co alloy, aging process, calorimetric studies *(Japanese)* 3−31066
Zr, oxygen and nitrogen saturated, strengthening mechanism *(Russian)* 3−24876
Zr-O alloys, strain aging parameters, dislocation cell struct., irrad. effects 3−27675
aging characteristics *see aging*
air
see also terrestrial atmosphere
acetylene-air flames, Ca atomic line-widths meas. by piezoelectric scanning Fabry-Perot interferometer 3−28779
acoustic generation by spherical expansion *(German)* 3−16333
adsorbed films, permeab. to air determ. using bubble shape theory 3−8015
air continued
air-glass-air system, verification of Fresnel and Airy equations 3−37
air-H$_2$O medium, droplet growth rate meas. using laser scatt. 3−18736
air-water mixture, two-phase flow, expansion from Laval nozzle 3−14496
air-water two-phase annular mist flow, droplet transfer 3−23780
anemometry, hot-wire of air/CO$_2$ and air/Ar turbulent gas mixtures 3−22564
arc, a.c., high current, free burning 3−20672
atmospheric gases, Cs$^+$ clustering and drift velocities 3−9053
breakdown and plasma mirror formation in CO$_2$ laser cavity *(Russian)* 3−1527
breakdown at 10.6 micron, loss mechanisms 3−23665
bremsstrahlung ionization, energy expended per ion pair *(German)* 3−25853
bubble effect on vapour bubble growth and collapse near solid surface, photographic study 3−23769
bubble nucleus spectrum, influence on cavitation inception, scattered light counting method investigation 3−26046
buffer, acoustic impedance *(German)* 3−16332
convection in small cells heated from below, heat transfer expts. 3−7351
convective heat transfer improvement with artificially modified turbulence 3−26789
corona discharge between point and disk, volt-ampere characts. 3−23933
cryotrapping by water condensates, press. depend. 3−15071
density, instrument for meas. rel. deviation from normal value 3−35552
atdewpoint, continuous supply *(Japanese)* 3−17972
discharge, audio frequency, cathode fall of potential 3−30028
discharge, cooled hollow-cathode, elec. and opt. characts. *(Russian)* 3−7577
discharge, nsec. region, electron-optical study *(Russian)* 3−17685
discharge development in strongly overvoltaged gaps, low press. *(Russian)* 3−26909
discharge pulses in air at low pressures, potential variation 3−38510
discharges, similarity laws, validity *(German)* 3−17683
dust in air, hydraulic resistance meas. during flow 3−4622
electric breakdown, pulsed interferometric holography of laser-produced breakdown 3−33189
flow, vibrations induced in flat plates in rectangular passage 3−16337
flow in axial flow inducer, visualisation study 3−26858
flowing turbulently in sooth annuli at high temp., heat transfer and friction coeffs. 3−23698
flows in planar nozzles, expt. study 3−1335
forced convection heat and mass transfer from humid air to frost surface 3−1363
frost formation on air coolers rel. to natural convection conditions for cooled plate 3−1780
heat transfer for turbulent flow with suction in a porous tube 3−20295
heat transfer to the atmosphere from the surface of thermal electric power plant cooling ponds 3−29847
n-hexane-air flame, temp. meas. using spectrum of scatt. laser light *(German)* 3−9868
history of meteorological exploration in the upper air over Australia 3−9298
humid air, adiabatic and isobaric mixing with water or ice *(French)* 3−31379
hypersonic air streams, multiple-orifice liquid injection 3−38415
hypersonic flow past blunt-nosed ablating graphitic body, heat transfer 3−1403
injection in compressible turbulent boundary layers 3−7365
intensive blowing through a permeable surface, nature of flow 3−33303
introduction of air into liquid by low-speed water jet *(German)* 3−7314
ionization by shock wave, from electron density O formation calc. 3−7397
jet, escape into dead end tube 3−4523
jets, from entry holes of high-intensity combustion-liner, mass flows 3−17494
laminar free convection in heated vertical corner 3−4561
microwave generated ionised sheath in coaxial transmission lines 3−17694
oceanic, salt particles in bubbles 3−12692
oscillatory flow, past an infinite, vertical, porous plate with constant suction, free convection effects 3−33211
oscillatory flow past an infinite, vertical, porous plate with constant suction, free convection effects 3−33212
planar jet striking a concave surface, heat transfer 3−23704
plasma, high frequency flare discharge, thermal expansion, atomic absorption measurements 3−33405
plasma, viscosity meas. 3−23904
plasma shock waves in an e.m. shock tube, shadow photography obs. 3−29986
plasmatron, low precision for spectral analysis of pf solutions *(Russian)* 3−30021
pollutant gases and air-water interfaces, Raman scattering 3−37534
positive corona formation 3−33410
pressure fluctuations on a membrane at 1 atmosphere 3−17486
Rayleigh scatt. coeffs. rel. to CO$_2$ and freon 3−14417
refractive index, rel. to corrections in optical pyrometry and photometry 3−22281
reverberant chamber for sound power meas. 3−99
rheology of air-liquid dispersions *(German)* 3−14505
roll waves entrainment in air-liquid flow 3−33263
shock waves, expt. study of rate of ionisation *(Russian)* 3−33248
shock waves, weak, vibr. relax. effects and sonic bang struct. 3−36121
shock-compressed, electroconductance depend. on piston material *(Russian)* 3−29826
solubility, in highly viscous liquids, measurement *(Russian)* 3−10199
solubility, in viscous liquids, measurement *(Russian)* 3−10200

air continued
sound pulses radiated in air by creeping waves on rigid spheres and cylinders 3−5726
sparks, nanosecond, breakdown and channel production 3−30037
subsonic flow, heat exchange in the critical zone ahead of a cylindrical step *(Russian)* 3−29857
subsonic jet, for noise field 3−3652
supersonic flow over leading edge of blunted flat plate, numerical solution for two-dimensional laminar compressible flows with embedded shock waves 3−26822
thermal conductivity measurement at atmospheric pressure 3−23659
transducer at air-water surface, radiation resistance, effect of spherical scatterers 3−37566
Trichel discharge, mechanism *(German)* 3−36210
turbine stage cooling by injection into flow paths 3−1379
turbulent boundary layer injection 3−1386
two phase air-water nozzle flow 3−23806
two-phase solids-in-air turbulent flow, friction effects 3−1433
unsteady flow rates in channels, meas. by hot-wire anemometer method 3−32269
wetting hysteresis effect on equations of state of air trapped by water in glass capillary 3−20925
Ar-air high-temp. jets with Ti dispersive particles, electroconductivity *(Russian)* 3−11455
CO_2-N_2-He system, amplification rel. to temperature 3−19605
Cs^+ clustering with atmospheric gases, drift velocities 3−9053
Mg-air flow, local void fraction measurement by optical fibre glass probe 3−16576
N/air mixtures heterogeneous oxidation of H_2S below 1000 ppm over metal oxide catalysts 3−37198
O_2-air mixture, viscosity meas. 3−38342
Rn daughters meas. using α disintegration data 3−9266

air bases *see airports*

air bubbles *see bubbles*

air cleaning, electrostatic *see electrostatic precipitation*

air compressors *see compressors*

air conditioning
see also ventilation
acoustics 3−25625
nonlocally reacting noise control materials, acoustic impedance meas. 3−3704
quiet, development 3−25624

air permeability *see permeability*

air pollution
see also smoke
abatement processes, effect on steam generation control 3−25618
airborne particulate matter examination, photomicrographic technique 3−35312
albedo and thermal effects of particle increase 3−31366
atmospheric ^{85}Kr, dosimetry studies 3−5683
atmospheric aerosol meas. from optical radar total scatt.-backscatt. ratio 3−9263
atmospheric ions, mobility spectrum rel. to pollution 3−28041
atmospheric particulate pollutants measurements 3−39816
Belgium, SO_2 and smoke pollution during 1 April 1969 to 31 March 1970 period *(French, Dutch)* 3−28401
biosphere, CO_2 and dust, effect on man 3−5511
buoyant plumes, vehicular and aircraft wakes 3−33325
cascade impactor adapted to collect particulate matter from town air 3−25331
Central London, air quality monitoring and O_3 levels 3−21953
climatic influence of human activities since Industrial Revolution *(French)* 3−21956
control, for high temp. industrial processes 3−37544
Denver, meteorology, transport equations 3−9276
diffusion eqn. for nonlinear chemical reactions, appl. of K-theory 3−39817
dilution factors for effluents diffused from elevated continuous point source 3−28051
dispersion of pollutants, effect of first order chemical reaction 3−37199
dispersion of pollutants, effect of horizontal impervious layer caused by temp. inversion 3−25210
dust emission suppression and control methods in cement industry 3−37537
dust meas. and control in mining, to reduce work-related diseases 3−25609
emission to air, conference, London, (1972) 3−37204
emission to air reduction in power generation industry, best practicable control means 3−37538
extreme urban air pollution rel. to frequency of surface inversion formation 3−37215
ferromagnetic particles, conc. and size distrib. meas. technique 3−37260
flue gas SO_2, alkali scrubbing test facility instrumentation 3−25619
fluorescent particle atm. tracer, possible toxicity hazard 3−39819
fluorides in stack gases, continuous on-site measurement method 3−37250
fog formation by steaming of warm-water lagoon used for power station cooling 3−39511
gaseous dispersion, concentration meter for wind tunnel studies 3−13522
Gaussian plume model modifications rel. to long averaging times 3−5492
generating plant stack plume, Raman scatt. by SO_2, optical radar obs. 3−39504
Great Plains, pollution from duststorms 3−39510
high-volume sampling system using cellulose filters 3−39818
Hudson River Valley, low wind turbulence statistics and pollutant diffusion estimates 3−25211
Hungarian theoretical meteorological studies of air pollution *(German)* 3−12704
in-situ monitor, for HF and HCl, using nondispersive i.r. technique 3−37753
industrial control, electrostatic precipitation applications 3−4062
inorganic effluents, atomic absorption anal. 3−5691
i.r. spectroscopy detection methods, review 3−32076
i.r. techniques for analysis 3−21977

air pollution continued
laser Raman backscattering technique, detection improvement 3−28399
laser Raman scattering detection, using Fabry-Perot periodic filter 3−3192
laser-Raman radar detection, using sampling technique 3−3190
marine aerosols, interaction with polluted continental air, S. California 3−12747
measurement, laser application *(German)* 3−34895
measurement, Mie scattering techniques with lasers, review 3−3188
measurement, using i.r. tunable laser, review 3−3187
measurement systems and techniques 3−25614
meteorology, fluid models 3−2971
Mie scatt. props. of aerosols., size distribs., Los Angeles Basin 3−2967
monitor 3−16328
monitoring, microwave rotational spectroscopy 3−37540
monitoring applic. of press.-broadened linewidths of SO_2 and NO_2 3−1245
monitoring by dye laser meas. of differential absorpt. of elastic backscatt. 3−37248
Netherlands power stations, SO_2 concentration meas. *(German)* 3−9734
optimal distribution of air pollution sources rel. to airshed simulation model 3−25213
particle size distribution measuring apparatus 3−28400
particle-sulphate in background air, amplification method of determination 3−37249
particulate material, neutron activation analysis with computer resolution of gamma ray spectra 3−18871
particulates, multielement analysis by energy-dispersive X-ray fluorescence 3−32253
photochemical smog, aerosol formation, significance of SO_2 photosensitized cis-trans isomerization of butene-2 3−5407
plume path of gases emitted by stack, new calculation method 3−16055
plume rise effect on ground level pollution, plume breakup model 3−25208
pollutant averaging times, statistical model 3−39506
pollutant behaviour, radioactive isotopes, aerosols, cosmic ray spallation products *(German)* 3−12862
pollutant gases and air-water interfaces, Raman scattering 3−37534
polynuclear aromatic hydrocarbons in Teheran atmosphere 3−15957
power plant stack gas, analysis for SO_2 and NO using i.r. analyser 3−25617
quality and abatement 3−37543
quality simulation modelling, applic. to air pollution control 3−28405
radioactive waste disposal and air cleaning facilities, soln. *(French)* 3−32958
Raman spectroscopy, remote spectroscopic analysis of p.p.m level 3−18897
rapid gas chromatograpy, application, atmosphere, flue gas and engine exhaust analysis 3−28398
regulations, Ringelmann Chart 3−25615
remote detection and analysis, laser-Raman radar, review 3−3189
remote sensing, using laser and i.r. heterodyne radiometer 3−3193
remote sensing methods 3−9736
sample analysis, location and identification of small particles within large samples 3−37774
sampling, use of differential flow controllers 3−37746
San Francisco Bay Area, trace element concentrations in aerosols 3−25214
small radioactive particles examination, reversal autoradiography 3−16060
source location, single fixed point, mathematical modelling 3−16327
specific gaseous constituents, remote mapping, tunable laser techniques 3−3191
surface aerosols rel. to atmospheric elec. parameters, Poona, India 3−28042
Sydney, visibility, humidity and smoke meas. in 1930-1935, 1951-1956, and 1963-1970 periods 3−39508
Toronto, meteorological interpretation of daily suspended particulate values 3−39509
trace element origin, air, rain and dry deposition sampling 3−18866
trace metals source, Hawaiian marine atm. 3−12754
transport model, appl. to dispersion in atm. boundary layer 3−12758
transport of diffusing material over thin wind-break 3−25212
transportation generated, modelling and computer implementation 3−28404
tritium removal from laboratory 3−39821
United Kingdom, economic and technical appraisal of air pollution, report 3−18870
urban air pollution modelling rel. to U.S. cities and SO_2 data 3−25215
urban atmosphere, pollution of lowest 100 m. from solar radiation attenuation 3−15973
urban atmospheric pollution, zoning by condensation nuclei concentrations 3−5494
visibility reduction due to aerosols, simulation 3−37235
wind direction persistence rel. to air pollution 3−15954
CCl_3F concentrations and atmospheric turbidity in rural S. England and S. Ireland 3−15955
CO monitoring, i.r. fluorescence analytical technique 3−26028
H_2S, heterogeneous oxidation below 1000 ppm in N/air mixtures over metal oxide catalysts 3−37198
Hg fall-out on snow surrounding Swedish chlor-alkali plants 3−37200
NH_3 and related atmospheric pollutants at Harwell, correlation of hourly sampling results 3−34904
NH_3 and related atmospheric pollutants at Harwell, technique for hourly sampling and analysis 3−37234
NO catalytic reduction in automobile exhaust gases using Fe-containing materials 3−37535
NO catalytic reduction in automobile exhaust gases, reactions with CO and O_2 on oxidized stainless-steel 3−37536
NO monitor 3−3918
NO_2, laser induced fluorescence obs. 3−3018

air pollution continued
NO_x, photometric measurement in emission source monitoring, associating oxidation of NO to NO_2 3−25616
Na_2SO_4 atmospheric summer and winter fallout near kraft mill 3−15956
^{22}Na in food chain, lichen-reindeer-man 3−3634
Rn daughters activity measurement by gamma counting 3−37722
S over Sweden during 1969 to 1970 3−12737
SO_2, absorption by fog forming cloud nucleus size particles 3−15970
SO_2, at Harwell, technique for hourly sampling and analysis 3−37234
SO_2, in stack plume, laser-Raman radar obs. 3−787
SO_2 and hydrocarbon gases, remote meas. by u.v. laser induced fluorescene 3−37541
SO_2 and particulate conc., smoke stack effluents, remote meas. 3−35313
SO_2 at Harwell, correlation of hourly sampling results 3−34904
SO_2 dispersal, stack design and siting *(Spanish)* 3−15959
SO_2 ground-level concentrations around modern power stations 3−25209
T, portable monitor 3−13431

air pumps *see compressors*

air terminals *see airports*

aircraft
see also aerospace control; aerospace instrumentation
atmospheric pollution, buoyant plumes, vehicular and aircraft wakes 3−33325
C-5, fail-safe strap panels testing employing transversing i.r. inspection system 3−37599
civil, heading indicating and automatic flight control systems, reliability 3−32116
Concorde, cosmic radiation rates, rel. to health hazard *(French)* 3−37533
fatigue and crack propagation analyses under stationary random excitation 3−553
fog dissipation by jet wakes 3−25216
non-conical delta wings, flow over, applic. of shock expansion theory 3−11418
potential flow about rotation-symmetric fuselages, air intakes and propellor inlets, calc. *(German)* 3−23753
rolling up characteristics of trailing vortex sheet in transport aircraft 3−26817
rotating blades in forward flight, boundary layer separation 3−38373
slender-wing, nonlinear lateral oscillations investigation 3−11377
stratospheric flight, meteorology, SST operation, aircraft dynamics, passenger comfort, environmental impact, Concorde, initial results *(French)* 3−18853
supersonic flight, optimum configurations for bangless sonic booms 3−4594
vortex by modified Newton-Raphson methods 3−7391

aircraft communication
acoustic alterations in speech when processed through Air Force aircraft communication systems 3−3646
optimal and preferred listening levels in aircraft acoustical environments 3−3488
U.S. Navy aircraft radios, nasality, sibilation and voicing 3−3489

aircraft instrumentation
nuclear instrument landing system using frequency-modulated gamma-radiation 3−19346
radiometer-scatterometer for ocean surface wind sensing, antenna calibration 3−39568
static discharger system, charged condensation droplets 3−662

airfields *see airports*

airglow
see also atmospheric spectra; aurora; nightglow; sky brightness; twilight
atmospheric cooling near mesopause, energy loss due to molecular deexcitation 3−34889
Balmer line emission from geocorona, nongalactic component meas. 3−28286
clouds, noctilucent, spectrophotometric meas. of near i.r. spectra, airglow hydroxyl rotational temps. 3−28010
dayglow spectral emission intensity, role of N_2 column density in control 3−9270
F-region neutral temp. meas., O 6300 angstrom emission line profile 3−16025
F-region tropical u.v. airglow intensity, theoretical calculations 3−12804
Mercury, Ar u.v. dayglow lines in atmosphere, models and predicted intensities 3−31616
OH contribution in emission line meas. in filter photometry 3−9311
photometer calibration 3−37247
spectrometer calibration 3−37247
summary of Japanese daily obs. results for Oct. 1969 to Dec. 1971 period 3−39610
twilight 6300 A, changes in thermospheric O_2 abundance 3−9308
H I Lyman-α airglow, spatial and temporal var. rel. to H I distributions 3−31399
N and O atom and ion reactions in an ultra high vacuum plant *(German)* 3−9306
O III 304 Angstoms emission in e.u.v. airglow 3−16003
OH, i.r. airglow, diurnal variation, balloon borne spectroscopic obs. 3−31392
OI emission line meas. in early morning ionosphere 3−16021

airports
noise modelling for statistical analysis of sound pressure wave propagation 3−28426

alarm systems
nuclear power plants, radiation detection system 3−23452

albedo
anisotropic slab albedo problem, new method for calc. of emergent distribs., soln. of integral eqns. 3−22757
balloon satellites orbital accel. effects of earth-reflected radiation 3−35222
cosmic ray albedo electrons, energy spectrum determ. from shielded gas-discharge detectors data 3−22446
global, effect of increase in air pollution 3−31366

albedo continued
ground albedo effects on sky brightness increase, sea surfaces *(German)* 3−12711
Jovian Galilean satellites, obs. at 1-4 μ 3−31581
Lake Ontario surface, dependence on solar zenith angle 3−2845
lunar maria albedo distrib. at 0.62 μ rel. to maria origin 3−37339
Mars, photometry and topography, by Mariner 9 n.v. spectrometer experiment 3−12977
Mars, variable features, Mariner 9 television results 3−16150
Martian violet clouds, meas. of southern hemisphere cloud 3−35063
Neptune, UBV photoelectric photometry of magnitude and geometric albedo 3−35058
planetary albedo γ-rays, model for scanning-angle distrib. 3−31485
planetary atm. spherical albedo determ. appl. to Venus 3−28157
Saturn's rings, u.v. absorption in 3300 to 4800 Å region 3−35065
Uranus' geometric albedo, rel. to cloud structure 3−28150

alclad *see aluminium alloys*

Alfven waves *see magnetohydrodynamic waves; solid-state plasma*

algebra
see also Boolean algebra; linear algebra; matrix algebra
φ^2:(x), field, selfadjointness of field algebra representations 3−32283
biquaternion representation for noumenon, a generalization of relativistic events and space-time 3−19494
book, Lie groups and Lie algebras 3−10236
C*-algebra, asymptotically abelian, spectra of states 3−484
C*, in quantum statistical mechanics, local normality of K.M.S.-states 3−28971
canonical anticommutation relation, Fourier transformation and Weyl relations 3−28817
continuity props. of additive meas. of continuous von Neumann factor 3−22705
correlated fermion state, construction of excitation operator algebra 3−10346
Duffin bracket for nonconservative systems, algebraic nature 3−28818
excitations, elementary, in Liouville space, statistics and interactions 3−26156
fermion field, algebraic equivalence of quasi-free states, C*-algebra *(French)* 3−13786
kernel G_1 calc. on stationary space-time *(French)* 3−28807
Lie, infinitely divisible projective representations 3−6181
Lie infinite-dimensional, subideal struct. and nilpotency considerations 3−16591
maximal simple Lie algebras from two pairs of Fermi operators, calc. of complete list *(Russian)* 3−28810
mixing transformations on metric spaces 3−19390
modern, in elementary physics courses 3−6
Neveu-Schwarz model, spectrum-generating algebra and no-ghost theorem 3−26328
nuclear C*-algebras, extension property for tensor products 3−28815
parastatistics from the Schwinger action principle 3−10233
physical theories, mathematical model 3−481
polytopes *(German)* 3−26052
quantum field theory Thirring model, conformal algebra in two space-time dimensions 3−13792
quantum lattice system, time evolution in automorphism of quasi-local algebra 3−28977
quantum mech. observables as positive-operator-valued measures, transformation props. 3−10345
real roots of algebraic eqn., method for determination *(Italian)* 3−28823
Regge residues, algebraic structure 3−38065
scale transformations for free scalar field of zero mass 3−4138
scattering theory, non-relativistic relation between cross-section and asymptotic condition 3−10343
topological *-algebra, props. of commutant of field representation 3−32284
von Neumann, spectra of modular operators 3−483
Weyl algebra, infinite vol. limit of canonical free Bose states 3−10386
Weyl and Gel'fand-Kirillov associated algebras 3−22578
Witt's theorem for quadratic forms on local rings, proof *(German)* 3−13530

algorithms *see subroutines*

aliphatic compounds *see organic compounds*

alkali metal compounds
see also alkali metal halides; caesium compounds; francium compounds; lithium compounds; potassium compounds; rubidium compounds; sodium compounds
alkali graphite intercalation compounds, C_8M, $C_{24}M$ (M = K, Rb, Cs), molecular sieve type sorption obs. 3−33732
aluminosilicate and aluminogermanate melts and glasses, iso-structural relations *(German)* 3−21735
alumosilicates, thermionic ion emission, pulse characteristics *(Russian)* 3−12207
bisulphates, $MHSO_4$, M = alkali metal or NH_4, growth from soln. or H_2SO_4 *(German)* 3−8716
complex polymetaphosphates, i.r. n.m.r. and magnetochemical studies 3−17454
dichromates, vibr. spectra, comparison 3−21416
e.p.r. spectral linewidth of hole centres in alkali silicate glass *(Russian)* 3−39029
glass systems, density *(Japanese)* 3−21747
halide crystals, electric breakdown mechanism in presence of microroughness on the cathode *(Russian)* 3−8514
halides, luminesc. impurity centres, energy transfer excitonic mechanisms *(Russian)* 3−27537
hydride molecules, vibrational, rotational consts., dipole moment and binding energy calc. using model potential functions 3−38271
hydrides, floating type wave functions in molecular pseudopotential calculations 3−38260
nitrates, specific conductances up to 12 Kbar *(German)* 3−11901
oxides, i.r. spectra and geometries, matrix reaction study of alkali metal and N_2O 3−17432
silicate glass, u.s velocity, temp. depend., liq. He temps. 3−36368
TCNQ salts, thermal cond., 80-410K *(Russian)* 3−7981
tellurite glasses, e.p.r. spectra, irrad. effects *(Russian)* 3−21309
ternary sulphides with transition metals, cryst. struct. 3−14749

alkali metal compounds continued
CdF_4MF, M=alkali metal, structures of compounds formed *(French)* 3−14819
$Zn(PO_3)_2$-MPO_3:Co (M=Na, K, Cs), glasses and melts, molar props., softening temp. and structure *(Russian)* 3−14695

alkali metal halides
see also compounds of individual alkali metals, e.g. sodium compounds
absorption bands, In^+ or Sn^{2+} doped crysts., high press. 3−39166
absorption spectra and phosphorescence spectra depend. on lattice parameters and refractive index *(Russian)* 3−30875
absorption spectra in vacuum u.v. due to excitons, ligand field theory calcs. 3−27509
adsorption, of Au, surface diffusion and cluster migration rel. to thin film growth 3−1888
alkali halide-Cu halide, excitonic doublets, test for coherent-potential approximation 3−30436
Anderson-Gruneisen parameter 3−1714
anharmonicities and reststrahlen frequencies 3−38631
aqueous solutions, with SCN^- impurity, Raman spectra *(Russian)* 3−15498
binary liq. mixtures, enthalpies of mixing 3−9039
Borelius' equation of state, high press. behaviour 3−20844
bound Frohlich polarons, induced i.r. absorption 3−36886
chlorides, electronic absorption spectra of Pt(II) centres, 325°-800°C 3−39167
colour centres, ENDOR in presence of external stresses, theory 3−27442
coloured crystals, kinetics of F-F' transitions 3−33528
compression to 32 kbar, neutron diffr. study for NaCl and CsCl 3−4808
crystals, surface, non-radiative electronic transitions *(Russian)* 3−38876
defect absorpt. strength, f-sum rule, Smakulas eqn. effective fields, review 3−12160
dichroism, periodic, plastic deformation induced 3−36894
dislocations in nonmetals, review 3−24126
electron affinities of F, Cl, I and Br 3−1117
electron avalanche breakdown induced by ruby laser light 3−30757
electronic polaron resonance, optical absorption 3−36570
electronic states, theory 3−11855
emission spectrum of O_2^-, phonon sidebands 3−39182
e.p.r. obs. of hyperfine and g-components of V_k centres 3−18369
e.s.r. studies of radiation induced defects 3−4769
exciton bands of D_{2h} model, nearly orthogonal basis 3−33857
exciton optical line shape, theory 3−38815
extended breathing shell model 3−33629
F_{2a}^+ centres in alkali halides, low lying states, pseudopotential calcs. 3−33831
F-centre, relaxed excited state, nearly degenerate states of bound lattice polaron 3−21040
F-centre, spin-lattice relax. in relaxed excited state, e.p.r. optical detection 3−18368
F-centre formation Rabin and Klick diagram 3−33525
F-centres, e.s.r. of relaxed excited states, review *(Japanese)* 3−15421
Gruneisen parameters, optic mode, rel. to anharmonic interactions 3−27094
hydrofluorides, electrostatic energies, Madelung parameters, lattice energies 3−1593
impurity vibration bands, temp. depend. of half-widths and integral absorpt. 3−21450
impurity-doped, review of Z-centres 3−8624
indentation hardness theory rel. to resist. to dislocation motion 3−24203
interstitial and trapped hole centres review 3−4754
ion, ratio of shell charges electrical and mechanical polarisability 3−1152
ionic radii determ. from second nearest neighbour repulsive energy ratio 3−1591
ionic Rydberg potential function 3−38549
i.r. absorpt. theory for alkali halide crystals 3−18444
irradiation defects, electron microscopy technique 3−1546
isotherms, calc. from shock wave data 3−27067
Kerr effect, due to paraelec. defects, in stress-free crysts. 3−21386
Kerr effect, due to paraelec. defects, stress effects 3−21387
laser damage, bulk, self-focusing elimination 3−29147
laser destruction mechanisms and multiphoton ionization of impurity centres 3−5162
laser induced bulk damage due to electron avalanche breakdown 3−35705
laser radiation self-focusing with alkali halide single crystals, focus of damage displacement 3−32600
as laser window material, intrinsic and impurity absorpt. at 10.6 micron 3−28580
lattice structure, stability under hydrostatic pressure 3−7930
luminescence centres, reson. secondary glow, polarisation theory *(Russian)* 3−36918
luminescent impurity centres, energy transfer, excitonic mechanisms *(Russian)* 3−27537
magnetically quenchable positron state 3−36545
mechanical properties of crystals with centres of colloid type *(Russian)* 3−14855
metal-insulator transition at pressures up to 2000 kbar *(Russian)* 3−38804
microhardness of NaCl-type crystals, rel. to dislocation rosette length 3−17837
molecular beams, collision reactions with Li atoms, beam kinetics 3−25058
molten, surface energy., temp. coeff., calc. *(Russian)* 3−20923
Mossbauer study of implanted ^{129}I ions 3−34261
nucleation of evaporated Ag deposits, effect of substrate vibr. 3−15100
paraelectric relax., low temp., Orbach process 3−2491
phosphors, photolum., 10-40 eV 3−27558
photoelectron spectra and zone structure 3−34464
photoelectron X-ray spectra, config. interaction, comment 3−34461
photoemission under soft X-ray bombardment, yield, statistical distrib. 3−12211

alkali metal halides continued
photoluminescence, analogue computer modelling *(Russian)* 3−21461
photomechanical effect and dislocation motion, i.r. irrad. crysts. *(Russian)* 3−38595
photostimulated luminescence, method of varying spatial distrib. of defects and effect *(Russian)* 3−5227
piezo-hyperfine interaction concept., rel. to ENDOR of impurity centres 3−2466
point defects formation and stabilization by u.v. irradiation dose dependence 3−7750
polarisability, electronic, calc. 3−30746
polaron effective masses, electron-phonon coupling constants 3−36569
positron annihilation, positron-anion bound state existence, Wigner-Seitz approx., γ-ray angular correlation curve 3−24157
positron annihilation 3−33551
reflection spectra, high-resolution, in far u.v., interband transitions 3−21437
relative stability, short-range three-body potential in first-order exchange energy 3−1595
solid solns., binary, Debye freq., Iosilevskii relation validity 3−30269
solid solutions, Debye temp. *(Russian)* 3−38648
surface excitations, exptl. obs. using attenuated total reflection 3−24493
surface faults, painting with Au *(French)* 3−15074
surface structure of electron beam sputtered ions 3−30313
T-centre form. by electrolysis in alkali halide: Pb^{2+}, Sn^{2+}, Ge^{2+} *(French)* 3−20738
tribo-photostimulated exoelectron emission, yield limit emission criterion 3−30925
U-centres, magneto-refl., Faraday rot., ellipticity 3−15476
vacancies, interstitials, Jahn-Teller distortions, molecular orbital models 3−33837
in water, temp. corresponding to sound veloc. max., effect of electrolytes 3−37592
X-irradiated, time-lag of photostimulated luminesc. *(Russian)* 3−18483
zero-phonon transitions of dissolved O_2^-, S_2^-. Se_2^- and SeS^- mols. 3−27556
CrO_4^{2-} doped, vibr. and electronic spectra 3−27091
K halides, T-centres, photoluminesc. meas. *(Russian)* 3−36919
KBr cryst. with PO_2^- mol. centre, low temp. luminesc., absorpt. and excitation spectra 3−15549
KCl cryst. with PO_2^- mol. centre, low temp. luminesc., absorpt. and excitation spectra 3−15549
KCl:Pb, Sn, microdistribution inhomogeneity, electron microscopic obs. 3−1636
KX:CrO_7^{2-}, (X=Br,I), optical and i.r. spectra, fine struct. meas. 3−12132
NaCl quenched crystals, influence of impurity distrib., applic. of electron microscopic decoration method and microhardness meas. 3−1676
NaCl quenched crystals, microhardness rel. to quenching temp. and contamination, obs. 3−1677
NaCl quenched single crystals, charge developed by local plastic deform., rel. to quenching temp. and contamination 3−2155
NaCl whisker surface structure, electron microscopic obs. and interpretation of evaporation processes 3−1964
Tl^+ impurity centre, many photon excitation of laser irradiation 3−5230

alkali metals
see also caesium; francium; lithium; potassium; rubidium; sodium
atom collisions with halogen molecules fragmentation of halogen negative ions 3−26715
critical properties, applications of significant liquid structure theory 3−20862
D-region ions, gas clustering reaction rates 3−3105
elastic constants, second and third order, calc. 3−27050
electrical resistivity, phonon drag effect on low-temperature form 3−2045
electronic transitions and structure, review 3−33814
evaporation from discharge tube wall, Rozhdestvenskii hook method appl. 3−14619
Fermi liquids, anisotropic simple models 3−33770
film and bulk, struct. model for abnormal optical props. verification *(French)* 3−30365
films, on W(100), quantitative AES and LEED study 3−38704
Hawaiian marine atmosphere, chemical fractionation of alkali and alkaline Earth metals 3−12748
impurity hydrogen conc., methods of determ. 3−445
intense radiation sources for alkali and alkaline earth metals, preparation methods 3−32262
interaction potentials between alkali metal and inert gas atoms 3−17385
intercalates of MoS_2, stoichiometries and X-ray data 3−17787
ion collisions with atomic Cd from threshold to 1000 eV 3−20065
ion source 3−28637
ion-atom collisions, wavefunctions and pseudopot. for charge transfer 3−1126
ionization of alkali atoms, determ. of cross-section by freq. doubling with dye laser *(Dutch)* 3−29492
ionizer for plasma production 3−11507
Knight shift, press. effect, calc. by KKR method 3−36806
Knight shifts, Pauli susceptibilities, from contact density in pseudopotential 3−34234
Landau Fermi liquid parameters anisotropy, electron-phonon interactions 3−27203
liquid, cooling, K vapour condensation 3−14987
liquid, electronic density of states calc. and comparison with free electron model 3−18054
liquid, ion-ion interaction calc. 3−33441
liquid, optical absorpt. and Ziman theory 3−21430
liquid pseudopotential form factor rel. to elec. resist. and thermoelec. power 3−21051
lunar poverty 3−3311
matrix reactions with N_2O, i.r. spectral study of resultant oxides 3−17432

- **alkali metals** continued
  - optical absorpt., phonon-assisted processes, direct interband absorpt., Drude absorpt. 3—34335
  - paramagnetic spin susceptibility, local pseudopot. calc. 3—8337
  - phonon dispersion, axially symmetric model for lattice dynamics, effect of conduction electrons 3—7881
  - phonon drag thermopower calc. 3—30461
  - photoionization cross sections using Hellmann-like pots. 3—17363
  - plasma containment in corrugated mag. field 3—38484
  - positive ions, bombardment of solid surfaces, negative ion source *(Russian)* 3—6061
  - positron annihilation, solid and liquid metals, thermal smearing Fermi surface, angular correlation 3—30393
  - relativistic effects in the hyperfine struct. 3—17341
  - solutions in liq. amines, pulse radiolysis, species identification 3—27881
  - vapour-inert gas mixture, optical third harmonic generation 3—26246
  - vapours, tunable coherent i.r. source from four wave parametric conversion 3—35712
  - Zeeman fine and hyperfine components, off-diagonal element phases of optical absorption matrix 3—33028
  - in Xe lattice, e.p.r. line broadening 3—36792
- **alkaline earth compounds**
  - *see also barium compounds; beryllium compounds; calcium compounds; magnesium compounds; radium compounds; strontium compounds*
  - alkaline earth sulphates, Eu^{2+} activation, fluorescence and excitation spectra 3—39172
  - difluorides, nonempirical LCAO MO SCF studies, bonding trends 3—20096
  - fluoride crysts., band struct. and optical props. 3—33793
  - fluoride-CdF_2 systems, comparative study *(French)* 3—14978
  - fluorite-type cryst., band struct. from space group theory 3—18078
  - fluorite-type crystals, activation of electron excitations by Er^{3+} ions, Stark splitting 3—36941
  - fluorites:Yb^{2+}, f-d transitions, investigation 3—24682
  - group II difluorides, ^{19}F chem. shift tensor and nonionic bonding . 3—12070
  - growth of alkaline earth orthophosphates in gelatin gel 3—24783
  - halides, luminesc. impurity centres, energy transfer excitonic mechanisms *(Russian)* 3—27537
  - hydrides, floating type wave functions in molecular pseudopotential calculations 3—38260
  - oxide crystals, effective ionic charge 3—20706
  - oxides, effect on optical and e.p.r. spectra of γ-irradiated glass *(Russian)* 3—15479
  - phosphates, cryst. growth in gelatin gels 3—15610
  - scheelite type cryst. containing Pr^{3+}, line broadening and vibr. spectra study 3—15526
  - sulphides, luminescence spectra *(Russian)* 3—27553
  - transparent refractory ceramics, high temperature baking process *(Russian)* 3—24972
  - tungstates, growth from LiCl melt, crystn. kinetics 3—24045
- **alkaline earth metals**
  - *see also barium; beryllium; calcium; magnesium; radium; strontium*
  - electronic transitions and structure, review 3—33814
  - evaporation from discharge tube wall, Rozhdestvenskii hook method appl. 3—14619
  - Hawaiian marine atmosphere, chemical fractionation of alkali and alkaline Earth metals 3—12748
  - intense radiation sources for alkali and alkaline earth metals, preparation methods 3—32262
  - ion collisions with atomic Cd from threshold to 1000 eV 3—20065
  - pseudopotential calcs., localized d-states 3—8116
- **alkalinity** *see pH*
- **allotropism** *see polymorphism*
- **alloys**
  - *alloys such as Au-Cu, Au-Cu-Zn are indexed under components of the named elements i.e. gold alloys; copper alloys; zinc alloys in these examples*
  - *see also actinide alloys; aluminium alloys; antimony alloys; arsenic alloys; bismuth alloys; cadmium alloys; dilute alloys; gallium alloys; indium alloys; lead alloys; liquid alloys; lithium alloys; magnesium alloys; mercury alloys; noble metal alloys; rare earth alloys; solid solutions; thallium alloys; tin alloys; transition metal alloys; zinc alloys*
  - A15 compounds with linear chains, superconductivity and lattice instabilities 3—2203
  - activity meas., comparison of e.m.f. and vapour press. methods 3—36999
  - additivity rule conformity in shock compression *(Russian)* 3—31102
  - aligned composite prod. by up-transform. 3—39324
  - amorphous, close packed random struct. model 3—14689
  - analysis and synthesis theory of alloys and materials, inhomogeneous in their physical properties *(Russian)* 3—2698
  - atomised powder method of alloy production for good high temp. props. 3—18681
  - b.c.c., screw dislocation retardation mechanism *(Russian)* 3—30988
  - binary, cryst. growth from melt 3—12272
  - binary, diffusion controlled phase transform. kinetics, X-ray analysis 3—34508
  - binary, disordered tight binding, theory for different constituent bandwidths 3—8087
  - binary, kinetic crystn. diagrams *(Russian)* 3—11724
  - binary, local order effect on electronic states 3—20994
  - binary, off-diagonal randomness, theoretical approaches 3—30384
  - binary, order-disorder transitions, behaviour of Gibbs free energy 3—36399
  - binary, solid/liquid interfacial tension, statistical calculation *(French)* 3—18018
  - binary alloys, substitutional, equilibrium solution of Vineyard's equation for the kinetics of long range order 3—34494
  - binary disordered, size effect and multisite correlations 3—17761
  - binary eutectic, phase separation by ultracentrifugation during solidification *(French)* 3—2715
  - binary ordered alloy, derivation of isotope diffusion coeff. for vacancy mechanism by path probability method 3—4874
  - binary system with excess vacancies, microscopic theory of interdiffusion *(Russian)* 3—15028
- **alloys** continued
  - binary systems, interdiffusion coefficients calc., computer program 3—30292
  - binary systems, statistical constitution anal., logical decision pattern *(German)* 3—8774
  - casting, binary, non-equil. thermodynamic approach to solidification process *(Japanese)* 3—34499
  - circumboundary free zone width, assessment method 3—18575
  - coarsening of compound precipitates, activation energy and rate constant 3—15679
  - corrosion fatigue of materials for biomedical applics. 3—27657
  - corrosion resistant, development 3—21683
  - creep rupture under multi-axial states of stress 3—5309
  - creep strength, conf., Sheffield, England (Sept. 1972) 3—8911
  - creep with weak strengthening under nonsteady temp. and force conditions 3—31100
  - cryogenically worked, properties 3—31037
  - crystal chemistry and physics, book 3—11586
  - deposit prep. by continuous electron beam evaporation from single rod-fed source 3—27715
  - diffusion creep inhibition by precipitates 3—20799
  - diffusional dissolution kinetics of spherical precipitate of second phase *(Russian)* 3—37016
  - dislocation model for critical flow stress calc., effect of solute atom conc. 3—24188
  - dislocations, by X-ray crystallography *(German)* 3—30123
  - disordered, config. entropy and solute correl. 3—36996
  - disordered, electronic spectrum, band-edge behaviour, short-range order effects 3—27202
  - disordered, electronic struct., iteration scheme, IATA 3—30389
  - disordered, localization criteria, single site coherent potential approximation 3—2019
  - disordered, role of 3-body potentials in quasibinary alloys 3—4820
  - disordered, second-order phase transition, long range order stability 3—33669
  - disordered binary, random transfer integrals and electronic struct. 3—36519
  - disordered substitutional alloy, calc. of extended potentials in CPA 3—24371
  - disordered ternary, coherent potential approximation and diagrammatic equivalent, electronic theory 3—38775
  - disperse phases in metallic alloy, kinetics of non-diffusional coalescence 3—31008
  - dispersed particles, size stability in the diffuse interface limit 3—18608
  - dispersion hardened, work hardening theory 3—37065
  - elastic constants, electrostatic contribs. in calcs. 3—17893
  - elastic elements of machines and instruments, mech. characteriz. 3—21684
  - electron density, model calc. approx. for strong scatt. binary alloy 3—24366
  - electronic averaged density of states, density of states in disordered systems 3—38777
  - electronic structure of binary alloy, short-range order effects 3—38774
  - eutectic, and pure liquids, melting or freezing in a wedge shaped enclosure 3—14982
  - eutectoid, transform. processes obs. by photoemission electron microscope 3—18568
  - eutectoid decomposition, λ-R relationship 3—8813
  - fatigue crack growth, effects of loading freq. and nonreactive external media 3—31234
  - fatigue crack growth, plastic strip method 3—21766
  - f.c.c., irradiated, nature of low temp. self-interstitial 3—14849
  - f.c.c., substitutional, influence of solute pairs on solute diffusion 3—5290
  - f.c.c. alloy, two vacancy interactions influence on substitutional solute diffusion 3—17997
  - f.c.c. substitutional, crit. strain associated with dynamic strain ageing 3—39373
  - ferromagnetic, anomalous Hall effect, cond. electron scatt. on magnons *(Russian)* 3—36589
  - ferromagnetic, plastically deformed single cryst., mag. anisotropy and dislocation struct. *(Russian)* 3—36729
  - ferromagnetic disordered, Went's theory modification using correlation range 3—15315
  - films, characterization by nuclear microanalysis 3—37754
  - fracture, inter- and transcrystalline fracture rel. to stress corrosion *(Russian)* 3—8801
  - heat resistant, anodic precipitation, quantitative X-ray analysis 3—25952
  - heterophase system with ordered segregation, phase boundaries *(Russian)* 3—15681
  - high-coercive, temp. hysteresis of residual induction *(Russian)* 3—8387
  - high-strength, fracture toughness role in low-cycle fatigue crack propag. 3—31047
  - interband effects in coherent potential approximation 3—20986
  - intermetallic lightweight cpds., dynamic yield strengths, compressional and Hugoniot elastic parameters 3—17927
  - Invar type, mag. exchange contrib. to elastic consts., rel. to anomalous elastic props. 3—24597
  - kinetics of ordering and antiphase domain growth vs. the kinetics of spinodal decomposition and coarsening 3—18609
  - $L2_0$ type, antiphase area energy created by dislocation slip 3—14913
  - large-grain, resistance to rupture 3—31062
  - Laves phase in $ZrFe_2$, $ZrCo_2$, $ZrNi_2$, $HfFe_2$, $HfCo_2$ and $HfNi_2$ *(Russian)* 3—12334
  - long period superstructures and their interpretation 3—14729
  - long-time strength test results, extrapolation method 3—34688
  - martensitic transformations, reconciliation of the phenomenological theory with mechanisms of diffusional nucleation and growth 3—15660
  - materials science and technology treatise 3—2621
  - metal-graphite alloys, nucleation and growth of spheroidal graphite 3—8789
  - metal-H system, in presence of applied stress field, thermodynamic anal. 3—5292
  - metallic, electron theory treatment of relaxations around lattice of point defects 3—1971

alloys continued
metallic alloys for high temperature gas-cooled reactors, status 3−23445
metastable, effect of overheating on creep resistance 3−21707
multialkali photocathode, optical props. and processing parameters 3−30835
neutron diffraction effects, assignment to struct. components 3−27640
nondestructive testing, computerized X-ray fluorescence spectrometer 3−10138
optic axis of optically uniaxial crystals, orientation determ. using polarized light microscopy 3−24858
order-disorder transformations in generalised Ising model 3−36401
ordered, interfaces study *(French)* 3−17855
ordered, phase transition within phase boundary 3−1716
ordered, type $L1_2$ superstruct., dislocation barriers *(Russian)* 3−30986
ordered and disordered, work hardening 3−39359
ordered $L1_0$ structure, new types of superdislocations 3−17845
phase diagrams, computer information processing 3−27619
Portevin-Le Chatelier effect, interaction of impurity atm. with moving dislocations 3−17912
powders new preparative processes 3−5363
precipitation hardening, a strengthening parameter 3−21704
precipitation of γ'-phase, moderate deformation influence 3−24936
quasi-binary alloys, disordered, theory 3−7864
random binary alloys, amorphous semiconductors, theoretical foundation of existing models 3−38778
random cubic binary solns., atomic pots. applic. to heat of mixing, lattice parameter and compressibility 3−24814
random lattice, coherent potential approx. improvements 3−36518
recrystallisation of dispersion hardened alloy with b.c.c. lattice 3−31011
recrystallisation of dispersion hardened alloys 3−5311
scanning electron microscope studies 3−12360
shape memory (‘Marmem’) effect, review 3−8872
short-range ordered, self-consistent single-site approx. 3−18067
soft X-ray absorpt. edges calcs. 3−30895
solidification, dendritic and laminar heterogeneity formation *(Russian)* 3−8778
spinodal decomposition without diffuse interface, theory 3−24844
splat-cooling apparatus for non crystalline solids preparation 3−9005
stability of precipitates in an irradiation environment 3−5310
stress corrosion cracking 3−15713
stress corrosion cracking via surface diffusion, interface morphology development 3−34570
stress corrosion test methods 3−9025
structural strength concepts and methods of determ. 3−21679
substitutional semiconductor, effect on spin-orbit splitting, test of virtual-crystal approximation 3−2008
substitutional-interstitial interactions in b.c.c. alloys 3−2704
super-refractory, mechanism of σ phase precipitation *(French)* 3−21602
super-refractory, unidirectional solidification *(French)* 3−27621
superalloy model, disruption peculiarities in high pressure gaseous oxidiser, sparks, arcs *(Russian)* 3−26911
superconducting, Josephson tunnel effect with local states within the gap 3−21184
superconducting, with overlapping energy bands, freq. depend. of u.s. absorpt. *(Russian)* 3−36676
superconducting dilute magnetic alloys, e.p.r. induced transitions 3−18265
superplastic, stress relaxation technique applic. to superplastic materials 3−37101
superplastic aggregates, diffusion 3−27639
superplasticity, electron theory and kinetic theory of dislocations 3−27057
symmetrical mixing enthalpy, statistical investigation *(French)* 3−7913
ternary b.c.c., anisotropy of substitutional-interstitial internal friction peaks 3−36365
ternary composite growth from melt 3−39315
thermo-e.m.f., irrad. effects *(Russian)* 3−8151
thermoelectricity, book 3−24414
two-dimensional ω phase transform., Monte Carlo simulation 3−15657
two-phase, cross slip mechanism, dislocation config. energy 3−33597
two-phase lamellar structs., thermal stability 3−37012
vacuum deposition, theoret. and practical considerations 3−25717
X-ray diffuse scatt., errors in analysis 3−36234
$Ca_{1-x}Sr_xPb_3$, supercond. critical temp. rel. to lattice deform., Brillouin zone effects 3−34008
$CeCu_2$ structure, crystal chemistry 3−20715
Cs_3Bi, valence band density of states determ. from photoemission and electron scatt. 3−24773
Cs_3Sb, valence band density of states determ. from photoemission and electron scatt. 3−24773
Cu_3Au-type, ordering, Monte Carlo calc. *(Russian)* 3−30970
Ge-Se system, current-voltage characteristics and temp. depend. of low-field conductivity 3−38843
Ge-Si, cryst. growth from melt 3−12272
Ge-Si, Gruneisen parameters determ. from inertial thermoelastic stress meas. 3−24278
Ge-Si, local and resonance modes from Raman scattering 3−24702
Ge-Si:Ga,Li, temp. depend. of Li solubility *(Russian)* 3−14974
Ge-Si-Sb phase diagram study *(French)* 3−17959
Ge-Sn amorphous film, energy pseudogap from d.c. cond. temp. depend. 3−18055
Ge-Ti-Nb superconducting sheets, applied magnetic field vs. critical current density characteristics *(Japanese)* 3−8298
$Ge_{0.5}Si_{0.5}$ amorphous film, struct. and Raman scatt. 3−36501
Ge_xSn_{1-x}, amorphous, $x \geqslant 0.5$, struct., optical props., optical gaps 3−7627
K-Rb(Cs), Hume-Rothery’s 15% rule and pseudo-alloy-atom model 3−24817
Na-Cd, crystal structure obs. for $NaCd_2$, Na_2Cd_{11} samples 3−24062
Na-K, interphase surface tension, 20-160°C 3−20924
Na-K-Rb ternary alloy, solid-liquid phase equilibria 3−24243

alloys continued
Na-K(Rb)(Cs), Hume-Rothery’s 15% rule and pseudo-alloy-atom model 3−24817
Rb-Cs, Hume-Rothery’s 15% rule and pseudo-alloy-atom model 3−24817
Se-Te, cryst. growth from melt 3−12272
Se-Te, struct., perturbed ang. γ-γ correl. study 3−14740
Si-Ge, e.p.r. of surface, temp. behaviour, Fermi level change rel. to surface states 3−5047
Si-Ge, local and resonance modes from Raman scattering 3−24702
n-Si-Ge alloys, Si-rich electron magnetic susceptibility and band structure 3−36530

alnico alloys *see iron alloys*

alpha decay
see also alpha-decay theory; alpha-particle spectra; radioactivity
absolute energy meas. for obtaining set of accurate standards 3−10940
short range fragment emission from K^- interactions 3−11028
superheavy isotopes, z=112, 114, 126, calc. of half-life, Winslow model 3−10937
$^{8}Be \rightarrow {}^{4}He + {}^{4}He$, following $^{11}B(p,\alpha)^{8}Be$, $E_p < 1.4$ MeV, mechanism 3−10938
^{9}Be excited state decay props. from four-body breakup of $d + {}^{11}B$ 3−26465
Bi isotopes *(French)* 3−6789
^{252}Cf ternary fission, post-scission α-particle emission 3−14240
^{244}Cm, calorimetric meas. of alpha half-life 3−6790
^{257}Fe, alpha-to-spontaneous-fission decay ratio and total half-life 3−35921
^{148}Gd, α-particle energy absolute meas. *(French)* 3−38145
^{248}Md, ^{249}Md, ^{250}Md, ^{251}Md, ^{252}Md, half-lines detn. and α-energies 3−19820
^{20}Ne, fractional branch and width ratio meas. for α-decay to ^{16}O 3−10939
$^{18}O(p, t)^{16}O$, α-decay modes in T=2 state to ^{12}C and ^{15}N 3−19819
^{169}Os, prodn. from ^{20}Ne bombardment of ^{150}Dy 3−14181
Pb, light isotopes *(French)* 3−6789
$^{188}Pb \rightarrow {}^{184}Hg$, search for rotational fine structure in ^{184}Hg 3−29368
Po-α energy scale, comparison with ^{198}Hg energy scale 3−10943
^{232}Pu decay, gamma-ray and alpha spectroscopy, half lives determ. 3−23263
^{233}Pu decay, gamma-ray and alpha spectroscopy, half lives determ. 3−23263
^{234}Pu decay, gamma-ray and alpha spectroscopy, half lives determ. 3−23263
Tl, light isotopes *(French)* 3−6789

alpha-decay theory
see also alpha decay
superfluid correlations in calc. of decay of odd and odd-odd nuclei *(Russian)* 3−19821
α particle emission and orthodox quantum mechanics 3−23282

alpha-particle absorption
see also nuclear reactions and scattering due to alpha-particles
1 to 5.476 MeV particles, energy loss in tissue equivalent plastics 3−5685

alpha-particle angular distribution
see also alpha-particle spectra
$^{8}Be \rightarrow {}^{4}He + {}^{4}He$, following $^{11}B(p,\alpha)^{8}Be$, $E_p < 1.4$ MeV, mechanism 3−10938
^{252}Cf, α-particle accompanied spontaneous fission, trajectory calcs. of correlations 3−1024
^{252}Cf, spontaneous fission, ang. distrib. of α-particles 3−17260
^{52}Cr, ^{53}Cr, cross-sections for elastic and inelastic α-particle scattering, 13-29 MeV 3−32882
Fe: ^{220}Rn, ^{224}Ra, hyperfine interactions of Rn and Ra, alpha decay PAC obs. 3−2270
$^{6}Li(\alpha,\alpha)^{6}Li$, two-nucleon transfer reaction, cross-section meas. *(French)* 3−11005
$^{26}Mg(^{3}He,\alpha)^{25}Mg$, 9-11 MeV, meas. of excitation functions, angular distrib., differential cross section, spectroscopic ratios 3−32877
^{58}Ni, cross-sections for elastic and inelastic α-particle scattering, 13-29 MeV 3−32882
$^{16}O(\alpha,\alpha)^{16}O$, backward scattering at 20 and 29 MeV, angular distrib. meas., Regge pole analysis 3−29409
$^{31}P(d,\alpha)^{29}Si$, $E_d = 2.8$-4 MeV, ang. distribs., excited states, cross sections *(Russian)* 3−17253
^{48}Ti, cross-sections for elastic and inelastic α-particle scattering, 13-29 MeV 3−32882
^{235}U thermal-neutron fission, correl. between energies and angles of emitted α-particles 3−1027
$^{89}Y(d,\alpha)$, 16 MeV, two-nucleon pick-up reaction, meas. of angular distribs., comparison with DWBA and ^{90}Zr reaction data 3−23335

alpha-particle attenuation *see alpha-particle absorption*

alpha-particle detection and measurement
see also alpha-particle spectrometers; dosimetry; particle detectors; radioactivity measurement
absolute energy meas. for obtaining set of accurate standards 3−10940
colour film, autoradiography applic. *(German)* 3−37715
heavy ion reactions and sum analysis 3−13425
position sensitive surface barrier array type detector 3−10080
thin film detector, position sensitive response 3−3849
tracks through mica backed with ^{241}Am source, in situ mass spectrometry 3−25895
Si surface barrier detector, comparative pulse-height anomaly at 9,500 MeV 3−10055
Si surface barrier detector, power resolution, effect of charge collection efficiency 3−19294

alpha-particle effects
see also nuclear reactions and scattering due to alpha-particles
mica backed with ^{241}Am source, in situ mass spectrometry of α-particle tracks 3−25895
Ar solid, electric currents and bubbles 3−30505
Cu, interstitial and vacancy props. rel. to Cu_3Au 3−14898
Cu foil, irrad. at 78K, internal friction and Young’s modulus *(German)* 3−7851
Cu_3Au, interstitial and vacancy props. rel. to Cu 3−14898
GaAs, photocond. in mag. field, 2 MeV α-particle irrad. effects at 300K 3−21108

alpha-particle effects continued
Si paramagnetic centre generation, e.s.r. study 3–34211
V, irrad., He gas bubble nucleation and distrib. 3–33572
W, deformed, α-ptcle. irradiated and annealed, presence of He bubbles 3–18656

alpha-particle interactions
see also nuclear reactions and scattering due to alpha-particles
No entries

alpha-particle model *see nuclear cluster model*

alpha-particle scattering
see also nuclear reactions and scattering due to alpha-particles
energy straggling, as fn. of atomic number of absorber 3–16502
SiO$_x$ thin films, Rutherford scattering, stoichiometry, impurity content investigation 3–7788

alpha-particle spectra
see also alpha-particle angular distribution
diffusion in solids, nondestructive method of study using alpha-particle spectrometry 3–25921
mathematical model to meas. gas props. with alpha particle gauges 3–335
^{12}C, α-particle spectroscopic amplitudes, harmonic oscillator shell model with SU(3) classification 3–35919
^{12}C(^{16}O, ^{4}He)^{24}Mg, residual nuclear level density effects on σ-particle spectrum 3–6908
^{12}C(n,n)3α obs. in kinematically complete expt. 3–26452
^{252}Cf, spontaneous fission, alpha-particle formation probability calc. 3–35922
^{148}Gd, α-particle energy absolute meas. *(French)* 3–38145
^{16}O, α-particle spectroscopic amplitudes, harmonic oscillator shell model with SU(3) classification 3–35919
(U, Pu)C, α-particle stopping power and range, application to self-diffusion meas. using alpha-spectroscopy 3–11664
UC, α-particle stopping power and range, application to self-diffusion meas. using alpha-spectroscopy 3–11664
^{235}U, thermal neutron fission, alpha-particle formation probability calc. 3–35922

alpha-particle spectrometers
see also alpha-particle spectra
Apollo 15 and 16, design and circuitry 3–31803
Argonne double focusing magnetic, position sensitive surface barrier array type detector, addition 3–10080

alpha-particles
see also cosmic ray alpha-particles and helium nuclei
geomagnetically trapped, off-equator particles in outer zone 3–12819
organic liquids, stopping power for alpha particles, 1-8 MeV 3–20773
standard source, checking 3–22459
α-particles acceleration, space radiation effects laboratory synchrocyclotron 3–35458
^{252}Cf fission, five-parameter correlation expt. 3–17272
^{235}U, fast and thermal neutron, tritium and α-part. yields 3–14238

alpha-radiation *see alpha-particles*

alpha-rays *see alpha-particles*

alpha-rhythm *see electroencephalography*

altitude measurement *see height measurement*

aluminium
adsorption effect in drawing with organic lubricants, oxide film form. 3–33604
alloying effect on neutron-irradiation hardening of Cu 3–18630
anelasticity, amplitude dependent, role of dislocation motion in single crystals *(German)* 3–24214
anelasticity, amplitude-dependent during and after plastic deformation *(German)* 3–34611
anharmonic thermal scattering of X-rays 3–38524
atom, K-shell Coulomb ionization cross-section, impact parameter depend with 0.3-3.0 MeV protons 3–23487
Auger electron and charact. energy loss spectra from clean and slow oxidized surfaces 3–34452
Auger-electron and photoelectron structure in secondary electron energy distributions, high reduction meas. 3–8691
axisymmetric extrusion, plastic flow, substructure exam. 3–39360
beveling process, etching, anodic oxidation, for multilayer metal circuitry 3–38739
Bordoni relax., secondary features 3–33608
brittle fracture change of tensile strength with temp., determ. of critical inflexion temp. 3–21699
cast, mirrors, dimensional stability on thermal cycling 3–5920
casting textures, influence of mould shape and melt feed method *(German)* 3–8900
cathode, dynamics of precathodic region at various rates of changing current in impulse discharges *(Russian)* 3–30046
cathode in medium voltage spark discharge, cathode spot formation obs. by high speed photography 3–30032
chondrules, vapour fractionation 3–2864
composite material from bonding with B 3–21732
conduction e.s.r., frequency dependence interpreted as new many-body effect in metals with g anisotropy 3–2394
conduction e.s.r. line detection using refl. spectrometer 3–265
contact on Si, specific contact resist. 3–27311
core binding energy in silicate minerals, ESCA technique 3–5431
coupled thermoelastoviscoplasticity, finite-element formulation 3–38612
cracks in space vehicle cabin wall panels, detection by u.s. techniques 3–31227
creep, high temp., internal stresses and dislocation structure 3–7832
creep, steady state, strain transient dip test obs. 3–7833
creep, substruct. formation kinetics 3–39344
creep characteristics, correl. with substruct. misorientation and stacking fault energy *(Russian)* 3–8837
creep under intermittent loading 3–37103
creep-deformed, dislocation struct. of subgrain boundaries 3–24121
crystalline ultrathin films, superconducting props. 3–18238
d.c. sputtered, low resistivity films 3–39225
deformed, neutron irrad. effects on anelastic behaviour *(French)* 3–30207
deformed in tension, flow stress and latent hardening 3–5316

aluminium continued
dense phase gas solid suspension, positive expulsion fluidization tank 3–4619
dielectric screening and phonon dispersion 3–38633
diffusion freq. factor and activation energy correl. 3–18002
diffusion in ZnSe, optical props. 3–24712
diffusion of Fe, surface barrier to diffusion, Mossbauer obs. 3–38684
dislocation annihilation mechanism by deformation 3–17823
dislocation damping at high strain rates, high-velocity compression tests 3–36301
disordered polycrystals, distortion waves 3–17926
dynamic stress/strain behaviour in torsion 3–21779
elastic behaviour under very weak stresses of single crysts. *(French)* 3–30169
elastoresistance relaxation in thin film 3–33866
electrical resist. meas. at low temp., temp. depend. of T^3 form 3–18114
electro-displacement deposition method for Zn on Al surface, Zn diffusion 3–11766
electron backscatt., angular distrib. 3–15580
electron backscatter and backemission yields, bombarded by 0.4 to 1.4 MeV electrons 3–18514
electron diffr. studies using fast electron diffractor with energy filter *(French)* 3–20683
electron diffraction obs., calc. of exchange effects on Kikuchi band and abnormal absorpt. 3–23999
electron emission, very low energy, following machining *(German)* 3–18535
electron energy loss analysis by thermomodulation procedure *(German)* 3–28640
electron irradiation damage, 3 MV electron microscope, voltage dependence 3–36333
electron radiation and surface roughness 3–27593
e.m. attenuation of shear waves near superconducting transition temp. 3–2213
embrittlement by Hg, role of solute additions 3–34566
equation of state, semiempirical, rel. to mech. props. *(Russian)* 3–27618
evaporation from discharge tube wall, Rozhdestvenskii hook method appl. 3–14619
exoelectrons, intensity and energy, simultaneous meas. after low temp. deform. *(Russian)* 3–21522
extrusion load calc., temp. rise meas. 3–37046
fatigue cracks, substruct. form. and propag. 3–21610
fatigue damage, visual display by means of exoelectron emission 3–12468
fatigue damage monitoring by u.s. attenuation meas. 3–13232
fatigue props. of pure specimens, microstruct. influence 3–31110
fatigue strength, low-cycle, determ. under axial and reversed torsional strain cycling 3–5299
fatigued, internal friction peak behaviour and dislocation-point defect interaction *(French)* 3–11685
Fermi surface, OPW model for pressure depend. 3–33788
Fermi surface, third-zone, uniaxial compression effects 3–8093
field-ion microscopy, for surface investigation 3–28734
film, conditions for vapour growth on mica substrate 3–15620
film, effect of charact. energy losses on electron diffraction intensities 3–24156
film, electromigration, quantitative mass distrib., scanning electron microscope obs. 3–7977
film, electron scatt., ang. distrib. of secondary electrons *(German)* 3–18521
film, granular, depression of vortex flow resist. helow H$_{c2}$ 3–30574
film, granular supercond., transition to zero dimensionality 3–30562
film, He ion pre-injected, electron irradiation effect on void form. 3–20967
film, in contact with Au film, interaction *(Russian)* 3–4871
film, influence of deposition substrate temp. and partial disorder on optical props. 3–24715
film, microstruct. and electromigration, laser irrad. effects 3–20974
film, optical radiation on passage of electrons up to 100 keV 3–24771
film, polycrystalline, dynamical effects in electron scatt. for structure obs. 3–24014
film, pure and oxidized, X-ray photoelectron spectra analysis 3–30923
film, refl., 1000-1600 Å, substrate roughness effects 3–12152
film, size effect parameters rel. to electron transport 3–30448
film, supercond. nonlinear elec. field depend. near T$_c$ 3–8302
film, supercond. transition temp. depression by Ar(Ne) overlayers, surface phonon contrib. 3–34017
film, vacancy influence on transversal magnetoresist. at 4.21 K 3–30460
film, vacuum deposition, source contrib. to O$_2$ contamination 3–15621
film deposition, thickness meas. by microbalance 3–37588
film stripes, electromigration rel. to anodic Al$_2$O$_3$ coating 3–38906
flaws during heat treatment, X-ray obs. of sources *(French)* 3–15057
foil, dislocations due to friction, lubrication and oxide layer effects 3–27063
foil, tensile and fatigue crack growth obs. electron microscope examination of materials 3–21761
foil, X-ray television method for grain growth obs. under heat and stress treatment 3–26936
foils, electron microscope search for foreign inclusions and their role in crack and pin hole formation 3–21608
on glass substrate, spectral specular reflectance, standard reference materials, preparation and calibration 3–19143
grain boundary fine structure, bright and dark field transmission electron microscopy 3–1632
grain boundary viscosity and rigidity modulus of neutron irradiated wire 3–1668
grown by recryst., dislocation density and distrib., annealing effects *(French)* 3–24885
heat transfer mechanism of contacting Al surfaces rel. to thermal contact resistance 3–2174

aluminium continued
hot rolled surfaces, ESCA exam. 3−24957
hypervelocity impacts, metallic plasma, flash, spectral line radiation 3−1484
impulse loading by subnanosecond laser pulses 3−29109
impurity atom interaction with vacancy, pseudopotential approach 3−36293
impurity in W wires, recrystallisation effect on mechanical properties *(Japanese)* 3−31065
impurity-vacancy pair, binding energy, pseudopotential calc. 3−30133
inertial-to-gravit. mass ratios for Al, Pt, torsion balance meas. 3−16742
intergranular corrosion in pressurized water, hydrogen/grain boundary interactions *(French)* 3−1909
interionic potential 3−33787
ion beam, relativistic, heavy, meas. of range in Al 3−33583
ion implantation in n^+- and p^+-Si, ohmic contact characts. 3−18214
ionisation balance, calc. for collisional ionisation, autoionisation, radiative recombination and dielectric recombination 3−11458
ionisation equilib. calc. for solar atm. ions 3−18960
k dependent potential calc. for band struct. and Fermi surface 3−8086
K X-ray spectra, ion-excited, effect of chemical environment of emitting atom 3−4365
laser irrad., plasma emission as light source 3−13301
laser-induced stress-wave and impulse augmentation 3−756
lattice parameter changes, by X-ray diffraction 3−13479
layer of Au substrate, backscatter coefficients, when bombarded with average-speed electrons *(German)* 3−8696
LEED, (110) and (111) surfaces, calc. and expt. 3−36465
LEED, elastic and inelastic, from (100) surface, absolute intensity meas. 3−36464
liquid, temp. dependence of surface tension and density *(Russian)* 3−11798
liquid, thermoelectric props., temp. depend., m.p.-1200K 3−24408
liquids, dielectric screening and resistivity 3−5000
localised orbital wave functions, comparison between theory and expt. 3−8082
longitudinal magnetoresistance, temp. and weak deform. effects 3−2056
lubricant trapping under cold compression *(Japanese)* 3−30990
magnetisation, spontaneous, when immersed in liquid nitrogen 3−36762
magnetothermoelectric power at low temps. 3−2058
matrix, B fibre reinforced composites, transverse tensile props. 3−18716
matrix composites, environment, application, cost and future, review 3−24977
matrix composites, mechanical props., review 3−15776
matrix composites, survey of fabrication methods 3−8997
mesa solid-phase growth from Al metallization 3−21542
microautoradiographs, effect of sort and surface roughness 3−9033
moderator, low energy positron emission in backscatt. mode 3−30926
molten foil, electron diffr. short term persistence of diffuse remnants of reflections 3−38532
Mossbauer effect obs. of dynamical props. of dissolved ^{57}Fe 3−34258
Mossbauer effect study of lattice dynamics of ^{57}Fe impurities, 4-1000 K 3−4835
Mossbauer spectroscopy studies of properties of Fe impurity 3−36822
neutron irrad., radiation damage, postirradiation annealing effects 3−11661
neutron irradiated and deformed at low temp., internal friction and modulus anomaly *(French)* 3−14935
neutron spectra, time-energy study using fast neutrons 3−6968
n.m.r. of ^{27}Al, thermometric detection 3−30680
oxidation mechanism, electron microscope obs. of fine particles 3−38744
oxide film removal by brazing flux and reaction soldering *(Japanese)* 3−31071
particles, cylindrical, attenuation factors calc. for i.r. radiation scatt. 3−24698
particles, oxid., electron microscope obs. of oxide-metal boundary 3−15076
phonon damping due to electron-phonon coupling, calcs. 3−38638
photoelectric emission, effect of gaseous desorption 3−15589
photoemission due to soft X-rays, model 3−18526
photoemission variation after plastic deformation *(Russian)* 3−8700
photostimulated exoelectron emission decay rel. to oxide growth 3−8704
pitting corrosion, alloying elements effect 3−8046
plasmon damping, volume, momentum dependency 3−2123
plasmon decay effects in Auger, secondary and electron energy loss spectra 3−5026
plasmon thresholds in the secondary electron yield, expt. 3−4976
plastically deformed, annealing of struct. discontinuities *(Russian)* 3−24854
plastically deformed, dislocation density, X-ray diffr. and n.m.r. obs. 3−24194
plastically deformed, fatigue damage detection by exoelectron emission 3−18534
plasticity effects in adhesive fracture 3−3973
plasticity of diffusion coatings on steel *(Russian)* 3−12371
polycrystalline strain-annealed, etch behaviour 3−18675
positron-dislocation interactions using independ. part. model and local screening theory 3−7791
powder, adsorption of hydrogen and moisture 3−1889
powder aggregates, strength characterisation, pressure-density data 3−8964
powder with Cu and Fe coating, scanning electron microscope obs. *(Russian)* 3−9022
quadrupolar n.m.r. line broadening obs. 3−34248
quenched-in vacancies 3−17806
recrystallisation of rolled plate, grain structure 3−15664
recrystallization of 99.85 wt% Al, effect of preceding recovery on nucleation *(Czech)* 3−31026

aluminium continued
reflection coeffs. meas. of ultrasonic interfaces using multitransducer configuration 3−9841
regrowth p^+ contacts, for HP Ge γ-ray spectrometer 3−35487
resonance series in vacuum u.v. absorption spectra of dense plasmas 3−17351
self-diffusion processes in different glasses 3−4882
sheet solution, eddy current conductivity meas. near solidus point 3−27830
sheet with cubic orientation, secondary workability obs. *(Japanese)* 3−8863
single edge notched specimens, influence of local variations of yield strength on plastic zones at crack tips 3−21623
slow secondary electron emission, role of bulk and surface plasmons 3−36966
soft X-ray absorpt. edges calcs. 3−30895
spall fracture, dislocation dynamics approach 3−14923
spalling, time dependence to the resistance 3−31095
specific heat anomaly and disorder *(German)* 3−24276
spin polarisation of electrons tunnelling from Fe(Co)(Ni)(Gd) ferromag. to Al superconducting film 3−15311
stacking fault and twin energies calc. 3−14881
straight circular elastic tubes, pulse propag. 3−22693
strain rate effect on ductility *(Japanese)* 3−12389
subgrain boundary misorientation, determ. from split Kikuchi lines 3−24009
superconducting, mag.-field dependence of microwave absorptivity near energy gap 3−18262
superconducting energy gap anisotropy, press. depend. 3−8287
superconducting film, fluctuation induced, paracond. above transition temp. 3−15304
superconducting films, angular dependence of resistive transitions in magnetic field 3−36683
superconducting thin film, interference effects in vortex structure and interactions 3−34034
superconducting transition, mag. field induced, volume change 3−36672
superconductor, zero-dimens. particles, fluctuation diamagnetism 3−34013
surface, bombardment with N^+, Na^+, Cu^+, Ag^+ and Au^+ ions, electron ejection, positive ion refl. 3−2608
surface, geometrical cavities development rel. to vol. diffusion of liq. Ga *(French)* 3−7999
surface, scatt. of H^+ and Ar^+ ions, negative ions energy distrib. 3−15583
surface morphology effect on LEED intensity from Al(110) 3−20915
surface oxidation, static method secondary ion mass spectrometry obs. 3−1906
surface photoelectric effect, modified form of Mitchell-Makinson time-depend. perturbative calc. 3−36978
surface plasmon calc. 3−36649
surface plasmon dispersion on Al(111) film via inelastic LEED 3−38701
surface preparation, by chemical methods 3−38736
surface resistance determ. in hyperfrequency region by transmission coefficient meas. *(Russian)* 3−9993
surface structure from LEED profiles, intensity evaluation 3−24323
surfaces pressed together under high loads, mean separation, real contact area 3−27064
texture influence on the yield loci 3−2733
thermal cond. in mag. fields to 50 kOe, 6K-57K *(Russian)* 3−4989
thermal contact conductance meas. in vacuo 3−10409
thermal diffuse scatt. in X-ray diffraction 3−24137
thermal expansion, linear coeff., 3-35 K, Gruneisen parameters 3−30273
thermal magnetoresistance, anisotropy meas. 3−24410
thermal oxidation, amorphous oxide film growth and cryst. island development during thermal oxidation of Al 3−8045
thermal resistivity at high temps. 3−33861
thermoelectric power in strong mag. field at low temp. 3−24409
thermoreflection, Bragg band-band transition range *(Russian)* 3−8590
thickness, beta versus X-ray measurement 3−22522
thin film, electron conc. and spectral line width from asymmetric self-reversed spectral lines 3−23941
thin film deposition, source-to-substrate distance effect on O_2 sorption 3−34478
thin films, ellipsometric thickness meas., udergraduate expt. 3−31992
titanomagnetite impurities, spinel structure 3−9142
twinning, mech., relation to strain to fracture 3−20808
type II superconducting film, Tinkham's formula for ang. depend. of critical field 3−15296
uniform tensile deformation degree, correl. with strengthening coeff. *(Russian)* 3−8835
vacancy diffusion, activation energy proportional to latent heat of melting *(Russian)* 3−24295
vacuum evaporation to form m.o.s. structure, effect of Si pre-oxidation on surface impurity charge density 3−15267
valence electron redistrib. and positron trapping at vacancies 3−21026
valence electronic charge density, calc. from wave functions obtained via Ashcroft's pseudopotential 3−27209
vaporisation under pulse heat flux in vacuum 3−27108
vertical cones, calc. of free convective heat transfer 3−10414
vertical section geometry of surfaces, studied by embedded Al layer 3−22508
wear due to dry friction, stacking fault energy and elastic modulus effects *(Russian)* 3−7844
work softening obs. and mechanism in polycryst. 3−37066
X-ray emission under O^{+n} bombardment, charge-state depend., dynamic screening 3−24768
X-ray induced photoemission, absolute yields 3−18524
X-ray Kα satellites, ion-energy depend. 3−1106
X-ray photoemission 3−21516
X-ray prod. by electron irrad. 3−16540
X-ray scattering by Al and Al^+, intensity calc. *(Russian)* 3−11132
X-ray technique for crystallography obs. behind shock wave front 3−26930
X-ray topography technique for structure obs. 3−26933

aluminium continued

- X-ray total attenuation coefficients of 25.8 keV photons, meas. 3-39198
- yield locus curves determ. with the aid of knoop hardness measurements *(German)* 3-2732
- Al I bound-free absorpt. importance in A-G type stars flux discrepancies 3-22047
- Al Schottky barrier height determination 3-18215
- Al VI to X e.u.v. and soft X-ray spectra 3-14301
- Al:^{57}Fe, Mossbauer spectroscopy studies 3-36822
- Al:Al_2O_3, dispersion strengthened, obs. of recrystallisation 3-18573
- Al:Gd(Dy)(Er), e.s.r. meas. of exchange integral 3-15413
- Al:Si, annealing near melting temp., effect on substructure *(Russian)* 3-12355
- Al:Ti, film, diffusion from Ti sublayer during Al vacuum condensation 3-30079
- Al:Ti, film, impurity distrib. and diffusion coeff. determ. by elec. method 3-30290
- Al/Al_2O_3 contact, electron injection into anodic oxide 3-8261
- Al/B composite, matrix fatigue behaviour under repeated tensile loads 3-31154
- Al/Cu lamellar cpd., dynamic compressibility *(French)* 3-1686
- Al/Si evaporated films, diffusion-limited Si precipitation 3-39237
- Al-Al_2O_3, electrical and structureal props. of amorphous system 3-38840
- Al-Al_2O_3-Al capacitor, dielec. inhomogeneities, visualization by liq. cryst. layers 3-15284
- Al-Al_2O_3-Al diodes, effect of electropolishing on tunnelling current 3-18230
- Al-Al_2O_3-Au m.i.m. system, electron emission, angular distributions 3-21160
- Al-Al_2O_3-Au m.i.m. systems, electron emission, energy distributions 3-21161
- Al-Al_2O_3-Au m.i.m. system, electron emission, discussion of processes in cathode 3-21162
- Al-Al_2O_3-Au sandwich cathodes, energy ang. distrib. of electrons emitted *(Russian)* 3-30550
- Al-Al_2O_3-Au structure, transmission coeff., applied field depend. 3-8280
- Al-Al_2O_3-electrolyte system electro- and photoluminescence 3-39190
- Al-Al_xO_y-Al(Pb), junction, ellipsometrical determ. of tunnelling barrier thickness 3-34004
- Al-CeF_3-Al structure, isothermal dielec. relax. curents 3-36666
- Al-CeF_3-Al thin film capacitor system, stimulated dielectric relaxation currents 3-8277
- Al-Formvar-Pb junction, logarithmic derivative curves and trap-assisted current transport 3-24544
- Al-I-Al, m.i.m. structure, tunnelling results with Ni doped electrodes prepared at 80K 3-34003
- Al-insulator-Al junctions doped with Fe impurities, conductance reduction 3-2217
- Al-n-Si Schottky contacts, semiconductor-metal boundary, preparation, characteristics *(German)* 3-15254
- Al-polydimethyl siloxane-Al, metal-dielectric-metal assemblies, γ-ray effects on capacitance and loss tangent *(Russian)* 3-39083
- Al-Si barriers, I-V and C-V characts. 3-24507
- Al-SiO_2-Si m.i.s. structure, potential barriers, height measurement, photoemission *(German)* 3-15240
- Al-SiO-Al struct., elec. breakdown of SiO film *(Russian)* 3-15280
- Al-SiO-CdSe system, semicond. insulator interface state density control 3-15268
- Al-ZnP_2-Si structure, surface charge control by wide-gap ZnP_2 semicond. film 3-38903
- Al^+, total cross sections for charge transfer and stripping in He and N_2 3-11181
- $AlNe^+$ collisions, K-shell ionization cross sections 3-23503
- ^{26}Al formation in Fe and Si targets by 0.6 and 24 GeV proton bombard., captive cross section determ. and astrophysical appl. 3-23315
- $^{27}Al^+$ implantation in SiC, effects 3-1633
- B/Al composite, reinforcement of Ti alloy, compressive strength 3-39390
- B/Al composites, fusion welding, microstructure 3-12361
- $BaTiO_3$:Al ceramic, piezo-electric effect 3-21363
- in Be film, effect on supercond. temp. range *(Russian)* 3-11979
- Be/Al filamentary composite, yield pt. phenomena, Luders band propag. 3-34639
- Fe, Armco, microfracture and structural failure under dynamic loading for 1145Al 3-2722
- in GaP, rel. to green light emitting diode appl. 3-8734
- Ge:Al, implanted acceptor levels, rel. to carrier generation at room temp. 3-2083
- Ge/Al thin film system, surface mass transfer mechanism, diffusion phenomena *(Russian)* 3-11836
- γ-ray attenuation coeffs., $E_\gamma=6$-10 MeV 3-17329
- in MgO, irradiated, inducing V_{al} and V^- centres 3-24113
- Se-Al electrode boundary, compound formation, energy levels, vacuum photoemission study 3-38893
- Si:Al, Czochralski growth, impurity striation struct. 3-17860
- Ta-oxide-Al superconducting tunnel junction, search for stimulated emission 3-27333
- YIG:Al epitaxial film, chemical vapour deposition for bubble domain devices 3-33746
- Zn diffusion meas. using the backscatter method 3-18000
- ZnS:Ag, Al, photocond. caused by redistrib. of charge carriers over trapping centres *(Russian)* 3-15220
- ZnS:Cu,Al, electrolum., Gaussian component intensity, alternating voltage freq. depend. *(Russian)* 3-21486

aluminium alloys

- *see also aluminium compounds*
- 7075-T6, fatigue damage accumulation 3-12470
- 7075-T6, vacuum environment effects on fatigue and fracture 3-27678
- braze alloy, presence in Ti honeycomb sandwiches, detection by eddy current testing 3-21767
- brittle rupture, crack propag. resist. study *(Russian)* 3-27669
- corrosion fatigue in aqueous solns., fractographic studies 3-27656
- crack closure obs. using simple strain gauge technique 3-24202
- creep, long-term strength, deform. criterion 3-31233

aluminium alloys continued

- creep rupture tesging 3-21652
- cyclic elasto-plastic notch stresses, graphical procedure 3-12469
- dilute, metal impurities, additional electrical resistivity, experimental results, Ashcroft pseudopotential theory *(Russian)* 3-30452
- ductile fracture, near tip strain concept 3-31052
- Duralumin, fatigue crack growth 3-18750
- duralumin, quenched, serrations in stress-strain curves 3-37058
- Duralumin D1, D16, increase in resistance to recrystallization of extruded bars 3-18603
- as electrical conductors, trace element, heat treatment and cooling effects on conductivity *(Norwegian)* 3-5304
- embrittlement by Hg, role of solute additions 3-34566
- endurance testing 3-22257
- fatigue, at room temp. and 300 F, low-cycle axial strain 3-21653
- fatigue crack closure at positive stresses, plastic deform. in crack wake 3-14922
- fatigue life, high vacuum effect on low cycle fatigue law 3-39423
- fatigue limit, effect of residual stresses caused by metal plating 3-37072
- fatigue strength, low-cycle, determ. under axial and reversed torsional strain cycling 3-5299
- fatigue strength obs. using push-pull testing under high press. *(Japanese)* 3-12486
- fatigue tests, stresses during vibr. of plates under acoustic loads 3-31236
- fracture resist. improvement through thermomech. processing 3-31048
- grain refinement by addition of Ti and B 3-18597
- high temp. aging effect on hardness *(Bulgarian)* 3-15655
- high-strength, hydrogen embrittlement and stress corrosion cracking 3-5336
- inclusions in rolled sheets, volume determ. methods 3-24861
- inclusions role in ductile fracture and fracture toughness 3-30984
- interaction with $MoSi_2$ ceramic, cermet formation, properties 3-8967
- low-cycle fatigue under high hydrostatic pressure, obs. *(Japanese)* 3-8861
- for machine construction, mechanisms of strengthening 3-21685
- nuclear fuel reprocessing, highly active wastes, solidification 3-35944
- phase equilibrium diagram, with Ti, B additives 3-18598
- plasma oscillations and electron energy losses in transition metal-Al alloys 3-33584
- precipitation phenomena, magnetic balance obs. 3-32115
- rare earth compounds RNiAl and RCuAl, struct. and mag. props. 3-20725
- resistance to torsional deform., strain-rate and temp. effect 3-2718
- resistivity, residual, multiple plane wave pseudopotential calc. and iterative soln. of Boltzmann equation 3-24406
- shells, cylindrical, elastic deformation under internal pressure 3-18611
- stress corrosion cracking initiation *(French)* 3-31083
- structural, artificial slow crack growth under const. stress, R-curve concept in plane stress 3-31218
- Ticonal, high-coercivity, characteriz. after isothermal thermomag. treatment 3-24943
- umklapp effect on low temp. thermal resistivity 3-1751
- viscoplastic cylindrical shells loaded by radial pressure impulse, dynamic buckling 3-37810
- voids in irradiated Al alloys 3-20769
- welded, distortion and residual stresses, rel. to use as struct. material 3-31108
- wrought, solution kinetics 3-37047
- βAg-Al splat quenched alloys, martensitic transformation 3-2695
- AgI-Mg commercial alloys, stress corrosion cracking and its prevention *(Japanese)* 3-18635
- Al bronze recrystallization kinetics, obs., effect of prior deformation 3-27627
- Al bronzes mechanical properties, casting properties, effect of iron *(Polish)* 3-31033
- Al bronzes transformations, structure and phase, iron effect *(Polish)* 3-30962
- Al high tensile alloys, fractographic investigation 3-27807
- Al Zn Mg Cu alloy, fibrous struct. and susceptibility to contact corrosion *(German, English)* 3-24354
- Al:Ag, very dilute, lattice sp. ht. rel. to force consts. changes 3-33683
- Al:Ag(Au)(Gd), spin scatt. cross sections 3-18300
- Al/Al_3Ni unidirectional fibre composite, elastic consts., u.s. vel. meas. 3-34637
- Al-3% Cu processed from double-oriented ingots, cold rolling and annealing textures *(Japanese)* 3-18640
- Al-3d transition metal, quadrupolar n.m.r. line broadening obs. 3-34248
- Al-(Ni,Cu,Be,Fe,Co) eutectics, directionally solidified, struct. morphology and microhardness *(Russian)* 3-39328
- Al-Ag (20wt.%), γ'-phase formation mechanism *(Russian)* 3-8780
- Al-Ag (4,5 at.%) alloys, surface superconductivity, magnetisation measurements 3-38920
- Al-Ag alloy, Guinier-Preston zones, electron diffraction effects *(French)* 3-18604
- Al-Ag alloys, quenched from liquid state, preprecipitation, small angle X-ray diffraction obs. 3-15667
- Al-Ag(1wt.%), work softening, polycryst. 3-37066
- Al-Al_2O_3 recrystallisation, effects of particle content, distribution and cold deformation 3-18581
- Al-Al_3Ni, two phase alloy, electron scatt. on precipitate boundaries, low temp. resist. meas. 3-36580
- Al-Al_3Ni aligned eutectic alloy, fatigue fracture behaviour 3-21658
- Al-Al_3Ni directionally solidified eutectic, elec. cond. *(Russian)* 3-24826
- Al-Al_3Ni eutectic, rod to blade transition 3-39313
- Al-Al_3Ni eutectic comp., thermal stability of microstruct. *(Russian)* 3-24850
- Al-Cr, cold-worked, impurity resistivity from 78 to 300 K 3-14886
- Al-Cr, dil., n.m.r. spectra. satellite struct. interpret. 3-2431
- Al-Cr, supersaturated solid solns., annealing and diffusion kinetics 3-36438

aluminium alloys continued
Al-Cr-Zr, granulated and supersaturated, decomposition mechanism and kinetics *(Polish)* 3−31032
Al-Cu, $AlCu_3$ phase, cryst. struct. 3−14733
Al-Cu, eutectic spherulites, electron microscope obs. 3−27638
Al-Cu, heat treatment effect on strain ageing 3−31080
Al-Cu, in various metallurgical states, mag. susceptibility, 10-300K *(French)* 3−24559
Al-Cu, liquid state, elec. conductivity, temp. depend. *(Russian)* 3−2054
Al-Cu, metastable equilib. study 3−39326
Al-Cu, oxidation kinetics, 475-575°C, γ-Al_2O_3 film formation, O_2 diffusion 3−33743
Al-Cu, serrated yielding and strain gradients occurrence 3−21700
Al-Cu, solvus curve of Guinier-Preston zones *(Japanese)* 3−30998
Al-Cu (4 at wt.%), diffuse scattering topography and struct. analysis of G.P. zones 3−18570
Al-Cu alloy, structural and phase changes in welded joints 3−24832
Al-Cu alloy, structural transformations and mechanical props. 3−12413
Al-Cu and Al-Cu-Mg directionally solidified eutectics, ageing response 3−34581
Al-Cu film, secondary grain growth 3−1956
Al-Cu oriented bicrysts., intergranular precip. *(French)* 3−27626
Al-Cu system impurity trapping during crystallisation from melts 3−33466
Al-Cu-Li, resist. obs. of Al_2CuLi precip. 3−21660
Al-Cu-Li, $T_1(Al_2CuLi)$ precip. 3−8798
Al-Cu-Mg-Ag, heat treatment, struct. of metastable precip. 3−15662
Al-Cu-Ni system, ternary composite growth from melt 3−39315
Al-Cu-Ni system, ternary composite growth from melt 3−39316
Al-$CuAl_2$ lamella eutectics and fibrous eutectics, unidirectionally solidified, microstructure *(Japanese)* 3−18592
Al-$CuAl_2$-$FeCu_2Al_7$ ternary eutectic composite, mechanical props. and thermal stability *(Japanese)* 3−15701
Al-$CuAl_2$-$NiCu_3Al_6$ ternary eutectic composite, mechanical props. and thermal stability *(Japanese)* 3−15701
Al-$CuAl_2$-Si ternary eutectic composite, mechanical props. and thermal stability *(Japanese)* 3−15701
Al-Cu(4 at wt.%), precipitation study by internal friction, hardness and electron microscopy meas. *(French)* 3−15687
Al-Cu(4.5 wt.%), surface relief effects associated with $CuAl_2$ rod form. 3−37006
Al-Fe, dil., cold-worked, internal friction and Young's modulus, heat treatment effects 3−27703
Al-Fe alloys, oxide films, X-ray photoelectron spectra 3−8701
Al-Fe bicrysts., grain boundary precipitate exam. by Ga embrittlement technique 3−37025
Al-Fe powders, cold worked and annealed, magnetisation, temperature and field dependence 3−12040
Al-Fe-Mn, splat quenched, decomposition mechanism 3−2712
Al-Fe(3.6 at.%), supersaturated solid solns., annealing and diffusion kinetics 3−36438
Al-Ge, incoherent Ge precipitates, vacancies and nucleation influence *(German)* 3−34550
Al-Ge alloys, vacancies influence on nucleation of incoherent Ge precipitates 3−2702
Al-Ge amorphous films, crystn. and decomp. *(German)* 3−24819
Al-Li, decomp. of solid soln., resist. obs. 3−21606
Al-Mg, Al-MgMn alloys, horizontal strip costing in stationary d.c. moulds, properties 3−12417
Al-Mg, dil., neutron irrad. at 4.6K, resist. study 3−27042
Al-Mg, dilute alloy, recovery after neutron irradiation at 4.6K, elec. resist. obs. 3−11658
Al-Mg, effect of addition of Bi on stress-corrosion cracking *(Japanese)* 3−18634
Al-Mg, Portevin-Le Chatelier phenomena *(French)* 3−31092
Al-Mg, soft X-ray absorpt. edges calcs. 3−30895
Al-Mg (1 wt.%), work softening, polycryst. 3−37066
Al-Mg (5 at %) solution annealed, material variability, low temp. resistivity obs. 3−24871
Al-Mg alloy, Guinier-Preston zones, electron diffraction effects *(French)* 3−18604
Al-Mg dilute solid solution, plasma energy loss rel. to band models of alloying 3−7803
Al-Mg stress-corrosion resistance, improvement by Bi additions 3−12382
Al-Mg work-hardened sheet, forming-limit diagrams in biaxial tension 3−12381
Al-Mg-Si, plastic deformation effect on precipitation *(Japanese)* 3−15699
Al-Mg-Si, quench-aged, step-wise yielding and unlocking serrations 3−31093
Al-Mg-Si:Cu, aging, effects of Mg loss, elec. resistance meas. 3−39361
Al-Mg-Ti-Zr-Mo, AL8 cast alloy, alloying additions influence on Failure under tensile stresses 3−31085
Al-Mg-Zn, microstruct. influence on mech. props. and stress corrosion susceptibility 3−39342
Al-Mg(0.13 wt.%) prismatic dislocation loop rotation and self-climb phenomena 3−36317
Al-Mg(0.8 wt.%), rolling textural stability role of deform. and shear banding 3−21582
Al-Mg(5 wt.%), grain size effect on fatigue 3−34594
Al-Mn, cold-worked, impurity resistivity from 78 to 300 K 3−14886
Al-Mn, dil., n.m.r. spectra, satellite struct. interpret. 3−2431
Al-Mn, supersaturated solid solns., annealing and diffusion kinetics 3−36438
Al-Mn:Fe, dilute alloy, temp. depend. of impurity resist. 3−21048
Al-Ni(3.6 at.%), supersaturated solid solns., annealing and diffusion kinetics 3−36438
Al-Pd, soft X-ray band spectra, localised electron states 3−15573
Al-Si, cyclic hardening and microstructure effects on fatigue 3−15708
Al-Si, liq. state cluster existence, rel. to hypo- and hyper-eutectic behaviour 3−34498
Al-Si, precip., liq. quenching effect on age-hardening 3−39371
Al-Si system ternary eutectic, unidirectionally solidified, microstructures *(Japanese)* 3−18593
Al-Si-Mg, Mg effect on Sn and Pb distrib. 3−21572

aluminium alloys continued
Al-Sn, changes in composition and structure due to friction and wear *(Japanese)* 3−8768
Al-T phonon resistivity, concetrated alloys 4.2 to 100 K, (T=V, Fe, Co, Ni, Cu) 3−38822
Al-Ti, dilute alloys, solid effect between pure quadrupolar nuclear transitions 3−34243
Al-Ti (0.16 at wt.%) yield point phenomenon *(Japanese)* 3−18644
Al-Ti(V)(Fe)(Cu)(Zn), temp. depend. of impurity resist. between 78 and 930K 3−11876
Al-transition metal, microhardness variation with comp. 3−31087
6Al-V(4)-Ti, metal diffusion bonding, fracture surface characteristics 3−15702
Al-W, phase transforms. on rapid quenching 3−12331
Al-Zn, Al-Zn-Mg, axisymmetric extrusion, plastic flow, substructure exam. 3−39360
Al-Zn, Al-Zn-Mg, extrusion load calc., temp. rise meas. 3−37046
Al-Zn, α-phase, enthalpies of form. 3−21600
Al-Zn, concentrated, solvus curves for Guinier-Preston zones *(Japanese)* 3−30997
Al-Zn, form. of aligned composite material by solid state decomposition 3−24976
Al-Zn, hard non-ordered, electrical resistivity concentrational dependence *(Russian)* 3−11883
Al-Zn, metastable solvus for Guinier-Preston zones 3−31022
Al-Zn, ordering, behaviour of f.c.c. and b.c.c. phases 3−11585
Al-Zn alloy, Guinier-Preston zones, electron diffraction effects *(French)* 3−18604
Al-Zn alloys, decomposition, effect of high temp. aging 3−37015
Al-Zn alloys, precipitation *(Czech)* 3−31030
Al-Zn eutectoid, crystallographic slip in superplastic deformation 3−20795
Al-Zn liq. solns., thermodynamic props. 3−21556
Al-Zn solid soln., thermodynamic props. 3−21555
Al-Zn-Mg, corrosion fatigue inhibition, crack growth rate meas. 3−39352
Al-Zn-Mg, grain boundary corrosion and stress corrosion cracking relationship *(Japanese)* 3−31072
Al-Zn-Mg, mech. props. and fine struct. changes on alloying and ageing 3−21671
Al-Zn-Mg, SCC, soln. chem. influence on repassivation kinetics, alloying effect 3−27652
Al-Zn-Mg, stress corrosion cracks, h.v. microscope studies 3−30981
Al-Zn-Mg-Cu, thermomech. treatment processed, age hardening mechanisms 3−24897
Al-Zn-Mg-Zr, recryst. temp., effect of heat treatment *(Russian)* 3−2716
Al-Zn-Si alloy, activity coeff. of Zn *(Czech)* 3−30980
Al-Zn(Zn 15 at.%) alloy, ageing at elevated temp., microhardness, structure transformations 3−2714
Al-Zn(15 at.%), spinodal-like decomp. kinetics, effect of random fluctuations 3−15666
Al-Zn(6.8 at wt.%), Ag, Si and Mg effect on solvus temp. of G.P. zones *(Japanese)* 3−18591
Al-Zr solid solution, crystal structure of new metastable phase 3−18599
AlMg5, diffusion coeff. during plastic deform. *(German)* 3−21611
AlMn, superconducting critical fields, effect of Mn concentration 3−11972
$AlNi_{1-x}$ non-stoichiometric, ordering of n-type vacancies during heat treatment 3−11614
$Al_{89}Si_{11}$, liquid, nuclear spin-lattice relaxation meas. for ^{27}Al 3−5145
AlZnMgCu, crack behaviour under static loading, processes at crack tip, fractographic obs. 3−24200
AlZn50, supersaturated solid soln., rolling texture development 3−21577
AlZn(6) alloy, effect of Zn-vacancy complexes on Guinier-Preston zone prod. *(German)* 3−12358
$CeAl_2$ single crystal preparation by Czochralski method 3−21541
Co-Al enthalpy meas. on the allotropic transformations *(French)* 3−17976
Co-CoAl-Ni, oriented eutectic, morphology rel. to Ni addition *(French)* 3−34523
β-CoAl, low temp. magnetic behaviour 3−34098
Cr_2Al_{11}, temperature dependence of magnetic susceptibility and Knight shift 3−36807
Cu- $\gamma_2(Cu_9Al_4)$-Ni mixed powder compacts sintering characteristics study using Ni plated composite powders *(Japanese)* 3−15730
Cu-Ag-Al, constitution and phase relationships, metallographic and X-ray examination 3−34512
Cu-Ag-Al solid solns., isothermal recrystn. kinetics 3−21592
Cu-Al, anomalous shift in interconduction band optical absorption, values for band gaps 3−30837
Cu-Al, Bauschinger effect and stacking fault energy 3−36352
Cu-Al, disordered polycrystals, distortion waves 3−17926
Cu-Al, elastic consts., solute conc. depend. *(French)* 3−39302
Cu-Al, elastic stiffness, comp. depend. 3−4780
Cu-Al, estimation of quasielastic force and anharmonic coeffs. from X-ray diffraction meas. 3−30209
Cu-Al, form. of aligned composite material by solid state decomposition 3−24976
Cu-Al, influence of precipitation of γ_2 phase on order-disorder transformation 3−27617
Cu-Al, stacking fault energy obs. using weak beam method of electron microscopy 3−1541
Cu-Al, stacking fault role in martensite phase formation form fcc struct. *(Russian)* 3−2699
Cu-Al, swaged, dislocation density, from flow stresses and stored energies 3−18633
Cu-Al, twinned γ_1' martensite h.c.p. phase, invariant plane strain 3−31021
Cu-Al (15.6 wt.%), multiple dislocation, stacking fault arrays, stability 3−17824
Cu-Al (15at.%), deformation temp. and annealing influence on structure and strength props. 3−31086
Cu-Al (2%) single crystals, edge-pit observations of dislocation motion 3−21609
Cu-Al alloys, annealing twins formation 3−2701

aluminium alloys continued
Cu-Al β-type martensite, stress-induced transformation to fcc structure 3−21569
Cu-Al solid solns., high temp. steady state creep deform. behaviour *(Japanese)* 3−31076
Cu-Al solid solution, hardening mechanism in microdeform. stage *(Russian)* 3−21633
Cu-Al-Mn, martensitic alloy, X-ray obs. of twin structure *(Russian)* 3−24130
Cu-Al-Mn, martensitic transform., β′-phase deform. influence *(Russian)* 3−18560
Cu-Al-Ni, acoustic emission in thermoelastic martensite transform. 3−5318
Cu-Al-Ni, martensitic thermoelastic transform., electron work function change 3−36346
Cu-Al-Zn, solid soln. elongated dislocation tangles and Al and Zn solubility *(French)* 3−31004
Cu-Al-Zn β-type martensite, stress-induced transformation to fcc structure 3−21569
Cu-Al(1 at wt.%), internal oxidation, effect of alloying elements, Ag, Pd, As and In *(Japanese)* 3−15700
Cu-Al(15 at.%), ordering and disordering kinetics after sudden annealing changes, residual resist. obs. 3−37062
Cu-Al(5.8 at.%), deformed, soft surface effect 3−24866
Cu-Al(7.9 wt.%), corrosion fatigue crack initiation 3−27661
Cu-Au-Al, plastic deform., electron microscope study *(Russian)* 3−5306
Cu-Ni(15 wt.%)-Al(3.5 wt.%)-Cr(2 wt.%)-Mn (3 wt.%), age-hardened, microstructural characts. rel. to elastic limit and yield pts. *(Russian)* 3−15668
Cu_3Au alloy, disordering process study by electrical resistivity meas. 3−8896
Cu_2MnAl Heusler alloy, β phase form. *(French)* 3−30964
Cu_2MnAl Heusler alloy, order-disorder transform., crit. temps. determ. *(French)* 3−39306
$Cu_{2\|x}MnAl_{1-x}$, mag. props. obs. by Lorentz microscopy 3−1545
$DyAl_2$-$DyFe_2(Co_2)$, struct. and mag. studies 3−18323
Fe-Al, Kossel interference patterns evaluation by computer *(German)* 3−4693
Fe-Al, superlattice dislocations, fourfold dissociation in DO_3 type order 3−17839
Fe-Al clusters in Alnico type alloy, Mossbauer obs. 3−8491
Fe-Al-C alloy, mag. after effects, directional ordering of interstitial atoms 3−12013
Fe-Al(40 at%), quenched-in vacancies annealing kinetics 3−37039
Fe-Al(40 at.%), ordered, quenched defect recovery *(French)* 3−24839
Fe-Ni-Al, b.c.c., Mossbauer obs. of Al impurities effect on Fe and Ni mag. moments 3−15444
Fe-Ni-Al, microstructure and fracture *(Japanese)* 3−15672
Fe-Ni-Al, subspinodal, hardening obs. and mechanism *(Czech)* 3−31103
Fe-Ni-Co-Al-Ti, temp. depend. of mag. moment, superparamag. props. *(Russian)* 3−8342
FeAl alloys, localised magnetic moment effects on positron annihilation parameters 3−38599
Fe_3Al, annealing effects on compression induced mag. anisotropy 3−30642
Fe_3Al, determination of order parameters by Mossbauer spectroscopy methods 3−39070
Fe_3Al, ordering mechanism and kinetics 3−37013
$Fe_{1-x}Co_xAl$ solid solns., lattice parameter, elec. resist., Hall coeff., thermo-e.m.f., mag. susceptibility *(Russian)* 3−30087
$Fe_{1-x}Ni_xAl$ solid solns., elec. resist., thermo-e.m.f., Hall effect, 80-300K *(Russian)* 3−18121
$Ga_xAl_{1-x}As$ obs. of disorder-activated acoustic phonon mode in Raman spectrum 3−2542
(La, Ce)Al_2 dilute alloy with Ce impurities, superconducting-Kondo system, specific heat 3−5072
$LaAl_2$-$GdAl_2$, mag. ordering, Curie temp. depend. on Gd conc. 3−34122
$LaAl_2$-$GdAl_2$, specific heat jump at supercond. transition 3−34022
Mg-Al alloy, transgranular stress corrosion cracking 3−30983
MgAl thin films, for optical storage, preparation method and characterization 3−36987
Mn-Al binary system, shape and energy position of $K\alpha$ and $K\beta$ bands *(Russian)* 3−2602
Mn-Al powders, comp. and defects influence on mag. props. *(Russian)* 3−24587
Mn-Al-B, magnetis. and coercive force, composition depend. 3−36744
Mn-Al(44 at.%), metastable phase form. *(Russian)* 3−30968
Nb-Al, Nb-rich, sputtered films and quenched samples, superconductivity 3−5082
Nb-Al, surface layer on Nb, supercond. transition temp. meas. of 14K 3−36671
Nb-Al alloys, σ-phase, superconductivity *(German)* 3−36691
NbAl, Knight shift obs. and rigid-band model approach 3−18381
Nb_3Al, Ni additive effect on crit. temp., magnetiz. curves and crit. mag. field *(Russian)* 3−15288
Ni-Al, mag., thermal and elec. props. showing phase transition *(French)* 3−8361
Ni-Al, plasticity of diffusion coatings on steel *(Russian)* 3−12371
Ni-Al and Ni-Co(Fe)-Al, phase transform. on heating *(Russian)* 3−8831
Ni-Al solid soln., Ni-rich, diffusion at 1260°C, effect of thoria dispersion 3−38686
Ni-Cr-Al, internal and external oxidation mechanism 3−31115
Ni-Cr-Al, internal oxidation 3−31116
Ni-Cr-Al, oxidation resist. and mech. strength 3−18027
Ni-Cr-Al with ThO_2 dispersion, hydrogen pretreatment effect on oxidation behaviour 3−39367
Ni-Cr-Al-Cu, Evanohm, thermal cond., 0.4-77K 3−18112
Ni-Ti-Al, heat resistant, effect of copper additions on mech. props. 3−24949
β′NiAl, thermoelastic behaviour of martensitic transformation 3−21573
NiAl, void and dislocation loop formation following annealing, 700-900°C 3−18658

aluminium alloys continued
Ni_3Al, dislocation struct. at various deform. stages *(Russian)* 3−37019
Ni_3Al, low temp. elec. resist. and spin density fluctuation theory 3−21046
Ni_3Al, mech. props. conc. depend. *(Russian)* 3−12364
Ni_3Al, precipitation influence on creep rate and dislocations 3−15680
Ni_3Al, relative bond energies from field ion images 3−36272
Ni_3Al-Ni_3Ta system, interaction of phases, form. of Ni_6TaAl ternary phase 3−34510
$(Ni_{74.5}Al_{25.5})_{100-x}Fe_x$, ferromag., neutron obs. of giant moments 3−36717
Ni_3Mn-Al, atomic distrib., rel. to electronic struct. *(Russian)* 3−26990
Pd-Al alloy, mechanical strength 3−24879
in n-Si, thermomigration of Al-rich liquid droplets 3−7966
Ti-Al, with isomorphous β-stabilizing elements, mech. props. characteriz. 3−24940
Ti-Al system, interdiffusion phenomena 3−24820
Ti-Al system, interdiffusion phenomena 3−24821
Ti-Al-Co ternary system, Ti rich region, annealing, melting points, structure 3−24836
Ti-Al-Mn alloys, effect of hydrogen on fatigue behaviour and low strain rate embrittlement 3−24882
Ti-Al-Mo, with metastable β-phase martensitic transform. during deform. 3−24833
Ti-Al-Mo-V, cleavage cracking in gaseous hydrogen 3−31044
Ti-Al-V, β transformed, absorbed hydrogen behaviour 3−37033
Ti-Al-V, stress corrosion crack propag., fractographic obs. 3−31043
Ti-Al-V, surface effects during fretting fatigue 3−15814
Ti-Al-V, susceptibility to brittle fracture of simulated weld seams 3−24942
Ti-Al-V alloy, fracture toughness specimen thickness depend. 3−24881
Ti-Al-V and Ti-Al-V-Sn, corrosion fatigue crack propag., freq. and wave form effects 3−27659
Ti-Mo-Al, microstruct. and phase relations, Al additions influence 3−34509
TiAl containing Nb, oxidation resist. at 800 and 1000°C *(Russian)* 3−15716
V-Al binary alloys, martensitic transformation and supercond. props. 3−36673
V_3X-V_3Al, X=Si, Ge, Sn, Ga, Sb, ternary ‘β-W’ phase, martensitic transformation and supercond. props. 3−36673
YAl_2:Er(Dy)(Tm), crystal field ground states, EPR obs. 3−30418
$YbAl_2$, ambiguous mag. behaviour, susceptibility meas. 3−30609
Zn-Al, pressure effect during solidification on structure and tensile strength *(Japanese)* 3−27680
Zn-Al (22 wt.%), superplastic, room temp. creep behaviour under bending and plane conditions 3−34678
Zn-Al eutectoid base alloy, superplastic deformation, ductile-brittle fracture 3−39362
Zn-Al sheet, superplastic forming, anisotropy *(German)* 3−2730
Zn-Al superplastic, effect of strain-rate and drawing temp. on drawing force and mechanical properties *(Japanese)* 3−18636
Zr-Al bulk getter, secondary electron emission 3−19182

aluminium compounds
see also aluminium alloys; ruby
: 3−39119
p- AlSb, mechanisms of carrier scattering 3−24455
alumina, e.p.r. determ. of nature of sites responsible for chemisorption of toluene *(French)* 3−1894
alumina, fast-neutron damage, 60-1230°C 3−26514
alumina permittivity meas. using TM_{020} mode resonant cavity at 9.34 GHz 3−6026
β-aluminia type phase identification in refractories 3−39387
aluminophosphate glass, struct. obs. using ^{57}Fe Mossbauer effect 3−24636
aluminosilicates, computed optimized model structs. 3−14761
aluminosilicates, radiation produced e.s.r. centres, model 3−21312
barrier anodic films, elec. equivalent 3−15831
cordierite glass, crystn., as nucleating agent for prod. of cordierite glass-ceramics 3−34643
cordierite glass, crystn., oxide additive effects on devitrification characts. 3−34644
corundum ceramic, densely sintered, third-stage creep *(Russian)* 3−15744
corundum cryst., high energy photon polariser, possible appl. *(Russian)* 3−5867
corundum crystals grown by Verneuil method, OH absorption bands *(Russian)* 3−24706
leucosapphire, grown by Czochralski method, u.v. transmission spectra 3−22326
metal-Al_2O_3-SiO_2-Si structures, instability mechanisms, flatband voltage shifts 3−38899
oxides, growth of dielectric layers *(German)* 3−20951
oxyanions, X-ray emission, ESCA spectral shifts, approx. molecular orbital theory 3−26986
sapphire, dispersion of acoustic phonons 3−27085
sapphire, elec. cond., press. effect 3−21066
sapphire, epitaxy of Si, ion erosion appartus for sample prep. for electron microscopy 3−1939
sapphire, far i.r. optical consts., room temp. and 1.5 K 3−24669
sapphire, lattice thermal cond. from 0.4 to 4K 3−7980
sapphire, spheroidization of tubular pores at high temps., reln. to surface diffusion 3−17921
sapphire, synthetic cryst., vacuum u.v. transmission props. rel. to chem. purity and polishing 3−22322
sapphire, theral cond., 0.15-2K *(French)* 3−4890
topaz, $Al_2SiO_4F_2$:Fe^{3+} e.p.r. spectrum, ^{19}F ENDOR study for hyperfine struct. tensors 3−21342
zeolite, decationized, geometrical arrangement and thermal mobility of struct. OH groups *(German)* 3−4470
AlN, commercial ceramic, thermal conductivity meas. 3−15739
Al silicate, coexisting phases in contact metamorphic aureoles 3−15871
Al-Al_2O_3, electrical and structural props. of amorphous system 3−38840

aluminium compounds continued
Al-Al_2O_3-Au sandwich cathodes, energy ang. distrib. of electrons emitted *(Russian)* 3−30550
Al-Al_2O_3-Au structure, transmission coeff., applied field depend. 3−8280
Al-Al_2O_3-electrolyte system electro- and photoluminescence 3−39190
Al-Al_xO_y-Al(Pb), junction, ellipsometrical determ. of tunnelling barrier thickness 3−34004
Al-Mg_2Si, effect of Fe on nucleation and zone formation 3−8884
AlAs, band struct. and pseudopotential form factors 3−15128
AlAs, impurity electron binding energy, using dielectric theory *(German)* 3−15159
AlAs, Lindemann-Gilvarry melting law and Debye temps. 3−36393
AlAs, optical critical point analysis using pseudopotential calculation of band structure 3−36863
$AlAu_x$ (x=0.5,2), heats of atomisation, high temp. Knudsen cell mass spectrometric determ. 3−15821
AlB_{12}, crystallisation from Al-Ga-B melt, effect of impurities 3−12284
AlB_{12}, dynamic yield strength. compressional and Hugoniot elastic parameters 3−17927
AlB_{12} dense phase gas solid suspension, positive expulsion fluidization tank 3−4619
AlB_2, cryst. growth, elec. cond., carrier conc. 3−11878
Al_2Br_6, in liq. phase from triple point to critical point, calc. of degree of dissociation *(Russian)* 3−25066
Al_4C_3, heat of dissociation determ. by atomic absorption method *(Russian)* 3−11648
Al_2Cl_6, in liq. phase from triple point to critical point, calc. of degree of dissociation *(Russian)* 3−25066
$Al(ClO_4)_3$, in H_2O and trimethylphosphate, ^{27}Al n.m.f. study, solvated species obs. 3−29720
AlF exploding-wire laser giving 12.5 to 13.5 μ pulses 3−19597
$Al_2Ga_{1-x}As$, local and collective phonon modes, Raman scatt. 3−5200
$Al_xGa_{1-x}As$, etching in strong alkaline soln., Al content dependency 3−38740
$Al_xGa_{1-x}As$, growth by zone melting method with temp. gradient *(Russian)* 3−15638
n-$Al_xGa_{1-x}As$, luminescence, exciton bands *(Russian)* 3−36931
$Al_xGa_{1-x}As$, molecular beam epitaxy 3−2677
$Al_xGa_{1-x}As$, p- and n-type, epitaxial film, solid soln., luminesc. depend. on comp. 3−39187
$Al_xGa_{1-x}As$, reson. Raman scatt., 2K 3−34359
n-$Al_xGa_{1-x}As$, temp. depend. of elec. resist. and Hall coeff. 3−30478
$Al_xGa_{1-x}As$, tunnel breakdown and photocurrent in reverse-biased p-n junctions 3−24503
$Al_xGa_{1-x}As$ graded heterojunction, phenomena, review 3−24512
$Al_xGa_{1-x}As$ semiconductor, radiative transition kinetics, luminescence spectra, 4.2-77K, influence of temperature 3−34422
$Al_xGa_{1-x}As$:Ge epitaxial film, photolum., 1.1-2 eV *(Russian)* 3−2589
$Al_xGa_{1-x}As$:Mg, molecular beam epitaxy 3−18553
p-$Al_xGa_{1-x}As$−n-GaAs, photodiode, excess noise rel. to flow of current mechanism 3−38888
AlH_3 mols., electronic struct. calc. *(Russian)* 3−11213
$Al(IO_3)_3.2HIO_3.6H_2O$, piezoelec., elastic, thermoelastic and optical props. *(German)* 3−8524
AlLi, LCAO-MO-SCF calc. using Gaussian basis functions, configuration interaction calc. 3−23524
$AlMgBO_4$, sinhalite, olivine type structure, hydrothermal synthesis at high pressure *(French)* 3−38571
Al_2MgO_4 lattice dynamics at zero wave vector and elastic constants of spinel in the rigid ion approximation 3−7875
$Al_2Mn_3(SiO_4)_3$ spessartite type garnet, obs. of rhombohadral mag. structure 3−21247
AlN, cubic, thermal cond. at room temp. impurity effects 3−30294
AlN, epitaxial growth, obs. of optical bandgap 3−11831
AlN, O centres, luminesc. study *(Russian)* 3−36921
AlN, pressureless sintering to high density 3−21720
AlN, refl. and luminesc. excitation spectra, 3-40 eV 3−18493
AlN film, epitaxial growth, props., optical band gap 3−21004
AlN film, for solid state electronics, chemical, mech. and electrical properties *(German)* 3−15281
AlO, $(C^2\Sigma^+ - X^2\Sigma^+)$ system, pot. energy curves, Franck-Condon factors and r-centroids calcs. 3−20106
AlO, dissoc. energy determ. from crossed-beam chemilum. 3−7241
AlO, $F^2\Sigma^+ - A^2\Pi_i$ electronic transition 3−26658
AlO_4^{n-}-, tetrahedral anion, bond length variation 3−14332
Al_2O_3, AlN semicond.-insulator boundaries in m.i.s. structures, surface charge, hysteresis curve, frequency response advantages of aluminium compounds *(German)* 3−15261
α-Al_2O_3, $Al(OH)_3$, AlO(OH), $MgAl_2O_4$, struct. effects on chem. shift, X-ray photoelectron spectra 3−30920
Al_2O_3, alumina, dynamic behaviour, impurity effects *(German)* 3−34669
Al_2O_3, alumina, mech. and elec. props., applications 3−34626
Al_2O_3, alumina, polycrystalline, thermal stability, sustained electrical potentials effects 3−12423
Al_2O_3, alumina, straight dislocations elastic energy, 0-900 K 3−17832
Al_2O_3, alumina ceramics, characterisation, analytical techniques 3−8961
Al_2O_3, alumina ceramics, surface defects, scanning electron microscope examination 3−12420
reactive Al_2O_3, alumina powder, characterisation for thin film circuit tape cast substrates 3−8951
Al_2O_3, alumina powder, particle size, agglomeration, sedimentation and X-ray obs. 3−34618
Al_2O_3, anodic film, on Al, breakdown and repair, electron microscope obs. 3−8060
Al_2O_3, anodic oxide, photodecomposition 3−39445
Al_2O_3, anodic thin films on prehydrated Al, structure 3−8065
Al_2O_3, bayerite + water system, phase transitions under various temperatures and pressures 3−7923
Al_2O_3, boehmite, X-ray obs. of polytypic structures 3−14997
Al_2O_3, boehmite + water system phase transitions under various temperatures and pressures 3−7923

aluminium compounds continued
Al_2O_3, cakes, formed by slip casting, compression permeability 3−8974
Al_2O_3, chemical vapour deposition, X-ray diffraction microscopic obs. of surface structure 3−11790
Al_2O_3, corundum, grinding using diamond wheel *(Russian)* 3−5912
Al_2O_3, corundum + water system, phase transitions under various temperatures and pressures 3−7923
Al_2O_3, diaspore + water system, phase transitions under various temperatures and pressures 3−7923
α-Al_2O_3, edge-defined film-fed cryst. growth 3−12279
Al_2O_3, electrophoretic mobilities determ. by microelectrophoresis method 3−5393
Al_2O_3, formation on oxidation of Al-Cu alloy in dry O_2, 475-575°C 3−33743
Al_2O_3, fused to glassy substrate, boundary layer formation *(German)* 3−12425
Al_2O_3, gibbsite + water system, phase transitions under various temperatures and pressures 3−7923
Al_2O_3, glazed substrate, uniformity of elec. resist. for evaporated Ni-Cr film 3−24794
Al_2O_3, grain size rel. to density during sintering 3−2754
Al_2O_3, growth of amorphous and epitaxial layers *(German)* 3−8056
Al_2O_3, growth of $La(OH)_3$ from two component nutrient La_2O_3 and Al_2O_3 system below 425°C 3−12281
Al_2O_3, h.v. insulator for vacuum apparatus, surface charging 3−140
Al_2O_3, in m.a.s. and m.a.o.s. structures, deposition temp. effect on charge storage and retention 3−2188
Al_2O_3, influence of electric field on parameters of impurity centre 3−36951
Al_2O_3, internal friction peaks due to adsorbed and capillary water 3−21754
β-Al_2O_3, ionic cond., Na- and Mg-content depend. 3−11758
Al_2O_3, ionic self diffusion activation energies, graphical method determ. from previous results 3−15035
Al_2O_3, Lucalox, thermal conductivity meas. at high temps., using heat pipe technique 3−16399
Al_2O_3, microimpurities, spectral determ. 3−16568
Al_2O_3, octahedral and tetrahedral, vibr. spectra *(Russian)* 3−12140
Al_2O_3, photocond. near intrinsic absorpt. edge, exciton nature of absorpt. band 3−5032
Al_2O_3, plasma-deposited coating, effective thermal conducting, struct. and temp. effects 3−24359
α-Al_2O_3, polycryst., sintering and shaping process effects on form, topotaxy and texture *(German)* 3−12424
γ-Al_2O_3, positronium Zeeman transition obs. 3−17872
Al_2O_3, pure and Mg-doped, thermal cond., 1.3-100 K, possible obs. of Fe^{4+} 3−30293
Al_2O_3, reacting with graphite, avalanche reaction postulate 3−18785
Al_2O_3, sapphire, edge-defined film-fed growth, cine-film 3−15636
Al_2O_3, sapphire, gradient furnace growth method, X-ray topography obs. 3−11572
Al_2O_3, sapphire, ion irrad. damage, comparison with results for $LiNbO_3$ 3−17880
Al_2O_3, sapphire, pressure effect on dielectric strength 3−27464
Al_2O_3, sapphire, substrate for epitaxial Si, film/substrate orientation, theoretical model 3−11832
Al_2O_3, sapphire, substrate for epitaxial Si, interface cpd. formation rel. to deposition conditions 3−11834
Al_2O_3, sapphire, substrate for Nb, effect of dislocation density on r.f. sputtering 3−20954
Al_2O_3, sapphire filaments, yielding and flow at 1750 to 1875°C 3−7817
Al_2O_3, sapphire laser damage, surface, plasma formation 3−29117
Al_2O_3, sapphire laser damage, surface threshold, ion beam polishing 3−29118
Al_2O_3, sapphire single crystal, obs. of Kikuchi line doubling rel. to block structure 3−24364
Al_2O_3, sapphire whiskers, Ni coated, stability 3−30377
Al_2O_3, spheres and powders plastic flow during hot-pressing 3−39381
Al_2O_3, substrate for epitaxial Si, symmetry rel. to film Hall mobility 3−11967
Al_2O_3, surface grain size estimation by optical scatt., application to microelectronics industry 3−4906
Al_2O_3, thermally shocked, strength degradation and crack propagation 3−2752
Al_2O_3, time decay of d.c., modelling using nonlinear regression analysis, comparison with experiment 3−8509
Al_2O_3, wetting by FeC melt, C content effect *(Russian)* 3−8883
Al_2O_3, wetting by molten metallides 3−34627
Al_2O_3, X-ray and u.v. irrad., activation energies 3−34435
Al_2O_3 alumina ceramics, flexural strength, high temperature impact resistance, effects of quenching 3−8960
Al_2O_3 alumina ceramics, mirror dimensions in fracture surfaces 3−8959
Al_2O_3 amorphous film, Poole-Frenkel cond., calc. including hot electron effects 3−5015
Al_2O_3 amorphous thin films, electrical inhomogeneity in m.i.m. structures, residual polarisation measurement *(Russian)* 3−11960
Al_2O_3 anodic film growth on Si 3−39246
Al_2O_3 anodic films, branching colony pore structure, electron microscope examination 3−1948
Al_2O_3 cables, radiation tolerance for instrumentation systems in LMFBR 3−26512
Al_2O_3 ceramics for implantation in living tissue *(German)* 3−27795
Al_2O_3 composite, metal fibre reinforced, fabrication and fracture toughness 3−18718
Al_2O_3 corundum crystal, coherent e^-e^+ pair production and bremsstrahlung *(Russian)* 3−35806
Al_2O_3 fibres, h.v. electron microscopy 3−1537
Al_2O_3 film, anodised, comparison of step and ramp voltage breakdown 3−8518
Al_2O_3 film, for solid state electronics, chemical, mech. and electrical properties *(German)* 3−15281
Al_2O_3 film, i.r. transmission spectra, boundary interaction with substrate *(Russian)* 3−15102
Al_2O_3 film, in m.i.m. capacitor, inhomogeneities, visualization by liq. cryst. layers 3−15284

aluminium compounds continued
Al_2O_3 film, made from evaporated sapphire behaviour in m.i.s. and m.i.m. structs. 3−27317
Al_2O_3 film, on Al, thickness meas. 3−36500
Al_2O_3 film, on Si, electronic charge trapping, photoinjection-photodepopulation and C-V studies 3−5066
Al_2O_3 film, preparation and structure *(German)* 3−15608
Al_2O_3 film, r.f. sputtered, surface charge density rel. to H_2 annealing 3−2187
Al_2O_3 foil, electron energy loss analysis by thermomodulation procedure *(German)* 3−28640
Al_2O_3 inclusions in Cu coatings, microhardness 3−18670
Al_2O_3 layer, on Al, thickness determ. by proton-induced X-ray fluoresc. 3−4935
Al_2O_3 molten alumina, radial distrib. function anal. of structure at 2200°C 3−26962
γ-Al_2O_3 powder, adsorption of hydrogen and moisture 3−1889
Al_2O_3 powder aggregates, strength characterisation, pressure-density data 3−8964
Al_2O_3 powder coatings, plasma jet efficiency in spraying *(Russian)* 3−27724
Al_2O_3 powders, high pure reactive, chemical and powder density 3−15792
Al_2O_3 pyrolytic layer, in m.o.s. capacitor, trap struct. 3−18220
Al_2O_3 reinforced Ti alloy composite, reactivity and interface struct. 3−31136
Al_2O_3 single crystal layer, carrier photo-injection from metal films and Poole-Frenkel transport 3−5054
Al_2O_3 sintering using a d.c. glow discharge 3−18695
β-Al_2O_3 solid electrolyte, e.m.f. meas. 3−39449
Al_2O_3 substrates, texture orientations, exam. 3−18769
Al_2O_3 TSEE activator in BeO, dosimetric characteristics 3−28671
Al_2O_3 thin films, electroforming and dielec. breakdown *(Russian)* 3−30530
η-Al_2O_3 water vapour heat of adsorption *(French)* 3−27187
α-Al_2O_3:Co^{2+}, H^+ e.s.r. spectra and magnetic consts. g and A 3−5131
Al_2O_3:Cr^{2+}, Jahn-Teller effect of ^5E ground state 3−30688
Al_2O_3:Cr^{2+}(Mn^{3+}), acoustic e.p.r. spectra obs. 3−8427
Al_2O_3:Cr^{2+}(Mn^{3+}), elec. field effect on acoustic e.p.r. spectra 3−8428
Al_2O_3:Cr^{3+}, electron spin echo for high Cr^{3+} concs. 3−8435
Al_2O_3:Cr^{3+}, exchange coupled ionic pairs, e.s.r. study of coupling force *(German)* 3−15418
Al_2O_3:MgO, grain boundary segregation 3−27739
Al_2O_3:Mn^{2+}, e.p.r., angular variation, forbidden transitions, spin Hamiltonians *(French)* 3−27404
Al_2O_3:Mn^{3+}, Cr^{2+}, acoustic paramagnetic resonance at high magnetic fields 3−2346
Al_2O_3:Ni, thermal conductivity at low temps. *(French)* 3−1845
Al_2O_3:V^{3+} phonon spectroscopy on the resonant scattering of V^{3+} and other impurities by tuning the 'Bremsspectrum' of a superconducting tunnel junction 3−1768
Al_2O_3:V^{4+}, acoustic paramagnetic resonance 3−2347
Al_2O_3/Al contact, electron injection into anodic oxide 3−8261
Al_2O_3/Nb thin cermet films, hopping conduction through localised states 3−11895
Al_2O_3-based, insulating fire-proof concrete, electrical cond. erosion and heat resistance in plasma jet 3−36206
Al_2O_3-NH_4Cl powder mixture, aluminizing 3−24963
Al_2O_3-Na_2O-SiO_2 glass, improvement of mech. props. *(Polish)* 3−8989
Al_2O_3-SiO_2, diffusion and reaction studies at high temps. 3−17994
Al_2O_3-TiO_2 powder, high freq. plasma oxidation prep., electron microscopy, X-ray diffr. 3−31122
$(Al_2O_3)_3$ $(SiO_2)_2$, mullite, ceramic powder, stoichiometric, synthesis and mechanical props. 3−27736
$Al(OH)_3$, secondary nucleation in seeded caustic aluminate soln. 3−2627
$Al_2O_3-Cr_2O_3$ modulated structures formation 3−4846
$Al_2O_3-Cr_2O_3-Fe_2O_3$, modulated structures formation 3−4846
AlP, band struct. and pseudopotential form factors 3−15129
AlP, impurity electron binding energy, using dielectric theory *(German)* 3−15159
AlP, Lindemann-Gilvarry melting law and Debye temps. 3−36393
AlSb, impurity electron binding energy, using dielectric theory *(German)* 3−15159
AlSb, resonant Raman scatt. 3−5201
AlSb film, X-ray and u.v. photoemission spectra, core levels, valence band electrons plasma freq. 3−15590
$(AlSb)_x(CdTe)_{1-x}$ solid solutions, optical absorption edge, coefficient, photoelectric method, band structure 3−34376
AlSe molecule, the $A^2\Sigma$-$X^2\Sigma$ system 3−20129
AlSiO, reflecting protective coating, for telescope mirrors, environmental evaluation 3−5893
$Al_6Si_2O_{13}-Al_2O_3$ controlled ceramic microstructures by solidification from melts 3−5344
Al_2TiO_5, structure obs. rel. to thermal expansion using high temp. X-ray diffraction furnace 3−26944
$AlVO_4$, thermoluminescence *(Russian)* 3−15565
$Al(urea)_6(ClO_4)_3$:$Cr(urea)_6(ClO_4)_3$ second order phase transformations, e.s.r. meas. 3−17975
$BaPO_3F$-AlF_3-Li(Na)(K)(Zn)(Cd)(Pb)F_x, glass vitrification and crystallisation capacity *(Russian)* 3−14698
BeO spheres, Al_2O_3 coated, neutron irradiation effects 3−4338
BeO-Al_2O_3-SiO_2-MgO glass, thermographic and X-ray study of struct. transforms. *(Russian)* 3−11547
$(CH_3NH_3)AL(SO_4)_2.12H_2O$, ferroelectric, electro-optical and thermo-optical props. 3−34328
CsCl-$AlCl_3$ melt, Raman spectra study of influence of species formation on stability 3−36868
Cs_2O-Al_2O_3-SiO_2, areas for glass form. 3−7629
Cu-Al_2O_3, internally oxidised, brittleness during annealing in H_2 *(Japanese)* 3−12395
Fe-Ni:Al_2O_3, dispersion strengthened composite, alloying additions effect on structural stability 3−15782
Fe-Si (3 at wt.%), Al_2O_3 dispersed, Newtonian viscous creep 3−31094
Fe_2O_3-Al_2O_3 mixed oxides, conc. depend. of lattice parameters *(French)* 3−7679

aluminium compounds continued
$Ga_{1-x}Al_xAs$, liq. phase epitaxy, variation of solid comp. with temp. 3−12258
GaAs-$Al_xGa_{1-x}As$, heterojunction, p-n-p-n structure electroluminesc. props. 3−18500
GaAs-AlAs solid solution, polarised luminescence due to optical orientation of electrons *(Russian)* 3−36934
$HoAl_2$, e.m. decay populating ^{166}Er 6^+ rot. states, g-factor meas. 3−26377
KCl-$AlCl_3$ melt, Raman spectra study of influence of species formation on stability 3−36868
LiCl-$AlCl_3$ melt, Raman spectra study of influence of species formation on stability 3−36868
Li_2O-Al_2O_3-SiO_2 glasses, Gd^{3+} doped, e.s.r. meas. during crystn. 3−27403
MgC-Al_2O_3, stoichiometric spinel, floating zone growth method in arc-image furnace 3−15639
MgO-Al_2O_3-SiO_2-TiO_2 glass-ceramic, crystn. and struct. 3−31161
Nb/Al_2O_3 cermet film, superconductivity, normal state elec. and struct. props. *(Russian)* 3−30482
Ni:Al_2O_3, Mg, effect of Mg additions on high temp. mech. props and microstructure 3−15711
Ni/Al_2O_3 composite, electrodeposition, phys. and mech. props. 3−37059
Ni-Co-(2.5 wt.%) Al_2O_3 alloys creep behaviour 3−8870
Si_2N_4-Al_2O_3, hot-pressing, exam. *(Japanese)* 3−8992
Si_3N_4-Ga_2O_3-Al_2O_3 solid soln., solubility limits, comp. 3−39378
SiO_2-Al_2O_3 thin film, splat cooling prepn. for transmission electron microscopy 3−18537
UO_2, Si, Al_2O_3, Fe, U, impurities, effect on fracture stress 3−39384

a.m. (modulation) *see amplitude modulation*

ambient temperature *see temperature*

americium
solid-state phase transitions investigation 3−12387
Am^{3+}, in CaF_2, optical Zeeman rot. spectra 3−18467
^{241}Am, neutron irradiated, presence of ^{238}Pu and ^{242}Pu, depend. of mass ratio on cooling period 3−32943
^{241}Am α-source for studying tracks in mica 3−25895
$CaWO_4$:Am^{3+}, fluoresc. emission props. 3−34405
Pu-Am spectra analysis for meas. of Pu contamination 3−3895

ammeters
digital nanoammeter, Siberian Instruments 1971 Exhibition *(Russian)* 3−9900
logarithmic picoammeter for exposure and dose meas. in electron microscopy of polymer crystals 3−346

ammonia
absorption bands of Jupiter and Saturns discs *(Russian)* 3−16145
anharmonic force constant 3−4416
atmospheric pollutant at Harwell, correlation of hourly sampling results 3−34904
atmospheric pollutant at Harwell, technique for hourly sampling and analysis 3−37234
condensed layer, adsorption characteristics, cryopumping 3−8022
dimer model systems, perturbation energies calc. 3−29758
effects on electrification of freezing and splashing water drops 3−27106
emission spectrum of silent electric discharge *(German)* 3−11270
far i.r. rotational spectrum in liquid SF_6 3−20151
ion-molecule reactions, positive and negative ions, ion cyclotron resonance study of thermal rate consts. 3−1273
i.r. spectra of mol. trapped in Ar matrix, rot. transitions 3−11259
i.r.-microwave double resonance in presence of high-field Stark effect 3−4440
Jupiter's atmosphere, ν_2 band and 8-13 μm spectrum 3−5578
liquid, optical constants in i.r. 3−30791
metal-NH_3 solutions, two electron cavity species study 3−39428
moderator, solid, time-depend. leakage neutron spectrum study 3−14263
molecular beam maser, principles and review of advances 3−32530
molecular spectra, band and total emissivity 3−23566
molecular Zeeman effect, inversion transitions 3−20209
molecule, degree of orbital delocalisation, comparison with canonical SCF solns. 3−23531
molecule, electron spectra, vibr. struct. and Jahn-Teller effects 3−38280
molecule, inversion spectra, relax. mechanisms 3−29753
molecule, microwave i.r. four-level system, efficiency of collisions 3−36056
molecule, potential energy surfaces calc. 3−23635
optical pumping of CO_2 TEA laser, submillimeter laser action 3−13731
orbital calc., atomic contrib. to symm. orbital integrals 3−35955
photodissociation, two-step, ^{14}N and ^{15}N isotope separation 3−38196
plane layer, radiant-conductive heat transfer 3−23711
positron annihilation, −19°C, 22.5°C and 95°C 3−20204
Schuster band structure, 5600-5700 Å *(German)* 3−11269
solvated electrons, semi-empirical UHF treatment 3−4402
trapped dielectron at 77K, semicontinuum model 3−38813
$(H_3N$-$H...NH_3)^+$, SCF calc. of hydrogen bonds 3−17400
$K-NH_3$ dilute solutions, u.s. velocity 3−33609
Li/ND_3 solutions of metallic conductivity, electrical explosion, obs. of neutron emission 3−38483
Li-ND_3 solns., velocity of 10 MHz compressional waves, metal conc. and temp. depend. 3−1695
ND_3, liquid, density and viscosity, +30 to −25°C, rel. to molecular volume 3−1814
NH_3, pyrolysis by CO_2 laser radiation 3−12509
NH_3-H^+ collisions, first order orientation dependent forces 3−4487
$(NH_3)_n$, H-bond energy, INDO calcs. 3−4412
NH_2D, optical free induction decay concept 3−4428

ammonia clocks *see atomic clocks*

ammonium compounds
ADP-KDA mixed crysts., X-ray and γ-ray irrad., paramag. centres e.s.r. 3−15422
ammonium oxalate monohydrate, isotope and bonding effects, analysis using combined neutron and X-ray diffraction analysis 3−7731
bisulphates, $MHSO_4$, M = alkali metal or NH_4, growth from soln. or H_2SO_4 *(German)* 3−8716

ammonium compounds continued
- metal halide-NH_4NSC aq. soln., mol. anion addition, luminesc. spectral effects *(Russian)* 3−36922
- metal-ammine complexes, NH_3 rocking vibration *(German)* 3−29618
- sodium tartrate:Cu^{2+}, cryst. field at Na site, e.s.r. 3−2349
- tartrate, cryst. struct., X-ray determ. 3−27014
- tetramethyl ammonium halides, proton magnetic resonance and internal motions 3−8460
- Al_2O_3-NH_4Cl powder mixture, aluminizing 3−24963
- $(CH_3NH_3)AL(SO_4)_2.12H_2O$, ferroelectric, electro-optical and thermo-optical props. 3−34328
- $CaAl_2$-NH_4Cl powder mixture, aluminizing 3−24963
- $Co(NH_4)_2(SO_4)_2.6H_2O$, spin-lattice relax. times, field-depend. Raman processes 3−15411
- $DH_4H_2AsO_4$, antiferroelec., X-irrad., e.p.r. of defect centres 3−2388
- ND_4Br, theory of inelastic neutron scattering in orientationally disordered mol. crystals 3−20726
- ND_4Br, volume-temp. hysteresis loop in transitions calc. 3−38668
- ND_4Br molecular crystal structure, orientationally disordered, analysis 3−38546
- ND_4Cl, theory of inelastic neutron scattering in orientationally disordered mol. crystals 3−20726
- ND_4Cl lattice dynamics at 85K, rigid ion−rigid molecule and shell model calcs. 3−11698
- $ND_4D_2AsO_4$, antiferroelec., X-irrad., e.p.r. of defect centres 3−2388
- $(ND_4)DSO_4$, ferroelectric, deuteron spin-lattice relaxation 3−8477
- NH, stratospheric, identification, absorption spectra 3−9294
- $(NH_4)_2BeF_4$ optical properties, digressions from phenomenological theory 3−18423
- NH_4Br, anomalous Raman mode near lambda transition 3−1715
- NH_4Br, Fm3m to Pm3m transform. orientation relations 3−7921
- NH_4Br, h.p. disorder-order transitions, Raman spectra 3−38654
- NH_4Br, in disordered phases I and II, low frequency Raman spectra 3−34347
- NH_4Br, ordered tetragonal phase, NH_4^+ libration study by Raman spectroscopy 3−34346
- NH_4Br, single cryst., order disorder transitions, Raman scatt. obs., 45-410 K 3−33646
- NH_4Br, volume-temp. hysteresis loop in transitions calc. 3−38668
- NH_4Br in phases II and III, u.v. reflection spectra 3−24711
- $NH_4Br:Cu^{2+}$, e.p.r. spectral interpretation from spin Hamiltonian parameters calc. 3−18357
- NH_4CNS photo-degradation, stability by pH control with succinic acid buffer 3−27904
- $(NH_4)_2C_2O_4.H_2O$, γ-irradiated single crystals, e.p.r. study of saturation effects 3−8415
- $(NH_4)_2Cd_2(SO_4)_3$, dielec., optical and domain props. 3−24662
- NH_4Cl, critical opalescence 3−24667
- NH_4Cl, disordered, vibr. modes from low freq. Raman spectra 3−24704
- NH_4Cl, epitaxial growth and substrate elec. props. 3−1927
- NH_4Cl, h.p. disorder-order transitions, Raman spectra 3−38654
- NH_4Cl, in disordered phases I and II, low frequency Raman spectra 3−34347
- NH_4Cl, nuclear mag. relax. induced by random molecular reorientation 3−34239
- NH_4Cl, order-disorder transform., Raman scatt., T_λ region, lattice and internal modes 3−24688
- NH_4Cl, orientational quadrupole relax., deuterium nuclei longit. relax. time 3−8483
- NH_4Cl, phonon system with disordered force consts., Raman scatt., optical absorpt. 3−34349
- NH_4Cl, spin-lattice relax. and mol. reorientations near T_c 3−21335
- NH_4Cl, tricritical points, critical exponents notation 3−13664
- NH_4Cl, undoped and divalent cation doped, ionic thermal currents 3−33917
- NH_4Cl, volume-temp. hysteresis loop in transitions calc. 3−38668
- NH_4Cl crystals without additives, growth from melt by Bridgman-Stockbarger method *(German)* 3−8740
- NH_4Cl releasing effect on Cr absorpt. in air-acetylene flame 3−14291
- $NH_4Cl:Co^{2+}$, Ni^{2+}, Cu^{2+}, light absorpt. by impurity centres, cryst. field parameters 3−21456
- NH_4Cl-H_2O soln., undercooled, crystal multiplication model 3−33467
- $NH_4Cl(Br)$, soln. growth under highly controlled conditions 3−12236
- $NH_4Cl_{1-x}Br_x$, solid soln. system, optical determ. of phase diagram 3−33656
- $NH_4Cl(Br)(I)$, proton mag. resonance line shape of NH_4^+ ions with tunnelling influence 3−15429
- NH_4ClO_3, radiation induced dislocations and thermal decomposition kinetics 3−4771
- NH_4ClO_4, proton spin-lattice relax., second moment and magnetisation study, 1.5 to 100K 3−18384
- NH_4ClO_4, pure and doped, temp. depend., elec. cond. mechanism 3−2081
- $(NH_4)_2CuCl_4(Br_4).2H_2O$, n.m.r., ferromag. behaviour 3−2420
- $(NH_4)_2Cu(SO_4)_2.6H_2O$, e.s.r., down to 37 mK 3−36785
- NH_4F, etchant, Al beveling, anodic oxidation, for multilayer metal circuitry 3−38739
- NH_4FeCl_3, temp. depend., 2 to 250K, interpretation using antiferromag. linear-chain model 3−21220
- $(NH_4)_3FeF_6$, Mossbauer obs. of phase transition 3−7933
- $(NH_4)_xFeF_3$, Mossbauer effect study *(French)* 3−8488
- $NH_4H_2AsO_4$ ferroelectrics, e.p.r. study of Slater configurations 3−2389
- $NH_4H_2PO_4$, soln. growth under highly controlled conditions 3−12236
- $NH_4H_2PO_4$, stress-optical and strain-optical consts. 3−36854
- $NH_4H_2PO_4$, X-ray diffraction contrast due to lattice distortions 3−30048
- $NH_4H_2PO_4$ crystals, ultraviolet refl. and absorpt. for electronic transition studies 3−2562
- $NH_4H_2PO_4$ four-sublattice theory of phase transitions, ferroelec.-antiferroelec. 3−8534

ammonium compounds continued
- $NH_4H_2PO_4:{}^{57}Fe^{3+}$, antiferroelec. transition, Mossbauer obs. 3−15468
- NH_4HSO_4, cryst. struct., ferroelectric phase and transition 3−8526
- $NH_4H_3(SeO_3)_2$, crystal structure, H-bonding, X-ray obs. 3−27002
- NH_4I, in disordered phases I and II, low frequency Raman spectra 3−34347
- NH_4I, kinetics of low temp. phase transformations 3−38667
- NH_4I, Raman spectra, one-phonon density-of-states and spatial correl. 3−39137
- $NH_4IN(SO_4)_2.12H_2O$, ${}^{115}In$ n.q.r. coupling const., temp. depend. 3−24629
- NH_4LiBeF_4 and NH_4LiSO_4, cryst. struct. and polymorphism 3−14751
- NH_4LiBeF_4 determ., space groups and symmetry 3−11598
- $(NH_4)_2MnF_5$, linear chain antiferromagnet, weak ferromagnetism and anisotropy 3−30643
- $(NH_4)_2MoO_2S_2$ with ${}^{92}Mo$, ${}^{100}Mo$, Raman spectra, force consts. *(German)* 3−4451
- $NH_4NH_2SO_3$, cryst. struct. 3−14759
- NH_4NO_3, allotropic transforms., kinetic study *(French)* 3−24268
- NH_4NO_3, cubic, X-ray diffuse scatt. of molecular rotation 3−24037
- NH_4NO_3, ND_4NO_3, calorimetric study of phase transitions between room temp. and melting points 3−27119
- NH_4NO_3, stress corrosion cracking, mild steel, effect of C content 3−39354
- NH_4NO_5, ${}^{15}N$ n.m.r. 3−5140
- $(NH_4)_2SO_4$, ${}^{15}N$ n.m.r. 3−5140
- $(NH_4)_2SO_4$, elastic anomaly near ferroelectric transition 3−30763
- $(NH_4)_2SO_4$, elastic compliance functions, electrostrictive consts., anomalies at ferroelec. transition 3−15453
- $(NH_4)_2SO_4$, ferroelectric transition, analysis of long wavelength lattice vibrs. 3−27476
- $(NH_4)_2SO_4$, hydrostatic pressure effect on ferroelec. transition temp. 3−2501
- $(NH_4)_2SO_4$, i.r. refr. index 3−31293
- $(NH_4)_2SO_4$, optical properties, digression from phenomenological theory 3−18423
- $(NH_4)_2SO_4$ aqueous solns., solidified, time depend. *(French)* 3−24646
- $(NH_4)_2SO_4$ elastic compliance and dielec. meas. rel. to ferroelec. transition 3−30781
- $(NH_4)_2SO_4:CrO_4^{2-}$, vibr. freqs., optical and i.r. absorpt. studies 3−14954
- $NH_4SO_3NH_2$, space group, unit cell dimensions 3−7722
- $(NH_4)_2SbCl_5$, e.p.r. of VO^{2+} and Cr^{3+}, site symmetry 3−24606
- $(NH_4)_2SeO_4$, $(ND_4)_2SeO_4$, Raman and i.r. spectra hydrogen bonding, ion distortion 3−39144
- $(NH_4)SnCl_5$, thermal expansion coeffs. determ. with Stoe precession camera 3−1808
- NH_4SnF_3, cryst. struct. 3−14748
- $NH_4UO_2(NO_3)_3$ oscillator strengths for four low-lying electronic states *(Russian)* 3−30843
- $(NH_4)_xWO_3$, ionic motion, n.m.r. obs. 3−7968

amorphous semiconductor materials
- amorphous layers, produced by ion irrad., interdiffusion with Pd film 3−27142
- Annual review of materials science vol. 2, 1972 3−24778
- band gap, rel. to struct. homogeneity 3−30387
- band structure, completely compensated crystalline semiconductor as model 3−18063
- band structure calcs. using self consistent, adhoc and empirical techniques 3−2007
- book 3−11941
- chalcogenide film, switching, room temp. and 77K 3−21129
- chalcogenide film, switching and memory effects 3−18198
- chalcogenide glass, electronic conductivity and switching 3−18134
- chalcogenide glass, reversible thermal breakdown as a switching mechanism 3−18197
- chalcogenide glass alloys, thermal and non thermal processes threshold structures 3−8236
- chalcogenide glass film, threshold switching 3−30523
- chalcogenide thin film devices, threshold switching, surface temp. changes 3−27294
- d.c. cond., diffusion type transport eqn. 3−8177
- doped highly compensated cryst. semiconductor model for switching and memory 3−36644
- electrical conduction mechanisms, comparison with conductivity meas. on SnS_2 3−18155
- electrical consuctivity in disordered system 3−18148
- electron transport by energy depend. diffusivity 3−2053
- electronic phenomena, reviews 3−24415
- film, pre- and postswitching phenomena 3−18196
- film, variable-range hopping cond., theory 3−30476
- fluctuation levels in semicond. with chain or layered structure 3−15115
- group-IV, phonon spectra, rel. to cryst. state 3−4825
- Hall constant, low temp. behaviour 3−33900
- hopping conduction, single phonon contrib. 3−2082
- hopping Hall effect, single phonon contribution 3−27274
- hopping low-field magnetoresistance 3−36626
- instabilities in temp. depend. conductors, review 3−27290
- liquid, review of electrical properties 3−30385
- localised states, e.s.r. study 3−18058
- memory-type, switching phenomena, electron microscope obs. 3−2151
- phonon assisted interband optical transitions 3−21433
- photoconductivity, photon stimulated hopping conduction mechanism *(Russian)* 3−2131
- polymer, electric conduction mechanism 3−11891
- production of oxides, nitrides and glass materials for IC *(German)* 3−21552
- pseudogap in density of states determ., multiple scattering theory 3−20991
- recent developments in research, book 3−38798
- refractive index, dispersion and magnitude 3−36851
- semiconductors, ion and electron irrad., clustering of defects 3−33576
- switching effect at discontinuous changes in heat transfer 3−30528
- switching obs. using oscillation circuit 3−8238

amorphous semiconductor materials continued
theoretical foundation of existing models 3–38778
thin film, space charge generation *(Russian)* 3–30491
transition metal oxide glass, switching delay time measurement 3–18199
transition metal semiconducting phosphate glasses, transport props. 3–8175
transport processes, size effect theory 3–30465
trinitrofluorenone-poly-n-vinylcarbazole charge-transfer complex, film, drift mobilities 3–21068
trinitrofluorenone-poly-n-vinylcarbazole mixture, film, densities of complexed and uncomplexed molecules 3–18038
vitreous oxides, structural defect equilibria based on the structon model 3–4723
$3As_2Se_3$-$2Sb_2Se_3$ film, recombination and trapping processes, photoconductivity obs., 278-308K 3–21094
Al_2O_3/Nb thin cermet films, hopping conduction through localised states 3–11895
As, photoelec. emission *(French)* 3–21512
As-Se-Ge amorphous films, photo-darkening effect 3–5212
$As_{30}Ge_{10}S_{12}Te_{48}$, film, switching props. *(German)* 3–15229
As_2S_3 glasses, magnetic susceptibility 3–8334
$As_2(S_xSe_{1-x})_3$ film, lattice phonons, i.r. spectra study 3–36382
$As_2(S_xTe_{1-x})_3$ film, lattice phonons, i.r. spectra study 3–36382
$As_{1-x}Se_x$ films, Poole-Frenkel effect *(French)* 3–11963
As_2Se_3, elec. field enhanced phase separation and memory switching 3–5042
As_2Se_3, radiative recomb. 3–24737
As_2Se_3, vitreous, chaotic potential field, optical absorption edge shift, deformation potentials 3–20993
As_2Se_3 glassy, optical absorpt. rel. to press. *(Russian)* 3–8608
As_2Se_3 glassy, photocond. spectra rel. to optical absorpt. spectra *(Russian)* 3–8224
As_2Se_3:B(Al)(In)(Ga)(Tl), vitreous, a.c. cond. and dielec. const. depend. on freq. and temp. 3–30742
$As_2Se_3:Fe^{3+}$ glass, e.s.r. *(Russian)* 3–5133
As_2Se_7, thin film, d.c. elec. cond. before switching 3–8239
$As_2(Se_xTe_{1-x})_3$ film, lattice phonons, i.r. spectra study 3–36382
As_2Te_3, glassy, electronic properties 3–1972
$AsTe_2Si$ chalcogenide film, localised states, thermally stimulated depolariz. current obs. 3–2020
B, hopping conduction at low temp. rel. to local order 3–21075
C, glassy, switching phenomena, correlation between memory time and resistivity 3–33966
CdTe, optical props. 3–2526
CdTe, struct. and elec. cond. 3–1942
Cu-As-Se glass, light-induced memory effect 3–16895
$FeSi_2$, new amorphous material, structural, electrical and optical props. 3–36419
GaAs, radiation annealing of amorphization on ion bombardment 3–33553
GaAs:He(N,S,Zn), ion implantation, elec. conduction due to defect centres 3–33906
GaAs:Te, amorphous layer form. on doping by Te ions bombard. 3–18062
GaAs:Zn, H^+ ion bombardment, channelling expts., annealing behaviour of disorder density 3–33578
GaP amorphous film, ohmic, hopping cond. and Poole Frenkel behaviour obs. 3–36604
Ge, cohesive energy and density of states 3–36521
Ge, d.c. cond. and pseudogap struct. 3–38839
Ge, electron spectra, effect of valence angles deform., LCAO calcs. *(Russian)* 3–8084
Ge, epitaxial, polycryst., amorphous, Hall mobility, carrier conc., cond., noise, 100-400 K 3–38855
Ge, evaporated film, elec. resist. meas. to distinguish amorphous from polycrystalline structure 3–30372
Ge, film, impurity effects on structure with different preparation methods 3–20968
Ge, sputtered layer, effect of deposition rate on physical props. 3–4934
Ge, struct., electronic and optical props., comparison witn Ge 3 and Ge 4 3–30095
Ge, thermoelec. power and low field conduction 3–8174
Ge, thin film, amorphous-crystal boundary, electron diffraction pattern 3–11839
Ge film, a.c. cond., contactless meas. in microwave region 3–15189
Ge film, density, effects of annealing 3–1958
Ge film, electronic structure, elec. and optical props. study 3–15116
Ge film, hopping transport, thickness depend. 3–38838
Ge film, magnetoresist. in fields up to 25 kG, impurity level effects 3–21095
Ge film, structure, electron microscope obs. 3–1949
Ge film, thermopower, comparison with crystalline film 3–2116
Ge film, Zeeman splitting of localized levels model approach to magnetoresist. 3–15213
Ge sputtered film, annealing activation energies, elec. cond. study 3–30369
Ge temp. depend. of conductivity, spectral depend. of absorption 3–18131
Ge thin films, absorption and transport study of the pseudo gap 3–33775
Ge thin films, optical props. 3–15575
Ge:As system, phase separation, X-ray photoemission study 3–36421
Ge-Se system, current-voltage characteristics and temp. depend. of low-field conductivity 3–38843
Ge-Sn film, energy pseudogap from d.c. cond. temp. depend. 3–18055
$(GePbSn)_{0.5}Te_{0.5}$ film, photocond., temp. and intensity depend. 3–18186
GeSbSe film, elec. and optical props. 3–21080
GeSe film, elec. and optical props. 3–21080
$Ge_{0.5}Si_{0.5}$, sputtered, struct. and Raman scatt. 3–36501
GeTe, crystalline and amorphous, similarities in valence bands, X-ray photoemission determ. 3–33796
GeTe, film, switching and memory effects 3–18206
GeTe film, thermopower, comparison with crystalline film 3–2116

amorphous semiconductor materials continued
$Ge_{15}Te_{81}S_2As_2$, IV characts., hydrostatic press. depend. 3–38830
HgSe film, Hall mobility obs. 3–5009
InSe film, crystallisation and decomposition, electron microscope obs. 3–7936
Nb_2O_5, in m.i.m. struct., cond. mechanisms and bistable switching 3–18135
PSe, P_2Se_3 and P_2Se_5 amorphous layers, photoconductivity *(Russian)* 3–8220
S-Se-Te system, amorphous thin film, memory switching phenomena 3–36642
Sb_2O, crystalline and amorphous, photoconductivity measurements 3–38870
Sb_2O_3, optical props. rel. to band structure 3–8602
Se, comparison of radial distrib. functions with those for liq. and crysts. 3–17732
Se, electronic energy struct., molecular orbital studies 3–36520
Se, hole mobility rel. to conductivity hysteresis at vitrification temp. 3–30529
Se, parameters of trapping levels 3–24451
Se, vacuum evaporated layer, amorphous and crystalline phase obs. 3–20970
Se, X-ray irrad., electrophotographic layer, fatigue mechanism *(Russian)* 3–33947
Se, X-ray irrad., electroradiographic layers discharge mechanism *(Russian)* 3–36638
Se based glass, photoreceptor performance and applic. to xerography 3–16455
Se film, photocond., temp. and applied field depend. *(French)* 3–27289
Se glassy, elec. cond., density and crystn. rate rel. to S and Te additions 3–33887
Se-As glassy, local states, photoelectric properties, structure and composition 3–33812
$Se_{0.98}Te_{0.02}$, ^{125}Te Mossbauer obs. of amorphous and trigonal phases 3–34267
$Se_{87}Te_{13}$, elec. switching in glass transition range 3–33970
$Se_{50}Te_{20}As_{20}Ge_{10}$, stress thermally induced by switching 3–27293
Si, amorphous layers formation by Si^+ implantation 3–17888
Si, cohesive energy and density of states 3–36521
Si, film, impurity effects on structure with different preparation methods 3–20968
Si, insulating amorphous layer form. on Si^+ bombard., props. on annealing 3–7798
Si, ion implantation, radiation damage 3–33585
Si, ion implanted, defect formation 3–33586
Si, neutron damage, 14 MeV, transient annealing 3–33566
Si, optical consts. meas. rel. to structure and energy states 3–21380
Si, radiation annealing of amorphization on ion bombardment 3–33553
Si, thin films, crystallisation 3–8063
Si film, structure, electron microscope obs. 3–1949
Si film, structure, sputter-ion source mass spectrometry obs. 3–1950
Si films, electronic transport and state distribution 3–8172
Si films, ion-implanted, circular etch pits 3–33752
Si high energy C^+ bombarded damage profiles, annealing props. of resulting subsurface amorphous layers 3–17887
Si layers, current-voltage characts. 3–15200
$Si_{1.2}Ge_{1.0}As_{3.0}Te_{4.8}$, chalcogenide glass film, switching rel. to breakdown mechanism 3–38874
SiO film, Al and/or Ag electrodes, conductivity, field and temp. depend., memory effect switching 3–21124
SiO_2, film, thermal oxidation, transport processes 3–21157
SiO_2, noncrystalline, defect struct. and irradiation behaviour 3–4770
SiO_2 film, amorphous, on Si, electron trap distrib. from transient photodepopulation meas. 3–18163
Te based chalcogenide film as memory material, crystallisation after short laser pulse 3–30524
Te chalcogenide, Mossbauer obs. rel. to switching action *(German)* 3–15230
Te film, struct., electron diffr. obs. 3–20964
Te-As-Ge-Si film, accumulation effects in switching 3–18200
Te-As-Ge-Si film, freq. depend. cond. and capacitance 3–2092
Te-As-Ge-Si thin film capacitors, frequency dependence of capacitance and conductance 3–27321
$Te_{50}As_{30}Ge_{10}Si_{10}$ glass film, differential capacitance 3–21361
$Te_{81}Ge_{15}As_4$, amorphous-cryst. phase transition, Mossbauer obs. 3–18395
$Te_{1-x}Se_x$, Mossbauer obs. of order-disorder transform. 3–15445
$TlAsSe:Fe^{3+}$ glass, e.s.r. *(Russian)* 3–5133
$TlSbSe_2$ film, prep., elec. and optical props. *(Russian)* 3–18235
$Tl_2SeAs_2Te_3$, macroscopic inhomogeneities using contactless-conductivity technique and comp. homogeneity from probe obs. 3–11896
Tl_2Te film, low temp. conduction recrystallisation at 261-289K 3–27249
V_2O_5-P_2O_5 glass, d.c. cond. by polarons 90-520K 3–33886
WO_3 thin films, optical and photoelectric props. and colour centres 3–36899
ZnTe, O_2 chemisorption effect on electrical conductivity 3–27320
ZnTe, optical props. 3–2526
ZnTe, struct. and elec. cond. 3–1942

amorphous state
see also vitreous state
acetylcellulose in diethylene ethyl ether, metastable solution, separation of amorphous phases 3–39402
alloy, binary, local order effect on electronic states 3–20994
alloy, binary, short-range order rel. to electronic structure 3–38774
alloy, disordered, substitutional, calc. of extended potentials in CPA 3–24371
alloy, disordered binary, CPA validity in elec. cond. theory 3–21050
Anderson three dimensional disordered model, localisation degree 3–18056
brittle amorphous materials, curves on fracture surfaces 3–38617
close packed random struct. model, for amorphous metallic alloys 3–14689
density of bound states calc. for one dimensional disordered array 3–18059
dielectric, Poole-Frenkel cond., calc. including hot electron effects 3–5015

amorphous state continued
  dielectric intermediate layer on NaCl substrate, condensation and epitaxial growth of evaporated thin films 3−38746
  differential thermal microanalysis study of differentiation between amorphous and microcryst. struct. *(French)* 3−7937
  disordered system, strong correlations effects 3−33777
  disordered system electronic energy spectrum 3−33774
  electron scatt. form amorphous material, transition matrix approach 3−7792
  electronic structure of disordered network 3−30388
  electronic theory of disordered materials, Bethe-Peierls approx. 3−38769
  epoxy adhesive, glass transition temp. relation to adhesive strength 3−5353
  ferromagnet, Heisenberg model, spin-wave spectrum, calc. 3−30593
  ferromagnet, molecular field theory 3−18279
  ferromagnetic film, weakly amorphous, density of spin wave states, Heisenberg model calc. 3−30636
  film, electron micrograph interpretations 3−17723
  glasses, inorganic, structure, separation of amorphous phases and uniform crystallisation, review 3−24032
  growth of Te film on amorphous substrate *(Russian)* 3−15108
  ice, i.r. absorpt. spectrum analysis 3−2541
  Ising ferromagnet, connection between amorphous and anisotropic models 3−38942
  magnet, constant coupling approx. for Ising and Heisenberg models 3−11998
  metal film, elec. cond. meas. showing negative temp. coeff. of resist. 3−33870
  microcrystallite and random network models to interpret electron micrographs and diffraction patterns 3−17744
  nylon 11, 66 and 12, deform. behaviour near glass transition temp. 3−20233
  Ostwald's rule, appl. to amorphous materials 3−24028
  poly(ethylene terephthalate) fibre, X-ray struct. obs. 3−24033
  polyamide fibre, small angle X-ray obs., polystyrene graft effect, intrafibrillar amorphous regions *(Russian)* 3−30077
  polyethylene, small angle X-ray scattering before and after irradiation 3−38541
  polyethylene terephthalate, small-angle X-ray scatt. 3−4506
  polymer, low temp. equation of state 3−4499
  polymer, oriented, elasticity of intercrystallite zones and mech. props. 3−26758
  polymers, surface tension rel. to solubility parameter 3−39400
  rare earth-transition metal alloy amorphous films, magneto-optic props., applications 3−36857
  reactions in vitreous and amorphous solids 3−5389
  silica, crystallization of powder effect of alkali halides and silver nitrate 3−18740
  splat-cooling apparatus for non crystalline solids preparation 3−9005
  thermoplastic, crazing, fracture, electron microscopy 3−34650
  tight-binding model of electronic structure, application to liquid metals 3−38773
  transition metal-C alloy film, polyconductivity *(Russian)* 3−8145
  Weaire model, electronic density of states 3−15114
  X-ray double diffr. *(French)* 3−36241
  Ag-Te films, amorphous state-polycryst. Ag_2Te-monocrystr. Te transform. *(Russian)* 3−36496
  Al film, influence of deposition substrate temp. and partial disorder on optical props. 3−24715
  Al-Al_2O_3, electrical and structural props. of amorphous system 3−38840
  Al-Ge films, crystn. and decomp. *(German)* 3−24819
  Al-Zn, hard non-ordered electrical resistivity concentrational dependence *(Russian)* 3−11883
  Al_2O_3, growth of amorphous and epitaxial layers on Si *(German)* 3−8056
  As_2S_3, film, kinetics of photo-induced edge shift in light transmission 3−24714
  BeO film, prep. by reactive evaporation of Be *(German)* 3−21534
  Bi, thin layer, transition from amorphous to crystalline state under mag. field *(Russian)* 3−15015
  C film, antiferromag. transition, e.s.r. obs. 3−18317
  C film, electron microscopy dark field images 3−14688
  C graphitisation of diamond, high pressure and temp., nucleation and planar growth 3−12450
  β- carotene films, amorphous, refractive and absorption indices *(Russian)* 3−36895
  CrSi, condensation, platelet structure, 300-1020°C, X-ray study *(Russian)* 3−7919
  Cu-As-Se-Au glass, memory effect rel. to Au content 3−33969
  (Fe-Ni)-P-C alloy, low temp. resist. and Curie temp. 3−21234
  $Fe_{75}P_{15}C_{10}$ alloy, crystallite morphology during crystn. 3−21595
  GaAs, radiation annealing of amorphization on ion bombardment 3−33553
  GaAs amorphous films, electron diffraction investigation of struct. *(Russian)* 3−8059
  GaP amorphous films, electron diffraction investigation of struct. *(Russian)* 3−8059
  Ge, l.f. Raman scatt., freq. depend. coupling const., elastic continuum limit 3−8586
  GeO_2, vitreous scattering of low frequency phonons at low temps. 3−1769
  GeS, black P struct. model 3−33457
  GeSe, black P struct. model 3−33457
  $Ge_{0.5}Sn_{0.5}$ l.f. Raman scatt., freq. depend. coupling const., elastic continuum limit 3−8586
  Ge_xSn_{1-x}, alloy, $x \geqslant 0.5$, struct., optical props., optical gaps 3−7627
  GeTe, black P struct. model 3−33457
  $Ge_{0.175}Te_{0.825}$, struct. of amorphous and liq. state from neutron scatt. 3−33456
  InSb, l.f. Raman scatt., freq. depend. coupling const., elastic continuum limit 3−8586
  Ni-NiO, electrical and structural props. of amorphous system 3−38840
  $Ni_{41}Pd_{41}B_{18}$:Cr, amorphous, elec. resist. meas. showing Kondo effect 3−33869
  Pb-In hard non-ordered, electrical resistivity concentrational dependence *(Russian)* 3−11883

amorphous state continued
  Pb-Sn, hard non-ordered, electrical resistivity concentrational dependence *(Russian)* 3−11883
  Pd-Ni-P alloy, effect of P conc. on atomic distrib. function 3−24027
  Sb_2Se_3, reflectivity, meas. rel. to electronic structure 3−8104
  Si, formation of disordered layers by Ar^+, Ne^+ and B^+ ion bombardment 3−24167
  Si, radiation annealing of amorphization on ion bombardment 3−33553
  SiO_2 fused below 1K, nonlinear phonon propag. 3−17952
  SiO_2 thermally grown on Si, electron trapping levels 3−8262
  Sn-SnO_2, electrical and structural props. of amorphous system 3−38840
  Ta-Ta_2O_5, electrical and structural props. of amorphous system 3−38840
  Te, atomic arrangement, transmission electron diffr. obs. 3−14687
  $Y(NO_3)_3$-$KNbO_3$(K_3NbO_4)-H_2O, X-ray obs. of amorphous $YNbO_4$ phase below 600°C *(Russian)* 3−14969
  Yb, thin layer, transition from amorphous to crystalline state under mag. field *(Russian)* 3−15015

amplification
  see also acoustic wave amplification; amplifiers
  benzene emission amplifier based on forced Raman effect with lateral pumping *(Russian)* 3−35717
  bulk viscosity effects on amplification function of Stokes signal interacting with laser beam in fluid 3−32588
  cylinders, rapidly heated, vibration amplification by repetitive pulsing 3−3986
  diocotron, in M-type devices *(Russian)* 3−16922
  dye amplifier, flash pumped, amplification gain eqn. 3−29084
  e.m. wave amplification in total internal refl. from region of inverted population *(Russian)* 3−10326
  explosion waves in biphase medium, secondary reaction effects *(Russian)* 3−14468
  hearing aids, amplitude compression and distortionless amplification 3−3459
  laser, Rhodamine 6G in ethanol, gain curve and triplet-triplet absorpt. study 3−13736
  laser, with resonator frequencies displaced relative to amplification contour of active medium *(Russian)* 3−22928
  magnetostatic echo in ferrites 3−15427
  parametric gain in birefringent crystals , optimum focusing conditions 3−781
  ruby laser, active quality modulation by extra-generative amplification *(Russian)* 3−13737
  three-frequency interaction of oscillations, amplitude amplification and frequency transformation *(Russian)* 3−770
  u.h.f. quantum amplification in ruby *(Russian)* 3−735
  v.l.f. signal in magnetosphere, by Cherenkov resonance interaction 3−9345
  CO flame laser, P-branch i.r. transitions in C_2H_2-O_2 flame, optical gain 3−10473
  CO_2 laser, electron beam controlled, current, voltage, gain meas. 3−10519
  CO_2 laser, TEA, translational temp. and vibr. temp. from gain spectral behaviour 3−19602
  CO_2 laser discharge, gain correl. with sidelight and plasma impedance props. 3−13729
  CO_2-N_2-He system, amplification rel. to temperature 3−19605
  GaAs laser, n-type and undoped active layers, optical gain coeff. rel. to current 3−16860
  HF laser, gain, relax., spatial and temporal depends. 3−10486
  N_2 laser amplifier, gain measurements 3−6473
  Nd:glass laser, mode locked pulses, pumped by Nd:$POCl_3$:$ZrCl_4$ liquid laser, effect of freq. shift on power gain 3−13746
  Nd-doped laser glass, nonlinear loss, two-photon absorption process 3−767

amplification measurement *see gain measurement*

amplifiers
  see also amplification; d.c. amplifiers; differential amplifiers; fluidic amplifiers; microwave amplifiers; operational amplifiers; preamplifiers; radiofrequency amplifiers; ring lasers; video amplifiers
  buffer, pH meas. application 3−35538
  charge amplifier, field effect transistor applic. 3−28684
  filter amplifier, for timing experiments 3−25911
  for i.r. spectrophotometers, with thermocouple detector 3−25758
  logarithmic, autoranging in apparatus for plotting log σ against 1/T *(German)* 3−37663
  logarithmic for photoelectric photometer 3−25752
  for nerve action potential recording, signal/noise ratio 3−28338
  photodiode detector, for Fourier transform spectrometer 3−9950
  prosthetic devices, charact. effect on control system design 3−28753
  slow bioelectric process recording, amplifier design 3−32236
  unity gain, monolithic IC impedance convertor for biomedical meas. apparatus 3−37741
  Nd: glass fibre, threshold characteristics of receivers *(Russian)* 3−740

amplifying *see amplification*

amplitude modulation
  see also pulse amplitude modulation
  e.m. waves in plane-bounded plasma, nonlinear modulation 3−17585
  hearing, beats of sinusoidally a.m. signal with tone near modulation frequency 3−3461
  low frequency plasma oscillations investigation by amplitude modulation of VHF radiation *(Russian)* 3−17596

analogue computer applications
  see also simulation
  chemical reaction kinetics 3−5378
  distributed flow systems, analogue simulation technique 3−33307
  forced vibrations of nonlinear dynamic absorber, analogue computer analysis 3−16680
  impact, of two masses along line of centres, modelling *(German)* 3−32302
  physics teaching tool 3−32009
  sampling distortion correction, in catheter-densitometer and thermistor systems 3−25993

analogue computer applications continued
- styrene-methylmethacrylate-CCl_4, cooligomerisation system, kinetic features, computer simulation 3—39440
- ventricular pressure, rate of proportional rise determination 3—13485

analogue computer circuits
- *see also differentiating circuits; function generators; integrating circuits; operational amplifiers*
- atmospheric relative humidity, analogue circuit calculation from dew point and temp. 3—37258
- operational amplifier, for modelling impact of two masses along line of centres *(German)* 3—32302
- preprocessor, for digital computer meas. of e.c.g. R-R interval and R wave width 3—25991
- pulse height analysis 3—19312

analogue computer methods
- crystal electron states simulation, using three-dimensional resistance network *(French)* 3—20979
- crystallography, solution of integral eqns. of structural analysis 3—33421
- e.e.g. signals analysis exponentially weighted running statistics 3—5640
- Ekman drift velocity, analogue computer simulation of equations 3—2957
- modelling of alkali halide photoluminescence *(Russian)* 3—21461
- subharmonic resonance of order 1/2 with asymmetrical restoring force 3—22675

analogue computers
- *see also analogue-digital conversion; digital-analogue conversion*
- Fourier analyser for n.m.r. 3—28616
- optical, Fourier transformation of i.r. interferogram 3—29048
- Siberian Instruments 1971 Exhibition *(Russian)* 3—9900

analogue digital computers *see hybrid computers*

analogue-digital conversion
- *see also digital-analogue conversion*
- data-logging analogue data in digital form 3—25964
- digital counting, reversible, to follow reversing signals 3—32179
- i.r. spectral analysis, automatic, numerical data, alcoholic solutions, Perkin Elmer 521, circuits *(French)* 3—13503
- isocon TV camera/mag. tape recorder system for fast oscilloscope trace analysis 3—3856
- GaAs laser diode, pulse position modulation technique for point-point voice communication 3—26209

analogue-digital convertors *see analogue-digital conversion*

analogues, direct *see direct analogues*

analytical chemistry *see chemical analysis*

anaphoresis *see electrophoresis*

anechoic chambers
- acoustic measurements, reflections and diffractions 3—104
- small portable, construction and performance 3—28419

anelasticity
- *see also creep; damping; internal friction*
- crystalline solids, relax., book 3—7852
- metals, unit for torsion investigations at room and high temps. 3—35358
- relaxation, real structure and migrational props., magnetic after-effect obs. *(Polish)* 3—24212
- soil, dynamical treatment 3—27957
- soil, rel. to structure destruction 3—31300
- steel, austenitic stainless, Nb-stabilized, stress varied creep behaviour 3—8925
- steel, low-C, pressurization and quenching effects on yield behaviour 3—24867
- Ag solid solutions, Zener relaxation strength 3—14852
- Al, anelasticity, amplitude-dependent during and after plastic deformation *(German)* 3—34611
- Al, single crystals, amplitude dependent, role of dislocation motion *(German)* 3—24214
- Cu, anelasticity, amplitude-dependent during and after plastic deformation *(German)* 3—34611
- Cu, single crystals, amplitude dependent, role of dislocation motion *(German)* 3—24214
- Cu-Al, estimation of quasielastic force and anharmonic coeffs. from X-ray diffraction meas. 3—30209
- Fe—Co(3.18-42.5 wt%) alloy, Zener relax. 3—24213
- Ge crystal, dislocations, internal friction meas. 3—17847

anemometers
- ambiguity noise in turbulent flow 3—28798
- constant temperature, appl. to intra-arterial blood flow meas. 3—9646
- d.c. hot wire thermoanemometer for determining water flow conditions 3—32272
- Doppler anemometer, meas. of electrohydrodynamic motion 3—164
- Doppler laser anemometer *(French)* 3—16577
- dynamics characteristics of vanes and cups 3—9395
- electronic, constant current, constant temperature, probes, operation, applications, analysis techniques 3—16581
- fluid flow, viscous shear sensor 3—463
- for fluid flow measurement, laser Doppler method 3—19654
- fluidic, for meas. of velocity of very slow currents 3—16582
- fringe, light scattering by clinder situated in interference pattern 3—22566
- gas mixtures in turbulent flow, hot-wire anemometry 3—22564
- Gill propeller, requirements for eddy correlation meas. 3—9400
- heat pulse, veloc. meas. in inhomogeneous turbulent flow 3—26042
- hot-wire, calibration for velocity perturbation expts. 3—22565
- hot-wire, meas. of air unsteady flow rates in channels 3—32269
- hot-wire, sensor resolution, errors occurring due to turbulence, estimation *(Russian)* 3—32274
- laser, broadening of meas. freq. spectrum due to interference plane gradients 3—13529
- laser, EUROMECH 36 report 3—3925
- laser, hot wire and film, literature review 3—450
- laser Doppler anemometer, velocity and turbulence meas. of turbulent swirling flow in water 3—794
- laser Doppler anemometry, fluid measurement 3—22577
- laser Doppler anemometry of electric arcs, fluid velocity meas. 3—795

anemometers continued
- optical-anemometry signals, light source and geometrical requirements for optimisation 3—163
- propeller, as atmospheric turbulence sensor 3—28082
- RADSCATT satellite, oceanographic parameter variation with wind speed 3—3233
- rotating vane, flow measurement and control, electronic system design 3—464
- sonic anemometer-thermometers, for wind velocity and temp. fluctuations over ice floes 3—12728
- sonic three-component anemometer *(Russian)* 3—39564
- thermoanemometer, constant temp., r.f., Siberian Instruments 1971 Exhibition *(Russian)* 3—9900
- thermoanemometer-Langmuir probe method for plasma parameters determ. 3—20613
- turbulence meas. in sludge-blanket by hot-wire anemometer *(Japanese)* 3—37780
- for water velocity measurement 3—16580
- wind speed measurements, by computer-controlled data acquisition system 3—28751
- CO_2 laser anemometer for long range wind velocity determination 3—3196

angle measurement *see angular measurement*

angular correlation techniques
- γ-γ-γ method for study of 308→296→316 keV cascade in ^{192}Pt 3—10918
- angular correlations of final particles and γ-quanta, sensitivity to mechanism-type *(Russian)* 3—19832
- atomic excited states lifetimes meas. method *(French)* 3—16503
- brass, Fermi surface study by positron annihilation 3—15117
- Compton polarimeter, for γ-ray linear polarization angular correlations 3—13417
- electron scattering effects 3—16504
- gamma-ray perturbed, angular correlation meas. applications, review 3—34275
- molecular reorientation in crystals and liquids, exptl. angular correlation functions 3—33437
- nuclear acoustic hypersuperradiance phenomena detection 3—2453
- nuclear quadrupole interactions determ. in metals and insulators by PAC 3—39062
- number distribution measurements, effect of detector geometry 3—19288
- numerical control and positioning system *(French)* 3—13418
- perturbation of γ-γ ang. correls. by coherent acoustic vibrs. in cryst. lattice 3—2474
- perturbed ang. correl. method applic. to mag. 3—25857
- perturbed meas. of excited states of magnetic tracer *(Hungarian)* 3—6062
- sum coincidence method with Ge(Li) detectors, applic. to ^{169}Yb, geom. correction factors calc. *(French)* 3—3846
- γ-γ apparatus with on-line irradiation system for short-lived isotopes 3—37685
- γ-γ measurements, algorithm for background corrections 3—37686
- γ-ray experiments, inherent ambiguities rel. to Legendre coefficients 3—22442
- γ-rays and charged particles, equipment description 3—22441
- ^{10}B(α,d)^{12}Cγ, calc. of angular correlations of final particles and γ-quanta *(Russian)* 3—19832
- ^{10}B(d,nγ)^{11}C, ang. correlation meas. of nγ at 0°, direct mode reaction 3—10999
- ^{11}B(α,t)^{12}Cγ, calc. of angular correlations of final particles and γ-quanta *(Russian)* 3—19832
- ^{11}B(d,nγ)^{12}C, ang. correlation meas. of nγ at 0°, non-direct mode interpretation 3—10999
- Cr, incommensurate antiferromag., hyperfine field meas. using time differential perturbed angular correlation 3—11993
- Cu-Ge(Ni), positron annihilation study of Fermi surfaces 3—15119
- Cu-Ni, positron annihilation study of Fermi surface necks 3—15118
- Fe:^{175}Lu(^{175}Yb), meas. of hyperfine fields at impurity nuclei 3—15141
- Fe:Tm, ferromag., perturbed angular correlation for localised moments 3—15359
- Ge(Li)-Ge(Li) asymmetric linear sum-peak coincidence spectrometer, use in γ-γ coincidence and directional correlation expts. 3—22489
- Ni:^{175}Lu, meas. of hyperfine fields at impurity nuclei 3—15141
- ^{a}Os, A=186, 188, 190, 192, recoil implanted in Ni, mag. dipole moments of first 2^+ states 3—14119

angular measurement
- *see also angular velocity measurement*
- Coma cluster of galaxies, size determ. from X-ray flux 3—28279
- dihedral angles on small specimens by optical system 3—16386
- e.m. field vehicle guidance system, patent 3—10426
- helical surface, cylindrical cavity, angular coeffs. of radiation 3—35634
- methods and instruments, review *(Czech)* 3—13227
- optical contacting by interference line with measuring microscopes 3—28468
- optical triaxial system 3—16406
- orientation determ. of observatory satellite with unfixed orientation 3—25535
- parallaxes for 25 stars using Thaw refractor 3—35134
- parallaxes of 23 stars from plates taken with McCormick 26-inch refractor 3—35133
- photoelectric microscope, optimal operating conditions for scanning device 3—19187
- radio sources (astronomical), lunar occultation meas. 3—28308
- reference standard, the radian 3—19141
- rocket pitch and yaw meas. by laser-optical lever system 3—32055
- survey of modern angle meas. *(Slovak)* 3—22261
- units, rationalisation in SI system 3—19136
- variable star X Cancri, angular diameter determ. from lunar occultation reappearance 3—9546

angular momentum
- Eulerian dynamics of rotating rigid body, construction in Hilbert space, reln. to time-independent Schrodinger eqn. 3—19489
- fusion reactions, complete: ^{11}B + ^{158}Tb ^{12}C + ^{158}Gd, ^{16}O + ^{154}Sm, ang. momentum role 3—11019
- nuclear angular momentum boundary of the VMI law 3—6710

- **angular momentum** continued
  - nuclear deformation energy, effect of angular momentum conservation in Strutinsky method 3−14110
  - rotating magnetically suspended spheres, slowing-down 3−22598
  - units, comment on nomenclature 3−28454
  - units, SI proposed nomenclature, comment 3−9819
  - vector props., teaching demonstration 3−9802
- **angular momentum theory**
  - *see also quantum theory; Regge poles and trajectories*
  - atomic structure, relativistic program to calc. angular momentum coefficients 3−35957
  - basis states for general j^n configuration, calc. in terms of Gel'fand patterns of SU_{2j+1} 3−4007
  - branch cuts in ang. momentum plane, discontinuities 3−10742
  - Clebsch-Gordan coefficients review of mathematical aspects *(Russian)* 3−590
  - nuclear projection model with anisotropy, study of quadrupole excitation 3−23239
  - off-diagonal operator equivalents 3−16707
  - reduced rotation matrix elements, plots and zeros, evaluation using computer program 3−19488
  - Regge symmetry application to Wigner (9-j) symbol 3−29179
  - transformation matrix, U_n group, unitary and orthogonal subgroups *(Russian)* 3−35848
  - ^{160}Dy, moment of inertia, Coriolis Antipairing effect and angular momentum projection 3−38104
  - ^{162}Er, moment of inertia, Coriolis Antipairing effect and angular momentum projection 3−38104
  - ^{16}O − ^{16}O scattering, 40-65 MeV, study of angular momentum effects via reaction channels 3−6865
- **angular velocity measurement**
  - with impulse discs, pulse frequency and variable-velocity time function harmonic relationship *(German)* 3−9818
- **anisotropy, magnetic** *see magnetic anisotropy*
- **anisotropy, magnetocrystalline** *see magnetic anisotropy*
- **annealing**
  - *see also work hardening*
  - Al, grain boundary fine structure, bright and dark field transmission electron microscopy 3−1632
  - alloy, dil., vacancy decay, analytical discrete lattice calc. 3−1619
  - austenite formation during hardening of high speed steel tools, grain size formation rel. to annealing 3−18655
  - composite, C fibre reinforced, Ni matrix, elevated temp. stability, morphological and mech. prop. degradation 3−31138
  - composite, fibre-reinforced M-M_7C_3 eutectic, ($M = Fe + Co + Cr$), $M_7C_3 \rightarrow M_{23}C_6$ transform. 3−31143
  - diamond:Li, implanted, elec. cond., after annealing at 1400°C *(Russian)* 3−2070
  - diamond crystals, electrical props. and cathodoluminescence, proton irradiation effects 3−24437
  - disordered polycrystals, distortion waves, comparison between cold worked and annealed samples 3−17926
  - ferrite, intermediate phase obs. during form. *(Russian)* 3−15736
  - glass, etched laser filament track fading 3−19642
  - graphite, reactor-grade neutron-irradiated, annealing at 350°C, effect on electrical resistivity and thermal conductivity 3−11060
  - graphite, thermoelectric power at temps. above 5 K, electron irrad. effects, annealing effects 3−27278
  - Inconel 718 solution annealed, material variability, low temp. electrical resistivity obs. 3−24871
  - martensite, electron irradiated, lattice tetragonality increases under low temp. annealing 3−33648
  - metal, proton radiation damage annealing, effects of film struct. and substrate *(Russian)* 3−7796
  - m.o.s. structures, energy distribution of charge 3−18223
  - optical glass, control of refractive index during annealing *(Polish)* 3−5174
  - Permalloy, ferromag. resonance line width obs. with annealing 3−5139
  - permalloy film, uniaxial mag. anisotropy rl. to annealing 3−18333
  - permalloy single cryst. film, uniaxial mag. anisotropy rel. to annealing *(Russian)* 3−15383
  - poly(ethylene terephthalate), bulk, effect of strain history on crystallization behaviour 3−1576
  - poly(ethylene terephthalate), cryst., annealing during polymerisation 3−31169
  - polyacrylonitrile, drawn, struct. changes during annealing 3−20236
  - polycaprolactam, doubly oriented, morphological changes during annealing 3−20235
  - polyethylene, drawn, effect on monomer vapour transport props. 3−15027
  - polyethylene, oriented, h.p. annealing effect on struct. 3−20247
  - polymer, etched laser filament track fading 3−19642
  - polymer, glassy, morphology 3−20230
  - polyolefins, cold-drawn, reversibility of deform. 3−25009
  - polystyrene, sound speeds from stimulated Brillouin scatt., annealing effects, laser induced damage 3−1307
  - quenched and irradiated metals, role of interstitials and vacancies in recovery 3−24104
  - rutile, abraded, electron microscope study of structure before and after annealing 3−15753
  - sapphire, spheroidization of tubular pores at high temps., reln. to surface diffusion 3−17921
  - semiconductor, ion and electron irrad., clustering of defects 3−33576
  - steel, 30Kh2GSN2VM, isothermal holding time of forgings 3−24933
  - steel, A286 stainless solution annealed, material variability, low temp. electrical resistivity obs. 3−24871
  - steel, AISI 316 solution annealed, material variability, low temp. electrical resistivity obs. 3−24871
  - steel, brittleness depend. on cooling rate after annealing *(Russian)* 3−24905
  - steel, cast heat resistant, with low Ni content, characteriz. 3−27696
  - steel, cold-rolled, singularities of softening phenomena *(Russian)* 3−8833
  - steel, diffusion-controlled coagulation process of globular cementite, expt. confirmation 3−5293
  - steel, hypereutectoid Si type, austenite decomp. *(Russian)* 3−15717
- **annealing** continued
  - steel, low-C, low-Mn, Nb additions effect on plastic anisotropy 3−37054
  - steel, martensite annealing, carbide precip., thermal stability, Si conc. influence *(French)* 3−21619
  - steel, Mossbauer obs. of strengthening mechanisms *(Russian)* 3−24875
  - steel, pipe, 15Kh1M1F, plastic deform. mechanism 3−21688
  - steel, stainless, stabilized, void form. due to fast neutron irrad. 3−26503
  - steel, stainless, type 304, deform. induced twin boundary crack form. 3−24857
  - steel, strengthening by directional transform, 3−31113
  - steel, tempered hardened, rapid heating and plastic deform., magnetometric exam. *(Russian)* 3−8876
  - steel sheet, cold-rolled, annealing-induced changes in texture in cross section *(Russian)* 3−30987
  - steel with C, Cr and 1% of Nb, Ni, W, V, physical changes caused by clustering *(Russian)* 3−12408
  - transformer steel, grain size and form control *(Russian)* 3−12342
  - transition metals, b.c.c., group VA, stage III annealing mechanism 3−34592
  - transition metals, b.c.c., group VA, stage III recovery mechanism 3−34593
  - triglycine sulphate, effect on critical region behaviour 3−15455
  - of vacanices, during cooling of crystal, analyt. eqns. 3−7752
  - α-Fe, recrystallization dependence on deformation and annealing, following high temp. torsion deformation 3−15707
  - Ag, epitaxially grown film, annealing rel. to dislocation density 3−11830
  - Ag film, partially disordered, anomalous absorpt. prior to annealing 3−36888
  - Ag film, recrystallisation and excess free energy obs. 3−1953
  - Ag film, temp. coeff. of resist. meas. in annealed and agglomerated states 3−21047
  - Ag-Al thin film contacts, degradation mechanism during annealing 3−15241
  - Ag-Te films, amorphous state-polycryst. Ag_2Te-monocrystr. Te transform. *(Russian)* 3−36496
  - Ag-Zn(27.6 wt.%) optical and electron microscope investigation of bainitic transformation in 180° to 260°C *(Japanese)* 3−18564
  - Al, deformed, struct. discontinuities *(Russian)* 3−24854
  - Al, dislocation annihilation mechanism by deformation 3−17823
  - Al, grown by recryst., dislocation density and distrib., annealing effects *(French)* 3−24885
  - Al, neutron irrad., radiation damage, postirradiation annealing effects 3−11661
  - Al, neutron irradiated and deformed at low temp., internal friction and modulus anomaly, influence of annealing *(French)* 3−14935
  - Al 2024 solution annealed, material variability, low temp. electrical resistivity obs. 3−24871
  - Al:Si, annealing near melting temp., effect on substructure *(Russian)* 3−12355
  - Al-3%Cu alloy processed from double-oriented ingots, cold rolling and annealing textures *(Japanese)* 3−18640
  - Al-Al_3Ni eutectic comp., thermal stability of microstruct. *(Russian)* 3−24850
  - Al-Cr(3.6 at.%), supersaturated solid solutions, decomposition rel. to diffusion, activation energy calcs. 3−36438
  - Al-Cu(4.5 wt.%) alloy, surface relief effects associated with $CuAl_2$ rod form. 3−37006
  - Al-Fe(3.6 at.%), supersaturated solid solutions, decomposition rel. to diffusion, activation energy calcs. 3−36438
  - Al-Ge alloys, vacancies influence on nucleation of incoherent Ge precipitates 3−2702
  - Al-Mg (5 at %) solution annealed, material variability, low temp. electrical resistivity obs. 3−24871
  - Al-Mg alloy, isotropic charged Guinier-Preston zone reversion at 100°C *(French)* 3−18604
  - Al-Mn(3.6 at.%), supersaturated solid solutions, decomposition rel. to diffusion, activation energy calcs. 3−36438
  - Al-Ni(3.6 at.%), supersaturated solid solutions, decomposition rel. to diffusion, activation energy calcs. 3−36438
  - Al-Ti (0.16 at wt.%) alloy, yield point phenomenon *(Japanese)* 3−18644
  - Al_2O_3, sapphire whiskers, Ni coated, stability 3−30377
  - Al_2O_3 film, r.f. sputtered, surface charge density rel. to H_2 annealing 3−2187
  - Au, epitaxially grown film, annealing rel. to dislocation density 3−11830
  - Au film, (001) oriented, recrystn. into (111) orientation 3−20973
  - Au films, recovery process for films vacuum deposited on substrate at liquid He temp. 3−2720
  - $BaTiO_3$, effect on positive temp. coeff. of resist., near Curie temp. *(Russian)* 3−18130
  - Be, hydrostatically extruded, elec. resist. changes during annealing *(Russian)* 3−18110
  - Bi, effect on twinning rate *(Russian)* 3−31057
  - C, isotropic pyrolytic, poorly crystalline, microstructure and mech. props., electron microscopy 3−24993
  - CdSe films in air, structure and electrical resistance obs. *(Russian)* 3−38752
  - $CdSnAs_2$, point defects, heat treatment effects, elec. props. study *(Russian)* 3−14853
  - Co films, rot. mag. moments changes due to oxidation and reduction *(Russian)* 3−30641
  - Co-Fe-Be, mag. and mech. props with annealing and cold drawing *(Japanese)* 3−12398
  - Co-Fe-Nb semihard mag. alloy development 3−21261
  - Co-Fe-Nb semihard mag. alloy characteriz. 3−21279
  - $CoCr_2S_4$, effect on resist. and magnetoresist., 77-450 K 3−27258
  - Cu, annealability testing 3−34675
  - Cu, plastically deformed, angular correlation of positron annihilation comparison with annealed specimens 3−17869
  - Cu torsionally fatigued wires, strain amplitude changes effect on stress amplitude and resistivity, intermediate annealing 3−27054
  - Cu-Ag-Al solid soln. alloys, isothermal recrystn. kinetics 3−21592
  - Cu-Al (15at.%), deformation temp. and annealing influence on structure and strength props. 3−31086
  - Cu-Al alloys, annealing twins formation 3−2701

annealing continued
Cu-Al_2O_3(MgO)(TiO_2), internally oxidised, brittleness during annealing in H_2 *(Japanese)* 3−12395
Cu-Al(15 at.%) alloys, ordering and disordering kinetics after sudden annealing changes, residual resist. obs. 3−37062
Cu-Ge, deformed alloy, lattice thermal cond. recovery with annealing 3−15174
Cu-Pt alloys, short-range order and atom displacement parameters *(Russian)* 3−39329
Cu-Ti, obs. of precipitation morphology on annealing *(Russian)* 3−12356
Cu-W fibre composite, thermal expansion *(Japanese)* 3−18703
$Cu_{2\|x}MnAl_{1-x}$, Heusler alloy, effects on mag. domain struct., Lorentz microscopy 3−1545
Fe, ferromag. resonance line width obs. with annealing 3−5139
Fe, high purity, quenched, resist. study 3−4749
Fe, malleable, Bi-containing, trace element effects on malleabilization kinetics and mech. props. 3−39357
Fe alloys, heat treatment practice in engineering, review 3−31053
Fe and Ni carbonyl powders, hot pressing method with subsequent annealing for production of permalloy *(Russian)* 3−27723
Fe coarse magneto soft powder, sintering effect on coercive force, recrystallisation annealing effect *(Russian)* 3−27718
Fe:^{175}Lu(^{175}Yb), annealing props. rel. to hyperfine fields at impurity nuclei 3−15141
Fe-Al(40 at%) alloy, quenched-in vacancies annealing kinetics 3−37039
Fe-Al(40 at.%) alloy, ordered, quenched defect recovery *(French)* 3−24839
Fe-Co-V alloys, effect on mag. transform. of γ phase *(Russian)* 3−30731
Fe-Cr-Ni alloys, austenitic, hydrogen charging and effects *(French)* 3−2747
Fe-Ni alloys, change in saturation magnetisation 3−12034
Fe-Ni alloys, effect on struct. and props. of soft-mag. alloy tapes 3−21275
Fe-Ni alloys, invar-type, Young's modulus, temp. depend., recovery and recrystn. influence *(Russian)* 3−36773
Fe-Ni-C alloy, reverted austenite, prior deform. effects on strength and annealing behaviour 3−37048
Fe-Ni-Cr-Mo alloy, effect on struct. changes, Mossbauer obs. *(Russian)* 3−31056
Fe-Ni-Mn alloy, martensite morphology depend. on isothermal transform. temp. *(Russian)* 3−24878
Fe-Pt (32-35 at.%) alloys, isothermal annealing depend. of mag. props. *(Russian)* 3−15389
Fe-Si, 480-680°C, effect of mag. field on softening process *(Russian)* 3−27673
Fe-Si, polygonization, influence of bending orientation during annealing *(Russian)* 3−8834
Fe-Si single cryst., texture formation during recrystallization, struct. changes during annealing *(Russian)* 3−12341
Fe-Si(3 wt.%) single crysts., deform. twins influence on rolling and recrystn. textures *(Russian)* 3−24848
Fe-Si(3 wt.%) texture variations at recovery stage with recrystallisation annealing 3−31012
Fe-Si(3.25 wt.%) alloy, impurity effects on grain growth in strain-anneal and secondary recrystn. 3−37041
Fe-Si(5.3 at.%), alloys, deformed screw dislocations and prismatic loops, annealing effects 3−18632
Fe_3Al, effects on compression induced mag. anisotropy 3−30642
$FeCr_2S_4$, effect on resist. and magnetoresist., 77-450 K 3−27258
n-GaAs, electron irradiated, defect annealing, cluster formation 3−33558
GaAs, point defects, precision lattice parameter measurements after quenching and annealing 3−33523
GaAs, radiation annealing of defects formed by ion bombardment 3−33553
GaAs, surface damage induced by 50 keV Zn^+ ions, study by isochronal annealing expts. 3−24168
GaAs:Cu, supersaturated solid solution, dislocation decoration on decomp. 3−33542
GaAs:He(N,S,Zn), ion implantation, elec. conduction due to defect centres 3−33906
GaAs:Si, free carrier conc. rel. to annealing 3−18141
GaAs:Sn(Si, Zn), electron irrad., 'near-edge' absorption, annealing 3−33846
GaAs:Zn, H^+ ion bombardment, channelling expts., annealing behaviour of disorder density 3−33578
Ga_3Te_4 thin films, crystal microstructure during annealing *(Russian)* 3−33754
Gd, hardness vs. annealing temp. behaviour rel. to O_2 content 3−24884
GdO, form. of superlattices and domain substructures 3−8067
Ge, amorphous, effect. on thermoelectric power 3−8174
p-Ge, annealing of radiation induced defects rel. to recovery and defect energy levels 3−15158
n-Ge, electron bombardment induced annealing stage 3−38598
Ge, H^+, O^+, B^+, ion bombardment, divacancy-like optical absorption 3−34394
Ge, n- and p-type impurities electron irrad., annealing, Frenkel pair model, vacancy release 3−33561
Ge, O doped and Li diffused, effect of annealing on carrier concentration and mobility 3−18136
Ge, single crystal discs, 200 to 800°C in vacuum, transmission electron microscope obs. 3−38705
Ge amorphous sputtered film, annealing activation energies, elec. cond. study 3−30369
Ge film, amorphous, effect on density 3−1958
Ge: group V (O,Te), electron irrad., E_c-0.2 eV level, defect model 3−33842
Ge:B and undoped, neutron irradiated, high temp. annealing, X-ray obs. 3−17876
Ge:Cu, effect of impurity on kinetics of annealing of radiation defects 3−24111
p-Ge:Ga, gamma irrad., role of Li in annealing processes 3−33844
InAs, electron irradiation damage studies 3−33555
$KBr_{0.5}I_{0.5}$, effect on microhardness 3−7843
KCl, γ-irradiated crystals, thermoluminescence, plastic deformation effect, thermal annealing of F-centres 3−8677

annealing continued
KCl, precip. of supersaturated solid of Ba, light scatt. obs. 3−33540
KCl, with centres of colloid type, mech. props. on annealing *(Russian)* 3−14855
KCl:Sr^{2+}(Ba^{2+}), effect on microhardness 3−7843
KH_2PO_4, effect on optical anomalies *(Russian)* 3−15470
LiF, annealing kinetics of radiation defects 3−4757
LiF, cold-worked, recovery of u.s. props. during annealing, dislocation behaviour 3−11624
LiF, dislocation density rel. to thermal treatment *(French)* 3−36306
LiF film epitaxially grown on NaCl, structure form. on annealing in air 3−1929
LiF glow peak growth due to annealing 3−291
LiF:Mg^{2+}, neutron irrad., annealing of radiation defects *(Russian)* 3−11656
MgO, creep-deformed, dislocation structures, cause of deformation, diffusion controlled 3−38593
Mn-Cu-Co nonmag. Elinvar-type alloys characteriz. 3−37074
Mn-Ni, multiphase structure form. on annealing 3−18594
MnBi thin film rel. to electric resistivity *(Japanese)* 3−34005
$Mn_xFe_{3-x}O_{4\|y}$, spinel, miscibility gap obs. 3−30265
Mo, annealing behaviour after electron irradiation 3−4772
Mo, deformed, subgrain growth during annealing 3−31014
Mo, prequenched, 1.7 MeV electron irrad., stage-I recovery 3−27039
Mo, purity effect on struct. and mech. props. 3−18602
Mo, removal of C by annealing under low press. oxygen *(French)* 3−21590
Mo alloys, deformed, interstitial solid soln. decomp. during recrystn. *(Russian)* 3−37018
Mo fibre, annealing temp. effects on props. rel. to composite fabrication *(Czech)* 3−31153
Mo:Ti, Zr, texture changes with high and low. temp. rolling and intermediate anneals *(Russian)* 3−24902
Mo-Ti-C, impurity braking influence on subgrain growth during annealing 3−31014
NaCl, annealing of γ-irradiation induced hardening 3−36330
NaCl crystals, reverse deformation comparison with annealing, polygonisation 3−17903
NaCl crystals, thermal annealing of radiation damage, positron annihilation techniques 3−33543
NaCl:$BaCl_2$, flow stress depend. 3−20786
NaCl:Ca, impurity induced Raman spectra of annealed and quenched crystals 3−21409
NaCl:Tl, annealed and quenched, thermoluminescence 3−15568
Nb, electron irradiated, annealing studies, H_2 contamination following UHV degassing 3−15723
Nb, neutron irradiated at low temp., annealed and cold worked, internal friction 3−17875
Nb plastically deformed, stage III recovery analysis 3−34591
Nb-Al alloy, Nb-rich, sputtered films and quenched samples, rel. to superconductivity 3−5082
Ni, 99.999%, pure, hardness max. following annealing after plastic deformation *(German)* 3−27711
Ni, cyclic endurance, and dislocation struct., initial state and after programmed strengthening *(Russian)* 3−5308
Ni, quenched, elec. resistivity exam. of point defects *(French)* 3−11611
Ni, structure stabilisation by multiple thermal cycling and isothermal annealing *(Russian)* 3−24903
Ni, u.s. irrad., struct. changes *(Russian)* 3−15718
Ni alloys, metallo-ceramic production, annealing of calcinal production hydrogen *(Russian)* 3−12380
Ni alloys, thoria dispersion influence on preferred orientation 3−21599
Ni:^{175}Lu, annealing props. rel. to hyperfine fields at impurity nuclei 3−15141
Ni:Hf, lattice-location of implanted impurity in ferromag. host, channelling obs. 3−18305
Ni-(50% wt.)Fe, melting process effect on coercive force *(Korean)* 3−5120
Ni-Mn alloy, Ni_3Mn, influence of annealing under load on struct. and props. *(Russian)* 3−15729
Ni-Mo alloy N70M27, corrosion resist. after ordering 3−21604
Ni-P coatings on steel, struct. and props. rel. to annealing temp. and time 3−27691
Ni-P thin films, optical and photoelectric props. rel. to structure *(French)* 3−36959
NiAl, void and dislocation loop formation following annealing, 700-900°C 3−18658
Ni_3(Fe,V), V atom redistrib. obs., Mossbauer spectra *(Russian)* 3−12080
NiO-Cr_2O_3 solid soln. prep., homogeneity 3−18787
Pb film, supercond., effect on crit. temp. *(Russian)* 3−18251
$Pb_{1-x}Sn_xTe$, single-zone annealing, n.m.r. meas. for sample characterisation 3−24619
PbTe, single-zone annealing, n.m.r. meas. for sample characterisation 3−24619
Pt, electron irrad., recovery during stage II annealing, interstitial rearrangement 3−11618
Pt, electron irrad., recovery during stage III annealing, vacancy migration mechanism 3−11619
Pt wire, thermal chock of annealed sample on cryogenic immersion 3−4746
Pt-Au alloy, electron irrad., recovery during stage II annealing, interstitial rearrangement 3−11618
Pt-Sn alloy, surface composition rel. to annealing O_2 chemisorpt., H_2 reduction, Auger spectra obs. 3−30318
Pu-Ga (1 wt.%) cold rolled 3−12384
Si, amorphous, evidence for Mott model of hopping conduction 3−5007
Si, amorphous layers formation by Si^+ implantation, damage obs. after annealing 3−17888
Si, amorphous thin films, crystallisation, voids removal by annealing 3−8063
Si, annealing twin form. at (111) (111) boundary in pulled crysts. 3−36323
Si, electron irrad., 130 K annealing stage of divacancy, i.r. transmission spectra 3−33559
p-Si, electron irrad., illum. induced annealing 3−21547

annealing continued

- Si, electron irradiated, charge state dep. of defects 3−33554
- Si, electron irradiation at 0.5K, a.c. conductivity changes, annealing up to 300K 3−7794
- Si, high energy C^+ bombarded, damage profiles, annealing props. of resulting amorphous subsurface layers 3−17887
- Si, i.r. absorpt. meas. after neutron irradiation and annealing 3−15496
- Si, insulating amorphous layer form. on Si^+ bombard., props. on annealing 3−7798
- Si, ion implantation, radiation damage 3−33585
- Si, ion implanted, defect formation 3−33586
- Si, irrad. and annealed, diffusion, role of defects, other semiconductors materials 3−33701
- Si, neutron damage, 14 MeV, transient annealing 3−33566
- Si, proton irradiated, recombination centres, photoconductivity measurements 3−33575
- p-Si, pulled, float-zone, carrier lifetime doping, annealing processes 3−39274
- Si, radiation annealing of defects formed by ion bombarment 3−33553
- Si, radiation damage in p-type with H impurity and high purity n-type, hole density, annealing 3−33546
- Si, shallow donor formation by proton bombardment, temp. effects on electron traps 3−17861
- Si, striations detn. by chem. etching and resistivity meas. after annealing *(German)* 3−2068
- p-Si electron irradiated, recovery stages, minority carrier lifetime obs. 3−33549
- Si film, monocryst. on sapphire, rel. to surface state density and film struct. *(Russian)* 3−24489
- p-Si:Al,(B), (Ga), electron irrad., annealing, effect of O and acceptor impurities 3−33560
- Si:B, ion implantation, defect centre studies 3−33587
- Si:Cu, Cu precip. colony dissolution during annealing, particle drag by climbing dislocations 3−20758
- Si:Cu precip. colony dissolution during annealing, dislocation processes 3−20757
- Si:Li, neutron irradiated solar cells, defect cluster obs. by electron microscopy 3−33569
- Si-Ge:P alloy, electron micro. exam. using replica technique *(Russian)* 3−12346
- SiC, effect on Hall effect and elec. cond. *(Russian)* 3−8211
- SiC, ion bombardment, annealing, intrinsic luminescent defects 3−34430
- SiC, structural transforms. on annealing 3−14791
- SiC temp. monitors, neutron irrad., postirrad. isochronal annealing behaviour 3−7004
- SiO_2 films on Si, annealing of degradation by Ar^+ ion bombardment 3−17879
- SiO_2 formation from SiN_4 thin films annealed in O_2 3−5416
- $Sm(Co, Cu)_5$, permanent mag. material, coercive force rel. to annealing 3−30658
- SmO, form. of superlattices and domain substructures 3−8067
- Sn-Cd alloy, eutectic lamellar microstructs., ripening by controlled annealing 3−12348
- Ta thin film resistor, proton irrad. at 30K and isochronal annealing 3−18232
- Te, electron irrad., recovery steps, isochronal and isothermal annealing expts. 3−33562
- Ti alloys, vacuum annealing influence on struct. and mech. props. 3−24938
- Ti alloys, vacuum annealing influence on operating characts. 3−24939
- Ti-Al-Co system, Ti-rich region, melting points, structure 3−24836
- TiAl containing Nb, oxidation resist. at 800 and 1000°C *(Russian)* 3−15716
- UO_2, ordered reduction and crystallographic shear, microscope obs. 3−7776
- UO_2 thin films, ion beam sputtering preparation technique, annealing, structural investigations 3−33756
- U_3Si, thermal conductivity and postirrad. densification, effects of swelling porosity 3−1058
- W, chemical vapour deposition studies 3−1960
- W, deformed, α-ptcle. irradiated and annealed, presence of He bubbles 3−18656
- W, radiation-induced defects, nature and thermal stability *(Russian)* 3−1649
- W, wires, doped, recrystallisation and annealing effect on brittleness *(Japanese)* 3−31065
- W fibre, annealing temp. effects on props. rel. to composite fabrication *(Czech)* 3−31153
- W lamps filaments void formation 3−27636
- W wire, doped temp. gradient effect on bubble growth 3−37087
- W-Zr-C alloy, dispersion struct. changes during annealing and recrystalln., electron microscope obs. *(Russian)* 3−8875
- WC, neutron irrad. damage, recovery *(Russian)* 3−30161
- $Y_{2.4}Eu_{0.6}Ga_{1.2}Fe_{3.8}O_{12}$, garnet film, annealing effects on mag. anisotropy and lattice consts. 3−30640
- YIG, polycryst. ceramic, reactively hot pressed, conversion to garnet phase 3−31123
- Y_2O_3 film, transparency, long wavelength absorpt. edge, refr. index, annealing effects 3−24763
- ZnO, ion-implanted, anneal characts. 3−30955
- ZnTe, atomic displacement energies, cathodoluminescence edge emission spectroscopy, monoenergetic electron irrad. 3−33556
- ZrO_2-CaO system, e.p.r. of Gd^{3+} and Yb^{3+}, ordered phase obs. *(French)* 3−18356

anodes

- anodic film on Pt electrode, ellipsometric and refl. obs. 3−5243
- for field desorption mass spectrometry, high temp. activation *(German)* 3−37709
- wire wall proportional X-ray counters, coaxial anodes for non-X-ray background suppression 3−25949
- Hg, low pressure high current discharge, anode region phenomena *(Russian)* 3−14624
- Ni, O_2-overvoltage in a neutral oxidising electrolyte 3−15834

anodes, electrochemical *see electrochemical electrodes*

anodic machining *see electrolytic machining*

anolytes *see electrolytes*

anomalous skin effect

- plasma, current penetration in toroidal turbulent heating expt. 3−4659
- plasma, with diffuse boundary 3−33350
- Tokamak, rel. to electron temp.-gradient instability 3−4678
- Bi, second harmonic generation rel. to anomalous effect 3−18179

antenna accessories

- magnetic sensor booms, near-field of scattering of semi-infinite cylinder, by Wiener-Hopf technique 3−22823
- Radio Astronomy Explorer B antenna aspect data processor 3−35218

antenna arrays

see also antenna phased arrays; microwave antenna arrays

- capacitor-transducer array for real-time acoustic holographic data recording 3−209
- continental slope of ocean meas., bottom boundary layer and internal wave field determ. using array meas. 3−27976
- microwave, numerical analysis applications 3−32492
- piezoelectric, review of development 3−72
- stacked Yagi, satellite automatic picture transmission reception 3−3161
- turnstile, radiation props. in warm plasma 3−36157

antenna components *see antenna accessories*

antenna lobe patterns *see antenna radiation patterns*

antenna patterns *see antenna radiation patterns*

antenna phased arrays

- 90°-phased crossed-dipole array in cold multicomponent magnetoplasma, v.l.f.-e.l.f. radiation characteristics 3−12842

antenna radiation patterns

- dielectric layers around 10 GHz *(German)* 3−19558
- far field, determ. by machine reconstruction of microwave hologram in aperture *(Russian)* 3−35421
- flanged parallel plate waveguide 3−674
- near-field hazard rel. to elliptical polarization 3−4055
- TE surface wave scatt. by semi-infinite grounded dielectric slab, horizontally polarised antenna 3−37932
- turnstile aerial, in warm plasma, e.m. and plasma wave field patterns 3−36157
- t.w. circular loop antenna in compressible electron plasma 3−36156

antenna theory

see also antenna radiation patterns

- aperture near-field calc., accuracy of Kirchhoff boundary values *(German)* 3−37922
- coplanar loops, h.f. e.m. coupling over inhomogeneous ground 3−32478
- dipole antennas over stratified anisotropic media, e.m. fields determ. 3−34885
- electric and mag. dipoles in dielectric sphere surrounded by sphere, ionospheric and magnetospheric appl. 3−34926
- flanged parallel plate waveguide 3−674
- h.f. coupling in computer circuits and components, applic. 3−29002
- Kirchhoff integral equation, for e.m. wave propagation 3−10429
- magnetic sensors, near-field of scattering of semi-infinite cylinders 3−22823
- metallic half-plane, diffraction fields of impulsive plane cylindrical or spherical waves 3−22830
- near-field of scattering due to semi-infinite cylinders by Wiener-Hopf techniques, applic. to sensor booms 3−22823
- radiation patterns of electric dipole and vibrator near perfectly conducting cylinder edge 3−22811
- spherical, plasma coated, effects of pseudosonic and electroacoustic waves 3−1493
- thin cylindrical, in lossy magnetoplasma, calculation of current distribution and impedance by method of moments 3−33352

antennas

see also dipole antennas; directive antennas; microwave antennas; mobile antennas; radar antennas; receiving antennas; reflector antennas; television antennas

- in cold magneto plasma, current distributions 3−7498
- cross-polarization characteristics, using microwave holography 3−22367
- cylindrical, radiating in weakly ionized plasma, radiation resistance 3−7501
- infinite tubular, in cold collisional plasma, current distribution 3−11482
- l.f. interferometer dish set up and pattern *(Japanese)* 3−16435
- linear, electromagnetic wave scattering, from perfectly conducting rotational bodies of arbitrary form. 3−19562
- magnetoplasma, input impedance 3−7497
- Radio Astronomy Explorer B Earth station antenna noise temp. prediction 3−35219
- turnstile, radiation props. in warm plasma 3−36157

antibaryons *see baryons*

antiferroelectric materials

see also antiferroelectricity; ferroelectric materials

- copper formate tetrahydrate, antiferroelectric phase, approximate struct. determ. by neutron diffraction 3−12100
- copper formate tetrahydrate, cryst. struct., neutron diffr. obs. 3−17797
- copper formate tetrahydrate, phase transition, X-ray diffr. obs. 3−15005
- copper formate tetrahydrate, proton orientation freqs. rel. to Raman and i.r. spectra 3−5199
- copper formate tetrahydrate, weak extra Bragg reflections in antiferroelec. phase 3−30769
- copper formate tetrahydrate crysts., antiferroelec. phase transition theory 3−30770
- order-disorder type, dynamics 3−30236
- pyrochlore type compounds, dielectric polarisation, relaxation character, antiferroelectric transitions 3−36836
- thiourea, elastic props. near IV-V phase transition 3−21371
- $AsO_4H_2NH_4$, proton spin-lattice relax. mechanism in paraelec. and antiferroelec. phases 3−2451
- $BaTiO_3$, polycryst. film with ferroelec. and antiferroelec. props., deposition by electrophoresis 3−39220
- $KNbO_3$-$NaNbO_3$, phenomenological theory of ferro- and antiferroelectricity 3−18421
- $ND_4D_2AsO_4$, X-irrad., e.p.r. of defect centres 3−2388

antiferroelectric materials continued
- $NH_4H_2AsO_4$, X-irrad., e.p.r. of defect centres 3–2388
- $NH_4H_2PO_4$ crystals, ultraviolet refl. and absorpt. for electronic transition studies 3–2562
- $NH_4H_2PO_4$:$^{57}Fe^{3+}$, antiferroelec. transition, Mossbauer obs. 3–15468
- $NaNO_2$, dipole-lattice relax. time near Neel temp. 3–15454
- $NaNO_2$, specific heat near paraelectric transition point 3–12103
- $NaNbO_3$, phenomenological theory of ferro- and antiferroelectricity 3–18421
- $NaNbO_3$, soft modes and superlattice struct. 3–39105
- $(Pb,La)(Zr_y,Ti_z)O_3$, PLTZ ceramics, $y=0.60$ to 1.0, $z=0.4$ to 0, antiferroelectric-ferroelectric phase boundary, temperature, d.c. field dependence 3–8525
- $PbHfO_3$, electric quadrupole interaction from $\gamma-\gamma$ ang. correl. and Mossbauer spectroscopy 3–21353
- $PbTiO_3$, polycryst. film with ferroelec. and antiferroelec. props., deposition by electrophoresis 3–39220
- $PbZrO_3$, polycryst. film with ferroelec. and antiferroelec. props., deposition by electrophoresis 3–39220

antiferroelectricity
- *see also antiferroelectric materials; ferroelectricity*
- cubic spinel compounds, possible antiferroelec. behaviour, rel. to cryst. struct. 3–30773
- F model, spontaneous staggered polarisation 3–30775
- phenomenological theory, appl. to $NaNbO_3$ and $KNbO_3$-$NaNbO_3$ 3–18421
- pyrochlore type compounds, dielectric polarisation, relaxation character, antiferroelectric transitions 3–36836
- $NH_4H_2PO_4$:$^{57}Fe^{3+}$, antiferroelec. transition, Mossbauer obs. 3–15468

antiferromagnetic properties of substances
- *see also antiferromagnetism*
- alkali metal iron fluoride, M_xFeF_3, $(M=K, Rb, Cs)$, Mossbauer effect study *(French)* 3–8488
- amorphous magnet, constant coupling approx. for Ising and Heisenberg models 3–11998
- Er_2O_2S:Er^{3+}, mag. suscept., rel. to crystal field effects in electronic ion structure *(French)* 3–30411
- haematite-ilmentite solid solution series, Mossbauer spectra 3–34819
- Heisenberg antiferromagnet, dynamical props., comparison of equation of motion and diagrammatic techniques 3–21198
- Heisenberg antiferromagnet, rutile structure CoF_2, two-magnon neutron scattering 3–21197
- Heisenberg antiferromagnet, rutile structure MF_2, $(M=Ni, Fe, Co)$, two-magnon light scattering 3–21196
- Heisenberg antiferromagnet, two-magnon correlations, equation of motion study 3–21195
- Heisenberg antiferromagnets with arbitrary interaction range, zero-point effects 3–15326
- Hubbard's simple decoupling scheme, absence of antiferromag. ordering 3–15342
- Hubbard model, tenfold d-electron degenerate, antiferromag. to paramag. (ferromag.) transitions 3–21207
- Kondo temp. for ferromag. and antiferromag. impurity pairs 3–21217
- magnon density of states calc. for canted antiferromagnet with substitutional impurities 3–8331
- metal, magnetoresist. due to electron-spin-scattering by s-d interaction 3–11886
- metal, magnon thermal cond. depend. on temp. and mag. field 3–36727
- Mossbauer diffraction by antiferromagnet, kinematical theory 3–24632
- oxides, M_xO-$M'O$, $(M=Co, Ni, Fe, Mn; M'=Mg, Ca, Sr, Zn, Al)$, Neel temp. comp. depend., bonding *(French)* 3–8363
- rare earth alloys, heavy, effect of hydrostatic pressure 3–36708
- rare earth intermetallics, $LnIn_3$ and $LnSn_3$, metamagnetism, spin-flopping and ordered struct. *(French)* 3–24563
- rare earth orthoferrites, Heisenberg superexchange and Dzyaloshinskii-Moriya interactions 3–34107
- semiconductor organic molecular crysts., mag. excitations 3–2230
- sound velocity mag. field depend. 3–21290
- spin wave reson. surface modes of antiferromag.-ferromag. surface coupled film 3–39033
- tetramethyl-2,2,6,6,piperidinol-4, oxyl-1 free radical, low temp. sp.ht. study 3–18314
- tetramethylammonium manganese chloride, tri-dimensional long range ordered state at low temp. 3–27432
- transfer of magnetic excitons between antiparallel spin sites, model 3–11868
- transition metals, 3d, relative stability of ferro- and antiferromagnetic state, models 3–36701
- 3d transition metals, impurity suppression of Neel temp. by paramag. impurities 3–8352
- $\{Cr_3O(CH_3COO)_6(H_2O)_3\}Cl.6H_2O$ Mossbauer study on the magnetism 3–2262
- $\{Fe_3O(CH_3COO)_6(H_2O)_3\}Cl.6H_2O$ Mossbauer study on the magnetism 3–2262
- Au-Cr, elec. resist. min. at low temp. rel. to antiferromag. long range order 3–30449
- Au-Fe alloys, mag. ordering rel. to Fe conc. (1-22 at.%) 3–2287
- Au_2Mn:^{119}Sn, mag. hyperfine interaction, Mossbauer study *(Russian)* 3–12088
- $Ba_3Fe_2TeO_9$, struct. and antiferromagnetism at low temps. *(French)* 3–7690
- $BaMnF_4$, two-dimensional mag. ordering in isotropic Heisenberg antiferromagnet 3–36725
- Ba_2NiF_6 susceptibility, single crystals, low temp. measurements 3–36714
- $BaTbO_3$, G-type collinear, neutron diffraction examination 3–7677
- $BiFeO_3$, internal mag. field obs. by Mossbauer effect 3–27447
- $BiFeO_3$ magnetic and structural props. 3–39064
- $Bi_2Fe_4O_9$, spin orientation, Mossbauer obs. 3–36724
- C film, amorphous, antiferromag. transition, e.s.r. obs. 3–18317
- $(CH_3NH_3)_2MnCl_4$, magnetic susceptibility meas., a quasi two-dimensional Heisenberg antiferromagnet 3–5098
- $Ca_2Fe_{2-x}Al_xO_5$, magnetic structures 3–12023
- $CdIn_{2(1-x)}Cr_{2x}S_4$, mag. susceptibility meas. 3–2263

antiferromagnetic properties of substances continued
- $CeMg(NO_3)_5$, search for ground state by extented Luttinger-Tisza method 3–34056
- $CoBr_2.6H_2O$, antiferromagnetic, spin-flop and paramagnetic phases, mag. susceptibility meas. 3–38977
- $CoCO_3$, magnetisation density and magnetic structure at 4.2 K 3–38984
- $CoCl_2.2H_2O$, AC susceptibility meas., mag. phase diagram and relax. times at antiferromag.-ferrimag. transition 3–30626
- $CoCl_2.2H_2O$, proton spin lattice relax. by Ising spin excitation 3–21337
- $CoCl_2.6H_2O$, magnetic susceptibility and antiferromagnetic, spin flop and paramagnetic transitions 3–18313
- $CoCl_2.6H_2O$, magnetic transition rounding and Pippard's relations 3–30619
- $CoNb_2O_6$, mag. struct., neutron diffr. obs. *(German)* 3–21249
- Cr, incommensurate antiferromag., hyperfine field meas. using time differential perturbed angular correlation 3–11993
- Cr, influence of mag. field on thermal hysteresis of mag. struct. *(Russian)* 3–8371
- Cr, mag. hysteresis, fields to 20 kOe, 77-450K 3–2310
- Cr, mathematical theory 3–18276
- Cr, obs. of antiferromagnetic domains by X-ray and neutron topography 3–30647
- Cr, pressure depend. of Neel temp., band calc. 3–18293
- Cr u.s. attenuation due to polarisation domain relaxation processes in transverse spin density wave phase 3–30675
- Cr-Pd dil. alloys, susceptibility, Neel temp., solute effects 3–34111
- Cr-Re alloys, coexist. of antiferro. and superconduct. *(Russian)* 3–8358
- $CrAs_{0.5}Sb_{0.5}$ crystal distortion at Neel temp., antiferromag. NiAs to helimag. MnP type structure 3–33671
- $CrCl_3$, anhydrous, layered antiferromagnet, specific heat between 4.5 and 20 K in mag. field 3–38974
- Cr_2O_3, u.s. attenuation freq. depend. in Neel pt. region *(French)* 3–5106
- Cr_2O_3-Fe_2O_3, Mossbauer obs. of mag. structure 3–8490
- $CrPt_3$, paramag. type behaviour as kind of antiferromag. on transition from ferrimag. phase 3–21237
- Cr_2S_3, rhombohedral single crystal 3–12021
- $CsCoCl_3.2H_2O$, mag. struct., magnetization, and short-range spin correl., neutron diffr. obs. 3–24568
- $CsFeCl_3$, susceptibility, 2-250K 3–21220
- Cs_xFeF_3, $0<x<1$, low temp. antiferromagnetic temp., evolution of Neel temp. *(French)* 3–12017
- $CsMnCl_3.2D_2O$ magnetic phase diagram, 2-20K, zero-field Neel temp. 3–5100
- $CsMnF_3$, magnetoelastic coupling and sound velocity 3–15400
- $Cs_{0.4}Mn_{0.4}Fe_{1.6}F_6$, magnetic struct. 3–5108
- $CsNiCl_3$, antiferromagnetic-paramagnetic transitions 3–34115
- $CsNiCl_3$, specific heat meas. from 1.5 to 10 K rel. to mag. transitions 3–30617
- $Cs_{0.4}Ni_{0.4}Fe_{1.5}F_6$, magnetic struct. 3–5108
- $Cu(C_6H_5COO)_23H_2O$, temp. and ang. depend. of e.s.r. line in linear chain antiferromag. 3–8426
- $Cu_3(CO_3)(OH)_2$, magnetic transition rounding and Pippard's relations 3–30619
- $CuCl_2.2H_2O$, spin spin relax. time meas. near Neel temp. 3–12054
- $Cu(NO_3)_2.2\frac{1}{2}H_2O$, specific heat and n.m.r. at the high-field phase transition 3–27370
- $Cu_2P_2O_7$, ^{31}P n.m.r. obs. 3–21322
- $Cu_2P_2O_7$, mag. struct. using neutron diffr. method 3–18322
- $CuWO_4$, mag. susceptibility and e.p.r. spectrum, 4.2-300 K, short-range order effects 3–34104
- $Cu_{12-x}Zn_xSb_4S_{12.7}$, synthetic tetrahedrite, antiferromag. ordering due to Cu atoms below 130K 3–27444
- Dy, hysteresis of ferromag.-antiferromag. transform., elec. resist. and thermal expansion obs. *(Russian)* 3–15363
- Dy helical phase, spin wave energy 3–5110
- $DyVO_4$, rel. to relax. of Mossbauer spectra, temp. depend. 3–36825
- $DyVO_4$, thermal conductivity at low temps. 3–1847
- Er, antiferromag. sinusoidal, magnetostrictive variation of lattice parameter *(French)* 3–27388
- Er, mag. struct., neutron diffr. obs. 3–24576
- $ErZn_{12}$, spin disorder resist., crit. effects and derivations from Matthiessen's rule 3–30450
- EuTe, ordering rel. to photoluminescence props. *(German)* 3–18495
- EuTe thin films, spin polarized photoelectrons *(German)* 3–18531
- $Eu_xYb_{1-x}Sn_3$, Mossbauer effect and magnetisation meas. *(German)* 3–24594
- Fe-Rh (52 at.%) alloy, antiferromag.-ferromag. transition, optical behaviour *(Russian)* 3–18439
- Fe-Rh alloy, Fe-Rh-Ir alloy, electron sp. ht. obs. 3–34128
- FeAs, obs. of helimagnetic structure below Neel temp. 77K 3–15370
- $FeBr_2$, $FeCl_2$, susceptibility, uniaxial tension at 4.2°K, metamagnetic properties *(French)* 3–27390
- $FeBr_2$, metamag. transition, magnetiz. variation with temp., press. and mag. field *(French)* 3–30615
- $FeBr_2$, metamagnetic phase transition *(French)* 3–27368
- $FeCO_3$, exciton-magnon transitions, effect of strong mag. field on intensity *(Russian)* 3–8558
- $FeCO_3$, siderite, rel. to Raman scatt., 4.2-300K, freqs. up to 2000 cm^{-1} 3–34366
- $FeCl_2$, antiferromagnetic resonance, high-pressure effects 3–18374
- $FeCl_2$, thermal conductivity 3–20843
- $FeCr_2S_4$, low temp. transition, Mossbauer obs. 3–5151
- FeF_2, calc. of pressure and temp. depend. of hyperfine mag. field 3–34059
- FeF_2, magnetoelastic waves and selection rules for magnon-phonon interaction 3–34131
- β-$FeF_3.3H_2O$, Mossbauer obs. of antiferromag. ordering below 14.7 K *(French)* 3–27449
- FeGe, susceptibility meas. and magnetic ordering 3–18326
- FeGe Fermi surface electrical resistivity and magnetic ordering 3–18327
- FeGe hexagonal single crystals, magnetoresistance between 4.2 K and 30 K 3–18328

antiferromagnetic properties of substances continued

- FeGe hexagonal single crystal, electrical resistivity meas., around Neel temperature 3-21239
- $FeGe_2$, elastic consts. temp. depend. rel. to antiferromag. transition 3-5105
- Fe_2GeS_4, cryst. and mag. structs. at 85 K and 4.2 K, mag. transitions *(French)* 3-27373
- FeMnP, mag. struct., neutron diffr. obs. 3-30629
- $Fe_xMn_{2-x}P$, mag. props. of different phases, Neel and Curie temps. 3-30608
- FeO, wustite, formed below 570°C, Mossbauer spectra 3-24638
- Fe_2O_3, angular depend. of field-induced antiferromag. to weak ferromag. transition 3-21228
- ϵ-Fe_2O_3, fine particle behaviour 3-27361
- α-Fe_2O_3, hematite, nonlinear susceptibility and anisotropy to Morin temp. 3-2261
- Fe_2O_3, magnetic hyperfine field at ^{57}Fe *(Korean)* 3-27452
- FeOCl, mag. susceptibility, 300-4.2 K, antiferromag. order *(French)* 3-30604
- $Fe_2(OH)_3$ amorphous, gel, characterisation and phase transformations 3-5383
- $Fe(Pt_cPd_{1-c})_3$ Neel temp. calc. for antiferromag. subsystem 3-12018
- FeRh alloys, positron annihilation study of electron structure of ferromagnetic and antiferromagnetic phases 3-7754
- $Fe_{1+\delta}Sb$, obs. of mag. superstructure lines below and above Neel point 3-12022
- FeSn, electrical resistivity 4.2-420 K 3-21240
- β-Ga_2O_3-Fe_2O_3 solid solution, mag. interactions, e.p.r. obs. 3-27406
- Gd-Y alloys, hydrostatic pressure effect on transition temp. at ferromag. to antiferromag. transition 3-2273
- $GdAlO_3$, spin dynamics near spin flops transition, antiferromag. reson. obs. 3-2401
- $Gd_3Fe(Co)(Ni)$, Neel metamagnetism theory and exchange interactions 3-21232
- $Gd(OH)_3$, cooperative transitions rel. to mag. specific heat 3-34117
- Ho, susceptibility, temp. depend. near Neel point *(Russian)* 3-12012
- $HoCo_2$, hyperfine specific heat meas., mag. moment determ. 3-34123
- $HoFeO_3$, magnetiz., anisotropy, spin reorientation, 50-120 K *(French)* 3-27380
- $HoMnO_3$, paramag Curie temp., mag. susceptibility, 4.2-400 K 3-34103
- $KCoF_3$ antiferromagnetic crystals, vibrational spectrum and dispersion of optical constants 3-18450
- $KCo_xMn_{1-x}F_3$, disordered, spin wave dispersion relns. 3-18332
- $KCrS_2$, mag. structure, ferromag. sheets with antiferromag. coupling 3-34132
- $KCuF_3$, anisotropic exchange interactions between pairs of Cu^{2+} ions 3-2264
- $KFeF_3$ Mossbauer spectroscopy, stressed single crystal 3-27454
- K_xFeF_3, $0<x<1$, low temp. antiferromagnetic temp., evolution of Neel temp. *(French)* 3-12017
- $KMgF_3$:Mn and $KZnF_3$:Mn, bilinear and biquadratic exchange interactions, effect on mag. susceptibility 3-27363
- $KMnF_3$, excited-state exchange interaction, molecular orbital theory 3-36718
- $KMnF_3$ antiferromagnetic crystals, vibrational spectrum and dispersion of optical constants 3-18450
- K_2MnF_4, neutron diffr. obs. of two-dimens. mag. behaviour 3-15371
- K_2MnF_4, two-dimens. antiferromagnet, e.p.r. linewidth, crit. point anomaly 3-30691
- K_2MnF_4 and K_2NiF_4, specific heat of two-dimensional Heisenberg antiferromagnets 3-34114
- $KNiF_3$, excited-state exchange interaction, molecular orbital theory 3-36718
- $KNiPO_4$, susceptibility and effective mag. moment *(Russian)* 3-11603
- $LaFe_{1-x}Cr_xO_3$, antiferromagnetic perovskite, obs. of ferromagnetic interaction by Mossbauer effect 3-39065
- $LiCuCl_3.2H_2O$, magnetic transition rounding and Pippard's relations 3-30619
- Mg_6MnO_8, paramag. structure with weak antiferromag. interaction, susceptibility and optical reflectance meas. 3-34091
- Mn-V(Cr)(Fe)(Ru), anomalies in elec. resist. meas. rel. to Neel temp. determ. 3-34119
- $Mn_3Al_2Ge_3O_{12}$ garnet, mag. struct., neutron diffr. obs. *(French)* 3-21248
- Mn_2As-Mn_2Sb system neutronographic investigation of magnetic transformations *(Russian)* 3-2291
- $MnBr_2.4H_2O$, heat capacity meas. near Neel temp., effect of chem. impurities 3-15367
- $MnCO_3$, interaction of hypersonic waves and spin waves in antiferromagnet 3-39008
- $MnCO_3:Fe^{2+}$, spin system and moment exam., reln. to concentration 3-2289
- $MnCl_2.4H_2O$, antiferromagnetic, temp. dependence of proton spin-lattice relaxation time 3-39054
- MnF_2, excited-state exchange interaction, molecular orbital theory 3-36718
- MnF_2, mag. susceptibility near T_n and Fisher's relation 3-38967
- MnF_2, magnetic transition rounding and Fippard's relations 3-30619
- MnF_2, spin flop domains, n.m.r., Faraday rotation, photographs and optical-absorption spectroscopy investigation 3-34113
- MnF_2 high frequency acoustic waves attenuation on low-temp. side of Neel point 3-34112
- Mn_3Ge_2, pulsed mag. field effects *(Russian)* 3-12015
- $MnGeN_2$, mag. struct., moments orientation *(French)* 3-8370
- Mn_2Hg_5 neutron diffraction obs. of antiferromag. coupling 3-18329
- $Mn_{3-x}Ni_xB_4$, spontaneous and saturation magnetization, and transitions *(Russian)* 3-8396
- MnO, inelastic neutron scattering obs. of antiferromag. spin waves 3-24580
- MnO, optical absorpt. spectrum, role of magnons and phonons *(Russian)* 3-15522
- MnO-MgO solid solns., susceptibility, exchange phenomena between Mn^{2+} ions *(French)* 3-38964
- $Mn_2P_2O_7$, mag. struct. using neutron diffr. method 3-18322

antiferromagnetic properties of substances continued

- $MnSn_2$, effective mag. fields at diamag. Sn atoms 3-5153
- $MnTa_2O_6$, mag. struct., neutron diffr. obs. *(German)* 3-21249
- MnTe, antiferromag. semicond., optical phonon spectrum obs. over Neel temp. 3-5104
- MnTe, transition from paramagnetism, susceptibility obs. 3-15365
- $MnWO_4$-$FeWO_4$, mixed crystal, coexistence of two antiferromag. phases 3-34124
- $MnWO_4$-$FeWO_4$, spontaneous magnetisation irregularities, modified effective field model 3-34060
- $MnWO_4$-$FeWO_4$, wolframite, mag. phase diagram, molecular field approx. 3-34125
- $Mn(pyrazole)_2Cl_2$, antiferromag. interaction determ. 3-30612
- N-methyl phenazinium tetracyanoquinodimethan, nuclear relax. study of spin fluctuations 3-15432
- NH_4FeCl_3, susceptibility, 2-250K 3-21220
- $(NH_4)_xFeF_3(M=K, Rb, Cs, NH_4)$, Mossbauer effect study *(French)* 3-8488
- $(NH_4)_2MnF_5$, linear chain antiferromagnet, weak ferromagnetism and anisotropy 3-30643
- Nd, thermal cond. below Neel pt. 3-2044
- $NdFe_2Si_2$, antiferromag. structure of Nd(2a) sublattice, ferromag. sheets, neutron diffraction obs. 3-34135
- $NdFe_2Si_2$, mag. struct., neutron diffr. obs. 3-24570
- NdP(As)(Sb), mag. ordering, neutron diffr. obs. 3-30630
- NdS ordering, spin configurations, neutron diffraction study 3-27374
- $NdZn_2$, ordering and struct., neutron diffr. obs. 3-27372
- $NiBr_2.2H_2O$, sp. ht., 1.2-23 K, anomalous behaviour 3-36722
- $NiCl_2$, spin arrangement rel. to temp. depend. of antiferromag. reson. 3-21316
- $NiCl_2.4H_2O$, antiferromag.-paramag. transition, molecular field model 3-34120
- $NiCl_2.6H_2O$, magnetic transition rounding and Pippard's relations 3-30619
- NiF_2, excited-state exchange interaction, molecular orbital theory 3-36718
- $Ni(IO_3)_2.2H_2O$, heat capacity maxima, exchange parameter, 1-30 K 3-8360
- NiO, crystal structure determined by X-ray topography 3-30646
- NiO, LEED, depend. of exchange refl. on diffr. conditions 3-23995
- NiO, low energy electron exchange diffraction by 3d electrons in crystal 3-30156
- NiO, obs. of domain walls using X-ray transmission topography 3-30645
- NiS, antiferromag. semimetal to paramag. metal transition 3-36540
- $Pb(Fe_{2/3}U_{1/3})O_3$, Neel temp. and saturation mag. moment 3-21231
- $Pb(Fe_{2/3}W_{1/3})O_3$, Neel temp. and saturation mag. moment 3-21231
- PdMn, dilute, ferromag., antiferromag. coupling with interimpurity Mn-Mn interaction 3-15184
- $(Pr, Nd, Sm, Tb, Dy, Ho)Pb_3$, low-field susceptibility, magnetisation, 3-300K *(French)* 3-18302
- PuX_3, X=Rh, Pd, Pt, cubic , mag. susceptibility obs. 3-38966
- $RbFeCl_3$, ferromagnetic chain existence, EFG temp. depend. obs. 3-18282
- $RbFeCl_3$, susceptibility, 2-250K 3-21220
- Rb_xFeF_3, $0<x<1$, low temp. antiferromagnetic temp., evolution of Neel temp. *(French)* 3-12017
- α-$RbMnCl_3.2H_2O$, anisotropy fields, antiferromag. reson. study 3-36796
- $RbMnF_3$, Jahn-Teller and exciton-exciton interaction energies 3-11867
- $RbMnF_3$, neutron scatt. function, spin correlations, at 1.17 T_n, expt. and simulation 3-24578
- $RbMnF_3$, reorientation of sublattice moments, effects on exciton absorpt. spectrum 3-30817
- $RbMnF_3$ with K^+, Co^{++}, Ni^{++}, Fe^{++} and Mg^{++} impurities, ^{19}F nuclear acoustic resonance 3-34225
- Rb_2MnF_4, two-dimens. antiferromagnet, e.p.r. linewidth, crit. point anomaly 3-30691
- Ru alloy, Pauli susceptibility with localised moments contrib., weak antiferromag. coupling 3-34097
- Sm, mag. struct., neutron diffr. obs. 3-5107
- Sm, neutron diffr. study 3-24577
- $SmFe_{0.67}Ge_{1.33}:Sm^{3+}$ antiferromagnetic ordering of Sm^{3+} 3-2290
- $SmSn_3$, crystal field effect on susceptibility and Knight shift 3-15322
- spin wave theories in the linear approximation 3-21251
- $SrFe_xMo_{1-x}O_{3-y}$, Neel temp., heat treatment effects 3-21345
- $Sr_3Fe_2TeO_9$, struct. and antiferromagnetism at low temps. *(French)* 3-7690
- $Sr(Fe_{2/3}U_{1/3})O_3$, Neel temp. and saturation mag. moment 3-21231
- Tb_8-$La(Pr)_2$, ordering in antiferromag. layer structure at 124K for Tb_8-La_2 and 131K for Tb_8-Pr_2 3-18321
- TbAl antiferromag. garnet, molecular field approx. of two-singlet model for metamag. transition 3-27341
- $TbAsO_4$, paramag.-antiferromag. transition, optical absorpt. study 3-2560
- $TbAsO_4$, paramag.-antiferromag. transition, sp. ht. study 3-18316
- $TbPO_4$ ordering of mag. moments 3-12019
- $TlCoF_3$, mag. struct., sp. ht. anomaly *(French)* 3-38983
- $TlFeCl_3$, susceptibility, 2-250K 3-21220
- Tm, antiferromag. sinusoidal, magnetostrictive variation of lattice parameter *(French)* 3-27388
- UAs_2, spin disorder resist., temp. depend. 3-2106
- $UAs_{0.75}Se_{0.25}$, metamagnetic transition 3-38975
- $UAs_{1-x}Se_x$, ferromag. and antiferromag. props. with different x comps. in field up to 80 kOe 3-21227
- USb_2, spin disorder resist., temp. depend. 3-2106
- V_2O_3, pure and doped, metal-insulator transitions 3-33820
- $V_{1-x}W_xO_2$, susceptibility, 80-400K, rel. to semicond.-metal transition 3-18205
- $YCrO_3$:Fe, impurity-host Fe^{3+}-O-Cr^{3+} antiferromag. superexchange, ^{57}Fe hyperfine field meas. 3-30611
- $YFe_xCr_{1-x}O_3$, obs. from 78 K to Neel temp., exchange interaction for Fe^{3+} and Cr^{3+} ions 3-5103
- $YMnO_3$, paramag. Curie temp., mag. susceptibility, 4.2-400 K 3-34103

antiferromagnetic properties of substances continued
$YbMnO_3$, paramag. Curie temp., mag. susceptibility, 4.2-400 K 3−34103

antiferromagnetic resonance
spin wave-dislocation scatt. effects in easy axis type antiferromagnets 3−2405
Suhl inverse stability processes by optical pumping 3−24616
$BaMnF_4$, 4.2K 3−34219
EuTe, reson. field angular depend., 9.2-33.99 GHz 3−30699
$FeCl_2$, high-pressure effects, phase change 3−18374
α-Fe_2O_3, high field, theory and expt. comparison 3−27420
$GdAlO_3$, spin dynamics near spin flop transition 3−2401
$KMnF_3$, resonance frequencies and sublattice magnetiz. for antisymmetric exchange interaction 3−8351
MnF_2, temp. dependence of linewidth 3−18373
$Mn_2P_2O_7$ single crysts., 1.2 to 14K 3−8447
$NiCl_2$, spectra spitting, 27-43 GHz *(Russian)* 3−15424
$NiCl_2$, temp. depend., rel. to spin arrangement 3−21316
α-$RbMnCl_3.2H_2O$, below 4.56K 3−36796

antiferromagnetism
see also antiferromagnetic properties of substances; exchange interactions (electron); metamagnetism
anisotropic antiferromagnet, Green's function theory 3−30584
anisotropy constants, low temp. 3−38988
chain, uniform, instability, Heisenberg, interaction in Hartree Fock approx. 3−38943
critical isotropic antiferromag., linewidth scaling function 3−21253
crystal with ferromag.-antiferromag. transition, magnetoacoustic waves 3−21289
cubic antiferromagnetic insulator, lifting of degeneracy of $^4E_{1g}$ level of Mn^{2+} *(Russian)* 3−11994
disordered system, spin wave dispersion relns. 3−18332
exactly soluble model for two coinciding lattices with interaction, dynamical rotational symmetry 3−15314
exciton-magnon transitions, effect of strong mag. field on intensity *(Russian)* 3−8558
Heisenberg alternating linear antiferromagnet, exciton interactions rel. to susceptibility 3−34075
Heisenberg ferromagnet, exchange interaction of surface spins causing surface antiferromagnetism 3−38951
Heisenberg linear chain (nearly one-dimens.) system, interchain coupling effects on e.p.r. 3−18354
Heisenberg model, two-dimensional 3 × 3 square lattice, antiferromag. coupling 3−38944
Heisenberg one-dimensional antiferromagnet, determ. of spin-wave spectrum when long-range order is absent 3−27348
Heisenberg susceptibilities, calcs. using lattice Green's function 3−22752
Hubbard model, non-existence of selfconsistent solns. 3−5093
Hubbard model, paramag. spin susceptibility, antiferromag. ordering 3−21209
Husimi-Temperley model, distrib. of zeros of partition function above and below critical temp. 3−5084
Husimi-Temperley model, distrib. of zeros of partition function 3−24548
hypersound, parametric excitation by large amplitude homogeneous oscills. 3−34176
Ising antiferromagnet, b.c.c., near critical field, phase transitions, Monte Carlo study 3−5089
Ising lattice with superexchange, phase transitions 3−24555
Ising model, three-dimensional, exact solution for finite continuous spins and non-zero external field 3−30588
Ising solvable decorated model combined with superexchange antiferromag. model 3−34073
Ising spin system, equilib. state uniqueness in phase transition region 3−21194
itinerant, above Neel temp., paramagnetic susceptibility and u.s. attenuation 3−12001
itinerant, thermodynamic props. near Neel temp. 3−5101
itinerant antiferromagnets in mag. fields, theory 3−12002
magnetism, introduction to the theory, monograph 3−2224
metal, reson. between spin and MHD waves 3−34145
model for an antiferromagnet 3−18289
molecular field approx. for phase diagram and metamag. transition in antiferromag. two-singlet system 3−27340
neutron critical scattering, cross section calc. for antiferromagnet 3−34136
noncollinear magnetic sublattice structure, spin-wave energy and mean value of Hamiltonian 3−2227
one-dimensional spin systems with two sublattices, phase transforms., mag. field effects *(Russian)* 3−21188
perturbation expansion of ground state, computer generation and calc. of higher-order diagrams 3−21199
polarons, small, role in metal-insulator transition, antiferromagnetic exchange interactions 3−30420
random-walk method application to theory of magnetism 3−18288
semiconductor, elec. resist., sample boundary and domain wall effects 3−34170
semiconductor, inhomogeneous ferro-antiferromag. state 3−21223
semiconductor, reson. between spin and MHD waves 3−34145
solvable model for two-dimensional antiferromagnet combining Fisher and Syozi-Miyazima models 3−18275
spin ordering, rel. between thermoelectric power and thermal cond. 3−34129
spin wave spectrum, localized, of antiferromagnet with two different impurities 3−30639
Cr_2O_3, magnon energies temp. depend., Bloch and Nagai methods calcs. 3−12028
O_2 solid, antiferromag. and light absorpt. due to mol. interaction 3−24549

antihyperons *see hyperons*

antimony
diffusion, in Ge, diffused layer production 3−24810
diffusion in liq. Cd *(Russian)* 3−1811
diffusion in Ni-Sb system, rate of reaction, high press. eff. *(Russian)* 3−7962
diffusion in SiO_2, summary of data 3−21546
Fermi surface, de Haas-van Alphen effect study 3−36527
film, elec. resist. rel. to thickness 3−18233

antimony continued
films, i.r. dispersion properties *(Russian)* 3−15500
Hall coefficient and electrical resistivity, low temp. depend. 3−36625
$L_{\gamma 4}$ X-ray emission bands in InSb, GaSb and AlSb *(German)* 3−15569
magnetoconductivity tensor coefficients, temp. depend., 4.2-30K 3−15183
specific heat anomaly and disorder *(German)* 3−24276
in CrV steel, grain boundary segregation and free energy of Sn and Sb *(Czech)* 3−31027
steel austenitizing treatment effect on temper embrittlement, search for Sb segregation at grain boundaries 3−34544
thermomagnetic phenomena in phonon drag region 3−33932
in Ag and Cu, alpha solid solns., thermodynamic activities determ. procedure *(German)* 3−21794
Ag:^{124}Sb, grain boundary electromigration of ^{124}Sb *(French)* 3−8806
CaO:Bi, Sb, Te phosphors, photoluminescence, radical-recombination luminescence of the O atoms *(Russian)* 3−30876
GE:Sb, high frequency monochromatic phonon spectroscopy 3−1765
Ge:Mn; Sb, recomb. wave current instability rel. to mag. field *(Russian)* 3−8180
Ge:Sb, Cu, kinetics for Cu precipitation, interaction with Sb 3−14979
Ge:Sb, direct absorp. edge, exciton plasma resonance obs. *(Russian)* 3−5211
Ge:Sb, dislocation mobility study, depend. on temp. and loading *(Russian)* 3−24120
Ge:Sb, luminesc. spectra due to electron-hole radiative recomb., virtual bound state, 2K 3−8632
Ge:Sb, reson. scatt. of phonons by bound donor electrons 3−30223
n-Ge:Sb far i.r. cyclotron reson. 3−15127
Sb/Cs photocathode photoemission in u.v., multielectron nature 3−18529
Sb + Se, enthalpy of mixing in liquid state 3−14976
Sb(II), atomic spectra from Hartree-Fock calcs., need of LS-depend. parameters 3−7035
Si:Sb, impurity photocond. oscills., 4.2-10K *(Russian)* 3−2134
SnO_2:Sb, film, Sb doping during vapour growth, effect on elec. props. 3−15627
SnO_2:Sb film, r.f. sputtered, transparency and elec. cond. 3−12200

antimony alloys
see also antimony compounds
Bi-Sb, alloying effect on twinning rate of Bi *(Russian)* 3−31057
Bi-Sb, cryst. growth from melt 3−12272
Bi-Sb, film, deposition by steady state evaporation 3−24787
Bi-Sb, narrow band gap semiconductors, zero bandgap transition 3−38800
Bi-Sb, quantum oscillations of thermoelectric power 3−8206
Bi-Sb, single crystal, dislocation study using etch pit technique 3−17836
Bi-Sb supercond. amorphous films, fluctuations near transition temp. of heat capacities 3−2200
Bi-Sb:Te,Se, calc. of thermoelec. figure of merit in mag. field 3−15176
Bi-Sb(12 at.%) powder compacts, transport and thermoelec. props., 300-77 K 3−36593
Bi-Sb(30%), with and without Te,Sn impurities electrical transport props., 8-300 K *(German)* 3−11916
Bi_xSb_{1-x} film, quantum size effects, elastoresistance, thermoelectric power and conductivity obs. 3−4997
Cd-Sb system, crystallisation conditions influence on props. *(Russian)* 3−8769
Cs_3Sb, valence band density of states determ. from photoemission and electron scatt. 3−24773
Cu-Sb-Sn, liq., Sn solvent activity equations, by stirred H-cell e.m.f. meas. 3−31269
β-Cu_3Sb, electrotransport obs. and mechanism *(German)* 3−24298
Fe-Sb polyphase pulverulent, sintering *(French)* 3−21715
Ge-Si-Sb phase diagram study *(French)* 3−17959
In-Sb, liquid, nuclear spin-lattice relaxation meas. for ^{115}In and ^{121}Sb 3−5145
Mn_2As-Mn_2Sb system, neutronographic investigation of magnetic transformations *(Russian)* 3−2291
$MnBi_{0.9}Sb_{0.1}$, mag. struct., neutron diffr. obs. 3−24573
MnSb, and related compounds, electronic struct., zero-field n.m.r. obs. 3−27440
MnSb, distrib. of unpaired electrons, neutron diffr. obs. 3−24574
Nd-Sb, anal. of phase diagram and alloy props. *(Russian)* 3−12338
Nd-Sb system alloys, physical props. and correlation with the phase diagram *(Russian)* 3−11882
$Ni_{1-x}Cu_xMnSb$, ferromag., anomalous line shift in n.m.r. 3−30704
Pb-2% Sb, spheres, plastic flow during hot-pressing 3−39381
Sb-Bi, transverse striations on top free surface, triangular features on cleavage plane 3−11786
Sb-Cu liq., struct. from combined neutron and X-ray diffr. 3−14676
Sb-In, liq., self-diffusion coeffs., conc. depend. *(French)* 3−30275
Sb-In, liq., self-diffusion coeffs., temp. depend. at equiatomic comp., ionic salt concept *(French)* 3−30276
Sb-Se composition region Sb to Sb_2Se_3, new melting diagram determ. by differential thermal analysis *(Russian)* 3−11723
Sb-Sn, Fermi surface, de Haas-van Alphen effect study 3−36527
Sb-Sn, Sb-Pb-Sn, columnar crystals, dendrite spacing *(Japanese)* 3−8792
Sb-Sn-As-Pb alloys, grain growth and microstructure 3−8785
Zn_3Sb_2, phase comp. and decomposition reactions *(Russian)* 3−15671

antimony compounds
see also antimony alloys
SbSI, near phase transition, effect of light on parameters 3−27479
$3As_2Se_3$-$2Sb_2Se_3$, amorphous film, recombination and trapping processes, photoconductivity obs., 278-308K 3−21094
Bi_2Te_3-Sb_2S_3, liquid, specific resist. and thermal e.m.f. meas., phase diagram study *(Russian)* 3−15192
Cr steel, retained austenite detection using vapour phase Sb_2S_3 deposited interference layers 3−8810
In-Ga-Sb system, liquidus and solidus data at 500C 3−1775

- **antimony compounds** continued
  - In_2Se_3-Sb_2Te_3, X-ray obs. of phase diagram, elec. props. depend. on comp. *(Russian)* 3–14964
  - Sb^{3+} oxides, fluorides and oxide fluorides, calcs. of bond lengths and angles 3–33073
  - $SbBr_3$, intramol. parameters sensitivity to intermol. interaction *(Russian)* 3–7202
  - $SbCl_3$, intramol. parameters sensitivity to intermol. interaction *(Russian)* 3–7202
  - $SbCl_5$ quick-frozen non-aqueous solutions, solvent effects on Mossbauer parameters, isomer-shift values 3–12082
  - $SbCl_5$-ClCN addition complex, nuclear quadrupole resonance spectrum *(French)* 3–7228
  - SbF, emission spectrum, new band system 3–33111
  - SbF, rot. analysis of 2550-2750 Å band system 3–7178
  - SbF, rotational structure of C_3 system 3–20132
  - SbF_5, association in vapour phase, molecular beam mass spectra 3–25924
  - $SbF_3(Cl_3)(Br_3)(I_3)$, centrifugal extension consts., calc. *(Russian)* 3–20104
  - SbI_3, absorpt., magnetooscillatory effect *(Russian)* 3–34329
  - Sb_2O, crystalline and amorphous, photoconductivity measurements 3–38870
  - Sb_2O_3, amorphous and crystalline, optical props. rel. to band structure 3–8602
  - Sb_2O_3-SbI_3 compounds, synthesis and vapour transport growth 3–30938
  - Sb_2S_3, photosemicond., crystallisation under hydrothermal conditions *(Russian)* 3–15633
  - Sb_2S_3 colloid, ^{99m}Tc-labelled, for linear scintigraphy 3–35286
  - Sb_2S_5 thin films, optical props. meas. 3–21501
  - SbSI, absorpt. edge shift rel. to elec. polarization 3–15507
  - SbSI, Barkhausen effect, rel. to state of defects 3–39114
  - SbSI, deep centres and photopolarization 3–24649
  - SbSI, elec. cond. mechanism determ. 3–33955
  - SbSI, electromechanical hysteresis and photo deformation effect 3–34300
  - SbSI, ferroelec. phase transition entropy from temp. depend. sp. ht. obs. *(Russian)* 3–8542
  - SbSI, photo-e.m.f. spectra *(Russian)* 3–8227
  - SbSI, photodomain effect and deformation 3–34311
  - SbSI, pleochroism associated with domain struct. 3–36852
  - SbSI, semiconductor-ferroelectric, domain structure rel. to local states 3–5172
  - SbSI based piezoceramic, prep. technology 3–34301
  - SbSI multiple domain effect, illumination induced, hysteresis loop 3–34299
  - SbSI-SbSeI mixed crysts., far-i.r. reflectivity, l.f. ferroelec. mode behaviour 3–39135
  - $SbSI_xBr_{1-x}$, ferroelec. semicond., nonequilib. carrier density influence on phase boundary form. 3–39113
  - $SbSI_xBr_{1-x}$ solid soln., photoelectret and ferroelec. polarization, mechanism *(Russian)* 3–8539
  - SbSe type cpds., gaseous phase, ioniz. pots. and dissoc. energies *(French)* 3–7240
  - Sb_2Se_3, amorphous and crystalline, reflectivity meas. rel. to electronic structure 3–8104
  - Sb_2Se_3, photosemicond., crystallisation under hydrothermal conditions *(Russian)* 3–15633
  - Sb_xSe_y thin films, electron irradiation effect on crystal growth 3–15097
  - SbSeI, deep centres and photopolarization 3–24649
  - SbSeI, semiconductor-ferroelectric, domain structure rel. to local states 3–5172
  - SbSi cryst., mid-i.r. absorpt. and indirect transitions 3–24697
  - $Sb(TaNb)O_4$, intrinsic absorpt. and thermal props. rel. to ferroelec. phase change 3–5171
  - Sb_2Te_3, Mossbauer effect of ^{129}I *(Russian)* 3–12087
  - Sb_2Te_3, Mossbauer spectra, verification of two different states of ^{119}Sn atoms 3–36823
  - Sb_2Te_3:Ge, reflectivity meas. with different Ge content 3–8605
  - Sb_2Te_3:I, reflectivity obs. rel. to band structure and transport props. 3–8607
  - Si:Sb, Czochralski pulled single crysts., doping stacking fault pyramids 3–20756
  - L-SIOF, crystal structure obs. 3–33495
- **antineutrinos** *see neutrinos*
- **antineutrons** *see neutrons*
- **antinucleons** *see nucleons*
- **antiphase domains** *see alloys; crystal microstructure; solid structure*
- **antiprotons** *see protons*
- **antireflection coatings** *see optical films*
- **aperture cards** *see microforms*
- **API gravity** *see density*
- **apodisation** *see acoustic imaging; optical images*
- **apparatus** *see instrumentation; instruments*
- **apparent porosity** *see porosity*
- **appearance potential** *see ionisation potential*
- **Appleton layer** *see ionosphere*
- **approximation theory**
  - *see also function approximation; interpolation; least squares approximations*
  - corona discharge, field distrib., charged disperse phase effect 3–33402
  - corona discharges, motion of aerosol particles, eqn. *(Russian)* 3–36213
  - error estimation of approx. solns. for motion of nonlinear viscous liquids and twisting of inelastic bars *(Russian)* 3–29837
  - heat transfer by radiation, two stream approximation *(Russian)* 3–35641
  - nuclear radiation, co-axial detectors *(Rumanian)* 3–32136
  - plasmatron, arcing characteristics, approximation *(Polish)* 3–11509
  - waveguide, periodic, e.m. wave propagation, computation *(Russian)* 3–10431
- **apr** *see acoustic paramagnetic resonance*
- **arc discharges** *see arcs (electric)*
- **arc furnaces**
  - heaters, heat flux measurement, null point calorimetry, heat conduction analysis 3–131
  - transfer furnace for cryst. growth, furnace design and operation 3–12263
- **arc heaters** *see arc furnaces*
- **arc lamps**
  - high power, Illuminating Engineering Society, Annual conference 3–5930
- **arc welding**
  - *see also welding equipment*
  - submerged, mild steel plates cladded by, residual welding stress, thermal stress *(German)* 3–2783
  - Ar-shielded, radiation spectrum 3–33401
  - B/Al composites microstructure 3–12361
- **archaeology**
  - archaeological secular inclination var. in USSR, archaeomagnetic maps 3–25177
  - archaeomagnetism in Georgian SSR, pole position over last 1700 years 3–34847
  - archeomagnetic geomagnetic inclination data rel. to spherical analyses of main field during 1550-1800 period 3–34843
  - geomagnetic field direction meas. 3–37183
  - obsidian prehistoric artefacts, fission track dating 3–34820
  - solar system, hard rock cosmic ray archaeology 3–34981
- **architectural acoustics**
  - *see also anechoic chambers; echo; reverberation*
  - absorbing materials, edge effect 3–19117
  - acoustic field in irregular rooms, finite difference analysis 3–5733
  - acoustic frequency respoase in theatres and dubbing rooms 3–9769
  - air conditioning, quiet, development 3–25624
  - air conditioning systems 3–25625
  - auditorium, increasing reverberation time, electro-acoustical system 3–19116
  - circular enclosure, sound field and characteristic frequencies *(French)* 3–9768
  - closed circuit subsonic wind tunnels, noise sources 3–5735
  - concert hall acoustics, computer model 3–31962
  - correlation and Fourier transform techniques 3–3696
  - diffuse sound field, continuous spatial averaging 3–35331
  - double glazing, sound insulation when partially open 3–35330
  - echograms, numerical calculation, images and sound rays *(French)* 3–22201
  - edge effect of sound absorbing materials 3–19117
  - enclosures, acoustic wave transmission, radiated power insertion loss, sabine absorption 3–3703
  - field sound transmission loss measurements, room size effects 3–3702
  - hospitals, practical approach to acoustic design 3–28423
  - impedance measurements, absorption coefficients, ground impedance, correlation technique 3–103
  - intensity growth and decay in rooms, by geometric acoustics theory 3–37559
  - linear system approach 3–3697
  - linear system impulse response of room, review of techniques 3–3692
  - medium sized music auditorium design, speech reinforcement systems 3–5730
  - modulation transfer function as predictor of speech 3–22200
  - music hall, multivariate analysis of subjective and physical measures 3–9770
  - NHK concert hall design *(Japanese)* 3–28418
  - office, open-plan, sound attenuation 3–35329
  - panels, transmission coefficients, acoustic measurements, infinite duration pulse trains 3–104
  - partition wall sound insulation efficiency auditory assessment *(Japanese)* 3–5734
  - rectangular reverberation chamber, acoustic power of point dipole source 3–9771
  - reverberant field, place dependence of timbre of complex tones 3–19118
  - reverberant room, probability density function of time average of sound pressure level obs. 3–3694
  - reverberant room acoustic test facility 3–3695
  - reverberation time characteristics meas. of domestic rooms 3–5731
  - reverberation time measurement, acoustic quality, techniques and equipment, rangefinding *(German)* 3–28417
  - right parallelepiped, perfectly reflecting walls, acoustical Green's function, acoustic potential 3–3687
  - room geometry, noise reduction in spaces, field measurement, noise isolation class 3–102
  - room-acoustics, in radio and television broadcasting 3–31963
  - rooms, sound insulation dependent on transmission, wall and floor areas 3–5732
  - rooms with open windows, response to airborne sounds 3–25627
  - singing voices, acoustic analysis, samples and room responses 3–9737
  - small room responses, real-time digital filter for modelling 3–3693
  - sonic boom signals, transmission into rooms through open windows 3–25628
  - testing of structures, time delay spectrometry 3–3699
  - transmission loss characteristics, double panel constructions, interpanel connections, absorption material, mechanical properties 3–3700
  - transmission loss of plasterboard walls, studs and cavity absorption effects 3–3701
  - vibration and sound in building structures caused by vibrating machinery 3–3762
- **arcing** *see arcs (electric)*
- **arcing, switches** *see circuit-breaking arcs*
- **arcs (electric)**
  - *see also arc furnaces; arc lamps; arc welding; circuit-breaking arcs*
  - a.c., constrained in granular insulating medium model *(German)* 3–23948
  - a.c., stability assessment method *(Russian)* 3–14601
  - air high current free burning a.c. arcs, spectroscopic analysis 3–20672
  - air plasma, viscosity meas. 3–23904

arcs (electric) continued
  atom spectral lines determ. in arcs and sparks, degree of ionisation determ. *(Russian)* 3–29482
  cathode spot, directional motion due to asymmetrical conditions at its boundaries *(Russian)* 3–1529
  cold cathode arcs, evidence of dynamic field emission in cathode spots 3–27598
  conical arc driver for high energy test facilities 3–38506
  constant current, containing evaporated mols. from minerals, plasma temp. and ionisation meas. for spectral anal. *(Russian)* 3–21908
  constant property arc discharge, canal model 3–36214
  controlled plasma, for energy transmission to high-speed vehicles 3–23931
  current density in electrode spots of arc with metal electrodes 3–20675
  cylindrical columns, temp. variations during current-zero period 3–23937
  d.c., energy equation 3–14627
  decaying wall stabilised, computation 3–36230
  discharge in turbulent gas flow, intermittent behaviour 3–7585
  disconnection vacuum arc, investigation of initial stage 3–17707
  disconnection vacuum arc characteristics in magnetic field, effect on arc direction 3–17708
  displacement speeds in transverse mag. field, calc. and expt. *(German)* 3–23947
  driver operation for efficient energy transfer or high current generation 3–38505
  electrode stable temp. conditions of const. current arc *(Russian)* 3–6158
  electrolyte surface, propagation 3–7581
  erosion plasma, reduced pressure *(Russian)* 3–11498
  flashover on polluted surface having uniform and time-invariant resistivity 3–7571
  gaseous electronics, modern view of classical problems *(German)* 3–36232
  glow discharge transition, measurement using IC device *(Japanese)* 3–20676
  heat exchange in discharge chamber of arc gas heater with boundary conditions in wandering speck *(German)* 3–4688
  high current generator, arc driver operation 3–11521
  high pressure arc with a refractory cathode, behaviour as function of current, pressure and gas *(Russian)* 3–7587
  high-current pulsed, anode current density meas. 3–17690
  hollow cathode arc discharge for generation of intense ionic resonance lines 3–1112
  h.v. insulators, plasma, characteristics *(Hungarian)* 3–30025
  impurities, easily ionised, effect on distribution of particles of natural samples *(Russian)* 3–35544
  laser Doppler anemometry of electric arcs, fluid velocity meas. 3–795
  low-current d.c., obs. of new transition 3–14616
  low-pressure three dimensiona, with cylindrical symmetry, cathode region props. 3–36222
  magnetically rotated, heat transfer in plasma systems 3–26866
  magnetoplasmadynamic arc used as plasma source, pressure and current effects on thermal efficiency 3–36204
  magnetoplasmadynamic arcs, anode losses, influence of magnetic fields 3–36203
  metal vapour arc, non-stationary 3–36229
  metal vapour arc, unified analysis 3–36228
  moving arc, boundary conditions for electrode surface in the arc spot *(Russian)* 3–23949
  plasma, deviations from local thermodynamic equilib., spectroscopic study 3–17662
  plasma, vaporiz. consts. of small metal particles 3–23938
  plasma arc melting system design 3–27714
  plasma arc spraying technology, book contrib. 3–11511
  plasmatron, arcing characteristics, approximation *(Polish)* 3–11509
  pulse-arc generator as source for spectral analysis *(Russian)* 3–9947
  pulsed, temperatures meas. using intensities of Cu spectral lines 3–23932
  quasistationary pulsed arcs, high power, in strong axial gasflow *(German)* 3–4691
  stabilisation by a rotating magnetic field *(French)* 3–30033
  standard sources and detectors for absolute spectroradiometric measurements, review 3–25646
  Steenbeck minimum principle, comparison with const. prop. arc model 3–36215
  superalloy model in high pressure gaseous oxidiser, discharge characteristics *(Russian)* 3–26911
  temperature variation, spectrographic obs. *(Russian)* 3–1522
  thermal arc plasmas as radiation sources for light intensity calibration in astrophysics 3–4681
  unified positive column theory of gas discharge phenomena 3–23944
  vacuum, modelling of field-amplification processes on cathode protuberances 3–17706
  wall stabilised, Lyman α profiles rel. to local thermodynamic equilib. 3–20432
  wall-stabilized arc meas. for absolute scale for Si I g f-values 3–4356
  weak-current switches, analysis *(German)* 3–30031
  Ar, electrical conductivity determ. from electric arc meas. 3–33187
  Ar, high current free burning a.c. arcs, spectroscopic analysis 3–20672
  Ar, steady-state fully ionized plasma column, magnetically confined arc 3–4656
  Ar, wall-stabilised low-pressure, radial gain profile of 4880 Å ionic laser line and distrib. of charge carriers *(German)* 3–23951
  Ar discharge with hollow cathode, meas. of spectral intensities *(Dutch)* 3–30030
  Ar electric arc chamber, heat transfer to a biased wall 3–33417
  Ar plasma, local thermodynamic equilib. in stabilised arcs 3–33387
  Ar plasma, Rayleigh scattering determ. of radial gas density and temp. distributions 3–30009
  Ar plasma turbulent flow in arc constrictor, equilibrium laminar flow model 3–38439
  Ar plasma under press., as high temp. reference source *(French)* 3–5939
  Ar-N_2 mixture, wall-stabilised arc, potential gradient meas. 3–17687

arcs (electric) continued
  C plasma, electron density determination using laser beam interferometry 3–11504
  Cs vapour in low voltage arc discharge, striation production 3–30035
  D_2 arc, explosively driven, as plasma energy source 3–36186
  He, high pressure discharge, spectroscopic and plasma characteristics, afterglow and arc periods 3–30029
  Hg, current limitation 3–14617
  Hg arc, steady-state, low pressure, velocity of neutral atoms emanating from cathode 3–23935
  Hg lamp, effect of single pulse ruby laser radiation 3–23917
  Hg plasma, VI characts. and power relation in transverse mag. field 3–36212
  Mg discharge, pulsed, low press., vapour press. variations under pulsed arc conditions 3–1523
  N_2, atmospheric, discharge activated, nature and decay of long-lived species 3–33414
  N_2, electrical conductivity determ. from electric arc meas. 3–33187
  N_2, electrode dominated with W anode and Cd or Zn cathode, power balance eqns. 3–1524
  N_2 plasma, viscosity meas. 3–23904
  Pd, low current atmospheric arc, voltage fluctuations 3–4685
  Xe, electrical conductivity determ. from electric arc meas. 3–33187
  Xe 1 kW arc as continuous spectrum source for atomic fluorescence flame photometer *(Russian)* 3–10211

area measurement
  metallic specimens of size a few cm^2, by sorption and desorption 3–32031

argon
  adsorbed on BPO_4 surface, adsorption isotherm meas. 3–8014
  adsorption and desorption on Mo in glow discharge 3–15072
  adsorption on exfoliated graphite, adsorption isotherms 3–36480
  adsorption on graphite 3–38712
  adsorption on graphite with preadsorbed NO, 77.5 K 3–38720
  adsorption on minerals, determ. by BET method *(French)* 3–15065
  adsorption on Pyrex, anomalous Dubinin-Radushkevich plots 3–27177
  afterglow, disappearance of 2p state *(French)* 3–17358
  anisothermal plasma, veloc. distrib. fn. and balance quantities of electrons 3–7484
  arc, a.c., high current, free burning 3–20672
  arc, wall-stabilised low-pressure, radial gain profile of 4880 Å ionic laser line and distrib. of charge carriers *(German)* 3–23951
  arc discharge with hollow cathode, mea. of spectral intensities *(Dutch)* 3–30030
  atom, 1048 and 1067 Å reson. lines, electron impact excitation, 10 to 2000 eV 3–38231
  atom, autoionizing state detection using mathematical technique 3–29500
  atom, collision with ^{87}Rb, broadening of level-crossing signals in $5^2P_{3/2}$ state 3–29496
  atom, collisions, with Fl ions at 35.7 MeV, dependence of X-ray production cross sections on ionic charge state 3–1129
  atom, correlation energy calc. using many body perturbation theory 3–11124
  atom, elastic scatt. of K ions, collision polarizing character *(Russian)* 3–14316
  atom, electron impact ionization energy and ang. correlation of ejected electrons 3–26600
  atom, electron scatt., 100 eV, optimal model 3–20041
  atom, electron scatt., elastic, 100 eV, optical model 3–26596
  atom, excited state, quadrupole moment calc. 3–29487
  atom, inner-shell ioniz. cross sections by 1.5-5.0 MeV protons 3–33047
  atom, metastable, collision with N_2, product internal state distributions 3–1288
  atom, metastable, collisions with HCN, dissoc. excitation of CN radical 3–20128
  atom, modified effective electron model for interaction energy calc. 3–7088
  atom, photoabsorption cross section, 180-700 Å 3–20014
  atom, photoionisation absorption coeffs. in 60–230 eV energy range 3–11152
  atom, polarisability and shielding factors, effective-field calc. 3–29488
  atom, proton scatt., total differential cross section 3–33059
  atom collisions with H_2^+ ions in $1s\sigma_g$ state, dissociation *(German)* 3–38310
  atomic, Rb ion collision, quasimolecular state interference 3–20066
  atomic beam meas. of Pt surface roughness 3–27595
  breakdown at 10.6 micron, loss mechanisms 3–23665
  breakdown initiated by u.v. photoionisation in presence of spark, laser interaction 3–17492
  charge changing and electron loss cross section for C^{4+}(N^{4+}) ions in Ar gas 3–11178
  clusters, struct. obs. using a supersonic beam method 3–14799
  collision with beams of C^{6+}, N^{7+}, O^{8+}, F^{9+} at 1 to 2 MeV/amu, charge dependence of K-shell ionisation 3–20067
  collision with He^- ions, detachment cross sections 3–14312
  collisions with H isotopes, hyperfine pressure shift meas. 3–35982
  collisions with He atoms, electron loss 3–11166
  collisions with Hg atoms, depolarisation of Hg resonance radiation 3–33060
  collisions with K in cross supersonic molecular beams, differential scattering cross sections meas. *(German)* 3–26737
  collisions with Tl atoms, excitation transfer between the $6^2D_{3/2}$ and $6^2D_{5/2}$ states 3–14318
  condensed layer, adsorption characteristics, cryopumping 3–8022
  cover gas bubbles in fast reactor coolant, number and size determ. 3–1070
  critical region, gravitational effects on small-angle X-ray scatt. 3–20867
  cryotrapping by water condensates, press. depend. 3–15071
  crystal, epitaxially grown on Nb (100), inelastic scatt. and energy loss spectra 3–11655
  crystal epitaxially grown on Nb (100), low energy electron diffraction and desorption 3–11654
  crystalline filamentary media for particle counters *(Russian)* 3–296

argon continued
- crystals, force constants and phonon dispersion, theoretical parameters 3−38645
- c.w. gas laser, pumping Ba_2NaNbO_{15} doubly resonant parametric oscillator 3−755
- cylindrical hollow cathode negative glow discharge, plasma diagnostics *(German)* 3−4675
- dense gas, depolarised light scattering 3−33190
- dense plasma production in plug-shaped mag. field by an electron beam *(Russian)* 3−17628
- dipole and quadrupole three-body interactions, virial coeffs. 3−20072
- discharge, fluctuations and oscillatory phenomena *(German)* 3−14602
- discharge, HF vortex, rotational temperature determ. method 3−16413
- discharge, high-current low press., electron conc. estimation *(Russian)* 3−7579
- discharge, laser induced, electron density growth dependence on magnetic field 3−7310
- discharge, low-power, h.f., optical and probe investigs. at atmos. pressure 3−23905
- discharge gas in Al hollow cathode discharge tube *(German)* 3−3779
- electric arc chamber, heat transfer to a biased wall 3−33417
- electrical cond. from arc meas., trial function technique 3−33187
- electron distribution determ. by holographic electron laser microscope 3−4714
- electron impact excitation of $3p^54s$ I and $3s3p^6$ II states 3−17374
- energy loss of fission fragments having selected masses 3−29455
- fast atoms and ions, impact dissoc. into ions of O_2, CO and NO molecules 3−23621
- flow, condensation of Cs vapour in admixture 3−1345
- fluorescence yields, K-shell 3−26570
- foreign hot dense gas, shift and broadening of resonance lines of Ca, Sr, Ba 3−17345
- gas, ionised, transport coeffs. calc., 0.001 to 1000 atm and temp. to 35000K 3−38347
- gas, meas. of low-energy $K\beta$ spectrum, evidence of radiative Auger transitions 3−29490
- gas thermodynamic energy per unit mass improvement by oblique shock waves 3−17534
- glacial composition variation 3−2842
- glow discharges, electron energy in Faraday dark space 3−30040
- h.f. discharge stability at 95-105 MHz rel. to industrial trace gas chromatography *(French)* 3−432
- high density gaseous, intermediate scattering functions obtained by quasielastic neutron scattering studies 3−17485
- high temp. flow in pipe, heat transfer, during cooling 3−14408
- high-current pulsed discharge, plasma properties of ionized gas *(Russian)* 3−7586
- hollow cylindrical cathode, elec. field distrib. in cathode fall, radial model *(German)* 3−4690
- hot compressed, pressure shift and broadening of resonance lines of alkali and singly ionised alkine earth atoms 3−33033
- hypersonic wakes behind models moving in Ar, meas. of electronic and gasdynamic parameters *(Russian)* 3−7316
- impulse discharge emission in vacuum u.v. region *(Russian)* 3−30044
- impurity in HfSi film, use in diffusing species determ. during growth on Si 3−20958
- inert gas-Br_2 systems, energy transfer collisions, trajectory studies of atomic recombination reactions 3−26732
- ion bombardment of field ion microscope specimens, in situ cleaning 3−23963
- ion laser, pulsed, multistep electron collision excitation mechanism, coherence length *(German)* 3−16839
- ionisation, electron-impact, in eikonal and Born approxs. 3−38240
- ionisation balance, calc. for collisional ionisation, autoionisation, radiative recombination and dielectric recombination 3−11458
- ionisation equilib. calc. for solar atm. ions 3−18960
- ionisation meas. behind shocks with microwaves and a pulsed Langmuir probe *(German)* 3−14594
- ionization by metastable atoms, electron energy spectra 3−33053
- ionized, supersonic flow induced by shock wave *(French)* 3−29957
- ions, penetration profiles in Ta, determ. by (p, γ) reaction 3−26010
- isotopic thermal diffusion factors from column meas. 3−23663
- laser, effect of laser field on contours of lines amplified by neighbouring transitions *(Russian)* 3−22889
- laser, neutral, line competition, transition uncertainties 3−4087
- laser, output power saturation with discharge current 3−32553
- laser, pulsed, multi-mode operation *(German)* 3−29073
- laser, radiation self-focusing in $Bi_{12}GeO_{20}$ by Raman scattering 3−4128
- laser beam, spatial coherence in water 3−339
- Lennard-Jones liquid near triple point, computer expt. on 864 particles 3−38657
- liquid, density fluctuations, generalized hydrodynamic approach 3−24172
- liquid, dilute solution of H_2, i.r. absorption spectra 3−21412
- liquid, ion drift vel. 3−24283
- liquid, non-linearity parameter, temp. depend. 3−4857
- liquid, pair pot. from neutron diffr. at low density 3−7614
- liquid, polyatomicity, acoustic method 3−7613
- liquid, press., energy and sp. ht., Monte Carlo calc. 3−38650
- liquid, transport properties, test of Davis-Rice-Sengers square-well theory using Yvon-Born-Green pair correlation functions 3−4862
- liquid, triplet correlations 3−14670
- liquid and dense gaseous, calc. of self-diffusion coeffs. 3−1809
- liquid gas target system for medium energy electron scatt. facility 3−3842
- liquid incoherent neutron scattering, self motion response function 3−11537
- localised orbital wave functions, comparison between theory and expt. 3−8082
- longitudinal diffusion of electrons, influence of Ramsauer-Townsend minimum 3−1324
- low pressure hollow cathode discharge pendel effect expt. evidence *(German)* 3−14631

argon continued
- magnetoplasma column, low density, ion temperature and steady-state characteristics meas. 3−23920
- Mercury, Ar u.v. dayglow lines in atmosphere, models and predicted intensities 3−31616
- mesosphere and lower thermosphere, r.f. quadrupole spectrometer obs. 3−3045
- metastable atom de-excitation cross sections by gases 3−23630
- metastable beam, scattering, from O_2 covered (100) surface of Ge 3−39204
- metastable formation, excitation functions, comment on previous report 3−7080
- methane-Ar solid mixture, heat capacity near consolute point 3−7938
- MHD generator with K-seeded Ar plasma in nonequilibrium ionization state, determ. of characts. 3−33388
- molar volume along melting curve up to 10 kbar 3−27105
- muonium hyperfine interval, precision meas. 3−33067
- nonadditive effects due to long range dispersion forces on m-6−8 potential function, calcs. of third virial coeff. 3−4838
- overdense glow discharge, energy of positive ions in the hollow cathode *(Russian)* 3−7590
- pair potential from second virial coeffs. 3−7268
- Percus-Yevick integral equation for dense fluid, soln. with Kihara potential 3−17483
- photoionisation, 3s subshell, threshold region, photoelectron spectroscopy study 3−29508
- photoionisation cross section, threshold to 50 eV, calc. by many-body perturbation theory 3−29510
- plasma, absorption lines, determ. of relative transition probabilities using resonant Faraday effect 3−11473
- plasma, Ar and O_2 mixture, intense electron beam interaction *(Russian)* 3−14582
- plasma, Ar-Cs two-temperature, in a disc MHD generator channel, flow assuming nonuniform reactions of ionisation and recombination *(Russian)* 3−26874
- plasma, continuous, sustained by focused high-power CO_2 laser 3−36187
- plasma, continuum radiation meas. Kramers-Unsold model in region 1000-9000 Å 3−7489
- plasma, cylindrically confined, radiation absorption 3−20427
- plasma, dense beam discharge in strong magnetic fields, heating, electron temperature dependence and measurement *(Russian)* 3−33382
- plasma, experimental and analytical aspects of heat transfer 3−33343
- plasma, meas. of real and imaginary part of cond. using skin effect *(German)* 3−7556
- plasma, non-axisymmetric Alfven wave propagation 3−38445
- plasma, O_2-He-Ar mixture, external high frequency modulation of an electron beam, heating effect of ions *(Russian)* 3−17627
- plasma, pulse-discharge, elec. cond. obs. of electron-atom collisions 3−23907
- plasma, pure, shock tube produced, equil. electron density and temp. *(French)* 3−26896
- plasma, sheath admittance, meas. by floating voltage swept double probe 3−17658
- plasma, shock heated flow, parameters variation 3−26876
- plasma, two-temperature partially ionised, transport props. calc. 3−33339
- plasma, weakly ionised, turbulence 3−4639
- plasma column, steady-state fully ionised, magnetically confined arc 3−4656
- plasma diagnostics, tuned GaAs laser diode 3−4670
- plasma flow, stagnation point streamline, electron temp. meas. 3−20616
- plasma helical microwave source in high density high magnetic field regime, operating props. 3−29993
- plasma local thermodynamic equilib. in stabilised arcs 3−33387
- plasma sheath, collision-dominated, elec. breakdown meas. 3−36198
- plasma surrounding W refractory metal, spectral surface temp. meas. method 3−25693
- plasma turbulent flow in arc constrictor, equilibrium laminar flow model 3−38439
- plasma under press., as high temp. reference source *(French)* 3−5939
- plasma-beam discharge laser 3−32555
- positronium in Ar gas, 3γ annihilation 3−29514
- proton ionization, meas. of ion pair prod. as function of press. 3−7309
- radiative lifetime meas. for neutral atoms and ions by beam foil spectroscopy at low initial ion energies 3−17348
- Rayleigh scattering determ. of radial gas density and temp. distributions 3−30009
- r.f. plasma, spectral meas. in laminar sonic flow region 3−7557
- saturated liquid properties from Mie (n,6) potential and Barker-Henderson perturbation theory 3−4715
- shock waves structured by nonequilibrium ionizing and thermal phenomena 3−29884
- solid, Brillouin scatt., adiabatic elastic consts. determ. near triple pt. 3−4781
- solid, compressed, X-ray diffr. technique and lattice parameter meas. 3−20678
- solid, elastic consts. from interatomic potential for Ar_2 3−20779
- solid, electric currents and bubbles induced by α particle source 3−30505
- solid, excitonic effects on valence absorption edge 3−33849
- solid, i.r. and Raman spectra of formaldehyde atoms, matrix conc. and temp. depend. 3−29676
- solid, luminesc. spectra *(Russian)* 3−5236
- solid, Mittleman parametric polarization potential, use for calc. electron-atom scattering cross-sect. *(French)* 3−11136
- solid, nonmetal to metal transition, APW and pseudopotential study 3−21021
- solid, phonon dispersion interpretation 3−7878
- solid, phonon spectra, specific heat calc. 3−27079
- solid, press., energy and sp. ht., Monte Carlo calc. 3−38650
- solid, Raman two-phonon spectra, mol. dynamics 3−34353
- solid, temp. and vol. dependence of thermal conductivity 3−36395

argon continued
spark discharges jet guided, electrode erosion electrode spot formation 3—1526
sputtering of fused silica, rates, ion energies 12 to 32 keV, ion incidence dependence 3—36964
superconducting transition temp. depression of metal film by Ar(Ne) overlayers 3—34017
supersonic plasma, effect of electrode processes on volt-ampere characteristics of discharge 3—17709
Townsend coeff. meas. *(German)* 3—4682
Townsend discharge, electron distrib. functions calc. 3—33415
vapour, imperfect, phys. clusters, Monte Carlo simulation and theory 3—37915
X-ray spectra, proton bombardment 3—17353
X-ray spectra from collisions of Ar ions with solid state targets 3—34440
Ar, effect of c.w. laser on pulsed gas breakdown threshold 3—17491
Ar I, transition probability of 6032 Å line, spectrophotometry of plasmas *(French)* 3—33386
Ar I resonance lines at 1048 and 1067 Å at normal pressure in vacuum u.v. 3—17352
Ar IX solar spectrum, further identifications 3—28143
Ar plasma, local thermodynamic equilib. in stabilised arcs 3—33387
Ar:^{57}Fe, Mossbauer isomer shift in inert gas matrix, covalency versus overlap distortion 3—18398
Ar:H_2, solid, lattice excitation assignment to reson. mode of H_2Ar mol. 3—24237
Ar:Kr, far. i.r. absorpt. spectra at 2K 3—2574
Ar:Ne, far. i.r. absorpt spectra at 2K 3—2574
Ar/air turbulent gas mixture, hot-wire anemometry 3—22564
Ar-air high-temp. jets with Ti dispersive particles, electroconductivity *(Russian)* 3—11455
Ar-Ar interaction, collision diameter and well depth calc. 3—29539
Ar-Cs atomic collisions, absorption coefficients, long and short-range forces 3—20074
Ar-HCl rotationally inelastic scattering semi-classical calcs. using computer program implemented algorithm 3—11305
Ar-I_2 interactions Raman spectra, resonance, laser induced, vibrational frequencies 3—23620
Ar-K whole-rock dating of basalts, electron microprobe evaluation 3—12572
Ar-Kr coagulator, basics 3—32245
Ar-Kr liquid mixtures, shear viscosity calcs. 3—38677
Ar-Kr mixed ion cw laser, current depend. of spontaneous emission 3—32539
Ar-Kr mixture, thermal diffusion, temp. and comp. depend. 3—36070
Ar-methyl chloride system, thermal diffusion, temp. and comp. depend., inelastic collision effects 3—36069
Ar-N mixture, calc. correlation coefficients and Baxter's equation of state used to determ. P-V-T information 3—17484
Ar-N_2, intermolecular pot. calc., orientational averaging of rot. transition probabilities 3—17407
Ar-N_2 mixture, wall-stabilised arc, potential gradient meas. 3—17687
Ar-N_2 mixtures, pulse radiolysis, energy transfer induced postluminesc. 3—23629
Ar-N_2 system, rot. relax., temp. depend. 3—11297
Ar-N_2-O_2 vapour-liquid equilibria, equation of state 3—30249
Ar-Na two-phase flow in vertical channel, void fractions and heat transfer coefficients 3—1434
Ar-Xe, Ar-Kr solid solutions, cathodoluminescence 3—18504
Ar + CsF, integral total cross sections meas., attractive pot. investigation 3—38324
Ar + H_2 discharge deionisation process 3—30041
Ar + H_2O discharge, deionisation process 3—30041
Ar + H_2O steady-state hollow cathode discharges, rate consts. determ. 3—15829
Ar + HCl collisions, semi-classical approach to inelastic cross sections calc. 3—38323
Ar + K^+ interaction pot. from mobility and diffusion coeffs. meas. 3—38246
Ar + methane, energy per ion pair for photons below 8 keV 3—38225
Ar + N_2 plasma, calc. of inelastic loss factor for collisions between slow electrons and N mols. *(Russian)* 3—7479
Ar + NO collisions, vibr. relax. mechanism 3—26718
Ar + propane, energy per ion pair for photons below 8 keV 3—38225
Ar^+, bombardment of Al surface, negative ions energy distrib. 3—15583
Ar^+, mutual influence of two laser transitions at 4880 and 5145 Å *(German)* 3—37962
Ar^+, sputtering of Au 3—8692
Ar^+, transition probability values 3—23471
Ar^+ cw laser, excitations of laser states 3—4096
Ar^+ impact on solid surface, secondary electron emission 3—36968
Ar^+ ion laser discharge at high current 3—16834
Ar^+ laser, with berrylia discharge channel *(Russian)* 3—13727
Ar^+-Ar collision, 50-200 keV, X-ray production 3—29526
Ar^+-Ar collision, X-ray yield dependence on final charge state 3—29527
$Ar^{(+)}$ + Ar, ioniz. processes in slow collisions 3—26605
ArI, meas. of absorpt. coeff. in arc plasma 3—7041
Ar^+ — Ar violent collisions, extended ion-electron coincidence meas. 3—11184
^{8}Ar/^{39}Ar ages of chondritic meteorites, determ. of cosmogenic rare gas production rates 3—5428
^{36}Ar, in terrestrial materials 3—5429
^{37}Ar/^{39}Ar activity ratios, in Lost City stone meteorite, spatial constancy of cosmic radiation 3—9138
CO_2-Ar mixtures, relaxation of bending vibration 3—23537
Cd mixture, third harmonic generation, phase matching, v.u.v. generation 3—780
Cs-Ar, spectral line profiles, satellite structures, theory 3—35959
H^+ + Ar, elastic differential scattering expts., investigation of one state molecular system 3—11185
HF-Ar, vibr. relax., quasiclassical trajectory study 3—38318
He-Ar, modified Stefan cell for diffusion measurements 3—32214
He-Ar atom pairs, interacting, dipole moment 3—29538
MgO:Ar, ion implanted, photolum. from damage related defect centres 3—21463
Ne-Ar atom pairs, interacting, dipole moment 3—29538

argon continued
Ne-Ar ionized beam collisions, 60 to 80 MeV, projectile structure effects on K X-ray production 3—11180
Ne-Ar mixtures, pressure dependence of primary ionisation in Townsend discharge 3—17702
O + Ar, ion-atom high-energy collisions, electron loss 3—38247
O^+-Ar scatt., atomic pots. calc. using form factor techniques 3—29540
O_2-Ar mixture, viscosity meas. 3—38342
O_2-Ar mixtures, vibrational excitation and dissociation in diffusion approx. *(Russian)* 3—7258
Xe-Ar phase-matched mixture, generation of 1182 Å radiation 3—32535

argon compounds
Ar-Cu film, metal-nonmetal transition 3—27291
Ar-O_2 cryst., luminesc. spectrum of paired O_2 centres *(Russian)* 3—18496
ArF_2, hypothetical, bond length 3—29550

aromatic compounds *see organic compounds*

arrays (antenna) *see antenna arrays.*

arsenic
alloying element in Cu-Al (1 at wt.%) alloy effect on internal oxidation *(Japanese)* 3—15700
amorphous, photoelec. emission *(French)* 3—21512
deposition on hydrogen reduction of $AsCl_3$, rate determ. 3—8723
diffusion in Ge substrate during GaAs epitaxial growth *(Russian)* 3—27606
diffusion in Si, effect of complex formation 3—20886
diffusion in Si, through SiO_2 layer, arsenosilicate glass source 3—39260
diffusion in Si and $SiO_{2,3}$ using $As_2O_3SiO_2$ source 3—21545
diffusion in SiO_2, summary of data 3—21546
evaporation, expt. and computer-simulated studies, effect of surface morphology 3—38665
ion, possible beam sources 3—22428
molecular spectra, u.v. vacuum, absorpt. bands, transitions, vibr. consts. *(French)* 3—4439
multiply charged ions, atomic lifetimes of low-lying levels 3—11156
powder, microimpurities, spectral determ. 3—16568
semiconductor doping, diffusion comparison of closed ampoule and gas stream *(Russian)* 3—24811
in Ag and Cu, alpha solid solns., thermodynamic activities determ. procedure *(German)* 3—21794
As-Se-Ge amorphous films, photo-darkening effect 3—5212
As^+ c.w. laser oscillation in He-As mixture, charge transfer reaction 3—37959
As_2 mol., $A(^1\Sigma_u{}^+)$ state data *(French)* 3—17418
As_n-S_n mixtures, gas-phase laser Raman spectra as function of composition up to 800°C 3—7195
As(II), atomic spectra from Hartree-Fock calcs., need of LS-depend. parameters 3—7035
$As_4(g)=2As_2(g)$, heat of dissociation and formation determ. 3—31256
CdTe:As valence band structure investigations near gamma point 3—36531
Ge:As, Ga, indirect semicond., direct transition probability in impurity luminesc. 3—15554
Ge:As, luminesc. spectra due to electron-hole radiative recomb., virtual bound state, 2K 3—8632
Ge:As system, phase separation, X-ray photoemission study 3—36421
LiH:As, excitation and luminesc. spectra *(Russian)* 3—21462
Se-As semiconductor, glassy, photoelectric properties, structure and composition, local states 3—33812
Si:As, As diffusion from doped oxide, effects of $N_2(O_2)$ atmosphere 3—30281
Si:As, bulk resist. vs. As doping curves rel. to diffusin temp. 3—21024
Si:As, impurity photocond. oscills., 4.2-10K *(Russian)* 3—2134
Si:As, Zeeman splitting of photoluminescence of excitons 3—38809
Si-As n-p-n structs., retarded base diffusion, theory 3—21544

arsenic alloys
see also arsenic compounds
As-Pb-Sb-Sn alloys, grain growth and microstructure 3—8785
As-Se thin films, vacuum deposited, vitreous state, vibrational reflectivity spectra 3—8057
$AsSe_{1.5}Pb_{0.13}$ glassy alloys, consecutive crystallisation of PbSe and As_2Se phases, meas. of density of quenched patterns *(Russian)* 3—7634
Cu-As system, phase diagram and Cu_5As_2 phase props. *(Russian)* 3—12329
Ga-As-impurity ternary systems, rapid method for triangulating phase diagrams *(Russian)* 3—12330
Mn_2As-Mn_2Sb system, neutronographic investigation of magnetic transformations *(Russian)* 3—2291
Pb-As phase diagram, Pb rich portion 3—21568
Sn-Pb-Sn_4As_3 pseudoternary system, thermalanalysis, metallographic and X-ray methods 3—34497
V-As system, V_4As_3 phase, struct. determ. using direct methods 3—17759

arsenic compounds
see also arsenic alloys
arsenosilica spun on films as diffusion sources for high conc. Si doping 3—21550
$3As_2Se_3$-$2Sb_2Se_3$, amorphous film, recombination and trapping processes, photoconductivity obs., 278-308K 3—21094
As-S-I:Mn^{2+} glasses, e.p.r. study 3—30686
As-Se-Ge, glass film, optical transmission, refractive index, laser irradiation effect 3—19639
As-Te, melt system, phase diagram study rel. to growth methods 3—30243
As-Te-I:Mn^{2+} glasses, e.p.r. study 3—30686
$AsCl_3$, hydrogen reduction and deposition rate of As 3—8723
$AsCl_3^-$ radical produced by γ-irradiation of $AsCl_3$, determ. of e.s.r. parameters 3—4462
AsF_3^- radical produced by γ-irradiation of AsF_3, determ. of e.s.r. parameters 3—4462
$AsF_3(Cl_3)(Br_3)(I_3)$, centrifugal extension consts., calc. *(Russian)* 3—20104

arsenic compounds continued
- $As_{30}Ge_{10}S_{12}Te_{48}$ amorphous film, switching props. *(German)* 3−15229
- AsH_3, effect on Si film deposition from SiH_4-H_2 mixture 3−21529
- As_2O_3-SiO_2, vapour deposited, characts. and use in Si device fabrication 3−2657
- As_2O_3-SiO_2 glass, diffusion source for As in Si and SiO_2 3−21545
- As_2O_3-SiO_2 glass diffusion sources, effect of heat-treatment on comp. 3−20963
- $AsO_4H_2NH_4$, proton spin-lattice relax. mechanism in paraelec. and antiferroelec. phases 3−2451
- AsP-FeP solid solutions, Mossbauer studies 3−36818
- As_2S_3, amorphous, refr. index, dispersion and magnitude 3−36851
- As_2S_3, amorphous film, kinetics of photo-induced edge shift in light transmission 3−24714
- As_2S_3, laminar semicond., Raman scatt., absorption spectrum, vibr. levels splitting *(Russian)* 3−21425
- γ-As_2S_3, melt for In_2S_3 growth *(German)* 3−8741
- As_2S_3 amorphous film, optical transmission edge, anomalous photo-induced shift 3−8687
- As_2S_3 glass, clearing coatings production *(Russian)* 3−5904
- As_2S_3 glass and crystalline phases, magnetic susceptibility 3−8334
- As_2S_3 layer cryst., edge refl. spectrum, exciton peculiarities 3−2559
- As_3S_2 crystal photosynthesis from As-As_2S_2 mixture 3−27898
- AsSI, AsSeSI semiconducting glasses, i.r. transmissivity, instability at softening temp. *(Russian)* 3−2552
- $As_2(S_xSe_{1-x})_3$ film, lattice phonons, i.r. spectra study 3−36382
- $As_2(S_xTe_{1-x})_3$ film, lattice phonons, i.r. spectra study 3−36382
- $AsSe_x$ glasses, x=1-20 electrical conductivity between 300-700K *(Russian)* 3−8160
- $As_{1-x}Se_x$ amorphous films, Poole-Frenkel effect *(French)* 3−11963
- As_2Se_3, amorphous, elec. field enhanced phase separation and memory switching 3−5042
- As_2Se_3, amorphous, radiative recomb. 3−24737
- As_2Se_3, vitreous, chaotic potential field, optical absorption edge shift, deformation potentials 3−20993
- As_2Se_3, vitreous, refractive index determ. 3−37621
- As_2Se_3 glassy, optical absorpt. rel. to press. *(Russian)* 3−8608
- As_2Se_3 glassy, photocond. spectra rel. to optical absorpt. spectra *(Russian)* 3−8224
- As_2Se_3:B(Al)(In)(Ga)(Tl), vitreous, a.c. cond. and dielec. const. depend. on freq. and temp. 3−30742
- $As_2Se_3:Fe^{3+}$ glass, e.s.r. *(Russian)* 3−5133
- As_2Se_3-As_2Te_3:^{119}Sn, glass-crystal transition, Mossbauer obs. of ^{119}Sn impurity atoms local surroundings 3−4722
- As_2Se_7, amorphous semiconductor film, d.c. elec. cond. before switching 3−8239
- $As_2(Se_xTe_{1-x})_3$ film, lattice phonons, i.r. spectra study 3−36382
- As_2Te_3, glassy, electronic properties 3−1972
- As_2Te_3 melt, DTA method for evaluation of glass-forming tendency 3−1575
- As_2Te_3:^{119}Sn, glass-crystal transition, Mossbauer obs. of ^{119}Sn impurity atoms local surroundings 3−4722
- $AsTe_2Si$ chalcogenide film, localised states, thermally stimulated depolariz. current obs. 3−2020
- Cu-As-Se glass, light-induced memory effect 3−16895
- Cu-As-Se-Au glass, memory effect rel. to Au content 3−33969
- Ge-As-Te-Si, Ge-As-Te amorphous films, switching and memory effects 3−18198
- H_2AsO_4, arsenic acid and its anions, vibrational and normal coordinate analysis 3−29555
- H_2AsO_4, arsenic acid and its anions, Raman spectra and vibrational analysis 3−29671
- Se:As, As_2S_3, Bi, SiO, doping in vacuum growth to produce semicond. film for electrophotography 3−15623
- $Se_{50}Te_{20}As_{20}Ge_{10}$, amorphous, stress thermally induced by switching 3−27293
- Te-As-Ge-Si film, accumulation effects in switching 3−18200
- Te-As-Ge-Si film, freq. depend. cond., and capacitance 3−2092
- Te-Ge-As alloy film, laser writing and erasing 3−4113

articulation (speech) *see speech*

artificial hearts *see artificial organs*

artificial kidneys *see artificial organs*

artificial limbs
- control system design, amplifier charact. effects 3−28753

artificial organs
- *see also prosthetics*
- visual prosthesis, current progress 3−13134

artificial satellites
- 24 hour synchronous satellites, electric propulsion, low thrust parameters, analytic partial derivatives 3−3283
- absolute orientation of satellite triangulation rel. to geograv coordinate system 3−34758
- aerodynamic forces factors theoretical analysis, spatial impulsive interaction model, results *(Italian)* 3−20342
- AEROS, adaptation of German polar ground station 3−16065
- AEROS test results 3−16066
- Aerosat programme *(French)* 3−28083
- applications, review 3−27970
- Ariel 4 for ionospheric plasma-wave particle interactions 3−25337
- atmospheric temp. structure determ., radiometric techniques 3−25332
- close Earth satellite orbits, precession, nutation and reference system 3−39578
- comparison of effects of gravitational interaction torques on body and gravity torques exerted by body 3−10265
- density layer models in satellite geodesy, error propagation in computed orbits 3−34769
- Dial, geopotential zonal harmonics determ. 3−34774
- dynamics, spinning space station, counterweight, multiple cables, analysis 3−22597
- Earth gravitational model, computation methods from combination of terrestrial and satellite data 3−34766
- Earth polar motion determ. using Doppler satellite data 3−34778
- Earth resources remote sensing systems, cost-effectiveness 3−3199
- Earth Resources Technology satellite, obs. of New York Bight 3−34873

artificial satellites continued
- Earth Resources Technology Satellite, photographic and sensing systems 3−9386
- Earth Resources Technology Satellite 3−9385
- Earth Resources Technology Satellite (ERTS-A), equipment and obs. desctiption 3−25323
- Earth Resources Technology Satellite expts., a collection of summaries 3−18892
- Earth surveillance spacecraft, long term stability in longitude of 12 hour eccentric orbit satellites 3−12939
- Echo 1, physical and optical properties rel. to precise geometric geodesy 3−34781
- elliptical orbit satellites, orientation and resonance locks during deployment 3−37298
- Explorer 31, ionospheric satellite, ion flux angular distrib. in wake 3−25276
- Faraday fading rate of beacon satellite transmissions across off-zenith transverse point 3−12790
- general relativity theory test application *(French)* 3−35603
- geodesy, internal geometric accuracy from simultaneous laser range measurements to satellites 3−34757
- geodesy, laser ranging appl. to polar motion and interstation distance meas. 3−34779
- geodesy gravity anomalies determ. by least squares method 3−34777
- geodetic applications, symposium (Washington D.C., 15-7 April 1971) 3−34755
- geodetic research *(German)* 3−34752
- geodetic satellite timing using Loran C, atomic clocks and very-long-base line interferometry 3−34970
- geophysical, electronic design and instrumentation 3−5530
- geopotential in satellite geodesy, simple layer model 3−34768
- GEOS 1 and 2 mean orbital elements from optical flash data 3−39581
- Geos 1 and Geos 2 optical flash data, tracking-station coordinates 3−34764
- Geos 1 Secor observations in Pacific area (Solution SP 7) 3−34762
- Geos C, geodetic survey improvement and calibration analysis for AFETR 3−34765
- Geos C altimetry experiment, mini-arc orbit determination 3−34763
- geostationary environmental satellites, infrared radiometer 3−13121
- geostationary weather system METEOSAT, ground control system *(German)* 3−3166
- global geoid mapping using satellite altimetry in high-inclination orbit 3−34969
- gravitational stabilization by flywheel, system parameters optimization 3−25374
- gravity anomaly satellite-determination, mathematical model 3−34767
- gravity field resolution using satellite-to-satellite Doppler tracking 3−34772
- gravity-stabilised gyrostat satellites, non-linear resonant attitude motions, Hamiltonian mech. 3−22596
- HELIOS, micrometeoroid experiments 3−25536
- HEOS 2, micrometeoroid experiments 3−25536
- HEOS I, payload and launching description, solar wind obs. *(French)* 3−18929
- Imp 4, tesseral resonance of orbit due to commensurability 3−9447
- inclination changes due to longit.-depend. part of geopotential 3−25147
- Intercosmos 2, nighttime ionosphere obs. 3−34933
- ionospheric plasma flow past semi-infinite cylinder 3−9323
- ionospheric satellite wake, distribution of electron density 3−18878
- laser tracking to determ. Goddard Space Flight Center latit. var. due to polar motion 3−12628
- launched in 1972, tabulated orbital and other data 3−35216
- luni-solar short period perturbations, appl. to Intelsat 3F3 3−37300
- Mariner 9 photographs of Mars' surface *(German)* 3−9490
- meteorological, pictures, gridding and interpretation 3−3162
- meteorological applications, conference, Poona, India (April 1970) 3−2977
- meteorological measurement, review 3−5529
- METEOSAT system *(French, English)* 3−16057
- Molniya 1 satellite neutron monitor, solar proton intensity and energy spectrum determ. 3−22490
- motion of heavy flexible string attached to satellite in central gravitational field 3−16102
- motion of synchronous satellite using approx. computation method 3−25368
- motion parameters, accuracy of estimates using astronomical meas. with correlated errors 3−25371
- motion under influence of tesseral harmonies of earth potential *(Russian)* 3−16097
- multilateration, satellite geodetic measurement system 3−31464
- NASA's second decade in space 3−5618
- network precision, numerical investigation using doppler, laser and photographic obs. *(German)* 3−28080
- nutational oscillations, damping with internal flywheel 3−25375
- OAO-A2 ground systems and mission operations 3−31817
- for ocean data collection 3−21984
- optimal manoeuvre for transition from orbit to landing path, two dimensional calcs. *(Russian)* 3−26070
- optimal orbit characteristics of artificial planetary satellite in elliptical orbit rel. to hyperbolic approach flight 3−25379
- orbit determ. by range-only data 3−37244
- orbit determ. from range meas. for planet-orbiting satellites 3−35003
- orbit evolution due to solar radiation press. *(Russian)* 3−18914
- orbit selection *(Japanese)* 3−39584
- orbital eqn. of motion, soln. to first order 3−26067
- orbital trajectory and attitude dynamics, unified state model 3−37299
- orbiting astronomical observatory, program and mission 3−16296
- orbits, operational calc. *(French)* 3−37302
- orbits on programmable calculator, computer instructional use 3−9809
- orientation determ. of observatory satellite with unfixed orientation 3−25535
- oscillations with two-position attitude-control system 3−25376
- OSO-3, diffuse X-ray background meas., comparison with S-11 rocket data 3−32135
- OSO-5, two-component temp. anal. of X-ray flare data 3−31566

artificial satellites continued
OSO-7, anal. of X-ray flare spectra of 1971 November 16 event 3—31567
Pageos, physical and optical properties rel. to precise geometric geodesy 3—34781
Peole, geopotential zonal harmonics determ. 3—34774
perturbation of coordinates in Earth's standard gravitational field *(Russian)* 3—16099
plasma, magnetised flow plate simulating conditions encountered by earth satellites 3—29962
radio ranging of satellites, correction for troposphere and stratosphere 3—34905
ranging, tropospheric refraction effects, atmospheric model, local meteorological conditions 3—21935
SAS, geopotential zonal harmonics determ. 3—34774
satellite-to-satellite tracking for determ. of geopotential coeffs. 3—34773
secular perturbations in orbital elements due to asphericity of earth *(Russian)* 3—16115
secular radiational perturbations *(Russian)* 3—16100
Small Astronomy Satellite (SAS-B), self deployable light shade for astronomical sensors 3—31824
small astronomy satellite B, γ-ray studies 3—31813
Small Astronomy Satellites, star sensor/mapper 3—31823
SOLRAD, effects on detectors of solar X-ray spectrum 1.9 Å line 3—31413
special satellite orbit-points prediction, analytical iterative algorithm, Brouwer theory 3—39583
surface interaction with gas atoms, effects on motion 3—25381
tracking data used for error model of SAO 1969 Standard Earth 3—34776
transfer from hyperbolic to nearly circular orbit round planet using aerodynamic braking 3—25378
UK5 satellite for X-ray astronomy 3—25537
upper atmosphere pressure prediction for duration of flight 3—31363
USA weather satellite projects *(German)* 3—31466
weather research *(German)* 3—34903
worldwide geometric satellite triangulation programme, data reduction and analysis methods 3—34759

asbestos
alignment of fibres by magnetic field 3—18737
chrysotile asbestos fibre, mean inner potential, electron interference microscopy 3—24060
precoked, thermal diffusivity at elevated temps. 3—24978

asdic *see sonar*

aspherical lenses
adaptability to manufacturing technology 3—16423
aspherical surfaces machining method 3—13284
double plane symmetric systems, aberration coeffs. 3—35679
figuring miniature asphérics, ion polishing technique 3—28530
focusing lenses with one aspherical surface used in lasers, analysis and calc. 3—22321
interference testing methods using spherical and aspherical test glasses *(Russian)* 3—5918
light scattering by single cylindrical lens, numerical result from rigorous theory 3—19579
optical system design, introduction of higher order equalising coefficients for known aberration magnitudes *(Russian)* 3—32056
surace meas. using IZS-7 spherometer 3—16424
surface decentering meas. by interferometric method 3—13290
synthesisation by optical means 3—9931
thin double-plane-symmetric lenses, third order aberrations 3—32524

association
see also association of gases; association of liquids
indole-pyridine systems, association constants by i.r. intensity meas. 3—29730
metal atom + O_2 crossed beams, assoc., reactive and electron transfer ioniz. 3—29746
metal nitrites in N,N′-dimethyl formamide, ion pairing role in photolysis 3—5404
9-methyl anthracene molecules, photoassociation 3—31281
molecular, study by matrix isolation spectroscopy *(German)* 3—20119
phenols, chlorosubstituted, self-assoc., i.r. spectra and OH hydrogen bonding study 3—33130
pyrrole-pyridine systems, association constants by i.r. intensity meas. 3—29730
solvation, ionic, spectroscopic study, ^{23}Na n.m.r. meas. in mixed solvents 3—26703
N + O assoc. reaction, rate consts. for O(^{3}P) recomb. 3—27858
N + O radiative recombination investigation using photodissociation of NO 3—20192

association factor (liquids) *see association of liquids*

association of gases
Clausius-Clapeyron equation, case of association in vapour phase *(German)* 3—14957
inorganic pentafluorides, saturated vapours, molecular beam mass spectra 3—25924

association of liquids
see also colloids
aliphatic alcohols, n.m.r. of association processes, H-bond enthalpy 3—27433
benzodioxane-1,4 soln. in n-octane, self-association, proton magnetic resonance spectra *(Russian)* 3—34709
di-T-butyl carbinol, near i.r. heteroassociation study and choice of mol. complex equilib. conc. scale 3—23575
liquified gases, polyatomicity, acoustic method 3—7613
phthalocyanine dyes in soln., self-association obs. by electron spectra and e.s.r. 3—31252
triphenylalkylidenephosphoranes, hydrogen bonding ability 3—12516
D_2O-dioxane system, u.s. study of molecular association 3—21790
5-oxybenzodioxane-1,4 solution in CCl_4, intermolecular action *(Russian)* 3—37116

associative memories *see associative storage*

associative storage
multiparameter data acquisition 3—28626

associative stores *see associative storage*

astatine
sticking coeffs. for on-line anal. of mol. beam with short-lived nuclides 3—10205

astatine compounds
No entries

asteroids
Alinda (887) resonances and encounters with Earth, Venus, Mars and Jupiter 3—9461
1221 Amor, resonance and libration with Earth 3—35102
Amor (1221), resonances and encounters with Earth, Venus, Mars and Jupiter 3—9461
813 Baumeia, position rel. to background stars, 1970 opposition 3—35101
(1559) 1942 BF, photographic position near Jupiter (25 January 1968) 3—31577
collisions, period depend. on size, orbital effects 3—31636
commensurable motion secular effects, appl. to Hecuba Gap and Hilda Group 3—31634
Crimean Astrophysical Observatory observations, USSR *(Russian)* 3—16194
data elements calculated using system of computer programs *(Russian)* 3—16195
433 Eros, Amor asteroid, resonance and libration with Earth 3—35102
evolutionary stages rel. to mean daily motion 3—37342
1620 Geographos, Apollo asteroid, resonance and libration with Earth 3—35102
1627 Ivar, Amor asteroid, resonance and libration with Earth 3—35102
459 Jessonda, position rel. to background stars, 1970 opposition 3—35101
(53) Kalypso, photographic positions near Jupiter (25 March 1968) 3—31577
meteor stream statistical model showing asteroid-meteor assoc. 3—31635
observations, Crimean Astrophysical Observatory *(Russian)* 3—16197
orbits, stability of solar system 3—18994
origin, possibility of remains of exploded planet 3—31637
photographic obs., Nikolayev observatory (1969) *(Russian)* 3—16196
photographic positions of six objects near Jupiter 1967-8 period 3—31577
position meas. of 26 southern asteroids during 1968-1969 period *(Italian)* 3—37341
spectral reflectivities for 32 objects rel. to orbital and physical parameters 3—35100
1685 Toro, Apollo asteroid, resonance and libration with Earth 3—35102
Toro (1685), resonances and encounters with Earth, Venus, and Mars 3—9461
619 Triberga, position rel. to background stars, 1970 opposition 3—35101

astigmatism *see aberrations*

astronautics *see space research*

astronomical instruments
see also astronomical observations; astronomical techniques; astronomical telescopes; radiotelescopes
35mm camera for a balloon borne solar telescope *(Japanese)* 3—19082
9558 Angstroms photomultiplier performance improvement, astronomical applications 3—25526
Aerospace-NASA videomagnetograph-based two-dimensional photon counting 3—31843
airborne Hadamard-Transform Spectrometer, i.r. obs. of Mars during 1971 opposition 3—35221
alpha spectrometer, in Apollo 15 and 16 3—31803
astrolabe, Czech circumzenithal VUGTK 100/1000 mm., Time and Latitude Services 3—35207
astrolable (Danjon), Jupiter obs., use for correction of ephemerides *(French)* 3—22031
automatic dynamic spectrum analyser for video tape recorded signals 3—39750
Becker's Iris Photometer, electric control system *(Italian)* 3—35209
CAMAC as standard for astronomical instrumentation 3—31842
circular polarimeter, appl. 3—39680
coherence interferometer 3—13112
Coude spectrum scanner for Lowell Observatory 42-inch telescope 3—39757
crystal spectrometer for cosmic X-ray detection by rocket and satellite expts. 3—28303
Danjon's astrolabe, installation at Merate Observatory, Italy *(Italian)* 3—37503
Dollfus polarisation modulator, development of wide-band version for starlight spectropolarimetry 3—25534
for Earth orbital and rotational motion 3—3743
electronographic cameras for space astronomy in far u.v. region 3—31833
energy calibration using synchrotron radiation 3—19079
far u.v. combination camera and spectrograph, Apollo 16 mission 3—9626
far u.v. stellar spectrograph for 200 to 900 Å region, design and aberrations 3—31840
Fourier spectrometer, monitoring by real time computer, airborne i.r. astronomy 3—3385
heliostat, for solar flux spectrum, stellar spectrophotometric reference 3—13119
historical, 18th century Russia 3—3390
image intensifier systems, established and recently developed devices, review 3—9629
image intensifier systems, recent developments in applications to astronomy 3—31832
i.r. interferometer for solar obs. 3—16292
i.r. scanning system and maps of Jupiter 3—9496
large aperture rocket camera 3—3396
l.f. interferometer, receiver and antenna set-up and circuit diagrams *(Japanese)* 3—16435
lunar surface u.v. spectrographic camera 3—25539
Mars Viking Lander cameras, implementation 3—31830

astronomical instruments continued
- Michelson interferometer used on Mariner 9 3−3384
- Michelson stellar interferometer, monochromator coherence length rel. to visibility drop 3−31808
- monochromators for nebular studies, Fabry-Perot, Pepsios and Sisam types 3−25528
- Monte Carlo method for calibration of γ-ray detectors 3−13113
- neutron monitor aboard Molniya 1 for solar proton intensity and energy spectrum determ. 3−22490
- new observatory at Chapel Hill, North Carolina 3−9633
- open-structure channel electrón multiplier, use in sounding rocket expts. 3−31811
- orbiting astronomical observatory, program and mission 3−16296
- OSO-7 1-60 keV X-ray detector 3−28243
- photo-optical instrumentation, conference (Tucson, Arizona March 1972) 3−31816
- photoelectric micrometer mounted on meridian circle for stellar tracking *(French)* 3−31800
- photoelectric phase apparatus, calc. of time delay *(Russian)* 3−16295
- photographic zenith tube, light attenuating plate *(Japanese)* 3−19087
- photographic zenith tube timing device, accuracy determ. *(Japanese)* 3−19086
- photon-counting Stokes vector polarimeter for solar studies of corona and disk 3−31835
- position sensitive X-ray detector, for HEAO-A satellite 3−31804
- radial velocity measurement, polarimetric method 3−13118
- rocket grazing incidence grating spectrograph with resolution and wavelength accuracy improvement 3−18954
- scanning measurement system, relative coordinates of astronomical objects, superorthicon TV camera, deflection circuits *(German)* 3−9631
- semiconductor image devices for spectroscopy, autoguiding and photometry 3−39756
- signal-generating optical image sensors for Large Space Telescope 3−31831
- slitless short wave stellar spectrograph 3−19028
- smoothing dissector, intensifier addition to image dissector 3−31834
- solar chromatograph, design and props. 3−37499
- solar energy collector, linear, heat transfer characts. 3−25529
- solar magnetograph using fibre optics 3−31826
- solar simulator, lens projection system, design equations 3−25530
- solar spectrograph for extreme u.v., rocket borne, design, performance 3−31798
- solar subtractive double pass spectrograph 3−39759
- spectroheliograph, multichannel Fabry-Perot configuration 3−25540
- spectrophotometer, automated two-channel scanning system with computer control 3−31829
- star tracking interferometer 3−9636
- u.v. and X-ray, high resolution position sensitive detector 3−28645
- X-ray proportional counters, coaxial anode for background suppression 3−35213
- PbS detectors, photoresponse variations without use of Fabrylens 3−31801

astronomical observations
- *see also infrared astronomical observations; radioastronomical observations; ultraviolet astronomical observations; visible astronomical observations; X-ray astronomical observations*
- 1973 Astronomical Ephemeris 3−9634
- 1973 Astronomical Handbook for Southern Africa 3−19088
- 1973 Observer's Handbook (for Canada) 3−16298
- asteroid data elements calculated using system of computer programs *(Russian)* 3−16195
- asteroids, spectral reflectivities for 32 objects rel. to orbital and physical parameters 3−35100
- bright stars, catalogue of dimensions 3−9530
- cosmic ray electron spectrum, modulation near solar max. 3−12911
- diffuse cosmic gamma ray flux observed at equatorial balloon altitude 3−25349
- heliocentric corrections, tables for light time corrections 3−28117
- Hercules X-1, position and spectrum meas. during high intensity phase, satellite obs. 3−13079
- HZ Herculis, optical properties, X-ray source on surface of collapsed star 3−13078
- high resolution observations, comments on paper by Couteau *(Italian)* 3−31797
- high resolution observations, image deterioration factors and resolution limits *(Italian)* 3−31796
- Kiev University Observatory, solar physics 3−39631
- Large Magellanic Cloud, comparison between Sanduleak and Fehrenbach-Duflot catalogues *(French)* 3−5612
- late type stars, Balmer emission and H and K emission 3−13036
- M 92 giants with enhanced CN and CH bands and strong metallic lines, membership of cluster *(Russian)* 3−16270
- Mars, from earth, 1965-69 3−31585
- Mexico, cloudiness meas. and suitability for astron. sites 3−37203
- occulting body diameter determ. from single observation using Fresnel diffraction 3−9625
- Royal Observatory, Cape Town, S. Africa, origin of bad seeing conditions 3−15978
- soft X-rays, supernovae remnants and diffuse background 3−13034
- The Sun and the amateur astronomer, book 3−31574
- time and latitude bulletins, (Jan 1972) 3−9619
- Tonantzintla lists, near South Galactic pole, photometry 3−9618
- Uhuru catalogue of 125 X-ray sources 3−19045
- velocity of light, three centuries of observations of Jupiter's satellite Io rel. to possible var. 3−32504

astronomical spectra
- *see also atmospheric spectra; solar-spectra; stellar spectra*
- Abell 194, cluster of galaxies, low-dispersion spectra, colour-magnitude diagram 3−39736
- absorption lines of PSR pulsars (0628-28, 2021,51, 1929+10, 1707-16) 21 cm 3−9583
- absorption spectra of Ca_2 in solid benzene 3−7179
- absorption-line systems in quasars, radiation pressure effects 3−16244

astronomical spectra continued
- black hole accretion from interstellar gas, emergent radiation spectrum 3−39586
- 4C 05.34, quasar absorption spectra rel. to surrounding gas density 3−16245
- CD −42° 14462, spectroscopy of Southern Hemisphere 3−9548
- CGCG 1439+5344, extremely compact galaxy 3−5614
- Coma cluster, spectroscopy and redshifts of outlying faint galaxies 3−39719
- comet Bennett (1969i), scattered light continuum, reddening 3−12999
- compact nebulae with very-low-excitation nebular component in spectra 3−16287
- cosmic ray differential spectrum meas., instrument characts. use 3−32137
- cosmic ray energies, charge dependence 3−21989
- cosmic ray nuclei energies, observational evidence 3−21990
- Cygnus X-1, energy spectrum and time variations of hard X-rays 3−25488
- e.m. radiation source moving in circular orbit around moving black hole *(Russians)* 3−16092
- emission-like objects, consistency of distribution with the randomness hypothesis 3−22088
- enhancement by digital convolution 3−35203
- formaldehyde in interstellar dust clouds, anomalous hyperfine lines 3−22119
- Galactic central region, energy spectrum of gamma rays 3−28265
- galactic nuclear regions, blueness, metal-line strength 3−13081
- Galaxy, spiral, anomalous radio emission line in spectrum of W49A 3−37465
- Hercules X-1, satellite obs. during high intensity phase 3−13079
- hot universe, effect of energy release on emission spectrum 3−25389
- interstellar gas, chemical composition from X-ray attenuation meas. 3−28287
- ion energy spectra of Mars-solar wind interaction region 3−31584
- isocyanic acid, interstellar emission line from Sgr B2 at 1.4 centimeters 3−16274
- isocyanic acid interstellar line, detection from Sgr B2 and W51 directions 3−16273
- Large Magellanic Cloud spectra of continuum radiosources, determ. of spectral indices 3−3350
- line blanketing in giants of disc population, comparison with 47 Tucanae obs. 3−28198
- line identification problems for ground based photographic spectroscopic instruments 3−3395
- lunar regolith from Mare Foecunditatis, i.r. reflection, emission and transmission spectra 3−31622
- M31, Andromeda galaxy radio spectrum at 2695 MHz rel. to spiral arms and nucleus 3−35183
- M31, spectrum of pointlike nucleus rel. to velocity dispersions and mass 3−37450
- M31, variation of emission-line strengths for H II regions 3−39717
- Markarian 78, galaxy with u.v. excess, spectroscopic observations of mass motions 3−28259
- Markarian 8, galaxy, morphological and dynamical structure *(Russian)* 3−37440
- Markarian galaxies, emission lines present *(Russian)* 3−16254
- Mars, air glow, study by Mariner 9 u.v. spectrometer 3−16154
- Mars, O_2 A band line meas. 3−25411
- Mars, u.v. emissions of upper atmosphere 3−16156
- methyl alcohol, new interstellar emission line from 5_1-4_0(E_2) transition 3−16271
- methyl alcohol interstellar line, detection of 4_1-3_0 (E_2) transition line from Sgr B2 clouds 3−16272
- NGC 1614, emission line inclinations, galactic rotation effects 3−19052
- NGC 3516, Seyfert nucleus, spectral var. rel. to spectroscopic observations 3−22105
- NGC 3699 (292+1°1), planetary nebula, image tube spectrogram 3−39748
- NGC 4151, gas motions in nucleus of Seyfert galaxy, image-tube spectra 3−39723
- NGC 5253, 0.33 to 2.2 μ spectrophotometric obs. and interpretation 3−37395
- Ohio radio sources, flux densities at u.h.f. 3−13065
- Orion nebula, kinematics of Huyghenian region from O II 3726 Å and O III 5007 Å radial-velocity measures 3−37490
- Parkes 2700 MHz survey, spectra of sources in the ±4° declination zone 3−16238
- Parkes 2700 MHz survey, spectra of sources in the ±4° declination zone, statistical analysis 3−16239
- PHL 957, digicon spectrometric meas. 3−16243
- PKS0123-01, obs. at 5000, 408, 80 MHz, determ. of spectral index and galactic effects on emission spectrum 3−3345
- planetary atmospheres, semi-infinite diffuse, spectral lines formation and curves of growth *(French)* 3−35071
- planetary nebulae, spectra of 8 southern objects in 3400-7200 Å region 3−39747
- PSR 0833-45, linear polarisation and spectrum scattering effects 3−16247
- QSOs, ionization potential-redshift correlations in absorption line spectra 3−19040
- quasar absorption spectra, statistical anal. of objects with multiple red shifts systems 3−31721
- quasar emission line red shift distrib., search line availability in 3300-6900 Å window 3−28234
- quasar emission spectra, simplified photoionisation analysis 3−39703
- quasars, absorption spectra, ionization and density of absorbing gas 3−31724
- radiation transport in spectral lines, book 3−14305
- radio source interplanetary scintillations, non-Gaussian spectra anal. 3−37411
- radiosource flux density calibration and spectra determ. at radiofrequencies 3−37408
- radiosource spectra, cosmological implications 3−37306
- reflection nebulae, strong 4430 Angstroms interstellar absorption in backscattered light 3−28295
- scintillation spectra characts. depend. on meteorological conditions 3−39513

astronomical spectra continued
Seyfert galaxies, rapid var. of $H\alpha$ intensity in nuclei 3−35182
Seyfert galaxies, variability of optical radiation from nuclei *(Russian)* 3−37439
solar cosmic-ray spectrum determ. using ionospheric data 3−25352
supernova remnants and HII regions, classification from recombination line emission 3−3334
Ton 1530, quasar, absorpt. line obs. 3−22089
u.v. atomic and molecular, recent advances 3−19078
X-ogen, unidentified interstellar microwave line in four new galactic sources 3−37484
D absorption line at 327 MHz in direction of galactic centre 3−31716
astronomical spectroscopy *see astronomical spectra; spectroscopy*
astronomical techniques
see also radioastronomical techniques
21 cm H line, calibration profiles 3−39751
1973 Astronomical Ephemeris 3−9634
absorption spectroscopy, ultra long optical path, technique using laboratory atmosphere 3−37502
Aerospace-NASA videomagnetograph-based two-dimensional photon counting 3−31843
age indicator for galactic clusters, significance of second bluest star 3−35204
asteroid data elements calculated using system of computer programs *(Russian)* 3−16195
high resolution observations, image deterioration factors and resolution limits *(Italian)* 3−31796
high resolution spectrometry, use of Michelson interferometers 3−13117
hook and absorption techniques for oscillator strength meas. 3−11147
infrared astronomy progress and development of planetary and stellar i.r. emission, popular survey *(French)* 3−22133
intensity interferometry, in spatial domain, for stellar observation 3−31807
interplanetary low-temp. plasma meas. using electron beams 3−18893
K-giants from IRC catalogue, luminosity functions determ. method 3−39677
laser lunar ranging, effect of ephemeride errors *(French)* 3−31505
lunar particle size meas. 3−16293
lunar retroreflectors, laser ranging meas. of Earth crustal movements 3−34971
Mariner 9, star photography Mars picture information decalibration 3−25531
Mars, laboratory obs. of simulated planet for determ. of surface optical parameters 3−35066
Mars Viking Lander cameras, implementation 3−31830
monochromatic extinction determ. from BV photometric obs. 3−34877
night time seeing, large telescope resolving power determ. using polar star trails 3−28302
objective-prism techniques for faint stars in Large Megellanic Cloud *(French)* 3−16290
occulting body diameter determ. from single observation using Fresnel diffraction 3−9625
photoelectric micrometer mounted on meridian circle for stellar tracking *(French)* 3−31800
photoelectric photometry, digitisation using the direct current method *(Japanese)* 3−19083
photoelectric photometry digital recording system *(Japanese)* 3−19084
photographic zenith tube, reduction method for star's coordinates *(Japanese)* 3−19085
photography of faint stars, recording at plate limit on different emulsions 3−37508
planetaria, historical review 3−13116
polar star trail classification rel. to seeing, Walker traces *(Italian)* 3−35211
position determination, geodetic stars, e.d.p. by Minsk 22 computer *(Russian)* 3−3394
rocket i.r. obs., H II regions 3−13102
seeing discs, model computations, i.r. appl. 3−39505
smoothing operator, estimation of mean response charact. 3−39752
solar electrograph for predicting electric fields during pre-flare energy build-up 3−37317
solar flare patrols, data uncertainty and service reliability 3−35053
solar telescopes, instrum. polarisation effects on magnetographic meas. 3−39758
solar weak white-light flares, time-wise photographic cancellation search method 3−22022
spectra enhancement by digital convolution 3−35203
spectroscopy, resolution enhancement of line spectra by deconvolution 3−35205
stellar occultations by moon, double image principle *(French)* 3−39753
Stokes parameters, Lorentz transformation properties 3−9627
u.v. obs. and methods, a review 3−19078
u.v. obs. from lunar based instruments 3−9623
astronomical telescopes
see also radiotelescopes
250 mm reflector construction 3−13115
γ-ray, using double Compton process 3−28306
achromatic Schmidt telescope, 131 cm, $f/3.5$, construction, props. 3−9622
array of small telescopes rel. to one large telescope, observations and cost 3−9624
balloon-borne solar, temp. variations meas. during flight, circuit diagrams *(Japanese)* 3−19082
balloon-borne u.v. stellar spectrometer telescope, Mg II 2800 Å doublet meas. 3−35220
balloon-borne u.v. stellar spectrometer telescope, pointing and guidance 3−31839
Cassegrain type, aberration correcting system *(Italian)* 3−25525
computer controlled, 150 inch, Siding Spring Observatory, CAMAC modular data system 3−3392
computer-controlled 24-inch telescope and on-line data processing system 3−31841
cosmological deceleration parameter accuracy derived from red-shift-magnitude relation for various telescopes 3−28130
astronomical telescopes continued
Coude system, polarisation effects on spectrometer transmission 3−37501
diffraction limited large space telescope, use of image quality criteria 3−31820
field correctors, review 3−13122
gamma-ray telescope for observing NP0532 (Crab pulsar) 3−37510
'Grand Schmidt', Liege, new improvements, comet and nebulae obs. *(French)* 3−31802
image quality, image motion compensation by secondary mirror control 3−13110
image read-out system for space appl. 3−25527
image structure and value of very large telescopes 3−39755
large orbital space stations, long term prospects *(German)* 3−35217
Large Space Telescope, 3m aperture, configuration and mission objectives 3−25538
Large Space Telescope, laser interferometric alignment sensor 3−31822
large space telescope, optical systems considerations 3−31818
Large Space Telescope, study of signal-generating optical image sensors 3−31831
low optical quality, diffr. limited imaging 3−31809
mirror figure control of spaceborne telescope by modal control 3−31819
multiple mirror, six 1.8 m aperture cassegrainian telescopes with common focal surface, design 3−9628
multiple mirror project, optical, electronic and mechanical subsystems 3−31828
multiple-mirror telescope project, 180 inch-equivalent 3−31827
observational, online computer aids 3−5622
offset guiding through large space telescopes 3−31821
optical surfaces, soft X-ray scatt., X-ray telescope mirror design 3−16289
paraboloid mirrors, field correctors, image spread, transmission 3−3391
reflecting, using Pe, French developments 3−3388
resolving power evaluation using polar star trails 3−28302
Schmidt, anastigmatism along axis, aspherical dioptres *(French)* 3−22128
Schmidt all-reflecting telescope, improved geometry 3−37500
solar telescopes, instrum. polarisation effects on magnetographic meas. 3−39758
star guiders, star simulator for checking, design 3−25541
Stratoscope II, Uranus photography with high-resolution imagery 3−22029
three mirror, closed form soln., spherical aberration, coma, astigmatism, field curvature 3−13111
three-mirror objectives with 4-fold reflection and increased field of view *(Russian)* 3−22134
two conic reflecting aplanats, analysis, design 3−9621
weak zone plate fabrication and evaluation 3−32092
X-ray monochromator for flare emission obs. 3−19077
Yerkes 40-inch refractor, effect on thermal condition of lens on plate scale, Vasilovskis theory 3−28301
Yerkes Observatory 40-inch refractor, determ. trigonometric parallaxes and proper motions 3−31662

astronomy and astrophysics
see also astronomical instruments; astronomical observations; astronomical spectra; cosmology; galaxies; gamma-ray astronomy; infrared astronomy; radioastronomy; radiosources (astronomical); solar system; stars; ultraviolet astronomy; X-ray astronomy
1973 Astronomical Handbook for Southern Africa 3−19088
1973 Observer's Handbook (for Canada) 3−16298
accretion onto a rotating magnetic monopole, sub-Alfven flow 3−12930
Annual Review of Astronomy and Astrophysics, Volume 10, book 3−16089
astronomical aspects of gravitational waves rel. to Weber's results *(Japanese)* 3−3280
Astronomical Soc. of Pacific, conference (Santa Cruz, USA, June 1972) 3−9617
astronomy, historical aspects, book 3−34994
astronomy data book 3−34995
astronomy teaching organization and conference, review 3−28430
axisymmetric, incompressible velocity turbulence, appl. of Cramer's theorem, astrophysical appl. 3−29840
baryon-antibaryon phase transition at high temp. 3−28114
black hole, relativistic conditions for kinematic magnification of tidal accel. 3−6324
charged particle distribution in random force field, Fokker-Planck and quasilinear approach 3−37891
coherent emission of radiowaves, by relativistic electrons 3−3351
coherent gyromagnetic emission from non relativistic electrons as a radiation mechanism 3−39587
collapsed objects, e.m. structure of magnetized rotating sphere 3−25358
core-halo config., thermal equilib. states of classical hard-sphere gas with gravit. 3−35643
cosmic dust astronomy and space research *(German)* 3−22124
cosmic radio emission prod. by relativistic electron scatt. by plasma turbulence 3−23859
cosmic rays, primary energy spectrum above 10^4 GeV and astrophysical implications 3−28097
cosmic-rays in random magnetic field, breakdown of quasilinear derivation of kinetic equation 3−31480
cylindrical sources, radial distrib. of emitters calc. using computer program 3−36209
educational material in astronomy and astrophysics 3−37576
e.m. radiation effects on motion of astrophysical objects 3−37293
fluctuation-dissipation theorem, mag. field regeneration, kinematic-dynamo activity 3−12928
general relativity related to energy release in stars 3−9453
Generalised Roche Model, self-similar isothermal flow behind spherical shock waves 3−25360
gravitating fluid layer stability with mag. field perpendicular to boundary 3−33357
group theory and dimensional analysis, use in reducing differential equations 3−12942
HI regions, excited atom population, low energy cross sections 3−3378

astronomy and astrophysics continued
- high energy, current status of gamma-ray astronomy 3−3397
- high energy astrophysics, conference (Pasadena USA, 23-25 October 1972) 3−[illegible]
- isentropic plasma flow near rotating magnetised spheres, appl. to planets 3−23935
- Kiev University Observatory, solar physics 3−39631
- magnetic fields origin, turbulent dynamo mechanism 3−31503
- magnetic neutral sheet system surrounded by cold, collisionless plasma 3−24071
- magnetic polytropes, hydromag. oscills. and stability determ. using variational method 3−31498
- mathematical astronomy for amateurs, book 3−31493
- MHD phenomena in rot. fluids, NATO Advanced Study Institute meeting 3−26839
- new horizons, introductory book 3−35000
- new observatory at Chapel Hill, North Carolina 3−9633
- new physics, based on new astronomical observations, methodological problems (Russian) 3−22209
- nonlinear and inverse Compton effects rel. to astrophysics and Crab pulsar 3−23099
- nuclear statistical equilibrium, composition changes in adiabatically cooling gas 3−28111
- observational online computer aids 3−5622
- old neutron stars, nuclear gamma rays and redshifted positron annihilation radiation 3−28169
- orbiting bodies, matter ejection and gravitational radiation 3−25362
- origin of microwave background, origin rel. to ordinary astronomical processes 3−28123
- photon absorpt. at super-high energies in Universe *(Russian)* 3−37280
- plasma expts., phys. parameters and general props. 3−3042
- plasma phenomena, models for radiation emitters, review 3−3286
- plasma turbulence and collisionless shocks, appls. 3−1501
- polytrope with toroidal mag. field, non-radial oscill. and convective instability 3−37285
- polytropes, weakly distorted under external press., stability against radial perturbations 3−28106
- polytropic differentially rotating fluids, appl. of post-Newtonian eqns to determ. equilib. config. 3−28104
- project options in an astronomy course 3−37573
- quantum theory of dielectric constant of magnetized plasma, astrophysical appl. 3−12933
- quasiradical pulsation of rotating relativistic polytropes *(Russian)* 3−16091
- r-processes, delayed-neutron emission at final stage, application of gross theory 3−25365
- radiative losses in magnetostatic and e.m. field, appl. to pulsars 3−31497
- relativistic astrophysical objects, external gravitational field *(Polish)* 3−25363
- relativistic astrophysics, hydrodynamical equations and relativistic shock waves *(Polish)* 3−25364
- relativistic corotating magnetosphere model for magnetized object 3−31499
- relativistic shocks in fluid, anal. of Taub adiabat, astrophysical appl. 3−29920
- relativistic theory of elasticity, appl. to neutron star vibrs. 3−599
- self gravitating non-rotating gas layer with stellar, mag. and cosmic ray components, linear stability anal. 3−28101
- short time constant phenomena, lower limit to e.m. energy pulse duration 3−37284
- solar neutrinos, observations and theoretical predictions 3−35027
- space physics and space astronomy, book 3−16090
- specific luminosity, note on terminology for use in astrophysics 3−31666
- spectroscopy of laboratory plasmas rel. to astrophysics, review 3−18917
- superheavy elements rela. to astrophysical beta decay formulas 3−32818
- thermal arc plasmas as radiation sources for light intensity calibration in astrophysics 3−4681
- thermonuclear reaction rates, weak screening theory for nondegenerate plasmas 3−25357
- transition radiation from relativistic electrons rel. to source of cosmic X-rays 3−31500
- ultralow temperature techniques, application 3−35383
- uv and X-ray spectroscopy of astrophysical and laboratory plasmas, symposium (Utrecht, August 1971) 3−18916
- viscous accretion flow, uniqueness of solution curves 3−29834
- weak interactions, implications of second-order effects in V-A theory 3−31668
- X-ogen 89190 GHz, CCH radical 3−3278
- C-O plasma crystallization rel. to white dwarf star interiors 3−31494
- CNO Ne cycle, β-decay rates rel. to nucleosynthesis 3−28108
- Fe(p,X)^{26}Al excitation function, cross section determ. for ^{26}Al formation in Fe and Si by proton bombard. 3−23915
- Mg$^+$, Ca$^+$ oscillator strengths and ground state photoionisation cross sections 3−11146
- ^{205}Pb as chronometer for s-process nucleosynthesis, cosmochronology 3−37567

asynchronous motors *see induction motors*

atmosphere *see* ***solar atmosphere; terrestrial atmosphere; upper atmosphere***

atmosphere (terrestrial) *see* ***terrestrial atmosphere***

atmospheric acoustics
- acoustic Doppler radar scattering equation, in turbulent atmosphere 3−9272
- ionosphere F-region, infrasound generated by severe thunderstorms 3−16024
- line-of-sight signals, spectra of short term fluctuations 3−37552
- noise in urban areas, multipath propagation 3−3659
- noise propagatin, effect of ground 3−3660
- noise propagation 3−3025
- noise propagation over open terrain from source near ground 3−3026
- ray tracing, computer program 3−3027
- shock wave distortion, by layers with weak thermal fluctuations 3−25241
- sounding, refraction by wind and temp. inhomogeneities 3−9273

atmospheric acoustics continued
- sounding of meteorological phenomena in planetary boundary layer 3−37256
- three-dimensional ray tracing, using Hamiltons equations 3−31365
- thunder from cloud-ground flashes 3−12744
- u.s. fading, in simulated rainfall, by air bubbles in water tank 3−16343

atmospheric composition
- *see also atmospheric structure*
- adiabatic and isobaric mixing with humid air *(French)* 3−31379
- aerosol composition above Atlantic Ocean, sea-salt particles *(German)* 3−25243
- aerosol content, as function of relative humidity, lidar obs. 3−3017
- aerosol microstructure in atm. surface layer, statistical characts. *(Russian)* 3−28016
- aerosol variability, humidity and condensation effects *(Russian)* 3−28015
- aerosols, chemical comp. of tropospheric aerosol *(Russian)* 3−39525
- air like gas mixtures, nature of negative ions 3−28040
- air pollutant averaging times, statistical model 3−39506
- Antarctic stratosphere, submicron particulate water meas. 3−12774
- atmospheric ions, mobility spectrum rel. to pollution 3−28041
- auroral heating of neutral atmosphere by particles rel. to thermospheric composition 3−34917
- Central London, air quality monitoring and O_3 levels 3−21953
- condensation nuclei and small ion conc. over sea near land 3−28039
- D and E-region, negative ion composition 3−3102
- D- and E-region ion-neutral reactions 3−3104
- D-region, dependence of positive ion composition on O and H concentration 3−3097
- D-region, negative ion chemistry 3−3101
- D-region, negative ion conc. 3−3103
- electron precipitation, 2.14 MHz absorption in winter 3−18862
- exosphere, H abundance, diurnal variation rel. to exospheric temperature 3−34923
- extensive dust layer in northern hemisphere due to a volcanic eruption 3−9289
- ferromagnetic particles, conc. and size distrib. meas. technique 3−37260
- ferromagnetic particles, size depend. rel. to ice crystal formation 3−37227
- fission and spallation products variation, correlation with vertical austausch variation 3−15981
- Greenland tropospheric aerosol measurements 3−34894
- Hawaiian marine atmosphere, chemical fractionation of alkali and alkaline Earth metals 3−12748
- high-energy charged particles rel. to v.l.f. radiation, Interkosmos 3 meas. 3−31444
- high-volume air sampling system using cellulose filters 3−39818
- India, turbidity meas. 3−37231
- ion density and composition rel. to time varying model aurora 3−34916
- ion-hydrates in ionosphere, reaction mechanisms and bonding energies 3−3066
- ionic ratio var. between reference seawater and marine aerosols 3−12683
- ions, symmetrical aspiration capacitor for simultaneous recording 3−28086
- kinetic cooling time constant, water vapour conc. depend., interferometric obs. 3−39503
- laser-Raman radar detection, using sampling technique 3−3190
- lateral and vertical atmospheric dispersion coefficients, continuous functions 3−5493
- lidar observations of tropospheric aerosols, comments and critique 3−5495
- liquid H_2O content in cumuli *(Russian)* 3−12717
- low energy γ-rays near geomag. equator 3−5509
- low-energy radiation belt protons observed by Molniya 1 satellite, July-August 1970 period 3−31443
- magnetosphere proton density determ. from Pc 3 type geomag. pulsations *(French)* 3−39552
- marine aerosols, experimental sea salt profiles 3−12685
- marine air, Hawaii, Aitken and giant nuclei conc. 3−28026
- mesosphere and lower thermosphere, seasonal effects on minor neutral component distrib. 3−3046
- mesosphere and lower thermosphere neutral composition meas. using r.f. quadrupole spectrometer 3−3045
- mesospheric ozone meas. by u.v. obs. of stellar occultation by Earth's atm. 3−25261
- metal-ion concentrations in marine atmospheric aerosol samples in Hawaii 3−12680
- methane, mixing ratio 3−12736
- moisture profile, optimal conditions for indirect probing *(Russian)* 3−3184
- monitors, stable ozone source, calibration 3−3186
- neutral composition in thermosphere, Ogo 6 satellite measurements 3−12784
- neutral species, latitudinal variation calc. using transport coeffs. 3−3030
- neutron flux in energy range $50<E<350$ MeV 3−5525
- NO_2 concentration, stratosphere, i.r. absorption measurements 3−5507
- oceanic aerosols, chemical comp. for determ. of wind transport 3−12753
- particle size distribution, restoration using scattering phase function *(Russian)* 3−16798
- particle-sulphate in background air, amplification method of determination 3−37249
- particulate material, neutron activation analysis with computer resolution of gamma ray spectra 3−18871
- photochemistry of minor constituents in troposphere 3−34901
- pollutants, laser Raman scatt. obs. using Fabry-Perot periodic filter 3−3192
- pollution analysis by laser-Raman radar 3−3189
- polynuclear aromatic hydrocarbons in Teheran atmosphere 3−15957
- precipitation, pH rel. to chemical comp. 3−37226
- radiation comp. below radiation belt region at middle latitudes 3−25254

atmospheric composition continued

- rain, Delhi, 1964-67 period, chemical anal. for NO_3^-, NH_4^+ and SO_4^{2-} ions 3−37228
- rapid gas chromatography, application 3−28398
- remote sensing, using laser and i.r. heterodyne radiometer 3−3193
- Saharan dust, vertical and areal distribution over western equatorial North Atlantic ocean 3−12751
- salt particles in bubbles, oceanic air 3−12692
- sampling, use of differential flow controllers 3−37746
- San Francisco Bay Area, trace element concentrations in aerosols 3−25214
- slow neutrons in lower layers of atmosphere, aircraft-borne meas. 3−34888
- specific gaseous constituents, remote mapping, tunable laser techniques 3−3191
- stratosphere, cosmic radiation as odd N source 3−15976
- stratospheric 'sulphate layer', scattering of sunlight by fine particles 3−3021
- stratospheric aerosol, bistatic optical probing, conc., layer struct. optical thickness 3−25205
- stratospheric Aitken nuclei counts, measurement errors due to a 'volatile' fraction 3−15971
- stratospheric sub-mm. far i.r. emission spectrum, Concorde 002 measurements 3−25248
- surface aerosols rel. to atmospheric elec. parameters, Poona, India 3−28042
- Sydney, visibility, humidity and smoke meas. in 1930-1935, 1951-1956, and 1963-1970 periods 3−39508
- thermosphere, two-component diffusion model of diurnal variations 3−31395
- thoron meas., ioniz. current calibration *(Japanese)* 3−3011
- trace element origin, air, rain and dry deposition sampling 3−18866
- trace metals abundance, Hawaiian marine atm. 3−12754
- tropospheric aerosol particle removal time by precipitation scavenging 3−28050
- tropospheric H_2O abundances, microwave meas. 3−15964
- upper, ozone temporary decrease at sunrise *(French)* 3−31393
- urban atmospheric pollution, zoning by condensation nuclei concentrations 3−5494
- u.v. spectrograph study from Apollo-16 3−3300
- water vapour dimers in upper troposphere, rotation spectral lines in microwave region *(Russian)* 3−28017
- B, seawater as source 3−12688
- Br, gaseous and particulate, marine atm. 3−12755
- CCl_3F concentrations and atmospheric turbidity in rural S. England and S. Ireland 3−15955
- CO, isotopic composition 3−2973
- CO, mixing ratio 3−12736
- CO production in rain water from aldehydes photodecomposition by sunlight 3−21948
- CO_2, large-scale flux in Southern Hemisphere troposphere 3−34900
- CO_2, mixing ratio 3−12736
- CO_2 profiles, control and readout system 3−18899
- H I distributions rel. to spatial and temporal var. of Lyman-α airglow 3−31399
- HNO_3 vapour distrib. in stratosphere, determ. by i.r. emission meas. 3−25233
- $H_3O^+.(H_2N)_n$ recombination with electrons in D-region 3−3107
- He budge, ion pumping by solar wind during geomagnetic field reversals 3−12757
- I enrichment of atm. sea salt particles prod. by bubbles in sea 3−12693
- I_2 gas and particles in marine atmosphere at Oahu, Hawaii 3−12750
- N_2, discharge activated, nature and decay of long-lived species 3−33414
- N_2^+ auroral emission parameters and electron excitation 3−9307
- N_2^{++} vibrational excitation in upper atmosphere, processes of formation and disappearance 3−34909
- NH identification, absorption spectra 3−9294
- NO, 75-80 km altitude global satellite obs. 3−3029
- NO, mesospheric concentration during polar cap absorption event 3−3085
- NO, vertical distribution in 60-170 km altitude region 3−3044
- NO in lower E-region, from electron density and X-ray flux obs. 3−3086
- NO_2, laser induced fluorescence obs. 3−3018
- N_2O production from the reaction of $O(^1D)$ with N_2 3−15999
- Na abundance in upper atmosphere effects on seasonal variation 3−21958
- Na_2SO_4 atmospheric summer and winter fallout near kraft mill 3−15956
- O auroral emission parameters and electron excitation 3−9307
- O measurements by rocket-borne mass spectrometers 3−16063
- O profiles in lower thermosphere 3−3050
- O^+_2/NO^+ in E-region, photochemical activity 3−3098
- O_2, photodissociation rates by solar radiation in 1025-2500 Å range in mesosphere and lower thermosphere 3−3047
- O_2 in lower thermosphere, stellar u.v. occultation meas. from OAO-2 satellite 3−31400
- O_2 in thermosphere, abundance changes from twilight 6300 A airglow 3−9308
- O_2^+ as source of ionisation in D-region 3−16026
- O_3, mesospheric, meas. from 1.27 μband 3−3049
- O_3 aqueous solution, oxidation of atmospheric gases 3−9292
- O_3 concentration under thunderclouds 3−12738
- O_3 fluxes over snow surfaces 3−12734
- O_3 photochemical neutral reactions below 100 km 3−3033
- $O(^1D)$ in upper atm. *(Russian)* 3−3078
- OH, mesosphere, vertical profile, electronic transition obs. 3−3048
- OH airglow structures, i.r. photography of night sky 3−34915
- OH contribution in emission line meas. in night airglow filter photometry 3−9311
- $O(2^1D_2)$ collisional quenching by atmospheric gases, time-resolved atomic absorption spectroscopy 3−18867
- ^{222}Rn, ^{220}Rn, at McMurdo and South Pole Stations 3−12773
- ^{222}Rn, CO, methane, continental dust meas. in air over Norwegian and Greenland seas 3−9288
- S over Sweden during 1969 to 1970 3−12737

atmospheric density *see atmospheric pressure and density*

atmospheric disturbances *see atmospheric movements; thunderstorms*

atmospheric duct *see atmospheric electromagnetic wave propagation*

atmospheric dynamics *see atmospheric movements*

atmospheric electricity

see also atmospheric electromagnetic wave propagation; atmospheric ionisation; atmospherics; aurora; electrojets; ionosphere; lightning; thunderstorms

- air ion, image interaction with conductive fluid droplet *(Russian)* 3−34893
- auroral ionosphere, electron intensity rel. to Ba cloud, rocket flight obs. 3−12785
- auroral particle acceleration, electric double layers 3−3041
- auroral zone, electric fields meas. 3−12812
- charge and relaxation time distribution, effects of convection 3−31376
- cloud droplets and drizzle drops over Mauna Loa-Mauna Kea saddle road of Hawaii, USA, electric charge 3−12726
- clouds, electrostatic field within structure of uniformly spaced coaxial conducting loops 3−31382
- DP1 and DP2 current systems, oscillations rel. to ionospheric conductivity 3−34939
- dust cloud electrification on dispersion into air 3−18735
- dust storms, potential gradient meas. 3−15966
- dust storms electrification, visual observation of electric sparks from New Mexico gypsum dunes 3−3015
- eddy diffusion coeff. over open ocean, meas. by atmospheric elec. meas. 3−28025
- electric field rel. to magnetospheric storms and charged-particle distrib. 3−25304
- electric fields, global variations 3−28034
- electrification of thunderstorms and formation of precipitation 3−37220
- electrojet, kinetic theory of electron density fluctuations 3−15996
- electrojet irregularities, parametric coupling for production and stabilisation 3−15997
- electron deposition in water vapour, atmospheric applications 3−12746
- electron precipitation, longitudinal extension during magnetospheric substorms 3−15983
- electron precipitation event accompanying sudden impulse in geomagnetic field, X-ray and radio observations 3−16019
- electrostatic field horizontal component in lower atmosphere, daily drift meas. *(German)* 3−37233
- enhanced particle precipitation in auroral zone morning sector, pitch angle distrib. of energetic electrons and protons *(German)* 3−16012
- equatorial current sheet in magnetosphere 3−12841
- equatorial electrojet, magnetic field fluctuations 3−16001
- equatorial electrojet, origin of small-scale type II irregularities 3−16004
- equatorial electrojet rel. to polar magnetic variations on moderately disturbed days 3−15930
- field in lower atm., field mill for tethered balloons 3−9403
- field measurements by balloons 3−12756
- fundamental problem, review 3−28033
- India, elec. cond., potential gradient 3−28038
- Indian Ocean, Feb-March, (1963) 3−31380
- ionospheric currents induced by solar wind interaction with planetary atmospheres 3−31421
- ions, effects on living systems, obs. *(Spanish)* 3−5625
- land stations, electric potential gradient and conductivity power and cross power spectra 3−15972
- longitudinal currents, polar magnetic substorms *(Russian)* 3−3120
- magnetospheric electric fields, INJUN 5 obs. 3−3146
- magnetospheric field fluctuations and penetration of solar protons to low geomag. latitude 3−5527
- magnetospheric plasma convection, at geosynchronous orbit altitudes 3−3147
- magnetotail current system, pressure and magnetic field considerations 3−12827
- magnetotelluric model rel. to micropulsation field obs. 3−2927
- nuclear explosion effects, electrostatic field meas. 3−15965
- point-discharge current density rel. to worldwide thunderstorm activity 3−31377
- Polar regions, meas. 3−28037
- polar-cap electric field distributions, rel. to interplanetary magnetic field direction 3−12829
- potential gradient, positive and negative, radiosonde meas. technique 3−28085
- potential gradient variation during aurora 3−28057
- precipitating electrons, magnetic local time dependence, spectral index 3−12818
- radiation belts, electric field induced by slowly decaying ring current 3−12828
- ring current, self-consistent model rel. to dipole field and magnetopause 3−25300
- ring current and geomagnetic storms rel. to Pc 1 micropulsations 3−18838
- seasonal variations of air-earth current density, columnar resistance, ionospheric potential 3−28035
- shadowing of electron azimuthal-drift motions near noon magnetopause 3−3124
- surface aerosols rel. to atmospheric elec. parameters, Poona, India 3−28042
- thundercloud electrification, polarization charging effects 3−5506
- thunderstorm clouds, differential charge transport 3−12739
- tornado initiation, geo-electromagnetic aspects 3−31381
- tornadoes, Venice lagoon, Sept. 1970, electrical theory *(Italian)* 3−34876
- v.l.f. hiss, analysis of multistation obs. 3−21959
- v.l.f. region, sudden changes in integrated intensity of atmospherics 3−21949
- O_2^+ as source of ionisation in D-region 3−16026

atmospheric electromagnetic wave propagation

see also atmospheric light propagation; ionospheric electromagnetic wave propagation; tropospheric electromagnetic wave propagation

- absorption, 4 to 6 millimetre wavelength band 3−12724
- absorption of mm-waves, spectral measurements 3−15952
- auroral v.h.f. signal scattering, region configuration *(Russian)* 3−3035

atmospheric electromagnetic wave propagation continued
conditions affecting models of atmospheric noise resulting from lightning discharges 3−12769
D-region sluggishness, comparisons of direct and indirect solar X-ray emissions 3−16023
dipole antennas over stratified anisotropic media, e.m. fields determ. 3−34885
directional analysis of e.m. variations, comments *(Russian)* 3−12646
diurnal var. of surface refractivity over India 3−12723
Earth-to-satellite links, rain attenuation, path diversity 3−28044
e.l.f. signal generation rel. to geomagnetic disturbance and solar protons 3−21976
gases, atmospheric, e.m. props. meas. by pressure-scanning microwave spectrometer 3−37236
internal acoustic-gravity waves, geometrical acoustics approximation 3−15963
line-of-sight signals, spectra of short term fluctuations 3−37552
magnetoacoustic channel under dome of plasmasphere *(Russian)* 3−3121
magnetospheric v.l.f. phenomena rel. to wave-particle interactions 3−3153
microwave atmospheric temperatures, variation with meteorological conditions 3−37238
radar sounding in clear sky conditions in UHF *(Russian)* 3−39518
radiowaves, attenuation and phase rotation due to rain, at 19.3 and 34.8 GHz 3−28045
rainfall-induced blackouts of mm.-wave Earth-satellite communications systems, reduction by space diversity 3−37217
sea evaporation duct effect on microwave propag. *(German)* 3−9405
turbulent microstructure from microwave propagation experiments *(German)* 3−34886
Venus atmosphere model for radiowave attenuation and S/N, wavelength dependence 3−35077
v.l.f. modal interference patterns observed on transequatorial paths 3−18881
v.l.f. radio emissions from magnetospheric regions during 25-27 May 1967 magnetic storm 3−21975
v.l.f. region, sudden changes in integrated intensity of atmospherics 3−21949

atmospheric energetics *see atmospheric movements*

atmospheric humidity
see also hygrometers
aerosol content, as function of relative humidity, lidar obs. 3−3017
aerosol particle growth rel. to relative air humidity *(Russian)* 3−39525
aerosol variability, effect on spectra depend. of scatt. coeff. *(Russian)* 3−28015
charged particle collision and coagulation efficiencies determ. *(Russian)* 3−39527
climatological relationships among precipitable water, saturation thickness and precipitation 3−37214
condensation nuclei with continuous flux, meas. counter *(French)* 3−12858
dew point temps., relation to cloudiness over tropics 3−2979
lower troposphere, satellite obs. 3−3002
moisture content, indirect vertical profile determ. *(Russian)* 3−39524
planetary air-sea boundary layer, numerical simulations 3−2936
relative humidity, analogue circuit calculation from dew pont and temp. 3−37258
sea-air interaction, model of long-term heat and moisture exchange processes *(Russian)* 3−39495
Singapore region, convective development dependence 3−34897
spectral dependence of extinction coefficient rel. to relative humidity *(German)* 3−9283
surface absolute humidity rel. to total precipitable water in vertical column 3−37213
Sydney, meas. during 1930-1935, 1951-1956, and 1963-1970 periods 3−39508
Si, humidity role in atmospheric oxidation *(Russian)* 3−8036

atmospheric ionisation
see also atmospheric radioactivity; ionosphere
air like gas mixtures, nature of negative ions 3−28040
atmospheric ions, mobility spectrum rel. to pollution 3−28041
collision and coagulation efficiencies in moist atm. *(Russian)* 3−39527
D-region, charges in ion chemistry during solar flares 3−3109
D-region, continuous monitoring of celestial X-ray sources 3−3360
D-region, contribution of hard solar X-radiation 3−21967
D-region ionization charges and electron densities from partial reflection differential absorption experiment 3−5521
E-layer diurnal variation in ionization from F_0E data 3−21970
E-region, atm. wave-induced instability 3−9333
E-region radiowave focusing by irregularlities 3−9330
electron scattering by stable atmospheric species, distrib. of secondary electron energies 3−29738
energetic electron precipitation as source of night-time D-region ionization 3−31431
expansion of charged particles from atmosphere, theory of electric field polarisation under gravity 3−29935
Gaussian sporadic E-layers as model ionization density, gradient instability 3−25283
ion and electron kinetics in disturbed ionosphere at 100 to 200 km. height 3−28059
ion chemistry study, mass spectrometer use 3−444
ionosphere irregularity structure, two beam obs., at Arecibo 3−28064
ions, symmetrical aspiration capacitor for simultaneous recording 3−28086
mesosphere, charged particle concentration and mobility measurements 3−3031
mesosphere, supersonic and subsonic meas. 3−3032
night sky, ionizing radiations, rocket study 3−3051
nighttime D-region, ionization contribution 3−3091
non-equilibrium, collisional and radiative, blunt body stagnation region, relaxation phenomena *(Italian)* 3−20350
sporadic-E layer, nighttime, ionization movement 3−9334

atmospheric ionisation continued
thermal plasma, spatial and temporal var. between 3000 to 5700 km. height 3−12557
tidal theory of ionospheric intermediate layer rel. to dynamics and ionization 3−21966
v.l.f. region, sudden changes in integrated intensity of atmospherics 3−21949
N_2/O_2 mixtures, electron bombardment in simulated disturbed ionosphere 3−3067
OI dayglow emission line obs. 3−16021

atmospheric light propagation
astronomical refraction near horizon, seasonal variation 3−39512
day sky light polarisation angle altitude depend., meas. in O 1.27 micron emission band *(Russian)* 3−39519
laser beam propagation in absorbing atm. 3−21947
laser beam reduction in surface layer due to temperature changes in wavelength *(Russian)* 3−28053
partially coherent light beam propagation theory in turbulent atmosphere *(Russian)* 3−689
photocount statistics in turbulent medium *(Russian)* 3−39515
photocounting detection of radiation passed through turbulent atmosphere 3−37945
scattering matrix rel. to 4-type weather classification *(Russian)* 3−39520
turbid medium, dispersion and centre of gravity determ. from refl. and transmission meas. *(Russian)* 3−37206
turbulence, optical investigation, exposure time choice 3−16053
turbulent, photon counting statistics of superposition of coherent and chaotic light of arbitrary spectrum 3−688
visibility reduction due to aerosols, simulation 3−37235

atmospheric motion *see atmospheric movements*

atmospheric movements
see also wind
5-day pressure waves, amplitude depend. on latitude 3−31368
advection, finite element approach 3−28024
advective accelerations, coupling between boundary layer and free atmosphere 3−31370
advective accelerations in low latitude planetary boundary layer, numerical anal. 3−31369
airflow over mountains, lee waves theory rel. to arbitrary profile height *(Russian)* 3−34892
anomalous circulation over N. Hemisphere used for forecasting seasonal rainfall and temp. for England and Wales 3−28029
atmospheric shear layer stability, effect of planetary vorticity and vertical entropy gradients 3−12708
austausch variation, fission and spallation products variation cause 3−15981
balloons, response to wind shear layers 3−12732
baroclinic wave flow patterns, direct temp. meas. 3−25234
barotropic atmosphere, large scale disturbances determ. using method of rays *(Russian)* 3−39528
bulk transfer coefficients over water 3−28007
buoyancy-induced flows, instability transition and turbulence, review 3−33217
cable equilibrium when connected to free floating body placed in fluid stream 3−5498
CAT, detection by lidar 3−25206
circulation anal. reference dates, zonal winds rel. to solar activity 3−28046
circulation changes in January in 20th century 3−9282
cloud photographs, motion computation 3−3172
cloud tracking, digital picture processing 3−3198
convection effects on relaxation time and charge distribution 3−31376
convective storms, updraft shape determ. using horizontal momentum changes 3−28022
displacement layer width and roughness parameter determ. for forest meas. *(Russian)* 3−21943
disturbances during 1951-1970, stability 3−9295
dust devil formation, stability of vortex sheet flow 3−28013
dynamics, rel. to lower ionosphere obs. and theories 3−3063
E-region, atm. wave-induced instability 3−9333
Earth-atmosphere-ocean system, intransitive model 3−9281
eddy correlation meas., instrument requirements 3−9400
Ekman turbulent boundary layer 3−28002
energy and water balances over land, inclusion of snowfall term 3−12761
equations of motion, numerical approxs. 3−3024
equatorial planetary wave propag., stratospheric penetration and effects of wind on diurnal tides 3−31367
explosion in atmosphere, self similar solns. stability 3−34902
feedbacks turbulent cellular convection *(Russian)* 3−12718
fog dissipation by jet aircraft wakes 3−25216
free atmosphere, energy transfer through the turbulence spectrum 3−34884
frictional forces over N.Atlantic and Europe during 1962 Hamburg stormy weather situation *(German)* 3−25242
geostrophic model, meridional form of baroclinic waves 3−12764
global circulation, rel. to monsoons and tropospheric convection 3−21951
gravity wave generation during solar eclipses, supersonic motion of Moon's shadow and Earth's terminator 3−25249
gravity waves, internal, ducting on stable layer with shear 3−12727
Gulf of Genoa, cyclogenesis, numerical expts. 3−18855
heavy convective clouds, spectral structure of the turbulence 3−34883
Helmholtz-Rayleigh instabilities in barotropic atmospheric non-divergent horizontal stream *(German)* 3−12707
hydrothermodynamic eqns. discretisation using integro-interpolative method *(Russian)* 3−28014
inertia tensor determ. and rel. to variations in earth's rotation *(Russian)* 3−39523
inertial waves in low latitudes, theory *(Russian)* 3−3006
internal gravity waves, integrated ionospheric response 3−31415
internal wave propagation in rotating stratified fluid with random stability freq. 3−33275
large-scale turbulence, Eulerian-Lagrangian time scale transformation 3−25238
laser Doppler velocimeter analysis, comments 3−9392
laser Doppler velocimeter analysis, reply to comments 3−12857

atmospheric movements continued
lee wave meas. using radiosonde data 3–37230
low pressure areas, waves, satellite pictures 3–5501
lower layer, low-frequency limit of the inertial interval in boundary layer 3–34882
mesosphere and lower thermosphere, minor neutral constituents, photochemistry and transport 3–3043
meteorological dynamics, introductory book 3–9302
model of general atmospheric circulation rel. to removal of Arctic ice-cap 3–15980
natural atmospheric ions, mobility spectra and meas. methods *(German)* 3–15984
northeast India, mountain waves 3–2990
perturbations, appl. of space-time tensor calculus, stability criteria determ. *(French)* 3–28032
planetary boundary layer unstable, circulations in transverse and longit. planes 3–25220
planetary boundary layers, universal functions in resistance law 3–18854
planetary wave long-range forecasting, hydrodynamic model using meteorological information 3–37222
planetary waves, vertical propag. in stratified atm. 3–28020
plasmasphere, model development of supersonic trough wind with shocks 3–5526
pollution, buoyant plumes, vehicular and aircraft wakes 3–33325
propagation tracks of atmospheric impulses *(German)* 3–12705
Singapore region, convective development rel. to humidity, wind and positive energy available 3–34897
snow transport in low level drifting snow 3–31364
solar semidiurnal tide in dissipative atmosphere, equivalent gravity mode approx. 3–34890
sporadic-E layer, ionization movement due to wind shear mechanism 3–9334
stationary zonal circulation in equatorial atmosphere, numerical simulation *(Russian)* 3–34891
stratospheric-ionospheric interaction during movement of deep planetary wave 3–3034
striations onset in barium clouds in ionosphere 3–9318
surface layer turbulence, spatial correlation functions of vel. components and temp. *(Russian)* 3–39516
system heated from below, stability 3–18865
thermal wave propag. inducing mean flow, perturbation method soln. 3–29891
thermally radiating stratified shear layer, stability anal. 3–36094
tidal meas. at 50 km from constant altitude balloon 3–12760
tidal theory of ionospheric intermediate layer rel. to dynamics and ionization 3–21966
tide, effects of Ampere force 3–5503
tropical wave disturbances, applic. of satellite data on cloud brightness 3–25236
tropics, large scale flow patterns, Indian southwest monsoon, mean cloudiness meas. 3–2980
tropics, large scale flow patterns, satellite determined cloudiness 3–2981
turbulence, effect on laser beam propagation, scintillations 3–21946
turbulence, long wave radiative transfer effects on wind and temp. determ. from model *(Russian)* 3–21941
turbulence, optical heterodyning processing with u.s. light modulators 3–3195
turbulence, optical investigation, exposure time choice 3–16053
turbulence, stability of finite amplitudes internal waves in shear flow 3–26781
turbulence, superboom development, laboratory simulation 3–37207
turbulent boundary layer above nonhomogeneous surface 3–31361
turbulent characts. of boundary layers with thermal stratification *(French)* 3–20333
turbulent diffusion, book 3–29858
turbulent diffusion eqn. with finite rel. for 3-dimens. case *(Russian)* 3–21925
two dimensional turbulence, numerical simulation, stability and predictability 3–5499
upper air circulation, 6-day brightness patterns, 1967 southwest monsoon 3–2982
upper tropospheric outflow, severe cyclonic storms, satellite pictures 3–2985
vertical laser paths, scintillation and transmitter aperture averaging 3–37208
wind vel. spectra in meteor region *(Russian)* 3–3037
CO_2, large-scale flux in Southern Hemisphere troposphere 3–34900

atmospheric noise *see atmospherics*

atmospheric optics
see also airglow; atmospheric light propagation; sky brightness; sunlight; twilight
aeosol light scatt. props. rel. to Mie scatt. theory 3–13696
aerosol optical thickness at high transparency *(Russian)* 3–39529
aerosol particles, extinction coeff. to mass ratio, humidity depend. 3–17493
aerosol scattering, analytical representation of polydispersion coeffs. *(Russian)* 3–12719
aerosols, refractive index model *(Russian)* 3–39525
air pollution measurement, Mie scattering techniques using lasers 3–3188
air pollution monitoring by dye laser meas. of differential absorpt. of elastic backscatt. 3–37248
albedo increase due to air pollution 3–31366
anomalous atmospheric optical phenomena associated with Tunguska meteorite fall *(Russian)* 3–35106
astronomical refraction, introduction to practical computation 3–28304
astronomical seeing, photometric weather at Toronto 3–9274
astronomical seeing conditions rel. to polar star trail classification *(Italian)* 3–35211
atmospheric aerosol meas. from optical radar total scatt.-backscatt. ratio 3–9263
atmospheric aerosols, optical absorpt. 3–37197
average spectral statistical dependences of the aerosol attenuation coeff. in the region 0.59-10 μm *(Russian)* 3–9267
Chapman's grazing incidence integral, numerical evaluation for a nonexponential model 3–15962

atmospheric optics continued
cloud spectral brightness, probability distribution in 2-5 micron range *(Russian)* 3–39522
clouds, plane-stratified, optical sounding, statistical estimation of light pulse deform. *(Russian)* 3–29041
distance meas. by optical modulation 3–6518
gravity centre shift. of focused light beam in turbulent atmosphere *(Russian)* 3–29047
haze spectral attenuation, characteristics in visible and i.r. *(Russian)* 3–15961
heating of turbulent atmosphere by light beam, intensity fluctuations *(Russian)* 3–3019
intensity interferometry, in spatial domain, for stellar observation 3–31807
i.r. spectral transmittance meas., instruments and techniques *(Russian)* 3–21981
irradiance fluctuations, plane waves 3–31373
ISP-28 spectrograph photometric attachment for atmospheric optics meas. *(Russian)* 3–39563
Lake Ontario surface albedo, dependence on solar zenith angle 3–2845
Las Vegas, hourly turbidity meas. during Fall months 3–39507
laser beam, long high path, deflection and spread 3–21933
laser beam propagation, effect of finite transmitter apertures on scintillations 3–21946
laser beam scintillation meas., at high altitudes 3–31374
laser beam transmission, beam spreading 3–18852
laser beams, angular divergence and refraction *(Russian)* 3–3020
laser communications in lower atmosphere, noise problem 3–19656
light scattering matrix and aureol part of phase function, complex measurements *(Russian)* 3–15960
linear polarization by mist haze, aerosol attenuation in i.r., distinction from haze *(Russian)* 3–3008
meteor flares, shock wave interactions 3–16192
Mie scatt. props. of aerosols., size distribs., Los Angeles Basin 3–2967
multiple scatt. by atmospheric aerosol, polarisation, Monte Carlo calcs. 3–6421
multiple scatt. by homogeneous cloud layers, polarization, Monte Carlo calcs. 3–6420
multiple scattering of laser pulses transmitted through clouds 3–22844
night time seeing, large telescope resolving power determ. using polar star trails 3–28302
nightglow, nonthermalized spectral features, Michelson interferometer obs. 3–16058
normal incidence radiation trends on Mauna Loa, atmospheric transmission 3–12763
optical thickness meas. from Kosmos 149 at 0.72 and 0.74 microns *(Russian)* 3–39562
origin of bad seeing conditions at Royal Observatory, Cape Town, S. Africa 3–15978
partially coherent light beam propagation theory in turbulent atmosphere *(Russian)* 3–689
polarisation of radiation emerging from spherical shell atmospheres, backward Monte Carlo calcs. 3–685
propagation through clouds, low angle approx. *(Russian)* 3–3009
pulsed lidar reflectance from clouds, comments 3–25207
pulsed lidar reflectance from clouds, discrepancy between meas. and calcs. 3–21934
radar reflectivity and refractive index spectra in clear air convection 3–9401
rainbows, glories, explanation using scalar field approach, limitations 3–18856
Rayleigh scatt. in planetary atmospheres, matrix operator theory 3–25204
refraction, theory 3–5496
scattering of sunlight by fine particles in stratospheric 'sulphate layer' 3–3021
scattering phase function for restoration of particle size distribution by statistical regularization *(Russian)* 3–16798
seeing discs, model computations, i.r. appl. 3–39505
single-scattering approximation, influence of Lidar geometrical parameters *(Russian)* 3–12720
sky radiation, multiple scatt., verification of approx. method 3–2968
solar radiation attenuation through lowest 100 m. of urban atmosphere rel. to pollution 3–15973
spectral dependence of extinction coefficient rel. to relative humidity *(German)* 3–9283
spectrometer for remote sensing, correlation mask techniques, signal modification 3–5944
spectrum of aerosol at 0.7 microns from meas. of clear sky during daytime *(Russian)* 3–39521
stellar extinction due to aerosol light scatt., blue moon phenomena 3–18850
stellar image motions, distribution law 3–39514
stellar monochromatic extinction determ. from BV photometric obs. 3–34877
stratospheric aerosol, bistatic optical probing, conc., layer struct. optical thickness 3–25205
turbulence degraded light, far field diffraction by circular apertures 3–5513
turbulent media, light beam spectra, outer scale effects 3–6424
two-laser optical distance-measuring instrument with atmospheric refractive index correction 3–16917
upper troposphere, stellar light scintillation, multilayer structure of air turbulence 3–31375
vertical laser paths, scintillation and transmitter aperture averaging 3–37208
CO laser, radiation absorpt. by water vapour 3–19627
He-Ne, propagation through atmosphere, beam spread 3–10576
MgI emission in night sky spectra 3–9290
OH bands, 6861 and 7273 Å, nightglow, intensity obs. 3–12721

atmospheric pollution *see air pollution*

atmospheric precipitation
see also ice; rain; snow
aerosol cations, Na concs. in Hawaiian atmosphere 3–12752
Bergen, statistical prediction of 12-hour amount from radiosonde obs. in UK using regression analysis 3–34878

atmospheric precipitation continued
- chemical composition meas. using station network, ion concentrations 3−28048
- climatological relationships among precipitable water, saturation thickness and precipitation 3−37214
- cloud droplets and drizzle drops over Mauna Loa-Mauna Kea saddle road of Hawaii, USA, electric charge 3−12726
- cloud modelling, press. perturbation effect., cumulus cell life cycle rel. to precipitation 3−25224
- cloud seeding, downwind and upwind effects, Arizona, USA 3−39531
- congelation of large drops in contact with AgI particles *(French)* 3−12768
- droplet growth kinetics by condensation with adiabatic expansion of air *(Russian)* 3−14507
- energy and water balances over land, inclusion of snowfall term 3−12761
- fission and spallation products variation, correlation with vertical austausch variation 3−15981
- formation, electrification of thunderstorms 3−37220
- full velocity determ. of spatial crystals and aggregates 3−28021
- geochemistry of ocean water bubble spray rel. to salts in precipitation 3−12681
- hail suppression, Project Climatite 3−12767
- ice cryst. terminal vel. meas. at varying altitude 3−25230
- ice crystals (rimed), fall patterns and velocities rel. to crystal dimensions 3−25229
- India, active monsoon, satellite radiation data 3−3000
- mean annual precipitation rel. to var. in mean annual sediment yield 3−39474
- meso-to-subsynoptic scale rainfall pattern rel. to cloud brightness data 3−28047
- pH, rel. to chemical comp. 3−37226
- rainbows, glories, explanation using scalar field approach, limitations 3−18856
- sea-air interface ion fractionation, tropospheric background and continental aerosols 3−12691
- Southern Norway, distrib. of monthly precipitation in reln. to H. Johansen weather types 3−34879
- temporal and spatial structure of heavy precipitation in Alpine regions *(German)* 3−25244
- total precipitable water in vertical column rel. to surface absolute humidity 3−37213
- tropospheric aerosol particle removal time by precipitation scavenging 3−28050
- water, zenith attenuation coefficients 3−12724
- western disturbances, winter season, cloud systems 3−2994
- NH_3 effects on electrification of freezing and splashing water drops 3−27106

atmospheric pressure *see atmospheric pressure and density*

atmospheric pressure and density
- aerohydrochannel, air pressure var. above wavy water surface *(Russian)* 3−15936
- air density near 200 km from Cosmos 268, 1969-20B orbital data 3−9310
- baroclinicity effects on wind structure rel. to stationary planetary boundary layer *(German)* 3−12710
- barotropic atmosphere, large scale disturbances determ. using method of rays *(Russian)* 3−39528
- circulation changes in January in 20th century 3−9282
- cloud model, perturbation effects rel. to temp. and saturation v.p. 3−25224
- density variations between 200 and 400 km from Aug. 1969 to May 1970, exospheric temp. meas. 3−25260
- England and Wales, mean-sea-level press. for 1950-69 period 3−34896
- height variation rel. to zonal wind components, 60-130 km 3−9297
- inertia tensor determ. and rel. to variations in earth's rotation *(Russian)* 3−39523
- linear statistical forecast, influence of sampling connectedness on accuracy *(Russian)* 3−12715
- long-period pressure-field variations in N.Hemisphere rel. to solar activity cycles 3−25218
- monthly data used for forecasting seasonal rainfall and temp. for England and Wales 3−28029
- oceanic western boundary currents, baroclinic and bottom topography effects on transport 3−34865
- planetary-scale fluctuations in pressure in E-layer rel. to f-min and stratosphere 3−21969
- predictive error distrib. of pressure gradients rel. to S_1 forecast score 3−37218
- pressure var. above mesopause, effect on seasonal anomalies in lower ionosphere radio wave absorption 3−12775
- radio ranging of satellites, correction for troposphere and stratosphere 3−34905
- stratospheric pressure meas. rel. to planetary-scale fluctuations in pressure in E-layer and f-min 3−21969
- surface, diurnal variation 3−5508
- symmetric baroclinic instability, verification by direct temp. meas. 3−25234
- upper atmosphere prediction for duration of flight of artificial earth satellies 3−31363
- vertical variations in temp. and press., simplified thermodynamic model *(Portuguese)* 3−28011

atmospheric propagation *see atmospheric electromagnetic wave propagation*

atmospheric radiation
- *see also aurora*
- air pollution, atmospheric ^{85}Kr, dosimetry studies 3−5683
- ARWG recommendations and evaluations rel. to future scientific programmes 3−27998
- auroral luminosity var. pulsations and X-rays, cross-correlation analysis 3−31398
- auroral-zone X-rays, balloon observations in conjugate regions 3−25257
- charged particle background, 200-300 km, space flight obs. *(Russian)* 3−12776
- clear and overcast, spectral radiance in S20-range, luminance 3−18851

atmospheric radiation continued
- clear sky and minimal smoke and dust content, prediction equation 3−12771
- cloud layers in atmosphere, radiation properties rel. to temp. distribution *(Russian)* 3−18859
- cloud parameters determ. by Kosmos 384 meas. in i.r. *(Russian)* 3−39517
- composition below radiation belt region at middle latitudes 3−25254
- day sky light polarisation angle altitude depend., meas. in O 1.27 micron emission band *(Russian)* 3−39519
- Earth-atmosphere system, radiation balance, satellite meas. 3−2999
- Earth-atmosphere system, radiation balance from satellite meas. *(German)* 3−37232
- Egypt, solar intensity in short wave spectral region *(French)* 3−12766
- e.l.f. signal generation rel. to geomagnetic disturbance and solar protons 3−21976
- excess radiation at small heights rel. to solar cycle var. 3−25353
- excess radiation in equatorial region between 200 and 350 km. 3−34910
- fog, conductive-radiative model of growth and formation 3−28004
- gamma-rays hard, balloon-borne acoustic spark chamber investigation *(Russian)* 3−12713
- h.f. radio noise, Radio Astronomy Explorer I observations 3−31288
- high-energy charged particles rel. to v.l.f. radiation, Interkosmos 3 meas. 3−31444
- India, active monsoon, satellite radiation data 3−3000
- lightning flashes, photoelectric observations of emitted light 3−25239
- low energy γ-rays near geomag. equator 3−5509
- Nimbus II measurements, comparative study 3−3001
- nonstationary diffusion in a semiinfinite isotropically scattering medium *(Russian)* 3−12716
- stratospheric O_2 emission at 53 GHz, temp. determ. 3−37219
- surface layer and soil, radiative exchange 3−28006
- temperature profiles from i.r. measurements during 750 radiosonde ascents *(Russian)* 3−18898
- tropospheric dust heating effects, dust storms 3−25247
- urban area, Tokyo Univ. Obs. *(Japanese)* 3−12700
- v.l.f. radio emissions from magnetospheric regions during 25-27 May 1967 magnetic storm 3−21975
- water vapour line contours in rotational spectrum of upper troposphere *(Russian)* 3−28017
- X-ray substorms, high resolution energy meas. and temporal variations 3−3155

atmospheric radioactivity
- *see also fallout*
- automatic radioactive inventory system 3−28775
- Bucharest, daily variation 3−5510
- fission and spallation products variation, correlation with vertical austausch variation 3−15981
- natural background rel. to nuclear power plant radiation 3−5504
- Prague, obs. at Bulovka 1971 3−15977
- small radioactive particles examination, reversal autoradiography 3−16060
- spallation products, cosmic radiation, atmospheric aerosols, applications to the study of tracers and pollutants *(German)* 3−12862
- terrestrial environment, behaviour, identification *(French)* 3−32792
- thoron meas., ioniz. current calibration *(Japanese)* 3−3011
- ^{210}Bi/^{210}Pb ratios and application to aerosol residence time determination 3−15975
- ^{137}Cs fallout as tracer in obs. of lake sediments 3−34898
- ^{210}Po/^{210}Pb ratios and application to aerosol residence time determination 3−15975
- Rn daughters, uncombined, in U mines 3−9398
- Rn daughters meas. using α disintegration data 3−9266
- ^{220}Rn emanation from soil deduced from atmospheric vertical profile meas. 3−15974
- ^{222}Rn, meas. of air content over Norwegian and Greenland seas 3−9288
- ^{222}Rn daughter small ions, mobility distribution in laboratory air 3−15967
- ^{222}Rn short-lived daughter ions' behaviour in atmospheric processes 3−15968

atmospheric spectra
- *see also atmospheric optics*
- 6-14 μm spectrum model 3−3022
- absorption bands rel. to dust particle shape and orientation *(Russian)* 3−18860
- absorption of mm-waves, spectral measurements 3−15952
- aerosol optical thickness at high transparency *(Russian)* 3−39529
- aerosol spectrum at 0.7 microns from meas. of clear sky during daytime *(Russian)* 3−39521
- air pollution, laser measurement *(German)* 3−34895
- auroral emission parameters and electron excitation 3−9307
- auroral u.v. intensity height profiles and rocket spectrograph sensitivity rel. to magnetospheric acceleration mechanisms 3−31447
- auroral X-rays, balloon obs. at Syowa Station, Antarctica *(Japanese)* 3−31402
- auroral-zone X-rays, balloon observations in conjugate regions 3−25257
- average spectral statistical dependences of the aerosol attenuation coeff. in the region 0.59-10 μm *(Russian)* 3−9267
- cloud spectral brightness, probability distribution in 2-5 micron range *(Russian)* 3−39522
- clouds, noctilucent, spectrophotometric meas. of near i.r. spectra 3−28010
- day sky light polarisation in 1.25-2.42 μ region, clear sky obs. *(Russian)* 3−21944
- e.u.v emissions from aurora, rocket-borne photometer meas. 3−12783
- F-region tropical u.v. airglow intensity, theoretical calculations 3−12804
- far i.r. background radiation meas. at balloon altitude 3−37221
- far i.r. emission, obs. of periodic signal 3−12762
- far i.r. spectra of stratosphere, high resolution aircraft measurements 3−21955
- ionospheric oblique and oblique-backscatter sounding, characts. of signal level fluctuations 3−25269

- **atmospheric spectra** continued
  - ionospheric scintillation obs. of Cygnus A, power-law wavenumber spectrum 3-12803
  - i.r. transmittance meas., instruments and techniques *(Russian)* 3-21981
  - magnetosphere, electron precipitation spectra, pitch angles in outer zone 3-3138
  - mass spectrometer ion source filament lifetimes in the présence of O_2 for rocket-borne mass spectrometers 3-25929
  - minor gases spectra, bibliography details 3-31359
  - model using computer weather forecasting data for Canada 3-37202
  - natural atmospheric ions, mobility spectra and meas. methods *(German)* 3-15984
  - spectral dependence of extinction coefficient rel. to relative humidity *(German)* 3-9283
  - stratospheric sub-mm. far i.r. emission spectrum, Concorde 002 measurements 3-25248
  - telluric Fraunhofer lines, differential shift, possible depend. on zenith distance of sun 3-28147
  - total photoabsorption cross sections at 584 Å for several atmospheric gases 3-12745
  - visible radiance of atm. over ocean water 3-3236
  - water vapour, transmission near i.r. spectra, effect of dimerisation 3-31378
  - water vapour absorption spectrum in vicinity of He I 10830 Angstroms triplet 3-31387
  - water vapour line contours in rotational spectrum of upper troposphere *(Russian)* 3-28017
  - BaO, $A^1\Sigma$-$X^1\Sigma$ band system, electronic transition moment, fluorescent scattering of sunlight at 106 km 3-17424
  - CO, u.v. photoionization, absolute cross sections 3-11282
  - CO_2, microwave discharge, CO_2^- form 3-20670
  - H I Lyman-α airglow, spatial and temporal var. rel. to H I distributions 3-31399
  - HNO_3 vapour distrib. in stratosphere determ. 3-25233
  - H_2O vapour and vapour dimers, radiowave absorption in 1.15-1.5 mm. band *(Russian)* 3-3003
  - H_2O vapour monomers and dimers, radiowave absorption in 0.71-0.76 mm band *(Russian)* 3-3004
  - H_2O-vapour 6.3 μ absorpt. band, determ. of atm. moisture content *(Russian)* 3-39524
  - N_2, u.v. photoionisation, absolute cross sections 3-11282
  - N_2^+ Meinel auroral spectra in 1.5μ region, Jan. 1972 3-25252
  - $N_2(A^3\Sigma_u^+)$ to $O(^1S)$ energy transfer in pulsating aurora, comments 3-34925
  - NH identification, absorption spectra 3-9294
  - N_2O, u.v. photoionization, absolute cross sections 3-11282
  - O 1.27 μ emission band meas. for determ. of altitude depend. of brightness index and day sky light polarisation angle *(Russian)* 3-39519
  - O 6300 Å emission, nighttime intensity variations during quiet geomag. conditions 3-34912
  - O III 304 Angstoms emission in e.u.v. airglow 3-16003
  - O_2, u.v. photoionization, absolute cross sections 3-11282
  - O_2 in thermosphere, changes in abundance from twilight 6300 A airglow 3-9308
  - O_4^- photodetachment cross section meas. at high pressure rel. to upper atmosphere 3-16002
  - OH, i.r. airglow, diurnal variation, balloon borne spectroscopic obs. 3-31392
  - OH contribution in emission line meas. in night airglow filter photometry 3-9311
  - OH rotational and vibrational excitation in laboratory and night airglow 3-31396
  - OI 5577 and 6300 Å emissions rel. to upper atmosphere temps. and auroral electron fluxes 3-34919
  - OI 6300 Angstroms emission above polar cap, rel. to precipitated low energy electrons 3-25258
  - $O(2^1D_2)$ collisional quenching by atmospheric gases, time-resolved atomic absorption spectroscopy 3-18867
- **atmospheric structure**
  - *see also atmospheric composition*
  - adiabatic and isobaric mixing with humid air *(French)* 3-31379
  - adjustment of atmospheric statistics to satisfy physical conditions 3-37211
  - aerosols, optical props. and chemical comp. *(Russian)* 3-39525
  - air mass seasonal redistrib., effect on earth's rotation *(Russian)* 3-39523
  - atomic Na layer, density decrease near the mesopause 3-18872
  - cloud drops and aerosols, particle size distrib. formula *(Russian)* 3-21942
  - displacement layer width and roughness parameter determ. for forest meas. *(Russian)* 3-21943
  - India, turbidity meas. 3-37231
  - of lower layer above sea 3-34881
  - lower thermosphere thermal structure and O and O_2 transport 3-31397
  - natural boundary layer lower portion, wind tunnel simulation 3-37201
  - observation techniques up to 150 km 3-16056
  - radar sounding in clear sky conditions, atm. fine structure determ. *(Russian)* 3-39518
  - Saharan dust layer, vertical and areal distribution over western equatorial North Atlantic ocean 3-12751
  - surface layer, statistical characts. of aerosol microstructure *(Russian)* 3-28016
  - troposphere, determination using spaced radio refractometers 3-12863
  - turbulent microstructure from microwave propagation experiments *(German)* 3-34886
  - variable parameters, large-scale and long-term fluctuations 3-5491
  - vertical variations in temp. and press., simplified thermodynamic model *(Portuguese)* 3-28011
- **atmospheric temperature**
  - *see also atmospheric thermodynamics*
  - acoustic soundings in refractive atmosphere 3-9273
  - atm. surface layer model, radiative heat transfer effects on profiles *(Russian)* 3-21941
  - buoyant thermal, strongly heated, temperature field structure 3-9296
- **atmospheric temperature** continued
  - Central Alaska during winter, surface inversion 3-12765
  - credible interval temperature forecasts 3-28000
  - D-region radiowave absorption rel. to temp. during IQSY 3-9331
  - dew point temps., relation to cloudiness over tropics 3-2979
  - dispersion of pollutants, effect of horizontal impervious layer caused by temp. inversion 3-25210
  - dust devils, frequency and diameter rel. to atmospheric temperature 3-25237
  - dust storms, ground level meas. 3-15966
  - exosphere, temp. rel. to diurnal var. of H abundance 3-34923
  - exospheric temp. meas. for density variations determ. between 200 and 400 km. during Aug. 1969 to May 1970 period 3-25260
  - heat-island above very small urban units 3-9285
  - height variation rel. to zonal wind components, 60-130 km 3-9297
  - ionospheric electron temp. meas., comparison of modulation Langmuir probe and incoherent scatter radar techniques 3-25272
  - ionospheric radiowave absorption rel. to stratospheric temperature, Winter anomaly 3-3071
  - lower layer inversion over Karlsruhe *(German)* 3-5505
  - lower thermosphere thermal structure and O and O_2 transport 3-31397
  - mean temp. estimation from incomplete data 3-28052
  - measurement, RIM-901 on Cosmos 320 *(Russian)* 3-3183
  - mesosphere at middle latitudes, rel. to intensity of corpuscular radiation *(Russian)* 3-3036
  - microwave, variation with meteorological conditions 3-37238
  - northeast India, mountain waves 3-2990
  - planetary wave formation by temp. disturbance at base of stratified atm. 3-28020
  - profile vertical resolution, Backus-Gilbert theory applied to remote radiation meas. 3-25221
  - profiles from i.r. measurements during 750 radiosonde ascents *(Russian)* 3-18898
  - quantitative temp. data from direct-readout i.r. pictures from satellites 3-37257
  - quaternary hypsithermals rel. to $^{18}O/^{16}O$ ratio of deep-sea cores, 3-39542
  - radiation properties between cloud layers in atmosphere rel. to temp. distributions *(Russian)* 3-18859
  - relative humidity, analogue circuit calculation from dew point and temp. 3-37258
  - satellite radiometric techniques for temp. structure determ. 3-25332
  - stochastic model of temperature variations at weather stations in Britain 3-18849
  - stratosphere mesosphere interaction in winter rel. to temperature changes 3-25235
  - stratospheric O_2 emission at 53 GHz, temp. determ. 3-37219
  - surface, diurnal variation 3-5508
  - surface layer turbulence, spatial correlation functions of vel. components and temp. *(Russian)* 3-39516
  - surface temp., cloudiness effects on climate 3-28019
  - thermospheric kinetic temp. time lag behind heat source max. 3-25256
  - troposphere, microwave radiometric meas. 3-15964
  - tropospheric-stratospheric compensation in high southern latitudes *(German)* 3-12709
  - upper air anal. using variational method, thermal wind relationship 3-37223
  - upper atmosphere at 90 km altitude, diurnal and seasonal variations 3-12781
  - upper atmosphere polar region, empirical models and exospheric temperature 3-31401
  - upper atmosphere temperatures and auroral electron fluxes from OI 5577 and 6300 Å emissions 3-34919
  - variations effects on concrete temp. distribution 3-2758
  - vertical distrib., Nimbus III SIRS meas. 3-2998
  - N_2, enhanced vibrational temps. in thermosphere 3-5515
  - N_2 vibrational temp. in F-region, determination from O^+ reaction rate constant 3-3100
- **atmospheric thermodynamics**
  - *see also atmospheric temperature*
  - air pollution effects on thermal regime, radiative transfer eqn. soln. 3-31366
  - atmospheric boundary layer energy exchange from kinetic loss considerations *(German)* 3-12706
  - boundary layer, urbanization and industrialization thermal effects 3-28008
  - buoyant thermals, radiative cooling by longwave radiation 3-25222
  - Central Alaska during winter, surface inversion 3-12765
  - cloudiness as climatic feedback mechanism, effects on radiation balance and surface temp. 3-28019
  - cooling near mesopause, airglow effects on de-excitation of molecules 3-34889
  - countergradient vertical heat flux, planetary boundary layer meas. and theoretical expression 3-15969
  - Earth-atmosphere system, radiation balance from satellite meas. *(German)* 3-37232
  - electron gas heat flux at heights > 180 km, cooling and heating sources 3-25270
  - evaporation from high latitude upland sites 3-9277
  - heat-island above very small urban units 3-9285
  - kinetic cooling time constant, water vapour conc. depend., interferometric obs. 3-39503
  - lower layer above sea, structural features, turbulent heat transfer, wind speed 3-34881
  - morning convective layer in bright sky, thickening mode *(French)* 3-25217
  - ocean-atmosphere system of mid-latitude N. Pacific, servomechanism 3-9240
  - radiative heat transfer effects on atmospheric surface layer model *(Russian)* 3-21941
  - radiative transfer eqn., implications of quadratic stream definition 3-31372
  - sea-air interaction, model of long-term heat and moisture exchange processes *(Russian)* 3-39495
  - surface inversion formation rel. to extreme urban air pollution 3-37215
  - temp. profile vertical resolution, Backus-Gilbert theory applied to remote radiation meas. 3-25221

atmospheric thermodynamics continued
thermospheric diurnal heat budget rel. to O_2 photo-dissociation 3−34918
thermospheric kinetic temp. time lag behind heat source max. 3−25256
zonal mean radiative heating rates meas. from surface to 10 mb., seasonal profiles 3−25223
zonally averaged state, simulation of annual variation 3−2974
atmospheric turbulence *see atmospheric movements*
atmospheric wind *see wind*
atmospherics
see also atmospheric electromagnetic wave propagation; dawn chorus; whistlers
astronomical scintillation spectra characts. depend. on meteorological conditions 3−39513
auroral VLF-LF hiss during polar substorms 3−39547
h.f. signal, statistical anal. of records of field amplitude *(Russian)* 3−2975
laser communications in lower atmosphere, noise problem 3−19656
location, waveform recorder and cathode ray direction finder, synchronised operation 3−21950
noise from lightning discharges, models based on thunderstorms distribution and propagation conditions 3−12769
plasmasphere, v.l.f. and e.l.f. noise 3−5522
radio noise level variation with sunspot number 3−15982
turbulent air flow, refractive index meas. by laser correlation technique 3−37259
v.l.f., diurnal and seasonal variation, Roburent, Northern Italy 3−28043
v.l.f., location of thunderstorms 3−31386
v.l.f., measurement and interpretation *(German)* 3−18868
v.l.f. hiss, analysis of multistation obs. 3−21959
v.l.f. noise spectrum, model of global thunderstorm activity *(Russian)* 3−2976
v.l.f. noise spectrum characts. during cosmic excitation of Earth-ionosphere resonator 3−34931
v.l.f. region, sudden changes in integrated intensity of atmospherics 3−21949
atomic beams
see also particle velocity analysis
alkali ion-inert gas potentials, mol. beam determ. 3−17383
alkaline earth metal atoms collisions with ICl, crossed beams product angular distributions 3−27864
alkaline earth metal beams collision with Cl_2 and Br_2 beams, chemical reactions 3−21803
cavity resonator, frequency shift due to Ramsey-type interrogation 3−10107
complexes, long-lived, formed in crossed beams of K, Rb, Cs, $SnCl_4$ and SF_6 3−17476
detection, using residual gas analyzer 3−28711
hollow cathode source for matrix isolation studies 3−29531
metal atom + O_2 crossed beams, assoc., reactive and electron transfer ioniz. 3−29746
scattering by pyrolytic graphite, scatt. energy, phase shifts 3−5251
Ag^- photodetachment by Ar-ion-laser beam, electron affinities 3−29502
Ar, radiative lifetime meas. for neutral atoms and ions by beam foil spectroscopy at low initial ion energies 3−17348
Ar, scattering from rough Pt surface 3−27595
Ar clusters, struct. obs. using a supersonic beam method 3−14799
C^{6+} beam collision with Ar at 1 to 2 MeV/amu, charge dependence of K-shell ionisation 3−20067
Cs, reson. multiphoton ionisation by Nd-glass laser 3−23489
Cu^- photodetachmnet by Ar-ion-laser beam, electron affinities 3−29502
F^{6+} passed through foil, yield of excited autoionized metastable states 3−20033
F^{9+} beam collision with Ar at 1 to 2 MeV/amu, charge dependence of K-shell ionisation 3−20067
^{19}F, one-electron atoms, oriented nuclei obs. 3−23504
H, impact excitation of He 3−26607
H, scatt. by LiF cryst., obs. of surface Debye temp. 3−8010
H beams, charge changing processes in gases and alkali metal vapours, review 3−35983
He, low temperature nozzle beam source 3−20070
He + He collisions, total cross section, energy depend., 0.30 to 3.00 keV 3−29536
^{3}He, hyperfine structure studies by zero-field quantum beats 3−17357
^{4}He, fine struct. intervals meas. by level crossing *(French)* 3−38216
Hg, scattering of light atomic projectiles, differential scatt. cross sections, ang. distribs. 3−29529
K supersonic, collisions with Ar, N_2, methane, fluoromethane, difluoromethane, carbon tetrafluoride, differential scattering cross sections meas. *(German)* 3−26737
Kr, radiative lifetime meas. for neutral atoms and ions by beam foil spectroscopy at low initial ion energies 3−17348
Li, for plasma heating in closed mag. traps *(Russian)* 3−1510
N^{7+} beam collision with Ar at 1 to 2 MeV/amu, charge dependence of K-shell ionisation 3−20067
Na, radiative lifetime meas. of $3p^2P^0$ level by beam foil spectroscopy 3−17348
Ne, radiative lifetime meas. for neutral atoms and ions by beam foil spectroscopy at low initial ion energies 3−17348
O^{5+} passed through foil, yield of excited autoinized metastable states 3−20033
O^{8+} beam collision with Ar at 1 to 2 MeV/amu, charge dependence of K-shell ionisation 3−20067
S, beam-gas v.u.v. spectrum 3−29478
^{166}Tm, hyperfine struct. and mag. and elec. moments, atomic beam meas. 3−10847
Xe, radiative lifetime meas. for neutral atoms and ions by beam foil spectroscopy at low initial ion energies 3−17348
atomic clocks
see also frequency measurement; time measurement
geodetic satellite timing to accuracy of 0.1 to 1.0 μsec 3−34970
synchronisation via ATS-1 and ATS-3 satellites 3−22238
Ca beam, absolute frequency standard 3−3747
atomic clocks continued
Cs, Rb and H, state-of-the-art report *(French)* 3−25652
H storage beam, frequency standard, low-Q cavity maser 3−3749
Mg beam, absolute frequency standard 3−3747
atomic collision processes
see also atomic electron scattering; atomic forces
activated ion-mol. reactions in strong electric fields, rate calc. 3−11299
alkali ion-atom, wavefunctions and pseudopot. for charge transfer 3−1126
alkali metal collisions with halogen molecules fragmentation of halogen negative ions 3−26715
alkaline earth metal beams collision with Cl_2 and Br_2 beams, chemical reactions 3−21803
anharmonic oscillator, vibrational relaxation, quantum mech. calcs., mol.-inert gas atom collision 3−36051
atom-atom and -ion scatt., theory from separated atom and ion props. 3−29540
atom-atom scatt., low energy, scaling rule derivation 3−29521
atom-diatom collinear reactions, classical mechanics and transition state theory 3−25057
atom-diatom scatt., semiclassical three-dimens. model for vibr. relax. 3−7253
atom-diatomic mol., quantum vibr. transition probabilities, three-dimens. model 3−7254
atom-molecule, collision-induced dissoc., differential energy transfer probabilities 3−26730
broadening and displacement cross sections of atomic lines calc. by the sewing method 3−17379
classical binary encounter approx. approach 3−33054
collinear atom-diatom collisions, distorted wave variational approach 3−26723
collinear atom-Morse oscillator, exact quantum mech. results 3−11331
collision broadening of Zeeman component of hyperfine optical line *(French)* 3−38302
Coulomb excitation by heavy charged particles application of semi-classical model in adiabatic projectile region 3−23492
Coulomb ionisation by heavy, charged particles, simultaneous ejection of K- and L-shell electrons 3−1130
cross sections calc., second Born approx., plane-wave and final-state Green functions 3−20043
diffraction of ^{7}Li ion beam at atoms rel. to scatt. undulations 3−14314
double-electron ejection, internal and external, direct collision amplitudes 3−26584
elastic scatt. from singular pot. *(French)* 3−7070
electron production mechanisms in ion-atom collisions 3−26601
elementary excitation transfer events, involving simultaneous quantum emission and absorpt. 3−32528
exchange matrix element calcs. for differential eqns., computer program 3−35969
excitation of Xe^+ in collisions with metastable Xe and He atoms 3−17380
excitation transfer process in self-broadening, linear transport equation 3−11162
glory scattering data analysis for the extraction of information on the interatomic potential well 3−23505
grazing collision of high-energy charged particles, bounds on mean excitation energies 3−20038
Hanle effect meas. technique for fast ions 3−25765
heavy charged particle induced K-shell ioniz., universal cross sections 3−29537
heavy ion collisions, electronic effects 3−6791
heavy ion-heavy ion scattering, study of electron shells in over-critical external fields 3−6604
heavy particle induced K-shell ioniz. 3−38250
heavy-particle, extraction of elastic scattering matrix element from impact parameter version of Born approx. 3−1118
homonuclear diatom-atom collisions, rotational-vibrational scattering 3−29749
hydrogenic ions and atoms highly excited, charged particle excitation 3−38235
impact parameter theory defined as a constant collision velocity semi-classical limit of a complete quantum scattering picture 3−20068
inelastic, of fast multi-electron atoms, theory *(Russian)* 3−29517
inelastic, quantum-mech. transport eqn. 3−4381
inelastic, threshold behaviour, extension of Wigner's treatment 3−33061
inelastic, two-state model problem, theoretical study 3−29518
inert gas atom pairs, interacting dipole moment 3−29538
inert gas ions and atoms, reson. charge exchange and fine struct. of levels *(Russian)* 3−4393
inert gas scattering of inert gas ions, singularities involving inner shell excitation 3−20064
inert gas-hydrogen cyanide mixtures, rot. transitions study 3−17471
inert gases;, spectrum due to ternary collisions in pure rare gases, simplified model 3−29515
interaction potential, anisotropy, infl. on broadening and displacement of lines *(French)* 3−7089
interaction potentials between alkali metal and inert gas atoms 3−17385
ion scattering, elastic small angle, high energy region 3−33056
ion-atom, inner-shell vacancy production, review 3−35979
ion-atom collisions, vacancy occupation probabilities 3−38245
ion-atom collisions at moderate nuclear velocities, ionization of inner shells 3−1131
ion-polar mol. collision theory, comparison with expt. charge transfer reaction data 3−33152
ions, drifting, asymptotic behaviour of the velocity distribution in strong electric fields 3−11298
ions, negative, electron binding energy determ. from charge exchange cross sections 3−38242
laser, chemical, atom-diatomic mol. reactions suitable for laser action 3−10495
laser spectroscopy study 3−1105
Lyman-α satellite line prod. due to protons 3−29475
metal surfaces, inelastic scattering of neutral atoms 3−36967
metal surfaces, low energy e^+ enhanced emission, time of flight method 3−10088

atomic collision processes continued

- metal total absorpt. cross sections for 450-1000 MeV photons 3-11163
- metal vapours in hot hollow carbon cathodes *(Russian)* 3-11520
- metastable, atom impact on metal surfaces, flux determination by measurement of secondary electron ejection coefficients 3-19324
- metastable atom collision with production of excited atom *(Russian)* 3-7072
- methyl halide-halogen, energy losses of hot atoms 3-7263
- molecular theory, fine struct. transitions 3-29519
- molecule-atom collisions, calc. of anisotropic glories 3-17381
- narrowing and foreign gas broadening of spectral line shapes, calc. using propagator technique of many body theory 3-11161
- parabolic cylinder functions of large order and argument, asymptotic expansions 3-4378
- positive and negative ions, mutual neutralization *(Russian)* 3-11177
- positron autoionization in heavy ion collisions 3-7087
- proton inelastic scatt. at intermediate energies, Eikonal distorted wave theory 3-33050
- proton-atomic H scattering, theoretical study 3-11179
- R-matrix methods, computer programs 3-11171
- rainbow scattering angle approximate formula *(Japanese)* 3-26608
- rare gas atoms and He metastable atoms, Penning ionization spectra, curve crossing mechanisms 3-11154
- rare gas mixtures, absorption coeff. detn. by quantum mech. description of translational motion *(French)* 3-7071
- reactive, simple model for endoergic and exoergic collisions 3-27863
- resonance interaction, multipole relax. and transfer rates in impact approx. 3-26585
- resonance transfer contributions to resonance line broadening in the impact limit 3-17475
- saturated resonance fluorescence, non quenching collisions influence 3-14298
- scattering from crystal surface, determ. of surface structure, study of physical and chemical interactions 3-1862
- scattering from surface of moving spheres 3-36963
- screening effects in pair production at photon energies from threshold to 5 MeV 3-4379
- semiclassical scattering matrix for two-state exponential model 3-37860
- slow, interference effect in energy distrib. of electrons due to two-fold passage of quasistationary term *(Russian)* 3-7073
- slow atom-ion cross sections, oscillatory structure in energy dependence of total cross sections 3-17378
- spectral line broadening, quantum kinetics equation method *(Russian)* 3-7045
- Stark broadening, non-Markovian treatment, cutoff expression *(French)* 3-33018
- stimulated by other atomic collisions *(German)* 3-11167
- stopping power of atomic matter for relativistic ions, mesons, electrons and positrons, Born approx. energy-loss formulas 3-7082
- symmetrical charge transfer cross section, ioniz. pot. depend. 3-20060
- three body problem, collinear, Fadeev approach with numerical results 3-1275
- total elastic scattering cross section data, optimal utilization for determ. of interatomic potentials 3-11168
- two-atom rotator, weak inelastic collisions with atom, time-dependent couple effect *(Dutch)* 3-29744
- two-level system in strong radiation field, coupled eqn. approach 3-1119
- universal function for collisional ionization of atoms by structureless charged particles 3-17365
- X-ray emission following nucl. reactions due to protons and alpha-particles 3-38161
- X-ray prod. by protons, cross sections for $K\alpha$ and $L\ \alpha$ X-rays 3-33046
- X-ray spectra of highly stripped ions in collisions 3-7048
- Al metal, oxide, nitride, He and Ne ion excitation of K X-ray spectra, chemical effects 3-4365
- Al^+, total cross sections for charge transfer and stripping in He and N_2 3-11181
- Ar, (Kr), (Xe)-CsF, integral total cross sections meas., attractive pot. investigation 3-38324
- Ar, fast atoms and ions, impact dissoc. into ions of O_2, CO and NO molecules 3-23621
- Ar, inner-shell ioniz. cross sections by 1.5-5.0 MeV protons 3-33047
- Ar, ioniz. by He metastables, electron energy spectra 3-33053
- Ar, K ion elastic scatt., collision polarizing character *(Russian)* 3-14316
- Ar, metastable, with HCN, dissoc. excitation of CN radical 3-20128
- Ar, metastable beam, scattering from O_2 covered (100) surface of Ge 3-39204
- Ar, proton scatt., total differential cross section 3-33059
- Ar, with Fl ions at 35.7 MeV, dependence of X-ray production cross sections on ionic charge state 3-1129
- Ar collision with beams of C^{6+}, N^{7+}, O^{8+}, F^{9+} at 1 to 2 MeV/amu, charge dependence of K-shell ionisation 3-20067
- Ar dense gas, depolarised light scattering 3-33190
- Ar metastable atom de-excitation cross sections by gases 3-23630
- Ar-Ar interaction, collision diameter and well depth calc. 3-29539
- Ar-HCl rotationally inelastic scattering semi-classical calcs. using computer program implemented algorithm 3-11305
- Ar-I_2 interactions Raman spectra, resonance, laser induced 3-23620
- Ar-methyl chloride system, thermal diffusion, temp. and comp. depend., inelastic collision effects 3-36069
- Ar-N_2 (metastable Ar), product internal state distributions 3-1288
- Ar-N_2 mixtures, pulse radiolysis, energy transfer induced postluminesc. 3-23629
- Ar-N_2 system, rot. relax., temp. depend. 3-11297
- Ar + NO, vibr. relax. mechanism 3-26718
- Ar^+-Ar, 50-200 keV, X-ray production 3-29526
- Ar^+ -Ar, X-ray yield dependence on final charge state 3-29527
- $Ar^{(+)}$ + Ar, ioniz. processes in slow collisions 3-26605
- Ar^+ − Ar violent collisions, extended ion-electron coincidence meas. 3-11184
- B, u.v. spectra, by beam-foil technique 3-29534

atomic collision processes continued

- Ba, line broadening for excited state transitions in rare gases *(German)* 3-4368
- Br_2-inert gas systems, energy transfer collisions, trajectory studies of atomic recombination reactions 3-26732
- C + C atomic collision, 19-240 keV, X-ray spectra from C_2 system 3-26568
- C^+-C collision, K-shell ionisation in keV-MeV range, Fano-Lichten theory 3-26603
- C^{4+} ions in He, Ne, Ar, Kr and Xe gases, charge changing and electron loss cross section 3-11178
- C_{IV}, 0.2 to 2.0 MeV beam energy, spectra between 30 and 500 Å 3-29532
- Ca reson. line, collision broadening and shift using inert gases 3-7090
- Ca^+, electron impact excitation anomaly for 4s→np transition rel. to oscillator strength 3-23494
- Cd, reson. excitation by slow Cd^+ ions *(Russian)* 3-7086
- Cd atoms, excitation transfers between 5^3D_1, 5^3D_2, 5^3D_3 excited levels, cross section detn. *(French)* 3-11143
- Cd^+ collisions with Mg^+, Mg ions, excitation of resonance levels 3-17377
- $Cl + HCl(v=1,2) = ClH + Cl$, vibr. relax., classical Monte Carlo trajectory study 3-23619
- Cr^+, total cross sections for charge transfer and stripping in He and N_2 3-11181
- Cs-Ar atomic collisions, absorption coefficients, long and short-range forces 3-20074
- Cu, X-rays from Ne^+ collision with solid target 3-27585
- μD, μ transfer to gaseous Xe in collisions 3-20077
- $D + F_2 \rightarrow DF + F$, Monte Carlo calc. of reaction rates and energy distributions of products 3-31255
- $D + H_2 = DH + H$, low temp. rate consts. using e.p.r. detection 3-39437
- D_2 vibrational relaxation in ^3He and ^4He mixtures 3-23628
- Er^+ and Er^{2+}, total cross sections for charge transfer and stripping in He and N_2 3-11181
- Eu with spin polarised 4f shell, collisions with rare gas atoms, relaxation processes *(German)* 3-35980
- $F + H^+$, molecular theory, cross sections calc. 3-29520
- $F + H^+$, molecular theory approach 3-29519
- Fe collisions with neutral He in glow discharge, Van der Waal's broadening 3-35981
- H, atoms in 2S, 2P states, dissociation from photon collisions *(German)* 3-33155
- H, fast atoms and ions, impact dissoc. into ions of O_2, CO and NO molecules 3-23621
- H, H^+ collisions with planetary atmosphere constituents, 1-25 keV, cross-sections for Lyman-α emission 3-33151
- μH, μ transfer to gaseous Xe in collisions 3-20077
- H, quenching of 2S state by inert gas collisions 3-11164
- H, zero-field quantum beats of Lyman-α radiation subsequent to beam-foil interaction 3-7062
- H beams, charge changing processes in gases and alkali metal vapours, review 3-35983
- H ionisation impact of $He(1s^2)$ and $Li^+(1s^2)$ 3-20063
- H isotopes collisions with Ar, hyperfine pressure shift meas. 3-35982
- H metastable atoms, collisional quenching by inert gases 3-17382
- H-H^+ collisions, closed-form Glauber cross sections 3-26597
- H-H^+ scattering in coupled state approx., impact parameter formulation 3-11176
- H-He potential determ. from molecular beam expts. 3-11165
- $H + C_2H_4$, press., stoichiometry and third body species effects 3-37118
- $H + ClH(v=1,2) = H + HCl$, vibr. relax., classical Monte Carlo trajectory study 3-23619
- $H + H_2$, exchange reaction probability calc. using quasi-classical trajectory calc. 3-27859
- $H + H_2$ collinear isotopic systems, exchange reactions, quantum mech. studies 3-31262
- $H + H_2$ collinear reaction, semi-classical, exact quantum and quasi-classical transition probabilities 3-31248
- $H + H_2$ three dimensional collisions, complex-valued classical trajectories for reactive tunneling 3-25056
- $H + H_2(v=1,2) = H_2 + H$, vibr. relax., classical Monte Carlo trajectory study 3-23619
- $H + H_2 \rightarrow H_2 + H$ collinear exchange reactions, analytical energy surfaces 3-20205
- $H + I_2 \rightarrow HI + I$, HI vibr. population inversion 3-29074
- H + proton electron-transfer collisions, second-order Born terms 3-4394
- H^+, H_2^+, bombardment of helium, He autoionisation and He^- autodetachment study 3-23490
- H^+ and H^- ion recombination in slow collisions 3-7085
- H^+ charge transfer collisions with H atoms, Faddeev approach 3-35977
- H^+ collision with HeH^+ isotopes, quasibound states theory, comparison with experiment 3-26714
- H^+ scattering in the weakly screened Coulomb field of Au nuclei 3-11182
- H^+-H^- collisions, charge transfer 3-14315
- H^+-Kr charge exchange collisions, spin polarisation 3-35978
- H^+ + Ar, elastic differential scattering expts., investigation of one state molecular system 3-11185
- H^+ + H scatt., hydrogenic expansion convergence 3-1128
- $H^+ + H_2$ inelastic scatt., differential cross sections, rainbow max., semiclassical treatment 3-33153
- H^+ + Kr, elastic differential scattering expts., investigation of one state molecular system 3-11185
- H_2, total inelastic cross section for collisions with fast charged particles 3-11303
- H_2-He, classical s-matrix elements for vibrational excitation in three dimensions 3-7251
- H_2^+ collisions with Ar atoms, dissociation *(German)* 3-38310
- $H_2^+ + He \rightarrow HeH^+ + H$, 1-25 eV, cross beam studies 3-39439
- He, 3^1P excitation transfer cross section, temp. depend. 3-23502
- He, autoionisation and He^- autodetachment following bombardment by H^+, H_2^+, He^+, He atoms 3-23490

atomic collision processes continued
- He, electron emission spectra excited by proton impact, 2s(^{1}S) autoionisation state 3−7067
- He, excitation by fast protons, charge exchange study 3−38244
- He, fast atoms and ions, impact dissoc. into ions of O_2, CO and NO molecules 3−23621
- He, metastable beam, scattering from O_2 covered (100) surface of Ge 3−39204
- He, proton excitation, time-dependent studies of vacuum u.v. emissions 3−29530
- He, proton scatt., total differential cross section 3−33059
- He, X-ray coherent scattering amplitude 3−4377
- He atom scatt. from Ag surface, one-phonon contrib. 3−11791
- He atom scatt. from metal surface, two-phonon terms 3−11792
- He atoms collisions with inert gases and molecular H_2, N_2, and O_2, electron loss 3−11166
- He collisions with CO_2, shock widening and probability of P20(00°1-100) CO_2 transition *(Russian)* 3−29754
- He excitation by H atoms, spectroscopic analysis of radiation emitted during decay of products 3−26607
- He I, beam-foil excitation, zero-field oscillations in 3p $^3P \rightarrow 2s^3S$ transition 3−29533
- He scatt. from surfaces, Debye-Waller theory 3−8002
- He-He_2^+ collisions near threshold, He^+ prod. 3−38248
- He-He^+, 80-1100 keV, cross sections for excitation of 4^1S-, 4^1D- and 3^1P-levels 3−4395
- He-Li^+, mechanism of inelastic transitions in collisions 3−20061
- He-Ne laser, influence of elastic collisions on intensity of natural fluctuations *(Russian)* 3−22888
- He-Ne low energy potential structure in total transfer cross sections 3−26586
- He + He, metastable, ionizing collision, rate coeff. 3−29528
- He + He, total cross section, energy depend., 0.30 to 3.00 keV 3−29536
- He + He scatt., low energy, scaling rule derivation 3−29521
- He + LiF, atom-solid elastic scatt., theoretical study 3−34445
- He + N_2^+, 0.5 to 3 keV, elastic scatt. and vibro-rot. dissoc., classical theory 3−38320
- He^- ions, detachment cross sections in He, H_2 and Ar gases 3−14312
- He^+, low-energy elastic scatt. by Ne, curve crossing 3−20062
- He^+ collision with methane mol. rainbow phenomena meas. in differential elastic cross section 3−29535
- He^+ collisions with Zn, Cd, Se charge transfer into excited states 3−14313
- He^+ near resonant charge transfer collisions with K, Rb and Cs, long-range forces effect 3−35976
- He^+ scattering in the weakly screened Coulomb field of Au nuclei 3−11182
- He^+-Ne inelastic collisions, uniform WKB theory 3−20069
- He^+ + He collisions, direct and exchange excitations, u-g symmetry effect 3−38243
- He^+ + Ne, differential scatt. cross section for Ne excitation 3−33055
- He^+ + Ne, elastic differential scattering expts., investigation of two state molecular system 3−11185
- He^+ + Ne, semiclassical collision theory within Feynman path integral formalism 3−28951
- He^{++}-He low-energy elastic differential scatt., 4 to 75 eV 3−38249
- He^{2+} + H, electron transfer and excitation coupled-state calcs. 3−26602
- He^{2+} + He, electron capture and excitation 3−26604
- $He^{(+)}$ + He, ioniz. processes in slow collisions 3−26605
- $HeH^+ + H \rightarrow H_2^+ + He$, 1-25 eV, cross beam studies 3−39439
- ^{3}He collisions between 0.25 keV and 3 keV, nuclear symmetry effect 3−14317
- ^{4}He collisions between 0.25 keV and 3 keV, nuclear symmetry effect 3−14317
- ^{4}He-^{4}He, repulsive pot. up to 0.14 eV, from inversion of total cross-section meas. 3−38254
- ^{4}He + ^{4}He scatt., Ramsauer-Townsend effect 3−20036
- He($1s^2$), ionisation by H impact 3−20063
- He(2^1S) and He(2^3S) metastable atoms collisions with H atoms, cross sections for chemiionisation 3−38253
- He(2^3S) and He(2^1S) metastable atoms collisions with H and H_2, chemiionisation 3−38252
- Hg + light atomic projectiles, differential scatt. cross sections, ang. distribs. 3−29529
- Hg collisions with buffer gases, collisional depolarisation of resonances radiation 3−33060
- Hg with H_2, D_2, N_2, NO, and CH_4, de-excitation of metastable state, electronic to vibronic energy conversion 3−20057
- Hg-N_2, determ. of cross section for 6^3P_1-6^3P_0 excitation transfer by method of delayed coincidences 3−4380
- Hg^+, hyperfine struct. Zeeman splitting, multi-step exchange collision obs. 3−23482
- K, 4044/7 Å line broadening by impact with Ar and Kr 3−4357
- K collisions with inert gases and molecules, coherence transfer between $^2P_{1/2}$ and $^2P_{3/2}$ states 3−26606
- K supersonic beams collisions with Ar, differential scattering cross sections meas. *(German)* 3−26737
- K-Br_2, quantization of vibrational coordinates in electron jump model 3−4392
- $K + NaCl \rightarrow KCl + Na$, classical trajectory studies of long-lived collision complexes 3−25059
- K^+ in N_2 and CO_3, gases, mobility, diffusion and clustering 3−29827
- k^+-inert gas potentials, molecular beam determination 3−17383
- K^+-K^+, repulsive potential calc. from particle beam scattering data 3−33062
- K^+-Li^+, repulsive potential calc., from particle beam scattering data 3−33062
- Kr, fast atoms and ions, impact dissoc. into ions of O_2, CO and NO molecules 3−23621
- Kr, inner-shell ioniz. cross sections by 1.5-5.0 MeV protons 3−33047
- Kr, with Fl ions at 35.7 MeV, dependence of X-ray production cross sections on ionic charge state 3−1129
- $Kr + CO^+ \rightarrow CO + Kr^+$, 0.04-3 eV 3−20058
- Kr^+-Kr, 50-200 keV, X-ray production 3−29526
- $Kr^+ + CO \rightarrow Kr + CO^+$, 0.04-3 eV 3−20058

atomic collision processes continued
- $Kr^+ + Kr \rightarrow Kr + Kr^+$, 0.04-3 eV 3−20058
- $Kr^{(+)}$ + Kr, ioniz. processes in slow collisions 3−26605
- Li collision reactions with alkali halide mol. beams, beam kinetics 3−25058
- Li-He, (Ne), collision-induced absorpt., model pot. calcs. at 300 and 1000 K 3−38230
- Li-inert gas systems, absolute total scatt. cross sections, pot. parameters 3−1127
- $Li + F_2 \rightarrow LiF + F$, pot. energy surfaces calc. 3−23637
- $Li + H_2 \rightarrow LiH + H$ collinear exchange reactions, analytical energy surfaces 3−20205
- Li^+, on H_2, vibr. quantum transitions, differential cross sections meas. 3−14396
- Li^+ scattering in the weakly screened Coulomb field of Au nuclei 3−11182
- Li^+-Li^+, repulsive potential calc., from particle beam scattering data 3−33062
- Li^+ + He, charge exchange, rot. coupling 3−20059
- $Li^+(1s^2)$, ionisation by H impact 3−20063
- Mg^+, Mg collisions with Cd^+ ions, excitation of resonance levels 3−17377
- N_2 second positive (0, 0) transition, emission cross sections for H, H^+, He and He^+ impact 3−11327
- N^{4+} ions in He, Ne, Ar, Kr and Xe gases, charge changing and electron loss cross section 3−11178
- $N_2(A^3\Sigma_u^+)$ to O(^{1}S) energy transfer in pulsating aurora, comments 3−34925
- NH_3-H^+, first order orientation dependent intermolecular forces 3−4487
- Na, $3^2P_{1/2}$-$3^2P_{3/2}$ states, coherence transfer induced by inert gas collisions 3−38229
- Na, fluoresc. quenching by N_2, energy depend. cross sections 3−33030
- Na/He atom pair, avoided crossings among excited states 3−20037
- Na-He, (Ne), collision-induced absorpt., model pot. calcs. at 300 and 1000 K 3−38230
- Na-Hg(6^3P_1), atomic collisions, induced sensitized fluorescence, excitation transfer to Na 3−26569
- Na^+-inert gas potentials, molecular beam determination 3−17383
- Ne, fast atoms and ions, impact dissoc. into ions of O_2, CO and NO molecules 3−23621
- Ne, low-energy elastic scatt. of He^+, curve crossing 3−20062
- Ne, metastable beam, scattering from O_2 covered (100) surface of Ge 3−39204
- Ne-Ar ionized beam, 60 to 80 MeV, projectile structure effects on K X-ray production 3−11180
- Ne-Ar mixtures, pressure dependence of primary ionisation in Townsend discharge 3−17702
- Ne-methyl chloride system, thermal diffusion, temp. and comp. depend., inelastic collision effects 3−36069
- Ne-O^{7+} 30 MeV, effect of multiple ionisation on fluorescence yields 3−11145
- Ne^+ collisions with Mg charge transfer into excited states 3−14313
- Ne^+-Al, K-shell ionization cross sections 3−23503
- Ne^+-C, K-shell ionization cross sections 3−23503
- Ne^+-Ne, 50-200 keV, X-ray production 3−29526
- $Ne^{(+)}$ + Ne, ioniz. processes in slow collisions 3−26605
- O ^{1}S state quenching by ^{3}P state atoms, rate calc. 3−29516
- O + Ar, ion-atom high-energy collisions, electron loss 3−38247
- O + CH chemi-ionisation, cross section and rate const. calc. 3−14397
- $O + HBr \rightarrow OH + Br$, collinear H transfer probability calcs. 3−21802
- $O^- + D_2 \rightarrow OD^- + D$, prohibited autodetachment 3−23616
- $O^+ + D_2$, below 4 eV, production of excited OD^+ 3−29747
- O^+ + He, low energy collisions, pot. curves and inelastic cross sections 3−35986
- O(^{1}S) quenching by O_2, temp. depend. 3−11139
- O(2^1D_2) collisional quenching by atmospheric gases, time-resolved atomic absorption spectroscopy 3−18867
- P-H_2 (O_2 PCl_3), collisional deactivation rate consts. for P(3^2D_j) and P(3^2P_j) states 3−17359
- Pb, L- and M-shell X-rays, from 0.5 to 14.0 MeV proton beams 3−38228
- Rb II ion, excitation in thermal collisions with metastable He atoms 3−33057
- Rb with H_2, HD, D_2, N_2, CH_4, CD_4, study of excitation transfer between 6^2P fine-structure substates in Rb 3−23477
- ^{87}Rb, $5^2P_{3/2}$ state, broadening of level-crossing signals by collision with Ar 3−29496
- Sr^+ collisions with rare gas atoms, $5^2S_{1/2}$ ground state spin depolarisation 3−38251
- T collisions with H_2, HD and D_2, hard sphere reactions, chattering 3−38321
- Ta ions stripped in He, Ar, Kr, Xe, C, Au with energies 2-15 MeV, equilib. charge-state distributions 3−11183
- Tl, line broadening for excited state transitions in rare gases *(German)* 3−4368
- U ions shipped in He, Ar, Kr, Xe, C, Au with energies 2-15 MeV, equilib. charge-state distributions 3−11183
- Xe, inner-shell ioniz. cross sections by 1.5-5.0 MeV protons 3−33047
- Xe, ioniz. by He and Ne metastables, electron energy spectra 3−33053
- Xe, with Fl ions at 35.7 MeV, dependence of X-ray production cross sections on ionic charge state 3−1129
- $Xe + He \rightarrow Xe^+ + He + e$, metastable atom collision with excited ion production *(Russian)* 3−7072

atomic collisions *see atomic collision processes*

atomic electric moments
- tensor polarizabilities and quadrupole coupling constants 3−29485
- two-level atom interacting with single radiation mode, continued fraction solution in elec. dipole approx. 3−17360
- Ar, excited state, quandrupole moment calc. 3−29487
- $^{163}Dy^+$ and $^{161}Dy^+$, hf.s. of spectrum, quadrupole moments 3−20025
- Kr, excited state, quadrupole moment calc. 3−29487
- Na, nucl. moments determ. using h.f.s. consts. *(Russian)* 3−7056
- Ne, excited state, quadrupole moment calc. 3−29487
- Sm, electric quadrupole hyperfine interaction consts. 3−4359

atomic electric moments continued
- Xe, excited state, quadrupole moment calc. 3-29487

atomic electron correlations
- Be, theoretical oscillator strengths for $1s^2\,2s^2\,{}^1S - 1s^2\,2s2p\,{}^1P^0$, $1s^2\,2s2p\,{}^1P^0 - 1s^2\,2p^2\,{}^1D$ and $1s^2\,2s2p\,{}^1P^0 - 1s^2\,2p^2\,{}^1S$ isoelectronic sequences 3-14285
- configuration $(d+s)^n p$, algebraic matrices, checking parameters 3-20009
- configuration interaction calcs., iterative method for determ. of eigenvalues and eigenvectors 3-23465
- correlation effects on KLL transtions 3-11155
- $d^3.d$ and $d^7.d$ electronic configurations matrices for interaction energies *(Spanish)* 3-38207
- Hund's rule for jj coupling 3-33015
- many electron atoms, orbit-orbit interactions 3-33013
- many-electron systems, correlated wavefunctions and energies, variational calcs. 3-26562
- mixed configurations, effective electrostatic interactions 3-26563
- multiconfiguration wavefunctions, two-by-two rot. method applic. 3-7038
- plasma, truncation technique for real time two-particle Green function 3-26861
- potential function derivation, comparison with Hartree Fock pot. props. 3-11123
- quantum chemistry, review 3-34715
- rare earth metals, $4f^n 6s^2$ config., orbit-orbit interactions *(Russian)* 3-33012
- spin doublets, X-ray spectra, singly and multiply ionised atoms, new analogy 3-35962
- spin orbitals, energy-optimised in accurate electronic calculations 3-11120
- wavefunctions form calc. 3-20008
- Ar, electron-impact, energy and angular correlations 3-26600
- Ar, polarisability and shielding factors effective-field calc. 3-29488
- Ar correlation energy calc. using many body perturbation theory 3-11124
- B^{2+}, ${}^2S$ state, natural orbital config. interaction expansions 3-26561
- Be, correlation energy using many-body perturbation theory calc. 3-20010
- Be ions, distribution function for angular correlation 3-4354
- Be^{1+} ${}^2S$ and Be ${}^3S$ states, natural orbital config. interaction expansions 3-26561
- Be^{2+} Coulomb holes and expectation values, explicitly correlated wavefunctions 3-23464
- C^{3+}, ${}^2S$ state, natural orbital config. interaction expansions 3-26561
- CI, lifetimes of metastable ${}^5S_2{}^0$ states 3-11140
- Cd I, emission spectra, autoionisation resonances and configuration-mixing 3-7044
- Cd ion, two electron transitions, $4d^9 5s^2$ to $4d^{10} 5p$ config. *(Russian)* 3-33014
- H^-, Coulomb holes and expectation values, explicitly correlated wavefunctions 3-23464
- He, accurate correl. energies computation using strong-orthogonal correl. functions 3-7037
- He, Coulomb holes and expectation values, explicitly correlated wavefunctions 3-23464
- He, excited state wavefunctions calc. 3-38205
- He, excited states, Coulomb hole calc. 3-38206
- He, polarisaibility and shielding factors, effective-field calc. 3-29488
- He atoms, zero energy electron scattering, simplified model 3-14309
- He ions, distribution function for angular correlation 3-4354
- Kr, polarisability and shielding factors, effective-field calc. 3-29488
- Li, ${}^2S$ state, natural orbital config. interaction expansions 3-26561
- Li, Fermi-contact h.f.s., MC SCF wavefunctions 3-33010
- Li, ions, ${}^2S$ and ${}^2P$ states, natural anal. 3-29473
- Li^+ Coulomb holes and expectation values, explicitly correlated wavefunctions 3-23464
- MgIV, even configurations, reevaluation of parameters 3-33011
- Ne, polarisability and shielding factors effective-field calc. 3-29488
- OI, lifetimes of metastable ${}^5S_2{}^0$ states 3-11140
- ${}^{129}Xe$, far configuration interactions, importance *(French)* 3-11125
- ${}^{131}Xe$, far configuration interactions, importance *(French)* 3-11125
- Zn I, emission spectra, autoionisation resonances and configuration-mixing 3-7044

atomic electron scattering
- *see also electron ionisation*
- $-f^2/r^4$ potential, Mathieu function solns. to radial Schrodinger eqn. 3-29522
- atmospheric species, cross sections for elastic and inelastic scattering 3-29738
- bremsstrahlung, linear polarisation 3-20052
- coupled eqns. asymptotic solns. for case of some channels closed 3-33049
- cross section calcs., general formulation of computer programs 3-7075
- cross sections calc., second Born approx., plane-wave and final-state Green functions 3-20043
- double ioniz. cross sections, wavefunction 3-20044
- effective pot., limiting form, Born approx. 3-1123
- electron, confined, ang. distrib. of bremsstrahlung 3-20050
- energy deposition in gaseous mixtures due to excitation and ionisation, computer program 3-35970
- exchange integrals, numerical evaluation using anal. basis set 3-26588
- Fredholm determinant and Jost function application, comparison with standard computational methods 3-1120
- Furry Sommerfield Maue wave functions in pair production and bremsstrahlung 3-20051
- HI regions, excited atom population, low energy cross sections 3-3378
- hydrogenic atoms, differential cross section for ionisation by electron impact 3-7078

atomic electron scattering continued
- hydrogenic ions and atoms highly excited, charged particle excitation 3-38235
- inelastic collision of fast charged particles with arbitrary-levelled hydrogen-like atoms 3-20049
- inelastic scatt. at intermediate energies, Eikonal distorted wave theory 3-33050
- inert gas collisions with very slow electrons, pressure shifts of high series spectral lines and scattering cross sections, calc. 3-35975
- ion multiple ionisations and transition probabilities by high energy electron impact 3-20053
- ionization, Born II approx., scatt. amplitude, phase factors 3-26589
- multichannel process, noniterative integral-eqn. approach 3-38239
- neutral atoms in dense discharge, excitation and ionisation by electron impact 3-23497
- non-exchange type integral evolution program using Slater-type orbitals as basis functions 3-23496
- optical sums extraction from generalized oscillator strengths and X-ray incoherent scatt. factor determ. 3-20040
- polarisation correlation in atomic-field bremsstrahlung 3-35974
- positron -He scattering length, variational calc. using approximate target wavefunctions 3-14310
- positron annihilation, screening and shell-ratio effects 3-33052
- positron elastic scattering by He atoms, phase shifts 3-17375
- power series expansion of collision amplitude 3-1121
- quantum chemistry, review 3-34715
- R-matrix methods, computer programs 3-11171
- radiation polarization from atoms excited by electron impact 3-7081
- solar corona polarisation, vel. effect of scatt. electrons 3-35047
- two-level system in strong radiation field, coupled eqn. approach 3-1119
- variation principle approach 3-26587
- X-ray emission cross sections and fluorescence yields for light atoms and molecules by electron impact 3-17468
- Ar, 100 eV, optical model 3-20041
- Ar, 100 eV elastic scatt., optical model 3-26596
- Ar, 1048 and 1067 Å reson. lines, electron impact excitation, 10 to 2000 eV 3-38231
- Ar, electron-impact ionisation, in eikonal and Born approxs. 3-38240
- Ar, impact ioniz., energy and ang. correls. of ejected electrons 3-26600
- Ar electron impact excitation of $3p^5 4s$ I and $3s3p^6$ II states 3-17374
- Ar ionisation meas. behind shocks with microwaves and a pulsed Langmuir probe *(German)* 3-14594
- Ar metastable formation, excitation functions, comment on previous report 3-7080
- Ar solid, Mittleman parametric polarization potential, use for calc. electron-atom scattering cross-sect. *(French)* 3-11136
- Be, photoioniz. cross sections calc. 3-26594
- Ca, 4227 Å reson. line, excitation, threshold to 1400 eV electron energies 3-38238
- Ca, excitation cross sections using Born approx. 3-1122
- Cd, extrema in generalized oscillator strengths of resonance transitions, 255 eV electron kinetic energy 3-7055
- Cd excited atoms in discharge effective slow electron collision cross sections 3-17699
- Cd-Ne afterglow plasma, $Cd(5^3P_1)$ and $Cd(5^1P_1)$ atom density decay due to e-Cd collisions 3-4687
- Ce autoionising states, excitation by electron impact *(Russian)* 3-26599
- Cs, electron impact excitation of autoionizing level 3-35972
- Cs, electron momentum-transfer cross section 3-4386
- Cs electron ionisation by impact, 6s and 5p, cross-section, Born approximation, threshold, Hartree method *(Russian)* 3-26598
- H, close coupled calcs. using noniterative integral eqn. technique 3-4382
- H, close coupled calcs. using noniterative integral eqn. technique 3-4383
- H, collisional excitation function, threshold behaviour 3-20046
- H, differential cross sections, off-shell Coulomb T matrix 3-7079
- H, electron transmission spectroscopy, resons. in total scatt. cross section 3-7083
- H, ioniz., Glauber theory 3-29524
- H, least squares method applic. 3-20042
- H, long-range dipole interactions, threshold law for $n \rightarrow n+1$ transitions 3-7076
- H, microscopic optical-model analysis 3-4388
- H, positron scatt., inelastic S-wave variational calcs. 3-4389
- H, S state elastic scattering resonances in absence of degeneracy 3-7077
- H, S-state expansion convergence at intermediate energies 3-20048
- H, singlet s-wave scattering below first excitation threshold 3-38236
- H atoms, highly excited, effective cross sections of electron collisions *(German)* 3-14307
- H atoms and electrons collisions at intermediate energies, classical cross sections calc. 3-14308
- H calc. in coupled state approx., impact parameter formulation 3-111'6
- H Glauber exchange amplitude, reduction 3-11170
- $H\text{-}e^-$ collisions, closed-form Glauber cross sections 3-26597
- $H\text{-}e^+$ collisions, calc. of S-wave phase shift and positronium formation cross sections using close-coupling method 3-4384
- $H\text{-}e^+$ collisions, Faddeev approach investigation 3-23501
- H^-, double ioniz. cross sections calc. 3-20045
- H^-, electron detachment, Born-Ochkur approx. 3-35973
- He, 2^1P state, electron-impact excitation, differential and integrated cross-sections by distorted-wave approx. 3-23500
- He, autoionization by low energy electron impact, 42-48 eV 3-7065
- He, Compton scatt. of 25 keV electrons 3-38237
- He, Coulomb effects in final state of ionizing collision 3-26595
- He, double ioniz. cross sections calc. 3-20045
- He, elastic electron-neutral atom interaction meas. of ultralow energies 3-29525
- He, elastic scatt., optical pot. model 3-20047
- He, elastic scatt., second order pots. 3-26590
- He, elastic scatt., variational calcs. 3-4387
- He, electron impact double ionisation, classical collision theory appl. 3-38234

atomic electron scattering continued
He, electron impact excitation of forbidden transition in range 300 to 500 eV 3−38233
He, exchange excitation cross sections, calc. using Ochkur approx. 3−11172
He, excitation of (1s, nd)^{1}D and (ns, mp)^{1}P states 3−26591
He, generalized oscillator strengths and excitation cross-sections 3−23495
He, polarization role in intermediate energy range 3−1125
He afterglow, decay of 2^3S_1 state, cross section determ. 3−14620
He atoms, zero energy electron scattering, simplified model 3−14309
He excitation of p-levels *(German)* 3−1124
He excited by electrons, polarisation of the 492.2 nm line at energies near 60 eV 3−17376
He gas, mean energy loss per ion pair and stopping power for electrons 3−26592
He I and II transitions, electron impact excitation rates 3−38241
He metastable formation, excitation functions, comment on previous report 3−7080
He states excited by electron impact, alignment relaxation meas., collisions and cascades influence *(German)* 3−14311
Hg, $6^1S_0 \rightarrow 6^1P_1$,$(7^1S_0)$,$(7^1P_1)$ transitions, generalised oscillator strengths 3−35971
Hg, 6s6p$^1P_1$ state, electron-impact excitation, spin polarisation and differential cross section 3−20054
Hg, impact excited, near-threshold polarization of 6^1S_0-$6^3\mathbf{P}_1$ line 3−7059
Hg, low energy scatt. amplitudes, free-electron-gas exchange approx. validity 3−33051
Hg, optimization of low energy electron scattering for producing beam of spin-polarized electrons 3−11175
K, excitation cross sections using Born approx. 3−1122
Kr excitation of p-levels *(German)* 3−1124
Kr I, meas. of lifetimes of levels excited by short electron pulse using delayed coincidence technique 3−4361
Kr II, meas. of lifetimes of levels excited by short electron pulses using delayed coincidence technique 3−4361
Li, excitation cross sections using Born approx. 3−1122
Li atoms, beyond the ionisation threshold, excitation functions 3−17373
Li$^+$, double ioniz. cross sections calc. 3−20045
Li$^+$, electron impact double ionisation, classical collision theory appl. 3−38234
Li$^+$, singly ionized by electron impact, lifetime and polarization of 2 ^{3}P term 3−29499
Mg, excitation cross sections using Born approx. 3−1122
Mg, photoioniz. cross sections calc. 3−26594
Na, elastic and inelastic scattering, Glauber approximation 3−23498
Na, electron impact excitation of 3p state 3−29523
Na, electron-excitation cross sections by close coupling method 3−20055
Na, excitation cross sections using Born approx. 3−1122
Na atoms, beyond the ionisation threshold, excitation functions 3−17373
Ne, autoionization by low energy electron impact, 42-48 eV, 57-65 eV 3−7065
Ne, electron-impact ionisation, in eikonal and Born approxs. 3−38240
Ne, resonance scatt. rel. to spin polarisation 3−33048
Ne, spin polarization by electron reson. scatt., energy depend. 3−26593
Ne I, Ne II lines, cross-sections for excitation by electron collision in 2700-3700 A region 3−35960
Ne solid, Mittleman parametric polarization potential, use for calc. electron-atom scattering cross-sect. *(French)* 3−11136
O, distorted wave calculation of electron impact excitation 3−20056
O, impact excitation and ioniz., cross sections 3−4390
OI(^{3}P-3s ^{3}S^0) calc. of excitation cross sections in unitarized Born nonexchange, and close-coupling approx. 3−4385
Rb total electron impact ionisation cross section from threshold to 250 eV 3−38232
Sr$^+$-electron spin exchange cross-section 3−1112
Tl, excitation of the 6s electron 3−17372
We excitation of p-levels *(German)* 3−1124
Xe, optical meas. of electron-impact excitation function in threshold region with high energy resolution *(German)* 3−4391
Xe, quasi-classical calc. of the elastic scattering parameters of electrons *(Russian)* 3−7074
Zn, extrema in generalized oscillator strengths of resonance transitions, 255 eV, electron kinetic energy 3−7055
atomic energy *see nuclear power*
atomic excitation
see also atomic collision processes; atomic metastable states; atomic spectra; Auger effect; ionisation of atoms
Bethe sums for Lamb shift calcs. in higher excited states 3−23467
charge density anal. 3−7034
coherence resonances in elec. field induced atomic alignment-orientation coupling 3−11142
coherence transfer, interatomic, in mag. fields 3−29541
collisional transfer process in self-broadening, linear transport equation 3−11162
core level, application to solid surface electronic structure determ. 3−38768
Coulomb excitation by heavy charged particles application of semi-classical model in adiabatic projectile region 3−23492
electron energy deposition in gaseous mixtures due to excitation and ionisations, computer program 3−35970
elementary excitation transfer events, involving simultaneous quantum emission and absorpt. 3−32528
excitation potential, solar equivalent width, damping, atmospheric microturbulence 3−3333
in flames, distribution in different zones of free atoms of various elements *(Russian)* 3−12520
fluorescence transitions, definitions 3−7050
Hanle effect, press. dependence in sensitised fluorescence 3−29494
Hanle effect, saturation by intense broad band laser radiation 3−29493
HI regions, excited atom population, low energy cross sections 3−3378

atomic excitation continued
hole-excitation spectrum, struct. 3−20024
hollow cathode arc discharge for generation of intense ionic resonance lines 3−1112
hydrogenic ions and atoms highly excited, charged particle excitation 3−38235
impact parameter version of Born approx., extraction of elastic scattering matrix element 3−1118
inert gas, atomic scattering of ions, singularities involving inner shell 3−20064
ion-atom collisions, inner-shell vacancy production, review 3−35979
laser saturated atomic reson. fluoresc., theory 3−1111
lifetime meas., using tunable flashlamp pumped dye laser 3−14390
lifetimes of excited states meas. using analog correlator *(French)* 3−16503
multielectron atom, transition-matrix calc. of excitation spectrum 3−20006
multielectron system, variational principle for direct calc. of excitation energy 3−20007
multiphoton absorpt. of laser photons 3−33036
multiphoton transition amplitude for high-order e.m. transitions, momentum translation approx. 3−26579
neutral atoms in dense discharge, excitation and ionisation by electron impact 3−23497
optical separation of isomeric nuclei by laser radiation 3−29506
photon and particle joint diffusion in a semi-infinite vacuum, concentration of excited atoms ahead of a plane shock front *(Russian)* 3−23479
photon echo on homogeneously broadened spectral line 3−35716
photons and particles joint diffusion in a semi-infinite vacuum, excited atoms distribution kinetic eqn. *(Russian)* 3−23478
quasi-Landau spectrum of hydrogen-like system in strong mag. field 3−33038
resonance interaction, multipole relax. and transfer rates in impact approx. 3−26585
secondary radiation from gas system, polarization characts. 3−23484
sputtering, quantum mechanical model 3−27594
stopping power of atomic matter for relativistic ions, mesons, electrons and positrons, Born approx. energy-loss formulas 3−7082
two-level, interacting with single radiation mode, continued fraction solution in elec. dipole approx. 3−17360
Yb quantum beats, pulsed dye laser excitation, fluorescence, determination of relaxation times and splitting factors 3−22968
Ar, 1048 and 1067 Å reson. lines, electron impact excitation, 10 to 2000 eV 3−38231
Ar, Rb ion collision, quasimolecular state interference 3−20066
Ar electron impact excitation of 3p^{5}4s I and 3s3p^6 II states 3−17374
Ar metastable formation, excitation functions, comment on previous report 3−7080
Ba, line broadening for excited state transitions in rare gases *(German)* 3−4368
Be, (1s^{2}2s2p^{3}p) excited state, magnetic hyperfine interaction many-body perturbation theory 3−35952
CI, lifetimes of metastable $^5S_2^0$ states 3−11140
Ca, 4227 Å reson. line, threshold to 1400 eV electron energies 3−38238
Ca, electron excitation cross sections using Born approx. 3−1122
Ca, optical pumping, metastable levels, prod. of large no. of atoms 3−33031
Ca$^+$, electron impact excitation anomaly for 4s→np transition rel. to oscillator strength 3−23494
Cd, extrema in generalized oscillator strengths of resonance transitions, 255 eV electron kinetic energy 3−7055
Cd, inelastic collisions with slow alkali and alkaline earth ions, spectral line excitation function 3−20065
Cd, reson. excitation by slow Cd$^+$ ions *(Russian)* 3−7086
Cd I, atomic lifetime meas. by the beam-foil technique 3−20013
Cd$^+$ collisions with Mg$^+$, Mg ions, excitation of resonance levels 3−17377
Ce autoionising states, excitation by electron impact *(Russian)* 3−26599
Cs, highly excited D and F levels, hyperfine struct. 3−38221
F^{6+} passed through foil yield of excited autonised metastable states 3−20033
Fe XIII spectrum excitation in solar corona, statistical equilibrium equations 3−37318
H, electron collisional excitation function, threshold behaviour 3−20046
H, electron scatt., S-state expansion convergence at intermediate energies 3−20048
H, in intense e.m. fields, 1S→2S transition, relativistic correction 3−29474
H, quenching of 2S state by inert gas collisions 3−11164
H, zero-field quantum beats of Lyman-α radiation subsequent to beam-foil interaction 3−7062
H atoms, highly excited, effective cross sections of electron collisions *(German)* 3−14307
H in metastable 2S state; 2 photon spontaneous emission, momentum-translation approximation 3−11110
H lines used in determ. of Rydberg const., dependence of line structure on excitation conditions 3−13206
H-electron S state elastic scattering resonances in absence of degeneracy 3−7077
H(2s) cross section meas., prequench losses 3−7060
He, 2^{1}P state, electron-impact excitation, differential and integrated cross-sections by distorted-wave approx. 3−23500
He, 3^{1}P excitation transfer cross section, temp. depend. 3−23502
He, 3^{3}D-4^{3}D levels, electron impact excitation transfer 3−23499
He, autoionizing states, low energy electron impact, 42-48 eV, 57-65 eV, excitation struct. 3−7065
He, by fast protons, charge exchange study 3−38244
He, by H atoms, spectroscopic analysis of radiation emitted during decay of products 3−26607
He, electron excitation of (1s, nd)^{1}D and (ns, mp)^{1}P states 3−26591
He, electron impact, exchange excitation cross sections, calc. using Ochkur approx. 3−11172
He, electron impact excitation of p-levels *(German)* 3−1124
He, electron impact excitation, generalized oscillator strength and cross-section 3−23495

atomic excitation continued
He, electron impact excitation of forbidden transition in range 300 to 500 eV 3—38233
He, excitation energy of 1^1S-2^1S, transition-matrix calc. 3—20006
He, proton excitation, time-dependent studies of vacuum u.v. emissions 3—29530
He, scattering and bound-state props., many-body Green's functions appl. 3—11122
He excited by electrons, polarisation of the 492.2 nm line at energies near 60 eV 3—17376
He gas, mean energy loss per ion pair and stopping power for electrons 3—26592
He I and II transitions, electron impact excitation rates 3—38241
He II lines used in determ. of Rydberg const., dependence of line structure on excitation conditions 3—13206
He metastable formation, excitation functions, comment on previous report 3—7080
He states excited by electron impact, alignment relaxation meas., collisions and cascades influence *(German)* 3—14311
He-He^+ collisions, 80-1100 keV, cross sections for excitation of 4^1S-, 4^1D- and 3^1P-levels 3—4395
He^+ coherent excitation in passage through Ag crystal film 3—24170
He^+ ions, by transmission through Au cryst., absence of channelling effect 3—1110
$He^+ + He$ collisions, direct and exchange excitations, u-g symmetry effect 3—38243
$He^{2+} + H$ collisions, electron transfer and excitation, coupled-state calcs. 3—26602
$He^{2+} + He$ collisions, electron capture and excitation 3—26604
^4He, fine struct. intervals meas. by level crossing *(French)* 3—38216
^4He, zero-field level-crossing resons. and weak mag. field meas. 3—7058
^4He fine-structure meas. by zero-field quantum beats 3—11130
Hg, $6^1S_0 \rightarrow 6^1P_1$,($7^1S_0$),($7^1P_1$) transitions, generalised oscillator strengths 3—35971
Hg, $6s6p^1P_1$ state, electron-impact excitation, spin polarisation and differential cross section 3—20054
Hg, ang. distrib. of photoelectrons from 5d-subshell 3—29501
Hg, by CO mols., time-of-flight sensitized fluoresc. vel. depend. of Hg excitation 3—11312
Hg, electron impact excited, near-threshold polarization of 6^1S_0-6^3P_1 line 3—7059
Hg-N_2 collisions, determ of cross section for 6^3P_1-6^3P_0 excitation transfer by method of delayed coincidences 3—4380
I photodissociation laser, luminesc. of $^2P_{1/2}-{}^2P_{3/2}$ transition 3—32554
K, electron excitation cross sections using Born approx. 3—1122
K, rel. to multiphoton resonance ionization 3—23491
Kr, resonance transitions, self broadened absorption linewidths 3—29491
Kr electron impact excitation of p-levels *(German)* 3—1124
Kr I, meas. of lifetimes of levels excited by short electron pulse using delayed coincidence technique 3—4361
Kr II, meas. of lifetimes of levels excited by short electron pulses using delayed coincidence technique 3—4361
Li, electron excitation cross sections using Born approx. 3—1122
Li atoms, beyond the ionisation threshold, excitation functions 3—17373
Li II (III), lifetimes of excited states by beam-foil technique 3—1109
Li^+, singly ionized by electron impact, lifetime and polarization of 2 ^3P term 3—29499
$^{6,7}Li$ II, 1snp ^3P terms, hyperfine struct. 3—38222
Mg, electron excitation cross sections using Born approx. 3—1122
Mg I, atomic lifetime meas. by the beam-foil technique 3—20013
Mg II, atomic lifetime meas. by the beam-foil technique 3—20013
Mg^+, Mg collisions with Cd^+ ions, excitation of resonance levels 3—17377
N, fluoresc. produced by photoabsorpt. of extreme u.v. radiation by N_2 3—33029
Na, 3s-3p transition, electronic excitation cross-sections calc. 3—35966
Na, electron excitation cross sections using Born approx. 3—1122
Na, electron impact excitation of 3p state 3—29523
Na, electron-excitation cross sections by close coupling method 3—20055
Na, fluoresc. quenching by N_2, energy depend. cross sections 3—33030
Na, photoabsorption in v.u.v., energy range 30 to 150 eV 3—11135
Na atoms, beyond the ionisation threshold, excitation functions 3—17373
Na excitation in supersonic gas flow, vibrational temp. meas. 3—36116
Na-$Hg(6^3P_1)$, atomic collisions. induced sensitized fluorescence, excitation transfer to Na 3—26569
Nd^{3+}:glass, estimation of electron excitation migration, time variation of ion luminescence 3—19621
Ne, autoionizing states, low energy electron impact, 42-48 eV, excitaion struct. 3—7065
Ne, optically pumped, double reson. meas. of Lande factors *(French)* 3—35964
Ne, population of excited levels in positive column 3—14618
Ne, spectral lines, $2p^55s^1P_1$, $^3P_{0,1,2}$ upper levels, optical excitation functions 3—26572
Ne, spin polarization by electron reson. scatt., energy depend. 3—26593
Ne absolute line strengths by analysis of Lu-Fano plots with application to excited state transitions 3—14275
Ne excitation in discharge tube with hollow cathode, intensity depend. on press. and dimensions *(Bulgarian)* 3—33407
Ne I, Ne II lines, excitation cross-sections in 2700 to 3700 angstroms region 3—35960
Ne III spectral lines 3—7057
Ne VIII lines, excitation rate coeffs. 3—33032
$Ne + He^+$ collisions, differential scatt. cross section for Ne excitation 3—33055
NeI, optical cross sections at max. of excitation functions 3—23481
O, distorted wave calculation of electron impact excitation 3—20056
O, electron impact excitation and ioniz., cross sections 3—4390

atomic excitation continued
O electron levels fine structure, ionospheric electron gas cooling effects 3—25270
O^-, autodetachment states 3—29511
O^{5+} passed through foil, yield of excited autoinized metastable states 3—20033
OI, lifetimes of metastable $^5S_2^0$ states 3—11140
OI(^3P-3s $^3S^0$), calc. of electron-impact excitation cross sections in unitarized Born nonexchange and close-coupling approx. 3—4385
O(^1S) quenching by O_2, temp. depend. 3—11139
^{187}Os excitation state effects on Clayton's Os/Re chronology for Galactic age determ. 3—28126
P(3^2D_j), P(3^2P_j), collisional deactivation rate consts. for H_2, O_2 and PCl_3 3—17359
Rb, excitation transfer between fine structure components of states, collision study 3—23477
Rb, highly excited D and F levels, hyperfine struct. 3—38221
Rb II ion, excitation in thermal collisions with metastable He atoms 3—33057
^{87}Rb, $5^2P_{3/2}$ state, broadening of level-crossing signals by collision with Ar 3—29496
Tl, excitation of the 6s electron 3—17372
Tl, excitation transfer between the $6^2D_{3/2}$ and $6^2D_{5/2}$ states by collisions with inert gas atoms 3—14318
Tl, line broadening for excited state transitions in rare gases *(German)* 3—4368
Tl, relative excitation functions *(Russian)* 3—14299
We electron impact excitation of p-levels *(German)* 3—1124
Xe, atomic photoabsorption spectra, collective resonance in the $4d^{10}$ shell 3—14295
Xe, in low pressure gas discharge tube, O_2 molecule, OI line emission 3—20197
Xe, ionisation relaxation behind a shock-wave front 3—36180
Xe, optical meas. of electron-impact excitation function in threshold region with high energy resolution *(German)* 3—4391
Xe oscillator strength of resonance lines 3—38218
$Xe + He \rightarrow Xe^+ + He + e$, metastable atom collision with excited ion production *(Russian)* 3—7072
Xe^+, in collisions of metastable Xe and He atoms 3—17380
XeI, optical cross sections at max. of excitation functions 3—23481
Zn, extrema in generalized oscillator strengths of resonance transitions, 255 eV electron kinetic energy 3—7055

atomic explosions *see nuclear explosions*

atomic forces
alloy, random cubic binary, atomic pots. applic. to heat of mixing, lattice parameter and compressibility 3—24814
benzene, hexamethylbenzene molecular crystals, phonon frequency calculations *(French)* 3—33626
closed shell systems, interaction pots., theory 3—26609
coherence transfer, interatomic, in mag. fields 3—29541
coherent potential approximation, matrix formulation 3—8074
exchange interactions, Rayleigh-Schrodinger perturbation theory applic. 3—7084
inert gas atom pairs, interacting dipole moment 3—29538
inert gas atoms, modified effective electron model for interaction energy calc. 3—7088
interaction potentials between alkali metal and inert gas atoms 3—17385
interatomic potential well, glory scattering data analysis 3—23505
interatomic potentials, extended Thomas-Fermi-Dirac approximation, quantum correction 3—38255
long range interactions in noniterative integral eqn. formalism 3—4383
metallic lattices, Lennard-Jones type potentials 3—38630
methane, determ. of energy parameters in Lennard-Jones potential between atoms from second virial coefficient 3—14402
partial-wave amplitudes, threshold behaviour 3—4397
potentials, ion-atom and atom-atom, using form factor techniques 3—29540
rare gas, Morse-6 hybrid potentials for pair interactions 3—1132
rare gas atoms, repulsive interaction potential in the Fermi-Amaldi model 3—14320
retarded interatomic potential energy, multipole expansion, derivation with use of a dispersion relation 3—26612
satellite structures on spectral line profiles, interatomic potentials 3—35959
short-range, determination by scattering of fast particle beams 3—36057
two-photon exchange pot. between neutral spinless systems, higher-multipole contribs. 3—4396
K^--nucleus optical potential 3—20075
Ar, (Kr), (Xe) + CsF, integral total cross sections meas., attractive pot. investigation 3—38324
Ar, dipole and quadrupole three-body interactions, virial coeffs. 3—20072
Ar-Ar interaction, collision diameter and well depth calc. 3—29539
Ar_2, interatomic pot., calc. of elastic consts. of solid Ar 3—20779
Au_3Cu ordered alloys use of Morse potential function to detn. nearest neighbour distances 3—7868
CO, determ. of energy parameters in Lennard-Jones potential between atoms from second virial coefficient 3—14402
Cs-Ar atomic collisions, absorption coefficients, long and short-range forces 3—20074
Cu_2Au ordered alloys, use of Morse potential function to detn. nearest neighbour distances 3—7868
H, long-range interactions, finite-difference approach 3—35985
H atom-electron system state in an intense e.m. field, interaction scalar potentials 3—35953
H retarded interactomic potential energy of 2 ground state H atoms, Dirac theory 3—20073
H_2, determ. of energy parameters in Lennard-Jones potential between atoms from second virial coefficient 3—14402
He atom hyperfine pressure shift, long-range contribution 3—11186
He^+ near resonant charge transfer collisions with K, Rb and Cs, long-range forces effect 3—35976
HeH, long-range hyperfine shift computation 3—26611
^4He-^4He, repulsive pot. up to 0.14 eV, from inversion of total cross-section meas. 3—38254
K^+-inert gas potentials, molecular beam determination 3—17383

atomic forces continued
K$^+$-K$^+$, repulsive potential calc. from particle beam scattering data 3-33062
K$^+$ + Ar interaction pot. from mobility and diffusion coeffs. meas. 3-38246
Li$^+$-K$^+$, repulsive potential calc. from particle beam scattering data 3-33062
Li$^+$-Li$^+$, repulsive potential calc. from particle beam scattering data 3-33062
Mn u.v. absorption linewidths and lineshifts, pressure broadening and foreign gases effect, interatomic potentials *(French)* 3-17344
N_2, determ. of energy parameters in Lennard-Jones potential between atoms from second virial coefficient 3-14402
N_2 system, mol. orbital calcs. for close collisions 3-26610
NH_3-H^+ collisions, first order orientation dependent forces 3-4487
NO, determ. of energy parameters in Lennard-Jones potential between atoms from second virial coefficient 3-14402
Ne_2, interatomic pot. from elastic scatt. cross sections 3-20071
Ne_2, interatomic pots. from scatt. data and cryst. props. 3-35984
O_2, determ. of energy parameters in Lennard-Jones potential between atoms from second virial coefficient 3-14402
Rb systems of 250 and 686 atoms, molecular-dynamics calcs. near melting temperature, liquid structure study *(German)* 3-4849

atomic magnetic moment
see also gyromagnetic ratio
Hamiltonian for atom in constant magnetic field, nuclear mass and other correlations 3-19999
hydrogenic 1-electron atom calc. 3-11137
resonance interaction, multipole relax. and transfer rates in impact approx. 3-26585
Ar, excited state, quadrupole moment calc. 3-29487
Fe-Pd alloy, f.c.c., ave. moment conc. depend. *(Russian)* 3-8343
Kr, excited state, quadrupole moment calc. 3-29487
Li-He, (Ne), collision-induced absorpt., ground state pot. curves and overlap dipole moments calc. 3-38230
Na, nucl. moments determ. using h.f.s. consts. *(Russian)* 3-7056
Na-He, (Ne), collision-induced absorpt., ground state pot. curves and overlap dipole moments calc. 3-38230
Ne, excited state, quadrupole moment calc. 3-29487
Sm, magnetic dipole hyperfine interaction consts. 3-4359
Xe, excited state, quadrupole moment calc. 3-29487

atomic mass
see also isotopes; mass spectra
1971 evaluation, meaning of values and given precision estimates 3-10843
1971 evaluation, problems connected with calcs. from exptl. data 3-10842
A=45-58, mass spectroscopic with highly accurate control measurements 3-10838
beta-unstable nuclei with $5 \leqslant A \leqslant 40$ 3-10834
conference, Teddington, England (Sep 1971) 3-11106
difference determ. with new mass spectrometer using second-order focusing theory 3-10096
electric field effects on precision meas. with r.f. spectrometer 3-14112
far unstable light nuclei produced in high energy nuclear reactions, on-line mass spectroscopic analysis 3-10837
Hamiltonian for atom in constant magnetic field, nuclear mass and other correlations 3-19999
intermediate mass range, mass extrapolation and mass formulae 3-10841
liquid-drop mass law, sheel model and deformation corrections 3-10893
low charge atomic nuclei, construction of mass formula 3-10839
medium and heavy nuclei, energy determ. using new generation of cyclotrons 3-10835
neutron excessive nuclei, determ. by (^{11}B,^{8}B) reaction 3-11022
nuclear fission, mass asymmetry and shell effects 3-11033
nuclear reaction ground-state Q-values, calc. from atomic mass evaluation, targets with A=9-251 3-19824
precise mass differences determ. from peak-matching mass spectrometer using computer 3-25922
radioactive isotopes, short half-life, feasibility study of mass meas. 3-10836
tables of standard data for spectroscopists 3-11111
Bi, volumetric mass determination *(French)* 3-27855
^{35}Cl, ^{37}Cl, mass spectroscopic determ., meas. of doublet mass differences using peak matching techniques 3-11107
^{35}Cl, atomic mass determ. 3-32998
^{37}Cl, atomic mass determ. 3-32998
D, atomic mass determ. 3-32998
D, mass spectroscopic determ., meas. of doublet mass differences using peak matching techniques 3-11107
H, atomic mass determ. 3-32998
H, mass spectroscopic determ., meas. of doublet mass differences using peak matching techniques 3-11107
^{3}H mass excess, electric field effects on precision meas. with r.f. spectrometer 3-14112
^{3}He mass excess, electric field effects on precision meas. with r.f. spectrometer 3-14112
^{4}He mass excess, electric field effects on precision meas. with r.f. spectrometer 3-14112
^{36}K mass determ. from thresholds for ^{36}Ar(p,n)^{36}K reaction, Coulomb energy systematics near A=36 3-14113
^{11}Li produced in high energy nuclear reactions, on-line mass spectroscopic analysis 3-10837
^{29}Mg, neutron excessive nucleus, mass determ. by (^{11}B,^{8}B) reaction 3-11022
^{14}N, atomic mass determ. 3-32998
^{a}Na, A=27-31, produced in high energy nuclear reactions, on-line mass spectroscopic analysis 3-10837
^{16}O, atomic mass determ. 3-32998
^{80}Rb, ^{82}Rb mass determ. from thresholds for ^{80,82}Kr(p,n)^{80,82}Rb reaction 3-14113
^{29}S, meas. from ^{32}S(τ,^{6}He) 3-19752
Se, from density of CdSe and Avogadro's constant 3-15614
^{232}Th, mass spectrometric meas. of mass doublets using peak matching techniques 3-10836
^{235}U, ^{238}U, mass spectrometric meas. of mass doublets using peak matching techniques 3-10836

atomic mass continued
Zn, volumetric mass determination *(French)* 3-27855

atomic metastable states
heading is late addition, see also atomic excitation
Ar, de-excitation cross sections by gases 3-23630
Ar, energy transfer to N_2, pulse radiolysis obs. 3-23629
Be, metastable $^{3}P_0$ states, double and triple photon decay 3-35965
CI, lifetimes of metastable $^{5}S_2^0$ states 3-11140
Ca, optical pumping, prod. of large no. of atoms 3-33031
Cd excited atoms in discharge, effective electron collision cross sections, conc. of atoms in 5^3P_0 and 5^3P_2 metastable states 3-17699
H, metastable 2S state, two photon spontaneous emission 3-11110
H, multi-photon ionisation of 2S state 3-26582
He, ioniz. of Ar and Xe, electron energy spectra 3-33053
He, metastable atom density calc., fine struct. effect *(French)* 3-38198
He, photoioniz. meas. near threshold 3-38226
He (1s2s:^{3}S) atoms in He (1s^2:^{1}S), hyperfine press. shift 3-11186
He afterglow, decay of 2^3S_1 state 3-14620
He(2 ^{3}S) Penning ioniz. reactions with diatomic mols. 3-29731
He(2^{1}S) and He(2^{3}S) metastable atoms collisions with H atoms, cross sections for chemiionisation 3-38253
He(2^{3}S) and He(2^{1}S) metastable atoms collisions with H and H_2, chemiionisation 3-38252
Hg de-excitation in molecular collisions, electronic to vibronic energy conversion 3-20057
Ne, ioniz. of Xe, electron energy spectra 3-33053
O I(^{1}S-^{1}P^0) transition, 1217.6 Å, oscillator strength meas. 3-33023
O^{5+} beam passed through foil, yield of excited autoionised metastable states 3-20033
O^{6+} beam passed through foil, yield of excited autoionised metastable states 3-20033
OI, lifetimes of metastable $^{5}S_2^0$ states 3-11140
O(^{1}S) quenching by O_2, temp. depend. 3-11139

atomic orbitals
see also atomic structure; orbital calculation methods
1S^{2}2S^{2}2p^{n}3d config., extended method of calc. *(Russian)* 3-33005
analytical radial orbitals, calc. method approximating Hartree-Fock solns. *(Russian)* 3-29471
coherent states for r-level atoms 3-23455
core integrals, one-centre calc. from config. average energies 3-29467
correlated wavefunctions form calc. 3-20008
electrons, complex configurations, extended method of calc., theory generalisation *(Russian)* 3-11117
exponents derivation from Hartree-Fock functions *(French)* 3-23458
gauge invariance, current conservation and GIAO's 3-23459
Gaussian-based model pots. and Gaussian basis functions for valence electron studies 3-1095
Gaussian-based model pots. and Gaussian basis functions for valence electron studies 3-1144
generalised H-like radial orbitals application to the normal configuration of Na and Al type atoms *(Russian)* 3-11116
group VIII elements, analytical wavefunctions for ions 3-20005
Hartree-Fock method, multiconfig., with non-orthogonal orbitals, generalized version 3-23457
Hund's rule for jj coupling 3-33015
integrals contrib. to symm. orbital integrals 3-35955
many electron atoms, orbit-orbit interactions 3-33013
matrix elements of atomic quantity operators using non-orthogonal radial orbitals *(Russian)* 3-11115
multiconfiguration wavefunctions, two-by-two rot. method applic. 3-7038
muonic atoms, nuclear motion effect on energy eigenvalues 3-17387
open-shell SCF procedures not satisfying stationary energy conditions 3-26558
orthonormality-constrained variation method 3-4350
point group degenerate wavefunctions construction 3-4351
rare earth atoms and ions, 4f^n config., applic. of extended method of calculation *(Russian)* 3-29472
rare earth metals, 4f^{n}6s^2 config., orbit-orbit interactions *(Russian)* 3-33012
Slater orbitals modification for heavier elements 3-33001
Slater-Condon parameters, semi- and nonempirical values, one-centre electron repulsion parametrization 3-1096
spin-dependent one- and two-electron operators, matrix elements 3-29464
spin-orbit coupling of p electrons 3-11119
transcorrelated wavefunctions, explicit formula solns. of contraction conditions 3-17340
transition series, second, self-consistent-field calc. 3-35954
transition-metal atoms calc. of analytic SCF wave functions by Hartree-Fock-Roothaan method 3-4352
X-ray scattering by Al and Al$^+$, intensity calc. *(Russian)* 3-11132
Al, localised orbital wave functions, comparison between theory and expt. 3-8082
Ar, localised orbital wave functions, comparison between theory and expt. 3-8082
Be projected Hartree producted wavefunctions, relationship of DODS and SCF orbitals 3-20004
C, X-ray scattering factors by anal. radial orbitals *(Russian)* 3-33006
Cd ion, two electron transitions, 4d^{9}5s^2 to 4d^{10}5p config. *(Russian)* 3-33014
Cs autoionising states, energies, wave functions, Hartree method *(Russian)* 3-26580
Er, incoherent scatt. by K-shell electrons, cross-sect. detn. 3-17337
FI, atomic spectra, 2p^{4}3d and 2p^{4}4d configs., energy levels calc. 3-17346
H, Gaussian wave functions *(French)* 3-23515
H, in intense e.m. fields, 1S→2S transition, relativistic correction 3-29474
H atom matrix elements off diagonal, continuum wave functions in calc. 3-17339
He, Hartree-Fock orbitals derivation from resolvent of hydrogen atom 3-7031
He, scattering and bound-state props., many-body Green's functions appl. 3-11122

atomic orbitals continued
- He constrained density matrix study of simple basis sets of 1s-type orbitals 3-29469
- K, atom and isoelectronic series, valence electron, descriptive function *(French)* 3-29468
- Li, atom and isoelectronic series, valence electrons, descriptive function *(French)* 3-29468
- Li ^{2}S ground state, natural spin orbitals and geminals 3-7030
- Mg IV, ionic spectra, 2p^{4}3d and 2p^{4}4d configs., energy levels calc. 3-17346
- Na, atom and isoelectronic series, valence electrons, descriptive function *(French)* 3-29468
- NaIII, ionic spectra, 2p^{4}3d and 2p^{4}4d configs., energy levels calc. 3-17346
- NeII, ionic spectra, 2p^{4}3d and 2p^{4}4d configs., energy levels calc. 3-17346
- S, X-ray scattering factors by anal. radial orbitals *(Russian)* 3-33006
- Sc I and V III, 3d^3 config., extended method of calc. *(Russian)* 3-33004
- Si, X-ray scattering factors by anal. radial orbitals *(Russian)* 3-33006
- V III and Sc I, 3d^3 config., extended method of calc. *(Russian)* 3-33004
- W, incoherent scatt. by K-shell electrons, cross-sect. detn. 3-17337

atomic photoelectric effect *see photoemission*

atomic polarisability
- alkali halides, ratio of shell charges, electrical and mechanical polarizabilities 3-1152
- depolarized light scatt. in atomic fluids 3-11138
- dipole, freq. depend., from time depend. Hartree-Fock theory 3-23463
- dynamic polarisabilities, computation method 3-35963
- electron photon coincidence technique for atomic radiation polarisation studies 3-7081
- Hartree-Fock polarisabilities calc. 3-29486
- interacting system, nonadditive polarizability 3-14294
- ionisation, multiphoton, spin-orbit coupling and photoelectron polarisation effect 3-23488
- noble metal halides, ratio of shell charges, electrical and mechanical polarizabilities 3-1152
- one- and two-electron systems, rigorous upper and lower limits and semiempirical approximation 3-23476
- optical pumping polarisation of ions in buffer gases 3-1112
- quantum mechanics for molecules of 6,7 and 8 residual at. polarisability degrees of freedom 3-26626
- R-matrix methods, computer programs 3-11171
- static elec. polarisability, ground and excited state atoms, using Coulomb-like approx. 3-17356
- tensor polarizabilities and quadrupole coupling constants 3-29485
- Ar, K ion elastic scatt., collision polarizing character *(Russian)* 3-14316
- Ar, polarisability and shielding factors effective-field calc. 3-29488
- Ar solid, Mittleman parametric polarization potential, use for calc. electron-atom scattering cross-sect. *(French)* 3-11136
- He, polarisability and shielding factors, effective-field calc. 3-29488
- He, static hyperpolarizability 3-11121
- He$^+$ near resonant charge transfer collisions with K, Rb and Cs, cross sections determ. from polarisability and ionisation potential 3-35976
- Kr, polarisability and shielding factors, effective-field calc. 3-29488
- Ne, polarisability and shielding factors, effective-field calc. 3-29488
- Ne solid, Mittleman parametric polarization potential, use for calc. electron-atom scattering cross-sect. *(French)* 3-11136

atomic power *see nuclear power*

atomic reactors *see nuclear reactors*

atomic scattering factors *see crystal atomic structure; crystallography; lattice dynamics*

atomic spectra
- *see also atomic excitation; atomic structure; Russell-Saunders coupling; Stark effect*
- A-G type stars, Al I bound free absorpt. importance in flux discrepancies 3-22047
- absorption and fluorescence of microwave-excited electrodeless discharge lamp, line broadening 3-3920
- absorption lines in plasma, determ. of relative transition probabilities using resonant Faraday effect 3-11473
- absorption spectra interferences in spectrochemical analysis *(French)* 3-13502
- absorption spectrometry, mechanisms of interference and releasing action 3-14291
- absorption spectrometry for the testing laboratory *(French)* 3-13500
- alkali metal atoms, relativistic effects in the hyperfine struct. 3-17341
- Balmer lines from low-density HF discharge, Stark broadening *(German)* 3-38515
- Be, theoretical oscillator strengths for $1s^2\ 2s^2\ ^1S-1s^2\ 2s2p\ ^1P^0$, $1s^2\ 2s2p\ ^1P^0-1s^2\ 2p^2\ ^1D$ and $1s^2\ 2s2p\ ^1P^0-1s^2\ 2p^2\ ^1S$ isoelectronic sequences 3-14285
- Bethe sums for Lamb shift calcs. in higher excited states 3-23467
- bound-bound multiphoton transitions, use of momentum-translation approx. 3-11110
- coherent states for r-level atoms 3-23455
- collision broadening of Zeeman component of hyperfine optical line *(French)* 3-38302
- Cygnus Loop, coronal line (Fe XIV) emission line search 3-22122
- d^3.d and d^7.d electronic configurations matrices for interaction energies *(Spanish)* 3-38207
- elements with Z=79 to 88, relative intensities of K-series X-rays *(Russian)* 3-4363
- emission and absorption spectrometers *(French)* 3-13300
- emission flame, atomic absorpt. meas. of distrib. of ground state atoms 3-14292
- fine structure constant determ. by electron spectroscopy 3-13198

atomic spectra continued
- in flames, distribution in different zones of free atoms of various elements *(Russian)* 3-12520
- fluorescence transitions, definitions 3-7050
- grazing collision of atom with high-energy charged particle, Lamb shift 3-20038
- group II elements, two-photon absorpt. spectra, intercombination transitions cross sections calc. 3-22953
- group V elements, spectra from Hartree-Fock calcs., need for LS-depend. parameters 3-7035
- H, first order Stark effect calc. in low elec. field 3-11127
- Hanle reson., zero field level crossing, longitudinal pumping with r.f. field *(French)* 3-11144
- He^{2+}, 4686 and 3203 lines, temp. determ. from relative line-to-continuum intensity 3-14303
- high-Z region, Coster-Kronig and fluoresc. yields for L$_2$ and L$_3$ subshells 3-26571
- highly ionized atoms of fifth period elements, energy levels and classification 3-17368
- hole-excitation spectrum, struct. 3-20024
- Hund's rule and Z expansion for energy, electron repulsion and electron nucl. attraction 3-29460
- hydrogenic ions, in static elec. field, Stark profiles, plasma diagnostic applications *(French)* 3-1102
- inert gas atom pairs, interacting dipole moment 3-29538
- inert gas collisions with very slow electrons, pressure shifts of high series spectral lines and scattering cross sections, calc. 3-35975
- inert gases, ternary colision translational spectrum simplified model 3-29515
- interaction potential, anisotropy, infl. on broadening and displacement of lines *(French)* 3-7089
- ions, r.f. spectroscopy using optical pumping technique 3-1116
- ions, two-electron, singlet-triplet expectation value differences 3-23466
- isotope effects, study by optical spectroscopy *(Rumanian)* 3-11129
- Lamb shift, value change 3-14281
- laser applications to saturation, level-crossing and double-resonance spectroscopy 3-1105
- level crossings and Back-Goudsmit effect, computer program for soln. of secular matrix 3-11141
- level-crossing signals, shape and amplitude 3-17361
- level-crossing signals, shape and amplitude 3-17488
- lifetimes and transitions, high luminosity technique 3-26567
- line broadening, quantum kinetic equation method *(Russian)* 3-7045
- line formation in magnetic field, quantum theory 3-38203
- many-electron atoms, calc. of energies and widths of autoionizing states 3-4373
- many-electron systems, correlated wavefunctions and energies, variational calcs. 3-26562
- mean-life theory of Wilhelm Wien, predictions 3-20018
- multielectron atom, transition-matrix calc. of excitation spectrum 3-20006
- multiplet square arrays obtained by computer program 3-38211
- muonium energy levels for n=2, relativistic recoil corrections, determ. of Lamb shift 3-38256
- muonium hyperfine structure splitting, determ. of Sommerfeld fine structure const. 3-13197
- mutlipets and periodic system of elements *(Spanish)* 3-38212
- narrow resonance in nuclear transition from absorpt. saturation of electron transition 3-26573
- optical double reson. line shape rel. to pulsed oscills. 3-7052
- photon time correl. for excited level lifetimes meas. *(French)* 3-1094
- plasma, turbulent, spectroscopy of H lines 3-29944
- Pleione, Balmer progression during the shell phase 3-22059
- positronium, $2^3\ S_1-1^3\ S_1$ photon-plasma transition 3-23506
- positronium, level shift and lifetime 3-20076
- Pr I energy levels 3-20017
- proton-atomic H scattering, theoretical study 3-11179
- quasi-Landau spectrum of hydrogen-like system in strong mag. field 3-33038
- radiation damping of atomic states in presence of external time dependent potential, determ. of lineshapes 3-7054
- radiation transport in spectral lines, book 3-14305
- radiative decay of multilevel system, neoclassical and q.e.d. theories 3-37946
- rare earth atoms and ions, energy level structures 3-38213
- rare gas mixtures, absorption coeff. detn. by quantum mech. description of translational motion *(French)* 3-7071
- relativistic effects on transition probabilities, hyperfine structure, isotope mass shifts 3-1098
- resonance, interpretation of Lomakina-Sheibe formula *(Russian)* 3-23485
- resonance scatt. by isolated atom, nonstationary phenomena 3-14276
- Rydberg constant, new measurement 3-13204
- Rydberg constant determination from He$^+$ spectrum 3-20022
- satellite structures theory 3-35959
- secondary radiation from gas system, polarization characts. 3-23484
- Sommerfeld fine structure constant, review of exptl. meas. 3-14280
- Sommerfeld fine-structure const. determ. from muonium HFS splitting 3-13197
- spectral lines determ. in arcs and sparks, degree of ionisation determ. *(Russian)* 3-29482
- splitting constants signs determ. using level crossing techniques 3-17362
- spontaneous emission in laser fields 3-1119
- Stark broadening, non-Markovian treatment, cutoff expression *(French)* 3-33018
- tables of atomic energy levels and multiplets of H, D and T 3-29483
- tables of standard data for spectroscopists 3-11111
- 28 Tauri (Pleione), Balmer progression during the shell phase 3-22059
- tensor polarizabilities and quadrupole coupling constants 3-29485
- three-electron atoms, Feshbach-type resonance states, variational calculations 3-38217
- transition attenuation in atomic collisions *(German)* 3-11167

atomic spectra continued
- transition metals, 3d4p isoelectronic sequence, spectral study *(Russian)* 3−11109
- transition metals, oscillator strengths for $3d^n4s \rightarrow 3d^n4p$ transitions 3−23470
- transition wavelengths and probabilities, theoretical studies 3−17367
- two electron systems, Rydberg corrections *(Russian)* 3−1103
- two-level atoms, frequency shifts in emission and absorption by resonant systems 3−33000
- vacuum u.v. absorption of dense plasmas with resonance series of light elements 3−17351
- X-ray spectra of highly stripped ions in collisions 3−7048
- X-rays, chemical energy shift calc., free ion configurations 3−11131
- Zeeman effect and stimulated Raman scattering, atomic levels in stationary mag. field 3−32605
- Zeeman transitions in magnetoactive plasma *(Russian)* 3−29476
- Ag I, atomic lifetimes of isoelectronic sequences 3−17338
- Ag quadratic Stark constants of spectral lines in LS coupling-Coulomb approximation 3−23469
- Al VI to X e.u.v. and soft X-ray spectra 3−14301
- Ar, absorption lines in plasma, determ. of relative transition probabilities using resonant Faraday effect 3−11473
- Ar, muonium hyperfine interval, precision meas. 3−33067
- Ar, photoabsorption cross section, 180-700 Å 3−20014
- Ar, proton-reduced L X-ray spectrum 3−17353
- Ar, radiative lifetime meas. for neutral atoms and ions by beam foil spectroscopy at low initial ion energies 3−17348
- Ar, Rb ion collision, quasimolecular state interference 3−20066
- Ar afterglow, disappearance of 2p state *(French)* 3−17358
- Ar arc, wall-stabilised low-pressure, radial gain profile of 4880 Å ionic laser line and distrib. of charge carriers *(German)* 3−23951
- Ar arc discharge with hollow cathode, meas. of spectral intensities *(Dutch)* 3−30030
- Ar collisions with Fl ions at 35.7 MeV, dependence of target X-ray production cross sections on ionic charge state 3−1129
- Ar electron impact excitation of $3p^54s$ I and $3s3p^6$ II states 3−17374
- Ar I, transition probability of 6032 Å line *(French)* 3−33386
- Ar I resonance lines at 1048 and 1067 Å at normal pressure in vacuum u.v. 3−17352
- Ar impulse discharge emission in vacuum u.v. region *(Russian)* 3−30044
- Ar^+, transition probability values 3−23471
- Ar^+-Ar collision, X-ray yield dependence on final charge state 3−29527
- ArI, meas. of absorpt. coeff. in arc plasma 3−7041
- As, multiply charged ions, atomic lifetimes of low-lying levels 3−11156
- Au I, atomic lifetimes of isoelectronic sequences 3−17338
- B, u.v. spectra, by beam-foil technique 3−29534
- Ba, line broadening for excited state transitions in rare gases *(German)* 3−4368
- Ba, shift and broadening of resonance lines in hot dense Ar and He 3−17345
- Ba vapour, stimulated anti-Stokes radiation 3−33021
- Be, $(1s^22s2p^3p)$ excited state, magnetic hyperfine interaction many-body perturbation theory 3−35952
- Be, first order Stark effect calc. in low elec. field 3−11127
- Be, metastable $^3P_0$ states, double and triple photon decay 3−35965
- Be I and II, energy levels and radiative lifetimes, beam foil studies 3−11159
- Be III ionized species, far u.v. absorpt. spectra *(French)* 3−20030
- BeI isoelectronic sequences, energy levels and spectra meas. 3−17369
- Bi IV, application of Slater-Condon theory with configuration interaction to various odd configurations 3−4360
- C+C atomic collision, 19-240 keV, X-ray spectra from C_2 system 3−26568
- C_{IV}, 0.2 to 2.0 MeV beam energy, spectra between 30 and 500 Å 3−29532
- Ca, shift and broadening of resonance lines in hot dense Ar and He 3−17345
- Ca^+, electron impact excitation anomaly for $4s \rightarrow np$ transition rel. to oscillator strength 3−23494
- Ca^+, oscillator strengths and ground state photoionisation cross sections 3−1146
- Cd, extrema in generalized oscillator strengths of resonance transitions, 255 eV electron kinetic energy 3−7055
- Cd, inelastic collisions with slow alkali and alkaline earth ions, excitation functions of lines 3−20065
- Cd, reson. excitation by slow Cd^+ ions *(Russian)* 3−7086
- Cd and Cd^+, atomic transition probabilities determ. 3−29479
- Cd I, atomic lifetimes of isoelectronic sequences 3−17338
- Cd I, emission spectra, autoionisation resonances and configuration-mixing 3−7044
- Cd vapour, optical reson. for forbidden lines 3076 and 3261 Å *(French)* 3−7051
- Cd-Ne afterglow plasma, $Cd(5^3P_1)$ and $Cd(5^1P_1)$ atom density decay due to e-Cd collisions 3−4687
- Cd^+, optical pumping meas. of hyperfine structure of ground state 3−29480
- Ce^{2+}, $4f^2$-4f5d lines 3−17350
- Co, Auger and photoelectron spectra, L_2 and L_3 vacancy states width 3−29512
- Cr^{3+} spectra, low terms. determ. 3−33025
- Cr^{4+} atomic spectra, term values determ. 3−33026
- Cs, highly excited D and F levels, hyperfine struct. 3−38221
- Cs, photoabsorption 3−20035
- Cs doublet lines, circular polarization considerations 3−16430
- Cs-Ar atomic collisions, absorption coefficients, long and short-range forces 3−20074
- Cu, Auger and photoelectron spectra, L_2 and L_3 vacancy states width 3−29512
- Cu I, v.u.v. absorption spectrum, autoionized resonances 3−29504
- Cu quadratic Stark constants of spectral lines in LS coupling-Coulomb approximation 3−23469
- D Balmer series, wavelength meas., determ. of Rydberg constant 3−13203
- $^{163}Dy^+$ and $^{161}Dy^+$, hf.s. of spectrum, quadrupole moments 3−20025

atomic spectra continued
- Er III, level structure, spin orbit parameters 3−29505
- FI, $2p^43d$ and $2p^44d$ configs., energy levels calc. 3−17346
- FI lines, Stark broadening and shift 3−7047
- Fe and related elements, regularities in spectra 3−38210
- Fe group ions, optical interaction spectra *(Russian)* 3−1104
- Fe highly ionized states, X-ray spectra in 1 to 2 Angstroms region 3−17354
- Fe I, emission lines, Van der Waal's broadening induced by neutral He in glow discharge 3−35981
- Fe I, line strengths determ. for intermediate coupling, solar Fe abundance 3−38208
- Fe I Fraunhofer lines, saturation effects rel. to solar curve of growth 3−22016
- Fe IX to Fe XVI emission lines and isoelectronic lines in laboratory and solar spectra 3−18952
- Fe XI to Fe XIV multiplet lines in solar spectrum in 200 to 400 Angstroms region, identifications 3−18969
- Fe XV e.u.v. spectrum of solar flare in 200 to 500 Å region, line identifications 3−31522
- Ga, multiply charged ions, atomic lifetimes of low-lying levels 3−11156
- Ge, multiply charged ions, atomic lifetimes of low-lying levels 3−11156
- Ge I and II, neutral and singly ionized, absolute transition probabilities 3−33024
- H, 14 lowest states spectrum in strong mag. field, 10^6-10^8 G 3−23456
- H, atoms in 2S, 2P states, dissociation from photon collisions *(German)* 3−33155
- H, Balmer and Lyman lines, tables of Stark broadening 3−35951
- H, line broadening, Stark effect, of first excited level and Lyman α line in 3 dimens. stochastic fields 3−17342
- H, Lyman-α, Stark broadened profile, unified calc. 3−33019
- H, seventh series 3−23468
- H atom, emission or absorption Raman of 1 or 2 Raman photons, transition amplitude calc. 3−11128
- H atom bound-bound transitions in field of 10^7-10^8 gauss, astrophysical appl. 3−26564
- H atom in plasma medium, 2S-1S photon-plasmon transition 3−23473
- H atoms, highly excited, effective cross sections of electron collisions *(German)* 3−14307
- H in metastable 2S state; 2 photon spontaneous emission, momentum-translation approximation 3−11110
- H lines, Stark-broadened, odd Balmer line shifts in Sirius 3−20012
- H lines used in determ. of Rydberg const., dependence of line structure on excitation conditions 3−13206
- H maser, automatic relaxation rate meas. and spectrum recording methods *(German)* 3−10459
- H plasma ionisation, recombination and population of excited levels 3−29938
- H(2S), H(2P) formation in H collision with planetary atmosphere constituents, Lyman-α emission cross-sections 3−33151
- He, 2^3P state, fine struct. calc. 3−33016
- He, electron impact excitation of forbidden transition in range 300 to 500 eV 3−38233
- He, first order Stark effect calc. in low elec. field 3−11127
- He, metastable atom density calc., fine struct. effects *(French)* 3−38198
- He, optical dipole transition oscillator strengths, perturbative corrections 3−11126
- He, spontaneous emission, forbidden $2^3S_1 \rightarrow 1^1S_0$ line, obs. and transition rate meas. 3−38220
- He, time-dependent studies of vacuum u.v. emissions 3−29530
- He excited by electrons, polarisation of the 492.2 nm line at energies near 60 eV 3−17376
- He high-pressure, irradiation by α-particles, meas. of optical line intensities from atomic and molecular states 3−20552
- He I, beam-foil excitation, zero-field oscillations in 3p $^3P \rightarrow 2s^3S$ transition 3−29533
- He I, off-diagonal matrix elements in Stark-broadening of neutral lines in plasma 3−4358
- He I 4026 2^3P-5^3D, 5^3F profile at low electron densities, non-adiabatic ion dynamic contribs. 3−20019
- He II, determ. of Rydberg constant from n=3-4 (4686 Å) line complex 3−13205
- He II lines used in determ. of Rydberg const., dependence of line structure on excitation conditions 3−13206
- He II resonance lines, plasma polarization shift at 304 and 256 Angstroms 3−17355
- He in high intensity laser field, perturbation atomic levels near ionization threshold 3−1114
- He-^{20}Ne laser with absorption cell, 0.63 μ line shift, line broadening *(Russian)* 3−7026
- He-Ne discharge, meas. of Ne 3.39μ transition decay rates using laser Faraday rotation 3−29079
- He^+, Rydberg constant derivation 3−20022
- He^+, $S_{1/2}$-$P_{1/s}$ Lambshift in n=5 state 3−26566
- He^+ collisions with Zn, Cd, Se, charge transfer into excited states 3−14313
- ^{3}He, hyperfine structure studies by zero-field quantum beats 3−17357
- ^{4}He fine-struct. meas. by zero-field quantum beats 3−11130
- ^{4}He I, fine structs. from intensity modulations in radioactive decays *(French)* 3−17336
- Hg, adsorbed on Ni(100), orbital energy spectra 3−39206
- Hg, electron impact excited, near-threshold polarization of 6^1S_0-$6^3\mathbf{P}_1$ line 3−7059
- Hg and Hg^+, atomic transition probabilities determ. 3−29479
- Hg I, atomic lifetimes of isoelectronic sequences 3−17338
- Hg I absorpt. spectrum meas. between 370 and 900 angstroms 3−35958
- Hg line for student obs. of Zeeman effect 3−16371
- Hg^+, hyperfine struct. Zeeman splitting 3−23482
- HgI, application of Slater-Condon theory with configuration interaction to various odd configurations 3−4360
- ^{202}Hg, forbidden transition 6^2S_0-6^3P_0 in mag. field *(French)* 3−23472

atomic spectra continued
- I, $^2P_{1/2}$-$^2P_{3/2}$ hyperfine struct. transition, induced emission spectra 3−32547
- In, doubly and triply ionized, obs. of forbidden transitions in electrodeless discharge, 340-2440 Å 3−7043
- In IV, triply ionized, emission spectrum, configs. identification 3−1099
- K, 4044/7 Å line broadening by impact with Ar and Kr 3−4357
- K, laser-excited, field splitting of violet lines *(Russian)* 3−7061
- K, oscillator forces of lines *(French)* 3−19998
- K excited vapour, in presence of strong electric field, electro-magneto-optical effects 3−17347
- K isoelectronic sequences, comments on electric quadripole transition probability 3−20020
- K^{2+}, radiative mean lifetimes of levels, beam foil spectra 3−11158
- Kr, muonium hyperfine interval, precision meas. 3−33067
- Kr, radiative lifetime meas. for neutral atoms and ions by beam foil spectroscopy at low initial ion energies 3−17348
- Kr, resonance transitions, self broadened absorption linewidths 3−29491
- Kr collisions with Fl ions at 35.7 MeV, dependence of target X-ray production cross sections on ionic charge state 3−1129
- Kr I, meas. of lifetimes of levels excited by short electron pulse using delayed coincidence technique 3−4361
- Kr II, meas. of lifetimes of levels excited by short electron pulse using delayed coincidence technique 3−4361
- Kr X-ray absorption spectrum, 8-0.8 keV, determ. of mass-attenuation coeffs. by continuous analysis 3−4364
- KrI, ioniz. pot. and 4s4p^{6}nl levels 3−26576
- Li, first order Stark effect calc. in low elec. field 3−11127
- Li, h.f.s. of 2^2P, 3^2P and 4^2P states, SCF and HF calcs. 3−33007
- Li, I and II daily excited states, transitions, 100 to 2000 Å, classification 3−29481
- Li, plasma, spectral line broadening *(Russian)* 3−30015
- Li, radial, bounds for energies 3−10357
- Li, Stark effect in hyperfine struct. 3−14293
- Li II (III), lifetimes of excited states by beam-foil technique 3−1109
- Li^+, singly ionized by electron impact, lifetime and polarization of 2 ^3P term 3−29499
- LiI isoelectronic sequences, energy levels and spectra meas. 3−17369
- ^{6,7}Li II, 1snp ^3P terms, hyperfine struct. 3−38222
- Mg atom, Hartree-Fock calculations of principal configurations 3−20023
- Mg IV, ionic spectra, 2p^{4}3d and 2p^{4}4d configs., energy levels calc. 3−17346
- Mg^+, oscillator strengths and ground state photoionisation cross sections 3−11146
- Mg^{2+}, spectra, ground term combinations 3−33027
- Mg^{3+}, extended analysis of spectrum 3−17349
- MgIV, even configurations, reevaluation of parameters 3−33011
- Mn u.v. absorption linewidths and lineshifts, pressure broadening and foreign gases effect *(French)* 3−17344
- Mn vapour, determination of absolute conc. of atoms by atomic absorption *(Russian)* 3−23474
- N, green glow phenomena of N_2 exposed Na_2SO_4 3−17343
- N VI 2s $^1S_0$-2p $^1P_1$ transition, weak lines 3−33022
- Na, high-resolution, using c.w. dye laser 3−37634
- Na, hyperfine struct. meas. using c.w. dye laser and atomic beam 3−37963
- Na, magnetooptical meas. of equivalent width of D_2-line as function of magnetic field and optical depth *(German)* 3−4362
- Na, photoabsorpt. in vacuum u.v. 3−7046
- Na, radiative lifetime meas. for the 3p$^2P^0$ level by beam foil spectroscopy 3−17348
- Na atoms in flame, radiation intensity, HNO_3 interfering effect, calc. 3−16565
- Na D_1-reson. radiation, forward scatt. by Na vapours in mag. field 3−38215
- Na isolectronic sequences, comments on electric quadrupole transition probability 3−20020
- Na-D-doublet, quenching by N_2, temp. depend. 3−14319
- NaIII, ionic spectra, 2p^{4}3d and 2p^{4}4d configs., energy levels calc. 3−17346
- Ne, 5s'[1/2[$^0_1$-4p]3/2]$_2$ transition, spectral characts. meas. 3−16840
- Ne, radiative lifetime meas. for neutral atoms and ions by beam foil spectroscopy at low initial ion energies 3−17348
- Ne absolute line strengths by analysis of Lu-Fano plots with application to excited state transitions 3−14275
- Ne emission spectra study between 3.5 and 5.5 μm with a grid spectrometer *(French)* 3−16434
- Ne excitation in discharge tube with hollow cathode, intensity depend. on press. and dimensions *(Bulgarian)* 3−33407
- Ne I, absolute transition probabilities for 2p^{5}3s-2p^{5}3p transition array 3−20015
- Ne I, odd-even isotope shift in 6096 and 6074 Å lines, h.f.s. coupling consts. 3−33020
- Ne I, redetermination of mean life of $2p_9$ level using cascade analysis 3−20016
- Ne II, ionic spectra, 2p^{4}3d and 2p^{4}4d configs., energy levels calc. 3−17346
- Ne III spectral lines, excitation 3−7057
- Ne VIII lines, excitation rate coeffs. 3−33032
- Ne^+ collisions with Mg, charge transfer into excited states 3−14313
- Ne^+ collisions with solid Cu target, X-ray spectra 3−27585
- ^{20}Ne-^{22}Ne isotope shift in i.r. spectrum 3−26565
- Ni, Auger and photoelectron spectra, L_2 and L_3 vacancy states width 3−29512
- Ni highly ionized states, X-ray spectra in 1 to 2 Angstroms region 3−17354
- Ni XVII and Ni XVIII resonance lines in solar spectrum in 200 to 400 Angstroms region, identifications 3−18969
- NiI lines in 3000 to 4000 Å range, Stark broadening rel. to electron density 3−17366
- O, beam-foil obs. below 2000 Å, mean lives 3−1100
- O, i.r. radiation, free-free electron transitions *(Russian)* 3−7042
- O ground state and first metastable state populations, instrument for simultaneous detection 3−5948
- O I (^1S-$^1P^0$) transition, 1217.6 Å, oscillator strength meas. 3−33023
- O VII 2s $^1S_0$-2p $^1P_1$ transition, weak lines 3−33022

atomic spectra continued
- OI 1304 Å multiplet, Doppler broadening in dissoc. excitation of CO_2 and O_2 3−23583
- OI 6300 Angstroms atmospheric emission above polar cap, rel. to precipitated low energy electrons 3−25258
- OI line at 5577 Å, O_2 molecule reacting with excited Xe 3−20197
- O(^1S) quenching by O_2, temp. depend. 3−11139
- O(2^1D_2) collisional quenching by atmospheric gases, time-resolved atomic absorption spectroscopy 3−18867
- P XII and P XIII, e.v.u.v. spectra, energy levels 3−29484
- Pb III, application of Slater-Condon theory with configuration interaction to various odd configurations 3−4360
- ^{208}Pb, lifetimes, oscillator strengths and coherence narrowing 3−20021
- Rb, highly excited D and F levels, hyperfine struct. 3−38221
- Rb III, obs. in 370 to 3500 Å range rel. to energy levels 3−14289
- Rb^{2+}, radiative mean lifetimes of levels, beam foil spectra 3−11158
- Rb(III), atomic spectra in sliding spark discharge, energy levels 3−7040
- S, beam-gas v.u.v. spectrum 3−29478
- SI photoionisation cross-section, absorption spectrum using flash-pyrolysis technique 3−17370
- Sc, hyperfine splitting constant determ. for stellar spectral analysis 3−26557
- Sc III, spectrum and energy levels, using vacuum sliding spark 3−29477
- Sc Rydberg series and autoionisation resonances in absorption spectrum 3−33042
- Se, multiply charged ions, atomic lifetimes of low-lying levels 3−11156
- Se II transitions in He-Se discharge laser 3−32544
- Si I g f-values, wall stabilized arc meas. 3−4356
- Sm, analysis of hyperfine structure of 4f^{6}6s^2 ^7F multiplet including meas. for $^7F_6$ state 3−4359
- Sn, isotope shift and hyperfine struct. 3−14277
- Sr shift and broadening of resonance lines in hot dense Ar and He 3−17345
- Tb, h.f.s., in 4f^{9}6s^2 and 4f^{8}5d6s^2 configs. *(French)* 3−1101
- Ti I, Ti II, shock-tube meas. of gf values, solar abundance of Ti 3−26574
- Tl, excitation of the 6s electron 3−17372
- Tl, excitation transfer between the $6^2D_{3/2}$ and $6^2D_{5/2}$ states by collisions with inert gas atoms 3−14318
- Tl, line broadening for excited state transitions in rare gases *(German)* 3−4368
- Tl, relative excitation functions *(Russian)* 3−14299
- Tl II, application of Slater-Condon theory with configuration interaction to various odd configurations 3−4360
- Tl vapour, spontaneous Raman scatt. cross section and linewidth 3−38219
- V, hyperfine splitting constant determ. for stellar spectral analysis 3−26557
- Xe, atomic photoabsorption spectra, collective resonance in the 4d^{10} shell 3−14295
- Xe, continuous spectrum, absorption coefficients calc. *(Russian)* 3−35961
- Xe, radiative lifetime meas. for neutral atoms and ions by beam foil spectroscopy at low initial ion energies 3−17348
- Xe collisions with Fl ions at 35.7 MeV, dependence of target X-ray production cross sections on ionic charge state 3−1129
- Xe emission spectra study between 3.5 and 5.5 μm with a grid spectrometer *(French)* 3−16434
- Xe impulse discharge emission in vacuum u.v. region *(Russian)* 3−30044
- Xe oscillator strength of resonance lines 3−38218
- Xe X-ray absorption spectrum, 8-0.8 keV, determ. of mass-attenuation coeffs. by continuous analysis 3−4364
- Xe^+ excitation in collisions of metastable Xe and He atoms 3−17380
- ^{129}Xe, hyperfine structure study and importance of relativistic effects *(French)* 3−11125
- ^{131}Xe, hyperfine structure study and importance of relativistic effects *(French)* 3−11125
- Y, Rydberg series and autoionisation resonances in the absorption spectrum 3−33043
- Y(VI), emission spectra 3−14288
- Zn, Auger and photoelectron spectra, L_2 and L_3 vacancy states width 3−29512
- Zn, extrema in generalized oscillator strengths of resonance transitions, 255 eV electron kinetic energy 3−7055
- Zn and Zn^+, atomic transition probabilities determ. 3−29479
- Zn I, emission spectra, autoionisation resonances and configuration-mixing 3−7044
- Zn vapour, optical reson. for forbidden lines 3076 and 3261 Å *(French)* 3−7051

atomic structure

see also atomic metastable states; atomic orbitals; atomic polarisability; atomic spectra; Hartree-Fock method; Russell-Saunders coupling
- alkali halides, ratio of shell charges, electrical and mechanical polarizabilities 3−1152
- alkali metal atoms, relativistic effects in the hyperfine struct. 3−17341
- Aufbau scheme, geometrical realisation, hidden symmetries search 3−38201
- bound states, critical review of computer programs 3−29466
- bound-bound multiphoton transitions, use of momentum-translation approx. 3−11110
- closed-shell atoms, relativistic Hartree-Fock eqns., local exchange pot. 3−33008
- coherent states for r-level atoms 3−23455
- electron effects on nuclear reaction energies 3−10942
- electron shells in over-critical external fields, quantum electrodynamical processes 3−6604
- electron stability and Pauli principle 3−7027
- energy level shift in low pressure hydrogen discharge on CO_2 laser beam irradiation 3−14290
- energy variational principle for variable number of particles 3−20001
- excited state energies, coordinate free analysis of modified Hylleraas functionals for bounds 3−29459

atomic structure continued
Fermi-Segre formula, rederivation of nonrelativistic approximation 3−4349
Feynman diagrams for energy of state with two electrons (holes) in unfilled (filled) shell 3−20002
fractional parentage coefficients for equivalent electrons in jj-coupling, computer calculation 3−19483
Gaussian-based model pots. and Gaussian basis functions for valence electron studies 3−1095
generalised H-like radial orbitals application to the normal configuration of Na and Al type atoms *(Russian)* 3−11116
Hamiltonian for atom in constant magnetic field, nuclear mass and other correlations 3−19999
Hartree-Fock results for configuration energies, He to Rn 3−11112
Hund's rule for jj coupling 3−33015
Hylleraas−Scherr−Knight variational perturbation eqns. soln. 3−7028
integrands containing spherical harmonics, evaluation by summing Legendre series 3−11108
ionic soft sphere parameters from Hartree-Fock charge densities 3−26559
level-crossing signals, shape and amplitude 3−17361
level-crossing signals, shape and amplitude 3−17488
light atoms, K electron binding energy by Braunbeks method 3−7036
magnetic coefficients of internal conversion in M-shell, dynamic struct. corrections *(Russian)* 3−20011
many-electron atoms, mass variation and Darwin relativistic corrections 3−7039
many-electron systems, correlated wavefunctions and energies, variational calcs. 3−26562
metal, connection with polymorphism 3−11577
model-potential theory and annihilation characteristics of positron-alkali-atom bound states 3−33066
modified Thomas-Fermi eqn., determ. of total atomic energy 3−7025
multiconfigurational approximation *(Russian)* 3−23462
muon binding energy in various atoms 3−11188
noble metal halides, ratio of shell charges, electrical and mechanical polarizabilities 3−1152
one-electron system, mag. h.f. interactions, Schrodinger, Dirac and QED perturbation calcs. 3−33017
opacity calculations, simplified Hartree-Fock method 3−33003
positron transmission and scattering meas. using superposition of annihilation lineshapes, backscatter coeffs. depend. on atomic number 3−11653
positron-alkali-atom bound states, ground-state energy detn. from model-potential theory 3−33065
rare earth atoms and ions, energy level structures 3−38213
Rayleigh scatt. of γ-rays by K-shell electrons, Z-depend. of linear polarization 3−26556
relativistic, program to calc. angular momentum coefficients 3−35957
relativistic energies, perturbation analysis of current calc. methods 3−14286
relativistic energies of first- and second-row atom isoelectronic sequences 3−35956
relativistic wavefunctions in central field approx., parametric pot. approach *(French)* 3−4355
second irreducible integral, for three atoms with unsaturated electron shells *(Russian)* 3−11114
slow collisions, interference effect in energy distrib. of electrons due to two-fold passage of quasistationary term *(Russian)* 3−7073
splitting constants signs determ. using level crossing techniques 3−17362
SU_{2j+1} Gel'fand patterns for angular-momentum basis states of general j^n configuration 3−4007
ten-electron system, perturbation theory calc. of diamagnetic susceptibility 3−23534
Thomas-Fermi equation, high density expansions 3−36506
Thomas-Fermi model, derivation from Lagrangian 3−1097
Thomas-Fermi model, shell structure effects on eqn. of state of matter at geophysical pressures 3−32435
Thomas-Fermi model with quantum corrections, X-ray scatt. obs. 3−29461
three-electron atoms, Feshbach-type resonance states, variational calculations 3−38217
time-reversal in the impact parameter method 3−38202
transition metals, numerical Hartree-Fock functions 3−33009
two electron atom, 1^1S ground state, expectation values, lower bounds 3−29457
two electron systems, Rydberg corrections *(Russian)* 3−1103
two-electron atomic systems, variational perturbation theory, comparative studies of different sets of basis functions 3−14279
U(nm) spin down U(n) × U(m) reduction, application to hadron, atomic and nuclear physics 3−37785
wavefunction, all-pair for many electron states with highest multiplicity 3−23460
μ-mesic energy levels for nuclear polarisation in adiabatic approximation 3−23507
Ar, electron distribution determ. by holographic electron laser microscope 3−4714
Ba muon binding energy in various atoms 3−11188
Be I and II, energy levels and radiative lifetimes, beam foil studies 3−11159
Cd(I), autoionising d^9s^2np level, intermediate coupling calcs. 3−7063
CsI, relativistic wavefunctions in central field approx. *(French)* 3−4355
Er III, level structure, spin orbit parameters 3−29505
Eu, screening ratios, relativistic contributions 3−14287
Fe group ions, optical interaction spectra *(Russian)* 3−1104
H, in intense magnetic field 3−1093
H atom second level populations in plasma medium 3−23473
H-like multielectrons atoms, empirical effective parameters based on ionisation potential and radius 3−29458
He, excited state wavefunctions calc. 3−38205
He, excited states, Coulomb hole calc. 3−38206
He, odd-parity D state positions, variational calc. 3−4347

atomic structure continued
He, perturbative corrections to Hartree-Fock oscillator strengths 3−11126
He, second-order corrections to fine structure, ^3P contributions 3−20000
He adsorbed on graphite calc. of ground state energy for superlattice states 3−38723
He atom hyperfine pressure shift, long-range contribution 3−11186
He variational calc. of third harmonic coefficient 3−11121
^{4}He 5^1D_2 state, lifetime and alignment meas. by beam-foil level crossing 3−23483
Hg(I), autoionising d^9s^2np level, intermediate coupling calcs. 3−7063
In IV, triply ionized, emission spectrum, configs. identification 3−1099
Li, Fermi-contact h.f.s., MC SCF wavefunctions 3−33010
Li, h.f.s. of 2^2P, 3^2P and 4^2P states, SCF and HF calcs. 3−33007
Li 2s wavefunction calc. by Messmer method 3−7029
Li isoelectronic sequence, spin density of ns^2S states 3−32999
Li-like ions, energy levels in solar and laboratory X-ray satellite spectra 3−23475
Mg atom, Hartree-Fock calculations of principal configurations 3−20023
Mn, electronic configuration in crystal, X-ray spectral obs. on Mn-Al system *(Russian)* 3−2602
Na atom, wavefunctions and pseudopotential calc. using Schrodinger equation 3−29470
Nd^{3+}, energy levels in $GdAlO_3$ *(Russian)* 3−24731
Ne absolute line strengths by analysis of Lu-Fano plots with application to excited state transitions 3−14275
O muon binding energy in various atoms 3−11188
^{16}O highly ionized atoms, time-differential meas. of hyperfine structure of 6.13 MeV state 3−32761
P XII and P XIII, e.v.u.v. spectra, energy levels 3−29484
Pb muon binding energy in various atoms 3−11188
Rb, excitation transfer between fine structure components of states, collision study 3−23477
Rb(III), energy levels from atomic spectra 3−7040
Tl muon binding energy in various atoms 3−11188
Xe, atomic photoabsorption spectra, collective resonance in the $4d^{10}$ shell 3−14295
Xe^+ excitation in collisions of metastable Xe and He atoms 3−17380
Zn(I), autoionising d^9s^2np level, intermediate coupling calcs. 3−7063

atomic structure, crystals *see crystal atomic structure*

atomic weight *see atomic mass*

atoms
see also exotic atoms; helium atoms; hydrogen neutral atoms; mesic and muonic atoms; positronium
bound states, initial integral equations of perturbation theory *(Russian)* 3−17335
coherent states in quantum optics 3−4077
fundamental natural standards for time and length 3−22239
interaction with radiation field, destruction of coherence 3−29064
model for students, electromagnetic 3−16368
principles of atomic and nuclear physics, textbook 3−9805
quantum theory of interaction of atoms and mols. with e.m. fields, review 3−19699
two-level, in closed cavity, source-field approach 3−4079
two-level, interacting with single radiation mode, continued fraction solution in elec. dipole approx. 3−17360
two-level system in sinusoidal field, Liouville eqn. soln. 3−704
Mn vapour, determination of absolute conc. of atoms by atomic absorption *(Russian)* 3−23474

attaching *see joining processes*

attenuation *see absorption*

attenuation measurement
see also loss measurement
film waveguide light attenuation, meas. apparatus 3−35403
irradiance attenuation rel. to conc. of suspended matter in sea, least squares method soln. 3−25187
photographic zenith tube plate, image diameter correlation with photographic magnitude *(Japanese)* 3−19087

attenuators
see also waveguide attenuators
acoustic, for brass wind instruments 3−5696

attitude control
astronomical instrumentation, conference (Tucson, Arizona, March 1972) 3−31816
balloon-borne u.v. stellar spectrometer telescope, pointing and guidance 3−31839
orientation determ. of observatory satellite with unfixed orientation 3−25535
satellite nutational oscillations, damping with internal flywheel 3−25375
spacecraft oscillations with two-position attitude-control system 3−25376
spacecraft reorientation, optimal control 3−6188
star sensor/mapper for Small Astronomy Satellites 3−31823

audio acoustics
see also audio recording; audio systems; hearing; speech
acoustic alterations in speech when processed through Air Force aircraft communication systems 3−3646
loudness, hearing, measurable dimensions of sound, audio reproduction, compensation 3−9656

audio equipment
see also gramophones; loudspeakers; microphones; pick-ups
Bekesy audiometer, calibration *(German)* 3−13233

audio recording
electrostatic, expt. 3−648

audio systems
see also acoustic devices; acoustic equipment
stereophony theory, relationship with human directional hearing theories *(German, French)* 3−25575

auditory activity *see hearing*

auditory perception *see hearing*

Auger effect
- *see also atomic spectra*
- adatom conc. profiler, Auger plasmon satellite intensities vs. depth 3—30904
- adsorbed gas on solid, structure from LEED and Auger emission spectroscopy 3—24341
- alkali metal overlayers on W(100), quantitative study 3—38704
- angular dependence of emission from single crystal, Cu(111) obs. 3—30916
- atomic correlation effects on KLL transitions 3—11155
- Auger electron spectroscopy, primary electron beam attenuation rel. to Auger currents 3—30905
- Auger spectroscopy, cylindrical mirror analyser, design 3—32221
- calculated transitions, catalogue 3—39205
- crystal surface structure obs. by electron spectroscopy 3—18008
- display type LEED-Auger apparatus, work for change meas. 3—35494
- electron production mechanisms in ion-atom collisions 3—26601
- electron spectroscopy technique, applic. to surface analysis, book contrib. 3—10106
- elements, complete list of Auger transitions and resulting energy, 10 to 30000eV energy range 3—2612
- elements with $Z=29$ to 94, KLL transitions, absolute probabilities dependence on atomic number *(Russian)* 3—4370
- elements with $Z=30$ to 94, absolute probabilities dependence of KLL transitions on atomic number *(Russian)* 3—4371
- emission electron microscopes using Auger spectroscopy to analyse surface chem. comp. 3—13470
- energy analyzer 3—28715
- film on metal surface, composition determ. by Auger electron spectroscopy 3—21553
- grain boundary activity, determ. by Auger spectroscopy 3—7767
- inert gas atoms, electron impact double ionisation, possible Auger emission study 3—11169
- $K\beta$ low-energy spectrum in P, S, Cl, CaO, CaF_2, Sc, Sc_2O_3, Ti, TiO, interpretation of structure 3—30892
- KLL energies including static relaxation, theory 3—35967
- mesic atom, mechanism of μ depolarisation in molecular condensed matter 3—17388
- Nimonic 80A, oxidation, low O_2 press., 800°C 3—30358
- Penning ion source, high charge state output, analysis 3—35464
- rare earth metal surfaces, Auger spectra obs. of ionisation losses 3—5252
- rare earth metals, electron spectra up to 530 eV *(Russian)* 3—15579
- p-s-n rectifiers, band-to-band Auger recombination and carrier-carrier scattering 3—5019
- relaxation effects of Auger energies 3—11149
- rel. to scanning electron microscopy 3—11536
- semiconductor, compound, state density determ. by Auger and photoemission electron spectroscopy 3—24381
- Si insulating compounds, AES 3—30917
- solid surface, relative escape depth of Auger and photoelectrons 3—21505
- spectrometer, cylindrical mirror type, construction and operation 3—19325
- spectroscopy, combined with s.e.m. 3—38700
- spectroscopy, electronic superposition of sample current and secondary-electron images 3—10099
- spectroscopy, L-shell ionization cross sections 3—39209
- spectroscopy, using 2-grid LEED system, and photoelectron multiplier *(Japanese)* 3—35492
- spectroscopy and electron ranges 3—30915
- substrate surface, structure obs. during sputtering and vapour deposition 3—24324
- surface electronic structure determ. 3—38768
- surface texture, corrosion, absorption 3—1864
- surface-vacuum interface, conference, Enschede, Netherlands, June (1972) 3—30316
- thin film anal., metals, semiconductors and insulators 3—1946
- thin film analysis by Auger spectroscopy 3—10207
- trace analysis techniques for solids, and instrumentation, review 3 - 22555
- Ag, Auger spectra, quasi-atomic fine struct. 3—30907
- Ag-Pd alloys, Auger electron spectroscopy for CO adsorption study 3—1885
- Al, Auger-electron and photoelectron structure in secondary electron energy distributions, high resolution meas. 3—8691
- Al, clean and slow oxidized surface, electron and charact. energy loss spectra obs. 3—34452
- Al, plasmon decay effects Auger, secondary and electron energy loss spectra 3—5026
- Al_2O_3:MgO, grain boundary segregation fracture in high vacuum Auger spectrometer, sputtering profiles 3—27739
- Ar gas, meas. of low-energy $K\beta$ spectrum, evidence of radiative Auger transitions 3—29490
- Ar^+ — Ar violent collisions, extended ion-electron coincidence meas. 3—11184
- Au, clean and black surface, electron and charact. energy loss spectra obs. 3—34452
- Au, substrate with Pb monolayers, spontaneous alloying, LEED and Auger obs. 3—36463
- Au-Si film-substrate system, diffuse interface obs. 3—38751
- Au(111), (100), (110), faces, LEED and Auger obs. of S adsorption *(French)* 3—20940
- BaF_2 core band-conduction band excitons, temp. depend., Auger effect 3—2036
- Be, clean and slow oxidized surface, electron and charact. energy loss spectra obs. 3—34452
- Be spectrum, clean and oxidised surfaces, band structure interpretation 3—30902
- Be:Si surface, and ionisation loss spectra meas. before and after oxidation 3—21508
- C fibre surface study 3—5346
- Ca, $K\alpha$ low energy satellite lines, with and without electron emission 3—15571
- CaF_2 of core band-conduction band excitons, temp. depend., Auger effect 3—2036
- Co, Auger and photoelectron spectra, L_2 and L_3 vacancy states width 3—29512

atomic structure continued
Auger effect continued
- Cr, core electron binding energies of bulk atoms, comparison with surface atoms 3—39210
- Cu, Auger and photoelectron spectra, L_2 and L_3 vacancy states width 3—29512
- Cu, Auger electron spectra and electron spectra, 25-400°C 3—30910
- Cu, Auger-electron and photoelectron structure in secondary electron energy distributions, high resolution meas. 3—8691
- Cu, clean and black surface, electron and charact. energy loss spectra obs. 3—34452
- Cu, spin splitting in electron spectrum 3—21504
- Cu Auger spectrum, fine struct. 3—34447
- CuO, Auger electron spectra and electron spectra, 25-400°C 3—30910
- Cu_2O, Auger electron spectra and electron spectra, 25-400°C 3—30910
- FE(111) surface structure determination using electron spectroscopy 3—15054
- Fe, Auger spectra rel. to oxidation 3—30908
- Fe, clean and slow oxidized surface, electron and charact. energy loss spectra obs. 3—34452
- Fe, initial oxidation obs. 3—38741
- Fe/O adsorbed layer, correl. of proton-excited X-ray and Auger spectroscopy anal. 3—1879
- Fe-Si alloy, initial oxidation obs. 3—38741
- GaAs:F^-, ion implantation profile, Auger spectroscopy determ. 3—12309
- n-GaAs/Ni/Au-Ge ohmic contact, Auger electron spectroscopy and sputter etching 3—4903
- GaP, states with two bound particles, Auger transitions at defects 3—36546
- GaP:Te, photocond. due to Auger recomb. of bound excitons 3—27283
- Ge, adsorbed C(N)(O)(P)(S)(Cl), Auger electron yields 3—2611
- Ge, laser excited, radiative transition, Auger recomb. processes 3—5233
- Ge, wafers, cleaning procedures, Auger analysis of residual surface contamination 3—39252
- GeO, relative escape depth of Auger and photoelectrons 3—21505
- $({}^4He\ \mu)_{2s}^+$ ionic system, meas. of Auger effect, contribution to deexcitation of system 3—26613
- n-$Hg_{1-x}Cd_xTe$, Auger limited band to band and Shockley-Read recomb., photocond. meas. 3—36634
- In, Auger spectra, quasi-atomic fine struct. 3—30907
- Kr, high resolution $L_{2,3}MM$ and $M_{4,5}NN$ 3—17364
- Li, high energy satellites in spectra 3—18519
- Li and Li_2O, proper assignment of Auger energy for Li 3—36969
- Mg, Auger spectra rel. to oxidation 3—30908
- Mg, High energy satellites in spectra 3—18519
- Mg Auger and photoelectron spectra of partially oxidised surface, abnormal chem. shift 3—30909
- Mg_2Sn, valence band electron density of states determ. by Auger and photoemission spectroscopy 3—24381
- Mo overlayer on W substrate, escape length of Auger electrons 3—36961
- N, chemisorbed, line shape, in different chemical environment 3—39207
- Na_2SO_4, $Na_2S_2O_5$, LMM spectra obs., correlation with molecular orbital structure 3—21509
- Ne, fluorescence yield, multiple ionisation effect 3—11145
- Ni, (110), investigation of chemisorption of CO 3—38721
- Ni, (110) surfaces, CO interaction, electron spectral study 3—38716
- Ni, Auger and photoelectron spectra, L_2 and L_3 vacancy states width 3—29512
- Ni, Auger-electron and photoelectron structure in secondary electron energy distributions, high resolution meas. 3—8691
- Ni, core electron binding energies of bulk atoms, comparison with surface atoms 3—39210
- Ni, electrodeposited, chem. analysis of Ni-Ni interface bonds by Auger electron spectroscopy 3—436
- P_2 adsorption and desorption kinetics on Si(111) surface, AES obs. 3—1883
- Pt, (100) surface, chemisorption of unsaturated mols., spectral and LEED study 3—11808
- Pt, reactivity of low index and stepped single cryst. surfaces 3—11787
- Pt, study of S adsorption *(French)* 3—36483
- Pt-Sn alloy, surface composition rel. to annealing O_2 chemisorpt., H_2 reduction, Auger spectra obs. 3—30318
- S, chemisorbed, line shape, in different chemical environment 3—39207
- S on Ni surface, spectral fine struct., origin 3—11810
- Si, adsorbed C(N)(O)(P)(S)(Cl), Auger electron yields 3—2611
- Si, Auger recomb., impact ionization, ionizing collisions transition rate rel. to electron energy 3—2103
- Si, core electron spectra, $L_{III,II}$ electron loss spectra and optical absorpt., comparison 3—34449
- Si, surface, LEED and Auger spectroscopy examination methods 3—15061
- Si, surface struct. obs. 3—15062
- Si surface, rel. to electron beam-adsorbate interactions 3—20939
- SiO_2 film, HCl- or Cl_2-grown, Auger anal. of Cl 3—38597
- SrF_2 core band-conduction band excitons, temp. depend., Auger effect 3—2036
- Ta, sputtered thin film, surface and in-depth analysis 3—37767
- Ti, core electron binding energies of bulk atoms, comparison with surface atoms 3—39210
- Ti, $K\alpha$ low energy satellite lines, with and without electron emission 3—15571
- Ti oxidation, marker expts. with Auger spectroscopy 3—36492
- V, Auger electron emission spectra, chem. shifts, ionisation and plasma losses 3—30906
- V_2O_5, Auger electron emission spectra, chem. shifts, ionisation and plasma losses 3—30906
- W overlayer on Mo substrate, escape length of Auger electrons 3—36961
- Xe, high resolution $M_{4,5}NN$ and $N_{4,5}OO$ 3—17364
- Zn, Auger and photoelectron spectra, L_2 and L_3 vacancy states width 3—29512

atomic structure continued

Auger effect continued

  Zr-Al bulk getter, secondary electron emission 3−19182

Auger electrons *see Auger effect*

Auger showers *see cosmic ray showers and bursts*

Auger spectra *see Auger effect*

Auger spectroscopy *see Auger effect*

aurora

  see also airglow; atmospheric spectra

  30 March, 3-4 April 1971 auroral events *(Russian)* 3−12875

  absorption region global motion, electron drift effects 3−34907

  acceleration of auroral electrons by electric field of pulsations 3−34914

  arc alignment, delineation of oval distribution pattern 3−15998

  arcs, electron intensities 3−3040

  arcs, electron intensity meas., source plasma identification 3−25259

  atmospheric potential gradient variation during aurora 3−28057

  auroral bay magnitude, freq. and period relationships with P12 micropulsations 3−31332

  auroral ionosphere, electron intensity rel. to Ba cloud, rocket flight obs. 3−12785

  auroral zone morning sector, pitch angle distrib. of energetic electrons and protons during enhanced particle precipitation *(German)* 3−16012

  bremsstrahlung X-rays rel. to auroral glow and shape during Jan. 21 and Feb 3 1969 storm and substorm 3−34887

  Cherenkov radiation emission from low energy electrons, broad band hiss source 3−15995

  conjugate balloon observations of auroral-zone x-rays 3−25257

  electric fields meas. and obs. 3−12812

  electrojet, separate ring current systems for eastward and westward types 3−16009

  electron precip., e.l.f. noise bands, polar cusp 3−12778

  electron precipitation, angular distributions 3−3139

  electron precipitation by artificial plasma injection 3−25296

  electron spectrum space-time dynamics during 1968 March-April magnetospheric substorms 3−25255

  electrons, 0.8 to 16 KeV, pitch-angle distributions 3−12788

  emission parameters and electron excitation 3−9307

  emissions and particle precipitation in the noon sector 3−15993

  e.u.v emissions from aurora, rocket-borne photometer meas. 3−12783

  German obs. between 1880 and 1964, seasonal freq. 3−16010

  heating of neutral atmosphere by auroral particles rel. to thermospheric composition 3−34917

  heating of upper atmosphere during aurora and auroral ray length 3−34906

  integral emission bursts of brief duration, temporal variations 3−34911

  ion density and composition rel. to time varying model aurora 3−34916

  ionosphere, ion velocity distrib. 3−9322

  ionosphere, plasma drifts, Ba cloud data 3−3061

  ionospheric total electron content meas. during visible auroras over Macquarie Island 3−31418

  low altitude particle precipitation, a local-time survey 3−15994

  luminosity var. pulsations and X-rays, cross-correlation analysis 3−31398

  magnetic disturbances, rel. to Pc5 pulsations *(Russian)* 3−3122

  magnetospheric electric field variations and geomagnetic perturbations, relationships 3−16047

  magnetospheric electron precipitation phenomena dynamics 3−28070

  midday auroras, behaviour during auroral substorms, all-sky photographs 3−34924

  morphology of auroral-zone X-ray events, early morning electron precipitation 3−31445

  morphology of auroral-zone X-ray events, electron precipitation in midnight-morning sector 3−31446

  oval, Alaskan meridian chain of stations, morphological obs. 3−12779

  particle acceleration, electric double layers 3−3041

  particle precipitation, Fermi acceleration, convection in geomagnetic tail 3−12777

  particle precipitation and electric fields, review of observational data 3−31391

  particle precipitation patterns 3−3039

  particle soft precipitation, photometric meas. 3−3141

  pinch effect development in magnetosphere rel. to auroral breakup 3−34955

  plasma drift velocity meas., magnetospheric convection process 3−16000

  polar-cap auroras rel. to intensity of disturbance field due to solar corpuscular flux 3−28056

  proton-excited, H beta emission and N_2^+ first negative band intensity ratio meas. 3−15990

  pulsating, spatial coherency 3−5514

  radio, aspect sensitivity 3−9305

  radio absorption and stratospheric temp. distrib., activity effects 3−18862

  red arcs, satellite and ground based obs. of electron temp. and flux and ion temp. and density 3−15989

  regular intensity fluctuations rel. to magnetic field pulsations at Pc4 periods 3−34913

  rocket-borne instrument for X-ray measurements 3−21983

  scanner, dual wavelength ground based 3−5538

  scattering of radiowaves, dependence of back-scattering on aspect ratio 3−31390

  Southern auroral zone, total electron content enhancement rel. to magnetospheric substorms 3−31419

  sporadic-E auroral-type layer in winter, reflection meas. from Dixon 3−28068

  stable red arcs, observation from Southern Africa 3−34922

  type A, electron influx meas. during a mag. storm, rocket meas. 3−12787

  u.v. intensity height profiles and rocket spectrograph sensitivity rel. to magnetospheric acceleration mechanisms 3−31447

  v.h.f. power spectra of radar aurora rel. to classifications 3−12782

aurora continued

  v.h.f. signal scattering, region configuration *(Russian)* 3−3035

  VLF-LF hiss during polar substorms 3−39547

  X-ray aurora observations of electron precipitation event rel. to sudden impulse in geomagnetic field 3−16019

  X-ray background behaviour at balloon heights, electron precipitation effects 3−15850

  X-rays, balloon obs. at Syowa Station, Antarctica *(Japanese)* 3−31402

  X-rays meas. rel. to longitudinal extension of electron precipitation during magnetospheric substorms 3−15983

  ^{4}He, precipitation from mass spectrometry of exposed Al and Pt foils 3−16007

  N_2^+ Meinel auroral spectra in 1.5μ region, Jan. 1972 3−25252

  $N_2(A^3\Sigma_u^+)$ to $O(^1S)$ energy transfer in pulsating aurora, comments 3−34925

  OI 5577 and 6300 Å emissions rel. to upper atmosphere temps. and auroral electron fluxes 3−34919

auroral ionisation *see aurora*

austenite *see iron alloys; steel*

autoionisation

  see also Auger effect

  acetylene, photoionisation near threshold, autoionisation features 3−26711

  anthracene anion radicals, autoionisation in photoelectron emission 3−18528

  astronomical u.v. obs. of effects, a review 3−19078

  Ce excitation by electron impact, atomic states *(Russian)* 3−26599

  electron production mechanisms in ion-atom collisions 3−26601

  in electron-capture decay, model 3−19813

  positron autoioniz. in heavy ion collisions 3−7087

  Ar, detection of states, mathematical technique 3−29500

  Ar, ioniz. processes in slow collisions 3−26605

  Cd(I), autoionising d^{9}s^{2}np level, intermediate coupling calcs. 3−7063

  CdI, emission spectra, reson. and configuration mixing 3−7044

  Cs, electron impact excitation of autoionizing level 3−35972

  Cs atomic states, wave functions, energies, Hartree method *(Russian)* 3−26580

  Cu, local thermodynamic equil. of autoionizing levels 3−33393

  Cu I, v.u.v. absorpt. spectrum, autoionized resons. 3−29504

  H_2, autoionizing transitions produced by electron impact 3−33156

  H_2, reson. struct. in ioniz. function *(Dutch)* 3−29733

  HOF, photoionisation with mass analysis, vibrational and electronic autoionization 3−26713

  He, and autodetachment of He$^-$ after bombardment by H^+, H_2^+, He$^+$ and He 3−23490

  He, electron emission spectra excited by proton impact, 2s(^{1}S) autoionisation state 3−7067

  He, ioniz. processes in slow collisions 3−26605

  He(2^{1}S) and He(2^{3}S) metastable atoms collisions with H atoms, autoionisation widths 3−38253

  Hg(I), autoionising d^{9}s^{2}np level, intermediate coupling calcs. 3−7063

  Mg, rel. to photoioniz. cross section near threshold 3−33039

  N_2, autoionizing transitions produced by electron impact 3−33156

  NO, photoelectron spectra obs. *(Russian)* 3−7247

  NO, threshold region vibr. autoioniz. fine struct. obs. 3−17462

  O^{5+} beam passed through foil, yield of excited autoionised metastable states 3−20033

  O^{6+} beam passed through foil, yield of excited autoionised metastable states 3−20033

  ^{147}Pm β decay, inner shell vacancy creation 3−4369

  Rb, total electron impact ionisation cross section from threshold to 250 eV 3−38232

  Sc, Rydberg series and autoionisation resonances in absorption spectrum 3−33042

  ^{185}W β decay, inner shell vacancy creation 3−4369

  Y, Rydberg series and autoionisation resonances in the absorption spectrum 3−33043

  Zn(I), autoionising d^{9}s^{2}np level, intermediate coupling calcs. 3−7063

  ZnI, emission spectra, reson. and configuration-mixing 3−7044

automatic checkout *see automatic testing*

automatic control

  acrylonitrile process, automatic mass spectrometer analyser 3−22556

  astronomical automatic dynamic spectrum analyser for video tape recorded signals 3−39750

  astronomical spectrophotometer, two channel scanning system 3−31829

  camera, using monolithic integration 3−37658

  clinical-chemical analyses *(German)* 3−10204

  crystal growth by Czochralski method, automatic control of crystal diameter 3−12264

  cyclotron facility at Indiana University, computer applic. 3−13376

  Eindhoven A.V.F. cyclotron, automatic control, measurements 3−13380

  Eindhoven A.V.F. cyclotron, automatic control, measuring instruments 3−13379

  environmental water, radioactivity monitoring system 3−26553

  flight controls for civil aircraft, reliability characteristics 3−32116

  foils, thin, non-magnetic, electropolishing for electron microscopy *(German, English)* 3−24350

  interferograms, automatic processing algorithm *(Russian)* 3−32518

  laboratory oven, linear temp. cycling, using programmable proportional regulator *(German)* 3−32046

  laser processing apparatus for automatic workpiece shaping, patent 3−6530

  lung cancer from chest radiograms, automatic computer diagnosis 3−39811

  mass spectroscopic chemical analysis, accessories *(French)* 3−19362

  modern measurement techniques, noise rejection properties 3−56

  nondestructive testing of semifinished products *(German)* 3−15809

  ORIC, isochronous cyclotron, computer control system 3−13377

  pupillary light reflex, systems approach *(Korean)* 3−31873

  river water quality monitoring 3−22186

  semiconductor diffusion system, computer control 3−34488

  spectrometer shielding, circuit description 3−28687

automatic control continued
  transistorised automatic two-wavelength pyrometer applic. *(Polish)* 3—22292
automatic data processing *see data processing*
automatic frequency control
  lasers, using Lamb dip *(Russian)* 3—13723
  sweep frequency laser, mode selection using Michelson interferometer *(Russian)* 3—10556
  He magnetometers *(Russian)* 3—16464
automatic gain control
  Model OC2-2 optical communication link, laser beam system, minimization of atmospheric changes effects 3—798
  scintillation counting systems in space experiments 3—35478
  u.s. distance amplitude correction unit, patent 3—9843
automatic test equipment
  Kjeldahl nitrogen determination for aqueous dispersible samples 3—37745
  magnetic particle inspection 3—27831
  microcircuit pattern inspection, gated optical comparator 3—4133
  programmed static testing machine for polymers 3—22265
  X-ray diffractometer for pressure vessel inspection, residual stress measurement 3—6121
automatic testing
  electrooculography, computer automated 3—25581
  fatigue data, stochastic function plots by computer 3—2776
  many-component substances analysis *(Russian)* 3—13509
  Al alloy rolled sheets, volume determ. methods 3—24861
automation, social aspects *see social aspects of automation*
automobile industry
  holography applic. to ear design conversion into numerical coordinates 3—34671
automobiles
  acoustic field in irregular rooms, finite difference analysis 3—5733
  oscillations of front suspension relative to body conditions for shimmy occurrence *(Russian)* 3—502
avalanche diodes
  see also electron avalanches; IMPATT devices
  avalanche breakdown delay *(Russian)* 3—8255
  TRAPATT for short-pulse modulation in double heterostructure, GaAs laser 3—32569
avalanches, electron *see electron avalanches*
avogadro's number *see constants*
axicons *see lenses*
backscatter
  see also particle backscattering
  circular wire loop, backscattered field, geometrical theory 3—4068
  Debye expansion, residue contribution, numerical calc. 3—37931
  elliptic metal plate, h.f. backscattering 3—10438
  of e.m. waves from rough surface model 3—10432
  e.m. waves from snow, ice, and sea ice, 26 to 40 GHz 3—37269
  exponential surfaces, two-dimensional density and correlation coefficient 3—22822
  ionospheric oblique and oblique-backscatter sounding, energy spectra characts. of signal level 3—25269
  Lake Ontario surface albedo, dependence on solar zenith angle 3—2845
  laser-Raman scatt. methods for air pollution detection 3—3189
  Moon and Venus, surface roughness meas. and backscatter diagrams from radar meas. 3—25409
  plasma wave spectrum, line enhancement by ionospheric heating 3—18879
  positron transmission and scattering meas. using superposition of annihilation lineshapes, backscatter coeffs. depend. on atomic number 3—11653
  radar from sea, applications in physical oceanography 3—2955
  Raman polarisation in back-scatter mode 3—3810
  reflection nebulae, strong 4430 Angstroms interstellar absorption in backscattered light 3—28295
  rough-surface, subsurface effect on depolarisation 3—670
  sea surfaces, noncoherent model for the cross section including a Fresnel reflection coeff. modification 3—15939
  semi infinite hollow cylinder, h.f. fields 3—35656
  stars, time-depend. transfer in infinite cylindrical shell media 3—37355
backward wave oscillations *see backward wave tubes; electromagnetic oscillations*
backward wave tubes
  see also carcinotrons
  charged particle beam interaction with one-dimensional periodic slow-wave system 3—13770
  microwave spectrometer, autodyne mode, tuned backward wave tube 3—183
bagging *see packaging*
balanced amplifiers *see differential amplifiers*
balanced input amplifiers *see differential amplifiers*
balances
  see also weighing
  1 kg, NBS, for comparison of standards 3—37775
  automatic scales with pre-weighing features, theory *(Russian)* 3—5765
  automatic with electrical compensators *(Russian)* 3—6023
  electromechanical scales, mounting and applic. *(German)* 3—13228
  formetal nucleation kinetics determ. on single crystal mica substrates 3—26033
  micro thermobalance, Shimadzu TGA-20B, applications *(Japanese)* 3—13519
  microbalance using 5 MHz quartz crystal, digital, linearity with heavy loading 3—37588
  millidyne film balance for intermol. energy meas. 3—10142
  thermobalance with magnetic suspension *(Russian)* 3—9832
  thermogravimetric, using Hall effect 3—3915
  top-loading, micromanometer applic. 3—3775
  translation balance for mag. susceptibility meas. at high temp. *(French)* 3—6030
ball lightning *see lightning*
ballistics
  see also Impact; military equipment
  Medium Artillery Delivered Sensors antennas for seismic detection systems, optimum design 3—34831
balloons
  see also aircraft
  atmospheric far i.r. background radiation balloon meas. using liquid He-cooled radiometer 3—28239
  meteorological sounding, solar cell array power supply applications 3—5542
  orbital accel., earth albedo and H drag effects 3—35222
  pointing and guidance of balloon-borne u.v. stellar spectrometer telescope 3—31839
band gap *see energy gap*
band model of magnetism
  alloy, dilute, phenomenological theory rel. to paramag.-ferromag. transition 3—21233
  Anderson model, physical props. from mag. Hartree-Fock soln. 3—36700
  Anderson model for dilute alloys, heuristic treatment for one-electron properties 3—2246
  antiferromagnet with substitutional impurities, magnon density of states calc. 3—8331
  antiferromagnetism on Hubbard model, non-existence of selfconsistent solns. 3—5093
  bandwidth renormalization by interatomic interactions between electrons 3—15337
  divergence in the RKKY interaction 3—18299
  ferromag. phase, collective spin excitation in narrow d band 3—5092
  ferromagnet, collective model, spin wave spectrum, RPA approach *(Russian)* 3—36698
  ferromagnet, current-carrying states rel. to spin polarization in photoemission 3—18533
  ferromagnet, use of Green's function for s-d interaction 3—2245
  ferromagnet weak itinerant film-paramag. proximity sample, Hubbard model calc. of Curie temp. 3—34086
  ferromagnetic disordered alloy, theory for residual resistivity 3—15340
  ferromagnetism in degenerate bands 3—38953
  ferromagnetism in transition metals and alloys, modified Zener model and Curie temp. calc. 3—34085
  ferromagnetism itinerant electron model, spin wave energy at low temps. 3—34082
  Friedel-Anderson model for electron distrib. around mag. impurity in nonmag. host 3—15351
  half-filled-band Hubbard model, statistical mechanics 3—34083
  heavy rare earth metals, electrons and spin waves, review 3—8327
  Hubbard, description of small polarons role in metal-insulator transition 3—30420
  Hubbard, high temp. sp. ht. and entropy of interacting electrons 3—18295
  Hubbard's simple decoupling scheme, absence of antiferromag. ordering 3—15342
  Hubbard mag. insulator, exciton spectra, moments and lattice walks rel. to spin configuration 3—15341
  Hubbard model, ferromagnetism 3—21210
  Hubbard model, one-dimensional half-filled band, calc. of thermodynamic properties using grand canonical method 3—15336
  Hubbard model, paramag. spin susceptibility, antiferromag. ordering 3—21209
  Hubbard model, spin waves in ferromag. state of narrow band 3—15343
  Hubbard model, tenfold d-electron degenerate, antiferromag. to paramag. (ferromag.) transitions 3—21207
  Hubbard model with infinite Coulomb repulsion, zero temp. mag. props. 3—38954
  Hubbard narrow-energy-band model, moment-generated solution 3—2247
  impurity interactions, noble or transition metal alloys, transition impurities, pair description, magnetic properties 3—30596
  itinerant and gap eqn. models for ferro-and antiferromagnetic states in 3d transition metals 3—36701
  itinerant antiferromagnetism, paramag. susceptibility and u.s. attenuation above Neel temp. 3—12001
  itinerant antiferromagnets in mag. fields, theory 3—12002
  itinerant electron ferromag. rel. to spin fluctuations 3—27353
  itinerant electron ferromagnet, electron-magnon interaction 3—21204
  magnetic insulators, one-electron Green function of Hubbard model in atomic limit 3—15334
  magnetite, multiple mag. ordering rel. to metal insulator transition 3—15369
  magnetoelastic waves and magnon-phonon interaction selection rules, inelastic neutron scattering 3—34131
  narrow band electrons, correlation effects on spin susceptibility 3—12000
  neutron scattering from itinerant electron ferromagnets 3—18294
  nondegenerate narrow band, interatomic electron correlation effects on ferromag. and paramag. states 3—21206
  one-dimensional Hubbard model, analytic props. of ground state energy 3—34087
  orbital diamagnetism of electron gas in infinite band *(Russian)* 3—34081
  paramagnetic instability in orbitally nondegenerate narrow band, interatomic correlation effect 3—8330
  rare earth metals, contribution of 5d electrons to mag. hyperfine fields 3—24564
  rare earth transition intermetallics, struct. relationships, Friedel's d-band mag. model 3—2248
  semiconductor, doped, CPA treatment of s-d model at high temp. 3—24557
  TCNQ salt, Li⁺TCNQ⁻, paramag. spin susceptibility meas., symmetry-split band theory 3—34084
  thin films magnetisation direction distribution in band model 3—27352
  tight-binding single band model. calcs. of electronic struct. of ferromag. alloys 3—8328
  3d transition metals, impurity effects, Hubbard's model 3—8352
  two-band model, spin susceptibility and Korringa relation 3—21208
  Bi, diamagnetism theory 3—8338
  Cr, pressure depend. of Neel temp., band calc. 3—18293

band model of magnetism continued
Cu:M, dil. alloy, M=transition metal, pair description 3−30596
Fe, ferromagnetic, energy band calc. 3−38784
Fe, paramag. and ferromag. states, self-consistent band calc. 3−21205
GaAs, magnetization of charge carriers and excitons by polarized light 3−4956
Gd, neutron mag. form factor calc. using Dirac-Fock equation 3−21244
NbAl alloys, Knight shift obs. and rigid-band model approach 3−18381
Ni, spontaneous magnetisation anisotropy from band theory, spin-orbit interaction 3−34150
Ni, with Cr impurity, rel. to high field susceptibility 3−21225
Ni alloys, conc., elec. resist. tests of validity 3−4993
Ni-Pt alloy, rel. to high press. and high field props., near crit. concn. for ferromagnetism 3−30622
Ni$_3$Al(Ga), low temp. elec. resist. and spin density fluctuation theory 3−21046
Pd, exchange-enhanced generalized susceptibility, tight binding model for d-bands 3−2253
(U$_x$Th$_{1-x}$)S, electronic props., models, mag. susceptibility, sp. ht. and elec. resist. obs. 3−2249
V-B-N, rel. to mag. susceptibility and antiferromag. Curie temp. meas. *(Russian)* 3−15333
VO$_2$, metallic, Coulomb interactions 3−24556
V$_2$O$_3$:Cr, Hubbard model, phase stability 3−15344
VS, V$_3$S$_4$-V$_2$S$_3$ and V$_5$S$_8$, rel. to mag. susceptibility and n.m.r. studies 3−27355

band-pass filters
see also crystal filters
100 cm^{-1} region, using metallic mesh grids 3−16405
ALPA seismic system, filter selections 3−28077
complex waveform generation using device with D/A convertor followed by low pass filter 3−28482
noise spectra measurement application 3−22402
optical narrow bandpass, for near u.v. and i.r., prep. method *(French)* 3−3785

band structure
see also Brillouin zones; conduction bands; energy gap; Fermi surface; valence bands
actinide monoputides and monochalcogenides 3−2006
actinides, electronic structure 3−1988
adsorbed layers of He atoms on graphite study by plane wave method *(Italian)* 3−30531
alkali halides, analogue computer modelling, rel. to photolum. *(Russian)* 3−21461
alkali halides, reflection spectra in far u.v., interband transitions 3−21437
alloy, disordered, band-edge behaviour, short-range order effects 3−27202
alloy, disordered binary, CPA validity in elec. cond. theory 3−21050
alloys, long period superstruct. and their interpretation 3−14729
alloys binary, disordered tight binding, theory for different constituent bandwidths 3−8087
amorphous semiconductor, rel. to refr. index 3−36851
amorphous semiconductor materials, completely compensated crystalline semiconductor as model 3−18063
amorphous semiconductors, electronic phenomena, review 3−24415
binary alloys, f.c.c. and b.c.c., energy expressions rel. to ordering, applic. to In-Mg, Li-Mg, Al-Zn 3−11585
binary alloys, IVA-VIA, phase diagrams and electron struct. of component atoms *(German)* 3−8775
collective pairing bands 3−19765
combined KKR-discrete variational method 3−36513
current and electron-phonon interaction in a strong electric field 3−38853
de Haas-van Alphen effect, review of future trends, determ. of relaxation times and spin properties of conduction electrons 3−1993
diamond, Hartree-Fock formalism for crystalline ground state computations 3−18052
dielectric films, thin disordered, Kronig-Penney-type calculations for electron tunnelling 3−8254
disordered system electronic energy spectrum 3−33774
electroabsorption, two-photon transitions, theory 3−15480
electron pairing, phonon-induced 3−38770
electronic transitions observed by inelastic electron tunnelling spectroscopy 3−8279
electroreflectance studies, state-of-the-art 3−15473
e.m. wave scattering and transformation by fluctuations in nonequilibrium plasma in semiconductor 3−18180
engineering rel. to predicting optimum semiconductor 3−1992
excitonic transitions at forbidden interband edge 3−33854
Fe, Compton profile and electron distribution, meas. using Kα X-rays 3−1982
fluorite type crysts., band struct. and optical props. 3−33793
free electron exchange approximation study by many body perturbation theory for metals 3−8085
g-factor of conduction electron, expression for orbital average as meas. in de Haas-van Alphen effect 3−24369
glass, rel. to refr. index 3−36851
graphite, electrical transport props. assuming acoustical phonon scattering 3−11897
graphite, Landau levels, effect of trigonal warping 3−1996
graphite, optical props., dispersion relations for π-bands 3−30785
graphite, theory and determination of the degree of band warping 3−8100
heavy rare earth metals, electrons and spin waves 3−8327
heterojunctions, phenomena, review 3−24512
III-V different semicond. layers forming superlattice, light absorpt. rel. to complex band structure 3−15519
insulating thin films, electronic transport processes 3−18237
interacting linear chains, electron network model description 3−26162
interband absorption, in field of intense acoustic flux, theory *(Russian)* 3−27488
interband effects in coherent potential approximation 3−20986
intermetallic compounds with linear chains, theoretical model for large critical superconducting temps., lattice instabilities 3−2203

band structure continued
ion neutralisation spectroscopy for solid surfaces, derivation of band energy 3−2613
ionic crysts., theory, energy bands, electron-phonon coupling 3−11855
liquid metals, development of electron states in disordered system 3−1971
liquid metals and semiconductors, review of electric properties 3−30385
magnetite, rel. to Verwey transition 3−8117
marked examples, book 3−18048
metal, correlation with chemisorption and electrocatalysis in H evolution reaction 3−38735
metal, k dependent pot., applic. to Ca and Al 3−8086
metal, k dependent pot., theory 3−8085
metal, meas. by photon enhanced field emission, electron and hole scatt. effects 3−27205
metal, pseudoatom props. derived from Shaw model potential 3−21000
metal, quasi one dimensional, interrupted strand model 3−20996
metal film, very thin, screening, random phase approx. 3−8090
metallic alloys, development of electron states in disordered system 3−1971
metallic pseudopotential, energy dependence and nonlocality 3−20997
metals, conduction electrons, quasiparticles, energy structure, electrical properties, general theory 3−24367
metals, d-bands splitting, high resolution photoelectron studies 3−30414
modulation spectroscopy, scalar perturbations, review 3−27487
molecular crystal in contact with metal, charge transfer states 3−8252
molecular crystal in contact with metal, quantum mechanical model of electronic states 3−8252
molecular crystals, temp. dependence of absorption bands intensities of the spectra at Fermi resonance, mass operator and band shape 3−2538
multiple scatt. theory, scatt. by non-muffin tin pots. 3−1967
noble metals, optical constants 3−8548
nucleic acid bases, thin layers, photoelectric props. 3−24465
one-dimensional crystal, Wannier-Stark ladders and electron energy spectrum 3−30409
periodic systems, LCAO functions applic. *(French)* 3−1965
perovskite-type crystals, strong-bonding method, interpolation formulae *(Russian)* 3−30399
photoconductors with adsorbed dyes rel. to spectral sensitization 3−27906
phthallocyanine, metal free, Stark effect of electronic levels 3−12142
polyanilines, linear, band struct. and limiting behaviour 3−33792
polymer, local derivatives, LCAO calcs. *(French)* 3−1966
polyvalent metals, thermorefl., Bragg band-band transition range *(Russian)* 3−8590
rare earth film, rel. to absorpt., 2000-8000 Å 3−12153
rare earth metal oxides, state distributions of 4f and 5d6s states *(French)* 3−1990
rare earth metals, band electrons, number 3−1989
rare earth metals, state distributions of 4f and 5d6s states *(French)* 3−1990
rare earth metals, superconductivity, effect of narrow partly filled band 3−34007
rare earth monoputides and monochalcogenides 3−2006
rare earth pnictides, optical electrical and magnetic props., review 3−11848
rare earth sesquisulphides 3−34370
rare earth solids, book 3−11523
rare earths, electronic struct. 3−1988
rare-earth chalcogenides, determination from specific heat, thermal expansion and conductivity data 3−15019
rutile structure, symmetry props., anal. for energy band calc. 3−24053
semiconducting alloys, narrow band gap semiconductors, zero bandgap transition 3−38800
semiconducting chalcogenides, intrinsic piezobirefringence obs. 3−12110
semiconducting crystals, I-III-VI$_2$, formation, stoichiometry and props. 3−5269
semiconductor, A^{II}B^{V} cpds., review 3−18084
semiconductor, absolute energies, rel. to band edge displacement in heterojuncs. and mixed crystals *(German)* 3−15139
semiconductor, crit. point determ. in 4-9 eV region, thermoreflectance study 3−2005
semiconductor, cubic, selection rules for optical transitions 3−36555
semiconductor, degenerate, Einstein relations modified for band tails at very low temps. 3−8164
semiconductor, E(k) relation for two-band scheme and appl. to metal-semicond. contact 3−1999
semiconductor, interband magneto-optical transitions rel. to isotropic excitons 3−11869
semiconductor, interband transitions of hot holes, and cyclotron reson. of light holes *(Russian)* 3−8109
semiconductor, magnetoresistance, quantum and ultra quantum fields *(French)* 3−38860
semiconductor, many valley, carrier conc. effect on short wavelength phonons self energy 3−30407
semiconductor, momentum representation of hydrogenic ground states derived from complicated band extrema 3−1998
semiconductor, multivalley, fluctuations due to intervalley transitions 3−33880
semiconductor, recent developments in research, book 3−38798
semiconductor, tetrahedrally coordinated *(German)* 3−15138
semiconductor, two-photon interband transitions, joint matrix element 3−34337
semiconductor, with famatinite lattice, group theoretical study *(Russian)* 3−30397
semiconductor, with famatinite lattice, pseudopotential calc. *(Russian)* 3−30398
semiconductor heterojunction *(Russian)* 3−27306
semiconductor with Kane-type band struct., internal quantum efficiency, spectral depend. 3−34338

band structure continued
semiconductor-metal and mag. phase transitions, Hamiltonian model 3—38806
semiconductor-metal boundaries, potential barrier of Schottky junction 3—15252
semiconductor-metal junction, many-body effects, self energy and band structure distortion 3—38890
semiconductors, calcs. using self consistent, adhoc and empirical techniques 3—2007
semiconductors, direct and indirect gap, and their appl. to electroluminescent devices 3—18499
semiconductors, electron-hole liquids, ground state energy 3—21009
semiconductors, electroreflectance study in low-field limit 3—2518
semiconductors, microwave Faraday rotation 3—15475
semimetal, mag. field depend. of elec. cond. for nonellipsoidal nonparabolic band struct. 3—33927
semimetals and narrow gap semiconductors, band struct. and electronic props. 3—33790
solids, electronic transitions and structure, review 3—33814
symmetrised computer calculation of energy bands electronic structure of solids 3—20981
transition metal, approximate calc., application to Pd 3—21001
transition metal dichalcogenides, layered, chemical bonding and struct. 3—4729
transition metal-hydrogen solid solns., X-ray emission spectra interpret. 3—2603
transition metals, 3d, and their solid solns., rel. to X-ray K-absorpt. spectra *(Russian)* 3—18509
transition metals, electrical resistivity at high temp. 3—36588
transition metals, superconductivity, effect of narrow partly filled band 3—34007
Van Hove singularities and zero point slopes in crystals 3—30382
Van Hove singularities and zero-point slopes in mag. crystals 3—30383
Ag, optical interband transitions 3—8088
Ag, relation to electron energy loss functions to transverse and longitudinal e.m. excitation 3—21030
Ag, u.v. photoemission from clean, Cs and Cs + O_2 coated surfaces, band theory 3—12215
$AgInSe_2$, electronic structure from electroreflectance and photoluminescence meas. 3—39183
Al, interionic potential 3—33787
Al, k dependent potential calc. 3—8086
Al, valence electronic charge density, calc. from wave functions obtained via Ashcroft's pseudopotential 3—27209
Al-Mg dilute solid solution, plasma energy loss rel. to band models of alloying 3—7803
AlAs, pseudopotential calculation, optical critical point analysis 3—36863
AlAs, pseudopotential method and kp-method 3—15128
AlN, band-to-band transitions, rel. to refl. and luminesc. excitation spectra 3—18493
AlP, band struct. and pseudopotential form factors 3—15129
$(AlSb)_x(CdTe)_{1-x}$ solid solutions, optical absorption edge, coefficient, photoelectric method 3—34376
As_2Te_3, glassy, electronic properties by Mott-CFO model 3—1972
Au, electron model for thermoelec. props. 3—38781
Au, photoemission from polycryst., ang. anisotropy phenomena 3—5258
Au, relation of electron energy loss functions to transverse and longitudinal e.m. excitation 3—21030
$B_{12}N_{12}H_{12}$, hexagonal, band width, band gap, charges, equilib. distance, sublimation energy, from Huckel calcs. 3—15136
BaF_2 films spectra of electronic excitations in 8-150 eV range 3—2032
Be, influence of non-locality of Shaw's model potential 3—1979
Be, optical absorpt., 0.12-45 eV, interpretation 3—36869
Bi, cyclotron resonance in far i.r., quantum aspects and electrodynamics 3—33786
Bi:Sn, hole g-factor meas. 3—8089
BiOBr, luminesc., photocond., energy levels *(Russian)* 3—8108
BiOCl, luminesc., photocond., energy levels *(Russian)* 3—8108
BiOI, luminesc., photocond., energy levels *(Russian)* 3—8108
Bi_2S_3, Hall effect data *(French)* 3—36406
Ca, APW calc. as function of lattice const. 3—18070
Ca, calc. from muffin tin pot., photoemission energy distrib. meas. and calc. 3—34462
Ca, k dependent potential calc. 3—8086
CaF_2, films spectra of electronic excitations in 8-150 eV range 3—2032
$CaTl_3$, density of states curve calc. compatible with oscillatory curve of Cu_3Au 3—1984
$CdCr_2S_4$, energy level model and band-to-band transitions in photocond. and luminesc. spectra 3—8222
$CdGa_2S(Se)_4$, refl. spectra obs. in polarized light 3—8604
$Cd_xHg_{1-x}Te$, electroreflectance obs. 3—12114
$Cd_xHg_{1-x}Te$, rel. to refl. spectra *(Russian)* 3—2548
$CdIn_2S_4$, calc. on symmetry lines by empirical-pseudopotential method 3—8101
CdO, APW calc., depend. on ionicity degree 3—30406
CdO film, band struct., optical props. 3—15134
CdS, electron-phonon interactions, first principles energy band calcs. 3—36535
CdS, spin orientation by optical pumping 3—2594
CdS conduction band effective mass anisotropy rel. to uniaxial compression *(Russian)* 3—15137
CdS thin films, shallow trapping levels, structure defects, photoconductivity relaxation 3—33833
$(CdS)_{3x}$-$(In_2S)_{1-x}$, optical and photocond. obs. 3—18085
CdTe, amorphous, transitions involving energy states, disorder effects 3—2526
CdTe, Monte Carlo calcs. on high field electron transport 3—8191
CdTe, recrystallised thin film,s exciton-phonon interaction *(Russian)* 3—11871
CdTe:In, absorption band edge of compensated crystals 3—24717
$(CdTe)_{1-x}(AlSb)_x$ solid solutions, optical absorption edge, coefficient, photoelectric method 3—34376
Ce hydrides, temp. dependent electronic transition, resistivity meas. 3—8237

band structure continued
CsI, photoemission calc., tight-binding approximation and pseudopotential fit 3—21519
CsI, photoemission obs. 3—21518
Cu, calc. using non-local screened exchange 3—1980
Cu alloy, magnetoresist. and dHvA meas. rel. to impurity scatt. of electrons 3—21055
CuCl, energy band calc. using mixed basis method of Kunz 3—33798
CuCl, Faraday rotation near absorpt. edge, interband and exciton effects 3—15474
$CuInSe_2$, electronic structure from electroreflectance and photoluminescence meas. 3—39183
Cu_2O, from two photon absorption spectrum 3—2567
p-Cu_2S, carrier effective mass from refl. spectra 3—36534
p-Cu_2Te, carrier effective mass from refl. spectra 3—36534
Dy, rel. to hydrostatic press. derivatives of elastic moduli 3—27051
Er, rel. to hydrostatic press. derivatives of electric moduli 3—27051
Er, rel. to photoemission, 4-21 eV 3—8702
Eu chalcogenides, ferromagnetic, semiconducting, band structure 3—38859
Eu chalcogenides, optical electrical and magnetic props., review 3—11848
$Eu_{1-x}Gd_xO$, refl. in visible and i.r. spectra rel. to band nature of elec. cond. 3—5214
Fe, contact charge density of 4s electrons, internal conversion expt. 3—15124
Fe, ferromagnetic, energy band calc. 3—38784
Fe, paramag. and ferromag. states, self-consistent band calc. 3—21205
Fe base bcc ferromagnetic alloys, coherent potl. approx. calc. 3—11999
Fe_3O_4, magnetite from optical props. at Verwey transition 3—2506
FeRh alloys, positron annihilation study of electron structure of ferromagnetic and antiferromagnetic phases 3—7754
$FeSi_2$, new amorphous material, structural, electrical and optical props. 3—36419
GaAs, band struct. and effective masses, combined pseudopotential-k.p calc. 3—18079
GaAs, cond. band effective mass anisotropy rel. to uniaxial compression *(Russian)* 3—15137
GaAs, laser focusing, intervalley transfer mechanism 3—10552
GaAs, pressure depend., combined pseudopot. calc. 3—27214
p-GaAs, reflection spectra obs. of temp. depend. of hole effective mass 3—24382
GaAs, rel. to low temp. Hall meas. and scattering mechanisms 3—21097
GaAs, subsidiary indirect cond. minima, donor levels 3—2027
GaAs heavily doped, electron mobility rel. to electron-electron scatt. and nonparabolic energy band shape 3—18139
GaAs oscillation band periodicity, temperature dependence *(Russian)* 3—30408
p-GaAs:Zn, optical orientation of electron spins, surface influence, recomb. radiation study *(Russian)* 3—8662
GaAs-GaP, energy band calc. by combining empirical pseudopotential method with virtual crystal approximation *(Korean)* 3—27213
$GaAs_{1-x}P_x$:N, photopumped thin films, luminescence, variable energy bandstructure, l.e.d. applications 3—39175
$Ga_xIn_{1-x}P$:S, from Hall effect and resistivity meas. 3—15215
GaN, calc. from muffin tin potential 3—11850
GaSe layer compound, band structure calc. using empirical pseudopotential method, charge densities and bonding 3—30404
Gd, rel. to hydrostatic press. derivatives of elastic moduli 3—27051
$Gd_xLa_{1-x}Al_2$, superconductivity and e.p.r. 3—21172
Ge, cond. band effective mass anisotropy rel. to uniaxial compression *(Russian)* 3—15137
Ge, crystalline and amorphous phases, band struct. and density of states 3—33776
Ge, electron states under uniaxial stress, pseudopotential calc. 3—33801
Ge, energy band calculations from a nonlocal separable potential model 3—33797
Ge, interband transitions of hot holes, and cyclotron reson. of light holes *(Russian)* 3—8109
Ge, laser excited, radiative transition 3—5233
Ge, nonlocal pseudopotential calc. 3—38792
Ge, optical absorp. var. with mag. field intensity, determ. of band struct. *(German)* 3—34332
n-Ge, rel. to hot electron Hall transport, calc. 3—38848
Ge, two-phonon deformation potential 3—7883
Ge amorphous, electron spectra, effect of valence angles deform., LCAO calcs. *(Russian)* 3—8084
Ge amorphous film, rel. to elec. cond. 3—15116
Ge amorphous thin films, optical props. 3—15575
Ge polytype, pseudopotential calcs. rel. to form factor 3—21005
GeO_2, interband optical transitions strengths 3—34362
$GeSb_2Te_4$, three valley model, re. to single cryst. characterization 3—5279
H, cubic atomic crysts., electronic struct., Bloch functions, Fermi surfaces, exact Hartree-Fock calcs. 3—33800
H_2, metallic, random-phase-approx. correl. energy using Hartree-Fock Bloch functions 3—36525
^4He, liquid, ground state wavefunction calc. 3—11774
$HfS_2(Se_2)$, octahedral coordination, transmission spectra obs. 3—12144
$Hg_{1-x}Cd_xTe$, and charge density calcs. using representative k points 3—18080
HgSe, determ. from magneto-quantum effects 3—2003
n-Hgs, cubic, band inversion, optical absorpt. and intra-band refl. rel. to carrier conc. and temp. 3—2002
In, magnetoacoustic geometrical resons., interpretation 3—4945
InAs, energy band struct., refl., modulated refl., dielec. function, pseudopot. calc. 3—30403
InAs, rel. to structural transition and Hall effect meas. to 90 kbar 3—21096
$In_{1-x}Ga_xP$:N, photopumped thin film, luminescence, variable energy band structure, l.e.d. applications 3—39175
InP, n- and p-type spin orientation by optical pumping 3—2593
InP, subsidiary indirect cond. minima, donor levels 3—2027
n-InSb, deformation potential parameters calc. 3—8105

band structure continued
InSb, energy band struct., refl., modulated refl., dielec. function, pseudopot. calc. 3−30403
n-InSb, heavily doped, Kane band model for dispersion law 3−21007
p-InSb, reflection spectra obs. of temp. depend. of hole effective mass 3−24382
InSb, two-phonon deformation potential, on electronic spectrum 3−7882
Ir, variations with crystal potentials, relativistic APW exam. 3−4944
K, interband optical cond. calc. in range 1 to 10 eV 3−24375
KCl, luminescence lifetime of α, F and F′ centres 3−21475
$KMoO_3$, energy bands, APW and LCAO calcs. 3−11852
$KNiF_3$, energy bands, APW and LCAO calcs. 3−11852
$KTaO_3$, energy bands, APW and LCAO calcs. 3−11852
LaF_2, crystalline, vacuum u.v. reflectivity meas. 3−34374
Li-Mg, alloys optical properties, optical and soft X-ray spectra, ellipsometry, Fermi surface 3−30836
LiF, electron excitations resulting from photoionisation *(Russian)* 3−8611
LiF, LEED intensity profile for (100) surface, and bulk energy bands, calc. 3−36466
LiF, self-consistent energy bands 3−21010
LiH, energy bands in Hartree Fock approximation 3−30401
Mg-Li, alloys optical properties, optical and soft X-ray spectra, ellipsometry, Fermi surface 3−30836
Mg_2Sn, logarithmic derivative refl. spectra, 1.3-3.2 eV 3−2561
$MnFe_2O_4$, rel. to permittivity tensor, visible region *(Russian)* 3−8551
MnSb, and related compounds, zero-field n.m.r. obs. 3−27440
Mo-Re alloy crystals Hall effect, Mo electron configuration changes due to Re addition 3−8155
MoS_2, 2H-, energy band calc. 3−38791
MoS_2, layered, u.v. photoemission obs. 3−5256
MoS_2, rel. to refl. spectra anal. *(Russian)* 3−5213
MoS_2, u.v. stimulated photoemission obs. 3−2615
$MoS_2(Se_2)(Te_2)$, trigonal prismatic coordination, transmission spectra obs. 3−12145
$MoSe_2$, 2H polytype, spectral obs. for photon energy range 0.5 to 3.8 eV 3−12151
$MoTe_2$, 2H polytype, spectral obs. for photon energy range 0.5 to 3.8 eV 3−12151
NaCl, optic phonon deform. effects, APW calcs. 3−15135
NaCl, rel. to F-centre absorpt. 3−4755
$NaClO_3$, phonon-assisted electronic transitions, 50-368K 3−21431
Nb, absorpt. or refl. meas. from 0.1 to 36.4 eV, interband effects 3−39159
$NbSe_2$, 2H-, energy band calc. 3−38791
$NbSe_2$, layered, u.v. photoemission obs. 3−5256
Ni, d-band wave functions *(Russian)* 3−30390
Ni alloys, conc., elec. resist. meas. rel. to electronic structure 3−4993
Ni base fcc ferromag. alloys with Co, Fe, Mn and Cr, coherent potential approx. calc. 3−8328
Ni_3Mn-based, ternary alloys, atomic distrib., rel. to electronic struct. *(Russian)* 3−26990
NiO, valence-electron ionization and optical excitation energies 3−27219
Ni_3P, density of states curve, band struct. calcs. 3−4950
PbI_2, temp. and press. effects on exciton spectrum 3−21436
p- $Pb_{1-x}Mn_xTe$ solid solutions, energy band scheme from spectra 3−24716
PbN_6, pure and doped thin films, photodecomposition and electronic struct. 3−25084
β-PbO_2, from Kohn-Korringa-Rostoker method calcs. 3−8107
PbPo, electron and hole effective masses, calc. 3−30400
PbS-GaAs p-n heterojunction, rel. to near i.r. detection 3−22283
PbS(Se)(Te), secondary band extrema, effect of strain 3−38793
PbSe, band inversion under hydrostatic press., elec. resist. and galvanomag. obs. 3−2004
PbSe, k.P perturbation calc. 3−1997
$Pb_{1-x}Sn_xSe$, $0 \leqslant x \leqslant 0.3$, band inversion under hydrostatic press., elec. resist. and galvanomag. obs. 3−2004
PbTe-SnTe, absorpt. coeff. calc. in nonparabolic region using two-band model 3−15520
Pd, enhancement effect in isochromat spectroscopic investigations 3−39202
Pd, using augmented-plane-wave method 3−1983
Pd-Ag-Gd solid solution, magnetic and crystallographic characteristics 3−8793
PrF_3, crystalline, vacuum u.v. reflectivity meas. 3−34374
α-Pu, model and explanation of anomalous physical props. *(French)* 3−8345
RbCl, rel. to X-ray Kβ emission and absorpt. spectra 3−39199
Rh, calc. and rel. to energy distrib. curve for photoemitted electrons 3−15121
Rh, enhancement effects in isochromat spectroscopic investigations 3−39202
Sb_2Te_3:I, six valley model used rel. to transport props. 3−8607
ScCo, stability investigation by self-consistent KKR method 3−15335
ScCu, stability investigation by self-consistent KKR method 3−15335
Se:Na, polycrystalline, i.r. photoconductivity 3−5029
Se-electrode (Cu, Ag, Al) metal-semiconductor boundary, compound formation, energy levels, vacuum photoemission study 3−38893
Si, cond. band effective mass anisotropy rel. to uniaxial compression *(Russian)* 3−15137
Si, crystalline and amorphous phases, band struct. and density of states 3−33776
Si, electrodistrib., X-ray structure factor interpret. 3−30106
Si, electron states under uniaxial stress, pseudopotential calc. 3−33801
Si, energy band calculations from a nonlocal separable potential model 3−33797
Si, heavily doped, rel. to transport eqns. 3−24419
n-Si, hole generation in anodic dissolution rel. to surface generation currents 3−18160
Si, optical absorp. var. with mag. field intensity, determ. of band struct. *(German)* 3−34332

band structure continued
Si, optical absorpt. near indirect band gap, fine structure 3−18082
Si, parametric study of surface potential and band bending 3−36654
Si electroreflectance obs. of E_0 and $E_0 + \Delta_0$ transitions 3−4948
Si inversion layers, electron exchange energy 3−21132
n-Si-Ge alloys, Si-rich and electron magnetic susceptibility 3−36530
Si-SiO_2, interface band struct., O and Si vacancies energy levels 3−18228
SiO_2, interband optical transitions strengths 3−34362
Sm, rel. to photoemission, 4-21 eV 3−8702
Sn, white mass calculations, PW and APW formalisms, one electron crystal potential parameters, Fermi surface 3−30392
SnO_2, interband optical transitions strengths 3−34362
SnS_2, from pseudopot. model 3−18086
SnS_xSe_{2-x} solid soln., from pseudopot. model 3−18086
$SnSe_2$, elec. props. under pressure rel. to band structure 3−8176
$SnSe_2$, from pseudopot. model 3−18086
SnTe, secondary band extrema, effect of strain 3−38793
SrF_2 films spectra of electronic excitations in 8-150 eV range 3−2032
$SrTiO_3$, differential optical spectra and band struct. 3−36891
$SrTiO_3$, distortion enhanced optical absorption at the cubic to tetragonal transition 3−12149
$SrTiO_3$, energy bands, APW and LCAO calcs. 3−11852
Te, electron mag. levels from electric field modulated magnetoreflectance 3−2524
p-Te, energy struct. of Landau levels from longit. magnetoresist. 3−7874
Te, inactive mode cyclotron resonance absorption 3−8106
p-Te, magnetoresist., transverse and longit., impurity band like states 0.4-4.2K 3−27275
Te-Se liquid alloys, band spectrum from thermal conductivity meas. 3−36632
TiFe, stability investigation by self-consistent KKR method 3−15335
TiO, band struct. of oxides crystallizing in the rocksalt struct., theoretical study 3−8102
TiO_2, interband optical transitions strengths 3−34362
Ti_2O_3, resistivity and one dimensional energy bands 3−21008
$TiS_2(Se_2)$, octahedral coordination, transmission spectra obs. 3−12144
TlCl, band edge temp. dependence, two-photon absorption and multiphonon processes 3−12148
γ-U, relativistic energy band structure and props. 3−38788
UFe_2-UAl_2 alloy, chem. ordering, electronic struct., ^{57}Fe Mossbauer obs. 3−1987
UFe_2-UGa_2 3−1987
$(U_xTh_{1-x})S$, electronic props., models, mag. susceptibility, sp. ht. and elec. resist. obs. 3−2249
V, Compton profile of single crystal 3−21019
VMn, stability investigation by self-consistent KKR method 3−15335
VO, by augmented-plane-wave method 3−2016
VO_2, calc. using tight-binding interpolation 3−24379
VO_2, metallic, calc. 3−36541
VO_2, metallic, Coulomb interactions 3−24556
VO_2, metallic phase, APW calc. 3−1975
VO_2, parametrized bands, method of obtaining 3−24384
VO_2, semicond., calc. 3−36542
$WS_2(Se_2)$, trigonal prismatic coordination, transmission spectra obs. 3−12145
WSe_2, 2H polytype, spectral obs. for photon energy range 0.5 to 3.8 eV 3−12151
WSe_2, line shape of electro-reflectance excitonic structure 3−2038
Y, rel. to optical absorpt., 4.2 K, 0.15-4.4 eV 3−39161
Zn, energy level struct. in mag. field, using single-band effective Hamiltonian 3−36526
$ZnIn_2S_4$ single crystals, response to illumination 3−18181
ZnO, interband magnetoreflection obs. 3−27513
$ZnS_{1-x}Se_x$, meas. of electron transitions and energy bands by optical reflection techniques *(German)* 3−34339
ZnSe, electronic struct. of zinc blende phase and rock salt phase 3−21011
ZnTe, amorphous, transitions involving energy states, disorder effects 3−2526
$ZrS_2(Se_2)$, octahedral coordination, transmission spectra obs. 3−12144

band theory models
see also band model of magnetism; band structure
$A^2B^4C^5_2$ compounds with chalcopyrite structure, energy gap approximation 3−36532
actinides, hybridized 6d-5f virtual bound states theory model 3−1986
alloys, disordered, electronic struct., iteration scheme, IATA 3−30389
antiresonance in exciton spectrum, phonon contrib. 3−8128
coherent potential approximation test with excitonic doublets in mixed crystals 3−30436
combined KKR-discrete variational method 3−36513
crystals with zinc blende symmetry, second order nonlinear optical susceptibility, energy band theory 3−8550
diamond, gamma-ray Compton profiles, comparison with Si band calculations 3−11649
dilute alloy, test of virtual-level, Friedel-Anderson model 3−38786
disordered system, strong correlations effects 3−33777
Hubbard, band narrowing and T-matrix pole 3−8075
Hubbard, high temp. sp. ht. and entropy of interacting electrons 3−18295
Hubbard band, half-filled, mobility gap due to spin random distrib. 3−15148
Hubbard model, classical, linear-chain, metal-insulator transition 3−38765
Hubbard model, critical intra-atomic interaction to bandwidth ratio 3−30422
Hubbard model, Mott transition and Lifshits instability 3−8118
Hubbard model, narrow half filled band, electrical conductivity and thermodynamics, semiconductor-metal transition investigation 3−11842
Korringa-Kohn-Rostoker energy band method, with the speed of empirical pseudopotential methods 3−8078

band theory models continued
  Kronig Penney model, soln. using T-matrix, educational example 3−28433
  magnetic semiconductors, valence bond approach conceptual phase diagrams 3−38803
  metals, d states from plane waves, multicomponent theory of hybridised energy bands 3−38783
  metals, d states from plane waves transformed plane-wave method 3−38782
  molecular cryst., substitutionally disordered, interacting bands, coherent pot. theory 3−30379
  molecular crystal in contact with metal, quantum mechanical model of electronic states 3−8252
  noble metal, electronic model for Au, rel. to thermoelec. props. 3−38781
  nonlocal separable potential model, applic. to energy band calcs. on Si and Ge 3−33797
  nonparabolic bands, evaluation of transport integrals for conduction 3−36573
  one-dimens. band hypothesis rel. to low temp. sp. ht. 3−8103
  open shell band energies at symmetry points rel. to cryst. field and superexchange energies 3−24373
  optical absorpt. spectra of half filled narrow band, Hubbard model, metal insulator transition region 3−30804
  periodic structs., unidimensional chain band parameters, calc. method *(Russian)* 3−21002
  semiconducting alloys, narrow band gap semiconductors, zero band-gap transition 3−38800
  semiconductor, Penn's model, dielec. function calc. 3−2000
  tetracyanoquinodimethan, semicond., Hubbard's third model for elec. cond. calc. 3−11893
  transition metal, muffin tin d-resonances and tight binding narrow d-band models 3−36523
  two-band model approach to nucl. spin-lattice relax. rate in excitonic state 3−30717
  two-band model instability w.r.t. annihilation scatt. of carriers, metal-insulator transition 3−36543
  two-photon exciton transitons in semiconductors, phonon-assisted, band models 3−18105
  Wannier function construction for simple and composite bands 3−38767
  Ag, u.v. photoemission from clean, Cs and Cs + O_2 coated surfaces, band theory 3−12215
  Ag-Pd, dilute alloy, test of virtual-level, Friedel-Anderson model 3−38786
  Al, uniaxial compression effects on the third-zone Fermi surface, NFE and OPW models 3−8093
  CdS/Cu_2S solar cell, band model 3−4946
  Cu, local exchange correlation potentials and the Fermi surface 3−8091
  Fe_3O_4, magnetite, based on Goodenough pair states below Verway temp. 3−2012
  Fe_3O_4, Verwey transition, model 3−4958
  Ge gamma-ray Compton profiles, comparison with Si band calculations 3−11649
  n-$Hg_{1-x}Cd_xTe$, Auger limited band to band and Shockley-Read recomb., photocond. meas. 3−36634
  γ-Mn, Hamiltonian, magnetic susceptibility, d electron, instability criterion 3−30602
  PbTe-MgTe alloy system, physical props., Seebeck coefficient explanation by two-valence band model 3−7904
  Si gamma-ray Compton profiles, comparison with Si band calculations 3−11649
  SnTe, band structure and Jones zone 3−4949
  $(U_xTh_{1-x})S$, electronic props., models, mag. susceptibility, sp. ht. and elec. resist. obs. 3−2249
  VO_2, c/a ratio in crysts. with rutile structure, rel. to metallic V-V bonding in band model of metal-insulator transition 3−18092
band theory of solids *see band theory models*
bands (kink) *see dislocations*
bandwidth compression
  optical images, review 3−10449
bang-bang control
  discrete linear systems, transient response to bang-bang type forcing functions 3−3662
  spacecraft oscillations with two-position attitude-control system 3−25376
Bardeen-Cooper-Schrieffer theory *see BCS theory*
barium
  abundance, isotopic, in ^{238}U fast fission spectrum 3−17269
  abundance in Luna 20 samples from Apollonius crater region *(French)* 3−12987
  adsorbed atoms, on metal, interaction with cond. electrons, rel. to transverse magnetoresist. 3−15186
  adsorbed on W, electron interaction obs. by static skin effect method 3−20937
  atom, line broadening for excited state transitions in rare gases *(German)* 3−4368
  atom, muonic, screening correction to binding energy 3−11188
  atomic emission spectra, shift and broadening of resonance lines in hot dense Ar and He 3−17345
  auroral ionosphere, plasma drifts, Ba cloud data 3−3061
  clouds in ionosphere, onset of striations 3−9318
  coating on GaAs, photoemission 3−15592
  desorption kinetics for Ba ad-particles on W surface with variation of O_2 surface coverage 3−24346
  exchange reactions with N_2O and NO_2, reaction products electronic states distrib. 3−9062
  ion cloud experiment, cylindrical shell computer model 3−34920
  ionisation, cross section meas. by energy resolved electrons 3−11173
  kaonic atom X-rays, determ. of K^- mass and K^- polarisability 3−29542
  localised d states for pseudopotential calcs. 3−8116
  neutron scatt. amplitudes 3−7604
  oxidation of Ba vapour with upper atmosphere O_2, BaO formation 3−16011
  phonon dispersion and binding energy, pseudopotential method 3−27208
barium continued
  photoemission spectra for u.v. illumination 3−18532
  plasma clouds, phys. parameters and general props. 3−3042
  plasma in Stellarator Wendelstein W II a, transit time magnetic pumping 3−20574
  purification by reactive distillation in Mo column 3−18536
  Q-plasma, ion temp., optical meas. 3−1519
  reaction with Cl_2 and Br, crossed beams chemistry 3−21803
  reactive collision with ICl, crossed beams product angular distributions of BaCl and BaI 3−27864
  reactive collisions with BrCN, crossed beams product angular distributions of BaCN and BaBr 3−27864
  superconductivity in h.p. phases 3−30561
  ultrapure single crystals preparation by ultrahigh vacuum reactive distillation *(German)* 3−8733
  upper atmosphere clouds, sampled spatial resolution spectrograph 3−16059
  vapour, stimulated anti-Stokes radiation 3−33021
  Ba cloud in auroral ionosphere rel. to electron intensity, rocket flight obs. 3−12785
  Ba II stars amongst Am- and Ap-types, uvby photometry 3−31661
  $Ba + Cl_2 \rightarrow BaCl + Cl$, collision dynamics, hermaphroditism 3−25047
  $Ba + O_2$ reaction, prod. of electronically excited BaO 3−12504
  Ba^+, pressure shift and broadening of resonance lines in hot compressed Ar and He 3−33033
  Cs-Ba thermionic converter under overneutralised Knudsen conditions, plasma diagnostics 3−30013
  $KBr:Ba^{2+}$, kinetics of conc. decrease of nonequilib. cation vacancies 3−38585
  $KCl:Sr^{2+}(Ba^{2+})$, microhardness, heat treatment effects 3−7843
barium compounds
  see also barium titanate
  ferrite, preferred orientation during hot pressing, X-ray investigation *(Russian)* 3−15743
  monoxide or hydroxide visible bands in flames, identification method 3−22547
  perovskites, ordered, pseudotriclinic cell deform. induced by displacement of ion 3−17766
  silicophosphates, preparation and characterization *(Russian)* 3−11597
  stearate 'built up' films, d.c. destructive breakdown field, temp. depend. 3−5161
  stearate multilayer films, breakdown field temp. depend. 3−27469
  BaB_6 mixtures for cathodes in electron optical instruments 3−805
  $BaBiO_3$, i.r. spectral determ. of Bi valency state, charge distrib. 3−34363
  δ-$BaCO_3$, metastable phase, props. study 3−4855
  $BaCaTlNb_5O_{15}$, lattice parameters, permittivity temp. depend. *(French)* 3−38566
  $BaCl_2$, electric dipole moment determ., bond angle 3−23552
  $BaCl_2$, holographic storage, efficiency, inscription duration *(French)* 3−35437
  $BaCl_2$ in NaCl, flow stress, annealing depend., dislocation-impurity interactions 3−20786
  $Ba(ClO_3)_2.H_2O:O^-{}_3$ single crystals, e.s.r. 3−5134
  $BaCl_2.2H_2O$, nuclear quadrupole resonance Zeeman study of ^{137}Ba 3−27437
  $BaCoF_4$, low freq. magnetoelectric resonances 3−18170
  $Ba_2Co_2Fe_{12}O_{22}$, mag. anisotropy, n.m.r. study 3−36801
  $Ba_3Co_{2-x}Fe_{24}O_{41}$, mag. anisotropy, n.m.r. study 3−36801
  $Ba_3Co_2Fe_2O_4$ ferrite film, arc plasma deposited, mag. props. 3−36772
  $Ba_3Co_2Fe_{24-x}Sc_xO_{41}$, Sc ions influence on hexaferrite magnetic structure *(Russian)* 3−15372
  $BaCu_4S_3$, $\alpha \rightarrow \beta$ phase transform atom at 640°C and crystal structure 3−11599
  BaF, green band system 3−33117
  BaF_2, ^{19}F chem. shift tensor and nonionic bonding 3−12070
  BaF_2, calc. of H^- impurity vibr. 3−36390
  BaF_2, changes in real structure due to compressive impact 3−33503
  BaF_2, e.p.r. of U^{3+}, discrete saturation phenomena 3−2366
  BaF_2, F-centres absorpt. bands in neutron irrad. cryst. 3−1623
  BaF_2, high-freq. acoustic harmonic generation by Bragg light scatt. 3−7859
  BaF_2, hopping motion of V_k centres 3−20735
  BaF_2, radiation induced transform. of defects, e.p.r. and optical absorpt. obs. *(Russian)* 3−30694
  BaF_2, shell model calc. of formation energy of point defects 3−38583
  BaF_2, static optical and spin resonance props. of V_k centres 3−20734
  BaF_2, temp. effect on X-ray luminesc. spectra, Eu^{2+} impurity effect *(Russian)* 3−8650
  BaF_2, vacancies, interstitials and inert gases in fluorite structures 3−17814
  BaF_2 and $BaF_2:Mn$, thermoluminescence, glow curves, appl. to dosimetry 3−2600
  BaF_2 spectra of electronic excitations in 8-150 eV range 3−2032
  $BaF_2:Eu^{2+}$, impurity-induced Raman scatt. 3−39147
  $BaF_2:H^-$ ions, impurity induced far infrared absorption 3−34387
  $BaF_2:Sm^{2+}$ shell model, sensitivity to high frequency dielectric constant 3−1737
  $BaF_2:U^{3+}$, linear elec. field effect in e.p.r. for U^{3+} tetragonal sites 3−34200
  BaF_2-NaF(KF) binary molten salt, specific electrical conductivity at 1000°C 3−36631
  $BaFe_{12}O_{19}$, ferrite with magnetoplumbite structure, anisotropy of hopping cond. and thermoelec. power 3−38829
  $BaFe_{12}O_{19}$, internal domain structure, power patterns and Faraday effect obs. in i.r. 3−38990
  $BaFe_{12}O_{19}$ ferrite film, arc plasma deposited, mag. props. 3−36772
  $BaFe_{12}O_{19}$ substituted ferrite, coercivity 3−34165
  $Ba_4Fe_9O_{20}H_6$, hydrothermally synthesized, cryst. struct. 3−17767
  $Ba_8Fe_{13}O_{30}H_6$, cryst. struct. and antiferromag. 3−17768
  $Ba_3Fe_2TeO_9$, struct. and antiferromagnetism at low temps. *(French)* 3−7690
  $BaGa_2S_4:Ce,Na$, cathodolum., rel. to flying spot scanner appl. 3−12186
  BaH, BaD, close-lying $A^2\Pi$ and $B^2\Sigma^+$ states, fine struct. calc. 3−23572

barium compounds continued
$BaHPO_4$, growth in gelatin gel 3−24783
$Ba(H_2PO_2)_2$, radiocrystallographic and i.r. spectroscopic obs. *(French)* 3−7700
$BaIn_xFe_{12-x}O_{19}$ Ferrite, mag. struct., reson. fields temp. depend., torque angular depend. 3−21250
$Ba_2LaLiNa_2Nb_{10}O_{30}$, cryst. growth from melt, and characterization 3−12268
$Ba_2LaLiNa_2Nb_{10}O_{30}$, obs. of tetragonal tungsten bronze structure 3−38572
$Ba_{0.5}Mg_{0.5}SO_u:Eu^{2+}$, fluorescence and excitation spectra 3−39172
$Ba_{2-x}Mg_{2-y}Ti_{8-z}O_{16}$, rutile substructure obs. 3−7908
$BaMg_2Y_2Ge_3O_{12}$, e.s.r. of Nd^{3+}, g-factor, mag. ion symmetry 3−2384
$BaMnF_4$, antiferromag. reson. spectrum 3−34219
$BaMnF_4$, two-dimensional mag. ordering in isotropic Heisenberg antiferromagnet 3−36725
$BaMoO_4$, $BaWO_4$, coupled vibrations, i.r. reflection and Raman spectra obs. 3−30815
$BaMoO_4$, melt growth by flux pulling method 3−12283
$BaMoO_4$-BaO, X-ray and visual obs. of phase diagram *(Russian)* 3−14965
$Ba(NH_4)PO_4.6H_2O$, cryst. growth in gelatin gels 3−15610
$BaNH_4PO_4.8H_2O$, growth in gelatin gel 3−24783
$Ba(NO_3)_2$, elastic consts., 4-300K, u.s. meas., thermoelastic behaviour 3−17894
$Ba(NO_3)_2$, single cryst., i.r. and Raman study at 300 and 80K 3−27504
Ba_2NaNbO_{15}, doubly resonant parametric oscillator, c.w. Ar laser pumped 3−755
$Ba_2NaNb_5O_{15}$, continuously pumped doubly resonant optical parametric oscillator, performance 3−32585
$Ba_2NaNb_5O_{15}$, X-ray K-absorpt. edge of Nb 3−27584
$Ba_2NaNb_5O_{15}$ polaritons, biaxial crystal, vibration retardation effect, frequency shift, dispersion 3−38818
$Ba_2NaNb_5O_{15}$ segregation of impurities and striation rel. to growth speed 3−24804
$BaNb_2O_6$, X-ray K-absorpt. edge of Nb 3−27584
$Ba_3Nb_7Si_2O_{25-x}$, cryst. struct. 3−14745
Ba_2NiF_6 magnetic susceptibility, antiferromagnet, single crystals, low temp. measurements 3−36714
$Ba_2Ni_2Fe_{12}O_{22}$, mag. anisotropy, n.m.r. study 3−36801
BaO, $A^1\Sigma$-$X^1\Sigma$ band system, electronic transition moment 3−17424
BaO, effects of pressure on crystal structure and lattice parameters 3−7684
BaO, electronically excited, prod. in $Ba + O_2$ reaction 3−12504
BaO, optical phonons at centre of Brillouin zone at 300 and 17K *(French)* 3−8567
BaO, thermo-chemical determination of defect structure 3−11613
BaO activation of Au film, change in work function of isolated centres 3−36658
BaO formation by oxidation of Ba vapour with upper atmosphere O_2 3−16011
BaO-Bi_2O_3-B_2O_3 flux system, use in growth of ferrite spinels 3−2663
BaO-SrO-SiO_2, phase equilibria 3−39379
$BaO.P_2O_5$ glass, absorpt. spectra rel. to redox behaviour of Fe 3−24723
$BaO.2Fe_2O_3$, crystal structure obs. 3−36277
$mBaO.2UO_3.(4-2m)H_2O$, $O \leqslant m < 2$ indexing of X-ray powder patterns *(French)* 3−30091
$BaO.6\ Fe_2O_3$, texture and reaction mechanism in the formation 3−5413
$Ba(PO_3)_2$-$Cu(PO_3)_2$ system, phase diagram, cryst. struct. of $Ba_2Cu(PO_3)_6$ phase *(French)* 3−7901
$Ba_3(PO_4)_2$, growth in gelatin gel 3−24783
$Ba_3(PO_4)_2$ and $BaHPO_4$, cryst. growth in gelatin gels 3−15610
$BaPO_3F$-$Al(Ga)F_3$-$Li(Na)(K)(Zn)(Cd)(Pb)F_x$, glass, vitrification and crystallisation capacity *(Russian)* 3−14698
$BaPdF_4$, preparation, madelung part of lattice energy *(German)* 3−14814
BaS, addition in US, effect on sintering, 1500-1950°C 3−18692
$BaSO_4:Eu(Mn)$, radiational defects, thermoluminesc. study *(Russian)* 3−27581
$BaSb_2O_6:Bi^{3+}(Pb^{2+})$, fluorescence obs. for each excitation band 3−21478
$BaSiO_3$ film, for use in integrated optics ccts., r.f. sputtering prep. 3−36983
$BaSi_2O_5$-$Na_2Si_2O_5$, phase equilibria and crystallisation kinetic 3−24030
$Ba_{1-y}Sr_yFeO_{3-x}$ and $Ba_{1-y}Sr_yFe_{1-z}M_zO_{2.5}$ ($M = Ga$ or In), dielec. props. *(French)* 3−36831
$Ba_{1-y}Sr_yMnO_{3-x}$ system, subsolidus phase relations and crystal structure of phases 3−27124
$Ba_xSr_{1-x}Nb_2O_6$, longitudinal electro-optical effects 3−21385
$Ba_xSr_{1-x}Nb_2O_6$, segregation of impurities and striation rel. to growth speed 3−24804
$BaSrTlNb_5O_{15}$, lattice parameters, permittivity temp. depend. *(French)* 3−38566
$Ba_{3-x}Sr_xZn_2Fe_{24}O_{41}$, hexagonal type-Z, noncollinear mag. struct. *(Russian)* 3−8372
$BaTbO_3$, crystal and magnetic structure, neutron diffraction examination 3−7677
Ba_2Te_3, refl. spectrum structs. due to optical consts. critical transitions 3−21432
$BaTiO_3:Nb_2O_5$, synthesis, dielec. props. 3−39385
$BaWO_4$, growth by double decomposition in melt 3−21540
$BaWO_4$, growth in silica gel 3−21527
$BaWO_4:U$, $BaMoO_4:U$, spectrum of UO_4^{2-} *(Russian)* 3−8619
$BaYb_2F_8:Er$, X-ray sensitive upconversion phosphor, prep. 3−12260
$Ba_2Zn_2Fe_{12}O_{22}$ ferrite film, arc plasma deposited, mag. props. 3−36772
CaO-BaO-WO_3, isothermal section and phase equilibrium study 3−17955
$KBa_5ZrNb_9O_{30}$, cryst. growth from melt, and characterization 3−12268
KCl-$BaCl_2$, precipitation of supersaturated solid soln., light scatt. obs. 3−33540
$KI:BaCrO_4$, reson. Raman effect 3−8565

barium compounds continued
$Sr_{1-x}Ba_xTiO_3$, phase transitions, u.s. velocity and permittivity studies 3−27478

barium titanate
Barkhausen effect and stabilization of spontaneous polarization 3−34315
$BaTiO_3$, photodomain effect 3−8528
ceramic, doped, grain boundary resistance model *(German)* 3−33938
ceramic, effect of clay and dolomite additions 3−21721
ceramic, high temperature equilibrium cation nonstoichiometry 3−8956
ceramic, I-V characts., 110-400°C 3−27266
ceramic, new thermally stimulated electron emission dosimeter *(German)* 3−14271
ceramics, weak field permittivity, saturation under high d.c. bias, grain size effects 3−8519
compressive deformation, role of twin boundaries 3−38608
conduction bands, two-dimensional character 3−1995
cubic phase, lattice dynamics, wave vectors, dispersion curves, elastic consts. *(French)* 3−20826
current-voltage characteristics and capacitance 3−33937
deposition by electrophoresis of $BaTiO_3$ polycryst. film with ferroelec. and antiferroelec. props. 3−39220
dielectric dispersion of irradiated $BaTiO_3$ in phase transition region *(Russian)* 3−15464
dielectric permeability meas., to 1.5×10^{10}Hz, including phase transitions *(Russian)* 3−8504
α- domain, antiparallel switching 3−21376
domain struct. and phase transition, illumination influence 3−15460
domains, obs. by convergent electron beam diffr. method 3−24657
ferroelectric domains in low temp. phase, electron microscope obs. 3−30765
ferroelectric phase transition, dielectric dispersion 3−15467
ferroelectric switching, kinetics of domain wall motion 3−39102
film, ferroelec., vacuum-evaporated, comp., struct. and dielec. props. 3−34317
grain boundaries, dielectric behaviour from electron beam scanning obs. 3−36302
internal friction, influence of domain struct. 3−36845
lateral motion in a-domain crystals 3−34314
light emission, solid state phase transitions, polarisation switching 3−39111
nonlinear dielectric constant determination, apparatus 3−19235
nonlinear optical properties, model of polarizable ions 3−32601
nonlinear props. at high freq., permittivity meas. 3−24648
nonstoichiometry detn. 3−17810
phonon modes, 27-134°C, Raman scatt. study 3−30221
piezoelectric props. of polarized $BaTiO_3$ ceramics under uniaxial transverse compression 3−5164
positive temperature coefficient of resistance, near Curie temp. *(Russian)* 3−18130
positron annihilation, effect of ferroelectricity 3−36335
Raman scatt. by soft E polariton mode 3−15481
single crystal growth, floating zone growth 3−2668
spontaneous polarisation, stabilisation *(Russian)* 3−12105
static electric quadrupole interaction meas. using differential PAC and Mossbauer effect 3−12090
u.s. velocities near paraelect. ferroelec. transition 3−30772
$(Ba, Sr)\ TiO_3$, boundary layer dielectric, permittivity and dispersion 3−2485
$Ba_{1-x}Sr_xTiO_3$, O_2 diffusion const. meas. 3−17991
$BaTiO_3$ polycrystalline, constant electric field influence on dielectric props. *(Russian)* 3−8532
$BaTiO_3:Al$ ceramic, piezo-electric effect 3−21363
$BaTiO_3:CeO_2$, non piezoelec. dielec. ceramic, electromechanical bond coeff. *(Russian)* 3−21365
$BaTiO_3:La_2O_3$, catalytic activity study using CO oxidation 3−18788
$BaTiO_3:Nb$, Mn ceramic, semiconducting, application as positive temp. coeff. thermistor 3−2152
$BaTiO_3:Y_2O_3$ depend. on composition and cation siting structure and electrical props. 3−14813
$BaTiO_3$-$CaTiO_3$ (5 wt.%), large polarisation depend. photovoltages 3−33951
$BaTi(Zr)O_3$ ^{89}Zr half-life change at upper phase transition 3−36844
$(Sr_{1-x}Ba_x)TiO_3$ mixed cryst. system, phase transitions obs. 3−15456

Barkhausen effect
metallic ferromagnets, negative Barkhausen jumps in consecutive asymmetrical magnetization reversal 3−38993
$BaTiO_3$, stabilization of spontaneous polarization and Barkhausen effect 3−34315
Fe-Ni alloy film, modulation of mag. noise spectral distrib. *(Russian)* 3−12042
Ni, influence of mechanical stresses in elastic deformation region on inversible elementary magnetisation 3−38991
SbSI, rel. to state of defects 3−39114

Barnett effect *see gyromagnetic effect; magnetisation*

barometers
No entries

barometric pressure *see atmospheric pressure and density*

barrages *see dams*

barrel distortion *see aberrations*

baryon-baryon interactions
see also hyperon-nucleon interactions; nucleon-nucleon interactions
self consistent field theory of extra strong interactions 3−19708

baryon-baryon scattering
see also hyperon-nucleon scattering; nucleon-nucleon scattering
No entries

baryon decay
see also baryon hadronic decay; baryon leptonic decay; hyperon decay
resonances, strong decay rate in two-body composite baryon model 3−35808
$\Delta(1232)$, determ. of electroproduction coincidence cross sections from coupled multipole eqns. 3−13941
$n \rightarrow pe\nu$, oscillation in hollow in potential energy curve 3−14099

baryon hadronic decay

- $\Delta S=0$ and $\Delta N'=1$ interactions in new Nagoya model for urbaryons 3—26289
- hyperon, P-wave, Lee-Sugawara relation 3—833
- hyperon, role of final-state interactions in producing $\Delta I=1/2$ rules 3—35779
- negative parity decay rates, $SU(6)_w$ fit 3—10672
- new particle obs. by Niu group, effect of form factor on decay rate 3—32653
- S-wave, mechanism for octet enhancement 3—26291
- selection rule based on law of configuration conservation, decays of new particles 3—32652
- spin-half baryons, elementary couplings in compensation theory of strong interact. 3—32651
- $\Delta\to\pi\Delta(1236)$, duality constraints 3—6585
- $\Sigma^+\to p\pi^0$, test of $\Delta I=1/2$ rule and Lee-Sugawara relation by meas. of decay proton polarisation 3—16976

baryon interactions

- *see also hyperon interactions; meson-baryon interactions; nucleon interactions*
- bilocal wave eqn. for baryons lying on linear trajectories 3—6555
- relativistic composite model in terms of B-S amplitudes 3—14024
- $\gamma B\to VB^*$, double resonance photoprod., statistical tensors expression 3—26303

baryon leptonic decay

- semi-leptonic weak interactions, Cabibbo theory, current algebra and strong interaction theories 3—831

baryon photoproduction

- *see also hyperon production; neutron production; proton production*
- p, meas. of inclusive cross sections at 3.2 GeV, comparison with electroproduction 3—23089
- $\gamma B\to PB^*$, VB, VB^*, quark models for angular distrib. 3—13902
- $\gamma B\to VB^*$, double resonance photoprod., statistical tensors expression 3—26303
- $\gamma p\to K^+\Lambda^0(K^+\Sigma^0)$, 1.05 to 2.2 GeV at constant momentum transfer, meas. of differential cross sections 3—13886
- $\pi\Delta$, spin 3/2 calcs., role of off-mass-shell terms in propagator and interaction vertices 3—23067

baryon production

- *see also baryon photoproduction; hyperon production; neutron production; proton production*
- multibaryonic resonance production with strangeness equal to and different from zero 3—29259
- relativistic quark model, spin predictions for baryon decuplet production 3—29223
- $\Delta(1236)$, production cross sections and parameters in K^+p interactions at 4.27 GeV/c 3—29262
- $\Delta(1236)$ production in $K^+p\to KN\pi$ reactions at 7.3 GeV/c in quasi-two-body reactions 3—29272
- $\Delta^{++}\Delta^{--}$ peripheral production in $pp\to pp\pi^+\pi^-$, meas. of Δ decay correlation parameters 3—26350
- $ep\to e'\pi^+\Delta^0(1236)$, electroproduction, meas. of differential cross section 3—13990
- N^*, by neutrinos, density matrix elements *(Korean)* 3—26293
- N^*, diffractive, in quark model 3—6665
- N^*, diffractively produced, spin-parity and helicity 3—17119

baryon resonances

- *see also hyperon resonances*
- decay, effective temp. in statistical bootstrap model 3—26322
- decays involving vector mesons, quark model, study of $\pi N\to N\rho$ 3—32655
- diffractive production processes, t-channel helicity conservation 3—32691
- double resonance production and equal-phase hypothesis 3—29260
- dual model, resonance production and inclusive cross-sections 3—26326
- electron and neutrino inelastic scattering with nucleons 3—10948
- exotic, in modified phase-shift analysis of $I=0$ K-N system 3—35826
- heavy nucleon resonances, applic. of missing mass method to examine 3—10824
- hypercharge and strangeness of strongly interacting system, role in multibaryon reson. prod. 3—17084
- multi-Regge iteration of low-energy peripheral resonances, absorption picture 3—19707
- multibaryonic resonance production with strangeness equal to and different from zero 3—29259
- negative parity decay rates, $SU(6)_w$ fit 3—10672
- photon excitation in 0.275-4.225 GeV region, meas. of total cross sections 3—13984
- positive-parity nucleonic resonances, two-quantum excited, quark-model analysis, SU_6 assignment 3—4246
- reciprocal bootstrap of N and N^*, calc. using nonpolynomial Lagrangian 3—4212
- strong decay rate in two-body composite baryon model 3—35808
- SU(4) classification scheme 3—819
- $\Delta(1236)$, production cross sections and parameters in K^+p interactions at 4.27 GeV/c 3—29262
- $\Delta(1236)$ excitation in inelastic ed scatt. 3—13919
- $\Delta(1236)$ production in inelastic ep scattering, separation of σ_s and σ_t cross-sections 3—17039
- $\Delta(1236)$ production in $K^+p\to KN\pi$ reactions at 7.3 GeV/c in quasi-two-body reactions 3—29272
- $\Delta(1236)$ production in $np\to pp\pi^-$, one-pion exchange analysis 3—23165
- $\Delta(1236)$ production in S-channel in photodisintegration of ^3He 3—17221
- $\Delta^-(1236)K^{*0}(890)$ double resonance production in K^-d interactions at 3.4 GeV/c 3—32719
- $\Delta^{++}(1236)$ prod. in pp interactions at 303 GeV/c 3—10812
- Δ^{++} production cross section in electroproduction with stramer chamber $0.3<Q^2<1.5$ GeV², $m_p\leqslant W<2.8$ GeV 3—38047
- Δ^{++} production $\gamma p\to p\pi^+\pi^-$ at 9.3 GeV, meas. of cross section 3—13947
- Δ_{1236} production threshold in $\pi N\to\pi\pi N$, model for partial wave analysis including triangular diagram contrib. *(Russian)* 3—10773
- $\Delta^{++}\Delta^{--}$ peripheral production in $pp\to pp\pi^+\pi^-$, meas. of Δ decay correlation parameters 3—26350

baryon resonances continued

- eN, electroproduction of nucleonic resonances, relativistic quark model 3—13996
- eN inelastic scattering, resonance form factors, scaling and Regge behaviour 3—35799
- $ep\to e'\pi^+\Delta^0(1236)$, electroproduction, meas. of differential cross section 3—13990
- $\gamma N\to N^*(I={}^1\!/_2)$, meas. of transition amplitudes, nucleon isobar mass <2 GeV/c² 3—13926
- $\gamma n\to p\pi^-$, cross-section meas. in 1st and 2nd reson. regions up to 1 GeV 3—16998
- $\gamma n\to p\pi^-$, dispersion relations discrepancy in isovector amplitude in Δ reson. region 3—17019
- $\gamma N\to\pi\Delta$, anal. using nucleon reson., in gradient-invariant mechanism 3—4177
- $\gamma p\to\pi^-\Delta^{++}$, exptl. check of quark model relations 3—13982
- $K^+p\to KN\pi\pi\pi$, 5GeV/c, study of resonance production 3—14077
- N resonances, electroproduction in relativistic quark model 3—14002
- N^* prod. by neutrinos, density matrix elements *(Korean)* 3—26293
- N^*, electroproduction with polarized leptons, symmetric quark model 3—4182
- $N^*(1236)$ in $K^+p\to K^+p\pi^+\pi^-$, 5 GeV/c, spin density matrix element 3—29273
- N^* prod., diffractive, in quark model 3—6665
- N^* production in K^+p interactions, influence on π angular correlations 3—29275
- $N^*\to\pi N$, spin-parity and helicity of N^* 3—17119
- $(N^*N\gamma)$ couplings for resonances in pion photoproduction, continuous partial wave analysis, quark model predictions 3—19692
- $\nu p\to\mu^-\Delta^{++}$, comparison of various models using spin-density matrix data 3—23045
- $\nu p\to\mu^-\pi^+p$ reaction at 1 GeV by $\mu\Delta^{++}(1236)$ mechanism, experimental study 3—23044
- $\omega\Delta^{++}$ joint decay correlations in π^+p interactions at 3.7 GeV/c 3—35840
- $\omega\Delta^{++}$ production in π^+p interactions at 3.7 GeV/c, quark-model comparison 3—35841
- pd scatt. baryon resonance exchange in GeV region 3—26440
- $pn\to\Delta^{++}(1238)\Delta^-(1238)$, 5.9 GeV/c, cross-section, isobar design and decay spherical harmonic moments 3—35838
- $pp\to px$, nucleon resonance production at 24.0 GeV/c 3—23153
- π electroproduction at $N^*(1236)$, isobaric model calc. using Feynman diagrams 3—13930
- π^0 photoprod. in third nucleon reson. region at 0.8 to 1.4 GeV, differential cross section meas. 3—16999
- πd scatt. in $\Delta(1236)$ region, calc. of amplitude from Feynman diagrams *(Russian)* 3—19744
- $\pi^-d\to ppx^{--}$, 7 GeV/c, search for $I=2$ multipion resonances 3—29271
- $\pi\Delta(1236)$ electroproduction, invariant amplitudes, vector-meson dominance 3—6618
- $\pi\Delta(1236)$ electroproduction, vector meson dominance 3—14008
- $\pi^-\Delta^{++}(1236)$ cross sections for electroproduction at 1.9 GeV and $-k^2=0.7$ GeV², Born and vector-dominance models 3—17001
- $\pi^0\Delta^{++}$ joint decay correlations in π^+p interactions at 3.7 GeV/c 3—35840
- $\pi^\pm\Delta$ electroproduction in electric Born model 3—14007
- $\pi^-p\to e^+e^-n$, meas. of differential cross-sections close to $\Delta(1236)$ reson., pion energy=276 MeV *(Russian)* 3—19728
- $\pi^-\rho\to lln$, at $N^*(1236)$ energy, 'isobar plus Born term' model 3—14085
- $\rho^0\Delta^{++}$ production in π^+p interactions at 3.7 GeV/c, quark-model comparison 3—35841
- $x\to\eta\rho^0$, investigation precedure when production cross-section small 3—32119
- $x\to m\pi^0$, investigation procedure when production cross-section small 3—32119
- Y^* (1930 MeV) new resonance in K^-p elastic scatt. 3—10786
- $Y^{*\pm}$ (1385) production in π^-p interactions at 20 GeV/c 3—32722

baryon scattering

- *see also baryon-baryon scattering; hyperon scattering; meson-baryon scattering; nucleon scattering*
- No entries

baryons

- *see also baryon resonances; hyperons; nucleons*
- annihilation processes, particle production, multiperipheral concepts 3—10754
- baryonnc quark states, fractional parentage decomposition 3—869
- big band cosmology, galaxy formation from annihilation-generated supersonic turbulence 3—16093
- bound and resonant states, quark model *(Hungarian)* 3—32676
- classification in SU(3) Regge scheme 3—14036
- cold (neutron) stars props. determ., appl. of energy variational principle to baryon sphere 3—28103
- e.m. form factors, calc. using phenomenological mass operator for hadrons 3—10693
- exotic, quark model for occurrence near nn threshold 3—23102
- exotic baryon-antibaryon system, compulsory resonance formation 3—865
- level structure, analysis using two-body quark potential 3—4188
- mass, calc. for baryons of incomplete SU_3-multiplets with high spins *(Russian)* 3—38011
- mass difference, calc. in model of strong and c.m. interactions based on broken U(3) × U(1) invariance 3—26276
- non-strange, effects of radial wave function in symmetric quark model, calc. of rotational energy levels 3—10722
- non-strange, radial excitation modes in symmetric quark model 3—10723
- nucleosynthesis, big-bang, baryonic number and electron leptonic number in Universe, limits 3—25387
- quark model calc. of mag. moment 3—14025
- SU(3) × SU(3) chiral algebra 3—6562
- symmetric quark model for nonstrange baryons, radial effects 3—29222
- universe structure, entropy, averaged initial state, short waves, galaxy clusters 3—3289

barysphere *see earth core*

BASIC
nondestructive testing, support of a minicomputer using BASIC 3−31226

batteries *see cells (electric); solar cells*

Bauschinger effect
elastic-plastic circular plates, large deflection analysis considering Bauschinger effect 3−6242
relay spring material, after effects of plastic working and plastic hysteresis 3−2724
steel, austenitic stainless, Nb-stabilized, stress varied creep behaviour 3−8925
viscoplasticity model in local strains theory 3−26093
Be, cyclic effect at twin boundaries *(Russian)* 3−30179
Be, rel. to twinning study *(Russian)* 3−20753
Be-Cu alloy, rel. to twinning study *(Russian)* 3−20753
Cu, stacking fault energy 3−36352
Cu-Al alloys, stacking fault energy 3−36352

Bayes methods
counting, nuclear, optimal estimation of background 3−25873
nuclear medicine, tumour detection, Scan-Rescan process based on Bayesian approach posterior probabilities 3−28371
spectral analysis, recursive Bayes deconvolution 3−9938

bays (magnetic) *see geomagnetic variations*

BCS theory
see also many-body problems; nuclear theory; superconductivity
coexistence of superconductivity and magnetism 3−38914
FBCS for odd nuclei and inverse gap equations, applic. to N=50 isotones 3−10887
Lagrangian approach to supercond. encompassing BCS model 3−5068
many-body problems, book 3−20990
model Hamiltonian of BCS theory, determ. of partition function, Green's function method 3−27324
nuclear pairing-force, Lipkin-Nogami version for ground and 0^+ states 3−19790
pairing in mag. field, appl. to liquid ^{3}He thermal anomalies 3−15048
reduced density matrix interpret. 3−26400
superconductivity theory for rigid boundaries 3−38913
superconductor, temp. depend. calc. of electromagnetic coherence length 3−15294
Pb, plastic deform. kinetics at superconducting transition 3−8293

beam choppers
ion bursts with small energy spread for linac 3−10033
light choppers, mechanical, high speed, design information 3−35392

beam handling equipment
accelerators, circular, field configurations for particle focusing 3−16494
achromatic deflection system with adjustable nonisochronism for particles with different momenta 3−28636
betatron, beam extraction by parametric resonance 3−16493
betatron, electron capture during injection and beam parameters 3−16495
CAMAC serial crate controller 3−35457
charge monitor, for neutron generator 3−37675
current and position monitor for Astron accelerator 3−6056
cyclotron, AEG-compact, design of extraction system 3−10025
cyclotron, Indiana university, USA, design study for split beam operation 3−16486
cyclotron, isochronous, at Julich, Germany, double-monochromator system 3−16487
cyclotron, isochronous, at Julich, Germany, system for emittance measurements 3−19274
cyclotron, isochronous, at Karlsruhe, methods of beam pulsing 3−19271
cyclotron, isochronous, longitudinal motion of particles 3−19269
cyclotron, Michigan university, USA, beam quality improvement 3−19272
cyclotron, TRIUMF, effect of magnetic imperfections on beam quality 3−19270
cyclotron, TRIUMF, optimization of phase acceptance 3−16485
88-inch cyclotron at Berkeley, USA, for heavy ion acceleration 3−13391
cyclotron Indiana University, USA, resonant depolarization effects for polarized beams 3−19273
cyclotron with active monochromatization system, optimization of beam acceleration and extraction conditions 3−16484
double focusing uniform field magnet, with circular poles 3−19278
Eindhoven, second order calculations 3−16490
elastically scattered 70 GeV/c proton beam from Mirabelle bubble chamber, beam guidance channel 3−16492
electromagnet design and construction 3−28623
guide system of betatron 3−16497
injection buncher applic. in 30 MeV linear travelling-wave accelerator *(Russian)* 3−28632
injection system, for Birmingham cyclotron, England 3−13400
injection system, using injected beam for synchronization in proton synchrotron 3−32126
injectors for electron accelerators with Pierce and Kerst-type optics 3−16496
ion source, low divergence extraction systems, design 3−19285
isochronous cyclotron of Michigan State Univ. USA, field trimming computer program 3−13395
Langmuir-Taylor detectors for ion beams 3−16533
linac, variable frequency, for heavy ion injection for separated sector cyclotron 3−13393
magnetic lenses, determination of non-linear components in corpuscular optical elements by incremental Hall-probe measurement 3−16488
monitor for secondary emission in accelerators 3−22447
neutron guide tubes of circular cross section production, for swimming pool reactor 3−11083
Oak Ridge, USA isochronous cyclotron for heavy ion injection 3−13392
optimized multiparticle central region for Michigan State Univ. isochronous cyclotron, USA 3−13394
proton beam, positioning by computer control 3−275
SPEAR storage ring, beam feedback electronics 3−37701

beam handling equipment continued
spill control system for Los Alamos Meson Physics Facility, USA 3−19275
superconducting flux exclusion tube, mag. field distribs. 3−19276
synchrocyclotron, filling of phase space in central region 3−13389
synchrotron guide field imperfections, program for closed orbit minimization by analytic technique 3−25962
tandem-cyclotrons of JINR, Dubna, USSR, acceleration of Xe ions 3−13390
Texas A and M cyclotron, USA, for heavy ion beams with cold-cathode source 3−13402
Uppsala tandem Van de Graaff accelerator, ion beam transport system 3−32123
π^{10} beam-line for nuclear structure expts on Nimrod, 200-2000 MeV/c 3−32128
H^- injection system for TRIUMF 500 MeV cyclotron, Vancouver, Canada 3−13401
He II cryostat, for supercon. particle separator 3−5840

beam-lead devices
see also hybrid integrated circuits
Si, fabrication, vapour deposition of Pt using c.w. laser energy 3−5264

bearings (machine) *see machine bearings*

bells
see also musical instruments
special bell with horns, continuous change of characteristic freq. *(Japanese)* 3−31973
special bell with horns, continuous change of characteristic freq. *(Japanese)* 3−31974

bending
see also stress analysis; torsion
anisotropic beams, analytic solns. from variational methods 3−28864
bar, anisotropic, with end loads, coefficients related to moment of internal stresses *(Russian)* 3−16642
bars, dynamic buckling under high velocity impact 3−16620
bars, dynamic buckling under low velocity impact 3−16619
beam, castellated with hexagonal holes, elastic stress detn. *(Japanese)* 3−16652
beam having holes of arbitrary shape, stress conditions *(Japanese)* 3−16651
beams and plates, analysis by lumped finite element technique 3−32385
beams curved in plane of noncircular centre lines, torsion and deflection, determ. of bending moment and angle of twist 3−19440
bend and compact specimens, stress intensity factors 3−13565
bimetallic strip bending due to interstitial diffusion 3−1825
box beam, thin-walled, post-buckled behaviour 3−539
brittle rectangular beam weakened by an internal circular crack, bending *(Russian)* 3−6243
buckling, dynamic, of elastic bars, successive approximation solution 3−16619
buckling, dynamic, of elastic bars under high velocity impact 3−16620
buckling and postbuckling behaviour of steep compressible arches 3−13576
buckling and postbuckling behaviour of unstiffed and stiffened cylind. shells under axial compress. 3−32321
buckling of laterally loaded plates with initial curvature 3−3970
buckling of plate with internal support 3−3992
cantilever, elastoplastic problem 3−22659
cantilever beam, approx. for large deflection 3−32343
cantilever beams of variable cross-section, non-linear bending, numerical soln. 3−22612
ceramics, acoustic emission testing for cracks when mechanically stressed 3−27832
circular oriented plastic plates, states of stress and strain 3−22670
circular plate, proposal of nonlinear theory *(Russian)* 3−527
circular plate, thermal stresses, transverse shear influence 3−22650
clamped skew plates, stability analysis using bar buckling eigenfunctions 3−3958
closed cylindrical shells, approx. methods and Jakobsen-Girkmann eqn. 3−16636
composite, fibre reinforced plastics, lamination effect on flexure behaviour *(Japanese)* 3−18713
composite beam deflection, microstructure model 3−10272
concrete load deflection characteristics of rectangular reinforced slabs 3−27814
constant moment finite element methods, unification with constant strain problems 3−32322
contact problems in bending of plates on elastic multilayer foundation *(Russian)* 3−32325
curved laminated beams, tangential stress analysis *(Russian)* 3−10295
cylindrical shell with inclined stiffeners, buckling load under axial compression 3−26089
design element, fatigue life determ. on basis of fatigue failure mechanism concepts 3−37108
discs supported around periphery, for strength determ. of materials and welded joints 3−34685
eigenfunction analysis and Fadle-Papkovitch functions for clamped rectangular orthotropic plates 3−28862
elastic beams, random gravity loads as stochastic function with independent increments *(Polish)* 3−19436
elastic plates, shear and C^0 and C^1 finite elements 3−28861
elastic-plastic analysis of bar under repeated axial loading 3−32357
elastic-plastic plate bending, finite element analysis 3−10274
elasto-plastic, analytical method of soln. 3−3952
elastoplastic, of rectangular plates with large deflection 3−22673
elastoplastic cylinder, circular bending, application of Tresca's criterion *(French)* 3−37814
epoxy compositions subjected to cyclic loading, relief of fracture surfaces 3−27780
equilateral triangular plates, corner supported, uniformly loaded, approximate soln. 3−22610
fibre reinforced incompressible isotropic elastic materials, universal solns. by inverse methods 3−28865

bending continued
- finite elastic-plastic, hyperelastic to perfectly plastic transition 3−37819
- flexibility matrix for exact torsion bending finite element 3−546
- flexural damping capacity, meas. apparatus 3−9833
- flexural deformations of a material line in a continuous body 3−35568
- foam-light refractories, strength testing apparatus *(Russian)* 3−27812
- general variational methods with discontinuous fields, applic. to bending, buckling and vibration of beams 3−19459
- glass, fracture, stress waves 3−33606
- glass reinforced plastic cylindrical shell weakened by circular opening, cantilevered 3−31149
- glass reinforced plastic plates, finite difference method with allowance for creep 3−27762
- glass reinforced plastic plates, rectangular, with low shear strength 3−24985
- glass reinforced plastics, oriented, mech. characts. in shear 3−27779
- hybrid displacement method for statics, vibr. and stability of thin elastic plates 3−10282
- hybrid elements, for plate bending problems analysis 3−517
- ice crystals, dynamical behaviour of dislocations 3−20739
- isoparametric stress elements, basis 3−19425
- laminated glass beams in 4-point bending, experimental and theoretical study of strength 3−32354
- limit loads of rigid-plastic variable thickness circular plates in bending 3−549
- load-bearing capacity of specimens with stress concentrators under repeated loading, deform. effects 3−34686
- multilayer sandwich beams and plates, finite element displacement analysis 3−26075
- nodal stress concept, for plates and shells 3−19410
- optical ceramics, KO-1, KO-2, bending strength temp. depend. 3−16414
- oriented plastics, failure mechanism 3−31183
- orthotropic almost cylindrical beams, bending by transverse load 3−28856
- orthotropic materials, transverse strain coeffs. determ. from bending tests 3−27846
- pipe, straight, eff. of bending and internal pressure 3−16645
- plane frames, finite deflection analysis on basis of bending stiffnesses 3−28859
- plastic, reinforced, testing apparatus, nonuniform heating 3−32033
- plate, convergence of mixed finite element scheme 3−37803
- plate stability, vibration analysis 3−3983
- plate with internal support, buckling 3−3992
- plates, Fadle eigenfunction analysis 3−35570
- post-buckling and imperfection-sensitivity of wide integrally stiffened panel under compression 3−13590
- postbuckling behaviour of optimally designed columns and plates 3−13575
- precurved disk, finite elastic-plastic bending *(German)* 3−3945
- recording device, for small bending deform. of plane samples 3−18758
- rectangular plates with stepped variation of thickness, analysis by Bubnov-Galerkin method *(Russian)* 3−28877
- rectangular plates with unidirectionally variable rigidity, soln. of differential eqn. of bending *(Polish)* 3−19435
- reinforced material under uniaxial compression, applied theories applicability in stability problems 3−26084
- relay spring material, after effects of plastic working and plastic hysteresis 3−2724
- sandwich beams of unsymmetrical structure 3−6200
- shell of revolution, variable thickness orthotropic, suppressed bending 3−26088
- shells of revolution, linear bending theory, calc. by method of differences *(German)* 3−19430
- snap-buckling of curved membranes, simple math. model with 1 degree of freedom 3−22662
- stability of bending vibrations of elastic beams moving periodically in a longitudinal direction *(German)* 3−19466
- steel, carbon specimens in oil, fatigue crack propagation, numerical analysis 3−21614
- steel, structural, hysteretic behaviour under cyclic bending *(Japanese)* 3−39374
- steel EBR II control-rod thimble, assessment of postirradiation room-temperature fracture due to bending 3−23441
- steel wire, loading in tensile testing 3−9029
- straight beams, moments, algorithm calc. 3−19420
- stress in an impulsively loaded cylindrical shell of exponentially varying thickness 3−37798
- stress-strain relation, in bending fatigue specimen 3−28475
- test, production of fatigue cracks, for work of rupture 3−27803
- thin plates, creep bending analysis by finite element method 3−16653
- torispherical shells under localized loads 3−6264
- triangular plate bending element for contact problems 3−22620
- uniform elastic strip around cylindrical drum 3−6227
- uniformly loaded clamped sector plate 3−507
- welded specimens, device for testing for long-term bending using cantilever method *(Russian)* 3−12483
- Young's modulus meas. method using fibre bending oscillations *(German)* 3−25668
- CdS, polarity of bending strength and photoplastic effect 3−1669
- CdS, thin wafers, piezoelec. modulation of surface charges on bending 3−2161
- Fe, Armco, coarse- and fine-grained, fatigue crack formation and propag. *(Russian)* 3−27671
- Fe_2O_3 polycrystalline powder ceramic, stress, high temp., grain size, porosity and O_2 partial pressure effects on creep 3−27738
- $Ga_xIn_{1-x}As$ on GaAs substrates, anisotropic bending during epitaxial growth 3−15085
- NaCl crystals, reverse deformation comparison with annealing, polygonisation 3−17903
- Ni alloy, fatigue strength, test temp. influence 3−34687
- Si crystals, crack propagation disclosed by X-ray Pendellosung fringes 3−17917
- Zn-Al (22 wt.%), superplastic, room temp. creep behaviour under bending and plane conditions 3−34678

bending of light *see gravitation; light*

berkelium
- Bk^{4+} e.p.r. in ThO_2 3−2351

berkelium compounds
- No entries

beryllium
- ageing and microhardness of single crystals 3−24932
- aging, resist. to microplastic deform. 3−21672
- anisotropy in phonon scattering resistivity 3−7876
- atom, $(1s^22s2p^3p)$ excited state, magnetic hyperfine interaction many-body perturbation theory 3−35952
- atom, correlation energy using many-body perturbation theory calc. 3−20010
- atom, multiconfiguration wavefunctions, two-by-two rot. method applic. 3−7038
- atom, photoioniz. cross sections calc. 3−26594
- atomic Stark shift in low elec. field 3−11127
- atoms, correlated wavefunctions form, calc. 3−20008
- Auger electron and charact. energy loss spectra from clean and slow oxidized surfaces 3−34452
- Auger spectrum, clean and oxidised surfaces, band structure interpretation 3−30902
- band structure, influence of non-locality of Shaw's model potential 3−1979
- Bauschinger effect, cyclic, at twin boundaries *(Russian)* 3−30179
- bombarded with deuterons, neutron production 3−25852
- charge density, X-ray structure amplitudes obs. 3−7659
- composite, brittle matrix ductile fibre, fracture mechanics 3−31134
- Compton profile, multiple X-ray scattering effect 3−17867
- dimagnetic Knight shift and its anisotropy 3−18380
- dispersion relations, curves, h.c.p., Sharma-Joshi model 3−30220
- dynamic stiffness computation 3−22696
- elastic-plastic single crystals, thermally-induced plane waves 3−3985
- energy levels and radiative lifetimes in Be (I) and (II), beam foil studies 3−11159
- film, SEM obs. of laser damage 3−35708
- film, supercond. temp. range, effect of Al addition *(Russian)* 3−11979
- Hartree-Fock polarisabilities calc. 3−29486
- hydrostatically extruded, elec. resist. changes during annealing *(Russian)* 3−18110
- ions, distribution function for electron angular correlation 3−4354
- liquid, electronic density of states calc. 3−38776
- local logarithmic decrement, hysteresis loops with reversible displacement of single twin boundaries 3−27030
- mechanical twinning study *(Russian)* 3−20753
- metastable $^3P_0$ atomic states, double and triple photon decay 3−35965
- neutron moderation, variation method 3−4335
- neutron multi-group theory, energy-dependent buckling 3−1042
- neutron wave propag., interference phenomena calc. by eigenvalue expansion 3−1041
- n.m.r. line width rel. to self diffusion, 300-1200K 3−39040
- optical absorptivity, 0.12-4.5 eV 3−36869
- phonon damping due to electron-phonon coupling, calcs. 3−38638
- phonon dispersion curves for noncentral force model 3−33617
- plasma, high z, produced by high power laser 3−20546
- plasma, laser produced in stellarator 3−33374
- projected Hartree producted wavefunctions, relationship of DODS and SCF orbitals 3−20004
- resonance series in vacuum u.v. absorption spectra of dense plasmas 3−17351
- soft X-ray absorpt. edges calcs. 3−30895
- sputtered thick foil, effects of growth conditions on orientation and hardness 3−30935
- steel cladding and corrosion stability in molten Li *(Russian)* 3−12377
- theoretical oscillator strengths for $1s^22s^2\ ^1S-1s^22s2p\ ^1P^0$, $1s^22s2p\ ^1P^0-1s^22p^2\ ^1D$ and $1s^22s2p\ ^1P^0-1s^22p^2\ ^1S$ isoelectronic sequences 3−14285
- thin film fabrication, by vapour deposition processes 3−39230
- warm-swaged, tensile characteristics *(Japanese)* 3−31069
- X-ray prod. by electron irrad. 3−16540
- X-ray Raman scattering 3−30143
- Be III ionized species, far u.v. absorpt. spectra *(French)* 3−20030
- Be:Si surface, Auger and ionisation loss spectra meas. before and after oxidation 3−21508
- Be/Al filamentary composite, yield pt. phenomena, Luders band propag. 3−34639
- $Be^{1+}\ ^2S$ and Be ^3S states, natural orbital config. interaction expansions 3−26561
- Be^{2+} Coulomb holes and expectation values, explicitly correlated wavefunctions 3−23464
- BeI isoelectronic sequences, energy levels and spectra meas. 3−17369
- in CdS(Se), i.r. absorpt. due to localized vibr. mode 3−27523
- in GaP, rel. to green light emitting diode appl. 3−8734
- GaP:Be, homogeneous doping in vapour growth, elec. props. *(Russian)* 3−15644
- MgO:Be^{2+}, tracer diffusion meas. up to 2340°C 3−20891
- Pu-α-Be neutron source, low energy neutrons average cross sections 3−38157
- Pu-Be neutron source for continuous γ-ray for nuclear resonance fluorescence 3−3840
- SiC:Be p-n junction, ionizing radiation detection characts. *(Russian)* 3−309

beryllium alloys
- *see also beryllium compounds*
- Ag-Be, internal oxidation study 3−21712
- Al-Be eutectics, directionally solidified, struct. morphology and microhardness *(Russian)* 3−39328
- Be-Ag, contact resistance, internal oxidation effects *(Japanese)* 3−8253
- Be-Cu, mech. twinning *(Russian)* 3−20753
- Be_4B, BeB_2, dynamic yield strength, compressional and Hugoniot elastic parameters 3−17927
- Be_4B-BeO, dynamic yield strength, compressional and Hugoniot elastic parameters 3−17927

beryllium alloys continued
- Be_{22}(Mo,Re)-phases, superconducting properties, meas. of T_c *(German)* 3-38923
- Co-Fe-Be, age hardening, hardness-controlling additions *(German)* 3-8901
- Co-Fe-Be, mag. and mech. props with annealing and cold drawing *(Japanese)* 3-12398
- Cu-Be, eutectoid decomp., ordering with metastable solid soln. form. *(Russian)* 3-37001
- Cu-Be(2 wt.%), age-hardened, microstruct. characts. rel. to elastic limit and yield pts. *(Russian)* 3-15668
- Cu-Ni-Be-Si, aging characts. *(Japanese)* 3-12352
- Fe-Be (23 at%) alloy, aged above 400°C, Mossbauer study of hyperfine fields 3-34264
- Mn-Fe-Be system, n.m.r. of ^{9}Be in $Mn_{1-x}Fe_xBe_2$ 3-2436
- Ni-Be, age hardening, hardness-controlling additions *(German)* 3-8901

beryllium compounds
- B + O capillary, CO_2 waveguide laser 3-13732
- B_2O_3-BeO glass systems, i.r. spectra and structural analysis *(Russian)* 3-27508
- Be complex, bis(cyclopentadienyl), mol. struct. in crystal at −120° and in gas phase 3-23513
- $Be_3Al_2Si_6O_{18}$:V^{3+}, beryl, optical and i.r. absorpt. rel. to crystal field parameters 3-34389
- $BeBH_5$ and BeB_2H_8, ab initio calcs. of mol. struct. 3-29548
- BeF_2, crystalline and glassy, F^{19} n.m.r. 3-34224
- BeF_2, low lying states, nonempirical LCAO MO SCF studies 3-23529
- BeF_2, nonempirical LCAO MO SCF studies, bonding trends 3-20096
- BeF_2-KF-MF_2, BeF_2-KF-AlF_3-MF_2, BeF_2-KF-AlF_3-CaF_2-MF_2(M=Mg, Ca, Sr, Ba), phase compositions formed by heat treatment *(Russian)* 3-11545
- BeH, configuration interaction LCAO-MO calc. of the $X^2\Sigma^+$ and $A^2\pi$ states 3-26624
- BeH^+, distorted-atoms-in molecules model, spatial electronic wavefunction 3-38265
- BeH_2, potential energy surfaces calc. 3-23635
- BeO, absorption spectra, window in v.u.v. 3-28520
- BeO, cryst. or amorphous film, prep. by reactive evaporation of Be *(German)* 3-21534
- BeO, dissociation energies 3-20190
- BeO, exoelectron emission, effect of O adsorption centres 3-24776
- BeO, F^+-centre, interactions with next-nearest-neighbour Be nuclei, ENDOR obs. 3-39058
- BeO, far u.v. refl. and correl. with Penn-Phillips gap 3-39158
- BeO, grain size rel. to density during sintering 3-2754
- BeO, limit of dangling bond theory rel. to surface microtopography 3-15053
- BeO, neutron moderation, variation method 3-4335
- BeO, seed-grown, morphological features 3-14708
- BeO in water vapour, vaporisation, transpiration determ., postulated results using Au vaporisation as reference substance 3-26019
- BeO spheres, Al_2O_3 coated, neutron irradiation effects 3-4338
- BeO TSEE detector, dosiometric characteristics variation with surface impurities 3-28671
- BeO-Al_2O_3-SiO_2-MgO glass, thermographic and X-ray study of struct. transforms. *(Russian)* 3-11547
- $BeSO_4$, thermal decomposition kinetics 3-2804
- Be_2SiO_4, anharmonicity of i.r. vibr. modes, refl. study, 300-1500 K 3-14947
- BeTeI film, elec. props., substrate temp. effects *(Russian)* 3-21067
- K_2O-SiO_2-BeO system glasses and crystn. products, synthesis and characteriz. *(Russian)* 3-11551

Bessel differential equation *see Bessel functions*

Bessel functions
- heated thin wire, temp. distribution in gas flow 3-36077
- integrals, related to Webers second exponential integral 3-485
- sound radiation in elastic medium, nonlinear distortion as Bessel function series *(Russian)* 3-31969

beta-decay
- *see also beta-decay theory; beta-ray spectra; nuclear electron capture; radioactivity*
- (0d, 1s) shell nuclei with A=17-39 calc. of β transition rates, half-lives 3-32811
- A=11, 13, 15, 17, 19 and 21, effective nuclear renormalization of axial-vector coupling constant detn. 3-29302
- astrophysical formulae and reln. to superheavy elements 3-32818
- double, neutrino and neutrinoless, determ. of lifetimes and limits on lepton non-conserving amplitude 3-6787
- far unstable nuclei, determ. of decay energies using ISOLDE facility at CERN 3-10934
- Fermi, accurate meas. and magnitude of weak interaction coupling const. 3-10660
- finite nuclear size effects and phase-space factor 3-10927
- fission products, short-lived, meas. of total-absorption γ-spectra, determ. of β strength functions 3-29361
- Gamow-Teller mirror β-decay, possibility of second-class currents involved 3-14180
- internal conversion transitions, electron correlation effects *(Russian)* 3-19818
- K/β^+ and ε/β^- ratios for allowed transitions, critical comparison between expt. and theory 3-35883
- light exotic nuclei, β half-lives 3-938
- log-f value tables of calc. of half-lives, values of capture-to-positron ratios 3-973
- neutron deficient nuclei, half-life meas. 3-6777
- short range fragment emission from K^- interactions 3-11028
- solar neutrino archaeology by double β-decay effects in old rocks 3-5545
- $T_2=1/2$ nuclei, meas. of energy of β^+-delayed protons from T=3/2 analogue states, determ. of lowest T=3/2 level in ^{41}Sc 3-19779
- transitions probabilities, $(ft)^+/(ft)^-$ and K/β^+ ratios relation to second-class currents 3-10936
- Λ, polarised, beta decay, correlations in centre-of-mass system and p recoil spectrum 3-23032
- n, formula 3-4300

beta-decay continued
- n decay, meas. of coupling constant ratio, gA/gV *(German)* 3-32819
- n → peν, oscillation in hollow in potential energy curve 3-14099
- ^{108}Ag, gamma ray singles and coincidence meas. 3-32802
- ^{25}Al, positron decay half-lives, mirror β decay ft values 3-29355
- $^{26}Al^{m}$, half-life meas., β-decay 3-10928
- ^{76}As, determ. of ^{76}Se energy levels 3-26384
- ^{209}At → ^{209}Po, γ-γ coincidence spectra, level scheme of ^{209}Po *(French)* 3-10872
- ^{198}Au, 2^-2^+ β transition, matrix element detn. 3-32812
- ^{198}Au → ^{198}Hg, beta-(circularly polarized gamma) correlation, detn. as function of β energy 3-23279
- ^{200m}Au → ^{200}Hg β^- decay, level scheme of ^{200}Hg 3-6717
- ^{8}B → ^{8}Be, search for second class currents 3-10936
- ^{126}Ba → ^{126}Cs → ^{126}Xe, decay investig. using Ge(Li) detectors 3-26424
- ^{129}Ba → ^{129}Cs, level struct. 3-19766
- ^{10}Be, half-life corrections 3-14173
- ^{205}Bi, γ-γ directional correlation meas., determ. of ^{205}Pb energy levels 3-19807
- ^{74}Br → ^{74}Se, energy levels and spin of ^{74}Se 3-29350
- ^{48}Ca double β decay, apparatus for exptl. obs. 3-6788
- ^{115m}Cd, spectroscopic investigations *(German)* 3-29367
- ^{141}Ce, $^{7}.{}_{2}{}^{-}$ $^{5}.{}_{2}{}^{+}$ beta transition, nonunique first-forbidden decay, analysis 3-32813
- ^{32}Cl, β-branches, gamma lines and ^{32}S levels detn. 3-29360
- ^{33}Cl, positron decay half-lives, mirror β decay ft values 3-29355
- ^{34}Cl, half-life meas., β-decay mirror asymmetry 3-10928
- ^{34}Cl superallowed Fermi decay, meas. of half-life and β end-point energy, vector weak interaction 3-19817
- ^{40}Cl, half-life, consequent γ-rays, β-branching *(French)* 3-10924
- ^{61}Co parity violation in allowed Gamow-Teller β-decay, Mossbauer spectroscopy meas. of ^{61}Ni 3-35886
- ^{49}Cr, branching ratios and γ-ray intensity meas. 3-17162
- ^{125}Cs, levels meas. during β-decay 3-14171
- ^{127}Cs, levels meas. during β-decay 3-14171
- ^{129}Cs, levels meas. during β-decay 3-14171
- ^{134}Cs, decay study by beta-gamma-gamma angular measurements 3-29354
- ^{59}Cu → ^{59}Ni β^+ decay, meas. of γ transitions in ^{59}Ni, determ. of log ft values 3-32797
- ^{173}Er → ^{173}Tm, β^- decay, meas. of γ-γ and γ-β coincidences, determ. of levels in ^{173}Tm 3-23266
- ^{148}Eu decay, obs. of high-lying 2^+ states in ^{148}Sm 3-19786
- ^{152}Eu, coincidence studies of levels in ^{152}Sm and ^{152}Gd 3-6725
- ^{152}Eu, higher order effects in nonunique first forbidden beta decay 3-29358
- ^{152}Eu, low energy γ-rays meas. 3-14174
- ^{160}Eu, radioactive decay scheme, half-life meas. 3-32807
- ^{72}Gd, β spectra shape factors 3-14179
- ^{76}Ge, neutrinoless double β decay 3-26425
- ^{3}H, high-energy part of β-spectrum, meas. using magnetic spectrometer 3-29359
- ^{3}H-^{3}He transition, corrections to Goldberger-Treiman relation 3-6780
- ^{162}Ho decay scheme *(Russian)* 3-23273
- ^{168}Ho, decay to levels of ^{168}Er 3-29356
- ^{131}I → ^{131}Xe, β-γ ang. correls. *(Russian)* 3-23275
- ^{116}In ground state, decay to levels in ^{116}Sn, obs. of γ-ray spectra 3-32805
- ^{119}In → ^{119}Sn, spin and parity values of states of ^{119}Sn 3-14165
- $^{123g+m}$In, beta decay to ^{123}Sn excited states 3-23280
- $^{121g+m}$In → ^{121}Sn, levels studied 3-14177
- ^{192}Ir, γ-ray energies and intensities, log ft values, ^{192}Os, ^{192}Pt deduced levels 3-32808
- ^{192}Ir → ^{192}Pt, meas. of $\beta\gamma\gamma$ coincidences, determ. of lifetimes of 316 and 612 keV states of ^{192}Pt 3-23258
- $^{38}K^{m}$, half-life meas., β-decay 3-10928
- ^{40}K, detection of produced Cherenkov radiation in aqueous solns., determ. of amount of KCl 3-37755
- ^{44}K, to levels in ^{44}Ca, meas. of γ-ray spectra 3-26427
- ^{77}Kr decay scheme *(Russian)* 3-23274
- ^{87}Kr, branching to ground-state of ^{87}Rb 3-17205
- ^{89}Kr decay to levels in ^{89}Rb, γ-γ coincidence meas. 3-10855
- ^{140}La, β spectra shape factors 3-14179
- ^{8}Li → ^{8}Be, search for second class currents 3-10936
- ^{176m}Lu, beta decay 3-29366
- ^{20}Na, branching ratios and mirror $\beta^\pm$ decays 3-17206
- ^{22}Na, ^{24}Na production cross sections from 22-52 MeV protons on ^{27}Al 3-29384
- ^{26}Na → ^{26}Mg β^- decay, γ-ray meas., determ. of log ft values and half-life *(French)* 3-38142
- ^{89}Nb → ^{89}Zr, γ-γ coincidence spectra, level scheme of ^{89}Zr *(French)* 3-10872
- ^{147}Nd → ^{147}Pm, β-γ ang. correls. *(Russian)* 3-23275
- ^{147}Nd → ^{147}Pm β^- decay, γ-ray spectrum 3-6786
- ^{25}Ne, delayed γ-ray spectrum meas. from 9Be(^{18}O,2p) 3-32815
- ^{61}Ni, β-γ coincidence meas. and parity violation in allowed Gamow-Teller β-decay of ^{61}Co 3-35886
- ^{238}Np → ^{238}Pu obs. of new weak lines using anti-Compton spectrometer 3-6758
- ^{182}Os(22h) → ^{182}Re, excited states energies meas. 3-35858
- ^{191}Os M3 transition, K conversion coefficient near threshold 3-29348
- ^{29}P, positron decay half-lives, mirror β decay ft values 3-29355
- ^{30}P, weak positron decay to ^{30}Si, meas. of log ft for first excited state 3-23276
- ^{233}Pa → ^{233}U, coincidences meas., obs. of weak γ-transitions to low energy levels in ^{233}U 3-23212
- ^{234m}Pa, level scheme of ^{234}U *(French)* 3-29352
- ^{147}Pm, inner shell vacancy creation 3-4369
- ^{154}Pm, decay of isomers to levels of ^{154}Sm, determ. of γ-ray transitions, half-lives 3-35884
- ^{230}Po → ^{230}Th, meas. of γ and electron-singles spectra and γ-γ coincidences, determ. of levels in ^{230}Th 3-23211
- ^{81}Rb → ^{81}Kr, γ-singles, γ-γ and β-γ coincidence meas., determ. of branching ratios and log ft values 3-23265
- ^{84}Rb, energy-dependent β-γ circular polarization 3-17204

beta-decay continued
^{87}Rb, shape of β-spectrum at low energies measured as difference between isotopes ^{87}Rb and ^{85}Rb, half life estimation 3−23281
^{184}Re, vibrational band struct. detn. in ^{184}W 3−29343
^{184}Re isomers, γ-ray and conversion electron spectra *(Russian)* 3−23272
^{186}Re, higher order effects in nonunique first forbidden beta decay 3−2935[illegible]
^{106g}Rh, γ spectra, ^{106}Pd level scheme *(French)* 3−23264
^{106g}Rh→^{106}Pd, γ-γ directional correlation measurements 3−32817
^{95}Ru→^{95}Tc, level stuct. detn. 3−29364
^{37}S→^{37}Cl, gamma transitions study and comparison to ^{40}Cl decay modes 3−29363
^{125}Sb, first forbidden β-decay, matrix elements detn. 3−26426
^{125}Sb, higher order effects in nonunique first forbidden beta decay 3−29358
^{130}Sb→^{130}Te, 40 min decay, level struct. and props. of Te 3−10864
^{40}Sc, β-branches, gamma lines, branching ratios and log ft values detn. 3−29360
^{41}Sc, positron decay half-lives, mirror β decay ft values 3−29355
^{42}Sc, ground state branching to 0^+ state in ^{42}Ca, Coulomb mixing model calc. 3−23278
^{42}Sc, half-life meas., β-decay 3−10928
^{42}Sc ground state β^+ decay, search for branching 3−14178
^{42}Sc(7^+)→^{42}Ca(6^+), exchange current effects 3−6774
^{48}Sc, decay scheme 3−975
^{49}Sc, to 3.08 MeV $3/2^-$ and to 4.49 MeV $1/2^-$ levels 3−17213
^{50}Sc, to levels is ^{50}Ti, meas. of 6^+ state lifetime 3−26418
^{91}Sr→^{91}Y, continuous β-ray spectrum and internal conversion electron spectrum 3−29362
^{93}Sr→^{93}Y, β, γ-ray spectra *(German)* 3−14175
^{94}Sr, decay properties *(German)* 3−29349
^{172}Ta→^{172}Hf, conversion electron and γ-ray spectra, coincidence mes., Q^+, log ft and ^{172}Hf level determ. 3−38143
^{184}Ta→^{184}W, β^- decay, β and γ energies, intensities and coincidence meas., ^{184}W deduced levels 3−32756
^{186}Ta→^{186}W+β, level scheme 3−23208
^{149}Tb, γ-ray spectra, conversion electrons *(Russian)* 3−4296
^{149}Tb→^{149}Gd, decay scheme and γ-γ coincidence spectra *(Russian)* 3−4297
^{99}Tc, K-shell internal ionization probability meas. 3−14170
^{105}Tc→^{105}Ru, meas. of singles and coincidence spectra, study of low-lying levels in ^{105}Ru 3−23213
^{109}Te→^{109}Sb, meas. of coincidences between positrons and delayed protons *(Russian)* 3−29365
^{204}Tl, double internal bremsstrahlung, obs. 3−14172
^{170}Tm, first-forbidden matrix elements and directional correlation of β and γ-rays 3−32816
^{48}V(β^+), level structure and lifetimes, $E_x<3.5$ MeV 3−19784
^{48}V→^{48}Ti, β-γ ang. correls. *(Russian)* 3−23275
^{185}W, inner shell vacancy creation 3−4369
^{138}Xe→^{138}Cs, energy level detn. using on-line techniques 3−17164
^{162}Yb 19 min., γ-γ and e-γ coincidence meas., ^{162}Tm levels 3−4299
^{62}Zn, population of states in odd-odd ^{62}Cu, meas. of γ-ray spectra 3−29312

beta-decay theory
see also beta-decay; beta-ray spectra
Coulomb corrections to nuclear beta decay, elementary particle treatment 3−23277
Fermi decay, universality 3−35882
Fermi theory simplification *(Spanish)* 3−10922
gross theory application to r-process calcs., delayed-neutron emission at final stage 3−25365
impulse-approximation and elementary-particle treatment, comparison 3−14168
matrix element extraction in 1st-forbidden decay, comparison of two methods 3−10925
polarised nuclear β-decay, ang. distrib. of e and ν 3−4300
second class currents, induced tensor interaction 3−10935
strong meson-dominance model, for β-emission from polarized nuclei 3−14167
strongly hindered allowed β-transition characts. and high order effects *(Russian)* 3−23271
superallowed $0^+ \to 0^+$ decays, corrections in coupling constant calc. 3−38141
superallowed Fermi transitions, charge dependence of radiative corrections, conserved-vector-current hypothesis 3−974
^{166}Ho calc. of singular β transition observables using independent quasiparticle in strained Woods-Saxon potential *(Rumanian)* 3−19812

beta-particles *see beta-rays*

beta-radiation *see beta-rays*

beta-ray absorption
see also electron absorption
tissue-equivalent medium, absorbed energy distribution 3−19102

beta-ray angular distribution
see also beta-ray spectra
β-γ angular correlations, induced tensor interaction 3−10935
^{134}Cs, decay study by beta-gamma-gamma angular measurements 3−29354
^{131}I→^{131}Xe decay, β-γ ang. correls. *(Russian)* 3−23275
^{147}Nd→^{147}Pm decay, β-γ ang. correls. *(Russian)* 3−23275
^{48}V→^{48}Ti decay, β-γ ang. correls. *(Russian)* 3−23275

beta-ray detection and measurement
see also beta-ray spectrometers; dosimetry; particle detectors; radioactivity measurement
colour film, autoradiography applic. *(German)* 3−37715
dosimetry, response of Si avalanche detector 3−404
source substrate thickness effect on β-spectrum meas. *(Russian)* 3−3836
thin films, plastic and metal, thickness meas. 3−22468
^{198}Au, absorbed dose in vicinity of surface beta emitters by MIRD method *(Czech)* 3−32991

beta-ray effects
see also electron beam effects; nuclear reactions and scattering due to electrons
bremsstrahlung, external, produced by beta particles in Cu, Ag, Cd, Sn, Pb targets, reln. to target thickness 3−29454
mammalian cells, breaking survival curves 3−28384
p-GaAs, effect on magnetophotocond. 3−18185

beta-ray effects continued
ZnS:Cu, β-irrad. at 5K, fast light emission 3−24753

beta-ray polarisation
^{84}Rb, energy-dependent β-γ circular polarization 3−17204

beta-ray scattering
see also electron scattering
Sn-Pb alloys, composition test, using inversely scattered β-radiation 3−26016

beta-ray spectra
see also beta-decay theory; conversion electron spectra
end-point energy determ., improvements in meas. accuracy 3−10933
source substrate thickness effect on β-spectrum meas. *(Russian)* 3−3836
^{a}Bi decay, A=202, 200, 198, study of levels in ^{198,200,202}Pb by obs. of γ- and β-rays and γ-γ coincidences *(French)* 3−23252
^{207}Bi, meas. using 4π-β-spectrometer 3−10084
^{40}Ca(^{16}O,X), 41 MeV, meas. of γ and positron activities, determ. of isomeric ratios in ^{53}Fe and ^{53}Co 3−32809
^{137}Cs, meas. using 4π-β-spectrometer 3−10084
^{72}Ga decay, β spectra shape factors 3−14179
^{3}H end-point energy determ. improvements in meas. accuracy 3−10933
^{39}K(^{16}O,X), 41 MeV, meas. of γ and positron activities, determ. of isomeric ratios in ^{53}Fe and ^{53}Co 3−32809
^{77}Kr decay scheme *(Russian)* 3−23274
^{140}La decay, β spectra shape factors 3−14179
^{65}Ni, 2.6h, decay investigation, ^{65}Cu spin and parity assignments 3−6772
^{93}Sr→^{93}Y, β, γ-ray spectra *(German)* 3−14175

beta-ray spectrometers
see also beta-ray spectra
active sample anticoincidence guarded Ge(Li) spectrometer low level radionuclide analysis 3−28773
band-spectrograph, with permanent magnet and 75 cm. radius 3−25917
Compton-suppressed spectrometer, for internal conversion studies 3−25919
in-beam axial, for meas. of internal conversion electrons 3−10081
liquid scintillation counter, coupled to multichannel pulse height analyser 3−10076
magnetic, for on-line work 3−37706
permanent magnet spectrographs, line shape analysis of conversion electron spectra 3−325
positron transmission and scattering meas. using superposition of annihilation lineshapes, backscatter coeffs., Ge(Li) detector 3−11653
positrons, low energy 3−25913
sector-focusing magnetic type 3−25920
sector-type, lab. expt. 3−16362
β-γ coincidence spectrometer, 4π geometry using Si(Li) and NaI(Tl) detectors 3−10078
β-γ-γ, multidimensional, development and application 3−28692
Ge three-dimension camera, for positron emitting radioisotopes 3−32197
Si(Li) detector, use for 4π operation 3−10084

beta-rays
see also electrons
decay constant, exp. weighted least squares fit method for detn. 3−10926
dose distrib. near interface 3−22183
maximum range of T β-particles, gas concentration in lungs 3−5687
point source functions of β-radiation, boundary conditions 3−9698
standard source, checking 3−22459
Al thickness meas., comparison with X-ray meas. 3−22522

beta spectrometers *see beta-ray spectrometers*

betatrons
19 MeV, for X-ray therapy, construction description 3−16480
20 MeV, construction description 3−16479
25 MV, modification for whole body electron irradiation 3−410
25 MV, X-ray beam, radiation field flatness obs. 3−272
50 MeV, apparatus details *(Russian)* 3−19264
for activation analysis *(Russian)* 3−19374
beam extraction by parametric resonance 3−16493
beamguide system 3−16497
BETI, Romanian, nondestructive testing 3−19261
breast cancer, treatment by electron beam from betatron 3−16560
bremsstrahlung γ-rays for photonuclear cross-sections for different reaction channels 3−17229
cancer, preoperational irradiation therapy *(Russian)* 3−25598
compact with high specific characteristics *(Russian)* 3−22422
for defectoscopy *(Russian)* 3−19266
for defectoscopy *(Russian)* 3−19267
for defectoscopy *(Russian)* 3−19268
dose rate control, for medicine 3−22172
electromagnet, size dependence on machine parameters *(Russian)* 3−19265
electron beam attenuation after injection *(Russian)* 3−19280
electron capture during injection and beam parameters 3−16495
electron capture efficiency for different times within injection pulse *(Russian)* 3−277
electron trapping, influence of magnetic field decrement *(Russian)* 3−19279
explosive ultrahigh magnetic field accelerators, possible designs and applications 3−6051
field inhomogeneities, causes 3−16482
high current, electron acceeration processes, radiation of electromagnetic waves *(Russian)* 3−19281
high current, extraction of electron beam by pulsed single revolution and electrostatic methods *(Russian)* 3−19282
injectors with Pierce and Kerst-type optics 3−16496
lung tumours, betatron therapy, clinical considerations 3−22171
magnet, improvements to increase energy from 19 to 22 MeV 3−16481
magnetic field, compensation of amplitude nonuniformity 3−22420
magnetic field measurement *(Russian)* 3−19262
medical, for patient treatment, X-ray and electron beam characteristics 3−3575
for medical use, neutron meas., track etch technique 3−16561
particle focusing, field configurations 3−16494
photoactivation analysis, geological samples 3−18896

betatrons continued
photoactivation analysis, using 25 MeV betatron 3—19373
plasma betatron, high voltage, intense electron beam production *(Russian)* 3—17665
power supplies, efficiency improvement *(Russian)* 3—22424
stomach cancer treatment, results of preoperational irradiation *(Russian)* 3—25597
symposium, Bucharest, Rumania (1971) 3—16478
therapy, adaptation of 30 MeV IAP betatron 3—16483
transient current on injection, synchronization *(Russian)* 3—22423
Bethe-Salpeter equation
bound states calc. using quasisecular perturbative method, comparison with Bethe-Salpeter eqn. 3—10605
composite lepton states induced by neutrinos 3—29185
conductivity of disordered harmonic solids, thermal, Green's functions 3—27149
crossing symmetric eqn. in relativistic field theory 3—13785
dilation invariant field solns., scaling and asymptotic behaviour 3—13796
energy-independent kernels, $s=0$ scattering soln. 3—35739
free particle Green's function representation 3—35733
hydrogenlike atom, soln. to eqn. as test of numerical technique accuracy 3—29173
integral representation, eigenvalues of Wick eqn. in weak-binding limit in perturbation theory 3—35746
ladder-approximated dressed-rung and generalization of relativistic off-shell model 3—38015
meson e.m. decay as test of relativistic-constituent Fermi-quark model based on Bethe-Salpeter eqn. 3—19689
mesons on relativistic Fermi-quark-antiquark system with strong binding, use of Bethe-Salpeter eqn. 3—17066
O(3) invariant integral and solution in infinite momentum limit 3—22988
reciprocal bootstrap of N and N*, calc. using nonpolynomial Lagrangian 3—4212
relativistic quantum mechanics of two interacting particles 3—10590
relativistic quark model, vector-meson dominance in e.m. interactions 3—13791
scalar quarks interacting, algebraic equations for 3—10595
separation of variables in Minkowski space *(Russian)* 3—29176
two-nucleon systems, low energy, relativistic three dimensional equations 3—35865
Wick-Cutkosky model, amplitudes obtained by stereographic projection method 3—13794
NN scattering matrix Pade approximants 3—26342
$\pi\pi$ interactions at high energies, multiperipheral theory, properties of elastic and inelastic processes *(Russian)* 3—23190
Bethe-Uhlenbeck equations *see quantum statistical mechanics*
bevatrons
No entries
big-bang theory *see cosmology*
bimetallic strips *see bimetals*
bimetallic wire *see bimetals*
bimetals
electron microscope specimens, thin foils from zone of union of bimetal prep. by explosion welding 3—18577
Cr-Au film, Cr diffusion into Au, work function study 3—15030
binaries (stellar) *see binary stars*
binary adders *see adders*
binary sequences
see also number theory
pseudo-random pressure disturbances, for sonic velocity meas. in two-phase flow 3—1442
binary stars
2U0525-06, identification with ϑ^2 Orionis, possibility of black hole 3—13080
32 Cygni, UBV photometry during 1971 eclipse 3—9566
Σ1321 (ADS 7251), parallax, proper motion and orbital motion of visual binary 3—9547
ADS 6126—AB, determ. of physical and orbital elements 3—25451
Algol like, gaseous rings generated during mass transfer 3—16221
Am SB_2 systems, atmospheric abundances and evolutionary origin 3—25462
TW Andromedae, Algol-type variable, photometric light curve distortion by hot spots 3—35148
α Andromedae (HD358), spectroscopic binary, UBV photometry rel. to magnetism 3—22052
Ap stars, 62 northern brightest, spectroscopic binary frequency obs. 3—37386
Aurigae, eclipsing binary, differential UBV photometry during 1971-72 eclipse 3—28220
Aurigae, eclipsing binary, UBV obs. before and during eclipse 3—39694
Aurigae, eclipsing binary, UBV photometry during 1971-2 eclipse 3—39685
BD+16°516, Hyades white dwarf eclipsing binary, proper motion meas. 3—28207
BD+43°4305, parallax and orbital motion of unresolved astrometric binary 3—13044
BD +60°2522, possible spectroscopic binary, anomalous energy distribution *(Russian)* 3—16285
black hole appearance in binary systems 3—39588
i Bootis, eclipsing binary, min. epoch determ. using Kwee and van Woerden method 3—22054
VW Bootis, eclipsing variable, light var. and orbital elements 3—35144
Z Camelopardalis, variable, high-speed photometry and model 3—35142
53 Camelopardalis (AX Cam), variability of radial velocities rel. to possible binary properties 3—22063
α Canis Majoris (Sirius), photographic positions rel. to possible third component 3—31680
α Canis Majoris (Sirius), redshift meas. of odd Balmer lines 3—20012
AM Canum Venaticorum (HZ 29), triple system model from photoelectric observations 3—31683
GL Carinae, eclipsing binary, minimum light time at primary eclipse, UBV obs. 3—39691
binary stars continued
γ Cassiopeiae, comparison with possible X-ray source X Persei 3—31687
cataclysmic variable stars, hot spot, particle trajectories, thermal velocities, mass ratios 3—3330
SV Centauri, eclipsing binary, minimum light time at primary eclipse, UBV obs. 3—39691
V 745 Centauri, eclipsing binary confirmation 3—5599
α Centauri, visual binary, chemical composition of A and B components 3—9565
Centaurus X-3, pulsation of X-ray emission rel. to accretion by neutron star in binary system 3—22094
VW Cephei, eclipsing binary, min. epoch determ. using Kwee and van Woerden method 3—22054
VW Cephei, orbital period var. of eclipsing binary 3—13049
GK Cephei, W Ursae Majoris-type contact binary, line profile distortion and velocities 3—37384
CQ Cephei (W-R eclipsing binary), model obs. in monochromatic emission and continuum 3—28219
GK Cephei contact binary system, best-fit model 3—28205
close binary system with collapsed star, disk model of gas accretion, X-ray source 3—37362
close binary systems, evolution with mass loss 3—37364
contact binary evolution and models for cataclysmic binaries 3—25434
contact binary stars, opacity, rotation, Lucy theory, zero age 3—3331
contact binary systems, appl. to W Ursae Majoris systems 3—39663
RS CVn, eclipsing, i.r excesses, JHKL photometry 3—9557
MR Cygni, eclipsing binary, spectroscopic obs. giving mass ratio and luminosity ratio 3—31686
31 Cygni, eclipsing binary, UBV obs. before and during eclipse 3—39694
MR Cygni, eclipsing binary orbital eccentricity evidence from two-colour light wave 3—37388
V 1136 Cygni, eclipsing binary with eccentric orbit, elements and light curve 3—31685
V444 Cygni, eclipsing-binary Wolf-Rayet star, envelope emission stratification *(Russian)* 3—13061
BF Cygni, symbiotic star, props. and evolutionary model *(French)* 3—28209
32 Cygni K-type component, chromospheric structure 3—5604
Cygnus X-1, radial velocity period, B and V photometry 3—3362
degenerate dwarfs, rapidly rotating, as X-ray sources in binaries 3—37360
double stars, micrometer measures of 401 objects 3—19010
DQ Her, rapid blue variable, phase amplitude and shape of periodic variations 3—3338
dwarf stars, nova shell formation and interaction with circumstellar envelope *(Russian)* 3—16224
dwarfs stars close binary systems, shock waves in gaseous streams *(Russian)* 3—37344
eclipsing, light curve solution by the differential corrections method 3—19074
eclipsing binaries, circular polarimetry of 2 objects 3—39680
eclipsing binaries, min. epoch determ. using Kwee and van Woerden method 3—22054
eclipsing binary, elements from light curves using generalized method of least squares *(Russian)* 3—13062
eclipsing variables, light-curves for 11 objects 3—13050
RZ Eri, eclipsing, i.r. excesses, JHKL photometry 3—9557
evolution on dynamical time scale 3—9550
G61-29 white dwarf, photoelectric obs. of flickering and light curve 3—3337
G95-57A/B, obs. combined with obs. of G95-59, position on absolute magnitude-colour diagram 3—31676
HD25823 (41 Tauri), spectroscopic binary, UBV photometry rel. to magnetism 3—22052
HD358 (α Andromedae), spectroscopic, binary, UBV photometry rel. to magnetism 3—22052
HD 11860, spectroscopic binary, orbital elements determ. 3—37406
HD 21242, eclipsing binary, i.r. excesses, JHKL photometry 3—9557
Hd 30353, H-deficient, shift of Hα lines to violet *(French)* 3—5603
HD 37017, strong He line star, spectroscopic study, mass transfer possibilities 3—22050
HD 74375 spectroscopic binary, observation of spectral β CMa characteristics 3—25463
HD 90707, spectroscopic orbit determ. by radial velocity meas. 3—19022
HDE 226868, optical counterpart of Cygnus X-1, spectroscopic obs. 3—31693
HDE 226868, orbital elements for association with Cygnus X-1 3—9555
HDE 226868, spectroscopic binary, optical counterpart of Cygnus X-1, secondary possible black hole 3—31694
Z Her, eclipsing, i.r. excesses, JHKL photometry 3—9557
Her X-1, X-ray pulsar identified as optical pulsar by spectrophotometric obs. 3—13073
Hercules X-1, pulsation of X-ray emission rel. to accretion by neutron star in binary system 3—22094
HZ Herculis, eclipsing binary, optical observations and pulsation rel. to Her X-1 source 3—22073
HZ Herculis, eclipsing binary, period and light curve rel. to X-ray properties 3—19016
HZ Herculis, eclipsing binary, spectra of optical counterpart of Hercules X-1 pulsating source 3—19017
HZ Herculis, identification with X-ray pulsar Hercules X-1 3—28236
HZ Herculis, model of optical variations 3—28211
HZ Herculis, optical properties, X-ray source on surface of collapsed star 3—13078
4 Herculis (HD 142926), periodic radial velocity changes rel. to spectroscopic binary props. 3—25457
HR 1886 and HR 1887, visual, model atmospheres 3—9558
HR 5999/6000 system, rapid changes in shell star (HR 6000) 3—37383
Hyades cluster stars and field stars, mass-luminosity relationship 3—37471
HZ 22 (UX Canum Venaticorum), highly-evolved, low-mass, short-period binary 3—25458

binary stars continued
HZ 22 primary component, comparison with model of B-type stars with low surface gravity and mass 3−28176
interior models for uniformly rotating synchronous close binary systems 3−13045
AR Lac, eclipsing, i.r. excesses, JHKL photometry 3−9557
late-type dwarfs, wide moving pairs existence 3−35123
AM Leonis, W Ursae Majoris-type contact binary, line profile distortion and velocities 3−37384
AM Leonis contact binary system, best-fit model 3−28205
β Lyrae, eclipsing binary, differential UBV obs. from three observatories 3−39695
β Lyrae, further evidence for black hole 3−9452
models of uniformly rotating non-synchronous binary polytropes 3−13046
RW Monocerotis, eclipsing binary gravity-darkening of secondary component 3−13047
V 501 Monocerotis, eclipsing binary with eccentric orbit, elements and light curve 3−31685
nonthermal radio emission due to mass exchange between components 3−31711
Nova Delphini 1967, obs. of nebular stage, possible eclipsing binary *(French)* 3−35147
novae explosions time interval, envelope mass and energy determ. *(Russian)* 3−16225
V566 Ophiuchi, W Ursae Majoris-type contact binary, line profile distortion and velocities 3−37384
V566 Ophiuchi contact binary system, best-fit model 3−28205
RS Opiuchi, nova Fe II lines formation region 3−37389
orbits and dynamical parallaxes for 10 visual binaries 3−31681
BM Orionis, eclipsing binary, secondary component possibly collapsed star 3−31682
DI Pegasi, eclipsing variable, light var. in yellow and blue 3−35143
AG Pegasi, symbiotic star, UBVJHKL, Hβ and Hδ obs. 3−37399
LX Per, eclipsing, i.r. excesses, JHKL photometry 3−9557
RT Persei, eclipsing binary, minima times from UBV photometric obs. 3−28217
X Persei, possible X-ray source, comparison with γ Cassiopeiae 3−31687
b Persei, radio obs. at 2.695 GHz and 8.085 GHz 3−31707
43 Persei, spectroscopic binary in Hyades cluster, improved orbital elements from high-dispersion spectrograms 3−39690
β Persei (Algol), 5-microns emission 3−28213
β Persei (Algol), eclipsing binary, BV photometry and differential corrections analysis 3−37382
SZ Psc eclipsing, i.r. excesses, JHKL photometry 3−9557
Roche potential determ. including radiation pressure effects 3−37354
rotation rel. to asynchronism parameter and orbital period for B0-A3V binaries *(Polish)* 3−25448
rotational coupling in double stars, statistical anal. method 3−39670
U Sagittae, Algol-type variable, UBV obs. and explanation of light curves 3−35153
CV Ser, spectroscopic, photometric variability 3−9556
Wserpentis, eclipsing, photoelectric five colour obs. 3−31698
W Serpentis, peculiar eclipsing binary, intrinsic polarization, six colour photometry 3−31684
CV Serpentis, Wolf-Rayet eclipsing binary, comparison of spectroscopic and photometric data 3−28214
single-line spectroscopic binaries, search for new optical pulsars 3−39706
Sirius, redshift meas. of odd Balmer lines 3−20012
spectral energy distrib. of 6 stars in energy ranges 3300-7300 Å and 0.88-1.53 μ 3−37380
spectroscopic binaries, least square determ. of mass ratios 3−28190
surface incident radiation in model atmospheres rel. to eclipsing binaries 3−13014
SV Cen, eclipsing, photometric and spectroscopic study 3−13058
symbiotic object discovery behind Coalsack with combination spectum 3−25467
SZ Cam, UBV photoelectric light curves 3−13063
53 Tauri, spectroscopic binary, orbit 3−13030
41 Tauri (HD25823), spectroscopic, binary, UBV photometry rel. to magnetism 3−22052
tidal evolution in close binary systems rel. to secular perturbations of orbital elements 3−28116
X Trianguli, eclipsing binary, new photometric elements 3−39689
ultrashort periods, light curves 3−19015
W Ursae Majoris, contact binary, line profile distortion and velocities 3−37384
W Ursae Majoris contact binary system, best-fit model 3−28205
W Ursae Majoris contact binary systems, evolution 3−39663
W Ursae Majoris contact binary systems, modified Lucy model 3−31657
W Ursae Majoris type eclipsing binary systems, observations and models *(Polish)* 3−25447
RU Ursae Minoris, eclipsing binary, orbital period and spectral types 3−35145
Vela XR-1, observations of periodic intensity var. rel. to eclipsing-binary component possibilities 3−22095
S Velorum, Algol-type eclipsing binary, u.v. excess of secondary due to metal deficiency 3−25465
α Virginis, Algol-type variable, apsidal constant and evolution 3−37385
visual, formation, Roche densities 3−3336
EQ Vulpeculae, eclipsing binary with eccentric orbit, elements and light curve 3−31685
Wolf-Rayet systems, evolution into massive X-ray binaries 3−35172
X-ray binaries ($M > 15M_\odot$), evolution from Wolf-Rayet systems 3−35172
X-ray binary sources, optical identification criteria 3−16251
as X-ray sources, theories 3−5600

binding energy
see also lattice energy; nuclear binding energy; nuclear forces
atomic migration after radioactive bombard., effect of atomic bond strength *(Russian)* 3−11762
electron core-level shifts at nucleus from CNDO theory 3−1154
exciton with Coulomb pot. screening, mag. field depend. calc. 3−2034

binding energy continued
exciton-neutral donor complex, ionic and electronic polarization effects *(French)* 3−11866
excitonic molecules, binding energy calc. of complex 3−8125
H, small clusters of ${}^3\Sigma_u{}^+$ H and D atoms, calc. 3−17386
hydrogenlike atom, calc. as test of numerical techniques used in solving Bethe-Salpeter eqn. 3−29173
ionic crystals, calc. for surface polarons 3−2156
ions, negative, electron binding energy determ. from charge exchange cross sections 3−38242
light atoms, K electron binding energy by Braunbeks method 3−7036
metal, activation energy for melting correl. with binding energy *(Russian)* 3−14983
metal, H chemisorption, charge densities and binding energies calc. 3−33740
metals, pure, estimation of the liquid-vapour and solid-vapour tension by means of the cohesive energy *(French)* 3−27169
molecular core, ESCA, chemical shifts, minimal Slater basis set calculations 3−23550
molecular core, fluorobenzenes, ESCA 3−23547
nuclear matter, three-body correlation energy, soln. of integral equations in momentum space 3−14149
oxide films on pure Fe and Fe-Al alloy, from X-ray photoelectron spectra 3−8701
polyfluoroethylenes, CNDO/2 and extended Huckel charge distribs., rel. to ESCA chem. shifts 3−1300
polymer, neutron scatt. and polarization analysis 3−11350
tautomeric forms, electronic struct., bonding energy and absorpt. bands *(Russian)* 3−20122
tetracyanoquinodimethane and metal salts, core-level satellites in X-ray photoelectron spectra 3−12213
three-body system, numerical study 3−581
transition metal carbonyls, bonding rel. to substitution, core electron binding energy 3−7133
transition metal coordination compounds, donor-acceptor props. of ligands, X-ray photoelectron spectroscopy 3−17415
transition metal cpds., metal-like, nature *(Russian)* 3−11581
zincblende and wurtzite structure crystals, sum of covalent and ionic parts 3−36270
Al, impurity-vacancy pair, binding energy, pseudopotential calc. 3−30133
Al-Ge alloys, vacancies influence on nucleation of incoherent Ge precipitates 3−2702
α-Al_2O_3, $Al(OH)_3$, AlO(OH), $MgAl_2O_4$, struct. effects on chem. shift, X-ray photoelectron spectra 3−30920
Au_3Cu ordered alloys, use of Morse potential function calc. 3−7868
B compounds spectra, electron, vapour state, chemical correlations 3−23549
Cr, atoms, surface and bulk, core-electron binding energies 3−39210
Cs and binary alloys, pseudo-alloy-atom model and hume-Rotherys 15% rule 3−24817
Cs-Rb alloy system, calculation as a function of alloy composition 3−33481
Cu_3Au ordered alloys, use of Morse potential function calc. 3−7868
Fe, Mg, Al, Si and O in silicate minerals, ESCA technique 3−5431
Ge, amorphous, cohesive energy and density of states 3−36521
Ge, electron-hole drop binding energy from luminescence spectrum 3−21476
Ge, metallic state rel. to free excitons 3−21009
${}^2H$, Yamaguchi-type potentials with repulsion in ${}^3S_1$ eigenchannel 3−29318
${}^3He_\Lambda$, properties and decay branching ratios 3−17185
K and binary alloys, pseudo-alloy-atom model and hume-Rotherys 15% rule 3−24817
K complexes, hexachlorometallate photoelectron spectra, X-ray, core and valence orbitals 3−23544
K-Rb alloy system, calculation as a function of alloy composition 3−33481
$MgZn_2$ Madelung constant and energy, in terms of parameters of crystal type, calculation *(German)* 3−1598
Na and binary alloys, pseudo-alloy-atom model and hume-Rotherys 15% rule 3−24817
NaBr-KBr solid solution, interatomic bonds, energetic and strength characts. *(Russian)* 3−20722
NaCl:$MnCl_2$, kinetics of clustering 3−4750
NaCl-KCl solid solution, interatomic bonds, energetic and strength characts. *(Russian)* 3−20722
Ni, atoms, surface and bulk core-electron binding energies, comparison 3−39210
O atom and negative ion binding energies approach to chemisorption forces determ. 3−30352
Pd-Ag alloy, inner core electrons 3−36976
Pt-O, chemisorbed system, determ. from desorpt. spectra 3−4927
Rb and binary alloys, pseudo-alloy-atom model and hume-Rotherys 15% rule 3−24817
Si, amorphous, cohesive energy and density of states 3−36521
Si, group V impurity atom-vacancy, binding energy, diffusion 3−33836
Si, metallic state rel. to free excitons 3−21009
Te, acceptor states, theory 3−36544
Ti, atoms, surface and bulk, core-electron binding energies, comparison 3−39210
U clean surfaces, electron binding energies determ. by soft X-ray appearance-potential spectroscopy 3−36977
W, surface diffusion and clustering, interpretation of ion microscopy data 3−36475
W, surface diffusion and clustering, interpretation of field ion microscopy data 3−36476

Bingham plastics and solids *see rheology*

biocontrol
see also biocybernetics
closed loop control system model of pitch and formant frequency transitions 3−3429
electrochemical information and energy transfer in vivo 3−5630
eye movement control model 3−39796
eye movement model for human visual task 3−39799
eye-movement study in target tracking 3−39798
hydraulic microdrives, for micromanipulators remote control 3−16551

biocontrol continued
- layered tissues, temperature distribution calc. 3—25587
- oculomotor control system, predictive tracking mechanism 3—9683
- prosthesis, orthosis, EMG signals, reliability *(Croatian)* 3—13130
- skin temperatures in warm environments, control of sweat evaporation 3—3561

biocybernetics
- *see also brain models; learning systems; man-machine systems; neural nets*
- aneurysm of circle of Willis, mathematical model, qualitative analysis of Austin's differential equation 3—33322
- aorta parameters, determ. using cost function analysis 3—9637
- auditory system, simulation of information processing mechanism 3—31862
- biomechanics, hereditary processes, evolution in terms of difference-differential equations 3—35229
- electrically excitable membranes, generalised model, systems theoretical approach 3—35240
- human vision, multiple-channel models, bandwidth consideratons 3—35261
- living cell as microcybernetic polymaser *(Spanish)* 3—25548
- pupillary light reflex, systems approach *(Korean)* 3—31873
- retina input system modelling, curvilinear images *(Russian)* 3—16319
- sensory receptors, intensity characteristic generalised function 3—35243
- simulated aortic valvular stenosis in pulsatile quasiphysiological flow, loss consideratons 3—3901

bioelectric potentials
- *see also contact potential*
- action potentials from single neurons of auditory cortex of unanesthetized macaque monkeys 3—3521
- alpha motoneurone activity obs. using motor unit studies 3—5639
- animals, chronic and asymmetrical cortical foci rel. to bilateral synchrony of epileptic discharge 3—28333
- anterior cingulate gyrus, stereo-EEG 3—28332
- association cortex potentials, reaction time in auditory discrimination 3—28325
- auditory evoked potentials, effects of long onset ramp 3—3415
- auditory evoked response to simultaneously and successively presented stimuli, frequency specificity 3—5633
- auditory evoked responses to speech and music stimuli, cerebral asymmetry 3—3414
- auditory evolved potentials, selective attention 3—19095
- average evoked, on-line circuit for extraction from periodic noise 3—3899
- average evoked potentials from auditory nerve region and brain cortex in waking monkeys 3—3410
- averaged evoked potentials, in rabbit, effects of fractionated X-ray irradiation 3—28328
- beta bursts in human frontal cortex, rel. to psychological parameters 3—5631
- brain stem potential changes rel. to stimuli 3—35245
- brain tissue using compound powder electrodes 3—3401
- brain tumor patient, delta activity during rapid eye movement sleep 3—37522
- cat, olfactory pathway, efferent evoked responses 3—28331
- cat, polysensory responses and sensory interaction in pulvinar and related posterolateral thalmic nuclei 3—39774
- cats, brain steady potential, β adrenergic mechanisms 3—28344
- cats, factor analysis of evoked potentials 3—31848
- cats, simultaneous d.c. and multiple unit responses from lateral geniculate 3—37729
- cats anesthetized, middle ear muscle contractions rel. to bone conduction 3—31856
- cells, axially symmetric, finite difference solution 3—35246
- cells, single, Fredholm integral equation solution 3—35247
- cephalic skin potentials, potential shifts 3—16309
- cortical, intensity function, evoked by electrical stimulation of VIIIth nerve 3—3412
- cortical auditory evoked potentials in dogs, electrogenetical differences 3—3407
- dog, sympathetic nerve stimulation on pulmonary vascular resistance 3—37517
- dorsal root, modifications during respiratory acidosis 3—28341
- eccentric dipole concept 3—25551
- e.e.g., photic response by focal lesions 3—31850
- e.e.g. alpha rhythm rel. to Schumann resonance 3—9652
- e.e.g. pattern recovery under photic stimulation by light of different colours 3—5638
- electrical activity of visual system, saccadic displacements of retinal image 3—9677
- electrocortical activity rel. to voluntary movement in man *(French)* 3—19092
- electromyogram waveform changes in postural muscle fatigue 3—28335
- electromyograph waveform analyser sensitivity 3—25982
- electromyographic analysis, interfacing of Olivetti P101 programmable calculator and Biomac 500 computer 3—16554
- e.m.g. activity, signal processing techniques 3—3408
- e.m.g. obs. of intrinsic and extrinsic laryngeal muscles in patients with spasmodic dysphonia 3—3409
- e.r.g. current source, rel. to potential, single cell obs. and tissue impedance *(German)* 3—3889
- evoked cortical response, early component, effects of frequency and phase reversal 3—3413
- evoked potential variability, age, amplitude, and measurement method effects 3—37520
- eye, computerised psychological experimentation 3—5657
- eye glissade, electrophysiological explanation 3—39788
- frog, early receptor pot., urea effect 3—31897
- guinea pig, sympathetic adrenergic transmission, mechanism of enhancement by angiotensin II 3—9650
- guinea pig taenia coli membrane potential rel. to extracellularly applied ATP and related nucleotides *(Japanese)* 3—37514
- hippocampus, averaged evoked brain potentials, component analysis 3—35241
- human, visual discrimination problem 3—31847
- human and adults, variability of visual evoked potentials 3—37519
- human brainstem electrical responses to acoustic signals 3—3411

bioelectric potentials continued
- human muscle motor units, volume conduction of potentials 3—3405
- human muscles, extraterritorial potential field of impulses from separate motor units 3—28334
- isolated carp retina, horizontal cell membrane potential, effects of amino acids 3—39791
- man, extracellular firing patterns of deep temporal lobe structures 3—39766
- marine, ocean engineering, conference, New York (1972) 3—3228
- measuring systems, in-phase interference immunity 3—32237
- medial rectus eye muscle, spectral analysis 3—25582
- monkey brain, slow potentials during preparatory interval 3—16308
- Monkey cores and rods, time courses of late receptor potentials 3—9674
- motor unit discharge, differentiated electromyography obs. 3—25976
- muscle artifact, in electroencephalographic recording 3—35236
- muscles, quadriceps and gastrocnemius, H reflex 3—19091
- nerve action potentials, in human, signal/noise ratio during recording 3—28338
- neurons recording, spike segregation technique 3—25980
- normal children, visual evoked response to language stimuli 3—37521
- online multi unit sorting with resolution of superposition 3—25979
- pigeon, photic evoked pot. in optic tectum, rel. to flash intensity and background illumination 3—31877
- pigeon, visual projections to wulst, electrophysiology 3—28342
- preterm newborn infants, visual and somatosensory evoked responses 3—37523
- primary auditory cortex in unanesthetized macaque monkeys, variation of excitability of neurons 3—3522
- primate retina, prominal negative response 3—39781
- prosthesis, orthosis, control, EMG signals, reliability *(Croatian)* 3—13130
- pure tone and speech-evoked response in normal and noise-exposed squirrel monkeys 3—3513
- quantitative, e.e.g. during hypnosis 3—19090
- rat retina, isolated, electroretinogram fast components, ionic environment depend. 3—31892
- Rhesus monkeys, brain steady potential, β adrenergic mechanisms 3—28344
- slow processes, multichannel recording, amplifier interaction 3—32236
- slow vertex potentials, in human, interactions among auditory, tactile, electric, and visual stimuli 3—28324
- somatosensory cortical evoked potential, effect of aging on wave form 3—5637
- somatosensory cortical evoked potentials, modification during action and rest *(French)* 3—5632
- somatosensory evoked response, travelling waves, human scalp recorded, recording technique and sleep effects 3—28326
- somatosensory evoked responses to tactile tap in man 3—28329
- spinal electrograms, evoked, recorded from epidural space in man 3—28336
- turtle retina, e.r.g. obtained with flickering light 3—9680
- vertex potentials and eyeblink, comparison of response plasticity 3—5634
- visual cortex of rabbit, single unit reactions to light plastics of different intensities 3—39767
- visual evoked cortical potentials, during pressure-blinding 3—31900
- visual evoked potential, of short latency, recorded from human mastoid process and auricle 3—28323
- visual evoked response using rapid flash rates technique 3—28330
- visual motion evoked potentials in man 3—13131

bioelectrical phenomena
- acoustically evoked potential, recovery cycle 3—25566
- Aplysia neurons, intracellular conductance 3—28315
- artificially segmented giant axon, in lobster, electronic modification of external current 3—28337
- cat, evoked responses from facial nucleus, background noise content 3—28339
- cat hippocampus, CA3 region recurrent excitation 3—28343
- cats, motoneurons, accommodation to current ramps 3—28340
- chemoreceptor discharge patterns, theoretical models 3—9651
- chronic animals, intracellular recording in cerebral cortex 3—35521
- discharge of cells in posterior colliculus of chinchilla, effect of stimulus intensity at different interaural phases 3—3520
- discharges of cells in posterior colliculus of chinchilla, effect of interaural phase at different frequencies 3—3519
- dog stomach, recorded with suction electrodes in monopolar lead *(Japanese)* 3—35239
- dogs, gastric smooth muscle, e.m.g. study, location of pacemaker *(Japanese)* 3—35238
- e.e.g. as index of orienting response in children 3—5635
- e.e.g. psychology-oriented analysis, circadian rhythms, sensory deprivation, computer program 3—9653
- electric fish communication, lightning as background noise source 3—31851
- electrochemical information and energy transfer in vivo 3—5630
- excitable membranes, generalised model, systems theoretical approach 3—35240
- frog muscle contractile behaviour under magnetic field *(Russian)* 3—16310
- galvanic skin response in sleep experiments 3—25978
- galvanic transmissions, electronic programmed control system *(Russian)* 3—37524
- gating currents assoc. with Na channels 3—35244
- heart, isolated rabbit, spread of excitation in atrioventricular mode, multiple microelectrode recording study 3—22145
- hippocampal electrical activity, in monkey, during delayed alteration problems 3—28327
- hippocampus, averaged evoked brain potentials, component analysis 3—35241
- isometric contractions, motor unit action potential trains, analysis of results 3—35242
- membranes, solutions of time-dependent electrodiffusion equations 3—25549
- nerve impulses, Na ion movement rel. to temp. 3—35230
- nerve tissue stimulation, using magnetic fields 3—16558
- nervous system of vertibrates, book 3—28311
- neural constants of motion 3—35249

bioelectrical phenomena continued
  pacemaker activity and atrioventricular conduction, vagal and stellate nerve stimulation effects in dog 3−35237
  Schumann resonance, rel. to alpha rhythm patterns in e.e.g. 3−9652
  sensory receptors, as transmitters of entropy 3−35250
  sensory receptors, intensity characteristic generalised function 3−35243
  skeletal muscle excitation-contraction coupling rel. to voltage depend. charge movement 3−31845
  skin impedance, effects on surface electrode meas. between 5 and 2000 Hz 3−31846
  squid axon, intracellular conductance 3−28315
  squirrel monkeys, awake and sitting, inputs to cingulate cortex 3−28345
  ventricular depolarisation, multiple dipole model 3−19093
biographical dictionaries *see biographies*
biographies
  see also history
  Giordano Bruno (1564-1600), scientist or heretic 3−9782
  Linus Pauling, his contribution to materials science 3−9783
  Luke Howard, cloud physics 3−9299
  Max Planck, by Hermann 3−3740
  Rankine, W.J.M., 1820-1872, short biography 3−5739
  William Gregor (1761-1817) discoverer of Ti, account of his scientific work 3−19128
biological cybernetics *see biocybernetics*
biological effects of radiation
  a.c. electric fields, 100 to 200 kV/m., effects on mice, modified growth of progenies 3−9716
  a.c. electric fields, from h.v. transmission lines, service personnel protection 3−9717
  a.c. electric fields in h.v. substations, PAT phenomena 3−9715
  acoustic impulses, 40 μsec impulses, audiometric and histological effects 3−3608
  acoustical overstimulation, behavioural and anatomic manifestations 3−3607
  artenia eggs, neutron irradiation, protective effect of β-mercaptoethylamine 3−28379
  audiometric effects of continuous and impulse noises 3−3514
  Australian Atomic Energy Commission, 20th Annual Report (1971-72) 3−14242
  averaged evoked potentials, in rabbit, effects of fractionated X-ray irradiation 3−28328
  bacteria dried on glass or plastic surfaces, sterilized by heat or γ-rays, pyrogenic activity 3−13157
  beta dose on skin rel. to gamma exposure from surfaces contaminated with aged fission products 3−9705
  bone marrow damage following total model irradiation in Hodgkin's disease patients 3−25601
  bone marrow stem cells, X-ray effects 3−31941
  breast cancer, treatment by electron beam from betatron 3−16560
  caloric vestibular stimulation by u.h.f. microwave irradiation 3−25602
  cancer, preoperational irradiation therapy, from 25 MeV betatron *(Russian)* 3−25598
  cancer treatment using π^- beam calcs. for producing desired depth-dose distribs. 3−25607
  carcinoma and leukemia resulting from whole body irradiation in fast neutron therapy 3−5679
  cell survival, molecular theory 3−28382
  cosmic radiation rates and Concorde, rel. to health hazard *(French)* 3−37533
  damage in cells, recovery of cell surface charge rel. to colony forming ability 3−3591
  diagnostic medical X-rays, genetically significant dose determ. 3−9706
  diagnostic medical X-rays, population mean marrow dose and leukaemia significant dose determ. 3−13152
  diagnostic radiography methodology for obs. of retakes 3−13143
  DNA, x-irradiation, effect of cyclic AMP on production of single-strand breaks in E. coli B/r CSH 3−28374
  DNA base-pairs, competition among biprotonic phototautomerism, excimer formation and proton tunnelling, radiation mutagenesis, review 3−11337
  DNA chain elongation and joining after U.V. irradiation of human cells 3−5677
  dose levels discrimination in whole-body irradiated mice by counts of bone marrow samples 3−31935
  dose protraction by fractionation and by continuous exposure, comparative effects 3−9732
  drosophila melanogaster, life-span shortening and age-related structural alterations 3−28366
  e.m. fields and waves, 2nd. International Colloquium of the International Section of ISSA for Prevention of Occupational Risks due to Electricity 3−9713
  e.m. fields and waves, physiological damage, mechanisms 3−9714
  e.m. radiation effects on human body, review *(Dutch)* 3−31934
  e.m. radiations, health hazards and safety regulations 3−9701
  endothelial cells of capillaries, radiosensitivity 3−25600
  escherichia coli, postirradiation degradation properties 3−28383
  eye, opacification due to fractionated X-ray and proton irradiation 3−35291
  eye exposure by Th containing lenses 3−9708
  fission neutrons, early transient incapacitation in monkeys 3−3598
  flour beetle pupae, X-irradiation, age at pupation and population effects 3−3589
  fractionated high energy radiation therapy, optimum treatment schedules 3−22170
  fruit, coloured, i.r. refl. rel. to ripening 3−9702
  grape seeds, effect of u.s. on diffusion of P 3−28310
  guinea pigs, enhancement of primary immune response by X-irradiation 3−9709
  haemopoietic stem cells of mouse, late effects 3−28377
  hamster cells, enhancement of X-ray damage by hypertonic treatments 3−31944
  hamster cells, lethal and sublethal X-ray irradiation, repair of damage 3−31943
  hamster cells, X-ray irradiation, radiosensitivity and chromatin dispersion during cell cycle 3−31945
biological effects of radiation continued
  heavy particle treatment for acromegally, Cushing's disease Nelson's syndrome and nonfunctioning pituitary adenomas 3−3587
  histological effects of continuous and impulse noise interaction 3−3515
  human brainstem electrical responses to acoustic signals 3−3411
  human damage by picosecond impacts of high-output laser systems 3−31937
  human lymphocytes, chromosome aberration yield as indication of dose 3−13156
  human lymphoid cells, synchronized populations, radiation response 3−28373
  incapacitation and postirradiation effects, report 3−3565
  injuries to exposed radiation workers, chromosome aberration dosimetry 3−16304
  inoculated cells, concentrations and shapes of doze-response curves 3−28380
  interference of sleep by noise 3−3524
  irradiated tooth enamel, e.p.r. study 3−9712
  isotope cisternography, development of neurogenic bladder 3−3592
  kidney, of mice, X-ray irradiation effects 3−31942
  laser effects on eye 3−28385
  left ventricular dimensions measurement in dogs, using cineradiography 3−3568
  leukocytes, of swine, γ-irradiation effects 3−31940
  lung tumours, betatron therapy, clinical considerations 3−22171
  mammalian and avian cells, effect of ion sputtering, s.e.m. study 3−22174
  mammalian cells, electron irradiation, breaking survival curves 3−28384
  mammalian cells in tissue culture, effects of irradiated medium on growth characteristics 3−9641
  mammalian embryo heart rate, prompt effects of X-radiation 3−25605
  mammalian fibroblasts, plateauphase in growths induced by hypoxia, radiation-survival curves 3−28376
  mammalian intestine, response to ionisation 3−9710
  marine ecosystems contamination 3−9232
  marine lymphoma cell in vitro, short-term effects on volume regulation, influence of H_2O_2 3−28378
  medical physics, therapy, conference (Chicago, USA, Dec 1971) 3−3574
  mice, exposed to r.f. e.m. fields, life span 3−39812
  mice, relative effectiveness of fission neutrons for gastrointestinal damage 3−3601
  mixed γ-n-radiation, acute mortality response in dogs 3−3599
  monkey, γ-n irradiation, e.e.g. and behaviour 3−3604
  monkeys, drug responsiveness, on radiation induced performance decrement 3−3600
  monkeys, early transient incapacitation, blood PO_2 and pH, brain hypoxia 3−3602
  monkeys, physiology and behaviour, injection of radioprotective agents prior to irradiation 3−3603
  neutron-produced single-event spectra, calculation and measurement 3−9711
  nuclear radiation and environment, protection 3−32997
  nuclear science, conference, Miami USA, (1972) 3−28622
  optical radiation hazards evaluation, safety exposure criteria, control measures 3−19101
  osteosarcoma induction, dose-time relations, rel. to maximal permissible ^{90}Sr burden in man 3−9704
  protons, molecular dissociation, charge transfer 3−35292
  pulsed γ-n-radiation, performance decrement of trained beagles and miniature pigs 3−3597
  pulsed u.s. radiation effects 3−3588
  radiation therapy, interactive computer program for standardization of prescriptions 3−31923
  radiotherapy with high low-energy-transfer radiations 3−3586
  radiowave, on human body, admissible field strength *(Polish)* 3−31938
  rat liver mitochondria, oxidation cell membranes 3−3605
  rat-spleen lysosomes, comparative effects of electron and neutron irradiation on relase of enzymes 3−28375
  rats, suppression of acetylcholinesterase 3−3606
  rats, X-ray induced pathophysiologic changes 3−31939
  replicative form DNA, φX-174, heavy ion induced single- and double-strand breaks 3−3590
  retina, radiant heating by nonuniform light sources, injury threshold temperature 3−9664
  safe tracer dose in medical investigation 3−3585
  skin, considerations for using thermal techniques for determination of damage 3−3595
  solar activity effects on biological processes, comparison with geophysical effects 3−22173
  space travellers *(German)* 3−35293
  spore growth, electron irrad. effects, electron microscope obs. 3−25599
  spores, germinating, DNA degradation 3−31946
  stomach cancer, results of preoperational irradiation from 25 MeV betatron *(Russian)* 3−25597
  superficial layers of skin in X-ray therapy, effect of shadow trays 3−3594
  temperature rise in biological tissue during focused u.s. irradiation 3−5678
  therapy, adaptation of 30 MeV IAP betatron 3−16483
  thyroid cancer, long-term radioisotope scanning 3−25604
  thyroid uptake test, normal range estimation 3−3582
  tissue-like media, quasi-elastic nuclear interactions 3−3593
  u.s., physiological effect 3−35294
  u.s., shear stress and cell disruption 3−25603
  u.s. B-mode scanning, radiation therapy 3−3577
  u.v., i.r., health lamps, history, development, use, benefits 3−3572
  X-ray damage in living cells, influence of energy metabolism on repair 3−13151
  X-rays, divided doses, hair regrowth in mouse 3−31936
  yeast, liquid-holding reactivation, effect of respiratory inhibitors and glucose 3−13151
  ^{252}Cf radiocytogenetic studies, chromosomal analysis of hamster ovary cells, irradiation under aerobic and anaerobic conditions 3−28381

biological effects of radiation continued
^{60}Co radiation therapy effect on plasma levels of cortisol and corticosterone in humans 3—16324
^{131}I treatment of thyroid cancer 3—3584
Rn exposure, rel. to bronchial epithelium thickness 3—9707
T, long-term evaluation 3—9697
biological macromolecules *see macromolecules*
biological sciences *see biology*
biological techniques and instruments
see also biology; biomedical engineering; biomedical equipment
air turbine viscometer, rheological testing of biological materials 3—22529
arterial blood pressure changes obs. using arterial tonometry 3—3897
bacteria size and concentration, determ. by spectral method and cloudiness *(Russian)* 3—26003
binocular low vision telescopic spectacles 3—28524
biochemical and biophysical morphology, book 3—26004
biotelemetry employing thick film technology *(German)* 3—32238
biplane X-ray videometry, visual-display unit with simultaneous data presentation 3—3906
blood, red cells moving towards orifice, holographic verification of model 3—28760
blood electroacidification 3—22527
blood flow monitor system 8, low limb circulation obs. 3—419
blood pressure and flow transmitter, FM telemetering 3—397
blood pressure catheter system requirements for arterial pressure wave processing 3—28320
blood vessel imaging in cerebral angiography, computer simulation 3—10158
bone phosphorus, neutron activation analysis 3—37730
botanical specimen prep. technique for SEM 3—35530
capacitor energy storage X-ray equipment, exposure factors rel. to conventional high tension transformer 3—10160
cardiac output calc. from dilution curve area estimation, compartmental hypothesis 3—6126
cardiac pacemakers, bioelectric energy sources 3—6125
carotid artery diameter and flow, noninvasive technique using Doppler effect 3—37733
cat's retina, method for projecting pattern, direct visual control 3—28767
catheter type blood flowmeter, three electrode probe 3—400
cell membranes, employing micropositioner in closed-loop control systems 3—22528
cerebral blood flow studies, HP Ge detector array 3—28759
Cherenkov detector for energy calibration of 9-22 MeV electron beams 3—10153
chronic animals, intracellular recording in cerebral cortex 3—35521
clinical spectrophotometric and fluorometric meas., need for standardisation 3—25648
coherent data processors, improved estimation techniques of blood cell counts 3—3402
comparison eyepiece, for slide mounted insects 3—25989
computer aided radiotherapy treatment, automation and patient repositioning 3—10167
coronarography, 70 mm intensifier fluorography with 6 inch image intensifier 3—6129
cryosurgery, effects of low temps. on tissues 3—6146
cutaneous electrical simulation mimicking touch 3—6141
cyclotron as short lived radionuclides and positron emitter source for medicine 3—273
cytophotometry, electronic systems for microspectrophotometer 3—25999
d.c. defibrillators, indicated and delivered energy 3—6123
defibrillator performance, instrument for evaluation 3—6124
diagnostic radiography, re-take procedures 3—13144
diagnostic X-ray machines, precise calibration with portable apparatus 3—415
diagnostic X-ray machines with voltage dividers 3—10151
dynacamera, device for recording time reference markers 3—10177
e.c.g. electrodes, insulated, with integrated impedance transformer 3—3905
echoencephalography using Automatic Midline Computer, clinical evaluation 3—16553
egg shells, radial fracture surfaces, s.e.m. study 3—19359
elastic and plastic props. of biological objects in the microsphere, meas. device 3—28754
electrical conductance of moving and stationary blood, effect of frequency changes 3—3904
electromyograph waveform analyser sensitivity 3—25982
electromyographic analysis, interfacing of Olivetti P101 programmable calculator and Biomac 500 computer 3—16554
electromyographic recording, apparatus for unanaesthetised free swimming fish 3—25997
electron beam therapy, review 3—6131
electron microscope environmental specimen chamber for examining biological ultrastructure in wet state 3—358
electron microscopy, review 3—423
electron microscopy of biological materials, image profiles 3—10143
electron probe analysis, computer program for quantitative microanalysis of thin specimens 3—37739
electron probe analysis, specimen preparation, review 3—37738
electronic drinkometer, circuit to operate during footshock 3—6140
electronic radiography for pelvimetry and intra-uterine transfusions 3—10172
e.m. flowmetry in anaesthetized rats 3—3562
e.m.g. obs. of intrinsic and extrinsic laryngeal muscles in patients with spasmodic dysphonia 3—3409
e.m.g. obs. of musculus depressor, anguli oris 3—3893
e.m.g. obs. of tones of Thai 3—3428
e.m.g. sensor design for use with externally powered prosthetic arm 3—6127
force transducer, low drift, for crayfish stretch receptor obs. 3—25985
galvanic skin response in sleep experiments 3—25978
gamma camera, count rate loss correction method 3—10174
gamma camera, parallel hole collimator design using optimization theory 3—10148
gamma camera uniformity 3—10178
high-pressure optical cell, for biochemical reactions 3—28525

biological techniques and instruments continued
histomechanics of Chordae tendineae of human heart *(German)* 3—3754
Hodgkin's therapy, lapjoint of opposed adjacent fields 3—10164
h.v. electron microscopes, effects of beam on biological and polymeric specimens 3—389
h.v. electron microscopy, biological applications 3—353
image formation by induced local interactions, zeugmatography 3—28617
image intensified fluoroscopic equipment, proper X-ray beam collimation 3—10154
impediography, u.s. technique 3—93
induction coil system for preventing air embolism during hemodialysis *(German)* 3—3888
insects, respiration meas., null balance O_2 analyser and i.r. CO_2 analyser 3—13484
intensifier fluorography in vascular examinations 3—6132
intracranial pressure measurement, using coplanar transmembrane pressure transducer 3—3903
i.r. spectrophotometer, modified for nerve excitation study 3—401
L-phase streptococci, s.e.m. techniques 3—19360
larynx height obs. during speech using thyro-umbrometer 3—3421
laser microprobes, analysis of biological specimens *(German)* 3—28762
linear accelerator, trip-out circuit for arcing or free-running trigger pulses 3—10176
linear motion generator, for physiological research 3—25986
lingual articulation, cinefluorographic analysis 3—19094
liquid surface acoustic holography, history and current status 3—210
liquid surface holographic u.s. imaging unit for soft tissue structures 3—10162
living organs, multicomponent spectra evaluation in presence of inhomogeneous optical paths, optical path invariants *(German)* 3—6133
low light level sensor for obs. of bioluminescence of fish schools 3—3208
lower urinary tract obstruction evaluation by transduction and signal processing 3—6145
magnetic gradiometer based on superconducting quantum interference device, construction 3—28499
marine mammals, underwater electric field telemetry using ingestible telemetry pills 3—428
medical treatment planning, using interactive graphics terminal 3—10169
megavoltage therapy machines, build-up characteristics, TLD obs. 3—9727
microelectrophoresis assembly, for cellular surface studies 3—25998
micromanometer for implantation in ventricles of dogs 3—3902
millidyne film balance for intermol. energy meas. 3—10142
mineralized tissues, high resolution surface scanning electron microscopy 3—3910
modulated light stimuli, device 3—25981
motor end-plate growth and degeneration in mammalian skeletal muscle 3—13139
multisensor cryogenic temp. probe 3—6147
muscle-pulling system for neural function studies 3—16570
National Accelerator Laboratory medical programme 3—409
neuromuscular testing device for extremities 3—3892
neuronal pulse spectrometry, similarity with nucler systems, applications of computers and mathematical models 3—28755
neurons recording, spike segregation 3—25980
neurophysiological data, computer-aided spectral analysis, using intermediate magnetic tape storage 3—28756
neutron diffractometer, for low angle studies 3—35528
neutron radiography, stroboscopic, using 35 MeV linac 3—6136
nondispersive X-ray fluorescence, techniques for in vitro studies 3—31927
nuclear medicine, computerized image improvement using selected frequency band enhancement 3—416
nuclear medicine, imaging and image improvement 3—417
on-line circuit for extraction of average evoked potentials from periodic noise 3—3899
operational amplifiers as electrometers 3—10152.
palatoglossus function in normal speech production, electromyographic implications 3—3420
perfusion chamber, in vitro investigations under microscopic control *(German)* 3—28764
perfusion fixation equipment with automatic pressure control 3—3909
photoelectric matrix method for two-dimens. eye movement recording 3—28766
photoretinoscopy, study of vision from a distance 3—6142
Picker 500 scanner, paper tape interface 3—10175
portable pneumophone for Eustachian tube patency determ. 3—28347
radiation exposure in dental panographic roentgenology 3—13158
radiation therapy, conference (Chicago, USA, Dec 1971) 3—3574
radiation treatment planning optimisation, decision-theoretic approach 3—13154
radioautography, rapid image generation using microchannel plate electron image amplifiers 3—35526
radiographic for medical image processing 3—6130
radiographic viewboxes, information capacity 3—10159
radionuclide imaging, three-dimensional 3—10146
radiotherapy, appls. of small computers 3—10183
radiotherapy, using RAD-8 treatment planning system 3—13153
radiotherapy machine connection to computer 3—3913
rapid eye movement analyser 3—39775
reflection coeffs. meas. of ultrasonic interfaces using a multitransducer configuration 3—9841
respiratory flow transducers, characteristics 3—6144
scanning electron microscopy, appl. to biological materials 3—10185
scree-film systems for cerebral angiography 3—414
short-lived isotopes, production using charged particle accelerators 3—32870
signal delivery and monitoring system for obs. of vibrotactile sensitivity of tongue 3—6139
silver grain yields in autoradiograms by scintillators in embedding media *(German)* 3—35527
simulated aortic valvular stenosis in pulsatile quasiphysiological flow, loss consideratons 3—3901

biological techniques and instruments continued

- SKAT, automated self-administered preschool auditory screening test 3−3508
- spark chamber gamma camera, computer simulation 3−10173
- specimen preparation for s.e.m., critical point drying *(German)* 3−28763
- spectrophotometric standards, role in clinical chemistry laboratory 3−25649
- spirometer and elec. impedance plethysmograph meas., computer-aided analysis 3−25975
- stomatology, materials shrinkage examination 3−25972
- strain gauge transducer system, meas. of jaw and lip movement 3−424
- taut-band meter for assessment of human heat stress 3−6134
- telemetry systems, implantable, for cardiovascular phenomena obs. 3−6122
- teletherapy, selection of optimum treatment, linear and non-linear discriminant anal. 3−3581
- teletherapy treatments, comparison of techniques using goodness-of-fit statistics 3−3580
- therapy planning aids and computer appls. 3−3579
- therapy unit timer error and instrument nonlinearities 3−10180
- thermal techniques for delineation of radiation damage in skin, considerations for using 3−3595
- thermographic ancillary devices for focusing and surface defect location 3−3898
- thermophysical properties, determination by probe method 3−114
- thyroid uptake test, normal range estimation 3−3582
- time lapse cinemicrography apparatus 3−19361
- tissue holder, for formaldehyde vapour induced fluoresc. 3−35525
- tomography and zonography of kidneys 3−6128
- tomosynthesis, holographic method for variable depth display 3−28765
- transmission electron microscopy for thickness and mass thickness meas. 3−37740
- transmission scanning, using continuous X-ray source 3−31928
- two-vessel manometry and substrate determinations, computer programs for numerical and graphic evaluation 3−3884
- ulnar resonant frequency measurement 3−32241
- ultra microtone for transmission electron microscopy 3−33436
- u.s. appl. in medical laboratory practice 3−25973
- u.s. B-mode scanning, radiation therapy 3−3577
- u.s. imaging systems, review 3−425
- u.s. transducer design, biological objects exam. 3−25974
- vocal tract area function, input impedance singularities from speech, determination 3−3416
- wind-tunnel metabolism chamber for small animals 3−25983
- X-ray complete treatment film, radiographic quality enhancement 3−13166
- X-ray films of vocal tract, computer aided measurement system 3−426
- X-ray image intensifier tube E5703, description 3−32232
- X-ray image processing, evaluation 3−3900
- X-ray imaging using proportional wire chambers, rel. to conventional photography 3−6137
- π^- therapy beam at TRIUMF 3−10182
- ^{252}Cf medical sources, storage and handling facility 3−10170
- ^{252}Cf sources, solid geometry versus plane geometry 3−10179
- Co radiation therapy unit, computer-controlled kinematic simulator 3−10166
- ^{60}Co γ-ray instrument calibration using collimated photon beam 3−10149
- ^{60}Co hospital sterilizers, developments 3−6135
- ^{60}Co mantle field therapy, lead block shaped fields, radiation field and optical shadow 3−10165
- ^{127}Cs and ^{129}Cs, production of curie amounts for medical use 3−13142
- ^{137}Cs line source, radiation distrib. 3−9700
- ^{52}Fe, preparation of medically useful amounts by spallation 3−13141
- ^{125}I-fibrinogen technique for venous thrombosis detection 3−3908
- NaI imaging systems, reduction of scattered radiation 3−10147
- Si(Li) detectors, application to clinical problems 3−28758
- ^{85}Sr bone scans in periosteal new bone formation 3−3571
- Ta dust persistence following accidental ingestion, rel. to that following canine bronchography 3−10161
- ^{133}Xe multibolus fractionation technique for human cerebral blood flow distribution meas. 3−22526

biology

- *see also blood; medicine; physiology*
- causality and anticipation, reference to phenomena of life 3−9784
- exobiology, review of extraterrestrial organic compound anal. 3−35016
- human lung transport processes, computation of boundary conditions 3−28319
- physics, conference (Edmonton, Canada, June 1972) 3−9699
- physics, its role in biology, comment 3−25544
- physics applied to biology, comment 3−25543
- $Q\beta$ RNA, sequencing algorithm 3−35226
- tobacco mosaic virus polymerized proteins, crystal dislocations 3−5623
- urine, radiochemical determ. of ^{35}S *(Czech)* 3−13505

biomedical electronics

- *see also electrocardiography; electroencephalography; microelectrodes; patient monitoring; patient treatment; prosthetics; sensory aids*
- blood, canine, specific resistance measurement 3−3406
- blood pressure signal conditioners, automatic calibration 3−398
- cardiac resuscitator, patent 3−35248
- catheter-densitometer and thermistor systems, analogue computer correction of sampling distortion 3−25993
- clinical radiometer, for dynamic processes using radioisotope method 3−35271
- cutaneous electrical simulation mimicking touch 3−6141
- digital thermometer *(German)* 3−37595
- drinkometer operation during footshock using contact relay circuit 3−6140
- dry electrode e.c.g., transmitter for rapid acquisition from moving subject 3−25970
- electroconvulsive shock generator, design description 3−37736

biomedical electronics continued

- electromedical instruments, faults due to poor design and maintenance, rectification, international standards 3−10141
- f.m. blood pressure and flow transmitter, FM telemetering 3−397
- heartrate indicator, IC application 3−25994
- impedance convertor, monolithic IC realisation, for membrane pot. meas. 3−37741
- microelectrode recording, d.c. level compensation 3−399
- nerve action potential recording, signal noise ratio 3−28338
- on-line circuit for extraction of average evoked potentials from periodic noise 3−3899
- ophthalmology, visual prosthesis 3−13134
- prosthesis, orthosis, control, EMG signals, reliability *(Croatian)* 3−13130
- rapid eye movement analyser 3−39775
- slow bioelectric process recording, amplifier design 3−32236
- spirometer and elec. impedance plethysmograph meas., computer-aided analysis 3−25975
- variable heartrate electronic simulator, for some haemodynamic signals 3−25995

biomedical engineering

- *see also patient treatment; prosthetics*
- 25 MV betatron, modification for whole body electron irradiation 3−410
- clinical laboratory electronic instrumentation, book 3−10184
- conference on medical instrumentation, Washington (1973) 3−39802
- electro-oculography, dry silver electrodes 3−19098
- human electro-oculogram, linearity of horizontal component 3−19099
- 25 MeV linear accelerator, X-ray and electron beam characteristics 3−3575
- National Accelerator Laboratory medical programme 3−409
- neurophysiological data, computer-aided spectral analysis, using intermediate magnetic tape storage 3−28756
- osseous attachment of non-porous metals by composite bonding 3−2794
- scintillation image enhancement, two-dimensional filtering 3−313
- stereotoxic neurosurgery on deep cerebral structures, computer graphics displayed maps of brain cross-section 3−3890
- tracer data, dynamic statistical analysis, parameter estimation 3−3567
- ultrasonic applications *(Polish)* 3−16393

biomedical equipment

- *see also artificial organs; biomedical electronics; defibrillators; pacemakers; X-ray apparatus*
- accelerators, meeting of Danesbury-Rutherford working party 3−32125
- automated microscope with optical analyzer for diagnostic cytology 3−159
- bandwidth selector, for EMG activity 3−32247
- Bekesy audiometer, calibration *(German)* 3−13233
- bioelectric measuring system, in-phase interference immunity 3−32237
- blood cell spectrometer, transit time 3−32244
- blood flow monitor system 8, low limb circulation obs. 3−419
- blood flow sensors for internal and external chronic use, ultrasonic 3−37777
- blood pressure and flow transmitter, implantable, FM telemetering 3−397
- blood pressure and flow transmitters, implantable, FM telemetering 3−397
- blood-gas analysers, review 3−16550
- body plethysmograph, factors affecting phase lag of airflow behind pressure 3−13138
- breathing gas pressure regulator, adjustable, patent 3−10190
- capacitor energy storage X-ray equipment, exposure factors rel. to conventional high tension transformer 3−10160
- cardiac pacemakers, bioelectric energy sources 3−6125
- Cherenkov detector for energy calibration of 9-22 MeV electron beams 3−10153
- coherent data processors, improved estimation techniques of blood cell counts 3−3402
- conference on medical instrumentation, Washington (1973) 3−39802
- cutaneous electrical simulation mimicking touch 3−6141
- cyclotron, TRIUMF, medical uses 3−22164
- cyclotron as short lived radionuclides and positron emitter source for medicine 3−273
- cyclotron size for medical applications 3−22165
- d.c. defibrillators, indicated and delivered energy 3−6123
- defibrillator performance, instrument for evaluation 3−6124
- detector probes, application in nuclear medicine 3−32141
- diagnostic X-ray machines, precise calibration with portable apparatus 3−415
- diagnostic X-ray machines with voltage dividers 3−10151
- digital tape recorder, portable, data acquisition and retrieval system for field operation 3−25990
- dosimetric, conference, Philadelphia, Pa., USA (1972) 3−13136
- dynacamera, device for recording time reference markers 3−10177
- e.c.g. electrodes, insulated, with integrated impedance transformer 3−3905
- electromedical instruments, faults due to poor design and maintenance, rectification, international standards 3−10141
- electronic drinkometer, circuit to operate during footshock 3−6140
- e.m.g. sensor design for use with externally powered prosthetic arm 3−6127
- eye, human, accommodation, continuous objective measuring apparatus, i.r., lag and transfer function 3−37735
- eye movement detector, photoelectric method 3−3907
- fatigue measurement, computerized data processing system 3−32246
- flicker photometer, automatic synchronised, evaluation and applications *(German)* 3−28538
- gamma camera, count rate loss correction method 3−10174
- gamma camera, parallel hole collimator design using optimization theory 3−10148
- gamma camera uniformity 3−10178
- gamma camera with large field of view 3−28370
- gamma scintillation camera, new method for design optimisation of parallel-hole collimators 3−22521
- gamma-ray camera using coaxial Ge(Li) detector 3−402
- gas exchange and respiratory function measurement system 3−25984

biomedical equipment continued
- gross motor movement detection device for human subjects, using Crime Alert CA-2 3—37737
- hydraulic microdrive, for micromanipulation 3—16551
- image intensified fluoroscopic equipment, proper X-ray beam collimation 3—10154
- image recording system for γ-camera 3—418
- impedance change measuring instrument, for physiological event obs. 3—25996
- induction coil system for preventing air embolism during hemodialysis *(German)* 3—3888
- infusion controller 3—32243
- for intensifier fluorography in vascular examinations 3—6132
- kinesiometer, for reflex measurement 3—25969
- linear accelerator, trip-out circuit for arcing or free-running trigger pulses 3—10176
- liquid surface holographic u.s. imaging unit for soft tissue structures 3—10162
- megavoltage therapy machines, build-up characteristics, TLD obs. 3—9727
- microcalorimeter, isothermal titration 3—37600
- mitotic cells searching by machine, computer applic. 3—6143
- multi-level scan display systems, analysis 3—35284
- multidetector instrumentation and data analysis, for regional pulmonary function studies using ^{133}Xe 3—32239
- multiwire proportional chambers 3—16559
- neuromuscular testing device for extremities 3—3892
- operational amplifiers as electrometers 3—10152
- perfusion fixation equipment with automatic pressure control 3—3909
- Picker 500 scanner, paper tape interface 3—10175
- for pulmonary imaging 3—22531
- radiation therapy, conference (Chicago, USA, Dec 1971) 3—3574
- radiographic viewboxes, information capacity 3—10159
- radiotherapy machine connection to computer 3—3913
- random time interval generator 3—13482
- respiratory flow transducers, characteristics 3—6144
- Scinticamera IV, gamma camera for brain scanning 3—16552
- scintillation camera, meas. of resolving time 3—10145
- scree-film systems for cerebral angiography 3—414
- sleep analyser, hybrid system *(French)* 3—16555
- soft ended u.s. probe for echo-encephalography 3—3887
- spark chamber gamma camera, computer simulation 3—10173
- standardisation 3—22246
- stereotoner, reading aid for blind people 3—3911
- taut-band meter for assessment of human heat stress 3—6134
- telemetry systems, implantable, for cardiovascular phenomena obs. 3—6122
- therapy unit timer error and instrument nonlinearities 3—10180
- thermal instruments, for blood flow 3—32242
- thermographic ancillary devices for focusing and surface defect location 3—3898
- three-electrode probe for catheter type flowmeters 3—400
- transistorised electronic stimulator 3—16556
- turbidity cell, for monitoring bacterial growth 3—32240
- u.s. imaging systems, review 3—425
- u.s. radiometer, portable 3—91
- u.s. scanning apparatus with transducer scanning rate responsive transmitter, patent 3—10186
- u.s. therapeutic transducer, scanning system for beam profile meas. 3—90
- ventricular pressure, rate of proportional rise determination, on-line computer applic. 3—13485
- visual display unit for biplane X-ray videometry, with simultaneous data presentation 3—3906
- X-ray image intensifier for indirect radiography 3—16548
- X-ray image intensifier tube E5703, description 3—32232
- π^- therapy beam at TRIUMF 3—10182
- Ar-Kr coagulator, basics 3—32245
- CdTe detector probes, application in clinical environment 3—32142
- ^{60}Co hospital sterilizers, developments 3—6135
- NaI imaging systems, reduction of scattered radiation 3—10147
- Si target storage tube, fluoroscopic dose reduction and image manipulation 3—411
- Tc imager, scintigraphic display 3—10144

biomedical measurement
- abdominal aortic aneurysm, ultrasonographic and radionuclide angiographic study 3—37732
- aortic-wall thickness in living dogs 3—16557
- arterial blood pressure changes obs. using arterial tonometry 3—3897
- blood circulation obs. in lower extremities using blood flow monitor system 8 3—419
- blood flowmeter, e.m., and use 3—395
- blood flowmeter, e.m. pulsed-field, design 3—396
- carotid artery diameter and flow, noninvasive technique using Doppler effect 3—37733
- chest clearance of inhaled ^{60}CoO 3—9696
- conference (Edmonton, Canada, 1972) 3—9699
- cortical thickness of bone obs. using photon absorption 3—3576
- differentiated electromyography, motor unit discharge abnormality detection 3—25976
- echoencephalography using Automatic Midline Computer, clinical evaluation 3—16553
- electromyographic recording, in free swimming unanaesthetised fish 3—25997
- gait recording, using tranistorised e.c.g. 3—22525
- gas exchange and respiratory function, continuous meas., computer analysis 3—25984
- internal structure calculation from multiple radiograms ' 3—5675
- internal tissue density, Compton effect applications 3—25596
- intracranial pressure measurement, using coplanar transmembrane pressure transducer 3—3903
- lower urinary tract obstruction evaluation by transduction and signal processing 3—6145
- marine mammals, underwater electric field telemetry using ingestible telemetry pills 3—428
- membrane potential, probe mounted integrated impedance convertor applic. 3—37741
- microscope spectrophotometer, radiation patterns of rod photoreceptors 3—3912

biomedical measurement continued
- nuclear diagnostic medicine, book 3—11101
- nuclear medicine, computerized image improvement using selected frequency band enhancement 3—416
- oxyhaemoglobin dissociation curves, computer-aided data reduction 3—28360
- phase lag of airflow behind pressure in meas. using a body plethysmograph 3—13138
- phenomena subject to severe artifactual distortion, histogram data selection algorithm for filtering 3—10168
- physiological events, instrument for measuring impedance changes 3—25996
- radioautography, rapid image generation using microchannel plate electron image amplifiers 3—35526
- reflexes, biomechanical profile using kinesiometer 3—25969
- thyroid uptake test, normal range estimation 3—3582
- underwater physiology, conference (Freeport, British Bahamas, Aug. 1972) 3—3566
- u.s. B-mode scanning, radiation therapy 3—3577
- visual motion evoked potentials in man 3—13131
- X-ray attenuation methods of bone mineral mass obs., effect of beam size 3—3596
- X-ray films of vocal tract, computer aided measurement system 3—426
- X-ray therapy, effect of shadow trays on dose to superficial layers of skin 3—3594
- xeroradiography, review 3—26000
- zero field size tissue-air ratio calc. for 4 MV X-rays produced by linac 3—3629

biomedical phenomena
- human acceleration tolerance, effects of elevated body temp. 3—28362
- muscle contraction effects of Ca ionophore, X-537A 3—35266
- optical absorption, quantisation eff. with elec. field dependence 3—36009

biomolecules *see macromolecules*

bionics *see biocybernetics*

biophysics
- *see also cellular biophysics; hearing; molecular biophysics; speech*
- Achromobacter s.p., luminesc. thermal variations 3—22136
- atria, guinea pig, effects of electrical stimulation on membrane potentials during hypothermia 3—22140
- bacteria dried on glass or plastic surfaces, sterilized by heat or γ-rays, pyrogenic activity 3—13157
- bacterial luminescence, transient suppression by H_2O_2, mechanism 3—16300
- bioenergetics, relation between radiation, soil type and vegetation 3—5626
- bioluminescence of fish schools, low light level sensor for obs. 3—3208
- biomembrane phase transitions theory 3—22142
- blocked purkinje tissue, passive conduction delay, numerical delay 3—13129
- blood pressure regulation by sympathetic nerve fibres and adrenal medulla in normotensive and hypertensive rats 3—22135
- canine circulatory response to graded stimulation of carotid chemoreceptors 3—9688
- canine mitral complex, ultrastructure and electromechanical properties 3—9687
- converence, Finland, 4 to 5 Jan. 1973 3—35224
- counterdiffusion, supersaturation, bubble formation, isobaric inert gas urticaria and vertigo 3—35232
- directional reversible currents of blood flow in spinal cord arteries 3—3404
- dynamic systems, mathematical models *(German)* 3—25546
- echinosphaerium, particle movement 3—16305
- energy absorption coeff. of bone and muscles 3—5674
- erythrocytes, light beating spectrum, active transport mechanism 3—19089
- expiration, physical model 3—26854
- fish muscle, analysis of bimodal diffusion of water 3—22143
- flagellar movement, small amplitude motion of sliding filament model 3—16301
- flagellar waves form and speed according to sliding filament model 3—16302
- health physics, multipurpose radiation monitoring system, ionization chamber and air monitoring, book 3—31921
- health physics, nuclear reactors, weapons and accelerators, book 3—35267
- health physics training, decontamination and radiation, book exposure 3—31922
- heat defect of ionizing radiation absorbed in tissue equivalent plastic 3—5676
- hemorheology, flow obs. *(German)* 3—5672
- human aortic valve, stress analysis, for design of prosthetic valve 3—35223
- human brain tissue in shear, rheological response 3—26002
- human lung transport processes, computation of boundary conditions 3—28319
- impairment of lung clearance mechanism by respiratory infection 3—9689
- lipid bilayer spheres, deform. and birefr. in mag. fields 3—37515
- lung, gas transport 3—10397
- membrane, book 3—28321
- membrane, excitable, physiochemical model of permeability 3—35233
- membrane transport, continuum mechanical approach to flow equations 3—35234
- memory components of skilled escape reaction in rat. heterogeneity 3—3398
- molecular biology and biophysics progress, book 3—9638
- monkeys, drug responsiveness, on radiation induced performance decrement 3—3600
- monkeys, physiology and behaviour, injection of radioprotective agents prior to irradiation 3—3603
- multicompartmental systems, tracer distribution equations 3—28318
- multiple transport systems, kinetic analysis of two component systems in transmembrane transport 3—9644

biophysics continued
- myosin location in physarum polycephalum and role in cytoplasmic streaming 3-16306
- nerve excitation study, using modified infrared spectrophotometer 3-401
- nervous system of vertibrates, book 3-28311
- osseous attachment of non-porous metals by composite bonding 3-2794
- particles in given volume, function rel. size distribution 3-25971
- periodontal ligament of maxillary central incisor, model, stress anal. 3-9692
- pyrimidine bases and derivatives, electronic aspects of photodimerization 3-21836
- quality factor for biological substances, track structure analysis 3-3861
- representation of activity determination in three dimensional regions *(German)* 3-5673
- respiratory physiology, recent advances, book 3-13123
- skin temperatures in warm environments, control of sweat evaporation 3-3561
- small blood vessels, mechanics *(German)* 3-25545
- trace elements, effects on mammalian life 3-3564
- vertebrates central nervous system, relation of axon sheath thickness to fibre size 3-28313
- vesicles bounded by single phospholipid bilayers and loaded with acetylcholine, preparation in suspension 3-13127
- Ca ions and muscle contraction 3-5628

Biot-Savart law *see electromagnetism*

biotite *see mica*

bipolar transistors
- n-p-n reverse biased, for charge injection into SiO_2 3-34006
- neutron irrad., limiting design parameters 3-33991
- As based diffision, closed ampoule and gas stream, comparison *(Russian)* 3-24811
- Si, common emitter type, current compressive stress depend. 3-21145
- n-p-nSi, ion implantation appl. 3-8761
- Si, leakage causing defects, electrochem. decoration and elec. microscope obs. 3-38581
- Si n-p-n, anodic oxidation, diffusion pipe decoration 3-38582
- Si n-p-n, enhanced P emitter diffusion, correlation with elec. props. 3-39291
- Si transistor emitter diffusion, effects of Sn on base impurity 3-39290
- Si-As n-p-n structs., retarded base diffusion, theory 3-21544

bipoles *see network analysis*

birefringence
- *see also electro-optical effects; flow birefringence; light polarisation; magneto-optical effects; mechanical birefringence; optical constants; optical rotation*
- acoustic image detection using nematic liquid crystal birefringence 3-35362
- Babinet compensator for anomalous dispersion meas. in birefringent media 3-13314
- Cherenkov radiation in biaxial crystals, Fourier integrals 3-33547
- Cherenkov radiation in biaxial crystals, generalized universality condition 3-33548
- cholesteric liquid crystals, circular dichroism and rotatory dispersion near i.r. absorption bands 3-30830
- colloids, electrical double refraction *(Rumanian)* 3-22848
- epoxy resin, cured, relax. and optical props. 3-31175
- ferroelectric, anisotropic, at submillimetre wavelengths *(Russian)* 3-12197
- ferroelectric materials, digression from phenomenological theory 3-18423
- freons, CF_2Br_2, CF_2Cl_2 and $CFCl_3$, temp. depend., sign change *(French)* 3-39120
- Fresnel rhomb, for quarter wave retardation in i.r. 3-35396
- illumination distribution of point in optical system with axial symmetry *(Russian)* 3-5879
- lens, spatial filtering applications 3-3796
- lipid bilayer spheres, deform. and birefr. in mag. fields 3-37515
- liquid cryst., nematic, elec. controlled birefringence, field alignment rel. to pulsed voltage *(French)* 3-8553
- liquid cryst., smectic and cholesteric, light scatt. by plane texture deform. 3-12111
- liquid crystal, cholesteric, compensated, temp. depend. 3-30796
- liquid crystal nematic, transverse field electro-optical effects 3-24676
- liquid crystals, their educational use for illustration 3-16366
- magnetic material, optical contrast of inclined boundaries 3-18436
- magnetised crystals and isotropic bodies, nonlinear changes in magneo-optical birefringence 3-37978
- nonmonochromatic light, effect of birefringent plate on polarisation 3-22842
- optical glass, control of refractive index during annealing *(Polish)* 3-5174
- parametric gain, optimum focusing conditions 3-781
- pentachlorodiphenyl, liq., relax. of elec. birefringence, temp. depend. *(French)* 3-24674
- phenomenological theory of optical props. of crystals 3-34320
- polymer, spectroscopic method for local stress meas. at stress raisers 3-28472
- polymer stiff-chain molecules in solution 3-21383
- polypropylene, hydrostatic extrusion and characteriz. 3-21744
- Rochelle salt, temp. variation of optic angle, +35 to −165°C 3-36853
- semiconducting chalcogenides, intrinsic piezobirefringence obs. 3-12110
- semiconductors, optical magnetisation 3-24593
- solutions, standard solvent choice for studying oscillatory dynamic birefringence *(Russian)* 3-26751
- streaming double refraction in dil. suspension of rigid spheroids, subject to weak Brownian motion 3-7457
- synthetic sapphire, refractive index meas. 3-5926
- wedge interference band displacement method of electro-optical voltage meas. *(Czech)* 3-3829
- wideband optical f.d.m. communications, birefringent branching filters 3-22307

birefringence continued
- $AgGaSe_2$, three freq. collinear phase matching 3-4120
- $(CH_3NH_3)AL(SO_4)_2.12H_2O$, ferroelectric, electro-optical and thermo-optical props. 3-34328
- CdS, dispersion *(Russian)* 3-2511
- GaP, spatial dispersion induced 3-2512
- GaSb, spatial dispersion induced 3-2512
- GaSe, rel. to nonlinear optical props. *(Russian)* 3-2505
- Ge, spatial dispersion induced 3-2512
- n-InAs, i.r. birefringence due to hot electrons, 80K *(Russian)* 3-8555
- KH_2PO_4, effect of annealing on anomalous biaxiality *(Russian)* 3-15470
- $(K_2O)_{0.3}(Li_2O)_{0.7}(Nb_2O_5)_x$, dielec. const., refr. index, electrooptic coeff., spontaneous polarisation, birefringence, pyroelec. props. 3-30798
- Mn-Bi film, birefringent, mag. domain patterns, polarisation microscope obs. 3-21283
- $(NH_4)_2Cd_2(SO_4)_3$, temp. depend. 3-24662
- NaCl structure crystals, piezo-optic birefringence, calc. 3-24675
- $Pb(Zr,Ti)O_3$, La_2O_3-modified, temp. depend. 3-5168
- $RbNiF_3$, acoustic birefr. due to magnetoelastic interaction 3-34177
- $SrTiO_3$, 105K structural phase transition, birefringence study of anisotropic fluctuations and order parameter 3-2510
- TeO_2, paratellurite, rel. acousto-optical light deflection 3-5176
- $Y_3Fe_5O_{12}$, garnet Cotton-Mouton effect, internal stress effects, anisotropy 3-39128
- $ZnGeP_2$, refinement of structural characteristics, structural depend. of birefringence 3-21382
- $ZnSiAs_2$ refinement of structural characteristics, structural depend. on birefringence 3-21382
- ZnTe, spatial dispersion induced 3-2512

bismuth
- amorphous film, supercond. transition temp. depression by Ar(Ne) overlayers, surface phonon contrib. 3-34017
- chemisorption on (111) surface, LEED obs. of layer struct. 3-30356
- chemisorption on Cu (100) surface, LEED obs. of layer struct. 3-30355
- cyclotron resonance in far i.r., quantum aspects and electrodynamics 3-33786
- diamagnetism theory 3-8338
- dislocation pile-ups due to polygonization 3-7757
- elastic properties, up to 32 kbar, determ. from press. depend. of u.s. velocity *(Russian)* 3-7806
- elastoresistance relaxation in thin film 3-33866
- electronic heat capacity calc. using ellipsoidal nonparabolic model 3-30270
- elimination rate of ^{214}Bi, ^{222}Rn rich water, radiation exposure 3-5682
- exciton phase transition in strong mag. field, u.s. absorption obs. 3-27230
- Fermi hole surface anomalies, giant quantum oscillations in ultrasonic attenuation 3-18068
- film, amorphous, crystn. temp. thickness depend. 3-20972
- film, Hall coeff. anomalous temp. depend. 3-30551
- film, oscill. in longitudinal magnetoresistance 3-33875
- film, quantum size effects, elastoresistance, thermoelectric power and conductivity obs. 3-4997
- film, transition from amorphous to crystalline state under mag. field *(Russian)* 3-15015
- film growth mechanism, condensation in vacuum, electrical resistivity, electron microscope examination 3-33758
- film melting and freezing, obs. in electron microscope 3-14980
- films, scattering processes investigation 3-2194
- galvanostatic oxidation, in aqueous oxalic acid soln. 3-8038
- grain boundary energy, and solid-liq. interfacial energy 3-4762
- lattice dynamics, five neightbours Born-von Karman model 3-20821
- lattice dynamics, phonon dispersion freq. spectra, sp. ht. 3-30215
- liquid, struct. microheterogeneities, kinetic viscosity, temp. depend. *(Russian)* 3-17729
- liquid, thermoelectric props., temp. depend., m.p.-1200K 3-24408
- local logarithmic decrement, hysteresis loops with reversible displacement of single twin boundaries 3-27030
- magnetoresistance, under pulse conditions in strong crossed elec. and mag. fields 3-24453
- magnetoresistance meas. at digital nitrogen temp. and high pressures rel. to polymorphic transitions 3-18122
- molecular beam, determ. of diatomic:atomic ratio from ESCA 3-29745
- muonic, elec. quadrupole X-ray transitions 3-7095
- phonon drag region, size dependence of the transport props. 3-8139
- plastic deform. behaviour of single crysts. 3-7818
- pseudocubic, second easy slip system obs. *(French)* 3-20741
- rare earth iron garnet: Bi substituted, Faraday effect 3-34330
- rethermalization of neutrons in graphite-Bi system 3-19895
- second harmonic generation during anomalous skin effect 3-18179
- semimetal-semiconductor transition under press. 3-33822
- single crystals, plastic deformation and dislocation etch-pit distribution *(Japanese)* 3-30993
- solution growth of $CdGeAs_2$ with Bi solvent 3-12286
- sound propag. in strong mag. field, phonon spectra singularities 3-30672
- target, picosecond light pulses absorption 3-20553
- thin film growth, gravimetric investigation of growth kinetics 3-36269
- thin films, longitudinal magnetoresistance meas. *(Korean)* 3-27246
- transport and thermoelec. props., 300-77 K 3-36593
- twinning and untwinning, kinetics 3-24133
- twinning rate, quenching, alloying and surface oxidation effects *(Russian)* 3-31057
- u.s. attenuation in single crystals, pulse echo technique at 20°C, dislocation damping 3-11690
- viscosity meas. by vibration method 3-4869
- volumetric mass determination *(French)* 3-27855
- B_2O_3-SiO_2, vapour deposited, characts. and use in Si device fabrication 3-2657
- Bi additions to Al-Mg alloys for improvement of stress-corrosion resistance 3-12382

bismuth continued
Bi IV, application of Slater-Condon theory with configuration interaction to various odd configurations 3–4360
Bi:Sn, hole g-factor meas. 3–8089
Bi-In(Sn)(Cd) systems, contact melting in mag. field *(Russian)* 3–15698
Bi + Se, enthalpy of mixing in liquid state 3–14976
Bi_2, potential energy curves and molecular dissociation energies 3–20189
Bi^{2+}:oxide glass, absorpt., fluoresc., excitation and decay time meas. 3–12168
Bi^{3+} in MSb_2O_6, (M = Ca, Sr, Ba), fluorescence obs. for each excitation band 3–21478
Bi(II), atomic spectra from Hartree-Fock calcs., need of LS-depend. parameters 3–7035
Bi(V), crystal structure at high pressure 3–11584
CaO:Bi, Sb, Te phosphors, photoluminescence, radical-recombination luminescence of the O atoms *(Russian)* 3–30876
CaS:Bi^{3+}, Pd^{2+} phosphorescence decay characteristics 3–30856
La_2O_3:Bi^{3+}, photoluminescence props. *(Russian)* 3–36930
MnBi films, apparatus for co-deposition 3–15607
inNa_2O-B_2O_3, Na_2O-NaCl-B_2O_3 glasses u.v. absorption of Bi(III) rel. to stoichiometry of complexes 3–24724
Pb:Bi superconducting thin films, surface impedance *(German)* 3–21165
PbN_6:Bi, thin films, photodecomposition, optical absorpt. and cond. meas. 3–25084
Se:As, As_2S_3, Bi, SiO, doping in vacuum growth to produce semicond. film for electrophotography 3–15623
Si:Bi, impurity photocond. oscills., 4.2-10K *(Russian)* 3–2134
SrS:Bi phosphors, activator conc. depend. of luminesc. characts. 3–27564
$SrSb_2O_6$:Bi^{3+}, photoluminescence props. *(Russian)* 3–36930

bismuth alloys
see also bismuth compounds
Bi-Cd, temp. and conc. dependence of mag. susceptibility 3–27362
Bi-Cd(Sb), alloying effect on twinning rate *(Russian)* 3–31057
Bi-Pb system, structure of metastable phase 3–18569
Bi-Sb, cryst. growth from melt 3–12272
Bi-Sb, film, deposition by steady state evaporation 3–24787
Bi-Sb, narrow band gap semiconductors, zero bandgap transition 3–38800
Bi-Sb, quantum oscillations of thermoelectric power 3–8206
Bi-Sb, single crystal, dislocation study using etch pit technique 3–17836
Bi-Sb, transverse striations on top free surface, triangular features on cleavage plane 3–11786
Bi-Sb supercond. amorphous films, fluctuations near transition temp. of heat capacities 3–2200
Bi-Sb:Te,Se, calc. of thermoelec. figure of merit in mag. field 3–15176
Bi-Sb(12 at.%) powder compacts, transport and thermoelec. props., 300-77 K 3–36593
Bi-Sb(30%), with and without Te,Sn impurities electrical transport props., 8-300 K *(German)* 3–11916
Bi-Sn, liq., n.m.r. linewidths, conc. depend. 3–2412
Bi-Sn liq. system, partial heats of mixing 3–37007
Bi-Zn, liquid, volumetric mass determination *(French)* 3–27855
Bi_{50}-X_{50}, liquid X = In, Sn, Sb, Pb, nuclear-spin-lattice relaxation meas. for ^{209}Bi 3–5145
BiMn, single crystal platelets formed by vacuum deposition, flux reversal, study using Kerr effect 3–2308
BiMn thin film formation study by elec. resistivity and X-ray diffraction *(Japanese)* 3–34005
$Bi_{0.9}Sb_{0.1}$ crystals, magnetoplasma wave dispersion *(Russian)* 3–11922
$Bi_{1-x}Sb$, gapless state, magnetoresist., semicond.-semimetal-semicond. transition 3–33791
Bi_xSb_{1-x} film, quantum size effects, elastoresistance, thermoelectric power and conductivity obs. 3–4997
BiSn, body centred tetragonal structure, obs. under high pressure 3–4732
Cs_3Bi, valence band density of states determ. from photoemission and electron scatt. 3–24773
CuBi, liq., mag. susceptibility *(Japanese)* 3–30600
In-Bi, liquid, nuclear-spin-lattice relaxation meas. for ^{115}In and ^{209}Bi 3–5145
In-Bi supercond. foils, eff. of a.c. mag. fields on flux-flow states *(Japanese)* 3–24547
InBi, intermetallic, chem. etchants for characterisation 3–11817
Mg-Bi, liquid, conc. fluctuations calc. using cluster model 3–36255
MnBi and $MnBi_{0.9}Sb_{0.1}$, mag. struct., neutron diffr. study 3–24573
MnBi fil, domain patterns, Faraday effect obs. 3–21272
MnBi film, low temp. mag. props. 3–27384
$Ni_{41}Pd_{41}B_{18}$:Cr, amorphous, elec. resist. meas. showing Kondo effect 3–33869
Pb-Bi, peritectic, heat of non-equilibrium solidification 3–39323
Pb-Bi, single-crystals, plasticity in superconducting and normal states at 4.2 K 3–36353
Pb-Bi film, inhomogeneous, supercond., critical currents and pinning effect 3–15306
Pb-Bi liquid solns., self-interaction parameters, limiting activity coeffs. temp. depend. 3–21793
Sn-Bi, controlled solidification in melt growth 3–11562
Sn-Bi liquid system, concentration dependence analysis of magnetic susceptibility *(Russian)* 3–8347

bismuth compounds
see also bismuth alloys
$Bi_2Bi_4Ti_3Fe_2O_{18}$, perovskite layer type ferroelec., ^{57}Fe Mossbauer obs. from 80 to 1150 K 3–27443
$Bi_{3-2x}Ca_{2x}Fe_{5-x}V_xO_{12}$, neutron diffraction obs. of structure 3–8369
$Bi_{3-2x}Ca_{2x}Fe_{5-x}V_xO_{12}$ garnet system, porosities, hysteresis, resonance linewidths, inhomogeneity effects 3–18342
$BiCl_3$ molten salts, supercritical temp. range, continuous density transition, electrical conductance, experimental 3–11728
$BiCl_3$ Raman spectra, method for resonance fluorescence effect elimination 3–28542
$BiCl_n$ $(N\text{-}3)^-$ complexes i.r. band intensities, combinatorial diffusion *(Russian)* 3–2832

bismuth compounds continued
$BiCl_3.H_2O$, n.q.r. obs. of two nonequivalent ^{35}Cl resonances at 25°C meas. of temperature dependence down to 196K 3–8480
BiF_5, association in vapour phase, molecular beam mass spectra 3–25924
$BiF_3(Cl_3)$, centrifugal extension consts., calc. *(Russian)* 3–20104
$BiFeO_3$, internal mag. field obs. by Mossbauer effect 3–27447
$BiFeO_3$ magnetic and structural props. 3–39064
$BiFeO_8$, superparamagnetic phase investigation by means of Mossbauer effect 3–24640
$Bi_2Fe_4O_9$, spin orientation, Mossbauer obs. 3–36724
$Bi_{12}GeO_{12}$, growth by Czochralski method from Pt crucible of Bi_2O_3 *(German)* 3–8737
$Bi_{12}GeO_{20}$, a self-focusing of A laser radiation by Raman scattering 3–4128
$Bi_{12}GeO_{20}$, acoustic surface waves, harmonic generation 3–17932
$Bi_4Ge_3O_{12}$, refr. index and electrooptic coeff. 3–21427
BiI_3, bielectron and bi hole luminesc. radiation, 1.6-10K 3–18490
BiI_3, bielectron and bihole energy levels, doublet fine struct. 3–21020
n-BiI_3 single crystals, photoconductivity and photoluminescence *(Russian)* 3–11932
$Bi_2In_4S_9$, crystal structure, chemistry 3–7673
$Bi_\alpha(MO)_\beta MO_3$, (M = Ta, W and Nb, W) new phases, struct. *(French)* 3–7697
$Bi_2(MoO_4)_3$, melt growth by flux pulling method 3–12283
BiO, mol., pot. energy curves, dissociation energies, calc. by Rydberg-Klein-Rees-Vanderslice method 3–14394
BiO_2, emission spectrum 3–33118
Bi_2O_3 glasses, refractive index > 1.75, correlation of refractive index and density, Newton-Drude relation 3–5902
Bi_2O_3 high-resistance anodic film formation on Bi 3–8038
Bi_2O_3-BaO-B_2O_3 flux system, use in growth of ferrite spinels 3–2663
Bi_2O_3-TeO_2 system at 450°C radiocrystallographic investigation *(French)* 3–27100
Bi_2O_3-TiO_2-KF-H_2O, crystallisation, form. and props. of $Bi_2Ti_4O_{11}$, $Bi_4Ti_3O_{12}$, $Bi_{12}TiO_{20}$ 3–24048
BiOBr, i.r. transmission, two phonon absorpt. processes 3–21424
BiOBr, long wavelength fund. absorpt. edge rel. to press. and elec. field *(Russian)* 3–8609
BiOBr, luminesc., photocond., energy levels *(Russian)* 3–8108
BiOBr, thermal cond. meas. 3–4891
BiOCl, i.r. transmission, two phonon absorpt. processes 3–21424
BiOCl, luminesc., photocond., energy levels *(Russian)* 3–8108
BiOCl, thermal cond. meas. 3–4891
BiOCl(Br)(I), two-phonon processes 3–15491
BiOI, i.r. transmission, two phonon absorpt. processes 3–21424
BiOI, long wavelength fund. absorpt. edge rel. to press. and elec. field *(Russian)* 3–8609
BiOI, luminesc., photocond., energy levels *(Russian)* 3–8108
BiOI thermal cond. meas. 3–4891
BiS, mol., pot. energy curves, dissociation energies, calc. by Rydberg-Klein-Rees-Vanderslice method 3–14394
Bi_2S_3, dissociation pressure meas. in 806-904K range, determ. of heat of formation from thermodynamic laws *(Russian)* 3–12511
Bi_2S_3, photosemicond., crystallisation under hydrothermal conditions *(Russian)* 3–15633
Bi_2S_3, sintered, electronic props. and range of existence *(French)* 3–36406
Bi_2S_3 crystals, thermostimulated electron emission *(Russian)* 3–12206
Bi_2Se_3 Hall effect magnetometer, for low temp. work 3–35446
Bi_2Se_3:Ge, lattice defects, reflectivity meas. at plasma resonance 3–33824
$Bi_{12}SiO_{20}$, growth by Czochralski method from Pt crucible of Bi_2O_3 *(German)* 3–8737
$Bi_{12}SiO_{20}$, light scatt. by optical phonons *(Russian)* 3–8591
$Bi_{12}SiO_{20}$, self-focusing of Ar laser radiation 3–32602
$Bi_4Si_3O_{12}$, refr. index and electrooptic coeff. 3–21427
Bi_2Te_3, Mossbauer effect of ^{129}I *(Russian)* 3–12087
Bi_2Te_3, thermoreflectivity spectrum, 2.7-3.8 eV, at 80°K 3–8598
Bi_2Te_3-Sb_2S_3, liquid, specific resist. and thermal e.m.f. meas., phase diagram study *(Russian)* 3–15192
BiTeI film, prep., struct. and mech. props. *(Russian)* 3–18033
$Bi_2Te_{2.4}Se_{0.6}$ and $Bi_{0.52}Te_3Sb_{1.48}$ cold pressed semielements, anisotropy of phys. props. *(Russian)* 3–11919
$Bi_{12}TiO_{20}$, nonlinear optical props. *(Russian)* 3–8552
$Bi_4Ti_3O_{12}$, solid solution, ferroelectric, solubility limits and structural stability 3–4841
$Bi_4Ti_3O_{12}$ film, electrooptical quality, epitaxial growth by r.f. sputtering 3–12252
$Bi_4Ti_3O_{12}$ single-domain epitaxial films, electro-optic contrast obs. 3–18431
MnBi-Bi eutectic, directionally solidified, mag. props. 3–36748
PbS-Bi_2S_3 system phases, cryst. struct. 3–15858

bistable multivibrators *see flip-flops*

bitter patterns *see magnetic domains*

bitumen *see materials*

black holes
see also gravitational collapse
2U0525-06, X-ray source, identification with ϑ^2 Orionis 3–13080
accretion from interstellar gas, emergent radiation spectrum 3–39586
in binary systems, obs. appearance 3–39588
3C273 (quasar), interpretation of light variations autocorrelation function 3–25477
charged rotating, invariant measures of surface geometry 3–28113
close binary system with collapsed star, disk model of gas accretion, X-ray source 3–37362
collapsed Schwarzschild fields and the second law of thermodynamics 3–25361
dynamics, parallels with thermodynamics, entropy 3–28112
e.m. radiation sources moving in stable circular orbit *(Russians)* 3–16092
energy and charge extraction and scattering of massless wave fields 3–37287
energy extraction and scalar synchrotron radiation from rotating black holes 3–18911

black holes continued
- energy removal by lowering rope into ergosphere, conditions on rope 3—9451
- existence, discussion *(French)* 3—39591
- expanding universe, propagation of light in a Friedmann model 3—16112
- galactic gravitational radiation model involving central black hole 3—13094
- galactic nuclei model, plasma turbulence effects 3—34996
- galaxies with central black hole rel. to Newtonian analysis of initial cosmological perturbation 3—13091
- gravitational radiation of falling particle, 4-dimens. Green's function approach 3—37885
- gyromagnetic factor of massive body with large space-time curvature 3—35610
- HDE 226868, spectroscopic binary, optical counterpart of Cygnus X-1, secondary possible black hole 3—31694
- HDE 226868, spectroscopic binary optical counterpart of Cygnus X-1, secondary possible black hole 3—31693
- Kerr, mass formula and comparison to rotating liquid drop 3—16113
- β Lyrae, further evidence for black hole 3—9452
- Maxwell eqns. for radiation by moving charge falling radially into hole 3—12945
- BM Orionis, eclipsing binary, secondary component possibly collapsed star 3—31682
- radial motion of spinning test body in field of black hole, analysis of gravitational radiation 3—12947
- Reissner-Nordstrom black hole due to collapsed electrically charged star, scalar perturbation method 3—19001
- relativistic disks at centres of galaxies rel. to gravitational wave production 3—22728
- rotating charged bodies and Kerr-Newman solns. of Einstein-Maxwell eqns. 3—35609
- Schwarzschild, gravitational radiation from mass projected inside with nonzero kinetic energy 3—35614
- Schwarzschild. vector and tensor radiation from relativistic circular geodesics 3—37288
- secondary star in HDE 226868 binary system 3—9555
- solar models, opacity, thermal instability and central black hole rel. to neutrinos 3—16125
- spinning test bodies, orbital motion anal. 3—16114
- stellar distribution in cluster with collapsed object 3—19055
- synchrotron radiation from relativistic Schwarzschild circular geodesics, polarisation 3—37289
- tidal accel. near black hole conditions for kinematic magnification 3—6324
- universe, behaviour as black hole, confined closed structure 3—5557
- vacuum metrics, axisymmetric system stability, Carter's theorem 3—10364
- X-ray sources, mass rel. to neutron stars and black holes 3—31733

Bloch walls *see domain walls*

blood
- *see also hemodynamics*
- abdominal aortic aneurysm, ultrasonographic and radionuclide angiographic study 3—37732
- acute fibrinous pericarditis, diagnosis using ^{125}I labelled fibrinogens 3—28363
- aortic blood flow meas., pulsed Doppler technique 3—37734
- aortic velocity and acceleration by u.s. device 3—37731
- arterial pressure changes obs. using arterial tonometry 3—3897
- brachial artery flow velocity meas. after cardiac surgery 3—39803
- canine, specific resistance measurement against hematocritic conditions at body temperature 3—3406
- carotid artery diameter and flow, noninvasive technique using Doppler effect 3—37733
- cats, left ventricle rel. to flow and pressure source 3—36141
- cats, normal myocardial function and energetics in volume overload hypertrophy 3—37512
- cell counts, improved estimation techniques in coherent data processors 3—3402
- cell spectrometer, transit time 3—32244
- cerebral flow, cerebral, HP Ge detector array 3—28759
- coagulation factor, electrochem. behaviour, obs. on fibrinogen 3—39764
- coagulation factor, electrochem. behaviour, obs. on prothrombin and thrombin 3—39763
- coagulation method and apparatus, patent 3—10191
- electrical conductance of moving and stationary blood, effect of frequency changes 3—3904
- electroacidification 3—22527
- extracorporeal irradiation 3—35288
- flow, by thermal instruments 3—32242
- flow sensors, Doppler, for internal and external chronic use 3—37777
- gas analysis, review 3—16550
- human myocardial blood flow meas. using ^{133}Xe 3—35269
- leukocytes, of swine, γ-irradiation effects 3—31940
- monkeys, PO_2 and pH, after radiation induced early transient incapacitation 3—3602
- n.m.r., relaxation times 3—35268
- oxyhaemoglobin dissociation curves, computer-aided data reduction 3—28360
- peripheral circulation, rheodynamic model for Fahraeus-Lindquist effect and flow in capillaries 3—17497
- plasma renin activity after renal artery constriction 3—22141
- polyelectrolyte red cell system, energy flow mediation 3—39765
- pressure regulation by sympathetic nerve fibres and adrenal medulla in normotensive and hypertensive rats 3—22135
- pressure signal conditions, automatic calibration 3—398
- red bllod cells in the mesenteric capillaries, dimensions arrangement and density 3—13125
- red cells moving towards orifice, holographic verification of model 3—28760
- volume and red cell density in capillaries of rapidly frozen lungs 3—13126
- ^{60}Co radiation therapy effect on plasma levels of cortisol and corticosterone in humans 3—16324
- Tc labelled red cells for determ. of red blood cell volume in man 3—3569

blood circulation *see hemodynamics*

blood dynamics *see hemodynamics*

blood flow *see hemodynamics*

blood platelets *see blood*

blue brittleness *see brittleness*

Bode diagrams
- *see also frequency response*
- pupil control system, analogue simulation *(Korean)* 3—31873

boilers
- nuclear industries, conference, Basel, Switzerland, 1972 3—1033
- nuclear steam generator shell behaviour under plastic deformation, relations for limiting pressure or thickness 3—23408

boiling
- *see also boiling point*
- apparatus for boiling equilibrium curves determination *(German)* 3—28793
- benzene boiling under free convection, heat transfer crisis 3—24256
- binary liquidmixtures, pool boiling data 3—1783
- boundary-layer film boiling, effect of radiation 3—23733
- carbon tetrachloride, transient film boiling, on horizontal cylindrical surface 3—24261
- carbon tetrachloride boiling hysteresis, electric field effect 3—38664
- crossed rod matrix, press. effect on departure from nucleate boiling 3—1068
- dielectric fluids, ponderomotive forces, electrostatic fields, heat transfer 3—1801
- from downward facing surface, surface tension effects 3—27113
- drop-form liquid, flow out of a Laval nozzle, accel. meas. 3—36142
- elementary theory of processes in a boiling layer *(Russian)* 3—30255
- film boiling, on vertical surfaces 3—24262
- film boiling, oscillation effects of sphere 3—27115
- film boiling heat tafer, correlation method 3—11732
- film boiling of aqueous binary mixture with volatile component 3—1788
- flow instability in boiling channel systems 3—1419
- forced-convection film boiling heat transfer from horizontal cylinder to saturated liquids *(Japanese)* 3—38369
- free convection boiling, Freons, heat transfer, refrigerator tube material 3—1786
- Freon-113, transient film boiling, on horizontal cylindrical surface 3—24261
- Freon-12 flowing vertically upwards in heated tube, meas. of temp. distrib. at and beyond dryout 3—32934
- Freons, heat transfer, refrigeration, finned tubes, shell exchangers 3—117
- fully developed nucleate boiling, heat transfer, microgeometry, heating surface, adhesive properties 3—1787
- heat transfer, refrigerants, film flow, liquid NH_3, NH_3 evaporators, heat exchangers 3—1438
- hemispherical bubble growth in binary mixture at liquid solid interface 3—4611
- hydrodynamic transition in electrolysis, analogy with boiling 3—25073
- hydrodynamics of gas-liquid systems 3—4616
- incipient-boiling superheat in turbulent channel flow, heat flux and flow rate effects 3—36085
- laminar flow boiling on inclined isothermal flat plates 3—36411
- liquid He boiling transition, cryostatic stabilization 3—8313
- liquid metals, influence of velocity on wall superheating due to turbulence in boundary layer 3—17970
- liquids, heat transfer crisis 3—14990
- mechanism of boiling heat transfer rel. to growth of vapour bubbles 3—7917
- metals, liquid, inert-gas transport during boiling expts., diffusion model soln. 3—19904
- $N_2O_4 \rightarrow NO_2$, heat transfer *(Russian)* 3—12507
- nuclear reactors, liquid cooled/moderated, acoustic and optical methods for boiling detection *(Spanish)* 3—35928
- nucleate, at high heat fluxes, forces acting on heated surface 3—30251
- nucleate, dynamic bubble growth 3—7462
- nucleate boiling heat transfer mechanism rel. to boiling liquid films 3—1785
- peak pool boiling heat flux from sphere, hydrodynamic prediction 3—7916
- pool boiling, flat heaters, first critical heat flux, contact angle 3—1366
- pool boiling, statistical characteristics determ. of temp. fluctuation 3—20856
- pool-boiling systems, graphical anal. method 3—20858
- pressure waves propag. characts. in steam-water system 3—6990
- Pt wire, natural convective boiling, heat transfer to binary mixtures *(Japanese)* 3—24274
- salt solutions, heat transfer rate determ. using similarity theory and mol. characts. 3—20864
- single component liquids, pool boiling data 3—1782
- surface film boiling under free convection, eff. of cylinder diameter 3—20869
- temperature fluctuation in two phase boiling boundary layer 3—14500
- temperature fluctuations of the heated surface at one active nucleation site 3—27110
- transient nucleate boiling, steady-state nucleate boiling, quasi-steady phenomena, meas. of heat flux 3—11733
- two-phase channel flow, heat transfer in nucleate boiling region 3—29849
- two-phase channel flow patterns, and heat transfer 3—29908
- two-phase flow of liquid in slotted channel *(Russian)* 3—11450
- vapour film boiling around spheres, destabilisation and energy transfer 3—20859
- water, bubble boiling, influence of the thermal props. of the heating surface on the heat transfer *(German)* 3—33661
- water, pseudoboiling, heat transfer 3—14989
- water, subcooled, pool boiling heat transfer study 3—30253
- water, subcooled, vapour bubble growth rate in boiling 3—27109
- water on wire, dynamics of unstable film boiling, process transfer function 3—20865
- water-ethanol mixture, pool nucleate boiling 3—30252
- water-ethylene glycol mixture, pool nucleate boiling 3—30252
- water-n-butanol mixture, pool nucleate boiling 3—30252

boiling continued
Cs boiling under free convection, heat transfer crisis 3−24256
H_2O, surface boiling, hydraulic resistance in a tube, arbitrary heat flux distribution 3−36081
He I, bubbling crises *(Russian)* 3−20902
He I, forced flow in vertical tube 3−9894
K, in pipes, heat transfer, effect of nonuniformity of heat supply on critical heat flows 3−14986
K boiling under free convection, heat transfer crisis 3−24256
KCl(I), boiling and convection in solvent inclusions rel. to movement 3−11610
N film boiling crises and transient boiling 3−9892
N film boiling in tubes, disperse regimes 3−9891
Na, continuous boiling phenomena under forced convection by direct heating 3−23398
Na, in fast reactor overheating, radii of surface nucleation sites 3−38181
Na, incipient boiling by direct heating under forced convection 3−17968
Na in LMFBR, incipient boiling press. pulses under forced convection 3−32927
NaCl, boiling and convection in solvent inclusions rel. to movement 3−11610
PuO_2, separation of Mo for fuel recovery 3−17291

boiling point
see also boiling; heat of vaporisation
K, saturated vapour press. meas., high b.p. substances 3−35384
O_2, pure and impure 3−36408

bolometers
chalcogenide glass thin film bolometers, props. 3−13235
low temp. a.c. capacitance bolometer, responsivity and detectivity 3−5798
standard sources and detectors for absolute spectroradiometric measurements, review 3−25646
Bi, thin film, nanosecond response time, responsivity and sensitivity characts. improvement 3−16395

Boltzmann equation
see also transport processes
activated ion-mol. reactions in strong electric fields, rate calc. from asymptotic velocity distribution expressions 3−11299
alkali dimers in supersonic nozzle beams, internal state distribution, Boltzmann distribution at stagnation pressure 3−17477
amplifying phonon system, Boltzman eqn. for phonon distrib. 3−33628
Boltzmann's constant, student experiment for determ. 3−22223
Boltzmann-Vlasov eqns., electrodynamic acceleration of partially ionized plasma 3−20428
collision duration correction, quantum mech. derivation 3−6369
collisions, long-lived, effects on eqn. 3−6368
collisions involving chemical reactions, application of Bhatnagar-Gross-Krook approximation 3−27866
cosmic ray transport eqn., solar modulation of electron spectrum 3−12911
Couette flow nonlinear rarefied with heat transfer, gas statistical models with and without internal energy states 3−33259
dense plasma, moment equations and Ohm's law 3−14523
density matrix, improved classical path matrix 3−22756
diatomic molecules, population of vibrational levels under stationary pumping conditions, Boltzmann distribution *(Russian)* 3−29712
diffusion of monoenergetic neutrons, tensor formulation 3−32918
dilute alloy, transport props., solubility for localised defects 3−27238
disparate-mass binary gases, energy and momentum eqns. 3−14474
electron energy distribution in hollow cathode 3−30038
for gas, monatomic, derivation with adiabatic switching-off of interactions 3−4043
gas laser, optically pumped, theory, Boltzmann eqn. description of three level gas 3−22878
generalized, projection-operator method applic. 3−6375
hard sphere fluid, nonlinear Enskog-Boltzmann eqn. 3−32456
hypersonic spherical source flow with finite back press. 3−1413
hyperthermal flow at large Knudsen no., asymptotic theory 3−14472
ions, drifting, asymptotic behaviour of the velocity distribution 3−11298
ions, drifting in gas, in an electric field, energy partitioning 3−33332
k, Boltzmann's constant, student laboratory expt. for meas. 3−22224
linear, structural properties and finite-range polynomial solutions 3−26170
metal, electrical conduction at 0°K, solution for constant relaxation case 3−18109
metallic thin films, low field magnetoresist. and Hall effect *(Russian)* 3−30463
mixture of gas and small spherical solid particles, flow, Boltzmann eqn. calc., kinetic theory 3−33290
monoenegetic neutrons in systems with one or more dimensions, solutions 3−17276
nearly-free molecular flow, nature of first iterate 3−14473
neutrino gas, determ. of transport coeffs. 3−32441
neutron integral Boltzmann eqn. in three-dimensional systems convergence in mean of solns. 3−29427
neutron thermalization in indefinite homogeneous multiplicative medium, soln. of Boltzmann eqn. 3−32914
neutron transport, second-order eqn., determ. from invariant imbedding theory 3−23389
Newton's method for solving nonlinear eqns. 3−22760
noncanonical forms, theory 3−26171
nonlinear, existence theory *(German)* 3−37904
nonsteady transport problem soln. by flux method 3−22762
particle density in M space, new derivation 3−32457
plasma, classical non-ideal 3−33334
plasma, quasineural system, scaling laws 3−23812
plasma, relativistic degenerate, electrical and thermal conductivities calc. by solving Boltzmann eqn. 3−30022
plasma, turbulently flowing, transport effects, momentum relations 3−38430
plasma probe characteristics, solving Boltzmann eqn. for electron-electron collisions 3−30019

Boltzmann equation continued
Poisson-Boltzmann eqn., bounds on soln. near infinite dilution 3−619
Poisson-Boltzmann eqn., lower bounds on solns., near limit of infinite dilution 3−618
radiation transport calcs., Monte Carlo method 3−6366
reaction gas mixture, approx. soln. *(Russian)* 3−7299
residual resistivity calcs., multiple plane wave calcs. and iterative soln. of Boltzmann eqn. 3−24406
rigid sphere suspension, molecular collisions with solid particles 3−37903
rigid spheres, derivation from Liouville equation 3−4044
secondary electron emission, work function and Fermi energy depend., calc. 3−5253
semiconductor, electron-phonon interaction and intervalley scatt. 3−5005
semiconductor, rel. to acoustic wave attenuation and amplification in strong fields 3−5036
semiconductor and semimetal, soln. with Fermi statistics for electron galvanomagnetic theory 3−21098
sparks, nanosecond, breakdown and channel production, Boltzmann particle distribution 3−30037
surface plasmons, Boltzmann eqn. hydrodynamic soln. 3−30533
Ar, plasma, two-temperature partially ionised, transport props. calc. 3−33339
Bi films, scattering processes investigation 3−2194
GaAs and GaP ellipsoidal ⟨100⟩ valleys, Hall and drift mobility 3−33883
He, variational soln. for Navier-Stokes coeffs. at 1-20K 3−6367
HgSe, iterated solns. with Fermi statistics 3−36598
HgTe, iterated solns. with Fermi statistics 3−36598
K film, calc. of electron-phonon interactions at low temp. 3−4994
K^+ mobility in He-Ne mixtures calc. 3−38424
$N + NO \rightarrow N_2 + O$, i.r. chemiluminescence, Boltzmann distribution approximation 3−25061
Ne plasma, electron-atom collisions calc. using Boltzmann and Fokker-Planck eqns. *(German)* 3−36150
α-Sn, iterated solns. with Fermi statistics 3−36598

bonds (adhesive) *see adhesion*

bonds (chemical)
see also binding energy; hydrogen bonds; intermolecular forces; lattice energy; molecular bonds
aliphatic alcohols, n.m.r. of association processes, H-bond enthalpy 3−27433
alkali metal complex polymetaphosphates, i.r., n.m.r. and magnetochemical studies 3−17454
alkaline earth oxide crystals, effective ionic charge 3−20706
amides, interaction of II^+ 3−11239
arylazonaphthols, crystalline, hydrogen bonding, electronic and vibrational spectra investigation 3−11580
1,4,8,11-tetra-azacyclotetradecanes, i.r. spectra and hydrogen bonding study 3−23576
benzene, average mol. structure, n.m.r. data, comparison with electron diffraction and Raman spectroscopy 3−36045
bromoacetic acid, vibr. spectra, cyclic hydrogen bonded dimer evidence 3−36028
carbazole, quenching mechanism due to hydrogen bonding *(Russian)* 3−8652
carboxylic acid single crysts., irrad., proton tunnelling from positive hole through intramol. hydrogen bond 3−5400
carboxylic acids, monomers, dimers mixed complexes, photoelectron spectra of H-bonded systems 3−7173
CdO-Cr_2O_3-Al_2O_3, phase relations and optical studies 3−5385
cellulose copolymers from cellulose reaction with aromatic epoxypropylamines, i.r. spectra, strong intramolecular H-bonds *(Russian)* 3−31265
charge densities, difference maps, net atomic charges and population parameters, comparison of expt. and theoretical 3−4709
charge redistribution obs. using LEED and Auger emission spectroscopy 3−24341
chloranhydrides of unsaturated phosphoric acids, Raman and n.q.r. studies *(Russian)* 3−20141
clathrate hydrates, double, monomer conc. in liq. water determ. from i.r. spectra 3−34343
crystal, bond perturbation effect on Stark ladders 3−27217
crystal chem. aspects of A_3B, β-W type structure, stability rel. to supercond. crit. temp. 3−33480
crystal forces effects on bond lengths, calc. of charge distribs. 3−14724
cyanoacetic acid, H-bond structure from vibr. spectra 3−15483
diamond, extended Huckel theory, total energy curve minimum 3−20707
diazaphospholane-1,3,2 derivatives, NH valance vibr. mode and intermol. hydrogen bond study *(French)* 3−17442
diazaphosphorinane-1,3,2 derivatives, NH valence vibr. mode and intermol. hydrogen bond study *(French)* 3−17441
4,4' dichloro diphenyl sulphone, n.q.r. of ^{35}Cl, field gradients, bond characters 3−30724
L-3, 5- diiodotyrosine, I bonding, obs. of ^{129}I Mossbauer 3−21350
diortho-hydroxybenzoic acid study of conformers by CNDO/2 method, intramolecular hydrogen bonds 3−17398
electron densities, conference, Albuquerque, N. Mex., USA, April 1972 3−4706
energies, semiempirical calc. method 3−29600
excitonic mols., stability, bonding mechanism 3−8126
ferroelectrics and antiferroelectrics, X-irrad., e.p.r. of defect centres, hydrogen bonding 3−2388
formation, heating effects, demonstration model 3−28441
glass, alkali borate, bonding of N_2 *(German)* 3−7628
glasses, inorganic, structure, review 3−24032
glasses, liquid chalcogenide, atomic reorientation rates, n.m.r. in Se and As_2Se_3 3−5143
glycine silver nitrate, ferroelectric crystal struct. 3−17798
graphite structure from angles and length determ. 3−17793
group II difluorides, ^{19}F chem. shift tensor and nonionic bonding 3−12070
group IV cpds., MX_4 type, core binding energies for analogous gaseous cpds. of C, Ge and Si 3−14340
group IV tetrahalides, general and orbital valence force field constants calc. 3−29609

bonds (chemical) continued
guaiacol derivatives, dipole moments, expt. and theoretical, comparison giving intramol. hydrogen bond details 3—29558
hemoglobin-O_2 bonding, Heitler-London calc. for singlet states 3—11336
N—heterocycles, H-bonding, ^{14}N chemical shift, H-^{14}N mag. double resonance 3—33146
p-hexyloxybenzoic acid liquid crystal, coupling of H bonding to orientational fluctuation modes 3—1571
hydrides, triatomic, potential energy surfaces calc., directional nature of chemical bonds 3—23635
hydrocarbons, halogenated, CH group hydrogen bonding ability, n.m.r. meas. metod limitations for XH_2 and XH_3 groups 3—20186
hydrogen bond, mol. orbital calcs. of ROH...OCH_2 dimers (R=H, CH_3, NH_2, OH, F) 3—38262
hydrogen bonded solids, theory of proton transfer 3—11583
hydrogen bonding of t-butanol and phenol in electron donating solvents, i.r. spectra *(Russian)* 3—23554
hydrogen bonding rel. to anharmonicity influence on i.r. intensities 3—1170
hydrogen bonds, charge-transfer theory 3—20207
hydrogen bonds, transfer of vibrational energy of the proton 3—36001
hydrogen-bonded systems in rock-forming silicates, valence balance 3—15859
ice IX, nearly proton-ordered structure, hydrogen bonding 3—17786
insulator, photoemission-determined valence band gaps and ionicity parameters, relation 3—24380
i.r. spectroscopy, chemical bonding detection between sulphonamide azo-dyes and albuminous polyacrylate film *(Russian)* 3—29658
lanthanide and actinide π sandwich complexes 3—14338
localization, and equivalent orbitals; 3—33077
macromolecule, high ionic strength, competitive cooperative binding, linear Ising model 3—38326
metal carbide (nitride) (oxide), electron config. influence on wetting props. *(German)* 3—8766
metal-oxygen pi bonding of heavy metals 3—26984
metals, crystalline electric field, physical aspects 3—30582
microwave spectrum, conformation, dipole moment and centrifugal distortion, weak intramolecular hydrogen bond 3—14386
Mossbauer isomer shift, covalency versus overlap distortion 3—18398
multibond cpds., bond susceptibilities, ionicities, d-electron effects 3—30086
nitroxide radical hydrogen bond, ^1H, ^{13}C contact shifts and mol. orbital studies 3—38305
noble metal halides, bond susceptibilities, ionicities, d-electron effects 3—30086
noncentral interaction in crystals and molecules, valence bond model, Slater wave functions 3—36383
nonlinear optical susceptibilities, localised bond charge model 3—29139
ortho-hydroxybenzoic acid, study of conformers by CNDO/2 method, intramolecular hydrogen bonds 3—17398
phenol complexes, influence of H-bond on luminesc. *(Russian)* 3—29703
phenols, chlorosubstituted, self-assoc., i.r. spectra and OH hydrogen bonding study 3—33130
polar crystals, limit of dangling bond theory rel. to surface microtopography 3—15053
polyatomic mols., polarizability calc. using δ-function model of chem. binding 3—20123
polyethylene, molten, p.m.r., double bonds anal. *(Japanese)* 3—4489
polyribonucleic acid, intramol. hydrogen bonding 3—31279
pyrazine, quenching mechanism due to hydrogen bonding *(Russian)* 3—8652
relative bond strengths in ion-molecule clustering reactions 3—26720
resonance integral distance depend. generaliz. 3—20088
semiconductor, I-III-VI_2, effective charges of atomic constituents 3—2001
semiconductor, photoemission-determined valence band gaps and ionicity parameters, relation 3—24380
semiconductors, III-V, effective charge transfer and covalent bonding 3—7656
semiconductors, vacancies formation, macroscopic model, covalent bonding 3—17813
semiconductors, X-ray atomic scattering functions, influence of tetrahedral covalent bonds *(Russian)* 3—11582
simple molecules, electronic charge distributions and chemical bonding 3—4707
small molecules, mol. momentum distributions, Compton profiles, effects of bonding 3—17393
sodium cupric nitrilotriacetate monohydrate 3—14832
sodium cyanoacetate, H-bond structure from vibr. spectra 3—15483
starch, n.m.r. of binding of adsorbed H_2O 3—30354
sucrose, X-ray data refinement, comparison with neutron diffraction data 3—4711
tautomeric forms, electronic struct., bonding energy and absorpt. bands *(Russian)* 3—20122
tetrachlorohydroquinone hydrogen-bonded cryst., mol. packing 3—14822
tetracyanoethylene oxide, charge density distribution by difference Fourier techniques and population refinement of the diffraction data 3—4710
thermal neutron scattering by magnetic interaction, covalency of chemical bond 3—30627
thermally excited ions, decomposition, bond energy calcs. 3—36975
L- thyroxine, I bonding, obs. of ^{129}I Mossbauer 3—21350
transition metal borides, metal-boron bonding, ESCA obs., oxidation effects 3—30911
transition metal carbonyls, bonding rel. to substitution, core electron binding energy 3—7133
transition metal cpds., bond susceptibilities, ionicities, d-electron effects 3—30086
transition metal cpds., metal-like, nature *(Russian)* 3—11581
transition metal dichalcogenides, layered, chemical bonding and struct. 3—4729
transition metal dichalcogenides, layered cpds., of IVA and VIA metals, i.r. refl. study 3—39146

bonds (chemical) continued
transition metals, electron conc. concept, rel. to hydrogen effects 3—1599
triphenylalkylidenephosphoranes, hydrogen bonding ability 3—12516
Zintl phase, stabilisation and chem. bonding rel. to structure form. 3—17754
Al oxyanions, X-ray emission, ESCA spectral shifts, approx. molecular orbital theory 3—26986
$AlAu_x$ (x=0.5,2), heats of atomisation, comparison with bond strengths and Pauling model 3—15821
Al_2O_3 film, i.r. transmission spectra, boundary interaction with substrate *(Russian)* 3—15102
B_2H_6 electron density problem, experimental and theoretical aspects 3—4708
Ba, localised d states for pseudopotential calcs. s-d hybridisation 3—8116
C-N and C-O, hybridation of atoms 3—20097
CO chemisorbed on W, ESCA obs., chem. shift 3—38732
Ca localised d states for pseudopotential calcs., s-d hybridisation 3—8116
$CaF_2:Tm^{2+}$, covalency contribution on the values of $g\Gamma_7$ and $g\Gamma_{7'}$ *(Russian)* 3—11861
$CaO-Cr_2O_3-Al_2O_3$, phase relatins and optical studies 3—5385
CdS, cubic, electron density, potential distribution *(Russian)* 3—30085
Cl-O, double bond character in chlorates 3—8481
Cr^{3+} thenoyl tri-fluoro acetonate, diffuse reflectance spectrum 3—18469
Cu(II) complex, tetrasodium dicopper-dl-tartrate dehydrate, H-bonds in H_2O mols. from cryst. and mol. struct. anal. 3—7696
$Cu_2SnS(Se)(Te)_3$, ^{119}Sn and ^{125}Te nuclear gamma resonance *(Russian)* 3—36821
Eu perrhenate tetrahydrate single crystals, absorption spectra, spin-orbit interactions evaluation for symmetry of crystal field and bonding of Eu^{3+} *(Russian)* 3—30844
Fe_2O_3, Mossbauer study of chemical binding of ^{59}Fe *(Korean)* 3—27452
GaSe layer compound, band structure calc. using empirical pseudopotential method, charge densities and bonding 3—30404
$H_{3\|x}CO_x{}^{II}CO_{1-x}{}^{III}(CN)_6.yH_2O$, H-bonding and hydronium ion effects *(French)* 3—14806
HF-HCN, hydrogen bonding through lone pair and π system 3—23530
$H_{3\|x}Fe_x{}^{II}Fe_{1-x}{}^{III}(CN)_6.yH_2O$, H-bonding and hydronium ion effects *(French)* 3—14806
$(H_3N\text{-}H...NH_3)^+$, SCF calc. of hydrogen bonds 3—17400
H_2O, hydrogen bonding rel. to liquid state self-diffusion down to −31°C 3—7953
H_2O, liquid, hydrogen bonded mols., i.r. spectral evidence 3—36031
H_2O molecule in field of Na^+ or K^+, complex structure and energy surfaces calc. 3—25044
Ir organometallic, π-bonding of butadiene to Ir 3—14825
Ir(I) complex, five-coordinated, X-ray photoelectron and Mossbauer spectroscopy 3—21343
KH_2AsO_4 ferroelectric, e.p.r. study of Slater configurations 3—2389
KH_2PO_4-KD_2PO_4 system, study in paraelectric phase 3—1614
$LiVO_3$, atomic structure, least squares refinement, bond lengths and strength 3—30094
$MgFe_4((OH)_2|(SO_4)_6).20\ H_2O$, copiapite, crystal structure and H bonding 3—7716
$MgHAsO_4.7H_2O$, Roesslerite, struct. rel. to hydrogen bonding 3—20717
MnO, electron diffraction study of the nature of the chemical bond *(Russian)* 3—4728
N, chemisorbed, Auger line shape, different chem. environment 3—39207
$NH_4H_2AsO_4$ ferroelectric, e.p.r. study of Slater configurations 3—2389
$NH_4H_3(SeO_3)_2$, crystal structure, H-bonding, X-ray obs. 3—27002
Na_2SeO_3, $NaHSeO_3$, H_2SeO_3, $NaH_3(SeO_3)_2$, vibr. spectra and hydrogen bonding effects 3—34341
Ni, electrodeposited, chem. analysis of Ni-Ni interface bonds by Auger electron spectroscopy 3—436
Ni_3Al alloy, relative bond energies from field ion images 3—36272
Ni_3Fe alloy, relative bond energies from field ion images 3—36272
Ni_3Mn alloy, relative bond energies from field ion images 3—36272
OsO_4, dispersion in centrosymmetric structs. 3—14741
OsO_x, metal-oxygen bond order and length, i.r. spectra obs. 3—30083
Pb oxides, partial covalent character rel. to thermal expansion *(French)* 3—17984
Pb^{2+} oxides, fluorides and oxide fluorides, calcs. of bond lengths and angles 3—33073
$Pb_2V_2O_7$, synthetic chervetite, structure refinement 3—30093
Pt, (100) surface, chemisorption of unsaturated mols., spectral and LEED study 3—11808
$RbH_3(SeO_3)_2$, crystal structure, hydrogen bond lengths 3—33496
ReO_x, metal-oxygen bond order and length, i.r. spectra obs. 3—30083
RuO_x, metal-oxygen bond order and length, i.r. spectra obs. 3—30083
S, chemisorbed, Auger line shape, different chem. environments 3—39207
Sb-In alloys, liq., ionic nature *(French)* 3—30276
Sb^{3+} oxides, fluorides and oxide fluorides, calcs. of bond lengths and angles 3—33073
Sb_2Se_3, crystalline and amorphous, valence bonding model 3—8104
$(Sc(CO_3)_4)^{5-}$ ion in aqueous soln., dicoordination of carbonate ion *(French)* 3—1214
ScCu, electronic structure stability investigation, importance of ionic bonds 3—15335
Si K X-ray emission, bonding effects on intensities 3—12193
Si oxyanions, X-ray emission, ESCA spectral shifts, approx. molecular orbital theory 3—26986
SiO_2, K_β X-ray spectra, effect of local bonding electronic states 3—21012
SiO_2, noncrystalline, defect struct. and irradiation behaviour 3—4770
SiO_2 K X-ray emission, bonding effects on intensities 3—12193

- **bonds (chemical)** continued
  - SiO_2 on Si, rel. to noncrystalline struct. and elec. behaviour 3−21157
  - Sn-As system, nature of bonding, Mossbauer effect studies 3−36828
  - Sr localised d states for pseudopoential calcs., s-d hybridisation 3−8116
  - TcO_x, metal-oxygen bond order and length, i.r. spectra obs. 3−30083
  - Te (II) and (IV) ethylenethiourea derivatives, ^{125}Te Mossbauer absorption spectra, bonding scheme 3−12078
  - Te (II) and (IV) tetramethylthiourea derivatives, ^{125}Te Mossbauer absorption spectra, bonding scheme 3−12078
  - Te (II) and (IV) thiourea derivatives, ^{125}Te Mossbauer absorption spectra, bonding scheme 3−12078
  - Te^{4+} oxides, fluorides and oxide fluorides, calcs. of bond lengths and angles 3−33073
  - Ti, strengthening by O_2, bonding 3−15725
  - TiO_2, ionicity of bonds 3−14725
  - $VN_{(1-x)}$, x=0, 0.18, $K\beta_2$ emission bands investigation by electron microprobe and computer processing, fine struct. and bonding *(French)* 3−28780
  - $ZnSiP_2$, degree of ionicity from analysis of refl. and absorpt. spectra *(Russian)* 3−8572
  - $Zr(HPO_4)_2$, n.m.r. study, proton position and P-H length *(French)* 3−27428
- **bone** *see materials*
- **Boolean algebra**
  - *see also formal logic*
  - No entries
- **Boolean functions**
  - Fourier transform, symbolic computation 3−486
- **Boolean lattices** *see Boolean algebra*
- **bootstrap models** *see bootstrapping*
- **bootstrap theory** *see bootstrapping*
- **bootstrapping**
  - action-at-a-distance theories and dual models 3−26284
  - analytical solution of truncated statistical eqn. with step-function kernel 3−17067
  - correlation functions in multiperipheral models, unitarity and the Pomeron, bootstrap calc. 3−29243
  - cut effects in multi-Regge bootstrap 3−10745
  - doubly closed shell nuclei states study 3−26380
  - dual multiperipheral model, Pomeranchukon generation from background, bootstrapping pot. discussion 3−32682
  - hadron mass spectrum, statistical approach 3−38069
  - inclusive reactions, bootstrap model, formation of fireball and leading particle 3−917
  - inclusive reactions, extended bootstrap model to include quantum numbers 3−38098
  - inclusive single particle spectra and strong thermodynamic bootstrap soln. 3−914
  - infinitely composite model of hadrons, equivalence to parton model 3−10720
  - multiparticle processes, statistical description 3−26336
  - multiperipheral bootstrap of the intercept-one pomeron pole 3−17076
  - N/D bootstrap, predictions for internal symmetrics, symmetry breaking 3−821
  - nonlinear bootstrap in dual models and $f\pi\pi$ coupling 3−10727
  - reciprocal bootstrap of N and N*, calc. using nonpolynomial Lagrangian 3−4212
  - reciprocal bootstrap on light cone, deep-inelastic electron scattering on polarised deuterons 3−10652
  - resonance decay, effective temp. in statistical model 3−26322
  - six-pion amplitude as modification of general chiral pion amplitudes 3−23103
  - statistical bootstrap, explicit solution 3−23014
  - statistical bootstrap eqn., truncated, for fireballs in two-body interactions 3−32679
  - statistical bootstrap theory, relation to dual resonance model in statistical approach to heavy resonance decay 3−17073
  - thermodynamic inclusive spectra, possible bootstrap origin 3−4239
  - $e^+e^-\to\pi^+\pi^-\pi^+\pi^-$, few GeV, statistical bootstrap model, one-photon mechanism 3−29210
  - KK scattering, bootstrap calc. of φ and f' using effective-potential method 3−32680
  - π-π resonance parameters, self-consistent calc. in potential model of Balazs 3−10756
  - $\pi\pi$ scattering, ρ-dominance and model for partial s- and p-waves *(Russian)* 3−19716
- **bootstraps** *see bootstrapping*
- **Bordoni effect** *see internal friction*
- **boron**
  - β rhombohedral, Poole-Frenkel effect, current-voltage characteristics 3−36619
  - atmospheric composition, seawater as source 3−12688
  - composite, effect of specimen geometry on fatigue strength 3−21770
  - composite material from bonding with Al 3−21732
  - crystal growth of polymorphs, vapour phase deposition, reaction conditions, polymerisation, nucleation and crystal growth, processes *(German)* 3−34474
  - dense phase gas solid suspension, positive expulsion fluidization tank 3−4619
  - diamond: B, dominant acceptor in semiconductor 3−38810
  - p-diamond:B, seed crystal, growth by vapour deposition 3−36986
  - diffusion, in Si, optimisation for semicond. devices *(Hungarian)* 3−18552
  - diffusion, in Si, orientation dependent, effects of oxidation 3−39300
  - diffusion in Si, effect of inert gas 3−39257
  - diffusion in SiO_2, summary of data 3−21546
  - diffusion in SiO_2 film deposited on n-Si in r.f. glow discharge, 1100-1200°C 3−27144
  - distribution in Incoloy-800, heat treatment effect 3−12386
  - equilibrium charge distributions of ions after passage through C foil 3−11662
  - fibre compatibility with W substrate and Ti matrix *(Russian)* 3−15784
  - fibre reinforced Al matrix composites, transverse tensile props. 3−18716
- **boron** continued
  - fibre reinforced epoxy composites, discontinuous, impact toughness 3−31137
  - fibre/W substrate, diffusion barrier establishment *(French)* 3−12440
  - field effect meas. rel. to transport phenomena in beta-rhombohedral boron 3−18158
  - filament, gauge length influence on mechanical strength *(Japanese)* 3−18704
  - gauges, Monte Carlo study of neutrons in materials 3−2780
  - hopping conduction at low temp. rel. to local order 3−21075
  - implanted in Si, depth distrib. of defects and impurities 3−17890
  - ion, possible beam sources 3−22428
  - ion effects on Si, spatial distrib. of radiation defects 3−24166
  - isotopic comp. of low energy cosmic ray particles *(German)* 3−9413
  - magnetic susceptibility of β-rhombohedral boron, temp. depend. 3−38960
  - microadditions in steel, heat resist. increase 3−21607
  - reactivity worths in fast reactor spectrum 3−11063
  - resonance series in vacuum u.v. absorption spectra of dense plasmas 3−17351
  - β-rhombohedral, relax. of non-equilib. cond. 3−27255
  - semiconductor, thermoelectric properties, thermal and electrical conductivity, temperature dependence 3−36630
  - inshim rods of reactor, meas. of energy liberation in 1 3−14247
  - steel:VN, B, stainless austenite, precipitation hardening rel. to creep resist. 3−15697
  - surface saturation diffusion into Ti(V)(Zr)(Cr)(Mo)(W), obs. of borated layer structure *(Russian)* 3−11763
  - target, picosecond light pulses absorption 3−20553
  - TSEE activator in BeO, dosimeter characteristics 3−28671
  - u.v. spectra, by beam-foil technique 3−29534
  - vapour growth of B tetragonal filaments on carbon fibre substrate, pyrolysis and morphology 3−21532
  - in Al alloys, grain refinement 3−18597
  - in Al alloys, grain refinement 3−18598
  - B/Al composite, matrix fatigue behaviour under repeated tensile loads 3−31154
  - B/Al composite, reinforcement of Ti alloy, compressive strength 3−39390
  - B/Al composites, fusion welding, microstructure 3−12361
  - B^{2+}, ^2S state, natural orbital config. interaction expansions 3−26561
  - $^{11}B^+$, implantation into 6H-SiC, phosphor prep. 3−30956
  - $^{11}B^+$ implantation in SiC, effects 3−1633
  - GaAs, GP, electron, neutron irrad., B, C, impurities, i.r. local mode abs. 3−34395
  - Ge, H^+, O^+, B^+, ion bombardment, divacancy-like optical absorption 3−34394
  - Ge:B, excitation spectra, Zeeman effect with linearly polarized light 3−2566
  - Ge:B, neutron irradiated, X-ray obs. 3−17876
  - Mo ingot, ductility effects of complex additions of 0.15 wt% Ru with C or B *(Japanese)* 3−31073
  - in Si, diffusion from shallow ion implants 3−7784
  - p-Si:B, cyclotron reson., effect of positively charged acceptor centres 3−36528
  - Si:B, deformation potentials and g-values from Zeeman splitting of Raman spectra 3−38809
  - Si:B, implanted through thermal SiO_2 films, resist. 3−24523
  - Si:B, impurity photocond. oscills., 4.2-10K *(Russian)* 3−2134
  - Si:B, ion implantation, defect centre studies 3−33587
  - Si:B, magneto-Raman scatt., g-value determ. for acceptor ground state 3−5203
  - Si:B, neutron irradiated, X-ray obs. 3−17876
  - Si:B, u.s. attenuation by neutral acceptors, mag. field depend. 3−4967
  - Si:B, X-ray topographic obs. of dislocation contrast after boron diffusion 3−17835
  - Si:B hole lifetime, capture rate, impurity concentration, 18-4.2K 3−30495
  - Si:B implanted, radiation damage distribution meas. 3−4766
  - Si:B ion implanted, W film mask 3−30949
  - β-SiC:B, low temp. luminesc. due to donor-acceptor pair emission 3−34419
  - β-SiC:B diffused p-n junction, V-I and C-V characts. and electrolum. response, 293 to 800 K *(Russian)* 3−18211
  - SiC:O, B, enhancement of luminescence brightness by O_2 3−39173
  - SiGe:P, B dopant in thermoelectric alloys, precipitation, Lifshitz and Slyozov model 3−5023
- **boron compounds**
  - boracite crystals, lattice strain review *(Japanese)* 3−14845
  - boracites, $T_d{}^5$ symmetry group, phase transitions, group theoretic analysis 3−20876
  - borate planar anion, polarisability from refractivity data using Lorentz local field method 3−30747
  - borates, multilayer shields for neutron attenuation in radiotherapy 3−3622
  - borides, high melting, thermal conductivity, as fn. of characteristic temp. *(Russian)* 3−12427
  - borosilicate films, Vickers microhardness characteriz. 3−39377
  - borosilicate glass, ion exchange chemical strengthening 3−15789
  - glass, borosilicate, ion diffusion and influence of two-site mechanism 3−14699
  - hydrides and derivatives, relative abundances of doubly charged ions in mass spectra 3−26707
  - sodoborate glasses with ZnO, X-irrad., e.p.r. of Zn^+ centres, g-factor anisotropy *(French)* 3−30684
  - spectra, electron, vapour state, binding energies, chemical correlations 3−23549
  - sulphurhydroxohalogenoborane, BX_2SH, struct. and mol. force field determ. from vibrational spectra *(French)* 3−14348
  - AlB_{12} semiconductor, thermoelectric properties, electrical and thermal conductivity, hopping conduction, temperature dependence 3−36630
  - B/epoxy plates, post-buckling behaviour 3−27756
  - BBC, and BCB, ab initio electronic struct. calcs., optimum bond lengths determ. 3−20093

boron compounds continued

- BBr_3, collision with K_2, KX reactive scatt., ang. distrib. meas. 3−29751
- BC_x, enthalpy and ht. capacity, 273-2600K 3−24964
- BC_x semiconductor, thermoelectric properties, hopping conduction, thermal and electrical conductivity, temperature dependence 3−36630
- $B_{12}C_3$, elec. cond., temp. depend. 3−24429
- B_4C, cryst. struct. 3−14742
- B_4C, fast-neutron irradiated, study of defect microstructure due to He, Li disposition 3−26528
- B_4C, neutron irradiated, meas. of He gas release rate at 750 to 950°C 3−26529
- B_4C nuclear reactor absorber materials, powder production process, properties, hot pressability 3−6977
- B_4C powder fast reactor irradiation 3−1077
- B_xC, growth, 1450-1500°C, thermal etching, morphology 3−24781
- B_xC_y, thermal conductivity meas. of irradiated absorber pellets 3−26526
- B_xC_y fast-reactor irradiated pellets, examination of microstructure 3−26527
- BCC, and CBC, ab initio electronic struct. calcs., optimum bond lengths determ. 3−20093
- BCN, and BNC, ab initio electronic struct. calcs., optimum bond lengths determ. 3−20093
- $B(C_xN_{1-x})$ refractory, physical, mechanical and chemical props. *(Russian)* 3−31124
- BCl_3, dispersion of resonant optico-acoustical effect in gas 3−38339
- BCl_3, i.r. double reson. study, vibr. relax. meas. 3−38316
- BCl_3, ioniz. pots., ab initio SCF calcs. 3−23609
- BCl_3, vibr.-rot. energy transfer data, comparison with near-reson. theory 3−38317
- B_2Cl_4, mol. consts., Green's function analysis 3−14343
- BF, reson. fluoresc., vibronic transition probabilities 3−29699
- BF_2 radical, bond angle determ. from e.s.r. 3−20081
- BF_3, ioniz. pots., ab initio SCF calcs. 3−23609
- BF_3, pot. barrier to electron passage through electronegative atoms 3−1196
- BF_3 multi-counter neutron detection system, flatness of response verification 3−16513
- BF_4^- anions in solution, temperature dependence of ^{19}F n.m.r. spectra 3−34231
- B_2F_4, mol. consts., Green's funcion analysis 3−14343
- $BF_3(Cl_3)(Br_3)(I_3)$, centrifugal extension consts., calc. *(Russian)* 3−20104
- BF_2OH, CNDO/2 and INDO calcs. of total charges, Wiberg populations of effective chemical bonds and total dipolar moment components *(French)* 3−7127
- BH mol., orbital approach and props. 3−7116
- BH_2, potential energy surfaces calc. 3−23635
- B_2H_6, effect on Si film deposition from SiH_4-H_2 mixture 3−21529
- B_2H_6 electron density problem, experimental and theoretical aspects 3−4708
- $BH_3.NH_3$ and perfluoro derivatives, electronic structure, CNDO/2 calc. *(French)* 3−17403
- BI, u.v. absorpt. spectrum, 265 to 280 nm 3−36013
- BN, cubic, thermal cond. at room temp. impurity effects 3−30294
- BN, growth of hexagonal crystal in SiB melt 3−12285
- BN, planar sources, diffusion in Si, effect of inert gas 3−39257
- BN, pyrolytic, wetting by molten metallides 3−34627
- BN crystalline, Compton profiles calc. 3−18508
- BN pyrolytic, shock-compressed, X-ray diffraction, evidence for phase transition 3−1687
- BN twinning *(Russian)* 3−1631
- BN_x, cubic, SEM obs., anomalous contrast effects 3−36471
- $B_{12}N_{12}H_{12}$, hexagonal, band width, band gap, charges, equilib. distance, sublimation energy, from Huckel calcs. 3−15136
- $B_3N_3H_6$, boronimide and dimeric boronimide, electronic structures and energies, ab initio calculations 3−7142
- fused B_2O_3, enthalpy meas. at high temps. *(Russian)* 3−11722
- B_2O_3, vitreous, struct. detn. by X-ray Fourier analysis 3−7633
- B_2O_3 glass, static and dynamic PVT obs. using acoustic densitometer 3−1774
- B_2O_3 i.r. spectra in terms of OH absorption and H bonding 3−1230
- B_2O_3 surface tension measurement, cylinder pulling method, 950-1950°C, corrections for cylinder thickness and meniscus contraction 3−11797
- B_2O_3-BeO glass systems, i.r. spectra and structural analysis *(Russian)* 3−27508
- B_2O_3-Bi_2O_3-BaO flux system, use in growth of ferrite spinels 3−2663
- $B(OH)_3$, i.r. spectra in terms of OH absorption and H bonding 3−1230
- $B_2O_3-Li_2O(Na_2O)(K_2O)$, glass, effect of adding N_2 at different temps. *(German)* 3−7628
- BP, cubic, thermal cond. at room temp. impurity effects 3−30294
- BP, Lindemann-Gilvarry melting law and Debye temps. 3−36393
- $B_{14}P$, prep. of monoclinic B-P phase *(German)* 3−12243
- BPO_4, adsorption isotherm meas. for A gas 3−8014
- BS_2, visible and i.r. absorpt. spectra at 4K 3−33128
- BX_3, X=H, F, Cl, CNDO/2 calcs. of electronic properties, comparison with BX_4^-, valence force field modifications 3−7130
- BX_4^-, X=H, F, Cl, CNDO/calcs. of electronic properties, comparison with BX_3, valence force field modification 3−7130
- $BeBH_5$ and BeB_2H_8, ab initio calcs. of mol. struct. 3−29548
- BiI_3, surface excitation effect on trapping and recombination processes 3−27271
- Mn-Al-B alloy, magnetis. and coercive force, composition depend. 3−36744
- MnO-Fe_2O_3-B_2O_3 glassy system, prepn. and mag. props. 3−18726
- PbO-B_2O_3 glasses, i.r. refl., band positions, conc. depend. *(Russian)* 3−12139
- Pd-B-H system, statistical thermodynamics, electron interaction energy *(German)* 3−30240
- Sm-B, phase behaviour 3−7925

Borrmann effect *see X-ray crystallography; X-ray diffraction*

Bose-Einstein statistics *see quantum statistical mechanics*

Bose gas *see boson systems*

boson fluids *see boson systems*

boson systems

see also liquid helium-4; quantum statistical mechanics

- Beliaev-Zelivinsky boson expansion and particle-vibration coupling methods, exactly soluble model 3−10388
- bilinear boson Hamiltonian diagonalised by Bogolyubov transformation, positive spectrum condition 3−26158
- binary boson solns., description of ground and low excited states 3−4031
- Bogoliubov and Brueckner-Sawada approx. compared 3−22738
- Bogoliubov excitation spectrum, second-order perturbation expansion 3−1850
- Bose condensation of fermion pair composites 3−38121
- Bose gases, charged and neutral, calc. of critical exponents above λ-transition points 3−1851
- Bose liquid, scaling laws and specific heat 3−15039
- Bose liquid phase transition, calc. of thermodynamical functions 3−36448
- canonical free Bose states on Weyl algebra, infinite vol. limit 3−10386
- chaotic beams, study of detection and emission processes in wave-packet formalism 3−26154
- charged Bose gas, crictical indices 3−26157
- charged Bose gas, excitation spectrum and liq. struct. function 3−15042
- condensation density, fluctuation 3−613
- condensed Bose liquid, scaling laws and critical exponents 3−36449
- current algebra representations for infinite free Bose or Fermi systems at finite temp. 3−28973
- excitations, elementary, in Liouville space, statistics and interactions 3−26156
- gas of spinless bosons, one-dimensional, with random impurities, Bose-Einstein condensation 3−19512
- ground-state energies of 2 and 3 bosons, validity conditions for inequality $E_0(3) \leqslant 3E_0(2)$ 3−10392
- hard-sphere Bose system, reformulation and condensed part based on cluster expansion 3−13645
- ideal gas in external scalar potential, properties in infinite volume thermodynamic limit 3−32437
- liquids three-particle variational wave function for ground state 3−4035
- low-lying energy spectrum of a one-dimensional disordered system in presence of random fixed finite-ranged repulsive potentials 3−19511
- many boson hamiltonian, matrix elements in correlated basis function 3−36446
- many boson theory, application of the Brillouin-Wigner perturbation method *(Dhfakx)* 3−22739
- many-particle system interaction with strong forces, ground state energy 3−13644
- pairwise-interacting particles ground state energies, set of inequalities 3−22741
- para-Bose operators, construction of system of n oscillators using new quantisation method 3−13615
- phase transition is Bose liquid, determ. of excitation energy anal. Landau f-functions 3−15040
- quantised vortex vibrs. in long wavelength limit, for weakly interacting fluid 3−24305
- quantum hydrodynamics 3−38692
- strongly interacting fluid, surface props., statistical mech. calcs. 3−22740
- superconductor, type II, magnetic props. using boson characteristic function 3−11974
- superfluids, reduced density matrices 3−7982
- vortex-ring model of Bose condensation 3−38691
- wave function in force field 3−11770
- weakly interacting Bose gas, excitation spectrum, method of correlated basis functions 3−15041
- CdSe, Bose condensation of excitonic molecules, luminesc. obs. 3−30437
- He, struct., pair correl. function determ. procedure 3−35621
- ^4He, solid, linked-cluster t-matrix perturbation theory 3−7991
- Ne, struct., pair correl. function determ. procedure 3−35621

bosons

see also alpha particles; boson systems; deuterons; gravitons; intermediate bosons; meson resonances; mesons; photons

- π^+d, higher-mass boson prod. with mass in T region 3−14079
- antisymmetric, in nucl. struct., four particle system investigation 3−19796
- Bogoliubov transformation coefficients, linear, series expansion to connect Fock states 3−35624
- dyons, dyonium and parastatistics 3−35771
- Goldstone, and low energy aspects of broken scale invariance 3−16947
- pseudo-Goldstone approximate symmetries in theories with spontaneously broken local symmetries 3−6556
- higher-mass, production from π^+d 7.87 GeV/c interaction 3−14079
- inverse scattering for L^2-dependent potentials, calc. from S-matrix at fixed energy 3−17142
- nonrelativistic quark model of bosonic spectrum and Regge trajectories 3−29219
- nucleon-K_a-boson model of hadrons, quantum-field formalism *(Russian)* 3−13827
- odd-particle systems, nuclear, boson expansion 3−32775
- one boson exchange pot., determ. of infinite nucl. matter props. 3−10904
- radiative decays, model 3−13867
- realization of Lie algebra of unitary symplectic group in terms of boson operators 3−28812
- Regge trajectories with left-hand cut, properties 3−29240
- resonances, intermediate, correspondence to intermediate structures in nuclear reactions 3−4214
- resonating group method, test in three-boson elastic scattering 3−38149
- semicoherent states, closure relation description of operators 3−35586
- strangeness-one, production in 1200-1600 MeV mass region in $\pi p \rightarrow \Lambda X_0$ reaction 3−4222
- transition-operator boson concept, application to monopole vibration model 3−29332

bosons continued
- triality selection rule, formal description by means of boson operator 3—16956
- $K^0_l \to \mu^+\mu^-$, CP nonconserv. and excess μ anomaly, unified model 3—16951

boundaries *see boundary layer flow; boundary layers; boundary value problems; grain boundaries; metal-insulator boundaries; semiconductor-insulator boundaries; semiconductor-metal boundaries*

boundary layer flow
- *see also boundary layers*
- advective accelerations, coupling between boundary layer and free atmosphere 3—31370
- advective accelerations in low latitude planetary boundary layer, numerical anal. 3—31369
- aerosols, particle eddy diffusivities and turbulent deposition velocities for isothermal flow and smooth surfaces 3—33298
- air flow and heat transfer to the atmosphere from the surface of thermal electric power plant cooling ponds 3—29847
- air flow in axial flow inducer, visualisation study 3—26858
- air subsonic flow, heat exchange in the critical zone ahead of a cylindrical step *(Russian)* 3—29857
- air supersonic flow over leading edge of blunted flat plate, numerical soln. of Navier Stokes eqn. for two-dimensional laminar compressible flows with embedded shock waves 3—26822
- airfoils, press. distrib. prediction for inviscid. pot. and real fluid flow 3—7386
- airfoils with spoilers, linearised pot. flow theory 3—29870
- atmosphere, lower layer, low-frequency limit of the inertial interval in boundary layer 3—34882
- atmospheric natural boundary layer lower portion, wind tunnel simulation 3—37201
- axisymmetric and two-dimensional, with attached shock waves 3—33237
- Black Sea, bottom layer, turbulence, vortex formation obs. 3—34862
- blades with fluctuating lift, flow through moving cascades 3—26809
- bounded shear flow, forces on flat plate, local circulation and global circulation 3—23741
- breaking bubbles, fluid flow patterns 3—11409
- buoyancy-induced flows, instability, transition and turbulence, review 3—33217
- Cassonian fluid, vel. distrib., press. flow characts. and residence-time distrib. eqns. 3—17508
- channel entry flow, uniform stream inlet 3—29871
- chemical reaction on catalytic surface in laminar incompressible hydrodynamic flow field 3—17498
- compressible laminar boundary layer flow at a three-dimensional stagnation point with intensive suction or injection 3—33234
- compressible laminar flow on moving continuous surfaces, parametric study 3—26805
- compressible turbulent layers at moderately large Reynolds no., higher order theory 3—20337
- along concave wall, laminar flow instability, development of turbulence *(German)* 3—26815
- condensate liquid film flow down inclined wall, stability characteristics 3—33233
- convection, combined free and forced, past a porous vertical circular cylinder 3—38355
- convection, free, in open ended vertical channels, numerical soln. 3—36089
- convection, Nusselt-Prandtl relationships 3—20281
- convective flow and transpiration, vertical-flat-plate problem 3—20306
- past cylinder, soln. of general heat-transfer problem by Tolubinskii integral method 3—23688
- de Saint Venant's eqn. for free surface flow, limits of integration 3—33230
- detachment forces for particles submerged in laminar layer 3—33294
- dilute aqueous polymer soln. pipe flows, viscous sublayer and adjacent wall region 3—20278
- domains, multiconnected, conformal representation 3—20332
- drag reduction in rotational viscoelastic boundary layer flow in polymer solutions 3—26810
- drag-reducing channel flow, near-wall region flow visualization 3—11410
- drops, deformable, approaching plane interface, creeping flow model 3—11446
- ducts, square, heated laminarizing gas flow 3—36082
- Ekman-Hartmann layers, nonlinear hydrodynamic and hydromag. spin-up 3—23732
- entrance region flows, inelastic fluids loss coeffs., prediction method 3—17506
- Falkner-Skan flows with slip, numerical method and soln. 3—1394
- falling film stability, asymptotic soln. 3—7369
- falling liquid films stagnant band analysis 3—33228
- fine solid particle gaseous suspension, fully developed turbulent boundary layer flow 3—33297
- fish-like forms, generalised slender-body theory 3—29869
- flat plate boundary layer, transitional flow characteristic, model *(Italian)* 3—36105
- fluids, three-dimensional boundary layer flow, regular solid surfaces, ducts, review 3—36113
- forced convection boundary layer flow in film boiling 3—23733
- free convection along lower surface of heated horizontal place, boundary layer approx. 3—1317
- free convection from vertical semi infinite flat plate to liquid under maximum density conditions 3—17526
- free-stream vorticity effect on boundary layer stability 3—33231
- gas, weakly rarefied, flow struct. exam. *(Russian)* 3—7378
- gas layer, nongray radiative transfer 3—36086
- generalised Couette flow of an elastico-viscous liquid between two co-axial porous circular cylinders 3—38378
- Hall currents effect on hydromagnetic flow near an accelerated plate 3—29898
- heat and mass transfer in mixed convection conditions, analytical soln. for binary boundary layer 3—1319
- heat conduction, turbulent mixing at boundary of parallel flows 3—29844
- heat transfer of heated plate in sinusoidally oscillating flows, applic. to internal combustion engine 3—1360

boundary layer flow continued
- heat transfer to strongly accelerated turbulent boundary layer, expt. obs. 3—38360
- high Reynolds number steady separated flow past negative angle wedge 3—11411
- hydromagnetic stability of elec. conducting fluid along flat plate *(German)* 3—11444
- hypersonic boundary layers, displacement interaction and surface curvature effects 3—38372
- hypersonic flows around blunt bodies, convective and radiative heating study *(Russian)* 3—26788
- hypersonic layer turbulence, hot-wire meas. 3—20340
- hypersonic slip-flow, viscous interaction region, effect of accommodation coeffs. 3—23755
- incompressible conducting laminar flow along a vertical wall, transverse mag. field effect 3—17546
- incompressible flow with mild adverse pressure gradient, over moving boundaries, boundary-layer separation 3—33236
- incompressible fluid, unsteady boundary layer flows at three dimensional stagnation points 3—11408
- incompressible turbulent, calculation of separation points 3—11394
- on infinite plate, boundary conditions determ. in exptl. investig. of unsteady state heat transfer 3—23693
- initial flow past impulsively started circular cylinder in viscous liq. 3—26811
- intensive blowing through a permeable surface, nature of flow 3—33303
- isobaric laminar, vectored injection 3—26814
- Jarvis Island, high Reynolds number flow, survey 3—37193
- jet, confined, nonseparated mixing, theoretical model 3—1373
- jet turbulence influence on flow of a boundary layer *(Russian)* 3—29931
- jets, isothermal turbulent, two-dimensional, at a curved porous wall 3—33311
- jets, turbulent, diffusion and vortex models, velocity profiles in turbulent boundary layer 3—33315
- jets, turbulent cocurrent, mixing in ducts with profiled walls, minimum losses determ. 3—33309
- jets, unsteady viscous flow into stationary surroundings, numerical calc., boundary layer approximations 3—33308
- jets semiconstrained turbulent submerged, integral method 3—33310
- laminar, approx. solns. of layer eqns. in presence of blowing 3—23736
- laminar, at crit. pt. of indestructible body washed by flow of ionized air 3—23737
- laminar, disturbance propagation 3—38382
- laminar, on flat plate, chock wave induced 3—7375
- laminar, rear stagnation point on cylinder 3—4581
- laminar, temperature field near two dimensional stagnation point 3—14462
- laminar, unsteady, with suction or blowing 3—33223
- laminar, with vibr. non-equilib., approx. soln. of eqns. *(French)* 3—23731
- laminar and turbulent, over ablating surfaces, nonsimilar soln. 3—1341
- laminar and turbulent jet mixing flow with boundary layer growth 3—1354
- laminar convection, unsteady, in uniformly heated vertical pipes 3—20308
- laminar flow over small hump on flat plate 3—29872
- laminar inlet flow, boundary layer velocity profile 3—11374
- laminar unsteady along flat plate, similarity solution 3—11413
- laser anemometry, meas. of mean velocity and turbulence in supersonic boundary layers 3—478
- leading edge effects on Nusselt number for vertical plate in free convection 3—20291
- liquid film falling on sphere, gas absorption 3—4535
- liquid film flow, entrance effects 3—36107
- liquid in channel, complex heat transfer calcs. 3—23692
- liquid surface motion, press. and accel.-induced distortion, computation 3—1391
- magnetic inhibition of thermal convection 3—14442
- mass-transfer effects on higher-order boundary layer solns., the leading edge of a swept cylinder 3—14460
- MHD, incompressible, separation parameter, dimension theory determ. 3—26806
- MHD duct flows, fully insulated, variable-area rectangular ducts with small divergences, strong transverse mag. fields 3—11441
- MHD free convection laminar flow of an elastico-viscous fluid along an infinite porous wall 3—20375
- MHD oscillatory flow along infinite flat plate with variable suction 3—20392
- MHD pipe flow, extremum principles, determ. of bounds for flow-rate 3—23776
- micropolar fluids, boundary layer equations 3—26803
- mixed convection above heated horizontal surface, between near and far surfaces 3—23697
- mixing length derivation from Karman's similarity hypothesis 3—20276
- molecular gas dynamics, boundary conditions, surface shocks, continuum flows, review 3—33261
- moving boundary stability at which fog forms or vaporises, heat and mass transfer 3—29865
- natural convection, influence of various surface roughness 3—20297
- natural convection boundary layer flow over horizontal and slightly inclined surfaces 3—38379
- Navier-Stokes equations, numerical treatment 3—36109
- non-Newtonian falling liquid films, gas absorption 3—36108
- non-Newtonian liquids, entrained on a vertical surface drainage 3—29875
- non-Newtonian pseudoplastic fluid, laminar two-dimens. free jet 3—23728
- nonequilibrium, three dimensional flow on highly swept hypersonic wings 3—23730
- oscillatory flow, past an infinite, vertical, porous plate with constant suction, free convection effects 3—33211
- oscillatory flow past an infinite, vertical, porous plate with constant suction, free convection effects 3—33212
- parabolic flow over flat plate with main stream wave disturbance 3—20339

boundary layer flow continued

- parametric excitation of Tolmin-Schlichting waves in boundary layer *(Russian)* 3—23770
- on permeable plate, turbulent, velocity profile obs. 3—23690
- perturbation response and propagation of disturbances 3—38381
- perturbed, influence of a boundary layer on a wavy surface *(Russian)* 3—26807
- plane turbulent mixing layer, experimental study 3—36104
- planetary, unstable, circulations in transverse and longit. planes 3—25220
- plasma, radiating, nonviscous nonconducting flow over flat boundary 3—26879
- plate in model testing tank, transition from laminar to turbulent flow 3—4577
- plate-separated two fluid system, thermal flux and temp. distrib. calc. 3—23689
- polymer solutions, adsorbed entangled layer in drag reduction 3—29864
- power-law fluids flow behaviour in entrance region of annuli 3—36106
- pseudoplastic power law flow, inlet region of porous tube 3—38418
- rarefied gases mixture flow between two parallel plates with sinusoidal concentration distribution at the boundary 3—23756
- rarefied hypersonic flow, surface press. meas. interpretation method 3—38385
- with reverse flow, finite difference method 3—1385
- rotating disc in fluid, hydrodynamic boundary layers, analysis 3—23722
- second order viscous fluid flow in a circular tube under pressure gradients varying exponentially with time 3—17510
- shear, pressure meas. made with holes, kinematic calc. of intrinsic errors 3—29874
- shock protuberance, visualization, optical surface indicator technique 3—6171
- similarity soln. for laminar boundary layer on continuous, moving, porous surface 3—11412
- slender foil unsteady motion near interface between two different fluids, numerical soln. 3—33272
- slot injection into a supersonic laminar boundary layer 3—14463
- stationary vortices behind a flat plate normal to the freestream in incompressible flow 3—38370
- stratified, unbounded, over vertical barrier 3—38380
- suddenly started laminar flow of power-law fluids in the entrance region of a straight channel 3—20335
- supersonic, on permeable plate *(Italian)* 3—23745
- supersonic detached flow between two bodies, turbulent jet theory application 3—33316
- supersonic flow, method of characteristics in intrinsic coordinates *(French)* 3—26820
- supersonic flow past large-angle pointed cones 3—38375
- supersonic laminar, plate-injection study 3—36111
- supersonic turbulent boundary layer subjected to adverse pressure gradients 3—36103
- surface roughness change rel. to turbulent-energy and momentum eqns., appl. to wind 3—26808
- surface waves, short wavelength, generation, Miles mechanism 3-29894
- temperature fluctuation in two phase flow 3—14500
- thermal boundary layer growth in the entrance region of an annulus 3—14459
- thermal eqns., known temp. gradient at moving flat plate in parabolic flow, solns. 3—7372
- thermal wave propag. in horizontal fluid layer, mean flow determ., appl. to planetary atm. 3—29891
- three dimensional turbulent boundary layer, momentum integral solution 3—26813
- three-dimensional model, flow past spheres 3—29868
- transition on cone in supersonic flow *(French)* 3—29863
- transitions, hypersonic He flow, freestream disturbances effects 3—11417
- transonic wind tunnel corrections method 3—36115
- turbulence intermittency, nonhomogeneous flows 3—33216
- turbulent, asymptotic analysis 3—14451
- turbulent, calc. at flat plate, and diff. eqns. for turbulence scale 3—4553
- turbulent, conditionally sampled measurements 3—4559
- turbulent, flow separation anal. ahead of step 3—1390
- turbulent, in compressible gases with suction, calc. method 3—33224
- turbulent, in incompressible fluids with longitudinal pressure gradients 3—4579
- turbulent, incompressible, explicit numerical soln. 3—1357
- turbulent, internal problem, approx. soln. 3—23738
- turbulent, off sharp edge, acoustic wave diffraction 3—5715
- turbulent, on circular cone, locally similar solns. *(French)* 3—20334
- turbulent, over rough and smooth surfaces, wind profile model *(German)* 3—17524
- turbulent, pulse excitation, jet mixing flow 3—1395
- turbulent, response of cylindrical shell 3—6277
- turbulent, separated flow past bluff bodies attached to plane wall, free streamline theory 3—7329
- turbulent, sink-flow, asymptotic, acceleration obs. 3—7371
- turbulent, three dimens., EUROMECH 33 report 3—36112
- turbulent, velocity distribution at porous surface 3—4557
- turbulent, vibration response of liquid-loaded structures 3—3675
- turbulent at a permeable surface 3—33225
- turbulent boundary layer, pressure fluctuations meas. with correlation micro-pickup 3—32271
- turbulent channel flow, struct. effects due to spanwise rot. 3—11398
- turbulent characts. of layers with thermal stratification *(French)* 3—20333
- turbulent compressible flow along curved surface, particular solns. of energy eqn. 3—1402
- turbulent flow adjacent wall 3—4555
- turbulent flow of macromol. solns., momentum and heat transfer 3—17518
- turbulent flow with negligible wall stress at high Reynolds number, singular-perturbation theory 3—14461
- turbulent layer in adverse press. gradient, effect of transpiration 3—1387
- turbulent open and confined flow experiments 3—33203
- turbulent pulsations in free boundary layers with equilibrium MHD flow in square tube *(Russian)* 3—7433
- turbulent shear flows, low Reynolds number phenomena, two-equation model 3—38356
- turbulent thermally stratified, effect of sharp change in surface roughness 3—4580
- turbulent tubular flow involving endothermic chemical reaction, calc. of heat transfer coeffs. *(Dutch)* 3—29926
- two dimensional gas particle flow, derivation of momentum integral equations 3—7379
- two dimensional steady flow, incompressible fluid medium, review 3—33235
- uniform streams of identical charged particles over a surface, existence conditions 3—29963
- velocity distribution in boundary layers with suction, application of Shvets-Targ calc. method 3—33226
- vertical shear layers in flow past circular cylinder in uniformly rotating frame 3—23729
- viscoelastic fluid layer in mag. field, oscillatory convection 3—14479
- viscous flow past circular cylinder, numerical study 3—26772
- viscous flows past circular cylinders, numerical calc. 3—33222
- viscous fluid, stability of oscillatory Stokes layers, energy theory approach 3—20367
- viscous fluid flow past permeable body at small Reynolds number 3—26846
- viscous fluids around and through porous bodies 3—11379
- viscous incompressible turbulent flow in axisymmetric channel under conditions of preliminary swirl in the entry zone 3—33317
- viscous sublayer in a channel flow, 3 dimensional study by mass transfer meas. *(French)* 3—14435
- wall pressure field, flat plate, flow noise, intermittency factor, bursts 3—1397
- wall region, mixing length theory 3—20275
- water and aqueous surfactants, thinning of oil films, rupture, flow velocity dependence 3—39465
- water laminar free convection flow at 4°C from a vertical plate with variable wall temperature 3—29843
- wedge flow with variable props., variational technique application 3—38374
- Ar supersonic plasma, effect of electrode processes on volt-ampere characteristics of discharge 3—17709
- H_2O sheet, fan-shaped, absorption of CO_2 3—4536

boundary layers

- *see also boundary layer flow*
- acoustic protuberance noise environments, role of boundary layers 3—5706
- acoustic wave diffraction by wedge and cone, study of unsteady boundary layer, determ. of stress tensor *(Russian)* 3—22199
- atmospheric, dispersion, numberical air pollution transport model 3—12758
- atmospheric, energy exchange from kinetic loss considerations *(German)* 3—12706
- atmospheric, urbanization and industrialization thermal effects 3—28008
- atmospheric research, atmospheric boundary-layer research, airborne instrument system 3—3181
- atmospheric turbulent boundary layer above nonhomogeneous surface 3—31361
- benzene, shear elasticity determ., dynamic method *(Russian)* 3—30167
- blunt body, three dimensional effects on electron density 3—11404
- boiling, influence of velocity on wall superheating due to turbulence in boundary layer 3—17970
- catalytic reactions with volume change 3—12500
- clamped rectangular plates in uniform subsonic flow, stability 3—38376
- coastal boundary layers of lake, effect of finite vertical Ekman number 3—27995
- compressible, at thermally isolated plate, energy eqn. 3—23735
- compressible laminar and turbulent, heat transfer and steady state disturbances 3—38354
- compressible turbulent, heat transfer meas. 3—22273
- compressible turbulent 2D with arbitrary press. gradient, theory for anal. 3—1392
- compressible turbulent boundary layers with air injection, two prediction methods 3—7365
- conical diffusers experiments 3—33313
- continental slope of ocean, array meas. of bottom boundary layer 3—27976
- curved surface, second order solns. 3—1393
- cylindrical fluid layer, waves generated by time-periodic source *(Russian)* 3—20369
- cylindrical shell, nonlinear multiple-scale soln. to Reissner's eqns. using perturbation technique 3—32342
- diffusion in a time-dependent three-dimensional layer 3—17527
- doubly periodic convection in horizontal fluid layer heated from below *(Russian)* 3—29854
- duct, acoustically treated rectangular, transmission of sound 3—16341
- earth-atmosphere surface layer, stability parameters 3—5497
- Ekman turbulent layer, height determ. 3—28002
- Ekman-Hartmann, steady nonlinear 3—7441
- electrostatic surface waves propagation at boundary of inhomogeneous plasma 3—14560
- equatorial Ekman layer singularity, rotating gravitating sphere 3—7370
- equilibrium turbulent, in presence of pressure gradient 3—29866
- flat nonisothermal bed, radiation flux impinging on surface of bed 3—22773
- flat plates, second order stability theory eqns., soln. by numerical methods 3—14464
- fluidised bed coating of thin plates, heat transfer with a moving boundary 3—14501
- forced turbulent convection in circular tubes, turbulent boundary layers 3—38359
- free convection from semi-infinite inclined flat plate, series soln. 3—26794

boundary layers continued
Hartmann-Sprenger tube, thermal phenomena, mass exchange at boundary layer separating the two gases *(French)* 3−20292
heat and mass transfer on the surface of glass-graphite materials in high temperature gas stream *(Russian)* 3−26786
heat flux and temp. distribs. in turbulent equilib. layers 3−1388
heat transfer through an unsteady laminar boundary layer on a semi-infinite flat plate 3−20293
hypersonic turbulent, heat transfer with blowing of coolant gas through slit *(Russian)* 3−11405
isotropic plasma flow near rotating magnetised sphere, boundary layer formation 3−23835
laminar, natural instabilities, rel. to wall deform. *(French)* 3−7367
laminar, on flat plate, shock wave induced 3−7375
laminar, on moving circular cylinder, mass transfer eqns. 3−29867
laminar, spectral analysis of instantaneous signals of vel. fluctuations *(French)* 3−7368
laminar film condensation on porous horizontal tube with uniform suction 3−11407
laminar film condensation with suction 3−11414
laminar flow boiling on inclined isothermal flat plates 3−36411
liquid crystals, nematic, orientation by suitable boundary surfaces 3−1572
liquids, sharply separated, resistance coefficient at interface *(Japanese)* 3−23784
lower troposphere, global operational model 3−2970
lubricant boundary layers, elec. props. and domain struct. 3−4509
magnetic boundary layer theory 3−38377
magnetic Rayleigh problem, variational solution for a non-Newtonian power law conducting fluid, thickness increase of boundary layers in absence of mag. field 3−20377
Magnus effect, influence of boundary-layer stability 3−36102
membranes of revolution, flattening by large stretching, asymptotic soln. with boundary layer 3−32339
mixed flow impeller, negative velocity gradients in, diffusion losses due to 3−4582
mixing length near a wall, theory 3−20336
moving boundary transport problems in finite media, freezing, integral transforms 3−34703
natural convection heat transfer from downward-facing horizontal surfaces with uniform heat flux 3−20296
natural convection in a sound field giving large streaming Reynolds numbers, boundary layer theory 3−38358
oscillating slender cone in viscous hypersonic flow 3−1339
perturbation solns. at high Schmidt nos., applic. to cont. system for desalination by reverse osmosis 3−1384
plane moving boundary problems, freezing and melting, integral transforms 3−34702
plane turbulent wake, conditional sampling, structure of turbulent boundary 3−23801
plane-parallel duct with artificially roughened walls, heat transfer and hydraulic resist. 3−20311
planetary, air-sea, numerical simulations 3−2936
planetary, universal functions in resistance law 3−18854
plasma, Langmuir probe, meas. *(Japanese)* 3−23922
plasma, magnetopause motions at lunar distance by Explorer 35 3−12839
plasma, oblique incidence light absorpt. 3−17562
plasma on nonconducting walls of MHD channel *(Russian)* 3−14536
1/N power law, sheared flow acoustic transmission 3−5707
radiation-layer on hot plate, Olfe's modified differential approximation 3−635
radiative energy transfer at laminar boundary layer 3−23734
re-entrainment of small particles from flat surfaces 3−17528
Rivlin-Ericksen fluid containing rotating heated sphere, calc. of thermal boundary layers 3−26812
rotating blades in forward flight, boundary layer separation 3−38373
sea-air interactions *(German)* 3−9262
separation in flow field, perturbation technique 3−7373
shock tube walls, formed after detonation 3−4589
spatial stability of stagnation H_2O layer with heat transfer 3−7374
stability of cable in axial stream of viscous incompressible liquid *(Russian)* 3−29838
stationary planetary boundary layer, effect of atmospheric baroclinicity on wind structure *(German)* 3−12710
superheated boundary layer, statistical characteristics determ. of temp. fluctuation in pool boiling 3−20856
supersonic viscous flow over a yawed circular cone, boundary layer separation 3−38384
surface pressure fluctuations calc. from velocity fluctuations 3−4576
temperature and thickness meas. by holographic interferometer 3−22375
temperature boundary layer, boundary-value problem for system of equations 3−33232
thermal, schlieren TV method of obs. 3−124
thermal, solution of equation for arbitrary distrib. of temp. of fairing surface *(Russian)* 3−7377
three dimensional laminar coefficient of restoration of the enthalpy *(Russian)* 3−33227
three dimensional turbulent boundary layer, momentum integral solution 3−26813
three-dimensional, in generalized Stokes fluid, similarity criterion 3−20338
thrust nozzle optimisation, using numerical relaxation scheme 3−1333
turbulent, effect of high-rate injection of air and CO_2 3−1386
turbulent, noise radiation 3−33208
turbulent, nonequilibrium, compressible generalised integral computation technique using moment equations 3−7376
turbulent, Reynold's stress, statistical characts. 3−23739
turbulent, statistical characteristics of Reynolds stress 3−29873
turbulent convection at isotheraml vertical plate *(Russian)* 3−11391
turbulent Ekman, asymptotic formulae for thickness *(Russian)* 3−1389
turbulent pressure fluctuations, transduction into rigid walled rectangular cavity, modal coupling effects 3−1396

boundary layers continued
turbulent with freestream pressure gradients, wall pressure fluctuations 3−1377
turbulent with suction 3−4578
two-dimensional incompressible turbulent boundary layer separation, wall pressure distrib. 3−7366
unsteady laminar boundary layer on a semi-infinite plate, experimental results from an oscillating plate 3−20294
unsteady state, interaction of convection and radiation *(Russian)* 3−11406
viscous fluid, surface and internal long waves *(Russian)* 3−33229
water, pure, boundary layer, drag reduction by ejecting additive solutions 3−23740
water, shear elasticity determ., dynamic method *(Russian)* 3−30167
weakly ionised gas, analysis of positive ion current in region of highly negative probe, boundary layer approx. 3−20610
Cu ammine complex, from a cation exchange resin, elution kinetics using integral transform techniques to soln. of moving boundary problems 3−34704

boundary-value problems
see also numerical analysis
acoustic press. fields in finite container 3−1425
acoustical Green's function, right parallelepiped, perfectly reflecting walls, Laplace transforms, acoustic potential 3−3687
aperture near-field calc., accuracy of Kirchhoff boundary values *(German)* 3−37922
bending of rectangular plates with stepped variation of thickness, analysis by Bubnov-Galerkin method *(Russian)* 3−28877
cavitation phenomena in lubricated bearings, solns. of Reynolds eqn. 3−17538
contact problem of nonplane punch on elastic layer, initial value method soln. 3−32317
differential eqn. with integral constraints, variational approach 3−28833
diffraction coeff. of conducting wedge loaded with cylindrical dielectric slab at apex 3−37928
diffraction of plane shear elastic wave by circular rigid disc and penny shaped crack 3−3990
edge crack, normal to edge of strip, calc. of stress distrib., Fredholm integral eqn. 3−13571
elastic anisotropic 3-d bodies, soln. for stress states using successive approximation method *(Russian)* 3−13579
elastic cylinder, dislocations, iterational method of soln. 3−26087
elastic layer, semi-infinited, mixed problems 3−19444
elastic perturbed boundary problems, soln. using small parameter method *(Russian)* 3−19445
elastic torsional and longitudinal wave growth in 2nd order material 3−32372
elastic wave reflection in superseismic region in presence of alternating boundary conditions *(Russian)* 3−34818
elasticity theory, dynamical problem *(Russian)* 3−16647
elasticity theory, using potential methods involving Green's matrices 3−13558
elastoplasticity, dual extremum theorems of boundary value problems in deformation theory 3−32362
elliptic systems, existence and uniqueness theorem for soln. of boundary problem *(Russian)* 3−13535
e.m. field at perfectly conducting wedge with exterior region divided by resistive sheet 3−22825
e.m. scattering, nonuniqueness consequences of integral equations 3−35663
exterior e.m. problem of wedge, use of Laplace, Fourier and Kontonovich-Lebedev transforms 3−19480
finite element method, natural boundary conditions 3−22651
finite element stiffness matrix, influence of Poisson's ratio on spectral condition number for nearly incompressible solid 3−22617
Galerkin's method, coord. function selection 3−22589
gas, potential flow theory *(Russian)* 3−11432
general relativity, e.m. boundary conditions, covariant derivation 3−13629
generalized axially symmetric potential theory, soln. of boundary problems *(Russian)* 3−13540
generalized finite element method 3−16601
geodetic boundary value problem using known surface of Earth 3−27938
Green's function formalism for acoustic response, scalar wave functions 3−3690
grid consisting nonparallel and nonrectilinear conductors on nonplane surface 3−26197
heat conduction, differential equation boundary value problem, extremum principles and error bounds 3−28988
heat conduction, nonstationary, simulation by elec. models 3−22782
heat conduction in elliptical cylinder 3−19533
heat conduction with time-variable heat exchange coeff., exact soln. 3−22779
heat transfer calcs., boundary extrapolation 3−35638
Helmholtz eqn. in cubic region, nodal surfaces of eigenfunctions 3−28914
hydraulic mains dynamical charact. *(Russian)* 3−20355
hyperbolic eqn. with boundary and initial conditions, soln. by elliptic problem with parameter 3−28822
hysteroelastic theory, dynamic, linear, general solns. for composite media *(Russian)* 3−28883
incompressible fluid with constant viscosity, flow around arbitrary obstacle, Navier-Stokes equations 3−36109
infinite tubular antenna in cold collisional plasma, current distribution 3−11482
initial value, quasilinear hyperbolic differential equations, solution by explicit second order method of characteristics 3−10252
initial-value, general, numerical solution 3−16706
isotropic rigid-plastic and viscoelastic continuous media, minimum principle in dynamics 3−6250
Korteweg-de Vries, in weak nonlinear dispersive waves propagation 3−10240
laminated beam, free vibrations by microstructure and effective modulus theories 3−37846
Langmuir probe in dense plasma 3−14592
linearized elastodynamics, displacement boundary-value problem, uniqueness 3−32336

boundary-value problems continued
liquid oscillations in cylindrical cavities, soln. of boundary problem by Bubnov-Galerkin method *(Russian)* 3—14486
long waves generated by wavemakers in non-linear dispersive systems, mathematical model 3—20366
mixed, asymptotic approximate solns. in multifrequency vibratory regimes *(Russian)* 3—13541
mixed, numerical solution using numerical Green's functions 3—22770
moment-method solutions, convergence improvement technique 3—3932
multidimensional bounded domain, asymptotic formula for eigenvalues of self-adjoint extensions of Schrodinger operator *(Russian)* 3—[illegible]
neutron thermalization in indefinite homogeneous multiplicative medium, soln. of Boltzmann eqn. 3—32914
non-linear viscoelastic rod, asymptotic soln. of initial value problem 3—32314
non-self-adjoint systems of elliptic partial differential equations, finite element analysis 3—28852
non-stationary free convection in close convex region, classical solns. of second boundary problem *(Russian)* 3—29855
nonlinear, use of initial value method 3—6189
nonlinear diffusion problem involving Arrhenius reaction rates, variational soln. and error bound 3—27867
nonlinear two-point, algorithm to solve using quasilinearisation method and invariant imbedding *(Japanese)* 3—22590
orthotropic bodies, symmetric deform. obs. by approx. method *(Russian)* 3—6214
Oseen streaming flow past semi-infinite needle 3—4574
parabolic, semidiscrete-least squares approximation 3—10259
peristaltic motion of non-Newtonian fluid 3—7335
Petrov theorems for large deviations *(German)* 3—35563
plasticity theory, extremal boundary problems *(Russian)* 3—6248
plate vibration, by improved finite difference method 3—565
Poiseuille flow, simulation 3—7337
pseudo-viscous methods for steady supersonic flow past waisted body 3—1405
quantum statistical mech., thermodynamic limit of boundary conditions 3—6354
quasilinear elliptic and parabolic eqns., soln. using projection-difference schemes *(Russian)* 3—10244
quasilinear elliptic eqns. in plane, regularity of solns. *(Russian)* 3—13536
quasilinear parabolic eqns., regularity of solns. of first boundary problem *(Russian)* 3—13534
regularization method for asymptotic expansions 3—16597
representation formula in a disc in terms of arithmetic means on boundary 3—[illegible]
rigid plastic structure, impulsively loaded, mode approximation 3—6241
scattering of plane waves by infinite grating on anisotropic medium *(Japanese)* 3—22818
sea level surface and mass transfer function calc. for north Atlantic *(Russian)* 3—12675
second order eqn. with turning point, uniqueness of asymptotic solns. by WKBJ method 3—32290
semiclassical collision theory within Feynman path integral formalism 3—28951
short range weather forecasting using a baroclinic atm. model *(Russian)* 3—21939
solids, spherical and cylindrical, melting, boundary and initial value problems 3—6384
spinning of axially-symmetric anisotropic body with mixed boundary conditions on side surface *(Russian)* 3—16646
static magnetic field calculations in nonlinear ferromagnetic medium *(Russian)* 3—34050
steady heat conduction in regions with generation 3—32463
storm surge eqns. for wind effects is Adriatic sea, numerical soln. by difference scheme 3—2935
surface wave incidence on plane structure having multi-mode discontinuity in impedance 3—3998
surface waves on shallow water, nonlinear interactions 3—4596
temperature boundary layer, boundary-value problem for system of equations 3—33232
thermoviscoelastic, correspondence principle 3—13572
thin-walled pipes with curved axes, calculation *(Russian)* 3—19432
transport processes, computer solns. by finite difference methods 3—10398
trapped modes of rotating viscous fluids in spherical shells, numerical simulation 3—20329
two earthed spheres, by image potentials *(German)* 3—4052
unbounded plate with collinear cracks, dynamic stress intensity factor 3—21760
uniqueness and Holder continuous dependence for linear micropolar fluid motion 3—23675
unsteady heat conduction in solids, with moving boundary, soln. to 1-D problem *(Russian)* 3—22789
vibrating beam, determ. of optimal frequencies using finite element displacement method 3—22684
vibrations of rectangular plates of micropolar elastic materials, three-dimensional analysis, series soln. 3—16665
vibrations of thick elastic shells, soln. using Cinelli's method 3—19464
vibratory motion of body on orthotropic half plane 3—22696
viscoelastic anisotropic half-space, surface shear stress pulse action 3—22632
viscoelasticity, linear theory, approximation with rational functions *(Russian)* 3—16650
viscoelasticity, quasistatic problems for media with time-varying props., method of soln. 3—26079
waves, slightly unstable nonlinear systems, initial-value problem, asymptotic soln. 3—36125
weather forecasting error anal. by solution of two-point problems 3—25219
wedge, anisotropic, plane soln. under normal and shear loading 3—22644

bowing *see bending*

Bragg reflection *see X-ray crystallography*

brain
animals, chronic and asymmetrical cortical foci rel. to bilateral synchrony of epileptic discharge 3—28333
anterior cingulate gyrus, stereo-EEG investigation 3—28332
cat, polysensory responses and sensory interaction in pulvinar and related posterolateral thalmic nuclei 3—39774
cats, factor analysis of evoked potentials 3—31848
chronic animals, intracellular recording in cerebral cortex 3—35521
e.e.g., interpretation, blood circulation, electric currents and metabolism of the brain *(Swedish)* 3—13486
hippocampus, averaged evoked brain potentials, component analysis 3—35241
human brain tissue in shear, rheological response 3—26002
man, extracellular firing patterns of deep temporal lobe structures 3—39766
scanning, with Scinticamera IV 3—16552
scanning in children 3—16325
stem electric potential changes rel. to stimuli 3—35245
visual cortex of rabbit, single unit reactions to light plastics of different intensities 3—39767
visual evoked response using rapid flash rates technique 3—28330

brain models
see also learning systems; neural nets
human memory storage efficiency improvement schemes 3—39761
plasma model of brain dynamics, memory plateau prediction 3—5624
visual cortex in higher mammals, using theory of generalised functions *(Russian)* 3—13135

brakes
eddy-current, relativistic electrodynamics *(German)* 3—37877

braking
planetary satellite transfer from hyperbolic to nearly circular orbit using aerodynamic braking 3—25378

brass
γ-type, tetrahedrally close packed struct. 3—14731
β-brass, multiple dislocation, stacking fault arrays, stability 3—17824
α-brass powder, cold-worked and stored at liquid N temp., increase in particle size 3—27642
disordered binary, electronic struct. 3—11856
elastic shear modulus, determ. during quantized parabolic strain hardening 3—21651
erosion due to water jet impact, damage threshold vel. prediction 3—1681
f.c.c., grain boundaries and surface tensions meas. by zero creep method 3—34543
Fermi surface study by positron annihilation 3—15117
film, protective, production by cathode sputtering 3—8726
frequency effects on enhanced diffusion during cyclic straining 3—20889
metallurgical factors in fretting fatigue behaviour 3—37076
microautoradiographs, effect of sort and surface roughness 3—9033
nucleation, electrolytic, brass on Pt cathode, pulse method investigation 3—1945
phase change correlation with stress corrosion fracture 3—27648
plasticity and strength characteristics, influence of grain size in presence of Hg *(Russian)* 3—12369
precipitates, massive, selected area electron channelling obs. 3—21576
self diffusion of ^{65}Zn in heterogeneous biphase brass 3—18001
serrated flow in alpha beta phases 3—31091
stress corrosion cracking, fractographic obs. 3—31042
stress corrosion cracking in citrate soln. 3—39358
superplastic, stress strain curves, flow stress, microstruct. 3—34556
thermal conductivity, low temp. measurement in presence of extraneous heat currents 3—25690
vacancy equilib. density from positron trapping meas. 3—17809
wear resistance in friction against filled polyethylene 3—25013
Au modified, β-phase, order-disorder transformation 3—5284
α-brass, Zn rate of removal by means of X-ray microanalyser *(German)* 3—12328
Cu-Zn, β-α massive transform. kinetics 3—39319
α-Cu-Zn, electron irrad., short range order, interstitial diffusion 3—11617
Cu-Zn, γ-phase, grain boundary diffusion, 25°C *(German)* 3—24840
Cu-Zn:Fe, Mossbauer effect isomer shift meas. 3—15441
Cu-Zn(30 wt.% Zn), relaxation during short range ordering, internal friction variation with annealing temp., ordering activation energy 3—4818
β-CuZn, Fermi surface props. by the APW method, agreement with dHvA expts. 3—809
CuZn ordered solid solution, size effect theory *(Russian)* 3—7658

Bravais lattice *see crystal atomic structure*

braze bonding *see brazing*

brazing
see also soldering
braze material, determ. of diffusion effect on thermal cond. of thin Cu fins 3—9855

breakage *see fracture*

breakdown (electric) *see electric breakdown*

breakdown (mechanical) *see mechanical strength*

breakdown diodes *see avalanche diodes*

breaking strength *see mechanical strength*

breeder reactors *see nuclear reactors*

bremsstrahlung
see also electron radiation; gamma-ray spectra; gamma-rays; X-ray emission spectra; X-rays
20 to 35 MeV, effects of collimators on spectral distribution 3—354[illegible]
60 to 120 MeV, energy expended for ion pair in air *(German)* 3—25853
activation analysis, use of electron accelerator 3—19372
atomic-field bremsstrahlung polarisation correlations 3—35974
attenuation meas. in ilmenite loaded concrete 3—1087
auroral-electron spectrum dynamics during magnetospheric substorms, X-ray data use 3—25255
betatron, determ. of photon distrib. by ^{2}H(γ,p)n reaction 3—10048
betatron γ-rays for photonuclear cross-sections for different reaction channels 3—17229

bremsstrahlung continued
black hole accretion from interstellar gas, electron-electron and electron-proton radiation mechanisms 3−39586
cluster of galaxies, X-ray source in hot gas 3−25491
coherent produced by relativistic electrons on diamond monocrystal, determ. of polarization degree *(Russian)* 3−38056
coherent production on corundum crystal *(Russian)* 3−35806
cosmic ray μ, e.m. interactions in Fe 3−18910
deuterium plasma, temp. meas. from quantum bremsstrahlung using filter method and Si detector 3−36197
electromagnetic processes at 1 GeV/c and production-rate limits 3−23070
electron, confined in magnetic mirrors, ang. distribution 3−20050
electron, from atomic scatt., linear polarisation 3−20052
electron, pair production 3−6613
electron bremsstrahlung in medium with an external electric field 3−30034
electron spectra from double inverse pinch device 3−20652
electron velocity distribution meas. in an electron cyclotron resonance plasma by bremsstrahlung intensity and polarisation methods 3−14589
external, produced by beta particles in Cu, Ag, Cd, Sn, Pb targets, reln. to target thickness 3−29454
Furry Sommerfield Maue wave functions in pair production and bremsstrahlung 3−20051
hadronic collisions, inclusive photon distributions 3−23189
inclusive photon spectra and high-energy multiplicities 3−4234
insulator, electric pot. obs. using bremsstrahlung and charact. X-ray spectra 3−36970
inverse, i.r. laser heating at dense arc plasmas 3−7544
laser-plasma interaction, one-photon inverse bremmsstrahlung process *(Japanese)* 3−1504
Lorentz-Dirac eqn. soln., results tested using electron beams in intense mag. fields 3−10703
lower ionosphere, impact and bremsstrahlung photoionisation due to precipitating electrons 3−34945
magnetospheric electron precipitation phenomena dynamics 3−28070
mass-attenuation coeffs. in Kr and Xe by continuous analysis between 8 and 0.8 keV using bremsstrahlung 3−4364
meson multiplicity in bremsstrahlung model for pp→ppX 3−17089
neutron spectra, non-Maxwellian, self-consistent transformation of bremsstrahlung of monochromatic photoneutron mean energies 3−37705
non-thermal, white dwarf flare production *(Russian)* 3−16208
plasma, hot electron, density axial distribution by bremsstrahlung meas. 3−38477
plasma, weakly ionized, bremsstrahlung radiation 3−7485
plasma energy balance, thermal conductivity and bremsstrahlung in a thermonuclear reactor 3−38472
plasma heating by multiphoton inverse Bremsstrahlung 3−29994
plasmas, high-frequency power absorption by inverse bremsstrahlung 3−38479
proton-proton bremsstrahlung at 156 MeV, rel. to nucleon-nucleon pots. *(French)* 3−6730
Puppis A, supernova remnant, origin of X-ray spectrum 3−35149
radiation damping, spectrum and polarization measurements and calcs. *(Russian)* 3−19687
radiative decay behind strong shock 3−4592
Razin-Tsytovich effect for bremsstrahlung from electrons rel. to synchrotron radiation 3−26905
solar flare lifetime in coronal storage regions, energy loss mechanisms 3−39627
solar flare X-ray prod. by bremsstrahlung of accel. electrons 3−39625
thermal emission from Coma cluster of galaxies 3−28279
X-rays, rel. to auroral glow and shape during Jan. 21 and Feb. 3 1969 storm and substorm 3−34887
α-α scattering, calc. of coplanar bremsstrahlung with Feshbach-Yennie model, 6-22 MeV 3−26444
$e^{\pm}p \to e^{\pm}\gamma$ + anything, meas. of deep inelastic bremsstrahlung in scaling region, test for fractional charged partons 3−4180
(γ, en) reaction using bremsstrahlung spectrum, yield curves 3−17227
$\gamma p \to \varphi p$ with unpolarised bremsstrahlung meas. 3−17002
μ cosmic ray e.m. interactions in Fe, 6-200 GeV, momentum dependence of interaction probabilities 3−5550
n distribution in nuclei from bremsstrahlung-weighted cross-section meas. 3−32789
NN interactions at large momentum transfer, hadronic bremsstrahlung production, correlation tests 3−29293
p, target, deep inelastic Compton scattering, expt. 3−13925
pp data at 42 MeV, determ. of off-shell t-matrix parameters 3−10767
pp inclusive scattering cross section, hadronic bremsstrahlung model for single-particle distribs. 3−4241
^{209}Bi, photofission by 1 GeV bremsstrahlung, spallation background 3−1029
Fe slab, transmitted energy spectra of radiation produced in Fe and Au targets 3−17328
Fe(γ,n), meas. of spectra prod. by 15 MeV electrons using activation detectors 3−23303
^{1}H(p,p'γ), 51.8 MeV, meas. of pp bremsstrahlung cross section 3−29375
^{204}Tl, β-decay, double internal bremsstrahlung, obs. 3−14172
W(γ,n), meas. of spectra prod. by 15 MeV electrons using activation detectors 3−23303

brick industry
clay mineral composition of Melbourne brickmaking clays 3−15762

bridge circuits
see also bridge instruments
a.c., for four terminal resistance thermometry 3−5808
continuously scanning, calibration, using on-line data 3−35352
galvanic skin response in sleep experiments 3−25978
Si planar transducer bridge, for pressure meas. 3−25706

bridge instruments
see also bridge circuits
automatic, errors in temp. difference meas. using resistance thermometers 3−25686
biological active macromolecules in aqueous solutions, dielectric permeability meas., modified Nernst's bridge 3−32234

bridge instruments continued
Kelvin bridge, for temp. measurement and control of desorption filaments *(Spanish)* 3−32040
operational amplifiers as electrometers 3−10152
semi-automatic, capacity ratio measurement of an m.o.s. structure *(German)* 3−15262
thermal conductivity measurement of air at atmospheric pressure 3−23659

brightness
see also sky brightness
cloud brightness data applied to tropical wave disturbances 3−25236
cloud brightness data rel. to meso-to-subsynoptic scale rainfall pattern 3−28047
coloured flashes, background effects, vision research 3−31920
coloured lights, luminance rel. to brightness 3−25585
elliptical galaxies with high surface brightness, tidal origin 3−28260
illumination distribution of point in optical system with axial symmetry under birefringence conditions *(Russian)* 3−5879
intrinsic light brightness and equivalent intensity 3−31885
irradiance, NBS scale 3−35347
Moon, integrated brightness, surface photometry 3−18987
Moon's surface, photometric and polarimetric study 3−18982
ocean water and overlying atm. 3−3236
plasma displays, rel. to choice of multiplex methods 3−23927
powder layer with opaque particles, brightness matrix in single scatt. approx. *(Russian)* 3−6427
solar granulation brightness fluctuations, new interpretation of power spectra 3−16124
Sun, distrib. at 8.6 mm. 3−5566
temperature distribs. defined by measured intensity interferograms, radio and optical astron. sources 3−28305
threshold stimuli, peripheral visual field 3−37531
visual perception, two stage model 3−5663

Brillouin scattering *see Brillouin spectra*

Brillouin spectra
absorbing liquids, stimulated thermal scattering picosecond light pulses 3−4127
absorbing materials, intrinsic width of phonons 3−15488
anisotropic media, polarisation and frequency shift effects of Brillouin scattering *(German)* 3−8564
anisotropic media, polarisation and frequency shifts *(German)* 3−8564
anisotropic media, scattering, geometrical situation *(German)* 3−5185
bulk viscosity effects on amplification function of Stokes signal interacting with laser beam in fluid 3−32588
dicalcium strontium propionate, Brillouin scatt., vibr. modes, elastic consts. 3−30814
glass, induced Mandelstam-Brillouin scatt. power 3−19645
inelastic light scattering and the Raman effect, review 3−33133
isotropic polymeric solids, theory 3−4505
laser resonators, stimulated Raman radiation and Mandel'stam-Brillouin radiation 3−22945
liquid crystals, smectic, Brillouin scattering 3−34354
liquids, light scattering from thermal shear waves 3−30821
magnetised ferrites, construction and applic. 3−22829
microwave ultrasonics in solid-state physics, book 3−20819
molecular fluids, density fluctuations calc. 3−4030
molecular fluids, Rayleigh-Brillouin scatt. expts. rel. to generalised transport coeffs. 3−32599
optical fibres, power handling capacity rel. to stimulated Raman and Brillouin scatt. 3−766
plasmas, laser irradiated, nonlinear behaviour of stimulated Brillouin and Raman scattering 3−36159
plastic, induced Mandelstam-Brillouin scatt. power 3−19645
polariton resonant Brillouin scattering, spatial dispersion effects 3−8131
polyethylmethacrylate, expt. confirmation of theory 3−4505
polystyrene, sound speeds from stimulated Brillouin scatt., annealing effects, laser induced damage 3−1307
quartz, fused, induced Mandelstam-Brillouin scatt. power 3−19645
rough surfaces, rel. to sound refl. coeff. determ. *(Russian)* 3−39151
semiconductor, acoustoelec. domains, piezoelec. potential and carrier distrib., microwave absorpt. study 3−5040
stimulated Mandelshtam-Brillouin emission in optical resonator 3−22956
stimulated scatt. meas. of elastic const. variations *(French)* 3−14904
stimulated scattering, gases, gain and line widths *(Russian)* 3−1326
thin films, structure in Brillouin spectra 3−12135
X-ray scattering, long wavelength phonon investigation 3−30146
Ar single crysts., adiabatic elastic consts. determ. near triple pt. 3−4781
CdS, acoustoelec. gain and lattice attenuation, Brillouin scatt. obs. 3−33961
CdS, acoustoelec. multi-peak domain propag. obs. 3−24481
CdS, acoustoelectric effect *(German)* 3−30521
CdS, Brillouin scatt. by propag. acoustoelec. domains 3−33960
CdS, harmonic conversion of acoustoelectrically amplified phonons, Brillouin scattering study 3−2141
CdS, Mandelstam-Brillouin scatt. obs. of parametric interaction of sound signals 3−36640
CdS, scatt. from acoustoelectrically amplified flux domains, dispersion spectrum 3−34352
CdS thermal, acoustoelectrically interacting and built-up phonon studies by laser Brillouin scattering 3−1749
$Ce_2Mg_3(NO_3)_{12}.24H_2O$, e.p.r. saturation of Ce^{3+}, light scatt. obs. of nonequil. phonon system 3−2370
$Ce_2Mg_3(NO_3)_{12}.24H_2O$, phonon system under e.p.r. saturation conditions *(Russian)* 3−8438
$Ce(NO_3)_2$, Mandelshtam Brillouin scatt. intensification at e.s.r. saturation 3−8417
GaAs, reson. Brillouin scatt. and absorpt. edge modulation by intensely amplified phonon beams 3−5204
He-Kr gas mixture, hypersonic vel. and absorpt. meas. 3−1322
^{4}He, liquid, second sound contrib. near λ transition 3−24308
KCl, temp. depend., 100-300 K 3−24700
KCl-KBr, mixed crysts. 3−39143

Brillouin spectra continued

- $LiNbO_3$, room temp. obs., elastic consts., elastooptical moduli *(French)* 3−36864
- NaCl, temp. depend., 100-300 K 3−24700
- $NaNO_3$, elastic and photoelastic consts., determ. from Mandelshtam-Brillouin scatt. spectra 3−33593
- Ne single crysts., adiabatic elastic consts. determ. near triple pt. 3−4781
- SF_6 hypersound speed meas., by spontaneous Brillouin scattering 3−5780

Brillouin zones

see also band structure

- crystals of D^7_{4h} symmetry, rel. to two-phonon processes 3−15491
- crystals with zinc blende symmetry, second order nonlinear optical susceptibility, energy band theory 3−8550
- density of states numerical calc. within Brillouin zone 3−8080
- graphite, optical props., dispersion relations for π-bands 3−30785
- hexagonal metals, anisotropy in phonon scattering resistivity 3−7876
- interpolation versus extrapolation in Brillouin zone integration schemes 3−18071
- interpolation versus extrapolation in Brillouin zone integration schemes 3−18072
- magnon-phonon selection rules, inelastic neutron scattering 3−34131
- metal, cubic, rel. to anharmonic thermal scatt. of X-rays 3−38524
- rhombohedral crystals, symmetry props. of energy bands *(Russian)* 3−11843
- scattering by elastic waves in cubic crystal 3−18448
- spectral props. of solids, numerical calcs. by integration over Brillouin zone 3−20983
- BaO optical phonons at centre of Brillouin zone at 300 and 17K *(French)* 3−8567
- Bi, diamagnetism theory 3−8338
- CaO optical phonons at centre of Brillouin zone at 300 and 17K *(French)* 3−8567
- $Ca_{1-x}Sr_xPb_3$ alloy, supercond. critical temp. rel. to lattice deform., Brillouin zone effects 3−34008
- $CaTl_3$, effect on density of states curve from band structure calc. 3−1984
- Cu_3Au, effect on electron props. oscillatory depend. 3−1984
- $Fe_{1-x}Ni_xAl$ solid solns., degree of occupation interpret. of magnetoelec. and thermoelec. effects *(Russian)* 3−18121
- K, interband optical cond. calc. in range 1 to 10 eV 3−24375
- KNCS, i.r. and Raman spectra, lattice mode analysis and order-disorder transition 3−5189
- LiD, phonon study in first zone using Raman and phonon spectra 3−2546
- NaI, rel. to one-phonon far i.r. absorp. obs. on cryst. powder 3−27502
- Ni, ferromagnetic, self-consistent calculation of energy bands 3−18073
- SnTe, band structure and Jones zone 3−4949
- SrO optical phonons at centre of Brillouin zone at 300 and 17K *(French)* 3−8567

bristles *see fibres*

brittle materials *see brittleness*

brittleness

see also mechanical strength

- amorphous materials, curves on fracture surfaces 3−38617
- brittle material, fracture toughness and specific fracture energy 3−36357
- brittle rectangular beam weakened by an internal circular crack, bending *(Russian)* 3−6243
- composite materials, containing second phase dispersions, strength 3−7841
- crack formation at segregation rel. to fracture theory and precipitation thickness *(German)* 3−7837
- crack initiation at elastic/plastic interface 3−33601
- electrolytic coatings, laboratory method 3−25657
- fractography, state-of-the-art review 3−30982
- fracture, near stress concentrations, limiting equilibrium state for infinite plate *(Russian)* 3−28887
- fracture, rail specimen resistance assessment in impact machine tests using rolled grid *(Russian)* 3−12476
- fracture toughness parameter calc., engineering method 3−34600
- hydrgen embrittlement cracking, lattice dilatation, complete elastic soln. 3−39353
- lacquer coating, crack form., coating thickness influence *(Japanese)* 3−18729
- material failure theory, classical approach rel. to damage accumulation 3−37105
- metal, b.c.c., plastic crack propag. *(Russian)* 3−20802
- metal, stat. eval. of strength at brittle fracture 3−31097
- metal, subcrit. crack branching implications 3−4796
- metals, brittle fracture 3−18662
- metals, H embrittlement 3−2723
- polymer, glassy, tensile strength rel. to stress crazing and brittle fracture *(Japanese)* 3−7280
- polymer, h.p. effects on mech. behaviour 3−31187
- radiation damage in structural materials 3−29449
- reactor weld metals, radiation and temper embrittlement processes 3−8889
- refractory metals of group VIa, nature of cold brittleness 3−18694
- reinforcement of brittle matrices by glass fibres 3−31140
- rupture of brittle bodies in surface-active medium, crack growth kinetics *(Russian)* 3−27059
- steel, AISI 4340, stress corrosion crack growth, stress history effect on incubation time 3−34585
- steel, ausformed, electron-beam weld props. 3−21645
- steel, austenitic, type 304L, hydrogen embrittlement 3−2745
- steel, brittleness depend. on cooling rate after annealing *(Russian)* 3−24905
- steel, delayed failure mechanism, hypotheses *(French)* 3−5329
- steel, dispersion-strengthened ferritic alloys for high-temp. applics. 3−8936
- steel, dynamic fracture toughness, material props. influence 3−31049
- steel, effective surface energy of fracture and brittle rupture *(Russian)* 3−8842

brittleness continued

- steel, for reactor vessels, radiation embrittlement sensitivity to Cu and Va, temp. depend. 3−26540
- steel, high-strength, static and dynamic embrittlement in water 3−5324
- steel, high-strength, tensile ductility, gaseous hydrogen influence 3−5323
- steel, hydrogen, embrittlement, industrial consequences *(French)* 3−2735
- steel, hydrogen embrittlement, diffusivity effects 3−5325
- steel, hydrogen embrittlement, temp. depend. *(French)* 3−5333
- steel, hydrogen embrittlement *(French)* 3−8905
- steel, hydrogen embrittlement meas. methods *(French)* 3−5327
- steel, hydrogen embrittlement rel. to hydrogen/dislocation interaction 3−2744
- steel, hydrogen embrittlement sensitivity, thermal processing depend. *(French)* 3−5328
- steel, hydrogen induced cracking, effect on weld microstructures 3−39364
- steel, hydrogen penetration and embrittlement, effect of electrolytic charging conditions 3−5326
- steel, lead embrittlement, comp. depend. 3−21648
- steel, low-alloy 18Gps, susceptibility to brittle fracture 3−21663
- steel, martensite, for machine construction, resist. to brittle fracture 3−24937
- steel, mild, config. of moving crack tip zones 3−30196
- steel, mild, micromechanisms due to the influence of cementite on the embrittlement *(French)* 3−31005
- steel, Ni-Cr-Mo, rare earth treated, temper embrittlement response and toughness 3−34584
- steel, pearlitic, hydrogen embrittlement, strength and struct. influence 3−27654
- steel, rail-grade, hydrogen effects in prod. and service performance 3−5335
- steel, stainless, hydrogen diffusion through oxide films 3−21644
- steel, stainless, influence of deoxidation on ductility 3−24919
- steel, stainless, stress corrosion cracking and hydrogen embrittlement 3−5330
- steel, stress corrosion cracking, role of hydrogen embrittlement 3−2736
- steel, structural, delayed and premature fractures *(French)* 3−5331
- steel, study at low temp. 3−24916
- steel, workability improvement considerations 3−21681
- steel austenitizing treatment effect on temper embrittlement, search for Sb segregation at grain boundaries 3−34544
- steel for dies, effect of double tempering on brittle fracture 3−18672
- steel weld, hydrogen-induced cracking, microstruct. effect 3−34567
- steels, high-strength, comparison of hydrogen embrittlement and stress corrosion cracking 3−21622
- transition metals, group V, hydrogen embrittlement and hydride form. 3−34530
- weld heat affected zones, martensite tempering rel. to hydrogen cracking 3−8910
- Zircaloy-2, polycrystalline, H_2 embrittlement by aqueous lithia soln. corrosion, hydride orientation *(French)* 3−12385
- Al, embrittlement by Hg, role of solute additions 3−34566
- Al alloys, high-strength, hydrogen embrittlement and stress corrosion cracking 3−5336
- Al alloys, tendency to brittle rupture *(Russian)* 3−27669
- Al bronzes, casting and wear props., effect of iron *(Polish)* 3−31033
- Al-Fe bicrysts., grain boundary precipitate exam. by Ga embrittlement technique 3−37025
- Cu-1.9 wt pct Co, age-hardened, Hg embrittlement at room temp. 3−18647
- Cu-3.6 wt pct Ti, age-hardened, Hg embrittlement at room temp. 3−18647
- $Cu-Al_2O_3(MgO)(TiO_2)$, internally oxidised, brittleness during annealing in H_2 *(Japanese)* 3−12395
- Fe, Armco, ductile-to-brittle transition, effect of cold deform. and subsequent heat treatment *(Russian)* 3−5307
- Fe, Armco, embrittlement by hydrogen *(French)* 3−1830
- Fe, Armco, hydrogen charging influence on yield stress and ultimate strength *(French)* 3−5321
- Fe, high purity, hydrogen embrittlement low carbon additions influence *(French)* 3−5322
- Fe, hydrogen embrittlement, industrial consequences *(French)* 3−2735
- Fe, hydrogen embrittlement rel. to hydrogen/dislocation interaction 3−2744
- Fe-C alloys, permeability and embrittlement by cathodic hydrogen *(French)* 3−21661
- Fe-Cr-Ni, 475°C embrittlement, microstructural change *(Korean)* 3−5291
- Fe-Cr-Ni embrittled alloys, aging effect, Mossbauer obs. *(Japanese)* 3−27634
- Fe-Ni alloys, hydrogen embrittlement of austeno-martensitic struct. *(French)* 3−5320
- Fe-S-Mn alloys, hot and cold brittleness, Mn conc. depend. *(French)* 3−27645
- Fe-Ta alloys, Laves phase precip. phenomena 3−37049
- Ge single crystals, slow loading effects *(Russian)* 3−30181
- Mo, fracture energy calc. based on phonon theory of brittle fracture 3−17923
- Mo, polycryst., low temp. props., surface oxidation effect 3−24896
- Mo prestraining effect on brittleness, ductility of dislocation containing specimens *(Japanese)* 3−31070
- Mo:Ti, Zr, low temp. rolling effect on ductile-brittle transition temp. *(Russian)* 3−24902
- Mo-Re alloys, effect of C 3−18663
- Nb, embrittlement at low temp. by hydride phase precip. 3−8818
- Ni and Nichrome, thoria dispersed, l.p. hydrogen gas influence on fatigue crack growth 3−39347
- Ni-Cr(50 50 wt.%) alloy, resist. to service embrittlement, high-creep strength, development 3−21636
- Pu-Ga, plastic deformation, mechanical props. influence of homogeneity *(French)* 3−34589
- Si crystals, crack propagation disclosed by X-ray Pendellosung fringes 3−17917
- Ta, electrodeposited from fused salt electrolyte 3−24362
- Ta, hydrogen embrittlement and hydride form. 3−34530

brittleness continued
- Ti alloy, TA6V, stress corrosion cracking and hydrogen embrittlement *(French)* 3−8907
- Ti alloy, TA6V6EZ, hydrogen and oxygen influence *(French)* 3−5334
- Ti alloys, cleavage cracking mechanism under loading hydrogen embrittlement 3−18653
- Ti alloys, vacuum annealing influence on struct. and mech. props. 3−24938
- Ti alloys, vacuum annealing influence on operating characts. 3−24939
- Ti-5Al-2.5Sn, gaseous hydrogen induced cracking, kinetics study 3−15704
- Ti-Al-Mn on fatigue behaviour and low strain rate embrittlement 3−24882
- Ti-Al-V alloy, β transformed, absorbed hydrogen behaviour 3−37033
- Ti-Al-V alloys, susceptibility to brittle fracture of simulated weld seams 3−24942
- Tu, hydrogen embrittlement mechanism *(French)* 3−5337
- V, hydrogen embrittlement and hydride form. 3−34530
- W, chemical vapour deposited, mech. behaviour, 800-1600°C 3−37085
- W wires, doped, recrystallisation effect on brittleness *(Japanese)* 3−31065
- Zr, hydride embrittlement behaviour 3−8909

broadcasting
- *see also radio broadcasting; television broadcasting*
- forecasting conditions rel. to solar activity effect *(German)* 3−35057

bromine
- atom, excited, gas-phase e.p.r. spectrum of $^2P_{1/2}$ state 3−1108
- dimer, collision with K_2, reactively scatt. K atoms, ang. distrib. meas. 3−29750
- electron affinity in alkali metal compound 3−1117
- inert gas-Br_2 systems, energy transfer collisions, trajectory studies of atomic recombination reactions 3−26732
- ions, response of Si surface barrier detector 3−13428
- marine atmosphere, sea salt particles as sources 3−12755
- pyrocarbon saturated with Br, temp. dependence on resistivity between 90-298 K and thermoelectric power *(French)* 3−8214
- reactions with alkaline earth metals, crossed beams chemistry 3−21803
- solid, phonn dispersion and symmetry 3−24236
- tektites, Br concentrations rel. to obsidians and impact glasses 3−16199
- Br^-, diffusion in KCl-KBr mixed crystals, 519-599°C 3−30285
- Br_2, gaseous, mol. dissoc. energies 3−20188
- Br_3^-, i.r. and Raman spectra, determ. of fundamental vibrations and splitting of bands 3−1224
- Br(I)-$H_2(D_2)$, reaction mechanism, classical dynamical study 3−37119
- in hydrocarbons, chem. effects of ^{80m}(I.T.)^{80}Br reactions 3−12541
- K-Br_2 collisions, quantization of vibrational coordinates in electron jump model 3−4392
- K_2-Br_2 collisions, quantization of vibrational coordinates in electron jump model 3−4392
- KCl:Pb, Br, X- or γ-irrad., $BrCl^-$ and associated centres, e.s.r. and optical absorpt. 3−39031
- NaCl:Br, absorpt. and luminesc. of Br^- clusters 3−21464

bromine compounds
- group IV tetrabromides, Raman spectra, 20 to 420°C, Coriolis and force const. determ. 3−29662
- BF_3, anharmonicity effects on force constants 3−20103
- $BrCL_2^-$, i.r. and Raman spectra, determ. of fundamental vibrations and splitting of bands 3−1224
- BrCN, collision with K_2, reactively scatt. K atoms, ang. distrib. meas. 3−29750
- BrCN collisions with Ba, crossed beams product angular distributions of BaCN and BaBr 3−27864
- Br_2CO, vibr. intensities, dipole moment derivatives 3−26640
- BrCl, Raman spectra, vibrational hot bands of isotopic species 3−20140
- BrF, electronic structure by photoelectron spectra 3−1161
- BrF_3, electronic structure by photoelectron spectra 3−1161
- BrF_5, mm wave spectrum, K-type doubling 3−29691
- BrHBr, computed bond energies and vibr. freq., including isotope effects 3−1181

Brownian motion
- *see also colloids*
- aerosols, particle eddy diffusivities and turbulent deposition velocities for isothermal flow and smooth surfaces 3−33298
- aerosols meas. by laser Doppler spectroscopy for particle size determ. 3−16428
- Brownian particles sedimentation in gravity and ultracentrifugal fields 3−10401
- classical spin interacting with surroundings, determ. of eqn. of motion and Fokker-Planck eqn. 3−13648
- coherent macroscopic motion from systems of Brownian particles 3−6361
- compressible and incompressible fluids, equipartition theorem 3−19516
- demonstration, using smoke cell 3−16369
- diffusion const., mol. theory of translational Stokes-Einstein relation 3−16754
- disordered systems, electronic excitation diffusion at zero temp., kinetic equations 3−18049
- electrolyte solns., liq. struct. effects on d.c. transport 3−2065
- electrons in weakly ionized plasma, effect of time-dependent magnetic fields 3−11469
- Fokker-Planck equation, retarded one-dimensional solution 3−16753
- Fokker-Planck operator, weakly-coupled, spectrum 3−16757
- glycerol:$CoSn(OH)_6$ colloidal suspension, Mossbauer study of Brownian motion, effect of ethanol and water dilution 3−5361
- harmonic oscillator with stochastic frequency 3−37897
- homogeneous isotropic, determ. of coeffs. of kinetic eqn. in linear-cubic approx. *(Russian)* 3−22750
- hydrodynamic models 3−6359
- kinetic eqns. for weak coupling motion in stationary temp. gradient 3−22746

Brownian motion continued
- molecular solution, fluorescence depolarization, computer simulation 3−26748
- Mossbauer effect of Brownian particles with axial symmetry *(Russian)* 3−12089
- nitroethane-iso-octane, diffusion coeff. of particles near critical phase transition 3−15509
- non-isothermal solid 3−1818
- nonlinear oscillators, weakly coupled, Mori's theory 3−35618
- particles of arbitrary shape, simultaneous translational and rotational motion 3−13649
- plasma oscillations, line shape, Kubo-Mori Brownian motion theory application 3−38456
- rheology of dilute suspension of dipolar spheres with weak Brownian couples 3−14508
- rodlike macromolecules dilute suspensions with Brownian motion, stress tensor for arbitrary flows 3−33172
- rotational motion, Fokker-Planck eqn. for joint probability density of orientation and ang. vel. 3−4038
- solid in stationary temp. gradient, kinetic equations 3−1817
- spherical particle in a compressible fluid 3−37896
- statistical problem of E.A. Milne, involving Brownian motion soln. 3−6350
- suspension, particles with weak Brownian rots., time-depend. shear flows 3−29911
- suspension of dipolar spherical particles in external field, rotary Brownian motion effects on rheology 3−31199
- teaching model, criticism 3−38
- velocity autocorrelation function calc., modification 3−16756
- velocity autocorrelation function calc. 3−16755
- Au epitaxial growth, influence of decoration of monatomic surface steps on crystallite mobility *(French)* 3−36495

Brownian movement *see Brownian motion*

brush discharges *see discharges (electric)*

bubble chambers
- bubble nucleation in superheated water by fission fragments, meas. of thresholds between 380 and 440°F 3−23374
- charged particle tracks, turning angles 3−19309
- computer-aided processing of bubble chamber pictures 3−6077
- dissector, for processing of photographs 3−28677
- event pattern measurement spiral reader, symposium, Stockholm (1972) 3−10072
- image plane digitizing of bubble chamber pictures by magnetostrictive wire 3−25901
- liquid hydrogen, vacuum sealing, cryogenics, low pressure 3−141
- Mirabelle, formation of beam of 70 GeV/c elastically scattered protons 3−16492
- photographs, pattern recognition, global transformation 3−6080
- recognition of events by Heidelberg automatic system 3−19306
- scanner, for chamber photographs 3−25898
- small angle deflection detection in beam track on bubble chamber photographs 3−6079
- superconductors for, Cu-stabilised, electron beam welding *(German)* 3−317
- track meas., semiautomatic machine 3−6078
- track sensitive H_2 target for 500 litre Ne-H_2 chamber 3−10071
- track sensitive target, in bubble chamber, performance 3−25850
- tracks, errors in momentum and direction considering energy loss 3−32173
- u.s., using liquid H_2, track formation 3−25896
- H, vapour bubble dynamics 3−4614
- H track sensitive target in Ne-H cryogenic bubble chamber, physics pictures 3−28639
- H_2, liquid, effect of u.s. field 3−25904
- Ne-H, operation 3−25847

bubble point *see boiling point*

bubble points *see bubbles*

bubbles
- *see also foams*
- acoustic cavitation, growth and decay *(Japanese)* 3−20364
- adiabatic gas-liquid bubble flow in convergent-divergent nozzle 3−7458
- adsorbed films, permeab. to air determ. using bubble shape theory 3−8015
- adsubble processes, foam and bubble fractionation 3−12464
- air in water, emission of harmonic and combination freq. waves 3−26830
- atm. sea salt particles, I enrichment anal. 3−12693
- boiling heat transfer mechanism rel. to growth of vapour bubbles 3−7917
- boiling two-phase channel flow patterns, and heat transfer, bubble, slug and annular flows 3−29908
- cavitation nucleus spectrum, influence on cavitation inception, scattered light counting method investigation 3−26046
- convective diffusion with chem. reaction, effect of multicomponent bubble collapse 3−7954
- dodecylamine soln., max. bubble pressure meas. of surface tension 3−5760
- dynamic growth in nucleate boiling 3−7462
- dynamics in H bubble chambers 3−4614
- electric field induced motion in KCl and NaCl rel. to impurities and X-ray irrad. *(Russian)* 3−20730
- expansion of spherical cavity in compressible liquid 3−4603
- film boiling of aqueous binary mixture with volatile component, action of vapour bubbles 3−1788
- fission fragment induced nucleation in superheated water 3−23374
- fluid flow patterns in breaking bubbles 3−11409
- fluidised bed catalytic reactors, countercurrent backmixing model, applicability to simplified solns. 3−7448
- fluidised bed reactors, two phase models which allow for bubble size variations 3−7464
- in fluidised beds, break-uo mechanism 3−26843
- fluidised beds, bubble chain coalescence 3−7460
- fluidised beds, gas transfer from bubbles to the dense phase 3−29905
- fluidised beds, two and three phase, hydrodynamics, bubble size and rising vels. 3−23782
- fluidised beds, volume changes accompanying bubble splitting 3−36124

bubbles continued
- fluidised particle trajectories about rising bubble, model 3−17552
- formation at nozzles *(German)* 3−26840
- formation at single submerged orifice under constant pressure, model 3−4613
- formation of orifice in fluidized bed 3−1477
- gas, in glass, anal. using quadrupole mass spectrometer 3−13504
- gas, in liquid subject to surface tension, collapse and expansion 3−26829
- gas fluidised beds, delayed bubbling 3−33285
- gas-liquid mixtures, bubble type supersonic flows 3−33286
- growth, by diffusion, in 11 kHz sound field 3−7401
- growth due to microlayer evaporation, influencing factors *(Japanese)* 3−24015
- growth in binary mixture at liquid solid interface 3−4611
- growth law of fast moving spherical second phase, heat and mass transfer limitations 3−24245
- heat and mass transfer in pulsed bubbling columns 3−26782
- inclusions effect on mechanical properties of cast poly-methyl metacrylate 3−27789
- inert gas bubble growth in solids, non uniform size effect 3−7744
- interactions with particles in gas fluidized bed 3−7443
- liquids, gas generation during initial stages of pulse discharge formation *(Russian)* 3−14614
- motion in liquids 3−26036
- nonspherical, dynamics 3−1444
- ocean water bubble spray, geochemistry rel. to salts in precipitation 3−12681
- particulate systems, real conc., high Reynolds number fluid dynamics and transfer processes 3−36136
- pressure fluctuations in separated flow, analysis and correlation of data 3−11395
- in quartz veins, distrib. 3−39484
- salt particles in oceanic air, transition from jet to film source of droplets 3−12692
- size distrib. in boiling water reactors 3−1069
- sodium cooled fast reactors, cover-gas bubbles in coolant, number and size determ. 3−1070
- sodium dodecyl sulphate soln., max. bubble pressure meas. of surface tension 3−5761
- spark induced cavitation bubble collapse, photographic study 3−26831
- spherical capped gas bubbles rising in aqueous media, mass transfer coefficients calc. 3−29921
- spherical-cap bubbles, wake structure, review 3−33324
- steel, stainless Type 316, obs. of He bubble growth following cyclotron implantation 3−27043
- surfactant soln., max. bubble press. meas. of surface tension 3−5761
- surfactant soln., max. bubble pressure meas. of surface tension 3−5760
- surfactant soln., surface tension meas. by mas. bubble press. method 3−5759
- temperature fluctuations of the heated surface at one active nucleation site 3−27110
- two-dimensional, in slow viscous flows, behaviour 3−36137
- u.s. cavitation research, mathematical treatments and recent progress *(Japanese)* 3−7407
- vapour, effect of air bubbles on growth and collapse near solid surface, photographic study 3−23769
- vapour bubble collapse temp. var. and collapse time at condensation 3−1420
- vapour growth patterns for bulk-liquid superheated Na at temp. greater than 10°C 3−11730
- vapour-bubble separation as function of bubble size 3−4615
- void fraction data, correl. 3−11447
- void fraction meas. by single type probe 3−20404
- in W wire, doped, temp. gradient effect on bubble growth 3−37087
- water, bubble boiling, influence of the thermal props. of the heating surface on the heat transfer *(German)* 3−33661
- water, subcooled, vapour bubble growth rate in boiling 3−27109
- Ar solid, induced by α particle source 3−30505
- H_2, liquid, bubble chamber, effect of u.s. field 3−25904
- H_2 bubble technique used for flow visualisation of planar jets 3−23804
- He at low temperatures, dielectric breakdown rel. to gas bubble formation 3−7987
- He gas, in irrad. V, nucleation and distrib. 3−33572
- N_2-Ar-O_2, equation of state prediction of bubblepoint 3−30249
- Na effervescence, maximum superheating in reactor *(Russian)* 3−11057
- UC fission-gas swelling, temp. depend., analytical evaluation 3−11066

buffer circuits
- amplifier, pH meas. application 3−35538

buffers (circuits) *see buffer circuits*

building
- *see also civil engineering*
- earthquake responses of nonlinear structures, hybrid computer simulation 3−12571

bulk density *see density*

bundling *see packaging*

Burgers vector *see dislocations*

burning *see combustion*

burnout *see combustion*

BWT *see backward-wave tubes*

C invariance
- charge-conjugator invariance violation and the isotensor current with mixed transformation props. 3−13805
- charged particle multiplicity distrib., predictions for higher moments from charge conservation constraints 3−10630
- lepton charge conservation, milliweak and superweak violation, astronomical consequences 3−6561
- lepton conservation law, possible effects of violation, Gribov-Pontekorov model *(Russian)* 3−38006
- strong interactions, C-invariant but P- and T-violating test using $\eta \rightarrow \pi\pi$ decay 3−13838
- $e^+e^- \rightarrow \mu^+\mu^-\gamma$, obs. of C-violating effects from $\gamma\gamma\gamma$ vertex 3−38042
- $e^+e^- \rightarrow \rho^0\gamma$, obs. of C-violating effects from $\rho\gamma\gamma$ vertex 3−38042

cable insulation
- *see also insulating oils*
- coaxial line, attenuation charact. rel. to permittivity and dielectric thickness *(Japanese)* 3−26107
- h.v., polyethylene for, breakdown strength determ. method for small test pieces *(German)* 3−15806
- polyethylene and polar materials, dielectric loss angle variation 3−39087
- radiation tolerance for instrumentation systems in LMFBR 3−26512

cable jointing
- encapsulation material and joint box, R&D, ECRC Capenhurst 3−1521

cables (electric)
- *see also coaxial cables; power cables; submarine cables; superconducting cables; telecommunication cables; underground cables*
- manufacturing machine, noise abatement by design analysis 3−35343
- radiation tolerance for instrumentation systems in LMFBR 3−26512
- remotely selective seismic cable variational depth controller, patent 3−39557

cadmium
- anisotropy in phonon scattering resistivity 3−7876
- atom, analytical radial orbitals, calc. method approximating Hartree-Fock solns. *(Russian)* 3−29471
- atom, extrema in generalized oscillator strengths of resonance transitions, 255 eV electron kinetic energy 3−7055
- atom, reson. excitation by slow Cd$^+$ ions *(Russian)* 3−7086
- atomic emission spectra, autoionisation resonances and configuration-mixing 3−7044
- atomic excitation transfers between 5^3D_1, 5^3D_2, 5^3D_3 excited levels, cross section detn. *(French)* 3−11143
- atomic inelastic collisions with slow alkali and alkaline earth ions 3−20065
- atomic lifetimes of isoelectronic sequences 3−17338
- atoms, charge-exchange phenomena with He ions, spectroscopic study 3−33058
- atoms and Zn$^+$ ions, atomic transition probabilities determ. 3−29479
- collisions with He$^+$, charge transfer into excited states 3−14313
- diffusion in Cu, 760-1070°C *(Russian)* 3−11756
- diffusion in Si, p-n junction formation by Cd diffusion 3−20896
- dislocation description of twin dynamic behaviour 3−20748
- electron emission, very low energy, following machining *(German)* 3−18535
- e.m. waves, l.f., spectrum and wave damping, Fermi surface 3−8216
- evaporation from discharge tube wall, Rozhdestvenskii hook method appl. 3−14619
- excited atoms in plasma, effective slow electron collision cross sections 3−17699
- Fermi surface, de Haas-van Alphen effect 3−30396
- Fermi surface changes under uniaxial compression, dHvA meas. 3−20998
- film, deposition on Ge substrate, initial stages of adsorption and clustering 3−18036
- film, deposition on Ge substrate, nucleation, growth and evaporation 3−18037
- Hookes law, deviations due to third order elastic consts. 3−17895
- ion, two electron transitions, $4d^95s^2$ to $4d^{10}5p$ config. *(Russian)* 3−33014
- isotopic effect on magnetic shielding 3−36804
- lattice dynamics, 80K, X-ray diffuse scatt. study 3−1731
- liquid, struct. microheterogeneities, kinetic viscosity, temp. depend. *(Russian)* 3−17729
- liquid, surface tension, temp. depend. 3−38710
- liquid, thermal diffn. of Ag, Zn, Sb and Tl *(Russian)* 3−1811
- magnetic field induced pseudo phase transition 3−24376
- magnetic surface states 3−8243
- magnetoelectric, magnetothermal and thermoelectric behaviour *(Russian)* 3−8154
- magnetoresistance at 78K, comparison with new theoretical predictions *(German)* 3−33876
- particles containing up to 30 atoms, molecular orbital calc. 3−27911
- phase transformations under hydrostatic press., compressibility, elec. resist. and elastic wave vel. meas. *(Russian)* 3−15013
- plasma, 5^3P_1 excited atoms in Kr, Xe, diffusion cross section investigation 3−23918
- positron trapping rate at lattice vacancies, temp. depend. 3−33550
- self-diffusion, temp. depend. activation volumes, 250-320°C, 0-8 kbar 3−30291
- size effect, radio frequency *(Russian)* 3−11847
- static nuclear quadrupole interaction produced by 247 keV level of ^{111}Cd, in-beam meas. 3−2476
- thermal resistivity anisotropy calc. using Mannari-Ziman-Baym theory 3−20840
- third harmonic generation, phase matching, v.u.v. generation 3−780
- u.s. phonons, transverse, breakdown of e.m. screening 3−24218
- vapour, equation of state for sublimation *(French)* 3−20871
- vapour, optical reson. for forbidden lines 3076 and 3261 Å *(French)* 3−7051
- vapour deposition, critical temp. of glass substrate 3−15622
- whisker and island growth on (211) Ge surface, relative growth conditions 3−11840
- X-ray L_{III} absorpt. limits, chem. combination effect 3−21497
- AgBr:Cd, ionic thermocurrents meas. rel. to interstitial-vacancy complex form. 3−33518
- Bi-Cd system, contact melting in mag. field *(Russian)* 3−15698
- CaF_2:Cd^{3+}, Pr^{3+}, Yb^{3+}, luminescence, energy transfer from Cd^{3+} to Pr^{3+} and Yb^{3+} *(Russian)* 3−36905
- Cd I, atomic lifetime meas. by the beam-foil technique 3−20013
- Cd lasing lines and possible appls. 3−22885
- Cd-He cataphoresis-laser, determ. of plasma charged-particle densities and electron temp. 3−16846
- Cd-Ne afterglow plasma, Cd(5^3P_1) and Cd(5^1P_1) atom density decay due to e-Cd collisions 3−4687
- Cd-Te detection, development and applications 3−37687
- Cd$^+$, optical pumping meas. of hyperfine structure of ground state 3−29480
- Cd$^+$ collisions with Mg$^+$, Mg ions, excitation of resonance levels 3−17377
- Cd^{2+} in NaCl crystals, diffusion from volume to surface 3−33692

cadmium continued
Cd(I), autoionising d^9s^2np level, intermediate coupling calcs. 3−7063
CdTe, electron and neutron irrad., excess, dissociative Cd pressure, defect behaviour, photoluminescence spectra 3−34431
^{107}Cd, nuclear hyperfine structure obs., orientation by optical pumping 3−11862
^{114}Cd hot cathode spectral lamp, as secondary standard, for interferometry 3−3748
GaAs:Cd epitaxial layer, near band-edge photoluminesc. 3−34406
InSb:Cd, acceptor excitation spectra, obs. of Zeeman splitting 3−24728
InSb:Cd, p-n technique 3−34489
KCl:Cd, Pb, reorientation of $Cd^{2+}(Pb^{2+})$-vacancy complex rel. to dielec. relax. 3−34293
KCl:Cd^+, X-ray irrad., e.s.r., hyperfine coupling const., g-factor, 77-300 K 3−27402

cadmium alloys
see also cadmium compounds
multicomponent impurities influence on density change during thermocyclic treatment *(Russian)* 3−8844
rare earth-Cd, phase diagram and crystal structure obs. 3−30972
Ag-Cd, dil., internally oxidized, strengthening mechanisms 3−24842
Ag-Cd, dil., partially internally oxidized, deform. and substruct. characts. 3−24841
β′ AgCd, marmem effect 3−30979
Au-Cd, thermoelastic martensite, lattice softening, ferroelasticity and shape memory effect 3−14907
Au-Cd-In, double h.c.p., liquisol quenching effect on struct. 3−34559
Au-Cd(47.5 at.%), martensitic pretransformation phenomena 3−18561
Bi-Cd, alloying effect on twinning rate of Bi *(Russian)* 3−31057
Cd-Bi, temp. and conc. dependence of mag. susceptibility 3−27362
Cd-Hg, n.m.r. of ^{113}Cd, Knight shifts, alloying depend. 3−2433
Cd-Mg, n.m.r. of ^{113}Cd, Knight shifts, alloying depend. 3−2433
Cd-Mg, superconducting transition temp. determ. 3−34020
Cd-Pb, zone refining, breakdown of regular laminations during growth *(Russian)* 3−24807
Cd-Pb dil. solns., equil. distrib. coeff. 3−21557
Cd-Sb system, crystallisation conditions influence on props. *(Russian)* 3−8769
Cd-Sn, eutectic lamellar microstructs., ripening by controlled annealing 3−12348
Cd-Sn, zone refining, breakdown of regular laminations during growth *(Russian)* 3−24807
Cd-Zn, melt growth of aligned eutectic film . 3−24802
Cd-Zn, zone refining, breakdown of regular laminations during growth *(Russian)* 3−24807
Cu-Cd, hardening effect, transmission electron microscope examination 3−4805
DyCd, CsCl type compound, field depend. of magnetisation, ferromag. model 3−36758
$Hg_{1-x}Cd_xTe$, band structure and charge density calcs. using representative k points 3−18080
In-Cd, superconductivity and hysteresis 3−34009
In-Cd, superconductivity and hysteresis, secondary properties 3−34010
La-Cd, phase diagram 3−21567
Mg-Cd, temp. and concentration depend. of electrical resistivity, phase diagrams *(German)* 3−34551
Mg_3Cd, stoichiometric, thermodynamic description of ordering process 3−21574
Na-Cd, crystal structure obs. for $NaCd_2$, Na_2Cd_{11} samples 3−24062
Na-Cd dilute alloys, state of Cd impurities, temp. dep. of elec. resistivity 3−33868
Pb-Cd, single crystals, plasticity in superconducting and normal states at 4.2 K 3−36353
Pb-Cd eutectic; Sn interface instability 3−39309
Pb-Sn-Cd, eutectic, anomalous structures 3−37005
Zn-Cd dil. solns., equil. distrib. coeff. 3−21557
ZnCdS pellets, electroluminesc. and stimulated conductivity study *(Russian)* 3−21492
$Zn_xCd_{1-x}Te$ solid solution, evaporation, vapour composition determ. and X-ray phase analysis *(Russian)* 3−11734

cadmium compounds
see also cadmium alloys
L-aspartatocadmium (II) trihydrate, neutron anomalous dispersion, phase ambiguity resolved by tangent formula 3−23985
dimethyl cadmium, vibrational spectra 3−38295
electron-phonon interaction, far i.r. cyclotron resonance absorption 3−36388
ethylxanthate, cryst. struct. 3−14830
fluorescent particle atm. tracer, possible toxicity hazard 3−39819
nuclear quadrupole interactions of ^{117}In, ^{111}Cd excited states 3−12085
picosecond light pulses *(Russian)* 3−2517
rare earth chalcogenide spinels, crystallographic, magnetic and electrical properties 3−7685
scheelite type cryst. containing Pr^{3+}, line broadening and vibr. spectra study 3−15526
tartrate pentahydrate, cell parameters, space group 3−4743
Al-SiO-CdSe system, semicond. insulator interface state density control 3−15268
CDS, Debye charact. temp., rel. to lattice oscillation spectra *(Russian)* 3−24221
$(Cd,Te)_{1-x}(AlSb)_x$ solid solutions, optical absorption edge, coefficient, photoelectric method, band structure 3−34376
Cd dihalide complexes with pyridine, pyrazine, dioxan and aniline, stretching mode assignments from i.r. and Raman spectra 3−11262
Cd-Ln_2-S_4, ternary sulphides, prep., elec. and opt. props. 3−39243
Cd-Te system, phase equilibrium diagram, calc. of liquidus line *(Russian)* 3−14963
$CdAs_2$ melt, DTA method for evaluation of glass-forming tendency 3−1575
Cd_3As_2, resistivity and Hall effect under high press. 3−27272
$Cd_3B_7O_{13}Cl(Br)(I)$, growth by chem. transport reaction, effect of different growth conditions *(Russian)* 3−15606
$CdBr_2$, lattice vibrations, i.r. and Raman spectra 3−30813

cadmium compounds continued
$CdCO_3$-kaolinite, reactions up to 1000°C 3−15754
$CdCl_2$, lattice vibrations, i.r. and Raman spectra 3−30813
$CdCl_2$, thermal conductivity 3−20843
$CdCl_2$ molten binary mixtures with KCl, $PbCl_2$, $SnCl_2$, and CdO, minima of absorption edge frequencies 3−2558
$Cd_{1-x}Co_xFe_2O_4$, paramag. region, elec. field gradients, Mossbauer obs. 3−34268
$CdCrS_4$:In photoluminescence spectra, emission and excitation, single crystals 3−36935
$CdCr_2S_4$, anomalies in mag. anisotropy and f.m.r. linewidth due to impurities 3−21318
$CdCr_2S_4$, closed tube vapour transport conditions, cryst. perfection 3−12244
$CdCr_2S_4$, critical broadening of e.p.r. line near Curie point 3−21294
$CdCr_2S_4$, exchange interactions rel. to e.p.r. and mag. susceptibility 3−21314
$CdCr_2S_4$, ferromag. semicond., heat treatment in sulphur atmosphere, variation of Curie constant and temp. 3−30621
$CdCr_2S_4$, photoconductivity and luminescence caused by band-band and band-to-band and Cr^{3+} crystal field absorptions 3−8222
$CdCr_3S_4$ single crystals gas transport and characterisation *(German)* 3−8730
n-$CdCr_2S_4(Se_4)$:Ga, cond. min. and negative magnetoresist. 3−27267
$CdCr_2Se_4$, exchange interactions rel. to e.p.r. and mag. susceptibility 3−21314
$CdCr_2Se_4$, ferromag. reson., photocond., and permeability 3−5033
$CdCr_2Se_4$, Ferromag. semicond., high-field transport props. above Curie temp. 3−5017
$CdCr_2Se_4$, mag. semicond., conductivity switching effects 3−33967
$CdCr_2Se_4$, production and properties *(Russian)* 3−14811
$CdCr_2Se_4$, refl., mag. ordering effect of low freq. i.r.-active phonon 3−15492
$CdCr_2Se_4$, transport props. of non-degenerate ferromagnetic semiconductor below Curie temp. 3−15205
CdF_2, ^{19}F chem. shift tensor and nonionic bonding 3−12070
CdF_2, changes in real structure due to compressive impact 3−33503
CdF_2, cooperative luminesc. of Yb^{3+} and Er^{3+} *(French)* 3−30855
CdF_2, insulating to semicond. transition rel. to lattice defect statistical thermodynamics 3−4947
CdF_2:$^{169}YbF_3$, Stockbarger technique growth, optical props. of radioactive and nonradioactive samples 3−2664
CdF_2:Er^{3+}, i.r. quantum counter, optical parameters for Er^{3+} sites of $C_{2v}(C_{3v})$ symmetry 3−35397
CdF_2:Fe, point defects, Mossbauer and mag. investigation 3−39063
CdF_2:Gd^{3+}, e.p.r., fluorine superhyperfine struct. 3−18363
CdF_2:Gd^{3+}, spin lattice interactions 3−8429
CdF_2:Gd^{3+}. orthorhombic ESR spectra 3−30690
CdF_2:In, semiconductor, optical absorpt. and elec. cond. meas. 3−21448
CdF_2:In^{3+}, semicond., resonance Raman spectra 3−36871
CdF_2:Mn^{2+}, ligand ENDOR obs. for F and Cd lattice nuclei 3−18394
CdF_2:$Na^+(La^{3+})$, F self diffusion, depend. on doping 3−7972
CdF_2:Pr^{3+}. line structure obs. in cathodoluminescence spectrum 3−30885
CdF_2-MF_2 systems, M=alkaline earth metal, comparative study *(French)* 3−14978
CdF_3:Er^{3+}, C_{3v} local-site symmetry from correlated e.p.r. and optical obs. 3−21305
$CdGa_2S_4$:Mn^{2+}, e.p.r. spectra meas., spin Hamiltonian description, g-values hyperfine constants, covalent bonding effect 3−12059
$CdGa_2S(Se)_4$, refl. spectra obs. in polarized light 3−8604
$CdGa_2Se_4$ photoconductivity, steady state thermally stimulated, single crystals, trapping, recombination, photoluminescence 3−33953
$CdGa_2Se_4$:Mn^{2+}, e.p.r. spectra meas., spin Hamiltonian description, g-values hyperfine constants, covalent bonding effect 3−12059
n-$CdGeAs_2$, magnetoresist., temp. and mag. field depend. *(Russian)* 3−2112
$CdGeAs_2$, phase matching, second and third harmonic generation 3−782
$CdGeAs_2$, solution growth using Bi as solvent 3−12286
Cd_2GeO_4, $Cd_3Ge_3O_9$, $Cd_5Ge_2O_9$, crystal structure *(Russian)* 3−17745
$Cd(H_2PO_2)_2$, radiocrystallographic and i.r. spectroscopic obs. *(French)* 3−7700
$CdHg(SCN)_4$, gel growth of single crysts. 3−34470
$Cd_xHg_{1-x}(SCN)_2$, gel growth 3−15611
$Cd_xHg_{1-x}Te$, anomalous temp. dependence of Hall coefficient 3−24458
$Cd_xHg_{1-x}Te$, electron mobility anomalous temp. depend. 3−2095
$Cd_xHg_{1-x}Te$, electroreflectance meas. rel. to alloy comp. and band structure 3−12114
$Cd_xHg_{1-x}Te$, films, elec. cond. *(Russian)* 3−24433
$Cd_xHg_{1-x}Te$, hot electron interaction with phonons rel. to photocond. oscillations 3−18159
$Cd_xHg_{1-x}Te$, mag. susceptibility temp. depend. 3−8339
$Cd_xHg_{1-x}Te$, refl., comp. and electron density depend., rel. to band struct. *(Russian)* 3−2548
$Cd_xHg_{1-x}Te$, spin effects on Shubnikov-de Haas oscillations, semimetal-semicond. transition 3−33795
$Cd_xHg_{1-x}Te$ film, sputtering in Hg vapour plasma 3−8727
$Cd_xHg_{1-x}Te$ magnetoresistance, Shubnikov-de Haas oscillations, 77-120K 3−36628
$Cd_xHg_{1-x}Te$ monocrysts., comp. distrib. from absorpt. spectrum *(Russian)* 3−12158
CdI_2, arcing of X-ray diffr. spots in X-ray photographs 3−23973
CdI_2, far i.r. lattice vibr. spectrum 3−2544
CdI_2, polytype growth by cleavage 3−7643
CdI_2, polytypic struct. series, layer transposition mechanism, struct. geometrical schemes 3−7719
CdI_2 and $CdI_2(Pb)$, trapping centre characts., thermoluminescence *(Russian)* 3−34437
CdI_2 X-ray diffraction spots, streaking and arcing, c-axis oscillation photographs, stacking faults and tilt boundaries 3−38521
$CdIn_{2(1-x)}Cr_{2x}S_4$, mag. susceptibility, Hall effect and elec. resistivity meas. 3−2263
$Cd_{1-x}In_xCr_2Se_4$, ferromag. semicond., transport props. 3−33881

cadmium compounds continued

- $CdIn_2S_4$, band struct. calc. on symmetry lines by empirical-pseudo-potential method 3−8101
- $CdIn_2S_4$ single crystal, DC cond., Hall effect and magnetoresist. meas. 3−33894
- $CdIn_2S_4:Fe^{2+}$, effect of weak Jahn-Teller coupling 3−21455
- $CdIn_2Se_{4x}Te_{4(1-x)}$, solid soln., forbidden zone width from absorpt. and Hall coeff. meas. *(Russian)* 3−15126
- $CdIn_2Te_4$, thin films electronmicroscopic and electron diffraction investigations *(Russian)* 3−30371
- CdM_2O_4, (M=Rh, Mn, V, Fe, Cr), interionic metal-oxygen distances, formulae *(Russian)* 3−17784
- $CdMoO_4$, ultrasonic technique for meas. of photoelastic coeff. absolute sign 3−28462
- $Cd(NH_3)_2.Ni(CN)_4.2C_6H_6:Cu^{2+}$, e.s.r. of isolated ions and exchange coupled pairs 3−39018
- $CdNaAsO_4$, crystal structure obs. *(French)* 3−30101
- $CdNaPO_4$, crystal structure obs. *(French)* 3−30101
- $CdNb_2O_6$, X-ray K-absorpt. edge of Nb 3−27584
- $Cd_{1-x}Ni_xFe_2O_4$, paramag. region, elec. field gradients, Mossbauer obs. 3−34268
- CdO, APW calc. of band structure, depend. on ionicity degree 3−30406
- CdO, anal. of vapour growth conditions rel. to surface and vol. supersaturation *(Russian)* 3−15617
- CdO, crystal growth by sublimation 3−2636
- CdO, high temp. elec. cond. and Hall effect 3−2080
- CdO, vapour growth, growth conditions effect on structure and morphology *(Russian)* 3−15616
- CdO film, band struct., optical props. 3−15134
- CdO single crystal, degenerate semicond., vapour phase growth and electrical props. 3−2087
- $CdO-Cr_2O_3-Al_2O_3$ phase relations and optical studies 3−5385
- $CdO-GeO_2-Na_2O-H_2O$ system, crystallisation under hydrothermal conditions at constant temperature 3−33508
- CdO-NaCl heterojunction, colour centres *(Russian)* 3−8627
- CdO(S)(Se)(Te), far u.v. refl. and correl. with Penn-Phillips gap 3−39158
- n- and p-CdP_2, impurity photolum. *(Russian)* 3−8658
- $Cd_3P_2:Cu$, deep impurity levels, effect on optical props. 3−30794
- $Cd(PO_3)_2$, orthorhombic, cryst. struct. *(French)* 3−11591
- $Cd_5(PO_4)_3Cl$, twinned, crystal structure obs. 3−38556
- $Cd_5(PO_4)_3Cl$, twinning rel. to structural detail 3−36275
- $Cd_2PO_4F:Mn$, Mn activated luminescence 3−2586
- $Cd_3(P_3O_9)_2.14H_2O$, cryst. data 3−7724
- CdS, acoustoelec. domains, piezoelec. potential and carrier distrib., microwave absorpt. and Brillouin scatt. 3−5040
- CdS, acoustoelec. gain and lattice attenuation, Brillouin scatt. obs. 3−33961
- CdS, acoustoelec. multi-peak domain propag., Brillouin scatt. study 3−24481
- CdS, acoustoelectric effects in homogeneous crystals with trapping centres 3−24482
- CdS, acoustoelectric effect, by Brillouin scattering *(German)* 3−30521
- CdS, adsorbent, adsorption kinetics of polar polymers 3−36486
- CdS, angular dispersion effects in acoustoelectric interaction 3−30522
- CdS, antistokes exciton luminesc. study *(Russian)* 3−27536
- CdS, birefringence, uniaxial stress depend., room temp., 0.1-2.3 eV 3−15511
- CdS, Brillouin scatt. by propag. acoustoelec. domains 3−33960
- CdS, Brillouin scatt. from acoustoelectrically amplified flux domains, dispersion spectrum 3−34352
- CdS, CdSe, heat treated epitaxial films, structure, composition, photoelec. props. *(Russian)* 3−33948
- CdS, contamination of heteroepitaxial layers vapour grown on GaAs substrates 3−2653
- CdS, cubic, electron density, potential distribution *(Russian)* 3−30085
- CdS, curent fluctuations under sound amplification conditions *(Russian)* 3−2144
- n- CdS, deviations from Ohm's law at 77 K 3−30485
- CdS, dielec. relax. time exceeding minority carrier diffusions lifetime, evidence from photocond. meas. 3−30756
- CdS, diffusion of noble metals, 300-800°C, u.s. study 3−30286
- CdS, dispersion of birefringence *(Russian)* 3−2511
- CdS, dispersion of Raman cross section over wide energy range 3−36872
- CdS, elec. field induced Raman scattering 3−21407
- CdS, electroluminesc. from controlled splits 3−24746
- CdS, electron field emission, energy distrib. 3−36980
- CdS, electron irrad., Cd displacement threshold at liq. He temp., cathodoluminesc. obs. 3−5247
- CdS, electron traps distribution *(Japanese)* 3−18183
- CdS, electron-phonon interactions, first principles energy band calcs. 3−36535
- CdS, exciton gas degeneracy after single photon excitation *(Russian)* 3−11870
- CdS, exciton luminesc. spectra obs. for free exciton lifetime 3−8659
- CdS, exciton luminescence and photoconductivity at high densities of excitation *(Russian)* 3−27531
- CdS, field emission under pulse conditions, periodicity effect 3−27599
- CdS, green edge luminesc. rel. to exciton emission, 20.4K *(Russian)* 3−21482
- CdS, Hall and thermoelec. effects under thermal equilib. conditions 3−18172
- CdS, high carrier and exciton conc., low temp. emission recomb. study *(Russian)* 3−27541
- CdS, hot-pressed, low temp. thermal conductivity 3−1848
- CdS, in $Cu-Cu_2S-CdS-Au$ sandwich struct., switching and filament migration obs. 3−2150
- CdS, interface reactions rel. to growth by spontaneous nucleation 3−2645
- CdS, isoelectronic Ni impurity, absorpt. spectra *(Russian)* 3−8618
- CdS, LA-phonon exciton interaction, luminesc. study *(Russian)* 3−36916
- CdS, laser pulse duration control, nonlinear absorption *(Russian)* 3−215

cadmium compounds continued

- CdS, luminesc. line shape due to elastic collision of anisotropic excitonic molecules 3−24738
- CdS, luminescence from impurities and fast neutron radiation defects 3−5224
- CdS, new luminesc. line due to inelastic collision of excitonic molecules 3−24739
- CdS, noncollinear, parametric 4-photon interaction 3−10572
- CdS, nonlinear interaction of Bleustein-Gulyaev waves 3−8004
- CdS, oxygen photodesorption, influence of nonequilib. minority carriers 3−15210
- CdS, photocond., acoustoelectric aftercurrent obs. 3−2129
- CdS, photocond., i.r. quenching, spectral response 3−18189
- CdS, photocond. and stimulated emission under intense electron beam excitation 3−8223
- CdS, photoconductive, current instability due to elastic surface waves 3−34297
- CdS, photoconductive, harmonic conversion of acoustoelectrically amplified phonons 3−2141
- CdS, photocurrent, saturation and acoustoelectric oscillations *(Russian)* 3−11930
- CdS, photoelectron spectral response, surface recomb. layer thickness 3−18525
- CdS, photoluminescence at high exciton densities at 4.2K 3−39184
- CdS, photosensitive, modulation of absorption by field effect 3−24679
- CdS, piezoelectric scattering anisotropy *(Russian)* 3−2078
- CdS, polarity of bending strength and photoplastic effect 3−1669
- CdS, recomb. waves induced by optical quenching 3−38866
- CdS, refl. phase spectrum in exciton region at 4.2 K 3−15517
- CdS, relax. time and cathodolum. efficiency *(Russian)* 3−5237
- CdS, spin orientation by optical pumping 3−2594
- CdS, subharmonic generation of surface and bulk acoustic waves at high pump amplitudes 3−1869
- CdS, thin wafers, piezoelec. modulation of surface charges on bending 3−2161
- CdS, topochemical conversion, Cu_2S single cryst. prep. 3−18540
- CdS, transverse acoustoelec. effect 3−33965
- CdS, two step current saturation on application of high voltage pulse and illumination 3−8195
- CdS, two-photon interband transitions, joint matrix element 3−34337
- CdS, u.s absorpt. and velocity, transport theory *(Russian)* 3−1704
- CdS, u.v. excited at 4.2K, recomb. processes in stimulated emission 3−15523
- CdS, X-ray atomic scattering factors, electronic structure, correl. atoms, crystal *(Russian)* 3−33625
- CdS acoustoelectric platelet oscillators, current saturation rel. to illum. 3−11936
- CdS and CdTe, refractive indices in far i.r. 3−32592
- CdS and glass multilayer film, light-intensity modulation 3−12198
- CdS coating on $LiNbO_3$ piezoelec. crystal, Rayleigh acoustic surface wave amplification and dispersion, calc. 3−11794
- CdS conduction band effective mass anisotropy rel. to uniaxial compression *(Russian)* 3−15137
- CdS crystal growth from melt using induction furnace 3−15630
- CdS crystals, d.c. and microwave-biased photoconductive response at 22 GHz 3−15221
- CdS crystals, X-ray wide angle diagrams with anomalous weak absorption *(German)* 3−7597
- CdS film, bulk compensation effect on chemisorption dependent semiconductivity 3−33889
- CdS film, cubic forms in surface morphology *(Russian)* 3−30376
- CdS film, evaporated, in m.i.s. struct. with SiO_2, positive flat band voltage obs. 3−5058
- CdS film, evaporated, resist. and Hall mobility rel. to prep. conditions 3−27322
- CdS film, photocond., effect of cryst. struct. after recrystn. 3−15226
- CdS film, polycryst., elec. cond., ambient O_2 depend. 3−8185
- CdS films, photoconductivity *(Russian)* 3−24474
- CdS films on Ge, epitaxial growth and struct. 3−36493
- CdS monocrystals, cathodoluminescence, investigation using electron microprobe scanning technique *(German)* 3−8674
- CdS needles and platelets, growth mechanism 3−11574
- CdS phosphors, Mossbauer spectrum measurements *(Russian)* 3−27448
- CdS platelets, acoustoelectric effects 3−33727
- CdS platelets, growth mechanisms and morphology 3−2635
- CdS single crystal, persistent internal polarisation variation with illumination intensity 3−34289
- CdS single crystals, electric field effect on optical quenching 3−15223
- CdS surface photovoltage spectroscopy 3−37714
- CdS thermal, acoustoelectrically interacting and built-up phonon studies by laser Brillouin scattering 3−1749
- CdS thin film, acoustoresistance, surface acoustic wave 3−38872
- CdS thin film, structural defects and epitaxial growth 3−18032
- CdS thin film formation by reactive sputtering with sublimated vapours *(Japanese)* 3−34475
- CdS thin films, shallow trapping levels, structure defects, photoconductivity relaxation 3−33833
- CdS thin films, textures, oblique, growth electron bombardment evaporation, reflection electron diffraction study 3−38758
- CdS type crystal, spontaneously polarised semicond. electrical cond. anisotropy 3−39110
- CdS with adsorbed dyes, spectral sensitization 3−27906
- CdS:Be, i.r. absorpt. due to localized vibr. mode 3−27523
- $CdS:Ce^{3+}$, Ag, Cu fluorescence spectra, probability of emission calc. *(Russian)* 3−27546
- $CdS:Cu^{2+}$, photosensitive e.s.r. spectra of Cu^{2+} impurity ions 3−2357
- CdS:Li single crystals, doped and undoped, photoluminescent props. at low temps., effects of doping and heat treatment *(Japanese)* 3−8656
- CdS:Li(Na)(Ag), furnace doping, rel. to bound exciton spectra 3−12184
- $CdS:Ni^{2+}$ absorpt. spectrum obs. of linear Stark effect 3−8625
- CdS:S system as photoelectret electrophotographic layer, photopolarisation study 3−36833

cadmium compounds continued
CdS:Te, piezoemission study 3−18492
CdS/Cu$_2$S solar cell, band model 3−4946
CdS-CdTe system, mutual solubility *(Russian)* 3−24273
CdS-Cu contact, elec. and photoelec. props. 3−8265
CdS-Cu$_{2-x}$S polycryst. heterojunction, coord. sensitive photocell 3−15242
CdS-Cu$_{2-x}$S heterojunctions, impurity photoeffect 3−27309
CdS-CuGaS$_2$ n-p diode, green electrolum. 3−39188
CdS-M^{I}M^{III}S$_2$, (M^I=Ag, Cu, M^{III}=Al, Ga, In), prep. and phase relations, mutual solid solubility regions 3−33678
CdS-metal contact at high current densities 3−21149
CdS-PVK, internal photoemission of holes 3−18217
(CdS)$_{3x}$-(In$_x$S$_3$)$_{1-x}$, optical and photocond. props. rel. to band structure 3−18085
CdS(Se) laser, pumping using pulsed elec. discharge in vacuum 3−37971
CdS$_{1-x}$Se$_x$, electro-absorption reduced effective mass 3−15471
CdS$_{1-x}$Se$_x$ film, photocond., effect of cryst. struct. after recrystn. 3−15226
CdS$_x$Se$_{1-x}$, epitaxial, growth of graded gap crystal layer, luminesc. obs. 3−8053
CdS$_x$Se$_{1-x}$, peculiarities of reflection spectra in exciton absorption region *(Russian)* 3−34381
CdS(Se)(Te) film, on amorphous substrate, conditions of formation of stable and metastable structs. *(Russian)* 3−15101
CdS; bound exciton form. kinetics 3−8133
n-CdSb, anisotropy factor rel. to surface states, absorpt. effects *(Russian)* 3−8246
p-CdSb, elec. cond. and Hall coeff., rel. to technology applic. *(Russian)* 3−24430
n-CdSb, photoresistors, recombination centres governing high sensitivity *(Russian)* 3−24476
CdSe, Bose condensation of excitonic molecules, luminesc. obs. 3−30437
CdSe, electroluminesc. from controlled splits 3−24746
CdSe, electrophyscial props., influence of growth conditions 3−24428
CdSe, films, structure and electrical resistance, electron microscope examination *(Russian)* 3−38752
CdSe, impact ionisation, breakdown, photoinduced switching, meas. of cond., Hall coeff., mobility, 4.2-300K 3−30487
CdSe, luminesc. line shape due to elastic collision of anisotropic excitonic molecules 3−24738
CdSe, luminescence from impurities and fast neutron radiation defects 3−5224
CdSe, new luminesc. line due to inelastic collision of excitonic molecules 3−24739
CdSe, photocurrent, saturation and acoustoelectric oscillations *(Russian)* 3−11930
n-CdSe, shallow donor states, cyclotron reson., Zeeman splitting, cond. electrons effective masses 3−2026
CdSe, vapour deposition, critical temp. of glass substrate 3−15622
CdSe, X-irrad., traps, photocond. study 3−30426
CdSe at low temps., S-type negative resistance due to electron scattering by ionised impurity pairs 3−33911
CdSe barrier in supercond. tunnel junction, photosensitivity 3−36688
CdSe coating on LiNbO$_3$ piezoelec. crystal, Rayleigh acoustic surface wave amplification and dispersion, calc. 3−11794
CdSe crystal growth on SiO$_2$ seed plate at 1225°C 3−15614
CdSe electron scattering mechanism, Hall effect measurements 3−30466
CdSe epitaxial film, electrodispersion and electroabsorpt. spectra obs. 3−30801
CdSe film, acoustoelectric effect as cause of current saturation *(German)* 3−15228
CdSe film, polycryst., elec. props., field effect, capacitance and C-V characts. obs. 3−15279
CdSe film, surface elec. props., surface doping effects *(Russian)* 3−2192
CdSe film, with Schottky barriers as contacts, photoconductive gain greater than one 3−21107
CdSe laser pulse duration control, nonlinear absorption *(Russian)* 3−215
CdSe layers on Y-Z-LiNbO$_3$ substrate, piezoelec. coupling of Rayleigh acoustic surface waves 3−30761
CdSe single crystals, memory props. 3−24484
CdSe single crystals self-diffusion of Cd and Se investigation 3−33689
CdSe thin film deposition, nucleation conditions, molecular cloud vapour density *(German)* 3−38757
CdSe thin film formation by reactive sputtering with sublimated vapours *(Japanese)* 3−34475
CdSe vapour phase epitaxial growth on sapphire substrate, growth conditions 3−30362
CdSe:Be, i.r. absorpt. due to localized vibr. mode 3−27523
CdSe:Co, degenerate discrete excited states, absorpt. and photocond. spectra obs. 3−2024
CdSe:Cu,In and undoped, high temp. defect equilibria 3−7745
CdSe:Ni, degenerate discrete excited states, absorpt. and photocond. spectra obs. 3−2024
CdSe-CdTe thin films, solid solns., comp. and elec. charact. depend. on method of deposition 3−33762
CdSe-Dy$_2$O$_3$ thin-film structure, elec. and interface props. 3−15265
CdSe-DyO$_3$ film struct., elec. props. 3−27312
CdSe-electrolyte interface, current multiplication noise *(Russian)* 3−5051
CdSe-PVK, internal photoemission of holes 3−18217
CdSe-Si$_x$O$_y$ film struct., elec. props. 3−27312
CdSe-ZnSe solid solution, identity periods and mean-square displacements of ions *(Russian)* 3−4739
CdSe$_x$Te$_{1-x}$ solid solution, evaporation, vapour composition determ. and X-ray phase analysis *(Russian)* 3−11734
n-CdSiP$_2$, majority carrier trapping, trap parameters, photocurrent obs., 100-400 K *(Russian)* 3−21082
CdSiP$_2$, melting and soln. growth, optical absorpt. meas. *(Japanese)* 3−12146
CdSiP$_2$, pure and doped crystal, long wavelength fund. absorpt. edge 3−39163

cadmium compounds continued
CdSnAs$_2$, point defects, heat treatment effects, elec. props. study *(Russian)* 3−14853
Cd$_x$Sr$_{1-x}$O, reflection spectra, calc. of optical consts. and LO-mode freq. 3−2547
CdTe, amorphous, optical props. 3−2526
CdTe, amorphous, struct. and elec. cond. 3−1942
CdTe, cathodoluminescence from lattice defect centres, quenching mechanism 3−15561
CdTe, crit. pt. determ of band structure, thermoreflectance study 3−2005
CdTe, defect struct., transmission electron microscope obs. 3−17830
CdTe, edge emission spectra, electron irrad. effects 3−18488
CdTe, elastic consts. and thermal expansion, 4.2-300 K 3−30170
CdTe, elec. cond., high temp. relax. *(Russian)* 3−2071
CdTe, electron and neutron irrad., defect behaviour, photoluminescence spectra, excess, dissociative Cd pressure 3−34431
CdTe, electron diffusion, applied field depend., Monte Carlo study 3−18149
CdTe, growth by chem. transport in Cd-Te-H-Cl-N system 3−34472
CdTe, growth from Te rich soln., from 480°C to 750°C 3−11567
CdTe, γ-ray and X-ray detectors, current evaluation and potential application 3−19304
CdTe, high power i.r. laser window materials, state-of-the-art review 3−5980
CdTe, hole mobility, Poole-Frenkel effect, 130-430K, 5-50kV/cm 3−21086
CdTe, hot pressing 3−27742
CdTe, hot pressing for high power laser windows at 10.6 μm 3−5983
CdTe, impurities, high temp. elec. cond. study *(Russian)* 3−27031
CdTe, investigation of doubly charged acceptors 3−24478
CdTe, modified Bridgman growth for high power laser windows at 10.6 μm, optical properties 3−5984
CdTe, Monte Carlo calcs. on high field electron transport 3−8191
CdTe, photoluminescence, lattice defect investigation with use of heat treatment, neutron and electron irradiation *(Russian)* 3−27550
CdTe, physical vapour deposition for high power laser windows at 10.6 μm 3−9960
CdTe, second harmonic generation, nonlinear susceptibility, at 28.0 μ by comparison with Te 3−19637
n-CdTe, shallow donor states, cyclotron reson., Zeeman splitting, cond. electrons effective masses 3−2026
CdTe, sonic casting for high power laser windows at 10.6 μm 3−5982
CdTe, thin films, photovoltaic effect dep. on mech. stress *(Russian)* 3−30518
CdTe, vacuum deposited film, mech. strain meas. as function of growth conditions 3−4939
CdTe, X-ray diffuse scatt. to observe dispersion curves of phonons *(Russian)* 3−7892
CdTe compensated doped crystals, density of states tails, conductivity, Hall mobility, conduction band 3−33832
CdTe detector, γ-ray efficiency 3−28658
CdTe detector probes, application in clinical environment 3−32142
CdTe detectors, rate of ionisation loss and intrinsic resolution 3−37683
n-CdTe films, cond., trap and free carrier density, Fermi level position *(French)* 3−27262
CdTe films, photoelectric properties *(Russian)* 3−24475
CdTe films, structure of complex particles in condensate islets 3−33760
CdTe γ-ray spectrometer, for nondestructive analysis of nuclear fuels 3−32198
CdTe low resistivity films, d.c. e.m.f. in a.c. fields *(Russian)* 3−11964
CdTe monocrystals, undoped and doped with Na, As, preparation by direct solidification, electrical properties *(Czech)* 3−21061
CdTe nucleonic system, for fuel gauging 3−32143
CdTe p-n junctions, photomagnetic effect, general relationships 3−33990
CdTe recrystallized thin films, exciton-phonon interaction *(Russian)* 3−11871
CdTe valence band structure investigations near gamma point 3−36531
n- CdTe with Au rectifying contacts, elec. props. meas. 3−18216
CdTe:Cd, thin films, electrical conductivity *(Russian)* 3−33891
CdTe:Cd oblique deposited films, rectification effect *(Russian)* 3−33936
CdTe:Cd thin films, V-A characteristics, anisotropy *(Russian)* 3−33892
CdTe:Cu single cryst. prep. and characteriz. 3−15632
CdTe:Fe, Hall effect and photocond. meas. rel. to impurity absorption 3−15531
CdTe:In, absorption band edge of compensated crystals 3−24717
CdTe:Ti, degenerate discrete excited states, absorpt. and photocond. spectra obs. 3−2024
CdTe:V, degenerate discrete excited states, absorpt. and photocond. spectra obs. 3−2024
CdTe-InAs solid solutions, absorption band structure from absorption spectra 3−24383
Cu$_2$S-CdS single crystal cell, optical degradation and thermal restoration 3−5034
Cu$_x$S-CdS solar cell, surface potential local distribution 3−5035
HgTe-CdTe, narrow bandgap semiconductor, zero bandgap transition 3−38800
KCl-CdCl$_2$, precip. of solid soln., light scatt. obs. 3−33541
Mg$_3$Cd and MgCd, Young's modulus, temp. changes proportional to long-range order *(Russian)* 3−7809
(NH$_4$)$_2$Cd$_2$(SO$_4$)$_3$, dielec., optical and domain props. 3−24662
Na$_2$O-CdO-GeO$_2$-H$_2$O system, hydrothermal crystallisation *(Russian)* 3−17745
Ni$_x$Cd$_{1-x}$Fe$_2$O$_4$, temp. dependence of intensity of resonance field, line width due to resonant damping and g-factors' 20-360°C *(Russian)* 3−12064
PbS-CdS system, obs. of phase equilibrium diagram *(French)* 3−20851
SrO-CdO-V$_2$O$_5$, phase equilibria detn. from DTA data, quenching and solid-state react. expts. 3−18690

cadmium compounds continued

- (Zn, Cd)S-Cu phosphors, long wave photolum. rel. to CdS conc. and temp., −150°C to 200°C 3−27526
- (Zn,Cd)S-Cu phosphor, short wave emission spectra rel. to CdS conc., -150°-70°C 3−21458
- Zn_3As_2, crystals, growth from Cd_3As_2 3−8758
- ZnS-CdS phosphors, activation by Cu diffusion at low temperature *(Russian)* 3−36943
- ZnTe−CdS heterojunction light emitting diodes 3−2659

caesium

- abundance, isotopic, in ^{238}U fast fission spectrum 3−17269
- adsorbed layer on Si single crystal surface, heat of evaporation and ionization coeff. of atoms and ions 3−15069
- adsorption on GaAs (110) surface, 77-450 K 3−20941
- adsorption on Si, prod. of surface negative electron affinity 3−30536
- adsorption on W(100) surface, variation of work function *(French)* 3−27300
- atom, 6^2P reson. levels, photoionisation by 488 nm light 3−23486
- atom, $8^2P_{1/2}$ ionizing transitions in a low temperature plasma *(Russian)* 3−11160
- atom, electron momentum-transfer cross section 3−4386
- atom, highly excited D and F levels, hyperfine struct. 3−38221
- atom, optical doublet lines, circular polarization considerations 3−16430
- atomic beam, reson. multiphoton ionisation by Nd-glass laser 3−23489
- atoms near resonant charge transfer collisions with He^+, long-range forces effect 3−35976
- autoionising states, wave functions, energies, Hartree method *(Russian)* 3−26580
- boiling under free convection, heat transfer crisis 3−24256
- compressibility from Fermi surface cross section press. depend. 3−33778
- condensation of vapour in Ar flow 3−1345
- elastic constants, second and third order, calc. 3−27050
- electron impact excitation of autoionizing level 3−35972
- electron ionisation by impact, 6s and 5p, cross-sections, Born approximation, threshold, Hartree method *(Russian)* 3−26598
- gaseous diagnostics, tuned GaAs laser diode 3−4670
- ion bombardment influence on n-Si and p-Si single crystal secondary electron emission 3−21506
- ion bombardment of metal and semiconductor targets, meas. of electron and photon spectra 3−12203
- ion plasma, departures from thermodynamic equilib., collisional-radiative mechanisms *(French)* 3−20419
- ion range in Ni rel. to preliminary low-energy bombardment 3−14901
- Knight shift, press. effect, calc. by KKR method 3−36806
- lamp, high press., pulsed i.r. source 3−5938
- liquid, absolute thermoelectric power and electrical conductivity in metal-nonmetal transition range 3−27247
- liquid, density and thermal expansion to 1300°C 3−4859
- liquid, electronic density of states calc. differs from free electron model 3−18054
- liquid, phonon freq. and elec. resist. calcs. using optimised model potential 3−20828
- liquid, pseudopotential form. factor rel. to elec. resist. and thermoelec. power 3−21051
- liquid, resist. and thermoelec. power calcs. under 40 kbar pressure 3−36586
- phonon damping due to electron-phonon coupling, calcs. 3−38638
- phonon dispersion and binding energy, pseudopotential method 3−27208
- photoabsorption 3−20035
- plasma, Ar-Cs two-temperature, in a disc MHD generator channel, flow assuming nonuniform reactions of ionisation and recombination *(Russian)* 3−26874
- plasma, electron distrib. function, Langmuir probe obs. 3−4669
- plasma, nonideal, equation of state by dynamical method 3−36201
- plasma, two-stream ion acoustic wave instability obs. 3−38458
- plasma, weakly ionised damping of ion acoustic waves *(French)* 3−14558
- primary ion source for sputtering mass spectrometer 3−25931
- self oscillating Cs vapour magnetometer, shift in output freq. 3−28612
- spectral line profiles, satellite structures theory 3−35959
- superconducting transition temp. calc. from electron-phonon coupling constant variations 3−8290
- surface ionization on SiC single crystal 3−34455
- surface tension meas. by combined method for temp. range 600 to 1100°C 3−4920
- thermal expansion and density near fusion-solidification point 3−4858
- Townsend discharge, breakdown potential and first ionisation coeff. 3−14415
- u.s. attenuation, mag. field depend. 3−8094
- vapour, efficient parametric conversion, laser beam effect 3−16903
- vapour, excited by light of 852.1-894.3 nm reson. lines, fluoresc. spectrum 3−23480
- vapour, interaction with a ZnS:AgCl polycryst. screen, induced capillary condensation 3−39464
- vapour, thermal conductivity coeff. 3−11352
- vapour in low voltage arc discharge, striation production 3−30035
- vapour pressure, boiling-point method obs. 3−24252
- viscosity det. 200-300°C above fusion pt. by vibration viscosimeter, effects of O_2 3−4867
- on Ag, u.v. photoemission from clean, Cs and Cs + O_2 coated surfaces 3−12215
- Cs/O on Si, negative electron affinity, struct. and electronic models 3−24339
- Cs-Ar, spectral line profiles satellite structures theory 3−35959
- Cs-Ar atomic collisions, absorption coefficients, long and short-range forces 3−20074
- Cs-Ba thermionic converter under overneutralised Knudsen conditions, plasma diagnostics 3−30013
- Cs-Rb-graphite system, mixed sorption models and isotherms at high temps. 3−20927
- Cs-Xe, spectral line profiles, satellite structures theory 3−35959
- Cs^+ clustering with atmospheric gases, drift velocities 3−9053

caesium continued

- Cs^+ ion bombardment of coated metal surfaces, probability distributions of emitted electrons *(German)* 3−27591
- Cs^+ scattered from surface of W crystal, meas. of fine structure in energy spectra 3−18520
- CsI, relativistic wavefunctions in central field approx. *(French)* 3−4355
- ^{133}Cs free atoms, g-factor ratios determ. 3−29489
- GaAs-Cs layer, effect on electron backscatter coeff. 3−5248
- Si-Cs interface, Schottky barrier height meas. 3−24505

caesium clocks *see atomic clocks*

caesium compounds

- acetate, cryst. struct., phase transform. 3−7726
- caesium hydrogen trifluoroacetate, i.r. and Raman spectra study of O-H-O bonding 3−11261
- Cs(V) complex, caesium oxobisoxalatobisaquoniobate (V) dihydrate, crystal structure obs. 3−38559
- Cs halides:Pb, Cd, dielectric loss meas. of impurity-vacancy dipoles, 90-180°C 3−11612
- halides, far i.r. absorpt. due to U-centres, defect model 3−15529
- halides, peak positions and half-widths of cadmium bands 3−39168
- $3CsCl.LaCl_3.3H_2O:Nd^{3+}$, absorption spectra *(Russian)* 3−24730
- $Co(PO_3)_2$-$CsPO_3$, glasses and melts, effect of water on molar props. *(Russian)* 3−14696
- Cs halide, study of impurity induced first order Raman spectrum 3−21411
- Cs leucites, thermal expansion, ionic substitution effects 3−36431
- Cs-O, CsF-Cs activated GaAs:Si epitaxial layers, photoemission 3−2620
- Cs-Rb alloy system, perturbation theory and pseudo alloy atom model appl. 3−33481
- CsBr, collisional dissoc. by Ar and Xe total cross sections for ion form. 3−4476
- CsBr, g_j-factor meas. with high temp. microwave spectrometer *(German)* 3−35411
- CsBr, U_2 centres, e.p.r. and ENDOR investigation *(German)* 3−30696
- CsCl, compression to 32 kbar, neutron diffr. study 3−4808
- CsCl, elastic consts., press. derivatives, calc. 3−1664
- CsCl, g_j-factor and magnetic susceptibility anisotropy meas. with high-temp. microwave spectrometer *(German)* 3−35411
- CsCl, quadrupole hyperfine structure *(German)* 3−7236
- CsCl, U_2 centres, e.p.r. and ENDOR investigation *(German)* 3−30696
- CsCl mass spectra, effects of vibrational-rotational excitations *(Russian)* 3−11220
- CsCl:$SrCl_2$, mobility of cation vacancies in f.c.c. phase 3−30480
- CsCl-$AlCl_3$ melt, Raman spectra study of influence of species formation on stability 3−36868
- CsCl-NaCl binary system, pressure effect on temperature of eutectic minimum 3−18813
- CsCl(Br)(I), Pb-centres, optical absorpt., elec. cond. and dielec. loss studies 3−24725
- CsCl(Br)(I), phonon dispersion, modified-rigid-ion model calc. 3−36381
- $CsClO_3$, n.q.r. study of ClO_3 ion 3−8481
- $CsCoCl_3.2H_2O$, mag. struct., magnetization, and short-range spin correl., neutron diffr. obs. 3−24568
- $CsCuCl_3$, absorpt. spectra obs., dielec. loss meas. at structural transition 3−21414
- Cs_2CuCl_4, struct., crystal forces and charge distribution determ. 3−17785
- $Cs_2CuCl_4.2H_2O$, Heisenberg b.c.c. ferromagnet, nuclear quadrupole resonance obs. of magnetic interactions 3−27439
- $Cs_2CuCl_4.2H_2O$, n.m.r., ferromag. behaviour 3−2420
- CsF, g_j-factor and magnetic susceptibility anisotropy meas. with high-temp. microwave spectrometer *(German)* 3−35411
- CsF:Tl single crystals, luminescence props. *(Russian)* 3−12175
- CsF-InF_3 systems, preparation and crystallographic data *(French)* 3−7699
- CsF + Ar, (Kr), (Xe), integral total cross sections meas., attractive pot. investigation 3−38324
- $CsFeCl_3$, temp. depend., 2 to 250K, interpretation using antiferromag. linear-chain model 3−21220
- Cs_xFeF_3, $0<x<1$, low temp. antiferromagnetic temp., evolution of Neel temp. *(French)* 3−12017
- Cs_xFeF_3 Mossbauer effect study *(French)* 3−8488
- $CsGa(SO_4)_2.12H_2O$, e.s.r. of Cr^{3+} at 4.2 and 300 K 3−2354
- $CsGa(SO_4)_2.12H_2O:^{53}Cr^{3+}$, ENDOR meas. at 4.2 K 3−2465
- CsH_2AsO_4, ferroelec., order of phase transform. 3−30782
- CsH_2AsO_4, ferroelec., X-irrad., e.p.r. of defect centres 3−2388
- CsH_2AsO_4, partially deuterated samples, ^{75}As n.q.r. study 3−30725
- CsH_2AsO_4, soft mode optical phonon interaction dynamics, Raman scatt. 3−5170
- CsH_2AsO_4 and CsD_2AsO_4, ferroelec., ^{75}As spin-lattice relax. and n.q.r., phase transition phenomena 3−30715
- Cs_2HgI_4, cryst. struct. 3−33506
- CsI, dislocation struct., volume decoration 3−18024
- CsI, dynamic polarisation of ^{133}Cs nuclei by u.s. excitation of forbidden transition 3−18376
- CsI, field effect on excitonic luminescence 3−33850
- CsI, g_j-factor meas. with high temp. microwave spectrometer *(German)* 3−35411
- CsI, phonon dispersion curves from neutron scatt. *(Russian)* 3−20836
- CsI, photoemission, band structure 3−21518
- CsI, photoemission calc. 3−21519
- CsI, space charge effects in electroluminescence 3−21489
- CsI, temp. depend. of half-widths and integral absorpt. of impurity vibration bands 3−21450
- CsI:Tl fluorescence, polarisation effects *(German)* 3−24742
- CsI:Wo^{2-}(MoO^{2-}), i.r. absorpt. and local symmetry 3−8621
- CsI(Na) detector, decay const. 3−25872
- CsI(Tl), 3″ × 3″ crystal, relative photopeak efficiencies 3−32162
- $CsLiBeF_4$ and $CsLiSO_4$, cryst. struct. and polymorphism 3−14751
- $CsLiBeF_4$ determ., space groups and symmetry 3−11598
- $CsMSi(Ge)_2O_6$, M = Al, Fe, B, Cr, synthesis and thermal expansion 3−2753
- $CsMnCl_3$, crystal structure obs. 3−36274

caesium compounds continued
- $CsMnCl_3.2D_2O$ magnetic phase diagram, 2-20K, zero-field Neel temp. 3−5100
- $CsMnCl_3.2H_2O$, interchain coupling effects on e.s.r. 3−18354
- $CsMnF_3$, antiferromag., magnetoelastic coupling and sound velocity 3−15400
- $Cs_{0.4}Mn_{0.4}Fe_{1.6}F_6$, magnetic struct. 3−5108
- $CsNO_2$, anomalous thermal effects, differential thermal analysis and electrical conductivity meas. 3−15010
- $CsNiCl_3$, antiferromag., specific heat meas. from 1.5 to 10 K rel. to mag. transitions 3−30617
- $CsNiCl_3$, antiferromagnetic-paramagnetic transitions 3−34115
- $CsNiF_3$, one dimensional Ferromagnet, spin wave meas. 3−30638
- $Cs_{0.4}Ni_{0.4}Fe_{1.5}F_6$, magnetic struct. 3−5108
- Cs_2O-activated $In_{1-y}Ga_yAs_{1-x}P_x$, photoemission 3−34456
- $Cs_2O-Al_2O_3-SiO_2$, areas for glass form. 3−7629
- Cs_2O-III-V ternary semiconductor, photoemission, heterojunction barrier model 3−2619
- Cs_2O-TeO_2 glass, e.p.r. spectra, irrad. effects *(Russian)* 3−21309
- $CsPO_3-Cu(PO_3)_2$ system, phase diagram *(French)* 3−17958
- $CsPbCl_3$, pulse ultrasonic investig. of elastic props. and detn. of phase transform. *(Russian)* 3−7813
- $Cs_2SO_4:Mn^{2+}$, e.s.r. spectrum, temp. depend. *(Russian)* 3−8437
- Cs_2Sb (IV) Cl_6, semiconducting crystals, diamagnetism and superexchange electron interaction 3−36705
- Cs_3Sb, secondary electron emission, Monte Carlo calc. 3−24767
- Cs_2SbCl_6, mixed valence of Sb, cooperative tunnel effect, Mossbauer obs. *(Russian)* 3−4943
- $Cs_3Sb_2Cl_9$, crystallisation behaviour and polytypism 3−14794
- $CsSbWO_6$, pyrochlore, isolation and cubic cell cation position detn. *(French)* 3−30104
- $Cs_6Ti_2O_7$, new alkali metal titanates and germanates, lattice consts. determ. *(German)* 3−36288
- CsU_2F_9, atomic struct., X-ray determ. 3−26994
- $Cs_2UO_2Cl_4$, oscillator strengths for four low-lying electronic states *(Russian)* 3−30843
- $Cs_4(UO_2)_2F_82H_2O$, crystal structure *(Russian)* 3−26993
- $CsUO_2(NO_3)_3$, oscillator strengths for four low-lying electronic states *(Russian)* 3−30843
- $CsVOF_4$ (V), crystl. struct. determ. 3−11588
- $Cs_2WO_4-Ln_2(WO_4)_3$ reactions in the melt, where Ln=Nd, Er *(Russian)* 3−15825
- GaAs-CsO layer, effect on electron backscatter coeff. 3−5248

caesium generators *see plasma diodes*

caesium plasma diodes *see plasma diodes*

calcium
- abundances in G- and K-type giant stars from narrow-band photometry 3−9554
- atom, electron excitation cross sections using Born approx. 3−1122
- atom, K-shell Coulomb ionization cross-section, impact parameter depend with 0.3-3.0 MeV protons 3−23487
- atom, optical pumping, metastable levels, prod. of large no. of atoms 3−33031
- atomic beam, absolute frequency standard 3−3747
- atomic emission spectra, shift and broadening of resonance lines in hot dense Ar and He 3−17345
- atomic line-widths meas. by piezoelectric scanning Fabry-Perot interferometer in air-acetylene and N_2O-acetylene flames 3−28779
- atoms in flames, absorption linewidth use of channelled spectra produced with a continuum source 3−32260
- Auger radiative effect, $K\alpha$ low energy satellite lines, with and without electron emission 3−15571
- collision broadening and shift in reson. line using inert gases 3−7090
- de Haas-van Alphen effect 3−36522
- desorption kinetics for Ca ad-particles on W surface with variation of O_2 surface coverage 3−24346
- electron excitation of 4227 Å reson. line 3−38238
- electronic structure as function of lattice const., APW calc. 3−18070
- H and K emission lines in late type stars with grain material in their atmospheres 3−13036
- interstellar line radial vels. meas. for galactic structure determ. *(French)* 3−28266
- ionisation balance, collisional ionisation, autoionisation, radiative recombination and dielectric recombination 3−11458
- ionisation degree calc. in acetylene-air and propane-butane-air flames *(Russian)* 3−31264
- ionisation equilib. calc. for solar atm. ions 3−18960
- ionophore, X-537A, muscle contraction effects 3−35266
- ions and muscle contraction 3−5628
- k dependent potential calc. for band struct. and Fermi surface 3−8086
- K-line wing solar brightness fluctuations in quiet region near centre of disc 3−35035
- localised d states for pseudopotential calcs. 3−8116
- photoemission energy distrib. meas. and calc. rel. to electron states 3−34462
- purification by reactive distillation in Mo column 3−18536
- reaction with Cl_2 and Br, crossed beams chemistry 3−21803
- reactive collision with ICl, crossed beams product angular distributions of CaCl and CaI 3−27864
- self-diffusion processes in different glasses 3−4882
- ultrapure single crystals preparation by ultrahigh vacuum reactive distillation *(German)* 3−8733
- urinary obs. in children, long-term obs. 3−3615
- $Al_2O_3:MgO$, Ca, Al and Mg segregation at grain boundaries 3−27739
- Ca I 4227 Å line polarization at Sun's limb, theoretical study 3−35031
- Ca I 6103 Angstroms line core for time-averaged spectroheliograms 3−19076
- Ca II, interstellar line profile in spectra of Ophiuchi 3−35150
- Ca II H and K emission lines in coronal spectrogram taken at 1970, March 7 eclipse 3−18941
- Ca II H and K line wings, obs. of solar disc emission lines 3−31571
- Ca II H and K lines in solar spectra, correlations of fluctuations with Mg b and $H\beta$ lines 3−39629
- Ca II H- and K-line obs. of Stephenson-Sanduleak 3378, He-rich B-type star 3−25453
- Ca II high-velocity interstellar gas near Gum Nebula 3−19073

calcium continued
- Ca II interstellar K-lines in spectra of γ Pegasi and ι Herculis 3−31675
- Ca II K, H and i.r. triplet lines, chromospheric plage obs. 3−5568
- Ca II K emission arches near solar limb 3−31535
- Ca II K_2 line width in late type stars, rel. to gravity and effective temp. 3−35135
- Ca II K-line emission core widths in sunspot umbra and penumbra 3−35037
- Ca II K-line strength determ. in B-stars by soln. of transfer eqns. 3−28166
- Ca II resonance lines in stellar spectra, meas. of brightness temp. rel. to stellar model chromospheres 3−37349
- Ca II solar H and K line oddities on spectrograms of good spatial resolution 3−39616
- Ca-Xe system, population inversion calc. using near-reson. charge exchange as pumping mechanism 3−37953
- Ca^+, electron impact excitation anomaly for 4s→np transition rel. to oscillator strength 3−23494
- Ca^+, oscillator strengths and ground state photoionisation cross sections 3−11146
- Ca^+, pressure shift and broadening of resonance lines in hot compressed Ar and He 3−33033
- Ca_2 in solid benzene, ground state, excited state and potential energy curves analyses 3−7179
- Ca^{2+} in MgO crystal, cation diffusion studies using a sectioning technique 3−33694
- Ca^{2+} in NaCl crystals, diffusion from volume to surface 3−33692
- Ca^{2+} replaced by ions of d^9 config., $CaCO_3$ crystals, e.p.r. and luminescence studies 3−36790
- Mg-Ca mixed layers on calcite, cationic distrib. and structural changes 3−15849
- NaCl:Ca, impurity induced Raman spectra of annealed and quenched crystals 3−21409
- NaCl:Ca, vacancy diffusion, ^{23}Na spin-lattice relax. time obs. 3−12074
- $YIG:Ca^{2+}$, mag. after-effect, electronic hopping processes 3−24591

calcium compounds
- apatite, oxygen-containing, synthetic, radical obs., e.p.r. *(French)* 3−36782
- $calcite:Mn^{2+}$, e.p.r. study of forbidden hyperfine transitions 3−2355
- calcite, CO_3^{--} ions Einstein coeff. spectra calc. 3−24696
- calcite, etched, dislocations obs. by polaroid photomicrography, undergraduate expt. 3−9813
- calcite, nucleation and motion of twinning dislocations rel. to twin layer broadening 3−14856
- calcite, vacuum u.v refl. spectra, dielec. consts. determ., dichroic absorpt. band 3−27510
- colemanite, ferroelectric, n.m.r. relax. studies 3−39047
- dicalcium strontium propionate, Brillouin scatt., vibr. modes, elastic consts. 3−30814
- dicalcium strontium propionate, proton spin-lattice relax. time, anomaly near Curie point 3−39103
- dicalcium strontium propionate, temp. depend. of sound velocity 3−1699
- fibrous calcite beds in Middle Devonian beds rel. to stratigraphy and formation 3−12569
- fluorapatite single crystals, frictional behaviour and surface failure investigations 3−36363
- fluorite, X-ray and optical obs. of planar defects as growth boundaries 3−7778
- fluorophosphate, e.p.r. study of luminescent and colour centre defects 3−34212
- gypsum, habit faces growth rates rel. to crystn. conditions 3−34468
- hydroxyapatite, hydrothermal growth and characterization 3−12282
- monoxide or hydroxide visible bands in flames, identification method 3−22547
- omphacite, cryst. struct. 3−15868
- silicophosphates, preparation and characterization *(Russian)* 3−11597
- sulphoaluminate and sulphosilicate, hydraulic hardening process *(Russian)* 3−15742
- tetraphosphonate, $Ca_2C_4H_8O_{12}P_4.10H_2O$, crystal struct. *(French)* 3−7737
- tobermorite, synthetic, pore struct., adsorpt. study 3−39421
- $3CaO-SiO_2$, solubility in $3SrO-SiO_2$, X-ray diffraction and i.r. spectroscopic obs. *(Russian)* 3−14972
- $\{Ca_2La\}[Zr_2](Ga_3)O_{12}$, lattice constants meas., 296-1400 K 3−11753
- $\{Ca_{2.5}Zr_{2.5}\{[Zr_2](Ga_3)O_{12}$, lattice constants meas., 296-1400 K 3−11753
- $BaTiO_3-CaTiO_3$ (5 wt.%), large polarisation depend. photovoltages 3−33951
- CVBIG, stress birefringence measurement 3−21381
- $Ca-Ln_2-S_4$, ternary sulphides, prep., elec. and opt. props. 3−39243
- $CaAl_2-NH_4Cl$ powder mixture, aluminizing 3−24963
- $CaAl(B_3O_7)$, johachidolite, crystallographic structure 3−1612
- $CaAl_2(NH_2)_8.NH_3$, monoclinic, cryst. struct. *(French)* 3−1607
- CaAs crystal structure 3−20724
- $Ca_2B_5O_9Br$, crystal structure obs. *(French)* 3−33494
- $CaB_3O_4(OH)_3.H_2O$, colemanite, n.m.r. and diffraction meas. rel. to atomistic mechanism of Ferroelec. behaviour 3−27424
- $CaB_3O_4(OH)_3.H_2O$, n.m.r. lineshape, quadrupole interaction tensor 3−2411
- $CaCO_3$, calcite, dislocation description of twin dynamic behaviour 3−20748
- $CaCO_3$, calcite, growth in gelatin gel 3−24783
- $CaCO_3$, calcite, hydrothermal growth, phase equilib. determ. 3−18538
- $CaCO_3$, calcite, slightly deformed, anomalous transmission of X-rays 3−24139
- $CaCO_3$, cryst. growth in aqueous solns. 3−12233
- $CaCO_3$, cryst. growth in gelatin gels 3−15610
- $CaCO_3$, i.r. refl. from longit. modes 3−39138
- $CaCO_3$, Iceland spar, elastic Rose channel formation *(Russian)* 3−14882
- $CaCO_3$, phonon densities and dispersion curves of external and internal modes 3−33630
- $CaCO_3$, spin-lattice relax. of CO_3^{3-} mol.-ion., phonon modulation of s.h.f. interaction 3−2350

calcium compounds continued
$CaCO_3$, twinning dislocations, macroscopic pileup config. *(Russian)* 3−7768
$CaCO_3$ calcite (synthetic), cathodothermoluminescence, low-temp. effects 3−18502
$CaCO_3$ crystals, containing ions of d^9 config., e.p.r. and luminescence studies 3−36790
$CaCO_3$ single crysts., plastic deform. in compression along 111 *(French)* 3−1667
$CaCl_2.4H_2O$, cryst. struct., X-ray determ. 3−24079
$Ca_3Cr_2(GeO_4)_3$, mag. struct., neutron diffr. obs. 3−24569
CaF:Na crysts., coloration centres, photoluminesc. meas. *(Russian)* 3−36920
CaF_2 3 23955
CaF_2, ^{19}F chem. shift tensor and nonionic bonding 3−12070
CaF_2, anharmonic lattice vibr., calc. and neutron diffr. obs. 3−24222
CaF_2, anisotropy in Knoop indentation hardness and friction of diamond cones 3−20788
CaF_2, changes in real structure due to compressive impact 3−33503
CaF_2, charge density from struct. amplitudes nonspherical analysis, atomic nonsphericities 3−27005
CaF_2, clc. of H^- impurity vibr. 3−36390
CaF_2, doped, interstitial anion clusters, formation mechanism 3−30113
CaF_2, doped, n.m.r. of ^{19}F, thermometric detection 3−30680
CaF_2, ENDOR of Ho^{2+}, hyperfine lines, spin Hamiltonian parameters 3−2468
CaF_2, e.p.r. of U^{4+} ions in trigonal sites, uniaxial stress effects 3−2360
CaF_2, electron diffr. structure factor determ. using Bloch wave analysis 3−24004
CaF_2, growth from vapour, transparency rel. to growth conditions 3−18547
CaF_2, hardening due to contamination by atmospheric O 3−4806
CaF_2, high-freq. acoustic harmonic generation by Bragg light scatt. 3−7859
CaF_2, hopping motion of V_k centres 3−20735
CaF_2, lattice vibrs. symmetry props., from space group representation of wave vector groups 3−14944
CaF_2, M^+ centre, prod., absorption and luminesc. obs. 3−27023
CaF_2, multiple charge states of Fe, Mossbauer obs. of isomer shift 3−27455
CaF_2, n.m.r., free-induction decay and line shape 3−24624
CaF_2, nonempirical LCAO MO SCF studies, bonding trends 3−20096
CaF_2, powder X-ray diffr. line integrated intensity changes, effective Debye parameter rel. to lattice strain 3−33424
CaF_2, radiation induced transform. of defects, e.p.r. and optical absorpt. obs. *(Russian)* 3−30694
CaF_2, refractive index, calc. from oscillator parameters and refl. spectra meas. 3−30840
CaF_2, shell model calc. of formation energy of point defects 3−38583
CaF_2, space-charge electret, bilinear depolarisation dynamics 3−39094
CaF_2, static optical and spin resonance props. of V_k centres 3−20734
CaF_2, surface excitations, exptl. obs. using attenuated total reflection 3−24493
CaF_2, temp. effect on X-ray luminesc. spectra, Eu^{2+} impurity effect *(Russian)* 3−8650
CaF_2, thin film, electron irradiation effects 3−38748
CaF_2, under reducing conditions, mixed cond. 3−21122
CaF_2, vacancies, interstitials and inert gases in fluorite structures 3−17814
CaF_2 containing heavy metal impurities, i.r. absorption and thermal conductivity 3−36898
CaF_2 crystals, X-ray topographs of dislocations 3−17825
CaF_2 overlay, surface depletion of InSb film 3−18219
CaF_2 spectra of electronic excitations in 8-150 eV range 3−2032
$CaF_2:Am^{3+}(Cm^{3+}, Nd^{3+})$, optical Zeeman rot. spectra 3−18467
$CaF_2:Cd^{3+}$, Pr^{3+}, Yb^{3+}, luminescence, energy transfer from Cd^{3+} to Pr^{3+} and Yb^{3+} *(Russian)* 3−36905
CaF_2:Ce,Na, near u.v. absorpt. spectra obs. of defect centres 3−12161
$CaF_2:Er^{3+}$, effect of dislocations on perturbed angular correlations in paramagnets 3−34256
$CaF_2:Er^{3+}$, luminesc., two-photon excitation by dye laser *(Russian)* 3−12181
CaF_2:Eu crystals, thermoluminescence and X-ray stimulated luminescence 3−27580
CaF_2:Gd, thermal depolarisation spectra before and after O contamination 3−24652
$CaF_2:GdF_3$, density, rel. to impurity incorporation 3−20759
$CaF_2:H^-$, impurity induced far infrared absorption 3−34387
$CaF_2:H^-$ i.r. relectivity study of high concs. of H^- ions 3−4836
CaF_2:Mn, cathode ray coloration, alpha and beta centre form. 3−30121
CaF_2:Mn, thermal and u.v. bleaching characts. of colour centres 3−7755
CaF_2:Mn teflon phosphor, for neutron dosimetry 3−35299
CaF_2:Mn thermoluminescent dosimeter response to β-rays 0.43-3.54 and γ-rays 8 keV to 1.25 MeV 3−311
CaF_2:Mn(Ce,Mn), cathodoluminescence, trapped hole diffusion 3−39197
$CaF_2:NaYF_4$, e.p.r. 3−24613
$CaF_2:Nd^{3+}(U^{3+})$, linear elec. field effect in e.p.r. for $Nd^{3+}(U^{3+})$ tetragonal sites 3−34200
$CaF_2:Np^{3+}(:Pu^{3+},:Am^{3+},:Cm^{3+})$, effect of γ-irradiation on actinide ions obs. in optical absorption and thermoluminescence meas. 3−5238
CaF_2:R, R = Ce, Pr, Sm, Eu, Tb, ionic thermocurrent obs. of reorientational properties 3−7787
CaF_2:Sm, X-ray or u.v. excited, thermolum 3−24758
$CaF_2:Sm^{2+}$, luminesc., nonradiative transition stimulation by intense optical excitation effects *(Russian)* 3−15539
$CaF_2:Sm^{2+}$, stimulation of nonradiating transitions by strong light excitation *(Russian)* 3−36925
$CaF_2:Tm^{2+}$, covalency contribution on the values of $g\Gamma_7$ and $g\Gamma_7$ *(Russian)* 3−11861

calcium compounds continued
$CaF_2:U^{3+}$, e.p.r., discrete saturation spectrum, r.f. field effect 3−21299
$CaF_2:X^{3+}$, X = Ce, Pr, Sm, Eu, Tb, polarisation storage 3−18406
$CaF_2:XF_3$ (X = Pr,Tb,Nd), gamma-induced luminescence 3−24732
$CaF_2:YF_3$, conc. and mobility of interstitial fluorine ions rel. to intrinsic cond. 3−30489
$CaF_2:Yb^{3+}$, covalency, ab initio calc. 3−2009
CaF_2-NaF(KF) binary molten salt, specific electrical conductivity at 1000°C 3−36631
CaF_6, thermal vibrs. of atoms, 300-1000 K *(Russian)* 3−27078
$Ca_5F(PO_4)_3$, of ^{19}F, exptl. obs., line shape calcs. for linear chain of spins 3−21331
$Ca_2Fe_{2-x}Al_xO_5$, magnetic structures 3−12023
$Ca_2Fe_{2-x}Al_xO_5$ with $x = 0.57, 0.72$, crystal structure 3−7675
$Ca_3Fe_2(GeO_4)_3$, mag. struct., neutron diffr. obs. 3−24569
$Ca_2Fe_2O_5$, elec. field gradient tensors at two nonequivalent ferric sites 3−24386
$Ca_3Fe_2Si_3O_{12}$, andranite garnet, magnetic structure, indirect exchange interaction 3−34137
$CaGa_2S_4$:Ce,Na, cathodolum., rel. to flying spot scanner appl/ 3−12186
$CaH(AsO_4),H_2O$, haidingerite, morphology rel. to bond assemblage 3−14789
$CaHAsO_4.3H_2O$, cryst. struct. and hydrogen bonding 3−14762
$CaHAsO_4.3H_2O$, hydrogen bonding, three-circle diffraction study 3−17756
$Ca(H_2PO_2)_2$, radiocrystallographic and i.r. spectroscopic obs. *(French)* 3−7700
$CaHPO_4.2H_2O$, brushite, growth in gelatin gel 3−24783
$CaHPO_4.2H_2O$, cryst. growth in gelatin gels 3−15610
$CaKAsO_4.8H_2O$, cryst. struct., density 3−7664
$CaLGa_3S_7$, $CaLAl_3S_7$, (L = La, Ce, Pr, Nd), sulphurized compound family of melilite type *(French)* 3−30102
$Ca_2Ln_8(SiO_4)_6O_2$, (Ln = Y, Gd or La), laser material, melt growth 3−12296
$CaMg\{B_3O_4(OH)_3\}_2.3H_2O$, n.m.r. lineshape, quadrupole interaction tensor 3−2411
$CaMoO_4$, for tunable acousto-optic filters, Czochralski growth 3−12300
$Ca_xN_{1-x}Fe_2O_4$, dielectric losses and dielectric constant 3−15451
$Ca(NO_3)_2$, polycryst., i.r. and Raman study at 300K 3−27504
$Ca(NO_3)_2$, stress corrosion cracking of mild steel, effect of C content 3−39354
$Ca_{2-2x}Na_{1\|x}Eu_xMg_2V_3O_{12}$, Eu^{3+} fluoresc., energy levels, point symmetry *(French)* 3−18480
$Ca_{2-2x}Na_{1\|x}Eu_xMg_2V_3O_{12}$, fluoresc. of Eu^{3+}, temp. and conc. depend. *(French)* 3−21460
$CaNaHSiO_4$ crystal atomic structure from examination of single crystals 3−17796
$CaNaP_3O_9.3H_2O$, anhydrous salt crystallographic data *(French)* 3−11593
$Ca(NbO_3)_2:Nd^{3+}$, stimulated emission in $^4F_{3/2} \rightarrow {}^4I_{13/2}$ transition 3−27516
$CaNb_2O_6$ and $CaNb_2O_7$, X-ray K-absorpt. edge of Nb 3−27584
$Ca_2Nb_2O_7$, lattice parameters *(French)* 3−1606
$Ca_xNi_{1-x}Fe_2O_4$ system, magnetic properties, phase equilibrium 3−8379
CaO, electric arc-fusion growth method to produce clear crystals 3−12265
CaO, F-centre Stark effect 3−30858
CaO, magnetic circular dichroism of F band 3−21451
CaO, multiphonon i.r. absorpt. spectra, lattice vibrs. i.r. active sum modes 3−24693
CaO, multiple charge states of Fe, Mossbauer obs. of isomer shift 3−27455
CaO, optical phonons at centre of Brillouin zone at 300 and 17K *(French)* 3−8567
CaO, polycrystalline, thermoelectric force meas. between 1200 to 1650°C *(German)* 3−15740
CaO, r.f. sputtered films, pure and Sm- and Tm-doped, X-ray excited fluoresc. 3−27568
CaO, r.f. sputtering, glow discharge anal. by spectroscopic method 3−5244
CaO, solid state reaction with β-quartz, anisotropy and water vapour influence 3−7924
CaO stabilised ZrO_2, creep 3−27740
CaO TSEE activator in BeO, dosimetric characteristics 3−28671
CaO:Bi, Sb, Te phosphors, photoluminescence, radical-recombination luminescence of the O atoms *(Russian)* 3−30876
CaO:Co, Fe, Mossbauer study of ^{57}Fe rel. to dynamical Jahn-Teller effect 3−24639
$CaO:Cr^{2+}$, acoustic paramagnetic resonance at high magnetic fields 3−2346
CaO:K, radiation induced K^0 centres, e.p.r., spin Hamiltonian parameters 3−34210
CaO:Mg, e.p.r. of colour centres 3−36791
CaO/MgO, in lunar rock 12039 3−5586
CaO-BaO-WO_3, isothermal section and phase equilibrium study 3−17955
CaO-Cr_2O_3-Al_2O_3, phase relations and optical studies 3−5385
CaO-MgO-P_2O_5-SiO_2 glass, effect of fluorine addition on crystallisation 3−20698
CaO-Nb_2O_5-TiO_2-SiO_2, liquidus temp. determ. in 25% SiO_2 plane 3−1781
CaO-Pt system, phase relations 3−8771
CaO-SiO_2 system, physicochem. props., effect on spectral line intensity in d.c. carbon arc *(Russian)* 3−28772
$Ca(OD)_2:Cu^{++}$, trigonal Jahn-Teller effects in e.p.r. 3−39024
$CaO_xNiO_{1-x}Fe_2O_3$, dielectric props. *(French)* 3−34284
2 $CaO.B_2O_3$, X-ray diffr. anal. of crystalline state 3−8969
$CaO.FeO.Fe_2O_3$, chrm. comp. and precip. microstruct. *(French)* 3−8986
$CaO.P_2O_5$ glass, absorpt. spectra rel. to redox behaviour of Fe 3−24723
$CaO.P_2O_5$ glass:Cu^+, fluoresc. 3−30869
$CaO.2B_2O_3-CaO.B_2O_3$, X-ray diffr. anal. of crystalline state 3−8969
$mCaO.2UO_3.(4-2m)H_2O$, $O \leqslant m < 2$, indexing of X-ray powder patterns *(French)* 3−30091

calcium compounds continued
CaP crystal structure 3–20724
$Ca_{10}(PO_4)_6Cl_2$, colour centres produced by X-rays, optical absorption measurements, e.p.r. 3–8442
$Ca_{10}(PO_4)_6F_2$, defect centres 3–8623
$Ca_{10}(PO_4)_6F_2:Sn$, luminescence, electronic transitions, substitutional sites 3–39174
$Ca_{10}(PO_4)_6F_2:Sn$, oxidation and reduction of Sn, luminescence effect of O_2 partial pressure 3–39470
$Ca_5(PO_4)_3F$, fluorapatite, dielectric loss for various fluoride vacancy concs. 3–39088
$Ca_5(PO_4)_3F$, synthetic and mineral, crystal structure compared 3–11601
$Ca_5(PO_4)_3F$: $Nd(Nd_2O_3)(NdF_3)$, fluorapatite, structure and location of dopant 3–17789
$CaPdF_4$, preparation, madelung part of lattice energy *(German)* 3–14814
CaS phosphors, F^- aggregate centre formation due to S^{2-} vacancies, e.s.r. obs. 3–39028
$CaS:Bi^{3+}$, Pd^{2+} phosphorescence decay characteristics 3–30856
$CaSO_4$, crystal structure, phase transformations and thermal decomposition 3–14809
$CaSO_4$, Raman spectra, comparison with gypsum 3–18457
$CaSO_4:Eu^{2+}$, fluorescence and excitation spectra 3–39172
$CaSO_4:Eu(Mn)$, radiational defects, thermoluminesc. study *(Russian)* 3–27581
$CaSO_4$:V, Ln, (Ln=Y, Dy, Sm, Tb), energy transfer by sensitizer-activator pairing 3–30868
$CaSO_4$-Mn phosphor, thermoluminesc., excitation by low- and middle-energy protons 3–24757
$CaSO_4(Tm)$, optical and thermal effects on thermoluminescence response 3–290
$CaSO_4.2H_2O$ dunes in New Mexico, visual observation of electric sparks 3–3015
$CaSb_2O_6:Bi^{3+}(Pb^{2+})$, fluorescence obs. for each excitation band 3–21478
Ca_2SiO_4, struct., from room temp. to over 1400°C 3–14798
$Ca_3Sn_3Ga_2O_{12}$, lattice constants meas., 296-1400 K 3–11753
$CaSo_4.2H_2O$, symmetry of $SO_4{}^{2-}$ ion 3–1611
$CaTi_2O_5$, formation, structure and props. deter. *(Russian)* 3–11596
$CaTl_3$, density of states curve calc. compatible with oscillatory curve of Cu_3Au 3–1984
$CaWO_4$, heteroepitaxial layers, growth on sapphire substrate *(German)* 3–8736
$CaWO_4$, temp. broadening of Nd^{3+} energy levels *(Russian)* 3–8617
$CaWO_4$, X-irrad., trap depth and charge carriers from optically and thermally stimulated conductivity *(German)* 3–2105
$CaWO_4:Am^{3+}$, fluoresc. emission props. 3–34405
$CaWO_4:Nd^{3+}$, crystal field parameters, calc. using MO LCAO method *(Russian)* 3–8112
$CaWO_4:Nd^{3+}$, stimulated emission in $^4F_{3/2}\rightarrow{}^4I_{13/2}$ transition 3–27516
$CaWO_4:Nd^{3+}$ film, epitaxial growth and lasing props. 3–29094
$CaWO_4:U$, $CaMoO_4:U$, spectrum of $UO_4{}^{2-}$ *(Russian)* 3–8619
$CaWO_4:Yb^{3+}$, crystal field parameters, calc. using MO LCAO method *(Russian)* 3–8112
$CaY_2Mg_2Ge_3O_{12}$, top-seeded soln. growth using borate fluxes 3–15637
$CaZrO_3$, formation by solid state reaction between CaO and ZrO_2 3–8977
$CaZrO_3$ properties of Dy^{3+} ion in lattice, luminescence spectra *(Russian)* 3–39171
CdS, Mandelstam-Brillouin scatt. obs. of parametric interaction of sound signals 3–36640
KBr-$CaCl_2$, solubility of $CaCl_2$ rel. to hardening 3–11719
NiO-CaO system, eutectic directional solidification, floating zone technique *(French)* 3–17965
$Sr_{1-x}Ca_xTiO_3$, phase transitions, u.s. velocity and permittivity studies 3–27478
V_2O_5-P_2O_5-CaO glass based m.i.m. structure, elec. characts. *(Russian)* 3–27318
ZrO_2-CaO system, e.p.r. of Gd^{3+} and Yb^{3+}, ordered phase obs. *(French)* 3–18356
ZrO_2-$CaO:Gd^{3+}$, e.s.r. spectral obs. rel. to structure 3–8432

calculating *see calculation*

calculating apparatus
see also computers
HP 9800 series programmable calculators, input/output structure 3–25939
programmable calculator, HP 9800 model 10 3–25936
programmable calculator, model 20 of HP 9800 series 3–25937
programmable calculator, model 30 of 9800 series 3–25938
programmable calculators, HP 9800 series 3–25935
slide rule, electron microscopy, for calc. of sizes, magnifications 3–19338
slide rule for close up photography 3–32107

calculation
see also graphs; nomograms
anharmonic force constant 3–4416
benzene, lower excited levels by Green's function method 3–4410
cyclotron, TRIUMF, effects of axial misalignment of dees 3–19249
cyclotron, TRIUMF, optimization of phase acceptance 3–16485
efficient computation of radiant interchange configuration factors within the enclosure 3–10412
liquid surface motion, press. and accel.-induced distortion 3–1391
molecular coordinates, high precision method for computer programming *(French)* 3–7098
optical systems calculation, automation *(Czech)* 3–5905
seismometric system identification, recorded signal connection 3–2904
Stokes component in Raman spectra, simple formula *(Russian)* 3–25772
H_2-He collisions, classical S-matrix elements for vibrational excitation in three dimensions 3–7251

calculus
see also differentiation; integration; variational techniques
spinor, formalisation without use of fibre bundles 3–591
symbolic, applic. to nonlinear viscoelasticity *(French)* 3–3954

calculus continued
tensor calculus, determ. on curvilinear coordinates, appl. to rheostatic lubrication *(German)* 3–28854

calibration
see also measurement standards; standardisation
absolute intensity, branching ratio technique 3–16545
absolute pressure gauge for high-pressure calibration 3–35385
absolute spectroradiometric measurements 3–25646
acoustic emission transducers, frequency response characteristics calibration 3–25671
airglow photometer calibration 3–37247
airglow spectrometer calibration 3–37247
astronomical apparatus, using synchrotron raiation 3–19079
automatic volumetric measuring tank for metering solid-water flow in pipelines, absolute calibration 3–22573
blood pressure signal conditioners 3–398
channel electron multipliers, calibration using standard omnidirectional electron beams 3–25943
comparator, computerised method 3–3788
continuously scanning bridge circuit, using on-line data 3–35352
d.c. vernier potentiometer, using inductive voltage divider 3–35351
differential pressure transmitters, span-shift errors with static pressure 3–25709
echo ranging transducers, self-reciprocity calibration 3–92
electron beams, 9-22 MeV energy range, with Cherenkov detector 3–10153
electrostatic analysers, calibration using standard omnidirectional electron beams 3–25943
field ion microscopy, field calibration using energy distribution of field ionization 3–28726
field strength meters, having loop and dipole antennas *(Russian)* 3–19237
gamma-ray precision energy meas. standards 3–3858
gas analyser, prep. and certifying gas mixtures 3–19371
high pressure gas meters with sonic nozzles 3–6164
hot-wire anemometers, for velocity perturbation expts. 3–22565
hydrophone, multiple interference smoothing 3–5782
instrument standards 3–13192
ionization current sources, capacitor charging method *(Russian)* 3–9995
large aperture i.r. radiometers, vacuum system 3–37597
line hydrophone array, l.f. technique for underwater calibration 3–3732
manometric transducers absolute calibration by comparison with compression manometer in cryostated installation 3–19177
MI-10 ionization convertor, vacuum measurement *(Russian)* 3–5856
MI-1305 mass spectrometer, meas. of water vapour pressure 3–25930
microwave antenna aperture efficiency, flux density scale 3–37498
mobile communication equipment 3–35348
moisture measuring equipment 3–9853
Monte Carlo method for calibration of γ-ray detectors 3–13113
neutron spectra, non-Maxwellian, self-consistent transformation of bremsstrahlung of monochromatic photoneutron mean energies 3–37705
oceanographic research velocimeters 3–37262
optical recording system, for partial discharges in air, soln. *(Russian)* 3–14613
optical self-beating spectometer, by polystyrene latex spheres 3–34659
optical systems, intensity calibration in u.v., mol. branching ratio method 3–5943
ozone source, stable, for atmospheric monitors, calibration 3–3186
photoelectron spectrometers, calibration procedures 3–22497
plasma pyrometer, use of reference monochromatic radiators 3–20614
PTB standard, for adjusting vertical magnification of optical instruments *(German)* 3–32061
radiometer-scatterometer for ocean surface wind sensing, antenna calibration 3–39568
radiometers, microwave, temperature reference, target design, technique 3–19139
receiver calibration of correlation micro-pickup for meas. of pressure fluctuations in turbulent boundary layer 3–32271
residual stress measurement, hole drilling method 3–22267
scintillation counter, liquid, energy calibration ^{113}Sn decay 3–32153
specimen-heating stage calibration in electron microscope 3–10114
spectral specular reflectance, standard reference materials, preparation and calibration 3–19143
spectrochemical analysis, spectrophotometric accurate measurement of molar absorptivities 3–26018
spectrofluorometry, emission standards, spectrometer calibration methods 3–35532
spectrometer, vacuum u.v., 50 to 120 nm, absolute intensity calibration method using electron impact excitation 3–37637
spectrophotofluorometer calibration for organic analysis of lunar and geological samples 3–32268
thermal arc plasmas as radiation standard for light intensity calibration in astrophysics 3–4681
thermal calibration for radiometers 3–16396
thermocouple vacuum-meter 3–19181
thermocouples, high temperature, calibration equipment for *(German)* 3–35377
turbine flowmeters, for supercritical helium 3–6175
vibration and shock effect test equipment, problems, periods *(Polish)* 3–19156
weighing scales, by electronic means 3–22254
Weissenberg rheogoniometer, using Newtonian fluids 3–6172
X-ray diagnostic machines, precise calibration with portable apparatus 3–415
^{60}Co γ-ray instrument, collimated photon beam 3–10149
^{57}Fe exact determ. of energies of 122 and 136 keV lines for calibration of high resolution Ge(Li) and Si(Li) spectrometers 3–13480
Ge(Li) detectors, absolute efficiency, $^{108}Ag^m$ as calibrating source 3–32164
O_3 calibration source for analysers and inlet-sample air systems 3–32252
Pt-Pt Rh thermocouples, automatic calibration in temperature range 0° to 1100°C 3–107

californium
^{252}Cf, fission neutron multiplicity meas. using a Gd-filled liquid scintillator *(French)* 3−10064
^{252}Cf, neutron activation analysis, oceanography, simulated ore samples, sea floor 3−3212
^{252}Cf radiocytogenetic studies, chromosomal analysis of hamster ovary cells, irradiation under aerobic and anaerobic conditions 3−28381
implantable ^{252}Cf sources, neutron dose rate calculations 3−13168

californium compounds
CfCl$_3$, X-ray diffraction study of hexagonal and orthorhombic forms 3−36282
CfCl$_3$ thin films, absorption spectrum in range 6000-46000 cm^{-1} 3−27497

calorimeters
see also calorimetry
absorbed dose obs. in C from ^{60}Co γ-rays 3−6070
a.c. high sensitivity meas. of specific heat *(Japanese)* 3−13237
adiabatic differential, Shimadzu, stored energy in twisted Cu bar *(Japanese)* 3−13254
automatic bomb calorimeter CA-3, Shimadzu-Nenken type, improvement of characts. *(Japanese)* 3−13255
detector for meas. of enthalpy of high-temperature gas media *(Russian)* 3−9869
differential, polymer monomer interactions, heat of mixing 3−37596
differential conduction microcalorimeter of high sensitivity *(French)* 3−35374
dosimetry, absolute meas. of gamma ray absorbed dose 3−28390
double layer calorimetric probe, temp. and pressure meas. far high temp. flow *(Russian)* 3−9870
drop calorimeter, calibration and thermal study at high temp. *(French)* 3−5816
flow calorimeter for heat capacity determ. of compressible fluids at high pressures 3−22284
graphite, construction and testing 3−22289
heat exchange gas filling method 3−25681
heat of mixing of binary liquid systems, determ. by thermometric titration *(German)* 3−22285
high-pressure, constant volume heat capacity meas. of ^{4}He in h.c.p. phase 3−30309
isothermal, heating pulse control, construction and meas. techniques *(German)* 3−16394
isothermal titration microcalorimeter 3−37600
for low temp. measurements 3−16401
Peltier effect meas., construction and operation of calorimeter *(Dutch)* 3−28492
radioactive sources, microcalorimetric measurement of γ-radiation *(French)* 3−28659
rotating bomb, general purpose, reaction solution, meas. at 400 K and 800 kPa 3−32255
single-step isoperibol deformation calorimeter, for stored energy determ. in deformed Cu 3−4787
throttling, wet air water droplet content measurement *(German)* 3−25675
u.s. power meas. at milliwatt levels, differential microcalorimeter 3−129
u.s. radiation meas. 3−128
CO$_2$ lasers, energy output measurement 3−35428
Si dosimeter 3−26550

calorimetry
see also calorimeters; specific heat
catalytic reaction rates, by calorimetric bead system 3−28489
differential scanning, application to diallyl phthalate resin molding, curing 3−5797
dosimetry of fast neutron beam 3−3623
DTA, measuring head *(French)* 3−28490
heater lead error, radiation effects 3−5809
heats of mixing, continuous determ. method by quasi-isothermal heat flow calorimetry *(German)* 3−9858
laser beams power and energy meas., calorimetric method 3−13337
liquids and gases, thermal cond. meas., high pressure 3−35369
metal, quenched-in vacancy parameters determ. in calorimetric studies 3−39348
nondestructive assay of Pu n scrap, calorimetric and γ spectrometric method 3−21783
rhodamine 6G solutions, calorimetric determ. of fluorescence energy yields using Ar$^+$ laser *(Russian)* 3−30846
specific heat measurement, at low temps. 3−5849
turbogenerator, efficiency, field test, calorimetric method *(Japanese)* 3−5796
u.s. intensity det. 3−82
^{244}Cm, calorimetric meas. of alpha half-life 3−6790
NaF in NaF-ZrF$_4$ mixtures, enthalpies of dissolution, calorimetric study at 1030°C *(French)* 3−7907
ZrF$_4$, specific heat of the solid as a function of temp. and enthalpy of the liquid meas. *(French)* 3−5816
ZrF$_4$ in NaF-ZrF$_4$ mixtures, enthalpies of dissolution, calorimetric study at 1030°C *(French)* 3−7907

caloristers *see calorimeters*

camera lenses *see photographic lenses*

cameras
see also coronagraphs; television cameras
control system monolithic integration 3−37658
convolution square camera for analysis of scanning electron micrographs of soil structure 3−379
diffusing screens for photolithographic camera illum. systems 3−217
dual camera attachment for scanning electron microscope 3−9975
electron diffraction, sectoral device 3−345
electron-optical streak, picosecond time-resolution, appls. 3−796
electronic, for high electron density plasma investigation *(French)* 3−9971
electronic, ultrahigh speed, with 2-500 ns exposure times, description *(French)* 3−9970
electronographic cameras for space astronomy in far u.v. region 3−31833
film, synchronisation with TV receiver image frequency *(Danish)* 3−3821
film exposure uniformity rel. to focal plane shutter parameters 3−16458
film flattening in aerial cameras 3−3823

cameras continued
focal plane shutters, mechanisms, developments, review *(Russian)* 3−6004
gamma, count rate loss correlation method 3−10174
gamma, with large field of view, for diagnosis 3−28370
gamma camera uniformity 3−10178
gamma ray, image recording system for vascular obs. 3−418
gamma ray Anger scintillation camera, resolution improvement using signal processing and movable filter 3−25858
gamma ray Anger scintillation system, collimation 3−25867
gamma scintillation, new method for design optimisation of parallel-hole collimators 3−22521
high speed cine cameras, highspeed photography, electronic imaging systems, pulsed light sources 3−228
infrared, surface temp. meas. application to nondestructive testing *(German)* 3−18778
Lang camera, optical attachment for selection of photographed region on crystal 3−25957
Lang camera with monochromatized convergent beam for X-ray topography obs. 3−26932
large aperture rocket camera 3−3396
lens change device for 'convas-automat' *(Russian)* 3−3827
lunar surface u.v. spectrographic camera 3−25539
Mars Viking Lander cameras, implementation 3−31830
movie camera for recording holographic images of objects in motion 3−35419
objectives, spectral transmittance evaluation *(Czech)* 3−22395
optical bar camera, Apollo 15 panoramic photography anal. 3−31825
PDO-1, unevacuated optical cryostat 3−25726
pinhole array, self imaging techniques 3−32523
pinhole arrays, multiple image formation 3−6453
Polaroid, catadioptric reflex viewfinder design 3−6010
Polaroid, reflex viewfinder optical component design 3−6011
Polaroid SX-70, evaluation 3−37654
remotely controlled Snorkel camera system 3−35434
resolution determination using large scale target 3−37653
scanning laser recording system, image quality, system evaluation 3−227
shutters, use of image takes in high speed photographic systems review 3−9984
simple camera attachment for vacuum u.v. monochromator 3−6001
spark chamber gamma camera, computer simulation 3−10173
step oscillation camera for X-ray data collection from large unit cells 3−26937
X-ray, scanning Lang camera modification for scanned Berg-Barrett topography 3−1534
X-ray scattering, small-angle, extra-fine cuvettes 3−28742
zoom lenses for amateur movie cameras, design problems 3−22399

candoluminescence *see luminescence*

capacitance
cholesterol-hexadecyltrimethylammonium bilayer, membrane, capacitance rel. to voltage 3−3403
concentric spheres 3−31
cylindrical conducting plane, dielectric-covered 3−13673
deep level impurity determination, Schottky barrier capacitance meas. 3−24510
Josephson junctions, parametric capacitance 3−21183
liquid crysts., nematic, optical transmission threshold and capacitance threshold for alignment in mag. field 3−20695
m.o.s. capacitor, transient response for depleted surface space charge layer 3−5055
m.o.s. structure, nonuniformly doped, h.f. capacitance minimum 3−24525
m.o.s. structure, recomb. characts., photocapacitive effect obs. *(Russian)* 3−24520
p-n heterojunction, nondegenerate, capacitance, elec. field, mode *(Russian)* 3−8258
p-n junction, double diffused, depletion layer transition capacitance calcs. 3−27308
p-n junction, thermally stimulated capacitance for shallow majority carrier traps in edge region 3−36661
parallelepiped of arbitrary dimensions 3−13670
plasma sheath capacitance, resonance behaviour 3−23909
spindle, infinite integral of Legendre function calc. 3−29007
standard, circular four electrode capacitors 3−22240
between three-dimensional electrodes, digital computer techniques 3−19478
transducer, for fluidised bed concentration obs. 3−458
unit in COMECON-countries 3−22241
Al-polydimethyl siloxane-Al, metal-dielectric-metal assemblies, γ-ray effects *(Russian)* 3−39083
GaP, p-n junction with deep centres, space charge capacitance 3−33989
Ge, amorphous, reactor irradiation expts., resistivity var. with heat treatment 3−15195
Hg-Si contact capacitance-voltage characteristic 3−2182
In-PbTe tunnel junction *(French)* 3−24545
KH$_2$PO$_4$, dielec. const., capacity, compressive stress effects, 20-210°C, dielec. anomaly 3−21360
Pb-polydimethyl siloxane-Pb, metal-dielectric-metal assemblies, γ-ray effects *(Russian)* 3−39083
Si-SiO$_2$-electrolyte system, voltage-capacity characts. *(Russian)* 3−24522
Sn-polydimethyl siloxane-Sn, metal-dielectric-metal assemblies, γ-ray effects *(Russian)* 3−39083
Te-As-Ge-Si thin film capacitors, frequency dependence of capacitance and conductance 3−27321
Te$_{50}$As$_{30}$Ge$_{10}$Si$_{10}$ glass film 3−21361
ZnSe phosphors, photocapacitive changes 3−8499

capacitance measurement
biological active macromolecules in aqueous solutions, dielectric permeability meas., modified Nernst's bridge 3−32234
contactless capacitive method for variable and mean thickness obs. of conducting thin films *(Russian)* 3−5766
farad, USSR standard *(Russian)* 3−5749
m.o.s. structure, capacity ratio, semi-automatic bridge *(German)* 3−15262
reference air capacitor, high freq. value detn. 3−19142
solutions of low cond., differential capacitance meas 3−6013

capacitance measurement continued
- $BaTiO_3$ single grain boundaries 3—33937
- GaAs, p^+-n photodiodes, electron irrad., defect studies, differential capacity, conductance measurements 3—33845
- $GeSiO_2$, $Ge\text{-}SiO_2\text{-}Si_3N_4$, semiconductor-insulator boundaries, variation with applied potential, low temps., 77K, surface states *(German)* 3—15264
- Si, impurity gradients, diffusion constant, capacitance meas., nondestructive technique 3—39284
- Si, radiation effects, obs. using junction-capacitance techniques 3—33926

capacitance meters *see capacitance measurement*

capacitor storage
- No entries

capacitor stores *see capacitor storage*

capacitors
- *see also electrolytic capacitors; thin film capacitors; varactors*
- air, constant and variable for electrometer cct. 3—22408
- air, reference standard, high freq. value detn. 3—19142
- alpha-dimethylolpropionic acid based electrolytes, patent 3—18790
- axisymmetric electrostatic fields calculation by numerical method *(Russian)* 3—32475
- circular four electrode, for capacitance standard 3—22240
- cylindrical, electron energy spectrum computation 3—19316
- metallized paper, internal discharges *(Japanese)* 3—26912
- m.o.s., bulk lifetime determ. from current and capacitance transient response 3—24448
- polytetrafluoroethylene film, r.f. sputtering system and film characts. *(Russian)* 3—30941
- $BaTiO_3.MnO$ ceramics, sintered in N_2, monolithic thick films 3—8952
- (HCl) m.o.s. capacitors, oxide stability, surface state density and substrate generation lifetime obs. 3—24513

capillarity
- *see also bubbles; contact angle; drops; foams; liquid films; surface tension*
- binary diffusion through heterogeneous medium, pore size distribution and capillary effects, bounds using moment and transport constraints 3—29917
- Burnett theory of thermal transpiration with wall accommodation 3—29824
- capillary wave interaction with gravity waves on liquid surface, appl. to oceanography *(Russian)* 3—27978
- capillary waves, optical method of detecton *(Russian)* 3—22575
- cement paste, hardened, capillary porisity 3—34668
- cylinder, thin-walled hollow viscous, capillary instability 3—8008
- drying of hygroscopic capillary porous solids, liquid capillary flow, vapour diffusion and heat transfer 3—20409
- dynamic meniscus profiles shape in free coating 3—30335
- entrainment of a liquid by a thin cylindrical filament moving through an interface 3—30334
- flow in packed homogeneous fluidised beds 3—1452
- gas trapped by liquid in a capillary, effect of wetting hysteresis on equations of state 3—20925
- ice compression in freezing of supercooled water in capillaries 3—24247
- jet break-up of non-Newtonian liquid, yield stress effect 3—4521
- liquid film remaining on internal surface of horizontal capillary, thickness determ. *(Russian)* 3—30337
- liquid flow rates in capillary grooves, meas., forced convection mass transfer 3—26800
- nucleation, heterogeneous, from vapour phase onto substrate, capillarity theory 3—1585
- nucleation, homogeneous, capillarity approx. in rate theory 3—26978
- polyacrylamide, meas. of axial normal stress in capillary flow, determ. of viscoelastic props. 3—29813
- polystyrene soln., viscometric study, upper Newtonian region, capillary end-correction 3—29803
- self-diffusion of gases through capillaries, transport equation *(German)* 3—14413
- surface tension, criticism of usual explanations in text books 3—32
- surface waves, nonlinear gravity-capillary, in study varying current, propag. 3—29893
- thermocapillary flow in thin layers, determ. of film profile 3—1349
- thermodynamics of gas/liquid interfaces in a porous medium, condensation/evaporation processes, viscous flow 3—26847
- two-phase granular media, effect of capilliary attraction, rel. to study of static problems 3—17554
- vapour-gas mixture, in a capillary, convective diffusion with evaporation 3—26784
- water vapour heats of adsorption on $\eta\text{-}Al_2O_3$, capillary condensation on dehydroxylated samples *(French)* 3—27187

capillary phenomena *see capillarity*

capture cross-sections, nuclear *see nuclear reactions and scattering*

Caratheodory's principle *see thermodynamics*

carbon
- *see also carbon fibres; charcoal; diamond*
- ablation layers, radiative transfer, Jupiter and Earth entry 3—33336
- absorbed dose of ^{60}Co γ-rays, obs. using calorimeter 3—6070
- adamantane, pressure-induced phase transition 3—20872
- adsorbed monolayer on clean and S, Na, Cs or O_2-covered f.c.c. Ni, vib. properties 3—24340
- amorphous, paramagnetic spin centres from e.s.r. investigations 3—34182
- amorphous dielectric intermediate layer on NaCl, epitaxial growth and condensation of evaporated thin films 3—38746
- amorphous film, electron microscopy dark field images 3—14688
- atom, effects of multiple ionisation on fluorescence yield 3—4366
- atomic, dissociatively prod., pulsed laser emission in elec. discharge 3—10520
- atoms, correlated wavefunctions form, calc. 3—20008
- in austenite, lattice parameter C content depend. at 1100°C *(Russian)* 3—12345
- black, e.p.r., 4.2-300K, paramagnetism, g-factor *(French)* 3—24614
- carbyne, crystalline structure charact. by X-ray and electron diffraction 3—33485

carbon continued
- channel black, adsorbent, adsorption kinetics of polar polymers 3—36486
- chemical transport, deposition mechanism in non-isothermal plasma 3—2644
- columnar growth by pyrolytic deposition, microstruct. 3—1581
- contaminant on W, effect on secondary emission characts. *(Russian)* 3—8693
- crystallite, preferred orientation in soft and hard C heat-treated under pressure 3—9002
- diffusion in Fe samples with dynamic hot pressing *(Russian)* 3—8945
- diffusion in Fe-metal-C system, successive *(Russian)* 3—7963
- diffusion in steel, austenite grain size influence *(Russian)* 3—39331
- epitaxial growth of Cu on Au(111) platelet, influence of intermediate amorphous C layer 3—24357
- evaporated C coatings, Formvar films, homogeneity, wettability hydrophilia, separation phenomena *(German)* 3—1961
- fibres, density meas., small samples, float-sink method 3—28476
- fibres, examination of structure after oxidation, carbonization or graphitization 3—15778
- film, amorphous, antiferromag. transition, e.s.r. obs. 3—18317
- film resistor, low temp. characts. 3—24529
- films, perforated, prep. using u.s. vibration for electron microscopy 3—3879
- foil, passage of 50 MeV protons, energy loss through δ-rays 3—287
- graphitisation of diamond, high pressure and temp., nucleation and planar growth 3—12450
- graphitisation under high press. 3—14999
- hexagonal crystal form suggestion 3—7702
- isotopic comp. of low energy cosmic ray particles *(German)* 3—9413
- K-shell photoionisation cross section and threshold energy determ. 3—14300
- lampblack films, i.r. dispersion properties *(Russian)* 3—15500
- liquid, model approach to melting of graphite and diamond at h.p. *(Russian)* 3—14981
- lunar C chemistry, effects on terrestrial organic chemistry 3—35088
- metal aggregates on C substrate, catalytic props. 3—37142
- molecular Cartesian force consts., computer calc. 3—4423
- negative ion source, bombardment of solid surfaces by positive alkali ions *(Russian)* 3—6061
- neutron spectra, time-energy study using fast neutrons 3—6968
- nuclear reactors, C transfer in Na systems, rate meas. by tab equilibration 3—26532
- plasma, high z, produced by high power laser 3—20546
- pyrocarbon saturated with Br, temp. dependence on resistivity between 90-298 K and thermoelectric power *(French)* 3—8214
- pyrocarbon whiskers, growth during pyrolysis of methane *(German)* 3—15111
- pyrolytic, deposition of fluidized bed particles, microstructure, electron microscopy 3—24994
- pyrolytic, graphite layers preferred orientations, integrated intensities rel. to uniaxial orientation 3—4734
- pyrolytic, isotropic, irrad. effect on mech. props. 3—32945
- pyrolytic, isotropic poorly crystalline, microstructure and mech. propos., annealing effect 3—24993
- pyrolytic rods, formation in gydrocarbon atmos. heated by focused laser beam 3—2807
- quasi-elastic scattering cross sections in tissue like media 3—3593
- radiocarbon dating of vegetable matter and hard-water error 3—15904
- resonance series in vacuum u.v. absorption spectra of dense plasmas 3—17351
- solidification of C in naphthalene, pushing of foreign particles 3—11570
- solubility in Au, Ag and Cu *(French)* 3—38689
- solubility in Rh, Ru, Ir and Re 3—8812
- stars, meas. of total to selective absorpt. ratio by numerical integration of photoelectric spectral scans 3—28200
- stars in Northern Milky Way, coords. and photographic magnitudes 3—31665
- stars with peculiar spectra 3—9541
- in steel, martensite, γ-irrad., redistribution *(Russian)* 3—5288
- stellar ignition of ^{12}C in degenerate cores 3—37359
- sublimation in flow of inert gas, 2800-3500K 3—26845
- substrate, Pd and Pt atomically dispersed thin film, H_2 isoteric adsorption enthalpy *(German)* 3—27921
- supernovae detonation resulting in neutron star remnant 3—28183
- switching phenomena, correlation between memory time and resistivity 3—33966
- thermal diffusivity meas. at high temp. by modulated electron beam technique 3—28495
- thermal vibrational displacement of C atoms in petroleum coke 3—7943
- in transition metal amorphous films, polyconductivity *(Russian)* 3—8145
- u.h.v. outgassing meas. up to 2200K 3—38731
- vitreous, fibre polarised emission of the K-band 3—34438
- X-ray appearance potential spectroscopy, soft X-rays, plasmons, electronic excitations, degree of disorder 3—27586
- X-ray prod. by electron irrad. 3—16540
- X-ray scattering factors by anal. radial orbitals *(Russian)* 3—33006
- B ion equilibrium charge distributions after interaction with C foil 3—11662
- C high strength fibres, h.v. electron microscopy 3—1537
- C IV, vacuum u.v. laser emission 3—37954
- C IV resonance doublets, quasar Ton 1530 absorpt. line spectrum obs. 3—22089
- C stars, spectra and C-classifications 3—39672
- C-burning in stellar Population I conc., p-process nuclei prod. 3—28179
- C-O plasma solidification rel. to white dwarf star interiors 3—31494
- C + C atomic collision, 19-240 keV, X-ray spectra from C_2 system 3—26568
- C^+ diffusion in CO, mobilities and longitudinal diffusion coefficients 3—20262
- C^+ high energy implantation in Si, damage profiles 3—17887
- C^+-C collision, K-shell ionisation in keV-MeV range, Fano-Lichten theory 3—26603
- C_2, comet Bennett, microwave spectrophotometry 3—16190

carbon continued
C_3, quantum model for bending vibrations and thermodynamic props. 3−33095
C_3 molecule, ht. of formation and entropy 3−27852
C^{3+}, ^2S state, natural orbital config. interaction expansions 3−26561
C^{4+} ions in He, Ne, Ar, Kr and Xe gases, charge changing and electron loss cross section 3−11178
C^{6+} beam collision with Ar at 1 to 2 MeV/amu, charge dependence of K-shell ionisation 3−20067
CI, lifetimes of metastable $^5S_2^0$ states 3−11140
CIII 5696 Å line in Wolf-Rayet stars rel. to temperature stratification 3−37369
CIV, spectra between 30 and 500 Å using 0.2 to 2.0 MeV beams 3−29532
CNe^+ collisions, K-shell ionization cross sections 3−23503
^{11}C, short-lived isotope production by Van de Graaff accelerators 3−270
^{14}C, natural isotope, uses in science, review 3−17334
in Co-C alloy, reorientation, rel. to conc. depend. of disaccommodation 3−5121
inFe-Cr-Mo ferritic stainless steel, effect of C and N on toughness, ductility and corrosion resist. 3−27676
in Fe-Sn alloys, decarburation, effects on cpd. formation, phase diag. *(French)* 3−24830
GaAs, GP, electron, neutron irrad., B, C, impurities, i.r. local mode abs. 3−34395
in GaP, rel. to green light emitting diode appl. 3−8734
Mo, wire, recrystallised, alloyed with Ru and C, tensile properties *(Japanese)* 3−31074
Mo ingot, ductility effects of complex additions of 0.15 wt% Ru with C or B *(Japanese)* 3−31073
Nb_3Sn:C, transmission electron microscope examination of defect struct. *(German)* 3−21179
Ni-C carmet film, struct. and electrical props. 3−5063
Ni-Cr-Mo steel, C diffusion study 3−27633
Si:C, i.r. absorpt. spectra, local vibr. modes and defect vibr. modes 3−18475
UO_2-C-N_2, reaction kinetics at 1700C 3−39382
ZnS:Cr^+, Cu, C, e.p.r. and luminescence studies *(Russian)* 3−27552

carbon compounds
see also organic compounds
carbide phase in steel, Mossbauer obs. of carbide phase dissociation on straining 3−15722
carbides, high melting, thermal conductivity, as fn. of characteristic temp. *(Russian)* 3−12427
carbides, preparation rel. to cutting tools, review 3−8939
carbides, sintered, manufacturing process, review 3−5339
carbides, sintered, manufacturing processes, techniques and equipment 3−8971
carbonate planar anion, polarisability from refractivity data using Lorentz local field method 3−30747
coadsorption with O on W, consecutive interactions 3−30347
cyanide complexes, use of electron population parameter to distinguish between C and N 3−20716
lunar sample anal., biological significance rel. to cosmic evolution 3−35087
lunar samples anal. by gas chromatography and high resolution mass spectrometry 3−35089
propane, laminar flame in a discharge, elec. field effects, photography 3−36211
shell carbonate, ^{14}C dating of Late Pleistocene corals and molluscs, effects of partial recrystallisation 3−9196
CCH radical, X-ogen, astronomical 89.190 GHz emission line 3−3278
CCN, spin-orbit coupling consts., non-empirical calc. 3−23532
CH, formation in ion-molecule reactions 3−13100
CH, potential energy and rot. const. calc. by Taylor series expansion 3−7270
CH and CN, comet Bennet, microwave spectrophotometry 3−16190
CH spectrum in magnetic white dwarf G99-37, circular polarization caused by magnetic fields 3−26651
CH^+ formation in ion-molecule reactions 3−13100
CH_2 radical, spin-orbit integrals, evaluation by gaussian expansion method 3−1163
CN, dipole moments, CI calcs., for states of $^2\Sigma^+$ symmetry 3−4405
CN, rotational analysis of 7-4 band 3−20133
CN, shock tube determ. of CN ground state dissociation energy and CN violet electronic transition moment 3−20198
CN radical, lifetimes of A $^2\pi$ and B $^2\Sigma$ states 3−7224
CN radical mol., h.f.s. of $A^2\pi$ and $B^2\Sigma^+$ states 3−14382
CN red system, synthetic spectrum calc. for spectra of moderate resolution 3−13027
CN red system of lines in sunspots, polarization meas. 3−31557
CN violet and red band excitation by metastable Ar and Xe reactions with CN containing cpds. 3−31251
C_2N_2, electron excitation, CN u.v. spectrum and excitation cross sections 3−33114
C_2N_2, Raman and far i.r. spectra 3−33125
C_2N_2 emission spectrum, N_2 sensitised, anharmonicity consts. 3−14360
$C_2N_2^+$, low-energy photoelectron spectra, bond length changes 3−1141
$C_3N_3Cl_3$, i.r. vibrational spectra 3−29660
CO, adsorbed on Ni(100), orbital energy spectra 3−39206
CO, adsorbed on W(100), photoemission energy distrib. curves 3−39213
CO, adsorpt. and desorpt. on Ru 3−20936
CO, adsorpt. on Ni(110) surface decomp. 3−30346
CO, adsorption and decomposition on Pt(111) surface 3−38722
CO, adsorption and desorption on W surface, field emission microscope obs. *(Japanese)* 3−20933
CO, adsorption on graphite with preadsorbed NO, 77.5 K 3−38720
CO, adsorption on Mo(100) surface 3−30348
CO, adsorption on Ni and Cu film, effect on elec. conductivity 3−8144
CO, adsorption on Pd, Pt, Ti films, elec. resistivity obs. *(Japanese)* 3−20929

carbon compounds continued
CO, adsorption on polycryst. Ni surface, sticking probability and desorption spectrum obs. *(Japanese)* 3−20931
CO, adsorption on W and reduction by hydrogen, field emission microscope obs. *(Japanese)* 3−20934
CO, atmospheric, mixing ratio 3−12736
CO, Born-Oppenheimer approx., equilib. bond length calc. 3−33085
CO, CO_2, replacement of chemisorbed gases on metal surface, elec. cond. and mass spectrometry obs. *(Japanese)* 3−20928
CO, CO_2 in Apollo 14 lunar samples 3−31627
CO, CO_2 laser action, electrochemical organic molecule oxidation, directly excited CW 3−16831
CO, c.w. laser emission from flowing gas HCHO near i.r. laser 3−35687
CO, chemisorpt. on Mo, adsorbate depend. surface states, optical refl. obs. 3−38879
CO, collision with F^-, electron detachment rates meas. 3−11300
CO, cooling effect in atm. of late-type stars 3−31642
CO, desorption from Nb (111), electron stimulated 3−20944
CO, desorption from W(100) surface by electron stimulation, time-of-flight analysis of ions and neutrals 3−38730
CO, dissoc. into ions by impact of fast ions and atoms of H, He, Ne, Ar and Kr 3−23621
CO, dissolved in CCl_4, vibr. and rot. motion, fluctuations from i.r. and Raman spectra theoretical anal. *(French)* 3−38284
CO, elastic electron scatt., vibr. excitation, 6-80 eV 3−1286
CO, electron impact excitation cross sections and energy degradation 3−11307
CO, energy parameters in Lennard-Jones potential between atoms determ. from second virial coefficients 3−14402
CO, excited state computation using equations-of-motion method 3−20092
CO, excited states, elastic cross relax. 3−36042
CO, fine struct. and perturbation analysis of $a^3\pi$ state 3−14368
CO, generalized oscillator strengths for lowest $\Pi \leftarrow \Sigma$ transitions 3−4407
CO, inclusion in carbonyl Ni, evolved gas analysis *(Russian)* 3−10197
CO, interaction with (110) Ni surfaces 3−38716
CO, laminar flame in a discharge, elec. field effects, photography 3−36211
CO, laser excited vibr. energy transfer, relax. rates 3−10466
CO, laser induced desorption from Pd surface, rate *(German)* 3−11807
CO, meas. of air content over Norwegian and Greenland seas 3−9288
CO, microwave breakdown 3−23666
CO, Penning ioniz. reactions with metastable He, fluoresc., vibr. populations 3−29731
CO, perturbations in $a^3\pi$ and $A'\pi$ states 3−14342
CO, perturbed by inert gases, determ. of linewidths in $0 \rightarrow 2$ bands *(French)* 3−7214
CO, pot. energy functions and electronic charge densities 3−29611
CO, potential energy curves for excited states, equations of motion method 3−33084
CO, pressure-broadened by itself and foreign gases, linewidth and lineshifts meas. *(French)* 3−17449
CO, produced by CO_2 photodissociation population distribution of triplet vibrational level 3−26683
CO, radio obs. of H II regions W49 and W51 3−35197
CO, rotational diffusion in various liquids 3−4864
CO, Rydberg-Klein-Rees integrals eval. 3−1147
CO, scattering from (100) crystal face of Pt 3−8001
CO, second overtone band identification the variable star α Herculis 3−28216
CO, spontaneous polarization during condensation 3−20942
CO, translational energy meas. use in eval. of energetics for dissoc. attachment processes 3−23612
CO, transport coeffs. in static elec. field, model calcs. 3−38340
CO, u.v. photoionisation, absolute cross sections 3−11282
CO, V-V energy transfer rate from CO(v=2) using tunable parametric oscillator excitation 3−38314
CO, VT relax., meas. by vibr. pumping technique 3−10484
CO, V→V relaxation by laser fluorescence technique 3−33165
CO, vibr. energy transfer cross sections calc. without Born approx. 3−11323
CO, vibr. excited relative populations in pulse discharged CS_2-O_2-He mixtures 3−10496
CO, vibr. relax. at 85 ± 8 K 3−11319
CO, vibr. relax. by He 3−23617
CO, vibrational excitation by electron impact, 10 to 90 eV 3−7262
CO, vibrationally excited, reaction of O atoms with acetylene, methylacetylene and methane 3−39432
CO, volume viscosity u.s. determ. between 77 and 300 K 3−26766
CO adsorbed on H-Y zeolite, ioniz., CO^+ radical studies 3−21809
CO adsorption on Ag-Pd alloys, adsorption energy. and ordered structure form. 3−1885
CO adsorption states on Ni films, thermal desorption and elec. resist. obs. *(German)* 3−27184
CO and O_2/CO mixture, plasmoidal r.f. discharge, spatially resolved spectroscopic profiles 3−20671
CO band absorpt. importance in A-G type stars flux discrepancies 3−22047
CO Cameron bands in Martian airglow, limb intensity profiles 3−16155
CO chemical laser, using reaction $O + CSe \rightarrow CO^* + Se$ 3−6457
CO chemisorption on NiO, h.f. form 3−36488
CO chemisorption on Pt, thermal desorption methods 3−37143
CO collision with O^-, associative detachment 3−20201
CO collisions with K^+, K^+, mobility diffusion and clustering 3−29827
CO crystal, orientational disordering rel. to thermodynamics props. 3−7866
CO dissociation in pumped CO laser, study using i.r. absorption 3−16899
CO emission at 2.6 mm. from molecular clouds in the Galactic centre region 3−19068
CO fluorescence cross-section from photo-dissociation of CO_2 3−20193

carbon compounds continued
CO fund. bands, relative transition probabilities 3–1183
CO gas, mobilities and longitudinal diffusion coefficients of CO^+, C^+ and $CO^+.CO^-$ 3–20262
CO in photosphere and faculae, equivalent width calc., temp. sensitivity of molecule *(Russian)* 3–16140
CO laser, based on flash initiated reaction O_3-XCN, X=Cl, Br, I, CN 3–10523
CO laser, CW, chem., prod. in N_2-O_2-CS_2 fast flow system 3–10472
CO laser, c.w. power from $CS_2/O_2/N_2O$ flames 3–32534
CO laser, chem., based on a CS-O reaction, characts. 3–10512
CO laser, chem., CW, single line operation 3–10507
CO laser, chem., kinetic theory, computer model 3–10491
CO laser, fast flow, construction, characts. 3–10510
CO laser, gasdynamic, vibr. relax. in supersonic expansion, numerical model 3–10504
CO laser, intracavity breakdown threshold calc. 3–10477
CO laser, Lamb dip, vibrational-rotational lines 3–16828
CO laser, meas. of density and collision frequency of electrons in plasma using resonator method 3–16845
CO laser, model in pulsed and CW operation 3–10494
CO laser, N_2O detection, amplified absorption 3–29129
CO laser, operation kinetics calc., vibr. distrib. function 3–10474
CO laser, output characts. rel. to electronegative gaseous additions 3–10509
CO laser, P-branch i.r. transitions in C_2H_2-O_2 flame, optical gain 3–10473
CO laser, radiation absorpt. by water vapour 3–19627
CO laser, resonant i.r. absorption of laser light by magnetically tuned NO, pressure broadening of spectral lines 3–14388
CO laser, supersonic flow, elec. excited, mol. energy transfer processes 3–10511
CO laser, used for detection of NO 3–13308
CO laser, vibrational energy exchange *(Russian)* 3–23632
CO monitoring, i.r. fluorescence analytical technique 3–26028
CO on W single- and poly-cryst., chemisorption desorption spectra 3–8025
CO photodesorption from polycryst. Ni 3–24344
CO production in rain water from aldehydes photodecomposition by sunlight 3–21948
CO rotational cooling in dark interstellar clouds 3–31783
CO shock heated, variation in equilibrium i.r. fluorescence 3–4453
CO thin films, transmission and reflection in vacuum u.v. study of intermolecular interaction of excited species 3–2568
CO trapped in solid Ar, i.r. spectra, libration motion 3–8563
CO vibr. energy distrib. in transverse flow laser, long-range force theory calc. 3–37956
CO/N_2 molecular laser, energy-transfer processes, modelling 3–4091
CO-CO_2, vibr.-vibr. energy transfer rate, 175-350 K 3–11320
CO-induced chemisorption levels in a Ni(110) surface, energy loss spectroscopy 3–10103
CO-N_2 laser, radiative gain of CO vibr.-rotation transitions 3–6470
CO-water vapour, calc. radiation from two plane isothermal layers 3–36066
CO + Hg collisions, time-of-flight sensitized fluoresc. vel. depend. of Hg excitation 3–11312
$CO + Kr^+ \rightarrow CO^+ + Kr$, 0.04-3 eV 3–20058
CO + O_2 mixtures, coeff. as CO tends to zero 3–14414
CO^+, relative intensities for ionisation of lowest 3 electronic states by electron impact 3–33159
CO^+ diffusion in CO mobilities and longitudinal diffusion coefficients 3–20262
$CO^+ + 2CO \rightarrow CO^+.CO + CO$, rate-coefficient meas. in a drift-tube mass spectrometer 3–20202
$CO^+ + Kr \rightarrow CO + Kr^+$, 0.04-3 Ev 3–20058
$CO^+{}_2$, effective cross sections and excitation functions of spectral bands, excitation by 0.4 to 20 keV electrons 3–14400
CO_2, 9.33 and 10.18 μm molecular transitions used in laser stabilisation, accurate freqs. 3–22872
CO_2, accurate analysis in O_2-N_2 mixtures using i.r. absorp. 3–26008
CO_2, adsorption on Ti film, binding state detn., mass spectrometry and elec. resistivity obs. *(Japanese)* 3–20930
CO_2, ang. distrib. of photoelectron spectra 3–23545
CO_2, atmospheric, control and readout system for profiles 3–18899
CO_2, atmospheric, mixing ratio 3–12736
CO_2, atmospheric additions due to human activities since Industrial Revolution *(French)* 3–21956
CO_2, biosphere, industrial influences on atmosphere 3–5511
CO_2, CO, in atmosphere, laser-Raman radar detection, using sampling technique 3–3190
CO_2, c.w. laser emission from flowing gas HCHO near i.r. laser 3–35687
CO_2, collision with O_2 and N_2 mols., fluorescence of stretching vibration *(Russian)* 3–26736
CO_2, composition variation in temperate glaciers 3–2842
CO_2, compound states, study using electron transmission spectroscopy 3–17466
CO_2, condensed layer, adsorption characteristics, cryopumping 3–8022
CO_2, continuous absorpt. exponential decrease beyond 4.3μ band head due to far wings contour 3–29734
CO_2, core level electron spectra showing shake-up satellite lines 3–11294
CO_2, critical isotherm equation 3–17971
CO_2, crystal, orientational disordering rel. to thermodynamics props. 3–7866
CO_2, D-region, photoionization of O_2 3–3088
CO_2, discharge, nsec. region, electron optical study *(Russian)* 3–17685
CO_2, discharge current change due to CO_2 laser beam, mechanism 3–26914
CO_2, dissoc. excitation, Doppler broadening of OI 1304 Å multiplet 3–23583
CO_2, distrib. in Martian atmosphere, i.r. absorption obs. 3–31588
CO_2, E-region content, mass spectral obs. 3–3084
CO_2, efficient elec. laser using preionization by u.v. radiation 3–16826

carbon compounds continued
CO_2, electron beam pumped amplifier, nanosecond pulse amplification 3–26217
CO_2, electron energy deposition rel. to Mariner u.v. data for Mars 3–12981
CO_2, energy fluxes from nonisothermal layer of selectively radiating gas *(Russian)* 3–11353
CO_2, Fermi reson., density effect, Raman scatt. meas. 3–33124
CO_2, glow discharge, vibr. translation rates for (10^00) and (00^01) levels 3–36054
CO_2, h.f. discharge excitation at low press. *(Russian)* 3–7593
CO_2, heat transfer in turbulent flow with combined forced and free convection *(Russian)* 3–11392
CO_2, helical TEA laser 3–35689
CO_2, i.r. general absorptance, polynomial representation 3–36015
CO_2, in atmosphere, remote sensing using i.r. heterodyne radiometer 3–3193
CO_2, integral spectrum absorpt. coeffs., calc. 3–35636
CO_2, l.p. decomp., non-equil. effects rel. to activation energy 3–12503
CO_2, large-scale flux in Southern Hemisphere troposphere 3–34900
CO_2, laser, chem., based on h-O_3 and OH-CO pumping reactions 3–10525
CO_2, line intensities in 2.0 μ region 3–29696
CO_2, liquid, u.s. velocity, thermodynamic data determ. 3–17930
CO_2, Martian atmosphere, rel. to water vapour exchange with surface 3–31595
CO_2, microwave discharge, $CO_2{}^-$ form 3–20670
CO_2, photodissociation, cross-sections for fluorescence of CO 3–20193
CO_2, photoionisation and photoabsorption cross-sections at 584 Å of solar radiation 3–11291
CO_2, pot. energy functions and electronic charge densities 3–29611
CO_2, potential parameters and combination rules, determ. from diffusion data 3–1293
CO_2, pulsed gas laser, kinetics *(German)* 3–6459
CO_2, Raman spectra for meas. in air at p.p.m level 3–18897
CO_2, Rayleigh scatt. coeff. rel. to that of air 3–14417
CO_2, relax. rates of lower laser levels 3–37952
CO_2, relaxation of bending vibration 3–23537
CO_2, reliable high efficiency atm. press. laser 3–16843
CO_2, replacement of H on a W surface *(Russian)* 3–8021
CO_2, respiratory acidosis, dorsal root potential modifications 3–28341
CO_2, sound scatter near critical pt. 3–4514
CO_2, sound velocity in pressure range 1-40 kg/cm², frequency range 450-3470 Hz, temps. 3–4513
CO_2, spatial distrib., on reflection and sublimation from cold surface 3–39203
CO_2, spherical capped gas bubbles rising in aqueous media, mass transfer coefficients calc. 3–29921
CO_2, supercritical, laminar forced convective heat transfer, buoyancy effects *(Japanese)* 3–20323
CO_2, TEA, optically pumped by NH_3 laser, submillimeter laser action 3–13731
CO_2, translational energy meas. use in eval. of energetics for dissoc. attachment processes 3–23612
CO_2, trapped electron technique for inelastic cross-section meas. 3–7260
CO_2, turbulent boundary layer injection 3–1386
CO_2, turbulent flow at supercrit. press., local worsening of heat transfer obs. 3–23691
CO_2, vibr. and rot. energy transfer with HF, DF and HCl 3–26734
CO_2, vibr.-vibr. energy transfer of ν_3 mode 3–33161
CO_2, waveguide laser, gain and saturation intensity meas. 3–26222
CO_2 15 μm bands, foreign-gas-broadening effects 3–7213
CO_2 absorption into monoethanolamine water mixtures by oscillating jet, interfacial tension meas. 3–11795
CO_2 adsorbed layer detection using attenuated total reflection 3–25714
CO_2 and H_2O elimination as O_2 transport species in mixed oxide fuel pins 3–17323
CO_2 at 1 atmosphere, pressure fluctuations on a membrane 3–17486
CO_2 atmospheric pressure pulsed laser with semiconducting plastic electrodes 3–10464
CO_2 atmospheric temp. profiles in 15 micron absorpt. band, vertical resolution of remote radiation meas. 3–25221
CO_2 blowing in air, heat and mass transfer obs. 3–1319
CO_2 clusters formed via homogeneous nucleation in nozzle beams, struct. obs. 3–26735
CO_2 diluted in Ar, vibr. energy transfer 3–29743
CO_2 dissociative attachment, CO fragments vibr. excitation 3–23613
CO_2 electric-discharge convection lasers, unstable resonators 3–16883
CO_2 extinction coefficients, temperature and pressure dependence rel. to Martian atmosphere 3–16164
CO_2 flux from lithosphere in Bohemian Massif 3–9190
CO_2 frost deposit on Mars 3–16149
CO_2 gas absorption by rapid laminar fan-shaped water sheet 3–4536
CO_2 gas lasers, chemical pumping, lasing mechanism, discharge and rapid expansion pumping, high pressure pulsed chemical laser 3–19600
CO_2 gas with H_2O impurity, CO_2 gas laser, vibrational relaxation *(Russian)* 3–4515
CO_2 glow discharge, vibr.-vibr. energy transfer 3–6458
CO_2 helical TEA laser, performance characts. 3–712
CO_2 high pressure laser powered by slow compression heater *(French)* 3–26228
CO_2 high-power electric-discharge laser, closed cycle performance 3–715
CO_2 high-pressure c.w. waveguide laser, mode locking 3–714
CO_2 in mesosphere and lower thermosphere, r.f. quadrupole spectrometer obs. 3–3045
CO_2 in venusian atmosphere intensities and spectroscopic compounds for weak bands 3–3302
CO_2 isotope ratio analysis with double focusing, double collecting mass spectrometer 3–25928
CO_2 laser, 300-J multigigawatt, transverse electric discharge 3–16829

carbon compounds continued

- CO_2 laser, asymmetric stretch mode vibr. temp. rel. to laser action 3−16837
- CO_2 laser, chem., based on CO-N_2O reaction catalyzed with NA 3−10514
- CO_2 laser, effect of proton beam on generation power *(Russian)* 3−6472
- CO_2 laser, gas, high current electron beam controlled, current, voltage, gain meas. 3−10519
- CO_2 laser, high press., pulsed, chem. transfer, props. 3−10470
- CO_2 laser, high press., TEA gain and power, theory rel. to expt. 3−10476
- CO_2 laser, intracavity breakdown threshold calc. 3−10477
- CO_2 laser, modulation of c.w. He-Ne laser, using ultrafast Kerr effect in CS_2 3−32581
- CO_2 laser, optical pumping with blackbody radiation *(Russian)* 3−6468
- CO_2 laser, output power rel. to cavity length 3−4085
- CO_2 laser, population inversion, role of CO 3−721
- CO_2 laser, pulsed discharge and electron beam controlled, performance comparison 3−35686
- CO_2 laser, radial mode, performance 3−26221
- CO_2 laser, TEA, dynamical processes, giant pulse form. 3−718
- CO_2 laser, TEA, small signal gain distrib. 3−717
- CO_2 laser, TEA, translational temp. and vibr. temp. from gain spectral behaviour 3−19602
- CO_2 laser, transition freqs., standard deviations 3−10537
- CO_2 laser, transversely sustained, photoinitiated, props. rel. to discharge parameters 3−22869
- CO_2 laser, unstable confocal resonator modes spatial props. 3−4086
- CO_2 laser, volume excited TEA, operational characteristics 3−4092
- CO_2 laser, wavelength and velocity of light meas. 3−9923
- CO_2 laser, with varying Q-factor, population inversion and radiation density *(Russian)* 3−29081
- CO_2 laser amplifier, cold-cathode electron-beam controlled 3−716
- CO_2 laser amplifier, electron beam controlled, performance 3−10478
- CO_2 laser anemometer for long range wind velocity determination 3−3196
- CO_2 laser discharge, stability and output rel. to nitrogen oxide impurities 3−10499
- CO_2 laser for thick film resistors trimming *(German)* 3−32607
- CO_2 laser Michelson interferometer, phase relations, obs. 3−13318
- CO_2 laser oscillator with unstable resonator cavity, performance 3−26218
- CO_2 laser pulse shaping with saturable gas absorbers 3−35714
- CO_2 lasers, calorimeter for energy output measurement 3−35428
- CO_2 lasers, double discharge TEA, powerful nanosecond pulses by stable passive mode-locking 3−26219
- CO_2 lower laser level, relax. of excess populations 3−1247
- CO_2 mixing into supersonic N_2, continuous lasing action 3−22882
- CO_2 molecular dissociative and non-dissociative photoionization at 304 and 584 Å 3−33149
- CO_2 P20 (00°1-100) transition probability, shock widening with collisions with N_2 and He *(Russian)* 3−29754
- CO_2 photodissociation, $O(^1S)$ prod. 3−9085
- CO_2 photodissociation population distribution of triplet vibrational level of CO 3−26683
- CO_2 quenching of vibr. excited N_2 3−4483
- CO_2 singularities in behaviour of interphase boundary near critical point 3−4840
- CO_2 spectral bands in Venus atmosphere, scattering layers 3−35072
- CO_2 spectral bands in Venus atmosphere, evidence for two scattering layers 3−35073
- CO_2 stability in Martian atmosphere and under radiolysis 3−22034
- CO_2 TEA double discharge grid amplifier, performance characs. 3−26220
- CO_2 TEA laser, output-power pulse shape, theory 3−16835
- CO_2 TEA laser, triggering characs., output optimisation 3−32541
- CO_2 TEA laser pulses, interaction with metals enhanced with liquid layers 3−18518
- CO_2 transverse discharge pulsed chemical transfer laser 3−32533
- CO_2 vibr. deactivation using laser induced fluoresc. in CO_2; $CO_2+{}^{14}N_2$, $CO_2+{}^{15}N_2$; CO_2+He 3−11280
- CO_2 vibrational-rotational bands, i.r. absorpt. and emission in Venusian mesosphere 3−28153
- CO_2 waveguide laser operated in flowing gas configuration, characteristics 3−727
- CO_2:N_2:He c.w. waveguide laser, using B+O capillary tube 3−13732
- CO_2/air gas mixtures, turbulent, hot wire anemometry 3−22564
- CO_2/H_2 system, ion-molecule reaction rates meas. by ion cyclotron resonance 3−26721
- CO_2/O_2 mixtures, acoustic absorption vibrational relaxation 3−1323
- CO_2-DF laser, chem., pulsed transfer 3−10469
- CO_2-DF laser, chem. transfer, efficiency rel. to gas flow rates and static press. 3−10503
- CO_2-DF laser, pulsed chem. transfer, kinetic model, computer simulation, review 3−10471
- CO_2-He laser, similarity law, disturbing electrodes effect 3−13730
- CO_2-inert gas mixtures, relaxation of bending vibration 3−23537
- CO_2-N_2, gas dynamic laser pulse amplifier, idealized rate eqn. analysis 3−10505
- CO_2-N_2 gas dynamic laser, model 3−10506
- CO_2-N_2 mixtures, electrodeless induction high-freq. discharge for laser pumping 3−32550
- CO_2-N_2-He system, amplification rel. to temperature 3−19605
- CO_2-N_2(He) (N_2-He) plasmas, stationary state, small signal gain coeffs. for rot.-vibr. transitions *(French)* 3−7223
- CO_2-O_3-D_2 laser, 10.6 μ, vibr. energy transfer from OD to CO_2 3−19603
- $CO_2+p\text{-}H_2(0\text{-}H_2)$ collisions, simultaneous vibr.-translation, vibr.-rot. and rot.-translation exchanges *(French)* 3−23614
- CO_2^- radical, bond angle determ. from e.s.r. 3−20081
- CO_2^+, fluorescence spectra, cross-section meas. 3−1249
- CO_2^+, spin-orbit coupling consts., non-empirical calc. 3−23532
- CO_3^- and $CO_3^-.H_2O$, photodetachment cross sections 3−1271
- $CO_2H^+ + CH_4 \rightarrow CH_5^+ + CO_2$, proton transfer reactions in flowing afterglows, kinetics 3−39438
- $CO_2{}^+N_2{}^+$He mixture expanding in supersonic jet, light amplification factor 3−19607
- COS, ang. distrib. of photoelectron spectra 3−23545
- COS, core level electron spectra showing shake-up satellite lines 3−11294
- COS, pot. energy functions and electronic charge densities 3−29611
- COS laser, photodissociation, lasing due to S_2, onset of inversion *(Russian)* 3−4458
- COS^+, spin-orbit coupling consts., non-empirical calc. 3−23532
- $CO^+.CO^-$ diffusion in CO mobilities and longitudinal diffusion coefficients 3−20262
- $CO(d^3\Delta)_{v=5}$, spin multiplet relax. and radiative lifetimes 3−20177
- CP_4, etching of Si, effect of u.s. agitation 3−39264
- CS, emission spectrum after excitation in energy transfer collisions 3−1212
- CS, high resolution photoelectron spectrum, ioniz. pots. 3−4427
- CS, radio obs. of H II regions W49 and W51 3−35197
- CS mol., Zeeman effect, dipole moment 3−23580
- CS_2, ang. distrib. of photoelectron spectra 3−23545
- CS_2, core level electron spectra showing shake-up satellite lines 3−11294
- CS_2, correl. of a, $^3A_2$ state with linear states 3−17435
- CS_2, crossed polariser system for base-line noise reduction in laser pulse trains 3−28582
- CS_2, liquid, Kerr consts. meas. 3−39121
- CS_2, liquid, Raman spectra, dilution and temp. var. effects 3−36030
- CS_2, pot. energy functions and electronic charge densities 3−29611
- CS_2, pure and dissolved in CCl_4, i.r. spectrum, mol. anharmonicity in liquid 3−20161
- CS_2, ultrafast Kerr effect, 10.6 μ, appl. to laser beam modulation 3−32581
- CS_2 light wave retardation in elec. field *(Russian)* 3−24678
- $CS_2/O_2/N_2O$ flame, c.w. laser power from vibr. excited CO 3−32534
- CS_2-O_2 laser, chemical flow, CW, operation, flash photolysis 3−10508
- CS_2-O_2-He, pulsed discharged mixture, relative populations of vibr. excited CO 3−10496
- CS_2-O_2-N_2, flast flow system for prod. of CO CW chem. laser 3−10472
- CS_2+O_2 chemical laser, reaction mechanisms 3−16836
- CSe, microwave spectrum, mol. Stark and Zeeman effects, dipole moment, g-values 3−23580
- CS emission system in vacuum and near u.v., vibr. and rot. consts. 3−14367
- $^{12}C^{16}O$, Rydberg-Klein-Rees eval. for $X'\Sigma^+$ state 3−1148
- $^{12}C^{32}S_2$, vibr. level calcs. *(French)* 3−1169
- $^{13}C^{16}O/^{12}C^{18}O$ ratios from line emission from nine H II regions 3−19072
- ^{14}CO in galactic ^{12}CO sources, obs. at 105871.11 MHZ 3−13099
- $^{14}CO_2$ expiratory gas continuous counting scintillation probe 3−25869
- Co, chemisorption of Ni(110), investigation by probe methods 3−38721
- Co_2, vibr. relaxation mechanism 3−19606
- 12%Cr-Fe-C-N, structural diagrams and phase reactions, 1300-700°C 3−8772
- 7%Cr-Fe-C-N, structural diagrams and solid phase reactions, 1300-700°C 3−8773
- Cs molecule, collisional vibr. relax. in presence of Ar, energy transfer probability calcs. *(French)* 3−20208
- Cs_2 mol., small angle electron diffraction from molecule 3−29545
- Fe-Al-C alloy, mag. after effects, directional ordering of interstitial atoms 3−12013
- Fe-C martensite, carbon multiplet creation during deform. obs. *(French)* 3−8829
- Fe-Ga-C alloys, f.c.c., interactions between insertion and substitution atoms *(French)* 3−8777
- Fe-W-C alloys, morphology of eutectic 3−18567
- He-CO_2 laser, absorpt. coeffs. of emission by CO_2, NH_3 and water vapour *(Russian)* 3−6474
- N_2 molecules in positive discharge column of CO_2+N_2 mixtures, excitation *(Russian)* 3−4474
- NaCl:CN^{-1}, mol. lattice relax. of CN^-, dynamic heat capacity meas., 0.3−4 K 3−7867
- Nb-C system, phase diag. 3−2692
- Nb-Mo-Zn-C cast alloys, ductility increase by heat treatment 3−18664
- $O+CS_2$ transverse flow laser, CO vibr. energy distrib., long-range force theory calc. 3−37956
- $O+CS_2 \rightarrow SO+Cs$ reaction obs. using crossed mol. beams 3−12505
- PyC-SiC-PyC, electrolytic etching of SiC in coated particles *(German, English)* 3−23438
- W-Zr-C alloy, dispersion struct. changes during annealing and recrystalln., electron microscope obs. *(Russian)* 3−8875

carbon fibres

- a-axis preferred orientation in commercial fibres, quantitative estimates 3−31171
- anisotropic, molecular struct., X-ray and electron diffr. obs. 3−27788
- composite, elastic consts. 3−27757
- composite, Ni-matrix, elevated temp. stability, morphological and mech. prop. degradation 3−31138
- composite material of polymer matrix with C fibres for high heat resist. 3−18697
- composite of C fibre in resin, crack propag. energy 3−8994
- composites, high-temp. strength up to 2000°C 3−31135
- dark field electron micrographs, interpretation of microfibrils 3−18731
- fillers in polyacetal, effects on friction and wear *(Japanese)* 3−18727
- fracture mechanisms 3−15781
- fractures, local, matrix and interface modification effect 3−5348
- growth from vapourized benzene, thermal decomposition, 1150-1290°C 3−24996
- heat treatment effects, analysis of structure after oxidation, carbonization or graphitization 3−15778
- high strength, h.v. electron microscopy 3−1537

carbon fibres continued
- hybrid composite, C and glass fibre reinforced epoxy resin, mech. props. *(Japanese)* 3—18708
- Kaiser effect in stresswave emission testing of type II composites 3—15783
- liquid suspension, alignment in magnetic field 3—5347
- micromorphology stability and interstitial compounds 3—31172
- polyacrylonitrile based, high-modulus, three-phase struct. obs. 3—27771
- Pyrex glass, carbon fibre reinforced 3—18700
- reinforced composites, review *(Japanese)* 3—18706
- reinforced composites, thermal expansion, 80-400 K 3—18702
- reinforced epoxy resin, impact and fracture props. 3—31142
- reinforced polymers, nondestructive testing, fatigue performance 3—31213
- sandwich composite with glass fibre, Izod impact props. 3—31131
- structural examination by different techniques 3—15779
- structure and physical props., X-ray and electron diffr. study after graphitization 3—15780
- structure obs. using polarized light microscopy 3—3793
- surface, Auger and secondary electron emission spectroscopy 3—5346
- surface, growth of n-alkane crysts. 3—20703
- tensile strength and modulus of elasticity, meas. method 3—18752
- vapour growth of B tetragonal filaments on carbon fibre substrate, pyrolysis and morphology 3—21532
- wettability measurement, wicking method 3—39394
- K intercalation compounds, colour, structure, elec. cond. 3—24995

carbon microphones *see microphones*

carbon tetrachloride, CCl_4 *see organic compounds*

carcinotrons
- No entries

cardiology
- *see also electrocardiography*
- acute fibrinous pericarditis, diagnosis using ^{125}I labelled fibrinogens 3—28363
- aneurysm of circle of Willis, model, qualitative analysis of Austin's differential equation 3—33322
- aorta parameters, determ. using cost function analysis 3—9637
- arterial pressure waves, ventricular ejection, computer-aided analysis 3—28320
- biomechanics, hereditary processes, evolution in terms of difference-differential equations 3—35229
- blood pressure signal conditioners, automatic calibration 3—398
- brachial artery flow velocity meas. after cardiac surgery 3—39803
- canine mitral complex, ultrastructure and electromechanical properties 3—9687
- cats, left ventricle rel. to flow and pressure source 3—36141
- cats, normal myocardial function and energetics in volume overload hypertrophy 3—37512
- d.c. defibrillators, indicated and delivered energy 3—6123
- defibrillator performance, instrument for evaluation 3—6124
- denervated transplanted human heart, electrophysiological studies 3—37518
- dilution curve area estimation by procedure based on compartmental hypothesis 3—6126
- dog common carotid artery, transport of ^{14}C-4-cholesterol between serum and wall 3—37513
- elastic modulus of canine cardiac muscle, in vivo technique 3—22532
- electric shocks, coronary circulation effects, possibility of myocardial infarction 3—9694
- electrocardiogram as a teaching example of electrostatics 3—37575
- electrophysiological, pacemaker activity and atrioventricular conduction, vagal and stellate nerve stimulation effects in dog 3—35237
- human aortic valve, stress analysis, for design of prosthetic valve 3—35223
- left ventricular volume calc. from X-ray obs. 3—3578
- left-ventricular function, mathematical model 3—28309
- muscle contraction effects of Ca ionophore, X-537A 3—35266
- muscle models and mechanics 3—22139
- ventricular depolarisation, multiple dipole model 3—19093
- ventricular pressure, rate of proportional rise determination, on-line computer applic. 3—13485
- ^{99}Tc, quantitative radioisotope method for in vivo evaluation of cephalic circulation in the rat 3—31932

carrier density
- *see also current density; electron density*
- distribution in semiconductor or insulator with small p.d. applied to long specimen *(French)* 3—33895
- excitation of carrier density oscillations by light 3—15217
- impurity level activation energy, estimation from carrier conc. temp. depend. *(Russian)* 3—33828
- kinetics under weak excitation for trapping levels and recombination centres *(Russian)* 3—24450
- m.i.s., from C/V meas. 3—24514
- m.i.s.i.m. structure, assumption of quasi-steady screening state *(Russian)* 3—30540
- over higher temperatures 3—33897
- plasma gradient-induced instabilities of single carrier stream in presence of carrier density gradient 3—36633
- p-s-n rectifiers, band-to-band Auger recombination and carrier-carrier scattering 3—5019
- semiconductor, deformation-concentration instability 3—33901
- semiconductor, Faraday effect with allowance for carrier density elec. field depend. 3—5180
- semiconductor, many valley, carrier conc. effect on short wavelength phonons self energy 3—30407
- semiconductor, many-valley, charge density fluctuation in strong elec. field 3—5003
- semimetal film, carrier conc. and mag. moment behaviour in semimetal semicond. transition region *(Russian)* 3—18064
- TCNQ charge transfer complexes, current carrier effective mass determ. from Hall mobility 3—2368
- AlB_2, metallic cond., carrier conc., cryst. growth 3—11878
- BeTeI film, substrate temp. depend. *(Russian)* 3—21067
- Bi and Bi-Sb alloy powder compacts characteriz., 300-77 K 3—36593
- Bi-Cd melt, conduction electron states density at fermi level rel. to mag. susceptibility 3—27362

carrier density continued
- CdO single crystal, degenerate semicond., Hall effect obs.. 3—2087
- CdS, heteroepitaxial layer, meas. rel. to contamination by GaAs substrate 3—2653
- CdSe-Dy_2O_3 thin-film structure 3—15265
- n-CdTe films, high field phenomena *(French)* 3—27262
- $Ga_{1-x}Al_xAs$:Si, L.P.E. growth, depend. of carrier conc. profiles on growth conditions 3—27190
- n-GaAs, electrochemical characterization, automatic plotting system 3—30953
- GaAs, epitaxial, characterisation for microwave devices 3—2685
- GaAs, epitaxially grown, electrical props. depend. on $AsCl_3$ temp. 3—8756
- GaAs, high resistivity film, dominant oxygen contrib. to compensation 3—15156
- p-GaAs, i.r. plasma refl., carrier conc. determ. 3—18454
- GaAs inhomogeneous crystals, temp. depend., 80-300K *(Russian)* 3—18133
- p-GaAs:Ge, epitaxial layer, electron diffusion length variation with hole conc. 3—24449
- GaAs:Si, free carrier conc. rel. to annealing 3—18141
- n-GaAs:Sn, epitaxial layer, hole diffusion length variation with electron conc. 3—24449
- $GaAs_{1-x}P_x$, meas. for malt grown crystals 3—24805
- $Ga_xIn_{1-x}Sb$, vertical freeze grown material characterisation 3—5280
- n-GaN(:Zn) film, vapour phase grown, Hall meas., carrier conc. 3—33884
- Ge, epitaxial, polycryst., amorphous, Hall mobility, carrier conc., cond., noise, 100-400 K 3—38855
- n-Ge, high purity, γ-irrad., carrier-conc.-depend., mobility 3—36627
- Ge, O doped and Li diffused, photon irradiation and annealing studies 3—18136
- Ge, radiation defects due to 45-50 MeV electrons, temp. depend. obs. *(Russian)* 3—36332
- n-Ge, surface hole mobility and density, scatt. in surface inversion channels, Hall meas. *(Russian)* 3—27299
- Ge:Al, implanted, rel. to carrier generation at room temp. 3—2083
- $GeSb_2Te_4$, single cryst. characterisation 3—5279
- n-Hgs, cubic, band inversion, optical absorpt. and intra-band refl. rel. to carrier conc. and temp. 3—2002
- InP epitaxial, carrier concentration profiles 3—24808
- n-InSb, acoustic gain optimum freq. depend. on carrier density 3—8231
- n-InSb, magnetic freeze out, in strong mag. field, theory 3—30498
- LaS, from i.r. refl. spectra obs. *(Russian)* 3—8595
- PbS epitaxial film, low conc. by quasi static growth 3—2674
- PbSe, effect on carrier mobility, 0.3 to 800K 3—27252
- $SbSI_xBr_{1-x}$, ferroelec. semicond., nonequilib. carrier density influence on phase boundary form. 3—39113
- Si, illuminated, effect on Young's modulus *(Russian)* 3—1665
- Si, optically inhomogeneous, surface free carrier reflectivity 3—5210
- Si, radiation defects due to 45-50 MeV electrons, temp. depend. obs. *(Russian)* 3—36332
- p-Si, rel. to double injection currents 3—33909
- n-Si m.o.s. capacitors, minority carrier generation and density 3—38898
- SnTe, i.r. refl. spectra, carrier effective mass. relax. time and density *(Russian)* 3—8588
- SnTe-PbSe system, comp. and temp. depend. *(Russian)* 3—11918
- Te, acoustoelec. non-ohmic conduction, carrier conc. depend. 3—33959
- Te, inactive mode cyclotron resonance absorption 3—8106

carrier mean free path
- from Boltzmann eqn. soln. using iterative technique 3—24406
- copper phthalocyanine, photoelectric emission, density of states, electron-electron m.f.p. 3—18527
- disordered one-dimens. system, localisation distance, m.f.p., backward scatt. 3—24385
- DNA periodic models, mobilities and m.f.p. calcs. 3—8171
- p-Si, rel. to double injection currents 3—33909
- Si surface barrier radiation detector, electron beam radiation damage effects 3—32157
- W, temp. depend. of electron m.f.p., determ. using r.f. size effect 3—36596

carrier mobility
- *see also carrier mean free path; carrier relaxation time; current density; electron-hole recombination; electron mobility; electron-phonon interactions*
- actinides, comparison across series 3—2049
- alkali metal nitrates, specific conductances up to 12 Kbar *(German)* 3—11901
- alloy, ferromag. anomalous Hall effect, cond. electron scatt. on magnons *(Russian)* 3—36589
- p- AlSb, mechanisms of carrier scattering 3—24455
- amorphous semiconductors, electronic phenomena, review 3—24415
- anthracene, perdeuterated, drift mobilities, 260 to 400K 3—30467
- anthracene, singlet-oxygen-induced hole current 3—2126
- anthracene, surface bands and assoc. mobilities calc. 3—30532
- charge carrier drag by transverse electromagnetic waves 3—21063
- chlorinated diphenyls, temperature behaviour in ionic conduction range *(German)* 3—36610
- complex semiconductor chalcogenides, physical props. *(Russian)* 3—8168
- cubic semiconductors in hot carrier range, symmetry relations between mobility and differential mobility-tensor components 3—8190
- cuprous halides, luminesc. during laser excitation, H band emission, electron and hole effective masses 3—27557
- defect photoconductor, charged centre scattering effect on photoexcited carriers mobility 3—18190
- deformed crystals, effective mass, perturbatin theory *(Russian)* 3—20982
- DNA periodic models, charge drift mobility calcs. 3—8171
- electron gas motion in conducting solids 3—2041
- epoxy resin, d.c. cond., transverse elec. field effects, majority carrier polarity 3—18143
- ferromagnetic semiconductors, max. resistivity due to carrier scattering by giant moments of mag. clusters 3—18145
- graphite:Fe, oscillatory magnetoresist., charged impurity selective scatt. 3—11864

- **carrier mobility** continued
  - n-hexane, rel. to impurities, nanosecond X-ray ionization pulses obs. 3 – 2084
  - holes, band gap width determ. from Hall constant meas. 3 – 18060
  - insulator, double injection for spherical and cylindrical geometry 3 – 21077
  - insulator, double injection negative resist., diffusion effects 3 – 21092
  - i.r. transmission through the diffusion, sheet resistance and junction depth meas. 3 – 39286
  - MBBA, isotropic phase, chem. and electrochem. activity rel. to d.c. conduction 3 – 15203
  - metal, liquid and vapour states, Hall mobility meas. up to 1600°C and 2000 atm. 3 – 36590
  - methane, liquid, excess electron and positive charge carrier drift velocities 3 – 36609
  - m.i.m. structure, zero bias anomalies, due to paramag. impurities, theory 3 – 30548
  - naphthalene, surface bands and assoc. mobilities calc. 3 – 30532
  - naphthalene single crystals, drift mobilities of holes and electrons 3 – 21073
  - organic dielectric films, charge transport 3 – 38834
  - p-i-n diode, transient process after current reversal 3 – 15243
  - paramagnetic spin polaron, self-trapped, mobility 3 – 30433
  - polar semiconductor, scattering mechanism from Hall coeff. factor obs. 3 – 11909
  - polar semiconductors, III-V, drag of carriers by other carriers 3 – 33899
  - polymer, book contrib. 3 – 11891
  - polymer, related a.c. effects 3 – 12093
  - polymers, charge trapping, role of unsaturated groups 3 – 30468
  - protonic, relation to frictional relax. drag 3 – 27134
  - quartz crystals, cause of anisotropy of elec. conduct. *(Russian)* 3 – 8161
  - semiconductor, book 3 – 21065
  - semiconductor, carrier fluctuations in current saturation region, time depend. *(Russian)* 3 – 8197
  - semiconductor, conductivity and thermodynamic props., effect of fluctuons 3 – 21079
  - semiconductor, deep impurity levels influence on double injection and recombination 3 – 8203
  - semiconductor, degenerate, diffusivity-mobility ratio at very low temps. 3 – 8164
  - semiconductor, degenerate, Einstein relations approximations rel. to diffusivity-mobility ratio 3 – 8163
  - semiconductor, doped periodically, carrier mobility, elec. cond. anisotropy *(Russian)* 3 – 8178
  - semiconductor, electron diffusion, in const. elec. field, with exponentially varying mobility and lifetime 3 – 33903
  - semiconductor, electron-phonon interaction and intervalley scatt. 3 – 5005
  - semiconductor, highly degenerate, diffusivity-mobility ratio, influence of band tails 3 – 24423
  - semiconductor, homogeneous, rel. to space charge induced by hot carrier regime 3 – 36617
  - semiconductor, low freq. e.m. wave propag., under inelastic carrier-phonon scatt. conditions *(Russian)* 3 – 8166
  - semiconductor, monopolar, V-I characts., admittance analysis *(Russian)* 3 – 27256
  - semiconductor, periodic impurity distrib., diffusion scatt. theory *(Russian)* 3 – 8209
  - semiconductor, polar, free polaron optical absorpt. const., velocity depend. 3 – 27505
  - semiconductor, polar, resonance interaction between carriers 3 – 33877
  - semiconductor, strongly compensated, hopping mobility 3 – 33900
  - semiconductor, thermal fluctuations of e.m. field, effect of drift 3 – 33878
  - semiconductor, with two types of carrier, rel. to Hall effect and magnetoresist. *(Russian)* 3 – 2111
  - semiconductor boundary layer, reflectivity with non-normal incidence and surface plasmon 3 – 27302
  - semiconductor devices, neutron irrad., limiting design parameters 3 – 33991
  - semiconductor surface, chemisorption thermodynamics rel. to surface scattering 3 – 5004
  - semiconductor surface, thermodynamics of chemisorption rel. to surface scattering of carriers 3 – 36489
  - semiconductor with deep traps, ambipolar mobility variation rel. to injection current theory 3 – 30488
  - semiconductors, carrier scattering by screened surface charges 3 – 21133
  - semiconductors, degenerate, in large magnetic field diffusivity-mobility ratio, temp. dependence 3 – 27273
  - semiconductors, in an external electric field, anisotropy in diffusion-noise temp. and differential mobility 3 – 27269
  - semiconductors, low-mobility, mol. excitons and charge carrier mobility 3 – 30514
  - semiconductors, offset, screening effect on charge carrier mobility *(Russian)* 3 – 8167
  - semiconductors, transport noise decomposition under space charge conditions, diffusion and hot electron effects 3 – 33915
  - semiconductors, with deep traps, ambipolar mobility and injection currents 3 – 27254
  - solid state plasma e.m. wave propag. rel. to carrier drift *(Russian)* 3 – 11921
  - trinitrofluorenone-poly-n-vinylcarbazole charge-transfer complex, amorphous film 3 – 21068
  - tunnel junction, with mag. impurities, effect of exchange scatt. by mag. moments 3 – 30547
  - n-$Al_xGa_{1-x}As$, mobility anal. from band structure and lattice vibration spectrum 3 – 30478
  - Ar, ion drift vel. 3 – 24283
  - BeTeI film, substrate temp. depend. *(Russian)* 3 – 21067
  - Bi and Bi-Sb alloy powder compacts characteriz., 300-77 K 3 – 36593
  - CdS, heteroepitaxial layers, meas. rel. to contamination by GaAs substrate 3 – 2653
  - CdS film, evaporated, resist. and Hall mobility rel. to prep. conditions 3 – 27322
- **carrier mobility** continued
  - $CdS_{1-x}Se_x$, electro-absorption reduced effective mass 3 – 15471
  - p-CdSb, rel. to technology applic. *(Russian)* 3 – 24430
  - CdSe, influence of growth conditions 3 – 24428
  - CdSe film, field effect mobility, In surface doping effects *(Russian)* 3 – 2192
  - CdSe-CdTe, solid solns., comp. and elec. charact. depend. on method of deposition 3 – 33762
  - CdSe-Dy_2O_3 thin-film structure 3 – 15265
  - CdTe, hole mobility, Poole-Frenkel effect, 130-430K, 5-50kV/cm 3 – 21086
  - CdTe:Cd, thin films, electrical conductivity *(Russian)* 3 – 33891
  - Cu_2Te, n and p type, electrical props. *(Russian)* 3 – 8170
  - FeS_2, pyrite, natural, resist., Hall effect, rel. to energy gap and mobility 3 – 38837
  - GaAs, band struct. and effective masses, combined pseudopotential-k.p calc. 3 – 18079
  - GaAs, depend. on heat treatment temp., thermal conversion rel. to impurities *(Russian)* 3 – 38832
  - GaAs, epitaxial, characterisation for microwave devices 3 – 2685
  - GaAs, epitaxial growth over wide range of crystallisation conditions, carrier mobility data for n and p type films *(Russian)* 3 – 8051
  - GaAs, for transferred electron devices 3 – 24424
  - GaAs, Hall meas. on X_{1c} electrons at low temp., scattering mechanisms and band structure 3 – 21097
  - GaAs, heavily doped, neutron displacement damage, i.r. optical reflectivity studies 3 – 33568
  - p- GaAs, heavily doped, neutron irradiation effects, elec. conductivity, Mott transition 3 – 33823
  - n-GaAs, interzone scattering study by specific resistance at high press. meas. *(Russian)* 3 – 8162
  - p-GaAs, rel. to i.r. plasma refl. 3 – 18454
  - GaAs, semiconductor, heteroepitaxial film growth, optical props., carrier transport characteristics 3 – 39266
  - GaAs, thin film, flash-evaporated, doping characts. 3 – 27611
  - GaAs anomalously high at room temp., resist. and Hall meas. 3 – 18140
  - GaAs film, epitaxial, hole diffusion length rel. to heterostruct. 3 – 36667
  - n-GaAs LSA diode, purity, evaluation determ. by low field temp. depend. mobility 3 – 2085
  - n-GaAs magnetoresistance, transverse, Gunn diodes, 300 to 800 K, electron transfer between conduction bands 3 – 36624
  - GaAs:Sn(Si, Zn), electron irrad., 'near-edge' absorption, annealing 3 – 33846
  - GaAs:Zn, H^+ ion bombardment, channelling expts., annealing behaviour of disorder density 3 – 33578
  - $Ga_xIn_{1-x}Sb$, vertical freeze grown material characterisation 3 – 5280
  - GaP, epitaxial growth over wide range of crystallisation conditions, carrier mobility data for n and p type films *(Russian)* 3 – 8051
  - GaP, thin film, determination from Hall constant 3 – 39298
  - GaP:Be, homogeneous doping during vapour growth, hole mobility meas. *(Russian)* 3 – 15644
  - GaSe, photoelec. props. rel. to minority carrier diffusion length and mobility 3 – 21112
  - Ge, charge carrier capture and reemission by shallow levels, field depend. 3 – 21091
  - n-Ge, effect of lattice and impurity scatt. rel. to Voigt magnetoabsorption 3 – 30802
  - Ge, epitaxial, polycryst., amorphous, Hall mobility, carrier conc., cond., noise, 100-400 K 3 – 38855
  - Ge, O doped and Li diffused, photon irradiation and annealing studies 3 – 18136
  - n-Ge, surface hole mobility and density, scatt. in surface inversion channels, Hall meas. *(Russian)* 3 – 27299
  - Ge hole scattering by acoustic and optical phonons in homogeneously deformed sample *(Russian)* 3 – 24417
  - Ge:Al, implanted, rel. to carrier generation at room temp. 3 – 2083
  - $Ge_{15}Te_{81}S_2As_2$, amorphous, IV characts, hydrostatic press. depend. 3 – 38830
  - HgSe film, amorphous, Hall mobility obs. 3 – 5009
  - InAs, InP, InP_xAs_{1-x} solid soln., neutron and gamma irrad., elec. and optical props. 3 – 33907
  - $In_{1-x}Ga_xP$:N, soln. growth, mobility depend. on comp. 3 – 24797
  - n-InP, scattering factor measurement 3 – 36599
  - p-InSb, injected carrier oscillations, trapping and recombination 3 – 11908
  - n-InSb, microwave props. in d.c. mag. field, hot electron effect, scatt. mechanism, 4-300K 3 – 21087
  - InSb based mixed crystal film, Hall coeff. and mobility meas. 3 – 36622
  - InSb:Fe, elec. and galvanomag. props., impurity levels and hole scatt. mechanisms 3 – 38844
  - InSb:Te, Se, S, transport phenomena, 77-300K, press. to 15k bar 3 – 2096
  - $K_2SO_4:Co^{2+}$, cond. by cation vacancies 3 – 36607
  - $Mn_zFe_{3-x}O_4$, 100-1000K 3 – 5010
  - Mo-Re alloy crystals Hall effect, Mo electron configuration changes due to Re addition 3 – 8155
  - Nb-S system cpds., nonstoichiometry rel. to elec. props. at thermodynamic equil. *(French)* 3 – 2113
  - Ne, ion drift vel. 3 – 24283
  - NiO, undoped, drift mobility of excess holes 3 – 18147
  - PbSe, carrier conc. and temp. depend., 0.3 to 800K 3 – 27252
  - $Pb_{1-x}Sn_xSe$, grown from vapour, ionized impurity and phonon scattering 3 – 24438
  - ^{222}Rn daughter small ions distribution in laboratory air 3 – 15967
  - Sb, hole mobility, temp. depend., calc. from galvanomagnetic meas. 3 – 15183
  - Se, amorphous, hole mobility rel. to conductivity hysteresis at vitrification temp. 3 – 30529
  - Se, amorphous, X-ray irrad., electrophotographic layers, fatigue mechanism *(Russian)* 3 – 33947
  - Se, barrier model of electric conduction, calc. of mobility *(German)* 3 – 33905
  - Se, X-ray irrad., electroradiographic layers discharge mechanism *(Russian)* 3 – 36638
  - Se liq., charge transport by hopping, hole photogeneration *(Russian)* 3 – 8179

carrier mobility continued
- Si, charge carrier capture and reemission by shallow levels, field depend. 3—21091
- Si, electron irrad., 130 K annealing stage of divacancy, i.r. transmission spectra 3—33559
- Si, grown on spinel, hole mobility limited by impurities 3—8720
- Si, hole mobility meas. for Si on sapphire film grown by dual rate technique 3—2656
- Si, mobility decreases at very high carrier conds. *(German)* 3—2089
- Si, mutual scattering of free carriers and eff. on charge mobility *(German)* 3—2088
- Si, radiation effects, obs. using junction-capacitance techniques 3—33926
- Si, surface layers in m.o.s. transistor, charge carrier scatt. and mobility calcs. 3—18227
- Si film, epitaxial, elec. effects of clustered defects 3—24434
- Si film, impurity centres, carrier mobility meas. by m.o.s. Hall technique 3—18094
- Si film, on insulating substrate, rel. to density of early growth islands 3—11833
- Si inversion layers, role of scattering by surface roughness 3—27315
- Si on sapphire, thin films surface charge effects, surface depletion 3—2185
- p-Si:Al, (B), (Ga), electron irrad., annealing, effect of O and acceptor impurities 3—33560
- Si:Co, thermal emission rates and activation energies of electrons and holes 3—15154
- Si:Ge(Sn), O electron irrad., selective trapping of vacancies, migration of interstitials 3—33925
- Si:Li, neutron irrad., defect interactions, Hall effect, i.r. absorption studies 3—33570
- Ta_2O_5, polycrystalline, 900 to 1400°C 3—8213
- Te, Dember, Hall and elec. cond. meas. rel. to carrier mobility anisotropy 3—21111
- Te, electron irrad., recovery steps, isochronal and isothermal annealing expts. 3—33562
- p-Te film, vacuum-deposited, temp. and crystallite size depend. *(Russian)* 3—30481
- TiO_2, photo-induced carrier behaviour from photoconductivity meas. 3—2128
- ZnO, displacement threshold, electron beam irradiation 3—20765
- ZnSe, undoped, p-type cond. 3—36602
- ZnTe, acceptor defect levels, elec. transport 3—18096

carrier motion *see carrier mobility*

carrier relaxation time
- chalcogenide threshold switches, thermal and nonthermal relax. processes 3—21127
- electronic lifetime anisotropy determ., mosaic spread enhancement of dHvA-Dingle temp. 3—11845
- frequency dep., current carrier heating technique, warm electron region *(Russian)* 3—33939
- graphite, lifetime anisotropy, Shubnikov-de Haas effect meas. 3—18168
- metals, free charge decay, theory 3—15187
- semiconductor, electron diffusion, in const. elec. field, with exponentially varying mobility and lifetime 3—33903
- semiconductor, electron elastic scatt., OPW wave function 3—2079
- semiconductor, hot carrier energy relaxation time measurement, elec. field effects *(Russian)* 3—36615
- semiconductor, nondegenerate, crossed field acoustic amplification in strong mag. fields, relaxation time for acoustic-phonon scattering 3—11937
- semiconductors, piezoelectric scattering, lattice vibration interactions, screening, conduction electron mobility 3—33898
- surface states, temp. dependence, kinetics of pulse field effect 3—24498
- Cu alloy, magnetoresist. and dHvA meas. rel. to impurity scatt. of electrons 3—21055
- DH-(GaAl)As laser, pulse modulation at 200 Mbits/s, spontaneous carrier lifetime 3—16878
- p-GaAlAs:Ge, electron diffusion lengths Al content depend. 3—18165
- GaAs, electron energy relaxation time, determination from 34 GHz complex conductivity measurements in presence of d.c. field 3—2118
- GaAs, electron energy relax. time as function of elec. field 3—24420
- p-GaAs:Ge, epitaxial, electron diffusion length, recomb. lifetime 3—18164
- GaAs:Ge, solution-grown electron diffusion length 3—21093
- GaP:Zn,O, Czochralski-grown photoluminesc., minority carrier lifetime, effect of heat treatment 3—39176
- Ge, electron energy relaxation time, as function of lattice temp. 3—30472
- Ge, radiation defects due to 45-50 MeV electrons, carrier density and minority carrier lifetime obs. *(Russian)* 3—36332
- Ge, resistivity and lifetime changes during deform. before fracture 3—27279
- Ge surface states, temp. dependence, kinetics of pulse field effect 3—24499
- Ge:Sb, relaxation processes involving trapping levels in bistable microplasmas 3—24452
- InP, electron energy relaxation time, determination from 34 GHz complex conductivity measurements in presence of d.c. field 3—2118
- InP, electron energy relax. time as function of elec. field 3—24420
- KCl:Li, cond. electron scatt. by tunnelling states of defects 3—33920
- Pb, freq. and temp. depend. rel. to electron-phonon interaction, high freq. cyclotron reson. meas. 3—38787
- n-PbSe, electron relax. time, i.r. refl. and magnetorefl. study 3—5207
- Si, electron energy relaxation time, as function of lattice temp. 3—30472
- n-Si, hot electron energy relaxation time measurement, elec. and microwave field effects *(Russian)* 3—36616
- Si, i.r. refl. spectra obs., temp. depend. *(Russian)* 3—8182
- Si, minority carrier lifetime meas. using m.o.s. capacitor transient response 3—38847
- Si, radiation defects due to 45-50 MeV electrons, carrier density and minority carrier lifetime obs. *(Russian)* 3—36332

carrier relaxation time continued
- n-Si m.o.s. capacitors, minority carrier generation and density 3—38898
- Si:B hole lifetime, capture rate, impurity concentration, 18-4.2K 3—30495
- Si-SiO_2, carrier lifetime in depletion region near interface 3—21158
- Si_3N_4, reactively sputtered, dielectric breakdown 3—34295
- SnTe, i.r. refl. spectra, carrier effective mass. relax. time and density *(Russian)* 3—8588

carrier scattering *see carrier mobility; electron-phonon interactions*

carriers (charge) *see charge carriers*

carry circuits *see adders*

cars *see automobiles*

cartography
- aerial mapping lenses, optical transfer function meas. standards 3—226
- Arctic sea ice, underside mapping, by backscattered sound 3—37190
- civil engineering design, digital photo map applic. 3—5998
- geophysical fields representation methods 3—25321
- hydrographic, computerised data acquisition and processing system 3—3240
- lunar crater nomenclature extended to far side 3—31623
- Moon, selenodetic reference frame precision and coordinate transformations 3—39643
- projection routines for displaying geophysical data 3—25318

cascade showers *see cosmic ray showers and bursts*

casting
- Al bronzes effect of iron, casting and wear properties *(Polish)* 3—31033
- chill casting in vacuum from 2500°C *(Russian)* 3—13257
- magnetic casting mould powder development *(Russian)* 3—27726
- metal, continuous casting, thermal fluxes determ. in mould walls 3—24891
- metal, product quality *(German)* 3—25035
- solidification research impact on metals processing 3—31114
- Al, alloys, horizontal strip costing in stationary d.c. moulds, properties 3—12417
- Al, casting textures, influence of mould shape and melt feed method *(German)* 3—8900
- Al alloys, wrought, solution kinetics 3—37047
- Al matrix composites, survey of fabrication methods 3—8997
- Cu alloys, binary, solidification characts. 3—21559
- Cu alloys, binary, solidification characts. 3—21560
- Fe, grey cast, induction furnace melting, mech. props. 3—24960
- Fe, malleable, Bi-containing, trace element effects on malleabilization kinetics and mech. props. 3—39357

castings
- Ni-Cr base alloy, weldable, stress rupture and ductility props. for use above 100°C 3—31063

catalysis
- *see also catalysts; reaction kinetics*
- Belousov-Zhabotinsky reaction, rel. to periodic heat evolution during temporal chemical oscillations 3—27869
- carboxylic acids and hydrogen, deuterium isotope exchange 3—27861
- electrocatalysis, electronic effects in H evolution reaction 3—38735
- fluidised bed catalytic reactors, countercurrent backmixing model, applicability to simplified solns. 3—7448
- graphite, enhanced reactivity at struct. faults, microscopic studies 3—11788
- heterogeneous, at line defects, active sites in periodic adlayers 3—9095
- heterogenous, at line defects, simple boundary-controlled reactions anal. 3—9096
- metal aggregates on C substrate 3—37142
- polystyrene sulphonate, ion-exchanged, para-hydrogen conversion 3—9066
- pseudo-fluidised bed, transverse nonuniformity in inhomogeneity distrib. 3—20398
- reaction rates, by calorimetric bead system 3—28489
- volume change reactions boundary layer effects 3—12500
- $BaTiO_3$:La_2O_3, catalytic activity study using CO oxidation 3—18788
- CO chemisorption on Pt, thermal desorption methods 3—37143
- Ge alloy surface of p-n junction, frmic acid catalytic decomposition products 3—8257
- H_2S, heterogeneous oxidation below 1000 ppm in N/air mixtures over metal oxide catalysts 3—37198
- I to I_2, photochemical oxidation 3—15839
- MoS_2, enhanced reactivity at struct. faults, microscopic studies 3—11788
- NO catalytic reduction in automobile exhaust gases using Fe-containing materials 3—37535
- NO catalytic reduction in automobile exhaust gases, reactions with CO and O_2 on oxidized stainless-steel 3—37536
- NO molecule, adsorbed on ZnO, reduction, doping depend., i.r. absorption obs. *(German)* 3—39463
- Ni, of H_2, on polycryst. wires, heat of adsorption correl. with reaction kinetics 3—11809
- Pt, reactivity of low index and stepped single cryst. surfaces 3—11787
- W of H_2, on polycryst. wires, heat of adsorption/reaction kinetics correl. 3—11809

catalysts
- *see also catalysis*
- atomically dispersed Pt and Pd thin film on C substrate, H_2 isoteric adsorption enthalpy *(German)* 3—27921
- diamond synthesis with non-conventional catalyst-solvents 3—20875
- finely divided, ferromag., granulometry and metallic mass. from magnetisation/mag. field curve *(French)* 3—34171
- fluid cracking, fluidised bed, interaction of gas jets 3—1457
- fluidized bed, solids entrainment obs. 3—1450
- highly dispersed catalytic materials, review 3—25069
- metal oxide, heterogeneous oxidation of H_2S below 1000 ppm in N/air mixtures 3—37198
- stainless-steel oxidized surface for NO catalytic reduction in automobile exhaust gases 3—37536
- Ag, obs. of adsorpt. complexes formed in N_2O and O_2 3—8020
- Fe-containing materials for NO catalytic reduction in automobile exhaust gases 3—37535

catalysts continued
N_2 adsorption measurements for the determination of pore size 3−37097

cataphoresis *see electrophoresis*

cathode-ray oscilloscopes
see also oscillographs
No entries

cathode-ray tube displays
electron probe X-ray microanalyser, scan modulation system for improved spatial displays 3−10109
photography 3−6002

cathode-ray tube screens *see cathode-ray tubes; fluorescent screens*

cathode-ray tubes
see also image intensifiers; image storage tubes; television picture tubes
cathode spot, directional motion due to asymmetrical conditions at its boundaries *(Russian)* 3−1529
direction finder, atmospherics location, waveform recorders, synchronised operation 3−21950
flying spot, suitability of Ce^{3+}-activated alkaline earth thiogallate phosphors 3−12186
IBM 2250 c.r.t. between man and computer for interrogating oceanographic data files 3−3209
testing, impact of steel ball, pulsed holographic study 3−5773

cathode rays
No entries

cathodes
see also electron emission; oxide coated cathodes; thermionic cathodes
Al hollow cathode discharge tube, use with vacuum grating spectrograph in u.v. region *(German)* 3−3779
alkali halide crystals, electric breakdown mechanism in presence of microroughness on the cathode *(Russian)* 3−8514
bakeable hollow device for plasma diagnostics 3−7564
cathodes, theory of high pressure arcs *(Russian)* 3−7587
cold-cathode operation at low pressures, formation of gas-focussed electron beam 3−17671
critical cathode potential drop and current density at the arc transition in MHD pole generators 3−26903
double hollow, with separated evaporation and excitation zones, spectral characteristics *(Russian)* 3−30043
double-cathode effect, boundary conditions *(German)* 3−14622
dynamic field emission in cathode spots of cold cathode arcs 3−27598
electron field-emitters, Au whisker single crystals emitting surface, vapour phase growth, electric field effects *(Russian)* 3−12245
fall of potential in audio frequency discharge 3−30028
field emission, W and LaB_6, for electron probes 3−13474
gas laser, patent 3−6475
glow discharge, obs. of cathode sputtering *(Russian)* 3−7574
glow discharge with circular luminescent cathode *(Russian)* 3−23954
high current field-emission cathodes, refractory metals *(Russian)* 3−8711
hollow, discharge effects on throttled ion thruster 3−38514
hollow, for mercury discharge, thrust meas. 3−11522
hollow carbon, discharge mechanism in presence of metals and salts *(Russian)* 3−11520
hollow cathode of an overdense glow discharge, energy of positive ions *(Russian)* 3−7590
hollow cathode source for matrix isolation studies 3−29531
hollow cylindrical cathode, elec. field distrib. in cathode fall, radial model *(German)* 3−4690
ion laser, special cathode design for pulsed and CW operation 3−13338
ionizer for alkali metal plasma production 3−11507
m.i.m. cathodes, field emitted electron angular distrib. rel. to electron traps 3−15602
plasma phase shifter with cylindrical hollow cathode 3−20456
pressed, operation in He-Ne lasers 3−22389
sandwich cathodes, m.i.m. systems, (Al-Al_2O_3-Au), electron emission, energy distributions 3−21161
sandwich cathodes, m.i.m. systems (Al-Al_2O_3-Au), electron emission, angular distribution 3−21160
sandwich cathodes, m.i.m. systems (Al-Al_2O_3-Au), electron emission, discussion of processes in cathode 3−21162
semiconductor cathode, with high anisotropic distribution function, thermoelectronic emission 3−27601
thin film, field emission characteristics calc. 3−21523
thin layer emitters with low or negative electron affinity, secondary electron emission 3−15582
vacuum arc, modelling of field-amplification processes on cathode protuberances 3−17706
Al, dynamics of precathodic region at various rates of changing current, in impulse discharges *(Russian)* 3−30046
Al in medium voltage spark discharge, cathode spot formation obs. by high speed photography 3−30032
Al-Al_2O_3-Au structure, transmission coeff., applied field depend. 3−8280
Al-LiF-Au sandwich cathode, electron emission characts. 3−15603
Ar cylindrical hollow cathode negative glow discharge, plasma diagnostics *(German)* 3−4675
Ar low pressure hollow cathode discharge pendel effect expt. evidence *(German)* 3−14631
BaB_6 mixtures for cathodes in electron optical instruments 3−805
Fe, dynamics of precathodic region at various rates of changing current in impulse discharges *(Russian)* 3−30046
Hg arc, steady-state, low pressure, velocity of neutral atoms emanating from cathode 3−23935
LaB_6 cathodes in electron optical instruments 3−805
Ne excitation in discharge tube with hollow cathode, intensity depend. on press. and dimensions *(Bulgarian)* 3−33407
Pt, dynamics of precathodic region at various rates of changing current in impulse discharges *(Russian)* 3−30046
Sn, dynamics of precathodic region at various rates of changing current in impulse discharges *(Russian)* 3−30046
Ta autocathode, structure changes on He ion bombard. *(Russian)* 3−8689

cathodes continued
W cathode, surface props. in Cs-Ba thermionic converter under overneutralised Knudsen conditions 3−30013
Zn, dynamics of precathodic region at various rates of changing current in impulse discharges *(Russian)* 3−30046

cathodes, electrochemical *see electrochemical electrodes*

cathodoluminescence
aromatic liquid solns., radioluminescence, scintillations decay law *(French)* 3−39196
cathode ray phosphors electron hole pair prod. by plasmon decay 3−18177
diamond crystals, proton irradiation effects 3−24437
diamonds, type I and IIa, pulse irradiation 3−8673
electron microscopy, scanning, high resolution images, spectroscopic cathodolum. images 3−28722
glass containing adenine, electron induced emission spectra at low temp. 3−30887
glasses, borate, phosphate, tungstate, Tb^{3+} doped, surface fluorescence study 3−2598
glow discharge with circular luminescent cathode *(Russian)* 3−23954
homogeneity testing of single crystals using raster electron microscope + X-ray spectrometer *(German)* 3−7789
inert gas solid solutions, atomic, molecular and heteroatomic centres 3−18504
metal and semiconductor bombardment by Cs and Na ions, meas. of electron and photon spectra 3−12203
metallized thin films, passage of primary electrons evaluation 3−27578
phosphor films, transmission microscopy and cathodoluminescent studies 3−1551
rel. to scanning electron microscopy 3−11536
semiconductors, 0.5 to 11 μ waveband, appl. as radiation detectors and lasers *(Russian)* 3−27576
semiconductors, system for measurement *(German)* 3−28548
β-SiC, with radiation defects, mechanism and efficiency *(Russian)* 3−2599
ZnTe, atomic displacement energies, cathodoluminescence edge emission spectroscopy, monoenergetic electron irrad. 3−33556
Ar solid, spectra *(Russian)* 3−5236
$BaGa_2S_4$:Ce,Na, rel. to flying spot scanner appl. 3−12186
$CaCO_3$, calcite (synthetic), Mn emission and low-temp. effects 3−18502
$CaCe_2S_4$, green-yellow emission 3−39243
CaF_2:Mn(Ce,Mn), cathodoluminescence, trapped hole diffusion 3−39197
$CaGa_2S_4$:Ce,Na, rel. to fyling spot scanner appl. 3−12186
CdF_2:Pr^{3+}. line structure obs. in cathodoluminescence spectrum 3−30885
CdS, electron irrad., Cd displacement threshold at liq. He temp. obs. 3−5247
CdS, relax. time and cathodolum. efficiency *(Russian)* 3−5237
CdS monocrystals, investigation using electron microprobe scanning technique *(German)* 3−8674
CdTe, cathodoluminescence from lattice defect centres, quenching mechanism 3−15561
CdTe, edge emission spectra, electron irrad. effects 3−18488
Cu, clean surface, light emission induced by H^+ and He^+ impact 3−18501
n-$Ga_{1-x}Al_xAs$:Si, catholum. obs. rel. to energy gap meas. 3−30886
GaAs, deuteron irrad., defect distrib. determ. *(Russian)* 3−1655
GaAs, $GaAs_xP_{1-x}$, temp. depend., 27-300K 3−36949
GaAs, plastically deformed, dislocations, i.r. cathodolum. study 3−38699
GaAs p-n junction, photo-e.m.f., under action of self-recomb. radiation *(Russian)* 3−27303
GaAs:Si, epitaxial layers, characterisation of p-n structure, etching, cathodoluminescence 3−39195
GaP, $GaAs_xP_{1-x}$, temp. depend., 27-300K 3−36949
n-GaP, liq.- encapsulated-Czochralski-grown, deep hole traps 3−5235
GaP:N, isoelectronically doped, radiative recombination 3−24754
GaSe, intense excitation by electron beam 3−15563
He(II), $0.3<T<4.2K$, luminesc. prod. by weak α-particle sources 3−15045
$InAs_{1-x}P_x$, vapour phase epitaxial material 3−2680
$In_{1-x}Ga_xAs_{1-y}P_y$ alloys, electron zones, luminesc. struct. study *(Russian)* 3−36946
InP, vapour phase epitaxial material 3−2680
Kr solid, spectra *(Russian)* 3−5236
La_2O_2S, rare-earth activated thin films 3−8671
α-$LiAlSi_2O_6$:Mn^{2+}, single crystal, polarised cathodoluminescence emission 3−39194
Ne solid, spectra, fine struct. splitting *(Russian)* 3−5236
SiC, proton irradiation and form. of luminesc. large defect centres 3−15562
SiON, thin insulating film from NO-NH_3-SiH_4 reaction 3−39244
$SrGa_2S_4$:Ce,Na, rel. to fyling spot scanner appl. 3−12186
TbF_3, ZnS-TbF_3, ($^5D_3 \rightarrow {}^7F_j$) transition obs., luminescence centre symmetry *(French)* 3−18503
Xe solid, spectra *(Russian)* 3−5236
YAG:Ce^{3+} and its solid solutions 3−30883
YAG:Nd, testing of the homogeneity of single crystals by means of cathodoluminescence *(German)* 3−7789
$ZnLu_2S_4$, blue-green emission 3−39243
ZnS, extinction of emission region by introducing extinction and luminescent centres *(Russian)* 3−12187
ZnS, u.v., temp. depend., 80-400K *(Russian)* 3−15560
ZnS monocrystals, investigation using electron microprobe scanning technique *(German)* 3−8674
ZnS:Cu, β-irrad. at 5K, fast light emission 3−24753
ZnS-TbF_3, ZnS:Tb^{3+}, ($^5D_3 \rightarrow {}^7F_j$) transition obs., luminescence centre symmetry *(French)* 3−18503
ZnSe layers, heteroepitaxy, luminescence centres 3−18546
Zn_2SiO_4:Mn powder, quantitative chem. anal. and luminesc. spectra 3−30854
ZnTe, cathodoluminescence of the donor-double-acceptor pairs *(Russian)* 3−27577
ZnTe, electron irradiated, Zn displacement threshold, Zn vacancy luminescence 3−33557

- **cathodoluminescence** continued
  - ZnTe, interpretation of asymmetric band shapes in terms of bound exciton complexes 3−36948
  - ZnTe, time resolved spectroscopy involving ionisable donor acceptor states 3−36947
  - ZnTe:Cu, electron-beam excited, visible luminesc. 3−30884
  - Zr phosphors, activated by Eu^{3+}, Dy^{3+} and Sm^{3+}, spectral, kinetic and colour characteristics *(Russian)* 3−27579
  - ZrSiO$_4$:Eu^{3+}, Eu^{2+}, scintillation characts. *(Russian)* 3−8672
- **cathodophosphorescence** *see cathodoluminescence*
- **cathodothermoluminescence** *see cathodoluminescence*
- **catholytes** *see electrolytes*
- **causality** *see physics fundamentals*
- **causticity** *see pH*
- **cavitation**
  - *see also bubbles; vortices*
  - acoustic, growth and decay of bubbles *(Japanese)* 3−20364
  - acoustic cavitation, luminosity, radioactivity, scintillation systems, sonoluminescence, radioluminescence 3−298
  - acoustic pressure fields in finite container, mixed boundary value problem, incipient cavitation analogue 3−1425
  - aerosols, u.s. atomisation, disintegration mechanisms, photographic study sonoluminescence and cavitation 3−31202
  - air bubble effect on vapour bubble growth and collapse near solid surface, photographic study 3−23769
  - bubble nucleus spectrum, influence on cavitation inception, scattered light counting method investigation 3−26046
  - diffusion of point defects to propagating crack tip, rel. to creep rupture by cavitation 3−7842
  - fluidised beds, volume changes accompanying bubble splitting 3−36124
  - gas bubble in liquid subject to surface tension, collapse and expansion 3−26829
  - heavy liquid flow past a curvilinear obstacle, numerical soln. *(Russian)* 3−29930
  - interference between body and permeable walls in water tunnel test section, supercavitated flow 3−33271
  - lubricant behaviour in cylindrical bearings, solns. of Reynolds eqn. 3−17538
  - metals, damage, depend. on temp. and cavitating liquid 3−2786
  - migration of gas filled cavities in inhomogeneous sound field 3−4602
  - noise spectrum in water, sonoluminescence dependence on acoustic pressure of u.s. field meas. 3−26825
  - screw pumps operating below capacity, improvement of anticavitation props. 3−3922
  - spark induced cavitation bubble collapse, photographic study 3−26831
  - steel, erosion study using water tunnel system and magnetostriction vibratory unit 3−2785
  - supercavitated flow past profiles, effect of water tunnel wall 3−4600
  - supercavitated flow past slender profiles in a finite flow 3−33267
  - supercavitating airfoil cascade calc. 3−33270
  - supercavitating bodies, inverse problems 3−33268
  - supercavitating foil with a finite cavity direct boundary value problem 3−33269
  - underwater explosions, computer program for analysis of test data on cavity explosion *(Russian)* 3−26066
  - u.s. cavitation research, mathematical treatments and recent progress *(Japanese)* 3−7407
  - water, swirling cavity flow, through straight circular pipe 3−36100
  - water, swirling cavity flow through straight circular pipe 3−36101
  - Fe, erosion study using water tunnel system and magnetostriction vibratory unit 3−2785
  - H$_2$, liquid, bubble chamber, effect of u.s. field 3−25904
  - He, liq., cavitation stability due to electron bubbles 3−33710
- **cavity resonators**
  - *see also acoustic resonators; laser cavity resonators*
  - atomic beam, frequency shift due to Ramsey-type interrogation 3−10107
  - complex permittivity meas. device with resonating cavity *(French)* 3−25793
  - cylindrical, for e.s.r. gaskinetic measurements up to 1000 K *(German)* 3−37670
  - Earth-ionosphere resonator excited by cosmic sources, v.l.f. noise spectrum characts. 3−34931
  - Helmholtz, generalized theory, jet flow model 3−31972
  - Helmholtz, nonlinear damping by acoustic liners *(Italian)* 3−22203
  - Josephson junction e.m. radiation emission, freq. pulling 3−5080
  - linear accelerators, cavity field calculation, by finite element method 3−32120
  - microwave, for studying chemical laser reactions 3−26239
  - microwave, meas. of electron density of plasma in shock tube 3−23912
  - open in one or two directions *(Rumanian)* 3−22702
  - open periodic structure with single iris, dispersion charact. determ. using variable length cavity *(French)* 3−29011
  - plasma temperature effects on the frequency shift in resonant cavities 3−23855
  - resonant freq. in neighbourhood of reson. in gas 3−22817
  - scatter calculation of retarding system of resonator chains with mixed excitation *(Russian)* 3−32402
  - semiinfinite iris-loaded waveguide, radiation of moving charged particle *(Russian)* 3−6302
  - SIN cyclotron, r.f. system 3−13373
  - slot-coupled toroidal resonators, scatter calculation by computer *(Russian)* 3−32401
  - spherical standard sound source, internal impedance *(Japanese)* 3−28481
  - TE$_{01n}$, complex permittivity meas. of low loss liquids 3−25806
  - He-Ne visible gas laser design, r.f. excited 3−37958
- **celestial mechanics**
  - *see also N-body problems; stellar motion*
  - accretion problem for protocluster of protostars, mass effects or velocity *(Russian)* 3−13059
  - anisotropic Kepler problem in two dimensions 3−9450
  - annual aberration, series expansion with respect to fundamental arguments 3−37303
- **celestial mechanics** continued
  - artificial satellite motion, stationary solutions *(Japanese)* 3−18921
  - artificial satellite surface interaction with gas atoms, effects on motion 3−25381
  - artificial satellites, suitable orbits *(Japanese)* 3−39584
  - asteroid belt, commensurable motion secular effects, appl. to Hecuba Gap and Hilda Group 3−31634
  - asteroid orbits, stability of solar system 3−18994
  - asteroidal collisions, period depend. on size, orbital effects 3−31636
  - asteroids, improved data elements calculated using system of computer programs *(Russian)* 3−16195
  - Bode's Law, sequence of random numbers with constraint 3−35014
  - canonical perturbation method for non-conservative dynamical systems 3−37791
  - circular orbit stability, secular variations in restricted problem 3−5552
  - close binary systems, tidal evolution rel. to secular perturbations of orbital elements 3−28116
  - close Earth satellite orbits, precession, nutation and reference system 3−39578
  - colliding bodies, mass distribution, Monte Carlo technique 3−12935
  - comets, nongravitational forces rel. to heliocentric distance, effects on orbits of long period 3−31633
  - Cosmos 268 rocket (1969-20B) orbit analysis, wind speed data 3−9309
  - disturbing function expansion using summation theorem for assoc. Legendre functions 3−25383
  - dynamical evolution of stellar cluster with initial subclustering 3−9445
  - dynamical evolution of triple star systems, numerical study 3−9444
  - dynamical var. of latitude and time rel. to Earth's pole of figure 3−35001
  - Earth satellite coordinate perturbation in standard gravitational field *(Russian)* 3−16099
  - Earth satellite motion parameters, accuracy of estimates using astronomical meas. with correlated errors 3−25371
  - earth satellite secular radiational perturbations *(Russian)* 3−16100
  - earth satellites, motion under influence of tesseral harmonics of earth potential *(Russian)* 3−16097
  - earth satellites, secular perturbations in orbital elements due to asphericity of earth *(Russian)* 3−16115
  - eccentric and concentric two-body systems 3−9454
  - elliptic orbit satellite, stability of planar oscill. 3−39593
  - elliptical orbit satellites, orientation and resonance locks during deployment 3−37298
  - Enceladus-Dione system, anal. using Poincares canonical variables and a modification of von Zeipal's method *(French)* 3−22007
  - ephemeride error effects on lunar laser ranging *(French)* 3−31505
  - escape from ecliptic plane along heliocentric orbit using Jupiter's gravitational field 3−25369
  - explosive disintegration and simultaneous collision of n-material gravitating points 3−35004
  - finite body motion equations *(Japanese)* 3−18920
  - force function expansion for two homogeneous spheroids with non-coincident symmetry planes *(Russian)* 3−16116
  - four-dimensional mapping of dynamical systems rel. to C-systems 3−22008
  - galaxies, motions in spherically symmetric clusters rel. to instabilities 3−37473
  - galaxies, tidal interaction anal. *(Russian)* 3−5615
  - galaxies, tidal interaction on close passage, computer simulation *(Russian)* 3−16265
  - GEOS 1 and 2 mean orbital elements from optical flash data 3−39581
  - gravitation clustering of galaxies, kinetics 3−39716
  - heliocentric corrections, tables for light time corrections 3−28117
  - Hohmann transfer ellipses, launch windows to the planets 3−12941
  - Huang formulation, four-body problem, perturbation region *(Polish)* 3−25382
  - hyperbolic and heliocentric orbits in flyby manoeuvres 3−9448
  - hyperbolic re-entry velocities into Earth's atmosphere, range interval of landing phase 3−31508
  - Ideal Resonance Problem, soln. using parallel perturbations method 3−37792
  - inertial motions on rotating sphere *(Russian)* 3−495
  - inner planets, absence of satellites rel. to tidal friction 3−28154
  - interaction of stars with local dust formations, densities and motion *(Russian)* 3−13108
  - interplanetary orbit determination, nonlinear estimation theory applic. 3−39585
  - interplanetary orbit optimisation using invariant nomographic scales 3−31510
  - interplanetary spacecraft trajectories, methods of improving accuracy of calculations 3−25370
  - isolated and non-isolated stellar systems, numerical experiments 3−22116
  - jetstreams, numerical simulation of two-dimensional case 3−12931
  - Jupiter's family of comets, original orbits determ. using Tisserand's constants 3−35002
  - Jupiter orbiter trajectories, moving gravitational field of Galilean satellites 3−9449
  - Kepler's eqn., optimised numerical soln., computer program 3−9456
  - Kepler's equation for elliptic and hyperbolic orbits, exact analytical solution 3−16104
  - Kepler motion stability, numerical procedure based on Floquet's theorem 3−3282
  - Kerr matric, astrophysical consequences 3−25367
  - latitude variations, analytic expression for diurnal term 3−28120
  - libration points stability of rotating triaxial ellipsoid 3−16101
  - lunar gravity field determ. from long-period satellite motion 3−39594
  - lunar physical librations due to third and fourth harmonics of lunar gravity potential 3−39639
  - lunar rotation element determ. using narrow-angle TV camera on lunar surface 3−28307
  - luni-solar theory, short-period perturbations of artificial satellites 3−37300
  - Mach Einstein doctrine, some secular consequences *(German)* 3−12593

celestial mechanics continued
  major planets, orbital elements, treatment of observations *(Russian)* 3−16147
  Mars, satellites orbit precession discrepancy rel. to shape of primary 3−31593
  Moon, orbital motion, secular accelerations, Earth rotation 3−18977
  motion of heavy flexible string attached to satellite in central gravitational field 3−16102
  motion of pulsating dumbbell (gravitocraft), optimal control 3−25380
  near-orbiting satellites, relative motion about primary determ. 3−39592
  normal places, formation method *(Russian)* 3−16096
  optimal orbit characteristics of artificial planetary satellite, coplanar impulse transition 3−25379
  orbital low thrust parameters, analytic partial derivatives, elliptical orbits, perturbations, synchronous satellite, electric propulsion 3−3283
  orbital spacecraft, trajector and attitude dynamics, unified state model 3−37299
  orbits, difference equations for estimation of biases in filtering problem *(Russian)* 3−16098
  orbits, operational calc. *(French)* 3−37302
  out-of-plane motion about libration points in elliptic restricted three-body problem 3−39580
  particle motion in equatorial plane of gravit. monopole-quadrupole field, classifcation 3−35564
  plane three-body problem, phase space *(French)* 3−31506
  planet X, hypothetical trans-Plutonian planet, case against 3−9494
  planetary disturbing function, secular terms 3−3279
  planetary problems, expansions of derivatives of disturbing function 3−16107
  planetary satellite transfer from hyperbolic to nearly circular orbit using aerodynamic braking 3−25378
  planetary system stability rel. to commensurabilities 3−37296
  Poisson Series Processor, design and appl. 3−39595
  precession, nutation, polar axes displacement, earth rotation, earth structure *(French)* 3−3285
  precession and nutation in rectangular equatorial coordinates, computer calculation *(Russian)* 3−16094
  resonance rotation of celestial bodies and Cassini's laws rel. to Moon and Mercury 3−16110
  resonances and encounters between minor planets and major planets 3−9461
  resonances and librations of Apollo and Amor asteroids with Earth 3−35102
  resonant stellar orbits in spiral galaxies 3−37294
  restricted elliptical problem, stability of triangular equilibrium points *(French)* 3−16105
  restricted problem of 3 bodies, periodic orbits around L_4 libration point 3−37297
  restricted three-body problem, comparison of Encke and Cowell integration methods 3−39596
  restricted three-body problem, periodic solutions and stability 3−39579
  review of recent results and developments in theoretical mechanics and mathematical physics 3−16584
  rotating liquid configuration of three or more components, determ. of stability *(Russian)* 3−26071
  satellite gravitational stabilization by flywheel, system parameters optimization 3−25374
  satellite motion in non-central field, determ. by perturbing function expansion *(Russian)* 3−9455
  satellite nutational oscillations, damping with internal flywheel 3−25375
  satellite orbit determ. from range meas. for planet-orbiting satellites 3−35003
  satellite orbit-orbit reson. capture in solar system, model 3−28118
  satellites, artificial, orbit evolution due to solar radiation press. *(Russian)* 3−18914
  self-gravitating n-body systems, thermodynamics rel. to stellar dynamics 3−37295
  spacecraft hyperbolic return-paths, analytical estimates of landing range 3−31507
  spacecraft motion parameters, linear estimates with a priori information 3−25372
  spacecraft oscillations with two-position attitude-control system 3−25376
  spacecraft rendezvous manoeuvres, iterative technique using coasting trajectories 3−31509
  spatially homogeneous gravitating medium, kinetic theory of small perturbations 3−37311
  special satellite orbit-points prediction, analytical iterative algorithm, Brouwer theory 3−39583
  spinning satellite in circular orbit, general equilibria 3−16103
  stellar gravit. systems, probability distrib. of random force 3−31741
  stellar triple systems of equal mass, stability criteria 3−16106
  symplectic mappings, stability theory *(Japanese)* 3−18919
  synchronous artificial Earth satellite motion using approx. computation method 3−25368
  tesseral resonance of Imp 4 orbit due to commensurability 3−9447
  third integral of motion in stellar dynamics 3−31664
  three body problem, isoenergetic escapes and variations, dynamic characs. of escaping body 3−22006
  three-axial ellipsoid, stability of libration points in first approximation under perturbations *(Russian)* 3−16095
  three-body problem, classification and single-valued definition of states *(Russian)* 3−28121
  restrictedthree-body problem, global stability 3−18922
  three-body problem, sufficient conditions for return of ejected particle 3−16109
  tidal evolution in planet-satellite systems 3−31504
  transfer of spacecraft from hyperbolic to closed orbit round planet by atmospheric drag 3−25377
  two-body orbits, exact analytical solutions from theory of complex variables 3−39582
  two-body problem, comparison of recurrence relations with Runge-Kutta integration 3−37301
  two-body problem, elliptic to hyperbolic orbit by slow loss of mass 3−16108

celestial mechanics continued
  two-body problem with corpuscular radiation, effects of particle trajectory curvatures 3−28119
  Universe expansion mechanics, Hubble's law *(French)* 3−9446
cell model (liquids) *see liquid theory*
cells (electric)
  see also fuel cells; photoelectric cells
  continuous voltage pulsing using a rotating bipolar electrode 3−13352
  dielectric, for u.h.f. meas. of liq. permittivity 3−6017
  electrochemical cell, microscopic observation of electrodeposition and dissolution of metals 3−5864
  ionic transport in solids with tunnel and layer structures 3−5018
  solid-state thermodynamics at elevated temperatures, point defects and galvanic cells, review 3−24112
  solutions of low cond., differential capacitance meas 3−6013
  AgZn batteries, oceanograph8c applications, lifetime, Hg contamination, resistance to ground problems 3−3213
cellular biophysics
  Allium cepa nuclei, s.e.m. study 3−31844
  Aplysia neurons, intracellular conductance 3−28315
  automated cell structure determination, from electron micrographs 3−9643
  blood, red cells moving towards orifice, holographic verification of model 3−28760
  cardiac muscle models and mechanics 3−22139
  carp retina, bipolar-amacrine transmission 3−31881
  carp retina, membrane resist. changes underlying bipolar cell response 3−31880
  cat, visual cortex, cell structure and formation correlation determ. by fluorescent dyeing 3−22153
  cell as microcybernetic polymaser *(Spanish)* 3−25548
  cell membrane, physical forces for adhesion 3−9640
  chromosome aberration yield in human lymphocytes as indicator of radiation dose 3−13156
  complementation and RNA synthesis by temp. sensitive mutants of VS virus 3−9642
  computerised analysis techniques 3−5629
  cooperativity in biomembranes *(German)* 3−37516
  DNA, bacterial and episomal, model for the regulation of replication 3−39762
  electrochemical information and energy transfer in vivo 3−5630
  electrochemical processes at biological interfaces 3−25550
  guinea pig taenia coli membrane potential rel. to extracellularly applied ATP and related nucleotides *(Japanese)* 3−37514
  Helix pomatia, amino acids in single nerve cells 3−28316
  histological thin section meas. quantitative analysis *(German)* 3−37511
  mammalian cells in tissue culture, effects of irradiated medium on growth characteristics 3−9641
  microelectrophoresis assembly, for cellular surface studies 3−25998
  motion of motile and non-motile single cells, photon correlation spectroscopy 3−5947
  muscles, smooth, contraction and excitation *(Japanese)* 3−35228
  percentage labelled mitoses experiments numerical inversion of Laplace transforms 3−25547
  potential of brain tissue using compound powder electrodes 3−3401
  radiation damage, recovery of cell surface charge rel. to colony forming ability 3−3591
  radiation effect on cell survival, molecular theory 3−28382
  rat, ventral horn cells, monosynaptic terminals 3−28314
  rat brain, quantitative synaptic changes with differential experience 3−28317
  rat liver mitochondria, effect of ionizing radiation 3−3605
  red bllod cells in the mesenteric capillaries, dimensions arrangement and density 3−13125
  retinal cells, characterization of different classes 3−3546
  skate retina, effect of Mg on horizontal cell activity 3−28357
  squid axon, intracellular conductance 3−28315
  twisting and mechanochemical energy conversion at dislocations in cylindrical crystals 3−14864
  volume and red cell density in capillaries of rapidly frozen lungs 3−13126
  Th atoms, monomolecular layer exam. by electron microscopy 3−24333
cement industry
  clinker coolers, electrostatic precipitator applications 3−13674
  concrete, microwave nondestructive testing of concrete strength 3−12471
  crack growth and fracture toughness meas. methods 3−27813
  dust emission suppression and control methods 3−37537
  mortar strength results using ASTM standard test method C348 and C349 3−34673
  transistorised automatic two-wavelength pyrometer applic. *(Polish)* 3−22292
centrifuges
  particle separation method 3−32216
  peeling type, approx. empirical eqn. and design *(German)* 3−6150
  for U enrichment, development in Netherlands, review *(Dutch)* 3−19901
ceramals *see cermets*
ceramic industry
  sintered carbide manufacture, review 3−5339
  u.s. cleaning *(Czech)* 3−34467
ceramic refractories *see refractories*
ceramics
  see also ceramic industry; refractories
  acoustic emission testing for cracks when mechanically stressed 3−27832
  American Ceramic Society meeting, Basic Science, Electronics and Nuclear Division (Sept. 1972) 3−8948
  arc plasma deposition of NiZn ferrite powders 3−8378
  borosilicate films, sintered, Vickers microhardness characterisation 3−39377
  brittle, strength loss with thermal shock 3−8985
  ceramic-metal soldered joints, mechanical stability research 3−28496
  in ceramics at Victoria, Australia 3−13185

ceramics continued
cermets-UO_2-metal applic. of Fricke's relationship to thermal conductivity 3-26513
chrome-magnesia fired bricks, electron microprobe analysis of failure 3-15755
coating with tungsten by reduction of WS_2 3-37084
coatings, thermal shock resistance testing 3-22256
coatings on metals, heat-resistant, high-temp. volatility *(Russian)* 3-12432
composite, metal fibre reinforced ceramics, fabrication and fracture toughness 3-18718
conference, Sydney, Australia, (Aug. 1972) 3-15747
cordierite glass, crystn., oxide additive effects on devitrification characts. 3-34643
cordierite glass, crystn., oxide additive effects on devitrification characts. 3-34644
corundum, densely sintered, third-stage creep *(Russian)* 3-15744
creep test, evaluation method, computer appl. *(German)* 3-31214
α- cristobalite thermal conductivity meas. 3-27741
dielectric breakdown of ceramic porous layer in vacuum and in air *(Russian)* 3-15452
dielectrics, properties, applications 3-2749
dielectrics, thermal diffusion of injected impurities, props. 3-20901
dielectrics for microelectronic packaging, laser micromachining 3-8954
as electrolytes and operation of oxygen concentration cells 3-15758
electron microscopy specimens, prep. and ion beam machining 3-24008
feldspar, modified, wetting of ceramics *(Polish)* 3-5342
ferrite permanent magnets, remanence, X-ray determination, technique, applications *(German)* 3-12006
ferrite-titanate substrate, composite formation, hot pressing 3-37079
ferroelectric, phase change induced by hydrostatic press. *(French)* 3-2497
ferroelectric, prepolarized, remanent polarization determ. *(French)* 3-2486
fibre reinforced composites, strength, theories 3-15777
fine-granular contact development for l.v. apparatus design *(Russian)* 3-27749
friction and wear rel. to structure, deformation and surface chemistry 3-34617
glass, struct. and props. 3-5355
glass, transmission electron microscope exam., thin foil prep. technique, microstruct. characteriz. 3-34645
glass bead compact, sintering obs. of neck growth and closed pores 3-15749
glass ceramics, tetrasilicic mica, strength depend. on mica grain size 3-8982
glass ceramics, texture development 3-5343
glass-ceramic microstructures formation by two stage heat treatment, high nucleation density 3-12439
glass-ceramics, solid state reactions 3-15786
grain boundaries, dielectric behaviour from electron beam scanning obs. 3-36302
grain boundary sliding deform. mechanism 3-8979
grinding, electropolishing methods, ion beam thinning for transmission electron microscopy 3-33436
impact data rel. to fracture 3-8995
intermetallic lightweight cpds., dynamic yield strengths, compressional and Hugoniot elastic parameters 3-17927
kaolinite-Cd(Sr)CO_3, reactions up to 1000°C 3-15754
kaolinite-illite-quartz mixtures, high-temp. refiring and ceramic props. 3-15751
machining, arc, laser beam and electron beam techniques, review 3-31128
machining, chemical, electrochemical and electrical discharge techniques and mechanisms, review 3-34630
mechanical strength, microstructure dependence, measurement and analysis techniques 3-12422
mechanical testing, fracture probability, stress density function, Weibull's statistical theory of mechanical strength *(German)* 3-12429
metal-ceramic system, microprobe meas. of diffusion 3-7964
microstructure, indirect shape factor 3-31015
mixed-oxide nucl. reactor microstructure, modification of three-region model 3-26536
molten salt additions during manufacture, applications *(Polish)* 3-27751
mullite, polycryst., ultra fine grain, creep kinetics, four point bending obs. 3-2755
new, mech. props., material texture depend. 3-5341
nuclear fuel, 1700°C sintering kiln *(French)* 3-34625
nuclear fuel pellets, comp. control in manufacture by sintering *(French)* 3-34622
nuclear reactor fuels, mixed oxides, cracking behaviour prediction using basic deformation characteristics, brittle-to-ductile transition temperature 3-6976
nuclear reactor fuels 3-6982
optical, KO-1, KO-2, bending strength temp. depend. 3-16414
optical glass, control of refractive index during annealing *(Polish)* 3-5174
particle morphology in real dimensions *(French)* 3-15796
Pb, La(Zr, Ti)O_3, acoustic pulse-echo detect. of ferroelec. phase transitions 3-18689
piezoceramic body stress-induced temp. increase demonstration by encapsulated liquid crystals 3-67
piezoelectric, properties and methods of determining 3-15748
piezoelectric plate, propag. of transverse electroacoustic waves 3-1870
plasma spraying of oxide ceramic materials *(German)* 3-23925
polymer-impregnated porous ceramics, elastic behaviour 3-39380
pore-size distributions, detn. for three dim. pore networks 3-15752
porosity, meas. by vibration method *(Russian)* 3-9830
porous, destroying press. determ. *(Russian)* 3-27750
powder prep. and treatment, review 3-39388
powders, ultrafine <100 Å, sintering in air up to 1500°C 3-8949
processing and fabrication for electronic applications, economics, quality, properties, developments and trends 3-18687
PZT 65/35 ferroelec. ceramic, dielec. breakdown under shock loading 3-18416

ceramics continued
radiating capacity of materials obtained by powder and plasmic metallurgy methods *(Russian)* 3-15767
raw materials, particle size measurement methods, conference 3-15793
resistor materials, Poland, alkali content, ionic current, surface state, crystallographic structure, life tests, laser trimming *(Polish)* 3-21722
sintering, conf., Villars-de-Lans, France (May 1971) *(French)* 3-34619
sintering, technical and fundamental aspects *(French)* 3-34620
strength, grain size dependence, Orowan-Petch and Knudsen eqns. 3-2751
strength behaviour, Rumpf's physical fracture theory, Griffith and critical crack length, cell size, experimental *(German)* 3-12430
strength characts., review 3-5340
ternary oxides high temperature equilibrium cation nonstoichiometry 3-8956
thermal insulating materials, electric heating equipment, pipes, requirements, applications *(German)* 3-12431
thermal shock resist. on heating rel. to failure 3-8984
transducer, ferroelectric nonlinearities 3-18686
transparent, based on alkaline earth oxides, high temperature baking process *(Russian)* 3-24972
uniaxial strength, porosity effects, working model 3-39383
u.s. cleaning *(Czech)* 3-34467
wetting by silicate melts, angle determ. by drop method, 'neck' phenomena *(Polish)* 3-27752
zirconia, preparation and props. 3-15760
AlN, commercial thermal conductivity meas. 3-15739
AlN, pressureless sintering to high density 3-21720
Al_2O_3, alumina, characterisation, analytical techniques 3-8961
Al_2O_3, alumina, dynamic behaviour, impurity effects *(German)* 3-34669
Al_2O_3, alumina, high temperature impact resistance, effects of quenching 3-8960
Al_2O_3, alumina, mech. and elec. props., applications 3-34626
Al_2O_3, alumina, mirror formation in fracture surfaces, dimensions dependence Young's modulus, fracture energy, temperature 3-8959
Al_2O_3, alumina, solid state bonding to metals, mechanism 3-8966
Al_2O_3, alumina, surface defects, scanning electron microscope examination 3-12420
Al_2O_3, alumina powder, particle size, agglomeration, sedimentation obs. 3-34618
Al_2O_3, alumina substrates, glazed, dynamic camber measurement technique 3-8963
Al_2O_3, alumina substrates containing rare earth oxides, fluorescent under u.v. 3-8965
Al_2O_3, cakes, formed by slip casting, compression permeability 3-8974
Al_2O_3, corundum, grinding using diamond wheel *(Russian)* 3-5912
Al_2O_3, fused to glassy substrate, boundary layer formation *(German)* 3-12425
Al_2O_3, h.v. insulator for vacuum apparatus, surface charging 3-140
α-Al_2O_3, polycryst., sintering and shaping process effects on form, topotaxy and texture *(German)* 3-12424
Al_2O_3, sapphire, pressure effect on dielectric strength 3-27464
Al_2O_3, thermally shocked, strength degradation and crack propagation 3-2752
$(Al_2O_3)_3(SiO_2)_2$, mullite, powder, stoichiometric synthesis and mechanical props. 3-27736
Al_2O_3 ceramics for implantation in living tissue *(German)* 3-27795
Al_2O_3 powder aggregates, strength characterisation, pressure-density data 3-8964
Al_2O_3 powders, high pure reactive, chemical and powder density 3-15792
Al_2O_3 sintering using a d.c. glow discharge 3-18695
Al_2O_3:MgO, grain boundary segregation 3-27739
Al_2O_3-TiO_2 powder prop. by h.f. oxidation, electron microscopy and X-ray diffr. 3-31122
B_4C, fast-neutron irradiated, study of defect microstructure due to He, Li disposition 3-26528
B_xC_y, thermal conductivity meas. of irradiated absorber pellets 3-26526
B_xC_y fast-reactor irradiated pellets, examination of microstructure 3-26527
$Ba_{2-x}Mg_{2-y}Ti_{8-z}O_{16}$, rutile substructure obs. 3-7908
BaO-SrO-SiO_2, phase equilibria 3-39379
$Ba_{1-x}Sr_xTiO_3$, O_2 diffusion constant meas. 3-17991
$BaTiO_3$, current-voltage characteristics and capacitance 3-33937
$BaTiO_3$, effect of clay and dolomite additions on sinterability 3-21721
$BaTiO_3$, I-V characts., 110-400°C, negative resist. 3-27266
$BaTiO_3$, new thermally stimulated electron emission dosimeter *(German)* 3-14271
$BaTiO_3$, polarized, piezoelec. props. under uniaxial transverse compression 3-5164
$BaTiO_3$, weak field permittivity saturation under high d.c. bias, grain-size effects 3-8519
$BaTiO_3$ doped, grain boundary resistance model *(German)* 3-33938
$BaTiO_3$ polycrystalline, constant electric field influence on dielectric props. *(Russian)* 3-8532
$BaTiO_3$:CeO_2, non piezoelec. dielec. ceramic, electromechanical bond coeff. *(Russian)* 3-21365
$BaTiO_3$:Y_2O_3 depend. on composition and cation siting structure and electrical props. 3-14813
$BaTiO_3$-$CaTiO_3$ (5 wt.%), large polarisation depend. photovoltages 3-33951
$BaTiO_3$.MnO, sintered in N_2, thick film monolithic capacitor applications 3-8952
BeO TSEE detector, dosiometric characteristics variation with surface impurities 3-28671
$BeSO_4$, thermal decomposition kinetics 3-2804
CaO, polycrystalline, thermoelectric force meas. between 1200 to 1650°C *(German)* 3-15740
$CaZrO_3$, formation by solid state reaction between CaO and ZrO_2 3-8977
CdO, high temp. elec. cond. and Hall effect 3-2080
CdTe, hot pressing 3-27742

- **ceramics** continued
  - CoO, pressure sintered, nonstoichiometry, final stage densification kinetics 3–8955
  - CoO, sintered, oxidation to Co_3O_4, kinetics, mechanism 3–8957
  - Cr_2O_3, final sintering rel. to grain growth 3–8981
  - $Dy_3Ga_5O_{12}$, garnet, influence of initial comp. and firing temp. in prep. *(Russian)* 3–15746
  - Fe_2O_3 polycrystalline powder, high temp. deformation 3–27738
  - $Gd_3Ga_5O_{12}$, garnet influence of initial comp. and firing temp. in prep. *(Russian)* 3–15746
  - $HfTiO_4$, $Hf_{1.26}Ti_{0.74}O_4$, thermal expansion coeffs., compressibility, polymorphism, X-ray diffr. obs. 3–8976
  - $LaGaO_3$, garnet, influence of initial comp. and firing temp. in prep. *(Russian)* 3–15746
  - LiF, optical quality, production by method of explosive compression of powdered inorganic compounds *(Russian)* 3–12434
  - Li_2O-K_2O-SiO_2-Al_2O_3:Sr^{2+} photopyrocerams, dislocation struct. and dielec. props. 3–27753
  - $MgAl_2O_4$, synthesis by thermal decomposition of hydrated nitrate mixtures 3–8968
  - $MgAl_2O_4$, transition due to hot-pressing 3–18688
  - MgO, polycrystalline, thermoelectric force meas. between 1200 to 1650°C *(German)* 3–15740
  - MgO ceramic, polycrystalline function representing planar distribution of grain size 3–24970
  - MgO-Al_2O_3-SiO_2-TiO_2 glass-ceramic, crystn. and struct. 3–31161
  - MgO-SnO_2, firing, binding props. and compressive strength *(Russian)* 3–15745
  - $MnFe_2O_4$, sintering in continuous kilns *(French)* 3–34623
  - $MnZnFe_2O_4$, comp. variations during sintering *(French)* 3–34624
  - $MoSi_2$, interaction with several metals and alloys, cermet formation, mechanical properties 3–8967
  - γ-Na_2BeF_4, orthorhombic to monoclinic phase transition investigation 3–27743
  - NiO, pressure sintered, nonstoichiometry, final stage densification kinetics 3–8955
  - (Pb,La)(Ti,Zr)O_3 ceramics, A-site and B-site vacancies distrib. 3–1618
  - (Pb,La)(Zr_y,Ti_z)O_3, PLTZ ceramics, y=0.60 to 1.0, z=0.4 to 0, antiferroelectric-ferroelectric phase boundary, temperature, d.c. field dependence 3–8525
  - Pb, La(Zr, Ti)O_3, elastic and piezoelectric props., La dependence 3–18691
  - Pb_xLa_{1-x}(Zr, Ti)O_3 powder, cold pressing and low temperature sintering 3–27734
  - PbO, polycrystalline ceramics, pyroelectric current obs. 3–5166
  - $PbTiO_3$, piezoelectric props., effect of additives *(Japanese)* 3–2495
  - Pb(Zr, Ti)O_3, pyroelec. props., comp. and phase struct. depend., i.r. detector characteriz. 3–39098
  - Pb(Zr,Ti)O_3, La substituted, PLZT, isothermal grain growth, dielectric and ferroelectric properties 3–8950
  - Pb(Zr,Ti)O_3, La_2O_3-modified, temp.-depend. ferroelec. domain alignment 3–5168
  - Pb(Zr,Ti)O_3 ceramic pyroelectric detector transient thermal analysis 3–8523
  - Pb(ZrTi)O_3 piezoelectric ceramics, stabilization effects by addition of Mn, Cr or U oxides 3–8507
  - $PbZr_{1-x}Ti_xO_3$ solid solns., press. induced ferroelec.-antiferroelec. transform., depolarization behaviour *(French)* 3–36842
  - $PbZr_{1-x}Ti_xO_3 + 0.8\%\ WO_3$, ferroelec. transition temp.–comp. phase diagram *(French)* 3–5167
  - Pu_2C_3, specific heat meas. between 35 and 300 K, entropy determ. *(French)* 3–23431
  - PuO_2 fuel for space vehicles, thermophysical and thermomechanical properties 3–19958
  - PuO_2 fuel form, He migration and release, heat treatment expts. 3–19957
  - PuO_2 spherical fuel form development for use in space flight, hot pressing technique 3–19955
  - ^{238}Pu isotopic fuels, large-scale production processes for heat source applications 3–19956
  - SbSI based piezoceramic, prep. technology 3–34301
  - SiC, fracture surface energy depend. on microstucture 3–8983
  - SiC, reaction bonded, neutron irradiated, reduction of mechanical properties 3–24968
  - Si_2N_4-Al_2O_3, hot-pressing, exam. *(Japanese)* 3–8992
  - Si_3N_4, fracture surface energies meas. 3–15738
  - Si_3N_4, high density, mechanical strength, effects of diamond grinding 3–8953
  - Si_3N_4, high temperature strength, slow crack propagation prior to fracture 3–8958
  - Si_3N_4, hot pressed, microstructure 3–12421
  - SiO_2-Al_2O_3-Na_2O glasses, containing TiO_2 as nucleation agent, props. and struct. *(Polish)* 3–4721
  - Si_2ON_2, neutron irrad. behaviour rel. to high temp. nucl. reactor applics. 3–7005
  - SnO_2:Sb_2O_3, effect of additives on sintering *(Japanese)* 3–8991
  - $SrTiO_3$, (Ba, Sr) TiO_3, boundary layer dielectrics, permittivity and dispersion 3–2485
  - $SrTiO_3$, O_2 diffusion constant meas. 3–17991
  - $SrTiO_3$-$MTiO_3$, (M=Pb, Ba, Ca), phase transitions, u.s. velocity and permittivity studies 3–27478
  - ThC-UC solid solutions, thermodynamic props. *(Japanese)* 3–31120
  - TiB_2, sintering under press. *(Polish)* 3–8990
  - TiC powder, creep during hot pressing *(Russian)* 3–27747
  - UC, U vacancy formation and migration, resistivity meas. 3–24966
  - UC-PuC, fuel rods, void deployment by irradiation to 77000 MWd/T 3–26539
  - U_2C_3, thermal diffusivity and cond., 1000-2200 K 3–37082
  - U_xC_y, high temp. enthalpy 3–23428
  - UN, porosity dependence of thermal conductivity 3–24965
  - UO_2, nonstoichiometric, sintering kinetics under nonisothermal conditions 3–37081
  - UO_2, porosity changes during sintering at 1700 to 2200 °C rel. to grain growth 3–24969
  - UO_2, sintering of grain boundary cavities 3–12437
  - UO_2 composite fuels, assessment of heat conduction effectiveness 3–23443
  - UO_2 powder activity determ. by DTA 3–34628
- **ceramics** continued
  - UO_2 sintered reactor fuel, temp. density and porosity effects on thermal conductivity 3–26516
  - UO_2-PuO_2 nucl. fuel, linear heat rating for incipient fuel melting, effect of cladding gap size 3–26537
  - UO_2-PuO_2 nucl. reactor fuels, vapour-transport mechanism for U and Pu migration 3–26538
  - $UO_{2\pm x}$, $0 \leqslant x \leqslant 0.25$, fracture stress and Young's modulus, porosity, grain size and excess O_2 effect 3–24967
  - US, with UOS or BaS addition, sintering, 1500-1950°C, in presence of liquid phase 3–18692
  - $VC_{0.76}$ monocrystals, TEM obs. of coherent precipitate 3–31119
  - $(V_{1-x}Cr_x)_2O_3$, prep. and electronic props. 3–27744
  - WC-Co hard alloy strength depend. on Co content *(Russian)* 3–15768
  - $Y_3Al_5O_{12}$, synthesis by thermal decomposition of hydrated nitrate mixtures 3–8968
  - $Y_3Ga_5O_{12}$, garnet, influence of initial comp. and firing temp. in prep. *(Russian)* 3–15746
  - YIG, polycryst., reactive hot pressing 3–31123
  - Y_2O_3 powder, sintering rel. to densification 3–12436
  - ZnO, thermally shocked, strength rel. to Hasselman theory 3–8978
  - ZnS, hot pressing 3–27742
  - ZrB_2, sintering under press. *(Polish)* 3–8990
  - ZrC, high-temp. creep characts. 3–37088
  - ZrO_2, CaO stabilised, creep 3–27740
  - ZrO_2:Y_2O_3, sintering, effect of CO_2 3–15761
  - $ZrTiO_4$, thermal expansion coeffs., compressibility, polymorphism, X-ray diffr. obs. 3–8976
- **Cerenkov counters** *see Cherenkov counters*
- **Cerenkov radiation** *see Cherenkov radiation*
- **cerium**
  - abundance, isotopic, in ^{238}U fast fission spectrum 3–17269
  - autoionising states, excitation by electron impact *(Russian)* 3–26599
  - cast iron:Ce, Ce effect on mech. strength with quenching *(Russian)* 3–12411
  - electrical resist., low temp., of alpha-Ce under pressure 3–30451
  - electrical resist. meas. on α-Ce, temp. depend. rel. to mag. impurities 3–33862
  - impurity in supercond. transition temp. press. depend. 3–8303
  - Kondo effect when impurity in alloys, cryst. field effects 3–2256
  - liquid, spectral emissivity obs. 3–27126
  - liquid, thermoelectric props., temp. depend., m.p.-1200K 3–24408
  - phase transition, α-γ, La impurity effects 3–38669
  - phase transition, α-γ, La impurity effects 3–38670
  - soft X-ray absorption, theory *(Russian)* 3–12192
  - surface, energy loss spectra of reflected electrons *(Russian)* 3–12205
  - thermal diffusivity and heat capacity, meas. and apparatus *(Russian)* 3–9864
  - thermoelectric power, room temp. to m.p. 3–2062
  - thermoelectric power meas. near melting point 3–18128
  - α-γ transition, effect of impurities 3–21238
  - wear and friction in air 3–18625
  - CaF_2:Ce,Na, near u.v. absorpt. spectra obs. of defect centres 3–12161
  - CaF_2:Ce^{3+} polarisation storage 3–18406
  - CaF_2:Mn(Ce,Mn), cathodoluminescence, trapped hole diffusion 3–39197
  - CdS:Ce^{3+}, Ag, Cu fluorescence spectra, probability of emission calc. *(Russian)* 3–27546
  - α-Ce, magnetisation, 1.7-80 K, elec. resist., 1.4–25 K 3–8143
  - Ce^{2+}, $4f^2$-4f5d lines 3–17350
  - Ce^{3+}, in H_2SO_4 vitreous aq. soln., effect on spin-lattice relax. of H atoms 3–34186
  - Ce^{3+}-activated alkaline earth thiogallates, cathodolum., rel. to flying spot scanner appl. 3–12186
  - (La, Ce)Al_2 dilute alloy with Ce impurities, superconducting-Kondo system, specific heat 3–5072
  - YAG:Ce^{3+} and its solid solutions, cathodolum. 3–30883
- **cerium compounds**
  - hydrides, temp. dependent electronic transition, resistivity meas. 3–8237
  - phosphates, $Me_{0.5}{}^{2+}Ce_{0.5}{}^{4+}PO_4$ type, synthesis, struct. props. 3–1616
  - silicates $Me^{2+}Ce^{4+}Si_2O_7$ type, synthesis, struct. props. 3–1616
  - Al-CeF_3-Al thin film capacitor system, stimulated dielectric relaxation currents 3–8277
  - $BaTiO_3$:CeO_2, non piezoelec. dielec. ceramic, electromechanical bond coeff. *(Russian)* 3–21365
  - CdF_4MF, M=alkali metal, structures of compounds formed *(French)* 3–14819
  - Ce complex, CDP, g-tensors from e.p.r. 3–15416
  - Ce complexes, π sandwich type, struct. 3–14338
  - Ce Mg nitrate, thermal contact with liquid ^3He at low temp. 3–36459
  - CeC_2-UC_2 solid solutions, composition dependence of cubic→tetragonal phase transformations 3–11739
  - $CeCo_2$, thermopower and sp. ht. at low temps. 3–2063
  - $CeCr_2B_6$, crystal structure 3–33505
  - CeF_2, Pr^{3+} absorpt. spectra and energy levels *(Russian)* 3–12157
  - CeF_3, symmetry, struct., screening consts. 3–7662
  - CeF_3 film, between Al electrodes, isothermal dielec. relax. currents 3–36666
  - Ce_2F_6(g), stabilities rel. to dimerization 3–27851
  - $Ce_{10/3}Ga_6S_{14}$, sulphurized compound family of melilite type *(French)* 3–30102
  - CeH_2, low temp. specific heats 3–11744
  - $Ce_2Me_3(NO_3)_{12}.24H_2O$, Me=Mg, Mn, Zn, Co, Ni spectra, substitution on vibration bands of water, Stark splitting of Ce^{3+} *(Russian)* 3–8571
  - $CeMg(NO_3)_5$, search for ground state by extented Luttinger-Tisza method 3–34056
  - $CeMg_3(NO_3)_{12}$, powdered, adiabatic susceptibility tensor, mag. field depend. 3–12003
  - $Ce_2Mg_3(NO_3)_{12}$, thermal cond., 0.2-1.5 K 3–36444
  - $Ce_2Mg_3(NO_3)_{12}.12H_2O/{}^3He$ boundary resist., nucl. spin-electron spin dipolar interaction 3–30303

- **cerium compounds** continued
  - $Ce_2Mg_3(NO_3)_{12}.24H_2O$, e.p.r. saturation of Ce^{3+}, light scatt. obs. of nonequil. phonon system 3-2370
  - $Ce_2Mg_3(NO_3)_{12}.24H_2O$, mag. field depend. of spin-spin relax. 3-8478
  - $Ce_2Mg_3(NO_3)_{12}.24H_2O$, magnetothermodynamics, heat capacity, entropy, magnetic moment, 0.5-4.2K, 90 kG 3-30616
  - $Ce_2Mg_3(NO_3)_{12}.24H_2O$, phonon system under Ce^{3+} e.p.r. saturation conditions, Mandelshtam-Brillouin study *(Russian)* 3-8438
  - $Ce_2Mg_3(NO_3)_{12}.24H_2O$, thermal expansion coefficients between 10 K and 300K 3-17986
  - $Ce_2Mg_3(NO_3)_{12}.24H_2O$ temperature scale, implications of new data on W specific heat 3-28457
  - $Ce(NO_3)_2$, phonon induction effects at e.s.r. saturation 3-8417
  - Ce_2NiSi, $P6_3/m$ group, struct. detn. X-ray anal. 3-7705
  - CeO_2, thermal expansion by an X-ray diffraction method 3-30272
  - $CeO_2:Gd^{3+}$, S-state, e.p.r. anal. method and g value determ. 3-27401
  - $CeO_2:Gd^{3+}(Cm^{3+})$, zero-field splittings 3-18358
  - Ce_2O_2S, long wave i.r. spectra *(Russian)* 3-30825
  - CeP, anomaly in n.m.r. shift of ^{31}P 3-18379
  - $Ce_{1-x}R_xAl_3(R=Y,La)$, n.m.r. and mag. susceptibility 3-27434
  - CeS, anomaly in n.m.r. shift of ^{75}As 3-18379
  - $Ce_{4.67}[SiO_4]_3O$ cry. struct. of TR analog by X-ray diffr. 3-7703
  - UO_2-CeO_2, sintered pellets, elec. resist. and Seebeck coeff. meas. 3-18132
  - $Y_{3-x}Ce_xFe_5O_{12}$, temp. depend. of magnetostriction, ferromag. reson. study *(Russian)* 3-12046
- **cermets**
  - ceramic-metal soldered joints, mechanical stability research 3-28496
  - compact cermet prep. by impregnation of porous blanks with FeB_x alloys *(Russian)* 3-27730
  - ferrites, wear resistant hot pressing production methods *(Russian)* 3-27746
  - fine-granular contact development for l.v. apparatus design *(Russian)* 3-27749
  - measurement methods and instruments 3-27745
  - porous materials, workability in hot steam environment *(Russian)* 3-15769
  - steel, insoluble residue in starting powder, effect on props. *(Russian)* 3-8946
  - steel, stainless, powders, pore size calcs. *(Russian)* 3-27748
  - surface oxide films, microstructure 3-24855
  - technology rel. to preparation and applications *(German)* 3-8973
  - thermal conductivities, obs. *(Russian)* 3-4987
  - two phase materials, elec. resist. computation *(German)* 3-8993
  - Ag-SiO, thin films, struct. and elec. cond. *(Korean)* 3-27198
  - Al_2O_3/Nb thin cermet films, hopping conduction through localised states 3-11895
  - Au-glass film, strain sensitivity and t.c.r. 3-5065
  - Au-SiO_x, cermet film, structure and elec. props. with heat treatment 3-15201
  - Au-SiO_x film, structural and electrical changes during heat treatment 3-5064
  - Cr_2O_3-Cr cermet, sintering and obs. of props. *(Russian)* 3-8944
  - Fe coarse magneto soft powder, sintering effect on coercive force *(Russian)* 3-27718
  - Fe powder with P additive, sintering conditions effect on shrinkage on magnetic props. *(Russian)* 3-27720
  - Fe powders with 1% P additives, sintering conditions effect on magnetic and mechanical props. *(Russian)* 3-27719
  - Mn/SiO film, elec. resist. and struct. 3-27754
  - $MoSi_2$-based, interaction of $MoSi_2$ with several metals and alloys 3-8967
  - Nb/Al_2O_3 film, superconductivity, normal state elec. and struct. props. *(Russian)* 3-30482
  - Ni powders, pore size calcs. *(Russian)* 3-27748
  - Ni-C, expt. confirmation of resist. calc. for two phase materials *(German)* 3-8993
  - Pb-dielectric cermet film, refr. indices, ellipsometric meas. rel. to Maxwell Garnet theory 3-8544
  - ThO_2-Mo cermet radioisotopic heat source, metallographic image analysis 3-18693
  - Ti cermet blanks, hot strain *(Russian)* 3-27732
  - Ti powders, pore size calcs. *(Russian)* 3-27748
  - TiC containing, heat cond. *(Russian)* 3-15766
  - TiC/Co(Ni), Vickers hardness under reduced charge, comp. depend. *(French)* 3-24971
  - TiC-Nb(Ta)(Mo)(W), electrophysical props. *(Russian)* 3-8988
  - VC-Co, grain growth during liquid phase sintering 3-18683
  - W-Re, electroresist. meas. *(Russian)* 3-8141
  - WC/Co, sintered, carbide phase recovery *(Japanese)* 3-31121
  - WC/Co, Vickers hardness under reduced charge, comp. depend. *(French)* 3-24971
  - WC/Co alloy, aging process, calorimetric studies, Co_3W precipitation *(Japanese)* 3-31066
- **cesium** *see caesium*
- **change of state** *see phase transformations*
- **channel capacity**
  - of ear as function of frequency 3-3484
  - laser beam communications 3-26249
- **channeling** *see channelling*
- **channelling**
  - *see also energy loss of particles*
  - atomic collision chains, vacancies, focusing influence, computer calcs. 3-20777
  - charged particles in perfect crysts., analysis for Born-Mayer interaction potentials 3-11665
  - Cherenkov structure radiation for particle channelled in crystal 3-26916
  - complex continuum potential, for channelling due to non-local inelastic scatt. 3-20772
  - crystalline defect anal., ion beam techniques 3-33577
  - crystalline structures, theory of channelling and of shadow effects *(Russian)* 3-1661
  - electron, high energy, transmission profiles, string effect 3-1658
  - electron pattern analysis by computer 3-1555
  - fast charged particles, wave-particle duality 3-27044
- **channelling** continued
  - impurity atom, location exact determ. by means of channelling effect *(Russian)* 3-1660
  - inelastic collisions, stopping power, dependence on atomic number of projectile atom 3-13416
  - ions in crystals, multiple scattering by electrons or thermal vibrations of lattice 3-17886
  - momentum transfer cross sections and Z_1 oscillations in stopping power 3-36338
  - nondegenerate semiconductor surface inversion layer, electron scattering by surface oxide charges theory 3-11954
  - phosphosilicate glass layers, analysis by Rutherford backscatt. and channelling meas. 3-38539
  - polar lattices, critical angle, blocking effects 3-11666
  - quantum mechanical treatment 3-30163
  - review of theory applic. to study of crystal imperfections and impurities *(Hungarian)* 3-7802
  - scanning electron microscope patterns, effect of dislocations 3-1553
  - scanning electron microscope patterns and crystalline contrast 3-1559
  - scanning electron microscope selected-area technique, metallurgical application 3-2713
  - selected area patterns and micrographs, simultaneous display using s.e.m. 3-1558
  - Si single crystal, back scatter energy spectra for 1.0 and 1.5 MeV protons 3-20774
  - Si single crystals, with 3.0 MeV protons 3-20775
  - single crystals, channelling and blocking, review *(Japanese)* 3-14900
  - thick single cryst., dechannelling, planar shadow shape 3-20776
  - Au, of electrons, electron microscopy study 3-24169
  - Au film, light ion channelling 0.5-2 MeV, scatt. and transmission probabilities, light emission *(French)* 3-20771
  - Fe, of 1.9 MeV He^+ ions, oscillating trajectories backscatt. obs. 3-4778
  - GaAs:Zn, H^+ ion bombardment, channelling expts., annealing behaviour of disorder density 3-33578
  - Ge, lattice disorder induced by 0.3 MeV D^+ random bombardment, 1.5 MeV D^+ channelling measurements 3-1656
  - Ge single crystals, fast-neutron-induced damage studies using channelling of 1 MeV protons 3-24163
  - He ion backscatt. spectra in planar channelling, oscillations stochastic model approach *(French)* 3-27589
  - He^+ ions excited by transmission through Au cryst., absence of channelling effect 3-1110
  - KCl, effect of atomic displacement on dechannelling 3-38601
  - KI(Tl), scintillation response to channelled ions 3-34434
  - LiF, blocking effect observation by (n,t) reaction 3-37684
  - NaCl, channelling effect on positron annihilation 3-7795
  - NaI(Tl), scintillation response to channelled ions 3-34434
  - Nb, effects on morphology of blisters due to 0.5 MeV ^4He ions impact 3-1653
  - Nb-D(2 at.%), interstitial location determ. by channelling of deuterons *(German)* 3-27017
  - Ni:Hf, lattice-location of implanted impurity in ferromag. host, chanelling obs. 3-18305
  - Pb-Sn superplastic alloys, scanning electron microscope deformation studies 3-1549
  - Si, 110 axis, of 1 GeV positrons *(Russian)* 3-1657
  - Si, axial to planar transition for protons 3-38602
  - Si, lattice disorder induced by 0.3 MeV D^+ random bombardment, 1.5 MeV D^+ channelling measurements 3-1656
  - Si, proton irradiated, defect studies by channelling backscattering measurements 3-33579
  - Si epitaxial layer, crystalline perfection from ion channelling and backscatt. meas. 3-18039
  - Si heteroepitaxial layers, crystalline perfection from ion channelling and electron microscopy, comparative evaluation 3-18040
  - Si irradiated with B and P ions, spatial distrib. of radiation defects 3-24166
  - Si monocrystal, channelling of fission-prod. ^{140}Ba 3-7801
  - Si overlaid with Au films, energy dependence of He^+ and H^+ channelling 3-33581
  - Si oxidised surface, m.o.s. electron surface mobility in inversion layers at room temp. 3-8268
  - Si single crystals, fast-neutron-induced damage studies using channelling of 1 MeV protons 3-24163
  - ThO_2, axial channelling of 6.5-MeV $^3He^{2+}$ ions 3-17883
  - ZnS, polarity of structure rel. to high energy ion blocking 3-30164
- **character recognition**
  - *see also optical character recognition*
  - information morphological invariants extraction by optical correlation and spatial filtering *(French)* 3-29049
- **character recognition equipment**
  - holographic recognition, spatial filtering technique 3-28574
  - nondestructive testing equipment with multi-channel signals 3-18765
- **character sets**
  - segmented master character for electronic display apparatus, patent 3-33455
- **characteristic temperature** *see specific heat*
- **characteristics measurement**
  - *see also headings for specific characteristics, e.g. gain measurement; viscosity measurement*
  - cyclohexane, self-diffusion measurement, high pressure, diaphragm cell, theory, results, analysis 3-10100
  - h.f. electrical characteristics semiconductors, thermostat 3-250
  - STL ionophone transducer and appls. 3-96
  - volt-ampere characteristics of periodic pulse discharges by probe method, recording on oscillograph *(Russian)* 3-6024
  - n-GaAs, electrochemical characterization, automatic plotting system 3-30953
  - Hg-Si contact capacitance-voltage characteristic 3-2182
  - n-InP, velocity/field characteristics from dipole domain measurements 3-8186
  - W, arc cast thermophysical props., direct heating method, TPRC multi-property apparatus 3-12426

charcoal
- *see also carbon*
- adsorbed methane, neutron scatt. study 3−27178

charge (electric) *see electric charge*

charge carriers
- *see also carrier mobility; electron-hole recombination; hot carriers; minority carriers*
- alkyd resin in acetone, elec. cond., potential distribution increase of charge carriers at anode 3−39408
- anthracene, delayed fluoresc. quenching due to triplet exciton-hole interaction 3−2587
- auramine hydrochloride, majority, sign and mean lifetime in photoconduction 3−33949
- crystals with zinc blende symmetry, second order nonlinear optical susceptibility, energy band theory, virtual electronic processes 3−8550
- diamond, semiconducting p type, high field magnetoresistance, hole conduction in uncoupled valence bonds 3−11912
- dilute mag. alloy, coupled local moment-conduction electron Bloch equation, e.s.r. obs. 3−34213
- echo signals of conduction electrons, Lowe and Norberg theorem 3−36793
- electron-hole liquids in semiconductors 3−21009
- ferromagnet, Seebeck coeff. at Curie temp., sp. ht. of charge carriers 3−18319
- ferromagnet, Seebeck coeff. at Curie temp., sp. ht. of charge carriers 3−18320
- graphite, electrical transport props. assuming acoustical phonon scattering 3−11897
- graphite, Shubnikov de Haas meas. rel. to carrier lifetime anisotropy 3−18168
- heating technique, warm electron region *(Russian)* 3−33939
- III-V semiconductors, small-gap, spin props. of conduction electrons 3−38845
- low mol. wt. organic solids, studies using electrical conductivity 3−5395
- low-density inversion layers, possible crystn. of charge carriers *(Russian)* 3−8273
- poly-N-vinylcarbazole complexed with trinitrofluorenone film, bulk recomb. of charge carriers 3−30513
- polymer, origin, book contrib. 3−11891
- semiconductor, electron cooling by static elec. field *(Russian)* 3−8202
- semiconductor, many-valley, charge density fluctuation in strong elec. field 3−5003
- semiconductors phonon scattering by electrons and holes 3−1748
- Ag halides, photoholes and photoelectrons formation 3−34744
- Ag halides electrons, holes and excitons at low temperature 3−27218
- Ar solid, holes and electrons induced by α particle source 3−30505
- C, black, e.p.r., localized centres, conduction electrons, 4.2-300K *(French)* 3−24614
- CaF$_2$:Mn(Ce,Mn), cathodoluminescence, trapped hole diffusion 3−39197
- CaWO$_4$, X-irrad., optically and thermally stimulated conductivity obs. *(German)* 3−2105
- CdTe:Cd, thin films, electrical conductivity *(Russian)* 3−33891
- GaAs, excess Ga and As in the vapour phase influence on epitaxial growth, hole mobility effect on growth rate *(Russian)* 3−8749
- GaAs, p$^+$−n photodiodes, electron irrad., defect studies, differential capacity, conductance measurements 3−33845
- GaAs:He(N,S,Zn), ion implantation, elec. conduction due to defect centres 3−33906
- p-GaP, hole effective mass, cyclotron reson. determ. 3−27215
- p-GaSb, phonon-phonon and phonon-charge carrier interactions *(French)* 3−1706
- p- Ge, galvanomagnetic effects in high electric fields, hole energy surfaces warping *(Russian)* 3−11910
- Ge hole scattering by acoustic and optical phonons in homogeneously deformed sample *(Russian)* 3−24417
- InAs, electron irradiation damage studies 3−33555
- n-InSb, phonon-phonon and phonon-charge carrier interactions *(French)* 3−1706
- n-InSb, reson. hole-TO and hole-LO phonon coupling, magnetooptical study 3−4831
- Pb(ZrTi)O$_3$ piezoelectric ceramics, stabilization effects, charge carrier trapping mechanism for polarization ordering above Curie temp. 3−8507
- Se liq., charge transport by hopping, hole photogeneration *(Russian)* 3−8179
- p-Si, pulled, float-zone, carrier lifetime doping, annealing processes 3−39274
- Si, radiation damage in p-type with H impurity and high purity n-type, hole density, annealing 3−33546
- Si:Au diode, field independence of thermal emission rate of holes 3−4964
- Si:Zn, thermal ionization rates and hole energies at double acceptor centres 3−15193
- Te, rel. to effect of elec. field and illumination on plasticity *(Russian)* 3−14912
- ZnO, Li doped and undoped, single crystals, baked layers, electrophotographic discharge mechanism *(Russian)* 3−30517
- ZnTe, electron irradiated, Zn displacement threshold Zn vacancy luminescence 3−33557

charge compensation
- *see also crystal field theory; crystallography*
- LiF:U^{6+}, e.s.r. obs. of charge compensation effects 3−2383

charge conservation *see C invariance*

charge-coupled devices
- image sensors, sensitivity and resolution at low light levels 3−29058
- Si-SiO$_2$ boundary, interface states *(German)* 3−34001

charge exchange
- *see also electron capture; ionisation*
- 1,4-dimethoxybenzene, acetonitrile soln., fluorescence quenching, charge transfer interaction 3−34401
- aerosols, hot beta-active particles in air, kinetics of unipolar charging 3−20264
- alkali ion-atom collisions, wavefunctions and pseudopot. for charge transfer 3−1126

charge exchange continued
- anthracene, mag. field modulation of prompt electrolum., charge transfer exciton fission 3−24747
- atoms, symmetrical charge transfer cross section, ioniz. pot. depend. 3−20060
- blood coagulation factor, electrochem. behaviour, obs. on fibrinogen 3−39764
- blood coagulation factor, electrochem. behaviour, obs. on prothrombin and thrombin 3−39763
- complex formation of I$_2$ with pyridine in cyclohexane soln. effect on positronium I$_2$ reaction 3−25100
- dye interacting with protons in aqueous soln. *(Russian)* 3−39427
- electrolytes, charge separation at phase boundary 3−9089
- electron production mechanisms in ion-atom collisions 3−26601
- hadron-hadron collisions, high-energy, charge transfer in fragmentation model 3−38070
- hydrogen-bonded complexes, charge transfer theory and relation between dipole moment energy and enhancement 3−20207
- hydroquinone charge-transfer complexes, i.r. spectra 3−36032
- hyperchange-exchange reactions, application of Ringland-Roberts-Roy-Tran Thanh Van Reggeized absorption model 3−10795
- impurity molecules, energy transfer during excitation 3−27899
- inert gas ions, charge transfer rate consts. to difluorobenzene and dichloroethylene 3−33152
- inert gas ions and atoms, reson. charge exchange and fine struct. of levels *(Russian)* 3−4393
- interatomic and intermol. exchange interactions, Rayleigh-Schrodinger perturbation theory applic. 3−7084
- ion-polar mol. collision theory, comparison with expt. charge transfer reaction data 3−33152
- ions, negative, electron binding energy determ. from charge exchange cross sections 3−38242
- Li$^+$ + He collisions, rot. coupling 3−20059
- meson-baryon charge- and hypercharge exchange reactions, fixed poles in t-channel helicity-flip amplitude 3−14049
- mutual neutralization in positive negative ion collisions *(Russian)* 3−11177
- organic molecular crystal, charge separation at phase boundary 3−9089
- organic semiconductor film, Stark effect and charge-transfer excitons 3−36538
- pseudoscalar meson-baryon scattering, amplitude analysis using dual absorptive model 3−4223
- pyrene charge-transfer complexes, i.r. spectra 3−36032
- pyridine and methyl derivatives in iodine soln., out-of-plane deform. vibrs. *(Russian)* 3−11232
- pyrometallic dianhydride, flash photolysis, anion formation 3−27889
- sodalite, damage mechanism, ESCA obs. 3−36298
- stannic-phthalocyanine, charge-transfer like structure 3−2583
- TCNQ, potassium salt, ^{14}N n.q.r., charge transfer phenomena 3−24628
- tetracyanobenzene-biphenyl complex, delayed charge-transfer fluoresc. in cryst. state 3−21820
- tetraphenylenediamine charge-transfer complexes, i.r. spectra 3−36032
- water drops, falling and colliding in elec. field 3−649
- K$^\pm$N interactions, search for Q^0 and Q^{++} production 3−35830
- K$^-$p→K^{0}n, meas. of charge-exchange cross sections at 25 and 35 GeV/c 3−17116
- np, at high energy, calc. of differential cross-sections in weak cut model 3−32717
- np scattering, charge exchange from 6-29 GeV/c, meas. of differential cross-sections, study of shape and momentum dependence 3−899
- pp, at high energy, calc. of differential cross-sections in weak cut model 3−32717
- pp→nn, 5.0 and 7.76 GeV/c, charge exchange, meas. of differential cross section near forward region 3−23160
- πN interactions, energy >6 GeV, complex angular momentum theory with cut contribution *(Russian)* 3−38080
- πN scattering, simultaneous fit to forward and backward data using dual resonance model 3−29263
- π^-p charge exchange scattering, peripheral absorption model 3−14066
- π^-p→π^0n, duality and Bessel-function model from Regge-theory viewpoint 3−6664
- π^-p→π^0n, 22.6, 32.9 and 42.6 MeV, meas. of charge exchange cross section 3−23134
- Ar, proton scatt., total differential cross section 3−33059
- Ar$^+$-Ar, X-ray yield dependence on final charge state 3−29527
- As$^+$ c.w. laser oscillation in He-As mixture, charge transfer reaction 3−37959
- C$^+$-C collision, K-shell ionisation in keV-MeV range, Fano-Lichten theory 3−26603
- Ca-Xe system, population inversion calc. using near-reson. charge exchange as pumping mechanism 3−37953
- Cd$^+$ collisions with Mg$^+$, Mg ions, excitation of resonance levels 3−17377
- Fe(CN)$_6$, Co$_3${Fe(CN)$_6$}$_2$, fast intramolecular electron transfer, γ-resonance spectroscopy obs. *(Russian)* 3−2472
- H beams, charge changing processes in gases and alkali metal vapours, review 3−35983
- H + H$_2$→H$_2$ + H collinear exchange reactions, analytical energy surfaces 3−20205
- H + proton electron-transfer collisions, second-order Born terms 3−4394
- H$^+$ charge transfer collisions with H atoms, Faddeev approach 3−35977
- H$^+$-Kr charge exchange collisions, spin polarisation 3−35978
- He, excitation by fast protons, charge exchange study 3−38244
- He, proton scatt., total differential cross section 3−33059
- He ions, charge-exchange phenomena with Zn, Cd, Hg, Te spectroscopic study 3−33058
- He$^+$ + He collisions, direct and exchange excitations, u-g symmetry effect 3−38243
- He$^+$ + Ne collisions, differential scatt. cross section for Ne excitation 3−33055
- He^{2+} + H collisions, electron transfer and excitation, coupled-state calcs. 3−26602
- He^{2+} + He collisions, electron capture and excitation 3−26604

charge exchange continued
  I_2 dissolved in hydroxylic solvents, photolysis, atom charge transfer complex identification 3−34736
  $Kr + CO^+ \rightarrow CO + Kr^+$, 0.04-3 eV 3−20058
  $Kr^+ + CO \rightarrow Kr + CO^+$, 0.04-3 eV 3−20058
  $Kr^+ + Kr \rightarrow Kr + Kr^+$, 0.04-3 eV 3−20058
  $Li + H_2 \rightarrow LiH + H$ collinear exchange reactions, analytical energy surfaces 3−20205
  Mg^+, Mg collisions with Cd^+ ions, excitation of resonance levels 3−17377
  $^{a}Mo(p, np)$ 1A reaction (A=94, 95, 66) study of (p, n) charge exchange 3−14206
  N_2, double charge transfer spectroscopy using 4 keV protons 3−14401
  NO, double charge transfer spectroscopy using 4 keV protons 3−14401
  O_2, double charge transfer spectroscopy using 4 keV protons 3−14401
  Si^+, with triethylamine, neutralisation study 3−23615
  SiO_2/electrolyte interface, mobile ion transfer from contaminating aqueous solutions 3−39241
  Ta oxidation, transport nos.of metal and O_2, obs. using noble gas tracers 3−38743

charge measurement
  see also electrometers
  application to testing of manufactured materials for static proneness 3−2787
  cosmic ray muons, latitude dependence at sea level 3−16088
  on cotton fibres, apparatus 3−6012
  dynamic systems, a.c. method 3−665
  electret, vacuum apparatus for meas. and sample fabrication 3−39082
  nuclei, (Z>26) in emulsions, photometric method *(Russian)* 3−10044

charge storage diodes
  optical modulation in step recovery diode *(Germany)* 3−37647

charge transfer *see charge exchange*

charring *see combustion*

Chebyshev approximation
  plasma physics integrals involving Chebyshev polynomials, soln. by Olver's algorithm 3−19396

checkout *see testing*

checkout, automatic *see automatic testing*

chelates *see coordination complexes*

chemical adsorption analysis
  see also chromatography
  precious metal films, gas content by neutron activation anal. *(German, English)* 3−10202

chemical analysis
  see also chemical adsorption analysis; chemical analysis by nuclear reactions and scattering; electrochemical analysis; electron probe analysis; mass spectroscopic chemical analysis; microanalysis; polarimetry; polarography; radioactive chemical analysis; spectrochemical analysis; X-ray chemical analysis
  alkali metals, methods for hydrogen conc. determ. 3−445
  Apollo 15 mare basalts, petrogenetic relationships 3−35081
  atmospheric pollutant at Harwell, correlation of hourly sampling results 3−34904
  atmospheric precip., pH rel. to chemical comp. 3−37226
  atmospheric sampling, use of differential flow controllers 3−37746
  Auger electron analysis of thin films 3−10207
  automated Kjeldahl nitrogen determination, for aqueous dispersible samples 3−37745
  automatic methods and measuring equipment *(Hungarian)* 3−19368
  basaltic komatiite and ocean-floor type basalts from N.E. Newfoundland, a comparison 3−25110
  brine hole in Red Sea, comparison with anoxic fjord sample 3−27992
  carbonyl Ni, included gas analysis *(Russian)* 3−10197
  centrifuges, peeling type, approx. empirical eqn. and design *(German)* 3−6150
  clay mineral composition of Melbourne brickmaking clays 3−15762
  clinical-chemical, automation *(German)* 3−10204
  coal slurries and polymetallic ores, spectrophotometric technique *(Russian)* 3−28771
  composition, ocean sediments, sea floor prospecting, γ ray backscattering 3−3170
  computer control of potentiometric titration 3−22524
  DIMA, discrete multiple analysers 3−19367
  p-dimethylamino-p'-nitrostilbene, surface fluorescence *(German)* 3−36938
  ESCA studies of dielectric films 3−39245
  extraterrestrial organic compounds, review 3−35016
  field-ion atom probe analysis 3−28778
  filter fluorimeter, meas. of weak luminescent signals 3−3921
  flame photometer for analysis in picogram range, using lock-in multiplier *(German)* 3−177
  fluorides in stack gases, continuous on-site measurement method 3−37250
  gas analyser, calibration gas mixture, prep. and certifying 3−19371
  gas analysis, by paramagnetic resonance 3−35537
  gas composition, alpha particle gauging, mathematical model 3−335
  gas composition meas., standard 3−22243
  gas mixture concentrations in supersonic flow, hot-wire technique 3−28795
  gas mixtures, binary, fluidic-electronic composition analyser 3−6153
  glass, soda borosilicate composition determ. by tie-line plotting 3−10203
  granites and biotites, flamephotometric analysis of Rb traces *(German)* 3−6157
  high melting metals, determ. of gas inclusion by electron microprobe *(Russian)* 3−6106
  lunar fines, pyrolysis of Apollo 11, 12 and 14 samples 3−32264
  lunar orange soil, chemical comp. and origin 3−37335
  lunar organic anal., extraction and hydrolysis techniques, review 3−32265
  lunar organic anal., ion-exchange chromatography 3−32267

chemical analysis continued
  many-component substances, automatic analyser *(Russian)* 3−13509
  Moon, chemistry, review 3−35097
  nuclear reactor fuel, irradiated, adjustment of burn-up code for chemical and isotopic analysis 3−19936
  oceanic aerosols, wind transport to ocean 3−12753
  Pacific Ocean deep water at 43 and 28°S, SCORPIO Expedition 3−37185
  particle-sulphate in background air, amplification method of determination 3−37249
  pharmaceutical tablet off-line computer analysis program, in FOCAL-12 3−394
  phosphosilicate glass layers, analysis by Rutherford backscatt. and channelling meas. 3−38539
  plastic, book contrib. 3−12457
  polarographic analytical instrument, with diffusion layer membranes electrodes *(German)* 3−16563
  rain in Delhi, 1964-67 period, anal. for NO_3^-, NH_4^+ and SO_4^{2-} ions 3−37228
  reaction probing using chem. lasers 3−10196
  real-time data processing, minicomputer applications *(French)* 3−19363
  residual gas analyzer, application to atomic beam detection 3−28711
  structural determ. for characterizing matter by combining spectral techniques 3−37760
  surface, by ion scattering and electron spectrometry 3−32259
  thermogravimetric, 3 instruments incorporating electronic microbalances 3−37756
  thermogravimetric balance using Hall effect 3−3915
  thin uniform target prep. for trace elemental analysis by laser evaporation 3−16916
  tie-line plotting determ. of phase compositions in glass 3−10203
  BeO in water vapour, transpiration determ., postulated results using Au vaporisation as reference substance 3−26019
  Mg, H_2 content by vacuum heating method 3−26017
  $Mo_{1-x}B_3$, anal. of structure rel. to comp. 3−33498
  NH_3 and related atmospheric pollutants at Harwell, technique for hourly sampling and analysis 3−37234
  Na contamination by H_2, determ. of content to 0.1 ppm amalgamation method 3−32942
  O_2 chemical detectors *(Russian)* 3−32248
  O_3 calibration source for analysers and inlet-sample air systems 3−32252
  Pb phosphates, i.r., X-ray and chem. anal. of apatite structure and comp. *(German)* 3−33497
  Pu, hydrogen impurity conc. determ. by hot vacuum extraction *(French)* 3−2746
  Pu reprocessing using tertiary amine extractants, analysis of process solvent 3−32950
  SO_2 determination, modified Monier-Williams apparatus 3−19366
  $TiCl_4$, continuous determination of impurities by optical method during purification *(Russian)* 3−26031
  UN, sintered, unsintered powder, 1.572 powder, gravimetric, inert gas fusion and combustion methods 3−6978
  UrF_6, purification *(Spanish)* 3−18781

chemical analysis by mass spectrometry *see mass spectroscopic chemical analysis*

chemical analysis by nuclear reactions and scattering
  see also chemical effects of nuclear reactions and scattering
  activation analysis, bibliography through 1971 3−16572
  activation analysis, by bremsstrahlung, use of electron accelerator 3−19372
  activation analysis, computer controlled study *(German)* 3−13508
  activation analysis, transfer system adaptable to neutron generator *(French)* 3−26025
  activation analysis by betatron *(Russian)* 3−19374
  activation analysis by photoneutron counting 3−10195
  airborne particulate material, neutron activation analysis with computer resolution of gamma ray spectra 3−18871
  chondrites, cosmogenic nuclides, instrumental activation analysis of principal progenitors 3−16200
  continuous activation logging, optimal velocities 3−25325
  cyclical activation analysis with neutron generator *(Russian)* 3−35879
  gamma-ray spectra, computer assisted analysis 3−431
  geological samples, instrumental activation analysis 3−22538
  impurity depth profiles determ. by reson. reactions 3−17859
  instrumental activation analysis using high-resolution γ-spectrometer and automated data analysis 3−37743
  minerals, comparison of radiative capture and decay γ-ray methods in borehole logging 3−439
  14 MeV neutron activation, determ. of short-lived isotopes, improved pneumatic tube system 3−26029
  neutron activation anal., ^{131}I tracer, I enrichment of atm. sea salt particles 3−12693
  neutron activation anal., Br in marine atm. 3−12755
  neutron activation analysis, ^{252}Cf, oceanographic techniques, simulated ore samples, sea floor 3−3212
  neutron activation analysis, computer oriented system 3−22536
  neutron activation analysis using isotopic neutron sources 3−22537
  neutron nondestructive active assay techniques for nuclear reactor fuel 3−23427
  non destructive activation analysis of W in steel and low grade wolframites by neutron activation analysis and γ-ray spectrometry 3−13512
  photoactivation analysis, geological samples, 25 MeV betatron 3−18896
  photoactivation analysis, using 25 MeV betatron 3−19373
  photopeak integration, peak boundary selection 3−22535
  precious metal films, gas content by neutron activation anal. *(German, English)* 3−10202
  solutions, activation analysis using Cherenkov counter 3−22551
  solutions, aqueous, concentration of main component using neutron source 3−37749
  solutions, fast neutron activation analysis 3−22552
  sum peak coincidence method for activation analysis 3−10193
  superficial carbon determ. from $^{12}C(d,p_0)^{13}C$ excitation function meas. *(French)* 3−11000

chemical analysis by nuclear reactions and scattering continued
- surface regions of solids, microanalysis by direct obs. of nuclear interactions at low energies 3-447
- trace element analysis, by particle and photon excited X-ray fluorescence in environmental samples 3-26024
- X-ray fluorescence, proton induced, trace element analysis 3-37750
- α and X-ray induced X-ray emissions, comparative study of techniques 3-37759
- Au alloys, neutron activation analysis, matrix components, rapid determ. 3-28769
- Ca mass determination in body by neutron activation analysis using cyclotrons 3-22163
- ^{252}Cf n.source for activation analysis of short half-life isotopes by cyclic-counting scheme 3-26026
- Co, neutron capture γ-rays, spectral enhancement 3-5455
- ^{1}H(^{19}F,$\alpha\gamma$)^{16}O, resonance, H_2 conc. versus depth in solid samples meas. 3-35539
- N in wheat grain, photonuclear activation analysis 3-32251
- Nb, impurities, neutron activation analysis, using semiconductor γ detectors *(Russian)* 3-10198
- NbO_5, impurities, neutron activation analysis, using semiconductor γ detectors *(Russian)* 3-10198
- P in human bone, neutron activation analysis 3-37730
- Se in organic and inorganic cpds., quantative analysis by proton bombardment 3-3914
- ^{77m}Se determ. in biological specimens, optimum procedure using neutron activation analysis 3-22533
- SiO_2 surface layer, anal. of oxygen atom amounts by nuclear reactions ^{16}O(d,p_1)^{17}O* and ^{16}O(d,α)^{14}N 3-30315
- Ta, F contamination by chem. polishing, nuclear reactions study 3-11812
- Ta, penetration profiles of Ar ions determ. by (p, γ) reaction 3-26010
- ^{235}U content in natural U determ. with solid state track detector, undergraduate expt. 3-9814
- Zn, natural, excitation functions for deuteron induced reactions 3-27917

chemical association *see association*

chemical batteries *see cells (electric)*

chemical bonding *see bonds (chemical)*

chemical bonds *see bonds (chemical)*

chemical composition *see chemical analysis*

chemical effects of nuclear reactions and scattering
- *see also chemical analysis by nuclear reactions and scattering; radiation chemistry*
- Br_2 in hydrocarbons, chem. effects of ^{80m}(I.T.)^{80}Br reaction 3-12541
- I_2 in hydrocarbons, chem. effects of (n,γ) reactions 3-12540
- I_2 in hydrocarbons, chem. effects of ^{127}I(n,2n)^{126}I and ^{130m}I(I.T.)^{130}I reactions 3-12541

chemical effects of radiation *see radiation chemistry*

chemical elements *see elements (chemical)*

chemical engineering *see chemical technology*

chemical equilibrium
- *see also chemical reactions; reaction kinetics*
- di-T-butyl carbinol, near i.r. heteroassociation study and choice of mol. complex equilib. conc. scale 3-23575
- cementite, influence of matrix on Cr contents 3-8790
- computational method, EQUIL, appl. to mixed metal complex form. system 3-2791
- constant estimation and model distinguishability 3-9049
- isopolyassociation and dissociation, acido-basic equilibriums, non linear regression of constants determ. *(French)* 3-9044
- kinetics with regard to the equilibrium of processes studied by non-isothermal techniques 3-12519
- organic dye molecules in aqueous soln. intermolecular reactions study by fluorescence quenching and difference absorption spectrophotometry 3-2806
- plasma chemical reactions, thermodynamic calc. *(German)* 3-15817
- Cu-diethydithiocarbamate and Cu-diethyldithiophosphate complexes, e.s.r. studies, kinetics of ligand substitutions 3-39441
- 5-oxybenzodioxane-1,4 solution in CCl_4, intermolecular action *(Russian)* 3-37116
- W solid with H and halogen gases 10^{-1} to 10^{-6} atm, 500 to 3600 K *(German)* 3-25101
- Zr-O-C system, thermodynamical study at high temp. *(French)* 3-9043

chemical exchanges
- *see also ion exchange; isotope exchanges*
- carboxylic acids and hydrogen, deuterium isotope exchange 3-27861
- collinear three-body exchange scatt., reaction rate consts. 3-12506
- ethanol, ^{17}O n.m.r. studies for slow and fast exchanges of hydroxyl proton 3-11285
- methanol, ^{17}O n.m.r. studies for slow and fast exchanges of hydroxyl proton 3-11285
- nuclei spin 3/2, effect on nucl. mag. relax., eqns. including nonexponential relax. 3-7232
- paramagnetic solns., deuteron relax. study, chem. exchange effect 3-21336
- scattering, reactive, direct interaction with product repulsion model derivation 3-21801
- spin relax. times, nondilute case, approx. solns. 3-30719
- thioamino acids, intramolecular proton transfer reactions by double-beam pulse method *(German)* 3-28478
- Ba(g) + N_2O or NO_2, reaction products electronic states distrib. 3-9062
- $Cl + HCl(v=1,2) = ClH + Cl$, vibr. relax., classical Monte Carlo trajectory study 3-23619
- $ClH(v=1,2) + H = HCl + H$, vibr. relax., classical Monte Carlo trajectory study 3-23619
- (H_2, D_2) exchange reaction mechanism potential barrier 3-25054
- $H + H_2$ collinear isotopic systems, quantum mech. computational studies 3-31262
- $H + H_2$ collinear reaction, semi-classical, exact quantum and quasi-classical transition probabilities 3-31248

chemical exchanges continued
- $H + H_2(v=1,2) = H_2 + H$, vibr. relax., classical Monte Carlo trajectory study 3-23619
- $H + I_2 \rightarrow HI + I$, classical trajectory anal. 3-29074
- $HBr + O \rightarrow Br + OH$, collinear H transfer probability calcs. 3-21802
- $H_2(D_2)$-Br(I), reaction mechanism, classical dynamical study 3-37119
- I^- reson. in I_3^- aq. solns., exchange study from n.m.r. line broadening obs. 3-25050
- $Li + F_2 \rightarrow LiF + F$, pot. energy surfaces calc. 3-23637
- $Li_2O.Al_2O_3.2SiO_2$, internal friction 3-1693
- $N_2^+ + N_2 \rightarrow N_3^+ + N$, ion cyclotron mass spectrometric study 3-26724
- $O + BHr \rightarrow OH + Br$, collinear H transfer probability calcs. 3-21802
- $O + HBr \rightarrow OH + Br$, collinear H transfer probability calcs. 3-21802

chemical industry
- chlor-alkali plants in Sweden, airborne Hg fall-out on surrounding snow 3-37200
- continuous leacher for dissolution of spent nuclear fuels 3-17304
- high temperature materials characteriz. 3-8919
- mass spectrometers, on-line monitoring, simultaneous multiple component 3-10192

chemical kinetics *see reaction kinetics*

chemical reactions
- *see also catalysis; chemical exchanges; chemiluminescence; chemisorption; corrosion; heat of reaction; oxidation; photochemistry; radiolysis; reaction kinetics*
- 2-naphthylamine, deactivation by proton transfer in the excited state 3-12543
- air glow and N and O atom and ion reactions in an ultra high vacuum plant *(German)* 3-9306
- alkali earth metals reactive collisions with ICl and BrCN, crossed beams product angular distributions 3-27864
- alkali halide mol. beams collision reactions with Li atoms, beam kinetics 3-25058
- alkaline earth metal beams collision with Cl_2 and Br_2 beams, chemical reactions 3-21803
- atmospheric pollutants, effect of first order chemical reaction on turbulent diffusion 3-37199
- atmospheric pollution, K-theory appl. to diffusion problems in non-linear chemical reactions 3-39817
- atom-diatom collinear reactions, classical mechanics and transition state theory 3-25057
- automotive emissions, ultraviolet irradiation analysis *(Japanese)* 3-27895
- benzophenone-d, in paraffin solvents, ketyl radical e.p.r. emission spectra decay for electron spin-lattice relax. times 3-25063
- benzylchlorides, substituted, with n-BuLi, chem. induced dynamic nucl. polarization effects 3-2813
- bimolecular, reactant vibr. energy effect on spectator stripping product distribs. 3-37117
- binary mixture, T-X diagram calculation, computer solution *(Spanish)* 3-35531
- binary mixture with chemical reaction, freezing curve 3-34710
- Boltzmann eqn. collisions involving chemical reactions, application of Bhatnagar-Gross-Krook approximation 3-27866
- bromination of pyrocarbon, temp. dependence on resistivity between 90-298 K and thermoelectric power *(French)* 3-8214
- carbene, MINDO/2 calc. of ground state and for reactions with methane and ethylene 3-29571
- carbonyl compounds, excited triplet, photochemically produced radicals, general theory 3-25083
- cellulose reaction with aromatic epoxypropylamine, i.r. spectra of reaction products *(Russian)* 3-31265
- chemically induced dynamic nuclear polarisation 3-2805
- combustible jets, turbulent diffusion flame, aerodynamic and thermodynamic analysis 3-23799
- complexing powers of phenylhydrazine derivatives, spectroscopic study *(Russian)* 3-27874
- consecutive metastable decay reaction, explanation of fine structure in metastable peaks 3-435
- convective diffusion with chem. reaction, effect of multicomponent bubble collapse 3-7954
- D- and E-region ion-neutral reactions 3-3104
- D-region, gas clustering to alkali metal ions, rate constants 3-3105
- diacyl peroxide decomposition reactions, chem. nucl. polarisation study 3-31258
- diatomic mol. form. in interstellar clouds 3-19069
- dissociation of asymmetric two-centre two-electron system, unrestricted Hartree-Fock theory 3-27870
- electron polarisation, chemically induced, theory 3-34723
- equations of state, mixture of nonideal, chemically reacting gases 3-34722
- ethyl radicals, chem. and thermal activation, unimol. reactions theory appl. 3-34724
- ethylene, during CO_2 laser irrad. 3-39430
- ethylene and O_2, i.r. laser induced reactions 3-2831
- explosion waves in biphase medium, amplification due to secondary reactions *(Russian)* 3-14468
- fluidised bed reactor, design based on mass transfer coeff. and mixing coeffs. 3-459
- fluidised bed reactor simulation and identification, frequency domain approach 3-1466
- fluids, confined exothermically reacting, dynamic stability 3-15823
- fluorination of MCl-CeO_2 mixtures, M = alkali metal, structures of compounds of MF-CeF_4 system *(French)* 3-14819
- free radical, magnetic field effects 3-25062
- free radicals, chemically induced dynamic nucl. and electron polarization, hydrodynamic theory 3-27865
- gas, chemically reacting, turbulent isobaric flow in a heated tube 3-33321
- gas kinetics, unimolecular reactions, neutral and ion-molecule reactions in mol. beams, review 3-34728
- gas-solid, investig. by modulated molecular beam mass spectrometry 3-26020
- glass-ceramics, solid state reactions 3-15786
- growth of pyrocarbon whiskers during pyrolysis of methane *(German)* 3-15111
- hard sphere reactions, chattering 3-38321

chemical reactions continued
heterogeneous reactions, method for determ. of effective thermokinetic constants 3 − 18789
high-temperature gas-solid reactions, review 3 − 25068
hydrodynamic mode damping and scattered light spectrum effects 3 − 11358
hydrolysis of bonds, silicate glass surface, influence of mechanical stress 3 − 39469
hydrolysis of high molec. wt. alkenyl succinic anhydrides, studied by i.r. spectra *(Russian)* 3 − 25067
III-V semiconductor, chemical vapour deposition, mass spectrometric and thermodynamic studies 3 − 2639
impulse model for atom-diatom reactive scattering 3 − 12521
interstellar molecule formation by chemical reactions involving negative ions 3 − 39738
ion-hydrates in ionosphere, reaction mechanisms and bonding energies 3 − 3066
ionic, in sporadic E-layer associated with formation and removal of M[illegible] 3 − 34943
iron phosphate glass formation 3 − 20697
isopolyassociation and dissociation, acido-basic equilibriums, non linear regression of constants determ. *(French)* 3 − 9044
isothermal, on catalytic surface in boundary layer flow 3 − 17498
kaolinite-Cd(Sr)CO_3, reactions up to 1000°C 3 − 15754
light scattering from coupled nonlinear reactions for steady states far from equilibrium 3 − 2803
liquid residence time and flow cycles, distrib. func. 3 − 6168
master eqn. soln. formulation 3 − 2796
MBBA, isotropic phase, chem. and electrochem. activity rel. to d.c. conduction 3 − 15203
mesic atom, mechanism of μ depolarisation in molecular condensed matter 3 − 17388
metal atom + O_2 crossed beams, assoc., reactive and electron transfer ioniz. 3 − 29746
methane pyrolysis in low current d.c. discharge 3 − 1528
p-methoxybenzilidene p-butylaniline, liquid crystal, hydrolysis *(French)* 3 − 36260
p-methoxybenzilidene p-butylaniline, liquid crystal hydrolysis, electrochem. props. of products *(French)* 3 − 36261
methyl iodide mol. beam interaction with K, energy depend. of reactive cross section 3 − 9060
methyl radical interaction with methane and ethylene, molecular orbital calc. 3 − 29574
methyl radical reactive scatt. ang. distrib. meas. 3 − 12502
mixed sulphides, synthesis by H_2S sulphuration of IB and IIB metals *(French)* 3 − 18539
nitriding, relationships in initial stages *(Russian)* 3 − 24907
organic dye molecules in aqueous solution, intramolecular reactions study by fluorescence quenching and difference absorption spectrophotometry 3 − 2806
organic solids, self diffusion, kinetics of solid state reactions 3 − 4885
periodic heat evolution during temporal chemical oscillations 3 − 27869
permalloy, ferromag. film, grain size rel. to chem. deposition conditions 3 − 8402
phenylhydrazine derivatives, complexing powers, spectroscopic study *(Russian)* 3 − 27874
plane moving boundary problems, freezing and melting, integral transforms 3 − 34702
plasma chemical reactions, thermodynamic calc. *(German)* 3 − 15817
poly(ethylene terephthalate), cryst., etching by hydrolysis 3 − 31168
polymer thermal degradation 3 − 11348
polystyrene sulphonate, ion-exchanged, para-hydrogen conversion 3 − 9066
premixed burning, large activation energy, asymptotic analysis 3 − 4526
propane unimol. decay into $C_3H_7^+ + H$, electron-impact-induced, time depend. 3 − 21797
pyrolysis of Apollo 11, 12 and 14 lunar samples 3 − 32264
reactive mol. collisions product energy distrib. determ. of temp. and entropy deficiency 3 − 9059
reactive scattering, simple model for endoergic and exoergic collisions 3 − 27863
reactive scattering, uncoupled channel operator eqns. for rearrangement 3 − 27862
recoil hot atom systems, collision density, effect of reactive events 3 − 21837
semiconductor compounds, $A^VB^{VI}C^{VII}$ where $A^V = Sb$, Bi, $B^{VI} = S$, Se, Te, $C^{VII} = T$, Br, crystallisation under hydrothermal conditions, preparative methods *(Russian)* 3 − 8750
short-lived reaction intermediates, gas phase molecular electron diffraction obs. 3 − 25046
simple substitution reactions theory 3 − 39434
sintering, chemical aspects, general considerations *(French)* 3 − 34621
solid reactivity, (conference, Bristol, England, July 1972) 3 − 5379
solid reactivity, (conference Bristol, England, July, 1972) 3 − 5386
solid reactivity (conference, Bristol, England, July 1972) 3 − 2810
solid state reaction paths and microstructure in crystals 3 − 5387
solid state reactions, role of dislocations 3 − 5390
solid-gas, effect of solid shape on diffusion model 3 − 34716
steel, nitriding by ion bombardment of 18-10 stainless steel *(French)* 3 − 24908
steel, stainless, type 304 and Nitralloy 135M, glow-discharge nitriding 3 − 8851
sulphuration of thin metal wires, cavity formation at metal-S interface during growth of thick layers of S 3 − 4753
synthetic resin cross-linked in strong elec. field, thermal decomposition obs. 3 − 2097
ternary mixture, total conc. fluctuations, microscopic study 3 − 39435
thermodynamic compensation law and thermal death 3 − 2795
transport of Ta by I, chemical transport reaction thermodynamics 3 − 2641
turbulent second order reaction, reactant and product structure at large wave nos. 3 − 21800
turbulent tubular flow involving endothermic chemical reaction, calc. of heat transfer coeffs. *(Dutch)* 3 − 29926

chemical reactions continued
two-stage thermal decomposition of solids in convention-type packed beds 3 − 2800
unimolecular, non-equil. effects rel. to activation energy 3 − 12503
uranyl acetate, thermal decomp., final product identification 3 − 37122
in u.s. field, effect of temp. and pressure on kinetics 3 − 27871
vitreous and amorphous solids, reactions 3 − 5389
zeolites, deammination at high temperatures, i.r. spectra study *(German)* 3 − 39152
Ag_2Se, reaction controlled growth of single crystal in solid/gas system 3 − 15605
$AsCl_3$, hydrogen reduction and deposition rate of As 3 − 8723
$Ba + Cl_2 \rightarrow BaCl + Cl$, collision dynamics, hermaphroditism 3 − 25047
$Ba + O_2$, prod. of electronically excited BaO 3 − 12504
δ-$BaCO_3$, props. study of metastable phase, substitutional reaction between $BaCO_3$ and additives 3 − 4855
BaO.6 Fe_2O_3, texture and reaction mechanism in the formation 3 − 5413
$BaWO_4$, growth by double decomposition in melt 3 − 21540
$BeSO_4$, thermal decomposition kinetics 3 − 2804
Bi_2S_3, complex form. in crystallisation and chain structure *(Russian)* 3 − 15633
Bi_2S_3, dissociation pressure meas. in 806-904K range, determ. of heat of formation from thermodynamic laws *(Russian)* 3 − 12511
C, pyrolytic rods, formation in hydrocarbon atmos. heated by focused laser beam 3 − 2807
CH + O chemi-ionisation, cross section and rate const. calc. 3 − 14397
$CH_3I + N_2F_4$ chemical laser, HF laser transitions 3 − 22871
$CO^+ + 2CO \rightarrow CO^+,CO + CO$, rate-coefficient meas. in a drift-tube mass spectrometer 3 − 20202
CO_2, l.p. decomp., non-equil. effects rel. to activation energy 3 − 12503
$CS_2 + O_2$ chemical laser, reaction mechanisms 3 − 16836
Ca sulphoaluminate and sulphosilicate, hydraulic hardening process *(Russian)* 3 − 15742
CaO-Cr_2O_3-Al_2O_3, phase relatins and optical studies 3 − 5385
$CaSO_4$, initial thermal decomposition temp. meas. 3 − 14809
CdO-Cr_2O_3-Al_2O_3 phase relations and optical studies 3 − 5385
$Cl + DI \rightarrow ClD + I$, distribution of reaction products 3 − 18786
$Cl + HI(DI) \rightarrow I + HCl(DCl)$ temperature parameter for rotational state of product 3 − 31245
$Cl + HI \rightarrow ClH + I$, distribution of reaction products 3 − 18786
Co-Si system, rate of reactive diffusion, high press. eff. *(Russian)* 3 − 7962
$Co_xFe_{3-x}O_4$, preparation and characterization 3 − 18741
Cr oxide gel systems, formation and interconversion of CrOOH and Cr_2O_3 3 − 5382
Cs^+ clustering with atmospheric gases, drift velocities 3 − 9053
Cu-Ti alloy, boriding, Ti content effects *(German)* 3 − 8902
$E + D_2$ reaction, dynamics, on a semiempirical valence-band potential energy surface, Monte Carlo trajectories 3 − 25052
$F + H_2(D_2) \rightarrow H(D) + HF(DF)$, temperature parameter for rotational state of product 3 − 31245
$FE(CN)^{3-}$ reduction to $Fe(CN)_6{}^{4-}$ by electron irradiation, Mossbauer study 3 − 2822
F_2O thermal decomposition kinetics 3 − 9048
Fe dispersion of carbides and nitrides, gas-solid reaction, thermal stability, homogeneous distributions *(French)* 3 − 34526
Fe-Ni-O, system, activities, thermodynamics, equilib. O_2 press., comp., at 1000°C 3 − 2793
$FeCO_3$, siderite, decomp. rel. to Mossbauer linewidth anomalous temp. depend. 3 − 34277
$Fe_2(OH)_3$ amorphous gel, characterisation and transformation to α-FeOOH 3 − 5383
GeH_4 thermal decomposition, Ge film growth 3 − 8719
GeO, thermogram at high temps. obs. of endo and exo-effects *(Russian)* 3 − 12512
H, hard sphere model of hot atom reactions, computer simulation 3 − 9061
H atom sources for H halide pulsed lasers 3 − 10501
$H + F_2 \rightarrow HF + F$, potential energy surface calc. 3 − 25053
$H + F_2 \rightarrow HF + H$, vibrational energy distribution determ. 3 − 1280
$H + H_2$ three dimensional collisions, complex-valued classical trajectories for reactive tunneling 3 − 25056
H_2-F_2, reaction behind shocks 3 − 11317
$H_2^+ + He \rightarrow HeH^+ + H$, 1-25 eV, cross beam studies 3 − 39439
$H(D) + Cl_2 \rightarrow Cl + HCl(DCl)$ temperature parameter for rotational state of product 3 − 31245
HF diffusion type chemical laser, numerical study 3 − 37955
$H_2O^+ + H_2 \rightarrow H_3^+ + OH$, and deuterium counterpart, cross section, H_2 proton affinity determ. 3 − 2802
^3H and alkanes or halocarbons, molecular beam studies 1-200 eV 3 − 25060
$HeH^+ + H \rightarrow H_2^+ + He$, 1-25 eV, cross beam studies 3 − 39439
$He^* + H_2 \rightarrow HeH^+ + H + e$, 0.05 to 10 eV, cross-sections 3 − 9052
2-In(e) + 3NiO(s) = In_2O_3(s) + 3Ni(s) thermodynamic properties 3 − 27856
$K + CH_3I \rightarrow KI + CH_3$, classical trajectory calc. of energy dependence of total reaction cross-section 3 − 31246
$K + NaCl \rightarrow KCl + Na$, classical trajectory studies of long-lived collision complexes 3 − 25059
$K_2 + Br_2(IBr)(BrCN)(SnCl_4)$, reactively scattered, ang. distrib. meas., product K atoms 3 − 29750
K_2 + cyclohexane(allyl halides)(alkyl halides), KX reactive scatt., ang. distrib. meas. 3 − 29752
$K_2 + SnCl_4(CCl_4)(SiCl_4)(PBr_3)(PCl_3)(BBr_3)(CH_2Br_2)$, KX reactive scatt., ang. distrib. meas. 3 − 29751
$KY(MoO_4)_2$, thermal decomposition of the melt *(Russian)* 3 − 2809
$Ln_2(WO_4)_3$-M_2WO_4 reactions in the melt, where Ln = Nd, Er and M = Rb, Cs *(Russian)* 3 − 15825
Mo, chemical vapour deposition by reduction of hexafluorides 3 − 8718
$MoO_3.2H_2O$, topotactic dehydration 3 − 9063
$N + NO \rightarrow N_2 + O$, i.r. chemiluminescence 3 − 25061
NH_3, pyrolysis by CO_2 laser radiation 3 − 12509
NH_4ClO_3, radiation induced dislocations and thermal decomposition kinetics 3 − 4771

chemical reactions continued

- $NO_2+O(^3P)\rightarrow NO+O_2$, absolute rate consts. meas. from 230 to 339K 3—18796
- N_2O+O^-, low energy, rate const., temp. depend. 3—39436
- $N_2O_4\rightarrow NO_2$, heat transfer *(Russian)* 3—12507
- $NaIn(MoO_4)_2$, melt growth, cryst. struct. and thermal stability 3—33507
- Ni, hexagonal, formed by Ni_3C decomposition 3—5384
- Ni-Sb system, rate of reactive diffusion, high press. eff. *(Russian)* 3—7962
- NiO-Cr_2O_3 solid soln. prep. 3—18787
- $O^-+D_2\rightarrow OD^-+D$, prohibited autodetachment 3—23616
- $O^++D_2\rightarrow OD^++D$, collisions below 4 eV, production of excited OD^+ 3—29747
- O_2 and ethylene, i.r. laser induced reactions 3—2831
- O_3 photochemical neutral reactions in atm. below 100 km 3—3033
- $O(^3P)+NO_2\rightarrow NO+O_2$, absolute rate consts. meas. from 230 to 339K 3—18796
- $PbTiO_3$:Nb_2O_5 solid solution, incorporation of Nb_2O_5 into the perovskite lattice 3—5381
- Pd atoms with CO, co-condensation, matrix isolated spectra 3—7192
- Pt atoms with CO, co-condensation, matrix isolated spectra 3—7192
- PuF_6, thermal decomposition 3—9050
- S_3^- formed on MgO surface, e.p.r. characteriz. 3—27919
- SO_2 with $CaCO_3$, rate of diffusion 3—21799
- $Sb_2S(Se)_3$, complex form. in crystallisation and chain structure *(Russian)* 3—15633
- Si plates masked with amorphous SiO_2, in H_2, Si and SiO_2 interaction during heat tretment *(Russian)* 3—11815
- SiC high temp. reactions with UO_2 3—2811
- SiH_4 bimol. reactions with NH_2^+, $C_2H_3^+$, $C_2H_6^+$ and $C_3H_8^+$, form. of SiH_5^+, proton affinity 3—39433
- Sr_3N_2, existence, possible mechanism for nitriding Sr *(French)* 3—15830
- SrO-CdO-V_2O_5, phase equilibria detn. from DTA data, quenching and solid-state react. expts. 3—18690
- Ta compatibility with graphite, UO_2 and UC at high temperature 3—35932
- Ti and alloys, nitriding by ion bombardment *(French)* 3—24909
- Ti oxides, solid state reactions, departures from stoichiometry and order 3—5388
- $TiCl_4$ reacting with methane to produce TiC refractory powder 3—18685
- TiO_2 anatase surfaces, model, interpretation of some interface processes 3—5414
- UO_2, high temp. reactions with SiC 3—2811
- VN on V_2N, growth rate at 1500°C 3—5415
- W, chemical vapour deposition by reduction of hexafluorides 3—8718
- W solid with H and halogen gases, 10^{-1} to 10^{-6} atm. and 500 to 3600 K *(German)* 3—25101
- W-halogen-O systems, gas phase composition and chem. transport reactions *(German)* 3—21792
- W-O_2-H_2 system, thermodynamics, gas phase composition, chemical transport reactions *(German)* 3—34712
- Y_2O_3, chlorination in presence of C, chemical vapour deposition of garnets 3—8717
- ZnO-NiO solid solution, Ni-Zn ferrite formation 3—2812
- Zn_3Sb_2, decomposition reactions rel. to phase comp. *(Russian)* 3—15671

chemical reactivity *see chemical reactions*

chemical shift

- acetonitrile in non-polar solvents, reaction field contribution to proton magnetic shielding 3—8467
- acetylene, ^{13}C-enriched, n.m.r., isotopic substitution 3—26692
- acetylene in nematic phase of liquid crystal, ^{13}C chemical shift anisotropy 3—8469
- acetylene in nematic phase of liquid crystal, ^{13}C-n.m.r. spectrum 3—8469
- aliphatic alcohols, n.m.r. of association processes, H-bond enthalpy 3—27433
- alkal metal complex polymetaphosphates, i.r., n.m.r. and magnetochemical studies 3—17454
- aqueous solns. of Cu^{2+} ions, relative demagnetizing and chem. n.m.r. field shift, conc. depend. 3—39043
- benzodioxane-1,4 soln. in n-octane, self-association, proton magnetic resonance spectra *(Russian)* 3—34709
- benzonitrile-nitromethane, ^{23}Na n.m.r. meas. for ionic solvation study 3—26703
- benzophenone single cryst., ^{13}C anisotropic chem. shift, axis orientations determ. 3—2429
- 2,4-dicarbaheptaborane(7), rel. to ground-state charge distrib. 3—26616
- 4,5-dicarbahexaborane(8), rel. to ground-state charge distrib. 3—26632
- meso and dl 2,5-dichlorohexanes, coupling constants and chemical shifts rotational isomerism 3—26697
- dimethylcycloheptanes, molecular geometry, conformations, p.m.r. obs. 3—35988
- dimethylsulphoxide-(acetonitrile),(nitromethane), ^{23}Na n.m.r. meas. for ionic solvation study 3—26703
- ESCA, molecular core binding energies, minimal Slater basis set calculations 3—23550
- ethylene carbonate oriented in the lyotropic nematic phase, proton magnetic resonance, chemical shifts 3—26698
- ethylene monothiocarbonate, oriented in the lyotropic nematic phase, proton magnetic resonance, chemical shifts 3—26698
- fluoroethylenes and fluoroacetylene, ^{13}C n.m.r. shifts 3—11287
- group II difluorides, ^{19}F chem. shift tensor and nonionic bonding 3—12070
- group IV cpds., MX_4 type, core binding energies for analogous gaseous cpds. of C, Ge and Si 3—14340
- heavy atom, absolute basis for paramagnetic contribution 3—20182
- N—heterocycles, H-bonding, ^{14}N chemical shift, H-^{14}N mag. double resonance 3—33146
- hydrocarbons, ^{13}C chemical shifts calc. 3—23598
- imidazobenzimidazoles, p.m.r. data 3—20098
- isotropic and anisotropic shifts in solids, resolution, applic. of multiple-pulse techniques 3—8466

chemical shift continued

- lanthanide-induced shifts in p.m.r. spectra, scavenging effects, problem and soln. 3—7235
- macromolecular structure, high-resolution n.m.r. 3—38328
- methylmercuric halides in isotropic and nematic liquid solutions, proton magnetic resonance 3—24622
- molecular struct. determ. using ^{13}C studies by Fourier transform. n.m.r. spectroscopy 3—1262
- molecule, small, temp. and freq. depend. ^{13}C relax. mechanisms 3—2446
- n.m.r., sweeped multiple pulse sequence technique for shift meas. in solids 3—2332
- n.m.r. and ESCA, relationship, electron binding energies, spin-rotation constants 3—23599
- n.m.r. spectral narrowing in solids by high-speed specimen rotation and resolution of chem. shift and spin multiplet structures 3—8465
- non-metallic compounds, X-ray induced photo-electron spectra, chemical shift of ionisation energy 3—39215
- nuclear mag. relaxation times, calc. under anisotropy of chem. shift 3—4469
- organosilicon compounds, ^{29}Si chemical shielding anisotropy 3—2430
- phenylacetylenes, CNDO/2 electron charge densities and ^{13}C chemical shifts *(German)* 3—14393
- polyfluoroethylenes, CNDO/2 and extended Huckel charge distribs., rel. to ESCA chem. shifts 3—1300
- polytetrafluoroethylene:^{19}F, symmetrized multipulse n.m.r. obs. of chem. shift shielding tensor 3—15433
- porphyrins, ring currents and n.m.r. chemical shifts 3—20099
- pyridine-(nitromethane),(acetonitrile),(dimethylsulphoxide), ^{23}Na n.m.r. meas. for ionic solvation study 3—26703
- semiconductor, shallow donor impurities, shift parameters 3—27224
- Si insulating compounds, AES 3—30917
- toluene, liq., ^{13}C and ^2D relax. times, mol. motion obs. 3—2445
- toluene, protonated and deuterated, mol. motion, ^{13}C, ^2D relaxation times 3—36815
- tricyclic heteroaromatic systems, p.m.r. data 3—20098
- very near phenomenon, calc. of paramagnetic components of ^{19}F shielding tensor 3—20183
- X-rays, calc. by free ion configurations 3—11131
- zeolites, chemical shift of ^{205}Tl *(German)* 3—15435
- $AgNa(NO_2)_2$, ferroelec. transition, ^{23}Na n.m.r. obs. 3—21370
- Al metal, oxide, nitride, He and Ne ion excitation of K X-ray spectra, chemical effects 3—4365
- α-Al_2O_3, $Al(OH)_3$, $AlO(OH)$, $MgAl_2O_4$, struct. effects on chem. shift, X-ray photoelectron spectra 3—30920
- Au, adsorption of H_2O, CO_2, CO, surface sensitivity of photoelectron spectroscopy 3—11944
- BF_4^- anions in solution, temperature dependence of ^{19}F n.m.r. spectra 3—34231
- BeF_2, crystalline and glassy, F^{19} n.m.r. 3—34224
- CO chemisorbed on W, ESCA obs., chem. shift 3—38732
- ^{13}C spectra, collection of data, book 3—23608
- Cr, atoms, surface and bulk, core-electron binding energies, comparison for surface chem. shifts calc. 3—39210
- GeX_4, where x=halogen, ^{73}Ge n.m.r., coordination depend. 3—29715
- HOF, meas. of ^{19}F chemical shift for low temp. liquid, determ. of atomic charge 3—4460
- HOF, proton and ^{19}F n.m.r. meas. for low temp. liquid and room temp. gas, determ. of atomic charge 3—4460
- Mg Auger and photoelectron spectra of partially oxidised surface, abnormal chem. shift 3—30909
- $MgCl_2.6H_2O$, powder proton n.m.r. shift 3—12071
- Ni, atoms, surface and bulk, core-electron binding energies, comparison for surface chem. shifts calc. 3—39210
- Ni and compounds, X-ray K-absorption edge, chemical shift meas. 3—5240
- OPF_2H_2, ^1H, ^{19}F, ^{31}P n.m.r. studies, chem. shifts and coupling consts. determ. 3—23600
- Pt complexes, mixed and partial oxidation states from photoelectron spectroscopic meas. 3—15585
- ^{85}Rb, Larmor frequency n.m.r., meas., atomic reference scale for liquid and solid state 3—12072
- S, and S containing compounds, meas. of shift in photoelectron spectra 3—30922
- SPF_2H, ^1H, ^{19}F, ^{31}P n.m.r. studies, chem. shifts and coupling consts. determ. 3—23600
- Se single crystals, anisotropic, n.m.r. 3—34233
- $SePF_2H$, ^1H, ^{19}F, ^{31}P, ^{77}Se n.m.r. studies, chem. shifts and coupling consts. determ. 3—23600
- Sn-As system, nature of bonding, Mossbauer effect studies 3—36828
- Te single crystals, anisotropic, n.m.r. 3—34233
- Ti, atoms, surface and bulk, core-electron binding energies, comparison for surface chem. shifts calc. 3—39210
- V, Auger electron emission spectra, chem. shifts, ionisation and plasma losses 3—30906
- V_2O_5, Auger electron emission spectra, chem. shifts, ionisation and plasma losses 3—30906
- Zn_3P_2:^{31}P, symmetrized multipulse n.m.r., obs. of chem. shift shielding tensor 3—15433

chemical structure

- *see also bonds (chemical); crystal atomic structure; crystal chemistry; molecular configurations and dimensions*
- 4-alkoxybenzylidene-2′-alkoxy-5′-aminopyridines, effect of heterocyclic N on mesomorphic behaviour 3—17738
- automatic compiling of descriptions of molecules from their fragments *(Russian)* 3—23541
- automatic methods and chemical structure *(Hungarian)* 3—19368
- monohydric alcohols in dioxane and cyclohexane, dielectric and thermodynamic behaviour 3—2490
- phosphate glasses, lanthanide activated, chain lengths of P-O-P groups and luminescence *(Russian)* 3—24733
- polyenes, struct. and electron spectra relation *(German)* 3—14404
- polymer, rel. to degradation processes 3—11348
- polymers, rel. to bulk props. 3—7272
- spectroscopic determ. by combining techniques 3—37760
- superadditive effectiveness on photographic development, formation of a stable semiquinone, phenidone 3—5409

chemical structure continued
- trinitrofluorenone-poly-n-vinylcarbazole mixture, amorphous film, densities of complexed and uncomplexed molecules 3−18038
- KH_2PO_4-KD_2PO_4 system, study in paraelectric phase 3−1614
- $Mg_7B_4O_{13}.7H_2O$, i.r. spectra interpretation *(Russian)* 3−36883
- UFe_2-UAl_2 alloy, chem. ordering, electronic struct., ^{57}Fe Mossbauer obs. 3−1987
- UFe_2-UGa_2 alloy chem. ordering, electronic struct., ^{57}Fe Mossbauer obs. 3−1987

chemical technology
- *see also chemical industry; chemical variables control; chemical variables measurement*
- $A^{II}B^{III}{}_2X_4$ compounds, production method *(Russian)* 3−14811
- fluidised bed catalytic reactors, countercurrent backmixing model, applicability to simplified solns. 3−7448
- fluidised beds, gas, grid leakage studies 3−23781
- fluidised beds, two and three phase, hold-up and axial mixing characts. 3−23782
- hot cells for processing ^{252}Cf, neutron shielding 3−17332
- microelectrode applications *(French)* 3−27875
- nuclear fuel reprocessing, Midwest Fuel Recovery Plant, remote control 3−17302
- nuclear waste processing plant, solidification improvements 3−35944
- polymerization of styrene with n-butyllithium in cyclohexane, math. model 3−1306
- rapid reaction rate meas., technique for rapid reactant introduction 3−9064
- vibrated fluidised beds appls. 3−1464
- SO_2 in flue gas, alkali scrubbing test facility instrumentation 3−25619

chemical variables control
- emission to air reduction in power generation industry, best practicable control means 3−37538
- potentiometric titration, application of computer operated system 3−22524
- $TiCl_4$, continuous determination of impurities by optical method during purification *(Russian)* 3−26031

chemical variables measurement
- *see also chemical analysis; moisture measurement*
- aqueous solution, dissolved O_2 measurement, electrochemical methods, review *(German)* 3−32256
- electron microscopic study of gas-solid systems study during reactions, controlled atmosphere 3−32226
- environmental pollution, systematic measurement methods 3−37539
- irradiated fuel elements, O_2 determination, remote equipment for 3−17307
- partition detector, piezoelectric quartz crystal digital sensor 3−37744
- pH scale of aqueous solutions 3−22244
- power plant stack gas, analysis for SO_2 and NO using i.r. analyser 3−25617
- pulse method for thermoactivity meas. of dielec. liqs. 3−22499
- river water quality 3−22186
- salinity, statistical anal. of thermohaline structure of ocean *(Russian)* 3−27977
- salinity calculations, from in situ measurements of low temperature seawater 3−16072
- salinity determination, from measures of electrical conductivity and temperature of seawater 3−16071
- u.v. absorption, using flow cell and suspended solids sensors 3−22188
- waste gas monitoring, continuous *(German)* 3−25608
- water pollution meas., conference, London (1973) 3−22185
- water quality, using electric sensors 3−22189
- water quality monitoring, using ion-selective and gas-permeable electrodes 3−22187
- NH_3, in water, on-line monitoring 3−22191
- NO_x, photometric measurement in emission source monitoring, associating oxidation of NO to NO_2 3−25616
- SO_2 concentration in flue gases, by ionisation chamber 3−3860
- SO_2 concentrations from Netherlands power stations *(German)* 3−9734

chemiluminescence
- acetaldehyde, ozone-induced chemilum. oxidation, Meinel bands of OH 3−2797
- acetylene + O_2 reaction, continuum chemilum. during induction period 3−9055
- ethylene, $O(^3P)$ addition, flash photolysis reson. fluoresc. study 3−25088
- ethylene and ethylene-d_4 and O atoms reactions, absolute rate consts. 3−12514
- fluorescence kinetics in photochemical reactions *(Russian)* 3−25099
- laser, chem., visible wavelength, based on metal oxides and nitrides chemilum. 3−10518
- lithium phosphides (organic), molecular structure depend. 3−30853
- phenanthrene, electochemiluminescence intensity, mag. field enhancement 3−18799
- tetracene−TMPD system, electrogenerated chemilum., mag. field effects, triplet-triplet annihilation 3−34719
- Al + O_3 crossed-beam chemilum., AlO dissoc. energy determ. 3−7241
- CN violet and red band excitation by metastable Ar and Xe reactions with CN containing cpds. 3−31251
- CO, vibrationally excited, reaction of O atoms with acetylene, methylacetylene and methane 3−39432
- $H + F_2 \rightarrow HF + F$, determ. of energy distribution among products using arrested relaxation variant of i.r. chemiluminescence technique 3−5377
- $H + F_2 \rightarrow HF + H$, vibrational energy distribution determ. 3−1280
- HF produced in $H + F_2 \rightarrow H + HF$, i.r. chemiluminescence, determ. of initial vibrational energy distributions 3−1280
- HF product of abstraction reaction between F atoms and org. cpds., energy partitioning and i.r. chemilum. 3−31253
- HF product of abstraction reaction between F atoms and hydrides, energy partitioning and i.r. chemilum. 3−31254
- $N + NO \rightarrow N_2 + O$, i.r. chemiluminescence 3−25061
- N + O assoc. reaction, rate consts. for $O(^3P)$ recomb. 3−27858

chemiluminescence continued
- N + O radiative recombination investigation using photodissociation of NO 3−20192

chemisorption
- alumina, of toluene, e.p.r. determ. of sorption sites *(French)* 3−1894
- American Vacuum Society, symposium, Chicago, USA (1972) 3−37608
- anthracene, singlet-oxygen-induced hole current 3−2126
- Auger electron spectroscopy, L-shell ionization cross sections 3−39209
- band-energy band-order model 3−38733
- charge redistribution obs. using LEED and Auger emission spectroscopy 3−24341
- electronic effects in H evolution reaction 3−38735
- graphite, of atomic oxygen on basal faces, photoelectron spectra 3−24347
- Kapron-highly dispersed Fe, Co and Ni, ferromag. resonance, chemisorption effect 3−39409
- metal, H chemisorption, charge densities and binding energies calc. 3−33740
- metal film, replacement of chemisorbed gases, elec. cond. and mass spectrometry obs. *(Japanese)* 3−20928
- metal surface with chemisorbed atom, field emission and total energy distrib. 3−1895
- metallic thin films, Hall effect rel. to H_2 and O_2 chemisorption 3−15278
- Ni polycrystalline surfaces, H_2 adsorption states at different temps., chemisorption states 3−11801
- phosphors, radical recombination luminescence 3−27572
- photo-induced, energy for one and two adatoms 3−30353
- polyceproamide-highly dispersed Fe, Co and Ni, ferromag. resonance, chemisorption effect 3−39409
- quantum mechanical model calculations of simple chemisorption processes at solid surfaces, chemisorption of an atom at a linear atomic chain *(German)* 3−15073
- semiconductor surface, thermodynamics of chemisorption rel. to surface scattering of carriers 3−36489
- semiconductor surface, thermodynamics rel. to carrier scattering 3−5004
- starch, n.m.r. of binding of adsorbed H_2O 3−30354
- transition metals, of hydrogen, review *(French)* 3−1897
- Ag, of O_2, low energy backscattered electron spectra, surface atom energetics, chem. bonding 3−24349
- Al thin film deposition, source-to-substrate distance effect on O_2 sorption 3−34478
- η-Al_2O_3 water vapour heat of adsorption *(French)* 3−27187
- Au, of H_2O, CO, CO_2, surface sensitivity of photoelectron spectroscopy 3−11944
- Ba surface, effect of chemisorbed oxygen 3−18532
- CdS film, bulk compensation effect on chemisorption dependent semiconductivity 3−33889
- Cu, of Bi on (100) surface, LEED obs. of layer struct. 3−30355
- Cu, of Bi on (111), LEED obs. of layer struct. 3−30356
- Cu (100) face, of Cl, electron diffr. obs. *(French)* 3−1893
- Cu film, epitaxial, electron diffr. obs. of adsorbed oxygen layer *(French)* 3−27188
- Eu surface, effect of chemisorbed oxygen 3−18532
- Fe, of O_2, photoelec. work function and Auger spectroscopy study 3−38741
- Fe-Si alloy, of O_2, photoelec. work function and Auger spectroscopy study 3−38741
- MO, of O_2 and CO, adsorbate dependent surface states, optical refl. obs. 3−38879
- Mo, of C and O, causing precipitation at surface and grain boundaries *(French)* 3−21590
- Mo(110) chemisorption of H_2 and N_2 3−11811
- N, Auger line shape, in different chemical environments 3−39207
- Ni, (110), Co adsorption, investigation by electron probe methods 3−38721
- Ni, (110) surface, of CO, LEED obs. 3−38716
- Ni, adsorption of benzene and cyclohexane 3−27922
- Ni, molecular orbital levels, CO-induced on a (110) surface 3−10103
- Ni, of H_2, on polycryst. wires, heat of adsorption correl. with reaction kinetics 3−11809
- Ni, of N, evidence for 'end-on' bonding in formation of NiN_2 3−23553
- Ni, of S, Auger spectral fine struct. origin 3−11810
- Ni/chemisorbed Na system, LEED intensity meas. 3−30312
- Ni-O system, cpd. formation, elucidation by ESCA 3−24348
- NiO, h.f. form of chemisorbed CO 3−36488
- NiO adsorption of benzene and cyclohexane 3−27922
- O atom and negative ion binding energies approach to forces determ. 3−30352
- Pb surface, ESCA obs. of atomic oxygen layer 3−33741
- Pt, (100) surface, chemisorption of unsaturated mols., Auger spectroscopic and LEED study 3−11808
- Pt, of CO, thermal desorption methods 3−37143
- Pt, of H_2, crystal field surface orbital−bond energy bond order model 3−4926
- Pt, of O_2 at low press., desorption spectra sticking probability, isobars, bonding energies 3−4927
- Pt, reactivity of low index and stepped single cryst. surfaces 3−11787
- Pt-Sn alloy, surface composition rel. to annealing O_2 chemisorpt., H_2 reduction, Auger spectra obs. 3−30318
- PuO_2, of water vapour, rel. to three-step model for total adsorption 3−38719
- Ru, of CO 3−20936
- S, Auger line shape, in different chemical environments 3−39207
- SiO, sticking coefficient of Pb, effect of water vapour 3−38734
- SnO_2 film, chemisorption of O_2 and H_2, var. of electrical conductance *(Japanese)* 3−8024
- TiO_2, interaction of sodium oleate with TiO_2 surface, i.r. studies 3−39410
- W, adsorbed 5d transition atom, theory and surface mol. 3−1896
- W, of CO, and desorption spectra of single and polycrystals 3−8025
- W, of CO and O_2, ESCA obs. of fractional monolayer quantities 3−38732

- **chemisorption** continued
  - W of H_2, on polycryst. wires, heat of adsorption/reaction kinetics correl. 3—11809
  - W(100) of H_2, absolute sticking probability, coverage and electron stimulated desorption 3—36490
  - ZnO single crystal surface, surface donor states influence on oxygen chemisorption kinetics, theory 3—33738
  - ZnO single crystal surface, surface donor states influence on oxygen chemisorption kinetics, experimental results 3—33739
  - ZnS:AgCl, interaction of Ce vapours, induced capillary condensation 3—39464
  - ZnTe, amorphous thin films, O_2 chemisorption effect on electrical conductivity 3—27320
- **chemistry**
  - accelerator applications 3—19252
  - clinical, automatic series analysis equipment *(Hungarian)* 3—19368
  - lunar C chemistry, effects on terrestrial organic chemistry 3—35088
- **chemistry, physical** *see physical chemistry*
- **Cherenkov counters**
  - cosmic ray isotope analysis with cryogenic magnet 3—6075
  - for electron and π meson separation over wide energy range 3—22448
  - electron beam energy calibration from 9-22 MeV, medicine 3—10153
  - gamma-ray telescope for observing NP0532 (Crab pulsar) 3—37510
  - gas, applic. as high-energy particle detectors 3—10056
  - gas, with large phase space acceptance 3—35475
  - gas-Cherenkov γ-ray telescope, performance 3—39754
  - hodoscope, large-aperture, for multi-particle state identification 3—10058
  - neutrino detector Cherenkov system, Utah, USA 3—32160
  - with organic wavelength shifter, performance 3—25891
  - simulation of missed counts by light pickups 3—22457
  - stabilization of spectrometric channel 3—22449
  - Pb silicate glasses, radiation induced colouring 3—35476
- **Cherenkov detectors** *see Cherenkov counters*
- **Cherenkov radiation**
  - *see also Cherenkov counters; electron radiation*
  - auroral electron emission in dayside polar-cusp region 3—15995
  - beam-plasma instabilities excited by anomalous Doppler effect and Cerenkov effect 3—23865
  - in biaxial crystals, Fourier integrals 3—33547
  - in biaxial crystals, generalized universality condition 3—33548
  - charged particle moving in dielectric along plane boundary with periodically changing density *(Russian)* 3—35650
  - charged particle moving through radially inhomogeneous medium 3—35652
  - drifting magnetoplasma, radiation from electrons 3—20449
  - electron beam injection into ionosphere, beam front depend. of coherent emission *(French)* 3—39548
  - electron beam injection into ionosphere, longit. wave prod. 3—28058
  - electron beam modulation by stimulated Cherenkov absorpt. 3—10582
  - ionosphere, radiated power calcs., e.l.f. and v.l.f. regions 3—21960
  - liquid crystal, cholesteric, coherent radiation emission 3—1639
  - magnetosphere, v.l.f. signal amplification 3—9345
  - particle channelled in crystal, Cherenkov structure radiation for structure anal. 3—26916
  - in photomultiplier windows, time shift effect in delayed coincidence time spectra 3—10060
  - in photomultipliers, induced by high energy electrons (245 MeV), noise pulses 3—10082
  - plasma, coherent radiation on injection of relativistic electron beam 3—30007
  - plasma-beam interaction, inhomogeneity effect on Cherenkov surface wave-beam resonance 3—14520
  - proton energy, by achromatic method using Vavilov-Cherenkov radiation 3—25886
  - reflection and capture of charged particle, by plane e.m. wave *(Russian)* 3—579
  - superluminal source motion in vacuum, Vasilov-Cerenkov effect and Doppler effect 3—29216
  - by tachyons, Lorentz-invariant formulation 3—10829
  - Vavilov Cherenkov, of charged particle moving along axis of channel in laminar medium *(Russian)* 3—35649
  - Vavilov-Cherenkov, in detection of 657 MeV proton energy by apochromatic method 3—3855
  - X-ray range in low-energy nuclei 3—4186
  - ^{40}K β-decay, detection of produced Cherenkov radiation in aqueous solns. 3—37755
  - Pb glass Cherenkov X-ray spectrometer, energy resolution for electron beam 3—28701
- **chilling** *see cooling*
- **chirality**
  - *see also SU_n theory*
  - σ commutator with isospin T=2, analysis 3—23005
  - (8,8) model of chiral-symmetry breaking, SU(3) violations and σ terms 3—23133
  - broken chiral symmetry and sigma commutators 3—16952
  - Cabbibo rotation in models of chiral-symmetry breaking 3—10638
  - chiral field, classical, solutions dependent on one space-time variable *(Russian)* 3—19673
  - chiral symmetry, algebraic realization on light cone 3—26277
  - chiral symmetry breaking, restrictions, calc. of meson-meson scattering lengths 3—26274
  - covariant perturbation theory and chiral superpropagators 3—6566
  - dual pion model, chiral dynamics as zero-slope limit, nonlinear σ-model 3—29230
  - Lagrangians, covariant perturbation theory 3—35742
  - non-conservation of unitary-singlet axial-vector current, possible role of Fujii boson 3—32639
  - nonrenormalisation theorem in the chiral symmetry limit 3—32635
  - pion model, chiral invariant, coordinate-independent Green's functions 3—35752
  - quantum mechanical model of chiral invariance rel. to order of non-commuting factors 3—22998
  - quark model, relativistic, chiral symm. breaking and meson decays 3—32678
  - spontaneously-broken gauge theory of strongly-interacting bosons based on SU(2) × SU(2) group, chiral invariance and e.m. mass difference 3—17085
- **chirality** continued
  - $SU_2 \times SU_2$ broken chiral symmetry in quark model of mesons 3—38059
  - SU(2) × SU(2) invariant phenomenological Lagrangians for πN interaction, minimal interaction principle 3—29251
  - $SU(2) \otimes SU(2)$, chiral, mixing, and quark model of hadrons 3—26320
  - SU(3) × SU(3), (6,6) + (6,6) symmetry breaking 3—10637
  - SU(3) × SU(3) chiral algebra for baryons 3—6562
  - SU(6) breaking, to determ. form of chiral SU(3) breaking 3—22999
  - superpropagator construction from SU(2) × SU(2) invariant Lagrangian 3—4247
  - symmetry breaking, connection to Cabbibo angle 3—19672
  - symmetry breaking and σ terms 3—23004
  - symmetry breaking and of $SU(3) \otimes SU(3)$ 3—19671
  - symmetry breaking and $SU_3 \times SU_3$ reln. to $SU_6 \times O_3$ 3—23000
  - symmetry violation in π-nuclear scattering 3—6922
  - U(3) x U(3) symmetry breaking and $X \rightarrow \eta\pi\pi$ decay amplitude 3—35757
  - $K \rightarrow \pi\mu(e)\nu$, chiral-limit theorems and PCAC corrections for scalar divergence form factor 3—29187
  - $K \rightarrow \pi\mu(e)\nu$ form factors, chiral symmetry breaking 3—13832
  - π Lagrangian, chiral invariant, single-loop calcs. 3—35747
  - π lagrangians, chiral-invariant, second-order effects, use of superpropagators 3—22980
  - $\pi - \pi$ phase shifts from covariant perturbation theory for chiral invariant field theoretic model 3—23146
- **chlorine**
  - adsorption on Cu (100) face, electron diffr. obs. *(French)* 3—1893
  - adsorption on Ti 3—1882
  - atom, in $KClO_3$, $KClO_4$, X-ray spectra, ClO_3^- and ClO_4^- electronic struct. determ. 3—29598
  - atomic, dissociatively prod., pulsed laser emission in elec. discharge 3—10520
  - chemisorbed monolayer, Auger spectra, L-shell ionization cross sections 3—39209
  - electron affinity in alkali metal compound 3—1117
  - fluorescence yields, K-shell 3—26570
  - gas environment, high strength steel slow crack growth 3—18680
  - gaseous, press. induced fundamental i.r. band intensity 3—33121
  - ion fractionation at sea-air interface, enrichment values 3—12691
  - ionisation balance, calc. for collisional ionisation, autoionisation, radiative recombination and dielectric recombination 3—11458
  - ionisation equilib. calc. for solar atm. ions 3—18960
  - liquid, molecular reorientation 3—24626
  - molecule, electron impact ionization cross section, 15-100 V 3—1284
  - negative ion source, bombardment of solid surfaces by positive alkali ions *(Russian)* 3—6061
  - Penning ioniz. reaction with metastable He, fluoresc., vibr. populations 3—29731
  - plasma-beam discharge laser 3—32555
  - reactions with alkaline earth metals, crossed beams chemistry 3—21803
  - tektites, Cl concentrations rel. to obsidians and impact glasses 3—16199
  - turtle photoreceptors, effect of ions on intracellular responses 3—22152
  - vacuum u.v. absorption, 105 to 550 nm, at atmospheric pressure *(Russian)* 3—7181
  - X-ray K spectrum of 30 MeV ion beam 3—7049
  - $Ba + Cl_2 \rightarrow BaCl + Cl$, collision dynamics, hermaphroditism 3—25047
  - Br/Cl ratio in oceanic rain 3—12755
  - Cl-HBr laser, vibr. rot. state populations, output spectra 3—10479
  - Cl-HI laser, vibr. rot. state populations, output spectra 3—10479
  - $Cl + DI \rightarrow ClD + I$, distribution of reaction products 3—18786
  - $Cl + H_2 \rightarrow HCl + H$ reversible reaction, rate const. ratio 3—21795
  - $Cl + HCl(v=1,2) = ClH + Cl$, vibr. relax., classical Monte Carlo trajectory study 3—23619
  - $Cl + HI(DI) \rightarrow I + HCl(DCl)$ temperature parameter for rotational state of product 3—31245
  - $Cl + HI \rightarrow ClH + I$, distribution of reaction products 3—18786
  - Cl^{12+} to Cl^{17+}, K_α satellite and hypersatellite and K_β satellite transitions 3—38214
  - Cl_2, Raman spectra, vibrational hot bands of isotopic species 3—20140
  - ^{35}Cl, ^{37}Cl atomic mass determ. 3—11107
  - ^{35}Cl, atomic mass determ. 3—32998
  - $^{35}Cl_2$, rotational laser Raman spectrum 3—1232
  - ^{37}Cl, atomic mass determ. 3—32998
  - $H(D) + Cl_2 \rightarrow Cl + HCl(DCl)$ temperature parameter for rotational state of product 3—31245
  - O_2-Cl_2, thermal oxidation of Si, electrically stable SiO_2-Cl 3—39287
  - in SiO_2, O_2:HCl grown, distrib. determ. 3—30951
  - ZnS:Cl, e.p.r. signal and self-activated luminesc. from A-centre, Zn vacancy-Cd donor pair 3—33529
  - ZnS:Cl, luminescence spectra *(Russian)* 3—27548
  - ZnS:Cu, Mn, Cl, film, doping in vacuum growth rel. to electrolum. props. 3—15559
  - ZnS:Cu,Cl film, stimulated cond., quenching by elec. pulses *(Russian)* 3—2069
  - ZnS:Mn, Cl, thermal quenching of luminesc., elec. field effects *(Russian)* 3—27555
- **chlorine compounds**
  - group IV tetrachlorides, Raman spectra, 20 to 420°C, Coriolis and force const. determ. 3—29662
  - perchloric acid glass, u.v.-irrad., hydronium radical obs. 3—34735
  - tetrachlorides, $XCl_4(X=C, Si, Ti, Sn)$, fluidity, general theory 3—7961
  - $[H_2O...Cl]^-$ complex, SCF LCAO MO calcs. of hydrogen bond 3—29587
  - Cl_2CO, vibr. intensities, dipole moment derivatives 3—26640
  - Cl_2CS, vibr. intensities, dipole moment derivatives 3—26641
  - ClF, dipole polarity and field gradient deriv. from Hartree Fock functions calc. 3—35998
  - ClF, elec. dipole moment sign determ. 3—33107
  - ClF, electronic structure by photoelectron spectra 3—1161
  - ClF_3, electronic structure by photoelectron spectra 3—1161
  - ClF_4 radical, e.p.r. spectrum 3—34739
  - ClHCl, computed bond energies and vibr. freq., including isotope effects 3—1181

chlorine compounds continued
  ClN_3 laser, chem., excited N_2 source 3−10522
  ClO, vacuum u.v. absorpt. spectrum 3−33119
  ClO_2, isotopic species quantum mech., spectroscopic and statistical thermodynamic studies 3−7208
  ClO_2-salts, luminesc., coloration appearance study *(Russian)* 3−37137
  ClO_4^-, X-ray photoelectron spectrum, line intensities 3−36048
  ClO_4^{n-}, tetrahedral anion, bond length variation 3−14332
  Cl_2O_7, valence force field calc. *(French)* 3−17412
  Cl_2O_7, vibrational spectrum 3−20148
  Cl_3PO, microwave spectrum, determ. of rotational consts. and structural parameters 3−1242
  H_2-ClF_3, possible chain-branching chem. -laser, comment on results 3−22875
  H_2-ClF_3, possible chain-branching chem. laser, reply to comments on results 3−22876
  Si-H-Cl system, thermodynamic evaluation 3−11716

cholesteric phase *see liquid crystals*

chondrites *see meteorites*

chopping *see cutting*

chromatic aberration *see aberrations*

chromatography
  see also adsorption; chemical adsorption analysis
  adsorbent, polyarylate F-1 thin layer on macroporous silica gel 3−38714
  amino acids and peptides at the picomole level, fluorescent reagent development, application to automated assay 3−35524
  aromatic amines, gas-liquid chromatography, adsorption activity of metallic supports 3−22542
  automatic detection of chromatographic peak in spectrum by deterministic methods *(Russian)* 3−443
  automatic sampling accessory 3−3916
  p,p′- azoxyphenetole, and eutectic mixtures, gas chromatographic study of phase transitions 3−24025
  function simulator 3−22540
  gas, application of correlation techniques 3−32250
  gas, automatic methods and equipment *(Hungarian)* 3−19368
  gas, computer acquisition and anal. of data 3−429
  gas, detection system *(German)* 3−19370
  gas, lunar fines, contamination problems in search for amino acids 3−35095
  gas, organic insulation degradation analysis applications *(French)* 3−13510
  gas, thermal conductivity detector, constant filament temp. 3−22544
  gas impurity analysis, review 3−22541
  gas liquid, data analysis by computing integrator 3−10206
  gas-liquid chromatography of lunar organic compound anal. 3−32266
  gases in crystal inclusions, gas chromatographic analysis technique 3−32254
  industrial trace gas analysis using 95-105 MHz discharge stability *(French)* 3−432
  ion-exchange, use in lunar organic anal. 3−32267
  liquid, detection based on differences in partial heat contents 3−22543
  liquid, detection system, refractometers and photometers *(German)* 3−19370
  liquid column, apparatus description *(German)* 3−13506
  mass spectrometry-gas chromatography system, capability evaluation 3−434
  memory cct. for, patent 3−10214
  overlapping gaussian and skewed peaks, resolution computer programs 3−3931
  partition detector, piezoelectric quartz crystal digital sensor 3−37744
  polymer analysis, applications of gas chromatography/mass spectrometry 3−37752
  pyroelectric katharometer, gas chromatography applications 3−22277
  rapid gas chromatography, atmosphere flue gas and engine exhaust analysis 3−28398
  Rf values, direct reading, mixtures 3−438
  separation scheme optimisation, multicomponent samples, graphical application 3−26007
  solar chromatograph, design and props. 3−37499
  transient phenomena, chromatographic meas., flow-proportional counter for radioactive tracers 3−6161
  $Ca(PO_4)_x$, composition exam. by paper chromatography *(Russian)* 3−11546
  Ni benzene and cyclohexane adsorption meas. by chromatography 3−27922
  NiO benzene and cyclohexane adsorption meas. by chromatography 3−27922

chromium
  absorption in air-acetylene flame, releasing effect of NH_4Cl 3−14291
  alloying element in Al-Zn-Mg alloys, grain boundary corrosion and stress corrosion cracking relationship *(Japanese)* 3−31072
  anodic behaviour of monocrystalline and polycrystalline Cr electrodes in H_2SO_4 *(French)* 3−9077
  antiferromagnet, incommensurate, hyperfine field meas. using time differential perturbed angular correlation 3−11993
  antiferromagnetic, mag. hysteresis, fields to 20 kOe, 77-450K 3−2310
  antiferromagnetic domain obs. by X-ray and neutron topography 3−30647
  antiferromagnetism, mathematical theory 3−18276
  aquatic frontal systems, element enrichment in films and foams 3−12690
  atomic mean square displacements, calc. for volume, (110) and (100) surface atoms 3−30218
  atoms, surface and bulk, core-electron binding energies, comparison 3−39210
  in British pillow lavas petrogenic affinities 3−2872
  composite, metal matrix/fibre reinforced, solidified, Piobert-Luders band deform. *(French)* 3−39391
  desorption of remanent gases by laser-probe method 3−26250

chromium continued
  diffusion coating layer form. on stainless steel surface *(Japanese)* 3−12397
  diffusion in NiO, 1192-1642°C, tracer sectioning study 3−27137
  faceting in dilute O_2 atm., l.e.e.d. and r.h.e.e.d. studies 3−11818
  film, electron energy loss spectrum 3−17885
  grating lines on optical diffraction gratings, X-ray total reflection and diffraction *(German)* 3−10131
  ionisation balance, calc. for collisional ionisation, autoionisation, radiative recombination and dielectric recombination 3−11458
  ionisation equilib. calc. for solar atm. ions 3−18960
  lattice parameter variation in thin films 3−26992
  magnetic structure, thermal hysteresis, influence of external field *(Russian)* 3−8371
  Mossbauer effect of ^{57}Fe, impurity lattice dynamics 3−33638
  Neel temperature, band calc. of pressure depend. 3−18293
  oxidation of (100) and (110) surfaces, RHEED study 3−1903
  plating on Cu crysts., plastic constraint as film strengthening mechanism 3−21613
  precipitation of N, early stage 3−37038
  reflection spectra, optical characteristics calc. using Kramers-Kronig relations 3−34372
  ruby:Cr^{4+}, elimination of Cr^{4+} ions as source of strong resonant phonon scattering *(French)* 3−1846
  small crysts., diameter $\leqslant 30$ Å, cryst. struct. 3−14735
  sputtered deposit, hardness and microstruct. substrate bias and deposition temp. effects 3−4936
  structure factor determ. by vanishing Kikuchi line method 3−24002
  superconducting film deposited with noble gases, supercond. transition temp. variation 3−36670
  surface oxidation, static method secondary ion mass spectrometry obs. 3−1906
  surface resistance determ. in hyperfrequency region by transmission coefficient meas. *(Russian)* 3−9993
  surface saturation diffusion of B, obs. of borated layer structure *(Russian)* 3−11763
  thin film deposition, in rotary drum evaporator 3−37609
  in transition metal-Be alloy, hardness-controlling addition *(German)* 3−8901
  u.s. attenuation due to polarisation domain relaxation processes in transverse spin density wave phase 3−30675
  vacuum-diffusion coating, effect on corrosion fatigue of steel *(Russian)* 3−27665
  wettability of melt on graphite and glasslike carbon substrates, catalytic graphitisation 3−11796
  wire drawn to 0.4-0.5 mm with Y, La, Ce or Gd impurities, mech. testing *(Russian)* 3−8878
  X-ray K-absorption spectra *(Russian)* 3−18509
  X-ray $L\alpha_{1,2}\beta_1$-bands *(Russian)* 3−34439
  Al_2O_3:Cr^{2+}, acoustic e.p.r. spectra obs. 3−8427
  Al_2O_3:Cr^{2+}, elec. field effect on acoustic e.p.r. spectra 3−8428
  Al_2O_3:Cr^{3+}, electron spin echo for high Cr^{3+} concs. 3−8435
  Al_2O_3:Cr^{3+}, electron spin-lattice time by continuous saturation method 3−34201
  α-Al_2O_3:Cr^{3+} direct optical excitation into excited states of Cr^{3+} pairs 3−8657
  δ-Cr, thin films, prod. conditions, electron diffr. data anal. 3−36502
  δ-Cr, thin films, prod. conditions, substrate and deposition rate effect 3−36503
  Cr IX 4566 Å line in solar corona, luminosity conditions 3−39606
  Cr-Au bimetallic film, Cr diffusion into Au, work function study 3−15030
  Cr-Si junctions, barrier height, cryst. orientation depend. *(French)* 3−27310
  Cr^+, total cross sections for charge transfer and stripping in He and N_2 3−11181
  Cr^+ in II-VI semiconductors, g-shift 3−2377
  Cr^{3+}, e.s.r., exact eigensolutions calc. 3−24609
  Cr^{3+}; in MgO, e.s.r. absorp. spectrum, strain broadening 3−27412
  Cr^{3+} e.p.r. in $(NH_4)_2SbCl_5$, site symmetry 3−24606
  Cr^{3+} e.p.r. in K_2SbF_5 site symmetry 3−24607
  Cr^{3+} e.p.r. in $ZnWO_4$, interaction with Li defects 3−2379
  Cr^{3+} in glass, interference states in absorption spectrum *(Russian)* 3−8620
  Cr^{3+} in $RbGa(SO_4)_2.12H_2O$ and $CsGa(SO_4)_2.12H_2O$ e.s.r. at 4.2 and 300 K 3−2354
  Cr^{3+} in $RbGa(SO_4)_2.12H_2O$ and $CsGa(SO_4)_2.12H_2O$, ENDOR meas. at 4.2 K 3−2465
  Cr^{3+} in trigonal symmetry, zero field splitting, effect of spin-spin contribs. 3−34054
  Cr^{3+} in $ZnGa_2O_4$ and $MgAl_2O_4$, e.s.r. and nearest-neighbour exchange interactions 3−2380
  Cr^{3+} spectra, low terms. determ. 3−33025
  Cr^{3+}-Cr^{3+} pairs in guanidinium aluminium sulphite, e.p.r., satellite lines 3−2381
  Cr^{4+} atomic spectra, term values determ. 3−33026
  $^{53}Cr^{3+}$ ENDOR at different sites in SnO_2 3−2467
  ^{54}Cr, synthesis in supernovae 3−13097
  n-GaAs:Cr, magnetoresist. and recombination instability in mag. field 3−30500
  GaAs:Cr, photocond. after 0.8 MeV electron irradiation, induced impurity trap levels 3−36637
  GaAs:Cr, recomb. radiation, carriers generated in vicinity of surface 3−34426
  GaAs:Cr, semiinsulating, photocond., electric field and thermal quenching *(Russian)* 3−5031
  MgO:Cr, ion implanted, photolum. from damage related defect centres 3−21463
  MgO:Cr^{3+}, absorpt. meas. rel. to tetragonal field splitting of levels 3−15513
  MgO:Cr^{3+}, obs. of optical absorpt. strengths for transition lines 3−15512
  MgO-Al_2O_3 synthetic spinel, spectra, luminesc. of Cr and Mn in impurities, comp. depend. 3−34429
  Mg_2TiO_4:Mn^{4+}, Cr^{3+}, phosphors, luminescence *(Russian)* 3−36928
  in Ni, effect on high field susceptibility 3−21225
  ruby:Cr^{2+}, Cr^{3+}, Cr^{4+} luminescence, quantum losses *(Russian)* 3−36929

chromium continued
- VO_2:Cr, structure obs. rel. to metal-insulator transition 3−27220
- V_2O_3:Cr, Hubbard model, phase stability 3−15344
- V_2O_5:Cr, e.p.r., h.f.s., γ-irrad. influence 3−2382
- $ZnGa_2O_4$, e.p.r. spectra of nearest neighbour Cr^{3+} pairs 3−34199
- ZnS:Cr, e.p.r. obs. of cubic and axial sites 3−15414
- ZnS:Cr^{+}, Cu, C, e.p.r. and luminescence studies *(Russian)* 3−27552
- ZnS:Cr^{2+}, excitation spectra interpretation by fitting eigenvalues of Tanabe-Sugano matrices 3−2588

chromium alloys
- *see also chromium compounds*
- carbide and boride strengthened, phase stability and mech. props. 3−34568
- cementite, influence of matrix on Cr contents 3−8790
- dispersion hardening, high-temp. stability of refractory metal borides 3−18626
- Elinvar, ageing effect on Young's modulus temp. depend. *(Russian)* 3−31055
- Elinvar, Cr type, tempering influence on Young's modulus and its temp. depend. 3−31084
- Elinvar, thermal expansion and elastic props. *(German)* 3−34610
- eutectic composite, fibre-reinforced M-M_7C_3, (M = Fe + Co + Cr), $M_7C_3 \rightarrow M_{23}C_6$ transform. 3−31143
- Incoloy-800, B distribution, heat-treatment effect 3−12386
- Inconel, X-750, precip. parameters role upon creep rupture props. 3−37024
- mechanical characteristics, rare earth metal additions effect 3−34604
- Mn-Cu-Cr, Elinvar props. 3−21291
- Mu-metal, magnetomechanical props. by shear strain meas. technique *(German)* 3−35447
- nichrome, deformation hardening, velocity dependence *(Russian)* 3−2727
- nichrome film, elec. resist. variation during deposition 3−21536
- Nimonic, age-hardening, temp. depend. of strengthening characts. *(Russian)* 3−8839
- protective coating of Y, La and Hf 3−18657
- stainless steel, 18% secondary workability obs. *(Japanese)* 3−8862
- steel plate, diffusion chromizing, effect of alloying elements 3−27689
- Al-Cr, dil., n.m.r. spectra, satellite struct. interpret. 3−2431
- Al-Cr, supersaturated solid solns., annealing and diffusion kinetics 3−36438
- Al-Cr-Zr, granulated and supersaturated, decomposition mechanism and kinetics *(Polish)* 3−31032
- Au-Cr, high concentrated alloy, elec. resist. min. at low temp. 3−30449
- Au-Cr, paramag.-antiferromag. critical composition, anisotropic diffuse scatt. of neutrons 3−38973
- AuCr, (3.3, 10.6 at. % Cr), elec. resist., $T^{3/2}$ depend. of impurity resist. 3−36581
- Co-Cr, sigma phase detection by electron microscopy 3−8811
- Co-Cr based superalloys, dispersion strengthening for high temp. applics. 3−31112
- Co-Cr-C system, crystallisation of 2-4 phase composite structures *(German)* 3−8776
- Co-Cr-Ni-Ta, directional solidification, interdendritic structures 3−37031
- Co-Cr-W alloys, phase equilibrium at 1350°C, with emphasis on R-phase 3−15659
- Co-Cr(21 wt.%) with Y_2O_3 dispersion, Cr diffusion, substruct. influence 3−39343
- Co-Nd, Co-(Nd,R) (R = rare earth), magnetic coercivity, effects of sintering with Pr, Sm additives 3−2309
- Cr alloy:Pr(La), zone refining rel. to low temp. ductility *(Russian)* 3−12305
- Cr steel, retained austenite detection using vapour phase deposited interference layers 3−8810
- Cr-C amorphous film, polyconductivity *(Russian)* 3−8145
- 12%Cr-Fe-C-N, structural diagrams and phase reactions, 1300-700°C 3−8772
- 7%Cr-Fe-C-N, structural diagrams and solid phase reactions, 1300-700°C 3−8773
- Cr-Fe(1%), phonon dispersion relation anomalies, neutron scatt. obs. 3−14948
- Cr-Mn, melt growth using directional solidification in ZrO_2 crucible 3−12291
- Cr-Mn alloy, equiatomic, paramagnetic scattering of neutrons 3−2254
- Cr-Mn-N austenitic stainess steel partial shape memory effect obs. 3−18677
- Cr-Mn-Ni, Elinvar type alloys, Young's modulus, thermal expansion, hardness, heat treatments, cold working effects *(Japanese)* 3−8858
- Cr-Mo-C ternary system, phase relationships and chromium carbide phase stabilities 3−34502
- Cr-Mo-Zr structural steel, weld joints, crack restraining properties *(German)* 3−2782
- Cr-Ni, interaction with $MoSi_2$, cermet formation, mechanical properties 3−8967
- Cr-Ni, two-phase, creep failure 3−27697
- Cr-Ni alloys, corroded, obs. using combined microprobe/opt. interferometry technique 3−39350
- Cr-Pd, dil., mag. props., solute effects 3−34111
- Cr-Re alloys, antiferromag. and superconductivity, coexistence *(Russian)* 3−8358
- Cr-Sn, Cr-rich, Neel temp., elec. resist., thermal expansion anomaly 3−15364
- Cr-W, dilute, force-constant changes influence on phonon frequency shifts 3−1736
- Cr_2Al_{11}, temperature dependence of magnetic susceptibility and Knight shift 3−36807
- CrMnNiN austenitic steel, planar slip during plastic deformation *(German, English)* 3−24132
- $CrPt_3$, transition from ferrimag. to paramag. type behaviour with cold working 3−21237
- $Cr_{0.30}Pt_{0.70}$, ordered and disordered, sp. ht., 1.2-4.2K 3−24567
- Cu-Cr, aging phenomena *(Japanese)* 3−31067
- Cu-Cr, dil., n.m.r. of ^{63}Cu, spin-lattice relax. mechanism 3−2443
- Cu-Cr, dilute, in supercond. sandwich, mag. props. from supercond. proximity meas. 3−8341

chromium alloys continued
- Cu-Cr base, precip. growth and nucleation, resist. study 3−24865
- Cu-Cr composite, fibre reinforced, deform. and fracture behaviour *(Japanese)* 3−34634
- Cu-Cr dilute, h.f. magnetoresist., 1.6-4.2K mag. field depend. 3−8156
- $Cu_{1-x}Au_x$-Cr, mag. field depreciation of Kondo magnetoresist. 3−33872
- Fe, cast, containing Cr and Cr-Mo, electrochem. props., rare earth additive effects *(Russian)* 3−27666
- Fe, oxidation in air and wet hydrogen at elevated temps. for sealing of soft glass, growth of whiskers *(Japanese)* 3−18590
- Fe-Cr, deviation from additivity rules, X-ray absorpt. obs. *(Russian)* 3−12337
- Fe-Cr, ferromag. reson., anisotropy const. determ. 3−2403
- Fe-Cr, low C and N content, gamma region *(French)* 3−27620
- Fe-Cr, ordering process, mass spectrometric obs. of secondary ion emission *(Russian)* 3−33490
- Fe-Cr, sigma phase detection by electron microscopy 3−8811
- Fe-Cr, solubility of N, nitriding characts. *(Russian)* 3−15719
- Fe-Cr, stress corrosion cracking 3−31039
- Fe-Cr, X-ray absorpt. spectra obs. of polymorphism *(Russian)* 3−12336
- Fe-Cr platings, electrodeposition *(German)* 3−9072
- Fe-Cr spinel, magnetoresist. anomalies at Curie point 3−30462
- Fe-Cr-Co containing Si, permanent mag. material, mag. props. 3−36746
- Fe-Cr-Co-Mo alloy, precipitation, structural and kinetic features 3−8787
- Fe-Cr-Ni, austenitic, hydrogen charging and effects *(French)* 3−2747
- Fe-Cr-Ni, embrittled, Mossbauer obs. *(Japanese)* 3−27634
- Fe-Cr-Ni alloy system, microstructural change study using selective etching *(Korean)* 3−5291
- Fe-Cr-Ni liq. system, thermochem. parameters 3−25045
- Fe-Cr(1 wt.%), creep strength 3−21640
- Fe-Cr(1 wt.%), high temp. tensile props. 3−21639
- Fe-Ni-Cr, grain boundary internal friction spectra, relax. phenomena 3−37028
- Fe-Ni-Cr, martensitic transform. kinetics, external factors influence *(Russian)* 3−37002
- Fe-Ni-Cr, stress corrosion cracking susceptibility, nuclear reactor water environments 3−39351
- Fe-Ni-Cr-Mo, deform. and heat treatment effect on struct. changes, Mossbauer obs. *(Russian)* 3−31056
- FeCr, Mossbauer effect, α-σ phase transitions obs. *(Russian)* 3−2479
- $Fe_{1-x}Cr_x$, bcc alloy, electronic struct., CPA calc. 3−11999
- Mn-Cr, antiferromag., Neel temp. determ., elec. resist. meas. 3−34119
- Ni-Cr, shock deform. of K-state, ordering kinetics 3−21697
- Ni-Cr, Sn alloying effect on mech. props. 3−21668
- Ni-Cr (2% Cr), optical constants *(Russian)* 3−15469
- Ni-Cr (20 wt.%) with Y_2O_3 dispersion, Cr diffusion substruct. influence 3−39343
- Ni-Cr (20%) alloy, influence of defects and short range order on recovery after deformation *(Russian)* 3−8877
- Ni-Cr base, precip. hardened, struct. factors influence on creep strength behaviour 3−8930
- Ni-Cr base alloy, weldable, stress rupture and ductility props., for use above 100°C 3−31063
- Ni-Cr based superalloys, dispersion strengthening for high temp. applics. 3−31112
- Ni-Cr disordered, mag. props., thermodynamic analysis near critical conc. *(Russian)* 3−2272
- Ni-Cr film, evaporated on glazed Al_2O_3 substrate, uniformity of elec. resist. 3−24794
- Ni-Cr-Al, internal and external oxidation mechanism 3−31115
- Ni-Cr-Al, internal oxidation 3−31116
- Ni-Cr-Al, oxidation resist. and mech. strength 3−18027
- Ni-Cr-Al with ThO_2 dispersion, hydrogen pretreatment effect on oxidation behaviour 3−39367
- Ni-Cr-Al-Cu, Evanohm, thermal cond., 0.4-77K 3−18112
- Ni-Cr-Mo martensitic steel, fatigue crack propagation law in water *(Japanese)* 3−18642
- Ni-Cr-Mo steel, C diffusion study 3−27633
- Ni-Cr-Nb heat resistant spring alloy characteriz. 3−24944
- Ni-Cr-ThO_2, dispersion strengthened, prep. by Cr diffusion in Ni-ThO_2 granule 3−8941
- Ni-Cr-ThO_2, Na_2SO_4 coated, oxidation, dispersion effect 3−39366
- Ni-Cr(50 wt.%), resist. to service embrittlement, high-creep strength, development 3−21636
- $NiCr_3$ K-states, X-ray absorption spectra study *(Russian)* 3−34441
- Ni_3Cr, X-ray K-absorpt. spectra *(Russian)* 3−18509
- NiCrTaC, directionally solidified eutectic, etching technique for orientation determ. 3−18701
- PdCr, interimpurity interaction effects below spin fluctuation temp., elec. resist. meas. 3−15348
- V-Cr, effect of oxygen in static indium 3−18030
- Zr-Cr system, $ZrCr_2$ interaction with ZrV_2 and $ZrMo_2$ *(Russian)* 3−27623

chromium compounds
- *see also chromium alloys*
- carbide fibre-reinforced composite, M-M_7C_3 eutectic, (M = Fe + Co + Cr), $M_7C_3 \rightarrow M_{23}C_6$ transform. 3−31143
- chrome-magnesia fired bricks, electron microprobe analysis of failure 3−15755
- chromocene, proton mag. reson., 1.6-20K, temp. independent paramag. 3−21329
- complex, quadri-nuclear, mag. spec. ht. and magnetization, analysis *(Japanese)* 3−18345
- μ- hydroxobis[pentaamminechromium(III)] chloride monohydrate, struct. and magnetic susceptibility of the acid rhodo complex 3−18301
- oxalate, hydrothermal synthesis 3−2629
- polynuclear complex salts, luminescence of extra-exchangeable Cr^{3+} ions *(Russian)* 3−36927
- $\{Cr_3O(CH_3COO)_6(H_2O)_3\}Cl.6H_2O$ Mossbauer study on the magnetism 3−2262

chromium compounds continued
$Al(urea)_6(ClO_4)_3$:$Cr(urea)_6(ClO_4)_3$ second order phase transformations, e.s.r. meas. 3−17975
Cr complex, $2[Cr(en)_3Cl_3].KCl.6H_2O$, magnetic circular dichroism of first spin-forbidden transition 3−8600
Cr complex, $[Cr(atp)_6]X_3$, atp=antipyrene, $X=so_3F$, BF_4, SCN, ClO_4, anion effects on luminesc. *(German)* 3−8679
Cr complex, acetylacetonate chromium (III), LCAO calc. of u.v. and visible absorption spectra 3−20137
Cr complex, tri(ethylenediamine) chromium(III) ion, polarized cryst. spectra 3−18447
Cr complex, trispyrrolidylcarbodithioate:Fe Mossbauer spectra 3−24635
Cr oxide gel systems, formation and interconversion of CrOOH and Cr_2O_3 3−5382
Cr-Pu-N system, phase behaviour 3−1776
Cr^{3+} thenoyl tri-fluoro acetonate, diffuse reflectance spectrum 3−18469
$CrAs_2$, high-pressure, determ. of $OsGe_2$ type structure, crystal chem. 3−38555
$CrAs_{0.5}Sb_{0.5}$ crystal distortion at Neel temp., antiferromag. NiAs to helimag. MnP type structure 3−33671
$CrBr_3$:^{53}Cr, low temp. n.m.r. obs. of ferromagnetic props. 3−15431
$Cr_{23}C_6$, cryst. struct., space group, cell dimensions 3−7669
$CrCl_3$, anhydrous, layered antiferromagnet, specific heat between 4.5 and 20 K in mag. field 3−38974
$CrCl_3$, specific magnetic rotation in crystal field bands 3−5179
CrF_3, X-ray $L\alpha_{1,2}\beta_1$-bands *(Russian)* 3−34439
Cr_2GeO_5, cryst. struct. *(French)* 3−7681
Cr(III) complex, $2Cren_3Cl_3KCl6H_2O$, linear dichroism in spin forbidden region 3−12130
Cr(III) complex, hexamminechromium(III) chlorocuprates(I,II), 10/3 effect in e.p.r. 3−27400
$Cr(IO_3)_2$, cryst. growth, boiling solvent technique 3−12235
$CrK(SO_4)_2.12H_2O$, deuterated and undeuterated, ultrasonic attenuation, phonon-phonon scatt. 3−4812
CrMn tellurides electrical conductivities under high pressure *(German)* 3−12594
CrN, X-ray $L\alpha_{1,2}\beta_1$-bands *(Russian)* 3−34439
$CrO_4{}^{2-}$, in orthorhombic sulphates, vibr. freqs., optical and i.r. absorpt. obs. 3−14954
$CrO_4{}^{2-}$ in alkali halides, vibr. and electronic spectra 3−27091
$CrO_8{}^{3-}$ ion, nature of metal-ligand bonding in K_3CrO^8 *(French)* 3−7715
Cr_2O_3, final sintering rel. to grain growth 3−8981
Cr_2O_3, $K_2Cr_2O_7$, KCr_3O_8 spectra, X-ray photoelectron, electronic structure relations 3−23548
Cr_2O_3, magnon energies temp. depend., Bloch and Nagai methods calcs. 3−12028
Cr_2O_3, u.s. attenuation freq. depend. in Neel pt. region *(French)* 3−5106
Cr_2O_3, X-ray $L\alpha_{1,2}\beta_1$-bands *(Russian)* 3−34439
Cr_2O_3-Cr cermet, sintering and obs. of props. *(Russian)* 3−8944
Cr_2O_3-Fe_2O_3, Mossbauer obs. of mag. structure 3−8490
CrP_2, high-presure, determ. of $OsGe_2$ type structure, crystal chem. 3−38555
Cr_3P, crystallographic study 3−11602
Cr_2S_3, rhombohedral single crystal, sublattice magnetisation 3−12021
Cr_2SSeTe, meas. of molar susceptibility and molar spontaneous magnetisation, 80-600 K, determ. of Curie point *(Russian)* 3−12010
CrSi, condensation, platelet structure, 300-1020°C, X-ray study *(Russian)* 3−7919
Cr(111) complex, $(Cr_3O(CH_3COO)_6(H_2O)_3)Cl.6H_2O$, luminesc. spectroscopic study, ground state parameter determ. 3−12165
$CuCr_2Te_3I$, internal fields at ^{129}I, Mossbauer effect obs. 3−30735
p-$EuCr_2Se_4$, doped, hysteresis, magnetization and coercive force 3−27385
NiO-Cr_2O_3 solid soln. prep., homogeneity 3−18787
$Sr_3Cr_2WO_9$, perovskite type, cryst. struct. and mag. props. *(French)* 3−24080
$Ti_{n-2}Cr_2O_{2n-1}$, shear struct., electron diffr. and electron microscope obs. 3−24127
UC, compatibility of Ta with UC at high temp. 3−35932
$YFe_xCr_{1-x}O_3$, antiferromag. props., exchange interaction for Fe^{3+} and Cr^{3+} ions 3−5103

chromosphere
brightness and effective temps. rel. to stellar model chromospheres 3−37349
brightness distrib. at 8.6 mm 3−5566
chromosphere-corona transition region, electron temp. and density meas. from rocket e.u.v. obs. 3−25393
chromosphere-corona transition region, temperature structure and conductive flux 3−9474
disk, spectra of near-vertical structures 3−31534
energy balance in chromosphere-corona transition region 3−39621
energy flux from 5-minute oscillations at 450 km. level 3−35018
equator-pole differences in chromospheric from Lyman-continuum spectroheliograms 3−18938
e.u.v. quiet spectrum meas., transition region emission measures 3−22012
heating by acoustic pulse propagation 3−16121
heating rel. to absence of flares at 3835 Angstroms 3−18943
models, rel. to outer layer models 3−9473
mottles, size from Hα scans 3−31536
mottles in fine structure and model of overall chromospheric structure 3−35034
oscillations, tunnelling in solar atm. 3−5567
photosphere-chromosphere transition region, line source functions, β_l values and microturbulence 3−9472
plage regions, velocity oscillations 3−9478
plages, Ca II K, H and i.r. triplet lines profiles 3−5568
polar chromosphere-corona transition layer model from OSO-4 e.u.v. obs. 3−39622
radio optical depth where electron temp. equals brightness temp. 3−31543
rotation rates determ. from OSO-4 e.u.v. spectroheliograms 3−39612
surges, dynamics and localisation from Hα line meas. 3−35048

chromosphere continued
temp. reduction by inclusion of Lyman-band absorpt. in a solar model 3−25438
temperature structure in chromosphere and corona, e.u.v. rocket experiment 3−18964
temperature structure of chromosphere-corona transition region 3−18950
Ca II K emission arches near solar limb 3−31535
He D_3-line study of chromosphere during 1968, Sept 22 total eclipse *(Russian)* 3−12972
He^+ 4686 Angstroms line search in low chromosphere and studies of He I 4713 Angstroms line 3−31555
Mg II doublet profiles of chromospheric inhomogeneities at centre of solar disc 3−28137

chronographs *see chronometers*

chronometers
No entries

cinefilming *see cinematography*

cinematography
see also cameras; telefilming
cinefluorographic analysis of lingual articulation 3−19094
cinemicrography of living cells, electronic devices 3−25784
cineradiography, for left venticular dimensions measurement in dogs 3−3568
colour characteristics of new discharge lamps for TV and film lighting 3−9979
colour positive developing control and printer tape preparation by minicomputer 3−35433
dye fading of motion picture film 3−220
holographic movie camera, using c.w. laser illumination 3−35419
impulse water jets at high press., obs. *(Russian)* 3−454
light source for continuous printing of black and white films *(Russian)* 3−3825
plasma, with high electron density, investigation, framing camera use *(French)* 3−9971
recording of high-speed phenomena, advanced techniques 3−35435
remotely controlled Snorkel camera system 3−35434
time lapse cinemicrography apparatus, biological applic. 3−19361
ultrahigh speed, proximity focusing shutter applic. *(French)* 3−9972
X-ray, of laser produced plasma, obs. *(French)* 3−9974
zoom lenses for amateur movie cameras, design problems 3−22399

circuit analysis *see network analysis*

circuit breakers
see also circuit breaking arcs
breakdown due to lightning *(German)* 3−15979
vacuum, arc cathode spot, retrograde motion, obs. 3−17684
vacuum power interrupter, mats. develop. and evaluation 3−25718

circuit-breaking arcs
see also circuit breakers; sparks
physical behaviour, theory and expt. *(German)* 3−23946
plasma physics principles and diagnostics *(German)* 3−23945
in vacuum, arc cathode spot, retrograde motion, obs. 3−17684

circuit oscillations
No entries

circuit reliability
see also quality control
reactor protection system components *(German, English)* 3−7020

circuit resonance
see also circuit oscillations
phase, measurement of magnetic susceptibility of rock in a.c. field, design and testing *(Russian)* 3−3158

circuit theory
see also filters; lumped parameter networks; network analysis
INPUT response to single-turn conductive circuit 3−5470

circuits
see also amplifiers; analogue computer circuits; demodulators; detector circuits; digital circuits; equivalent circuits; integrated circuits; magnetic circuits; modulators; oscillators; power supply circuits; printed circuits; pulse circuits; switching circuits
aerospace instrumentation, radiation effects, conference, Seattle, Wash., USA (1972) 3−17864
contact sparks and vacuum interruption arcs as light sources for vacuum u.v. spectra, improved Akimow circuitry *(German)* 3−14630
for cw n.m.r. measurements 3−16469
d.c. level compensation, microelectrode recording 3−399
deflection, partial linearity correction, superorthicon TV camera scanning meas. system, relative coordinates of astronomical objects *(German)* 3−9631
deflector-generator circuit, of proton synchrotron 3−32127
f.m. telemetering, blood pressure and flow transmitters implantable 3−397
high speed photographic recording for materials shock testing *(German)* 3−15803
Mossbauer spectrometer, electronic block for controlling moving system 3−28700
for neutrons beam pulsing, EG-2.5 electrostatic accelerator 3−32194
nuclear, using p-i-n diodes 3−37700
servo system, analogue-controlled, blood presssure calibration 3−398
spectrometer shielding, automatic control circuit 3−28687
squaring device, for mean-square value measurement of noise signal 3−25640
stabilizing circuit, for intensity of Ar continuous wave laser 3−9964

circular polarisation *see polarisation*

circular waveguides
cut off wavelength, of TE and TM modes 3−10332
H_{21} wave excitation 3−19557
with stratified dielectric filling, parametric radiation of relativistic electron bundles 3−29161

civil engineering
see also building; dams
digital photo map applic. to design problems 3−5998
end-loaded cantilevers with circular, triangular holes, calc. of plane strain plastic yielding 3−32355
laminated glass beams in 4-point bending, experimental and theoretical study of strength 3−32354

civil engineering continued
- multilayer sandwich beams and plates, bending and vibration, finite element analysis 3−26075
- reinforced concrete members, short-time and long-time deflections, calculations 3−6239
- stress, dislocation systems, finite element analysis 3−27027
- structural analysis computer program ISTRAN/PL *(Japanese)* 3−26078
- structures, numerical solution of quadratic matrix equations 3−28906
- underground hydroelectric power plant positioning, rock property determ. using seismic wave velocities 3−9116

classical algebra *see algebra*

classical field theory
- *see also classical mechanics; electromagnetic field theory; gravitation; special relativity*
- $\lambda\varphi^4$ theory, scattering analysis and $SO(4) \times SO(2)$ invariant solns. 3−35753
- acceleration in Minkowski space and generalized version of Newton's second law 3−35584
- Born-Infeld, quantization 3−813
- canonical formalism, finite-dimensional, based on calculus of variations 3−28929
- Coulomb's law and Biot-Savart law, heuristic derivation for teaching approach 3−26
- cylinder with tangential boundary conditions, external magnetic field *(Russian)* 3−10325
- dielectric elastic hollow sphere, large amplitude oscill. 3−556
- inverse square laws, autocorrelation function 3−6298
- non-linear, Poisson bracket definition in multisymplastic formulation 3−28933
- non-relativistic and Euclidean, functional description *(French)* 3−10320
- random field generated by point source random distrib., trajectory characteristics *(Russian)* 3−3997
- SU(2, 2), field representations of conformal group with continuous mass spectrum 3−37782
- transverse tensile stress waves, postulated existence 3−16685
- unbounded field problems, finite element solution, free-space Green's functions 3−6296
- Yang-Mills fields and the minimal electromagnetic interaction principle 3−10586

classical mechanics
- *see also classical mechanics of continuous media; classical mechanics of discrete systems; classical theories of fluid structure*
- analytical, algorithm for problems analysis *(Russian)* 3−22600
- Buckingham π theorem and dimensional analysis 3−20
- centripetal force experiment for students using coat hanger and pennies 3−22221
- conformal invariance of equations of motion in curved spaces 3−22592
- conservation laws, invariant geometrical characterization of ignorable coordinates 3−16604
- dimensional analysis and Buckingham π theorem 3−20
- drag racing, its physics 3−22213
- Fermi quantum systems, classical analogue 3−6310
- general logical scheme of physical systems containing classical and quantum mechanics 3−37790
- impact, of two masses along line of centres, analogue computer modelling *(German)* 3−32302
- inertial motions on rotating sphere *(Russian)* 3−495
- interaction pots. between particles of system, distrib. and true masses *(French)* 3−28841
- invariance groups in classical and quantum mechanics 3−35599
- motion on a half-line, comparison of quantum and classical treatment 3−10337
- nonholonomic systems, generalized inertia forces, kinetic energy applic. 3−19405
- nonlinear problems, extended Kantorovich method applic. 3−19406
- nonlinear systems with transformed argument *(Russian)* 3−28849
- pucks, CO_2 supported, using dry ice, for studying mechanics 3−22226
- quotient spaces 3−35598
- reformulation using Lie derivatives of functions of non-commutating variables 3−13612
- rock thrown in air problem, illustration of L'Hospital's rule for students 3−22220
- systems with Coulombic friction, stagnation conditions *(Russian)* 3−32298
- torque, gravitational between two bodies expressed in terms of external potential fields 3−22595
- transmission angle problem of Alt, for four-bar linkages, computer applic. 3−35565
- turntable system, orbital motion study, demonstration expt. 3−31993

classical mechanics of continuous media
- adhesive fracture analyzed using continuum mechanics 3−7840
- asymptotic theory of thin rectilinear elastic and plastic panels 3−32345
- conservative systems, stability, energy method 3−16617
- continuum model unsuitability for machining description 3−21656
- discretization by finite element anal., determ. of constitutive eqn. and eqns. of motion 3−28844
- doubly curved finite elements for analysis of thin shallow shells with large displacements 3−16616
- echo signal from elastic spherical shell in ideal liq., approx. calc. *(Russian)* 3−19110
- echo signal struct. from rigid sphere in liquid *(Russian)* 3−19111
- elastic laminates, wave propagation using multi-continuum theory 3−3977
- equation of motion soln. of mech. system, nonlinear couplings influence 3−6194
- equation of motion soln. of mech. system with irregular perturbations 3−6193
- film, electrical conduction, continuum percolation theory and Monte Carlo techniques 3−8281
- fluid mixtures, inviscid mechanical theory 3−3942
- geometrically nonlinear plane frames, analysis for finite displacements 3−28860
- heterogeneous systems, spatial macroscopization 3−28851
- least squares criterion in finite element formulation 3−26072

classical mechanics of continuous media continued
- meas. stress calc. method for surfaces oriented in all directions 3−32348
- mechanical interaction, relation between power additivity and stress principle 3−6195
- molecular gas dynamics, boundary conditions, surface shocks, continuum flows, review 3−33261
- non-self adjoint systems of partial differential equations, finite element analysis 3−28852
- nonelastic media thermodynamic and shock phenomena *(French)* 3−6263
- nonlinear eqns. for non-shallow spherical shells stability, limits of applicability for shallow shells *(Russian)* 3−6209
- nonlinear problem for plane continua in Euler's coords. *(Russian)* 3−10271
- orthotropic axisymmetric plates, exact solutions in design 3−3939
- polymer melts, viscoelasticity, continuum mechanics approach 3−7295
- potential operators in Hilbert space, application to conservative systems 3−32305
- pretwisted curved beams of thin-walled open section 3−6197
- rectangular plates of variable thickness, deflection and moment data 3−6198
- review of recent results and developments in theoretical mechanics and mathematical physics 3−16584
- in Riemannian spaces, intrinsic coordinates and integration of indefinite equations 3−16731
- rock masses, continuum mechanical considerations 3−12626
- sandwich beam analysis 3−6228
- snap-buckling of curved membranes, simple math. model with 1 degree of freedom 3−22662
- solids elasticity theory, stability theory and plasticity theory, review 3−16614
- spatial and planar problems, relationship and transition 3−32306
- statistical treatment of macroscopic props., depend. on degree of order *(German)* 3−13573
- thermoviscoplasticity, non-linear variational principle 3−537
- thin plate theory, polygon-circle paradox and convergence 3−10285
- two-liquid systems with asymmetric stress tensors, model construction *(Russian)* 3−28853
- variational principles of thermodynamics and mechanics for stable equilibrium states *(German)* 3−3941
- WC-Co, sintered, cemented carbide, fracture behaviour, continuum mechanics analysis 3−14921

classical mechanics of discrete systems
- *see also N-body problems*
- anisotropic Kepler problem in two dimensions 3−9450
- artificial satellite, calc. of optimal manoeuvre for transition from orbit to landing path *(Russian)* 3−26070
- artificial satellite, soln. of eqn of motion to first order 3−26067
- canonical perturbation method for non-conservative dynamical systems 3−37791
- collisions, elastic, time-reversal invariance, demonstration 3−28439
- comparison of effects of gravitational interaction torques on body and gravity torques exerted by body 3−10265
- composite spacial pendulum, eqns. of motion *(Russian)* 3−13552
- conservative systems, stability and bifurcation of equil. 3−16607
- constitutive eqns. and eqns. of motion 3−19398
- Coriolis effect, demonstration for students by simple problem 3−28
- coupled Duffing eqns., analytic soln. for forced oscillations, Kryloff-Bogoliuboff technique 3−26068
- discretization by finite element anal., determ. of constitutive eqn. and eqns. of motion 3−28844
- dissipative systems, soln. of Hamilton-Jacobi eqn. 3−28847
- disturbing function expansion using summation theorem for assoc. Legendre functions 3−25383
- dynamics of angular motion of solid body with rotating rotor accounting for energy dissipation *(Russian)* 3−13545
- elastic lattice-type shell linear theory, consistant approx. 3−3949
- elasticity, lattice-type shell structs. 3−3948
- Euler eqns. of rigid body motion, simple matrix formulation 3−29
- Eulerian dynamics of rotating rigid body, construction in Hilbert space, reln. to time-independent Schrodinger eqn. 3−19489
- gravity-stabilised gyrostat satellites, non-linear resonant attitude motions, Hamiltonian mech. 3−22596
- Ideal Resonance Problem, soln. using parallel perturbations method 3−37792
- isotropic discretized bodies, wave propag. problems 3−19456
- lever as impedance machining device 3−33
- linear Hamiltonian system, algorithm for canonical transform. to normal form *(Russian)* 3−497
- motion of a heavy particle near Earth's surface, integration of differential equation system 3−19404
- multiple degree of freedom mechanical systems, steady-state forced vibration amplitude determination 3−22678
- multipolar bodies, elasticity theorems 3−19414
- non-linear cascaded spring syst., determ. of response *(French)* 3−494
- non-linear springs connecting unequal masses, calc. of free vibrs. by perturbation method 3−19399
- non-linear two degree of freedom dissipative system, calc. of forced vibrs., and stable regions 3−19400
- nonlinear systems, periodic solns. near to rectilinear normal vibration modes *(Russian)* 3−16613
- normal modes for 2 spring-connected masses with 2 degrees of freedom 3−493
- particle motion in equatorial plane of gravit. monopole-quadrupole field, classifcation 3−35564
- particles with identical masses, integrals for relative motion *(Russian)* 3−500
- restricted problem of 3 bodies, periodic orbits around L_4 libration point 3−37297
- restricted three-body problem, comparison of Encke and Cowell integration methods 3−39596
- review of recent results and developments in theoretical mechanics and mathematical physics 3−16584
- rotating liquid configuration of three or more components, determ. of stability *(Russian)* 3−26071
- rotational dynamics, torque free rigid body, passive stability, discrete tip masses, Skylab 3−496

classical mechanics of discrete systems continued
- sliding mode of motion in systems with collisions *(Russian)* 3−499
- stabilisation of stationary motion by controlling part of variables *(Russian)* 3−16612
- stability of positional equil. of solid body with cavity containing fluid *(Russian)* 3−498
- steel ball on oscillating brass plane, periodic impact 3−26069
- structure calcs., static and dynamic analysis, new approach 3−16608
- surge waves in stranded springs 3−6192
- systems of solid bodies, eqns. of motion *(Russian)* 3−13551
- three-axial ellipsoid, stability of libration points in first approximation under perturbations *(Russian)* 3−16095
- three-body problem, classification and single-valued definition of states *(Russian)* 3−28121
- two finite body problem. first order perturbations 3−3937
- two-body problem with corpuscular radiation, effects of particle trajectory curvatures 3−28119
- uniform disc motion, application of extended Hamilton-Jacobi integration method *(Russian)* 3−16602
- variable length pendulum, stability under support-point acceleration *(Russian)* 3−32300

classical theories of fluid structure
- *see also kinetic theory*
- hard sphere fluid with attractive square wells, spatial struct. and thermodynamic props. 3−26182
- Percus-Yevick integral eqn. for dense fluids (Ar, Kr, Xe) using Kihara potential 3−17483
- Percus-Yevick theory, with Kihara potential, determ. of correlation functions 3−17484
- three-dimensional fluids, asymptotic props. of autocorrelation functions and Enskog expansion 3−28995
- van der Waals interaction between inert gas atoms in dense classical fluid 3−17384

classification
- *see also indexing*
- BCD stellar classification system rel. to spectral type and absolute magnitudes *(French)* 3−25443
- electro-optical media suitable for frequency-shift devices 3−19644
- Feynman diagrams in high energy phys. 3−816
- low energy electron diffraction theory *(Czech)* 3−11784
- phase transitions, using struct. stability math. theory 3−7905
- polarography, stationary electrode, doublet peak detection, pattern classification 3−22400
- sound envelope/frequency connection 3−25620
- uniform cosmological models 3−3290

clathrates *see molecules; organic compounds*

clay
- aluminosilicates, statistical mechanics and anomalous swelling rel. to electrolytes 3−21752
- bentonite clay, internal friction peaks due to adsorbed and capillary water 3−21754
- clay-water systems, thermal and elec. props., press. induced changes 3−2856
- determination of quartz by X-ray diffraction *(French)* 3−13496
- determination of quartz by X-ray diffraction *(French)* 3−13498
- disperse systems, sand-water, clay-water, state of water, n.m.r. studies 3−39396
- fault clay, chracteristics and origin 3−27959
- initial stage of chemical explosions with ejection in moist clay *(Russian)* 3−12510
- kaolin deposit from Tanzfleck/Oberpfalz, geological and petrographic investig. *(German)* 3−12565
- kaolinite minerals, thermodynamics aspects of montmorillonite formation 3−15763
- kaolinite-illite-quartz mixtures, high-temp. refiring and ceramic props. 3−15751
- kaolinites of good brightness, viscosity meas. 3−15791
- mineral composition of Melbourne brickmaking clays 3−15762
- mineralogy of N. Sea drift 3−2949
- minerals, dioctahedral layer silicates crystallochem. 3−15860
- minerals in late Quaternary deposits of Sea of Azov 3−31354
- sandy-clay deposits, hydrogeologic investigations using induced potentials method for finding groundwater 3−25315
- specific surface determ., review *(Polish)* 3−25149
- undrained clay strength, deep sea vane shear device for torque meas. 3−3250
- $BaTiO_3$ ceramics, sinterability improvement 3−21721

cleaning *see surface treatment*

cleanliness *see hygiene*

cleavage, crystal *see crystal cleavage*

Clebsch-Gordan coefficients
- *see also elementary particle theory; nuclear theory*
- complex ang. momentum coeffs. 3−26278
- reduction to binomial expansion 3−4272
- review of mathematical aspects *(Russian)* 3−590
- SL(2,C), determ. of coeffs. for tensor products of irreducible unitary representations 3−32418
- transformation matrix, U_n group, unitary and orthogonal subgroups *(Russian)* 3−35848
- vector coupling coefficients as products of prime factors, computer program 3−10258
- Wigner (9-j) symbol, application of Regge transposition symmetry 3−29179

climatology
- *see also atmospheric humidity; atmospheric precipitation; sunlight; wind*
- agrotopoclimatology, meteorological criteria for mobile surveys 3−9284
- air mass seasonal redistrib., effect on earth's rotation *(Russian)* 3−39523
- airblast propagation effects, long range 3−3028
- asynoptic reports from satellites, minimization of data set for global analysis and macroscale weather forecasting 3−9394
- atmospheric large scale response to 1964-65 Pacific equatorial warming 3−27980
- climatic influence of human activities since Industrial Revolution *(French)* 3−21956
- cloudiness as climatic feedback mechanism, effects on radiation balance and surface temp. 3−28019

climatology continued
- Early Tertiary climate dependence on continental position 3−3014
- East Africa, consequences of climate cycles 3−34899
- England and Wales, cyclonic-type rainfall and atm. mean-sea-level press. for 1950-69 period 3−34896
- glacial cycle and geological records of climatic events 3−39533
- glaciological responses to climate in easter Baffin Island 3−39534
- global climate effects of ice sheet growth, dynamics of ocean-cryosphere system 3−39501
- global climate rel. to stratospheric aerosol meas. 3−25205
- global future climate, effect of man's activities 3−18869
- Gulf of Mexico cores, faunal evidence of abrupt palaeoclimatic change 3−39538
- Holocene period in South Atlantic, climatic fluctuations rel. to diatoms in deep-sea cores 3−39535
- Hudson River Valley, turbulence climatology concept rel. to low wind turbulence statistics and pollutant diffusion estimates 3−25211
- India, palaeoclimate from palaeobotanical evidence in Tertiary period 3−31384
- interglacial and postglacial climates rel. to pollen records 3−39532
- interglacial climates, Antarctic ice surges and sea level rises 3−39540
- magnetic intensity variations correlated with climatic changes in the 1925 to 1970 period 3−25250
- North Atlantic deep-sea core V23-82 rel. to interglacial climatic events 3−39537
- North Atlantic Ocean, salinity reduction rel. to next Glacial period 3−39502
- palaeoclimatic significance of $^{18}O/^{16}O$ ratio in deep ice cores at Camp Century, Greenland 3−39539
- paleoclimate and historic climate, multiple thermometry 3−9275
- paleoclimatology, review 3−9291
- Present Interglacial, conference (Rhode Island, 26-7 January 1972) 3−39570
- Present Interglacial and Future Ice Age, climatic conditions 3−39536
- qualitative theory of climate behaviour, based on system theory 3−39544
- quaternary hypsithermals rel. to $^{18}O/^{16}O$ ratio of deep-sea cores 3−39542
- relationships among precipitable water, saturation thickness and precipitation 3−37214
- secular climatic changes rel. to variable solar output, gravity and geomagnetism 3−39541
- subtropical region, solar radiation climate, estimates 3−28031
- Tatra Mountains, climatic zoning from Czech observations *(German)* 3−12703
- tropospheric dust heating effects, dust storms 3−25247
- urban thermal regimes, mapping and modelling of land use effects 3−37216
- zonally averaged macroclimate of southern hemisphere, global equilibrium solutions 3−12733

clock paradox *see special relativity*

clocks
- *see also atomic clocks; chronometers; time measurement*
- circumnavigating, relativistic behaviour 3−19503
- counter MH 7490 comprising flip-flops *(Czech)* 3−16525
- electric, loudness evaluation 3−3453
- watch mechanisms, historical development 3−16532

closed loop control systems *see closed loop systems*

closed loop systems
- *see also feedback*
- laser pulse duration control, nonlinear absorption in semiconductors *(Russian)* 3−215
- micropositioner, for cell membranes 3−22528
- optical tracking telescope, combined open/closed loop and adaptive compensation 3−39760
- pitch and formant frequency transitions, model 3−3429
- spaceborne telescope mirror figure modal control 3−31819

cloud chambers
- computer-controlled, expts. on search for quarks in EAS 3−16086
- diffusion, design and construction for demonstration purposes 3−28680

cloud physics *see clouds*

clouds
- *see also atmospheric precipitation; nucleation; sky*
- Arabian Sea, during winter 3−2996
- Arabian Sea, southwest monsoon, average forenoon cloud cover 3−2991
- artificial, anal. of upper atm. clouds prod. by rocket expts. 3−39543
- artificially ionized clouds in upper atm., motion determ. 3−34932
- Asia and Africa, tropical belt, satellite radiometric meas. 3−2993
- atmosphere, artificial formation 3−12770
- Bay of Bengal, mean clouding during 1968 and 1969 July and August 3−2992
- brightness data applied to tropical wave disturbances 3−25236
- brightness data rel. to meso-to-subsynoptic scale rainfall pattern 3−28047
- brightness patterns, upper air circulation, 1967 southwest monsoon 3−2982
- cirriform, over India, during winter 3−2995
- cirrus canopy, upper tropospheric outflow, severe storms, satellite pictures 3−2985
- cirrus generating cells, props. determ. from particle size spectra 3−25231
- climatic feedback mechanism, cloudiness effects on radiation balance and surface temp. 3−28019
- cloud physics, a biography of Luke Howard 3−9299
- convective, evolution effects of vertical wind shear *(Russian)* 3−21940
- convective cloud elements, characteristic scaling for rain clouds *(Russian)* 3−18858
- cumuli, liquid H_2O content, cloud characteristics *(Russian)* 3−12717
- cumulonimbus, electrification of thunderstorms and formation of precipitation 3−37220
- cumulus, drag coeff. determ. *(French)* 3−2972
- cumulus and cumulonimbus in high latitudes, Greenland photographs 3−9301

clouds continued
depression movements, southwest monsoon, cloud distrib. patterns 3-2988
droplet growth, stochastic coalescence model 3-31371
droplet spectra, Monte-Carlo simulation model for temporal development 3-25225
droplets and drizzle drops over Mauna Loa-Mauna Kea saddle road of Hawaii, USA, electric charge 3-12726
electrical stimulation of warm clouds for droplet coalescence *(Polish)* 3-25330
electrostatic field within structure of unfirformly spaced coaxial conducting loops 3-31382
over equatorial Indian Ocean, distributions 3-5500
Europe/Northeast Atlantic region, satellite and surface estimates of cloud cover above 4/8, sources of error *(German)* 3-9287
heavy convective clouds, spectral structure of the turbulence 3-34883
Hungarian theoretical meteorological studies of cloud physics *(German)* 3-12704
ice and water contents, remote meas. from Raman scattering 3-9399
ice cryst. formation in supercooled regions at warm temps. 3-25227
ice cryst. growth in supercooled H_2o droplets by diffusion, numerical simulation 3-25226
ice-forming ability rel. to formation conditions of AgI nuclei, stoichiometric ratio effects 3-25228
India, active monsoon, satellite radiation data 3-3000
over India, annular formation, satellite obs. 3-2978
i.r. meas. by Kosmos 384 at 0.8 cm. and 10-12 μ *(Russian)* 3-39517
large scale systems, vertical motion, diagnostic study 3-2986
latent heat of condensation from cloud clusters in atmospheric intertropical convergence zone *(Russian)* 3-34891
light propagation, low angle approx. *(Russian)* 3-3009
macron clouds, charging and discharging, role of gas breakdown 3-35657
mapping, automatic, from cloud cover pictures 3-5541
Mexico, cloudiness meas. and suitability for astron. sites 3-37203
monsoon depression, satellite pictures, cloud patterns 3-2987
monsoon depression centre, satellite picture determ. 3-2989
motion computation from photographs 3-3172
multiple scattering of laser pulses transmitted through clouds 3-22844
NASA-MPE Ba ion cloud experiment, cylindrical shell computer model 3-34920
noctilucent, brightness contrast and visibility in twilight sky *(German)* 3-12712
noctilucent, spectrophotometric meas. of near i.r. spectra 3-28010
particle diffusive ion charging, kinetic eqn. *(Russian)* 3-39526
particle size distrib. formula, comparison with Γ-distrib. *(Russian)* 3-21942
plane-stratified, optical sounding, statistical estimation of light pulse deform. *(Russian)* 3-29041
pressure perturbation rel. to temp. and saturation v.p., numerical modelling 3-25224
pulsed lidar reflectance, comments 3-25207
pulsed lidar reflectance, discrepancy between meas. and calcs. 3-21934
radiation properties between cloud layers in atmosphere rel. to temp. distributions *(Russian)* 3-18859
rainfall mechanism from droplet clouds *(Russian)* 3-3010
satellite observations, conference, Poona, India (April 1970) 3-2977
satellite pictures, upper tropospheric winds 3-5502
seeding, downwind and upwind effects, Arizona, USA 3-39531
seeding using Portland cement 3-37229
spectral brightness, probability distribution in 2-5 micron range *(Russian)* 3-39522
streaming media, size of stationary space charge clouds 3-651
thundercloud electrification, polarization charging effects 3-5506
tracking, digital picture processing 3-3198
transparency, nephelometric determination *(Russian)* 3-13291
tropics, large scale flow patterns, Indian southwest monsoon 3-2980
tropics, large scale flow patterns, satellite determined cloudiness 3-2981
tropics, satellite obs., relation to dew point temps. 3-2979
western disturbances, winter season 3-2994
AgI particles, freezing action on water drops in aerosol *(Bulgarian)* 3-9303
Ba, in ionosphere, onset of striations 3-9318
Ba cloud in auroral ionosphere rel. to electron intensity, rocket flight obs. 3-12785
BaO fluorescent scattering by sunlight at 106 km, electronic transition moment of the $A^1\Sigma$-$X^1\Sigma$ band system 3-17424
NH_3 effects on electrification of freezing and splashing water drops 3-27106

Clusius-Dickel columns *see isotope separation*

cluster model (nuclear) *see nuclear cluster model*

clusters, stellar *see stellar clusters*

coal
see also mining
coal measure rocks, weathering influence on composition and engineering properties 3-5443
dynamic deformation due to sorption processes *(Russian)* 3-13223
SEM exam., 'organically bound' iron concept 3-37771
slurries, quality control by spectrophotometric method *(Russian)* 3-28771
Vicker's indentation hardness, effect of load 3-5445

coating processes *see coating techniques*

coating techniques
see also corrosion protection; electrodeposition; electrophoresis; electroplating; protective coatings
airless spray painting, safety measures to avoid igniting sparks 3-661
antireflection coatings on glass, high vacuum *(Rumanian)* 3-22337
ceramic, tungsten coating by reduction of WS_2 3-37084
chemical vapour deposition, applic. to W 3-1960
corrosion and oxidation 3-8035
fused salt diffusion, book contrib. 3-11814

coating techniques continued
glass, invisible, layered systems 3-19190
glass, non-silicate, coating with antireflection and water vapour protecting layers 3-25744
IFS25, IKS27 glass protective coatings for optical filters vacuum deposition *(Russian)* 3-5916
photochromic, in nondestructive testing 3-27827
plasma flame spraying for hard coating of critical surfaces 3-38503
polymer substrates, principles of adhesive bonding 3-12456
powder coatings, plasma jet efficiency in spraying *(Russian)* 3-27724
vapour deposition in vacuum, heat transfer 3-2631
As_2S_3 glass, clearing coatings production MgF_2 film deposition by thermal evaporation *(Russian)* 3-5904
Si_3N_4 pyrolytically deposited film passivation of GaAs and Si substrates 3-18555
TiO_2, reflective layers on glass, aerosol spray deposition technique 3-22339
ZrC, coating microspheres of nuclear reactor fuel, technique 3-11059

coatings, protective *see protective coatings*

coaxial cables
errors caused by radiation and temp. on d.c. readout 3-17289
gas-discharge noise generator loaded with helical coaxial line, theory 3-26902
layered dielectrics, attenuation charact. rel. to permittivity and dielectric thickness *(Japanese)* 3-26107

coaxial lines *see coaxial cables*

cobalt
Apollo 15 lunar soil samples, metallic particles of high Co content 3-35080
atom, Auger and photoelectron spectra, L_2 and L_3 vacancy states width 3-29512
composite, metal matrix/fibre reinforced, solidified, Piobert-Luders band deform. *(French)* 3-39391
Curie temp., pressure variation 3-2276
densities of unfilled one-electron levels, X-ray continuum isochromat study 3-36536
diffusion and solubility in GaAs 3-33699
diffusion in Co-Si system, rate of reaction, high press. eff. *(Russian)* 3-7962
diffusion in Cu, isotope effect 3-7965
electrodeposited, effect of I^- ions on phase structure and preferred orientation of crystallites *(Bulgarian)* 3-30366
electrodeposited films, effect of I^- ions on mag. props. *(Bulgarian)* 3-30670
electrodeposition, influence of organic additives *(German)* 3-12523
electronic structure calcs. for paramag. and ferromag. Co., exchange energy contrib. 3-36515
ferromagnet, current-carrying states rel. to spin polarization in photoemission 3-18533
film, effect of ang. dispersion of anisotropy on reson. linewidth *(Russian)* 3-8452
film, electroless, nucleation and growth, electron microscope obs. 3-11837
film, electron energy loss spectrum 3-17885
film, Hall effect rel. to H_2 and O_2 chemisorption 3-15278
film, monocryst., Hall effect and elec. cond. *(Russian)* 3-18120
film, oxidation mechanism 3-27196
film, perpendicular anisotropy, rot. moments, superparamag. particles *(Russian)* 3-30641
internal friction peak at 300°C rel. to lattice defects 3-30208
liquid, electrolytic deoxidation at 1600°C 3-5313
magnetoresistance and open orbits domain, rel. to Fermi surface 3-18074
in Mundrabilla meteorite shower, X-ray fluorescence spectrometry 3-5452
neutron capture γ-rays, spectral enhancement 3-5455
particles, oxid., electron microscope obs. of oxide-metal boundary 3-15076
photographic development by deposition on layers containing precious metals *(Russian)* 3-238
quartz: Co^{2+}, impurity absorpt. near 78μ band 3-5216
scanning electron microscopy, Kossel lines, magnetic domain contrast 3-2320
single-domain powders with cubic anisotropy, mag. props. *(Russian)* 3-15390
spin polarisation of electrons tunnelling from Co ferromag. to Al superconducting film 3-15311
sublimation, in range including Curie point, 1320-1410K *(Russian)* 3-8365
thermoelectric power meas. near melting point 3-18128
thin fulm, electrical resistivity, Mayadas-Shatzkes model 3-27240
vapour press. and heat of vaporization 3-4851
wettability of melt on graphite and glasslike carbon substrates, catalytic graphitisation 3-11796
X-ray K-absorption spectra *(Russian)* 3-18509
CaO:Co, Fe, Mossbauer study of ^{57}Fe rel. to dynamical Jahn-Teller effect 3-24639
CdSe:Co, degenerate discrete excited states, absorpt. and photocond. spectra obs. 3-2024
β-Co, stacking fault role in martensite phase formation from FCC struct. *(Russian)* 3-2699
$Co{:}^{51}V(^{103}Rh)$, meas. of relaxation rates rel. to impurity band structure 3-5147
Co-WC, sintered, cemented carbide, fracture behaviour, continuum mechanics analysis 3-14921
Co^{2+}, in H_2SO_4 vitreous aq. soln., effect on spin-lattice relax. of H atoms 3-34186
Co^{2+} ions, relaxation in $Mg_{1-y}Co_yFe_2O_4+\gamma'$, ferrite single crystals with different inversion degrees 3-15379
Co^{3+} ions in garnets, spin Hamiltonians for $3d^n$ ions in tetrahedral symmetry 3-38934
^{59}Co films, nuclear mag. levels inverted state 3-30628
^{60}Co contamination in pharmaceutically prepared ^{59}Fe solutions 3-407
^{60}Co gamma radiation build-up effects, use of LiF dosimetry *(German)* 3-5681

cobalt continued
^{60}Co tangential breast therapy, analysis of skin reactions 3−13150
Fe:Co, ^{57}Fe c.w. n.m.r. spectra obs. of hyperfine field at impurities 3−21326
Fe:Co, temp. depend. of hyperfine fields, c.w. n.m.r. obs. 3−21327
Fe-Zn supersaturated solid solution, influence on the precipitation behaviour *(German)* 3−2694
$FeSi_2$:Mn, Co, semiconductor-metal transition resist., thermoelec. and Hall effect obs., 300-1400 K 3−33973
KCl:^{57}Co, ^{57}Fe, Mossbaur obs. of colour centres 3−15447
K_2SO_4:Co^{2+}, cond. by cation vacancies 3−36607
NH_4Cl:Co^{2+}, Ni^{2+}, Cu^{2+}, light absorpt. by impurity centres, cryst. field parameters 3−21456
NaCl:^{57}Co, ^{57}Fe, Mossbauer obs. of colour centres 3−15447
inSi, gettering by ion-damaged surface layers 3−5276
β-, substrate for Cu epitaxial growth, lattice defects *(Russian)* 3−8049
TiC/Co cermets, Vickers hardness under reduced charge, comp. depend. *(French)* 3−24971
WC/Co, aging process, calorimetric studies *(Japanese)* 3−31066
WC/Co, sintered, carbide phase recovery *(Japanese)* 3−31121
WC/Co cermets, Vickers hardness under reduced charge, comp. depend. *(French)* 3−24971

cobalt alloys
(rare earth-misch metal)-copper-cobalt, chill cast, heat treatment effect on permanent magnet props. *(Japanese)* 3−34562
Alnico, domain structure variation in partial hysteresis cycles 3−30664
enthalpy meas. on the allotropic transformations *(French)* 3−17976
eutectic composite, fibre-reinforced M-M_7C_3, (M=Fe+Co+Cr), $M_7C_3 \rightarrow M_{23}C_6$ transform. 3−31143
hard rare earth-Co_5 alloys, physical quantities, manufacturing methods *(German)* 3−15384
Inconel alloy films, optical constants meas. 3−30790
Kovar, thermal expansion and magnetostriction, below 50K 3−5123
oxidation, chemical composition of oxide scale, X-ray fluoresc. obs. 3−36491
Permendur, 2V, hot-rolled sheet, order-disorder transform. mechanism *(Japanese)* 3−8865
rare earth Co_{17}, ferrimag., rare earth contrib. to mag. anisotropy 3−34151
rare earth Co_5, ferrimag., rare earth contrib. to mag. anisotropy 3−34151
rare earth cobalt permanent magnet alloys, magnetisation, anisotropy and coercivity, review 3−24595
rare earth-cobalt compounds, Ho_2Co_{17} and Er_2Co_{17}, cryst. struct. 3−17760
relaxation, real structure and migration props., magnetic after-effect obs. *(Polish)* 3−24212
superalloys, σ-phase susceptibility prediction using modified system 3−37029
Superinvar, thermal expansion, alloying effect, γ-phase stability 3−27699
Superinvar prep. and characteriz. 3−24945
Ticonal, high-coercivity, characteriz. after isothermal thermomag. treatment 3−24943
Ticonal alloy, lattice conjugation of metastable tetragonal phases 3−31009
Vicalloy, domain structure variation in partial hysteresis cycles 3−30664
Vicalloy 1, phase transforms. *(Russian)* 3−30965
Al-Al_9Co_2 eutectics, directionally solidified, struct. morphology and microhardness *(Russian)* 3−39328
Au-Co, quasielastic neutron scattering cross section for paramag. impurities 3−5095
$(Co, Fe)_{17}R_2$ [R=rare earth, La, Y], magnetic symmetries and domains 3−18340
Co-(20)Ni-(18)Cr-(2)ThO_2, microstructure and mech. props. on dispersion hardening 3−8782
Co-(20)Ni-(18)Cr-(4)ThO_2, microstructure and mech. props. on dispersion hardening 3−8782
Co-(2)ThO_2-(0.2)Zr, microstructure and mech. props. on dispersion hardening 3−8782
Co-(4)ThO_2, microstructure and mech. props. on dispersion hardening 3−8782
Co-C, h.c.p., disaccommodation, mag. aftereffect study 3−5121
Co-CoAl-Ni, oriented eutectic, morphology rel. to Ni addition *(French)* 3−34523
Co-Cr based superalloys, dispersion strengthening for high temp. applics. 3−31112
Co-Cr sigma phase detection by electron microscopy 3−8811
Co-Cr-C system, crystallisation of 2-4 phase composite structures *(German)* 3−8776
Co-Cr-Ni-Ta, directional solidification, interdendritic structures 3−37031
Co-Cr-W alloys, phase equilibrium at 1350°C, with emphasis on R-phase 3−15659
Co-Cr(21 wt.%) with Y_2O_3 dispersion, Cr diffusion, substruct. influence 3−39343
Co-Elinvar, meas. of thermal expansion and Young's moduli in 150-500°C range, obs. rigidity modulus of polycrystal *(Japanese)* 3−17896
Co-Er intermetallic, struct., disordered substitutions 3−1603
Co-Fe, double h.c.p. structure from X-ray diffraction study, rel. to mag. props. 3−1600
Co-Fe, mag. moments depend. on comp., effect of h.c.p. to double h.c.p. structural transition 3−30607
Co-Fe, X-ray K-absorpt. spectra *(Russian)* 3−18509
Co-Fe-Be, age hardening, hardness-controlling additions *(German)* 3−8901
Co-Fe-Be, mag. and mech. props with annealing and cold drawing *(Japanese)* 3−12398
Co-Fe-Nb, semihard mag., anisotropy 3−21261
Co-Fe-Nb, semihard mag., characteriz. 3−21279
Co-Fe-Nb, semihard magnetic, anisotropy *(Japanese)* 3−18334
Co-Fe-Ni mated film (bifilm) plated wire element, effects of process variables 3−12041
Co-Fe(Co-rich) alloys, temp. dependence of single crystal elastic constants 3−38605

cobalt alloys continued
Co-Ni, Curie temp., pressure variation 3−2276
Co-Ni, flow stress rel. to mag. field, domain wall dislocation interactions 3−5125
Co-Ni, photostimulated exoelectron emission, temp. depend. 3−30921
Co-Ni-P layers, chem. deposited, mag. anisotropy field *(French)* 3−8404
Co-Ni-Ti, morphology and decomp. kinetics, electron diffr. obs. *(Russian)* 3−21581
Co-Ni(10)-(2)ThO_2-(0.2)Zr, microstructure and mech. props. on dispersion hardening 3−8782
Co-P film, high-coercivity, domain struct. and reversal processes 3−24592
Co-Pd, interdiffusion coeff., Curie temp. phenomena 3−20899
Co-Pt, high coercivity rel. to struct., electron microscope study *(Russian)* 3−8779
Co-Sn, dilute ferromag., two current cond. and impurity resist. 3−36719
Co-Ti, preliminary study by field ion microscope 3−27635
Co-Ti(Zr)(Fe) systems, TiCo, ZrCo and FeCo phases, X-ray emission study *(Russian)* 3−15572
Co-W-Ti, second phase precip. phenomena *(Russian)* 3−24846
Co-WC, deform. phenomena meas. using new electron microscope replica locating technique 3−18674
Co-Y-Fe, mag. props., moment values at 4.2K 3−2294
Co-Y-Ni, mag. props., moment values at 4.2K 3−2294
Co_5-Sm permanent magnet alloy, sintered anisotropy parameters and coercivity 3−5097
β-CoAl, low temp. magnetic behaviour 3−34098
$CoFe_2$ film, oxidation mechanism, ferrite film form. 3−27196
β-CoGa, low temp. magnetic behaviour 3−34098
Co_3Nb, phase thermodynamic stability, electrochem. determ. 3−2691
CoNi:Mn, n.m.r. of ^{55}Mn, local moments obs. 3−36799
CoNiFe film, domain wall motion rel. to low freq. creep 3−36738
Co_5Pr, splat-cooled, obs. of dislocations 3−8791
CoPt, ordered, plastic deform. influence on structural state and coercive force *(Russian)* 3−18338
$CoPt_3$, long-range order and ordering kinetics 3−34506
$CoPt_3$, partially ordered, field-ion microscopy and X-ray diffr. obs. 3−14738
$Co_{17}R_2$ [R=rare earth, La, Y], magnetic symmetries and domains 3−18340
Co_7R_2 [R=rare earth, La, Y], magnetic symmetries and domains 3−18340
CoSb, elec. resist., Seebeck coeffs., rel. to comp. defect clustering 3−18124
$CoSb_3$, crystal-chemical props., detn. by Mossbauer spectroscopy *(Russian)* 3−7660
CoTi phase, density comp. depend. 3−39337
Co_5X, X=rare earth, domain wall energy, polarized light metallography obs. 3−5118
Cu/Kovar/Cu three-layer band, expansion coeffs. determ. 3−27700
Cu-Co, cell structure formation with Bridgeman growth method 3−11571
Cu-Co, precipitation hardened, mech. props., effect of Nb additions 3−8881
$DyCo_2$-$DyAl_2$, struct. and mag. studies 3−18323
Fe-^{57}Co dilute alloy, hyperfine field nonalignment under mag. saturation, meas. at 25 mK 3−24565
Fe-Co, alloying effect on hydrogen diffusion in α-Fe 3−1829
Fe-Co, deviation from additivity rules, X-ray absorpt. obs. *(Russian)* 3−12337
Fe-Co, ordering process, mass spectrometric obs. of secondary ion emission *(Russian)* 3−33490
Fe-Co alloys, Si influence on friction and wear 3−7846
Fe-Co single-domain powders with cubic anisotropy, mag. props. *(Russian)* 3−15390
Fe-Co-Mn, cold worked, strain gauge factor and elec. resist. meas. *(Japanese)* 3−12399
Fe-Co-Ni-Al-Ti-Cu, thermomag. treatment effects *(Russian)* 3−8386
Fe-Co-V, Mossbauer spectra temp. depend., mag. transform. of γ phase *(Russian)* 3−30731
Fe-Co-V, permendur type alloy, long-range order effect on low temp. deform. 3−30189
Fe-Co-V(2 wt.%), ordered, h.p. prestrain effect on fracture stress and yielding 3−37061
Fe-Cr-Co containing Si, permanent mag. material, mag. props. 3−36746
Fe-Cr-Co-Mo alloy, precipitation, structural and kinetic features 3−8787
Fe-Mn-Co, cold rolled, heat treatment effect on mag. props. *(Japanese)* 3−31077
Fe-Ni-Co, Mossbauer study of Fe mag. moment 3−2471
Fe-Ni-Co and Fe-Ni-Co-Mo(W), redistrib. of alloying element atoms, effect of Co, Mossbauer obs. *(Russian)* 3−5294
Fe-Ni-Co-Al-Ti, temp. depend. of mag. moment, superparamag. props. *(Russian)* 3−8342
$Fe_{1-x}Co_x$, bcc alloy, electronic struct., CPA calc. 3−11999
$Fe_{1-x}Co_xAl$ solid solns., lattice parameter, elec. resist., Hall coeff., thermo-e.m.f., mag. susceptibility *(Russian)* 3−30087
Fe−Co(3.18-42.5 wt%), Zener relax. 3−24213
Gd_3Co, antiferromag. props. and structure 3−21232
Ge-Co, liquid state, resistivity, theory 3−8147
$HfCo_2$, Laves phase, single phase region, mag. suscept. 3−27360
$HfCo_2$, occurrence of Laves phases, X-ray, differential and microstruct. analysis *(Russian)* 3−12334
$HoCo_2$, hyperfine specific heat meas., mag. moment determ. 3−34123
$Ho(Fe_{1-x}Co_x)_2$, Mossbauer obs. of Laves phases 3−36820
L-605 at 1180°F, cyclic creep-rupture behaviour 3−18650
Mn-Cu-Co nonmag. Elinvar-type alloys characteriz. 3−37074
Mn-Ni-Co elinvar-type alloys, meas. of Young's moduli at −150-400°C and rigidity moduli and hardness at room temp. *(Japanese)* 3−17897
Ni-Co, cyrstalline, athermal weakening effect during cold plastic deform. 3−33599
Ni-Co, f.c.c., stacking fault effect on cyclic deform. curve 3−7825

cobalt alloys continued
Ni-Co, superlattice form. in fatigue specimens 3−8808
Ni-Co, wear due to dry friction, stacking fault energy and elastic modulus effects *(Russian)* 3−7844
Ni-Co alloys, dislocations by X-ray crystallography *(German)* 3−30123
Ni-Co film, electrodeposited, stripe domains *(Russian)* 3−30667
Ni-Co layers covering Cu wires, mag. and mech. treatment effect on mag. props. *(Rumanian)* 3−12043
Ni-Co-Al, phase transform. on heating *(Russian)* 3−8831
Ni-Co-Fe-SiO system, bilaminar ferromag. films, field of interaction *(Russian)* 3−21267
Ni-Co-P film, cylindrical, anisotropy dispersion meas. *(French)* 3−25819
Ni-Co-(2.5 wt.%)Al_2O_3 alloys, creep, behaviour 3−8870
Ni-Zn-Co ferrites, mag. permeab. and losses, freq. and temp. depend. 3−15395
Pd-Co, dil., ferromag. transition temp., resist. study 3−30624
Pd-Co dil. alloys, ^{57}Fe hyperfine field press. depend. up to 180 kbar 3−18306
ScCo, electronic structure, stability investigation by self-consistent KKR method 3−15335
$SmCo_4$, cryst. growth, Bridgman technique 3−12269
$SmCo_5$ powder, coercivity, grinding duration and method influence *(Russian)* 3−27731
Sm_2Co_{17}, Czochralski growth in thermal imaging furnace 3−12295
$Sm_{0.5}Pr_{0.5}Co_5$ strongly textured magnet prep. from magnetically anisotropic powders *(Russian)* 3−39375
Ta-Co, anal. of phase diagram *(Russian)* 3−12339
Ti-Al-Co ternary system, Ti rich region, annealing, melting points, structure 3−24836
VC-Co, grain growth during liquid phase sintering 3−18683
WC-Co, struct. changes on heating, emission electron microscope obs. 3−18574
WC-Co alloy, transition metal carbides as grain growth inhibitors *(German)* 3−24973
WC-Co hard alloy strength depend. on Co content *(Russian)* 3−15768
Y_2Co_{17}, Czochralski growth in thermal imaging furnace 3−12295
$Y(Fe_{1-x}Co_x)_2$, Mossbauer obs. of Laves phases 3−36820
$ZrCo_2$, occurrence of Laves phases, X-ray, differential and microstruct. analysis *(Russian)* 3−12334

cobalt compounds
see also cobalt alloys
boracite, growth by modified Schmid three crucible technique 3−2634
carbide fibre-reinforced composite, M-M_7C_3 eutectic, (M = Fe + Co + Cr), $M_7C_3 \rightarrow M_{23}C_6$ transform. 3−31143
$Co_xNi_{(1-x)}O$, single crystals, thermal diffusivity in the region of continuous phase transition 3−4892
complexes, 2p photoelectron lines, multiplet splitting evidence 3−12209
garnet, mag. ordering in octahedral lattice *(Russian)* 3−12024
nitrosyl complexes, crystal struct. *(French)* 3−7701
silicides, ultra-soft X-ray spectra analysis *(Russian)* 3−30893
Tutton salts, direct and Raman spin-lattice relaxation 3−27410
$[Co(NH_3)_4](ReO_4)_2$, crystal structure, vibrational and electronic spectra, magnetic properties *(German)* 3−30099
CaO, long-range magnetic order from neutron scattering meas. and theory comparison 3−2288
$Cd_{1-x}Co_xFe_2O_4$, paramag. region, elec. field gradients, Mossbauer obs. 3−34268
$(Co_x,K_{1-x})M_2(SO_4)_2.6H_2O$, field depend. Raman relax. processes 3−2364
Co complex, $[Co(NH_3)_6][Ge(C_8H_6O_5)_3]_3$, i.r. spectra *(Russian)* 3−26673
Co complex, acetylacetonate cobalt (III), LCAO calc. of u.v. and visible absorption spectra 3−20137
Co complex, $Co_3(C_5H_5)_3S_2$, cryst. struct., 293 and 130K 3−14770
Co complex, $CoNO(S_2CNMe_2)_2$, cryst. struct. 3−14776
Co complex, $Co(NO_3)_2.10CO(NH_2)_2$, cryst. struct. *(Russian)* 3−4737
Co complex, $Co(NO_3)_2.2CO(NH_2)_2.4H_2O$, cryst. struct. *(Russian)* 3−4738
Co complex, trispyrrolidylcarbodithioate:Fe Mossbauer spectra 3−24635
Co-Si, form. of aligned composite material by solid state decomposition 3−24976
$CoAl_2O_4$ powder, X-ray diffr. line integrated intensity changes, effective Debye parameter rel. to lattice strain 3−33424
Co_2B, n.m.r. study, hyperfine field and quadrupole coupling meas. for Co^{59} 3−12077
$Co_3B_7O_{13}Cl(Br)(I)$, growth by chem. transport reaction, effect of different growth conditions *(Russian)* 3−15606
CoBr molecule, visible emission spectrum 3−20130
$CoBr_2.6H_2O$, antiferromag., isotope effects, p.m.r. 3−2421
$CoBr_2.6H_2O$, magnetic susceptibility meas. 3−38977
$CoCO_3$, magnetisation density and magnetic structure at 4.2 K 3−38984
$CoCl_2$, lattice vibrations, i.r. and Raman spectra 3−30813
$CoCl_2.2H_2O$, AC susceptibility meas., mag. phase diagram and relax. times at antiferromag.-ferrimag. transition 3−30626
$CoCl_2.2H_2O$, proton spin lattice relax. by Ising spin excitation 3−21337
$\alpha CoCl_2.2py$, cryst. phase transition, Mossbauer obs. 3−21344
$CoCl_2.6H_2O$, magnetic susceptibility and antiferromagnetic, spin flop and paramagnetic transitions 3−18313
$CoCl_2.6H_2O$, magnetic transition rounding and Pippard's relations 3−30619
$CoCr_2S_4$, hot pressed, ferrimagnetic spinel, refractive index, Faraday rotation 3−18435
$CoCr_2S_4$, hot pressed, magneto-optic props., digital memory application 3−36858
$CoCr_2S_4$, resist. and magnetoresist., 77-450 K 3−27258
CoD, A-X band system, rotational analysis 3−11245
CoD, absorption spectra between 290 and 700 nm behind reflected shock waves 3−14365
CoD, band spectrum, new sub-system, rotational analysis, spin-orbit interactions 3−33115

cobalt compounds continued
CoF_2, Heisenberg antiferromagnet, rutile structure, two-magnon light scattering 3−21196
CoF_2, Heisenberg antiferromagnet, rutile structure, two-magnon neutron scattering 3−21197
$Co_{0.98}Fe_{0.02}S_2$, pyrite, transferred hyperfine field at ^{57}Fe 3−8487
$Co_xFe_{3-x}O_4$, preparation and characterization 3−18741
$Co_xFe_{3-x}O_4$ film prep. by oxidation, electron microscope exam. of microstruct. 3−27196
CoH absorption spectra between 290 and 700 nm behind reflected shock waves 3−14365
Co(II) complex, Co(PNNP)Br, where PNNP = N,N′-bis(2-diphenyline, cryst. struct. 3−17780
Co(III) complex, $[Co(3,2,3\text{-tet})\times_2]^+$, $X = Cl^-$ and NO_2^-, $42NH(CH_2)_3NH_2$, struct. and optical activity 3−17774
Co(III) complex, hexamminecobalt (III) hexacyanocobaltate (III) and hexacyanochromate (III), cryst. struct. 3−14765
Co(III) complex, hexamminecobalt(III) chlorocuprates(I,II) 10/3 effect in e.p.r. 3−27400
Co(III) complex, hexamminecobalt (III) hexacyanocobaltate (III), crystal structure obs. 3−36276
Co(III) complex, trigonal tris(diphenyltriazine)cobalt(III), crystal structure obs. 3−38554
$Co(IO_3)_2$, anhydride and di- and tetrahydrates, cryst growth, boiling solvent technique 3−12235
$CoIn_2S_4$, cation distrib., mag. susceptibility temp. depend. 3−34102
$Co_3La_2(NO_3)_{12}.24H_2O$, direct and Raman spin-lattice relaxation 3−27411
$Co_{0.5}Mg_{0.5}O$ powder, X-ray diffr. line integrated intensity changes, effective Debye parameter rel. to lattice strain 3−33424
$Co_xMn_{2.9-x}Fe_{0.1}O_4$, Mossbauer obs. of Jahn-Teller distortion 3−8492
$CoMn_2O_4$, chem. transport growth 3−39224
$Co(NH_3)_6Cl_2$, phase transition and far i.r. spectrum 3−11741
$Co(NH_4)_2(SO_4)_2.6H_2O$, spin-lattice relax. times, field-depend. Raman processes 3−15411
$Co(NH_4)_2(SO_4)_2.6H_2O{:}Mn^{2+}$, e.p.r. study 3−15406
$CoNb_2O_6$, mag. struct., neutron diffr. obs. *(German)* 3−21249
$Co_xNi_{1-x}Fe_2O_{4\mp y}$, magnetic anisotropy temp. depend. 3−36728
CoO, pressure sintered, nonstoichiometry, final stage densification kinetics 3−8955
CoO, sintered, oxidation kinetics, mechanism 3−8957
CoO diffusion of ^{35}S 3−1821
CoO powder, X-ray diffr. line integrated intensity changes, effective Debye parameter rel. to lattice strain 3−33424
CoO-M′O, (M′ = Mg, Ca, Sr, Zn, Al), Neel temp. comp. depend. *(French)* 3−8363
CoO-MgO-GeO_2, spinel-olivine and olivine-phenacite transitions, thermodynamic and vol. relations 3−27122
CoO-ZnO-GeO_2, thermodynamic relations among olivine, spinel and phenacite structures 3−27123
Co_2O_3 distribution coefficient in NaCl single crystals 3−30947
Co_3O_4, electron diffraction anal. of superstructure *(Russian)* 3−7712
Co_3O_4, low-spin cpd., cryst. struct. 3−20720
CoP-FeP solid solutions, Mossbauer studies 3−36818
$Co(PO_3)_2$-$CsPO_3$, glasses and melts, effect of water on molar props. *(Russian)* 3−14696
Co_3S_4, n.m.r. of ^{59}Co at A and B sites 3−21330
$CoS_{2-x}Se_x$, pyromagnetic obs. of magnetic phase transition 3−34110
$CoSiF_6.6H_2O$, direct and Raman spin-lattice relaxations 3−27409
$CoSn(OH)_6$, colloidal suspension in glycerol, Mossbauer study of Brownian motion, effect of ethanol and water dilution 3−5361
Co_2Te_3, ^{125}Te Mossbauer obs. of quadrupole splitting 3−21354
$Co_6Te_5O_{16}$, crystal structure determ. *(German)* 3−36285
$CoTiO_3$, in ferrite-titanate composite substrate, hot pressing 3−37079
$Co_xZn_{1-x}Cs_3Cl_5$, random Ising spin system, calorimetric obs. 3−8359
$Co_xZn_{1-x}Fe_2O_4$, mag. permeability, freq. and temp. depend. *(Russian)* 3−8349
$Fe(CN)_6$, $Co_3\{Fe(CN)_6\}_2$, fast intramolecular electron transfer, γ-resonance spectroscopy obs. *(Russian)* 3−2472
TiO-CoO, mag. susceptibility, 100-1000 K, composition and temp. depend. *(Russian)* 3−12008

cochlea *see ear*

codes
see also encoding; error correction codes
mass spectra, computer identification, highly compressed spectral codes, Aldermaston collection 3−28702

coding *see encoding*

coefficient of thermal expansion *see thermal expansion*

coercive force
see also hysteresis
ferrimagnet, coercivity behaviour nr. compensation temp. 3−36750
ferrite spinels, anomalies in compensation temp. region 3−8394
ferrofluid, Ni-Fe alloy particles in Hg, coercive force 3−2321
garnet, mixed rare earth iron type, epitaxial film, domain wall coercivity temp. depend. 3−21257
permanent magnetic materials *(Dutch)* 3−21276
rare earth cobalt permanent magnet alloys, magnetisation, anisotropy and coercivity, review 3−24595
rare earth cpds., ferromagnetic, thin wall coercivity 3−2317
single domain particles in nonmag. matrix, hysteresis, remanence, antihysteresis susceptibility, coherence field 3−30668
steel, rel. to expt. confirmation of diffusion-controlled coagulation process of globular cementite 3−5293
Ticonal alloy, high-coercivity, characteriz. after isothermal thermomag. treatment 3−24943
triglycine sulphate thin film deposited by low temp. spinning technique, rel. to switching 3−39107
$BaFe_{12}O_{19}$ substituted ferrite, intrinsic coercivity 3−34165
$CeCo_5$, powder, coercive force rel. to strain 3−39005
Co alloy, spin config. and intrinsic coercive field of narrow domain walls 3−8391
Co single-domain powders with cubic anisotropy *(Russian)* 3−15390
Co-Fe-Be, rel. to annealing and cold drawing *(Japanese)* 3−12398
Co-Fe-Nb, semihard mag. alloy characteriz. 3−21279

coercive force continued
Co-P film, high-coercivity, domain struct. and reversal processes 3—24592
Co-Pt alloy, high coercivity rel. to struct. *(Russian)* 3—8779
CoPt alloy, ordered, plastic deform. influence *(Russian)* 3—18338
Co_5Sm permanent magnet alloy, sintered 3—5097
$ErFe_2$, near mag. compensation temp. *(Russian)* 3—8380
p-$EuCr_2Se_4$, doped, temp. depend. 3—27385
$(Fe, Ti, \square)_3O_4$, cation deficient, magnetic props. 3—4735
Fe coarse magneto soft powder, sintering effect on coercive force *(Russian)* 3—27718
Fe single-domain powders with cubic anisotropy *(Russian)* 3—15390
Fe-Co-Ni-Al-Ti-Cu, thermomag. treatment effects *(Russian)* 3—8386
Fe-Co(Ni) alloy single-domain powders with cubic anisotropy *(Russian)* 3—15390
Fe-Cu-Mn system, semihard mag. reed switch material, heat treatment and cold drawing effects 3—36757
Fe-Ni alloys, change in saturation magnetisation 3—12034
Fe-Ni thin films, crystal structure, phase dependence 3—8376
Fe-Pt (32-35 at.%) alloys, isothermal annealing depend. *(Russian)* 3—15389
FePd alloy, ordered, plastic deform. influence *(Russian)* 3—18338
FePt alloy, ordered, plastic deform. influence *(Russian)* 3—18338
FePt alloy powders, ordered *(Russian)* 3—30652
$HoFe_3$, near mag. compensation temp. *(Russian)* 3—8380
KNO_3, coercive field of ferroelectric phase III single crystals 3—27473
Mn-Al alloy powders, comp. and defects influence *(Russian)* 3—24587
Mn-Al-B alloy, composition depend. 3—36744
Mn-Ga alloy powders, high-anisotropy, mag. reversals, domain boundary displacement *(Russian)* 3—36737
Mn-Ga alloys, plastically deformed, mag. hardness *(Russian)* 3—36735
MnBi film, high and low temp. phases, temp. depend. 3—27384
Nd-Co, (Nd,R)-Co alloys (R=rare earth), magnetic coercivity, effects of sintering with Pr, Sm additives 3—2309
Nd-Co_5, effects of sintering with Pr, Sm additives 3—2309
Ni, aerosol particles, coercive force and saturation magnetisation from 4.2 to 300 K 3—39006
Ni single-domain powders with cubic anisotropy *(Russian)* 3—15390
Ni-(50% wt.)Fe, melting process effect on coercive force *(Korean)* 3—5120
Ni_3Mn, influence of annealing under load *(Russian)* 3—15729
$(Pr,Sm)Co_5$, intrinsic coercive force rel. to Sm content 3—24585
$Sm(Co, Cu)_5$, permanent mag. material, coercive force rel. to annealing 3—30658
$SmCo_5$, powder, coercive force rel. to strain 3—39005
$SmCo_5$ permanent magnet materials *(French)* 3—36753
$SmCo_5$ powder, coercivity, grinding duration and method influence *(Russian)* 3—27731
$Sr_2Nb_2O_7$, ferroelectric single cryst., coercive field determ. 3—21373
YCo_5, powder, coercive force rel. to strain 3—39005

coercivity *see coercive force*

coherence
see also light coherence
apparent image enhancement, through coherent defocusing 3—28717
atomic coherent states in quantum optics 3—4077
dispersive media, coherent nonlinear waves 3—28949
higher order coherence of the electromagnetic field 3—16820
NMR, multiple-pulse, reson. offset processes, quantitative aspects of coherent averaging 3—7233
partially coherent light beam propagation theory in turbulent atmosphere *(Russian)* 3—689
radiometry, partial, generalisation of basic laws 3—22815
radiosources, astronomical, emission mechanism, by relativistic electrons 3—3351
signal, noise and reverberation meas. in sea 3—3224
superposed coherent and chaotic radiation, photocount statistics, closed form solutions 3—4076

cohesive energy *see binding energy*

coils
see also inductors; windings
30 kOe superconducting coil with reduced external field 3—6038
blood flow transducer, n.m.r. obs., pickup coil space filling coefficient calculation *(Russian)* 3—19248
circular, group, magnetic fields calc. *(Czech)* 3—4054
cylindrical with flat conductive shielding, magnetic field analysis using magnetic vector potential *(Russian)* 3—32476
magnetic flux and field, circular and rectangular coils *(French)* 3—32487
rotating superconducting field coils for superconducting machines, cryogenic aspects 3—5845
superconducting, large scale applications, review 3—7016

coincidence circuits
see also counters
4 $\pi\beta$-γ coincidence method for radionuclides standardization 3—13443
active sample anticoincidence guarded Ge(Li) spectrometer low level radionuclide analysis 3—28773
coincidence-anticoincidence circuit based on current switch 3—22479
delayed system, using NaI(Tl) and surface-barrier detectors, prompt timing response 3—25888
digitally controlled fast logic modules, CAMAC interface 3—28685
multichannel differential circuit to nsec range 3—32195
multifold and of serial structure, statistical model 3—35483
quadrupole unit, for positron annihilation studies 3—37699
β-γ spectrometer, 4π geometry using Si(Li) and NaI(Tl) detectors 3—10078

coincidence counters *see coincidence circuits; counters*

cold-cathode tubes
see also counting tubes; photomultipliers; phototubes
gas laser, patent 3—6475

cold forming *see cold working*

cold reduction *see cold working*

cold shortness *see brittleness*

cold working
see also bending; plastic deformation; slip; work hardening
α-brass powder, cold-worked and stored at liquid N temp., increase in particle size 3—27642
brittle metal, central cracking during cold-extrusion, prevention by hydrostatic back pressure 3—24869
disordered polycrystals, distortion waves, comparison between cold worked and annealed samples 3—17926
Elinvar, thermal expansion, elastic props., influence of heat treatment and cold working *(German)* 3—34610
Invar, thermal expansion, elastic props., influence of heat treatment and cold working *(German)* 3—34610
metal, crystalline, athermal weakening effect during cold plastic deform. 3—33599
polyolefins, cold-drawn, reversibility of deform. 3—25009
positron annihilation for dislocation density estimation in f.c.c cold-worked polycrystal 3—30159
stainless steel, microhardness with different cold work percentages 3—31224
steel, austenitic, Cr-Ni-Mo, Ti-stabilized, creep strength behaviour 3—8928
steel, cold-rolled, singularities of softening phenomena during annealing *(Russian)* 3—8833
steel, cold-worked, dislocation struct. stability during high-temp. ageing *(Russian)* 3—8838
steel, effect on notch toughness *(German)* 3—27685
steel, influence of high temp. austenitization on ductility 3—24935
steel, martensite, effect of cold work on tempering *(Russian)* 3—5305
steel, stainless, type 316, irrad. temp. depend. of void form. 3—26506
steel, stainless, under press., yield effects 3—2728
steel, transformer, recrystallisation matrix depend. on cold rolling and initial structure, secondary recrystallisation 3—31013
steel for dies, working capacity for cold deformation 3—18667
steel sheets, low carbon, effects of Ni on cold-rolling and recrystallization textures *(Japanese)* 3—18589
strip rolling, asymmetry effects in cold rolling 3—31106
transformer steel, grain size and form control *(Russian)* 3—12342
Ag, cold-worked and γ-irrad., modulus defect and internal friction during recrystn. 3—5314
Al, effects on quadrupolar n.m.r. 3—34248
Al for alloys, machine construction, mechanisms of strengthening 3—21685
Al-3%Cu alloy processed from double-oriented ingots, cold rolling and annealing textures *(Japanese)* 3—18640
Al-Al_2O_3, effects on recrystallisation 3—18581
Al-Fe dilute alloy, cold-worked, internal friction and Young's modulus, heat treatment effects 3—27703
Al-Ti (0.16 at wt.%) alloy, yield point phenomenon *(Japanese)* 3—18644
Au, cold-worked, stage II and III recovery, internal friction and modulus defect, trace impurity effects 3—5315
Au-Ag alloys, short-range ordering upon quenching and cold-work, calorimetric and resistometric study 3—21713
Au-Pd alloys, short-range order destruction 3—39372
$Bi_2Te_{2.4}Se_{0.6}$, and $Bi_{0.52}Te_3Sb_{1.48}$ cold-pressed semielements, effects on phys. props. *(Russian)* 3—11919
Co-Fe-Be, mag. and mech. props with annealing and cold drawing *(Japanese)* 3—12398
Co-Fe-Nb semihard mag. alloy development 3—21261
Co-Fe-Nb semihard mag. alloy characteriz. 3—21279
$CrPt_3$, transition from ferrimag. to paramag. type behaviour with cold working 3—21237
Cu, internal friction, dislocation pinning by hydrogen *(French)* 3—2740
Cu, stability on cold rolling deform. *(Japanese)* 3—12390
Cu-Al alloy, swaged, dislocation density, from flow stresses and stored energies 3—18633
Cu-Fe alloys, ageing characts., precipitate transform. 3—37075
Cu-Ni-Zn microduplex nickel silver, effect on tensile props. 3—34571
Fe, Armco, cold deform. and subsequent heat treatment, effect on mech. props. *(Russian)* 3—5307
Fe alloy, E1437B, ageing/deformation treatments influence on struct. and mech. props. *(Russian)* 3—24873
Fe and alloys, internal friction, hydrogen influence, interaction with dislocations *(French)* 3—2739
Fe-Co-Mn, strain gauge factor and elec. resist. meas. *(Japanese)* 3—12399
Fe-Cu-Mn system, semihard mag. reed switch material, cold drawing effect on mag. props. 3—36757
Fe-Mn-Co alloys, effect on mag. props. *(Japanese)* 3—31077
Mg central cracking during cold-extrusion, prevention by hydrostatic back pressure 3—24869
Mg hydrostatic extrusion, critical back pressure to prevent central cracking 3—21615
Mn-Cu-Co nonmag. Elinvar-type alloys characteriz. 3—37074
Mn-Cu-Cr alloys, Elinvar props. 3—21291
Mn-Cu-Ni alloys, Elinvar props. 3—21292
Mn-Ni-Cr alloys, Elinvar type effects on Young's modulus, rigidity, hardness *(Japanese)* 3—8858
Mn-Ni-Fe, Elinvar type, effects on Young's modulus, rigidity, thermal expansion and hardness *(Japanese)* 3—8859
Nb, neutron irradiated at low temp., annealed and cold worked, internal friction 3—17875
Nb superconductor, effects on power frequency losses 3—11980
Pt wire, thermal shock of cold worked sample on cryogenic immersion 3—4746
Ti sheet, cold rolling rel. to deep drawability *(Japanese)* 3—12393
Ti sheet, elastic anisotropy laws and texture form. *(Russian)* 3—24851
Ti sheet, texture dispersion and thermo-e.m.f. anisotropy *(Russian)* 3—24852

collections of physical data
artificial satellites launched in 1972, tabulated orbital and other data 3—35216
atomic energy levels and multiplet tables of H, D and T 3—29483
Auger transitions for elements, calculated, catalogue 3—39205

collections of physical data continued
  Auger transitions in 10 to 3000eV energy range, complete list 3−2612
  elementary particle data bank, Durham, data analysis and model comparison project 3−29256
  elementary particle inclusive spectra 3−10817
  epitaxy, planes, directions periods and misfits for 3700 systems 3−8055
  even-even nuclei, members of quasi-ground, quasi-beta and quasi-gamma bands in spherical and deformed regions 3−19777
  gamma-gamma directional correlation coeffs. for states of high angular momenta, tables 3−967
  log-f value tables for β-decay 3−973
  metallic materials specification handbook 3−37000
  molecular laser-emissions in the i.r., rotational and vibrational-rotational transitions 3−11267
  molecular vibration frequencies for 223 molecules, from U.S. department of commerce 3−11235
  normalized Legendre functions and tesseral harmonics of 7th order for calcs. of energy levels of rare earth ions in crystals 3−4953
  nuclear internal conversion coeffs. for high-energy transitions 3−19809
  nuclear optical model parameters determ. by fitting of elastic scattering angular distribs. 3−19827
  nuclear reaction ground-state Q-values, calc. from atomic mass evaluation, targets with A=9-251 3−19824
  nuclear reaction list for charged-particle induced reactions (july 1971-June 1972) 3−19823
  organic compounds structural data compilation from 1960-5 publications 3−30109
  reduced rotation matrix elements, plots and zeros, evaluation using computer program 3−19488
  SCF mol. wavefunctions and properties, tables 3−26623
  tables of standard data for spectroscopists 3−11111
  thermocouple reference tables (0 to 280 K) 3−9862
  uranium carbides, thermodynamic functions 3−23428
  $\pi^\pm$ reactions on p,n,d, compilation of cross-sections and variation with incident momentum 3−882
  ^{13}C, n.m.r. spectra, collection of data, book 3−23608
  DBF_2, thermodynamic props. 3−39426
  HBF_2, thermodynamic props. 3−39426
  Pt10Rh/Pt and Pt13Rh/Pt, thermocouples, improved tables 3−3770

collision processes
  see also atomic collision processes; charge exchange; elementary particle interactions; intermolecular mechanics; molecular collision processes; particle scattering; plasma collision processes; quantum field theory
  atmospheric charged particles, collision and coagulation efficiencies determ. *(Russian)* 3−39527
  binary mixtures, Thorne's modified eqn., transport coefficients 3−28983
  Boltmann density matrix, improved classical path matrix 3−22756
  classical binary collision operator estimate 3−22755
  cloud collision processes, energy source for driving the interstellar gas 3−19071
  direct simulation of mutually colliding bodies, mass distribution, Monte Carlo technique 3−12935
  DWBA approx. for vibrationally inelastic collisions, averaging procedures 3−26110
  inverse s-wave scattering for energy-dependent potential 3−584
  kinetic equation for hard sphere correlation functions 3−26148
  mechanical systems, transition conditions using Hamilton functions *(German)* 3−32301
  modified Korteweg-de-Vries equation 3−37905
  numerical calculation of the classical deflection function 3−16712
  one particle distribution function, kinetic eqn. *(Russian)* 3−10384
  outer solar corona, MHD wave dissipation and collisionless protons and collisional electrons 3−31520
  plasma-filled transversely magnetized rectangular waveguide charact. 3−1491
  radiation damage 3−4779
  rearrangement and exchange collisions, semiclassical theory 3−16700
  rigid sphere suspension, molecular collisions with solid particles 3−37903
  scattering theory, the quantum theory of nonrelativistic collisions, book 3−16713
  semiclassical theory within Feynman path integral formalism 3−28951
  sliding mode of motion in systems with collisions *(Russian)* 3−499
  solar wind, quiet and collisionless, parallel heat flux through collision transition region 3−31527
  surface composition by analysis of neutral impact radiation 3−36973
  three-body problem, separable approximations t off-shell two-body t and K matrices at positive energies 3−6316
  water drops falling in elec. field, charge transfer 3−649

collision sequences, focused *see sputtering*

collisions, atomic *see atomic collision processes*

colloid chemistry *see colloids*

colloids
  see also Brownian motion; electrophoresis; electroviscous effect; emulsions; gels; photophoresis; thixotropy
  acetylcellulose in diethylene glycol ethyl ether, metastable solution, separation of new disperse phases, light scattering 3−39402
  alkyd resin in acetone, elec. cond., potential distribution 3−39408
  aluminosilicate clay, statistical mechanics and anomalous swelling rel. to electrolytes 3−21752
  birefringence electrical *(Rumanian)* 3−22848
  Boltzmann's constant, student experiment for determ. 3−22223
  clay-water, different phases of water, n.m.r. studies 3−39396
  copper dodecyl sulphate micelle surface, local conc. of counterions, obs. of Cu^{2+} e.p.r. 3−34656
  dense colloidal suspensions of spherical particles, light scattering cross sections 3−29045
  elec. interaction, constant surface-charge density 3−39401
  electric double-layer force between unlike spheres, calc. 3−31200
  ferrite particle solution, osmotic press., mag. field gradient 3−27792

colloids continued
  glycerol:$CoSn(OH)_6$ colloidal suspension, Mossbauer study of Brownian motion, effect of ethanol and water dilution 3−5361
  glycerol and aqueous-glycerol solns., Mossbauer parameters, diffusion constants and viscosity coeffs. for dispersed Fe^{2+} 3−5360
  graphite colloidal suspensions, rheological props. 3−31192
  inhomogeneous media, study by ultrasonic methods 3−25669
  irreversible coagulation criteria in elec. field 3−34657
  micellar systems, nonradiative energy transfer rates 3−20174
  polyarylate F-1, adsorption on macroporous silica gel, chromatographic adsorbents 3−38714
  polydimethylsiloxane monolayers, thermodynamic properties, surface viscosity, at water-air interface 3−39406
  polyelectrolyte solns., stability determ. by laser Doppler spectroscopy 3−34661
  polystyrene latex spheres, dil. aqueous solns., optical self-beating spectrometer calibration, Stokes-Einstein formula 3−34659
  small metallic particles, quantum microscopic approach to electric-dipole absorption 3−26207
  sodium oleate, interaction with TiO_2 surface, chemisorption, i.r. studies 3−39410
  spectra, absorpt., band intensities, effect of particle shapes 3−18739
  stability and classification of colloidal systems, review 3−34653
  superconducting, applic. to particle detection 3−10050
  Van der Waals and double layer forces, interdepend. 3−31191
  Van der Waals attraction between particles having adsorbed layers, Vold effect 3−39413
  Van der Waals attraction between particles having adsorbed layers, interaction curve calc. 3−39414
  water-in-oil emulsion coagulation in strong electric field *(Russian)* 3−9016
  AgCl particles in water, mass motion, observation using light-beating spectroscopy 3−180
  FeS_x, ageing 3−2770
  H_2O-$Na_2CO_3(NaOH)$-SiO_2, quartz hydrothermal growth, nature of nonstruct. admixture in heavy phase 3−31197
  $Mg(OH)_2$, disperse porous structure, strength, influence of dehydration 3−39420
  Na colloid due to proton bombardment in NaF crystal, average projected range meas. 3−1654
  Sb_2S_3 colloid, ^{99m}Tc-labelled, for linear scintigraphy 3−35286
  SiO_2 colloidal suspensions, sound velocity 3−34658

color *see colour*

colorimeters
  see also colorimetry
  colour TV picture tubes colour meas. 3−25748

colorimetry
  see also colorimeters; spectrochemical analysis; spectrophotometry
  automated analysis, optimum working range, calibration curve, errors, statistical analysis 3−28783
  colour shifts, subjective measurement using various light sources 3−9684
  colour specification, CIE system 3−25749
  metameric spectral reflectance functions numerical calcs. 3−5929
  small samples, apparatus and method 3−22344
  spectral colour matching, minimax approx., computer algorithm 3−3805
  spectral masks techniques, accuracy *(Russian)* 3−5934
  standard colour samples, metamerism and selection 3−35405
  tetrachromatic colour match as colorimetric technique 3−9685

colour
  see also colour vision
  3D spectrum locus, CIE chromaticity diagram, region of realisable colours in tristimulus space 3−6450
  cholesteryl ω-phenylalkanoates, synthesis and mesomorphic characterization 3−24023
  cholesteryl n-alkyl carbonates, synthesis and mesomorphic characterization 3−24022
  copper phthalocyanine pigments, α and β forms, adsorption props., optical props., effect of heating 3−38713
  diamond, synthetic, charact. growth on cryst. faces 3−20702
  early-type stars, i.r. excesses, free-free emission explanation 3−9536
  films, transmission-type and reflection types, comparison of colour reproduction quality 3−28597
  liquid crystal, cholesteric, shear effects on colour intensity and reflectance wavelengths 3−24709
  liquid crystal tapes, ambient light effect on colour/temp. response 3−24710
  multicolour holograms, white light reconstruction 3−28567
  quartz, blackness determ. 3−24666
  rare earth sesquisulphides 3−34370
  transparencies on coloured supports 3−28596
  $AgInS_2$-ZnS system, wurtzite vapour-grown cpds. 3−18545
  C fibre, K intercalation compounds, structure, elec. cond. 3−24995

colour blindness *see colour vision*

colour centres
  see also F-centres
  ADP-KDA mixed crysts., X-ray and γ-ray irrad., paramag. centres e.s.r. 3−15422
  alkali halide: Pb^{2+}, Sn^{2+}, Ge^{2+}, T-centre form. by electrolysis *(French)* 3−20738
  alkali halide, e.p.r. obs. of hyperfine and g-components of V_k centres 3−18369
  alkali halide, impurity doped, review for Z-centres 3−8624
  alkali halide, review of interstitial and trapped hole centres 3−4754
  alkali halide, X-coloration dichroism, plastic deformation induced 3−36894
  alkali halide, X-irrad., rel. to time-lag of photostimulated luminesc. *(Russian)* 3−18483
  alkali halides, ENDOR in presence of external stresses, theory 3−27442
  alkali halides, point defects formation and stabilization by u.v. irradiation, dose dependence 3−7750
  alkali halides, U-centres, magneto-refl., Faraday rot., ellipticity 3−15476
  aluminosilicates, radiation produced e.s.r. centres, model 3−21312
  anthracene single cryst., low temp. radiation and meas. of absorpt. 3−132

colour centres continued
calcium fluorophosphate, e.p.r. study of luminescent and colour centre defects 3−34212
diamond, H3 zero-phonon line, luminescence quenching obs. 3−30860
glass, La-silicate, radiation centres investigation by e.p.r., absorption spectra and thermal decolourising *(Russian)* 3−30697
insulator, defect absorpt. strength, f-sum rule, Smakulas eqn. effective fields, review 3−12160
KCl, α and F' centres, luminescence lifetime, band structure 3−21475
leucine halide salts, X-irrad., free radical form. and trapping 3−2367
n-paraffin matrix, impurity mols., linear spectra and impurity centre theory *(Russian)* 3−36896
phosphors, radical recombination luminescence 3−27572
potassium halide crysts., T-centres, photoluminesc. meas. *(Russian)* 3−36919
ruby with vanadium impurities, γ-irrad., absorpt. obs. *(Russian)* 3−12156
SiC, cathodoluminesc. and form. of large defect centres on proton irradiation 3−15562
titania-silica glass, optical attenuation, bleaching, H_2 evolution 3−21447
X, optical information storage in KCl and KBr crystals, conversion of F and X centres 3−13329
AlN, O centres, luminesc. study *(Russian)* 3−36921
$Ba(ClO_3)_2.H_2O:O^-_3$, u.v. photolysis of X-irradiated single crystal, e.s.r. 3−5134
BaF_2, hopping motion of V_k centres 3−20735
BaF_2, static optical and spin resonance props. of V_k centres 3−20734
CaF_2, hopping motion of V_k centres 3−20735
CaF_2, M^+ centre, prod., absorption and luminesc. obs. 3−27023
CaF_2, static optical and spin resonance props. of V_k centres 3−20734
CaF_2:Mn, cathode ray coloration, alpha and beta centre form. 3−30121
CaF_2:Mn, theraml and u.v. bleaching characts. 3−7755
CaF_2:Mn(Ce,Mn), cathodoluminescence, trapped hole diffusion 3−39197
$CaF_2:XF_3$ (X=Pr,Tb,Nd), gamma-induced luminescence of X^{3+} centres 3−24732
CaO:K, radiation induced K^0 centres, e.p.r., spin Hamiltonian parameters 3−34210
CaO:Mg, e.p.r. as function of visible irradiation 3−36791
$Ca_{10}(PO_4)_6Cl_2$, e.p.r. investigation 3−8442
$Ca_{10}(PO_4)_6Cl_2$, optical absorption measurements, e.p.r. 3−8442
$Ca_{10}(PO_4)_6F_2$, defect centres 3−8623
CdO-NaCl heterojunction, optical absorpt. *(Russian)* 3−8627
Cs halides, far i.r. absorpt. due to U-centres, defect model 3−15529
Cs halides, peak positions and half-widths of cadmium bands 3−39168
CsBr, U_2 centres, e.p.r. and ENDOR investigation *(German)* 3−30696
CsCl, U_2 centres, e.p.r. and ENDOR investigation *(German)* 3−30696
CsCl(Br)(I), Pb-centres, optical absorpt., elec. cond. and dielec. loss studies 3−24725
$Fe_{1-x}S$, semiconducting uniaxial ferroelectric model 3−8531
$H_2N.NH_3Cl_2(Br_2)$, γ-irrad., e.p.r., V-centres and H atom spectra 3−2393
K halides, quantum mechanical calcs. of i.r. props of H^- ions 3−21453
KBr, additively coloured, M- and R-centres, photoemission study 3−2617
KBr, additively coloured, loss tangent, temp. and freq. depend. 3−39092
KCl, additively coloured, M- and R-centres, photoemission sutdy 3−2617
KCl, additively coloured, photochem. F→M centre conversion *(Russian)* 3−33526
KCl, i.r. absorpt. of aligned H^--Na^+-H^- complex 3−24727
KCl, M-centre, singlet to triplet conversion 3−5219
KCl, M-centre form. and destruction by ionising radiation 3−4756
KCl, plastically deformed, rel. to luminesc. flashes on unloading 3−5232
KCl, with centres of colloid type, mech. props. on annealing *(Russian)* 3−14855
KCl crystals, hole centres, structure and conversion *(Russian)* 3−11621
KCl V_k-centre on (001) external surface, simple theoretical model 3−36296
KCl:^{57}Co, ^{57}Fe, formed by X-ray irradiation and impurity addition, Mossbauer obs. 3−15447
KCl:Au^-, study of absorption bands and related luminescence centres 3−12167
KCl:Mg^{2+}, study of Mg electron centre 3−20737
KCl:OH^-, u.v. irrad., Y- and Y′-centres, absorpt. 3−18477
KCl:Pb, Br, X- or γ-irrad., $BrCl^-$ and associated centres, e.p.r. and optical absorpt. 3−39031
KCl:Sr, Z centres, photochem. transforms. 3−34741
KCl:Tl, Ga, In, absorp. bands and luminesc. of Tl^0, Ga^0, and In^0 centres 3−27024
KCl:Tl, optical delocalization of holes from Tl^{2+} centres 3−34390
KCl:U, trapping of H_2 molecules by M-centres 3−20732
KCl-KI, light absorpt. by second harmonics of U-centre oscill., calc. *(Russian)* 3−15533
KCl-KI:Ag, X-irrad., e.s.r. and optical absorpt. spectra 3−8445
KCl+NaCl crystals, hole centres, structure and conversion *(Russian)* 3−11621
KCl(Br):$Eu^{++}(Sm^{++})(Yb^{++})$, thermoluminesc. of Z_1 centres 3−8678
KI, optical reorientation of V_k centres 3−17817
KI M-centres, polarised light absorption spectra, anisotropies 3−27520
$KMgF_3$, impurity and defect centres, thermoluminesc. 3−34436
LiH, capture sites and high temperature luminescence *(Russian)* 3−12190
$LiNbO_3$, formation under p and d bombardment, 140 keV 3−2571
Lif, neutron irrad., zero-phonon lines in M-band region 3−1622
MgF_2, electron, colour centre prod. mechanism 3−34479
MgF_2, electron and proton irrad., thermolum. *(Russian)* 3−18505

colour centres continued
MgO, hypersonic attenuation, impurity and defects effect 3−1701
MgO, neutron irrad., thermal cond., 0.4-80 K, quasilocalized modes, defect centre prod. 3−30295
MgO, neutron irradiated, isotropic e.s.r. line of V^- centre at room temp. 3−34209
MgO, paramagnetic defects at the surface 3−5048
MgO, trapped-hole centre displaying orthorhombic symmetry, ESR spectra 3−8440
MgO, V_{al} and V^- centres 3−24113
$Mg_2TiO_4:Mn^{4+}$, Cr^{3+}, phosphors, luminescence, R and N-centres study *(Russian)* 3−36928
$NH_4Cl:Co^{2+}$, Ni^{2+}, Cu^{2+}, light absorpt. by impurity centres, cryst. field parameters 3−21456
NaCl, positron annihilation study of concentration of colour centres, meas. of lifetime and of dynamics of A centres 3−7754
NaCl:^{57}Co, ^{57}Fe, formed by X-ray irradiation and impurity addition, Mossbaur obs. 3−15447
NaCl:Mg^{2+}, study of Mg electron centre 3−20737
NaCl:Mn, e.p.r. study of Mn centres 3−8441
NaF:Li^+, e.s.r. study of F_3^{2-} molecule ion with Li impurity forming di-interstitial centre 3−2390
Na_2SiO_3:La photochromic glass, darkening characteristics caused by u.v. emission and colour centres formation *(Russian)* 3−30852
Pb silicate glasses, radiation induced colouring in Cherenkov counters 3−35476
$PbBr_2$ single crystals, luminescence and e.p.r. of u.v. irradiated crystals 3−8640
$PbCl_2$ single crystals, luminescence and e.p.r. of u.v. irradiated crystals 3−8640
Rb halides, peak positions and half-widths of cadmium bands 3−39168
Si, ion beam irrad., VV centre prod., e.s.r. *(Russian)* 3−8444
$SrCl_2$, form. of F, V_k, V_{ka} centres on X-irradiation 3−17816
SrF_2, form. of F, V_k, H centres on X-ray irradiation, temp. depend. 3−17815
SrF_2, hopping motion of V_k centres 3−20735
SrF_2, static optical and spin resonance props. of V_k centres 3−20734
SrO:K, radiation induced K^0 centres, e.p.r., spin Hamiltonian parameters 3−34210
WO_3 thin films, wavelengths shorter than 3500 A 3−36899
ZnO, electron irrad., displacement thresholds 3−20765
ZnS:Cl, e.p.r. signal and self-activated luminesc. from A-centre, Zn vacancy-Cd donor pair 3−33529
$ZnWO_4$, defect distrib. near paramag. centre from e.s.r. lineshape 3−21311

colour filters *see optical filters*

colour perception *see colour vision*

colour photography
cine film, colour positive developing control and printer tape preparation by minicomputer 3−35433
colography, photoselective polymerization 3−37655
computer simulation of optimum combinations of colour dyes to produce selective greys 3−223
dye fading of motion picture film 3−220
film, autoradiography applic. *(German)* 3−37715
film for water penetration photography 3−245
film quality rel. to reciprocity failure, exposure plane temp. and solar altitude 3−22394
Gemini V and Apollo VII data, colour separation and electronic analysis 3−224
Kodacolor II, improved colour negative film 3−6009
light source filtration 3−37652
reversal film CO-32D *(Russian)* 3−37656
telecine, colour balance of film, spectral characteristics, densitometer 3−5994
transparency duplicates, applications 3−37651
TV flesh colour 3−219

colour television
discharge lamps, colour characteristics of new equipment for TV and film lighting 3−9979
Kell-type camera, spatial frequency filter 3−147
picture tubes screens colour meas. by direct-reading colorimeter 3−25748

colour tv *see colour television*

colour vision
see also eye
anomalous trichromats, photopigment absorption spectra 3−31913
brightness of coloured flashes, background effects 3−31920
California ground squirrel, visual sensitivity 3−5667
cat, behavioural and neurophysiological studies 3−28359
chromatic filters for vision 3−16321
chromatic rod vision, theoretical survey 3−31918
chromaticity coordinates, neural adaptation 3−31914
colour blind observers, spectral sensitivity, cone photopigments 3−5670
colour shifts, subjective measurement using various light sources 3−9684
coloured lights, luminance rel. to brightness 3−25585
congenital tritanopia and tritanomaly, colour naming and hue discrimination 3−31916
dichoptically presented colour and form, orientation-sensitive after effects 3−35264
and form perception in visual information processing 3−28351
foveal spectral sensitivity, heterochromatic additivity 3−35263
history and diagnosis methods 3−31915
human, violet sensitivity rel. to age *(German)* 3−16323
minimally distinct border, chromaticity comparison 3−5671
observer with unilateral defective colour vision, spectral response 3−5669
photopic luminosity, by critical frequency method 3−5668
red and green blindness, reference to visibility of electrolum. diodes 3−3558
retinal in visual pigment, optical property theory and Schiff base binding 3−11333
spatial frequency channels, contrast thresholds 3−3560
spatial summation in colour-receptive pathways 3−31917
spectral sensitivity, by const. CFF, chromatic adaptation effect 3−31912

colour vision continued
spectral sensitivity and visual pigment absorbance 3−39801
stereopsis, colour perception and pattern recognition 3−31919
temporal response props. of individual colour mechanisms, reaction time 3−9686
tests, pseudo-isochromatic and matching 3−35265
tetrachromatic colour match as colorimetric technique 3−9685
TMC and HRR tests as to red-green defectiveness, statistical analysis 3−16322
turtle retina, L- and C-type S-potentials, physiological and morphological identification 3−31891
wavelength discrimination from colour naming 3−22155

columbium *see niobium*

COM *see computer output to microfilm*

coma *see aberrations*

combinational mathematics *see combinatorial mathematics*

combinatorial mathematics
see also graph theory
hypergeometric functions for SU(n) states, structure of combinatorial generalisation 3−26275

combustion
see also explosions; flames; heat of combustion; reaction kinetics
gaseous mixtures acted on by magnetic field, stability *(Russian)* 3−2808
gases, spectrometric temp. and conc. distrib., probe system 3−35379
gases, thermal radiation 3−14419
glass-graphite disintegration in hypersonic gas stream, evaporation and combustion, heat and mass transfer on the surface *(Russian)* 3−26786
luminous flame, mean emissivity from spray combustion of liquid fuel 3−2801
n-pentane droplets, expt. at high pressures 3−3777
plasma of combustion products, statistical properties of parameter fluctuations for subsonic flow 3−17591
propane-air flames, combustion nuclei production and electrostatic precipitation 3−5391
solid rocket propellants, acoustic pressure wave amplification 3−35344
sound propagation, axial temp. and density gradients 3−9758
turbulent diffusion flame of combustible jet, aerodynamic and thermodynamic analysis 3−23799
turbulent media, chem. prod. rate *(French)* 3−21798
U-water reactors, four-group scheme for calc. of isotopic composition of fuel *(Russian)* 3−29435
Zr droplets, combustion in N_2/O_2 mixtures, thermochem., microbubble formation, 3000-4000 K 3−31249

comets
Apollo 16 sample 66095, possible origin by comet impact 3−37331
Bennett, determ. of tail orientation from obs. 3−9515
Bennett 1969i, dust and gas motion in head rel. to type II tail 3−28160
Bennett 1969i, type I ion tail axes rel. to kinematics and irregularities 3−28159
Bennett (1969i), scattered light continuum, mean particle size meas. 3−12999
Bennett (1970 II), dust comet model applic. 3−39651
Comet Bennett, central coma, 1.1 μ spectrogram 3−13002
comet Bennett, microwave spectrophotometry 3−16190
Earth-comet collisions rel. to geological periods 3−25145
Encke, Na twilight emission increase after Earth's crossing of orbital plane 3−18875
extraterrestrial organic compounds, anal., review 3−35016
P/Grigg-Skjellerup (1972 b), obs. of associated radio meteors 3−39650
Halley, Na twilight emission increase after Earth's crossing of orbital plane 3−18875
Halley's, orbit and problems concerning trans-Plutonian planet 3−25427
Halley's, perihelion passage time rel. to Brady's theory of trans-Plutonian planet 3−25412
Halley 1910, comparison with Comet Bennett 1969i rel. to type II tail 3−28160
ionic (type I) comet tail orientations rel. to solar wind vel. meas. 3−39652
Jupiter's family, original orbits determ. using Tisserand's constants 3−35002
lunar carbon source via C-cycle in lunar atmosphere 3−35085
lunar impact, possible evidence from volatile-rich soil exam. 3−31630
mass influx into Solar System dust cloud 3−5591
meteor stream statistical model showing comet-meteor assoc. 3−31635
nongravitational forces rel. to heliocentric distance, effects on orbits of long period 3−31633
observations during 1971 with 'Grand Schmidt' telescope *(French)* 3−31802
polarisation of cometary radiation rel. to orientation of interplanetary dust grains 3−28300
Reinmuth 1 periodic comet, orbit and ephemeris for 1972-73 apparition 3−9512
Tago-Sato-Kosaka 1969 IX, kinematical behaviour of plasma tail 3−5590
type I ion tail axes, kinematics rel. to Comet Bennett 1969i double axis 3−28159
type I tail model, Kelvin-Helmholtz instability and growth rate of MHD waves 3−28164
type-1 tails, non-linear waves rel. to Kelvin-Helmholtz instability 3−35107
CO^+_2 tail bands, effective cross sections and excitation functions, excitation by 0.4 to 20 keV electrons 3−14400
H atmosphere model for Lyman-α radiation with multiple scattering effects 3−28161

commissioning
see also installation
reprocessing plants, decommissioning of Eurochemic installations *(French)* 3−38185

communication channels
progress at MIT electronics research lab. 3−1

communication networks
international standards 3−59

communication overhead lines
see also telecommunication cables
telephone cable supports, steel strand, fatigue testing, comparison of UG and EHS strands 3−12492

communication overhead transmission lines *see communication overhead lines*

communication systems *see telecommunication systems*

communication theory *see information theory*

communications applications of computers
see also telephony; television
antenna array design 3−32492
digital signal processor using MSI logic circuits, use for sonar, seismic and underwater telemetry systems 3−3178
radio-sky map, 136-400 MHz, for system noise temp. detn. in satellite links 3−31810
speech and pause analysis, computer program monitoring 3−28425

community planning *see town and country planning*

commutation
see also commutators
switch, injection semiconductor laser *(Russian)* 3−789

commutators
see also commutation
h.v. plasma, d.c. to multiphase a.c. *(Czech)* 3−23924

compacting *see densification*

compasses
see also navigation
astro-, for civil aircraft, structure, operating precision 3−32116
gyrocompass, suitable for undergraduates 3−28448

compensation
see also error compensation
adaptive, open loop and closed loop, of optical tracking telescope 3−39760
conductometric granulometers, temp. compensation errors 3−37665
electron probe nonlinearities, for image storage system 3−37721
interferometry, apochromatic path-difference compensator *(Russian)* 3−9951
pressure-compensated cables for deep submergence search vehicle 3−3206
temperature, in thermostat elements 3−32041

complementarity
No entries

complete computer programs
see also subroutines
axisymmetric electrostatic collector design problems, direct numerical solution, in Fortran 3−32490
dispersed seismic surface wave, spectrum and dispersion analysis 3−21979
ephemerides, FXS procedure use *(Japanese)* 3−19081
furnaces, temperature profile calculation, in FORTRAN 3−9866
gas, computer program for fitting time of arrival and shock peak overpressure data, in FORTRAN 3−36123
line profiles and continuum fluxes, numerical methods and computer programs in FORTRAN 3−35118
pharmaceutical tablet on off-line auto-analysis, in FOCAL-12 3−394
spectral multiplet square arrays, generation 3−38211
time-of-flight spectrometer, Fortran programs for data reduction 3−32203

complex angular momentum plane
see also angular momentum theory; Pomeranchuk poles and trajectories; Regge poles and trajectories
Crichton's phase-shift ambiguity, features of elastic unitarity constraint 3−38018
direct channel, Veneziano eikonal approx. approach 3−10750
fixed and moving poles, HNZ construction 3−17078
fixed poles in pion Compton scatt. 3−10706
fixed poles in the t-channel helicity-flip amplitude in charge- and hypercharge-exchange reactions 3−14049
harmonic moments and amplitude zeros in $\pi\pi$ and Kπ scattering, resolution of anomalies 3−17096
Linear Absorption Models, fund. constraints 3−10749
resonances and echoes in nuclear scattering and related processes 3−26434
singularities in complex ang. momentum and helicity 3−10743
spinor ladder model of π^0 photoproduction and NN scatt., asymptotic behaviour 3−13898
virtual Compton scattering, fixed poles, perturbative approach to parton model 3−29211
virtual Compton scattering, presence of fixed singularities in T_1 3−35800
weak-cut model for high-energy np and pp charge exchange scattering 3−32717
zeros in differential cross sections at high energies 3−14039
πN elastic scattering and change exchange, analysis including cut contribution *(Russian)* 3−38080
ρ, charged, photoproduction, parity asymmetry, differential cross-section *(Russian)* 3−6615
ρ photo prod., presence of J=0 fixed pole in vector meson amplitudes, using dispersion relations 3−17062

composite insulating materials
liquid mixture, permittivity and loss factor, calc. 3−2484
R&D, ECRC Capenhurst, ceramics, plastic compound materials 3−1521

composite materials
see also cermets; composite insulating materials; fibres
acrylonitrile-butadiene-styrene/glass bead, stress-strain behaviour, crazing, permeability 3−24986
adhesion between glass fibres and resins *(German)* 3−21730
aligned composite form. by solid state decomposition 3−24976
n-alkane cryst. growth on graphite and C fibre surfaces 3−20703
alloy, aligned composite prod. by up-transform. 3−39324
anisotropic shells, geometrically nonlinear theory variant and transverse shear 3−22668
Annual review of materials science vol. 2, 1972 3−24778
bending and torsion of anisotropic beams, analytic solns. from variational methods 3−28864

composite materials continued
bi-material plates, collocated interfaced elastic stress intensity factors 3—21724
boron-epoxy laminates, stress wave propagation under impulsive loads 3—18698
brittle matrices, reinforcement by glass fibres 3—31140
brittle matrix ductile fibre, fracture mechanics 3—31134
brittleness, materials containing second phase dispersions 3—7841
butadiene-styrene copolymer based filled systems, temp. effect on fracture surfaces 3—25005
carbon fibre reinforced, thermal expansion, 80-400 K 3—18702
carbon texolite, thermal diffusivity at elevated temps. 3—24978
concrete, plain and reinforced, ductility 3—5345
concrete tubes thick-walled, steel wire reinforced, limit analysis under dynamic internal pressure 3—39389
concrete-polymer materials and solid-waste polymer composites, development, properties and uses 3—21733
creep mechanisms and fibre strengthening 3—15773
Cu-Cu$_6$Ce and Cu-Cu$_6$La eutectics, unidirection of growth, microstructure 3—39310
cylinder, helically wound, burst fracture strength under internal press. *(Japanese)* 3—8998
cylinder, helically wound, torsional fracture strength *(Japanese)* 3—5349
cylindrical anisotropic composite plastic shells, filled with incompressible fluid, load anal. 3—22664
cylindrically anisotropic body, under two-dimensional surface traction, stress field 3—6230
elastic laminates, wave propagation using multi-continuum theory 3—3977
elastic moduli, slender rigid inclusions at dil. concs. 3—11671
elastic wave propagation theory 3—2761
elasticity, effects of shape of dispersed particles 3—2750
elasticity, stochastic green functions 3—37794
epoxy laminate, glass reinforced, coupling agents 3—37090
epoxy resin, C fibre reinforced, impact and fracture props. 3—31142
epoxy resin/powder composites, thermal conductivity at low temps. 3—9887
fabrication techniques, book contrib. 3—12445
failure theory, classical approach rel. to damage accumulation 3—37105
fibre composite, review of creep theories 3—15774
fibre composite materials fracture phenomena 3—37089
fibre composite with metallic matrix for use above 800°C 3—18696
fibre reinforced, carbon, review *(Japanese)* 3—18706
fibre reinforced, continuum mixture theory of wave propagation including microstructure 3—24975
fibre reinforced, elastic stiffness analysis, structural design 3—31130
fibre reinforced, fatigue, book contrib. 3—21714
fibre reinforced, matrix fatigue behaviour under repeated tensile loads 3—31154
fibre reinforced, nondestructive prediction of engineering props. 3—34672
fibre reinforced by unidirectional short fibres, elastic properties *(Russian)* 3—24987
fibre reinforced ceramic composites, strength, theories 3—15777
fibre reinforced composites, variational bounds of bulk, shear and Young's moduli 3—18699
fibre reinforced incompressible isotropic elastic materials, universal solns. by inverse methods 3—28865
fibre reinforced mat., continuum theory development 3—34640
fibre reinforced metal, bond strength between fibre and matrix 3—37093
fibre reinforced metal matrix, deform. and fracture behaviour *(Japanese)* 3—34634
fibre reinforced plastic, impact data rel. to fracture 3—8995
fibre reinforced plastic bonded struct. *(Japanese)* 3—18712
fibre reinforced plastics, design problems analysis 3—15790
fibre reinforced plastics, impact resist. *(Japanese)* 3—18705
fibre reinforced plastics, lamination effect on flexure behaviour *(Japanese)* 3—18713
fibre reinforced plastics, strength reliability and design *(Japanese)* 3—18709
fibre-reinforced, elasticity theory with microstruct. 3—530
fibre-reinforced, plates, constant thickness, optimal layouts 3—24974
fibre-reinforced M-M$_7$C$_3$ eutectic, (M = Fe + Co + Cr), M$_7$C$_3$ → M$_{23}$C$_6$ transform. 3—31143
fibre-reinforced materials, acoustic wave reflection 3—16670
fibre-reinforced plates, comment on paper by Lowe and Melchers on optimisation 3—32356
fibre-reinforced plates, constant thickness, optimisation 3—22607
fibrous, multiple fracture, theory 3—34633
fibrous, tensile strength, review 3—24992
filament Nb-Ti superconductor for use in pulsed magnets 3—11992
filamentary, elastic wave propag. characts. 3—6272
filamentary reinforced metals, mech. prop. considerations 3—31155
fracture 3—2760
fracture control technique 3—21726
fracture mechanism based on change in Poisson's ratio *(Japanese)* 3—18710
fracture problems and solns. 3—21725
glass epoxy effect of specimen geometry on fatigue strength 3—21770
glass epoxy plates, post-buckling behaviour 3—27756
glass fabric laminate reinforced, compressive strength *(Japanese)* 3—18715
glass fabric laminate reinforced, torsional strength and void effects *(Japanese)* 3—18714
glass fibre composite, fracture surface energy and transverse fracture 3—12443
glass fibre reinforced polyester laminates, mech. props. *(Japanese)* 3—18707
glass fibre statistical strength distrib. functions 3—31147
glass fibre-resin composites of high strength 3—34638
glass microsphere/epoxy resin, adhesion, hydrolytic stability, thermomechanical props. *(Russian)* 3—31152
glass reinforced plastic cylindrical shell weakened by circular opening, cantilevered, bending 3—31149

composite materials continued
glass reinforced plastic cylindrical shells, creep stability under long-term external press. 3—31144
glass reinforced plastic plates, bending, finite difference method with allowance for creep 3—27762
glass reinforced plastic plates, rectangular, with low shear strength, bending 3—24985
glass reinforced plastic plates with central metal layer, elastoplastic stability 3—24984
glass reinforced plastic rings, temp. deform. 3—27764
glass reinforced plastic rings, wound, residual stresses determ. 3—24983
glass reinforced plastic rings, wound, transverse characts. variation over thickness 3—31150
glass reinforced plastic shell, orthotropic, effect of local load 3—31145
glass reinforced plastic shells, anisotropy of props. 3—24979
glass reinforced plastic shells, cylindrical, stability 3—24982
glass reinforced plastic shells, stability and shear stresses 3—24980
glass reinforced plastic shells, two-way reinforcing system effect on load-carrying capacity 3—27760
glass reinforced plastics, oriented, mech. characts. in shear 3—27779
glass reinforced plastics, residual stresses determ. 3—27763
glass reinforced plastics, tensile deform. analysis 3—31148
glass reinforced plastics, wound, resist. to failure by unwinding 3—24981
glass reinforced plastics in conical shells, stability of strength 3—31146
glass-epoxy laminates, stress wave propagation under impulsive loads 3—18698
graphite epoxy plates, post-buckling behaviour 3—27756
graphite fibre composite, friction and wear 3—39392
graphite filament protective coating development 3—15771
graphite-graphite heatshields, filament wounds 3—37091
hybrid, C and glass fibre reinforced epoxy resin, mech. props. *(Japanese)* 3—18708
hysteroelastic theory, dynamic linear, general solns. with mixed boundary-value problems *(Russian)* 3—28883
in situ production by unidirectional crystalline recomposition of non-crystalline solids 3—18717
laminate composites, fracture mechanism transitions 3—31141
laminated, three-dimensional finite element analysis 3—10275
laminated orthotropic elastic spheres, study of natural vibrations using Rayleigh-Ritz technique 3—22682
laminates, continuum mixture theory of wave propagation including microstructure 3—24975
laminates, glass reinforced epoxy and polyester, creep mechanism 3—9000
layered, harmonic elastic wave propag. 3—6293
lubricant/metal systems, comp. effect on tribological props. 3—15785
materials science and technology treatise 3—2621
metal fibre reinforced ceramics, fabrication and fracture toughness 3—18718
metal matrix/fibre reinforced, solidified, Piobert-Luders band deform. *(French)* 3—39391
metal pressure vessels reinforced with unidirectional glass-reinforced plastic, elastoplastic deform. 3—27761
multi-plate structures in compression, influence of orthotropy, computer-aided analysis 3—21723
multilayer sandwich beams and plates, bending and vibration, finite element analysis 3—26075
multilayer slab system, j_n method for neutron transport problems 3—19896
nylon, glass fibre reinforced, tensile strength 3—2759
oblique fibre sparsely reinforced matrix, constitutive eqns., impact-deflection 3—24990
organic fibre/epoxide, evaluation 3—31132
oriented plastics, failure mechanism 3—31183
osseous attachment of non-porous metals by composite bonding 3—2794
plastic reinforced with carbon fibres, erosion under liq. impact 3—27765
plates, monolithic grid stiffened, steady-state frequencies of vibration 3—16669
polyester resin, casts and laminates, fracture toughness, crack propag. 3—12454
polyester resin and glass fibre strand, investigation for strength improvement 3—15772
polyethylene, filler surface state effect on props. 3—27759
polyethylene coated paper, vapour permeability 3—34667
polyethylene filled with glass fibre and plasticized with rubrax, chemical stability in HCl and H$_2$SO$_4$ *(Russian)* 3—12441
polymer, two-component heterogeneous composition, composite specimen method of dynamic props. simulation 3—27784
polymer based, thermal expansion, review 3—34632
polymer fibre PRD-49 reinforcement, aircraft appl. 3—31133
polymer matrix with C or B fibres for high heat resist. 3—18697
polymeric, crack propag. vel. 3—21727
polymers, molten, composite formation during extrusion, viscoelastic fluids in flow dispersion modes 3—2762
polystyrene, Silas-balloon filled, mech. props. *(Japanese)* 3—21728
Pyrex glass, carbon fibre reinforced, mechanical props., strength 3—18700
reinforced, analogies, modelling and similarity criteria 3—27758
reinforced, strengthening mechanisms 3—21731
reinforced material under uniaxial compression, applied theories applicability in stability problems 3—26084
reinforced plastics, fabrication, design, book contrib. 3—12444
reinforced plastics, matrix materials, reinforcements and fabrication 3—5351
reinforced plastics, testing apparatus, nonuniform heating 3—32033
reinforced plastics with short randomly distributed fibres, failure mechanisms 3—24988
reinforced spherical shells with external pressure, stability and weight optimisation *(Russian)* 3—28873
scanning electron microscope studies 3—12360
secondary fabrication problems 3—12418

composite materials continued
- shell of revolution, variable thickness orthotropic, suppressed bending 3−26088
- shells, optimal design subject to natural frequency constraints 3−32367
- soil mechanics, model for dynamical treatment of anelasticity 3−27957
- solid-solid interface, moving load, steady-state solution for supersonic velocities 3−37796
- steel/mylar composite, dynamic stiffness computation 3−22696
- stiffened flat plates with multilayered composite reinforcement, compressive buckling analysis 3−32308
- stress distrib. in two half-planes due to prescribed forces 3−32331
- stress distribution near tip of array of screw dislocations piled up against an inclusion 3−1625
- stress wave attenuation, geometric dispersion and spatial attenuation 3−26100
- stress wave propagation in laminated plate under impulsive loads 3−18698
- switching materials, conducting particles in semicryst. matrix 3−18201
- tensile testing, application of rule of mixing *(German)* 3−24991
- testing for static proneness, appl. of charge and resist. meas. 3−2787
- thermal sensing, indirect, rheoretical calc. 3−35639
- thermoelectric moduli determination 3−34631
- thermoplastic, fibre reinforced, deformation behaviour rel. to fibre length and orientation 3−8996
- transversely isotropic annular plates with low shear resist., stability 3−22669
- transversely isotropic fibre-reinforced, Saint-Venant's principle for plane deformation 3−32333
- transversely isotropic spherical shell coupled with elastic foundation, stability 3−28870
- twisted superconducting conductors, matrix loss meas. from magnetisation meas. 3−11987
- two-component, initial stages of rupture, effect of form of inclusion *(Russian)* 3−27755
- two-component layered material, analytical determ. of uniform strain *(Russian)* 3−12442
- with viscous third inclusions, bulk elastic consts. and Q-factor 3−26074
- wave propagation, continuum theory in laminated composites, elastodynamic model 3−26095
- Al bonded with B fibres, strength characts. 3−21732
- Al matrix composites, environment, application, cost and future, review 3−24977
- Al matrix composites, mechanical props., review 3−15776
- Al matrix composites, survey of fabrication methods 3−8997
- Al/Al_3Ni unidirectional fibre composite, elastic consts., u.s. vel. meas. 3−34637
- Al/B, matrix fatigue behaviour under repeated tensile loads 3−31154
- Al-$CuAl_2$ lamellar eutectics and fibrous eutectics, unidirectionally solidified, microstructure *(Japanese)* 3−18592
- Al-$CuAl_2$-$FeCu_2Al_7$ ternary eutectic, mechanical props. and thermal stability *(Japanese)* 3−15701
- Al-$CuAl_2$-$NiCu_3Al_6$ ternary eutectic, mechanical props. and thermal stability *(Japanese)* 3−15701
- Al-$CuAl_2$-Si ternary eutectic, mechanical props. and thermal stability *(Japanese)* 3−15701
- Al-Si system ternary eutectic alloys, unidirectionally solidified, microstructures *(Japanese)* 3−18593
- B epoxy, effect of specimen geometry on fatigue strength 3−21770
- B fibre compatibility with W substrate and Ti matrix *(Russian)* 3−15784
- B fibre reinforced Al matrix, transverse tensile props. 3−18716
- B fibre reinforced epoxy, discontinuous, impact toughness 3−31137
- B fibre/W substrate, diffusion barrier establishment *(French)* 3−12440
- B filament, gauge length influence on mechanical strength *(Japanese)* 3−18704
- B/Al composite, reinforcement of Ti alloy, compressive strength 3−39390
- B/Al composites, fusion welding, microstructure 3−12361
- B/epoxy plates, post-buckling behaviour 3−27756
- Be/Al filamentary composite, yield pt. phenomena, Luders band propag. 3−34639
- C fibre, elastic consts. 3−27757
- C fibre, Ni-matrix, elevated temp. stability, morphological and mech. prop. degradation 3−31138
- C fibre reinforced, type II, Kaiser effect in stress wave emission testing 3−15783
- C fibre reinforced polymers, nondestructive testing, fatigue performance 3−31213
- C fibre reinforced resin, crack propag. energy 3−8994
- C fibre/glass fibre sandwich structure, Izod impact props. 3−31131
- C fibres in epoxy, matrix and interface modification effect on local fractures 3−5348
- C-C composites, high-temp. strength up to 2000°C 3−31135
- Cu/W fibre, thermal cycling 3−37092
- Cu-W fibre composite, thermal expansion *(Japanese)* 3−18703
- Fe/Cu single-fibre composite, multiple yield phenomena 3−34636
- Fe-Fe_2B fibrous eutectic alloy, thermal stability 3−8999
- Fe-Ni:Al_2O_3, dispersion strengthened, alloying additions effect on structural stability 3−15782
- Mg/MgO, effect of dispersed particles on structural stability 3−39376
- MgO-C, elasticity, effects of shape of dispersed particles 3−2750
- Mo fibre, annealing temp. effects on props. rel. to composite fabrication *(Czech)* 3−31153
- Nb-Ti superconducting wires, clad in Cu, effect on mag. instability 3−11989
- Ni plated composite powders addition in sintering process study of Cu-γ_2 (Cu_9Al_4)-Ni mixed powder compacts *(Japanese)* 3−15730
- Ni/Al_2O_3, electrodeposition, phys. and mech. props. 3−37059
- Pb impregnated porous glass, Pb morphology, elec. microscope obs. 3−8315
- SiO_2, silica, fibre fabric, influence of heat treatment on props. *(Russian)* 3−15775

composite materials continued
- TaC fibres and nichrome matrix binary eutectic, orientation determ. by etching 3−18701
- Ti/Al_2O_3, filament reinforced, reactivity and interface characts. 3−31136
- Ti/W, solid-state interfacial reactions 3−31139
- UO_2 composite fuels, assessment of heat conduction effectiveness 3−23443
- W composite cast heat resistant alloys, creep rupture strength 3−24989
- W fibre, annealing temp. effects on props. rel. to composite fabrication *(Czech)* 3−31153
- W fine wire with thoria dispersion, creep behaviour 3−37086
- W wire reinforcement, creep and durability 3−31151
- W-3Re:2ThO_2, dispersion hardened fibres in Ni superalloy matrix 3−15696
- W-vinyl powder composites, for acoustic dissipation 3−19106

composite models of hadrons
- *see also parton model; quarks*
- $A+B \rightarrow C+X$ (A, B, C=l, γ or hadron) e.m. interaction at high energies, parton model 3−17059
- Adler inelastic lepton-hadron sum rule saturation in quark-parton model 3−849
- Adler sum rule for neutrino processes, analysis 3−6586
- baryon two-body model for strong decay rates of baryon resonances 3−35808
- Bogolyubov transformation for oscillator levels of composite particle interacting strongly with boson field 3−26321
- charge distrib. of partons and scaling in deep inelastic scatt. 3−10725
- charge distrib. of partons and scaling in $pp \rightarrow ll$ anything 3−10726
- collisions at high transverse momentum, point-like interaction behaviour, parton-model calcs. 3−38092
- compulsory resonance formation 3−865
- dual parton dynamics and distribs. reln. to hadron level struct. 3−29220
- dual parton model of elementary particle interaction, string model 3−26318
- dual-parton model for high-energy πN scattering in forward and backward regions 3−32702
- equal-time correlations in hadrons 3−23007
- Fermi model, convergence function and e.m. form factors in time like region 3−13852
- fields, light cone dominance of vertex structures and asymptotic behaviour of elastic form factors 3−37992
- fireball decay, explicit solution of integral equation 3−16969
- fractionally charged partons, test by meas. of deep-inelastic bremsstrahlung in scaling region 3−4180
- gluon model in three dimensions, scaling 3−38051
- inclusive reactions at large transverse momenta, bound-state model 3−918
- lepton-hadron scattering, Han-Nambu partons and internal symm. 3−863
- multichannel interaction of particles with identical quantum numbers including composite particles 3−32627
- new Nagoya model of urbaryons, study of $\Delta S=0$ and $\Delta N'=1$ non-leptonic decay processes 3−26289
- new particle obs. by Niu group, effect of form factor on decay rate 3−32653
- non-perturbative parton model for two-photon semi-inclusive reactions 3−10709
- nonlocality in high energy ν expts., internal particle mass effect 3−10676
- parton clusters and order parameters 3−864
- parton model, applic. to e.m. processes 3−38055
- parton model, equivalence to bootstrap theories 3−10720
- parton model, Galiean invariance in infinite momentum frame 3−14026
- parton model, Regge cuts, reggeon coupling functions, review 3−6632
- parton model, relevance of short distances and light cone behaviour of currents 3−13816
- parton model, reln. between multiplicities in lepton-hadron, lepton-lepton and hadron-hadron processes 3−26315
- parton model and Bjorken scaling in deep inelastic ep scatt. 3−4172
- parton model approach to inclusive neutrino scatt. 3−6596
- parton model for $\nu_\mu p \rightarrow \mu^- e^+ e^- +$ hadrons in deep inelastic region 3−35780
- parton model for deep inelastic ep scatt. 3−13923
- parton model for electroproduction, semi-inclusive, Drell-Yan scaling 3−38053
- parton model for two-photon processes 3−38050
- parton model predictions for azimuthal dependence of semi-inclusive deep inelastic electroproduction cross section 3−23087
- parton model relations for deep inelastic structure functions, light cone analysis 3−29213
- parton model study of t/s scaling in strong interactions 3−6658
- parton model with variable intermediate state mass for photon absorpt., changing after photon absorpt. 3−13896
- parton-model, role in deep-inelastic processes 3−13938
- phenomenological mass operator for internal dynamics, application to baryon e.m. form factors 3−10693
- phenomenological mass operator leading to same slope of meson and baryon trajectories and invariant form factors 3−10719
- photoproduction amplitudes sum rule, deep-inelastic limit, covariant parton model discussion 3−32668
- quark parton model for polarisation effects in ν and ν scattering 3−10680
- quark-gluon chain model of nucleon 3−4187
- quartet model of hadrons, review *(Japanese)* 3−14023
- relativistic composite model for interactions of baryons in terms of B-S amplitudes 3−14024
- scaling breakdown at 10^{-15} cm, speculations 3−38004
- selection rule of weak processes based on law of configuration conservation, decays of new particles 3−32652
- softened-parton-field model for deep inelastic Compton scattering 3−23083
- statistical bootstrap, explicit solution 3−23014
- string model interaction, construction of general vertex operator 3−26319

composite models of hadrons continued
urbaryon rearrangement and breaking of line reversal relations 3−35807
ep→e′AB, reaction with highly virtual photons, parton model 3−13965
π^+n inelastic collisions at 60 GeV/c, data anal. by fireball, fragmentation and quark models 3−17117

composite particles
see also alpha-particles; deuterons; nuclei with A ≤ 5; tritons
bosons, radiative decay model, three particle formalism for unstable composite particles 3−13867
fermion pair composites, Bose condensation 3−38121

composition measurement *see chemical analysis*

compressibility
see also compressibility of gases; compressibility of liquids; compressive strength
alkali halides, isotherms, calc. from shock wave data 3−27067
alloy, random cubic binary solns., atomic pots. applic. 3−24814
alloys, additivity rule conformity in shock compression *(Russian)* 3−31102
eclogites, at high pressure and temp. *(Russian)* 3−9132
elements, V and VI, Gruneisen parameters, from thermal expansion, compressibility and Morse function 3−17983
equations of state of solids formulation method using shock compression data and second law of thermodynamics, Monte Carlo simulation *(Russian)* 3−30239
graphite electrical resistivity change during compressive tests 3−23432
hard sphere fluid with attractive square wells, spatial struct. and thermodynamic props. 3−26182
ice, linear compressibility at low hydrostatic pressures, meas. technique 3−16051
ice compression in freezing of supercooled water in capillaries 3−24247
intermetallic lightweight cpds., dynamic yield strengths, compressional and Hugoniot elastic parameters 3−17927
ionic solids, Rao-Keer constant and compressibility, relation to Gruneisen constant 3−15025
metal, isothermal compression relation 3−15721
metal and alloy, statistical thermodynamic properties crystal binding, charge neutrality 3−30084
metals, verification of Thomas-Fermi model under high pressure 3−20816
partial, isotropic and anisotropic media, tensorial expansions for plastic flow 3−24182
phenol, I and II, under press., vol. compressibilities at 10°C and phase diagram at 0°C 3−24269
polymer, shock-compressed, physicomech. props. variation with loading 3−30204
polymethyl methacrylate Gruneisen parameter calc., comparison with data 3−20221
polystyrene, Gruneisen parameter calc., comparison with data 3−20221
polytetrafluoroethylene, Gruneisen parameter and interchain specific heat, pressure dependences, compressibility and u.s. velocity meas. 3−27129
quantum crystals, Fermi-type, phenomenological theory 3−24238
shock wave propag. in medium with variable acoustic characts., conversion to isentropic compression *(Russian)* 3−4810
solids, universal equation of state *(Russian)* 3−7898
X-ray diffraction photographic technique for thermal expansion and compressibility meas. 3−26934
Ag, isothermal compression meas. using NaCl phase transform. as internal pressure calibrant 3−36349
Al/Cu lamellar cpd., dynamic compressibility *(French)* 3−1686
Al_2O_3, cakes, formed by slip casting, compression permeability 3−8974
Br_2, solid, phonon dispersion and symmetry, intramolecular degrees of freedom influence on compressibility and elastic constants 3−24236
CaF_2 type fluorides, changes in real structure due to compressive impact 3−33503
Cd, under hydrostatic press., search for first and second order phase transforms. *(Russian)* 3−15013
CdTe, thin films, photovoltaic effect dep. on mech. stress *(Russian)* 3−30518
Cs, from Fermi surface cross section press. depend. 3−33778
CsCl, compression to 32 kbar, neutron diffr. study 3−4808
Fe_2O_3 polycrystalline powder ceramic, stress, high temp., grain size, porosity and O_2 partial pressure effects on creep 3−27738
GaSe, anisotropic linear expansion and isothermal compressibility 3−4860
H_2, at densities 0.5-2 gm/cm^3, 0.4-8 Mbar, metallization, eqns. of state determ. *(Russian)* 3−11713
H_2 solid, ground state energy, compressibility, press. 3−33479
^{3}He solid, pair interaction from press. and compressibility 3−33718
^{4}He solid, pair interaction from press. and compresssibility 3−33718
$HfTiO_4$, $Hf_{1.26}Ti_{0.74}O_4$, thermal expansion coeffs., compressibility, polymorphism, X-ray diffr. obs. 3−8976
I_2, solid, phonon dispersion nd symmetry, intramolecular degrees of freedom influence on compressibility and elastic constants 3−24236
InBi, elastic behaviour, u.s. wave velocity meas. 3−27048
NaCl, compression to 32 kbar, neutron diffr. study 3−4808
$(U,Pu)O_{2-x}$ fuel pellets, compressive creep 3−6991
$UO_{2\pm x}$, polycrystalline, stoichiometry influence on compression creep 3−6992
$ZrTiO_4$, thermal expansion coeffs., compressibility, polymorphism, X-ray diffr. obs. 3−8976

compressibility of gases
see also high pressure phenomena and effects
flow-resistance gas heater 3−19173
fluids and fluid mixtures, prediction of thermodynamic props., applications 3−34699
hypersonic turbulent flow at wedge compression corner, heat transfer 3−14465
methane, compressed, adiabatic, density depend., from u.s., velocity obs. *(Russian)* 3−11354

compressibility of gases continued
methane, compressibility factor calc. for pseudo Lennard-Jones system representation 3−38531
tube, unidirectional closed, piston motion under high initial pressure *(German)* 3−23655
Ar, crit. region, gravitational effects on small-angle X-ray scatt. 3−20867
N_2, compressibility factor calc. for pseudo Lennard-Jones system representation 3−38531
Xe, compressibility factor calc. for pseudo Lennard-Jones system representation 3−38531

compressibility of liquids
acoustic wave propagation in viscous compressibile liquids confined in elastic tubes 3−23767
alloy, random cubic binary solns., atomic pots. applic. 3−24814
barker-Henderson local-compressibility approx., anal. and comparison with other theories 3−24171
bubbles, nonspherical, effect on motion 3−1444
chemical systems, adiabatic compressibility expressions for complex sound vel. derivation 3−17892
computation using Henderson's partition function, temp. depend. 3−30268
glycerin, viscous low compressibility medium *(Russian)* 3−4870
heavy water, excess u.s. absorpt., excess, from relax. times and relaxing compressibility 3−4813
nonlinear, interaction of vibr. enhancement and orientational Kerr effect 3−32590
seawater, bellows-type differential compressimeter, testing to 900 bars 3−28090
seawater, isothermal compressibility rel. to temp. dependent data for sea salts 3−37189
ternary mixtures, u.s. study, free volume 3−7853
water, calc. using scaled particle quasilattice model 3−36256
water, compression by strong shock waves *(Russian)* 3−7804
Ar, crit. region, gravitational effects on small-angle X-ray scatt. 3−20867
C, complex relation with press., model approach *(Russian)* 3−14981
CO_2, liquid, u.s. velocity, thermodynamic data determ. 3−17930
KNO_3, aqueous dilute solutions, u.s. velocity measurements 3−38621
$NaNO_3$, aqueous dilute solutions, u.s. velocity measurements 3−38621
Pb-Sn alloys, from u.s. velocity obs. 3−24215

compressible flow
see also compressibility
aerofoil, scattering of sound 3−9759
automated streamline analysis, optimum interpolation, maps, field parameters 3−3163
boundary layer laminar flow on moving continuous surfaces, parametric study 3−26805
circular aerofoils with asymptotic critical Mach number, numerical results in relation to transonic similarity rule 3−17533
convergent conical nozzles, compressible flow investigation 3−23808
corner flow, viscous, subsonic and supersonic theory 3−14466
diffusers, truncated conical, performance 3−11421
dissipative gas dynamics, evolution of finite disturbances 3−29877
elastico-viscous fluid flow in a circular tube under pressure gradients varying with time 3−33264
finite element soln. of 3D flow problem and Reynold's eqn. 3−1351
gas at reduced ambient press., flow through fibrous filter 3−17511
gas high pressure flows with and without heat transfer 3−38389
heat capacity determ. of compressibile fluids at high pressures by flow calorimetry 3−22284
heat transfer, between semi-inifinite surface and incoming flow, temp. field determination 3−631
heat transfer, hydrodynamic resistance, turbulent and laminar flow in circular tube 3−36080
heat transfer between semi-infinite surface and flow, analytical solution 3−630
high speed flows heat transfer steady state disturbances in compressible laminar and turbulent boundary layers 3−38354
hydraulic mains dynamical charact. *(Russian)* 3−20355
hypersonic spheres, ionized turbulent wake structure study using survey arrays of ion probes 3−11356
inviscid three-dimensional, extremum principle 3−11424
jet-like exhaust flow, refraction of acoustic duct waveguide modes 3−33244
laminar boundary layer flow at a three-dimensional stagnation point with intensive suction or injection 3−33234
laminarizing nozzle flows, design 3−23807
low Mach number free convective flow, general elliptic method for computational soln. 3−20347
Mach reflection of shock waves, slip stream behaviour *(Japanese)* 3−38393
mixing, heterogeneous, turbulent transport coeffs. 3−36143
nonstationary flows of general gas, determ. of time-invariant parameters *(Russian)* 3−29878
one dimensional flow of gas with arbitrary internal rate processes, thermodynamic relaxation *(German)* 3−20346
one-dimensional frictional unsteady flow with heat transfer, numerical procedure for solution 3−11420
penetration of cone into compressible fluid, analytic soln. for subsonic case *(Russian)* 3−29879
relativistic Navier-Stokes eqn., plane solns. for laminar incompressible and compressible flows 3−17556
stationary, of perfect fluid, variational inequality *(French)* 3−20269
steam generator tube plate, convective heat flow *(Russian)* 3−16768
subsonic stream under acoustic radiation, instability of vortex sheet 3−7387
transonic, about circular cones with incidence, pressure measurements 3−17531
transonic, analogies between inert viscous and non-equilibrium steady flows 3−17532
transonic aircraft compressor, unsteady *(French)* 3−26044

compressible flow continued
  transonic flow, nonlinear wave propag. 3 — 29876
  turbulent 2D boundary layer with arbitrary press. gradient, theory for anal. 3 — 1392
  turbulent boundary layer, thermally stratified, effect of surface roughness change 3 — 4580
  turbulent boundary layer flow along curved surface, particular solns. of energy eqn. 3 — 1402
  turbulent boundary layer in compressible gases with suction, calc. method 3 — 33224
  turbulent boundary layers at moderately large Reynolds no.; higher order theory 3 — 20337
  two dimensional supersonic sails in high-Mach number airstreams, centred compressions 3 — 20345
  two-dimensional laminar compressible flows with embedded shock waves, Navier Stokes eqns. numerical soln. 3 — 26822
  viscous flow problems, cell type finite difference methods 3 — 33241
  viscous fluids flow analysis by finite-element method 3 — 38348
  water compressible flow, discharge velocity issuing from nozzles 3 — 33318
  wings with blunt trailing edges, lift and drag meas. *(German)* 3 — 23754

compression, bandwidth *see bandwidth compression*

compressive strength
  see also compressibility
  acrylic resin, tensile and impact strength, 4.2-300 K 3 — 25010
  alkali halides, single crystals, solute strengthened 3 — 7835
  cement mortar strength results using ASTM standard test method C348 and C349 3 — 34673
  ceramic, reinforced composites strength, theories 3 — 15777
  cermet steel, effect of insoluble residue in starting powder *(Russian)* 3 — 8946
  composite, glass fabric laminate reinforced *(Japanese)* 3 — 18715
  concrete, compressive and tensile props. 3 — 5350
  concrete, strengths and elasticity, effect of long time exposure to elevated temperatures *(Japanese)* 3 — 5352
  foam-light refractories, strength testing apparatus *(Russian)* 3 — 27812
  glass reinforced plastic shells, anisotropy of props. 3 — 24979
  glass reinforced plastics in conical shells, stability of strength 3 — 31146
  martensite, work hardening origins, strength-differential effect 3 — 37067
  plastic, temp. effect on stat. characts. 3 — 31177
  PMMA, cast, bubble inclusions effect on mechanical props. 3 — 27789
  polyformaldehyde blocks, stress relax. props. in tension and compression, supermol. struct. influence 3 — 25004
  polymer, macroscopic yield criteria 3 — 31162
  polymer compositions based on silicone adhesives, antifriction and mech. props. 3 — 25012
  polystyrene composite, Silas-balloon filled *(Japanese)* 3 — 21728
  post-buckling and imperfection-sensitivity of wide integrally stiffened panel under compression 3 — 13590
  shear stress equation in compressed crystal 3 — 20790
  steel, carbon *(Japanese)* 3 — 24870
  steel, carburized, impact-fatigue strength, effect of structurally-free ferrite in core 3 — 21691
  steel, fatigue strength, small plastic deform. effect. 3 — 27688
  steel, maraging, strength differential between uniaxial compressive and tensile flow stresses, and dislocation interactions 3 — 18652
  steel, prestress effect on low-cycle fatigue failure 3 — 21758
  steel, strength differential effect, test temp. and microstruct. influence 3 — 39370
  stress/strain test data analytical evaluation 3 — 25024
  testing, device for sheet materials 3 — 18759
  C fibres in epoxy, matrix and interface modification effect on local fractures 3 — 5348
  Cd, Fermi surface changes under uniaxial compression 3 — 20998
  Cu, fatigue strength, small plastic deform. effect 3 — 27688
  Cu, malleability and plastic anisotropy study 3 — 18651
  Fe, cast, shear, compressive and tensile characts., comparison 3 — 27674
  Fe alloys, strength-differential effect, effective modulus interpret. 3 — 37063
  Fe alloys, strength-differential effect, effective modulus interpret. 3 — 37064
  Ge, ⟨100⟩, ⟨110⟩ and ⟨111⟩ axes, uniaxial shock-wave loading 3 — 4807
  Ir, malleability and plastic anisotropy study 3 — 18651
  MgO-SnO_2, ceramic, pressure and comp. depend. *(Russian)* 3 — 15745
  Ti alloy skin-stringer panels selectively reinforced with B/Al composite 3 — 39390
  Ti alloys, fatigue strength, small plastic deform. effect. 3 — 27688
  Ti alloys, strength differential effect, test temp. and microstruct. influence 3 — 39370
  Zn, Fermi surface changes under uniaxial compression 3 — 20998

compressors
  adiabatic compression units, double-chamber 3 — 22563
  intake duct, acoustic modes propagation and determ. of acoustic field 3 — 5787
  recirculation, for hot gases 3 — 28803
  $LaNi_5$-hydride, thermal absorption compressor for H refrigerator *(German)* 3 — 28503

Compton effect
  see also electron scattering
  analytic invariant amplitudes for photon-hadron interactions with discrete symmetry 3 — 26310
  clusters of galaxies, X-ray emission rel. to cluster vel. dispersion 3 — 37463
  coherent photon beam induced, quantum model and classical interpret. *(French)* 3 — 35794
  condensed unbounded medium, photo-Compton currents 3 — 36636
  deep inelastic scattering using 18 and 20.5 GeV bremsstrahlung 3 — 13925
  derivation for non-stationary and bound electrons 3 — 36956
  diamond Compton profiles 3 — 11649

Compton effect continued
  dual currents with cut-off, construction of amplitudes 3 — 17071
  duality results for p-n electroprod. struct. function difference 3 — 13870
  educational demonstration apparatus 3 — 45
  electron momentum distrib. measurement using γ-ray Compton scattering 3 — 30150
  electroproduction, inelastic, Regge pole model 3 — 23071
  Fe, Compton profile and electron distribution, meas. using Kα X-rays 3 — 1982
  finite energy sum rules for forward scatt. on N, determ. of Regge behaviour 3 — 13897
  first-order non-Abelian determ. of generalized Cabibbo-Rad cati theorem 3 — 26307
  fixed poles in Compton scattering, relevance of short distances and light cone behaviour of currents 3 — 13816
  fixed poles in pion Compton scatt. 3 — 10706
  fixed-pole residues and operator Schwinger terms, connection 3 — 35791
  forward polarized, positivity, subtractions and the moduli of scattering amplitudes 3 — 23090
  gauge invariance for vector meson scatt. of pseudoscalar mesons 3 — 35797
  graphite, X-ray plasmon and Compton scattering 3 — 30144
  helicity structure functions, scaling behaviour 3 — 17032
  high intensity radiation, stimulated Compton scatt. by free electrons 3 — 23075
  integral bounds on total cross sections, determ. using analyticity crossing symmetry and unitarity 3 — 13868
  internal at nuclear transition energies comparable with electron mass *(Russian)* 3 — 23262
  inverse, wave scattering in magnetoactive plasma 3 — 1487
  inverse Compton scattering of synchrotron radiation, circular polarisation and astrophysical appl. 3 — 37281
  ionic crystals, calc. of Compton profile 3 — 33544
  isobar prod. and peripheral scatt. models for cross-section of inelastic Compton effect on ρ 3 — 17053
  isotropic X-ray background, inverse Compton models and hot intergalactic gas 3 — 13082
  laser-plasma interaction, plasma heating, inverse bremsstrahlung 3 — 23887
  medical applications, internal tissue density measurement 3 — 25596
  molecular Compton scatt., $C_4H_8O_2$ isomer profiles 3 — 38301
  molecular X-ray Compton scattering, comparison of line profiles 3 — 20170
  moving electron gas, Compton scattering effects 3 — 37291
  non-Abelian second order, and generalized magnetic-moment radius theorem 3 — 23066
  non-forward scattering amplitude, relevant to two-photon correction, generalization of Bjorken-Feynman scaling 3 — 14026
  non-linear and inverse Compton effects rel. to astrophysics and Crab pulsar 3 — 23098
  nonforward scattering at high energies, study using Regge model with fixed poles 3 — 10704
  nonlinear inverse radiation from the Crab nebula 3 — 13070
  nuclear correlations and isovector current-current processes 3 — 17143
  nucleon scatt., Regge model satisfying scale-invariance 3 — 13904
  off-shell absorptive amplitudes and positivity restrictions for asymmetry effect 3 — 29206
  paraffin, Compton profiles 3 — 33806
  photon-hardon diffractive interactions, vector-meson dominance and coupled Pomeranchukon model 3 — 23095
  photoproduction amplitudes from local current commutators, sum rule 3 — 32668
  plasma scattering of laser beam, electron temp. and diffusion 3 — 17581
  profile measurement, using solid-state detector, optimum conditions 3 — 25956
  recoil-proton polarisation in neutral-pion photoproduction and in proton Compton scattering 3 — 10701
  Regge model for on and off shell scattering, nonleading energy behaviour and breaking of scaling in νW_2 3 — 13915
  Regge pole model, connecting with deep inelastic scatt. 3 — 16994
  Reggeization and gauge invariance in photoproduction and compton scatt. 3 — 13970
  relativistic electron scatt. by plasma turbulence, polarisation of h.f. radiation 3 — 23859
  scattering, existence of right signatured fixed poles with polynomial residues, nonleading Regge behaviour 3 — 13914
  scintillators, liquid, Compton edge determination 3 — 25881
  small molecules, mol. momentum distributions, Compton profiles, effects of bonding 3 — 17393
  Sn transport code for X-ray Compton scatt. from Maxwellian distrib. of electrons 3 — 26169
  supernovae expanding shell, effect on line spectrum 3 — 28171
  synchrotron radiation polarisation by inverse Compton scattering, astrophysical appl. 3 — 25359
  Teflon, Compton profiles 3 — 33806
  transition metals, anisotropy of Compton profile 3 — 30136
  unpolarized scattering, contribution of spin-dependent forward Compton amplitude 3 — 4167
  vector meson dominance, light cone expansion and corrections 3 — 13920
  virtual Compton scattering, presence of fixed singularities in T_1 3 — 35800
  virtual scattering, fixed poles, perturbative approach to parton model 3 — 29211
  in X-ray anomalous transmission through perfect Si crystals 3 — 24149
  X-ray background radiation, inverse Compton origin 3 — 25489
  X-ray inelastic scattering, electron momentum distribution in solids, low energy 3 — 30135
  X-ray scattering, Compton profile meas. with solid state detector 3 — 30137
  X-ray scattering, Compton profile using solid state detector 3 — 30138
  X-ray scattering in solids 3 — 30141
  γd, comparison between photoproduction and Compton scattering using VDM 3 — 13993

Compton effect continued
  $\gamma d \to \gamma d$, high-energy, generalised vector meson dominance model in relativistically extended quark model 3−26314
  γd scattering, 8 and 16 GeV, vector dominance model prediction difference in p and n cross sections 3−13882
  γe, scattering amplitude determ. including radiative correction, calc. of polarization coeff. *(Russian)* 3−23076
  γn, residue of J=0 fixed pole, ratio for γn to γp, finite energy sum rule study 3−23068
  $\gamma N \to \gamma +$ hadrons, connection with deep inelastic electroproduction in softened-parton-field model 3−23083
  γN scattering, determ. of couplings of f, σ, η, A_2 and π to photons and nucleons 3−846
  γN scattering, review 3−13876
  γp, comparison between photoproduction and Compton scattering using VDM 3−13993
  γp, residue of J=0 fixed pole, ratio for γn to γp, finite energy sume rule study 3−23068
  $\gamma p \to \gamma p$, 650-1350 MeV, Compton scatt., 60-140° CM 3−10702
  $\gamma p \to \gamma p$, high-energy, generalised vector meson dominance model in relativistically extended quark model 3−26314
  $\gamma p \to p'\gamma'$, differential cross sect. meas. in first resonance region 3−13924
  γp scatt. at 2.2 GeV, verification of Kramers-Kronig relation 3−23084
  γp scattering, 8 and 16 GeV, vector dominance model prediction 3−13882
  p Compton scattering, 2-5 GeV, meas. of forward cross sections, comparison with vector meson dominance model 3−13878
  p Compton scattering of 3.5 GeV polarised photons, asymmetry measurement 3−13879
  p-n mass difference, Compton amplitude representation, scale-invariance of A_2 meson 3−13863
  pγ nonforward scattering at high energies, study using Regge model with fixed poles 3−10704
  pγ scattering in region of second πN resonance, polarisation of recoil protons 3−10700
  π Compton scatt., Regge pole and scale invariant model 3−13899
  Al, localised orbital wave functions, comparison between theory and expt. 3−8082
  Ar, localised orbital wave functions, comparison between theory and expt. 3−8082
  BN crystalline, Compton profiles calc. 3−18508
  Be, multiple X-ray scattering effect on Compton profile 3−17867
  Ge, Compton profiles 3−11649
  H plasma, underdense, Compton scatt. of laser radiation by ions 3−20431
  He, scatt. of 25 keV electrons 3−38237
  Li, Compton profile compared with RPA approx. for conduction electron interactions 3−20762
  LiH, profile meas. using 59.54 keV γ rays of ^{241}Am 3−11650
  Na, Compton profile compared with RPA approx. for conduction electron interactions 3−20762
  Na, core-orthogonalization effect and Compton profile 3−33780
  Ni electron momentum distrib. measurement using γ-ray Compton scattering 3−30150
  NiO, Compton profile anisotropy 3−20763
  O_2, Compton spectra compared with Hartree-Fock calcs. 3−20762
  Si, Compton profiles 3−11649
  Ti electron momentum distrib. measurement using X-ray Compton scattering 3−30150
  TiO, Compton profile 3−30140
  V, anisotropy of Compton profile on single crystal 3−27036
  V, single crystal, band structure 3−21019
  V electron momentum distrib. measurement using γ-ray Compton scattering 3−30150
  VO, VO_2, V_2O_3 and V_2O_5, localised electron states from Compton profile meas. 3−30139
Compton scattering *see Compton effect*
computation *see calculation*
computational physics
  see also numerical analysis
  Algol program for crystal structure illustrations on digital plotter 3−14636
  analog-digital integrator for soln. of partial differential equations in mathematical physics *(Russian)* 3−13542
  anisotropic slab albedo problem, new method for calc. of emergent distribs., soln. of integral eqns. 3−22757
  antiferromagnetic ground state perturbation expansion, computer generation and calc. of higher-order diagrams 3−21199
  atmospheric acoustic ray tracing, computer program 3−3027
  atomic collision chains, vacancies, focusing influence, computer calcs. 3−20777
  atomic collisions, computer program for soln. of differential eqns. for exchange matrix elements 3−35969
  atomic energy R&D aspects applic. 3−4341
  atomic structure, relativistic program to calc. angular momentum coefficients 3−35957
  atomic structure for bound states, critical review of computer programs 3−29466
  atomic structure of face of growing crystal, computer simulation 3−33472
  axially symmetric electron optics systems, e.s. field computation 3−802
  Ball-Zachariasen scatt. eqn., analyticity of soln. Riemann surface, numerical determ. 3−16593
  basis-set optimising SCF program OPIT, job control and scheduling for large applications programs 3−29565
  binary systems, interdiffusion coefficients calc. 3−30292
  bubble chamber events recognition by Heidelberg automatic system 3−19306
  bubble chamber photographs, pattern recognition, global transformation 3−6080
  bubble chamber photographs, small angle deflection detection in beam track 3−6079
  bubble chamber pictures, automatic processing 3−6077
  burnup optimisation using modal expansion method 3−6986
  Cartesian force consts. determ. 3−4423
  chemical laser, numerical formulation for constant-gain calcs. 3−22877
computational physics continued
  collisionless plasma with point particles, variational techniques for numerical simulation 3−20663
  collocation constant calc. 3−4042
  combustion gases, thermal radiation 3−14419
  condensing annular-mist flow, integral anal. 3−1432
  configuration interaction calcs., iterative method for determ. of eigenvalues and eigenvectors 3−23465
  conformational anal. method for O-containing heterocycles 3−29559
  control rod drop for pressurized water reactor, hybrid simulation 3−6999
  Cosmos 268 rocket (1969-20B) orbit analysis, wind speed data 3−9309
  Coulomb wavefunctions, remarks on computation 3−10253
  coupled-reaction-channels study of (^{3}He,t) reactions, computer program analysis 3−32883
  crystal defect, atomic vibrational behaviour, time averaged atom arrangement, computer simulation 3−33512
  crystal dissolution morphology, computer simulation 3−4847
  crystal electronic states simulation, using analogue computer with three-dimensional resistance network *(French)* 3−20979
  crystal model simulation by computer, SDMPLT 3−27092
  crystal structure anal. using interactive graphics in hierarchical computing system 3−26923
  crystal structure lacking symmetry centre, calc. of structure amplitude phases 3−23964
  crystallographic fast Fourier transforms 3−23959
  crystallography, electron diffraction data reduction and structure analysis, DEC-PDP-9, techniques 3−26956
  crystallography, IUCr Commission, objectives, experience, developments, report 3−26927
  crystallography, localisation of atoms on three dimensional electron density syntheses 3−33422
  crystallography, organic structures, computer-aided systematic search 3−33420
  crystallography, solution of integral eqns. of structural analysis 3−33421
  cylindrical sources, radial distrib. of emitters calc. using computer program 3−36209
  d.c. heated conductor, computer calc. of thermophysical props. *(German)* 3−30442
  digital computer control algorithm for diameter control of Czochralski grown garnet 3−12289
  digitally controlled double crystal X-ray spectrometer 3−32231
  discs, hollow and solid, with loadings having rotational symmetry, stress and strain calc. *(German)* 3−32349
  dislocation motion, point obstacles, stress, geometric statistics, simulation 3−34517
  dislocation networks and cells, stress distrib. mapping by computer, rot. stress field obs. 3−11626
  Doppler effect laser velocimeters, evaluation of systematic error by computer simulation *(Russian)* 3−16573
  dye laser, electronically tuned by acoustooptic filter, transient analysis, computer simulation 3−4098
  EAS electron component, Monte Carlo simulation for single and multi-cored showers 3−12917
  Einstein tensor, computation from covariant tensor, FORMAC program 3−10365
  electron energy deposition in gaseous mixtures due to excitation and ionisations, computer program 3−35970
  electron gun design computational problems 3−807
  electron scatt., analytic evaluation of integrals in variational calcs. suitable for computer solns. 3−19486
  electron scattering amplitude precise determ. from crit. voltage obs. 3−24003
  electron-atom collision cross section calcs., general formulation of computer programs 3−7075
  electron-atom scattering theory, non-exchange type integral evolution program 3−23496
  electrostatic energy matrix calc. by computer in Racah-Slater method 3−26185
  elementary particle scatt., program for integration of phase-space to determine cross-section 3−10657
  energy spectrum of inelastically scattered neutrons, calc. using Monte Carlo program *(German)* 3−35926
  e.s.r. data, paper tape recording and use of computers for signal improvement 3−27393
  excitation spectra interpretation by fitting eigenvalues of Tanabe-Sugano matrices 3−2588
  expansion equation of state subroutine for one-phase and two-phase behaviour of material 3−27131
  experimental data gathering and processing and control, DESY on-line system 3−19353
  Feynman diagrams, computer calculation, using REDUCE package 3−10684
  finite sized plates bonded to elastic half space, finite element analysis 3−508
  fluid dynamics, numerical solution, extensions to Eulerian methods 3−20266
  fluid transport algorithm, flux corrected, for soln. of continuity eqn. 3−23668
  Fourier contouring and molecular modelling using three dimensional computer graphics 3−26925
  Fourier transform spectroscopy with PDP 11/20 computer 3−28549
  gamma camera, parallel hole collimator design using optimization theory 3−10148
  gas, computer program for fitting time of arrival and shock peak overpressure data 3−36123
  gas dynamics problems, numerical methods of soln. 3−1416
  Genap III, random binary digit generator 3−37727
  graphic display driven by mini-computer for crystallography applications 3−26924
  group overlap integrals for crystals and coordination compounds, program for calc. *(Russian)* 3−1590
  growth kinetics and surface structure, computer simulation 3−11556
  hadronic cascades at high energies, Monte Carlo anal. in 3 dimensions and computer simulation 3−10801
  Hartree-Fock method, computer program for multiconfiguration eqn., bound state atoms 3−11113

computational physics continued
heat of mixing of binary liquid systems by thermometric titration, ALGOL program *(German)* 3−22285
helicopter rotor tips, synthesis of shape for noise suppression 3−33210
high intensity proton beams, two-dimensional computer simulation of transverse behaviour 3−22426
high-energy scattering to two particle final states, Durham data bank, analysis and model comparison project 3−29256
high-energy two-body reactions, computation of effective Regge trajectories 3−29234
hologram synthesis 3−16812
holograms, synthesis and restitution, computer simulation *(Russian)* 3−19576
hyperbola, curve fitting and iteration, instructional paper 3−13183
improper problems 3−10250
inelastic cross-sections calc. using Hauser-Feshbach program ELIESE-2 *(German)* 3−35889
interactive computer studies 3−3933
interatomic forces in crystals and molecules, computer program for calc. 3−26922
inverse vibrational problem, computational method based on common solns. of vibrational eqns. of two isotopic species 3−14346
isocon TV camera/mag. tape recorder system for fast oscilloscope trace analysis 3−3856
iterative method for g tensors determ. from crystal e.s.r. data 3−24603
Kepler's eqn., optimised numerical soln., computer program 3−9456
Kepler motion stability, numerical procedure based on Floquet's theorem 3−3282
kinetic theory of the space instability of a radial-limited plasma-electron stream system with preset plasma radial-heterogeneous configuration *(Russian)* 3−11463
laboratory experiments, hierarchical computing for data acquisition, data reduction and control 3−19354
laminar flow of viscous incompressible liquid in channel with step, numerical solution 3−4544
laser atmospheric windows, computer study of transmittance, 2.7-3.2 μ 3−5977
lattice parameters calc. for orthogonal cryst. unit cell, program 3−300[illegible]0
Laue pattern comparison with computed pattern to determine crystal orientation 3−14634
Lennard-Jones liquid near triple point, computer expt. on 864 particles 3−38657
level crossings and Back-Goudsmit effect, computer program for soln. of secular matrix 3−11141
liquid crystal, nematic, deformation in elec. field 3−14681
liquid metal, nearly-free-electron, computer program calc. of form factor and electrical resistivity 3−36585
liquid state, computer simulation studies 3−26958
Lorentz invariant momentum-space integral for particles of equal masses, computer approximation method 3−29182
magnetic probe, three coil, optimisation 3−6029
magnetoplasma toroidal systems, computer simulation of evolution 3−11500
many-particle interaction problems, computation by special purpose processors 3−28972
medial rectus eye muscle, spectral analysis 3−25582
medical applications, conference, Philadelphia, Pa., USA (1972) 3−13136
melting of microcrystals in two dimensions, molecular dynamics simulation 3−27102
metallic thin films, complex refr. index, numerical evaluation 3−16419
metals research, book contrib. 3−10263
MHD code for calc. of decay of linear plasmas 3−20657
microwave, numerical analysis applications 3−32492
molecular coordinates, high precision method for computer programming *(French)* 3−7098
molecular crystals, external modes of vibration, symmetry properties calculation 3−11702
molecular orbital program OPIT, file-handling scheme for data in large applications program 3−29564
molecular vibration, program for calculating frequencies and forms *(Russian)* 3−1193
molecules, linear triatomic, spin-orbit coupling consts., non-empirical calc. 3−23532
moment-method solutions, convergence improvement technique 3−3932
multi-plate structures in compression, influence of orthotropy 3−21723
multidimensional nonlinear subsonic incompressible flow, computer simulation methods 3−23727
multilayer systems, improved integral transport theory by means of space polynomial approx., use of SHADOK code 3−19897
multiple dislocation, stacking fault arrays, stability 3−17824
Navier-Stokes eqns. in inlet regions, numerical solns. for two-dimens. flow 3−20273
neutron beam experiments for HERALD reactor, on-line computer applic. 3−19931
neutron cross sections, role of systematics in data evaluation 3−35907
neutron physics experiments, computer control system, High Flux Reactor at Petten 3−25825
neutron spectra measurements, unfolding methods in foil activation technique 3−3848
neutron transmission through matter, calc. 3−1044
n.m.r. spectrometer, digital data processing 3−6040
nonlinear problems, numerical solution 3−10251
nuclear data ND-160 pulse height analyser modification for high capacity two-parameter analysis 3−23195
nuclear energy level calculations with AROVMI model 3−10257
nuclear Hartree-Fock intrinsic wavefunction projection, program 3−10901
nuclear level-densities for $f_{7/2}$-shell and $d_{5/2}$-subshell nuclei with $A \leqslant 130$ *(German)* 3−35861
nuclear magnetic resonance, polarization target experiment, computer data handling *(French)* 3−13361

computational physics continued
nuclear optical model, OPTICS program for small computers 3−26433
nuclear reactions, neutron-induced, on medium mass nuclei, analysis using computer code THRESH 3−32844
nuclear reactor experiments in ZEBRA fast reactor, on-line computer applic. 3−19930
nuclear reactor fuel elements, deformation effects on temp. distrib., computer anal. 3−26515
nuclear reactor plates inhomogeneous uranium distribution *(German)* 3−11051
nucleation kinetics, electron micrograph evaluation using Quantimet 720 image analysing computer 3−26979
on-line control of intensity meas. accuracy from single crystal diffractometer 3−26921
on-line minicomputer system for control of KUR research reactor 3−1049
optical filter production, computer simulation 3−9934
optical props. and thickness of thin layers, ALGOL 60 procedure 3−683
organic molecule structure solution, Fourier map interpretation, computer produced connectivity diagrams, interactive display system 3−26926
overlapping gaussian and skewed peaks, resolution computer programs 3−3931
partial differential eqns. computer soln. by finite difference method, automatic generation of programmes 3−13538
particle analysis by electron probe, correction program 3−37765
particle beams, cylindrical, numerical graphs of envelopes in presence of space-charge effects and uniform acceleration 3−35459
phonon spectra of superconductors determ. from tunnelling characteristics 3−2204
photonuclear cross section calc. using unfolding distribution theory, soln. by computer *(Rumanian)* 3−23306
photonuclear cross-sections, computer program 3−17231
plane Couette-Poiseuille flows, application of special form of Galerkin's method to heat transfer problem 3−23699
plasma confinement, design and modelling on toroidal surfaces of various types of spiral windings *(Russian)* 3−17646
plasma confinement, numerical simulation of evolution with conversational program 3−11499
plasma models, comparison with electrical network problem, analytical and numerical method combinations 3−1478
plasma of combustion products, statistical properties of parameter fluctuations for subsonic flow 3−17591
plasma physics integrals involving Chebyshev polynomials, soln. by Olver's algorithm 3−19396
plasma simulation nonphysical noises and instabilities due to spatial grid. depend on Debye length 3−20664
plasma theory, nonlinear dynamical problems, simulation 3−20662
plasma turbulent heating, phase space flow, Lagrangian description, computer study 3−38476
plasmas, computer simulation using PIC model, behaviour of hot plasma and turbulent electrical resistivity 3−1479
plastic flow during hot-pressing relative-density of the compact vs temp. 3−39381
Poiseuille flow, simulation 3−7337
polarity correl. method, appl. to graphite moderated reactor 3−6988
protein three-dimensional structures, comparison using computer program 3−4488
proteins, folding process simulation, pseudo free energy, interactive computer graphics 3−26742
quantum electrodynamics, radiative correction 3−10692
R-matrix methods for atomic collision processes, computer programs 3−11171
radiation damage and defects in crystals, computer simulation 3−27033
radiative transfer, transformation of eqn. for numerical soln. of steep source gradient problems 3−19521
radioactive wastes, computer calc. long-term heat generating rates 3−19927
rapid-convergence algorithm for quantum mech. cryst. binding energies 3−1594
Rayleigh scattering computer program 3−4067
reactors, thermal heterogeneous, u-graphite, enriched u and u-water lattices 3−4339
real-time experiments, multi-user on-line computer data-handling system 3−19355
reduced rotation matrix elements, plots and zeros, evaluation using computer program 3−19488
relativistic kinematics for three-body final states 3−10255
relativistic kinematics for two-body final states 3−10254
resistivity pseudosections of buried spherical conductor body 3−9354
Schrodinger eqn., radial type differential eqns., integrating procedure 3−28450
Schrodinger equation, normalised Morse functions, computer subroutine 3−10256
seismic prospecting, refraction data study on first arrivals, digital processing 3−9350
seismic reflectors detection under ocean aboard R/V Atlantis II 3−3179
SHEBA shell element with variable curvature 3−509
shielding and related calcs., computer programs 3−1091
simple cubic crystal, dissolution morphology, simulation 3−1898
simulation of phase transition dynamics 3−645
simulation of plasmas, recent developments 3−17558
simulation of spiral structure of galaxies 3−3376
single-crystal diffractometer data, online control of precision of intensity meas. 3−23961
Sn transport code for X-ray Compton scatt. from Maxwellian distrib. of electrons 3−26169
space groups, FORTRAN computer programs for cosine seminvariants 3−26920
spark chamber gamma camera, computer simulation 3−10173
spark source mass spectrometric photoplates, determination of ion intensities 3−13492
spectral props. of solids, numerical calcs. by integration over Brillouin zone 3−20983
spectrometer misalignment, automatic feedback correction 3−13493

computational physics continued
- stiffness coefficients of plane elastic frames with continuous or noncontinuous girders *(Greek)* 3−6237
- stochastic generator, appl. to neutronic system kinetic response determ. 3−6967
- streamer chamber pictures, computer-controlled measurements 3−19356
- subgrid resolution of flow and force fields 3−26768
- subsonic and supersonic flows, numerical solution 3−4586
- supercritical He for cooling superconducting devices *(Japanese)* 3−15038
- synchrotron guide field imperfections, program for closed orbit minimization by analytic technique 3−25962
- techniques for metals research, book 3−9825
- terrestrial biaxial ellipsoid, reln. between coeffs. of spherical and ellipsoidal resoln. of gravitational force, computer soln. *(Russian)* 3−25160
- transonic airfoils, transonic flow, computational methods airfoil design, review 3−33247
- transport integral eqn. with anisotropic scatt. as linear system computer calc. of matrix elements 3−19522
- transport processes, computer solns. by finite difference methods 3−10398
- TRIUMF cyclotron, CAMAC control applications 3−13375
- TRIUMF cyclotron, control system 3−13374
- two-nucleon effective range parameters with tensor forces, computer program for wavefunction 3−10880
- underwater explosions, computer program for analysis of test data on cavity explosion *(Russian)* 3−26066
- vector coupling coefficients as products of prime factors, computer program 3−10258
- vibrating string wave motion, computer simulation for teaching purposes 3−13181
- VIPUNEN programming system for analysis of large amounts of physical data, especially nuclear physics 3−23194
- viscous compressible flow problems, cell type finite difference methods 3−33241
- viscous flow, two-dimensional, through T-junction, finite difference method 3−11369
- wave propagation in viscous compressible liquids, dispersion reln. soln. using method of eigenvalleys 3−23760
- wear, simulation 3−4802
- Weibel instability, second order effects 3−11493
- Weyl's problem solution 3−10340
- Wilson parameters, binary systems, non-linear regression 3−37115
- X-ray crystallography, program for struct. refinement by least-squares using diffr. from polycryst. aggregate 3−33427
- X-ray diffractometer, automatic, powder samples, computer programmed, pattern file retrieval 3−26946
- X-ray diffractometer, computer controlled, data collection, structure determination, hardware and software 3−26947
- X-ray line broadening analysis by interfacing powder diffractometer with time shared computer 3−4697
- X-ray scattering, two-centre integral evaluation using analytical procedure 3−23514
- X-ray transmission factors, Monte Carlo calculation method, computer analysis 3−38520
- Ar-HCl rotationally inelastic scattering semi-classical calcs. using computer program implemented algorithm 3−11305
- CoD, A-X band system, rotational analysis 3−11245
- Cu, occupied valence bands computation incorporating pseudopotential methods and Korringa-Kohn-Rostoker energy band method 3−8078
- Fe-Si Kossel patterns evaluation *(German)* 3−4693
- field-ion image simulation, Ni_4Mo alloys 3−8804
- $Gd_3Ga_5O_{12}$, garnet, computer controlled Czochralski growth 3−12290
- Ge(Li) detectors, relative efficiencies by Monte Carlo computer program 3−300
- ^4He, numerical calc. of 2-nucleon correlation function 3−6733
- InAs, electron irradiation damage studies 3−33555
- $O_2^+ b^4\Sigma^-_g - a^4\Pi_u$ band system, rotational line strengths computation including spin-orbit interaction 3−11238
- Si, computer calc. of impurity profiles and diffusion 3−20760
- Si, impurity profile, computer calc. 3−24134
- Si, proton irradiated, defect studies by channelling backscattering measurements, computer simulation calcs. 3−33579
- Si crystal with superimposed oxide film, calc. of X-ray diffraction topographs 3−24317
- Si oxidised crystal, computational procedures rel. to X-ray diffraction topographs 3−24152

computer-aided analysis
- *see also computer-aided design*
- acoustic analysis, applic. to speech pathology 3−9654
- Adriatic sea dynamics computer simulation, forecasting of floods in Venice 3−27975
- aerotriangulation of photogrammetric and geodetic observations, SAPGO program, in FORTRAN IV 3−5532
- alloys, information processing of phase diagrams 3−27619
- antenna far field pattern determ. by machine reconstruction of microwave hologram in aperture *(Russian)* 3−35421
- arterial pressure waves 3−28320
- atmospheric ray tracing 3−3027
- automated chemical structure analysis of small-sized organic compounds 3−1142
- axisymmetric buckling of uniformly loaded spherical caps undergoing plastic deformation, numerical soln. 3−37820
- axisymmetric clamped plates subject to displacement and stress constraints, weight minimisation 3−16626
- axisymmetric electrostatic collector design problem, direct numerical solution 3−32490
- binary mixture, T-X diagram calculation *(Spanish)* 3−35531
- biological, $Q\beta$ RNA, sequencing algorithm 3−35226
- breathing, spirometer and elec. impedance plethysmograph meas. 3−25975
- bubble chamber photographs, pattern recognition, global transformation 3−6080
- bubble chamber pictures, automatic processing 3−6077
- cell picture processing 3−5629

computer-aided analysis continued
- chemical analysis, real-time data processing, minicomputer applications *(French)* 3−19363
- chemical analysis by nuclear activation, automated data analysis 3−37743
- chemical reaction, $H + C_2H_4$, stoichiometry effects, rate consts. determ., simulation 3−37118
- classical transmission angle problem of Alt, for four-bar linkages 3−35565
- cloud photographs, motion computation 3−3172
- cloud tracking, digital picture processing 3−3198
- contour search technique for complex roots of transcendental eqns., method of eigenvalleys 3−23760
- corona discharge, in coaxial cylinder, field distribution calc. 3−14605
- creep analysis of transversely isotropic bodies subjected to time-dependent loading 3−39368
- crystallographic fast Fourier transforms 3−23959
- digitised photographs, multiband and multiemulsion automated data handling 3−5999
- dye laser, electronically tuned by acoustooptic filter, transient analysis 3−4098
- e.e.g. patient diagnosis, review 3−25968
- e.e.g. psychology-oriented analysis, circadian rhythms, sensory deprivation, computer program 3−9653
- e.e.g. signals, exponentially weighted running statistics 3−5640
- elastic boundary method for complex structures *(Italian)* 3−19426
- electromyographic analysis, interfacing of Olivetti P101 programmable calculator and Biomac 500 computer 3−16554
- electron channelling pattern analysis 3−1555
- electron microprobe X-ray analysis 3−6119
- electron probe quantitative microanalysis of thin biological specimens 3−37739
- electrooculography, computer automated 3−25581
- e.m.g. activity, signal processing techniques 3−3408
- energy spectrum of inelastically scattered neutrons, calc. using Monte Carlo program *(German)* 3−35926
- fatigue data, stochastic function plots by computer 3−2776
- flow of drying particles in pipe, coupled momentum, heat and moisture transfer 3−1467
- fluidised beds, local particle concentration fields data 3−1447
- furnaces, temperature profile calculation, thermocouple with shunting errors 3−9866
- gamma-ray spectra, computer assisted analysis 3−431
- gamma-ray spectra from semiconductor detectors *(Japanese)* 3−28752
- gas chromatographic data analytical system 3−429
- gas exchange and respiratory function measurement system 3−25984
- geophysical prospecting induced polarisation method *(Spanish)* 3−31463
- guided missile cell-like structures, static magnetic fields, CALCOMP plotting routine 3−32491
- implanted dosimetry method for source localisation 3−13164
- inelastic cross-sections calc. using Hauser-Feshbach program ELIESE-2 *(German)* 3−35889
- ion microprobe mass analyzer, quantitative correction procedure, CARISMA program 3−37768
- isocon TV camera/mag. tape recorder system for fast oscilloscope trace analysis 3−3856
- $K\beta_2$ emission bands *(French)* 3−28780
- laser Doppler velocimeter systems, simulation 3−22965
- linear elasticity problems solving programs ELAS 3−6205
- lung cancer diagnosis from chest radiograms 3−39811
- magnetic system, field distributions calc. *(Polish)* 3−24584
- matrix method for local instability in plates, stiffened panels and columns 3−515
- measuring equipment data *(Croatian)* 3−25961
- metal forming process, visioplasticity solution 3−15727
- mitotic cells searching by machine, computer applic. 3−6143
- molecular structure relating to the biological function, computer program for the conformational analysis 3−22138
- Mossbauer spectra for effective spin $S = ^1/_2$ hamiltonian, computer simulation 3−30730
- multi-plate structures in compression, influence of orthotropy, computer-aided analysis 3−21723
- multilayer systems, improved integral transport theory by means of space polynomial approx., use of SHADOK code 3−19897
- neurophysiological data, spectral analysis, using intermediate magnetic tape storage 3−28756
- neutron activation analysis, spectral analysis by ICPEAX program 3−22536
- nuclear data ND-160 pulse height analyser modification for high capacity two-parameter analysis 3−23195
- nuclear material anal. and monitoring, portable systems for nondestructive assay, computer control 3−21784
- nuclear optical model, OPTICS program for small computers 3−26433
- nuclear reactor, pulsed, application of j_n method for neutron transport problems to moderator optimisation 3−19896
- nuclear reactor fuel, irradiated, adjustment of burn-up code for chemical and isotopic analysis 3−19936
- nuclear reactor fuel-cladding materials 3−26517
- nuclear reactor pressure vessels, history of applications 3−11052
- optical surfaces testing, computer fitting of mechanical probe meas. 3−3803
- oxyhaemoglobin dissociation curves, computer-aided data reduction 3−28360
- particle physics problems, curve fitting of statistical distributions, subroutine suite OPTIME 3−28966
- pharmaceutical tablet auto-analysers, off-line FOCAL-12 program 3−394
- photoelastic fringe data, elastic circular ring 3−12493
- photonuclear cross section calc. using unfolding distribution theory, soln. by computer *(Rumanian)* 3−23306
- pinhole lenses for s.e.m., low aberration 3−360
- potentiometric titration, application of computer operated system 3−22524
- power spectral density analysis 3−37728
- pulmonary function studies, multidetector instrumentation using ^{133}Xe 3−32239

computer-aided analysis continued
radiation film badge densitometer, integrated semiautomatic system using minicomputer 3—28673
radiation therapy, interactive computer program for standardization of prescriptions 3—31923
radiotherapy treatment, automation and patient repositioning 3—10167
railway wagons computer investigation of nonlinear horizontal oscillations *(Russian)* 3—492
relaxation time meas. in H and Rb masers 3—22866
reliability and availability of reactor systems, new method for approx. calc. *(German, English)* 3—19907
rotating shells, non-linear deformation, numerical soln. *(Russian)* 3—37799
semi-automated hydrographic survey system, computer facility for collection and processing of depth and position data 3—3240
slot-coupled toroidal resonators, scatter calculation by computer *(Russian)* 3—32401
small angle deflection detection in beam track on bubble chamber photographs 3—6079
spectrographs, permanent magnet, line shape analysis of conversion electron spectra 3—325
speech recognition, based on pitch contours 3—25633
speech recognition of complex sounds 3—25557
spherical shells, thin, non-shallow, with wind loading, study of stress state *(Russian)* 3—28875
stability of transversely-isotropic cylindrical shells in nonhomogeneous subcritical states, numerical calculations *(Russian)* 3—22639
steel austenitic, explosive bonded and hot rolled clad flat plates, residual stresses *(German)* 3—27837
stress relaxation data based on the Johnston-Gilman equation 3—34595
structural analysis computer program ISTRAN/PL *(Japanese)* 3—26078
synchrotron closed orbit minimisation program 3—25962
Tokamak fluid codes, generation by PL/1-FORMAC interpreter 3—17667
two-vessel manometry and substrate determinations, computer programs for numerical and graphic evaluation 3—3884
ventricular pressure, rate of proportional rise determination, on-line computer applic. 3—13485
vibrations, natural axially symmetrical, of open spherical layer, freq. calc. *(Russian)* 3—37838
VIPUNEN programming system for analysis of large amounts of physical data, especially nuclear physics 3—23194
visual neural networks simulation 3—39771
X-ray, laboratory automation for steel research *(Japanese)* 3—28740
X-ray diffraction data online evaluation computer program 3—14659
X-ray films of vocal tract 3—426
X-ray line broadening analysis by interfacing powder diffractometer with time shared computer 3—4697
NH_3, in water employing on-line membrane electrode 3—22191
$Pu(NO_3)_4$ solutions containing borated raschig rings, criticality safety limits, expts. and calcs. using Monte Carlo code 3—19940
PuO_2-UO_2 homogeneous mixtures containing 8.15 and 30 wt% Pu, critical expts., use of diffusion and transport theory codes 3—19939
V, $K\beta_2$ emission bands investigation by electron microprobe and computer processing *(French)* 3—28780

computer-aided circuit design
e.l.f. radio receiver design 3—3232

computer-aided design
see also computer-aided analysis
acoustic lenses for u.s. imaging 3—79
acoustics of concert hall 3—31962
complex enclosures 3—37924
elastic boundary method for complex structures *(Italian)* 3—19426
electron and ion guns 3—22523
electron gun design computational problems 3—807
experiment design, student exercise 3—35
holographic mass memory *(French)* 3—5967
NHK concert hall design *(Japanese)* 3—28418
nuclear reactors, heat exchanger resonators *(French)* 3—16347
optical systems, automatic design based on minimising wave aberrations 3—32068
plastic design problems for plane frame 3—541
spectroscopic light sources 3—13305
tethered vehicle for deep ocean viewing 3—3223

computer-aided instruction
see also education
analogue computer as a physics teaching tool 3—32009
in a chemical instrumentation course 3—9791
experiment design, student exercise 3—35
Fourier analysis using fast Fourier transforms 3—32019
Huckel mol. orbital computer programs 3—46
kinetic analysis, undergraduate expt. 3—47
nuclear phys. topics, instructional uses of computers 3—22228
on-line computing and digital electronics, undergraduate course 3—42
physical teaching material production 3—9816
physics, graphic display applic. 3—13187
physics student design expt. by computer simulation 3—31994
ray tracing, an interactive instruction session 3—37577
satellite orbits on programmable calculator 3—9809
Science Faculty of Univ. Paris, 1965-70 expt. *(Spanish)* 3—22230
statistical mechanics, illustration for students using Monte Carlo computer program 3—22227
therapy planning aids 3—3579
thermodynamics course for first and second year college students 3—16354
visualisation of molecular orbitals 3—3742

computer applications
see also aerospace applications of computers; analogue computer applications; communications applications of computers; computational physics; computer-aided analysis; computer-aided design; computer-aided instruction; engineering applications of computers
activation analysis *(German)* 3—13508
Airy-Fock function, calc. in complex variable domain, Algol 60 subroutine *(Polish)* 3—29000

computer applications continued
AS-11A stereoplotter for radar photographs, coordinate transformation, using computer program 3—3885
aspheric wavefront testing using computer generated holograms 3—5899
asteroids, improved data elements *(Russian)* 3—16195
astronomical ephemerides, a programme *(Japanese)* 3—19081
astronomical spectrophotometer, two-channel scanning system with automatic control and data handling 3—31829
astronomy, differential curve-of-growth analysis for stellar spectra, computer programmes 3—9632
automated microscope with optical analyzer for diagnostic cytology 3—159
automatic program for seismic coherent three dimensional velocity distrib. determ. 3—9112
barotropic and multilevel baroclinic models of weather system for South Pacific, computer requirements 3—28055
basilar membrane, computer simulation of nonlinear model, determ. of distortion products 3—3472
blocked purkinje tissue, passive conduction delay, numerical delay 3—13129
blood vessel imaging in cerebral angiography, simulation 3—10158
bubble chamber event pattern measurement spiral reader, symposium, Stockholm (1972) 3—10072
CAMAC as standard for astronomical instrumentation 3—31842
cartography, projection routines for displaying geophysical data 3—25318
chemical dynamics in complex imaging system, computer simulation 3—15846
chemical equilib. solution, EQUIL program 3—2791
clinical e.e.g. laboratory 3—392
comparator calibration technique 3—3788
computer aided optical surfacing 3—5895
computer simulation of optimum combinations of colour dyes to produce selective greys 3—223
CONVERGE-part of MULTAN program system for phase determ. of acentric cpds. 3—14652
creep test, evaluation method *(German)* 3—31214
crystal symmetry, FORTRAN IV program 3—1587
current rainfall data processing 3—9387
data acquisition methods, for seismic data 3—9368
diffusion bonding, computer pulse echo u.s. meas. of bondwidth 3—25963
direct solar radiation estimation 3—12772
display, anal. of epenthetic stops between l and following sibilants 3—5643
dosimetry, generation of isodose contours from external X-ray sources, appl. to treatment planning 3—13161
earthquake focal plane solutions using maximum-likelihood method 3—25319
e.c.g. R-R interval and R wave width measurement, analogue preprocessor 3—25991
echoencephalography using Automatic Midline Computer, clinical evaluation 3—16553
eclipsing binary light curve solution using the differential corrections method 3—19074
electrode kinetic studies, overpotential meas., review 3—12531
e.p.r., analysis of anisotropic spectra 3—34184
estuarine pollution monitoring system using multivariate prediction techniques 3—3244
exploration geophysics, conference, Paris, France (1972) 3—9347
fast track following system, PDP-15 directed interactive control 3—25965
galaxies, tidal interaction on close passage, simulation *(Russian)* 3—16265
gas exchange and respiratory function measurement system 3—25984
geomagnetic field models, scalar and vector potential, induction vector and gradient tensor calculation by computer program 3—21911
geomagnetism, thick plate model, automatic interpretation 3—12638
geophysical data, computer graphics 3—25314
geophysical data acquisition and pocessing at sea, digital systems 3—3176
geophysical exploration 3—9124
geophysical prospecting, digital data processing, seismology, Geocom and Sperry Univac, oil 3—21902
geophysics joint interpretation of two-dimensional gravity and magnetic anomalies 3—12589
gravitational attraction of three-dimensional bodies in spherical or ellipsoidal earth, computing method 3—18804
heat pulse anemometer, veloc. meas. in inhomogeneous turbulent flow 3—26042
high speed computer controlled mask making techniques for optical diffractometer studies of disorder 3—16549
hologram generation, book 3—19577
holograms, computer generated, coding techniques for recording on computer controlled c.r.t. 3—198
human lung transport processes, computation of boundary conditions 3—28319
human respiratory system, digital computer simulation 3—28361
human visual system, experimentation 3—5657
hurricanes weakening, simulation study *(German)* 3—21957
image improvement in nuclear medicine using selected frequency band enhancement 3—416
imanco systems for picture processing by conventional digital computers 3—16805
instrument calibration 3—13192
integral form of Green's function for computer evaluation, acoustic propagation study 3—3690
intense acoustic signals of arbitrary waveform, algorithm for propagation prediction 3—9764
ionospheric and cosmic ray measuring systems, minicomputer applications, Institut Royal Meteorologique, Belgium *(French)* 3—21980
isochronous cyclotron of Michigan State Univ. USA, field trimming computer program 3—13395
kinetic data analysis, renal ^{133}Xe washout in dogs and man applic. 3—35273
left ventricular volume calc. from X-ray obs. 3—3578
loudness calculation from third-octave band levels or from critical band levels *(German)* 3—16329

computer applications continued
magnetotelluric sounding, computer processing of data *(Russian)* 3−5473
marine seismic data, digital processing 3−3177
mass spectra identification, highly compressed spectral codes, Aldermaston collection 3−28702
mass spectra low resolution, computer calc. of ionic formulae and monoisotopic spectrum 3−7024
mass spectrometer, precise atomic mass differences using peak matching 3−25922
medical treatment planning, using interactive graphics terminal 3−10169
medical X-ray spectra correction for Alderson phantom 3−13145
medicine, nuclear, computer-based scanning system 3−35275
Meteorological Office IBM 360/195 computing system 3−28028
meteorology, Canadian weather forecasting 3−37202
minicomputer psychoacoustic system 3−3460
molecular solution, fluorescence depolarisation, Brownian motion effect, simulation 3−26748
molecular structure, from data on their fragments *(Russian)* 3−23541
molecules, nonempirical SCF LCAO MO calculations, program 3−33078
Mossbauer spectra, thick absorber correction 3−25955
Mossbauer spectroscopy, data handling *(German)* 3−22520
NE102A plastic scintillator, Monte Carlo evaluation of fast response to neutrons 3−3852
neuronal pulse spectrometry, similarity with nuclear systems, applications of computers and mathematical models 3−28755
neutron detector with organic scintillator, program for detection efficiency *(German)* 3−25885
noise level, by Stevens Mark VII method 3−35334
nondestructive assay of nuclear fuel automated neutron interrogation systems 3−19302
nondestructive testing, support of a minicomputer using BASIC 3−31226
nuclear counting systems in Pu recovery, computerization of data handling 3−19357
nuclear medicine, imaging and image improvement 3−417
nuclear physics investigation technique, three-dimensional system tests and calibration 3−25905
nuclear plants effluent monitoring, on-line gamma spectroscopy 3−29452
nuclear power plant effluent monitoring, using digital computer and γ-ray spectroscopy 3−32229
nuclear reactions with spin 1/2 particles only, calculation of cross sections and polarisations 3−19825
open-shell SCF program for ab initio Gaussian-type calcs. 3−26619
optical surfaces testing, computer fitting of mechanical probe meas. 3−3803
organic molecules, simulated mass spectra generation by computerised pattern recognition technique 3−28703
oscillatory pipe flow simulation 3−7334
particle percolation, computer determination of path 3−31207
particle size distrib. by area analysis, Saltykov method modifications and extensions 3−35520
particle size measurement and counting *(French)* 3−15801
penetrant testing, automatic control, sytems approach 3−27826
photoelectric photometry digitisation *(Japanese)* 3−19083
plates, circular with stepped thickness, vibration mode 3−32389
polarography, stationary electrode, doublet peak detection, pattern classification 3−22400
polymer crystallinity, computerisation of Rulands X-ray method 3−36242
positive streamer propagation, computer model, calc. of measurable quantities 3−1525
potentiometric titration, automatic control 3−22524
powder flow, in storage bins, simulation by computer graphics display 3−4617
proton correlation spectroscopy using PDP-9 computer 3−5947
radiation dosimetry, cancer treatment, minicomputers 3−9728
radiation treatment planning optimisation, decision-theoretic approach 3−13154
radiative transfer model of light scattering in earth's atm., comparison with Monte Carlo method 3−31372
radiographic data processing, computer-generated holograms 3−22856
radiographic image enhancement 3−32233
radiotherapy, integrated interactive computerized treatment planning system 3−31930
radiotherapy using small computers 3−10183
reactor core, deformation due to stainless steel swelling and thermal bowing 3−6998
seismic profiling system, appl. to signal to noise ratio meas. 3−31462
seismic wave velocity analysis, summational type, algorithm for digital processing program 3−31458
seismic wavelet processing, continuous velocity estimation, computer program 3−9123
seismology, continuous velocity estimation and computerized seismic wavelet processing 3−25313
semiconductor thin films, manufacturing process control 3−39229
simulation approach to dendritic growth phenomenon 3−34500
simulation of dither appl. to quantization of speech signals 3−3640
solar mm. radial brightness distrib., computer program with standard antenna patterns 3−35043
spectral colour matching, minimax approx., computer algorithm 3−3805
spectrofluorimeter-spectrophotometer combination, computer centred 3−28770
stellar atmospheres, line profiles and continuum fluxes, numerical methods and computer programs 3−35118
stress analysis by force method and use of computer program for prismatic shells 3−6262
stress determ. by X-ray diffraction, on-line 3−27825
system sciences, conference, Honolulu (1973) 3−28403
terrestrial hand and computer processing 3−9211
tone intonation and segmental duration in Serbo Croatian, model 3−3430

computer applications continued
two coordinate digital recording, broad n.m.r. lines, radio spectroscopy 3−184
underwater propagation path prediction, exptal. digital system 3−37565
underwater sound, geometrical acoustics, ray paths for velocity profiles 3−31964
unfolding and simulating meas. distrib., interactive graphical computing 3−10140
u.s. pulse echo, computer based data-processing system to improve 3−31225
whistler instabilities in anisotropic collisionless plasmas 3−7519
wind speed measurements 3−28751
wire chamber ferrite core readout with software decoding 3−323
wire chamber spectrometer, two-arm, for 30 to 50 MeV protons, connected on-line to two computers 3−322
wire chamber spectrometer with on-line two-computer system for data analysis 3−324
γ-ray spectra by semiconductor detectors *(French)* 3−6064
As, expt. and computer-simulated studies of surface morphology effect on evaporation 3−38665
BaF_2, shell model calc. of formation energy of point defects 3−38583
CaF_2, shell model calc. of formation energy of point defects 3−38583
Ge(Li) detector, Monte Carlo calculation of efficiencies and response functions of thick disc γ-ray sources 3−3853
Ge(Li) detector γ-ray spectra, evaluation 3−37689
H, hard sphere model of hot atom reactions, computer simulation 3−9061
NaI(Tl) detector, Monte Carlo calculation of efficiencies and response functions for thick disc γ-ray sources 3−3853
Pu, body content estimation, SEBEACH, digital computer program 3−22176
SrF_2, shell model calc. of formation energy of point defects 3−38583
computer architecture
on-board data processing system MLCB, design considerations 3−3243
computer graphic equipment
see also plotters
man-computer graphic interaction, IBM 2250 c.r.t. as interface for interrogating oceanographic data files 3−3209
physics teaching application 3−13187
computer graphics
atmospheric acoustic ray tracing, computer program 3−3027
beam optics design 3−10580
CAI physical teaching material production 3−9816
crystal structure anal. using interactive graphics in hierarchical computing system 3−26923
Fourier contouring and molecular modelling using three dimensional computer graphics 3−26925
geophysical data representations 3−25314
holographic memory *(French)* 3−5967
kinetic theory of the space instability of a radial-limited plasma-electron stream system with preset plasma radial-heterogeneous configuration *(Russian)* 3−11463
medical treatment planning, using interactive graphics terminal 3−10169
organic molecule structure solution, Fourier map interpretation, computer produced connectivity diagrams, interactive display system 3−26926
powder flow, in storage bins, simulation 3−4617
protein three-dimensional structures, comparison using computer program 3−4488
proteins, folding process simulation, pseudo free energy, interactive computer graphics 3−26742
seismic data interpretation, colour sonagrams 3−39559
stereotoxic neurosurgery on deep cerebral structures, computer graphics displayed maps of brain cross-section 3−3890
three dimensional graphics with mini-computer and television raster display 3−26924
unfolding and simulating meas. distrib., interactive computing 3−10140
computer interfaces
see also computer peripheral equipment
astronomy, observational online computer aids 3−5622
CAMAC, for computer control of spectrometer 3−35519
CAMAC, fundamentals and specification status 3−32188
CAMAC, review 3−32186
CAMAC, specifications 3−32187
CAMAC as standard for astronomical instrumentation 3−31842
CAMAC magnetostrictive readout, with Schottky memories, for use with spark chambers 3−28676
CAMAC scalers, modular readout system 3−32190
CAMAC system, for remote data acquisition 3−32189
CAMAC system, software 3−32191
electromyographic analysis, interfacing of Olivetti P101 programmable calculator and Biomac 500 computer 3−16554
experimental beam line control, CAMAC serial crate controller 3−35457
IBM 2250 c.r.t. between man and computer for interrogating oceanographic data files 3−3209
neurophysiology, pulse height discriminator 3−16524
ORIC, isochronous cyclotron, computer control system 3−13377
Picker 500 scanner, paper tape interface 3−10175
pulse counting experiments, general purpose interfacing for PDP-8 minicomputer 3−393
radioisotope disintegration counting data processing 3−3883
radiotherapy machine connection 3−3913
X-ray line broadening analysis by interfacing powder diffractometer with time shared computer 3−4697
computer internal arrangement *see computer architecture*
computer operator training *see training*
computer output to microfilm
laser microform recording system, patent 3−13764
computer peripheral equipment
see also character recognition equipment; computer graphic equipment; printers; punched tape equipment
laser microform recording system, patent 3−13764

- **computer peripheral equipment** continued
  - Meteorological Office IBM 360/195 computing system 3−28028
- **computer peripherals** *see computer peripheral equipment*
- **computer printers** *see printers*
- **computer programs, complete** *see complete computer programs*
- **computer science education** *see education*
- **computer software**
  - *see also complete computer programs; subroutines*
  - CAMAC system 3−32191
  - depth dose determ. for neutrons and γ-rays, Monte Carlo program and standard man phantom 3−28393
  - for graphic display, rel. to physics teaching 3−13187
  - interferometric test data analysis, computer program 3−5896
  - radiating shielding and related calcs., computer programs 3−1091
  - seismic imaging, program for interpretation of discontinuities 3−2900
  - X-ray diffraction data online evaluation computer program 3−14659
- **computer storage devices** *see storage devices*
- **computer subroutines** *see subroutines*
- **computers**
  - *see also analogue computers; computer architecture; computer peripheral equipment; computer software; data handling; data processing; digital computers; digital storage; file organisation; general purpose computers; hybrid computers; satellite computers; special purpose computers*
  - engineering, conference, Ilmenau, Germany, 16-21 Oct. (1972) 3−15645
- **concrete**
  - *see also cement industry*
  - bremsstrahlung attenuation meas. in ilmenite loaded concrete 3−1087
  - cement pastes and mortars, fracture toughness meas. methods 3−27813
  - concrete-polymer materials and solid-waste polymer composites, development, properties and uses 3−21733
  - coupled neutron and secondary γ-ray transport through concrete for incident neutrons 15-75 MeV 3−19899
  - ductility of plain and transversally reinforced concrete 3−5345
  - early shrinkage measurements 3−34635
  - load deflection characteristics of rectangular reinforced slabs 3−27814
  - load props., crack propagation, compressive and tensile strength 3−5350
  - microwave nondestructive testing 3−12471
  - neutron attenuation, half-value thickness 3−38192
  - nuclear reactor pressure vessel, meas. on protective covering *(German)* 3−17284
  - nuclear reactor pressure vessels, prestressed concrete, design, testing and operational behaviour 3−35929
  - reinforced beams, inelastic analysis, math. programming methods 3−16658
  - reinforcing steel elastic characts. at low temp. 3−21678
  - shielding n and γ-irrad., exptl. results *(Rumanian)* 3−17330
  - strengths and elasticity, effect of long time exposure to elevated temperatures *(Japanese)* 3−5352
  - temperature distribution, atmos. temp. variations effects 3−2758
  - tensile failure under water pore pressure 3−27815
  - testing model rel. to physical characteristics of coupled shear wall *(Japanese)* 3−3943
  - thermal diffusivity, coarse aggregate approach *(Japanese)* 3−21729
  - tubes, thick-walled, steel wire reinforced, limit analysis under dynamic internal pressure 3−39389
  - Al_2O_3-based, insulating fire-proof concrete, electrical cond. erosion and heat resistance in plasma jet 3−36206
  - MgO-based, insulating fire-proof concrete, electrical cond. erosion and heat resistance in plasma jet 3−36206
- **condensation**
  - *see also clouds; drops; fog*
  - aerosols, condensation, coagulation and size distribution 3−31201
  - atmospheric aerosols, humidity effects on transformation *(Russian)* 3−28015
  - atmospheric condensation nuclei with continuous flux, meas. counter *(French)* 3−12858
  - binary mixtures of miscible vapours, codensation on cooled vertical plates 3−20860
  - Bose condensation, vortex ring model 3−38691
  - Bose liquid, fluctuation of condensation density 3−613
  - charged droplets from aircraft discharger system 3−662
  - cloud clusters, latent heat in atmospheric intertropical convergence zone *(Russian)* 3−34891
  - computer simulation rel. to surface structure and growth kinetics 3−11556
  - drop, condensing, thermal resistance calc. 3−27116
  - droplet growth kinetics by condensation with adiabatic expansion of air *(Russian)* 3−14507
  - drops, condensation growth and nonsteady evaporation 3−34749
  - of drops, nonsteady state theory 3−24259
  - dropwise, drop size distrib. model 3−24254
  - dropwise condensation, drop size distributions and heat transfer 3−20857
  - evaporated thin films on NaCl covered by an amorphous dielectric intermediate layer 3−38746
  - film condensation on a downward-facing horizontal rippled surface 3−11731
  - films, vapours, laminar flow, turbulent flow, heat transfer coefficient, pressure gradient 3−1347
  - filmwise condensation on a surface with uniform heat flux and body force convection 3−29850
  - flow of a condensate film down a vertical wall, stability 3−14433
  - freon 12 and 12, condensation study 3−27111
  - gas, one-dimensional, linear potential model 3−33659
  - gas mixtures, surface potential theory of multilayer adsorption when vapour near to condensation 3−33733
  - gases, with elec. dipole moment, spontaneous polarization during condensation 3−20942
  - growth rate of water drops during condensation 3−14992
  - homogeneous nucleation in steam nozzle condensation 3−7910
  - laminar film, on porous horizontal tube with uniform suction, boundary layer analysis 3−11407
- **condensation** continued
  - laminar film condensation due to rotating disc 3−14439
  - laminar film condensation with suction 3−11414
  - laminar films, vapour flow, momentum transfer, hydrodynamics 3−1346
  - liquid film flow down inclined wall, stability characteristics 3−33233
  - local heat transfer, water vapour, vertical pipes 3−629
  - meteorite formation, Allende carbonaceous phase, s.e.m. exam. 3−18995
  - mist droplets, passivation of condensation growth, cetyl alcohol vapour adsorption 3−39399
  - mixed beds, interpretation of meas. of heat of adsorption *(French)* 3−27181
  - mixed beds, properties of isotherms *(French)* 3−27180
  - one-dimensional gas with long-range linear attractive pot., phase transition 3−6387
  - presence of noncondensing gas, heat and mass transfer 3−36413
  - refrigerator, for 90-100 K region 3−5831
  - shock form. mechanism 3−20352
  - solar corona, electron density distrib. 3−37327
  - spherical droplet condensation in an isothermal vapour diffusing through a heavy background gas 3−20861
  - steam, drop behaviour and surface temp. fluctuation correspondence 3−20855
  - steam, dropwise condensation, effect of condenser material thermal props. 3−24255
  - steam, heat transfer during condensation at a rotating disc 3−26785
  - steam, steam-gas mixture, heat transfer 3−628
  - steam flow in vertical tube, heat transfer and pressure drop 3−17517
  - thermodynamics of gas/liquid interfaces in a porous medium, condensation/evaporation processes, viscous flow 3−26847
  - trail of aircraft, ice budget growth meas. 3−25232
  - vapour deposition in vacuum, heat transfer 3−2631
  - of vapour flowing inside a vertical cylinder 3−24257
  - water, condensation coeff. obs. for water evaporated in different gas atmospheres *(Russian)* 3−14995
  - water, in droplets *(German)* 3−17967
  - water organic solvent binary mixtures mass transfer and condensation heat transfer coeffs. 3−1784
  - water vapour, non-steady-state nucleation on gaseous ions, multistate kinetics 3−24258
  - water vapour during unsteady discharge in a long tube *(French)* 3−14993
  - water vapour heats of adsorption on η-Al_2O_3, capillary condensation on dehydroxylated samples *(French)* 3−27187
  - Al:Ti, film, diffusion from Ti sublayer during Al vacuum condensation 3−30079
  - CO, spontaneous polarization during condensation 3−20942
  - Ce vapours, interaction with a ZnS:AgCl polycryst. screen, induced capillary condensation 3−39464
  - CrSi, platelet structure, 300-1020°C, X-ray study *(Russian)* 3−7919
  - Cs vapour in Ar flow 3−1345
  - ^{4}He superfluid, search for Bose-Einstein condensation using neutron inelastic scattering 3−4898
  - K vapour, in pipe cooled by liquid alkali metal 3−14987
  - KCl, condensation coeff. rel. to sub- and supersaturation, mol. beam method obs. 325-425°C *(German)* 3−1792
  - KCl, relax. effects of (100) face during condensation *(German)* 3−1793
  - KOH vapour, mass transfer, MHD generator 3−36414
  - Kcl, crystals subjected to molecular beams, condensation and vaporisation kinetics investigation *(German)* 3−7920
  - Li_2F_2, Li_3F_3 crystals subjected to molecular beams, condensation and vaporisation kinetics investigation *(German)* 3−7920
  - NaCl oriented single cryst., $Na_xCl_x(x=1,2)$ mol. beams, coeffs. for condensation, 185 to 700 K 3−17973
  - PbS films, growth on cleavage surf of NaCl cry. containing macrodefects *(Russian)* 3−8068
- **condensers (electric)** *see capacitors*
- **condensing** *see condensation*
- **conducting materials**
  - *see also bimetals; metals; superconducting materials*
  - cylindrical conducting shells, motion under magnetodynamic compression *(Russian)* 3−6395
  - $C_5H_6NI.8AgI$, superionic, ionic Hall effect 3−38875
  - Fe-Si steels, electrical and magnetic props., manufacturing processes, development, applications to electrical power 3−15173
- **conduction, electric** *see electric conduction*
- **conduction, heat** *see heat conduction*
- **conduction bands**
  - *see also electric conduction; fermi level; semiconductor materials*
  - carrier energy in mag. field, determ. using continuous fractions 3−33803
  - crystals with zinc blende symmetry, second order nonlinear optical susceptibility, energy band theory 3−8550
  - diamond structure, Wannier function construction 3−38767
  - III-V semiconductors, small gap, spin props. of conduction electrons, small-gap semiconductors 3−38845
  - inert gas solid mixtures, extreme u.v. spectra, electron energy states effects of dilute mixing 3−21452
  - magnetic semiconducting crystals, electron ground-state, coherent states 3−38799
  - magnetic semiconductors, band structure, transport properties 3−38858
  - metal and alloy, statistical thermodynamic properties compressibility, crystal binding, charge neutrality 3−30084
  - metal carbide (nitride) (oxide), electron config. influence on wetting props. *(German)* 3−8766
  - polar semiconductor, nonparabolic, role in state mechanism, Hall coeff. factor obs. 3−11909
  - self-trapped states in conduction band of gases and liquids 3−38772
  - semiconductor, electromag. field effect on valence band ionisation by cond. electron collision 3−4951
  - semiconductor, electron heating in elec. field, effect of finite width of cond. band 3−33921
  - semiconductor, highly degenerate, diffusivity-mobility ratio, influence of band tails 3−24423
  - semiconductors, Raman scattering by electronic excitations 3−39153

conduction bands continued
superconductivity in cubic and hexagonal struct. 3−30555
thin conductors, Shubnikov-de Haas effect 3−21054
transiton metal perovskites, two-dimensional character 3−1995
transparent dielectric, rel. to excitation of cascade ionization by strong alternating e.m. field *(Russian)* 3−8517
AlAs, effective masses for cond. band minima, calc. 3−15128
n-$Al_xGa_{1-x}As$, impurity conc. and effective masses from cond. band electron conc. 3−30478
Au, structure study by photoelectron spectrometer 3−28716
CdTe compensated doped crystals, density of states tails, conductivity, Hall mobility 3−33832
Cu, Cu-Al alloys, interband transitions 3−30837
Cu, positron annihilation, band structure calculation of momentum densities 3−18065
Fe, ferromagnetic, positron annihilation, band structure calculation of momentum densities 3−18065
Fe, magnetised with polarised positrons, positron annihilation, investigation of spin and momentum density 3−18066
FeS_2, rel. to low temp. resist. and Hall effect 3−21070
p-$Ga_xAl_{1-x}As$, creation of spin-polarized electrons, optical study 3−2596
n-GaAs, effective masses in cond., valence and spin orbit split bands, electroabsorpt. meas. 3−39123
n-GaAs magnetoresistance, transverse, Gunn diodes, 300 to 800 K, electron transfer between Γ and X bands 3−36624
$GaAs_{(1-x)}P_x$, optically induced paramag. by distrib. change in cond. electron spins on recombination 3−2513
p-GaSb, optical pumping of spin polarised conduction electrons and inelastic scattering by neutral acceptors 3−34398
GaSb:Te, role in low temp. thermal cond. *(French)* 3−4893
GaSe, symmetry, rel. to magnetooptical props. 3−30803
Ge: group V (O,Te), electron irrad., E_c-0.2 eV level, defect model 3−33842
n-InAs, nonparabolicity, confirmed by optical absorpt. study *(Russian)* 3−38797
InAs and InAs-CdTe solid solutions, absorption band structure from absorption spectra 3−24383
n-InSb, strongly compensated, potential distortion of band rel. to low temp. elec. cond. 3−15216
PbSe, k.P perturbation calc. 3−1997
Si, Bloch states mixing 3−33794
SiO_2 thermally grown on Si, electron trapping levels 3−8262
$SrTiO_3$, effect of 110K structural phase transition 3−11853
TlBr, linear combination of atomic orbitals calc. 3−18083
V_2O_3, enhancement effect in cond. band, electron-hole interaction change through metal insulator transition, positron lifetime spectra obs. 3−27212

conduction electron mobility
see also conduction bands; electron-phonon interactions
adsorption, surface scatt., obs. by static skin effect 3−20937
amorphous semicond. d.c. cond., diffusion type transport eqn. 3−8177
dilute mag. alloy, coupled local moment-conduction electron Bloch equation, e.s.r. obs. 3−34213
dilute non-mag. alloy, kinetic equation for cond. electron scatt. 3−30603
Hubbard band, half-filled, mobility gap due to spin random distrib. 3−15148
II-IV-V_2 compounds, preparation in layer form, properties and heterojunctions based on them 3−8747
III-V semiconductor solid solution, disorder scattering 3−30470
III-V semiconductors, small gap, spin props. of conduction electrons, small-gap semiconductors 3−38845
ionic crystals, expt. obs. using photoconductivity 3−36601
magnetic semiconductors, band structure, transport properties 3−38858
metal, internal electron refl. rel. to angle of incidence *(Russian)* 3−11879
metal, transverse magnetoresist., interaction of conduction electrons with adsorbed atoms 3−15186
relaxation times and spin properties of conduction electrons determ. from oscillatory amplitudes of de Haas-van Alphen effect 3−1993
semiconductor, degenerate, the Einstein relation 3−30464
semiconductor, generalised Einstein relation 3−38827
semiconductor, high field domain modes, due to field depend. carrier diffusion 3−33908
semiconductor, rel. to second harmonic generation 3−30509
semiconductors, piezoelectric scattering, lattice vibration interactions, screening 3−33898
semiconductors, polar, II-VI and III-V, spherical conduction band calc. 3−21074
Au, electron-impurity scatt., anisotropy study using de Haas-van Alphen effect 3−11881
Au thin films, conduction electron diffusion by surface defects *(French)* 3−36584
$Cd_xHg_{1-x}Te$, anomalous temp. depend. 3−2095
CdSe, impact ionisation, breakdown, photoinduced switching, meas. of cond., Hall coeff., mobility, 4.2-300K 3−30487
CdTe compensated doped crystals, density of states tails, conductivity, Hall mobility 3−33832
Fe, scatt. rel. to Hall and Nernst-Ettingshausen effects, anomalies near Curie pt. *(Russian)* 3−12014
GaAs heavily doped, electron mobility rel. to electron-electron scatt. and nonparabolic energy band shape 3−18139
n-GaN(:Zn) film, vapour phase grown, Hall meas., carrier conc. 3−33884
GaP, electron effective mass *(Russian)* 3−5008
GaSb, diffusion current, rel. to impurity density-of-states tails 3−11844
GaSb, electron mobility in Γ_{1c} band, temp. and press. depend. 3−24422
n-GaSb, heavily doped density-of-states tails associated with L-minima of conduction band 3−30425
n-Ge, elec. cond. anisotropy, hot electron drift velocity temp. depend. *(Russian)* 3−8196
Ge n-type, warm electron anisotropy 3−2102
n-Ge transport props., negative differential cond., impurity effects at 20K 3−21085

conduction electron mobility continued
Ge: group V (O,Te), electron irrad., E_c-0.2 eV level, defect model 3−33842
Ge:Sn, heavily doped single cryst., impurity conc. depend., Hall effect obs. 3−33885
HgSe, calculation from iterative soln. of Boltzmann eqn. and first Born approximation for scattering 3−36598
HgTe, anomalous temp. depend. 3−2095
HgTe, calculation from iterative soln. of Boltzmann eqn. and first Born approximation for scattering 3−36598
n-InP, velocity field characs., microwave obs. 3−30484
n-InSb, photocond., LO phonons emitted in inelastic scatt. of conduction electrons 3−24477
Ni, scatt. rel. to Hall and Nernst-Ettingshausen effect, anomalies near Curie pt. *(Russian)* 3−12014
Ni solid soln., giant moments, cond. electron scatt. by Ni clouds 3−36716
Ni thin film, elastic scattering of conduction electrons by adsorbed H_2 3−27301
Si epitaxial film, on sapphire, effects of vacuum deposition conditions *(Russian)* 3−24813
Si film, monocryst. on sapphire, rel. to imperfection effect on surface state density *(Russian)* 3−24489
Si n-type, warm electron anisotropy 3−2102
α-Sn, calculation from iterative soln. of Boltzmann eqn. and first Born approximation for scattering 3−36598
W/Ba(Cu), surface scatt. obs. by static skin effect method 3−20937
ZnO:In temp. depend. 5 to 300K *(German)* 3−11899

conduction electron scattering *see conduction electron mobility*

conduction in solids, ionic *see ionic conduction in solids*

conductivity, electrical *see electrical conductivity*

conductivity, thermal *see thermal conductivity*

conductors (electric)
see also bimetals; wires (electric)
d.c. heated conductor, computer calc. of thermophysical props. *(German)* 3−30442
dielectric covered, e.s. capacitance 3−13673
elliptic cross-section, magnetic field calc. *(Polish)* 3−29001
isolated stranded, electric field distribution, comments 3−37923
laser beam welding of winding conductors in their insulation *(Russian)* 3−6523
magnetic bubble domain propag. arrangement, patent 3−18346
shielded conductor, time domain e.m. response, theory 3−29014
terminal characts. and thermal stability of composites 3−30569
twisted superconducting composites, matrix loss meas. 3−11987
two dimensional electrostatic field, calculation *(Russian)* 3−10424
underground conductors, position determ. by e.m. induction method *(Polish)* 3−22401
Al, for cryogenic devices, purity, u.s. nondestructive test *(Polish)* 3−68

confinement, plasma *see plasma confinement*

connecting *see joining processes*

connectors (electric) *see electric connectors*

conservation laws
see also C invariance; CP invariance; CPT invariance; elementary particle symmetry; T invariance
classical mechanics, invariant geometrical characterization of ignorable coordinates 3−16604
for coherent optical pulse propag. in inhomogeneously broadened medium 3−4071
diffractive processes, exptl. status of helicity conservation 3−14058
dilation invariance, conformal algebra and conformally covariant operator product expansion, tensor representation 3−26257
e.m. fields, conservation theorems 3−4060
general relativistic particle conservation, Christoffel symbols 3−4019
helicity violation in s- and t-channels from LPS analysis of diffraction dissociation in $\pi p \rightarrow \pi\pi\pi p$ 3−10803
inclusive reactions, isospin invariance constraints and rapid scaling criteria for degeneracy 3−17130
inequality relating cross sections to polarization from isospin conservation 3−13826
isospin conservation in strange-particle production 3−29280
isospin constraints between three cross sections and two polarization density matrices 3−6559
isospin invariance, inequalities in pp interaction 3−14047
lepton conservation and exotic muon capture in nuclei 3−4305
nonlocality in high energy ν expts., internal particle mass effect 3−10676
P, T invariance rel. to polarisation of lunar and planetary radiation 3−28155
parity conservation rel. to polarization in 3-body break-up reactions 3−10953
parity-violating internucleon one-meson-exchange pots., rel. to models of weak Hamiltonian 3−23121
s-channel helicity, conservation in ρ^0 photoproduction 3−13959
s-channel helicity conservation of pomeron and tensor meson dominance, pomeron-f-meson couplings 3−23113
scale invariance, broken, presence of Goldstone boson 3−16947
scaling breakdown at 10^{-15} cm, speculations 3−38004
scaling law, elastic particle scatt. on protons, 5-25 GeV/c 3−26345
t-channel helicity conservation in diffractive production processes 3−32691
$e^+e^- \rightarrow$ hadrons, $U(3) \times U(3)$ symmetry breaking, determ. of sum rules for T=0, T=1 3−13963
$\gamma N \rightarrow O^- N$, s-channel helicity conservation and Regge cuts in t-channel 3−13901

constant current modulation *see amplitude modulation*

constant voltage diodes *see avalanche diodes*

constants
see also elastic constants; gravitational constant; lattice constants; optical constants; thermal critical constants
2e/h, NPL determination using a.c. Josephson effect 3−22248
2e/h determ. comparison of point-contact and thin film Josephson junctions 3−13199
2e/h measurements at NBS using D.C. Josephson effect, implications for fine structure constant 3−13202

constants continued
2e/h measurements at NPL using a.c. Josephson effect, monitoring of voltage standard 3−13201
2e/h measurements at PTB using point contact junctions 3−13200
μ_p/μ_n precision meas. in terms of n.m.r. frequency and cyclotron resonance frequency, error elimination 3−13208
anomalous magnetic moment of muon, precise meas. rel. to hyperfine structure const. determ. 3−13861
Avogadro's number, high accuracy detn. through absolute ampere meas. 3−32025
Avogadro's number determ. from lattice spacing meas. using new X-ray interferometry techniques 3−13212
Faraday, determ. by means of iodine coulometer, preliminary results 3−13213
fine struct. fermi coupling constants rel. to boson mass 3−14109
fine structure constant determ. by electron spectroscopy 3−13198
fundamental, conference, Teddington, England (Sep 1971) 3−11106
fundamental physical, reevaluation 3−13216
g-factor anomalies of electron and positron 3−13860
gas, new determ. using acoustic interferometry 3−13215
Lamb shift, value change 3−14281
magnetic moment of proton, meas. at NPL in terms of cyclotron frequency by omegatron method 3−13207
proton gyromagnetic ratio, precision meas. at NBS 3−13211
proton gyromagnetic ratio meas. using magnetically isolated cable solenoid 3−13210
proton gyromagnetic ratio meas. with NPL weak-field apparatus 3−13209
Rydberg, Avogadro's number, electron's Compton wavelength, scale of γ-ray wavelengths and X-ray wavelengths, relations 3−13195
Rydberg, determ. from He II n=3-4 (4686Å) line complex 3−13205
Rydberg, determ. from wavelength meas. on Balmer series of deuterium 3−13203
Rydberg, new measurement 3−13204
Rydberg excitation-dependent characteristics of H and He II lines used in determ. of const. 3−13206
Sommerfeld fine structure const. determ. from muonium HFS splitting 3−13197
Sommerfeld fine structure constant, review of exptl. meas. 3−14280
tables of standard data for spectroscopists 3−11111

constitution diagrams *see phase diagrams*

construction *see building*

constructional engineering *see civil engineering*

contact angle
see also capillarity; surface tension; wetting
formamide on glass, velocity effect on dynamic contact angles 3−8007
glycerol on glass, velocity effect on dynamic contact angles 3−8007
metal melts on graphite and glasslike carbon substrates, sessile drop method, free energy 3−11796
methylene iodide on glass, velocity effect on dynamic contact angles 3−8007
nonpolar solids, of nonpolar liqs. 3−1874
pool boiling, flat heaters, first critical heat flux 3−1366
refractory materials wetting by molten metallides 3−34627
ternary liquid system of acetone, toluene and H_2O 3−5412
water on glass, velocity effect on dynamic contact angles 3−8007
wetting by silicate melts, determ. by drop method, 'neck' phenomena *(Polish)* 3−27752
Ag, on clean W substrate, rel. to heterogeneous nucleation theory *(Japanese)* 3−20699
Au, on clean W substrate, rel. to heterogeneous nucleation theory *(Japanese)* 3−20699
Ge wettability by Au alloys *(Russian)* 3−8006
Si, wettability by Au alloys *(Russian)* 3−8006

contact e.m.f. *see contact potential*

contact potential
see also contact resistance
measurement by dynamic capacitor method, effects of stray capacitive coupling 3−33984
metal plates, force between them arising from contact pot. 3−10422
m.o.s., dielec. breakdown rel. to nonuniform contact barriers, Na effects 3−21155
semiconductor surface, measuring instrument *(Russian)* 3−22409
transition metal carbide, work function, comparison of contact potential difference and thermionic emission obs. *(Russian)* 3−12208
CdS, thin wafer, shift in steady state contact pot. difference on bending 3−2161
Si-Au, Si-Al, intersection and differential capacitance obs. 3−5053
Te thin films, work function and Fermi level results obtained by CPD method 3−15130
W(112), meas. rel. to Li adsorption 3−20938

contact resistance
see also contact potential
measurement method, metal-semiconductor ohmic contacts *(German)* 3−15253
metal surfaces in contact, heat transfer mechanism rel. to thermal contact resistance 3−2174
Ag-Be alloys, internal oxidation effects *(Japanese)* 3−8253
n-GaAs evaporated silver contacts, surface cleaning by ion bombardment, experimental results 3−15250

contacts, electrical *see electrical contacts*

continuous creation hypothesis *see cosmology*

continuum hypothesis *see set theory*

continuum mechanics *see classical mechanics of continuous media*

contours, surface *see surface contours*

control engineering applications of computers
see also control systems; digital control; numerical control
astronomical telescope, Siding Springs Observatory, CAMAC modular data system 3−3392
astronomy, observational online computer aids 3−5622
atomic flame spectroscopy, computer controlled sampler 3−6149
cine film, colour positive developing control and printer tape preparation by minicomputer 3−35433
Eindhoven A.V.F. cyclotron, automatic control, measurements 3−13380

control engineering applications of computers continued
Eindhoven A.V.F. cyclotron, automatic control, measuring instruments 3−13379
epitaxial growth, computer control 3−12231
epitaxial growth process, direct digital control, process and layer parameters 3−12221
experimental beam line control, CAMAC serial crate controller 3−35457
Gentilly nuclear power station, reactor power system control 3−14254
Indiana Univ. cyclotron facility, computer control 3−13376
irradiated fuel elements, nondestructive examination, new gamma scanning system 3−17305
neutron physics experiments, computer control system, High Flux Reactor at Petten 3−25825
neutron spectrometer control by minicomputer *(Japanese)* 3−10089
n.m.r. spectrometer, pulsed, automatic meas. of spin-lattice relax. times 3−267
nondestructive analysis of alloys, computerized X-ray fluorescence spectrometer 3−10138
nuclear fuel handling, position control system for Hot Fuel Examination Facility 3−17313
nuclear fuel rod fabrication plant, automatic Pb spectrometer for control of fissile material output 3−19990
on-line minicomputer system for control of KUR research reactor 3−1049
ORIC, isochronous cyclotron, computer control system 3−13377
proton beam positioning 3−275
semiconductor diffusion system, computer control 3−34488
semiconductor growth, automated, monitoring lateral dimensions 3−12312
SIN cyclotron, computer control, standard control components 3−13378
spectrometer control, using CAMAC interface to Honeywell 316 computer 3−35519
telescope, 24 inch 3−31841
TRIUMF cyclotron, CAMAC control applications 3−13375
TRIUMF cyclotron, control system 3−13374
vibration test, digital control and analysis 3−34697
X-ray diffractometer 3−23980
X-ray double crystal spectrometer, digitally controlled 3−32231
Co radiation therapy unit, computer-controlled kinematic simulator 3−10166
Si crystal growth production process 3−12323

control equipment
see also actuators; controllers; electric control equipment; nonelectric final control devices; relays; telecontrol equipment; thermostats; valves
coherent e.m. waves beam control, patent 3−37933
LMFBR, instrumentation 3−32192
SIN cyclotron, computer control, standard control components 3−13378

control gear, electric *see electric control equipment*

control of specific variables
this heading is restricted to those variables which are not covered by other specific headings. See also acoustic variables control; chemical variables control; electric variables control; frequency control; magnetic variables control; mechanical variables control; optical variables control; thermal variables control
vapourization rate, chem. vapour deposition instrumentation 3−12250

control system analysis
see also Bode diagrams; correlation methods; frequency response; linearisation techniques; phase space methods; sensitivity analysis; stability; step response; transfer functions
linear elastic systems on Hilbert space, energy-like Lyapunov functionals 3−32341

control system synthesis
see also Bode diagrams; correlation methods; frequency response; linearisation techniques; phase space methods; sensitivity analysis; stability; step response; transfer functions
prosthetic devices 3−28753

control systems
see also adaptive systems; closed loop systems; discrete time systems; distributed parameter systems; multivariable control systems; optimal control; sampled data systems
camera, using monolithic integration 3−37658
cyclotrons, conference, Vancouver, Canada (1972) 3−10010
digital, for high resolution spectrograph 3−3808
Eindhoven A.V.F. cyclotron, automatic control, measurements 3−13380
Eindhoven A.V.F. cyclotron, automatic control, measuring instruments 3−13379
for electron probe system for quantitative mineral anal. 3−369
galvanic transmissions, programmed control *(Russian)* 3−37524
immersion technique device for automatic non-destructive ultrasonic testing of nuclear fuel rod cladding tubes 3−19163
neural function studies 3−16570
nuclear reactor, stability analysis by Tsypkin Locus method 3−32922
nuclear science conference, Miami USA (1972) 3−28622
optical beams, oblique cut $LiNbO_4$ electrooptical elements *(Russian)* 3−693
real dynamical systems, observability and measurement theory 3−16373
steam generation control, effect of pollution abatement processes 3−25618
TRIUMF cyclotron, CAMAC control applications 3−13375
TRIUMF cyclotron 3−13374
X-ray diffractometer associating punched paper tape program 3−23980

controllers
see also control of specific variables; cryostats; instruments; servomechanisms; thermostats
breathing gas pressure regulator, adjustable, patent 3−10190
chemical vapour deposition instrumentation 3−12250
cryogenic temp. controller for use with resistance thermometers from 0.3 to 6 K 3−5820
digital electrode controller, for r.f. spark source mass spectrometer 3−25932

controllers continued
- fractional glow curves measurement, automatic controlled apparatus 3—3809
- infusion controller 3—32243
- liquid N level control in dewars, automatic device 3—5821
- Mossbauer spectrometer, electronic block for controlling moving system 3—28700
- nuclear magnetic resonance probe, temp. control 3—13245
- precision temperature regulator in dislocation-free crystals growth 3—24779
- remotely selective seismic cable variational depth controller, patent 3—39557
- stabilizing circuit, for intensity of Ar continuous wave laser 3—9964
- voltage control device used for synchrotron accel. cavities *(Russian)* 3—6053

convection
- *see also convection in liquids*
- air, heat transfer improvement with artificially modified turbulence 3—26789
- air in small cells heated from below, heat transfer expts. 3—7351
- atmospheric charge and relaxation time distribution, effects of convection 3—31376
- atmospheric convective development in Singapore area 3—34897
- axial heat transfer witrturbulent flow in a tube, dynamics *(German)* 3—14446
- beam-plasma system, linear and nonlinear props. of convective and absolute instabilities 3—20510
- Benard convection in non-linear region, minimum principle 3—1404
- Bingham plastic, transient free convection on vertical flat plate 3—26796
- boiling Freons, heat transfer, refrigerator tube material 3—1786
- boundary layer, Nusselt-Prandtl relationships 3—20281
- boundary layer unsteady state, interaction of convection and radiation *(Russian)* 3—11406
- boundary-layer film boiling, radiation and convection interaction 3—23733
- bounds for heat transport in a porous layer 3—26790
- buoyant plume above horizontal line heat source 3—23696
- clouds, characteristic scaling for convective elements *(Russian)* 3—18858
- combined free and forced, past a porous vertical circular cylinder 3—38355
- compressible free convective flow, general elliptic method for computational soln. 3—20347
- conductive heat and mass transfer in a dynamic two-phase layer meas. 3—26783
- core-He-burning in massive stars, effects of semiconvection 3—13013
- cosmic ray transport theory, with anisotropic particle scatt. and convection using Fokker-Planck eqn. *(Russian)* 3—12871
- crystal growth, and mass transfer in chem. vapour transport process 3—24793
- cumulus clouds, drag coeff., determ. *(French)* 3—2972
- diffusion-convection equation, finite element soln. 3—14429
- dilute aqueous polymer solns., laminar natural convection heat transfer 3—4542
- disperse material, convective drying, in agitated layer in cross flow of coolants 3—25022
- dispersed liquid metal-gas packed bed heat exchanger 3—39303
- double diffusive convection, transport and profile meas. of diffusive interface 3—20305
- doubly diffusive, finite amplitude, temp. and salinity gradients 3—7357
- doubly periodic, in horizontal fluid layer heated from below *(Russian)* 3—29854
- earth, plume convection with upper mantle temperature inversion 3—12618
- in Earth, rel. to gravity anomalies and bathymetry 3—37150
- Earth, tectonic plate motion rel. to convection process between elastic lithosphere and viscous asthenosphere 3—15896
- Earth mantle, a laboratory model with temp.-dependent viscosity 3—25108
- external natural convection about two-dimensional bodies with constant heat flux 3—17520
- film boiling heat transfer from horizontal cylinder to saturated liquids *(Japanese)* 3—38369
- filmwise condensation on a surface with uniform heat flux and body force convection 3—29850
- finite amplitude occurring in a modulated gravity field *(Russian)* 3—26787
- flow in inclined homogeneous porous layer *(French)* 3—7348
- flows started from rest, stability 3—4564
- fluid in rectangular region heated from below, effect of wall conduction on stability 3—26797
- fluid subjected to vibration, heat transfer 3—26798
- fluids, confined exothermically reacting, dynamic stability 3—15823
- forced, heat transfer for flow in pipes, past flat plates and for flow in packed beds 3—11365
- forced, heat transfer problems, direct variational methods of soln. *(German)* 3—20289
- forced, spatiotemporal reconstitution of instantaneous vel. component near cylinder wall *(French)* 3—26777
- forced convection heat and mass transfer from humid air to frost surface 3—1363
- forced convection mass transfer from wetted grooves 3—26800
- forced turbulent convection in circular tubes, effects of buoyancy and acceleration due to thermal expansion 3—38359
- free, from vertical plate, leading edge effects on Nusselt number 3—20291
- free, heat transfer, schlieren TV method for thermal boundary layer obs. 3—124
- free, in open ended vertical channels, numerical soln. 3—36089
- free convection, variation of fluid properties *(Japanese)* 3—20324
- free convection along lower surface of heated horizontal place 3—1317
- free convection from semi-infinite inclined flat plate, series soln. 3—26794
- frost formation on air coolers rel. to natural convection conditions for cooled plate 3—1780

convection continued
- Gibbs adsorption effects on Marangoni instability in penetration mass transfer 3—7342
- growth system, vapour phase, effect of natural and forced convection 3—2647
- Hartmann-Sprenger tube, thermal phenomena, forced convection *(French)* 3—20292
- heat and mass transfer 3—11388
- heat and mass transfer between two phases, effects of convection *(French)* 3—2840
- heat transfer, convective, forced, effect of 2-dimens. roughness 3—22765
- heat transfer, free convective, between parallel plates, anal. 3—20279
- heat transfer from stripwise heated surface 3—22275
- heat transfer in porous layer heated from below 3—1361
- heat transfer in rod clusters with turbulent axial coolant flow *(German)* 3—23720
- heated fluid layers, natural oscill. 3—26828
- between heated planes, non-uniform, natural convection stability 3—36084
- heavy convective clouds, spectral structure of the turbulence 3—34883
- high Prandtl number heat transfer in Blasius flow 3—20280
- horizontal annular air layers at low Grashof numbers *(Russian)* 3—7354
- horizontal tubes in transition regime, interaction of free and forced convection 3—23700
- hypersonic flows around blunt bodies, convective and radiative heating study *(Russian)* 3—26788
- ice-fre zone length correction in a convectively cooled pipe 3—20300
- instability of layer of binary gas mixture heated below 3—20309
- isotropic plasma convective motion near rotating magnetised sphere, appl. to planets 3—23835
- laminar, combined free and forced, in inclined tubes, numerical soln. 3—23681
- laminar, from rotating radial plate 3—23718
- laminar, in closed spherical containers 3—23716
- laminar, unsteady, in uniformly heated vertical pipes 3—20308
- laminar boundary layer, radiative transfer, viscous dissipation, convection and heat conduction 3—23734
- laminar forced convective flow and heat transfer in triangular ducts 3—1343
- laminar free, Gortler-type series for non-isothermal vertical plate 3—4563
- laminar free, in heated vertical corner 3—4561
- laminar free convection stagnation heat transfer, isothermal cylinder with internal sources/sink 3—26774
- laminar free convective flow over isothermal nonconducting plate in transverse magnetic field 3—38403
- laminar layer on hot plate, Olfe's modified differential approximation 3—635
- liquids, boiling, heat transfer crisis 3—14990
- magnetic fields generation, nonlinear hydromagnetic dynamo problem 3—26837
- magnetic inhibition of thermal convection 3—14442
- magnetospheric interrelations 3—3127
- mass transfer, convective, from stationary and moving surfaces using a Hg evaporation technique 3—20286
- mass transfer, from single sphere *(Japanese)* 3—22764
- mass transfer in sublimation by laminar free convection *(German)* 3—26801
- MHD channel, convective heat loss and elec. cond. calc. 3—36131
- MHD free convection laminar flow of an elastico-viscous fluid along an infinite porous wall 3—20375
- MHD free convective flow in vertical channel, stability analysis 3—38401
- micropolar free convection flow, heat-transfer and flow characts. 3—20288
- mixed, heat and mass transfer obs. 3—1319
- mixed convection above heated horizontal surface, buoyancy effects 3—23697
- mixed convection in porous media *(French)* 3—20287
- mixed laminar, problems 3—1356
- models for simulating transport processes in convective flow, book 3—11400
- molecular gas dynamics, boundary conditions, surface shocks, continuum flows, review 3—33261
- naphthalene circular discs, forced convective mass transfer meas. 3—33214
- natural, between horizontal concentric cylinders *(French)* 3—26778
- natural, mass transfer adjacent to horizontal plates 3—36088
- natural convection, influence of various surface roughness 3—20297
- natural convection boundary layer flow over horizontal and slightly inclined surfaces 3—38379
- natural convection heat transfer from downward-facing horizontal surfaces with uniform heat flux 3—20296
- natural convection in a sound field giving large streaming Reynolds numbers, boundary layer theory 3—38358
- natural convection in vertical cells of rectangular cross section, expt. study 3—14447
- natural flow and transpiration, vertical-flat-plate problem 3—20306
- natural laminar, around plane plate in incompressible fluid *(French)* 3—26776
- natural turbulent convection on an isothermal vertical wall; transition *(French)* 3—14449
- non-stationary free convection in close convex region, classical solns. of second boundary problem *(Russian)* 3—29855
- nonlinear, conducting Boussinesq fluid, in magnetic field 3—7442
- nonlinear Benard convection with rotation 3—23702
- nonlinear heat conduction equations solutions by numerical method, convective heating and cooling tests simulation of Tylose samples 3—19527
- nonstationary heat transfer, for turbulent flow in tubes *(Russian)* 3—11393
- ocean, driven by surface stress and non-uniform horizontal heating, numerical model 3—9248
- one-dimensional heating with time-depend. heat-transfer coeff. 3—22786

convection continued
oscillatory flow, past an infinite, vertical, porous plate with constant suction, free convection effects 3−33211
oscillatory flow past an infinite, vertical, porous plate with constant suction, free convection effects 3−33212
parked beds, forced convection mass transfer at low Reynolds numbers 3−33200
Penning discharge under rotational instability, convective particle transport across mag. field *(Russian)* 3−33373
periodic struct. flow, Lagrangian description rel. to conc. gradient *(French)* 3−1359
planetary atmospheres, convective vortex sheet in fluid heated from below 3−31618
plasma, rotating, inertial e.m.f. due to thermal convection 3−29945
plasma linear and nonlinear properties of convective and absolute instabilities in a beam-plasma system 3−23869
plume swaying due to free convective heat transfer from horizontal cylinder *(Japanese)* 3−23684
pollutant transport, stochastic processes 3−1375
polytrope with toroidal mag. field, non-radial oscill. and convective instability 3−37285
porous layer, horizontal, heat transfer by natural convection *(French)* 3−29916
Pt wire, natural convective boiling, heat transfer to binary mixtures *(Japanese)* 3−24274
rarefied gas between two parallel plates, flow mode 3−23757
Rayleigh-Benard, two-dimens., confined Boussinesq fluid 3−38364
rolls, strong mag. fields in dark filaments in sunspot penumbrae 3−35020
rotating annulus uniformly heated from below, nonlinear results 3−23701
rotating magnetic stars, Coriolis force effects on convective motions origin 3−35112
saturated porous media, thermal field visualisation by Christiansen effect 3−19377
sea-air interaction, convective motion in two-dimensional extended rectangular basin model *(Russian)* 3−25203
slab, with radiative and convective heating, transient temp. distrib., variational method calc. 3−35635
sloping porous layer, natural convection 3−20307
in slot, slightly slanted, instabilities 3−23695
solar circulations, large scale nonlinear Boussinesq convective model 3−31533
solar convective zone hydrodynamics *(Russian)* 3−16130
solar global convection, dynamo action explaining sunspot proper motions and magnetic activity longitude 3−22014
stability, between two parallel vertical walls 3−36075
star of 0.5 $M_\odot$ during core H burning, pulsational instability rel. to convection 3−37357
stationary, correction near the critical Rayleigh numbers for an almost vertical temperature gradient *(Russian)* 3−33206
stellar atmospheres, effect in solar atm. determ. using mixing-length formalism 3−39660
stellar atmospheres, in presence of magnetic fields 3−22058
stellar atmospheres, semiconvection rel. to general opacity law and thermal He flashes 3−13015
stellar interior convective motion, exponential growth rates in advanced red giant 3−37350
stellar magnetised isothermal atm., thermal convective instability 3−39589
sunspot cooling rel. to convection zone models and magnetic power supply 3−39620
supernovae, Urca neutrino losses driven by post-ignition convection 3−28183
surface film boiling under free convection, eff. of cylinder diameter 3−20869
temperature field structure in strongly heated buoyant thermal 3−9296
terrestrial, plume convection, synchronous discharge evidence from volume estimates and age dating of igneous deposits 3−12616
thermo-acoustic oscillations in forced convection heat transfer to supercritical pressure water 3−20282
transient heat transfer to walls of cylindrical channel filled with liq. 3−19531
turbulent, at isothermal vertical plate *(Russian)* 3−11391
turbulent cellular convection in the atmosphere, feedbacks *(Russian)* 3−12718
turbulent flow, multicomponent mass transfer 3−7341
turbulent free flow 3−4556
turbulent wake behind optically heated sphere, temp. fluctuations 3−20317
unsteady convective diffusion with interphase mass transfer, miscible dispersion theory 3−33292
unsteady flow, produced by temp. fluctuations at horizontal boundaries, numerical study 3−1365
vapour-gas mixture, in a capillary, convective diffusion with evaporation 3−26784
viscoelastic fluid layer in mag. field, oscillatory convection 3−14479
viscous dissipation effects in free convection 3−17519
vortices, pressure and velocity fields 3−36098
water, subcooled, vapour bubble growth rate in boiling under slightly forced convection conditions 3−27109
water in enclosed rectangular cavity, effect of inversion temp. 3−4562
CO_2, heat transfer in turbulent flow *(Russian)* 3−11392
CO_2, supercritical, laminar forced convective heat transfer, buoyancy effects *(Japanese)* 3−20323
H_2O, forced and free, heat transfer in vertical tube 3−4550
He, supercritical liquid, meas. of forced convection heat transfer 3−9893
KCl(I), boiling and convection in solvent inclusions rel. to movement 3−11610
Na, continuous boiling phenomena under forced convection by direct heating 3−23398
Na, incipient boiling by direct heating under forced convection 3−17968
NaCl, boiling and convection in solvent inclusions rel. to movement 3−11610

convection continued
Si, vapour deposition, surface transient effects, instabilities due to convection, Si devices 3−39275

convection in liquids
buoyancy-induced flows, instability, transition and turbulence, review 3−33217
Czochralski growth method, forced convection theory 3−11568
ditolilmethane and diphenyl mixture, electric field effect, electrodes, Schlieren pictures *(Russian)* 3−27146
Earth core thermal history, macroscopic convection at melting point 3−34817
flow regimes in a periodic external force field *(Russian)* 3−29856
free convection under maximum density conditions from vertical semi infinite flat plate in liquid 3−17526
glass melts with high fluoride content, F loss to atmosphere effects *(German)* 3−27161
natural convection in shallow pools, free-surface deformations 3−26792
nematic liquid crystals, heated from above heat convection 3−36443
Rayleigh-Benard, two-dimens., confined Boussinesq fluid 3−38364
reverse osmosis 3−7950
rotating deep annulus convection, thermal fields in high amplitude wave regime 3−26802
saline solutions, freezing, salt rejection, absence of free convection 3−34701
supercritical water flowing in tubes, heat transfer 3−1370
thermal equilib. near crit. point, effect of convection instability on thermal conductivity 3−36442
thermohaline structure of ocean, formation and evolution *(Russian)* 3−27977
turbulence intermittency, nonhomogeneous flows 3−33216
water, secondary convection between parallel vertical plates at diff. temps., calc. 3−11768
water laminar free convection flow at 4°C from a vertical plate with variable wall temperature 3−29843
H_2SO_3 dilute soln., surface tension gradient stabilisation of density driven convection 3−34747
^{4}He, liquid, superfluid, cooling by convective heat transport 3−27152
K, convective heat transfer, during turbulent flow 3−14445

convergence
see also convergence of numerical methods
homogeneous Markov chains, multidimensional central limit theorem, speed of convergence *(Russian)* 3−13537
Legendre series, nonlinear Pade approximants 3−26057
measure theoretic convergences of observables and operators 3−26117
neutron integral Boltzmann eqn. in three-dimensional systems convergence in mean of solns. 3−29427
of semigroups, $A^{n,a}$ $(n=0,1,2,\ldots;\ 0\leqslant a<1)$, theorems *(Russian)* 3−13532
sum rules of cluster functions in φ^3 ladder model 3−26281
t matrix, convergence of seperable expansions 3−28813

convergence of numerical methods
complementary energy method, application to non-conservative elastic stability problems 3−32330
far scattered magnetic field equations of cylinder of arbitrary cross-section 3−22831
finite element, convergence rate in problems with singularities 3−22616
high subsonic flow, parabolic substitution in Euler eqns. 3−23751
iterative sequences, extrapolation method 3−20003
mixed finite element scheme for bending of plates 3−37803
moment-method solutions, convergence improvement technique 3−3932
non-uniform elastic circular region, iterative soln., convergence *(Russian)* 3−28867
rapid-convergence algorithm for quantum mech. cryst. binding energies 3−1594
successive approx. method for soln. of non-linear integral eqn. for strain hardened zone *(Russian)* 3−28898
Timoshenko beam finite element 3−564
vortex by modified Newton-Raphson methods 3−7391

conversion electron spectra
β-decay, internal conversion transitions, electron correlation effects *(Russian)* 3−19818
line shape analysis by computer 3−325
spectrometer, beta-ray, in-beam axial, for detection of 3−10081
^{209}At → ^{209}Po decay, excited states of ^{209}Po *(Russian)* 3−23267
^{129}Ba → ^{129}Cs decay, level struct. 3−19766
^{252}Cf, prompt electrons from neutron-induced fission 3−6949
^{154}Eu → ^{154}Gd decay 3−6771
^{57}Fe, internal conversion of 4s electrons in Fe 3−15124
^{157}Gd, thermal neutron capture, conversion electron and γ-ray spectra *(Russian)* 3−10969
^{177}Hf, quasiparticle isomeric states, decay obs. 3−14162
^{197}Hg decay, transitions of ^{197}Au *(Russian)* 3−17191
^{76}Kr → ^{76}Br, β- and γ-ray spectroscopy, determ. of spin-parity assignments for ^{76}Br states 3−19758
^{191}Os, relative conversion line intensities meas. and nuclear structure effect 3−29341
^{228}Pa, decay to levels of ^{228}Th 3−38107
^{230}Po → ^{230}Th, meas. of γ and electron-singles spectra and γ-γ coincidences, determ. of levels in ^{230}Th 3−23211
^{197}Pt decay, transitions of ^{197}Hg *(Russian)* 3−17191
^{184}Re isomers, and γ-ray spectra *(Russian)* 3−23272
^{150}Sm, internal conversion spectrum emitted by ^{149}Sm(n,γ) reaction *(Russian)* 3−32795
^{117}Sn, upper intensity limit of direct transition between $h^-{}_{11/2}$ and $S^+{}_{1/2}$ states, internal conversion electron spectra *(Russian)* 3−10912
^{91}Sr → ^{91}Y, continuous β-ray spectrum and internal conversion electron spectrum 3−29362
Ta β decay to ^{172}Hf levels, $\beta^+\gamma$ coincidence meas. 3−38143
Ta decay, 25-300 keV *(Russian)* 3−17203
Tb → ^{148}Gd decay scheme obs. *(Russian)* 3−23269
Tb decay, γ-ray spectra *(Russian)* 3−4296
^{150}Tb → ^{150}Gd decay scheme obs. *(Russian)* 3−23269

conversion electron spectra continued
^{121}Te, upper intensity limit of direct transition between $h^-_{11/2}$ and $S^+_{1/2}$ states, internal conversion electron spectra *(Russian)* 3−10912
^{123}Te, upper intensity limit of direct transition between $h^-_{11/2}$ and $S^+_{1/2}$ states, internal conversion electron spectra *(Russian)* 3−10912
^{125}Te, upper intensity limit of direct transition between $h^-_{11/2}$ and $S^+_{1/2}$ states, internal conversion electron spectra *(Russian)* 3−10912
^{194}Tl decay modes *(Russian)* 3−976
^{235}U, prompt electrons from neutron-induced fission 3−6949

converters *see convertors*

convertors
see also analogue-digital conversion; digital-analogue conversion; frequency convertors; magnetohydrodynamic convertors; phase convertors
amplitude-time, nonlinearity compensation 3−28688
impedance, monolithic IC for biomedical meas. apparatus 3−37741
parametric, for crystal hygrometers 3−37779
start-stop time-to-amplitude, interaction between correlated and uncorrelated time-interval distributions 3−10057
voltage-to-frequency, current integrator with digital read-out, student apparatus 3−28452

convex programming
plastic strains in shake-down of structs. subjected to cyclic loads, upper bounds 3−16660
plates of minimum weight under given load, optimisation *(Russian)* 3−10287
shakedown of plastic struct., mimimax principle for calc. of upper limits to strains 3−32363
shells of minimum weight under given load, optimisation *(Russian)* 3−10287

conveyors
bistable fluid device, solid particle flows 3−1471
dense phase gas solid suspension, positive expulsion fluidization tank 3−4619
dynamics of two-dimensional particle on vibrating conveyor 3−16682
solid particle transportation, bistable fluid device 3−4618

cooling
see also Joule-Thomson effect; low-temperature production; refrigeration; supercooling
air injection into flow path of turbine stage 3−1379
atmosphere, near-mesopause, airglow effects on energy loss due to molecular de-excitation 3−34889
BWR emergency core cooling system for loss of coolant accident 3−4337
convectively cooled pipe, correction on the length of ice-free zone 3−20300
crossed rod matrix, press. effect on departure from nucleate boiling 3−1068
of crystal, annealing of vacancies, analyt. eqns. 3−7752
dilution refrigerator for precooling Pomeranchuk cell, design and construction 3−25698
electrically conductive laser beam reflector cooling, patent 3−35431
electronic apparatus design *(German)* 3−25676
enhanced cooling of cryogenic electrical leads, comments and critique 3−5822
evaporative air coolers, internal heat transfer, flow turbulization, boiling Freons 3−1439
fin effectiveness, effect of thermal conductivity and base temperature depression 3−9856
finely dispersed material in fluidised beds 3−2763
fog formation by steaming of warm-water lagoon used for power station cooling 3−39511
frost formation on air coolers rel. to natural convection conditions for cooled plate 3−1780
glass melts with high fluoride content, F loss to atmosphere effects *(German)* 3−27161
glass reinforced plastic rings, wound, residual stresses determ. 3−24983
heat transfer to a cooling coil in an agitated vessel 3−23714
helical cooling coils in agitated vessels, turbulent heat transfer 3−1364
hypersonic turbulent boundary layer, blowing of coolant gas through slit *(Russian)* 3−11405
IC chips, fluidised powder cooling, 1.5 to 2.0 watts at room temp. 3−11451
ionospheric electron gas cooling by excitation of O electron levels fine structure 3−25270
large-scale He refrigerator-liquefier system 3−25703
laser optical element, strongly anisotropic, nonlinear cooling, approximation calculation method 3−22868
late-type stars, CO i.r. opacity effects, appl. to Sun and grain formation 3−31642
layered tissues, temperature distribution calc. 3−25587
liquid, evaporative cooling in a rarefied gas 3−14991
LMFBR, coolant mixing in fuel pin assembly using helical wire wrap spacers 3−38177
of locked form in V-belt-vulcanisation, transient heat conduction calc., application of finite element solution technique *(German)* 3−22790
low-pressure dischrge tubes vessel for cooling with liquid N_2 *(Czech)* 3−25934
mist, establishment of definite heat transfer regions 3−20854
modular type packaging, using thermoelectric heat exchanger 3−19167
molten fuel-sodium interaction in fast reactors, theoretical model 3−1066
natural cooling of Rhine water rel. to thermal pollution by power stations and plants *(German)* 3−9226
nonlinear heat conduction equations solutions by numerical method, convective heating and cooling tests simulation of Tylose samples 3−19527
Pomeranchuk, ultralow temperature production, review 3−35383
porous media by fluid flowing through 3−627
pure He white dwarf stars (mass $0.15M_\odot$), cooling sequence 3−31648
quenching bodies of complex shape, cooling time calc. 3−21694
quenching liquid metal, cooling power, general definition *(French)* 3−15720

cooling continued
radiative, buoyant thermals by longwave radiation, applic. to troposphere, Mars and Venus 3−25222
radiative decay behind strong shock 3−4592
radio-electronic devices, low-temperature cooling *(Russian)* 3−9875
reactor core spray cooling after loss of coolant, numerical soln. of Yamanouchi model 3−11074
reactor systems, heat-transfer coeff. during rewetting of hot dry patch, anal. 3−1067
refractory metals, high-speed crystallisation apparatus *(Russian)* 3−12327
saturated vapour-gas mixtures heat and mass exchange 3−23656
shock waves, radiating-conducting flowfield 3−4591
sodium cooled fast reactors, cover-gas bubbles in coolant, number and size determ. 3−1070
solute escape from droplet cooled by vaporization and radiation, liq.-phase diffusion-controlled 3−27849
splat cooling, cooling rate indicators 3−8855
steel, austenite residual percentages prediction from transformation curves *(French)* 3−24910
steel, brittleness depend. on cooling rate after annealing *(Russian)* 3−24905
sulphide minerals, effect of temp. on magnetic susceptibility during continuous heating and cooling, phase change obs. *(Russian)* 3−12009
sunspot cooling mechanism rel. to Carnot cycle and hydromagnetic interactions 3−39619
sunspot cooling rel. to convection zone models and magnetic power supply 3−39620
superconducting devices employing supercritical He *(Japanese)* 3−15038
supernovae remnants, of different ages 3−16218
temperature fields produced in a workpiece by repeated applications of a source of heating, numerical calc. 3−24962
thermal design of evaporative coolers, calc. method 3−112
thermoelectric, for variable low temperature test chamber *(Polish)* 3−121
transpiration cooling, heat and mass transfer equations 3−26168
transpiration cooling, heat transfer phenomenon 3−7918
viscous dissipation effects in free convection 3−17519
Yerkes 40-inch refractor, effect on thermal condition of lens on plate scale, Vasilovskis theory 3−28301
Zircaloy-2, corrosion in hot water and steam at different cooling rates 3−37021
Al alloy as electric conducting wire, effect on conductivity *(Norwegian)* 3−5304
Ar, high temp. flow in pipe, heat transfer 3−14408
Cd-Sb system, crystallisation conditions influence on props. *(Russian)* 3−8769
Cu-Al alloys, influence of precipitation of γ_2 phase on order-disorder transformation 3−27617
^{4}He, liquid, superfluid, cooling by convective heat transport 3−27152
Ni-rich alloys, superrefractory, instability aspects, cooling effect on creep strength, crystallization, precipitation and microtoughness *(French)* 3−18660
Pt wire, elec. resist. change on immersion in liquid He, thermal shock 3−4746
SiO_2-Al_2O_3 thin film, splat cooling prepn. for transmission electron microscopy 3−18537
Ti-Pu dilute alloys, influence of $\beta \to \alpha$ transformation and of O_2on Pu distribution, segregation after cooling *(French)* 3−18601
Zr-Pu dilute alloys, influence of $\beta \to \alpha$ transformation and of O_2 on Pu distribution, segregation after cooling *(French)* 3−18601

cooling towers
air flow and heat transfer to the atmosphere from the surface of thermal electric power plant cooling ponds 3−29847
computer code for thermal design 3−17285
vibrations of shells of revolution with variable thickness 3−37849

Cooper Hewitt lamps *see mercury vapour lamps*

coordination complexes
inorganic complexes are indexed under the appropriate metal compound headings
ten coordination, equal sized ligands, calc. geometry, repulsion energy minimisation 3−29546

copper
absorption cross section for 450-1000 MeV photons 3−11163
acoustic wave resonant interactions, slowness diagrams 3−32391
adsorbed on W, electron interaction obs. by static skin effect method 3−20937
adsorption effect in drawing with organic lubricants, oxide film form. 3−33604
adsorption of Cl on (100) face, electron diffr. obs. *(French)* 3−1893
adsorption of SF_6, stepwise adsorption isotherms, application to study of surface phases *(French)* 3−27176
adsorption of Xe, adsorbed layer struct., LEED obs. 3−30345
alkali halide phosphor, Cu-activated, X-irrad., time-lag of photostimulated luminesc. *(Russian)* 3−18483
alloying element in Al-Zn-Mg alloys, grain boundary corrosion and stress corrosion cracking relationship *(Japanese)* 3−31072
amino acid:Cu^{2+}, ligand hyperfine interaction 3−24605
anelasticity, amplitude dependent, role of dislocation motion in single crystals *(German)* 3−24214
anelasticity, amplitude-dependent during and after plastic deformation *(German)* 3−34611
angular correl. anisotropy of γ annihilation radiation at 925°C 3−5150
annealability testing 3−34675
aquatic frontal systems, element enrichment in films and foams 3−12690
atom, Auger and photoelectron spectra, L_2 and L_3 vacancy states width 3−29512
Auger electron and charact. energy loss spectra from clean and black surfaces 3−34452
Auger electron spectra and electron spectra, 25-400°C 3−30910
Auger electron spectrum, spin splitting 3−21504
Auger emission from (111) face, angular dependence 3−30916
Auger spectrum, fine struct. 3−34447

copper continued

- Auger-electron and photoelectron structure in secondary electron energy distributions, high reduction meas. 3−8691
- backscattering of H and ^{4}He, ion fraction, 25-150 keV 3−30912
- band profile in Fermi surface neck region of k-space 3−30837
- band structure, calc. using non-local screened exchange 3−1980
- chemisorbed monolayer, Auger spectra, L-shell ionization cross section 3−39209
- chemisorption of Bi on (100) surface, LEED obs. of layer struct. 3−30355
- chemisorption of Bi on (111), LEED obs. of layer struct. 3−30356
- cladding of Nb-Ti composite wires, effect on mag. instability 3−11989
- coating on supercond. Nb alloy wire, crit. current density depend on coating thickness 3−34036
- coatings, current density and temp. influence on morphology and predominating orientation 3−1943
- cold rolling, slip system and orientation changes obs. *(Japanese)* 3−12390
- cold-worked, mech. after-effect caused by dumb-bell interstitials *(German)* 3−1663
- composite, fibre reinforced, deform. and fracture behaviour *(Japanese)* 3−34634
- composite with solid lubricants, comp. effect on tribological props. 3−15785
- conduction electron g-factor, meas. by de Haas-van Alphen effect 3−1977
- conduction e.s.r., frequency dependence interpreted as new many-body effect in metals with g anisotropy 3−2394
- corrosion, in electrolytic environment, photopotential obs. of surface layer 3−8044
- corrosion fatigue, crit. corrosion rate considerations 3−27655
- corrosion fatigue crack initiation 3−27661
- creep characteristics, correl. with substruct. misorientation and stacking fault energy *(Russian)* 3−8837
- creep deform., obs. of dislocations and grain boundaries 3−14880
- creep of electrodeposited films, rate and strain thickness dependence *(Russian)* 3−11674
- critical hardening of germination and migration *(French)* 3−8826
- crystals dispersed with SiO_2, re-examination of recrystallisation data 3−15688
- de Haas-van Alphen scatt. temp., lattice dislocations effect 3−18069
- defect production temp. depend. by electron irradiation 3−7749
- deformation hardening, velocity dependence *(Russian)* 3−2727
- deformational anisotropy study using plasticity theory *(Russian)* 3−536
- deformationless cutting of single crystals 3−27712
- deformed, neutron bombardment influence on recrystn. *(Russian)* 3−15693
- densities of unfilled one-electron levels, X-ray continuum isochromat study 3−36536
- diffusion in CdS, 300-700°C 3−30286
- diffusion in CdTe, single cryst. prep. and characteriz. 3−15632
- diffusion of Ag, Cd, In, 760-1070°C *(Russian)* 3−11756
- diffusion of Ag adatoms, Fick's eqn., soln. *(French)* 3−11804
- diffusion of Co, isotope effect 3−7965
- diffusion of Rh, temp. depend., 750-1075°C *(Russian)* 3−15029
- dislocation attenuation and acoustic emission during deformation of single crystals 3−11629
- dislocation dynamics, interaction with lattice phonons and electrons 3−14857
- dislocation line kinetics, effect of high temp. pulse irradiations 3−36300
- dislocation loops, interstitials and vacancies, X-ray meas. of neutron beam effects 3−14895
- dislocation pinning after neutron irrad. at liq. He temp., internal friction and dynamic modulus obs. 3−38600
- dislocations, vibrating string model, damping and modulus effects 3−17935
- disordered polycrystals, distortion waves 3−17926
- dissolution in liq. Sn, alloy layer growth 3−21709
- ductility, temp. depend., grain boundary migration *(Russian)* 3−39355
- elastic anisotropy of Cu with (001) (100) texture under biaxial stress *(German)* 3−2731
- elastic constants, rel. to third and fourth order anharmonic coeffs. of Cu-Ni alloys *(Russian)* 3−33619
- elastic constants, third order, long wave calc. method 3−17898
- elastic consts., third order, pseudopotential calcs. 3−33590
- electrochemical microsectioning technique 3−2815
- electrode, morphological changes of low-index planes, near equilib. 3−9075
- electrodeposited coatings, morphology and preferred orientation, current density and temp. effects 3−9070
- electrodeposition from pyrophosphate solutions, interfacial metal-electrolyte resistance 3−6152
- electron backscatter and backemission yields, bombarded by 0.4 to 1.4 MeV electrons 3−18514
- electron scattering, angular distrib. of secondary electrons *(German)* 3−18521
- electron-phonon interaction, interpolation scheme calc. 3−30222
- electronic spectra and density of states, cluster calc. 3−36516
- electroplating using Sn, Zn and Ti 3−9073
- electroreflection phenomena interpret. rel. to surface electron density *(French)* 3−18432
- electrothermal analyzer, Shimadzu, for resistivity meas. *(Japanese)* 3−13253
- epitaxial film, electron diffr. obs. of adsorbed oxygen layer *(French)* 3−27188
- epitaxial growth on Au(111) platelet, influence of intermediate amorphous C layer 3−24357
- equation of state, semiempirical, rel. to mech. props. *(Russian)* 3−27618
- etchants for exposing dislocations, and mechanism *(Russian)* 3−8033
- exploding wire in strong axial mag. field, discharge damping 3−36218
- extended X-ray absorption fine struct., meas. of shielding of impurities 3−18511
- fatigue failure, vacuum influence *(Russian)* 3−24874

copper continued

- fatigue strength, low-cycle, determ. under axial and reversed torsional strain cycling 3−5299
- fatigue strength, small plastic deform. effect 3−27688
- fatigued, recovery of shear modulus and internal friction 3−7811
- Fermi surface stress derivatives, oscillatory magnetostriction 3−33779
- field-ion microscopy, for surface investigation 3−28734
- film, adhesion, scratch test apparatus obs. *(Japanese)* 3−20959
- film, elec. conductivity, effect of CO adsorp. 3−8144
- film, elec. resist., γ-irrad. effects *(Russian)* 3−18231
- film, electrolytic, ductility and tensile strength, thickness depend. *(Russian)* 3−7820
- film, electron energy loss spectrum 3−17885
- film, epitaxial growth on β-Co *(Russian)* 3−8049
- film, far-u.v. transmission, N_2 press. influence *(French)* 3−12199
- film, Hall effect rel. to H_2 and O_2 chemisorption 3−15278
- film, optical radiation on passage of electrons up to 100 keV 3−24771
- film, polycrystalline, dynamical effects in electron scatt. for structure obs. 3−24014
- film, thermoelec. power and temp. coeff. of resist. 3−27243
- film deposition, thickness meas. by microbalance 3−37588
- films on n-Si, structure obs. 3−33751
- fine particles, n.m.r. linewidth field depend. 3−34221
- fluorescence resistograms using an atomic fluorescence photometer *(Russian)* 3−28791
- foil, α-irrad. at 78K, internal friction and Young's modulus *(German)* 3−7851
- fracture surfaces produced by high temp. creep of continuously cast specimens 3−34535
- fracture surfaces produced by high temp. creep of continuously cast specimens 3−34536
- friction during working, effects of crystalline structure and single cryst. orientation *(Russian)* 3−8873
- gamma-ray scatt., total cross sections, 60-1400 keV 3−29462
- grain boundary energy, 1030°C 3−36308
- grain boundary friction with neutron irradiation and fatigue 3−24117
- grown by Czochralski method, cryst. perfection, absence of dislocations 3−1601
- Hall effect, temp. dependence in dilute alloys, intermediate field condition 3−21057
- heat transport, between electrons and phonons below 0.2 K 3−27237
- heavy ion bombardment, shadow effect 3−33574
- impulse lasers, expt. obs. *(Russian)* 3−35690
- impurity scattering, phase-shift anal. 3−33863
- indirect nuclear interaction coupling constants 3−27216
- induced torque, magnetic field and temp. dependence, anisotropy of closed-orbit torque 3−11884
- internal friction, dislocation pinning by hydrogen *(French)* 3−2740
- internal friction, freq. depend. for technical purity metal *(Russian)* 3−1691
- internal friction Bordoni peak, cold worked crystals and polycrystalline specimens, 20 to 200 K, 10 to 25 kHz 3−36364
- ion beam, relativistic, heavy, meas. of range in Cu 3−33583
- ion production for vacuum deposition, high rate system 3−25716
- Knoop hardness meas. *(Japanese)* 3−12391
- lattice dynamics, modified Bhatia's model 3−38635
- light emission induced by H$^+$ and He$^+$ impact on clean surface 3−18501
- liquid, acoustic wave velocity, new meas. technique using e.m. detection 3−11688
- liquid, diffusivity of hydrogen 3−36433
- liquid, electrolytic deoxidation at 1600°C 3−5313
- liquid, surface tension, 1100-1500°C, temp. coeff. *(French)* 3−1872
- local exchange correlation potentials and the Fermi surface 3−8091
- lubricant trapping under cold compression *(Japanese)* 3−30990
- macroscopic yielding of highly perfect crysts. *(Japanese)* 3−30184
- magnetoacoustic open-orbit antiresonances, obs. and mechanism 3−27207
- magnetostriction meas. rel. to stress depend. of Fermi surface necks 3−18350
- malleability and plastic anisotropy study 3−18651
- mechanical strength, calc. using semiempirical equation of state *(Russian)* 3−8836
- moderator, low energy positron emission in backscatt. mode 3−30926
- negative ion source, bombardment of solid surfaces by positive alkali ions *(Russian)* 3−6061
- negative positron work function calc. 3−15151
- negative secondary ionic emission adsorpt. and oxidation effects 3−30913
- neutron irrad., damage due to radioactive decay 3−11660
- neutron irradiation hardening, effect of alloying elements Si and Al 3−18630
- n.m.r., low temp. obs. using SQUID magnetometer 3−2328
- nucleation, electrolytic, Cu on Pt cathode, pulse method investigation 3−1945
- occupied valence bands computation incorporating pseudopotential methods and Korringa-Kohn-Rostoker energy band method 3−8078
- open orbit resonance, polarisation of shear-wave attenuation 3−8092
- optical constants 3−8548
- oxidation, i.r. reflection studies, inhibition by benzotriazole *(Japanese)* 3−18639
- oxidation, low temp., very thin oxide film form., contact pot. meas. 3−4928
- oxidation mechanism, electron microscope obs. of fine particles 3−38744
- particles, cylindrical, attenuation factors calc. for i.r. radiation scatt. 3−24698
- particles, oxid., electron microscope obs. of oxide-metal boundary 3−15076
- permeability of hydrogen, stress and elec. field effects 3−1824
- phonon freqs. at 80 K from neutron diffr., Debye temp. 0-300 K 3−33632
- phonon viscosity, dislocation drag, and u.s. attenuation 3−38625
- photoemission, two-photon high-probability, from metals in electrolyte solutions 3−39214

copper continued
  - photographic development by deposition on layers containing precious metals *(Russian)* 3−238
  - plasma, local thermodynamic equil. of autoionizing levels 3−33393
  - plastic aftereffect, vibr. stimulation *(French)* 3−21618
  - plastic constraint as mechanism for film strengthening 3−21613
  - plastic deformation mechanism, low temp., in polycrysts. 3−24193
  - plastically deformed, angular correlation of positron annihilation 3−17869
  - plastically deformed at room temperature, stored energy 3−4786
  - plastically deformed at room temperature, stored energy 3−4787
  - plasticity increase phenomenon with prestressing in vacuo rel. to hydrogen content 3−30187
  - point defects due to cyclotron irradiation rel. to Cu$_3$Au 3−14898
  - polishing, electrolytic vibration, advantages 3−30357
  - polycrystal surface layers, structure under cyclic loading *(Russian)* 3−36991
  - polycrystalline, ideal rolling texture *(French)* 3−37022
  - positron annihilation, band structure calculation of momentum densities 3−18065
  - positron annihilation, Fermi surface, long slit angular distributions, analysis 3−30394
  - positron annihilation, in annealed single crysts., ang. correl. meas. 3−27206
  - positron annihilation for dislocation density estimation in f.c.c cold-worked polycrystal 3−30159
  - potentiostatic controlled etching and polishing, rel. to metallography 3−37127
  - powder, drying, heat cond. change *(Russian)* 3−27727
  - powder aggregates, strength characterisation, pressure-density data 3−8964
  - powders, pore characteristics, reln. to compacting behaviour 3−2748
  - precipitation, in GaAs, electron microscope examination 3−36329
  - proton bombardment, charact. X-ray prod., charact./continuous radiation ratio 3−27583
  - pulsed arc temperatures meas., using intensities of Cu spectral lines 3−23932
  - pyramidal growth during electrocrystallisation *(Japanese)* 3−24063
  - quadratic Stark constants of spectal lines in LS coupling-Coulomb approximation 3−23469
  - radiation damage anisotropy, u.s. attenuation due to dislocation damping 3−17865
  - recrystallization kinetics, obs., effect of prior deformation 3−27627
  - relaxation, real structure and migration props., magnetic after-effect obs. *(Polish)* 3−24212
  - residual element effect on radiation strengthening in Fe-alloys, press. vessel steels, and welds 3−18645
  - ribbons, cryst. perfect, gliding dislocation loops preceding slip line form. *(French)* 3−4761
  - secondary electron emission, unified treatment by Monte Carlo method *(French)* 3−27592
  - secondary electron emission for e. beam bombardment, 200 eV, theoretical aspects *(French)* 3−12202
  - self-diffusion, effect of iron solute, vacancy jumps *(French)* 3−24289
  - sheet with cubic orientation, secondary workability obs. *(Japanese)* 3−8863
  - shock wave propagation, deform. energy and collision velocity determ. *(Russian)* 3−27066
  - single and polycrystals, deformation at high strain rates 3−8897
  - single crystal (100) film, (100) NaCl, oxidation 3−1907
  - single crystals, dislocation motion after tensile stress and unloading *(Japanese)* 3−7760
  - single crystals, electrodeposition of Ni *(Japanese)* 3−2819
  - single crystals, plastic deformation, u.s. obs. 3−14906
  - sintered, nucl. cooling system for liquid ^{3}He, sp. ht. meas. below 3 mK 3−38695
  - sintering, grain size rel. to density 3−2754
  - slip line struct., surface effect 3−17913
  - sodium ammonium tartrate:Cu^{2+}, cryst. field at Na site, e.s.r. 3−2349
  - soft-metal coatings and linings, effect on contact thermal resistance 3−24889
  - solid-liquid interface shape determ. method during Czochralski growth 3−8735
  - solubility of carbon, impurity effects *(French)* 3−38689
  - spalling, time dependence to the resistance 3−31095
  - stacking fault energy, weak beam electron microscopic obs. 3−1542
  - steel, for reactor vessels, radiation embrittlement sensitivity to Cu and Va, temp. depend. 3−26540
  - stored energy in twisted bar, meas. with Shimadzu adiabatic differential calorimeter *(Japanese)* 3−13254
  - surface, (100), He$^+$ bombarded, energy spectrum of secondary electrons 3−2609
  - surface and vol. self-diffusion meas. 3−7974
  - surface diffusion of Ag on (001), (111) and (110) Cu planes and vicinal surfaces *(French)* 3−36477
  - surface oxidation, static method secondary ion mass spectrometry obs. 3−1906
  - surface polariton propag. at Cu-air interface at optical freq. 3−24397
  - surface structure formed on oxidation of (311) face, RHEED study 3−1904
  - surface waves, noncollinear, interactions, 5-7 MHz 3−18013
  - texture influence on the yield loci 3−2733
  - thermal expansion, at elevated temps., Fizeau system 3−13243
  - thermal expansion at low temps. ($T < 10$ K) specimen depend. effects 3−36430
  - thermal props. of Cu condenser, effect on steam dropwise condensation 3−24255
  - thin Cu fins, determ. of diffusion effect of braze material on thermal cond. 3−9855
  - thin film, Hall coefficient rel. to temperature and magnetic field *(German)* 3−24413
  - torsionally fatigued, strain amplitude changes effect on stress amplitude and resistivity 3−27054
  - transport props. meas. for very pure Cu below 8.5 K 3−18113
  - triglycine fluoroberylate:Cu^{2+} single crystals, e.p.r., high-pressure influence 3−34191
  - true-stress/true-strain of heavily deformed Cu rel. to hardness and subgrain size 3−12383

copper continued
  - twinning, mech., relation to strain to fracture 3−20808
  - ultrasonic vibration effect on resistance to plastic deformation 3−4789
  - uniform tensile deformation degree, correl. with strengthening coeff. *(Russian)* 3−8835
  - u.s. three-phonon processes 3−17943
  - vacancy diffusion, activation energy proportional to latent heat of melting *(Russian)* 3−24295
  - vacancy equilib. density from positron trapping meas. 3−17809
  - vacancy form. energy, positron annihilation meas. 3−17811
  - valence band, X-ray photoemission study 3−11846
  - vaporisation under pulse heat flux in vacuum 3−27108
  - vapour laser, supersonic elec. discharge 3−10462
  - very thin overlayers on Ag substrates, photoemission obs. of resonant d levels, d-band formation 3−18530
  - void form. on fast neutron irrad. *(French)* 3−26504
  - water saturated sintered fibre wicks, effective thermal conductivity meas. 3−15802
  - wear due to dry friction, stacking fault energy and elastic modulus effects *(Russian)* 3−7844
  - whisker, anisotropy of dislocation internal friction 3−8071
  - whisker, glide motion up to upper yield point 3−24365
  - whisker, nonlinear elasticity and lattice anharmonicity 3−15112
  - whisker, primary recrystallisation nuclei formation kinetics on torsional straining *(Russian)* 3−12365
  - whiskers, stretch deformed, dislocation struct., X-ray obs. *(Russian)* 3−8072
  - wire, instabilities with elec. explosion 3−36217
  - wires with electrodeposited Cu coatings, diffusional creep *(Russian)* 3−31059
  - work function of (100) surface, determ. by field emission retarding potential method 3−21137
  - work hardening characts. of a single crystal, Ni content effects 3−18673
  - X-ray emission spectra measurements 3−36976
  - X-ray induced photoemission, absolute yields 3−18524
  - X-ray K-absorption spectra *(Russian)* 3−18509
  - X-ray L$_3$-emission spectra, cluster calc. 3−36954
  - X-ray prod. by electron irrad. 3−16540
  - X-ray total attenuation coefficients of 25.8 keV photons, meas. 3−39198
  - X-rays from Ne$^+$ collision with solid target 3−27585
  - yield locus curves determ. with the aid of knoop hardness measurements *(German)* 3−2732
  - AgCl:Cu^{2+}, blue light irrad., growth and decay of self-trapped holes, e.s.r. obs. 3−39019
  - Al/Cu lamellar cpd., dynamic compressibility *(French)* 3−1686
  - Al-Mg-Si:Cu, aging, effects of Mg loss, elec. resistance meas. 3−39361
  - Au/Cu planar couples, mass diffusion of base metal to electroplate surface 3−38685
  - Ca(OD)$_2$:Cu^{++}, trigonal Jahn-Teller effects in e.p.r. 3−39024
  - CaO.P$_2$O$_5$ glass:Cu$^+$, fluoresc. 3−30869
  - Cd$_3$P$_2$:Cu, deep level effects on optical props. 3−30794
  - CdS:Ce^{3+}, Ag, Cu, fluorescence spectra, probability of emission calc. *(Russian)* 3−27546
  - CdS:Cu^{2+}, photosensitive e.s.r. spectra of Cu^{2+} impurity ions 3−2357
  - CdSe:Cu,In and undoped, high temp. defect equilibria 3−7745
  - Cu, Bauschinger effect and stacking fault energy 3−36352
  - Cu I, v.u.v. absorption spectrum, autoionized resonances 3−29504
  - Cu:Fe and Cu:Mn, temp. dependence of Hall effect, spin component of mag. solute 3−21058
  - Cu:Mn, dilute mag. alloy, coupled local moment-conduction electron Bloch equation 3−34213
  - Cu/Fe single-fibre composite, multiple yield phenomena 3−34636
  - Cu/Kovar/Cu three-layer band, expansion coeffs. determ. 3−27700
  - Cu/Teflon contact, static electrification 3−2170
  - Cu/W fibre composites, thermal cycling 3−37092
  - Cu-CdS contact, elec. and photoelec. props. 3−8265
  - Cu-Cu$_2$O, single crystal and polycrystalline contacts, photovoltaic props. and barrier heights 3−36663
  - Cu-liquid ^{3}He interface, meas. of Kapitza thermal boundary resistance from 10-160 mK 3−33712
  - Cu-mild steel roll bonded combinations, study of deformation properties using equal strain hypothesis 3−24880
  - Cu-Pb N-S sandwich, electron interference effects, tunnelling study 3−18269
  - Cu-Sn diffusion couple, Kirkendall effect 3−4876
  - Cu-SrTiO$_3$ boundary, surface barrier energy determ. 3−5052
  - Cu$^-$ beams, photodetachment by Ar-laser beam, electron affinities 3−29502
  - Cu$^+$, orthorhombic e.s.r. spectra, angular variation 3−24608
  - Cu$^+$ diffusion over interstitial sites in Si 3−33700
  - Cu^{++} pair indirect nucl. spin coupling, ^{63}Cu n.m.r. in copper acetate monohydrate 3−23603
  - Cu$_2$, Cu$_2^+$ particles, ab initio study 3−11201
  - Cu^{2+}, e.p.r. in anatases *(French)* 3−36783
  - Cu^{2+}, impurities in NH$_4$Br, e.p.r. spectral interpretation from spin Hamiltonian parameters calc. 3−18357
  - Cu^{2+}, in Cd(NH$_3$)$_2$.Ni(CN)$_4$.2C$_6$H$_6$ 3−39018
  - Cu^{2+}, in H$_2$SO$_4$ vitreous aq. soln., effect on spin-lattice relax. of H atoms 3−34186
  - Cu^{2+} in NaCl crystals, diffusion from volume to surface 3−33692
  - Cu^{2+} octahedrally coordinated, low temperature ligand field reflectance spectra *(German)* 3−36877
  - Cu(Ni), Cu(Fe), Cu(Al), impurity scattering anal. in terms of s, p and d partial waves 3−8135
  - CuO(Cl)(S)(SO$_4$), X-ray photoelectron spectra obs. *(French)* 3−8705
  - Fe, Armco, microfracture and structural failure under dynamic loading of OFHC Cu 3−2722
  - GaAs, surface contamination due to Cu atoms in resist film stripper during photo-etching 3−8757
  - n-GaAs:Cu, 1.26-1.30 eV photolum. band rel. to recombination centres 3−39186
  - GaAs:Cu, electron absorpt. obs. rel. to impurity energy levels *(Russian)* 3−15532

copper continued
- GaAs:Cu, photolum. of excitons bound to Cu complex centres 3−34418
- GaAs:Cu, supersaturated solid solution, dislocation decoration on decomp. 3−33542
- GaP:Cu, luminesc. bands at 2.179 eV and 1.922 eV due to diffused Cu 3−2592
- GaP:Cu, red pair luminesc. 3−15544
- n-Ge:Cu, current fluctuations, 77-200 K *(Russian)* 3−27257
- Ge:Cu, effect of impurity on kinetics of annealing of radiation defects 3−24111
- Ge:Cu, space charge limited currents rel. to photoelec. amplification 3−15198
- Ge:Sb, Cu, kinetics for Cu precipitation, interaction with Sb 3−14979
- γ-ray attenuation coeffs., E_γ=6-10 MeV 3−17329
- KCl:Cu, optical props. of complex centres 3−15528
- NH_4Cl:Co^{2+}, Ni^{2+}, Cu^{2+}, light absorpt. by impurity centres, cryst. field parameters 3−21456
- in Na_2O-PbO-SiO_2 glass, redox behaviour rel. to absorption spectra 3−24722
- $PbMoO_4$:Cu, Czochralski growth and site occupancy 3−12301
- Se-Cu electrode boundary, compound formation, energy levels, vacuum photoemission study 3−38893
- inSi, gettering by ion-damaged surface layers 3−5276
- Si:Cu, Cu precip. colony dissolution during annealing, particle drag by climbing dislocations 3−20758
- Si:Cu, Cu precipitation, obs. with Cameca ion analyser 3−7785
- Si:Cu precip. colony dissolution during annealing, dislocation processes 3−20757
- inSn, white, single crystals, dislocation etch hillock formation, due to Cu impurity precipitation from etching solution 3−8030
- YIG:Cu, octahedrally coordinated Cu^{2+} ions contrib. to magnetocryst. anisotropy 3−2304
- ZnO(:Cu), elec. cond. and Hall effect, 5 to 300 K *(German)* 3−33933
- $Zn_2(OH)PO_4$, tarbuttite, Cu^{2+} e.s.r., hyperfine structure 3−36784
- ZnS:Ag, Cu fluorescence spectra, probability of emission calc. *(Russian)* 3−27546
- ZnS:Cr^+, Cu, C, e.p.r. and luminescence studies *(Russian)* 3−27552
- ZnS:Cu, β-irrad. at 5K, fast light emission 3−24753
- ZnS:Cu, Mn, Cl, film, doping in vacuum growth rel. to electrolum. props. 3−15559
- ZnS:Cu,Cl film, stimulated cond., quenching by elec. pulses *(Russian)* 3−2069
- ZnS:Cu and ZnS:Cu,Al, electrolum., Gaussian component intensity, alternating voltage freq. depend. *(Russian)* 3−21486
- ZnS:Ni, Cu crystal, phototransfer of holes from Ni^{2+} to Cu^+ ions 3−34411
- ZnS-CdS phosphors, activation by Cu diffusion at low temperature *(Russian)* 3−36943
- ZnTe:Cu, electron-beam excited, visible luminesc. 3−30884

copper alloys
- *see also brass; copper compounds*
- (rare earth-misch metal)-copper-cobalt, chill cast, heat treatment effect on permanent magnet props. *(Japanese)* 3−34562
- base alloys with B metals, concentration dependence of the lattice constant and its relation to the lattice modulus *(German)* 3−1666
- binary, solidification characts. 3−21559
- binary, solidification characts. 3−21560
- coatings with corundum inclusions, microhardness 3−18670
- constantan wire, instabilities with elec. explosion 3−36217
- Cu-Cu_6Ce and Cu-Cu_6La eutectics, unidirection of growth, microstructure 3−39310
- dilute, collective recrystn., excess grain boundary energy determ. *(Russian)* 3−8832
- dilute, elec. quadrupole tensor parameters from n.m.r. 3−30726
- dislocation model for critical flow stress calc., effect of solute atom conc. 3−24189
- fatigue strength obs. using push-pull testing under high press. *(Japanese)* 3−12486
- internal friction, grain boundary behaviour *(Russian)* 3−24210
- magnetoresistance and dHvA meas. rel. to impurity scatt. of electrons 3−21055
- manganin type, characteriz. for precision resistors 3−24946
- Mn-Cu-Cr, Elinvar props. 3−21291
- polishing, electrolytic vibration, advantages 3−30357
- potentiostatic controlled etching and polishing, rel. to metallography 3−37127
- rare earth compounds RCuAl, struct. and mag. props. 3−20725
- relay spring material, after effects of plastic working and plastic hysteresis 3−2724
- solution hardening rate derived from flow stresses on tensile deform. 3−15712
- stacking fault probability, size factor depend. 3−34538
- strength loss, absorption induced during selective transfer in boundary friction 3−21706
- void form. on fast neutron irrad. *(French)* 3−26504
- X-ray scatt. by binary Cu alloy, secondary peak due to superlattice structure 3−30089
- Ag-Cu, liquid, thermodynamic props. of dilute solns. of oxygen 3−27850
- Al bronze recrystallization, obs., kinetics, effect of prior deformation 3−27627
- Al bronze recrystallization kinetics, obs., effect of prior deformation 3−27627
- Al Zn Mg Cu alloy, fibrous struct. and susceptibility to contact corrosion *(German, English)* 3−24354
- Al-Al_2Cu eutectics, directionally solidified, struct. morphology and microhardness *(Russian)* 3−39328
- Al-Cu, $AlCu_3$ phase, cryst. struct. 3−14733
- Al-Cu, eutectic spherulites, electron microscope obs. 3−27638
- Al-Cu, heat treatment effect on strain ageing 3−31080
- Al-Cu, in various metallurgical states, mag. susceptibility, 10-300K *(French)* 3−24559
- Al-Cu, liquid state, elec. conductivity, temp. depend. *(Russian)* 3−2054
- Al-Cu, metastable equilib. study 3−39326

copper alloys continued
- Al-Cu, oxidation kinetics, 475-575°C, γ-Al_2O_3 film formation, O_2 diffusion 3−33743
- Al-Cu, serrated yielding and strain gradients occurrence 3−21700
- Al-Cu, solvus curve of Guinier-Preston zones *(Japanese)* 3−30998
- Al-Cu (4 at wt.%), diffuse scattering topography and struct. analysis of G.P. zones 3−18570
- Al-Cu alloy, structural and phase changes in welded joints 3−24832
- Al-Cu alloy, structural transformations and mechanical props. 3−12413
- Al-Cu and Al-Cu-Mg directionally solidified eutectics, ageing response 3−34581
- Al-Cu film, secondary grain growth 3−1956
- Al-Cu oriented bicrysts., intergranular precip. *(French)* 3−27626
- Al-Cu system, impurity trapping during crystallisation from melts 3−33466
- Al-Cu-Li, resist. obs. of Al_2CuLi precip. 3−21660
- Al-Cu-Li, $T_1(Al_2CuLi)$ precip. 3−8798
- Al-Cu-Mg-Ag, heat treatment, struct. of metastable precip. 3−15662
- Al-Cu-Ni system, ternary composite growth from melt 3−39315
- Al-Cu-Ni system, ternary composite growth from melt 3−39316
- Al-$CuAl_2$ lamella eutectics and fibrous eutectics, unidirectionally solidified, microstructure *(Japanese)* 3−18592
- Al-$CuAl_2$-$FeCu_2Al_7$ ternary eutectic composite, mechanical props. and thermal stability *(Japanese)* 3−15701
- Al-$CuAl_2$-$NiCu_3Al_6$ ternary eutectic composite, mechanical props. and thermal stability *(Japanese)* 3−15701
- Al-$CuAl_2$-Si ternary eutectic composite, mechanical props. and thermal stability *(Japanese)* 3−15701
- Al-Cu(3 wt.%), processed from double-oriented ingots, cold rolling and annealing textures *(Japanese)* 3−18640
- Al-Cu(4 at wt.%) precipitation study by internal friction, hardness and electron microscopy meas. *(French)* 3−15687
- Al-Cu(4.5 wt.%), surface relief effects associated with $CuAl_2$ rod form. 3−37006
- Al-Zn-Mg-Cu, thermomech. treatment processed, age hardening mechanisms 3−24897
- Au-Cu, wear due to dry friction, stacking fault energy and elastic modulus effects *(Russian)* 3−7844
- Au-Cu (25-33%Au), fine struct., X-ray diffr. obs. *(French)* 3−14739
- Au-Cu alloys electrodepositing from cyanide free acid solution *(French)* 3−9071
- Au-Cu binary disordered, size effect and multisite correlations 3−17761
- Au-Cu film, order-disorder transformation obs. 3−1800
- β-Au-Cu-Zn alloys, lattice softening, phase stability and elastic anomaly 3−2719
- Au-Cu-Zn martensite, cryst. struct., electron diffr. obs. 3−1604
- β-Au-Sn alloys, martensitic transformations 3−8895
- $AuCu_3$ ordered solid solution, size effect theory *(Russian)* 3−7658
- Au_3Cu, I and II-type superlattice structure 3−8805
- Au_3Cu ordered alloys, use of Morse potential function to determ. harmonic props. 3−7868
- $Au_{50}Cu_{50-x}Ga_x$, thin specimens study of AuCu II phase with periodic antiphases and AuCu III phase *(French)* 3−31003
- $AuCuZn_2$, soft acoustic phonons near martensitic transition 3−14942
- $AuCuZn_2$, thermoelastic martensite, lattice softening, ferroelasticity and shape memory effect 3−14907
- Be-Cu, mech. twinning *(Russian)* 3−20753
- (Cu, Ga)-V, supercond. V_3Ga layers at interface, growth and props. *(German)* 3−8311
- Cu, recrystallization kinetics, obs., effect of prior deformation 3−27627
- Cu:As(Sb), alpha solid solns., thermodynamic activities determ. procedure *(German)* 3−21794
- Cu:M, dilute, M=transition metal, pair description of magnetic props. 3−30596
- Cu- $\gamma_2(Cu_9Al_4)$-Ni mixed powder compacts sintering characteristics study using Ni plated composite powders *(Japanese)* 3−15730
- Cu-Ag, Cu-Fe and Cu-Zn whiskers, X-ray topography of internal structure 3−15110
- Cu-Ag-Al, constitution and phase relationships, metallographic and X-ray examination 3−34512
- Cu-Ag-Al solid solns., isothermal recrystn. kinetics 3−21592
- β-Cu-Ag-Zn, phase stability, absolute thermoelec. power, cond. electron mag. susceptibility, comp. depend. 3−33871
- Cu-Al, anomalous shift in interconduction band optical absorption, values for band gaps 3−30837
- Cu-Al, Bauschinger effect and stacking fault energy 3−36352
- Cu-Al, disordered polycrystals, distortion waves 3−17926
- Cu-Al, elastic consts., solute conc. depend. *(French)* 3−39302
- Cu-Al, elastic stiffness, comp. depend. 3−4780
- Cu-Al, estimation of quasielastic force and anharmonic coeffs. from X-ray diffraction meas. 3−30209
- Cu-Al, form. of aligned composite material by solid state decomposition 3−24976
- Cu-Al, influence of precipitation of γ_2 phase on order-disorder transformation 3−27617
- Cu-Al, stacking fault energy obs. using weak beam method of electron microscopy 3−1541
- Cu-Al, stacking fault role in martensite phase formation form fcc struct. *(Russian)* 3−2699
- Cu-Al, swaged, dislocation density, from flow stresses and stored energies 3−18633
- Cu-Al, twinned γ_1' martensite h.c.p. phase, invariant plane strain 3−31021
- Cu-Al (15.6 wt.%), multiple dislocation, stacking fault arrays, stability 3−17824
- Cu-Al (15at.%), deformation temp. and annealing influence on structure and strength props. 3−31086
- Cu-Al (2%) single crystals, edge-pit observations of dislocation motion 3−21609
- Cu-Al alloys, annealing twins formation 3−2701
- Cu-Al β-type martensite, stress-induced transformation to fcc structure 3−21569
- Cu-Al solid solns., high temp. steady state creep deform. behaviour *(Japanese)* 3−31076
- Cu-Al_2O_3, internally oxidised, brittleness during annealing in H_2 *(Japanese)* 3−12395

copper alloys continued
Cu-Al-Mn, martensitic alloy, X-ray obs. of twin structure *(Russian)* 3−24130
Cu-Al-Mn, martensitic transform., β'-phase deform. influence *(Russian)* 3−18560
Cu-Al-Ni, acoustic emission in thermoelastic martensite transform. 3−5318
Cu-Al-Ni, martensitic thermoelastic transform., electron work function change 3−36346
Cu-Al-Zn, solid soln. elongated dislocation tangles and Al and Zn solubility *(French)* 3−31004
Cu-Al-Zn β-type martensite, stress-induced transformation to fcc structure 3−21569
Cu-Al(1 at wt.%), internal oxidation, effect of alloying elements, Ag, Pd, As and In *(Japanese)* 3−15700
Cu-Al(15 at.%), ordering and disordering kinetics after sudden annealing changes, residual resist. obs. 3−37062
Cu-Al(5.8 at.%), deformed, soft surface effect 3−24866
Cu-Al(7.9 wt.%), corrosion fatigue crack initiation 3−27661
Cu-Ar film, metal-nonmetal transition 3−27291
Cu-As system, phase diagram and Cu_5As_2 phase props. *(Russian)* 3−12329
Cu-Au, effect of press. on phase transition and ordered structs. of CuAu 3−18610
Cu-Au, press, depend. of long period of CuAuII 3−20712
Cu-Au and Cu-Au-Al, plastic deform., electron microscope study *(Russian)* 3−5306
β-Cu-Au-Zn, phase stability, absolute thermoelec. power, cond. electron mag. susceptibility, comp. depend. 3−33871
Cu-Au(Fe), Kodon effect in dilute magnetic α-phase alloys 3−21218
Cu-Be, eutectoid decomp., ordering with metastable solid soln. form. *(Russian)* 3−37001
Cu-Be(2 wt.%), age-hardened, microstructural characts. rel. to elastic limit and yield pts. *(Russian)* 3−15668
Cu-Cd, hardening effect, transmission electron microscope examination 3−4805
Cu-Co, cell structure formation with Bridgeman growth method 3−11571
Cu-Co, precipitation hardened, mech. props., effect of Nb additions 3−8881
Cu-Co(1.9 wt.%), age-hardened, Hg embrittlement at room temp. 3−18647
Cu-constantan Peltier effect meas. *(Dutch)* 3−28492
Cu-Cr, aging phenomena *(Japanese)* 3−31067
Cu-Cr, dil., n.m.r. of ^{63}Cu, spin-lattice relax. mechanism 3−2443
Cu-Cr, dilute, in supercond. sandwich, mag. props. from supercond. proximity meas. 3−8341
Cu-Cr base, precip. growth and nucleation, resist. study 3−24865
Cu-Cr composite, fibre reinforced, deform. and fracture behaviour *(Japanese)* 3−34634
Cu-Cr dilute, h.f. magnetoresist., 1.6-4.2K mag. field depend. 3−8156
Cu-CuZrSi pseudo-binary eutectic alloys, directionally solidified, tensile props. 3−34565
Cu-Fe, ageing characts., mech. props. 3−37075
Cu-Fe, dil., n.m.r. of ^{63}Cu, spin-lattice relax. mechanism 3−2443
Cu-Fe, dil., oscill. of cond. electron density near solute atoms, ^{63}Cu n.m.r. obs. 3−2462
Cu-Fe, dil., resist. and thermo-e.m.f., 4.2-273K *(Russian)* 3−8152
Cu-Fe, dilute, in supercond. sandwich, mag. props. from supercond. proximity meas. 3−8341
Cu-Fe, dilute, Kondo temp. conc. depend. 3−21216
Cu-Fe, sp. Lt., magnetisation, effect of ordering and precip. 3−34166
Cu-Fe, spin-scatt. anisotropy and exchange coupling energy meas. using de Haas-van Alphen effect 3−33781
Cu-Fe Kondo system, eqn. of state from phenomenological model 3−5096
Cu-Ga, liq., mag. susceptibility *(Japanese)* 3−30600
Cu-Ge, deformed alloy, lattice thermal cond. recovery with annealing 3−15174
Cu-Ge, liq., mag. susceptibility *(Japanese)* 3−30600
Cu-Ge, positron annihilation study of Fermi surfaces 3−15119
Cu-Ge (0.5 at wt.%), vacancy-impurity complexes study by positron annihilation 3−17868
Cu-In, form. of aligned composite material by solid state decomposition 3−24976
Cu-M alloy, polycrystalline, collective recrystallisation rel. to excess valence of alloying addition, M, resistivity obs. *(Russian)* 3−12366
Cu-Mg-Ni, monovariant eutectic, unidirectional solidification, aligned microstructs., interface stability criteria 3−12347
Cu-MgO, internally oxidised, brittleness during annealing in H_2 *(Japanese)* 3−12395
Cu-Mn, dil., n.m.r. of ^{63}Cu, spin-lattice relax. mechanism 3−2443
Cu-Mn, dilute, in supercond. sandwich, mag. props. from supercond. proximity meas. 3−8341
Cu-Mn dilute alloy single crystals, strain rate and temp. depend. of the flow stress 3−8898
Cu-Mn-Sn, ferromag. beta phase, crystal structure and ordering 3−18324
Cu-Mn(0.5 at wt.%), vacancy-impurity complexes study by positron annihilation 3−17868
Cu-Ni, comparison of Bridgman, Czochralski and zone levelling growth methods 3−12291
Cu-Ni, density, depend. on composition 3−26991
Cu-Ni, dependence of density on composition, determ. using absolute hydrostatic method *(German)* 3−37014
Cu-Ni, diffusional creep 3−24195
Cu-Ni, dislocation motion in alternating mag. field, oscill. domain wall interactions 3−30674
Cu-Ni, disordered polycrystals, distortion waves 3−17926
Cu-Ni, magnetostriction, forced 77K to Curie temp., 12-20 kOe 3−15398
Cu-Ni, phase diagram calc. from thermodynamic data 3−21562
Cu-Ni, positron annihilation study of Fermi surface necks 3−15118
Cu-Ni, positron annihilation study of Fermi surfaces 3−15119
Cu-Ni, spontaneous volume magnetostriction, lattice const., 4.2-1000 K 3−30671

copper alloys continued
Cu-Ni, third and fourth order anharmonic coeffs., X-ray determ. *(Russian)* 3−33619
Cu-Ni, weld cracking and ductility-trough phenomenon 3−21637
Cu-Ni (10 wt.%), stress corrosion resist. in ammoniacal environment, effect of Fe 3−31041
Cu-Ni (20 wt.%)-Mn(20 wt.%), age-hardened, microstructural characts. rel. to elastic limit and yield pts. *(Russian)* 3−15668
Cu-Ni alloys, dissociation-conditioned line broadening of X-ray interference *(German)* 3−15661
Cu-Ni alloys, photoelectron spectroscopy of oxide films 3−11826
Cu-Ni Peltier effect meas. *(Dutch)* 3−28492
Cu-Ni-Au, mag. hyperfine structure coupling and Mossbauer isomer shift of ^{197}Au 3−34257
Cu-Ni-Be-Si, aging characts. *(Japanese)* 3−12352
Cu-Ni-Fe, mag. anisotropy and magnetis. reversal 3−36745
Cu-Ni-Mg, monovariant eutectic alloy, microstructure obs. in unidirectional solidification 3−21589
Cu-Ni-Zn microduplex nickel silver, tensile props. 3−34571
Cu-Ni(Zn)(Al)(Ge) solid solutions, hardening mechanism in microdeform. stage *(Russian)* 3−21633
Cu-Ni(0.5 at wt.%), vacancy-impurity complexes study by positron annihilation 3−17868
Cu-Ni(15 wt.%)-Al(3.5 wt.%)-Cr(2 wt.%)-Mn (3 wt.%), age-hardened, microstructural characts. rel. to elastic limit and yield pts. *(Russian)* 3−15668
Cu-Pd, ordering process, mass spectrometric obs. of secondary ion emission *(Russian)* 3−33490
Cu-Pd, plastic deform., electron microscope study *(Russian)* 3−5306
Cu-Pd system, long period superlattice form. 3−14737
Cu-Pd(Pt), short range order, electron microscope and diffr. obs. 3−14734
Cu-Pt, atomic motion under action of laser pulse, X-ray obs. *(Russian)* 3−29111
Cu-Pt, long-period ordered alloy Cu_3Pt, existence range 3−15656
Cu-Pt, short-range order and atom displacement parameters *(Russian)* 3−39329
Cu-Pt system, existence range of long-period ordered Cu_3Pt, X-ray study 3−21565
Cu-Sb liq., struct. from combined neutron and X-ray diffr. 3−14676
Cu-Sb-Sn, liq., Sn solvent activity equations, by stirred H-cell e.m.f. meas. 3−31269
Cu-Si(5.09 at wt.%), aged, internal friction meas. 3−18678
Cu-Sn, diffusional creep 3−24195
Cu-Sn, elastic stiffness, comp. depend. 3−4780
Cu-Sn, liquid, thermodynamic props. of dilute solns. of oxygen 3−27850
Cu-Sn, twinned γ_1' martensite h.c.p. phase, invariant plane strain 3−31021
Cu-Sn base self-lubricating composites, comp. effect on tribological props. 3−15785
Cu-Sn-Pb, changes in composition and structure due to friction and wear *(Japanese)* 3−8768
Cu-Th system, intermediate phase formation in liq. Na, struct., 200-700°C 3−2690
Cu-Ti, boriding, Ti content effects *(German)* 3−8902
Cu-Ti, obs. of precipitation morphology on annealing *(Russian)* 3−12356
Cu-Ti (4 at wt.%), X-ray small angle scattering study during early stages of spinodal decomposition *(Japanese)* 3−30995
Cu-Ti (4 at wt.%), X-ray small angle scattering study on later stages of aging after spinodal decomposition *(Japanese)* 3−30996
Cu-TiO_2, internally oxidised, brittleness during annealing in H_2 *(Japanese)* 3−12395
Cu-Ti(3.6 wt.%), age-hardened, Hg embrittlement at room temp. 3−18647
Cu-Ti(4 wt.%), early stage side-bands, model *(Japanese)* 3−31000
Cu-Ti(4 wt.%), side-bands, X-ray obs. *(Japanese)* 3−30999
Cu-Ti(4.3 wt.%), age-hardened, microstructural characts. rel. to elastic limit and yield pts. *(Russian)* 3−15668
Cu-W fibre composite, thermal expansion *(Japanese)* 3−18703
Cu-Zn (0.5 at wt.%), vacancy-impurity complexes study by positron annihilation 3−17868
Cu-Zn-Si, shape memory effect and pseudoelasticity 3−21702
Cu-Zr, Cu-rich phase diagram 3−21563
Cu-Zr, eutectic and hypo-eutectic, directionally-solidifed, characteriz. 3−34558
$CuAu_3$, phase diagram similar to order-disorder diagram calc. for f.c.c. solid solns. 3−4821
$Cu_{1-x}Au_x$-Fe(Cr), mag. field depreciation of Kondo magnetoresist. 3−33872
Cu_3Au, electron props. oscillatory curve, compatible with $CaTl_3$ density of states curve calc. 3−1984
Cu_3Au, phase diagram similar to order-disorder diagram calc. for f.c.c. solid solns. 3−4821
Cu_3Au, point defects due to cyclotron irradiation rel. to Cu 3−14898
Cu_3Au, temperature depend. of flow stress in range 4 K to 300 K 3−36351
Cu_3Au, type ordering, short range and long range, energy, second coordination sphere 3−38551
Cu_3Au alloy, disordering process study by electrical resistivity meas. 3−8896
Cu_3Au order-disorder transition temp. 3−36400
Cu_3Au ordered alloys, use of Morse potential function to determ. harmonic props. 3−7868
Cu_3Au ordering effect on lattice thermal conductivity 3−2048
CuBi, liq., mag. susceptibility *(Japanese)* 3−30600
CuMn:^{63}Cu, spin-lattice relax., nuclear spin diffusion 3−36800
Cu_2MnAl Heusler alloy, β phase form. *(French)* 3−30964
Cu_2MnAl Heusler alloy, order-disorder transform., crit. temps. determ. *(French)* 3−39306
$Cu_{2-x}MnAl_{1-x}$, mag. props. obs. by Lorentz microscopy 3−1545
CuPt, ordered, deformation twinning and slip electron microscope obs. 3−1670
$CuPt_3$, ordered struct., electron microscope and diffr. obs. 3−14803
β-Cu_3Sb, electrotransport obs. and mechanism *(German)* 3−24298
Cu_3Ti, charact. defect struct., electron microscope obs. 3−11606
Fe-Cu, phase change in microdomain, field ion microscope images 3−18563

copper alloys continued
Fe-Cu-Mn system, semihard mag. reed switch material, heat treatment effect on mag. props. 3−36757
Fe-Cu(1.7 wt.%) alloy Cu precipitation from α-Fe in pre-peak and peak hardness range of ageing 3−8797
Fe-Ni-Cu ferrite, internal friction, delta E-effect and stress sensitivity in alternating magnetic field 3−39009
Mn-Cu, martensitic transform., shape memory effect *(Russian)* 3−5317
Mn-Cu-Co nonmag. Elinvar-type alloys characteriz. 3−37074
Mn-Cu-Ni, Elinvar props. 3−21292
Ni steels, 9%, modified, thermomech. treatment effects on low-temp. hardness and tensile strength, obs. *(Japanese)* 3−8860
Ni-Cr-Al-Cu, Evanohm, thermal cond., 0.4-77K 3−18112
Ni-Cu, comparison of photoelectron spectra with results of density of state calcs. 3−36976
Ni-Cu, ferromag., neutron diffraction obs. of mag. moments distrib. 3−15374
Ni-Cu, mag. form. factor, neutron diffr. obs. 3−24575
Ni-Cu, mag. moment in pulsed fields, Pauli susceptibility *(Russian)* 3−30606
Ni-Cu, magnetocryst. anisotropy consts. at 0°K, conc. depend. 3−21258
Ni-Cu, X-ray K-absorpt. spectra *(Russian)* 3−18509
Ni-Cu alloys, temp. dependence of mag. susceptibility 3−18303
Ni-Ti-Al, heat resistant, effect of copper additions on mech. props. 3−24949
NiCu, ferromag. disordered alloy, band theory for residual resistivity 3−15340
$Ni_{1-x}Cu_xMnSb$, ferromag., anomalous line shift in n.m.r. 3−30704
Ni_3Mn-Cu, atomic distrib., rel. to electronic struct. *(Russian)* 3−26990
$Pd_{0.775}Cu_{0.06}Si_{0.165}$ glass, localized shear deform. 3−5312
ScCu, electronic structure, importance of ionic bonds for stability 3−15335
Sn-Cu layer form. between solid Cu and liq. Sn, rel. to soldering 3−21709
$ThCu_{3.6}$, crystal structure obs., comparison with $GdAg_{3.6}$ structure 3−17763
Ti-Cu, X-ray emission spectra obs. rel. to band structure 3−21498
YCu:Gd, wave vector depend. of exchange interaction, e.s.r. obs. 3−34202
$YbCu_2$, ambiguous mag. behaviour, susceptibility meas. 3−30609

copper compounds
see also copper alloys
alkali halide-Cu halide, excitonic doublets, test for coherent-potential approximation 3−30436
aqueous solns. of Cu^{2+} ions, relative demagnetizing and chem. n.m.r. field shift, conc. depend. 3−39043
complex, $CaCu(OAc)_4 6H_2O$, absorption spectra, electronic transition in dodekahedral crystal field 3−39156
copper dodecyl sulphate micelle surface, local conc. of counterions, obs. of Cu^{2+} e.p.r. 3−34656
copper formate tetrahydrate, liquid air and room temp. vibr. spectral comparison 3−5199
copper formate tetrahydrate, weak extra Bragg reflections in antiferroelec. phase 3−30769
copper phthalocyanine:vanadyl phthalocyanine, energetic trap distrib. rel. to impurity 3−38811
copper phthalocyanine, electrical transport phenomena, model for bulk defects 3−21062
copper phthalocyanine, photoelectric emission, density of states, electron-electron m.f.p. 3−18527
cupric acetate monomers in acetic acid-water mixtures, e.s.r. study 3−27408
cuprous halides, luminesc. during laser excitation, H band emission, electron and hole effective masses 3−27557
diluted Tutton salts, proton dynamic polarisation and cross relaxation 3−39050
formate tetrahydrate, antiferroelectric phase, approximate struct. determ. by neutron diffraction 3−12100
formate tetrahydrate, cryst. struct., neutron diffr. obs. in antiferroelec. phase 3−17797
formate tetrahydrate, phase transition, X-ray diffr. obs. 3−15005
formate tetrahydrate, Raman spectra 90-250 K, water modes 3−24692
halides, electrical pulsed-discharges in vapour, model for population inversion 3−726
halides, electronic states, theory 3−11855
hexadecachloro-copper-phthalocyanine, electron microscopy, molecular image resolution determ. 3−17390
oxinate, photocond. props. 3−21109
phthalocyanine, absence of near i.r. emission of single crysts. and films 3−21465
phthalocyanine, near i.r. emission of single crysts. and films 3−21465
sodium cupric nitrilotriacetate monohydrate, cryst. struct. 3−14832
sulphide minerals, effect of temp. on magnetic susceptibility during continuous heating and cooling, phase change obs. *(Russian)* 3−12009
$(Ag_xCu_{1-x})_2Se$, electronic and ionic cond. 3−21123
$Ba(PO_3)_2$-$Cu(PO_3)_2$ system, phase diagram, cryst. struct. of $Ba_2Cu(PO_3)_6$ phase *(French)* 3−7901
CdS/Cu_2S solar cell, band model 3−4946
CdS-$CuM^{III}S_2$, (M^{III}=Al, Ga, In), prep. and phase relations, mutual solid solubility regions 3−33678
$(Cu_x,Zn_{1-x})M_2(SO_4)_2.6H_2$, electron and proton relax. 3−2361
Cu (II) complex, bis-(N,N′-di-n-propyldithiocarbamate), cryst. and mol. struct. 3−24073
Cu ammine complex, from a cation exchange resin, elution kinetics 3−34704
Cu complex, α-bis-(N-methylsalicylaldiminato)-Cu(II) structure, mag. props. and linear chain behaviour 3−2286
Cu complex, mesoporphyrin, triplet-triplet absorption *(Russian)* 3−9088
Cu complex, Shiff base derivatives of iminoxy radicals copper (II), e.p.r. and mag. susceptibilities 3−21214
Cu complex $((CH_3)_3NH)CuCl_3.2H_2O$, crystal struct. and mag. props. 3−1613

copper compounds continued
Cu complex with octamethylporphins, combinational dispersion spectra *(Russian)* 3−11284
Cu complex with porphin, i.r. spectra and normal coord. analysis 3−1217
Cu complexes of 1,3-dipheyltriazine, struct. chem. 3−14766
Cu $SnCl_6.6H_2O$, proton magnetic resonance study of internal motions 3−27426
Cu-As-Se glass, light-induced memory effect 3−16895
Cu-As-Se-Au glass, memory effect rel. to Au content 3−33969
Cu^{2+} complexes in single crystals of dl serine and l-lycine DCl $2D_2O$, e.p.r. obs. 3−8419
$Cu_{2-x}Ag_xSe$, metal-nonmetal transition, elec. cond., energy gap 3−38805
$CuAl_2O_4$, spinel, equilib. cation distrib., X-ray diffr. analysis 3−7687
$CuAlS_2:Fe^{3+}$, ternary semicond., ESR and X-ray anal. of crystal structure 3−30693
$CuAlS_2(Se_2)$, single crystals, semiconductors, growth from melt, structure, p-type conductive 3−39265
$CuAlSe_2$, refr. index, second harmonic generation coeffs. 3−4120
$Cu_7As_6Se_{13}$, partial Patterson method application and the thirteenfold hexagonal superstructure 3−4741
$Cu_4Bi_4S_9$, cryst. struct., rel. to simple sulphide structs. 3−14763
CuBr, elastic and piezoelec. consts. 3−1662
CuBr, magneto-optical spectra due to excitons 3−8556
CuBr, nonlinear dielec. props. rel. to sphalerite crystal structure, obs. *(French)* 3−2482
CuBr two photon absorption, exciton region 3−10570
$Cu(C_6H_5COO)_2 3H_2O$, temp. and ang. depend. of e.s.r. line in linear chain antiferromag. 3−8426
$Cu_3(CO_3)(OH)_2$, magnetic transition rounding and Pippard's relations 3−30619
CuCl, absorpt. spectra 3−13301
γ-CuCl, calc. of energies of formation of point defects by method of Mott and littleton 3−27018
CuCl, elastic and piezoelec. consts. 3−1662
γ-CuCl, energies of formation of point defects, calc. 3−30114
CuCl, energy band calc. using mixed basis method of Kunz 3−33798
CuCl, Faraday rotation near absorpt. edge, interband and exciton effects 3−15474
CuCl, high carrier and exciton conc., low temp. emission recomb. study *(Russian)* 3−27541
CuCl, magneto-optical spectra due to excitons 3−8556
CuCl, nonlinear dielec. props. rel. to sphalerite crystal structure, obs. *(French)* 3−2482
CuCl, oscillator strength for interband transitions, valence bands 3−38795
CuCl, polariton fusion, selection rules and freq. depend. 3−18107
CuCl, two photon absorption, at 4.2K, creation of excitons 3−10571
CuCl Frenkel defects, relaxation obs. 3−27022
CuCl-AgCl photochromic coatings for optical instrument protection *(Russian)* 3−5883
$CuCl_2$, absorpt. spectra in aq. and organic soln., energy bands and levels, cryst. field parameter determ. 3−5215
$CuCl_2$-$PbCl_2$ electrodes, use in salt water batteries 3−3265
$CuClO_3$, n.q.r. temp. depend., motional averaging of elec. field gradients 3−21341
$CuCl_2.2D_2O$, zero field deuteron mag. reson., quadrupole consts., internal field, fine struct. *(French)* 3−21339
$CuCl_2.2H_2O$, spin spin relax. time meas. near Neel temp. 3−12054
$CuCl_2.2NC_3H_5$, interchain coupling effects on e.s.r. 3−18354
$CuCr_{2-2x}Ga_{2x}O_4$, spinel, mag. structure and cooperative Jahn-Teller distortion 3−30632
$CuCr_2O_4$, structure changes under high pressure, Jahn-Teller effect 3−27118
$CuCr_2S_{4-x}Se_x$ solid soln., lattice parameter, Curie temp., mag. moment and effective mag. moment 3−21241
$CuCr_2S(Se)(Te)_4$, paramagnetic susceptibility temp. depend. 380-650K *(Russian)* 3−15345
$CuCrSe_2$, mag. props. *(Japanese)* 3−38968
$CuCr_2Se_4$, production and properties *(Russian)* 3−14811
$CuCr_2Te_3I$, internal fields at ^{129}I, Mossbauer effect obs. 3−30735
$CuCr_{2-2x}Zn_xTi_xO_4$, spinel, mag. structure and cooperative Jahn-Teller distortion 3−30632
$CuCs_2(SO_4)_2.6H_2O$, hydrogen bonding, coordination polyhedron around cation 3−17757
$CuFe_{2-2x}Ga_{2x}O_4$, spinel, mag. structure and cooperative Jahn-Teller distortion 3−30632
$CuFe_2O_4$, cubic-tetragonal transform. and induced uniaxial anisotropy *(French)* 3−15382
$CuFe_2O_4$, elec. switching, memory phenomena 3−18202
$CuFeS_2$, chalcopyrite, cryst. struct. refinement 3−26998
Cu_5FeS_4, bornite, superstructs. determ. by mofified Patterson method 3−15865
$Cu_9Fe_9S_{16}$, mooihoekite, cryst. struct. 3−18805
$CuFe_{2-2x}Zn_xGe_xO_4$, spinel, mag. structure and cooperative Jahn-Teller distortion 3−30632
$CuFe_{2-2x}Zn_xTi_xO_4$, spinel, mag. structure and cooperative Jahn-Teller distortion 3−30632
$CuGaS_2$, absorpt. and refl. spectra, low temp. 3−15510
$CuGaS_2$, absorpt. and refl. obs. rel. to excitons and spin orbit splitting 3−18108
$CuGaS_2$, dielec, dispersion, phonon freqs., i.r. refl. spectrum 3−8585
$CuGaS_2$, formation, stoichiometry and props. 3−5269
$CuGaS_2$, grown by I_2 transport, p-type cond. and green photolum. 3−30474
$CuGaS_2:Fe^{3+}$, chalcopyrite, e.s.r. obs. of magnetically inequivalent metal sites 3−30689
$CuGaS_2$-CdS p-n diode, green electrolum. 3−39188
$CuGaSe_2$, refr. index, second harmonic generation coeffs. 3−4120
$CuGaTe_2$, semicond., elec. and thermal. cond. meas. in liquid and solid states *(Russian)* 3−15191
$Cu_2Ga_4Te_7$, phase in Cu_2Te-Ga_2Te_3 system, band and transport props. 3−38660
Cu_2GeS_4, precipitation from HCl:Ge,Cu soln. on addition of H_2S *(Russian)* 3−14975
β-Cu_2HgI_4, disorder phenomena 3−1718

copper compounds continued
Cu_2HgI_4, thermochromic, i.r. recording, image recording sensitivity, refl. vs. temp. phase transition hysteresis 3—108
Cu(I), Cu(II) complexes of 2,2′-bipyridine and 1,10-phenanthroline, determ. of structural information from i.r. spectra 3—1227
CuI, elastic and piezoelec. consts. 3—1662
CuI, film growth by Cu tarnishing in I atmosphere, estimation of ionic cond. 3—38683
CuI, nonlinear dielec. props. rel. to sphalerite crystal structure, obs. *(French)* 3—2482
Cu(I) complexes, with 1,5-cyclooctadiene, i.r. and Raman spectra 3—26668
γ-CuI disorder phenomena 3—1718
CuI film, electrical and luminescent props. *(Russian)* 3—24432
p-CuI-n-ZnS:Mn film, low voltage electroluminesc. *(Russian)* 3—24748
Cu(II) complex, chelate of N-3-hydroxypropylsalicylideneimine, cryst. struct. 3—17775
Cu(II) complex, copper(II) bis(N,N′-di-n-propyldithiocarbamate), struct. 3—17778
Cu(II) complex, di-μ-thiocyanato-bis di(2-aminoethyl)amine copper(II), cryst. struct. 3—17779
Cu(II) complex, dichloromonoaquopyridine-N-oxide, singlet-triplet separation from proton spin-lattice relax. meas. 3—8475
Cu(II) complex, e.p.r. meas. for Cu(II) ion in distorted tetrahedral environment 3—21295
Cu(II) complex, tetrasodium dicopper-dl-tartrate dehydrate X-ray anal. 3—7696
Cu(II) complex perchlorate tris-octamethylpyrophosphoramide, e.s.r. study 3—30685
Cu(II) complexes, cross relaxation and e.p.r. of trapped H atoms in γ-irradiated glasses 3—8414
$Cu(IO_3)_2$ and $3Cu(IO_3)_2.2H_2O$, cryst. growth, boiling solvent method 3—12235
$CuInS_2:Fe^{3+}$, ternary semicond., ESR and X-ray anal. of crystal structure 3—30693
$CuInSe_2$, electronic structure from electroreflectance and photoluminescence meas. 3—39183
CuInTe-CdTe, complex semiconductor chalcogenide, phase diagram and physical props. *(Russian)* 3—8168
$CuInTe_2$, semicond., elec. and thermal cond. meas. in liquid and solid states *(Russian)* 3—15191
$CuK_2(SO_4)_2.6H_2O$, hydrogen bonding, coordination polyhedron around cation 3—17757
$Cu_{12-x}M(II)_xSb_4S_{13}$, (M=Fe, Zn, Ag), synthetic tetrahedrite, Mossbauer spectra and mag. props. 3—27444
$CuM^{III}S_2-ZnS$, M^{III}=In, Ga, Al, preparation and phase relationships 3—7909
$Cu_xMn_{3-x}O_4$ spinels, crystal structure and tetragonal-cubic transition investigations 3—38575
$Cu_3Mo_2O_9$, centrosymmetric struct. space group 3—7667
$Cu(NH_3)SO_4.H_2O$, temperature dependent correlations meas. by e.p.r. 3—39016
$Cu(NH_3)_4SO_4.H_2O$, interchain coupling effects on e.s.r. 3—18354
$Cu(NO_3)_2.2^1._2H_2O$, specific heat and n.m.r. at the high-field phase transition 3—27370
CuNSal, Cu complex, mag. susceptibility meas. for spin $^1/_2$ linear chain 3—15355
$Cu_{1-x}Ni_xFe_2O_4$ ferrite, extraordinary Hall const., resist., 293-550K 3—24459
CuO, Auger electron spectra and electron spectra, 25-400°C 3—30910
$CuO-TeO_2$ system, phase diagram 3—20847
Cu_2O, Auger electron spectra and electron spectra, 25-400°C 3—30910
Cu_2O, dielec. const., Cu inclusions effect 3—34282
Cu_2O, excitonic transitions at forbidden interband edge 3—33854
Cu_2O, magneto-optical study, diamag. effect on exciton line splitting in mag. field 3—12123
Cu_2O, modulated excitonic absorption in elec. and mag. fields 3—2037
Cu_2O, optical absorpt. spectra obs. of Mott excitons in elec. field 3—8129
Cu_2O, photoluminescence, existence of excitonic molecules 3—5228
Cu_2O, Raman scattering, luminescence, exciton-phonon coupling 3—8581
Cu_2O, resonance Raman scattering at the forbidden yellow exciton 3—21408
Cu_2O, two photon absorption spectrum 3—2567
Cu_2O film form. by low temp. oxidation of Cu, contact pot. meas. 3—4928
Cu_2O nucleation and growth near (100) face of Cu 3—15088
Cu_2O thin films, electrophysical properties *(Russian)* 3—38833
Cu_2O-Cu, single crystal and polycrystalline contacts, photovoltaic props. and barrier heights 3—36663
Cu_xO layer, on Cu, thickness determ. by proton-induced X-ray fluoresc. 3—4935
$Cu(OH_2)_6^{++}$ complex in aqueous perchloric media, behaviour *(French)* 3—8434
x CuO(1-y-x)PbO.y SiO_2, infl. of CuO content on conductivity *(Russian)* 3—11889
$Cu(PO_3)_2-CsPO_3$ system, phase diagram *(French)* 3—17958
$Cu_2P_2O_7$, antiferromagnetic, ^{31}P n.m.r. obs. 3—21322
$Cu_2P_2O_7$, mag. struct. using neutron diffr. method 3—18322
$Cu_3PS_4(Se_4)$, and other ternary normal tetrahedral struct. cpds. with comp. 1_356_4, cryst. struct. 3—24078
CuS particles on or in surface of supercooled H_2O drops, icebuilding activity *(Russian)* 3—21945
Cu_2S, chalcosite, djurleite, minority charge carrier, recombination diffusion length 3—11907
Cu_2S, chalcosite thin crysts., unusual form, absorpt. and refr., 0.5-1.1μ 3—24701
Cu_2S, in $Cu-Cu_2S$-CdS-Au sandwich struct., switching and filament migration obs. 3—2150
Cu_2S thin single crystals, prep. by topochemical conversion of CdS crystals 3—18540
Cu_2S:S, thermal e.m.f. coeff., conductance, Hall constant meas. 3—36577
Cu_2S-CdS single crystal cell, optical degradation and thermal restoration 3—5034

copper compounds continued
Cu_2S-CuS system, specific heat, thermal disorder, phase transformations *(German)* 3—38673
Cu_2S-FeS liquid quasi-binary mixtures, temp. dependence of density and surface tension 3—30168
$Cu_{2-x}S$-CdS polycryst. heterojunction, coord. sensitive photocell 3—15242
$Cu_{2-x}S$-CdS heterojunctions, impurity photoeffect 3—27309
Cu_xS, electrical resistivity and optical transmission as function of composition 3—33904
Cu_xS-CdS solar cell, surface potential local distribution 3—5035
$CuSO_4$ doped gelatin, X-ray coherent emission under laser irrad. 3—24759
$CuSO_4$ liquid electrolyte, calc. of Hall coeff. and H^+ ion mobility 3—11755
$CuSO_4$:gelatin, collimated X-ray emission on laser irrad. 3—13721
$Cu_3SbS_4(Se_4)$, and other ternary normal tetrahedral struct. cpds. with comp. 1_356_4, cryst. struct. 3—24078
CuSe, X-ray K-absorpt. spectra, fine struct. *(Russian)* 3—21495
Cu_2Se, phase transition enthalpy, structural order, specific heats, temp. depend. *(German)* 3—38672
Cu_2Se-CuSe system, specific heat, thermal disorder, phase transformations *(German)* 3—38673
Cu_3SmS_3 single crystal preparation by gas transport method, X-ray structure determ. *(Russian)* 3—12241
Cu_2SnS_3, Cu_2SnSe_3, Cu_2SnTe_3, semiconductors, ^{119}Sn, ^{125}Te, nuclear gamma resonance spectra *(Russian)* 3—36821
Cu_2SnSe_3, variation of lattice parameter with temp. and thermal expansion 3—14815
p-Cu_2Te, carrier effective mass from refl. spectra 3—36534
Cu_2Te, n and p type, electrical props. *(Russian)* 3—8170
Cu_2Te, phase transition enthalpy, structural order, specific heats, temp. depend. *(German)* 3—38672
Cu_2Te:Te, thermal e.m.f. coeff., conductance, Hall constant meas. 3—36577
$Cu_2Te-Ga_2Te_3$ system, phase diagram showing $Cu_2Ga_4Te_7$ phase, band and transport props. 3—38660
$Cu_2Te(c)$, dissociation pressures and thermodynamic props. 3—15828
$Cu_3V_2O_8$, new form, unit cell dimensions, octahedral networks 3—30092
$CuVO_3(I)$, distorted ilmenite type derivative, cryst. struct. determ. 3—7695
$CuWO_4$, mag. susceptibility and e.p.r. spectrum, 4.2-300 K, short-range order effects 3—34104
$(Cu_xZn_{1-x})M_2(SO_4)_2.6H_2O$, electron spin-lattice relax. processes 3—2362
Cu(11) complexes, $Cu[(C_2H_5)_2NCS_2]_2$ and $Cu[(C_2H_5O)_2PS_2]_2$, e.p.r. studies 3—20181
p-cu_2S, carrier effective mass from refl. spectra 3—36534
$GuGa_{1-x}In_xS_2$, band gap comp. depend. from transmission wavelength modulation 3—38789
$Na_2CuSi_4O_{10}$, cryst. struct., X-ray determ. 3—27013
$Pb(PO_3)_2-Cu(PO_3)_2$ system, phase diagram *(French)* 3—7901
$Sr(PO_3)_2-Cu(PO_3)_2$ system, phase diagram *(French)* 3—7901

copper-oxide rectifiers
No entries

copper zinc alloys *see brass*

Corbino effect
see also Hall effect
In, electronic component of linear magnetoresist. in thermal cond., Corbino geometry study 3—11880
In, very pure, lattice thermal conductivity 3—1725

core stores (magnetic) *see magnetic core stores*

Coriolis force
see also rotation
charged point-mass motion, Coriolis force derivation from vector pot. 3—28928
demonstration for students 3—16363
magnetic field origin as Coriolis force from Thomas rotation 3—37853
Maxwell theory (in media) and quantum theory in a rotating reference frame 3—35600
molecular coupling constants of cis- and trans-1,2-dichloroethylene 3—7154
plasma, rotating, inertial e.m.f. due to thermal convection, Coriolis acceleration 3—29945
plasma wave dispersion and stability 3—11496
prestressed cylindrical shells with arbitrary boundary conditions, effect on free vibration 3—10303
rotating mag. stars, stability dependence 3—13035
rotating magnetic stars, effects on stability and convective motions origin 3—35112
FeF_6^{3-}, force constants and Coriolis coupling constants calc. 3—33103
FeF_6^{3-}, force consts., Coriolis coupling consts., mean amplitues of vibration 3—29622
GaF_6^{3-}, force constants and Coriolis coupling constants calc. 3—33103
GaF_6^{3-}, force consts., Coriolis coupling consts., mean amplitudes of vibration 3—29622
$InCl_6^{3-}$, coriolis coupling constants 3—33102
SO_3, assignment of ν_2 and ν_4, gas phase Raman spectrum 3—36021
ScF_6^{3-}, force constants and Coriolis coupling constants calc. 3—33103
^aW, A=179, 181, 183, 185, 187, study of energy levels and Coriolis coupling by (d,p) and (d,t) reactions 3—29308

cornea *see eye*

corona
see also electric breakdown; flashover; solar corona
in air, optical recording system, calibration, soln. *(Russian)* 3—14613
air discharge between point and disk, volt-ampere characts. 3—23933
air positive corona formation 3—33410
coaxial cylinders, field strength distribution, calc. 3—14605
compressed air, breakdown charact. of highly nonuniform long gaps 3—7582
d.c. and a.c. noises from double conductor in foul weather 3—14610

corona continued
discharge, conductors between planes, characteristics, calc. 3−14607
discharge, field distrib. charged disperse phase effect, calc. 3−33402
discharges, motion of aerosol particles, approximation *(Russian)* 3−36213
Dust figure technique to study corona streamer development 3−36216
gas-particulate systems, meas. of surface area 3−32213
homopolar, stationary in plane fields, space-charge density distribution, numerical method 3−14609
location, by detection of u.v. emission 3−17713
metallized paper capacitors *(Japanese)* 3−26912
multichannel pulse height analysis 3−17688
negative near sparkover, fine particle charging rel. to free electrons 3−4692
point-to-plane devices with coated electrodes, modelling 3−26186
power transformers, high voltage, oil environment, u.s. measurement 3−17710
power transformers, oil environment, u.s. spectrum signature 3−17711
power transmission, cost of energy losses *(Russian)* 3−11516
similarity criteria, current and mean power losses, comparison with experimental results *(Italian)* 3−7573
subsonic airstream effects 3−14608
two-phase aerodisperse medium, electric field analysis rel. to electron-ion equipment 3−13671
SiO_2, high elec. fields produced by corona charging, surface pot. meas. rel. to dielec. breakdown 3−24654

coronagraphs
see also solar corona
electronic camera adaptation to coronography *(French)* 3−3387

corpuscular streams *see cosmic rays; solar corpuscular radiation*

correlation methods
see also correlators
application to gas chromatography 3−32250
application to partial discharge measurement 3−16375
in architectural acoustics 3−3696
atmospheric surface layer turbulence, spatial correlation functions of vel. components and temp. *(Russian)* 3−39516
autocorrelations functions for mag. and gravity anomalies, character of variation 3−25129
circular discs, binary array, optical correl. analysis 3−686
cross-correlation techniques for detection of spectral information 3−37631
dielectric characteristics determ. by correl. function analysis of noise voltage *(French)* 3−34281
diffuse object arrays, optical correlation using single lensless Fresnel hologram 3−19214
digital beamformer, output autocorrelation fn., quantizer fns. 3−37569
evoked brain potential of hippocampus, transient wave/peak amplitude correlation 3−35241
Fourier combined, for acoustic parameter determ. 3−3698
ideal digital correlation computer, design, for light beating spectroscopy 3−32074
ionospheric drift records, errors in correlation analysis 3−28084
liquid flow measurement, by cross-correlation of temperature fluctuations 3−10222
low bit-rate coding from autocorrelation method of linear prediction 3−3639
mass spectrometer, correlation type, resolving power *(Russian)* 3−6090
noise correl. thermometer for meas. of Pt wire temp. 3−5806
oceanographic depth sounding, processing methods 3−3262
optical, using diffuse objects 3−6438
pattern classification, holographic cross-correlation of training patterns with random mask 3−692
polarity, appl. to graphite moderated reactor 3−6988
seismic data autocorrelation functions, adaptive estimation 3−5535
seismic data processing, autocorrelation matrix techniques 3−9366
signal recording in correlation mass spectrometer *(Russian)* 3−6089
solids for obs. 3−341
spectrochemical analysis, application to determination of chemical composition *(Russian)* 3−10210
spectrometer for remote sensing, correlation mask techniques, signal modification 3−5944
technique for film boiling heat transfer 3−11732
three-dimensional spatial correlation function estimation for Abell clusters of galaxies 3−28280
velocity flow measurement, analysis of method *(Polish)* 3−26252

correlation theory
see also correlators; information theory
autocorrelation function for quasar 3C273 light variations 3−25477
seismic time-varying autocorrelation function, estimation 3−34807

correlators
see also correlation methods; correlation theory; information theory
digital interference correlation meter with high storage time 3−22132
for e.e.g., on-line 3−25977
flow measurement, time delay 3−465
in gamma ray Anger scintillation camera, resolution improvement 3−25858
holographic, ground glass, autocorrelation function, automatic displacement and distortion detection 3−22374
incoherent optical correlator 3−6439
noise correl. thermometer for meas. of Pt wire temp. 3−5806
optical, sensitivity enhancement with additional filters 3−35391
optical cross-path real-time correlator and ambiguity-function processor 3−32520
$CdS_{0.6}CdSe_{0.4}$, picosecond light pulses *(Russian)* 3−2517

correspondence principle
muon decay, equivalence of gravitational and magnetic fields 3−19501

corrosion
see also corrosion protection; electrochemistry; surface chemistry
AISI type 304 stainless steel pipe, eff. of exposure to liquid sodium 3−20949

corrosion continued
Al bronzes effect of iron, casting and wear properties *(Polish)* 3−31033
alloy, corrosion resistant, development 3−21683
alloy, inter- and transcrystalline fracture rel. to stress corrosion *(Russian)* 3−8801
alloy system, stress corrosion cracking 3−15713
alloys, stress corrosion test methods 3−9025
alloys for biomedical applics., corrosion fatigue 3−27657
β-brass, stress corrosion cracking, fractographic obs. 3−31042
brass, stress corrosion cracking in citrate soln. 3−39358
α-brass phase change correlation with stress corrosion fracture 3−27648
brittle bodies, rupture in surface-active medium, crack growth kinetics *(Russian)* 3−27059
BWR fuel rods, Zircaloy-clad, internal hydride formation, review 3−14267
chrome-magnesia fired bricks, electron microprobe analysis 3−15755
conference, Anaheim, USA (Mar. 1973) 3−27614
constructional materials and compressor components, fatigue strength under fretting corrosion conditions 3−34605
failure of welded joints, residual stress effects 3−21718
fatigue, crit. corrosion rate considerations 3−27655
film on metal surface composition determ. by Auger electron spectroscopy 3−21553
fractography, state-of-the-art review 3−30982
fracture mechanics and stress corrosion cracking 3−8034
glass surface properties, review 3−25017
glue metal interfaces 3−8042
manganin type alloy characteriz. for precision resistors 3−24946
metal, subcrit. crack branching implications 3−4796
metals, in high purity water, test assemblies *(Russian)* 3−12472
metals, thermal fatigue, under mechanical loading in corrosive medium 3−27798
metals in liquid media, apparatus for long-term strength testing in corrosional cracking conditions *(Russian)* 3−9826
naphthalene rods in organic solvents, effects of pressure and atmospheres 3−15756
potentiostat and its applications, book 3−12534
refractories in molten glass, model studies 3−15756
specimen for testing, loaded spring in corrosive fluid 3−34670
stainless steel in PFR liquid Na coolant, mass transport 3−14252
stainless steel weld metal, resistance 3−20950
steel, AISI 4340, stress corrosion crack growth, stress history effect on incubation time 3−34585
steel, austenitic, index of susceptibility to stress corrosion cracking, electromech. model 3−27643
steel, austenitic, performance of inhibitor-protector against corrosion fatigue failure *(Russian)* 3−4929
steel, austenitic stainless, fracture surfaces in stress corrosion cracking *(Japanese)* 3−34561
steel, austenitic stainless, intergranular corrosion, microstruct. and microsegregation effects 3−37032
steel, austenitic stainless, stress corrosion crack propag. in hot chloride media 3−27651
steel, austenitic stainless, stress induced cracking in HCl solutions 3−34553
steel, austenitic stress corrosion cracking, fractographic obs. 3−31042
steel, C, stress corrosion cracking, in nitrate and alkaline solns., temp. and inhibitors effect 3−27649
steel, cast heat resistant, with low Ni content, characteriz. 3−27696
steel, corrosion resistant, development 3−21683
steel, durability, effect of fretting after thermochem. treatment *(Russian)* 3−27668
steel, ferritic stainless, stress corrosion cracking, heat treatment and comp. effects 3−31040
steel, high-strength, internal stress effects on susceptibility to stress corrosion 3−21692
steel, high-strength, stress-corrosion and corrosion-fatigue crack vels. 3−5324
steel, high-strength Type 4140, corrosion fatigue behaviour 3−37051
steel, HY-130, corrosion fatigue crack propag., temp. and freq. effects 3−27660
steel, inter- and transcrystalline fracture rel. to stress corrosion *(Russian)* 3−8801
steel, maraging, nitriding, nonbrittle case form. 3−27690
steel, martensitic, stress corrosion cracking, interplay of hydrogen dissoc. and comp. 3−8904
steel, mild, stress corrosion cracking, in nitrate solns., effect of C content 3−39354
steel, Ni-Co-C, roll-extruded, effect of degrees of rolling reduction 3−31050
steel, pearlitic, hydrogen embrittlement, strength and struct. influence 3−27654
steel, specimens with cappings, corrosion fatigue strength, heat treatment and rolling effects *(Russian)* 3−27667
steel, stainless, ferritic, intergranular corrosion and chromium depletion 3−27653
steel, stainless, pitting and stress corrosion *(French)* 3−24913
steel, stainless, stress corrosion cracking 3−31039
steel, stainless, stress corrosion cracking and hydrogen embrittlement 3−5330
steel, stainless, surface prep, and pit propag. 3−11822
steel, stainless, type 403, corrosion fatigue metallography 3−27658
steel, stainless ferritic, intergranular corrosion 3−20946
steel, stress corrosion, inhibiting action of mineral iodides *(French)* 3−1901
steel, stress corrosion cracking, role of hydrogen embrittlement 3−2736
steel, Ti stabilised austenite stainless, intergranular corrosion, carbide morphology and composition effect 3−8853
steel 1Kh17N2, mech. props. after vacuum heat treatment 3−21676
steel austenitic, explosive bonded and hot rolled clad flat plates, residual stresses, sensitivity to stress corrosion cracking *(German)* 3−27837
steels, high-strength, comparison of hydrogen embrittlement and stress corrosion cracking 3−21622

corrosion continued
- stress corrosion, adsorption-electrochemical hypothesis *(Russian)* 3—27670
- stress corrosion crack propag., film rupture model 3—27663
- stress corrosion cracking, acoustic emission applic. 3—31216
- stress corrosion cracking, film rupture model 3—27662
- stress corrosion cracking by H_2 embrittlement, lattice dilatation, complete elastic soln. 3—39353
- stress corrosion cracking via surface diffusion, interface morphology development 3—34570
- stress corrosion cracks, h.v. microscope studies 3—30981
- stress cracking, test methods development 3—15808
- stress-corrosion fracture of structures under random loading 3—21627
- surface coating methods development 3—8035
- surface texture, adsorption, Auger electron spectroscopy, slow electron diffraction, field ion microscopy 3—1864
- thin film instability rel. to substrate corrosion 3—15275
- u.h.v.-t.e.m. corrosion studies, in situ sputter cleaning of thin film metal substrates 3—38737
- X-ray variable focus tube, for studying stress corrosion cracking 3—28744
- Zircaloy-2, cooled from β phase temp. with different cooling rates in hot water and steam 3—37021
- Zircaloy-2, H_2 embrittlement by aqueous lithia soln. corrosion *(French)* 3—12385
- Zircaloy-2 in methanol-I_2 solutions, stress-corrosion cracking 3—24886
- Zircaloy-4, transmission electron microscopy of ion-thinned oxides during corrosion 3—11825
- Zircaloys acoustic emission during stress corrosion cracking, correl. with fractography of cracking 3—31045
- Agl-Mg commercial alloys, stress corrosion cracking and its prevention *(Japanese)* 3—18635
- Al, intergranular corrosion in pressurized water, hydrogen/grain boundary interactions *(French)* 3—1909
- Al, pitting corrosion, alloying elements effect 3—8046
- Al alloy, stress corrosion cracking initiation *(French)* 3—31083
- Al alloys, corrosion fatigue in aqueous solns., fractographic studies 3—27656
- Al alloys, high-strength, hydrogen embrittlement and stress corrosion cracking 3—5336
- Al alloys for aircraft structures, thermomech. processing effects 3—31048
- Al matrix composites, corrosion, erosion, thermal stability, review 3—24977
- Al Zn Mg Cu alloy, fibrous struct. and susceptibility to contact corrosion *(German, English)* 3—24354
- Al-Mg alloy, effect of addition of Bi on stress-corrosion cracking *(Japanese)* 3—18634
- Al-Mg alloys, stress-corrosion resistance, improvement by Bi additions 3—12382
- Al-Mg-Zn alloy, microstruct. influence on stress corrosion susceptibility 3—39342
- Al-Zn-Mg, corrosion fatigue inhibition, crack growth rate meas. 3—39352
- Al-Zn-Mg alloys, grain boundary corrosion and stress corrosion cracking relationship *(Japanese)* 3—31072
- Al-Zn-Mg alloys, SCC, soln. chem. influence on repassivation kinetics, alloying effect 3—27652
- Al-Zn-Mg alloys, stress corrosion resist., alloying and ageing depend. 3—21671
- Ca sulphoaluminate and sulphosilicate, hydraulically hardened, corrosion stability *(Russian)* 3—15742
- CrMnNiN austenitic steel, planar slip during plastic deformation *(German, English)* 3—24132
- Cu and Cu-Al(7.9 wt.%) alloys, corrosion fatigue crack initiation 3—27661
- Cu electrode, in chloride soln., photopotential obs. of surface layer 3—8044
- Cu-Ni (10 wt.%) alloy, stress corrosion resist. in ammoniacal environment, effect of Fe 3—31041
- Fe, cast, containing Cr and Cr-Mo, corrosion stability, rare earth additive effects *(Russian)* 3—27666
- Fe, cast, pipe, u.s. inspection 3—31223
- Fe, inhibiting action on hydrogen adsorption in sulphuric acid solns. *(French)* 3—1911
- Fe-Cr alloys, stress corrosion cracking 3—31039
- Fe-Cr-Mo ferritic stainless steel, vacuum melted, effect of C and N on toughness, ductility and corrosion resist. 3—27676
- Fe-Ni-Cr, stress corrosion cracking susceptibility, nuclear reactor water environments 3—39351
- Ge, growth form and soln. form relation, corrosion of hollow half spheres in acidic soln. *(German)* 3—9079
- Mg-Al alloy, transgranular stress corrosion cracking 3—30983
- Nb, corrosion in liq. Li, effect of O_2 addition at 600°C 3—26533
- Nb alloys, corrosion-erosion strength *(Russian)* 3—12375
- NdSb, analysed from Nd-Sb alloy phase diagram, resist. to corrosion compared with other phases *(Russian)* 3—12338
- Ni electrode, in sulphate soln., photopotential obs. of surface layer 3—8044
- Ni-Cr-Nb heat resistant spring alloy characteriz. 3—24944
- Ni-Cr-ThO_2, Na_2SO_4 coated, dispersion effect 3—39366
- Ni-Cr(50 50 wt.%) alloy, resist. to service embrittlement, high-creep strength, development 3—21636
- Ni-Mo, on exposure to HBr 3—8041
- Ni-Mo alloy N70M27, corrosion resist. after ordering 3—21604
- Ni-Mo-W corrosion resistant hard alloy development 3—21667
- Ni-Ti-Al alloys, heat resistant, effect of copper additions 3—24949
- $SrTiO_3$, Sr_2TiO_4, SrO, compatibility with superalloys at 900 and 1100°C 3—19946
- Ta, corrosion in liq. Li, effect of O_2 addition at 600°C 3—26533
- Ta, sputtered film, 6-20 μ, on stainless steel, prep., mech. props. and corrosion resist. 3—27677
- Ti, stress corrosion cracking in methanol/HCl mixture, fracture 3—27650
- Ti alloy, TA6V, stress corrosion cracking and hydrogen embrittlement *(French)* 3—8907
- Ti alloy, TA6V6EZ, hydrogen and oxygen influence on tensile props. *(French)* 3—5334

corrosion continued
- Ti alloys, corrosion fatigue in aqueous solns., fractographic studies 3—27656
- Ti and alloys, hydrogen adsorption processes 3—1910
- Ti-Al-Mo-V alloy, cleavage cracking in gaseous hydrogen 3—31044
- Ti-Al-V alloy, stress corrosion crack propag., fractographic obs. 3—31043
- Ti-Al-V and Ti-Al-V-Sn alloys, corrosion fatigue crack propag., freq. and wave form effects 3—27659
- Ti-Ni (2 at. wt%) alloy influence of microstructure on corrosion behaviour in hot acidic chloride solns., application to weld regions 3—27647
- W, H promoted, by O_2 in elec. field, surface topography changes 3—30359
- W-Ni-Mo, corrosion resist. compared with Fe alloys 3—8783
- Zn, effect of surface-active Hg melt on electroplastic deform. *(Russian)* 3—24186
- Zr alloy, fuel element sheath, stress corrosion cracking in J_2 3—29447
- Zr alloy, stress induced cracking, environmental effects 3—31082

corrosion control *see corrosion protection*

corrosion prevention *see corrosion protection*

corrosion protection
- *see also corrosion; packaging; pH control; protective coatings*
- coated materials strength and creep testing apparatus for temps. above 1400°C 3—32047
- magnet, machined, method of protection during heat treatment 3—24956
- mirror, silvered, protective coatings for preventing atmospheric tarnishing 3—13273
- steel, 1KH18N9T, cladding with Be and corrosion stability in molten Li *(Russian)* 3—12377
- steel, austenitic, performance of inhibitor-protector against corrosion fatigue failure *(Russian)* 3—4929
- steel, corrosion fatigue, effect of vacuum-diffusion coating *(Russian)* 3—27665
- steel, mild, nitrate solns., stress corrosion cracking, effect of C content 3—39354
- thin metal films on ceramic substrates, two layer, vibratory finishing, occlusion of pinholes 3—11819
- Zircaloy-2 corrosion in hot water and steam, oxide film growth 3—37021
- BeO spheres, Al_2O_3 coated, neutron irradiation effects 3—4338

cosmic dust
- *see also meteoroids*
- in astronomy and space research *(German)* 3—22124
- Comet Bennett 1969i, dust and gas motion in head rel. to type II tail 3—28160
- R Coronae Borealis, i.r. measurements rel. to dust clouds surrounding star 3—22074
- coupling of dust grains to gas in circumstellar envelopes 3—18998
- dusty Stromgren spheres, analytic approximations from far i.r. observations 3—13104
- formaldehyde in interstellar dust clouds, anomalous hyperfine lines 3—22119
- interaction of stars with local dust formations, densities and motion *(Russian)* 3—13108
- intergalactic filaments, formation, tidal forces, computer simulation 3—3370
- IR sources, ionised gases, H II region W_3, H_2O maser emission 3—3358
- mass distribution of colliding particles, effects of erosion and fragmentation 3—9613
- metagalactic X-ray prod. by relativistic dust grains 3—31487
- mineralogical comp. variation of dust clouds as function of galaxy age 3—37333
- orientation of interstellar and interplanetary dust grains rel. to polarised radiation 3—28300
- planetary nebulae, dust effects on dynamics and thermal stability 3—31794
- static charged dust distribs. with plane symmetry 3—28962
- symbiotic object behind Coalsack, discovery with combination spectrum 3—25467
- ^{26}Al and ^{53}Mn produced by solar flare particles 3—9502

cosmic radiation *see cosmic rays*

cosmic radiations, radiofrequency *see radiofrequency cosmic radiation*

cosmic radio waves *see radiofrequency cosmic radiation*

cosmic ray absorption
- negative muons stopping rate near sea level, radiochemical meas. method 3—12913
- Pb-glass, origin of fission fragment tracks 3—24135

cosmic ray alpha-particles and helium nuclei
- interplanetary deceleration and source spectra 3—9432
- light flashes due to α-particles seen aboard high altitude planes, prediction 3—22151
- modulation within solar cavity (1965-1970) 3—3275
- source spectrum, Fermi mechanism 3—3271
- α-N jets with primary energy 0.1-1 TeV, production of fireballs, detection using DW and target plots 3—12923
- He, rigidity spectrum above 17 GV, search for high energy anti-nuclei in primary cosmic rays 3—9437
- He/medium nuclei abundance ratio, nuclear emulsion meas. and Explorer 35 solid state detector meas., a comparison 3—16077
- ^{4}He auroral precipitation from mass spectrometry of exposed Al and Pt foils 3—16007

cosmic ray apparatus
- *see also particle detectors*
- anomalous barometer coeff. of neutron monitor at Mt. Norikura 3—12914
- atmospheric γ-ray spectrum in 40-1500 GeV range, meas. using Pb-emulsion sandwich detector 3—12899
- Cherenkov hodoscope, large-aperture, for multi-particle state identification 3—10058
- cosmic X-rays, low energy, detection by proportional counter 3—32163
- crystal scintillators for meas. of diffuse X-ray spectrum, radioactive spallation errors 3—37274

cosmic ray apparatus continued
- detector telescopes, geometrical aspects of performance in non-isotropic particle distributions 3−301
- differential spectrum meas., instrument characts. use 3−32137
- diffuse X-ray background meas., collimator corrections, comparison of S-11 and OSO-3 data 3−32135
- digital sonde measuring systems, minicomputer applications, Institut Royal Meteorologique, Belgium *(French)* 3−21980
- EAS, search for charge e/3 quarks using flash-tube chamber 3−31486
- EAS, study of radio pulses in 30-140 MHz region using Geiger-Muller counter and v.h.f. receiver 3−12918
- isocon TV camera/mag. tape recorder system for fast oscilloscope trace analysis 3−3856
- isotope analysis with cryogenic magnet 3−6075
- isotope and charge comp. meas. using counters 3−6074
- isotope determ. by tracks in plastics 3−6081
- large area γ-ray detector, Pb scintillator sandwich with optical spark chambers 3−32161
- multiple neutron distributions in cosmic ray neutron monitors 3−6086
- muon specific ionisation meas. in 5 to 500 GeV/c region using Cosmic Ray Spectrograph 3−12926
- neutrino detector Cherenkov system, Utah, USA 3−32160
- neutron monitor data for IGY, barometer-corrected data from Deep River (1961) 3−34988
- ocean wave and tide recording system using cosmic rays 3−16074
- proportional beam hodoscope system 3−28650
- rigidity spectra meas. between 5 and 100 GeV/c 3−37270
- scintillation hodoscope spectrometer, for spatial coordinates of high energy photons 3−22493
- spark chambers for charge spectrum 3−28693
- spectrograph, Elbrus, in the Caucuses for obs. of neutron, hard and electron-photon components *(Russian)* 3−12874
- thick section technique for meas. fossil tracks 3−9630
- n supermonitor, optimization of observational data *(Russian)* 3−12878
- n supermonitor at Krasnaya Parkha *(Russian)* 3−12877
- He hodoscope, for particle density measurements 3−37690

cosmic ray composition
- *see also cosmic ray alpha-particles and helium nuclei; cosmic ray deuterons; cosmic ray electrons; cosmic ray mesons; cosmic ray muons; cosmic ray neutrinos; cosmic ray nucleons*
- atmospheric components ratios, hadronic scaling predictions 3−28099
- chemical and isotopic comp. determ. from balloon flights 3−9438
- energetic very heavy nuclei, propag. 3−21999
- galactic, Li overabundance and heating of H I regions 3−9421
- galactic, N flux 3−9420
- galactic cosmic ray chemical composition rel. to diffuse model 3−31482
- galactic cosmic rays with energies between 10 and 30 MeV per nucleon 3−39573
- HEAO satellite proposal on chem. and isotopic comp. 3−9439
- heavy nuclei enrichment, charge dependence of energy spectra 3−21989
- isotope analysis with cryogenic magnet 3−6075
- isotope analysis with nucl. emulsions 3−6082
- isotope and charge comp. meas. using counters 3−6074
- isotope comp. meas. using geomag. field 3−9431
- isotope determ. by tracks in plastics 3−6081
- isotopic, in interstellar space, rel. to electron component 3−9422
- isotopic comp., conf., Lyngby, Denmark (Mar. 1971) 3−9414
- isotopic comp. of low energy boron, carbon, nitrogen and oxygen particles *(German)* 3−9413
- leptonic quarks, search in cosmic radiation near sea level 3−31491
- low energy, chemical compositions of particles of charges from $Z=12$ to $Z=28$ using plastic detectors *(German)* 3−28681
- nuclei abundance ratios, leakage path length dependence on energy 3−21991
- propagation and source distrib. effects 3−9423
- rigidity spectra meas. for H to Fe elements between 5 and 100 GeV/c 3−37270
- solar cosmic rays with $6\leqslant Z\leqslant 26$, satellite meas. of charge comp. 3−37277
- solar flare, differential energy spectra of ^{1}H, ^{3}He and ^{4}He 3−39601
- solar particle Fe-group abundances in 1971 Jan. 24 and 1971 Sept. 2 event 3−37278
- Be isotopic comp. interpret. 3−9419
- ^{7}Be destruction by electron capture in interstellar medium 3−9417
- He/medium nuclei abundance ratio, nuclear emulsion meas. and Explorer 35 solid state detector meas., a comparison 3−16077

cosmic ray deuterons
- interplanetary deceleration and source spectra 3−9432

cosmic ray effects and interactions
- *see also nuclear reactions and scattering due to cosmic rays*
- atmospheric neutrino induced muon flux and neutrino nucleon high energy interactions 3−9443
- atmospheric spallation, aerosols, applications to the study of tracers and pollutants *(German)* 3−12862
- burner surface interaction 3−25421
- clusters of galaxies, heating of X-ray emitting cloud 3−25491
- cosmogenic radionuclides in Allende and Murchison carbonaceous chondrites 3−9513
- depth-intensity curve for muon-produced neutrons *(Russian)* 3−22002
- fluxes in atmosphere, effect of collision parameters 3−9435
- fossil tracks from extinct radioactivity and ancient cosmic rays in lunar minerals 3−28096
- fragmentation region and multiparticle production, expt. 3−19721
- galactic, Li overabundance and heating of H I regions 3−9421
- galactic, secondary nuclei/primary nuclei effects at high energies, galactic disc trapping 3−25351
- galactic, upper atmosphere capture by ionization loss *(Russian)* 3−12889
- galactic ray bombardment of interstellar gas, element prod. 3−9418
- hadron multiple production, review 3−22001
- hadronic cascades at high energies, Monte Carlo anal. in 3 dimensions and computer simulation 3−10801
- IGY neutron monitor data 3−12915

cosmic ray effects and interactions continued
- interstellar gas, sound vibrations in presence of mag. field *(Russian)* 3−37478
- interstellar medium heating by ionisation, turbulence in intercloud medium 3−37489
- interstellar molecular cloud heating by low-energy cosmic rays 3−31782
- ionization sources of D- and E-regions 3−3087
- light flashes due to α-particles seen aboard high altitude planes, prediction 3−22151
- moon, dating of mechanical events by deformation induced erasure of particle tracks 3−9505
- noise in rocket borne proportional counters for X-ray astronomy, reduction 3−13429
- Pb-glass, origin of fission fragment tracks 3−24135
- redshift limits due to e.m. interaction of photons with interstellar radiation field 3−19066
- scaling model of Feynman, relevance of cosmic ray data above 10^{12} eV 3−31488
- scintillations of cosmic rays inside magnetosphere, broad-band fluctuations 3−16081
- solar cosmic ray scattering in interplanetary space, anisotropic propagation *(Russian)* 3−13004
- spallation induced prod. of elements 3−9415
- stratosphere, cosmic radiation as odd N source 3−15976
- transport theory, with anisotropic particle scatt. and convection using Fokker-Planck eqn. *(Russian)* 3−12871
- ultra-high-energy interaction processes 3−9434
- underground high energy leptonic processes search 3−9442
- α-N jets with primary energy 0.1-1 TeV, production of fireballs, detection using DW and target plots 3−12923
- μ, vision stimuli 3−22154
- μ e.m. interactions in Fe, 6-200 GeV, search for charge asymmetry 3−5549
- μ e.m. interactions in Fe, 6-200 GeV, momentum dependence of interaction probabilities 3−5550
- μ-e collision cross section dependence on Z/A of target material 3−12927
- ν expt., high energy 3−9440
- p primaries, 14 GeV interactions with nucleons in nuclear emulsion, identification of shower particles 3−9436
- H I region heating and ionisations, props. determ. 3−28293

cosmic ray electrons
- albedo electrons spectrum characts. determ. from studied gas discharge detectors data 3−22446
- anisotropy and diffusion due to streaming motion of particles 3−3277
- galactic cosmic ray secondary electron prod. 3−31481
- interstellar space, rel. to isotopic comp. 3−9422
- modulation within solar cavity (1965-1970) 3−3275
- muon/electron abundance ratio and muon lateral distrib. in inclined showers, calc. 3−34989
- origin contrib. of π production by primary nucleons to interstellar e^-e^+ flux 3−37279
- secondary and return albedo, differential energy spectra, 2-35 MeV, balloon meas. in upper atmosphere *(German)* 3−3274
- secondary electron prod. from pulsar nebula complexes 3−37273
- solar and galactic, 30-35 keV rocket and stratospheric obs. *(Russian)* 3−12896
- spectrum, modulation near solar max. 3−12911
- spectrum modulation and origin of low energy interplanetary particles 3−21994
- synchrotron radiation in geomagnetic field, meas. technique 3−21995

cosmic ray jets *see cosmic ray showers and bursts*

cosmic ray mesons
- hadron interaction characteristics of high-energy cosmic rays, basis of model for break in primary spectrum at $\sim 10^{15}$ eV 3−9433
- Weinberg W-meson, possible observation in anomalous cosmic ray events 3−16087
- π energy spectra at top of atm. from expt. μ spectrum 3−12921
- π production by primary nucleons, contrib. to interstlar e^-e^+ flux 3−37279

cosmic ray muons
- atmospheric neutrino induced muon flux and neutrino nucleon high energy interactions 3−9443
- background effects in solar neutrino expts. 3−9427
- boson pair model unification with $K^0_l \rightarrow \mu^+\mu^-$ and excess μ anomaly 3−16951
- charge ratio at sea level, 10 to 1500 GeV, zenith angles 0 to 90° 3−39577
- depth-intensity curve for muon-produced neutrons *(Russian)* 3−22002
- EAS, meas. of momentum spectrograph, survey of track-fitting methods, theoretical model calcs. 3−12924
- e.m. interactions in Fe, 6-200 GeV, momentum dependence of interaction probabilities 3−5550
- e.m. interactions in Fe, 6-200 GeV, search for charge asymmetry 3−5549
- fluxes of stopping muons at various levels underground 3−12925
- intensity predictions, effects of proton-atmospheric nuclei interaction processes 3−5551
- interaction cross sections, positive and negative μ 3−18910
- low momentum integral muon spectrum at sea level near geomagnetic equator 3−31490
- momentum spectra and charge ratio meas. of sea-level latitudes 3−16088
- muon/electron abundance ratio and muon lateral distrib. in inclined showers, calc. 3−34989
- negative, stopping rate near sea level, radiochemical method of meas. 3−12913
- sea-level energy spectrum and scaling hypothesis, derivation of primary nucleon spectrum 3−5547
- specific ionisation meas. in 5 to 500 GeV/c region using Cosmic Ray Spectrograph 3−12926
- total cross section values of high energy expts., analysis 3−9441
- underground high energy processes search 3−9442
- zenith-angle distrib. in Mont Blanc tunnel, comparison with intermediate vector boson decay distrib. 3−31492

cosmic ray muons continued
μ-e collision cross section dependence on Z/A of target material 3−12927
μ^+/μ^- ratio at sea level, hadronic scaling predictions 3−28099
$(\mu^+ + \mu^-)$/p ratio at sea level, hadronic scaling predictions 3−28099
n production at 4300 m w.e. 3−22000

cosmic ray neutrinos
atmospheric neutrino induced muon flux and neutrino nucleon high energy interactions 3−9443
energy spectra calc. in expanding universe 3−3273
high energy interaction expt. 3−9440
penetrating ability in solar matter *(Russian)* 3−16078
solar, background effects in detection expts. 3−9427
solar, discrepancy between theoretical and exptl. production rates, possible explanations 3−9428
solar, effect of partial wave contrib. to ^{7}Be(n,γ)^{8}B reaction cross section 3−29395
solar, investigation of background in proportional counters 3−6073
solar, mixing model, stellar evolution considerations 3−9468
solar, review of theory and discrepancies with exptl. results 3−9426
solar, search for related M1 transitions in ^{6}Li using 180° electron scattering 3−39574
solar core mixing, ^{8}B neutrino flux 3−9469
solar neutrino detection using ^{37}Cl(ν,e$^-$)^{37}Ar reaction 3−9425
solar neutrino flux, prod. by ^{6}Li isobaric analogue state reactions 3−25399
solar-neutrino expts., existence of resonance in ^{3}He + ^{3}He system 3−12973
stars, thermonuclear reactions, review *(Russian)* 3−5553
total cross section values of high energy expts., analysis 3−9441
underground high energy processes search 3−9442

cosmic ray neutrons
27-day variations of diurnal anisotropy using neutron component data 3−34985
anomalous barometer coeff. of neutron monitor at Mt. Norikura 3−12914
energetic flux leakage from top of atmosphere 3−5548
interactions with C, Fe, Pb, 600-3000 GeV, comparison with p induced interactions *(Russian)* 3−12920
latitude distribution 1967-9, relationship to solar activity cycle *(Russian)* 3−12910
monitor for IGY, barometer-corrected data from Deep River (1961) 3−34988
Moon, surface composition, cosmic-ray produced neutron equilibrium spectra 3−5580
multiple neutron distributions in cosmic ray neutron monitors 3−6086
partial coefficients and specific yield functions, altitude-latitude dependences *(Russian)* 3−12876
solar neutrons, correlations between intensity changes and sun-spots and mag. storms *(Bulgarian)* 3−34986
solar neutrons, statistical anal. of continuous intensity measures *(Russian)* 3−34987
supermonitor, optimization of observational data *(Russian)* 3−12878
supermonitor at Krasnaya Parkha *(Russian)* 3−12877

cosmic ray nucleons
see also cosmic ray neutrons; cosmic ray protons
energy spectra at top of atm. from expt. μ spectrum 3−12921
hadron interaction characteristics of high-energy cosmic rays, basis of model for break in primary spectrum at $\sim 10^{15}$ eV 3−9433
heavy nuclei enrichment in 17 April 1972 solar flare 3−12898
inelasticity of interaction with Pb nuclei, 1-10 TeV *(Russian)* 3−31489
interactions with Fe nuclei, total coefficient of nucleon inelasticity 0.6-10 TeV *(Russian)* 3−29400
interstellar relativistic plasma containing immobile and cosmic ray protons and thermal neutrons 3−14537
neutron intensity at barometric pressure at Syowa station, Antarctica, effect of high winds 3−21996
primary, contrib. of π production to interstellar e$^-$e$^+$ flux 3−37279
primary spectrum from sea-level muon energy spectrum using scaling hypothesis 3−5547
secondary nuclei prod. from pulsar nebula complexes 3−37273
α-N jets with primary energy 0.1-1 TeV, production of fireballs, detection using DW and target plots 3−12923

cosmic ray origin
see also cosmology; element origin
acceleration in strong e.m. fields, appl. to pulsars 3−22091
constellation Cygnus, γ-quanta flux meas. *(Russian)* 3−12885
deuterons and ^{3}He formation and destruction in proton induced spallation of light ($Z \leqslant 8$) nuclei 3−21987
energies $> 10^{21}$ eV, generation in superstrong e.m. fields 3−18907
evolution due to interactions with self excited relativistic plasma waves 3−25348
extragalactic and big bang theories 3−16076
Galactic, near centre, metagalactic origin 3−3368
galactic distribution model *(Russian)* 3−12886
galactic mag. field effects on cosmic rays above 10^{17} eV 3−25350
galactic nucleus species, phenomenological study of propag. 3−28094
rel. to gamma ray astronomy 3−34982
high energy gamma rays, celestial distribution showing galactic and extragalactic components 3−12880
magnetic stars interaction with interstellar gas 3−39572
pulsar, acceleration of charged particles in e.m. fields, numerical study 3−35167
pulsar nebular matter, path length distrib. 3−37273
pulsed galactic nuclei rel. to origin of cosmic rays 3−13086
relativistic, $Z \geqslant 74$ nuclei, r-process source 3−12919
secondary nuclei lifetime rel. to ^{54}Mn decay 3−39575
source spectrum, Fermi mechanism 3−3271
supernova generation nonplanar relativistic flow 3−7478
theories since the discovery of pulsars 3−37276
transition radiation from relativistic electrons rel. to source of cosmic X-rays 3−31500
universal cosmic-ray theory for gamma-ray astronomy 3−21988

cosmic ray photons
see also cosmic ray X-rays; solar cosmic ray photons
atmospheric γ-ray spectrum in 40-1500 GeV range, meas. using Pb-emulsion sandwich detector 3−12899
Cherenkov bursts, cosmic ray point source determ., γ-quanta flux meas. from constellation Cygnus *(Russian)* 3−12885
diffuse cosmic gamma ray flux in 100 keV to 8.5 MeV range 3−25349
energy spectra for γ-rays, ν, calcs. using black and greybody photons 3−3273
extragalactic, interactions with universal radiation, absorption due to hadron production 3−34983
Galactic, near centre, metagalactic origin 3−3368
Galactic central region, energy spectrum of gamma rays 3−28265
gamma quanta, polarisation and energy spectra determ. method *(Russian)* 3−12893
gamma rays from ^{7}Li nuclear de-excitation rel. to cosmic radiation from galactic centre 3−18905
pulsars, flux origin, calc. 3−12890
redshift limits due to e.m. interaction of photons with interstellar radiation field 3−19066
secondary differential energy spectra, 1-44 MeV, balloon meas. in upper atmosphere *(German)* 3−3274
γ-ray line feature from Galactic centre direction 3−28110

cosmic ray protons
astronaut, calc. of radionuclide production and delayed photon leakage, solar protons 3−3611
evolution due to interactions with self excited relativistic plasma waves 3−25348
geomagnetic cutoff for particles of energy between 1.2 and 39 MeV 3−16080
idealised extensive air showers, rapidly using proton-proton total cross sections effect 3−16085
interactions with atmospheric nuclei, effects on predicted muon intensities 3−5551
interactions with C, Fe, Pb, 600-3000 GeV, comparison with n induced interactions *(Russian)* 3−12920
interactions with nuclear emulsion, 70 GeV/c, characteristics of nuclear decay *(Russian)* 3−34992
isotropic spectrum deviation for energies over 1 MeV 3−18906
modulation within solar cavity (1965-1970) 3−3275
solar, stratospheric meas. of energy spectra *(Russian)* 3−12895
solar and galactic, 0.5 MeV rocket and stratospheric obs. *(Russian)* 3−12896
solar flare protons, 1969, March 30, rel. to two-component cosmic ray injection 3−22026
solar flare protons, polar-cap meas. down to 12.4 keV 3−12897
solar injection into magnetosphere 3−3131
solar low energy protons, adiabatic energy loss in interplanetary space during cosmic ray event decay 3−22028
solar proton entry into magnetospheric tail 3−3133
solar proton flux, 12.5-minute periodicity at balloon altitude 3−16082
solar proton transport in interplanetary space, numerical studies 3−18931
solar relativistic protons before Hα maximum phase of solar flare, direct detection 3−21993
source spectrum, Fermi mechanism 3−3271
$(\mu^+ + \mu^-)$/p ratio at sea level, hadronic scaling predictions 3−28099
p primaries, 14 GeV interactions with nucleons in nuclear emulsion, identification of shower particles 3−9436
pp collision cross-section, exam. to 5×10^{13} eV 3−18909

cosmic ray showers and bursts
see also cosmic ray electrons; cosmic ray X-rays
Cherenkov bursts, cosmic ray point source determ., γ-quanta flux meas. from constellation Cygnus *(Russian)* 3−12885
EAS, muon component, meas. of momentum spectrograph, survey of track-fitting methods, theoretical model calcs. 3−12924
EAS, search for charge e/3 quarks using flash-tube chamber 3−31486
EAS, search for quarks using computer-controlled cloud chamber 3−16086
EAS, study of radio pulses in 30-140 MHz region using Geiger-Muller counter and v.h.f. receiver 3−12918
EAS and Feynman scaling above 1000 GeV 3−18908
EAS and primary cosmic radiation, experimental aspects 3−34990
EAS electron component, Monte Carlo simulation for single and multicored showers 3−12917
EAS event of energy 4×10^{21} eV 3−12916
electronic component of extensive air showers, spatial distribution *(Russian)* 3−21998
hadron induced interactions in condensed matter, determ. of mean energy 3−12922
hadronic cascades at high energies, Monte Carlo anal. in 3 dimensions and computer simulation 3−10801
idealised extensive air showers, rapidly using proton-proton total cross sections effect 3−16085
lateral distribution of u.h.f. radio emission rel. to cosmic ray showers 3−21997
multiple prod. law for secondary particles *(French)* 3−25355
muon/electron abundance ratio and muon lateral distrib. in inclined showers, calc. 3−34989
shower particles, in jets produced by interaction of 14 GeV protons with nucleons in nuclear emulsion, identification 3−9436
α-N jets with primary energy 0.1-1 TeV, production of fireballs, detection using DW and target plots 3−12923

cosmic ray solar modulation
27-day variations of diurnal anisotropy using neutron component data 3−34985
diffusion models based on hypothesis of scattering centres in solar wind *(Russian)* 3−3272
electron energy spectrum, force field approximation to transport eqn. 3−12911
interplanetary electron spectrum, origin and time variations 3−21994
low-energy galactic cosmic rays, solar max. period obs. 3−16083
off ecliptic control, interplanetary magnetic field 3−9429
protons, electrons and He nuclei, (1965-1970) 3−3275
rigidity dependence of modulation function relative to solar min. for rigidities > 2 Gv 3−16079
storm from August 1972 solar activity 3−21902

cosmic ray variations

- *see also geomagnetism*
- 27-day cycle explained by solar activity 1957-70 *(Russian)* 3−12905
- 27-day variations of diurnal anisotropy using neutron component data 3−34985
- 30 March, 3-4 April 1971 events *(Russian)* 3−12875
- 1969, June 8, Forbush decrease and change in 11-year modulation 3−12912
- aeonic flux, detn. from lunar rocks 3−39576
- anisotropy, three dimensional, during disturbance 25 Oct-10 Nov 1968 *(Russian)* 3−12906
- anisotropy in Galaxy, interpretation 3−9416
- anomalous recurrent diurnal anisotropy rel. to garden hose direction 3−25354
- density gradients in interplanetary space, for various propag. models *(Russian)* 3−12904
- diurnal anisotropy, long-term modulation by interplanetary magnetic field 3−31484
- diurnal anisotropy, quiet and enhanced characteristics 3−5546
- flux direction changes due to Earth motion through solar wind *(Russian)* 3−12900
- Forbush decreases, linear and nonlinear cosmic ray modulation theory *(Russian)* 3−12902
- Forbush decreases and connection with solar activity and interplanetary medium parameters *(Russian)* 3−12907
- Forbush effects, 7 Nov. 1970, 27 Jan. 1971, recorded *(Russian)* 3−12909
- galactic mag. field effects on cosmic rays above 10^{17} eV 3−25350
- intensity variation for types I and II meteor showers 3−3270
- long-term and short-term modulations 3−12891
- magnetic storm effects on intensity N-S asymmetry 3−34984
- magnetospherical and interplanetary origin, polar coupling coefficients *(Russian)* 3−12908
- modulation, residual, at 1954 solar minimum 3−9430
- neutron intensity at barometric pressure at Syowa station, Antarctica, effect of high winds 3−21996
- planetary orbital motion effects *(Russian)* 3−12873
- radiocarbon content of dated specimens, past cosmic ray var. study *(Russian)* 3−12901
- solar neutrons, correlations between intensity changes and sun-spots and mag. storms *(Bulgarian)* 3−34986
- solar neutrons, statistical anal. of continuous intensity measures *(Russian)* 3−34987
- solar wind, anisotropic, galactic cosmic ray modulation *(Russian)* 3−12903
- spatial, ^{37}Ar/^{39}Ar activity ratios, in Lost City stone meteorite 3−9138
- spatial var. from radioactivity data of meteorites in known orbits *(Russian)* 3−12887
- n component, calc. of partial coefficients and specific yield functions, altitude-latitude dependences *(Russian)* 3−12876
- n latitude distribution 1967-9, relationship to solar activity cycle *(Russian)* 3−12910

cosmic ray X-rays

- clusters of galaxies, relic radiation obs. as test of X-ray radiation nature 3−35171
- crystal spectrometer for rocket and satellite expts. 3−28303
- diffuse background meas., collimator corrections, comparison of S-11 and OSO-3 data 3−32135
- diffuse spectrum shape, origin of features at 40 keV and 1 MeV 3−37274
- low energy, detection by proportional counter 3−32163
- low energy diffuse radiation, galactic latitude dependence, correlation with interstellar hydrogen 3−12882
- low energy diffuse radiation at high galactic latitude, contamination-free results 3−12881
- metagalactic X-ray prod. by relativistic dust grains 3−31487
- nighttime D-region, ionization contribution 3−3091
- supernova remnants in the Lupus Loop and the diffuse background 3−13034
- transition radiation from relativistic electrons rel. to source of cosmic X-rays 3−31500
- X-ray spectra, review 3−18904

cosmic rays

- *see also cosmic ray absorption; cosmic ray apparatus; cosmic ray composition; cosmic ray effects and interactions; cosmic ray origin; cosmic ray showers and bursts; cosmic ray solar modulation; cosmic ray variations; galactic cosmic rays; nuclear reactions and scattering due to cosmic rays; primary cosmic rays; radiofrequency cosmic radiation; solar cosmic ray particles; solar radiation*
- book, tracing history of cosmic ray physics 3−12879
- differential spectrum meas., instrument characts. use 3−32137
- diffusion coeff. in interplanetary space, rigidity and heliocentric distance dependence 3−16075
- diffusion of charged particles in random magnetic field 3−31495
- diffusion theory, resonance integrals 3−37271
- gamma-ray flux meas., power law spectrum deviation, theoretical interpretation 3−18906
- hard rock cosmic ray archaeology 3−34981
- Japanese daily obs., summary of results for Oct. 1969 to Dec. 1971 period 3−39610
- kinetic equation for cosmic-rays in random magnetic field, breakdown of quasilinear derivation 3−31480
- lifetime of secondary nuclei rel. to ^{54}Mn decay 3−39575
- non-relativistic heavy cosmic ions, photometric charge discrimination in nuclear emulsion 3−315
- nuclei energy spectra differences, observational evidence 3−21990
- particle injection at $25<E<250$ MeV 3−3132
- radiation rates and Concorde, rel. to health hazard *(French)* 3−37533
- relativistic heavy ($Z\geqslant 74$) nuclei propagation 3−12919
- self-gravitating, non-rotating gas layer with stellar, mag. and cosmic ray components, linear stability anal. 3−28101
- storm of cosmic rays from August 1972 solar activity 3−21992
- transport props. in one dimension, random electric field effects 3−23813

cosmic X-rays *see cosmic ray X-rays*

cosmogony *see cosmology*

cosmology

- *see also black holes; element origin; general relativity; red shift*
- 3°K blackbody radiation, search for fluctuations at 2.8 cm 3−37305
- anisotropic cosmological model, hydrodynamic motions and vacuum stage 3−35010
- anisotropic cosmology and cosmic structure 3−28131
- anisotropic universe with torsion, Einstein-Cartan theory 3−22724
- astronomical rotation, conference, Bologna, Italy (1971) 3−25356
- big-bang, galaxy formation from annihilation-generated supersonic turbulence 3−16093
- big-bang nucleosynthesis rel. to cosmological models 3−28122
- black hole behaviour of universe, confined closed structure 3−5557
- black holes in an expanding universe 3−16112
- Brans-Dicke, solar rotation 3−25391
- Brans-Dicke and general relativistic cosmologies comparative study rel. to observationally measurable quantities 3−12943
- Brans-Dicke field equation, position-depend. Robertson-Walker solns. 3−22723
- Brans-Dicke flat space, observational constraints 3−37310
- Brans-Dicke theory and anisotropic cosmologies, Bianchi types I and IX, solns. 3−39598
- clusters of galaxies at different redshifts, core radii rel. to cosmological model 3−37449
- clusters of galaxies rel. to cosmic background light 3−31737
- cosmic numbers relative to models of the universe 3−25386
- cosmogony, planetary formation, floccule theory 3−12949
- CPT conservation in an oscillating universe model 3−16120
- De Sitter type cosmological models, consequences of field quantization 3−35006
- diffuse cosmic X-ray spectrum shape, astrophysical implications 3−37274
- Dirac's principle and variability of fund. consts. 3−6339
- Einstein's cosmology, Copernican character 3−22009
- Einstein equation, general cosmological soln. with time singularity 3−35011
- evolutionary corrections to q_0, effect of rate of change of stellar population turnoff magnitude 3−28282
- expanding radiation-filled universe, redshift magnitude relation 3−18925
- expanding universe, development of correlation of galaxies in Abell clusters 3−31515
- expanding universe, high-energy cosmic ray energy spectra 3−3273
- expanding universe, Hubble constant 3−9604
- expanding universe with matter injection from negative phase substratum 3−5558
- Faraday rotation of polarised radio waves from extragalactic sources 3−18924
- finite photon rest mass, difficulties rel. to cosmological redshift 3−22003
- Friedmann model evolution with radiation 3−12944
- Friedmann universe, dynamics using Regge calculus 3−37309
- Galactic age determ. using Clayton's ^{187}Os/^{187}Re chronology, ^{187}Os excitation state effects 3−28126
- galaxies and galaxy clusters, primordial random motions in expanding universe 3−37447
- galaxies with central black hole rel. to Newtonian analysis of initial cosmological perturbation 3−13091
- galaxy counts effects on evolution 3−18923
- galaxy formation, primordial turbulence in a Friedmann universe 3−16259
- gravitating sphere model, motion induced by internal stress 3−3288
- gravitation, Einstein theory generalization using $T^{\nu}_{\mu;\nu}=\lambda R$ 3−22726
- gravitation and relativity theory *(German)* 3−35012
- gravitation theory, solar system expts. 3−32433
- gravitational aberrations in stellar images 3−16220
- gravitational origin of strong interactions from general relativity rel. to universal creation 3−9457
- hadron era in cosmology for first 100 μ seconds in life of universe 3−28124
- Hot Big Bang model and properties of elementary particles in cosmic plasma 3−9460
- hot universe, effect of energy release on emission spectrum 3−25389
- Hoyle-Narlikar, magnitude-redshift relation for galaxies 3−28125
- integrated background light from distant galaxies, information content 3−35007
- intergalactic nongaseous H rel. to missing cosmological mass, critique 3−19054
- introductory book on astronomy 3−35000
- isotropy of universe rel. to initial arbitrary conditions and cosmological models 3−37304
- large numbers, cosmological significance 3−35008
- light element origin, review 3−31512
- lunar sample anal., biological significance rel. to cosmic evolution 3−35087
- magnetic fields origin in the early Universe 3−18926
- mixmaster universe, h.f. sound waves to eliminate horizon 3−25388
- mixmaster universe, tensor perturbation equations 3−9459
- model universe filled with magnetofluid 3−39590
- models, singularity and matter creation 3−39599
- multiple universes, props. of closed universe 3−25384
- neutrinos of nonzero mass, effect on gravit. dynamics 3−35005
- Noerdlinger hypothesis on diffuse X-radiation, comments 3−31511
- nonlinear gravitational growth in expanding gases 3−12937
- nucleosynthesis, big-bang, baryonic number and electron leptonic number in Universe, limits 3−25387
- opaqueness of various models, assessment of Wheeler-Feynman absorber theory 3−5556
- origin of microwave background, origin rel. to ordinary astronomical processes 3−28123
- particle size barriers 3−35009
- photographic plate information rel. to expansion of universe, deceleration parameter accuracy obtained using various telescopes 3−28130
- photon rest mass rel. to quasar and other abnormal redshifts 3−22004
- primeval adiabatic perturbations evolution, neutrino effects 3−31513
- primordial irregularities in early Universe 3−9458
- principle of reciprocity, consequences for red-shift test by search for blue-shifted lines in galactic spectra 3−16118
- protogalaxies, density fluctuations due to turbulence in self-gravitating media 3−34999

cosmic ray muons continued
cosmology continued
quantization of gravit. charge, from gauge invariance, solar neutrino discrepancy and QSO's 3—10379
quasars, angular diameters 3—3354
radio source counts in cosmology 3—28127
radiosource spectra, implications 3—37306
regular model universes, gravitational instability in modified theory of general relativity 3—28129
review of recent results and developments in theoretical mechanics and mathematical physics 3—16584
scalar tensor theory, vacuum solutions 3—3287
simpler cosmological models, derivation of differential equation 3—37308
singularity in Yilmaz-Tupper theory of gravitation 3—26141
space-time singularity, local structure, gravitational collapse 3—34997
spatially homogeneous gravitating medium, kinetic theory of small perturbations 3—37311
spinor field eqns. construction, in cosmological space *(Russian)* 3—5555
stars and gas, combined system, energy conservation for gravitational interaction 3—12938
steady state theory, radiosource counts and redshifts 3—12946
steady-state, Hoyle's electrodynamic version, evaluation of constants 3—39597
steady-state and Einstein-de Stitter, radio wave absorption 3—5559
structure in Universe, chaos 3—5554
superfluidity and superconductivity in Universe, fully covariant theory of charged superfluids 3—12940
thermal behaviour of matter and e.m. radiation in the universe 3—16119
transformation, model 3—5560
uniform models, classification 3—3290
Universe creation, use of red shift as age indicator 3—37312
universe model, using spin and torsion to avert gravitational singularities 3—28128
universe structure, entropy, averaged initial state, short waves, galaxy clusters, cold baryon 3—3289
universes with some intergalactic matter, distance-redshift relations 3—31514
Weinberg model, and hot Universe 3—16970
ν field-particle aspects, role of gravitational field 3—12948
ν_μ rest mass, calc. of cosmological limit 3—10827
^{205}Pb as chronometer for s-process nucleosynthesis, cosmochronology 3—37307
Re-Os cosmochronology, effect of recycling r-process elements through stars 3—28181
cosmotrons
No entries
Costa Ribeiro effect *see dielectric phenomena; phase transformations*
Cotton-Mouton effect *see birefringence; magneto-optical effects*
Cottrell atmosphere *see dislocations*
Couette flow
see also jets
absolute surface shear viscosity in Couette surface viscometers, finite ring thickness effects 3—1350
annular Couette flow of a suddenly pressurised viscoelastic fluid 3—33296
bounded shear flow, forces on flat plate, local circulation and global circulation 3—23741
generalised Couette flow of an elastico-viscous liquid between two co-axial porous circular cylinders 3—38378
laminar, nonrotationally symmetric modes excitation interval 3—14438
MHD, between conducting walls with heat transfer 3—4609
MHD, heat transfer 3—29897
nonlinear rarefied with heat transfer, gas statistical models with and without internal energy states 3—33259
oscillatory, stability investigation using linear theory *(German)* 3—11383
oscillatory, stability investigation using nonlinear anal. 3—11382
plane, in rarefied gas, heat transfer 3—14471
plane, stability to infinitesimal disturbances 3—23677
plane Couette-Poiseuille flows, application of special form of Galerkin's method to heat transfer problem 3—23699
plane flow with viscous heating, stability 3—26771
polarizable liq., induced viscosity changes theory 3—14441
stability of two-dimens. flow, Taylor-Goldstein eqn., Howard's technique 3—23676
stability of viscoelastic fluids, fluid model, overstability and disturbance form 3—11362
suspension, dil., of rigid spherical particles, stability of motions 3—20402
counter accessories
see also counting circuits
X-ray proportional counters, thin window supports 3—28666
counters
see also Cherenkov counters; counting tubes; crystal counters; Geiger counters; proportional counters; radiation detectors; scintillation counters; semiconductor counters; spark counters
active sample anticoincidence guarded Ge(Li) spectrometer low level radionuclide analysis 3—28773
astronomical instrumentation, conference (Tucson, Arizona March 1972) 3—31816
atmospheric condensation nuclei with continuous flux, meas. counter *(French)* 3—12858
cascade impactor, general expression of functional collector efficiency 3—16508
crystalline filamentary, development, expts. on Ar and Xe *(Russian)* 3—296
differential counter for changes in decay rate 3—19314
false peaks and resonance narrowing due to variable resolution 3—13444
gas flow, resolving time measurement, using time to amplitude convertor 3—318
halogen parallel plate, short dead time 3—25863
histological thin section meas. quantitative analysis *(German)* 3—37511
counters continued
ion pulse counting technique with a quadrupole mass filter *(Japanese)* 3—28508
lifetime expts. and pile up corrections 3—6050
multiple neutron distributions in cosmic ray neutron monitors 3—6086
neutron multiplication effects in coincidence well counter for Pu assay 3—19303
neutrons, track etch technique, betatrons for medical use 3—16561
nuclear radiation measurements, radiation detectors, particle detectors 3—297
particle size measurement and counting using television camera and computer *(French)* 3—15801
photographic process considered as a photon counting device 3—9978
pulse, rapid statistical test *(German)* 3—13423
radioisotope disintegration counting data processing, computer applic. 3—3883
shielded gas-discharge detectors, cosmic ray albedo electron spectrum characts. determ. 3—22446
time-of-flight resonance, Mossbauer effect meas. applic. 3—35515
timing system, digitally stabilized 3—10074
β-γ coincidence spectrometer, 4π geometry using Si(Li) and NaI(Tl) detectors 3—10078
counters (circuits) *see counting circuits*
counting circuits
see also coincidence circuits; pulse height analysers; scaling circuits
alpha spectrometer, in Apollo 15 and 16 3—31803
ballistic galvanometer, Si photoconvertor dosimeter, for X-ray examinations 3—35270
charge amplifier, field effect transistor applic. 3—28684
clinical radiometer, for dynamic processes using radioisotope method 3—35271
computer interfacing for real time data acquisition to PDP-8 minicomputer 3—393
cosmic rays, spark chambers for charge spectrum 3—28693
digital, reversible, to follow reversing signals 3—32179
digital arithmetic devices, for small angle scattering experiments 3—32182
digital processor, for high-energy experiments 3—37704
digitally controlled fast logic modules, CAMAC interface 3—28685
display network for multidigit counting devices 3—22478
ECL and TTL ICs 3—37698
eight-channel sample-and-hold unit, with multiplexed analogue output 3—32180
electron multiplier, 4500 V bias supply, for satellite use 3—28683
fast nuclear electronic modules, in CAMAC system 3—13441
flip-flops applications *(Czech)* 3—16525
four-stage synchronous counters *(German)* 3—10073
for ionisation chamber currents measurement, using MOS FET circuitry 3—32181
linear adding circuit, for Ge(Li) detectors 3—32196
multi-decade ferrite-transistor reversing counter 3—22477
multiwire proportional chambers, proceedings of meeting 3—32169
multiwire proportional counter, hybrid IC 3—28649
multiwire proportional counter, with integral readout delay line 3—28646
multiwire proportional counters, digitizing electronics 3—28652
multiwire proportional counters, high spatial resolution using e.m. delay line readouts 3—28647
nanosecond α-decays, fast pulsed beam meas. technique 3—35486
nuclear fuel, nondestructive assay, neutron interrogation system 3—19301
nuclear science, conference, Miami USA, (1972) 3—28622
photon counter and monochrometer drive for studies of optical spectra of gases irradiated by ionising radiation 3—19315
proportional beam hodoscope system 3—28650
proportional wire chamber readout, delay lines 3—19313
proportional wire chambers, electronics and readout systems 3—28648
pulse radiolysis expts., signal-compiling differential preamplifier 3—35535
random tail pulse generator, controlled voltage transitions 3—28686
ratemeter, strongly fluctuating pulse count rates, design *(German, English)* 3—6085
rocket borne astronomical X-ray obs., reduction of cosmic ray induced noise 3—13429
sequential, forwards counter in 8-4-2-1 code *(German)* 3—19311
stabilisation system, remotely controlled, for γ-ray spectrum 3—3862
supermonitor neutron recording channel, input circuit parameters and resolution time 3—32178
termination of electroanalytical expts. and resetting of instrument 3—6151
time analyser with high speed plated wire memory for pulsed neutron experiments 3—13440
timing system for high resolution time spectroscopy 3—3864
trigger device for fast events *(German)* 3—16523
tunnel diode ring counter 3—28689
γ-spectrum, on-line monitoring of specific-lines 3—13439
Ge(Li) detectors, counting circuit 3—13442
NaI(Tl) pulse timing, noise suppressed leading edge trigger technique 3—28651
T low-level counting, risetime discriminator 3—28682
counting tubes
see also dekatrons
No entries
country planning *see town and country planning*
county planning *see town and country planning*
coupled circuits
computer circuits and components, high-frequency effects, analysis for distribution of current and electric potential 3—29002
coupled networks *see coupled circuits*
coupled superconductors *see superconducting junctions*
couplers (electric connectors) *see electric connectors*
couplers (waveguide) *see waveguide couplers*
coupling (process) *see joining processes*
coupling circuits *see coupled circuits*

CP invariance
- boson pair model unification with $K^0{}_l \to \mu^+\mu^-$ and excess μ anomaly 3−16951
- five-dimensional theories approach 3−16948
- hyperon-antihyperon nonleptonic decays, upper limit on violation effects 3−19669
- lepton number nonconservation, influence on CP violation *(German)* 3−4148
- nonconservation in $K \to ll\gamma$ decays 3−4158
- relativistic wave eqns. of 2-component neutrino, CP and CPT noninvariance 3−16937
- renormalizable guage field model of weak and e.m interactions with CP-violation 3−10616
- time-reversal violating Lagrangian for nucl. reactions with e.m. interaction 3−16949
- violation, macroscopic effects of geometric scheme *(Russian)* 3−6560
- violation in dyon model 3−32630
- violation of e.m. states and field-current identity, connection with nonchiral SU(2) × SU(2) classification of hadron states 3−14037
- weak interaction renormalizable theory, CP-violation 3−35773
- weak interactions with maximal CP violation, W boson model 3−6575
- K decay, CP preserving phenomenology 3−10673
- K^0, nonlinear theory, time reversal and combined inversion *(Russian)* 3−38007
- $K^0 \to 2\pi$, self-contained determ. of phase of CP-invariant parameter η_{+-} 3−4162
- K^0 CP-violating decay, nonlocality and unitary transformation 3−38024
- $K^0 \to \pi\mu\nu$, CP-violating charge asymmetry 3−10670
- $K^\pm \to \pi^\pm\pi^0\gamma$, test of CP invariance 3−26290
- $K_l \to \mu^+\mu^-$, review of models and predicted branching ratio 3−32647
- $K_{s,l} \to \gamma\gamma$, CP violation 3−16992
- $K^0_s \to \mu^+\mu^-$ branching ratio for T, CP and CPT invariances 3−10664
- $K^0_s \to \pi^+\pi^-\pi^\circ$, search for CP violation 3−6583

CPT conservation *see CPT invariance*

CPT invariance
- arbitrary spin-wave eqns., proper Poincare invariance and invariance under discrete transformation and quantization 3−10619
- neutral-kaon decay test 3−19668
- P, T violating but C = PT conserving strong interactions, possibility of existence, Schwinger's dyon theory 3−14041
- parity and time reversal in gravitational interaction and existence of massless scalar particle 3−32629
- parity-violating e.m. interaction for hadrons 3−32663
- Poincare invariant eqns. for massive particles, P, T, C properties 3−19667
- relativistic wave eqns. of 2-component neutrino, CP and CPT noninvariance 3−16937
- strong interactions, C-invariant but P- and T-violating test using $\eta \to \pi\pi$ decay 3−13838
- universe, oscillating model, CPT conservation 3−16120
- validity in relation to $K^\circ{}_l \to \mu^+\mu^-$ puzzle 3−10668
- $K_l \to \mu^+\mu^-$ amplitude, effects of possible CPT violation 3−38022
- $K_{s,l} \to \mu\mu$, CPT constraints 3−4157
- $K^0_s \to \mu^+\mu^-$ branching ratio for T, CP and CPT invariances 3−10664
- K^0 decays, upper limit to T-conserving, CPT-violating amplitude 3−35775

crack detection
- *see also cracks*
- acoustic emission applic. to stress corrosion cracking 3−31216
- acoustic emission detection of flaws in steel, test 3−27824
- acoustic emission monitoring of end closure welds on Fast Flux Test Facility reactor fuel pin 3−27834
- acoustic emission technique for prediction of material failure *(Japanese)* 3−27843
- acoustic emission testing, following mechanical stress 3−27832
- acoustical holography for flaw detection in pressure vessel sections 3−27818
- alloys, computerized X-ray fluorescence spectrometer 3−10138
- angle probes for u.s. testing, resolution of flaw depth *(German)* 3−18777
- Armco iron, microcrack initiation in fatigued specimens 3−18745
- cement pastes and mortars, fracture toughness meas. methods 3−27813
- ceramics, acoustic emission testing for cracks when mechanically stressed 3−27832
- eddy current of cladding thickness of fuel rods 3−26510
- fatigue damage monitoring by u.s. attenuation meas. 3−13232
- fracture mechanics, role of nondestructive testing 3−27829
- liquid crystal application to temperature measurement for crack detection in aerospace industry 3−31222
- magnetic powder test with two alternating fields out of phase *(German)* 3−15810
- metal, thermoelectric method for determ. of specific work fracture, optimal placement of thermocouples *(Russian)* 3−8843
- nuclear reactor pressure vessels, acoustic stress-wave emission measurement 3−5790
- nuclear reactor pressure vessels, in-service inspection, u.s. techniques, equipment 3−5793
- nuclear reactor pressure vessels, remote inspection, u.s. techniques 3−5792
- photoelasticity dynamic in flaw detection analysis 3−27833
- polystyrene, injection-moulded, technique for demonstrating flaws at which fracture initiates 3−31164
- pressure vessles, residual stress measurement, automated X-ray diffractometer for 3−6121
- PWR pressure vessels, in-service inspection, u.s. instrumentation technique 3−5789
- reactor pressure vessel, hairline crack discovery by various methods 3−26495
- slow crack growth eval. technique 3−31217
- steel, 13 CrMoV 58, curing of fatigue cracks by local welding *(German)* 3−27684
- steel, reactor pressure vessel, deform. and fracture behaviour, acoustic emission meas. 3−34680
- steel, stainless, type 304, weldments at high temp., fatigue crack growth 3−34676
- structural (service) reliability, kinetic fracture models 3−21764

crack detection continued
- submerged arc weld testing device *(French)* 3−9036
- tubes for heat exchangers, eddy current testing by using an internal coil system *(German)* 3−18775
- tubing, steel clad, effect of small cracks on creep rupture props. 3−31221
- u.s., of dense ferrites for magnetic memory heads *(Polish)* 3−12491
- u.s. field meas. 3−2790
- welded bodies, meas. of damping coeff. by resonance method 3−18772
- X-ray, variation in radiographic parameters 3−27823
- X-ray variable focus tube, for studying stress corrosion cracking 3−28744
- Al, cracks in space vehicle cabin wall panels, detection by u.s. techniques 3−31227
- Al foils, electron microscope search for foreign inclusions and their role in crack and pin hole formation 3−21608
- Fe, cast, pipe, u.s. inspection 3−31223

crack inspection *see crack detection*

cracking *see fracture*

cracks
- *see also crack detection*
- acrylonitrile-butadiene-styrene/glass bead composite, stress-strain behaviour, crazing, permeability 3−24986
- aircraft structure, propagation analyses under stationary random excitation 3−553
- alloy, fatigue crack growth, effects of loading freq. and nonreactive external media 3−31234
- alloy, high-strength, fracture toughness role in low-cycle fatigue crack propag. 3−31047
- alloy system, stress corrosion cracking 3−15713
- alloys, stress corrosion test methods 3−9025
- anisotropic bimaterial plates, crack opening displacement, elastic const. depend. 3−17922
- biaxial cumulative fatigue damage, octahedral shear strain theory 3−31239
- β-brass, stress corrosion cracking, fractographic obs. 3−31042
- brass, stress corrosion cracking in citrate soln. 3−39358
- brittle, integral solns. for propagation at constant and accelerating speeds 3−32318
- brittle bodies, rupture in surface-active medium, crack growth kinetics *(Russian)* 3−27059
- brittle fracture, near stress concentrations, limiting equilibrium state for infinite plate *(Russian)* 3−28887
- brittle metal, central cracking during cold-extrusion, prevention by hydrostatic back pressure 3−24869
- brittle rectangular beam weakened by an internal circular crack, bending *(Russian)* 3−6243
- cast iron:Ce, Ce effect on resist. to cracking with quenching *(Russian)* 3−12411
- ceramic materials, Rumpf's physical fracture theory, Griffith and critical crack length, cell size, experimental *(German)* 3−12430
- outside circular inclusion, screw dislocation double pile-up treatment 3−20803
- inside circular inclusion, screw dislocation double pile-up treatment 3−24201
- closure obs. using simple strain gauge technique 3−24202
- composite, brittle matrix ductile fibre, fracture mechanics 3−31134
- composite material, two-component, initial stages of rupture, effect of form of inclusion *(Russian)* 3−27755
- composite materials, containing second phase dispersions, strength 3−7841
- composite materials, fracture problems and solns. 3−21725
- composite structures, fracture control technique 3−21726
- compressional modulus of material permeated by random distrib. of circular cracks 3−32340
- control by means of elastic waves *(Russian)* 3−11680
- coplanar, circular, in elastic solid, thermal stresses 3−22613
- cracklength, u.s. determ. during fracture toughness testing 3−13231
- creep rupture testing machine with electronic temp. control *(German)* 3−9834
- cylindrical shell with axial crack under skew-symmetric loading 3−22619
- damage induced by acoustic waves 3−2913
- dislocation pile ups against plane interfaces, anal. 3−17925
- Duralumin, fatigue crack growth 3−18750
- edge crack, normal to edge of strip, calc. of stress distrib., Fredholm integral eqn. 3−13571
- elastic body, rel. to wedge motion at constant super-Rayleigh subsonic velocity 3−22627
- elastic circular inclusion in infinite plate with two cracks, soln. 3−32316
- elastic disc edge crack, stress intensity factor by Mellin transform technique 3−13569
- elastic half space with embedded pennypshaped flaws 3−6229
- electrolytic coatings, brittleness testing 3−25657
- electron microscope examination of hot cracks 3−18577
- epitaxial growth, form. of cracks 3−11827
- extending, in elastic solid, energy flux into tip 3−32334
- extension force on deviating crack, detn. from infinitesimal dislocation considerat. 3−4793
- failure resistance curves *(Russian)* 3−7838
- fatigue, crack propagation, review 3−24961
- fatigue, growth rate estimation 3−27804
- fatigue, production for bending tests, work of rupture 3−27803
- fatigue, propagation rate analysis *(Japanese)* 3−11678
- fatigue crack growth, plastic strip method 3−21766
- fatigue crack growth behaviour under variable amplitude loading 3−21756
- fatigue crack growth data analysis 3−25028
- fatigue crack growth rate and theory, empirical laws *(Japanese)* 3−24815
- fatigue crack morphology at surfaces 3−31230
- fatigue growth monitoring, using acoustic emission technique 3−25040
- fatigue life estimation and crack propag. under stress *(Japanese)* 3−25030
- ferritic materials, fatigue crack propag., stress intensity and microstruct. influence 3−21580

cracks continued
finite rotating elastic disc, stress intensity factor and crack formation energy of edge crack 3—19428
finite strip problems, dynamic stress-intensity factors determ. 3—22626
formation at segregation rel. to fracture theory and precipitation thickness *(German)* 3—7837
fracture initiation criteria *(German)* 3—11679
fracture mechanics and stress corrosion cracking 3—8034
Griffith, perpendicular to 2-dim. elastic strip, soln. by Fredholm integral 3—22615
Griffiths crack in elastic strip, soln. of equilibrium eqn. by Fourier transforms 3—13567
growth rate obs., elevated temp. torsional fatigue testing future 3—5769
heat flow disturbed by 2-D crack in elastic strip, dual eqn. method 3—13566
homogeneous material, nucleation and propag., statistical features of time to break 3—1678
at interface of elastic half-spaces, opening displacement rel. to screw dislocation distrib. 3—24199
lacquer coating, brittle, crack form., coating thickness influence *(Japanese)* 3—18729
mechanical interaction between crack tip and point defect 3—36358
metal, b.c.c., plastic crack propag. *(Russian)* 3—20802
metal, cubic, cleavage in intrinsic dislocation dipoles 3—24204
metal, fatigue crack starter defects prod. by pulsed laser 3—21762
metal, plasticity effects in crack propag. 3—30195
metal, subcrit. crack branching implications 3—4796
metallic film, crevice formation during electromigration 3—4878
metals, H embrittlement 3—2723
metals b.c.c., cleavage crack nucleation at 'unlikely' twin intersections 3—17924
metals in liquid media, apparatus for long-term strength testing in corrosional cracking conditions *(Russian)* 3—9826
mica crystal, crack propag. using fracture mech. 3—7839
microcrack initiation, accommodation of stress field at grain boundary under heterogeneous shear 3—4792
nonlinear defect model of crack propag. in one-dimens. cryst. *(Japanese)* 3—20805
nozzle corner cracks in nucl. reactor vessel models, stress intensity factors 3—27847
nuclear piping systems, fracture mechanics applic. 3—19933
opening displacement and plasticity in shells 3—22666
optical material, transparent dielectric, laser induced damage rel. to cracks, pores, absorbing inclusions 3—35701
optical method of caustics for studying singularities due to uniform loads at crack tips 3—32320
Papkovitch-Neuber potentials, applic. *(Ddegae)* 3—32319
penny-shaped, diffraction of plane shear elastic wave 3—3990
penny-shaped, in homogeneous elastic sphere, stress distrib. 3—6206
photoelastic stress freezing technique for stress fields near crack tips, factors influencing data 3—19147
plane crack problems, convergence rate of stress intensity factor in finite element method 3—22616
plastic material, dynamic growth and fracture appl. 3—3972
plastic relax. at crack tip, influence of anisotropy and slip 3—24197
plate, uniformly stretched, plastic flow around expanding crack 3—13581
Plexiglas, elastic wave generation at crack tip rel. to energy reserve 3—20809
PMMA, cast, bubble inclusions effect on mechanical props., crack initiation at bubble surfaces 3—27789
PMMA, correl. of fracture data 3—20804
PMMA, fracture under complex stress, angled crack problem 3—24198
PMMA, growth, viscoelastic and thermal effects 3—24997
PMMA, spall cracks, microscopic obs. *(Japanese)* 3—21748
PMMA, stress crazing, statistical treatment 3—24998
PMMA sheets, growth of part-through thickness fatigue cracks 3—21734
point loaded disc, determ. of stress intensity factor of radial crack from soln. of Fredholm eqn. 3—19429
poly(ethylene terephthalate) film, linear fracture elastic mechanics, Dugdale model 3—34651
polycarbonate, delayed crack growth, environmental effect *(Japanese)* 3—21749
polycarbonate, statistical nature of craze formation process *(Japanese)* 3—7281
polyester resin, casts and laminates, fracture toughness, crack propag. 3—12454
polyethylene, fatigue test, propagation, stress depend., surface microscopy 3—31158
polyethylene, high and low mol. wt., struct. changes during deform. 3—20239
polyethylene in air and surface-active medium, crack propagation under creep conditions *(Russian)* 3—11676
polymer, fatigue, propagation and failure mechanism *(Japanese)* 3—12455
polymer, glassy, tensile strength rel. to stress crazing and brittle fracture *(Japanese)* 3—7280
polymer, morphology and macrocrack form. on fracture surfaces 3—20241
polymer, oriented, crack density increase rel. to tensile strain 3—31178
polymer, oriented cryst., morphology influence on submicrocrack form. 3—20240
polymer, stress ratio effect on fatigue crack growth *(Japanese)* 3—18728
polymer blocks, transparent, laser induced destruction 3—22936
polymeric composites, crack propag. vel. 3—21727
polymethyl methacrylate, statistical nature of craze formation process *(Japanese)* 3—7281
polymethyl methacrylate in surface-active medium, longevity dependence on rupture energy and crack size *(Russian)* 3—11677
polymethylmethacrylate, rel. to elec. breakdown *(Russian)* 3—2493
polypropylene film, isotactic, crazing, −210° to −140°C, environmental effects of N_2, O_2 and CO_2 3—27787
polystyrol, rel. to elec. breakdown *(Russian)* 3—2493
polyurethane soling, cut growth and fatigue 3—31156

cracks continued
propagating crack tip, point defect diffusion 3—7842
propagation between similar and dissimilar orthotropic media, nonlinear effect of initial stress 3—32338
propagation resistance, formation of angular cracks in cylindrical samples 3—27806
propagation under cyclic stress, fracture probability *(German)* 3—27060
propagation under nonstationary random excitation 3—574
Pyrex glass, carbon fibre reinforced, under stress 3—18700
quartz particles from post-glacial clay soils, h.v. electron microscope exam. 3—37161
Rayleigh pulses and boundary cracks interaction, investigation by a dynamic photoelasticity method *(Russian)* 3—30205
real engineering components, influence of local variations of yield strength on plastic zones at crack tips 3—21623
reinforced plastics with short randomly distributed fibres, failure mechanisms 3—24988
rock, propagation obs. using servo-controlled testing and miniature straddle packer 3—25329
rock beam, rel. to failure, exptl. 3—31308
rock beam, rel. to failure, theory 3—31307
sandwich plate, with part through debonding crack, stress analysis 3—13561
sapphire, spheroidization of tubular pores at high temps., reln. to surface diffusion 3—17921
seismic, longitudinal shear crack, cohesive force, Griffith's specific surface energy 3—9151
semi-infinite solid, infinite periodic sequence of relaxed cracks 3—36356
sharply notched plates, stress analysis technique and notch tip blunting meas. 3—19146
sheet materials, fracture kinetics, effect of order of applying fatigue crack and heat treatment 3—18621
slit-like, in anisotropic elastic media, fracture mech. 3—3959
stability and quasielastic concept 3—21759
under static loading, processes at crack tip, fractographic obs. 3—24200
steel:Cr, Ni, austenite, cracking due to high temp. creep 3—15694
steel, 13 CrMoV 58, curing of fatigue cracks by local welding *(German)* 3—27684
steel, 4340, fatigue crack growth rate, thickness and orientation effect 3—18646
steel, A-533-B, effects of crack size on gross-strain crack tolerance 3—8891
steel, AISI 4340, stress corrosion crack growth, stress history effect on incubation time 3—34585
steel, austenitic, fatigue crack initiation *(Japanese)* 3—12396
steel, austenitic, index of susceptibility to stress corrosion cracking, electromech. model 3—27643
steel, austenitic, type 304L, hydrogen embrittlement 3—2745
steel, austenitic stainless, fracture surfaces in stress corrosion cracking *(Japanese)* 3—34561
steel, austenitic stainless, stress corrosion crack propag. in hot chloride media 3—27651
steel, austenitic stainless, stress corrosion in HCl solns. 3—34553
steel, austenitic stress corrosion cracking, fractographic obs. 3—31042
steel, C, stress corrosion cracking, in nitrate and alkaline solns., temp. and inhibitors effect 3—27649
steel, carbon specimens in oil, fatigue crack propagation, numerical analysis 3—21614
steel, case hardened, effect of residual stress on fatigue strength *(Japanese)* 3—12400
steel, Cr-Mn, acoustic emission meas., crack tip plasticity characteriz. 3—34679
steel, Cr-Ni, wedge-crack growth during creep deformation 3—18582
steel, fatigue crack propag., microstruct. change at crack tip 3—21579
steel, ferritic stainless, stress corrosion cracking, heat treatment and comp. effects 3—31040
steel, He-implanted, annealed and cold-worked Type 316 stainless, fatigue crack growth 3—27706
steel, high strength, crack tip yielding during fatigue cycling 3—8882
steel, high-strength, crack vel. and fractography, heat treatment effect, stress intensity 3—5332
steel, high-strength, internal stress effects on susceptibility to stress corrosion 3—21692
steel, high-strength, stress-corrosion and corrosion-fatigue crack vels. 3—5324
steel, high-strength, tensile ductility, gaseous hydrogen influence 3—5323
steel, HY-130, corrosion fatigue crack propag., temp. and freq. effects 3—27660
steel, hydrogen embrittlement *(French)* 3—8905
steel, hydrogen induced cracking, effect on weld microstructures 3—39364
steel, influence of electrostatic field on rate of growth of fatigue cracks *(Russian)* 3—12368
steel, large forgings, primary heat treatment, shattercrack form. 3—24950
steel, low C, microcrack formation on machining unsuitability of continuum models 3—21656
steel, low carbon specimens, changes of residual stress due to slip band accumulation under fatigue loading 3—21578
steel, low-alloy high-strength, weld solidification cracking, O_2 role 3—21643
steel, low-C, effect of stress amplitude in fatigue processes in annealed and cold-rolled specimens *(Japanese)* 3—12405
steel, low-C, fatigue crack initiation process in notched specimens *(Japanese)* 3—21597
steel, low-C alloy, duplex microstruct. rel. to fracture behaviour 3—21646
steel, low-cycle fatigue properties, transformation of retained austenite and cracks 3—37060
steel, maraging for use in military bridge, fatigue crack growth and fracture 3—21626
steel, martensitic, stress corrosion cracking, interplay of hydrogen dissoc. and comp. 3—8904
steel, mild, config. of moving crack tip zones 3—30196

cracks continued
steel, mild, fatigue crack growth under crack opening displacement cycling 3−31046
steel, mild, grain size and stress distrib. effect on fatigue strength of notched specimens 3−8899
steel, Ni-Co-C, roll-extruded, effect of degrees of rolling reduction 3−31050
steel, notched, understressing and coaxing effects rel. to nonpropagating cracks *(Japanese)* 3−8866
steel, quenched U8, effect of various surface active media on the changes taking place in the strength *(Russian)* 3−2726
steel, rel. to fatigue curve discontinuities *(Russian)* 3−12367
steel, stainless, stress corrosion cracking 3−31039
steel, stainless, stress corrosion cracking and hydrogen embrittlement 3−5330
steel, stainless, type 304, deform. induced twin boundary crack form. 3−24857
steel, stainless, type 304, hold-time effects on fatigue crack propag. 3−8880
steel, stainless, type 304, intergranular crack propag., influence of deform. rate 3−21593
steel, stainless, type 403, corrosion fatigue metallography 3−27658
steel, stress corrosion, inhibiting action of mineral iodides *(French)* 3−1901
steel, stress corrosion cracking, role of hydrogen embrittlement 3−2736
steel, TRIP, subcritical crack growth in air under static loads 3−21629
steel austenitic, explosive bonded and hot rolled clad flat plates, residual stresses, sensitivity to stress corrosion cracking *(German)* 3−27837
steel balls, crack form. during quenching, effect of technological parameters 3−24951
steel for reactor applications, fatigue crack growth, effects of moisture, temp. and neutron irradiation 3−21596
steel weldments, crack growth, effect of synthetic seawater 3−15692
steels, high-strength, comparison of hydrogen embrittlement and stress corrosion cracking 3−21622
steels, influence of heat treatment *(Russian)* 3−12370
stress corrosion, test methods development 3−15808
stress corrosion crack propag., film rupture model 3−27663
stress corrosion cracking, acoustic emission applic. 3−31216
stress corrosion cracking, film rupture model 3−27662
stress corrosion cracking by H_2 embrittlement, lattice dilatation, complete elastic soln. 3−39353
stress corrosion cracking via surface diffusion, interface morphology development 3−34570
stress corrosion cracks, h.v. microscope studies 3−30981
stress intensity factor of crack in elastic solid, application of dual eqns. 3−32335
strip under uniaxial tension, central crack, stress intensity factor 3−13564
surface deformation and plastic yielding associated with deep semielliptical surface cracks in mode I loaded plates 3−21621
unbounded plate with collinear cracks, dynamic stress intensity factor 3−21760
uniformly moving, dilatation field, propag. velocity effects 3−4795
viscoelastic material, linear, crack propagation, comment on Cherepanov calc. 3−16622
weld heat affected zones, martensite tempering rel. to hydrogen cracking 3−8910
Westergaard eqns., modified, for plane crack problems, error 3−22625
Zircaloy, cracking due to localized texturing 3−34533
Zircaloy-2 in methanol-I_2 solutions, stress-corrosion cracking 3−24886
Zircaloys acoustic emission during stress corrosion cracking, correl. with fractography of cracking 3−31045
Ag, dislocation motion geometry at tip of spreading cracks 3−17918
Agl-Mg commercial alloys, stress corrosion cracking and its prevention *(Japanese)* 3−18635
Al, fatigue cracks, substruct. form. and propag. 3−21610
Al alloy, 7075-T6, vacuum environment effects on fatigue and fracture 3−27678
Al alloy, artificial slow crack growth under const. stress, R-curve concept in plane stress 3−31218
Al alloy, fatigue crack closure at positive stresses, plastic deform. in crack wake 3−14922
Al alloy, stress corrosion cracking initiation *(French)* 3−31083
Al alloys, corrosion fatigue in aqueous solns., fractographic studies 3−27656
Al alloys, crack propag. resist., −196 to +20°C *(Russian)* 3−27669
Al alloys, high-strength, hydrogen embrittlement and stress corrosion cracking 3−5336
Al alloys for aircraft structures, thermomech. processing effects 3−31048
Al foil, tensile and fatigue crack growth obs. 3−21761
Al Zn Mg Cu alloy, fibrous struct. and susceptibility to contact corrosion *(German, English)* 3−24354
Al-Mg alloy, effect of addition of Bi on stress-corrosion cracking *(Japanese)* 3−18634
Al-Mg-Zn alloy, microstruct. influence on stress corrosion susceptibility 3−39342
Al-Zn-Mg, corrosion fatigue inhibition, crack growth rate meas. 3−39352
Al-Zn-Mg alloys, grain boundary corrosion and stress corrosion cracking relationship *(Japanese)* 3−31072
Al-Zn-Mg alloys, SCC, soln. chem. influence on repassivation kinetics, alloying effect 3−27652
Al_2O_3, sapphire, gradient furnace growth method, crack nucleation 3−11572
Al_2O_3, thermally shocked, strength degradation and crack propagation 3−2752
BeO spheres, Al_2O_3 coated, neutron irradiation effects 3−4338
C, istropic pyrolytic, Young's modulus fracture stress, annealing effect, electron microscopy 3−24993
C fibre reinforced resin, crack propag. energy 3−8994
Cr-Ni alloys, two-phase, creep failure 3−27697

cracks continued
CrMnNiN austenitic steel, planar slip during plastic deformation *(German, English)* 3−24132
Cu, vacuum influence on stages of fatigue failure *(Russian)* 3−24874
Cu and Cu-Al(7.9 wt.%) alloys, corrosion fatigue crack initiation 3−27661
Cu-Ni (10 wt.%) alloy, stress corrosion resist. in ammoniacal environment, effect of Fe 3−31041
Cu-Ni alloys, weld cracking and ductility-trough phenomenon 3−21637
Fe, Armco, coarse- and fine-grained, fatigue crack formation and propag. *(Russian)* 3−27671
Fe, b.c.c., crack extension by bond rupture 3−15724
Fe, b.c.c., temp. effect on crack extension, model approach 3−30199
Fe, hydrogen-induced surface blisters and internal cracks 3−39349
Fe, microcrack form. around inclusions during solidification 3−34537
Fe, polycryst., failure mechanism under plane stress conditions at low temps. 3−31096
Fe-Cr alloys, stress corrosion cracking 3−31039
Fe-Cr-Ni alloys, austenitic, hydrogen charging and effects *(French)* 3−2747
Fe-Ni-Al alloy, microstructure and fracture *(Japanese)* 3−15672
$FeCl/H_2O$ frozen soln., glass transitions study by Mossbauer effect and DTA 3−38540
$Fe(ClO_4)/H_2O$ frozen soln., glass transitions study by Mossbauer effect and DTA 3−38540
GaP, rel. to liquid encapsulated Czochralski growth of constant diameter crystal 3−12319
Mg central cracking during cold-extrusion, prevention by hydrostatic back pressure 3−24869
Mg hydrostatic extrusion, critical back pressure to prevent central cracking 3−21615
Mg-Al alloy, transgranular stress corrosion cracking 3−30983
NaF crystal proton bombardment, average projected range meas. 3−1654
Ni, u.s. irrad. and annealed, struct. changes *(Russian)* 3−15718
Ni and Nichrome, thoria dispersed, l.p. hydrogen gas influence on fatigue crack growth 3−39347
Ni-Cr-Mo martensitic steel, fatigue crack propagation law in water *(Japanese)* 3−18642
Ni-Mo alloy electrolytic deposits, exptl. parameters depend. *(French)* 3−5287
Si crystals, crack propagation disclosed by X-ray Pendellosung fringes 3−17917
Si_3N_4, fracture surface energies meas. 3−15738
Si_3N_4 ceramics, high temperature strength slow crack propagation 3−8958
Ti, stress corrosion cracking in methanol/HCl mixture, fracture 3−27650
Ti alloy, TA6V, stress corrosion cracking and hydrogen embrittlement *(French)* 3−8907
Ti alloys, cleavage cracking mechanism under loading hydrogen embrittlement 3−18653
Ti alloys, corrosion fatigue in aqueous solns., fractographic studies 3−27656
Ti-Al-V alloy, stress corrosion crack propag., fractographic obs. 3−31043
Ti-Al-V and Ti-Al-V-Sn alloys, corrosion fatigue crack propag., freq. and wave form effects 3−27659
YIG:Ga, L.P.E. growth, effect of substituting Gd(Sm)(La) for Y 3−1924
Zr, hydride embrittlement behaviour 3−8909
Zr alloy, fuel element sheath, stress corrosion cracking in J_2 3−29447
Zr alloy, stress corrosion, environmental effects 3−31082

cranking model
moment of inertia in microscopic theory of nucl. rot. *(Russian)* 3−17174
muonic rotational nuclei, recalc. of hfs constants in cranking model 3−38113
phonon, axially deformed nucl., ground band rot. energies calc. 3−26408
rare-earth nuclei, change of radii due to rotation, calc. of Mossbauer and muonic isomer shifts 3−26368

creation hypothesis, continuous *see cosmology*

creation of electron pairs *see electron pair production*

creep
see also anelasticity; plastic deformation; slip
activation energy during creep and recovery mechanism 3−14917
Al, grain boundary fine structure, bright and dark field transmission electron microscopy 3−1632
alloy, AMG-3, creep with weak strengthening under nonsteady temp. and force conditions 3−31100
alloy, two-phase lamellar structs., thermal stability 3−37012
alloys, commercial, high temp. metallographic exam. 3−5309
alloys, high temp. Ti-, Co-, and steel, cyclic creep-rupture behaviour 3−18650
alloys, metastable effect of overheating on creep resistance 3−21707
brass, f.c.c., grain boundaries and surface tensions meas. by zero creep method 3−34543
ceramic, test evaluation method, computer appl. *(German)* 3−31214
chemical stress theory 3−17916
circular plates, influence of finite-deformations on creep behaviour 3−28896
coated materials strength and creep testing apparatus for temps. above 1400°C 3−32047
compliance and relaxation modulus improved numerical interconversion 3−534
constitutive eqns. for inelastic behaviour of components of fast breeder reactors 3−26524
corundum ceramic, densely sintered, third-stage creep *(Russian)* 3−15744
cylinders and spheres under internal pressure with steady radial heat flow, reference stresses and temps. 3−28893
damage rules, study 3−1675

creep continued
- deformation bounds for creeping structure approaching rupture, energy principle relation 3 – 30191
- diffusion creep inhibition by precipitates 3 – 20799
- diffusion of point defects to propagating crack tip, rel. to creep rupture by cavitation 3 – 7842
- discs, reference results for plane stress creep behaviour 3 – 10299
- domain wall creep rate under unipolar field action along axis of hand magnetisation 3 – 38994
- elevated temperature and slowly time varying loads, inelastic stress-strain law 3 – 25027
- fast-breeder and fusion reactors, neutron void swelling 3 – 17322
- f.c.c. metals, steady-state creep rate, correl. with substruct. misorientation and stacking fault energy *(Russian)* 3 – 8837
- fibre composite, review of creep theories 3 – 15774
- fibre composite with metallic matrix, creep props. above 800°C 3 – 18696
- fibre composites and dispersion hardening of alloys rel. to creep props. 3 – 15773
- flow, incompressible viscous fluid, past deforming sphere 3 – 4545
- glass reinforced plastic cylindrical shells, creep stability under long-term external press. 3 – 31144
- glass reinforced plastic plates, bending, finite difference method with allowance for creep 3 – 27762
- grain boundary sliding in polycryst. specimens, meas. methods 3 – 21601
- grain boundary sliding on deform. at high temp. to directional diffusion creep 3 – 14860
- grain boundary sliding role, phenomenological theory 3 – 33598
- graphite in reactor, irradiation induced creep at high temp., review 3 – 14896
- high temperature materials characteriz. for chem. industry 3 – 8919
- high temperature materials technology rel. to stress-rupture props. 3 – 8917
- Inconel alloy X-750, precip. parameters role upon creep rupture props. 3 – 37024
- ionic crystals, diffusion creep in pure, impure and non-stoichiometric materials 3 – 36355
- irradiation creep due to interstitial loop growth 3 – 17812
- laminates, glass reinforced epoxy and polyester, creep mechanism 3 – 9000
- loaded uniaxial tension panels containing holes under plane stress conditions, time hardening creep solution 3 – 22606
- mechanics, application of energy theorems, stress/strain relaxation 3 – 38615
- metal, cyclic creep fracture in low cycle fatigue *(Japanese)* 3 – 25029
- metal, diffusional creep in presence of independently acting vacancy source *(Russian)* 3 – 7830
- metal, dislocation creep, multi-axial and reversing stress effects, mech. eqn. of state 3 – 8916
- metal, dispersion strengthened, review of high temp. strength and creep mechanisms 3 – 15695
- metal, during supercond. transition, strain delay time 3 – 8304
- metal, hardness-temperature relationships, stress coeff. 3 – 34557
- metal, polycrystalline, hydrostatic press. effects at room temp. *(Japanese)* 3 – 12404
- metallic materials, creep behaviour of room temp. and stress-strain curve connection *(German)* 3 – 2734
- metallic springs, irrad. creep in materials testing reactor 3 – 27809
- metals, b.c.c., neutron irradiated creep mechanism 3 – 34541
- metals, empirical constants calc. in the Dorn equation 3 – 34547
- metals, unit for torsion investigations at room and high temps. 3 – 35358
- mullite, polycryst., ultra fine grain, four point bending obs. 3 – 2755
- neutron radiation enhancement mechanism 3 – 20800
- Nimonic alloy, notched creep strength, microstruct. effects 3 – 8932
- Nimonic PE16 alloy, neutron irrad. creep behaviour 3 – 8931
- non-fissile materials, neutron irradiated, theory of creep 3 – 17293
- nonfissile metals and alloys, high neutron exposures, effects, void swelling and radiation creep, review 3 – 24164
- nonlinear, integral eqns. for different load paths 3 – 30192
- nuclear fuel, hot cell testing, remote technique, equipment 3 – 17309
- nuclear fuels, in-reactor creep study at high fission rates using instrumented capsule 3 – 19945
- nuclear reactor, in-core component creep, prediction from post-irradiation data, life-fraction method 3 – 26523
- nuclear reactor materials, neutron irradiated, diffusion controlled creep process 3 – 24196
- nuclear reactors, inelastic materials in high-temp. structural anal., problems involved 3 – 26497
- permalloy cross-tie walls density influence on domain boundary creep *(Russian)* 3 – 2315
- pipe, straight, eff. of bending and internal pressure 3 – 16645
- plastic shells, creep stability, modelling 3 – 26092
- plastics, in air and NaCl solutions under bending and compression conditions *(Russian)* 3 – 12448
- polycaproamide fibres, creep behaviour during homogeneous cold drawing 3 – 21739
- polycrystalline solid, grain boundary sliding rel. to diffusional creep 3 – 17840
- polyethylene in air and surface-active medium, crack propagation under creep conditions *(Russian)* 3 – 11676
- polymer, glassy, delayed yielding, theoretical description 3 – 31165
- polymer, linear unoriented, creep in tension, compression and torsion 3 – 31176
- polypropylene, comparison of single-integral nonlinear viscoelasticity theories 3 – 519
- polystyrene, high-impact and blends with poly(2,6-dimethyl-1,4-phenylene oxide), strain damage 3 – 37094
- polystyrene-polyphenylene oxide plastics, rubber toughened 3 – 18724
- polyvinylchloride, comparison of single-integral nonlinear viscoelasticity theories 3 – 519
- pulsating stress creep rupture, nonlinear damage law proposal 3 – 31237
- rarefied gas between parallel plates, Poiseuille flow and thermal creep 3 – 38394
- reactor core, deformation due to irradiation enhanced and thermal creep 3 – 6998
- refractories, superplasticity *(Russian)* 3 – 2757

creep continued
- rigid-plastic shell, load carrying capacity *(Russian)* 3 – 19449
- rigidity of thin isotropic cylindrical shell of elliptic x-section *(Bulgarian)* 3 – 13584
- rubbery polymers, rheological props. at low shear stresses 3 – 27777
- rupture testing machine with electronic temp. control *(German)* 3 – 9834
- slightly redundant structures, stress field analysis 3 – 37816
- steel:Cr, Ni, austenite, cracking due to high temp. creep 3 – 15694
- steel:VN, B, stainless austenite, precipitation hardening rel. to creep resist. 3 – 15697
- steel, austenite, isothermal decomp. products characts. 3 – 21673
- steel, austenitic, γ' hardened, transient and steady state creep mechanisms 3 – 8913
- steel, austenitic, Cr-Ni-Mn, ageing and creep rupture behaviour 3 – 8927
- steel, austenitic, Cr-Ni-Mo, Ti-stabilized, creep strength behaviour 3 – 8928
- steel, austenitic, microstruct. changes during creep deform. at 600°C 3 – 8921
- steel, austenitic, Nb-stabilized, low stress creep behaviour 3 – 8926
- steel, austenitic, preliminary thermocycling influence on hot strength 3 – 31101
- steel, austenitic stainless, creep rupture props., niobium carbide effect 3 – 12415
- steel, austenitic stainless, Nb-stabilized, creep strain effect on stacking fault precip. 3 – 8924
- steel, austenitic stainless, Nb-stabilized, stress varied creep behaviour 3 – 8925
- steel, austenitic stainless, neutron irrad. creep behaviour 3 – 8931
- steel, austenitic stainless, stabilized, Nb conc. depend. of steady-state creep 3 – 8923
- steel, Cr-Mo-V, cyclic straining influence on creep behaviour 3 – 12416
- steel, Cr-Mo-V type rotor forgings, empirical relations between creep strain, stress, time and temp. 3 – 8918
- steel, Cr-Mo-V-Nb, nickel content influence on struct. and high temp. props. 3 – 8937
- steel, Cr-Ni, secondary creep deform. mechanism, stress and temp. depend. 3 – 8938
- steel, Cr-Ni, wedge-crack growth during creep deformation 3 – 18582
- steel, Cr-Ni type, dislocation distribs. during creep and recovery at 700°C 3 – 8920
- steel, Cr-Ni type, dispersed phase effect on creep strength 3 – 8914
- steel, dispersion-strengthened ferritic alloys for high-temp. applics. 3 – 8936
- steel, elec. resistivity and coercive force obs. *(German)* 3 – 34609
- steel, ferritic, Mo-containing, comp. and microstruct. effects on creep strength 3 – 8933
- steel, ferritic creep resistant, strengthening mechanisms 3 – 8934
- steel, fine struct. during deform. and ageing *(Russian)* 3 – 8838
- steel, Kh18N10T, study at low temp. 3 – 24917
- steel, low alloy, containing vanadium carbide, microstruct. effects 3 – 8935
- steel, maraging stainless, Almar 362, viscoelastic analysis of in-pile stress relaxation 3 – 18628
- steel, recovery creep model based on dislocation distribs. 3 – 8912
- steel, stainless, Cr-Ni, Nb-stabilized, steady state creep, temp. depend. 3 – 8922
- steel, stainless, time and cycle dependent failure at elevated temp. 3 – 31240
- steel, stainless, type 304, deform. induced twin boundary crack form. 3 – 24857
- steel, stainless 304, heat-to-heat variations of creep, in range 500 to 650°C 3 – 27708
- steel, stainless 304, hold-time effect in high temp. fatigue fracture 3 – 27707
- steel, stainless austenitic, behaviour under continuous or repeated stress *(French)* 3 – 24914
- steel, struct. stability during high temp. creep 3 – 8915
- steel, temperature depend., anelastic, effects on grain boundaries, interior of grain 3 – 31036
- steel, type 304(+15% Ti), post irrad. creep-rupture and tensile props. 3 – 17915
- steel and high temp. alloy creep strength, conf., Sheffield, England (Sept. 1972) 3 – 8911
- strain data analysis, numerical methods 3 – 34695
- structural hardening calc. procedures and thermal strength problems 3 – 32347
- structures subjected to steady load operating in creep region, bounds on life 3 – 28895
- superplastic metals determ. of deformation mechanism 3 – 1673
- test extrapolation, model considerations *(French)* 3 – 25032
- testing, compression and tension, with recording of deformation diagrams 3 – 27799
- testing machines, throughput capacity increase 3 – 25659
- thin plates, creep bending analysis by finite element method 3 – 16653
- time-hardening material under variable loading, deform., displacement and work bounds 3 – 22671
- torsional and tensile meas., apparatus 3 – 22258
- transversely isotropic bodies subjected to time-dependent loading 3 – 39368
- tubes, testing stand for strength and creep 3 – 27800
- tubing, steel clad, effect of small cracks on creep rupture props. 3 – 31221
- turbine blade materials, behaviour under asymmetric loading 3 – 31232
- viscoelastic hollow thick-walled cylinder under conditions of nonlinear creep, stressed state 3 – 35576
- viscous flow, through circular tube of nonuniform cross section 3 – 7338
- Zircaloy-2, in-reactor tubular creep, 260-300°C 3 – 32946
- α-Zr, high temp. creep interpretation in terms of effective stress and dislocation dynamics 3 – 27681
- Ag, grain boundary migration under compression at 500°C 3 – 37042
- Al, creep under intermittent loading 3 – 37103
- Al, creep-deformed, dislocation struct. of subgrain boundaries 3 – 24121
- Al, high temp., internal stresses and dislocation structure 3 – 7832

creep continued
Al, steady state, strain transient slip test obs. 3−7833
Al, subgrain boundary misorientation, determ. from split Kikuchi lines 3−24009
Al, substruct. formation kinetics 3−39344
Al alloy, long-term strength, deform. criterion 3−31233
Al alloys, creep rupture testing 3−21652
CoNiFe film, low-freq. rel. to domain wall motion 3−36738
Cr-Ni alloys, two-phase, creep failure 3−27697
Cu, continuously cast, fracture surfaces produced by high temp. creep 3−34535
Cu, continuously cast, high temp. creep cavitation mechanisms 3−34536
Cu, electrodeposited films, rate and strain thickness dependence *(Russian)* 3−11674
Cu, grain boundary influence in creep deform. 3−14880
Cu wires with electrodeposited Cu coatings, diffusional creep *(Russian)* 3−31059
Cu-Al solid solns., high temp. steady state creep deform. behaviour *(Japanese)* 3−31076
Cu-Ni(Sn) alloys, diffusional creep 3−24195
Fe, cast, spheroidal graphite austenitic, microstruct. effects on creep-rupture props. 3−8929
α-Fe, grain boundary sliding in creep, investigation 3−21612
Fe, high-purity, const. mag. field influence, dislocation-domain wall interaction *(Russian)* 3−36774
Fe alloys containing Mn, Mo and Cr, creep strength 3−21640
Fe-Ni-Cr alloy, grain boundary internal friction spectra, relax. phenomena 3−37028
Fe-Si (3 at wt.%), Al_2O_3 dispersed, Newtonian viscous creep 3−31094
Fe_2O_3 polycrystalline powder ceramic, stress, high temp., grain size, porosity and O_2 partial pressure effects on creep 3−27738
α-Hf, low temp. deformation, thermal activation parameters determ. by differential stress creep expts. 3−31088
LiF single crystal (pure and Mg-doped), temp. depend. of steady state deform. rate 3−17846
Mg dislocation creep 3−8871
Mg single crysts., high temp. creep, struct. changes *(Russian)* 3−14920
MgO, creep-deformed, dislocation structures, transmission electron microscopy 3−38593
MgO, secondary creep props., depend. on stress 3−14918
MgO single crystals, dependence on dislocation substructure 3−7829
MgO:Fe, polycrystalline, transient creep rate 3−7831
Mo, primary creep, high temp. analysis 3−34531
Mo single crysts., deform. and slip system type *(Russian)* 3−14919
Nb-Mo solid soln., Mo alloying effect on high temp. creep characts. 3−37069
Ni, neutron irrad. creep behaviour 3−8931
Ni alloy, 713C, effects of σ-phase formation 3−24883
Ni alloy, grain boundary pore form. correl. with internal friction *(Russian)* 3−24877
Ni alloy, Nimonic 80A, method of predicting creep life 3−15710
Ni alloys, struct. stability during high temp. creep 3−8915
Ni-Co-(2.5 wt.%)Al_2O_3 alloys, creep, behaviour 3−8870
Ni-Cr base alloys, precip. hardened, struct. factors influence on creep strength behaviour 3−8930
Ni-rich alloys, superrefractory, instability aspects, cooling effect on creep strength, crystallization, precipitation and microtoughness *(French)* 3−18660
Ni-W(6 wt.%) solid soln., environment and grain size effect on creep behaviour 3−37057
Ni_3Al(Ti), precipitation influence on creep rate and dislocations 3−15680
Pb-Sn alloy, superplastic, const. stress creep and const. true strain-rate tensile tests 3−21650
α-Pu, recovery creep and ductility transition 3−26508
Ti alloys, characts. under varying loads 3−37068
TiC powder, creep during hot pressing *(Russian)* 3−27747
$(U,Pu)O_{2-x}$ fuel pellets, compressive creep 3−6991
UC, device for creep meas. under axial compression and neutron irradiation up to 1150°C *(Italian)* 3−19148
$UO_{2\pm x}$, polycrystalline, stoichiometry influence on compression creep 3−6992
W, wire, elongation, creep tests, doping effects *(Hungarian)* 3−24894
W composite cast heat resistant alloys, rupture strength 3−24989
W fine wire with thoria dispersion, creep behaviour 3−37086
W wire, recrystallized, creep and durability 3−31151
W-Re(25 wt.%) alloy, l.p. oxygen effect on high temp. creep props. 3−34569
Zn, low temp., influence of quantum effects 3−1674
Zn, pure and impure, grain boundary migration role 3−34527
Zn-Al (22 wt.%), superplastic, room temp. creep behaviour under bending and plane conditions 3−34678
Zr alloys strengthening by mobile dislocations and gas bubble interactions 3−34615
ZrC, high-temp. creep characts. 3−37088
ZrO_2, CaO stabilised, expt. obs. 3−27740

crestatrons *see travelling-wave-tubes*

crevices *see cracks*

crimping
No entries

critical constants, thermal *see thermal critical constants*

critical mixtures *see solutions*

critical opalescence
macromolecular soln., critical slowing down and correl. of conc. fluctuations near crit. mixing pt. 3−2792
phenol-water binary mixtures in two-phase region, crit. light scatt. asymmetry 3−4844
thermostat for optical meas. near crit. unmixing pt. of solns. 3−22280
Ar, gravitational effects on small-angle X-ray scatt. 3−20867
^4He, critical opalescent light scatt. near gas-liquid critical point 3−1854
NH_4Cl, rel. to domain growth mechanism 3−24667

critical path analysis
see also project engineering; systems analysis
radioactive waste disposal, assessments, critical pathways and working limits 3−32994
radioactive waste disposal control, aquatic environment 3−32957
radionuclide discharges to atmosphere, critical pathways and working limits 3−32794

critical phenomena
heading is late addition, see also thermodynamics
see also magnetic transitions of substances; phase equilibrium; phase transformations
Bose-Einstein condensation of one-dimensional gas of spinless bosons with random impurities, thermodynamic treatment 3−19512
critical indices with long range interactions, interdimensional scaling laws 3−38656
electron mobility in simple fluid near critical point 3−21044
equation of state near critical point 3−22795
equations for critical indices, derived using liq.-droplet model 3−16778
exponents, critical, multivalued and unique aspects 3−19541
exponents and scaling relations in 1/n expansion 3−35648
external field influence on the interface position of two phases near the critical point *(Russian)* 3−26184
fluid parametric eqns. of state 3−32466
fluids free energy near critical point 3−16772
four dimensional restriction of critical exponent relation validity 3−32453
interdimensional scaling laws 3−19542
Ising model with dilute impurities, critical properties 3−27349
Ising model with spin $S>1/2$, low temp. behaviour 3−30591
Ising system, correlation length divergence along crit. isotherm 3−32468
isotherm, in Ising model, scaling theory test 3−18307
light propag. theory in systems with high spatial inhomogeneity 3−22846
liquid, long-range three-particle correlations at crit. point 3−22794
long-range interactions, critical exponents 3−35647
multicomponent fluid system, transport coeff. near crit. point 3−4047
order parameter dynamics, departures from Ornstein-Zernicke behaviour 3−19543
pair correl. function asymptotic near crit. pt. *(Russian)* 3−6390
perturbation theory application 3−35646
real gas, Carnahan-Starling eqn. of state, crit. parameters effect 3−37916
renormalization group, in large N limit 3−35626
scaled free energy in crit. region, divergent terms 3−6385
scaling eqn. of state for systems with tricrit. pt. 3−4051
scaling laws, analogy with high energy collisions 3−10780
scaling laws connecting tricrit. and normal crit. exponents 3−28997
series analysis, comparison of methods used in critical phenomena theory 3−32469
series analysis, generalised and extended methods, application ot Ising model 3−32470
skeleton graph expansion of critical exponents 3−16779
stochastic spherical model, critical behaviour 3−28993
symmetry of crit. exponents *(French)* 3−19536
thermodynamic scaling hypothesis, corrections for generalization around crit. point 3−6382
three-dimensional system, crit. parameter $\delta(=5)$ 3−32454
transitions with $n=-2$ components of order parameter, critical exponents 3−28994
tricritical points, double-power scaling functions 3−38661
tricritical points and type-three phase transitions 3−32467
Wilson type expansions of critical exponents for long range interactions 3−13661
$HgCr_2S_4$, critical broadening of e.p.r. line near Curie point 3−21294

CRO *see cathode-ray oscilloscopes*

crocidolite *see asbestos*

cross-sections (nuclear) *see nuclear reactions and scattering*

crowdions *see interstitials*

CRT *see cathode-ray tubes*

crushing strength *see compressive strength*

cryogenic pumps *see cryopumping*

cryogenics
see also cryopumping; cryoscopy; cryostats; cryotrons; Joule-Thomson effect; liquefaction of gases; low-temperature phenomena; low-temperature production; low-temperature techniques; refrigeration; superconductivity
appl. to refrigeration plant delivering 10 kW at 25 K, gas bearing cryogenic expansion turbines 3−5833
axial rubber seal, vacuum 3−143
closed-cycle refrigerator, for Ge γ-ray spectrometer 3−32199
cryochemical process, freezing droplets of aqueous solution 3−9872
cryorefrigerator, small capacity valveless piston expansion engine type 3−5838
cryotribometer, apparatus for meas. dry friction at low temperatures 3−5755
dewar, finger, for e.p.r. meas. 3−22296
dilution refrigerator for low temp. nucl. polarization expts. 3−9878
distillation of He isotopes 3−5841
engineering, conference (Eindhoven, Netherlands, May 1972) 3−5826
enhanced cooling of cryogenic electrical leads, comments and critique 3−5822
e.p.r. resonator for 8 mm band with specimen interchangeability at liquid He temps. 3−6043
expansion ejector use in 5-W refrigerator at 1.8 K 3−9883
gamma ray thermometry 3−9884
Gifford McMahon cycle, development and principles, self-operated cryocooler, development and operation 3−133
heat exchanger using sintered Cu, experiments with superfluid He 3−28501
heat exchangers for dilution refrigerator, phonon passage through thin foils 3−5844
heat exchangers for dilution refrigerators 3−5843
heat transfer and flow friction characteristics of dense mesh wire screen regenerator matrices 3−9881

cryogenics continued
insulating materials, physical properties, at cryotemperatures 3—9996
insulating moist capillary-porous multicomponent materials, thermophysical props. 80-400 K 3—134
Irtran 6, cryogenic window, for vacuum use, capable of temp. cycling 3—5825
liquid hydrogen, handling, transport and storage, experience 3—3774
liquid level indicator, design *(French)* 3—22297
liquid N level control in dewars, automatic device 3—5821
low temp. refrigeration, developments, review 3—5827
magnetic gradiometer based on superconducting quantum interference device, construction 3—28499
mechanical thermal switch for using cryostat between 4 and 650 K 3—5823
metals and alloys, cryogenically worked, properties 3—31037
multisensor temp. probe, for medial application 3—6147
reciprocating expansion engine 3—5835
remotely operated electromechanical switch 3—5848
rotating superconducting field coils for superconducting machines, cryogenic aspects 3—5845
sealing methods for repeated cooling 3—37602
shock tube development 3—22572
shuttle heat transfer problem 3—5839
spectrophotometric Cryotip 3—28546
steel for cryogenic technology 3—24916
support, low heat leak temp. stabilized column type 3—22295
systems for supercon. LINACS and particle separators 3—9882
temp. controller for use with resistance thermometers from 0.3 to 6 K 3—5820
thermal insulation, review 3—22293
turbine flowmeters, for supercritical He, operation and calibration 3—6175
turbo-expander as cryogenic tool in oil and gas industry 3—5834
two-stage expansion engine with differential piston 3—5837
two-stage Stirling cryogenerator with unbalanced refrigerators as precooler 3—5836
vacuum insulated cryocable installations, thermal and electrical insulation 3—5818
vacuum seal, current input lead 3—142
Al conductor, purity, u.s. nondestructive test *(Polish)* 3—68
H_2 refrigerator for 20 K region with $LaNi_5H_x$ thermal absorption compressor 3—5842
^3He dilution refrigerator with condensation pump 3—5819
^4He, PV isotherms at low temps., 2-20K 3—3773
$LaNi_5$-hydride, thermal absorption compressor for H refrigerator *(German)* 3—28503
Nb_3Al, Nb_3AlGe, fabrication studies, super conductors 3—8317

cryopumping
adsorption characteristics of condensed Ar, NH_3, CO_2 and ethane 3—8022
cryopumping, appls. and developments, review 3—5828
molecular flux distribution in cylindrical space simulation chamber with spherical gas source 3—9916
multiple cooling with one cryogenerator, distribution system 3—5846
review, of cryosorption and condensation pumps 3—37612
supercavitating pumps 3—22294
tests for Indiana Univ. 200 MeV cyclotron beam line 3—13368
ultrahigh vacuum pump with low liquid He consumption 3—35388
H_2, by adsorption on condensed gases 3—9917
^3He dilution refrigerator with condensation pump 3—5819

cryoscopes *see cryoscopy*

cryoscopy
No entries

cryosorption *see sorption*

cryostats
0.7 K using ^4He, evacuation by sorption pump 3—25701
anthracene single cryst., low temp. irradiation and meas. colour centres 3—132
continuous flow, high constancy temperature control 3—9898
cryogenic temp. controller for use with resistance thermometers from 0.3 to 6 K 3—5820
current leads for 4.2 K cryostat 3—28500
desorption, for 1.5-120 K expts. 3—35382
for detectors 3—25704
dilution refrigerator cryostat for high press. exprts. 3—9885
double ridged tapered waveguide transition 3—5847
foils, internal friction, resistance measurement 3—251
heat conducting and gas-flow types, for optical spectroscopy 3—5824
laboratory instruction low-cost cryostat, construction and operation 3—9808
mechanical testing of materials, in liquid He 3—5775
mechanical thermal switch for using cryostat between 4 and 650 K 3—5823
for m.i.s. studies, use of LN_2 to overcome water condensation 3—37604
for Mossbauer effect meas. after 4 K neutron irrad., lattice defect investig. 3—9879
optical, unevacuated, for PDO-1 camera 3—25726
optical camera-cryostat installation, for spectra of luminescent objects 3—25756
for optical meas. in far i.r., with pneumatic device 3—37620
orientation determ., external goniometer 3—25705
for scintillator-photodiode detector, for charged particles 3—37695
for ultrasonic attenuation study of solids down to 0.32 K 3—28502
vacuum-free optical cryostat 3—25702
vacuum-tight electrical leads *(Russian)* 3—9876
Ge, demountable high-vacuum tight high voltage feedthrough, description *(German)* 3—9912
He, for diffractometer 3—25700
He II, for supercon. particle separator 3—5840
He liquid, for optical absorption measurements 3—13277
^3He, 0.3 to 3 K *(German)* 3—28504
^3He-^4He dilution refrigeration, pressure induced superconductor search, mechanical press. up to 200 kbar 3—9902
^3He-^4He dilution refrigerator cryostat system, for nuclear orientation studies 3—37605

cryotrons
CROG thermometer for liquid helium temp. meas. 3—35381

crystal atomic structure
see also crystal atomic structure of alloys; crystal atomic structure of elements; crystal atomic structure of inorganic compounds; crystal atomic structure of organic compounds; crystal electron states; electron diffraction crystallography; lattice constants; neutron diffraction crystallography; space groups; X-ray crystallography
Algol program for structure illustrations on digital plotter 3—14636
analogue computers used to solve integral eqns. 3—33421
anisotropic defects in solid, dimension changes in lattice parameters 3—20754
atom displacements, reln. to rhombohedral deformation in certain compounds *(Russian)* 3—7653
binary closest-packed layers, tesselations and plane symmetry groups, space groups, Buerger derivatives 3—38544
coincidence site lattice, general conditions for occurrence 3—1589
crystal model simulation by computer, SDMPLT, simulation by computer, SDMPLT 3—27092
diamond configuration, distorted, with sphere packing character, effective range *(German)* 3—4726
diamond structure crystal, microhardness print mechanism on local phase transition 3—7931
dielectric materials, u.s. attenuation dependence on structural parameters 3—1705
difference reflections, intensities and Fourier transforms 3—23972
diffractometry, data evaluation, validity and accuracy of current methods, standard derivations, rejection criteria 3—26928
discrepancy factors for crystals with two heavy atoms 3—36233
extended X-ray absorption fine struct., meas. of shielding of impurities 3—18511
film, single crystal, transillumination proton diffraction for structure obs. 3—24363
forces effects on bond lengths, calc. of charge distribs. 3—14724
intensity project, I.U.C. type III, structure factor determ. 3—26919
layered stratified lattice, X-ray diffraction profile showing preferred orientation 3—11783
least squares refinement of highly covarying parameters 3—14651
localisation of atoms on three dimensional electron density syntheses 3—33422
metals, f.c.c. and h.c.p., atomic scattering factors, h.v. electron diffraction 3—38528
modulation spectroscopy, electric field and uniaxial stress effect, vector and tensor perturbations 3—34334
molecular packing determ., potential energy calcs. 3—24061
n-dimensional lattices, study via reduced bases for n=2, 3, 4 3—7651
octahedron, effects of geometry on structure of crystals 3—38548
paracrystal state theory *(German)* 3—20704
Patterson function, systematic anal., review 3—30081
perovskites, classification of tilted octahedra 3—7648
phase relations between reflection quartets to determine strengthened quartet relationships 3—14633
point groups, multi-coloured, construction 3—7649
point groups, singular matrix representation, comment 3—24052
point groups O and D_4, class sum operator approach 3—26049
polynomial method to determine statistical equations between structure factors *(French)* 3—11576
polytype transform. structure 3—14721
pyrophyllite, hydroxyl orientation 3—24083
rutile structure, symmetry props., anal. for energy band calc. 3—24053
semiconductors, lattice parameter changes on diffusion doping, meas. method 3—27032
site potential calc. for positions of hydrogen atoms 3—14711
stability, math. theory, appl. to phase transitions description and classification 3—7905
structure factors, conditional distributions and related expectation values 3—4694
superstructure determ. using partial Patterson functions 3—4705
triglycine sulphate, X-ray structure damage 3—30149
X-ray imaging device for rapid acquisition of structure factor data 3—26941
Zintl phase, stabilisation and chem. bonding 3—17754
GaAs, X-ray diffraction by perfect acentric crystals 3—30049
MnBi thin film *(Japanese)* 3—34005
$Mn_xfe_{3-x}O_4$ solid solution, cation distribution and local distortion 3—30729
ZrO_2-Sc_2O_3, X-ray obs. of rhombohedral and cubic phases and transitions 3—14786

crystal atomic structure of alloys
Am alloys, Laves phases 3—4731
austenite, lattice parameter C content depend. at 1100°C *(Russian)* 3—12345
book 3—11586
γ-brass, tetrahedrally close packed struct. 3—14731
complex intermetallic compounds, struct. relationships 3—14730
long period superstructures and their interpretation 3—14729
random cubic binary solns., atomic pots. applic., lattice parameters 3—24814
rare earth, Ln-Rh phases with Mn_5Si_3, $CaZn_5$ and $CeNi_3$ structures 3—20714
rare earth alloys, RXSn (R=Ho, Yb, Tm, Lu, Tb, X=Rh, Pd, Ir, Pt), X-ray and Mossbauer obs. 3—17762
rare earth compounds RNiAl and RCuAl 3—20725
rare earth MAu_2Si_2 compounds 3—20713
rare earth solids, book 3—11523
rare earth transition intermetallics, struct. relationships, Friedel's d-band mag. model 3—2248
rare earth-Cd, structure obs. for different phases 3—30972
rare earth-transition metal compounds, Th_2Ni_{17} type 3—17760
rare-earth-Rh, intermediate phases and crystal struct. 3—34513
solid solution, multicomponent, ordering theory 3—33489
stainless steel, austenitic, struct. changes in welded joints *(Czech)* 3—1062
steel, axially centred cubic to f.c.c. transition, internal energy reduction *(Russian)* 3—15728
steel, Z-phase NbCrN struct. 3—21564
transition metals, X-ray characteristic absorption spectra, atomic struct. determ. *(Russian)* 3—12194

crystal atomic structure of alloys continued
- two phase systems, X-ray diffr. pattern, use of symmetry in interpretation 3—4701
- Al-Cu, $AlCu_3$ phase 3—14733
- Al-Cu-Mg-Ag, heat treatment, struct. of metastable precip. 3—15662
- Al-Zr solid solution, crystal structure of new metastable phase 3—18599
- Au-Cu (25-33% Au), X-ray diffr. obs. *(French)* 3—14739
- Au-Cu-Zn martensite, electron diffr. obs. 3—1604
- Au-transition metal, short range order, eledtron microscope and diffr. obs. 3—14734
- $AuCu_3$ ordered solid solution, size effect theory *(Russian)* 3—7658
- Au_4Mn, micromagnetic to superparamag. transition, effect of atomic ordering 3—21229
- BiSn, body centred tetragonal structure, obs. under high pressure 3—4732
- Cd-Sb system, crystallisation conditions influence on props. *(Russian)* 3—8769
- Ce-Rh, intermediate phases and cryst. struct. 3—34513
- $CeOs_2$ lattice parameters, $MgCu_2$ type, polymorphic transition point, high pressure effects 3—33488
- Co-Cr-C system, crystallisation of 2-4 phase composite structures *(German)* 3—8776
- Co-Cr-W, discovery of 3 topologically close-packed phases 3—15659
- Co-Fe, double h.c.p. structure from X-ray diffraction study, rel. to mag. props. 3—1600
- $CoPt_3$, long-range order and ordering kinetics 3—34506
- $CoPt_3$, partially ordered, field-ion microscopy and X-ray diffr. obs. 3—14738
- 12%Cr-Fe-C-N, structural diagrams and phase reactions, 1300-700°C 3—8772
- 7%Cr-Fe-C-N, structural diagrams and solid phase reactions, 1300-700°C 3—8773
- Cu binary alloy, X-ray scattering secondary peak due to superlattice structure 3—30089
- Cu-Au, effect of press. on phase transition and ordered structs. of CuAu 3—18610
- Cu-Au, press, depend. of long period of CuAuII 3—20712
- Cu-Co, cell structure formation with Bridgeman growth method 3—11571
- Cu-Mn-Sn, and ordering in ferromag. beta phase 3—18324
- Cu-Ni, comp. effects on lattice parameter by density meas. 3—26991
- Cu-Pd, ordering process, mass spectrometric obs. of secondary ion emission *(Russian)* 3—33490
- Cu-Pd system, long period superlattice form. 3—14737
- Cu-Pd(Pt), short range order, electron microscope and diffr. obs. 3—14734
- Cu-Pt, long-period ordered alloy Cu_3Pt 3—15656
- Cu_3Au, type ordering, short range and long range, energy, second coordination sphere 3—38551
- Cu_3Au-type, ordering, Monte Carlo calc. *(Russian)* 3—30970
- $CuPt_3$, ordered struct., superlattice refls. 3—14803
- CuZn ordered solid solution, size effect theory *(Russian)* 3—7658
- Dy-Au, structure obs. for different intermetallic phases 3—30971
- $DyAl_2$-$DyFe_2(Co_2)$, struct. and mag. studies 3—18323
- Fe, b.c.c. crack extension by bond rupture, fracture toughness and crystal structure relation 3—15724
- Fe-Al, superlattice dislocations, fourfold dissociation in DO_3 type order 3—17839
- Fe-Co, ordering process, mass spectrometric obs. of secondary ion emission *(Russian)* 3—33490
- Fe-Cr, ordering process, mass spectrometric obs. of secondary ion emission *(Russian)* 3—33490
- Fe-Cr(V)(Ni)(Co), deviation from additivity rules, X-ray absorpt. obs. *(Russian)* 3—12337
- Fe-Mn-C, structural features of martensitic transform. 3—30976
- Fe-Ni, lattice const., spontaneous volume magnetostriction, 4.2-1000 K 3—30671
- Fe-Ni(V)(Cr), X-ray absorpt. obs. of polymorphism *(Russian)* 3—12336
- Fe-Si, long-range order, A_7B types, config. energies 3—38550
- Fe-V, ordering process, mass spectrometric obs. of secondary ion emission *(Russian)* 3—33490
- Fe_3Al, determination of order parameters by Mossbauer spectroscopy methods 3—39070
- $Fe_{1-x}Co_xAl$ solid solns., conc. depend. of lattice parameter *(Russian)* 3—30087
- FeCr, electron config. at α-σ phase transition, Mossbauer effect obs. *(Russian)* 3—2479
- FeV, electron config. at α-σ phase transition, Mossbauer effect obs. *(Russian)* 3—2479
- Gd-Rh, intermediate phases and crystal struct. 3—34513
- $Gd_3Fe(Co)(Ni)$, and antiferromag. props. 3—21232
- $GdPt_2$ (20-30% rare earth) structures 3—33487
- HoPtSn, X-ray and Mossbauer obs. 3—17762
- $LaOs_2$ lattice parameters, $MgCu_2$ type, polymorphic transition point, high pressure effects 3—33488
- Mg-base Friauf-Laves phases, struct. relation between stacking variants 3—14732
- Mo-Ga system, $MoGa_4$ phase, determ. using direct methods 3—17759
- Na-Cd, lattice const. determ. for $NaCd_2$, Na_2Cd_{11} samples 3—24062
- Nb-Al alloy, Nb-rich, sputtered films and quenched samples, lattice parameters rel. to superconductivity 3—5082
- Nb-Zr-H, n.m.r. exam. and H self-diffusion *(Russian)* 3—1815
- NbFe, Laves phase, comp. depend. of lattice parameter 3—27637
- Ni-Cu, lattice const., spontaneous volume magnetostriction, 4.2-1000 K 3—30671
- Ni-Fe, atomic size-modulus influence on cyclic deform. curve 3—7825
- $(Ni_{1-x}M_x)_2P$ solid solution, M=Co, Fe, Mn, Cr, inverted ordering near Ni_2P *(French)* 3—30088
- Ni_3Mn-based, ternary alloys, atomic distrib., rel. to electronic struct. *(Russian)* 3—26990
- Np alloys, Laves phases 3—4731
- Pb-Bi system, structure of metastable phase 3—18569
- Pd-Gd, solid solutions, magnetic and crystallographic characteristics 3—8793
- Pd-La(Ce)(Pr), lattice spacing variation with comp. 3—18298

crystal atomic structure of alloys continued
- Pt-Mn-Sn, X-ray analysis *(Japanese)* 3—8346
- Pu_3Pd_4, X-ray determ. 3—26989
- Rh-Pb system, cryst. struct. and stability of phases *(German)* 3—5286
- Ru-Mg system, intermetallic compounds, X-ray obs. 3—34495
- Se-Te, perturbed ang. γ-γ correl. study 3—14740
- Sm-Au, structure obs. for different intermetallic phases 3—30971
- Sm-Rh, intermediate phases and cryst. struct. 3—34513
- Ta-H system, X-ray obs. 3—20711
- Tb-Rh, intermediate phases and crystal struct. 3—34513
- Tb_8-$La(Pr)_2$, Sm type structure, ordering and symmetry rel. to mag. props. 3—18321
- $TbPt_3$ (20-30% rare earth) structures 3—33487
- $ThCu_{3.6}$, Debye-Scherrer powder pattern, comparison with $GdAg_{3.6}$ structure 3—17763
- Ti-Mo-H alloys, b.c.c., proton spin lattice relaxation time obs., struct. of H sublattice 3—12073
- Ti-Zr-O system, ω' phase *(French)* 3—18565
- V-As system, V_4As_3 phase, determ. using direct methods 3—17759
- V-D, neutron and X-ray diffr. 3—14728
- V_2C and VC_{1-x} phases *(French)* 3—7657
- V_2Hf, Laves phase cpd., low temp. struct., supercond. transition temp. rel. to impurities 3—18244
- V_3Rh_5 unit cell parameters, space group, lattice structure 3—33486
- V_3Si solid solution, lattice const. and supercond. crit. temp., comp. depend. *(Russian)* 3—8295
- $V_3Si_xGe_{1-x}$, lattice parameters, conc. depend. *(Russian)* 3—18242
- V_2Zr, Laves phase cpd., low temp. struct., supercond. transition temp. rel. to impurities 3—18244
- Y-Rh, intermediate phases and cryst. struct. 3—34513
- $Zr_{0.80}Mo_{0.20}Fe_2$, heat treatment effects 3—21649
- $Zr_{0.60}Nb_{0.40}Fe_2$, heat treatment effects 3—21649

crystal atomic structure of elements
- carbyne, charact. by X-ray and electron diffraction 3—33485
- graphite, band angles and length determ. 3—17793
- incoherent X-ray intensities of atoms with $Z \geqslant 20$, analytic approx. 3—11527
- metal, struct. factor, rel. to electron correlations and moment sum rules 3—38764
- metals, book 3—11586
- metals, lattice imaging at 10^6 magnification in electron microscope 3—7607
- periodic table position depend. of struct. regularities 3—14723
- rare earth metal film, electron microscope obs. of f.c.c. structure 3—18042
- rare earth solids, book 3—11523
- transition metals, X-ray characteristic absorption spectra, atomic struct. determ. *(Russian)* 3—12194
- Al, valence electronic charge density, calc. from wave functions obtained via Ashcroft's pseudopotential 3—27209
- Ar clusters, struct. obs. using a supersonic beam method 3—14799
- Au, lattice contraction due to quenching-in vacancies 3—30118
- Au thin platelets, lattice spacings, electron diffr. study 3—4730
- Bi(V), high pressure form 3—11584
- C, hexagonal form suggestion 3—7702
- Cr, small crysts., diameter $\leqslant 30$Å 3—14735
- D_2, as-frozen cubic struct. 3—15007
- Fe, small crysts., diameter $\leqslant 30$Å 3—14735
- Fe lattice distortion by vacancies, interaction energies, discrete lattice model 3—30116
- δ-Ga *(French)* 3—20710
- Gd, neutron mag. form factor calc. using Dirac-Fock equation 3—21244
- Ge, high press. phases, comparison with amorphous Ge 3—30095
- Ge polytype, pseudopotential calcs. rel. to band structure and form factor 3—21005
- Mo, lattice parameters, ion-irrad. effects *(Russian)* 3—4776
- Mo lattice distortion by vacancies, interaction energies, discrete lattice model 3—30116
- α-N_2, $P2_13$ struct., far-i.r. absorpt. obs. 3—7683
- Ni, hexagonal, formed by Ni_3C decomposition 3—5384
- Ni, rapid X-ray diffraction structure analysis with energy dispersive Si(Li) detector 3—30052
- Pt, lattice contraction due to quenching-in vacancies 3—30118
- S_{18}, cell constants and space group determ. 3—36283
- S_8, orthorhombic, constrained refinement and model for lattice dynamics 3—24074
- Se, hexagonal, bond distances and chain angle at high press. 3—7682
- Si, optimum crystallographic orientation, for semicond. device fabrication 3—30959
- Si, temp. depend. of forbidden (442) refl. 3—24064
- Sm, orthorhombic *(French)* 3—8353
- Ta film, r.f. sputtered, β and b.c.c. struct. obs. 3—1955
- Ta film, sputtered, electron microscopy and X-ray diffr. obs. 3—1954
- V, small crysts., diameter $\leqslant 30$Å 3—14735
- V lattice distortion by vacancies, interaction energies, discrete lattice model 3—30116
- Zn, anomalous X-ray transmission rel. to imperfect structure, dislocation and thickness effects 3—24145

crystal atomic structure of inorganic compounds
- $A^{II}B^{III}_2X_4$ compounds *(Russian)* 3—14811
- ABO_4 molybdates and tungstates, cell dimensions 3—7661
- alkali metal halide:Th, In phosphors, absorption and phosphorescence spectra depend. on lattice parameters and refractive index *(Russian)* 3—30875
- aluminosilicates, computed optimized model structs. 3—14761
- amphiboles, high-temp. cryst. chem. 3—15863
- analcime, cryst. struct., neutron diffr. obs. 3—7721
- anandite, 2O brittle mica 3—18808
- bis-dipivaloylmethane mercury *(German)* 3—14807
- chlorite, one-packet, dioctahedral, structureal features detn. by X-ray anal. 3—7709
- clathrate compounds of aromatic molecules in metal complex host lattices 3—14778
- Co (III) complex, hexamminecobalt (III) hexacyanocobaltate (III), X-ray obs. 3—36276
- complex semiconductor chalcogenides, physical props. *(Russian)* 3—8168

crystal atomic structure of inorganic compounds continued
  corundum, positions of O in lattice *(Russian)* 3−24706
  cubic spinel compounds, rel. to possible antiferroelec. behaviour 3−30773
  cyanide complexes, use of electron population parameter to distinguish between C and N 3−20716
  1,8-dichloroanthaquionne, X-ray diffr. study *(Russian)* 3−7738
  divalent metal complexes of 1,3-diphenyltriazine, struct. chem. 3−14766
  DO_9 type, bronze and tunnel structures, shear structures, examples 3−38545
  electrolyte, rel. to conductivity 3−27282
  enstatite, high-temp. cryst. chem. 3−15864
  feldspars, Al-Si ordering, X-ray obs. 3−14764
  ferrite, hexagonal, direct lattice imaging for stacking sequence recognition 3−38530
  ferroelectric crystal, three dimensional vacuum furnace for neutron diffraction structure obs. 3−17720
  group VIII polynucl. carbonyl complexes 3−14768
  β-hopeite, X-ray obs. 3−15862
  hornblende and ortho(clino)-pyroxenes, Fe^{2+} order-disorder in structure, Mossbauer obs. 3−27096
  hydrates, pentagonal dodecahedral water structure 3−11600
  hydrogen-bonded systems in rock-forming silicates, valence balance 3−15859
  μ- hydroxobis[pentaamminechromium(III)] chloride monohydrate, struct. and magnetic susceptibility of the acid rhodo complex 3−18301
  hypophosphites, $M(H_2PO_2)_2$, M=Cd, Ca, Sr, Pb, Ba, radiocrystallographic and i.r. spectroscopic obs. *(French)* 3−7700
  ice, structure obs. in different phases, molecular interpretation by model studies 3−27099
  ice IX, nearly proton-ordered structure 3−17786
  illite-montmorillonite mixture interstratified mineral struct. 3−7720
  kozulite, and tetrahedral Al content in amphiboles 3−15867
  $LiCl.H_2O$, space group, cell dimensions *(German)* 3−7672
  lunar breccias and vapour deposited crystals formed in their cavities 3−16171
  lunar rock 12053, cation order, domain struct. and exsoln. in pigeonite and augite 3−16170
  metal oxides, cation diffusion 3−4886
  mica group and related sheet silicates, electron energy loss spectra rel. to struct. 3−1608
  mica polytypes coexisting with pyroxene polymorphs 3−14792
  mineral groups, mica, amphibole and pyroxene, polytypism, polymorphism and subsolidus reactions 3−14790
  nacrite, structure refinement by high-voltage electron diffr. 3−7707
  omphacite, refinement 3−15868
  ore minerals, X-ray powder pattern calcs. 3−15861
  oxides, M_xO-M′O, (M=Co, Ni, Fe, Mn; M′=Mg, Ca, Sr, Zn, Al), Neel temp. comp. depend., bonding *(French)* 3−8363
  perovskites, atomic displacements, X-ray diffuse scatt. obs. 3−14802
  perovskites, ordered, pseudotriclinic cell deform. induced by displacement of ion 3−17766
  perovskites, tilting schemes approach 3−15002
  plagioclase, Patterson function of e and f satellites 3−24067
  polytype, correlation between stacking fault energy and atomic structure 3−17753
  prediction of structure types for AB_2X_4(x=S,Se,Te) compounds, crystal chem. 3−27011
  pyroxenes, high-temp. cryst. chem. 3−15863
  pyroxenes, natural, X-ray topography and electron petrography 3−18807
  pyrrhotites ($Fe_{1-x}S$), stability relations and structures 3−14743
  α-quartz, structure factor, absolute meas. by Pendellosung fringes 3−23967
  quartz powder, X-ray structure charact. after grinding 3−31208
  rare earth borates, vibr. spectra, struct. 3−2555
  rare earth chalcogenides, $EuLn_2S_4$ type, mag. interactions and isomer shift rel. to struct., Mossbauer obs. 3−2481
  rare earth cobaltide hydrides, RCo_5-H (R=La, Pr, Nd, Sm, Gd), rel. to hydrogen sorption 3−27357
  rare earth Ga garnets, substrate material for bubble domain films, thermal expansion of lattice parameters 3−34158
  rare earth hydrides, struct., dynamics, H diffusion, slow neutron scatt. obs. 3−1615
  rare earth silicates, structures for different comps. and polymorphism 3−14788
  $RbR(TO_4)_2$, R=Sc, In, T=Mo, W, systems crystallizing in $KAL(MoO_4)_2$ and $KIn(MoO_4)_2$ struct. types *(Russian)* 3−7710
  scheelite based structure obs. for $NaLu(WO_4)_2$, $Na_5Lu(WO_4)_4$ 3−24084
  semiconductor $A^{II}B^{V}$ compounds 3−18084
  silicate glasses, diffusion rates and solubilities of He and Ne as a function of SiO_2 content 3−4883
  silicate-germanate, $A_2(Si,Ge)O_4$, (A=Be,Zn,Ca,Cd,Sr,Ba) 3−7922
  silicates, dioctahedral layer, transformational alterations, crystallochem. 3−15860
  SmO, film, structure and defect substructure obs. 3−8067
  spinel solid solutions, cation distrib. determ. from temp. depend. of lattice consts. *(Russian)* 3−27003
  spinels, interionic metal-oxygen distances, formulae *(Russian)* 3−17784
  stibnite, struct. refinement 3−7723
  ternary silicides, homologous series including new struct. types 3−14781
  ternary sulphides of alkali and transition metals 3−14749
  tetrahedral-framework structs. of sulphates and fluoberyllates 3−14751
  titanites, cryst. chem. 3−18806
  transition metal complex, cluster compounds 3−14771
  transition metal complexes with fluorocarbons, zero oxidation state, struct. types 3−14773
  transition metal dichalcogenides, layered, chemical bonding and struct. 3−4729
  transition metal hydrides, 6- and 8-coordinate 3−14774
  transition metal oxides, oxyfluorides, oxyhydrides, high press. synthesis, struct. characterisation 3−14800
  transition metal oxides containing pentagonal columns 3−14750

crystal atomic structure of inorganic compounds continued
  valence forces between anions and cations, analysis of local balance 3−24059
  $[Co(NH_3)_4](ReO_4)_2$ *(German)* 3−30099
  $A^{II}B^{VI}$, rules for struct. formation and stable structures 3−7652
  Ag_2CrO_4, data from i.r. and Raman spectra 3−34364
  $AgGaS_2$:Fe^{3+}, ternary semicond., ESR and X-ray anal. of crystal structure 3−30693
  $AgInS_2$, in Ag_2S-In_2S_3 system, distorted wurtzite structure of high temp. polymorph 3−38574
  $AgIn_5S_8$, cubic spinel type phase in Ag_2S-In_2S_3 system 3−38574
  $AgNa(NO_2)_2$, accurate struct. analysis rel. to ferroelec. phase transition 3−14804
  $AgNaSO_3.2H_2O$, X-ray determ. 3−27000
  $Al_xGa_{1-x}As$, molecular beam epitaxial layer, HEED obs. 3−2677
  $AlMgBO_4$, sinhalite, olivine type structure, hydrothermal synthesis at high pressure *(French)* 3−38571
  Al_2TiO_5, structure obs. rel. to thermal expansion using high temp. X-ray diffraction furnace 3−26944
  As_2Se_3-As_2Te_3:^{119}Sn, glass-crystal transition, Mossbauer obs. of ^{119}Sn impurity atoms local surroundings 3−4722
  As_2Te_3:^{119}Sn, glass-crystal transition, Mossbauer obs. of ^{119}Sn impurity atoms local surroundings 3−4722
  B_4C, X-ray obs. 3−14742
  B_2H_6 electron density problem, experimental and theoretical aspects 3−4708
  $B_{12}N_{12}H_{12}$, hexagonal, equilib. distance, charges, from Huckel calcs. 3−15136
  δ-$BaCO_3$, metastable phase, props. study 3−4855
  $BaCaTlNb_5O_{15}$, lattice parameters *(French)* 3−38566
  $Ba_2Cu(PO_3)_6$, monoclinic *(French)* 3−7901
  $BaCu_4S_3$, unit cell parameters and space groups 3−11599
  $Ba_4Fe_9O_{20}H_6$, hydrothermally synthesized 3−17767
  $Ba_8Fe_{13}O_{30}H_6$, cubic three-dimens. network of FeO_4 tetrahedra with large cavities 3−17768
  $Ba_3Fe_2TeO_9$, struct. and antiferromagnetism at low temps. *(French)* 3−7690
  $Ba_2LaLiNa_2Nb_{10}O_{30}$, melt grown, characterization 3−12268
  $Ba_2LaLiNa_2Nb_{10}O_{30}$, obs. of tetragonal tungsten bronze structure 3−38572
  $Ba_4{}^{2+}La_6(SiO_4)_4(PO_4)_2O_2$, silicophosphate, preparation and characterization *(Russian)* 3−11597
  $Ba_3Nb_7Si_2O_{25-x}$, X-ray obs. 3−14745
  $BaO.2Fe_2O_3$, heavy atom determ. method 3−36277
  m $BaO.2UO_3.(4-2m)H_2O$, $O\leqslant m<2$, indexing of X-ray powder patterns *(French)* 3−30091
  $Ba_{1-y}Sr_yMnO_{3-x}$, structure of phases and subsolidus phase relations 3−27124
  $BaSrTlNb_5O_{15}$, lattice parameters *(French)* 3−38566
  $BaTbO_3$, neutron diffraction examination 3−7677
  $BaTiO_3$:Y_2O_3, struct. depends. on composition and cation siting 3−14813
  $BiFeO_3$ magnetic and structural props. 3−39064
  $Bi_2In_4S_9$, synthesized in gas phase 3−7673
  $Bi_\alpha(MO)_\beta MO_3$, (M=Ta, W and Nb, W) new phases, struct. *(French)* 3−7697
  Bi_2O_3-TeO_2 system at 450°C radiocrystallographic investigation *(French)* 3−27100
  CO(III) complex, $[Co(3,2,3\text{-tet})\times_2]^+$, $x=Cl^-$ and $No_2{}^-$, $42NH(CH_2)_3NH_2$ 3−17774
  Ca-Ln_2-S_4, ternary sulphides, prep., elec. and opt. props. 3−39243
  $CaAl(B_3O_7)$, johachidolite, X-ray diffraction obs. 3−1612
  $CaAl_2(NH_2)_8.NH_3$, monoclinic *(French)* 3−1607
  CaAs powder, X-ray data 3−20724
  $Ca_2B_5O_9Br$, determ. of pseudotetragonal orthorhombic symmetry *(French)* 3−33494
  $CaCl_2.4H_2O$, X-ray determ. 3−24079
  CaF_2, charge density from struct. amplitudes nonspherical analysis, atomic nonsphericities 3−27005
  CaF_2, integrated intensities of Laue and Bragg reflections, extinction and structure factor determ. 3−23955
  CaF_2 type fluorides, changes in real structure due to compressive impact 3−33503
  $CaH(AsO_4),H_2O$, haidingerite, morphology rel. to bond assemblage 3−14789
  $CaHAsO_4.3H_2O$, and hydrogen bonding 3−14762
  $CaHAsO_4.3H_2O$, hydrogen bonding, three-circle diffraction study 3−17756
  $CaHaHSiO_4$, examination of single crystals 3−17796
  $CaKAsO_4.8H_2O$, space group, cell dimensions 3−7664
  $CaLGa_3S_7$, $CaLAl_3S_7$, (L=La, Ce, Pr, Nd), sulphurized compound family of melilite type *(French)* 3−30102
  $Ca_4{}^{2+}La_6(SiO_4)_4(PO_4)_2O_2$, silicophosphate, preparation and characterization *(Russian)* 3−11597
  $CaNaP_3O_9.3H_2O$, anhydrous salt data *(French)* 3−11593
  $Ca_2Nb_2O_7$, lattice parameters *(French)* 3−1606
  m $CaO.2UO_3.(4-2m)H_2O$, $O\leqslant m<2$, indexing of X-ray powder patterns *(French)* 3−30091
  CaP powder, X-ray data 3−20724
  $Ca_5(PO_4)_3F$, synthetic and mineral, crystal structure compared 3−11601
  $Ca_5(PO_4)_3F$: $Nd(Nd_2O_3)(NdF_3)$, fluorapatite, structure and location of dopant 3−17789
  $CaSO_4$, X-ray obs. of α-phase 3−14809
  Ca_2SiO_4, struct., from room temp. to over 1400°C 3−14798
  $CaTi_2O_5$, formation, structure and props. deter. *(Russian)* 3−11596
  Cd rare-earth chalcogenide spinels, X-ray determ. of lattice, cation distrib. and u-parameters 3−7685
  Cd-Ln_2-S_4, ternary sulphides, prep., elec. and opt. props. 3−39243
  $CdCr_3S_4$ single crystals, gas transport and characterisation *(German)* 3−8730
  CdF_2-MF_2 systems, M=alkaline earth metal, comparative study *(French)* 3−14978
  CdF_4MF, M=alkali metal, structures of compounds formed *(French)* 3−14819
  Cd_2GeO_4, $Cd_3Ge_3O_9$, $Cd_5Ge_2O_9$, interplanar distances and lattice parameters *(Russian)* 3−17745
  $Cd_xHg_{1-x}(SCN)_2$, gel grown, characterization 3−15611
  $CdNaXO_4$, (X=P,As) orthorhombic structure obs. *(French)* 3−30101

crystal atomic structure of inorganic compounds continued
- $Cd(PO_3)_2$, orthorhombic *(French)* 3−11591
- $Cd_5(PO_4)_3Cl$, twinning rel. to structural detail 3−36275
- $Cd_5(PO_4)_3Cl$, X-ray obs. 3−38556
- $Cd_3(P_3O_9)_2.14H_2O$, cryst. data 3−7724
- CdS, X-ray atomic scattering factors, electronic structure, correl. atoms, crystal *(Russian)* 3−33625
- $CdS\text{-}M^{III}M^{I}M^{III}S_2$, ($M^I$=Ag, Cu, M^{III}=Al, Ga, In), solubility rel. to wurtzite and chalcopyrite structures 3−33678
- Ce hydrides, temp. dependent electronic transition, resistivity meas. 3−8237
- Ce silicates $Me^{2+}Ce^{4+}Si_2O_7$ type synthesis, struct. props. 3−1616
- $CeCr_2B_6$ 3−33505
- CeF_3, symmetry, struct., screening consts. 3−7662
- $Ce_{10/3}Ga_6S_{14}$, sulphurized compound family of melilite type *(French)* 3−30102
- Ce_2NiSi, $P6_3/m$ group, struct. detn. X-ray anal. 3−7705
- $Ce_{4.67}[SiO_4]_3O$ cry. struct. of TR analog by X-ray diffr. 3−7703
- $CfCl_3$, X-ray diffraction study of hexagonal and orthorhombic forms 3−36282
- Co (III) complex, hexamminecobalt (III) hexacyanocobaltate (III) and hexacyanochromate (III) 3−14765
- Co complex, $CoNO(S_2CNMe_2)_2$ 3−14776
- Co complex, $Co(NO_3)_2.10CO(NH_2)_2$ X-ray study *(Russian)* 3−4737
- Co complex, $Co(NO_3)_2.2CO(NH_2)_2.4H_2O$, X-ray obs. *(Russian)* 3−4738
- Co nitrosyl complexes, crystal struct. *(French)* 3−7701
- $Co_2Fe_{2-x}Al_xO_5$ with x=0.57, 0.72 3−7675
- Co(III) complex, tris(diphenyltriazine)cobalt(III), trigonal distortion 3−38554
- Co(II) complex, Co(PNNP)Br, where PNNP=N,N'-bis(2-diphenyl-ine 3−17780
- $CoIn_2S_4$, cation distrib., mag. susceptibility temp. depend. 3−34102
- $CoO\text{-}MgO\text{-}GeO_2$, spinel-olivine and olivine-phenacite transitions, thermodynamic and volume relations 3−27122
- $CoO\text{-}ZnO\text{-}GeO_2$, thermodynamic relations among olivine, spinel and phenacite structures 3−27123
- Co_3O_4, electron diffraction anal. of superstructure *(Russian)* 3−7712
- Co_3O_4, low-spin cpd. 3−20720
- $Co_6Te_5O_{16}$, lattice consts. determ. *(German)* 3−36285
- Co complex, $Co_2(C_5H_5)_3S_2$, 293 and 130K 3−14770
- $CrAs(P)_2$, high-pressure, determ. of $OsGe_2$ type structure, crystal chem. 3−38555
- $CrAs_{0.5}Sb_{0.5}$ crystal distortion at Neel temp., antiferromag. NiAs to helimag. MnP type structure 3−33671
- $Cr_{23}C_6$, space group, cell dimensions 3−7669
- Cr_2GeO_5, X-ray diffr. obs. *(French)* 3−7681
- Cr_3P, crystallographic study 3−11602
- Cs_2CuCl_4, struct., crystal forces and charge distribution determ. 3−17785
- $CsF\text{-}InF_3$ systems, preparation and crystallographic data *(French)* 3−7699
- Cs_2HgI_4 3−33506
- $CsLiBeF_4$ determ., space groups and symmetry 3−11598
- $CsMnCl_3$, Weissenberg data 3−36274
- $CsSbWO_6$, pyrochlore, isolation and cubic cell cation position detn. *(French)* 3−30104
- $Cs_6Ti_2O_7$, new alkali metal titanates and germanates, lattice consts. determ. *(German)* 3−36288
- CsU_2F_9, X-ray determ. 3−26994
- $Cs_4(UO_2)_2F_82H_2O$, lattice parameters and structure *(Russian)* 3−26993
- Cs(V) complex, caesium oxobisoxalatobisaquoniobate (V) dihydrate, X-ray obs. 3−38559
- $CsVOF_4$ (V), crystl. struct. determ. 3−11588
- Cu (II) complex, bis-(N,N′-di-n-propyldithiocarbamate), and mol. struct. 3−24073
- Cu complex, $((CH_3)_3NH)CuCl_3.2H_2O$, room temp. 3−1613
- Cu complex, α-bis-(N-methylsalicylaldiminato)-Cu(II) structure, mag. props. and linear chain behaviour 3−2286
- $CuAl_2O_4$, spinel, equilib. cation distrib., X-ray diffr. analysis 3−7687
- $CuAlS_2:Fe^{3+}$, ternary semicond., ESR and X-ray anal. of crystal structure 3−30693
- $Cu_7As_6Se_{13}$, partial Patterson method application and the thirteenfold hexagonal superstructure 3−4741
- $Cu_4Bi_4S_9$, rel. to simple sulphide structs. 3−14763
- $CuCr_2O_4$, spinel structure, structure changes under high pressure, Jahn-Teller effect 3−27118
- $CuCr_2S_{4-x}Se_x$ solid soln., lattice parameter, Curie temp., mag. moment and effective mag. moment 3−21241
- $CuFeS_2$, chalcopyrite refinement 3−26998
- Cu_5FeS_4, bornite, superstructs. determ. by mofified Patterson method 3−15865
- $Cu_9Fe_9S_{16}$, mooihoekite 3−18805
- Cu(II) complex, copper(II) bis(N,N′-di-n-propyldithiocarbamate) 3−17778
- Cu(II) complex, tetrasodium dicopper-dl-tartrate dehydrate X-ray anal. 3−7696
- Cu(II) complex, chelate of N-3-hydroxypropylsalicylideneimine 3−17775
- Cu(II) complex, di-μ-thiocyanato-bis di(2-aminoethyl)amine copper(II) 3−17779
- $CuInS_2:Fe^{3+}$, ternary semicond., ESR and X-ray anal. of crystal structure 3−30693
- $Cu_xMn_{3-x}O_4$ spinels, lattice parameters determ., tetragonal-cubic transition 3−38575
- $Cu_3Mo_2O_9$, centrosymmetric struct. space group 3−7667
- $Cu_3PS_4(Se_4)$, and other ternary normal tetrahedral struct. cpds. with comp. $1_35 6_4$ 3−24078
- $Cu_3SbS_4(Se_4)$, and other ternary normal tetrahedral struct. cpds. with comp. $1_35 6_4$ 3−24078
- Cu_3SmS_3 single crystal preparation by gas transport method, X-ray structure determ. *(Russian)* 3−12241
- Cu_2Te, n and p type, electrical props., struct. and preparation *(Russian)* 3−8170
- $Cu_3V_2O_8$, new form, unit cell dimensions, octahedral networks 3−30092

crystal atomic structure of inorganic compounds continued
- $CuVO_3(I)$, distorted ilmenite type derivative, cryst. struct. determ. 3−7695
- DI solid phases 3−15008
- $D_{0.53}WO_3$, cubic hydrogen tungsten bronze, powder neutron diffraction obs. 3−33501
- $DyAsO_4$, paramag. to antiferromag. transition, cryst. phase transition 3−2281
- $DyVO_4$, paramag. to antiferromag. transition, cryst. phase transition 3−2281
- $Dy_{4.67}[GeO_4]_3O$ apatite, cry. struct. of TR analog by X-ray diffr. 3−7703
- Er-Co intermetallic, struct., disordered substitutions 3−1603
- $ErCd_3$, space group, cell dimensions 3−7666
- Er_3GaS_6, and refinement *(French)* 3−20718
- Er(III) complex, tris-(2,2,6,6-tetramethylheptane-2,5-dionato)erbium(III) 3−14769
- $Er_9La_{10}S_{27}$, three dimensional X-ray data *(French)* 3−17782
- Eu complex, tetrakis(benzoylacetonate)europium, laser compound 3−21440
- EuAs powder, X-ray data 3−20724
- $EuEr_2Ga_xFe_{5-x}$, $Eu_xEr_{3-x}Ga_{0.7}Fe_{4.3}O_{12}$ bubble domain films, thermal expansion of lattice parameters 3−34158
- $EuLGa_3S_7$, $EuLAl_3S_7$, (L=La, Ce, Pr, Nd), sulphurized compound family of melilite type *(French)* 3−30102
- EuM_2Si_2, (M=Mn, Fe, Co, Ni, Cu, Ag), X-ray and Mossbauer obs. rel. to valency 3−14785
- EuTe, NaCl-CsCl structural type transform. at 100kbar pressure 3−27221
- $(Fe, Ti, \square)_3O_4$, cation deficient, magnetic props. 3−4735
- $(Fe,Ti)_3S_4$, X-ray diffr. obs. 3−14758
- Fe complex, clathrochelate, disorder 3−17773
- FeAs, MnP type structure, magnetic props. 3−15370
- $FeAsO_4$, type-I *(French)* 3−4733
- $FeCr_3S_4$ gas transport and characterisation *(German)* 3−8730
- $FeCr_2Se_4$ *(Russian)* 3−14811
- Fe_2GeS_4, cryst. and mag. structs. at 85 K and 4.2 K, mag. transitions *(French)* 3−27373
- Fe(III) complex, chlorobis-(N-n-propylsalicylaldiminato)iron(III), and mol. struct. 3−24076
- $FeIn_2S_4$, cation distrib., mag. susceptibility temp. depend. 3−34102
- $FeNiBO_4$, dense warwickite type formed by hydrothermal synthesis at high pressure *(French)* 3−38571
- $\alpha\text{-}Fe_2O_3$, hematite, equilib. form, from Hartman and Perdock method *(French)* 3−33492
- $Fe_2O_3\text{-}Al_2O_3$ mixed oxides, conc. depend. of parameters *(French)* 3−7679
- $Fe_2(OH)_3$ amorphous gel, characterisation and phase transformation 3−5383
- $FeTaO_4$, polymorphic transition from rutile to wolframite type structure under high pressure 3−33670
- GaAs, lattice parameter, temp. depend., 20-800°C 3−24279
- GaAs, molecular beam epitaxial layer, HEED obs. 3−2677
- $GaAs_{1-x}P_x$, superlattice, X-ray diffraction obs. of lattice distortion and structure 3−17788
- GaAs(P)(Sb), structure factor meas. rel. to electron distrib. and bonding 3−14784
- GaP, molecular beam epitaxial layer, HEED obs. 3−2677
- GaSe, needle cryst., growth by sublimation process, struct. 3−2633
- $(Ga_{1-x}Zn_x)Mn_3C$, meas. from 4.2 to 320 K rel. to mag. structure *(French)* 3−30631
- Gd complex, $Gd(DMP)_3Cl_3$, (DMP=2,6-dimethyl-4-pyrone) 3−17776
- GdGa garnet, lattice parameters in faceted regions, X-ray double cryst. analysis 3−1609
- GdGa garnet, macroscopic strain in facetted regions 3−33493
- GdO, film, structure and defect substructure obs. 3−8067
- $H_{3\|x}Co_x{}^{II}Co_{1-x}{}^{III}(CN)_6.yH_2O$, H-bonding and hydronium ion effects *(French)* 3−14806
- $H_{3\|x}Fe_x{}^{II}Fe_{1-x}{}^{III}(CN)_6.yH_2O$, H-bonding and hydronium ion effects *(French)* 3−14806
- $HK_8Rh_3Br_{18}.10H_2O$ 3−17769
- $HK_8Rh_3Br_{18}.10H_2O$, and mol. struct. 3−24072
- Hf-O system, near $HfO_{1/6}$, interstitial superstruct. and order-disorder transform. 3−14847
- $HfO_2\text{-}Dy_2O_3$ system of cubic solid solutions, dependence of lattice parameters on composition *(Russian)* 3−11715
- $HfTe_{2-x}$, x=0.061, preparation and X-ray characterization 3−7691
- $HgMoO_4$, determ. from single crystal counter data by Patternson and Fourier methods 3−38560
- $Hg(OH)NO_3$, neutron diffr. obs. 3−14755
- $\alpha\text{-}Hg_2V_2O_7$, X-ray determ. *(French)* 3−26997
- $InNbO_4$, cell data *(German)* 3−7668
- $In_2O_3\text{-}SnO_2$ transparent conducting films, structure obs. by electron diffraction and spectroscopy 3−33763
- InOF, X-ray determ. *(French)* 3−27001
- $\gamma\text{-}In_2S_3$ growth from melt of As_2S_3 *(German)* 3−8741
- In_4Se_3 *(French)* 3−7680
- $InTaO_4$, cell data *(German)* 3−7668
- $\beta\text{-}In_2Te_3$, X-ray investigation *(Russian)* 3−8724
- $KBa_5ZrNb_9O_{30}$, melt grown, characterization 3−12268
- $KBa_5ZrNb_9O_{30}$, obs. of tetragonal tungsten bronze structure 3−38572
- $K_2BiNb_5O_{15}$, crystal growth, structure, composition and dielectric props. 3−8535
- KCl, anomalous X-ray transmission rel. to imperfect structure, dislocation and thickness effects 3−24145
- KCl, of high press. high temp. phase at 100°C and 30 kbar 3−7671
- $K_3Co(CN)_6$, Raman spectra data 3−30816
- $K_6(Co_2O_7)$, new oxocobaltate (IV), lattice parameters determ. *(German)* 3−36287
- $K_2Cr_2O_7$, structure refinement 3−38570
- $K_2Cr_4O_{13}$, by systematic analysis of Patterson function on basis of crystal symmetry 3−33426
- K_3CrO_8, refinement of structure and bond nature of $CrO_8{}^{3-}$ ion *(French)* 3−7715
- $K_4Cu_4OCl_{10}$, lattice constants 3−7678
- $K_2Cu(SO_4)_2.2H_2O$, crystal struct., Patterson synthesis, tridimensional Fourier summations *(French)* 3−14820
- $K_{0.6}FeF_3$ pseudo-tetragonal bronze 3−14746

crystal atomic structure of inorganic compounds continued
$K_6Ge_2O_7$, new alkali metal titanates and germanates, lattice consts. determ. *(German)* 3-36288
$KH_5(PO_4)_2$ crystal struct. refinement by neutron diffraction *(French)* 3-27012
$KH_3(SeO_3)_2$, refined struct., H-bonding network 3-7670
$K_xLi_xTi_{4-x/2}O_8$. new structure type in K_2O-Li_2O-TiO_2 system, crystal chem. 3-38573
K_2MoO_4, high temp. phase, modulated struct. 3-26999
KNO_2 high pressure phases, X-ray diffraction, analysis 3-11595
KNO_3, alpha-phase, neutron diffraction obs. at 25 and 100°C 3-20723
$KNd(WO_4)_2$, monoclinic, refinement and cell parameter determ. 3-24090
$K_3Ni_2F_7$ antiferromagnetic, magneto-optical props. and struct. determ. 3-12119
$KNiPO_4$, X-ray determ. *(Russian)* 3-11603
$K_2O.2B_2O_3$, space group, cell dimensions 3-7665
$K_4P_8Ta_{12}O_{52}$ 3-14754
$KSbWO_6$, pyrochlore, isolation and cubic cell cation position detn. *(French)* 3-30104
K_2SeO_4, X-ray obs. 3-14805
$KTa_xNb_{1-x}O_3$, x=0.56, ferroelectric, soft modes and struct. 3-11594
$K_6Ti_2O_7$, new alkali metal titanates and germanates, lattice consts. determ. *(German)* 3-36288
$K_3(UO_2)_2F_9$, $K_3(UO_2)_2F_72H_2O$ and $K_5(UO_2)_2F_9$, lattice parameters and structure *(Russian)* 3-26993
K_2WO_4, high temp. phase, modulated struct. 3-26999
$KY(MoO_4)$:Nd, effect of Nd concentration on cell parameters *(Russian)* 3-11643
$K_2[Ru(NO)Cl_5]$, and mol. struct. 3-24071
KrF, X-ray diffraction meas. at −80°C 3-36289
La complex, $[La(DMP)_8](ClO_4)_3$, (DMP=2,6-dimethyl-4-pyrone) 3-17776
LaF_3, symmetry, struct., screening consts. 3-7662
$La_{10/3}Ga_6S_{14}$, sulphurized compound family of melilite type *(French)* 3-30102
La_2GeS_5, diffractometer data using Patterson and Fourier syntheses *(French)* 3-38557
$LaLiNb_4O_{12}$, rel. to tungsten bronze structure 3-38572
$La_3Li_3Nb_8Zr_2O_{30}$, rel. to tungsten bronze structure 3-38572
α-La_2S_3, cryst. struct. from X-ray diffr. meas. 3-30100
$LiAlSiO_4$, β-eucryptite, average struct. 3-7717
$LiAlSiO_4$, β-eucryptite, superstruct. 3-7718
$LiBO_2$, monoclinic characterisation *(French)* 3-14818
$Li_6B_4O_9$ characterisation *(French)* 3-14818
Li_4CoO_4, new oxocobaltate (IV), lattice parameters determ. *(German)* 3-36287
LiF, integrated intensities of Laue and Bragg reflections, extinction and structure factor determ. 3-23955
$LiLnMo_2O_8$, epitaxially grown on Ln_2GeMoO_8, X-ray diffr. obs. 3-1913
$LiMg_x(Zn_x)V_{2-x}O_4$ mixed oxides, phase comp., lattice parameters, spinel phases 3-38563
$Li_2Mo_4O_{13}$, $Li_4Mo_5O_{17}$, grown from Li_2MoO_4-MoO_3 system, X-ray diffr. obs. 3-2666
$LiNbO_3$, Czochralski grown, cryst. perfection, obs. of Pendellosung fringes 3-36279
Li_2O-Pd-O_2 system, synthesis, structure and stability of phases 3-33676
Li_2SO_4 3-20719
$LiTaO_3$, temp. depend. of ferroelec. phase and paraelectric phase at 940 K 3-30098
$LiTaO_2F_2$, single-crystal diffraction method for structure anal. 3-30103
$Li_4Te_2O_7$, lattice parameters *(French)* 3-38564
$LiVO_3$, least squares refinement, bond lengths and strength 3-30094
Li_2WO_4, phase transforms. at high pressure, structure obs. for III(IV) phases 3-33668
Lu-Fe intermetallic, X-ray and neutron diffr. obs. 3-1602
$LuAsO_4$, zircon type, X-ray analysis *(German)* 3-17783
$LuPO_4$, zircon type, X-ray analysis *(German)* 3-17783
Mg-Ln_2-S_4, ternary sulphides, prep., elec. and opt. props. 3-39243
$Mg_{8.5}As_3O_{16}$, structure analysis rel. to comp. 3-24082
$MgFe_{2-x}In_xO_4$, X-ray diffraction and γ-resonance obs. of spinel structure 3-24087
$MgFe_4((OH)_2|(SO_4)_6).20\,H_2O$, copiapite, crystal structure and H bonding 3-7716
$MgHAsO_4.7H_2O$, Roesslerite, rel. to hydrogen bonding 3-20717
$MgHAsO_4.7H_2O$, rosslerite, and hydrogen bonding 3-14762
$MgIn_2O_4$, X-ray diffraction and γ-resonance obs. of spinel structure 3-24087
$Mg_4{}^{2+}La_6(SiO_4)_4(PO_4)_2O_2$, silicophosphate, preparation and characterization *(Russian)* 3-11597
$MgNH_4AsO_4.6H_2O$, arsenstruvite, structure refinement, hydrogen bonding 3-38558
$MgNH_4AsO_4.6H_2O$, As-struvite, and hydrogen bonding 3-14762
MgO, lattice parameter, 2100°C 3-24225
MgO, X-ray integrated intensities, primary extinction effects 3-24068
MgO-ZnO, local order, diffuse X-ray scatt. obs. 3-4740
$Mg_2(PO_4)Cl$, and refinement 3-24069
$MgSO_3.6H_2O$, slightly distorted CsCl arrangement *(French)* 3-38553
Mg_2Sn, obs. in polymorphic phases at high pressure and temp. 3-24270
MgV_2O_6, cryst. struct. and e.s.r. of Mn^{2+} 3-11589
β-MgV_3O_8, lattice parameters, space group *(French)* 3-38567
$MnFe_{2-x}In_xO_4$, X-ray diffraction and γ-resonance obs. of spinel structure 3-24087
MnGaGe, ferromagnet, prep., struct., Curie temp., saturation magnetisation, mag. moments 3-21268
$MnGeN_2$, position parameters of Mn and N atoms, mag. struct., moments orientation *(French)* 3-8370
$MnIn_2O_4$, X-ray diffraction and γ-resonance obs. of spinel structure 3-24087
$MnIn_2S_4$, cation distrib., mag. susceptibility temp. depend. 3-34102

crystal atomic structure of inorganic compounds continued
MnO, electron diffraction study of the nature of the chemical bond *(Russian)* 3-4728
MnSe high pressure modification, NiAs structure type, X-ray diffraction data *(German)* 3-11737
$MnSiO_3$, pyroxmangite 3-17770
Mo complex, $K_4(CN)_8Mo.2H_2O$, neutron diffr. study 3-14780
$Mo_{1-x}B_3$, powder diffraction obs. rel. to comp. 3-33498
$Mo_3Ir_{1-x}Ru_x$, A-15 pseudo-binary type cpd., supercond. Transition Temp., room temp. lattice parameters 3-15308
MoO_3 type crystal structure, relation with ReO_3 type 3-11587
$MoO_3.2H_2O$, topotactic dehydration 3-9063
$Mo_3Os_{1-x}Ru_x$, A-15 pseudo-binary type cpd., supercond. Transition Temp., room temp. lattice parameters 3-15308
Mo_3Se_4, heavy atom method for structure soln. *(French)* 3-27008
NH_4HSO_4, cryst. struct., ferroelectric phase and transition 3-8526
$NH_4H_3(SeO_3)_2$, H-bonding, X-ray obs. 3-27002
NH_4LiBeF_4 determ., space groups and symmetry 3-11598
$NH_4NH_2SO_3$ 3-14759
$NH_4SO_3NH_2$, space group, unit cell dimensions 3-7722
NH_4SnF_3 3-14748
$Na_8(Al_6Si_6O_{24}).(OH)_2$, hydrosodalite, p.m.r. obs. of water molecules and hydroxyl groups positions 3-24086
$Na_2B_4O_6(OH)_2.3H_2O$, charge density and at 300K rel. to bonding 3-14833
$Na_2Ba_4Si_{10}O_{25}$ 3-24030
γ-Na_2BeF_4, crystal struct. and anisotropic thermal expansion at 25° and 74°C 3-7946
NaBr-KBr solid solution, interatomic bonds, energetic and strength characts. *(Russian)* 3-20722
NaCN, single crystal neutron diffr. obs. 3-27004
$Na_2Ca(Al_2Si_3O_{10})_2.6H_2O$ (gonnardite) crystal structure *(Russian)* 3-2886
$NaCa_2Co_2V_3O_{12}$, mag. and atomic struct., Co spin state *(Russian)* 3-12025
$NaCaHSiO_4$, unit cell, electron microscope and X-ray study 3-27006
NaCl, integrated intensities of Laue and Bragg reflections, extinction and structure factor determ. 3-23955
NaCl-KCl solid solution, interatomic bonds, energetic and strength characts. *(Russian)* 3-20722
α-$Na_2Cr_2O_7$, and alpha-beta phase transition 3-38561
$Na_2CuSi_4O_{10}$, X-ray obs. 3-27013
$NaD_3(SeO_3)_2$, room-temp. struct. detn. by heavy-atom method 3-7704
$NaH_3(SeO_3)_2$, phase II 3-39106
$Na_3HSiO_4,5H_2O$ 3-17765
$NaIn(MoO_4)_2$, melt growth, cryst. struct. and thermal stability 3-33507
$NaMn_7O_{12}$, high pressure syhnthesized, study of distorted perovskite structure 3-27007
$NaNbO_3$, soft modes and superlattice struct. 3-39105
Na_3NbO_4, cubic, i.r., Raman, and luminesc. spectra obs. of rocksalt struct. 3-5190
Na_2O-CdO-GeO_2-H_2O system, crystallisation under hydrothermal conditions at constant temperature 3-33508
Na_3P_{11}, phosphide with isolated $P_{11}{}^{3-}$ groups, lattice parameters determ. *(German)* 3-36286
Na_2S-GeS_2, struct. investigation of sodium thiogermanate with infinite $(GeS_3)^{2n-}{}_n$ chains *(French)* 3-14817
$Na_4Zr_2\,[SiO_4]_3$, structure from X-ray goniometry 3-17795
Nb suboxides, electron microscopy study 3-17794
NbGeX, (X=As, Sb), PbFCl-type pnictide, powder refinement of structure 3-33499
NbH, meas. of f.c.o. lattice parameters 3-30097
$Nb_{12}O_{29}$, oxidation, electron microscope assessment of the role of extended defects 3-5380
Nb_2O_5, electron microscope obs. of planar defects and structure at high temps. 3-11638
NbSiX, (X=As, Sb) PbFCl-type pnictide, powder refinement of structure 3-33499
NdF_3, symmetry, struct., screening consts. 3-7662
$NdFe_2Si_2$, and mag. structure, neutron diffraction obs. 3-34135
α-Nd_2S_3, cryst. struct. from X-ray diffr. meas. 3-30100
Nd_2TiO_5, X-ray diffraction determ. of lattice constants and space group *(German)* 3-36281
$NiAl_2O_4$, spinel, equilib. çation distrib., X-ray diffr. analysis 3-7687
NiAs, structure factors rel. to outer electrons density distrib. and bonding 3-14787
$NiCr_2O_4$, spinel structure, structure changes under high pressure, Jahn-Teller effect 3-27118
$NiFe_{2(1-c)}Cr_{2c}O_4$, crystal chem., lattice dimens. and cation lattice point distrib. *(Russian)* 3-38568
Ni(II) complex, bis(1-methyl-3-orthochlorophenyl triazene 1-oxide) nickel (II) 3-17777
Ni(II) complex, μ', μ'', μ'''-tris(dithioacetato)-μ_3-trithioorthoacetato-triangulo-trinickel(II) 3-17772
Ni(II) complex, Ni(PNNP)Br, where PNNP=N,N'-bis(2-diphenyl- 3-17780
Ni(II) complex, bis(2,4-dithiobiuret)nickel(II).glycol 3-14777
Ni(II) complex, bis(dithiocarbazato)nickel(II) 3-14767
$NiIn_2S_4$, cation distrib., mag. susceptibility temp. depend. 3-34102
$Ni_{0.33}Mo_3Se_4$, structure determ. by analogy with Mo_3Se_4 *(French)* 3-33500
Ni_4N, electron diffraction obs. of N interstitials and structure factors 3-14783
NiO, antiferromagnetic, crystal structure determined by X-ray topography 3-30646
NiO-MgO-GeO_2, spinel-olivine and olivine-phenacite transitions, thermodynamic and volume relations 3-27122
NiO-TiO_2-SiO_2 system, spinel phase formation, lattice constants determ. 3-36284
NiO-ZnO-GeO_2, thermodynamic relations among olivine, spinel and phenacite structures 3-27123
γ-o_2, paramag. cubic phase, crystal structure and mag. form factor 3-34092
OsO_4, dispersion in centrosymmetric structs. 3-14741
$PCl_4{}^+TeCl_5{}^-$ 3-14760

crystal atomic structure of inorganic compounds continued

Pb phosphates, i.r., X-ray and chem. anal. of apatite structure and comp. *(German)* 3-33497
Pb^{2+} oxides, fluorides and oxide fluorides, calcs. of bond lengths and angles 3-33073
$Pb_{26}Ag_9Cu_{24}Cl_{62}(OH)_{48}$, boleite mineral, obs. of Ag atom clusters 3-27009
$Pb(Fe_{2/3}U_{1/3})O_3$, lattice const. 3-21231
$Pb(Fe_{2/3}W_{1/3})O_3$, lattice consts. 3-21231
$Pb_5Ge_3O_{11}$, ferroelec., prototypic structure determ. 3-33502
$Pb_5Ge_3O_{11}$, ferroelec. 3-17764
$PbGeO_3$ single crystals in PbO-GeO_2 binary system, Czochralski pulling method 3-18549
Pb(II) complex, thiourea coordination compounds 3-14775
$Pb_{1-kx}La_xTiO_{3\|x(1.5-k)}$, with A-site and B-site vacancies, X-ray obs. 3-17792
$Pb_\alpha(MO)_\beta MO_3$, (M=Ta, W and Nb, W) new phases, struct. *(French)* 3-7697
$PbNb_4O_{11}$, $Pb_5Nb_4O_{15}$, $Pb_2Nb_2O_7$, unit cells, X-ray diffr. obs. *(French)* 3-4736
m $PbO.2UO_3.(4-2m)H_2O$, $o \leqslant m < 2$, indexing of X-ray powder patterns *(French)* 3-30091
$5PbO.3GeO_2$ single crystals in PbO-GeO_2 binary system, Czochralski pulling method 3-18549
$Pb_2P_2O_7$, Czochralski growth, crystal structure and dielec. props. 3-33470
$Pb_5P_4O_{15}$, and growth phase transform., dielec. props. 3-1727
PbS-Bi_2S_3 system phases 3-15858
PbTe-MgTe alloy system, physical props. 3-7904
$Pb_2V_2O_7$, synthetic chervetite, full matrix least squares refinement, bonds, interatomic distances 3-30093
$Pb_{2-x}Zn_yNb_{2-z}O_{7-x\|y-2,\,5z}$, unit cells, X-ray diffr. obs. *(French)* 3-4736
Pm_2O_3, polymorphic modifications of struct. 3-7688
PrF_3, symmetry, struct., screening consts. 3-7662
$(Pr^{-r})Ga$ garnets with R=small rare earths on two crystallographic sites, magnetic susceptibility meas. 3-7689
PrTe, NaCl-CsCl structural type transform. at 100kbar pressure 3-27221
PtP_2O_7, lattice parameters 3-14753
RbF-InF_3 systems preparation and crystallographic data *(French)* 3-7699
$Rb_6Ge_2O_7$, new alkali metal titanates and germanates, lattice consts. determ. *(German)* 3-36288
$RbH_3(SeO_3)_2$, chain structure, hydrogen bond lengths 3-33496
Rb_2MgCl_4, e.p.r study on Mn(II)-doped crysts. 3-27413
$Rb_2MgCl_2Br_2$, e.p.r. study on Mn(II)-doped crysts. 3-27413
Rb_2MgCl_3Br, e.p.r. study on Mn(II)-doped crysts. 3-27413
$RbSbWO_6$, pyrochlore, isolation and cubic cell cation position detn. *(French)* 3-30104
$Rb_6Ti_2O_7$, new alkali metal titanates and germanates, lattice consts. determ. *(German)* 3-36288
Rb_2WO_4, high temp. phase, modulated struct. 3-26999
Re(I) complex, μ-[tetraphenylporphyrin]-bis-[tricarbonyl-rhenium(I)] 3-14779
ReO_2, monoclinic, orthorhombic, crystal parameters precisions and Debye-Scherrer indexing *(French)* 3-14816
ReO_3, monoclinic, orthorhombic, crystal parameters precisions and Debye-Scherrer indexing *(French)* 3-14816
ReO_3 type crystal structure, relation with MoO_3 type 3-11587
Rh_2O_3, X-ray powder obs. of high temp. low pressure form. 3-17790
Ru complex, $(\varphi_3P)_2[(CF_3)_2C_2S_2]$-RuCO, orange and violet isomers 3-14772
$(SN)_n$, electron diffr. obs. 3-24065
$S_6(NH)_2$, isomer II, structure refinement, N-S bond lengths 3-38562
Sb^{3+} oxides, fluorides and oxide fluorides, calcs. of bond lengths and angles 3-33073
L-SbOF, determ. of orthorhombic symmetry and anion positions 3-33495
m $ScO.2UO_3.(4-2m)H_2O$, $O \leqslant m < 2$, indexing of X-ray powder patterns *(French)* 3-30091
$Sc_2Si_2O_7$, thortveitite, refinement and cell parameters determ. 3-24089
Se_3S_5, X-ray obs. 3-14757
SiC, structural transforms. on annealing 3-14791
$SiPb_2S(Se)_4$, X-ray diffraction obs., determ. of lattice dimensions and space group 3-27010
α-Sm_2S_3, cryst. struct. from X-ray diffr. meas. 3-30100
SmTe, NaCl-CsCl structural type transform. at 100kbar pressure 3-27221
Sn complex, $C_6H_{12}SnSO_2$, X-ray determ. *(French)* 3-26996
$SnCl_2.2H_2O$, X-ray and neutron diffr. obs. 3-14756
$SnCr_2S_4$, ferrimag., prep. by heating method, Curie temp. and cell dimensions meas. 3-31261
SnI_2, space group, cell dimensions 3-7663
SnP_3, crystal struct. determ. 3-7694
$Sn_2S(Se)I_2(Br_2)$ *(French)* 3-11590
β-$SnWO_4$, diamagnetic and semiconducting 3-7674
$Sn_{0.11}WO_3$, $Sn_{0.25}WO_3$, tetragonal struct., electron density maps 3-1610
$Sn_xZr_{1-x}S_2$, layer compound, vapour growth conditions and structure parameters 3-38543
SrAs powder, X-ray data 3-20724
$Sr_3Cr_2WO_9$, perovskite type *(French)* 3-24080
$SrFe_xMo_{1-x}O_{3-y}$, X-ray obs. 3-21345
$Sr_3Fe_2TeO_9$, struct. and antiferromagnetism at low temps. *(French)* 3-7690
$Sr(Fe_{2/3}U_{1/3})O_3$, lattice const. 3-21231
$SrLGa_3S_7$, $SrLAl_3S_7$, (L=La, Ce, Pr, Nd), sulphurized compound family of melilite type *(French)* 3-30102
$Sr_4{}^{2+}La_6(SiO_4)_4(PO_4)_2O_2$, silicophosphate, preparation and characterization *(Russian)* 3-11597
$SrLi_{0.25}Nb_{0.75}O_3$ and $SrLi_{0.25}Ta_{0.75}O_3$, perovskite structure and dielectric props. *(Russian)* 3-14810
$Sr(NO_3)_2.4H_2O$, crystal struct. *(German)* 3-4742
$2SrO.Al_2O_3.B_2O_3$, struct. detn. by Patterson and electron density synthesis *(Japanese)* 3-20727
SrP powder, X-ray data 3-20724

crystal atomic structure of inorganic compounds continued

$Sr_5(PO_4)_3OH$ 3-24077
$SrTiO_3$, lattice parameter var., 10 to 130K, neutron backscattering obs. *(German)* 3-30107
$Sr_2TlNb_5O_{15}$, lattice parameters *(French)* 3-38566
Ta oxides, orthorhombic, in thin films at. struct. detn. by electron diffraction 3-7706
$TaSe_2$, polymorphism, mag. and elec. props. of polymorphs at low temp. 3-14793
TaSiAs, PbFCl-type representative, structure and comp. from microanalysis 3-30096
Te^{4+} oxides, fluorides and oxide fluorides, calcs. of bond lengths and angles 3-33073
Te_2O_5, three dimensional X-ray obs. 3-38552
$TeVO_4$, monoclinic system, lattice parameters determ. *(French)* 3-24081
Th-Cu, of intermediate phases formed in liq. Na, 200-700°C 3-2690
Th-Ni intermetallic, struct., disordered substitutions 3-1603
Ti-C-O system crystallographic and metallographic obs. *(French)* 3-7698
Ti_4O_7, obs. in metallic and insulating phases rel. to metal-insulator transition 3-27220
Ti_4O_7, structural aspects of metal-insulator transition 3-33815
Tl_3AsS_4, Stockbarger-grown, characterization 3-12266
Tl_3BO_3, stereochem. role of Tl I doublet *(French)* 3-20721
TlF-InF_3 systems, preparation and crystallographic data *(French)* 3-7699
Tl_3FCO_3, X-ray diffr obs. 3-26995
TlI, mol. struct., anharmonicity, i.r. and Raman investigations 3-20825
$TlLTe_2$, L=rare earth *(French)* 3-11592
$Tl_3Na(SO_3)_2$, space group, lattice parameters *(French)* 3-38565
TlOF, cubic structure, space group, Patterson functions 3-7676
$TlSbWO_6$, pyrochlore, isolation and cubic cell cation position detn. *(French)* 3-30104
$UAs_{2-x}Se_x$, solid solution, X-ray diffraction, lattice parameters determ. 3-38985
UF_6, neutron diffraction analysis, deviations from ideal symmetry structure 3-17781
$U_2N_{3\|x}$ cubic, uranium positions 3-17791
α-UO_3, by neutron and electron diffr. 3-24075
U_4O_9, struct. below and above transition temp. 3-14744
γ-$UO_2(OH)_2$ 3-24070
β-$UO_2(OH)_2$, atom positional parameters rel. to thermal expansion, 21-260°C 3-7942
U_3S_5, orthorhombic *(French)* 3-14808
U_3Se_4, structure isomorphic to Th_3P_4, no mag. ordering at 77 K, neutron diffr. obs. 3-38959
V_6C_5, obs. of ordered arrangement of C vacancies 3-14782
V_3H_2, superstructure model for low temp. phase 3-30262
$V_xMn_{1-x}O$, lattice dimens. determ. by X-ray anal. *(Russian)* 3-12007
VO, structure interpretation from short range order scattering in electron diffraction 3-24066
VO_2, c/a ratio in crysts. with rutile structure, rel. to metallic V-V bonding in band model of metal-insulator transition 3-18092
VO_2:Cr, obs. in metallic and insulating phases rel. to metal-insulator transition 3-27220
V_2O_3 oxidation to V_3O_5, topotactic relation of crystal structure 3-14801
V_4O, interstitial superstructure, O long range order 3-30112
V_4O_7, obs. in metallic and insulating phases rel. to metal-insulator transition 3-27220
V_4O_7, structural aspects of metal-insulator transition 3-33819
V_nO_{2n-1}, n=2, 3, 4, 5 3-14747
β-VPO_5, crystal struct. 3-7693
W_2C, of α, β, γ and orthorhombic phases, supercond. critical temps. 3-2205
WO_3-Nb_2O_5, high resolution electron microscopy 3-24128
Y TaO_4, Y Ta_3O_9 formation in Y_2O_3-Ta_2O_5 system, X-ray interplanar distances *(Russian)* 3-12497
Y-Ni intermetallic, struct., disordered substitutions 3-1603
$YNiAl_2$, struct. detn. from Laue patterns *(Russian)* 3-7708
$YNiAl_4$, struct. detn. from Laue patterns *(Russian)* 3-7708
$Y_2O_3-YF_3$ system, intermediate fluorite related phases, examples of one dimensional ordered intergrowth 3-7692
Y_2ReB_6, Laue method exam. of crystal and analogs *(Russian)* 3-7711
YSeF polytypes, lattice parameters *(French)* 3-1605
YVO_4, zircon type, X-ray analysis *(German)* 3-17783
Zn phosphates, synthetic group, unit cell parameters of six phases, x-ray obs. 3-33657
Zn-Ln_2-S_4, ternary sulphides, prep., elec. and opt. props. 3-39243
$ZnAl_2O_4$, spinel, equilib. cation distrib., X-ray diffr. analysis 3-7687
$Zn_2AsO_4(OH).H_2O$, legrandite, structural interpretations 3-24088
$ZnCr_2Se_4$ *(Russian)* 3-14811
$ZnGeP_2$, refinement of structural characteristics, structural depend. of birefringence 3-21382
$Zn_xHg_{1-x}(SCN)_2$, gel grown, characterization 3-15611
Zn(II) complex, bis(dithiobenzoato)zinc(II), four-membered chelate ring obs. 3-17771
Zn(II) complex, trichloroadeniniumzinc (II), metal binding to nucleic acids 3-36278
$Zn_2In_3S_5$(II)a, Weissenberg X-ray goniometer exam. *(Russian)* 3-7714
$ZnIn_2S_4$(II)b, Weissenberg X-ray goniometer exam. *(Russian)* 3-7713
$ZnNb_2O_6$, $Zn_3Nb_2O_8$ unit cells, X-ray diffr. obs. *(French)* 3-4736
ZnO, film, d.c. diode sputtered, variation of c-axis orientation 3-33753
$Zn_2(OH)PO_4$, tarbuttite, Cu^{2+} e.s.r., hyperfine structure 3-36784
ZnS, Patterson method for layer sequence determ. of polytypes 3-14795
ZnS, study of polytypes using proton backscattering patterns 3-24085
ZnS films, electron microscopy, electron diffraction and X-ray analysis obs. 3-33759
ZnS:Cu electroluminophors in strong magnetic field, $\beta \rightarrow \alpha$ phase change *(Russian)* 3-8668

crystal atomic structure of inorganic compounds continued
- $ZnS-M^IM^{III}S_2$, M^i=Cu, Ag and M^{III}=In, Ga, Al, preparation and phase relationships 3—7909
- ZnSe-CdSe solid solution, identity periods and mean-square displacements of ions *(Russian)* 3—4739
- $ZnSiAs_2$ refinement of structural characteristics, structural depend. of birefringence 3—21382
- Zr-O solid solution, interstitial order-disorder transform., neutron diffr. 3—14848
- ZrO_2-Y_2O_3, review of structure and ordering *(Russian)* 3—14812
- $Zr(OH)_2CrO_4$ and $Zr_4(OH)_6(CrO_4)_5.H_2O$ 3—14752
- Zr_3P-H solid solution, crystallographic study 3—11602

crystal atomic structure of organic compounds
- π-endo-dicyclopentadiene Pt dichloride 3—14824
- acenaphthylene, polarised i.r. and Raman spectra, crystal structure 3—39134
- 1-acetyl 2-ethoxynaphthalene, X-ray diffr. obs. 3—7741
- L-N- acetylhistidine monohydrate, space group P1, X-ray crystallography direct calculation methods 3—7732
- alkane system, n-$C_{20}H_{42}$, $C_{22}H_{46}$ 3—14959
- α-amino acids, neutron diffr. obs. 3—24094
- ammonium oxalate monohydrate, isotope and bonding effects, analysis using combined neutron and X-ray diffraction analysis 3—7731
- ammonium tartrate, X-ray determ. 3—27014
- anthrone, $C_{14}H_{10}O$, struct. refinement 3—7740
- L-aspartatocadmium (II) trihydrate, neutron anomalous dispersion, phase ambiguity resolved by tangent formula 3—23985
- benzidine-TCNQ complex containing dichloromethane 3—24096
- benzylchromium tricarbonyl, charge density and at 77K rel. to bonding 3—14833
- biological systems, single cryst. studies importance 3—14821
- bis(cyclooctatetraene)iron, evidence for dynamic tautomerism 3—24091
- bis-(11-ammonio-undecanoic acid) chloro-cuprate, room temp. phase 3—14829
- bisdimethyl-2,3-benzothiazoline *(French)* 3—14326
- cadmium ethylxanthate, X-ray obs. 3—14830
- cadmium tartrate pentahydrate, cell parameters, space group 3—4743
- caesium acetate 3—7726
- calcium tetraphosphonate, $Ca_2C_4H_8O_{12}P.10H_2O$, crystal struct. *(French)* 3—7737
- carbon tetrachloride, high pressure polymorph at 10 kbar, crystal and molecular structure determ. 3—27016
- 5-chloro-2-pyridone, hydrogen bond study 3—7735
- compilation from 1960-5 publications 3—30109
- copper formate tetrahydrate, antiferroelec. phase 3—17797
- copper formate tetrahydrate, antiferroelectric phase, approximate struct. determ. by neutron diffraction 3—12100
- cyclododecane, inhomogeneous impurity distrib. and effect on molecular parameters 3—1634
- cyclohexane I and II, X-ray diffr. obs. 3—15004
- deuteromethane, three phases 3—24265
- dibenzofuran, crystal and molecular structure 3—38580
- 1,8-dichloro 10-methyl anthracene, photochemistry, cryst. struct. and fluorescence *(French)* 3—2830
- 1,8-dichloro 9-methyl anthracene, photochemistry, cryst. struct. and fluorescence *(French)* 3—2830
- 3,5-dichlorophenol, crystal struct. and bond character, n.q.r. Zeeman effect study 3—34242
- N,N'-diethyladipamide, Nylon 6.6 model cpd., cryst. struct. 3—14836
- diglycine sulphate, orthorhombic structure 3—17800
- 3,5-dimethyl-5-nitro-tetrahydro-1,3-oxazine hydrochloride, unit cell and space group 3—27015
- p-dimethylamino-phenyl-diphenylphosphins, space group, lattice consts. *(German)* 3—7743
- diphenylamine, lattice parameters *(French)* 3—20728
- dipicolinic acid derivative of monoperoxovanadate (V), —100°C 3—14828
- durene, constrained refinement 3—20080
- fluorine organic compound, structure rel. to determ. of covalent radius 3—14834
- 9α-1 fluorocortisol, structural determination using pair relationships 3—7730
- β-fluoronaphthalene, naphthalene, comparison *(French)* 3—7734
- L-glutamic acid hydrochloride, neutron diffr. obs. 3—24092
- glycine, derivation from ^{14}N nuclear quadrupole resonance 3—27438
- glycine silver nitrate, ferroelectric crystal struct. 3—17798
- hexafluorobenzene, X-ray analysis at 120 K 3—17801
- isocinchophyllamine, phase function determ. *(French)* 3—14842
- lanthanide and actinide π sandwich complexes 3—14338
- latifolin, cell parameters 3—4744
- lithium acetate dihydrate, single crystals, proton magnetic resonance study 3—7728
- lithium ammonium tartrate monohydrate, accurate struct. aalysis rel. to ferroelec. phase transition 3—14840
- lithium ammonium tartrate monohydrate, symbolic addition method, three dimensional X-ray intensity data 3—7729
- lithium formate monohydrate, determ. of all hydrogen atoms position 3—38579
- magnesium picolinate dihydrate, determ. by symbolic addition procedure *(French)* 3—38577
- malate dehydrogenase, X-ray data, improved background correction using partial ω-scan method 3—20677
- mercury diethyldithiophosphate 3—14831
- mercury ethylxanthate 3—14831
- mercury N,N'-diethylthiocarbamate 3—14827
- method for assessing number of molecules in unit cell 3—24051
- 1-methyl-4-nitro-5-chloro-imidazol, twinned crystals, unit cell dimensions, space group determ. 3—33510
- molecular crystals, doped, polarisation luminescence method for struct. determ. *(Russian)* 3—27525
- molecular crystals, potential energy and equilibrium structure using atom-atom potentials method 3—11604
- naphthalene, β-fluoronaphthalene, comparison *(French)* 3—7734
- octafluoronaphthalene, X-ray examination, lattice constants, Patterson's method 3—7736
- oestrogen, stereochemistry *(French)* 3—14327
- orthophenylene diamine monohydrobromide, struct. 3—7725

crystal atomic structure of organic compounds continued
- p-nitropyridine N-oxide, charge density and at 30K rel. to bonding 3—14833
- pentachlorotoluene, ^{35}Cl n.q.r. Zeeman effect studies 3—34241
- pentachlorotoluene, n.q.r. and X-ray struct. analysis rel. to rotator phase 'freezing' *(Russian)* 3—7640
- cyclopentadienylnickelnitrosyl, cryst., i.r. spectra in polarised light, space group assignments 3—18460
- pepsin, heavy-atom parameters determ. by X-ray study 3—7277
- perchlorofulvene, X-ray obs. 3—14837
- 2-phenyl-3-fluorenyliden-4-benzyliden-spiro cyclobutan-1,9-fluoren 3—14652
- phloroglucinol, wide line n.m.r. investigations of structure and molecular reorientation 3—30703
- polyethylene, small angle X-ray scattering before and after irradiation 3—38541
- polyethylene crystals, Moire fringes in triple lamellae 3—23965
- potassium acetate 3—7726
- n-propyl-4'-octyloxydiphenyl-4-carboxylate smectic liquid crystal, X-ray scattering 3—7619
- proteins, anomalous X-ray scatt. 3—14655
- pyroxenes, Ca-Mg-Fe, synthesis and unit cell parameters 3—27925
- pyrroles, rel. to i.r. and Raman spectra at —180°C *(French)* 3—2529
- α-resorcinol, neutron diffr. obs. 3—24093
- rhodium(III) etioporphyrin 3—14823
- Rochelle salt, accurate struct. analysis rel. to ferroelec. phase transitions 3—14839
- rubidium acetate 3—7726
- rubidium ammonium hydrogen fluorocitrate dihydrate, soln. from Patterson map 3—38578
- rubidium salt of homophthalic acid, X-ray diffr. obs. 3—7742
- salicylic acid, neutron diffr. obs. 3—24093
- selenoindigo, lattice constants, space group determ. by 3 dimens. Patterson and Fourier synthesis *(German)* 3—36291
- L-serine, derivation from ^{14}N nuclear quadrupole resonance data 3—27438
- sodium cupric nitrilotriacetate monohydrate 3—14832
- stemonone, cell parameters 3—4744
- strontium dipicolinate tetrahydrate 3—18428
- strontium violurate tetrahydrate, X-ray obs. *(French)* 3—14843
- systematic search of structures, computer appl. 3—33420
- TCNQ salt, NMP type, non-mag. semicond. phase obs. 3—2066
- 4,8,9,10-tetrachloro-2,6-dithiaadamantane, crystal and molecular struct. 3—7739
- tetrachloro-m(p-)xylene, n.q.r. and X-ray struct. analysis rel. to rotator phase 'freezing' *(Russian)* 3—7640
- tetrachlorohydroquinone hydrogen-bonded cryst., mol. packing 3—14822
- α-tetrafluoromethane 3—24097
- tetramethyl ammonium halides, proton magnetic resonance and internal motions 3—8460
- thieno-(2, 3-b)thiophene, space group 3—15490
- thiophene, four solid modifications, i.r. spectra 3—27494
- transition metal acetylenic complexes, X-ray obs. 3—14826
- tribenzylamine, three dimensional X-ray analysis at —70°C 3—7733
- 2,4,6-tribromo aniline, wide line n.m.r. investigations of structure and molecular reorientation 3—30703
- triglycine fluoroberyllate, ferroelec. and paraelec. phases 3—14841
- triglycine sulphate, accurate struct. analysis rel. to ferroelec. phase transition 3—14838
- L-tyrosine, and HCl salt, cryst. and mol. struct. comparison 3—30108
- uranyl oxalate trihydrate, monoclinic lattice parameters 3—7727
- α-, p-bromodiazoaminobenzene, and mol. struct. 3—33511
- CH_4 solid, in phases I and II, i.r. spectra and cryst. struct. 3—12128
- CH_3CCl_3, methylchloroform, crystal structure relationship with CX_4(x=Cl, Br, I) 3—14835
- CO_4 solid, in phases I and II, i.r. spectra and cryst. struct. 3—12128
- 11-chloro-indazole(2,3-9)(3,1)benzoxazin-5-one, lattice parameters, X-ray meas. 3—36290
- p-chloroaniline, ^{35}Cl n.q.r. Zeeman effect studies 3—34241
- $Hg(CH_3CONH)_2$, derivative of DF trypsin, determ. of heavy atom coordinates 3—24098
- Ir organometallic, π-bonding of butadiene to Ir 3—14825

crystal binding
- *see also binding energy; lattice energy*
- alkali halide, electronic polarisability calc. 3—30746
- alkali halide ionic radii determ. from second nearest neighbour repulsive energy ratio 3—1591
- alkali halides, relative stability, short-range three-body potential in first-order exchange energy 3—1595
- alkali halides, Rydberg potential function 3—38549
- alkaline earth oxides, effective ionic charge 3—20706
- benzylchromium tricarbonyl, charge density and at 77K rel. to bonding 3—14833
- borate planar anion polarisability, effect on crystn. environment 3—30747
- carbonate planar anion polarisability, effect on crystn. environment 3—30747
- charge density analysis, effect of models for thermal motion and two-centre scatt. 3—14654
- covalence in elemental structures and AB compounds, band structure *(French)* 3—26985
- covalent systems, quantum dielectric theory of electronegativity 3—20709
- critical ionicity of A^nB^{8-n} compounds 3—1596
- effective charges and ionicity, empirical correl. 3—36271
- elastic constants, electrostatic contribs. in calcs. 3—17893
- electrostatic potential of point charge in dielectric solid, shell model 3—18407
- finite ionic crystal, electrostatic potential 3—11579
- hydrogen bonded solids, theory of proton transfer 3—11583
- ice, hexagonal, mol. orbital calcs. 3—17758
- inorganic structure, analysis of local balance of valences 3—24059
- insulator, photoemission-determined valence band gaps and ionicity parameters, relation 3—24380
- LCAO-HMO study 3—1592
- metal, calc. of stable cryst. structs. with pseudopotentials 3—1597
- metal, irrad., plasmon cohesive energy of voids and void lattices 3—36554

crystal binding continued
metal, simple, pseudopotential method 3—27208
metal and alloy, thermodynamics, statistical, charge neutrality, compressibility 3—30084
molecular packing anal. with lattice energy minimisation, internal rotations about bonds 3—14710
monatomic solid regularities, semi-theoretical models 3—14723
nitrate planar anion polarisability, effect on crystn. environment 3—30747
p-nitropyridine N-oxide, charge density and at 30K rel. to bonding 3—14833
potential energy calcs. rel. to mol. packing determ. 3—24061
radial distrib. of electrons rel. to cryst. chem. *(Russian)* 3—14726
resonating valence bonds, insulating state 3—30415
rigid ion crystal, short range forces, static equilib. conditions 3—33483
second nearest neighbour electron interaction 3—33482
semiconductor, photoemission-determined valence band gaps and ionicity parameters, relation 3—24380
semiconductor, relation to band models 3—2007
short-range three-body potential in first-order exchange energy 3—1595
transition metal coordination compounds, donor-acceptor props. of ligands, X-ray photoelectron spectroscopy 3—17415
valence struct. from coherent X-ray scatt. 3—14653
zeolites, chemical shift of ^{205}Tl, binding and Tl^+ ions arrangement *(German)* 3—15435
Zn(II) complex, trichloroadeniniumzinc (II), crystal structure, metal binding with nucleic acids 3—36278
Al, interionic potential 3—33787
$BaBiO_3$, i.r. spectral determ. of Bi valency state, charge distrib. 3—34363
CaF_2, Fe multiple charge states, isomer shift, Mossbauer obs. 3—27455
$CaF_2:Yb^{3+}$, covalency, ab initio calc. 3—2009
$CaH(AsO_4).H_2O$, haidingerite, crystal morphology rel. to bond assemblage 3—14789
CaO, Fe multiple charge states, isomer shift, Mossbauer obs. 3—27455
CdTe, rel. to elastic consts. and thermal expansion, 4.2-300 K 3—30170
CsCl, ionic radii difference, rel. to press. derivatives of elastic consts. 3—1664
$CuCs_2(SO_4)_2.6H_2O$, hydrogen bonding, neutron diffraction study 3—17757
$CuK_2(SO_4)_2.6H_2O$, hydrogen bonding, neutron diffraction study 3—17757
Dy, electrostatic model, rel. to hydrostatic press. derivatives of elastic moduli 3—27051
Er, electrostatic model, rel. to hydrostatic press. derivatives of elastic moduli 3—27051
Fe-Co system, FeCo, X-ray emission study *(Russian)* 3—15572
GaAs(P)(Sb), structure factor meas. rel. to electron distrib. and bonding 3—14784
Gd, electrostatic model, rel. to hydrostatic press. derivatives of elastic moduli 3—27051
H_2 solid, ground state energy, compressibility, press. 3—33479
KCl, interatomic interaction potential, plotting by radiographical data *(Russian)* 3—14727
KI, interionic potentials, force const. models 3—26987
LiF, interionic potentials, force const. models 3—26987
$Li(NH_4)SeO_4$, Raman and i.r. spectra hydrogen bonding, ion distortion 3—39144
$MgHAsO_4.7H_2O$, Roesslerite, struct. rel. to hydrogen bonding 3—20717
$MgNH_4AsO_4.6H_2O$, arsenstruvite, structure refinement, hydrogen bonding 3—38558
MgO, interionic potentials, force const. models 3—26987
$(NH_4)_2SeO_4$, $(ND_4)_2SeO_4$, Raman and i.r. spectra, hydrogen bonding, ion distortion 3—39144
Na chemically motivated pseudopotential 3—20708
$Na_2B_4O_6(OH)_2.3H_2O$, charge density and at 300K rel. to bonding 3—14833
NaBr-KBr solid solution, interatomic bonds, energetic and strength characts. *(Russian)* 3—20722
NaCl, interionic potentials, force const. models 3—26987
NaCl, ionic radii difference, rel. to press. derivatives of elastic consts. 3—1664
NaCl-KCl solid solution, interatomic bonds, energetic and strength characts. *(Russian)* 3—20722
NiAs, structure factors rel. to outer electrons density distrib. and bonding 3—14787
$S_6(NH)_2$, isomer II, structure refinement, N-S bond lengths 3—38562
Se, hexagonal, bond distances and chain angle at high press. 3—7682
Si, bonding electron distrib., rel. to struct. factor 3—24064
Si_3N_4, optical props. and bonding model 3—30829
Ti-Fe(Co)(Ni) systems, TiFe, TiCo and TiNi phases, X-ray emission study *(Russian)* 3—15572
TiO_2, ionicity of bonds and dielectric susceptibility 3—14725
VO_2, c/a ratio in crysts. with rutile structure, rel. to metallic V-V bonding in band model of metal-insulator transition 3—18092
$W_4Nb_{26}O_{77}$, upper limits of ionicity, n-beam lattice images 3—24005
ZnS, ionic radii difference, rel. to press. derivatives of elastic consts. 3—1664
Zr-Co system, ZrCo, X-ray emission study *(Russian)* 3—15572

crystal chemistry
see also crystallography
adamite, Fe^{3+} paramagnetic resonance, co-substitution of Cu^{2+} and Fe^{3+} in Zn sites 3—15415
c- 3—30729
chromium oxalate, rel. to hydrothermal synthesis 3—2629
effective charges and ionicity, empirical correl. 3—36271
ferrite spinels, mixed, nonstoichiometry of aging of mag. props. 3—21222
metal systems, book 3—11586
pyroxene stoichiometry and omphacite breakdown 3—27926
rare earth alloys, and thermodynamic props., 4f electron valence config. model 3—1985

crystal chemistry continued
silicate-germanate, $A_2(Si,Ge)O_4$, (A=Be,Zn,Ca,Cd,Sr, and Ba), cryst. chem. and polymorphism 3—7922
structure types for AB_2X_4(x=S,Se,Te) compounds, prediction method 3—27011
$AgReO_4$, n.q.r., point-charge field-gradient tensors, ions struct., bonding 3—39056
$BaO.P_2O_5$ glass, absorpt. spectra rel. to redox behaviour of Fe 3—24723
$Bi_2In_4S_9$, synthesized in gas phase 3—7673
$CaO.FeO.Fe_2O_3$, chem. comp. and precip. microstruct. *(French)* 3—8986
$CaO.P_2O_5$ glass, absorpt. spectra rel. to redox behaviour of Fe 3—24723
$CeCu_2$ type structure 3—20715
$CoSb_3$, crystal-chemical props., detn. by Mossbauer spectroscopy *(Russian)* 3—7660
Cs_2SbCl_6, mixed valence of Sb, cooperative tunnel effect, Mossbauer obs. *(Russian)* 3—4943
$CuVO_3(I)$, distorted ilmenite type derivative, cryst. struct. determ. 3—7695
FeO, wustite, formed below 570°C, Mossbauer spectra 3—24638
$HfTe_{2-x}$, $x=0.061$, preparation and X-ray characterization 3—7691
KIO_4, n.q.r., point-charge field-gradient tensors, ions struct., bonding 3—39056
Li in octahedrally coord. structures, $K_xLi_xTi_{4-x/2}O_8$ near structure type 3—38573
$Li_{0.5-\alpha}Fe_{2.5}O_{4-\alpha/2}$, nonstoichiometric, point defects, X-ray diffr. obs. 3—33520
$LiNb(Ta)O_3$, stiochiometry variations from Raman powder spectroscopy 3—2536
$Mg_{0.9}Fe_{2.1}O_4$ ferrite, cation redistrib. rates, oxidation effects, saturation magnetisation obs. 3—15387
$MgO-Al_2O_3$ synthetic spinel, spectra, luminesc. of Cr and Mn in impurities, comp. depend. 3—34429
$MgO.P_2O_5$ glass, absorpt. spectra, rel. to redox behaviour of Fe 3—24723
$Mn_xFe_{3-x}O_4$, i.r. spectra and cation distrib. 3—30807
NH_4ReO_4, n.q.r., point-charge field-gradient tensors, ions struct., bonding 3—39056
$Na_2CuSi_4O_{10}$, X-ray obs. 3—27013
$NaIO_4$, n.q.r., point-charge field-gradient tensors, ions struct., bonding 3—39056
$Na_2O-B_2O_3$, $Na_2O-NaCl-B_2O_3$ glasses, u.v. absorption of Bi(III) rel. to stoichiometry of complexes 3—24724
$Na_2O-PbO-SiO_2$, absorpt. spectra rel. to redox behaviour of Fe and Cu 3—24722
$NaReO_4$, n.q.r., point-charge field-gradient tensors, ions struct., bonding 3—39056
$NiFe_{2(1-c)}Cr_{2c}O_4$, spinel solid soln., rel. to mag. and elec. props. *(Russian)* 3—38568
NiS, non-stoichiometry effects on elec. and mag. props. 3—2017
$RbSbCl_6.2Rb_3SbCl_6$, mixed valence of Sb, cooperative tunnel effect, Mossbauer obs. *(Russian)* 3—4943
Re complex, chem. effects on fine struct. of L_{III} absorpt. edge of Re 3—27582
SnSb single crysts., stoichiometry *(Russian)* 3—30264
$Sr_2Nb_2O_7$ ferroelectric single cryst., stoichiometry, homogeneity 3—21373
$SrO.P_2O_5$ glass, absorpt. spectra rel. to redox behaviour of Fe 3—24723
Ti oxides, solid state reactions, departures from stoichiometry and order 3—5388
$UO_{2\pm x}$, polycrystalline, stoichiometry influence on compression creep 3—6992
V_2O_3, metal/antiferromagnetic insulator transition, effect of non-stoichiometry 3—18091

crystal classes *see crystal symmetry*

crystal cleavage
ferritic materials, fatigue crack propag., stress intensity and microstruct. influence 3—21580
fractography, state-of-the-art review 3—30982
metal, cubic, cleavage in intrinsic dislocation dipoles 3—24204
metals b.c.c., cleavage crack nucleation at ‘unlikely’ twin intersections 3—17924
quartz particles from post-glacial clay soils, h.v. electron microscope exam. 3—37161
radiation damage in structural materials 3—29449
steel, mild, config. of moving crack tip zones 3—30196
Al_2O_3, sapphire, obs. of cleavage planes for gradient furnace grown crystals 3—11572
CdI_2, polytype growth by cleavage 3—7643
Cu_5As_2 single cryst. characteriz. *(Russian)* 3—12329
α-HgS, cinnabar, single crystals, Berg-Barrett X-ray topographic study of small angle boundaries 3—38525
$KNbO_3$, cleavage planes, superposed linear relief patterns, orientation 3—7996
Mg-Al alloy, transgranular stress corrosion cracking 3—30983
NaF crystal proton bombardment, average projected range meas. 3—1654
SiC-6H, polished single crystals, mechanical breaking effect on absorption in near i.r. spectral region *(Russian)* 3—30827
Ti alloys, cleavage cracking mechanism under loading hydrogen embrittlement 3—18653
Ti-Al-Mo-V alloy, cleavage cracking in gaseous hydrogen 3—31044
Ti-Al-V alloy, stress corrosion crack propag., fractographic obs. 3—31043
TiO_2 anatase surfaces, model, interpretation of some interface processes 3—5414

crystal counters
see also particle detectors; radiation detectors
Compton profile measurement, using solid-state detector, optimum conditions 3—25956
heavy ion tracks, etch kinetics 3—3845
CsI(Tl), 3″×3″ crystal, relative photopeak efficiencies 3—32162

crystal defects
see also crystal impurities; crystal microstructure; dislocations; grain boundaries; point defects; semiconductor defects; stacking faults; twinning
active sites in periodic adlayers, heterogeneous catalysis at line defects 3−9095
alkali halide photoluminescence, method of varying spatial distrib. of defects and effect *(Russian)* 3−5227
alkali halides, irradiation, electron microscopy technique 3−1546
alkali silicate glass, e.p.r. spectral linewidth of hole centres *(Russian)* 3−39029
anisotropic defects in solid, dimension changes in lattice parameters 3−20754
Annual review of materials science vol. 2, 1972 3−24778
atomic vibrational behaviour, time averaged atom arrangement, computer simulation 3−33512
Bloch electron additional scattering, simultaneous impurity and lattice interactions 3−20831
boracite crystal lattice strains, review *(Japanese)* 3−14845
bounded rotation faults, concept and examples 3−7775
cavities, spontaneous facing 3−20729
channelling, theory, use for study of imperfections *(Hungarian)* 3−7802
circular twist disclination loop moving in 2 phase material, calc. of elastic field 3−14863
computer simulation studies of damage mechanism 3−27033
crushed material, rel. to dust electrification 3−2167
defect crystal lattices, phonon-radiation force 3−7888
disclination, Volterra, movement and associated mechanical forces 3−20744
disclinations rel. to folded structures in rock and geological strata 3−2869
dislocation motion kinetics for crystal containing local obstacles 3−20750
electron irradiation induced void studies in metal in h.v. electron microscope 3−1640
film, ion sputter deposited, polygonization patterns, illumination effect on mech. stability 3−15106
fluorite, X-ray and optical obs. of planar defects as growth boundaries 3−7778
formation due to growth method, review 3−17748
garnet, influence on bubble domain motion 3−36742
glass, bubble form. on electron bombard. 3−7790
glass, phosphate, irrad., radiational capture centre, e.p.r. *(Russian)* 3−27415
graphite, in-pile irradiation damage, temp. rel. to flux density *(French)* 3−29443
high resolution scanning electron microscopy, direct obs. of defect contrast 3−23988
high-resolution X-ray topographic techniques, review 3−17716
ice, cavity form., electron microscope obs. 3−7746
image plane crystallographic technique for structural spatial resolution 3−24010
imperfect crystals, electronic structure determ. by MO method *(Russian)* 3−27201
imperfect crystals, perturbation treatment of high energy electron diffraction 3−7793
inert gas bubble growth in solids, non uniform size effect 3−7744
initial plastic deformations corresponding to defects, determ. of displacement field 3−30110
internal friction, obs. of interaction between point defects and dislocations 3−7766
KCl, bubble motion, elec. field induced, X-ray and impurity effects *(Russian)* 3−20730
KH$_2$PO$_4$, X-ray diffraction contrast due to lattice distortions 3−30048
lattice, electron microscopic obs. using weakly excited beams 3−1539
line, heterogenous catalysis at defects, simple boundary-controlled reactions anal. 3−9096
line defects in high-symmetry cases, anisotropic elastic solns. 3−24116
liquid crystal, nematic, existence of even indexed disclinations 3−20693
magnetic bubble materials, melt grown, stoichiometry and perfection 3−12277
melting, defect model for three-dimensional crystal 3−17964
metal, irrad., plasmon cohesive energy of voids and void lattices 3−36554
metal systems, real structure and migrational props., magnetic aftereffect obs. *(Polish)* 3−24212
metallic strands interrupted with insulating lattice defects, model 3−20996
metallic thin films, effect on optical props., theory 3−36958
migration of supersaturated constituents to line sinks 3−24296
Mossbauer study and cryostat description 3−9879
non-metallic crystals heat conductivity, phonon interactions and effect of lattice imperfections 3−33643
nonfissile metals and alloys, high neutron exposures, effects, void swelling and radiation creep, review 3−24164
nonlinear defect model, microscopic, local fracture and residual strain *(Japanese)* 3−20806
nonlinear defect model of crack propag. in one-dimens. cryst. *(Japanese)* 3−20805
numerical method for computing X-ray diffraction contrast 3−36244
packing defects, infl. on graphite structures, X-ray diffr. study *(Russian)* 3−7779
phonon resonance absorpt. into vibrational modes, mass defect influence 3−17950
phonon scattering at high temperatures at lattice defects 3−1747
phonon scattering by lattice defects 3−1744
phonon scattering in solids, conference, Saclay, France (July 1972) 3−1739
photoinert organic solids with aromatic impurities, phosphorescence induced by u.v. and X-ray irradiation 3−5234
photoluminescence, method of varying spatial distrib. of defects and effect *(Russian)* 3−5227
plastic organic crystals, n.m.r. of translational mol. motion, solids with intermediate entropy of fusion 3−24109

crystal chemistry continued
crystal defects continued
pore isolated on grain boundary, volume diffusion controlled shrinkage 3−36292
pyroxenes, natural, X-ray topography and electron petrography 3−18807
radiation induced, direct observation by transmission electron microscopy 3−33434
rare earth garnet, rel. to liquid phase epitaxy for bubble domain devices 3−36770
rare-earth chalcogenides, determination from specific heat, thermal expansion and conductivity data 3−15019
rarefaction centre form during crystallisation of polycrystalline material 3−33514
refractories, mechanical properties and defects 3−31129
shear structure, generation mechanism for shear planes 3−30130
slightly deformed crystals, anomalous transmission of X-rays 3−7596
solid reactivity, (conference, Bristol, England, July 1972), 1st part 3−5379
solid reactivity, (conference Bristol, England, July, 1972), 3rd part 3−5386
solid solns., f.c.c., Portevin-Le Chatelier effect, grain size and vacancy annihilation influence *(German)* 3−21711
stainless, 316, proton-irradiated, effects of injected He on void formation in steel 3−11607
steel, austenitic stainless, voids and swelling on fast reactor irrad. *(Russian)* 3−11056
steel, electron microprobe analysis *(German)* 3−8794
steel, mild, 1 MeV electron irrad., void formation 3−11609
steel, solution-treated type 316 stainless, fast-neutron irradiation effects on defect development, microstructure 3−26520
steel, stainless, Type 304, cyclotron-injected helium effect on void form. characts. 3−35934
steel, stainless, Type 316, neturon irrad., defect development 3−35933
steel fuel claddings, cold-worked austenitic stainless, study of irradiation-induced void formation 3−26519
steel nondestructive testing of semi-finished products, development and present state, u.s. and radiation methods for internal defects *(German)* 3−18774
TEM study *(Rumanian)* 3−24013
thin and solid specimens, conditions for defect obs. in S.E.M. 3−23997
transparent dielectric, optical strength reduction due to macroscopic defects 3−5175
triglycine selenate, normal and deuterated, single crystals, γ radiation changes of dielectric props. in phase transition region *(Russian)* 3−8533
triglycine sulphate, growth defects, X-ray topographic obs. 3−1617
triglycine sulphate, X-ray topographic obs. of dislocations and volume defects 3−27026
vitreous oxides, structural defect equilibria based on the structon model 3−4723
void formation obs., cyclotron applications 3−20761
void lattice, b.c.c. form 3−33513
Al, rolled plate, after recrystallisation 3−15664
Al film, He ion pre-injected, electron irradiation effect on void form. 3−20967
Au thin films, conduction electron diffusion by surface defects *(French)* 3−36584
BaF$_2$, radiation-induced transform., e.p.r. and optical absorpt. studies *(Russian)* 3−30694
BaSO$_4$:Eu(Mn), radiational defects, thermoluminesc. study *(Russian)* 3−27581
BaTiO$_3$, nonstoichiometry detn. 3−17810
CaF$_2$, radiation induced transform., e.p.r. and optical absorpt. studies *(Russian)* 3−30694
CaF$_2$:NaYF$_4$, e.p.r. 3−24613
Ca$_{10}$(PO$_4$)$_6$F$_2$, defect centres 3−8623
CaSO$_4$:Eu(Mn), radiational defects, thermoluminesc. study *(Russian)* 3−27581
CdF$_2$, insulating to semicond. transition rel. to lattice defect statistical thermodynamics 3−4947
Cd$_x$Hg$_{1-x}$Te, paramag. susceptibility contrib. from complex lattice defects 3−8339
CdI$_2$, X-ray diffraction spots, streaking and arcing, c-axis oscillation photographs, stacking faults and tilt boundaries 3−38521
CdTe, cathodoluminescence from lattice defect centres, quenching mechanism 3−15561
CdTe, photoluminescence, lattice defect investigation with use of heat treatment, neutron and electron irradiation *(Russian)* 3−27550
Co, internal friction peak at 300°C rel. to lattice defects 3−30208
β-Co, substrate for Cu epitaxial film growth *(Russian)* 3−8049
Cu, heavy ion bombardment, shadow effect 3−33574
Cu, temp. depend. of defect production by electron irradiation 3−7749
Cu epitaxial film on β-Co *(Russian)* 3−8049
Cu-Pt alloy, atomic motion under action of laser pulse, X-ray obs. *(Russian)* 3−29111
Cu$_3$Ti, charact. defect struct., electron microscope obs. 3−11606
Fe microcrystals, substruct., X-ray obs. 3−36505
Fe-Re-C, defect cluster influence on martensite form. *(Russian)* 3−12353
Fe-Si alloys, thermomagnetic treatment, effects of inclusions and internal stresses *(Russian)* 3−8385
Fe$_3$B$_7$O$_{13}$I, crystal, lattice strain *(Japanese)* 3−14845
GaAs, photolum., regions damaged by laser beam 3−27571
GaAs, radiation annealing of defects formed by ion bombardment 3−33553
GaAs i.r. window, X-ray examination of defects and strains 3−9935
GdO, film, defect substructure obs. 3−8067
Ge proton radiation damage, single crystals, shadow effect, defect accumulation kinetics, radiation stability 3−33573
Ge single crystals, Na$^+$ induced lattice damage, effects on angular and energy distributions of scattered ions, E<5 keV *(Russian)* 3−11663
KCl, step lines, local struct., X-ray obs. 3−38596
KCl:Sm^{2+}, fluoresc. spectral meas. of ion-defect pair energies 3−24736

crystal chemistry continued
crystal defects continued
$KMgF_3$. reorientation and thermal motion of self-trapped hole 3−18100
LiH, high temperature luminescence and impurity defect dislocations *(Russian)* 3−12190
$LiNbO_3$, Czochralski growth conditions rel. to lattice defects and optical quality 3−21539
Mg ultramicrotomed thin slices, plastic deformation, recovery of defects and recrystallisation 3−17902
MgO, hypersonic attenuation, impurity and defects effect 3−1701
Mo, vapour deposited on Cu and Mo substrates 3−8718
MoO_3 crystal, X-ray microscopic study, earthworm patterns 3−17802
$NH_4H_2PO_4$, X-ray diffraction contrast due to lattice distortions 3−30048
$NaBF_4$, radiation induced defect centres, e.p.r. study 3−18366
NaCl, bubble motion, elec. field induced, X-ray and impurity effects *(Russian)* 3−20730
$NaF{:}Li^+$, electron irradiated, e.s.r. study of di-interstitial centre 3−2390
$NaNO_3$, calc. of migration enthalpies of Frenkel defects, application of Mott and Littleton methods 3−24294
$NbFe_2$, Laves phase, homogeneity range and defect struct. 3−27637
NbO_2-Nb_2O_5, phase equilibria, Wadslay intergrowth defects of nonequilib. nature 3−33655
$Nb_{12}O_{29}$, oxidation, electron microscope assessment of the role of extended defects 3−5380
Nb_2O_5, electron microscope obs. of planar defects and structure at high temps. 3−11638
Nb_2O_5, high resolution electron microscopy 3−24128
H-Nb_2O_5, training and defects study by electron microscopy 3−7774
Nb_3O_7F, double shear structure form. in electron microscope beam 3−33534
Nb_3Sn, transmission electron microscope examination of defect struct. *(German)* 3−21179
Nb_3Sn film, produced by O ion irradiation, effect on superconducting critical current density *(German)* 3−2210
Ni, dislocation influence on nucleation of voids with neutron irradiation 3−17803
Ni, neutron induced voids, low dose dependence at 400°C 3−8856
Ni, shapes of irradiation produced voids 3−30111
Ni, void prod. by ion irrad., electron stereomicroscopy analysis 3−11608
$NiNb_2O_6$-NiF_2 solid solution, columbite and trirutile transformation mechanisms *(French)* 3−7928
Pb-Au dilute alloys, dehancement of Au diffusivity, Au pairs motion 3−34546
Re, plastically deformed single crystal, defect influence on supercond. transition crit. temp. 3−30566
S, metallic, formation process of central cavities during growth of thick layers 3−4753
SbSI, rel. to Barkhausen effect 3−39114
Si, form. on plastic deform., electron microscope obs. 3−7747
Si, formation of disordered layers by Ar^+, Ne^+ and B^+ ion bombardment 3−24167
Si, oxygen precipitation at oxidation induced defects 3−33539
Si, radiation annealing of defects formed by ion bombardment 3−33553
Si, X-ray topography of deformation produced by indentation 3−17904
Si film, epitaxial, elec. effects of clustered defects 3−24434
Si proton radiation damage, single crystals, shadow effect, defect accumulation kinetics, radiation stability 3−33573
Si single crystals, Na^+ induced lattice damage, effects on angular and energy distributions of scattered ions, $E<5$ keV *(Russian)* 3−11663
Si:Ar ion-implanted, X-ray study of lateral strains 3−38603
Si:B, implanted single crystal, X-ray diffraction for defect structure obs. 3−38522
SiB, epitaxial layers, perfection enhancement by thermal oxidation *(German)* 3−18236
SiC, ion implanted, localised vibrational modes, luminesc. obs. 3−30227
SiO_2 glass films, r.f. sputtered 3−18045
SmO, film, defect substructure obs. 3−8067
SrF_2, radiation-induced transform., e.p.r. and optical absorpt. studies *(Russian)* 3−30694
$SrSO_4{:}Eu(Mn)$, radiational defects, thermoluminesc. study *(Russian)* 3−27581
$Ti_{n-2}Cr_2O_{2n-1}$, shear struct., electron diffr. and electron microscope obs. 3−24127
UO_2, crystallographic shear and ordered reduction, electron microscope obs. 3−7776
VO, defect ordering and structure from short range order scattering in electron diffraction 3−24066
V_nO_{2n-1}, shear struct., electron diffr. and electron microscope obs. 3−24127
W, fast neutron irrad., superlattice of voids 3−17878
W, heavy ion bombardment, shadow effect 3−33574
W, radiation-induced defects, nature and thermal stability *(Russian)* 3−1649
W, vapour deposited on Cu and Mo substrates 3−8718
WC, neutron irrad. damage, recovery, annealing *(Russian)* 3−30161
Zn ultramicrotomed thin slices, plastic deformation, recovery of defects and recrystallisation 3−17902
ZnS, cathodoluminescence and defect formation *(Russian)* 3−12187
ZnS, spectral investigation of luminescence centres *(Russian)* 3−27547
ZnTe, Bridgemann and solution grown, voids, microscopic obs. *(Japanese)* 3−11605
$ZnWO_4$, defect distrib. near paramag. centre from e.s.r. lineshape 3−21311
ZnZo, spectral investigation of luminescence centres *(Russian)* 3−27547
Zr, neutron irrad. induced void form. 3−33564
Zr, neutron irrad. induced void form. 3−33565
ZrO_2, oxide defect structure effect on elec. cond. 3−8235
crystal diffraction spectrometers *see X-ray spectrometers*
crystal diodes *see semiconductor diodes*
crystal dislocations *see dislocations*
crystal electron states
see also band structure; band theory models; carrier mobility; colour centres; electron gas; electron-phonon interactions; electronic density of states; excitons; Fermi level; fermi surface; helicons; impurity electron states and effects; localised electron states; metal-insulator transition; plasmons; polarons; positron states; pseudopotential methods; quasi-particles; surface electron states
alloys, binary, strong scatt., model calc. approximation 3−24366
alloys, disordered binary, random transfer integrals and electronic struct. 3−36519
alloys, disordered ternary, coherent potential approximation and diagrammatic equivalent, electronic theory 3−38775
amorphous semiconductors, book 3−11941
amorphous semiconductors, theoretical foundation of existing models 3−38778
anthracene, crystn., hole detrapping by singlet excitons or photons, photoenhanced current obs. 3−24470
bound electron-phonon state spectrum in quantizing mag. field 3−4980
bound electrons, magneto-ionic theory 3−21032
deformed crystals, perturbation theory *(Russian)* 3−20982
disorder-induced transition in one-dimensional finite Kronig-Penney model 3−18061
disordered network, electronic structure 3−30388
disordered system, d.c. cond. and Anderson transition 3−18057
disordered system, generalized cluster theory of coherent potential approx. 3−36512
disordered systems, electronic excitation diffusion at zero temp., kinetic equations 3−18049
disordered systems, equivalence of two approaches to random chain of oscillators 3−20988
disordered systems, multiple scattering formalism, generalised coherent potential approximation 3−24368
disordered systems, theory to interpret electronic props. of metal-molten salt mixtures 3−1970
electron correlation consideration in the second quantization method *(Russian)* 3−1968
electron-plasmon approx., single particle Green's function 3−20980
finite anisotropic crystalline array of polarisable dipoles, normal excitation modes 3−18104
finite linear chain, dynamic effective charge 3−36514
Gaussian wave packet dynamics in uniform mag. and quadratic potential fields 3−20987
imperfect crystals, electronic structure determ. by MO method *(Russian)* 3−27201
interacting systems decoupling, one electron energy matrix 3−20985
liquid alloys, electronic correlation functions at long wavelength 3−30386
liquid metals, Van Hove theory application 3−38771
many-body problems, book 3−20990
metal, electron correlations and moment sum rules 3−38764
metal, simple, pseudopotential method, binding energy detn. 3−27208
metal, small particles, static electronic props. 3−36517
metal, total energy, pseudopotential calcs. 3−33785
metal-nonmetal transition in dense media, numerical study of electronic and thermodynamic properties 3−27199
metals, conduction electrons, quasiparticles, energy structure, electrical properties, general theory 3−24367
metals and their compounds, photoelectron spectra, electron states, review *(Japanese)* 3−15120
network model of electrons, appl. to monatomic lattice with defects 3−20984
one-dimensional disordered systems, electronic wave functions 3−8083
optimized model pot. for 33 elements 3−36507
orthogonalised phase wave method for crystal potential and orbital shift calcs. 3−30381
orthonormalised and complete basis description 3−38762
polar liquids and solids, trapped dielectron, semicontinuum 3−38813
polar media, nonradiative transitions, processes with mixing of quantum and classical degrees of freedom 3−7865
polar media, nonradiative transitions, processes without mixing of quantum and classical degrees of freedom 3−1717
random lattice, coherent potential approx. improvements 3−36518
rare earths and actinides, conference, Durham, England, July (1971) 3−2223
resonating valence bonds, insulating state 3−30415
screened atomic potentials, Slater model calc. 3−18051
simulation by analogue computer with three-dimensional resistance network *(French)* 3−20979
Ag halides at low temperature 3−27218
Fe-Co system, FeCo, X-ray emission study *(Russian)* 3−15572
Fe(II) six coordinated compounds, spin $S=1$, low temp. magnetism, Mossbauer effect and electronic struct. 3−34250
Ge, distribution of donors and acceptors 3−28655
Ge, divacancies and single vacancies, statistical problem 3−15150
Hg-In alloys, liq., electronic spectra, 0.14 to 4 μm 3−39133
$K_2Pt(CN)_4X_{0.3}.nH_2O$, $X=Cl(Br)$, X-ray photoelectron obs. of energy levels 3−15587
$((NH_3)_4)$ $(PtCl_4)$, spectroscopic evidence for a delocalised excited state 3−18464
Pb/Zn-ZnO_2-Pb, tunnelling obs. of bound states 3−18270
$(Pd(NH_3)_4)(PdCl_4)$, spectroscopic evidence for a delocalised excited state 3−18464
$(Pt(NH_3)_4)$ $(PtCl_4)$, spectroscopic evidence for a delocalised excited state 3−18464
$(Pt(NH_3)_4)(PtCl_4)$, spectroscopic evidence for a delocalised excited state 3−18464
Si, divacancies and single vacancies, statistical problem 3−15150
Si(Li) detector, determ. of Fano factor 3−28641
SiO_2, electronic struct. of vitreous silica rel. to different crystn. forms 3−21298
Ti-Fe(Co)(Ni) systems, TiFe, TiCo and TiNi phases, X-ray emission study *(Russian)* 3−15572
U, monopnictides and monochalcogenides, review of electronic and mag. props. 3−2260

crystal electron states continued
- ZnTe, cathodoluminescence of the donor-double-acceptor pairs *(Russian)* 3–27577
- Zr-Co system, ZrCo, X-ray emission study *(Russian)* 3–15572

crystal energy *see lattice energy*

crystal etching *see etching*

crystal faces
- atomic structure of face of growing crystal, computer simulation 3–33472
- diamond, synthetic, internal struct., charact. growth on faces, growth history construct. 3–20702
- group VIA metals, faceting in dilute O_2 atm., l.e.e.d. and r.h.e.e.d. studies 3–11818
- Rochelle salt, temperature depend. of rates of growth of faces from aqueous solns. 3–33473
- GdGa garnet, macroscopic strain in facetted regions 3–33493
- KNO_3, temperature depend. of rates of growth of faces from aqueous solns. 3–33473
- $KNbO_3$, cleavage planes, superposed linear relief patterns, orientation 3–7996
- $NaNO_2$, $NaNO_3$, $NaClO_4$, temperature dependence of the rates of growth of the faces from aqueous solns. 3–33473
- Pt, field emission tip, crystal face specificity for N_2 adsorption 3–24342

crystal field theory
- *see also crystal hyperfine field interactions; crystal internal fields*
- actinide cpds, NaCl-type, hyperfine fields, crystal field and relativistic effects, angular wave function 3–2233
- aggregates of exchange-bonded paramag. ions, microscopic model 3–21193
- aggregates of exchange-bonded paramagnetic ions, effective Hamiltonian formalism 3–15318
- alkali halides, absorption spectra in vacuum u.v. due to excitons, ligand field theory calcs. 3–27509
- alloy with Ce and Yb impurities, effect on Kondo effect 3–2256
- amorphous ferromagnet, molecular field theory 3–18279
- Anderson model, symmetric, perturbation calc. of susceptibility 3–24551
- antiferromagnetic crystal, magnetic excitons transfer model between antiparallel spin sites 3–11868
- antiferromagnetic two-singlet system, molecular field approx. for phase diagram and metamag. transition 3–27340
- borate glasses:Ce^{3+} optical absorption, probe of crystal field and nature of impurity-ligand bond 3–8614
- cluster model approach to the evaluation of dynamic orbit-lattice parameters 3–39011
- $Co(NH_4)_2(SO_4)_2.6H_2O:Mn^{2+}$, e.p.r. study, coordination of H_2O ligands around the divalent ions 3–15406
- critical and tricritical transitions, logarithmic corrections to molecular field behaviour 3–13663
- cubic antiferromagnetic insulator, lifting of degeneracy of $^4E_{1g}$ level of Mn^{2+} *(Russian)* 3–11994
- dilute alloy, magnetic, e.s.r. spectra, cryst. field struct., theory 3–15423
- e.p.r., pair conc. and mag. parameters, spatial distrib. of centres 3–2385
- e.p.r. lineshape in presence of spin-phonon and dipole-dipole interactions 3–34206
- equilibrium correlation functions of current density and mag. moment 3–24388
- e.s.r. hyperfine transition probabilities for large cryst. field effects case 3–2345
- e.s.r. transition effects on time dependent perturbations 3–36779
- ferrimagnetic spinels, Curie points and Weiss molecular field coeffs. 3–30623
- ferromagnetic electron gas, spin polarisation due to mag. impurities 3–15339
- ferromagnetic metal, secondary spin thermal cond., molecular field approx. 3–30447
- glasses, electron correl. and susceptibility 3–15319
- hemin, zero-field splitting and low-temp. mag. susceptibility 3–30583
- II-VI semiconductor, g-shift of S-state ions 3–21016
- ionic mixed crystal, spontaneous magnetisation irregularities, modified effective field model 3–34060
- lanthanide ion, substituted, Slater parameter shifts 3–30412
- ligand field, equivalent quantum states in d^n and d^{5+n} electronic configurations 3–21015
- Ligand field parameters in trigonal Ligand fields 3–21017
- ligand field splitting parameters, comparison of angular overlap model and point charge crystal field model 3–8111
- Luttinger and Tisza conjecture, ordering of classical spins 3–34057
- magnetic crystal, uniaxial and biaxial quadrupolar ordering, molecular field theory 3–15321
- magnetic semiconductors, s-f exchange interactions, review 3–8350
- magnetic semiconductors, valence bond approach conceptual phase diagrams 3–38803
- magnetic systems with various cryst. field level schemes, excitations study and Hamiltonian anal. 3–21189
- metal, d-band splitting, high resolution photoelectron obs. 3–30414
- metals, crystalline electric field, physical aspects 3–30582
- metals, diagrammatic analysis of dynamics of localised moments 3–34058
- Mossbauer isomer shift, covalency versus overlap distortion 3–18398
- noble metal-rare earth, dilute alloy, effect of d-electrons on crystal field potentials 3–21014
- open shell band energies at symmetry points rel. to cryst. field and superexchange energies 3–24373
- paraelastic resonance of Jahn-Teller and off-centre ions 3–24387
- paramagnet, uniaxial, longitudinal magnetization by transverse high freq. mag. field 3–34061
- paramagnetic impurity levels, curvature in Orgel-Tanabe-Sugano diagrams 3–36694
- phosphate glasses:Ce^{3+} optical absorption, probe of crystal field and nature of impurity-ligand bond 3–8614
- rare earth, effect of d-electrons on crystal field potentials 3–21014
- rare earth beryllium intermetallics, ^9Be relax. and mag. moment dynamics 3–2444

crystal field theory continued
- rare earth compounds, with zircon struct., cryst. distortion and Zeeman effects, theory 3–38802
- rare earth hafnate pyrochlores, Eu^{3+} luminesc. spectra as indication of distortion 3–30865
- rare earth hydroxides, energy levels of Er^{3+}, optical spectra 3–2572
- rare earth ion spectra, deviations from perfect symmetry effects *(Russian)* 3–12127
- rare earth ions, Sternheimer shielding-antishielding parameters, calc. 3–30416
- rare earth ions in hexagonal field, calc. of energy levels, eigenfunctions and mag. moments 3–27343
- rare earth metal, 5d and 4f mixing coeffs. for rare earth ions 3–33810
- rare earth orthoferrites, paramag. susceptibility anisotropy, cryst. field parameters 3–34094
- rare earth solids, book 3–11523
- rare earth stannate pyrochlores, Eu^{3+} luminesc. spectra as indication of distortion 3–30865
- rare earth titanate pyrochlores, Eu^{3+} luminesc. spectra as indication of distortion 3–30865
- rare earth titanate-stannate pyrochlores, Eu^{3+} luminesc. spectra as indication of distortion 3–30865
- rare earth zirconate pyrochlores, Eu^{3+} luminesc. spectra as indication of distortion 3–30865
- rare earths and actinides, conference, Durham, England, July (1971) 3–2223
- rare-earth metal, rotationally invariant theory for magnetoelastic interactions effect on elastic consts. 3–15401
- relativistic, construction of approx. radial wavefunctions 3–30410
- RKKY interaction, electron conc., cryst. and magnetic struct. 3–24550
- single crystal with arbitrary crystal field and exchange interactions, paramag. susceptibility calc. 3–34089
- spin system with ferromagnetic exchange interaction, application of Abrikosov's pseduofermion technique 3–38970
- spin-phonon interaction, level struct. 3–2226
- spin-phonon interactions and rotational invariance 3–1760
- spinel ferrimagnet containing two types of ions, Weiss mol. field coeffs. 3–2229
- time-dependent spin correlations in anisotropic systems, solution of the high temp. kinetic eqns. in the presence of a crystal field 3–18281
- time-dependent spin-correlation functions in anisotropic systems, infinite temp. kinetic eqns. in the presence of a crystal field 3–18280
- transition metal complex, tetrahedral, oscillator strengths for ligand field transitions, d-d intensities 3–34333
- transition metal ions, octahedral and tetrahedral D^4 and D^6 configs., paramag. 3–2250
- two-iron ferredoxins, geom. and electronic props. of Fe-S site 3–33805
- Van Vleck ferro- and paramagnets, cryst. field ligands, model calcs. 3–34062
- zeolites, NaX and NaY type, e.s.r. of Gd^{3+}, nonequivalent position obs. 3–2386
- Ag, 5d and 4f mixing coeffs. for rare earth ions 3–33810
- $AgReO_4$, n.q.r., point-charge field-gradient tensors, ions struct., bonding 3–39056
- Au, 5d and 4f mixing coeffs. for rare earth ions 3–33810
- BaF_2 films, spin orbit splitting of electronic excitations in 8-150 eV range 3–2032
- $BaMg_2Y_2Ge_3O_{12}$, e.s.r. of Nd^{3+}, g-factor, mag. ion symmetry 3–2384
- $Be_3Al_2Si_6O_{18}:V^{3+}$, beryl, optical and i.r. absorpt. rel. to crystal field parameters 3–34389
- CaF_2, e.p.r. of U^{4+} ions in trigonal sites, uniaxial stress effects 3–2360
- CaF_2 films, spin orbit splitting of electronic excitations in 8-150 eV range 3–2032
- $CaF_2:Tm^{2+}$, covalency contribution on the values of $g\Gamma_7$ and $g\Gamma_{7'}$ *(Russian)* 3–11861
- $CaO-Cr_2O_3-Al_2O_3$, phase relations and optical studies 3–5385
- Cd rare-earth chalcogenide spinels, crystalline field effects on saturation magnetic moments 3–7685
- $CdCr_2S_4$, Cr^{3+} field transitions in photocond. and luminesc. spectra 3–8222
- $CdF_2:Er^{3+}$, C_{3v} local-site symmetry from correlated e.p.r. and optical obs. 3–21305
- $CdO-Cr_2O_3-Al_2O_3$ phase relations and optical studies 3–5385
- CeF_2, Pr^{3+} absorpt. spectra and energy levels *(Russian)* 3–12157
- CeH_2 low temp. specific heats, crystal field influence 3–11744
- $CeO_2:Gd^{3+}(Cm^{3+})$, zero-field splittings 3–18358
- $Co_xFe_{3-x}O_4$, preparation and characterization 3–18741
- Cr complex, tri(ethylenediamine) chromium(III) ion, polarized cryst. spectra 3–18447
- Cr^{3+} in trigonal symmetry, zero field splitting, effect of spin-spin contribs. 3–34054
- Cr^{3+} thenoyl tri-fluoro acetonate, diffuse reflectance spectrum 3–18469
- $CrCl_3$, specific magnetic rotation in crystal field bands 3–5179
- $CsCuCl_3$, absorpt. spectra obs. rel. to crystal field levels 3–21414
- Cu complex, $CaCu(OAc)_46H_2O$, absorption spectra, electronic transition in dodekahedral crystal field 3–39156
- Cu^{2+} octahedrally coordinated, low temperature ligand field reflectance spectra *(German)* 3–36877
- $CuCl_2$, distortion at Cu^{2+} and field parameters, comparison with Tutton salts 3–5215
- $Cu(OH_2)_6^{++}$ complex in aqueous perchloric media, crystal field theory analysis of Gaussian absorption curves *(French)* 3–8434
- d^2 and d^8 noncubic ligand field spectrum, I quadrate, trigonal and cylindrical ligand fields theory 3–15147
- Er^{3+}, in solids, C_{3h}, D_{2d}, O_h site symmetry, cryst. field parameters rel. to props. 3–2234
- EuB_4HP, pressure effects on electronic spectrum of Eu^{3+} *(Russian)* 3–8113
- $EuCl_3.6H_2O$, pressure effects on spectrum of Eu^{3+}, crystal field theory *(Russian)* 3–8113
- $Eu_2(SO_5)_3.8H_2O$, pressure effects on spectrum of Eu^{3+}, crystal field theory *(Russian)* 3–8113

crystal field theory continued
- FeO_4^{2-} diluted in NaOH, paramag. hyperfine interactions in e_g^2 config. of ^{57}Fe 3−2470
- Gd, second mag. phase transition, molecular field model to explain anomalies in props. 3−15366
- $GdNi_2$, ferromag., Landau model for critical susceptibility 3−15320
- Ge, two electron donor pair system, eigenvalue problem, Heitler-London method soln. 3−2579
- $K_3Fe(CN)_6$, temp. depend., 90 to 300K 3−11857
- KIO_4, n.q.r., point-charge field-gradient tensors, ions struct., bonding 3−39056
- $KNiF_3$, cubic field splitting parameter, MO-LCAO calc. *(Russian)* 3−11859
- K_2SbF_5, e.p.r. of Cr^{3+}, site symmetry 3−24607
- La:Ce, cubic crystalline field effect on magnetic susceptibility rel. to Kondo effect 3−24560
- La-zn double nitrate:Gd^{3+}, e.s.r. in trigonal crystal field, spin hamiltonian interpretation 3−36789
- $LaCl_3$:Sm^{3+} crystal field splitting with inclusion of J mixing 3−18087
- LaH_2 low temp. specific heats, crystal field influence 3−11744
- $LiNbO_3$:Gd^{3+}, e.p.r. and zero field resonance obs. of crystal field 3−34203
- $MgSO_4.7H_2O$:Mn^{2+}, zero-field splitting of Mn^{2+} ion S-state, spin-hamiltonian parameters 3−38935
- $MnWO_4$-$FeWO_4$, spontaneous magnetisation irregularities, modified effective field model 3−34060
- $MnWO_4$-$FeWO_4$, wolframite, mag. phase diagram, molecular field approx. 3−34125
- $(NH_4)_2MnF_5$, linear chain antiferromagnet, weak ferromagnetism 3−30643
- NH_4ReO_4, n.q.r., point-charge field-gradient tensors, ions struct., bonding 3−39056
- $(NH_4)_2SbCl_5$, e.p.r. of VO^{2+} and Cr^{3+}, site symmetry 3−24606
- $NaCa_2Ni(Co)_2V_3O_{12}$, garnet with octahedral mag. sublattice, absorpt. spectra obs. 3−21434
- $NaIO_4$, n.q.r., point-charge field-gradient tensors, ions struct., bonding 3−39056
- $NaReO_4$, n.q.r., point-charge field-gradient tensors, ions struct., bonding 3−39056
- Na_2SO_4, $Na_2S_2O_5$, LMM Auger spectra obs., correlation with molecular orbital structure 3−21509
- $NdAlO_3$, energy levels and crystal field theory, Raman scatt. and optical absorpt. meas. 3−34357
- NdH_2 low temp. specific heats, crystal field influence 3−11744
- NdN(P)(As)(Sb), rel. to mag. ordering 3−30630
- Ni complex, $Ni(pyrazole)_4\ Cl_2$, Br_2, zero-field splitting for spin triplet ground state 3−8366
- Ni ferrite, contribution of tetrahedral Ni^{2+} ion to magnetocrystalline anisotropy 3−2303
- $(NiCl_6)^{4-}$, semiempirical MO calc. choice of basis functions, crystal field parameter and spin-orbit coupling constant 3−4952
- $NiCl_2.4H_2O$, antiferromag.-paramag. transition, molecular field model 3−34120
- Np complex, $((C_2H_5)_4N)_2NpCl_6$, absorpt. spectra of inequivalent sites of Np^{4+} 3−2557
- Pd, e.p.r. of Dy^{3+} analysis 3−2352
- Pd-rare earth, paramag. dilute alloy, anal. of mag. props. 3−15349
- PrH_2, sp. ht. and related thermodynamic props., 23-342K, crystal field effects 3−24277
- PrH_2 low temp. specific heats, crystal field influence 3−11744
- $PrNI_5$, thermal, magnetic and electrical props. 3−8357
- $PtCl_4^{2-}$, ligand field transitions calc. by SCF $X\alpha$ scattered wave method 3−15140
- $RbFeCl_3$, linear chain, ferromagnetic interactions, from EFG temp. depend. obs. 3−18282
- Ru^{4+} in single cubic crystals, effect of config. interaction on mag. props. 3−30585
- Si two electron donor pair system, eigenvalue problem, Heitler-London method soln. 3−2579
- SiO_2 system, field strength and symmetry in crystn. and vitreous polymorphs, e.p.r. obs. 3−21298
- SnO_2, ENDOR of $^{57}Fe^{3+}$ and $^{53}Cr^{3+}$ at different sites, h.f. data interpret. 3−2467
- $SrCl_2$:$^{165}Ho^{2+}$, coupled nuclear-electronic spin system, low temp. relax. 3−18362
- SrF_2 films spin orbit splitting of electronic excitations in 8-150 eV range 3−2032
- SrF_2:Tm^{2+}, crystal field splitting *(Russian)* 3−11860
- TbAl antiferromag. garnet, molecular field approx. of two-singlet model for metamag. transition 3−27341
- ThO_2:$Gd^{3+}(Cm^{3+})$, zero-field splittings 3−18358
- $TiCl_4$, photoelectron and opt. spectra, Hartree-Fock-Slater model 3−27489
- TmF_8^{6-} cluster, shielding of crystal fields *(Russian)* 3−11858
- $Tm_3Ga_5O_{12}$, vibro-electronic Raman effect of Tm^{3+} 3−30809
- VCl_4, photoelectron and opt. spectra, Hartree-Fock-Slater model 3−27489
- YAl_2:Er(Dy)(Tm), crystal field ground states, EPR obs. 3−30418
- $YAlO_3$:Er^{3+}, optical spectra and energy levels 3−5225
- $Zn_xNiFe_{2-x}O_{4-x}F_x$, spinel structure, props. in paramag. domain, molecular field factors *(French)* 3−38962
- ZnO(S):Ni^{2+}, near i.r. absorpt. obs. of crystal field, dynamic Jahn-Teller effect in $^3T_2$ state 3−21446
- ZnS:Cr^{2+}, excitation spectra interpretation by fitting eigenvalues of Tanabe-Sugano matrices 3−2588
- ZnS:Cr(Mn)(Fe), e.p.r obs. of cubic and axial sites 3−15414

crystal fields *see crystal internal fields*

crystal filters
- $LiTaO_3$, for filter appl., Czochralski growth 3−12297

crystal growth
- *see also crystal growth from melt; crystal purification; crystallisation; dendrites; epitaxial growth; nucleation; semiconductor growth; zone melting and refining*
- alkaline earth orthophosphates, growth in gelatin gel 3−24783
- alkaline earth phosphates, in gelatin gels 3−15610
- n-alkane, on graphite and C fibre surfaces 3−20703
- atom assembly, thermodynamic and mech. stability rel. to crystal growth mechanism 3−1586

crystal growth continued
- atomic structure of face of growing crystal, computer simulation 3−33472
- autoclave, growth at high temp. and pressure 3−3776
- b.c.c., effect of adatom position, stability, binding energy 3−33468
- benzene thin film growth, microwave and radiofrequency plasma polymerisation 3−39221
- bisulphates, $MHSO_4$, M=alkali metal or NH_4, growth from soln. or H_2SO_4 *(German)* 3−8716
- camphene, holographic anal. of morphology in dendrite growth 3−11564
- cancrinite, solubility in aqueous solutions of NaOH under hydrothermal conditions *(Russian)* 3−7914
- β-carotene, large single cryst. growth, problems 3−24782
- CDP, trisodium tris(pyridine-2, 6-dicarboxylato)-cerate(III) 15-hydrate 3−2626
- ceramics, American Ceramic Society meeting, Basic Science, Electronics and Nuclear Division (Sept. 1972) 3−8948
- chkalovite, formation from beryl decomposition in NaOH solutions *(Russian)* 3−8715
- chromium oxalate, hydrothermal synthesis 3−2629
- computer simulation 3−11554
- computer simulation of growth kinetics and crystal surface structure 3−11556
- conference, Freiburg, Germany 21-23 Sept. (1972) 3−5261
- controllers, for temp. and position 3−12225
- corundum grown by Verneuil method, OH absorption bands *(Russian)* 3−24706
- crystalliser, well stirred isothermal, stability analysis 3−34717
- cyclododecane, hollow cryst. rod growth from soln., morphology 3−1583
- defects formation due to growth method, review 3−17748
- dendritic growth, nonlinear theory 3−11565
- diamond, catalyst-solvent process 3−12230
- diamond, natural, cubic habit, internal struct., X-ray topography obs. 3−7642
- diamond, natural, growth history obs. by X-ray topography, via disloc. struct. analysis 3−24041
- diamond, synthetic, internal struct., charact. growth on faces, growth history construct. 3−20702
- dislocation structure analysis using X-ray topography 3−24041
- end forms evolution caused by environmental inclusions *(Russian)* 3−36266
- eutectoid transformation, aligned lamellar, theory and expts. 3−4850
- garnet, mixed rare earth iron $RM_2Fe_5O_{12}$ type, growth induced noncubic mag. anisotropy 3−21256
- garnet, mixed rare earth iron type, growth induced noncubic mag. anisotropy 3−21255
- gel growth, advantages of using gelatin gels 3−15610
- gel growth, state-of-the-art 3−12222
- glass, needlelike crystal growth on electron bombard. 3−7790
- glass ceramics, texture development 3−5343
- graduate curriculum, interdisciplinary 3−12229
- growth disorder, two-dimens. model 3−36268
- heat and mass transfer effects on growth from soln. and melts 3−1579
- high temperature gel growth in pressurized chambers 3−12224
- impurity trapping by localized kinks at a step 3−7644
- interfacial energy between crystal and solution by inverted bubble method, morphology prediction 3−14707
- ion and plasma sputtering apparatus for film deposition 3−24784
- laboratory manual 3−9815
- metal-metal oxide system, binary and ternary, eutectic solidification 3−11561
- mixed sulphides of IB and IIB metals, H_2S sulphuration, morphology *(French)* 3−18539
- organic material, film of crystal growth morphology 3−11558
- orthoferrite mag. bubble materials *(German)* 3−5262
- polygonised growth spiral morphology rel. to advancement rates *(French)* 3−24046
- precision temperature regulator bath 3−24779
- pyromellite-acid-dianhydride anthracene, growth and zone refining *(German)* 3−8745
- quartz, high acoustic, growth at high rates by hydrothermal technique 3−24780
- quartz, high acoustic Q, hydrothermal, at high growth rates 3−12226
- quartz, study of growth morphology and cobble structures 3−14706
- rare earth orthovanadates, RVO_4, prep. by precip. from soln. 3−2630
- review on growth of single crystals, evaluation of single and multicomponent techniques *(Hungarian)* 3−27603
- Rochelle salt, temperature depend. of rates of growth of faces from aqueous solns. 3−33473
- saturated solution, model evaluation using special purpose computing registers 3−28972
- seed holding tip, designed for growing single crystals of nitrobenzene 3−1712
- SiC, effect of Si/C molar ratio in vapour phase on morphology 3−17750
- snow, appearance, formation conditions 3−25251
- solution growth, under highly controlled conditions, apparatus and appl. 3−12236
- solution growth, under simulated zero-gravity conditions 3−12228
- supersaturated system, nucleation in active centres, theory 3−1584
- surface-volume coupled diffusion currents rel. to growth rate, capture condition effect at steps 3−11559
- temperature gradient controlled growth in high temp. furnace 3−12232
- temperature gradient zone migration analysis 3−11759
- tetramethylammonium chloride, soln. growth under simulated zero-gravity conditions 3−12228
- thermal chamber for single cryst. growth, 0-45°C 3−5260
- thermal diffusion technique for soln. growth of single crystals 3−34469
- transition metal iodates, of 3d elements, boiling solvent technique 3−12235
- transition metal oxides, oxyfluorides, oxyhydrides, high press. synthesis, struct. characterisation 3−14800
- triglycine selenate, time depend. of specific resist., effect of growth conditions *(Russian)* 3−21367

crystal growth continued
triglycine sulphate, pyroelectric crystals growth for i.r. detector applications 3—31985
triglycine sulphate, time depend. of specific resist., effect of growth conditions *(Russian)* 3—21367
triglycine sulphate crystals, growth conditions effect on elec. domain structure 3—39100
triglycinsulphate growth, role of surface and volume diffusion 3—20700
twinned five-fold symmetry crystals, mechanism of formation 3—1588
whiskers, book 3—8073
Ag, crystal growth in meniscus region of electrolytic soln. 3—2817
Ag, electrodeposited, spiral growth rel. to impurities 3—1582
Ag halides, sheet cryst. prep. by modified Mitchell method 3—34471
Ag_3AsS_3, optimal conditions for obtaining perfect proustite crystals 3—26980
AgBr crystals in excess alkali solution 3—221
AgCl rhombic dodecahedra formation in photographic emulsion 3—37140
$AgNO_2$, growth from acetonitrile soln., domain struct. 3—30932
Ag_3SbS_3, optimal conditions for obtaining perfect pyrargyrite crystals 3—26980
Ag_2Se, reaction controlled growth of single crystal in solid/gas system 3—15605
Al by recryst., dislocation density and distrib., annealing effects *(French)* 3—24885
Al film, influence of deposition substrate temp. and partial disorder on optical props. 3—24715
AlB_2, and elec. cond., carrier conc. 3—11878
$AlMgBO_4$, sinhalite, olivine type structure, hydrothermal synthesis at high pressure *(French)* 3—38571
Al_2O_3, sapphire, gradient furnace growth method, X-ray topography obs. 3—11572
Al_2O_3 anodic film growth on Si 3—39246
$Al(OH)_3$, secondary nucleation in seeded caustic aluminate soln. 3—2627
Au particles along steps on NaCl surface 3—15098
B_xC, growth, 1450-1500°C, thermal etching, morphology 3—24781
$BaO.6Fe_2O_3$, texture and reaction mechanism in the formation 3—5413
$BaPdF_4$, preparation, madelung part of lattice energy *(German)* 3—14814
$BaTiO_3$, polycryst. film with ferroelec. and antiferroelec. props., deposition by electrophoresis 3—39220
$BaWO_4$, in silica gel 3—21527
BeO, seed-grown, morphological features 3—14708
Bi_2S_3 crystals, thermostimulated electron emission, curves depend. on cryst. growth and X-ray excitation dose *(Russian)* 3—12206
$CaCO_3$, calcite, hydrothermal, from carbonate soln., phase equilib. determ. 3—18538
$CaCO_3$, growth in aqueous solns. 3—12233
$CaPdF_4$, preparation, madelung part of lattice energy *(German)* 3—14814
$Cd_3B_7O_{13}Cl(Br)(I)$, growth by chem. transport reaction, effect of different growth conditions *(Russian)* 3—15606
$CdHg(SCN)_4$, gel growth of single crysts. 3—34470
$Cd_xHg_{1-x}(SCN)_2$, gel growth 3—15611
CdS, suitable for electron beam pumped laser *(Russian)* 3—748
$Co_3B_7O_{13}Cl(Br)(I)$, growth by chem. transport reaction, effect of different growth conditions *(Russian)* 3—15606
Cu, pyramidal growth during electrocrystallisation *(Japanese)* 3—24063
Cu_2S, prep. by topochemical conversion of CdS crystals 3—18540
Fe whiskers, production and properties 3—24796
$Fe_3B_7O_{13}Cl(Br)(I)$, growth by chem. transport reaction, effect of different growth conditions *(Russian)* 3—15606
$FeNiBO_4$, dense warwickite type formed by hydrothermal synthesis at high pressure *(French)* 3—38571
Fe_3S_4, greigite, stoichiometric 3—21525
GaAs single crystals, thermal conditions in the floating zone process, dislocation structure 3—33533
$Gd_{2.3}Tb_{0.7}Fe_5O_{12}$ garnet, single cryst. growth by grain growth technique 3—21526
Ge, growth form and soln. form relation *(German)* 3—9079
InBi whisker, growth by squeeze technique, morphology 3—1963
$KBr-CaCl_2$, Czochralski and Bridgman crystals solubility of $CaCl_2$ rel. to hardening 3—11719
KCl(I), boiling and convection in solvent inclusions rel. to movement 3—11610
KH_2PO_4, capture of random impurities, effect of soln. pH *(Russian)* 3—30078
KH_2PO_4, X-ray topographic study of dislocations *(Russian)* 3—7771
KH_2PO_4 state of soln. obs. using holographic interferometry 3—33475
KNO_3, temperature depend. of rates of growth of faces from aqueous solns. 3—33473
KNO_3 III, metastable rhombohedral polymorph, growth from soln. 3—12219
$KNbO_3$, orthorhombic, large single domain cryst. prep. 3—15463
$La_2Ti_2O_7$, for light modulation 3—27602
$LiIO_3$, growth from acid solns. 3—12234
$MgSO_47H_2O$ from soln.; resist. to growth using flow system 3—8713
Mo_nO_{2n-1}, by chem. transport reactions 3—15604
$NaBrO_3$, (+) and (−), variation of optical properties with crystal growth temperature 3—18425
NaCl, boiling and convection in solvent inclusions rel. to movement 3—11610
NaCl, segregation from NaCl aq. solns. during freezing, vibrs. effects 3—12220
NaCl whiskers, growth in polymer-doped solns. 3—11841
$NaNO_2$, ethyl alcohol effect on temp. depend. of rate of growth from aqueous soln. 3—33474
$NaNO_2$, $NaNO_3$, $NaClO_4$, temperature dependence of the rates of growth of the faces from aqueous solns. 3—33473
H- nB_2O_5, twinning and defects study by electron microscopy 3—7774
$Ni_3B_7O_{13}I$, ferroelectric and ferromagnetic props. 3—17746

crystal growth continued
PBi_2, in silica gels, growth habit and kinetics 3—12223
Pb dendrite, electrodeposited, habit and morphology rel. to growth parameters 3—33767
$Pb_5P_4O_{15}$, Czochralski technique growth and dielec. props. 3—1727
$PbPdF_4$, preparation, madelung part of lattice energy *(German)* 3—14814
PbS films on cleavage surf of NaCl cry. containing macrodefects *(Russian)* 3—8068
$PbTiO_3$, polycryst. film with ferroelec. and antiferroelec. props., deposition by electrophoresis 3—39220
$PbZrO_3$, polycryst. film with ferroelec. and antiferroelec. props., deposition by electrophoresis 3—39220
Pt, d.c. sputtering in diode system to produce Pt film thermoresistor 3—15612
S, metallic, formation process of central cavities during growth of thick layers 3—4753
Se, monoclinic, from soln. of methylene iodide 3—2628
Si, humidity role in atmospheric oxidation, retardation of surface film growth by γ irradiation *(Russian)* 3—8036
$(Sm, Tb)FeO_3$, surface crystal growth depression 3—33469
Sn dendrites, effect of anisotropic mobility of interphase boundary on kinetics 3—20978
$SrPdF_4$, preparation, madelung part of lattice energy *(German)* 3—14814
$SrWO_4$, in silica gel 3—21527
Ti_nO_{2n-1}, by chem. transport reactions 3—15604
$TlIO_3$, and properties *(Japanese)* 3—27605
V_nO_{2n-1}, by chem. transport reactions 3—15604
YIG film on GdGaG substrate, growth by hydrothermal synthesis 3—1922
$YMnO_3$ as-grown monocrystalline ferroelectric, surface effects 3—8527
$Y_2O_3-YF_3$ system, intermediate fluorite related phases, examples of one dimensional ordered intergrowth 3—7692
Zn_3As_2, crystals, growth from Cd_3As_2 3—8758
$Zn_3B_7O_{13}Cl(Br)(I)$, growth by chem. transport reaction, effect of different growth conditions *(Russian)* 3—15606
$Zn_xHg_{1-x}(SCN)_2$, gel growth 3—15611
$Zn(NH_4)_2(SO_4)_2.6H_2O$, supersaturation and impurities, infl. on stepped relief and uniformity *(Russian)* 3—7645
ZnO, hydrothermal, growth rate *(Japanese)* 3—27604
$Zn_3(PO_4).4H_2O$, high temp. gel growth in pressurized chambers 3—12224
$ZnSiO_4$ film, on Si substrate, electrolum. props. 3—21491
$ZrSiO_4$ large single crystals, hydrothermal growth 3—12227
crystal growth from melt
alloy, binary, factors controlling purity, heterogeneity, perfection and max. growth rate 3—12272
apparatus for growth under high vacuum conditions 3—24799
arc transfer furnace method, furnace design and operation 3—12263
benzil, preferential dislocation directions and elastic energy *(German)* 3—7765
Czochralski cryst. pulling apparatus, construction and operation *(German)* 3—5271
Czochralski growth, film showing use of vertical thermal-imaging furnace 3—12294
Czochralski method, automatic control of crystal diameter 3—12264
Czochralski method, flux, hydrothermal and water solution growth 3—11555
Czochralski method, forced convection theory 3—11568
Czochralski process, expts. on the dynamics of the phase limits *(German)* 3—8743
dislocation propag. and annihilation during epitaxial growth 3—1916
edge-defined film-fed growth, for controlled profile cryst. prep. 3—12279
faceted crystals, site selectivity 3—11560
ferrite single crystals, Bridgman method 3—12267
ferrites, flux growth of hexagonal single crysts. with Y struct. *(German)* 3—24800
film, aligned, eutectic, growth by withdrawing silica loop from eutectic melt 3—24802
garnet, Czochralski growth, automatic diameter control using digital computer control algorithm 3—12289
garnet, phase relations and growth conditions rel. to defects and mag. props. 3—2667
garnet film, LPE growth for substrate facet replication 3—38749
garnet substrate prep. by liq. phase homoepitaxy 3—34483
growth form, radii development rel. to external parameters, computer simulation *(German)* 3—7646
heat and mass transfer effects 3—1579
heat and mass transfer in liquid phase epitaxy 3—1923
heat conduction in rod of variable length drawn from melt with const. vel. 3—26176
hexamethylenetetramine, dislocation density rel. to growth methods from ethanol soln. 3—21538
hydrothermal growth method, review 3—24806
hydroxyapatite, hydrothermal growth and characterization 3—12282
I-III-VI_2 compounds, semiconductors, single crystals, growth from melt, structure, p-type conductive 3—39265
ice, morphology of solid-liquid interface, dendritic and planar growth 3—38542
ice, stable growth of single doped crystals *(German)* 3—8739
impurity trapping during crystallisation from melts 3—33466
instant crystal growth teaching demonstration 3—32018
magnetic bubble materials, stoichiometry and perfection 3—12277
orthoferrites, flux grown, induced nonperiodic growth striations, growth program 3—2662
polyethylene, growth rate study, conc. depend. 3—24801
polyoxyethylene films, supermolecular structure *(Russian)* 3—29781
polypropylene, isotactic, mechanism for lamellar branching 3—24044
pyrrhotite mono crysts., melt growth by modified Bridgman method 3—12262
rare earth Ga garnet, Czochralski growth to produce substrate, defect and strain elimination 3—12293
rare earth garnet, liquid phase epitaxy for bubble domain devices 3—36770
rare earth molybdates, $Ln_2(MoO_4)_3$, Czochralski growth 3—12302

crystal growth from melt continued
rare earth molybdates, $Ln_2(MoO_4)_3$ type, single cryst. growth by Czochralski method 3−34484
seed holding crystal growing tip 3−2665
silicate oxyapatite laser crystals, $Me_2Ln_8(SiO_4)_6O_2$, (Me=Ca or Sr, Ln=Y, Gd or La) 3−12296
solid-liquid interface, morphological stability near grain boundary groove 3−11557
spherical crysts. growth by freezing, interface growth stability 3−20701
stable growth in high temp. soln. *(German)* 3−8742
transition metal silicide, refractory, morphology and spontaneous crystallization in growth from Zn melt *(Russian)* 3−14709
tungsten bronzes, $X_cY_{10}O_{30}$, growth and characterization 3−12268
visibility improvement techniques 3−30943
$\{Gd_3\}[Gd_{0.03}Ga_{1.97}](Ga_3)O_{12}$, lattice constants meas. 296-1400 K, Czochralski grown crystal 3−11753
$AgGaS_2$, formation, stoichiometry and props. 3−5269
AlB_{12}, crystallisation from Al-Ga-B melt, effect of impurities 3−12284
α-Al_2O_3, edge-defined film-fed growth 3−12279
Al_2O_3, sapphire, edge-defined film-fed growth, cine-film 3−15636
As-Te, melt system, phase diagram study rel. to growth methods 3−30243
BN, growth of hexagonal crystal in SiB melt 3−12285
$BaMoO_4$, crystal growth by flux pulling method 3−12283
$Ba_2NaNb_5O_{15}$, segregation of impurities and striation rel. to growth speed 3−24804
BaO-Bi_2O_3-B_2O_3 flux system, use in growth of ferrite spinels 3−2663
$Ba_xSr_{1-x}Nb_2O_6$, segregation of impurities and striation rel. to growth speed 3−24804
$BaWO_4$, growth by double decomposition in melt 3−21540
$BaYb_2F_8$:Er, X-ray sensitive upconversion phosphor, prep. 3−12260
$Bi_{12}GeO_{20}$, by Czochralski method from Pt crucible of Bi_2O_3 *(German)* 3−8737
$Bi_2(MoO_4)_3$, crystal growth by flux pulling method 3−12283
Bi_2S_3, photosemicond., crystallisation under hydrothermal conditions *(Russian)* 3−15633
$Bi_{12}SiO_{20}$, by Czochralski method from Pt crucible of Bi_2O_3 *(German)* 3−8737
$CaMoO_4$, for tunable acousto-optic filters, Czochralski growth 3−12300
CaO, electric arc-fusion method to produce clear crystals 3−12265
$Ca_{10}(PO_4)_6F_2$, defect centres 3−8623
$CaY_2Mg_2Ge_3O_{12}$, top-seeded soln. growth using borate fluxes 3−15637
CdF_2:$^{169}YbF_3$, Stockbarger technique growth, optical props. of radioactive and nonradioactive samples 3−2664
$CdGeAs_2$, solution growth using Bi as solvent 3−12286
CdI_2, polytype growth by cleavage 3−7643
CdS and CdS+ZnS mixed crystals, investigation of composition and structure 3−15630
CdTe, growth from Te rich soln., from 480°C to 750°C 3−11567
CdTe, modified Bridgman growth for high power laser windows at 10.6 μm, optical properties 3−5984
CdTe, sonic casting for high power laser windows at 10.6 μm 3−5982
CdTe monocrystals, undoped and doped with Na, As, preparation by direct solidification, electrical properties *(Czech)* 3−21061
CdTe:Cu single crysts., by directional freezing and Cu diffusion 3−15632
$CeAl_2$ single crystal preparation by Czochralski method 3−21541
Cr-Mn, growth using directional solidification in ZrO_2 crucible 3−12291
Cu, by Czochralski technique, cryst. perfection, absence of dislocations 3−1601
Cu crystals solid-liquid interface shape determ. method during Czochralski growth 3−8735
Cu-Co, cell structure formation with Bridgeman growth method 3−11571
Cu-Ni, comparison of zone levelling, Bridgman and Czochralski methods 3−12291
$CuAlS_2(Se_2)$, single crystals, semiconductors, growth from melt, structure, p-type conductive 3−39265
$DyAlO_3$, $Dy_3Al_5O_{12}$, flux crystn., crucible size effect 3−34482
EuO crystal growth parameters relation to stoichiometry, determ. by i.r. and conductivity meas. 3−7641
$(EuY)_3(GaFe)_5O_{12}$, epitaxial growth on $Gd_3Ga_5O_{12}$ by tipping process 3−12278
$Eu_{1.1}Yb_{1.9}Fe_5O_{12}$, garnet film, LPE growth by isothermal dipping with axial rotation 3−30945
$Ga_{1-x}Al_xAs$:Si, L.P.E. growth, depend. of carrier conc. profiles on growth conditions 3−27190
GaAs, liq. phase epitaxial growth by rotating boat technique 3−34481
GaAs, review of methods 3−30948
GaAs, vertical gradient freeze growth, theory and practice 3−15635
GaAs growth in space, Skylab programme 3−12287
GaAs large diameter ingots, for i.r. window appl. 3−15634
GaAs:Sn, defect props. rel. to growth conditions, elec., luminesc. and lattice const. meas. 3−36267
GaAs-GaP system, correlation between miscibility and lattice parameter mismatch 3−11720
$GaAs_{1-x}P_x$, by pulling from Ga rich soln. using liquid encapsulation 3−24805
$Ga_xIn_{1-x}Sb$, vertical freezing technique, and elec. props. 3−5280
GaN, heteroepitaxial thermal gradient soln. growth 3−12257
GaP, constant diameter crystal, liquid encapsulated Czochralski growth 3−12319
GaP, large crystal, liquid encapsulated Czochralski growth 3−12317
GaP, liquid encapsulation and growth from Ga rich soln. 3−12320
GaP, pressure furnace system with modified Bridgeman technique 3−12318
GaP, single crystal, liq. encapsulation-Czochralski and vertical gradient freeze techniques 3−39247
GaP, uniform dia. crystals, liq. encapsulation Czochralski growth, X-ray imaging technique 3−39248
GaP:O, electrical props. of crystal 3−24442

crystal growth from melt continued
GaP:Te,O, liq. phase epitaxy, Te and O incorporation 3−39234
GaSe, Bridgman Stockbarger method 3−2671
Gd-Ga garnet crystal, X-ray topographic anal. of dislocations and growth bands 3−30946
GdF_3, impurity-conditioned solid-solid transition 3−12274
$Gd_3Ga_5O_{12}$, garnet, computer controlled Czochralski growth 3−12290
$Gd_3Ga_5O_{12}$ single cryst. dislocation-free growth 3−36989
$(GdY)_3(GaFe)_5O_{12}$, epitaxial growth on $Gd_3Ga_5O_{12}$ by tipping process 3−12278
$(GdYYb)_3(GaFe)_5O_{12}$, epitaxial growth on $Gd_3Ga_5O_{12}$ by tipping process 3−12278
Ge, shaped crystals, ribbons, tubes and filaments 3−15629
$GeSb_2Te_4$, and semicond. props. 3−5279
HCl, stress free single crystal 3−15631
HoF_3 and HoF_3-ErF_3, impurity-conditioned solid-solid transition 3−12274
$In_{1-x}Ga_xP$ cryst., liq. phase epitaxial growth by sliding method 3−30944
$In_{1-x}Ga_xP$:N, elec. props. and photoluminesc., effect of N-trap states 3−24797
InP, Bridgeman and Czochralski growth with liquid encapsulation 3−12321
InP, growth facility *(German)* 3−8738
InP, liquid encapsulation technique 3−2679
γ-In_2S_3 growth from melt of As_2S_3 *(German)* 3−8741
InSb melt, thermo-hydrodynamic effects 3−11563
InSb:Te, obs. of strain patterns 3−12315
InSb:Te,Se, liquid epitaxial growth, solubility and distrib. of Te and Se *(Russian)* 3−15093
$K_2BiNb_5O_{15}$, crystal growth and dielectric props. 3−8535
KCl-KBr, Czochralski growth in protective atmosphere, optical absorpt., hardness and thermal cond. meas. 3−12292
KCl-KBr mixed crystal, Czochralski growth, i.r. transmissivity 3−16453
$La(OH)_3$, growth from two component nutrient La_2O_3 and Al_2O_3 system below 425°C 3−12281
La_2O_2S, Czochralski growth 3−12298
$LiBaF_3$ by Czochralski and Bridgman methods, doped and pure, absorpt. spectra *(German)* 3−2661
$Li_2Mo_4O_{13}$, $Li_4Mo_5O_{17}$, Czochralski growth from Li_2MoO_4-MoO_3 system 3−2666
$LiNbO_3$, Czochralski growth conditions rel. to lattice defects and optical quality 3−21539
$LiNbO_3$, Czochralski grown, cryst. perfection, obs. of Pendellosung fringes 3−36279
$LiNbO_3$ single crystals, X-ray topographic studies, relation between growth conditions and lattice defects 3−17747
$LiNb_3O_8$, Czochralski method rel. to optimal props. 3−24803
$LiTaO_3$, for piezoelec. filter devices, Czochralski growth 3−12297
$LiTaO_3$ single crystals, X-ray topographic studies, relation between growth conditions and lattice defects 3−17747
$MgAl_2O_4$, nearly stoichiometric, gradient furnace technique 3−5267
Mg_2Ge, modified Bridgman method 3−12270
MgO, electric arc-fusion method to produce clear crystals 3−12265
MnF_2, pure and LiF-doped, modified Bridgman method 3−12273
NH_4Cl, epitaxial growth on NaCl and mica, substrate elec. props. 3−1927
NH_4Cl crystals without additives, growth from melt by Bridgman-Stockbarger method *(German)* 3−8740
NaCl melt, film of gas flow patterns above melt 3−11569
NaCl single crystals, growth from melt, Co_2O_3 impurities distribution coefficient 3−30947
NaCl-KCl polycrystalline window materials, Czochralski, Bridgman crystals, optical properties 3−5901
$NaIn(MoO_4)_2$, melt growth, cryst. struct. and thermal stability 3−33507
$NaNbO_3$, growth by top seeding from $NaBO_2$ flux, growth stability 3−11566
Nb-Ta, growth using electron beam float zoning method 3−12291
Pb-Sb-Sn-As alloys, grain growth and microstructure 3−8785
$PbGeO_3$ single crystals in PbO-GeO_2 binary system, Czochralski pulling method 3−18549
$PbMoO_4$, for acoustooptic light deflector 3−27609
$PbMoO_4$:Cu, Czochralski growth and site occupancy 3−12301
$5PbO.3GeO_2$ single crystals in PbO-GeO_2 binary system, Czochralski pulling method 3−18549
$Pb_2P_2O_7$, Czochralski growth, crystal structure and dielec. props. 3−33470
$(Pb_{1-x}Sn_x)_{1-y}Te_y$, Czochralski-grown, compositional striations 3−39242
PtSi, PtGe, self regulating growth method, and characterization 3−5268
$Sb_2S(Se)_3$, photosemicond., crystallisation under hydrothermal conditions *(Russian)* 3−15633
Si, bipolar wafers, Czochralski grown, props. rel. to growth conditions 3−39253
Si, dislocation free crystals, X-ray diffraction contrast of growth bandings, defect struct. 3−17749
Si ribbons, edge-defined film-fed growth 3−12280
Si:Al, Czochralski growth, impurity striation struct. 3−17860
Si:Al, Czochralski growth, study of impurity striations 3−12322
$SmCo_5$, Bridgman technique 3−12269
$SmCo_5$, by Bridgman technique 3−24798
Sm_2Co_{17}, Czochralski growth in thermal imaging furnace 3−12295
Sn supercooled melt, procedure for dendrite growth kinetics study at melt free surface 3−30378
Sn-Bi, controlled solidification 3−11562
Sn-Pb, controlled solidification 3−11562
SnTe:Mn, Bridgeman method, transport props. rel. to mag. impurities 3−33882
$Sr_2Nb_2O_7$ ferrolectric single crystal 3−21373
SrO, electric arc-fusion method to produce clear crystals 3−12265
Te, by Czochralski method 3−21537
Th-Cu system, intermediate phase formation in liq. Na, struct., 200-700°C 3−2690
TiO_2, chem. vapour growth 3−12254
TiO_2, growth by chem. vapour transport 3−12255
Tl_3AsS_4, Stockbarger technique 3−12266

crystal growth from melt continued
V_2O_3, $(V_{1-x}Cr_x)_2O_3$, tri-arc Czochralski method, paramagnetic insulating and metallic phases 3−18548
V_2O_5 single crystals, growth by Czochralski method and props. *(German)* 3−8744
YAG large crystals, laser quality, commercial growth, Czochralski process 3−12288
$YAlO_3$, rare earth doped, Czochralski growth 3−12299
$YAlO_3$:Nd^{3+}, single cryst. growth by Czochralski method *(German)* 3−5270
Y_2Co_{17}, Czochralski growth in thermal imaging furnace 3−12295
$Y_3Fe_{5-x}Ga_xO_{12}$ garnet, of single crysts. from liq. melt soln. *(German)* 3−5273
$YFeO_3$, top-seeded soln. growth using borate fluxes 3−15637
$Y_3(GaFe)_5O_{12}$, epitaxial growth on $(GdDy)_3Ga_5O_{12}$ by tipping process 3−12278
YIG, from soln. in PbO-PbF_2 *(Russian)* 3−30942
YIG, top-seeded soln. growth using borate fluxes 3−15637
YIG:Ga, L.P.E. growth, effect of substituting Gd(Sm)(La) for Y 3−1924
$Y_2Ti_2O_7$, top-seeded soln. growth using borate fluxes 3−15637
$ZnGeP_2$, phase relations in ZnP_2-Ge system 3−12271

crystal growth from vapour
L-alanine, whisker growth by evaporation through porous membrane 3−33768
alloy deposit prep. by continuous electron beam evaporation from single rod-fed source 3−27715
alloy vacuum deposition, theoret. and practical considerations 3−25717
anthracene-acridine binary system, single crystal growth 3−11718
boracites, modified Schmid three crucible technique 3−2634
chemical transport reaction thermodynamics, Ta transport by I 3−2641
chemical vapour deposition, heat transfer and temp. oscills. 3−12253
chemical vapour deposition, sensors and control elements 3−12250
chemical vapour transport method 3−11555
convection effects 3−2647
p-diamond:B, seed crystal, vapour deposition from methane gas mixture 3−36986
dislocation propag. and annihilation during epitaxial growth 3−1916
electronic materials, chemical vapour growth 3−39296
epitaxial films, review 3−24358
and epitaxy, conf., Jerusalem, Israel, (May 1972) 3−2637
film, grown near source axis in evaporation system, thickness uniformity meas. by multiple beam interferometry 3−36984
film deposition, in electron microscope 3−17722
film deposition, uniformity of the thickness on rotating planetary substrates *(Russian)* 3−30940
garnet, chemical vapour growth for bubble domain devices 3−36771
garnet, growth by chem. transport 3−24791
garnet film, chem. vapour deposition for substrate facet replication 3−38749
garnet film, control of product phases in chemical vapour deposition 3−12249
garnets, chemical vapour deposition, chlorination of Y_2O_3 in presence of C 3−8717
graphite, filamentary growth on metallic impurities 3−18047
group II-VI cpds., improved process *(Russian)* 3−12239
heat transfer for in vacuo situations 3−2631
ice grown on NaCl and mica, substrate elec. props. 3−1927
II-VI semiconductor epitaxial growth by vacuum sublimation *(French)* 3−5265
III-V semiconductor, chem. vap. deposition, mass spectrometric and thermodynamic obs. 3−2639
III-V semiconductor, vapour transport equation derivation 3−2651
III-V semiconductor compounds 3−8762
III-V semiconductors, chem. vapour deposition using organometallics 3−21531
γ-In_2S_3, crystals grown from vapour, X-ray and electron microscope investigation of struct. faults *(German)* 3−7781
lunar breccias and vapour deposited crystals formed in their cavities 3−16171
in lunar vugs, from microprobe analysis 3−39648
magnesia, fibrous, via vapour phase *(Japanese)* 3−8728
mass transfer and thermal convection in chem. vapour transport process 3−24793
nichrome film, elec. resist. variation during deposition 3−21536
non-isothermal plasma application to the preparation of crystals and thin films *(German)* 3−8731
organo-silicon polymer, film deposition by decomp. of $Si(OC_2H_5)_4$ in r.f. glow discharge 3−21535
phosphosilicate glass, chem. vapour deposition at low substrate temps. from SiH_4, O_2 and $POCl_3$ 3−2632
pyrocarbon whiskers, growth during pyrolysis of methane *(German)* 3−15111
rare earth iron garnet, chemical vapour deposition for bubble domain devices 3−24792
rare gas crystals, derivation of upper limit for Xe stacking fault energy 3−1925
semiconductors with chalcopyrite struct., by chem. transport through halogens *(German)* 3−5281
tetracene, structure of vacuum deposited thin films 3−15103
thin film, effect of substrate inhomogeneity on kinetics of heterogeneous nucleation 3−33765
thin film growth by ion beam sputtering, TEM obs. 3−39232
thin film processes for microelectronic applications, review 3−8712
vacuum apparatus, rotary, linear motion feedthrough 3−25713
vacuum deposition, high rate ion production system 3−25716
vacuum deposition high rate, effect of ion bombardment on microstructure of massive layers 3−27632
vacuum deposition of metallurgical systems, conf., Pittsburgh, USA, (June 1972) 3−27615
$AgInS_2$-ZnS system, wurtzite structure 3−18545
Al film, source contrib. to O_2 contamination 3−15621
Al films, conditions for growth on mica substrate 3−15620
Al thin film deposition, source-to-substrate distance effect on O_2 sorption 3−34478
Al:Ti, film, diffusion from Ti sublayer during Al vacuum condensation 3−30079

crystal growth from vapour continued
AlN, epitaxial growth, obs. of optical bandgap 3−11831
Al_2O_3, chemical vapour deposition, X-ray diffraction microscopic obs. of surface structure 3−11790
Al_2O_3, growth of amorphous and epitaxial layers on Si, tunnel characteristics *(German)* 3−8056
As, deposition on hydrogen reduction of $AsCl_3$, rate determ. 3−8723
Au, vacuum deposited on SiO_2 for surface structural defects obs. 3−8027
Au film, epitaxial growth on NaCl, influence of elec. field on orientation *(Russian)* 3−30364
Au film grown on NaCl, small-angle torsion boundary structure in (001) plane 3−4940
Au nuclei, vapour deposition on NaCl substrate, mobility and coalescence 3−2643
Au whisker single crystals for electron field-emitter cathodes, electric field effects *(Russian)* 3−12245
B, polymorphs reaction conditions, polymerisation, nucleation and crystal growth, processes *(German)* 3−34474
B tetragonal filaments on carbon fibre substrate, pyrolysis and morphology 3−21532
$B_{14}P$, prep. of monoclinic B-P phase *(German)* 3−12243
Ba, ultrapure single crystals preparation by ultrahigh vacuum reactive distillation *(German)* 3−8733
$BaSiO_3$ film, for use in integrated optics ccts., r.f. sputtering prep. 3−36983
Be, thick sputtered foil, effects of growth conditions on orientation and hardness 3−30935
BeO, cryst. or amorphous film, prep. by reactive evaporation of Be *(German)* 3−21534
Bi thin films, gravimetric investigation of growth kinetics 3−36269
Bi-Sb, film, deposition by steady state evaporation 3−24787
$Bi_2In_4S_9$, crystal structure, chemistry 3−7673
BiTeI film, optimum conditions of prep. *(Russian)* 3−18033
C, chemical transport, deposition mechanism in non-isothermal plasma 3−2644
C, columnar growth by pyrolytic deposition, microstruct. 3−1581
Ca, ultrapure single crystals preparation by ultrahigh vaccum reactive distillation *(German)* 3−8733
CaF_2 transparency rel. to growth conditions 3−18547
Cd, critical temp. of glass substrate 3−15622
Cd film, deposition on Ge substrate, initial stages of adsorption and clustering 3−18036
Cd film, deposition on Ge substrate, nucleation, growth and evaporation 3−18037
$CdCr_2S_4$, closed tube vapour transport conditions, cryst. perfection 3−12244
$CdCr_2S_4$ single crystals gas transport and characterisation *(German)* 3−8730
$Cd_xHg_{1-x}Te$ film deposition and characterisation *(Russian)* 3−24433
CdO, anal. of growth conditions rel. to surface and vol. supersaturation *(Russian)* 3−15617
CdO, growth conditions effect on structure and morphology *(Russian)* 3−15616
CdO, sublimation 3−2636
CdS, contamination of heteroepitaxial layers vapour grown on GaAs substrates 3−2653
CdS, interface reactions rel. to growth by spontaneous nucleation 3−2645
CdS needles and platelets, growth mechanism 3−11574
CdS platelets, growth mechanisms and morphology 3−2635
CdS_xSe_{1-x}, epitaxial, growth of graded gap crystal layer, luminesc. obs. 3−8053
CdSe, critical temp. of glass substrate 3−15622
CdSe, electrophyscial props., influence of growth conditions 3−24428
CdSe, epitaxial growth on sapphire substrate, growth conditions 3−30362
CdSe, on SiO_2 seed plate at 1225°C 3−15614
CdSe-CdTe, solid solns., comp. and elec. charact. depend. on method of deposition 3−33762
CdTe, by chem. transport in Cd-Te-H-Cl-N system 3−344[illegible]2
CdTe, physical vapour deposition for high power laser windows at 10.6 μm 3−9960
CdTe, vacuum deposited film, mech. strain meas. as function of growth conditions 3−4939
CdTe films, structure of complex particles in condensate islets 3−33760
$CoMn_2O_4$, chem. transport growth 3−39224
Cu epitaxial growth on β-Co *(Russian)* 3−8049
Cu-Ag, Cu-Fe and Cu-Zn whiskers, X-ray topography of internal structure 3−15110
Cu_3SmS_3 single crystal preparation by gas transport method, X-ray structure determ. *(Russian)* 3−12241
EuS, sublimation and high temp. chem. transport, kinetic and thermodynamic aspects 3−2638
Fe, phase relations for epitaxial intergrowth of nitrogenized Fe sheets and films *(German)* 3−1926
Fe film, prep. with aid of laser beam *(Russian)* 3−30934
$FeCr_2S_4$ single crystals, gas transport and characterisation *(German)* 3−8730
Fe_8N film, vapour deposition from nitrogen atmos., ultrahigh mag. moment *(Japanese)* 3−8403
Fe_9S_8, pentlandite, Ni-free, flash evaporation prep. 3−27608
GaAs, epitaxial, from $AsCl_3$-Ga-H_2, electrical props. depend. on $AsCl_3$ temp. 3−8756
GaAs, epitaxial, Ga-$AsCl_3$-H_2 system, Ga:As ratio, chemical thermodynamics calc. *(German)* 3−15095
GaAs, epitaxial growth from transport reaction with HCl *(Russian)* 3−8725
GaAs, excess Ga and As in the vapour phase influence on epitaxial growth in (111) direction *(Russian)* 3−8749
GaAs, homoepitaxial growth, transmission electron microscope obs. 3−15096
GaAs, parameters for epitaxial growth of high purity crystals 3−1918
GaAs, thin film, flash-evaporated, and doping characts. 3−27611
GaAs, V.P.E. growth, effect of As vapour pressure on elec. props. 3−27191

crystal growth from vapour continued
- GaAs film, growth on sapphire substrate in ultrahigh vacuum conditions 3−15619
- GaAs p-n junction, defect morphology and electrolum., gas-phase stoichiometry effects 3−11950
- $GaAs_{1-x}P_x$, pyrolytic epitaxial growth, analysis of growth rate 3−1914
- $GaAs_{1-x}P_x$ superlattice, layer spacing uniformity 3−2687
- GaP, open tube vapour phase epitaxy onto GaAs substrate, influence of liquid Ga 3−2652
- GaP films, lattice defects in epitaxial growth 3−15091
- GaP:Be, homogeneous doping during growth and elec. props. *(Russian)* 3−15644
- GaP:Zn, O, vapour phase epitaxial, form. of Zn-O radiation centre 3−2672
- GaS, layer struct., growth mechanism 3−1580
- $GaS_{0.4}Se_{0.6}$, layer struct., growth mechanism 3−1580
- GaSe, comparison of different growth methods 3−2650
- GaSe, layer struct., growth mechanism 3−1580
- GaSe, needle cryst., growth by sublimation process, struct. 3−2633
- GdN, by sublimation in sealed Mo crucibles 3−2642
- Ge, evaporated film, structure change and elec. resist. step, depend. on substrate temp. 3−30372
- Ge, growth in open iodide system, efficiency of Ge transport *(Russian)* 3−15615
- Ge homoepitaxial layers, dislocation struct., effect of crystn. conditions 3−24356
- Ge:Ga, distrib. coeffs. for Ga doping during growth in open iodide system *(Russian)* 3−15643
- GeSe, transport rate, growth mechanism and morphology 3−11573
- HfO_2, c.v.d. on Si, structure, optical and elec. characts. obs. 3−2658
- $HfTe_{2-x}$, $x=0.061$, preparation and X-ray characterization 3−7691
- HoN, by sublimation in sealed Mo crucibles 3−2642
- $InAs_{1-x}P_x$, $(0.7 \leqslant x \leqslant 1)$, vapour epitaxial growth and characterization 3−1917
- $InAs_{1-x}P_x$, vapour-grown epitaxial layers, electron microprobe characterization 3−20955
- InP layer prod. by Nicoll and Sirt short path transport method *(German)* 3−8729
- β-In_2Te_3, chem. gas transport method *(Russian)* 3−8724
- IrO_2, continuous flow method 3−12256
- KCl, condensation coeff. rel. to sub- and supersaturation, mol. beam method obs. 325-425°C *(German)* 3−1792
- KCl, relax. effects of (100) face during condensation *(German)* 3−1793
- Li-Cr ferrite film, LPE growth on MgO, Mossbauer obs. of substrate contamination 3−1928
- LiF film, epitaxially grown on NaCl, electron microscope obs. of annealed structures 3−1929
- MgO, growth of high quality crysts. by chem. vapour transport techniques 3−24789
- Mo, chemical vapour deposition, crystal orientation and defect structure obs. 3−8718
- Mo, growth using electron beam evaporation source 3−15626
- NaCl, growth conditions effect on electrical relief 3−33985
- NaCl, moving mask deposition on fused SiO_2 3−20961
- NaCl film, epitaxial growth on muscovite 3−27193
- Nb/Al_2O_3 cermet film preparation *(Russian)* 3−30482
- Ni-Cr film, evaporated on glazed Al_2O_3 substrate, uniformity of elec. resist. 3−24794
- NiO, epitaxial growth of high purity crystals 3−1915
- PbO, film, obs. of fracture edge, surface structure and higher oxides 3−15628
- PbS epitaxially grown on KCl, Pb form. 3−8052
- PbS film for photodetector, oxidant effects in chem. deposition 3−24360
- PbSe films, vapour phase deposits epitaxially grown 3−30360
- $Pb_{1-x}Sn_xSe$, resistivity and Hall mobility 3−24438
- $Pb_{1-x}Sn_xTe$, vertical epitaxial system for growth 3−2654
- Pd film, artificial ageing effect on elec. and galvanomag. props. 3−8159
- Pt film, epitaxial growh 3−34473
- $RbAg_4I_5$, thin solid electrolyte film, vacuum-deposited, and electrochem. charact. 3−39223
- $RbSnCl_3$, gaseous complex, thermodynamic stability rel. to chemical transport 3−2640
- ReO_x, continuous flow method 3−12256
- Sb_2O_3-SbI_3 compounds, synthesis and vapour transport growth 3−30938
- Se, critical temp. of glass substrate 3−15622
- Se, vacuum evaporated layer, amorphous and crystalline phase obs. 3−20970
- Se film, nucleation phenomena *(German)* 3−20976
- Se:As, As_2S_3, Bi, SiO, doping in vacuum growth to produce semicond. film for electrophotography 3−15623
- Si, epitaxial deposition in N_2, effect of prep. conditions 3−1921
- Si, epitaxial deposition on insulating subsrate, combination of two growth methods 3−2655
- Si, epitaxial growth, generation of growth nuclei 3−1919
- Si, epitaxial growth at high rates by chem. vapour deposition 3−24788
- Si, epitaxial growth by rotating disk method 3−12242
- Si, etch rate and deterioration of $MgAl_2O_4$ substrate in H_2 3−11816
- Si, from silane, initial mat. manuf. process 3−39295
- Si, grown on sapphire film, elec. props. rel. to dual rate technique 3−2656
- Si, growth using electron beam evaporation source 3−15626
- Si, homoepitaxial growth, transmission electron microscope obs. 3−15096
- Si, onto spinel, chem. interaction between deposition constituents and subtrate 3−8720
- Si, structure of isoepitaxial films made by condensation from a molecular beam in ultrahigh vacuum 3−33749
- Si, vapour deposition, surface transient effects, instabilities due to convection, Si devices 3−39275
- Si amorphous films, growth by silane decomposition in r.f. glow discharge, electronic transport 3−8172
- Si film, deposited from SiH_4-H_2, growth rate, influence of AsH_3, PH_3 and B_2H_6 3−21529

crystal growth from vapour continued
- Si film, epitaxial growth, impurity atom transfer from substrate 3−21530
- Si-Ge, epitaxial layer grown on Si substrate, crystal defects obs. 3−1920
- Si-Ge, solid soln., anal. of vapour grown homogenous crystals 3−2649
- β-SiC, vapour-phase deposition on Si 3−18543
- Si_3N_4, layer, effect of H_2 on growth rate *(Russian)* 3−15618
- Si_3N_4, pyrolytic, prep. and props. 3−8980
- Si_3N_4 film, deposition by microwave glow discharge 3−30937
- SiO, effects of substrate temp. on vac. deposited thin films 3−34490
- SiO film, vacuum deposition, props. of evaporated material used in prep. 3−15624
- SiO_2, silica, reaction kinetics for silane oxidation 3−24786
- SiO_2 film, deposition by decomp. of $Si(OC_2H_5)_4$ in r.f. glow discharge 3−21535
- SiO_2 film, growth in plasma microwave discharge 3−15625
- SiO_2 thin films growth on n-GaAs substrates 3−24785
- SiO_2-$B_2O_3(As_2O_3)(P_2O_5)$, characts. and use in Si device fabrication 3−2657
- SnO_2:Sb, film, Sb impurity influence on elec. props. 3−15627
- $(SnTe)_{1-x}(PbSe)_x$, $(SnTe_{1-x})(PbTe)_x$ thin layers, structure depend. on phase composition and prep. conditions 3−33761
- $Sn_xZr_{1-x}S_2$, layer compound, iodine vapour transport growth conditions and structure parameters 3−38543
- Sr, ultrapure single crystals preparation by ultrahigh vacuum reactive distillation *(German)* 3−8733
- Ta, chem. transport by iodine, demonstration expt. *(German)* 3−18544
- Ta, growth using electron beam evaporation source 3−15626
- Ta film nucleation and growth obs. from high energy electron diffraction 3−33766
- TiC, deposited by activated reactive evaporation, effect of substrate temp. on struct. 3−27631
- TiO film, vacuum deposition, props. of evaporated material used in prep. 3−15624
- TiO_2, c.v.d. on Si, structure, optical and elec. characts. obs. 3−2658
- $TlSbSe_2$ film, thermal evaporation and condensation *(Russian)* 3−18235
- UO_2, deposition from plasma 3−36985
- V_2O_3, $HCl(TeCl_4)$ chem. transport method, obs. of sharp insulator-metal transition *(French)* 3−30939
- V_6O_{13}, growth by chem. transport, semicond. semicond. transition 3−24790
- V_nO_{2n-1}, $(n=3, 4, 5, 6, 7, 8)$, by chem. transport, $TeCl_4$ as transport agent 3−2648
- W, chemical vapour deposition, annealing and mech. behaviour 3−1960
- W, chemical vapour deposition, crystal orientation and defect structure obs. 3−8718
- $Y_3Fe_{5-x}Ga_xO_{12}$, epitaxial garnet film, growth by chemical vapour deposition 3−12248
- Zn crystallites, growth by evap. on C-coated or preheated NaCl 3−15613
- $ZnMn_2O_4$, chem. transport growth 3−39224
- ZnO, evaluation of $HgCl_2$ as transport agent 3−39222
- ZnS, epitaxial growth on Si, condensation of vapour from electron beam heated source 3−24795
- ZnS:Cu, Mn, Cl, film, doping in vacuum growth rel. to electrolum. props. 3−15559
- ZnSe, chemical vapour deposition for high power laser windows at 10.6 μm 3−5981
- ZnSe, epitaxial growth of sphalerite and wurzite phases on Ge surface by sublimation 3−21528
- ZnSe on GaAs, heteroepitaxial, H_2 transport, luminescence centres 3−18546
- $ZnSe_xTe_{1-x}$ solid soln., cryst. growth by vapour phase sublimation 3−30936
- ZnTe, growth temp. depend. on carrier gas velocity in open tube transport 3−2646
- ZrO_2, c.v.d. on Si, structure, optical and elec. characts. obs. 3−2658

crystal hyperfine field interactions
see also crystal internal fields
- acoustic resonance absorption, paraelectric, quadrupole transitions, noncentral impurity ions 3−38624
- actinide cpds, NaCl-type, hyperfine fields, crystal field and relativistic effects, angular wave function 3−2233
- actinides magnetic hyperfine fields, relativistic effects 3−2228
- alkali halide, e.p.r. obs. of hyperfine and g-components of V_k centres 3−18369
- alkali metal, nuclear contact densities for electrons, calc. 3−36806
- alloy with Ce and Yb impurities, Kondo effect rel. to cryst. field 3−2256
- amino acid:Cu^{2+}, ligand hyperfine interaction, e.p.r. spectra 3−24605
- anthracene molecules crystal, Raman spectra, fine structure investigation 3−34342
- 9,10-anthraquinone molecular crystal, Raman spectra fine structure investigation 3−34342
- aromatic molecular crystals, Raman spectra, fine structure investigation 3−34342
- rel. to dynamic self-polarization of nuclei in solids 3−21325
- ENDOR, in presence of external stresses, theory 3−27442
- ENDOR freqs. and h.f.s. formulae 3−34249
- e.p.r. spectrum, exchange and dipole-dipole broadening of individual hyperfine components *(Russian)* 3−34189
- $Er_2O_2S:Er^{3+}$, absorption spectra, crystal field effects on electronic ion structure detn. *(French)* 3−30411
- e.s.r. hyperfine transition probabilities for large cryst. field effects case 3−2345
- exchange core polarisation in transferred hyperfine interaction of Li^+ with O^-, model calc. 3−21013
- ferroelectrics and antiferroelectrics, X-irrad., e.p.r. of defect centres 3−2388
- ferromagnetic insulators, nuclear spin interactions, excitation spectrum 3−34066
- ferromagnetic insulators, nuclear spin interactions, thermodynamic props. 3−30592

crystal hyperfine field interactions continued
ferromagnetic rare earth alloys, hyperfine field versus average spin 3—15317
ferromagnets, field sign determination by n.m.r. 3—22412
glass, phosphate, irrad., radiational capture centre, e.p.r. *(Russian)* 3—27415
glasses, kaolinite, pure and Fe doped, recrystallisation, Mossbauer obs. 3—7632
haematite-ilmentite solid solution series, Mossbauer spectra 3—34819
interacting systems decoupling, one electron energy matrix 3—20985
ionic crystal, effect on conduction electrons 3—36601
isotope separator implantation of radioactive ion for hyperfine interaction studies 3—32217
magnetic exchange interaction between two ions in cubic field *(French)* 3—36702
metals, crystalline electric field, physical aspects 3—30582
molecular cryst., optical nucl. polarization in high mag. fields 3—2425
molecular crystals, optical nuclear spin alignment in zero mag. field, mechanism 3—15146
molecular crystals, optimal Raman instrumentation for obs. of fine structure of vibrational modes 3—27493
Mossbauer spectra, partly resolved, calc. of hyperfine interactions using superposition of Lorentzians 3—8495
naphthalene molecular crystal, Raman spectra, fine structure investigation 3—34342
1,4-naphthaquinone molecular crystal, Raman spectra, fine structure investigation 3—34342
n.m.r., dipole-dipole and quadrupole interactions, parameters 3—36803
nuclear quadrupole interactions determ. in metals and insulators by PAC 3—39062
nuclear spin phonon coupling mechanism 3—1756
phonon-spin interactions of a dilute system 3—1752
piezo-hyperfine interaction concept. rel. to ENDOR of impurity centres in crysts. 3—2466
pseudo-tetrahedral ferrous compounds, quadrupole splitting and magnetic susceptibilities 3—21190
quadrupole coupling in complex radicals, determ. using e.s.r. probe in smectic A phase 3—17739
quadrupole interaction tensor of nuclei with half-integer spins and lineshape of polycrysts. 3—2411
rare earth ferromagnets, fields at Sn impurity atoms 3—21357
rare earth intermetallic compounds, orbital contributions to transferred mag. hyperfine fields 3—38937
rare earth metals, contribution of 5d electrons to mag. fields 3—24564
rare earth orthoferrite, and Neel temp. rel. to covalency parameters 3—21191
rare-earth iron garnets, nuclear quadrupole coupling constants 3—2010
Rochelle salt, temp. dependence of ^{23}Na quadrupole coupling constant 3—34245
ruby, rel. to inhomogeneous broadening of E-reson. lines *(Russian)* 3—15417
ruby, superhyperfine interactions on photon echo behaviour 3—34417
S-state ions with axial crystalline environments, line intensity ang. dependence 3—39023
singlet ground state systems, combined electron nuclear mag. ordering phenomena 3—38969
tensor A component estimation using e.s.r. probe in smectic A phase 3—17739
time differential perturbed angular correlation and Mossbauer spectra, imperfect crystal lattices, electric field gradient parameter 3—15440
transition metal cpds., core electron exchange splittings of 2s and 3s electrons, hyperfine fields 3—30417
transition metal/hydrogen systems, electron-nucl. interactions 3—2439
$\{Cr_3O(CH_3COO)_6(H_2O)_3\}Cl.6H_2O$ Mossbauer study on the magnetism 3—2262
$\{Fe_3O(CH_3COO)_6(H_2O)_3\}Cl.6H_2O$ Mossbauer study on the magnetism 3—2262
Al-Cr(Mn) dil. alloys, n.m.r. spectra, satellite struct. interpret. 3—2431
Al-Ti, dilute alloys, solid effect between pure quadrupolar nuclear transitions 3—34243
Au-Ni alloys, mag. hyperfine structure coupling and Mossbauer isomer shift of ^{197}Au 3—34257
AuCo dilute alloys, n.m.r. of ^{59}Co 3—34226
Au_2Mn:^{119}Sn, mag. hyperfine interaction, Mossbauer study *(Russian)* 3—12088
$BaTiO_3$:^{181}Ta(^{178}Hf), static quadrupole interaction 3—12090
$BiFeO_3$, Mossbauer effect, mag. h.f. interaction, quadrupole splitting, elec. field gradient 3—27447
$CaCO_3$, spin-lattice relax. of CO_3^{3-} mol.-ion., phonon modulation of s.h.f. interaction 3—2350
CaF_2, ENDOR of Ho^{2+}, hyperfine lines, spin Hamiltonian parameters 3—2468
CaF_2, e.p.r. of U^{4+} ions, elec. quadrupole coupling const. 3—2360
CaF_2:Er^{3+}, effect of dislocations on perturbed angular correlations in paramagnetics 3—34256
CaF_2:Yb^{3+}, rel. to covalency 3—2009
Cd, in-beam meas. of static quadrupole interaction produced by 247 keV level of ^{111}Cd 3—2476
Cd compounds: ^{117}In(^{111}Cd), excited state nucl. quadrupole interactions, PAC obs. 3—12085
CdF_2:Gd^{3+}, e.p.r., fluorine superhyperfine struct. 3—18363
CdF_2:Mn^{2+}, ligand ENDOR obs. for F and Cd lattice nuclei 3—18394
$CdGa_2S_4$:Mn^{2+}, e.p.r. spectra meas., spin Hamiltonian description, g-values hyperfine constants, covalent bonding effect 3—12059
$CdGa_2Se_4$:Mn^{2+}, e.p.r. spectra meas., spin Hamiltonian description, g-values hyperfine constants, covalent bonding effect 3—12059
$CdIn_2S_4$:Fe^{2+}, effect of weak Jahn-Teller coupling 3—21455
$Cd(NH_3)_2.Ni(CN)_4.2C_6H_6$:$Cu^{2+}$, isolated ion, e.s.r. obs. 3—39018
CdS:Cu ang. depend. of hyperfine structure const. from e.s.r. spectrum 3—2357

crystal hyperfine field interactions continued
^{107}Cd, nuclear hyperfine structure obs., orientation by optical pumping 3—11862
^{111}Cd nuclei, time-differential quadrupole interaction with cubic Ag lattice after implant. by (α, 2n) 3—33808
Co, hexagonal, from ^{59}Co n.m.r. obs. 3—8459
Co_2B, and quadrupole coupling, ^{59}Co n.m.r. obs. 3—12077
$Co_{0.98}Fe_{0.02}$ S_2, pyrite, transferred hyperfine field at ^{57}Fe 3—8487
Cr, incommensurate antiferromag., hyperfine field meas. using time differential perturbed angular correlation 3—11993
Cr^{3+}, e.s.r. exact eigensolutions calc., spin hamiltonian, electronic Zeeman, crystal field and hyperfine interaction terms 3—24609
Cu, indirect nuclear interaction coupling constants 3—27216
Cu diluted Tutton salts, dynamic polarization, cross relaxation, e.s.r. hyperfine splitting 3—39050
Cu-Ni-Au alloys, mag. hyperfine structure coupling and Mossbauer isomer shift of ^{197}Au 3—34257
$CuCr_2Te_3I$, Mossbauer effect obs. 3—30735
Cu(II) complex perchlorate tris-octamethylpyrophosphoramide, e.s.r. study, spin lattice and hyperfine interactions 3—30685
$DyVO_4$, middle i.r. absorpt. obs. at low temp. 3—18443
Er^{3+}, in solids, C_{3h}, D_{2d}, O_h site symmetry, hyperfine struct. parameters rel. to cryst. field parameters 3—2234
Eu complex, tetrakis(benzoylacetonate)europium, laser action 3—21440
Eu dibenzoylmethane complexes, ion-ion interaction effect on luminescence 3—27527
Eu^{2+}, primary and secondary solution spheres, effect on electric quadrupole transitions 3—15536
EuI, mag. hyperfine splitting meas. 3—15316
EuO(S), spin echo meas. of hyperfine interactions at ^{153}Eu nuclei 3—21324
$Eu_xYb_{1-x}Sn_3$, Mossbauer effect and magnetisation meas., paramagnetic Curie temp. and hyperfine fields depend. on Eu concentrations *(German)* 3—24594
$(Fe, Mg)_3Al_2(SiO_4)_3$ garnet, hyperfine interactions of ^{27}Al and ^{29}Si, quadrupole coupling const., paramag. shift 3—8482
Fe, mag. h.f. field at ^{99}Tc, perturbed ang. correl. obs. 3—5154
Fe alloyed with ^{54}Mn, ^{57}Co, ^{182}Ta, ^{191}Ir, nonalignment effects under mag. saturation at 25 mK 3—24565
Fe: ^{220}Rn, ^{224}Ra, hyperfine interactions of Rn and Ra, alpha decay PAC obs. 3—2270
Fe:^{175}Lu(^{175}Yb), ang. correlation meas. of hyperfine fields at impurity nuclei 3—15141
Fe:^{44}Sc, hyperfine field meas. using time differential perturbed angular correlation technique 3—34260
Fe:Hg, time-differential-perturbed-angular correlation meas. of hyperfine mag. field 3—39067
Fe:Tm, molecular field model of mag. hyperfine interactions rel. to localised moments 3—15359
Fe-Be (23 at%) alloy, aged above 400°C, Mossbauer study of hyperfine fields 3—34264
Fe-Ni-Co, Fe mag. moment from nuclear hyperfine field 3—2471
Fe-transition metal, dilute alloys, Mossbauer spectra, hyperfine field, isomer shift changes analysis 3—30733
Fe_2B, Mossbauer absorpt. obs. of elec. quadrupole interaction 3—15443
$FeCO_3$, siderite, Mossbauer linewidth anomalous temp. depend., obs. and mechanism 3—34277
$Fe(ClO_4)_3$, effect of weak mag. fields on paramag. hyperfine struct. of Mossbauer line *(Russian)* 3—8494
$FeCr_2S_4$, low temp. transition, Mossbauer obs. 3—5151
FeF_2, calc. of pressure and temp. depend. of hyperfine mag. field 3—34059
FeNi, (75 at. % Fe), transformation of fine particles from f.c.c. to b.c.c. structure with temp., mag. hyperfine field at Fe nuclei *(Korean)* 3—30734
FeO_4^{2-} diluted in NaOH, paramag. hyperfine interactions in e_g^2 config. of ^{57}Fe 3—2470
Fe_2O_3, magnetic hyperfine field at ^{57}Fe *(Korean)* 3—27452
$^{57}Fe^{3+}$ Mossbauer spectra in diamag. host lattice, hyperfine splitting 3—34253
Ga quadrupole interaction of Ge nuclei following nuclear reactions 3—34255
Gd, ^{155}Gd and ^{157}Gd n.m.r. study 3—24631
Gd^{3+} compounds, Mossbauer studies at very low temps. 3—2478
$GdAl_2$, transferred mag. induced ^{27}Al quadrupole interaction 3—34244
Ge, lattice defect obs. using ^{73}Ge, 13.3 keV Mossbauer effect 3—34279
GeO_2, hyperfine, superhyperfine and quadrupole interactions for V^{4+} 3—34198
H_2 solid, anisotropic intermolecular interactions in the rotation-vibration Raman spectrum, cryst. field quadrupole splitting 3—27492
$Ho(Fe_{1-x}Co_x)_2$, Laves phases, mag. hyperfine field and isomer shift, Mossbauer obs. 3—36820
KCl:Cd^+, X-ray irrad., e.s.r., hyperfine coupling const., g-factor, 77-300 K 3—27402
KD_2PO_4, domain influence on elec. field gradient, n.m.r. obs. 3—2413
$K_3Fe(CN)_6$, effects of electronic relaxation phenomena on Mossbauer spectra at very low temps. 3—27446
K_2IrCl_6, transferred hyperfine shift in n.m.r., unpaired spin distrib. 3—24620
$KNbO_3$, n.m.r. of ^{93}Nb, in single domain cryst., phase transition 3—2414
K_2ReCl_6, transferred hyperfine shift in n.m.r., unpaired spin distrib. 3—24620
K_2SO_4:Hg^+, X-irrad., e.s.r. 3—39026
LiF, dipole-dipole interactions role in acoustic saturation of n.m.r. 3—2423
$LiTaO_3$, ^{7}Li quad. coupling const. temp. depend. near Curie pt. 3—2415
Mg, nucl. quad. interaction, electronic and lattice contribs. to EFG, cryst. field l=2 component 3—21018
MgO, lattice distortion around F^+ centre, ENDOR obs. 3—27441
MgO, paramagnetic defects at the surface 3—5048
MgO containing Mn^{2+}, Cr^{3+} and Fe^{3+} impurities, ^{17}O transferred hyperfine interactions 3—30727

crystal hyperfine field interactions continued
MgO:Mn^{2+}, temp. depend. of hyperfine structure splitting 3—15143
Mo:^{161}Dy, Mossbauer effect, paramagnetic hyperfine structure 3—36824
MoO_3, rel. to localization of $4d^1$ electrons near protons, e.s.r. 3—2353
NH_4Br:Cu^{2+}, nondiagonal contribs. to hyperfine struct. anisotropy 3—18357
NaCN, ^{23}Na elec. quad. coupling const., cubic-orthorhombic transition phenomena 3—2416
NaCN, ^{23}Na quadrupolar coupling const. and relax. rate 3—36809
NaCl, dipole-dipole interactions role in acoustic saturation of n.m.r. 3—2423
NaCl-NaBr mixed crysts., pulsed double n.m.r., quadrupole freq. at ^{23}Na around Br^- impurities 3—34222
NaN_3, rel. to F-centre wave function calc. by point-ion method 3—38587
$Na_2O.11\,Al_2O_3$, n.m.r. study and effect of water on ^{23}Na quadrupole interaction 3—8457
NdAs, cryst. field splitting 3—2298
$Nd_{0.95}Ca_{0.05}Fe_{0.95}Sn_{0.05}O_3$ orthoferrite, reorientation of induced mag. field at diamag. Sn_2 atom 3—34252
NdP, cryst. field splitting 3—2298
NdSb, cryst. field splitting 3—2298
Ni, Mossbauer spectra of ^{181}Ta 3—18397
Ni alloy:^{57}Fe, mag. impurity interactions and hyperfine field, Mossbauer obs. at 4.2K 3—36819
Ni:^{175}Lu, ang. correlation meas. of hyperfine fields at impurity nuclei 3—15141
Ni:^{187}Re, hyperfine field meas. using time differential perturbed angular correlation technique 3—34260
Ni:^{192}Ir, elec. quadrupole interaction on ^{192}Ir, n.m.r. obs. 3—2461
$Ni_{1-x}Cu_xMnSb$, ferromag. rel. to anomalous line shift in n.m.r. 3—30704
$Ni_3(Fe,V)$, V atom redistrib. obs., Mossbauer spectra *(Russian)* 3—12080
$Ni_{75-x}Fe_xGa_{25}$ giant moment system, ^{57}Fe Mossbauer expt., determ. of hyperfine fields, isomeric structure, quadrupole splitting 3—39074
Np, inner Sternheimer shielding factor from Mossbauer spectra 3—2480
$PbHfO_3$ from γ-γ ang. correl. and Mossbauer spectroscopy 3—21353
$PbTiO_3$, ^{44}Sc probe, low temp. structure 3—39068
$PbTiO_3$:^{181}Ta(^{178}Hf), static quadrupole interaction 3—12090
Pd alloy:^{57}Fe, mag. impurity interactions and hyperfine field, Mossbauer obs. at 4.2K 3—36819
Pd-Co dil. alloys, ^{57}Fe hyperfine field press. depend. up to 180 kbar 3—18306
PrO_2, Mossbauer scattering, Pr^{4+} ion in magnetic cubic crystal 3—34259
Pt alloy:^{57}Fe, mag. impurity interactions and hyperfine field, Mossbauer obs. at 4.2K 3—36819
RbCl(:Na, :Ca), e.s.r. investigation of F-centres, obs. of hyperfine structure 3—27414
Rh-Fe dilute alloy, Mossbauer meas. of hyperfine field at ^{57}Fe 3—30739
SiO_2:Fe^{3+}, V^{4+}, α-tridimite, e.p.r., crystal field strength, symmetry 3—21298
$SnMn_3C$, $SnMn_3N$, Mossbauer obs. 3—34278
SnO_2, ENDOR of $^{57}Fe^{3+}$ and $^{53}Cr^{3+}$ at different sites, h.f. data interpret. 3—2467
SnTe:^{151}Eu, e.s.r. hyperfine splitting 3—5132
$SrCl_2$:$^{165}Ho^{2+}$, coupled nuclear-electronic spin system, low temp. relax. 3—18362
TbAl garnet, Tb^{3+} fundamental multiplet cryst. field splitting 3—27342
Te, electric field gradient and quadrupole interaction constant from Mossbauer spectra 3—21356
TiO_2:Cr^{3+}, dynamic nucl. polarization of ^{47}Ti, ^{49}Ti and ^{17}O, quad. coupling consts. 3—2424
$Tm_x\,Y_{1-x}Al_2$, cryst. elect. field transitions, susceptibility, inelastic neutron scatt. 3—18283
$TmBr_3.6H_2O$, meas. at low temp. in ^{3}He cryostat, determ. of crystal field splitting 3—27367
$TmCl_3.6H_2O$, specific heat meas. at low temp. in ^{3}He cryostat, determ. of crystal field splitting 3—27367
$Tm_2(SO_4)_3.8H_2O$, specific heat, meas. at low temp. in ^{3}He cryostat, determ. of crystal field splitting 3—27367
UP, cubic, hyperfine mag. fields, ^{238}U Mossbauer obs. 3—2473
US, cubic, hyperfine mag. fields, ^{238}U Mossbauer obs. 3—2473
VO_2, metallic phase, n.m.r. spectrum interpret, elec. field gradient 3—2432
V_2O_5:Cr, e.p.r., h.f.s., γ-irrad. influence 3—2382
V_3O_5, inelastic neutron scattering 3—38940
$YCrO_3$:Fe, impurity-host Fe^{3+}-O-Cr^{3+} antiferromag. superexchange, ^{57}Fe hyperfine field meas. 3—30611
$Y(Fe_{1-x}Co_x)_2$, Laves phases, mag. hyperfine field and isomer shift, Mossbauer obs. 3—36820
$YbNi_2$, ^{107}Yb Mossbauer obs. 3—30610
Zn, quadrupole interaction of Ge nuclei following nuclear reactions 3—34255
$ZnAl_2O_4$:Mn^{2+}, e.p.r., fine struct. *(French)* 3—24611
$Zn(Mn_{1-x}Fe_x)_2O_4$, quadrupole splitting due to Fe^{3+} pair interaction, Mossbauer obs. 3—39069
$Zn_xNi_{1-x}Fe_2O_4$:Fe^{3+}, n.m.r. study of supertransferred hyperfine fields of Fe^{3+} ions 3—2407
$Zn_2(OH)PO_4$, tarbuttite, Cu^{2+} e.s.r., hyperfine structure 3—36784
ZnS:Mn, phonon induced hyperfine fields, molecular orbital model *(German)* 3—15161
ZnS:Mn^{++}, spin lattice coupling coeffs. of $3d^5$ ion in trigonal symmetry 3—39025
ZnSe:Mn, phonon induced hyperfine fields, molecular orbital model *(German)* 3—15161
$ZrFe_2$, $ZrFe_2H_{0.3}$, effective mag. field acting on ^{57}Fe, nucl. γ-reson. method obs. *(Russian)* 3—12079
crystal imperfections *see crystal defects*
crystal impurities
see also impurity electron states and effects; magnetic impurity interactions
alkali halides, Jahn-Teller distortions, molecular orbital models 3—33837
alkali halides, single crystals, solute strengthening, effects on hardness 3—7835
alloy, ternary b.c.c., anisotropy of substitutional-interstitial internal friction peaks 3—36365
anatases, e.p.r. of Cu^{2+} and V^{4+} impurities, calculation of line shapes *(French)* 3—36783
anthracene single crystals with tetracene impurity, electroluminescence *(Russian)* 3—24751
b.c.c. metals, Neumann and Hirschwald's model for diffusion 3—33695
benzene mixed crystal, Raman spectra, phonon delocalization and trap depths 3—21403
Bloch electron additional scattering, simultaneous impurity and lattice interactions 3—20831
channelling, theory, use for study of impurities *(Hungarian)* 3—7802
corundum grown by Verneuil method, effect of additives (Ti, V etc.) on OH absorption bands *(Russian)* 3—24706
Cs halides:Pb, Cd, dielectric loss meas. of impurity-vacancy dipoles, 90-180°C 3—11612
cyclododecane, inhomogeneous distrib. and effect on molecular parameters 3—1634
defect anal., ion beam techniques 3—33577
defects formation due to growth method, review 3—17748
diamond:N, e.s.r., exchange broadening of hyperfine components *(Russian)* 3—8436
diamond, e.p.r. of low-symmetry impurity centres *(Russian)* 3—12058
diamond, neutron irrad., semiconducting interstitials, e.s.r. studies 3—33571
diffusion in semiconductors, infl. of inhomog. distrib. of vacancies *(Russian)* 3—11757
elastic wave attenuation in crysts. with linear defects, anharmonicity *(Russian)* 3—14932
to electron irradiation defect production rate at temperatures above stage I 3—30158
ferroelectric, impurity vibronic spectra, anomalies 3—30228
ferroelectric semiconductor solid solutions, concentration effects on physical props. in vicinity of phase transition point 3—34306
graphite, evaporation of impurities determ. by atomic absorption method *(Russian)* 3—11648
group IV, II-VI semiconductors, vacancies, interstitials, Jahn-Teller distortions, molecular orbital models 3—33837
harmonic lattice, entropy of binding between vacancies and solute atoms, lattice vibr. 3—33515
ice, pure and HF doped, X-ray topographical study of dislocations 3—17826
ice stable growth of single doped crystals *(German)* 3—8739
inclusions in elastically anisotropic media, strain fields for diffraction contrast calcs. 3—33538
interaction with screw dislocations, eval. of interaction energy *(French)* 3—11644
internal friction caused by impurity atom diffusion along dislocations *(Russian)* 3—1692
ion implanted, distrib., enhanced diffusion by vacancy mechanism 3—33537
ion-induced X-ray microanalysis, impurity detection, semiconductors 3—39281
ionic crystals, symmetry-dependent effective force const. changes around impurities 3—36391
i.r. absorption and X-ray diffraction obs. 3—30847
lattice with random substitutional impurities, lattice dynamics 3—14946
metal, b.c.c., dislocation pinning by impurities *(Russian)* 3—14866
metal, f.c.c., impurity diffusion, model 3—15031
metal, pseudopotential studies of vacancy-impurity and impurity-impurity interactions 3—36295
metal-graphite alloys, nucleation and growth of spheroidal graphite 3—8789
Mo wire, recrystallised, alloyed with Ru and C, tensile properties *(Japanese)* 3—31074
Mossbauer spectrum, impurity atom diffusion influence on Mossbauer spectrum 3—30738
optical material, transparent dielectric, laser induced damage rel. to cracks, pores, absorbing inclusions 3—35701
oxides, survey of deformation and physical props *(French)* 3—11672
paraelectric impurity, dipole-dipole relax. 3—8513
quartz: Fe^{2+}(Fe^{3+})(Co^{2+}), impurity absorpt. near 78μ band 3—5216
quartz: Na, Al, Fe, impurity distrib. rel. to crystal growth morphology 3—14706
ruby, laser irrad., damage threshold rel. to impurities *(Russian)* 3—13750
semiconductor diffusion profile meas. using pseudo Brewster angle method 3—39254
semiconductors, lattice parameter changes on diffusion doping, meas. method 3—27032
solid soln. supersaturated with impurities, form. of dislocation with liquid core 3—24124
solidification of C in naphthalene, pushing of foreign particles 3—11570
stainless, 316, proton-irradiated, effects of injected He on void formation in steel 3—11607
steel, martensitic stainless, influence of Cu, C, Ni, Mo impurities and heat treatment on mechanical props. and struct. *(French)* 3—34588
steel austenitizing treatment effect on temper embrittlement, search for Sb segregation at grain boundaries 3—34544
structure of defects in solids, review 3—24099
transport relaxation time for phonon-impurity scatt., rel. to thermal cond. 3—1836
trapping by localized kinks at a step during crystal growth 3—7644
trapping during crystallisation from melts 3—33466
tunnelling, molecular impurity assisted, many body theory 3—2176
vacancies, annealing during cooling of crystal, analyt. eqns. 3—7752
variable diffusion coeffs., Boltzmann-Matano analysis 3—39259

crystal hyperfine field interactions continued
crystal impurities continued
white, single crystals, dislocation etch hillock formation, due to impurities 3−8030
Zircaloy-2, polycrystalline, hydride precipitation, crystallographic orientation *(French)* 3−12385
zone melting multi-stage apparatus for purification of substances of high sublimation pressure *(German)* 3−8746
α--Fe, diffusion of Ag 3−17990
AlN, commercial ceramic, thermal conductivity meas., residual impurities effect 3−15739
Ag, deformed, recovery of elec. resist., effect of O *(Russian)* 3−7819
Ag, electrodeposited, spiral growth rel. to impurities 3−1582
AgBr impurity ions and vacancies, interactions 3−27227
AgBr:Cd, ionic thermocurrents meas. rel. to interstitial-vacancy complex form. 3−33518
AgCl impurity ions and vacancies, interactions 3−27227
AgN_3, rel. to elec. breakdown and explosion 3−36838
Al, impurity-vacancy pair, binding energy, pseudopotential calc. 3−30133
Al, interaction between impurity atoms and vacancies, pseudopotential approach 3−36293
Al, low-temp. diffusion of Zn meas. using the backscatter method 3−18000
Al, pitting corrosion, alloying elements effect 3−8046
Al alloy as electric conducting wire, effect on conductivity *(Norwegian)* 3−5304
Al:Ti, film, impurity distrib. and diffusion coeff. determ. by elec. method 3−30290
Al-Cr and Al-Mn cold-worked alloys, resistivity from 78 to 300 K 3−14886
Al-Zn-Mg alloys, Cr and Cu alloying element effect on grain boundary corrosion and stress corrosion cracking *(Japanese)* 3−31072
β-Al_2O_3, ionic cond., Na- and Mg-content depend. 3−11758
Al_2O_3, pure and Mg-doped, thermal cond., 1.3-100 K, possible obs. of Fe^{4+} 3−30293
Al_2O_3:MgO, grain boundary segregation 3−27739
$Al(urea)_6(ClO_4)_3$:$Cr(urea)_6(ClO_4)_3$ second order phase transormations, e.s.r. meas. 3−17975
Au, cold-worked, stage II and III recovery, internal friction and modulus defect, trace impurity effects 3−5315
BaF_2, calc. of H^- impurity vibr. 3−36390
BaF_2, vacancies, interstitials and inert gases in fluorite structures 3−17814
$Ba_2NaNb_5O_{15}$, segregation of impurities and striations in melt growth 3−24804
$Ba_xSr_{1-x}Nb_2O_6$, segregation of impurities and striations in melt growth 3−24804
Bi_2Te_3, Mossbauer effect of ^{129}I *(Russian)* 3−12087
$CaCO_3$ crystals, containing ions of d^9 config., e.p.r. and luminescence studies 3−36790
CaF_2, calc. of H^- impurity vibr. 3−36390
CaF_2, doped, interstitial anion clusters, formation mechanism 3−30113
CaF_2, vacancies, interstitials and inert gases in fluorite structures 3−17814
CaF_2 containing heavy metal impurities, i.r. absorption and thermal conductivity 3−36898
CaF_2:GdF_3, density, rel. to impurity incorporation 3−20759
CaF_2:H^- i.r. relectivity study of high concs. of H^- ions 3−4836
CaF_2:R, R=Ce, Pr, Sm, Eu, Tb, ionic thermocurrent obs. of reorientational properties 3−7787
$Ca_{10}(PO_4)_6F_2$:Sn, luminescence, electronic transitions, substitutional sites 3−39174
$Ca_5(PO_4)_3F$: $Nd(Nd_2O_3)(NdF_3)$, fluorapatite, structure and location of dopant 3−17789
Cd alloys, multicomponent impurities influence on density change during thermocyclic treatment *(Russian)* 3−8844
$CdCr_3S_4$ single crystals gas transport and characterisation *(German)* 3−8730
CdF_2:Fe, Mossbauer and mag. investigation 3−39063
CdF_2:$Na^+(La^{3+})$, F self diffusion, depend. on doping 3−7972
$Cd_xHg_{1-x}Te$ monocrysts., comp. distrib. from absorpt. spectrum *(Russian)* 3−12158
CdS:Be, i.r. absorpt. due to localized vibr. mode 3−27523
CdS:Li(Na)(Ag), furnace doping, rel. to bound exciton spectra 3−12184
CdSe:Be, i.r. absorpt. due to localized vibr. mode 3−27523
CdSe:Cu,In and undoped, high temp. defect equilibria 3−7745
CdTe, high temp. elec. cond. study *(Russian)* 3−27031
Co_2O_3 distribution coefficient in NaCl single crystals 3−30947
Cu single crystal work hardening characts., Ni content effects 3−18673
Cu-X (0.5 at wt.%) alloys, X=Mn, Ge, Zn, Ni, vacancy-impurity complexes study by positron annihilation 3−17868
Fe-Si (3.25 wt.%) alloy, impurity effects on grain growth in strain-anneal and secondary recrystn. 3−37041
$FeCr_3S_4$ single crystals, gas transport and characterisation *(German)* 3−8730
Ga(As, P):I highly doped mixed crystals, problems of growth *(German)* 3−8765
GaAs, epitaxial growth substrate, distribution obs. 3−1938
GaAs, epitaxially grown on Cr and Sn doped substrates, electrical props. depend. on $AsCl_3$ temp. 3−8756
GaAs, GaP, electron and neutron irrad., B, C impurities, i.r. local mode abs. 3−34395
GaAs, implantation of Kr and Tl, energetic ion collection, saturation effects 3−11646
GaAs, implantation of Kr and Tl, ion conc. profile and ion range probability distrib. 3−11647
GaAs, liquid phase epitaxial growth, impurity incorporation, depend. on growth rate and cryst. orientation 3−1638
GaAs, liquid phase epitaxial growth in silica boat, Si contamination control 3−2684
GaAs, parameters for epitaxial growth of high purity crystals 3−1918
GaAs, spectral determ. 3−16567
GaAs, surface contamination due to Cu atoms in resist film stripper during photo-etching 3−8757
GaAs film, epitaxial, Ga vacancies and impurity profiles 3−14883

crystal hyperfine field interactions continued
crystal impurities continued
n-GaAs LSA diode, purity, evaluation determ. by low field temp. depend. mobility 3−2085
GaAs layers, vapour phase epitaxially grown 3−34477
GaAs:Cu, dislocation decoration on decomp. of supersaturated solid soln. 3−33542
GaP, implantation of Kr and Tl, energetic ion collection, saturation effects 3−11646
GaP, implantation of Kr and Tl, ion conc. profile and ion range probability distrib. 3−11647
GaP, local strain fields due to impurities 3−2023
GaP, p-type dopants for green light emitting diodes 3−8734
GaP:O, epitaxial, O conc., nuclear microanalysis 3−39249
GaSb-InSb alloyed solid solns., distrib. coeffs. of Te and Zn *(Russian)* 3−11642
Ga_2Te_3 and GaTe, Mossbauer effect of ^{129}I *(Russian)* 3−12087
GdF_3, impurity-conditioned solid-solid transform., rel. to melt growth 3−12274
Ge, annealing processes after irradiation with 1 MeV electrons at 85K 3−11616
Ge, implantation of Kr and Tl, energetic ion collection, saturation effects 3−11646
Ge, implantation of Kr and Tl, ion conc. profile and ion range probability distrib. 3−11647
Ge, wettability by Au alloys, surface impurities influence *(Russian)* 3−8006
Ge: group V, defect formation under γ irradiation 3−33545
Ge: group V (O, Te), electron irrad., E_c-0.2 eV level, defect model 3−33842
Ge:Sn, highly doped single cryst., conc. effect on Hall mobiliity 3−33885
HoF_3 and HoF_3-ErF_3, impurity-conditioned solid-solid transform., rel. to melt growth 3−12274
In, thermotransport meas. for Ag tracer 3−17999
InAs-GaAs alloyed solns., Zn and Te impurity effect on crystallisation *(Russian)* 3−7782
InP:Ge,Sn,Te, liquid phase epitaxial growth, impurity distribution coeffs. 3−1637
In_2Te_3 and InTe, Mossbauer effect of ^{129}I *(Russian)* 3−12087
KBr:Ba^{2+}, rel. to kinetics of conc. decrease of nonequilib. cation vacancies 3−38585
KCl, bubble motion, elec. field induced, X-ray and impurity effects *(Russian)* 3−20730
KCl:Cd, Pb, reorientation of $Cd^{2+}(Pb^{2+})$-vacancy complex rel. to dielec. relax. 3−34293
KCl:Mn^{2+}, off centre position of Mn^{2+}, e.s.r. obs., 4.2-77K 3−21307
KCl:OH^-, Hg, study of Hg diffusion, effect of OH^- impurity 3−20892
KCl:OH^-, paraelec. relax., anomalous temp. depend., 0.025-0.3 K 3−8512
KCl:OH^-, paraelec. relax., appl. of theory for dipole-dipole relax. of impurities 3−8513
KCl:Pb, Sn, microdistribution inhomogeneity, electron microscopic obs. 3−1636
KCl:$PbCl_2$, flow stresses and relax. of stresses rel. to doping and temp. 3−20797
KH_2PO_4, cryst. growth, capture of random impurities, effect of soln. pH *(Russian)* 3−30078
$KY(MoO_4)_2$:Nd, effect of Nd concentration on cell parameters and limit of isomorphous penetration of Nd *(Russian)* 3−11643
Li:Na(Ag), isotope effect comparison for ^{22}Na, $^{24}Na(^{105}Ag$, $^{110m}Ag)$ diffusion 3−38688
LiF, Mg doping effects on steady state deform. and dislocation structure 3−17846
$LiNbO_3$, stretching vibr. band of OH^- defects, 2.87 μ 3−24729
$LiNbO_3$ single crystals, X-ray topographic studies, relation between growth conditions and lattice defects 3−17747
$LiNbO_3$:Fe, e.p.r. obs. of Fe impurities and n.m.r. obs. of stoichiometry 3−12060
$LiTaO_3$ single crystals, X-ray topographic studies, relation between growth conditions and lattice defects 3−17747
MgO single crystal, cation diffusion studies using a sectioning technique 3−33694
MgO:Sr^{2+} diffusion of Sr^{2+} 3−17993
$MnBr_2.4H_2O$, heat capacity meas. near Neel temp. 2.12 K, effect of chem. impurities 3−15367
Mo, Portevin Le Chatelier effect at high press. and temp. 3−30180
Mo ingot, ductility effects of complex additions of 0.15 wt% Ru with C or B *(Japanese)* 3−31073
Mo-Ti-C, impurity braking influence on subgrain growth during annealing 3−31014
Na:divalent cation rod-like imperfections, light scatt. orientation effect 3−15493
NaBr, potential of F^-, calc. 3−36834
NaBr, potential of F^-, theory 3−36835
NaCl, bubble motion, elec. field induced, X-ray and impurity effects *(Russian)* 3−20730
NaCl, Sr-doped, precip. meas. by study of bulk density variations 3−17862
NaCl crystals, diffusion to divalent impurities from volume to surface 3−33692
NaCl quenched crystals, influence of impurity distrib., applic. of electron microscopic decoration method and microhardness meas. 3−1676
NaCl quenched crystals, microhardness rel. to quenching temp. and contamination, obs. 3−1677
NaCl quenched single crystals, charge developed by local plastic deform., rel. to quenching temp. and contamination 3−2155
NaCl:$BaCl_2$, flow stress, annealing depend., dislocation-impurity interactions 3−20786
NaCl:$SrCl_2$, X-ray and ionic conductivity expts. comparison 3−17857
NaF, lattice thermal cond. due to impurities, calc. 3−27095
Nb, contamination vy H_2 following UHV degassing 3−15723
Nb, neutron activation analysis, using semiconductor γ detectors *(Russian)* 3−10198
Nb superconductor, interstitial impurities effects on power frequency losses 3−11980

crystal hyperfine field interactions continued
crystal impurities continued
Nb-H system, partial molar entropy of H in b.c.c. metal *(German)* 3−27616
NbO_5, neutron activation analysis, using semiconductor γ detectors *(Russian)* 3−10198
Nb_3Sn:C, transmission electron microscope examination of defect struct. *(German)* 3−21179
Ni, diffusion of Ag 3−17990
NiO, epitaxial growth of high purity crystals 3−1915
^{18}O diffusion conc. profiles from obs. of $^{18}O(p, \alpha)^{15}N$ reaction 3−1635
Pb:Bi superconducting thin films, surface impedance *(German)* 3−21165
Pb:Ni, pressure effect on Ni interstitial diffusion 3−17996
$Pb(ZrTi)O_3$ piezoelectric ceramics, stabilization effects by addition of Mn, Cr or U oxides 3−8507
Sb_2Te_3, Mossbauer effect of ^{129}I *(Russian)* 3−12087
Se:Na, polycrystalline, i.r. photoconductivity 3−5029
Se-Ag junction, asymmetric conduction changes under electric field influence, due to impurity redistribution *(Russian)* 3−11951
n-Si, 10 MeV proton irrad., point defect-impurity complexes and divacancy formation *(Russian)* 3−7799
Si, computer calc. of impurity profiles and diffusion 3−20760
Si, diffusion, effect of surface oxidation 3−7786
Si, diffusion, electrotransport and solubility of Mg, 1000-1350°C *(Russian)* 3−7975
Si, diffusion of Cu^+, Ag^+ and Au^+ ions over interstitial oxygen sites 3−33700
Si, diffusion of O_2, X-ray meas. of lattice strain 3−17858
Si, dislocation-free crystals, float-zone growth, growth striations, X-ray topography 3−39273
Si, effect on SiO_2 film formation by thermal oxidation 3−11823
Si, group V impurity atom-vacancy, binding energy, diffusion 3−33836
Si, grown on spinel, impurities formed from interaction between substrate and deposits 3−8720
Si, implantation of Kr and Tl, energetic ion collection, saturation effects 3−11646
Si, implantation of Kr and Tl, ion conc. profile and ion range probability distrib. 3−11647
Si, impurity cluster localisation and comp., influence on emission props. 3−30134
Si, impurity gradients, diffusion constant, capacitance meas., nondestructive technique 3−39284
Si, impurity incorporation phenomena, crystal growth 3−39271
Si, impurity profile, computer calc. 3−24134
Si, ion-damaged surface layers, gettering rates of fast-diffusing metal impurities 3−5276
Si, oxygen precipitation at oxidation induced defects 3−33539
Si, point defects, stress, semiconductor device characteristics 3−39279
Si, radiation damage in p-type with H impurity and high purity n-type, hole density, annealing 3−33546
Si, selectively ion implanted, X-ray obs. of fine diffr. effects 3−30132
Si, stacking faults and prismatic dislocation loops due to O_2 precipitation, X-ray topography 3−17829
Si, wettability by Au alloys, surface impurities influence *(Russian)* 3−8006
Si film, amorphous and crystalline, sputter-ion source mass spectrometry obs. 3−1950
p-Si:Al, (B), (Ga), electron irrad., annealing, effect of O and acceptor impurities 3−33560
Si:Al, Czochralski growth, impurity striation struct. 3−17860
Si:Al, Czochralski growth, study of impurity striations 3−12322
Si:As, As diffusion from doped oxide, effects of $N_2(O_2)$ atmosphere 3−30281
Si:Au, high resistivity, impurity conc., i.r. absorpt. study *(Russian)* 3−2673
Si:B, X-ray topographic obs. of dislocation contrast after boron diffusion 3−17835
Si:B(P), surface conc. in diffusion layer *(Russian)* 3−8751
Si:C, i.r. absorpt. spectra, local vibr. modes and defect vibr. modes 3−18475
Si:Cu, Cu precip. colony dissolution during annealing, particle drag by climbing dislocations 3−20758
Si:Cu, Cu precipitation, obs. with Cameca ion analyser 3−7785
Si:Cu precip. colony dissolution during annealing, dislocation processes 3−20757
Si:Ge, radioactive tracer meas. of ^{71}Ge diffusion 3−24293
Si:Ge(Sn), O electron irrad., selective trapping of vaccancies migration of interstitials 3−33925
Si:In, ion implantation, damage around ion tracks 3−33588
Si:Li, neutron irrad., defect interactions, Hall effect, i.r. absorption studies 3−33570
Si:O, crystal properties, O-complex formation, lifetime trapping levels 3−39262
Si:Sb, Czochralski pulled single crysts., doping stacking fault pyramids 3−20756
Si:Sb(As)(P)(B), epitaxial wafer, buried layers, impurity profile 3−39261
Si-SiO_2 interface, nonuniform lateral ionic impurity distrib., C-V characts. 3−8267
Si_3N_4, hot pressed, microstructure 3−12421
SiO_2, Al impurity depth profiles by $^{27}Al(p, \gamma)^{28}Si$ resonance reaction 3−17859
SiO_2, As glass source diffusion 3−21545
SiO_2, incorporation during r.f. sputtering 3−15104
SiO_2, noncrystalline, defect struct. and irradiation behaviour 3−4770
SiO_2, O_2:HCl grown, residual Cl distrib. determ. 3−30951
SiO_2 film, HCl- or Cl_2-grown, Auger anal. of Cl 3−38597
SiO_2:Cl_2Na, electrically stable, thermal oxidation of Si, O_2-Hcl, O_2-Cl_2 mixtures 3−39287
SiO_2/Si, ion bombardment effects, impurity ion transport, ^{22}Na radiotracer 3−39288
SiO_x thin films, examination using Rutherford scattering of MeV α-particles 3−7788
SrF_2, calc. of H^- impurity vibr. 3−36390

crystal hyperfine field interactions continued
crystal impurities continued
SrF_2:R, R=Ce, Pr, Sm, Eu, Tb, ionic thermocurrent obs. of reorientational properties 3−7787
Ta, F contamination by chem. polishing, nuclear reactions study 3−11812
Ta, Portevin Le Chatelier effect at high press. and temp. 3−30180
Ta:N_2 and pure metal, work hardening, ion purity content effect 3−31090
Ti, adsorption of Cl, segregation of Cl and S impurities from bulk 3−1882
Ti, hardening by O_2 3−15725
TiO_2, Fe-doped, Mossbauer spectra 3−18401
UO_2, Si, Al_2O_3, Fe, U, impurities, effect on fracture stress 3−39384
UO_4^{2-}, impurity in scheelite type crystals, energy structure and spectroscopic characteristics *(Russian)* 3−8619
W, wire, elongation, creep tests, doping effects *(Hungarian)* 3−24894
W, wires, doped recrystallisation effect on brittleness *(Japanese)* 3−31065
$ZnAl_2O_4$:Mn^{2+}, e.p.r. *(French)* 3−24611
$Zn(NH_4)_2(SO_4)_2.6H_2O$, supersaturation and impurities, infl. on stepped relief and uniformity *(Russian)* 3−7645
ZnO, rosette like precipitates of Mg and Pb, identification 3−33536
ZnS, extinction of emission region by introducing extinction and luminescent centres *(Russian)* 3−12187

crystal inclusions
anisotropic media, elastic fields, surface integral reduction to a line integral 3−17863
diamond, synthetic, comp. of inclusions, X-ray microanal. study *(Russian)* 3−4767
end forms evolution caused by environmental inclusions *(Russian)* 3−36266
gases in crystal inclusions, gas chromatographic analysis technique 3−32254
generation of large prismatic dislocation loops, mechanism 3−24122
martensite, work hardening origins, strength-differential effect 3−37067
rare earth-Ga garnets, inclusion elimination in Czochralski growth 3−12293
steel, inclusions rel. to crit. mech. props., metallurgical processing incl. vacuum melting 3−27629
steel, inclusions rel. to crit. mech. props., vacuum melting effects 3−27630
steel, maraging, non-metallic inclusions and fracture behaviour 3−21586
steel, MnS inclusions morphology 3−8788
steel, plastic deformation of MnS inclusions 3−8852
steel, stress field surrounding inclusions, photoelastic analogue 3−21585
urea trioxane inclusion compound, low temp. phase changes 3−7927
Zircaloy, slowly cooled, hydride distribution, precipitation 3−31001
Al alloy rolled sheets, volume determ. methods 3−24861
Al alloys, role in ductile fracture and fracture toughness 3−30984
Al foils, electron microscope search for foreign inclusions and their role in crack and pin hole formation 3−21608
Fe, effect on grain growth and secondary recrystn. 3−21591
Fe, microcrack form. around inclusions during solidification 3−34537
Gd-Ga garnet, growth of dislocation spirals about Ir inclusion 3−20751
KCl(I), boiling and convection in solvent inclusions rel. to movement 3−11610
NaCl, boiling and convection in solvent inclusions rel. to movement 3−11610
Ni-(50% wt.)Fe alloy, melting process and non-metallic inclusions effect on coercive force *(Korean)* 3−5120
Si_3N_4, hot pressed, distribution, analysis using transmission electron microscopy, electron microprobe, X-rays 3−12421
Ti honeycomb structure, presence of Al braze alloy determ. by eddy current testing 3−21767
YAG:Nd, obs. using transmission electron microscopy 3−36319
YIG, effect on mag. domains, Ferrimag. resonance and i.r. obs. 3−27379

crystal internal fields
see also crystal field theory
actinide cpds, NaCl-type, hyperfine fields, crystal field and relativistic effects, angular wave function 3−2233
alloy with Ce and Yb impurities, Kondo effect rel. to cryst. field 3−2256
amino acid:Cu^{2+}, ligand hyperfine interaction, e.p.r. spectra 3−24605
anisotropic, analysis *(Russian)* 3−32102
anthracene, internal electrostatic field meas. 3−19236
4,4' dichloro diphenyl sulphone, n.q.r. of ^{35}Cl, field gradients, bond characters 3−30724
rel. to dipole-dipole relaxation of paraelectric impurities 3−8513
electrostatic potential of point charge in dielectric solid, shell model 3−18407
ferrite sphere, internal mag. field *(Russian)* 3−24617
ferromagnetic plate, travelling wave excitation, steady state elliptical vector mag. field 3−18341
glass, aluminosilicate, transition metal ion substitution, kinetic model depend. on crystal field strength 3−7631
hexagonal lattice, potential field study *(French)* 3−26983
ionic crysts., far u.v. spectra, local-field effects on optical props. 3−39157
Ising ferromagnet, crystal field anisotropy effect on Curie temp. 3−8324
metals, empirical potentials and calc. of point defect energy 3−24103
microcrystal, mean inner potential, electron interference microscopy 3−24060
multiple scatt. theory, scatt. by non-muffin tin pots. 3−1967
potential energy calcs. rel. to mol. packing determ. 3−24061
quadrupolar spin echo, in polycryst samples excited by coherent resonance pulses, theory 3−34247
rare earth ions in D_2 symm. cryst. field, Zeeman effect theory and appl. to rare earth garnets 3−18466

crystal internal fields continued
rare earth metals, collective excitations, Heisenberg ferromag., effect of strong cryst. fields 3−2243
rare earth metals, crystal electric field, cond. electron contribs. 3−2231
rare earth metals, crystal electric field, cond. electron contribs., comments 3−2232
Rochelle salt, phase transitions, microscopic theory 3−2498
sodium ammonium tartrate:Cu^{2+}, cryst. field at Na site, e.s.r. 3−2349
superconductor, internal elec. fields induced by rot. and gravity 3−30581
thulium perrhenate tetrahydrate, absorpt. spectra and energy levels, cryst. field parameters from fine struct. *(Russian)* 3−20171
time differential perturbed angular correlation and Mossbauer spectra, imperfect crystal lattices, electric field gradient parameter 3−15440
trigonal field calc., degenerate localised levels in optical transitions theory 3−15535
$3CsCl.LaCl_3.3H_2O$:Nd^{3+}, parameters calc. from spectra *(Russian)* 3−24730
As_2Se_3, vitreous, chaotic potential field, optical absorption edge shift, deformation potentials 3−20993
$BaTi(Zr)O_3$ ^{89}Zr half-life change at upper phase transition, change in ligand field 3−36844
$BiFeO_3$, mag. fields, Mossbauer obs. 3−27447
CaF_2:X^{3+}, X=Ce, Pr, Sm, Eu, Tb polarisation storage, optical absorption for 4f-5d transition of rare earth in local crystal field 3−18406
$Ca_2Fe_2O_5$, elec. field gradient tensors at two nonequivalent ferric sites 3−24386
$CaWO_4$:Nd^{3+} field parameters calc. *(Russian)* 3−8112
$CaWO_4$:Yb^{3+} field parameters calc. *(Russian)* 3−8112
$Cd_{1-x}Co_xFe_2O_4$, paramag. region, elec. field gradients, Mossbauer obs. 3−34268
$Cd_{1-x}Ni_xFe_2O_4$, paramag. region, elec. field gradients, Mossbauer obs. 3−34268
CdS, cubic, electron density, potential distribution *(Russian)* 3−30085
Cr^{3+}, e.s.r. exact eigensolutions calc., spin hamiltonian, electronic Zeeman, crystal field and hyperfine interaction terms 3−24609
$CsClO_3$, electric field gradient at Cl nucleus in free ClO_3 ion 3−8481
Cs_2CuCl_4, struct., crystal forces and charge distribution determ. 3−17785
Cu alloys, dilute, elec. quadrupole tensor parameters from n.m.r 3−30726
$CuCl_2.2D_2O$, zero field deuteron mag. reson., quadrupole consts., internal field, fine struct. *(French)* 3−21339
$CuCr_2Te_3I$, Mossbauer effect obs. 3−30735
Eu perrhenate tetrahydrate single crystals, absorption spectra, spin-orbit interactions evaluation for symmetry of crystal field and bonding of Eu^{3+} *(Russian)* 3−30844
GaP, local strain fields due to impurities 3−2023
KD_2PO_4, influence of domain struct. near phase transition, n.m.r. study 3−24660
K_2ZnF_4:Ni^{2+}, cryst. field and exchange interaction of Ni^{2+}, lattice distortion effects, e.s.r. obs 3−15357
Mn^{2+} ion, Zeeman pattern calcs. in octahedral or tetrahedral crystal field 3−2011
$MnSn_2$, antiferromag., Mossbauer obs. of mag. fields at diamag. Sn atoms 3−5153
NH_4Cl:Co^{2+}, Ni^{2+}, Cu^{2+}, light absorpt. by impurity centres, cryst. field parameters 3−21456
NaF:Eu^{3+}, fields for luminesc. Eu^{3+} centres 3−5229
$NaNO_2$ ferroelectric, gradient-elastic tensor component measurement, acoustic n.m.r. technique 3−21321
Np, inner Sternheimer shielding factor from Mossbauer spectra 3−2480
$PbCl_2$:Nd^{3+} and $PbCl_2$:Pr^{3+}, Stark splitting of energy levels 3−15515
$PbMoO_4$:Nd^{3+}, field parameters *(Russian)* 3−8112
$PbMoO_4$:Yb^{3+}, field parameters *(Russian)* 3−8112
PbTe thin film, lowering of intergranular potential barriers, rel. to photocond. 3−30515
Pr, high field magnetisation, first order transition, nonmagnetic to metamagnetic phase due to crossing of crystal field levels 3−21221
Pr, magnetic resistivity meas., 4K-ice point, effects of crystalline field 3−8356
Pr-Tb alloy, exchange field at Pr ion rel. to comp. 3−2267
$RbClO_3$, electric field gradient at Cl nucleus in free ClO_3 ion 3−8481
$SrMoO_4$:Nd^{3+} field parameters calc. *(Russian)* 3−8112
$SrMoO_4$:Yb^{3+} field parameters calc. *(Russian)* 3−8112
TmNi, effect on mag. structure 3−15375
$YCl_3.6H_2O$:Yb^{3+}, proton polarisation and relaxation, hexagonal crystal field interaction 3−18388
ZnO, macroscopic elec. fields, induced double refr. study *(Russian)* 3−2515
ZnS, macroscopic elec. fields, induced double refr. study *(Russian)* 3−2515
ZnS:Mn^{2+}, wurtzite, optical and paramag. spectra, impurity site, cryst. field 3−21306
$ZrFe_2$, $ZrFe_2H_{0.3}$, effective mag. field acting on ^{57}Fe, nucl. γ-reson. method obs. *(Russian)* 3−12079
crystal interstitials *see interstitials*
crystal lattice structures *see crystal atomic structure*
crystal microphones *see microphones*
crystal microstructure
see also crystal defects; crystal inclusions; crystallites; grain boundaries; texture; X-ray examination of microstructure
actinide-Pt metal-C systems, occurrence of ordered phases of Cu_3Au struct. type 3−2710
alloy, ordered, antiphase slip boundaries and dislocation config., theory *(Russian)* 3−34522
alloy, rel. to inter- and transcrystalline fracture under stress corrosion *(Russian)* 3−8801
alloy with b.c.c. lattice, dispersion hardened, recrystallisation rate rel. to grain size 3−31011
crystal microstructure continued
alloys, kinetics of ordering and antiphase domain growth vs. the kinetics of spinodal decomposition and coarsening 3−18609
alloys, solidification, dendritic and laminar heterogeneity formation *(Russian)* 3−8778
armco iron, grain size and prestressing effects on props. in presence of Hg *(Russian)* 3−12369
austenite formation during hardening of high speed steel tools, grain size formation rel. to annealing 3−18655
brass, superplastic, fibrous struct. with elongated grains 3−34556
brass L62, grain size and prestressing effects on props. in presence of Hg *(Russian)* 3−12369
butadiene-styrene block copolymers, viscoelastic props. in tension shear, domain morphology effect 3−29802
calcite, etched, dislocations obs. by polaroid photomicrography, undergraduate expt. 3−9813
cast iron, spheroidal graphite form. 3−8816
ceramic, strength, grain size dependence, Orowan-Petch and Knudsen eqns. 3−2751
ceramics, American Ceramic Society meeting, Basic Science, Electronics and Nuclear Division (Sept. 1972) 3−8948
ceramics, mechanical strength dependence, measurement and analysis techniques 3−12422
coarsening of compound precipitates, activation energy and rate constant 3−15679
crystallite orientation distribution analysis, three-dimensional, estimation of reliability 3−26981
crystallographic orientation of components, determ. using polarized light microscopy 3−24858
Cu-Cu_6Ce and Cu-Cu_6La eutectics, unidirection of growth, microstructure 3−39310
dynamics of microstructural change 3−2705
ethylene-vinylidene chloride copolymers, determ. from proton n.m.r. *(German)* 3−12069
f.c.c. metals, steady-state creep rate, correl. with substruct. misorientation and stacking fault energy *(Russian)* 3−8837
ferritic materials, fatigue crack propag., stress intensity and microstruct. influence 3−21580
ferromagnetic solid solutions, anomalous microregions, Mossbauer obs. 3−34272
fuel cladding of EBR-II Mark II, swelling behaviour, axial formation 3−23440
glass ceramics based on tetrasilicic mica, strength depend. on mica grain size 3−8982
glass-ceramics, two stage heat treatment resulting in high nucleation density 3−12439
glasses, self-diffusion processes 3−4882
glasses, silicate 3−5355
grain boundary contrast in field ion microscope images, computer image simulation 3−17853
grain boundary contrast in field ion microscope images, rel. to tilt and twist 3−17852
grain boundary contrast in field ion microscope images 3−17851
grain shape, stochastic models 3−34521
graphite, in Ni-C alloy, unusual microstructure 3−31016
heterophase solid, domain structure caused by internal stresses 3−30266
γ-In_2S_3, crystals grown from vapour, X-ray and electron microscope investigation of struct. faults *(German)* 3−7781
Inconel alloy X-750, precip. parameters role upon creep rupture props. 3−37024
intermetallic compounds, sigma phase detection by electron microscopy 3−8811
Invars, dispersion-hardening, Guinier-Preston zone form., conc. heterogeneity increase *(Russian)* 3−21631
lamellar eutectic structure growth, kinetics for solidification, diffusion and solid phase boundary formation *(Japanese)* 3−30975
laminates, glass reinforced epoxy and polyester, creep mechanism 3−9000
limestones, deformed, preferred orientation patterns, stability field boundaries 3−37160
local deformation redistribution in plastic forming of polycrystallites *(Bulgarian)* 3−15690
martensite:C, polycrystals, two-phase decomposition and static distortions 3−31010
martensite, twinned γ_1' phase, invariant plane strain approach 3−31021
martensite, u.s. attenuation for nondestructive testing, applic. to Fe-Ni alloys *(German)* 3−12490
massive deposits produced by high rate vapour deposition process, effects on ion bombardment 3−27632
material design with specific props. using powder metallurgy 3−15677
materials science and technology treatise 3−2621
metal, dispersion strengthening rel. to microstructure and creep mechanisms 3−15695
metal, polycryst., plastic deform. during low-cycle tensile, stressing, X-ray obs. of struct. change *(Japanese)* 3−8868
metal, polycrystalline, elastic deform., grain shape effects on stress-strain distribs. in grains 3−5300
metal, refinement during u.s. interaction with crystallizing melt *(Bulgarian)* 3−8893
metal-graphite alloys, nucleation and growth of spheroidal graphite 3−8789
metallography, stereological analysis, materials preparation, instrumental techniques 3−34516
metals, fatigue failure, structural-energetic analysis *(Russian)* 3−8841
metals and alloys, method of assessing width of circumboundary free zone 3−18575
Mullite reusable surface insulation (HCF) for space shuttle characterisation, analytical techniques 3−8962
multiply twinned particles, 1000 kV electron microscope study 3−7606
Nimonic, rel. to temp. depend. of strengthening characts. *(Russian)* 3−8839
Nimonic alloy, notched creep strength, microstruct. effects 3−8932
nondestructive investigation, use of surface prints 3−18746
oxides, vitreous, structural defect equilibria based on the structon model 3−4723

crystal microstructure continued
parallel plate shaped coherent precipitates arrangement, influence of strain energy 3—18607
particulate structure evolution, growth paths 3—34520
permalloy, ferromag. film, grain size rel. to chem. deposition conditions 3—8402
polyethylene, melt-crystallized, lamellar and interlamellar struct. 3—21743
polygonization, rel. to dislocation interactions under hydrostatic press. *(Russian)* 3—4763
pyroxenes, natural, X-ray topography and electron petrography 3—18807
recrystallised grain nucleation, survey of theories *(German)* 3—27641
refractory metals, conference, Atlanta, USA (May 1971) 3—34493
rutile, abraded, electron microscope study of structure before and after annealing 3—15753
scanning electron microscopy applications 3—12360
shape factor, indirect, in metals and ceramics 3—31015
solid state reaction paths and microstructure in crystals 3—5387
solidification, review of process and structural implications 3—24249
steel, 000N18K9M5T, influence of heating on phase content and structure 3—24831
steel, 4340, fatigue crack growth rate, thickness and orientation effect 3—18646
steel, (36.1 wt.% Ni, 2.5 wt.% Ti, 2.1 wt.% Al), kinetics of gamma'-phase precip. *(Russian)* 3—39334
steel, austenite, shape of $M_{23}C_6$ particles after ageing 3—15689
steel, austenitic, changes during martensitic transformation with increased stacking fault energy *(Russian)* 3—8781
steel, austenitic, thermomech. hardening effect *(Russian)* 3—37045
steel, austenitic, type 304L, hydrogen embrittlement 3—2745
steel, carbonitrided, dislocation and fatigue meas. 3—18605
steel, cold-worked, dislocation struct. stability during high-temp. ageing *(Russian)* 3—8838
steel, cold-worked, rel. to singularities of softening phenomena during annealing *(Russian)* 3—8833
steel, Cr-Mn-N stainless, grain size variation rel. to tensile flow stress and hardness 3—8825
steel, deformed by tension, orientation depend. of carbide cracking 3—34539
steel, ferrous martensite, as-quenched and tempered, fine struct. 3—34540
steel, high strength, fracture toughness enhancement by microstruct. control 3—31051
steel, high-C ferrite-pearlite, struct./prop. relationships 3—21647
steel, highly deformed, microcavity, form. from dislocation clusters *(Russian)* 3—24900
steel, hydrogen induced cracking, effect on weld microstructures 3—39364
steel, hypoeutectoid, grain refinement by thermal cycling 3—34563
steel, low C, and chem. homogeneity rel. to $\delta \rightleftharpoons \gamma$ transition *(Russian)* 3—8803
steel, low carbon specimens, changes of residual stress due to slip band accumulation under fatigue loading 3—21578
steel, low-alloy, fracture toughness of martensitic and martensitic-bainitic microstructs. 3—21641
steel, low-alloy, struct. and phase comp. changes during prolonged ageing 3—21687
steel, low-C, As-bearing, laminated struct., As diffusion *(Russian)* 3—37020
steel, low-C, effect of stress amplitude in fatigue processes in annealed and cold-rolled specimens *(Japanese)* 3—12405
steel, low-C alloy, duplex microstruct. rel. to fracture behaviour 3—21646
steel, low-C non-alloy type, grain size effect on yield strength *(German)* 3—34606
steel, low-cycle fatigue properties, transformation of retained austenite and cracks 3—37060
steel, martensit, low-C, anomalous microstruct., electron diffr. obs. 3—39339
steel, martensite, ferrous, double twinning 3—39341
steel, martensite obtained under h.p. and in pulse mag. fields, struct. singularities *(Russian)* 3—39330
steel, martensitic, high C, electron diffuse scattering 3—15663
steel, medium-C, quenched and tempered, effect of Si additions 3—21584
steel, metastable 2Kh15N5AM3, explosive loading effects on struct. and props. *(Russian)* 3—39308
steel, microsegregation, electron microprobe analysis *(German)* 3—8794
steel, mild, micromechanisms due to the influence of cementite on the embrittlement *(French)* 3—31005
steel, mild, slack-quenched, effect of process parameters 3—8847
steel, nickel-free complex-alloyed, struct. recrystn. 3—24952
steel, pearlitic, tendency to grain growth on remelting 3—27698
steel, pearlitic, yield strength rel. to heterogeneous struct. dispersion 3—31099
steel, phase transitions during hot working, obs. of C and SiC segregation *(Russian)* 3—12354
steel, precip. of silicon nitrides and manganese-silicon nitrides 3—21588
steel, quenched, X-ray determ. of retained austenite vol. fraction 3—12349
steel, recrystn. diagrams, influence of rare earth metal additions 3—21605
steel, rel. to inter- and transcrystalline fracture under stress corrosion *(Russian)* 3—8801
steel, rel. to notch toughness in heated zone *(Japanese)* 3—27644
steel, retained austenite, volume percentage and distrib., scanning electron metallography obs. 3—8800
steel, solution-treated type 316 stainless, fast-neutron irradiation effects on defect development, microstructure 3—26520
steel, stainless, martensitic, influence of composition and heat treatment on mechanical props. and struct. *(French)* 3—34588
steel, stainless maraging, influence of alloying elements on properties, low temp. study 3—24925
steel, strength differential effect depend. 3—39370
steel, struct. stability during high temp. creep 3—8915

crystal microstructure continued
steel, transformer, dislocat. density and grain growth for secondary recrystallisation *(Russian)* 3—1624
steel, transformer, recrystallisation matrix depend. on cold rolling and initial structure, secondary recrystallisation 3—31013
steel fuel claddings, cold-worked austenitic stainless, study of irradiation-induced void formation 3—26519
steel weld, hydrogen-induced cracking, microstruct. effect 3—34567
steels containing Cr, Ni, Mo, Mn, V and C, carbide formation with X-ray exam. *(Russian)* 3—8802
tetracene, structure of vacuum deposited thin films 3—15103
tetrahedral crystalline compounds, theory of nonlinear dielec. props. *(French)* 3—12106
Ticonal alloy, lattice conjugation of metastable tetragonal phases 3—31009
transformer steel, grain size and form control *(Russian)* 3—12342
of transition metal oxide scales, techniques for examination compared 3—24859
triglycine selenate, normal and deuterated, rel. to ferroelec. props. near Curie point *(Russian)* 3—8537
vitreous and amorphous solids, reactions 3—5389
α-Fe, recrystallization dependence on deformation and annealing, following high temp. torsion deformation 3—15707
Ag, intermediate stage sintering correlation of grain size and density 3—27713
βAg-Al splat quenched alloys, martensitic transformation 3—2695
Ag-Ni alloys extrusion effect on texture and Ni grain size *(Russian)* 3—27702
Ag-Zn alloys growth rates of bainite plates *(Japanese)* 3—15658
Ag-Zn(27.6 wt.%) β-phase alloy transmission electron microscopic investigation of bainite formation in 180-260°C range *(Japanese)* 3—18587
Ag-Zn(27.6 wt.%) optical and electron microscope investigation of bainitic transformation in 180° to 260°C *(Japanese)* 3—18564
Al, creep, substruct. formation kinetics 3—39344
Al, fatigue cracks, substruct. form. and propag. 3—21610
Al, pure, grain size influence on fatigue props. 3—31110
Al, refinement during u.s. interaction with crystallizing melt *(Bulgarian)* 3—8893
Al, subgrain disloc. struct. rel. to high temp. creep 3—7832
Al alloy, stress corrosion cracking initiation, corrosion pits shape depend. on crystal struct. *(French)* 3—31083
Al alloys, grain refinement by addition of Ti and B 3—18597
Al alloys, grain refinement by additions of Ti and B 3—18598
Al alloys, rel. to tendency to brittle rupture *(Russian)* 3—27669
Al and Al alloys, axisymmetric extrusion, plastic flow, substructure exam. 3—39360
Al and Al alloys, extrusion load calc., temp. rise meas., based on substructure meas. 3—37046
Al bronze recrystallization, obs., kinetics, effect of prior deformation 3—27627
Al foil, X-ray television method for grain growth obs. under heat and stress treatment 3—26936
Al:Si, annealing near melting temp., effect on substructure *(Russian)* 3—12355
Al-(Ni,Cu,Be,Fe,Co) eutectics, directionally solidified, struct. morphology and microhardness *(Russian)* 3—39328
Al-Ag alloy, Guinier-Preston zones, electron diffraction effects *(French)* 3—18604
Al-Ag alloys, quenched from liquid state, preprecipitation, small angle X-ray diffraction obs. 3—15667
Al-Al_3Ni, two phase alloy, electron scatt. on precipitate boundaries, low temp. resist. meas. 3—36580
Al-Al_3Ni eutectic comp., thermal stability of microstruct. *(Russian)* 3—24850
Al-Cu alloy, eutectic spherulites, electron microscope obs. 3—27638
Al-Cu alloy, solvus curve for Guinier-Preston zones *(Japanese)* 3—30998
Al-Cu alloy, structural and phase changes in welded joints 3—24832
Al-Cu alloy film, secondary grain growth 3—1956
Al-Cu alloys, Guinier-Preston zone and θ'' phase, metastable solvus curves 3—39326
Al-Cu and Al-Cu-Mg directionally solidified eutectics, ageing response 3—34581
Al-Cu-Ni system, ternary composite growth from melt 3—39316
Al-$CuAl_2$ lamellar eutectics and fibrous eutectics, unidirectionally solidified *(Japanese)* 3—18592
Al-Cu(4 at wt.%) alloys, diffuse scattering topography and struct. analysis of G.P. zones 3—18570
Al-Mg alloy, Guinier-Preston zones, electron diffraction effects *(French)* 3—18604
Al-Mg alloy, rel. to effect of Bi on stress-corrosion cracking *(Japanese)* 3—18634
Al-Mg-Si:Cu, aging, effects of Mg loss, elec. resonance meas. transmission electron microscopy 3—39361
Al-Mg-Zn alloy, influence on mech. props. and stress corrosion susceptibility 3—39342
Al-Mg(5 wt.%) alloy, grain size effect on fatigue 3—34594
Al-Si, cyclic hardening and microstructure effects on fatigue 3—15708
Al-Si system ternary eutectic alloys, unidirectionally solidified *(Japanese)* 3—18593
Al-Sn rel. to friction and wear *(Japanese)* 3—8768
Al-Ti (0.16 at wt.%) alloy, yield point phenomenon, subgrains and dislocation density *(Japanese)* 3—18644
Al-Zn alloy, concentrated, solvus curves for Guinier-Preston zones *(Japanese)* 3—30997
Al-Zn alloy, Guinier-Preston zones, electron diffraction effects *(French)* 3—18604
Al-Zn alloys, metastable solvus for Guinier-Preston zones 3—31022
Al-Zn-Mg, corrosion fatigue inhibition, anal. of fracture surface features 3—39352
Al-Zn-Mg alloys, fine struct. changes on alloying and ageing 3—21671
Al-Zn(6.8 at wt.%) alloy, Ag, Si and Mg effect on solvus temp of G.P. zones *(Japanese)* 3—18591
Al_2CuLi alloys, Ti precipitation, electron microscope examination of microstructure 3—8798
Al_2O_3, grain size rel. to density during sintering 3—2754

crystal microstructure continued
- α-Al_2O_3, polycryst., sintering and shaping process effects on form, topotaxy and texture *(German)* 3−12424
- Al_2O_3, thermally shocked, grain size rel. to strength degradation and crack propagation 3−2752
- $Al_2O_3-Cr_2O_3$, modulated structures formation 3−4846
- $Al_2O_3-Cr_2O_3-Fe_2O_3$ modulated structures formation 3−4846
- AlZn(6) alloy, effect of Zn-vacancy complexes on Guinier-Preston zone prod. *(German)* 3−12358
- Au_3Cu, I and II-type superlattice structure 3−8805
- B/Al composites, fusion welding, microstructure 3−12361
- B_4C, fast-neutron irradiated, study of defect microstructure due to He, Li disposition 3−26528
- B_4C powder fast reactor irradiation effects 3−1077
- BN twinning *(Russian)* 3−1631
- $Ba_{2-x}Mg_{2-y}Ti_{8-z}O_{16}$, rutile substructure obs. 3−7908
- Be, warm-swaged, tensile characteristics, depend. on grain size *(Japanese)* 3−31069
- BeO, grain size rel. to density during sintering 3−2754
- C fibres, micromorphology stability and interstitial compounds 3−31172
- CaO.FeO.Fe_2O_3, chem. comp. and precip. microstruct. *(French)* 3−8986
- CdTe, hot pressing, grain size determ. 3−27742
- β-Co, diffr. pattern and reciprocal lattice exam. of martensite phase formation from fcc struct. *(Russian)* 3−2699
- Co alloy, dispersion hardened 3−8782
- Co-Cr based superalloys, dispersion strengthening for high temp. applics. 3−31112
- Co-Cr-Ni-Ta alloy, directional solidification, interdendritic structures 3−37031
- Co-Cr(21 wt%) alloy with Y_2O_3 dispersion, Cr diffusion, substruct. influence 3−39343
- Co-Ni-Ti alloy, rel. to decomp. processes *(Russian)* 3−21581
- Co-Pt alloy, rel. to high coercivity, electron microscope study *(Russian)* 3−8779
- CoPt alloy, ordered, plastic deform. influence on structural state *(Russian)* 3−18338
- Cr sputtered deposit, substrate bias and deposition temp. effects 3−4936
- Cr steel, retained austenite detection using vapour phase deposited interference layers 3−8810
- Cr-Ni alloys, corroded, obs. using combined microprobe/opt. interferometry technique 3−39350
- Cu, grain size recrystallization, obs., kinetics, effect of prior deformation 3−27627
- Cu, grain size rel. to density during sintering 3−2754
- Cu alloys, age-hardened, rel. to elastic limits and yield pts. *(Russian)* 3−15668
- Cu single and polycrystals deformation at high strain rates 3−8897
- Cu-Al alloys, diffr. pattern and reciprocal lattice exam. of martensite phase formation from fcc struct. *(Russian)* 3−2699
- Cu-Mg-Ni alloy, monovariant eutectic, unidirectional solidification, aligned microstructs., interface stability criteria 3−12347
- Cu-Ni-Mg, monovariant eutectic alloy, microstructure obs. in unidirectional solidification 3−21589
- Cu-Ni(Zn)(Al)(Ge) solid solutions, rel. to hardening mechanism in microdeform. stage *(Russian)* 3−21633
- Cu-Pb-Sn, rel. to friction and wear *(Japanese)* 3−8768
- Cu-Pt alloy, rel. to atomic motion under action of laser pulse *(Russian)* 3−29111
- Cu-Ti, obs. of precipitation morphology on annealing *(Russian)* 3−12356
- $CuPt_3$ alloy, ordered struct., antiphase boundaries 3−14803
- Fe, Armco, Fatigue crack formation and propag., grain size effects *(Russian)* 3−27671
- Fe, cast, high-Mn malleable, isothermal transform. to austenite 3−24834
- α-Fe, diffusion of sulphur, temp. and grain size depend. *(Russian)* 3−24292
- Fe, grain growth and secondary recrystn. 3−21591
- Fe, gray, hypo-eutectic, eutectic solidification, metallographic struct. and melting conditions *(Japanese)* 3−27679
- Fe, high-purity, fatigue deform., cryst. orientation depend. *(Japanese)* 3−18595
- Fe, hydrogen-induced surface blisters and internal cracks 3−39349
- Fe, oxidation in air and wet hydrogen at elevated temps. for sealing of soft glass, growth of whiskers *(Japanese)* 3−18590
- Fe, single crystals at 78 and 4K, gliding, twin formation, fracture *(German)* 3−34612
- Fe alloys, martensite morphology and deform. of cryst. form during athermal transform. *(Russian)* 3−24824
- Fe-Al liquid alloys, specific electrical resistance, microinhomogeneities explanation of behaviour *(Russian)* 3−8146
- Fe-Al-C steel, precipitates of perovskite structure obs. by electron diffraction 3−18600
- Fe-C liquid alloys, impurities removal and structure control *(German)* 3−2729
- Fe-Cr-Ni alloy system, microstructural change study using selective etching *(Korean)* 3−5291
- Fe-Cu alloy, phase change in microdomain, field ion microscope images 3−18563
- Fe-Fe_2B fibrous eutectic alloy, thermal stability, rapid degradation of microstructure 3−8999
- Fe-Ni-C alloy, reverted austenite, prior deform. effects on strength and annealing behaviour 3−37048
- Fe-Ni-C alloys, morphology of thin plate-like martensite 3−37043
- Fe-Ni-C alloys, strain-induced martensite and thermally transformed martensite morphology 3−21575
- Fe-Ni-Cr-Mo alloy, deform. and heat treatment effect on struct. changes, Mossbauer obs. *(Russian)* 3−31056
- Fe-Ni-Ti alloy morphology after annealing *(Russian)* 3−15684
- Fe-Ni-Ti-Al-Nb alloys, in two-phase $(\alpha+\gamma)$ states, effects on props. and struct. *(Russian)* 3−12363
- Fe-Re-C, defect cluster influence on martensite form. *(Russian)* 3−12353
- Fe-Si, polygonization, influence of bending orientation during annealing *(Russian)* 3−8834
- Fe-Si (3.25 wt.%) alloy, impurity effects on grain growth in strain-anneal and secondary recrystn. 3−37041
- Fe-Si alloy, X-ray meas., cryst. struct. *(German)* 3−8809
- Fe-Si single cryst., texture formation during recrystallization, struct. changes during annealing *(Russian)* 3−12341
- Fe-Si single crysts., deformed, substruct. *(Russian)* 3−24847
- Fe-Zn supersaturated solid solution, alloying elements influence on the precipitation behaviour. *(German)* 3−2694
- FePd alloy, ordered, plastic deform. influence on structural state *(Russian)* 3−18338
- FePt alloy, ordered, plastic deform. influence on structural state *(Russian)* 3−18338
- GaTe thin films, structure, elec. and photoelec. props. *(Russian)* 3−33755
- Ga_3Te_4 thin films, during annealing *(Russian)* 3−33754
- Ge epitaxial layer, tripyramid growth obs. *(Japanese)* 3−1931
- Ge film, vacuum deposited, island radius and grain size 3−18542
- InSb-NiSb eutectic alloy, structure by unidirectional solidification *(Japanese)* 3−15673
- α-IrW, diffr. pattern and reciprocal lattice exam. of martensite phase formulation from fcc struct. *(Russian)* 3−2699
- KBr, press forged, for laser window applications 3−5979
- KCl, press forged, for laser window applications 3−5979
- KCl, step lines, local struct., X-ray obs. 3−38596
- Li_2O-K_2O-SiO_2-Al_2O_3:Sr^{2+} photopyrocerams, dislocation struct. and dielec. props. 3−27753
- Mg, creep, dislocation pipe diffusion 3−8871
- Mg-Zr (0.5 at wt.%) alloy metallography of ZrH_2 precipitation 3−18585
- MgO ceramic, polycrystalline function representing planar distribution of grain size 3−24970
- Mo, deformed, subgrain growth during annealing 3−31014
- Mo, effect of purity 3−18602
- Mo, elasticity limit depend. on grain size rel. to Petch law 3−30171
- Mo-Ti-C, impurity braking influence on subgrain growth during annealing 3−31014
- MoC_x, f.c.c., crystallite size, electron diffr. obs. 3−15737
- Nb/Al_2O_3 cermet film, superconductivity, normal state elec. and struct. props. *(Russian)* 3−30482
- Nb-H system, internal friction, domain boundary effects 3−38620
- Nb-Sn system intermetallics, constitution diagram singularities *(Russian)* 3−30967
- Nb-Ti-Zr superconducting sheets, relation between microstructure and applied magnetic field vs. critical current density characteristics *(Japanese)* 3−18257
- Nb-Zr alloy, unevenly distributed deformation 3−18256
- Nb_2O_5, grain growth during sintering 3−37083
- H-Nb_2O_5, training and defects study by electron microscopy 3−7774
- Ni, structure stabilisation by multiple thermal cycling and isothermal annealing *(Russian)* 3−24903
- Ni alloy, IN 100, γ' prime eutectic elimination 3−24856
- Ni alloys, struct. stability during high temp. creep 3−8915
- Ni alloys, thoriated, grain struct. effect on Kirkendall porosity appearance 3−37034
- Ni superalloys, constitution and microstructure 3−39312
- Ni:Al_2O_3, Mg, effect of Mg additions 3−15711
- Ni-base superalloy coherent particle strengthening, stress coarsening effect 3−18648
- Ni-Co, superlattice form. in fatigue specimens 3−8808
- Ni-Co-(2.5 wt.%)Al_2O_3 alloys creep behaviour, dislocation pipe diffusion mechanisms 3−8870
- Ni-Cr base alloys, precip. hardened, struct. factors influence on creep strength behaviour 3−8930
- Ni-Cr based superalloys, dispersion strengthening for high temp. applics. 3−31112
- Ni-Cr(20 wt.%) alloy with Y_2O_3 dispersion, Cr diffusion, substruct. influence 3−39343
- Ni-In aligned eutectics, phase morphology 3−39318
- Ni-Mo, transmission electron microscope obs. rel. to corrosion on exposure to HBr 3−8041
- Ni-Ti (Ni rich) alloy, precipitation and its hardening effect *(Japanese)* 3−30992
- Ni-Ti alloy, relation between modulated structure and yield strength *(Japanese)* 3−12350
- Ni_3Al, order and APB development rel. to onset of dynamic weakening stress *(Russian)* 3−12364
- Ni_3Al-Ni_3Ta system, interaction of phases, form. of Ni_6TaAl ternary phase 3−34510
- NiCrTaC, directionally solidified eutectic, etching technique for orientation determ. 3−18701
- Ni_3Fe, antiphase slip boundaries and dislocation config. *(Russian)* 3−34522
- Ni_3Mn, annealed under load, dislocation struct. *(Russian)* 3−15729
- Ni_4Mo, ordered, domain structs. and hardening 3−37026
- Ni_4Mo alloys, ordered, field-ion image interpretation, computer simulation procedure 3−8804
- Pb oxides, layer structures rel. to thermal expansion coeffs. *(French)* 3−17984
- Pb-Sb-Sn-As alloys, grain growth and microstructure 3−8785
- Si, small crystallite array, intercrystalline interference contrib. to X-ray scatt. 3−4695
- Si, striations, detection by chemical etching after annealing *(German)* 3−2068
- Si:Cu, Cu precipitation, obs. with Cameca ion analyser 3−7785
- SiC, fracture surface energy depend. on microstucture 3−8983
- Sn, chemically polished, grain contrast, investigation using scanning electron microscope *(German)* 3−8000
- Sn-Cd alloy, eutectic lamellar microstructs., ripening by controlled annealing 3−12348
- Sn-Sb, Sn-Pb, Sn-Sb-Pb alloys, columnar crystals, dendrite spacing *(Japanese)* 3−8792
- Ta_2O_5 film, anodic, rel. to mechanical props. and electrolytic breakdown 3−1684
- Ti alloy, welded joint struct. and props. affected by e.m. agitation of weld pool 3−21717
- Ti alloys, strength differential effect depend. 3−39370
- Ti-Mo-Al alloy, Al additions influence 3−34509
- Ti-Mo-Zr-Sn β-III titanium, thermomech. treated 3−34582
- Ti-Ni (2 at. wt%) alloy influence of microstructure on corrosion behaviour in hot acidic chloride solns., application to weld regions 3−27647

crystal microstructure continued
Ti-Ni alloys, B_2 phase region, stacking modulated structs. 3-14878
Ti-Ni alloys, near-equiatomic, diffusion controlled phase transform. structures 3-39311
Ti-Si(1 wt%) alloy, Mo effect on quenched and aged struct. 3-31064
Ti-Ti_5Si_3 alloy, oriented eutectic, crystallography of phases *(French)* 3-34525
TiC, deposited by activated reactive evaporation, effect of substrate temp. on struct. 3-27631
$UC_{1.86}$, twin struct., transmission electron microscope obs. 3-11639
UO_2 fuel pellets, surface cracking during hydrogen sintering 3-14259
$UO_{2\pm x}$, $0 \leqslant x \leqslant 0.25$, porosity, grain size and excess O effect on Young's modulus and fracture strength 3-24967
V-D alloys, interstitial superstructure exam. by neutron and X-ray diffraction and sp. ht. meas. 3-18606
VC-Co, grain growth during liquid phase sintering 3-18683
$VC_{0.76}$ monocrystals, TEM obs. of coherent precipitate 3-31119
W, chemical vapour deposition studies 3-1960
W lamps filaments void formation 3-27636
W wire, spherical micropore network formation, GK props. *(Hungarian)* 3-24892
W-Ni-Mo, two phase structure obs., mech. props. 3-8783
W-Re (22 wt.%) alloy, chem. vapour deposited, grain growth 3-37023
WC-Co alloy, transition metal carbides as grain growth inhibitors *(German)* 3-24973
YAG:Nd, testing of the homogeneity of single crystals by means of cathodoluminescence *(German)* 3-7789
Zn-Al alloy, pressure effect during solidification on structure and tensile strength *(Japanese)* 3-27680
Zn-Al eutectoid base alloy, superplastic deformation, ductile-brittle fracture 3-39362
Zn-Al sheet, superplastic forming, anisotropy *(German)* 3-2730
Zn-Sn alloy, dilute, segregation substruct. evolution during solidification 3-34524
Zn-$TiZn_{15}$ eutectic, lamellar and rod morphologies 3-37004
$Zn(NH_4)_2(SO_4)_2.6H_2O$, supersaturation and impurities, infl. on stepped relief and uniformity *(Russian)* 3-7645
ZnO, grain size rel. to density during sintering 3-2754
ZnS, hot pressing, grain size determ. 3-27742
Zn_3Sb_2, phase comp. and decomposition reactions *(Russian)* 3-15671
Zr, neutron damage to microstructure, electron microscope obs. 3-11657
Zr ion-thinned oxides formed during corrosion of Zircaloy-4, transmission electron microscopy 3-11825
Zr-H system, formation of the γ phase by a peritectoid reaction 3-18586

crystal morphology
butadiene-styrene block copolymers, viscoelastic props. in tension shear, domain morphology effect 3-29802
camphene, holographic anal. of morphology in dendrite growth 3-11564
copper phthalocyanine pigments, α and β forms, adsorption props., optical props., effect of heating 3-38713
crystal geometry shape from X-ray silhouette photos, least squares determ. 3-4703
Cu electrodeposited coatings, morphology and preferred orientation, current density and temp. effects 3-9070
cyclododecane, hollow cryst. rod growth from soln. 3-1583
diamond, natural, cubic habit, internal struct., X-ray topography obs. 3-7642
end forms evolution caused by environmental inclusions *(Russian)* 3-36266
ice, grown from melts, morphology of solid-liquid interface, dendritic and planar growth 3-38542
interfacial energy between crystal and solution by inverted bubble method, morphology prediction 3-14707
magnesia, fibrous, grown via vapour phase *(Japanese)* 3-8728
metal films, ultra thin, pseudomorphism, nucleation 3-30374
p-methoxybenzylidene, p-n-butylaniline with cholesterol benzoate or Canada balsam, exam. of mesomorphic state *(French)* 3-7618
mixed sulphides, synthesis by H_2S sulphuration of IB and IIB metals *(French)* 3-18539
nylon 6, morphological changes and effect on dynamic mech. props. 3-20243
organic material, film of crystal growth morphology 3-11558
perovskites, ordered, pseudotriclinic cell deform. induced by displacement of ion 3-17766
point groups, four-coloured, study of diamorphism 3-14719
polar crysts., absolute configuration assignment 3-33476
poly(ethylene oxide) fractions, mol. wt. depend. 3-20223
poly(ethylene terephthalate), cryst., etching by hydrolysis 3-31168
poly-ω-undecane-amide morphology and spherulitization kinetics in isothermal crystallisation *(Russian)* 3-36062
poly-p-xylylene, crystallisation from gas phase during polymerisation, 77 to 473K 3-29800
polycaprolactam, doubly oriented, morphological changes during annealing 3-20235
polyethylene, minimum pot. energy of folds and kinks 3-20244
polyethylene, n- and γ-irradiation, effect on degree of crystallinity *(Russian)* 3-7636
polyethylene nascent, prep. using $VOCl_3/(C_2H_5)_2AlCl$ catalyst 3-7283
polyethylene spherulites, lamellar struct., scanning electron microscopy 3-20248
polygonised growth spiral morphology rel. to advancement rates *(French)* 3-24046
polymer, conf., Prague, Czechoslovakia (Aug.-Sep. 1971) 3-20222
polymer, elongation ratio of deformed spherulites, small-angle light scatt. 3-20229
polymer, oriented cryst., morphology influence on submicrocrack form. 3-20240
polymer, semicryst., supermol. struct. form. under mol. orientation 3-20227
polymer, spherulite-fibril transform., model 3-33180
polymers, discussion 3-5357
polyoxymethylene, morphology and growth kinetics of supermol. structs. from molten mixtures 3-20225

crystal morphology continued
polyoxymethylene supermol. structs., growth rate and morphology 3-20224
polypropylene, quenched, struct. changes during aging 3-27772
quartz, study of growth morphology and cobble structures 3-14706
quartz particles from post-glacial clay soils, h.v. electron microscope exam. 3-37161
rare earth transition intermetallics, struct. relationships, Friedel's d-band mag. model 3-2248
rare gas, epitaxially grown on Nb (100), LEED obs. 3-11654
SiC growth, effect of Si/C molar ratio in vapour phase 3-17750
simple cubic crystal, computer simulation of dissolution morphology 3-1898
solid-liquid interface, morphological stability near grain boundary groove 3-11557
steel, martensite cryst. steric form and size determ. *(Russian)* 3-37017
transition metal silicide, refractory, morphology and spontaneous crystallization in growth from Zn melt *(Russian)* 3-14709
triglycine sulphate thin films deposited by low temp. spinning technique 3-39107
two phase systems, X-ray diffr. pattern, use of symmetry in interpretation 3-4701
$A^{II}B^{VI}$, rules for struct. formation and stable structures 3-7652
Ag, electrodeposited, spiral growth rel. to impurities 3-1582
βAg-Al splat quenched alloys, martensitic transformation 3-2695
Al-Al_3Ni eutectic, rod to blade transition 3-39313
AlN, epitaxial growth by vapour phase reaction, growth morphology 3-11831
B tetragonal filaments vapour grown on carbon fibre substrate 3-21532
B_xC, growth, 1450-1500°C, thermal etching, morphology 3-24781
BeO, seed-grown, flux composition, temp., impurity and orientation effects 3-14708
C, columnar growth by pyrolytic deposition 3-1581
C fibres, micromorphology stability and interstitial compounds 3-31172
$CaH(AsO_4).H_2O$, haidingerite, rel. to bond assemblage 3-14789
CdO, vapour growth, growth conditions effect on structure and morphology *(Russian)* 3-15616
CdS, whiskers, needles and platelets, rel. to growth mechanisms 3-2635
CdS film, cubic forms in surface morphology *(Russian)* 3-30376
Co-CoAl-Ni alloy, oriented eutectic, morphology rel. to Ni addition *(French)* 3-34523
Co-Ni-Ti alloy, electron diffr. obs. *(Russian)* 3-21581
Cu, grown by Czochralski method, cryst. perfection, absence of dislocations 3-1601
Cu alloys, binary, solidification characts., cryst. growth habits 3-21559
Cu coatings, electrodeposited, current density and temp. influence on morphology and predominating orientation 3-1943
Cu electrode, morphological changes of low-index planes, near equilib. 3-9075
Fe-Ni-C alloys, morphology of thin plate-like martensite 3-37043
GaAs, parameters which influence morphology of epitaxial layers in vapour growth 3-1918
p-GaAs, surface micromorphology, effect of surface treatment *(Russian)* 3-18009
GdGa garnet, macroscopic strain in facetted regions 3-33493
GeSe, cryst. growth, transport rate, growth mechanism and morphology 3-11573
InBi whisker, grown by squeeze technique 3-1963
Nb suboxides, electron microscopy study 3-17794
Pb dendrite, electrodeposited, habit and morphology rel. to growth parameters 3-33767
Pb dendrites, grown by electrolysis, crystallographic features 3-4942
Pb impregnated porous glass, Pb morphology, elec. microscope obs. 3-8315
PbI_2, cryst. growth in silicon gels, habit and kinetics 3-12223
Si, etching, electrochem. displacement technique, specific crystallographic directions 3-39277
Ti-Ti_5Si_3 alloy, oriented eutectic, crystallography of phases *(French)* 3-34525
Zn dendrites, electrolytic, crystallographic and morphological characts. 3-20977
ZnO, hydrothermally grown *(Japanese)* 3-27604

crystal orientation
Cu electrodeposited coatings, morphology and preferred orientation, current density and temp. effects 3-9070
cubic bicrystal, tilt and twist boundaries 3-11622
cubic crystal, determ. from {111} surface traces, analytical method 3-23958
direct method for orientation matrix determ. on diffractometer *(French)* 3-26953
Laue pattern comparison with computed pattern to determine crystal orientation 3-14634
layered stratified lattice, X-ray diffraction profile showing preferred orientation 3-11783
sheet and fibres, orientation distrib. calc. 3-17752
single, to incident X-ray beam axis in diffraction measurements, single Laue photograph, accuracy, method *(Greek)* 3-14661
standard projections for triclinic system of arbitrary orientation 3-14650
substrate orientation influence on purity of vapour grown GaAs epitaxial layers 3-1918
Zircaloy-2, polycrystalline, hydride precipitation, crystallographic orientation *(French)* 3-12385
Ba ferrite, preferred orientation during hot pressing, X-ray examination *(Russian)* 3-15743
C, pyrolytic, graphite layers preferred orientations, integrated intensities rel. to uniaxial orientation 3-4734
C fibres, a-axis preferred orientation in commercial fibres, quantitative estimates 3-31171
Co electrodeposited, effect of I^- ions on preferred orientation of crystallites *(Bulgarian)* 3-30366
Cu coatings, electrodeposited, current density and temp. influence on morphology and predominating orientation 3-1943
Fe-Al Kossel interference pattern computation *(German)* 3-4693

crystal orientation continued
Fe-Si Kossel interference pattern computation *(German)* 3—4693
GaAs substrate, influence on InAs$_{1-x}$P$_x$ vapour epitaxial growth 3—1917
GaP, substrate, influence on InAs$_{1-x}$P$_x$ vapour epitaxial growth 3—1917
InAs substrate, influence on InAs$_{1-x}$P$_x$ vapour epitaxial growth 3—1917
KH$_2$PO$_4$, effect of annealing on anomalous biaxiality and on plane of optic axes *(Russian)* 3—15470
Mo, vapour deposited on Cu, Mo and stainless steel substrates 3—8718
NH$_4$Br, Fm3m to Pm3m transform. orientation relations 3—7921
Pt, nucleation rate of Cu and brass on Pt, depend. on substrate orientation 3—1945
Si, diffusion of O$_2$, X-ray meas. of lattice strain, depend. on crystal orientation 3—17858
Si etching, KOH, H$_2$O and isopropyl alcohol, effect of wafer orientation and composition 3—39278
W, vapour deposited on Cu, Mo and stainless steel substrates 3—8718

crystal oscillators *see crystal resonators*

crystal properties
see also crystal chemistry
cirrus clouds generating cells, particle size spectra meas. 3—25231

crystal purification
see also crystal growth
Ba, by reactive distillation in Mo column 3—18536
Ca, by reactive distillation in Mo column 3—18536

crystal resonant gamma-ray interactions *see Mossbauer effect*

crystal resonators
see also piezoelectric oscillations
digital frequency sweeps for ENDOR exps. 3—19243
e.m. radiation linear equations 3—6398
film deposition, thickness monitoring by oscillating quartz resonators with large mass load 3—3780
quartz, continuous elec. field effect on reson. freq. *(French)* 3—34296
quartz, nonlinear eval. of moving elements of equiv. scheme *(French)* 3—27470
thickness measurement accuracy, temp. effects 3—25662
PbTiO$_3$ ceramic, V.H.F. resonator for video i.f. circuits *(Japanese)* 3—2495

crystal structure
see also crystal atomic structure; crystal microstructure; crystal morphology; crystal orientation; crystal symmetry; crystallography; granular structure; polymorphism
absorption correction in structure refinement, empirical method 3—23956
alkali halide lattice, stability under hydrostatic pressure 3—7930
Cherenkov structure radiation for particle channelled in crystal rel. to structure anal. 3—26916
computerised graphics in hierarchical computing system for crystal structure anal. 3—26923
diolefinic compound, X-ray obs. of structure changes during photopolymerisation 3—15820
ethyleneimine quinone, valence electron distrib. exhibiting bent bond 3—24095
glassy crystalline state 3—14692
gumbelite, ditrigonal rotation of tetrahedra in structures of layer silicates 3—9198
Harker Kasper criterion for structure determ. in centrosymmetric symmorphic space groups 3—11575
ice, cavity model hydrated electron absorpt. spectral peak press. shift at high press. 3—12141
lizardite, ditrigonal rotation of tetrahedra in structures of layer silicates 3—9198
nacrite, ditrigonal rotation of tetrahedra in structures of layer silicates 3—9198
packing, radius of sphere inscribed between four different spheres arbitrarily separated, calculation 3—38547
paragonite, ditrigonal rotation of tetrahedra in structures of layer silicates 3—9198
polymers, discussion 3—5357
polytypism, syntaxy and nonstoichiometry in layered structures *(French)* 3—33677
spinels, i.r. spectrum, interpretation 3—5198
surface layer, electron diffraction study *(Russian)* 3—7993
AgGaS$_2$, chalcopyrite structure rel. to nonlinear dielec. props. *(French)* 3—2482
BaO, effects of pressure on crystal structure and lattice parameters 3—7684
C fibres, obs. using polarized light microscopy 3—3793
Cu halides, sphalerite structure rel. to nonlinear dielec. props. *(French)* 3—2482
graphite-CrO$_2$Cl$_2$, lamellar compound, electric conductivity and thermal stability 3—33491
HCN, orthorhombic to tetragonal transition rel. to acoustic phonons 3—7873
KBr$_{1-x}$I$_x$, Raman scatt., X-ray scatt., struct. 3—33504
KCl$_{1-x}$I$_x$, Raman scatt., X-ray scatt., struct. 3—33504
K$_{1-x}$Rb$_x$Cl, Raman scatt., X-ray scatt., struct. 3—33504
Mo film, on W, Ir and Re, grown from vapour, struct., field in microscope obs. 3—38753
Se, vacuum evaporated layer, amorphous and crystalline phase obs. 3—20970
UO$_2$-UO$_3$ region, nonstoichiometric phases, review *(Japanese)* 3—32944
ZrO$_2$-CaO:Gd^{3+}, e.s.r. spectral obs. 3—8432

crystal surface and interface vibrations
adsorbed layer on f.c.c. crystals, vib. props. 3—24340
alkali halide crystal surface, non-radiative electronic transitions, optical vibrations excitation *(Russian)* 3—38876
atomic particles interaction with surfaces of solids, model *(Russian)* 3—33731
atomic scattering from surface of moving spheres 3—36963
dispersion forces between macroscopic bodies, surface polariton response function approach 3—38325

crystal surface and interface vibrations continued
eigenvalue problem of finite monoatomic linear chain with asymmetrical boundary conditions 3—24495
electron scattering by surface excitations 3—8003
free energy alteration of phonon system accounting for surface effects *(Russian)* 3—33725
i.r. absorption by surface phonons and plasmons in small crysts., continuum model 3—24705
Kapitza resist. of thin metallic films *(French)* 3—4998
layered substrates, piezoelec. waves, acoustic surface wave vel., computer programs 3—19107
localised surface phonons due to adsorbed atoms monolayers, resonant states 3—33729
metal slabs, vacancy relaxation energies, free surface effects 3—24110
metal surface, long wavelength phonon generation by e.m. waves 3—27167
metal surface, scattering of He atoms, two-phonon terms 3—11792
methane adsorbed layer on activated charcoal, obs. by cold neutron scattering 3—27178
phonon behaviour at interfaces, theory 3—24330
phonon radiation from heated NaF crystal face into liquid ^{4}He, meas. of angular distrib. 3—1855
phonon scattering in solids, conference, Saclay, France (July 1972) 3—1739
phonons, exptl. obs. using attenuated total reflection 3—24493
piezosemiconductors, acousto-plasmic transformations *(Russian)* 3—20922
polar crystal, optical phonons and phonon-plasmon modes 3—24326
polar semiconductor, magnetoplasmon-optical phonon interaction 3—24328
polaritons, response functions 3—24327
polaritons in semi-infinite anisotropic media 3—24329
quartz, OH groups, i.r. internal reflection spectra 3—39132
reconstructed surfaces, optical phonons 3—20920
surface modes calc. for finite lattices, Louck's method extension 3—17941
surface phonon h.f. generation rel. to surface defects, emission into dielec. substrates 3—15064
transducer cylindrical, in piezoelec. medium of hexagonal symmetry, diffr. 3—28410
Ag surface, scattering of He atoms, one-phonon contrib. 3—11791
C adsorbed layer on clean and S, Na, Cs or O$_2$-covered f.c.c. Ni, vib. properties 3—24340
CdS, photoconductive, current instability due to elastic surface waves 3—34297
Cr, mean square displacements for (110) and (100) atoms 3—30218
Cu, noncollinear surface wave interactions, 5-7 MHz 3—18013
He scatt. from surfaces, Debye-Waller theory 3—8002
He solid-liquid boundary, phonon transmission, microscopic theory 3—1763
KBr slab, anharmonic effects on surface mode absorpt. 3—18014
MgF$_2$ uniaxial crystal, surface optical phonons 3—20827
NaCl slab, anharmonic effects on surface mode absorpt. 3—18014
Pt(100) crystal face, localized surface modes due to scattering of diatomic and polyatomic molecules 3—8001
Si, (111) surface, spectral oscills. of photocond., role of surface phonons 3—18015
Si, glancing incidence HEED study 3—24331
Si, photocond. oscills. due to surface phonons 3—30519
TiO$_2$ uniaxial crystal, surface optical phonons 3—20827
YIG substrate, dielectrically induced surface wave 3—27471
ZnO, photocond. oscills. due to surface phonons 3—30519

crystal symmetry
see also crystallography; group theory
Belov space groups with colour symmetry, derivation from irreducible representation tables 3—24055
centrosymmetry degree and statistical distribution of X-ray intensities 3—26982
close packing structure, less dense, condensed model for stacking cubic and hexagonal layers 3—14720
colour space groups, generalisation of symmetry concepts and mag. structure 3—14716
electron diffraction pattern of skew structure, coincident reflection 3—24058
equilibrium and non-equilibrium structures, generalisation of concepts 3—14712
Fedorov group, cross sections of doubled Patterson function for structure near symmetry elements 3—24057
Fedorov group, symmetrical cross sections of the doubled Patterson function 3—24056
Fedorov symmetry group, isogons method for analysis of vector systems 3—24054
hexagonal canonical form representation for symmetric functions of 3-vectors 3—33477
intensity statistics, symmetry considerations with respect to space-group extinctions and weights 3—23960
invariant point group transform., zero component Cartesian tensors, determ. 3—17751
ion scattering study to confirm classification of crystal struct. *(Dutch)* 3—30082
lattice vibrations and their symmetry groups 3—14717
magnetic crystals, symmetry props. of transport coeffs. 3—34051
molecular crystals, theoretical derivation of degree of abundance of structural classes 3—33478
molecular packing anal. with lattice energy minimisation 3—14710
monoclinic crystal, i.r. dichroism of lattice vibrations of the B$_u$ species 3—2539
octahedron, effects of geometry on structure of crystals 3—38548
Patterson function, systematic anal. and use of peak rhombohedra to det. struct. fragments 3—7599
Patterson function, systematic analysis on basis of crystal symmetry 3—33426
and piezoelectricity under hydrostatic pressure 3—8521
and piezoelectricity under hydrostatic pressure 3—8522
point group symmetry in R4, representation and colour symmetry 3—14718
point groups, four-coloured, study of diamorphism 3—14719
quantum mechanics non-symmetric multiplicative wave function approx. *(Russian)* 3—10355

crystal symmetry continued
- rhombohedral crystals, symmetry props. of energy bands *(Russian)* 3−11843
- rotation functions in quaternion representation, symmetry *(Russian)* 3−4725
- rutile structure, anal. for energy band calc. 3−24053
- statistical methods 3−1587
- structure lacking symmetry centre, computational calc. of structure amplitude phases 3−23964
- subgroup, index list to determine colour and black-white symmetries 3−14714
- symbols for symmetry operations 3−14713
- tetrahedrally close packed layered planar structs., generating and coding schemes 3−7647
- two phase systems, X-ray diffr. pattern, use of symmetry in interpretation 3−4701
- $Ca_{2-2x}Na_{1+x}Eu_xMg_2V_3O_{12}$, point symmetry of dodecahedral site *(French)* 3−18480
- CeF_3, and struct. and screening consts. 3−7662
- $CsLiBeF_4$ determ., space groups and symmetry 3−11598
- $Cu_3Mo_2O_9$, centrosymmetric struct. space group 3−7667
- LaF_3, and struct. and screening consts. 3−7662
- NH_4LiBeF_4 determ., space groups and symmetry 3−11598
- Na_2Co_3, four dimensional space group of modulated structure 3−14715
- NdF_3, and struct. and screening consts. 3−7662
- PrF_3, and struct. and screening consts. 3−7662
- SbSI, single cryst., polycryst. and ceramic, comparison rel. to piezoceramic prep. 3−34301

crystal whiskers *see whiskers (crystal)*

crystallisation
- *see also crystal growth; dendrites; heat of crystallisation; nucleation; recrystallisation*
- alkaline earth tungstates, from LiCl melt, crystn. kinetics 3−24045
- anomalous water, refractive index meas., crystallisation, vapour pressure meas. 3−39466
- of Au on the (111) face of fluorite, condensation conditions *(Russian)* 3−8069
- basanite magma, high temp. and press. meas. of garnet peridotite 3−21857
- bulk, interrelation between crystal size distribution and degree of separation *(Dutch)* 3−2622
- bulk, mixing criterion in cooling crystallizers *(Dutch)* 3−2624
- bulk, production of large crystals by continuous ripening in stirred tank 3−2625
- bulk, secondary nucleation in stirred vessel cooling crystallizer 3−2623
- chalcogenide films, laser beam writing 3−22930
- convection and interface movement effects on heat and mass transfer *(French)* 3−2840
- by cooling, supersaturation, nucleation, specific crystal surface area and grain size rel. to temp. and time 3−33465
- crystallization of alloy powders obtained by liq. phase pulverization *(Russian)* 3−27728
- electrochemical aspects *(German)* 3−9080
- glass, cordierite, oxide additive effects on devitrification characts. 3−34643
- glass, cordierite, oxide additive effects on devitrification characts. 3−34644
- glass, cordierite, review of differential thermal and i.r. spectrophotometry anal. methods 3−12453
- glass, effect on spin-lattice relax. time, Mossbauer spectra h.f.s. 3−36826
- glass, Na_2O-CaO-SiO_2 system, crystallization process study by i.r. spectroscopy *(Russian)* 3−30248
- glass, stoichiometric diopside, microscopic study *(Russian)* 3−30074
- glasses, inorganic, structure, separation of amorphous phases and uniform crystallisation, review 3−24032
- gypsum, habit faces growth rates rel. to crystn. conditions 3−34468
- high-speed, of refractory metals, apparatus *(Russian)* 3−12327
- II-IV-V_2 compounds, preparation in layer form, properties and heterojunctions based on them 3−8747
- in situ composites production by unidirectional crystalline decomposition of non-crystalline solids 3−18717
- inert gas mixtures, mixed cryst. form., electron diffr. diagrams *(French)* 3−24043
- kinetic crystallization diagrams *(Russian)* 3−11724
- lanthanide oxide-silicate glasses, occurrence of crystallization on standing 3−5187
- metal, u.s. experiments, time duraton reduction *(Bulgarian)* 3−8893
- methaemoglobin water sorbed cryst., relax. times, temp. and regain depend. 3−12075
- molecular kinetics of sedimentation, model *(German)* 3−4724
- molybdates and tungstates, double, crystallization study *(Russian)* 3−7710
- monatomic system, molecular dnynamic study of freezing 3−11726
- nuclei formation in liquids with incomplete wetting of cryst. 3−15958
- nylon 6, pressure-induced, obs. 3−18732
- phased composite materials with prop. variations through thickness *(German)* 3−5263
- phosphate glasses, compositional effects 3−26974
- phosphate glasses, refining time effect on crystn. rate and viscosity 3−26975
- poly(2,6-dimehtyl 1,4-phenylene oxide) toluene mixture, induced by liquid-liquid phase separation 3−29798
- poly(ethylene oxide) fractions, mol. wt. depend. 3−20223
- poly(ethylene terephthalate), crystn. kinetics, influence of temp., mol. wt. and additives 3−33179
- poly(ethylene terephthalate) effect of strain history on behaviour 3−1576
- poly-ω-undecane-amide morphology and spherulitization kinetics in isothermal crystallisation *(Russian)* 3−36062
- poly-p-xylylene, from gas phase during polymerisation, 77 to 473K 3−29800
- polyamide 6, crystn. kinetics from glassy state 3−20226
- polyethylene, from xylene, conc. influence, crit. turbidity 3−33178

crystallisation continued
- polyethylene, high-strength transparent, morphology, controlled prep. conditions 3−4502
- polyethylene, n- and γ-irradiation, effect on kinetics and morphology *(Russian)* 3−7636
- polyethylene fibrillar crysts., hydrodynamically induced crystn. from soln., tensile props. 3−21738
- polyethylene melt, flow induced, fibrous struct. 3−25014
- polyethylene terephthalate electret, effect on homocharge and thermally stimulated currents 3−26976
- polyetyleneoxides, segmented, crystn., features due to steric hindrance of urethane linkages 3−14703
- polymer, branched, substitutional soln. of side chains 3−20245
- polymer, branching model 3−29780
- polymer, bulk-crystallized, morphological changes during melting 3−20237
- polymer, elongation ratio of deformed spherulites, small-angle light scatt. 3−20229
- polymer, semicryst., supermol. struct. form. under mol. orientation 3−20227
- polymer, spherulites, crystn. kinetics, light scatt. method 3−32060
- polymers, crystn. kinetics universal relationship 3−7284
- polymers, isothermal kinetics *(Polish)* 3−7637
- polyoxymethylene, morphology and growth kinetics of supermol. structs. from molten mixtures 3−20225
- polyoxymethylene supermol. structs., growth rate and morphology 3−20224
- trans-polypentenamer, strain-induced crystn., kinetics study 3−29801
- polypropylene spherulite, crystallisation temp. effect on deform. 3−9003
- polyvinylidene fluoride, rel. to temp. depend. of elec. cond. 3−33462
- rarefaction centre form from liquid phase continuity breaks in intercrystalline regions 3−33514
- rubber, Nairit, relative degree of crystallinity for different polymerisation temps. *(Russian)* 3−7635
- rubber film, uncrosslinked, morphology of strain-induced crystn. 3−4501
- semiconductor compounds, $A^VB^{VI}C^{VII}$ where A^V=Sb, Bi, B^{VI}S,Se, Te, C^{VII}=I, Br, crystallization under hydrothermal conditions *(Russian)* 3−8750
- silica, crystallization of powder effect of alkali halides and silver nitrate 3−18740
- Spol'ski's method for spectral luminescence analysis of mixtures by fast crystallisation *(Russian)* 3−28786
- supercooled melts and glasses, statistical thermodynamics 3−30073
- supercooling at face developing on rounded crystallisation front 3−33471
- tartaric acid, supersaturated soln., crystal dispersity, effect of u.s., latent period of mass crystn. 3−39404
- twinned five-fold symmetry crystals, mechanism of formation 3−1588
- water, processes in freely suspended microcrystals *(German)* 3−17967
- Ag, dislocation free plane multinuclear growth by electrocrystallisation 3−2816
- Ag noncrystalline thin films, resistivity study of crystallisation process 3−8062
- Al, u.s. experiments, time duration reduction *(Bulgarian)* 3−8893
- Al-Ge amorphous films, crystn. and decomp. *(German)* 3−24819
- AlB_{12}, crystallisation from Al-Ga-B melt, effect of impurities 3−12284
- Al_2O_3 thin films, electroforming and dielec. breakdown *(Russian)* 3−30530
- As_3S_2 crystal photosynthesis from As-As_2S_2 mixture 3−27898
- $AsSe_{1.5}Pb_{0.13}$ glassy alloys, consecutive crystallisation of PbSe and As_2Se phases, meas. of density of quenched patterns *(Russian)* 3−7634
- Au noncrystalline thin films, resistivity study of crystallisation process 3−8062
- $BaPO_3F$-Al(Ga)F_3-Li(Na)(K)(Zn)(Cd)(Pb)F_x, glass, vitrification and crystallisation capacity *(Russian)* 3−14698
- Bi film, amorphous, crystn. temp. thickness depend. 3−20972
- Bi_2O_3-TiO_2-KF-H_2O, study by hydrothermal method, form and props. of $Bi_2Ti_4O_{11}$, $Bi_4Ti_3O_{12}$, $Bi_{12}TiO_{20}$ 3−24048
- CaO-MgO-P_2O_5-SiO_2 glass, effect of fluorine addition 3−20698
- Cd-Sb system, crystallisation conditions influence on props. *(Russian)* 3−8769
- Co-Cr-C system, crystallisation of 2-4 phase composite structures *(German)* 3−8776
- $Cs_3Sb_2Cl_9$, rel. to polytypism 3−14794
- Cu, pyramidal growth during electrocrystallisation *(Japanese)* 3−24063
- Fe-C liquid alloys, impurities removal and structure control *(German)* 3−2729
- $Fe_{75}P_{15}C_{10}$ alloy, amorphous, crystallite morphology during crystn. 3−21595
- GaAs, epitaxial film, produced by vapour transport reactions, crystallization condits. *(Russian)* 3−8725
- GaAs, epitaxial growth over wide range of crystallisation conditions, comparison with GaP *(Russian)* 3−8051
- GaP epitaxial growth over wide range of crystallisation conditions, comparison with GaAs *(Russian)* 3−8051
- Ge-Te glass quenched, oxygen effect on struct. props. 3−33458
- InAs-GaAs alloyed solns., Zn and Te impurity effect on crystallisation *(Russian)* 3−7782
- InS film, amorphous, electron microscope obs. 3−7936
- InSb film, hot wire zone refining, bulk props. 3−2669
- K_2O-SiO_2-Al_2O_3 system of glasses, phases produced *(Russian)* 3−24031
- K_2O-SiO_2-BeO system glasses and crystn. products, synthesis and characteriz. *(Russian)* 3−11551
- LiBr saturated solution, anhydrous and hydro-crystalline solid state phases *(Russian)* 3−12517
- LiCl saturated solution, anhydrous and hydro-crystalline solid state phases *(Russian)* 3−12517
- $LiNO_3$ saturated solution, anhydrous and hydro-crystalline solid state phases *(Russian)* 3−12517

crystallisation continued
Li$_2$O-Al$_2$O$_3$-SiO$_2$ glasses, Gd^{3+} doped, e.s.r. meas. during crystn. 3—27403
Li$_2$O-SiO$_2$ glass, liq. phase separation and crystal nucleation 3—30075
MgCl$_2$-UCl$_3$-CaCl$_2$ fusibility, differential thermographic study *(Russian)* 3—24042
MgCl$_2$-UCl$_4$-CaCl$_2$, fusibility, differential thermographic study *(Russian)* 3—24042
MgO-Al$_2$O$_3$-SiO$_2$-TiO$_2$ glass-ceramic, crystn. and struct. 3—31161
NH$_4$Cl-H$_2$O soln., undercooled, crystal multiplication model 3—33467
Na$_2$O-CdO-GeO$_2$-H$_2$O system, hydrothermal crystallisation *(Russian)* 3—17745
Na$_2$O-CdO-GeO$_2$-H$_2$O system, under hydrothermal conditions at constant temp. 3—33508
Na$_2$Si$_2$O$_5$-BaSi$_2$O$_5$, phase equilibria, and crystallisation kinetics 3—24030
Ni-Au film couple, rel. to surface diffusion, electron microscope obs. 3—1878
Ni-rich alloys, superrefractory, instability aspects, cooling effect on creep strength, crystallization, precipitation and microtoughness *(French)* 3—18660
RbLn(WO$_4$)$_2$, hydrothermal synthesis *(Russian)* 3—8714
Sb$_x$Se$_y$ thin films, electron irradiation effects 3—15097
Se glassy, elec. cond., density and crystn. rate rel. to S and Te additions 3—33887
Si, amorphous thin films, crystallisation 3—8063
Si, high energy C$^+$ bombarded, damage profiles, crystallisation of resulting amorphous layer between 500 and 700°C 3—17887
Si-saturated tholeiite and basaltic andesite, crystallisation at high water pressures 3—15884
SiO$_2$ glass, superstruct., internal struct., morphology, in early crystn. 3—14693
SiO$_2$-Al$_2$O$_3$-Na$_2$O glasses, containing TiO$_2$ as nucleation agent, surface crystallisation effects on props. *(Polish)* 3—4721
SrSO$_4$, inhibiting effects of triphosphates and pyrophosphates 3—12218
Te based chalcogenide film as memory material, crystallisation after short laser pulse 3—30524
Y$_2$O$_3$-K$_2$O-WO$_3$, crystallisation of KY(WO$_4$)$_2$ phase, X-ray and differential thermal analysis *(Russian)* 3—14970

crystallite texture *see texture*

crystallites
see also crystal microstructure
ballas diamond, structure and texture 3—30090
carbon-graphite materials, crystallite size effect on strength 3—34652
cellulose, orientation in cotton fibres, X-ray meas. 3—31166
cotton fibres, X-ray diffraction study of crystallite orientation, determ. of average spiral angle 3—31157
ethylene-trifluoropropylene copolymers, chain microstruct. and crystallizability *(Russian)* 3—23654
nylon 11, 66 and 12, deform. behaviour near glass transition temp. 3—20233
orientation distribution analysis, three-dimensional, estimation of reliability 3—26981
oxide cathodes, high-field elec. cond. through pores and grains, theory and obs. 3—15207
poly, plastic forming local deformation redistribution *(Bulgarian)* 3—15690
poly(ethylene oxide) fractions, morphology 3—20223
polyethylene, annealed, structural transformations, reorientation, X-ray obs. *(Russian)* 3—31184
polyethylene, oriented, h.p. annealing effect on struct. 3—20247
polymer, oriented, elasticity of intercrystallite zones and mech. props. 3—26758
polymer, semicrystalline, orientation distrib. function of crystallites with cryst. lamella 3—33463
polyoxymethylene, morphology and growth kinetics of supermol. structs. from molten mixtures 3—20225
polyoxymethylene, size in chain direction 3—14705
polyoxymethylene supermol. structs., growth rate and morphology 3—20224
powders, hexagonal close-packed, corrections of integrated X-ray intensities for preferred orientation 3—30050
steel sheet, cold-rolled, annealing-induced changes in texture in cross section *(Russian)* 3—30987
transformer sheets, orientation distribution of crystallites *(Polish)* 3—18571
Au epitaxial growth, influence of decoration of monatomic surface steps on crystallite mobility *(French)* 3—36495
Co electrodeposited, effect of I$^-$ ions on preferred orientation *(Bulgarian)* 3—30366
Fe-Si (3.25 wt.%) alloy, impurity effects on grain growth in strain-anneal and secondary recrystn. 3—37041
Fe$_{75}$P$_{15}$C$_{10}$ alloy, amorphous, crystallite morphology during crystn. 3—21595
Ge-Te glass quenched, oxygen effect on struct. props. 3—33458
MoC$_x$, f.c.c., crystallite size, electron diffr. obs. 3—15737
Sb$_x$Se$_y$ thin films, electron irradiation effects 3—15097

crystallography
see also crystal atomic structure; electron diffraction crystallography; isomorphism; lattice constants; neutron diffraction crystallography; space groups; X-ray crystallography
absorption correction in structure refinement, empirical method 3—23956
Buerger algorithm for separating fundamental system from vector system 3—17755
coincidence site lattice, general conditions for occurrence 3—1589
coincidence-site lattices, math. characterization 3—24049
computer graphics and television raster display 3—26924
computer program for calc. of interatomic forces in crystals and molecules 3—26922
computerised graphics in hierarchical computing system for crystal structure anal. 3—26923
computing, IUCr Commission, objectives, experience, developments, report 3—26927
conference, Kyoto, Japan (Aug.-Sept. 1972) 3—14632
cubic crystal orientation, determ. from {111} surface traces, analytical method 3—23958

crystallography continued
deuteromethane orientationally disordered molecular structures, analysis 3—38546
dictionary, English-German-French-Russian 3—9787
electron microscopy, spatial measurements 3—22504
extinction effects, method for experimental reduction 3—26917
fast Fourier transforms, for use with Cooley-Tukey algorithm 3—23959
flameless mounting of crystals in capillaries 3—17715
Fourier contouring and molecular modelling using three dimensional computer graphics 3—26925
information services, system features, review 3—26915
intensity meas. from single crystal diffractometer, on-line control of accuracy 3—26921
intensity project, I.U.C. type III, structure factor determ. 3—26919
intensity statistics, symmetry considerations with respect to space-group extinctions and weights 3—23960
Kossel patterns, lattice parameter computation 3—1547
large mosaic crystal, integrated intensities of Laue and Bragg reflections 3—23955
lattice parameters calc. for orthogonal cryst. unit cell, program 3—30080
least squares refinement of crystal structure, effect of second derivative of F$_c$ 3—14635
low temp. equipment for automatic four circle diffractometer used for crystal studies 3—25674
modelling, macromolecular, interactive display system, electron density maps 3—26741
molecular structures, orientationally disordered coherent scattering length density, analysis method 3—38516
monatomic solid regularities, semi-theoretical models 3—14723
multidimensional, number theory applic. *(Russian)* 3—20705
n-dimensional lattices, study via reduced bases for n=2, 3, 4 3—7651
n.m.r. and diffraction techniques, complementarity 3—27424
organic crystal, method for assessing number of molecules in unit cell 3—24051
organic structures, computer-aided systematic search 3—33420
orientation of single crystals, by shadow effect, improvement using streak-camera *(Russian)* 3—11524
pair formulas, applic. to struct. determ. of 9α-fluorocortisol 3—7730
Patterson function, systematic anal., review 3—30081
Patterson superposition-Σ_2 technique, combined method for phase determ. 3—23962
periodic close packings of identical spheres 3—7650
phase relations between reflection quartets to determine strengthened quartet relationships 3—14633
probability-plot comparison of crystallographically independent molecules 3—23512
projections of crystallographic directions and planes on semicylindrical and plane scanning surfaces 3—33423
proton beam techniques, book contrib. 3—11526
realtime obs. of changing reflection profiles 3—26918
single-crystal diffractometer data, online control of precision of intensity meas. 3—23961
standard projections for triclinic system of arbitrary orientation 3—14650
structure invariants determination, quadrupoles and their uses 3—24050
symbolic-addition procedure, modification involving phase function 3—23957
tetrahedrally close packed layered planar structs., generating and coding schemes 3—7647
p-D$_2$ orientationally disordered molecular structures, analysis 3—38546
Fe-Al Kossel interference pattern computation *(German)* 3—4693
Fe-Ni, Fe-Ni-C, martensite, crystallographic aspects 3—18566
Fe-Si Kossel interference pattern computation *(German)* 3—4693
ND$_4$Br orientationally disordered molecular structures, analysis 3—38546

crystals
see also crystal structure; crystallography; dendrites; liquid crystals; plastic crystals; whiskers (crystal)
group overlap integrals for crystals and coordination compounds, program for calc. *(Russian)* 3—1590

Curie point *see Curie temperature*

Curie temperature
see also ferroelectric phenomena; ferromagnetic properties of substances; ferromagnetism
alloy, strongly paramag., dilute, phenomenological theory 3—21233
amorphous magnet, constant coupling approx. for Ising and Heisenberg models 3—11998
apparatus for investigating the electrical props. of ferroelectrics *(Russian)* 3—6016
BaTiO$_3$, dielec. permeability meas., to 1.5×10^{10}Hz, including phase transitions *(Russian)* 3—8504
dicalcium strontium propionate, proton spin-lattice relax. time, anomaly near Curie point 3—39103
dipole-dipole interactions, critical point behaviour 3—30625
ferrimagnetic spinels, Curie points and Weiss molecular field coeffs. 3—30623
ferrite, small size using differential test device 3—37667
Ferroelectric, wide band, depend. on nonequilib. carrier-conc. 3—24664
ferromagnet, amorphous, mixed, Heisenberg and Ising models 3—27350
ferromagnet, Seebeck coeff. at Curie temp., sp. ht. of charge carriers 3—18319
ferromagnet, Seebeck coeff. at Curie temp., sp. ht. of charge carriers 3—18320
ferromagnet, temp. increase by spin-phonon interaction 3—38971
ferromagnet weak itinerant film-paramag. proximity sample, Hubbard model calc. of Curie temp. 3—34086
ferromagnets, isotropic, resistive anomalies at the critical point 3—21236
Heisenberg ferromagnet, anisotropic 3—24553
Invar, magnetovolume, effects, Curie temp. press. depend., localised electron model 3—38979

Curie temperature continued
- Ising and Heisenberg ferromag. model nonmag. impurity effect at Curie temp. 3−8323
- Ising ferromagnet, crystal field anisotropy effect on Curie temp. 3−8324
- magnetic reversal nuclei, thermal activation 3−18277
- magnetically dilute ferromagnet, conc. depend. *(Japanese)* 3−38981
- NiSpan C, Invar range, precip. hardening effect on phys. props. 3−39345
- rare earth-Fe compound, Curie temp. pressure depend. 3−36720
- Rochelle salt, two-dimensional pressure effect on Curie point 3−2500
- spinel ferrimagnet containing two types of ions, Weiss mol. field coeffs. 3−2229
- surface effects near ordering temp. 3−34118
- teaching-aid demonstration 3−19131
- Tomita-Tanaka approx. validity in limit of spin 112 Ising ferromagnet 3−34067
- transition metals and alloys, modified Zener model and Curie temp. calc. 3−34085
- triglycine selenate, normal and deuterated, ferroelec. props. near Curie point *(Russian)* 3−8537
- triglycine sulphate thin films deposited by low temp. spinning technique 3−39107
- triglycine sulphate two-dimensional pressure effect on Curie point 3−2500
- Ag-Gd, alloy metastable, vapour quenching preparation, properties, thin films 3−30370
- $BaTiO_3$, ferroelec., domain struct. and phase transition, illumination influence 3−15460
- $BaTiO_3$, positive temp. coeff. of resist., near Curie temp. *(Russian)* 3−18130
- $BaTiO_3$:Al ceramic, piezo-electric effect, maximum peak open circuit voltage near Curie temp. 3−21363
- $BaTi(Zr)O_3$ ^{89}Zr half-life change at upper phase transition 3−36844
- $Bi_2Bi_4Ti_3Fe_2O_{18}$, perovskite layer type ferroelec., Mossbauer meas. of 1075 K 3−27443
- $Ca_xNi_{1-x}Fe_2O_4$ system, phase structure determinations, phase equilibrium 3−8379
- $CaO_xNiO_{1-x}Fe_2O_3$, $0 \leqslant x \geqslant 0.7$, variation with concentration of Ca ions *(French)* 3−8362
- $CdCr_2S_4$, critical broadening of e.p.r. line near Curie point 3−21294
- $CdCr_2S_4$, ferromag. semicond., effect of heat treatment in sulphur atmosphere 3−30621
- Co, pressure variation 3−2276
- Co, sublimation, in range including Curie point, 1320-1410K *(Russian)* 3−8365
- Co-Ni, pressure variation 3−2276
- Co-Pd alloys, interdiffusion coeff. behaviour 3−20899
- Cr_2S_3, rhombohedral single crystal, sublattice magnetisation 3−12021
- Cr_2SSeTe, meas. of molar susceptibility and molar spontaneous magnetisation, 80-600 K, determ. of Curie point *(Russian)* 3−12010
- $Cs_2CuCl_4.2H_2O$ Heisenberg b.c.c. ferromagnet, nuclear quadrupole resonance obs. of magnetic interactions, spin-orbit distortions at T_c 3−27439
- Cu-Cr alloy, dilute, in supercond. sandwich, T_c thickness meas. 3−8341
- Cu-Fe alloy, dilute, in supercond. sandwich, T_c thickness meas. 3−8341
- Cu-Mn alloy, dilute, in supercond. sandwich, T_c thickness meas. 3−8341
- $CuCr_2S_{4-x}Se_x$ solid soln., ferromag. and paramag. Curie points 3−21241
- ErGa, ferromag. props. 3−2319
- $Er_xY_{1-x}Al_2$, magnetic ordering, linear depend. of Curie temp. on ordering *(German)* 3−12027
- $EuEr_2Ga_{0.7}Fe_{4.3}O_{12}$ epitaxial film, for bubble domains, variation with growth temp. 3−34157
- EuO, weak crit. scatt. rel. to mag. order effect on thermal cond. 3−7979
- $Eu_xYb_{1-x}Sn_3$, Mossbauer effect and magnetisation meas., paramagnetic Curie temp. and hyperfine fields depend. on Eu concentrations *(German)* 3−24594
- Fe, Hall and Nernst-Ettingshausen effects, anomalies near Curie pt. *(Russian)* 3−12014
- Fe, pressure variation 3−2276
- Fe, self diffusion coeff. temp. depend. at Curie point *(Russian)* 3−11761
- Fe-Cr spinel, magnetoresist. anomalies at Curie point 3−30462
- Fe-Ni, f.c.c. alloy, pressure effect on Curie temp., rel. to magnetostriction anomalies 3−34126
- Fe-Ni, pressure variation 3−2276
- Fe-Ni (fcc) alloys, C_p meas. in 300-1000K range, obs. of behaviour at Curie temp. *(Japanese)* 3−18312
- (Fe-NI)-P-C amorphous alloy 3−21234
- Fe_2B, Mossbauer absorpt. obs. of mag. hyperfine field, isomer shift discontinuity at transition 3−15443
- $Fe_xMn_{2-x}P$, mag. props. of different phases, Neel and Curie temps. 3−30608
- $Fe_{1-x}Pt_x$ alloy, $0.25 \leqslant x \leqslant 0.3$, ferromag. Curie temp. rel. to atomic ordering 3−30618
- $Fe(Pt_cPd_{1-c})_3$ calc. for ferromag. subsystem 3−12018
- Gd-Ag, alloy metastable, vapour quenching preparation, properties, thin film 3−30370
- $Gd_{3-x}Ca_xFe_{5-x}Sn_xO_{12}$ ferrite-garnets, temp. dependence of EMR and FMR linewidths *(Russian)* 3−36795
- $Gd_2(MoO_4)_3$, neutron irrad. effects 3−36847
- $Gd_xTh_{1-x}PdIn$, comp. depend. 3−27364
- $Gd_xY_{1-x}PdIn$, comp. depend. 3−27364
- $HfCo_2$, Laves phase, single phase region, mag. suscept. obs. 3−27360
- $HgCr_2S_4$, critical broadening of e.p.r. line near Curie point 3−21294
- $HgCr_2Se_4$, critical broadening of e.p.r. line near Curie point 3−21294
- $HgCr_2Se_4$, magnetoabsorpt. obs., temp. and field depend. at Curie point 3−12122
- $HoMnO_3$, paramag. Curie temp., mag. susceptibility, 4.2-400 K 3−34103

Curie temperature continued
- $K_2BiNb_5O_{15}$, crystal growth, dielectric constants anomalies at Curie temp. 3−8535
- $KCrS_2$, meas. of 112K showing ferromag. dominant over antiferromag. interaction 3−34132
- $KD_{2x}H_{2(1-x)}PO_4$, deuterium conc. depend. 3−34318
- KH_2PO_4, in vicinity of Curie point, ionic motion effect on refractive index 3−29141
- $KNbO_3$, soft lattice vibr. modes, spontaneous polarisation and Curie constants 3−34303
- $LaAl_2$-$GdAl_2$, mag. ordering, Curie temp. depend. on Gd conc. 3−34122
- $LiTaO_3$, ^7Li quad. coupling const. temp. depend. near Curie pt. 3−2415
- MnAlGe, nonstoichiometric film, low Curie temp. meas. of 190°C 3−36497
- $Mn_3Cr_2Ge_3O_{12}$ garnet, 3.68K, ferrimagnetic props. *(Russian)* 3−2266
- $Mn_3GaC{:}^{57}Fe$, Mossbauer obs. of paramag. and ferromag. spectra 3−12081
- MnGaGe, ferromagnet, prep., struct., Curie temp., saturation magnetisation, mag. moments 3−21268
- MnGaGe, sputtered film, ferromag. and magneto-optical props., Curie temp. depend. on comp. 3−36861
- MnGaGe film, Curie point writing with laser pulse, thermal and mag. profiles comparison 3−36860
- $NaNO_2$ single crystal γ-irradiated, dielectric const. and Curie temp. variation 3−27477
- Ni, Hall and Nernst-Ettingshausen effects, anomalies near Curie pt. *(Russian)* 3−12014
- Ni, magnetization singularities near Curie temp. *(Russian)* 3−8383
- Ni, photo-thermostimulated exoelectron emission, shift at Neel and Curie points, strain effects 3−30918
- Ni, pressure variation 3−2276
- Ni, spin wave excitations, 4.2-715K, temp. depend., change in character above Curie point 3−30637
- $Pb_5Ge_3O_{11}$, ferroelec. behaviour, enantiomorphism and optical activity 3−18419
- $Pb(ZrTi)O_3$ piezoelectric ceramics, stabilization effects, polarization ordering above Curie temp. 3−8507
- Pd-Mn(Fe)(Co) dilute alloys, resist. study 3−30624
- $(PrBi)Bi_4Ti_3Fe_2O_{18}$, perovskite layer type Ferroelec., Mossbauer meas. of 1050K 3−27443
- $Pr_2Bi_4Ti_3Fe_2O_{18}$, perovskite layer type ferroelec., Mossbauer meas. of 900K 3−27443
- Pt-Mn-Sn alloys, 313 to 365°K *(Japanese)* 3−8346
- $Rb_2CuCl_4.2H_2O$, Heisenberg b.c.c. ferromagnet, nuclear quadrupole resonance obs. of magnetic interactions, spin-orbit distortions at T_c 3−27439
- $SnCr_2S_4$, ferrimag., prep. by heating method, Curie temp. and cell dimensions meas. 3−31261
- $Sr_2Nb_2O_7$, ferroelectric single cryst. 3−21373
- $SrT.TeO_2$, ferroelec., phase transition 3−15457
- TbGa, ferromag. props. 3−2319
- Tm_6Fe_{23}, meas. using thermodynamic method 3−21273
- U_3Se_4, cubic, from magnetisation obs. from fields up to 80 kOe and temps. to above T_c 3−15356
- UTe, U_3Te_4, cubic, from magnetisation obs. from fields up to 80 kOe and temps. to above T_c 3−15356
- U_7Te_{12}, Curie point meas. of 73K 3−12011
- U_3X_4, Th_3P_4 type struct., mag. props., mag. moments, Curie point, remnance magnetization 3−2318
- V-B-N, antiferromag. Curie temp. meas. rel. to band structure *(Russian)* 3−15333
- YIG, magnetization near Curie point 3−38980
- $YMnO_3$, paramag. Curie temp., mag. susceptibility, 4.2-400 K 3−34103
- $YbMnO_3$, paramag. Curie temp., mag. susceptibility, 4.2-400 K 3−34103
- $YbNi_2$, crystal field effects, Mossbauer obs. 3−30610

Curie-Weiss law *see paramagnetism*

curium
- Cm^{3+}, in CaF_2, optical Zeeman rot. spectra 3−18467
- Cm^{3+}, in $CeO_2(ThO_2)$, zero-field splittings 3−18358

curium compounds
- Cm_2O_3, one-kilowatt heat source test 3−19961

current (electric) *see electric current*

current algebra
- ***see also elementary particle theory; hadron current; quantum field theory***
- $\pi\pi$ scattering amplitude calcs. 3−19732
- anomalous dimensions in Wilson's expansion of two currents near lightcone, exptl. limits from deep inelastic ep scattering 3−23009
- Araki's theorem and perturbation theory in current formalism 3−26280
- axial vector current, influence on space-time 3−598
- axial vector current-two-photon triangle graph, unsubtracted dispersion relations, anomalous term 3−13822
- axial-vector current, inconsistency in value of D/F ratio shown not to occur 3−10649
- axial-vector-current anomaly in canonical formalism of quantum field theory 3−10608
- base current-quark masses inelastic reactions and light-cone algebra 3−29224
- bilocal algebra of Fritzsch and Gell-Mann, test in deep inelastic electro- and muoproduction of W-boson 3−6629
- bilocal current algebra in quark model testing by μ electroproduction 3−13812
- bilocal operators, test of algebra in massive muon pair production 3−16958
- broken scale invariance, review 3−32631
- canonical algebra approach to meson-baryon scatt. 3−4205
- chiral symmetry, algebraic realization on light cone 3−26277
- class of representations of bilocal currents on a light-like ray 3−6571
- commutators, local current, yielding photoprod. amplitudes sum rule 3−32668
- commutators, null plane restrictions 3−10646
- compactness and vector meson dominance 3−26279

current algebra continued
conservation of vector currents, necessary and sufficient conditions in relativistic quantum field theory 3−29164
conserved and partially conserved currents on the light cone 3−10647
covariant time-ordered products, generating functional 3−35764
deformed, and computation of Cabibbo angle 3−38013
deuteron, form factors of e.m. current of np system determ. in terms of Jost matrix 3−26301
dimensions and equal-time commutators of current components 3−35767
dual parton model and PCAC, reformulation 3−35765
dual resonance model, new scalar and conserved vector currents 3−6634
dynamic resonance model, with e.m. interactions, calc. of sum rules and factors 3−14021
equal-time commutators of charge and current sandwiched between states of unequal momenta, sum rules 3−4150
equal-time correlations in hadrons 3−23007
Fermion fields, covariant T-product and gauge-invariant vacuum polarisation amplitude 3−13809
fixed mass limits of amplitudes, reln. to light cone singularity of current commutators 3−32640
fixed poles in virtual Compton amplitude for octet currents 3−6569
Fritzsch-Gell-Mann, application to deep inelastic processes $eN \to e\gamma$anything and $\nu N \to l\gamma$anything 3−13933
Gamow-Teller mirror β-decay, possibility of second-class currents involved 3−14180
Goldstone's theorem for class of currents not covariant under translation 3−32638
Goldstone and Coleman theorems, generalizations in framework of Wightman field theory 3−4142
hard-pion, for low-energy π electroproduction and photoproduction 3−35796
inelastic electroproduction, range, light cone dominance and scaling at low Q^2 3−23080
isotensor electromagnetic current, reln. to dispersive calcs. on π photoprod. 3−13819
Landau's quantised hydrodynamics, current-algebra approach 3−32445
lepton currents, neutral 3−4155
lepton-nucleon, deep inelastic scatt., light-cone algebra and field-current identity 3−38052
leptonic decays of hadrons 3−831
light cone, and algebra of vertex strengths 3−13814
light cone, exotic application to inclusive reactions 3−17126
light cone expansion and Regge couplings 3−6642
light-cone bilocal algebra test in unified theory of weak and e.m. interactions 3−16957
light-cone commutators and bilocal operators 3−35762
light-cone expansion and conformal algebra 3−13800
light-cone ordering and current commutators, construction of Green functions, sea-gull terms 3−23008
light-cone structure and scaling in inelastic electron scattering, Mellin-transform analysis 3−10715
light-cone structure of infinite-component fields 3−6627
light-cone theory, algebra of fields 3−10648
non-canonical dimensions and current commutator matrix elements near light-cone 3−13801
non-leptonic hyperon decay amplitudes determ. 3−10675
nuclear β-decay, conserved-vector-current hypothesis for superallowed Fermi transitions 3−974
on-mass-shell pions, calc. 3−19675
partially conserved axial-vector current, dynamic formulation 3−13811
parton model relations for deep inelastic structure functions, light cone analysis 3−29213
PCAC, and soft pion theorems in nuclear physics, review 3−14234
PCAC, anomaly for world with one space and one time dimens. 3−23010
PCAC and light cones, application to π electroproduction 3−17003
PCAC and pion pole dominance deviations 3−23011
PCAC in $\pi^0 \to \gamma\gamma$, conflict with VMD 3−38037
PCAC triangle anomaly, nonperturbative evaluation of low energy theorem relating $\gamma \to 3\pi$ and $\pi \to 2\gamma$ 3−32637
photon fields, fundamental length and fine struct. consts. from equal time commutators 3−10624
pion photo-and electro-production, calc. of amplitude by soft-pion techniques and PCAC 3−13972
propagators for large and small momentum for free field and spectral representations 3−35768
relativistic dynamical system with variables defined on light-like surface derivation of new current algebra 3−22978
representations for infinite free Bose or Fermi systems at finite temp. 3−28973
scale breaking, colliding beams and light cone commutators 3−13813
scale dimensions of axial current components exploited in local saturation scheme 3−6570
scaling laws and equal-time commutators 3−35766
second class currents, role of meson exchanges 3−6573
short distance behaviour of currents, operator product and light cone expansions 3−13816
spectral representation treatment of primitive divergences in perturbation theory 3−13844
$SU_3 \times SU_3$ σ model, closed-loop corrections to one- and two-point functions 3−26266
$SU_3 \times SU_3$ σ model, renormalization procedure 3−26267
SU(3) × SU(3) algebra and Cabibbo angle 3−820
sum rules of Adler Cabibbo Radicatti, in field-theoretical models and algebra of equal-time current commutators *(Russian)* 3−10678
support properties of scaling functions for time-like virtual photons; perturbative model 3−16943
triplet model, current commutators near light cone 3−822
Ward identities, anomalous, divergence of currents 3−13810
weak and electromagnetic currents, connections 3−13815
$e^+e^- \to \sigma\gamma$, current algebra derivation of Ward identity 3−13817
$e^+e^- \to \sigma\gamma\gamma$, current algebra derivation of Ward identity 3−13817
eN deep inelastic electroproduction, inequalities for structure functions, tests of basic algebraic structures 3−13981

current algebra continued
ep deep inelastic scatt., asymptotic props. of amplitude rel. to Schwinger term sum rule 3−26316
$\gamma n \to p\pi^-$, dispersion relations discrepancy in isovector amplitude with isotensor e.m. current 3−17019
$K \to \pi\mu(e)\nu$, chiral-limit theorems and PCAC corrections for scalar divergence form factor 3−29187
$K \to \pi\mu(e)\nu$, determ. of form factors from hard meson current algebra 3−16974
$K \to \pi\mu(e)\nu$, theoretical study using current algebra, light cone algebra and related techniques 3−10671
$K \to \pi\pi$ decay, soft-pion limit 3−13834
$K_l \to \mu^+\mu^-$, neutral current contrib. 3−10669
μ decay current, normalization in V-A theory, inclusion of radiative corrections 3−23028
νN deep inelastic scattering, inequalities for structure functions, tests of basic algebraic structures 3−13981
$\nu_\mu p \to \mu^- e^+ e^-$ + hadrons, calc. of deep inelastic cross section using bilocal algebra, parton model 3−35780
$pp \to K^+K^-\pi^+\pi^-$, amplitude calc. for annihil. process 3−19722
$\pi + \alpha \to \pi + \beta$, current algebra sum rules for Reggeons, $SU_2 \times SU_2$ symmetry 3−13821
$\pi\pi$ phase-shift analysis in low-energy region 3−38077
$\pi\pi$ scatt. low energy model using current algebra and dispersion relations 3−14055
$\pi\pi$ scattering, unitarity corrections from current algebra, hard-pion amplitude 3−17095
^3H-^3He transition, corrections to Goldberger-Treiman relation 3−6780

current density
see also electron density
arc, high-current pulsed, anode current density meas. 3−17690
hollow cylindrical cathode, elec. field distrib. in cathode fall, radial model *(German)* 3−4690
insulating and electrode materials, elec. cond., erosion and heat resistance in plasma jet 3−36206
ion saturation currents in collision dominated flowing plasma, planar Langmuir probe meas. 3−14583
m.i.s. structures current transfer through dielectric after gamma-irradiation 3−24526
parallel superconducting wires in Meissner state, behaviour of superconducting cable wires 3−11988
solid or liquid, equilib. correlation functions in linear response to electromag. field 3−24388
superconducting film, two-zone, with paramag. additions, crit. current density and mag. field *(Russian)* 3−15287
toroidal mag. field, adiabatic compression of the E-layer 3−7549
Au films, electromigration, local variations of current density and temp. influence *(French)* 3−30282
GaAs laser, n-type and undoped active layers, optical gain coeff. rel. to current 3−16860
Nb-Ti superconductor in range 1.9 to 4.2 K, critical current density 3−8316
Nb-Ti-Zr ternary alloys with different compositions 3−11982
Nb-Zr, superconducting critical current density following annealing, transition temp. 3−18256
Nb_3Sn layer, O ion irradiation effect on superconducting critical current density *(German)* 3−2210
NbTi, superconducting wire, critical, E-J chracteristics 3−38930

current distribution
see also current density
cylindrical antenna in cold magneto plasma 3−7498
infinite tubular antenna in cold collisional plasma 3−11482
parallel superconducting wires in Meissner state, behaviour of superconducting cable wires 3−11988
resistive wire electrode 3−39446
superconducting cylinder, homogeneous type II superconductor 3−27332
thin cylindrical antenna, calculation of current distribution and impedance by method of moments 3−33352
tubular electrode 3−39447
in Z-pinch discharge in condensed molecular beams of N_2 *(German)* 3−4689

current fluctuations
see also noise
semiconductor, carrier fluctuations in current saturation region, time depend. *(Russian)* 3−8197
semiconductor electron equilib. distrib. instability *(Russian)* 3−8184
three cylinders, model for interaction between 3 conducting molecules, internal fluctuations 3−1295
n-Ge:Cu, 77-200 K *(Russian)* 3−27257
Ge:Mn; Sb, recomb. wave current instability rel. to mag. field *(Russian)* 3−8180

current measurement, electric *see electric current measurement*
current transients *see transients*
currents algebra *see current algebra*

curvature measurement
corneal radius, diffraction effects on precision 3−3886
small surface areas, interference methods *(Russian)* 3−22263

curvature of field *see aberrations*

cutting
see also machining; spark machining
carbide tools, review 3−8939
diamond drilling of glass, temp. field calc. 3−22780
diamond microtool electrolytically formed 3−25745
electric spark-cutting, foil prep. for electron microscopy 3−18576
hole formation by laser beam, workpiece material thermophysical properties *(Russian)* 3−10579
laser application to stainless steel sheet cutting 3−4131
machined surface layer strwture and thermal residual stress by grinding 3−21708
metal, residual stress analysis 3−521
metal single crystals, deformationless cutting 3−27712
metallic crystals, spark cutter using weak electrolyte 3−27704
metals, chip formation and operating conditions of machine tools 3−24958
metals, machine for deform. free chem. cutting 3−18620
plasma torch, ceramic nozzle wall, R&D, ECRC 3−1521

cutting continued
steel, high-speed tool, characterization 3—21682
steel, low C, microcrack formation, unsuitability of continuum models 3—21656
Ni, effect of plastic deform. in high-speed cutting on mech. props. of cut chips *(Russian)* 3—18617
CO_2 laser applications 3—22969

cyanogen, C_2N_2 *see carbon compounds*

cybernetics
see also biocybernetics; information theory; man-machine systems; pattern recognition
quantum field theory, mathematical model development and verification, cybernetic methodology 3—35729
quantum field theory math. models development and verification 3—35730

cyclotron frequency *see cyclotron resonance*

cyclotron resonance
see also diamagnetism
μ_p/μ_n precision meas. in terms of n.m.r. frequency and cyclotron resonance frequency, error elimination 3—13208
anomalous resistance due to cross-field electron ion streaming instabilities 3—7522
Azbel Kaner resonance in gaseous plasmas 3—17583
cold plasma, quasilinear particle acceleration in hydrodynamic cyclotron instability 3—17617
collisional cyclotronic instability in an ionized Ramsauer gas *(French)* 3—11485
dispersion of cyclotron waves in metals *(Japanese)* 3—24377
electron beam-plasma interaction, spiraling, enhanced emission around ion cyclotron harmonic freq. 3—1483
electron cyclotron drift instability, controlled steady-state experiment 3—14553
electron cyclotron drift instability 3—7523
electron cyclotron resonance heating, long time and stochastic effects 3—17637
electron velocity distribution meas. in an electron cyclotron resonance plasma 3—14589
electrons in mirrors, r.f. heating process, stochastic character 3—23895
electrostatic electron cyclotron harmonic waves in the magnetosphere 3—16035
ferromagnetic metals, electron and neutron scattering by coupled spin waves, near cyclotron resonance *(Russian)* 3—12031
Frohlich polarons, internal structure determined by optical absorption, cyclotron resonance 3—36561
in geomagnetic field, intrinsic bandwidth 3—5523
graphite, by using circularly polarized radiation, exam., 23 and 69 GHz 3—11849
graphite, theory and determination of the degree of band warping 3—8100
high density sheet plasma, RF plugging and heating, ion cyclotron motion 3—20568
inhomogeneous and non-uniformly magnetized plasma, harmonic generation of microwaves at cyclotron frequency 3—14590
inhomogeneous plasma, transverse e.m. wave 3—7503
instability in mirror machines 3—4644
ion, coil to plasma coupling, inhomogeneous effect 3—23863
ion, sheet plasma, characteristic oscillations, integral eqn. 3—20505
ion cyclotron resonance mass spectrometer construction *(Japanese)* 3—28705
ion spectrometer for determ. of rate consts. for ion-molecule reactions in ammonia 3—1273
ion-cyclotron whistlers, propagation in upper atmosphere 3—31403
ionic crystal, rel. to transport processes 3—36601
ionic crystals, effect on optical absorption, electron-phonon interaction 3—36885
Landau diamagnetism, surface modified cyclotron orbits 3—38956
magnetic field uniformity degree effect on radiation of harmonics of the electron cyclotron frequency from a plasma *(Russian)* 3—14568
magnetic moment of proton, meas. at NPL in terms of cyclotron frequency by omegatron method 3—13207
magnetosphere pitch angle scattering into loss cone by cyclotron resonance, whistler modes-electron interactions 3—25306
metallic crystal, ideal, low freq. resonance and electron-phonon interactions *(Russian)* 3—2043
microwave absorption in magnetoactive plasma at electron cyclotron resonance 3—20465
nonlinear theory of electron drift instability in high-β systems 3—23852
plasma, characteristics of electric field far and close to a radiating antenna in ionosphere around lower hybrid resonance 3—21962
plasma, electron-cyclotron wave, excitation by modulated helical electron beam 3—33367
plasma, hot electron, axial distribs. determ. for heating mechanism study 3—38477
plasma, magnetoactive, e.s. surface waves at transition layer, damping at electron cyclotron resonance 3—29966
plasma, microwave heating of electrons of dense column at freqs. higher than electron cyclotron freq. 3—38467
plasma beam reflection by HF supplemented magnetic mirror near electron cyclotron resonance, energy balance 3—20608
plasma column radial structure of oscills. of advanced cylcotron resonance instability in crossed fields *(Russian)* 3—33372
plasma cyclotron harmonic waves excitation 3—36173
plasma cyclotron instability in presence of suprathermal electrons 3—20541
plasma cyclotron oscillations in bounded systems, surface absorption effect 3—38451
plasma cyclotron resonance heating saturation 3—38478
plasma diagnostics by cyclotron radiation 3—20629
plasma drift instability, freq. entrainment by nonlinear effects at electron cyclotron resonance 3—26885
plasma drift waves, absorption of HF power at cyclotron resonance 3—20531
plasma electron and ion cyclotron harmonic waves dispersion curves for generalised Bernstein modes 3—29967
plasma electron cyclotron heating in Tokamak TM-3 3—20572
plasma electrostatic ion cyclotron and ion acoustic wave coupling 3—29974

cyclotron resonance continued
plasma e.m. fast wave damping at the second harmonic of the ion cyclotron frequency 3—20461
plasma e.m. waves, nonlinear generation of harmonics of the cyclotron frequency 3—20466
plasma heating, nonuniform magnetic field, stochastic character 3—4658
plasma in ionosphere 3—12793
plasma ion cyclotron drift loss-cone instability in a coexisting cold plasma 3—26886
plasma ion cyclotron instability in current-carrying plasmas with anisotropic temperatures 3—20488
plasma ion cyclotron wave heating, non linear theory 3—20557
plasma ion heating by mixing of e.m. waves near electron cyclotron resonance 3—20580
plasma ion-cyclotron oscillations, dispersion 3—36181
plasma kinetic instabilities at cyclotron resonance in Gabor magnetron, expt. obs. 3—26892
plasma microwave absorption and conversion at upper hybrid resonance, efficiency near cyclotron resonance 3—17582
plasma parametric instabilities at upper hybrid and cyclotron harmonic freqs., heating obs. 3—38480
plasma particle motion near electron cyclotron resonance 3—20418
plasma RF heating in Heliotron D 3—20554
plasma wave damping in the lower hybrid frequency range 3—23856
plasma waves, nonlinear modulation 3—23864
plasmas, cold inhomogeneous, energy absorption, Herlofson paradox 3—20452
polarons, plasma-phonon interactions 3—36572
reflection of charged particles by magnetic mirror at electron cyclotron resonance 3—20607
reflex discharge, cyclotron harmonic waves 3—38447
rotating plasma, resonant cyclotronic instability *(Russian)* 3—14544
semiconductor, interband transitions of hot holes, and cyclotron reson. of light holes *(Russian)* 3—8109
semiconductor, nondegenerate, mag. field depend. at i.r. freq. 3—36533
semiconductor, polar, nondegenerate, cyclotron phonon reson. linewidth, mag. field depend. 3—15132
AgBr, resonant electron-phonon interaction, crystal imperfections 3—36387
Bi in far i.r., quantum aspects and electrodynamics 3—33786
CO_2/H_2 system, ion-molecule reaction rates meas. 3—26721
n-CdSe, of shallow impurity states, cond. electron effective masses 3—2026
CdTe, electron-phonon interaction, far i.r. cyclotron resonance absorption 3—36388
n-CdTe, of shallow impurity states, cond. electron effective masses 3—2026
Ga acoustic geometric and acoustic cyclotron resonances 3—8096
n-GaAs, of shallow impurity states, cond. electron effective masses 3—2026
p-GaP, hole effective mass determ. 3—27215
Ge, interband transitions of hot holes, and cyclotron reson. of light holes *(Russian)* 3—8109
Ge, optically pumped, evaporation of metallic exciton droplets, excitons time decay monitored by cyclotron resonance method 3—18106
n-Ge:Sb far i.r. cyclotron reson. 3—15127
n-InP, of shallow impurity states, cond. electron effective masses 3—2026
InSb, i.r., in pulsed mag. fields up to 1.4 MG 3—30405
n-InSb, strongly compensated, radiation transmission depend. on mag. field and temp. 3—11851
n-InSb donor deionisation, impurity cond., CW laser cyclotron reson., magnetocond., temp. depend. 3—15149
n-InSb tunable far i.r. radiations from hot electrons 3—34442
K cyclotron phase resonance transmission at 116 GHz, Fermi-liquid effects 3—20999
N_2O/H_2 and N_2O/CH_4 mixtures, ion-molecule reaction rates meas. 3—26722
Na cyclotron phase resonance transmission at 116 GHz, Fermi-liquid effects 3—20999
Ni, study of Fermi surfaces and effective mass 3—15125
Pb, freq. and temp. depend. of electron-phonon interactions for freq. up to 500 GHz 3—38787
p-Si:B, effect of positively charged acceptor centres 3—36528
Te, electron-phonon interaction, far i.r. cyclotron resonance absorption 3—36388
Te, inactive mode cyclotron resonance absorption 3—8106
Te, valence band structure determ., consistent with k.p perturbation model 3—38794
ZnO:Ga, shallow bound states, cyclotron reson., Zeeman splitting, 30-100 cm^{-1}, 5-100K 3—2028

cyclotrons
see also microtrons; synchrocyclotrons
80 MeV variable energy, at Univ. of Louvain, status report 3—10022
200 MeV, variable energy, design study 3—10017
acceleration of heavy ions 3—10030
with active monochromatization system, optimization of beam acceleration and extraction conditions 3—16484
AEG-compact, design of extraction system 3—10025
axial injection system of Grenoble cyclotron, France 3—13399
beam handling, optimization for high resolution studies of nuclei 3—13397
Berkeley 88 inch, wide band driven r.f. system 3—13372
Berkeley 88-in cyclotron, USA, for heavy ion acceleration 3—13391
Calcutta, variable energy, status report 3—10021
compact, for physics, nuclear medicine and neutron therapy 3—19251
conference, Vancouver, Canada (1972) 3—10010
design, future trends, review 3—10012
Eindhoven A.V.F., automatic control, measurements 3—13380
Eindhoven A.V.F., automatic control, measuring instruments 3—13379
explosive ultrahigh magnetic field accelerators, possible designs and applications 3—6051
heavy ion acceleration, alternates to cyclotron 3—10013
Indiana Univ. 200 MeV cyclotron beam line, cryopumping tests 3—13368
Indiana Univ. facility, computer control 3—13376

cyclotrons continued
Indiana Univ. facility, current status 3—10011
Indiana university, USA, design study for split beam operation 3—16486
Indiana University, USA, resonant depolarization effects for polarized beams 3—19273
injection systems 3—13398
internal rotating target for 16 MeV cyclotron 3—25841
ion beams, neutrals formation 3—28633
isochronous, at Julich, Germany, double-monochromator system 3—16487
isochronous, at Julich, Germany, system for emittance measurements 3—19274
isochronous, horizontal motion and phase dilatation of internally injected ion beam 3—25838
isochronous, particle revolution frequency 3—28628
isochronous, separated-sector, comparison of various geometries 3—19250
medical applications, selection of size 3—22165
medical uses of cyclotron of Harvard university, USA 3—22158
Michigan university, USA, beam quality improvement 3—19272
nanosecond α-decays, fast pulsed beam meas. technique 3—35486
neutron pulsing by deflection bunching by cyclotron of Atomic Energy Institute, Moscow 3—28634
neutron therapy 3—22166
neutron therapy facility 3—22162
orbit studies of Indiana university cyclotron, USA 3—16472
particle bunches, reduction of repetition frequency 3—22427
particle orbits, computer programs for injection, acceleration and extraction 3—274
radionuclide production by cyclotron of Argonne cancer research hospital, USA 3—22161
separated sector cyclotron for heavy ion acceleration 3—13393
separated sector cyclotron of Oak Ridge, USA for heavy ion acceleration 3—13392
short lived radionuclides and positron emitter source for medicine 3—273
SIN, computer control, standard control components 3—13378
SIN, r.f. system, cavity and power amplifier 3—13373
SIN ring, status report, meson beam production 3—10023
spinning wheel target system, radioisotope production cross-section meas. 3—16499
split pole, heavy ions, combination with Van de Graaff accelerator 3—10015
tandem-cyclotrons of JINR, Dubna, USSR, acceleration of Xe ions 3—13390
Texas A&M cyclotron, freq. stabilization by injection locking 3—13369
Texas A and M cyclotron, USA, for heavy ion beams with cold-cathode source 3—13402
thin shield walls, radiation leakage 3—19255
transport processes study in discharge tubes 3—20668
TRIUMF, CAMAC control applications 3—13375
TRIUMF, control system 3—13374
TRIUMF, effect of magnetic imperfections on beam quality 3—19270
TRIUMF, effects of axial misalignment of dees 3—19249
TRIUMF, medical uses 3—22164
TRIUMF, optimization of phase acceptance 3—16485
TRIUMF, r.f. accelerating voltage control and stabilization 3—13370
TRIUMF, r.f. amplifier and resonator system 3—13371
TRIUMF, Victoria Univ., 300 MeV pion channel 3—25837
TRIUMF 500 MeV cyclotron, Vancouver, Canada, H^- injection system 3—13401
TRIUMF central region, progress report 3—10019
TRIUMF project, progress report 3—13364
d polarized ion source, for Birmingham cyclotron, England 3—13400
mass determination in body by neutron activation analysis 3—22163
Czochralski method *see crystal growth from melt*
D-layer *see D-region*
D-region
charges in D-region ion chemistry during solar flares 3—3109
differential-absorption, differential-phase partial-reflection experiments 3—12805
effective electron loss rate in lower D-region during solar X-ray flare events 3—3110
effective recombination coeff., theoretical estimate 3—3082
electron densities, during solar maximum and minimum 3—3089
electron densities from rocket meas. using l.f. radio propagation and d.c. probe techniques 3—16031
electron densities in midlatitude D-region diurnal and seasonal var. under quiet conditions 3—3115
electron density meas., comparison of two ground-based techniques 3—3112
electron density meas. by incoherent-scatter technique at Millstone Hill 3—3114
electron density profiles, comparison of two ground-based techniques 3—3113
electron density profiles, dependence on solar zenith angle *(Russian)* 3—3073
electron density profiles rel. to experimental techniques 3—3111
electron heating by a horizontal terrestrial current carrying wire 3—12813
energetic electron precipitation as source of night-time ionization 3—31431
equatorial, positive ion composition meas. 3—3093
f.m.c.w. partial reflection meas. of D-region, preliminary investigation 3—16032
gas clustering to alkali metal ions, rate constants 3—3105
h.f. radiowave absorption meas. at low latitude station 3—9332
ion chemistry, conference (Urbana, USA, July 1971) 3—3083
ion density model rel. to diurnal var. of electron density 3—3116
ion-neutral reactions 3—3104
ionisation, contribution of hard solar X-radiation 3—21967
ionisation at sunrise and during daytime, contribution of solar corpuscular streams 3—34946
ionization charges and electron densities from partial reflection differential absorption experiments 3—5521
ionization sources, cosmic and solar X-ray and u.v. radiation 3—3087
D-region continued
lower thermosphere, minor neutral constituents, photochemistry and transport 3—3043
lunar variations from long-path 10.2 kHz phase measurements 3—16027
negative ion chemistry 3—3101
negative ion composition 3—3102
negative ion conc. 3—3103
negative-ion changes during sudden ionospheric disturbances 3—25281
negative-ion composition of normal daytime D-region 3—25282
neutral gas winds, density changes and A3 absorption meas., correlation studies 3—3118
nightglow, precipitating energetic electrons 3—3090
nighttime, ionization contribution by cosmic X-rays 3—3091
nocturnal, ionization effects of celestial X-ray sources 3—3360
nonsolar related periodic variations, sources 3—9340
polar cap absorption events, solar electrons and alpha particle effects 3—16030
positive ion chemistry, ion-molecule reaction rates 3—3092
positive ion composition, dependence on O and H concentration 3—3097
positive ions and Winter anomaly of D-region ionization, conductivity measurements 3—3117
radiowave absorption rel. to 10-mb winds and temp. during IQSY 3—9331
recombination coefficients and X-ray flux during 1972, January 22 solar flare 3—31437
reflection effects on the differential phase expt. 3—18889
review of ionospheric D- and E-region studies, outstanding problems 3—3119
rocket sampling, Monte Carlo simulation 3—12859
sluggishness, comparisons of direct and indirect solar X-ray emissions 3—16023
solar cosmic ray bombardment at polar latitudes 3—25295
sudden field anomalies effect on 164 kHz waves rel. to D-region seasonal structure var. 3—25286
symmetric double probe, ionospheric plasma temperature 3—28087
wind meas. from fading of partially reflected radio waves 3—31432
H_2O cluster ions, shock layer meas. of decomposition reaction rate 3—3106
$H_3O^+.(H_2O)_n$ recombination with electrons 3—3107
NO concentration during polar cap absorption event 3—3085
O^-, O^-_2 and O^-_3 clustering rates with H_2O vapour 3—3108
O_2 photoionization rates, CO_2 absorption 3—3088
O_2^+ as source of ionisation in D-region 3—16026
O_2^+ as source of water cluster ions 3—3096
D/A conversion *see digital-analogue conversion*
damage, radiation *see radiation effects*
damming *see dams*
damping
see also internal friction
acoustic dampers, energy dissipation mechanism 3—31958
atmospheric microturbulence, solar equivalent widths, excitation potential, wavelength 3—3333
beam, monosymmetrical thin-walled, dynamic stability 3—19475
beams and plates, flexural mode absorbers, synthesis and investigation 3—26097
built-up structures 3—16672
conductors, nonlinear Landau damping of u.s. waves 3—24220
configurations with stabilizing influence on nonconservative systems 3—16666
dynamics of angular motion of solid body with rotating rotor accounting for energy dissipation *(Russian)* 3—13545
electron plasma oscills. in a uniform electric field, classical Ohmic heating effects 3—4645
electronic, in pendant accelerometers, operation, construction and static behaviour 3—13218
electrostatic oscills. in plasmas with cutoff distributions 3—4646
finite amplitude electron wave damping in plasma 3—20624
flexural damping capacity, meas. apparatus 3—9833
graphite, pyrolytic and single cryst., Alfven wave propag. and damping, 35 GHz 3—30510
gravity models of mirror field of collisionless plasma, stability of modes 3—7521
harmonic oscillator with stochastic frequency, Brownian motion 3—37897
hydrodynamic modes, effect of chemical reactions 3—11358
impact damper, response to stationary random excitation 3—28846
interacting particle system, Schrodinger type equation with damping 3—26152
ion acoustic waves, in a low density Cs plasma *(French)* 3—14558
ion Landau damping, drift wave stabilisation in a sheared magnetic field 3—20506
ion Landau damping of plasma drift wave in a sheared magnetic field 3—20523
ionic crystals, charge cloud dislocation damping 3—36320
Landau, in warm homogeneous plasmas, energy absorption in cold inhomogeneous plasmas, the Herlofson paradox 3—20452
Landau, of hydromagnetic waves, plasma heating and acceleration 3—4657
Landau, type III solar radiobursts, effect of radial density gradient 3—28136
Landau damping as dissipation mechanism in E-layer and resistors 3—7550
Landau damping of electron plasma wave, modulation instability 3—29965
large amplitude plasma oscillations, electron two-stream instability 3—7525
l.f. internal friction, measurement instrumentation system 3—28467
meas. of structure damping when subjected to a spatially-distributed random force 3—3753
meteorolgical data assimilation, h.f. motion damping in four-dimensional models 3—28023
MHD waves in astrophysical plasma 3—3281
multidegree of freedom structure, frictionally damped systems, linearized analysis 3—3936
neutron star models, pulsational damping rel. to magnetic field and structure 3—5594

damping continued
non-linear two degree of freedom dissipative system, calc. of forced vibrs., and stable regions 3−19400
optimum, for mass-spring accelerometer, minimum phase distortion 3−62
orthorhombic crystals, damped polaritons theory 3−14952
oscillating cylinders in fluid, Stokes' paradox 3−7409
oscillation damping by pulsed dynamic dampers 3−32394
plasma, inhomogeneous, nonlinear damping of potential monochromatic waves 3−17579
plasma, longitudinal ion oscillations, nonlinear damping 3−1499
plasma, magnetoactive, e.s. surface waves at transition layer, damping at electron cyclotron resonance 3−29966
plasma, nonlinear wave modulation, with account of nonlinear Landau damping 3−20481
plasma, rarefaction wave-propagation from growing sheath 3−7516
plasma electron waves in unbounded uniform magnetoplasma 3−33361
plasma e.m. fast wave damping at the second harmonic of the ion cyclotron frequency 3−20461
plasma finite amplitude electron wave damping 3−20534
plasma ion acoustic waves, dispersion and Landau damping 3−38463
plasma ion cyclotron wave heating, non linear theory 3−20557
plasma ion heating by geometrical Landau damping 3−20579
plasma MHD waves in dense plasma with nonequilibrium ions 3−26878
plasma mode, nonlinear 3−4642
plasma monochromatic waves, nonlinear damping, effect of plasma inhomogeneity 3−20487
plasma nonlinearly excited oscillations, saturation amplitude calc. taking into account collision damping 3−29975
plasma self consistent finite amplitude wave 3−7513
plasma surface waves propagation along plasma-vacuum channel, resonance effect 3−36169
plasma wave damping in the lower hybrid frequency range 3−23856
plasma waves, free-streaming, Hirshfield-Jacob criterion 3−1498
Pontryagin's maximum principle formulation, for structural mechanics problems 3−22680
pressure fluctuations on a membrane in gases of 1 atmosphere, acoustical radiation damping calc. through extended Nyquist theorem 3−17486
satellite nutational oscillations, damping with internal flywheel 3−25375
shells with openings, exptl. investigation of vibration attenuation *(Russian)* 3−28918
soliton in plasma 3−20491
spatial ion wave echoes, collisional damping increased by mag. mirror 3−23858
spherical standard sound source, internal impedance *(Japanese)* 3−28481
spinning elastic medium damped by conical shell, use of coupled pair of integral eqns. *(Russian)* 3−16649
stellar clusters, spherically-symmetric system, resonance damping of oscill. *(Russian)* 3−37441
structural members with inserts, damping characteristics improvement 3−37843
transmission of acoustic wave through circular plate, internal damping and vibrations *(Japanese)* 3−5694
uniaxial crystals, extraordinary i.r. spectrum, directional depend. of damping factors 3−18453
viscoelastic system, vibrating, method of averaging approach 3−22687
welded bodies, meas. of damping coeff. by resonance method, crack detection 3−18772
Cu, dislocations, u.s. attenuation, γ-radiation damage 3−17865
GaAs, i.r. refl., damping effects on plasmon-phonon spectrum *(Russian)* 3−8592
K plasma, drift waves, dispersion and damping, meas. 3−26882
Mo single crystal, dislocation damping of ultrasonic waves, internal friction study *(Russian)* 3−24211
SiC, i.r. refl., damping effects on plasmon-phonon spectrum *(Russian)* 3−8592
$YFeO_3$, of domain wall motion 3−30661

dams
see also civil engineering; hydroelectric power stations
water flow through porous media, equivalent nonlin. permeability coeff. calc. 3−7474

dark space *see discharges (electric)*

data acquisition
see also data handling; data processing; indicators; recorders
computer methods, for seismic data 3−9368
Coude spectrum scanner for Lowell Observatory, system for data acquisition and reduction 3−39757
digital tape recorder, portable, acquisition and retrieval system for field operation 3−25990
flue gas control system, alkali scrubbing facility instrumentation 3−25619
gas chromatographic data analytical system, computer-based 3−429
geophysical, digital systems for collecting and processing at sea 3−3176
laboratory experiments, hierarchical computing for data acquisition, data reduction and control 3−19354
for large aperture solenoid spectrometer at SLAC 3−28695
magnetic airborne recording system for collecting total field magnetic meas. and flight parameters 3−3174
measuring equipment, by computer *(Croatian)* 3−25961
meteorological non-synoptic observations, continuous data assimilation 3−28088
multiparameter system, at ORIC 3−28626
nuclear science, conference, Miami USA, (1972) 3−28622
ocean engineering, conference, New York (1972) 3−3228
on-line, of asymmetric interferograms 3−28549
photoelastic data 3−9837
in pulse counting experiments, general purpose interfacing for PDP-8 minicomputer 3−393
semi-automated hydrographic survey system, computer facility for collection and processing of depth and position data 3−3240
shore collection centre for marine data 3−3247
transient recorder 3−32113

data acquisition continued
TRIUMF cyclotron, control system 3−13374

data communication systems
see also computer peripheral equipment; data transmission systems
CAMAC as standard for astronomical instrumentation 3−31842

data compression
see also information theory
optical image transformation, in space frequency analysis system *(Russian)* 3−10450
Radio Astronomy Explorer B antenna aspect data processor 3−35218

data handling
see also codes; file organisation
automatic radioactive inventory system 3−28775
barotropic and multilevel baroclinic models of weather system for South Pacific, computer requirements 3−28055
digitised photographs, multiband and multiemulsion automated data handling 3−5999
marine meteorological data, international exchange 3−3023
for Mossbauer spectroscopy, velocity spectrometer *(German)* 3−22520
nuclear reactors, real-time experiments, multi-user on-line computer data-handling system 3−19355
windowing, energy loss in surface wave spectra 3−2938

data loggers
for atmospheric CO_2 profiles 3−18899
multichannel, using multiplexer, A/D convertor and minicomputer 3−25964
transient recorder 3−32113

data processing
see also administrative data processing; data handling; data reduction and analysis; medical information processing; optical information processing
absolute intensity determ. from X-ray scatt., data processing steps 3−4698
computer-controlled 24-inch telescope and on-line data processing system 3−31841
electronic calculator method, frequency-contrast characts. of film projector lenses *(Russian)* 3−9933
magnetotelluric sounding, computer processing of data *(Russian)* 3−5473
MAXIPULSE seismograms, debubbling data processing step 3−9122
Meteorological Office IBM 360/195 system, modelling and forecasting methods 3−28028
meteorology, using canonical decomposition and biplots 3−9278
NEL laser velocimeter, new developments and treatment of data 3−342
nuclear science, conference, Miami USA (1972) 3−28622
ocean engineering, conference, New York (1972) 3−3228
on-board system MLCB, design considerations 3−3243
optical, coherent, Fourier transform methods 3−6434
optical, of seismic data, deconvolution method 3−9363
optical radar, low order aberrations and apodization 3−6452
PHOENIX system for seismic data processing 3−9121
photoelastic data, measurement of isoclinic angle and isochromatic fringe number 3−9837
quantum field theory, model development and verification, cybernetic methodology 3−35729
seismic, autocorrelation matrix techniques 3−9366
seismic, review 3−9105
seismic appl. of interactive terminal systems to interpretation of computer-picked reflection information 3−12573
seismic data *(Japanese)* 3−25159
seismic exploration, review 3−37154
seismic wavelet processing, continuous velocity estimation, computer program 3−9123
terrestrial electrical soundings, automatic interpretation 3−9205
terrestrial tidal variations in gravity, data processing using Venedikov's method *(Russian)* 3−21978
wind speed, by computer-controlled system 3−28751
X-ray analysis for steel research *(Japanese)* 3−28740

data processing (administrative) *see administrative data processing*

data reduction and analysis
see also data acquisition
aircraft obs. of estuarine circulation and diffusion 3−3210
chemical analysis by nuclear activation, automated data analysis 3−37743
Coude spectrum scanner for Lowell Observatory, system for data acquisition and reduction 3−39757
cross-correlation techniques for detection of spectral information 3−37631
crystallography, electron diffraction data, structure analysis, computer aided, DEC-PDP-9, techniques 3−26956
diffractometry, structure analyses, validity and accuracy of current methods, standard derivations, rejection criteria 3−26928
elementary particle data bank, Durham, data analysis and model comparison project 3−29256
empirical meteorological data, computational procedure *(German)* 3−9286
e.s.r. data, paper tape recording and use of computers for signal improvement 3−27393
isometric contractions, motor unit action potential trains 3−35242
laboratory experiments, hierarchical computing for data acquisition, data reduction and control 3−19354
mean atmospheric temp. estimation from incomplete data 3−28052
measuring equipment, by computer *(Croatian)* 3−25961
meteorolgical data assimilation, h.f. motion damping in four-dimensional models 3−28023
meteorological non-synoptic observations, continuous data assimilation 3−28088
nuclear data ND-160 pulse height analyser modification for high capacity two-parameter analysis 3−23195
oxyhaemoglobin dissociation curves, computer-aided data reduction 3−28360
spectrometric measurements, Hilbert space algorithm 3−5940
structural analysis, powder diffraction photography, systematic data indexing, accuracy 3−26949
vibration test, digital control and analysis 3−34697

data reduction and analysis continued
  VIPUNEN programming system for analysis of large amounts of physical data, especially nuclear physics 3—23194
  wire chamber spectrometer, two-wire, 30-50 MeV protons, complete reduction of data on-line 3—322
  worldwide geometric satellite triangulation programme, data reduction and analysis methods 3—34759
  X-ray diffractometer, computer controlled, data collection, structure determination, hardware and software 3—26947
  $^{129}I_2$, data reduction method for hyperfine parameters from Mossbauer spectra 3—12084
data security *see security of data*
data tables *see collections of physical data*
data transmission equipment
  see also telemetering equipment
  Radio Astronomy Explorer B antenna aspect data processor 3—35218
data transmission systems
  see also data communication systems; telemetering systems
  CAMAC, fundamentals and specification status 3—32188
  CAMAC, review 3—32186
  CAMAC, specifications 3—32187
  CAMAC scalers, modular readout system 3—32190
  CAMAC system, for remote data acquisition 3—32189
  ionospheric scatter link digital data system with automatic interrogation *(Russian)* 3—3194
  optical communication link with subcarrier PCM and frequency multiplexing of digital data channels, noise immunity analysis 3—29051
  optical techniques, equipment availability, reliability, capacity analysis 3—797
dating, earth *see earth age*
dating, radioactive *see radioactive dating*
dawn *see twilight*
dawn chorus
  see also ionosphere
  No entries
dayglow *see airglow*
d.c. amplifiers
  chopper stabilized, flow meas. spontaneous heterogeneous character of flowing material 3—466
d.c. generators
  Faraday dynamo, demonstration model construction 3—9810
DDC *see direct digital control*
de Haas-van Alphen effect
  see also diamagnetic properties of substances; diamagnetism
  Dingle temp. for quantum oscills., phonon collisions effects *(Russian)* 3—4985
  in dislocated crystals 3—38779
  electronic lifetime anisotropy determ., mosaic spread enhancement of dHvA-Dingle temp. 3—11845
  field inhomogeneity requirements, absolute amplitude meas. 3—24372
  g-factor meas. in conduction electrons in Cu and K 3—1977
  g-factor of conduction electron, expression for orbital average as meas. in de Haas-van Alphen effect 3—24369
  metallic electrons, internal energy and susceptibility under de Haas-van Alphen conditions 3—24374
  semiconductor, oscills. appearance conditions *(Russian)* 3—8336
  Al, uniaxial compression effects on the third-zone Fermi surface 3—8093
  Au, electron-impurity scatt., anisotropy study using de Haas-van Alphen effect 3—11881
  Ca, band structure and Fermi surface 3—36522
  Cd, dHvA meas. of Fermi surface changes with uniaxial compression 3—20998
  Cd, Fermi surface 3—30396
  Cu, lattice dislocations effect on de Haas-van Alphen scatt. temp. 3—18069
  Cu alloy, meas. rel. to impurity scatt. of electrons 3—21055
  Cu-Fe alloy, spin-scatt. anisotropy and exchange coupling energy meas. 3—33781
  β′-CuZn, Fermi surface props. by the APW method, agreement with dHvA expts. 3—8097
  InSb, degenerate, oscillations, rel. to u.s. attenuation minima in mag. fields *(French)* 3—5041
  InSb oscillations, u.s. attenuation, degenerate crystals, direction of propagation and magnetic field, relaxation time *(French)* 3—27389
  Ir, Fermi surface, press. effect determ. 3—15123
  Ir, study of Fermi surface and cyclotron masses 3—38785
  Mo, Fermi surface, press. effect determ. 3—15122
  Mo-W dil. alloys, anisotropic point-scatt. lifetimes, Landau-level lifetimes 3—4962
  Os, Fermi surface, press. effect determ. 3—15123
  Pd, determ. of frequencies using augmented-plane-wave method 3—1983
  Pd, L-centred pocket of Fermi surface existence, magnetoacoustic evidence 3—8095
  Pd, press. dependence of external cross sectional area of Fermi surface 3—18075
  Re, Fermi surface, press. effect determ. 3—15122
  Ru, Fermi surface, press. effect determ. 3—15123
  Sb-Sn alloys, Fermi surface determ. 3—36527
  W, Fermi surface, press. effect determ. 3—15122
  Zn, dHvA meas. of Fermi surface changes with uniaxial compression 3—20998
Debye-Huckel theory
  see also electrical conductivity of electrolytic liquids
  LiF:MgF_2, Debye-Huckel interactions and solubility 3—4881
Debye-Scherrer cameras *see cameras; X-ray crystallography apparatus*
Debye temperature
  see also specific heat
  alkali halide solid solns., binary, Debye freq., Iosilevskii relation validity 3—30269
  alkali halide solid solutions, calculation from elastic constants *(Russian)* 3—38648
  alkali halides, calc. from ionic Rydberg potential function 3—38549
Debye temperature continued
  elastic Debye temp. calc. by averaging elastic stiffness coeffs. 3—36340
  metal, cubic, from elastic consts. 3—4817
  metal, rel. to monovacancy form. energy 3—36294
  metallic hexaborides, X-ray determ. *(Russian)* 3—27078
  metallic lattices, Lennard-Jones type potentials, Debye temps. calc. 3—38630
  powder, X-ray diffr. line integrated intensity changes, effective Debye parameter rel. to lattice strain 3—33424
  pyrocarbon saturated with Br, temp. dependence on resistivity between 90-298 K and thermoelectric power *(French)* 3—8214
  Al with dissolved ^{57}Fe, determination from temp. dependence of Lamb-Mossbauer factor 3—34258
  AlAs, Lindemann-Gilvarry melting law and Debye temp. 3—36393
  AlP, Lindemann-Gilvarry melting law and Debye temp. 3—36393
  Au_3Cu ordered alloys, use of Morse potential function calc. 3—7868
  Bi, up to 32 kbar, determ. from press. depend. of u.s. velocity *(Russian)* 3—7806
  Bp, Lindemann-Gilvarry melting law and Debye temp. 3—36393
  CdS, charact. temp., rel. to lattice oscillation spectra *(Russian)* 3—24221
  CdTe, determ. from elastic consts. extrapolated to 0 K 3—30170
  Cu, phonon freqs. at 80 K from neutron diffr., Deby temp. 0-300 K 3—33632
  Cu_3Au ordered alloys, use of Morse potential function calc. 3—7868
  D, inelastic coherent neutron scattering from solid 3—20832
  Fe, general force const. model calc. 3—30234
  H, inelastic coherent neutron scattering from solid 3—20832
  He adsorped films near monolayer densities, structure, estimation of exchange effects and Debye temp. 3—20910
  ^{4}He, solid, in h.c.p. phase at low densities, Debye temp. heat capacity and entropy meas. 3—30309
  In, lattice dynamics 3—20830
  InBi, elastic behaviour, u.s. wave velocity meas. 3—27048
  KCl, X-ray study 3—24224
  KCl-RbCl solid solutions, Debye temp. and lattice energy calcs. *(Russian)* 3—7862
  KCl(Br), X-ray diffraction determ. of temp. depend., thermal expansion contrib. 3—11694
  KI, calc. from elastic moduli 3—36394
  KI-KBr solid solutions, Debye temp. and lattice energy calcs. *(Russian)* 3—7862
  $LaNbO_4$, determ. from temp. depend. of spin-lattice relax. of Mo^{5+} 3—34207
  LiF, calc. from elastic moduli 3—36394
  LiF, of surface, H atom beam scatt. obs. 3—8010
  MgO, anal. of X-ray data at 2100°C 3—24225
  Mo, general force const. model calc. 3—30234
  NaBr-KBr solid solution *(Russian)* 3—20722
  NaCl, X-ray study 3—24224
  NaCl-KCl solid solution *(Russian)* 3—20722
  NaF, calc. from elastic moduli 3—36394
  Pb, and lattice dynamics using local model pseudopotential 3—17946
  PbS, room temp., X-ray determ. 3—27077
  RbCl, X-ray diffraction determ. of temp. depend., thermal expansion contrib. 3—11694
  Ta, general force const. model calc. 3—30234
  Ti_2O_3, determ. from low temp. sp. ht. 3—36428
  TiC_xO_y and TiN_xO_y, correl. with thermal expansion coeff. *(Russian)* 3—11751
  W, general force const. model calc. 3—30234
  YZn alloy, phonon dispersion curves determ. by inelastic neutron scattering 3—7886
  ZnSe, Debye temp. obtained by X-ray diffraction 3—1804
Debye-Waller factors
  see also lattice dynamics
  atomic mass. depend. of Debye-Waller temp. factors 3—14938
  Invar, 'magnetic anomaly', Mossbauer effect 3—39071
  liquid metal, Debye-Waller correction to theoretical interference function 3—24016
  semiconductor, sound instability conditions, hard photon and slow neutron scatt. *(Russian)* 3—7893
  Ag(111), LEED, thermal diffuse scattering, at low temp. 3—38702
  Au, crystallites, Debye-Waller factor rel. to size 3—36247
  Au thin films, temperature dependence, electron diffraction determination *(Russian)* 3—33637
  Cd, calc. from phonon dispersion studies 3—1731
  Fe, general force const. model calc. 3—30234
  H, inelastic coherent neutron scattering from solid 3—20832
  He absorbed films near monolayer densities, structure prediction of structure factor, pair-distribution function and Debye-Waller factor 3—20910
  He scatt. from surfaces, Debye-Waller theory 3—8002
  KCl, temp. depend., X-ray study 3—24224
  KCl Mossbauer γ-ray diffraction, anharmonic coupling constant 3—39059
  MgO, from thermal vibr. and dissociation at 2100°C 3—24225
  MgO, X-ray diffraction meas. 3—14939
  Mo, general force const. model calc. 3—30234
  NaCN, single crystal neutron diffr. obs. 3—27004
  NaCl, temp. depend., X-ray study 3—24224
  Nb:H, rel. to quasi-elastic neutron scatt. intensity 3—30230
  Ta, general force const. model calc. 3—30234
  W, general force const. model calc. 3—30234
decay periods (radioactive) *see radioactive decay periods*
decay schemes (radioactive) *see radioactive decay schemes*
decay theory (nuclear) *see nuclear decay theory*
decision theory *see decision theory and analysis*
decision theory and analysis
  see also Bayes methods; dynamic programming
  equivalent criteria for modularity of lattice of all physical decision effects 3—28835
decoding
  see also demodulation
  colour signals 3—22853
decomposition *see dissociation; precipitation*
decomposition, thermal *see chemical reactions*
defects, crystal *see crystal defects*

defibrillators
see also patient care; patient treatment
cardiac resuscitator, patent 3−35248
recent developments, applications, review 3−427

deformation
see also aging; bending; creep; elastic deformation; ferroelasticity; plastic deformation; recovery
atom displacements, reln. to rhombohedral deformation in certain compounds *(Russian)* 3−7653
coals, dynamic, due to sorption processes *(Russian)* 3−13223
fast reactor fuel assemblies, channel deformation analysis for swelling and thermal bowing 3−11077
holographic interferometry test specification for deform. and fault testing *(German)* 3−19154
homogeneous nonpiezoelectric anisotropic dielectric due to electric fields and mechanical traction 3−6269
lipid bilayer spheres, deform. and birefr. in mag. fields 3−37515
liquid cryst., smectic and cholesteric, light scatt. by plane texture deform. 3−12111
liquid crystal, cholesteric, shear effects on colour intensity and reflectance wavelengths 3−24709
liquid crystal, nematic, in elec. field 3−14681
Moire method for deformation meas. of spatial complicated elements *(German)* 3−19210
multilayer plates, stress analysis *(Russian)* 3−10288
planar structures, effect of transverse shear deformation on vibrations 3−28908
poly(ethylene terephthalate), bulk, effect of strain history on crystallization behaviour 3−1576
pretwisted curved beams of thin-walled open section 3−6197
reactor core, deformation due to stainless steel swelling and thermal bowing 3−6998
reinforced concrete members, short-time and long-time deflections, calculations 3−6239
residual stresses in a gently sloping spherical shell *(Russian)* 3−6208
rock beam, force-displacement curve rel. to failure, exptl. 3−31308
rock beam, force-displacement curve rel. to failure, theory 3−31307
rock test models with rigid and deformable inclusions, compression and simple shear 3−34829
rocks, geometric effects of vol. changes during tectonic processes 3−25157
shear, columns with variable rigidity and mass, frequency equations using associative matrices *(Russian)* 3−567
space photographic images, detection and correction 3−3822
transverse shear, composite beam deflection, microstructure theory 3−10272
Al alloys, resist. to torsional deform., strain-rate and temp. effect 3−2718
CdTe, thin films, photovoltaic effect dep. on mech. stress *(Russian)* 3−30518
Ni-Cr, shock deform. of K-state, ordering kinetics 3−21697

dekatrons
No entries

delay circuits
see also delay lines; phase shifters
automatic recording device for delayed coincidence curves 3−3865

delay elements (circuits) *see delay circuits*

delay lines
see also acoustic delay lines
high spatial resolution spark chambers, e.m. delay line readout 3−28675
multiwire proportional counter, with integral readout delay line 3−28646
multiwire proportional counters, high spatial resolution using e.m. delay line readouts 3−28647
optical modulation of coherent light beams for information processing *(Russian)* 3−19573
for proportional wire chamber readout 3−19313
supermonitor neutron recording channel, dead time reduction using short-circuited delay lines 3−32178

delays
see also delay circuits; distributed parameter systems
dispersion theory construction on basis of the delay-time concept *(Russian)* 3−684
photoelectric phase apparatus for transit time meas. *(Russian)* 3−16295
time, optimal regulator for metropolitan storm-sewer system 3−28408
transition metal oxide glass device, switching delay time measurement 3−18199
TV sync. pulse method for time and frequency comparisons, accuracy 3−22236
Te-As-Ge-Si thin film switch, accumulation effects 3−18200

Delbruck scattering *see nuclear reactions and scattering due to photons*

demagnetisation
see also magnetisation
film, ferromag., demagnetising factor, method of rot. moments *(Russian)* 3−21265
film, hypercritical, mag. field influence on ground state *(Russian)* 3−36699
Kapitza thermal boundary resistance between ^{3}HE and Cu, meas. from 10-160 mK 3−33712
Kittel structure and magnetic thin film, computer aided field distrib. calc. *(Polish)* 3−24584
nuclear, ultralow temperature production, review 3−35383
paramagnetics, strong, demagnetising effects *(Czech)* 3−12052
α-Fe, low temp. mag. relax. rel. to mag. aftereffect, susceptibility meas. 3−34168
^{3}He cooling by adiabatic solidification 3−25699
MnAlGe film, self-demagnetisation during thermomag. writing 3−24407
$(NH_4)_xWO_3$, ionic motion, n.m.r. obs., adiabatic demagnetisation method for correlation time for ionic jumps 3−7968

demagnetisation, adiabatic *see demagnetisation*

demagnetization *see demagnetisation*

Dember effect *see photoelectromagnetic effects*

demodulation
see also demodulators; modulation
broadband, of Doppler signals, gated zero crossing detector 3−476
heterodyne detection processing for atm. turbulence using u.s. light modulators 3−3195
particle beams, at optical frequencies 3−37990

demodulators
see also demodulation; discriminators
optical heterodyne imaging device, hologram instead of lens 3−5973
sampling, f.m. wideband, for laser Doppler velocimeter 3−6103

demonstrations
air-glass-air system, verification of Fresnel and Airy equations 3−37
angular momentum, vector props. 3−9802
atomic model 3−16368
bond formation, heating effects, model 3−28441
Bragg diffr. of μ-waves 3−9812
Brownian motion, using smoke cell 3−16369
classical mech., time-reversal invariance 3−28439
Coriolis force, demonstration for students 3−16363
critical angle refl., optics and electromagnetism 3−28436
crystal growth cine-film, edge-defined film-fed growth of sapphire 3−15636
crystal growth from melt 3−32018
Curie pt. 3−19131
diffraction patterns, random multiple aperture, obs. technique 3−31998
Doppler effect, interference and radiation resistance using a 'Sonalert' 3−32014
Doppler effect demonstration in classroom with laser *(Russian)* 3−52
electronics, diodes and transistors, digital appls. 3−28437
Faraday dynamo, construction 3−9810
film of gas flow patterns above NaCl melt 3−11569
film of liquid floating zones in simulated zero gravity 3−11360
film on crystal growth morphology 3−11558
film showing use of vertical thermal-imaging furnace Czochralski crystal growth 3−12294
fluidity meas. in metal casting 3−12487
gamma spectroscopy expts. using ^{116}In source 3−28443
Gaussian beam propagation, using rotation of a collimated laser beam 3−28449
Gedanken experiment, action and reaction in relativistic system 3−36
heat conduction, using liquid crystals 3−16370
inductor core 3−19132
interference effect in glass tube between reflections from inner and outer surfaces 3−16788
interference with polarised light 3−28442
kinematics, air track relative motion car 3−28440
lever as impedance machining device 3−33
light interference and coherence 3−32002
magnetic induction heating using linear air track 3−9806
magnetostatic field and induction law characts. using heavy bar electromagnet 3−28438
mechanics problem, turntable system, orbital motion 3−31993
MHD power generator for student laboratory 3−16359
Mossbauer effect meas., simple arrangement 3−9811
operators, noncommuting, optical demonstration 3−22217
optical props., using liquid crystals 3−16366
plane waves, interference, production of stationary waves 3−50
satellite navigation system, laboratory model expt. 3−31995
semiconductor diode characts., direct obs. technique 3−9798
sinusoidal oscillations, superposition 3−49
small pulse-operated X-ray apparatus for schools and laboratories *(German)* 3−37726
stationary waves, quantum theory of radiation 3−30
statistical mechanics, illustration for students using Monte Carlo computer program 3−22227
steam engine, room temp., for demonstration of second law of thermodynamics 3−32013
ultrasonic wave, standing, in liquid 3−36068
velocity of light, simple student equipment 3−16367
wave optics, simple demonstration using He-Ne laser *(Russian)* 3−13184
Zeeman effect, normal and anomalous, laboratory conditions for obs. 3−22218
$\gamma \to e^+e^-$, experiment for students 3−9794

dendrites
see also crystal growth
alloy powders obtained by liq. phase pulverization, crystn. *(Russian)* 3−27728
camphene, holographic anal. of morphology in dendrite growth 3−11564
growth, nonlinear theory 3−11565
ice, grown from melts, morphology of solid-liquid interface, dendritic and planar growth 3−38542
inhibition of dendritic electrocrystn. of Zn from doped alkali zincate soln. 3−12525
solidification, dendritic growth phenomenon, computer simulation 3−34500
spatial crystals (unrimed), free-fall patterns in atm. precip. 3−28021
steel, Ti stabilised austenitic stainless, intergranular corrosion, TiC, $Cr_{23}C_6$ dendritic precipitation 3−8853
Ag, twinned, disclination model and mismatch 3−33769
Al-Cu-Ni system, ternary composite growth from melt 3−39316
Bi-Sb alloy, growth on cleavage plane rel. to transverse striations on surface 3−11786
CdTe, isothermal growth from Te rich soln., dendritic growth with constitutional supercooling 3−11567
Co-Cr-Ni-Ta alloy, directional solidification, interdendritic structures 3−37031
Cu-Ni, dendrite growth using Bridgman, Czochralski and zone levelling growth methods 3−12291
InBi, dislocation density 3−11817
Mg-Zn alloys, non-homogeneity, Zn distribution, electron microprobe examination 3−8796
$NaNbO_3$, dendritic growth resulting from instability in growth from $NaBO_2$ flux melt 3−11566
Pb, grown by electrolysis, crystallographic features 3−4942

dendrites continued
  Pb electrodeposited, habit and morphology rel. to growth parameters 3−33767
  Pb-Sn-Cd alloys, eutectic, anomalous structures 3−37005
  Sn, effect of anisotropic mobility of interphase boundary on kinetics of growth 3−20978
  Sn supercooled melt, procedure for dendrite growth kinetics study at melt free surface 3−30378
  Sn-Pb alloys, off-eutectic, hysteresis in composite-dendrite transition 3−34507
  Sn-Sb, Sn-Pb, Sn-Sb-Pb alloys, columnar crystals, dendrite spacing *(Japanese)* 3−8792
  YIG, effect on mag. domains, Ferrimag. resonance and i.r. obs. 3−27379
  Zn, electrolytic, crystallographic and morphological characts. 3−20977

dendritic crystals *see dendrites*

densification
  see also density; powders; sintering
  borosilicate films, effect on Vickers microhardness 3−39377
  cermets, particle size effect on densification during compaction and sintering *(German)* 3−8973
  compact cermet prep. by impregnation of porous blanks with FeB_x alloys *(Russian)* 3−27730
  electrical contact material compacting by explosive powder metallurgy *(German)* 3−31117
  ferrite, hot pressing, for device appl. *(Polish)* 3−8972
  group VIII metal oxides, hot pressing *(Russian)* 3−15734
  metal powders, compaction at up to 10 kbar, hardness, electrical resistivity 3−12379
  porous solid, volume-diffusion-controlled final stage, anal. 3−5365
  powder, heterogeneous mixtures, compactibility during rolling *(Russian)* 3−27729
  Al_2O_3, spheres and powders, plastic flow during hot-pressing 3−39381
  $CoCr_2S_4$, vacuum hot pressing, magneto-optic material 3−18435
  CoO, press.-sintered, final stage densification kinetics 3−8955
  Cu powders, pore characteristics, reln. to compacting behaviour 3−2748
  Fe powders, particle shape effect on compactability *(Russian)* 3−27717
  Ge, hot pressing effects on neutron topographs 3−23983
  $MgAl_2O_4$, transition due to hot-pressing 3−18688
  Nb_2O_5, grain growth during sintering 3−37083
  Ni spheres, plastic flow during hot-pressing 3−39381
  Ni-Zn ferrite, hot pressing for mag. heads 3−2756
  Pb-2% Sb, spheres plastic flow during hot-pressing 3−39381
  SiO_2, noncrystalline, defect struct. and irradiation behaviour 3−4770
  ThO_2 and ThO_2-Y_2O_3 with NiO, sintering, effect of additives 3−18742
  UO_2 powders, u.s. treatment effect on sinterability 3−12438
  U_3Si, thermal conductivity and postirrad. densification, effects of swelling porosity 3−1058
  Y_2O_3 powder, sintering rel. to densification 3−12436

densimeters *see densitometry*

densitometers *see densitometry*

densitometry
  see also photometry
  atmospheric, meas. using transmission-type alpha particle gauge, math model for optimum design 3−335
  beam-width effects in high-resolution neutron radiography 3−23391
  black and white, colour materials, Soviet sensitometric instruments for, review *(Russian)* 3−6005
  catheter-densitometer system, analogue computer correction of sampling distortion 3−25993
  cement paste, γ-ray densitometer for particle settling obs. 3−9019
  cine film, colour positive developing control and printer tape preparation by minicomputer 3−35433
  film, thickness meas. by microdensitometric interoferogram method 3−13229
  flying-spot microdensitometry, anal. of radioactive resin standard radiographs 3−3792
  gamma ray densitometers, bulk density, seafloor soils, geotechnical probes 3−3217
  high temp. density measuring apparatus, using photon attenuation technique 3−26034
  microdensitometer, frequency contrast characteristics, black and white photographic materials *(Russian)* 3−19229
  microdensitometer using ITV cameras for intensity meas. of Weissenberg photograph 3−26943
  particle size distribution in air 3−28400
  radiation film badge densitometer, integrated semiautomatic system using minicomputer 3−28673
  X-ray diffraction power photograph analysis, digital microdensitometer, pattern recognition 3−26948
  B_2O_3 glass, static and dynamic PVT obs. using acoustic densitometer 3−1774
  $TiCl_4$, continuous determination of impurities during purification, using i.r. absorption *(Russian)* 3−26031

density
  see also atmospheric pressure and density; density measurement; density of gases; density of liquids; density of solids
  Apollo 11 fines, methane and carbide distrib. 3−18989
  bulk density of seafloor soils, obs. using geotechnical probes, and gamma-ray densitometer 3−3217
  cement paste density meas. rel. to settling of particles 3−9019
  Dirac delta function and density of states of several systems 3−3741
  Earth, density differentiation of matter and processes at core-mantle interface 3−15902
  Earth, density distribution limits in lower mantle *(Russian)* 3−12608
  Earth, heterogeneous, equation defining variation of density with depth *(Russian)* 3−5434
  Earth, modelling, by Monte Carlo inversion 3−12583
  Earth, modelling, by Monte Carlo inversion 3−12584
  electron density, electronic and gasdynamic properties of hypersonic wakes behind models moving in Ar *(Russian)* 3−7316
  galactic mass, orbit computational viewpoint 3−3371
  lunar fines bulk densities, effect on spectral emittance 3−12997

density continued
  molecular fluids, translational hydrodynamics and light scatt. 3−4030
  protogalaxies, density fluctuations due to turbulence in self-gravitating media 3−34999
  radiation energy density and heat flux in small rectangular cavities 3−10402
  solar corona density distrib., effect of solar wind 3−31570
  solar coronal active regions, X-ray obs. 3−35049
  weakly associated liquids, molecular theory of vibrational relaxation *(Russian)* 3−4477
  NaCl:Sr, bulk density, impurity precip. meas. 3−17862

density, atmospheric *see atmospheric pressure and density*

density, vapour *see density of gases*

density measurement
  see also gravimetry; hydrometers
  air, instrument for meas. rel. deviation from normal value 3−35552
  in high speed arc heated flows 3−28797
  ionospheric density profiles, manual processing of ionograms *(Russian)* 3−3182
  literature survey 3−450
  magnetic float densimeter, construction and applic. to organic liq. mixtures 3−22557
  Mars, by optical means 3−16158
  metals, using photon attenuation technique 3−26034
  n-pentane, at high press., u.s. technique 3−25672
  nonequilibrium low-density plasma, meas. density of charged particles, Langmuir probe 3−36196
  particle size, number density and velocity meas. using laser interferometry 3−4129
  powders, meas. apparatus, trapped air removal 3−3756
  single particles, immersed in paramagnetic fluid between electromagnet poles 3−19376
  small samples, paramagnetic technique 3−37776
  soil density gauge, gamma-ray backscatter, Monte-Carlo simulation 3−37724
  subsurface gamma density gauge, Monte Carlo calcs. 3−37725
  thin films, density profiles and changes with temp. 3−18043
  two-dimensional distrib. using dual hologram interferometry 3−208
  X-ray and gamma-ray absorption applic. *(Italian)* 3−35514
  C fibres, small samples, float-sink method 3−28476

density of gases
  air, instrument for meas. rel. deviation from normal value 3−35552
  freon-II, density meas., 110-200°C, determ. of eqn. of state *(Russian)* 3−20259
  stellar atm., search for density and press. inversions in high-temp., low gravity models 3−37345
  Kr, self diffusion coefficient, density depend. 3−17489

density of liquids
  see also hydrometers
  alkali borate system melts *(Japanese)* 3−21747
  cyclohexane-benzene mixture, determ. using magnetic float densimeter 3−22557
  fluorescein dye, molar volume determ. *(Russian)* 3−12179
  hydrodynamic approach to density fluctuations in simple liquids 3−7611
  measurement standard, standard liquids and measurement methods 3−32024
  phenylphosphine, 220 to 350 K 3−8476
  ternary mixtures, u.s. study, free volume 3−7853
  thermal conductivity of liquids density dependence in simplified model 3−1835
  thermal equilib. near crit. point, effect of convection instability on thermal conductivity 3−36442
  Al, temp dependence *(Russian)* 3−11798
  Ar, fluctuations, generalized hydrodynamic approach 3−24172
  Ar, molar volume along melting curve up to 10 kbar 3−27105
  Cs, near fusion-solidification point, and thermal expansion 3−4858
  Cs temps. to 1300°C, and thermal expansion 3−4859
  Cu_2S-FeS quasi-binary mixtures, temp. dependence 3−30168
  D_2O, effects on dynamic struct. 3−1566
  Ga, temp. dependence *(Russian)* 3−11798
  ^3He, liquid, sound propagation 3−11778
  ^4He, superfluid density under pressure near λ point 3−36452
  In, temp. dependence *(Russian)* 3−11798
  KCl, molten molar volumes meas. 3−15022
  KCl-TlCl, molten molar volumes meas. 3−15022
  KNO_3 aqueous dilute solutions 3−38621
  ND_3, +30 to −25°C, rel. to molecular volume 3−1814
  Na-In alloys, dil., 170-400°C, comparison with Na-Cd alloys 3−36994
  $NaNO_3$ aqueous dilute solutions 3−38621
  $Ni + NiCl_2$, liquid mixtures at 1323 K, determ. by γ-ray absorption 3−15020
  Rb temps. to 1300°C, and thermal expansion 3−4859
  RbCl, molten molar volumes meas. 3−15022
  RbCl-TlCl, molten molar volumes meas. 3−15022
  Sn, temp. dependence *(Russian)* 3−11798
  TlCl, molten molar volumes meas. 3−15022

density of solids
  alkali borate glasses *(Japanese)* 3−21747
  composite, C fibre reinforced Ni-matrix, elevated temp. stability, morphological and mech. prop. degradation 3−31138
  fibre, porosity, dependence of mech. props. *(Polish)* 3−31174
  glasses, radn. damage eff. due to electrons, neutrons or γ-rays *(Russian)* 3−11548
  ionic crystals, new method of calculation *(Russian)* 3−1685
  metals, verification of Thomas-Fermi model under high pressure 3−20816
  oxide glasses, correlation with refractive index, Newton-Drude relation 3−5902
  poly(ethylene terephthalate), cryst., annealing during polymerisation 3−31169
  polyethylene, oriented, h.p. annealing effect on struct. 3−20247
  polyethylene, single-textured, anisotropy of physicochem. props. rel. to morphology 3−20231
  PtSi, PtGe, characterization of single crystals 3−5268
  reactor core materials, radiation-induced void form. 3−29450

density of solids continued
steel, austenitic stainless, dispersion hardened, inhibited void form. during electron irrad. 3—26505
steel, maraging, quenching and ageing effect on change in dimensions 3—21666
steel, stainless, stabilized, void form. due to fast neutron irrad. 3—26503
steel, stainless, type 316, irrad. temp. depend. of void form. 3—26506
steel 1Kh17N2, mech. props. after vacuum heat treatment 3—21676
Superinvar alloy prep. and characteriz. 3—24945
trans-1,4-polyisoprene spherulite, deformation, small angle X-ray diffr. 3—27786
weathering influence on coal measure rocks 3—5443
Ag, intermediate stage sintering correlation of grain size and density 3—27713
Al, deformed, annealing of struct. discontinuities *(Russian)* 3—24854
Al_2O_3, rel. to grain size during sintering 3—2754
BeO, rel. to grain size during sintering 3—2754
Bi, up to 32 kbar, determ. from press. depend. of u.s. velocity *(Russian)* 3—7806
CaF_2:GdF_3, rel. to impurity incorporation 3—20759
$CaKAsO_4.8H_2O$, from X-ray data and refr. index 3—7664
$CaTi_2O_5$, formation, structure and props. deter. *(Russian)* 3—11596
Cd alloys, multicomponent impurities influence on density change during thermocyclic treatment *(Russian)* 3—8844
CoTi phase, comp. depend. 3—39337
Cu, rel. to grain size during sintering 3—2754
Cu and alloys, void form. on fast neutron irrad. *(French)* 3—26504
Cu-Ni alloy, depend. on composition 3—26991
Cu-Ni alloys, dependence of density on composition, determ. using absolute hydrostatic method *(German)* 3—37014
Cu_5As_2 single crysts. characteriz. *(Russian)* 3—12329
x CuO(1-y-x)PbO.y SiO_2, glass, infl. of CuO content *(Russian)* 3—11889
Fe, high-purity, influence of slip and mech. twinning *(Russian)* 3—7826
Fe-Si, influence of slip and mech. twinning *(Russian)* 3—7826
Fe-Si alloys, 0-24%Si, effects of furnace cooling and water quenching 3—36776
GaAs single crystals, point defects, nature and struct., density and X-ray meas. *(Russian)* 3—7753
Ge amorphous sputtered layer, effect of deposition rate 3—4934
Ge film, amorphous, effects of annealing 3—1958
$K_2O.2B_2O_3$, from struct. data 3—7665
LiF:Mg^{2+}, neutron irrad., annealing effect *(Russian)* 3—11656
$Na_2Ba_4Si_{10}O_{25}$ 3—24030
NiTi phase, comp. depend. 3—39337
Se glassy, elec. cond., density and crystn. rate rel. to S and Te additions 3—33887
SnO_2:Sb_2O_3 ceramics, effect of additives *(Japanese)* 3—8991
ThO_2-Mo cermet radioisotopic heat source, determ. by metallographic image analysis 3—18693
Ti cermet blanks, hot strain *(Russian)* 3—27732
$YTaO_4$, formation in Y_2O_3-Ta_2O_5 system *(Russian)* 3—12497
YTa_3O_0, formation in Y_2O_3-Ta_2O_5 system *(Russian)* 3—12497
ZnO, rel. to grain size during sintering 3—2754
density of states, electron *see electronic density of states*
deperming *see demagnetisation*
depolarisation *see polarisation*
desalination
fresh water production from sea, present state and trends in development *(German)* 3—7947
sea ice, stalactites growing beneath pack ice, observations, laboratory experiments, processes 3—9098
design aids
see also design engineering; nomograms
No entries
design engineering
see also project engineering; systems engineering
cable making machinery, noise abatement 3—35343
electronic apparatus, cooling *(German)* 3—25676
fusion reactor with pulsed system 3—4343
ion beams production, apparatus for, practical problems 3—6536
modular design principle, expt. facilities development *(German, English)* 3—1064
prestressed elastic structures, optimal design 3—513
structural, fibre composite material, stiffness 3—31130
desk-top computers *see minicomputers*
desorption
alkali halides photoinduced evaporation, exciton-phonon decay *(German)* 3—27186
cryostat, for 1.5-120K expts. 3—35382
crystal surface, phonon induced desorption of adatoms, computations for model system 3—18023
crystal surface, theory of phonon induced desorption of adatoms 3—18022
diffusion theory adsorption and desorption rate constants with experimental lifetimes, comparison 3—33736
electron stimulated desorption of ions from crystal surfaces, meas. apparatus 3—334
filaments, temp. measurement and control by Kelvin bridge method *(Spanish)* 3—32040
film, phase transform. rel. to work function and heat of desorption 3—20971
gas atoms at solid surface, diffusion theory 3—24336
gas release apparatus, for solid targets 3—28713
glass, surface water release in environmental effects on strength 3—24999
isotherm meas., fully automatic apparatus *(German)* 3—16531
metallic specimens of size a few cm^2, means of area meas. 3—32031
minerals, of N or Ar by BET method *(French)* 3—15065
packed spherical particles, pore-size distrib. from desorption isotherm 3—39412
refractory metal systems with N, O and C, mechanisms and kinetics of absorption and desorption 3—37035
replacement of H by CO_2 on a W surface, mechanism proposal *(Russian)* 3—8021
desorption continued
solid surface, mol. beam scattering 3—24769
steel, of hydrogen, kinetics *(French)* 3—1892
water vapour, by γ-irradiation 3—22306
zeolites, of pyridine at high temperatures, i.r. spectra study *(German)* 3—39152
Al, gaseous desorption, effect on photoelectric emission 3—15589
C, u.h.v. outgassing meas. up to 2200K 3—38731
CO, adsorption states on Ni films, elec. resist. obs. *(German)* 3—27184
CdS, oxygen photodesorption, influence of nonequilib. minority carriers 3—15210
Cr surfaces, remanent gases by laser-probe method 3—16250
Cu, photodesorption and thermodesorption of K *(French)* 3—27185
Fe, of hydrogen, kinetics *(French)* 3—1892
Ge, of H and D cooperative, (111) faces, pulsed time of flight mass spectrometry, exchange reactions, kinetics 3—36485
γ-MnO_2, of water, energetics 3—38729
Mo, anomalous photodesorption under intense u.v. light 3—33737
Mo, of Ar ion in glow discharge 3—15072
Mo(110) chemisorption of H_2 and N_2 3—11811
NaCl, diffusion and solubility of He, desorpt. study 3—33698
Nb, rare gas crystals epitaxially grown on (100) face, low energy electron diffraction and desorption 3—11654
Nb (111), of CO, electron stimulated 3—20944
Ni, of CO, thermal desorption spectrum, adsorption props. detn. *(Japanese)* 3—20931
Ni, polycryst., photodesorption of CO 3—24344
Ni polycrystalline surfaces, H_2 adsorption states at different temps., thermal desorption spectra 3—11801
Ni-Fe alloys, dil., Mossbauer obs. of hydrogen desorption *(French)* 3—1891
P_2 on Si(111) surface, desorption kinetics, AES and LEED obs. 3—1883
Pd surface of CO, induced by Nd laser, rate *(German)* 3—11807
Pt, of CO, thermal desorption method investigation of chemisorption 3—37143
Pt, of O_2, determ. of binding energy 3—4927
Rh, of O_2, reaction rate and state at high temp. and low press. *(French)* 3—36487
Ru, of CO 3—20936
Si, of H and D cooperative, (111) faces, pulsed time of flight mass spectrometry, exchange reactions, kinetics 3—36485
Si, surfaces, H and H_2O adsorption, desorption spectrometric results 3—11805
Ta, adsorption of O_2, thermodesorption effects *(Russian)* 3—15070
Ta, of hydrogen, kinetics, elec. resist. obs. *(French)* 3—1890
^{235m}U isomeric nucleus, as probe for surface adsorption and desorption studies 3—28714
W, adsorbed O_2, electron stimulated desorption 3—1886
W, desorption of SiO_2, autoelectronic microscope obs. *(Russian)* 3—8023
W, field evaporation, model and expt. 3—27600
W, of N_2, and adsorpt., λ-state of N_2 3—8019
W polycrystalline filament, mean residence time of K *(Japanese)* 3—24345
W surface, kinetics for CA(Sr)(Ba) ad-particles with variation of O_2 surface coverage 3—24346
W surface, of CO, field emission microscope obs. *(Japanese)* 3—20933
W(100), meas. of chemisorption of H_2 by electron stimulated desorption 3—36490
W(100) surface, electron stimulated desorption of CO, time-of-flight analysis of ions and neutrals 3—38730
detection (demodulation) *see demodulation*
detector circuits
see also demodulation; demodulators
i.r. radiation detectors with thermistors, theory of operation *(Russian)* 3—9851
l.f. synchronous detector, SD-1 modification *(Russian)* 3—10003
on-line, for extraction of average evoked potentials from periodic noise 3—3899
detectors
see also electric sensing devices; hydrophones; microwave detectors; nonelectric sensing devices; particle detectors; radiation detectors
characteristics, voltage standing wave ratio meas. *(Russian)* 3—6022
electric field, for space, circuit and testing *(Spanish)* 3—28606
electrical discharge, insulation testing, method 3—24644
electrochemical gas detectors, review 3—35551
Langmuir-Taylor detectors for ion beams 3—16533
l.f. synchronous detector, SD-1 modification *(Russian)* 3—10003
magnetic, in e.m. field vehicle guidance system, patent 3—6397
photometers, for liquid chromatography detection *(German)* 3—19370
polymer electret time-of-arrival detector for shock and detonation waves 3—22260
refractometers, for liquid chromatography detection *(German)* 3—19370
viscosity meas. system, continuous detection, patent 3—6174
determinants
see also matrix algebra
probability laws connected with Karle-Hauptman determinants in phase determs. 3—14645
tridiagonal secular, evaluation, coupled vibrating systems 3—6180
detonation
see also explosions; shock waves
blast wave propagation, analytic methods, review 3—33250
blasting, with and without presplitting, practical obs. of vibrations 3—9118
electrical contact material compacting by explosive powder metallurgy *(German)* 3—31117
electrical pulse from pulsations of explosion products vol. 3—33252
explosions gasdynamics, detonation, shock-wave, blast-wave studies, review 3—33253
heterogeneous systems, non-premixed phases, model *(Russian)* 3—27860
jet formation by explosives with lined trumpet cavities 3—11427
laser-supported detonation wave, lateral expansion 3—38466

detonation continued
point blasts in explosive gas with variable initial density *(Russian)* 3−29885
relaxation region, integral variational method 3−29881
seismic effects, a comparison with falling weights 3−18836
shock wave interaction with matrix discontinuities prod. acoustic oscillations and detonation *(German)* 3−29886
spherical detonation waves, propagation, finite steady-state velocities <Chapman-Jouguet value 3−33256
supernovae C-detonation with neutron star remnant 3−28183

deuterium
adsorption, on Si and Ge, cooperative, (111) faces, pulsed time of flight mass spectrometry, exchange reactions, kinetics 3−36485
anomalous ion heating in a laser heated deuterium plasma, neutron yield 3−14565
arc plasma channel from exploding metal tube, formation 3−20547
atom, Vibr. relax. of HF and DF 3−1290
atomic energy levels and multiplet tables 3−29483
atomic mass determ. 3−11107
atomic mass determ. 3−32998
Balmer series, wavelength meas., determ. of Rydberg constant 3−13203
collisions with F_2, Monte Carlo calc. of reaction rates and energy distributions of products 3−31255
collisions with laser excited methyl fluoride, vibrational relaxation 3−33162
collisions with methyl chloride, laser fluorescence study of vibrational energy transfer 3−33163
collisions with O^+, production of excited OD^+ 3−29747
collisions with T, hard sphere reactions, chattering 3−38321
concentration determ. with automatic mass spectrometer 3−32212
diffusion isotope effects in isotope mixtures, β-PdH$(D)_n$ 3−27136
electromigration in transition metals *(French)* 3−1823
electron impact ioniz. cross section meas. 3−33158
Galactic abundance, relevance to stellar nucleo-synthesis 3−22043
galactic centre, 327 MHz obs. and possible detection of D absorption line 3−31716
hyperfine pressure shift measurements in Ar buffer gas 3−35982
interstellar, obs. of DCN and HCN in Orion cloud, atomic abundances determ. 3−37486
lamps, suitability as short u.v. spectral irradiance standard *(Japanese)* 3−28551
laser beam interactions, anomalous heating of plasma 3−4662
liquid target for 400 MeV γ-ray interactions *(French)* 3−284
low-mass stars, min. mass for D main sequence evolution 3−31646
molecules in interstellar medium, radiative lifetime as function of vibrational quantum number 3−13098
nuclear spin relax. in rotating frame in solid D_2 3−34228
nuclear spin-lattice and spin-spin relax. in h.c.p. D_2 3−34227
plasma, collision of blobs ejected from theta pinch guns, compression expts. 3−20644
plasma, produced by fast rise time laser pulses 3−20562
plasma, temp. meas. from quantum bremsstrahlung using filter method and Si detector 3−36197
plasma arc, explosively driven, as energy source 3−36186
plasma confinement in magnetic mirror well 3−17656
plasma in megavolt theta pinch, shock heating to thermonuclear temps. 3−20561
plasma toroidal Z pinch ZT-1, plasma temperature, magnetic probe data, gross stability 3−20630
polarized negative beam production 3−22431
polarized particle beams, current state of physics and technology for prodn. 3−35727
Q branch Raman band, J depend. of the depolarization ratio of the rotational components 3−17430
quasi-elastic scattering cross sections in tissue like media 3−3593
on silica gel, adsorbed O_2, paramagnetic relaxation 3−37144
solid, cryst. struct. and phase transitions 3−15007
solid, librational anharmonicity effects 3−38641
solid, phonon dispersion relations from inelastic coherent neutron scattering 3−20832
solubility in metals and alloys *(French)* 3−2708
sorption, molecular sieve type, on alkali graphite intercalation compounds 3−33732
thermal diffusion in H_2 and HD at 85°C composition depend. *(German)* 3−14412
transport in LiH cryst., press. depend. 3−38681
vibrational relaxation in $HCl/D_2/{}^3He$ and $HCl/D_2/{}^4He$ mixtures 3−23628
ed→$e\pi^\pm\Delta(1236)$, coincidence meas. and nucleon cross-sect. detn. for Δ channels 3−17041
$\pi^\pm$ electroproduction from deuterium, coincidence expts. 3−14012
CO_2-O_3-D_2 laser, 10.6 μ, vibr. energy transfer from OD to CO_2 3−19603
μD, μ transfer to gaseous Xe in atomic collisions 3−20077
D/H ratio determ. for Jupiter, first extraterrestial obs. 3−28148
D-He scattering, H-He potential determ. from molecular beam expts. 3−11165
D-T plasma, concentric conduction type laser heating 3−36184
D-T plasma, energy balance instability in a thermonuclear reactor 3−38472
D-T targets, laser-driven implosion yielding thermonuclear burn conditions 3−14564
D-T two temperature plasma, laser concentric conduction heating 3−36185
$D + Cl_2 \rightarrow Cl + DCl$, temperature parameter for rotational state of product 3−31245
D_2, solid, specific heat, 0.5 to 5K 3−11747
p-D_2 molecular crystal structure, orientationally disordered, analysis 3−38546
D_2-H_2-inert gas mixtures, permeation through Pd tubes, model 3−7305
D_2 + Ne excitation and dissociation only observed 3−1274
D_2^+ and D^+ trapping in confined plasmas, calc. 3−17567
$F + D_2$ reaction, dynamics on a semiempirical valence-bond potential energy surface, Monte Carlo trajectories 3−25052
$F + H_2(D_2) \rightarrow H(D) + HF(DF)$ temperature parameter for rotational state of product 3−31245
(H_2, D_2) exchange reaction mechanism potential barrier 3−25054

deuterium continued
H-D ion mixture, plasma, h.f. heating under ion-ion hybrid resonance conditions *(Russian)* 3−1511
H-D three metre liquid nuclear target of stabilized density 3−32129
H_2 and D_2, ionisation shift between energy thresholds, meas. using new mathematical technique 3−29500
H_2-D_2 solid mixture, specific heat, 0.5 to 5K 3−11747
HD, depolarised Rayleigh lineshape, mol. reorientation rot. depend. 3−4433
He-D_2 total scatt. cross sections, 760-2600 m/sec 3−1294
NH_4Cl, orientational quadrupole relax., deuterium nuclei longit. relax. time 3−8483
$O^- + D_2 \rightarrow OD^- + D$, prohibited autodetachment 3−23616
in Pd-Ag alloy, effect on supercond. transition temp. 3−36675
$VD_{.5}$, vibrational and diffusional motions of deuterium in α and β phases 3−1820

deuterium compounds
see also heavy water
quinoxaline and quinoxaline-d_6, in durene, durene-d_{14}, naphthalene and naphthalene-d_{10}, mixed crystal electronic polarisation spectra 3−39141
sound velocity with increasing mol. wt. at 20°C *(German)* 3−11689
$CL + HI(DI) \rightarrow I + HCl(DCl)$, temperature parameter for rotational state of product 3−31245
$Cl + DI \rightarrow ClD + I$, distribution of reaction products 3−18786
DBF_2, thermodynamic props. calc. 3−39426
DBr, obs. of monomolecular and collision-induced predissociation in mass spectrum, radiative lifetimes 3−4471
DBr, Raman spectra, lattice modes in molecular crystal 3−5183
DBr spectra, photoelectron, ionisation energies, predissociation 3−23546
DCN, line emission from M42 (Orion Nebula) 3−31785
DCN hyperfine structure obs. in Orion Nebula, enrichment by chemical fractionation 3−31781
DCN in interstellar matter, obs. of Orion molecular cloud 3−37486
DCN-HCN isotopic pair inverse vibrational problem, intensity calc. 3−14347
DCP, deuterium quadrupole coupling const. 3−20168
DCl, Raman spectra, lattice modes in molecular crystal 3−5183
DCl, V→T, R and V→V relaxation, by laser fluorescence technique 3−33165
DCl crystal, molecular rotational vibr., neutron diffr. study 3−24036
DCl dimers trapped in monatomic solids, far-i.r. spectra, orientational motions 3−39139
DF, F-atom vibr. relax. rates, Monte Carlo calcs. 3−1289
DF, H- and D-atom vibr. relax. rates, Monte Carlo calcs. 3−1290
DF, vibr. and rot. energy transfer with HF, HCl and CO_2 3−26734
DF, vibr. relax., shock tube study 3−23626
DF, vibr. relax. rates in presence of deactivating gases 3−11316
DF, vibr. relax. times calc. 3−11315
DF laser, chem., CW, performance in unstable cylindrical confocal oscillators 3−10490
DF laser, diagnostic techniques, cavity characts. 3−9961
DF-CO_2 laser, chem., pulsed transfer 3−10469
DF-CO_2 laser, chem. transfer, efficiency rel. to gas flow rates and static press. 3−10503
DF-CO_2 laser, pulsed chem. transfer, kinetic nodel, computer simulation, review 3−10471
DF-HF laser, CW combustion/mixing laser, construction., props 3−10534
DF_2^-, vibr. struct. and equil. geom., ab initio calcs. 3−1171
DI, cryst. struct. and phase transition 3−15008
DNCO and DNCS, far-i.r. matrix isolated spectra, vibr. mode assignment 3−29656
D_2O, anharmonic force constant calc. *(Russian)* 3−1191
DOF, centrifugal distortion analysis of rot. spectrum 3−1237
D_2S^+ ion radical, rot. anal. of emission spectra, 400-500 nm 3−1207
$D_{0.53}WO_3$; cubic hydrogen tungsten bronze, crystal structure determ. 3−33501
HDO, Stark splitting of millimetre wave transitions, meas. technique 3−25763
V-D system, cryst. struct. and phase transitions 3−14728

deuteron effects
see also nuclear reactions and scattering due to deuterons
anthacene, fluorescence, polarisation effects, activation by 27.5 MeV deuterons *(German)* 3−24742
CsI:Tl, fluorescence, polarisation effects, activation by 27.5 MeV deuterons *(German)* 3−24742
polarisation effects of fluorescence light emitted by plastic NE 102A, activation by 27.5 MeV deuterons *(German)* 3−24742
Be, bombarded with deuterons, neutron production 3−25852
GaAs, irrad., defect distrib., luminesc. study *(Russian)* 3−1655
KI:Tl, fluorescence, polarisation effects, activation by 27.5 MeV deuterons *(German)* 3−24742
$LiNbO_3$, 140 keV bombardment, colour centre production, absorption band 3−2571
Nb-D(2 at.%), interstitial location determ. by channelling of deuterons *(German)* 3−27017
Ni-Fe film, oblique incidence evap., mag. anisotropy 3−34148
TiD, production and dependence of neutron yield on deuteron irradiation time 3−35465
TiT, production and dependence of neutron yield on deuteron irradiation time 3−35465

deuteron interactions
see also hyperon-deuteron interactions; nuclear reactions and scattering due to deuterons
asymptotic nucleon cross section excitation from deuterium data, effect of Fermi motion 3−29294
$dd \rightarrow \alpha + (mm)^0$, ABC effect obs., E=2.49 geV/c 3−32713
$dp \rightarrow dp\pi^+\pi^-$, s- and t-channel helicity nonconservation at 25 GeV/c 3−14078
ed deep inelastic scattering in continuum region, validity of scaling and sum rules 3−13936
γd, comparison between photoproduction and Compton scattering using VDM 3−13993
γd, photoproduction of ρ^0 and ω at 4.3 GeV 3−13945
γd multipion photoproduction up to 5 GeV, meas. of partial cross sections 3−13946
$\gamma d \rightarrow pp\pi^-$, anal. of expt. data to determine cross-section for $\gamma n \rightarrow \pi^- p$ 3−17052

deuteron interactions continued
- $\gamma d\to\pi^0 d$, coherent production of π^0 near first resonance *(French)* 3−6616
- $\gamma d\to\rho^0 d$, 6, 12 and 18 GeV, determ. of total and differential rho-nucleon cross sections 3−13881
- $\gamma d\to\rho^\circ d$, $\rho^- p$ meas. of cross-sections at 1-5 GeV 3−13929
- $K^- d$, 4.56 eV/c, study of final states with three charged particles and visible Λ 3−35839
- $K^- d$, 5.5 GeV/c, to $\Sigma^\pm\pi^\pm\pi^-(\pi^0)$, $\Sigma^- K^+ K^-$, $K^-\pi^- p$ final states in which hyperon is produced 3−29274
- $K^- d$, to $K^-\pi^+\pi^- d$ and $K^-\pi^+\pi^- n$ final states, 3.4 GeV/c, cross sections and resonance production 3−32719
- $K^- d$, total cross-sections, 15-65 GeV/c with Glauber correction *(Russian)* 3−26360
- $K^- d\to p\pi^-\Lambda$, polarization, matrix elements, double scattering terms 3−38074
- $K^- d\to\pi^\pm\Sigma^\pm n$ at rest, study of low-energy $\Sigma^\pm n$ interaction 3−29248
- $K^+ d\to K^0\pi^+ d$, coherent reaction at 2 GeV/c, determ. of cross section and parameters of ω trajectory 3−23166
- $nd\to nnp$, nucleon spectra analysis *(Russian)* 3−23128
- $\nu d\to\mu^- pp$, calc. of differential cross section, determ. of axial vector nucleon form factor 3−10682
- pd, 1.51-2.90 GeV/c, study of resonance production cross-sections in non-strange annihilation channels 3−17132
- pd, 5.55 GeV/c coherent interactions, inclusive features of π^+ spectra 3−4236
- pd, total cross-sections, 15-65 GeV/c with Glauber correction *(Russian)* 3−26360
- pd 1.09-3.45 GeV/c, study of reaction and resonance cross-sections, formation of storage particles 3−19747
- $pd\to(p_s)pp\pi^-$, 28 GeV/c, two-cluster form. obs. 3−4224
- $pd\to(p_s)pp\pi^-\pi^-\pi^+$, 28 GeV/c, two-cluster form. obs. 3−4224
- $pd\to ppn$, rescatt. effects on cross-section calcs. at 600 MeV *(Russian)* 3−4206
- pd topological and reaction cross sections, 1.51-2.90 GeV/c formation study 3−17131
- π^0 coherent photoproduction on deuterons in first resonance region, meas. of differential cross sections 3−13985
- π^0 coherent photoproduction on deuterium in first resonance region 3−29209
- π^0 single photoproduction on d in forward direction at 4 GeV meas. of cross-section ratio for $\gamma d\to(\pi^0 n)p/\gamma d(\pi^0 p)n$ 3−17024
- $\pi^- d$, total cross-sections, 15-65 GeV/c with Glauber correction *(Russian)* 3−26360
- $\pi^- d\to nn\gamma$, determ. of n-n scattering length using nonrelativistic graphical technique *(Russian)* 3−10772
- $\pi^- d\to pp\pi^-\pi^-$, 7 GeV/c, study of $\pi\pi$ scattering in isotopic-spin-2 channel 3−29278
- $\pi^- d\to ppx^{--}$, 7 GeV/c, search for I=2 multipion resonances 3−29271
- $\pi^+ d$, higher-mass boson prod. with mass in T region 3−14079
- $\pi^+ d\to K\pi\Lambda^0 p_s$, 7 GeV/c, obs. of $K^{*0}(890)$ production and decay modes, isospin conservation 3−29280
- $\pi^\pm d$, compilation of cross sections, variation with incident momentum over wide range 3−882

deuteron photodisintegration
- cross section dependence on off-shell T-matrix 3−35896
- electromagnetic structure by inclusion of virtual particle effects 3−6606
- isobar configuration effects, nonrelativistic calc. below threshold 3−29378
- $\gamma d\to\pi^- pp$, near first resonance study *(French)* 3−6628

deuteron polarisation
- application in $(d,p\gamma)$ angular correlation measurements 3−19874
- $K^- d\to p\pi^-\Lambda$, polarization, matrix elements, double scattering terms 3−38074
- nd scattering, 77-300 MeV, calc. of tensor moments of d polarisation 3−26341
- $^{16}O(d,d)$, $E_d=1.9$-3.0 MeV *(Russian)* 3−4318

deuteron reactions *see deuteron interactions*

deuteron scattering
- *see also hyperon-deuteron scattering; nuclear reactions and scattering due to deuterons; proton-deuteron scattering*
- asymptotic hadron scattering, Doppler effect in extraction of total neutron cross sections 3−6674
- breakup, in elastic scattering of projectile particle by neutron, determ. of low momentum transfer 3−10765
- ed elastic scatt., two-photon-exchange contribution to cross section 3−19691
- impact-factor representation for completely relativistic scattering, determ. of Lorentz-contracted wave function 3−890
- shadow and antishadow effects in scatt. of particles on deuterons 3−6681
- total cross section measurement, targets, protons, elementary particles *(Russian)* 3−282
- dd quasi-electric, quadrupole moment effect study in framework of Glauber theory 3−880
- ed, elastic, reviews 3−13875
- ed, inelastic, smearing effects due to deuteron structure ambiguities 3−29322
- ed, polarised target, reciprocal bootstrap on light cone 3−10652
- ed deep inelastic scatt., quark exclusion principle effects on structure functions 3−17023
- eD elastic scatt., calc. of deuteron e.m. form factors 3−16989
- $ed\to epn$, coincidence meas. of cross sections, determ. of e.m. form factors of n. 3−17055
- ed quasi elastic scatt., final state interaction effects at large t 3−17022
- ed scatt., inelastic, cross section meas. and excitation of $\Delta(1236)$ resonance 3−13919
- γd Compton scattering, 8 and 16 GeV, vector dominance model prediction 3−13882
- $K^+ d$, extraction of stable neutron scattering cross sections from deuteron expts. 3−26343
- $K^+ d$, total cross sect. meas., 0.57-1.16 GeV/c 3−19731
- N-d scattering at intermediate energies, multiple scattering series, S-wave separable model 3−38154
- nd, 77-300 MeV, calc. of tensor moments of d polarisation 3−26341

deuteron scattering continued
- Nd, elastic, comparison of exact and approx. calc. of single-scattering integral 3−35823
- Nd high-energy elastic, calc. using linearized propagator 3−6540
- pd, azimuthal correlations, protostatistical model analysis 3−14082
- pd elastic scatt. at 5 GeV, meas. of cross-sections in Coulomb interference range *(Russian)* 3−19738
- pd elastic scattering below 1.0 GeV/c, differential cross sections 3−23130
- πd, at high energies, application of Glauber theory including spin and isospin 3−32708
- $\pi d\to pp\eta'$, $\eta'\to\pi^+\pi^-\eta$, obs. for beam momenta 1.1-2.4 GeV/c 3−14081
- $\pi d\to\pi d$, determ. of recoil form factor for double-scattering term using eikonal approximation 3−4210
- $\pi d\to\pi d$, eikonal scatt. T-matrix 3−16927
- $\pi d\to\pi d$, Fermi motion and deuteron recoil in relativistic covariant, eikonal formalism 3−13823
- πd scatt. in $\Delta(1236)$ region, calc. of amplitude from Feynman diagrams *(Russian)* 3−19744

deuterons
- *see also cosmic ray deuterons*
- e.m. form factor, reln. to physical S matrix, relativistic parametrization 3−23060
- form factors, relationship with physical S matrix of n p scattering 3−29203
- form factors of e.m. current of np system determ. in terms of Jost matrix 3−26301
- gyromagnetic ratio determ. using n.m.r. in D_2O 3−4251
- magnetic moment, meson exchange effects 3−6610
- polarized ion source, for Birmingham cyclotron, England 3−13400
- structure ambiguities, smearing effects in inelastic and scattering 3−29322
- Yamaguchi-type potentials with repulsion in $^3S_1$ eigenchannel 3−29318
- $np\to d\pi^+\pi^-$ below 3.5 GeV/c, determ. of cross-sections, d production features and enhancements 3−32720
- $^2H(^3He,p)^4He$, proton asymmetry with polarised ^3He beam 3−35895
- $^2H(d,d)^2H$, 10 MeV, ang. distrib. of analyzing powers 3−10959
- $^2H(\mu,n\nu_\mu)n$, n-n interaction and possible off-shell effects 3−29376
- ^3He-d overlap function and ^3He charge form factor 3−29321
- KH_2PO_4-KD_2PO_4 system, isotope effects on deuteron orientation distrib. in short O-O bonds 3−1614
- $^{15}N(\gamma,d)^{13}C$, meas. of energy distrib. in giant resonance region *(Russian)* 3−35901

developers (photographic) *see photographic materials*

development, photographic *see photographic process*

development management *see research and development management*

diagnosis, patient *see patient diagnosis*

diagnostics, plasma *see plasma diagnostics*

diagrams
- *see also Bode diagrams; Feynman diagrams; flowcharting; nomograms; phase diagrams*
- insertions in hole and particle lines, nuclear matter calcs. 3−32788

diamagnetic properties of substances
- *see also de Haas-van Alphen effect; diamagnetism*
- inert gases, diamag. susceptibility, free-electron gas exchange correlation calc. 3−38204
- liquid crystal, nematic, susceptibility and anisotropy, temp. depend. *(French)* 3−38955
- superconducting dirty films, diamag. susceptibility rel. to fluctuating Cooper pairs 3−21170
- superconductor, thermal fluctuation induced diamagnetism above transition temp. 3−30575
- Ag-Ga alloys, liq., susceptibility, diamag. peak, temp. and comp. depend. *(Japanese)* 3−30600
- β-B, rhombohedral, susceptibility, temp. depend. 3−38960
- Be, value of diamagnetic Knight shift and its anisotropy 3−18380
- Bi, diamagnetism theory 3−8338
- Cd, magnetostriction, rel. to mag. field induced pseudo phase transition 3−24376
- $Cd_xHg_{1-x}Te$, diamag. susceptibility contrib. from crystal lattice 3−8339
- Cs_2Sb (IV) Cl_6, semiconducting crystals, superexchange electron interaction calc. 3−36705
- Cu-Ga(Ge)(Bi) alloys, liq., susceptibility, diamag, peak, temp. and comp. depend. *(Japanese)* 3−30600
- Cu_2O, obs. of exciton line splitting in mag. field, diamag. effects 3−12123
- $^{57}Fe^{3+}$ Mossbauer spectra in diamag. host lattice, hyperfine splitting 3−34253
- n-Ge, temp. depend. of anisotropy parameter *(Russian)* 3−24558
- Ge specific susceptibility rel. to disorder 3−30599
- Li, diamagnetic susceptibility 3−34096
- Mn_nSi_{2n-m}, obs. of metallic MnSi precipitates in diamag. matrix, mag. behaviour 3−27356
- $MnSn_2$, antiferromag., effective mag. fields at diamag. Sn atoms 3−5153
- Ni_xB, (x=1,2,3), mag. susceptibility, 100-1100K *(Russian)* 3−8333
- Pb-Sb-S, semicond., diamag. and paramag. terms in mag. susceptibility 3−8335
- PtSi, PtGe, molar susceptibility, characterization of single crystals 3−5268
- Se specific susceptibility rel. to disorder 3−30599
- n-Si, temp. depend. of anisotropy parameter *(Russian)* 3−24558

diamagnetic resonance *see cyclotron resonance*

diamagnetism
- *see also cyclotron resonance; de Haas-van Alphen effect; diamagnetic properties of substances*
- atomic, astronomical u.v. obs. of effects 3−19078
- Dirac theory for electron diamagnetism interpretation *(French)* 3−27354
- dirty superconductors, fluctuation induced diamagnetism 3−34012
- electrons confined by pot. barrier, diamag. susceptibility depend. on surface pot. 3−38957
- fluctuation-induced, in superconductor, theory and experiment comparison 3−2208

diamagnetism continued
- geomagnetic tail plasma sheet, spatial distrib. of magnetic field, diamagnetic effects 3—12824
- hydrocarbons, monocyclic unsaturated, mol. diamag. susceptibility, Hartree-Fock calc. 3—29601
- Landau diamagnetism, role of field induced surface currents 3—38956
- low density inversion layers, two-dimens-charge carrier lattice *(Russian)* 3—8273
- magnetism, introduction to the theory, monograph 3—2224
- molecules, diamag. susceptibility ab initio calc. 3—29567
- molecules, neutral, theory of diamagnetism 3—23509
- orbital diamagnetism of electron gas in infinite band *(Russian)* 3—34081
- semiconductor, of electron gas *(Russian)* 3—8336
- ten-electron system, perturbation theory calc. of diamagnetic susceptibility 3—23534
- $\{Ga_3\}[SnSb](Fe_3)O_{12}$ magnetic fields, induced diamagnetic tin atoms in antiferromagnetic garnets, Mossbauer effect 3—34270
- $\{GdCa_2\}[Sn_2](Fe_3)O_{12}$ magnetic fields, induced, diamagnetic tin atoms in antiferromagnetic garnets, Mossbauer effect 3—34270
- Al supercond. particles, zero-dimens., fluctuation diamagnetism 3—34013

diamond
- adamantane, pressure-induced phase transition 3—20872
- ballas, structure and texture 3—30090
- bonding, extended Huckel theory, total energy curve minimum 3—20707
- carbonado type, usefulness at high press., 2.5-3 megabar *(Russian)* 3—3778
- coherent bremsstrahlung, electron induced, determ. of polarisation degree *(Russian)* 3—38056
- crystal growth, catalyst-solvent process 3—12230
- cubic face, etch pit orientation changes 3—8032
- defect deep levels, molecular orbital treatment 3—30429
- p-diamond:B, seed crystal, growth by vapour deposition 3—36986
- diamond tool, spherical, designing for lens grinding 3—25746
- drilling of glass, temp. field calc. 3—22780
- electrical conductivity, transition to metallic state at 1 Mbar 3—18204
- electrical props. and cathodoluminescence, proton irradiation effects 3—24437
- e.p.r. of low-symmetry impurity centres *(Russian)* 3—12058
- e.s.r. of N impurity, exchange broadening of hyperfine components *(Russian)* 3—8436
- exciton energy spectrum *(Russian)* 3—11874
- gamma-ray Compton profiles, band structure test 3—11649
- growth history via dislocation struct. analysis, X-ray topography 3—24041
- Hartree-Fock formalism for crystalline ground state computations 3—18052
- high-resolution X-ray topographic techniques, review 3—17716
- intermediate type, defect associated with B1 absorpt. bands *(Russian)* 3—5220
- ion implanted with Si ions, SiC prep. *(Russian)* 3—8764
- luminescence quenching and zero-phonon line broadening associated with defect interactions 3—30860
- mech. of defect production 3—33521
- melting, h.p. characts. and nature of liq. carbon, model approach *(Russian)* 3—14981
- microtools, electrolytically formed 3—25745
- natural, cubic habit, internal struct., X-ray topography obs. 3—7642
- neutron irrad., semiconducting interstitials, e.s.r. studies 3—33571
- proton irradiated, cond. in disordered regions *(Russian)* 3—2072
- pulse irradiation of type I and type IIa 3—8673
- semiconducting, B as dominant acceptor 3—38810
- semiconducting, high field magnetoresistance 3—11912
- semiconducting, thermolum. excited by elec. field 3—21494
- semiconductor, defect energies and states, defect-molecule method, extended Huckel calc. 3—33838
- semiconductor, vacancies, electronic levels, defect-molecule model, extended Huckel approx. 3—33839
- semiconductor defect calc., LCAO-MO methods, extended Huckel theory 3—33840
- shock conversion from graphite *(Polish)* 3—24217
- spectra, absorption and luminescence, red region, neutron irradiation effects 3—36901
- structure type, elastic consts. temp. depend. 3—20785
- synthesis with non-conventional catalyst-solvents 3—20875
- synthetic, comp. of inclusions, X-ray microanal. study *(Russian)* 3—4767
- synthetic, internal struct., charact. growth on faces, growth history construct. 3—20702
- thermal cond. at room temp., impurity effects 3—30294
- transformation from graphite under high static pressure 3—33672
- type IIa, boundary scattering 3—1866
- type IIb, natural resonant scattering 3—1841
- types Ia and IIa, thermally stimulated currents, 20-400°C 3—30473
- u.v. and i.r. absorption spectra *(Russian)* 3—2578
- valence bands, bonding mol. orbitals applic. 3—24378
- Wannier function construction of band structure 3—38767
- C graphitisation of diamond, high pressure and temp., nucleation and planar growth 3—12450
- Li-implanted, elec. cond. after annealing at 1400°C *(Russian)* 3—2070

diaphragms
- *see also valves*
- human respiratory system, digital computer simulation 3—28361
- resonant, for pressure sensing, design 3—5852

dichroism
- *see also pleochroism*
- : 3—39119
- aliphatic amino acids, mag. circular dichroism, pH depend. *(French)* 3—12494
- alkali halide, coloured, periodic, plastic deformation induced 3—36894
- aminoquinolines, electronic spectra and nitrogen parameters from dichroism analysis 3—7180
- ammonium uranyl oxalate crysts., dichroism of i.r. absorpt. *(Russian)* 3—12178

dichroism continued
- benzene and derivatives, magnetic circular dichroism spectra 3—23567
- calcite, vacuum u.v. refl. spectra, dielec. consts. determ., dichroic absorpt. band 3—27510
- carbonyl compounds, aromatic, mag. circular dichroism study 3—26657
- chlorophylls in soln., circular dichroism spectra assignments 3—1301
- cholesteric liquid crystals, circular dichroism and rotatory dispersion near i.r. absorption bands 3—30830
- coupled chromophore system, absolute configuration by u.v. and circular dichroism spectra 3—17425
- cyclic, crystals with helical axis of symmetry, quantum mechanical and classical formulae *(Czech)* 3—32514
- cytochromes, oxidised, low-temp. mag. circular dichroism 3—8554
- trans-cisdiacetamide, and C- and N-deuterated derivatives, i.r. dichroism and out-of-plane vibr. 3—20165
- 1, 3-diazaazulene, allowed and forbidden n-π^* transition bands, dichroism analysis 3—11247
- 1, 3-diazaazulenes, π-π^* and n-π^* transition assignment by dichroism analysis 3—11246
- dielectric cylindrical particles, attenuation factors calc. for i.r. radiation scatt. and max. dichroism conditions 3—24698
- 2,2'-dimethyl-1,1'-binaphthyl anion radical circular dichroism and electronic spectra 3—29639
- p-dimethylamino-p'-nitrostilbene, circular measurements, surface fluorescence *(German)* 3—36938
- ferroelectric, anisotropic, at submillimetre wavelengths *(Russian)* 3—12197
- ionic cryst., magneto-optical spectra of colour centres 3—2580
- linear dichroism, adjunct to polarized cryst. spectroscopy 3—12130
- liquid crystal, cholesteric, i.r. circular dichroism, mol. vibrs. 3—5184
- measurement of fast changes, using double beam optical system *(German)* 3—32062
- metal cylindrical particles, attenuation factors calc. for i.r. radiation scatt. and max. dichroism conditions 3—24698
- monoclinic crystal, i.r. dichroism of lattice vibrations of the B_u species 3—2539
- monomolecular layers, pigment distribution, linear dichroism study 3—5887
- Orange II, electronic transitions polarisation by dichroism method 3—17417
- oscillating stress-plate polarization modulator for magnetic circular dichroism meas. 3—151
- particles, cylindrical, dichroism in light scatt., optical consts. depend. 3—13698
- phase plate, high-chromatic meas. technique for linear and circular dichroism 3—13280
- L-phenylalanine, mag. circular dichroism, pH depend. *(French)* 3—29638
- polymer, fully retarded expression for circular dichroism and Frenkel exciton model 3—12109
- polyvinylformal highly stretched films, polarised i.r. spectra, struct. 3—7273
- R-(+)-propylen sulphide, circular dichroism study 3—23560
- ring resonator, losses induced by nonequivocal Faraday phase shifter *(Russian)* 3—6493
- semiconductor cylindrical particles, attenuation factors calc. for i.r. radiation scatt. and max. dichroism conditions 3—24698
- sodium uranyl acetate, interpretation of Cotton effect 3—30797
- tryptophan, mag. circular dichroism, pH depend. *(French)* 3—17419
- tyrosine, mag. circular dichroism, pH depend. *(French)* 3—17419
- Au particles, cylindrical, dimensions depend. *(Russian)* 3—6426
- CaO, magnetic circular dichroism of F band 3—21451
- Cr complex, $2[Cr(en)_3Cl_3].KCl.6H_2O$, magnetic circular dichroism of first spin-forbidden transition 3—8600
- Cr(III) complex, $2Cren_3Cl_3KCl6H_2O$, linear dichroism in spin forbidden region 3—12130
- CuBr(Cl), mag. circular dichroism spectra obs. rel. to excitons 3—8556
- EuS thin films, mag. circular and linear dichroism spectra 3—2323
- $GaAs_{(1-x)}P_x$, optically induced paramagnetism obs. 3—2513
- KBr:Tl, mag. circular dichroism in C-band meas. of g-factors and electron-lattice coupling 3—18430
- KCl:Tl, stress induced dichroism and energy shifts in A, B and C absorption bands 3—21454
- KI with trapped S_2^-, S_3^- and Se_2^- mols., stress-induced linear dichroism 3—30848
- $K_3Ni_2F_7$, mag. circular dichroism meas. 3—12119
- $MnBr_4^{2-}$, magnetic circular dichroism studies on d-d transitions 3—26662
- $MnCl_4^{2-}$, magnetic circular dichroism studies on d-d transitions 3—26662
- Sm chalcogenide film, absorpt. spectra, mag. circular dichroism 3—2606
- UO_2 ion, in $(Bu_4N)UO_2(NO_3)_3$, mag. circular dichroism and electronic spectra, 18000 to 33000 cm^{-1} 3—24708
- YIG:Si, an torque data, analysis using small polaron theory 3—24398
- YIG(Si) photoinduced dichroism, role of first-order dichroism 3—18429

dictionaries *see glossaries*

dielectric breakdown *see electric breakdown*

dielectric breakdown diodes *see space-charge limited devices*

dielectric constant *see permittivity*

dielectric depolarisation
- polyglycine I(II), depolarisation thermocurrents rel. to dielec. relax. 3—30749

dielectric devices
- *see also capacitors; ferroelectric devices; insulators; piezoelectric devices; space-charge limited devices*
- pyroelectric detector arrays, characts. of high power lasers 3—25779
- pyroelectric katharometer, gas chromatography applications 3—22277

dielectric function *see dielectric properties of substances; optical constants*

dielectric hysteresis
- apparatus for investigating the electrical props. of ferroelectrics *(Russian)* 3—6016

dielectric hysteresis continued
liquid single crystal, study of hysteresis loop, spontaneous polarisation and coercive field 3–24026
triglycine sulphate thin film deposited by low temp. spinning technique, rel. to switching 3–39107
$BaTiO_3$, domain struct. and phase transition, illumination influence 3–15460
$BaTiO_3$ film, ferroelec., vacuum-evaporated 3–34317
$BaTiO_3$ polycrystalline, constant electric field influence on dielectric props. *(Russian)* 3–8532
KH_2PO_4, dielec. const. and 'hysteresis' loop rel. to γ irrad. 3–34304
KH_2PO_4, ferroelec., phase transition meas. 3–15459
KH_2PO_4, thermal hysteresis of ferroelec. transition 3–21372
KNO_3, coercive field of ferroelectric phase III single crystals 3–27473
$Pb(Zn_{1/3}Nb_{2/3})O_3$ and $Pb(Cd_{1/3}Nb_{2/3})O_3$, microdomain behaviour in diffuse phase transition region 3–15462
SbSI multiple domain effect, illumination induced, hysteresis loop 3–34299
$Sr_2Nb_2O_7$, ferroelectric single cryst., D-E loop at room temp. 3–21373
$SrT.TeO_2$, ferroelec., phase transition 3–15457
dielectric loss angle *see loss angle*
dielectric losses
see also loss-angle measurement
acrylonitrile-butadiene polymers, dielec. relaxation and losses 3–39091
alkali halide, impurity doped, review of meas. for Z-centres 3–8624
analyser, loss tangent, high voltage bridge method 3–24644
bromoform dil. solns. in nonpolar solvents, dielec. meas. and complex form. 3–8511
chlorinated diphenyls, temperature behaviour of loss factor in ionic conduction range *(German)* 3–36610
chloroform dil. solns. in nonpolar solvents, dielec. meas. and complex form. 3–8511
α, ω-dichloroalkanes, meas. at radio and visible freq. 3–12094
fluoroanisols in solution, microwave meas. 3–39075
fluorophenols in solution, microwave meas. 3–39075
iso-octyl phenoxy polyethoxy ethanol in dilute solutions of benzene, dielectric relaxation and losses 3–20220
liquid dielectrics, moisture content effects *(Russian)* 3–25020
liquids, element for obs., design *(Russian)* 3–6025
multilayer specimen, meas. of dielectric constant and loss tangent 3–8498
nonpolar liqs., microwave region meas., Debye expression 3–2489
1-phenyl-1-propanol, liquid, temp., pressure and freq. dependences 3–15450
phthalocyanines, microwave dielectric constant and conductivity 3–8501
polar materials, dielectric loss angle variation 3–39087
polyethylene, dielectric loss angle variation 3–39087
polymer, book contrib. 3–12092
polymer, nondestructive determ. using external capacitive probes 3–25805
polymer, pulsed gamma-neutron irrad. effects *(Russian)* 3–20256
polymer-diluent system, rel. to plasticization 3–4500
polyoxymethylenes, dielec. absorpt. and melting behaviour 3–30754
polyvinyl chloride, radiation eff. on dielec. strength, permittivity, loss and resistivity 3–18405
pyridines N-substituted long chains in dilute benzene solns., microwave absorption, determ. of dielectric permittivity and losses 3–15574
thiourea, 1.6 Hz to 20 MHz, near ferroelec. transition 3–30774
trichlorobenzene in solution, microwave meas. 3–39075
triglycine selenate, deuterated, ferroelec. and pyroelectric props. in phase transition region 3–34319
AgBr, photographic emulsion grains, ionic cond., dielec. loss, meas. 3–31283
$BaTiO_3$, depend. on freq., temp., and fast neutron irradiation rel. to phase transitions *(Russian)* 3–15464
$BaTiO_3$ polycrystalline, constant electric field influence on dielectric props. *(Russian)* 3–8532
$Ca_xN_{1-x}Fe_2O_4$ ferrite compounds, dependence on temp. and Ca ion conc. 3–15451
$CaO_xNiO_{1-x}Fe_2O_3$, dielectric props. *(French)* 3–34284
$Ca_5(PO_4)_3F$, fluorapatite, dielectric loss for various fluoride vacancy concs. 3–39088
Cs halides:Pb, Cd, meas. of impurity-vacancy dipoles, 90-180°C 3–11612
CsCl(Br)(I), Pb-centre studies 3–24725
$CsCuCl_3$, anomaly in meas. at structural transition 3–21414
Ge, amorphous, reactor irradiation expts., resistivity var. with heat treatment 3–15195
$KBr{:}OH^-$, dielec. loss due to tunnelling paraelec. defects reorientation, caloric meas. 3–36837
$NaCl{:}Mn^{2+}$, Fe, bulk crystals, phase transformations 3–4768
$Pb(Zr, Ti)O_3$, pyroelec. props., comp. and phase struct. depend., i.r. detector characteriz. 3–39098
SbSI, single cryst., polycryst., ceramic, comparison rel. to piezoceramic prep. 3–34301
Si, electron irradiation at 0.5K, a.c. conductivity changes dopant dependent 3–7794
Te-As-Ge-Si film, freq. depend. cond. and capacitance 3–2092
Te-As-Ge-Si thin film capacitors, frequency dependence of capacitance and conductance 3–27321
Y_2O_3, electron beam evaporated film, step response and bridge dielec. loss meas. 3–24320
dielectric materials
see also antiferroelectric materials; electrets; ferroelectric materials; insulating coatings; insulating materials; insulation; piezoelectric materials
alkali halide crystals, electric breakdown mechanism in presence of microroughness on the cathode *(Russian)* 3–8514
amorphous, Poole-Frenkel cond., calc. including hot electron effects 3–5015
anisotropic cantilever, deformation due to electric fields and mechanical traction 3–6269
book 3–8496
ceramics, properties, applications 3–2749
ceramics, thermal diffusion of injected impurities, props. 3–20901
dielectric materials continued
characterisation by thermal analysis techniques 3–39076
charge carriers, dynamical props., polaron theory 3–36559
dielectric crystals, thermal conductivity in the boundary scattering region 3–1723
electrochemical conference, Chicago, USA (1973) 3–38760
electron scattering by optical surface phonons 3–8003
electron-phonon interaction at very low temps. 3–1762
ferromagnetic dielec. plate, instability of magnetoelastic oscillations 3–36777
films, thin disordered, Kronig-Penney-type calculations for electron tunnelling 3–8254
free liquid surface, radiation pressure 3–13754
gap boundaries, electric discharge with formation of thin semiconductor layer *(Russian)* 3–7589
i.r. and Raman spectra for analysis of dielectric and insulating materials 3–39140
liquid breakdown, photographic study with picosecond time resolution 3–244
noise temperature and noise coefficient of temperature, measurement technique *(Russian)* 3–27459
nonstationary currents, and analogues from nonlinear wave theory 3–27259
organic, a.c. and d.c. conduction 3–38861
organic dielectric films, charge transport 3–38834
oxides of Al and Ta, growth of dielectric layers *(German)* 3–20951
phonon-phonon collisions and entropy fluctuations 3–1740
phonons interacting with high frequency sound, kinetic and hydrodynamic eqns. 3–1743
secondary electron emission, dispersion of emission time *(Russian)* 3–8695
space-charge-perturbed transient currents following time depend. injection 3–36605
spin phonon spectrometer 3–1754
spin-lattice relax. in dielec. with paramag. defects 3–5135
thin films, thermal conductivity and Poiseuille flow of phonons 3–1722
transparent, excitation of cascade ionization by strong alternating e.m. field *(Russian)* 3–8517
transparent, laser irrad., energy balance and dynamics of damage *(Russian)* 3–6498
transparent, laser surface damage, morphological asymmetry 3–757
transparent, optical strength reduction on laser radiation due to macroscopic defects 3–5175
transparent sphere, electromagnetic field intensity calc. *(Russian)* 3–37920
u.s. attenuation dependence on structural parameters 3–1705
u.s. thermo-absorption and nonlinear absorption, in hydrodynamic region 3–33613
$BaTiO_3{:}CeO_2$, non piezoelec. dielec. ceramic, electromechanical bond coeff. *(Russian)* 3–21365
KH_2PO_4, in vicinity of Curie point, ionic motion effect on refractive index 3–29141
KH_2PO_4-KD_2PO_4 system, structural studies and bonding in paraelectric phase 3–1614
$LiTaO_3$, paraelectric phase, struct. at 940 K, neutron diffr. obs. 3–30098
NaBr, paraelec. cryst., potential of F^-, calc. 3–36834
NaBr, paraelec. cryst., potential of F^-, theory 3–36835
NaCl, breakdown strength, temp. depend., −40 to +100°C *(Russian)* 3–18414
Pb-dielectric cermet film, refr. indices, ellipsometric meas. rel. to Maxwell Garnet theory 3–8544
RbH_2PO_4 in paraelectric and ferroelectric phases, Raman and vibration spectra of $(PO_4)^{3-}$ *(Russian)* 3–5191
$SrTiO_3$, (Ba, Sr) TiO_3, boundary layer dielectrics, permittivity and dispersion 3–2485
dielectric measurements
see also capacitance measurement; loss-angle measurement; permittivity measurement
correlation function analysis of noise voltage *(French)* 3–34281
Gopala Krishna's method for relax. time of polar solute in nonpolar solvent 3–12095
layer thickness, optical method *(Czech)* 3–22359
multilayer specimen, meas. of dielectric constant and loss tangent 3–8498
nonmagnetic material, meas. of dielectric const. in waveguide system with unknown movable reflecting load 3–16462
open-resonator technique 3–22925
dielectric phenomena
see also dielectric hysteresis; dielectric losses; dielectric relaxation; dielectric resonance; electric strength; ferroelectric phenomena; loss angle; piezoelectricity; solvated electrons
boiling dielectric fluids, ponderomotive forces, electrostatic fields, heat transfer 3–1801
book 3–8496
cavity field in nonlinear dielectric, calc. 3–22701
colloid particles, elec. interaction, constant surface-charge density 3–39401
deconvolution techniques for data analysis 3–24645
dielectric, semi-infinite, reflectivity and surface polaritons, rel. to spatial dispersion 3–34322
dipole interactions in liquid phase, statistical theory *(French)* 3–18402
electron liquid, dielectric response in generalised random phase approximation 3–38761
flexural deformation of an initially curved cuboid dielectric 3–28866
forces between parallel dielectric surfaces 3–33974
hereditary media, electrostatics, variational principle *(Italian)* 3–30740
in insulating substances *(French)* 3–30759
least squares analysis of complex weighted data, dielectric applications 3–34280
'memory waves' in homogeneous transparent dielec., exact soln. *(Russian)* 3–10294
naphthalene, Costa Ribeiro effect, rel. to resist 3–24426
Onsager theory of dipole moments for radially inhomogeneous permittivity 3–37126
photon momentum in dielectrics 3–859

dielectric phenomena continued
rectangular waveguide dielectric loaded bends, reflection coefficients 3−16690
semiconductor, organic, Costa Ribeiro effect, rel. to resist. 3−24426
theory, analogy with superfluidity theory 3−27153
transient currents rel. to relaxation time and sample to Debye length ratio *(French)* 3−34294
$CuGaS_2$, dielec. dispersion, phonon freqs., i.r. refl. spectrum 3−8585
H_2O, thermodielectric effect in vapour-ice transition 3−5156

dielectric polarisation
aftereffect in coaxial geometry, model 3−31980
crystals with large nonlinear optical effects *(German)* 3−6515
dioxane-water solns., nonlinear polarization 3−36832
electrostatic potential of point charge in dielectric solid, shell model 3−18407
ferroelectric, phase change induced by hydrostatic press. *(French)* 3−2497
ferroelectric displacement type, dispersion of dielec. nonlinearity 3−34313
gases, with elec. dipole moment, spontaneous polarization during condensation 3−20942
laser beam induced, reversible, ferroelectric memories, triglycine sulphate *(French)* 3−22967
perspex electrets in nonuniform fields 3−21362
1-phenyl-1-propanol, liquid, temp., pressure and freq. dependences 3−15450
PMMA, thermally stimulated current obs., −80°C to +130°C *(German)* 3−27280
PMMA solns., effect of chem. nature of solvent *(Russian)* 3−20257
polyethylene terephthalate electret, effect of crystallisation on homocharge and thermally stimulated currents 3−26976
pyrochlore type compounds, relaxation character, antiferroelectric transitions 3−36836
theoretical analysis, using principle of field superposition *(Russian)* 3−30744
thermally stimulated depolarization, phenomenological anal. *(Russian)* 3−34288
thermoelectret, volume polarization determ., sectioning technique 3−2488
thermoelectret charge of sealing wax, prep. temp. effect, barrier and bulk polarisation 3−39080
triglycine fluoroberylate: $Cu^{2+}(Cr^{3+})$, ferroelec. props., spontaneous polarisation 3−39099
triglycine selenate, deuterated, ferroelec. and pyroelectric props. in phase transition region 3−34319
triglycine sulphate, temp. effects in applied alternating field *(Russian)* 3−39097
triglycine sulphate thin film deposited by low temp. spinning technique, rel. to switching 3−39107
Ag_8GeS_6, argyrite, electret state *(Russian)* 3−34287
Ag_8SnS_6, canfieldite, electret state *(Russian)* 3−34287
$BaTiO_3$, 180° polarization reversal 3−34314
$BaTiO_3$, Barkhausen effect and stabilization of spontaneous polarization 3−34315
$BaTiO_3$, stabilisation of spontaneous polarisation *(Russian)* 3−12105
$BaTiO_3$ film, ferroelec., vacuum-evaporated 3−34317
$BaTiO_3$ polycrystalline, constant electric field influence on dielectric props. *(Russian)* 3−8532
$BaTiO_3$-$CaTiO_3$ (5 wt.%), large polarisation depend. photovoltages 3−33951
CO, spontaneous polarization during condensation 3−20942
CaF_2, space-charge electret, bilinear depolarisation dynamics 3−39094
CaF_2:X^{3+}, X=Ce, Pr, Sm, Eu, Tb polarisation storage 3−18406
CdS single crystal, persistent internal polarisation variation with illumination intensity 3−34289
CdS:S system as photoelectret electrophotographic layer, photopolarisation study 3−36833
KCl, dipolar complexes resulting from 1.5 MeV electron bombardment 3−12096
KCl:Cd, Pb, double crystal d.c. polarisation meas. rel. to $Pb^{2+}(Cd^{2+})$-vacancy dipole relax. 3−34293
KD_2PO_4, and phase transition behaviour 3−34290
KH_2PO_4, ferroelec., phase transition meas. 3−15459
$KNbO_3$, soft lattice vibr. modes, spontaneous polarisation and Curie constants 3−34303
$LiNbO_3$, z-cut, strain depend. of piezoelec. polarisation 3−30762
$(NH_4)_2Cd_2(SO_4)_3$, spontaneous polarization, temp. depend. 3−24662
$(NH_4)_2SO_4$, and elastic compliance at ferroelec. transition 3−30781
$Na(D_xH_{1-x})_3(SeO_3)_2$, and xT phase diag. refinement 3−34285
$NiFe_2O_4$ with CaO additions and $Ca_xNi_{1-x}Fe_2O_4$, Verwey mechanism of electronic cond. and dielec. polarisation *(French)* 3−34286
$Pb_5Ge_3O_{11}$, ferroelec. behaviour, enantiomorphism and optical activity 3−18419
$Pb_5Ge_3O_{11}$ and $Pb_5Ge_2SiO_{11}$, spontaneous polarisation, temp. depend. 3−18420
PbO, polymorphic, current inversion study of photoelectret state dark depolarisation 3−21113
$Pb(Zn_{1/3}Nb_{2/3})O_3$ and $Pb(Cd_{1/3}Nb_{2/3})O_3$, microdomain behaviour in diffuse phase transition region 3−15462
$Pb(Zr,Ti)O_3$, La_2O_3-modified, temp. depend. 3−5168
$Pb(ZrTi)O_3$ piezoelectric ceramics, stabilization effects, polarization ordering above Curie temp. 3−8507
$PbZr_{1-x}Ti_xO_3$ solid solns., press. induced ferroelec.-antiferroelec. transform., depolarization behaviour *(French)* 3−36842
SbSI, single cryst., polycryst. and ceramic, comparison rel. to piezoceramic prep. 3−34301
SbSeI, deep centres and photopolarization 3−24649
SbSi, deep centres and photopolarization 3−24649
$(Sr_{1-x}Ba_x)TiO_3$ mixed cryst. system, phase transitions obs. 3−15456
$Sr_2Nb_2O_7$, ferroelectric single cryst., spontaneous polarization 3−21373
$SrT.TeO_2$, ferroelec., phase transition 3−15457
TiO_2, dielectric susceptibility and ionicity of bonds 3−14725
TiO_2, freq. and temp. depend., 100 Hz to 500 kHz, 500-1000°C 3−30745
TiO_2, thixotropic and dilatant dispersions, elec. cond., rheology, polarisation 3−39407

dielectric polarisation continued
ZnF_2:LiF, and relaxation using vacancy and interstitial models 3−24650

dielectric properties of gases
discharges, equivalent circuits *(Polish)* 3−20667
electric strength, acceleration or retardation effects 3−26913
electronegative gases, in uniform field, dielectric strength, obs. *(Russian)* 3−36071
fluoroform, dielec. relax. density depend., r.f. meas. at const. temp. 3−23664
methyl fluoride, dielec. relax. density depend., r.f. meas. at const. temp. 3−23664

dielectric properties of liquids and solutions
acrylate (monomer) solns. in microwave region 3−34292
alcohols in neutral solvents, linear dielec. effect, domain theory 3−12091
p-azoxyanisole, isotropic melt, relax. data interpret., effect of reorienting methoxy groups 3−34291
binary liquid mixture, permittivity and loss factor, calc. 3−2484
biological active macromolecules in aqueous solutions, dielectric permeability meas., modified Nernst's bridge 3−32234
chloro alcohols, complex dielec. consts. and relax. time distrib. meas. 3−8500
chloroform, dielec. relax. and far i.r. dispersion 3−21398
chloroform, relaxation, theoretical interpretation of experimental results *(French)* 3−36829
complex permittivity meas., reflecto-interferometer setup *(French)* 3−25792
complex permittivity meas. device with resonating cavity *(French)* 3−25793
dioxane-water solns., nonlinear polarization 3−36832
emulsion, polydispersed system, prop. determ. method *(French)* 3−25018
epoxy oligomer ED-5 solns., dipole relax. behaviour *(Russian)* 3−20252
fluoroanisols in solution, microwave meas. 3−39075
fluorophenols in solution, microwave meas. 3−39075
glycerol, Debye effect, relax. time distrib., 0-180°C *(French)* 3−30750
glycine in aqueous soln., relax., complex permittivity, Argand diagrams *(French)* 3−30751
heterogeneous aromatic compounds in dilute solution, dielectric relaxation 3−39084
hexane, transient current flow, obs. 3−2494
liquid cryst., cholesteric-nematic transition, elec. field induced, rel. to dielec. anisotropy 3−4717
liquids, electrical properties, moisture content effects *(Russian)* 3−25020
monohydric alcohols in dioxane and cyclohexane, dielectric and thermodynamic behaviour 3−2490
nitrobenzene/ethane dihalogenoderivatives, dielec. permittivity rel. to elec. field 3−30741
m-nitrotoluene/ethane dihalogenoderivatives 3−30741
nonpolar liqs., loss meas. in microwave region 3−2489
permittivity, u.h.f. meas. using coaxial line 3−6017
PMMA solns., effect of chem. nature of solvent *(Russian)* 3−20257
polar liquids dissolved in different non-polar solvents, RF conductivity meas. 3−38862
polar liquids in solution, rate process, thermodynamic props., free energy of activation for dipole relaxation *(Greek)* 3−15021
poly(oxypropylene glycol) solns., dipole relax. behaviour *(Russian)* 3−20252
poly-eta-N-carbobenzoxy-L-Lysine, chloroform solution, critical dispersion freqs., molecular weight depend. *(Russian)* 3−30743
polyvinyl acetate, in toluene and carbon tetrachloride, transition phenomena obs. 3−38333
pyridines, substituted in CCl_4, dipole moments 3−39425
quinolines, substituted, relax. times, microwave region meas. 3−8510
rising effect at high voltage electrode rel. to elec. field 3−39089
statistical theory of dielectric constant *(French)* 3−18402
1,1,1-trichloro tert-butyl alcohol in benzene solution, dielectric dispersion behaviour 3−39085
trichlorobenzene in solution, microwave meas. 3−39075
viscosity frequency dependence effect on dielectric relaxation 3−39086
viscous solutions of substituted ethanes, viscoelastic relax. determ. from microwave meas. 3−36435
water, optical constant, calc. using Kramers-Kronig method *(Russian)* 3−5173

dielectric properties of solids
calcite, vacuum u.v refl. spectra, dielec. consts. determ., dichroic absorpt. band 3−27510
cubic crystal with substitutional impurities, i.r. absorpt. and dielec. susceptibility 3−18478
ferroelectric, improper, dielec. anomaly near phase transition temp. 3−15465
glass, low and high frequency relaxation regions 3−24651
ice, impure specimens obtained by solidification of $(NH_4)_2SO_4$ aqueous solns., complex permittivity model *(French)* 3−27463
ice, impure specimens obtained by solidification of $(NH_4)_2SO_4$, km. wave behaviour *(French)* 3−36830
ice, optical constant, calc. using Kramers-Kronig method *(Russian)* 3−5173
Mo, reflection spectra, optical characteristics calc. using Kramers-Kronig relations 3−34372
phthallocyanine, metal free, Stark effect, aligned dipole effect 3−12142
phthalocyanines, microwave dielectric constant and conductivity 3−8501
piezoelectric, pyroelec., and paraelec. crystals, low freq. props. 3−18403
polyethylene, effect of surface and internal discharges *(French)* 3−27468
polyethylene terephthalate electret, effect of crystallisation on homocharge and thermally stimulated currents 3−26976
polyglycine I(II), depolarisation thermocurrents rel. to dielec. relax. 3−30749
polymer, book contrib. 3−12092
polymer, mol. theory, book contrib. 3−12093

dielectric properties of solids continued
- polymer, nondestructive determ. using external capacitive probes 3−25805
- polymer, under d.c. bias, complex dielec. const. ionic contrib. 3−27465
- polyvinyl chloride, radiation eff. on dielec. strength, permittivity, loss and resistivity 3−18405
- polyvinylalcohol, skewed circular arc method analysis of dielectric data 3−2483
- PVC, low freq. dielec. const. meas., continuous voltage superposition influence *(French)* 3−21358
- rocks, dielectric properties at 500 MHz rel. to SiO_2 content *(Russian)* 3−9129
- sea ice, millimetre wave reflectivity 3−2956
- tetrahedral crystalline compounds, theory of nonlinear dielec. props. *(French)* 3−12106
- transition metal semiconducting phosphate glasses, transport props., dielectric props. 3−8175
- triglycine fluoberyllate, dielec. const. and hysteresis loop meas. rel. to ferroelec. transition 3−34310
- Ag halides, anharmonicity, low frequency dielectric response 3−8502
- $AgGaS_2$, nonlinear props. rel. to chalcopyrite crystal structure *(French)* 3−2482
- $Ba_{1-y}Sr_yFeO_{3-x}$ and $Ba_{1-y}Sr_yFe_{1-z}M_zO_{2.5}$ (M=Ga or In) *(French)* 3−36831
- $BaTiO_3$, neutron irradiated, dielectric dispersion near phase transition 3−15467
- $BaTiO_3$:Nb_2O_5, synthesis, dielec. props. 3−39385
- $BaTiO_3$-$CaTiO_3$ (5 wt.%), large polarisation depend. photovoltages 3−33951
- $C_{16}H_{10}$, pyrene, electron energy loss meas. at dielec. tensor 3−8547
- CdS, dielec. relax. time exceeding minority carrier diffusions lifetime, evidence from photocond. meas. 3−30756
- CdS single crystal, persistent internal polarisation variation with illumination intensity 3−34289
- CdS:S system as photoelectret electrophotographic layer, photopolarisation study 3−36833
- Cr, reflection spectra, optical characteristics calc. using Kramer-Kronig relations 3−34372
- CsCl(Br)(I), Pb-centres, dielec. loss studies 3−24725
- CuBr, nonlinear props. rel. to sphalerite crystal structure obs. *(French)* 3−2482
- CuCl, nonlinear props. rel. to sphalerite crystal structure, obs. *(French)* 3−2482
- $CuGaS_2$, dielec. dispersion, phonon freqs., i.r. refl. spectrum 3−8585
- CuI, nonlinear props. rel. to sphalerite crystal structure obs. *(French)* 3−2482
- GaSb, reflectivity spectra, Kramers-Kronig analysis *(French)* 3−30831
- HfS_2, elec. props. and memory effects 3−30527
- HgTe, dielec. function, refl. spectra in far i.r., 8K-300K 3−2565
- $(K_{3/4}Bi_{1/4})(Zn_{1/6}Nb_{5/6})O_3$, dielec. relax., thermally stimulated current 3−30752
- KCl, static dielec. consts., press. and temp. depend., 15-295 K 3−39078
- KCl:Cd, Pb, double crystal d.c. polarisation meas. rel. to $Pb^{2+}(Cd^{2+})$-vacancy dipole relax. 3−34293
- $KCoF_3$ antiferromagnetic crystals, vibrational spectrum, dispersion of refractive index, Kramers-Kronig analysis 3−18450
- KH_2PO_4, dielec. const., capacity, compressive stress effects, 20-210°C, dielec. anomaly 3−21360
- $KMnF_3$ antiferromagnetic crystals, vibrational spectrum dispersion of refractive index, Kramers-Kronig analysis 3−18450
- LiF, static dielec. consts., press. and temp. depend., 15-295 K 3−39078
- MgO, static dielec. consts., press. and temp. depend., 15-295 K 3−39078
- $(NH_4)_2SO_4$, and elastic compliance at ferroelec. transition 3−30781
- $(NH_4)_2So_4$ aqueous solns., solidified, time depend. *(French)* 3−24646
- NaCl, static dielec. consts., press. and temp. depend., 15-295 K 3−39078
- $NiFe_2O_4$ with CaO additions and $Ca_xNi_{1-x}Fe_2O_4$, Verwey mechanism of electronic cond. and dielec. polarisation *(French)* 3−34286
- $PB(Zr,Ti)O_3$, La substituted, PLZT ceramic, pressure-sintered samples 3−8950
- $PbMo_2O_4$, single crystal *(Russian)* 3−8397
- $Pb_2P_2O_7$, Czochralski growth, crystal structure and dielec. props. 3−33470
- $Pb_5P_4O_{15}$, Czochralski technique growth and dielec. props. 3−1727
- $SrLi_{0.25}Nb_{0.75}O_3$ and $SrLi_{0.25}Ta_{0.75}O_3$, perovskite structures *(Russian)* 3−14810
- $SrTiO_3$, dielec. nonlinearity coeff., Devonshire coeffs., near 110 K transition 3−21374
- $SrTiO_3$-$MTiO_3$, (M=Pb, Ba, Ca), phase transitions, permittivity obs. 3−27478
- $Te_{50}As_{30}Ge_{10}Si_{10}$ glass film, differential capacitance 3−21361
- TiO_2, freq. and temp. depend., 100 Hz to 500 kHz, 500-1000°C 3−30745
- Tl halides, anharmonicity, low frequency dielectric response 3−8502
- W, reflection spectra, optical characteristics calc. using Kramers-Kronig relations 3−34372
- Xe reflectivity, Kramers-Kronig analysis 3−30788
- Y_2O_3, electron beam evaporated film, permittivity and dielec. loss meas. 3−24320
- ZnF_2:LiF, relax. and polarisation using vacancy and interstitial models 3−24650

dielectric properties of substances
- *see also antiferroelectricity; coercive force; Curie temperature; dielectric depolarisation; dielectric materials; dielectric measurements; dielectric phenomena; dielectric polarisation; dielectric properties of gases; dielectric properties of liquids and solutions; dielectric properties of solids; electric strength; ferroelectricity; permittivity; piezoelectricity; pyroelectricity*
- amino compounds dielectric absorption 0.3-135 GHz, intramolecular dipole orientation 3−11335
- Kramers-Kronig anal. of reflection spectrum 3−2547
- liquid crystals, nematic Schiff base, dielec. anisotropy 3−1570

dielectric properties of substances continued
- relative refl. spectra, optical consts. determ. by Kramers-Kronig analysis 3−18426
- surface conductivity effect on e.s. field *(Russian)* 3−6393

dielectric relaxation
- *see also dielectric resonance*
- acrylate (monomer) solns. in microwave region 3−34292
- acrylonitrile-butadiene polymers, dielec. relaxation and losses 3−39091
- alkali halides, paraelec. relax., low temp., Orbach process 3−2491
- N-alkyl and N-aryl polymaleimide, freq. and temp. ranges 10^{-5} to 10^6Hz and −80° to 230°C 3−1314
- alternating styrene-maleic anhydride copolymer, molecular motion 3−26750
- p-azoxyanisole, isotropic melt, relax. data interpret., effect of reorienting methoxy groups 3−34291
- bromoform dil. solns. in nonpolar solvents, dielec. meas. and complex form. 3−8511
- chloro alcohols, complex dielec. consts. and relax. time distrib. meas. 3−8500
- chloroform, liq., 0 to 112 GHZ 3−21398
- chloroform, theoretical interpretation of experimental results *(French)* 3−36829
- chloroform dil. solns. in nonpolar solvents, dielec. meas. and complex form. 3−8511
- dipolar relax. times distrib. meas. by thermally stimulated currents 3−39090
- epoxy oligomer ED-5 solns., dipole relax. behaviour *(Russian)* 3−20252
- ferroelectric, polydispersive nature 3−39104
- fluoroanisols in solution, microwave meas. 3−39075
- fluoroform, density depend. r.f. meas. at const. temp. 3−23664
- fluorophenols in solution, microwave meas. 3−39075
- glass, low and high frequency relaxation regions 3−24651
- glycerol, Debye effect, relax. time distrib., 0-180°C *(French)* 3−30750
- glycine in aqueous soln., Argand diagram construct., temp. and conc. depend. *(French)* 3−30751
- Gopala Krishna's method for relax. time of polar solute in nonpolar solvent 3−12095
- heterogeneous organic compounds in dilute solution 3−39084
- insulating oils, at low temps., glass transition and supercooling 3−18408
- iso-octyl phenoxy polyethoxy ethanol in dilute solutions of benzene, dielectric relaxation and losses 3−20220
- liquid, rising effect at high voltage electrode rel. to elec. field 3−39089
- liquid crystal, nematic, dipole relax. behaviour, mol. ordering depend. 3−18412
- liquids, polar, various theories 3−5158
- liquids, viscosity frequency dependence effect on dielectric relaxation 3−39086
- methyl fluoride, density depend., r.f. meas. at const. temp. 3−23664
- m.i.m. systems, dielectric relaxation effect on isothermal electrical characteristics of defect insulators 3−11959
- m.i.m. systems, dielectric relaxation effect on thermal electric characteristics 3−8276
- monohydric alcohols in dioxane and cyclohexane, dielectric and thermodynamic behaviour 3−2490
- $Na_2O.3SiO_2$ glass, mech. and ionic relaxation meas. 3−18410
- noble metals, optical constants 3−8548
- paraelectric impurities, dipole-dipole relax. 3−8513
- PMMA solns., effect of chem. nature of solvent *(Russian)* 3−20257
- polar liquid, Cole-Cole relation, complex dielec. const. angular freq. depend. 3−27467
- polar liquids dissolved in different non-polar solvents, RF conductivity meas. 3−38862
- polar liquids in solution, rate process, thermodynamic props., free energy of activation for dipole relaxation *(Greek)* 3−15021
- poly(N-substituted maleimides), comparison with n.m.r. data 3−5142
- poly(oxypropylene glycol) solns., dipole relax. behaviour *(Russian)* 3−20252
- polyamide 66, v.l.f. meas. by a noncontact method at room temp. 3−18413
- polychloroprene, dipole relax. under external press. *(Russian)* 3−20251
- polyethylene, low temp. peaks 3−30755
- polyglycine I(II), depolarisation thermocurrents rel. to dielec. relax. 3−30749
- polymaleimide, freq. and temp. ranges 10^{-5} to 10^6Hz and −80° to 230°C 3−1314
- polymer, model, dynamic susceptibility in several limits 3−1305
- polymer, mol. theory, book contrib. 3−12093
- polymeric chain, time dependent Ising model 3−1312
- polymers, nonisothermal relax., equiv. model theory breakdown 3−30753
- quinolines, substituted, microwave region meas. 3−8510
- rel. to thermally stimulated depolarization, phenomenological anal. *(Russian)* 3−34288
- theory, dynamic reaction field *(French)* 3−36829
- transient currents rel. to relax. time *(French)* 3−34294
- 1,1,1-trichloro tert-butyl alcohol in benzene solution, dielectric dispersion behaviour 3−39085
- trichlorobenzene in solution, microwave meas. 3−39075
- viscous solvents, viscoelastic relaxation determ. from microwave dielectric meas. 3−36435
- vitreous ionic conductors, role of long range diffusion process in dielec. relax. 3−30748
- $AgNa(NO_2)_2$, determ. by step-function method 3−18409
- Al-CeF_3-Al structure, isothermal dielec. relax. curents 3−36666
- Al-CeF_3-Al thin film capacitor system, stimulated dielectric relaxation currents 3−8277
- CaF_2:Gd, F- and O-compensated dipoles, reorientation kinetics 3−24652
- CdS, dielec. relax. time exceeding minority carrier diffusions lifetime, evidence from photocond. meas. 3−30756
- $(K_{3/4}Bi_{1/4})(Zn_{1/6}Nb_{5/6})O_3$, dielec. relax., thermally stimulated current 3−30752

dielectric relaxation continued
KBr, additively coloured 3−39092
KCl, dipolar complexes resulting from 1.5 MeV electron bombardment 3−12096
KCl, paraelec. reson. of Li^+, relax. behaviour at high dipole conc. 3−2492
KCl:Cd, Pb, reorientation of Cd^{2+}(Pb^{2+})-vacancy complex rel. to dielec. relax. 3−34293
$KCl:OH^-$, paraelec. relax., low temp., Orbach process 3−2491
$KCl:OH^-$, paraelec. relax., anomalous temp. depend., 0.025-0.3 K 3−8512
$KCl:OH^-$, paraelec. relax., appl. of theory for dipole-dipole relax. of impurities 3−8513
NH_4ClO_4, pure and doped, temp. depend., elec. cond. mechanism 3−2081
$NaNO_2$, libration mode temp. depend. rel. to dielec. relax. 3−38642
$Na_2O.3SiO_2$ glass electrical relax. and alkali diffusion 3−18411
$PbTiO_3$, dissipation factor, effect of additives *(Japanese)* 3−2495
$SrTiO_3$, (Ba, Sr) TiO_3, boundary layer dielectrics, permittivity and dispersion 3−2485
Te-As-Ge-Si film, freq. depend. cond. and capacitance 3−2092
Te-As-Ge-Si thin film capacitors, frequency dependence of capacitance and conductance 3−27321
$Te_{50}As_{30}Ge_{10}Si_{10}$ glass film, differential capacitance 3−21361
TiO_2, a.c. cond., freq. and temp. depend., 100 Hz to 500 kHz, 500-1000°C 3−30745
ZnF_2:LiF, and polarisation using vacancy and interstitial models 3−24650

dielectric resonance
see also dielectric relaxation
acoustic paraelectric resonance in crystals with noncentral impurity ions 3−38624
paraelectric, at 10, 35 and 70 GHz, microwave cavities 3−3831
paraelectric resonance lineshape, theory 3−27460
semiconductors, paraelectric resonance of excitons 3−24400
KCl, paraelec. reson. of Li^+, relax. behaviour at high dipole conc. 3−2492

dielectric strength *see electric strength*

dielectric triodes *see space-charge limited devices*

dielectrics *see dielectric materials*

diesel engines *see internal combustion engines*

difference amplifiers *see differential amplifiers*

difference equations
axisymmetric buckling of uniformly loaded spherical caps undergoing plastic deformation, numerical soln. 3−37820
finite, for numerical solution of diffusion and heat conduction equations 3−10399
finite difference approxs. of eqns. of atmospheric motion 3−3024
finite difference soln. to elastoplastic wave propagation and reflection *(Russian)* 3−37841
fluid dynamics, numerical solution, extensions to Eulerian methods 3−20266
flux-corrected finite-difference algorithm for fluid transport 3−23668
heat conduction, transient nonlinear, with temperature dependent thermal properties, finite difference method of soln. 3−19524
heat flow problems transient, educational example 3−28434
inhomogeneous regions, mathematical modelling of regions with spatial variation in cond. 3−10261
inverse scattering, discrete version with difference eqn. 3−35589
iterative methods 3−3957
loaded flat plate containing holes, finite-difference relations and correction routine for stress and deformation history 3−22606
moment theory of elasticity for one-dimensional continuous medium with nonunform periodic structure *(Russian)* 3−16681
multi-beam slabs supported by flexible edge beams, model and closed form solution 3−28863
nonlinear analysis by combined finite element-finite difference methods 3−10269
plate vibration, by improved finite difference method 3−565
pseudo-viscous method, for steady supersonic flow calculation past waisted body 3−1405
second order equations with discontinuous coeffs., difference soln. *(Russian)* 3−13539
spectral theory of Kodaira's type for ordinary linear difference operators of second order 3−13651
storm surge eqns. for wind effects is Adriatic sea, numerical soln. by difference scheme 3−2935
temperature distribution in layered tissues 3−25587
turbulent flow, pressure driven, in square duct, finite difference approach to solution 3−20304
two-dimensional nonlinear Poisson eqn., finite difference eqns., mag. lense calcs. *(French)* 3−22974
viscous compressible flow problems, cell type finite difference methods 3−33241
viscous flow, two-dimensional, through T-junction, finite difference method 3−11369
viscous flow in circular pipe orifice, numerical study of fluid motion 3−33197
viscous flows past circular cylinders, numerical calc. 3−33222
wave equation solution, generalizations allowing weak and strong discontinuities 3−10260

differential amplifiers
for magnetophonon studies 3−18126
signal convertor and amplifier, for additive flow metering, patent 3−10226

differential calculus *see differentiation*

differential equations
see also Boltzmann equation; boundary-value problems; difference equations; Green's function methods; integro-differential equations; linear differential equations; Navier-Stokes equations; nonlinear differential equations; partial differential equations; wave equations
Adelphic integrals, applic. to non- and partially-degenerate dynamic systems, using Hamiltonian functions 3−22581
aneurysm of circle of Willis, qualitative analysis of Austin's differential equation 3−33322
argument periodic transformation *(Russian)* 3−37787
astrophysical differential equations, reduction 3−12942

differential equations continued
axisymmetric plates, static, vibration and buckling analysis, finite element method 3−32310
beams curved in plane of noncircular centre lines, torsion and deflection, determ. of bending moment and angle of twist 3−19440
belt type radiator, thermal analysis by method of matched asymptotic expansions 3−37908
boundary value problem for 2nd order eqn. with turning point, uniqueness of asymptotic solns. 3−32290
boundary value problem for natural frequencies of thin rotating cylinder 3−32373
Cauchy-Poisson media, mech. models 3−16638
conductor with nonlinear heat source, rel. to nonstationary temp. behaviour *(Russian)* 3−32461
constitutive eqns. for finite strains of granular materials 3−18744
Coulomb wavefunctions, remarks on computation 3−10253
coupled Duffing eqns., analytic soln. for forced oscillations, Kryloff-Bogoliuboff technique 3−26068
d.c. heated conductor, computer calc. of thermophysical props. *(German)* 3−30442
dynamical theory of electron diffraction within a distribution formalism 3−33432
EHD unipolar fluid flow in channel with electrode walls, exact solns. *(Russian)* 3−29900
elastic rod, equil. problem soln. in terms of generalized stresses and displacements 3−16637
e.m. wave scatt. by radially inhomogeneous spheres 3−37930
equation of motion for particle in mag. field, numerical soln. 3−26253
equations of motion for macroscopic quantities *(Russian)* 3−10243
first-order linear, for one-loop generalized Feynman integrals 3−28830
geometrically nonlinear plane frames, analysis for finite displacements 3−28860
Hill's eqn., charact. exponents and stability near transition curves 3−26060
Lagrange eqn. of second kind, generalised form *(Russian)* 3−28848
linear coupled, computer program 3−35969
Lyapunov functions, for boundedness and global existence of solutions 3−22583
monotonicity conditions for ordinary differential linear operators in problems of theory of elastic structures 3−16631
motion of a heavy particle near Earth's surface, integration of differential equation system 3−19404
neutron diffusion in reactor, method for evaluating local variations 3−1040
neutron multigroup diffusion eqn., errors arising in soln. from use of perturbation calcs. 3−23388
Newtonian, of Kepler motion, numerical stabilising procedure based on Floquet's theorem 3−3282
ordinary, multi-step method for numerical integration 3−10262
orthotropic plates, postbuckling anal. and determ. of load-shortening and effective width 3−22608
PHOEBUS-2 reactor, thermal balance and stress stationary limit conditions, calc. *(Italian)* 3−35927
prolate spheroidal functions, asymptotic expressions and eigenvalues 3−10238
quantum field theory, Thirring's model, scatt. props. of differential eqn. defining model 3−13787
quasilinear parabolic, regularity of solns. of first boundary problem *(Russian)* 3−13534
rotating disc, vibr., eqn. of motion soln. 3−26098
Schrodinger eqn., coupled one-dimensional, direct numerical integration 3−10338
Schrodinger eqn., time dependent, numerical soln. 3−10339
second order equations with discontinuous coeffs., difference soln. *(Russian)* 3−13539
seismic waves, inhomogeneous anisotropic Earth's crust, rays and travel time curves 3−2906
self-gravitating fluids, Cauchy soln. with press. equal to energy density 3−7475
shell, thin, large deform., inverse problem 3−22641
shell equations for stress distribution in corrugated tube or bellows 3−3955
simpler cosmological models, derivation of differential equation 3−37308
solar wind two-fluid eqns., asymptotic behaviour of supersonic 3−39630
solutions for prescribed means of boundary 3−28825
stochastic, perturbation series solns. and Green's function for Markovian systems 3−35560
stochastic, renormalized projection operator technique 3−28836
strain gradient elasticity theory of arbitrary order, analytic props. of solns. 3−28857
surface heat shock effects, differential equations for thermoelastic state of shell *(Russian)* 3−28882
turbulent dynamo, rel. to functional approach 3−23713
vibrating constrained-layer damping sandwich plates and beams, governing eqns. 3−22697
waveguide, periodic, e.m. wave propagation, soln. *(Russian)* 3−10431
^{222}Rn short-lived daughter ions' behaviour in atmospheric processes 3−15968

differentiating circuits
for derivative spectroscopy, electronic differentiator design 3−5941

differentiation
see also differential equations
No entries

diffraction
see also acoustic wave diffraction; diffraction gratings; diffractometers; electromagnetic wave diffraction; electron diffraction; neutron diffraction
defocused optical syst. with slit aperture, effect of partial coherence 3−677
edge diffraction cone detection, laser beam use, obs. 3−4070
elastic waves, diffraction at spherical cavities *(Russian)* 3−570
fast charged particles, wave-particle duality in crystals 3−27044
fast MHD waves diffraction by plasma layer of a periodically varying density 3−17588

- **diffraction** continued
  - gravity surface waves, diffraction in harbour, SOGREAH method *(Polish)* 3−25199
  - hadron interactions, applic. of Huygens' principle at high-energy 3−23150
  - Kirchhoff diffraction of longit. elastic waves, tensor pot. 3−37834
  - optical images, calc. of intensity distrib. with image motion and sinusoidal vibrs. 3−29055
  - partially coherent images of object with linear motion and transverse vibrs., far-field diffraction method 3−29056
  - plane elastic waves by cylindrical cavity, polarity effect, stress field determ. 3−32396
  - plane shear elastic wave by circuilar rigid disc and penny shaped crack 3−3990
  - plate affected by shock-wave, calc. *(Russian)* 3−10318
  - powder patterns, Joint Committee on Powder Diffraction Standards, data collection and search 3−26929
  - shock waves incident on fixed sphere and on cylinder *(Russian)* 3−14469
  - water waves, theory 3−20811
- **diffraction gratings**
  - application of telescope objective gratings to faint star photometry 3−13120
  - corrugated structures, asymmetry and blazing effects 3−32507
  - double, diffraction and polarization of plane e.m. wave 3−668
  - echelette, diffraction anomalies 3−3795
  - echelette type, perfectly cond., surface currents calc. by approx. analysis techniques 3−5868
  - ellipsoidal, for Seya-Namioka monochromators, parameters and optical props. 3−32069
  - ellipsometry, generalised 3−5870
  - e.m. wave diffraction, applic. of conformal mappings 3−6403
  - Fourier transform spectroscopy, far i.r., diffraction limitations of lamellar grating interferometer 3−28562
  - gaussian beam, one dimens., diffr. by amplitude sinusoidal grating of zero thickness 3−10442
  - ghost lines 3−5872
  - grating spectrographs, elliptic polarisation by metallic grating 3−13298
  - hologram, with modulation, diffraction efficiency 3−29030
  - human vision, multiple-channel models, bandwidth consideratons 3−35261
  - large plane gratings for high-resolution i.r. spectrographs 3−9954
  - modulating, increase in dynamic range of coherent optical filters 3−19218
  - optical, X-ray total reflection and diffraction *(German)* 3−10131
  - periodic, image in coherent light produced by optical system 3−26204
  - photographic gratings for linear measurement, moire fringe measuring system 3−22358
  - plane grating, dynamic dispersion formulae 3−35668
  - polarisers, deposition of metallic coatings, method 3−16422
  - profile preparation rel. to gelatin lenticular rasters *(German)* 3−32105
  - radiation of plane wave from active grating for given near field amplitude behind grating 3−5710
  - review, appl. of e.m. laws to gratings 3−32502
  - Rowland system with concave holography gratings, stigmatism conditions *(French)* 3−35676
  - ruling defects, effects on spectral lines *(Japanese)* 3−5889
  - S-polarization anomalies in gratings with sinusoidal and triangular profiles 3−680
  - semiconductor injection heterojunction laser with diffraction grating on contact surface, light propag. theory 3−13741
  - shallow ruled blazed, X-ray diffraction properties 3−3882
  - spectrograms, grating, Taylor series expansion for plate distance and wavelength relation 3−9939
  - surface plasmon obs. 3−24493
  - thick, periodically stratified, with complex dielectric constant, diffraction computation 3−19568
  - triangular profile, blaze optimisation 3−22315
  - tuning dye lasers, angular dispersion 3−22379
  - vibrating, far field diffraction images 3−19565
  - v.u.v. meas. of grating efficiency using two Seya-Namioka monochromators 3−155
  - wire, suitable for student construction in spectroscopic studies 3−32015
  - $Mg_xMn_{1-x}Fe_2O_4$ film, use as phase diffr. grating 3−36862
- **diffraction instruments** *see diffractometers*
- **diffractometers**
  - data evaluation, structure analyses, validity and accuracy of current methods, standard derivations, rejection criteria 3−26928
  - Dumond-type, high-resolution, for meas. of (n,γ)-lines 3−10091
  - Fresnel zone plate, optical image formation using VUV radiation 3−19184
  - laser, for electron micrograph analysis 3−378
  - low temp. equipment for automatic four circle diffractometer used for crystal studies 3−25674
  - neutron, for low angle biological studies 3−35528
  - neutron single crystal diffractometer with 100 movable detectors 3−26955
  - for online diffractograms of electron microscope images 3−32223
  - optical, for analysis of high resolution electron micrographs 3−5876
  - single crystal diffractometer, on-line control of intensity meas. accuracy 3−26921
  - single-crystal diffractometer data, online control of precision of intensity meas. 3−23961
  - for surface structure examination, on Si slices *(German)* 3−15060
  - vidicon diffractometer system for registration of X-ray reflection profiles 3−26942
  - X-ray, automatic, power samples, computer programmed, pattern file retrieval 3−26946
  - X-ray, computer controlled, data collection, structure determination, hardware and software 3−26947
  - X-ray, He cryostat description 3−25700
  - X-ray, URS-50I, with BSV-11 sharp focusing tube 3−25951
  - X-ray diffractometer, high pressure unit up to 100 kbar for powder samples 3−13475
  - X-ray non-dispersive diffractometer for critical scatt. meas. 3−26935
  - He cryostat, for X-ray diffractometer 3−25700
- **diffusion**
  - *see also acoustic wave diffusion; diffusion in gases; diffusion in solids; electromagnetic wave diffusion; neutron diffusion; osmosis; surface diffusion; thermal diffusion*
  - adsorbed molecules on metals, semiconductors or insulators, surface diffusion 3−27183
  - adsorption, partially mobile, of gases on homogeneous solid surfaces, statistical mechanics 3−30342
  - agar gel, of UO_2^{2+} ions, inverse mass depend. 3−38676
  - alkali halide cleavage plane, of Au, adatom surface diffusion rel. to thin film growth 3−1888
  - alloy oxide scales, diffusion and partitioning of elements 3−2696
  - Bi-In(Sn)(Cd) systems, contact melting in mag. field *(Russian)* 3−15698
  - binary diffusion through heterogeneous medium, pore size distribution and capillary effects, bounds using moment and transport constraints 3−29917
  - concentration-dependent, existence and uniqueness analysis, use of shooting methods 3−32458
  - with concentration-dependent diffusion coefficients, numerical solution of equations 3−6371
  - conformal mapping soln. of diffusion eqn. in arbitrary doubly connected domain 3−6374
  - cosmic radiation, galactic, modulation by anisotropic solar wind *(Russian)* 3−12903
  - cosmic ray diffusion theory, resonance integrals 3−37271
  - cosmic rays, in radially diverging flux of magnetic inhomogeneities *(Russian)* 3−3272
  - coupled diffusion eqns., general solns. in integral transform theory, eigenvalue problem 3−19520
  - desorption rate constants and diffusion theory adsorption comparison with experimental lifetimes 3−33736
  - diffusion-convection equation, finite element soln. 3−14429
  - diffusophoresis velocity of large nonvolatile aerosol particles *(Russian)* 3−7466
  - double diffusive convection, transport and profile meas. of diffusive interface 3−20305
  - electrodiffusion of divalent ions (Ca^{2+}, Sr^{2+}, Cd^{2+}, SO_4^{2-}) determ. in gels by radiotracers 3−39451
  - fluid, of tagged particles, long time behaviour 3−35631
  - fluidized beds, turbulence, calc. *(Japanese)* 3−23787
  - fused salt diffusion coating technique, book contrib. 3−11814
  - gas atoms adsorption and deorption at solid surfaces, diffusion theory 3−24336
  - harmonic particle weakly coupled to lattice, diffusion jump rate calc. 3−22746
  - heat or mass transfer with axial diffusion rel. to boundary conditions 3−20285
  - heterogeneous medium, transport equation solution 3−10397
  - human lung, computation of boundary conditions 3−28319
  - integral analog method for diffusion coeffs. determ. 3−22761
  - jets, turbulent, diffusion and vortex models 3−33315
  - jets, vibrating, adsorption and diffusion limited surface aging 3−29923
  - Kirkwood theory applic. to rigid assemblies of beads 3−26747
  - lamellar eutectic structure growth, kinetics for solidification, diffusion and solid phase boundary formation *(Japanese)* 3−30975
  - liquid crystal, nematic, neutron scatt. study 3−1812
  - liquid crystal, smectic A, self-diffusion const. meas. 3−1813
  - Lorentz gas, logarithmic terms in density expansion of diffusion coeff. 3−6376
  - motion of small spheres in gases, diffusion coeff. of porous membranes 3−33258
  - nondeforming fluid media, anisotropic transport processes 3−620
  - nonlinear, partial differential equation numerical solution 3−13655
  - nonlinear rate processes, first order diffusive effects 3−37123
  - nonsteady transport problem soln. by flux method 3−22762
  - numerical solution of equations, survey 3−10399
  - particle diffusion across a mag. field, large scale hydromag. turbulence effects, appl. to interplanetary mag. field 3−25428
  - planar turbulence free interfacial diffusion layer, condensation nuclei deposition 3−17550
  - plane moving boundary problems, freezing and melting, integral transforms 3−34702
  - plasma in magnetic field, density diffusion and temp. perturbations *(Russian)* 3−38425
  - porous materials, converging-diverging pore model, computational simulation 3−27172
  - radial, inner zone electron repopulation 3−12820
  - radiation belt particles, parasitic pitch angle diffusion by ion cyclotron waves 3−12836
  - random walk derivation of diffusion coefficient 3−16353
  - self-diffusion, fully renormalized kinetic theory 3−10383
  - silica surface, of adsorbed water, test of Resing model for spin-spin relaxation 3−38727
  - spin diffusion rel. to interchain coupling effects in Heisenberg linear chain (nearly one-dimens.) system 3−18354
  - spread on surface, in zero gravity *(Russian)* 3−11799
  - stress corrosion cracking via surface diffusion, interface morphology development 3−34570
  - strong pitch angle, within polar cusps, magnetosheath plasma 3−3123
  - surface, self diffusion coeffs. relationship, electrostatic field and impurity effects 3−18021
  - surface diffusion coeff. determ. from healing kinetics of isolated scratch *(Russian)* 3−30340
  - surface film growth rate-controlling factor, true substrate ion current 3−20969
  - surface self diffusion mechanisms, temperature dependence 3−15066
  - time-dependent three-dimensional boundary layer 3−17527
  - transport, enhancement by u.s. 3−29851
  - transverse nuclear spin relaxation, mol. diffusion through locally inhomogeneous mag. fields 3−36814
  - triglycinsulphate growth, role of surface and volume diffusion 3−20700
  - tubular flow chemical reactors, variational soln. and error bound for nonlinear diffusion problem 3−27867
  - turbulent, eqn. with finite vel. for 3-dimens. case *(Russian)* 3−21925

diffusion continued
unsteady convective diffusion with interphase mass transfer, miscible dispersion theory 3−33292
unsteady state diffusion equation, quasilinearization technique for numerical soln. 3−19523
Wagner approximations compatibility with the heterogeneous kinetics equations of a diffusion regime *(French)* 3−27920
Cu, comments on vol. and surface self-diffusion meas. by thermal surface smoothing 3−7974
Cu, of Ag adatoms, Fick's eqn., soln. *(French)* 3−11804
Cu, surface diffusion of Ag on (001), (111) and (110) planes and vicinal surfaces *(French)* 3−36477
Ni, surface self-diffusion in vacuum and dry H_2 3−27179
Ta autocathode, low temp. surface diffusion on He ion bombard. *(Russian)* 3−8689
Ta compatibility with graphite, UO_2 and UC at high temperature 3−35932
Ta surface, hydrogen absorpt. kinetics, surface barrier influence *(French)* 3−4921
Ta surface, of hydrogen, kinetics, elec. resist. obs. *(French)* 3−1890
W, surface diffusion and clustering, interpretation of ion microscopy data 3−36475
W, surface diffusion and clustering, interpretation of field ion microscopy data 3−36476
W, surface diffusion of Sb, adsorpt. of Cs, work function changes 3−15067
W-Re alloy, surface self-diffusion in field-emission electron microscope 3−36982
diffusion columns *see isotope separation; thermal diffusion in gases*
diffusion in gases
see also flow of gases; fugacity; thermal diffusion in gases
acceleration waves in gases, effect of diffusion on growth and decay 3−29823
aerosols, particle eddy diffusivities and turbulent deposition velocities for isothermal flow and smooth surfaces 3−33298
air pollution meteorology, fluid models 3−2971
n-alkane + N_2 mixtures, diffusion coeffs. meas., 300 to 700K 3−38341
anharmonic oscillator, vibrational relaxation, diffusion theory, classical statistics 3−36051
atmospheric dilution factors for effluents diffused from elevated continuous point source 3−28051
atmospheric dispersion of pollutants, effect of horizontal impervious layer caused by temp. inversion 3−25210
atmospheric pollution, K-theory appl. to diffusion problems in nonlinear chemical reactions 3−39817
atmospheric transport of diffusing material over thin wind-break 3−25212
binary, coeff., definition *(German)* 3−17490
charged particle anisotropic diffusion in neutral gas in an electric field, thermodynamic treatment 3−14515
clouds, particle ion charging, kinetic eqn. *(Russian)* 3−39526
cyclone, reverse-flow, steady-state model 3−17523
electron stream diffusing in a gas, theory 3−38344
finite mean free path effect on diffusion around convex obstacle 3−20349
inert gas potentials, tables of collision integrals 3−26739
interaction pot. from mobility and diffusion coeffs. meas. 3−38246
ionospheric F-region electron-ion gas nonstationary distrib. for pure ambipolar diffusion 3−34948
lateral and vertical atmospheric dispersion coefficients, continuous functions 3−5493
Loschmidt diffusion experiment, interferometric method 3−32077
Loschmidt diffusion experiment, perturbation analysis 3−33186
mass transfer in turbulent flow, formulation of diffusion eqn. 3−14448
mixed flow impeller, diffusion losses due to negative velocity gradients in boundary layer 3−4582
moderately dense mixtures, binary diffusion coeff. 3−20261
monodeuteromethane, compressed gaseous, rot. diffusion 3−33185
polar gas mixtures, binary diffusion coeffs. prediction 3−7306
pollutant diffusion estimates rel. to low wind turbulence statistics in Hudson River Valley 3−25211
self-diffusion through capillaries, transport equation *(German)* 3−14413
spherical droplet condensation in an isothermal vapour diffusing through a heavy background gas 3−20861
star formation in rotating cloud with mag. field, ambipolar diffusion effects 3−35120
Stefan cell, modified, for gas diffusion measurements 3−32214
thermo-osmosis of refrigerant gases through permeable, non-porous membranes 3−7307
tropospheric diffusion coeffs., meas. from isotope conc. in rain samples *(German)* 3−5512
turbulent, in pipe core with uniform transverse wall flow 3−11386
turbulent diffusion of atmospheric pollutants, effect of first order chemical reaction 3−37199
upper atmosphere, ambipolar diffusion coeff. determ. by radar obs. of meteor trails 3−34908
vapour-gas mixture, in a capillary, convective diffusion with evaporation 3−26784
Ar, calc. of self-diffusion coeff. using method of molecular dynamics and Barker-Bobetic pair potential 3−1809
Ar, longitudinal diffusion of electrons, influence of Ramsauer-Townsend minimum 3−1324
Ar high density gaseous, intermediate scattering functions obtained by quasi elastic neutron scattering studies 3−17485
C^+ in CO, mobilities and longitudinal diffusion coefficients 3−20262
CO^+ in CO, mobilities and longitudinal diffusion coefficients 3−20262
CO^+,CO^- in CO, mobilities and longitudinal diffusion coefficients 3−20262
H_2 purification by diffusion through Pd membranes at high pressure *(Russian)* 3−9905
HF diffusion type chemical laser, numerical study 3−37955
He^{2+}, diffusion limited destruction of metastable states 3−11470
^3He gas density dependence of the diffusion constant and nuclear spin-lattice relaxation time by spin echo meas. 3−26699
diffusion in gases continued
^4He gas, viscosity, thermal conductivity self-diffusion coefficient calc. 3−14409
K^+ mobility, diffusion and clustering in gases 3−29827
kr, self diffusion coefficient, density depend. 3−17489
Kr at intermediate density , self-diffusion 3−14410
PuO_2 fuel form, He migration and release, heat treatment expts. 3−19957
UO_2-C-N_2, reaction kinetics at 1700 C 3−39382
diffusion in liquids
see also flow of liquids; thermal diffusion in liquids
alcohols, primary, in nitrobenzene and CS_2, viscous drag studies by quasielastic light scatt. 3−24282
alloy, binary, ionic motion rel. to nucl. spin relax. 3−2441
alloy, of hydrogen, rel. to metallurgical processes 3−4865
anisotropic-diffusion model calculation of spin lattice relaxation time due to spin-rotation interaction 3−27398
aqueous soln., protonic, relation to frictional relax. drag 3−27134
aqueous solutions, of UO_2^{2+} ions, inverse mass depend. 3−38676
benzenes, ^{14}C-substituted, meas. of tracer-diffusion coeffs., isotope effects 3−24285
binary-liquid phase transition, decoupled-mode theory of critical diffusion 3−4843
Brownian particles, mol. theory of translational Stokes-Einstein relation 3−16754
bubble growth, in 11 kHz sound field 3−7401
carbon tetrachloride, liq., ^{13}C and ^{35}Cl relaxation, J-diffusion model for molecular reorientation 3−12066
Caribbean Sea, diffusivity of suspended matter, gravimetric analysis 3−15947
coefficients of gases in liquids, eqn. for their prediction 3−7952
computer simulation studies of liquid state 3−26958
convective diffusion with chem. reaction, effect of multicomponent bubble collapse 3−7954
cyclohexane, self-diffusion under pressure, measurement, diaphragm cell, theory, results, analysis 3−10100
1,2-dichloroethane, liquid, proton spin relaxation time and self-diffusion coefficient 3−18383
dilute solution of H_2 in liquid Ar i.r. absorption spectra, absorption line shapes depend. on H_2 diffusion 3−21412
effect on obs. of transient conductivity induced in irradiated aqueous solutions 3−5397
egg albumen soln., real and simulated, self-diffusion coeffs. comparison 3−28975
electrolytes, sea and brackish water, osmotic coefficients 3−9068
estuary, obs. using aircraft 3−3210
ethers of carbonic acids and their solutions in CCl_4, meas. of self-diffusion coeffs. by spin-echo technique *(Russian)* 3−7957
extended M- and J-diffusion model for symmetric top mols. in liqs. 3−7610
falling liquid films, Taylor diffusion 3−1962
fluid mechanics aspects of environmental protection, research program *(German)* 3−36147
gas diffusion to a liquid film flowing down inclined surface, asymptotic eigenvalues for heat or mass transfer 3−26779
glycerol, self-diffusion coeff., temp. depend., pulsed n.m.r. study 3−30710
glycerol and aquesus-glycerol soln. Mossbauer determ. of diffusion consts. for dispersed Fe^{2+} 3−5360
ice cryst. growth in supercooled H_2O droplet clouds, numerical simulation 3−25226
inert gas transport in liquid metals during boiling expts. 3−19904
isothermal differential diffusion coeffs. determ. using holographic interferometry and computer simulation *(French)* 3−2814
liquid crystal, lyotropic, deuteron relax. obs. of D_2O motions at soap-water interface 3−27173
liquid crystal, nematic, self-diffusion in isotropic phase near nematic-isotropic transition 3−33446
liquid crystals, self-diffusion, meas. by multiple-pulse n.m.r. method 3−30712
longitudinal dispersion of ink in turbulent flow of water, electro-optical measurement 3−1376
metal, molten, self diffusion coeff. calc. from effective interionic pot. calc. *(Japanese)* 3−11539
metal, of hydrogen, rel. to metallurgical processes 3−4865
metal, small fluctuation theories 3−36432
metal alloys, liquid, reactive diffusion and electron transfer, multipoint semiautomatic unit *(Russian)* 3−9909
methane in hexane, heptane, octane, dodecane, hexadecane, molecular size and shape effects 3−4863
methylamines, mol. reorientation mechanisms, n.m.r. obs. 3−18386
molecular, in two-dimensional stagnation flow *(French)* 3−36076
molecular liquids, neutron spectroscopy study 3−1652
monatomic, self-diffusion coeff., temp. and density depend. 3−7955
multicomponent diffusion in liquid systems, approx. theories 3−37114
$NaNO_3$, pure molten, equation for numerical computation of self diffusion coefficient of Ag ion 3−7956
nitroethane-iso-octane, diffusion coeff. of Brownian particles near critical phase transition 3−15509
obstacle effect study, random-walk method 3−28975
open-channel flow, longitudinal dispersion, turbulent mixing, review 3−33215
n-paraffins, using theorem of corresponding states 3−9038
phenol, liquid and solid, nuclear spin-lattice relaxation, diffusive molecular motion 3−34237
point defects and diffusion, monograph 3−1621
polyelectrolytes equilibrium theory, transport props., review 3−34731
polymer mols. in dil. solns., dynamics 3−23648
polymers, molten, sorption apparatus for diffusion studies 3−32215
polyoxypropylene polyols and CCl_4 solns., self-diffusion, spin echo obs. *(Russian)* 3−20249
self motion in classical liquids 3−30059
shear effect diffusion in shallow open seas 3−31339
solute escape from droplet cooled by vaporization and radiation, liq.-phase diffusion-controlled 3−27849
solutions, diffusion and solvation 3−36253
trichlorofluoromethane, rot. diffusion, nucl. relax. data interpret. 3−30274

diffusion in liquids continued
turbulent diffusion in the sea meas. by fluorescent tracer method 3−34973
water, quasi-elastic scattering of slow neutrons near density maximum, determ. of self-diffusion coeff. 3−24159
water, self-diffusion coeff. down to −31°C 3−7953
water jump diffusion, cold neutron scatt. obs. 3−1810
Al:Ti, film, diffusion from Ti sublayer during Al vacuum condensation 3−30079
Ar, calc. of self-diffusion coeff. using method of molecular dynamics and Barker-Bobetic pair potential 3−1809
Ar, ion drift vel. 3−24283
CO in various liquids, rotational diffusion 3−4864
Cu, diffusivity of hydrogen 3−36433
Fe, mass transfer coefficients 3−31034
Ga, of O, 750-950°C, potentiostatic electrochem. study 3−30278
H ion mobility in water in glass pores of 15 μm diam. 3−1567
H self-diffusion in sodium-ammonia and lithium-ammonia solutions, n.m.r. meas. 3−20883
^{3}He-^{4}He isotopic mixtures, ^{3}He diffusion, 3 to 0.4K 3−11780
^{3}He-^{4}He solution, diffusion constant at high temp. 3−24311
^{4}He, of ^{3}He, near λ-line 3−24310
In, of O, 750-950°C, potentiostatic electrochem. study 3−30278
Li self-diffusion in lithium ammonia solutions, n.m.r. meas. 3−20883
$LiNO_3 + AgNO_3$ melt, interdiffusion coefficients determ. *(German)* 3−36434
Na, of Cd, electrotransport, 130-530°C, 0.001-2.3 at.% conc. 3−33868
Na self-diffusion in sodium ammonia solutions, n.m.r. meas. 3−20883
Na-K alloys, electrotransport, drag coeff. 3−24284
$NaNO_3 + AgNO_3$ melt, interdiffusion coefficients determ. *(German)* 3−36434
Ne, ion drift vel. 3−24283
Ni, diffusivity of hydrogen 3−36433
Pb, liq., and solubility of O_2, electrochem. obs. 3−27133
Pb-Ag (0.25-2.5%) alloy, molten, temp. depend. of internal adsorption *(Russian)* 3−11541
Sb-In alloy, self-diffusion coeffs., conc. depend. *(French)* 3−30275
Sb-In alloys, self-diffusion coeffs., temp. depend. at equiatomic comp., ionic salt concept *(French)* 3−30276
Sn-Pb system, conc. depend. of pseudopots., atom scatt. cross section, electrotransport *(Russian)* 3−30277
Tl-Te molten alloys, electrotransport *(Russian)* 3−24370
TlCl melt, conductance, transport modes, temp. depend. 3−27132

diffusion in plasma *see plasma transport processes*

diffusion in solids
see also mechanical permeability; thermal diffusion in solids
alloy, binary, diffusion controlled phase transform. kinetics, X-ray analysis 3−34508
alloy, rel. to superplasticity 3−27639
alloys stability of precipitates in an irradiation environment 3−5310
anodic oxidation at const. pot. of permeated H at bipolar electrode, detection of H uptake 3−12522
anodic oxide, O_2 and metal migration, obs. techniques 3−28708
arsenosilica spun on films as diffusion sources for high conc. Si doping 3−21550
atomic migration after radioactive bombard., effect of atomic bond strength *(Russian)* 3−11762
b.c.c. metal, self-diffusion, divacancy mechanism, correlation factor, isotope effects 3−30288
b.c.c. metals, impurity, Neumann and Hirschwald's model 3−33695
bimetallic strip bending due to interstitial diffusion 3−1825
binary ordered alloy, derivation of isotope diffusion coeff. for vacancy mechanism by path probability method 3−4874
binary system with excess vacancies, microscopic theory of interdiffusion *(Russian)* 3−15028
binary systems, interdiffusion coefficients calc., computer program 3−30292
brass, enhanced diffusion during cyclic straining, frequency effects 3−20889
brass, heterogeneous biphase, self diffusion of ^{65}Zn 3−18001
Cahn's equation, in presence of steep comp. gradient, additional term 3−4875
correlation factor, derivation of expression by simple arguments 3−33693
couples with fixed surface composition, effect of conc. dependent diffusion coeffs. 3−38680
creep, chemical stress by vacancy and interstitial supersaturations, diffusion 3−17916
crystal, impurity atom diffusion influence on Mossbauer spectrum 3−30738
cyclohexanol, diffusion and reorientation, n.m.r. study 3−24035
diamond, Si, mech. of defect production 3−33521
diamond struct., correlation factor for impurity diffusion, with electrostatic effects 3−4880
diffusion mobility of inert gases in metals *(Russian)* 3−24286
dislocation, edge, diffusion around cylindrical inclusions *(Russian)* 3−11635
dissolution kinetics of spherical precipitate of second phase *(Russian)* 3−37016
drying of hygroscopic capillary porous solids, liquid capillary flow, vapour diffusion and heat transfer 3−20409
electronic excitation, sensitized luminescence, energy transfer by resonance, impurity states 3−27566
f.c.c. alloy, substitutional, influence of solute pairs on solute diffusion 3−5290
f.c.c. alloy, two vacancy interactions influence on substitutional solute diffusion 3−17997
f.c.c. and b.c.c. metal, vacancy migration energy calc. using Morse function 3−7971
f.c.c. lattice, interstitial migration, molecular dynamics study 3−7748
f.c.c. metal, migrational jumps in long-range diffusion *(German)* 3−7823
$Fe_{1-x}O$, Mossbauer line broadening and diffusion mechanisms 3−4884
Fick's second law, analytical soln. for conc. depend. case 3−24288
fish muscle, analysis of bimodal diffusion of water 3−22143

diffusion in solids continued
glass, borosilicate, ion diffusion and influence of two-site mechanism 3−14699
glass, of Na, atmosphere effects 3−1816
glass, permeability of He, silica comp. depend. *(German)* 3−30284
glasses, diffusion interactions from anion conc. discontinuities 3−18723
glycerol, diffusion and reorientation, n.m.r. study 3−24035
graphite, evaporation of impurities determ. by atomic absorption method *(Russian)* 3−11648
harmonic lattice, entropy of binding between vacancies and solute atoms, lattice vibr. 3−33515
ice, jump diffusion, cold neutron scatt. obs. 3−1810
ice, pure and HF doped X-ray topographical study of dislocations, prismatic loops shrinkage depend. on HF diffusion coefficient 3−17826
II-VI compounds, phenomenological interpretation of anomalous diffusion processes *(German)* 3−15036
impurity, infl. of inhomog. distrib. of vacancies in semicond. *(Russian)* 3−11757
impurity atm. interaction with moving dislocations in metals and alloys 3−17912
intergranular corrosion in pressurized water, hydrogen/grain boundary interactions *(French)* 3−1909
internal friction caused by impurity atom diffusion along dislocations *(Russian)* 3−1692
ion mobility along grain boundaries 3−4877
ionic crystals, diffusion creep in pure, impure and non-stoichiometric materials 3−36355
ionic crystals, Teltow model generalisation of direct current conduction 3−38678
ionic crystals Teltow theory, generalised, models 3−36436
i.r. transmission through the diffusion, sheet resistance and junction depth meas. 3−39286
isotope effects, light interstitial electromigration and thermomigration, quantum theory 3−30287
IV-VI compounds, phenomenological interpretation of anomalous diffusion processes *(German)* 3−15036
Kirkendall shifts during neutron irrad. due to stress gradients 3−11767
loop annealing kinetics, diffusion equations soln. using physical electrostatic analogue 3−20755
marine sediments, diffusion of Mn in pore waters 3−2940
martensitic transformations, reconciliation of the phenomenological theory with mechanisms of diffusional nucleation and growth 3−15660
measurement, appl. of nuclear radiation absorpt. meas. 3−22463
metal, activation energy for vacancy diffusion proportional to latent heat of melting *(Russian)* 3−24295
metal, f.c.c., impurity diffusion, model 3−15031
metal, H_2 diffusion, quasielastic neutron scatt. theory considering finite jump times 3−38687
metal, hydrogen diffusivity meas., low temp., Gorsky effect 3−36440
metal, hydrogen uptake, detection method using anodic oxidation 3−12522
metal oxides, cation diffusion 3−4886
metal systems, real structure and migrational props., magnetic aftereffect obs. *(Polish)* 3−24212
metal-ceramic system, microprobe meas. of chem. and partial diffusion 3−7964
metal/hydrogen systems, conf., Paris, France (May-June 1972) 3−2688
metallic film, electromigration, review 3−4878
metallic film, groups I-IV, electromigration 3−4879
metals, contact areas, intermetallic diffusion obs. 3−4800
metals, diffusion of H_2, neutron spectroscopy study 3−1652
metals, neutron irradiated, deformation and diffusional void growth under stress 3−31020
metals, theory of vibr. props. of point defects 3−24232
migration of supersaturated constituents to point and line sinks 3−24296
misfit dislocations during interdiffusion, interaction forces 3−36472
mixed alkali glasses model based on short range electrodynamic interaction concept 3−11765
Mossbauer effect applics., book *(French)* 3−34276
neutron scattering law for self-diffusion in solids 3−20837
neutron spectroscopy study 3−1652
non-isothermal, brownian motion 3−1818
nondestructive method of study using alpha-particle spectrometry 3−25921
nuclear backscattering microanalysis, semiconductor surfaces, thin films, layered structures, dopant diffusion profiles 3−39280
nuclear reactor materials, neutron irradiated, diffusion controlled creep process 3−24196
organic solid, doped, exciton diffusion theory of luminesc. emission 3−21471
organic solid, doped, exciton diffusion theory of luminesc. emission 3−21472
organic solids, self diffusion 3−4885
Pd-V(Ti), microprobe meas. of chemical and partial diffusion 3−7964
phenanthrene single crystals, self-diffusion meas. 3−11760
phenol, liquid and solid, nuclear spin-lattice relaxation, diffusive molecular motion 3−34237
plastic crystalline cyclic ketones, mol. motion obs. by p.m.r. 3−24040
point defects and diffusion, monograph 3−1621
point defects behaviour study, stochastic processes application 3−17989
polyethylene, of monomer vapour, effect of annealing 3−15027
polyethylene, U diffusion determination by fission track detector 3−27141
pore isolated on grain boundary, volume diffusion controlled shrinkage 3−36292
pore shrinkage by vol. diffusion during final stage sintering 3−37080
precipitate inhibition of diffusion creep 3−20799
rare earth hydrides, hydrogen mobility mechanism *(French)* 3−1826

diffusion in solids continued
rare earth hydrides, struct., dynamics, H diffusion, slow neutron scatt. obs. 3–1615
sapphire, spheroidization of tubular pores at high temps., reln. to surface diffusion 3–17921
saturation parameters determ. procedure 3–20887
semiconductors, in an external electric field, anisotropy in diffusion-noise temp. and differential mobility 3–27269
semiconductors, multivalley, with screw dislocations, diffusion theory of electrical resistance 3–24416
silicate glasses, diffusion rates and solubilities of He and Ne as a function of SiO_2 content 3–4883
solid gas reactions, effect of solid shape on diffusion model 3–34716
solid reactivity, (conference, Bristol, England, July 1972) 3–5379
solid reactivity (conference, Bristol, England, July 1972) 3–2810
solid solution, supersaturated, precip. growth kinetics, effect of conc.-depend. diffusion coeffs. 3–8784
solid state reaction paths and microstructure in crystals 3–5387
steel, austenitic stainless, tritium diffusivity and solubility meas. *(French)* 3–1831
steel, Cr-Ni, secondary creep deform. mechanism, stress and temp. depend. 3–8938
steel, diffusion-controlled coagulation process of globular cementite, expt. confirmation 3–5293
steel, gas diffusivity and solubility meas. and calc. method *(French)* 3–1832
steel, heat treatment, application of the diffusion laws *(French)* 3–18659
steel, low-C, As-bearing, laminated struct., As diffusion *(Russian)* 3–37020
steel, low-C, austenite grain size influence on carbon and sulphur diffusion *(Russian)* 3–39331
steel, of hydrogen, effects on embrittlement 3–5325
steel, stainless, types 304 and 316, grain boundary diffusion of tritium 3–27628
steel, stainless Type 316, obs. of He bubble growth following cyclotron implantation 3–27043
steel plate, diffusion chromizing, effect of alloying elements 3–27689
steel surface, stainless, form. of Cr diffusion coating layer *(Japanese)* 3–12397
succinonitrile, diffusion and reorientation, n.m.r. study 3–24035
superconducting systems, diffusion layers method for construction of phase zones in phase diagrams by electron probe microanalysis *(German)* 3–11717
surface diffusion rel. to sintering kinetics 3–31125
surface-volume coupled diffusion currents rel. to growth rate, capture condition effect at steps 3–11559
transition metal hydrides and their alloys, of hydrogen, activation energy and conc. depend. *(French)* 3–4888
transition metals, hydrogen and deuterium electromigration *(French)* 3–1823
triethylenediamine, diffusion and reorientation, n.m.r. study 3–24035
triglycinsulphate growth, role of surface and volume diffusion 3–20700
trimethylacetic acid, diffusion and reorientation, n.m.r. study 3–24035
vacancy diffusion rel. to edge dislocation velocity in stress induced climb 3–17842
vacancy motion, integral methods in correlation factors calc. 3–17998
variable diffusion coeffs., Boltzmann-Matano analysis 3–39259
VN on V_2N, growth rate at 1500°C, chemical diffusivity of N_2 3–5415
Zircaloy-yttrium welded sheet, isothermal hydrogen diffusion obs. 3–26500
Ag, cold worked, inert gas diffusion and gas release meas. 3–24287
Ag, grain boundary migration under compression at 500°C 3–37042
Ag, point defect parameters determ. from self diffusion data 3–20890
Ag film, of Pb, Pb/Ag/Au and Pb/Ag/Pd layered struct. obs. 3–7976
Ag:^{124}Sb, grain boundary electromigration of ^{124}Sb *(French)* 3–8806
Ag-Be alloys, internal oxidation and hardening 3–21712
Ag-Li alloys, internal oxidation and hardening 3–21712
AgBr:Cd, ionic thermocurrents meas. rel. to interstitial-vacancy complex form. 3–33518
AgCl, of Mn^{2+}, substitutional and interstitial diffusion 3–20888
Al, dynamical props. of dissolved ^{57}Fe, obs. by Mossbauer effect 3–34258
Al, electromigration rel. to anodic Al_2O_3 coating 3–38906
Al, freq. factor and activation energy correl. 3–18002
Al, low-temp. diffusion of Zn meas. using the backscatter method 3–18000
Al, of Fe, surface barrier to diffusion, Mossbauer obs. 3–38684
Al film, electromigration, laser irrad. effects 3–20974
Al film, electromigration, quantitative mass distrib., scanning electron microscope obs. 3–7977
Al glasses, self-diffusion processes 3–4882
Al surface, diffusion of Zn deposited by electro-displacement method 3–11766
Al surface, geometrical cavities development rel. to vol. diffusion of liq. Ga *(French)* 3–7999
Al:Ti, film, impurity distrib. and diffusion coeff. determ. by elec. method 3–30290
Al/Si evaporated films, diffusion-limited Si precipitation 3–39237
Al-Cr, supersaturated solid solns., volume, activation energy calcs. 3–36438
Al-Fe(3.6 at.%), supersaturated solid solns., volume, activation energy calcs. 3–36438
Al-Mn, supersaturated solid solns., volume, activation energy calcs. 3–36438
Al-Ni(3.6 at.%), supersaturated solid solns., volume, activation energy calcs. 3–36438
AlMg5, diffusion coeff. during plastic deform. *(German)* 3–21611
Al_2O_3, ionic self diffusion activation energies, graphical method determ. from previous results 3–15035
Al_2O_3-SiO_2, diffusion and reaction studies at high temps. 3–17994

diffusion in solids continued
As, in Si, effect of complex formation 3–20886
Au film, electromigration, void and hillock growth 3–36437
Au film, self-diffusion along dislocations 3–15032
Au films, electromigration, local variations of current density and temp. influence *(French)* 3–30282
Au/Cu planar couples, mass diffusion of base metal to electroplate surface 3–38685
Au-Al double film system, interaction *(Russian)* 3–4871
AuZn ordered alloys; activation volumes for self-diffusion 3–7973
B diffusion from doped oxide source, characterisation 3–21551
B fibre/W substrate, diffusion barrier establishment *(French)* 3–12440
B surface saturation diffusion into Ti(V)(Zr)(Cr)(Mo)(W), obs. of borated layer structure *(Russian)* 3–11763
$BaSrTiO_3$, O_2 diffusion const. meas. 3–17991
Be, n.m.r. line width rel. to self diffusive, 300-1200K 3–39040
BeF_2, diffusion in F, n.m.r. data 3–34224
α-brass, Zn rate of removal by means of X-ray microanalyser *(German)* 3–12328
Ca glasses, self-diffusion processes 3–4882
CaF_2:YF_3, conc. and mobility of interstitial fluorine ions rel. to intrinsic cond. 3–30489
Cd, self-diffusion, temp. depend. activation volumes, 250-320°C, 0-8 kbar 3–30291
CdF_2:Na^+(La^{3+}), F self diffusion, depend. on doping 3–7972
CdS, of noble metals, 300-800°C, u.s. study 3–30286
CdSe single crystals self-diffusion of Cd and Se investigation 3–33689
CdTe, of Cu, single cryst. prep. and characteriz. 3–15632
Co-Cr(21 wt%) alloy with Y_2O_3 dispersion, Cr diffusion, substruct. influence 3–39343
Co-Pd alloys, interdiffusion coeff., Curie temp. phenomena 3–20899
Co-Si system, rate of reactive diffusion, high press. eff. *(Russian)* 3–7962
CoO, diffusion of ^{35}S 3–1821
Cr-Au bimetallic film, Cr diffusion into Au, work function study 3–15030
(Cu, Ga)-V, supercond V_3Ga layers at interface, growth and props. *(German)* 3–8311
Cu, comments on vol. and surface self-diffusion meas. 3–7974
Cu, of Co, isotope effect 3–7965
Cu, of Rh, temp. depend., 750-1075°C *(Russian)* 3–15029
Cu, self-diffusion, effect of iron solute, vacancy jumps *(French)* 3–24289
Cu, vacancy capture radius for migrating interstitials 3–7749
Cu wires with electrodeposited Cu coatings, diffusional creep *(Russian)* 3–31059
Cu-Ni(Sn) alloys, diffusional creep 3–24195
Cu-Sn diffusion couple, Kirkendall effect 3–4876
Cu-Ti alloy, rel. to boriding *(German)* 3–8902
Cu-Zn alloys, γ-phase, grain boundary diffusion, 25°C *(German)* 3–24840
β-Cu_2HgI_4, disorder phenomena 3–1718
CuI, film growth by Cu tarnishing in I atmosphere, estimation of ionic cond. 3–38683
γ-CuI disorder phenomena 3–1718
β-Cu_3Sb, electrotransport obs. and mechanism *(German)* 3–24298
Er_2O_3, thermal expansion by an X-ray diffraction method, abnormal expansion due to O_2 self-diffusion 3–30272
Fe, Armco, of hydrogen, stress effects *(French)* 3–1830
Fe, hydrogen diffusion coeff. determ. from permeability meas. *(French)* 3–1827
α-Fe, of hydrogen, alloying additions influence 3–1829
α-Fe, of sulphur, volume and grain boundary diffusion, temp. and grain size depend. *(Russian)* 3–24292
Fe, P diffusion, radioactive tracer study *(French)* 3–31002
Fe, self diffusion coeff. temp. depend. at Curie point *(Russian)* 3–11761
Fe alloy, soft, of H_2 and degassing, main parameters *(German)* 3–8888
Fe and alloys, of hydrogen, conc. and temp. depend. 3–1828
Fe and Fe-Ni alloys, of hydrogen, effects of dislocation interactions 3–4887
Fe-C alloys, permeability and embrittlement by cathodic hydrogen *(French)* 3–21661
Fe-metal-C, successive diffusion *(Russian)* 3–7963
Fe-Mn, γ-solid solution, self-diffusion and interdiffusion determ. *(Japanese)* 3–30994
Fe-Ni-Al alloy, subspinodal, vacancy mechanism rel. to hardening process control *(Czech)* 3–31103
Fe-Ni-C alloys, internal friction meas., Snoek-peak, C interstitials diffusion towards dislocations mechanism 3–34542
Fe-Si (3 at wt.%), Al_2O_3 dispersed, Newtonian viscous creep, diffusion mechanism 3–31094
Fe-Si solid solns., of hydrogen, ordering influence *(Russian)* 3–30283
Fe_2O_3 polycrystalline powder ceramic, high temp. deformation rate controlled by stress directed or O_2 or Fe diffusion 3–27738
Ga diffusion, closed-tube, controlled surface conc. 3–39258
GaAs, of Co, temp. depend., 580 to 1160°C, conc. distrib. 3–33699
GaAs, of Zn vacancies, influence of As vapour pressure, distribution regions, surface treatment 3–33696
GaAs, rel. to impurity incorporation during liquid phase epitaxial growth 3–1638
GaAs:Sn, selective diffusion of Zn using SiO_2 layer 3–15244
Ge, of Li drift velocity, depth of drift, electric field configuration 3–33697
Ge, self-interstitials, geometrical config., migration energy 3–33522
Ge diffused layers, reproducibility 3–30954
Ge substrate, of Ga and As during epitaxial growth of GaAs *(Russian)* 3–27606
Ge/Al thin film system, surface mass transfer mechanism, diffusion phenomena *(Russian)* 3–11836
^{4}He:^{3}He, quantum diffusion of ^{3}He impurities 3–33719
HfSi film growth on Si, use of Zr and Ar impurities to determ. diffusing species 3–20958
HgTe, of Ag, Zn, In and Mn, 200-300°C 3–36441

- **diffusion in solids** continued
  - In, thermotransport of tracer Ag, saddle-point cooperation effects 3−17999
  - InSb:Cd, p-n technique 3−34489
  - KBr:Ba^{2+}, rel. to kinetics of conc. decrease of nonequilib. cation vacancies 3−38585
  - KCl, rel. to effect of atomic displacement on dechannelling 3−38601
  - KCl:OH^-, Hg, study of Hg diffusion, effect of OH^- impurity 3−20892
  - KCl:U, of H_2 molecules, rel. to trapping by M-centres 3−20732
  - KCl-KBr mixed crystals, Br^- diffusion, 519-599°C 3−30285
  - KCl + NaCl crystals, hole centres, struct. and conversion, alkaline vacancies diffusion *(Russian)* 3−11621
  - KI, of water molecules, F-band absorp. obs. 3−30120
  - KN_3, activation energy of cation vacancy migration, Born model calc. 3−17995
  - K_2O-SrO-SiO_2, multicomponent diffusion, mobility model, electrostatic effects 3−7967
  - Kcl, crystals subjected to molecular beams, condensation and vaporisation kinetics investigation *(German)* 3−7920
  - Li:Na(Ag), isotope effect comparison for ^{22}Na, ^{24}Na(^{105}Ag, ^{110m}Ag) diffusion 3−38688
  - LiF crystals, pure, anion diffusion, steady state deformation rate temp. depend. 3−17846
  - Li_2F_2, Li_3F_3 crystals subjected to molecular beams, condensation and vaporisation kinetics investigation *(German)* 3−7920
  - LiH, of H, exchange process, press. depend. 3−38681
  - Mg, creep, dislocation pipe diffusion 3−8871
  - $MgAl_2O_4$ single crystals, self-diff. coeff. of oxygen detn. 3−7978
  - MgO, creep-deformed, dislocation structures, cause of deformation, diffusion controlled 3−38593
  - MgO, polycryst., preferential O diffusion along grain boundaries 3−4873
  - MgO:Be^{2+}, tracer diffusion meas. up to 2340°C 3−20891
  - MgO:Fe, polycrystalline, transient diffusional creep mechanism 3−7831
  - MgO:$LiCo_3$ (LiF_2, MgF_2), ionic self-diffusion activation energies, effect on press sintering 3−15770
  - MgO:Sr^{2+} diffusion of Sr^{2+} 3−17993
  - Mo, dislocation-interstitial interactions using dislocation damping obs. 3−36312
  - Mo, interstitial migration on electron irradiation, recovery mechanism 3−11615
  - Mo, of hydrogen, 400-1200°C 3−1833
  - Mo-W system, heterodiffusion, temp. and conc. depend. *(Russian)* 3−4872
  - NH_4Cl, undoped and divalent cation doped, ionic thermal currents 3−33917
  - $(NH_4)_xWO_3$, ionic motion, n.m.r. obs. 3−7968
  - Na, energetics of divacancy diffusion 3−7970
  - Na, self-diffusion, defect energetics 3−36439
  - Na glasses, self-diffusion processes 3−4882
  - NaCl, of He, 300-500°C, desorpt. study 3−33698
  - NaCl:Ca, vacancies, ^{23}Na spin-lattice relax. time obs. 3−12074
  - NaCl-KCl equimolar mixed crystals, spinodal decomp., expt. rel. to diffusion theory 3−30261
  - $NaNO_3$, calc. of migration enthalpies of Frenkel defects, application of Mott and Littleton methods 3−24294
  - Na_2O-Cs_2O-SiO_2 glasses, self diffusion and interdiffusion coeffs. of alkali ions 3−11764
  - $Na_2O.11\ Al_2O_3$, diffusion, n.m.r. diffusion study of ^{23}Na and effect of water on quadrupole interaction 3−8457
  - Nb, of H, quasi-elastic neutron scatt. study 3−1819
  - Nb, of Ni, temp. depend., vacancy mechanism 3−20900
  - Nb, of nitrogen, activation energy temp. depend. 3−20898
  - Nb-Zr-H alloys, n.m.r. exam. and self-diffusion of H *(Russian)* 3−1815
  - Ni, neutron induced voids, low dose dependence at 400°C 3−8856
  - Ni, of Hf and Ti, temperature dependence *(German)* 3−7969
  - Ni, of hydrogen, anomalous mechanism and quantum diffusion *(French)* 3−1822
  - Ni alloys, thoriated, grain struct. effect on Kirkendall porosity appearance 3−37034
  - Ni-Al solid soln., Ni-rich, diffusion at 1260°C, effect of thoria dispersion 3−38686
  - Ni-Au film couple, surface diffusion, electron microscope obs. 3−1878
  - Ni-Co(2.5 wt.%)Al_2O_3 alloys creep behaviour, diffusion mechanisms 3−8870
  - Ni-Cr-Al alloys, internal and external oxidation mechanism 3−31115
  - Ni-Cr-Al alloys, internal oxidation 3−31116
  - Ni-Cr-Mo steel, C diffusion study 3−27633
  - Ni-Cr-ThO_2, dispersion strengthened, prep. by Cr diffusion in Ni-ThO_2 granule 3−8941
  - Ni-Cr(20 wt.%) alloy with Y_2O_3 dispersion, Cr diffusion, substruct. influence 3−39343
  - Ni-Fe film, oblique incidence evap., deuteron irrad. enhanced vacancy migration, effect on mag. anisotropy 3−34148
  - Ni-Sb system, rate of reactive diffusion, high press. eff. *(Russian)* 3−7962
  - $NiFe_{2-x}Al_xO_4$, spinel, cation transfer kinetics, during thermal treatment 3−20885
  - $NiNb_2O_6$-NiF_2 solid solution, columbite and trirutile transformation mechanisms *(French)* 3−7928
  - NiO, diffusion of ^{35}S 3−1821
  - NiO, of ^{51}Cr, 1192-1642°C 3−27137
  - P, in grape seeds, u.s. effects 3−28310
  - Pb:Hg alloys, modified interstitial vacancy-pair model for Hg diffusion 3−20894
  - Pb:Mg alloys, diffusion of Mg and Pb, interstitial-vacancy pair model 3−20893
  - Pb:Ni, pressure effect on Ni interstitial diffusion 3−17996
  - Pb-Au dilute alloys, dehancement of Au diffusivity, Au pairs motion 3−34546
  - Pb-Au solid soln., kinetics and morphology of $AuPb_3$ precip. 3−24843
  - Pb-Sn lamellar eutectic, fine struct. studies in Pb-rich phase *(French)* 3−24818
  - Pd alloys, of hydrogen, 300-900°C 3−1834

- **diffusion in solids** continued
  - Pd film, on cryst. and amorphous Si, interdiffusion and cpd. formation 3−27142
  - Pd/Rh alloys, absorption of H and possible existence of β-phase rhodium hydride 3−31006
  - β-$PdH(D)_n$ isotope mixtures, of D and T, rel. to mobility of surrounding isotope species 3−27136
  - PuO_{2-x}, elec. resist., vacancies, oxidation kinetics *(French)* 3−27139
  - Si, anomalous diffusion discussion 3−20895
  - Si, computer calc. of impurity profiles and diffusion 3−20760
  - Si, conc. depend. of diffusivity, rel. to impurity profile calc. 3−24134
  - Si, diffusion and electrotransport of Mg, 1000-1350°C *(Russian)* 3−7975
  - Si, diffusion of B from shallow ion implants 3−7784
  - Si, diffusion of O_2, X-ray meas. of lattice strain 3−17858
  - Si, from SiO_2 films doped with P and B, diffusional layer prod. *(Russian)* 3−8751
  - Si, granular phase formed by diffusion of O_2, optical consts. calc. *(Russian)* 3−24673
  - Si, group V impurity atom-vacancy, binding energy, diffusion 3−33836
  - Si, impurity gradients, diffusion constant, capacitance meas., nondestructive technique 3−39284
  - Si, irradiated and annealed, diffusion, role of defects, other semiconductor materials 3−33701
  - Si, multistage, conductivity of diffused layers *(Russian)* 3−18137
  - Si, of As, through SiO_2 layer, arsenosilicate glass source 3−39260
  - Si, of As, using As_2O_3-SiO_2 glass diffusion source 3−21545
  - n-Si, of Au, determ. from precip. kinetics of Si-Au solid soln. *(Russian)* 3−1779
  - Si, of Au deposited layer on thermal treatment 3−39289
  - Si, of B experiment-design method, highest slope, diffusion process from diborane source *(Hungarian)* 3−18552
  - Si, of Cu^+, Ag^+ and Au^+ ions over interstitial oxygen sites 3−33700
  - Si, of Ga, effect of oxide layer 3−18212
  - Si, of impurities, effect of surface oxidation 3−7786
  - Si, p-n junction formation by Cd diffusion 3−20896
  - Si, self-interstitials, geometrical config., migration energy 3−33522
  - n-Si, thermomigration of Al-rich liquid droplets 3−7966
  - Si diffused layers, reproducibility 3−30954
  - Si gettering of heavy metal impurities by ion damaged surface layers, Rutherford scatt. obs. 3−30961
  - Si photostimulated diffusion of Au 3−33691
  - Si slices, of Au, dislocation density effects, dissociative mechanism 3−39240
  - Si transistor emitter diffusion, effects of Sn on base impurity 3−39290
  - Si:As, As diffusion from doped oxide, effects of $N_2(O_2)$ atmosphere 3−30281
  - Si:As, bulk resist. vs. As doping curves rel. to diffusin temp. 3−21024
  - Si:B, anomalous B diffusion, effect of inert gas 3−39257
  - Si:B, orientation dependent, effects of oxidation 3−39300
  - Si:B, X-ray topographic obs. of dislocation contrast after boron diffusion 3−17835
  - Si:Ge, radioactive tracer meas. of ^{71}Ge diffusion 3−24293
  - Si:Ge(Sn), O electron irrad., selective-trapping of vacancies, migration of interstitials 3−33925
  - Si:Li, segregation of dissolved Li to surface, photoemission meas. 3−24297
  - Si-As n-p-n structs., retarded base diffusion, theory 3−21544
  - SiO_2, of As, using As_2O_3-SiO_2 glass diffusion source 3−21545
  - SiO_2, of B, Ga, P, As and Sb, summary of data 3−21546
  - SiO_2, vitreous, of Ne, 189-720°C, obs. and models 3−30289
  - SiO_2 film, deposited on n-Si in r.f. glow discharge of B, 1100-1200°C 3−27144
  - SiO_2 film, ion neutralization processes and impurity migration effects 3−34450
  - SiO_2 film, r.f. sputtered, Na^+ motion, meas. using thermally stimulated ionic currents 3−33688
  - SiO_2 film, silica, ion movement in applied field, diffusion eqn. calc. *(German)* 3−15037
  - $SrTiO_3$, O_2 diffusion const. meas. 3−17991
  - Ta, diffusion of H_2, coefficients determ. by X-ray meas. of lattice expansion 3−27145
  - Ta:H, H diffusion activation energy, elec. resist., 77-400K 3−38682
  - Th(C,N) scale on solid Th-C alloy 3−8770
  - ThN scale, on liq. Th 3−8770
  - Ti, adsorption of Cl, segregation of Cl and S impurities from bulk 3−1882
  - Ti-Al system, interdiffusion phenomena 3−24820
  - Ti-Al system, interdiffusion phenomena 3−24821
  - Ti-Mo-H alloy, b.c.c., proton motion, spin-lattice relax. time obs. 3−12073
  - Ti-Ni alloys, near-equiatomic, diffusion controlled phase transform. structures 3−39311
  - Ti-Si(1 wt%) alloy, Mo effect on quenched and aged struct. 3−31064
  - Ti-Sn alloys, scale resist., oxygen effect 3−24941
  - TiH_{2-x}, γ-phase, of H, model 3−27138
  - (U, Pu)C, α-particle stopping power and range, application to self-diffusion meas. using alpha-spectroscopy 3−11664
  - $(U,Pu)O_2$ fuel, irrad.-enhanced interdiffusion of U and Pu, shielded microprobe obs. 3−38179
  - $(U,Pu)O_{2-x}$ fuel pellets, compressive creep, diffusion of cation vacancies and interstitials 3−6991
  - UC, self-diffn. of C, meas. using tracers and sectioning techniques 3−17992
  - UC fission-gas swelling, temp. depend., analytical evaluation 3−11066
  - UC_2, U self-diffusion, 1670-2500 K 3−27143
  - UO_2, sintering of grain boundary cavities, grain boundary diffusion coeff. estimation 3−12437
  - UO_2-C-N_2, reaction kinetics at 1700 C 3−39382
  - $UO_{2\pm x}$, polycrystalline, stoichiometry influence on compression creep 3−6992
  - V-C supersaturated solid soln., carbon precip. obs. 3−37036
  - $VD_{.5}$, vibrational and diffusional motions of deuterium in α and β phases 3−1820

diffusion in solids continued
V_3Ga supercond. diffusion layers at V-(Cu, Ga) interface, growth and props. *(German)* 3−8311
W, of hydrogen, 400-1200°C 3−1833
W, of sulphur, vacancy mechanism *(Russian)* 3−24291
W fine wire with thoria dispersion, creep behaviour 3−37086
ZnO-NiO solid solution, Ni-Zn ferrite formation 3−2812
ZnS-CdS phosphors, activation by Cu diffusion at low temperature *(Russian)* 3−36943
ZnSe:Al, Ga and In, optical absorption, diffusion of impurities 3−24712
Zr, bulk diffusion of Mn in b.c.c. and h.c.p. phases 3−26507
Zr-Nb dil. alloys, β-phase, self- and solute-diffusion 3−27140
diffusion length *see diffusion*
diffusion pumps
review of technology 3−37610
diffusivity, thermal *see thermal diffusivity*
digital-analog convertors *see digital-analogue conversion*
digital-analogue conversion
see also analogue-digital conversion
complex waveform generation using device with D/A convertor followed by low pass filter 3−28482
ratemeter, strongly fluctuating pulse count rates, design *(German, English)* 3−6085
digital circuits
see also adders; counting circuits; digital integrated circuits; pulse circuits; switching circuits
for angle scattering experiments 3−32182
counter MH 7490 applications *(Czech)* 3−16525
current integrator with digital read-out, student apparatus 3−28452
frequency synthesizer, programmable for high resolution n.m.r. spectrometer 3−32117
galvanic transmissions, electronic programmed control system *(Russian)* 3−37524
h.f. coupling analysis 3−29002
on-line computing and digital electronics, undergraduate course 3−42
pulse generator, for n.m.r. experiments 3−25823
sine generator, for Mossbauer spectrometer 3−35517
smoothing, for infrared spectrophotometer 3−401
teaching expts., diodes and transistors, appls. 3−28437
digital communication systems
ionospheric scatter link, with automatic interrogation *(Russian)* 3−3194
laboratory on-line data transmission using PDP-15 and PDP-8/E 3−26005
optical, applications of quantum amplifiers 3−22851
optical, with subcarrier PCM and frequency multiplexing of digital data channels, noise immunity analysis 3−29051
optical binary signal detection optimisation, characteristic function method *(Russian)* 3−16802
optical binary system, coherent radiation detection in thermal noise 3−26211
GaAs laser diode, pulse position modulation technique for point-point voice communication 3−26209
digital computer applications *see computer applications*
digital computers
see also digital systems; general purpose computers; minicomputers; special purpose computers
IBM 360/195 system at Meteorological Office 3−28028
pollution sensing system, read out control, oceanic pollution 3−3214
digital control
see also direct digital control; numerical control
X-ray double crystal spectrometer, digitally controlled 3−32231
digital filters
see also signal processing
least squares smoothing operators, analysis in frequency domain 3−28838
real-time, for modelling small room responses 3−3693
seismic wave time-dependent frequency spectra detection and analysis *(Spanish)* 3−34967
digital instrumentation
see also digital readout; digital voltmeters
electrometers, measurement problems in measuring very small voltages and currents *(Polish)* 3−25812
frequency meter, l.f., Siberian Instruments 1971 Exhibition *(Russian)* 3−9900
interference correlation meter with high storage time 3−22132
ionosonde for automatic readout of electron density profiles 3−12865
for magnetic field measurement *(German)* 3−13356
nanoammeter, Siberian Instruments 1971 Exhibition *(Russian)* 3−9900
nonstationary flow meter, Siberian Instruments 1971 Exhibition *(Russian)* 3−9900
Omega receiver for buoy location 3−3205
photoelectric photometry, digitisation using the direct current method *(Japanese)* 3−19083
piezoelectric quartz crystal digital sensor as partition detector 3−37744
signal processor using MSI logic circuits, use for sonar, seismic and underwater telemetry systems 3−3178
temperature measurement, magneto-thermal effect *(German)* 3−255
thermometer, for medical application *(German)* 3−37595
third order light intensity correlator 3−35401
transient recorder 3−32113
voltmeter, high speed, automatic, Siberian Instruments 1971 Exhibition *(Russian)* 3−9900
digital instruments *see digital instrumentation*
digital integrated circuits
signal processor using MSI logic circuits, use for sonar, seismic and underwater telemetry systems 3−3178
TTL and ECL for counting circuits 3−37698
digital readout
see also digital instrumentation
cryogenic liquid level indicator design *(French)* 3−22297
current integrator with digital read-out, circuit description 3−28452
reversible, to follow reversing signals 3−32179
digital readout continued
spectrophotometer, double-beam, with automatic sample system *(Japanese)* 3−25754
digital signals
optical binary signal detection optimisation, characteristic function method *(Russian)* 3−16802
digital storage
see also associative storage; cryotrons; magnetic storage systems; optical stores; read-only storage
ferroelectric memories, reversible domain polarisation by laser beam, triglycine sulphate plate *(French)* 3−22967
superconductive tunnelling and applications, monograph 3−2221
tape recorder, portable, data acquisition and retrieval system for field operation 3−25990
digital systems
see also digital computers; multiprocessing systems; parallel processing; real-time systems; sampled data systems
beamformers, influence of input quantizer step sizes on processing gain 3−86
geophysical data acquisition and processing at sea 3−3176
Meteorological Research Flight digital systems 3−9402
microscope for edge detection by digital probing of intensity distribution *(German)* 3−32064
minicomputer psychoacoustic system 3−3460
programmable digital pulser for pulsed n.m.r. applications 3−6047
digital to analogue convertors *see digital-analogue conversion*
digital voltmeters
leakage current measurement in decaying process *(Japanese)* 3−19234
photoelectric photometry, digitisation using the direct current method *(Japanese)* 3−19083
digitisers *see analogue-digital conversion*
dilatometers *see extensometers*
dilute alloys
see also impurity electron states and effects; Kondo effect; magnetic properties of dilute systems
Anderson model for dilute alloys, heuristic treatment for one-electron properties 3−2246
binary, residual resist. calc., pseudopot. form factors, impurity effects *(Russian)* 3−15172
Boltzmann transport eqn., solubility for localised defects 3−27238
conducting state, nonmag. impurity quasilocal vibration 3−4986
disordered binary, electronic struct. 3−11856
disordered binary, random transfer integrals and electronic struct. in dilute limit 3−36519
ferromagnetic, thermodynamic and kinetic props. 3−34109
Friedel-Anderson, virtual level model, test of validity 3−38786
inert gases, solid and liq., emission spectra of deep impurity states 3−2581
kinetic equation for cond. electron scatt. in dilute non-mag. alloy 3−30603
Kondo, thermoelec. power and Lorenz number temp. depend., from Anderson model 3−8138
magnetic, application of ultralow temperature techniques 3−35383
magnetic, e.s.r. spectra, cryst. field struct., theory 3−15423
metal-3d impurity, e.p.r. theory 3−30683
point defects, arbitrary set, statistical thermodynamic calc. of equilib. conc. 3−30115
polarised neutron scattering by impurities, Kondo effect, spin fluctuations, inelastic phenomena, survey 3−21224
residual resistivity, pseudopotential calcs. for volume depend. 3−36575
superconducting states using Anderson Hamiltonian 3−8286
umklapp effect on low temp. thermal resistivity 3−1751
vacancy decay, analytical discrete lattice calc. 3−1619
Ag-Pd, test of virtual-level, Friedel-Anderson model 3−38786
Ag-Sn, dislocations dynamic behaviour and yielding phenomena 3−17819
Al-Cr(Mn) n.m.r. spectra, satellite struct. interpret. 3−2431
Al-Fe, cold-worked, internal friction and Young's modulus, heat treatment effects 3−27703
Al-Mg, neutron irrad. at 4.6K, resist. study 3−27042
Al-Mg, recovery after neutron irradiation at 4.6K, elec. resist. obs. 3−11658
Al-Ti, dilute alloys, solid effect between pure quadrupolar nuclear transitions 3−34243
Au-Co, quasielastic neutron scattering cross section for paramag. impurities 3−5095
Au-V, quasielastic neutron scattering cross section for paramag. impurities 3−5095
Au-Yb(Ce)(Gd), negative s-f interaction 3−24561
AuCo alloys, n.m.r. of ^{59}Co 3−34226
Be-Cu, mech. twinning *(Russian)* 3−20753
Ce-La alloys, α-γ electronic transition, La impurity effects 3−38669
Ce-La alloys, α-γ electronic transition, La impurity effects 3−38670
Cu-base, collective recrystn., excess grain boundary energy determ. *(Russian)* 3−8832
Cu-Fe, oscill. of cond. electron density near solute atoms, ^{63}Cu n.m.r. obs. 3−2462
Cu-Fe, resist. and thermo-e.m.f., 4.2-273K *(Russian)* 3−8152
Cu-Mn dilute alloy single crystals, strain rate and temp. depend. of the flow stress 3−8898
Ge:As system, phase separation, X-ray photoemission study 3−36421
$(La, Ce)Al_2$ dilute alloy with Ce impurities, superconducting-Kondo system, specific heat 3−5072
Na-Cd dilute alloys, state of Cd impurities, temp. dep. of elec. resistivity 3−33868
Na-In, liq., density and surface tension, 170-400°C, comparison with Na-Cd alloys 3−36994
Ni:Hf, lattice-location of implanted impurity in ferromag. host, channelling obs. 3−18305
Ni-Fe, Mossbauer obs. of hydrogen desorption *(French)* 3−1891
Ni-Fe:H dilute alloy with high H conc., magnetoresistivity rel. to local mag. moments 3−8158
Pb-Ag (0.25-2.5%), molten, temp. depend. of internal adsorption *(Russian)* 3−11541
Pb-Au, dehancement of Au diffusivity 3−34546

dilute alloys continued
  Pb-Fe, spin-disorder resistivity meas. as function of temp. in 0-60 kOe 3 – 2057
  Pb-Sn system, supercond. dynamics of Sn impurity oscills., Mossbauer and u.s. velocity studies *(Russian)* 3 – 7894
  Pd-Co, ^{57}Fe hyperfine field press. depend. up to 180 kbar 3 – 18306
  Pd-Mn(Fe)(Co), ferromag. transition temp., resist. study 3 – 30624
  Pd-Ni, pressure effect on low temp. elec. resist. 3 – 15170
  Rh-Fe-Mn, Rh-Mn, Rh-Fe alloys, low temp. meas. and comparisons of elec. resist., magnetoresist. and magnetiz. 3 – 4990
  Sn, residual electrical resistance, impurity effects *(Russian)* 3 – 8137
  Sn-Zn, liq., Ag effect on Zn activity coeff., 803 K 3 – 36995
  Ti-Pu, influence of $\beta\to\alpha$ transformation and of O_2 on Pu distribution *(French)* 3 – 18601
  Zr-Nb, β-phase, self- and solute-diffusion 3 – 27140
  Zr-Pd(Ru), heat treated, mech. props. and microstruct. *(Japanese)* 3 – 31079
  Zr-Pu, influence of $\beta\to\alpha$ transformation and of O_2 on Pu distribution *(French)* 3 – 18601
dimensions
  temperature coefficient, in meas. of parametric and non-parametric quantities 3 – 25645
dimers *see molecules*
dineutrons *see neutrons*
diode lasers *see semiconductor lasers*
diode tubes *see diodes*
diodes
  see also plasma diodes; rectifier tubes; semiconductor diodes
  electron beam focusing using current carrying plasmas in high ν/γ diodes 3 – 17650
  W filament, effect of adsorbed O on work function, meas. in space charge region *(French)* 3 – 36648
dipole antennas
  10 GHz design for e.m. field distribution meas. 3 – 10423
  electric and magnetic transmitter/receiver system for detection of conducting object in lossy environment 3 – 3175
  e.m. fields for antennas over stratified anisotropic media 3 – 34885
  field strength meters, equipment for checking and calibrating *(Russian)* 3 – 19237
  plasma, characteristics of electric field far and close to a radiating antenna around lower hybrid resonance 3 – 21962
  plasma, hot isotropic system, current distrib. at surface of dipole antenna *(French)* 3 – 23825
  radiation props. improved by plasma or dielectric layer 3 – 29020
  resonances excitation by dipole antenna inside hollow cylindrical plasma 3 – 7495
  short dipole in drifting magnetoplasma, radiation resistance calc. 3 – 38433
  space wave field reflection from perfectly conducting sinusoidal ocean surface 3 – 4063
dipole moment, electric *see electric moments*
dipole moments, magnetic *see magnetic moments*
diquarks *see quarks*
Dirac electron theory *see Dirac equation; electron theory*
Dirac equation
  see also electron theory
  atom, one-electron, magnetic h.f. interactions, Schrodinger, Dirac and QED perturbation calcs. 3 – 33017
  bremsstrahlung, mag., Lorentz-Dirac eqn. soln., results tested using electron beams in intense mag. fields 3 – 10703
  Cauchy problem for Dirac eqn. in De Sitter space and anticommutator of spinor field 3 – 28965
  classical notion of spin 1/2 particles with zero anomalous magnetic moment 3 – 37851
  covariant solutions in e.m. field 3 – 19484
  diatomic crystals, heavy, relativistic effects on the surface states, Dirac eqn. solutions 3 – 27298
  electron diamagnetism, Dirac theory for interpretation *(French)* 3 – 27354
  electron in central-symmetry field, perturbation of bound states 3 – 22713
  electron motion in quantized electromagnetic field, rel. with Volkov solution 3 – 23050
  external symmetry group formation 3 – 23052
  heavy ion collisions, electronic effects, modification 3 – 6791
  Lorentz-Dirac eqn. for particle in uniform field, relativistic motion 3 – 35719
  Lorentz-Dirac equations of motion, for charged particles in const. e.m. field 3 – 29196
  Poincare invariance of alternative to eqn., reply to comment 3 – 6315
  propagation of spin-one-field in interaction with Dirac field 3 – 16938
  quasirelativistic eqns. reduction to subspace of positive energy states 3 – 582
  relativistic Coulomb Green function, Sturmian expansions 3 – 26121
  relativistic electron theory, pseudoscalar mass and its relation to scalar mass 3 – 6548
  relativistic electrons, movement in crossed mag. and elec. fields of focusing type *(Russian)* 3 – 19686
  relativistic eqns., classical origin 3 – 4000
  relativistic H atom, algebraic treatment based on SO(4,2) dynamical group 3 – 22707
  spinor field as fusion of tensor fields *(Russian)* 3 – 22994
  surface states, Dirac classification 3 – 24488
  two-component alternative 3 – 16692
  H retarded interactomic potential energy of 2 ground state H atoms, Dirac theory 3 – 20073
direct analogues
  inner ear, stapes-basilar membrane system, electrical and mechanical *(German)* 3 – 37527
direct coupled amplifiers *see d.c. amplifiers*
direct current amplifiers *see d.c. amplifiers*
direct current generators *see d.c. generators*
direct digital control
  see also control systems
  epitaxial growth process, computer control, process and layer parameters 3 – 12221
direct energy conversion
  see also cells (electric); magnetohydrodynamic conversion; plasma diodes; thermionic conversion; thermoelectric conversion
  angular-dependent transmission of ribbon grids, use for fusion reactors 3 – 17649
  direct pumping of lasers by exhaust plasma in fusion reactors 3 – 19971
  fusion reactor, direct-conversion collector, computed efficiencies 3 – 38188
  superconducting coil applications, review 3 – 7016
direct nuclear reactions and scattering
  see also pick-up reactions; stripping reactions
  angular correlations of final particles and γ-quanta, sensitivity to mechanism-type *(Russian)* 3 – 19832
  Hauser Feshbach formulas derived 3 – 10952
  Hauser-Feshbach's calc. of cross sections, modification by direct reaction channel coupling 3 – 17209
  heavy ion reactions, semiclassical theory 3 – 1017
  hole spectral function in continuum shell model 3 – 10889
  multistep processes, distorted wave theory 3 – 19826
  single-particle knock out reactions, hole states 3 – 19830
  single-particle transfer, new approach to recoil effects 3 – 38153
  two-particle transfer form factors, approximate calc. method 3 – 19831
  (n, 2n), E_n = 10-20 MeV, reaction mechanism *(Russian)* 3 – 23321
  $^{10}B(\alpha,d)^{12}C\gamma$, calc. of angular correlations of final particles and γ-quanta *(Russian)* 3 – 19832
  $^{11}B(\alpha,t)^{12}C\gamma$, calc. of angular correlations of final particles and γ-quanta *(Russian)* 3 – 19832
  $^9Be(^3He,p)^{11}B$, excitation functions, low energy, direct process 3 – 26469
directional antennas *see directive antennas*
directional patterns *see antenna radiation patterns*
directive antennas
  see also loop antennas
  stacked Yagi, satellite automatic picture transmission reception 3 – 3161
directors (programs) *see supervisory and executive programs*
discharge lamps
  see also arc lamps; flash lamps; fluorescent lamps; metal vapour lamps
  colour characteristics of new discharge lamps for TV and film lighting 3 – 9979
  dye laser pumping *(Russian)* 3 – 6481
  electrodeless microwave-excited, problems of line broadening for volatile elements 3 – 3920
  fluorescent, spectroradiometric measurements 3 – 22348
  hollow cathode, for spectrochemical analysis of solutions *(German)* 3 – 16569
  hollow cathode, intermittent high current operation, atomic fluorescence spectroscopy appl. 3 – 28540
  hollow cathode, program controlled, for emission analysis *(German)* 3 – 25771
  IFP-5000 lamp, emission characts. and reliability *(Russian)* 3 – 5950
  intense microsecond flash lamp for flash photolysis 3 – 6155
  intensified u.v. analyzing lamp for flash photolysis 3 – 6154
  metal halide, water-cooled, efficient pumping of c.w. garnet laser 3 – 22388
  multielement electrodeless discharge lamps for atomic fluorescence analysis 3 – 37742
  multiple element electrodeless discharge, temp. controlled, for atomic fluorescence spectrometry 3 – 26006
  quartz-Xe, tubular, maximum input energy *(Russian)* 3 – 1530
  u.v. source two-channel glow discharge lamp 3 – 22352
  ^2H lamps, suitability as short u.v. spectral irradiance standard *(Japanese)* 3 – 28551
discharge tubes *see gas discharge tubes*
discharges (electric)
  see also arcs (electric); electric breakdown; flashover; glow discharges; high-frequency discharges; lightning; plasma; positive column; sparks; surface discharges; Townsend discharge
  air, discharge development in strongly overvoltaged gaps, low press. *(Russian)* 3 – 26909
  air, microwave generated ionised sheath in coaxial transmission lines 3 – 17694
  air, nsec. region, electron-optical study *(Russian)* 3 – 17685
  in air, similarity laws, validity *(German)* 3 – 17683
  ammonia and hydrazine, schuster band structure *(German)* 3 – 11270
  Ar, impulse discharge emission in vacuum u.v. region *(Russian)* 3 – 30044
  Ar + H_2 mixture, deionization process 3 – 30041
  atmospheric point-discharge current density rel. to worldwide thunderstorm activity 3 – 31377
  atomic resonance, interpretation of Lomakina-Sheibe formula *(Russian)* 3 – 23485
  audio frequency, cathode fall of potential 3 – 30028
  capilliary narrow, spectral method of electrolyte solution analysis *(Russian)* 3 – 35546
  cathode, double hollow, with separated evaporation and excitation zones, spectral characteristics *(Russian)* 3 – 30043
  confined-discharge plasma generator with local fluid construction 3 – 26904
  cooled hollow-cathode, elec. and opt. characts. *(Russian)* 3 – 7577
  corona, conductors between planes, characteristics, calc. 3 – 14607
  corona, field distrib. charged disperse phase effect, calc. 3 – 33402
  corona, motion of aerosol particles, approximation *(Russian)* 3 – 36213
  current in pulsed plasma accelerators, potential drops near electrodes *(Russian)* 3 – 7569
  current trapping in toroidal, high current discharges 3 – 4667
  current-voltage characteristic of discharge between water and Cu cathode *(French)* 3 – 7570
  d.c., low current, methane pyrolysis 3 – 1528
  detection, rel. to power system apparatus, ramp and l.f.-a.c. voltage applic. 3 – 17712
  detectors, for insulation testing, method 3 – 24644
  dielectric degradation, equivalent circuits *(Polish)* 3 – 20667
  dielectric liquids, prebreakdown, obs. 3 – 2494

discharges (electric) continued
dielectric units on accelerators, two-stage development of discharge in space-charged medium, damage 3−16475
distortion of volt-coulomb characteristics in a gap with dielectric boundaries *(Russian)* 3−7589
electric breakdown initiation in vacuum, rel. to Mo electrodes 3−33411
electron beam energy broadening, one dimens. distrib. function in press. discharge 3−7490
electron bremsstrahlung at high overvoltages 3−30034
erosion of steel in different atmospheres, effect of tertiary elements *(Russian)* 3−23952
excitation and ionisation of neutral atoms in dense discharge by electron impact 3−23497
exploding wire formation of gas discharge zone, review *(German)* 3−11519
flame plasma, different calor-electric effect manifestations 3−23934
gas breakdown initiation, u.v. photoionisation and laser effects 3−17492
gaseous electronics, modern view of classical problems *(German)* 3−36232
gaseous pulsed nanosecond, mechanism 3−36220
halogen parallel plate counters, short dead time 3−25863
helical, excitation of static density structures 3−7592
Hg, vapour, 1 to 20 Torr press., positive discharge column study 3−17700
high voltage pulsed discharges, oscillograms, automatic initiation, streak photography 3−252
hollow, cathode, electron energy distribution 3−30038
hollow cathode, effects on throttled ion thruster 3−38514
hollow cathodes, cooled and heated, spectral characteristics *(Russian)* 3−28553
holograms of spark discharges produced by nsec. pulses 3−5970
hot cathode Penning discharge plasma, rotation of ion component *(Russian)* 3−14628
hot hollow cathode, for ion production for vacuum deposition 3−25716
impulse, distribution of ionic spectral line intensities *(Russian)* 3−36231
impulse, dynamics of precathodic region at various rates of changing current *(Russian)* 3−30046
impulse, emission measurements *(Russian)* 3−30045
inertial plasma instruments with inplatrons for meas. moving parameters *(Russian)* 3−9835
insulating materials, partial discharges recording method 3−32112
intense radiation sources for alkali and alkaline earth metals, preparation methods 3−32262
ion flux probe, low pressure discharge plasma 3−36199
ion source development using cathode sputtering technique for introduction of solid substances into discharge atmosphere *(Russian)* 3−10042
linear, production of a relativistic electron beam 3−23896
liquid dielectric breakdown under recurring discharge, high-voltage meas. 3−11514
liquids, gas generation during initial stages of pulse discharge formation *(Russian)* 3−14614
low frequency, a.c., sonic irradiation effect on discharge characteristics 3−30027
low-pressure, in a transverse magnetic field, anode sheath instability and high energy electrons 3−36226
low-pressure, radial distribution of neutrals 3−30042
low-pressure tubes, vessel for cooling with liquid N_2 *(Czech)* 3−25934
Lyman capillary discharge light source, spectral props. 3−7575
metallized paper capacitors *(Japanese)* 3−26912
molecular vapours, investigation of electrically pulsed discharges, search for laser media with high quantum efficiency 3−726
oscillating electron, dependence of current on system parameters *(Russian)* 3−11518
oscillation modes and cathode pot. drop meas. possibility *(French)* 3−7572
partial, in air, optical recording system, calibration, soln. *(Russian)* 3−14613
partial, measurement using correlation methods 3−16375
Penning, modified, ion heating mechanism 3−33383
Penning, modified, origin of hot ions 3−23943
Penning discharge in a strongly inhomogeneous magnetic mirror field, collective phenomena 3−20642
Penning discharge under rotational instability, convective particle transport across mag. field *(Russian)* 3−33373
plasma beam discharge with an anti cathode, instability and ionic heating investigation *(Russian)* 3−14542
plasma current heating in turbulent discharges, phenomenological model 3−20581
plasma diagnostics in a pulsed discharge in a mixture containing H_2 3−14587
plasma ionisation measurements at high d.c. voltage *(German)* 3−23930
plasma spatial density distributions in h.f. discharge with superimposed static magnetic field 3−7505
plasma/tube interaction, metal evaporation obs., Rozhdestvenskii hook method appl. 3−14619
plasmoidal r.f. discharge, spatially resolved spectroscopic profiles 3−20671
polyethylene, internal, rel. to dielectric performance *(French)* 3−27468
positive column, low pressure weak current, dynamic behaviour *(German)* 3−7483
positive streamer propagation, computer model, calc. of measurable quantities 3−1525
propane, laminar flame in a discharge, elec. field effects, photography 3−36211
pulses in air at low pressures, potential variation 3−38510
radiation emission from Hg vapour discharge and derived electron energy distribution *(German)* 3−14603
resistive electrode discharge system, for TEA CO_2 laser 3−25781
rhodamine-6G laser, rhodamine-6G, pinched discharge pumped, divergence time dependence *(Russian)* 3−729
self excited moving striations in longitudinal magnetic field, analysis 3−14611

discharges (electric) continued
short airgaps, predischarge phenomena 3−14612
spark, influence of subsonic airstream 3−14608
spectra of gas discharge plasma, effect of electrode materials *(Russian)* 3−23953
spectroscopic light sources, erosion of electrodes, dependence on physical properties of metal *(Russian)* 3−9948
stability of discharge surrounded by free vortex 3−7584
streamers in plasma displays, rel. to choice of multiplex methods 3−23927
tempeature distribution in heterogeneous medium with radiative heat transfer *(Russian)* 3−11515
tornado initiation, geo-electromagnetic aspects 3−31381
transport processes study by Eindhoven AVF cyclotron, Netherlands 3−20668
Trichel, in air, mechanism *(German)* 3−36210
triggering of gas discharge, utilizing transverse extension of normal glow discharge *(German)* 3−38508
turbulent, electron beam emission through mesh anode *(Russian)* 3−14623
turbulent, in longitudinal mag. field, energy balance of ions 3−23891
vacuum, rel. to breakdown triggered by low velocity microparticles 3−4683
in vacuum, surface processes on discharge-cleaned electrodes *(Russian)* 3−7588
vacuum, triggered by electron beam, characteristics *(Russian)* 3−14625
vacuum breakdown, dependence on cathode surface roughness 3−14626
vacuum discharge, duration of X-ray emission *(Russian)* 3−30026
water, circuit transient following a pulsed discharge 3−36227
in water, finite difference simulation 3−17693
in water, u.v. radiation dissipation 3−17692
xerographic discharge characts. of photoreceptors 3−16456
Z-pinch, low press. high voltage, formative phase obs. 3−1513
Z-pinch h.f. discharge, spectroscopic meas. of turbulent plasma parameters *(Russian)* 3−7537
Al, atoms and ions, in low-voltage pulsed discharge, spectral line contours 3−23941
Ar, cylindrical hollow cathode negative glow discharge, plasma diagnostics *(German)* 3−4675
Ar, high-current low press., electron conc. estimation *(Russian)* 3−7579
Ar, rotational temperature determ. method 3−16413
Ar discharge, fluctuations and oscillating phenomena *(German)* 3−14602
Ar high-current pulsed discharge, plasma properties of ionized gas *(Russian)* 3−7586
Ar low pressure hollow cathode discharge pendel effect expt. evidence *(German)* 3−14631
Ar supersonic plasma, effect of electrode processes on volt-ampere characteristics of discharge 3−17709
Ar + H_2O deionisation process 3−30041
Ar^+ ion laser discharge at high current 3−16834
CO, laminar flame in a discharge, elec. field effects, photography 3−36211
CO_2, current change due to CO_2 laser beam, mechanism 3−26914
CO_2, microwave discharge, CO_2^- form 3−20670
CO_2, nsec. region, electron-optical study *(Russian)* 3−17685
Cs, gaseous diagnostics, tuned GaAs laser diode 3−4670
Cs plasma, electron distrib. function, Langmuir probe obs. 3−4669
H cluster beams, electrical discharge effects on size 3−4661
H discharge, pulsed, plasma diagnostics, electron conc. determ. 3−17660
H_2, plasma-beam discharges, multiply charged ions plasma parameters determ. 3−23916
H_2 electron beam stabilized discharge, superfluorescence due to HF quenching 3−19599
HF low-density discharge, Stark broadened Balmer lines *(German)* 3−38515
H_2O pulsed laser discharge, gas temp. measurement, spectroscopic obs. 3−4090
He, high pressure spectroscopic and plasma characteristics 3−30029
He, plasma-beam discharges, multiply charged ions plasma parameters determ. 3−23916
He, positive column, transition from homogeneous to striated state 3−4686
He, pulsed, elec. and opt. meas. *(Russian)* 3−7578
He afterglow, decay of 2^3S_1 state, investigation in pulsed electric discharge 3−14620
He d.c. discharge, ion acoustic waves spontaneous excitation 3−23879
He positive column, improved probe curve analysis 3−4684
He-Hg mixture, weakly ionized, electron distrib. function 3−14604
He-Ne discharge, 3.39 μm Ne linewidth, mixture composition depend. 3−32546
He-Ne laser, relax. oscillations, range of existence, gas press. effect *(Russian)* 3−4094
He-Se^+, for positive-column lasers, electron temp. and density 3−16833
He-Xe mixture, pulsed discharge generation mechanism 3−17701
He-Xe mixture, pulsed laser action mechanism, excitation characteristics with external electrodes 3−33412
Hg, in thyratron, dielectric const. as function of freq. 3−17686
Hg, low pressure, high current, anode region phenomena *(Russian)* 3−14624
Hg, with hollow cathode, thrust meas. 3−11522
Hg vapour pulsed high-current, characteristics 3−36223
K, luminesc. in pulse discharge, H_2-addition effect 3−33413
in Kr, double-cathode effect, boundary conditions *(German)* 3−14622
Kr, plasma-beam discharges, multiply charged ions plasma parameters determ. 3−23916
Li plasma, high-current discharge struct. 3−33404
Mg, atoms and ions, in low-voltage pulsed discharge, spectral line contours 3−23941
N_2, impulse discharge emission in vacuum u.v. region *(Russian)* 3−30044
N_2, nsec. region, electron-optical study *(Russian)* 3−17685

discharges (electric) continued
- N_2, pulsed, vibr. temp. meas., microwave technique 3−38494
- N_2, SF_6, photoelectric processes in a uniform field *(Russian)* 3−7591
- N_2 condensed mol. beams, z-pinch discharge current distrib. *(German)* 3−4689
- N_2 electron beam stabilized discharge, superfluorescence due to HF quenching 3−19599
- N_2 molecules in positive discharge column of CO_2+N_2 mixtures, excitation *(Russian)* 3−4474
- Na, luminesc. in pulse discharge, H_2-addition effect 3−33413
- Ne, ^{20}Na, production and detection for use as radioactive tracer 3−37716
- Ne, column discharge, probe meas. at 77K *(Czech)* 3−9874
- Ne, positive column, population of excited levels 3−14618
- Ne, radial distrib. of excited atoms, 0.1-5 torr 3−23942
- Ne low pressure discharge, electron energy distribution 3−20669
- Ne plasma column light emission system *(German)* 3−14516
- O atoms through microwave discharge, reaction with acetylene, methylacetylene and methane, production of vibrationally excited CO 3−39432
- O_2 dissociation in a microwave discharge, model for the kinetics 3−33406
- Se, X-ray irrad., electroradiographic layers discharge mechanism *(Russian)* 3−36638
- Xe, impulse discharge emission in vacuum u.v. region *(Russian)* 3−30044
- Xe-He d.c. discharge, complex ion formation 3−17691
- Xe^+ excitation in collisions of metastable Xe and He atoms in afterglow of plasma discharge 3−17380
- ZnO, Li doped and undoped, single crystals, baked layers, electrophotographic discharge mechanism *(Russian)* 3−30517

discontinuous control systems *see sampled data systems*

discrete systems
- *see also discrete time systems; sampled data systems*
- collision processes, transition conditions *(German)* 3−32301
- linear elastic systems on Hilbert space, energy-like Lyapunov functionals 3−32341
- transient response of discrete linear systems to forcing functions rel. to optimal control 3−3662

discrete time systems
- *see also sampled data systems*
- optimal regulator for metropolitan storm-sewer system 3−28408

discriminators
- *see also demodulators*
- amplitude, millivolt range with two stable states 3−22482
- pulse-shape, minimal threshold 3−35484
- threshold device for time holding of pulses 3−22483
- Ge(Li) detectors, timing system 3−319

disintegration (radioactive) *see radioactivity*

disintegration energies *see radioactivity*

dislocations
- acoustic signal from uniformly moving edge dislocation, lattice normal mode expansion 3−36304
- acoustic wave field influence on equil. defect distrib. around dislocations *(Russian)* 3−30124
- ageing, thermal and volumetric effects *(Russian)* 3−39332
- alkali halide, indentation hardness theory rel. to resist. to dislocation motion 3−24203
- alkali halide, i.r. irrad., photomech. effect and dislocation motion *(Russian)* 3−38595
- alkali halide, NaCl-type, microhardness rel. to dislocation rosette length 3−17837
- alkali halides, painting with Au *(French)* 3−15074
- alloy, b.c.c., ordered, screw dislocation retardation mechanism *(Russian)* 3−30988
- alloy, binary, rel. to critical flow stress calc., effect of solute atom conc. 3−24188
- alloy, f.c.c. substitutional, crit. strain associated with dynamic strain ageing 3−39373
- alloy, ferromag., plastically deformed single cryst., rel. to mag. anisotropy *(Russian)* 3−36729
- alloy, network rel. to transcrystalline fracture under stress corrosion *(Russian)* 3−8801
- alloy, ordered, antiphase slip boundaries and dislocation config., theory *(Russian)* 3−34522
- alloy, ordered, type $L1_2$ superstruct., dislocation barriers *(Russian)* 3−30986
- alloy, ordered and disordered, work hardening model 3−39359
- alloy, two-phase, cross slip mechanism dislocation config. energy 3−33597
- alloys, kinetic theory, rel. to superplastic effect 3−27057
- alloys, ordered, interfaces study, grain boundaries, twinning, martensitic transformation, thermal antiphase walls *(French)* 3−17855
- alloys, with periodic antiphase domain struct., rel. to plastic deform. *(Russian)* 3−5306
- anisotropic b.c.c. crysts., glide dislocations, energy, stability and Peierls stress 3−33531
- anisotropic bimaterial plates, screw dislocation arrays, equilib. config. 3−17922
- antiferromagnet, easy axis type, spin wave-dislocation scatt. effects on antiferromag. reson. 3−2405
- ballas diamond, meas. of density in crystallites 3−30090
- benzil, preferential dislocation directions for growth and elastic energy *(German)* 3−7765
- calcite, etched, dislocations obs. by polaroid photomicrography, undergraduate expt. 3−9813
- calcite, nucleation and motion of twinning dislocations rel. to twin layer broadening 3−14856
- charged dislocation with surrounding charge cloud, nonlinear theory 3−7764
- continuously distrib., soln. method for fracture mech. of slit-like cracks in anisotropic elastic media 3−3959
- corundum, plastic deformation, dislocation model characterizing anisotropy *(Russian)* 3−7827
- cracks at interface of elastic half-spaces, opening displacement rel. to screw dislocation distrib. 3−24199
- cracks inside circular inclusion, screw dislocation double pile-up treatment 3−24201

dislocations continued
- cracks outside circular inclusion, screw dislocation double pile-up treatment 3−20803
- crystal, effect on ground state energy *(Russian)* 3−24119
- crystal containing local obstacles, dislocation motion kinetics 3−20750
- crystals, dislocated, de Haas-van Alphen effect 3−38779
- cubic crystal, long-range elastic interaction between dislocation and ellipsoidal inclusion 3−36303
- cubic crystals, small dislocations loops, diffuse X-ray scatt. study 3−1626
- cubic structure, rel. to general analysis of tilt boundaries 3−7761
- dark field images in transmission electron microscopy 3−36252
- density, theory of melting using pseudostatic computational model 3−36410
- diamond, natural, growth history obs. by X-ray topography, via disloc. struct. analysis 3−24041
- dipoles, termination mechanisms 3−1628
- disordered polycrystals, distortion waves, dislocation configurations 3−17926
- disordered short-range dislocation system, fluctuation region of electron energy spectrum *(Russian)* 3−8081
- duralumin, quenched, solute dislocation interaction in dynamic strain aging 3−37058
- dynamics, in nonmetals, review 3−24126
- dynamics and phonon interactions, stress pulse obs., review 3−11625
- dynamics of individual dislocations 3−14857
- edge, symmetric intersecting pile-ups, distribution function 3−36327
- edge dislocation, elastic interactions *(Russian)* 3−11635
- edge dislocation velocity in stress induced climb, vacancy diffusion 3−17842
- edge dislocations in surface layer, calc. of elastic fields, Peach-Kochler force 3−14861
- elastic cylinder, boundary value problem, iterational method of soln. 3−26087
- elastic interaction of dislocation array with phase boundary 3−38588
- elastic solns. for dislocation core fields in high-symmetry cases 3−24116
- electron micrography, sources of error, statistical analysis 3−34519
- electron microscope examination, diffraction contrast of a continuous set of dislocations, intensity distribution *(Russian)* 3−32227
- electron pulse irradiation at high temp., effect on dislocation line kinetics 3−36300
- epitaxial film, influence on alignment 3−1932
- epitaxial growth, form. of dislocations 3−11827
- epitaxial growth, propag. and annihilation of dislocations 3−1916
- epitaxial growth problem, dislocations at film/substrate interface 3−33747
- epitaxy, closely spaced misfit, moire image contrast 3−15082
- extended dislocation nodes, influence of elastic anisotropy 3−1627
- extension force on deviating crack, detn. from infinitesimal dislocation considerat. 3−4793
- externally deformed crystals, low temp., deformation description 3−36348
- f.c.c. cold-worked polycrystal, positron annihilation for dislocation density estimation 3−30159
- f.c.c. metal, mech. after-effect due to long range dislocation-interstitial interaction *(German)* 3−7823
- finite element stress field analysis 3−27027
- flow stress of recovered dislocation arrays, temp. depend. 3−20794
- garnet, dislocation free growth from supercooled melts 3−2667
- glass, ideal, flow via dislocations 3−17833
- glide controlled by linear elastic obstacles, thermodynamic analysis 3−20745
- grain boundary structure, planar matching model 3−20749
- graphite, enhanced reactivity at struct. faults, microscopic studies 3−11788
- group dynamics, equilib. of distrib. 3−36314
- group dynamics, general solns. of the continuum approximation 3−36313
- group dynamics, release of a pile-up 3−36315
- growth structure analysis for crystal growth history obs. by X-ray topography 3−24041
- hexagonal crystal, elastic interaction with point defect prismatic disloc. loop 3−4747
- hexagonal crystals, disclinations, elastic energies 3−17831
- hexagonal screw dislocation array, stresses of semiinfinite multipole 3−27029
- hexamethylenetetramine, dislocation density rel. to growth methods from ethanol soln. 3−21538
- high angle grain boundaries, applicability of the grain boundary (secondary) dislocation model 3−17848
- h.v. electron microscopy, contrast of dislocation images 3−20682
- ice: HF, X-ray topographical study 3−20746
- ice, obs. and interaction with cavities 3−7746
- ice, pure and HF doped, X-ray topographical study of dislocations 3−17826
- ice crystals, dynamical behaviour of dislocations 3−20739
- image profiles for scanning electron microscope 3−1554
- inhomogeneous structures, evolution during plastic deformation studied in one dimensional phenomenological model 3−36321
- interaction of substrate dislocations with epitaxially grown Y(Gd)(Sm)(La)IG:Ga film 3−1924
- interaction with impurity atm. during serrated flow, Portevin-Le Chatelier effect in alloys and metals 3−17912
- interaction with irradiation produced point defects in high voltage electron microscope 3−17844
- interactions, under hydrostatic press. *(Russian)* 3−4763
- internal friction, obs. of interaction between point defects and dislocations 3−7766
- internal friction caused by impurity atom diffusion along dislocations *(Russian)* 3−1692
- internal friction obs., book 3−20813
- rel. to ion mobility along grain boundaries 3−4877
- ionic crystals, charge cloud dislocation damping 3−36320
- ionic crystals, surface potential barrier variations and effect on mobility 3−33532
- isotropic medium, infinite, displacement field around shear disloc. loop 3−7762

dislocations continued
IV-V transition metal carbides, concentration dependence of hardness in terms of activation energy of dislocation motion *(Russian)* 3−12433
kink motion and internal friction, theory 3−14934
$L2_0$ type ordered alloys, antiphase area energy created by slip 3−14913
large prismatic dislocation loops, generation at inclusions in crysts. 3−24122
lattice resistance to motion under influence of hydrostatic press. *(Russian)* 3−36299
lattice sp. ht., dislocation strain field effects, higher order elasticity theory 3−27128
limestones, deformed, microstruct. exam. 3−37160
liquid crystal, smectic A, edge dislocations, elastic peak, inelastic light scatt. *(French)* 3−30065
magnetostrictive ferrite, u.s wave propagation consts., lattice deformation, relaxed electron diffusion 3−36367
martensite, work hardening origins, strength-differential effect 3−37067
metal, b.c.c., dislocation pinning by impurities *(Russian)* 3−14866
metal, b.c.c., macroscopic deform. characts, micromodel approach *(Russian)* 3−14911
metal, b.c.c. lattice, nonplanar dissociation of non-screw dislocations 3−38589
metal, crystalline, dislocation rearrangement rel. to athermal weakening on cold plastic deform. 3−33599
metal, cubic, cleavage in intrinsic dislocation dipoles 3−24204
metal, dislocation creep, multi-axial and reversing stress effects, mech. eqn. of state 3−8916
metal, f.c.c., dissoc. of $(a/2)\langle 110\rangle$ dislocations on $\{110\}$ planes *(French)* 3−20793
metal, f.c.c., hexagonal Frank loop dissoc. *(French)* 3−38590
metal, f.c.c., plastic deform., stability criterion *(French)* 3−17914
metal, grain boundaries influence on mech. props., review 3−37037
metal, stat. eval. of strength at brittle fracture 3−31097
metal, stress relaxation expts., dislocation behaviour 3−37104
metal single cryst., stress variations upon strain-rate changes *(German)* 3−14909
metal single crystal stress variation strain depend. effect of glide obstacles and dislocation multiplication *(German)* 3−4782
metal single crystal stress/strain relationship effect *(German)* 3−4783
metallic springs, irrad. creep in materials testing reactor 3−27809
metallography, stereological analysis, materials preparation, instrumental techniques 3−34516
metals, b.c.c., neutron irradiated creep mechanism from formation of dislocation loops 3−34541
metals, empirical constants calc. in the Dorn equation 3−34547
metals, f.c.c., statistical treatment 3−17822
metals, H embrittlement 3−2723
metals, large angle grain boundary structures, recrystallisation 3−38594
metals and alloys, X-ray crystallography *(German)* 3−30123
Mg, quenched, obs. of Bardeen-Herring sources *(French)* 3−20747
misfit dislocations during interdiffusion, interaction forces 3−36472
mobility of Cd and S dislocations on bending 3−1669
molecular crystals, painting with Sn *(French)* 3−15074
molecular crystals, trapping state formation 3−21072
Monte Carlo methods for theoretical study, review 3−20916
motion, point obstacles, applied stress, geometric statistics, computer simulation 3−34517
moving superdislocation, fine struct. calc. *(Russian)* 3−7769
nematic liquid crystals, propagating plane disinclination surfaces 3−20690
networks and cells, stress distrib. mapping by computer, rot. stress field obs. 3−11626
nonscrew, core structure, $1/2\langle 111\rangle$ on (110) planes in b.c.c. crystals, unstressed, atomistic calculations 3−36309
nonscrew core structure, $1/2\langle 111\rangle$ on (110) planes, b.c.c. crystals, Peierls stress, external stress effects 3−30125
nuclear reactor materials, neutron irradiated, diffusion controlled creep process, interstitials and vacancies flux into dislocation 3−24196
ordered $L1_0$ structure, new types of superdislocations 3−17845
organic crystals, straight line dislocations, calc. of preferred orientation directions *(German)* 3−7772
parallel line pair generation of stress components *(Russian)* 3−3997
passing, three pair behaviour, workhardening behaviour 3−11623
passing screw dislocation pair behaviour in presence of lattice frictional forces 3−14865
rel. to Peierls mechanism of deformation, atomic model 3−1671
Peierls stress, dynamic initial slip in a linear chain due to dislocation subjected to shock wave 3−7849
Peierls-Nabarro generalized model 3−38591
Peierls-Nabarro model, minimum of energy 3−20740
photoplasticity, orientation and dislocation type depend., stress and temp. effects 3−20796
pile ups against plane interfaces, anal. 3−17925
plane pile-ups, small-amplitude oscills., analysis by Eshelby-Frank-Nabarro method *(Russian)* 3−11630
rel. to plastic deformation, with deform.-induced supersaturation of point defects 3−4790
plastic deformation and dislocation cells 3−17821
plastic deformation of crystals, initial relationships, dislocation pile-ups 3−36354
point defects behaviour study, stochastic processes application, dislocation kinks diffusion 3−17989
polymethylmethacrylate, rel. to elec. breakdown *(Russian)* 3−2493
polystyrol, rel. to elec. breakdown *(Russian)* 3−2493
o-pyroxene, exsolution lamellae 3−37157
quartz particles from post-glacial clay soils, h.v. electron microscope exam. 3−37161
quartz rocks, deformed, dislocation substructures 3−18809
in quartz veins, distrib. 3−39484
quartzites, naturally-deformed, dislocation structures responsible for optical effects 3−37159
radiation damage in structural materials 3−29449
Rayleigh wave radiation on edge dislocation emergence at crystal surface 3−4912

dislocations continued
refractories, mechanical properties and defects, double kink nucleation mechanism for alloy softening 3−31129
refractory, obs. rel. to admixture effect *(Russian)* 3−8987
refractory material transport by dislocation motion in sintering 3−31127
ruby, rel. to inhomogeneous broadening of E-reson. lines *(Russian)* 3−15417
salol, monocryst., evap., X-ray topography obs. *(French)* 3−11633
scanning electron microscope channelling patterns 3−1553
screw, interaction with impurity atoms, eval. of interaction energy *(French)* 3−11644
screw dislocation hexagonal array, long-range rotational stresses of terminated multipoles 3−30129
SEM obs. using back-scattered electrons 3−35511
semiconductor, ion and electron irrad., clustering of defects 3−33576
semiconductor surface, edge, effects on surface nuclei formation 3−33722
semiconductors, multivalley, with screw dislocations, diffusion theory of electrical resistance 3−24416
shear stress effect on screw dislocation core struct. in b.c.c. lattices 3−14867
slip dislocations, merging, rel. to stress depend. of activation energy for rupture 3−33600
solid soln. supersaturated with impurities, form. of dislocation with liquid core 3−24124
solid state reactions, role of dislocations 3−5390
spirals, formation mechanism rel. to that for formation of interstitial loops 3−20751
stability of multiple dislocation, stacking fault arrays 3−17824
statistical treatment and plastic deform. charact. 3−14859
steady motion in lattice, formula for energy dissipated 3−20742
steel, γ-α transform., nonequil. struct. influence on start temp. *(Russian)* 3−21558
steel, austenitic, Cr-Ni-Mo, Ti-stabilized, creep strength behaviour 3−8928
steel, austenitic, microstruct. changes during creep deform. at 600°C 3−8921
steel, austenitic, penetration of fast electrons, dislocation image obs. *(French)* 3−39327
steel, austenitic, rel. to fatigue crack initiation *(Japanese)* 3−12396
steel, austenitic, structural changes during martensitic transformation with increased stacking fault energy *(Russian)* 3−8781
steel, austenitic stainless, creep rupture props., niobium carbide effect 3−12415
steel, austenitic stainless, Nb-stabilized, stress varied creep behaviour 3−8925
steel, carbonitrided, fatigue meas. 3−18605
steel, cold-worked, dislocation struct. stability during high-temp. ageing *(Russian)* 3−8838
steel, Cr-Ni type, dislocation distribs. during creep and recovery at 700°C 3−8920
steel, dislocation role in hydrogen transport *(French)* 3−2741
steel, fatigue crack propag., microstruct. change at crack tip 3−21579
steel, ferritic creep resistant, strengthening mechanisms 3−8934
steel, highly deformed, microcavity, form. from dislocation clusters *(Russian)* 3−24900
steel, hydrogen embrittlement rel. to hydrogen/dislocation interaction 3−2744
steel, hydrogen trapping sites *(French)* 3−2742
steel, low carbon specimens, changes of residual stress due to slip band accumulation under fatigue loading 3−21578
steel, low-C, effect of stress amplitude in fatigue processes in annealed and cold-rolled specimens *(Japanese)* 3−12405
steel, low-C, fatigue crack initiation process in notched specimens *(Japanese)* 3−21597
steel, low-C, pressurization and quenching effects on yield behaviour 3−24867
steel, lower yield strength depend. on grain size and temp. 3−37053
steel, maraging, dispersion hardening mechanism *(Russian)* 3−39333
steel, maraging, interaction with strain fields due to defects 3−18652
steel, medium-C, quenched and tempered, effect of Si additions on microstruct. 3−21584
steel, mild, low carbon, hydrogen-dislocation interaction *(French)* 3−2706
steel, mild, strain hardening exponent in Ludwik-Hollomon relation, dislocation model applic. 3−34576
steel, recovery creep model based on dislocation distribs. 3−8912
steel, stainless, Type 304, cyclotron-injected helium effect on void form. characts. 3−35934
steel, stainless, Type 316, neturon irrad., defect development 3−35933
steel, transformer, dislocat. density and grain growth for secondary recrystallisation *(Russian)* 3−1624
stress distribution near tip of array of screw dislocations piled up against an inclusion 3−1625
stress required to move dislocation from etch figure rosettes 3−4764
stress variation strain depend. effect of glide obstacles and dislocation multiplication *(German)* 3−4782
stress-fields of moving dislocation in elastic solid 3−14862
stress/strain relationship effect *(German)* 3−4783
structure obs. using weak beam method of electron microscopy 3−1541
structure of defects in solids, review 3−24099
superconductor, ideal, Frank-Read source behaviour under external stress, stress softening 3−24537
superconductors, type II, flux lattice dislocation motion in mixed state 3−24539
supercooling at face developing on rounded crystallisation front, growth mechanisms 3−33471
thin films, statistical calc. of dislocation movements 3−38592
thiourea, preferential rectilinear lines rel. to elastic anisotropy *(German)* 3−14868
tobacco mosaic virus polymerized proteins 3−5623
triglycine sulphate, growth defects, X-ray topographic obs. 3−1617

dislocations continued
- triglycine sulphate, X-ray topographic observations of lattice defects 3−27026
twin dynamic behaviour, dislocation description 3−20748
twinning dislocations, macroscopic pileup config. *(Russian)* 3−7768
twisting and mechanochemical energy conversion at dislocations in cylindrical crystals 3−14864
X-ray diffr. contrast, from Takagi eqns., expt. obs. 3−24123
X-ray diffuse scatt. by polycrystalline aggregates containing small dislocation loops 3−38526
X-ray topographic images of loops, Lang and double crystal method 3−30047
α-Zr, high temp. creep interpretation in terms of effective stress and dislocation dynamics 3−27681
Ag, cold worked, inert gas diffusion and gas release meas. 3−24287
Ag, dislocation motion geometry at tip of spreading cracks 3−17918
Ag, extended dislocation nodes, influence of elastic anisotropy 3−1627
Ag, phonon viscosity, dislocation drag, and u.s. attenuation 3−38625
Ag binary alloy, rel. to critical flow stress, effect of solute atom conc. 3−24189
Ag dendrites, twinned, disclination model and mismatch 3−33769
Ag film, epitaxial growth rel. to dislocation density, X-ray rocking curve obs. 3−11830
Ag single crystal films plastic deformation, dislocation struct. 3−17900
Ag single crystals, dislocations dynamic behaviour and yielding phenomena 3−17819
Ag-Cd(Mg) dil. alloys, internally oxidized, strengthening mechanisms 3−24842
Ag-Cd(Mg) dil. alloys, partially internally oxidized, deform. and substruct. characts. 3−24841
Ag-Sn dilute alloy single crystals dislocations dynamic behaviour and yielding phenomena 3−17819
AgBr, rel. to photographic sensitivity 3−37139
β' AgMg single crystals, operative slip systems and strain hardening 3−14915
Al, amplitude-dependent anelasticity during and after plastic deformation, dislocation struct. *(German)* 3−34611
Al, annihilation mechanism by deformation 3−17823
Al, Bordoni relax., secondary features 3−33608
Al, creep-deformed, dislocation struct. of subgrain boundaries 3−24121
Al, deformed, annealing of struct. discontinuities *(Russian)* 3−24854
Al, deformed, dislocation density, X-ray diffr. and n.m.r. obs. 3−24194
Al, deformed in tension, rel. to latent hardening 3−5316
Al, disloc. structure in high temp. creep 3−7832
Al, fatigue cracks, substruct. form. and propag. 3−21610
Al, fatigued, internal friction peak behaviour and dislocation-point defect interaction *(French)* 3−11685
Al, foil, due to friction, lubrication and oxide layer effects 3−27063
Al, grown by recryst., dislocation density and distrib., annealing effects *(French)* 3−24885
Al, high velocity dislocation damping at high strain rates 3−36301
Al, neutron irradiated and deformed at low temp., internal friction and modulus anomaly, dislocation and point defects interaction *(French)* 3−14935
Al, polycryst., strain-annealed, etch behaviour 3−18675
Al, positron-dislocation interactions using independ. part. model and local screening theory 3−7791
Al, rel. to interpretation of steady state creep 3−7833
Al, rolled plate, after recrystallisation 3−15664
Al, sources of flaws during heat treatment, X-ray obs. *(French)* 3−15057
Al, spall fracture, dislocation dynamics approach 3−14923
Al alloys, inclusions role in ductile fracture and fracture toughness 3−30984
Al and Al alloys, axisymmetric extrusion, plastic flow, modified dislocation model 3−39360
Al and alloys, polycryst., work softening obs. and mechanism 3−37066
Al single crystal, amplitude dependent, role of dislocation motion *(German)* 3−24214
Al:Si, rel. to substructure form. on annealing *(Russian)* 3−12355
Al-Cr and Al-Mn cold-worked alloys, rel. to impurity resistivity 3−14886
Al-Cu alloy film, misfit disloc. rearrangement, rel. to secondary grain growth 3−1956
Al-Cu-Li alloy, Al$_2$CuLi T$_1$ precipitation, electron microscope examination of microstructure 3−8798
Al-Fe dilute alloy, cold-worked, rel. to effect of heat treatment on mech. props. 3−27703
Al-Mg alloy, prismatic loop rotation and self-climb phenomena 3−36317
Al-Mg-Si alloy, plastic deformation on the precipitation, heterogeneous nucleation at dislocations *(Japanese)* 3−15699
Al-Ti (0.16 at wt.%) alloy, yield point phenomenon, subgrains and dislocation density *(Japanese)* 3−18644
Al-Zn-Mg-Cu alloy, thermomech. treatment processed, age hardening mechanisms 3−24897
Al$_2$O$_3$, alumina, straight dislocations elastic energy, 0-900 K 3−17832
Al$_2$O$_3$, sapphire, substrate for Nb, effect of dislocation density on r.f. sputtering 3−20954
Al$_2$O$_3$, sapphire, X-ray topographic obs. for gradient furnace grown crystal 3−11572
Au, phonon viscosity, dislocation drag, and u.s. attenuation 3−38625
Au, pure, deformed, point defect clusters at tangled dislocations 3−17807
Au, quench-hardened single crysts., yield stress and surface morphology, dislocation-stacking fault interaction 3−36350
Au binary alloy, rel. to critical flow stress, effect of solute atom conc. 3−24189
Au film, epitaxial growth rel. to dislocation density, X-ray rocking curve obs. 3−11830

dislocations continued
Au film, self-diffusion along dislocations 3−15032
Au film grown on NaCl, boundary formed by screw dislocations 3−4940
Au-Ag alloys, high dislocation density influence on ordering process 3−21713
β'AuZn single crystals, operative slip modes and dislocation mechanism 3−31023
Be, hydrostatically extruded, elec. resist. of dislocations *(Russian)* 3−18110
Be, rel. to twinning *(Russian)* 3−20753
Be-Cu alloy, rel. to twinning *(Russian)* 3−20753
Bi, energy factor, rel. to absolute solid-liq. and grain boundary energies 3−4762
Bi, Granato-Lucke damping, u.s. attenuation obs. 3−11690
Bi, pile-ups due to polygonization 3−7757
Bi, plastic deform. behaviour of single crysts. 3−7818
Bi, thermally activated mechanism of barrier surmounting by twinning dislocations *(Russian)* 3−31057
Bi single crystals, plastic deformation and dislocation etch-pit distribution *(Japanese)* 3−30993
Bi-Sb, single crystal, study using etch pit technique 3−17836
CaCO$_3$, twinning dislocations, macroscopic pileup config. *(Russian)* 3−7768
CaF$_2$, rel. to hardening due to contamination by atmospheric O 3−4806
CaF$_2$ crystals, X-ray topographs of dislocations 3−17825
CaF$_2$:Er^{3+}, effect on perturbed angular correlations in paramagnets 3−34256
CdS, cathodoluminescence investig. using electron microprobe scanning *(German)* 3−8674
CdTe, transmission electron microscopy 3−17830
Co-Cu substrate-epitaxial film interface *(Russian)* 3−8049
Co$_5$Pr, splat-cooled, transmission electron microscope obs. 3−8791
CsI, volume decoration 3−18024
Cu, amplitude-dependent anelasticity during and after plastic deformation *(German)*—34611
Cu, dislocation pinning after neutron irad. at liq. He temp., internal friction and dynamic modulus obs. 3—38600
Cu, dislocations at grain boundaries in creep deform. 3—14880
Cu, etchants and their mechanism *(Russian)* 3—8033
Cu, fatigued, rel. to discovery of shear modulus and internal friction 3—7811
Cu, internal friction, dislocation pinning by hydrogen *(French)* 3—2740
Cu, lattice dislocations effect on de Haas-van Alphen scatt. temp 3—18069
Cu, macroscopic yielding of highly perfect crysts. *(Japanese)* 3−30184
Cu, neutron irradiated, X-ray meas. 3−14895
Cu, phonon viscosity, dislocation drag, and u.s. attenuation 3−38625
Cu, ribbons, cryst. perfect, gliding dislocation loops preceding slip line form. *(French)* 3−4761
Cu, single crystal, u.s. attenuation and acoustic emission during deformation 3−11629
Cu, structure, effects of friction coeff. during working *(Russian)* 3−8873
Cu, u.s. attenuation, γ-radiation damage 3−17865
Cu, vibrating string model, damping and modulus effects 3−17935
Cu, weak beam electron microscopic obs. 3−1542
Cu alloys, age-hardened, role in high elastic limit and yield pt. behaviour *(Russian)* 3−15668
Cu binary alloy, rel. to critical flow stress, effect of solute atom conc. 3−24189
Cu crysts., plastic constraint as mechanism for film strengthening 3−21613
Cu film, electrolytic, rel. to thickness depend. of ductility and tensile strength *(Russian)* 3−7820
Cu foil, α-irrad., rel. to internal friction and Young's modulus *(German)* 3−7851
Cu polycrystals, rel. to low temp. deform. mechanism 3−24193
Cu single crystal, amplitude dependent, role of dislocation motion *(German)* 3−24214
Cu single crystal, density effects on work hardening characts. 3−18673
Cu single crystals, motion after tensile stress and unloading *(Japanese)* 3−7760
Cu single crystals, plastic deformation, u.s. obs. 3−14906
Cu torsionally fatigued wires, strain amplitude changes effect on stress amplitude and resistivity, dislocation and point-defect density 3−27054
Cu whisker, anisotropy of dislocation internal friction 3−8071
Cu whisker, behaviour rel. to primary recrystallisation nuclei formation on torsional straining *(Russian)* 3−12365
Cu whisker, motion in preyield region 3−24365
Cu whiskers, stretch deformed, dislocation struct., X-ray obs. *(Russian)* 3−8072
Cu-Al (2%) single crystals, edge-pit observations of dislocation motion 3−21609
Cu-Al alloy, swaged, dislocation density, from flow stresses and stored energies 3−18633
Cu-Al-Ni, dislocation mechanisms rel. to twinning and martensite transform. 3−5318
Cu-Al-Zn, solid soln. elongated dislocation tangles and Al and Zn solubility *(French)* 3−31004
Cu-Al(5.8 at.%) alloy, deformed, soft surface effect 3−24866
Cu-Fe alloys, ageing characts., precipitate transform. 3−37075
Fe, Armco, hydrogen trapping sites *(French)* 3−2742
Fe, Armco, hydrogen-dislocation interaction *(French)* 3−1830
Fe, Armco, tested at fatigue limit *(Russian)* 3−7758
α-Fe, at elevated temps. unstable glide dislocations, elastic anisotropy factors calc. 3−31024
Fe, deform. resist., temp. and strain rate depend. *(Russian)* 3−31058
Fe, dislocation multiplication rate in polycrysts. 3−38611
Fe, edge and screw motion, low temp. obs. using HVEM 3−11631
Fe, Fe-Mn and Fe-Ni, stress exponent of dislocation vel. from strain rate cycling tests *(Japanese)* 3−31078

dislocations continued
Fe, high-purity. creep. const. mag. field influence, dislocation-domain wall interaction *(Russian)* 3—36774
Fe, hydrogen embrittlement rel. to hydrogen/dislocation interaction 3—2744
α-Fe, Peierls-Nabarro barrier and stress of $a/2\langle 111\rangle$ edge dislocation 3—14858
Fe, single crystal foil, motion under tensile test in high voltage electron microscope 3—11628
Fe, single crystals, tensile test of foil specimens at room and low temp., dislocation motions 3—17820
Fe, single crystals at 78 and 4K, gliding, twin formation, fracture *(German)* 3—34612
Fe, under fatigue loading, plastic deform. of surface and internal layers 3—27056
Fe (100) single crystal film, rel. to magnetisation ripple 3—8399
Fe alloys, martensite morphology and deform. of cryst. form during athermal transform. *(Russian)* 3—24824
Fe and alloys, interactions with hydrogen *(French)* 3—2739
Fe and Fe-Ni alloys, hydrogen-dislocation interactions 3—4887
α-Fe lower yield strength depend. on grain size and temp. 3—37053
Fe microcrystals, substruct., X-ray obs. 3—36505
Fe zone melted crystals under tensile stress, dislocations and magnetic domain walls, X-ray topographic study 3—17828
Fe-Al, superlattice dislocations, fourfold dissociation in DO_3 type order 3—17839
Fe-Cr-Co-Mo alloy, precipitation, structural and kinetic features 3—8787
Fe-Mo-Ni alloys, continuously cooled carbon-free microstruct. 3—39317
Fe-N alloys, rapid strain aging, Snoek ordering, conc. depend. 3—24868
Fe-Ni (2.86 wt.%), solid solution softening, Peierls mechanism 3—34545
Fe-Ni invar alloys, effect of mag. props. on plastic deformation 3—14914
Fe-Ni-C alloy, reverted austenite, prior deform. effects on strength and annealing behaviour 3—37048
Fe-Ni-C alloys, internal friction meas., Snoek-peak, C interstitials diffusion towards dislocations mechanism 3—34542
Fe-Ni-C alloys, strain-induced martensite and thermally transformed martensite morphology 3—21575
Fe-Ni-Cr alloy, grain boundary internal friction spectra, relax. phenomena 3—37028
Fe-Si (2.94 wt.%), solid solution softening, Peierls mechanism 3—34545
Fe-Si (3 at wt.%) single crystals, tensile test of foil specimens at room and low temp., dislocation motions 3—17820
Fe-Si(12.1 at.%) alloy, screw dislocation retardation mechanism *(Russian)* 3—30988
Fe-Si(3.2 wt.%) alloy, normal stress influence on yielding behaviour 3—14908
Fe-Si(5.3 at.%), alloys, deformed screw dislocations and prismatic loops, annealing effects 3—18632
Fe-Ta alloys, Laves phase precip. phenomena 3—37049
n-GaAs, deformed crystal, positron lifetime meas. for electric charge on dislocations 3—11863
GaAs, epitaxial growth over wide range of crystallisation conditions, dislocation density data for n and p type films *(Russian)* 3—8051
GaAs, epitaxial growth substrate, density and config. obs. 3—1938
GaAs, plastically deformed, i.r. cathodolum. study 3—38699
p-GaAs luminesc. reduction due to dislocations introduced during polishing 3—27559
GaAs obs. by X-ray refl. topography, optimum refl. 3—4760
GaAs single crystals, structure rel. to thermal conditions in the floating zone growth process 3—33533
GaAs:Cu, decoration on decomp. of supersaturated solid soln. 3—33542
$Ga_xAs_{(1-x)}P$, epitaxial growth on GaAs, lattice mismatch strain rel. to dislocation equilib. 3—11828
GaP, epitaxial growth over wide range of crystallisation conditins, dislocation density data for n and p type films *(Russian)* 3—8051
GaP films, in vapour- and liquid-phase epitaxial growth 3—15091
GaP-GaAs heterojunction, TEM obs. of misfit dislocations caused by lattice mismatch 3—36305
Gd-Ga, melt grown garnet, X-ray topographic anal. of dislocations and growth bands 3—30946
Gd-Ga garnet dislocation spirals mechanism for formation 3—20751
$Gd_3Ga_5O_{12}$ single cryst. dislocation-free growth 3—36989
β'-$Gd_2(MoO_4)_3$, dislocation etchants 3—8028
Ge, dislocation relax., internal friction meas. 3—17847
n-Ge, edge, rel. to polarisation of photocond. 3—27287
Ge, n- and p-type, influence of single dislocations on electrical props. 3—24439
Ge, plastic deformation, work-beam high-resolution micrographs 3—36318
Ge, rel. to effect of preliminary deform. on plasticity *(Russian)* 3—4788
Ge crystals, deformed, internal friction from 4.2 to 150 K 3—14936
Ge homoepitaxial layers, dislocation struct., effect of crystn. conditions 3—24356
Ge radiative recombination, influence of electron irradiation and annealing 3—34423
Ge whisker, rel. to elastic props. and torsional strength 3—38759
Ge:Sb, dislocation mobility study, depend. on temp. and loading *(Russian)* 3—24120
Ge/Si interface, dislocation network via mismatch on Ge epitaxy, t.e.m. obs. 3—1941
^{4}He-solid interface, Kaptiza resistance reduction through surface dislocation scattering 3—1764
In, normal and supercond., flow stress and yield pt. obs. 3—5076
In, normal and supercond., rel. to amplitude-depend. internal friction 3—36679
InBi, intermetallic, chem. etchants for revealing dislocation sites 3—11817
InP, crystal quality rel. to liquid encapsulation growth 3—2679
In_2S_3, and stacking faults, X-ray topograph and electron microscope obs. *(German)* 3—17834
KCl, anomalous X-ray transmission rel. to imperfect structure, dislocation and thickness effects 3—24145

dislocations continued
KCl, dislocation effect on anomalous X-ray transmission 3—4704
KCl, interaction with 5 MHz ultrasonic waves, plastic deform. 3—24190
KCl, kinetics of motion and multiplication *(Russian)* 3—33530
KCl, luminesc. flashes on unloading deformed crystal rel. to dislocation motion 3—5232
KH_2PO_4, X-ray topographic study, during growth *(Russian)* 3—7771
KH_2PO_4 interdomain and domain defect interactions 3—8529
KI, defect clusters, planar dislocation loops produced by electron, γ-irradiation, obs. at 5 K with electron microscope 3—30126
LiF, cold-worked, recovery of u.s. props. during annealing, dislocation behaviour 3—11624
LiF, density rel. to thermal treatment *(French)* 3—36306
LiF, elastically stressed, dislocation density rel. to u.s. vibrs. 3—20752
LiF, interaction between dislocations and thermal phonons 3—1745
LiF, pure and Mg doped, steady state deform. dislocation struct., etch pit studies 3—36322
LiF, rel. to electromechanical effect 3—34298
LiF, slip band dislocation struct., influence of dislocation forest *(Russian)* 3—7770
LiF, yield stress minima and apparent isoelectric temp. relationship 3—20792
LiF single crystal (pure and Mg-doped), temp. depend. of steady state deform. rate 3—17846
Li_2O-K_2O-SiO_2-Al_2O_3:Sr^{2+} photopyrocerams, dislocation struct. and dielec. props. 3—27753
Mg dislocation creep 3—8871
Mg single crysts., dislocation struct. changes during basal slip *(Russian)* 3—24185
Mg-Ce alloy, precipitation on dislocations with aging *(Japanese)* 3—12351
Mg-Y(8.7 wt.%) alloy, elevated temp. precip. stages 3—39340
$MgAl_2O_4$, rel. to fracture 3—7836
$MgAl_2O_4$, spinel stoichiometric single crysts., stacking faults and dislocations, X-ray topographic obs. 3—17854
MgO, creep-deformed, dislocation structures, transmission electron microscopy 3—38593
MgO, dislocation damping in single crysts. 3—36324
MgO, dislocation dipole termination mechanisms 3—1628
MgO, erosion by fast moving particles, dislocations, obs. by thin film electron microscopy 3—27065
MgO, polycryst., microyield and fracture 3—20789
MgO, rel. to fracture 3—7836
MgO, rel. to secondary creep props. 3—14918
MgO crystal, dislocation-defects interaction, internal friction obs. 3—30117
MgO foil, stability of edge dislocation loops, effect of surface forces, electron microscope obs. 3—18011
MgO single crystals, rel. to creep properties 3—7829
Mg_2Si:Al alloy, dissolution and growth of precipitates β', electron micro. obs. 3—8814
$MgZn_2$, mobility, depend. on chemical composition and temperature 3—27028
Mn-Sn intermetallic cpd., crit. resolved shear stress, temp. depend. 3—34586
Mo, dislocation pinning after neutron irrad. at liq. He temp., internal friction and dynamic modulus obs. 3—38600
Mo, dislocation-interstitial interactions using dislocation damping obs. 3—36312
Mo, Portevin Le Chatelier effect at high press. and temp. 3—30180
Mo, primary creep, high temp. analysis 3—34531
Mo, single crystals, structure after deformation of 293 K and 400 K 3—36316
Mo, single crystals orientation dependence of shear stress 3—38613
Mo alloys, deformed, interstitial solid soln. decomp. during recrystn. *(Russian)* 3—37018
Mo prestraining effect on brittleness, ductility of dislocation containing specimens *(Japanese)* 3—31070
Mo single crystal, dislocation damping of ultrasonic waves, internal friction study *(Russian)* 3—24211
MoS_2, enhanced reactivity at struct. faults, microscopic studies 3—11788
MoS_2, molybdenite, high resolution scanning electron microscope obs. 3—7763
NH_4Cl, rel. to domain growth, crit. opalescence study 3—24667
NH_4ClO_3, radiation induced dislocations and thermal decomposition kinetics 3—4771
NaCl, dislocation mobility and work hardening on plastic deform. 3—20743
NaCl, quenching effect on dislocation motion 3—24125
NaCl, rel. to electromechanical effect 3—34298
NaCl, single crystals, anomalous amplitude depend. of elastic modulus rel. to dislocation pinning 3—30172
NaCl, strain rate change rel. to mobile dislocation conc. 3—4785
NaCl, u.s. effect on stress/strain relation *(German)* 3—14916
NaCl crystals, reverse deformation comparison with annealing, polygonisation, dislocations at sub-grain boundaries 3—17903
NaCl quenched crystals, generation mechanism rel. to impurity effects on microhardness 3—1677
NaCl single crystals, highly deformed, dislocation density 3—14869
NaCl single crystals, rel. to deform. energy 3—7824
NaCl:$BaCl_2$, flow stress, annealing depend., dislocation-impurity interactions 3—20786
NaCl:Mn^{2+}, meas. of charge acquired by dislocations and vacancy sweep-up 3—17843
NaCl:Tl, annealed and quenched, thermoluminescence, dislocation dipoles formation 3—15568
NaF, dislocation movement at various temp. *(Russian)* 3—27025
NaF(Cl)(I), n.m.r. line shape, effect of dislocation broadening *(Russian)* 3—8463
Nb, interaction between dislocations and thermal phonons 3—1745
Nb, neutron irradiated at low temp., internal friction, relaxation peaks due to dislocation and point defects interaction 3—17875
Nb, superconducting, effect on lattice thermal conductivity 3—11634
Nb alloy, softening rel. to interstitial interactions and dislocation motion 3—18627
Nb deformed crystals, study by electron microscope 3—1630

dislocations continued
Nb plastically deformed, stage III recovery analysis 3−34591
Nb-H system, rel. to internal friction max. 3−27069
Nb-O solid solns., dislocation dynamics 3−36311
Nb-Zr alloy, cross-slip of dislocations 3−18256
Ni, 99.999% pure, dislocation arrangement and density following plastic deformation at −196 and 25°C *(German)* 3−27711
Ni, cyclic endurance, and dislocation struct., initial state and after programmed strengthening *(Russian)* 3−5308
Ni, dislocation content rel. to structure stabilisation on heat treatment *(Russian)* 3−24903
Ni, dislocation influence on nucleation of voids with neutron irradiation 3−17803
Ni, ferromag. reson. linewidth depend. on dislocation density *(Russian)* 3−18370
Ni, hydrogen-dislocation interaction, binding energy *(French)* 3−1629
Ni, motion in alternating mag. field, oscill. domain wall interactions 3−30674
Ni, preliminary extensional fatigue deform., dislocation struct. changes *(Russian)* 3−27664
Ni (100) single crystal film, rel. to magnetisation ripple 3−8399
Ni film on (001) Cu substrate, transmission electron microscope obs. 3−33764
Ni flow stress rel. to mag. field, domain wall dislocation interactions 3−5125
Ni-Co alloy, flow stress rel. to mag. field, domain wall dislocation interactions 3−5125
Ni-Co-(2.5 wt.%)Al_2O_3 alloys creep behaviour, dislocation pipe diffusion mechanisms 3−8870
Ni-Cr base alloys, precip. hardened, struct. factors influence on creep strength behaviour 3−8930
Ni-Cu alloy, motion in alternating mag. field, oscill. domain wall interactions 3−30674
Ni-Fe (100) single crystal film, rel. to magnetisation ripple 3−8399
NiAl, void and dislocation loop formation following annealing, 700-900°C 3−18658
Ni_3Al, dislocation struct. at various deform. stages *(Russian)* 3−37019
Ni_3Al, superpartial motion rel. to onset of dynamic weakening stress *(Russian)* 3−12364
$Ni_3Al(Ti)$, precipitation influence on creep rate and dislocation 3−15680
Ni_3Fe, antiphase slip boundaries and dislocation config. *(Russian)* 3−34522
Ni_3Fe, elastic anisotropy effect 3−17838
Ni_3Mn, annealed under load, dislocation struct. *(Russian)* 3−15729
Ni_8Ta, Ni_8Nb alloys, ordered phases, triple dislocation analysis 3−4758
Pb, normal and supercond., flow stress and yield pt. obs. 3−5076
Pb, plastic flow in supercond.-normal transition region, 4.2K, dislocation model 3−30183
Pb, superconducting transition, plastic deform. rel. to dislocation motion 3−8293
Pb-Tl alloy 50/50 single crysts., activation area and strain-rate sensitivity, 78 K 3−24895
Pd-Ag(Ce) alloys, dislocation tangles after hydrogen cycling through α-β transform. 3−2737
Pt wire, dislocation movement rel. to elec. resist. on cryogenic immersion 3−4746
α-S, monocryst., grown from CS_2 soln., dislocation distrib., X-ray topography obs. *(French)* 3−11632
Si, dislocation generation at (111)(111) boundary in pulled crysts. 3−36323
Si, dislocation pile-up in deformed single crystal slice 3−17841
Si, dislocation structure on plastic deform. 3−7747
Si, displacement velocity, X-ray determ. *(French)* 3−15058
Si, epitaxial, Shockley loops 3−15094
Si, moving dislocations, X-ray topographic obs. 3−17827
Si, n- and p-type, influence of single dislocations on electrical props. 3−24439
Si, single dislocation mobility, X-ray topographic obs. 3−11627
Si, stacking faults and prismatic dislocation loops due to O_2 precipitation, X-ray topography 3−17829
n-Si, undoped, dislocation motion kinetics 3−4765
Si n-p-n transistor, rel. to diffusion pipes, anodic oxidation decoration 3−38582
Si slices, density effects on Au diffusion, dissociative mechanism 3−39240
Si slices, with and without dislocations, temp. quenching effects 3−4759
Si wafers, dislocations formed by thermal stresses 3−30122
Si:B, X-ray topographic obs. of dislocation contrast after boron diffusion 3−17835
Si:Cu, Cu precip. colony dissolution during annealing, particle drag by climbing dislocations 3−20758
Si:Cu precip. colony dissolution during annealing, dislocation processes 3−20757
n-Si:P, dislocation motion kinetics 3−4765
n-Si-Au solid solution, rel. to precip. kinetics *(Russian)* 3−1779
α-SiC, semicond., X-ray obs. of defects, single crysts. 3−36326
Si_3N_4, hot pressed. 3−12421
Sn, white, single crystals, dislocation etch hillock formation 3−8030
Ta, localized multiplication of mobile dislocations, rel. to cyclic yield pt. behaviour 3−21654
Ta, Portevin Le Chatelier effect at high press. and temp. 3−30180
Te, electron irrad., recovery steps, isochronal and isothermal annealing expts. 3−33562
Te, influence on absorpt. spectra near electronic band edge 3−21449
Te, rel. to effect of elec. field and illumination on plasticity *(Russian)* 3−14912
Te single crystals, cleaved Berg-Barrett X-ray topographic analysis, etch pit studies 3−11636
Te single crystals, low temp. substructure in early stage of deformation 3−14870
α-Ti, oxygen conc. influence on internal stress and dislocation arrangements 3−34534
Ti, single crystals, deformation kinetics for {1010} ⟨1120⟩ slip 3−17901

dislocations continued
Ti film, dislocation-enhanced elec. resist. 3−21049
Ti-Nb superconducting alloy, influence on crit. current density *(German)* 3−8308
Ti-Ni alloys, near-equiatomic, diffusion controlled phase transform. structures 3−39311
V, α-irrad., He gas bubble nucleation and distrib. 3−33572
V, high-purity, deform. mechanism at low temps. 3−37055
V wire, deformation, low temp. relaxation, damping peaks 3−30206
V-C system, carbide precip. behaviour 3−34529
W, electron-beam zone-melted single cryst., struct. obs. *(Russian)* 3−7759
W, neutron irrad., raft form. mechanism 3−33563
W crystal, etch pits, light figures 3−24352
W emitters, prepared from deformed wire, dislocation density *(Russian)* 3−30178
W fine wire with thoria dispersion, creep behaviour 3−37086
WC, networks, transmission electron microscopy 3−39386
YAG, in-grown dislocations, obs. by etching 3−24118
YAG:Nd, obs. using transmission electron microscopy 3−36319
$Y_3Fe_{5-x}Ga_xO_{12}$, high pressure effect on ferromag. resonance line width rel. to dislocations 3−5138
YIG, grown from soln. in PbO-PbF_2, characterization *(Russian)* 3−30942
Zn, anomalous X-ray transmission rel. to imperfect structure, dislocation and thickness effects 3−24145
Zn, basal screw dislocation, determ. of line energy 3−17818
Zn, dislocation effect on anomalous X-ray transmission 3−4704
Zn, low temp. creep, influence of zero-point vibrs. 3−1674
Zn, single crystals, anomalous amplitude depend. of elastic modulus rel. to dislocation pinning 3−30172
Zn bulk crystal, X-ray topographic obs. of dislocation loop ground 3−11637
ZnS, and stacking faults rel. to structural transforms. 3−17856
ZnS, cathodoluminescence investig. using electron microprobe scanning *(German)* 3−8674
ZnS-CdS phosphors, activation by Cu diffusion due to dislocations at low temp. *(Russian)* 3−36943
Zr, slip dislocation incorporation in {1102} twins 3−36310
Zr single crysts., basal slip mechanism, critical resolved shear stress 3−24183
Zr-O alloys, strain aging parameters, dislocation cell struct., irrad. effects 3−27675
Zr-Pd(Ru) dil. alloys, heat treated, microstruct. of martensite plates *(Japanese)* 3−31079

disordered systems, vibrational states *see vibrational states in disordered systems*

disperse systems
see also aerosols; Brownian motion; colloids; dust; emulsions; foams; fog; gels; powders; smoke; sols; suspensions
adsorbent system, packed spherical particles, pore size distrib. 3−39412
air pollution samples, location and identification of small particles within large samples 3−37774
aniline in cyclohexane, depolarised light scattering near critical separation point 3−39416
anisotropic porous media, analysis of dispersion tensor using random walk model 3−7472
atmospheric pollution, buoyant plumes, vehicular and aircraft wakes 3−33325
catalysers, finely divided, ferromag., granulometry and metallic mass. from magnetisation/mag. field curve *(French)* 3−34171
characterization by particle size analysis *(German)* 3−25019
circular discs, binary array, optical correl. analysis 3−686
convective drying, in agitated layer in cross flow of coolants 3−25022
cooling in fluidised beds 3−2763
electron microscopy, specimen preparation 3−18734
electrophoresis of solid spherical particles with arbitrary conductivity 3−31198
gas-liquid, heat and mass transfer processes 3−639
gas-liquid, meas. of liquid solute concentrations 3−32275
gas-liquid dispersions, rheology *(German)* 3−14505
heat transfer in uniform mixture of two dispersed materials 3−23792
heterogeneous systems, spatial macroscopization 3−28851
homogenized fluid and sphere with finite interfacial transport coeffs., comment on transient mass transport 3−20405
hydrothermomagnet, elementary theory 3−12039
Kapron-highly dispersed Fe, Co and Ni, ferromag. resonance, chemisorption effect 3−39409
lean liquid-liquid dispersions, population balance model for mass transfer, droplet breakage processes 3−33293
light scattering, absorption and transmission, statistical particle layer model *(German)* 3−26208
liquid liquid systems, prediction of drop volume 3−9013
liquid-liquid, drop sizes in agitated system 3−9012
liquid-liquid, droplet size distribution determination 3−9014
marine sediments, shear strength determ. 3−3757
metal in finely dispersed state, thermodynamic characts. 3−33686
metallic alloy, kinetics of non-diffusional coalescence of disperse phases 3−31008
mist, cooling investigation 3−20854
mutual adhesion, unit for determining *(Russian)* 3−12462
mutual fixing of particles with different sizes and shapes 3−31194
nitrobenzene in n-hexane, depolarised light scattering near critical separation point 3−39416
ocean sediments, temp. coeff. of thermal conductivities 3−2939
orientable particle system, transport mechanics of arbitrary shaped particles 3−10401
particle analysis by electron probe, take-off angle effect 3−37765
particle analysis by ion microprobes 3−37766
particle concentration obs. using capacitance transducer 3−458
particle motion in crossed e.m. fields with large Reynolds no. in conducting medium *(Russian)* 3−7432
particle size, number density and velocity meas. using laser interferometry 3−4129
particle size from low angle light scatt., refr. index effects 3−31190
particle size measurement and counting with computer *(French)* 3−15801

disperse systems continued
pneumatic transfer of dispersed solid material under piston conditions of motion in pipeline *(Russian)* 3−38406
polydisperse systems, size distrib. determ. by X-ray small angle scatt. *(German)* 3−12466
polyisobutylene, carbon black filled, meas. of rheological props. 3−12451
polymer concentrated solns., time dependent viscoelastic props. 3−29816
polymer dilute solns., internal viscosity effects on transient elongational behaviour, elastic dumbbell model 3−29817
polymer solutions, secondary and primary normal stresses, hole error, reservoir edge effects in cone-and-plate flow 3−29819
polymer solutions, viscoelasticity, finite amplitude dynamic motion 3−29818
polymers in abrasive media, dispersion on steel surface *(Russian)* 3−12373
polyvinyl chloride latex, particle size analysis by comparative methods 3−2768
powders, flow and storage, conference, Chicago, Ill., USA (1972) 3−1468
quartz-sand-water, different phases of water, n.m.r. studies 3−39396
sinusoidal field effect, elec. moment and dielec. permitt., theoretical determ. *(Russian)* 3−9015
statistical hydromechanics, pseudo-turbulent structure of homogeneous suspensions 3−7454
superconductor, in porous material, filamentary model 3−34037
switching materials, conducting particles in semicryst. matrix 3−18201
tartaric acid, supersaturated soln., crystal dispersity, effect of u.s., latent period of mass crystn. 3−39404
transparency, nephelometric determination *(Russian)* 3−13291
two-phase aerodisperse medium, corona discharge, limit conc. rel. to electron-ion equipment 3−13671
unsteady convective diffusion with interphase mass transfer, miscible dispersion theory 3−33292
water retention by plastic bodies, maximum quantity formulation *(French)* 3−39395
Cu fine particles, n.m.r. linewidth field depend. 3−34221
Cu-Al(1 at wt.%) alloy, alloying elements Ag, Pd, As and In effect on internal oxidation, dispersion particles formation *(Japanese)* 3−15700
Ga, detection of metastable phases 3−11740
In small particles in the quantum size regime in paraffin, magnetic moment 3−18347
TiO_2, thixotropic and dilatant dispersions, elec. cond., rheology, polarisation 3−39407

dispersion (wave)
see also acoustic dispersion; optical dispersion
atmospheric mm waves, simulation results 3−37236
conductivity tensor and dispersion equation for collisional magnetoactive plasma 3−17613
dielectric mirror, in obliquely incident light, theory 3−32513
direct measurement by a space Fourier analysis 3−19322
dispersion relation, theory of turbulent heating by the modified two-stream instability 3−7524
dispersion theory construction on basis of the delay-time concept *(Russian)* 3−684
electrostatic electron cyclotron harmonic waves 3−7510
electrostatic two-stream instability, symmetry properties, of longitudinal plasma wave 3−7512
e.m., generalized expressions in terms of bilinear concomitants 3−10437
ferromagnet, spin-wave spectrum, linear contribution to spatial dispersion 3−18330
flexural waves in elastic circular cylinder 3−6289
giant polariton dispersion and selfinduced transparency of Frenkel excitons 3−24402
ion surface waves on bounded warm plasma, dispersion eqn. 3−17612
ionospheric radio signal spreading, absorpt. dispersion effects in lower layers 3−34938
laser radiation dispersion characteristics of an aqueous medium subject to hydrodynamic disturbance, time variation *(Russian)* 3−29113
metal, laser-irrad., stress-pulse propag., dispersion 3−7847
monoatomic rarefied gases, study of sound propagation using modified Navier-Stokes eqn. 3−29822
nonlinear dielectric boundary surface waves, dispersion curves and mode patterns 3−32496
open periodic structure with single iris, dispersion charact. determ. using variable length cavity *(French)* 3−29011
oscillations of an inhomogeneous plasma slab, dispersion relation 3−17598
periodic waveguide delay structures with complex boundaries 3−13608
plasma, characteristics of electric field from a radiating antenna in ionosphere, quasi transverse waves dispersion 3−21962
plasma, electrostatic and e.m. wave nonlinear coupling, equations of motion, dispersion relations 3−33358
plasma, magnetoactive, e.s. surface waves at transition layer, dispersion eqns. 3−29966
plasma, Maxwellian, ballistic second-order wave echoes 3−33363
plasma, multicomponent, crossover frequencies, e.m. dispersion 3−38436
plasma, non-Maxwellian, electronic longitudinal modes, dispersion curves 3−20486
plasma, warm random, electrostatic wave propagation 3−36171
plasma Bernstein mode excitation in inhomogeneous collisionless plasma 3−36173
plasma electron and ion cyclotron harmonic waves dispersion curves for generalised Bernstein modes 3−29967
plasma electron waves in unbounded uniform magnetoplasma 3−33361
plasma electron waves resonant interaction with an ion wave, complex ion wave dispersion 3−20535
plasma electrostatic waves, cyclic canonical variables calc. method 3−23840
plasma e.m. wave absorption and amplification considering spatial dispersion *(Russian)* 3−29948
plasma e.m. wave dispersion, covariant formulation 3−14530

dispersion (wave) continued
plasma e.m. wave dispersion equations for waves in multilayer structures 3−36161
plasma e.m. waves, propagating along mag. field 3−7502
plasma gravitational instability dispersion relation, effect of collisions and gyroviscosity 3−20490
plasma ion acoustic waves, dispersion and Landau damping 3−38463
plasma ion-acoustic coil-excited low freq. waves in single-ended Q machine 3−33366
plasma ion-cyclotron oscillations, dispersion 3−36181
plasma Langmuir wave dispersion, kinetic eqns. *(Russian)* 3−29987
plasma MHD waves, effect of high frequency collisions 3−36168
plasma oscillations, line shape, Kubo-Mori Brownian motion theory application 3−38456
plasma surface waves propagation along plasma-vacuum channel, resonance effect 3−36169
plasma wave, finite amplitude, dispersion relations 3−4638
plasma wave damping in the lower hybrid frequency range, dispersion eqn. 3−23856
plasma wave phase velocity rel. to beam velocity 3−17614
plasma waves, in presence of Coriolis force 3−11496
plasma waves *(Russian)* 3−7534
plasma waves and echoes *(German)* 3−14541
plasma-beam system, stable electrostatic fluctuations lineshape 3−38460
rotating stratified fluid, phase speed change and spatial growth rate of internal waves 3−17544
semiconductor, polar, magnetoplasma surface waves 3−2160
SH waves in infinite elastic plate with Cauchy's inverse transverse stress 3−12622
sodaniter and calcite, i.r. reflectance spectra 3−8545
surface waves guided by slit in isotropic elastic solid 3−22695
time-dependent dispersion equation, numerical solution for nonlinear freq. shift of plasma mode 3−4648
waveguide with limited comb *(Russian)* 3−13610
weak nonlinear dispersive waves, Korteweg-de Vries equations 3−10240
Ar plasma, non-axisymmetric Alfven wave propagation 3−38445
GaP, surface plasmons, phonons and polaritons 3−2554
InSb, surface plasmons, phonons and polaritons 3−2554
K plasma, drift waves, dispersion and damping, meas. 3−26882
Pd, dispersion of lattice waves 3−17942

dispersion hardening
$Al:Al_2O_3$, obs. of recrystallisation behaviour 3−18573
alloy, precip. hardening, specific strengthening parameter characteriz. 3−21704
alloy, recrystallization 3−5311
alloy, work hardening theory 3−37065
alloy with b.c.c. lattice, disperse particles influence on recrystallisation 3−31011
alloys, rel. to high temp. strength and creep props. 3−15773
C alloy, solution hardening rate derived from flow stresses on tensile deform. 3−15712
composite material strengthening mechanisms 3−21731
Cr alloy, high-temp. stability of refractory metal borides 3−18626
Invars, rel. to Young's modulus anomaly *(Russian)* 3−21631
metal, review of high temp. strength and creep mechanisms 3−15695
$Ni:Al_2O_3$, Mg, effect of Mg additions on high temp. mech. props. and microstructure 3−15711
$Ni:ThO_2$, study of high temp. strength mechanisms using explosion techniques 3−18615
Ni alloys, thoria dispersion influence on preferred orientation 3−21599
NiSpan C, Invar range, precip. hardening effect on phys. props. 3−39345
solid solution hardening, crit. resolved shear stress, conc. depend. 3−24898
steel:VN, B, stainless austenite, precipitation hardening rel. to creep resist. 3−15697
steel, 110G13L, strain hardening, modifier effects 3−18668
steel, austenitic, Cr-Ni-Mn, niobium carbide precip. rel. to creep behaviour 3−8927
steel, austenitic stainless, inhibited void form. during electron irrad., dispersion effect 3−26505
steel, austenitic stainless, solid soln. hardening effects of niobium carbide precip. 3−12415
steel, Cr-Mo-V, carbide hardening 3−21686
steel, dispersion-strengthened ferritic alloys for high-temp. applics. 3−8936
steel, durability of superheater tubing at elevated temps. 3−27701
steel, ferritic, Mo-containing, precip. and solid soln. hardening effects on creep strength 3−8933
steel, ferritic creep resistant, precip. strengthening mechanisms 3−8934
steel, low alloy, containing vanadium carbide, due to isothermal transform. 3−8935
steel, maraging, hardening mechanism *(Russian)* 3−39333
steel, Mossbauer obs. of strengthening mechanisms *(Russian)* 3−24875
$W-3Re:2ThO_2$, rel. to high temp. strength for use as fibre reinforcement 3−15696
Ag-Cd(Mg) dil. alloys, internally oxidized, strengthening mechanisms 3−24842
Ag-Cd(Mg) dil. alloys, partially internally oxidized, deform. and substruct. characts. 3−24841
Al alloys for machine construction, mechanisms of strengthening 3−21685
$Al-Al_2O_3$, recrystn., particle content, distrib. and cold deform. effects 3−18581
Al-Cu-Li alloys, resist. obs. of Al_2CuLi precip. 3−21660
Co alloy, microstructure and mech. props. 3−8782
Co-Cr based superalloys, strengthening mechanisms for high temp. applics. 3−31112
Co-Cr(21 wt.%) alloy with Y_2O_3 dispersion, rel. to Cr diffusion 3−39343
Cr alloys, carbide and boride strengthened, phase stability and mech. props. 3−34568
Cu coatings with corundum inclusions with high microhardness 3−18670

dispersion hardening continued
- Cu crystals dispersed with SiO_2 re-examination of recrystallisation data 3–15688
- Cu neutron irradiation hardening, effect of alloying elements Si and Al 3–18630
- Cu-Al_2O_3(MgO)(TiO_2), internal oxidation method, brittleness during annealing in H_2 *(Japanese)* 3–12395
- Cu-Cd single crysts., transmission electron microscope obs. 3–4805
- Cu-Mn dil. alloy single crysts., Friedel's solid soln. hardening theory rel. to dynamical deform. 3–8898
- Cu-Ni(Zn)(Al)(Ge), solid solutions, hardening mechanism in microdeform. stage *(Russian)* 3–21633
- Fe alloys containing Mn, Mo and Cr additions, precip. hardening 3–21640
- Fe alloys with Mo and Cr additions, solid soln. hardening 3–21639
- Fe carbonizing and nitriding, gas-solid reaction, thermal stability, homogeneous distrib. *(French)* 3–34526
- Fe-Cr-Co-Mo alloy, via R-phase precipitation 3–8787
- Fe-Ni:Al_2O_3, composite, alloying additions effect on structural stability and cohesion between phases 3–15782
- Fe-Ni-Al alloy, subspinodal, obs. and mechanism *(Czech)* 3–31103
- Fe-Ni-Sn Invar alloy, precip. hardening by Sn additions, Mossbauer obs. 3–21634
- Fe-Ni-Ti-Al-Nb alloys, resulting from ageing in two-phase $(\alpha+\gamma)$ state *(Russian)* 3–12363
- Fe-Si (3 at wt.%), Al_2O_3, dispersed, Newtonian viscous creep 3–31094
- Fe-Ta alloys, Laves phase precip. phenomena 3–37049
- Mg/MgO composites, effect of dispersed particles on structural stability 3–39376
- Mg-Al spinel crystal, kinetics, potential energy model 3–30930
- Nb, embrittlement at low temp. by hydride phase precip. 3–8818
- Nb-H solid solns., solute interactions role 3–2743
- Nb-Mo-Zr-C cast alloys, precip. hardening, heat treatment effect on ductility 3–18664
- Ni, with ThO_2 dispersion, recrystn. 3–21669
- Ni/Al_2O_3 composite, electrodeposition and hardness 3–37059
- Ni-Cr alloy, ThO_2 dispersion effect on oxidation of coated specimens 3–39366
- Ni-Cr alloys, Sn alloying effect, precip. hardening 3–21668
- Ni-Cr base alloys, precip. hardening and creep strength behaviour 3–8930
- Ni-Cr based superalloys, strengthening mechanisms for high temp. applics. 3–31112
- Ni-Cr-Al alloy with ThO_2 dispersion, rel. to oxidation behaviour 3–39367
- Ni-Cr-ThO_2, prep. by Cr diffusion in Ni-ThO_2 granule 3–8941
- Ni-Cr(20 wt.%) alloy with Y_2O_3 dispersion, rel. to Cr diffusion 3–39343
- Ni-Mo-W corrosion resistant hard alloy development 3–21667
- Ni-P coatings on steel, precip. hardening 3–27691
- Ni-ThO_2, prep. from organic metal compounds *(French)* 3–8940
- Ni-Ti-Al alloys, heat resistant, effect of copper additions on mech. props. 3–24949
- Pb-Ca alloy, rel. to appl. as grid material for Pb-acid battery 3–21635
- VC-Co alloys, carbide grain growth during liquid sintering 3–18683
- W fine wire with thoria dispersion, creep behaviour 3–37086
- Zr, saturated with oxygen and nitrogen *(Russian)* 3–24876

dispersion power, rotatory *see optical rotation*

dispersion relations
- *see also Mandelstam representation; N/D method; S-matrix theory*
- analyticity in quantum field theory, causality and dispersion relations 3–32628
- boundary, extension to interior of physical regions 3–16963
- causality-violation at high energies, use of once-subtracted dispersion relations, Brookhaven expts. 3–14094
- cochlear mechanics, guided interfacial waves 3–3443
- Compton scattering, couplings of f, σ, η, A_2 and π to photons and nucleons 3–846
- contour fixed-t for πN partial wave amplitudes in low-energy region and below threshold 3–10771
- electric wave propag. in warm plasma, effect of non-zero photon mass 3–25515
- electronic surface excitations via analysis of inelastic LEED 3–20914
- e.m. wave propag. in random media, dispersion relations due to dielec. fluctuations 3–6401
- finite-contour, test at fixed t in πN scattering 3–16962
- finite-energy sum rules for five-point amplitudes and duality 3–35812
- fixed poles in pion Compton scatt. 3–10 06
- fluctuation-dissipation theorem, mag. field regeneration, kinematic-dynamo activity 3–12928
- Fourier-Bessel expansion of scatt. amplitude at zero momentum transfer for unequal mass particles 3–29238
- hadron photoprod., dispersion theory for unknown partial wave amplitudes 3–13969
- high-energy contribs. to integrals for photoproduction of $\pi^{\pm}$ up to 450 MeV, isotensor e.m. current contrib. *(Russian)* 3–23078
- hydrodynamic waves, ffects of Coriolis force, rotating magnetic astronomical bodies 3–33282
- microelastic wave propag., restrictions on dispersion relations and elastic moduli 3–13592
- nonleptonic weak decays, role of final-state interactions in producing $\Delta I=1/2$ rules 3–35779
- nonlinear, for square of scattering amplitude 3–13820
- off-mass-shell, calc. of σ term in $K^{\pm}p$ scattering 3–29252
- optical potential, dispersion relation derivation 3–35892
- phenomenological, determ. of substitute using expansion of scattering amplitude in terms of analytic functions 3–4152
- plasmas, nonuniform streaming, drift instabilities 3–14531
- rectangular waveguide, filled with homogeneous lossy anisotropic drifting plasma 3–23830
- rectangular waveguide filled with homogeneous anisotropic plasma 3–26867
- relativistic five-particle amplitudes, analyticity props. and dispersion relations 3–16940
- retarded interatomic potential energy, multipole expansion, derivation with use of a dispersion relation 3–26612

dispersion relations continued
- rotating stratified fluid, phase speed change and spatial growth rate of internal waves 3–17544
- Schur Pick Nevanlinna interpolation theory as alternative to N/D method 3–29181
- surface plasmon dispersion rel., model-independent, by electromag. anal. 3–2035
- surface polaritons in spatially dispersive medium 3–24487
- technique for mass struct. investigation using gravitons 3–608
- trade-winds east of Barbados, wave shapes 3–12677
- two-pion exchange contrib. to N-N potential, calc. using dispersion relation technique and πN and $\pi\pi$ interaction data 3–6650
- unsubtracted, for convergence of Cottingham formula for p-n mass difference 3–10695
- unsubtracted study of axial vector current-two-photon triangle graph, anomalous term 3–13822
- $ep \to en\pi^+$, 2 GeV, analysis using Chew-Low extrapolation and fixed t dispersion relations, determ. of π form factor 3–13987
- $\gamma\gamma \to \gamma\gamma$, dispersion method study, contribution of intermediate KK state *(Russian)* 3–23077
- $\gamma\gamma \to KK$, dispersion method study including two-pion intermediate state, cross-sections for s- and d-waves *(Russian)* 3–23077
- $\gamma\gamma \to \pi\pi$, cross-section determ. from dispersion relations *(Russian)* 3–4174
- $\gamma\gamma \to \pi\pi$, low energy cross section determ. from dispersion relations and unitarity 3–13916
- $\gamma N \to \pi^{\pm}N$, $\pi^{\pm}\Delta$ high energy, S-channel dominance and charge ratios from quark model or duality diagrams 3–13911
- γp Compton scatt., at 2.2 GeV, verification of Kramers-Kronig relation 3–23084
- KN scatt., rel. to nucleon coupling of ω and φ mesons 3–10761
- K^+p scattering below 2 GeV/c 3–35825
- N, evaluation of e.m. form factors using method of sideways dispersion relations 3–6605
- π e.m. form factor, dispersion sum rules for behaviour in asymptotic domain, heavy ρ-meson existance *(Russian)* 3–23061
- $\pi^{\pm}$ photoproduction amplitudes at high energy construction from dispersion relations and local density 3–38040
- $\pi\Lambda \to \pi\Sigma$, dispersion sum rules for $\Sigma\Lambda$ transition magnetic moment 3–23138
- $\pi\Lambda$ scattering, partial wave relations and $\Sigma\Lambda\pi$ coupling constant, determ. using dispersion relations and Regge poles 3–14063
- πN, p and d-wave scattering lengths, forward constraints 3–6655
- πN backward dispersion relations and sum rules, determ. of f^0NN and gNN coupling constants 3–881
- πN dispersion relation approach to study of low energy $\pi\pi$ interactions 3–10778
- πN scatt. amplitude, modified Goldberger Miyazawa Oeheme sum rule 3–23015
- πN scattering, 10-500 GeV, real-imaginary amplitude ratio and e.m. corrections *(Russian)* 3–38079
- πN scattering amplitudes, extrapolation to unphysical region, using unitarity 3–17090
- π^-p charge exchange in double Regge pole model, application of dispersion sum rules 3–17107
- π^-p charge exchange reaction in double Regge poles model, application of dispersion sum rules 3–26347
- $\pi^{\pm}p$ scattering amplitudes, determ. of coupling const. f^2 and s-wave scattering lengths from once subtracted forward dispersion relations 3–4216
- $\pi\pi$ scatt. crossing props. of s- and p-wave phases, using fixed t dispersion relations 3–14053
- $\pi\pi$ scatt. low energy model using current algebra and dispersion relations 3–14055
- $\pi\pi$ scattering, low-energy, four-parameter solns. to partial wave dispersion relations 3–29253
- $\pi^-\pi^0$ elastic scattering in low-energy region, forward dispersion relations 3–29254
- ρ photo prod., presence of $J=0$ fixed pole in vector meson amplitudes, using dispersion relations 3–17062
- D, lattice phonons from inelastic coherent neutron scattering 3–20832
- H, lattice phonons from inelastic coherent neutron scattering 3–20832
- In, lattice dynamics 3–20830
- Mo, phonon dispersion relation Δ_1 branch meas. for Kohn anomaly temp. depend. 3–11700

dispersions *see disperse systems*

dispersoids *see disperse systems*

displacement measurement
- circular cylinder, radial eigenfunctions 3–3976
- continuous creep meas. in UC under axial compression and neutron irradiation up to 1150°C *(Italian)* 3–19148
- diffusely refl. surfaces, holographic interferometry 3–28461
- elastic displacement, as result of excavations related to pillar stresses 3–3975
- holographic interferometry, production testing 3–5966
- interferometers, patent 3–22362
- mechanical oscill. analysis by speckling in Fourier transform plane 3–5754
- moire fringe method, photographic gratings 3–22358
- opticoelectronic system for contactless obs. *(Russian)* 3–5768
- thermal expansion, optical microtelescopes, high temp. target config. and fiducial marks, experimental aspects 3–9863
- Al_2O_3 glazed substrates, dynamic camber measurement technique 3–8963

display equipment
- *see also computer peripheral equipment; screens (display)*
- circuit for display of peak of transient signal applic. to integrated laser pulse 3–214
- fatigue damage, obs. by exoelectron emission, appl. to Al 3–12468
- ferroelectric film applications 3–8543
- for time resolved mass spectrometry, offset raster unit 3–13448
- u.s. nondestructive testing, applic. of graphic display 3–21787

display instruments
- *see also cathode-ray oscilloscopes*
- CAMAC magnetostrictive readout, with Schottky memories, for use with spark chambers 3–28676

display instruments continued
- high spatial resolution spark chambers, e.m. delay line readout 3−28675
- holographic optical element, off-axis, off-bisector refl. type, visual display applications 3−19213
- LEED-Auger apparatus, work for change meas. 3−35494
- MI-10 ionization converter, calibration curve *(Russian)* 3−5856
- multiwire proportional counter, with integral readout delay line 3−28646
- for transient phenomena 3−32113

display systems
- *see also cathode-ray tube displays*
- Aerospace-NASA videomagnetograph-based two-dimensional photon counting 3−31843
- biplane X-ray videometry, visual-display unit with simultaneous data presentation 3−3906
- conference, Lausanne (1972) 3−22250
- digital, liquid crystal devices, physical principles, types *(German)* 3−7622
- encapsulated liquid crystals for obs. of temp. increase due to stresses in piezoceramic bodies 3−67
- h.f. acoustic holography, display using liquid crystals 3−19165
- holography appl. 3−22376
- interactive, macromolecular modelling, electron density maps 3−26741
- i.r. sensitive vidicon in TV camera for i.r. microscopy 3−25723
- liquid crystal, influence of contacts on scattering props. 3−14686
- liquid crystal, laser beam applic., development 3−6524
- liquid crystal, new nematic compounds 3−30066
- liquid crystal, visualisation of u.s. waves 3−77
- liquid crystal filled, degradation mechanism 3−21796
- liquid crystals appl. *(German)* 3−11543
- multi-level, improved optical images for non-optical hologram distributions 3−32088
- multi-level scan display systems, analysis 3−35284
- physics applic., heat exchanger resonator design *(French)* 3−16347
- plasma, choice of multiplex methods 3−23927
- segmented master character for electronic display apparatus, patent 3−33455
- seismic, multivariable, section analysis 3−9365
- stereoscopic, holographic materials for, characterisation and device feasibility 3−28576
- storage, for scanning electron microscope 3−372
- u.s. imaging, real-time, by Bragg diffraction 3−71
- video display, high-resolution, of X-ray optically magnified topographs 3−26931
- ZnS powdered phosphor systems, d.c. electroluminescence 3−24752
- Zn_2SiO_4 film, growth on Si substrate, electrolum. props., monolithic display device applications 3−21491

display tubes, television *see television picture tubes*

disruptive voltage *see electric breakdown*

dissipation (heat) *see cooling*

dissociation
- *see also electrolytic dissociation; heat of dissociation; ionisation; molecular dissociation; molecular dissociation energies*
- alloys, kinetics of ordering and antiphase domain growth vs. the kinetics of spinodal decomposition and coarsening 3−18609
- beryl decomposition in NaOH solutions forming chkalovite *(Russian)* 3−8715
- chkalovite, formation from beryl decomposition in NaOH solutions *(Russian)* 3−8715
- dispersed particles, size stability in the diffuse interface limit 3−18608
- iodine perfluoralkyl photodissociative laser, selective pumping effect *(Russian)* 3−10540
- Kirkwood-Westheimer theory of electrostatic effects, effective dielec. const. calc. 3−9054
- molecules, optical separation of isomeric nuclei by laser radiation 3−29506
- nozzles, contact interaction hypothesis accuracy, relative momentum for dissociating particles 3−33319
- oxyhaemoglobin dissociation curves, computer-aided data reduction 3−28360
- phenylalanine in aqueous soln., biphotonic photodissoc., 20°C, pH depend. 3−21822
- photodissociation in planetary thermosphere, appl. to Venus 3−31613
- steel, austenitic stainless, solid soln. decomp. kinetics 3−21603
- steel, hypereutectoid Si type, austenite decomp., isothermal annealing effect *(Russian)* 3−15717
- thermally excited ions, decomposition, statistical theory of mass spectra 3−36975
- Ag_2Te(c), $Ag_{1.9}Te$(c) and $Ag_{1.64}Te$(c), dissociation pressures 3−15828
- Al-Li alloys, decomp. of solid soln., resist. obs. 3−21606
- Al-Zn(15 at.%) alloy, spinodal-like decomp. kinetics, effect of random fluctuations 3−15666
- Al_2Br_6, in liq. phase from triple point to critical point, calc. of degree of dissociation *(Russian)* 3−25066
- Al_2Cl_6, in liq. phase from triple point to critical point, calc. of degree of dissociation *(Russian)* 3−25066
- Bi_2S_3, dissociation pressure meas. in 806-904K range, determ. of heat of formation from thermodynamic laws *(Russian)* 3−12511
- CO_2, O I 1356A emission line source in Martian atm. 3−16163
- Cu_2Te(c), dissociation pressure 3−15828
- H_2O, irradiation effects at high temps. and press. 3−18792
- H_2O cluster ions, shock layer meas. of reaction in D-region 3−3106
- InSe film, amorphous, electron microscope obs. 3−7936
- LiBr concentrated water solution, n.m.r. study of relaxation times and structural transitions *(Russian)* 3−12517
- LiCl concentrated water solution, n.m.r. study of relaxation times and structural transitions *(Russian)* 3−12517
- $LiNO_3$ concentrated water solution, n.m.r. study of relaxation times and structural transitions *(Russian)* 3−12517
- MgO, thermal vibr. and dissociation at 2100°C 3−24225
- O_2, photodissociation rates by solar radiation in 1025-2500Å range in mesosphere and lower thermosphere 3−3047
- O_2 in thermosphere, changes in abundance from twilight 6300 A airglow 3−9308

dissociation continued
- PbN_6, pure and doped thin films, photodecomposition, optical absorpt. and cond. meas. 3−25084

dissolution *see dissolving*

dissolving
- *see also solubility; solutions*
- autoclave, crystal growth and dissolution at high temps. and high pressure 3−3776
- crystal dissolution morphology, computer simulation 3−4847
- diffusion in a time-dependent three-dimensional boundary layer, dissolution of a thin surface layer 3−17527
- electric potential set up by phase change on single crystal membrane meas. *(German)* 3−9080
- microscopic obs. improved by electrochemical cell use 3−5864
- quartz, single cryst. spheres, in acid alkali fluoride melts, polyhedra form 3−20877
- simple cubic crystal, computer simulation of dissolution morphology 3−1898
- thin platelet preparation from bulk single crystal, dissolving technique 3−28529
- Zircaloy-2, in methanol-I_2 solutions, stress-corrosion cracking, dissolution activation energy due to I_2 adsorption 3−24886
- $Fe_2(OH)_3$ amorphous gel, characterisation and transformation to α-FeOOH by dissolution of gel particles 3−5383
- Ge, growth form and soln. form relation, corrosion of hollow half spheres in acidic soln. *(German)* 3−9079
- Mg_2Si:Al alloy, dissolution and growth of precipitates β', electron micro. obs. 3−8814
- NaF in NaF-ZrF_4 mixtures, enthalpies of dissolution, calorimetric study at 1030°C *(French)* 3−7907
- Sn, liq., dissolution of solid Cu, alloy layer growth 3−21709
- ZrF_4 in NaF-ZrF_4 mixtures, enthalpies of dissolution, calorimetric study at 1030°C *(French)* 3−7907

distance measurement
- *see also height measurement; thickness measurement*
- DNR-06 autoreduction rangefinder head, 20-200 m range 3−16388
- Cygnus X-3 radio source, neutral H obs. 3−35161
- galactic centre region, radiosource distances rel. to H I absorption 3−25498
- Galactic X-ray sources 3−19006
- irradiated fuel elements, optical profilometer system for in-cell measurement 3−17314
- laser interferometers *(Czech)* 3−16440
- laser interferometry applic. *(Japanese)* 3−213
- laser Moon-ranging for physical libration meas. *(French)* 3−28158
- modulated beam rangers 3−6519
- by optical means 3−25735
- optical method, patent 3−790
- by optical modulation 3−6518
- optical rangefinders, freq. conversion, double modulation of light 3−22319
- piezoelectric laser beam deflector *(German)* 3−19225
- reactor fuel element spacing, in-core eddy current measurements 3−23402
- reverberation time measurement, architectural acoustic quality, techniques and equipment *(German)* 3−28417
- satellite orbit determ. from range meas. for planet-orbiting satellites 3−35003
- satellite ranging, tropospheric refraction effects, atmospheric model, local meteorological conditions 3−21935
- Scorpius X-1, parallax and proper motion rel. to Sco-Cen association 3−22096
- Sculptor group of galaxies, H I obs. 3−28274
- thunderstorms, field strength spectral components ratio method 3−25336
- two colour, geodesy applications 3−157
- two-laser optical distance-measuring instrument with atmospheric refractive index correction 3−16917
- W51 galactic radiosource, 21 cm H line absorpt. meas. 3−35163

distillation
- *see also isotope separation*
- adsubble processes, foam and bubble fractionation 3−12464
- fractionation of alkali and alkaline Earth metals in Hawaiian marine atmosphere 3−12748
- ion fractionation at sea-air interface, alkali metals and halogens 3−12691
- ion fractionation at surface of aqueous inorganic salt solutions, film centrifuge 3−12555
- polymer solutions, liq.-liq. phase relns., fractionation 3−11344
- Ba, by reactive distillation in Mo column 3−18536
- Ba, ultrapure single crystals, preparation by ultrahigh vacuum reactive distillation *(German)* 3−8733
- Ca, purification by reactive distillation in Mo column 3−18536
- Ca, ultrapure single crystals, preparation by ultrahigh vacuum reactive distillation *(German)* 3−8733
- ^2H_2O enrichment, Sulzer rectifying plants 3−23439
- Sr, ultrapure single crystals, preparation by ultrahigh vacuum reactive distillation *(German)* 3−8733

distortion *see deformation*

distortion, electric *see electric distortion*

distortion measurement, electric *see electric distortion measurement*

distributed parameter systems
- linear elastic systems on Hilbert space, energy-like Lyapunov functionals 3−32341
- multiregion slab reactor, control rod programming and loading pattern optimisation 3−11069
- nonlinear, optimal control computational methods 3−6191

distributions, statistical *see statistics*

diversity reception
- *see also fading*
- Earth-to-satellite microwave links, path diversity expt. 3−28044

dividers, voltage *see voltage dividers*

DNA
- bacterial and episomal, model for the regulation of replication 3−39762
- base-pairs, competition among biprotonic phototautomerism, excimer formation and proton tunnelling, review 3−11337

DNA continued
- bases, CNDO/2 calcs., total and electronic energies, dipole moments, normal and tautomeric forms 3−36059
- bases, mol. radiation damage using scanning ion microscope 3−28730
- chain elongation and joining after U.V. irradiation of human cells 3−5677
- chromosome aberration dosimetry in case of over-exposure to radiation 3−16304
- cytosine, i.r. and laser-Raman spectra, planar vibr. 3−29773
- escherichia coli, postirradiation degradation properties 3−28383
- inverse problem, melting curves rel. information recorded *(Russian)* 3−1313
- mobilities, charge carrier, in periodic DNA models 3−8171
- photochemistry, formation of thymine free radicals 3−21836
- polyribonucleic acid, adenine containing subunits, phosphoresc. spectra 3−31279
- radiation-induced degradation, in germinating spores 3−31946
- replicative form DNA, φX-174, heavy ion induced single- and double-strand breaks 3−3590
- ribonucleic acid, appl. of detailed balancing approach to disordered copolymeric Ising chains 3−23640
- u.v. irradiation at high temp. with high doses, photoproduct formation 3−27893
- x-irradiation, effect of cyclic AMP on production of single-strand breaks in E. coli B/r CSH 3−28374

document retrieval *see information retrieval*

domain walls
- *see also domains*
- Bloch wall films, wall contraction 3−30656
- bubble, hard ferromag., translational mobility 3−8390
- bubble collapse method, for wall mobility meas., anal. 3−38995
- bubble domain lattices, elastic consts. and elastic waves, domain wall damping 3−21269
- bubbles, extraordinary, wall energy, statics 3−34163
- circular, wall energies, exchange and anisotropy contribs., numerical soln. 3−12036
- creep of domain boundaries with transverse constrictions, model approach *(Russian)* 3−18337
- creep rate under unipolar field action along axis of hand magnetisation 3−38994
- ferroelectric, local electron states *(Russian)* 3−8538
- ferroelectric semiconductors, localised electron states in domain walls 3−24663
- ferromagnet, Bloch walls, eqn. of motion from Landau-Lifshitz eqn. 3−8389
- ferromagnetic bulk material, transient wall motion, transient solns. 3−30655
- ferromagnetic film, domain wall creep in nonuniform fields, intrinsic fields influence *(Russian)* 3−36736
- garnet mixed rare earth iron type, epitaxial film, anisotropy field and domain wall coercivity temp depend. 3−21257
- magnetic, boundary movement, model verification *(Russian)* 3−21266
- magnetic, motion, eddy current limited, bowing and merging, segmented model 3−12035
- magnetic bubble film domain walls, static props. of film thicker than wall width 3−36761
- magnetic bubble film domain walls, theory of static props. 3−36760
- magnetic elliptical bubbles, dynamics, domain wall anisotropy effects 3−36759
- magnetic film and platelet, theory of domain wall motion 3−36754
- magnetic semiconductor, effect on elec. resist. 3−34170
- magnetic thick-walled cylindrical domains, props. in uniaxial platelet 3−36755
- magnetically soft materials, Bloch walls, basic properties 3−8377
- nematics, behaviour above Freedericks transition 3−4719
- ordered L1_0 structure, interaction of superdislocations with domain boundaries 3−17845
- permalloy cross-tie walls density influence on domain boundary creep *(Russian)* 3−2315
- permalloy electrodeposited films micron thickness, reversal of magnetisation by domain wall creep 3−38992
- Permalloy film, l.f. oscillating movement *(Russian)* 3−24586
- permalloy film, transit time limited nonlinear domain wall motion 3−36733
- permalloy thin films, Bloch line motion, behaviour at inhomogeneities, Lorentz electron microscope study 3−12038
- rare earth cpds., ferromagnetic, thin wall coercivity 3−2317
- triglycine sulphate, interaction with defects 3−27026
- two-dimensional domain wall structures, Lorentz microscopy anal. 3−24590
- $BaTiO_3$, ferroelec. switching, kinetics of domain wall motion 3−39102
- $BaTiO_3$ single crystals, rel. to compressive deform. 3−38608
- Co, hexagonal, resonance peak in ^{59}Co n.m.r., hyperfine field anisotropy 3−8459
- Co alloy, spin config. and intrinsic coercive field of narrow domain walls 3−8391
- $DyAl_2$-$DyFe_2(Co_2)$, rel. to complex mag. behaviour 3−18323
- Eu-Y-Ga-Fe garnet, low-field mobility and saturation velocity measurements 3−36765
- Fe, high-purity, creep, const. mag. field influence, dislocation-domain wall interaction *(Russian)* 3−36774
- Fe, zone-melted, X-ray diffr. obs. 3−17828
- Fe whiskers, X-ray topographic obs. of fir-tree branch and rectangular domains 3−30648
- KD_2PO_4, phase transitions, domain influence on elec. field gradient and spin-phonon interactions 3−2413
- $KNbO_3$, orthorhombic, domain struct. and single domain cryst. characteriz. 3−15463
- MnBi film, Faraday effect obs. 3−21272
- Ni, dislocation motion in alternating mag. field, oscill. domain wall interactions 3−30674
- Ni, flow stress rel. to mag. field, domain wall dislocation interactions 3−5125
- Ni, pulsed n.m.r. of ^{61}Ni, Bloch wall effects *(French)* 3−30702
- Ni, two-dimens. domain wall struct., Lorentz microscopy anal. 3−24590

domain walls continued
- Ni-Co alloy, flow stress rel. to mag. field, domain wall dislocation interactions 3−5125
- Ni-Cu alloy, dislocation motion in alternating mag. field, oscill. domain wall interactions 3−30674
- NiFe, distrib. function of forces exerted by defects on mag. domain walls 3−36756
- NiO, obs. of antiferromagnetic domain walls using X-ray transmission topography 3−30645
- Y-Eu garnet, epitaxial film, magnet domain wall velocity 3−36734
- $YFeO_3$, domain wall mobility, nonlinear applied field depend. 3−30661
- YIG, Ga substituted, nearly compensated, compensation magnetic domain walls 3−36732

domains
- *see also crystal microstructure; domain walls; electric domains; magnetic domains*
- active sites in periodic adlayers, heterogeneous catalysis at line defects 3−9095
- anorthite, temp. depend., model 3−24131
- ferroelectric crystals, phase transition and domain structure change obs. 3−778
- heterogenous, at line defects, simple boundary-controlled reactions anal. 3−9096
- heterophase solid, domain structure caused by internal stresses 3−30266
- internal friction obs., book 3−20813
- liquid crystals, twisted nematic, electric field induced domains 3−26970
- magnetoelastic theory of soft ferromagnetic elastic solids of multidomain struct. 3−34155
- rotating magnetic field control for bubble-domain experiments 3−6033
- semiconductors, influence of adhesions on characteristics of domain recombination *(Russian)* 3−11905
- CdS, Brillouin scatt. by propag. acoustoelec. domains 3−33960
- $CoPt_3$, antiphase domain struct. 3−34506
- β'-$Gd_2(MoO_4)_3$, dislocation domain wall interaction, etchants 3−8028
- $K_2PbCu(NO_2)_6$, rel. to Jahn-Teller effect 3−30687
- NH_4Cl, critical opalescence study 3−24667
- Pb, supercond., Landau domain struct. growth 3−15297
- $SrTiO_3$, monodomain charact. above struct. phase transition, birefringence obs. 3−2510

doping, semiconductors *see semiconductor doping*

Doppler broadening *see Doppler effect*

Doppler effect
- *see also atomic spectra; red shift; spectral line breadth*
- atmospheric laser Doppler velocimeter analysis, comments 3−9392
- atmospheric laser Doppler velocimeter analysis, reply to comments 3−12857
- attenuation method for nucl. lifetime meas. 3−17186
- beam-plasma instabilities excited by anomalous Doppler effect and Cerenkov effect 3−23865
- blood, aortic velocity and acceleration by u.s. device 3−37731
- blood flow ultrasonic sensor for internal and external chronic use 3−37777
- carotid artery diameter and flow, noninvasive technique using Doppler effect 3−37733
- demonstration in classroom with laser *(Russian)* 3−52
- differential Doppler laser velocity measuring instrument using a Fabry-Perot interferometer 3−16454
- Doppler anemometer, meas. of electrohydrodynamic motion 3−164
- Earth polar motion determ. using Doppler satellite data 3−34778
- flow measurement, jet, turbulence distribution, laser photon correlation spectroscopy 3−22570
- formamide, obs. from Sagittarius B2 in 6 cm region, hyperfine struct. Doppler shift meas. 3−39698
- gas laser, optically pumped, theory, Doppler broadening effect 3−22878
- gas mixtures, laminar, rotational, turbulent and exhaust jet flows, laser-Doppler velocimeter, review 3−32281
- heavy ion bombardment of titanium deuteride, Doppler-shift attenuation meas. of (2s-1d)-shell nuclei lifetimes 3−32891
- Lamb-dip spectroscopy, hyperfine struct. in electronic spectrum of I_2 3−11276
- laser anemometer *(French)* 3−16577
- laser anemometers for fluid flow measurement 3−19654
- laser Doppler anemometer, velocity and turbulence meas. of turbulent swirling flow in water 3−794
- laser Doppler anemometry of electric arcs, fluid velocity meas. 3−795
- laser Doppler spectroscopy of polyelectrolyte solns., colloid stability determ. 3−34661
- laser Doppler velocimeter signal for turbulent flow, spectral anal. 3−35553
- laser Doppler velocimetry, ambiguity noise level reduction with cross-correlation technique 3−791
- laser flow velocity meters *(French)* 3−32273
- laser spectroscopy, aerosol particle size meas., theory and expt. techniques 3−16428
- laser spectroscopy, operational limits, polydispersity effects, aerosol meas. appl. 3−16429
- laser techniques for flow velocity obs. 3−475
- laser velocimeter, anal. of simulators and tracking systems 3−340
- laser velocimeter, Doppler effect type, applications to gas and liquid streams *(Russian)* 3−13334
- laser velocimeter, dual beam, geometric anal. of probe volume 3−336
- laser velocimeter, Fourier optical model 3−473
- laser velocimeter, frequency shifting by electro-optic techniques 3−337
- laser velocimeter, reduction of const. component and noise in output signal *(Russian)* 3−13335
- laser velocimeter, turbulent transport obs. 3−338
- lunar topography, global determ. by radar interferometry and delay-Doppler stereoscopy 3−25422
- naval gun projectile, initial velocity measurement, laser Doppler velocimeter 3−32611

Doppler effect continued
non-stationary processes in ionosphere, magnetosphere and interplanetary space, elimination of electron current derivatives 3−25339
nonlinear absorpt. of separated light beams by Doppler broadened transition 3−13753
nuclear lifetime meas. with Doppler shift attenuation method 3−25826
photon rest mass, upper limit rel. to conventional Doppler shift departures 3−861
plasma particle motion near electron cyclotron resonance 3−20418
polystyrene latex charged particles in buffer solution, spectroscopy of scattered light 3−9018
saturated resonance fluorescence, non quenching collisions influence 3−14298
shallow seawater areas, Doppler spreading of reverberation 3−3730
spectral line collisional and Doppler broadening, mol. distribution effect on absorption 3−33141
stellar spectra, rapidly rotating objects, appl. to pulsars 3−35124
superluminal source motion in vacuum, Vasilov-Cerenkov effect and Doppler effect 3−29216
supersonic flow velocity meas. using laser Doppler meas. 3−4588
suspensions, laser velocimeter obs., Doppler signal correl. time rel. to conc. *(Russian)* 3−13336
teaching demonstration of Doppler effect, interference and radiation resistance using a 'Sonalert' 3−32014
total neutron cross section extraction from deuterium data, effect of nuclear Fermi motion 3−6674
tracking data for determ. of lunar gravity field 3−39594
tracking from satellite-to-satellite for gravity field resolution 3−34772
turbulence spectra meas. by laser velocimeter, Doppler ambiguity effect 3−22558
ultrasonic aortic blood flow meas. using pulsed Doppler flowmeter 3−37734
underwater modulation effects of Doppler system using Kirchoff-Huygen's integral 3−3729
upper troposphere, average wind speed estimation from 16 GHz scatter link Doppler shift obs. 3−39567
velocity measurement of working surfaces, laser technique *(Russian)* 3−22390
v.h.f. radar echoes, q-type sporadic-E meas., daytime disappearance 3−18888
wave normal direction of whistler mode signals in ionosphere, rocket-Doppler technique 3−34941
Ar low density magnetoplasma column, ion temp. by Doppler broadening of Ar II 4610 Å radiation meas. 3−23920
Cu, clean surface, light emission induced by H^+ and He^+ impact, Doppler broadening of emission lines 3−18501
Fe, rel. to Mossbauer γ-ray energy shift of ^{57}Fe 3−27451
OI 1304 Å multiplet, Doppler broadening in dissoc. excitation of CO_2 and O_2 3−23583

Doppler shift *see Doppler effect*

dosimeters
see also dosimetry
at AFRRI LINAC, electron irradiation techniques 3−3633
benzoid, as radiation dosimeter 3−35301
chloral hydrate system 3−19103
Con Rad 5100 thermoluminescence readers, effect of tray current on sensitivity variations 3−39815
detector accuracy, solid state detectors replacing film dosimeters 3−5686
dye-polychlorostyrene film, dose-rate response 3−16506
fluoride based radiophotoluminescent glass *(German)* 3−26545
intracavity scintillation counting system, conversion to dose-rate meter 3−408
ionisation chamber, for dose profiles 3−35306
linear accelerator, diode scanner recorder system for operating parameters monitoring 3−25894
logarithmic picoammeter for exposure and dose meas. in electron microscopy of polymer crystals 3−346
nuclear medicine, radiation detector materials 3−28396
paired ionization chambers, for reactor dosimetry, separation of γ and n dose 3−3632
photon survey meter, portable, 5-10 MeV 3−292
polyacrylamide, as radiation dosimeter 3−35301
polyhalostyrene thin-film dosimeters for high doses 3−35529
PTW/Keithley rel. to Baldwin Farmer 3−10150
radiation film badge densitometer, integrated semiautomatic system using minicomputer 3−28673
scintillation cell, determ. of Rn in U mine atmosphere 3−19358
succinic acid, solid, radiolytic decomposition, use as in-pile chemical dosimeter 3−29453
thermoelectret applications, review 3−8508
thermoluminescent, for X-ray beams comparison 3−35300
thermoluminescent personnel badge for student monitoring 3−293
whole-body monitors, absorption of oral dose of ^{57}Co and ^{58}Co labelled vitamin B_{12} 3−403
BaF_2 and BaF_2:Mn, thermoluminescence, glow curves 3−2600
$BaTiO_3$ ceramic, new thermally stimulated electron emission dosimeter *(German)* 3−14271
BeO TSEE detector, dosiometric characteristics variation with surface impurities 3−28671
CaF_2:Mn thermoluminescent dosimeter, response to β-rays 0.43-3.54 MeV and γ-rays 8 keV-1.25 MeV 3−311
$CaSO_4$(Tm), optical and thermal effects on thermoluminescence response 3−290
$FeSO_4$, molar extinction coeff. determ., radiotherapy appls. 3−6138
KCl:Eu radiothermoluminescence dosimeter for ionising radiations *(Russian)* 3−14270
$Li_2B_4O_7$:Mn thermoluminescent dosimeter, response to β-rays 0.43-3.54 MeV and γ-rays 8 keV-1.25 MeV 3−311
LiF, thermoluminescent, mailed, obs. of absorbed dose rel. to dose distrib. of X-rays 3−405
LiF glow peak growth due to annealing 3−291
LiF thermoluminescent dosimeter, response to β-rays 0.43-3.54 MeV and γ-rays 8 keV-1.25 MeV 3−311
Mg_2SiO_4(Tb), optical and thermal effects on thermoluminescence response 3−290
Si absolute dose calorimeter 3−26550

dosimeters continued
Si avalanche detector, response in beta, γ, X-ray and neutron dosimetry 3−404
Si photoconvertor, for X-ray examinations 3−35270
SrF_2 thermoluminescence, glow curves 3−2600

dosimetry
see also dosimeters; radiation monitoring; radioactivity measurement; X-ray detection and measurement
^{226}Ra faecal excretions after $ReSO_4$ dust contamination and alginate treatment 3−3617
absorbed dose and dose equivalent from protons and neutrons, 3.5 GeV to 1.0 TeV 3−35296
absorbed dose and tissue dose, revised recommendations 3−22182
absorbed dose at exit determ., film technique 3−13167
absorbed fraction for small objects, cube root of mass dependence 3−13160
adsorbed dose from γ-rays and fast neutron, assessment with surface dosemeter 3−9726
albedo fast neutrons and density, relation for cylindrical diffusers 3−22438
alpha absorpt. meas., lung dose from Rn daughters 3−9719
alpha particle energy loss in tissue equivalent plastic 3−5685
astronaut, calc. of radionuclide production and delayed photon leakage, solar protons 3−3611
atmospheric ^{85}Kr, bare skin and whole body doses 3−5683
beta dose on skin rel. to gamma exposure from surfaces contaminated with aged fission products 3−9705
beta radiation distrib. in tissue-equivalent material, transport theory based meas. method 3−9724
betatrons, control, for medicine 3−22172
biomedical instrumentation, conference, Philadelphia, Pa., USA (1972) 3−13136
biosatellite III, high-LET nuclear recoil particle exposure 3−3610
bladder dose from radioactive glomerular agents 3−13159
capacitor energy storage X-ray equipment, exposure factors rel. to conventional high tension transformer 3−10160
chromosome aberration dosimetry in case of over-exposure to radiation 3−16304
chromosome aberration yield in human lymphocytes as indicator 3−13156
clinical, techniques and machine performance checking 3−3627
collimator evaluation in presence of scattering medium 3−3630
computer generation of isodose contours from external X-ray sources, appl. to treatment planning 3−13161
continuous Compton recoil gamma-ray spectroscopy, in natural environment 3−31949
coupled neutron and secondary γ-ray transport through concrete, determ. of total and γ-ray dose equivalents 3−19899
depth dose determ., using standard man phantom and γ-sources 3−35298
depth dose determ. for neutrons and γ-rays, Monte Carlo program and standard man phantom 3−28393
depth-dose data for square and rectangular fields for Clinac-4 with lead flatness filter 3−13163
diagnostic medical X-rays, genetically significant dose determ. 3−9706
diagnostic medical X-rays, population mean marrow dose and leukaemia significant dose determ. 3−13152
dose equivalent and specification of ambient radiation limits 3−11102
dose equivalent index 3−9722
dose protraction by fractionation and by continuous exposure, comparative effects 3−9732
dose-fields, planar industrial irradiators, radiation modification of polymers, gamma ray *(Russian)* 3−26547
electron, for radiotherapy, conference (Teddington, England, Oct. 1971) 3−3621
electron kinetic energy flow through an interface 3−28394
e.m. fields and waves, instrumentation, developments 3−9714
entrance dose determ. for large irregular shaped fields in therapy 3−3628
environmental, for nuclear facilities 3−29451
epidermal thickness, new determ. method by weight determ. 3−22175
errors introduced by finite length of line sources 3−3631
exoelectron emission technique for personnel dosimetry 3−19973
fast neutron, estimation of S content of human hair and nail 3−3618
fast neutron contamination from 25 MV X-ray beam of clinical linear accelerator 3−13147
fractionated radiotherapy, simple formula for calc. of total dose 3−28386
Fricke, optical absorption for impurity detection at 224 and 304 nm 3−32257
gamma irradiation, dose-field characteristics, industrial cylindrical irradiator *(Russian)* 3−26548
gamma ray absorbed dose, absolute measurement, comparison of different calorimeters 3−28390
high energy, reactors and accelerators, report 3−3565
high energy particle accelerators, prediction of dose rate 3−1089
implanted, computer-aided method for source localisation 3−13164
introduction to luminescence dosimetry 3−31947
ionization, rel. to $FeSO_4$, for MeV electrons 3−406
isodose distribution, by Agfacontour film 3−35302
isodose representation in mantle therapy of Hodgkin's disease 3−9730
maximum range of T β-particles, gas concentration in lungs 3−5687
mean quality factor meas. by LET spectroscopy 3−3619
megavoltage therapy machines, build-up characteristics, TLD obs. 3−9727
mice, dose level discrimination by counts of bone marrow samples 3−31935
multiple beam X-ray treatment, computer program for planning 3−3625
neutron, using solid state fission track detectors *(Japanese)* 3−11093
neutron beam, using calorimetry and ionization techniques 3−3623
neutron beams, tissue air ratios, and scatter air ratios 3−13165
neutron fluence and those equivalent determination by moderating spheres containing fission track recorders 3−37696
neutron irradiation in man, over-conservatism in dose limits 3−3612

dosimetry continued
- nuclear industry contribs. to regional dose calc. using HERMES program 3—19984
- nuclear medicine, radiation detector materials 3—28396
- nuclear power reactor primary coolant system repair, environmental problems 3—38194
- personnel, fast neutron, integral methods, review *(Czech)* 3—3620
- personnel dosimetry, accuracy of detectors, monitoring methods 3—5686
- personnel service, organizational aspects 3—22181
- photons, from 200 GeV proton interaction with Fe-Pb beam stops 3—28397
- photons, monoenergetic X and γ ray 3—31948
- pion absorption in matter, Monte-Carlo calculations 3—31951
- proton interaction studies, dose composition in tissue-equivalent phantoms 3—5684
- proton synchrotron, radiation attenuation in tunnels 3—22180
- radiation, cancer treatment, appl. of minicomputers 3—9728
- radiation exposure from accelerator beams, NaI crystal gamma ray scintillation detector, beam size and energy 3—3894
- radiation exposure from diagnostic X-rays 3—5688
- radiation exposure meas. in 8-15 kVp X-ray range 3—3609
- radiation induced carcinoma and leukemia, whole body obs. 3—5679
- radiation levels and fluence conversion factors 3—3613
- radiation therapy, conference (Chicago, USA, Dec 1971) 3—3574
- radiation therapy, dose meas. associated with use of 7.5 MeV electrons 3—28387
- radiation unit proposal, for patients 3—37579
- radiologists, during X-ray fluoroscopy 3—13173
- radionuclide imaging, three-dimensional 3—10146
- radiotherapy, X-ray and electron beam characteristics from 25 MeV linear accelerator 3—3575
- reactor fuel reprocessing, offsite doses, review 3—32968
- relative health effects, medical and environmental radiation 3—13155
- safe tracer dose in medical investigation 3—3585
- scattered diagnostic X-rays, spectra, Alderson phantom 3—22179
- self-powered detector techniques for monitoring dose and position of intense bremsstrahlung pulses 3—9731
- simple phantom, X-ray pattern, photon energy and dose 3—13172
- simulation, industrial radiation sources, RK-M1 radiative loop model, construction, operation *(Russian)* 3—26546
- standards comparison 3—22242
- superficial layers of skin in X-ray therapy, effect of shadow trays 3—3594
- surface dose during spot-film radiography 3—9729
- thermal neutron dose meas. by fission track technique in u doped glasses 3—16507
- thermoluminescent, for fast neutron beams using CaF_2:Mn teflon phosphor 3—35299
- thermoluminescent materials characteriz., Al_2O_3 and MgO applic. 3—34435
- threshold detector meas., sealed tube DT neutron generators 3—13169
- tissue equivalent liquids, Standard Man and lean mammalian muscle 3—13171
- urinary ^{90}Sr and Ca in children, long-term obs. 3—3615
- water, pion depth-dose curves, Monte-Carlo program 3—31950
- X-ray and 10-40 MeV electrons, comparison of dosimetry methods 3—13170
- X-ray beam, 6 MeV, analytical model 3—3624
- X-ray complete treatment film, radiographic quality enhancement 3—13166
- X-ray doses from cervical applicators, film and cavity chamber obs. 3—3626
- X-ray object pattern, calc. rel. to radiographic image energy flux density pattern 3—28395
- X-ray radiotherapy, 33 MeV, mathematical model for influence of lung tissue on depth dose curve 3—28388
- X-ray spectrum measurements, superficial therapy X-ray unit, f-factor comparison 3—13137
- X-rays, correction of percentage depth dose for varying source to skin distance 3—13162
- X-rays, rap, proposed unit 3—22184
- zero field size tissue-air ratio calc. for 4 MV X-rays produced by linac 3—3629
- β radiation, using end window counter 3—9725
- β radiation absorbed energy distribution in tissue-equivalent medium 3—19102
- β-rays, distrib. near interface 3—22183
- γ-rays, absorption, track length distribution 3—9718
- γ-rays, cylindrical phantom, Monte Carlo method 3—22178
- π^- beam for cancer treatment, calcs. for producing desired depth-dose distribs. 3—25607
- π^- beam in water, depth-dose distrib. 3—11100
- ^{198}Au, absorbed dose in vicinity of surface beta emitters by MIRD method *(Czech)* 3—32991
- C, absorbed dose of ^{60}Co γ-rays, obs. using calorimeter 3—6070
- ^{144}Ce-Pr, airborne, evaluation of two indirect exposure pathways to humans, determ. of dose equivalent 3—19983
- ^{252}Cf, skeletal content, alternative technique to whole body counting 3—9720
- implantable ^{252}Cf sources, neutron dose rate calculations 3—13168
- ^{60}Co fields, derivative of scatter-air ratio 3—35303
- ^{60}Co irregularly shaped fields, comparison of theoretical and experimental dose calculations 3—35304
- ^{252}Cp, radiation control for clinical implants 3—3614
- Cs 134/137 mixtures from power reactors, comparison with ^{60}Co source parameters and dose uniformity ratios 3—19992
- ^{137}Cs, airborne, evaluation of two indirect exposure pathways to humans, determ. of dose equivalent 3—19983
- $FeSO_4$, molar extinction coeff. determ., radiotherapy appls. 3—6138
- $FeSO_4$, rel. to ionization, for MeV electrons 3—406
- ^{125}I source, personnel exposures due to inadequate beta tests 3—39814
- ^{192}Ir γ-rays emergent dose meas. in humans accidentally exposed 3—9721
- KCl:Eu radiothermoluminescence dosimeter for ionising radiations *(Russian)* 3—14270
- ^{85}Kr, dosage device *(Slovak)* 3—15848
- LiF, thermolum. response of rad. of X-rays and γ-rays 3—28392

dosimetry continued
- LiF, type 7, irrad. with low energy X-rays and γ-rays 3—28391
- LiF dosimetry, use in meas. of build-up effect of ^{60}Co gamma radiation *(German)* 3—5681
- ^{54}Mn, airborne, evaluation of two indirect exposure pathways to humans, determ. of dose equivalent 3—19983
- ^{55}Mn(n,2n)^{54}Mn, average cross-section in fission neutron spectrum, use for fast neutron dosimetry 3—23326
- ^{22}Na in food chain, lichen-reindeer-man 3—3634
- ^{210}Pb skeletal levels rel. to Rn daughter exposures 3—9723
- Pu, body content estimation, SEBEACH, digital computer program 3—22176
- Pu contamination, analysis of Pu-Am spectra by a Xe proportional counter 3—3895
- ^{220}Pu, monomeric and polymeric, metabolism in rat and mouse 3—3616
- ^{222}Rn ridi H_2, elimination rate of ^{214}Bi and radiation exposure 3—5682
- Si surface barrier detectors, for X- and γ-ray dosimetry, temp. influence on sensitivity 3—32166
- Si target storage tube, fluoroscopic dose reduction and image manipulation 3—411
- ^{90}Sn, retention in human bone 3—35297
- ^{90}Sr-^{90}Y β-ray source bonded in Al measurements 3—32132
- T, assimilated, theoretical dose to human system 3—22177
- Tc imager, scintigraphic display 3—10144
- ^{99m}Tc lung scan of mother, radiation dose to breast feeding child 3—28389

double refraction *see birefringence*

double refraction, electric *see electro-optical effects*

double refraction, magnetic *see magneto-optical effects*

double resonance, electron nuclear *see ENDOR*

doublet antennas *see dipole antennas*

DPPH, diphenylpicrylhydrazyl *see organic compounds*

drawability *see ductility*

drawing (mechanical) *see forming processes*

drives
- *see also electric drives*
- electron microscope 3—19341
- hydraulic, for remote control of micromanipulation 3—16551

drop model (nuclear) *see nuclear liquid drop model*

droplets *see drops*

drops
- aqueous solution, freezing for cryochemical process 3—9872
- boiling drop-form liquid, flow out of a Laval nozzle, accel. meas. 3—36142
- charged condensation droplets from aircraft discharger system 3—662
- cloud droplet growth, stochastic coalescence model 3—31371
- cloud droplet spectra, Monte Carlo simulation model for temporal development 3—25225
- cloud droplets and drizzle drops over Mauna Loa-Mauna Kea saddle road of Hawaii, USA, electric charge 3—12726
- coalescence in warm clouds and fog induced by electrical stimulation *(Polish)* 3—25330
- condensation, drop size distrib. model 3—24254
- condensation, drop size distributions and heat transfer 3—20857
- condensation growth and nonsteady evaporation 3—34749
- condensing, thermal resistance calc. 3—27116
- conductive fluid droplet, image interaction with air ion *(Russian)* 3—34893
- congelation in contact with AgI particles *(French)* 3—12768
- damage due to liq. drop high speed impacts 3—18622
- deformable, approaching plane interface, creeping flow model 3—11446
- deformation of liq. drop at small Reynolds number, asymptotic expansion 3—26855
- dichlorethane, motion through water contaminated with surface-active agent 3—1474
- dielectric, rotating, spherical, equilibrium shape in electric field 3—7453
- drying characteristics of single drops containing solids rel. to sprays 3—2764
- electrohydrodynamically sprayed liquid droplets, charge-to-mass relationships, fissionability concept 3—29914
- electrohydrodynamically sprayed liquid droplets charge-to-mass relationships 3—29913
- electrohydrodynamics of liquid drops, time-depend. problem 3—7440
- evaporation in two-phase system with evolution of heat *(Russian)* 3—11449
- fluidropper, device for forming uniform drops 3—26041
- fog droplets, explosive vaporisation by 10.6 μm laser pulse 3—37196
- forced oscillations in a viscous medium 3—29890
- formation in non-Newtonian fluids 3—7446
- glycerine in water, in collision, stability *(Russian)* 3—7467
- growth and evaporation, nonsteady-state theory 3—24259
- growth law of fast moving spherical second phase, heat and mass transfer limitations 3—24245
- growth rate in air-H_2O medium using laser scatt. meas. 3—18736
- kinetics of droplet growth by condensation with adiabatic expansion of air *(Russian)* 3—14507
- lean liquid-liquid dispersions, population balance model for mass transfer, droplet breakage processes 3—33293
- liquid crystal, centrifugal spreading, thin layer production 3—14685
- liquid in liquid, sizes in agitated system 3—9012
- liquid liquid systems, prediction of drop volume 3—9013
- liquid metal, study of liquid-gas interface at different temps. *(Russian)* 3—24260
- metal, formation during pulverisation *(Russian)* 3—27722
- mist droplets, passivation of condensation growth, cetyl alcohol vapour adsorption 3—39399
- n-pentane, combustion at high pressures 3—3777
- Newtonian liquid drops falling through viscoelastic liquid, tailing phenomena 3—1441
- oscillation of viscous drop in viscous field 3—7461
- particulate systems, real conc., high Reynolds number fluid dynamics and transfer processes 3—36136

drops continued

- pentane, iso and cyclo, droplet evaporation in glycerine-water solns., average heat transfer coeffs. 3—24250
- polystyrene monodisperse aerosols production with a spinning disc, drop formation process obs. 3—28800
- rainbows, glories, explanation and droplet size calc. using scalar field approach, limitations 3—18856
- raindrop empirical distrib. laws, coherence tests *(French)* 3—12699
- rebounding drop study, surface tension depend. on length *(Korean)* 3—27171
- size distribution determination in liquid-liquid dispersions 3—9014
- size measurement *(German)* 3—22255
- solution droplets, diffusiophoresis and thermophoresis, thermodynamic calc. 3—31204
- spherical droplet condensation in an isothermal vapour diffusing through a heavy background gas 3—20861
- sprays, photographic analysis of drop formation 3—31203
- steam, condensation, drop behaviour and surface temp. fluctuation correspondence 3—20855
- steam, dropwise condensation, effect of condenser material thermal props. 3—24255
- two-phase annular mist flow, droplet transfer 3—23780
- in two-phase flow, mixing of jet of fluid 3—14498
- viscoelastic fluids, breakup in simple shear fields 3—7447
- water, condensation coeff. obs. for water evaporated in different gas atmospheres *(Russian)* 3—14995
- water, effects of NH_3 on electrification of freezing and splashing drops 3—27106
- water, evaporation regimes, heating by optical radiation 3—27112
- water, falling and colliding in elec. field, charging 3—649
- water, growth rate during condensation 3—14992
- water, supercooled, freely suspended, freezing in wind tunnel 3—9280
- water, surface temp. during vaporization, interfacial tension during mass transfer 3—1875
- water, vaporization by i.r. laser 3—6496
- water used for self-excited high voltage generation 3—16358
- wetting by silicate melts, angle determ. by drop method, 'neck' phenomena *(Polish)* 3—27752
- Ge, optically pumped, evaporation of metallic exciton droplets 3—18106
- H_2O water drops in superheated steam atmosphere, thermal and dynamic interaction, theory and experiment *(French)* 3—4621
- Mg, pumping by travelling electric potential wave 3—10098

drying

- concrete, early drying shrinkage measurements 3—34635
- disperse material, convective drying, in agitated layer in cross flow of coolants 3—25022
- freezing, critical point drying, electron microscopy, biological specimen preparation 3—421
- granular materials equilibrium water content at different temps. 3—5362
- hygroscopic capillary porous solids, mathematical model 3—20409
- nuclear reactor, irradiated fuel treatment, waste products *(French)* 3—38183
- photochemicals, apparatus for photochemical treatment and drying *(Russian)* 3—28599
- porous solids, drying rate rel. to heat and mass transfer 3—2774
- single drops containing solids, drying characteristics rel. to sprays 3—2764
- through-circulation dryer, math. model and optimisation 3—11457
- Cu powder, heat cond. change *(Russian)* 3—27727

dual resonance model *see duality and dual models*

duality (mathematics)

- dual eqns., application in elasticity theory 3—32335
- equivalent criteria for modularity of lattice of all physical decision effects 3—28835
- spin-$^1/_2$ lattice system, duality transformation and correlation functions 3—37899

duality and dual models

see also Veneziano model

- absorption model of structure of elastic scattering 3—10785
- absorptive model, amplitude analysis of charge-exchange and strangeness-exchange processes in pseudoscalar meson-baryon scattering 3—4223
- absorptive model, existence of new absorption effect, structure of πN helicity amplitude 3—38064
- absorptive model, rel. to elastic p—p scattering around $t=-0.8(GeV/c)^2$ 3—879
- action-at-a-distance theories and dual models 3—26284
- algebra of Regge residues based on duality 3—38065
- backward π^+ photoproduction using narrow reson. model, absence of dip 3—6654
- baryon-exchange Regge residues, rel. to absence of Macdowell doublets and duality soln. 3—870
- compensated fields in dual theory *(Russian)* 3—26330
- current models, rubber-band field of Virasoro-Shapiro model and complex field 3—35813
- deep inelastic e and ν scatt., parton and dual model approach 3—13960
- deep inelastic reactions, application of duality principles 3—13932
- degenerate trajectory splitting 3—10733
- dimension of hadronic matter with harmonic forces in infinite-momentum plane, estimate 3—38062
- dual absorptive model, calc. of interaction range real part of helicity scatt. amplitudes 3—17069
- dual amplitude behaviour with Mandelstam analyticity, large angle scatt. and reln. to S-matrix *(Russian)* 3—29232
- dual amplitude construction with cuts using two-reggeon cut discontinuity 3—10740
- dual amplitude with Mandelstam analyticity, high-energy and Regge asymptotic behaviour 3—4191
- dual amplitudes with Mandelstam analyticity, dynamical representation, large angle and Regge behaviour 3—29231
- dual currents with cut-off, construction of amplitudes 3—17071
- dual hadrodynamics application to meson photoproduction, statistical approach 3—13869
- dual parton dynamics and distribs. reln. to hadron level struct. 3—29220

duality and dual models continued

- dual parton model of elementary particle interaction, string model 3—26318
- dual pion model, chiral dynamics as zero-slope limit, nonlinear σ-model 3—29230
- dual pion model, magnetic moments, e.m. problems and general formula 3—19703
- dual Pomeron and diffraction dissociation 3—38063
- dual resonance model, dynamical averages 3—29227
- dual resonance model, factorisation of pomeron sector and currents 3—10728
- dual resonance model for heavy resonance decay in statistical approach, relation to statistical bootstrap theory 3—17073
- dual resonance model for simultaneous fit for forward and backward πN charge exchange 3—29263
- dual resonant model, transverse momentum distrib., exponential cut-off 3—14030
- dual-parton model for high-energy πN scattering in forward and backward regions 3—32702
- dual-Pomeron amplitude, single-particle spectrum and scaling 3—26324
- dual-resonance amplitudes, connections between smoothed and narrow-resonance discontinuities 3—29229
- dual-resonance model for massive μ-pair production in hadron-hadron interactions 3—14035
- dual-resonance model for production of meson resonances with high masses and spins 3—29226
- dual-resonance models, four-dimensional interpretation of associated internal space 3—35811
- dual-resonance models, Lorentz covariance and physical states 3—4192
- dynamic resonance model, scaling and fixed poles of e.m. current 3—14021
- effective Regge trajectory in entire complex angular momentum plane, duality implications 3—32684
- electroproduction, two-component framework with dual reson. contribution 3—19700
- ep inelastic scatt. in low q^2 region 3—6635
- for exotic peaks and exotic cross-sections in K^-p and pp scatt. 3—17105
- field theory of dual resonance model, by second-quantisation of hadron string model 3—4195
- finite-energy sum rules for five-point amplitudes and duality 3—35812
- free bose field, duality, using von Neumann algebra 3—6541
- functional calculus for neutral scalar field theory with duality, applic. to Veneziano model 3—19702
- gauge identities in dual field theory 3—10600
- group structure for spin-1/2 lattice system, duality transformation generalization 3—10396
- hadron mass spectrum, statistical approach, dual theories 3—38069
- hadron scatt., unitary symmetry and duality 3—10732
- Harari-Freund two component duality in baryon inclusive spectra, quark topologies 3—17070
- hardon currents, strong and electromagnetic, dynamical Lagrangian theory 3—16959
- inclusive photon-hadron reactions, limiting fragmentation hypothesis and duality, Regge formalism 3—13997
- inclusive two-body reactions, finite mass sum rules and duality 3—32735
- inelastic lepton-hadron collisions, scaling and dual amplitudes 3—853
- internal symmetry predictions, baryon transformations, symmetry breaking 3—821
- Jacobi imaginary transformation and critical dimension, physical interpretn. 3—23104
- light-cone asymptotic props. of hadrons, analogy with duality 3—14028
- meson-baryon scattering, exact duality, spectroscopic consequences 3—23105
- meson-meson scatt., unitary symmetry and duality 3—10731
- multiparticle theory with nonlinear trajectories, manifestly dual quark-like operator formulation 3—35814
- multiperipheral model, dual, Pomeranchukon generation from background 3—32682
- n-particle inclusive distribs. in dual reson. model, cluster decomposition 3—14029
- Nakanishi decomposition, Feynman-like rules, extension to general loop amplitudes 3—14033
- Neveu-Schwarz model, spectrum-generating algebra and no-ghost theorem 3—26328
- nonlinear bootstrap in dual models and $f\pi\pi$ coupling 3—10727
- off-shell dual amplitudes and currents 3—867
- parton model and PCAC, reformulation and current algebra 3—35765
- Pomeranchuk branchings in dual resonance model and total cross sections at high energies *(Russian)* 3—23106
- Pomeron in dual models with Mandelstam analyticity 3—38060
- projective invariance of dual-resonance model from spin analyticity and Lorentz invariance 3—38061
- quark-symm. four-point-function without parity doublets, test using NN processes 3—32683
- resonance model with nonlinear trajectories, triple-Regge vertex 3—10729
- resonance production and inclusive cross-sections, model 3—26326
- resonance spins distrib. function and mass depend. of reson. elastic widths *(Russian)* 3—868
- scalar and conserved vector currents, new derivation 3—6634
- six-pion amplitude as modification of general chiral pion amplitudes 3—23103
- string model, Virasoro conditions and trajectory equation, derivation 3—14031
- string model interaction, construction of general vertex operator 3—26319
- $SU_{1,1}$ representations, dual amplitudes constructed on $J>0$ integer point 3—19701
- SU_3 derivation from dual models 3—29228
- $SU(6)\times O(3)$ quark model, relativistic extension, consequences of duality and exchange degeneracy 3—10724
- two new classes of dual models with spontaneous symmetry breaking 3—6636

duality and dual models continued
two-body and inclusive processes, average nonlinear duality and Pomeron 3−10741
two-body phenomenology at high energies 3−6649
unitarity corrections to dual resonance models 3−17068
vector meson inclusive production in dual resonance model 3−23188
Veneziano amplitudes, semi-local duality props. for total and one-particle cross sections 3−23179
Virasoro case, transformation props. of asymmetrical general vertex under projective group 3−14032
Virasoro conditions and Plateau's problem in duality theory 3−4194
Virasoro symmetry and simple loop graphs without tachyons *(Russian)* 3−19705
zero-slope dual reson. model, equivalence with $\varphi 3$ theory 3−10736
$A_1\pi\to\pi\pi$, crossing-symmetric dual geometrical amplitude model 3−26327
$e^+e^-\to e^+e^-$ + hadrons, dual frame loops diagram and scaling behaviour 3−848
$\gamma N\to\pi^\pm N$, $\pi^\pm\Delta$ high energy, S-channel dominance and charge ratios from quark model or duality diagrams 3−13911
K^+ photoproduction, duality diagrams and Regge cuts 3−13968
K^+ photoproduction, polarisation predictions from pion data and duality, Reggeized absorption model 3−26305
$KN\to K\pi N$, isospin conservation and choice of B_5 amplitudes 3−901
KN scatt., reson. and background amplitudes, dual absorptive model 3−23178
$NN\to\pi\pi\pi$, dual quark model for annihilation at rest 3−862
νN inelastic interactions, determ. of threshold relations from scaling and duality 3−13841
p-n electroprod. struct. function difference, duality results 3−13870
π photo- and electroproduction in dual relativistic quark model, U_6 symm. breaking 3−13931
π^0 photoproduction in weak-Regge-cut model with duality SU(3) and vector dominance constraints 3−32669
$\pi^\pm$ photoproduction amplitudes at high energy construction from dispersion relations and local density 3−38040
πN scatt., dual model with second-sheet resonances 3−19726
πN scatt., reson. and background amplitudes, dual absorptive model 3−23178
$\pi^-p\to\pi^-p(\pi^+\pi^-)$, diffraction dissociation and dual model 3−19704
$\pi^-p\to\pi^0n$, duality and Bessel-function model from Regge-theory viewpoint 3−6664
$\pi\pi$ amplitude of modified CHKZ type, analysis 3−26325
ρ meson diffractive photoproduction dual model study 3−23072
ρ' photoproduction suppression, in terms of multiperipheral and duality models 3−17054

ductility
Al bronzes effect of iron, casting and wear properties *(Polish)* 3−31033
concrete, plain and reinforced, ductility 3−5345
fracture strain, criteria from theory of plasticity 3−22661
Hastelloy alloy X, elevated temp. ductility min. and associated props. 3−15705
Inconel alloy X-750, precip. parameters role upon creep rupture props. 3−37024
metal, b.c.c., plastic crack propag. *(Russian)* 3−20802
metal, ductile fracture, development of surfaces, unstable cavity expansion 3−38618
metal, hardness-temperature relationships, stress coeff. 3−34557
metal, plasticity effects in crack propag. 3−30195
metal, rel. to strain-hardening coeff. *(Russian)* 3−39356
nuclear reactors, inelastic materials in high-temp. structural anal., problems involved 3−26497
polymer, glassy, delayed yielding, theoretical description 3−31165
polymer, h.p. effects on mech. behaviour 3−31187
radiation damage in structural materials 3−29449
steel, austenitic, preliminary thermocycling influence on hot strength 3−31101
steel, austenitic, type 304L, hydrogen embrittlement effects 3−2745
steel, austenitic Cr-Mn, cold-worked unstable, heating effect on martensitic transforms. *(Russian)* 3−30966
steel, austenitic stainless, creep rupture props., niobium carbide effect 3−12415
steel, carbon, high-temp. plasticity change rel. to pearlite struct. 3−21689
steel, characteriz. for cryogenic technology, stress concentrators influence 3−34603
steel, cold worked, influence of high temp. austenitization 3−24935
steel, Cr-Mo-V, carbide hardening and characteriz. 3−21686
steel, Cr-Mo-V, cyclic straining influence on creep behaviour 3−12416
steel, dispersion-strengthened ferritic alloys for high-temp. applics. 3−8936
steel, ductile state produced by fast cooling after annealing *(Russian)* 3−24905
steel, durability of superheater tubing at elevated temps 3−27701
steel, heavily alloyed, resistance to failure 3−34601
steel, high-speed tool, characterization 3−21682
steel, high-strength, tensile ductility, gaseous hydrogen influence 3−5323
steel, inclusions rel. to crit. mech. props., metallurgical processing incl. vacuum melting 3−27629
steel, inclusions rel. to crit. mech. props., vacuum melting effects 3−27630
steel, lead embrittlement, comp. depend. 3−21648
steel, low alloy, containing vanadium carbide, microstruct. effects on creep props. 3−8935
steel, lower yield strength depend. on grain size and temp. 3−37053
steel, maraging N18K9M5T, carbon effect 3−21664
steel, metastable austenitic Cr-Mn, warm rolling effect *(Russian)* 3−18612
steel, N14Kh5M3TYu, heat treatment effect 3−21665
steel, near tip strain as ductile fracture criterion 3−31052
steel, Ni-Co-C, roll-extruded, effect of degrees of rolling reduction 3−31050
steel, stainless, influence of deoxidation on mechanical properties 3−24919
steel, stainless, type 316, annealed, tensile props. after EBR-II irrad. 3−34560

ductility continued
steel, stainless 304, hold-time effect in high temp. fatigue fracture 3−27707
steel, stainless 304 and 316, post-irradiation ductility meas. for fuel rod design 3−26525
steels containing Mn, Cr, V, wear resistance and mech. props. 3−24928
Superinvar alloy prep. and characteriz. 3−24945
transition metals, group V, hydrogen embrittlement and hydride form. 3−34530
W wires, doped, recrystallisation effect on mechanical properties *(Japanese)* 3−31065
Zircaloy-2, hydrogenated, deformability testing method based on high vel. deform. *(French)* 3−9035
Al, strain rate effect on ductility *(Japanese)* 3−12389
Al alloy, long-term strength, deform. criterion 3−31233
Al alloy, near tip strain as ductile fracture criterion 3−31052
Al alloys, inclusions role in ductile fracture and fracture toughness 3−30984
Cr. rare earth metal additions effect 3−34604
Cr alloy:Pr(La), zone refining rel. to low temp. ductility *(Russian)* 3−12305
Cr-Ni alloys, two-phase, creep failure 3−27697
Cu, temp. depend., grain boundary migration *(Russian)* 3−39355
Cu film, electrolytic, thickness depend. *(Russian)* 3−7820
Cu-Ni alloys, weld cracking and ductility-trough phenomenon 3−21637
Fe, Armco, effect of cold deform. and subsequent heat treatment *(Russian)* 3−5307
Fe, Fe-Mn and Fe-Ni, stress exponent of dislocation vel. from strain rate cycling tests *(Japanese)* 3−31078
α-Fe, lower yield strength depend. on grain size and temp. 3−37053
Fe, polycryst., failure mechanism under plane stress conditions at low temps. 3−31096
Fe alloys, binary substitutional, b.c.c., wire drawing and alloy content effects 3−34572
Fe-Cr-Mo ferritic stainless steel, vacuum melted, effect of C and N on toughness, ductility and corrosion resist. 3−27676
Fe-Ni-Ti-Al-Nb alloys, ageing in two-phase $(\alpha+\gamma)$ states, effects on props. and struct. *(Russian)* 3−12363
Fe-Si, annealing, 480-680°C, effect of mag. field on softening process *(Russian)* 3−27673
Fe-Ta alloys, Laves phase precip. phenomena 3−37049
Fe-Ti solid solns., temp. and conc. depend. of mech. props. *(French)* 3−31038
Gd, meas. from 78 to 675 K 3−18624
Mo, polycryst., low temp. props., surface oxidation effect 3−24896
Mo, wire, recrystallised, alloyed with Ru and C, tensile properties *(Japanese)* 3−31074
Mo ingot, ductility effects of complex additions of 0.15 wt% Ru with C or B *(Japanese)* 3−31073
Mo prestraining effect on brittleness, ductility of dislocation containing specimens *(Japanese)* 3−31070
Mo:Ti, Zr, low temp. rolling effect on ductile-brittle transition temp. *(Russian)* 3−24902
Nb-Mo-Zn-C cast alloys, ductility increase by heat treatment 3−18664
Ni, electrodeposited from ethylene glycol electrolyte 3−25071
Ni electrode, intergranular cracking at cathodic potentials 3−31266
Ni-Cr base alloy for use above 100°C 3−31063
Ni-Cr-Nb heat resistant spring alloy characteriz. 3−24944
Ni-Cr(50 50 wt.%) alloy, resist. to service embrittlement, high-creep strength, development 3−21636
α-Pu, recovery creep and ductility transition 3−26508
Pu-Ga (1 wt.%), cold rolled, annealing, yield strength, strain hardening and ductility meas. by tensile tests 3−12384
Ta, electrodeposited from fused salt electrolyte 3−24362
Ta, hydrogen embritlement and hydride form. 3−34530
Ti alloy, TA6V6EZ, hydrogen and oxygen influence on tensile props. *(French)* 3−5334
Ti-Mo-Zr-Sn, βIII alloy, combined high and low temp. deform. processing effects 3−34578
Ti-Mo-Zr-Sn β-III titanium, thermomech. treated 3−34582
U, hydrogen contamination effects 3−8908
V, high-purity, deform. mechanism at low temps. 3−37055
V, hydrogen embrittlement and hydride form. 3−34530
W, chemical vapour deposited, mech. behaviour, 800-1600°C 3−37085
W, Ni, Fe doped, heat treatment effects *(Japanese)* 3−8857
Zr, hydrided, quenching effect on slow-bend behaviour 3−18631
Zr-Pd(Ru) dil. alloys, heat treated *(Japanese)* 3−31079

dusk *see twilight*

dust
see also cosmic dust
Arizona haboob of 16 July 1971, general characteristics 3−27997
atmospheric, turbidity meas. over India 3−37231
atmospheric dust in Bucharest, daily variation of natural radioactivity 3−5510
atmospheric spectral absorption bands rel. to dust particle shape and orientation *(Russian)* 3−18860
biosphere, industrial influences on atmosphere 3−5511
continental dust, meas. of air content over Norwegian and Greenland seas 3−9288
dusty gas, weak shock wave propagation, perturbation study 3−11428
electrification, influence of lattice defects in crushed material 3−2167
electrification on dispersion into air 3−18735
electrostatic precipitation from high PbO waste gases, optimum conditions *(German)* 3−19550
extensive dust layer in northern hemisphere due to a volcanic eruption 3−9289
flowing gas, dust content determ. *(German)* 3−22562
macron clouds, charging and discharging, role of gas breakdown 3−35657
Mars, dust-storms, occurrence frequency 3−12980
Martian, wind, water, volcanism, Mariner 9 obs. 3−35075
Martian dust storms, photometric obs. by remote serving 3−31597
Martian dust storms, review 3−31594

dust continued
  mining dust meas. and control to reduce work-related diseases 3−25609
  NGC 4151, Seyfert galaxies, i.r. variability of dust model 3−13087
  Sahara dust, i.r. refr. index 3−31293
  Sahara mineral dust in Atlantic marine aerosol 3−12749
  Saharan, vertical and areal distribution over western equatorial North Atlantic ocean 3−12751
  shirlwinds, dust devil frequency and diameter rel. to atmospheric temperature 3−25237
  stability of vortex sheet flow rel. to dust devil formation 3−28013
  storms, long-wave aerosol heating effects 3−25247
  Fe anionic species in interstellar dust 3−13107
dust storms *see storms*
dyeing
  cat, visual cortex, cell structure and formation correlation determ., using Procion yellow 3−22153
dynamic braking *see braking*
dynamic programming
  nuclear medicine, tumour detection, Scan-Rescan process 3−28371
  spacecraft motion parameters, linear estimates with a priori information 3−25372
dynamic stability *see stability*
dynamic testing
  alloy, fatigue crack growth, effects of loading freq. and nonreactive external media 3−31234
  alloy, high-hot-strength, fatigue strength under nonsteady state loading 3−37106
  alloy, high-strength, fracture toughness role in low-cycle fatigue crack propag. 3−31047
  alloys, low yield strength fatigue crack propagation using plastic strips 3−21766
  bending tests, production of fatigue cracks, for work of rupture 3−27803
  biaxial cumulative fatigue damage, octahedral shear strain theory 3−31239
  cement mortar strength results using ASTM standard test method C348 and C349 3−34673
  composites, effect of specimen geometry on fatigue strength meas. 3−21770
  compression and tension, with recording of deformation diagrams 3−27799
  constructional materials and compressor components, fatigue strength under fretting corrosion conditions 3−34605
  corrosion fatigue, crit. corrosion rate considerations 3−27655
  crack propagation resistance, formation of angular cracks in cylindrical samples 3−27806
  creep test extrapolation, model considerations *(French)* 3−25032
  creep testing machines, throughput capacity increase 3−25659
  design element, fatigue life determ. on basis of fatigue failure mechanism concepts 3−37108
  Duralumin, fatigue crack growth 3−18750
  elevated temperature and slowly time varying loads, inelastic stress-strain law 3−25027
  energy dissipation determ. from log. decrement of torsional oscillations of compound rod 3−37111
  fatigue, apparatus for testing plastics 3−18757
  fatigue, apparatus for testing plastics in biaxially stressed condition 3−18756
  fatigue, axial vibrations in nonuniformly heated rod, amplitude distrib. 3−31235
  fatigue, overhead telephone cable supports, steel strands, comparison of UG and EHS strands 3−12492
  fatigue, plastic, study of torsion specimens *(German)* 3−21785
  fatigue, probability of faults during cyclic loading, estimation method 3−34694
  fatigue crack growth behaviour under variable amplitude loading 3−21756
  fatigue crack growth data analysis 3−25028
  fatigue cracks, growth rate estimation 3−27804
  fatigue life, high vacuum effect on low cycle fatigue law 3−39423
  fatigue life estimation and crack propag. under stress *(Japanese)* 3−25030
  fatigue test machines TsDM-10-Pu, features of use and modernization *(Russian)* 3−12479
  fatigue testing, low-cycle, on machines with pendulum load measuring devices 3−18755
  fatigue testing, metal hardening, recording at elevated temps. 3−28465
  fatigue testing, temp. meas. of rotating specimens 3−18751
  fatigue testing machine, push-pull type for high pressure operation *(Japanese)* 3−12486
  fatigue testing method *(German)* 3−31229
  fatigue testing unit, with pulsating load at specified force and deflection 3−18754
  fin, from shipping cask, plastic impact testing, energy absorption characteristics 3−39424
  fracture toughness, repeated determ. with one specimen 3−27805
  friction welded high speed steel, annealed steel *(German)* 3−31118
  graphite, Poco and RC4, dynamic fatigue behaviour and general fatigue design criterion 3−32951
  high-speed methods analysis 3−37110
  load-bearing capacity of specimens with stress concentrators under repeated loading, deform. effects 3−34686
  metal, cyclic creep fracture in low cycle fatigue *(Japanese)* 3−25029
  metal, preliminary plastic strain effect on form of mech. hystersis loop 3−34599
  metal, stress relaxation expts., dislocation behaviour 3−37104
  metal hoses, failure resist. under low cycle loading 3−34684
  metals, thermal fatigue, under mechanical loading in corrosive medium 3−27798
  metals, unit for torsion investigations at room and high temps. 3−35358
  piano wires, low-cycle torsional fatigue under const. strain amplitude at elevated temps. *(Japanese)* 3−18771
  plastics, fatigue tests, rational test piece geometry for cyclic tension-compression tests 3−25033
  polymer, apparatus for dynamic characts. meas. 3−18761
  polymers, dynamic properties obs. by resonance method 3−27801
dynamic testing continued
  polymers and composites, servo-controlled axial fatigue machine with strain rate feedback 3−25665
  polystyrene, failure in tensile and cyclic deform. 3−21740
  programed loading and testing machine 3−32032
  programming unit for low cycle testing with holding at high temperature *(Russian)* 3−12478
  pulsating stress creep rupture, nonlinear damage law proposal 3−31237
  rail specimen plasticity assessment in impact machine tests using rolled grid *(Russian)* 3−12476
  reactor materials and components subjected to time-dependent loading, creep analysis 3−39368
  rock, fatigue failure as stochastic process under pulsating tensile stress *(Japanese)* 3−21771
  rotor hydropulsators for use with fatigue testing machines, 'floating zero' effect and kinematic distortions *(Russian)* 3−12475
  SGHWR pressure tubing, pressure cycling tests, defect growth analysis 3−14250
  special impact test specimen *(Russian)* 3−12484
  steel, bainitic, notch acuity effect on fracture toughness testing 3−25031
  steel, fatigue strength of standard steel specimens with varying percentages of carbon, under reversed bonding loads 3−24888
  steel, fracture toughness in cyclic loading, rel. to fractographic peculiarities 3−34689
  steel, load-bearing capacity of specimens with stress concentrators under repeated loading 3−34598
  steel, low-cycle fatigue testing, transformation of retained austenite and cracks 3−37060
  steel, maraging for use in military bridge, fatigue crack growth and fracture 3−21626
  steel, mild, fatigue crack growth under crack opening displacement cycling 3−31046
  steel, pearlitic, low cycle fatigue, heat treatment type depend. 3−37070
  steel, prestress effect on low-cycle fatigue failure 3−21758
  steel, stainless, stabilized, strain rate effect on high strain fatigue props. 3−34564
  steel, stainless, time and cycle dependent failure at elevated temp. 3−31240
  steel, stainless, type 403, corrosion fatigue metallography 3−27658
  steel, structural, hysteretic behaviour under cyclic bending *(Japanese)* 3−39374
  steel, structural, influence of rest periods on fatigue strength 3−21755
  steel, work hardened, impact strength under cyclic loading at low temp. 3−34682
  steel components, contact fatigue kinetics obs. using inductive sensor 3−34692
  steel machine parts, notch sensitivity under alternating loads, machining methods influence 3−34693
  steel plate, mild, performation by flat-ended cylindrical projectile 3−25026
  steel pressure vessels, cumulative fatigue damage tests, cyclic stress, strain and energy variations 3−34677
  stress relaxation technique applic. to superplastic materials 3−37101
  stress/strain test data analytical evaluation 3−25024
  structural (service) reliability, kinetic fracture models 3−21764
  tension grips used on testing machines GSM-50, GRM-1, GRM-2 for thin-walled tubes 3−12485
  thin plates dynamic testing with sinusoidal pneumatic excitation *(Japanese)* 3−25036
  turbine blade materials, behaviour under asymmetric loading 3−31232
  two-dimensional stress state testing device 3−35357
  unbounded plate with collinear cracks, dynamic stress intensity factor 3−21760
  vibration and shock effects, mechanical equipment, calibration, periods, problems *(Polish)* 3−19156
  vibration test, digital control and analysis 3−34697
  vibrations, digital incremental oscillator analyser systems, inherent limitations 3−5762
  Weissenberg rheogoniometer, calibration using Newtonian fluids 3−6172
  weld joints, fracture strength testing *(German)* 3−31231
  welded specimens, programmed fatigue testing 3−37107
  wire reinforcement metal, fatigue tests *(Russian)* 3−12474
  Young's modulus, flexural damping capacity, meas. apparatus 3−9833
  Al, creep under intermittent loading 3−37103
  Al, dynamic stress/strain behaviour in torsion 3−21779
  Al alloy, long-term strength, deform. criterion 3−31233
  Al alloy, stresses during vibr. of plates under acoustic loads 3−31236
  Al_2O_3, alumina, impurity effects *(German)* 3−34669
  Fe, deform. resist., temp. and strain rate depend. *(Russian)* 3−31058
  Ni alloy, fatigue strength, test temp. influence 3−34687
  Ni based superalloy, elevated temp. fatigue behaviour of single crysts., environment effects 3−39365
  Ti alloys, creep characts. under varying loads 3−37068
  Zn-Al (22 wt.%), superplastic, room temp. creep behaviour under bending and plane conditions 3−34678
dynamics
  see also ballistics; fluid dynamics; force; friction; hemodynamics; impact; kinematics; resonance; rotating bodies; rotation; vibrating bodies; vibrations
  approximately relativistic Lagrangians for classical interacting point particles 3−22720
  bidimensional system with infinite number of degrees of freedom, dynamical theory 3−10381
  building structures, method for prediction of dynamical behaviour 3−3762
  dense stellar systems, dynamics rel. to galactic nuclei, review 3−39734
  elastic fibre suspension, turbulent dynamics rel. to drag reduction 3−20407
  elasticity theory spatial problem, operators and permissible dynamic eqns. *(Russian)* 3−16643
  elastodynamics, numerical integration methods, evaluation 3−22604

dynamics continued
- explosive volcanic eruptions, atmospheric trajectories of pyroclasts 3−34811
- ice sheets in Antarctic 3−12563
- Kepler motion, numerical stabilising procedure based on Floquet's theorem 3−3282
- laboratory apparatus for double spark source on linear air track 3−39
- Lagrange's equations of second kind, generalisations and modifications *(Russian)* 3−28850
- linearization of dynamical rotor system 3−16606
- mechanical systems with random forces, Gauss principle appl. *(Russian)* 3−10267
- oscillating system, delinearization *(Russian)* 3−10309
- rigid-plastic bodies, variational methods for dynamic loading 3−28891
- stellar, probability distrib. of random force in gravit. systems 3−31741

dynamometers
- *see also force measurement*
- hydraulic tensometric, eccentricity allowance 3−25660

dynamos *see d.c. generators*

dysprosium
- antiferromagnetic helical phase, spin wave energy 3−5110
- Auger electron spectra, up to 530 eV *(Russian)* 3−15579
- elastic moduli, hydrostatic press. derivatives, electrostatic model and band struct. contrib. 3−27051
- ferrimagnetic reson. theory, spin system time evolution 3−2406
- ferromagnetic-antiferromagnetic transform., elec. resist. and thermal expansion obs. *(Russian)* 3−15363
- film, obs. of f.c.c. structure and oxidation 3−18042
- heat of soln. in Sn, calorimetric meas. *(French)* 3−4839
- ionisation loss in inelastic electron refl. from Gd surface 3−5252
- isotopes, X-ray transitions, isotope shifts 3−1107
- magnetic domain patterns obs. 3−21274
- magnetostriction, bulk and surface magnetoelastic waves 3−21285
- nitrate glass; Eu, Sm, Gd, Tb, Dy absorption, luminescence, excitation spectra *(Russian)* 3−30878
- wear and friction in air 3−18625
- $AgCl:Dy^{3+}$, photoluminesc. spectrum, meas. at 77K 3−5223
- Al:Dy, e.s.r. meas. of exchange integral 3−15413
- $CaSO_4$:V, Dy, energy transfer by sensitizer-activator pairing 3−30868
- $CaZrO_3:Dy^{3+}$ luminescence spectra, transition energies and relative intensities *(Russian)* 3−39171
- Dy, hydrostatic pressure effect on spin disorder resistivity 3−2284
- Dy^{3+}, in $LaH_3(H=Cl,Br)$, electronically excited ions, radiationless relax., multi-quantum scatt. processes 3−24390
- Dy^{3+} e.p.r in Pd 3−2352
- Dy^{3+} in polyphosphoric acid and polyphosphate glass, exchange interaction role in energy transfer *(Russian)* 3−8651
- $^{163}Dy^+$ and $^{161}Dy^+$, hf.s. of spectrum, quadrupole moments 3−20025
- YAl_2:Dy, crystal field ground states, EPR obs. 3−30418

dysprosium compounds
- $DyVO_4$ crystallographic and mag. phase transitions, molec. field approx. 3−2277
- $DyAlO_3$, $Dy_3Al_5O_{12}$, flux crystn., crucible size effect 3−34482
- $DyAsO_4$, paramag. to antiferromag. transition, cryst. phase transition 3−2281
- $DyCl_3.6H_2O$, caloric and mag. props. 3−38976
- $DyFeO_3$, magnetostriction, low temp. 3−34175
- $DyFeO_3$, paramag. susceptibility, room temp. and 77K 3−21213
- $Dy_3Ga_5O_{12}$, garnet, ceramic, influence of initial comp. and firing temp. in prep. *(Russian)* 3−15746
- $Dy_3Ga_5O_{12}$, substrate material for bubble domain film, lattice parameter thermal exp. 3−34158
- Dy_2O_3, elec. cond., high temp. variations, equil. oxygen press. depend. *(French)* 3−38831
- Dy_2O_3-CdSe film struct., elec. props. 3−27312
- Dy_2O_3-CdSe thin film structure, elec. and interface props. 3−15265
- Dy_2O_2S, long wave i.r. spectra *(Russian)* 3−30825
- $DyPO_4$, mag. susceptibility curves anomalies at high temps., n.m.r. obs. 3−30707
- DySb, shear elastic const. meas. near mag. and structural phase transition 3−33591
- $Dy_2Ti_2O_7:^{161}Dy$, Mossbauer effect, quadrupole interactions and relax. effects 3−34265
- $DyVO_4$, elastic anomalies near cooperative Jahn-Teller transitions 3−2014
- $DyVO_4$, i.r. absorpt. obs. at low temp. rel. to crystal field splitting 3−18443
- $DyVO_4$, paramag. to antiferromag. transition, cryst. phase transition 3−2281
- $DyVO_4$, relax. of Mossbauer spectra, temp. depend. 3−36825
- $DyVO_4$, soft acoustic mode and the strain dependence of the g factor 3−1761
- $DyVO_4$, struct. transition, due to spontaneous Jahn-Teller distortions 3−24266
- $DyVO_4$, thermal conductivity at low temps. 3−1847
- $Dy_{4.67}[GeO_4]_3O$ apatite, cry. struct. of TR analog by X-ray diffr. 3−7703
- HfO_2-Dy_2O_3 system, of cubic solid solutions, phase diagram determ. by X-ray analysis at temps. 1000-1700°C *(Russian)* 3−11715

E-layer *see E-region*

E-region
- *see also sporadic-E layer*
- after sunrise state of E-layer rel. to max. electron concentration *(Bulgarian)* 3−9339
- Appleton E-layer seasonal anomaly, world morphology 3−21971
- auroral and ring current precipitation effects caused by artificial plasma injection 3−25296
- auroral E-layer, electron intensity rel. to Ba cloud, rocket flight obs. 3−12785
- conductivity effects on F region ionisation motion due to meridional wind 3−18886
- density var. with freq. of e.m. wave 3−1490
- drift meas., skewness of correlation functions of fading records 3−25288
- E-layer diurnal variation in ionization from F_0E data 3−21970

E-region continued
- effect of geomagnetic storms on nighttime E-layer during increasing maximum solar activity *(Bulgarian)* 3−9338
- electric field reversal causing q-type sporadic-E disappearance during daytime 3−18888
- electric fields, small scale struct. and a.c. fields 3−12812
- electrojet irregularities, parametric coupling for production and stabilisation 3−15997
- electron collision frequency from rocket and ground-based measurements, v.h.f. absorption 3−25279
- electron densities, during solar maximum and minimum 3−3089
- electron densities from rocket meas. using l.f. radio propagation and d.c. probe techniques 3−16031
- electron density, at night-time at auroral lattitudes in sunspot maximum 3−31435
- electron density, nighttime ionospheric model 3−3099
- electron density, semi annual variation 3−5520
- electron density meas. by incoherent-scatter technique at Millstone Hill 3−3114
- electron density peak, solar activity dependence 3−34950
- electron density profiles rel. to experimental techniques 3−3111
- equatorial, positive ion composition meas. 3−3093
- equatorial scintillation, effect of irregularities 3−9335
- field aligned irregularities, oblique backscatter obs. 3−37241
- h.f. radiowave absorption meas. at low latitude station 3−9332
- ion chemistry, conference (Urbana, USA, July 1971) 3−3083
- ion composition and photochemistry 3−3098
- ion composition during sunrise and sunset above Kiruna, mass spectroscopy meas. 3−25292
- ion concentration and compos. obs. using incoherent scatter radar 3−3095
- ion-neutral reactions 3−3104
- ionization sources, cosmic and solar X-ray and u.v. radiation 3−3087
- irregularities, phase path measurements 3−3081
- irregularities over magnetic equator, characteristics determ. from spaced fading records of radio wave echoes 3−34944
- Lagrange invariant in MHD geophysical aspects rel. to E-region magnetic parameter *(Russian)* 3−17548
- magnetic field vertical component diurnal variations, interplanetary mag. field East-West component depend. *(French)* 3−39551
- negative ion composition in lower part of region 3−3102
- nighttime, atm. wave-induced instability 3−9333
- nighttime electron density rel. to 40 kHz wave phase shift due to X-radiation from Scorpius XR-1 source 3−25275
- nonlinear interaction of radiowaves *(Russian)* 3−3072
- penetration critical frequency and winter anomaly rel. to sunspot minimum 3−12798
- planetary-scale fluctuations in pressure in E-layer rel. to f-min and stratosphere 3−21969
- positive ion chemistry, ion-molecule reaction rates 3−3092
- positive ions, mass spectral obs. 3−3094
- radiowave focusing by irregularities 3−9330
- review of ionospheric D- and E-region studies, outstanding problems 3−3119
- seasonal variation of height and thickness rel. to model 3−21973
- slant sporadic-E at high latitudes in summer 3−18887
- type I instability, nonlinear saturation by wave energy transfer to electrons 3−15991
- BaO, $A^1\Sigma$-$X^1\Sigma$ band system, electronic transition moment, fluorescent scattering of sunlight at 106 km 3−17424
- CO_2, mass spectral obs. 3−3084
- N, NO, mass spectral obs. 3−3084
- N_2^+ dominated afterglows, dissociative recomb. at elevated temps. 3−11293
- NO, vertical distribution in 60-170 km altitude region 3−3044
- NO concentration from electron density and X-ray flux obs. 3−3086

[illegible]
- *see also hearing*
- acoustic impulses, 40 μsec impulses, audiometric and histological effects 3−3608
- acoustical overstimulation, behavioural and anatomic manifestations 3−3607
- action potentials, influence of hair-cell nomrmalcy 3−25563
- artificial, acoustic impedance obs. 3−98
- auditory nerve evoked potential, changes following intense sound stimulation 3−3483
- basilar membrane, computer simulation of nonlinear model, determ. of distortion products 3−3472
- basilar membrane, integrable model 3−35255
- basilar membrane motion, nonlinear phenomenological model 3−3471
- basilar membrane motion, temporal relationship with initation of nerve impulses in auditory nerve fibres 3−3474
- bat's middle ear, dynamical mechanical model 3−3473
- cats anesthetized, muscle contraction rel. to bone conduction 3−31856
- channel capacity as function of frequency 3−3484
- cochlea, effects of ethacrynic acid 3−3479
- cochlea, new boundary conditions for Peterson-Bogert model 3−25558
- cochlea of guinea pigs, ethacrynic acid ototoxicity, potentiation by Kanamycin 3−3478
- cochlear harmonics, effects of d.c. polarization 3−25635
- cochlear injury in chinchilla, whole-nerve action potentials as index of severity 3−3480
- cochlear mechanics, guided interfacial waves 3−3443
- cochlear partition, comparison of effects of biasing with electrical current and sound stimulation of DIF SP responses 3−3477
- cochlear potentials of guinea pig, modelling and simulation 3−25561
- cochlear whole-nerve response to acoustic transients, origin of negative deflection N_2 3−3476
- cortex, unanesthetized macaque monkeys, action potentials from single neurons 3−3521
- dichotic listening, shift of ear superiority to temporally patterned nonverbal stimuli 3−31859
- eardrum displacement following stapedius muscle contraction 3−3444
- electrode placement for activation of VIIIth nerve by electrical stimulation in cases of sensorineural hearing loss 3−3482

ear continued
equal loudness pressure and normal ear, normal ear and perfect average ear 3—3455
Eustachian tube patency determ. employing portable pneumophone 3—28347
evoked cortical response, early component, effects of frequency and phase reversal 3—3413
external, electrical analogue network representation for transfer characteristics 3—25631
hearing mechanism research, potential appl. of engineering science disciplines 3—9658
human click action potentials and click loudness, postmasking recovery 3—25556
in-ear microphone meas. of ear protective devices, reliability and validity 3—3465
in-ear monitoring of noise exposure 3—3525
intracochlear, multimicroelectode for differential electrical stimulation of cochlear nerve in human sensory deafness 3—3481
intraoral air pressure rel. to vocal effort 3—3419
microphonics, electric network effects 3—31857
noise effect evaluation, damaging *(German)* 3—16311
noise reduction ear enclosures 3—3467
nonlinear ear protectors, evaluation using constant temporary threshold shift technique 3—3466
perception, dichotically presented vowels 3—31860
posterior colliculus, internal organization, electrophysiological obs. 3—3518
posterior colliculus of chinchilla, effect of interaural phase at different frequencies on cell discharge 3—3519
posterior colliculus of chinchilla, effect of stimulus intensity at different interaural phases on cell discharge 3—3520
potential response at round window membrane of cat 3—25565
primary auditory cortex in unanesthetized macaque monkeys, variation of excitability of neurons 3—3522
protectors, review 3—25573
single cochlear nerve fibres, response patterns to click stimuli for cat 3—25562
stapes-basilar membrane system, modals and unified theory *(German)* 3—37527
three-tone complexes, second effect of pitch shift 3—31861
tunnel of Corti, recording of local potentials using microelectrodes 3—3475
two tone inhibition, interference, nonlinear effects 3—35253
tympanic, submicroscopic vibration, obs. by stroboscopic holography 3—3446
visual evoked potential, of short latency 3—28323

ear microphones *see microphones*

earphones
No entries

earth
see also earth age; earth composition; earth rotation; earth structure; geochemistry; geodesy; geomagnetic variations; geomagnetism; terrestrial atmosphere; terrestrial electricity; terrestrial heat
apparatus for orbital and rotational motion 3—3743
Archaean craton of North Atlantic region 3—21882
Archaean crust, granulite facies rocks and partial melting, review 3—21879
Archaean crust, plate tectonic model 3—21877
atmosphere study by u.v. spectrograph in Apollo-16 3—3300
centre of mass from satellite triangulation, absolute orientation rel. to geograv words 3—34758
Colorado plateau crustal-upper mantle model from Moses Rock dike intrusive breccia 3—18815
continental crust, problems concerning evolution, review 3—21873
continental drift, rel. to paleomagnetic data *(Russian)* 3—2919
continental positions rel. to S. American shear zone before opening of Bay of Biscay 3—25120
continents and oceans distrib. rel. to mantle convection 3—34816
crust and m-boundary, models, review 3—2890
crust discontinuities rel. to P-wave amplitudes 3—2892
crust waveguide rel. to dipole excitation of u.l.f. e.m. waves 3—18819
crustal evolution in Bay of Biscay rel. to Iberian sub-continent 3—15876
crustal seismic meas. over Appalachian front from shots in Labrador and Quebec 3—2846
crustal thickness determ. from seismic refr. data from S.E. Alaska-W. British Columbia region 3—27942
density layer models in satellite geodesy, error propagation in computed orbits 3—34769
dynamical var. of latitude and time rel. to Earth's pole of figure 3—35001
early Precambrian crust evolution of southern Africa rel. to greenstone belts 3—21875
early Proterozoic continental margin evolution rel. to coronation geosyncline 3—21885
Earth-atmosphere-ocean system, intransitive model 3—9281
Earth-Moon mass ratio from Mariner 9 radio tracking data 3—22035
electrical conductivity, effect of radial distrib. on geomagnetic S_q-variations 3—25174
electrical conductivity, overall distrib. rel to external magnetic fields 3—34851
e.m. propagation in earth crust idealised waveguide, mode characts. 3—31335
e.m. propagation in earth crust idealised waveguide 3—31334
e.m. response of permeable inhomogeneous conducting sphere 3—25130
e.m. wave propagation, electric field attenuation and myriametric wave propagation *(Rumanian)* 3—27974
Eurasian plate, lines of volcanoes rel. to concentric plume traces 3—21870
geodynamic models and undation theory, book 3—15916
geopotential model, from satellite Doppler data 3—9140
geopotential representations by buried masses 3—34770
gravitational attraction of three-dimensional bodies in spherical or ellipsoidal earth 3—18804
gravitational model, computation methods from combination of terrestrial and satellite data 3—34766
Great Basin, Cenozoic volcano-tectonic evolution 3—15877

earth continued
Hercynian continental collision rel. to palaeogeography of south west England 3—21871
h.f. radio noise, Radio Astronomy Explorer I observations 3—31288
Indian-Antarctic-Pacific plates triple junction 3—15878
Insubric Line displacement rel. to Pennine and Southern Alps 3—21869
Lake Superior basin, stratigraphy of Quaternary sediments 3—27941
Ligurian country, seismic refraction profiles *(French)* 3—31323
Limpopo mobile belt in southern Africa, geology and evolutionary aspects 3—21880
Limpopo orogenic belt, southern Africa, structural interpretation of northern margin 3—21881
lithospheric plate motion rel. to mantle plume traces, palaeomagnetism and polar wandering 3—25142
lithospheric plates, displacement of dipping oceanic slabs, flow movements 3—15875
lithospheric plates, relative motions and earthquake mechanisms in east Pacific 3—15882
lithospheric slabs (subducted), comparison of temp. distrib. to muscovite stability ranges 3—25119
Love wave propagation in non-homogeneous isotropic layer of finite depth on infinite non-isotropic layer 3—31321
Mineral Bluff formation, natural folds rel. to fold model for quartzite and marble 3—39473
model based on current physical and petrological theories 3—9154
Moho-discontinuity, deep seismic sounding in Czechoslovakia 3—2893
Mohorovicic discontinuity determ. from deep seismic sounding and outer gravity field 3—27939
Mount Etna, meas. of archaeomag. variation over past 600 years 3—21920
New Hebrides, descending lithospheric slab, evidence from seismic waves and earthquakes 3—27963
normal mode data from quartz torsion accelerometers, review 3—27953
ocean crust origin of Troodos Massif rocks 3—39483
ocean floor origin, volcanic processes evidence from Troodos Massif, Cyprus 3—25144
oceanic crust, age rel. to tectonics and Deep Sea Drilling Project 3—9100
oscillations, free, determ. method knowing earthquake source mechanism 3—31289
P-wave investigation of lateral inhomogeneity in crust and mantle 3—31322
Pacific plate northward movement, evidence from Midway Atoll lavas palaeomagnetism 3—15917
polar wobble anomaly in 1930 rel. to variations of earth's rotational velocity 3—5419
Portugal earthquake 1969 rel. to thrust faulting at lithospheric plate boundary 3—34795
Pre-Ordovician polyphase structure in Burlington Peninsula of Newfoundland Appalachians 3—21868
Precambrian crustal development rel. to oldest Archaean rocks 3—21874
Precambrian crustal evolution, conference (London, 22-3 March 1972) 3—21872
Precambrian of northern West Greenland, recumbent folding and flat-lying structure 3—21884
Proterozoic mobile belts in Greenland, tectonic displacements and thermal activity 3—21883
proto-Gulf of California, Miocene volcano-tectonic rift zone 3—15879
resonances and librations of Apollo and Amor asteroids 3—35102
Rhodesian Archaean craton rel. to cratonic evolution and greenstone belts 3—21876
SAO 1969 Standard Earth, error model using satellite tracking data 3—34776
satellite-determined gravity anomalies, mathematical model 3—34767
spherical $\alpha\omega$-dynamos by variational method rel. to Earth dynamo model 3—37180
surface radiation temp. determ. in 0.8-8 cm region *(Russian)* 3—39475
thermal history, simplified mathematical model for unsteady temp. distrib. *(Italian)* 3—31290
tidal effects on sunspots 3—3293
two-layer Earth model, Argand representation of mutual e.m. coupling of loops 3—5432
undulations, gravity anomaly 3—9139

earth (soil) *see soil*

earth age
see also radioactive dating
Bay of Biscay formation, use of Pyrenean geological data 3—25116
British Tertiary igneous province, K-Ar ages of dykes and lavas from Mull, Scotland 3—34812
core thermal history, macroscopic convection at melting point 3—34817
Lewisian gneiss from Outer Hebrides, U-Pb ages rel. to geochronology 3—15887
Nigerian mesozoic granites, sequential age trends 3—27968
oceanic crust, age rel. to tectonics and Deep Sea Drilling Project 3—9100
Ubeidiya Formation, Jordan Valley, K-Ar meas. of olivine basalt 3—31311

earth atmosphere *see terrestrial atmosphere*

earth composition
see also earth structure
andesite origin rel. to volcanism and organic belts 3—37173
lithosphere in Bohemian Massif, CO_2 flux 3—9190
lower mantle, polycrystalline stishovite, elastic wave velocity 3—9146
magma origin in oceanic and circium-oceanic regions 3—37172
Mount Etna, 1971 eruption, anal. of composition of magma 3—21888
Mount Etna, 1971 eruption, petrography of the lavas 3—21889
Mount Etna, 1971 eruption, quenching and melting experiments on lavas 3—21890
Mount Etna, struct. and petrology of volcanic system 3—21887

earth composition continued
- Mount Etna, viscosity meas. of lava, depend. on bubble content 3−21893
- Mount Etna, volcanic gas collection and analysis during 1970 and 1971 activity 3−21896
- Mount Etna 1971, composition and size of ash deposits from new crater 3−21899
- Mount Etna 1971, direct meas. of O_2 on S_2 fugacities in active vents 3−21898
- Mount Etna evolution of volcanic gas characteristics up to 1971 eruption 3−21897
- origin of simple inorganic compounds in the Earth *(Japanese)* 3−5449
- submarine pillow lavas in Catania, study of development and morphology 3−21900

earth core
- core-mantle boundary, PKP wave precursors rel. to seismic wave scattering 3−12620
- density differentiation of matter and processes at core-mantle interface 3−15902
- discontinuities and structure, hypotheses development 3−2895
- e.m. core-mantle coupling, shell model 3−21864
- e.m. coupling with mantle, during geomag. dipole field variations 3−2857
- mantle-core discontinuity using equations of state for silicates in metallic form 3−31317
- MHD of rotating fluids, review, applications to dynamics of Earth's core 3−20393
- motion, inferred from drifting and standing nondipole fields 3−21919
- temperatures, melting relations of Fe 3−12581
- thermal history, macroscopic convection at melting point 3−34817

earth crust
- *heading is late addition, see also earth*
- *see also geology*
- age of oceanic crust rel. to tectonics and Deep Sea Drilling Project 3−9100
- Algeria, structure determ. from seismic meas. *(French)* 3−34783
- Archaean crust, plate tectonic model 3−21877
- Atlantic floor, tropical western region, tectonics rel. to geomorphological features 3−31351
- average rate of continental crust determ. by K-Ar ages and paleomagnetic meas. 3−9180
- Baffin Basin, seismic refraction studies rel. to tectonic development of ocean basin and oceanic crust 3−25126
- Colorado plateau crustal-upper mantle model from Moses Rock dike intrusive breccia 3−18815
- conducting layers, by e.m. methods 3−12641
- continental, trace metals source, Hawaiian marine atm. 3−12754
- continental crust, problems concerning evolution, review 3−21873
- diurnal tidal waves in tilts of crust along Sumy-Kherson profile *(Russian)* 3−21907
- early Precambrian crust evolution of southern Africa rel. to greenstone belts 3−21875
- e.m. propagation in earth crust idealised waveguide 3−31334
- e.m. propagation in idealised earth crust waveguide, mode characts. 3−31335
- heat flow and elevation of marginal basins of western Pacific 3−9177
- Hercynian continental collision rel. to palaeogeography of south west England 3−21871
- Iberian Peninsula, crust-mantle seismic velocities rel. to tectonics and seismicity 3−12591
- Iberian sub-continent, crustal evolution in Bay of Biscay 3−15876
- Iberian variscan orogen, a tectonic model 3−15912
- Ligurian country, seismic refraction profiles *(French)* 3−31323
- lithosphere, myriametric wave propagation and electric field *(Rumanian)* 3−27974
- lithospheric plate motion rel. to mantle plume traces, palaeomagnetism and polar wandering 3−25142
- lithospheric plates, displacement of dipping oceanic slabs, flow movements 3−15875
- lithospheric plates, relative motions and earthquake mechanisms in east Pacific 3−15882
- Love wave propagation in non-homogeneous isotropic layer of finite depth on infinite non-isotropic layer 3−31321
- Mediterranean crustal structure and plate tectonics *(German)* 3−31325
- Mohorovicic discontinuity determ. from deep seismic sounding and outer gravity field 3−27939
- movement of crust from laser ranging to lunar retroreflectors 3−34971
- muscovite dehydration and melting, stability ranges compared to subducted lithospheric slabs' temp. distrib. 3−25119
- New Hebrides, descending lithospheric slab, evidence from seismic waves and earthquakes 3−27963
- North Sea Cainozoic subsidence, lateral transfer of crustal material 3−34802
- ocean floor origin, volcanic processes evidence from Troodos Massif, Cyprus 3−25144
- ocean ridge crustal creation, thermal model 3−39480
- ocean ridges, positive free-air gravity anomalies rel. to lithospheric model 3−12588
- oceanic basalts from layer 2, viscous remanent magnetization 3−39487
- oceanic crust, evidence for short geomagnetic polarity intervals during early Cenozoic 3−18839
- oceanic crust fusion in subduction zones rel. to high pressure granite melting 3−25121
- oceanic crust origin of Troodos Massif rocks 3−39483
- oceanic crustal layer, progressive thickening with age in Pacific Ocean 3−31344
- P-wave investigation of lateral inhomogeneity 3−31322
- Peru-Bolivia altiplano, seismic low velocity zones 3−21860
- plate motion rel. to convection process between elastic lithosphere and viscous asthenosphere 3−15896
- Precambrian crustal evolution conference (London, 22-3 March 1972) 3−21872
- Precambrian crystal development rel. to oldest Archaean rocks 3−21874

earth crust continued
- Protoarchean crust development, use of trace element distrib. coeff. models 3−31296
- Puget Sound region crustal model, tectonics and seismicity determ. 3−21843
- Rayleigh and low-velocity channel seismic waves in crust 3−25127
- seaflor spreading and tectono-eustatic changes in sea level 3−39477
- shallow crustal depth and high heat flow in southwestern Pacific due to recent magma intrusion 3−9176
- thickness determ. for S.E. Alaska-W. British Columbia region from seismic refr. data 3−27942
- tilt measurements at Daryevka rel. to block structure of crust *(Russian)* 3−21905
- u.l.f. wave dipole excitation in earth crust waveguide 3−18819
- vertical crustal movements in Israel, geodetic network survey 3−25146
- vertical movement along E. coast of United States 3−15890
- vertical movement determinations, percentile accuracy *(German)* 3−12595
- waveguide e.m. attenuation, e.l.f. to v.l.f. 3−34855
- western British Isles, evidence for crustal low-velocity seismic zone 3−12592

earth electricity *see terrestrial electricity*

earth heat *see terrestrial heat*

earth interior
- *see also earth core; earth crust; earth mantle; tectonics; volcanology*
- Birch-Murnaghan equation of states for rocks and minerals under high pressure *(German)* 3−34814
- fine structure, seismic wave analysis, solid kernel 3−39485
- heterogeneous, equation defining variation of density with depth *(Russian)* 3−5434
- isostasy, deformations of gravitational potentials *(German)* 3−12602
- magmatic glass, crystal chemistry and differentiation 3−15869
- seismicity, objective representation 3−12598

earth lower mantle *see earth mantle*

earth magnetic field *see geomagnetism*

earth magnetic field variations *see geomagnetic variations*

earth mantle
- Afar mantle plume, rare earth pattern zonation evidence 3−27967
- Algeria, crust structure determ. from seismic meas. *(French)* 3−34783
- alkaline igneous rock lineaments rel. to transform directions in Africa and S. America 3−34800
- basaltic komatiite and ocean-floor type basalts from Newfoundland, magma origin comparison 3−25110
- basanite magma, crystallisation behaviour meas. of garnet peridotite at high press. and temp. 3−21857
- central Arctic Ocean, geomagnetic variations, statistical analysis *(Russian)* 3−2918
- Colorado plateau crustal-upper mantle model from Moses Rock dike intrusive breccia 3−18815
- composition, polycrystalline stishovite, elastic wave velocity 3−9146
- cond. determ. by meas. of mineral props. 3−15928
- convection rel. to distrib. of continents and oceans 3−34816
- convective motions, a laboratory model with a temp.-dependent viscosity 3−25108
- core-mantle boundary, PKP wave precursors rel. to seismic wave scattering 3−12620
- crystal structures, elasticity 3−9158
- deep magnetotelluric sounding in Sakhalin *(Russian)* 3−5472
- deformation, global ocean tides 3−12672
- density differentiation of matter and processes at core-mantle interface 3−15902
- density distribution limits in lower mantle *(Russian)* 3−12608
- discontinuities, seismological evidence 3−2889
- electrical conductivity distrib. rel. to external magnetic fields 3−34851
- e.m. core-mantle coupling, shell model 3−21864
- e.m. coupling with core, during geomag. dipole field variations 3−2857
- fault dimensions, corner frequency relation 3−9150
- force field in ocean ridge formation, models 3−15910
- global movements of earth's crust, Wegener's theory, research method and measuring techniques *(German)* 3−34830
- high pressure solid phases, equations of state determ. for minerals, appl. to elasticity studies 3−25118
- Iberian Peninsula, crust-mantle seismic velocities rel. to tectonics and seismicity 3−12591
- Iceland hot mantle plume, geochemical study of Rejkjanes Ridge 3−37163
- Ichinomegata volcano, rocks and minerals from upper mantle *(Japanese)* 3−5450
- lateral inhomogeneities of deep mantle, seismic travel time data 3−34822
- Lesser Antilles island arc, undersaturated magma assoc. 3−34799
- longitudinal shear cracks cohesive force, Griffith's specific surface energy 3−9151
- Love wave propagation in non-homogeneous isotropic layer of finite depth on infinite non-isotropic layer 3−31321
- magma chamber depth rel. to gas press., volcanic activity 3−34787
- magma processes rel. to muscovite dehydration and melting in deep crust 3−25119
- magma spraying causing alkali volatilisation, Na and K losses, appl. to Moon 3−27965
- magmas, viscosity at various pressures, melt meas. 3−21867
- mantle-core discontinuity using equations of state for silicates in metallic form 3−31317
- Mohorovicic discontinuity determ. from deep seismic sounding and outer gravity field 3−27939
- North Sea Cainozoic subsidence, initiation rel. to Mesozoic extensional tectonics 3−34802
- oceanic crust fusion in subduction zones rel. to high pressure granite melting 3−25121
- P-wave attenuation 3−2896
- p-wave investigation of lateral inhomogeneity 3−31322
- partial fusion in seismic low vel. zone of upper mantle changes in electrical conductivity of basalt 3−5446

earth mantle continued
PcP waves, character of core-mantle boundary 3−2847
peritite, anatexis rel. to origin of andesites 3−37173
plume convection, synchronous discharge evidence from volume estimates and age dating of igneous deposits 3−12616
plume convection with upper mantle temperature inversion 3−12618
plume hypothesis, rel. to seismic refl. profile of Reykjanes Ridge 3−25113
plume traces rel to palaeomagnetism, polar wandering and lithospheric plate motion 3−25142
Protoarchean crust development, trace element distrib. coeff. models 3−31296
pyrolite upper mantle under mid oceanic ridges, stable crusts and island arcs, melting relations 3−37177
Rayleigh wave dispersion in mantle rel. to tectonic provinces and earthquake data 3−15901
seismic P-waves azimuth anomalies, velocity lateral var. rel. to deep mantle 3−15881
seismic zone thickness, Tonga region meas. 3−31312
Southern Scandinavia, isostasy, eustasy and crustal sensitivity 3−37169
strain tides in Yorkshire, single wire strainmeter 3−12585
structure, toroidal-free oscillations, spectral splitting 3−9161
tectonic plate motion rel. to convection process between elastic lithosphere and viscous asthenosphere 3−15896
temperature profiles determ. from cond.-depth models, dependence of Fe oxidation state in elec. cond. of olivine 3−25114
Tonga-Fiji region, low velocity zone in upper mantle behind Tonga Island arc 3−15899
unstable tetrahedral mantle-convection model rel. to continental drift and polar ice sheets 3−34827
upper, conducting layers, by e.m. methods 3−12641
upper, reflection of seismic waves from velocity gradient anomalies 3−2902
upper, rocks, anisotropy 3−2898
upper mantle compressional velocity distrib. from Nevada explosions 3−12587
upper mantle transition zone, electrical conductivity, olivine-spinel transformations of orthosilicates 3−12606
vertical crust movement determinations, accuracy *(German)* 3−12595
vertical crustal movements between Dead Sea Rift and Mediterranean, geodetic anal. 3−25146
Western Pacific, seismic wave anal. at Guam, travel time anomalies 3−34786
Si-saturated tholeiitic magma production in island arcs rel. to hydrous mantle peridotite 3−15884

earth rotation
air mass seasonal redistrib. effects *(Russian)* 3−39523
annual aberration, series expansion with respect to fundamental arguments 3−37303
magnetotelluric method theory rel. to daily rotation of Earth 3−25179
MHD of rotating fluids, review, applications to dynamics of Earth's core 3−20393
polar motion determ. using Doppler satellite data 3−34778
polar motion meas. using laser ranging to satellites 3−34779
polar wandering rel. to mantle plume traces, palaeomagnetism and lithospheric plate motion 3−25142
precession, nutation, polar axes displacement, Earth structure *(French)* 3−3285
rate, effect of change in geomag. dipole moment 3−2857
secular acceleration, Moon's orbital motion 3−18977
shock waves in the rotating atmosphere 3−21938
solar wind effects on angular velocity *(German)* 3−12603
solar wind torque effects, upper limit for rotational slowing 3−12558
spin rate, discontinuous change following August 1972 great solar storm 3−39471
tidal variations, Love number determ. *(Russian)* 3−5485
variations from A.D. 1663-1972 rel. to the constancy of G 3−25103
variations of velocity rel. to polar wobble 1930 anomaly 3−5419

earth satellites *see artificial satellites; Moon*

earth structure
see also earth composition; earth interior
Afar mantle plume, rare earth pattern zonation evidence 3−27967
Archaen Basement, uniformitarian evolutionary models 3−37166
China Basin, tectonic evolution rel. to Mesozoic palaeography of Borneo 3−34806
continental drift rel. to ring structures in Indo-Gangetic Basin 3−39482
continental margins, granite cycle triggering mechanisms 3−15909
crust and Moho, seismic observations 3−34792
crustal structure, Faeroe Islands, from seismic deep soundings 3−18833
density differentiation of matter and processes at core-mantle interface 3−15902
density modelling, by Monte Carlo inversion 3−12583
density modelling, by Monte Carlo inversion 3−12584
Early Tertiary climate dependence on continental position 3−3014
Eastern Mediterranean Basin structure, seismic reflection data 3−34794
Europe, continental fracture patterns, palaeomagnetic determ. of poles of rotation *(German)* 3−12596
flattening transformation for point source waves 3−21846
geological, rel. to diurnal distrib. of weak earthquakes *(Russian)* 3−5437
Great Valley, Pennsylvania, faulting sequence 3−27931
Hebrides and Irish Sea, relation of Palaeogene ridge, basin structures and volcanicity 3−2848
Laguna Guatavita, salt collapse crater 3−2862
large impact crater doublets rel. to simultaneous impacts 3−39636
lava flow, depend. of length on rate of effusion and initial viscosity rel. to 1971 Etna eruption 3−21895
Limpopo orogenic belt, southern Africa, structural interpretation of northern margin 3−21881
Mediterranean crustal structure and plate tectonics *(German)* 3−31325
Mediterranean island arcs, origin of high potash volcanoes 3−9103
Mount Etna, 1971 eruption rel. to ENE tectonic fault system 3−21892

earth structure continued
Mount Etna, conditions and changes in activity at summit prior to 1971 eruption 3−21891
Mount Etna, depend. of volcanic activity on tectonic motion 3−21901
Mount Etna, review of struct. and evolution 3−21886
Mount Etna, struct. and petrology of volcanic system 3−21887
Mount Etna 1971 lavas, rheological study 3−21894
Oslo Graben, permian, crustal structure from gravity obs. 3−9191
plate tectonics and continent origin approach to expansion *(French)* 3−12566
rotation, precession, polar axes displacement *(French)* 3−3285
Sea of Japan, Fe_2S in sediment cores, geophysical implications 3−2850
South Atlantic, mag. smooth zones 3−2929
South-Western Iceland, thickness of magnetic crustal layer 3−2854
Southern Scandinavia, isostasy, eustasy and crustal sensitivity 3−37169
unsteady temp. distrib., determ. of struct. props. *(Italian)* 3−31290

earth third layer *see earth mantle*

earth upper layer *see earth mantle*

earthquake recorders *see seismometers*

earthquakes
see also seismology
1966, Parkfield California, focal depths 3−9152
1969, March 28, meas. of crust mantle seismic velocities in Iberian Peninsula 3−12591
Adirondack, 1971, field study and tectonic stress meas. 3−21854
Aleutian, 1969, May 14, focal plane solutions using maximum-likelihood method 3−25319
Australian, mechanisms rel. to contemporary stress in Indian Ocean plate 3−34805
body wave focal plane solutions, fiducial regions from max. likelihood method 3−25320
Cape Province, S. Africa, seismological study 3−5456
Central Asian events, M_s:m_b diagram anal. 3−27954
coupled internal-rotational foundation-soil interaction of building structures, soln. of Lamb problem 3−19439
deconvolution of teleseismic events by homomorphic filtering 3−21852
deep soundings, inhomogeneity obs. 3−2897
East Africa region, seismic activity meas. 3−21847
elastic wave radiation, comparison with underground explosion 3−12582
engineering, review 3−27956
Fairview Peak area at time of BENHAM nuclear explosion, freq., distrib. and focal mechanism meas. 3−21849
faulting, implications of rock fracture at pressures up to 7kbar 3−5461
Fennoscandia, seismicity, review *(German)* 3−12597
focal mechanisms and plate tectonics of S.W. Pacific 3−9171
focal plane solutions for earthquakes using maximum-likelihood method 3−25319
Garm region, travel-time variations due to rock dilatancy and pore pressure effects 3−21848
Gediz, 1970, March 28, seismotectonic aspects 3−25125
Glenalmond series Feb 1970-March 1972 3−5454
Greece, seismic activity for 1966 to 1969 period 3−34784
high-gain long-period seismograph expt. results 3−27952
hybrid computer simulation of uncertainty in earthquakes responses of nonlinear structures 3−12571
Imperial Valley, 1940, source theory predicting body wave spectra shape 3−21853
Kurile earthquake data rel. to mantle Rayleigh wave dispersion and tectonic provinces 3−15901
mechanism at faults rel. to frictional sliding characteristics of granite 3−15895
mechanisms of earthquakes and plate motions in east Pacific 3−15882
Mediterranean region, active tectonics 3−21858
microearthquake clustering near Fairview Peak, Nevada and in Nevada seismic zone 3−18817
microtremors, underground amplitude distrib. 3−27958
Mid-Atlantic Ridge, microearthquake survey 3−12619
multi-element seismic zoning rel. to Indian Peninsula *(Russian)* 3−12609
New Hebrides, descending lithospheric slab, evidence from seismic waves and earthquakes 3−27963
NORSAR discrimination results for central Asia and W. Russia 3−28078
nuclear power plant structures, effect of foundation rotation on seismic inertia forces 3−19917
P_n and Rayleigh waves, comparison with explosions and afterevents 3−25128
Pahute Mesa underground nuclear explosions, seismicity meas. 3−21855
Parkfield 1966, geodetic network deformation predicted by rock dilatancy model 3−21856
Peru-Bolivia earthquake data rel. to mantle Rayleigh wave dispersion and tectonic provinces 3−15901
Portugal, 1969, rel. to thrust faulting at lithospheric plate boundary 3−34795
prediction at Japan's Earthquake Research Institute 3−5453
prediction rel. to premonitory changes in seismic wave velocities 3−18820
Pribaykal area, stresses in foci of weak earthquakes *(Russian)* 3−9130
Puget Sound region, seismicity, structure and tectonics determ. and crustal model generation 3−21843
Rat Island earthquake data rel. to mantle Rayleigh wave dispersion and tectonic provinces 3−15901
recurrence relation log N=A-BM, prediction method independent of population size 3−25104
Reykjanes Ridge, distrib. of earthquakes rel. to seismicity 3−25117
seismic background temporal var. in Garm seismic region 3−25132
seismic wave discrimination from explosions, spatial and freq. depend of Q 3−27951
seismic zone thickness, Tonga region meas. 3−31312
seismicity, objective representation 3−12598

earthquakes continued
  short-period seismic energy, time depend. 3—27949
  Sino-Soviet area, seismic wave analysis of earthquakes and explosions, 1966 period report 3—21909
  soil, skin friction, static and dynamic, meas. for wave eqn. analysis 3—21768
  source characterisation using LP surface waves 3—27948
  source mechanism, Earth's free oscills. determ. method using high-resolution spectroscopy 3—31289
  source time-function, scaling law modification 3—27943
  spectral treatment of actions of three earthquake components on structures 3—19920
  stress drop, long strike-slip fault model with horizontal discontinuity 3—25105
  Tokyo, strong earthquakes in history examined 3—27955
  travel times and epicentre estimation 3—21859
  Tuscania, 1971, epicentral parameters and focal depth determ. *(Italian)* 3—34785
  weak, diurnal distrib., rel. to geological structure *(Russian)* 3—5437
  Western Pacific, seismic wave anal. for mantle phases recorded at Guam 3—34786
EAS *see cosmic ray showers and bursts*
Eberhard effect *see photographic materials*
ebullition *see boiling*
e.c.g. *see electrocardiography*
echelons *see diffraction gratings*
echo
  see also anechoic chambers; architectural acoustics; reverberation; sonar
  acoustically rigid stationary spheres in ideal compressible liquid, structure of echo signal *(Russian)* 3—35316
  echo signal from elastic spherical shell in ideal liq., approx. calc. *(Russian)* 3—19110
  echo signal struct. from rigid sphere in liquid *(Russian)* 3—19111
  elastic spherical shell in ideal compressible liquid, determ. of thickness and radius by echo signals *(Russian)* 3—22197
  explosive, ranging, by underwater sound signal source, patent 3—19119
  ionospheric sporadic-E thin layers, mode coupling process rel. to echoes on ionograms 3—25285
  magnetospheric propagation modes of radioelectric whistlers and gyroelectric echoes received at middle latitudes *(French)* 3—31441
  ophthalmology, u.s. diagnosis 3—32235
  parametric acoustic array, echograms and bottom profiling capability 3—9780
  photon echo on homogeneously broadened spectral line 3—35716
  photon echoes, focusing, radius of curvature expressions 3—37984
  plasma, Maxwellian, ballistic second-order wave echoes 3—33363
  plasma spatial echo and non-linear interaction between waves *(Russian)* 3—14543
  pulse echo u.s. systems, registration errors, beam deformation, rel. to medical diagnostics 3—19115
  pulse-echo u.s. system, registration errors, rel. to medical diagnostics 3—19114
  salt formations, ECHO-LOG determination of form of leached cavities *(German)* 3—9356
  sea-surface waves, waveheight meas. system using transducer as echo-sounder 3—3226
  sonar, optimum signal and filter design 3—3736
  spatial ion wave echoes, collisional damping increased by mag. mirror 3—23858
  v.h.f. radar auroral echoes and power spectra rel. to classifications 3—12782
  weather radar system 3—9304
  MgO:Fe ultrasonic spin echo obs. 3—15407
eclipses
  see also solar eclipses
  1971, February 10, total lunar eclipse, effect of solar photons on lunar photoelectron layer 3—16181
  Aurigae, eclipsing binary, differential UBV photometry during 1971-72 eclipse 3—28220
  Aurigae, spectrophotometric obs. during the 1971-72 period 3—22078
  MR Cygni, eclipsing binary star, orbital eccentricity evidence 3—37388
  32 Cygni, spectrophotometric obs. during the 1971-72 period 3—22078
  Europa, thermal model from 10 μ obs. 3—31609
  Galilean satellites, thermal props. determ. from 20 μ obs. 3—31608
  Ganymede, thermal model from 10 μ obs. 3—31609
  Io, eclipses rel. to velocity of light, three centuries of observations 3—32504
  Io, thermal model from 10 μ obs. 3—31609
  Jupiter's satellites, mutual eclipses and occultations (1973-74) 3—31621
  lunar, brightness of future eclipses *(Russian)* 3—16172
  lunar, total eclipse of August 6, 1971 *(Russian)* 3—16173
  theoretical treatment in antiquity 3—3389
economic and sociological effects
  see also social aspects of automation
  environmental resource packets, teaching aids 3—9796
  mechanical science, role in contemporary knowledge of world *(Russian)* 3—22208
  Plowshare, assessment of technological, environmental and economic effects 3—19889
economics
  control valve, noise pollution 3—25638
  Earth resources prospecting, high altitude remote sensing systems 3—3199
  ENEL's power station, fuel management exprience 3—26501
  Hungarian meteorological activities, economic efficiency *(German)* 3—12704
  industrial use of ^{137}Cs and power reactor 134/137 mixtures 3—19994
  losses rel. to corona *(Russian)* 3—11516
  modelling and optimisation of controlled thermonuclear fusion reactor system 3—38180
  nuclear fast reactors, optimal fuel enrichment distrib. for minimising fuel cycle costs 3—19941
  nuclear fission product solutions, solidification *(French)* 3—38186
economics continued
  nuclear fuel cycle industry, in Germany, overview 3—19942
  nuclear fuel cycle logistics, anticipated U.S. requirements over next 30 years 3—19922
  nuclear fuel industry planning in Australia 3—23425
  nuclear fuel reprocessing, high activity liquid waste, solidification and storage 3—32980
  nuclear fuel reprocessing waste disposal, in deep underground cavities, advantages 3—32983
  nuclear reactor, irradiated fuel treatment *(French)* 3—38183
  nuclear reactor, thermodynamic cycles, optimum parameter selection *(Spanish)* 3—1050
  nuclear reactor fuel, high activity liquid effluents, storage *(French)* 3—38182
  Plowshare project, cost analysis of environmental impact 3—19891
  radioactive waste storage, industrial facility, design 3—35947
  scheduling system in radiology department 3—22167
  standards of measuring instruments 3—37580
  United Kingdom, economic and technical appraisal of air pollution, report 3—18870
  water quality management, OR applic. 3—35307
  Cs-134/137 power reactor mixtures, feasibility and prospects for private separation and marketing 3—19996
eddy current losses
  in ferromagnetic sheets, calc. 3—21262
  solid cylinder movement in magnetic field *(German)* 3—13665
  steel plates with nonlin. magnetisation characteristics, calc. 3—2313
eddy currents
  see also induction heating
  in axially symmetric a.c. current carrying conductors, fields calculations by computer *(Russian)* 3—32485
  bearing shells testing applic. *(Polish)* 3—27844
  brake, relativistic electrodynamics *(German)* 3—37877
  e.m. coil encircling 2-conductor rod, solution to induction problem 3—27821
  ferromagnetic cylindrical specimens under the influence of field strength dependent permeability eddy-current distribution *(German)* 3—18776
  ferromagnetic plate, travelling wave excitation, steady state elliptical vector mag. field 3—18341
  fuel rods, eddy current study of irradiation effects 3—26509
  magnetic domain wall motion, eddy current limited, bowing and merging, segmented model 3—12035
  NDT method for hydride and alpha-case detection in Ti alloys, evaluation 3—27836
  reactor control rods, evaluation of thickness cladding and crack detection 3—26510
  reactor fuel element spacing, in-core eddy current measurements 3—23402
  semiconductors, resistivity measurement 3—248
  superconducting hollow cylinder, magnetic fields prod. by induced eddy currents, shielding props. 3—18243
  transportation system, eddy currents effect on torques and forces on moving coil 3—35651
  tubes for heat exchangers, eddy current testing by using an internal coil system *(German)* 3—18775
  vector density of eddy flux, in thin plates and conducting spherical shells *(Russian)* 3—32473
  Al sheet solution, eddy current conductivity meas. near solidus point 3—27830
  Ti honeycomb structure, presence of Al braze alloy determ. by eddy current testing 3—21767
education
  see also computer-aided instruction; educational aids; training
  astronomy, teaching organization and conference, review 3—28430
  calcite, etched, dislocations obs. by polaroid photomicrography, undergraduate expt. 3—9813
  ceramics at Victoria, Australia 3—13185
  consortium for the advancement of physics education 3—16350
  electron microscopy for metallography 3—31017
  Faraday's law problem, solution including a nonlinear term 3—31982
  general physics instruction, Keller versus lecture method 3—31978
  general physics instruction, Keller vs. lecture method, comments 3—31977
  health physics technicians 3—8
  interdisciplinary course for the physical scientist 3—37571
  log normal distribution function, use in undergraduate teaching 3—9804
  marked examples, book 3—18048
  microstructure in metallics and ceramics, indirect shape factor, description 3—31015
  nuclear engineering, role of NEPA environmental assessment 3—19892
  nuclear engineering, self-study course in radiation measurements and analysis 3—19130
  nuclear power, summer school for high school teachers 3—19893
  ocean engineering program for undergraduates 3—10
  on-line computing and digital electronics, undergraduate course 3—42
  ophthalmic optics, at 1 and research at UMIST 3—19129
  physics research laboratory, educational and training in electronics and mechanical technology for untrained personnel 3—28627
  power engineering, American Power Conference, Chicago, USA (1972) 3—14273
  program for studying man's reaction in water 3—11
  stratospheric O_3 shield, effects of H_2O and nitrogen oxides, chemical kinetics presentation for students 3—9803
  ^{235}U content in natural U determ. with solid state track detector, undergraduate expt. 3—9814
educational aids
  analogue computer as a physics teaching tool 3—32009
  astronomy and astrophysics educational material 3—37576
  Compton scatt. expt., teaching apparatus 3—45
  eye model for demonstrating ocular refraction 3—28451
  focal length of diverging lens, simple method of meas. 3—43
  holographic equipment, low-cost 3—40
  interferometric device for demonstration of electron interference 3—32010
  laboratory apparatus for double spark source on linear air track 3—39

educational aids continued
- laboratory exercises in crystal growth, book 3-9815
- leaf electrometer with charge polarity discrimination 3-44
- synchrotron radiation, film loop 3-37578
- velocity of light meas. from Apollo 15 recordings 3-41
- wide range laboratory spark timer 3-32017
- Young's modulus determination via dynamic modulus apparatus 3-32011

e.e.g. *see electroencephalography*

effusion
- Knudsen method applied to determ. of dissociation pressures of Cu and Ag tellurides 3-15828

EHD *see electrohydrodynamics*

eigenfunctions *see eigenvalues and eigenfunctions*

eigenvalues and eigenfunctions
- anharmonic oscillator, evaluation of eigenvalues and eigenfunctions 3-35595
- bounds, in vibration and stability problems, by finite element analysis 3-563
- Casimir operators of U(n) and SU(n) for totally symmmetric and antisymmetric representation, eigenvalues 3-32415
- coordinate relaxation method for iterative calc. of eigenvalues and eigenvectors of very large symmetric matrices 3-23465
- coupled diffusion eqns., general solns. in integral transform theory, eigenvalue problem 3-19520
- density matrix, reln. to dynamics of quantum correlations 3-32404
- eccentric ring, nonstationary thermal conductivity calc. 3-35633
- eigenchannel treatment of particle hole states and related nuclear reaction models 3-29371
- eigenfunction analysis and Fadle-Papkovitch functions for bending of clamped rectangular orthotropic plates 3-28862
- eigenvalley method, contour search technique for complex roots of transcendental eqns. 3-23760
- eigenvalue distrib. in ensemble of random particles, spectrum of random matrices 3-22747
- eigenvalues of λx^{2m} anharmonic oscillators 3-10359
- eigenvectors and transfer matrices for Ising model, representation 3-18287
- eight-vertex model in lattice statistics and 1-d anisotropic Heisenberg chain, fundamental eigenvectors 3-26160
- eight-vertex model in lattice statistics and Heisenberg chain, eigenvectors of transfer matrix and Hamiltonian 3-26161
- elastic layer/half-space receding contact problems 3-22645
- elasticity, two-dimensional theory, eigenvalues 0 and −1 of spectra of integral operators *(German)* 3-13559
- electronic states in solids, orthonormalised and complete basis description 3-38762
- e.m. diffraction theory, eigenfunctions, generalised method, stationary functionals calc. *(Russian)* 3-10436
- energy eigenvalues of charged particles in homogeneous magnetic field, Foldy-Wouthuysen transformation 3-35792
- exciton, calc. for coupled coherent and incoherent motion 3-15165
- Fadle eigenfunction analysis of bending of plates 3-35570
- fluids, light scatt. spectra, anal. 3-32446
- Graetz extended problem, higher eigenvalues determ. 3-10415
- harmonic oscillator, simple energy quantisation, soln. by operator method 3-32000
- Heisenberg Hamiltonian, symmetric, exact solution in spin-wave representation 3-11996
- Helmholtz eqn. in cubic region, nodal surfaces of eigenfunctions 3-28914
- infinite-momentum frame, eigenvalues of Wick eqn. in weak-binding limit in perturbation theory 3-35746
- Krons eigenvalue procedure, generalization 3-16671
- laminar-turbulent transition as Sturm-Liouville eigenvalue problem 3-33199
- laminated orthotropic elastic spheres, study of natural vibrations using Rayleigh-Ritz technique 3-22682
- laser cavity resonator, excitation problem, soln. *(Russian)* 3-10558
- laser mode-locking process, eigenfunction anal. 3-35682
- least-squares method of solns. 3-6190
- Lorentz transforms, theory of eigenvalues and eigenvectors *(Hungarian)* 3-26130
- magnetic domain wall, eigenvalue equation for excitation modes 3-15394
- mass eigenvalue problem in SU$_2$-invariant pseudoscalar meson theory 3-13793
- mass eigenvalues from infinite-component particle wave eqn. with widely spaced mass spectrum 3-16708
- Maxwell's eqn. solved for dielectric slab waveguides with inhomogeneous core, soln. of Maxwell's eqn. 3-10328
- molecular dynamics, numerical soln. for infinite matrices 3-11219
- multidimensional bounded domain, asymptotic formula for eigenvalues of self-adjoint extensions of Schrodinger operator *(Russian)* 3-19493
- multigroup transport eqn., half-range completeness of vector eigenfunctions 3-29432
- non-Newtonian falling liquid films, gas absorption 3-36108
- non-self adjoint systems of partial differential equations, finite element analysis 3-28852
- plasma surface waves, axially symmetric, in cylindrical cavity with magnetised plasma, exact eigenvalues *(Japanese)* 3-36155
- polaron, eigenvalue determ. of effective Hamiltonian in external mag. field 3-21035
- potential distrib. on sphere with longit. depend. cond., soln. by separation of variable, magnetosphere appl. 3-25302
- prolate spheroidal functions, asymptotic expressions 3-10238
- prolate spheroidal wave functions, eigenvalue computation program, in FORTRAN 3-37861
- quantum electrodynamics, electron and muon as eigensolns. under Green function $\delta(x^2+l^2)$, quantization 3-35785
- rare earth ions in hexagonal field, calc. from modified Hamiltonian 3-27343
- recurrence relations, transmission electron diffraction 3-36251
- resonant vibrations of annular beam, disc and fibre, field parameters *(German)* 3-10306
- S-matrix eigenphases at high energy, concept of resonant state 3-29177

eigenvalues and eigenfunctions continued
- Schrodinger eqn., bound state energies, contact interactions influence 3-32411
- Schrodinger eqn., coupled one-dimensional, direct numerical integration 3-10338
- Schrodinger equation, normalised Morse functions, computer subroutine 3-10256
- singular eigenfunction expression of soln. of slab albedo problem, soln. of coupled Fredholm eqns. 3-22757
- sloshing frequencies of incompressible inviscid fluid in half-space, eigenvalue determ. 3-23771
- structural mechanics eigenvalue problems, solution methods comparison 3-32377
- SU(3) in O(3) basis, calc. of eigenvalues with no l degeneracy 3-22997
- Thomas-Fermi density matrix, simple harmonic oscillator 3-32410
- time eigenvalues of neutron-transport eqn. for fast subcritical assemblies 3-29430
- two nuclei with one electron system, energy level calc. 3-36000
- wave equation in finite domain, eigenvalue distribution, Weyl's problem computational solution 3-10340
- wave system in non-linear dissipative medium, solns. 3-14464
- waveguide of doubly connected cross-section 3-32400

eigenvectors *see eigenvalues and eigenfunctions*

Einstein-de Haas effect
- *see also gyromagnetic ratio*
- No entries

einsteinium
- No entries

einsteinium compounds
- No entries

elastic constant measurement
- asphalt, elastic modulus and loss factor meas. 3-32028
- dynamic properties obs. by resonance method 3-27801
- impulse method for high temp. meas. *(French)* 3-13217
- modulus of canine cardiac muscle, in vivo technique 3-22532
- orthotropic materials, transverse strain coeffs. determ. from bending tests 3-27846
- polymer, two-component heterogeneous composition, composite specimen method of dynamic props. simulation 3-27784
- resonating bar method for Young's modulus and Poisson coeff. determ. *(French)* 3-22253
- stimulated Brillouin scatt. meas. of press. variations *(French)* 3-14904
- stress/strain test data analytical evaluation 3-25024
- Young's modulus determination via dynamic modulus apparatus 3-32011
- C single filaments, thread or braided form 3-18752

elastic constants
- *see also compressibility; stress/strain relations; Young's modulus*
- alkali halide solid solutions, calculation of Debye temp. *(Russian)* 3-38648
- alkali metals, second and third order, calc. 3-27050
- anisotropic bimaterial plates, crack opening displacement, elastic const. depend. 3-17922
- benzene boundary layers, shear elasticity determ., dynamic method *(Russian)* 3-30167
- bituminous mix, stiffness moduli, computer simulation of Van der Poel's nomograph 3-27810
- brass, elastic shear modulus, determ. during quantized parabolic strain hardening 3-21651
- bronzite, meas. of single-crystal elastic constants of orthopyroxene 3-15893
- bubble domain lattices, elastic consts. and elastic waves, domain wall damping 3-21269
- bulk modulus, covalent crystals, obs. using regenerative feedback loop and composite oscillator 3-5770
- cellular-porous material, porosity influence 3-37098
- composite, carbon fibre 3-27757
- composite, fibre-reinforced M-M$_7$C$_3$ eutectic, (M = Fe + Co + Cr), effect of M$_7$C$_3$→M$_{23}$C$_6$ transform. 3-31143
- composite, fracture mechanism based on change in Poisson's ratio *(Japanese)* 3-18710
- composite material, effects of shape of dispersed particles 3-2750
- composite material, with viscous fluid inclusions 3-26074
- composite materials, slender rigid inclusions at dil. concs. 3-11671
- composites, fibre reinforced, nondestructive prediction of engineering props. 3-34672
- composites, fibre reinforced, variational bounds of bulk, shear and Young's moduli 3-18699
- cylindrical shell with axial crack under skew-symmetric loading 3-22619
- de Gennes's theory of smectic state, anisotropic u.s. properties of liquid crystal 3-1703
- Debye temp. calc. by averaging elastic stiffness coeffs. 3-36340
- diamond structure type, elastic consts. temp. depend. 3-20785
- dicalcium strontium propionate, Brillouin scatt., vibr. modes, elastic consts. 3-30814
- disordered materials, effective elastic consts., bounds, variational treatment 3-33594
- electrostatic contribs. in calcs. 3-17893
- epoxy resin, effect of fillers 3-27781
- fibre composite material, stiffness, structural design 3-31130
- fibre reinforced materials, by unidirectional short fibres, elastic properties *(Russian)* 3-24987
- fourth order nonlinear eqn. of state applic. to press. depend. determ. *(French)* 3-7805
- glass fibre reinforced polyester laminates, mech. props. *(Japanese)* 3-18707
- glass reinforced plastic rings, wound, transverse characts. variation over thickness 3-31150
- granular materials, propagation of u.s. elastic waves 3-34666
- graphite, phonon dispersion curves and elastic constants 3-38639
- hercynite spinel, high-pressure mantle phase 3-9158
- ofheterogeneous materials, linear integral equation 3-37801
- incompressible BKZ elastic fluid theory, relation between dynamic moduli 3-6221
- intermetallic lightweight cpds., dynamic yield strengths, compressional and Hugoniot elastic parameters 3-17927

elastic constants continued
- Invar alloys, mag. exchange contrib. to elastic consts., rel. to anomalous elastic props. 3—24597
- liquid crystal, nematic to smectic A transition, pretransitional anomaly in elastic bend const. 3—30069
- liquid films, complex shear modulus 3—27045
- mass and stiffness matrix synthesization, from experimental vibration modes 3—28926
- metal, bulk modulus, calc. using Lennard-Jones potential 3—38630
- micropolar elasticity, ‘second’ axial-symmetric problem, elastic potential 3—35567
- multicomponent polymeric compositions, dynamic mech. props. 3—31180
- nearly incompressible solid, influence of Poisson’s ratio on condition of finite element stiffness matrix 3—22617
- nematic liquid crystals, Frank elastic constants theory 3—20778
- nematic liquid crystals, splay and bend elastic constants determ. 3—36264
- NiSpan C, Invar range, precip. hardening effect on phys. props. 3—39345
- perchlorovinyl film, quartz conc. and dispersivity effect on physico-mech. props. 3—27782
- pleonaste spinel, high-pressure mantle phase 3—9158
- PMMA, stimulated Brillouin scatt. meas. of press. variations *(French)* 3—14904
- Poisson’s ratio, for central-force polycrysts. 3—27052
- Poisson’s ratio, Young’s modulus of media, characteristic equation for a layer—half-space system *(Russian)* 3—5714
- polycrystal, soln. for effective tensor of elastic consts. and analytical approx. 3—20783
- polycrystals, influence of elastic anisotropy on size effect in diffuse X-ray scatt. *(Russian)* 3—20679
- polymer, crystalline, theoretical estimates of shear moduli temp. depend. 3—24178
- polymer, structure/property relationships rel. to engng. material applics. 3—31186
- polymer compositions based on silicone adhesives, antifriction and mech. props. 3—25012
- polymer plates, flexural oscillations, dynamic parameters 3—26761
- polymer-impregnated porous ceramics, elastic behaviour 3—39380
- polymeric cylinder, mech. props. influence on temp. stresses, edge effect 3—26082
- polystyrene composite, Silas-balloon filled *(Japanese)* 3—21728
- PVC, partly plasticized, filler effect 3—31179
- PVC, plasticized and antiplasticized *(Russian)* 3—20250
- quartz, stimulated Brillouin scatt. meas. of press. variations *(French)* 3—14904
- quartz, X-cut impact loaded alpha, strain depend. of longitudinal piezoelectric, elastic and dielectric consts. 3—12098
- rare earth metal, rotationally invariant theory for magnetoelastic interactions effect on elastic constants 3—15401
- relationship at finite temperatures 3—38606
- sapphire, transverse components of elastic-compliance tensor, calc. *(Russian)* 3—7814
- schistous rocks, modulus of elasticity, Poisson ratio *(Portuguese)* 3—9199
- semiconductor, cubic, Young’s modulus and Poisson’s ratio 3—20781
- spinel in the rigid ion approximation lattice dynamics at zero wavevector and elastic constants 3—7875
- steel, reinforcing, low temp. characts. 3—21678
- steel, structural, temp. effect on physical and mechanical properties 3—24927
- steel and alloy characteriz. for elements of machines and instruments 3—21684
- stiffness coefficients of plane elastic frames with continuous or non-continuous girders, by computer *(Greek)* 3—6237
- succononitrile, plastic cryst., u.s. dispersion, freq. elastic consts., reaction mechanism *(French)* 3—20814
- thick liquid films and threads, Gibbs elasticity, thermodynamic theory 3—38708
- thiourea, near IV-V phase transition 3—21371
- transition metal, rel. to anal. of thermal expansion in quasiharmonic approx. 3—33642
- transversely isotropic annular plates with low shear resist., crit. load parameter depend. 3—22669
- triphenylbenzene, elastic const., evaluation from X-ray thermal diffuse scatt. 3—11670
- u.s. continuous wave interferometer 3—35366
- viscoelastic medium, linear theory soln. rel. to elastic consts. 3—35571
- water boundary layers, shear elasticity determ., dynamic method *(Russian)* 3—30167
- wurtzite and zinc blende structure materials, relation between elastic tensors 3—7810
- AG, cold-worked and γ-irrad., modulus defect variation during recrystn. 3—5314
- Ag, anisotropy, influence on extended dislocation nodes 3—1627
- Ag, third order elastic consts., pseudopotential calcs. 3—33590
- Al wire neutron irradiated, meas. of modulus of rigidity 3—1668
- Al/Al_3Ni unidirectional fibre composite, u.s. vel. meas. 3—34637
- Ar, solid, from interatomic potential for Ar_2 3—20779
- Ar single crysts., adiabatic consts. determ. by Brillouin scatt. near triple pt. 3—4781
- Au, cold worked, stage II and III recovery, modulus defect, trace impurity effects 3—5315
- Au_3Cu ordered alloys, use of Morse potential function calc. 3—7868
- $Ba(NO_3)_2$, u.s. meas., 4-300K 3—17894
- $BaTiO_3$, cubic phase, from lattice dynamics *(French)* 3—20826
- Bi, up to 32 kbar, determ. from press. depend. of u.s. velocity *(Russian)* 3—7806
- Br_2, solid, phonon dispersion and symmetry, intramolecular degrees of freedom influence on compressibility and elastic constants 3—24236
- Cd, Hookes law, deviations due to third order elastic consts. 3—17895
- CdTe, temp. depend., 4.2-300 K 3—30170
- Co-Elinvar, meas. of thermal expansion and Young’s moduli in 150-500°C range, obs. rigidity modulus of polycrystal *(Japanese)* 3—17896

elastic constants continued
- Co-Fe(Co-rich) alloys, temp. dependence of single crystal elastic constants 3—38605
- CsCl, pressure derivatives, calc. 3—1664
- Cu, cold-worked, after-effect caused by dumb-bell interstitials *(German)* 3—1663
- Cu, dislocation pinning after neutron irrad. at liq. He temp., internal friction and dynamic modulus obs. 3—38600
- Cu, fatigued, recovery of shear modulus 3—7811
- Cu, long wave method for third order elastic consts. calc. 3—17898
- Cu, rel. to third and fourth order anharmonic coeffs., of Cu-Ni alloys *(Russian)* 3—33619
- Cu, third order elastic consts., pseudopotential calcs. 3—33590
- Cu-Al alloy, elastic stiffness, comp. depend. 3—4780
- Cu-Al alloys, solute conc. depend. *(French)* 3—39302
- Cu-Sn alloy, elastic stiffness, comp. depend. 3—4780
- Cu_3Au ordered alloys, use of Morse potential function calc. 3—7868
- CuCl(Br)(I), rel. to ionicity 3—1662
- Dy, hydrostatic press. derivatives, electrostatic model and band struct. contrib. 3—27051
- DySb, shear elastic const. meas. near mag. and structural phase transition 3—33591
- $DyVO_4$, elastic anomalies near cooperative Jahn-Teller transitions 3—2014
- $DyVO_4$, soft acoustic mode and the strain dependence of the g factor 3—1761
- Er, hydrostatic press. derivatives, electrostatic model and band struct. contrib. 3—27051
- α-Fe, at elevated temps. unstable glide dislocations, elastic anisotropy factors calc. 3—31024
- Fe alloys, strength-differential effect, effective modulus interpret. 3—37063
- Fe alloys, strength-differential effect, effective modulus interpret. 3—37064
- Fe base binary alloys, composition and temp. depend. 3—17899
- $FeGe_2$, temp. depend. rel. to antiferromag. transition 3—5105
- Ga, anisotropy rel. to thermal expansion 3—27053
- Gd, elastic and inelastic behaviour in spin reorientation region, pressure effects 3—34116
- Gd, hydrostatic press. derivatives, electrostatic model and band struct. contrib. 3—27051
- $Gd_3Ga_5O_{12}$ garnet, elastic and thermoelastic constants *(German)* 3—7816
- α-HgS, rel. to piezoelec. props., resonant method obs. 3—36840
- Ho, high purity single crystals, between 78 and 300 K, u.s. meas. 3—20780
- I_2, solid, phonon dispersion and symmetry, intramolecular degrees of freedom influence on compressibility and elastic constants 3—24236
- InBi, elastic behaviour, u.s. wave velocity meas. 3—27048
- InSb, press. depend., up to 5.5 kbar *(Russian)* 3—7812
- KH_2PO_4, u.s. absorption at high press. 3—17939
- KI, Debye temp. calc. from elastic moduli 3—36394
- Kr solid, elastic consts. from neutron diffr. by acoustic phonons, 77 K 3—27049
- LiBr(Cl), meas. rel. to pressure and temp. depend. 3—24175
- LiF, Debye temp. calc. from elastic moduli 3—36394
- $LiNbO_3$, room temp. Brillouin scatt. obs. *(French)* 3—36864
- $^7LiH(D)$, 298K, u.s. determ. 3—20782
- Mn-Cu-Co nonmag. Elinvar-type alloys characteriz. 3—37074
- Mn-Cu-Cr alloys, nonmag. Elinvar-type 3—21291
- Mn-Cu-Ni alloys, nonmag. Elinvar-type 3—21292
- Mn-Ni-Co elinvar-type alloys, meas. of Young’s moduli at −150-400°C and rigidity moduli and hardness at room temp. *(Japanese)* 3—17897
- Mo, dislocation pinning after neutron irrad. at liq. He temp., internal friction and dynamic modulus obs. 3—38600
- NaBr-KBr solid solution, rel. to energetic and strength characts. of interatomic bonds *(Russian)* 3—20722
- NaCl, pressure derivatives, calc. 3—1664
- NaCl-KCl solid solution, rel. to energetic and strength characts. of interatomic bonds *(Russian)* 3—20722
- NaF, Debye temp. calc. from elastic moduli 3—36394
- $Na_xK_{1-x}Br$, u.s. velocity determ. *(Russian)* 3—27046
- $Na_xK_{1-x}Cl$, u.s. velocity determ. *(Russian)* 3—27046
- $NaNO_3$, determ. from Mandelshtam-Brillouin scatt. spectra 3—33593
- Na_2O-SiO_2 glass, i.r. absorp. pressure depend. obs. 3—5186
- Ne single crysts., adiabatic consts. determ. by Brillouin scatt. near triple pt. 3—4781
- Ni, cold-worked, after-effect caused by dumb-bell interstitials *(German)* 3—1663
- Ni, rel. to third and fourth order anharmonic coeffs. of Cu-Ni alloys *(Russian)* 3—33619
- Ni, shear modulus, rel. to hydrogen-dislocation interaction *(French)* 3—1629
- Ni, third order, at 80 K, from u.s. wave vel. meas. 3—36345
- Ni, third-order elastic constants of single crystal at 298°K 3—36343
- $NiCr_2O_4$, elastic props. and cooperative Jahn-Teller phase transition 3—24181
- Ni_3Fe, dislocations, elastic anisotropy effect on dislocations 3—17838
- $Ni_xZn_{1-x}Cr_2O_4$, elastic anomalies near cooperative JAHN-Teller transitions 3—2014
- $Pb(NO_3)_2$, u.s. meas., 4-300K 3—17894
- $RbMnF_3$, third-order elastic constants 3—36344
- Sc, lattice dynamics and second order elastic consts. 3—30225
- Se, trigonal, rel. to lattice dynamics 3—24223
- Si, heavily doped, elastic consts. and Raman frequencies under uniaxial stress 3—30173
- Si, impulse meas. at high temp. *(French)* 3—13217
- SiO_2, fused silica, adiabatic third order elastic consts., u.s. wave meas. 3—36342
- $(Sr_{1-x}Ba_x)TiO_3$ mixed cryst. system, phase transitions obs. 3—15456
- $Sr(NO_3)_2$, u.s. meas., 4-300K 3—17894
- Ti, and lattice dynamics rel. to anisotropic thermal expansion 3—17987
- Ti-Nb, (40 at.% Nb), superconductor, meas. at 298 K 3—27047
- TiC_xO_y and TiN_xO_y, correl. with thermal expansion coeff. *(Russian)* 3—11751

elastic constants continued
- UO_2, elastic moduli, meas. by ultrasonic technique, effect of porosity 3—14905
- V, allotropy possibility, resist. meas. 3—34503
- Zn, Hookes law, deviations due to third order elastic consts. 3—17895
- ZnS, pressure derivatives, calc. 3—1664
- ZnS struct. type, anharmonic props. 3—20785
- ZnSe, C_{ij} consts., meas. 3—20784

elastic deformation
- *see also bending; elasticity; stress/strain relations; torsion*
- acoustic wave propagation in finitely deformed elastic material 3—37828
- anisotropic media conclusion fields, surface integral reduction to a line integral 3—17863
- axial compression of elastic cylinders, axisymmetric contact problem 3—6218
- bar, anisotropic, coefficients related to moment of internal stresses *(Russian)* 3—16642
- cantilever beam, approx. for large deflection 3—32343
- cantilever beams of variable cross-section, non-linear bending, numerical soln. 3—22612
- circular plate, nonlinear theory of bending *(Russian)* 3—527
- circular tube under combined axial and torsional shear, universal relations for components 3—26085
- composite, fibre reinforced metal matrix, deform. and fracture behaviour *(Japanese)* 3—34634
- composite solid of two half-planes, stress distrib. due to prescribed forces 3—32331
- composites transversely isotropic fibre-reinforced, Saint-Venant's principle 3—32333
- compressible BKZ fluid, decomposition theorem on scalar potential 3—22798
- compressible isotropic materials, theoretical aspects 3—6201
- consistant conjugate stresses computation for elastic finite elements 3—26076
- constant strain/constant moment finite element methods, unification 3—32322
- contact problem, effect of two semi-infinite stamps on elastic band *(Russian)* 3—32327
- contact problems, triangular plate bending element 3—22620
- contact problems in bending of plates on elastic multilayer foundation *(Russian)* 3—32325
- contact rough surfaces with parallel surface asperities 3—21617
- contacting rough surfaces, initial contact position estimation 3—5302
- contacting rough surfaces, new contact theory 3—5303
- contacting rough surfaces, topography 3—5301
- copolymer, PN-1, deform. effect on supermol. struct. 3—27785
- crack parallel to edge of strip, soln. of equilibrium eqn. by Fourier transforms 3—13567
- crack propagation between similar and dissimilar orthotropic media, nonlinear effect of initial stress 3—32338
- cylinder, infinitely thin nonlinear elastic, asymptotic approx. in curvilinear medium *(French)* 3—32307
- cylindrical shell, nonlinear multiple-scale soln. to Reissner's eqns. using perturbation technique 3—32342
- cylindrical shell with axial crack under skew-symmetric loading 3—22619
- cylindrical shells, prestressed, dynamic response study using Green's tensor technique 3—37835
- discrete structures, analysis by integrated force method 3—32323
- displacement boundary-value problem of linearized elastodynamics, uniqueness 3—32336
- displacements of rigid body, matrices calc. *(Rumanian)* 3—19419
- dynamic buckling of elastoplastic bars 3—19423
- edge crack, normal to edge of strip, calc. of stress distrib., Fredholm integral eqn. 3—13571
- elastic-plastic plate bending, finite element analysis 3—10274
- elastic-rigid bodies under repeated variable deformation, mathematical models, optimisation theory 3—37797
- elasto-plastic, in partly yield notched bar, assessment of finite element analysis programs 3—26077
- epitaxial growth problem, dislocations at film/substrate interface 3—33747
- externally deformed crystals, low temp., deformation description 3—36348
- fibre reinforced incompressible isotropic elastic materials, universal solns. by inverse methods 3—28865
- fibre-reinforced, plates, constant thickness, optimal layouts 3—24974
- finite strain theory of elastic-inelastic crystalline materials 3—37807
- flexural deformation of an initially curved cuboid dielectric 3—28866
- flexural deformations of a material line in a continuous body 3—35568
- half-space with steady periodic vibrations, dynamic contact problem 3—32397
- hollow cylinder, axial compression, analysis of friction effects on elastic-plastic deformation using finite element method 3—19424
- hollow sphere with spherical transversal isotropy, deformations and stresses under impulsive pressure 3—19422
- hybrid displacement method for statics, vibr. and stability of thin elastic plates 3—10282
- ice plates, floating 3—3944
- impulse transitional functions for stamp-semispace system *(Russian)* 3—32326
- incompressible materials, stability conditions 3—32376
- indentation of elastic half space by rigid punch, eigenvalue problem 3—10283
- inflation-extension and eversion of tube of incompressible isotropic elastic material 3—10280
- inhomogeneous half-plane, plane contact problem *(Russian)* 3—28878
- inhomogeneous half-plane, soln. by successive approx. method *(Russian)* 3—37800
- instability of incompressible elastic materials 3—532
- integral formulation of elastic equilibrium problem *(Italian)* 3—19412
- isochoric finite, two-parameter family of solutions 3—6231

elastic deformation continued
- junction deformation models for asperities in sliding interaction, comments 3—4803
- laminated composites, three-dimensional finite element analysis 3—10275
- laminated orthotropic shell theory including transverse shear deform. 3—19442
- laminates, propagation using multi-continuum theory 3—3977
- large deflection elastic-plastic response of certain structures to impulsive load, numerical solns. and exptl. results 3—22605
- leaf spring moment meas., fluidic sensor *(German)* 3—13224
- linear theory of thin shells based on conservation of non-normal straight line, tensor notation 3—16624
- mechanics of elastic bodies with internal gyrations *(Russian)* 3—22637
- membrane, finite axisymmetric deform. due to edge tractions and internal press. 3—535
- membrane, nonlinear viscoelastic, axisymmetric deform. due to spinning 3—22640
- membrane shells, isotropic and anisotropic, uniform stress analysis *(German)* 3—22656
- metal, polycrystalline, grain shape effects on stress-strain distribs. in grains 3—5300
- multilayer sandwich beams and plates, finite element displacement analysis 3—26075
- nonlinear, finite element methods, theoretical and numerical comparison 3—10276
- nonlinear shell theory with finite rot. and stress-function vectors 3—22642
- nonlinear theory of arches and beams with shear deform. 3—22649
- orthotropic almost cylindrical beams, bending by transverse load 3—28856
- orthotropic bodies, symmetric deform. obs. by approx. method *(Russian)* 3—6214
- planar problem for bodies with rectilinear orthoropy, method of initial functions *(Russian)* 3—32328
- plane deformation of plane beams in one-dimensional finite-strain beam theory 3—22655
- plane distortion problem of micropolar elasticity, singular solns. 3—3947
- plane frames, finite deflection analysis on basis of bending stiffnesses 3—28859
- planet Mercury, thermal elastic deformations with period of 176 days 3—16165
- polyethylene fibre, oriented, conform. transitions associated with elastic tension 3—29810
- polymer plates, flexural oscillations, dynamic parameters 3—26761
- prestressed elastic structures, optimal design 3—513
- rare gas solid, stress tensor depend. on deform. gradient 3—7808
- relativistic systems and generalization of Hooke's law 3—19434
- rigidity of gases, Maxwell's kinetic theory, application to simple shear problem 3—38337
- rotating shells, non-linear deformation, numerical soln. *(Russian)* 3—37799
- Saint-Venant torsion problem elastic-plastic analysis, by hybrid stress model 3—514
- sandwich beam analysis 3—6228
- schistous rocks, uniaxial compression tests *(Portuguese)* 3—9199
- sheet steel, determ. of transverse stresses produced by uniaxial tension *(Russian)* 3—2781
- shell, thin, large deform., inverse problem 3—22641
- shells of revolution, criteria for finite element discretisation 3—32324
- shells of revolution, finite symmetrical strain 3—22648
- shells of revolution, linear bending theory, calc. by method of differences, determ. of stresses and elastic deformation *(German)* 3—19430
- solid sphere, displacement and strain fields under large deformations 3—32311
- solid-solid interface, moving load, steady-state solution for supersonic velocities 3—37796
- sphere, hollow, deformation under pulsed loading, study by 3-dimensional elasticity theory and shell theory *(Russian)* 3—10286
- spherical shells, thin, non-shallow, with wind loading, study of stress state *(Russian)* 3—28875
- stability conditions for thermoelastic continua 3—16632
- stability of locally loaded cylindrical shell under axially symmetric deformation *(Russian)* 3—16648
- steel, annealed, postulate of isotropy consequence test 3—34690
- straight beams, bending moments and deflections, algorithm calc. 3—19420
- strains, elastic-plastic finite, kinematics 3—35574
- temperature and volume changes on loading 3—24179
- thermal, quasi-static, of sphere by radiation from point source 3—28888
- thermoviscoelasticity, prediction of residual deformations 3—6236
- thick-walled spherical shell, large deformation elastic-viscoplastic analysis 3—6226
- thin shell, Castigliano's variational and continuity relations *(Russian)* 3—28881
- three-dimensional theory of elastic stability under finite subcritical deformations, review *(Russian)* 3—22635
- torsion, hyperelastic, incompressible, second-order, reln. to deformation 3—22614
- torsion of half space with embedded penny-shaped flaws 3—6229
- transversely isotropic cylindrical shell in axial compression, stability 3—26081
- uniform elastic strip around cylindrical drum, bending and stretching 3—6227
- vibration of elastic medium deforming in time 3—6270
- viscoelastic anisotropic plates, large deflections, soln. of nonlinear integro-differential eqns. 3—37795
- viscoelastic fluids, meas. of normal stress difference using Barus effect and theory of finite elastic deformation 3—1309
- viscoelastic solid, propagation of plane sinusoidal wave 3—3991
- Al alloy cylindrical shell, under internal pressure 3—18611
- Al single crysts., nonlinear behaviour under very weak stresses *(French)* 3—30169
- Cu, ribbons, cryst. perfect, gliding dislocation loops preceding slip line form. *(French)* 3—4761

elastic deformation continued
- Cu-Al-Ni alloy, martensitic thermoelastic transform., electron work function change 3−36346
- Cu-W fibre composite, thermal expansion, matrix yielding *(Japanese)* 3−18703
- Ge whisker, elastic props. and torsional strength 3−38759
- Ni, influence of mechanical stresses in elastic deformation region on Barkhausen effect 3−38991
- Si, diffusion of Cu^+, Ag^+ and Au^+ ions over interstitial oxygen sites 3−33700

elastic fatigue *see fatigue*

elastic hysteresis
- glass fibres, static hysteresis from −78 to 196°C 3−38619
- rolling resistance components comparison for elastic bodies *(Russian)* 3−10296
- Au-Cd alloy, thermoelastic martensite, lattice softening, ferroelasticity and shape memory effect 3−14907
- $AuCuZn_2$, thermoelastic martensite, lattice softening, ferroelasticity and shape memory effect 3−14907
- Be, determination of local logarithmic decrement 3−27030
- Bi, determination of local logarithmic decrement 3−27030
- Zn, determination of local logarithmic decrement 3−27030

elastic limit
- *see also slip*
- dynamically loaded structures, mode responses characteriz. 3−19441
- fatigue S/N curve, shape analysis 3−31228
- f.c.c. polycrystalline metals rel. to grain interaction *(French)* 3−33592
- steel, austenite, isothermal decomp. products characts. 3−21673
- structures with random resistance variations, limit analysis, probabilistic interpret. 3−16634
- Be, resist. to microplastic deform. during aging 3−21672
- Cu alloys, age-hardened, microstructural effects *(Russian)* 3−15668
- p-Ge:Au whiskers, plastically deformed, 760°C *(Russian)* 3−27055
- Ni, rel. to hydrogen-dislocation interaction *(French)* 3−1629

elastic losses *see internal friction*

elastic relaxation
- *see also creep*
- creep compliance and relaxation modulus improved numerical interconversion 3−534
- cubic lattice, Wert-Marx law generalization and interstitial vibr. freq. *(French)* 3−1688
- dynamic properties obs. by resonance method 3−27801
- epoxy resin, cured, relax. and optical props. 3−31175
- ethyl acetate relaxation time, u.s. absorption *(Russian)* 3−4814
- gases, behind shock and detonation waves, integral variational method 3−29881
- glycerin, structural relaxation of shear and bulk viscosity meas. *(Russian)* 3−4870
- jet swelling, anal. for non-Newtonian flow 3−11371
- liquid-gas bubble mixtures, struct. of propagating shock wave, relaxation effects *(Dutch)* 3−29882
- magnetostrictive ferrite, u.s. wave propagation consts., acoustical relaxation 3−36367
- metal, stress relaxation expts., dislocation behaviour 3−37104
- metal films, relaxation of elastoresistance 3−33866
- multicomponent polymeric compositions, dynamic mech. props. 3−31180
- nylon 6, morphological changes and effect on dynamic mech. props. 3−20243
- oxide mixture, critical, composition fluctuation lifetimes, volume relaxation spectroscopy, u.s. obs. 3−20818
- polymer blends, freq., conc. and temp. depend. 3−31188
- polymethylmethacrylate, glassy, biaxial stress relax. 3−4507
- polystyrenes blended monodisperse, two-step plateau in rubbery region of stress relaxation spectrum 3−1310
- polytetrafluoroethylene, acoustical investigation 3−27074
- rubber, inhomogeneity characts. estimation from relax. spectra 3−25008
- steel, maraging stainless, Almar 362, viscoelastic analysis of in-pile stress relaxation 3−18628
- steel wire, acoustical characteriz. 3−22205
- stress relaxation data based on the Johnston-Gilman equation, computer analysis 3−34595
- stress relaxation time, temp. depend., calc. method *(Russian)* 3−30175
- viscoelastic system, method of averaging, damping determ 3−22687
- Al, neutron irradiated and deformed at low temp., internal friction and modulus anomaly, influence of stress and work hardening *(French)* 3−14935
- Cu-Zn (30 wt.% Zn) internal friction variation with annealing 3−4818
- Nb, neutron irradiated at low temp., internal friction, relaxation peaks due to dislocation and point defects interaction 3−17875
- Si_2O_3, fused ultrasonic attenuation at high frequencies and low temps. 3−1708
- Ta with interstitially dissolved H, meas. of elastic Curie const., 300 to 450 K 3−20812
- V wire, deformation, low temp. relaxation, Snoek peak, dislocation motion 3−30206

elastic waves
- *see also acoustic waves; Love waves; magnetoelastic waves; Rayleigh waves; seismic waves; vibrations*
- acceleration, in anisotropic thermoelastic materials with internal state variables 3−3978
- anisotropic elastic plates, transient response for cusped wave fronts 3−13593
- anisotropic medium with point source, wave fields and acute-angled edges on wave fronts *(Russian)* 3−3988
- application to crack control *(Russian)* 3−11680
- aquartz, energy flow direction by acoustoelectric probe 3−8005
- axially symmetric transient wave propagation in elastic circular rods with nonuniform section 3−28904
- Babinet's principle, seismic representation 3−32380
- bubble domain lattices, elastic consts. and elastic waves, domain wall damping 3−21269
- cantilever on rotating disc, elastic oscillations *(Russian)* 3−19472
- caustics formation, interaction of sound with shells 3−28414

elastic waves continued
- clamped isotropic circular cylindrical shell, low natural frequencies calc. by asymptotic method 3−32375
- composite material, filamentary, propag. characts. 3−6272
- composite materials, stress wave attenuation, geometric dispersion and spatial attenuation 3−26100
- composite materials elastic wave propagation theory 3−2761
- compressible elastic half-space, one-dimensional finite amplitude wave propagation, stable numerical soln. 3−22683
- conference, Boston, Mass., USA (1972) 3−16334
- conical rod, one dimensional propag. 3−10310
- conical shells, axisymmetric wave propag. 3−26104
- continuum theory in laminated composites, elastodynamic model 3−26095
- crystals of C_{3v} class, guided elastic waves in plates *(Russian)* 3−14933
- crystals with linear defects, l.f. wave attenuation and anharmonicity *(Russian)* 3−14932
- in cylindrical bar, moving load on internal surface 3−6275
- cylindrical shell in acoustic medium, dynamic stability 3−6276
- cylindrical shells, prestressed, dynamic response study using Green's tensor technique 3−37835
- cylindrical shells with discontinuous cross-sectional area, longit. impact 3−22692
- cylindrical tank filled with elastic medium, oscillations of elastic tap and bottom *(Russian)* 3−28916
- deformed viscoelastic solid, propagation of plane sinusoidal wave 3−3991
- diffraction at spherical cavities *(Russian)* 3−570
- diffraction of plane shear wave by circular rigid disc and penny shaped crack 3−3990
- disordered polycrystals, distortion waves 3−17926
- disordered substructure media, mean field dispersion spectra 3−27068
- elastic sphere in solid medium, scatt. of transverse wave 3−16667
- elastic-plastic stress wave propagation, finite element analysis 3−28905
- elastoplastic string, unloading boundary determ. in transverse impact 3−22689
- expanding spherical cavity and elastic radiation rel. to underground explosions 3−34813
- fibre reinforced composites, continuum mixture theory of wave propagation including microstructure 3−24975
- flexural, dispersion in elastic circular cylinder 3−6289
- flexural waves, propagation in elastic rectangular bars 3−13595
- flexure waves, in thin shells, geometrical theory 3−32381
- glass, bending, fracture, crack movement 3−33606
- gravitational wave detection by method of light scatt. from elastic waves *(Russian)* 3−37884
- half-space, computer simulation of nearfield 3−32383
- harmonic, in layered composites 3−6293
- hollow conical frustum, wave propag. 3−26102
- holographic imaging 3−37570
- hypersonic thermal wave, averaged props. of wave solns. 3−20544
- impact wave formation in elastic half-space with nonlinear transitional wave process excitation *(Russian)* 3−32378
- incompressible materials, stability conditions 3−32376
- infinite elastic medium with spheroidal cavity, torsional waves 3−22690
- in inhomogeneous elastic media, WKB solution 3−6283
- initial-boundary value problem numerical solution 3−16706
- instability of incompressible elastic materials 3−532
- isotropic discretized bodies, wave propag. problems 3−19456
- isotropic sphere, transient vibrations 3−10312
- junction of two noncollinear rods, generation of stress pulses 3−6288
- Kirchhoff diffraction of longit. elastic waves, tensor pot. 3−37834
- Korteweg-de Vries, in weak nonlinear dispersive waves propagation 3−10240
- laminated composites, continuum mixture theory of wave propagation including microstructure 3−24975
- laminated orthotropic elastic spheres, study of natural vibrations using Rayleigh-Ritz technique 3−22682
- laminated orthotropic plates, natural vibr. 3−6287
- laminates, propagation using multi-continuum theory 3−3977
- light scattering by elastic waves in cubic crystal 3−18448
- linear field with couple stresses, wave propag. 3−26099
- in liquids, longitudinal pulses, vel. meas. for students 3−22229
- longitudinal and transverse, nonlinear interaction in isotropic solid 3−26096
- longitudinal hypersonic waves, in solids, excitation by short laser pulses 3−7857
- materials science and technology treatise 3−2621
- mechanical systems, excitation by elastic shock waves for vibration characteristics meas. *(German)* 3−16339
- metal, laser-irrad., stress-pulse propag., dispersion 3−7847
- microelastic wave propag., restrictions on dispersion relations and elastic moduli 3−13592
- micropolar elasticity, forced vibrs. by time dependent loads and moments 3−13591
- moment theory for one-dimensional continuous medium with nonuniform periodic structure *(Russian)* 3−16681
- monochromatic, propagation in initially stressed infinite micropolar elastic plate 3−28902
- motion in solid due to nonuniformly moving line load 3−3989
- non-dispersive media, slowness diagrams for resonant wave interactions 3−32391
- nonlinear propagation in fluid-filled tubes steepening effect *(German)* 3−37826
- nonlinear transient stress waves, in cylindrical and conical shells 3−32382
- nonlinear wave propagation in elastic-plastic semi-space, due to moving and variable loading along boundary 3−37829
- olivine aggregates, numerical experiments on plane wave velocities 3−15894
- paraelastic resonance of Jahn-Teller and off-centre ions 3−24387
- piezoelectric crystal, elastic wave formulation for electroelastic waves 3−21364
- piezoelectric crystal, energy flow direction by acoustoelectric probe 3−8005

elastic waves continued
- piezoelectric half-space, elastic-e.m. wave excitation *(Russian)* 3—34302
- plane, diffraction by cylindrical cavity, polarity effect, stress field determ. 3—32396
- plane, thermally-induced, anal. in elastic-plastic single crystals 3—3985
- plane stress wave reflection in elastic-plastic medium with variable yield limit *(Polish)* 3—19470
- plane wave scatt. from objects near interface 3—22694
- plate-fluid system, spectrum of natural freq. 3—4599
- Plexiglas, elastic wave generation at crack tip rel. to energy reserve 3—20809
- polycrystalline solids and plates u.s. backscattering meas. 3—37555
- polycrystalline stishovite, velocity, lower mantle composition 3—9146
- polyethylene rod, longit. wave propag. analysis 3—30202
- polymer, compound vibrator method for determ. of complex deform. characts. 3—28471
- polymer, optically active, longit. stress wave propag. 3—30203
- polyurethane foam, compression wave behaviour 3—31205
- in prestressed incompressible hyperelastic material 3—10304
- propag. in 2nd order materials, torsional and longitudinal motions 3—32372
- propagation in elastic half space, action of nonstationary surface forces *(German)* 3—37827
- propagation in elastic half-strip, soln. using space characteristic method *(Russian)* 3—19469
- propagation in infinite cylindrical shell containing hollow elastic filling *(Russian)* 3—19468
- pseudospherical waves Schlieren investigation 3—2909
- random initial stress influence on propag. *(German)* 3—3980
- reflection in superseismic region in presence of alternating boundary conditions *(Russian)* 3—34818
- refraction at elastoplastic half-space, application to study of seismic wave refraction at earth's surface *(Russian)* 3—21862
- relativistic theory, formulation and application to small motions about stable equilib. configuration 3—16730
- rod, two-layered with imperfect bonding, transient compressional wave propagation 3—32387
- rods and pipes, e.m. generation 3—576
- rotating shells in presence of turning points, vibration and stability, stress-strain distrib. *(Russian)* 3—37837
- Sanbagawa metamorphic belt, Shikoku, velocities rel. to geological struct. 3—27962
- semiinfinite elastic cylinder containing one acoustic medium, dynamic response 3—6281
- SH-mode piezoelectric surface waves, on rotated cuts 3—17931
- shear, guided by cylindrical hole in finitely deformed elastic solid 3—6284
- shear waves, propagation in moving elastic medium with lubricating layer 3—35321
- shockless pulses at interface, reflection and transmission theory 3—14470
- soil, skin friction, static and dynamic, meas. for wave eqn. analysis 3—21768
- solid inclusions in medium, model investigations 3—571
- spherical, propagation, one boundary-value problem soln. *(Russian)* 3—37836
- spherical wave propagation in a viscoplastic medium 3—19465
- Stoneley wave propag. along perturbed interface 3—10311
- straight circular elastic tubes, pulse propag. 3—22693
- stress wave propagation in laminated plate under impulsive loads 3—18698
- stress waves, focusing, in elastic sphere 3—32379
- stress-induced polarization in slightly anisotropic materials 3—13594
- submerged rods, fluid influenced stress wave dispersion 3—16664
- surface, devices for processing radar, television and radio signals 3—3987
- surface elastopolarization waves at domain boundaries in ferroelectrics *(Russian)* 3—8540
- surface waves guided by slit in isotropic elastic solid 3—22695
- surface waves in anisotropic media, rapid numerical cals. 3—20921
- theory of propag. in inhomogeneous media 3—2899
- thermoelastic, plane unidimensional, propagation in an inhomogeneous semispace *(Russian)* 3—10315
- thermoelastic two-temperature theory, wave propagation 3—37824
- torsional oscillations of rigid spherical inclusion in elastic stratum 3—32392
- torsional waves in elastic cylinder with Cauchy initial stress 3—32370
- transient stress conc. in elastic medium with spherical cavity 3—22691
- turbulent fluid, waves with fluctuating stress proportional to strain field 3—26775
- unbounded medium generalized thermoelastic longtiudinal waves 3—28923
- u.s., propagation in granular media 3—34666
- vibrating string, computer simulation for teaching purposes 3—13181
- vibrations, radial, of circular cylinders of perfectly conducting elastic material 3—22676
- vibrations of rectangular plates of micropolar elastic materials, three-dimensional analysis, series soln. 3—16665
- vibrations of thick elastic shells, soln. using Cinelli's method 3—19464
- viscoelastic, energy velocity equal to phase velocity for Standard Linear Solid or Maxwell Model 3—32393
- viscoelastic, in half space, due to moving excitation source 3—32395
- viscoelastic materials, propagation *(Russian)* 3—568
- viscoelastic solid, wave front velocity 3—26094
- wave propagation and secular theory of calculation based on Hamilton-Jacobi theory 3—22677
- wave propagation in thermo-viscoelastic solid of Maxwell type 3—32369
- Al, cracks in space vehicle cabin wall panels, detection by u.s. techniques 3—31227
- Al, laser-induced stress-wave and impulse augmentation 3—756
- BaF_2, high-freq. acoustic harmonic generation by Bragg light scatt. 3—7859
- $Bi_{12}GeO_{20}$, acoustic surface waves, harmonic generation 3—17932

elastic waves continued
- CaF_2, high-freq. acoustic harmonic generation by Bragg light scatt. 3—7859
- Cd, propag. vel. meas. under hydrostatic press., search for first and second order phase transforms. *(Russian)* 3—15013
- Ge, energy flow direction by acoustoelectric probe 3—8005
- KH_2PO_4, boundary reflection phase shifts, nonlinear interaction 3—27073
- $LiNbO_3$, acoustic surface waves, harmonic generation 3—17932
- $LiNbO_3$ plates, guided elastic waves *(Russian)* 3—14933
- $LiTaO_3$ plates, guided elastic waves *(Russian)* 3—14933
- SrF_2, high-freq. acoustic harmonic generation by Bragg light scatt. 3—7859
- TiO_2, rutile, internal conical refr. 3—17928
- $ZnSiO_4$, zircon, internal conical refr. 3—17928

elasticity
- *see also anelasticity; elasticity of liquids; elastoplasticity; photoelasticity; rheology; thermoelasticity; viscoelasticity*
- aeroelastic optimisation os semi-infinite flat panel 3—11422
- anharmonic crysts., statistico-thermodynamic approach *(Russian)* 3—36371
- anisotropic 3-d bodies, soln. for stress states using successive approximation method *(Russian)* 3—13579
- anisotropic b.c.c. crysts., glide dislocations, energy, stability and Peierls stress 3—33531
- anisotropic bodies, elastic equil., systems of Fredholm integral eqns. 3—16639
- anisotropic elastic plates, transient response for cusped wave fronts 3—13593
- anisotropic shell theory 3—16640
- anisotropy, influence on extended dislocation nodes 3—1627
- asymmetric, Sommerfeld type radiation conditions 3—32332
- asymptotic theory of thin rectilinear elastic and plastic panels 3—32345
- axisymmetric clamped plates subject to displacement and stress constraints, weight minimisation 3—16626
- axisymmetric rigid body of arbitrary profile vibrations on a semi-infinite elastic solid 3—32390
- axisymmetrically loaded orthotropic shell of revolution, finite element analysis 3—10273
- beam, cantilever and clamped-hinged, elastic stability by complementary energy method 3—32330
- beam, infinitely long, rigid, resting on elastic base, soln. by Shtaerman's hypothesis *(Russian)* 3—28884
- beams, effect of force moving at variable speed 3—22603
- beams, stability by variational procedures 3—37802
- beams curved in plane of noncircular centre lines, torsion and deflection, determ. of bending moment and angle of twist 3—19440
- bending beams, random gravity loads as stochastic function with independent increments *(Polish)* 3—19436
- bending of beam, castellated with hexagonal holes, stress detn. *(Japanese)* 3—16652
- bending vibrations stability of elastic beams moving periodically in a longitudinal direction *(German)* 3—19466
- benzil, elastic anisotropy rel. to preferential dislocation directions for growth *(German)* 3—7765
- bi-material plates, collocated interfaced elastic stress intensity factors 3—21724
- bond failure between elastic plates and rigid bodies 3—533
- bones, viewed as anisotropic poroelastic bodies, flexure and torsion 3—9691
- bow shackles of circular section, tensile stresses 3—10268
- box beam, thin-walled, post-buckled behaviour under pure bending 3—539
- brittle cracks, integral solns. for propagation at constant and accelerating speeds 3—32318
- brittle elastic bodies, spallation theory, spall damage rel. to stiffness and thermal cond. 3—17920
- bronzitite, compressional and shear wave velocities rel. to anisotropic elasticity 3—18812
- buckling of rigidly clamped hemispherical shells, numerical study 3—32312
- Castigliano's principle applied to elastic parallelepiped, temp. stresses, calc. *(Russian)* 3—10292
- Cauchy-Poisson media, mech. models 3—16638
- Chordae tendineae of human heart, histomechanics *(German)* 3—3754
- circular inclusion in infinite plate with two cracks, soln. 3—32316
- closed cylindrical shells, approx. methods and Jakobsen-Girkmann eqn. 3—16636
- complex structures analysis and design by elastic boundary method *(Italian)* 3—19426
- composite, fibre reinforced, elasticity theory with microstruct. 3—530
- composite materials, effects of shape of dispersed particles 3—2750
- composition, stochastic Green functions 3—37794
- compressional modulus of material permeated by random distrib. of circular cracks 3—32340
- conical shells, 2nd order asymptotic soln. to Donnell-type eqns. 3—32313
- contact between elastic layer with slightly curved bottom and substrate 3—6234
- contact problem of nonplane punch on elastic layer, initial value method soln. 3—32317
- Cosserat medium with forced rotations, Green's function matrix integrals in inhomogeneous region 3—26073
- coupled internal-rotational foundation-soil interaction of building structures, soln. of Lamb problem 3—19439
- cracks, Griffith, perpendicular to 2-dim. elastic strip, soln. by Fredholm integral 3—22615
- cracks at interface of elastic half-spaces, opening displacement rel. to screw dislocation distrib. 3—24199
- cracks inside circular inclusion, screw dislocation double pile-up treatment 3—24201
- cracks outside circular inclusion, screw dislocation double pile-up treatment 3—20803
- crystals, elastic-plastic, at arbitrary strain, constitutive anal. 3—3960
- cubic crystal, long-range elastic interaction between dislocation and ellipsoidal inclusion 3—36303

elasticity continued
cylinder, dislocations, boundary value problem, iterational method of soln. 3−26087
cylinder, infinitely thin nonlinear elastic, asymptotic approx. in curvilinear medium *(French)* 3−32307
cylinder shrink-fitted to hollow cylinder, stress distributions and displacements 3−16618
cylindrical shell, axially loaded, with low shear stiffness, two-dimens. approach to stability 3−28871
cylindrical shell beams, centres of twist and shear 3−22643
cylindrical shell with circular opening, transverse shear effect on stress state 3−35572
cylindrical shell with filling under axial compression and external pressure, stability *(Russian)* 3−28880
cylindrical shell with one or two circular holes, stress concentration 3−3951
dielectric elastic hollow sphere, large amplitude oscill. 3−556
difference eqns. iterative methods 3−3957
discretized bodies, lattice type shells 3−3948
discretized multipolar bodies, elasticity theorems 3−19414
displacement-energy bound for elastic structures 3−6233
drag-reducing polymer solutions 3−7286
dunite, compressional and shear wave velocities rel. to anisotropic elasticity 3−18812
dynamic theory spatial problem, operators and permissible dynamic eqns. *(Russian)* 3−16643
dynamically loaded structures, mode responses characteriz. 3−19441
earth mantle, equations of state of high-pressure solid phases 3−25118
eclogites, at high pressure and temp. *(Russian)* 3−9132
edge crack in disc, stress intensity factor by Mellin transform technique 3−13569
elastic layer mixed boundary value problem, soln. by invariant imbedding 3−512
elastic-plastic circular plates with combined isotropic and kinematic hardening 3−3956
elasto-plastic bending problem, analytical method of soln. 3−3952
elastokinetics, method of large internal forces *(German)* 3−22654
elastoplastic analysis soln. by matrix displacement or finite element method 3−22652
elastoplastic problem, biharmonic solution to St. Venant's eqn. *(Russian)* 3−529
elastostatic circle theorem 3−10284
elastostatic invariance in composite field for perfectly bonded orthotropic half-planes 3−32315
electro-elastic interactions in dielectrics, oriented elastic continuum model *(German)* 3−37793
ellipsoidal inclusion, elastic field 3−28858
energy flux into tip of extending crack in elastic solid 3−32334
fibre reinforced mat., continuum theory development 3−34640
fibre-reinforced plates, constant thickness, optimisation 3−22607
finite element analysis of finite sized plates bonded to elastic half space 3−508
finite rotating disc, stress intensity factor and crack formation energy of edge crack 3−19428
finite strip problems, dynamic stress-intensity factors determ. 3−22626
flexible shells, state equations *(German)* 3−22653
general relativistic high-pressure theory of perfectly elastic solid 3−599
glasses, rel. to neg. Gruneisen gammas 3−12134
grillages of maximum strength and maximum stiffness optimality conditions 3−3935
half-plane, extremal stresses in first principal plane problem *(Russian)* 3−6213
half-space, strengthened by slabs, contact problems *(Russian)* 3−523
half-space, transversally-isotropic, external axially symmetric mixed problem *(Russian)* 3−3962
half-space with inhomogeneous inclusions, punch problem *(Russian)* 3−526
half-space/layer receding contact problems 3−22645
hexagonal crystal, elastic interaction between point defect and prismatic disloc. loop 3−4747
homogeneous isotropic hyperelastic solids, stress/strain relation 3−16641
hysteroelastic theory, dynamic, linear, general solns. for composite media *(Russian)* 3−28883
ice plates, floating, deformation and stress 3−3944
imbedding of one-dimens. bodies in constrained continuum 3−16633
impact, rigid cone and elastic half-space, Hertz's theory 3−32297
impact interaction of absolutely solid body with two-mass elastic system *(Russian)* 3−32299
inclusions in elastically anisotropic media, strain fields for diffraction contrast calcs. 3−33538
inertial foundation model, dynamic analysis 3−6210
infinite plate with circular hole, effect of couple stresses 3−28889
instability of incompressible elastic materials 3−532
invariant finite strain meas. 3−32329
isotropic, relative flow of multicomponent medium, dynamic theory *(Russian)* 3−10293
isotropic material, quasilinear and linear relations between stress tensors and finite deformations *(Russian)* 3−19431
Kelvin-Voigt solids, adjoint system for dissipative, nonconservative stability problems 3−32337
laminated orthotropic shell theory including transverse shear deform. 3−19442
lateral vibration and stability relationship of elastically restrained circular plates 3−37831
lattice-type shell linear theory, consistant approx. 3−3949
line defects in high-symmetry cases, anisotropic elastic solns. 3−24116
linear, c.-a.a. programs ELAS 3−6205
linear, equivalence method and finite element method *(French)* 3−3953
linear couple-stress theory, potential methods 3−13558
linear systems on Hilbert space, energy-like Lyapunov functionals 3−32341
linear theory, appl. to fine struct. calc. for moving superdislocation *(Russian)* 3−7769

elasticity continued
linear theory, reln. to piezoelectricity and crystal lattice dynamics, review 3−33615
linear theory of thin shells based on conservation of non-normal straight line, tensor notation 3−16624
magnetoelastic interactions in relativistic continua, constitutive theory 3−22722
Marguerre-Vlasov eqns. for nonshallow shells, solving functions *(Russian)* 3−10298
materials with microstructure, equations of motion using first law of thermodynamics 3−14931
matrix method for local instability analysis in plates, stiffened panels and columns 3−515
membranes of revolution, flattening by large stretching, asymptotic soln. with boundary layer 3−32339
'memory waves' in elastic liquid, exact soln. *(Russian)* 3−10294
micropolar, axi-symm. contact problem 3−19417
micropolar, axial shear vibrs. in elastic cylinders 3−3981
micropolar, linear theory, forced vibrations, determ. of displacements, rotations and stresses 3−16674
micropolar, plane problem, stress functions 3−19415
micropolar, second plane distortion problem 3−19413
micropolar, singular solns. of plane distortion problem 3−3947
micropolar, two dimens. problem. stress and displacement functions 3−19416
micropolar elasticity, 'second' axial-symmetric problem, elastic potential 3−35567
micropolar elasticity, forced vibrs. by time dependent loads and moments 3−13591
micropolar theory, axisymmetric Boussinesq problem 3−6204
moment theory for one-dimensional continuous medium with nonuniform periodic structure *(Russian)* 3−16681
monotonicity conditions for ordinary differential linear operators in problems of theory of elastic structures 3−16631
multiphase media theory, review *(Russian)* 3−6217
non-linear vibration of beams and membranes 3−22700
non-uniform elastic circular region, analysis of first kind and general boundary problems *(Russian)* 3−28867
nonlinear eqns. for non-shallow spherical shells stability, limits of applicability for shallow shells *(Russian)* 3−6209
nonlinear equations, derivation of linearized theory of transversely isotropic beams 3−6290
nonlinear magnetoelasticity, boundary problem *(Russian)* 3−3963
nonlinear oscillations, piece-wise linearization formulations and loss of stability *(Russian)* 3−13604
nonlinear problems reduction to discrete ones by finite element methods *(Russian)* 3−6212
nonlinear shell theory with finite rot. and stress-function vectors 3−22642
nonlinear theory, nonstationary eqns. in Euler coordinates *(Russian)* 3−28890
nonlinear theory of arches and beams with shear deform. 3−22649
nonlinearly elastic material, equi-area transforms. *(Russian)* 3−3965
nonlocal theories, Galerkin stress functions 3−6211
nonuniform isotropic media, harmonic functions applic. *(Russian)* 3−525
numerical integration methods in elastodynamics, evaluation 3−22604
open spherical layer, axially symmetrical natural vibrations, computer calcs. *(Russian)* 3−37838
optimal structural design for minimum deflection and maximum fundamental freq. and stability, approx. soln. 3−32344
orthotropic plates, postbuckling anal. and determ. of load-shortening and effective width 3−22608
oval ring with stiffeners 3−6223
perturbed boundary problems, soln. using small parameter method *(Russian)* 3−19445
physical determ. of fields of displacements and derivatives in continuous media 3−6224
piezo-elastic effects, polynomial solution of plane problem *(Russian)* 3−28879
plane, orthotropic problems, solution by integral method 3−6232
plane, problem for anisotropic inhomogeneous wedge *(Russian)* 3−10290
plane stress and strain in structures, finite element analysis 3−22628
plane stress wave reflection in elastic-plastic medium with variable yield limit *(Polish)* 3−19470
plate, longitudinally stiffened, lateral flexural rigidity 3−26090
plates, nonlinear theory and tractable problems 3−13577
plates, optimisation for minimum weight under given load *(Russian)* 3−10287
point loaded disc, determ. of stress intensity factor of radial crack from soln. of Fredholm eqn. 3−19429
polar elastic continuum, ambiguities in interpretation of terms in theorem of kinetic energy 3−16630
polycrystals, effects of stress induced anisotropy 3−7807
polymer, chain coiling, rel. to elasticity and viscoelasticity 3−7294
polymers, recovery on deformation, thermal properties 3−21737
precurved disk, finite elastic-plastic bending *(German)* 3−3945
prismatic shells, transmission of concentrated forces perpendicular and parallel to ridge 3−16625
quasi-linear bodies, mechanical behaviour 3−37811
radial field inhomogeneity, of symmetric springs in gyroscopes *(Russian)* 3−10319
random linearly elastic solid, correlation of field quantities 3−10279
rectangular plates with unidirectionally variable rigidity, soln. of differential eqn. of bending *(Polish)* 3−19435
reinforced material under uniaxial compression, applied theories applicability in stability problems 3−26084
reinforced spherical shells with external pressure, stability and weight optimisation *(Russian)* 3−28873
Reissner-Sagoci problem for non-homogeneous solid 3−10277
relativistic systems and generalization of Hooke's law 3−19434
relativistic theory, formulation and application to small motions about stable equilib. configuration 3−16730
ribbed cylindrical shells, under axial compression stability investigation *(Russian)* 3−22634
ribbon-like inclusion problems, interaction between inclusion and free boundary 3−19427

elasticity continued
rod, equil. problem soln. in terms of generalized stresses and displacements 3—16637
rods, stability in linear dynamical theory 3—13560
rolling resistance components comparison for elastic bodies *(Russian)* 3—10296
rubber, intermolecular obstruction theory 3—7278
safety domain of structures in load and strength parameter space 3—16659
semi-infinite crack with concentrated shears, Papkovitch-Neuber potentials, applic. *(Ddegae)* 3—32319
semi-infinite layer, mixed boundary-value problems 3—19444
semi-infinite plane cut analogue of Lamb's soln., mixed boundary problem soln. using Wiener Hopf method *(Russian)* 3—16647
semi-infinite plate with row of circular holes, stress distribs. 3—3950
semiconductors, III-V, effective charge transfer and covalent bonding 3—7656
shallow shell theory, construction of exact solutions in form of power series *(Russian)* 3—19433
SHEBA shell element with variable curvature, application 3—509
shell, thin, stability equations *(German)* 3—22658
shell equations for stress distribution in corrugated tube or bellows 3—3955
shell modelling by variational methods *(Russian)* 3—524
shell of revolution, variable thickness orthotropic, suppressed bending 3—26088
shell theory, comparison of solns. in first approx. 3—26086
shells, non-symmetric strongly convex thin and shallow, loss of stability due to turbuelnt stresses *(Russian)* 3—28868
shells, optimisation for minimum weight under given load *(Russian)* 3—10287
shells of revolution with variable thickness, free vibrations 3—37849
shells with openings, exptl. study of stability, determ. of critical axial compression *(Russian)* 3—28874
shock waves in materials with memory, calc. of growth and decay 3—13570
shock waves propagation in hyperelastic solids, approx. solution 3—7848
singularity problems, convergence of finite element method 3—22616
slanting spherical shells under dynamic load, initial potential state, numerical analysis *(Russian)* 3—22638
solids elasticity theory, stability theory and plasticity theory, review 3—16614
sound propagation speed in high-pressure elastic general-relativistic solid 3—37883
sphere in solid medium, scatt. of transverse elastic wave 3—16667
spherical rubber shell, determ. of characteristic frequencies and forms of vibration *(Russian)* 3—510
spherical shell, non-shallow, stability for finite displacements *(Russian)* 3—6215
spherical shell in ideal compressible liquid, determ. of thickness and radius by echo signals *(Russian)* 3—22197
spherical shell/rigid plate contact press., applanation tonometry applic. 3—19443
spinning elastic medium damped by conical shell, use of coupled pair of integral eqns. *(Russian)* 3—16649
stability of axially symmetrically loaded shallow closed conical shell, nonlin. problem *(Russian)* 3—28885
statistical treatment of macroscopic props., depend. on degree of order *(German)* 3—13573
strain gradient theory of arbitrary order, analytic props. of solns. 3—28857
stress distribution in homogeneous sphere containing penny-shaped crack 3—6206
stress distribution near tip of array of screw dislocations piled up against an inclusion 3—1625
stress field in cylindrically anisotropic body under two dimensional surface traction 3—6230
stress intensity factor of crack in elastic solid, application of dual eqns. 3—32335
structures, 3D, elasto-plastic anal. using isoparametric element 3—543
thick-walled elastic shells under external press., determ. of oscill. and stability 3—557
thin circular plate, non-linear tensor eqns. for large deflections 3—511
thin cylindrical shells collided with dampers, dynamic stress behaviour 3—19438
thin elastic nonuniform plate, nonlinear oscills., numerical soln. 3—558
thin elastic rings subjected to radial load sets 3—6222
thin plate theory, polygon-circle paradox and convergence 3—10285
thin plates dynamic testing with sinusoidal pneumatic excitation *(Japanese)* 3—25036
thin plates on elastic foundation with unilateral behaviour 3—16635
thin shells, deficiency in displacement finite elements 3—22618
thin-walled pipes with curved axes, calculation *(Russian)* 3—19432
thiourea, elastic energy and preferential rectilinear dislocation lines *(German)* 3—14868
three-dimensional wedge, mixed boundary problems *(Russian)* 3—3961
Timoshenko-type shell theory, complex eqns. and static-geometric analogy 3—22633
torsion, hyperelastic, incompressible, second-order, reln. to deformation 3—22614
torsion of cylindrical shafts made of micropolar material 3—35569
transmission of force between two half-planes 3—531
transversely isotropic spherical shell coupled with elastic foundation, stability 3—28870
transversely-isotropic cylindrical shells in nonhomogeneous subcritical states, stability, numerical calculations *(Russian)* 3—22639
Tresca-type plastic dielectric in simple shear, hypoelastic theory of optical props. 3—32352
two-dimensional half-space contact theory 3—22646
two-dimensional theory, eigenvalues 0 and −1 of spectra of integral operators *(German)* 3—13559
under fluctuating loads, regions of stability of 2nd-order system uniform pin-ended column 3—16683

elasticity continued
unidimensional momentless problem for elastic shell of variable thickness *(Russian)* 3—28886
variational principle of Hashin and Shtrikman 3—506
vibrations, nonlinear free, of elastic structures 3—32374
vibrations of cylindrical shells, effect of surface mass distrib. *(Russian)* 3—37839
wave propagation, continuum theory in laminated composites, elastodynamic model 3—26095
wedge, anisotropic, plane soln. under normal and shear loading 3—22644
wedge motion at constant super-Rayleigh subsonic velocity 3—22627
Westergaard eqns., modified, for plane crack problems, error 3—22625
work hardened elastic-plastic materials, dual-energy theorems 3—518
β' AgMg single crystals, operative slip systems and strain hardening 3—14915
Al(IO$_3$)$_3$.2HIO$_3$.6H$_2$O, piezoelec., elastic, thermoelastic and optical props. *(German)* 3—8524
Cd, Hookes law, deviations due to third order elastic consts. 3—17895
Cr wire drawn to 0.4-0,5 mm with Y, La, Ce or Gd impurities *(Russian)* 3—8878
CsPbCl$_3$, pulse ultrasonic investig. of elastic props. and detn. of phase transform. *(Russian)* 3—7813
Cu whisker, nonlinear elasticity and lattice anharmonicity 3—15112
Cu-Zn-Si alloys, pseudoelasticity and shape memory effect 3—21702
Fe-Ni invars influence of Mn on some physical props. *(Russian)* 3—8355
Ge amorphous, freq. depend. coupling const., elastic continuum limit l.f. Raman scatt. 3—8586
Ge$_{0.5}$Sn$_{0.5}$, amorphous, freq. depend. coupling const., elastic continuum limit, l.f. Raman scatt. 3—8586
InSb amorphous, freq. depend. coupling const., elastic continuum limit l.f. Raman scatt. 3—8586
MgO, hot-pressed, polycrystalline, ultrasonic meas. and distorted Kroner theory 3—36341
Mo, elasticity limit depend. on grain size rel. to Petch law 3—30171
(NH$_4$)$_2$SO$_4$ elastic compliance and dielec. meas. rel. to ferroelec. transition 3—30781
NaCl, single crystals, anomalous amplitude depend. of elastic modulus rel. to dislocation pinning 3—30172
Pb, La(Tz, Ti)O$_3$ ceramic, elastic and piezoelectric props., La dependence 3—18691
V$_3$Si, pressure induced elasticity changes 3—24176
Zn, Hookes law, deviations due to third order elastic consts. 3—17895
Zn, single crystals, anomalous amplitude depend. of elastic modulus rel. to dislocation pinning 3—30172

elasticity of liquids
see also compressibility of liquids
benzene, boundary layers, shear elasticity determ., dynamic method *(Russian)* 3—30167
film, Gibbs elasticity meas. technique and apparatus 3—28464
polyisobutylene, bubble inflation technique for obs. in equal biaxial extensional flow 3—453
thick liquid films and threads, Gibbs elasticity, thermodynamic theory 3—38708
water boundary layers, shear elasticity determ., dynamic method *(Russian)* 3—30167

elasto-optical effects
modulation and deflection phenomena, review 3—12112
polyethylene, optico-deformational absorption meas. *(Russian)* 3—5756
LiNbO$_3$, room temp. Brillouin scatt. obs. *(French)* 3—36864
NaF, light scatt. by second sound, thermo-optic and elastooptic parameters 3—34323
RbBr, stress-optical dispersion, 5750-2500Å 3—36889
RbCl, stress-optical dispersion, 5750-2500Å 3—36889

elastomers
see also rubber
adhesion theories, review 3—14926
friction in glass transition region, temp. and rate depends. on normal press. 3—27790
polyurethane soling, cut growth and fatigue 3—31156
rheological props. at low shear stresses 3—27777
thin section and replicas from it, low temp. and vacuum conditions 3—18719
viscoelasticity eqns., stat. derivation for homogeneous finite deform. 3—26757
Viton B fluorocarbon elastomer, chemorheology, long term aging 3—31185

elastoplasticity
axisymmetric buckling of uniformly loaded spherical caps undergoing plastic deformation, numerical soln. 3—37820
bar under repeated axial loading 3—32357
bending of rectangular plates with large deflection 3—22673
buckling of rectangular plates under edge loading, incremental theory, finite difference procedure 3—32353
cantilever bending and twisting 3—22659
circular bending of elastoplastic cylinder, application of Tresca's criterion *(French)* 3—37814
circular oriented plastic plates, states of stress and strain 3—22670
collapse mechanism of indefinite plate on elastoplastic continuum 3—32364
constitutive eqns. and directors in plastic and viscoplastic media 3—37821
constitutive eqns. for inelastic behaviour of components of fast breeder reactors 3—26524
crystalline solids, coupled thermoelastoviscoplasticity, finite-element formulation 3—38612
cyclic elasto-plastic notch stresses, graphical procedure, application to Al alloy 3—12469
deformation of thick-walled cylinder, non-linear integral eqn. for circular strain hardened zone *(Russian)* 3—28898
dual extremum theorems of boundary value problems in deformation theory 3—32362
elastic-plastic circular plates, large deflection analysis considering Bauschinger effect 3—6242

elastoplasticity continued
elastic-plastic medium subjected to temp. field and uniform tension, stress concentration around circular hole *(Russian)* 3—6238
elasto-visco-plastic media, ray method for soln. of shock wave propagation problem *(Russian)* 3—28897
elastoviscoplastic bodies, stability under compression *(Russian)* 3—544
elliptical plate, limit state determ. 3—37815
equi-area transformations, appl. to elastic-plastic rod torsion problem *(Russian)* 3—3965
fibre reinforced plastics, visco-plastic-elastic expression for stress/strain diagram under l.f. loads *(Japanese)* 3—18711
finite strain theory of elastic-inelastic crystalline materials 3—37807
finite strains, kinematics 3—35574
glass reinforced plastic plates with central metal layer, elastoplastic stability 3—24984
graphite, artificial generalization of theory of plasticity, stress-strain curves 3—39393
hyper elastic-plastic strip, finite bending 3—37819
limit state of indefinite plates on elastoplastic continuum, solution for collapse load 3—6253
metal pressure vessels reinforced with unidirectional glass-reinforced plastic 3—27761
nonhomogeneous pressure vessel, partially yielded, closed form soln. 3—19446
nonlinear wave propagation in elastic-plastic semi-space, due to moving and variable loading along boundary 3—37829
oscillator with geometrically nonlinear behaviour, forced vibrs. 3—16676
plate, bifurcation stress, uniaxial compression, yield surface corner lowering 3—32361
polymer, shock-compressed, physicomech. props. variation with loading 3—30204
pressure vessels, cyclic plasticity analysis, finite difference method 3—32925
prismatic semiinfinite rod, unloading wave *(Russian)* 3—10297
rigid-plastic spherical shell compressed by rigid plate 3—6254
rotating discs, exptl. verification of applicability of theory of small elastoplastic deformations *(Russian)* 3—28899
shakedown of plastic struct., mimimax principle for calc. of upper limits to strains 3—32363
sharply notched plates, stress analysis technique and notch tip blunting meas. 3—19146
steel, pearlitic, low cycle fatigue, heat treatment type depend. 3—37070
steel mild circular plate, large elasto-plastic deflection under cyclic loading 3—34613
strains in shake-down of structs. subjected to cyclic loads, upper bounds 3—16660
strengthened material, anti-plain strain around notch, mechanical failure *(Russian)* 3—37823
string, unloading boundary determ. in transverse impact 3—22689
thermodynamic constitutive theories *(Japanese)* 3—19450
time-hardening material under variable loading, deform., displacement and work bounds 3—22671
uniqueness of ideally elastoplastic problems for nonassociated flow rules case 3—19453
upper bounds on small displacements of structures under variable loading 3—22672
void growth under plane strain conditions 3—24959
wave propagation and reflection, finite difference soln. *(Russian)* 3—37841
work hardened elastic-plastic materials, dual-energy theorems 3—518
work hardening modes of elasto-plasto-viscous solids 3—21657

elastoresistance *see piezoresistance*

electrets
see also electrostatics
amorphous dielectric intermediate layer on NaCl substrate electret behaviour, epitaxial film growth 3—38746
anthracene, pressed polycryst., photoelectret state form., isopot. curves *(Russian)* 3—15449
anthracene, pressed polycrystalline photoelectret state formation *(Russian)* 3—2125
carnauba wax, produced under simultaneous effects of magnetic and electric fields, orientation phenomena *(German)* 3—8506
electret-key transducers, operation anal. 3—97
electrical cond. anisotropy 3—39110
epoxy resin, charge formation characteristics 3—39081
film, time-of-arrival detectors, for shock and detonation waves 3—22260
organic hydrocarbons thermophotoelectrets, depolarization currents 3—5157
perspex, dielectric breakdown in nonuniform fields 3—21362
perspex, polymethyl methacrylate, heterocharge decay 3—5155
perspex thermoelectret, variation in surface charge 3—2487
polyethylene terephthalate electret, effect of crystallisation on homocharge and thermally stimulated currents 3—26976
polyfluoroethylenepropylene foil, charging using liquid contacts 3—8505
polymer, book contrib. 3—11891
polymer foils, electron irrad., currents, charges, voltage buildup 3—36841
practical applications, review 3—8508
PVC, polarizing field effects on fabrication and characteristics, vacuum obs. 3—39082
thermoelectret, volume polarization determ., sectioning technique 3—2488
thermoelectret and photoelectret states of ZnO-Boswellia Glabra mixture used for electrophotographic coatings 3—22393
thermoelectret charge of sealing wax, prep. temp. effect, barrier and bulk polarisation 3—39080
Ag_8GeS_6, argyrite, depolarizing and thermodepolarizing state *(Russian)* 3—34287
Ag_8SnS_6, canfieldite, depolarizing and thermodepolarizing state *(Russian)* 3—34287
CaF_2, space-charge electret, bilinear depolarisation dynamics 3—39094
CdS single crystal, persistent internal polarisation variation with illumination intensity 3—34289

electrets continued
CdS:S system as photoelectret electrophotographic layer, photopolarisation study 3—36833
PSe, P_2Se_3 and P_2Se_5, photoelectret behaviour *(Russian)* 3—8220
SbSI, deep centres and photopolarization 3—24649
$SbSI_xBr_{1-x}$ solid soln., photoelectret and ferroelec. polarization, mechanism *(Russian)* 3—8539
SbSeI, deep centres and photopolarization 3—24649

electric actuators
linear motion generator, for physiological research 3—25986

electric admittance *see admittance*

electric amplifiers *see amplifiers*

electric arc furnaces *see arc furnaces*

electric arc welding *see arc welding*

electric arcs *see arcs (electric)*

electric breakdown
see also corona; discharges (electric); electric breakdown of gases; electric breakdown of liquids; electric breakdown of solids; electric strength; flashover; sparks; Zener effect
American Vacuum Society, symposium, Chicago, USA (1972) 3—37608
ceramic porous layer, breakdown in vacuum and in air *(Russian)* 3—15452
chlorobiphenyls with dissolved water and air, space charge effects 3—18415
dielectric insulation, thermal instability, transient d.c. and a.c. voltages *(Hungarian)* 3—12097
dielectric liquid breakdown, photographic study with picosecond time resolution 3—244
discharges in vacuum, surface processes on discharge-cleaned electrodes *(Russian)* 3—7588
gaseous gaps, high pressure, calc. 3—14606
high pressure discharge gaps, breakdown voltage meas. 3—28602
insulating materials, partial discharges recording method 3—32112
insulating materials *(French)* 3—30759
internal field emission and impact ionization in Zener diode for reverse field breakdown 3—2098
large sphere-plane gaps 3—7580
long air gaps under switching pulses *(Japanese)* 3—14621
nonuniform long gaps in compressed air 3—7582
p-n junction, heterogeneity influence *(Polish)* 3—24500
perspex electrets in nonuniform fields 3—21362
plasma sheath, collision-dominated, elec. breakdown meas. 3—36198
semiconductor diode, avalanche breakdown delay *(Russian)* 3—8255
surface breakdown in vacuum 3—21131
transformers and circuit breakers *(German)* 3—15979
u.h. vacuum, effect on current emission 3—9913
vacuum initiation with Mo electrodes 3—33411
voltage calc., gaseous liquid and solid insulating materials, Schumann's statement, power functions for α ionisation *(German)* 3—4517
Al_2O_3 film, anodised, comparison of step and ramp voltage breakdown 3—8518
Ar, laser induced, electron density growth dependence on magnetic field 3—7310
Cs Townsend discharge, breakdown potential and first ionisation coeff. 3—14415
Si, p-n, p-n-p structures, i.r. observation 3—24501
Ta_2O_5 film, anodic, rel. to mechanical props. and microstruct. 3—1684

electric breakdown of gases
air, in CO_2 laser cavity, and plasma mirror formation and effects *(Russian)* 3—1527
air, microwave generated ionised sheath in coaxial transmission lines 3—17694
air, pulsed interferometric holography of laser-produced breakdown 3—33189
air, spark discharges, nanosecond, breakdown and channel production 3—30037
electronegative, sparking voltage rel. to elec. field uniformity 3—17697
generation of sparks in air by mode locked laser pulses, single pulse mechanism 3—23939
high frequency flare discharge, elastic field effects, dep. air flow rate 3—33405
initiation mechanism, review 3—38346
laser induced, u.v., threshold intensity, focal volume dependence 3—23940
laser pulse breakdown 3—33409
laser-beam induced, focal spot size depend. arising from particulate ionization 3—38465
laser-induced gas breakdown with preionisation 3—29825
laser-induced initiated by u.v. photoionisation in presence of spark 3—17492
loss mechanisms in breakdown at 10.6 micron 3—23665
macron clouds, charging and discharging, role of gas breakdown 3—35657
pulsed nanosecond, mechanism 3—36220
superalloy model in high pressure gaseous oxidiser, characteristics, sparks, arcs *(Russian)* 3—26911
Townsend sparking formulae for uniform electric field in air 3—23936
vacuum, triggering, by low velocity microparticles 3—4683
Ar, effect of c.w. laser on pulsed breakdown threshold 3—17491
Ar h.f. discharge stability at 95-105 MHz rel. to industrial trace gas chromatography *(French)* 3—432
CO, microwave breakdown 3—23666
H_2, CO_2 laser-induced breakdown 3—17689
He h.f. discharge stability at 95-105 MHz rel. to industrial trace gas chromatography *(French)* 3—432
Ne-Ar mixtures, pressure dependence of primary ionisation in Townsend discharge 3—17702

electric breakdown of liquids
dielectric, prebreakdown, obs. 3—2494
dielectric breakdown under recurring discharge, high-voltage meas. 3—11514
insulating liq. photographic techniques 3—13342

electric breakdown of liquids continued
water, circuit transient following a pulsed discharge 3−36227
He at low temperatures, dielectric breakdown rel. to He pressure 3−7987

electric breakdown of solids
alkali halide crystal, electron avalanche breakdown induced by ruby laser light 3−30757
alkali halide crystals, electric breakdown mechanism in presence of microroughness on the cathode *(Russian)* 3−8514
alkali halide crystals, laser destruction mechanisms and multiphoton ionization of impurity centres 3−5162
barium stearate 'built up' films, d.c. destructive breakdown field, temp. depend. 3−5161
barium stearate multilayer films, breakdown field temp. depend. 3−27469
breakdown polarity effect, theory 3−30758
chalcogenide glass, reversible thermal breakdown as a switching mechanism 3−18197
epoxy resin, elec. cond. and dielec. breakdown mechanism *(Japanese)* 3−8516
insulating film, localized breakdown, review 3−5159
Langmuir thin molecular films, dielec. breakdown thickness depend. 3−39095
m.o.s., dielec. breakdown rel. to nonuniform contact barriers, Na effects 3−21155
organic insulators *(French)* 3−13510
p-n junction with double error function doping profile 3−36662
polyethylene, dielec. breakdown strength determ. method for small test pieces *(German)* 3−15806
polyethylene, voltage stabilised, bimodal distribution of logarithms of times to breakdown *(German)* 3−24653
polymer, book contrib. 3−11891
polymer films, initial behaviour of excess electrons 3−39093
polymethylmethacrylate, mech. aspects *(Russian)* 3−2493
polystyrol, mech. aspects *(Russian)* 3−2493
PZT 65/35 ferroelec. ceramic, dielec. breakdown under shock loading 3−18416
refractories for electric storage heaters 3−27733
semiconductor overheating instabilities, low-temp. impurity breakdown 3−24395
transparent dielectrics, excitation of cascade ionization by strong alternating e.m. field *(Russian)* 3−8517
trimethylethyltin-based polymer thin films breakdown voltage *(Russian)* 3−8187
AgN_3, elec. breakdown and explosion, high speed photography 3−36838
Al_2O_3 film, in m.i.m. capacitor, rel. to visualization of defects by liq. cryst. layers 3−15284
Al_2O_3 thin films, electroforming and dielec. breakdown *(Russian)* 3−30530
CdSe, impact ionisation, breakdown, photoinduced switching, meas. of cond., Hall coeff., mobility, 4.2-300K 3−30487
p-Ge, autoemission volt ampere characts. with O_2 adsorption rel. to elec. breakdown 3−8709
Ge, impurity breakdown, origin of S-shaped I-V charact. 3−24443
p-Ge field emitter, I-V characts. 3−39219
NaCl, breakdown strength, temp. depend., −40 to +100°C *(Russian)* 3−18414
NaCl, rock salt, thickness depend. on breakdown voltage *(Russian)* 3−8515
$NaNO_2$, ferroelectric, and high field elec. cond. 3−5160
Si_3N_4, reactively sputtered, dielectric breakdown 3−34295
SiO film, in m.i.m. struct. *(Russian)* 3−15280
SiO_2, high elec. fields produced by corona charging, surface pot. meas. rel. to dielec. breakdown 3−24654

electric cables *see cables (electric)*

electric capacity *see capacitance*

electric cells *see cells (electric)*

electric charge
see also space charge
accumulation on fabrics and explosives, temp. and relative humidity effects 3−658
airless spray painting, dangerous electrostatic charging 3−661
anthracene, surface charge determ. 3−19236
antigravitational effects in behaviour of neutral particle in field of charged particle *(Russian)* 3−22727
beta active hot particles, intrinsic sedimentation velocity effect on their steady-state electrical charge in the presence of an impurity of a contaminant aerosol *(Russian)* 3−2771
capacitor electrodes, determination of charge for specific potentials *(Russian)* 3−32475
dislocation charge and surrounding charge cloud, nonlinear theory 3−7764
electrostatic charges formed by reduction of sensitization of Ag halide emulsions 3−2837
generation during washing of tanks with water sprays, math. methods 3−654
generation during washing of tanks with water sprays, meas. and interpretation 3−653
generation during washing of tanks with water sprays, mechanism studies 3−655
generation during washing of tanks with water sprays 3−652
mica substrate, effect on epitaxial growth 3−1927
mica surface, decoration of elec. fields *(Russian)* 3−5050
molecule, electrical neutrality testing method 3−33070
moving, field in collisionless plasma 3−23820
polyfluoroethylenepropylene foil, charging using liquid contacts 3−8505
polymer, generation and decay of charge produced by frictional rubbing 3−2169
polymer foils, electron irrad., currents, charges, voltage buildup 3−36841
rubber-glass contact, elec. double-layer force meas. between liquid immersed contact surfaces 3−6020
on stainless steel surface, effects of H_2, charged particles, illum. and electric fields on work function 3−24496
surface activity centres revealed by electrical, magnetic and thermal diffusion decoration 3−15052

electric charge continued
AgCl(Br)(I), surface contacting water, zero charge point temp. depend. 3−8248
Au powder particle adhesion, charge contribution 3−5049
Cu/Teflon system, static electrification 3−2170
Ge, surface elec. contour changes on illumination, memory and photoepitaxy 3−8054
LiF, yield stress minima and apparent isoelectric temp. relationship 3−20792
NaCl, surface relief, cellular struct. obs. using sublimation of AgCl films *(Russian)* 3−8240
NaCl quenched single crystals, charge developed by local plastic deform., rel. to quenching temp. and contamination 3−2155
NaCl substrate, effect on epitaxial growth 3−1927
NaCl surface, cryst. growth conditions effect on electric relief 3−33985
Si, surface elec. contour changes on illumination, memory and photoepitaxy 3−8054
Si insulating cpds., charging-up phenomenon in Auger electron spectroscopy 3−30917

electric coils *see coils*

electric condensers *see capacitors*

electric conduction
chlorobiphenyls with dissolved water and air, space charge effects on breakdown 3−18415
cylinders, long thin conducting, effect on Van der Waals forces, appl. to long conjugated mols. 3−17479
liquid semiconductor, migration mechanism determ. 3−33902
m.i.m. structure, V_2O_5-P_2O_5 glass based, temp. depend. *(Russian)* 3−2190
m.i.m. structure, V_2O_5-P_2O_5-CaO glass based *(Russian)* 3−27318
polymer, book contrib. 3−11891
random lattice under potential gradient 3−4983
$B_{12}C_3$, mechanism determ. 3−24429
β-Cu_3Sb, electrotransport obs. and mechanism *(German)* 3−24298
SbSI, cond. mechanism determ. 3−33955
Se, barrier model of conduction for d.c. meas. depend. on temp. *(German)* 3−33905
Si_3N_4 layer, in m.n.o.s. struct., cond. mechanism 3−27316
SiO_2 layer, in m.n.o.s. struct., cond. mechanism 3−27316

electric conductors *see conductors (electric)*

electric connectors
see also cable jointing
Au/Cu planar couples, mass diffusion of base metal to electroplate surface 3−38685

electric control equipment
see also controllers; electric actuators; electric sensing devices; switches; telecontrol equipment; telemetering equipment
astronomical iris photometer (Becker's), control system *(Italian)* 3−35209

electric control gear *see electric control equipment*

electric current
see also arcs (electric); corona; current density; current fluctuations; discharges (electric); eddy currents; electrojets; fault currents; leakage currents; short-circuit currents; sparks
a.c., effect on steady-state characts. of a Josephson junction *(Russian)* 3−8310
current ratio in r.f. sputtering, det. by Langmuir's theory *(German)* 3−5245
current-eddy blobs, derivation of virial theorem 3−25172
dielectric materials, transient currents *(French)* 3−34294
discharge of oscillating electron, dependence of current on system parameters *(Russian)* 3−11518
electrojet, equatorial zone current determ. 3−34927
glow discharge, toroidal radial magnetic field effect on current-voltage characteristic 3−17682
induction in conducting thin plate *(French)* 3−32488
inert gas afterglow plasma, cylindrical Langmuir probe meas. 3−14584
magnetic field analysis of line currents, Biot-Savart modification 3−37921
parallelogram of linear currents, analysis of magnetic field *(French)* 3−4059
solar flare particle accel. mechanism determ. from X-ray spectra 3−28145
Ar solid, electric currents and bubble induced by α particle source 3−30505
Hg arc discharge, limitation 3−14617

electric current control
ion current of electron impact ion source 3−25842

electric current measurement
see also ammeters; galvanometers
electrometers, various types, problems in measuring very low values *(Polish)* 3−25812
fibre optic technique using Faraday rotation 3−6028
galvanometer, mirror type, over-damped, parameter meas. 3−35440
high resistivity materials, thermally stimulated currents 3−28601
h.v., optical technique based on Faraday effect 3−19655
ionisation current sources calibration, capacitor charging method *(Russian)* 3−9995
leakage current from decaying process *(Japanese)* 3−19234
logarithmic picoammeter for exposure and dose meas. in electron microscopy of polymer crystals 3−346

electric discharge machining *see spark machining*

electric discharges *see discharges (electric)*

electric distortion
see also fading
chirped Gaussian pulse, by ionosphere 3−39550
e.m. wave reflection from moving dielectric half-space 3−4064
hearing aids, amplitude compression and distortionless amplification 3−3459
intermodulation distortion produced by centre clipping 3−3638
mesa-stripe double-heterostructure laser, direct modulation up to 1 Gbit/s 3−16853

electric distortion measurement
perceptibility and meas. method of nonlinear distortion of speech and music *(Japanese)* 3−5784

electric domains
- *see also ferroelectric materials*
- acoustoelectric, rel. to interband absorpt. in field of intense acoustic flux *(Russian)* 3−27488
- $BaTiO_3$, photodomain effect 3−8528
- ferroelectric, domain walls, local electron states *(Russian)* 3−8538
- ferroelectric, microdomain behaviour ind diffuse phase transition region 3−15462
- ferroelectric, thermodynamic relations for domain struct. 3−34312
- ferroelectrics, surface elastopolarization waves at domain boundaries *(Russian)* 3−8540
- ferroic state shift, second order, optical discernibility between domains 3−12101
- Gunn, dynamics, in presence of field-independent trapping 3−18151
- liquid cryst., MBBA, nematic, domain formation threshold variation under d.c. dynamic scatt. 3−18422
- polarisation by laser beam, reversible, ferroelectric memories, triglycine sulphate *(French)* 3−22967
- semiconductor, acoustoelec. domains, piezoelec. potential and carrier distrib., microwave absorpt. and Brillouin scatt. 3−5040
- semiconductor, feasibility of suppression of Gunn domains *(Russian)* 3−8199
- semiconductor, high field domain modes, due to field depend. carrier diffusion 3−33908
- semiconductor, negative differential mobility, electric field profile rel. to formation 3−8188
- semiconductor, nonpiezoelec., acoustic wave generation by moving domains *(Russian)* 3−2145
- semiconductor, piezoelec., microwave absorpt. by bunched carriers in acoustoelec. domains 3−30896
- stibiotantalite, mineral, ferroelec. domain structure obs. 3−24665
- tri-glycine sulphate, ferroelec. domain struct., electron microscope obs. 3−30777
- triglycine fluoroberylate: $Cu^{2+}(Cr^{3+})$, ferroelec. props., domain structure 3−39099
- triglycine sulphate, ferroelec. domains, direct obs. by second harmonic generation by laser 3−24658
- triglycine sulphate crystals, growth conditions effect on domain structure 3−39100
- $AgNO_2$, growth from acetonitrile soln., domain struct. 3−30932
- $BaTiO_3$, a-domain, lateral motion 3−34314
- $BaTiO_3$, α-domain, antiparallel switching 3−21376
- $BaTiO_3$, electron microscope obs. of ferroelectric domains in low temp. phase 3−30765
- $BaTiO_3$, ferroelec., domain struct. and phase transition, illumination influence 3−15460
- $BaTiO_3$, ferroelec. switching, kinetics of domain wall motion 3−39102
- $BaTiO_3$, internal friction, influence of domain struct. 3−36845
- $BaTiO_3$, obs. by convergent electron beam diffr. method 3−24657
- $BaTiO_3$, rel. to stabilisation of spontaneous polarisation *(Russian)* 3−12105
- $BaTiO_3$ polycrystalline, constant electric field influence on dielectric props. *(Russian)* 3−8532
- $BaTiO_3$ single crystals, rel. to compressive deform. 3−38608
- CdS, acoustoelec. multi-peak domain propag., Brillouin scatt. study 3−24481
- CdS, Brillouin scatt. from acoustoelectrically amplified flux domains, dispersion spectrum 3−34352
- GaAs, acoustoelectric domains, on and off axis, observation by stroboscopic illumination 3−5037
- $Gd_2(MoO_4)_3$, ferroelastic-ferroelec., antiphase boundaries and their interactions with domain walls 3−24659
- $Gd_2(MoO_4)_3$, X-ray topographic study of ferroelec. phase transitions and domains 3−15461
- Ge, high-field domain in electron-hole plasma 3−24444
- N-Ge:Au, hysteresis of I-V characts., and props. of elec. domains *(Russian)* 3−2100
- n-InP, dipole domain measurements for determination of velocity/field characteristics 3−8186
- n-InP, velocity field characs., dipole-domain obs. 3−30484
- KD_2PO_4, influence on elec. field gradient and spin-phonon interactions, n.m.r. obs. 3−24660
- KD_2PO_4, phase transitions, domain influence on elec. field gradient and spin-phonon interactions 3−2413
- KH_2PO_4 interdomain and domain defect interactions 3−8529
- $KNbO_3$, orthorhombic, domain struct. and single domain cryst. characteriz. 3−15463
- $KNbO_3$ single cryst., domain struct., optical studies 3−21368
- $LiTaO_3$, ferroelectric domain reversal 3−8530
- $(NH_4)_2Cd_2(SO_4)_3$, optical distinguishability of domains 3−24662
- $NaH_3(SeO_3)_2$, optical obs. 3−39106
- $NaNO_2$, optical second harmonic generation during ferroelectric switching 3−15466
- $NaNO_2$, X-ray topographic study of ferroelec. phase transitions and domains 3−15461
- Nb supercond., domain pattern characts., flux line interaction, flux line lattice 3−2197
- $Pb_5Ge_3O_{11}$, ferroelec., antiparallel 180° domains, X-ray topographic obs. 3−12102
- $Pb(Zn_{1/3}Nb_{2/3})O_3$ and $Pb(Cd_{1/3}Nb_{2/3})O_3$, microdomain behaviour in diffuse phase transition region 3−15462
- $Pb(Zr,Ti)O_3$, La_2O_3-modified, temp.-depend. ferroelec. domain alignment 3−5168
- SbSI, photodomain effect and deformation 3−34311
- SbSI, pleochroism associated with domain struct. 3−36852
- SbSI, semiconductor-ferroelectric, domain structure rel. to local states 3−5172
- $SbSI_xBr_{1-x}$, ferroelec. semicond., nonequilib. carrier density influence on phase boundary form. 3−39113
- SbSeI, semiconductor-ferroelectric, domain structure rel. to local states 3−5172
- $Sr_2Nb_2O_7$, ferroelectric single cryst., single domain obs. from electromech. coupling factor 3−21373
- $SrTiO_3$, distortion enhanced optical absorption, via electron scattering at fluctuating domain boundaries, at the cubic to tetragonal transition 3−12149
- Te, acoustoelectric domain formation 3−33959

electric charge continued

electric domains continued
- Te, propag. and generation in the temp. range 77°K to 293°K 3−18156

electric double refraction *see electro-optical effects*

electric drives
- piezoelectric, for intracavity tilted etalon used for ion laser tuning *(German)* 3−32543

electric field effects
- *see also particle optics; Stark effect*
- a.c. fields, 100 to 200 kV/m, effects on mice, modified growth of progenies 3−9716
- acceleration of auroral electrons by electric field of pulsations 3−34914
- asymmetry effect on ionic field emission image formation 3−19661
- p-azoxyanisole, X-ray diffr. obs. under simultaneous action of electric and mag. fields 3−33454
- boiling dielectric fluids, heat transfer, ponderomotive forces 3−1801
- bubbles in KCl and NaCl, elec. field induced motion rel. to X-ray irrad. and impurities *(Russian)* 3−20730
- carbon tetrachloride boiling hysteresis, electric field effect 3−38664
- charged particle motion in free vortex flow field, applied electric field effects 3−33330
- charged particle transport props. in one dimension 3−23813
- charging of falling and colliding water drops 3−649
- colloid, irreversible coagulation criteria in elec. field 3−34657
- continuum polaron theory, equation of motion approach appl. to dynamical props. 3−36566
- D-region electron heating by a current carrying wire near earth's surface 3−12813
- damping of electron plasma oscills. with large phase vels. 3−4645
- deformation of homogeneous nonpiezoelectric anisotropic dielectric 3−6269
- dielectric liq., rising effect at high voltage electrode rel. to elec. field 3−39089
- ditolilmethane and diphenyl mixture, convection, electrodes, Schlieren pictures *(Russian)* 3−27146
- DR-currents belt, charged particle trajectory determ. for periodic fields 3−25303
- dye laser, rhodamine 6G in methanol, emission rel. to elec. field 3−6480
- electrets in carnauba wax, produced under simultaneous effects of magnetic and electric fields, orientation phenomena *(German)* 3−8506
- electrostatic field penetration into metal surfaces, analytic estimates 3−5045
- epoxy resin, d.c. cond., transverse elec. field effects, majority carrier polarity 3−18143
- exciton spectrum, elec. field depend. of line intensity and splitting 3−4979
- F-centre ENDOR spectra, effects of applied electrostatic fields and hydrostatic press. 3−18393
- fibre orientation in electrostatic field, statistical minimum angle determination *(Russian)* 3−29003
- field ionisation, temperature dependences 3−26575
- gaseous ions, energy partitioning 3−33332
- glass, low temp. thermal conductivity in electric and magnetic fields 3−1849
- harmonic settling transitional process appl. to disperse medium, investigation *(Russian)* 3−9015
- n- hexane, superheated absolute thermodynamic stability in perturbing elec. field, nucleation induction 3−20866
- high frequency flare discharge, electric field effects, atomic absorption 3−33405
- h.v. overhead line field strength, rel. to physiological effects *(German)* 3−9703
- ion velocity distrib. in weakly ionized gas in uniform electric field of arbitrary strength 3−4519
- ionospheric heating by transverse fields, night variations 3−25264
- ionospheric parametric plasma instabilities, effect of h.f. electric field 3−16020
- Knight shift oscillations and spin-lattice relax in crossed fields 3−18382
- liquid cryst., cholesteric-nematic transition, elec. field induced, rel. to dielec. anisotropy 3−4717
- liquid cryst. mixed, cholesteric-nematic transition, a.c. elec. field induced 3−17736
- liquid crystal, nematic, deformation in elec. field 3−14681
- liquid crystals, twisted nematic, electric field induced domains 3−26970
- liquid drop EHD, time-depend. problem 3−7440
- liquid surface stability 3−4607
- magnetised collision-dominated plasma, kinetic theory of density fluctuations 3−15996
- p-methoxybenzilidene p-butylaniline, liquid crystal, electrochem. props. *(French)* 3−36261
- multiple field ionisation mechanism 3−26709
- nitrobenzene/ethane dihalogenoderivatives, dielec. permittivity rel. to elec. field 3−30741
- m-nitrotoluene/ethane dihalogenoderivatives 3−30741
- p-n-nonyloxybenzoic acid, liquid cryst., mol. alignment, elec. and high mag. field effects 3−38535
- optical absorption, quantisation eff. with elec. field dependence 3−36009
- paraelectric resonance lineshape, internal field effect, theory 3−27460
- photographic emulsion sensitivity at low temps. *(Russian)* 3−241
- photographic emulsions, orientation of development centres in monocrystals by electric field *(Russian)* 3−230
- plasma acceleration in crossed electric and magnetic fields 3−29947
- plasma anaomalous heating induced by very strong high frequency electric field 3−29992
- plasma conversion of trapped charged particles into untrapped particles in h.f. electric field 3−17651
- plasma e.m. slow waves, excitation by longitudinal electric fields 3−29953
- plasma heating in CO_2-N_2-He laser 3−19596
- plasma induced electric field effect on propagation of relativistic electron beam 3−33341

electric field effects continued
plasma ion-ion instability induced by a.c. electric fields 3−38459
polaron energy levels, electron-phonon interactions, magnetic and Coulomb field effects 3−36563
polarons, electron-phonon interactions, ionic crystals, polar semiconductors, conf., Antwerp, Belgium (Aug. 1971) 3−36558
propane, laminar flame in a discharge, elec. field effects, photography 3−36211
pulsar model for electron-positron pair prod. 3−22090
resonance trapping and drift velocity in inert gases of electrons 3−23667
semiconductor, electron density of states calc. in external elec. field 3−1969
semiconductor, many-valley, charge density fluctuation in strong elec. field 3−5003
semiconductors, many-valley, electrical conductivity in strong alternating fields 3−24446
steel, stainless, effects on work function rel. to elec. charge 3−24496
steel, stainless, on work function 3−33984
styrene-methylmethacrylate copolymer, suspension, particle interaction, frequency effect of external elec. field 3−39403
superconducting film, conductivity, nonlinear external field effects 3−8301
surface self-diffusion coeff. parameters variation 3−18021
suspension, aggregation and paired interaction of particles in elec. field 3−34654
synthetic resin cross-linking, rel. to conductivity, optical and thermal props. 3−2097
triglycine sulphate alternating, pyroelectric coefficient and polarisation *(Russian)* 3−39097
tris-sarcosine calcium chloride:Mn^{2+}, influence on Mn^{2+} spectra 3−8433
water-in-oil emulsion coagulation *(Russian)* 3−9016
Al film, supercond. nonlinear elec. field depend. near T_c 3−8302
Al_2O_3, influence of electric field on parameters of impurity centre 3−36951
Al_2O_3:Cr^{2+}(Mn^{3+}), on acoustic e.p.r. spectra 3−8428
Au film, epitaxial growth on NaCl, influence of elec. field on orientation *(Russian)* 3−30364
Au film, vacuum deposition, orientation and particle arrangement 3−1934
BiOBr, long wavelength fund. absorpt. edge rel. to elec. field and press. *(Russian)* 3−8609
BiOI, long wavelength fund. absorpt. edge rel. to elec. field and press. *(Russian)* 3−8609
CO, laminar flame in a discharge, elec. field effects, photography 3−36211
CdS single crystals, effect on optical quenching 3−15223
CdTe low resistivity films, d.c. e.m.f. in a.c. fields *(Russian)* 3−11964
Cu_2O, modulated excitonic absorption in elec. and mag. fields 3−2037
Cu_2O, optical absorpt. spectra obs. of Mott excitons in elec. field 3−8129
GaAs, electron energy relax. time as function of elec. field 3−24420
GaAs:Cr, semiinsulating, photocond., electric field and thermal quenching *(Russian)* 3−5031
Ge, electro-optical effects on surface levels in external elec. field 3−2163
Ge diffusion of Li ions, drift velocity, depth of drift, electric field configuration 3−33697
n-Ge:Ni, local negative photoconductivity in strong electric fields 3−24479
n-Ge:Ni, surface domains in strong elec. field, 77-300K *(Russian)* 3−8245
H atom-electron system state in an intense e.m. field 3−35953
InP, electron energy relax. time as function of elec. field 3−24420
InSb, effect of weak, longit. static field on transverse e.m. wave propag. along magnetostatic field 3−2121
Mg drop pumping by travelling electric potential wave 3−10098
Ne flash tube, use of alternating clearing fields to reduce sensitive time 3−28670
PbI_2, rel. to excitons at band edge 3−33856
$PbMoO_4$:Mn^{2+}, electric field effect in paramagnetic resonance 3−34195
SbSI, absorpt. edge shift rel. to elec. polarization 3−15507
Se, X-ray irrad., electrophotographic layer, fatigue mechanism *(Russian)* 3−33947
Si p-n junctions, 1/f noise on surface, external field effects, source *(Russian)* 3−27305
SiO_2 film, silica, ion movement in applied field, diffusion eqn. calc. *(German)* 3−15037
Ti-butylalcohol suspension, particle interaction, frequency effect of elec. field LiCl conc. effect 3−39403
W, corrosion, H promoted, by O_2 in elec. field, surface topography changes 3−30359
W, field evaporation, model and expt. 3−27600
Zn, electroplastic deform., temp. and rate depend. *(Russian)* 3−24186
ZnS:Cl photoluminescence, effect of trapezoidal electric field *(Russian)* 3−36944

electric field measurement
see also field plotting
atmospheric electricity by balloons 3−12756
automatic equipment, study of acoustoelectric phenomena 3−35441
detector, saw-tooth and ramp generator circuits, testing *(Spanish)* 3−28606
electrostatic field horizontal component in lower atmosphere, daily drift meas. *(German)* 3−37233
electrostatic wave dispersion relation meas. technique 3−17604
internal electrostatic field, determ. for anthracene 3−19236
ionic and particulate clouds, ballistic probe system 3−666
ionosphere, electric component of e.l.f. hiss 3−16016
ionospheric v.l.f. obs. from satellites, high-latitude electrostatic emissions 3−16015
lightning discharges, oscillographic method 3−21936
magnetosphere, critical review 3−3145
photosensitive semiconductor, nonuniformities, obs. device *(Russian)* 3−6018

electric field measurement continued
plasma, h.f. field meas. by stimulated Raman scatt. and two-photon absorpt. on excited atoms 3−4672
plasma clouds, expts. 3−3042
radiofrequency d.c. field, meas. using paramag. system, classical theory *(French)* 3−7053

electric field strength measurement *see electric field measurement*

electric fields
see also crystal internal fields; electric field effects; electric field measurement; electromagnetic fields; electromagnetic waves; field plotting
a.c., from h.v. transmission lines, service personnel protection, protective clothing, screening devices 3−9717
anisotropic crystals, analysis *(Russian)* 3−32102
aperture near-field calc., accuracy of Kirchhoff boundary values *(German)* 3−37922
auroral latitude, review of observational data 3−31391
auroral zone, electric fields meas. 3−12812
axially symmetric electron optics systems, e.s. field computation 3−802
capacitors, axisymmetric electrostatic fields calculation by numerical method *(Russian)* 3−32475
chlorobiphenyls with dissolved water and air, static distribution rel. to breakdown 3−18415
corona discharge, in coaxial cylinder, field distribution calc. 3−14605
corona discharge, in two-phase aerodisperse medium, rel. to electron-ion equipment 3−13671
dielectric nonlinear, calc. of cavity field 3−22701
discharges, in gases gaps, high pressure, calc. 3−14606
distribution around isolated stranded conductor, comments 3−37923
due to double lamina, double circular disc and double spherical cap 3−4057
eddy currents calculation in axially symmetric a.c. current carrying conductors, by computer *(Russian)* 3−32485
electrojet, equatorial zone field determ. 3−34927
in electrolytes, calc. 3−27880
e.m. induction in infinite plane sheet with circular hole, varying mag. field 3−26187
geophysical fields, cartographic representation method 3−25321
helical e.s. field, motion of small charged particle 3−13768
hollow cylindrical cathode, elec. field distrib. in cathode fall, radial model *(German)* 3−4690
h.v. overhead line, strength at ground level and span centre rel. to physiological effects *(German)* 3−9703
inhomogeneous electric fields of plane electrodes, test for surface condition *(German)* 3−3830
inner radiation zone, electron transport mechanism 3−12820
ionospheric l.f. equatorial fluctuations and relation to turbulence 3−16017
ionospheric neutral gas, three-layer model of small scale dynamo 3−25265
ionospheric potential electric field eqns., iteration method 3−25266
magnetospheric, INJUN 5 obs. 3−3146
magnetospheric potential electric field eqns., iteration method 3−25266
magnetospheric variations, relationship with auroral activity and geomagnetic perturbations 3−16047
medium with nonlinear conductivity, thermal electric fluctuations under quasi-stationary conditions *(Russian)* 3−37919
m.o.s. structure, electrostatic attenuation of the longitudinal field in near-surface region *(Russian)* 3−24521
neutron star accretion, surrounding electric field appl. to X-ray source models 3−37283
p-n and Schottky junctions obs. by liquid crystal technique 3−38887
p-n heterojunction, nondegenerate, capacitance, elec. field, mode *(Russian)* 3−8258
in plasma, collisionless, due to moving test charge 3−23820
plasma, electric field anomaly of near wakes 3−26907
polar-cap electric field distributions, rel. to interplanetary magnetic field direction 3−12829
radiation belts, electric field induced by slowly decaying ring current 3−12828
seawater attenuation used as gradient sounding method 3−25342
semiconductor, negative differential mobility, form and stability of electric field profiles 3−8188
semiconductor or insulator with small p.d. applied to long specimen *(French)* 3−33895
spheroidal gas inclusion in dielectric, surface conductivity effect *(Russian)* 3−6393
spline fitting method for subgrid resolution of field due to current distrib. 3−26768
static, 3-dimensional, potential calculations *(Russian)* 3−32484
static, in homogeneous media for given source distribution, integral characteristics *(Russian)* 3−32486
static fields calculation in piece-wise-homogeneous anisotropic media *(Russian)* 3−32483

electric filters *see filters*

electric furnaces
see also arc furnaces; resistance furnaces
induction, construction, refractory concrete applic. *(German)* 3−15765
induction furnace for unidirectional solidification studies 3−13264
industrial, construction, refractory concrete applic., advantages *(German)* 3−15764
laboratory oven, programmable proportional regulator for temp. control *(German)* 3−32046
tank furnaces for melting of Pb containing glass 3−22340

electric generators
see also d.c. generators; magnetohydrodynamic convertors; turbogenerators; Van de Graaff generators
deflector-generator circuit, of proton synchrotron 3−32127
design by holographic technique *(German)* 3−37642
high current, arc driver operation 3−11521
low-current (10^{-10}A), using ionization chamber, for testing current meas. devices *(French)* 3−10008
for oceanographic buoys, patent 3−12870

electric glow *see corona*

electric heaters *see electric heating*

- **electric heating**
  - *see also drying; electric furnaces; heating elements; induction heating; radiofrequency heating*
  - ceramic insulating materials, pipes, requirements, applications *(German)* 3-12431
  - solid cylindrical Cu block, electric resistance heating for comparison of transient and steady-state nucleate boiling 3-11733
  - storage heaters, refractories, electric breakdown 3-27733
  - wire heater embedded in glass for heating glass tubes 3-9992
- **electric heating elements** *see heating elements*
- **electric ignition**
  - airless spray painting, safety measures to avoid igniting sparks 3-661
  - plasma jet generator, electrical characteristics, obs. *(Korean)* 3-11508
  - risk, due to static on outer clothing 3-657
- **electric machine testing** *see machine testing*
- **electric machine theory** *see machine theory*
- **electric machines**
  - *see also electric generators; machine bearings; machine testing; machine theory; rotors*
  - permanent magnet suspension systems, rotational decay experiments 3-35653
  - vibration, optimal parameters for minimal dispersion of mechanism *(Russian)* 3-28922
- **electric moments**
  - *see also atomic electric moments; molecular moments; nuclear electric moment*
  - acrylate (monomer) solns. in microwave region, dielectric props. 3-34292
  - alkali metal hydrides vibrational, rotational consts., dipole moment and binding energy calc. using model potential functions 3-38271
  - aromatic hydrocarbons, planewise summation of point dipole-dipole interactions 3-18102
  - benzene derivatives, π-dipole moments calc. by SCF-MO method 3-11209
  - benzoic acid, elec. dipole moment and hydrogen bonding 3-7174
  - carbazole, direction of the transition moment and dipole moment of the first excited singlet state *(German)* 3-26652
  - cyclohexene oxide, μ-wave spectra, rot. consts. and elec. dipole moment components 3-29690
  - diatomic mols., Born-Oppenheimer approx. breakdown, dipoles moment and nucl. quadrupole coupling const. effect 3-29596
  - diatomic mols., dipole moment and polarisability anisotropy calc. from Stark effect data 3-29632
  - dioxydinaphthyl film, vibr. excitation, dipole moment var. meas. 3 -23573
  - dipole scattering from perfectly conducting sphere in homogeneous lossy medium 3-3175
  - disperse medium, sinusoidal field effect, polarised particle moment determ. *(Russian)* 3-9015
  - formaldehyde, absorpt. spectra, vibronically induced transitions dipole moments calc. 3-33113
  - formaldehyde, CNDO calc. of dipole moment derivatives and i.r. intensities 3-29630
  - halofluorophosphines, dipole moments, polarization model 3-7176
  - Herżberg-Teller induced intensity, calc. approximation 3-14359
  - heterogeneous organic compounds in dilute solution, dielectric relaxation, dipole moments calc. 3-39084
  - hydrogen-bonded complexes, charge transfer theory and relation between dipole moment energy and enhancement 3-20207
  - methylphosphine boranes, dipole moments, polarization model 3-7175
  - molecular crystals, calc. and use of retarded and static dipole sums in mol. exciton theory 3-18103
  - neutron, dipole moment, review 3-4244
  - nuclear explosions, atmospheric electrical effects 3-15965
  - organic mol. changes in dipole moment upon excitation, CNDO calc. 3-29634
  - polyatomic mols., higher-order vibr. intensities, rel. to dipole moment 3-33099
  - propylphosphines, dipole moments, polarization model 3-11240
  - Rochelle salt, phase transitions, microscopic theory 3-2498
  - semiconductors, III-V, effective charge transfer and covalent bonding 3-7656
  - square non polar lattice, light reflection and transmission, dipole-dipole interactions calc. 3-26203
  - transport crystals, multiphonon absorption of i.r. due to higher-order electric moments 3-18452
  - triazolopyrazines and triazolopyrimidine dipole moments 3-4452
  - Van Vleck-Weisskopf gas, excitation by reson. μ-wave pulse, response calc. 3-14358
  - BH_2 radical, coupling consts., force consts., dipole moments 3-29605
  - BrO, radical, μ-wave spectrum, dipole moment calc. 3-29694
  - CH_2^+ radical, coupling consts., force consts., dipole moments 3-29605
  - CN, dipole moments, CI calcs., for states of $^2\Sigma^+$ symmetry 3-4405
  - CO_2, line intensities in 2.0 μ region, rotationless dipole moment matrix elements calc. 3-29696
  - CS mol., dipole moment 3-23580
  - CSe mol., dipole moment 3-23580
  - ClF, dipole polarity and field gradient deriv. from Hartree Fock functions calc. 3-35998
  - ClF, elec. dipole moment sign determ. 3-33107
  - Eu^{3+}, primary and secondary solvation spheres, effect on electric quadrupole transitions 3-15536
  - $H^{79}Br$, dipole moment coeffs. calc. 3-11241
  - NF, gas phase e.p.r. spectrum and dipole moments 3-29724
  - NH_2 radical, coupling consts., force consts., dipole moments 3-29605
  - SiS, electric dipole moment sign determ. *(German)* 3-11230
- **electric permeability** *see permittivity*
- **electric potential**
  - *see also contact potential; overvoltage; surface potential; voltage control; voltage measurement*
  - activity meas., comparison of e.m.f. and vapour press. methods 3-36999
  - alkyd resin in acetone, elec. cond., potential distribution 3-39408
- **electric potential** continued
  - Coulomb pot. perturbation by contact interaction 3-4009
  - crystallisation, electric potential set up by phase change on single crystal membrane meas. *(German)* 3-9080
  - discharge pulses in air at low pressures, potential variation 3-38510
  - distribution on sphere with longit. depend. cond., appl. to magnetosphere 3-25302
  - electrostatic potential of point charge in dielectric solid, shell model 3-18407
  - e.m.f. meas. on cells with β-Al_2O_3 solid electrolyte 3-39449
  - e.m.f. standard monitoring using a.c. Josephson effect 3-3750
  - image pot. for charged particle moving towards surface, surface mode wave function 3-15231
  - land stations, electric potential gradient and conductivity power and cross power spectra 3-15972
  - mass spectrometer, electrostatic, pot. distrib. approx. *(Russian)* 3-6088
  - metal-Al_2O_3-SiO_2-Si structures, instability mechanisms, flatband voltage shifts 3-38899
  - Poisson's equation, soln. in two dimens., charged-particle flux determ. *(Russian)* 3-10425
  - porous electrode double-layer capacity determ. by triangular voltage sweep method 3-39448
  - potential distrib. in a space-charge sheath meas. by a nonperturbing probe *(Russian)* 3-6027
  - potential ratios in r.f. sputtering, det. by Langmuir's theory *(German)* 3-5245
  - semiconductor, compensated, heavily doped, large-scale potential props., microwave absorpt. *(Russian)* 3-8165
  - Ar-N_2 mixture, wall-stabilised arc, potential gradient meas. 3-17687
  - CdTe low resistivity films, d.c. e.m.f. in a.c. fields *(Russian)* 3-11964
  - IrO_2, free energy of form. by solid electrolyte galvanic cell method 3-37124
  - PbO-SiO_2 melts, activity meas. by TIE method 3-36998
- **electric power generation**
  - *see also power stations*
  - emission to air reduction in power generation industry, best practicable control means 3-37538
  - nuclear power in USA, prospects for 1992 3-19964
  - superconductivity appl. 3-15286
  - ZrO_2 solid electrolyte applications 3-34729
- **electric reactors** *see reactors (electric)*
- **electric relays** *see relays*
- **electric resistance** *see resistance (electric)*
- **electric resistance furnaces** *see resistance furnaces*
- **electric resistors** *see resistors*
- **electric sensing devices**
  - *see also instruments; measurement*
  - Bozicevic-Everaets detector, microanalysis, design, operation, advantages, applications 3-10194
  - capacitive wavestaff for water surface wave measurements, low power circuits 3-2966
  - float-transformer gauge, to meas. liq. surface level in high press. vessel *(Russian)* 3-19176
  - fluid flowmeter, patent 3-455
  - image sensors, charge-coupled, sensitivity and resolution at low light levels 3-29058
  - laser beam scanning photometer 3-35429
  - laser interferometric alignment sensor for Large Space Telescope 3-31822
  - magnetic field, survey of methods *(German)* 3-13356
  - magnetic sensors, errors due to sensor booms, near-field of scattering of semi-infinite cylinders 3-22823
  - membrane electrode, on-line monitoring of NH_3 in water 3-22191
  - meteorological and oceanographic, for National Data Buoy Project 3-31467
  - oceanic pollution, digital computer control, purge solutions 3-3214
  - piezoelectric quartz crystal digital sensor as partition detector 3-37744
  - pressure, thin vibrating aneroid diaphragm, design 3-5852
  - river water quality monitors, installation problems 3-22192
  - river water quality monitors 3-22193
  - self deployable high attenuators light shade for spaceborne astronomical sensors 3-31824
  - star sensor/mapper for Small Astronomy Satellites 3-31823
  - tidal movements of the deep sea, sensors for press., temp. and current meas. 3-25202
  - trawl system for lobsters 3-9258
  - variable geometry cylindrical detector, for scanning electron microscopy 3-373
  - water pollution meas., conference, London (1973) 3-22185
  - water pollution monitoring 3-22188
  - water quality monitoring 3-22189
  - water using submersible monitor 3-22190
  - Ge thin film, appl. to detectors 3-15641
- **electric shocks**
  - *see also protection; safety*
  - 2nd. International Colloquium of the international Section of ISSA for Prevention of Occupational Risks due to Electricity 3-9713
  - coronary circulation effects, possibility of myocardial infarction 3-9694
  - nervous system effects, neurological symptoms and syndromes appearing during and after 3-9695
- **electric spark machining** *see spark machining*
- **electric sparks** *see sparks*
- **electric strain gauges** *see strain gauges*
- **electric strength**
  - *see also electric breakdown*
  - dielectric, theoretical anal., using principle of field superposition *(Russian)* 3-30744
  - gases subjected to acceleration or retardation 3-26913
  - insulating materials *(French)* 3-30759
  - liquid dielectric, moisture content effects *(Russian)* 3-25020
  - polyethylene, dielec. breakdown strength determ. method for small test pieces *(German)* 3-15806
  - polyvinyl chloride, radiation eff. on dielec. strength, permittivity, loss and resistivity 3-18405

electric strength continued
  NaCl, temp. depend., −40 to +100°C *(Russian)* 3−18414
  SiO_2 film, degradation, rel. to devitrification study 3−8752
electric transformers *see transformers*
electric variables measurement
  see also attenuation measurement; capacitance measurement; charge measurement; dielectric measurements; electric current measurement; electric distortion measurement; electric field measurement; electrical impedance measurement; frequency measurement; gain measurement; inductance measurement; loss measurement; noise measurement; phase measurement; power factor measurement; power measurement; Q-factor measurement; reactance measurement; resistance measurement; voltage measurement
  a.c. field effect, technique for organic semiconductor *(Russian)* 3−11946
  anodic stripping polarography, automatic peak meas. 3−26012
  arc, high-current pulsed, anode current density meas. 3−17690
  electrical signals, recording and reconstruction using one dimens. holograms 3−28604
  galvanomagnetic coefficients of semiconductors, determ. by one-point method 3−24454
  impurity resistivity, temperature dependence 3−22407
  l.f., using r.f. biased pont contact superconducting device 3−9999
  liquid dielectric breakdown under recurring discharge, high-voltage meas. 3−11514
  in measuring instruments, catalogue 3−5753
  partial discharges, using correlation methods 3−16375
  power transfer expt. for teaching purposes 3−22215
  semiconductor, surface mobility meas. using surface waves on adjacent piezoelec. 3−38828
  thermoelectric efficiency of semiconductor materials *(Russian)* 3−9994
electric welding
  see also arc welding; electron beam welding; resistance welding; welding electrodes
  plasma, improvements and applic. *(French)* 3−11510
electrical conductivity
  see also electrical conductivity of gases; electrical conductivity of liquids; electrical conductivity of solids; electrical conductivity transitions; hopping conduction; Kondo effect; mixed conductivity; negative resistance effects; photoconductivity; semiconductor materials; semiconductors; skin effect; space-charge-limited conduction; superconducting materials
  alkyd resins, wetting ability rel. to elec. cond. 3−34642
  blocked purkinje tissue, passive conduction delay, numerical delay 3−13129
  current-voltage problem, Feynman diagram approach 3−2075
  d.c. and Hall conductivities of system of interacting electrons, quantum effect, application of Wigner representation 3−27234
  Earth, anomalies, e.m. perturbation fields 3−21913
  Earth, dry valleys in Antarctica 3−12630
  Earth conductivity, effect of radial distrib. on geomagnetic S_q-variations 3−25174
  electrojet, equatorial zone integral cond. tensor charges 3−34927
  electronic and gasdynamic properties of hypersonic wakes behind models moving in Ar *(Russian)* 3−7316
  geophysical soundings, geometrical progression of depth 3−9209
  industrial minerals prospecting, with E-phaser 3−9210
  infinite dielectric, rel. to e.s. field *(Russian)* 3−6393
  ionosphere, oscillations of DP1 and DP2 current systems rel. to conductivity 3−34939
  Kilauea volcano, Hawaii, e.m. sounding survey 3−9167
  liquid crystal, nematic p-azoxyphenetole, temp. depend. 3−21071
  MHD channel, convective heat loss and elec. cond. calc. 3−36131
  moon, inversion method applied to data giving two layer moon 3−25417
  non-Debye plasma *(Russian)* 3−11466
  ocean ridge model, electrical conductivity rel. to geomagnetic variations 3−18840
  plasma, anomalous cond., exactly solvable electrodynamic model 3−36151
  plasma, Coulomb, quantum correction *(Russian)* 3−36154
  plasma, d.c. current induction by r.f. travelling wave in strong mag. field 3−26864
  plasma, low temp. *(Russian)* 3−11467
  plasma, non-Debye, collective effects, empirical factor 3−36152
  plasma, non-equilibrium, high frequency resistivity, numerical evaluations of wave-wave contributions 3−23822
  plasma, relativistic degenerate, appl. to neutron-star interiors 3−30022
  plasma, toroidal electrical conductivity, particle trapping 3−38428
  plasma, turbulent, effect of ion-acoustic oscill. 3−20502
  plasma electrical conductivity and collective interactions in strong electric fields 3−29940
  plasma longitudinal current, radial profile, temporal development 3−38427
  plasma turbulent resistivity, computer simulation 3−1479
  potential distrib. on sphere with longit. depend. cond., appl. to magnetosphere 3−25302
  stars, early-type, electrical conductivity in atmosphere rel. to models 3−35115
  terrestrial, Germany, Saar area, soln. of tectonical problems 3−9125
  two dimensional structure, direct interpretation of resistivity data 3−31460
  two-phase metal flows, hypothetical structures 3−15178
  Ar plasma, meas. of real and imaginary part of cond. using skin effect *(German)* 3−7556
  Ar supersonic plasma, effect of electrode processes on volt-ampere characteristics of discharge 3−17709
  Au, refractory exploding-wire measurement of heat of fusion and electrical conductivity during melting 3−30247
  CrMn tellurides under high pressure, Earth interior *(German)* 3−12594
  FeS, under high pressure, Earth interior *(German)* 3−12594
  Ir, refractory exploding-wire measurement of heat of fusion and electrical conductivity during melting 3−30247
  N_2 plasma, in terms of transport coefficients 3−33344
  TiO_2, thixotropic and dilatant dispersions, elec. cond., rheology, polarisation 3−39407
electrical conductivity measurement
  a.c. conductivity, contactless meas. in microwave region, appl. to amorphous Ge film 3−15189
  bulk and surface resistivities, a.c. meas. *(French)* 3−13353
  contactless method, using induced currents 3−37660
  cylindrical sample, conductivity meas. by RF induction method 3−37659
  device for use in different gas atmospheres up to 250°C *(Russian)* 3−9990
  difference field contactless method 3−22406
  earth resistivity surveying for Sanguine transmitter site selection 3−3173
  eddy current meas. of conductivity to determ. solidus point 3−27830
  ferroelectric materials, temp. dependence at low temp., method overcoming pyrocurrent interference *(Russian)* 3−8497
  Hall mobility, probe-bar and multiprobe methods, applic. to inhomogeneous-in-depth semiconductor layers *(Russian)* 3−6015
  impurity resistivity, temperature dependence 3−22407
  intracellular, Aplysia neurons and squid axon 3−28315
  land stations, electric potential gradient and conductivity power and cross power spectra 3−15972
  liquid metal elec. cond. meas. apparatus, 1000-2500 K 3−32111
  magnetotelluric soundings, processing and interpretation 3−34964
  metallic thin films in hyperfrequency region *(Russian)* 3−9993
  minerals, earth mantle elec. props. determ. 3−15928
  oceanography, salinity determination, from measures of electrical conductivity and temperature 3−16071
  resistivity determ. for homogeneous materials, test for surface condition of plane electrodes *(German)* 3−3830
  sea ice, in situ at v.l.f. 3−28091
  semiconductor, apparatus for plotting log σ against 1/T *(German)* 3−37663
  semiconductor, apparatus for simultaneous meas. with thermoelectric power up to 1000C 3−25803
  semiconductor, meas. with d.c. four point probe with nonpenetrating tip 3−27281
  semiconductor thin films, microwave freqs. 3−24463
  semiconductors, at microwave frequencies *(Russian)* 3−11925
  soil, resistivity, extension of Wenner's method *(Hungarian)* 3−12847
  specific cond. of pure unconsolidated sands, dependence on grain size *(German)* 3−5533
  stainless steel, meas. with Shimadzu electrothermal analyzer *(Japanese)* 3−13253
  synthetic basalt, changes due to partial fusion in seismic low vel. zone of upper mantle 3−5446
  thermoelectric materials, specimens with small cross sections between 80 and 400 K 3−116
  Al-Ge alloys, vacancies influence on nucleation of incoherent Ge precipitation 3−2702
  Cu wire, meas. with Shimadzu electrothermal analyzer *(Japanese)* 3−13253
  Ni wire, meas. with Shimadzu electrothermal analyzer *(Japanese)* 3−13253
  Si, characterisation with Hg probes 3−39256
electrical conductivity of electrolytic liquids
  see also electrochemical analysis; electrolytic ion velocity
  Brownian-like solns., liq. struct. effects on d.c. transport 3−2065
  equation for associated symmetrical electrolytes 3−27879
  KI/DMSO system, K^+ and I^- mobility determ. from conductivity and transport number meas. by interface diffusion method *(German)* 3−37130
  MBBA, isotropic phase, chem. and electrochem. activity rel. to d.c. conduction 3−15203
  p-methoxybenzilidene p-butylaniline, liquid crystal solutions of tetraisoamylammonium tetraphenylboride *(French)* 3−36260
  nematic electrolyte solns., electric props., influence of sample geometry *(German)* 3−37129
  polyelectrolytes equilibrium theory, transport props., review 3−34731
  AgBr membrane in aqueous solns., elec. cond. by ion transport 3−2841
  $CuSO_4$ soln., Hall coeff. meas., H^+ ion mobility 3−11755
  $KF-BaF_2(CaF_2)$ binary molten salt, meas. at 1000°C, determ. of ionic conducting species 3−36631
  $NaF-BaF_2(CaF_2)$ binary molten salt, meas. at 1000°C, determ. of ionic conducting species 3−36631
  TlCl melt, conduction and diffusive transport modes, temp. depend. 3−27132
electrical conductivity of gases
  air, shock-compressed, electroconductance depend. on piston material *(Russian)* 3−29826
  anomalous resistivity in plasma 3−17621
  electron mobility, in moderately dense gases *(Russian)* 3−11355
  marked examples, book 3−18048
  MHD power generators, thermal and electrical conductivity as function of temp. 3−26903
  partially ionized, in magnetic field. theory *(Czech)* 3−4518
  plasma anomalous resistivity 3−23877
  plasma anomalous resistivity and heating in high-amplitude intermediate-frequency electric fields 3−23899
  plasma anomalous resistivity caused by cross-field current driven instability development and saturation 3−23882
  plasma resistive pinch, linear and nonlinear perturbation theory 3−20476
  plasma resistivity of high beta diffuse pinch, numerical results of influence of axial antiparallel bias mag. field on energy transfer 3−20559
  trial function technique using elec. arc meas. 3−33187
  Ar, elec. arc meas., trial function technique 3−33187
  Ar, ionised, transport coeffs., 0.001 to 1000 atm and temp. to 35000K 3−38347
  Ar-air high-temp. jets with Ti dispersive particles *(Russian)* 3−11455
  He-Ne, glow discharge, sectionalised cathodes, cathode pot. step, current distrib. *(Russian)* 3−14629
  He^+ plasma, d.c. electric resistivity perpendicular to mag. surface, meas. 3−11471
  N_2, arc, electrode dominated with W anode and Cd or Zn cathode, power balance eqns. 3−1524

electrical conductivity of gases continued
- N_2, elec. arc meas., trial function technique 3–33187
- Xe, elec. arc meas., trial function technique 3–33187

electrical conductivity of liquids
- *see also electrical conductivity of electrolytic liquids*
- alkali metal, pseudopotential calc. of elec. resist. and thermoelec. power 3–21051
- alkali metal nitrates, specific conductances up to 12 Kbar *(German)* 3–11901
- alkyd resin in acetone, elec. cond., potential distribution 3–39408
- aqueous solutions, irradiated, transient conductivity induced using h.v. pulse 3–5397
- blood, moving and stationary, effect of frequency changes 3–3904
- cyclohexane, electron-pulse radiation induced *(Russian)* 3–5394
- dielectric, moisture content effects *(Russian)* 3–25020
- liquid chalcogenide semiconds., thermopower and cond. activation energy differences 3–21100
- liquid cryst., nematic phase of smectic C materials, elec. cond. temp. depend., short range order effects 3–14683
- metal, calc. using optimized model pot. 3–36508
- metal, nearly-free-electron, computer program calc. of form factor and resistivity 3–36585
- metal, nomogram for mat. testing 3–27816
- metal, temp. depend. calc. rel. to Debye-Waller correction to theoretical interference function 3–24016
- metal, theory, allowance for ion subsystem influence on electron scatt. *(Russian)* 3–8150
- metal, Ziman formula applic., kinetic eqn. for electrons soln. *(Russian)* 3–15177
- metal-molten salt systems, theoretical interpretation 3–1970
- metals and semiconductors, review of electric properties 3–30385
- polar liquids dissolved in different non-polar solvents, RF conductivity meas. 3–38862
- semiconductor, migration mechanism determ. 3–33902
- semiconductor melts, thermal cond. rel. to elec. cond. *(Russian)* 3–8181
- technique for obs. of kinetics of radiation-induced chemical reactions in aqueous solutions 3–5374
- thermodiffusion of semiconductors, bipolar, Wiedemann-Franz ratio, Mott model 3–36600
- transition metal, resistivity, theory 3–8147
- transition metals, electrical resistivity at high temp. 3–36588
- Al, dielectric screening and resistivity 3–5000
- Al-Cu alloy, temp. depend. *(Russian)* 3–2054
- Ar, ion drift vel. 3–24283
- Bi_2Te_3-Sb_2S_3, specific resist. and thermal e.m.f. meas. *(Russian)* 3–15192
- Cs, resist. and thermoelec. power calcs. under 40 kbar pressure 3–36586
- Cs liquid, absolute thermoelectric power and electrical conductivity in metal-nonmetal transition range 3–27247
- CuGa(In)Te_2, semicond., temp. depend. meas. *(Russian)* 3–15191
- Ga, resist. to 1000°C, temp. depend. 3–4999
- Ge-Co, Ge-Fe alloys, resistivity, theory 3–8147
- H_2O-N_2 two-phase mixture, meas. of elec. conductivity in bubbly and slug flow area 3–32941
- Hg-H_2O two-phase mixture, meas. of elec. conductivity in bubbly and slug flow area 3–32941
- Hg-In alloy, Lorenz number and thermal cond. 3–30453
- In-Tl liquid alloys, structure and electrical conductivity *(Russian)* 3–33443
- K, liquid, accurate resistivity and thermoelectric power calculations 3–8149
- K liquid, 2-parameter Brovman potential study 3–2052
- Na, liquid, 2-parameter Brovman potential study 3–2052
- Na, liquid, accurate resistivity and thermoelectric power calculations 3–8149
- Na-Cd dilute alloys, state of Cd impurities, temp. dep. of elec. resistivity 3–33868
- NaK-N_2 two-phase mixture, meas. of elec. conductivity in bubbly and slug flow area 3–32941
- Ne, ion drift vel. 3–24283
- Pb-Sn alloy, temp. dependence of resistivity 3–30454
- Rb, electrical resistivity calc. by optimized model potential method 3–7877
- Tl-Te, molten, electrotransport and density of states *(Russian)* 3–24370
- Zn, transport props. rel. to resonant d-levels 3–8148

electrical conductivity of solids
- *see also ionic conduction in solids; Poole-Frenkel effect; semiconductor materials; superconducting materials*
- actinides, comparison across series 3–2049
- alkali metals, phonon drag effect on low-temperature resistivity 3–2045
- alloy, binary, residual resist. calc., pseudopot. form factors, impurity effects *(Russian)* 3–15172
- alloy, dilute, thermoelec. power and Lorenz number temp. depend., from Anderson model 3–8138
- alloy, disordered binary, CPA validity in elec. cond. theory 3–21050
- amorphous metal film, meas. showing negative temp. coeff. of resist. 3–33870
- amorphous semicond. d.c. cond., diffusion type transport eqn. 3–8177
- amorphous semiconductor, switching obs. using oscillation circuit 3–8238
- amorphous semiconductor film, variable-range hopping cond., theory 3–30476
- amorphous semiconductors, electronic phenomena, review 3–24415
- amorphous thin film, non-ohmic behaviour *(Russian)* 3–30491
- anthracene, thermally stimulated current meas. of trapping level depth and frequences 3–18167
- barium stearate multilayer film, I.V characts. 3–27469
- basalts, physicomechanical and electrical properties at high pressurs and temp. 3–25134
- cellulose nitrate, elec. field depend. *(French)* 3–38846
- ceramic grain boundaries, cond. determ. from electron beam scanning obs. 3–36302
- chalcogenide film, noncryst., switching, room temp. and 77K 3–21129
- chalcogenide glass, electronic conductivity and switching 3–18134

electrical conductivity of solids continued
- chlorinated diphenyls, temperature behaviour of d.c. and a.c. conductivity in ionic conduction range *(German)* 3–36610
- compacted metal powders, pressures up to 2 kbar, piezometer measurement of resistivity 3–12379
- complex semiconductor chalcogenides, physical props. *(Russian)* 3–8168
- conducting particles in insulating matrix, theory of infinite chains 3–4984
- copper phthalocyanine, model with molecular stacks and bulk defects 3–21062
- current and electron-phonon interaction in a strong electric field 3–38853
- diamond:Li, implanted, after annealing at 1400°C *(Russian)* 3–2070
- diamond, proton irrad., cond. in disordered regions *(Russian)* 3–2072
- diamond, types Ia and IIa, thermally stimulated currents, 20-400°C 3–30473
- diamond crystals, proton irradiation effects 3–24437
- dielectrics, device for measurement in different gas atmospheres up to 250°C *(Russian)* 3–9990
- dilute alloy, spin-orbit interactions, induced spin anisotropy effect on elec. resist. 3–36711
- dilute alloys, pseudopotential calcs. of volume depend. for residual resistivity 3–36575
- dilute mag. alloys, elec. resist. rel. to localised mag. moment exchanges, RKKY s-d exchange model 3–30439
- disordered materials, inhomogeneous transport regime existence 3–33893
- disordered one-dimens. system, localisation distance, m.f.p., backward scatt. 3–24385
- disordered system, d.c. cond. and Anderson transition 3–18057
- Earth, e.m. anomaly enhancement by conducting overburden 3–9353
- Earth resistivity pseudosections of buried spherical conductor body, computer calc. 3–9354
- eclogites, at high pressure and temp. *(Russian)* 3–9132
- energy surface integral numerical calc. within Brillouin zone 3–8080
- epoxy resin, d.c. cond., transverse elec. field effects, majority carrier polarity 3–18143
- epoxy resin, elec. cond. and dielec. breakdown mechanism *(Japanese)* 3–8516
- excitonic fluctuations effects 3–33859
- ferrite oxyfluoride spinels, elec. cond., hopping mechanism *(French)* 3–27251
- ferrocene, ferricenium mixed valence semicond. polymers, elec. props. 3–2064
- ferroelectric semiconductors, localised electron states in domain walls 3–24663
- ferromagnetic disordered alloy, band theory for residual resistivity 3–15340
- ferromagnetic metal, electron-phonon and electron-magnon scatt. effects on resist. *(Russian)* 3–15181
- ferromagnetic semiconductors, max. resistivity due to carrier scattering by giant moments of mag. clusters 3–18145
- ferromagnetic semiconductors, non-degenerate, high field effects 3–8194
- film, continuum percolation theory and Monte Carlo techniques 3–8281
- film, quantum size effects in surface cond., practical application 3–2040
- GaAs:He(N,S,Zn), ion implantation, elec. conduction due to defect centres 3–33906
- generalised conductivity of a heterogeneous system from the structure and phase composition 3–36574
- glass, rel. to viscosity changes below vitrification temp. *(Russian)* 3–14697
- graphite, electrical transport props. assuming acoustical phonon scattering 3–11897
- graphite, polycrystalline, porous effects on electrical and thermal conductivity 3–27796
- graphite, reactor-grade neutron-irradiated, annealing at 350°C, effect on electrical resistivity and thermal conductivity 3–11060
- graphite electrical resistivity change during compressive tests 3–23432
- graphite thin crystal, residual resist. depend. on crystal thickness 3–30469
- Green function approach to hot electron conductivity 3–18153
- hexagonal metals, anisotropy in phonon scattering resistivity 3–7876
- Hubbard model, narrow half filled band, electrical conductivity and thermodynamics, semiconductor-metal transition investigation 3–11842
- II-IV-V_2 compounds, preparation in layer form, properties and heterojunctions based on them 3–8747
- III-V semiconductors, mm. wave investigation 3–21084
- insulating and electrode materials, elec. cond., erosion and heat resistance in plasma jet 3–36206
- insulator, with arbitrary trap distrib., isothermal currents and trap parameter determ. 3–36620
- insulator, with arbitrary trap distrib., thermally stimulated currents 3–36621
- ionic transport in solids with tunnel and layer structures 3–5018
- linear induction accelerator, parameters for conducting wall of accelerator tube 3–16474
- lithium disilicate glass, space-charge limited current 3–8173
- lunar interior, data evaluation *(Russian)* 3–9500
- lunar temp. determ. from meas. on olivine and pyroxene, melting point depth determ. 3–25420
- magnetic semiconductor, sample boundary and domain wall effects 3–34170
- metal, elec. resist. rel. to umklapp electron electron scatt. 3–30440
- metal, inhomogeneously strained, with impurities, calc. *(Russian)* 3–30443
- metal, internal electron refl. rel. to angle of incidence *(Russian)* 3–11879
- metal, Kondo effect, resist. due to 3d impurities, s-d interaction model 3–2042
- metal, magnetic, conductivity tensor calc. 3–8136

electrical conductivity of solids continued
metal, nearly ferromag., electron-paramagnon scatt. contrib., temp. depend. 3—27235
metal, nomogram for mat. testing 3—27816
metal, polyvalent, impurity scatt. and residual resist. 3—18115
metal, Stewart-Huebener method to determine deviations from Mattheissen's rule 3—18116
metal, strain coeffs. of resistance in bulk and thin film, comparison of longit. and transverse 3—38821
metal film, γ-irrad. effects *(Russian)* 3—18231
metal film, current noise, due to intergrain tunnelling 3—4996
metal film, replacement of chemisorbed gas obs. *(Japanese)* 3—20928
metal films, rel. to interaction of u.s. surface waves with conduction electrons 3—11793
metal films, relaxation of elastoresistance 3—33866
metal thin films, var. during vapour and gas adsorption 3—15276
metal with non-mag. impurities, I-V characts., analysis rel. to quasilocal vibs. 3—4986
metallic discontinuous film, elec. cond., electron emission and electrolum. rel. to hot electrons 3—15171
metallic film, groups I-IV, electromigration obs. 3—4879
metallic film, size effect model in strain coeff. of resist. 3—8142
metallic thin film, effect of superimposed dielec. layers 3—30552
metallic thin films, size effect 3—33867
metals, electron-phonon umklapp interaction anisotropy and deviations from Matthiessen's rule 3—38820
metals, polyvalent, umklapp electron-phonon scattering in low temp. resistivity 3—8140
metals, refractory, thermophysical props., Moscow State University research *(German)* 3—36579
metals, soln. of Boltzmann eqn. at 0°K for constant relaxation time 3—18109
m.i.m. systems, dielectric relaxation effect on isothermal electrical characteristics of defect insulators 3—11959
m.i.m. systems, dielectric relaxation effect on thermal electric characteristics 3—8276
m.i.s. structures on Si, scattering mechanisms in inversion channels 3—8271
moisture-saturated rocks, electrical conductivity at high pressures and temperatures 3—25141
m.o.s. structure, effect of electrostatic attenuation of the longitudinal field in near-surface region *(Russian)* 3—24521
naphthalene, effect of double space charge after solidification 3—24426
Ni, quenched, elec. resistivity exam. of point defects *(French)* 3—11611
nichrome film, variation during deposition 3—21536
noble metal, solid, resistivity, thermopower, calculations 3—30444
olivine, cond. meas. as function of temp. and O fugacity 3—25114
organic, low mol. wt., charge carrier obs. 3—5395
organic dielectric films, charge transport 3—38834
organic dielectrics, a.c. and d.c. conduction 3—38861
organic polymers, effects of vacuum *(Japanese)* 3—24469
oxide cathodes, high-field cond. through pores and grains, theory and obs. 3—15207
percolation theory, branching model 3—18142
PMMA, thermally stimulated current obs., −80°C to +130°C *(German)* 3—27280
polar semiconductors, inclusion of higher order terms for energy distribution function of hot carriers at high temp. 3—8193
poly-N-vinylcarbazole, amorphous film, cond. mechanism 3—27253
polyamide 66, v.l.f. meas. by a noncontact method at room temp. 3—18413
polyethylene films, d.c. conductivity measurements 1×10^7 to 3×10^7 Vm^{-1}, model, hexane treatment 3—36614
polyhexazocyclane PF, current instability 3—36618
polymer, book contrib. 3—11891
polymer film, d.c. glow discharge polymerisation and electronic conduction mechanisms *(German)* 3—15282
polymers, thermoluminescence and thermally stimulated cond. meas. 3—30889
polyvinyl chloride, radiation eff. on dielec. strength, permittivity, loss and resistivity 3—18405
polyvinylidene fluoride, rel. to crystallisation 3—33462
porous glass, C-impregnated, thermometric props. at low temps. 3—5807
porous glass, rel. to hygroscopicity and no dimming phenomena *(Japanese)* 3—20935
powders, compressed form, investigation *(German)* 3—12460
Precambrian rocks, electrical anisotropy determ. 3—34809
pyrocarbon saturated with Br, temp. dependence on resistivity between 90-298 K and thermoelectric power *(French)* 3—8214
quartz crystals, anisotropy due to mobility of current-carrier ions *(Russian)* 3—8161
quasi one-dimens. org. semicond., low temp. cond. 3—2067
rare earth alloy, spin disorder resistivity, theory 3—4988
rare earth hydrides, hydrogen mobility mechanism *(French)* 3—1826
rare earth pnictides, optical electrical and magnetic props., review 3—11848
rare earth-Fe compound, Curie temp. pressure depend., elec. resist. meas. 3—36720
refractory, obs. rel. to admixture effect *(Russian)* 3—8987
resistivity, noble metals, pseudopotential formalism 3—30445
sapphire, press. effect 3—21066
semiconducting transition metal oxides small polaron concept, d.c. and optical props. 3—36568
semiconductor, $A^{II}B^{V}$ cpds., review 3—18084
semiconductor, artificial, formed by alternating thin films of Au and SiO_2, characterization 3—38790
semiconductor, complex low freq. cond. in strong elec. field, imaginary part *(Russian)* 3—2101
semiconductor, conductivity and thermodynamic props., effect of fluctuons 3—21079
semiconductor, current flow, analogy with filtration *(Russian)* 3—11443
semiconductor, doped periodically, carrier mobility, elec. cond. anisotropy *(Russian)* 3—8178
semiconductor, electron cooling by static elec. field *(Russian)* 3—8202
semiconductor, high field domain modes, due to field depend. carrier diffusion 3—33908
semiconductor, monopolar, V-I characts., admittance analysis *(Russian)* 3—27256
semiconductor, organic, effect of double space charge after solidification 3—24426
semiconductor, spontaneously polarised, anisotropy of elec. cond. 3—39110
semiconductor, with arbitrary trap distrib., isothermal currents and trap parameter determ. 3—36620
semiconductor, with arbitrary trap distrib., thermally stimulated currents 3—36621
semiconductor film, surface cond. 3—8242
semiconductor overheating instabilities, low-temp. impurity breakdown 3—24395
semiconductor thin films, contactless meas., microwave freqs. 3—24463
semiconductor with non-parabolic dispersion law, in mag. field, high freq. cond. of hot carriers 3—2109
semiconductors, bounded, possessing negative differential conductivity, current-voltage characts. 3—18162
semiconductors, disordered systems 3—18148
semiconductors, high-resistivity, parameters of trapping levels 3—24451
semiconductors, many-valley, in strong alternating electric fields 3—24446
semiconductors, multivalley, with screw dislocations, diffusion theory of electrical resistance 3—24416
semiconductors, strong electric fields, arbitrary electron bandwidths and electron-thermostat coupling 3—38851
semiconductors device for measurement in different gas atmospheres up to 250°C *(Russian)* 3—9990
semimetal, elec. cond. for ultrasound propagating parallel to d.c. mag. field., calc. 3—33927
shaly sandstones, water-saturated 3—15874
n-Si, high field effects, velocity-field curve, space charge induced nonuniformities 3—5014
steel, creep process obs. *(German)* 3—34609
steel A286 stainless, solution annealed, material variability, low temp. resistivity obs. 3—24871
steel AISI 316 solution annealed, material variability, low temp. resistivity obs. 3—24871
sugarcane wax, subjected to high elec. fields and diff. temps., cond. mechanism 3—21083
synthetic resin, cross-linked in strong elec. field, obs. 3—2097
Ta, 1200-3000K *(Russian)* 3—11877
TCNQ salt, NMP type, non-mag. semicond. phase obs. 3—2066
TCNQ salts, impurity effects on electrical conductivity and activation energy anisotropy *(German)* 3—30504
$TEA(TCNQ)_2$, model of quasi metallic interrupted TCNQ chains 3—27236
teaching approach, pinball machine analogue 3—9800
tetracyanoquinodimethan, semicond., Hubbard's third model for elec. cond. calc. 3—11893
5,12-6,11-tetraoxotetracene with dioxytetracenchionone impurities, Poole-Frenkel effect *(Russian)* 3—11904
thermally stimulated, trap emptying model *(German)* 3—15162
thermally stimulated cond. and thermolum. maxima 3—24755
thin films, discontinuous, resistance, electrode and substrate considerations 3—38905
threshold switches, multicomponent chalcogenide glass alloys, thermal and non thermal processes 3—8236
transition metal semiconducting phosphate glasses, transport props. 3—8175
transition metal-C alloy amorphous film, polyconductivity *(Russian)* 3—8145
trap pot. well shape calc. using Frenkel thermal field effect 3—4966
trimethylethyltin-based thin polymer films, electrical conductivity *(Russian)* 3—8187
triphenylmethylphosphonium-7,7,8,8- tetracyanochinodimethane, anisotropy of the activation energy of the electrical conductivity *(German)* 3—11900
two phase materials, resist. computation *(German)* 3—8993
Ag, deformed, recovery of elec. resist., effect of O and excess vacancies *(Russian)* 3—7819
Ag, noncrystalline thin films, electron diffraction and resistivity study 3—8062
Ag film, detection of N atoms, electrical resistivity obs. 3—4925
Ag-Al thin film contacts, degradation mechanism during annealing 3—15241
Ag-SiO, thin films, struct. and elec. cond. *(Korean)* 3—27198
$(Ag_xCu_{1-x})_2Se$, electronic and ionic cond. 3—21123
Ag_2HgI_4, high pressure phases, pressure depend. 3—30471
β-AgI pellets, pure and PbI_2 doped, phase stability 3—14966
AgI(α and β), hydrostatic pressure effect on electrical conductivity 3—7686
AgO and Ag_2O thin films, specific resist. *(French)* 3—20960
Ag_2S chemically deposited films, change in resistivity with frequency and temp. for 0.02 to 0.2 μ thickness *(French)* 3—11962
Ag_5SbS_4, stephanite, in phase transition region *(Russian)* 3—30259
Ag_2Se-Ag_3PO_4 solid solution, mixed ionic and electronic cond. 3—11939
Al, dislocation annihilation mechanism by deformation, resistivity decay meas. 3—17823
Al, meas. at low temp., temp. depend. of T^3 form 3—18114
Al, quenched-in vacancies, resistivity meas., formation energy and entropy determ. 3—17806
Al, surface resistance determ. in hyperfrequency region by transmission coefficient meas. *(Russian)* 3—9993
Al 2024 solution annealed, material variability, low temp. resistivity obs. 3—24871
Al alloys, residual resistivity from multiple plane wave pseudopotential calc. 3—24406
Al film, sheet resist. meas. rel. to size effect parameters 3—30448
Al resistivity, additional due to metal impurity atoms, experimental results, Ashcroft pseudopotential theory *(Russian)* 3—30452

electrical conductivity of solids continued
Al sheet solution, eddy current conductivity meas. near solidus point 3−27830
Al thin film, d.c. sputtered, low resistivity, sputtering bias effects 3−39225
Al-Al_2O_3, electrical and structural props. of amorphous system 3−38840
Al-Al_3Ni, two phase alloy, electron scatt. on precipitate boundaries, low temp. resist. meas. 3−36580
Al-Al_3Ni directionally solidified eutectic, resist. meas. *(Russian)* 3−24826
Al-CeF_3-Al structure, isothermal dielec. relax. curents 3−36666
Al-CeF_3-Al thin film capacitor system, stimulated dielectric relaxation currents 3−8277
Al-Cr and Al-Mn cold-worked alloys, impurity resistivity from 78 to 300 K 3−14886
Al-Cu alloys, reversion phenomenon study, hardness and elec. resist. meas. 3−39326
Al-Cu-Li alloys, resist. obs. of Al_2CuLi precip. 3−21660
Al-Li alloys, decomp. of solid soln., resist. obs. 3−21606
Al-Mg. dilute alloy, recovery after neutron irradiation at 4.6K 3−11658
Al-Mg (5 at %) solution annealed, material variability, low temp. resistivity obs. 3−24871
Al-Mg dilute alloy, neutron irrad. at 4.6K, resist. study 3−27042
Al-Mg_2Si, meas. for Fe effect on nucleation and zone form. 3−8884
Al-Mn:Fe, dilute alloy, temp. depend. of impurity resist. 3−21048
Al-T phonon resistivity, concetrated alloys 4.2 to 100 K, (T=V, Fe, Co, Ni, Cu) 3−38822
Al-Ti(V)(Fe)(Cu)(Zn), dilute alloy, temp. depend. of impurity resist. 3−11876
Al-Zn, hard non-ordered electrical resistivity concentrational dependence *(Russian)* 3−11883
Al-Zn alloy, metastable solvus for G-P zones, electrical resistivity meas. 3−31022
AlB_{12} semiconductor, thermoelectric properties, thermal conductivity, hopping conduction, temperature dependence 3−36630
AlB_2, metallic cond., carrier conc., cryst. growth 3−11878
n-$Al_xGa_{1-x}As$, temp. depend. of elec. resist. 3−30478
AlN, elec. resist. of epitaxial layer 3−11831
AlN film, epitaxial growth, props., optical band gap 3−21004
Al_2O_3 single crystal layer, carrier photo-injection from metal films and Poole-Frenkel transport 3−5054
$AsSe_x$ glasses, x=1-20 electrical conductivity between 300-700K *(Russian)* 3−8160
As_2Se_7, amorphous semiconductor film, d.c. elec. cond. before switching 3−8239
As_2Te_3, glassy, electronic properties by Mott-CFO model 3−1972
$AsTe_2Si$ chalcogenide film, localised states, thermally stimulated depolariz. current obs. 3−2020
Au, elec. resist. vs. electron flux, stable interstitial at 300K 3−4748
Au, lattice contraction due to quenching-in vacancies, resist. study 3−30118
Au noncrystalline thin films, electron diffraction and resistivity study 3−8062
Au thin film, strain effect on electrical conduction 3−33865
Au thin film on glass plate, rel. to temperature and voltage under vacuum 3−18234
Au thin films, conduction electron diffusion by surface defects *(French)* 3−36584
Au-Al double film system, rel. to diffusion coeff. determ. *(Russian)* 3−4871
Au-Cd(47.5 at.%) alloy, martensitic pretransformation phenomena obs. 3−18561
Au-Cr, high concentrated alloy, elec. resist. min. at low temp. 3−30449
Au-Cu alloy film, rel. to order-disorder transformation 3−1800
Au-glass cermet film, strain sensitivity and t.c.r. 3−5065
Au-SiO_x, cermet film, meas. after heat treatment 3−15201
Au-SiO_x cermet film, resistivity changes on heat treatment 3−5064
Au-Yb(Ce)(Gd), negative s-f interaction 3−24561
AuCr, (3.3, 10.6 at. % Cr), elec. resist., $T^{3/2}$ depend. of impurity resist. 3−36581
AuMn(V), localised spin fluctuation and Kondo system, resist. temp. depend. 3−36582
B, BC_x semiconductor, thermoelectric properties, thermal conductivity, hopping conduction, temperature dependence 3−36630
β-B, rhombohedral, Poole-Frenkel effect, current-voltage characteristics 3−36619
β-B, rhombohedral, relax. of non-equilib. cond. 3−27255
$B_{12}C_3$, temp. depend. 3−24429
$BaFe_{12}O_{19}$, ferrite with magnetoplumbite structure, anisotropy of hopping cond. and thermoelec. power 3−38829
$Ba_{1-y}Sr_yFeO_{3-x}$ and $Ba_{1-y}Sr_yFe_{1-z}M_zO_{2.5}$ (M=Ga or In), semiconductivity and dielec. props. *(French)* 3−36831
$BaTiO_3$, I-V characts., 110-400°C, negative resist. 3−27266
$BaTiO_3$, positive temp. coeff. of resist., near Curie temp. *(Russian)* 3−18130
Be, hydrostatically extruded, resist. changes during annealing *(Russian)* 3−18110
BeTel film, specific resist., substrate temp. depend. *(Russian)* 3−21067
Bi, phonon drag region, size dependence of the transport props. 3−8139
Bi and Bi-Sb alloy powder compacts characteriz., 300-77 K 3−36593
Bi film, elastoresistance, conductivity, quantum size effect obs. 3−4997
Bi film growth mechanism, condensation in vacuum, electron microscope examination 3−33758
Bi films, scattering processes investigation 3−2194
Bi-Sb:Te,Se, meas. rel. to thermoelec. figure of merit calc. in mag. field 3−15176
Bi_xSb_{1-x} film, elastoresistance, conductivity, quantum size effect obs. 3−4997
$Bi_2Te_{2.4}Se_{0.6}$, and $Bi_{0.52}Te_3Sb_{1.48}$ cold-pressed semielements, anisotropy obs. *(Russian)* 3−11919
C fibre, K intercalation compounds, structure, colour, X-ray exam. 3−24995
CaF_2, under reducing conditions, mixed cond. 3−21122

electrical conductivity of solids continued
$CaO_xNiO_{1-x}Fe_2O_3, 0 \leqslant x \leqslant 0.7$, variation with Ca ion conc. *(French)* 3−8362
$CaWO_4$, X-irrad., trap depth and charge carriers from optically and thermally stimulated conductivity *(German)* 3−2105
Cd, resist. meas. under hydrostatic press., search for first and second order phase transforms. *(Russian)* 3−15013
Cd, temp. depend. *(Russian)* 3−8154
Cd rare-earth chalcogenide spinels, resistivity meas., superconductive behaviour 3−7685
Cd_3As_2, resistivity and Hall effect under high press. 3−27272
n-$CdCr_2S_4(Se_4)$, cond. min. in Ga-doped samples 3−27267
$CdCr_2Se_4$, 300-500 K *(Russian)* 3−14811
$Cd_xHg_{1-x}Te$, films *(Russian)* 3−24433
$CdIn_{2(1-x)}Cr_{2x}S_4$, meas. as function of temp. 3−2263
$Cd_{1-x}In_xCr_2Se_4$, ferromag. semicond., transport props. 3−33881
$CdIn_2S_4$ single crystal, DC cond., Hall effect and magnetoresist. meas. 3−33894
CdO, 970-1270K 3−2080
CdO single crystal, degenerate semicond. 3−2087
CdS, CdSe, heat treated epitaxial films, structure, composition, photoelec. props. *(Russian)* 3−33948
n- CdS, deviations from Ohm's law at 77 K 3−30485
CdS film, bulk compensation effect on chemisorption dependent semiconductivity 3−33889
CdS film, evaporated, resist. and Hall mobility rel. to prep. conditions 3−27322
CdS film, polycryst., ambient O_2 depend. 3−8185
CdS thin film, acoustoresistance, surface acoustic wave 3−38872
n-CdSb, anisotropy factor rel. to surface states. absorpt. effects *(Russian)* 3−8246
p-CdSb, rel. to technology applic. *(Russian)* 3−24430
n-CdSb, temp. depend. rel. to recombination and photoresistor applic. *(Russian)* 3−24476
CdSe, films, resistance obs., electron microscope examination *(Russian)* 3−38752
CdSe, impact ionisation, breakdown, photoinduced switching, meas. of cond., Hall coeff., mobility, 4.2-300K 3−30487
CdSe, influence of growth conditions 3−24428
CdSe film, surface cond., In surface doping effects *(Russian)* 3−2192
CdSe single crystals, memory props. 3−24484
CdSe:Cu,In and undoped, high temp. defect equilibria 3−7745
CdSe-CdTe, solid solns., comp. and elec. charact. depend. on method of deposition 3−33762
$CdSnAs_2$, point defects, heat treatment effects, elec. props. study *(Russian)* 3−14853
CdTe, amorphous, temp. depend. 3−1942
CdTe, high temp. relax. of cond. *(Russian)* 3−2071
CdTe, impurities, high temp. elec. cond. study *(Russian)* 3−27031
CdTe, Monte Carlo calcs. on high field electron transport 3−8191
CdTe compensated doped crystals, density of states tails, Hall mobility, conduction band 3−33832
n-CdTe films, high field phenomena *(French)* 3−27262
CdTe:Cd oblique deposited films, rectification effect *(Russian)* 3−33936
CdTe:Cd thin films, V-A characteristics, anisotropy *(Russian)* 3−33892
CdTe:Cd thin films *(Russian)* 3−33891
CdTe:Cu single cryst. characteriz. 3−15632
Ce, alpha phase, low temp. elec. resist. under pressure 3−30451
α-Ce, elec. resist. meas., temp. depend. rel. to mag. impurities 3−33862
α-Ce, magnetisation, 1.7-80 K, elec. resist., 1.4−25 K 3−8143
Ce hydrides, temp. dependent electronic transition, resistivity meas. 3−8237
$CeNi_5$, resistivity between 5 and 300K, rel. to entropy changes assoc. with mag. ordering 3−12016
Co film, monocryst., struct. depend. *(Russian)* 3−18120
Co thin film, electrical resistivity, Mayadas-Shatzkes model 3−27240
Co-Fe-Nb, semihard mag. alloy characteriz. 3−21279
Co-Sn, dilute ferromag. alloy, two current cond. and impurity resist. 3−36719
$CoCr_2S_4$, temp. depend., 77-450 K 3−27258
$Co_xFe_{3-x}O_4$, preparation and characterization 3−18741
CoSb, elec. resist., Seebeck coeffs., rel. to comp. defect clustering 3−18124
Cr, surface resistance determ. in hyperfrequency region by transmission coefficient meas. *(Russian)* 3−9993
Cr-Pd dil. alloys, Neel pt. phenomena, solute effects 3−34111
Cr-Sn alloy, Cr-rich, Neel temp., elec. resist., thermal expansion anomaly 3−15364
Cs, liquid, phonon freq. and elec. resist. calcs. using optimised model potential 3−20828
CsCl(Br)(I), Pb-centre studies 3−24725
$CsCuCl_3$, meas. rel. to structural transition at 423K 3−21414
$CsNO_2$, anomalous thermal effects due to solid-state transitions, differential thermal analysis and electrical conductivity meas. 3−15010
Cu, cyclotron irradiation effects 3−14898
Cu, high purity, quenched, lattice defects, resist. study 3−4749
Cu, very pure, meas. below 8.5 K 3−18113
Cu film, effect of CO adsorption 3−8144
Cu film, temp. coeff. of resist. 3−27243
Cu torsionally fatigued wires, strain amplitude changes effect on stress amplitude and resistivity 3−27054
Cu-Al(15 at.%) alloys, ordering and disordering kinetics after sudden annealing changes, residual resist. obs. 3−37062
Cu-Cr alloys, aging phenomena, electrical resistivity meas. *(Japanese)* 3−31067
Cu-Cr base alloys, precip. growth and nucleation, resist. study 3−24865
Cu-Fe alloy, dil., 4.2 to 273K *(Russian)* 3−8152
Cu-Fe alloys, resist., ageing characts. 3−37075
Cu-M alloy, polycrystalline, collective recrystallisation rel. to excess valence of alloying addition, M, resistivity obs. *(Russian)* 3−12366
Cu-Zn alloy, resist. obs. of β-α massive transform. kinetics 3−39319

electrical conductivity of solids continued
Cu-Zr alloys, eutectic and hypo-eutectic, directionally-solidified, characteriz. 3−34558
$Cu_{2-x}Ag_xSe$, metal-nonmetal transition, elec. cond., energy gap 3−38805
$CuAlS_2(Se_2)$, p-type cond. 3−39265
Cu_5As_2 single cryst. characteriz. *(Russian)* 3−12329
Cu_3Au, cyclotron irradiation effects 3−14898
Cu_3Au alloy, disordering process study by electrical resistivity meas. 3−8896
$CuGa(In)Te_2$, semicond., temp. depend. meas. *(Russian)* 3−15191
$CuGaS_2$, grown by I_2 transport, p-type cond. and green photolum. 3−30474
β-Cu_2HgI_4, disorder phenomena 3−1718
γ-CuI disorder phenomena 3−1718
CuI film, temp. depend. *(Russian)* 3−24432
$Cu_{1-x}Ni_xFe_2O_4$ ferrite, extraordinary Hall const., resist., 293-550K 3−24459
CuO-TeO_2 system, rel. to phase diagram 3−20847
Cu_2O thin films, temp. depend., activation energy calcs. *(Russian)* 3−38833
x CuO(1-y-x)PbO.y SiO_2, glass, infl. of CuO content *(Russian)* 3−11889
Cu_xS, electrical resistivity and optical transmission as function of composition 3−33904
β-Cu_3Sb, electrotransport obs. and mechanism *(German)* 3−24298
Cu_2Te, n and p type, electrical props. *(Russian)* 3−8170
Dy, resist., ferromag.-antiferromag. transform. behaviour *(Russian)* 3−15363
$DyAu_2$, elec. resist., thermal expansion, 4.2-60 K 3−33860
Dy_2O_3, high temp. variations, equil. oxygen press. depend. *(French)* 3−38831
Er film, elec. cond. change due to sorption of H_2 and O_2 3−30553
$ErZn_{12}$, antiferromag., crit. scatt. and low temp. deviations from Matthiessen's rule in resist. 3−30450
$ErZn_{12}$, spin disorder resist., 2K-300K 3−2051
Eu chalcogenides, optical electrical and magnetic props., review 3−11848
p-$EuCr_2Se_4$, doped, ferrimagnet 3−27385
EuO crystal growth parameters relation to stoichiometry, determ. by i.r. and conductivity meas. 3−7641
Eu_2O_3, high temp. variations, equil. oxygen press. depend. *(French)* 3−38831
Fe, pure, Lorenz number determ. at high temps. 3−18118
Fe alloy D16, aging effect 3−21677
Fe-Al(40 at.%) alloy, ordered, quenched defect recovery *(French)* 3−24839
Fe-Co-Mn, cold-worked, elec. resist. meas. *(Japanese)* 3−12399
Fe-Mn-C alloys, infl. of mag. transformations on resistivity *(Russian)* 3−2271
Fe-Ni(29.7 at.%) alloy, martensitic pretransformation phenomena obs. 3−18561
Fe-Si alloys, 0-24%Si, effects of furnace cooling and water quenching 3−36776
Fe-Sn, dilute ferromag. alloy, two current cond. and impurity resist. 3−36719
(Fe-Ni)-P-C amorphous alloy, low temp. resist. anomaly 3−21234
$Fe_{1-x}Co_xAl$ solid solns., conc. depend. of resist. *(Russian)* 3−30087
$Fe_{1-x}Co_xS_2$, narrow band ferromag., elec. resist. below Curie point, anomalous temp. depend. 3−4992
$FeCr_2S_4$, temp. depend., 77-450 K 3−27258
$FeCr_2Se_4$, 300-500K *(Russian)* 3−14811
FeGe hexagonal single crystal, electrical resistivity meas. at 411 K 3−21239
$Fe_{1-x}Ni_xAl$ solid solns., resist. temp. depend., 80-300K *(Russian)* 3−18121
Fe_3O_4 film, magnetite, low temp. conversion from α-Fe_2O_3, hematite obs. 3−34173
FeS_2, pyrite, natural, resist., Hall effect, rel. to energy gap and mobility 3−38837
FeS_2, temp. depend., down to 1.3K 3−21070
$FeSi_2$:Mn, Co, semiconductor-metal transition resist., thermoelec. and Hall effect obs., 300-1400 K 3−33973
FeSn, electrical resistivity 4.2-420 K 3−21240
Ga film, sheet resist. meas. rel. to size effect parameters 3−30448
p-type GaAs, after proton bombardment and subsequent annealing 3−21442
GaAs, characts. rel. to laser irrad. *(Russian)* 3−27248
GaAs, damage produced by fast neutrons 3−33567
GaAs, depend. on heat treatment temp., thermal conversion rel. to impurities *(Russian)* 3−38832
GaAs, film, dominant oxygen contrib. to compensation rel. to elec. resist. 3−15156
p-GaAs, heavily doped, neutron irradiation effects, elec. conductivity, Mott transition, Hall coeff. 3−33823
GaAs, high purity by liquid and vapour phase epitaxy, resistivity 3−2676
GaAs, ion irrad., cond. in disordered regions *(Russian)* 3−2072
GaAs, microwave study of hot electrons 3−27263
n-GaAs, millimeter wave freq. response of hot electrons 3−2119
GaAs, mobility, anomalously high at room temp., resist. and Hall meas. 3−18140
GaAs, p^+-n photodiodes, electron irrad., defect studies, differential capacity and conductance measurements 3−33845
GaAs, resist. meas. with d.c. four point probe with nonpenetrating tip 3−27281
p-GaAs:Zn, magnetoresist. meas. rel. to impurity cond. 3−11914
$Ga_xIn_{1-x}P$:S, band structure from Hall effect and resistivity meas. 3−15215
GaP, p- and n-type, after proton bombardment 3−21443
GaP, thin film, determination from Hall constant 3−39298
GaP amorphous film, ohmic, hopping cond. and Poole Frenkel behaviour obs. 3−36604
GaP:O, props. of crystal grown from melt 3−24442
GaSb, electron mobility in Γ_{1c} band, temp. and press. depend. 3−24422
GaSe, meas. for crystals grown from vapour by different methods 3−2650

electrical conductivity of solids continued
GaTe thin films, structure, elec. and photoelec. props. *(Russian)* 3−33755
Gd, anomaly in meas. near 226K rel. to second mag. phase transition 3−15366
Gd high-temp., thermal diffusivity 3−33864
Gd-Dy alloy, spin disorder resistivity theory 3−4988
$GdNi_5$, resistivity between 5 and 300K, rel. to entropy changes assoc. with mag. ordering 3−12016
Gd_2O_3, high temp. variations, equil. oxygen press. depend. *(French)* 3−38831
$GdZn_{12}$, spin disorder resist., 2K-300K 3−2051
Ge, amorphous, d.c. cond. and pseudogap struct. 3−38839
Ge, amorphous, hopping transport, thickness depend. 3−38838
Ge, amorphous, model for low field cond. 3−8174
Ge, amorphous, reactor irradiation expts., resistivity var. with heat treatment 3−15195
Ge, amorphous sputtered layer, effect of deposition rate on physical props. 3−4934
n-Ge, anisotropy, hot electron drift velocity temp. depend. *(Russian)* 3−8196
Ge, characts. rel. to laser irrad. *(Russian)* 3−27248
Ge, effect of high-field domain in electron-hole plasma 3−24444
n-Ge, effect of multiple deformations of alternating sign *(Russian)* 3−18129
Ge, epitaxial, polycryst., amorphous, Hall mobility, carrier conc., cond., noise, 100-400 K 3−38855
Ge, evaporated film, structure change and elec. resist. step, depend. on substrate temp. 3−30372
n-Ge, I-V characts., impurity breakdown characts. 3−18166
Ge, impurity breakdown, origin of S-shaped I-V charact. 3−24443
Ge, n- and p-type, influence of single dislocations 3−24439
Ge, resistivity and lifetime changes during deform. before fracture 3−27279
p-Ge, size effect rel. to elec. cond. and hole cooling length 3−18161
Ge, strong microwave field, third harmonic generation *(Russian)* 3−11924
Ge absorption coeff. rel. to resist. at 10.6 μm 3−30787
Ge amorphous film, a.c. cond., contactless meas. in microwave region 3−15189
Ge amorphous film, rel. to electronic struct. 3−15116
Ge amorphous sputtered film, annealing activation energy determ. 3−30369
p-Ge double layer film, Hall coeff., elec. cond., transverse magnetoresistance thickness effects *(Russian)* 3−8284
Ge film, amorphous, rel. to order-disorder transformation 3−1800
Ge film, electroresist. and resist. rel. to deposition conditions 3−38909
Ge film, vacuum deposited *(Russian)* 3−24431
Ge film, vacuum deposited on glass 3−18542
Ge n-type, warm electron anisotropy 3−2102
Ge single crystal, current-voltage characts. under strong injection conditions, mag. field effects 3−24447
Ge temp. depend. of conductivity, spectral depend. of absorption 3−18131
Ge:Al, implanted, rel. to carrier generation at room temp. 3−2083
Ge:Au, cond. depend. on high elec. field, impact ionisation 3−33918
N-Ge:Au, hysteresis of I-V characts., and props. of elec. domains *(Russian)* 3−2100
Ge:Mn; Sb, recomb. wave current instability rel. to mag. field *(Russian)* 3−8180
Ge-Sn amorphous film, energy pseudogap from d.c. cond. temp. depend. 3−18055
GeSbSe amorphous film, temp. depend. 3−21080
$GeSb_2Te_4$, single cryst. characterisation 3−5279
GeSe amorphous film, temp. depend. 3−21080
GeTe-A^{II}Te solid solution, thermoelectric properties, temperature dependence 3−30502
$Ge_{15}Te_{81}S_2As_2$, amorphous, IV characts, hydrostatic press. depend. 3−38830
graphite-CrO_2Cl_2, lamellar compound, crystal structure and thermal stability 3−33491
$Gu_2Ga_4Te_7$, phase in Cu_2Te-Ga_2Te_3 system, semicond. props. 3−38660
Hf, 1200-2000K 3−24404
HfS_2, a.c. cond. and memory effects 3−30527
$HgSe_xTe_{1-x}$ pressure induced phase transitions, resistivity meas. 3−15011
In film, sheet resist. meas. rel. to size effect parameters 3−30448
$InAa_xP_{1-x}$ solid solutions, compositions, transport properties, electron effective mass 3−33802
InAs, electron irradiation damage studies 3−33555
InAs, temp. depend., electron effective mass determ. *(Russian)* 3−27250
n- InAs transport phenomena, heavily doped 3−36608
$InAs_{1-x}P_x$, vapour phase epitaxial material 3−2680
In_2O_3:Sn film, r.f. sputtered, transparency and elec. cond. 3−12200
In_2O_3-SnO_2 transparent conducting films, structure obs. by electron diffraction and spectroscopy 3−33763
InP, vapour phase epitaxial material 3−2680
InSb, dependence of Hall voltage and electrical resistance on temperature and magnetic field 3−5021
n-InSb, magnetoresist. meas., impurity cond. effects 3−38857
n-InSb, strongly compensated, meas. at low temp. rel. to conduction band distortion 3−15216
p-InSb, thin crystals, current voltage characts., surface cond. effects *(Russian)* 3−2073
InSb, thin films, high field electrical conduction, breakdown, intercrystalline potential barriers 3−38852
n-InSb band tailing, hot electron magnetophotocond., cond. and Hall coeff. obs. 3−2138
InSb film, resist. change due to surface trapping *(Russian)* 3−30492
InSb films, electrical props. rel. to structure of size quantisation 3−24528
n-InSb impurity conduction, Hall coefficient, activation energies, impurity concentrations 3−30501
In_2Se_3-Sb_2Te_3, X-ray obs. of phase diagram, elec. cond. depend. on comp. *(Russian)* 3−14964

electrical conductivity of solids continued
Ir, 293-2275 K, meas. 3−21045
K, phonon drag and Matthiessen's rule 3−36583
K, phonon drag effect on low-temperature resistivity 3−2045
K complex, $K_2Pt(CN)_4Br_{0.3} \times 2.3H_2O$, elec. cond. at press. to 10^5 atm. 3−15180
K film, electron-phonon interactions at low temp. 3−4994
$K_2SO_4:Co^{2+}$, cond. by cation vacancies 3−36607
$LaNi_5$, resistivity between 5 and 300K, rel. to entropy changes assoc. with mag. ordering 3−12016
Mg-Cd alloys, temp. and concentration depend. of electrical resistivity, phase diagrams *(German)* 3−34551
Mg-Nd, dilute alloy, elec. resist. meas. rel. to precipitation of phases 3−18580
MgF_2 film, influence of prep. and measurement conditions *(French)* 3−2094
Mg_2Ge, melt-grown, characterization 3−12270
MgO, radiation degree of blackness, electrical resistance 3−36423
MgO high-porosity layer, secondary-electron conductivity 3−15206
Mn ferrites, temp. depend. 10-100K 3−5001
Mn/SiO cermet film, elec. resist. and struct. 3−27754
Mn-V(Cr)(Fe)(Ru), antiferromag., anomalies in elec. resist. meas. rel. to Neel temp. determ. 3−34119
MnBi thin film, changes during annealing *(Japanese)* 3−34005
$Mn_xFe_{3-x}O_4$, 100-1000K 3−5010
MnO_2, commercially electrodeposited, heat treatment effect on the semiconductor properties 3−2086
Mo, ion-irrad. effects *(Russian)* 3−4776
Mo and Mo-rich-Re and Mo-Nb alloys, 4.2-295 K 3−38824
Mo fibre, annealing temp. effects on props. rel. to composite fabrication *(Czech)* 3−31153
Mo-Rh alloys, elec. resistivity meas. at high temps. 3−36576
NH_4ClO_4, pure and doped, temp. depend. cond. mechanism 3−2081
NH_4I, kinetics of low temp. phase transformations, conductivity obs. 3−38667
$NaCl:Mn^{2+}$, meas. of charge acquired by dislocations 3−17843
$NaNO_2$, ferroelectric, high field, rel. to breakdown 3−5160
Na_2O-K_2O glasses, Na^+ and K^+ mobilities, 350-500°C *(French)* 3−5013
Nb, electron irradiated, anomalous resistivity due to H_2 contamination 3−15723
Nb and Nb-rich-Zr alloys, 4.2-295 K 3−38824
Nb/Al_2O_3 cermet film, superconductivity, normal state elec. and struct. props. *(Russian)* 3−30482
Nb/Al_2O_3 thin cermet films, hopping conduction through localised states 3−11895
Nb-N-O solid solutions, rel. to nitrogen conc. determ. *(Russian)* 3−39335
Nb-S system cpds., nonstoichiometry rel. to elec. props. at thermodynamic equil. *(French)* 3−2113
NbO, resist. and Hall coeff. meas. in high mag. field showing metallic behaviour 3−33888
Nb_2O_5, in m.i.m. struct., cond. mechanisms and bistable switching 3−18135
Nb_3Sn, density of states of phonons, energy gap harmonics and subharmonics, differential cond. obs. *(Russian)* 3−4823
Nd-Sb system alloys, physical props. and correlation with the phase diagram *(Russian)* 3−11882
Nd-Y alloys, 100 to 800 K, precip. depend. *(Russian)* 3−15683
$NdNi_5$, resistivity between 5 and 300K, rel. to entropy changes assoc. with mag. ordering 3−12016
Ni, pure, Lorenz number determ. at high temps. 3−18118
Ni alloys, conc., rel. to electronic structure and crit. cones. for mag. transitions 3−4993
Ni and alloys with 1-3% transition metal, press. coeff. of resist., 0-60 kbar *(French)* 3−30441
Ni film, CO adsorption states, thermal desorption *(German)* 3−27184
Ni film, effects of N_2 and CO adsorption 3−8144
Ni film, thickness depend. of resist., 77K 3−27244
Ni solid soln., giants moments, anomalous resist. due to cond. electron scatt. by Ni clouds 3−36716
Ni:Sn, meas. on deformation, defect accumulation effects *(Russian)* 3−12409
Ni-Al, temp. depend. meas. showing phase transition *(French)* 3−8361
Ni-C, expt. confirmation of resist. calc. for two phase materials *(German)* 3−8993
Ni-C carmet film, t.c.r. 3−5063
Ni-Cr, elec. resist. obs. of ordering with shock deform. of K-state 3−21697
Ni-Cr (20%) alloy, residual resistance, reln. to initial defect state, after deformation *(Russian)* 3−8877
Ni-Ge alloy film, conc. depend. *(Russian)* 3−18123
Ni-NiO, electrical and structural props. of amorphous system 3−38840
Ni-P alloys, change in resistivity due to tempering *(French)* 3−12359
Ni-P alloys, resist. decrease during tempering, hydrogen emission *(French)* 3−2738
Ni-P film, effect of oxidation 3−18028
Ni-Sn, dilute ferromag. alloy, two current cond. and impurity resist. 3−36719
$Ni_3Al(Ga)$, low temp. resist. and spin density fluctuation theory 3−21046
$NiFe_{2(1-c)}Cr_{2c}O_4$, depend. on comp. and cation lattice point distrib. *(Russian)* 3−38568
$NiFe_2O_4$ ferrite, effect of addition of CaO *(French)* 3−8362
$NiFe_2O_4$ with CaO additions and $Ca_xNi_{1-x}Fe_2O_4$, Verwey mechanism of electronic cond. and dielec. polarisation *(French)* 3−34286
NiO, at high temp., press. depend. 3−24421
NiO, high temp. cond., cationic vacancy conc. 3−36606
$Ni_{41}Pd_{41}B_{18}:Cr$, amorphous, elec. resist. meas. showing Kondo effect 3−33869
NiS, meas. at paramag. metal to antiferromag. semimetal transition 3−36540
NiSb, elec. resist., Seebeck coeffs., rel. to comp., defect clustering 3−18124
Ni_2SiO_4 measurements, phase equilibria, high temp. and pressure, olivine-spinel transformation 3−12606

electrical conductivity of solids continued
$NiVTi_2S_4$, resist. meas. ref. to order-disorder transition temp. of vacancies 3−33647
Pb, determ. from 80 to 400 K 3−24405
Pb restivity, additional due to metal impurity atoms, experimental results, Ashcroft pseudopotential theory *(Russian)* 3−30452
Pb:Bi superconducting thin films, surface impedance *(German)* 3−21165
Pb-Fe dilute alloys, spin-disorder resistivity meas. as function of temp. in 0-60 kOe 3−2057
Pb-In hard non-ordered, electrical resistivity concentrational dependence *(Russian)* 3−11883
Pb-Sn hard non-ordered, electrical resistivity concentrational dependence *(Russian)* 3−11883
$PbFe_{12}O_{19}$, ferrite with magnetoplumbite structure, anisotropy of hopping cond. and thermoelec. power 3−38829
PbN_6, pure and doped thin films, photodecomposition, optical absorpt. and cond. meas. 3−25084
PbO, between Pt electrodes, memory effect *(Russian)* 3−30525
PbS(Te), Lorenz number, 77K and lower, calc. 3−33877
PbSe, band inversion under hydrostatic press., elec. resist. and galvanomag. obs. 3−2004
$Pb_{1-x}Sn_xSe$, $0 \leqslant x \leqslant 0.3$, band inversion under hydrostatic press., elec. resist. and galvanomag. 3−2004
$Pb_{1-x}Sn_xSe$, grown from vapour, resistivity meas. 3−24438
PbTe-TlTe system, phase diagrams and electrical props. *(Russian)* 3−8169
Pd film, 1000 Å, looped I-V characts., obs. 3−27239
Pd film, CO adsorption obs. *(Japanese)* 3−20929
Pd-Mn(Fe)(Co) dilute alloys, ferromag. transition temp., resist. study 3−30624
Pd-Ni, dilute alloy, pressure effect on low temp. elec. resist. 3−15170
Pd-Ni, spin fluctuation resistivity, T-matrix calc. as function of temp. 3−4991
Pd-rare earth, paramag. dilute alloy, residual elec. resist. meas. rel. to scatt. mechanisms 3−15349
PdCr, interimpurity interaction effects below spin fluctuation temp., elec. resist. meas. 3−15348
$PrNI_5$, thermal, magnetic and electrical props. 3−8357
Pt, lattice contraction due to quenching-in vacancies, resist. study 3−30118
Pt, specific resist., 60-860°C, rel. to Fermi energy determ., two-zone model approx. *(Russian)* 3−30391
Pt film, CO adsorption obs. *(Japanese)* 3−20929
Pt wire, elec. resist. charge on immersion in liquid He, thermal shock 3−4746
PtSi, PtGe, resistivity, characterization of single crystals 3−5268
β-pu, elec. resist., $T<4.2K$, self irrad. damage effects 3−2050
β-Pu-Np alloy, elec. resist., $T<4.2K$, self irrad. damage effects 3−2050
PuO_2, sintered pellets, meas. from 20 to 1500°C 3−18132
PuX_n, ($X=Ru$, Rh, Ir, Pt, $n=2$ and $X=Rh$, Pd, Pt, $n=3$), and mag. susceptibility 3−38966
$RbNO_2$, anomalous thermal effects due to solid-state transitions, differential thermal analysis and electrical conductivity meas. 3−15010
Rh, elec. resistivity meas. at high temp. 3−36576
Rh-Fe-Mn, Rh-Mn, Rh-Fe alloys, low temp. meas. and comparisons 3−4990
Sb film, elec. resist. rel. to thickness 3−18233
Sb single crystals low temperature depend. Hall coefficient 3−36625
SbSI, cond. mechanism determ. 3−33955
$Sb_2Te_3:I$, I impurity influence on meas. 3−8607
Sc four probe potentiometric method, 290-1300 K, thermal diffusivity 3−38823
Se, hexagonal, polycrystalline layers, dark conductivity for high crurent densities *(Russian)* 3−30475
Se, trigonal single crystals, electroconductivity, current-voltage characteristics, temp. dependence *(Russian)* 3−33890
Se glassy, elec. cond., density and crystn. rate rel. to S and Te additions 3−33887
Se texture effects 3−33723
Se trigonal single crystal, photoconductivity, thermally stimulated currents, trap distrib. obs. *(Russian)* 3−30516
Se-Ag junction, asymmetric conduction changes under electric field influence, due to impurity redistribution *(Russian)* 3−11951
Se-Ge system, low-field, temp. depend., current-voltage characteristics 3−38843
Si, characts. rel. to laser irrad. *(Russian)* 3−27248
n-Si, current carrier heating technique, warm electron region *(Russian)* 3−33939
Si, diffused layers formed by multistage diffusion *(Russian)* 3−18137
p-Si, double injection currents 3−33909
Si, effect of thermal defects *(Russian)* 3−11890
p-Si, elec. resist. under shock wave compression 3−18138
Si, electron irradiation at 0.5K, a.c. conductivity changes 3−7794
Si, epitaxial thin film, spreading resistance meas., device applications 3−38835
Si, heavy doped, transport equations 3−24419
Si, high energy C^+ bombarded, damage profiles, resistivity profiling 3−17887
Si, high resistivity sample, current oscillations 3−11898
Si, in surface barrier radiation detector, electron beam radiation damage effects 3−32157
Si, insulating amorphous layer form. on Si^+ bombard., props. on annealing 3−7798
Si, n- and p-type, influence of single dislocations 3−24439
Si, polycryst. thin films, resistivity model 3−38836
Si, resist. meas. with d.c. four point probe with nonpenetrating tip 3−27281
Si, striations, detection by resistivity meas. after annealing *(German)* 3−2068
Si amorphous films, electronic transport and state distribution 3−8172
Si amorphous layers, current-voltage characts. 3−15200
Si film, deposited from SiH_4-H_2, influence of AsH_3, PH_3 and B_2H_6 3−21529

electrical conductivity of solids continued
Si film, doping conc. depend. 3−21069
Si film, epitaxial on sapphire, effects of vacuum deposition conditions *(Russian)* 3−24813
Si film, homogeneous, on sapphire, current filamentation, dynamic temp. config. 3−21102
Si implanted with B ions through thermal SiO_2 films, resist. 3−24523
Si n-type, warm electron anisotropy 3−2102
Si negative differential conductivity, inhomogeneous electric field, 77 K, critical drift rate *(Russian)* 3−33922
Si on sapphire, thin films surface charge effects, surface depletion 3−2185
p-Si:Al, (B), (Ga), electron irrad., annealing, effect of O and acceptor impurities 3−33560
Si:As, bulk resist. vs. As doping curves rel. to diffusin temp. 3−21024
Si:Pd, investigation of impurity level effects 3−24436
n-(221)Si/(1122)Al_2O_3 film, anisotropy 3−11961
SiC, rel. to annealing *(Russian)* 3−8211
SiGe resistivity, alloys as thermoelectric materials, Hall effect 3−5023
Si_3N_4 film, 50-100 Å, conduction mechanism 3−38910
Si_3N_4 film, identification of electronic cond. mechanisms *(German)* 3−15199
Si_3N_4 film, local, scanning low energy electron beam obs. *(German)* 3−15283
SiO film, Al and/or Ag electrodes, field and temp. depend., switching, memory effect 3−21124
SiO_2, film, thermal oxidation, transport processes 3−21157
SiO_2, radiation degree of blackness, electrical resistance 3−36423
SiO_2 film, in m.i.s. struct., tunnelling mechanisms *(German)* 3−15258
SiO_2 film, local, scanning low energy electron beam obs. *(German)* 3−15283
SiO_2 films on Si, annealing of degradation by Ar^+ ion bombardment 3−17879
SmS, metallic phase, 3-298K, high press. 3−38978
$SmZn_{12}$, spin disorder resist., 2K-300K 3−2051
Sn resistivity, additional due to metal impurity atoms, experimental results, Ashcroft pseudopotential theory *(Russian)* 3−30452
Sn-SnO_2, electrical and structural props. of amorphous system 3−38840
SnO_2 film, chemisorption of O_2 and H_2, var. of electrical conductance *(Japanese)* 3−8024
SnO_2:Sb film, r.f. sputtered, transparency and elec. cond. 3−12200
SnS_2 mechanisms, space charge injection prior to forming 3−18155
$SnSe_2$, meas. under pressure rel. to band structure 3−8176
SnTe:Mn, growth, transport props. rel. to mag. impurities 3−33882
SnTe-PbSe system, comp. and temp. depend. *(Russian)* 3−11918
$SrFe_{12}O_{19}$, ferrite with magnetoplumbite structure, anisotropy of hopping cond. and thermoelec. power 3−38829
$SrTiO_3$, (Ba, Sr) TiO_3, boundary layer dielectrics 3−2485
Ta film, β-phase and β-b.c.c. mixtures, temp. coeff., 4.2-380 K 3−27242
Ta film, r.f. sputtered, β and b.c.c. struct., resistivity and t.c.r. obs. 3−1955
Ta film, review 3−21533
Ta film, triode-sputtered in Ar-O_2 mixture *(Russian)* 3−30375
Ta thin film resistors reactively sputtered in O_2, effect of deposition temp. 3−39226
Ta wire, plastic deform. and neutron irradiation rel. to elec. resist. changes 3−18623
Ta:H, H diffusion activation energy, elec. resist., 77-400K 3−38682
Ta:N film, triode-sputtered, effect of N_2 flow rate 3−18111
Ta-H system, 77-300K 3−20711
Ta-Ta_2O_5, electrical and structural props. of amorphous system 3−38840
Ta_2O_5, polycrystalline, 900-1400°C, dependence on O_2 partial pressure 3−8213
Ta_2O_5 thin films, thermal currents, energy peaks, dipolar polarisation model, dipole moments and density *(French)* 3−38911
$TbZn_{12}$, spin disorder resist., 2K-300K 3−2051
Te, acoustoelec. non-ohmic conduction, carrier conc. depend. 3−33959
Te, meas. rel. to carrier mobility anisotropy 3−21111
Te-As-Ge-Si film, freq. depend. cond. and capacitance 3−2092
Te-As-Ge-Si thin film capacitors, frequency dependence of capacitance and conductance 3−27321
Th_3P_4-U_3P_4 solid solution, type of conduction, comp. depend. 3−5022
Ti film, adsorption of CO_2, binding state detn. *(Japanese)* 3−20930
Ti film, CO adsorption obs. *(Japanese)* 3−20929
Ti film, dislocation-enhanced elec. resist. 3−21049
Ti film, epitaxial, resistivity 3−4995
TiC-Nb(Ta)(Mo)(W), cermet, temp. depend. *(Russian)* 3−8988
Ti_2O_3, resistivity and one dimensional energy bands 3−21008
Tl film, sheet resist. meas. rel. to size effect parameters 3−30448
$TlIO_3$ single crystal, growth and props. *(Japanese)* 3−27605
Tl_xIn_xSe, temp. and comp. depend. 3−17957
$TlSbSe_2$ film, characterization *(Russian)* 3−18235
$Tl_2SeAs_2Te_3$, glassy, macroscopic inhomogeneities using contactless-conductivity technique and comp. homogeneity from probe obs. 3−11896
Tl_2Te amorphous film, low temp. conduction and recrystallisation 3−27249
UAs_2, antiferromagnet, temp. depend. of transverse resist. 3−2106
UAsY (Y=S, Se, Te), electrical resistivity rel. to temp. and mag. structure 3−15175
UC, neutron irradiated, recovery stages 3−17281
UC, U vacancy formation and migration, resistivity meas. 3−24966
UO_2-CeO_2(PuO_2), sintered pellets, meas. from 20 to 1500°C 3−18132
$UO_{2|x}$, sintered pellets, meas. from 20 to 1500°C 3−18132
USb_2, antiferromagnet, temp. depend. of transverse resist. 3−2106
$(U_xTh_{1-x})S$, electronic props., models, mag. susceptibility, sp. ht. and elec. resist. obs. 3−2249
V, allotropy possibility, resist. meas. 3−34503
V film, 1000 Å, looped I-V characts., obs. 3−27239
V-C supersaturated solid soln., carbon precip. obs. 3−37036

electrical conductivity of solids continued
$(V_{1-x}Cr_x)_2O_3$, ceramic, low temp. resist. meas. 3−27744
$V_{1-x}Mo_xO_2$, at metal-insulator, monoclinic-tetragonal transition 3−30424
V_2O_5, switching mechanisms, pressure and temperature dependence 3−8234
V_2O_5-P_2O_5 glass, d.c. cond. by polarons 90-520K 3−33886
$V_{1-x}W_xO_2$, semicond.-metal transition study, 80-400K 3−18205
W, arc cast resistivity, measurement, direct heating method, TPRC multi-property apparatus 3−12426
W fibre, annealing temp. effects on props. rel. to composite fabrication *(Czech)* 3−31153
W film, r.f. sputtered, rel. to morphology 3−27241
W-Re, cermet alloy, meas. rel. to Nordgeim law *(Russian)* 3−8141
WO_3, electrical conductivity from −190° to +580°C, variation due impurities 3−27261
YIG:Si^{4+}(Ge^{4+})(Ca^{2+}), mag. after-effect, electronic hopping processes 3−24591
Y_2O_3, electron beam evaporated film, d.c. cond. meas. 3−24320
Yb, b.c.c., h.p. resist.-temp. behaviour 3−5074
Yb, phase transforms., resist. study, 300-1088 K 3−27125
Zn, temp. depend. *(Russian)* 3−8154
Zn thin films, sputtered, high stability resistance, Laville Saint Martin's theories *(French)* 3−38908
$ZnCr_2Se_4$, 300-500K *(Russian)* 3−14811
$Zn_xHg_{1-x}Se(Te):Mn^{2+}$, temp. and comp. depend. 3−15409
ZnO, ion-implanted, anneal characts. 3−30955
ZnO:In temp. depend. 5 to 300K *(German)* 3−11899
ZnO:Li, thermally stimulated cond. associated with thermolum. 3−15566
ZnO(:Cu), elec. cond. and Hall effect, 5 to 300 K *(German)* 3−33933
ZnS, meas. from 1040 to 1170°C and additive coloration 3−21076
ZnS:Cu,Cl film, stimulated cond., quenching by elec. pulses *(Russian)* 3−2069
ZnSe, defect centres, energy levels and effective radii, thermally stimulated current obs. *(German)* 3−15160
ZnSe, undoped, p-type cond. 3−36602
p-$ZnSiAs_2$, 77-900 K 3−24425
$ZnSnAs_2$, chalcopyrite and sphalerite forms, neutron effects 3−15514
ZnTe, acceptor defect levels, elec. transport 3−18096
ZnTe, amorphous, temp. depend. 3−1942
ZnTe, amorphous thin films, O_2 chemisorption effect on electrical conductivity 3−27320
Zr-O, HCP alloy, meas. rel. to phase transform. 3−30973
ZrO_2, oxide defect structure effect on elec. cond. 3−8235

electrical conductivity transitions
see also metal-insulator transition
$A^{III}B^{VI}$, $A_2^{III}B_3^{VI}$, $A^{II}B_2^{III}C_4^{VI}$ type compounds, single crystals, switching, I-V characts. 3−38873
amorphous semicond., switching effect at discontinuous changes in heat transfer 3−30528
amorphous semicond. doped highly compensated cryst. semiconductor model for switching and memory 3−36644
amorphous semiconductor film, pre- and postswitching phenomena 3−18196
chalcogenide film, noncryst., switching, room temp. and 77K 3−21129
chalcogenide film, switching and memory effects 3−18198
chalcogenide glass, electronic conductivity and switching 3−18134
chalcogenide glass, reversible thermal breakdown as a switching mechanism 3−18197
chalcogenide glass film, threshold switching 3−30523
chalcogenide thin film devices, threshold switching, surface temp. changes 3−27294
chalcogenide threshold switches, thermal and nonthermal relax. processes 3−21127
diamond, metallic transition at 1 Mbar 3−18204
instabilities in temp. depend. conductors, review 3−27290
liquid metals in critical region of temperatures and pressures, metal-dielectric transition 3−30385
memory-type material, switching phenomena, electron microscope obs. 3−2151
Mott transition in transition metal compounds, influence of pressure, review 3−24485
rare earth monochalcogenide, pressure-induced semicond.-metal transition 3−27221
semiconductor, thermal switching, cooling parameter effects 3−27292
semimetal film, carrier conc. and mag. moment behaviour in semimetal semicond. transition region *(Russian)* 3−18064
switching materials, conducting particles in semicryst. matrix 3−18201
thermal instability, boundary conditions 3−21125
transition metal oxide glass, switching delay time measurement 3−18199
Ag-SiO_2-Co, reversible memory switching 3−11958
Al_2O_3 thin films, electroforming and dielec. breakdown *(Russian)* 3−30530
Ar-Cu film, metal-nonmetal transition 3−27291
$As_{30}Ge_{10}S_{12}Te_{48}$ amorphous film, switching props. *(German)* 3−15229
As_2Se_3, amorphous, elec. field enhanced phase separation and memory switching 3−5042
As_2Se_3:B(Al)(In)(Ga)(Tl), vitreous, a.c. cond. and dielec. const. depend. on freq. and temp. 3−30742
$BiCl_3$ molten salts, supercritical temp. range, continuous density transition, experimental investigation 3−11728
$Bi_{1-x}Sb$, gapless state, magnetoresist., semicond.-semimetal-semicond. transition 3−33791
C, glassy, correlation with memory time 3−33966
$CdCr_2Se_4$, mag. semicond., switching effects 3−33967
CdF_2, insulating to semicond. transition rel. to lattice defect statistical thermodynamics 3−4947
CdSe, impact ionisation, breakdown, photoinduced switching, meas. of cond., Hall coeff., mobility, 4.2-300K 3−30487
CdSe single crystals, memory props. 3−24484
Cs liquid, absolute thermoelectric power and electrical conductivity in metal-nonmetal transition range 3−27247

- **electrical conductivity transitions** continued
  - Cu-As-Se-Au glass, memory effect rel. to Au content 3−33969
  - Cu-Cu_2S-CdS-Au sandwich structure, switching and filament migration scanning elec. microscope obs. 3−2150
  - $CuFe_2O_4$, elec. switching, memory phenomena 3−18202
  - Cu_xS, electrical resistivity and optical transmission as function of composition 3−33904
  - $FeSi_2$, amorphous material, semiconducting to metallic transition 3−36419
  - $FeSi_2$:Mn, Co, semiconductor-metal transition resist., thermoelec. and Hall effect obs., 300-1400 K 3−33973
  - GaAs:O junction, duplex transport phenomena, switching and memory effect 3−2178
  - p-GaSe, light effect on switching props. at 77K 3−21126
  - GeTe, amorphous film, switching and memory effects 3−18206
  - HfS_2, elec. props. and memory effects 3−30527
  - Nb_2O_5, in m.i.m. struct., cond. mechanisms and bistable switching 3−18135
  - NiS_2, non-stoichiometry influence at insulator-metal transition 3−2017
  - PbO, between Pt electrodes, memory effect *(Russian)* 3−30525
  - S-Se-Te system, amorphous thin film, memory switching phenomena 3−36642
  - Se, amorphous, hole mobility rel. to conductivity hysteresis at vitrification temp. 3−30529
  - Se, liq., reversible switching effect above 720°C 3−36645
  - Se, low-conductance switching effect, delay time and conductivity expiration 3−30526
  - Se, metallic state stability under pressure 3−30419
  - Se amorphous film, optical memory laser induced, voltage bias effects 3−32610
  - Se-SnO_2 film system, polarized memory effect 3−2146
  - $Se_{87}Te_{13}$, elec. switching in glass transition range 3−33970
  - $Se_{50}Te_{20}As_{20}Ge_{10}$, amorphous, stress thermally induced by switching 3−27293
  - $Si_{1.2}Ge_{1.0}As_{3.0}Te_{4.8}$, chalcogenide glass film, switching rel. to breakdown mechanism 3−38874
  - $Si_{12}Ge_{10}Te_{48}As_{30}$, mechanism of threshold and memory switching in glassy chalcogenide alloy devices 3−36643
  - SiO film, Al and/or Ag electrodes, switching and memory effect 3−21124
  - $Sm_{1-x}Nd_xSe$, from semiconducting SmSe to metallic NdSe 3−2148
  - SmS-SmSe mixed crystals, semiconductor-metal transition 3−4957
  - Te based chalcogenide film as memory material, crystallisation after short laser pulse 3−30524
  - Te chalcogenide, switching action, Mossbauer obs. *(German)* 3−15230
  - Te-As-Ge-Si film, accumulation effects in switching 3−18200
  - TiO_2, threshold switching phenomena 3−18203
  - VO_2, Hall effect near semiconductor-to-metal transition 3−33971
  - VO_2 film, pyrolytic, switching effect, electrophysical characts. 3−21164
  - V_2O_3, semicond.-metal transition, heat capacity, integrated transition heat, 120-190 K 3−21128
  - V_6O_{13}, growth by chem. transport, semicond. semicond. transition 3−24790
  - V_nO_{2n-1}, $(n=3\rightarrow 8)$ meas. for crystals grown by chem. transport 3−2648
- **electrical contacts**
  - *see also contact potential; contact resistance; ohmic contacts; point contacts*
  - ASTM standards, Pt.8, annual book (1972) 3−35353
  - fine-granular ceramic contact development for l.v. apparatus design *(Russian)* 3−27749
  - liquid crystal display, influence on scattering props. 3−14686
  - material compacting by explosive powder metallurgy *(German)* 3−31117
  - metal, in pressed iron powder sintering *(Bulgarian)* 3−8947
  - metal point contacts, phonon generation 3−18209
  - metal-semiconductor, E(k) relation for two-band scheme of semicond. 3−1999
  - metal-semiconductor, electron currents, equations 3−24506
  - metal-semiconductor boundary, Imref behaviour, theory 3−30539
  - static electrification, physical models 3−2166
  - Ag-Al thin film contacts, degradation mechanism during annealing 3−15241
  - Al/Al_2O_3, electron injection into anodic oxide 3−8261
  - Au/glass or quartz, electrification, elec. field and temp. effects 3−2168
  - n-CdTe diodes with Au contacts, elec. props. meas. 3−18216
  - Cu/Teflon, static electrification 3−2170
  - Cu-CdS, elec. and photoelec. props. 3−8265
  - n-GaAs resistance, evaporated silver contacts, surface cleaning by ion bombardment, experimental results 3−15250
  - Hg on Si, for nondestructive C-V meas. 3−2182
  - $In_{2-x}Sn_xO_{3-y}$ film, transparent, highly conductive, prep. by d.c. diode sputtering 3−2193
  - Nb/Nb_2O_5, electron injection into anodic oxide 3−8261
  - Ni/glass or quartz, electrification, elec. field and temp. effects 3−2168
  - n- and p-Si, with Al and Pd_2Si, specific contact resist. 3−27311
  - Si pedestal growth by liquid phase epitaxy on planar diodes, selective growth 3−2670
  - Si-Au, Si-Al, contact potentials and barrier heights 3−5053
  - Ta/Ta_2O_5, electron injection into anodic oxide 3−8261
- **electrical engineering**
  - electronics education and training at physics research laboratory for untrained personnel 3−28627
  - papers for publication, principal requirements for manuscripts *(Russian)* 3−25639
  - SI units, relation with mechanical engineering *(German)* 3−19137
- **electrical engineering applications of computers**
  - *see also electronics applications of computers*
  - eddy currents calculation in axially symmetric a.c. current carrying conductors *(Russian)* 3−32485
  - electrostatic precipitator, example of c.-a.d. of complex enclosures 3−37924
  - nuclear reactor reliability and availability analysis *(German, English)* 3−19907
  - nuclear science conference, Miami USA (1972) 3−28622
- **electrical fault location** *see fault location*
- **electrical forming** *see electroforming*
- **electrical impedance**
  - *see also admittance; reactance; resistance (electric)*
  - cats, left ventricle rel. to flow and pressure source 3−36141
  - chalcogenide film, structure obs. rel. to switching from high to low impedance state 3−8061
  - cylindrical antenna in collisional magnetoplasma 3−7497
  - e.m. wave impedance and S-matrix definition, comments 3−13679
  - gap in waveguide 3−35664
  - loop antennas over inhomogeneous ground, mutual impedance between loops and dipole 3−32478
  - skin impedance, effects on surface electrode meas. between 5 and 2000 Hz 3−31846
  - superconducting weak links, with negligible capacity, r.f. impedance 3−18266
  - superconductor, type I, surface impedance in weak mag. field 3−15301
  - surface wave incidence on plane structure having multi-mode discontinuity in impedance 3−3998
  - thin cylindrical antenna, calculation of current distribution and impedance by method of moments 3−33352
  - Al barrier anodic films, elec. equivalent 3−15831
  - Al_2O_3 film, on Al, thickness meas. 3−36500
  - Cd, magnetic surface states, microwave surface impedance obs. 3−8243
  - Cu-Fe Kondo system, far.i.r. surface resist. 3−5046
  - Se thin film diodes, polarized memory effects 3−5043
  - ZnSe phosphors, photocapacitive changes 3−8499
- **electrical impedance measurement**
  - *see also reactance measurement; resistance measurement*
  - instrument for physiological event observation 3−25996
  - Lecher wire student expt., line termination study and complex impedance meas. 3−28453
  - plethysmograph, computer-aided analysis of quiet spontaneous breathing 3−25975
  - ratiometer, cct and applic. *(German)* 3−37664
  - sea ice, in situ at v.l.f. 3−28091
- **electrical insulation** *see insulation*
- **electrical noise** *see noise*
- **electrical power systems** *see power systems*
- **electrical properties of substances**
  - *see also carrier density; carrier mobility; crystal electron states; dielectric properties of substances; electric breakdown; electrical conductivity; photoconductivity; piezoelectricity; semiconductors; superconductivity; thermoelectricity*
  - alkalic rocks from Khibiny and Lovozero *(Russian)* 3−9136
  - ceramic dielectrics, thermal diffusion of injected impurities, props. 3−20901
  - clay-water systems, press. induced changes 3−2856
  - electrophotographic papers containing CdS, elec. and photoelec. props. 3−37648
  - ice, determ. using microwave radiometric technique 3−9157
  - igneous rocks, dependence of electrical props. on temp. and field frequency *(Russian)* 3−9135
  - insulating thin films, for solid state electronics *(German)* 3−15281
  - i.r. laser window materials, review 3−5980
  - liquids, element for obs., design *(Russian)* 3−6025
  - polymer, radiation-induced effects 3−11349
  - snow, determ. using microwave radiometric technique 3−9157
  - transition metal oxides, theory of props., review 3−15188
  - $BaTiO_3$:Y_2O_3, depend. on composition and cation siting 3−14813
  - Fe-Si steels, manufacturing processes, development, applications to electrical power 3−15173
  - MoS_2 sputtered films 3−8282
  - $PbMo_2O_4$, single crystal *(Russian)* 3−8397
  - SnO_2 (cassiterite) ores, frequency dispersion of electrical properties at audio frequencies *(Russian)* 3−12613
- **electrical resistance measurement** *see resistance measurement*
- **electricity**
  - *see also atmospheric electricity; electric charge; electric current; electrical impedance; electrical properties of substances; electromagnetism; terrestrial electricity; triboelectricity*
  - No entries
- **electro-optical devices**
  - *see also liquid crystal devices; optical modulation; Q-switching*
  - anisotropic crystals, electric field modelling *(Russian)* 3−32102
  - frequency-shift, classification of suitable media 3−19644
  - integrated ten element linear modulator array 3−9966
  - laser and Kerr cell for h.v. meas. 3−3787
  - layered structures, diffr. modulation of optical radiation *(Russian)* 3−25725
  - light beam deflector, using $Sr_{0.75}Ba_{0.25}Nb_2O_6$ prism 3−2514
  - optical signal regeneration system *(Russian)* 3−13272
  - phase shifters, elect. controlled dispersive, theory 3−16910
  - shutter with laser beam synchronisation, pulse formation *(Russian)* 3−5986
  - $Al_yGa_{1-y}As$-$Al_xGa_{1-x}As$ double heterostructures, electroabsorpt. 3−39119
  - $Bi_4Ti_3O_{12}$ single-domain epitaxial films, contrast obs. 3−18431
  - CdS film, light-intensity modulator 3−12198
  - KH_2PO_4 crystal laser beam deflection system, multiple-pass *(Russian)* 3−9967
  - $LiNbO_3$ prism deflector, appl. to optical multiplexing and demultiplexing 3−16407
- **electro-optical effects**
  - *see also birefringence; electroluminescence; electroreflectance; Kerr electro-optical effect*
  - cascade tripler, conversion efficiency at optical freq. 3−10573
  - cholesteric planar texture, imperfectly aligned, elec. field induced blue shift 3−15508
  - colloids, double refraction *(Rumanian)* 3−22848
  - disordered semiconductors in external electric field, determ. of coeffs. of absorption *(Russian)* 3−24681
  - electric-dipole induction and echo, intensities, particle concentration dependences 3−39124
  - electrochromic substances, device for electrooptical characteristics 3−22404

electro-optical effects continued
ferroelectric materials, digression from phenomenological theory 3−18423
frequency shifting of laser light in velocity obs. 3−337
gas laser frequency modulation technique 3−720
geodimeter meas. of strain accumulation 3−156
inert gases, third-order hyperpolarizabilities, quantum calcs. 3−38275
laser, ruby, monofrequency with elctro-optical modulation and smooth reforming of emission frequencies *(Russian)* 3−29097
layered structures, diffr. modulation of optical radiation *(Russian)* 3−25725
light wave retardation in CS_2 and toluene, polarization interferometric determ. *(Russian)* 3−24678
linear, study using transformation formulas of rectangular coordinates expressed in Euler angles *(Russian)* 3−5177
liquid cryst., nematic, elec. controlled birefringence, field alignment rel. to pulsed voltage *(French)* 3−8553
liquid crystal, cholesteric, voltage effect 3−15472
liquid crystal, N-(p-methyoxybenzylidene)-p-n-butylaniline, role of electrode reactions in dynamic scatt. 3−12113
liquid crystal, nematic, decay time reduction when driven by d.c. pulse 3−24677
liquid crystal, nematic, with positive dielec. anisotropy 3−27484
liquid crystal, nematic new compounds for display devices 3−30066
liquid crystal nematic, transverse field electro-optical effects 3−24676
liquid crystals, dynamic light scattering *(Russian)* 3−30799
liquid crystals, nematic Schiff base 3−1570
media suitable for frequency-shift, devices, classification 3−19644
multiple pass laser beam deflection system using KH_2PO_4 crystals with quadrupole electrode arrangement *(Russian)* 3−9967
nematic liquid crystals, visualisation of u.s. waves 3−77
meta- nitroaniline, linear electro-optic coeffs. 3−12116
meta-nitroaniline, linear electrochromic effect 3−27485
optical susceptibilities, higher order, rotational invariance 3−29125
phase shifters, elect. controlled dispersive, theory 3−16910
photosemiconductor, optical props. changing mechanism by photocond. i.r. quenching 3−21388
picosecond light pulses *(Russian)* 3−2517
platelet suspension, optical props. anisotropic changes on elec. field appl. 3−9017
polyethylene, high density, i.r. absorpt. intensity rel. to elec. field 3−34324
quadratic medium, circular light nonlinear interaction 3−13757
radioastronomy 3−37505
refractive index damage, optically induced, laser, electrooptic crystals, mechanisms, susceptibility reduction 3−29146
semiconductor, Franz-Keldysh effect, density of states explanation 3−1969
semiconductor, impurity absorpt. in strong elec. field below absorpt. edge 3−34391
semiconductor, interband absorpt. mechanism with Landau selection rules violation 3−21389
semiconductor film, electrodispersion and electroabsorpt. spectra obs. 3−30801
semiconductor thin films, optical absorption edge shift, electric field dependence, electron spectrum quantisation 3−39125
semiconductors, amorphous, glassy, electroabsorption 3−34325
shutter with laser beam synchronisation, pulse formation *(Russian)* 3−5986
solid, two-photon absorpt. coeff. in uniform elec. field 3−15480
three dimens. anharmonic oscill. model, nonlinear susceptibility, linear electrooptic coeffs. 3−29131
trinitrofluorenone-poly-n-vinylcarbazole mixture, amorphous film, complexing study 3−18038
waveguide, modulation using nematic liquid crystals 3−39118
Ag film, electro-transmittance 3−12154
$Al_yGa_{1-y}As$-$Al_xGa_{1-x}As$ double heterostructures, electroabsorpt. 3−39119
Au film, electro-transmittance 3−12154
$Ba_xSr_{1-x}Nb_2O_6$, longitudinal effects 3−21385
$Bi_4Ge_3O_{12}$, wavelength depend., visible region 3−21427
$Bi_{12}SiO_{20}$, self-focusing of Ar laser radiation 3−32602
$Bi_4Si_3O_{12}$, wavelength depend., visible region 3−21427
$Bi_4Ti_3O_{12}$ film, electrooptical quality, epitaxial growth by r.f. sputtering 3−12252
$Bi_4Ti_3O_{12}$ single-domain epitaxial films, contrast obs. 3−18431
$(CH_3NH_3)AL(SO_4)_2.12H_2O$, ferroelectric, and thermo-optical props. 3−34328
CdS, elec. field induced Raman scattering 3−21407
CdS, photosensitive, modulation of absorption by field effect 3−24679
CdS and glass multilayer film, light-intensity modulation 3−12198
$CdS_{1-x}Se_x$, electro-absorption reduced effective mass 3−15471
n-GaAs, electroabsorpt. meas. for transitions from spin orbit split to cond. band 3−39123
GaAs, thin film, index difference control by elec. field application 3−2605
Ge, on surface levels in external elec. field 3−2163
In_3Te_4, thin films, abs. spectra at fund. obs. edge, rel. to exciton transition *(Russian)* 3−30818
K excited vapour, in presence of strong electric field, electro-magneto-optical effects 3−17347
KH_2PO_4, transverse, Q-switching, ruby laser output control *(Russian)* 3−741
KIO_3, ferroelectric, piezoelec. moduli, electrooptic phase modulation *(German)* 3−39096
$(K_2O)_{0.3}(Li_2O)_{0.7}(Nb_2O_5)_x$, dielec. const., refr. index, electrooptic coeff., spontaneous polarisation, birefringence, pyroelec. props. 3−30798
$LiNbO_3$ electro-optic prism deflector, appl. to optical multiplexing and demultiplexing 3−16407
$LiNbO_4$ oblique cut crystals, optical beam control *(Russian)* 3−693
$LiTaO_3$ crystal, prècision machining for electro-optic elements 3−171
$Pb_5Ge_3O_{11}$ and $Pb_5Ge_2SiO_{11}$, quadratic electro-optic consts. 3−18420
$PbMg_{1/3}Nb_{2/3}O_3$, ferroelec. with smeared phase transition, electrooptical effect linearisation and coeffs. 3−24680

electro-optical effects continued
$PbMg_xNb_{1-x}O_3$, longit. electrooptic effect 3−34327
$PbMg_{1/3}Ta_{2/3}O_3$, ferroelec. with smeared phase transition, electrooptical effect linearisation and coeffs. , 3−24680
$5PbO.3GeO_2$, linear and quadratic coeffs. 3−18433
$PbTa_2O_6$, low freq. linear effect meas. 3−12115
$PbZn_{1/3}Nb_{2/3}O_3$, ferroelec. with smeared phase transition, electrooptical effect linearisation and coeffs. 3−24680
$Pb(Zn_{1/3}Nb_{2/3})O_3$-$PbTiO_3$, quadratic electro-optic effect, g coeffs. 3−39122
Si p-n junctions, electroabsorption, influence of polarised light 3−34326
Si-SiO_2 boundary, inter-extrinsic transitions, surface extrinsic photocond., electro-absorpt. obs. *(Russian)* 3−24518
$Sr_{0.75}Ba_{0.25}Nb_2O_6$ prism, light beam deflection obs. 3−2514
$Sr_2Nb_2O_7$ ferroelectric single cryst., linear props. 3−21373
$SrTiO_3$, electroabsorpt. and band struct. 3−36891
Te, optical rectification due to i.r. radiation at 10.6 μm 3−12117
ZnO, macroscopic elec. fields, induced double refr. study *(Russian)* 3−2515
ZnS, macroscopic elec. fields, induced double refr. study *(Russian)* 3−2515
ZnSe, cubic, wavelength depend. of linear electro-optical coeff. *(French)* 3−18463
ZnSe, microwave modulation of light *(Russian)* 3−2516
electroacoustic devices
auditorium, increasing reverberation time, electro-acoustical system 3−19116
electroacoustic units using verbo-tonal system for hearing-impaired people 3−3516
hearing aid, conical coupler for measurements *(German)* 3−37594
CdS platelet oscillators, current saturation rel. to illum. 3−11936
electroacoustic effects *see acoustoelectric effects*
electroacoustic generators *see acoustic generators*
electroacoustic transducers
see also loudspeakers
scattering matrix description and nearfield meas. 3−89
surface wave, theory and expt. *(German)* 3−15227
electrocaloric effects *see pyroelectricity*
electrocardiogram *see electrocardiography*
electrocardiography
see also cardiology
cardiac resuscitator, patent 3−35248
dry electrode, transmitter for rapid acquisition from moving subject 3−25970
eccentric dipole, surface potentials 3−25551
insulated electrodes with integrated impedance transformer 3−3905
R-R intervals and R wave widths, analogue preprocessor for digital computer measurement 3−25991
electrocataphoresis *see electrophoresis*
electrochemical analysis
see also electrochemistry
aqueous solution, dissolved O_2 content, review *(German)* 3−32256
Bozicevic-Everaets detector, microanalysis, design, operation, advantages, applications 3−10194
crystallisation, electrochemical aspects *(German)* 3−9080
fracture mechanics and stress corrosion cracking 3−8034
function generator for controlled current and controlled potential expts. 3−6151
gas detectors, review 3−35551
metal, hydrogen uptake, detection method using anodic oxidation at bipolar electrodes 3−12522
potentiostat and its applications, book 3−12534
semiintegral analyzer, analog implementation 3−28768
signal generator for analysis of mixtures of electroactive species 3−37747
Al, oxide film removal by brazing flux and reaction soldering *(Japanese)* 3−31071
Al, pitting corrosion, alloying elements effect 3−8046
Fe-Cr-Ni alloy system, microstructural change study using selective etching *(Korean)* 3−5291
electrochemical batteries *see cells (electric)*
electrochemical electrodes
see also electrochemistry
composite-poste, small surface area 3−27876
electrode processes and adsorption study, special techniques, review 3−12533
ion-selective and gas-permeable for water quality monitoring 3−22187
ionic double layer study and adsorption phenomena 3−12530
metal, oxide films formation, theory of voltage sweep method *(French)* 3−31270
metal/electrolyte interface, adsorption of hydrogen *(French)* 3−2820
metal/electrolyte solution interface, multireflexion ellipsometry 3−31267
overpotential meas., electrode kinetic studies, review 3−12531
porous battery electrode processes, microscopic obs. 3−5864
porous electrode double-layer capacity determ. by triangular voltage sweep method 3−39448
quantum chemical treatment of adsorbed species, review 3−25102
resistive wire, current distrib. 3−39446
reversible electrode potentials meas., review 3−12529
surface area and porosity meas., review 3−12532
surface state and diffusion layer 3−6152
techniques of electrochemistry, book Vol. 1 3−12528
tubular, current distrib. 3−39447
tubulus system for mass transfer obs. in laminar and turbulent flow conditions 3−1355
water quality monitoring 3−22189
Ag, oxidation of Fe(II) oxalate complex, investigation of photographic process *(Russian)* 3−234
Au electroreflection spectrum, influence of the potential 3−36855
Cr monocrystalline and polycrystalline electrodes in H_2SO_4, anodic behaviour *(French)* 3−9077
Cu, in chloride soln., photopotential obs. of surface layer 3−8044
Cu, morphological changes of low-index planes, near equilib. 3−9075

electrochemical electrodes continued
Ni, in sulphate soln., photopotential obs. of surface layer 3−8044
Ni, intergranular cracking at cathodic potentials 3−31266
Ni, porous, in alkaline electrolytes, oxidation and reduction *(German)* 3−5392
NiO:Li, potential distrib. between space charge region and electrolyte Helmholtz layer 3−31268
$PbCl_2$-$CuCl_2$, fusion-cast, salt water batteries 3−3265
Pt electroreflection spectrum, influence of the potential 3−36855
Pt-Fe^{2+}/Fe^{3+} system faradaic shot noise of charge transfer step 3−15835
Zn, inhibition of dendritic electrocrystn. of Zn from doped alkali zincate soln. 3−12525

electrochemical machining *see electrolytic machining*

electrochemical polishing *see electrolytic polishing*

electrochemistry
see also electrical conductivity of electrolytic liquids; electrochemical analysis; electrochemical electrodes; electrodeposition; electrolysis; electrolytic devices; electrophoresis
α-Ag_2S powder, electrochemical method for estimating surface energy *(German)* 3−8009
biological interfaces, electrochemical processes, review 3−25550
blood coagulation factor, electrochem. behaviour, obs. on fibrinogen 3−39764
blood coagulation factor, electrochem. behaviour, obs. on prothrombin and thrombin 3−39763
complex plane analysis in electrode modulated specular reflectance 3−25070
electric double-layer force between unlike spheres, calc. 3−31200
electrocatalysis, electronic effects in H evolution reaction 3−38735
electrochemical information and energy transfer in vivo 3−5630
electrode processes and adsorption study, special techniques, review 3 12533
electrode reactions on demetallized surfaces 3−9076
electrode-solution interface, elec. double layer, review 3−31272
electrodialysis hydrodynamics 3−9067
electrolytes, osmotic coefficients 3−9068
electron transfer process, theory 3−39444
equivalent circuits for electrochemical cells 3−27877
equivalent circuits for electrochemical cells containing an indifferent electrolyte 3−27878
Faraday, determ. by means of iodine coulometer, preliminary results 3−13213
fused salt diffusion coating technique, book contrib. 3−11814
ionic double layer study and adsorption phenomena 3−12530
large electrodialysis units, mapping Faradic efficiencies 3−9069
liquid crystal, N-(p-methyoxybenzylidene)-p-n-butylaniline, role of electrode reactions in dynamic scatt. 3−12113
MBBA, electrochem. stability, rel. to display device degradation 3−21796
MBBA, isotropic phase, chem. and electrochem. activity rel. to d.c. conduction 3−15203
metal/electrolyte interface, elec. double layer, electrode reactions and static 3−2821
metal/electrolyte solution interface, multireflexion ellipsometry 3−31267
p-methoxybenzilidene p-butylaniline, liquid crystal and products of hydrolysis *(French)* 3−36261
microelectrode applications *(French)* 3−27875
microsectioning technique 3−2815
Modern aspects of electrochemistry, No.8, monograph 3−25074
oscillatory behaviour in electrochemical systems, review 3−25075
overpotential meas., review 3−12531
polarization curve determination, two probe automatic compensation method 3−28605
potentiostat and its applications, book 3−12534
reaction kinetics, in metallurgy, potentiostatic method of investigation *(Russian)* 3−8767
reversible electrode potentials meas., review 3−12529
role in environmental control, review 3−25076
stainless steel polishing, electrolyte 3−25072
stress corrosion, adsorption-electrochemical hypothesis *(Russian)* 3−27670
techniques of electrochemistry, book Vol. 1 3−12528
Ag, dislocation free plane multinuclear growth by electrocrystallisation 3−2816
Ag^+/Ag system, obs. of mass transfer hydrodynamics from streaming solutions 3−1355
AgBr membrane in aqueous solns., elec. cond. by ion transport 3−2841
Al barrier anodic films, elec. equivalent 3−15831
Al_2O_3, anodic oxide, photodecomposition 3−39445
Bi_2O_3 high-resistance anodic film formation on Bi 3−8038
Co_3Nb, phase thermodynamic stability, electrochem. determ. 3−2691
Cr monocrystalline and polycrystalline electrodes in H_2SO_4, anodic behaviour *(French)* 3−9077
Cu-Sb-Sn liquid alloys, Sn solvent activity equations, by stirred H-cell e.m.f. meas. 3−31269
Cu^{2+}/Cu system, obs. of mass transfer hydrodynamics from streaming solutions 3−1355
Hg_2^{2+}/Hg system, obs. of mass transfer hydrodynamics from streaming solutions 3−1355
^6Li, ^7Li isotope exchange reactions in quadruple cell, thermodynamic props. 3−9074
$Ni(OH)_2$ film, growth and anodic oxidation, optical study 3−30368
Pb, liq., diffusion and solubility of O_2, electrochem. obs. 3−27133
$RbAg_4I_5$, thin solid electrolyte film, vacuum-deposited, prep. and electrochem. charact. 3−39223
Si humidity role in atmospheric oxidation, electrochemical mechanism for surface film growth *(Russian)* 3−8036
Ta, F contamination by chem. polishing and behaviour during anodic oxidation 3−11812

electrodeposition
see also electroforming; electroplating
anodic film on Pt electrode, ellipsometric and refl. obs. 3−5243
brass, nucleation Pt from cyanide electrolyte 3−1945
electrophoretic method 3−34730
microscopic obs. improved by electrochemical cell use 3−5864

electrodeposition continued
spiral growth rel. to impurities 3−1582
stainless steel electrochemical polishing, electrolyte 3−25072
Ag, dislocation free plane multinuclear growth by electrocrystallisation 3−2816
Ag cryst. in meniscus region of electrolytic soln. 3−2817
Au-Cu alloys from cyanide free acid solution *(French)* 3−9071
Co, effect of I^- ions on magnetic props. *(Bulgarian)* 3−30670
Co, effect of I^- ions on phase structure and preferred orientation of crystallites *(Bulgarian)* 3−30366
Co, influence of organic additives *(German)* 3−12523
Co single crystals, electrodeposition of Ni *(Japanese)* 3−2819
Cu, coating morphology and preferred orientation, current density and temp. effects 3−9070
Cu, from pyrophosphate solutions, interfacial metal-electrolyte resistance 3−6152
Cu nucleation from cyanide electrolyte on Pt cathode 3−1945
Fe, on Cu, epitaxy relationships *(French)* 3−24355
Fe-Cr platings *(German)* 3−9072
Ge, electrochem. behaviour in fused LiCl-KCl eutectic 3−21808
Ge, of H cathodic, hydrogen overvoltage mechanism, temperature effects 3−37128
Ni, fabrication problem, obs. of Ni-Ni interface bonds by Auger electron spectroscopy 3−436
Ni, from ethylene glycol electrolyte 3−25071
Ni, X-ray investigation of twinning processes *(Bulgarian)* 3−30367
Ni film on (001) Cu substrate, transmission electron microscope obs. 3−33764
Ni/Al_2O_3 composite, electrodeposition, phys. and mech. props. 3−37059
Ni-Fe, permalloy film, Watts type bath technique 3−12044
Ni-Mo alloys, internal stresses and crack form. *(French)* 3−5287
Pb dendrite, electrodeposited, habit and morphology rel. to growth parameters 3−33767
Ta, deposited from fused salt electrolyte, struct. and mech. props. 3−24362
Zn, from alkaline solns., morphology 3−20962

electrodes
see also cathodes; electrochemical electrodes; microelectrodes; welding electrodes
discharge in conducting gas effect of electrode processes on volt-ampere characteristics 3−17709
discharged cleaned electrodes, surface processes preceding breakdown in vacuum *(Russian)* 3−7588
disconnection vacuum arc, investigation of initial stage 3−17707
dry, for electro-oculography 3−19098
e.c.g., insulated, with integrated impedance transformer 3−3905
e.e.g., patient discomfort rel. to resistance meas. 3−35235
erosion in Ar jet guided spark discharges, electrode spot formation 3−1526
external, excitation mechanism of He-Xe gas discharge, pulsed laser action mechanism 3−33412
gas discharge plasma, effect of electrode materials on spectra *(Russian)* 3−23953
hemispherically capped rod and plane, electric fields calc. 3−13672
high frequency flare discharge, elastic field effects, dep. air flow rate 3−33405
h.v. conditioning, at large gaps in industrial vac. 3−13265
inhomogeneous electric fields of plane electrodes, test for surface condition *(German)* 3−3830
for isometric contraction recording in man 3−35242
magnetic flowmeters, using nonhomogeneous magnetic field, patent 3−456
membrane, diffusion layer, polarographic analytical instruments *(German)* 3−16563
moving electric arcs boundary conditions for electrode surface in the arc spot *(Russian)* 3−23949
oscillating, for surface wave excitation, anal. 3−33262
placement for activation of VIIIth nerve by electrical stimulation in cases of sensorineural hearing loss 3−3482
plasma coaxial accelerator with non uniform pressure distribution, radiation and conductivity front propagation along electrodes 3−30020
porous nickel with skeleton catalyst, electrooxidation of hydrazine 3−4930
powder, compound, for brain tissue potential determ. 3−3401
pulsed plasma accelerators, potential drop due to discharge current and geometry *(Russian)* 3−7569
rotating bipolar, continuous voltage pulsing for electro-chemical cells 3−13352
spectroscopic light sources, rate of erosion, dependence on physical properties of metal *(Russian)* 3−9948
steel, electrical erosion in different atmospheres, effect of tertiary elements *(Russian)* 3−23952
steel, stainless, electrodes, surface oxide layer growth, ellipsometric obs. 3−18029
Ag-Se metal-semiconductor boundary compound formation, energy levels, vacuum photoemission study 3−38893
Al-Se metal-semiconductor boundary compound formation, energy energy levels, vacuum photoemission study 3−38893
CO_2-He laser, similarity law, disturbing electrodes effect 3−13730
Cu-Se metal-semiconductor boundary, compound formation, energy levels, vacuum photoemission study 3−38893
Mo, initiation of electric breakdown in vacuum 3−33411
SiC:Mo(Cr)(Ti), electrodes, electrical cond. erosion and heat resistance in plasma jet 3−36206

electrodynamics
see also electron optics; electron tubes; ion beams; ion optics; ion sources; quantum electrodynamics
acceleration of charged particles in e.m. field of pulsar numerical study 3−35167
aggregate of point-like particles, inertia centre of motion in analytical mechanics 3−32399
anisotropic media, with space and time dispersion 3−6402
charge moving through capacitor gap, oscills. with self-regulating interaction time *(Russian)* 3−10584
charged particles, multi-stage bunching, theory 3−13772
charged point particle in uniform circular motion teaching approach 3−23

electrodynamics continued
  charged point-mass motion, Coriolis force derivation from vector pot. 3—28928
  Chu-Haus-Penfield principle of virtual power, criticism 3—28931
  classical charged particles in uniform magnetic field, comment on new eqn. of motion of Mo and Papas 3—10322
  classical notion of spin 1/2 particles with zero anomalous magnetic moment 3—37851
  classical relativistic, elimination of retarded time 3—28927
  conducting regions, discontinuities, eqn. *(Russian)* 3—10419
  coupled system of oscillators and e.m. fields excited by external charge 3—16684
  deflection of radiating electron traversing inhomogeneous magnetic field 3—35585
  dielectric elastic hollow sphere, large amplitude oscill. 3—556
  electron motion in constant and orthogonal e.m. fields *(Russian)* 3—3995
  electron motion in uniform magnetic field and field of plane e.m. wave, influence of radiation friction *(Russian)* 3—10324
  energy bounds of charged particle moving in alternating axisymmetric magnetic field *(Russian)* 3—6300
  equation of motion for particle in mag. field, numerical soln. 3—26253
  field-dynamic equilibrium equation, analogue *(Russian)* 3—28930
  generally covariant nonlinear electrodynamics with a tensor potential *(Russian)* 3—3996
  ionosphere, day/night side variability in cond., potential distrib. determ. 3—25302
  kinetic equation for charged particles, including radiative retardation *(Russian)* 3—10323
  Lorentz-Dirac eqn. for particle in uniform field, relativistic motion 3—35719
  marked examples, book 3—18048
  motion of charged particles in homogeneous alternating magnetic fields *(Russian)* 3—6299
  multipole Hamiltonian for time dependent fields, comment, semi-classical approach 3—37862
  multipole interaction Hamiltonian with time dependent fields, extension 3—10321
  multipole radiation from extended charge-current distrib., relativistic approach, e.m. field asymptotic props. 3—37987
  plasma electrodynamic acceleration in a coaxial accelerator 3—23914
  principle of virtual power, comment on Brevik's arguments 3—6297
  principle of virtual power of Chu-Haus-Penfield, criticism 3—28932
  progress at MIT electronics lab. 3—1
  radiation from electron, influence of vacuum moment and wave polarization *(Russian)* 3—577
  radiation of charge particle moving along axis of channel in laminar medium *(Russian)* 3—35649
  radiation of charged particle moving in dielectric along plane boundary with periodically changing density *(Russian)* 3—35650
  relativistic, of eddy-current brake *(German)* 3—37877
  relativistic acceleration of charged particles by superintense laser beams 3—22970
  screw beam formation in adiabatic magnetron-type gun 3—22976
  Smith Purcell effect, radiation emitted as an electron beam passes over a metal surface 3—19553
  steady-state cosmology, Hoyle's electrodynamic version, evaluation of constants 3—39597
  superluminal source motion in vacuum, Vasilov-Cerenkov effect and Doppler effect 3—29216
  transfer of fast electrons, differential flow in inhomogeneous plate *(Russian)* 3—26254
  transfer of fast electrons, under influence of homogeneous elec. field *(Russian)* 3—29159
  two-dimensional electron beam trajectories, mapping theorem 3—4137

electrodynamometers *see dynamometers*

electroencephalograms *see electroencephalography*

electroencephalography
  see also brain
  alpha rhythm rel. to Schumann resonance 3—9652
  association cortex potentials, reaction time in auditory discrimination 3—28325
  averaged response, effects of stimulus rate and number 3—25568
  blood circulation, electric currents and metabolism of the brain, interpretation of an e.e.g. *(Swedish)* 3—13486
  cat, polysensory responses and sensory interaction in pulvinar and related posterolateral thalmic nuclei 3—39774
  cephalic skin potentials, potential shifts 3—16309
  clinical, appls. of digital computers 3—392
  current source, rel. to potential, single cell obs. and tissue impedance *(German)* 3—3889
  electrode resistance rel. to patient discomfort 3—35235
  epileptic patients, anterior cingulate gyrus, study 3—28332
  frequency sensitivity rel. to photic stimulation, epoch averaging 3—31849
  index of orienting response in children 3—5635
  intrinsic supratentorial brain tumours determ. 3—5636
  magnetic tape recording 3—25967
  man, extracellular firing patterns of deep temporal lobe structures 3—39766
  monkey, after γ-n irradiation 3—3604
  muscle artifact reduction 3—35236
  nonstationary bioelectrical signals analysis, exponentially weighted running statistics 3—5640
  on-line correlator 3—25977
  patient diagnosis, computer aided, review 3—25968
  patient monitoring, during surgery, effect of morphine in open heart operations 3—25966
  pattern recovery under photic stimulation by light of different colours 3—5638
  photic response by focal lesions 3—31850
  psychology-oriented analysis, circadian rhythms, sensory deprivation, computer program 3—9653
  quantitative, during hypnosis 3—19090
  spike and wave patterns, hybrid computer system for detecting and quantifying 3—3891

electroendosmosis *see electrophoresis*

electroerosive machining *see spark machining*

electrofluidynamics *see electrohydrodynamics*

electrofluorescence *see electroluminescence*

electroforming
  see also metalworking
  No entries

electrogasdynamics *see electrohydrodynamics*

electrohydrodynamics
  see also magnetohydrodynamics
  agitation of liq. system in strong external elec. fields, instability condition 3—20362
  charge-to-mass relationships for electrohydrodynamically sprayed liquid droplets 3—29913
  charge-to-mass relationships for electrohydrodynamically sprayed liquid droplets, fissionability concept 3—29914
  Doppler anemometer, meas. of electrohydrodynamic motion 3—164
  dynamics of electromechanical flow structs. 3—29899
  electrical conductivity of Hg metal mixture in bubbly and slug flow regions 3—32941
  electrogasdynamic refrigeration 3—136
  electrostatic atomisation of liquids by discharge from capillary in electric field 3—4606
  electrostatic crop spraying, triboelectrogasdynamic generator system 3—656
  filtration, analogy with current flow in semiconductors *(Russian)* 3—11443
  fluidized bed particles, nonlinear relation between specific resist. and current density 3—23783
  heat pipes, design using polarisation electrohydrodynamic force effects 3—36127
  insulating dielectric liquids, interfacial parametric electrohydrodynamics 3—7412
  insulating fluid stability during transient region of unipolar space charge injection *(French)* 3—1426
  liquid crystal, cholesteric, storage effect *(French)* 3—30072
  liquid drop, time-depend. problem 3—7440
  liquid surface stability in electric field 3—4607
  lunar mag. fields, volcanic ash particle flow ionisation 3—12995
  multiphase media, one dimensional flow, discontinuous solns. and weak wave attenuation *(Russian)* 3—14491
  one-dimensional EGD flow with shock waves *(Russian)* 3—1431
  one-dimensional flows with shock waves *(Russian)* 3—1430
  shock wave struct. for large and small Prandtl numbers *(Russian)* 3—1429
  spreading of jet of uni-polarly charged particles in hydrodynamic flow, numerical soln. *(Russian)* 3—29901
  surface wave propagation in conducting fluid 3—38399
  unipolar fluid flow in channel with electrode walls, exact solns. *(Russian)* 3—29900
  viscous liquid, two-dimensional potential flow *(Russian)* 3—14488
  Ar-air high-temp. jets with Ti dispersive particles, electroconductivity *(Russian)* 3—11455
  Mg drop pumping by travelling electric potential wave 3—10098

electrojets
  see also ionosphere
  auroral, ring current systems 3—16009
  counter electrojet currents, afternoon depression in horizontal component of geomagnetic field at Trivandrum 3—31326
  E_s-q layer disappearance during mag. storms, electrojet current reversal effects 3—25291
  equatorial, abnormal depression of Sq(H) in afternoon 3—21915
  equatorial current, effect on ionosphere and influences of geophysical disturbances 3—12791
  equatorial current stoppage, sporadic-E effects 3—18888
  equatorial electrojet rel. to polar magnetic variations on moderately disturbed days 3—15930
  equatorial sporadic E layer, cross-field instability temporay reversal of electrojet current 3—25289
  equatorial zone electric fields and currents determ. 3—34927
  radiowave absorption by resonant coupling 3—18873

electrokinetic effects
  see also electrophoresis
  electrodiffusion of divalent ions (Ca^{2+}, Sr^{2+}, Cd^{2+}, SO_4^{2-}) determ. in gels by radiotracers 3—39451
  osmosis, isotonic, flux scheme for electrokinetic relations 3—7959
  powdered substances, device for determining props. *(Russian)* 3—12524

electroluminescence
  see also phosphors
  anthracene, breakdown electrolum. characts. *(Russian)* 3—12185
  anthracene, mag. field modulation of prompt electrolum., charge transfer exciton fission 3—24747
  anthracene, semiconductor, Π-shaped voltage pulse excitation 3—34433
  anthracene crystals, electroluminescence caused by field-induced minority carriers at moderate temps. 3—39189
  anthracene single crystals with tetracene impurity *(Russian)* 3—24751
  diamond, electrically excited thermolum. 3—21494
  Gunn device, i.r. light emission phenomenon 3—18498
  injection diodes, book 3—32575
  kinetics, electroluminescent diodes and injection lasers 3—29104
  metallic discontinuous film, elec. cond., electron emission and electrolum. rel. to hot electrons 3—15171
  modelling of electroluminescence processes *(Russian)* 3—8666
  phenanthrene, electochemiluminescence intensity, mag. field enhancement 3—18799
  semiconductors, direct and indirect gap, and their appl. to electroluminescent devices 3—18499
  solid state convertor screens, for X-radiography 3—19351
  spectral lines, $2p^55s^1P_1$, $^3P_{0,1,2}$ upper levels, optical excitation functions 3—26572
  Al-Al_2O_3-electrolyte system 3—39190
  Au film, with island struct., I-V characts. rel. to electrolum. 3—21488
  $BaTiO_3$, light emission, solid state phase transitions, polarisation switching 3—39111
  CdS(Se), from controlled splits, hole-tunnelling mechanism 3—24746

electroluminescence continued
- CdS_xSe_{1-x}, graded gap crystal layer, luminesc. obs. by electron beam excitation 3−8053
- CsI, space charge effects 3−21489
- $CuGaS_2$-CdS p-n diode, green electrolum. 3−39188
- p-CuI-n-ZnS:Mn film, low voltage operation *(Russian)* 3−24748
- GaAs, light emitting diodes, near-field intensity variation in Fabry-Perot structure by pulsed electron injection 3−39193
- GaAs, p-n junction, rel. to impurity atom parameters 3−15157
- GaAs p-n junction, optical absorpt. influence on near-field intensity 3−21490
- GaAs p-n junction, vapour-grown, gas-phase stoichiometry effects 3−11950
- GaAs:Si, injection diode, electrolum. line shift *(Russian)* 3−8669
- GaAs-$Al_xGa_{1-x}As$, heterojunction, p-n-p-n structure, recombination in base region 3−18500
- $GaAs_{0.2}P_{0.8}$ from controlled splits, hole-tunnelling mechanism 3−24746
- GaN, u.v. d.c. electrolum. generation by forward bias injection 3−15556
- GaN:Zn electro-luminesc. diodes, manufacture and characts. *(Russian)* 3−36945
- GaN-GaN:Mg light emitting diode, violet luminesc. 3−34432
- GaP red-emitting lamp, O content and electrolum. efficiency 3−30537
- GaP:N, Te(Zn), LPE layer, minority carrier lifetimes and electrolum. efficiencies 3−30493
- GaP:N diodes, influence of temp. on spectra 3−24750
- $In_{1-x}Ga_xP$ free electron-bound hole recomb. 3−2597
- Si, diffused p-n junction, avalanche breakdown luminesc. 3−15557
- β-SiC pn junctions, green band structure, measurement of spectra at ambient and nitrogen temperatures *(Russian)* 3−30881
- β-SiC:B diffused p-n junction, V-I and C-V characts. and electrolum. response, 293 to 800 K *(Russian)* 3−18211
- Ta-Ta_2O_5-ZnS:Tb^{3+}-Au film, electrolum., light emission voltage depend. 3−39192
- Ta_2O_5 powder, incorporated in polymer *(Russian)* 3−18497
- ZnCdS pellets, electroluminesc. and stimulated conductivity study *(Russian)* 3−21492
- ZnS, electroluminesc. intensity, origin of first peak *(Russian)* 3−21493
- ZnS powdered phosphor display systems, d.c. electroluminescence 3−24752
- ZnS:Cu, Mn, anisotropy reln. to degree of orientation of ZnS microcrystals *(Russian)* 3−8670
- ZnS:Cu, Mn, Cl, film, doping in vacuum growth rel. to electrolum. props. 3−15559
- ZnS:Cu, Pb crystals, electroluminescent streaks development, stroboscopic obs. *(Russian)* 3−8664
- ZnS:Cu and ZnS:Cu,Al, Gaussian component intensity, alternating voltage freq. depend. *(Russian)* 3−21486
- ZnS:Cu crystals, electroluminescent streaks development, stroboscopic obs. *(Russian)* 3−8664
- ZnS:Cu electroluminophors, magnetic field effect on structure and optical props. *(Russian)* 3−8668
- ZnS:Mn film, d.c. electrolum. 3−30882
- ZnS:Mn film, low voltage d.c. light source *(Russian)* 3−24749
- ZnS:TbF_3 thin films, d.c. electroluminescence 3−8667
- ZnS-Cu powder cells, electrolum. decay rel. to trapped electrons 3−21487
- ZnS(Cu, Cl) electroluminophores, shallow traps and deterioration 3−30880
- ZnSe, rel. to improved generation-recomb. processes in light emitting diodes *(German)* 3−15558
- ZnSe-SnO_2 heterojunction, injection electroluminescence *(Russian)* 3−27575
- Zn_2SiO_4 film, growth on Si substrate, electrolum. props., monolithic display device applications 3−21491
- ZnTe−CdS heterojunction light emitting diodes 3−2659

electrolysis
- *see also electrical conductivity of electrolytic liquids; electrolytic dissociation; electrolytic ion velocity; electrolytic machining; electrolytic polishing*
- dielectric liq., rising effect at high voltage electrode rel. to elec. field 3−39089
- electrolyte soln., aperiodic large signal equiv. circuits 3−31271
- electron transfer rate, quantum mechanical formulation 3−9078
- foil preparation from wires, electrolytic thinning 3−18579
- hydrodynamic transition 3−25073
- liquid metals, electrolytic deoxidation at 1600°C 3−5313
- non-faradaic, galvamoluminescence, co-liberation 3−39450
- α- quartz, thermoluminescence investigation by Ag ion exchange electrolysis *(German)* 3−15564
- steel, hydrogen penetration and embrittlement, effect of electrolytic charging conditions 3−5326
- tetracene−TMPD system, electrogenerated chemilum., mag. field effects, triplet-triplet annihilation 3−34719
- Au plating, puriy of Au deposits as function of metal concentration 3−12527
- Fe, Armco, hydrogen charging influence on yield stress and ultimate strength *(French)* 3−5321
- n-InAs, electroreflectance spectra, line shape, electrolyte method *(Russian)* 3−34371
- Nb-O solid solution, study using solid electrolytic cells 3−31025
- PbS, film, photographic image formation by internal electrolysis *(Russian)* 3−9091
- Si, electrolytically etched surfaces, transmission electron microscopy 3−18025
- UF_4 production by electrolytic reduction *(Spanish)* 3−35930

electrolytes
- *see also electrolysis*
- alpha-dimethylolpropionic acid based, for electric capacitor, patent 3−18790
- aluminosilicate clay, statistical mechanics and anomalous swelling rel. to electrolytes 3−21752
- aqueous soln. adjacent to charged nonmetallic interface, fluctuation pot. of ion in diffuse region 3−12556
- arc propagation along surface 3−7581
- ceramic use in oxygen concentration cells 3−15758
- charge separation at phase boundary 3−9089

electrolytes continued
- colloid stability in polyelectrolytes, laser Doppler spectroscopy 3−34661
- concentration determination by neutron absorption *(Russian)* 3−23383
- electric field calc. 3−27880
- for electropolishing Nb for TEM 3−36249
- equivalent circuits for electrochemical cells containing an indifferent electrolyte 3−27878
- Hall effect meas. in electrolytic solns. *(German)* 3−15832
- isothermal differential diffusion coeffs. determ. using holographic interferometry and computer simulation *(French)* 3−2814
- MHD transient effects in bounded electrolytes 3−36132
- $Na(H_2O)^+_n$ extended Huckel method study of complex 3−18780
- nematic electrolyte solns., electric props., influence of sample geometry *(German)* 3−37129
- neutral oxidising, O_2-overvoltage on an Ni anode 3−15834
- nonaqueous solns., heat of soln., conc. depend. 3−31259
- osmotic coefficients 3−9068
- polyelectrolytes, limiting law theory, rel. to Poisson-Boltzmann eqn. 3−619
- polyelectrolytes, limiting law theory, rel. to soln. of Poisson-Boltzmann eqns., lower bounds on solns. near limit of infinite dilution 3−618
- polyelectrolytes, mol. struct. rigidity rel. to physicochem. props. 3−11345
- polyelectrolytes equilibrium theory, transport props., review 3−34731
- pulse discharge, gas generation during initial stages of formation *(Russian)* 3−14614
- rubber-glass contact with sandwiched electrolyte film, elec. double-layer force meas. 3−6020
- solid, conductivity rel. to cryst. struct. 3−27282
- solid ionic conductor, piezogalvanic effect 3−30506
- solutions, analysis by spectral method using narrow capilliary discharge *(Russian)* 3−35546
- solutions, isotropic Rayleigh scattering based on ion-dipole system free energy 3−27507
- stainless steel, electrochemical polishing 3−25072
- surface potential of sea-air interface rel. to effect of salts in electrolyte solutions 3−12687
- water, electric discharge between electrolyte and Cu cathode, current-voltage characteristics *(French)* 3−7570
- zirconia, use in fuel cells 3−15833
- Al-Al_2O_3-electrolyte system electro- and photoluminescence 3−39190
- β-Al_2O_3 solid electrolyte, e.m.f. meas. 3−39449
- K_2CrO_4, boundary layer formation during electrolysis, anomaly in ionic migration 3−39443
- $K_2Cr_2O_7$, boundary layer formation during electrolysis, anomaly in ionic migration 3−39443
- $K(H_2O)^+_n$, extended Huckel method study of complex 3−18780
- $Li(H_2O)^+_n$ extended Huckel method study of complex 3−18780
- ZrO_2, solid, applications 3−34729
- ZrO_2:Y_2O_3, sintering, effect of CO_2, analysis 3−15761
- $ZrO_2.Y_2O_3$, solid solution, electrolyte, crit. temp. meas. 3−36420

electrolytic capacitors
- Al, prehydrated, anodic oxide film structure 3−8065

electrolytic conductivity of liquids *see electrical conductivity of electrolytic liquids*

electrolytic deposition *see electrodeposition*

electrolytic devices
- No entries

electrolytic dissociation
- *see also electrolytic ions*
- alkyd resin in acetone, elec. cond., potential distribution determined by acidic group dissoc. 3−39408
- heat and mass transfer in electrolyte solution, efff. of mag. field *(Russian)* 3−20313

electrolytic ion velocity
- *see also electrophoresis*
- H^+ ion mobility in $CuSO_4$ electrolyte solution 3−11755
- $K_2C_2O_7$, boundary layer formation during electrolysis, anomaly in ionic migration 3−39443
- K_2CrO_4, boundary layer formation during electrolysis, anomaly in ionic migration 3−39443

electrolytic ions
- *see also electrical conductivity of electrolytic liquids; electrolytic dissociation; electrolytic ion velocity*
- aqueous soln. adjacent to charged nonmetallic interface, fluctuation pot. of ion in diffuse region 3−12556
- in diffusion layer, meas. 3−6152
- effects on structure of liquid water 3−38621
- electrodiffusion of divalent ions in gels determ. by radiotracers 3−39451
- interfacial resistance meas. by probing *(Russian)* 3−2818
- BF_4^- anions in solution, temperature dependence of ^{19}F n.m.r. spectra 3−34231

electrolytic machining
- *see also electrolytic polishing*
- ceramic materials, techniques and mechanisms, review 3−34630
- diamond microtool manufacture 3−25745

electrolytic polishing
- *see also electrolytic machining*
- acid saw, possibilities for increasing the cutting speed 3−8885
- ceramic materials for transmission electron microscopy 3−33436
- electrolytic thinning apparatus for electron microscope specimens 3−17724
- foils, thin, non-magnetic, electropolishing for electron microscopy *(German, English)* 3−24350
- Al-Al_2O_3-Al diodes, effect on tunnelling current 3−18230
- Cu and alloys, potentiostatic controlled etching and polishing, rel. to metallography 3−37127
- Cu and Cu alloys, electrolytic vibration polishing 3−30357
- Ge, single crystal discs, KOH contamination of crystal surface transmission electron microscope obs. 3−38705
- Nb, for transmission electron microscopy, new electrolyte development 3−36249

electrolytic polishing continued
- Nb_3Sn, transmission electron microscope examination of defect struct., electropolishing technique for thinning HASTELLOY strips *(German)* 3−21179
- Ni alloys, thin film foil specimens for electron microscopy, electropolishing method 3−17726
- $Y_3Fe_5O_{12}$, in orthophosphoric acid, rates of action *(Russian)* 3−11820

electromagnetic corrections
- absence in anomaly of axial vector current Ward-Takahashi identity 3−38036
- atomic transition freqs., radiative corrections 3−23063
- dominance of e.m. effects in high energy hadron and photon induced reactions 3−23062
- electron scattering coincidence cross sections, correction for radiative effects 3−35803
- e.m. effects on hadron scatt., violation of Pomeranchuk theorem 3−841
- fourth-order vac. polarization, treatment of i.r. divergences by adiabatic switching 3−16990
- hadron scattering, high energy, particle and antiparticle, total cross sections *(Russian)* 3−912
- hadron weak form factor, calc. of electromagnetic corrections using gauge invariance *(Russian)* 3−10696
- hadronic atom particle physics aspects 3−7093
- meson-baryon scatt. e.m. effects in polarization at high energies, small t *(Russian)* 3−4168
- muon production massive-pair, light-cone presence and use of spectral representations 3−29268
- second-order weak and e.m. corrections to decay rate calc. from Weinberg's model 3−16972
- spontaneous symmetry breaking, radiative corrections as origin 3−35793
- two-nucleon pot., e.m. mass splitting effect of $I=1$ mesons 3−16986
- unified gauge theories, effective weak-interaction cutoff 3−38035
- ee ($e\mu,\mu\mu$) colliding beams, weak-e.m. processes and interference at high energies 3−17058
- e^+e^- elastic scatt., cross-section at 4 GeV/c, radiative correactions 3−26306
- $e^+e^- \rightarrow \mu^+\mu^-$, e.m. background in search for neutral weak currents 3−29207
- $ep \rightarrow ep\gamma$, investigation between elastic peak and pion threshold, exptl. test of higher order radiative corrections 3−13951
- γe, scattering amplitude determ. including radiative correction, calc. of polarization coeff. *(Russian)* 3−23076
- $K \rightarrow \pi\pi$, $\Delta I = {}^3/_2, {}^5/_2$ contributions to decay amplitudes and $(\delta_0\text{-}\delta_2)$S-wave $\pi\text{-}\pi$ phase shifts 3−35778
- $K_l \rightarrow \mu^+\mu^-$, models and reln. to CP invariance, review 3−32647
- K^-p interactions, low-energy, Coulomb and mass difference corrections in K-matrix treatment 3−32699
- μ decay current, normalization in V-A theory, inclusion of radiative corrections 3−23028
- p-n mass difference, Compton amplitude representation, scale-invariance of A_2 meson 3−13863
- π^- mass and vacuum polarization, meas. 3−32664
- $\pi^\pm$ photoproduction, threshold to 450 MeV, high-energy contribs. to dispersion integrals, isotensor e.m. current contribs. *(Russian)* 3−23078
- πN scattering, 10-500 GeV, dispersion relation analysis *(Russian)* 3−38079
- $e^+e^- \rightarrow e^+e^-$, acollinearity and radiative corrections 3−38038

electromagnetic decays
- bosons, radiative decay model 3−13867
- Burnett-Kroll soft-photon theorem to polarized cross sections, generalization 3−23100
- meson, as test of relativistic-constituent Fermi-quark model based on Bethe-Salpeter eqn. 3−19689
- meson, extended vector meson dominance model 3−32665
- $\eta \rightarrow \gamma\gamma$, $\eta' \rightarrow \gamma\gamma$, e.m. interaction and reln. to $SU(3) \times SU(3)$ *(Russian)* 3−29204
- $\eta\text{-}\eta$ mixing, study of two-photon decays to decide between linear and quadratic schemes 3−16991
- $\gamma \rightarrow 3\pi$ low-energy theorem, exptl. test using $e^+e^- \rightarrow \gamma \rightarrow \pi^+\pi^-\pi^0$ 3−26302
- $K_{s,l} \rightarrow \gamma\gamma$, CP violation 3−16992
- $K_s^0 \rightarrow \gamma\gamma$, unitarity relations for two-pion intermediate states 3−32666
- $K^{*+}(890)$ coherent production on nuclei, determ. of upper limit for radiative decay width $K^{*+} \rightarrow K^+\gamma$ 3−19741
- $\mu^- \rightarrow e^-\nu_1\nu_2\gamma$, longit. spin correls. *(Russian)* 3−23064
- ω radiative decay modes meas. with Orsay storage ring 3−16993
- ω^0 radiative neutral decay modes, expt. at Orsay Storage Ring 3−13872
- φ radiative decay modes meas. with Orsay storage ring 3−16993
- φ^0 radiative neutral decay modes expt. at Orsay Storage Ring 3−13872
- $\pi \rightarrow \gamma\gamma$, low-energy theorem reln. to $\gamma \rightarrow \pi\pi\pi$, nonperturbative evaluation 3−32637
- $\pi^0 \rightarrow \gamma\gamma$, conflict between VMD and PCAC 3−38037
- $\pi^0 \rightarrow \gamma\gamma$, detection following $\gamma p \rightarrow \pi^0 p$ process 3−13910
- $\pi^0 \rightarrow \gamma\gamma$, determ. of relative sign of decay constant in SU(3) symm. *(Russian)* 3−4169
- $\pi^0 \rightarrow \gamma\gamma$, e.m. interaction and reln. to $SU(3) \times SU(3)$ *(Russian)* 3−29204
- $\rho^+ \rightarrow \pi^+\pi^0\gamma$, comparison of hard-pion amplitude and low-energy expansion using KSRF-type relations 3−32661

electromagnetic energy *see electromagnetic waves*

electromagnetic field theory
- *see also electromagnetic waves; electromagnetism*
- atoms and molecules, interaction, quantum theory 3−19699
- bianisotropic media 3−35655
- boundary conditions for laminar regions, from Maxwell's eqns. formal integrals 3−646
- generalised singular e.m. field of Bel, Lapiedra and Montserrat, spinor approach 3−26105
- higher order coherence of the electromagnetic field 3−16820
- integral equations, for 3-dimensional quasistationary e.m. field calculation in homogeneous conducting media *(Russian)* 3−32482

electromagnetic field theory continued
- loop antennas, h.f. e.m. coupling over inhomogeneous ground, earth depth depend. 3−32478
- nonlinear, by adding one term to Lagrangian density 3−6391
- nonlinear, derivation of Lagrangians using inductive method *(French)* 3−37917
- relativistic representations, compatibility *(Hungarian)* 3−16688
- soft photon radiation in strong electromagnetic wave field *(Russian)* 3−580
- static, in homogeneous media for given source distribution *(Russian)* 3−32486
- unification with gravitational field in space of constant curvature 3−32432
- zero-point energy shift induced by conducting closed surfaces 3−19552

electromagnetic fields
- cable (infinite) on surface of anisotropic medium *(Russian)* 3−6392
- charge and current due to interaction with gravitational field 3−19500
- charged aerosol clouds, confinement and transportation via electric curtain *(Japanese)* 3−35654
- charged particle motion in superstrong electromag. field surrounding pulsar 3−16249
- conducting ferromagnetic materials, nonlinear, field distribution, power losses 3−15396
- conductive shells, thin, shielding characts., e.m. induction study 3−22802
- conductors (buried) position determ. by e.m. induction method *(Polish)* 3−22401
- cosmic ray generation, particles with energy $>10^{21}$ eV 3−18907
- cosmic ray particle accel. near pulsars, high particle loss effects on refractive index 3−22091
- cylindrical electromagnet parallel to metallic wall *(Polish)* 3−22801
- dielectric sphere, intensity calcs. *(Russian)* 3−37920
- dipole and loop antennas for 10 GHz meas. using light modulated scatt. technique 3−10423
- dipole antennas over stratified anisotropic media 3−34885
- divergent perturbation expansion for vacuum polarization by e.m. field 3−17063
- Einstein-Maxwell eqns., solns. for spinning particles at rest, balancing of e.m. and gravitational forces and torques 3−26140
- electron motion in uniform magnetic field and field of plane e.m. wave, influence of radiation friction *(Russian)* 3−10324
- elliptical polarization rel. to near-field radiation hazard 3−4055
- energy in field, determ. from repulsion between aerials 3−22
- exterior boundary value problem of wedge, use of Laplace, Fourier and Kontonovich-Lebedev transforms 3−19480
- finite circular loop, transient e.m. fields in the presence of a conducting half space 3−4056
- flux compression experiments analysis 3−10420
- gaussian beam near focus, field anomalies 3−32579
- geomagnetic field disturbance accompanied by nonstationary γ-quantum source, e.m. signal characts. 3−25169
- h.f. coupling in computer circuits and components, analysis of current and electric potential distributions 3−29002
- human body interactions, biological effects, mechanisms 3−9714
- meal forming, X-ray diffraction meas. of deformation rate 3−25959
- model structure in small cavity, determ. of thermal radiation field 3−10402
- multipolar represent. development *(French)* 3−37918
- multipole radiation from extended charge-current distrib., relativistic approach, e.m. field asymptotic props. 3−37987
- power cables, screened *(Russian)* 3−19549
- pulsar, acceleration of charged particles, numerical study 3−35167
- quantization of maximal flux of magnet *(French)* 3−4053
- quantum theory of particles and Maxwell group in homog. field 3−19484
- radiation and finiteness conditions *(German)* 3−19547
- radiative losses in magnetostatic and e.m. field, appl. to pulsars 3−31497
- reciprocity and conservation theorems 3−4060
- scattered field attainment, principal methods survey 3−32517
- scattering from round metal post and gap 3−35664
- semi infinite hollow cylinder, h.f. backscatt. 3−35656
- semiconductor, electromag. field effect on valence band ionisation by cond. electron collision 3−4951
- stigmatic lens, structure of field near focus 3−19580
- subterranean cylindrical inhomogeneity excited by line source, appl. to geophysical prospecting and mine rescue 3−32477
- superradiance in interaction of e.m. field with N atoms, semi-classical approach 3−16981
- vacuum pulsar model, determ. of e.m. torque in oblique rotator case 3−31726
- vehicle guidance system, patent 3−6397
- vehicle guidance system, patent 3−10426
- virtual particles as sources of gravit. field 3−16716

electromagnetic interference
- *see also radiofrequency interference*
- bioelectric measuring system, in-phase interference immunity 3−32237

electromagnetic lenses *see magnetic lenses*

electromagnetic oscillations
- *see also cavity resonators; lasers; masers; ring lasers*
- leaky corrugated optical waveguides, laser oscill. 3−22890
- open resonators 3−19554
- solar oscillations at 9.6 mm., observations allowing for atmospheric absorption effects 3−25401

electromagnetic radiation *see electromagnetic waves*

electromagnetic theory of light
- anisoropic thin-film optical waveguides, wave propagation 3−29039
- bianisotropic media, biorthogonality relations 3−29043
- nature of light, tutorial 3−32505

electromagnetic wave absorption
- *see also gamma-ray absorption; light absorption; X-ray absorption*
- anomalous microwave absorption near the plasma frequency 3−20622
- atmosphere, 4 to 6 millimetre wavelength band 3−12724

electromagnetic wave absorption continued
- atmospheric absorption of mm-waves, spectral measurements 3−15952
- atmospheric mm waves, simulation results 3−37236
- attenuation in Earth crust waveguide, e.l.f. to v.l.f. 3−34855
- attenuation of radiowaves during ionospheric propagation in 3-100 MHz range 3−28062
- bound free absorpt. of S I in B to K-stars rel. to u.v. opacity 3−28189
- 4C 05.34, quasar absorption spectra rel. to surrounding gas density 3−16245
- cloud of particles, radiative transfer 3−12461
- D-region, h.f. radiowave absorption meas. at low latitude station 3−9332
- D-region differential-absorption, differential-phase partial-reflection experiments 3−12805
- D-region ionization Winter anomaly, meas. using A1 and A3 radiowave absorption techniques 3−3117
- D-region neutral gas winds and A3 radiowave absorption meas., correlation studies 3−3118
- D-region radiowave absorption rel. to 10-mb winds and temp. during IQSY 3−9331
- dielectric layers in microwave antenna field *(German)* 3−19558
- diffusion dipole source, analytic soln. 3−29018
- E-region, v.h.f. absorption rel. to electron collision frequency from rocket and ground-based measurements 3−25279
- Earth-to-satellite links, rain attenuation, path diversity 3−28044
- electrojet radio wave absorption by resonant coupling 3−18873
- fluctuation-dissipation theorem, mag. field regeneration, kinematic-dynamo activity 3−12928
- hot plasma, at double the plasma frequency *(Russian)* 3−2120
- ionosphere, at 2.4 MHz, lunar effects 3−12792
- ionosphere, measuring method *(Russian)* 3−3056
- ionospheric A1 absorption ship-borne meas. at 2 MHz above North Atlantic during winter anomaly 3−31417
- ionospheric absorption, Winter anomaly above Kjeller during solar cycle 3−3070
- ionospheric absorption of 1.725 MHz radiowaves, Winter anomaly during sunspot minimum 3−3071
- ionospheric conjugate absorption observations of electron precipitation event rel. to sudden impulse in geomagnetic field 3−16019
- ionospheric radio signal spreading, absorpt. dispersion effects in lower layers 3−34938
- i.r., stratospheric NO_2 concentration 3−5507
- l.f., lower nighttime ionosphere, ionization processes *(Russian)* 3−3053
- lower ionosphere radio wave absorption, pressure var. above mesopause, effect on seasonal anomalies 3−12775
- magnetoactive, absorption and amplification of electromagnetic waves *(Russian)* 3−29948
- magnetoactive plasma, absorption of microwave energy 3−20623
- metal influence of magnetic breakdown 3−11887
- microwave absorption in magnetoactive plasma 3−20465
- microwave signals at 10 GHz interaction with electron density gradients 3−33351
- opaqueness of various cosmological models, assessment of Wheeler-Feynman absorber theory 3−5556
- optical absorption, quantisation eff. with elec. field dependence 3−36009
- plasma, magnetoactive, amplification considering spatial dispersion *(Russian)* 3−29948
- plasma anomalous microwave absorption near the plasma frequency 3−20464
- plasma column, hot magnetised, loading of a RF helix 3−20460
- plasma formed by moving ionization source, influence of collisions *(Russian)* 3−17574
- plasma ion heating by mixing of e.m. waves near electron cyclotron resonance 3−20580
- plasma microwave absorption and conversion at upper hybrid resonance, efficiency near cyclotron resonance 3−17582
- plasma microwave absorption at high magnetic fields 3−20447
- plasma RF absorption in a nonuniform hot magnetised column 3−20459
- plasmas, cold, nonlinear limits to the theory of resonant absorption 3−20463
- plasmas, cold inhomogeneous, energy absorption, the Herlofson paradox 3−20452
- polarimetric study of anomalous absorption of cosmic radio waves in midlatitude ionosphere 3−25262
- radio waves, in steady-state and Einstein-de Sitter, cosmology 3−5559
- radiowave, due to rain, at 19.3 and 34.8 GHz 3−28045
- receiving antenna 3−26190
- semiconductor, acoustoelec. domains, piezoelec. potential and carrier distrib., microwave absorpt. study 3−5040
- semiconductor, compensated, heavily doped, large-scale potential props., microwave absorpt. *(Russian)* 3−8165
- semiconductors, by hot electrons *(Russian)* 3−11906
- semiinfinite dielectric medium undergoing phase transition, velocity of phase front generated by e.m. wave absorption 3−16784
- solar Lyman-α control of 2775 kHz ionospheric absorption 3−31412
- superconducting dilute magnetic alloys, e.p.r. induced transitions 3−18265
- superconductor, type I, rel. to surface impedance in weak mag. field 3−15301
- total spectral absorptivity, black radiation, heat transfer, gases, nonisothermal medium 3−1325
- u.l.f. wave dipole excitation in earth crust waveguide 3−18819
- u.v. data, correl. with organic compound substituent consts. 3−20135
- Venus, radar attenuation rel. to chemical composition and altitude profile 3−25409
- Venus atmosphere model for radiowave attenuation and S/N, wavelength dependence 3−35077
- Al, superconducting, mag.-field dependence of surface resistance near energy gap 3−18262
- n-Ge, in Voigt config., microwave transmission 3−2522
- H_2O atmospheric vapour and vapour dimers, radiowave absorption in 1.15-1.5 mm. band *(Russian)* 3−3003

electromagnetic wave absorption continued
- H_2O atmospheric vapour monomers and dimers, radiowave absorption in 0.71-0.76 mm band *(Russian)* 3−3004
- Hg plasma, weakly ionised, negative absorpt. of r.f. waves 3−11476
- In superconducting film, conversion of electromag. into acoustic energy 3−15305
- Si, microwave transient absorp., exciton coeff. of formation obs. *(French)* 3−30434
- Te, inactive mode cyclotron resonance absorption 3−8106

electromagnetic wave diffraction
- *see also light diffraction; X-ray diffraction*
- Bragg diffr. of μ-waves, lab expt. 3−9812
- conducting half-plane 3−6406
- conducting wedge loaded with cylindrical dielectric slab at apex 3−37928
- cylinders with spiral slot *(Russian)* 3−16785
- by dielectric loaded wedge, E-polarized plane wave 3−26195
- dielectric step, plane wave scatt., amplitude and ang. distrib. expressions *(Russian)* 3−6407
- double circular irises rel. to elliptical reflector scatt. 3−6405
- by double grating 3−668
- double knife-edge diffraction in high freq. approx., comparison with ray theory 3−26194
- eigenfunctions, generalised method, stationary functionals calc. *(Russian)* 3−10436
- excitation coefficients of diffraction modes, Lorentz lemma application *(Russian)* 3−13683
- flanged parallel plate waveguide, radiation patterns 3−674
- free space and planar waveguide 3−26196
- Fresnel subzones demonstrations *(Russian)* 3−6413
- grating, conformal mappings appl. 3−6403
- grid consisting nonparallel and nonrectilinear conductors on nonplane surface 3−26197
- hologram grating, with modulation, diffraction efficiency 3−29030
- infinite array of finite parallel strips residue calculus method 3−19561
- infinitely conducting objects, Physical Optics Approximation validity in reson. region *(French)* 3−32501
- metallic half-plane, by impulsive plane cylindrical or spherical waves 3−22830
- N bodies, orthogonalization method 3−13687
- optical resonator with cylindrical mirrors, losses, calc. *(Russian)* 3−10557
- random phase screen effects, anisotropic case simulation 3−16786
- reactance plane, inverse problem of diffraction *(Russian)* 3−13684
- reflectors with periodically modulated surface impedance *(Russian)* 3−32500
- review, appl. of e.m. laws to gratings 3−32502
- scattering of plane waves by infinite grating on anisotropic medium *(Japanese)* 3−22818
- slit, polarised wave, interface of two isotropic dielectric media, distribution theory, numerical solution *(French)* 3−26193
- triangular obstacles, shadow zone diffraction patterns 3−4066
- two-dimensional e.m. field diffraction on an ideally conducting plane with an infinite straight slit 3−29024
- uniform bodies of revolution with arbitrary complex dielectric constant 3−13688
- v.h.f./u.h.f. signals, ionosphere 3−37239
- waveguide, dielectric loaded, integral eqn. 3−669

electromagnetic wave diffusion
- *see also electromagnetic wave scattering; light diffusion*
- quasi-monochromatic weakly dispersed beams in anisotropic dielec. medium, diffusion study *(Russian)* 3−19569
- nonstationary diffusion in a semiinfinite isotropic scattering medium *(Russian)* 3−12716
- nonstationary diffusion of radiation in medium of finite optical thickness *(Russian)* 3−32499

electromagnetic wave interference
- *see also atmospherics; electromagnetic wave interferometers; electromagnetic wave interferometry; light interference*
- coherent e.m. waves beam control, patent 3−37933
- X-rays, flash interferences in high compressed matter *(German)* 3−391

electromagnetic wave interferometers
- *see also electromagnetic wave interferometry; light interferometers*
- digital interference correlation meter with high storage time 3−22132
- Fabry-Perot with plane grating mirrors *(Russian)* 3−3814
- laser velocimeter system, for meas. of high velocity of reflecting surface 3−3872
- Mach Zehnder, for heat transfer obs. 3−123
- mirror position control by Fabry-Perot interferometer 3−16439
- polyethylene-terephthalate fibres, study of center sorption using X-band hyperfrequency interferometer *(French)* 3−8011
- reflecto-interferometer setup for complex permittivity meas. of liqs. with high losses *(French)* 3−25792

electromagnetic wave interferometry
- *see also light interferometry*
- brightness temp. distribs. defined by measured intensity interferograms, radio and optical astron. sources 3−28305
- Fabry-Perot analysis of simple spectral line profile, Voigt type, methods *(French)* 3−23584
- heat transfer obs. using motion picture camera 3−123
- laser, vibration obs., homodyne and heterodyne techniques 3−196
- magnetic field-aligned irregularities detected by phase interferometry, wavelike struct. 3−9326
- microwave, holographic synthetic aperture interferometry 3−9957
- Taurus A radiosource, VLBI obs. at 121.6 MHz indicating assoc. with pulsar NP 0532 3−39696
- velocity of light determ. by interference of mm waves using two-beam interferometer, in vacuo meas. 3−13325
- very long baseline interferometry of Crab pulsar at 196.5 and 111.5 MHz 3−31727
- very-long-baseline interferometry for geodetic satellite timing 3−34970
- C arc plasma, laser beam, electron density determination 3−11504

electromagnetic wave propagation
see also atmospheric electromagnetic wave propagation: atmospheric light propagation; backscatter; electromagnetic wave diffraction: electromagnetic wave diffusion: electromagnetic wave interference; electromagnetic wave propagation in plasma: guided electromagnetic wave propagation: radiowave propagation
2-D transmission and reflection at dielectric plane interfaces of 2-D Gaussian beam 3—26188
3-D transmission and reflection at dielectric plane interfaces of beam waves 3—22809
anisotropic media, with space and time dispersion 3—6402
anisotropic stratified media, radiation by arbitrary sources 3—26191
conducting medium, excitation of plane-polarised waves and structures 3—35662
conducting sphere, transient response excited by different input pulses 3—29012
coordinate independent dyadic formulation of wave normal and ray surfaces of general anisotropic media 3—6418
coordinate system with axial symmetry of revolution, propag. eqns. *(French)* 3—35659
cylindrical wave focusing in ducts 3—10430
Cytherean ionosphere, effective collision freq. and h.f. cond., refr. index 3—22033
dielectric layers in microwave antenna field *(German)* 3—19558
in dispersive media, generalized wave energy expression 3—10437
earth crust idealised waveguide, mode characts. 3—31335
earth crust idealised waveguide 3—31334
explosive instability of parametrically coupled waves 3—16783
fault zone, separating two media of high resistivity, transient response 3—31459
ferrite interactions, definitions 3—15353
fields of wide wave beam in inhomogeneous medium and vacuum, comparison *(Russian)* 3—29015
Gaussian beam propag. in planar and cylindrical inhomogeneous media, vector theory 3—760
irradiance fluctuations, in turbulent air, plane waves 3—31373
isotropic homogeneous medium, plane, uniform and heterogeneous waves, absorption effects *(French)* 3—16794
Kirchhoff integral equation, obstacles, antennas, and edges 3—10429
layered conducting earth, with dipping anisotropy, impedance of plane e.m. wave at surface 3—29013
in lens-like media, analysis by perturbation method 3—29017
light, propag. theory in high spatial inhomogeneous systems 3—22846
light pulses, short coherent, in linear amplifying and absorbing media, regular propag. study *(Russian)* 3—19632
in lithosphere, myriametric waves, theoretical methods for study of electric field and its attenuation *(Rumanian)* 3—27974
localized smoothly varying turbulence, wave fluctuations problem 3—6400
lossless positive bianisotropic media, wave normal and ray propagation 3—6399
lycopodium suspension, flux fluctuations of light in scattering medium *(Russian)* 3—37937
in magnetised ferrite medium, group velocity diagrams 3—22813
in magnetised ferrites, construction and applic. of Brillouin diagrams 3—22829
magnetospheric v.l.f. waves propagating in non-ducted mode 3—21974
magnetospheric whistler transmission in ionosphere and lower exosphere at high latitudes 3—5519
magnetotelluric soundings, mag.- and electric field variations transfer function 3—34964
in media varying slowly with position and time, study by WKB methods 3—22816
medium with random density, non-local theory, correl. approx. *(Russian)* 3—667
microwave transmission through inclined parallel wire gratings 3—32495
milk solution, flux fluctuations of light in scattering medium *(Russian)* 3—37937
in n-type GaAs, microwave study of hot electrons 3—27263
photons momentum in dielectrics 3—859
pulse propag., weakly dispersive, in lossy media 3—22808
pump wave, intense coherent, propag. in reson. media 3—32598
radiation and finiteness conditions for e.m. fields *(German)* 3—19547
radiation patterns of electric dipole and vibrator near perfectly conducting cylinder edge 3—22811
radiative transfer in isotropic medium using statistical perturbation theory *(Russian)* 3—37925
random media, dispersion relations due to dielec. fluctuations 3—6401
semiconductor, low freq., under conditions of inelastic scatt. of carriers by phonons *(Russian)* 3—8166
single-position scattering matrix 3—13681
stochastic Gaussian beam, propagation in strongly focussing medium with random deviations 3—6495
stratified media, multiplicity of wave numbers 3—26192
surface wave incidence on plane structure having multi-mode discontinuity in impedance 3—3998
surface wave propag. along various cuts of uniaxial crystals 3—24486
symmetric objects, reference polarization 3—13680
through-the-ground, buried dipole in presence of semiinfinite metallic tube 3—31337
time domain e.m. response of shielded conductor 3—29014
transformation of wave spectrum in medium with spatial-time fluctuations 3—22810
transient signal propagation in unbounded lossless dispersive moving media 3—35660
transition radn. of charge, hyrotropic media and vacuum boundary *(Russian)* 3—6599
travelling wave parametric interactions, phase bunching, amplitude bunching 3—6301
uniaxial crystals, plasma oscillations, optical phonons, interactions, spectra 3—33941
velocity modulation in medium varying in time and space 3—22814
v.l.f. propagation over long distances to study the lower ionosphere *(German)* 3—9337

electromagnetic wave absorption continued
electromagnetic wave propagation continued
waveguide, circular, with spirally conducting insertions *(Russian)* 3—16782
GaAs, doped, absolute instability of e.m. waves and microwave emission 3—24461
Ge layer, transverse mag. field influence *(French)* 3—18174
InSb, effect of weak, longit. static field on transverse e.m. wave propag. along magnetostatic field 3—2121

electromagnetic wave propagation in plasma
absorption of e.m. field energy in randomly inhomogeneous plasma 3—20457
accessibility to the lower hybrid resonance 3—36163
anisotropic cold plasma, transient radiation, index of refraction 3—26870
anomalous microwave absorption near the plasma frequency 3—20464
anomalous propagation, stability 3—20458
anomalous skin effect conditions, e.m. wave penetration 3—33350
argon-gas cylindrical guide, excitation experimental studies of e.m. and electroacoustic waves 3—23826
artificial transmission line simulation 3—11481
attenuation in plasma formed by moving ionization source, influence of collisions *(Russian)* 3—17574
axially symmetric surface, in cylindrical cavity with magnetised plasma, exact eigenvalues *(Japanese)* 3—36155
Azbel Kaner resonance, e.m. waves propag., refractive index calc. 3—17583
beam-plasma interaction, axial inhomogeneity effect on surface wave excitation 3—14520
bounded hot electron system, wave attenuation meas. 3—14528
Cerenkov radiation in a drifting magnetoplasma 3—20449
charged particle beam, interaction with running e.m. wave *(Russian)* 3—13386
circularly polarized waves producing a global magnetization *(French)* 3—11480
cold electron-ion system, e.m. instability 3—23831
collective processes in the universe 3—26906
collisional, multi-ion horizontal duct producing v.l.f. noise bands 3—16014
collisionless plasma, microwave stimulated Raman scattering *(Russian)* 3—1492
complete iso-thermalisation by collective e.m. interactions of strongly anisotropic magnetized collisionless plasmas 3—17578
compressible electron plasma, travelling wave circular loop antenna, radiation props. 3—36156
compression of wave power density in time varying medium 3—11475
compressional Alfven, electrostatic sound and RF wave coupling in ionospheric plasma, characteristics of electric field from radiating antenna 3—21962
counterstreaming electron-ion plasmas, e.m. instability 3—23851
coupled e.m. waves, inhomogeneous compressible magnetoplasma coupled wave equations 3—7511
covariant formulation of wave dispersion 3—14530
crossover freqs., polarisation coeff. var. 3—7504
crossover frequencies in a multicomponent plasma 3—38436
cyclotron resonance in inhomogeneous plasma 3—7503
cylindrical antenna, current distribution 3—7498
cylindrical antenna, weakly ionized plasma, radiation resistance 3—7501
d.c. current induction by r.f. travelling wave in strong mag. field 3—26864
density var. of plasma with freq., determ. for E-layer 3—1490
dipole sources, nonstationary radiation in plasma with diagonal dielectric permittivity tensor *(Russian)* 3—38432
direct nonlinear coupling of e.m. and electrostatic waves 3—33358
dispersion equations for waves in multilayer structures 3—36161
electric point dipole radiation 3—29956
e.m. instability in cold streaming plasma in presence of a magnetic field 3—26868
e.m. wake, of charged particle pulse, charge density profile effects 3—36148
energy absorption in cold inhomogeneous plasmas, the Herlofson paradox 3—20452
energy momentum tensor for plane quasimonochromatic wave packet 3—26869
excitation by longitudinal electric fields 3—29953
excitation by relativistic electron beam in magnetised plasma, two-stream instability 3—29954
excitation of anisotropic plasma by localized current source 3—14527
fast wave damping at the second harmonic of the ion cyclotron frequency 3—20461
fluctuations in a semi-bounded nonequilibrium plasma 3—23834
focusing of e.m. waves in inhomogeneous mag. field 3—23823
heating by beating of laser beams 3—33379
heating of ionic component, by collisional absorpt. of fast waves *(French)* 3—17625
high freq. waves, in electron plasma, stochastic kinetic theory 3—11478
homogeneous isotropic ionospheric 3—14532
homogeneous lossy anisotropic drifting plasma, in rectangular waveguide, dispersion relation 3—23830
hot isotropic system, current distrib. at surface of dipole antenna *(French)* 3—23825
incoherent reflection from plasma layer 3—36162
induction of d.c. current by an r.f. travelling wave in a strong mag. field 3—17584
infinite tubular antenna in cold collisional plasma 3—11482
instabilities in magnetised plasmas, computer simulation 3—20467
instabilities of a plasma with anisotropic ion temp. penetrated by the field of a helicon wave 3—33345
instability when propagating obliquely to double stream in plasma 3—23824
interplanetary, e.m. fluctuations, due to solar radio bursts *(Russian)* 3—3320
ion heating by geometrical Landau damping, lower hybrid frequency waves 3—20579
ion-sheathed spherical probe, r.f. impedance 3—30010

electromagnetic wave propagation in plasma continued
ionospheric group refractive index involving temp. and ion effects 3—18877
ions, counter-streaming, with anisotropic temps., ordinary-mode e.m. instability 3—29949
large volume microwave plasma generator 3—17632
laser irradiated plasmas, nonlinear behaviour of stimulated Brillouin and Raman scattering 3—36159
laser light absorption in dense plasma 3—33347
laser scattering, electron temp. and diffusion 3—17581
loading of a RF helix by a hot magnetised plasma column 3—20460
longitudinal, transmitted pulse shape determ. for both circularly polarised waves 3—16018
longitudinal and transverse e.m. waves nonlinear interactions, phase effects 3—33362
loss-cone instability rel. to whistlers 3—17577
lower-hybrid-resonance heating in parallel-plate waveguide 3—17576
magnetic fluctuation energy, thermodynamic bounds for anisotropic unstable plasma 3—29936
magnetic line source, excitation fields 3—20448
magnetically biased plasma, net-field polarization 3—23833
magnetized plasma, parametric excitation of circularly polarized and ion waves 3—23847
magnetoactive plasma, absorption and amplification considering spatial dispersion *(Russian)* 3—29948
magnetoactive plasma, kinetic theory of wave reflection on boundary 3—23829
magnetoactive plasma, nonthermal radiation in field of microwave pumping wave 3—33395
magnetoplasma, inhomogeneous, optimum second harmonic generation 3—29952
magnetoplasma, self-focussing of transverse waves 3—36158
magnetoplasma associating cylindrical antenna, input impedance 3—7497
microwave absorption and conversion, at upper hybrid resonance h.f. field distrib. density electron energy and wave propagation 3—17582
microwave absorption in inhomogeneous magnetoactive plasma 3—20447
microwave absorption in magnetoactive plasma 3—20465
microwave cavity partially filled with warm plasma, eigenvalues 3—20468
microwave heating, longitudinal electronic thermal conductivity in magnetic field 3—17639
microwave radiation effect on shock-produced electron precursor 3—20454
microwave signals at 10 GHz interaction with electron density gradients 3—33351
microwave-plasma interaction, electric field strength determ. by means of Stark effect 3—30012
modelling *(Russian)* 3—19556
motion and wave propagation along mag. field, stationary and moving plasma 3—7502
multicomponent plasma, static magnetic field 3—1488
multicomponent plasma with negative ions, crossover frequencies 3—11477
multilayered drifted solid-state magnetoplasma 3—14526
nonconcentric circular plasma cylinders with axial magnetic fields, scattering problem 3—7499
nonequilibrium gas discharge plasma, alternating mag. field struct. 3—33346
nonlinear, in weakly ionised plasma 3—36160
nonlinear damping of potential monochromatic waves in inhomogeneous plasma 3—17579
nonlinear generation of harmonics of the cyclotron frequency of e.m. waves 3—20466
nonlinear limits to the theory of resonant absorption in cold plasmas 3—20463
nonlinear modulation in plane-bounded plasma 3—17585
numerical analysis application 3—32492
optimum pulse transmission through exponential plasma inhomogeneity 3—7500
parallel whistler mode instability unified picture 3—37242
parametric backscatt. 3—33348
parametric excitation of circularly polarised and Langmuir wave in magnetised plasma 3—20453
parametric excitation of high frequency electrostatic oscillations in a cold magnetoactive plasma by an e.m. wave 3—29955
parametrically generated elctrostatic waves refraction by e.m. pump 3—33365
penetration, boundary conditions, reflection 3—14534
phase shifter with cylindrical hollow cathode 3—20456
photon hydrodynamics in inhomogeneous plasma 3—17580
plasma consisting of matter and antimatter e.m. and acoustic wave propag. 3—17561
plasma diagnostics 3—14591
plasma ion heating by mixing of e.m. waves near electron cyclotron resonance 3—20580
plasma-filled transversely magnetized rectangular waveguide charact., collision frequency effect 3—1491
polarisation of nonlinearly generated harmonic for oblique propagation 3—29951
pulsar detection by propagation of whistler mode in surrounding and interstellar plasmons 3—16248
radially inhomogeneous plasma, buildup of narrow plasma channel by microwave 3—1489
radiation from moving sources, complex effects *(Russian)* 3—38431
rarefied, in alternating mag. field 3—23827
rectangular waveguide with homogeneous anisotropic plasma, dispersion relations 3—26867
rectangular waveguides, fitted with lossy warm plasma, characteristics 3—20451
reflection and transmission props. 3—7496
relativistic plasma, self-focusing, analogy with electron gas of III-V semicond. *(Russian)* 3—8218
relativistically strong e.m. wave of circular polarisation in cold plasma, instability 3—11479
relaxation of anisotropic collisionless plasma distribs. due to whistler mode instabilities 3—14529

electromagnetic wave propagation in plasma continued
resonances excitation by dipole antenna inside hollow cylindrical plasma 3—7495
resonant Faraday effect use to determ. relative transition probabilities for absorption lines with Voigt profiles 3—11473
resonant interaction between ordinary e.m. modes 3—29950
RF absorption by hot ion-electron plasma cylinder excited by an arbitrary e.m. field 3—38481
r.f. absorption in a nonuniform hot magnetised plasma column 3—20459
RF feedback stabilisation of an ion-acoustic instability 3—38455
r.f. nonlinear effects near the lower hybrid resonance frequency 3—20462
r.f. response of non-uniform plasma slab-condenser system 3—4633
scattering, in magnetoactive plasma 3—1487
scattering of e.m. waves by plasma containers 3—38434
self focussing of laser light and supersonic ionization wave 3—17634
semi-infinite random media, total reflection of plane wave 3—4634
semiconductor plasma, propag. under crossed elec. and mag. fields 3—20455
short dipole in drifting magnetoplasma, radiation resistance calc. 3—38433
short-wave propag. in plane symmetric plasma waveguide, appl. to topside ionosphere inhomogeneities 3—34928
solid state plasma e.m. wave propag. rel. to carrier drift *(Russian)* 3—11921
source free region 3—29956
spatial e.m. echoes in a magnetoplasma, observation conditions *(French)* 3—38437
spherical antenna, plasma coated, effects of pseudosonic and electroacoustic waves 3—1493
stratified overdense plasma with high collision freq., microwave scatt., dnd refl. 3—17575
streaming nonuniform plasmas, drift instabilities 3—14531
strongly inhomogeneous weakly ionized plasma 3—23828
thermomagnetic effect 3—26888
thin cylindrical antenna, calculation of current distribution and impedance by method of moments 3—33352
TM-wave self focussing theory in an anisotropic plasma 3—38435
Tokamak FT-1, e.m. wave interaction and heating 3—20573
transient signal propagation 3—35660
turbulent-plasma scatt. theories, comments on critique 3—33349
two stream instability, bounded plasma, relativistic electron beam 3—14533
two-component magnetoplasma, attenuation and phase coefficients 3—9315
two-dimensional e.m. field diffraction on an ideally conducting plane with an infinite straight slit 3—29024
u.h.f. signal parametric amplification by beam-plasma interaction in mag. field *(French)* 3—11474
warm plasma, turnstile aerial radiation props. 3—36157
whistler waves, parametric instability and anomalous heating 3—4635
whistler waves in thermal simulation plasma 3—23832
$Bi_{0.9}Sb_{0.1}$ crystals, magnetoplasma wave dispersion, low frequency e.m. wave propag. *(Russian)* 3—11922
Hg plasma, weakly ionised, negative absorpt. of r.f. waves 3—11476

electromagnetic wave reflection
see also light reflection; X-ray reflection
2-dimensional Gaussian beam, at plane interface of dielectrics, two-dimensional solutions 3—26188
amplification in total internal refl. from region of inverted population *(Russian)* 3—10326
apparent reflection height, det. of phase information from l.f. field strength observations *(German)* 3—9313
auroral-type E_s-layer in winter, reflection meas. from Dixon 3—28068
beam waves at plane interface of dielectrics, 3-dimensional solutions 3—22809
critical angle refl., teaching expt. 3—28436
D-region differential-absorption, differential-phase partial-reflection experiments 3—12805
D-region wind meas. from fading of partially reflected radio waves 3—31432
dipole antenna coeffs. for stratified anisotropic media 3—34885
F-region e.m. wave reflection coefficients rel. to thickness of E_s-layer 3—25284
flux contours on a plane for parallel radiation specularly reflected from a cone, a hemisphere and a paraboloid 3—19526
FM pulses, from ionosphere 3—25278
f.m.c.w. partial reflection meas. of D-region, preliminary investigation 3—16032
Goos-Hanchen effect, simple anal. 3—24
heat radiation specular reflection from an arbitrary reflector surface to an arbitrary receiver surface 3—19525
from ionosphere, obs. of angles of arrival *(Russian)* 3—3055
ionospheric radio wave reflection, depend. of freq. correlation of fluctuations 3—34934
ionospheric reflection field distrib., verification using quantitative statistical confidence criterion 3—25267
ionospheric reflections, average field polarisation rel. to reflected wave fluctuation characts. 3—25268
ionospheric sporadic-E thin layers, mode coupling process rel. to echoes on ionograms 3—25285
l.f. radiowave reflection theory in ionosphere near critical coupling frequency 3—21963
magnetoactive plasma 3—23829
magnetospheric whistlers in ionosphere and lower exosphere at high latitudes 3—5519
metal, spectral radiating power meas. at high temperatures, analysis 3—22287
microwave reflectometers, tuned, refl. coeffs. meas. 3—35665
moving dielectric half-space, distortion 3—4064
multiple internal reflection rel. to e.m. wave transmission through conducting sheet 3—16687
nongray directional surfaces, wavelength and temp. dependence 3—22772
perfectly conducting sinusoidal ocean surface rel. to fading 3—4063
perforated flat plates, transmission charact. 3—10331

electromagnetic wave reflection continued
plane dioptre, uniform heterogeneous wave refl. and shift of reflected wave *(French)* 3−32493
plasma, anisotropic, boundary problem, interface with vacuum 3−23816
in plasma, boundary conditions for penetration 3−14534
plasma, stratified, overdense, with high collision freq., microwave scatt. and refl. 3−17575
plasma, total reflection of plane wave in semi-infinite random media 3−4634
plasma sphere, in terms of electron radius or plasma freq. 3−17563
plasma wave incoherent reflection from plasma layer 3−36162
pulse signal, from moving mirror *(Russian)* 3−29016
radio waves returned from ionosphere, double-peak amplitude distribution 3−18883
radiowaves, reflection from inhomogeneous layers in Fraunhofer zone, fluctuations in angles of arrival *(Russian)* 3−12797
rectangular waveguide, voltage-reflection coefficient and VSWR 3−16689
rectangular waveguide dielectric loaded bends, reflection coefficients 3−16690
semiinfinite dielectric medium undergoing phase transition, reflection of e.m. field energy 3−16784
total, filters of polarization states *(French)* 3−13677
total, photon inertial spin effect *(French)* 3−13678
total reflection of polarized light, calc. of transverse shift of spinning photons 3−16819
transmission and reflection at dielectric slab with inverse-square permittivity profile 3−22812
transverse shift during total refl. of circularly polarized wave, luminous intensity *(French)* 3−19555
u.h.f., from semiconductor plates of finite thickness, calc. of modulus and phase of reflection coeff. *(Russian)* 3−12196
uniaxial plasma slab relativistically moving 3−7496
Venus, radar reflection rel. to chemical composition and altitude profile 3−25409
water film on microwave antenna *(German)* 3−19558
WKB solutions, extension to any high order of accuracy 3−26189
Bi, second harmonic generation of u.h.f wave during anomalous skin effect 3−18179

electromagnetic wave refraction
atmospheric diurnal var. of surface refractivity over India 3−12723
atmospheric mm waves, simulation results 3−37236
gas lens, laminar flow type 3−37926
ionosphere, scale height determination from radiowave satellite signals 3−9319
satellite ranging error, tropospheric effects, atmospheric model, local meteorological conditions 3−21935
stigmatic lens, structure of e.m. field near focus 3−19580

electromagnetic wave scattering
see also backscatter; gamma-ray scattering; light scattering; X-ray scattering
auroral v.h.f. signal scattering, region configuration *(Russian)* 3−3035
backscatter from snow, ice, and sea ice, 26 to 40 GHz 3−37269
backscattering, from perfectly reflecting object situated near caustic surface 3−22820
backscattering, wave corrections for transfer equation 3−22821
backscattering from rough surface model 3−10432
boundary conditions, continuous wave inverse scatt. 3−10433
characteristic waves through infinite slab of irregularities in magneto-ionic medium 3−25271
circular wire loop, backscattered field, geometrical theory 3−4068
cloud of particles, radiative transfer 3−12461
convex conducting object, mean scattering cross section, relation to surface area *(Russian)* 3−10434
cosmic maser model with resonance-scattering feedback, appl. to OH and H_2O clouds 3−28290
cylindrical boundary of arbitrary shape, green function theory 3−29021
from dielectric bodies, state-space formulation, applic. to spherically symmetric objects 3−29020
diffusion dipole source, analytic soln. 3−29018
disturbance of coherence through interaction with hydrogen like atoms, group theory treatment of scattering *(German)* 3−13716
electric and magnetic dipole scattering from perfectly conducting sphere in homogeneous lossy medium 3−3175
elliptic metal plate, h.f. backscattering 3−10438
elliptical reflector rel. to diffraction by double circular irises 3−6405
Ewald-Oseen extinction theorem, general form and new interpretation 3−22832
from finite cone, backscattering 3−35666
by free electron, frequency drift *(Russian)* 3−10575
Helmholtz equation, three-dimensional inverse scattering 3−37854
highly conducting surface, stimulated scatt., nonlinear theory *(Russian)* 3−6408
hollow semi-infinite cylinder, near field of scattering, applic. to magnetic sensor boom 3−22823
hyperbolic dispersive partial differential equation, two-dimensional, inverse problem 3−16595
inhomogeneous media, remote probing by parameter optimization techniques 3−19563
inhomogeneous objects, computation 3−37929
inhomogeneous spherical lenses, numerical and asymptotic scattering 3−37855
inverse problem of scattering by smooth convex-shaped conductors for high frequency, system-synthesis approach 3−22833
inverse scatt. from perfectly cond. prolate spheroid, in quasi-static domain 3−22819
ionosphere, multistatic incoherent scatter meas. of drift velocity 3−28063
ionospheric incoherent radar scatter observations, mid-latitude F-region trough structure 3−31427
ionospheric inhomogeneity structure, magnetoionic component scatt. 3−34929
least-squares boundary residual method 3−13685
loaded N-port scatterers, modal analysis in both open- and short-circuit parameters 3−22824
in magnetoactive plasma, inverse Compton effect 3−1487

electromagnetic wave scattering continued
Mie theory for determ. of optical props. of zodiacal light models 3−31638
by non-Gaussian surfaces, physical and geometrical optics methods 3−22822
nonconcentric circular plasma cylinders with axial magnetic fields 3−7499
numerical analysis application 3−32492
numerical soln., nonuniqueness of integral equations 3−35663
ocean-like surfaces, integral equation determination of numerical method, comparison with optical and perturbation methods 3−32503
one-dimensional random media, Monte-Carlo computer technique 3−6404
plane wave at statistically uneven interface, second-order and multiple scatt. 3−13686
plane waves, obliquely incident on perfectly conducting rotational bodies of arbitrary form. 3−19562
plane waves by infinite grating on anisotropic medium *(Japanese)* 3−22818
inplasma, dense turbulent, density fluctuation effect on e.m. wave scatt. 3−20450
plasma, stratified, overdense, with high collision freq., microwave scatt. and refl. 3−17575
by plasma containers 3−38434
radar cross-sections calc. 3−6409
radar target, statistical modelling 3−13689
radially inhomogeneous spheres, numerical soln. 3−37930
radiowave, attenuation and phase rotation due to rain, at 19.3 and 34.8 GHz 3−28045
Rayleigh, cross sections, polarizability tensors 3−672
rectangular groove on metallic mirror, resonance scattering 3−29022
by refractive index radially moving spherical discontinuity 3−19560
reson. link radiation in a homogeneous sphere, planetary nebula appl. *(Russian)* 3−16286
resonators, toroidal, in slot coupled chain, scatter calc. *(Russian)* 3−32401
retarding system of resonator chains with mixed excitation, scatter calculation *(Russian)* 3−32402
rough surface, composite model compared with Kirchhoff method 3−22826
rough surface, Rayleigh-FFT approach 3−37927
rough-surface backscatter, effect of subsurface on depolarization 3−670
round metal post and gap in waveguide, gap impedance calc. 3−35664
r.w.. scattering by sea surface *(Russian)* 3−31341
semiconductor, many-valley, elec. field depend. of freq. and polarisation 3−5003
semiconductor with anisotropic energy band, by fluctuations in nonequilibrium plasma 3−18180
sphere, perfectly conducting, Lewis's (1969) inverse scatt. method, calc. and simulation 3−22828
sphere, perfectly conducting, size determ. from Mie scatt. intensity extrema 3−22827
spherical shell of arbitrary thickness, transient response 3−671
statistically inhomogeneous medium, radiative transfer equation deduction by theory of multiple wave scattering *(Russian)* 3−13682
statistically uneven surfaces, Kirchhoff's method, perturbation method and multiple scattering 3−29023
TE surface wave scatt. by semi-infinite grounded dielectric slab, horizontally polarised antenna 3−37932
Thomson, effect on emission spectrum of an optically semiopaque plasma, X-ray sources *(Russian)* 3−16117
transversely moving conducting cylinder of arbitrary cross section, e.m. wave scattering 3−32498
velocity dependent, by two thin dielectric cylinders 3−673
v.l.f. waves, nonlinear hydrodynamic scattering in magnetosphere 3−31452
waveguide, periodic, e.m. wave propagation, approximate computation *(Russian)* 3−10431
waveguide, periodic delay system, dispersion charact., calc. *(Russian)* 3−10435
waveguide junctions, moment method with mixed basis functions 3−37856
wedge, perfectly conducting, exterior region divided by resistive sheet edge condition 3−22825
^{3}He, liq., freq. power spectrum of density fluctuations 3−11779

electromagnetic waves
see also bremsstrahlung; Cherenkov radiation; electromagnetic field theory; electromagnetism; gamma-rays; light; microwaves; radiofrequency cosmic radiation; solar radiofrequency radiation; sunlight; synchrotron radiation; whistlers; X-rays
applications of Reciprocity Principle, book 3−28934
black holes, Schwarzschild, vector and tensor radiation from relativistic circular geodesics 3−37288
cosmic incoherent h.f. radiation from relativistic electrons with power energetic spectrum 3−12934
galvanomagnetic surface waves of short wavelength, nonlinear excitation theory 3−21060
human body interactions, biological effects, mechanisms 3−9714
instabilities produced by ionisation of interplanetary neutral particles 3−13007
ion cyclotron, parasitic pitch angle diffusion of radiation belt particles 3−12836
Maxwell eqns. in black-hole background, radiation from charge falling into hole 3−12945
media with spatial dispersion, integral relationship between elec. field and displacement field 3−29010
metal surface, long wavelength phonon generation by e.m. waves 3−27167
metallic scattering of He ions, cut off of l.f. radiation 3−27588
optical field, plane wave expansions 3−10327
piezoelectric half-space, elastic-e.m. wave excitation *(Russian)* 3−34302
point charges in weak gravitational fields, Green's function study, generation of e.m. waves in Riemann tensor 3−26128
polarisation, numerical method for measurement of degree *(Russian)* 3−22329

- **electromagnetic waves** continued
  - quartz plate, e.m. radiation 3—6398
  - radiance volume density concept 3—22807
  - radiation effects on motion of astrophysical objects 3—37293
  - radiation energy, determ. from repulsion between aerials 3—22
  - radiation fields in Schwarzschild background, study of Newman-Penrose quantities 3—6330
  - radiation from electron beams 3—13776
  - radiation of charged particle in semiinfinite iris-loaded waveguide *(Russian)* 3—6302
  - radiation pressure, Larmor and adiabatic theorems 3—37906
  - wave equation, solution, circularly cylindrical coordinates, homogenous isotropic regions containing coordinate axis 3—19479
  - wave impedance and S-matrix definition, comments 3—13679
- **electromagnetism**
  - *see also electric fields; electromagnetic field theory; electromagnetic oscillations; electromagnetic waves; inductance; magnetic fields; magnetism*
  - anisotropic media, e.m. props., relativistic treatment *(French)* 3—22732
  - Biot-Savart law modified for mag. fields due to line currents 3—37921
  - charged point-mass motion, Coriolis force derivation from vector pot. 3—28928
  - e.m. response of permeable inhomogeneous conducting sphere 3—25130
  - e.m. wave amplification in total internal refl. from region of inverted population *(Russian)* 3—10326
  - engineering electromagnetics, textbook 3—32472
  - general relativity, e.m. boundary conditions, covariant derivation 3—13629
  - horizontal dipole buried in 2-layer earth 3—22803
  - interaction between charged elements, thermal agitation influence *(French)* 3—19544
  - line splitting in differentially rotating slabs 3—13605
  - Lorentz force law implies Faraday's law of induction B time independ., proof 3—31997
  - magnetic field, origin as Coriolis force from Thomas rotation 3—37853
  - magnetostatic field and induction law characts. using heavy bar electromagnet, demonstration 3—28438
  - Maxwell's eqn., conducting spherical region, soln. *(Russian)* 3—10419
  - Maxwell's eqn. solved for dielectric slab waveguides with inhomogeneous core, soln. of Maxwell's eqn. 3—10328
  - Maxwell's equations, quantisation, determ. of generalized energy addition law 3—4143
  - Maxwell's equations new solns. by extension into complex Minkowski space 3—10368
  - Maxwell theory (in media) and quantum theory in a rotating reference frame 3—35600
  - moving charged particle in a dielectric, electromagnetic field theory 3—31981
  - nonrelativistic Galilean theory 3—37852
  - noumenon, a generalization of relativistic events and space-time, basis for e.m. interactions 3—19494
  - oblong nonmagnetic conducting body, orientation by homogeneous alternating mag. field *(Russian)* 3—32474
  - relativistic, transformation eqns. and objectivity principle 3—32428
  - rotating disc, in external d.c. electric and magnetic fields, relativistic theory 3—19545
  - SI units, conventions of nomenclature 3—16376
  - Smith Purcell effect, radiation emitted as an electron beam passes over a metal surface 3—19553
  - teaching approaches to classical theory 3—13186
  - transformation props. of e.m. quantities under space inversion, time reversal, charge conjugation 3—28998
  - transportation system, forces on moving coil due to eddy currents, Maxwell equation soln. 3—35651
  - two-layer Earth model, Argand representation of mutual e.m. coupling of loops 3—5432
- **electromagnets**
  - *see also coils; superconducting magnets*
  - betatron, size dependence on machine parameters *(Russian)* 3—19265
  - cylindrical electromagnet parallel to metallic wall, field distribution determ. *(Polish)* 3—22801
  - levitation system rel. to magnet design and technology 3—6036
  - for magnetic thin film testing, patent 3—10427
  - particle accelerator for nuclei research electromagnet design and construction 3—28623
  - proton beam switching system, for synchrotron 3—32121
- **electromechanical effects** *see electrostriction; piezoelectricity*
- **electromechanical filters**
  - lasers, rapid frequency tuning 3—3819
- **electrometers**
  - *see also charge measurement*
  - air capacitors, constant and variable for electrometer cct. 3—22408
  - contactless, Q-meter transducer with capacitance cell 3—6021
  - leaf electrometer with charge polarity discrimination, educational use 3—44
  - liquid, absolute voltage measurement *(Japanese)* 3—254
  - logarithmic, analytical fit of transfer function and correction for ambient temp. variations 3—25809
  - measurement problems in measuring very small voltages and currents *(Polish)* 3—25812
  - operational amplifiers, medical use 3—10152
  - vacuum tube, sensitivity improvement 3—35439
- **electrometry** *see electrometers*
- **electromotive force** *see electric potential*
- **electron absorption**
  - *see also beta-ray absorption; nuclear reactions and scattering due to electrons*
  - auroral electron spectrum dynamics during magnetospheric substorms rel. to X-ray bursts 3—25255
  - fast electrons, energy dissipation curves, fitting function 3—10043
  - inelastic dispersion rel. to absorption in electron diffraction 3—11652
  - Kikuchi patterns, dynamical theory allowing for absorpt. of scattered electrons 3—11532
- **electron absorption** continued
  - pseudo-Kikuchi patterns, meas. of ratio of abnormal to normal absorpt. coeff. in solids 3—23987
  - pseudo-Kikuchi patterns for detn. of normal/abnormal electron absorption ratio 3—11651
  - Ramsauer effect, apparatus for expt. demonstration, and theory *(Russian)* 3—17371
- **electron accelerators**
  - *see also betatrons; electron ring accelerators; microtrons*
  - activation analysis, by bremsstrahlung 3—19372
  - apparatus for producing relativistic electrons in rotating angular bunches *(Russian)* 3—10041
  - high current, in vacuum foil changer 3—19259
  - injectors with Pierce and Kerst-type optics 3—16496
  - linac with side-coupled struct., design, performance 3—28629
  - linear, development at Moscow Engng.-Phys. Inst. *(Russian)* 3—19253
  - linear, diode gun, production of beam single shots and pulse trains by pulse position modulation 3—10035
  - monitor for secondary emission 3—22447
  - pulsed high current, transient phenomena of beams 3—28635
  - superconducting linear and synchrotrons, meeting of Danesbury-Rutherford working party 3—32125
- **electron affinity**
  - *see also ionisation*
  - polyatomic mols., low energy electron attachment, temp. depend. 3—26712
  - Ag^-, dye-laser photodetachment studies 3—29503
  - Ag^- beams, photodetachment by Ar-ion-laser beam, electron affinities 3—29502
  - Au^-, dye-laser photodetachment studies 3—29503
  - Br in alkali metal compound 3—1117
  - Cl in alkali metal compound 3—1117
  - Cu^- beams, photodetachment by Ar-ion-laser beam, electron affinities 3—29502
  - F in alkali metal compound 3—1117
  - GeF_4, bond dissoc. energies, ioniz. pots. and electron affinities 3—20191
  - I in alkali metal compound 3—1117
  - N fluorides, molecules and ions, CNDO/2 calculation of atomization energies 3—7245
  - P fluorides, molecules and ions, CNDO/2 calculation of atomization energies 3—7245
  - Pt^-, dye-laser photodetachment studies 3—29503
  - PtN^-, dye-laser photodetachment studies 3—29503
  - SO_2, application to flue gas monitoring instrument 3—3860
- **electron annihilation** *see positron annihilation*
- **electron avalanches**
  - *see also avalanche diodes; discharges (electric); IMPATT devices; Zener diodes*
  - alkali halide crystal, electron avalanche breakdown induced by ruby laser light 3—30757
  - alkali halides, laser induced bulk damage due to electron avalanche breakdown 3—35705
  - m.i.s structure, rel. to n-channel enhancement realisation 3—34000
  - p-n junction with double error function doping profile 3—36662
  - p-n junctions multiple epitaxial, avalanche breakdown voltage, peak field at breakdown 3—27307
  - Si, diffused p-n junction, avalanche breakdown luminesc. 3—15557
  - n-Si, high field effects 3—5014
  - Si, p-n junction, obs. of photocurrent spectra under avalanche breakdown conditions 3—15247
- **electron beam absorption** *see electron absorption*
- **electron beam applications**
  - *see also electron beam welding*
  - alloy deposit prep. by continuous electron beam evaporation from single rod-fed source 3—27715
  - appearance potential spectroscopy, for surface studies 3—34446
  - betatron beam for defectoscopy *(Russian)* 3—19267
  - breast cancer, treatment by electron beam from betatron 3—16560
  - cancer, preoperational irradiation therapy, from 25 MeV betatron *(Russian)* 3—25598
  - ceramics, machining techniques, review 3—31128
  - channel electron multipliers, calibration using standard omnidirectional electron beams 3—25943
  - defectoscopy using betatron beam *(Russian)* 3—19268
  - electron and ion beam technolgoy, conference, Houston, Texas (1972) 3—13473
  - electrostatic analysers, calibration using standard omnidirectional electron beams 3—25943
  - evaporation, for deposition of multilayer films on glass substrate 3—37710
  - fluorescence probe measurements, apparatus and techniques 3—35493
  - hologram recording 3—13333
  - inductive energy storage, pumped electron beam switching circuit 3—25835
  - injection buncher applic. in 30 MeV linear travelling-wave accelerator *(Russian)* 3—28632
  - integrated optics circuit fabrication by electron beam technique 3—35390
  - lithography, negative electron resist exposure, voltage dependent parameters 3—35505
  - low power switching integrated circuit production 3—15653
  - low-temp. plasma meas. in the magnetosphere and interplanetary space 3—18893
  - medical therapy, review 3—6131
  - microfabrication, computer-controlled 3—35513
  - neutron production, by hot dense plasmas 3—29989
  - optical film deposition 3—34479
  - plasma, Z-pinch preionisation using pulsed relativistic electron beam 3—23884
  - scanning, for work function distribution measurement 3—30535
  - stomach cancer, results of preoperational irradiation from 25 MeV betatron *(Russian)* 3—25597
  - therapy, adaptation of 30 MeV IAP betatron 3—16483
  - therapy, field patching using computer 3—10163
  - thin films, thermal processing, development *(German)* 3—6534
  - tracing of microcircuits patterns of small Si chips 3—10583

electron beam applications continued
X-ray analysis, electron excitation, instrumentation 3−37757
zone, melting of Sn and Sn-Pb films, preliminary formation of refractory layer *(French)* 3−34486
C materials thermal diffusivity meas. at high temp. by modulated electron beam technique 3−28495
GaAs targets excitation for miniature pulsed laser 3−26237
Nb single crystal, electron beam float zone melting and vacuum degassing 3−27716
$YbFeO_3$, electron beam induced charge storage memory with read-out and erasure 3−35504

electron beam effects
see also beta-ray effects
absorption and inelastic dispersion in electron diffraction 3−11652
alkali halide ion sputtering, surface structure 3−30313
alkali tellurite glasses, e.p.r. spectra, irrad. effects *(Russian)* 3−21309
amorphous material, electron scatt. theory, transition matrix approach 3−7792
autoionic projector, thin films 3−344
beam specimen interaction in h.v. electron microscopy 3−351
Cherenkov radiation prod. by beam injection into ionosphere *(French)* 3−39548
Cherenkov radiation prod. in inosphere by beam injection 3−28058
defect production rate at temperatures above stage I 3−30158
dislocation interaction with irradiation produced point defects in high voltage electron microscope 3−17844
dislocation line kinetics, effect of high temp. pulse irradiations 3−36300
electro-ionization and pumping of highly compressed gases for generating laser pulses and freq. 3−6464
electron beam-plasma interaction, spiraling, enhanced emission around ion cyclotron harmonic freq. 3−1483
E × **B**electron drift instability in plasmas with $T_i \sim T_e$, nonlinear stabilisation 3−14557
electron irradiation induced void studies in metal in h.v. electron microscope 3−1640
energy loss spectra for V(Cr)(Fe)(Co)(Ni)(Cu) films 3−17885
exciton creation in strong mag. fields due to energy losses of fast electrons 3−36339
external high frequency modulation of an electron beam, heating effect of ions on interaction with a plasma *(Russian)* 3−17627
fast electrons as simulated photon source between 25-400 eV for meas. of photo-spectra *(Dutch)* 3−30897
glass, defect form. and crystal growth 3−7790
glasses, electrovacuum, density change meas. and mechanism of radn. damage *(Russian)* 3−11548
graphite, thermoelectric power at temps. above 5 K, electron irrad. effects, annealing effects 3−27278
graphite surface, electron irrad., momentum transfer, blow off vapour yield, 300-5000K 3−24765
halide film damage rel. to anomalous opt. absorpt. 3−34479
high current relativistic electron beam interaction with a plasma in a magnetic field 3−23923
high energy impacts, thin foils, secondary emission *(Russian)* 3−12201
interaction between intense electron beam and homogeneous and heterogeneous plasma *(Russian)* 3−14582
kinetic instability in plasma, nonlinear theory 3−33368
laser pumping, waveguide resonator structure, semiconductor laser, laser threshold 3−22926
lung tumours, betatron therapy, clinical considerations 3−22171
magnetoplasma-electron beams counterstreaming system, wave-wave coupling 3−17601
martensite, electron irradiated, lattice tetragonality increases under low temp. annealing 3−33648
metal, fine strength change of irradiated crystals 3−33552
metal radiation damage at 0.5-3MeV, effect of crystallographic conditions 3−14889
metal-polymer-silicon structure, C-V characts., irrad. effects 3−18221
metals, electron radiation and surface roughness 3−27593
microfission explosion by laser or relativistic electron-beam high-density compression, reactor prospects 3−32932
m.i.s. structure, annealing, bias-temp. stress effects on surface states and flatband voltage 3−15269
1-naphthol, H-randomization under electron impact 3−11193
noise pulses induced by high energy electrons (245 MeV), exam. 3−10082
penetration mechanism, for high power density beams 3−14894
planar p-n junctions, beam induced current 3−2179
plasma, electron-cyclotron wave, excitation by modulated helical electron beam 3−33367
plasma Cherenkov coherent radiation on injection of relativistic electron beam 3−30007
plasma nonlinear instabilities, phase-space evolution of trapped electron beam 3−14555
plasma oscillations incoherent excitation by almost monoenergetic relativistic electron beam 3−7539
plasma production, counter streaming 3−23839
plasma relativistic electron beams, induced fields and currents 3−29941
plasma-beam instability, nonlinear mode competition 3−14556
plasma-beam interaction fast electron prod. 3−38429
polycarbonate films, effect of energetic electron irradiation upon charged-particle track registration 3−19307
polyimides, mech. props. changes 3−27783
polymer film, in m.i.s. struct., radiation resistance obs. 3−5060
polymer foils, electron irrad., currents, charges, voltage buildup 3−36841
polymer particles in electron microscope, decrease in size 3−9006
polymeric materials operating in vacuum in presence of ionizing radiations, accelerated testing 3−27845
radiation therapy, dose meas. associated with use of 7.5 MeV electrons 3−28387
rare gas laser, electron beam excitation mechanism 3−10521
rat-spleen lysosomes, comparative effects of electron and neutron irradiation on relase of enzymes 3−28375
relativistic, excitation of e.m. waves in magnetised plasma, two stream instability 3−29954

electron beam effects continued
relativistic, plasma two-stream instability heating 3−36188
semiconductor, ion and electron irrad., clustering of defects 3−33576
semiconductor laser radiating mirror type, electron beam pumped, construction, props. 3−16869
sodalite, damage mechanism, ESCA obs. 3−36298
spectra, emission, produced by electron impact, instrument design for obs. *(Japanese)* 3−16436
spore growth, irrad. effects, electron microscope obs. 3−25599
stable intense electron beam heating of dense plasma 3−4660
steel, austenitic stainless, dispersion hardened, inhibited void form. during electron irrad. 3−26505
steel, irrad. effects on hardenability 3−24948
steel, mild, 1 MeV electron irrad., void formation 3−11609
steel, stainless, on work function rel. to elec. charge 3−24496
transmission electron microscopy, specimen temp. increases 3−24011
two stream instability, bounded plasma, e.m. wave excitation 3−14533
vacancy and interstitial formation and annihilation in metals 3−14851
vacuum discharge triggering, characteristics *(Russian)* 3−14625
X-ray prod. by electron irrad. of target, thickness and inclination effects 3−16540
Al film, He ion pre-injected, electron irradiation effect on void form. 3−20967
Al irradiation damage, 3 MV electron microscope, voltage dependence 3−36333
Ar dense plasma production in plug-shaped mag. field by an electron beam *(Russian)* 3−17628
Au, bremsstrahlung produced by 0.5-1.44 MeV electrons, energy spectra transmitted through Fe slab 3−17328
Au, electron irrad., stable interstitial at 300K 3−4748
Au-Ni thin film thermocouple, transmission electron microscopy, specimen temp. increases 3−24011
BaF_2, radiation induced transform. of defects, e.p.r. and optical absorpt. obs. *(Russian)* 3−30694
CO_2 laser, electron beam controlled, current, voltage, gain meas. 3−10519
CO_2 laser amplifier, cold-cathode electron-beam controlled 3−716
CO_2 laser amplifier, electron beam controlled, performance 3−10478
CaF_2, radiation induced transform. of defects, e.p.r. and optical absorpt. obs. *(Russian)* 3−30694
CaF_2, thin films, electron irradiation effects 3−38748
CaF_2:Mn, cathode ray coloration, alpha and beta centre form. 3−30121
CdS, Cd displacement threshold at liq. He temp., cathodoluminesc. obs. 3−5247
CdS_xSe_{1-x}, graded gap crystal layer, luminesc. obs. by electron beam excitation 3−8053
CdTe, electron and neutron irrad., defect behaviour, photoluminescence spectra, excess, dissociative Cd pressure 3−34431
CdTe, electron irrad., edge emission spectra 3−18488
CdTe, photoluminescence, lattice defect investigation with use of heat treatment, neutron and electron irradiation *(Russian)* 3−27550
CdTe, radiation damage rel. to cathodoluminescence from lattice defect centres, quenching mechanism 3−15561
Cu, temp. depend. of defect production by electron irradiation 3−7749
α-Cu-Zn alloy, electron irrad., short range order, interstitial diffusion 3−11617
$FE(CN)^{3-}$ reduction to $Fe(CN)_6^{4-}$ by electron irradiation, Mossbauer study 3−2822
F_2-H_2 laser, excitation by relativistic electron beam, energy characts. *(Russian)* 3−4093
Fe, bremsstrahlung produced by 0.5-1.44 MeV electrons, energy spectra transmitted through Fe slab 3−17328
GaAs, defect levels induced by electron irradiation 3−21022
n-GaAs, electron irradiated, defect annealing, cluster formation 3−33558
GaAs, GaP, electron and neutron irrad., B, C impurities, i.r. local mode abs. 3−34395
GaAs, non-spherical radiation damage regions, Hall field calcs. 3−38856
n-GaAs, optical absorpt. increase with electron irrad., selective bands 3−39164
GaAs, p^+-n photodiodes, electron irrad., defect studies, differential capacity and conductance measurements 3−33845
GaAs, radiation annealing of defects formed by ion bombardment 3−33553
GaAs laser, electron beam excited, internal Q-switching emission time resolved spectra 3−16866
GaAs:Cr, photocond. after 0.8 MeV electron irradiation, induced impurity trap levels 3−36637
GaAs:Sn(Si, Zn), electron irrad., 'near-edge' absorption, annealing 3−33846
GaSe, luminescence, intense excitation by electron beam 3−15563
p-Ge, annealing of radiation induced defects rel. to recovery and defect energy levels 3−15158
Ge, annealing processes after irradiation with 1 MeV electrons at 85K 3−11616
n-Ge, electron bombardment induced annealing stage 3−38598
Ge, n- and p-type impurities electron irrad., annealing, Frenkel pair model, vacancy release 3−33561
Ge, non-spherical radiation damage regions, Hall field calcs. 3−38856
Ge, radiation defects due to 45-50 MeV electrons, carrier density and minority carrier lifetime obs. *(Russian)* 3−36332
Ge: group V (O, Te), electron irrad., E_c-0.2 eV level, defect model 3−33842
Ge: groups III and V, electron irrad., unusual donors and acceptors 3−33843
Ge:Cu, effect of impurity on kinetics of annealing of radiation defects 3−24111
H plasma, heating by relativistic beam 3−7541
H_2 excitation, gas laser, VUV, four level 3−22883
$H^+(H_2)_n$, $H^+(H_2O)_n$ cluster production on solid H_2 and ice, models 3−36965

electron beam effects continued
- InAs, electron irradiation damage studies 3−33555
- KCl, dipolar complexes resulting from 1.5 MeV electron bombardment 3−12096
- KCl, irrad., F-centre formation efficiency, 10-80K 3−20733
- KCl, M-centre form. and destruction by electron irradiation 3−4756
- KI, defect clusters, planar dislocation loops produced by electron, γ-irradiation, obs. at 5 K with electron microscope 3−30126
- K_2SO_4, exoelectron energy meas. after X-ray irrad. and electron bombardment 3−24777
- MgF_2, electron, colour centre prod. mechanism 3−34479
- MgF_2, electron and proton irrad., thermolum. *(Russian)* 3−18505
- Mo, point defect production 3−4772
- Mo, prequenched, 1.7 MeV electron irrad., stage-I recovery 3−27039
- Mo, stage III recovery mechanism 3−11615
- Na_2O-B_2O_3 glass, irrad., optical absorpt. spectra *(Russian)* 3−18474
- Nb, electron irradiated, annealing studies, H_2 contamination following UHV degassing 3−15723
- Nb (111), desorption of CO 3−20944
- Nb_3O_7F, double shear structure form. in electron microscope beam 3−33534
- Pt, electron irrad., recovery during stage II annealing, interstitial rearrangement 3−11618
- Pt, electron irrad., recovery during stage III annealing, vacancy migration mechanism 3−11619
- Pt-Au alloy, electron irrad., recovery during stage II annealing, interstitial rearrangement 3−11618
- Sb_xSe_y thin films, crystal growth 3−15097
- Si, charge state dep. of defects 3−33554
- Si, electron irrad., 130 K annealing stage of divacancy, i.r. transmission spectra 3−33559
- p-Si, electron irrad., illum. induced annealing 3−21547
- Si, electron irradiation at 0.5K, a.c. conductivity changes 3−7794
- Si, irrad., neutron and electron, heat treated, i.r. absorption band, high order vacancy defects, uniaxial stress response 3−34393
- Si, irradiated and annealed, diffusion, role of defects, other semiconductor materials 3−33701
- Si, non-spherical radiation damage regions, Hall field calcs. 3−38856
- Si, radiation annealing of defects formed by ion bombardment 3−33553
- Si, radiation damage in p-type with H impurity and high purity n-type, hole density, annealing 3−33546
- Si, radiation defects due to 45-50 MeV electrons, carrier density and minority carrier lifetime obs. *(Russian)* 3−36332
- Si, radiation effects, obs. using junction-capacitance techniques 3−33926
- p-Si, recovery stages on annealing, minority carrier lifetime obs. 3−33549
- Si, vacancy interaction with Sn impurities 3−18093
- Si absorption of O_2, electron beam-adsorbate interactions 3−30317
- Si surface, electron beam-adsorbate interactions 3−20939
- Si surface barrier radiation detector, radiation damage 3−32157
- p-Si:Al,(B), (Ga), electron irrad., annealing, effect of O and acceptor impurities 3−33560
- Si:Ge(Sn), O electron irrad., selective trapping of vaccancies migration of interstitials 3−33925
- Si-SiO_2 interface, low energy irrad. effects 3−21159
- β-SiC, with radiation defects, cathodolum. mechanism and efficiency *(Russian)* 3−2599
- Si(Li), surface barrier detectors, negative resist. on electron irrad. 3−28668
- SrF_2, radiation induced transform. of defects, e.p.r. and optical absorpt. obs. *(Russian)* 3−30694
- Te, electron irrad., lattice defects, galvanomagnetic props. 3−33934
- Te, electron irrad., recovery steps, isochronal and isothermal annealing expts. 3−33562
- α-U thin foils, penetration of h.v. electrons rel. to electron microscopy 3−1536
- V_2O_5(010) surface work function change, V_6O_{13} surface formation 3−36657
- W, adsorbed O_2, electron stimulated desorption 3−1886
- W(100) surface, electron stimulated desorption of CO, time-of-flight analysis of ions and neutrals 3−38730
- ZnO, displacement thresholds 3−20765
- ZnO, electron irrad., O displacement energy, F^+ centre form. 3−4773
- ZnS, cathodoluminescence and defect formation *(Russian)* 3−12187
- ZnTe, atomic displacement energies, cathodoluminescence edge emission spectroscopy, monoenergetic electron irrad. 3−33556
- ZnTe, electron irradiated, Zn displacement threshold, Zn vacancy luminescence 3−33557

electron beam ionisation *see electron ionisation*

electron beam welding
- electron and ion beam technology, conference, Houston, Texas, (1972) 3−13473
- instabilities, two-stream and kite 3−29984
- penetration mechanism, for high power density beams 3−14894
- steel, ausformed, electron-beam weld props. 3−21645
- superconductors, Cu-stabilised, for large bubble chamber magnet *(German)* 3−317

electron beams
- *see also electron optics*
- angular distrib. of 12-25 MeV electrons beyond W, Cd abd Cu pils *(Russian)* 3−13412
- Astron type injection in magnetic mirror 3−20661
- azimuthal, in magnetic field, instabilities with thermal velocity spread 3−13775
- backscatter and backemission yields, from metals 3−18514
- backscattered, angular distrib. 3−15580
- beam-plasma discharge, collective props., coherent light emission study *(Russian)* 3−7531
- beam-plasma system, suppression of instabilities by beam modulation 3−20484
- betatron, acceleration processes and radiation of electromagnetic waves *(Russian)* 3−19281
- betatron, attenuation after injection *(Russian)* 3−19280

electron beams continued
- betatron, extraction by pulsed single revolution and electrostatic methods *(Russian)* 3−19282
- betatron at Prague, influence of magnetic field decrement on trapping *(Russian)* 3−19279
- bremsstrahlung, mag., Lorentz-Dirac eqn. soln., results tested using electron beams in intense mag. fields 3−10703
- capture efficiency for different times within injection pulse in betatron *(Russian)* 3−277
- cathode spot, directional motion due to asymmetrical conditions at its boundaries *(Russian)* 3−1529
- characteristics from 25 MeV linear accelerator 3−3575
- cold-cathode operation at low pressures, formation of gas-focussed electron beam 3−17671
- confined, in plasma, kinetic instability *(Russian)* 3−1496
- cylindrical beam, combined effects of space charge and external fields 3−37989
- deflection of radiating electron traversing inhomogeneous magnetic field 3−35585
- diffusing electron stream in a gas, theory 3−38344
- electromagnetic waves radiation 3−13776
- electrostatic lens for monochromatic electron beams production 3−35723
- e.m. field interaction with electron beams in wave guides with resistive walls *(French)* 3−32497
- emission through mesh anode in turbulent discharge *(Russian)* 3−14623
- energy broadening in l.p. discharge, one dimens. distrib. functions 3−7490
- in external field, nonlinear hydrodynamic motion *(Russian)* 3−13777
- focusing of high output beams, in mag. fields 3−13780
- focusing using current carrying plasmas in high v/γ diodes 3−17650
- generation and diagnosis of 1.87 TW/cm^2 beams 3−16491
- growth of Si(Mo)(Ta) using electron beam evaporation source 3−15626
- high energy channelling, transmission profiles, string effect 3−1658
- high-current accelerator with a plasma cathode, intense electron beam production *(Russian)* 3−17665
- high-current electron beam gas focusing 3−17652
- high-current transient phenomena 3−28635
- high-power, technique for measurement 3−19277
- hollow cylindrical, reversible focusing 3−13766
- injection of electron beam into plasma confined by conducting shell *(Russian)* 3−7554
- intense, production and focusing, expt. obs. 3−35724
- intense relativistic electron beams for nuclear fusion 3−23897
- Jupiter, electron streams in Jovian magnetosphere rel. to intense decametric radiation 3−25406
- Kapitza-Dirac effect at high laser intensities 3−35721
- l.f. beam-plasma interactions in finite sized plasma 3−7493
- light scattering by relativistic electrons, differential scattering cross section and plasma diagnostics 3−7560
- logarithmic picoammeter for exposure and dose meas. in electron microscopy of polymer crystals 3−346
- low-energy electron and X-ray interaction coeffs. for solids 3−36469
- in magnetoplasma, saturation of convective instability due to trapped particles 3−23845
- metallic thin films, optical radiation on passage of electrons up to 100 keV 3−24771
- modulated in crossed fields, h.f. perturbations analogous to parametric transmission-line wave processes 3−13771
- modulation and demodulation at optical frequencies 3−37990
- modulation by stimulated Cherenkov absorpt. 3−10582
- monitor for secondary emission in accelerators 3−22447
- National Accelerator Lab., USA, design presentation 3−25836
- nonlinear theory of interaction between bounded relativistic beam and plasma 3−20501
- optical information transfer by beam collective states 3−29050
- optical modulation and Schwarz-Hora effect 3−16926
- parametric instability in a spatially periodic electrostatic field *(Russian)* 3−14545
- plasma counterstreaming modification of resonant interactions between ordinary e.m. modes 3−29950
- plasma dynamic stabilisation by means of a high frequency modulated electron beam 3−23867
- plasma induced emission on interaction with relativistic beam *(Russian)* 3−20617
- plasma instability, excitation and interaction of low frequency oscillations *(Russian)* 3−17597
- plasma linear and nonlinear properties of convective and absolute instabilities in a beam-plasma system 3−23869
- plasma relativistic, hose instability in a plasma channel 3−29973
- plasma ST Tokamak discharges, high energy electron, X-ray meas. 3−20628
- plasma velocity diffusion, one and three dimensional, in an electron beam plasma interaction 3−23821
- plasma-beam discharge laser 3−32555
- plasma-beam interactions, strongly nonlinear, dynamics 3−23868
- plasma-beam quasilinear and nonlinear interactions 3−23870
- plasma-beam system, explosive instability computation 3−23871
- plasma-beam system, stable electrostatic fluctuations lineshape 3−38460
- plasma-electron beam system, detection of feedback *(Russian)* 3−38464
- plasmas, dynamic stabilisation using high-freq.-modulated electron beam, hydrodynamic model 3−38454
- polarised source construct. and operation 3−13409
- polarized, production using trap *(French)* 3−32617
- relativistic, in plasma, nonlinear theory of dissipative instability 3−26891
- relativistic, instability formation on interaction with plasma 3−20493
- relativistic, intense, cone focus trajectories, adiabatic envelope conservation 3−32616
- relativistic, intense, cone focusing 3−32615
- relativistic, intense, propagation through magnetic constriction 3−801
- relativistic, production in a linear discharge 3−23896
- relativistic astron E-layer axial compression during neutralisation 3−38489

electron beams continued
relativistic electron beam driven plasma instabilities in Astron-like systems 3−20530
relativistic electron bundles in circular waveguide with stratified dielectric filling, parametric radiation 3−29161
relativistic in plasmas, macroscopic equilibria 3−30002
relativistic pulses, propagation through plasma, induced axial electric field effect 3−33341
relativistic rings, radiation instability, calc. of nonlinear stage of development 3−23857
screw, formation in adiabatic magnetron-type gun 3−22976
single shots and pulse train prodn. by pulse position modulation 3−10035
Smith Purcell effect, radiation emitted as it passes over a metal surface 3−19553
solid-state plasma, microwave generation and amplification, using electron beam, possibility 3−33944
space charge, quasilinear wave theory assuming multifreq. excitation *(Russian)* 3−16921
spatial energy distrib. sensing using liq. cryst. films 3−35426
spin-polarized beam production by optimization of low energy electron scattering from Hg atoms 3−11175
synchronous waves, interaction with t.w. in electrodynamic structure, expt. 3−13773
target surfaces, backscatt. electron flux, scanning electron microscope obs. 3−34444
thermal scatt. influence on fast electrons anomalous absorpt. in thick crystals 3−24155
theta pinch, turbulence, hydrodynamic-type unstable oscillations obs., relativistic electron beam formation 3−20519
thin foils, ang. distrib. of transmitted electrons *(French)* 3−30157
transfer of fast electrons, differential flow in inhomogeneous plate *(Russian)* 3−26254
transfer of fast electrons, under influence of homogeneous elec. field *(Russian)* 3−29159
transition metals and their alloys with Al, energy losses 3−33584
two-dimensional image production, using KH_2PO_4 crystal electron beam modulator *(Russian)* 3−16529
two-dimensional trajectories, mapping theorem 3−4137
two-stream instability, in presence of trapped electrons 3−33371
ultrarelativistic, interaction with plasma, nonlinear effects 3−23861
$e\gamma$ inelastic scatt., expt. use of e^+e^- colliding beam 3−13962
Au film, electron energy loss spectra, surface excitations influence *(French)* 3−33580
CdS laser pumping, crystal growth technique *(Russian)* 3−748
Si, irradiated, electron slowing down spectrum 3−33582
W, refl. coeff. of electrons, energy depend., up to 30 eV *(Russian)* 3−18513

electron capture
see also charge exchange
autoionisation model 3−19813
betatron, capture efficiency for different times within injection pulse *(Russian)* 3−277
stellar internal processes, destruction of s process correlations after neutron irradiation 3−16212
^{159}Dy, K-electron capture probabilities and decays 3−38144
^{145}Eu, decay to levels in ^{145}Sm transition energies detn. 3−17197
GaAs, p^+-n photodiodes, electron irrad., defect studies, differential capacity, conductance measurements 3−33845
^{151}Gd, K-electron capture probabilities and decays 3−38144
H^+-H^- collisions, charge transfer, electron capture cross section calc. 3−14315
$^{166}Yb \rightarrow ^{166}Tm$ decay study 3−38139

electron capture, nuclear *see nuclear electron capture*

electron density
see also carrier density; current density; plasma
air, calc. of O formation behind shock waves 3−7397
antisymmetric wavefunction densities from coherent diffraction data 3−4712
atom, neutral with $A \leqslant 40$ ions, excited states, charge density anal. 3−7034
automatic profiles using a digital ionosonde 3−12865
blunt body boundary layer, three dimensional effects 3−11404
Cerenkov radiative power variation dependence on frequency, electron density and collision frequency models in drifting magnetoplasma 3−20449
CGCG 1439+5344, extremely compact galaxy 3−5614
charge densities, difference maps, net atomic charges and population parameters, comparison of expt. and theoretical 3−4709
circuit-breaking arc, physical principles and diagnostics *(German)* 3−23945
Compton scattering of γ-rays as method for determ. of electron momentum distrib. in solids 3−30150
conference, Albuquerque, N. Mex., USA, April 1972 3−4706
contraction on bond formation at H sites, expts. on sucrose 3−4711
cyanide complexes, use of electron population parameter to distinguish between C and N 3−20716
BF Cygni, symbiotic star, emission region size determ. *(French)* 3−28209
D region profiles during solar cosmic ray bombardment at polar latitudes 3−25295
D- and E-region, electron density profiles rel. to experimental techniques 3−3111
D-region electron density meas., comparison of two ground-based techniques 3−3112
D-region electron density profiles, comparison of two ground-based techniques 3−3113
D-region electron density rel. to charges in ion chemistry during solar flares 3−3109
D-region ion density model rel. to diurnal var. of electron density 3−3116
D-region ionization charges and electron densities from partial reflection differential absorption experiment 3−5521
daytime equatorial lower ionosphere above Thumba, electron density profiles 3−3069
difference density function w.r.t. diborane 3−4708
discharge, cooled hollow-cathode, characts. *(Russian)* 3−7577
disturbances of normal height distribution of electron density *(German)* 3−9337
E- and F-region, effect on equatorial scintillations 3−9335

electron density continued
E-region, at night-time at auroral lattitudes in sunspot maximum 3−31435
E-region, calc. of NO concentration 3−3086
E-region, semi annual variation 3−5520
E-region density peak, solar activity dependence 3−34950
E-region nighttime ionospheric model 3−3099
electron distributions determ. by electron diffraction 3−4714
F2 layer, semi annual variation 3−5520
F2-layer at noon, standard electron density profile 3−31434
F_1 layer, effect of solar activity on geometric parameters *(Russian)* 3−3075
F_1-region, electron density profile from rocket experiments 3−34951
F_2 layer, spatial and temporal manifestation of seasonal anomaly *(Russian)* 3−3074
F_2-layer and topside ionosphere variations during 1962 December mag. storm 3−25280
F-region, average scintillation, at u.h.f./v.h.f. 3−37240
F-region, behaviour during sunrise 3−9328
F-region equatorial anomaly, longitudinal variation 3−9336
F-region plasma cloud, diffusion model for electron density distrib. along geomagnetic field 3−31430
flames, meas. in far i.r. using laser beam 3−33390
global distrib. at mid-lititudes during quiet mag. periods, Ariel 3 obs. 3−18880
glow discharge, r.f. and d.c. probes 3−14615
H magnetised arc plasma, electron density distribution meas. with ion temp. deviating from electron temp. *(German)* 3−38500
He^{2+}, 4686 and 3203 lines, temp. determ. from relative line-to-continuum intensity 3−14303
inner magnetosphere variations, whistler dispersion obs. 3−18891
ionosphere, at medium latitude geomagnetically conjugate stations 3−9321
ionosphere, equatorial anomaly in F_2-region from vertical soundings above Pacific Ocean 3−28067
ionosphere, meas. radiowave technique, celestial polarization 3−3057
ionosphere, plasma-wave particle interactions 3−25337
ionosphere, seasonal anomaly below F_2-layer electron density max. rel. t latitude and time 3−28066
ionosphere, strong radiowave effects on electron density and inhomogeneous structure 3−28061
ionospheric and interplanetary matter meas. using quantum freq. standards 3−34972
ionospheric D- and E-regions, electron density meas. by incoherent-scatter technique at Millstone Hill 3−3114
ionospheric D-region, dependence on solar zenith angle *(Russian)* 3−3073
ionospheric D-region distrib., ionisation effects of solar corpuscular streams 3−34946
ionospheric E-layer, after sunrise state rel. to max. electron concentration *(Bulgarian)* 3−9339
ionospheric E-layer, electron density isopleth rel. to planetary-scale fluctuations of f-min 3−21969
ionospheric electron density meas. rel. to solar X-ray flare temp. determ. 3−31529
ionospheric equatorial electron density profile rel. to spatial resonance and internal gravity waves 3−31420
ionospheric f_0F_2 values rel. to electron loss rate 3−31426
ionospheric F_2-layer max. electron density, mag. storm disturbance variation with storm time on noon meridian 3−34949
ionospheric F-region non-stationary distrib. for pure ambipolar diffusion 3−34948
ionospheric meas. with h.f. quadrupole probe 3−9316
ionospheric profiles computation using min. number of parameter 3−34935
ionospheric research, use of VLF radiowaves, whistler mode, ion electron density and temperature studies, review 3−18900
ionospheric satellite wake, distribution of electron density 3−18878
linear polyatomic molecules, atomic charges calc. 3−17401
lower D-region, effective electron loss rate during solar X-ray flare events 3−3110
lower ionosphere, density increase rel. to movement of deep planetary wave 3−3034
lower ionosphere, var. with zenith angle, solar cycle and during eclipses 3−3068
lower ionosphere densities from rocket meas. using l.f. radio propagation and d.c. probe techniques 3−16031
magnetised collision-dominated plasma in an electric field, kinetic theory of fluctuations 3−15996
mid-latitude electron density trough and v.l.f. radio emission during 25-27 May 1967 magnetic storm 3−21975
mid-latitude F-layer electron concentration seasonal var. in magnetic storm effects 3−31433
mid-latitude topside ionosphere during local sunrise, electron density and scale height 3−31408
midlatitude D-region, diurnal and seasonal var. under quiet conditions 3−3115
midlatitude lower ionosphere, during winter 3−3064
midlatitude upper atmosphere, rocket meas. 3−3052
nighttime D-region, nightglow, precipitating energetic electrons 3−3090
non-Maxwellian electron energy distributions effects on orbital limited current-voltage characteristics of spherical and cylindrical Langmuir probes under collisionless conditions 3−14577
Nova Delphini 1967, nebular stage obs. in Dec. 1968 to June 1970 period *(French)* 3−35147
one-electron systems, electron density pointwise bounds and expectation value estimates 3−14274
phenylacetylenes, CNDO/2 electron charge densities and ^{13}C chemical shifts *(German)* 3−14393
pinch plasmas, development and props. of the halo *(German)* 3−20618
plasma, anodic, spectrometric study of emitted light, electron, ion and atomic densities *(French)* 3−26897
plasma, spatial electron distriution function, radial moments calc. *(Russian)* 3−11465
plasma, warm anisotropic, inhomogeneous in a mag. field., expression for electron density from microwave spectra 3−26901

electron density continued
  plasma, warm in microwave cavity, eigenvalues as function of density and thermal speed 3−20468
  plasma continuous flow pinch, temperatures and densities meas. 3−20633
  plasma cyclotron instability in presence of suprathermal electrons, inhomogeneities in electron density 3−20541
  plasma density in plasma with periodically varying parameters, probe circuit 3−30014
  plasma focus, neutron and electron density meas., holographic interferometry 3−20620
  plasma Focus machine, neutron fluences, electron density and deuteron temp. meas. 3−20637
  plasma formed in a shock tube, microwave cavity meas. 3−23912
  plasma guide, annular, azimuthal electron density variation, surface wave propag. 3−17564
  plasma high beta density profiles holographic interferometry technique at $\lambda=3\mu m$ 3−20634
  plasma in shielded volume *(Russian)* 3−4631
  plasma measured by using gas laer with nonlinear absorbing cell *(Russian)* 3−7567
  plasma spectroscopic measurement method of electron temp. and density in focus discharge *(French)* 3−26900
  plasma trapped in toroidal ringless quadrupole, spatial distribs. 3−1515
  plasmon threshold depend. on electron density in the secondary electron yield, dispersion laws 3−4977
  polyethylene, small angle X-ray scattering, two-phase electron density parallel layer model 3−38541
  relatavistic electron-beam current densities meas. in 1.87 TW/cm^2 beams 3−16491
  screw pinch discharge, electron density and Z-current radial distrib. control 3−14571
  semiconductor electron equilib. distrib. instability *(Russian)* 3−8184
  semiconductor intervalley population transfer in electric field 3−5012
  shock wave, decelerating in air, electron density meas. 3−38392
  simple molecules electronic charge distributions and chemical bonding 3−4707
  solar atmosphere, absorpt. line profile inversion showing LTE departures 3−31525
  solar chromosphere-corona transition region meas. from e.u.v. obs. 3−25393
  solar corona, densities and temperatures from monochromatic images in red and green lines 3−37322
  solar corona, determ. from obs. of Fe XI and Cr IX lines 3−39606
  solar corona, during Sept. 22 1968 eclipse 3−9476
  solar corona condensation, distrib. as function of distance from condensation knot 3−37327
  solar corona polar plumes, core density profiles 3−39624
  solar coronal distrib., three dimens. mapping 3−35045
  solar coronal holes, regions of low electron density rel. to coronal magnetic field 3−18940
  spatially defined fragments of mol. systems, virial relationship, mol. chrge distribution 3−17478
  spherically expanding envelopes of WR stars and Seyfert galaxies, electron scattering effects 3−16209
  spin densities, magnetic neutron scattering expt. methods 3−5109
  sporadic-E layer, nighttime 3−9334
  sporadic-E layer, redistribution theory 3−9327
  stable density fluctuations in plasma in presence of h.f. electric field 3−16020
  sucrose, X-ray data refinement, comparison with neutron diffraction data 3−4711
  Sun, adjustment of outer layer solar models 3−9473
  superstructure determ. using partial Patterson functions 3−4705
  tetracyanoethylene oxide, charge density distribution by difference Fourier techniques and population refinement of the diffraction data 3−4710
  p, m, o- toluidine, quantum mechanical calc. *(Russian)* 3−11202
  topside ionosphere, magnetic storms and seasonal anomaly rel. to electron distributions 3−25274
  topside ionosphere at high southern latitudes, Aerial 3 observations 3−31407
  topside ionospheric electron densities and scale heights rel. to shallow solar zenith angle 3−9317
  tropical F-region, spatial variations determ. 3−15988
  upper atmosphere, during solar maximum and minimum 3−3089
  X-ray generalised scattering factors, higher multipoles, electron population analysis 3−23981
  Al valence electron redistrib. and positron trapping at vacancies 3−21026
  Ar discharge, high-current low press., electron conc. estimation *(Russian)* 3−7579
  Ar plasma, pure, shock tube produced, equil. electron density and temp. *(French)* 3−26896
  B_2H_6 electron density problem, experimental and theoretical aspects 3−4708
  Be, X-ray structure amplitudes obs. 3−7659
  C arc plasma, laser beam interferometry 3−11504
  Co nitrosyl complexes, crystal struct. *(French)* 3−7701
  Cs_2CuCl_4, struct., crystal forces and charge distribution determ. 3−17785
  Cu_3Au, valence electron conc. oscillatory curve compatible with $CaTl_3$ density of states curve calc. 3−1984
  Eu, screening ratios, relativistic contributions 3−14287
  GaAs, change on fast neutron irrad. *(Russian)* 3−27041
  n-GaAs, electrochemical characterization, automatic plotting system 3−30953
  GaAs epitaxial layer, high purity for Gunn devices 3−2686
  GaAs:Te, implanted, influence of implantation temp. and surface protection 3−12310
  H beta line shape of transient plasma, fibre optics system 3−11502
  He, scattering and bound-state props., many-body Green's functions appl. 3−11122
  He constrained density matrix study of simple basis sets of 1s-type orbitals 3−29469
  He positive column, electron temp. and density meas. *(Japanese)* 3−30011

electron density continued
  He-Hg mixture, weakly ionized, electron distrib. function 3−14604
  He-Se$^+$ discharge, for positive-column lasers 3−16833
  InAs:Se(Te), rel. to temp. depend. of electron effective mass *(Russian)* 3−27250
  InP, vapour phase epitaxial layer 3−2681
  InP crystal, grown by liquid encapsulation technique, elec. props. 3−2679
  InP:Ge,Sn,Te, liquid phase epitaxial layer, carrier conc. and mobility 3−1637
  $K_2Pt(CN)_4X_{0.3}.nH_2O$, X=Cl(Br), between 2 Pt sites, and X-ray photoelectron obs. of energy levels 3−15587
  MnO, electron diffraction study of the nature of the chemical bond *(Russian)* 3−4728
  N_3^0 and N_3^{2-} anisotropic hyperfine interactions, p spin densities from e.s.r. spectrum 3−38308
  Na_2O-TiO_2-SiO_2 glasses, determ. of electron radial distribution curve by X-ray diffraction 3−11550
  Ne, afterglow, electron-diffusion supercooling, expt. verification 3−36219
  Ne positive column, electron temp. and density meas. *(Japanese)* 3−30011
  NiI lines in 3000 to 4000 Å range, Stark broadening rel. to electron density 3−17366
  O_4^- photodetachment cross section meas. at high pressure rel. to electron densities in upper atmosphere 3−16002
  Si, distrib., X-ray struct. factor determ. by Pendellosung method 3−30105
  Si, distrib., X-ray structure factor interpret. 3−30106
  n-Si, high field effects, space charge induced nonuniformites 3−5014
  Si, shallow donor form., profile determ. by the Copeland method 3−17861
electron device manufacture
  see also electron tube manufacture; semiconductor device manufacture
  electron beam microfabrication, computer-controlled 3−35513
electron diffraction
  see also electron diffraction crystallography; electron diffraction examination of materials; low energy electron diffraction
  Babinet's principle applications *(German)* 3−29160
  camera, sectoral device, molecular structure 3−345
  contrast calc. without column approximation 3−1540
  gas molecules, atomic scattering factors of heavy atoms for 40 keV electrons 3−29544
  high energy, formulation for elastic scattering 3−27037
  high energy, transition from quantum to classical theory 3−1646
  interferometric device for demonstration of electron interference 3−32010
  metal with convex Fermi surface, differential cross sections for scatt. on e.m. waves *(Russian)* 3−24151
  Mott scattering cross sections for calc. backscattering of 10-100 keV electrons 3−1645
  with supersonic molecular beam 3−35495
  surface texture, corrosion, adsorption 3−1864
  Yoshioka term, rel. to complex continuum potential for channelling 3−20772
electron diffraction crystallography
  see also crystal atomic structure; Debye-Waller factors
  amorphous film, electron micrograph interpretations 3−17723
  anomalous absorption, effect of non-systematic reflection 3−14668
  anomalous transmission 3−20767
  Bethe's second-order approximation, discussion and generalization 3−14667
  block structure kinetics, by microbeam method, error estimation 3−24007
  computer aided data reduction and structure analysis, DEC-PDP-9, techniques 3−26956
  crystal surface layer structure determ. *(Russian)* 3−7993
  crystallite volume and shape, dark field electron microscopy, microbeam method 3−24006
  diffraction pattern analysis, coincidence ambiguity 3−17725
  diffuse scattering from short-range order of defects 3−24066
  direct lattice imaging for stacking sequence recognition in hexagonal ferrites 3−38530
  dynamical theory, integral and differential eqns. within a distribution formalism 3−33432
  elastic scatt., rel. to single crystals and evaporated elemental thin films 3−1641
  electron distributions determ. by electron diffraction using holographic microscope 3−4714
  energy filtered patterns *(French)* 3−33431
  excess Kikuchi band, localization, many beam theory, for Ni 3−24012
  factor analytical technique applied to gas phase electron diffraction 3−23996
  fast electron diffractor with energy filter *(French)* 3−20683
  fine structure, for studying defects *(Rumanian)* 3−24013
  gas phase molecular electron diffraction obs. of short-lived reaction intermediates 3−25046
  h.c.p. crysts., dynamic theory *(French)* 3−17870
  high energy, many beam theory rel. to Berry theory 3−1647
  high energy, semi-classical behaviour 3−1648
  h.v., f.c.c. and h.c.p. metals, atomic scattering factors 3−38528
  h.v. microscopy, diffr. phenomena 3−20682
  h.v. microscopy, Kikuchi patterns 3−23989
  image plane technique for spatial resolution of structural defects 3−24010
  imperfect crystal, exact dynamical soln. 3−24142
  imperfect crystals, perturbation treatment of high energy electron diffraction 3−7793
  inclusions in elastically anisotropic media, strain fields for diffraction contrast calcs. 3−33538
  inelastic dispersion, in terms of optical potential 3−11652
  inelastic scattering, rel. to image formation in electron microscopy 3−1643
  inelastic scattering small angle, theory 3−1642
  Japan, past and present review 3−14665
  Kikuchi band and abnormal absorpt., exchange effect calc. 3−23999
  Kikuchi band contrast, variation through crit. voltage 3−23993

electron diffraction crystallography continued
Kikuchi band contrast reversal in transmission electron diffraction 3−24000
Kikuchi bands, contrast above and below crit. voltage 3−38529
Kikuchi diagrams, geometry, dynamic theory applic. *(French)* 3−30057
Kikuchi patterns, dynamical theory allowing for absorpt. of scattered electrons 3−11532
Kikuchi patterns, in h.v. electron microscopy 3−7608
Kikuchi patterns and anomalous absorption, dynamical theory 3−23998
lattice planes perpendicular to primary beam in texture pattern 3−33435
low angle, with Elmiskop 101 microscope 3−13460
nucleation, pentagonal structures, formation and growth, very small paracrystals *(French)* 3−38756
plural scattering, in electron energy anal. using electron microscope 3−1644
pseudo-Kikuchi patterns, meas. of ratio of abnormal to normal absorpt. coeff. for electrons 3−23987
pseudo-Kikuchi patterns for detn. of normal/abnormal electron absorption ratio 3−11651
scanning HEED patterns, interpretation and application to GaAs surface 3−36460
scattering amplitude precise determ. from crit. voltage obs. 3−24003
simulation of electron diffraction patterns of metallurgical structures by optical transforms 3−1550
skew structure type, coincident reflection in electron diffraction pattern 3−24058
state-of-the-art 3−20681
structure factor determ. by vanishing Kikuchi line method 3−24002
structure factor determ. methods 3−24001
structure factor determ. using Bloch wave analysis 3−24004
structure factors determ. by numerical analysis *(French)* 3−33433
subgrain boundary misorientation, determ. from split Kikuchi lines 3−24009
surface state resonances, calc. using Green functions 3−24497
surface state resonances, rel. to diffracted beam emergence, theory 3−24312
thermal diffuse scattering, theory 3−23994
tilted specimen, applic. to s.e.m. 3−1556
transmission, perturbation theory 3−36251
$MgFe_2O_4$, thin films, electron diffraction superlattice lines 3−38569
NaCl electron irradiation, Kikuchi pattern during sputtering 3−36250

electron diffraction examination of materials
acetyl halides, zero point average mol. struct., gas phase electron diffr. and microwave spectra obs. 3−14325
alkali metal overlayers on W(100), quantitative AES and LEED study 3−38704
amorphous material, microcrystallite and random network models to interpret diffraction patterns 3−17744
amorphous material, transition matrix approach 3−7792
amphiboles, fibrous, planar defects 3−37158
b.c.c. crystals, twinning partials, diffr. contrast behaviour 3−17850
benzene, ave. mol. structure, n.m.r. data, comparison with electron diffraction and Raman spectroscopy 3−36045
carbon tetrachloride, mol., small angle electron diffraction 3−29545
ceramic grain boundaries, dielectric behaviour from electron beam scanning obs. 3−36302
defect study by transmission microscopy *(Rumanian)* 3−24013
d,l-1,2,3,4-diepoxybutane, mol. struct. from electron diffraction data 3−11192
4,6- dimethyl trimethylene sulfite molecular geometry study by gas phase electron diffraction 3−14328
ferrite, hexagonal, direct lattice imaging for stacking sequence recognition 3−38530
ferromagnetic metals and semiconductors, fluctuations and scattering of electrons and neutrons by coupled magnons *(Russian)* 3−12032
ferromagnetic semiconductors and metals electron and neutron scattering by coupled spin waves *(Russian)* 3−12031
fibrous polymers and derivatives, progress 3−386
gas high temp. electron diffr. studies, photographic procedure 3−13457
graphite, surface thermal expansion determination 3−15023
group VIA metals, faceting in dilute O_2 atm., l.e.e.d. and r.h.e.e.d. studies 3−11818
imidazole, molecular structure obs. in gas phase 3−23511
inert gas mixtures, mixed cryst. form., phase studies *(French)* 3−24043
isobutane, zero point average struct., electron diffraction and microwave spectroscopy determ. 3−14384
martensitic, high C, electron diffuse scattering 3−15663
methane sulphonyl fluoride, electron diffraction study of mol. struct. 3−29554
1-methoxycyclohexene, gas-phase investigation 3−33072
methyl allenyl ether, determ. of bond lengths and bond angles by means of gas electron diffraction 3−1139
methylazine, determ. of bond lengths and angles by electron diffraction meas. of gas phase 3−7103
methylisocyanide, determ. of bond lengths and angles by electron diffraction meas. of gas phase 3−7103
methylisothiocyanide, determ. of bond lengths and angles by electron diffraction meas. of gas phase 3−7103
mica, monoclinic angle effect on texture electron diffraction patterns 3−24325
molecular structure, effects of systematic errors in intensities in gas-phase diffraction 3−29549
nacrite, structure refinement by high-voltage electron diffr. 3−7707
organometallics, atomic scatt. factors for heavy atoms by small-angle electron diffr. 3−26615
plasma oxide film, on $GaAs_{1-x}P_x$, composition obs. *(Japanese)* 3−11821
polyethylene, single crystal, obs. of stress induced twinning and phase transforms. 3−17977
polyethylene fibres drawn from single crysts., mol. struct. 3−33177
polypropylene, isotactic, obs. of lamellar branching in melt growth 3−24044
propynal, molecular structure determ. by gas electron diffraction 3−7100
pyrrole, molecular structure obs. in gas phase 3−23511

electron diffraction examination of materials continued
reaction intermediates, short-lived, gas phase molecular electron diffraction obs. 3−25046
rubber film, uncrosslinked, morphology of strain-induced crystn. 3−4501
semiconductor, nonpolar, rel. to electron mobility 3−15190
stacking faults, dark field images, contrast under weak beam conditions, mechanism 3−7777
steel, austenitic, deformed with participation of twinning and $\gamma \rightarrow \varepsilon$ conversion, diffr. pattern. anal. 3−18618
steel, austenitic, penetration of fast electrons, dislocation image obs. *(French)* 3−39327
steel, galvanized sheet, diffusion layer 3−18619
steel, martensite, low-C, anomalous microstruct. 3−39339
surface struct. from RHEED 3−30321
surfaces, medium energy electron diffr. with scanning microscopy 3−30320
1,4-thioxane, electron diffraction study of bond lengths and angles 3−7102
transition metal carbides, B-1 type, substoichiometric, short range order of vacancies 3−17808
trimethyldifluorophosphine, molecular structure 3−29550
Ag epitaxial growth on GaAs(110) 3−15087
Ag noncrystalline thin films, electron diffraction and resistivity study 3−8062
Ag polycrystalline film, dynamical effects in electron scatt. for structure obs. 3−24014
βAg-Al splat quenched alloys, martensitic transformation 3−2695
Ag(111), LEED, thermal diffuse scattering, at low temp. 3−38702
Al, (100) surface, elastic and inelastic LEED, absolute intensity meas. 3−36464
Al, (110) and (111) surfaces, LEED, calc. and expt. 3−36465
Al, calc. of exchange effects on Kikuchi band and abnormal absorpt. 3−23999
Al, inelastic scatt. using fast electron diffractor with energy filter *(French)* 3−20683
Al, subgrain boundary misorientation, determ. from split Kikuchi lines 3−24009
Al alloys, Guinier Preston zone effects due to coherent particles with lattice distortions *(French)* 3−18604
Al film, effect of charact. energy losses on electron diffraction intensities 3−24156
Al molten foil, electron diffr. short term persistence of diffuse remnants of reflections 3−38532
Al polycrystalline film, dynamical effects in electron scatt. for structure obs. 3−24014
Al-Zn alloys, metastable solvus for Guinier-Preston zones 3−31022
$Al_xGa_{1-x}As$, molecular beam epitaxial layer, struct., HEED obs. 3−2677
Al_2O_3, sapphire single crystal, obs. of Kikuchi line doubling rel. to block structure 3−24364
Au, (110) surface, diffuse LEED pattern, temp. depend. 3−24313
Au, crystallites, Debye-Waller factor rel. to size 3−36247
Au noncrystalline thin films, electron diffraction and resistivity study 3−8062
Au polycrystalline film, dynamical effects in electron scatt. for structure obs. 3−24014
Au thin films, Debye-Waller factor, temperature dependence *(Russian)* 3−33637
Au thin platelets, lattice spacings 3−4730
Au-Cd(47.5 at.%) alloy, martensitic pretransformation phenomena obs. 3−18561
Au-Cu alloy film, order-disorder transformation obs. 3−1800
Au-Cu-Zn martensite, structure obs. 3−1604
Au-SiO_x cermet film, structural changes on heat treatment 3−5064
Au-transition metal alloy, short range order 3−14734
$BaTiO_3$, domains, obs. by convergent electron beam diffr. method 3−24657
C fibre, molecular struct. obs. 3−27788
C fibres, heat treatment effects, analysis of structure after oxidation, carbonization or graphitization 3−15778
CS_2, mol., small angle electron diffraction 3−29545
CaF_2, structure factor determ. using Bloch wave analysis 3−24004
CaF_2, thin films, electron irradiation effects 3−38748
$CdIn_2Te_4$, thin films electronmicroscopic and electron diffraction investigations *(Russian)* 3−30371
CdS thin films, growth by electron bombardment evaporation, oblique textures 3−38758
Co-Ni-Ti alloy, morphology and decomp. kinetics *(Russian)* 3−21581
Co_3O_4 films, superstruct. detn. *(Russian)* 3−7712
Cr, oxidation of (100) and (110) surfaces, RHEED study 3−1903
Cr, structure factor determ. by vanishing Kikuchi line method 3−24002
δ-Cr, thin films, prod. conditions, diffr. data anal. 3−36502
Cu, surface structure formed on oxidation of (311) face, RHEED study 3−1904
Cu (100) face, Cl adsorption *(French)* 3−1893
Cu (100) single crystal film, on (100) NaCl, oxidation obs. 3−1907
Cu epitaxial film with adsorbed oxygen layer *(French)* 3−27188
Cu polycrystalline film, dynamical effects in electron scatt. for structure obs. 3−24014
Cu-Pd(Pt) alloy, short range order 3−14734
$CuPt_3$ alloy, ordered struct. 3−14803
Fe, oxidation of ideal clean surface, kinetics and struct. changes 3−8043
Fe, sheet and thin film, nitride phase form. obs. in epitaxial intergrowth *(German)* 3−1926
Fe complex, tetrafluoroethylene-tetracarbonyl iron, molecular struct., gas-phase electron diffr. 3−14324
Fe-Al-C steel, precipitates of perovskite structure obs. by electron diffraction 3−18600
Fe-Ni-Al alloy, fracture and microstructure, electron diffraction examination of precipitates *(Japanese)* 3−15672
Fe-V alloys, transformation twins 3−2711
Fe_3S_4, elec. field induced anisotropy 3−5163
Fe(111) surface structure determination using LEED 3−15054
GaAs, molecular beam epitaxial layer, struct., HEED obs. 3−2677
GaAs amorphous films, electron diffraction investigation of struct. *(Russian)* 3−8059

electron diffraction examination of materials continued
GaAs surface, interpretation of scanning HEED meas. 3−36460
GaP, molecular beam epitaxial layer, struct., HEED obs. 3−2677
GaP amorphous films, electron diffraction investigation of struct. *(Russian)* 3−8059
GaSe, LEED studies 3−38698
Ga_3Te_4 thin films, crystal microstructure during annealing *(Russian)* 3−33754
Ge, crit. voltage effect involving vanishing 3rd order Kikuchi lines 3−24003
Ge antireflection coating, characterization 3−3799
Ge film, amorphous, order-disorder transformation obs. 3−1800
Ge film, obs. of Kikuchi line doubling rel. to block structure 3−24364
Ge thin film, amorphous-crystal boundary, electron diffraction pattern 3−11839
Ge film, vacuum-deposited on Si, elastic strains 3−27194
H_2O, mol., small angle electron diffraction 3−29545
Hf-O system, near $HfO_{1/6}$, interstitial superstruct. and order-disorder transform. 3−14847
$InAs_{1-x}P_x$, vapour phase epitaxial material, quality monitoring 3−2680
In_2O_3-SnO_2 transparent conducting films, structure obs. by electron diffraction and spectroscopy 3−33763
InP, vapour phase epitaxial material, quality monitoring 3−2680
InTe, obs. of thermal expansion anisotropy 3−4861
LiF, LEED intensity profile for (100) surface, and bulk energy bands, calc. 3−36466
Mg ultramicrotomed thin slices, plastic deformation 3−17902
$Mn_{0.8}Fe_{0.2}[Mn_{0.2}Fe_{1.8}]O_4$, thin films, electron diffraction superlattice lines 3−38569
MnO, electron diffraction study of the nature of the chemical bond *(Russian)* 3−4728
MoC_x, f.c.c., crystallite size 3−15737
NSCl, gaseous, mol. struct. and vibr. study 3−26617
$NaCaHSiO_4$, selected area diffraction, unit cell detn. 3−27006
NaCl film, epitaxial growth on muscovite, RHEED obs. 3−27193
Nb suboxides, superstructure spots due to occupation of interstitial sites by Nb 3−17794
Ni, excess Kikuchi band localization, many beam theory 3−24012
Ni, Kikuchi band contrast, variation through crit. voltage 3−23993
Ni, Kikuchi bands, contrast above and below crit. voltage 3−38529
Ni, surface and other localized states 3−24312
Ni/chemisorbed Na system, LEED intensity meas. 3−30312
Ni-based alloys, glazes prod. by high-temp. wear and friction 3−34590
Ni-Cr-Al alloys, internal and external oxidation mechanism 3−31115
Ni-Cr-Al alloys, internal oxidation 3−31116
Ni-P alloys, existence of P microcrystals and amorphous regions during tempering *(French)* 3−12359
Ni_4N, obs. of N interstitials and structure factors 3−14783
$(SN)_n$, cryst. struct. determ. 3−24065
Si, amorphous layers formation by Si^+ implantation 3−17888
Si, calc. of exchange effects on Kikuchi band and abnormal absorpt. 3−23999
Si, crit. voltage effect involving vanishing 3rd order Kikuchi lines 3−24003
Si, effect of non-systematic reflection on anomalous absorption 3−14668
Si, epitaxial deposition in N_2, HEED obs. 3−1921
Si, glancing incidence HEED, temp. depend. of intensities 3−24331
Si, Kikuchi band contrast reversal in transmission electron diffraction 3−24000
Si antireflection coating, characterization 3−3799
Si film, obs. of Kikuchi line doubling rel. to block structure 3−24364
Si_2Cl_6, molecular struct. determ. *(German)* 3−35989
SiO_2 glass, superstruct., internal struct., morphology, in early crystn. 3−14693
β-Sn film 3−20957
Ta film nucleation and growth obs. from high energy electron diffraction 3−33766
Ta oxides, orthorhombic, in thin films, at struct. detn. 3−7706
Te, amorphous, atomic arrangement, transmission electron diffr. obs. 3−14687
Te, amorphous films, local atomic arrangement 3−36499
Te film, amorphous, struct. 3−20964
Ti-Ni alloys, B_2 phase region, stacking modulated structs. 3−14878
Ti-Ni alloys, near-equiatomic, martensitic phase studies 3−14879
Ti-Ni alloys, near-equiatomic, diffusion controlled phase transform. structures 3−39311
Ti-Ti_5Si_3 alloy, oriented eutectic, crystallography of phases *(French)* 3−34525
$Ti_{n-2}Cr_2O_{2n-1}$, shear struct. determ. 3−24127
TiO, disordered phase, structure factor determ. by vanishing Kikuchi line method 3−24002
Tl_2MoO_4, gas phase study 3−29557
α-UO_3, cryst. struct. by neutron and electron diffr. 3−24075
V structure factor determ. by vanishing Kikuchi line method 3−24002
VC, substoichiometric, short range order of vacancies 3−17808
V_2C and VC_{1-x} phases, cryst. struct. *(French)* 3−7657
V_6C_5, obs. of ordered arrangement of C vacancies 3−14782
VO, short range order scatt. rel. to defect ordering and structure 3−24066
V_nO_{2n-1}, shear struct. determ. 3−24127
V_nO_{2n-1} shear struct. cpds., metal-insulator transition 3−18090
W(001), relativistic LEED, spin polarisation effects 3−27164
Zn ultramicrotomed thin slices, plastic deformation 3−17902
ZnS crystal structure of thin layers 3−33759
Zr, h.c.p. α type, Kikuchi patterns 3−28707

electron emission
see also cathodes; electron field emission; photoemission; secondary electron emission; thermionic electron emission; work function
alkali halide crystal surfaces, non-radiative electronic transitions *(Russian)* 3−38876
alkali halides, tribo-photostimulated exoelectron emission, yield limit emission criterion 3−30925
atomic Coulomb ionization by heavy, charged 3−1130
conductor, theory of cold emission *(Russian)* 3−15593

electron emission continued
electronics and vacuum physics, conference, Kralovopolska, Czechoslovakia, Oct. (1972) 3−15576
emission microscope, construction 3−13468
exo-emission, thermally stimulated 3−15594
metal, exoelectron emission during oxidation 3−21524
metal, plastically deformed, fatigue damage detection by exoelectron emission 3−18534
metal, polycrystalline, surface, noble metal ion bombardment, electron ejection, positive ion refl. 3−2608
metal oxide, thermostimulated exoemission obs. of oxygen effects on electron trapping 3−30929
m.i.m. structure, hot electron emission, tunnel current equation *(German)* 3−15270
m.i.m. systems, (Al-Al_2O_3-Au), electron emission, energy distributions 3−21161
m.i.m. systems (Al-Al_2O_3-Au), electron emission, angular distribution 3−21160
m.i.m. systems (Al-Al_2O_3-Au), electron emission, discussion of processes in cathode 3−21162
semiconductor, theory of cold emission *(Russian)* 3−15593
p-Si very low energy following machining *(German)* 3−18535
solar flare non thermal radiation in X-ray region 3−18959
thermally stimulated exo-electron emission, trapping centre emptying model *(German)* 3−15162
thermally stimulated exoelectrons, channel electron multiplier detector 3−32154
Al, fatigue damage, visual display by means of exoelectron emission 3−12468
Al, low-temp. deformed, energy and intensity of exoelectrons, simultaneous meas. *(Russian)* 3−21522
Al, very low energy, following machining *(German)* 3−18535
Al moderator, low energy positron emission in backscatt. mode 3−30926
Al-Al_2O_3-Au sandwich cathodes, energy ang. distrib. of electrons emitted *(Russian)* 3−30550
Au, low-temp. deformed, energy and intensity of exoelectrons, simultaneous meas. *(Russian)* 3−21522
Au moderator, low energy positron emission in backscatt. mode 3−30926
BeO, exoelectron emission, effect of O adsorption centres 3−24776
Cd very low energy, following machining *(German)* 3−18535
Cu moderator, low energy positron emission in backscatt. mode 3−30926
GaAs, p^+-n photodiodes, electron irrad., defect studies, differential capacity, conductance measurements 3−33845
Ge, N_2^+ and Kr^+ bombarded, relax. *(Russian)* 3−8694
H_2^+ collisions with H_2 from 0.6 to 1.5 MeV, electron emission 3−36050
He, electron emission spectra excited by proton impact, $2s(^1S)$ autoionisation state 3−7067
He II liq., negatively charged vortex rings, electron escape from electronic bubble 3−7985
KCl:Tl, slow decay of exoelectron emission after X-ray irradiation 3−30928
K_2SO_4, exoelectron energy meas. after X-ray irrad. and electron bombardment 3−24777
Si, ion-electron emission, relax. effect, temp. and current depend. 3−21510
SiC, reverse biased p-n junction, electron emission current rel. to oxide film 3−24775
SiO_2 film, thermally stimulated exo-electron emission spectra, trapping centre obs. *(German)* 3−15596
Ti very low energy, following machining *(German)* 3−18535

electron energy bands *see band structure*

electron energy states
see also crystal electron states; electronic density of states
alkali metal, liquid, pseudopotential calc. of elec. resist. and thermoelec. power 3−21051
alloys, disordered ternary, coherent potential approximation and diagrammatic equivalent, electronic theory 3−38775
amorphous insulator, u.s. absorpt. by localized two-level systems 3−7861
amorphous semiconductor, theoret. foundation of existing models 3−38778
amorphous semiconductors, book 3−11941
analogue computer simulation, using three-dimensional resistance network *(French)* 3−20979
coherent potential approximation, matrix formulation 3−8074
concentrational broadening of energy spectrum in Poisson random field 3−16758
disorder-induced transition in one-dimensional finite Kronig-Penney model 3−18061
disordered network, determ. from modified free-electron model 3−30388
disordered system, d.c. cond. and Anderson transition 3−18057
disordered system, generalized cluster theory of coherent potential approx. 3−36512
disordered system, self-trapped states 3−38772
disordered system, strong correlations effects 3−33777
disordered systems, diffusion of electronic excitation 3−18049
disordered systems, equivalence of two approaches to random chain of oscillators 3−20988
disordered systems, forward scattering approximation 3−20992
disordered systems, multiple scattering formalism, generalised coherent potential approximation 3−24368
disordered systems, one-dimens., electron wave functions 3−8083
Gaussian wave-packet dynamics in uniform mag. and quadratic potential fields 3−20987
interband effects in coherent potential approximation 3−20986
liquid alloys, electronic correlation functions at long wavelength 3−30386
liquid metal, dielectric screening and resistivity 3−5000
liquid metal and binary alloy, short-range order effects 3−38774
liquid metals, binary, explanation of immiscibility gap 3−18583
liquid metals, Van Hove theory application 3−38771
magnetic semiconducting crystals, electron ground-state coherent states 3−38799
periodic systems, LCAO functions applic. *(French)* 3−1965
polymer local derivatives, LCAO calcs. *(French)* 3−1966

electron energy states continued
- Si, amorphous film, optical consts. meas. rel. to structures and energy states 3−21380
- As_2Se_3, vitreous, chaotic potential field opt. absorpt. edge, deform. pots. 3−20993
- Au, photoemission from polycryst., ang. anisotropy phenomena 3−5258
- Be, liq., density of states calc. 3−38776
- CdTe, amorphous, optical spectra interpret. 3−2526
- Hg-In alloy, electronic spectra, 0.14-4.0 μm 3−39133
- MoS_2, layered, u.v. photoemission obs. 3−5256
- $NbSe_2$, layered, u.v. photoemission obs. 3−5256
- SiO_2, electronic struct. of vitreous silica rel. to different crystn. forms 3−21298
- ZnTe, amorphous, optical spectra interpret. 3−2526

electron field emission
- cathodes, W and LaB_6, for electron probes 3−13474
- current fluctuation rel. to adsorpt. on surface 3−15597
- dynamic field emission in cathode spots of cold cathode arcs 3−27598
- electron microscope field emission tips, microcratering and destruction by microparticles 3−8707
- emission through double potential barriers, total energy distribs. 3−15601
- field emission illum. systems, performance estimates, design criteria, aberrations, defocus, stability 3−803
- high current field-emission cathodes, refractory metals *(Russian)* 3−8711
- illumination system, using optical congig. 3−16539
- insulating thin films, electronic transport processes 3−18237
- metal, band struct. meas. by photon enhanced field emission, electron and hole scatt. effects 3−27205
- metal surface with chemisorbed atom, total energy distrib. study 3−1895
- m.i.m. cathodes, field emitted electron angular distrib. rel. to electron traps 3−15602
- nanosecond pulse production of fast electrons, sealed two electrode tube *(Russian)* 3−10110
- neutron star surface, pulsar magnetosphere evolution relationship 3−19043
- space charge effects of relativistic electrons *(Russian)* 3−15595
- thin film cathode characteristics, calc. 3−21523
- work function determ. by field emission retarding potential method 3−21137
- Ag tip, clean and contaminated, field emission study of impurity adsorption 3−30927
- Al-Al_2O_3-Au structure, transmission coeff., applied field depend. 3−8280
- Al-LiF-Au sandwich cathode, electron emission characts. 3−15603
- CdS, energy distrib. 3−36980
- CdS, pulse conditions, periodicity effect 3−27599
- Cu-Al-Ni alloy, martensitic thermoelastic transform., electron work function change 3−36346
- p-Ge autoemission volt ampere characts. with O_2 adsorption rel. to elec. breakdown 3−8709
- p-Ge field emitters, breakdown 3−39219
- ^{4}He, liq., field emission and field ionization, press. up to 25 atm. 3−30299
- Pt, field emission tip, crystal face specificity for N_2 adsorption 3−24342
- Re, exchange and correlation force effects 3−39218
- Si, field emission as a criterion of the surface state *(Russian)* 3−12216
- Si, impurity cluster localisation and comp., influence on emission props. 3−30134
- Si, time depend. of field-emission current, transient effects *(Russian)* 3−8710
- Si_3N_4 film, internal rel. to electronic cond. mechanisms *(German)* 3−15199
- Ta, electron energy distrib. when coated with SiO 3−15600
- Ta, work function when covered with SiO, field emission microscope obs. 3−15239
- W, emitted electron energy rel. to electron-phonon interactions, 78-950 K 3−5259
- W, flicker noise, spectral density functions, adsorbed K effects 3−15598
- W emitters, prepared from deformed wire, dislocation density *(Russian)* 3−30178
- W tip, EuS-coated, electron spin polarization 3−8706
- W wire thermal emitter, as field emission gun 3−28732
- W-Re alloy, surface self-diffusion in field-emission electron microscope 3−36982
- W(110), work function in field emission 3−36981

electron gas
- *see also cathode ray tubes; electron optics*
- alkali metals, Landau Fermi liquid parameters anisotropy, electron-phonon interactions 3−27203
- bulk modulus calc. 3−18050
- Compton scattering effects on hot moving electron gas 3−37291
- degenerate, finite temps., polarization propagator and self-energy operator 3−6356
- degenerate, temp. corrections of specific heat *(German)* 3−35620
- degenerate, Thomas-Fermi equation, high density expansions 3−36506
- dielectric response of electron liquid in generalised random phase approximation 3−38761
- dye aggregates from polyene type monomers, light absorpt., electron gas model 3−37132
- electron gas, spin and charge susceptibility 3−15338
- electron-electron interaction, lowest order polarisation diagram 3−19509
- energy, very low temps., quantum strong-mag. field limit 3−8077
- exchange and correlation, dielec. response beyond random phase approx. 3−38766
- excitation energy, variational calc. 3−20007
- ferromagnetic electron gas, spin polarisation due to mag. impurities 3−15339
- ground state energy, singularity associated with Wigner lattice formation 3−8076
- ground-state, approx. Euler-Langrange eqns. description 3−37895

electron gas continued
- ground-state properties at metallic densities, use of Wu-Feenberg theory 3−4036
- inert gas atoms, diamagnetic susceptibility and orbital momentum, free-electron gas exchange correlation calc. 3−38204
- inhomogeneous, spin effects and ferromagnetism 3−33773
- ionospheric heat flux at heights >180 km, cooling and heating sources 3−25270
- magnetic, spin correlation and density response function 3−30586
- metal, fluctuations in electron Fermi liq., scatt. of slow neutrons 3−21043
- metal, interacting electron gas, thermal diffuse X-ray scatt., compressibility 3−33650
- metal, internal energy and susceptibility under de Haas-van Alphen conditions 3−24374
- metal film, very thin, screening, random phase approx. 3−8090
- metal film and whisker crysts., equil. props. *(Russian)* 3−18064
- metals, h.c.p., lattice dynamics using modified electron gas model 3−36373
- motion in conducting solids 3−2041
- orbital diamagnetism of electron gas in infinite band *(Russian)* 3−34081
- orbital susceptibility, wave vector and freq. depend. 3−2244
- plasma, rotating electron, internal instabilities 3−29970
- response functions and short-range correls. 3−38763
- semiconductor, III-V, possibility of simulating relativistic plasma *(Russian)* 3−8218
- in semiconductor, mag. susceptibility, dHvA oscills. appearance conditions *(Russian)* 3−8336
- semiconductor, multivalley, fluctuations due to intervalley transitions 3−33880
- semimetal film and whisker crysts., equil. props. *(Russian)* 3−18064
- rel. to semimetal-dielectric transition, in quantizing mag. field *(Russian)* 3−8119
- short range correlation between electrons with antiparallel spins, ladder interactions 3−8098
- theory, radiative corrections 3−33772
- thermodynamic props. in mag. field 3−27200
- $Cd_xHg_{1-x}Te$, mag. susceptibility contrib. 3−8339
- GaAs, magnetization bh polarized light 3−4956
- Pd, dispersion of lattice waves, angular force models, effect of presence of electron gas 3−17942

electron guns
- computation and design problems 3−807
- computer-aided design 3−22523
- diode, linear electron accelerator, single shots and pulse train prodn. 3−10035
- electron injectors, bunching and performance with linear accelerator 3−10026
- electron optical data, brightness, characts., 50-125 kV, 0.1-1 mA *(German)* 3−347
- space-charge-limited dispenser thermionic cathode, electron energy distrib. 3−18522

electron-hole recombination
- *see also carrier mobility; charge carriers*
- BiI_3, effect of surface excitation and O_2 adsorption 3−27271
- carrier density kinetics under weak excitation for recombination centres *(Russian)* 3−24450
- ethylene glycol/water glass, luminesc. and photo-induced cond. meas., trapped electron optical excitation study 3−12162
- excitons, self-localised, recomb. luminesc., magneto-optical effects *(Russian)* 3−27538
- $GaAs_{1-x}P_x$:N laser, photoexcited, reson. enhanced, electron-hole recomb. probability 3−16876
- II-VI semiconductors, recomb. luminesc. and photoconduction, review *(Russian)* 3−27545
- metal, band struct. meas. by photon enhanced field emission, electron and hole scatt. effects 3−27205
- n-p-i junctions in Si, current voltage characts. rel. to recomb. leakage *(Russian)* 3−8260
- optoelectronic devices, degradation mechanisms under ionising irradiation *(German)* 3−37974
- pair prod. by plasmon decay 3−18177
- p-s-n rectifiers, band-to-band Auger recombination and carrier-carrier scattering 3−5019
- semiconductor, biexcitons, electron-hole droplet for motion, radiant recombination, helium temp. *(Polish)* 3−38816
- semiconductor, deep impurity levels influence on double injection and recombination 3−8203
- semiconductor, multiple energy level defects, continuity and Poisson equations 3−24418
- semiconductor, slow recomb. waves, nonlinear theory *(Russian)* 3−8204
- semiconductor overheating instabilities, low-temp. impurity breakdown 3−24395
- semiconductor-metal and mag. phase transitions, Hamiltonian model 3−38806
- semiconductors in relaxation regime 3−38854
- $3As_2Se_3$-$2Sb_2Se_3$, amorphous film, trapping processes, photoconductivity obs., 278-308K 3−21094
- $Al_xGa_{1-x}As$ semiconductor, radiative transition kinetics, luminescence spectra, 4.2-77K, influence of temperature 3−34422
- As_2Se_3, amorphous, radiative recomb. 3−24737
- $CdGa_2Se_4$ photoconductivity, trapping, single crystals, photoluminescence, local centres 3−33953
- CdI and CdI_2(Pb) thermoluminescence, recombination kinetics *(Russian)* 3−34437
- CdS, high carrier and exciton conc., low temp. emission recomb. study *(Russian)* 3−27541
- CdS, recomb. waves induced by optical quenching 3−38866
- CuCl, high carrier and exciton conc., low temp. emission recomb. study *(Russian)* 3−27541
- Cu_2S, chalcosite, djurleite, minority charge carriers, recombination diffusion length 3−11907
- n-GaAs, optically excited, doping dependence of photon yield as function of excitation energy 3−8638
- GaAs, recomb. radiation, carriers generated in vicinity of surface 3−34426

electron-hole recombination continued
- p-GaAs:Ge, epitaxial, electron diffusion length, recomb. lifetime 3−18164
- p-GaAs:Zn, optical orientation of electron spins, surface influence, recomb. radiation study *(Russian)* 3−8662
- $GaAs_{1-x}P_x$:N, photopumped thin films, luminescence, variable energy bandstructure, l.e.d. applications 3−39175
- GaP, donor-acceptor radiative recomb. of C-S and Zn-S pairs *(Russian)* 3−8633
- GaP, recombination processes responsible for room-temp. near-band-gap radiation 3−34416
- GaP:O, donor deep states, capture cross sections, photocapacitance obs. 3−30428
- GaP:Zn, O, free hole to impurity centre bound electron recomb. at 300K 3−30494
- GaSb:Te, and undoped p-, acceptor radiative recomb., photoluminesc. spectral comparison *(Russian)* 3−36915
- GaTe:Ge, high-resistivity, radiative capture of holes by luminescence centres 3−24740
- n-Ge, breakdown and recombination kinetics connected with excited states shallow donor 3−18166
- Ge, laser excited, radiative transition, Auger recomb. processes 3−5233
- n-Ge, microwave photocond. and radiative recomb. under high optical excitation at low temp. 3−38871
- Ge, oscill. of recomb. radiation of electron-hole drops in strong mag. field *(Russian)* 3−2030
- n-Ge centres, properties and nature, τ, majority carrier density 3−33924
- Ge:As,Sb, luminesc. spectra due to electron-hole radiative recomb., virtual bound state, 2K 3−8632
- n-$Hg_{1-x}Cd_xTe$, Auger limited band to band and Shockley-Read recomb., photocond. meas. 3−36634
- InAs p-n junction, rel. to kinetics of photo-e.m.f. *(Russian)* 3−2177
- $In_{1-x}Ga_xP$, electroluminesc., free electron-bound hole recomb. 3−2597
- $In_{1-x}Ga_xP$:N, photopumped thin film, luminescence, variable energy band structure, l.e.d. applications 3−39175
- $In_{1-x}Ga_xP$:N laser operation, reson. enhancement of recomb. probability associated with isoelectronic trap states 3−18472
- InSb, anal. using wave function method in two-zone approx. *(Russian)* 3−15212
- n-InSb, microwave emission, sample geometry and surface condition depend. 3−5016
- p-InSb, negative differential resistivity region at 77°K, injected carrier oscillations 3−11908
- KI, recomb. luminesc. lifetimes rel. to self trapped excitons 3−21468
- RbI, recomb. luminesc. lifetimes rel. to self trapped excitons 3−21468
- Si, cross-section for recombination at group V donor impurity centres, 1.5-20K 3−27270
- n-Si, γ-irrad., recomb. levels 3−5020
- Si, p-n, p-n-p structure, i.r. obs. of breakdown behaviour 3−24501
- Si, proton irradiated, recombination centres, photoconductivity measurements 3−33575
- Si, transient absorp. of microwave obs. rel. to exciton formation *(French)* 3−30434
- Si surface recomb. velocity at 370 K in vacuum *(Russian)* 3−8244
- Te, enhancement of capture rate of excess carriers due to acoustoelec. amplification 3−2143
- YAG, rare earth activated, recomb. luminesc., thermolum. and photolum. obs. 3−21480
- ZnS, electroluminesc. emission peak, depend. on recomb. processes *(Russian)* 3−21493
- ZnSe, electroluminesc., rel. to improved generation-recomb. processes in light emitting diodes *(German)* 3−15558

electron interactions
- *see also nuclear reactions and scattering due to electrons; positron annihilation*
- asymptotic nucleon cross section excitation from deuterium data, effect of Fermi motion 3−29294
- coincidence electroproduction and hadronic channels at edge of deep continuum 3−14004
- deep inelastic electroproduction and colliding beam processes, final hadron states 3−13938
- deep inelastic scattering in continuum region, validity of scaling and sum rules 3−13936
- electron intensity enhancement at 100 km due to interaction with whistlers mode waves 3−25308
- electroproduction, scaling function and form factors, relationship 3−16979
- electroproduction, Schwarz inequality, relation to one-photon annihilation and two-photon processes 3−4181
- electroproduction, semi-inclusive, Drell-Yan scaling 3−38053
- electroproduction at high energy, diffraction-dissociation model 3−38048
- electroproduction coincidence cross sections in $\Delta(1232)$ region from coupled multipole eqns. 3−13941
- electroproduction cross sections in resonance region, consequences for σ_l/σ_t 3−13992
- electroproduction of single pion, vector meson dominance model 3−13890
- high energy conference, Ithaca, New York U.S.A., (August 1971) 3−13842
- inclusive electroproduction cross-section for π^+ in proton fragmentation region, prediction via factorization 3−17031
- inelastic electroproduction, range, light cone dominance and scaling at low Q^2 3−23080
- ionospheric photoelectron interaction with ambient electrons, Coulomb collision effects 3−31422
- low temp. targets 3−28638
- low-Q^2 electroproduction models 3−13939
- meson reson. electroproduction 3−17026
- parity and time reversal in gravitational interaction and existence of massless scalar particle 3−32629
- quantum transitions of relativistic electrons, in superstrong mag. field 3−23099
- space-time phenomenology of real and virtual photon absorption by nucleons, Regge-like behaviour 3−13913

electron interactions continued
- strange particle electroproduction on nucleons, Born approx. *(Russian)* 3−4183
- sum rules, parametric for electroproduction and tests of complex scaling 3−19677
- $ed \to e\pi^{\pm}\Delta(1236)$, coincidence meas. and nucleon cross-sect. detn. for Δ channels 3−17041
- $ee \to ee\Gamma$, two photon processes, determ. of differential cross sections for inclusive and exclusive channels 3−13978
- $ee \to eeKK$, cross-section determ. using dispersion relation method, reln. to $\gamma\gamma \to KK$ *(Russian)* 3−23077
- $ee \to ee\varepsilon(850)$, $eef(1260)$ cross sections, finite energy sum rules 3−13980
- $e^-e^- \to \mu^-\mu^-$, parity violation by neutral lepton currents 3−4155
- $e^-e^{\pm}$ high energy collisions, production of electron and muon pairs, total and differential cross section 3−13998
- e^+e^-, exptl. tests of quantum electrodynamics at Adone 3−13871
- e^+e^-, total cross sections and one- and two-particle distribs., theoretical models and exptl. results 3−6631
- e^+e^- colliding beams, hadron production in 1.4-2.0 GeV 3−13943
- e^+e^- colliding beams, study of QED processes and hadronic e.m. current 3−858
- e^+e^- collisions, hadron production, existence of new vector meson 3−13994
- $e^+e^- \to e^+e^-F$, F=electron, μ or π pairs, two photon annihilation processes at Adone storage rings 3−13944
- $e^+e^- \to e^+e^- +$ others, first observation at Frascati Storage Rings 3−13942
- $e^+e^- \to e^+e^- + X$, two photon reactions at Adone 3−13871
- $e^+e^- \to e^+e^-e^+e^-$, evidence for the, reaction in Novosibirsk colliding beam expt. 3−13873
- $e^+e^- \to e^{\pm}e^-A$, two-photon process, Schwarz inequality, relation to one-photon annihilation and electroproduction 3−4181
- $e^+e^- \to \mu^+\mu^-$ in colliding beams, polarization effects on cross sections *(Russian)* 3−4176
- $e^+e^- \to \nu\nu\gamma$ in colliding beams, polarization effects on cross sections *(Russian)* 3−4176
- $e \pm e^-$ colliding beams, two-photon processes, parton model 3−38050
- $e^{\pm}e^- \to e^{\pm}e^-X$ check on e.m. interactions of hadrons including two hadrons, review 3−13846
- $e\gamma$ state of 'magnetised' electrons at low quantum levels *(Russian)* 3−23101
- $e^-\gamma \to e^-\nu\nu$, photoneutrino energy losses, computation for 10^{13} G mag. field 3−35805
- eN, Be targets, production of K_l^0 and n above 10 GeV 3−29214
- eN, electroproduction cross sections, separation of resonant and nonresonant contribs., isotensor currents 3−13983
- eN deep inelastic electroproduction, structure functions in scaling limit, rel. to form factors 3−13865
- eN deep inelastic electroproduction, inequalities for structure functions, tests of basic algebraic structures 3−13981
- eN deep inelastic processes, hole fragmentation for large ω 3−23096
- $eN \to eX$ inclusive, neutral current effects 3−855
- $eN \to e\gamma$anything, deep inelastic processes, Fritzsch-Gell-Mann algebra applic. 3−13933
- $ep \to e'p\eta^o$, e.m. form factor meas. for $S_{11}(1535)$ reson., comparison with quark-model calc. 3−38034
- $ep \to en\pi^+$, 2 GeV, analysis using Chew-Low extrapolation and fixed t dispersion relations, determ. of π form factor 3−13987
- $ep \to epM_x$, electroproduction coincidence meas. in deep inelastic region, determ. of cross sections 3−13991
- $ep \to ep\pi^+\pi^-$, streamer chamber study for $0.3 < Q^2 < 1.5$ GeV^2 and $m_p \leqslant W < 2.8$ GeV, Δ^{++} and ρ^o production 3−38047
- $ep \to ep\pi^{\circ}$, coincidence meas. of backward production 3−17040
- $ep \to e\pi^+\Delta^0$, vector meson dominance 3−14008
- $ep \to e\pi^+M_y$, electroproduction coincidence meas. in deep inelastic region, determ. of cross sections 3−13991
- $e^-p \to e^-K + \Lambda$, coincidence meas., −0.17 to −1.2 GeV^2 3−14011
- $e^-p \to e^-\pi +$ anyting, low t theorems and minimal gauge invariant extension of one-pion exchange 3−38049
- $\mu^+e^- \to \nu_1\nu_2\gamma$, longit. spin correls. *(Russian)* 3−23064
- $\mu^+\mu^-$ production using PCAC and light cones 3−17003
- ω-meson electroproduction, model 3−10699
- π electroproduction at threshold, implications of gauge invariance 3−10714
- π electroproduction at threshold, calc. of axial nucleon and e.m. pion form factors 3−38044
- π electroproduction in scaling limit using PCAC and light cones 3−17003
- π^- electroproduction into bound state of mesoatom *(Russian)* 3−38054
- π^0 electroproduction at first resonance, multipole amplitude analysis, determ. of magnetic dipole amplitude 3−13940
- $\pi\Delta(1236)$ production, invariant amplitudes, vector-meson dominance 3−6618
- Be targets, production of K_l^0 and n above 10 GeV 3−29214

electron ionisation
- *see also atomic electron scattering; molecular electron scattering*
- Born II approx., scatt. amplitude, phase factors 3−26589
- double ioniz. cross sections, wavefunction 3−20044
- energy deposition in gaseous mixtures due to excitation and ionisation, computer program 3−35970
- Franck-Condon factors for transitions on ionization of diatomic molecules 3−23624
- hydrogenic atoms, inner shell ionisation by electron impact 3−7078
- inert gases, electron impact double ionisation, cross section calc. 3−11169
- inner-shell ionization of medium-heavy atoms by electrons, calc. of cross-section 3−11174
- ion multiple ionisations and transition probabilities by light energy electron impact 3−20053
- metallocenes, appearance pots., negative and positive ion form. 3−29739
- neutral atoms in dense discharge, excitation and ionisation by electron impact 3−23497
- propane unimol. decay into $C_3H_7^+ + H$, electron-impact-induced, time depend. 3−21797
- rare earth metal surfaces, ionisation losses in inelastic electron refl. spectra 3−5252
- Ar, elastic scatt., 100 eV, optical model 3−20041

electron ionisation continued
- Ar, electron impact, eikonal and Born approxs. 3−38240
- Ar, impact ioniz., energy and ang. correls. of ejected electrons 3−26600
- Ba, cross section meas. by energy resolved electrons 3−11173
- Be, photoioniz. cross sections calc. 3−26594
- CO$^+$, relative intensities for ionisation of lowest 3 electronic states by electron impact 3−33159
- Ce autoionising states, excitation by electron impact *(Russian)* 3−26599
- Cs, electron impact excitation of autoionizing level 3−35972
- Cs impact, 6s and 5p, cross-sections, Born approximation, threshold, Hartree method *(Russian)* 3−26598
- D_2, ioniz. cross section meas. 3−33158
- H, differential cross sections, off-shell Coulomb T matrix 3−7079
- H, Glauber theory 3−29524
- H^-, double ioniz. cross sections calc. 3−20045
- H^-, electron detachment, Born-Ochkur approx. 3−35973
- H_2, autoionizing transitions produced by electron impact 3−33156
- H_2, ioniz. cross section meas. 3−33158
- He, Coulomb effects in final state of ionizing collision 3−26595
- He, differential ioniz. cross section for slow electron ejection by fast charged particles 3−33045
- He, double ioniz. cross sections calc. 3−20045
- He, electron impact double ionisation, classical collision theory appl. 3−38234
- He, excitation of (1s, nd)^1D and (ns, mp)^1P states 3−26591
- Li^+, double ioniz. cross sections calc. 3−20045
- Li^+, electron impact double ionisation, classical collision theory appl. 3−38234
- Li^+, singly ionized by electron impact, lifetime and polarization of 2 ^3P term 3−29499
- Mg, photoioniz. cross sections calc. 3−26594
- N_2, autoionizing transitions produced by electron impact 3−33156
- N_2, electron impact vibrational excitation cross-sections 3−36052
- Na, electron impact excitation of 3p state 3−29523
- Ne, electron impact, eikonal and Born approxs. 3−38240
- Ne, ionisation by electron impact, Townsend coefficient 3−33403
- O, electron impact excitation and ioniz., cross sections 3−4390
- O_2, negative molecular ion formation in electron collision $E+O_2 \rightarrow O_2^{-*}$ 3−29741
- Rb total electron impact ionisation cross section from threshold to 250 eV 3−38232
- ^{50}Sn, inner-shell ionization, calc. of cross-section, relativistic effects 3−11174

electron lenses
- *see also electron microscopes; electron optics; electrostatic lenses; magnetic lenses*
- cathode lenses, image parameter determination method *(Russian)* 3−6535
- double quadrupole, electron optical props. 3−37991
- einzel lens, three diaphragm, monochromator 3−28721
- electron microscope objective, astigmatism measurement from spatial frequency spectrum of image *(Russian)* 3−6115
- focal props. of cylindrically symmetric microwave cavities 3−363
- magnetic, electron, for electron microscopes and probe forming systems, developments 3−1538
- magnetic, probe forming, low aberration for s.e.m., design 3−360
- magnetic and electrostatic quadrupole, achromatic, with minimum electric fields 3−361
- magnetic electron microscope, adjustment of polepiece system with initially non-coincident polepiece-bore axes *(German)* 3−6110
- objective−intermediate−projecter system design 3−364
- optical properties and practical realization, review 3−35722
- plane-symmetric two-dimensional, electric potential and field on the principal optical axis 3−29162
- quadrupole lens, fringing field calcs. 3−28723
- quadrupole lenses in five-electrode quadrupole-octupole elements generating electron microprobe, effective lengths *(Russian)* 3−6114
- round and cylindrical with field free object space, theory *(German)* 3−26256
- thin probe formation theory rel. to Maxwellian initial distrib. and spherical aberration 3−13774

electron mean free path *see carrier mean free path*

electron micrographs *see electron microscope examination of materials; electron microscopy*

electron microprobe analysers *see electron probe analysis*

electron microprobes *see electron probes*

electron microscope examination of materials
- *see also electron microscopy*
- alkali halide cleavage plane, Au adatom diffusion and cluster migration 3−1888
- alloy, eutectoid, transform. processes obs. by photoemission electron microscope 3−18568
- alloys, high-coercivity, ordered, plastic deform. influence on structural state *(Russian)* 3−18338
- alloys, ordered, interfaces study, grain boundaries, twinning, martensitic transformation, thermal antiphase walls *(French)* 3−17855
- alloys, with periodic antiphase domain struct., plastic deform. *(Russian)* 3−5306
- amorphous material, microcrystallite and random network models to interpret electron micrographs 3−17744
- amorphous thermoplastic, fracture processes, crazes 3−34650
- amphiboles, fibrous, planar defects 3−37158
- anorthite, domain temp. depend., model 3−24131
- Armco iron, microcracks and slip band structure in fatigued specimens 3−18745
- barium stearate 'built up' films, d.c. destructive breakdown field, temp. depend. 3−5161
- basalt, whole-rock K-Ar dating, electron microprobe evaluation 3−12572
- bimetal, zone of union prep. by explosion welding, thin foil prep. 3−18577
- butadiene-styrene latex, gelling, condensation structures, rheology, electron microscopy 3−39398
- carbide filaments development for graphite filaments 3−15771
- carbon fibres, dark field micrographs, interpretation of microfibrils 3−18731

electron microscope examination of materials continued
- carbon-graphite materials, crystallite size effect on strength 3−34652
- cathode surface erosion prod. by dynamic field emission 3−27598
- ceramic raw materials, particle morphology in real dimensions *(French)* 3−15796
- channelling pattern analysis by computer 3−1555
- channelling patterns in s.e.m. and crystalline contrast 3−1559
- coal, medium rank, SEM obs., 'organically bound' iron concept 3−37771
- complementary dark field dislocation images 3−36252
- computed and expt. micrographs, comparison for stability of multiple dislocation, stacking fault arrays 3−17824
- crack behaviour under static loading, processes at crack tip, fractographic obs. 3−24200
- cryptoperthitic alkali feldspar, complex exsolution textures 3−37156
- cubic materials, ferromagnetic, magnetic domain contrast 3−38998
- diffraction from tilted specimens, application to s.e.m. 3−1556
- dislocation effect on s.e.m. channelling patterns 3−1553
- dislocation interaction with irradiation produced point defects in high voltage electron microscope 3−17844
- dislocations, diffraction contrast of a continuous set, intensity distribution *(Russian)* 3−32227
- field ion microscopy specimen fracture 3−1533
- film, epitaxial growth, direct observation, review 3−1935
- fractography, state-of-the-art review 3−30982
- glass, stoichiometric diopside exam. *(Russian)* 3−30074
- glass-ceramics, thin foil prep. technique, microstruct. characteriz. 3−34645
- graphite, enhanced reactivity at struct. faults, microscopic studies 3−11788
- handbook for beginners 3−6117
- hexadecachloro-copper-phthalocyanine, molecular image resolution determ. 3−17390
- high current field emission cathodes of refractory metals *(Russian)* 3−8711
- ice, obs. of defect structure 3−7746
- γ-In$_2$S$_3$, crystals grown from vapour, X-ray and electron microscope investigation of struct. faults *(German)* 3−7781
- intermetallic compounds sigma phase detection 3−8811
- introductory paper, for metallography 3−31017
- IV-VI monolayer overgrowth on IV-VI substrate, effect of substrate temp. and orientation 3−15083
- Kikuchi diagrams, energy filter *(French)* 3−388
- Kikuchi patterns, in h.v. electron microscopy 3−7608
- lattice defect images for s.e.m. 3−1554
- lattice defects, using weakly excited beams 3−1539
- limestones, deformed, microstruct. 3−37160
- lunar breccias, SEM obs. 3−39648
- lunar grain radiation damage due to solar particles 3−37333
- lunar materials at 100 KV 3−3318
- magnetic domain contrast, Kossel lines 3−2320
- medium-range ordering studied by diffraction and imaging 3−14736
- memory-type material, switching phenomena obs. 3−2151
- metal, b.c.c., plastic crack propag. *(Russian)* 3−20802
- metal, crystalline, athermal weakening on cold plastic deform., TEM obs. 3−33599
- metal, electron irrad., void obs. 3−1640
- metal, quenched and neutron irrad., impurities role in damage form. 3−29448
- metal machining chips, microscopic plastic instabilities 3−34580
- metal particles, oxid., electron microscope obs. of oxide-metal boundary 3−15076
- metallic film, groups I-IV, electromigration obs., scanning elec. microscope 3−4879
- metallurgical application, s.e.m. selected-area channelling pattern technique 3−2713
- metals, f.c.c. and b.c.c., vacancy clusters 3−24107
- metals textures, status of research review 3−8799
- mica group and related sheet silicates, electron energy loss spectra rel. to struct. 3−1608
- micrographs and selected area channelling patterns, simultaneous display using s.e.m. 3−1558
- mineralized tissues, high resolution surface scanning electron microscopy 3−3910
- mullite, polycryst., ultra fine grain, creep kinetics, electron fractograph obs. 3−2755
- Mullite reusable surface insulation (HCF) for space shuttle, characterisation 3−8962
- multiply twinned particles, 1000 kV electron microscope study 3−7606
- natural latex, gelling, condensation structures, rheology, electron microscopy 3−39398
- Nb$_2$O$_5$, obs. of planar defects and structure at high temps. 3−11638
- Nimonic 80A, oxidation, low O_2 press. 800°C, Auger spectra 3−30358
- optically transparent dielectrics, study of laser induced surface damage, obs. of microstructure 3−16898
- perfect and imperfect crystals, backscattering of electrons in S.E.M. 3−23997
- permalloy cross-tie walls density influence on domain boundary creep *(Russian)* 3−2315
- Permalloy film, bubble domains, h.v. microscope obs. 3−30660
- permalloy thin films, Bloch line motion, behaviour at inhomogeneities, Lorentz electron microscope study 3−12038
- phase transitions at high temp. 3−14669
- phosphor films, transmission microscopy and cathodoluminescent studies 3−1551
- photographic emulsion, by Philips 300, equipped with goniometer storage and cooling holder 3−28725
- PMMA, morphology of fracture surface layer and fracture mechanism 3−20242
- polycaprolactam, doubly oriented, morphological changes during annealing 3−20235
- polyethylene, fatigue crack propagation, stress depend. 3−31158
- polyethylene, high and low mol. wt., struct. changes during deform. 3−20239
- polyethylene, high-strength transparent, morphology, controlled prep. conditions 3−4502
- polyethylene, low density bulk, gamma-irrad., morphology and tensile strength, SEM obs. 3−36331

electron microscope examination of materials continued
polyethylene, oriented, h.p. annealing effect on struct. 3—20247
polyethylene, oriented films, study of microfibrilar struct. *(Russian)* 3—7289
polyethylene fibres drawn from single crysts., mol. struct. 3—33177
polyethylene orientated, formation of kink band during compression 3—18725
polyethylene single crysts. on Cu and NaCl substrates, plastic deform. 3—33596
polyethylene spherulites, lamellar struct. 3—20248
polymer, glassy, morphology 3—20230
polymer, morphology and macrocrack form. on fracture surfaces 3—20241
polymer fibres and films, melt-crystallized, spherulitic struct. change during uniaxial stretching 3—20238
polymer mixtures, morphology of cast films 3—20246
polyoxymethylene supermol. structs., growth rate and morphology 3—20224
polystyrene, morphology of crazes formed in thin films and bulk specimens 3—27770
porous materials, pore-size determination by N_2 adsorption measurements 3—37097
pyrocarbon, thin film grown from methane on Pt, determ. of struct. *(Russian)* 3—11835
o-pyroxene, exsolution lamellae 3—37157
pyroxenes, natural, petrographic studies 3—18807
quartz particles from post-glacial clay soils, internal and surface struct. 3—37161
quartz rocks, deformed, dislocation substructures 3—18809
rare earth metal film, obs. of f.c.c. structure and oxidation 3—18042
replicas, lucite for electron fractography 3—21769
research with scanning electron microscope 3—10120
roughness meas. of heat transfer surfaces 3—20299
rubber film, uncrosslinked, morphology of strain-induced crystn. 3—4501
rutile, abraded, electron microscope study of structure before and after annealing 3—15753
sand grains, surface texture rel. to depositional history 3—34821
selected area diffraction in s.e.m., approaching 1 micron 3—1557
semiconductors, ion and electron irrad., clustering of defects 3—33576
sheet metal, high temperatures, sample deformation under observation by emission microscope, device for *(German)* 3—8795
single crystals, tensile test of foil specimens at room and low temp., dislocation motions 3—17820
sputtered thin film growth, in situ transmission electron microscope studies 3—6112
stainless steel, obs. of pseudo-subgrain boundaries 3—12357
steel, (36.1 wt.% Ni, 2.5 wt.% Ti, 2.1 wt.% Al), obs. of gamma'-phase precip. *(Russian)* 3—39334
steel, austenite, shape of $M_{23}C_6$ particles 3—15689
steel, austenitic, Cr-Ni-Mo, Ti-stabilized, creep strength behaviour 3—8928
steel, austenitic, fatigue crack initiation, transmission electron microscope obs. *(Japanese)* 3—12396
steel, austenitic, microstruct. changes during creep deform. at 600°C 3—8921
steel, austenitic, stress corrosion cracking, fractographic obs. 3—31042
steel, austenitic, thermomech. hardening effect *(Russian)* 3—37045
steel, austenitic CrMnNiN, stacking fault energy meas. by method of extended nodes *(Czech)* 3—31028
steel, austenitic stainless, fracture surfaces in stress corrosion cracking *(Japanese)* 3—34561
steel, austenitic stainless, intergranular corrosion, microstruct. and microsegregation effects 3—37032
steel, austenitic stainless, Nb-stabilized, stress varied creep behaviour 3—8925
steel, austenitic stainless, solid soln. decomp. kinetics 3—21603
steel, austenitic stainless, stabilized, Nb conc. depend. of steady-state creep 3—8923
steel, eutectoid, obs. of pearlite coarsening and spheroidization on deform. 3—15709
steel, ferritic, Mo-containing, comp. and microstruct. effects on creep strength 3—8933
steel, galvanized sheet, diffusion layer 3—18619
steel, low stacking-fault energy, deform. twinning 3—21594
steel, low-C, containing tungsten tempering behaviour and carbide form. 3—37050
steel, low-C, low-Mn, Nb additions effect on plastic anisotropy 3—37054
steel, low-C, precip. on grain boundaries 3—18577
steel, maraging, fractographic lines and fracture toughness 3—34573
steel, martensite cryst. steric form and size determ. *(Russian)* 3—37017
steel, medium-C, quenched and tempered, effect of Si additions on microstruct. 3—21584
steel, retained austenite, volume percentage and distrib., scanning electron metallography obs. 3—8800
steel, stainless, stabilized, void form. due to fast neutron irrad. 3—26503
steel, stainless, Type 304, cyclotron-injected helium effect on void form. characts. 3—35934
steel, stainless, Type 316, neturon irrad., defect development 3—35933
steel, tufftrided mild, fatigue strength and microstructure *(Japanese)* 3—30991
steel MnS inclusions morphology 3—8788
steel sheets, low carbon, effects of Ni on cold-rolling and recrystallisation textures *(Japanese)* 3—18589
stress corrosion cracks, h.v. microscope studies 3—30981
substoichiometric rutile, generation mechanism for shear planes, TEM obs. 3—30130
surface structure obs. 3—15055
surface topography, scanning and transmission microscope obs. 3—11789
surfaces, medium energy electron diffr. with scanning microscopy 3—30320
techniques and analysis, conference (Cambridge, England, June-July 1971) 3—1535

electron microscope examination of materials continued
tetracene, structure of vacuum deposited thin films 3—15103
thermally stimulated exoelectron emission spectroscopy applications 3—13466
thin crystals vacuum decoration technique, microstructure obs. *(Russian)* 3—38750
tri-glycine sulphate, ferroelec. domain struct., electron microscope obs. 3—30777
Zircaloy, fracture toughness characteriz. 3—8879
Zircaloy-2, hydride precip. distrib. 3—8820
Zircaloy-2, polycrystalline, hydride crystallographic orientation *(French)* 3—12385
Ag, dislocation motion geometry at tip of spreading cracks 3—17918
Ag film, annealed, recrystallisation obs. 3—1953
Ag particle rotation observation by electron microscopy during sintering 3—18684
Ag single crystal films plastic deformation, dislocation struct. 3—17900
Ag thin film surface obs. by electron microscopy *(French)* 3—33724
βAg-Al splat quenched alloys, martensitic transformation 3—2695
Ag-Zn alloys, massive precipitates study by selected area electron channelling 3—21576
Ag-Zn(27.6 wt.%) β-phase alloy transmission electron microscopic investigation of bainite formation in 180-260°C range *(Japanese)* 3—18587
Al, creep-deformed, dislocation struct. of subgrain boundaries 3—24121
Al, dislocation annihilation mechanism by deformation 3—17823
Al, foil, dislocations due to friction, lubrication and oxide layer effects 3—27063
Al, grain boundary fine structure, bright and dark field transmission electron microscopy 3—1632
Al, spall fracture, scanning microscope obs. 3—14923
Al alloys, corrosion fatigue in aqueous solns., fractographic studies 3—27656
Al alloys, inclusions role in ductile fracture and fracture toughness 3—30984
Al and alloys, polycryst., work softening obs. and mechanism 3—37066
Al film, electromigration, quantitative mass distrib., scanning electron microscope obs. 3—7977
Al film microstruct. and electromigration, laser irrad. effects 3—20974
Al fine particles, oxid. mechanism, electron microscope obs. 3—38744
Al foil, tensile and fatigue crack growth obs. 3—21761
Al foils, electron microscope search for foreign inclusions and their role in crack and pin hole formation 3—21608
Al irradiation damage, 3 MV electron microscope, voltage dependence 3—36333
Al powder with Cu and Fe coating, scanning microscope obs. *(Russian)* 3—9022
$Al:Al_2O_3$, dispersion strengthened, obs. of recrystallisation 3—18573
$Al-Al_2O_3$, dispersion strengthened, obs. of recrystallisation 3—18581
$Al-Al_3Ni$ aligned eutectic alloy, fatigue fracture behaviour 3—21658
$Al-Al_3Ni$ eutectic comp., thermal stability of microstruct. *(Russian)* 3—24850
Al-Cu alloy, eutectic spherulites 3—27638
Al-Cu oriented bicrysts., intergranular precip. *(French)* 3—27626
Al-Cu-Li alloy, Al_2CuLi T_1 precipitation, electron microscope examination of microstructure 3—8798
Al-Cu(4 at wt.%) alloy, precipitation study by internal friction, hardness and electron microscopy meas. *(French)* 3—15687
Al-Fe-Mn alloy, splat quenched, decomposition mechanism 3—2712
Al-Mg-Si alloy, plastic deformation on the precipitation *(Japanese)* 3—15699
Al-Mg-Si:Cu, aging, effects of Mg loss, elec. resistance meas. 3—39361
Al-Ti (0.16 at wt.%) alloy, yield point phenomenon *(Japanese)* 3—18644
Al-Zn alloys, metastable solvus for Guinier-Preston zones 3—31022
Al-Zn-Mg-Cu alloy, thermomech. treatment processed, age hardening mechanisms 3—24897
Al_xGa_{1-x}, molecular beam epitaxial layer, struct. 3—2677
Al_2O_3, alumina ceramics, characterisation 3—8961
Al_2O_3, alumina ceramics for IC substrates, pitting, burring 3—12420
Al_2O_3 anodic films, branching colony pore structure 3—1948
Al_2O_3 fibres, h.v. electron microscopy 3—1537
Al_2O_3 film, on Al, thickness meas. 3—36500
Al_2O_3-TiO_2 powder, high-freq. plasma oxidation prep. 3—31122
$(Al_2O_3)_3$ $(SiO_2)_2$, mullite, ceramic powder, stoichiometric, synthesis and mechanical props. 3—27736
$Al_2O_3-Cr_2O_3$ modulated structures formation 3—4846
$Al_2O_3-Cr_2O_3-Fe_2O_3$ modulated structures formation 3—4846
Al_2O_3 anodic film, on Al, breakdown and repair 3—8060
Ar, electron distribution determ. by holographic electron laser microscope 3—4714
As_2S_3 amorphous film, optical transmission edge, anomalous photo-induced shift 3—8687
Au, electron channelling obs. 3—24169
Au, h.v. electron microscopy, multi-beam imaging technique 3—23991
Au, pure, deformed, point defect clusters 3—17807
Au, quench-hardened single crysts., yield stress and surface morphology, dislocation-stacking fault interaction 3—36350
Au film, electromigration, void and hillock growth, TEM obs. 3—36437
Au film, vacuum deposition, effect of electric field on orientation and particle arrangement 3—1934
Au film grown on NaCl, obs. of small-angle torsion boundary structure 3—4940
Au island condensates, on NaCl chips, cross section determ. 3—18035
Au-Cu alloy film, order-disorder transformation obs. 3—1800
Au-Cu alloys deposition from cyanide free acid solution *(French)* 3—9071
Au-Ni thin-film thermocouple, transmission electron microscopy, specimen temp. increases 3—24011
$Au-SiO_x$, cermet film, structure obs. with heat treatment 3—15201

electron microscope examination of materials continued
Au-SiO$_x$ cermet film, structural changes on heat treatment 3−5064
Au-transition metal alloy, short range order 3−14734
Au$_{50}$Cu$_{50-x}$Ga$_x$, thin specimens study of AuCu II phase with periodic antiphases and AuCu III phase *(French)* 3−31003
BN$_x$, cubic, SEM obs., anomalous contrast effects 3−36471
B$_2$O$_3$-BaO-Fe$_2$O$_3$ glass, morphology of precipitate particles, X-ray scatt. and electron microscope examination 3−12020
BaTiO$_3$, electron microscope obs. of ferroelectric domains in low temp. phase 3−30765
Be film, SEM obs. of laser damage 3−35708
Bi film, melting and freezing, obs. in electron microscope 3−14980
Bi film growth mechanism, condensation in vacuum, electrical resistivity 3−33758
β-brass, stress corrosion cracking, fractographic obs. 3−31042
C, isotropic pyrolytic, microstructure, fracture stress, Young's modulus, annealing effect 3−24993
C, pyrolytic deposition on fluidized particles, microstructure 3−24994
C amorphous film, electron microscopy dark field images 3−14688
C fibres, heat treatment effects, analysis of structure after oxidation, carbonization or graphitization 3−15778
C fibres, polyacrylonitrile based, high-modulus, three-phase struct. obs. 3−27771
C fibres, structural study 3−15779
C high strength fibres, h.v. electron microscopy 3−1537
CaCO$_3$, twinning dislocations, macroscopic pileup config. *(Russian)* 3−7768
CaF$_2$, thin films, electron irradiation effects 3−38748
CdIn$_2$Te$_4$, thin films, electron microscopic and electron diffraction investigations *(Russian)* 3−30371
CdS films on Ge, epitaxial growth and struct. 3−36493
CdSe, films, structure and electrical resistance obs. *(Russian)* 3−38752
CdTe, defect struct., transmission microscope obs. 3−17830
Co film, electroless, nucleation and growth obs. 3−11837
Co-P film, high-coercivity, domain struct. and reversal processes 3−24592
Co-Pt alloy, struct. rel. to high coercivity *(Russian)* 3−8779
Co-W-Ti alloy, second phase precip. phenomena *(Russian)* 3−24846
Co-WC alloys, meas. using new electron microscope replica locating technique 3−18674
CoFe$_2$ film, oxidation mechanism, ferrite film form. 3−27196
CoO, sintered, oxidation to Co$_3$O$_4$, kinetics, mechanism 3−8957
Co$_5$Pr, splat-cooled, obs. of dislocations 3−8791
Cu, continuously cast, fracture surfaces produced by high temp. creep 3−34535
Cu, fine particles, oxid. mechanism, electron microscope obs. 3−38744
Cu, obs. of grain boundaries in creep deform. 3−14880
Cu, single cryst., slip line struct., surface effect 3−17913
Cu (100) single crystal film, on (100) NaCl, oxidation obs. 3−1907
Cu and alloys, void form. on fast neutron irrad. *(French)* 3−26504
Cu stacking fault energy obs. 3−1542
Cu-Al(1 at wt.%) alloy, alloying elements Ag, Pd, As and In effect on internal oxidation *(Japanese)* 3−15700
Cu-Al(5.8 at.%) alloy, deformed, soft surface effect 3−24866
Cu-Be alloys, eutectoid decomp., ordering with metastable solid soln. form. *(Russian)* 3−37001
Cu-Cd, hardening effect, transmission electron microscope examination 3−4805
Cu-Cu$_2$S-CdS-Au sandwich structure, switching filament migration, s.e.m. obs. 3−2150
Cu-Fe alloys, ageing characts., mech. props. 3−37075
Cu-Ni-Zn microduplex nickel silver, cold rolling and ageing effects 3−34571
Cu-Pd(Pt) alloy, short range order 3−14734
Cu-Ti, obs. of precipitation morphology on annealing *(Russian)* 3−12356
Cu-Zn alloys, massive precipitates study by selected area electron channelling 3−21576
Cu$_{2\|x}$MnAl$_{1-x}$, Heusler alloy, annealing effects on mag. domain struct., Lorentz microscopy 3−1545
CuPt, ordered, deformation twinning and slip obs. 3−1670
CuPt$_3$ alloy, ordered struct. 3−14803
Cu$_3$Ti, charact. defect struct. obs. 3−11606
Er films, He implanted, dimensional expansion and surface microstructure 3−7994
ErD films, He implanted, dimensional expansion and surface microstructure 3−7994
α-Fe, and 3% ferrosilicon, S content study *(French)* 3−32222
Fe, dislocation motion in stretched single crystal foil, high voltage electron microscope obs. 3−11628
Fe, edge and screw motion, low temp. obs. using HVEM 3−11631
Fe, fine particles, oxid. mechanism, electron microscope obs. 3−38744
Fe, hydrogen-induced surface blisters and internal cracks 3−39349
Fe, under fatigue loading, plastic deform. of surface and internal layers 3−27056
Fe-Al, weak beam obs. of superlattice dislocations, fourfold dissociation in DO$_3$ type order 3−17839
Fe-Cu(1.7 wt.%) alloy Cu precipitation from α-Fe in pre-peak and peak hardness range of ageing 3−8797
Fe-Mn-C alloy, thermally cycled, long period stacking order structs. and phase transitions 3−15665
Fe-Mo-Ni alloys, continuously cooled carbon-free microstruct. 3−39317
Fe-Ni alloy, martensite-austenite transform., stuct. mechanism *(Russian)* 3−24823
Fe-Ni-C alloys, strain-induced martensite and thermally transformed martensite morphology 3−21575
Fe-Si (3 at wt.%) single crystals, tensile test of foil specimens at room and low temp., dislocation motions 3−17820
Fe-Si alloy, X-ray and electron microscope meas. of struct. *(German)* 3−8809
Fe-Ta alloys, Laves phase precip. phenomena 3−37049
Fe$_{75}$P$_{15}$C$_{10}$ alloy, amorphous, crystallite morphology during crystn. 3−21595

electron microscope examination of materials continued
GaAs, microheterogeneities, study using surface decoration method 3−18010
GaAs, molecular beam epitaxial layer, struct. 3−2677
GaAs, vapour phase homoepitaxial growth, transmission microscope obs. 3−15096
GaAs precipitation of Cu 3−36329
GaP, molecular beam epitaxial layer, struct. 3−2677
GaP-GaAs heterojunction, TEM obs. of misfit dislocations caused by lattice mismatch 3−36305
Ga$_3$Te$_4$ thin films, crystal microstructure during annealing *(Russian)* 3−33754
GdFeO$_3$, etch patterns on (001) surface 3−8031
Ge, epitaxial growth on Ge in field-emission microscope 3−33750
Ge, single crystal discs, KOH contamination of crystal surface 3−38705
Ge antireflection coating, characterization 3−3799
Ge epitaxial layer, tripyramid growth obs. *(Japanese)* 3−1931
Ge film, amorphous, order-disorder transformation obs. 3−1800
Ge film, amorphous, structure obs. 3−1949
Ge film, emission microscope obs., fine electron beam broadening by multiple scatt. 3−14666
Ge/Al thin film system, surface mass transfer mechanism, diffusion phenomena *(Russian)* 3−11836
Ge/Si interface, dislocation network via mismatch on Ge epitaxy, t.e.m. obs. 3−1941
Ge-Te glass quenched, oxygen effect on struct. props. 3−33458
In$_2$S$_3$, obs. of dislocations and stacking faults *(German)* 3−17834
InSe film, amorphous, crystallisation and decomposition obs. 3−7936
KCl crystals, vaporised under new equilib. conditions, electron microscopy studies of surface struct. 3−4905
KCl:Pb, Sn, microdistribution inhomogeneity obs. 3−1636
KI, defect clusters, planar dislocation loops produced by electron, γ-irradiation, obs. at 5 K with electron microscope 3−30126
LiF film epitaxially grown on NaCl, obs. of annealed structures 3−1929
Mg single crysts., dislocation struct. changes during basal slip *(Russian)* 3−24185
Mg ultramicrotomed thin slices, plastic deformation 3−17902
Mg-Ce, obs. of precipitation process on aging *(Japanese)* 3−12351
Mg-Nd, dilute alloy, obs. of precipitation and structure of phases 3−18580
Mg-Zr (0.5 at wt.%) alloy, metallography of ZrH$_2$ precipitation 3−18585
MgO, creep-deformed, dislocation structures, transmission electron microscopy 3−38593
MgO, erosion by fast moving particles, dislocations, obs. by thin film electron microscopy 3−27065
MgO, foil, stability of edge dislocation loops, effect of surface forces, transmission microscope obs. 3−18011
MgO-Al$_2$O$_3$-SiO$_2$-TiO$_2$ glass-ceramic, crystn. and struct. 3−31161
Mo, cast, intercrystalline fracture by grain boundary precip. *(Russian)* 3−24853
Mo, Mo-Ti-C, subgrain growth during annealing 3−31014
Mo, primary creep, high temp. analysis 3−34531
Mo, recrystallization, emission microscope obs. 3−18574
Mo alloy, carbide precip., emission microscope obs. 3−18574
Mo alloy, partly dissolved precipitates of second phase *(Russian)* 3−15669
Mo alloys, deformed, interstitial solid soln. decomp. during recrystn. *(Russian)* 3−37018
MoO$_3$.2H$_2$O, topotactic dehydration 3−9063
MoS$_2$, enhanced reactivity at struct. faults, microscopic studies 3−11788
MoS$_2$, molybdenite, dislocation images, high resolution SEM obs. 3−7763
NaCl film, epitaxial growth on muscovite, transmission microscope obs. 3−27193
NaCl quenched crystals, influence of impurity distrib., applic. of electron microscopic decoration method and microhardness meas. 3−1676
NaCl whiskers, surface structure obs. and interpretation of evaporation processes 3−1964
NaCl:Mn^{2+}, Fe, bulk crystals, phase transformations 3−4768
Nb deformed crystals, dislocation bands 3−1630
Nb$_{12}$O$_{29}$, oxidation, electron microscope assessment of the role of extended defects 3−5380
Nb$_2$O$_5$, defects, high resolution electron microscopy 3−24128
H-Nb$_2$O$_5$, training and defects study by electron microscopy 3−7774
Nb$_3$Sn, transmission electron microscope examination of defect struct. *(German)* 3−21179
Ni, high voltage microscope obs. of void nucleation with neutron irradiation 3−17803
Ni, neutron induced voids, low dose dependence at 400°C 3−8856
Ni, two-dimens. domain wall struct., Lorentz microscopy anal. 3−24590
Ni, void prod. by ion irrad., electron stereomicroscopy analysis 3−11608
Ni alloy, PE-16, low stacking-fault energy, deform. twinning 3−21594
Ni based alloys, glazes prod. by high-temp. wear and friction 3−34590
Ni film, electroless, nucleation and growth obs. 3−11837
Ni film on (001) Cu substrate, transmission electron microscope obs. 3−33764
Ni superalloys, constitution and microstructure 3−39312
Ni-Au film couple, surface diffusion obs. 3−1878
Ni-C, unusual microstructure in graphite 3−31016
Ni-C carmet film, structure rel. to electrical props. 3−5063
Ni-Cr base alloys, precip. hardened, struct. factors influence on creep strength behaviour 3−8930
Ni-Mo, rel. to corrosion on exposure to HBr 3−8041
Ni-V (18.1 at.%) alloy, scanning electron microscope study of deformation and fracture 3−15703
Ni$_3$Fe, antiphase slip boundaries and dislocation config. *(Russian)* 3−34522
Ni$_3$Mn, annealed under load, dislocation struct. *(Russian)* 3−15729
p-n junction, obs. by out-of-focus technique 3−38886
Pb impregnated porous glass, delineation of Pb morphology 3−8315

electron microscope examination of materials continued
Pb-Au solid soln., kinetics and morphology of $AuPb_3$ precip. 3−24843
Pb-Sn lamellar eutectic, fine struct. studies in Pb-rich phase *(French)* 3−24818
Pb-Sn superplastic alloys, deformation studies 3−1549
PbO, vapour grown film, obs. of fracture edge and surface structure 3−15628
PbS, thin films, photoelectromotive force and thin layer structure depend. on substrate temperature and evaporation speed *(Russian)* 3−27323
$PbSe-Ge_{1.5}As_{0.5}Se_3$, pseudobinary system, immiscibility, liquidus temp. 3−20853
Pd-Ag(Ce) alloys, dislocation tangles after hydrogen cycling through α-β transform. 3−2737
ReO_2, monoclinic, crystal parameters precisions and Debye-Scherrer indexing *(French)* 3−14816
Se, vacuum evaporated layer, amorphous and crystalline phase obs. 3 20970
Si, amorphous layers formation by Si^+ implantation 3−17888
Si, defects, causing transistor leakage, electrochem. decorated 3−38581
Si, electrolytically etched surfaces, transmission microscopy 3−18025
Si, epitaxial, Shockley loops 3−15094
Si, high energy C^+ bombarded, damage profiles 3−17887
Si, obs. of microplastic deform. mechanisms 3−7747
Si, p-n junction, SEM obs. of currents 3−15249
Si, vapour phase homoepitaxial growth, transmission microscope obs. 3−15096
Si antireflection coating, characterization 3−3799
Si epitaxial surface, S.E.M. and T.E.M. obs. of stacking fault form. in thermal oxidation 3−24321
Si film, amorphous, structure obs. 3−1949
Si heteroepitaxial layers, crystalline perfection from ion channelling and electron microscopy, comparative evaluation 3−18040
Si layers prepared by ion beam thinning, t.e.m. examination of cross sections 3−1552
Si on sapphire, epitaxial layer sample prep. and defect obs. 3−1939
Si p-n junction, rel. to electrical effects near surface defects 3−38884
Si:B, ion implantation defect centre studies 3−33587
Si:Cu precip. colony dissolution during annealing, dislocation processes 3−20757
Si:Li neutron irradiated solar cells, defect cluster obs. by electron microscopy 3−33569
Si:Ni, precipitation of $NiSi_2$ phase, morphology from transmission electron microscope obs. 3−11640
Si-Ge:P alloy, exam. after annealing at 500°C *(Russian)* 3−12346
SiC, structure obs. using two step decoration *(Russian)* 3−7997
SiC whiskers, h.v. electron microscopy 3−1537
Si_3N_4, hot pressed microstructure 3−12421
SiO_2, transmission, structure defects, pyrolytic film on semiconductor substrate *(Russian)* 3−27197
SiO_2 glass, superstruct., internal struct., morphology, in early crystn. 3−14693
Sn, chemically polished, grain contrast *(German)* 3−8000
Sn grey, β→α transform. induced lattice defects 3−30974
Ta, field emission, electron energy distrib. when coated with SiO 3−15600
Ta, work function when covered with SiO, field emission microscope obs. 3−15239
Ta film, sputtered, structure obs. 3−1954
α-Ti, oxygen conc. influence on internal stress and dislocation arrangements 3−34534
Ti alloy VTZ-1, foil prep., elec. spark cutting technique 3−18576
Ti alloys, corrosion fatigue in aqueous solns., fractographic studies 3−27656
Ti-Al-Mo-V alloy, cleavage cracking in gaseous hydrogen 3−31044
Ti-Al-V alloy, stress corrosion crack propag., fractographic obs. 3−31043
Ti-Mo-Al alloy, microstruct. 3−34509
Ti-Nb (40 at.%) alloy, deformed and annealed, struct. obs., supercond. *(Russian)* 3−30989
Ti-Ni alloys, B_2 phase region, stacking modulated structs. 3−14878
Ti-Ni alloys, near-equiatomic, martensitic phase studies 3−14879
Ti-Ni alloys, near-equiatomic, diffusion controlled phase transform. structures 3−39311
$Ti_{n-2}Cr_2O_{2n-1}$, shear struct. determ. 3−24127
Ti_3Sn, slip systems and deform. substructure obs. 3−21698
α-U thin foils, penetration of h.v. electrons rel. to electron microscopy 3−1536
$UC_{1.86}$, twin struct., transmission electron microscope obs. 3−11639
UO_2, ordered reduction and crystallographic shear, microscope obs. 3−7776
UO_2, polycrystalline, deformed, grain boundaries 3−11050
UO_2, Si, Al_2O_3, Fe, U, impurities, effect on fracture stress 3−39384
U_3Si, twinning due to stresses induced at allotropic transformation at 765°C 3−7773
V, α-irrad., He gas bubble nucleation and distrib. 3−33572
V, grain boundary motion at 1400°C, emission microscope obs. 3−18574
V-C supersaturated solid soln., carbon precip. obs. 3−37036
V-C system, carbide precip. behaviour 3−34529
$VC_{0.76}$ monocrystals, TEM obs. of coherent precipitate 3−31119
V_6C_5, obs. of ordered arrangement of C vacancies 3−14782
V_nO_{2n-1}, shear struct. determ. 3−24127
W, chemical vapour deposited, mech. behaviour, 800-1600°C 3−37085
W, chemical vapour deposition studies 3−1960
W, desorption of SiO_2, autoelectronic microscope obs. *(Russian)* 3−8023
W, fast neutron irrad., superlattice of voids 3−17878
W, neutron irrad., raft form. mechanism 3−33563
W, r.f. sputtered, elec. resist., rel. to defect struct. 3−27241
W, SiO_2 epitaxial layer, obs. of growth and work function *(Russian)* 3−8251
W, Ta and SiO_2 covering layers, work function determ. *(Russian)* 3−8250
W lamp filaments, void formation 3−27636
W wire, doped temp. gradient effect on bubble growth 3−37087

electron microscope examination of materials continued
W-Re (22 wt.%) alloy, chem. vapour deposited, grain growth 3−37023
WC, dislocation network obs. 3−39386
WC/Co, sintered, carbide phase recovery *(Japanese)* 3−31121
WC/Co alloy, aging process, calorimetric studies *(Japanese)* 3−31066
WC-Co alloy, struct. change on heating, emission microscope obs. 3−18574
WC-Co alloys, meas. using new electron microscope replica locating technique 3−18674
$W_4Nb_{26}O_{77}$, upper limits of ionicity, n-beam lattice images 3−24005
$WO_3-Nb_2O_5$, intermediate phases, high resolution electron microscopy 3−24128
Xe epitactic growth on graphite, liquid He stage in transmission electron microscope 3−1940
YAG:Nd, obs. of inclusions and dislocations using transmission electron microscopy 3−36319
YAG:Nd, testing of the homogeneity of single crystals by means of cathodoluminescence *(German)* 3−7789
Zircaloy-4, transmission electron microscopy of ion-thinned oxides formed during corrosion 3−11825
Zn, electrodeposition from alkaline solns., morphology 3−20962
Zn dendrites, electrolytic, crystallographic and morphological characts. 3−20977
Zn ultramicrotomed thin slices, plastic deformation 3−17902
$Zn-TiZn_{15}$ eutectic, lamellar and rod morphologies 3−37004
ZnS crystal structure of thin layers 3−33759
α-Zr, hydride dissolution and precip. 3−8821
Zr, neutron damage to microstructure, electron microscope obs. 3−11657
Zr H, fuel rods, swelling due to irradiation, electron microscope examination 3−26522
Zr ion-thinned oxides formed during corrosion of Zircaloy-4, transmission electron microscopy 3−11825
Zr-O alloys, strain aging parameters, dislocation cell struct., irrad. effects 3−27675
ZrO_2, martensitic transform., metallographic obs. 3−24267
ZrO_2 fibres, h.v. electron microscopy 3−1537
ZrO_2:Y_2O_3, sintering, effect of CO_2, analysis 3−15761

electron microscopes
see also electron microscopy
astigmatism, prep. of perforated C films for checking 3−3879
Auger spectroscopy, cylindrical mirror analyser, design 3−32221
central wire beam-stopping aperture manufacture, capacitive discharge microwelder 3−25947
channel plates (fibre-optic electron multipliers) as image intensifiers in transmission electron microscope 3−356
composite boride cathodes in electron optical instruments 3−805
distortion free low-magnification stage 3−3878
dual camera attachment for scanning 3−9975
electron energy loss analyzer, v.h.v., adaptation *(French)* 3−35506
electron microscope environmental specimen chamber for examining biological ultrastructure in wet state 3−358
Elmiskop 101, low angle electron diffraction 3−13460
emission microscope with three stage optical system for selected area LEED 3−13469
emission microscopes, image contrast, initial electron velocity dependence *(Russian)* 3−10116
energy filter for 100 kV electrons, design 3−362
environmental specimen chamber for examining biological ultrastructure in wet state 3−358
exoelectron microscopes, surface characterization 3−19326
field emission tips, Mo, W, microcratering and estruction by microparticles 3−8707
flying-spot, with focus-assist device 3−22503
high voltage microscopes, design and applications 3−32228
high-powered, characteristics *(German)* 3−22511
Hitachi 650 kV, high angle tilting stage 3−32225
h.v. type, description *(Italian)* 3−6105
IC pattern generation, soft X-ray replication 3−13481
image resolution and contrast for elastic scatt. and incoherent illumination 3−16924
image resolution and contrast for elastic scatt. and incoherent illumination 3−16925
in-focus phase contrast arrangement 3−6104
limiting resolution, holographic reconstruction methods *(Russian)* 3−10118
low temperature electron microscope goniometer stage, design 3−22513
magnetic, adjustment of polepiece system with initially non-coincident polepiece-bore axes *(German)* 3−6110
microprobe, design description 3−28718
and microprobe analyser combination 3−19328
microtensometer for use in scanning electron microscopes 3−13464
mirror electron and u.v. emission microscopes using Auger spectroscopy 3−13470
objective lenses, astigmatism measurement from spatial frequency spectrum of image *(Russian)* 3−6115
one-dimensional sinusoidal magnetic microfield, image contrast *(Russian)* 3−10119
Philips 300, equipped with goniometer storage and cooling holder for photographic emulsion obs. 3−28725
Philips EM 300, coupling of energy dispersing X-ray detector 3−10137
pointed filaments as bright electron sources for scanning electron microscope 3−354
pressure cell design for studying condensed gases 3−359
qualitative straining stage with double tilting facilities for h.v. electron microscope 3−357
radiation protection 3−35295
resolving power, of microscope with single-pole condenser-objective *(Russian)* 3−3876
scanning, characterization and correction of distortions in micrographs 3−28719
scanning, design and use, book 3−35509
scanning, design and use, book contribution 3−10123
scanning, engineering and design considerations 3−370
scanning, fault recognition, book contribution 3−10126

electron microscopes continued
scanning, history, principle and advantages, book contribution 3—10122
scanning, in materials research 3—10120
scanning, low aberration probe forming lens, design 3—360
scanning, management, book contribution 3—10128
scanning, obs. of Fresnel fringes in transmission mode 3—343
scanning, photogeometry for surface microgeometry 3—28720
scanning, principles, construction and appl., book 3—12217
scanning, principles, description, magnification, resolution, applications *(German)* 3—10108
scanning, semiconductor material examination 3—13433
scanning, semiconductor type specimen detector, surface voltage meas. 3—390
scanning, storage display system 3—372
screen drive mechanism, patent 3—19341
SEM, conceptual development rel. to electron beam microfabrication 3—35513
SEM, image meas. and analysis, incl. image storage system requirements 3—37721
SEM collection of secondary electrons using small aperture probes 3—35512
Siemens, magnification reproducibility, digital voltmeter across intermediate lens 3—19336
specimen positioning assembly, patent 3—19340
techniques and analysis, conference (Cambridge, England, June-July 1971) 3—1535
transmission, field-emission illumination system, using new optical config. 3—16539
transmission 100 kV, three lens imaging system, design 3—364
transmission and scanning, using image intensifiers 3—22501
transmission scanning microscope combined with convergent beam diffraction camera 3—25944

electron microscopy
see also electron microscope examination of materials; electron microscopes; metallography; specimen preparation
alkali halides, irradiation defects 3—1546
amplitude and phase evaluation from micrograph intensity distrib. 3—11534
analysis of scanning micrographs of soil structure using convolution square camera 3—379
analytical, appls. pathology and pollution 3—367
apparent image enhancement, through coherent defocusing 3—28717
application to metal studies, new methods 3—18577
automad electron-probe system for quantitative mineral anal. 3—369
automated cell structure determination, from micrographs 3—9643
background energy loss *(French)* 3—387
beam specimen interaction in h.v. electron microscopy 3—351
Bethe's second-order approximation, discussion and generalization 3—14667
biological applications, review 3—423
biological applications of h.v. electron microscopy 3—353
biological materials, image profiles 3—10143
block structure kinetics, by microbeam method, error estimation 3—24007
channeltron image intensifier, operation results 3—22506
circumboundary free zone width determination in metals and alloys 3—18575
coating thickness evaluation for electron microscopy 3—17727
contrast transfer theory, isoplanatism 3—376
crystallographic analysis, spatial measurements 3—22504
cylindrical emission, book contrib. 3—10121
dark field, resolved cryst. lattice image 3—23986
darkfield, contract dependence in element 3—349
darkfield, glass microelectrode examination 3—13458
defects, radiation induced, direct observation by transmission electron microscopy 3—33434
double diffr. microscopy of grain boundaries *(French)* 3—7605
early history of Electron Microscopy and Analysis Group of the Institute of Physics 3—350
edge error correction in lineal analysis, reply to comment 3—28729
edge error correction in lineal analysis, using TV for solid structure examination 3—28728
electron channelling, obs. using electron microscopic imaging method 3—24169
electron irradiation induced void studies in metal in h.v. electron microscope 3—1640
electronographic phase analysis method 3—16536
EM 300 t.e.m., 27 million magnification obtained 3—37718
emission microscope, construction 3—13468
emission microscopy, appl. to high temp. studies of metals and alloys 3—18574
energy anal., using plural electron scattering 3—1644
epitaxial layer sample prep., applic. to Si on sapphire 3—1939
fatigue striations exam., SEM technique 3—37027
fibrous polymers and derivatives, progress 3—386
field emission, thin film and surface studies, review 3—27159
field emission illum. systems, performance estimates, design criteria, aberrations, defocus, stability 3—803
field-emission emitters and probes, electron microscope monitoring 3—10112
film deposition, in situ, for growth studies 3—17722
foil prparation from wires 3—18579
foils, thin, non-magnetic, electropolishing for electron microscopy *(German, English)* 3—24350
Fourier analysis of micrographs 3—375
fractographs, interpretation rel. to surface contamination 3—7995
gas high temp. electron diffr. studies, photographic procedure 3—13457
gas-discharge chamber for neutralization of charges on objects 3—16538
gas-solid systems study during reactions, controlled atmosphere 3—32226
graphic three dimensional representation, from serial sections 3—25945
grid-holder, for negative contrast serial investigations *(German)* 3—28724
grids, handling and straining techniques 3—22509
handbook for beginners 3—6117

electron microscopy continued
height meas. in t.e.m., artefact introduced during shadow casting technique 3—32220
high energy electron diffraction, transition from quantum to classical theory 3—1646
high resolution, image improvement using holographic image-deblurring deconvolution 3—25948
high resolution scanning, direct obs. of defect contrast 3—23988
Hitachi, modification of high angle goniometer stage, to reduce specimen contamination 3—13462
holography without fringes 3—6108
homogeneity testing, nondestructive, of single crystals using cathodoluminescence *(German)* 3—7789
h.v., absorpt. coeffs. for high energy electrons 3—23992
h.v., diffr. contrast characts. 3—23989
h.v., effects of beam on biological and polymeric specimens 3—389
h.v., electron diffr. phenomena 3—20682
h.v., for stress corrosion crack obs. 3—30981
h.v., multi-beam imaging technique 3—23991
h.v., of field ion specimens prior to ion microscopic examination for defect. location 3—385
h.v. electron microscopy in 1 to 10 MV range, theoretical assessments 3—352
h.v. scanning and fixed-beam, resolution and contrast 3—23990
image and techniques appl. 3—371
image contrast from metallic specimens 3—366
image formation, inelastic electron scattering 3—1643
image improvement, holographic image deblurring 3—3880
image improvement by holographic image deblurring deconvolution, contrast inversion removal 3—13465
image resolution and contrast, effect of lens aberrations for coherent illumination 3—10581
images recorded on thin polymer films, evaluation of object mass thickness 3—11535
introductory paper, for metallography 3—31017
island condensates, on NaCl chips, cross section determ. 3—18035
Japan, past and present review 3—14665
JEM 6A, heating stage, inclusion of thermocouple 3—13463
Kikuchi diagrams, energy filter *(French)* 3—388
Kossel line techniques, tensile testing 3—1548
Kossel patterns, lattice parameter computation 3—1547
light diffractometer allowing online diffractogram generation 3—32223
light pipe for s.e.m. 3—6113
logarithmic picoammeter for exposure and dose meas. in electron microscopy of polymer crystals 3—346
Lorentz, obs. of mag. props. of Heusler alloys 3—1545
Lorentz microscopy, improved in-focus method 3—13471
low current density microscopy with time integration, internal photography versus TV 3—355
magnetofluids, sample prep. by polymerisation 3—11533
maximum observable thickness, voltage depend. up to 3 MV 3—32219
metallographic specimen preparation, for study of surface layers 3—18578
metals, lattice imaging at 10^6 magnification 3—7607
microcrystal, mean inner potential, electron interference microscopy 3—24060
micrographs, high resolution, analysis by optical diffractometer 3—5876
micrographs analysis using high power laser diffractometer 3—378
micrographs and selected area channelling patterns, simultaneous display using s.e.m. 3—1558
microstructural obs. using EMMA-3 3—1543
microstructure, nondestructive investigation, use of surface prints 3—18746
molecular biology, optical techniques applied to electron micrograph analysis 3—9639
molecular image resolution determination 3—17390
n-beam lattice images, calc. of upper limits of ionicity in $W_4Nb_{26}O_{77}$ 3—24005
noise of electron photographic image in noncoherent illumination *(Russian)* 3—237
non-conducting materials, metallic layer deposition using ion gun for scanning electron microscopy *(German)* 3—6109
nucleation, pentagonal structures, formation and growth, very small paracrystals *(French)* 3—38756
nucleation kinetics, electron micrograph evaluation using Quantimet 720 image analysing computer 3—26979
open type field emission microscopes, in exptal. chamber *(Russian)* 3—10111
optical shadowing, surface topography studies 3—19332
optical transforms applic. 3—6436
optics, microanalysis applications, review 3—13474
perfusion fixation equipment with automatic pressure control 3—3909
phase transitions at high temp. 3—14669
photoemission, technique and application 3—19333
polycrystalline specimens, crystallite volume and shape, microbeam method 3—24006
polymer growth contamination, reduction using fluorocarbon oxide pump fluid 3—25946
polymer particles in electron microscope, decrease in size 3—9006
power surface, method of obtaining replicas 3—18748
primary impressions, use of adhesive films 3—18747
quantimet 720 with fully automated pattern recognition system for metallography 3—28727
replica locating technique, appl. for deform. phenomena meas. of high-strength WC-Co alloys 3—18674
replica mounting device, on specimen supporting grid 3—22507
replicas giving diffraction contrast of image, production 3—17721
scanning, appl. to biological materials 3—10185
scanning, appl. to fibre and polymer studies 3—12459
scanning, appl. to metallurgy 3—12360
scanning, book 3—12217
scanning, channelling patterns and crystalline contrast 3—1559
scanning, diffraction from tilted specimens 3—1556
scanning, dimensional measurements, book contribution 3—10127
scanning, direct obs. of backscatt. electron distribs. on surfaces 3—34444

electron microscopy continued
scanning, edge contrast rel. to object material and detector position 3−13467
scanning, future developments, book contribution 3−10129
scanning, high resolution images, spectroscopic cathodolum. images 3−28722
scanning, history and brief description, book contribution 3−10122
scanning, nature of electron interactions in solids, book contribution 3−11536
scanning, object shape determ. from one view in secondary electrons mode of operation 3−804
scanning, pseudo-Kikuchi patterns, meas. of ratio of abnormal to normal absorpt. coeff. for electrons in solids 3−23987
scanning, resolution and contrast, book contribution 3−10123
scanning, selected area diffraction approaching 1 micron 3−1557
scanning, simultaneous display of micrographs and selected area channelling patterns 3−1558
scanning, solid target, electron backscatt., penetration and X-ray production, Monte Carlo study 3−14891
scanning, specimen preparation, book contribution 3−10124
scanning, surface characterization 3−36468
scanning, use procedures, book contribution 3−10125
scanning and conventional, modes of image formation 3−19337
scanning electron microscope selected-area channelling pattern technique 3−2713
scanning electron microscope use for high resolution microautoradiographs, study of S in α-Fe and 3% ferrosilicon *(French)* 3−32222
scanning transmission of thick objects, resolution *(German)* 3−32224
s.e.m., Allium cepa nuclei 3−31844
SEM, botanical specimen prep. technique 3−35530
s.e.m., combined with Auger electron spectroscopy 3−38700
SEM, forensic science application 3−37720
s.e.m., of biological specimens, critical point drying *(German)* 3−28763
s.e.m., techniques for examination of L-phase streptococci 3−19360
SEM, using back-scattered electrons, conditions necessary to observe crystn. defects 3−35511
s.e.m. study of radial fracture surfaces of egg shells 3−19359
semiconductor cleaved surface roughness obs. 3−36470
slide rule, for calc. of sizes, magnifications 3−19338
specimen electrolytic thinning apparatus 3−17724
specimen heating method 3−16537
specimen holder for tensile deform. expts. at low temps. 3−19329
specimen prep. methods 3−33436
specimen preparation, dispersed materials 3−18734
specimen preparation, epoxy resins, cell constituents, microprobe analysis *(German)* 3−422
specimen preparation, freeze drying, critical point drying 3−421
specimen preparation, Ti VTZ-1 alloy foil, elec. spark cutting technique 3−18576
specimen thinning equipment with twin anode ion source 3−13459
specimen-heating stage calibration 3−10114
staining, dry specific gravity and section thickness 3−22510
steel, 316 stainless, proton irradiated, cross-section preparation technique for transmission electron microscopy 3−8026
stereo adaptor for use with s.e.m. 3−3877
Stereoscan stage modification, for large specimens 3−22505
surface scanning, low-loss image formation 3−35510
surfaces, vertical section geometry, embedded Al layer 3−22508
suspensions and emulsions study, cold fracture technique *(German)* 3−16535
techniques and analysis, conference (Cambridge, England, June-July 1971) 3−1535
TEM, crystal defect study *(Rumanian)* 3−24013
tensile test pieces, microwelding techniques 3−20684
theory of small angle inelastic scattering of electrons 3−1642
thermally stimulated exoelectron emission spectroscopy applications 3−13466
thin film thickness meas. *(Czech)* 3−32218
thin foil prep. technique for transmission studies of glass-ceramics 3−34645
time lapse photography, 16 mm cine film 3−374
transmission, complementary dark field dislocation images 3−36252
transmission, disc shaped specimen preparation 3−37719
transmission, electropolishing method for Nb 3−36249
transmission, ion thinning of fibres, sputtering of rough cylinders 3−36248
transmission, method for soln. of phase problem 3−30058
transmission, prep. and ion beam machining of ceramic specimens 3−24008
transmission, specimen temp. increases 3−24011
transmission, thickness and mass thickness meas. in biological specimens 3−37740
transmission scanning microscopy, review 3−26957
two-dimensional domain wall structures, Lorentz microscopy anal. 3−24590
u.h.v.-t.e.m. corrosion studies, in situ sputter cleaning of thin film metal substrates 3−38737
variable geometry cylindrical detector, theoretical analysis 3−373
weak beam method, of dislocation structure obs. 3−1541
He liquid stage for s.e.m. 3−348
Ni alloys, thin film foil specimens for electron microscopy, electropolishing method 3−17726
SiO_2-Al_2O_3 thin film, splat cooling prepn. for transmission electron microscopy 3−18537
Th atoms, monomolecular layer operation and micrographs 3−24333
α-U thin foils, penetration of h.v. electrons rel. to electron microscopy 3−1536

electron mobility
see also carrier mobility; conduction electron mobility
alloy, magnetic, dilute, Hall effect, s-d scatt., many body theory 3−8157
amorphous state, by energy depend. diffusivity 3−2053
anthracene, perdeuterated, drift mobilities, 260 to 400K 3−30467
band gap width determ. from Hall constant meas. 3−18060
cuprous halides, luminesc. during laser excitation, H band emission, electron and hole effective masses 3−27557
disordered system, Anderson model, mobility edges 3−18057

electron mobility continued
ferromagnetic semicond., anomalous Nernst-Ettingshausen theory, electron scatt. by spin waves 3−36629
fluid, simple, mobility near critical point 3−21044
n-Ge, impurity ionisation, hot electron mobility 3−8192
Hall mobility calc. 3−8207
III-V compounds, donor and acceptor conc. determ. from hot electron mobility 3−38812
magnetostrictive ferrite, u.s wave propagation consts., lattice deformation, relaxed electron diffusion 3−36367
methane, liq., mobility of excess electrons 3−15815
methane, liquid, excess electron and positive charge carrier drift velocities 3−36609
methane, liquid, quasifree electron mobility calc. 3−11892
nondegenerate semiconductor surface inversion layer, electron scattering by surface oxide charges theory 3−11954
resonance trapping and drift velocity in inert gases 3−23667
semiconductor, nonpolar, rel. to electron diffr. 3−15190
semiconductor, surface mobility meas. using surface waves on adjacent piezoelec. 3−38828
semiconductor, two-valley, contact thermalisation effects, importance in high freq. devices 3−30508
semiconductor, Wurzite struct., piezoelectric scattering anisotropy *(Russian)* 3−2078
transport equation in the presence of random impurities 3−11875
trinitrofluorenone-poly-n-vinylcarbazole charge-transfer complex, amorphous film 3−21068
Al-Al_3Ni, two phase alloy, electron scatt. on precipitate boundaries, low temp. resist. meas. 3−36580
BeTel film, effective mass, substrate temp. depend. *(Russian)* 3−21067
CdO single crystal, degenerate semicond., Hall effect obs. 3−2087
CdSe mechanism, Hall effect measurements 3−30466
CdTe, electron diffusion, applied field depend., Monte Carlo study 3−18149
CdTe, Monte Carlo calcs. on high field electron transport 3−8191
Cu film, scattering centres formed by CO adsorp. 3−8144
n-GaAs, Gunn oscillations, low field mobility temp. variation effects 3−18146
n-GaAs, scattering mechanisms *(Russian)* 3−2076
GaAs, V.P.E. growth, effect of As vapour pressure 3−27191
GaAs ellipsoidal $\langle 100 \rangle$ valleys, soln. of Boltzmann equation, Hall and drift mobility 3−33883
GaAs epitaxial film, anomalous magnitude and temp. depend. *(Russian)* 3−2091
GaAs inhomogeneous crystals, temp. depend., 80-300K *(Russian)* 3−18133
GaN, free-electron and intrinsic lattice dispersion 3−18455
GaP ellipsoidal $\langle 100 \rangle$ valleys, soln. of Boltzmann equation, Hall and drift mobility 3−33883
n-Ge, high purity, γ-irrad., carrier-conc.-depend. mobility 3−36627
Ge intervalley, hot electrons, impurity and phonon mechanisms, transition times 3−33919
Ge p-n junctions, tunnelling electrons effective mass, electron-hole pair prod. energy 3−18213
He gas, dense, as model for structurally disordered systems 3−33858
^{4}He, dense gas, electron mobility and localisation 3−38345
InAs:Se(Te), effective mass, determ. from temp. depend. of transport props. *(Russian)* 3−27250
n- InP 3−15202
InP, vapour phase epitaxial material 3−2680
InP:Ge,Sn,Te, liquid phase epitaxial layer, Hall effect obs. 3−1637
InSb, electron velocity field characts., negative differential mobility, meas. 3−33914
n-InSb, hot electron scatt. at 4.2 K 3−38850
InSb film, hot wire zone refined, Hall mobility 3−2669
InSb film, mobility and field effect 3−27260
InSb Monte Carlo calc. of hot electron mobility 3−36612
Ni film, scattering centres formed by CO and N_2 adsorp. 3−8144
O_2 electron transport coeffs., thermal and near-thermal, time-of-flight swarm technique 3−1482
n-PbTe, magnetophonon resonance, electron intravalley scatt. with phonon absorpt. 3−33931
Sb, temp. depend., calc. from galvanomagnetic meas. 3−15183
n-Si, anisotropy of electron scatt. by charged impurities, absorpt. study *(Russian)* 3−2077
n-Si, impurity core effect 3−11894
Si amorphous films, electronic transport and state distribution 3−8172
Si on sapphire film, meas. for fibres grown by dual rate technique 3−2656
Si oxidised surface, m.o.s. electron surface mobility in inversion layers at room temp. 3−8268
Si surface inversion layer, hot electron nonlinear transport and negative diff. mobility, m.o.s.f.e.t. obs. 3−11952
n-(221)Si/(1122)Al_2O_3 film, anisotropy 3−11961
Ti film, scattering, rel. to dislocation-enhanced elec. resist. 3−21049

electron multipliers
afterpulses, effect on atom probe field ion microscope identification of metal compound ions 3−19339
channel, calibration using standard omnidirectional electron beams 3−25943
channel, open structure, use in sounding rocket expts. 3−31811
channel, used as detectors in organic mass spectrometry 3−13450
channel plates (fibre-optic electron multipliers) as image intensifiers in transmission electron microscope 3−356
channel type, as detector of thermally stimulated electrons 3−32154
discrimination, meas. of multiplier yields for mass-analysed ions 3−6087
discrimination for atomic ions, comparison of yields for 61 atoms 3−26555
fatigue damage display, exoelectron emission obs. 3−12468
high performance 4500 V bias supply, for satellite use 3−28683
ion beam profiles meas. method using electron multiplier detector 3−25940
microchannel, applic. in X-ray cinematography of laser produced plasma *(French)* 3−9974
secondary electrons, MI-1305 mass spectrometer sensitivity 3−333

electron nuclear double resonance *see ENDOR*

electron optics
see also beta-ray spectrometers; ion optics; magnetic lenses; particle optics
apparent image enhancement, through coherent defocusing 3−28717
Astron resistor config. for electron focusing 3−16923
axially symmetric systems, e.s. field computation 3−802
azimuthal relativistic beam, in magnetic field, instabilities with thermal velocity spread 3−13775
Babinet's principle applications *(German)* 3−29160
channel plates (fibre-optic electron multipliers) as image intensifiers in transmission electron microscope 3−356
contrast transfer theory, isoplanatism 3−376
dispersion theory construction on basis of the delay-time concept *(Russian)* 3−684
electric potential and field on the principal optical axis of a plane symmetric two-dimensional lens 3−29162
electron beams, relativistic, intense, cone focus trajectories, adiabatic envelope conservation 3−32616
electron beams relativistic, intense, cone focusing 3−32615
electron guns, electron optical data, brightness, characts., 50-125 kV, 0.1-1 mA *(German)* 3−347
electron microscopy scanning, object shape determ. from one view in secondary electrons mode of operation 3−804
electronics and vacuum physics, conference, Kralovopolska, Czechoslovakia, Oct. (1972) 3−15576
electrostatic lens for monochromatic electron beams production 3−35723
emission microscopes, image contrast, initial electron velocity dependence *(Russian)* 3−10116
e.s. mirror spectrometer, with coaxial electrodes, for multidetector operation 3−32204
field emission illum. systems, performance estimates, design criteria, aberrations, defocus, stability 3−803
field-emission illumination system, using new optical config. 3−16539
focal props. of cylindrically symmetric microwave cavities 3−363
focus and astigmatism detection by scanning methods 3−365
focusing and production of intense electron beam 3−35724
focusing of high output beams, in mag. fields 3−13780
focusing systems, electrostatic, periodic 3−13781
Fourier analysis of micrographs 3−375
geometrical general central/trajectories, space charge optics 3−13779
half Maxwell distrib., change in accelerating electric field *(German)* 3−6532
h.v. electron microscopy in 1 to 10 MV range, theoretical assessments of image contrast 3−352
image meas. and analysis, incl. image storage system requirements, for SEM and probes 3−37721
image resolution and contrast, effect of lens aberrations for coherent illumination 3−10581
imaging features of e.m. field, first principal problem 3−13778
interference in electrostatic biprism, Fresnel integrals 3−22977
ion focusing, short duration intense electron beams *(Russian)* 3−6533
ion-electron image converter for ion microscopes *(Russian)* 3−6116
large angle, low energy loss electron scattering with retarding field analyzers 3−806
lenses, optical properties and practical realization, review 3−35722
microscope, image resolution and contrast for elastic scatt. and incoherent illumination 3−16924
microscope, image resolution and contrast for elastic scatt. and incoherent illumination 3−16925
microscopes, shadowing, surface topography studies 3−19332
mirror microscope, one-dimensional sinusoidal magnetic microfield, image contrast *(Russian)* 3−10119
multi-stage bunching, kinematic theory 3−13772
multicavity magnetron, trajectories allowing for space charge 3−13769
numerical computation of electrostatic fields, trajectories, abberations, space charge and lateral velocities at emission 3−807
pointed filaments as bright electron sources for scanning electron microscope 3−354
probes and microscopes, microanalysis applications 3−13474
quadrupole system, paraxial electron optical imaging, wave mechanical basis *(German)* 3−35720
rotating and deflecting a line focus, props. 3−37991
scanning electron microscope edge contrast rel. to object material and detector position 3−13467
scanning microscope, obs. of Fresnel fringes in transmission mode 3−343
stability regions in axially symmetric periodic focusing mag. field 3−26255
superconducting lens characts., saturation of iron influence *(French)* 3−22975
symmetric prism mass spectrometer, theoretical studies of electron-optics *(Russian)* 3−6095
three-dimensional problems, digital computer techniques 3−19478
transfer function rel. to astigmatism and field curvature 3−32614
transfer function rel. to coma 3−32613
two-dimensional image production, using KH_2PO_4 crystal electron beam modulator *(Russian)* 3−16529
unstable problems solution, potential distribution *(Russian)* 3−32612
BaB_6 mixtures for cathodes in electron optical instruments 3−805
LaB_6 cathodes in electron optical instruments 3−805
electron pair annihilation *see positron annihilation*
electron pair production
atomic-electron screening effects in pair production at photon energies from threshold to 5 MeV 3−4379
bremsstrahlung 3−6613
coherent e^-e^+ pair production on corundum crystal *(Russian)* 3−35806
electromagnetic processes at 1 GeV/c and production-rate limits 3−23070
Furry Sommerfield Maue wave functions in pair production and bremsstrahlung 3−20051
by muons, critical evaluation of theories 3−10698
polarized photons on nonpolarized nuclei with arbitrary spin, cross section *(Russian)* 3−4175
electron pair production continued
probability, in variable and homogeneous elec. field, oscillator problem 3−23074
pulsar model based on Maxwell's and quantum-hydrodynamical equations 3−22090
total pair prod. cross sections, 1.12 to 2.754 MeV 3−10697
in zeolite single crystals, possible transport *(Russian)* 3−14893
$e^-e^\pm$ high energy collisions, production of electron and muon pairs, total and differential cross section 3−13998
$e^+\mu^-$ direct production by neutrinos on nucleon, C, F, Br *(Russian)* 3−38028
$\gamma\to e^+e^-$, experiment for students 3−9794
$\gamma C\to Ce^+e^-$, meas. of photoproduction phase of φ meson at 7 MeV 3−17047
μ cosmic ray e.m. interactions in Fe, 6-200 GeV, momentum dependence of interaction probabilities 3−5550
$\pi N\to Ne^+e^-$ processes at high energies *(Russian)* 3−17125
$\pi^-p\to e^+e^-n$, meas. of differential cross-sections close to $\Delta(1236)$ reson., pion energy = 276 MeV *(Russian)* 3−19728
ρN forward scatt. amplitude and $\rho\omega$ prod. phase from e^-e^+ photoproduction at 4 GeV 3−17009
electron pairs
see also electron pair production; positron annihilation; positronium
relativistic system interaction with external time depend. elec. field *(Russian)* 3−19694
vacuum polarization in exotic atoms 3−1133
vector meson photoproduction in ρ-ω interference region, obs. by means of e^-e^+ pairs 3−13966
$e^-e^-\to\mu^-\mu^-$, parity violation by neutral lepton currents 3−4155
Fe_3O_4 magnetite, band theory of pair-localized electrons 3−2012
electron paramagnetic resonance *see paramagnetic resonance*
electron-phonon interactions
see also carrier mobility
alkali halides, polaron effective masses, electron-phonon coupling constants 3−36569
alkali metal, phonon drag thermopower calc. 3−30461
alkali metals, Landau Fermi liquid parameters anisotropy, electron-phonon interactions 3−27203
alkali metals, phonon drag effect on low-temperature resistivity 3−2045
amorphous semiconductors, hopping Hall effect, single phonon contribution 3−27274
amorphous solids, single-phonon contribution to hopping conductivity 3−2082
amplifying phonon system, Boltzman eqn. for phonon distrib. 3−33628
anthracene, perdeuterated, rel. to drift mobilities, 260-400K 3−30467
antiresonance in exciton spectrum, phonon contrib. 3−8128
band model, phonons, lattice distortion, metal-insulator phase transition 3−38807
bound electron-phonon state spectrum in mag. field 3−4980
classical lattice dynamics and localized potential method 3−30216
conduction band electron pairing, phonon-induced 3−38770
coupling strength relation to shifts in phonon frequencies 3−8292
current and electron-phonon interaction in a strong electric field 3−38853
dielectrics, charge carriers, dynamical props., polaron theory 3−36559
dilute alloys, effect of umklapp on low temp. thermal resistivity 3−1751
Dingle temp. for quantum oscills., phonon collisions effects *(Russian)* 3−4985
disordered systems, thermally assisted hopping transport 3−30483
electronic polaron resonance, optical absorption 3−36570
e.s.r. saturation conditions, reson. increase in kinetic temp., elastic scatt. effects *(Russian)* 3−8446
F-centre, relaxed excited state, nearly degenerate states of bound lattice polaron 3−21040
Fermi liquids, anisotropic simple models 3−33770
Fermi surface, nesting, spin density wave and soft phonon mode 3−36524
ferromagnetic metal, effect on elec. resist. *(Russian)* 3−15181
Feynman method application 3−36389
Frohlich polaron concept, charged particle interaction, ionic polarisation 3−36560
glass, hopping Hall effect, single phonon contribution 3−27274
graphite, low-temp. thermomag. effects, phonon drag 3−2107
Green's function approach, dynamical theory 3−36565
hexane matrix, 1, 12-benzphenylene and coronene impurities, fluorescence spectra 3−27567
hot-electron conductivity, Green function approach, interaction with phonons 3−18153
impurity and lattice interactions, additional scattering of Bloch electrons 3−20831
impurity crystals, phononless lines, thermal broadening and shift, adiabatic approximation 3−36900
inelastic scatt. theory for low energy electrons in multiphonon process 3−17874
influence on energy shift of donor-acceptor pair emission 3−36939
ionic cryst., effect on magneto-optical spectra of colour centres 3−2580
ionic crystals, effect on optical absorption 3−36885
ionic crysts., electron-phonon coupling theory 3−11855
ionic polarisation effects on shallow exciton at finite temp. 3−24399
ions in a crystal, vibrating struct. of luminescence spectra *(Russian)* 3−36913
lattice vibrs., microscopic theory 3−7870
light absorption by bound states of electron and phonon, in mag. field, calc. *(Russian)* 3−8560
low temp. interaction meas. 3−1762
magnetic semiconductors, valence bond approach, small polaron effects 3−38803
magnetophonon effect, oscillatory structure, resolvent analysis of longitudinal configuration 3−30497
many-body problems, book 3−20990
metal, elec. resist. rel. to umklapp electron electron scatt. 3−30440
metal, impure, electron-phonon interactions 3−38646
metal, phonon capture by electron from Fermi surface *(French)* 3−38780

electron-phonon interactions continued
metal, pure, low-temperature resistance *(Russian)* 3−2046
metal, rel. to phonon damping, calcs. 3−38638
metallic crystal, ideal, low freq. cyclotron resonance obs. *(Russian)* 3−2043
metals, polyvalent, umklapp electron-phonon scattering in low temp. resistivity 3−8140
metals, umklapp interaction anisotropy and deviations from Matthiessen's rule 3−38820
noble metals, interpolation scheme calc. 3−30222
nonlinear, bound electron and phonon states in strong mag. field 3−24401
nuclear spin phonon coupling mechanism 3−1756
optical lattice vibrations, longitudinal, effect on electronic excitations of solids 3−20833
optical pumping effect on phonon damping 3−14945
perturbation theory for bound polaron 3−21041
phase transitions, microscopic theory *(Russian)* 3−1778
phonon coupled states with impurity centres, multiplicity of dielectric local modes *(Russian)* 3−36924
phonon scattering in solids, conference, Saclay, France (July 1972) 3−1739
photon-drag, polar and piezoelectric crystals, photoconductivity 3−24471
piezosemiconducting crystals, new mechanism of acousto-optical interaction 3−39116
piezosemiconductor, transverse acoustoelec. effect 3−33965
polar crystals, bound polarons, Wannier excitons, perturbation approach 3−36562
polar semiconductor, phonon fluctuation effect on energy levels 3−36571
polaron energy levels, magnetic and Coulomb field effects 3−36563
polarons, ionic crystals, polar semiconductors, conf., Antwerp, Belgium (Aug. 1971) 3−36558
polarons plasma-phonon interactions, magnetic field effects 3−36572
rare-earth chalcogenides, determination from specific heat, thermal expansion and conductivity data 3−15019
rare-earth ions, luminesc. spectra, interaction effects *(Russian)* 3−36372
semiconductor, disordered, phonon assisted interband optical transitions 3−21433
semiconductor, heavily doped piezoelectric interaction with acoustic phonons 3−36567
semiconductor, III-V, rel. to drag of electrons by photons in intraband absorpt. of light *(Russian)* 3−2135
semiconductor, longit. Seebeck effect, damped magnetophonon struct. 3−24460
semiconductor, low freq. e.m. wave propag., under inelastic carrier-phonon scatt. conditions *(Russian)* 3−8166
semiconductor, magneto-optic props., appl. of reson. interaction theory 3−4832
semiconductor, magnetophonon oscills. of current due to drag of electrons by photons *(Russian)* 3−2136
semiconductor, many valley, carrier conc. effect on short wavelength phonons self energy 3−30407
semiconductor, non equilib. phonon distrib. and electron-phonon coupling 3−30224
semiconductor, nondegenerate, thermal e.m.f., two-stage entrainment of electrons by phonons *(Russian)* 3−11920
semiconductor, polar, nondegenerate, cyclotron phonon reson. linewidth, mag. field depend. 3−15132
semiconductor, pseudopotential theory, intervalley coupling consts. determ. 3−5005
semiconductor, rel. to acoustic wave attenuation and amplification in strong fields 3−5036
semiconductor, rel. to deformation-concentration instability 3−33901
semiconductor, u.s. amplification, theory *(Russian)* 3−7891
semiconductor, Wurzite struct., piezoelectric scattering anisotropy *(Russian)* 3−2078
semiconductor with Kane-type band struct., energy loss by hot carriers 3−34338
semiconductors, acoustoelectric effects, measurement by electron-photon-phonon interactions for hypersonic phonons 3−7871
semiconductors, heavily doped, temp. dependence of, density-of-states effective meas. in 1 to 20 K range 3−8121
semiconductors, piezoelectric scattering, lattice vibration interactions, screening, conduction electron mobility 3−33898
semiconductors, polar, resonant electron-optic mode coupling, magnetic fields 3−36564
semiconductors phonon scattering by electrons and holes 3−1748
solid-state theory, book *(German)* 3−17714
stimulated photon-electron-photon scatt. theory 3−1738
superconducting metal film, transition temp. depression by Ar(Ne) overlayers, surface phononcontrib. 3−34017
superconducting transition temperature, repulsive effect of low freq. phonons 3−27330
superconductor, phonon spectrum and Coulomb interaction effects on sp. ht. jump 3−2198
thallous halides, polaron effective masses, electron-phonon coupling constants 3−36569
thermoelectricity in metal alloys, book 3−24414
threshold singularity, electron optical phonon coupling spectrum, polarisation interaction 3−36385
transition metal, electron-phonon mass enhancement theory rel. to superconducting transition temp. 3−18246
transition metal carbides, phonon scattering by conduction electrons 3−2212
transition metal cpds., phonon Raman scatt. theory 3−15494
transition metal ions, luminesc. spectra, interaction effects *(Russian)* 3−36372
transition metals, interpolation scheme calc. 3−30222
transition metals, Y-Pd series, rel. to supercond. crit. temp. *(Russian)* 3−15299
Ag halides, polaron effective masses, electron-phonon coupling constants 3−36569
AgBr, cyclotron resonance, crystal imperfections 3−36387
Ag_2Te, electronic and lattice thermal conductivity 3−1843
Ag(111), LEED, thermal diffuse scattering, at low temp. 3−38702

electron-phonon interactions continued
Al, e.m. attenuation of shear waves near superconducting transition temp. 3−2213
Al-Al_2O_3-Au m.i.m. system, electron emission, discussion of processes in cathode, traps and optical phonons electron scattering in dielectric layer 3−21162
Al-T phonon resistivity, concetrated alloys 4.2 to 100 K, (T=V, Fe, Co, Ni, Cu) 3−38822
$BaF_2:Eu^{2+}$, rel. to impurity-induced Raman scatt. 3−39147
Bi, phonon drag region, size dependence of the transport props. 3−8139
Cd, breakdown of e.m. screening of transverse u.s. phonons 3−24218
$CdCr_2Se_4$, transport props. of non-degenerate ferromagnetic semiconductor below Curie temp. 3−15205
$Cd_xHg_{1-x}Te$, hot electron interaction with phonons rel. to photocond. oscillations 3−18159
CdS, first principles energy band calcs. 3−36535
CdS, LA-phonon exciton interaction, luminesc. study *(Russian)* 3−36916
CdS, photoluminesc., exciton-phonon interaction study *(Russian)* 3−27536
CdS:Te, piezoemission study 3−18492
CdTe, electron-phonon interaction, far i.r. cyclotron resonance absorption 3−36388
Cs, pressure induced, coupling constant variations, prediction of supercond. transition temp. 3−8290
Cu, interpolation scheme calc. 3−30222
Cu film, mean free path of dominant phonon mode 3−27243
Cu_3Au ordering effect on lattice thermal conductivity 3−2048
FeF_3, Fe Mossbauer line shift, electron-phonon contribs. 3−18399
Ga, electron-phonon scattering using heat pulse measurements 3−2047
GaAs, acoustic parametric processes discontinuities due to electron-phonon scattering near the Fermi surface 3−1750
n-GaAs, intervalley absorpt., LA and TA phonons contrib. *(French)* 3−24726
n-GaAs, phonon drag effect, electron-acoustic phonon interaction 3−11913
GaAs, phonon struct. of interband transition 3−2027
n-GaAs, rel. to temp. depend. of electron mobility *(Russian)* 3−2076
GaAs, rel. to temp. depend. of carrier mobility *(Russian)* 3−18133
p-GaSb, phonon-hole interactions, u.s. longitudinal wave attenuation due to 3−7858
GaSb:Te, low temp. phonon scatt., two cond. band role, Te doping depend. *(French)* 3−4893
Ge, electron energy relaxation time, as function of lattice temp. 3−30472
n-Ge, rel. to transverse magnetoresist. in quantizing mag. fields 3−15214
n-ge, thermoelectromotive force rel. to electron-phonon mutual entrainment *(Russian)* 3−21101
Ge, upper and lower bounds on the three-phonon umklapp resistances 3−27089
p-Ge substrates, optical phonon scattering, transverse magnetoresistance 3−8208
Ge:Sb, reson. scatt. of phonons by bound donor electrons 3−30223
Ge:Sb,(:As), phonon conductivity, determ. of density of states effective meas. in 1 to 20 K range 3−8121
^4He, umklapp phonon thermal resistivity anisotropy 3−1856
HgSe, iterated solns. of Boltzmann eqn. with Fermi statistics 3−36598
HgTe, iterated solns. of Boltzmann eqn. with Fermi statistics 3−36598
n-, high field effects, mean free path parameter 3−5014
n-InAs, rel. to drag of electrons by photons in intraband absorpt. of light *(Russian)* 3−2135
InP phonon struct. of interband transitions 3−2027
InSb, hot electron-phonon interaction in nonparabolic cond. band., 4.2K 3−33912
n-InSb, microwave props. in d.c. mag. field, hot electron effect, scatt. mechanism, 4-300K 3−21087
n-InSb, photocond., LO phonons emitted in inelastic scatt. of conduction electrons 3−24477
n-InSb non ohmic transport and phonon amplification 3−8189
K, phonon drag and Matthiessen's rule 3−36583
k, phonon drag effect on low-temperature resistivity 3−2045
K, thermal resistivity between 1.5 and 15 K, umklapp processes 3−20841
K film, low temp. electrical conductivity 3−4994
$LaBr_3:Dy^{3+}$, electronically excited ions, radiationless relax., multi-quantum scatt. processes 3−24390
$LaCl_3:Dy^{3+}(Nd^{3+})$, electronically excited ions, radiationless relax., multi-quantum scatt. processes 3−24390
$LaF_3:Er^{3+}$, electronically excited ions, radiationless relax., multi-quantum scatt. processes 3−24390
$LaF_3:Nd^{3+}$, stimulated emission study *(Russian)* 3−6487
$NaClO_3$, phonon-assisted electronic transitions, 50-368K 3−21431
Nb-Ta superconducting alloy resistivity meas., estimation of electron-phonon coupling, calc. of transition temp. 3−21173
Nb_3Sn, phonon linewidths, influence of the superconducting energy gap, electron transverse phonon interaction 3−17948
Pb, rel. to effective mass freq. and temp. depend., high freq. cyclotron reson. meas. 3−38787
PbSe, rel. to carrier conc. and temp. depend. of mobility 3−27252
n-PbTe, magnetophonon resonance, electron intravalley scatt. with phonon absorpt. 3−33931
Pd, press. dependence of Fermi surface and electronic structure 3−18075
Sb, thermomag. phenomena in phonon drag region 3−33932
Si, electron energy relaxation time, as function of lattice temp. 3−30472
n-Si, Raman scatt. study 3−4830
n-Si, thermoelectromotive force rel. to electron-phonon mutual entrainment *(Russian)* 3−21101
α-Sn, iterated solns. of Boltzmann eqn. with Fermi statistics 3−36598
$SrF_2:Eu^{2+}$, rel. to impurity-induced Raman scatt. 3−39147

electron-phonon interactions continued
Te, electron-phonon interaction, far i.r. cyclotron resonance absorption 3−36388
W, field emitted electron energy rel. to electron-phonon interactions, 78-950 K 3−5259
Xe, thermal diffuse scatt. of low energy electrons, one phonon contrib. 3−17873
$Y_3Al_5O_{12}$-Nd^{3+} point model of crystal field, Hamiltonians, shift and broadening of phononless lines 3−36384
Zn, phonon induced anisotropy theory 3−38629
ZnO, rel. to band struct., magnetoreflection obs. 3−27513
ZnO(S):Ni^{2+}, coupling in dynamic Jahn-Teller effect rel. to crystal field splitting 3−21446
p-ZnSiAs, rel. to temp. depend. of Hall mobility 3−24425

electron probe analysers *see electron probe analysis*

electron probe analysis
air pollution samples, location and identification of small particles within large samples 3−37774
biological samples, specimen preparation, review 3−37738
biological samples, thin, computer program for quantitative microanalysis 3−37739
carbide filaments development for graphite filaments 3−15771
chrome-magnesia fired bricks, electron microprobe analysis of failure 3−15755
coal, medium rank, energy dispersive X-ray analysis and SEM obs. 3−37771
conference, San Francisco, USA (Jul. 1972) 3−35497
correction procedures by Monte Carlo method, practicality test by inclined target method 3−35501
forensic science application 3−37720
general and historical background 3−36336
geological application, quantitative procedures 3−37769
high melting metals, determ. of gas inclusion *(Russian)* 3−6106
insulator, electric pot. obs. using bremsstrahlung and charact. X-ray spectra 3−36970
jet, supersonic of rarefied N_2 and N_2-H_2 mixtures, probe meas. of rotational temp. and concentration around blunt body *(Russian)* 3−29929
Kossel patterns, lattice parameter computation 3−1547
low-energy electron and X-ray interaction coeffs. for solids 3−36469
lunar breccias, energy dispersive X-ray analysis and SEM obs 3−39648
lunar ilmenites 3−3305
lunar pyroxenes, intracrystalline variations of major and minor elements 3−39647
lunar soil glasses 3−39646
metal ceramic system, chemical and partial diffusion 3−7964
microanalysis, by Monte Carlo technique 3−28782
microprobe, background corrections using Si(Li) detectors 3−22545
microprobe analyser and electron microscope combination 3−19328
microprobe X-ray analysis, with computer link-up 3−6119
oxide films, surface and interfacial, characterization by soft X-ray spectroscopy 3−36504
particle, take-off angle effect 3−37765
primary X-ray absorption correction factor 3−35498
quantitative microanalysis, accurate correction theory 3−446
quantitative microprobe obs. of thin specimens, using continuum method 3−368
quartz, obs. of growth morphology and cobble structures 3−14706
scanning, solid target, electron backscatt., penetration and X-ray production, Monte Carlo study 3−14891
scanning electron microscopy, Kossel lines, magnetic domain contrast 3−2320
silicate minerals, at 6 KeV, use of pure element standards 3−37770
sodalite, damage mechanism, ESCA obs. 3−36298
soft X-ray absorption correction factor 3−35549
soft X-ray techniques for materials characterization 3−35550
steel, austenitic stainless, intergranular corrosion, microstruct. and microsegregation effects 3−37032
steel, microstructure *(German)* 3−8794
superconducting systems, phase zones construction in phase diagrams by electron probe microanalysis *(German)* 3−11717
surface characterization using X-ray microanalyzer/s.e.m. combination 3−36468
thermionic convertor emitter, postirradiation microprobe examination 3−26521
thin film, application of ionization function 3−37763
thin film thickness meas. with electron microprobe 3−25667
trace analysis techniques for solids, and instrumentation, review 3−22555
ultra-thin sections, problems in quantitative analysis 3−37762
uranium ores, low grade, from US 3−39486
X-ray continuum fluorescence correction procedure 3−35499
X-ray energy dispersion using scanning electron microscope 3−13507
X-ray intensity data correction, geometry effects or $\varphi(\rho z)$ curves 3−35500
X-ray microanalysis, scan modulation system for improved spatial displays 3−10109
Al_2O_3, alumina ceramics, characterisation 3−8961
Al_2O_3 film, on Al, thickness meas. 3−36500
Au film, substrate, operating voltages and thickness effects 3−37764
CdS monocrystals, cathodoluminescence *(German)* 3−8674
Cr-Ni alloys, corroded, obs. using combined microprobe/opt. interferometry technique 3−39350
Cu-Mn-Sn, microprobe obs. of crystal structure and ordering in ferromag. beta phase 3−18324
Fe, hydrogen-induced surface blisters and internal cracks 3−39349
Fe-Ta alloys, Laves phase precip. phenomena 3−37049
GaAs, high ohmic, subthreshold, surface potential mapping *(German)* 3−8263
$GaAs_{1-x}P_x$-GaAs, alternate layers forming superlattice structure, obs. of comp. 3−12324
$InAs_{1-x}P_x$ vapour-grown epitaxial layers, characterization 3−20955
KBr-$CaCl_2$, rel. to $CaCl_2$ solubility 3−11719
α-$LiAlSi_2O_6$:Mn^{2+}, single crystal, polarised cathodoluminescence emission 3−39194
$LiLnMo_2O_8$, epitaxially grown on Ln_2GeMoO_8 3−1913

electron probe analysis continued
Mg-R system, with large Z correction, R=Gd, Tb, Dy, Ho, Er, Yb, determ. of solid solubility of R by electron probe analysis 3−37044
Mg-Zn alloys, Zn distribution, dendrite non-homogeneity 3−8796
MgO-Al_2O_3-SiO_2-TiO_2 glass-ceramic, crystn. and struct. 3−31161
Mn-Bi thin films, composition rel. to domain patterns 3−21283
Mn_nSi_{2n-m}, obs. of metallic MnSi precipitates in diamag. matrix, mag. behaviour 3−27356
$Mo_{1-x}B_3$, microprobe anal. of structure rel. to comp. 3−33498
Ni superalloys, constitution and microstructure 3−39312
Ni-based alloys, glazes prod. by high-temp. wear and friction 3−34590
PbS epitaxially grown on KCl, obs. of Pb blobs 3−8052
Pd-Ti(V), chemical and partial diffusion 3−7964
Si-Ge epitaxial layer, crystal defect obs. during growth process 3−1920
Si_3N_4, hot pressed microstructure 3−12421
SiO_n thin films, degree of oxidation *(German)* 3−8066
Ta:O system microprobe detection, oxygen absorption concentrations 3−35536
$Tl_2SeAs_2Te_3$, glassy, macroscopic inhomogeneities using contactless-conductivity technique and comp. homogeneity from probe obs. 3−11896
(U,Pu) oxide fuel, irrad., oxygen pot. determ. 3−37772
$(U,Pu)O_2$ fuel, irrad.-enhanced interdiffusion of U and Pu, shielded microprobe obs. 3−38179
$(U,Pu)O_2$ fuel, stainless steel clad, irrad., using shielded probe 3−37773
U, enriched fuel, zircalloy clad, irrad., using shielded probe 3−37773
V, $K\beta_2$ emission bonds investigation by electron microprobe and computer processing *(French)* 3−28780
$VN_{(1-x)}$, x=0, 0.18, $K\beta_2$ emission bands investigation by electron microprobe and computer processing *(French)* 3−28780
V_3Si homogeneity region determ. for single crystal growth 3−18550
W-Re(22 wt.%) alloy, chem. vapour deposited, lamellar comp. fluctuations 3−37023
ZnS monocrystals, cathodoluminescence *(German)* 3−8674
Zn_3Sb_2, microanalysis of phase comp. and decomposition reactions *(Russian)* 3−15671

electron probe microanalysis *see electron probe analysis*

electron probe microscopy *see electron probe analysis*

electron probes
see also electron probe analysis
automated system for quantitative mineral anal. 3−369
Cameca MS 46 electron microprobe, photographic attachment *(Russian)* 3−10113
charge memory application 3−35504
electron and ion beam technology, conference, Houston, Texas, (1972) 3−13473
electron beam fluorescence probe measurements, apparatus and techniques 3−35493
fast ionisation gauge, rarefied gas puff transient behaviour, electron beam fluorescence probe obs. 3−1507
field emission from surfaces, mapping 3−28735
field-emission emitters and probes, electron microscope monitoring 3−10112
image meas. and analysis, incl. image storage system requirements 3−37721
Kossel line techniques, tensile testing 3−1548
lithography application, negative electron resist exposure, voltage dependent parameters 3−35505
magnetic, electron, for electron microscopes and probe forming systems, developments 3−1538
microanalysis, by Monte Carlo technique 3−28782
microprobes, five-electrode quadrupole-octupole elements, effective length of quadrupole lenses *(Russian)* 3−6114
microprobes, for electron microscope 3−28718
microprobes, use in X-ray spectrometry *(French)* 3−32261
non-perturbing probe, meas. of potential distrib. in a space-charge sheath *(Russian)* 3−6027
nuclear reactor shielded for in-pile analysis, specifications 3−37773
optics, microanalysis applications 3−13474
resolution limits 3−35503
SEM collection of secondary electrons using small aperture probes 3−35512
spectrometer for quantitative meas. of surface voltages with electron microprobe instruments 3−35502
thin, formation theory rel. to Maxwellian initial distrib. and spherical aberration 3−13774
Na_2O-Cs_2O-SiO_2 electron microprobe analysis for profiles of Cs diffusion 3−11764

electron-proton scattering
amplitudes in resonance region, relativistic quark model 3−14002
Bjorken scaling and parton model 3−4172
deep inelastic, limits on anomalous dimension in Wilson's expansion of two currents near lightcone 3−23009
deep inelastic, resonance model using gneralized crossing relation and scaling prediction 3−32671
deep inelastic, structure functions νW_2 and $2MW_1$ construction 3−17008
deep inelastic, study of multiplicity fluctuations in inclusive spectra 3−854
deep inelastic scatt., asymptotic props. of amplitude rel. to Schwinger term sum rule 3−26316
duality of inelastic scatt. low q^2 region 3−6635
elastic, from polarised protons, determ. of rigorous bounds for transverse polarisation 3−13917
elastic, optimal positivity bounds to the up-down asymmetry 3−29206
elastic, polarized target, differential cross sections and weak neutral currents *(Russian)* 3−23081
elastic, reviews 3−13875
elastic scatt. at low momentum transfer, meas. of proton form factor and r.m.s. radius 3−17016
inelastic, generalized vector dominance and small ω' region 3−6624
inelastic, high energy, generalized vector meson dominance model 3−10758

electron-proton scattering continued
- inelastic, in region of $\Delta(1236)$ resonance for two values of q^2, coincidence expt. 3−14005
- inelastic, phase oscillation method and light cone dominance 3−26308
- inelastic, phenomenological comparison with pp inelastic scatt. 3−14043
- inelastic, separation of σ_s and σ_t cross-sections in the region of the $\Delta(1236)$ resonance 3−17039
- inelastic, separation of longitudinal and total cross sections at $q^2=1$ $(\mathrm{GeV}/c)^2$ in resonance region 3−4178
- inelastic, unitarity lower bound on the longitudinal contribution 3−17027
- inelastic cross section, meas. at four momentum transfers in region of $\Delta(1236)$ resonance 3−17035
- inelastic in massive quantum electrodynamics, calc. of leading contrib. to structure functions 3−13986
- inelastic scatt., twofold diffl. cross-sect. at small scatt. angles detn. 3−17043
- inelastic scattering, semi-inclusive and inclusive processes, phenomenological model based on statistical assumption 3−26312
- parity-violating e.m. interaction for hadrons, magnitude of effect 3−32663
- parton model for deep inelastic scatt. 3−13923
- polarization of the recoil protons in elastic scatt., isobar model 3−13903
- scaling behaviour in three dimensional gluon model 3−38051
- small angle, differential cross-sections 3−23097
- $e^- + p \rightarrow e^- + \pi^\pm + X$ inclusive electroproduction reactions, scaling 3−32670
- $ep \rightarrow 3p^1X$, inclusive reactions, scaling laws rel. to γp scatt. 3−13976
- $ep \rightarrow epX^0$, coincidence electroproduction in ρ mass region, meas. of cross sections for 0-1Gev/c^2 missing masses. 3−13956
- $ep \rightarrow ep\gamma$, investigation between elastic peak and pion threshold, exptl. test of higher order radiative corrections 3−13951
- $ep \rightarrow ep\pi^0$ coincidence cross sections, correction for radiative effects 3−35803
- $ep \rightarrow epx^0$ electroproduction, inclusive proton distribs. 3−851
- $e^\pm p \rightarrow e^\pm \gamma +$ anything, meas. of deep inelastic bremsstrahlung in scaling region, test for fractional charged partons 3−4180
- π^+ electroproduction, k^2-dependence of transverse cross section in generalized Born term model 3−10710
- ρ^0 electroproduction, transversely polarized cross-section meas. 3−13957

electron radiation
- Fermi-particles in field of two e.m. waves *(Russian)* 3−14017
- Fermi-particles in field of two e.m. waves *(Russian)* 3−14018

electron reactions *see electron interactions*

electron relaxation time *see carrier relaxation time*

electron resonance *see cyclotron resonance; paramagnetic resonance*

electron ring accelerators
- heavy ion acceleration, alternates to cyclotron 3−10013
- ion cluster acceleration, magnetic field shapes and lengths of accelerating stage 3−13383
- kite instability in two-component relativistic ring, stabilization by azimuthal magnetic field *(Russian)* 3−6057
- longitudinal coupling impedance, in cylindrical geometry 3−25833
- performance characteristics, proton energy gain 3−25834

electron scattering
- *see also atomic electron scattering; beta-ray scattering; electron-proton scattering; molecular electron scattering; nuclear reactions and scattering due to electrons*
- coincidence cross sections, correction for radiative effects 3−35803
- crystal, scatt., anomalous transmission 3−20767
- crystal transmission, nuclear disintegration 3−19287
- deep, inelastic, vector meson dominance, light cone expansion and corrections 3−13920
- deep inelastic, general threshold relation with deep inelastic electron-positron annihilation 3−845
- deep inelastic electroproduction, parton and dual model approach 3−13960
- deep inelastic electroproduction of W-bosons, test of bilocal algebra 3−6629
- deep inelastic on unpolarised targets, direct-channel resonance model, determ. of structure functions 3−13905
- deep inelastic structure function at small ω' and resonance form factors in quark model with broken SU(6) 3−29201
- deep-inelastic, direct-channel resonance model, spin dependence of cross section 3−13906
- ed elastic scatt., two-photon-exchange contribution to cross section 3−19691
- eikonal approximation, second-order, for potential scattering 3−22712
- in foils, 40 to 60 MeV optical transition radiation patterns *(French)* 3−13414
- hydrogenic ions with infinite Z, Coulomb-Born-Oppenheimer cross-sections 3−20039
- inelastic, deep, coincidence meas. of ρ electroproduction, Π and p production 3−14001
- inelastic, on hadrons at high energies, review of single-arm and coincidence expts. 3−857
- inelastic, proton structure functions 3−13917
- inelastic, resonance dominant model, analogies with excitation of nuclei, quark-parton model 3−13979
- inelastic deep scatt. scaling laws from limiting fragmentation, strength function behaviour 3−14015
- inelastic structure functions, Mellin-transform analysis of light-cone singularities and scaling behaviour 3−10715
- large angle, low energy loss electron scattering with retarding field analyzers 3−806
- light-cone behaviour and structure functions in perturbation theory 3−22985
- Mainz linac, description of scatt. expt. facilities *(German)* 3−10009
- metal films, thin, angular distrib. of secondary electrons *(German)* 3−18521
- Ramsauer effect, apparatus for expt. demonstration *(Russian)* 3−17371
- random array of strong scattering centres, algebraic technique for determ. of transport and optical coeffs. 3−6365

electron scattering continued
- solid target, electron backscatt., penetration and X-ray production, Monte Carlo study 3−14891
- spectra analysis without inclusion of nuclear model 3−32830
- thick targets, multiple scattering and energy loss 3−19286
- transition metals, electron refl., energy loss spectra characts., 30-70 eV 3−20768
- ed, deep inelastic, Doppler effect in extraction of total neutron cross sections 3−6674
- ed, elastic, reviews 3−13875
- ed, inelastic, smearing effects due to deuteron structure ambiguities 3−29322
- ed, polarised target, reciprocal bootstrap on light cone 3−10652
- ed deep inelastic scatt., quark exclusion principle effects on structure functions 3−17023
- eD elastic scatt., calc. of deuteron e.m. form factors 3−16989
- $ed \rightarrow epn$, coincidence meas. of cross sections, determ. of e.m. form factors of n. 3−17055
- ed quasi elastic scatt., final state interaction effects at large t 3−17022
- ed scatt., inelastic, cross section meas. and excitation of $\Delta(1236)$ resonance 3−13919
- $ee \rightarrow ee +$ anything, two-photon exchange approximation, general covarint formalism 3−38046
- e^+e^-, expts. at Adone storage ring, test of QED 3−13877
- $e^+e^- \rightarrow e^+e^-X \rightarrow e^+e^-\gamma\gamma(X=\pi^\circ,\eta$ or $\eta')$ coupling constants and vertices exam. 3−17036
- $e^+e^- \rightarrow e^+e^-X \rightarrow e^+e^-\gamma\gamma(X=\pi^\circ,\eta$ or $\eta')$ vertices study for one almost real photon and one highly virtual 3−17037
- $e^+e^- \rightarrow e^+e^- +$ hadrons, dual frame loops diagram and scaling behaviour 3−848
- e^+e^- elastic scattering 1.4-2.4 GeV, agreement with quantum electrodynamical predictions 3−4173
- $e^\pm e^-$ colliding beams, polarization effects on cross sections *(Russian)* 3−4176
- $e\gamma$ deep inelastic scatt., possibility of observation in $e^\pm e^-$ colliding beam expt. 3−13974
- $e\gamma$ inelastic scatt., expt. use of e^+e^- colliding beam 3−13962
- eN, deep-inelastic scatt., surface dominance 3−23094
- en, elastic, reviews 3−13875
- eN, electroproduction of nucleon resonances with polarized leptons, symmetric quark model 3−4182
- eN, inelastic, Bjorken's scaling laws, light-cone structure of infinite-component fields 3−6627
- eN, inelastic, generalized vector dominance and small ω' region 3−6624
- eN deep inelastic, violation of Bjorken scaling law, finite value of p-n mass difference 3−29202
- eN elastic scatt., departure from scaling laws, anal. by broken-symmetry 3−17010
- eN inelastic, resonance form factors, scaling and Regge behaviour 3−35799
- en scatt., inelastic, cross section meas. and excitation of $\Delta(1236)$ resonance 3−13919
- e^-N inelastic, positivity restrictions from e.m. hadronic tensor props. 3−13893
- $E\nu$, analytic renormalization approach 3−6626
- $e\pi$, inelastic, upper bounds on π form factor 3−10705
- γe, scattering amplitude determ. including radiative correction, calc. of polarization coeff. *(Russian)* 3−23076
- $\gamma\gamma$ collisions in $e^+e^- \rightarrow e^+e^-A^+A^-$ reactions in storage rings 3−13964
- ne scatt. length, neutron polarizability effect 3−4171
- ne scatt. length, neutron polarizability contrib. 3−6623
- νe, elastic, and neutral lepton current *(Russian)* 3−16978
- νe, energy spectra and ang. distribs. of recoil electrons *(Russian)* 3−23040
- νe, twistor theory applic. 3−6576
- νe scattering, e.m. props of neutrino and weak interaction variants 3−26294
- $\nu e^- \rightarrow \nu e^-\gamma$, ang. and energy distribs. *(Russian)* 3−4163
- $\nu_e e$ inelastic scattering, possibility of study in high energy neutrino beams *(Russian)* 3−38029
- $\nu_e e^- \rightarrow \nu_e e^-$, search for process in fission reactor expt. 3−6591
- Au, elastic and inelastic scattering from solid 3−30151
- $e^+e^- \rightarrow e^+e^-$, acollinearity and radiative corrections 3−38038
- $\mu^-\mu^+$ pair prod. in e^-e^- and e^-e^+ colliding beams, calc. of cross-section *(Russian)* 3−4185

electron spectra
- *see also Auger effect; electron spectroscopy; photoelectron spectra*
- acetylene, threshold electron impact excitation 3−26726
- alkali halide crystal, energy schemes and zone structure, photoelectron spectra obs. 3−34464
- alkali halides, X-ray photoelectron spectra, config. interaction, comment 3−34461
- anthracene anion radicals, autoionisation in photoelectron emission 3−18528
- auroral arc electron intensity meas., source plasma identification 3−25259
- auroral electrons, space-time dynamics during 1968 March-April magnetospheric substorms 3−25255
- backscattering factor determ. in X-ray emission microanalysis *(French)* 3−24766
- benzene, photoelectron spectra using polarised and unpolarised photons 3−26649
- benzenes, substituted, photoelectron spectra 3−33087
- carboxylic acids, monomers, dimers mixed complexes, photoelectron spectra of H-bonded systems 3−7173
- chloroethylenes, ionisation potentials determ. by photoelectron spectroscopy 3−11290
- cosmic ray albedo electrons, energy spectrum determ. from shielded gas-discharge detectors data 3−22446
- cosmic rays, modulation near solar max. 3−12911
- cyclooctatetraene, hydrogenated derivatives, photoelectron spectra, pi-orbitals spacing, conformation 3−33086
- double-mode X-ray source, for photoelectron spectroscopy 3−13476
- ESCA exam. of hot rolled Al surfaces 3−24957
- fluorobenzenes, molecular core binding energies 3−23547
- formic acid, vibr. structs. in photoelectron spectrum 3−36004

electron spectra continued
- graphite, chemisorption of atomic oxygen on basal faces, photoelectron spectra 3—24347
- group IV cpds., MX$_4$ type, X-ray photoelectron spectra determ. of d-orbital participation 3—14340
- hydrazine, photoelectron spectra, CNDO/2 and MINDO/2 analysis 3—35993
- from ion-atom collisions, production mechanisms 3—26601
- ion-neutralization vs u.v. photoelectron spectroscopy for metal-adsorbate obs. 3—39206
- magnetic storm with a type A aurora, rocket meas. 3—12787
- metal, d-band splitting, high resolution photoelectron obs. 3—30414
- metals and their compounds, photoelectron spectra, electron states, review *(Japanese)* 3—15120
- methane, electron impact spectra, oscillator strengths 3—23543
- methane, photoelectron spectrum from energy surface investigation 3—23521
- m.o.s. structure, oxide states, photoelectric spectroscopy, 79 K 3—38896
- naphthacene cryst., vacuum u.v. photoelectron spectra, energy distrib. curves, valence bands 3—21513
- non-metallic compounds, X-ray induced photo-electron spectra, chemical shift of ionisation energy 3—39215
- oxide films, surface and interfacial, characterization by soft X-ray spectroscopy 3—36504
- oxide films on pure Fe and Fe-Al alloy 3—8701
- photoelectron, u.v. and X-ray, surface sensitivity 3—11944
- photoelectron spectral intensities, importance of asymmetry parameter 3—26649
- photoelectron spectrometers, calibration procedures 3—22497
- photoemission, prediction of new multiplet struct. 3—39216
- phthalocyanine dyes in soln., self-association obs. 3—31252
- plasma, double inverse pinch device 3—20652
- polyenes, struct. and electron spectra relation *(German)* 3—14404
- polyethylene, photoelectron spectrum comparison with cryst. orbital calcs. 3—27597
- polyethylene, vacuum u.v. region photoemission spectra 3—12210
- polyfluoroethylenes, ESCA chem. shifts, rel. to charge distribs. 3—1300
- scattering, analysis without inclusion of nuclear model 3—32830
- semiconductor, compound, state density determ. by Auger and photoemission electron spectroscopy 3—24381
- sodalite, damage mechanism, ESCA obs. 3—36298
- solids, numerical calcs. by integration over Brillouin zone 3—20983
- surface electronic states detect., u.v. photoemission and ion-neutralisation spectroscopy comparison 3—12214
- surface structure, meas. of elastically backscattered electron current at charact. excitation threshold 3—16534
- tetracyanoquinodimethane and metal salts, core-level satellites in X-ray photoelectron spectra 3—12213
- tetrafluoromethane, electron impact spectra, oscillator strengths 3—23543
- thiocarbonyl fluoride photoelectron spectrum, obs. of vibrational structure and fluorine substitution shifts 3—7168
- transition metal coordination compounds, donor-acceptor props. of ligands, X-ray photoelectron spectroscopy 3—17415
- triatomic molecules, ang. distrib. of photoelectron spectra 3—23545
- 1,3,5-trifluorobenzene and deuterated analog, photoelectron spectra 3—11253
- tris-bridged cyclophane, photoelectron spectra and highly strained geometry 3—11206
- X-ray induced photoemission, absolute yields 3—18524
- Ag/O$_2$ chemisorbed layer, low energy backscattered electron spectra, surface atom energetics, chem. bonding 3—24349
- Al, plasmon decay effects Auger, secondary and electron energy loss spectra 3—5026
- Al film, pure and oxidized, X-ray photoelectron spectra analysis 3—30923
- Al oxyanions, X-ray emission, ESCA spectral shifts, approx. molecular orbital theory 3—26986
- Ar, 3s subshell, photoionisation in threshold region, photoelectron spectroscopy study 3—29508
- Ar, ioniz. by He metastables, electron energy spectra 3—33053
- Ar$^{(+)}$ + Ar collisions, ioniz. processes 3—26605
- B compounds binding energies, vapour state, chemical correlations 3—23549
- BaF$_2$, Auger effect in reflectance spectra 3—2036
- Bi, diatomic:atomic ratio in molecular beam determ. 3—29745
- CO, adsorbed on Ni(100), orbital energy spectra 3—39206
- CO, adsorbed on W(100), photoemission energy distrib. curves 3—39213
- CS, high resolution photoelectron spectrum, ioniz. pots. 3—4427
- CaF$_2$, Auger effect in reflectance spectra 3—2036
- ClO$_4^-$, X-ray photoelectron spectrum, line intensities 3—36048
- Cr$_2$O$_3$, K$_2$Cr$_2$O$_7$, KCr$_3$O$_8$ X-ray photoelectron, electronic structure relations 3—23548
- Cu, Auger electron spectra and electron spectra, 25-400°C 3—30910
- Cu-Ni alloys, photoelectron spectroscopy of oxide films 3—11826
- CuO, Auger electron spectra and electron spectra, 25-400°C 3—30910
- Cu$_2$O, Auger electron spectra and electron spectra, 25-400°C 3—30910
- Fe$_3$Si, FeSi, FeSi$_2$, electron struct. obs. *(Russian)* 3—24760
- GaSb, photoemission, core levels obs. *(French)* 3—30831
- GaSe, LEED studies, plasmon losses from secondary electron spectra 3—38698
- HBr, DBr photoelectron, ionisation energies, predissociation 3—23546
- HCNO, photoelectron spectrum, CNDO/2 calcs. 3—33089
- HOF, photoelectron spectrum, valence region orbitals analysis 3—36047
- He$^{(+)}$ + He collisions, ioniz. processes 3—26605
- Hg, adsorbed on Ni(100), orbital energy spectra 3—39206
- Hg, ang. distrib. of photoelectrons from 5d-subshell 3—29501
- Hg adsorbed on Au, surface sensitivity of ESCA for sub-monolayer quantities 3—24334
- Ir(I) complex, five-coordinated, bonding, X-ray photoelectron spectra 3—21343
- K complexes, hexachlorometallate photoelectron, X-ray, core and valence orbitals, binding energy 3—23544

electron spectra continued
- Kr, 4p photoelectron ang. distrib., far u.v., using synchrotron light source 3—29507
- Kr$^{(+)}$ + Kr collisions, ioniz. processes 3—26605
- Mg$_2$Sn, valence band electron density of states determ. by Auger and photoemission spectroscopy 3—24381
- MnF$_2$, photoemission, new multiplet struct. 3—36979
- Mo reflection, energy loss plasma peaks, scattering angle dependence 3—39211
- NO, photoelectron spectra obs. of autoioniz. process *(Russian)* 3—7247
- Ne$^{(+)}$ + Ne collisions, ioniz. processes 3—26605
- Ni, with chemisorped S, Auger spectral fine struct., origin 3—11810
- Ni-O system, cpd. formation, elucidation by ESCA 3—24348
- Ni(100) surface, influence of H$_2$, CO and O$_2$ adsorption on electron energy loss spectra *(German)* 3—36653
- O, adsorbed on W(110), photoemission energy distrib. curves 3—39213
- O + Ar, ion-atom high-energy collisions, electron loss 3—38247
- Pb diatomic:atomic ratio in molecular beam determ. 3—29745
- PbO layer formed by oxidation of Pb, ESCA obs. 3—33741
- Pt complexes, mixed and partial oxidation states from photoelectron spectroscopic meas. 3—15585
- S, and S containing compounds, meas. of chemical shift in photoelectron spectra 3—30922
- Se, amorphous and polycryst. electron energy loss spectroscopy and optical consts. determ. *(German)* 3—11668
- Se-electrode (Cu, Al, Ag) metal-semiconductor boundary, energy levels, compound formation, vacuum photoemission study 3—38893
- Si, rel. to doping, level bending 3—8690
- Si oxyanions, X-ray emission, ESCA spectral shifts, approx. molecular orbital theory 3—26986
- SiO$_2$ film, thermally stimulated exo-electron emission spectra, trapping centre obs. *(German)* 3—15596
- SrF$_2$, Auger effect in reflectance spectra 3—2036
- Te, amorphous and polycryst., electron energy loss spectroscopy and optical consts, determ. *(German)* 3—11668
- TiCl$_4$, photoelectron spectra, Hartree-Fock-Slater model 3—27489
- U clean surfaces, electron binding energies determ. by soft X-ray appearance-potential spectroscopy 3—36977
- VCl$_4$, photoelectron spectra, Hartree-Fock-Slater model 3—27489
- W, chemisorption of CO and O$_2$, ESCA obs. of fractional monolayer quantities 3—38732
- W, three single-cryst. faces, directional photoemission study, energy distrib. spectra 3—39217
- W/WO$_3$ surface, photoelectron spectrum as function of surface oxide layer thickness 3—12212
- Xe, 5p photoelectron ang. distrib., far u.v., using synchrotron light source 3—29507
- Xe, ioniz. by He and Ne metastables, electron energy spectra 3—33053
- XeOF$_4$, photoelectron spectra, electronic struct. 3—33088

electron spectroscopy
- *see also electron spectra*
- Auger, electronic superposition of sample current and secondary-electron images 3—10099
- Auger, sensitive high resolution (0.2%) three grid energy analyser 3—34452
- Auger, thin film analysis 3—10207
- Auger effect, L-shell ionization cross sections 3—39209
- Auger spectroscopy, cylindrical mirror analyser, design 3—32221
- Auger technique, applic. to surface analysis, book contrib. 3—10106
- betatron beam for defectoscopy *(Russian)* 3—19267
- chemical shifts, relationship with n.m.r., electron binding energies, spin-rotation constants 3—23599
- Compton wavelength of electron and fine structure const. determ. from eqn. for electron motion in magnetostatic field 3—13198
- cylindrical capacitor energy analysis 3—19316
- electron spectrometer for quantitative meas. of surface voltages with electron microprobe instruments 3—35502
- energy analyzer—gun system with retarding field and cylindrical mirror 3—37713
- e.s. mirror spectrometer, with coaxial electrodes, for multidetector operation 3—32204
- ESCA, new design of instrument 3—28784
- film on metal surface, composition determ. by Auger electron spectroscopy 3—21553
- magnetic-Si(Li) swept current spectrometer, for on-line internal conversion studies 3—32201
- molecular core binding energies, chemical shifts, minimal Slater basis set calculations 3—23550
- Penning ionization electron spectra of collisions between rare gas atoms and He metastable atoms 3—11154
- photoelectron, high resolution, bond structure of metals, d-bonds 3—30414
- photoelectron spectrometer, for band structure studies 3—28716
- photoelectron spectrometer, specimen holder, irregular solid specimens 3—22500
- photoelectrons, large aperture energy analyser 3—21521
- photoemission, of metals, v.u.v. 3—2618
- secondary electron yields, ion impacts on thin film oxide surfaces 3—28709
- semiconductor mat. and processing, ESCA applic. 3—39293
- spectrometer, coaxial-cylinder for beam-foil experiments to 10 keV 3—10085
- steel, obs. of internal energy reduction with axially centred cubic to f.c.c. transition *(Russian)* 3—15728
- surface analysis 3—32259
- transition metal borides, metal-boron bonding, ESCA obs., oxidation effects 3—30911
- u.v. photoelectron spectrometers, transmission fn. determ. 3—22498
- Al oxyanions, X-ray emission, ESCA spectral shifts, approx. molecular orbital theory 3—26986
- CO-induced chemisorption levels in a Ni(110) surface, energy loss spectroscopy 3—10103
- CO$_2$, ESCA studies to identify shake up satellite lines 3—11294
- COS, ESCA studies to identify shake up satellite lines 3—11294
- CS$_2$, ESCA studies to identify shake up satellite lines 3—11294

electron spectroscopy continued
  N_2, ESCA spectra compared with X-ray emission spectra fine structure 3−33120
  Ni, adsorption of O_2, ESCA obs. 3−8017
  Ni based alloys, glazes prod. by high-temp. wear and friction 3−34590
  Si oxyanions, X-ray emission, ESCA spectral shifts, approx. molecular orbital theory 3−26986
electron spin
  g-factor anomalies of electron and positron 3−13860
  ionic crystal, polarization effect on conduction electrons 3−36601
  magnetic moment, sixth-order radiative corrections 3−4165
  photoelectrons from ferromagnets, spin polarization 3−18533
  photoelectrons from non-crystalline magnetic materials, spin polarized *(German)* 3−18531
  photoemission, transitions from cond. band to states in band gap, electron spin polarization 3−5255
  pitch correction to $(g-2)$ precession freq. 3−6690
  state of 'magnetised' electrons at low quantum levels, electron-photon interactions *(Russian)* 3−23101
  Ni surface, magnetized, predominant electron spin orientation meas. 3−34448
electron spin-lattice relaxation *see spin-lattice relaxation*
electron spin relaxation *see spin-lattice relaxation*
electron spin resonance *see paramagnetic resonance*
electron states, crystal *see crystal electron states*
electron states, impurity *see impurity electron states and effects*
electron states, surface *see surface electron states*
electron states (solids) *see crystal electron states*
electron structure of solids (crystallography) *see crystal atomic structure*
electron structure of solids (energy structure) *see crystal electron states*
electron theory
  see also Dirac equation; quantum electrodynamics
  Dirac equation, covariant solutions in e.m. field 3−19484
  relativistic Dirac theory, pseudoscalar mass and its relation to scalar mass 3−6548
  H retarded interactomic potential energy of 2 ground state H atoms, Dirac theory 3−20073
electron theory of metals *see crystal electron states; metal theory*
electron traps
  see also colour centres; electron mobility; impurity electron states and effects
  aminobenzoic acids, thermolum., trap depths and density 3−15567
  anthracene, thermally stimulated current meas. of trapping level depth and frequences 3−18167
  brass, equilib. vacancy density from positron trapping meas. 3−17809
  captured electron lifetime in deep traps from tunnelling current 3−21141
  carrier density kinetics under weak excitation *(Russian)* 3−24450
  copper phthalocyanine:vanadyl phthalocyanine, energetic trap distrib. rel. to impurity 3−38811
  copper phthalocyanine, perturbation or trap level calcs. 3−21062
  defect photoconductor, charged traps effect on photo-excited carriers mobility 3−18190
  dependence of nonlinear properties of waves in cross-field electron-ion streaming instability 3−7523
  glass, La-silicate, radiation centres investigation by e.p.r., absorption spectra and thermal decolourising *(Russian)* 3−30697
  high-resistivity semiconductors, parameters of trapping levels 3−24451
  hydroxybenzoic acids, thermolum., trap depths and density 3−15567
  insulating thin films, electronic transport processes 3−18237
  insulator, tunnelling to traps from metal or semicond. 3−18225
  insulator, with arbitrary trap distrib., isothermal currents and trap parameter determ. 3−36620
  insulator, with arbitrary trap distrib., thermally stimulated currents 3−36621
  ionic crystals, rel. to theory of surface polarons 3−2156
  metal oxide surfaces, influence of O_2 3−30929
  m.i.m. cathodes, field emitted electron angular distrib. rel. to electron traps 3−15602
  molecular crystals, trapping state formation by structural defects 3−21072
  molecular solids, exponential carrier trap distributions 3−33825
  m.o.s. capacitor, recombination trapping centres in surface space charge layer 3−5055
  m.o.s. structure, charge trapping, slow state effects at Si-SiO_2 interface 3−5056
  oligoaniline derivatives, linear, photoelectric props., depend. on thermal releasing of charge carriers from traps 3−24466
  oxide layer, on superconductor, tunnelling calc. 3−30579
  paramagnetic spin polaron, self-trapped, mobility 3−30433
  p-quarterphenyl, photocurrent and discharging dark currents decay, trap struct. 3−21106
  self-trapped states in disordered systems (gases and liquids) 3−38772
  semiconductor, deep traps in quasi-classical random field, light absorpt. *(Russian)* 3−34385
  semiconductor, multiple energy level defects, continuity and Poisson equations 3−24418
  semiconductor, negative resist. due to trapping increase of deep centres with magneto-depletion 3−30490
  semiconductor, rel. to double injection, unified theoretical approach 3−24435
  semiconductor, wide-band monopolar, trapping centres, depth and conc. from photocurrent *(Russian)* 3−21081
  semiconductor, with arbitrary trap distrib., isothermal currents and trap parameter determ. 3−36620
  semiconductor, with arbitrary trap distrib., thermally stimulated currents 3−36621
  semiconductor devices, neutron irrad., limiting design parameters 3−33991
  semiconductor with deep traps, injection current theory 3−30488
  sodalite, damage mechanism, ESCA obs. 3−36298
  tetracene crystals, photoionisation of quasicontinuous traps 3−15194
  thermal emptying, model *(German)* 3−15162
electron traps continued
  thermionic emission, isolated box model 3−30919
  from thermoluminescenct glow curves, review 3−18506
  vanadates of group III elements, rel. to thermoluminescence *(Russian)* 3−15565
  well shape using Frenkel thermal field effect potential 3−4966
  $3As_2Se_3$-$2Sb_2Se_3$, amorphous film, recombination processes, photocond., 278-308K 3−21094
  Al-Al_2O_3-Au m.i.m. system, electron emission, discussion of processes in cathode, traps and optical phonons electron scattering in dielectric layer 3−21162
  Al-CeF_3-Al thin film capacitor system, obs. using stimulated dielectric relaxation currents 3−8277
  Al-Formvar-Pb junction, logarithmic derivative curves and trap-assisted current transport 3−24544
  Al_2O_3 film, on Si, photoinjection-photodepopulation and C-V studies 3−5066
  Al_2O_3 pyrolytic layer, in m.o.s. capacitor, trap struct. 3−18220
  BiI_3, effect of surface excitation and O_2 adsorption 3−27271
  Bi_2S_3 crystals, thermostimulated electron emission, ionisation energy of trapping centres calc. *(Russian)* 3−12206
  CaS:Bi^{3+}, Pd^{2+}, phosphorescence decay characteristics, trap depth calc. 3−30856
  $CaWO_4$, X-irrad., trap depth and charge carriers from optically and thermally stimulated conductivity *(German)* 3−2105
  CdI_2 and CdI_2(Pb), trapping centre characts, thermoluminescence *(Russian)* 3−34437
  CdS, acoustoelectric effects in homogeneous crystals with trapping centres 3−24482
  CdS, distribution *(Japanese)* 3−18183
  CdS thin films, shallow trapping levels, structure defects, photoconductivity relaxation 3−33833
  CdSe, X-irrad., photocond. study 3−30426
  n-$CdSiP_2$, majority carrier trapping, trap parameters, photocurrent obs., 100-400 K *(Russian)* 3−21082
  n-CdTe films, high field phenomena *(French)* 3−27262
  Cu, equilib. vacancy density from positron trapping meas. 3−17809
  GaAs:Cr, photocond. after 0.8 MeV electron irradiation; induced impurity trap levels 3−36637
  $GaAs_{1-x}P_x$:N, $In_{1-x}Ga_xP$:N, luminescence, l.e.d. applications 3−39175
  $GaAs_{1-x}P_x$:N, isoelectronic trap transitions in resonant enhancement region 3−30430
  GaP:O, donor deep states, capture cross sections, photocapacitance obs. 3−30428
  GaP:Zn, O, free hole to impurity centre bound electron recomb. at 300K 3−30494
  Ge, charge carrier capture and reemission by shallow levels, field depend. 3−21091
  Ge crystal grown for radiation detection, hole trapping rel. to etch figures 3−12314
  Ge p-n junction, trapping level influence on microplasma bistable state 3−15246
  Ge:Sb, relaxation processes involving trapping levels in bistable microplasmas 3−24452
  $In_{1-x}Ga_xP$:N, soln. growth, effect of N-trap states on photoluminesc. and elec. props. 3−24797
  $In_{1-x}Ga_xP$:N laser operation, reson. enhancement of recomb. probability associated with isoelectronic trap states 3−18472
  InSb film, carrier trapping at slow surface states *(Russian)* 3−30492
  $KMgF_3$. reorientation and thermal motion of self-trapped hole 3−18100
  LiF:Mg trap depth and supralinear thermolum. response 3−24756
  Se trigonal single crystal, photoconductivity, thermally stimulated currents, trap distrib. obs. *(Russian)* 3−30516
  Si, charge carrier capture and reemission by shallow levels, field depend. 3−21091
  Si, radiation effects, obs. using junction-capacitance techniques 3−33926
  Si, shallow donor formation by proton bombardment, annealing temp. depend. 3−17861
  Si:Ge(Sn), O electron irrad., selective trapping of vacancies, migration of interstitials 3−33925
  SiO_2 film, amorphous, on Si, electron trap distrib. from transient photodepopulation meas. 3−18163
  SiO_2 film, in m.o.s. struct., trapping due to avalanche currents 3−5057
  SiO_2 film, thermally stimulated exo-electron emission spectra, trapping centre obs. *(German)* 3−15596
  $SrTiO_3$, elec. and optical meas. rel. to oxygen vacancies as electron traps 3−27225
  ThO_2, thoria, pure, Ca^{2+} doped and Y^{3+} doped samples, u.v. excitation, γ-irradiation effects 3−8675
  Zn_2GeO_4:Mn^{2+}, luminesc. rel. to free carriers prod. by sub-band-gap excitation, trapping effects 3−21467
  ZnO, Li doped and undoped, single crystals, baked layers, electrophotographic discharge mechanism *(Russian)* 3−30517
  ZnS:Ag, Al, photocond. caused by redistrib. of charge carriers over trapping centres *(Russian)* 3−15220
  ZnS:Cu, β-irrad. at 5K, rel. to fast light emission 3−24753
  ZnS-Cu powder cells, electrolum. decay rel. to trapped electrons 3−21487
  ZnS(Cu, Cl) electroluminophores, shallow traps and deterioration 3−30880
  ZnTe, shallow donor level, field-assisted detrapping obs. 3−24391
  p-ZnTe:Ga(In), photoelectronic props., electron trap level rel. to Ga(In) impurities 3−36635
electron tube diodes *see diodes*
electron tube manufacture
  seal, cryogenics, current input lead 3−142
  welding, laser beam, anode-cathode assemblies, high melting point metals, technique, advantages 3−19652
electron tube rectifiers *see rectifier tubes*
electron tube testing
  c.r.t. testing, impact of steel ball, pulsed holographic study 3−5773

electron tubes
see also cold-cathode tubes; diodes; electron emission; microwave tubes; nuvistors; pentodes; tetrodes; thermionic tubes; triodes; ultra-high frequency tubes; X-ray tubes
field emission, space charge effects of relativistic electrons *(Russian)* 3—15595
marked examples, book 3—18048
two electrode, needle field emission cathode, nanosecond pulse production of fast electrons *(Russian)* 3—10110
vacuum breakdown, dependence on cathode surface roughness 3—14626
vacuum tube electrometer, sensitivity improvement 3—35439

electron tunnelling *see tunnelling*

electron valves *see electron tubes*

electron-wave tubes
see also klystrons; magnetrons; travelling-wave-tubes
M-type devices, diocotran amplification suppression *(Russian)* 3—16922

electronic calculators
heading is late addition, see also minicomputers
data processing of meas. results of lens frequency-contrast characts. *(Russian)* 3—9933

electronic component manufacture *see electron device manufacture*
electronic data processing *see data processing*
electronic density of states
alloy, binary, effect of local order 3—20994
alloy, disordered, band-edge behaviour, short-range order effects 3—27202
alloy, disordered, substitutional, density of states in impurity band, CPA calcs. 3—24371
alloys, binary, off-diagonal randomness, theoret. approach comparison 3—30384
alloys, binary, strong scatt., model calc. approximation 3—24366
alloys with short-range order, self-consistent single-site approx. 3—18067
amorphous covalent semicond., study using multiple scattering theory to show pseudogap 3—20991
amorphous solid, Weaire model 3—15114
charge density analysis, effect of models for thermal motion and two-centre scatt. 3—14654
charge density oscillation around resonant scatt. impurities 3—4961
copper phthalocyanine, photoelectric emission, density of states, electron-electron m.f.p. 3—18527
core level excitation techniques 3—38768
disordered material, calc. using Bethe-Peierls approx. 3—38769
disordered short-range dislocation system, fluctuation region of electron energy spectrum *(Russian)* 3—8081
disordered system, density of bound states in one dimensional array 3—18059
disordered system model 3—8079
disordered systems, averaged density of states 3—38777
electron-plasmon approx., single particle Green's function 3—20980
insulator, paramagnetic, single particle density of states in mag. field 3—15113
interacting linear chains, electron network model description 3—26162
IV-V transition metal carbides, concentration dependence of hardness in terms of density of states *(Russian)* 3—12433
liquid alkali metals, calc. and comparison with free electron model 3—18054
liquid metal, determ. from one-electron continuum Green's function, tight binding model 3—38773
liquid metals and semiconductors, review of electric properties 3—30385
metal, effect of singularities on thermodynamic props. *(Russian)* 3—8099
metals, 1-20K, and specific heats 3—1806
metals, V and Fe-Zn, unfilled one-electron levels, X-ray continuum isochromat study 3—36536
molecular solids, photoemission rel. to impurities and defects 3—15588
numerical calc. within Brillouin zone 3—8080
piezoelectric semiconductor, degenerately doped, rel. to acoustoelec. interaction 3—18194
semiconductor, compound, state density determ. by Auger and photoemission electron spectroscopy 3—24381
semiconductor, in external elec. field, direct calc. 3—1969
semiconductor, neutral, impurity density-of-states tails 3—11844
semiconductors, heavily doped, temp. dependence of, density-of-states effective meas. in 1 to 20 K range 3—8121
spectral props. of solids, numerical calcs. by integration over Brillouin zone 3—20983
superconductors, computation of phonon spectra from tunnelling characteristics 3—2204
surface states, network model of electrons in solids 3—27297
TCNQ complexes, low temp. mag. props. study *(Russian)* 3—8332
thin films, calcs. 3—27295
transition metal and alloy superconductivity, high press. effects on density and transition temp. *(German)* 3—34026
transition metal surface, electronic density of states model, application to ferromag. Ni 3—33981
Van Hove singularities and zero point slopes in crystals 3—30382
Wannier function construction 3—38767
Al, in valence band, from Auger spectra fine structure 3—34452
Be, in valence band, from Auger spectra fine structure 3—34452
Be, influence of non-locality of Shaw's model potential 3—1979
Be, liq., calc. 3—38776
C fibre, Auger and secondary electron emission spectroscopy 3—5346
Ca, APW calc. as function of lattice const. 3—18070
Ca, calc. from muffin tin pot., photoemission energy distrib. meas. and calc. 3—34462
CaTl$_3$ curve from band structure calc. compatible with oscillatory curve of Cu$_3$Au 3—1984
CdS, cubic, electron density, potential distribution *(Russian)* 3—30085
CdTe compensated doped crystals, density of states tails, conductivity, Hall mobility, conduction band 3—33832
α-Ce, elec. resist. and magnetisation obs. 3—8143

electronic density of states continued
Co, paramag. f.c.c. phase, KKR calc. with Gaspar like pot., exchange energy contrib. 3—36515
Co silicides, ultra-soft X-ray spectra analysis *(Russian)* 3—30893
Cs$_3$Bi(Sb), valence band density of states determ. from photoemission and electron scatt. 3—24773
Cu, electronic spectra determ., cluster calc. 3—36516
Cu:M, dil. alloy, M = transition metal, pair description 3—30596
Fe, electronic spectra determ., cluster calc. 3—36516
Fe, in valence band, from Auger spectra fine structure 3—34452
Fe, paramag. and ferromag. states, self-consistent band calc. 3—21205
p-GaAs-metal tunnel junction, heavily doped, effective mass and Fermi energy 3—33995
n-GaSb, heavily doped density-of-states tails associated with L-minima of conduction band 3—30425
Ge, amorphous, cohesive energy and density of states 3—36521
Ge, crystalline and amorphous phases, band struct. and density of states 3—33776
Ge, high press. phases, comparison with amorphous Ge 3—30095
Ge, hole density of states effective mass under stress and strain 3—18081
Hg, liquid and solid, photoemission meas. of density of states rel. to pseudogap 3—34463
HgSe at Fermi level, magneto-quantum effects, determ. of band struct. 3—2003
InSb, calculations for various magnetic fields at the metal-insulator transition 3—33829
InSb, rel. to spontaneous spin-flip Raman line shape 3—36870
Mg$_2$Sn, valence band electron density of states determ. by Auger and photoemission spectroscopy 3—24381
Mo and Mo-rich-RE Mo-Nb alloys, rel. to Hall effect and resist. 3—38824
Nb and Nb-rich-Zr alloys, rel. to Hall effect and resist. 3—38824
Nb$_3$Sn, i.r. absorptivity calc. 3—34360
Ni, electronic spectra determ., cluster calc. 3—36516
Ni, nucl. relax. rate of ^{101}Ru, rel. to virtual bound state 3—2442
Ni-Cu alloy, calculation, comparison with photoelectron spectra 3—36976
Ni-M alloys, f.c.c., ferromag., M = Co, Fe, Mn, Cr, at Fermi level, calc. 3—8328
Ni$_3$P, density of states curve, band struct. calcs. 3—4950
NiS, paramag. metal to antiferromag. semimetal transition, density of states at Fermi surface 3—36540
Pd, determ. using augmented-plane-wave method 3—1983
Pd, press. dependence, electron-phonon interactions 3—18075
Rh, calc. and rel. to energy distrib. curve for photoemitted electrons 3—15121
ScCo, stability investigation by self-consistent KKR method 3—15335
ScCu, stability investigation by self-consistent KKR method 3—15335
Se, amorphous, molecular orbital studies 3—36520
Si, amorphous, cohesive energy and density of states 3—36521
Si, crystalline and amorphous phases, band struct. and density of states 3—33776
Ti silicides, ultra-soft X-ray spectra analysis *(Russian)* 3—30893
TiFe, stability investigation by self-consistent KKR method 3—15335
TiNi, ordered, APW calc. of component local densities of states 3—18053
Tl-Te molten alloys, polygenic character, comp. and temp. depend. *(Russian)* 3—24370
V$_3$Au cpds., ^{51}V spin-lattice relax., rel to density of states at Fermi level 3—2211
VMn, stability investigation by self-consistent KKR method 3—15335
VO, determ. from augmented-plane-wave method calc. 3—2016
VO$_2$, metallic, calc. 3—36541
VO$_2$, semicond., calc. 3—36542
Yb, unoccupied 5d band 3—18532

electronic desk calculators *see electronic calculators*

electronic music
see also musical acoustics; musical instruments
No entries

electronic structure, atomic *see atomic structure*

electronic structure, molecular *see molecular electronic structure*

electronics applications of computers
axially symmetric electron optics systems, e.s. field computation 3—802
capacitance between three-dimensional electrodes, digital computer techniques 3—19478
electron beam therapy, field patching 3—10163
electron optics, three dimensional problems, digital computer techniques 3—19478
fractional parentage coefficients for equivalent electrons in jj-coupling, computer calculation 3—19483
Gunn device calc., using finite difference method for solving partial differential eqns. 3—27268
microfabrication using electron beams 3—35513
semiconductor diffusion system, computer control 3—34488
semiconductor growth, automated, monitoring lateral dimensions 3—12312
slot-coupled toroidal resonators, scatter calculation by computer *(Russian)* 3—32401
solids, energy bands and electronic structure calculation, symmetrised program 3—20981
Si crystal growth, production system 3—12323

electrons
see also beta-rays; cosmic ray electrons; positrons
aurora particle precipitation by plasma injection 3—25296
auroral, 0.8 to 16 KeV, pitch-angle distributions 3—12788
bremsstrahlung, ang. distrib. calc., confined in magnetic mirrors 3—20050
bremsstrahlung, linear polarisation, from atomic scatt. 3—20052
bremsstrahlung and pair production 3—6613
Crab Nebula, spatial distrib. of relativistic electrons, diffusion-loss model 3—16283

electrons continued
  electron motion in constant and orthogonal e.m. fields *(Russian)* 3-3995
  electrostatic electron cyclotron harmonic waves in the magnetosphere 3-16035
  field theory, gauge-invariant, nonlinear, in Clifford space 3-22984
  gyromagnetic ratio, anomalous, sixth-order contributions 3-836
  magnetic moment, anomalous, calc. and reln. to infinite momentum frame 3-14107
  magnetic moment computation by vertex graphs technique 3-35738
  motion in quantized electromagnetic field 3-23050
  polar cap and boundary of open geomagnetic field lines 3-12655
  propagator, average, in disordered system, correlation function expression 3-32440
  radiation belt slot region, pitch angle diffusion meas. 3-16033
  self-energy, second-order, in finite q.e.d. 3-10688
  solar flare plasma, electron acceleration and radiation processes 3-18947
  synchrotron radiation identification method in beams >50 GeV/c 3-10029
  Al, Al_2O_3 foils, energy loss analysis by thermomodulation procedure *(German)* 3-28640
electrooptics *see electro-optical effects*
electroosmosis *see osmosis*
electrophoresis
  deposition method 3-34730
  divalent ions (Ca^{2+}, Sr^{2+}, Cd^{2+}, SO_4^{2-}) electrodiffusion determ. in gels by radiotracers 3-39451
  microelectrophoresis assembly, for cellular surface studies 3-25998
  microelectrophoresis study of surface properties of insoluble metal oxides 3-5393
  overlapping gaussian and skewed peaks, resolution computer programs 3-3931
  polyelectrolyte solns., colloid stability detern. by laser Doppler spectroscopy 3-34661
  polystyrene latex charged particles in buffer solution, spectroscopy of scattered light 3-9018
  solid spherical particles with arbitrary conductivity 3-31198
  $BaTiO_3$, polycryst. film with ferroelec. and antiferroelec. props., deposition by electrophoresis 3-39220
  $PbTiO_3$, polycryst. film with ferroelec. and antiferroelec. props., deposition by electrophoresis 3-39220
  $PbZrO_3$, polycryst. film with ferroelec. and antiferroelec. props., deposition by electrophoresis 3-39220
electrophotography
  electronic copiers 3-25788
  electrophotographic papers containing CdS, elec. and photoelec. props. 3-37648
  metallic thin films, on photoconductive thermoplastic substrate, information recording 3-6007
  nip, pressure and film thickness around, numerical soln. 3-25785
  photocopying machine BD-34A 3-25790
  photoelectret and thermoelectret states of ZnO-Boswellia Glabra mixture used for electrophotographic coatings 3-22393
  thermoelectret applications, review 3-8508
  transfer of powder images, effects of pressure *(Russian)* 3-239
  xerographic discharge characts. of photoreceptors 3-16456
  xerographic image study, electric field, transfer and spread functions 3-36659
  xerography, amorphous Se-based photoreceptor applic. 3-16455
  xeroradiography, review 3-26000
  CdS:S system as photoelectret electrophotographic layer, photopolarization study 3-36833
  Se:As, As_2S_3, Bi, SiO, doping in vacuum growth to produce semicond. film for electrophotography 3-15623
  ZnO, Li doped and undoped, single crystals, baked layers, electrophotographic discharge mechanism *(Russian)* 3-30517
electrophotoluminescence *see electroluminescence; photoluminescence*
electrophysiology
  see also biomedical phenomena
  cardiac, pacemaker activity and atrioventricular conduction, vagal and stellate nerve stimulation effects in dog 3-35237
  cochlear partition, comparison of effects of biasing with electrical current and sound stimulation of DIF SP responses 3-3477
  cochlear whole-nerve response to acoustic transients, origin of negative deflection N_2 3-3476
  denervated transplanted human heart, electrophysiological studies 3-37518
  pigeon, visual projections to wulst 3-28342
  prosthetic arm, externally powered, e.m.g. sensor design 3-6127
  tunnel of Corti, recording of local potentials using microelectrodes 3-3475
electroplating
  applications, with physical development photographic development 3-27905
  boride coating form. of Fe-plated metals and alloys 3-27693
  over-critical films, domain structure 3-39000
  steel, 316 stainless, proton irradiated, cross-section preparation technique for transmission electron microscopy 3-8026
  Al surface, electro-displacement deposition method for Zn, Zn diffusion 3-11766
  Au plating, puriy of Au deposits as function of metal concentration 3-12527
  Ni, from ethylene glycol electrolyte 3-25071
  Sn in Fe and Cu bases 3-9073
  Ti on Fe bases 3-9073
  Zn on Fe bases 3-9073
electropolishing *see electrolytic polishing*
electroreflectance
  complex plane analysis in electrode modulated specular reflectance 3-25070
  III-V semiconducting alloys, spin-orbit splitting 3-2013
  metal, surface electron density interpret. *(French)* 3-18432
  modulation spectroscopy, electric field effects, vector and tensor perturbations, crystal structure 3-34334
  semiconductor, energy band structure in low-field limit 3-2518
  semiconductor, theory of phonon electroreflectance 3-27503
  semiconductor boundary layer, reflectivity with non-normal incidence and surface plasmon 3-27302
electroreflectance continued
  servosystems for electroreflectance meas. 3-32065
  state-of-the-art 3-15473
  Ag film, dielec. const. determ. 3-12154
  $AgInSe_2$, electronic structure from electroreflectance and photoluminescence meas. 3-39183
  Au, optical electromodulated properties in 1.3-7.3 eV photon energy range 3-30800
  Au film, dielec. const. determ. 3-12154
  Au spectrum, electrochemical electrode metals, influence of the potential 3-36855
  $Cd_xHg_{1-x}Te$, meas. rel. to alloy comp. and band structure 3-12114
  $CuInSe_2$, electronic structure from electroreflectance and photoluminescence meas. 3-39183
  GaAs, neutron irrad., electroreflectance obs. of metal-like plasma reson. 3-4973
  GaAs, study of radiation damage by obs. of shift in reflectance peaks by optical modulation spectroscopy 3-27040
  GaAs semiconductor surfaces, Schottky barrier effect, diffusion potential, impurity concentration 3-33982
  Ge, E_1 transition in low field limit, two or three dimensions 3-18434
  Ge, high resolution and uniaxial piezo-electroreflectance, using Ge-Cu_2S heterojunction 3-2520
  n-InAs, electroreflectance spectra, line shape, electrolyte method *(Russian)* 3-34371
  InP, spectra rel. to hydrostatic press. *(Russian)* 3-8610
  Mg_2Sn, logarithmic derivative refl. spectra, 1.3-3.2 eV 3-2561
  Pt spectrum, electrochemical electrode metals, influence of the potential 3-36855
  Se, study of radiation damage by obs. of shift in reflectance peaks by optical modulation spectroscopy 3-27040
  Si, doping inhomogeneities, electroreflectance meas. 3-39285
  Si, heavily doped, interpretation of spectra structure 3-2519
  Si electroreflectance obs. of E_0 and $E_0+\Delta_0$ transitions 3-4948
  Te, electroreflectance line due to interband magneto-optical transitions 3-2524
  WSe_2, line shape of electro-reflectance excitonic structure 3-2038
  $ZnSnAs_2$, chalcopyrite and sphalerite forms, neutron effects 3-15514
  ZnTe single crystal, excitons and Zn vacancies obs. *(Japanese)* 3-11605
electrospark machining *see spark machining*
electrostatic devices
  see also capacitors; electrostatic generators; electrostatic lenses
  analyser, 127°, performance as a spectrometer 3-28690
  analysers, calibration using standard omnidirectional electron beams 3-25943
  axisymmetric electrostatic collector design problem, electron steady-state flow, numerical solution and Fortran program 3-32490
  biprism, electron interference, Fresnel integrals 3-22977
  electron energy selector for ionisation meas. by crossed beam method 3-11173
  electron-ion equipment, limit concentrations of disperse phase 3-13671
  grid-type electrostatic precipitator, investigation and analysis 3-13669
  image of off-axis point source in cylindrical-mirror electrostatic analyzer *(Russian)* 3-6096
  mirror, toroidal, particle optical props. in plane of symmetry, cylindrical condenser application 3-16920
  neutralizer, spatial distrib. of ionizing process near radioactive surface *(Russian)* 3-22443
  precipitator, interelectrode flashover voltage meas. *(Polish)* 3-10421
  tandem accelerator, heavy ion acceleration, alternates to cyclotron 3-10013
  toroidal analysers, characteristics determ. *(French)* 3-13451
  transfer electrostatic printing system, patent 3-13676
  winding, four-pass, for sorting of molecules 3-19589
electrostatic fields *see electric fields*
electrostatic generators
  see also Van de Graaff generators
  liquid-immersed h.v., performance 3-664
  state-of-the-art 3-663
  thermoelectret applications, review 3-8508
  at Tomsk Polytechnic Institute *(Russian)* 3-19254
  triboelectrogasdynamic system for crop spraying expt. 3-656
electrostatic lenses
  see also focusing; particle beams
  achromatic system with minimum electric fields 3-361
  asymmetrized quadrupole lenses, paraxial chromatic aberration 3-13782
  line focusing of ion beams, for accelerators 3-25839
  monochromatic electron beams production 3-35723
  photoelectron spectrometers, three element cylindrical lens, constant focal position over wide kinetic energy range 3-10102
  quadrupole, potential for given axial gradient 3-13455
  quadrupole system, paraxial electron optical imaging, wave mechanical basis *(German)* 3-35720
  quadrupole-octupole lenses in electrostatic prism spectrometer, geometric aberrations 3-35488
  formed by two coaxial cylinders, field calculation 3-13456
  two electrode electrostatic cylindrical mirrors, numerical design 3-35725
electrostatic microphones *see microphones*
electrostatic precipitation
  cement industry applications, clinker coolers 3-13674
  dust from high PbO waste gases, optimum conditions *(German)* 3-19550
  grid-type electrostatic precipitator, investigation and analysis 3-13669
  industrial atmospheric pollution control applications 3-4062
  operating voltage optimal control method *(German)* 3-19551
  particulate matter collection from smokestacks using γ-ray ioniz. 3-17866
  point-to-plane devices with coated electrodes, corona modes, model 3-26186
  precipitator, example of c.-a.d. of complex enclosures 3-37924

electrostatic precipitation continued
precipitator, interelectrode flashover voltage meas. *(Polish)* 3−10421
propane-air flames, combustion nuclei production and electrostatic precipitation 3−5391
steam power stations, fossil fueled, flyash conditioning techniques 3−22806
voltage control by s.c.r. and analogue electronic networks 3−4061

electrostatics
see also electrets; electric charge; electric fields; electrostatic devices; static electrification; triboelectricity
aerosol deposition in polystyrene chamber 3−39415
aircraft discharger system, charged condensation droplets 3−662
airless spray painting, dangerous electrostatic charging 3−661
charge accumulation on fabrics and explosives, temp. and relative humidity effects 3−658
charge distribution on spherical zone, using Robin integral system *(Greek)* 3−6396
charge generation during washing of tanks with water sprays, meas. and interpretation 3−653
charge generation during washing of tanks with water sprays, math. methods 3−654
charge generation during washing of tanks with water sprays, mechanism studies 3−655
charge generation during washing of tanks with water sprays 3−652
charged dust distribs. with plane symmetry 3−28962
clothing, risks of ignition due to static 3−657
clouds, electrostatic field within structure of uniformly spaced coaxial conducting loops 3−31382
conductor, two dimensional electrostatic field calc. *(Russian)* 3−10424
Coulomb system with net charge 3−6394
crop spraying, and expts. with triboelectrogasdynamic generator system 3−656
current due to probe charge moving through static space charge 3−32480
cylindrical conducting plane, dielectric-covered, electric field calc. 3−13673
dielectric hereditary media, variational principle *(Italian)* 3−30740
dielectric sphere potential energy in an arbitrary quasistatic electric or magnetic field 3−35658
dimensional analysis, rel. to streaming currents and decay of apparent cond. 3−650
dynamic systems, charge meas., a.c. method 3−665
electrocardiogram as a teaching example of electrostatics 3−37575
emissions from the light latitude ionosphere, satellite v.l.f. obs. of electric fields 3−16015
energy matrix calc., by computer in Racah-Slater method 3−26185
fields in homogeneous media for given source distribution integral characteristics *(Russian)* 3−32486
fine particle charging in negative corona near sparkover 3−4692
flexural deformation of an initially curved cuboid dielectric 3−28866
Green's function and images in electrostatics problem 3−22799
hemispherically capped rod and plane electrodes 3−13672
induction problems, soln. by singular integral equations *(Russian)* 3−19546
interstellar grains, electrostatic potential rel. to H I ans H II regions and circumstellar envelopes 3−39749
macron clouds, charging and discharging, role of gas breakdown 3−35657
magnetospheric electrostatic waves interaction with local plasma particles, OGO 5 measurements 3−3152
metal plates, force between them arising from contact pot. 3−10422
metal/electrolyte interface, elec. double layer, electrode reactions and static 3−2821
metallic thin film, adhesion on insulating substrates, electrostatic contribution 3−8070
model for correlation between gaseous metal atom ionisation energy and solid work function 3−4376
multiwire proportional chambers, problems 3−10062
plasma wave dispersion relation, a meas. technique 3−17604
powders, separation and concentration, ponderomotive forces in nonuniform field, anal. *(Russian)* 3−21753
sound recording, expt. 3−648
spheroidal coord. systems, appl. to undergraduate physics problems 3−31991
streaming media, size of stationary space charge clouds 3−651
tank filling, estimation of electrostatic hazards 3−659
testing for static proneness, appl. of charge and resist. meas. 3−2787
theorem concerning average field value, proof 3−22800
turbulence, ion heating source in colliding solar wind streams 3−31517
two earthed spheres boundary value problem, solution by image potentials *(German)* 3−4052

electrostriction
see also piezoelectric materials; piezoelectricity
Love waves propagation in electrostrictive dielectric media 3−13596
self-focusing in optical glasses, relative contribution of Kerr effect and electrostriction 3−29149
vibration excitation in dielectric, method for meas. u.s. attenuation 3−5779
$AgNa(NO_2)_2$, anomalous temp. depend., rel. to improper ferroelectricity 3−24655
$BaTiO_3$:CeO_2, non piezoelec. dielec. ceramic, electromechanical bond coeff. *(Russian)* 3−21365
CaO, rel. to Stark effect of F-centre 3−30858
Fe_3S_4, elec. field induced anisotropy, electron diffr. studies 3−5163
LiF, electromechanical effect 3−34298
$(NH_4)_2SO_4$, and elastic compliance at ferroelec. transition 3−30781
$(NH_4)_2SO_4$, elastic compliance functions, electrostrictive consts., anomalies at ferroelec. transition 3−15453
NaCl, electromechanical effect 3−34298
$NaNO_2$, anomalous temp. depend., rel. to improper ferroelectricity 3−24655
$NaNO_2$, ferroelectric, rel. to elec. breakdown 3−5160
SbSI, electromechanical hysteresis and photo deformation effect 3−34300
SbSI multiple domain effect, illumination induced, hysteresis loop 3−34299

electrostriction continued
$SrTiO_3$ substrate, surface acoustic wave generation 3−4908

electrosynchronisation *see synchronisation*

electroviscous effect
see also colloids; viscosity
No entries

element origin
see also cosmic ray origin; cosmology
light elements in Universe, review 3−31512
r-processes, delayed-neutron emission at final stage, application of gross theory 3−25365
$^{12}C/^{13}C$ meas. in extragalactic sources and solar neighbourhood 3−25385

element relative abundance
see also isotope relative abundance
Apollo 16 and Luna 20 soils, chemical composition and trace element abundances 3−12989
basal metalliferous Pacific sediments from Deep Sea Drilling Project 3−34875
brine hole in Red Sea (Ostapoff's 4th), chem. anal. and comparison with anoxic fjord sample 3−27992
α Centauri, visual binary star, chemical composition of A and B components 3−9565
cosmic ray nuclei, leakage path length dependence on energy 3−21991
cosmic ray rigidity spectra meas. for H to Fe elements between 5 and 100 GeV/c 3−37270
δ Delphini, δ Scuti-type variable star, curve-of-growth anal. 3−35155
dolerite plugs (Late Tertiary) of S. Cariboo Region, British Columbia, petrology 3−37147
dunite from Almklovdalen, west Norway, element distribution between metal and silicate phase 3−2851
exosphere, H abundance, diurnal variation rel. to exospheric temperature 3−34923
G- and K-type supergiant stars, comparison with solar abundances 3−31667
giants of disc population, line blanketing in u.v. due to elements heavier than CNO group 3−28198
HD156074, C star, atomic and molecular spectra rel. to atmospheric abundances 3−22064
HD 116745, F-type giant star in ω Centauri, curve of growth anal. 3−31703
HR 646 (η Arietis), differential analysis of metal deficient star, heavy element abundances 3−25459
HR 860, differential analysis of metal deficient star, heavy element abundances 3−25459
Lake Superior basin Quaternary sediments, trace element concs. 3−27941
Luna 20 and Apollo 16 fines, large-ion lithophile trace-element abundances 3−12986
Luna 20 samples from Apollonius crater region, K, Rb, Sr, Ba and rare earth concentrations *(French)* 3−12987
lunar biogenic elements, origin and distrib. 3−35090
lunar glasses from Luna 20, major element composition 3−12985
RR Lyrae stars in M22 (globular cluster), metal abundance meas. 3−31753
metals in galaxies, time variations 3−16268
near-main sequence stars, secular stability and effect of perturbations in chemical abundances 3−28174
nucleosynthesis, big-bang, baryonic number and electron leptonic number in Universe, limits 3−25387
old Galactic disk G-type stars, age rel. to elemental abundances 3−13029
planetary nebulae, elemental abundances and ionisation distrib. rel. to theoretical models 3−39743
Population-II A-type stars, revised chemical abundances from spectral analyses 3−22056
protostars, cosmic maser sources from dense condensation and protoplanet formation 3−25445
rare earths in alkaline volcanic rocks from Campania, S.Italy 3−15885
RGO 70, second CH star in ω Centauri and $^{12}C/^{13}C$ ratio 3−3340
solar corona, elemental abundances and model of quiet Sun from radio and u.v. observations 3−18939
solar cosmic ray particle Fe-group abundances in 1971 Jan. 24 and 1971 Sept. 2 event 3−37278
solar e.u.v. quiet spectrum meas. rel. to relative abundances 3−22012
stellar nucleosynthesis r-process, abundance variations due to neutron flux 3−31640
stellar spectra, multiplet obs. 3−39676
super-heavy elements, production processes 3−23198
superheavy, reln. to astrophysical beta decay formulas 3−32818
trace elements in earth crust, use in models of Protoarchean crust development 3−31296
trace metal migration in snow in three environmental areas 3−25246
Ca abundances in G- and K-type giant stars from narrow-band photometry 3−9554
Eu in solar photosphere, Eu II lines, $^{151}Eu/^{153}Eu$ ratio and abundance from high resolution spectra 3−39614
F/Cl ratio in region south of Greenland 3−39500
Fe in δ Cephei, possibility of being super Fe-rich 3−37391
Fe solar abundance determ. from intermediate-coupling line strengths 3−38208
Fe/H variations in North Galactic Pole K-type giants, stars, UBVRI photometry 3−9543
Fe/S ratio determ. for pyrrhotite-bearing rocks rel. to remanence self-reversal 3−25171
^{64}Ge, nucleosynthesis, role of mass. 3−17146
H/Fe variations in North Galactic Pole K-type giants, stars, UBVRI photometry 3−9543
H/He surface ratio, C-stars, effect on spectra 3−13023
He, solar wind variations 3−16137
He content of metal-deficient star 99 Herculis 3−35146
He II underabundance in galactic centre, H and He radio recombination line obs. 3−35194
He in open cluster NGC 2264, II Scorpii, I Lacertae 3−39718

element relative abundance continued
He in RR Lyrae stars from pulsational blue edges of instability region 3−19008
He solar wind abundance, velocity and flux dependence 3−16131
Hf, solar system determ. using the ^{176}Lu-^{176}Hf pair 3−22010
Hg concentrations of Greenland icecap and Icelandic geothermal activity 3−25143
Hg dissolved in Irish Sea, distrib. rel. to pollution sources 3−25197
Li distrib. in Canadian granitoid rocks 3−37149
Mg^{2+}/Ca^{2+} molar ratio rel. to protodolomite formation 3−39481
Mn solar abundance from theoretical line profiles 3−39615
N in HD 188209, abundance anomalies in ON stars 3−9527
N in nitride form, occurrence and abundance rel. to silicate minerals 3−15905
Na in upper atmosphere, effects on seasonal variation 3−21958
Rb/Sr abundance ratio in Sun from Sr I photospheric lines and Rb abundances 3−18933
Ti in solar photosphere, gf-value meas. of Ti I, Ti II 3−26574
U abundance in HR 465 stellar spectra 3−19018
U content in Apollo 15 green soil and rock 3−35083
Xe in carbonaceous chondrite meteorites 3−9514
Zr, solar system determ. using the ^{176}Lu-^{176}Hf pair 3−22010

elemental semiconductors
see also germanium; silicon
defect deep levels, molecular orbital treatment 3−30429
p-diamond:B, seed crystal, growth by vapour deposition 3−36986
diamond:Li, implanted, elec. cond., after annealing at 1400°C *(Russian)* 3−2070
diamond, B as dominant acceptor 3−38810
diamond, defect energies and states, defect-molecule method, extended Huckel calc. 3−33838
diamond, electrical conductivity to metallic state at 1 Mbar 3−18204
diamond, gamma-ray Compton profiles, band structure test 3−11649
diamond, semiconducting, high field magnetoresistance 3−11912
diamond, semiconducting, thermolum. excited by elec. field 3−21494
diamond, types Ia and IIa, thermally stimulated currents, 20-400°C 3−30473
diamond crystals, electrical props. and cathodoluminescence, proton irradiation effects 3−24437
diamond crystals, spectra, absorption and luminescence, red region, neutron irradiation effects 3−36901
electron diffr. and mobility 3−15190
e.m. beam self focusing in inhomogeneous mag. fields 3−10568
heavy rare earth metals, electrons and spin waves 3−8327
optoelectronic properties and device applications, book 3−32574
particles, cylindrical, attenuation factors calc. for i.r. radiation scatt. 3−24698
phonon spectra, amorphous rel. to cryst. state 3−4825
α-Sn, zero bandgap transition, inverted band model, uniaxial stress studies 3−38800
X-ray atomic scattering, functions, influence of tetrahedral covalent bonds *(Russian)* 3−11582
As, amorphous, photoelec. emission *(French)* 3−21512
B, hopping conduction at low temp. rel. to local order 3−21075
β-B, rhombohedral, diamag. susceptibility, temp. depend. 3−38960
β-B, rhombohedral, relax. of non-equilib. cond. 3−27255
B thermoelectric props., thermal and elec. cond., temp. depend. 3−36630
C, glassy, switching phenomena, correlation between memory time and resistivity 3−33966
Ge, anisotropic semiconductors, light scattering calculation 3−8580
p-Ge, anisotropy of magnetothermal conductivity 3−1842
Ge p-n junctions, ionization energy of adhesion levels and thermogeneration centres in a volume of microplasma *(Russian)* 3−4960
Se, amorphous, electronic energy struct., molecular orbital studies 3−36520
Se, amorphous, hole mobility rel. to conductivity hysteresis at vitrification temp. 3−30529
Se, amorphous, refr. index, dispersion and magnitude 3−36851
Se, amorphous, X-ray irrad., electrophotographic layers, fatigue mechanism *(Russian)* 3−33947
Se, barrier model of conduction for d.c. meas. depend. on temp. *(German)* 3−33905
Se, hexagonal, polycrystalline layers, dark conductivity for high current densities *(Russian)* 3−30475
Se, liq., drift velocity, hole photogeneration, quantum efficiency *(Russian)* 3−8179
Se, resonant Raman scatt., 1.8-2.7 eV, room temp. 3−5202
Se, reversible switching effect above 720°C 3−36645
Se, trigonal single crystals, electroconductivity, current-voltage characteristics, temp. dependence *(Russian)* 3−33890
Se, vacuum evaporated layer, amorphous and crystalline phase obs. 3−20970
Se, X-ray irrad., electroradiographic layers discharge mechanism *(Russian)* 3−36638
Se amorphous film, photocond., temp. and applied field depend. *(French)* 3−27289
Se current saturation rel. to internal potential barrier, 77-290 K 3−30486
Se glassy, elec. cond., density and crystn. rate rel. to S and Te additions 3−33887
Se single crystal, p-n junction, props. *(Russian)* 3−11949
Se trigonal single crystal, photoconductivity, thermally stimulated currents, trap distrib. obs. *(Russian)* 3−30516
p-Si, anisotropy of magnetothermal conductivity 3−1842
Si, electron irradiation at 0.5K, a.c. conductivity changes 3−7794
Si oxidised surface, m.o.s. electron surface mobility in inversion layers at room temp. 3−8268
Si:Co, thermal emission rates and activation energies of electrons and holes 3−15154
Te, acceptor states, theory 3−36544
Te, acoustoelec. non-ohmic conduction, carrier conc. depend. 3−33959
Te, amorphous, refr. index, dispersion and magnitude 3−36851
p-Te, anisotropic phonon coupling in magnetophonon resonance 3−7874

elemental semiconductors continued
Te, current-stimulated emission of e.m. waves, mechanism *(Russian)* 3−8200
Te, defect induced absorpt. spectra obs. near electronic band edge 3−21449
Te, Dember, Hall and elec. cond. meas. rel. to carrier mobility anisotropy 3−21111
Te, electrical conductivity when highly-excited by laser beam, calc. 3−8221
Te, electron domain propag. in the temp. range 77°K to 293°K 3−18156
Te, electron irrad., lattice defects, galvanomagnetic props. 3−33934
Te, electron irrad., recovery steps, isochronal and isothermal annealing expts. 3−33562
Te, enhancement of capture rate of excess carriers due to acoustoelec. amplification 3−2143
Te, fast photoelectromagnetic effect, induced by 10.6μ laser radiation 3−27288
Te, inactive mode cyclotron resonance absorption 3−8106
Te, intervalence band transitions, absorpt. spectra calcs. 3−21006
p-Te, magnetoresist., transverse and longit., impurity band like states, 0.4-4.2K 3−27275
Te, resonant Raman scatt., 1.8-2.7 eV, room temp. 3−5202
p-Te film, vacuum deposited, carrier mobility *(Russian)* 3−30481

elementary particle decay
see also electromagnetic decays; hadron decay; leptonic decays; muon decay; semi-leptonic decays
exponential decay law of nonstable particles 3−6303
phase space 2-body, alternate calc. 3−23021
unstable composite particles, relativistic three-particle eqns. 3−826

elementary particle electromagnetic interactions
$A+B \to C+X$ (A, B, C=1, γ or hadron) e.m. interaction at high energies, parton model 3−17059
analytic invariant amplitudes for photon-hadron interactions with discrete symmetry 3−26310
charge-conjugator invariance violation and the isotensor current with mixed transformation props. 3−13805
clashing symmetries in unified description of weak and e.m. interactions, Han-Nambu model 3−35774
currents, connections between weak and electromagnetic 3−13815
cutoff vector-gluon model, scaling behaviour 3−35802
deep inelastic reactions, application of duality principles 3−13932
deep inelastic structure functions, symmetry principles and constraints 3−16955
dual parton model-string model 3−26318
dynamic resonance model, with e.m. interaction, calc. of elastic form factor 3−14021
electric Born term model with absorpt. effects for π electroproduction beyond resonance region 3−17061
fixed poles, scaling and Schwinger terms, two-current matrix elements 3−13977
fixed-pole residues and operator Schwinger terms, connection 3−35791
gauge field theory and Cabbibo angle 3−16945
gauge model, triplet realisation of weak and e.m. interactions 3−13795
gauge model of strong and e.m. interactions, baryon mass differences 3−26276
gauge theories, unified, of weak and e.m. interactions, G-G model 3−32643
gauge theory, O(4) treatment of electromagnetic weak synthesis 3−6565
hadron structure in weak and e.m. interactions, $U(1)\times SU(2)$ gauge models 3−32644
hadronic symmetries and gauge theories 3−23025
hadrons, using Regge pole exchange 3−16994
helicity structure functions, scaling behaviour 3−17032
high energy diagonalization over particle helicity *(Russian)* 3−10717
high-energy behaviour of particles, in quantum electrodynamics 3−13847
higher order corrections, renormalization 3−13848
inelastic e^- and μ scatt., positivity restrictions from e.m. hadronic tensor props. 3−13893
inelastic lepton scattering, inclusive reactions 3−6630
lepton-hadron symmetry breaking and Cabibbo rotation 3−10640
light-cone ordering and current commutators, construction of Green functions, sea-gull terms 3−23008
minimal interaction with spin-two particles, Lagrangian approach 3−860
model without neutral currents, muon g-2 and other constraints 3−13829
parity-violating e.m. interaction for hadrons 3−32663
particles with spin 3−6613
parton model, applic. to e.m. processes 3−38055
pseudoscalar meson decays, e.m. interact. in $SU(3)\times SU(3)$ symmetry *(Russian)* 3−29204
reducible scale invariance at short distances, conformal symmetry and canonical scaling 3−38005
relativistic quark model, vector-meson dominance in e.m. interactions 3−13791
renormalizable gauge model of weak and e.m. interactions, pseudo-Cabibbo structure 3−38020
renormalizable guage field model of weak and e.m interactions with CP-violation 3−10616
renormalization of unified theory of weak and e.m. interactions 3−16944
scaling functions of deep inelastic scattering and annihilation processes, generalized crossing relation 3−23085
scaling props. approach 3−6574
SO(3) gauge theory of weak and e.m. interactions with Han-Nambu quarks 3−26287
spontaneously broken gauge theories, generalized renormalizable gauge formulation 3−10641
structure functions for deep inelastic scattering and annihilation of current in ladder models 3−16946
T invariance, study using $\gamma n \to p\pi^-$ 3−16998
three triplet hadron model, broken weak and e.m. interaction symmetry 3−17074

elementary particle electromagnetic interactions continued
time-reversal violating Lagrangian for nucl. reactions with e.m. interaction 3–16949
U(3) nonet scheme with 6 heavy leptons 3–23026
unified gauge theories, effective weak-interaction cutoff of e.m. radiative corrections 3–38035
unified models of weak and e.m. interactions, μp scattering and effects of neutral currents in scaling region 3–10712
unified theories of weak and e.m. interactions from $\Delta I=112$ rule in nonleptonic weak interactions 3–35781
unified weak and e.m. interaction theory, test of light-cone bilocal algebra of currents 3–16957
Weinberg's gauge theory, calc. of divergences in weak and e.m. corrections to μ decay 3–10666
Weinberg's lepton model, compact version, construction of gauge fields as bound states of spinor fields 3–4154
Weinberg's model, anomaly-free version 3–818
Weinberg's model, overall coupling constant renormalization 3–29171
Weinberg's model, static quantities calc. 3–6557
Weinberg's $SU_2 \times U_1$ model, mixing angle determ. 3–32633
Weinberg's unified gauge model of leptons and hadrons, p-n mass difference 3–26299
Weinberg model of weak and e.m. interactions, calc. of soft-π and soft-k mass differences 3–26300
Weinberg model of weak and e.m. interactions, triplet representation of leptons 3–13828
Weinberg W-meson, possible observation in anomalous cosmic ray events 3–16087
μ cosmic ray interactions in Fe, 6-200 GeV, search for charge asymmetry 3–5549
μ cosmic ray interactions in Fe, 6-200 GeV, momentum dependence of interaction probabilities 3–5550
n-p mass difference calc. in semirealistic gauge model of weak and e.m. interactions 3–35789

elementary particle inclusive reactions
$A+B \rightarrow C+X$ (A, B, C=l, γ or hadron) e.m. interaction at high energies, parton model 3–17059
$ab \rightarrow c +$ anything, fragmentation in φ^3-theory ladder model 3–23186
bootstrap model, extension to include quantum numbers, determ. of distrib. functions 3–38098
bootstrap model for multiparticle processes, formation of fireball and leading particle 3–917
central region, particle and antiparticle spectra *(Russian)* 3–4231
characteristics in many Lorentz frames, two-dimensional plots 3–14098
charged particle production at CERN as a function of transverse momentum 3–17140
coherent hadron-nucleus collisions, inclusive particle spectra, diffraction excitation models 3–10819
composite theory of inclusive scattering at large transverse momenta 3–918
continuum electroproduction by coincidence meas., inclusive final states 3–13937
correlation functions, generating functional and sum rules 3–23182
correlation parameters of charged particles, single-excitation diffractive model 3–17129
correlations, hadronic scaling 3–6675
Deck model for triple-Regge couplings 3–4199
di-triple Regge expansion, photon Reggeization in massless quantum electrodynamics 3–32659
differential cross sections in pionization limit, study via Gribov-Feynman graphs and Mueller's generalized optical theorem 3–17137
diffraction peak slope and total cross section, general inequality *(Russian)* 3–17128
diffractive dissociation, domination of high energy total cross section 3–14091
diffractive models and high multiplicities 3–19713
diffractively excited cluster decay and exclusive components 3–35847
double pomeron exchange in inclusive and exclusive expts., multiperipheral model 3–23112
dual-Pomeron amplitude, single-particle spectrum and scaling 3–26324
electroproduction, semi-inclusive, Drell-Yan scaling 3–38053
electroproduction, semi-inclusive deep inelastic cross sections, azimuthal dependence 3–23087
electroproduction cross-section for π^+ in proton fragmentation region, prediction via factorization 3–17031
energy dependence of inclusive spectra at X=0 and x=0 3–14096
energy fragmentation distribs. and momentum integrals 3–6680
energy-momentum sum rules, derivation 3–19676
finite-energy sum rule, application to triple-Regge amplitude 3–14095
generalized optical theorem study of reactions with multi-Regge expansion, elimination of unwanted coupling schemes 3–10746
hadron collisions, cross-sections and correlations at very high energy, theory 3–29285
hadron collisions at high transverse momemtum, point-like interaction behaviour 3–38092
hadron scattering on nuclei at high-energy, momentum loss spectra 3–32851
hadronic scaling, predictions for ratios of cosmic-ray components in atmosphere 3–28099
Harari-Freund two component duality in baryon inclusive spectra, quark topologies 3–17070
high energies, analysis of pionization, scale invariance and limited fragmentation in terms of analyticity and unitarity 3–6683
high energy collisions, sealing of multiplicity distribs. 3–932
high transverse momentum, extension into kinematic region 3–17139
hypercharge and isotopic-spin conservation constraints 3–26356
inclusive photon distributions, π^0 and bremsstrahlung contributions 3–23189
inelastic lepton scattering 3–6630
isospin invariance constraints and rapid scaling criteria for degeneracy 3–17130
kinematical constraints, sum rules 3–17080
light cone, exotic application to inclusive reactions 3–17126
Muellerism and mean multiplicities 3–913

elementary particle inclusive reactions continued
multiparticle inclusive spectra, data compilation 3–10817
multiparticle production, unitarity bounds on angular distrib. 3–17133
multiparticle production processes, asymptotic behaviour 3–17127
multiparticle spectra, cluster-decomposition analysis of simple theoretical models 3–903
multiparticle spectra, dynamic models, cluster decomposition analysis 3–10760
multipion production model describing factorizable emission of pion pairs, cluster diagrams 3–38091
multiplicity cross sections, front-back asymmetries 3–920
multiplicity distrib. in central region, independent emission and fragmentation models 3–32694
multiplicity distributions and inclusive cross sections in Regge-pole and Regge cut models 3–38096
multipomeron production of showers at high energy, cross sections 3–38095
n^2 kinematic variable, usefulness 3–17104
n-particle inclusive distribs. in dual reson. model, cluster decomposition 3–14029
nonlinear duality and Pomeron 3–10741
nova model, analytically solvable, asymptotic behaviour for single and two-particle distribs. 3–32696
nova model, calc. of rapidity distribs. for two-particle inclusive reactions 3–4242
one-particle distrib., calc. of triple Regge limit in absorptive multiperipheral model 3–4203
one-particle distrib. in wee-x region, diffractive-excitation model, blackbody radiation 3–38097
one-particle leptonic induced inclusive reactions, applications of quark parton model in deep inelastic region, sum rules 3–17025
particle inclusive, limiting behaviour 3–933
particle production ratios, effects of e.m. and weak decays SU(3) breaking 3–38093
parton-like behaviour in bootstrap theory of infinitely composite hadrons 3–10720
photon induced, review of new data 3–13934
photon-hadron reactions, limiting fragmentation hypothesis and duality, Regge formalism 3–13997
pionization and correlations, uncorrelated jet model 3–35843
polarisation, two-particle correlation and triple-reggeon phenomenology 3–17135
polarisation effects, absorptive mechanism 3–934
production of particles and antiparticles in central region and resonance πN scattering *(Russian)* 3–10816
production of particles on nuclear target, use of Glauber's multiple scattering formation 3–17134
production rates and distinctive components of single-particle distributions, urbaryon rearrangement diagrams 3–4233
rank structure effects, urbaryon rearrangement diagrams 3–14097
Regge phenomenology, generalised optical theorem approach 3–6682
resonance production and inclusive cross-sections, dual model 3–26326
s-channel formation mechanism in ISR central region data 3–29286
scaling in strong interactions above 1 TeV 3–26357
semi-inclusive, induced by polarised leptons on unpolarised and spin 1/2 polarised targets 3–10711
semi-inclusive bubble chamber expts. 3–931
semi-leptonic reactions, neutral-current effects 3–855
shadow and antishadow effects in scatt. of particles on deuterons 3–6681
single particle distributions in small x region, multiperipheral model 3–35844
single-particle and two-particle $\pi^\pm$ p reactions 3–923
single-particle and two-particle processes, survey 3–14089
single-particle processes, analytic structure in complex helicity 3–10747
single-particle production spectra at ISR energies, pionization process 3–23181
thermodynamic inclusive spectra, possible bootstrap origin 3–4239
total cross sections, average behaviour from proof of Pomeranchuk theorem 3–10744
total cross-section meas. in momentum range up to 65 GeV/c by hodoscope method *(Russian)* 3–10814
triple-Regge scaling and behaviour of form factors for resonance couplings 3–35817
two-particle calc. of rapidity distribs. from nova model, study of correlations in production processes 3–4242
two-particle correlation function and multiplicity distrib. in uncorrelated jet model with two leading particles 3–26338
two-particle correlations, new characteristic 3–17081
two-particle correlations, shapes, model and energy dependences in thermodynamic model 3–29287
two-particle correlations in inclusive reactions on light nuclei in emulsion, 50-10^5 GeV 3–34991
two-particle processes, applications of Mueller theory 3–35846
two-photon semi-inclusive reactions in non-perturbative parton model 3–10709
unstable particle production kinematics, reconstruction of π^0 spectra from obs. of one decay γ 3–19748
vector meson production in dual resonance model 3–23188
Veneziano amplitudes, single particle distribs. determ. 3–4189
Veneziano amplitudes, single particle distribs. determ. 3–4190
$ee \rightarrow ee +$ anything, two-photon exchange approximation, general covarint formalism 3–38046
$e^+e^- \rightarrow$ hadrons, inclusive properties, hadronic structure of photon 3–10713
$ep \rightarrow ep^1X$, scaling laws rel. to γp scatt. 3–13976
$ep \rightarrow epx^0$ electroproduction, inclusive proton distribs. 3–851
ep inelastic scattering, semi-inclusive and inclusive processes, phenomenological model based on statistical assumption 3–26312
ep scattering, deep inelastic, study of multiplicity fluctuations in inclusive spectra 3–854
$e^-p \rightarrow e^-\pi +$ anyting, low t theorems and minimal gauge invariant extension of one-pion exchange 3–38049
$\gamma p \rightarrow \pi^- + X$, comparison with $K^+p \rightarrow \pi^+ + X$ and cross section meas. 3–17050

elementary particle inclusive reactions continued
$\gamma p \to \pi^- +$ (anything), inclusive reaction study for polarised photons. 2.8, 4.7 and 9.3 GeV 3−14003
$\gamma p \to \pi^- +$ anything, meas. of differential cross section in proton fragmentation region 3−13999
$\gamma p \to \pi^\pm X$ from H_2, cross-section meas. at 18 GeV, forward angles 3−17056
$\gamma p \to \pi^\pm +$ anything, minimal gauge-invariant extension of pion exchange 3−38045
K/π production ratio in central region, generalized f,f′- coupled Pomeron model 3−23183
K^-p, two-body, cross-sect. and correlation function, detn. at 9 GeV/c 3−23187
$K^-p \to K^0X$, 14.3 GeV/c, triple Regge analysis 3−29292
$K^-p \to \Lambda X$, 14.3 GeV/c, triple Regge analysis 3−29292
$K^+p \to K^0X^{++}$ inclusive reaction, 5.0 and 8.2 GeV/c, behaviour in terms of angular variables 3−6676
$K^+p \to K^0\pi^+X^+$ inclusive reaction, 5.0 and 8.2 GeV/c, behaviour in terms of angular variables 3−6676
$K^+p \to K^{*+}(890)X$, single particle spectra, pion pole effect in fragmentation region 3−26354
$K^\pm p \to \Lambda +$ anything, 13 GeV/c, role of diffractive processes 3−17136
NN interactions at large momentum transfer, hadronic bremsstrahlung production, correlation tests 3−29293
$\nu N \to h_\mu{}^c +$ anything, heavy-lepton production, Monte Carlo calc. 3−19683
νp, high-energy, spin-dependent sum rule relating inclusive cross section to axial-vector coupling const. 3−23046
P inclusive spectra at ISR energies, yield and rapidity distrib. 3−29290
$p + p \to p + X$ between 40 and 260 GeV/c using an internal H_2 jet target 3−35845
$\bar{p}n$ annihilations at rest, inclusive charged π spectra 3−29291
$pN \to XY$, strong and weak interact., interference effects *(Russian)* 3−19749
pp, determ. of average multiplicity for single particle production up to ISR energies 3−19746
$\bar{p}p$ annihilation in multiperipheral Regge model 3−4240
pp collisions, inclusive pion spectra in single- and double-excitation models 3−32725
pp collisions, inclusive thermodynamical spectra in the range 19-1500 GeV/c 3−26355
$pp \to \gamma +$ anything at 205 GeV and its implications for π^0 production 3−10811
pp interactions at 12 and 24 GeV/c 3−922
pp interactions in 23-53 GeV range at CERN ISR 3−927
$pp \to \Lambda/\Sigma^0 +$ anything, triple Regge limit interpretation at 5.7 GeV/c 3−29288
$pp \to pX$, 19 and 24 GeV/c determ. of normalized cross section, test of factorization near kinematical limit 3−4237
$pp \to pX$, 19.2 GeV/c, unitarity bounds on angular distrib. 3−17133
$pp \to p +$ anything study of t/s scaling using parton model 3−6658
$pp \to \pi^-\pi^- +$ anything, 28.5 GeV/c, correlations between $\pi^-\pi^-$ pairs 3−23180
$pp \to \pi^+\pi^- +$ anything, 24 to 1500 GeV/c, prediction using Landau's hydrodynamical model 3−38094
$pp \to \pi^\pm +$ anything, comparison of data at 28.5 GeV/c and 1000 GeV/c, scaling limit 3−919
pp scattering, hadronic bremsstrahlung model for single-particle distribs. 3−4241
pp semi-inclusive scaling of multiplicity distributions at ISR energies 3−32728
pp single-particle spectra, shapes and scaling characteristics in terms of clustering effects, nova model 3−4238
$p\pi^- \to pX$, 25 and 40 GeV/c determ. of normalized cross section, test of factorization near kinematical limit 3−4237
π production, multiplicity distrib. analysis by correlation integrals, two-component model 3−23191
$\pi^-p \to \pi^-p(\pi^+\pi^-)$, diffraction dissociation and dual model 3−19704
$\pi^-p \to \rho^0X$, single particle spectra, pion pole effect in fragmentation region 3−26354
π^-p semi-inclusive interactions, spectral symm. at p = 4 GeV/c *(Russian)* 3−4243
$\pi^\pm p$ inclusive single-particle distribs. at 8 and 16 GeV/c 3−32726
$\gamma p \to K^\pm X$ from H_2, cross-section meas. at 18 GeV, forward angles 3−17056

elementary particle interaction models
see also bootstrapping; composite models of hadrons; duality and dual models; peripheral models
cutoff vector-gluon model, scaling behaviour 3−35802
Deck model for diffractive dissociation, eikonal interpretation 3−32695
diffractive, and high multiplicities 3−19713
diffractive excitation mechanism for multiple production of hadrons 3−26352
diffractive processes, helicity conservation and Drell-Hiida-Deck effect 3−26339
diffractive single- and double-excitation models for inclusive spectra 3−32725
diffractive-excitation model for inclusive reactions in wee-x region, blackbody radiation 3−38097
double Pomeron exchange in high energy production processes 3−26351
fragmentation in high-energy hadron-hadron collisions, charge transfer 3−38070
gauge model of weak interactions, triplet-triplet realizations 3−38019
gauge models of weak interactions, physical constraints 3−26286
gauge theory of weak and e.m. interactions with Han-Nambu quarks 3−26287
generalised vector meson dominance model in relativistically extended quark model, application to high-energy photo-reaction 3−26314
hadron fireball, chain decay, integral equations for 3−29244
hadron structure in weak and e.m. interactions, U(1) × SU(2) gauge model 3−32644
hadronic bremsstrahlung production process in hadron reactions at large momentum transfer 3−29293
high energy scaling model of Feynman, relevance of cosmic ray data above 10^{12} eV 3−31488

elementary particle interaction models continued
impact parameter amplitude, analytic properties 3−35818
independent emission and fragmentation models of multiplicity distrib. in central region 3−32694
Landau's hydrodynamical model, appl. to inclusive pion spectrum, 24 to 1500 GeV/c 3−38094
Lee-Prentki-Zumino model calcs. of semi-leptonic processes involving charged Higgs-Kibble scalars, inconsistencies 3−16973
Lorentz contracted geometrical model 3−32693
multi-pion production, inclusive distrib., model describing factorizable emission of pion pairs 3−38091
nova model, analytically solvable, asymptotic behaviour 3−32696
optical model for πN scattering, 6 GeV/c, amplitude rotation reln. to Regge model 3−32688
optical model for diffractive resonance excitation 3−35819
parameter free Reggeized absorption model for meson baryon scattering 3−23111
parity-violating internucleon one-meson-exchange pots., rel. to models of weak Hamiltonian 3−23121
phenomenological model of Plahte and Roberts, elimination of spurious low-energy effects 3−26323
potential model, high-energy approx. 3−22989
Reggeized absoption model, parameter free, application to spin-2^+ production 3−29235
resonance model for deep inelastic e p scattering and e^+e^- annihilation 3−32671
semi-classical absorption model for multiplicity moments of hadronic collisions 3−19710
single-particle exchange models of weak lepton interactions *(Russian)* 3−29186
statistical isospin model and cross sections of $\pi^-p \to N + (2, \ldots, 6)x$ in 1-16 GeV range 3−38084
thermodynamical s-channel formation for ISR central-region data 3−29286
three-triplet hadron model, broken weak and e.m. interaction symmetry 3−17074
two-component model of multiparticle production, perturbative description of Pomeron 3−38068
two-component model of particle production for high energy multiplicity distrib. 3−17120
two-mechanisms model, exptl. test 3−38071
two-particle correlation functions for inclusive reactions 3−17081
uncorrelated jet model for pionization and correlations in inclusive reactions 3−35843
uncorrelated jet model with two leading particles, inclusive two-particle correlation function and multiplicity distrib. 3−26338
unified model of weak and e.m. interactions, test of light-cone bilocal algebra of currents 3−16957
unified models of weak and e.m. interactions based on spontaneously broken gauge symmetry, sum rule test 3−23046
Weinberg's model, and hadron and lepton struct. 3−19679
Weinberg's model, overall coupling constant renormalization 3−29171
Weinberg's model, renormalizable gauge calcs. of weak corrections to muon magnetic moment 3−23057
Weinberg's $SU_2 \times U_1$ model, mixing angle determ. 3−32633
Weinberg model, soft-π and soft-k mass differences 3−26300
ep inelastic scattering, semi-inclusive and inclusive processes, phenomenological model based on statistical assumption 3−26312
pp scattering, distorted wave theory, parity nonconserving asymmetry 3−35822
π^o correlations, test of production models 3−23169

elementary particle interactions
see also alpha-particle interactions; cosmic ray effects and interactions; deuteron interactions; elementary particle electromagnetic interactions; elementary particle inclusive reactions; elementary particle strong interactions; hadron interactions; helium-3 interactions; lepton interactions; nuclear reactions and scattering; photon interactions; quantum field theory of interactions; triton interactions
analyzer of high-level interactions, use of nuclear levels 3−16470
Burnett-Kroll soft-photon theorem to polarized cross sections, generalization 3−23100
collision probabilities for spherical shells in homogeneous medium 3−11067
inequality relating cross sections to polarization from isospin conservation 3−13826
Lorentz invariant momentum-space integral for particles of equal masses, computer approximation method 3−29182
many-prong events, ang. distrib. uniformity *(Rumanian)* 3−10823
multipion production, determ. of isospin bounds 3−902
multiple processes, scaling and hydrodynamical theory *(Russian)* 3−10659
multiproduction final state with resonances, approx. to mass distribs. 3−10804
Ogawa theory review *(Japanese)* 3−17141
parity and time reversal in gravitational interaction and existence of massless scalar particle 3−32629
precocious scaling and two-mechanisms model, experimental test 3−38071
production processes at large transverse momenta at high energies *(Russian)* 3−19735
scaling laws, analogy with crit. phenomena 3−10780
string model interaction, construction of general vertex operator 3−26319

elementary particle scattering
see also alpha-particle scattering; bootstrapping; deuteron scattering; hadron scattering; helium-3 scattering; lepton scattering; Mandelstam representation; photon scattering; Pomeranchuk poles and trajectories; Regge poles and trajectories; relativistic scattering theory; S-matrix theory; triton scattering
bounds on Pomeranchukon amplitudes and positions of zeros 3−32687
bounds on s-wave scattering length and amplitude in terms of d-wave scattering length 3−4147
box diagram amplitude, analytic properties, double spectral representation 3−22996
charged particles and coherent states, reduction formulas 3−38031
computer program for determ. of total cross-section, peripheral matrix elements 3−10657

elementary particle scattering continued
  Crichton's phase-shift ambiguity, features of elastic unitarity constraint 3−38018
  cross sections, forward and backward, integral Hankel representation *(Russian)* 3−38072
  deep inelastic structure functions, light cone analysis of parton model relations 3−29213
  diffraction peak slope and total cross section, general inequality *(Russian)* 3−17128
  diffractive models in nondiffractive regions 3−23120
  dual amplitude behaviour with Mandelstam analyticity, large angle scatt. and reln. to S-matrix *(Russian)* 3−29232
  elastic, bounds on phase of amplitudes due to positivity 3−10350
  elastic, light-cone variables and high-energy limit 3−17098
  elastic, scaling law, 5-25 GeV/c 3−26345
  elastic amplitudes, fundamental tachyon field role 3−37998
  elastic and inelastic S, P and D phase-shift analysis 3−23023
  elastic particle-antiparticle scatt., comments on testing quantum electrodynamics 3−16983
  few-particle scattering and analogous equations 3−10655
  forward polarized, positivity, subtractions and the moduli of scattering amplitudes 3−23090
  Fourier-Bessel expansion of scatt. amplitude at zero momentum transfer for unequal mass particles 3−29238
  gas analog of multiperipheral model, multiplicity distrib. 3−23118
  generalized wave operator, conditions for existence 3−811
  high-energy, commutator props. 3−13802
  high-energy, space-time analysis 3−29183
  infinite-momentum frame helicity scattering amplitudes, crossing relations 3−38017
  inverse s-wave scattering for energy-dependent potential 3−584
  inverse scattering for L^2-dependent potentials, calc. from S-matrix at fixed energy 3−17142
  light scattering, similarities and differences *(Dutch)* 3−824
  Lorentz contracted geometrical model 3−32693
  massive particles with spin, Mackey-state formulation 3−10654
  multiparticle amplitudes in complex helicity, analytic structure 3−10747
  multiple-scatt. formalism, generalized eikonal approx. at high energies 3−14060
  multiplicity processes, high energy, charge correlations 3−23151
  n^2 kinematic variable, usefulness 3−17104
  nonlinear dispersion relations for square of scattering amplitude 3−13820
  off-energy-shell impact parameter representation 3−23022
  operator droplet model at finite momenta, relation to Glauber theory 3−10656
  partial-wave representation, use in planning scattering meas. 3−10627
  phenomenological dispersion relations, determ. of substitute using expansion of scattering amplitude in terms of analytic functions 3−4152
  poles of an amplitude, analytic properties 3−17086
  quark light-cone algebra model, current-particle scattering amplitudes, real parts 3−23017
  radial s-wave Schrodinger equation and inverse scattering with energy-dependent potential 3−22706
  relativistic amplitudes, generalization for particles with arbitrary spin 3−23019
  S-matrix eigenphases at high energy, concept of resonant state 3−29177
  saturation of diffraction peak to unitarity bound 3−19711
  scaling laws and equal-time commutators 3−35766
  similarities and differences between particle and light scattering *(Dutch)* 3−10658
  spin 0-spin $^1/_2$ elastic scattering amplitudes, determ. from exptl. data and unitarity 3−35769
  stable extrapolation of low energy data using unitarity bounds 3−35827
  strong and e.m. interactions for scattering amplitude and Coulomb-nuclear interference 3−23126
  structure of elastic scattering, peripheral nature of tensor exchanges 3−10785
  sum rules and bounds on scattering amplitudes, derivation of relation between low and high energy scattering 3−10763
  three-body decays for particles with arbitrary spin 3−23020
  three-body nonrelativistic scattering amplitudes, unitary variational approximations 3−37869
  three-body problem, singular cores 3−35863
  three-particle nonrelativistic scattering, connected-kernel Heitler equations 3−23024
  three-particle scattering with three-particle interactions 3−35772
  ultralow temperature techniques, application 3−35383
  unitary analytic scattering construction for scalar particles 3−35770
  unstable, properties by Lee model and LSZ study 3−35735
  velocity space, discrete structure 3−823
  Veneziano amplitudes, semi-local duality props. for total and one-particle cross sections 3−23179
  Yukawa potential, infinite-range limit, high-energy approximations 3−22989
  Σ amplitudes and absorption pattern in two-body scatt. 3−23162
elementary particle strong interactions
  see also composite models of hadrons; duality and dual models; hadron classification schemes; peripheral models; quantum field theory of strong interactions
  $ab \to c +$ anything, fragmentation in φ^3-theory ladder model 3−23186
  absorption model for Regge cuts, application to phases of πN scattering amplitudes 3−6644
  absorptive corrections to Regge pole amplitudes compatible with unitarity 3−23108
  action-at-a-distance theories and dual models 3−26284
  annihilation processes, particle production, multiperipheral concepts 3−10754
  automodelity and dimensional anal. for hadron-hadron collisions 3−6647
  Bogolyubov transformation for oscillator levels of composite particle interacting strongly with boson field 3−26321
  broken symmetries, systematics of high energy collision including particle production 3−809
elementary particle strong interactions continued
  C-invariant but P- and T-violating strong interactions, test using $\eta \to \pi\pi$ decay 3−13838
  CERN intersecting storage rings and strong interactions at high energies 3−32701
  coherent diffractive production of multi-body states on nuclear targets at high energy 3−14074
  compensation theory, elementary couplings in nonleptonic decays of spin 1/2 baryons 3−32651
  correlation functions in multiperipheral models, unitarity and the Pomeron, bootstrap calc. 3−29243
  Deck model for diffractive dissociation, eikonal interpretation 3−32695
  diffraction models, test using pp elastic scattering up to ISR energies 3−17101
  diffractive dissociation, multiple counting in exptl. meas. 3−17123
  diffractive dissociation of particles through collective excitations 3−19715
  diffractive excitation of mesons, relativistic quark model 3−14073
  diffractive models and high multiplicities 3−19713
  diffractive processes, exptl. status of helicity conservation 3−14058
  diffractive processes, helicity conservation and Drell-Hiida-Deck effect 3−26339
  diffractive production processes, t-channel helicity conservation 3−32691
  diffractive production processes at high energies conference, Cracow, Poland (June 1972) 3−14057
  diffractive production processes on simple targets (nucleons) and composite targets (nuclei), unified description 3−13825
  diffractively produced 3π system, partial wave analysis using Ascoli method 3−14072
  dilation model, perturbation theory and spontaneously broken chiral symmetry limits 3−23123
  double pomeron exchange in inclusive and exclusive expts., multiperipheral model 3−23112
  dual parton model-string model 3−26318
  dual Pomeron and diffraction dissociation 3−38063
  fermion vertices and diffractive dissociation 3−10769
  Fourier-Bessel expansion of scatt. amplitude at zero momentum transfer for unequal mass particles 3−29238
  fragmentation and multiperipheral dynamics, connection through unitarity, Pomeron coupling 3−29245
  gauge field theory and Cabbibo angle 3−16945
  gauge model of strong and e.m. interactions, baryon mass differences 3−26276
  gauge model of vector-meson masses with broken U(3) × U(3) symmetry 3−35815
  generalised optical theorem, existence and uniqueness for unitarity eqn. 3−10752
  hadron correlation functions, integral equations 3−19718
  hadron-hadron scattering, effect of 'Van der Waals force' on scattering amplitudes 3−32697
  hadronic diffractive production, isospin analysis of cross-sections 3−14071
  high energy inelastic models 3−17080
  high energy theorems and comparison with exptl. data 3−19734
  high-energy two-body reactions, computation of effective Regge trajectories 3−29234
  hypercharge and strangeness of strongly interacting system, role in multibaryon reson. prod. 3−17084
  impact parameter amplitude, analytic properties 3−35818
  inclusive and exclusive data analysis in longitudinal phase space 3−6648
  inclusive single particle spectra and strong thermodynamic bootstrap soln. 3−914
  inelastic effects in vector meson dominance 3−10759
  internal symmetry properties, formulation on basis of permutational groups *(French)* 3−29246
  isovector scalar meson interactions with static source 3−23124
  large transverse momenta in multiperipheral model 3−23116
  localisability and single-particle exchange amplitudes, causal constraints on coupling constants 3−23114
  Lorentz contracted geometrical model 3−32693
  models for π^+N inelastic collisions, comparison with expts. at 60 GeV/c 3−17117
  multibody prod. at mediate energy 3−14040
  multiparticle processes, statistical description 3−26336
  multiparticle production, correlations between neutral and charged pions 3−35842
  multiparticle production, qualitative meas. of cluster formation 3−19714
  multiparticle production, two-component model, perturbative description of Pomeron 3−38068
  multiparticle production mechanisms in particle-nucleon collisions at high energies, particle-nucleus collision test 3−4204
  multiparticle spectra, cluster-decomposition analysis of simple theoretical models 3−903
  multiparticle spectra, dynamic models, cluster decomposition analysis 3−10760
  multiperipheral and diffraction excitation model analysis of $pp \to pp\pi^+\pi^+\pi^-\pi^-$ 3−17122
  multiperipheral dynamics, two-particle azimuthal correl. 3−4200
  multiperipheral model, distrib. rel. to transverse momentum 3−19709
  multiperipheral model, interference terms 3−10755
  multiperipheral model, multi-Regge amplitudes, rules and discontinuities 3−32685
  multiperipheral model, self-consistent diffractive, in strong-ordering limit failure 3−23119
  multiperipheral models, possibility of constant total cross-section *(Russian)* 3−23122
  multiple production of hadrons, role of diffractive excitation mechanism 3−26352
  multiplicity moments, cluster functions and symptotic behaviour of cross section 3−26268
  nova model, distributions for single-particle spectra in pp collisions 3−4238
  one-pion exchange reactions, density matrix elements and amplitudes determination 3−6684
  optical theorem tests for πp scattering above 1 GeV/c 3−4202

elementary particle strong interactions continued
P, T violating but C=PT conserving strong interactions, possibility of existence, Schwinger's dyon theory 3−14041
parity-violating internucleon one-meson-exchange pots., rel. to models of weak Hamiltonian 3−23121
peripheral dynamics, off-shell behaviour, inclusive sum rules 3−4201
phenomenology of diffractive production reactions 3−14059
Plahte and Roberts model, elimination of spurious low-energy effects 3−26323
polarisation meas. in high-energy physics, analysis in polarisation domain, spin 3/2 particles 3−26362
polarization density matrix properties in Regge-pole models 3−32686
Pomeranchuk branchings in dual resonance model and total cross sections at high energies *(Russian)* 3−23106
quark-quark strong interactions, relativistic model with strong coupling constant 3−38058
random star generation by expanding of multilaterals 3−873
Regge-cut model, consequences of t-channel unitarization 3−26332
Reggeized absorption model, parameter free, application to spin-2^+ production 3−29235
relativistic quantum many-body theory in Riemannian space-time 3−26139
relativistic quark model, chiral symmetry breaking 3−32678
resonant particle production, correlations in multiperipheral model 3−32690
Ringland-Roberts-Roy-Tran Thanh Van Reggeized absorption model for hypercharge-exchange reactions 3−10795
saturation of diffraction peak to unitarity bound 3−19711
scale invariance, vector meson dominance approach 3−847
scaling and hadron-nucleus collisions at high energies, diffractive dissociation model 3−10820
scaling in inclusive interactions above 1 TeV 3−26357
scattering amplitude and Coulomb-nuclear interference 3−23126
singularity and strong interaction theory 3−6639
spontaneously-broken gauge theory of strongly-interacting bosons based on SU(2) × SU(2) group, chiral invariance and e.m. mass difference 3−17085
superpropagators, matrix and computation of T-product 3−35734
t/s scaling, parton approach 3−6658
thermodynamic model, determ. of exclusive cross-sections 3−10753
thermodynamic single-particle spectra, kinematical cut-off 3−915
three-body processes, relations between differential cross sections from quark model 3−10721
two-body phenomenology at high energies 3−6649
two-component model of particle production for high energy multiplicity distrib. 3−17120
two-particle strong-interaction amplitudes, double-discontinuity 3−10625
uncorrelated jet model, grand partition function 3−874
universality test using $\pi^- p \rightarrow ne^+e^-$ process 3−14084
zeros in differential cross sections at high energies 3−14039
eN elastic scatt., examination of strong interactions by departure from scaling 3−17010
π-π resonance parameters, self-consistent calc. in potential model of Balazs 3−10756
π° correlations, test of production models 3−23169
$\pi\Delta(1236)$ electroproduction within vector-meson dominance 3−6618

elementary particle symmetry
see also conservation laws; nonlinear symmetries; SU_n theory
(8,8) model of chiral-symmetry breaking, SU(3) violations and σ terms 3−23133
Cabbibo rotation in models of chiral-symmetry breaking 3−10638
chiral symmetry, algebraic realization on light cone 3−26277
chiral symmetry breaking, relativistic quark model 3−32678
chiral symmetry breaking, restrictions, calc. of meson-meson scattering lengths 3−26274
chiral symmetry breaking and K_{l3} form factors 3−13832
chiral U(3) x U(3) symmetry breaking and $X \rightarrow \eta\pi\pi$ decay amplitude 3−35757
clashing symmetries in unified description of weak and e.m. interactions, Han-Nambu model 3−35774
classification criterion *(French)* 3−6558
conformal group in Poincare basis, principle discrete series 3−6179
conformal symmetry at lightlike distances and asymptotic behaviour of electromagnetic form factors 3−13853
covariant wave functions with invariant helicity for massless particles 3−13806
crossing-unitarity eqn., reformulation in terms of partial waves 3−10757
dilation model, perturbation theory and spontaneously broken chiral symmetry limits 3−23123
dynamical invariance groups of Kepler problem and harmonic oscillator 3−10644
dynamical symmetries and nonlinear realizations, geometric approach 3−10645
eigenvalues of Casimir operators of U(n) and SU(n) for totally symmetric and antisymmetric representations 3−32415
external symmetry group formation from Dirac's eqn. 3−23052
fermionic quarks with integral charge, heuristic model *(French)* 3−29178
gauge, spontaneous breaking with nonlin. realizations and gauge invariant massive vector-meson formulation 3−38012
gauge model of vector-meson masses with broken U(3) × U(3) symmetry 3−35815
generalized Clifford group 3−10643
generlised 3j- and 6j-coefficients and their symmetries 3−10636
H_4.SL(2,C) group, local represents. *(French)* 3−26047
hadron structure in weak and e.m. interactions, U(1) × SU(2) gauge models 3−32644
hadronic symmetry breaking due to weak interactons 3−35761
internal, predictions from N/D bootstraps and duality hypothesis, symmetry breaking 3−821
lepton-hadron symmetry breaking and Cabibbo rotation 3−10640
local, spontaneously broken, general formalism in unitarity gauge 3−35759
logarithmic scaling and spontaneous breaking 3−6568
non-conservation of unitary-singlet axial-vector current, possible role of Fujii boson 3−32639

elementary particle symmetry continued
O(3), triplet realisation of gauge model for weak and e.m. interactions 3−13795
octet dominance formulation of partial conservation of vector currents 3−35763
parametric dispersion representation with three-channel symmetry, derivation of sum rules 3−10651
perturbation theory, conformal-covariant Wilson expansion, at lightlike distances 3−37994
Poincare gauge invariance and dynamical role of spin in gravitational theory 3−22730
Poincare invariance in detn. of arbitrary-spin wave equations, constraints from discrete symmetries 3−29168
Poincare invariant eqns. for massive particles, P, T, C properties 3−19667
positivity and crossing symmetry, application of moment inequalities to unitarized π-π Veneziano model 3−4193
reducible scale invariance at short distances, conformal symmetry and canonical scaling 3−38005
Regge symmetry application to Wigner (9-j) symbol 3−29179
Regge-Regge cuts, symmetry constraints 3−872
self-consistent quantum field theory approach to symmetry breaking 3−19670
SL(3, R), hadronic Regge sequences as primitive realizations 3−6567
spontaneous symmetry breaking, radiative corrections as origin 3−35793
spontaneous symmetry breaking in new classes of dual models 3−6636
spontaneously broken, general gauge formulation 3−38010
spontaneously broken, quantization and gauge freedom 3−35760
spontaneously broken gauge model for higher-order contribution to muon decay 3−10665
spontaneously broken gauge symmetry and approximate mass formulas 3−10642
spontaneously broken gauge theories, calc. of finite n-p mass difference 3−35788
spontaneously broken gauge theories, divergence cancellations 3−35748
spontaneously broken gauge theories, generalized renormalizable gauge formulation 3−10641
strong interactions, internal symmetry properties, formulation on basis of permutational groups *(French)* 3−29246
strongly interacting particles, broken symmetries 3−809
SU(2) chiral breaking test, analog of Coleman-Glashow formula for pseudoscalar mesons 3−10639
SU(3) asymptotic, breaking model and produced particle ratios 3−23003
SU(4) as candidate for higher symmetry 3−819
U(3) × U(1) broken gauge-invariance theory with calc. of baryon masses 3−26276
Yang-Mills gauge mesons in theories with spontaneously broken symm., Reggeisation 3−37996
$e^+e^- \rightarrow$ hadrons, U(3) × U(3) symmetry breaking, determ. of sum rules for T=0, T=1 3−13963
$\eta \rightarrow \pi^0\gamma\gamma$, gauge invariance and chiral symmetry in closed-fermion-loop model 3−38026
$\eta' \rightarrow \eta\pi\pi$, symmetry breaking, calc. of matrix element of σ term 3−32656
$\pi\pi$ low-energy S- and P-wave models, test of crossing symmetry using crossing relations on physical region 3−23147
$\pi\pi$ scattering, unitarity corrections from current algebra, hard-pion amplitude 3−17095
$SO_0(p,1)$, multiplier representations of supplementary series 3−35557

elementary particle theory
see also Bethe-Salpeter equation; chirality; complex angular momentum plane; current algebra; dispersion relations; electron theory; elementary particle interaction models; elementary particle symmetry; Feynman diagrams; form factors; group theoretical schemes; Lee model; quantum field theory; S-matrix theory; sum rules
action-at-a-distance theories and dual models 3−26284
analyticity, statistical method of testing 3−16965
analyticity constraints on amplitudes at high energy given low-energy theorem 3−4167
box diagram amplitude, analytic properties, double spectral representation 3−22996
broken scale invariance, low-energy theorem test using $\varepsilon(700)$ 3−32636
correlation functions in multiperipheral models, unitarity and the Pomeron, bootstrap calc. 3−29243
currents, covariant time-ordered products, generating functional 3−35764
diffractive models in nondiffractive regions 3−23120
diffractive processes, helicity conservation and Drell-Hiida-Deck effect 3−26339
Durham data bank, data analysis and model comparison project 3−29256
dyon model, violation of CP invariance 3−32630
fragmentation and multiperipheral dynamics, connection through unitarity, Pomeron coupling 3−29245
gas analog of multiperipheral model, multiplicity distrib. 3−23118
generalized Cabibbo-Radicati theorem from first-order non-Abelian Compton effect 3−26307
generalized wave operator, conditions for existence 3−811
hadronic scaling, predictions for ratios of cosmic-ray components in atmosphere 3−28099
inelastic deep scatt. scaling laws from limiting fragmentation, strength function behaviour 3−14015
infinite component wave equations and mass splittings within SU(3) and SU(2) multiplets 3−13808
mass eigenvalues from infinite-component particle wave eqn. with widely spaced mass spectrum 3−16708
mass formula, universal, dynamically based theory 3−38016
multi-particle helicity amplitude regularization 3−26283
multiparticle processes, statistical description 3−26336
multiperipheral dynamics, semi-group approach 3−26337
N-interacting particles in configuration space, uncertainty 3−19678
non-abelian gauge groups, fields and statistics 3−4140

elementary particle theory continued
nonlinear spinor field theory of elementary particles, four-fermion model 3-16935
O(4) treatment of electromagnetic weak synthesis 3-6565
orthogonal transformations of multidimensional angular harmonics for particle permutation operators *(Russian)* 3-19391
phase oscillation method for asymptotic estimation of Fourier transforms 3-26308
Poincare group, unitary representations in octonionic Hilbert space 3-32632
Poincare invariance in detn. of arbitrary-spin wave equations, constraints from discrete symmetries 3-29168
precocious scaling and two-mechanisms model, experimental test 3-38071
relativistic, off-shell, analyticity and unitarity 3-38015
scaling breakdown at 10^{-15} cm, speculations 3-38004
single-particle exchange model of weak lepton interactions *(Russian)* 3-29186
singularities in complex ang. momentum and helicity 3-10743
size barriers, cosmological aspects 3-35009
$SL_{2,c}$ group, transformation function from jm-basis to z-basis for unitary representation 3-28819
spontaneously broken scale invariance model 3-26271
$SU(3)\otimes SU(3)$ and unified gauge theories of hadrons and leptons 3-38002
U(3) nonet scheme with 6 heavy leptons 3-23026
unified model based on leptons 3-16966
vertex graphs technique 3-35738
weak uncertainty relations in quantum theory from weak convergence in Hilbert space 3-13616
Zitterbewegung in relativistic spin-0 and -$^1/_2$ Hamiltonian theories 3-37997
$dp \to dp\pi^+\pi^-$, s- and t-channel helicity nonconservation at 25 GeV/c 3-14078
$\gamma N \to O^- N$, s-channel helicity conservation and Regge cuts in t-channel 3-13901
ρ^0 photoproduction, conservation of s-channel, helicity 3-13959

elementary particle weak interactions
see also quantum field theory of weak interactions
clashing symmetries in unified description of weak and e.m. interactions, Han-Nambu model 3-35774
Coulomb corrections to nuclear beta decay, elementary particle treatment 3-23277
currents, connections between weak and electromagnetic 3-13815
deep inelastic reactions, application of duality principles 3-13932
deep inelastic structure functions, symmetry principles and constraints 3-16955
dual parton model-string model 3-26318
gauge field theory and Cabbibo angle 3-16945
gauge model, triplet realisation of weak and e.m. interactions 3-13795
gauge models, physical constraints imposed by Higgs particle exchange and higher-order effects 3-26286
gauge models, triplet-triplet realizations, predictions for deep inelastic scattering 3-38019
gauge theory, O(4) treatment of electromagnetic weak synthesis 3-6565
hadron structure in weak and e.m. interactions, U(1) × SU(2) gauge models 3-32644
hadron weak form factor, calc. of electromagnetic corrections using gauge invariance *(Russian)* 3-10696
hadronic symmetries and gauge theories 3-23025
hadronic symmetry breaking due to weak interactons 3-35761
helicity structure functions, scaling behaviour 3-17032
high energy and higher order weak processes 3-6578
Hot Big Bang model and properties of elementary particles in cosmic plasma 3-9460
inelastic neutrino scattering, inclusive reactions 3-6630
inelastic neutrino-nucleon scatt., positivity restrictions from weak hadronic tensor props. 3-13893
Lee-Prentki-Zumino model calcs. of semi-leptonic processes involving charged Higgs-Kibble scalars, inconsistencies 3-16973
lepton-hadron symmetry breaking and Cabibbo rotation 3-10640
leptonic four-Fermion interactions, strength of diagonal part $(\mu\nu_\mu)$ $(\nu_\mu\mu)$ 3-16968
mass spectrum of elementary particles and weak interaction consts. 3-35345
model relationship to parity-violating internucleon one-meson-exchange pots. 3-23121
model without neutral currents, muon g-2 and other constraints 3-13829
neutral current detection, comparison of exptl. upper limits and Weinberg model predictions 3-10661
neutral currents, leptonic and semileptonic, Gargamelle bubble chamber expt. 3-10662
neutral weak current detection and isolation in $\mu^- p$ inelastic scattering 3-827
neutral weak currents, e.m. corrections to $e^+e^- \to \mu^+\mu^-$ 3-29207
neutral-current effects in class of gauge field theories 3-855
nonleptonic, $\Delta I = {}^1/_2$ rule, embedding in unified theories of weak and electromag. interac. 3-35781
nonleptonic weak decays, SU_3 breaking of strong coupling constant in quark density model 3-16967
nonlocality in high energy ν expts., internal particle mass effect 3-10676
renormalizable gauge model of weak and e.m. interactions, pseudo-Cabibbo structure 3-38020
renormalizable guage field model of weak and e.m interactions with CP-violation 3-10616
renormalization of unified theory of weak and e.m. interactions 3-16944
S-matrix approach and formulation 3-4153
scaling props. approach 3-6574
second class currents, role of meson exchanges 3-6573
second class currents 3-10663
second class currents in nuclear β-decay 3-10936
second class currents in nuclear beta decay 3-10935
second-order weak and e.m. corrections to decay rate calc. from Weinberg's model 3-16972

elementary particle weak interactions continued
self-coupling of weak lepton currents in high-energy neutrino and muon reactions 3-23038
single-particle exchange model of weak lepton interactions *(Russian)* 3-29186
SO(3) gauge theory of weak and e.m. interactions with Han-Nambu quarks 3-26287
spontaneously broken gauge theories, generalized renormalizable gauge formulation 3-10641
three triplet hadron model, broken weak and e.m. interaction symmetry 3-17074
twister theory applic. 3-6576
U(3) nonet scheme with 6 heavy leptons 3-23026
unified gauge theories, effective weak-interaction cutoff of e.m. radiative corrections 3-38035
unified models of weak and e.m. interactions, μp scattering and effects of neutral currents in scaling region 3-10712
unified weak and e.m. interaction theory, test of light-cone bilocal algebra of currents 3-16957
unstable composite particles, relativistic three-particle eqns. 3-826
V-A theory, astrophysical implications of second-order effects 3-34998
V-A theory, evolution of higher order terms 3-825
vector coupling const., magnitude 3-10660
virtual-boson effects in neutrino trident production 3-19680
weak currents, short-range interactions and scale invariance 3-16971
Weinberg's gauge theory, calc. of divergences in weak and e.m. corrections to μ decay 3-10666
Weinberg's lepton model, compact version, construction of gauge fields as bound states of spinor fields 3-4154
Weinberg's model, and hadron and lepton struct. 3-19679
Weinberg's model, anomaly-free version 3-818
Weinberg's model, overall coupling constant renormalization 3-29171
Weinberg's $SU_2 \times U_1$ model, mixing angle determ. 3-32633
Weinberg's unified gauge model of leptons and hadrons, p-n mass difference 3-26299
Weinberg model, consequences for a large system of thermodynamically weakly interacting particles 3-16970
Weinberg model of weak and e.m. interactions, calc. of soft-π and soft-k mass differences 3-26300
Weinberg model of weak and e.m. interactions, triplet representation of leptons 3-13828
Weinberg W-meson, possible observation in anomalous cosmic ray events 3-16087
$ee(e\mu,\mu\mu)$ colliding beams, weak-e.m. processes and interference at high energies 3-17058
ll colliding beams at 10^3 GeV, calc. of elastic scatt. cross-section 3-16980
$ll \to ll\nu\nu, l = e^\pm, \mu^\pm$, cross sections for inelastic weak processes at high energy *(Russian)* 3-38030
μ magnetic moment in Weinberg's model, renormalizable gauge calc. of weak corrections 3-23057
n-p mass difference calc. in semirealistic gauge model of weak and e.m. interactions 3-35789
$pN \to XY$, strong and weak interact., interference effects *(Russian)* 3-19749
pp scattering parity nonconserving asymmetry 3-35822
W boson model of interactions with maximal CP violation 3-6575

elementary particles
see also bosons; composite particles; cosmic rays; fermions; gamma-rays; hadrons; hypothetical particles; leptons; mass differences; particle detectors; quantum field theory; strange particles
antimatter, recent developments, review 3-29163
charged particle multiplicity distrib., predictions for higher moments from charge conservation constraints 3-10630
conference, CERN School of Physics, Geneva (May 1972) 3-6537
Eastern philosophy, unity of ideas with those of particle physics 3-16344
high energy physics conference, Bombay, India, (Dec. 1972) 3-10585
multiparticle aspects, conf., Schladming, Austria (Feb-Mar 1972) 3-13784
review of properties, Particle Data Group 3-35728
review of recent developments in high energy physics 3-809

elements (chemical)
for specific metals and non-metals see appropriate chemical names
see also element origin; element relative abundance; periodic system of elements
Auger transitions in 10 to 3000eV energy range complete list 3-2612
superheavy, search for, control experiments 3-6962
superheavy element calc. by Hartree-Fock and single-particle shell model, review 3-17172
superheavy nuclei, Hartree-Fock method study *(French)* 3-6963
superheavy nuclei cross section for formation in 450-500 MeV Kr collisions with U and Th *(French)* 3-6964

ellipsometers *see ellipsometry; polarimeters*

ellipsometry
anodic film on Pt electrode, ellipsometric and refl. obs. 3-5243
of diffraction gratings 3-5870
ellipsometer, photoelectric, very small thickness measurement, quarter wave plate compensator, null device *(German)* 3-13282
ellipsometers, generalised, fixed polariser nulling scheme 3-28523
epitaxial layer thickness meas. by far, i.r. ellipsometry 3-3797
films, highly absorbing, thickness meas. technique 3-24764
glass, optical, fund. polishing mechanism, ellipsometric obs. *(French)* 3-28534
Kerr effect, meas. of dynamic ellipticity of polarised light 3-22309
metal/electrolyte solution interface, electrochemical processes, multireflexion method 3-31267
optical and spectroscopic methods for the study of surfaces, review 3-22342
partially polarized Gaussian beam, average form of polarization 3-32509
plasma oxide film, on $GaAs_{1-x}P_x$, refractive index obs. *(Japanese)* 3-11821
randomly rough surface, calc. of parameters using Stratton-Chu-Silver integral 3-29037

ellipsometry continued
review 3−28527
Robinson's method for thin film studies, assessment and modification 3−5885
steel, stainless, electrodes, surface oxide layer growth, ellipsometric obs. 3−18029
surface examination applic. 3−37585
surface roughness meas. 3−13283
thin absorbing films, optical constants evaluation from ellipsometric parameters 3−37626
thin film studies, expt. and computing methods, choice of criteria 3−5886
thin film thickness meas., undergraduate expt. 3−31992
thin films, built-up, anisotropic effects in ellipsometry and optical constants 3−34443
two-layer dielectric thin films on semiconductor substrates, thickness meas. using ellipsometric method 3−13230
Al_2O_3, amorphous film growth and cryst. island development 3−8045
Fe, passive, passivating film, thickness, complex refr. index and absorpt. coeff. meas. *(German)* 3−27163
GaAs surface film evaluation 3−39239
Ge, adsorbed C(N)(O)(P)(S)(Cl), Auger electron yields 3−2611
In_2O_3, growth on In film, optical props. obs. 3−1908
Mo film, obs. of oxidation 3−8040
$Ni(OH)_2$ film, growth and anodic oxidation study 3−30368
Pb-dielectric cermet film, refr. indices, ellipsometric meas. rel. to Maxwell Garnet theory 3−8544
Si, adsorbed C(N)(O)(P)(S)(Cl), Auger electron yields 3−2611
Ti oxidation, Au marker expts. 3−36492
elliptical polarisation *see polarisation*
e.m. waves *see electromagnetic waves*
embrittlement *see brittleness*
e.m.f. *see electric potential*
emission nebulae *see nebulae*
emissivity
apparent directional emittance of V-groove and circular groove rough-surface 3−1858
cylindrical enclosures with and without diaphragms, apparent thermal emittance 3−636
gray body temperature measurement using black-body-calibrated radiometer, measurement errors *(Russian)* 3−5813
helical surface, cylindrical cavity, angular coeffs. of radiation 3−35634
luminous flame, mean emissivity from spray combustion of liquid fuel 3−2801
lunar fines spectral emittance for varying bulk densities 3−12997
metal, spectral radiating power meas. at high temperatures, analysis 3−22287
metallic plate, normal spectral emission factor using i.r. thermography *(French)* 3−30267
metallic thin films on dielectrics, thermal radiation properties 3−27127
metals, effect of surface roughness 3−33680
metals, refractory, thermophysical props., Moscow State University research *(German)* 3−36579
Planck radiation law, light bulb efficiency teaching expt. 3−28447
spectrum, integral, absorpt. coeffs. of medium 3−35636
total, determ. for nonblack bodies 3−28488
water, surface i.r. emissivity, laboratory determ., effect of surface oil films 3−36424
Ce liquid, spectral emissivity obs. 3−27126
Hf, 1200-2000K 3−24404
La, liquid, spectral emissivity obs. 3−27126
MgO, radiation degree of blackness, electric resistance 3−36423
Mo bodies, dependence on surface roughness 3−15016
NH_3 molecular spectra, band and total emissivity 3−23566
Pr, liquid, spectral emissivity obs. 3−27126
SiO_2, radiation degree of blackness, electric resistance 3−36423
Ta, spectral emissivity meas. visible region, 1200 to 2400K 3−35378
W, arc cast thermal, measurement, direct heating method, TPRC multi-property apparatus 3−12426
W, meas. of spectral emissivity using Fourier transform spectroscopy 3−28556
employment
No entries
emulsiods *see emulsions*
emulsions
see also nuclear track emulsions; photographic emulsions
disperse analysis, photoelectric sedimentometer 3−28706
electron microscope study, cold fracture technique *(German)* 3−16535
high internal phase ratio, complex-rheological behaviour 3−2767
polydispersed system, dielec. prop. determ. method *(French)* 3−25018
PVC particles, emulsion paste-forming, struct. changes on contact with plasticizer 3−21751
spherical double dispersion model applic. to change of state processes of dispersed phase *(French)* 3−27791
viscous flow under arbitrary shear fields, effect of surfactant impurities 3−29915
water-in-oil type, coagulation in strong electric field *(Russian)* 3−9016
Ag halides, digesting, technique for following photographic sensiometric props. 3−27903
emulsions (nuclear track) *see nuclear track emulsions*
encapsulation
see also packaging
^{60}Co heat source, use of Hastelloy X and C, Inconel 600 and Haynes 25 3−26552
encoding
see also codes; decoding
colour signals 3−22853
holograms, computer generated, coding techniques for recording on computer controlled c.r.t. 3−198
low bit-rate coding from autocorrelation method of linear prediction 3−3639
encoding continued
Radio Astronomy Explorer B antenna aspect data processor 3−35218
ENDOR
acetylglycine, X-irrad., primary radiation products identification 3−2827
2-adamantyl radical in γ-irrad. adamantane 3−12535
alkali halide, ENDOR obs. of H-centre in interstitial centres review 3−4754
alkali halide, impurity doped, review for Z-centres 3−8624
benzophenone, of $n\pi^*$ lowest triplet state 3−21832
benzophenone in soln., liq. phase ^{13}C obs., anisotropic h.f.s. interaction 3−1263
carbazyl radical, randomly oriented, proton hyperfine tensor 3−5402
cross-relaxation transitions in ENDOR dynamics, with inhomog. broadening of e.p.r. lines *(Russian)* 3−2336
m-dibenzoylbenzene radical anion, conformation, ENDOR obs. 3−26700
enhancement magnitude calc. from dispersion mode e.p.r. signal 3−30728
experiments employing crystal controlled signal generator 3−19243
external stress effect, theory 3−27442
F-centre, effects of applied electrostatic fields and hydrostatic press. 3−18393
free radicals, e.p.r. spectra, saturation and double reson. effects, theory, average ENDOR and ELDOR lines 3−34183
hydrocarbons, phenyl-substituted, twisted, π-σ delocalization 3−1264
hyperfine structure formulae and ENDOR freqs. 3−34249
microwave cavity, for high power spectroscopy 3−37668
naphthalene single crysts., X-irrad., α-hydronaphthyl radical obs. 3−12537
piezo-hyperfine interaction concept. rel. to impurity centres in crysts. 3−2466
radicals produced by X-irrad. of single crysts., proton hyperfine couplings 3−2826
review 3−30678
TCNQ ion radical salts, Overhauser effect and exciton motion 3−2469
topaz, $Al_2SiO_4F_2:Fe^{3+}$ e.p.r. spectrum, ^{19}F ENDOR study for hyperfine struct. tensors 3−21342
1,2,4-triazole crystal, ENDOR study of the radical created by gamma irradiation at room temp., proton hyperfine tensors and spin density distribution 3−21814
BeO, F^+-centre, interactions with next-nearest-neighbour Be nuclei 3−39058
CaF_2, of Ho^{2+}, hyperfine lines, spin Hamiltonian parameters 3−2468
$CdF_2:Mn^{2+}$, ligand ENDOR obs. for F and Cd lattice nuclei 3−18394
CsBr, U_2 centres, e.p.r. and ENDOR investigation *(German)* 3−30696
CsCl, U_2 centres, e.p.r. and ENDOR investigation *(German)* 3−30696
$CsGa(SO_4)_2.12H_2O:^{53}Cr^{3+}$, 4.2 K meas. 3−2465
1,1-cyclobutanedicarboxylic acid, EDNMR study 3−1256
H_3PO_4/H_2O glass γ-irradiated at 77K, ENDOR spectra of trapped H atom 3−25078
H_2SO_4/H_2O glass γ-irradiated at 77K, ENDOR spectra of trapped H atom 3−25078
KCl, optically detected F-centre pairs 3−21310
KH_2PO_4/H_2O matrix γ-irradiated at 77K ENDOR spectra of trapped H atom 3−25078
$KHSO_4/H_2O$ matrix γ-irradiated at 77K, ENDOR spectra of trapped H atom 3−25078
MgO, obs. of lattice distortion around F^+ centre 3−27441
MgO containing Mn^{2+}, Cr^{3+} and Fe^{3+} impurities, ^{17}O transferred hyperfine interactions 3−30727
$RbGa(SO_4)_2.12H_2O:^{53}Cr^{3+}$, 4.2 K meas. 3−2465
SnO_2, of $^{57}Fe^{3+}$ and $^{53}Cr^{3+}$ at different sites, h.f. data interpret. 3−2467
energies, molecular dissociation *see molecular dissociation energies*
energy, binding *see binding energy*
energy, lattice *see lattice energy*
energy, surface *see surface energy*
energy bands *see band structure*
energy bands, electron *see band structure*
energy gap
$A^2B^4C^5_2$ compounds with chalcopyrite structure, cubic tetrahedral model structure 3−36532
alkali halide crystal, forbidden zone width, photoelectron spectra obs. 3−34464
amorphous solid, Weaire model 3−15114
demarcation levels and occupancy of single and multiple-level centres 3−2133
finite linear chain, rel. to dynamic effective charge 3−36514
Hall constant meas., electron and hole mobility determ. 3−18060
II-VI semiconductors, far u.v. refl., and correl. with Penn-Phillips gap 3−39158
insulator, photoemission-determined valence band gaps and ionicity parameter, relation 3−24380
I 3−34404
metal/semiconductor interface, many body effects 3−2183
phase transitions, microscopic theory *(Russian)* 3−1778
photoemission, transitions from cond. band to states in band gap, electron spin polarization 3−5255
polyanilines, linear, band struct. and limiting behaviour 3−33792
polyethylene, from vacuum u.v. photoemission 3−12210
polymethylpolyarsine, determ. from elec. resist., intrinsic semicond. behaviour 3−30479
semiconducting alloys, narrow bandgap semiconductors, zero bandgap transition 3−38800
semiconductor, amorphous, rel. to struct. homogeneity 3−30387
semiconductor, artificial, formed by alternating thin films of Au and SiO_2 3−38790
semiconductor, elemental, rel. to covalence and dangling bonds *(French)* 3−26985
semiconductor, interband energy gap from thermoreflectance spectra 3−2005

energy gap continued
  semiconductor, photoemission-determined valence band gaps and ionicity parameter, relation 3—24380
  semiconductor organic molecular crysts., mag. excitations 3—2230
  semiconductors, intraband edge absorpt. of light, theory 3—15506
  sugarcane wax, subjected to high elec. fields and diff. temps., cond. mechanism and band gap meas. 3—21083
  superconductors with transition metal impurities, localised states in energy gap 3—15298
  u.s. induced in continuous spectra, acoustic forbidden band, conduction electron screening 3—33804
  Ag_2HgI_4, high pressure phases, pressure depend. 3—30471
  $AgInSe_2$, electronic structure from electroreflectance and photoluminescence meas. 3—39183
  Al, supercond. energy gap anisotropy, press. depend. 3—8287
  $Al_xGa_{1-x}As$, reson. Raman scatt. study 3—34359
  AlN film, epitaxial growth, props., optical band gap 3—21004
  $B_{12}N_{12}H_{12}$, hexagonal, band width, band gap, charges, equilib. distance, sublimation energy, from Huckel calcs. 3—15136
  $Bi_{1-x}Sb$, gapless state, magnetoresist., semicond.-semimetal-semicond. transition 3—33791
  $CdCr_2S_4$, in energy level model established from photocond. and luminesc. spectra 3—8222
  $CdIn_2S_4$, lowest indirect gap of 2.43 eV, direct gap of 2.50 eV, calc. 3—8101
  $CdIn_2Se_{4x}Te_{4(1-x)}$, solid soln., forbidden zone width from absorpt. and Hall coeff. meas. *(Russian)* 3—15126
  $CdSc_2S_4$, and synthesis 3—39243
  $CdSiP_2$, meas. from optical absorpt. *(Japanese)* 3—12146
  Cu-Al, anomalous shift in interconduction band optical absorption, values for band gaps 3—30837
  $Cu_{2-x}Ag_xSe$, metal-nonmetal transition, elec. cond., energy gap 3—38805
  $Cu_2Ga_4Te_7$, phase in $Cu_2Te-Ga_2Te_3$ system, defect sphalerite type semicond. with 1.08 eV gap 3—38660
  $CuInSe_2$, electronic structure from electroreflectance and photoluminescence meas. 3—39183
  Cu_2S, chalcosite thin crysts., unusual form, absorpt. and refr., 0.5-1.1μ 3—24701
  Fe_3O_4, magnetite, band splitting at Verwey transition with 0.11 eV gap 3—2506
  Fe_3O_4, magnetite, calc. from band theory of pair-localized electrons 3—2012
  FeS_2, pyrite, natural, resist., Hall effect, rel. to energy gap and mobility 3—38837
  n-$Ga_{1-x}Al_xAs$:Si, catholum. obs. rel. to energy gap meas. 3—30886
  $GaAs_{1-x}P_x$, indirect Γ_{8v}-X_{1c} band gap, absorpt. and photolum. studies 3—21003
  GaSb, Landau transitions at higher energy gaps, spin-orbit splitting 3—33809
  p-GaSb, optical pumping of spin polarised conduction electrons and inelastic scattering by neutral acceptors 3—34398
  GaSe, magnetooptical props. near band gap 3—30803
  Ge, amorphous, d.c. cond. and pseudogap struct. 3—38839
  Ge, H^+, O^+, B^+, ion bombardment, divacancy-like optical absorption 3—34394
  Ge amorphous film, optical gap 3—15116
  Ge amorphous thin films, absorption and transport study of the pseudo gap 3—33775
  Ge-Sn amorphous film, energy pseudogap from d.c. cond. temp. depend. 3—18055
  GeSbSe amorphous film, optical determ. 3—21080
  GeSe amorphous film, optical determ. 3—21080
  $GuGa_{1-x}In_xS_2$, band gap comp. depend. from transmission wavelength modulation 3—38789
  $Hg_{1-x}Cd_xTe$, linear variation with x over semimetal-semicond. transition 3—18080
  InAs, impact ionisation and scattering mechanisms in narrow gap semiconds. 3—21088
  InAs, reson. Raman scatt. near E_1 gap, uniaxial stress effects 3—5206
  $InAs_{1-x}P_x$, $(0.7 \leqslant x \leqslant 1)$, band gap variation meas. for vapour epitaxial grown crystals 3—1917
  $InAs_{0.07}Sb_{0.93}$ films, photoelectronic props. 3—33958
  $In_{1-x}Ga_xAs_{1-y}P_y$ alloys, electron zones, luminesc. struct. study *(Russian)* 3—36946
  $In_{1-x}Ga_xP$:N, soln. growth, photoluminesc. meas. rel. to band gap and N-trap states 3—24797
  InSb, Landau transitions at higher energy gaps, spin-orbit splitting 3—33809
  InSb, reson. Raman scatt. near E_1 gap, uniaxial stress effects 3—5206
  β-In_2Te_3, photocond. study *(Russian)* 3—8724
  $KClO_3$, indirect, fundamental absorp. obs. 3—30832
  La, d-h.c.p., supercond. energy gap from far-i.r. absorpt. 3—5069
  LiF, LEED intensity profile for (100) surface, and bulk energy bands, calc. 3—36466
  LiF, self-consistent energy bands 3—21010
  $NaBrO_3$, $NaIO_3$, indirect, fundamental absorp. obs. 3—30833
  $NaClO_3$, indirect, fundamental absorp. obs. 3—30832
  $NaClO_3$, temp. depend., absorpt. study 3—21431
  $NbSe_2$, supercond., gap anisotropy 3—18241
  $NbSe_2$, supercond. energy gap, tunnelling meas. 3—24536
  Nb_3Sn, phonon linewidths, influence of the superconducting energy gap 3—17948
  Pb-In system, superconducting energy gap from magnetization meas. 3—34014
  β-PbO_2, from Kohn-Korringa-Rostoker method calcs. 3—8107
  $Pb_{1-x}Sn_xTe$ alloys, two valence band model for Seebeck coeff. *(French)* 3—11854
  p-$Pb_{1-x}Sn_xTe$ solid soln., i.r. absorpt. spectra due to free carriers, valence bands energy gap *(Russian)* 3—8626
  SbI_3, rel. to magnetooscillatory effect of absorpt. *(Russian)* 3—34329
  Sb_2O_3, amorphous and crystalline, energy gaps corresponding to indirect transitions 3—8602
  SbSi cryst., mid-i.r. absorpt. and indirect transitions, phonon energy and energy gap calc. 3—24697
  $Sb(TaNb)O_4$, forbidden band width at ferroelec. transition, opt. absorpt. obs. 3—5171

energy gap continued
  Si, subbands energy level differences in surface quantization, piezoresist. meas. at 15 K 3—15133
  SiAs single crystal, optical consts. and energy gap, absorpt. meas. 3—36850
  αSiC(6H), photoionisation spectra of impurity centres at high temp. 3—36902
  SiO_2 thermally grown on Si, electron trapping levels 3—8262
  Sn-Te-PbSe system, forbidden band width, conc. depend. *(Russian)* 3—11918
  SnTe, band structure and Jones zone 3—4949
  TlBr indirect edge in luminesc. excitation spectra confirming indirect band gap 3—2584
  $TlSbSe_2$ film, characterization *(Russian)* 3—18235
  VO_2, semicond., calc. 3—36542
  V_2O_5-P_2O_5 glass absorpt. tail, fund. absorpt. edge, band gap, forbidden transitions 3—21444
  Zn, superconducting, critical mag. field and energy gap anisotropy 3—38918
  $ZnGeP_2$, meas. from optical absorpt. *(Japanese)* 3—12146
  $Zn_xHg_{1-x}Se(Te)$:Mn^{2+}, rel. to e.p.r. 3—15409
  ZnS-Te, variation of energy gap with composition 3—30402
  $ZnSc_2S_4$, and synthesis 3—39243
energy level crossing
  atomic splitting constants signs determ. using level crossing techniques 3—17362
  atomic systems, quantum-mech. transport eqn. 3—4381
  1,2-benzanthracene, activated intersystem crossing from fluorescent state 3—4457
  biacetyl, magnetic resonance expts. on triplet state, zero field splittings meas., zero field level assignment, intersystem crossing 3—27890
  computer program for soln. of secular matrix 3—11141
  Hanle effect, press. dependence in sensitised fluorescence 3—29494
  Hanle effect, saturation by intense broad band laser radiation 3—29493
  Hanle effect meas. technique for fast ions 3—25765
  microwave optical magnetic resonance, induced by electrons, line shape, level crossing and intensity considerations 3—29717
  pulsed excitation effects 3—7052
  rel. to secondary radiation from gas system 3—23484
  signals, shape and amplitude 3—17361
  signals, shape and amplitude 3—17488
  space of operators commuting with the Hamiltonian 3—16711
  CN radical, lifetimes of A $^2\pi$ and B $^2\Sigma$ states 3—7224
  CO, collision-induced interactions between excited states, elastic cross relax. 3—36042
  Cs, highly excited D and F levels, h.f.s. 3—38221
  Er^{3+}, Tm^{3+} doped phosphate and borate glasses, energy transfer processes, fluorescence obs. 3—21466
  p-H_2, 4p $^3\Pi_u$ level excited by electron impact, non-zero mag. field level-crossing 3—17453
  He states excited by electron impact, alignment relaxation meas., collisions and cascades influence *(German)* 3—14311
  He^+ + Ne low-energy elastic scatt., curve crossing 3—20062
  ^4He, fine struct. intervals meas. *(French)* 3—38216
  ^4He, zero-field level-crossing resons. and weak mag. field meas. 3—7058
  ^4He 5^1D_2 state, lifetime and alignment meas. by beam-foil level crossing 3—23483
  I_2, nonlinear level crossing in $X^1\Sigma_g{}^+$ state 3—1251
  $N_2{}^+$, Hanle effect obs. of electronic levels *(French)* 3—33142
  Na, nucl. moments determ. using h.f.s. consts. *(Russian)* 3—7056
  Na/He atom pair, avoided crossings among excited states 3—20037
  Na-D-doublet, quenching by N_2, ionic curve-crossing model theory, interaction pot. inclusion 3—14319
  Ne, K X-ray yields on Be, C, Mg, Al and Ti targets, electron promotion model 3—20029
  Ne, laser optically pumped, fluoresc. saturation resons. due to mag. mode crossing 3—20026
  No, optical reson. and Hanle effect *(French)* 3—14392
  $O_2{}^+$, Hanle effect obs. of electronic levels *(French)* 3—33142
  Rb, highly excited D and F levels, h.f.s. 3—38221
  ^{87}Rb, $5^2P_{3/2}$ state, broadening of level-crossing signals by collision with Ar 3—29496
energy level transitions, atomic *see atomic spectra*
energy level transitions, molecular *see molecular spectra*
energy level transitions, nuclear *see nuclear energy level transitions*
energy levels
  see also atomic structure; band structure; energy level crossing; molecular electronic structure; nuclear energy levels; population inversion
  Bohr-Sommerfeld orbits and quantizable symplectic manifolds 3—37868
  bound state energies, contact interactions influence 3—32411
  demarcation levels and occupancy of single and multiple-level centres 3—2133
  exciton, mag. field depend. of ground state energy with Coulomb pot. screening 3—2034
  oxide films on pure Fe and Fe-Al alloy, from X-ray photoelectron spectra 3—8701
  transition metals, 3d4p isoelectronic sequence, spectral study *(Russian)* 3—11109
  two nuclei with one electron system, energy level calc. 3—36000
  GaAs, photoelectron energy distrib. spectra, core levels 3—15591
  p-Ge:Ga, gamma irrad., role of Li in annealing processes 3—33844
  InSb, photoelectron energy distrib. spectra, core levels 3—15591
  Sc III, spectrum and energy levels, using vacuum sliding spark 3—29477
  Si, electron spectra rel. to doping, level bending 3—8690
  Si-SiO_2, interface band struct., O and Si vacancies energy levels 3—18228
  ZnSe:Mn, photocapacitance meas. of impurity created energy levels 3—15153
energy levels, atomic *see atomic structure*
energy levels, molecular *see molecular electronic structure*
energy levels, nuclear *see nuclear energy levels*
energy levels of electrons in solids *see band structure*

energy loss of particles
- *see also channelling; radiation effects*
- alpha particle gauging, gas property meas., mathematical model 3−335
- atomic collision chains, vacancies, focusing influence, computer calcs. 3−20777
- attenuation and energy deposition, application of binomial statistics 3−22419
- bremsstrahlung, external, produced by beta particles in Cu, Ag, Cd, Sn, Pb targets, reln. to target thickness 3−29454
- charged, energy loss through δ-rays from finite volumes 3−287
- charged, in Maxwellian plasmas 3−20429
- coupled system of oscillators and e.m. fields excited by external charge, creation of plasma wave 3−16684
- dE/dx calculations for electron pair production by muons 3−10698
- electron backscatt. factor determ. in X-ray emission microanalysis *(French)* 3−24766
- electron deposition in water vapour, atmospheric applications 3−12746
- electron energy loss analyzer, v.h.v., adaptation for electron microscope *(French)* 3−35506
- electron energy loss spectra for V(Cr)(Fe)(Co)(Ni)(Cu) films 3−17885
- electron penetration, in h.v. microscopy 3−23989
- electron scattering in metallic foils, 40 to 60 MeV optical transition radiation patterns *(French)* 3−13414
- electrons, 1.3 to 3.0 GeV/c, identification of individual particles by transition radiation in X-ray region 3−32134
- electrons, during turbulent heating of plasma 3−17636
- electrons, in solids, probes and resist exposure 3−14902
- electrostatic analyzer for energy analysis of secondary electrons emitted by ion bombarded targets *(French)* 3−28691
- energy loss in tissue equivalent plastics 1 to 5.476 MeV α-particles 3−5685
- exciton creation in strong mag. fields due to energy losses of fast electrons 3−36339
- fast electrons, energy dissipation curves, fitting function 3−10043
- fast electrons, through thick layers of matter 3−19286
- ferroelectric, transparent, energy loss of spirally moving charge *(Russian)* 3−30165
- fission fragment spectrum, calc. of energy deposited in various stopping materials 3−22440
- Franck-Hertz tube, energy loss of electrons in traversing gas, student experiment 3−16372
- graphite, pyrolytic, low energy electron energy loss spectrum and plasmon excitation *(French)* 3−7800
- heavy ion tracks in solid state detectors, etch kinetics 3−3845
- heavy ions, momentum transfer cross sections and Z_1 oscillations in stopping power 3−36338
- hydrocarbon compounds and mixtures stopping powers 3−25854
- inelastic collisions, stopping power, dependence on atomic number of projectile atom 3−13416
- interaction lengths of energetic pions and protons in Fe, 9.3-18 GeV 3−29456
- ion beam, relativistic, heavy, meas. of range in matter 3−33583
- ionization of energetic neutral atoms on metallic surface 3−33396
- ions, radiation damage, collision theory 3−4779
- Landau Vavilov straggling fns., for relativistic charged particles 3−17882
- metallic thin films, optical radiation on passage of electrons up to 100 keV 3−24771
- mica group and related sheet silicates, electron energy loss spectra rel. to struct. 3−1608
- microwave generation of fast charged particles *(Russian)* 3−308
- multple scattering in medium, with axisymmetric magnetic field 3−13415
- nuclear emulsions, relation with track width 3−288
- organic liquids, stopping power for alpha particles, 1-8 MeV 3−20773
- organic scintillators, luminescence response *(French)* 3−13434
- photoemission, energy loss rel. to plasmon and phonon excitation 3−21517
- range-energy dependence of charged particles, instrument description 3−32133
- rare gas crystal on Nb (100), inelastic scattering and energy loss spectra, LEED obs. 3−11655
- relativistic heavy nuclei, corrections to Bethe-Bloch formula for average ionization energy loss 3−22439
- semiconductor, atom recoil displacement effects, energy dependence 3−18515
- single crystals, channelling and blocking, review *(Japanese)* 3−14900
- solid target, electron backscatt., penetration and X-ray production, Monte Carlo study 3−14891
- solids, depolarization of negative muons 3−23508
- stopping power, higher-order corrections proportional to Z^3 3−1659
- stopping power of atomic matter for relativistic ions, mesons, electrons and positrons, Born approx. energy-loss formulas 3−7082
- thermal scatt. influence on fast electrons anomalous absorpt. in thick crystals 3−24155
- thin polymer films, electron beam exposure profiles 3−14903
- transition metals and their alloys with Al, of electrons 3−33584
- α-particles, energy straggling, as fn. of atomic number of absorber 3−16502
- $e^-\gamma\rightarrow e^-\nu\nu$, photoneutrino energy losses, computation for 10^{13} G mag. field 3−35805
- Ag, relation of electron energy loss functions to transverse and longitudinal e.m. excitation 3−21030
- Ag crystal film, coherent excitation of He$^+$ ions 3−24170
- Ag/O_2 chemisorbed layer, low energy backscattered electron spectra, surface atom energetics, chem. bonding 3−24349
- Al, Al_2O_3 foils, electron energy loss analysis by thermomodulation procedure *(German)* 3−28640
- Al, clean and slow oxidized surface, Auger electron and charact. loss spectra 3−34452
- Al film, effect of charact. energy losses on electron diffraction intensities 3−24156
- Al-Mg dilute solid solution, plasma energy loss rel. to band models of alloying 3−7803
- Ar, of fission fragments having selected masses 3−29455

energy gap continued

energy loss of particles continued
- Au, clean and black surface, Auger electron and charact. loss spectra 3−34452
- Au, relation of electron energy loss function to transverse and longitudinal e.m. excitation 3−21030
- Au film, electron energy loss spectra, surface excitations influence *(French)* 3−33580
- Au film, mean free path determ. for low energy electrons 3−15277
- BaF_2 films spectra of electronic excitations in 8 to 150 eV range 3−2032
- Be, clean and slow oxidized surface, Auger electron and charact. loss spectra 3−34452
- CO, electron impact excitation cross sections and energy degradation 3−11307
- CO_2, electron energy deposition rel. to Mariner u.v. data for Mars, 3−12981
- CaF_2 films spectra of electronic excitations in 8 to 150 eV range 3−2032
- CdTe detectors, rate of ionisation loss and intrinsic resolution 3−37683
- Ce, electrons reflected from surface *(Russian)* 3−12205
- Cu, clean and black surface, Auger electron and charact. loss spectra 3−34452
- Fe, clean and slow oxidized surface, Auger electron and charact. loss spectra 3−34452
- He gas, mean energy loss per ion pair and stopping power for electrons 3−26592
- ^{4}He ions, in Si, amorphous, polycrystalline and single crystal 3−17884
- La, electrons reflected from surface *(Russian)* 3−12205
- Mo, determ. of stopping power for 0.50-1.75 MeV protons with backscattering method 3−22437
- Mo, plasma loss peaks in spectra of reflected electrons 3−39211
- N_2 excitation of $W^3\Delta_u$, $w^1\Delta_u$, $B'^3\Sigma_u^-$, $a'^1\Sigma_u^-$ states by electron impact 3−17470
- Na$^+$ scattering by Si, Ge single crystals with ion beam induced lattice damage, angular and energy distributions of scattered ions, $E<5$ keV *(Russian)* 3−11663
- Nd, electrons reflected from surface *(Russian)* 3−12205
- Ni, range of Na$^+$ and Cs$^+$ ions, rel. to preliminary bombardment 3−14901
- Ni(100) surface, influence of H_2, CO and O_2 adsorption on electron energy loss spectra *(German)* 3−36653
- Pr, electrons reflected from surface *(Russian)* 3−12205
- Se, amorphous and polycryst., electron loss spectra and opt. const. determ. *(German)* 3−11668
- Si, irradiated, electron slowing down spectrum 3−33582
- Si, proton random stopping power, backscatter obs. 3−11667
- SrF_2 films spectra of electronic excitations in 8 to 150 eV range 3−2032
- Ta, determ. of stopping power for 0.50-1.75 MeV protons with backscattering method 3−22437
- Te, amorphous and polycryst., electron loss spectra and opt. const. determ. *(German)* 3−11668
- Ti, determ. of stopping power for 0.50-1.75 MeV protons with backscattering method 3−22437
- (U, Pu)C, α-particle stopping power and range, application to self-diffusion meas. using alpha-spectroscopy 3−11664
- UC, α-particle stopping power and range, application to self-diffusion meas. using alpha-spectroscopy 3−11664
- W, determ. of stopping power for 0.50-1.75 MeV protons with backscattering method 3−22437

energy measurement *see power measurement*

energy-range relations *see energy loss of particles*

energy resources
- *see also fuel*
- earth core, terrestrial heat flow from U, Th and K concentration profile 3−9183
- fusion, hydrogen-electric utility system, future trends 3−4346
- geothermal energy in Mexico, exploitation and utilization *(Spanish)* 3−31479
- geothermal reservoirs from ground-noise surveys in 0.5 to 5 Hz range 3−25124
- nuclear power industry in Sweden 3−1034
- solar energy received over Brazil, possibility of direct utilization *(Portuguese)* 3−28132
- U, supply and demand, future uses and prospecting 3−19935
- U for nuclear reactor fuel, economics *(Polish)* 3−23424

energy states in solids *see crystal electron states*

energy storage
- *see also capacitor storage*
- inductive, pumped electron beam switching circuit 3−25835
- superconducting coil applications, review 3−7016
- Ag-Zn encapsulated high energy density system for deep submergence vessel 3−31476

energy transfer collisions, molecular *see molecular energy transfer collisions*

engineering
- *see also biomedical engineering; civil engineering; design engineering; electrical engineering; environmental engineering; high-voltage engineering; maintenance engineering; mechanical engineering; project engineering; systems engineering*
- education, wave eqn., computer simulation 3−13181
- electromagnetics, text book 3−32472
- hydrographic engineering/marine environment training program 3−12
- materials technology, conf. Rio de Janeiro, Brazil (Aug. 1972) 3−30931
- ocean, education program for undergraduates 3−10
- production, conference, Ilmenau, Germany 16-21 Oct, (1972) 3−15645
- progress at MIT electronics research lab. 3−1
- ultrasonic applications *(Polish)* 3−16393

engineering applications of computers
- *see also electrical engineering applications of computers; electronics applications of computers*
- air pollution 3−28404
- civil engineering design, digital photo map applic. 3−5998

engineering applications of computers continued
- classical transmission angle problem of Alt, for four-bar linkages 3−35565
- compressible free convective flow, general elliptic method for computational soln. 3−20347
- coolant flow distribution in experimental breeder reactor, EBRFLOW program 3−26496
- distributed flow systems, analogue simulation technique 3−33307
- fast reactor fuel assemblies, channel deformation analysis for swelling and thermal bowing 3−11077
- fatigue data processing, stochastic function plots 3−2776
- interactive computer studies 3−3933
- metal forming process, axisymmetric extrusion 3−15727
- modal content of sound in annular and circular ducts, Fourier analysis 3−35368
- nonlinear structure earthquake responses, hybrid computer simulation 3−12571
- nuclear industry contribs. to regional dose calc. using HERMES program 3−19984
- nuclear reactor fuel releases, calc. of effect of fuel cycle parameters using HERMES computer program 3−19926
- nuclear reactor fuel-cladding materials selection 3−26517
- nuclear reactor pressure vessels, design history of applications 3−11052
- nuclear reactors, computer simulation of NPD using LATREP-PERIGEE codes 3−19929
- photoelasticity, measurement of isoclinic angle and isochromatic fringe number, data processing system 3−9837
- plane stress analysis, finite element computer program with automatic mesh generation *(Japanese)* 3−10270
- plastic design problems for plane frame 3−541
- sonar system, signal processing and operator response simulation 3−39569
- temperature fields produced in a workpiece by repeated applications of a source of heating, numerical calc. 3−24962
- tensile tests 3−19160
- Van der Poel's nomograph simulation, stiffness moduli of bituminous mixes 3−27810

engineering facilities
- application of modular design principle *(German, English)* 3−1064

engineering societies *see societies*

enthalpy
- *see also heat of adsorption; heat of crystallisation; heat of mixing; heat of reaction; heat of transformation*
- alloys, binary, symmetrical mixing enthalpy, statistical investigation *(French)* 3−7913
- boundary layer, three dimensional laminar coefficient of restoration of the enthalpy *(Russian)* 3−33227
- chemical reaction kinetics, temp. depend. activation parameters, isokinetic model 3−34720
- confined-discharge plasma generator with local fluid construction, energy conversion factor and mean enthalpy increase 3−26904
- dithiin complexes, with trinitrobenzene and tetracyanoethylene, enthalpies of complex formation 3−23593
- fluids and fluid mixtures, prediction of thermodynamic props., applications 3−34699
- freon-113, meas. of thermodynamic props. in 240-460 K and 25-300 bar ranges *(Russian)* 3−24240
- heat of atomization, effect on const. A_0 in Richardson-Dushman eqn. 3−21511
- high temperature gas media, calorimetric detector *(Russian)* 3−9869
- nonideal gas, deformation by intense light beam *(Russian)* 3−774
- nonpolar liquids, from analytic partition function 3−29785
- partial molar mixing enthalpy of binary liquid systems, ALGOL program *(German)* 3−22285
- phosphoryl halide molecule, calcs. using rigid rotator and harmonic oscillator model 3−27857
- polymer, light scatt., Smoluchowski-Einstein-Zernike theory used to determ. free enthalpy 3−29797
- polymer solutions, free enthaply of mixing 3−29789
- polymer solutions, function determ. rel. to quantitative treatment of phase relns. 3−11344
- polymer solutions, generalization of Flory-Huggins free enthalpy 3−29787
- radiative energy transfer at laminar boundary layer, radiation influence on enthalpy profile 3−23734
- steel, austenite, alloyed, dil. solns. with carbon and nitrogen, thermodynamic parameters *(Russian)* 3−24822
- thiophosphoryl halide molecule, calcs. using rigid rotator and harmonic oscillator model 3−27857
- vapour-liquid equilib. data in P-T-X space, consistency testing 3−11727
- water, anomalous, enthalpy of evaporation 3−1789
- weakly associated liquids, molecular theory of vibrational relaxation *(Russian)* 3−4477
- Ag_2Te(c), $Ag_{1.9}Te$(c) and $Ag_{1.64}Te$(c), enthalpies of formation 3−15828
- $As_4(g) = 2As_2(g)$, heat of dissociation, formation, second and third law enthalpies determ. 3−31256
- BC_x, and ht. capacity, 273-2600K 3−24964
- Bi + Se, mixing in liquid state 3−14976
- Co alloys, enthalpy meas. on the allotropic transformations *(French)* 3−17976
- Cu_2Se, Cu_2Te, phase transition, structural order, specific heats, temp. depend. *(German)* 3−38672
- Cu_2Te(c), enthalpy of formation 3−15828
- DBF_2, thermodynamic props. calc. 3−39426
- Dy partial enthalpy meas. in Sn *(French)* 3−4839
- Er partial enthalpy meas. in Sn *(French)* 3−4839
- $EuFeO_3$, equilib. reduction, thermodynamic props. *(Russian)* 3−15077
- Ga-Pb, liquid alloy, calc. of enthalpies and entropies of mixing 3−30271
- GaAs, point defects, precision lattice parameter measurements after quenching and annealing 3−33523
- $GdFeO_3$, equilib. reduction, thermodynamic props. *(Russian)* 3−15077
- H_2 isoteric adsorption enthalpy of Pd and Pt atomically disposed thin film on C substrate *(German)* 3−27921
- HBF_2, thermodynamic props. calc. 3−39426

enthalpy continued
- $HoFeO_3$, equilib. reduction, thermodynamic props. *(Russian)* 3−15077
- In_2O_3, standard molar free energy of formation, standard molar enthalpy 3−27856
- IrO_2, free energy of form. by solid electrolyte galvanic cell method 3−37124
- K-C (graphite) system, partial and total thermodynamic props. determ. *(French)* 3−9045
- $LaPO_4$, method of mixtures meas., and temp. depend. *(Russian)* 3−11745
- LiF, activation enthalpy of deformation 3−7822
- NaAg molecule, dissociation energies, third law enthalpies, heat of formation 3−29728
- NaF in NaF-ZrF_4 mixtures, enthalpies of dissolution, calorimetric study at 1030°C *(French)* 3−7907
- $NaNO_3$, calc. of migration enthalpies of Frenkel defects, application of Mott and Littleton methods 3−24294
- Nb-O solid solution, study using solid electrolytic cells, enthalpy and entropy determ. from solubility limit 3−31025
- $NdPO_4$, method of mixtures meas., and temp. depend. *(Russian)* 3−11745
- Ni-W system, integral molar excess free enthalpy, conc. depend., and activity coeffs. *(German)* 3−27624
- NiO-ZnO solid solns., enthalpy of mixing, activity meas. 3−36429
- PF_3(g), enthalpy of formation 3−15827
- RbI and RbI:Sr, ionic conductivity Schottky defect, positive-ion and negative-ion vacancy enthalpies and entropies 3−24290
- Sb + Se, mixing in liquid state 3−14976
- TaC, enthalpy and sp.ht. meas., 273-3600K 3−36426
- α-Ti single crysts., thermal activation parameters of plastic deform. *(Russian)* 3−24184
- γ-U-Mo solid solns., excess thermodynamic props. 3−32947
- UC, high temperature enthalpy meas. 3−23428
- UC_2, high temperature enthalpy meas. 3−23428
- U_2C_3, high temperature enthalpy meas. 3−23428
- UO_2, smoothed values in room temp. to melting pt. range 3−7003
- XeF_6(c), XeF_4(c), XeF_2(c), enthalpies of formation 3−15827
- YPO_4, method of mixtures meas., and temp. depend. *(Russian)* 3−11745
- Zn-In-Pb solns., liq., miscibility gap, zinc isoactivity and molar functions 3−38675
- ZrF_4, specific heat of the solid as a function of temp. and enthalpy of the liquid meas. *(French)* 3−5816
- ZrF_4 in NaF-ZrF_4 mixtures, enthalpies of dissolution, calorimetric study at 1030°C *(French)* 3−7907

entropy
- *see also entropy of substances*
- atmospheric shear layer stability, effect of planetary vorticity and vertical entropy gradients 3−12708
- black-hole dynamics, parallels with thermodynamics 3−28112
- chemical reaction kinetics, temp. depend. activation parameters, isokinetic model 3−34720
- dielectric crystals phonon-phonon collisions and entropy fluctuations 3−1740
- distribution function representation for homogeneous gas using maximum entropy principle *(Russian)* 3−26183
- entropy wake, schlieren visualisation 3−38414
- entropy waves in a Rijke tube influencing heat transfer *(Russian)* 3−5712
- f.c.c. Lennard-Jones system, form. entropy of point defects 3−4745
- flow-resistance gas heater 3−19173
- harmonic lattice, entropy of binding between vacancies and solute atoms, lattice vibr. 3−33515
- Hubbard model, high temp. sp. ht. and entropy of interacting electrons 3−18295
- inequality of states for quantum measurements 3−585
- rel. to information theory of measurement *(Polish)* 3−25641
- irreversible thermodynamics with internal inertia, principle of stationary total dissipation 3−37913
- layers in supersonic flow, numerical calc. 3−33242
- liquid-vapour systems critical point thermodynamic relations, behaviour of entropy along coexistence curve 3−6386
- Mie-Gruneisen materials, high press., equations 3−7897
- neoclassical thermodynamics, local form of entropy inequality 3−19535
- nonelastic media thermodynamic and shock phenomena *(French)* 3−6263
- nuclear shell correction energies, determ. from statistical temp. depend. of entropy 3−10890
- nucleation, heterogeneous, from vapour phase onto substrate, entropy contrib. 3−1585
- planar box, information theory and entropy 3−16352
- pressure polymorphism in solids 3−4842
- quantum measurements, inequality of states 3−585
- quantum-mechanical, strong subaddivity prop. 3−22744
- reactive mol. collisions product energy distrib. determ. of temp. and entropy deficiency 3−9059
- relaxing gas, vibrational-vibrational energy exchange *(Russian)* 3−23632
- second law of thermodynamics, alternative statement 3−32465
- sensory receptors, as transmitters of entropy 3−35250
- steady-state system far from equil. entropy changes 3−4039
- stimulated light scatt. from isobaric temp. excitations, electrocaloric effect in fluids 3−32597
- superconductors, energy currents, entropy current, heat flow, quasistatic time dependent order parameter 3−30571
- turbulent flow, asymmetric mechanics, energy and entropy *(Russian)* 3−29853
- two-level system, near-equil., thermalizing matter and radiation, entropy prod. 3−37943
- Al, quenched-in vacancies, resistivity meas., formation energy and entropy determ. 3−17806
- $Nb_{80}Mo_{20}$, $Nb_{85}Mo_{15}$, dirty supercond. in mixed state, transport entropy, two-band analysis 3−27337
- U-Rh-C system, phase equilib. study, entropy determ. *(German)* 3−12333

entropy of substances
- activation entropy for low temperature plastic flow 3−17911
- alloy, disordered, config. entropy and solute correl. 3−36996

entropy of substances continued
ammonium hydrogen chlorotartrate and deuterated analogue, ferroelec. and phase transitions 3—18418
freon-113, meas. of thermodynamic props. in 240-460 K and 25-300 bar ranges *(Russian)* 3—24240
liquid crystals, homologous series, nematic-smectic A transition entropies 3—30070
oxalyl fluoride from 13 K to its boiling point, thermodynamic props. 3—34705
phosphoryl halide molecule, calcs. using rigid rotator and harmonic oscillator model 3—27857
plastic organic crystals, n.m.r. of translational mol. motion in solids of intermediate energy of fusion 3—24109
polymer, deform., internal energy rel. to speed of sound 3—30188
polymer and solvent, entropy of mixing derivation from free volume concept 3—29786
powder surfaces study by ^{85}Kr adsorption, differential standard entropies and isotherm shape determ. *(French)* 3—27175
rare earth nickelides, $LnNi_5$, thermal props. over range of ordering, entropy and spin-disorder resistivity 3—12016
saturated liquids, prediction using Mie (n,6) potential and Barker-Henderson perturbation theory 3—4715
thiophosphoryl halide molecule, calcs. using rigid rotator and harmonic oscillator model 3—27857
trithiane, solid-state polymeriz. rate, temp. depend. 3—37121
water structural model based on intermolecular potential function, structural entropy contributions 3—30062
C_3 molecule, and ht. of formation 3—27852
$Ce_2Mg_3(NO_3)_{12}.24H_2O$, magnetothermodynamics, heat capacity, entropy, magnetic moment, 0.5-4.2K, 90 kG 3—30616
DBF_2, thermodynamic props. calc. 3—39426
$EuFeO_3$, equilib. reduction, thermodynamic props. *(Russian)* 3—15077
Ga-Pb, liquid alloy, calc. of enthalpies and entropies of mixing 3—30271
$GdFeO_3$, equilib. reduction, thermodynamic props. *(Russian)* 3—15077
HBF_2, thermodynamic props. calc. 3—39426
^3He-^4He mixtures, dynamical behaviour near tricritical pt. 3—7989
^4He, solid, in h.c.p. phase at low densities, Debye temp. heat capacity and entropy meas. 3—30309
$HoFeO_3$, equilib. reduction, thermodynamic props. *(Russian)* 3—15077
In_2O_3, standard molar free energy of formation, standard molar enthalpy 3—27856
IrO_2, free energy of form. by solid electrolyte galvanic cell method 3—37124
K-C (graphite) system, partial and total thermodynamic props. determ. *(French)* 3—9045
LiF, role in thermally activated deformation 3—7822
$LiF:MhF_2$, Debye-Huckel interactions and solubility 3—4881
MnTe, 300-700 K 3—15365
Nb, magnetocaloric behaviour 3—8291
Nb-O solid solution, study using solid electrolytic cells, enthalpy and entropy determ. from solubility limit 3—31025
Pb-In(4.56 wt.%) alloy, supercond., sign change in entropy flux associated with vortex motion *(French)* 3—38925
$PbFe_{12}O_{17}$, free energy, entropy, of parallel plate domain struct. 3—2314
Pu_2C_3, specific heat meas. between 35 and 300 K, entropy determ. *(French)* 3—23431
o-pyrocatechuic acid in water and water-methanol mixtures, ionisation consts. and related thermodynamic functions 3—18783
RbI and RbI:Sr, ionic conductivity Schottky defect, positive-ion and negative-ion vacancy enthalpies and entropies 3—24290
$ThCl_4$, sublim.-pressure meas. by Knudsen effusion method, 400-600°C *(German)* 3—11735
γ-U-Mo solid solns., excess thermodynamic props. 3—32947
V_4O_7, mag. entropy rel. to crystal structure of insulating phase 3—15368
XeF_2, standard entropy calc. from heat capacity meas. at 5-350K 3—1805

environmental engineering
see also air conditioning; cooling; lighting; safety; temperature control; ventilation
air quality simulation modelling, applic. to pollution control 3—28405
conference, New York, USA (1972) 3—34754
dust emission suppression and control methods in cement industry 3—37537
dust meas. and control in mining, to reduce work-related diseases 3—25609
emission to air, conference, London, (1972) 3—37204
emission to air reduction in power generation industry, best practicable control means 3—37538
fluid mechanics aspects of environmental protection, research program *(German)* 3—36147
industrial noise control, use of acoustical absorbents 3—9750
industrial plant noise control, criteria and design specifications 3—9749
NASA life-support system as model for pollution problems 3—31952
nuclear fusion reactors, anal. of environmental impact 3—19969
planning deep ocean mining, equipment size, equipment type 3—3169
Plowshare project, cost analysis of environmental impact 3—19891
pollution control by consumption optimisation 3—28407
simulated sea floor mining, open cut mining 3—3168
sound level estimation in industrial environments 3—5788
systems research into urban industrial liquid waste treatment 3—28409

environmental requirements *see environmental engineering*

environmental testing
continuous Compton recoil gamma-ray spectroscopy, radiation monitoring 3—31949
dosimetry, for nuclear facilities 3—29451
dust meas. and control in mining, to reduce work-related diseases 3—25609
nuclear power plant effluent monitoring, using digital computer and γ-ray spectroscopy 3—32229
solar generator, for Helios Sun Probe 3—5619

environmental testing continued
techniques for extreme environment, applic. to metals research, book 3—9825

ep scattering *see electron-proton scattering*

epitaxial growth
alignment, influence of misfit dislocations 3—1932
chemical vapour deposition, sensors and control elements 3—12250
chlorinated Cu phthalocyanine film, orientational adsorption 3—15086
computer contol system 3—12231
crystal growth conference, Freiburg, Germany 21-23 Sept. (1972) 3—5261
data compilation, planes, directions, periods and misfits for 3700 systems 3—8055
defect formation during growth 3—11827
direct observation, in situ transmission electron microscopy, review 3—1935
dislocation propag. and annihilation during epitaxy 3—1916
elastic deformation problem, dislocations at film/substrate interface 3—33747
evaporated thin films on NaCl covered by an amorphous dielectric intermediate layer 3—38746
f.c.c. metal films, epitaxy and recrystn. on mica and NaCl *(French)* 3—15092
ferrite film prep. by oxidation of metal films, electron microscope exam. of microstruct. 3—27196
film deposition, optimization, chem. thermodynamic anal. 3—12247
film growth, review 3—24358
garnet, chemical vapour growth for bubble domain devices 3—36771
garnet, phase relations and growth conditions rel. to defects and mag. props. 3—2667
garnet film, control of product phases in chemical vapour deposition 3—12249
garnet film, for substrate facet replication 3—38749
garnet film, mag., growth by liq. phase epitaxy on nonmag. substrate 3—1912
garnet magnetic bubble films 3—12276
garnet substrate prep. by liq. phase homoepitaxy 3—34483
heat and mass transfer in liquid phase epitaxy 3—1923
ice on muscovite mica and NaCl, substrate elec. props. 3—1927
II-VI semiconductor, growth by vacuum sublimation in sealed quartz tube *(French)* 3—5265
III-V semiconductor, comparison of liquid phase and chemical vapour phase methods 3—30363
III-V semiconductor alloy, lattice match in heteroepitaxy 3—4932
III-V semiconductors, chem. vapour deposition using organometallics 3—21531
island growth, pseudomorphic arrangement 3—15081
IV-VI monolayer overgrowth on IV-VI, substrate, effect of substrate temp. and orientation 3—15083
lattice matching quality, geometrical interpretation *(French)* 3—1930
liquid phase, state-of-the-art 3—12275
liquid-phase, for garnets, production and applic. to integrated optical components 3—27610
magnetic bubble material, liquid and vapour phase growth 3—11555
magnetic bubble materials, stoichiometry and perfection 3—12277
metal films, ultra thin, pseudomorphism, nucleation 3—30374
misfit dislocations, closely spaced, moire image contrast 3—15082
monocrystalline semiconductor layers on insulating substrate, epitaxial methods of prod. *(German)* 3—34491
nucleation, heterogeneous, from vapour phase onto substrate, atomistic and capillarity theories 3—1585
oxide films, quasi-homoepitaxy 3—15084
production process control, digital computer system 3—12221
rare earth garnet, liquid phase growth for bubble domain devices 3—36770
rare earth iron garnet, chemical vapour deposition for bubble domain devices 3—24792
rare gas crystal on Nb (100), inelastic scattering and energy loss spectra, LEED obs. 3—11655
rare gas crystals, derivation of upper limit for Xe stacking fault energy 3—1925
rare gas crystals on Nb (100), LEED and absorpt. 3—11654
semiconductor film, ion beam sputtering 3—9915
semiconductor film, on insulators, vapour phase epitaxy by reactions involving organometallics 3—12251
semiconductor homoepitaxial layer growth by sublimation in UHV, impurity density control 3—27613
substrates of Ag platelets, prep., cleanliness, perfection 3—20953
temperature gradient cell for liq. phase growth 3—12261
and vapour growth, conf., Jerusalem, Israel, (May 1972) 3—2637
ZnTe—CdS heterojunction light-emitting diode, epitaxial vapour growth 3—2659
Ag, adsorp. and nucleation on W(110) surface 3—1887
Ag film, growth method rel. to dislocation density, X-ray rocking curve obs. 3—11830
Ag on Au substrate, evidence of stresses at interface 3—36494
Ag on GaAs(110) obs. by LEED 3—15087
Ag thick single crystal films, plastic deformation, dislocation struct. 3—17900
AgCl on NaCl or PVC copies, determ. of NaCl surface relief *(Russian)* 3—8240
Al crystalline ultrathin films epitaxially grown on Si, superconducting props. 3—18238
$Al_xGa_{1-x}As$, molecular beam epitaxy 3—2677
$Al_xGa_{1-x}As$, molecular beam epitaxy 3—18553
AlN, by vapour phase reaction, obs. of optical bandgap 3—11831
AlN film, props., optical band gap 3—21004
Al_2O_3, growth of amorphous and epitaxial layers on Si *(German)* 3—8056
Au, on Ag single cryst., effect of amorphous intermediate layers 3—1933
Au, vacuum deposition, effect of electric field on orientation and particle arrangement 3—1934
Au film, growth method rel. to dislocation density, X-ray rocking curve obs. 3—11830
Au film, on NaCl, influence of elec. field on orientation *(Russian)* 3—30364

epitaxial growth continued
Au nuclei, vapour deposition on NaCl substrate, mobility and coalescence 3−2643
Au on KCl, influence of decoration of monatomic surface steps on crystallite mobility *(French)* 3−36495
$Bi_4Ti_3O_{12}$ single-domain films, electro-optic contrast obs. 3−18431
$Bi_4Ti_3O_{12}$ sputterred films, optimization of epitaxial quality 3−12252
CaF_2, thin films, electron irradiation effects 3−38748
$CaWO_4$, heteroepitaxial layers, growth on sapphire substrate *(German)* 3−8736
CdS, CdSe, heat treated epitaxial films, structure, composition, photoelec. props. *(Russian)* 3−33948
CdS, contamination of heteroepitaxial layers vapour grown on GaAs substrates 3−2653
CdS films, on Ge, growth and struct. 3−36493
CdS needles and platelets, growth mechanism 3−11574
CdS thin film, structural defects 3−18032
CdS_xSe_{1-x}, growth of graded gap crystal layer, luminesc. obs. 3−8053
CdSe, growth conditions for vapour growth on sapphire substrate 3−30362
CdTe, physical vapour deposition for high power laser windows at 10.6 μm 3−9960
Cu film, on β-Co *(Russian)* 3−8049
Cu films on n-Si, structure obs. 3−33751
Cu on Au(111) platelet, influence of intermediate amorphous C layer 3−24357
Cu_2O nucleation and growth near (100) face of Cu 3−15088
$(EuY)_3(GaFe)_5O_{12}$, liquid phase growth on $Gd_3Ga_5O_{12}$ substrate by tipping process 3−12278
$Eu_{1.1}Yb_{1.9}Fe_5O_{12}$, garnet film, LPE growth by isothermal dipping with axial rotation 3−30945
Fe, phase relations for epitaxial intergrowth of nitrogenized Fe sheets and thin films *(German)* 3−1926
Fe electrodeposition on Cu, epitaxy relationships *(French)* 3−24355
Fe_3S_4, oriented growth 3−15089
$Ga_{1-x}Al_xAs$, liq. phase epitaxy, variation of solid comp. with temp. 3−12258
$Ga_{1-x}Al_xAs$:Si, amphoteric behaviour of Si, effect of As soln. conc. 3−5278
$Ga_{1-x}Al_xAs$:Si, L.P.E. growth, depend. of carrier conc. profiles on growth conditions 3−27190
n-GaAs, by vapour phase process 3−1937
GaAs, effect of surface states on amphoteric behaviour of Sn 3−24393
GaAs, epitaxial growth over wide range of crystallisation conditions, comparison with GaP *(Russian)* 3−8051
GaAs, epitaxially grown, electrical props. depend. on $AsCl_3$ temp. 3−8756
GaAs, excess Ga and As in the vapour phase influence on the growth in (111) direction *(Russian)* 3−8749
GaAs, for Gunn devices, optimisation for high purity layers 3−2686
GaAs, Ga-$AsCl_3$-H_2 system, Ga:As ratio, chemical thermodynamics calc. *(German)* 3−15095
GaAs, heteroepitaxial film growth on spinel, optical props., carrier transport characteristics 3−39266
GaAs, high purity by liquid and vapour phase deposition 3−2676
GaAs, inhomogeneities in epitaxial layers *(Russian)* 3−8050
GaAs, liq. phase epitaxial growth by rotating boat technique 3−34481
GaAs, liquid phase, impurity incorporation, depend. on growth rate and cryst. orientation 3−1638
GaAs, liquid phase epitaxy from Ga free Sn melts *(German)* 3−4933
GaAs, molecular beam epitaxy 3−2677
GaAs, on Ge, diffusion of Ga and As in substrate *(Russian)* 3−27606
GaAs, parameters for vapour growth of high purity crystals 3−1918
GaAs, prep. and characterisation for microwave devices 3−2685
GaAs, review 3−27192
GaAs, review of methods 3−30948
GaAs, solution growth in silica boat, Si contamination control 3−2684
GaAs, temp. gradient cell for liq. phase growth 3−12261
GaAs, V.P.E. growth, effect of As vapour pressure on elec. props. 3−27191
GaAs, vapour phase homoepitaxial growth, transmission electron microscope obs. 3−15096
GaAs and related compounds, conference, Aachen, Germany, (Oct. 1970) 3−2675
GaAs epitaxial layers, micromorphology and electron distrib., effect of growth time in iodide system *(Russian)* 3−30933
GaAs film, produced by vapor transport reactions, crystallization condits. *(Russian)* 3−8725
GaAs film, small angle shadowing and chem. decoration obs. of growth surface 3−20956
GaAs layers, substrate surface orientation effect 3−33748
GaAs p-n junction, vapour-grown, defect morphology and electrolum., gas-phase stoichiometry effects 3−11950
GaAs substrate, characterisation, disloc., impurity, and precipitate obs. 3−1938
GaAs vapour phase epitaxial growth, rate of growth and purity of layers 3−34477
GaAs:Mg, molecular beam epitaxy 3−18553
GaAs:Si, epitaxial layers, characterisation of p-n structure, etching, cathodoluminescence 3−39195
GaAs-GaAlAs, profiling of periodic structures by nuclear backscattering 3−39238
GaAs-GaAlAs superlattice, ultra high vacuum epitaxy system 3−39297
$GaAs_{1-x}P_x$, by pyrolysis of $Ga(CH_3)_3$, AsH_3 and PH_3 3−15640
$GaAs_{1-x}P_x$, pyrolytic, growth rate analysis 3−1914
$GaAs_{1-x}P_x$, superlattice, X-ray diffraction obs. of lattice distortion and structure 3−17788
$Ga_xAs_{(1-x)}P$ on GaAs substrate, lattice mismatch strain rel. to dislocation equilib. 3−11828
$Ga_{1-x}In_xAs$, vapour phase, for i.r. photocathodes 3−2678
$Ga_xIn_{1-x}As$ on GaAs substrates, anisotropic bending 3−15085
GaN, heteroepitaxial thermal gradient soln. growth 3−12257

epitaxial growth continued
GaP, light emitting diode, materials prep., p-n junction formation, liquid phase epitaxy 3−39191
GaP, liquid phase, selectively through SiO_2 and Si_3N_4 masks 3−2683
GaP, molecular beam epitaxy 3−2677
GaP, open tube vapour phase epitaxy onto GaAs substrate, influence of liquid Ga 3−2652
GaP, p-type dopants for green light emitting diodes 3−8734
GaP, surface morphology of liquid-phase epitaxial layers 3−38747
GaP epitaxial growth over wide range of crystallisation conditions, comparison with GaAs *(Russian)* 3−8051
GaP films, lattice defects in growth from liquid and vapour 3−15091
GaP:Te,O, liq. phase epitaxy, Te and O incorporation 3−39234
GaP:Zn, O, chem. vapour deposition, Zn-O radiative centre form. 3−2672
GaP:Zn,O, liquid phase epitaxy, use of $Zn(PO_3)_2$ glass as doping source 3−8755
on Gd-Ga garnet substrate, chem. etching in prep. for mag. garnets liquid phase growth 3−8029
$(GdY)_3(GaFe)_5O_{12}$, liquid phase growth on $Gd_3Ga_5O_{12}$ substrate by tipping process 3−12278
$(GdYYB)_3(GaFe)_5O_{12}$, liquid phase growth on $Gd_3Ga_5O_{12}$ substrate by tipping process 3−12278
Ge, on Ge substrate, sputter deposition at low temps. 3−18554
p-Ge, solid-phase growth from Al-Ge 3−8759
Ge, surface memory effect of uniaxial texture form. rel. to photoepitaxy 3−8054
Ge film, vacuum-deposited on Si, elastic strains 3−27194
Ge homoepitaxial layers, dislocation struct., effect of crystn. conditions 3−24356
Ge on Ge, in field-emission microscope 3−33750
Ge or Si, interface dislocation struct., transmission electron microscope obs. 3−1941
Ge tripyramid growth obs. *(Japanese)* 3−1931
$InAs_{1-x}P_x$, $(0.7 \leqslant x \leqslant 1)$, vapour epitaxial growth and characterization 3−1917
$InAs_{1-x}P_x$, vapour phase, elec. props. 3−2680
$InAs_{1-x}P_x$, vapour-grown epitaxial layers, electron microprobe characterization 3−20955
$In_{1-x}Ga_xP$ cryst., liq. phase epitaxial growth by sliding method 3−30944
$In_xGa_{1-x}P$ solid solns., from gas phase *(Russian)* 3−12240
$In_xGa_{1-x}Sb$, rel. to solidus points of In-Ga-Sb system 3−1775
InP, vapour phase, elec. props. 3−2680
InP, vapour phase, photoluminesc. props. 3−2681
InP:Ge,Sn,Te, liquid phase, impurity distribution coeffs. 3−1637
InSb:Te,Se, liquid epitaxial growth, solubility and distrib. of Te and Se *(Russian)* 3−15093
Li-Cr ferrite film, LPE growth on MgO, Mossbauer obs. of substrate contamination 3−1928
LiF film grown on NaCl electron microscope obs. of annealed structures 3−1929
$LiLnMo_2O_8$, on Ln_2GeMoO_8 single cryst. substrate from $LiO_2.2MoO_3$ soln. 3−1913
$Lu_2EuMFe_4O_{12}$ (M = Al or Ga), growth-induced mag. anisotropy of epitaxial films 3−21259
NH_4Cl, on muscovite mica and NaCl, substrate elec. props. 3−1927
NaCl, on mica, prep. of dissolvable substrates 3−1936
NaCl film, on muscovite, RHEED and transmission electron microscope obs. 3−27193
Nb film, r.f. sputtering on perfect and imperfect sapphire 3−20954
Ni films on n-Si, structure obs. 3−33751
NiO, high purity crystals, details of starting materials and apparatus 3−1915
Pb epitaxial films growth on PbTe 3−18238
PbS film, quasi-static growth, and h.f. props. 3−2674
PbS grown on KCl in vitreous silica hot wall system, Pb form. 3−8052
PbSe films, vapour phase deposits epitaxially grown 3−30360
$Pb_{1-x}Sn_xTe$, vertical epitaxial system for growth from vapour 3−2654
PbTe layers, on CdTe *(French)* 3−8048
Pt, vacuum evaporated epitaxial films, preparation *(German)* 3−8732
Pt film 3−34473
Si, at high rates by chem. vapour deposition 3−24788
Si, by rotating disk method 3−12242
Si, deposition from SiH_4, 800-1150°C 3−12246
Si, epitaxial deposition on insulating subsrate, combination of two growth methods 3−2655
Si, epitaxial thin film, spreading resistance meas., device applications 3−38835
Si, etch rate and deterioration of $MgAl_2O_4$ substrate in H_2 3−11816
Si, etching effects with SF_6 during epitaxial growth 3−39268
Si, grown on sapphire film, elec. props. rel. to dual rate technique 3−2656
Si, grown over buried layer area, i.r. thickness meas. 3−11829
Si, in chloride process, kinetics *(Russian)* 3−12238
Si, on insulating substrate, density of early growth islands rel. to semicond. props. 3−11833
Si, on sapphire, elec. props., effect of vacuum deposition conditions *(Russian)* 3−24813
Si, on sapphire, interface cpd. formation rel. to deposition conditions 3−11834
Si, on sapphire, ion erosion apparatus for sample prep. for electron microscopy 3−1939
Si, on W surface, field emission microscope obs. *(Japanese)* 3−20952
Si, onto spinel, chem. interaction between deposition constituents and subtrate 3−8720
Si, pedestal growth by liquid phase epitaxy on planar diodes, selective growth 3−2670
Si, structure of isoepitaxial films made by condensation from a molecular beam in ultrahigh vacuum 3−33749
Si, surface memory effect of uniaxial texture form. rel. to photoepitaxy 3−8054
Si, using dichlorosilane 3−8760
Si, vapour epitaxial growth, generation of growth nuclei 3−1919

epitaxial growth continued
- Si, vapour phase homoepitaxial growth, transmission electron microscope obs. 3−15096
- Si epitaxial layers, thickness meas. using Michelson interferometer 3−30361
- Si film, impurity atom transfer from substrate 3−21530
- Si film, on Al_2O_3, Hall mobility anisotropy, rel. to substrate thermal expansion 3−11967
- Si in N_2, effect of carrier gas change from H_2 and low deposition temp. 3−1921
- Si layers, carrier lifetimes and diode characts., rel. to growth conditions 3−8754
- Si mesas, solid-phase from Al metallization 3−21542
- Si:B layers, thermal oxidation treatment, Hall mobility obs. *(German)* 3−18236
- Si:Sb(As)(P)(B), epitaxial wafer, buried layers, impurity profile 3−39261
- Si/sapphire film/substrate orientation, theoretical model 3−11832
- Si-Ge, epitaxial layer grown on Si substrate, crystal defects obs. 3−1920
- β-SiC, vapour-phase deposition on Si 3−18543
- SiO_2 on W substrate, work function determ. *(Russian)* 3−8251
- Ti film, vacuum deposition onto mica, elec. resistivity obs. 3−4995
- TiO_2, growth by chem. vapour transport 3−12255
- Xe, on graphite, liquid He stage in transmission electron microscope 3−1940
- YAG:Nd^{3+}, growth from flux, site selectivity 3−11560
- $Y_3Al_5O_{12}$, heteroepitaxial layers, growth on sapphire substrate *(German)* 3−8736
- $Y_{2.4}Eu_{0.6}Ga_{1.2}Fe_{3.8}O_{12}$, garnet film, growth-induced mag. anisotropy 3−30640
- $Y_2EuMFe_4O_{12}$ (M = Al or Ga), growth-induced mag. anisotropy of epitaxial films 3−21259
- $Y_3Fe_{5-x}Ga_xO_{12}$, for epitaxial films 3−11753
- $Y_3Fe_{5-x}Ga_xO_{12}$, epitaxial garnet film, growth by chemical vapour deposition 3−12248
- $Y_3Fe_{5-x}Ga_xO_{12}$ garnet film, growth by liq. phase epitaxy *(German)* 3−5274
- $Y_3(GaFe)_5O_{12}$, liquid phase growth on $(GdDy)_3Ga_5O_{12}$ by tipping process 3−12278
- YIG film on GdGaG substrate, growth by hydrothermal synthesis 3−1922
- YIG:Al, chemical vapour deposition for bubble domain devices 3−33746
- YIG:Ga, L.P.E. growth, effect of substituting Gd(Sm)(La) for Y 3−1924
- YIG:Gd,Ga uniaxial films, r.f. sputtering 3−12237
- Zn, electrodeposition from alkaline solns., morphology 3−20962
- ZnS, on Si, condensation of vapour from electron beam heated source 3−24795
- ZnS thin film, structural defects 3−18032
- ZnSe, of sphalerite and wurzite phases on Ge surface by sublimation 3−21528
- ZnSe on GaAs substrate, H_2 transport, luminescence obs. 3−18546

epitaxy *see epitaxial growth*

equalisers
- optical fibre double-reverse-scatter interference reduction 3−149

equations
- *see also Bethe-Salpeter equation; Boltzmann equation; differential equations; equations of state; functional equations; integral equations; nonlinear equations; Vlasov equation*
- No entries

equations of state
- *see also equations of state of gases; equations of state of liquids; equations of state of solids; phase transformations; thermodynamics*
- Baxter's for binary mixture, to determ. P-V-T information 3−17484
- Clausius, modified, prediction of vapour liquid equilibria 3−36403
- computer simulation of associated second order transition 3−645
- critical phenomena, perturbation theory application 3−35646
- near critical point, phenomenological approach 3−22795
- dense fluids, direct correl. function, first-order perturbation theory 3−611
- Dirac delta function and density of states of several systems 3−3741
- expansion equation of state subroutine for one-phase and two-phase behaviour of material 3−27131
- fluid parametric eqns. near crit. point 3−32466
- free energy calc. of fluids near critical point 3−16772
- gas-solid higher virial coeffs. rel. to heterogeneity 3−20845
- hard sphere fluid with attractive square wells, spatial struct. and thermodynamic props. 3−26182
- hard-core potentials, quantum corrections to virial coeffs. 3−19514
- hard-core-plus-attractive-well-potential model, high-temp. corrections to virial coeff. 3−19513
- irreversible thermodynamics with internal inertia, principle of stationary total dissipation 3−37913
- magnetic critical point, scaling law equation of state, free energy and magnetic field-temperature paths 3−27369
- mantle-core discontinuity using equations of state for silicates in metallic form 3−31317
- numerical models of ocean circulation 3−9256
- P, V, T boundary surfaces, comparison of exptl. and fitted, by simulation 3−14955
- plasma, nonideal, Cs, study using dynamical method 3−36201
- plastic and viscoplastic media, constitutive eqns. and directors 3−37821
- quasi-linear bodies, mechanical behaviour 3−37811
- scaling eqn. for thermodynamic systems with tricrit. pt. 3−4051
- second virial coeff. for free and metastably bound atoms interacting through Morse potential *(Russian)* 3−11330
- stellar interiors, approximation to Fermi Dirac integrals 3−31651
- stishovite and coesitelike phases, det. from shock wave and other data 3−9165
- third virial coefficient, second irreducible integral, for three atoms with unsaturated electron shells *(Russian)* 3−11114
- Thomas-Fermi model, shell structure effects at geophysical pressures 3−32435
- three-sort ion and dipole system, binary distrib. function curves in third virial coeff. approx. *(Russian)* 3−20846

equations of state continued
- virial relationship for spatially defined fragments of molecular systems 3−17478
- viscoplastic thin shells, approximate linear theory, constitute eqns. and stress, strain relns. 3−37817
- Xe, second virial coeffs. for three parameter pair potential determination 3−7268
- Yang-Yendall equation, inapplicability to ideal gas state 3−11710
- Ar, dipole and quadrupole three-body interactions, virial coeffs. 3−20072
- Ar, second virial coeffs. for three parameter pair potential determination 3−7268
- Kr, second virial coeffs. for three parameter pair potential determination 3−7268
- N_2-Ar-O_2 vapour-liquid equilibria 3−30249
- Ne + Kr, virial coefficients 3−14996

equations of state of gases
- binary gas mixtures, method for determination of second virial coefficients *(German)* 3−33181
- Carnahan-Starling eqn., real gas, crit. parameters effect 3−37916
- compressed gases, sound velocity calc. using virial series 3−26765
- condensation of one-dimensional gas, Van der Waals equation of state 3−33659
- critical isotherm equation for real gases 3−17971
- empirical equations which are consistent, recipe for development 3−24239
- ethylene, deuterated, intermolecular force parameters in the gas phase, calc. from virial coefficient data *(German)* 3−26740
- ethylene, deuterated, isotope effects in the second virial coefficients *(German)* 3−26763
- exact one-dimensional statistical model for thermodynamic behaviour of gas of identical particles 3−16776
- freon-II, density meas., 110-200°C, determ. of eqn. of state *(Russian)* 3−20259
- hard-sphere gas, thermal equilib. states of classical system with gravit., astrophysical appl. 3−35643
- inert gases, meas. of second virial coefficient of Lorentz-Lorentz function 3−11714
- inert gases, sublimation *(French)* 3−20871
- Lennard-Jones particles, fourth virial coeff. calc. 3−36064
- methane, methane-d, differences in second virial coeffs. rel. to intermol. pots. *(German)* 3−26738
- mixture of nonideal, chemically reacting gases 3−34722
- n-paraffins, P-V-T relations, press to 2500 atm., temps. to 120 °C *(Russian)* 3−14958
- polar, second virial coeffs., correlation with Stockmayer potential function 3−1772
- polyatomic gases, calc. of second virial coefficient from acoustic data *(Russian)* 3−26762
- second virial coeff., two-dimens. calc. for curved surfaces 3−7899
- second virial coefficients of H_2, O_2, N_2, NO, CO, methane, determ. of energy parameters in Lennard-Jones interatomic potential 3−14402
- wetting hysteresis effect on state of gas trapped by liquid in a capillary 3−20925
- Ar, nonadditive effects due to long range dispersion forces on m-6−8 potential function, calcs. of third virial coeff. 3−4838
- Cd vapour, sublimation *(French)* 3−20871

equations of state of liquids
- binary mixtures, polar and nonpolar fluids, interaction virial coeffs. calc. 3−26181
- dichlorodifluoromethane, law of corresponding states 3−11711
- freon-113, meas. of thermodynamic props. in 240-460 K and 25-300 bar ranges *(Russian)* 3−24240
- fused salts and molten metals, from u.s. velocity data 3−101
- liquid structure and Lennard-Jones (6,12) pair potential parameters, determ. from equation of state of liquids 3−1565
- polymer soln., dil., binary cluster integrals 3−23649
- seawater, determ. from sound velocity data 3−2954
- sound attenuation due to thermal relax., determ. from eqn. of state 3−1773
- thermodynamic properties using perturbation theory 3−1807
- water, determ. from sound velocity data 3−2954
- H_2, from compressibility data *(Russian)* 3−11713

equations of state of solids
- alkali halides, Borelius' law 3−20844
- alloys, additivity rule conformity in shock compression *(Russian)* 3−31102
- amorphous polymer glasses, low temp. 3−4499
- Birch-Murnaghan equation of states for rocks and minerals under high pressure *(German)* 3−34814
- Borelius' law, derivation, modification and appl. 3−20844
- bulk modulus of the electron gas calc. 3−18050
- formulation method using shock compression data and second law of thermodynamics, Monte Carlo simulation *(Russian)* 3−30239
- fourth order nonlinear eqn. applic. to elastic moduli determ. *(French)* 3−7805
- Heisenberg ferromagnet, Feynman graph expansion for equation of state near crit. point 3−15330
- high-pressure solid phases, appl. to minerals 3−25118
- Ising model, $(4-\varepsilon)$ dimensional *(Russian)* 3−5087
- materials intermediate to rubbers and glasses, equation of state calc. 3−33653
- metallic halides, one-parameter isothermal eqn. 3−7900
- metals, Gruneisen two coeff. model *(French)* 3−7896
- metals, one-parameter isothermal eqn. 3−7900
- metals, rel. to charact. collision velocity determ. *(Russian)* 3−27066
- Mie-Gruneisen materials, isentropic release from Hugoniot state 3−7897
- noble metals, rel. to mech. strength calc. *(Russian)* 3−8836
- nylon 6, pressure-induced crystallisation, obs. 3−18732
- pair potential microcrystals in two dimensions, molecular dynamics simulation using Lennard-Jones pair potential 3−27102
- universal equation *(Russian)* 3−7898
- Ag, semiempirical equation, rel. to mech. props. *(Russian)* 3−27618
- Al, semiempirical equation, rel. to mech. props. *(Russian)* 3−27618
- Au, semiempirical equation, rel. to mech. props. *(Russian)* 3−27618

equations of state of solids continued
B_2O_3 glass, static and dynamic PVT obs. using acoustic densitometer 3−1774
CsCl, rel. to compression to 32 kbar 3−4808
Cu, semiempirical equation, rel. to mech. props. *(Russian)* 3−27618
Dy, Murnaghan equation, rel. to elastic consts. 3−27051
Er, Murnaghan equation, rel. to elastic consts. 3−27051
Fe, of alpha and epsilon phases, empirical 3−33652
Gd, Murnaghan equation, rel. to elastic consts. 3−27051
H_2, from compressibility data *(Russian)* 3−11713
H_2, metallic phase 3−24271
NaCl, rel. to compression to 32 kbar 3−4808
Ne, 20 kbar, piston displacement equation of state 3−36405
Ni, semiempirical equation, rel. to mech. props. *(Russian)* 3−27618
Pb, semiempirical equation, rel. to mech. props. *(Russian)* 3−27618

equilibrium, chemical *see chemical equilibrium*

equilibrium, phase *see phase equilibrium*

equilibrium constants *see chemical equilibrium*

equilibrium diagrams *see phase diagrams*

equilibrium properties of superconductors
critical fluctuations in superconductors, functional integral approach 3−34016
crystal chem. aspects of A_3B, β-W type structure, stability rel. to supercond. crit. temp. 3−33480
dirty bulk superconductors, specific heat transition in mag. field, screening theory 3−30565
dirty films, diamag. susceptibility rel. to fluctuating Cooper pairs 3−21170
dirty superconductors, fluctuation induced diamagnetism 3−34012
electromagnetic coherence length, temp. depend. calc. 3−15294
film, two-zone, with paramag. additions, thermodynamic props. *(Russian)* 3−15287
Frank-Read source behaviour under external stress, stress softening 3−24537
hollow cylinder, magnetic fields prod. by induced eddy currents, shielding props. 3−18243
hysteretic supercond., magnetisation for complete field penetration, crit. state model 3−36669
II, flux density distrib., meas. with microfield probes 3−21174
Josephson junction, quasiparticle pair interf. rel. to current voltage characts., BCS theory 3−34021
layered anisotropic superconducting system, critical field calc. 3−21171
magnetic behaviour of type II superconductor with small Ginzburg Landau parameters 3−15293
magnetic impurity behaviour, thermodynamic props. near T_c 3−5073
microwave residual surface resistance, phonon generation and fluxoid models 3−34019
phonon spectra determ. from tunnelling characteristics 3−2204
phonon spectrum and Coulomb interaction effects on sp. ht. jump 3−2198
superconductors with transition metal impurities, Hartree-Fock calc. of props. 3−15298
Thomas Fermi screening in one dimension 3−15292
transition metal, electron-phonon mass enhancement theory rel. to superconducting transition temp. 3−18246
transition metal binary alloys, empirical correlations 3−18248
transition metal film deposited with noble gases, supercond. transition temp. variation 3−36670
transition metals, Y-Pd series, crit. temp. *(Russian)* 3−15299
transition metals and alloys, high pressure effects on transition temp. *(German)* 3−34026
transition temp. dependence on topology of Fermi surface 3−18250
transition-metal alloy amorphous films, supercond. transition temps. 3−15291
type I, normal thermoelec. power influence on heat carrying intermediate state 3−15289
type II, clean, isolated vortex structure and lower crit. field calcs. 3−30567
type II, magnetic props. using boson characteristic function 3−11974
type II, mixed to normal state specific heat discontinuity 3−34023
type II, variational treatment of isolated vortex tube 3−15290
type II, vortex interaction, behaviour near H_{c1} at arbitrary temp. 3−30568
type II superconductors containing magnetic impurities 3−11973
type II with anisotropic Fermi surface, flux-line lattices at $T \sim 0$ 3−27328
type-II, with first-order transition at lower crit. field, free energy calc. 3−30560
Al, volume change at mag. field induced transition 3−36672
Al film, granular, transition to zero dimensionality 3−30562
Al film, supercond. transition temp. depression by Ar(Ne) overlayers, surface phonon contrib. 3−34017
Al film, Tinkham's formula for ang. depend. of critical field 3−15296
AlMn alloys, critical fields, effect of Mn concentration 3−11972
Ba, press. depend. of transition temp. 3−30561
Be_{22}(Mo,Re)-phases meas. of T_c, new model *(German)* 3−38923
Bi amorphous film, supercond. transition temp. depression by Ar(Ne) overlayers, surface phonon contrib. 3−34017
$Ca_{1-x}Sr_xPb_3$ alloy, supercond. critical temp. rel. to lattice deform., Brillouin zone effects 3−34008
Cd-Mg alloys, superconducting transition temp. determ. 3−34020
Cs, pressure induced electron-phonon coupling constant variations, prediction of supercond. transition temp. 3−8290
Ga, type I, supercooling and superheating at transition 3−15295
Ga:Sn, in porous glass, ^{119}Sn Mossbauer, phonon spectrum, supercond. critical temp. 3−21355
In, thin films, critical thicknesses, magnetic field distributions 3−34011
In-Cd alloys, superconductivity and hysteresis 3−34009
In-Cd alloys, superconductivity and hysteresis, secondary properties 3−34010
$In_xSn_{1-x}Te_{1.02}$, type II, superconducting transition 3−30559
La transition temperature of superconductivity, pressure dependence, up to 250 kbar 3−38921
$LaAl_2$-$GdAl_2$, specific heat jump at supercond. transition 3−34022

equilibrium properties of superconductors continued
$La_{3-x}Ce_xAl$, specific heat jump of superconducting-Kondo system 3−30558
Nb, domain pattern characts., flux line interaction, flux line lattice 3−2197
Nb, thermo-electrostatic effects 3−38916
Nb-Al, surface layer on Nb, transition temp. meas. of 14K 3−36671
Nb-based alloys, deformed, mag. field penetration determ. 3−27331
Nb-Ti-Ge alloys, superconductivity, effect of Ge addition *(Japanese)* 3−30563
Nb_3Al, Ni additive effect on crit. temp., magnetiz. curves and crit. mag. field *(Russian)* 3−15288
$Nb_3Al_{0.75}Ge_{0.25}$, mag. susceptibility, 19-300K 3−18245
Nb_3Sn, phonon linewidths, influence of the superconducting energy gap 3−17948
$Nb_{0.26}Zr_{0.74}$ alloy, disordered and cryst., heat capacity, rel. to supercond. T_c 3−2199
Pb, residual microwave surface resist. 3−27325
Pb, superconducting film, temp. and thickness depend. of crit. mag. fields 3−34018
Pb, thermo-electrostatic effects 3−38916
Pb, volume change at mag. field induced transition 3−36672
Pb grains, sp. ht. below 5k 3−27329
Pb thin films, critical thicknesses, magnetic field distributions 3−34011
Pb-In system, superconducting energy gap from magnetisation meas. 3−34014
$Pb_{0.9}Bi_{0.1}$, thermodynamic props. 3−34015
PbTe with excess Pb, supercond. above 7.2K *(French)* 3−38915
Re, plastically deformed single crystal, defect influence on supercond. transition crit. temp. 3−30566
Sn, Mossbauer effect and superconductivity, press. effects *(Russian)* 3−8296
Sn, thin films, critical thicknesses, magnetic field distributions 3−34011
Sn film, supercond. transition temp. depression by Ar(Ne) overlayers, surface phonon contrib. 3−34017
SnTe-MnTe alloy, critical temp. particle size depend. 3−27327
$Ta(S, Se)_2$ layer cpds., anisotropic superconductivity 3−18247
Te, transition temp. and crit. mag. fields, 260 kbar 3−34024
Ti-Nb(22 at.%) alloy, crit. field strength 3−34025
Tl film, supercond. transition temp. depression by Ar(Ne) overlayers, surface phonon contrib. 3−34017
Tl_5Te_3, specific heat meas. from 1.8 to 4.2 K 3−27326
γ- U alloys, isotope effect in superconducting transition 3−38919
V, type II, anisotropic, null-deflection magnetometer meas. of torque 3−24534
V_2Hf, Laves phase cpd., low temp. struct., supercond. transition temp. rel. to impurities 3−18244
$V_3Si_xGe_{1-x}$, crit. temp., Knight shift, lattice parameters, conc. depend. *(Russian)* 3−18242
V_2Zr, Laves phase cpd., low temp. struct., supercond. transition temp. rel. to impurities 3−18244
W, rel. to $Ce_2Mg_3(NO_3)_{12}.24H_2O$ temp. scale 3−28457
Zn-Mn quench condensed films, transition temp. depression 3−34027

equivalent circuits
see also network analysis
acoustic equivalent networks, planar interfaces 3−9763
acoustic waves in isotropic media, microwave network formalism 3−9762
dielectric degradation *(Polish)* 3−20667
electrically excitable membranes, generalised model, systems theoretical approach 3−35240
electrocapillary accelerometer *(Polish)* 3−19155
electrochemical cells containing an indifferent electrolyte 3−27878
electrolyte soln., aperiodic large signal circuits 3−31271
equivalent circuits for electrochemical cells 3−27877
ferromagnetic material models, Coulomb law of magnetism *(German)* 3−13666
ionisation current sources calibration, capacitor charging method *(Russian)* 3−9995
reference air capacitor, rel. to high freq. value detn. 3−19142
slot-coupled toroidal resonators, scatter calculation by computer *(Russian)* 3−32401

erbium
antiferromagnetic sinusoidal structure, magnetostrictive variation of lattice parameter *(French)* 3−27388
atoms, incoherent scatt. by K-shell electrons, cross-sect. detn. 3−17337
elastic moduli, hydrostatic press. derivatives, electrostatic model and band struct. contrib. 3−27051
4f-electron energy rel. to Fermi level, u.v. photoemission obs. 3−1991
film, elec. cond. change due to sorption of H_2 and O_2 3−30553
film, obs. of f.c.c. structure and oxidation 3−18042
heat of soln. in Sn, calorimetric meas. *(French)* 3−4839
isotopes, X-ray transitions, isotope shifts 3−1107
magnetic structure, neutron diffr. obs. 3−24576
photoemission, 4-21 eV, rel. to band structure 3−8702
thin film, f.c.c., oxidation 3−20966
Ag:Er, dilute mag. alloy, coupled local moment-cond. electron Bloch equation 3−34213
Al:Er, e.s.r. meas. of exchange integral 3−15413
$BaYb_2F_8$:Er, X-ray sensitive upconversion phosphor, prep. 3−12260
$CdF_2:Er^{3+}$, i.r. quantum counter, optical parameters for Er^{3+} sites of $C_{2v}(C_{3v})$ symmetry 3−35397
$CdF_3:Er^{3+}$, C_{3v} local-site symmetry from correlated e.p.r. and optical obs. 3−21305
Er, hydrostatic pressure effect on spin disorder resistivity 3−2284
Er III, level structure, spin orbit parameters 3−29505
Er^+ and Er^{2+}, total cross sections for charge transfer and stripping in He and N_2 3−11181
Er^{2+} in CaF_2, luminesc., two-photon excitation by dye laser *(Russian)* 3−12181
Er^{3+}, impurity luminescent centre, Monte Carlo method for solving excitation transfer 3−34412
Er^{3+}, in Er_2O_2S, crystal field effects on electronic ion structure detn., optical absorp. obs. *(French)* 3−30411

erbium continued
Er^{3+}, in fluorite-type crystals, electron excitations 3−36941
Er_3^+. in LaF_3. electronically excited ions, radiationless relax., multiquantum scatt. processes 3−24390
Er^{3+}, in solids, C_{3h}, D_{2d}, O_h site symmetry, cryst. field parameters rel. to props. 3−2234
Er^{3+}, in YPO_4 and $YAsO_4$, pair interactions, e.p.r. study 3−15408
Er^{3+}, soft X-ray absorption by 4d-electrons, theory *(Russian)* 3−11133
Er^{3+} and Yb^{3+} in CdF_2, cooperative luminesc. *(French)* 3−30855
Er^{3+} doped fluorides, i.r. excited visible luminesc. 3−21469
Er^{3+} in borate and phosphate glasses, energy transfer to Tm^{3+}, fluorescence decay times 3−21466
Er^{3+} in CaF_2, effect of dislocations on perturbed angular correlations in paramagnets 3−34256
Er^{3+} in rare earth hydroxides, optical spectra, energy levels 3−2572
Er^{3+} in $YAlO_3$, optical spectra and energy levels 3−5225
Er^{3+} supersensitive transitions in complexes with different numbers of ligands *(Russian)* 3−12180
films, He implanted, dimensional expansion and surface microstructure 3−7994
Mg:Er, dilute mag. alloy, coupled local moment-cond. electron Bloch equation 3−34213
$NaLnF_4$:Yb^{3+}, Er^{3+}, (Ln=Y,Gd,La), efficient green-emitting i.r. excited phosphor, prep. 3−8639
α-$NaYF_4$:Yb^{3+}, Er^{3+}, phosphors, visible luminescence during i.r. excitation *(Russian)* 3−36906
YAl_2Er, crystal field ground states, EPR obs. 3−30418
$Y_3Al_5O_{12}$:Er resonance phonon scattering at average and high temps. 3−1767
YF_3: Yb, Er phosphor, i.r. to visible conversion, determ. of host parameters 3−39179
YIG:Er^{3+}, ferromag. reson. and e.s.r. linewidths and g-factor, temp. depend. *(Russian)* 3−8454

erbium compounds
Er_3GaS_6, crystal struct. determ. and refinement *(French)* 3−20718
ErB_{12}, high temp. enthalpy, 1300 to 2200 K 3−11750
$ErCl_3.6H_2O$, caloric and mag. props. 3−38976
ErD films, He implanted, dimensional expansion and surface microstructure 3−7994
ErF_3-HoF_3, impurity-conditioned solid-solid transform., rel. to melt growth 3−12274
$ErFeO_3$, intrinsic Faraday rotation temp. depend. 3−21390
$ErFeO_3$, paramag. susceptibility, room temp. and 77K 3−21213
$ErFeO_3$, spin reorientation, n.m.r. of ^{57}Fe 3−21332
Er(III) complex, tris-(2,2,6,6-tetramethylheptane-2,5-dionato)erbium(III), cryst. struct. 3−14769
$Er_9La_{10}S_{27}$, structure determ., three dimensional X-ray data *(French)* 3−17782
$ErMn_2O_5$, helimagnetic order of Mn, neutron diffr. obs. *(French)* 3−36723
Er_2O_3, thermal expansion by an X-ray diffraction method 3−30272
Er_2O_3 layer, on ErD_2, thickness determ. by proton-induced X-ray fluoresc. 3−4935
ErOF phase transitions, rhombohedral/cubic, high pressure effects 3−33666
$Er(OH)_3$, energy levels of Er^{3+}. optical spectra 3−2572
Er_2O_2S:Er^{3+}, absorption spectra, crystal field effects on electronic ion structure detn. *(French)* 3−30411

ergodic theorem *see statistical mechanics*

error analysis
see also error correction; error detection
acoustic reduction meas., ultimate and systematic errors *(Russian)* 3−3765
approximate solns. for motion of nonlinear viscous liquids and twisting of inelastic bars *(Russian)* 3−29837
Doppler effect laser velocimeters, evaluation of systematic error by computer simulation *(Russian)* 3−16573
elastodynamics, numerical integration methods, evaluation 3−22604
electron diffraction determ. of molec. struct. in gas phase, error matrices, systematic errors 3−29549
emission spectra meas. of bodies at temps. 40-80°C *(Russian)* 3−35375
fluxmeter, employing Hall generator *(Polish)* 3−258
focusing, in a line focus, electron optical props. 3−37991
liquid scintillator, minimisation of systematic errors by optimal adjustments *(French)* 3−10064
Mariner 6 and 7 occultation expts., Martian atmosphere 3−31620
molecular force consts. by rot. method 3−33101
noise signal, analysis of accuracy of mean-square value by squaring device based on f.e.t. 3−25640
nonlinear diffusion equation, numerical solution 3−13655
nonlinear diffusion problem involving Arrhenius reaction rates, variational soln. and error bound 3−27867
pendulum with vibrating suspension, error due to finite rod stiffness *(Russian)* 3−28845
Photoelectric Catalogue of Stars 3−39674
plasma emission coefficient calc., influence of random errors *(Russian)* 3−7494
pulse counting statistics 3−25879
radiation damage function unfolding procedure, error estimation 3−23454
reflection coefficient meas. on VSWR magnitude 3−22233
shell vibrations, calc. using triangular finite element scheme *(Russian)* 3−10316
weather forecasting, solution of two-point boundary value 3−25219

error compensation
see also error correction
amplitude-time convertor, nonlinearity compensation 3−28688
measurement errors, applic. of materials with temp. dependent magnetisation and permeability *(German)* 3−15385
twofold spectral-ratio pyrometry, selective radiation, error elimination 3−35370

error correction
bubble chamber tracks, errors in momentum and direction considering energy loss 3−32173
crystallographic struct. analysis by direct methods, error correction using translation function 3−14638
dynamic meas. instrument errors due to inertia *(Polish)* 3−25642

error correction continued
Fourier spectroscopy. phase errors multiplicative correction procedure 3−19212
NMR spectrometers modulated absorpt. lines, error correction for large amplitudes 3−6042

error correction codes
median algorithm for data processing of parallel measurements having differing accuracy *(Russian)* 3−13188
noisy acoustic channel 3−3738

error detection
see also error analysis
beam transport system, method for calc. of error effects 3−3838

error statistics
atmospheric twin-channel optical link, error probability rel. to signal scintillation and modulation depth 3−19572
meteorology, probability forecasts, predictive error distrib. of pressure gradients rel. to S_1 forecast score 3−37218
optical communication link with subcarrier p.c.m. frequency multiplexing of digital data channels 3−29051
pulse counting rate 3−25879

errors
see also measurement errors
alignment in high energy laser system 3−5992
alloys, X-ray diffuse scatt., errors in analysis 3−36234
calorimetry, from heater leads, radiation effects 3−5809
coaxial signal cables, effect of radiation and temp. on d.c. readout 3−17289
flatness errors of machined surfaces, techniques for meas. 3−3874
geodesy, random error propagation model for weakly constrained angular networks 3−27936
gravity meas. on surface ship 3−9155
intensity-dependent, oscillator strength meas. of Fe I resonance lines 3−11147
local meas. error of calorimetric detector *(Russian)* 3−9869
maximum permissible total errors as function of radiation dose, solid state detectors for high accuracy 3−5686
m.i.s. capacitor for doping profile meas. with minimal interface state error 3−30541
optical coherence area estimation 3−13692
pressure measurement 3−57
pulse echo u.s. systems, registration errors, beam deformations, rel. to medical diagnostics 3−19115
pulse-echo u.s. system, registration errors, rel. to medical diagnostics 3−19114
seismic data autocorrelation functions, adaptive estimation 3−5535
surface roughness meas. by stylus method, orientation and sampling errors 3−4907
thickness measurement, microscope manipulation, error sources 3−25732

Esaki effect *see tunnelling*

ESCA *see electron spectra; electron spectroscopy; spectrochemical analysis*

estimation theory
see also information theory
Earth satellite motion parameters, accuracy of estimates using astronomical meas. with correlated errors 3−25371
impulsive methods of estimation of phase coords. of linear system with Gaussian noise *(Russian)* 3−28837
interplanetary orbit determination, nonlinear estimation theory applic. 3−39585
least square method for residence time distrib. anal. 3−17507
phase meas., multi-scale, unambiguous optimal estimate of parameter varying linearly with time 3−13190
reflection seismology velocity analysis by nonparametric estimation 3−5465
seismic data autocorrelation functions, adaptive estimation 3−5535
spacecraft motion parameters, linear estimates with a priori information 3−25372

etalons *see interferometers*
etchants *see etching*
etching
see also crystal defects; integrated circuit production
calcite, etched, dislocations obs. by polaroid photomicrography, undergraduate expt. 3−9813
ceramic materials, chemical machining techniques and mechanisms, review 3−34630
diamond, cubic face, etch pit orientation changes 3−8032
dislocation movement starting stress from etch figure rosettes 3−4764
epitaxial structures, microcell and chamber for spectrochemical analysis 3−26013
field emission microscope emitter, technique for preparing fine tip *(Japanese)* 3−19327
glass, etched laser filament tracks, self-focusing 3−19642
glass-ceramic thin foil prep. technique for transmission electron microscopy 3−34645
heavy ions measurement using solid state glass detectors, particle energy depend. on etching time *(German)* 3−35482
Incoloy-800, heat treatment effect on B distribution, detection by fission-track etching at grain boundaries 3−12386
lunar glass bulk etching rate, Apollo 15 samples 3−35083
particle tracks 3−22474
photo-etching techniques *(French)* 3−15075
photoengraving process for microelectronics applications, review 3−8712
poly(ethylene terephthalate), cryst., etching by hydrolysis 3−31168
polycarbonate charged particle detectors by aqueous NaOH 3−32174
polymer, etched laser filament tracks, self-focusing 3−19642
sputter-etching processes, spectroscopic monitor 3−37712
steel, MnS inclusions morphology, etched and fractured surfaces examination 3−8788
steel 1Kh17N2, mech. props. after vacuum heat treatment 3−21676
transition metal oxide scales, study of grain structure 3−24859
Ag, grain boundary migration under compression at 500°C 3−37042
Ag dendrites, twinned, disclination model and mismatch 3−33769
Al, beveling process, etching, anodic oxidation, for multilayer metal circuitry 3−38739
Al, polycryst. strain-annealed, etch behaviour 3−18675

etching continued
$Al_xGa_{1-x}As$, in strong alkaline soln., Al content dependency 3−38740
B_xC, growth, 1450-1500°C, thermal etching, morphology 3−24781
$BaTiO_3$, effect on positive temp. coeff. of resist., near Curie temp. *(Russian)* 3−18130
Bi single crystals, plastic deformation and dislocation etch-pit distribution *(Japanese)* 3−30993
Bi-Sb, single crystal, dislocation study using etch pit technique 3−17836
$CdCr_3S_4$ single crystals, gas transport and characterisation *(German)* 3−8730
Cu, etchants, for exposing dislocations, and mechanism *(Russian)* 3−8033
Cu and alloys, potentiostatic controlled etching and polishing, rel. to metallography 3−37127
Cu-Al (2%) single crystals, edge-pit observations of dislocation motion 3−21609
Cu_5As_2 single cryst. characteriz. *(Russian)* 3−12329
Fe-Cr-Ni alloy system, microstructural change study using selective etching *(Korean)* 3−5291
$FeCr_3S_4$ single crystals, gas transport and characterisation *(German)* 3−8730
p-GaAs, effect on surface micromorphology *(Russian)* 3−18009
GaAs, mesa-etching technique, Gunn diode fabrication 3−36990
GaAs, surface contamination during photo etching 3−8757
GaAs substrates, surface contaminations, spectrochemical analysis 3−26014
GaAs:Si, epitaxial layers, characterisation of p-n structure, etching, cathodoluminescence 3−39195
n-GaAs:Te, effect on photolum. at 80 K 3−27570
n-GaAs/Ni/Au-Ge ohmic contact, Auger electron spectroscopy and sputter etching 3−4903
Gd-Ga garnet substrate, chem. etching 3−8029
$GdFeO_3$, etch patterns on (001) surface 3−8031
β'-$Gd_2(MoO_4)_3$, dislocation etchants 3−8028
InBi, intermetallic, chem. etchants for characterisation 3−11817
LiF, pure and Mg doped, steady state deform. dislocation struct., etch pit studies 3−36322
LiF, thermal etching and effect on atomic beam scatt. 3−1900
$LiLnMo_2O_8$, epitaxially grown on Ln_2GeMoO_8 3−1913
$LiNbO_3$, growth of craters during ion etching 3−1859
$MgAl_2O_4$, etch rate and deterioration in H_2, rel. to appl. as substrate for epitaxial Si 3−11816
MoO_3 crystal, X-ray microscopic study of struct. effect of etching 3−17802
NaCl crystal, etching kinetics using organic acids and alcohols as solvents 3−24351
NaOH anisotropic etch for discontinuities detection in glasses on Si substrates 3−11968
Nb_3Sn superconducting thin film, micromachining by electron beam microetching 3−15285
NiCrTaC, directionally solidified eutectic, etching technique for orientation determ. 3−18701
PbS, photodiode fabrication 3−30952
$PbS_{1-x}Se_x$, photodiode fabrication 3−30952
PyC-SiC-PyC, electrolytic etching of SiC in coated particles *(German, English)* 3−23438
Si, effect of u.s. agitation 3−39264
Si, electrolytically etched surfaces, transmission electron microscopy 3−18025
Si, etching, electrochem. displacement technique, specific crystallographic directions 3−39277
Si, etching, KOH, H_2O and isopropyl alcohol, rate limiting mechanism 3−39278
Si, etching effects with SF_6 during epitaxial growth 3−39268
Si, high angle grain boundaries in pulled crysts. 3−36323
Si, striations, detn. after annealing *(German)* 3−2068
Si, surface prep., optically flat, damage-free surfaces 3−39263
Si, swirl etch pits due to small stacking faults 3−36328
Si amorphous film, ion-implanted, circular etch pits 3−33752
Si by CF_4 plasma 3−18026
Si nuclear radiation detector, rel. to surface props. *(Russian)* 3−22464
Si plates masked with amorphous SiO_2, in H_2, Si and SiO_2 interaction during heat tretment *(Russian)* 3−11815
Si substrates, surface contaminations, spectrochemical analysis 3−26014
Si-on-sapphire films, anisotropic etching 3−39267
α-SiC, thermal etching in Ar, 1800-2650°C 3−1899
SiON, thin insulating film from NO-NH_3-SiH_4 reaction, rate obs. 3−39244
Sn, investigation of grain contrast using scanning electron microscope *(German)* 3−8000
Sn, white, single crystals, dislocation etch hillock formation 3−8030
Ti alloy surface, vacuum annealing induced 3−24939
W, surface orientation, meas. by orientation sensitive colour etching technique 3−18012
W crystal, dislocation etch pits, light figures 3−24352
YAG, in-grown dislocations, obs. by etching 3−24118
$Y_3Fe_5O_{12}$, in orthophosphoric acid, rates of action *(Russian)* 3−11820
ZnO, to reveal stacking at inversion boundaries 3−14871
ether drift *see special relativity*
Ettingshausen effect *see magnetothermal effects*
europium
alkali halide phosphor, Eu-activated, X-irrad., time-lag of photostimulated luminesc. *(Russian)* 3−18483
alkaline earth sulphates, Eu-doped, radiational defects thermoluminesc. study *(Russian)* 3−27581
atom, relaxation with spin polarised 4f shell in rare gas atmospheres *(German)* 3−35980
4f-electron energy rel. to Fermi level, u.v. photoemission obs. 3−1991
glass:Yb, Tb(Eu) luminescence, cooperative processes *(Russian)* 3−36907
high-field magnetisation 3−21221
nitrate glass: Eu, Sm, Gd, Tb, Dy absorption, luminescent and excitation spectra *(Russian)* 3−30878
photoemission spectra for u.v. illumination 3−18532

europium continued
pyroxene, glass. Eu^{3+}, effect of thermal working on luminescence spectra *(Russian)* 3−30874
reactivity worths in fast reactor spectrum 3−11063
screening ratios, relativistic contributions 3−14287
$BaF_2:Eu^{2+}$, impurity-induced Raman scatt. 3−39147
CaF_2:Eu crystals, thermoluminescence and X-ray stimulated luminescence 3−27580
$CaF_2:Eu^{3+}$, polarisation storage 3−18406
Eu II solar photospheric lines, $^{151}Eu/^{153}Eu$ ratio and abundance from high resolution spectra 3−39614
Eu^{2+} activation, fluorescence and excitation spectra, alkaline earth sulphates 3−39172
Eu^{2+} in BaF_2 and CaF_2, effect on X-ray luminesc. *(Russian)* 3−8650
Eu^{2+} ion, conditions for narrow line luminesc. emission 3−21473
Eu^{3+}, luminesc. spectra in rare earth pyrochlores, $Ln_2B_2^{4+}O_7$ 3−30865
Eu^{3+}, luminescence spectra in presence of charge transfer *(Russian)* 3−36926
Eu^{3+}, primary and secondary solvation spheres, effect on electric quadrupole transitions 3−15536
Eu^{3+} electronic spectrum in EuB_4HP, $EuCl_36H_2O$ and $Ru_2(SO_4)_3.8H_2O$, pressure effects *(Russian)* 3−8113
Eu^{3+} fluoresc. in $Ca_{2-2x}Na_{1\|x}Eu_xMg_2V_3O_{12}$, energy levels *(French)* 3−18480
Eu^{3+} fluoresc. in $Ca_{2-2x}Na_{1\|x}Eu_xMg_2V_3O_{12}$ *(French)* 3−21460
Eu^{3+} in D_2O, secondary fluorescence quenching rate constants for ethanol, acetic acid and H_2O 3−34421
Eu^{3+} in polyphosphoric acid and phosphate glass, exchange interaction role in energy transfer *(Russian)* 3−8651
$KBr(Cl):Eu^{++}$, thermoluminesc. of Z_1 centres 3−8678
KCl:Eu, thermoluminesc., cryst. light-sum storage 3−32595
$NaF:Eu^{3+}$, Eu^{3+} luminesc. centres, spectral anal. 3−5229
$SnTe:^{151}Eu$, e.s.r. hyperfine splitting 3−5132
$SrF_2:Eu^{2+}$, impurity-induced Raman scatt. 3−39147
Y_2O_3:Eu phosphor, Eu determ., absorpt. spectrophotometric and flame photometric anal. 3−16566
YVO_4:Eu phosphor, Eu determ., absorpt. spectrophotometric and flame photometric anal. 3−16566
$YVO_4:Eu^{3+}$, photoluminescence, concentration and temp. characteristics *(Russian)* 3−30872
$ZrSiO_4:Eu^{3+}$, Eu^{2+}, radioluminescence *(Russian)* 3−8672
europium compounds
chalcogenides, optical electrical and magnetic props., review 3−11848
Er_2O_3 on thin Er film, ion microprobe obs. 3−20965
$(Eu,Y)_3(Fe,Ga)_5O_{12}$ film, epitaxial growth 3−12276
Eu chalcogenides, ferromagnetic, semiconducting, band structure 3−38859
Eu chalcogenides, magnetic semiconductors, s-f exchange interactions, review 3−8350
Eu complex, tetrakis(benzoylacetonate)europium, laser compound, crystal structure 3−21440
Eu complexes, with tenoyltrifluoroacetone and 1, 10-phenanthroline, luminesc. extinction by impurity lanthanide ions *(Russian)* 3−21483
Eu dibenzoylmethane complexes, ion-ion interaction effect on luminescence 3−27527
Eu perrhenate tetrahydrate single crystals, absorption spectra *(Russian)* 3−30844
Eu-Y-Ga-Fe garnet, dynamics of magnetic bubble domain arrays 3−36765
EuAs crystal structure 3−20724
EuB_4HP, pressure effects on energy state of $4f^6$ electrons, spectrum of Eu^{3+} *(Russian)* 3−8113
$EuBr_3^-$, phase equilibria, vaporisation behaviour and thermodynamic props. 3−34707
$EuCl_3.6H_2O$, pressure effects on energy state of $4f^6$ electrons, spectrum of Eu^{3+} *(Russian)* 3−8113
p-$EuCr_2Se_4$, doped, hysteresis, magnetization and coercive force 3−27385
$EuEr_2Ga_xFe_{5-x}$, $Eu_xEr_{3-x}Ga_{0.7}Fe_{4.3}O_{12}$ bubble domain films, thermal expansion of lattice parameters 3−34158
$EuEr_2Ga_{0.7}Fe_{4.3}O_{12}$ epitaxial film, for bubble domains, variation of magnetiz., Curie temp., and Ga/Fe ratio, with growth temp. 3−34157
$Eu_2ErX_{0.7}Fe_{4.3}O_{12}$, (X=Al,Ga), garnet, refractive index meas. 3−27481
EuF_2, magnetic semiconductors, s-f exchange interactions, review 3−8350
$EuFeO_3$, equilib. reduction, enthalpy and entropy, O_2 press. *(Russian)* 3−15077
$Eu_{2.2}Gd_{0.8}Al_{0.6}Fe_{4.4}O_{12}$, garnet, growth induced uniaxial anisotropy 3−2305
$Eu_{1-x}Gd_xO$, refl. in visible and i.r. spectra rel. to band nature of elec. cond. 3−5214
EuI, mag. hyperfine splitting meas. 3−15316
EuI_2, vaporization thermodynamics 3−30250
Eu(II) silicates, photoluminescence comparison with EuS, EuSe and EuTe *(German)* 3−18495
$EuLGa_3S_7$, $EuLAl_3S_7$, (L=La, Ce, Pr, Nd), sulphurized compound family of melilite type *(French)* 3−30102
EuM_2Si_2, (M=Mn, Fe, Co, Ni, Cu, Ag), X-ray and Mossbauer obs. rel. to valency 3−14785
EuO, EuS, dipole-dipole interactions, critical point behaviour 3−30625
EuO, Hall coeff. insulator-metal transition rel. to mag. order 3−2147
EuO, mag. order effect on thermal cond. 3−7979
EuO, press. induced electronic collapse and semicond.-metal transition 3−7929
EuO, spin echo meas. of hyperfine interactions at ^{153}Eu nuclei 3−21324
EuO crystal growth parameters relation to stoichiometry, determ. by i.r. and conductivity meas. 3−7641
EuO Heisenberg ferromagnet, spin polarization and existence of paramagnetic surface sheet 3−8368
EuO:Fe film, thermomag. writing, optimum thickness calc. 3−16915

europium compounds continued
- Eu_2O_3, elec. cond., high temp. variations, equil. oxygen press. depend. *(French)* 3 − 38831
- Eu_2O_3 and europium silicate glass, Mossbauer effect, recoilless fraction 3 − 21348
- EuO(S)(Se)(Te), magneto-Raman scatt. 3 − 5208
- $Eu_2O_3.SrO.Fe_2O_3$ phase in Eu_2O_3-SrO-Fe_2O_3 system 3 − 20849
- EuS, effect of mag. structure on thermoreflectance spectra 3 − 27512
- EuS, EuSe and EuTe photoluminescence props. *(German)* 3 − 18495
- EuS, EuSe and EuTe thin films, spin polarized photoelectrons *(German)* 3 − 18531
- EuS, spin echo meas. of hyperfine interactions at ^{153}Eu nuclei 3 − 21324
- EuS, sublimation and high temp. chem. transport, kinetic and thermodynamic aspects 3 − 2638
- EuS coated W tips, electron spin polarization in field emission 3 − 8706
- EuS thin films, magneto-optical props., study of spin-orbit coupling and exchange field 3 − 2323
- EuS-FeS, partial phase diagram 10 to 70 mole % EuS 3 − 20850
- $Eu_2(SO_4)_3.8H_2O$, pressure effects on energy state of $4f^6$ electrons, spectrum of Eu^{3+} *(Russian)* 3 − 8113
- EuTe, antiferromag. reson. field angular depend., 9.2-33.99 GHz 3 − 30699
- EuTe, NaCl-CsCl structural type transform. at 100kbar pressure 3 − 27221
- EuTe, Raman scatt. by coupled plasmon-LO phonon mode, 2K 3 − 5209
- $EuWO_4$, ferrimagnetism of single crystal 3 − 30605
- $(EuY)_3(GaFe)_5O_{12}$, liquid phase epitaxial growth on $Gd_3Ga_5O_{12}$ substrate by tipping process 3 − 12278
- $Eu_{1.1}Yb_{1.9}Fe_5O_{12}$, garnet film, LPE growth by isothermal dipping with axial rotation 3 − 30945
- Y-Eu garnet, epitaxial film, magnet domain wall velocity 3 − 36734

evaluation
- *see also function evaluation*
- flicker photometer, automatic synchronised, evaluation and applications *(German)* 3 − 28538
- hearing damage due to acoustic noise *(German)* 3 − 16311
- nuclear reactor pressure sections, acoustic holography applications, evaluation 3 − 6447

evaporation
- *see also drying*
- alkali halides photoinduced evaporation, exciton-phonon decay *(German)* 3 − 27186
- benzene, from porous bodies, obs. of simultaneous heat and mass transfer 3 − 1790
- bubble growth due to microlayer evaporation, influencing factors *(Japanese)* 3 − 24015
- n-butanol, from porous bodies, obs. of simultaneous heat and mass transfer 3 − 1790
- carbon tetrachloride, from porous bodies, obs. of simultaneous heat and mass transfer 3 − 1790
- ceramic coatings on metals, heat-resistant, high-temp. volatility *(Russian)* 3 − 12432
- computer simulation rel. to surface structure and growth kinetics 3 − 11556
- drops, condensation growth and nonsteady evaporation 3 − 34749
- of drops, nonsteady state theory 3 − 24259
- drops in vapour, with evolution of heat *(Russian)* 3 − 11449
- effect on temperature and humidity of air currents in mines 3 − 4587
- evaporator tubes, fluid flow regimes, semireversed flow 3 − 1331
- falling film evaporators, performance prediction 3 − 26045
- film, of liquid patches, heat transfer coeff. determ. 3 − 30254
- flow of evaporating two-phase mixtures in smooth tubes and channels, pressure gradients due to friction 3 − 20397
- forced convection and evaporation mass transfer, liquid flow rate in capillary grooves meas. 3 − 26800
- fusion reactors, first-wall erosion effects 3 − 14598
- glass melts with high fluoride content, F loss to atmosphere effects *(German)* 3 − 27161
- glass-graphite disintegration in hypersonic gas stream, evaporation and combustion, heat and mass transfer on the surface *(Russian)* 3 − 26786
- graphite, evaporation of impurities determ. by atomic absorption method *(Russian)* 3 − 11648
- heat transfer, mass transfer, porous walls, multiphase flow 3 − 1437
- heat transfer across turbulent falling films 3 − 20301
- high latitude upland sites, model 3 − 9277
- high radioactivity residues treatment *(Spanish)* 3 − 17279
- ice cryst. formation in cloud supercooled region at warm temps. 3 − 25227
- interstellar cloud collisions and statistical theory rel. to evaporation 3 − 37482
- interstellar dirty ice particles surrounding early type stars, size distrib. 3 − 35202
- liquid, evaporative cooling in a rarefied gas 3 − 14991
- liquid film evaporation into turbulent gas flow, mass transfer model 3 − 29842
- liquid from porous bodies, obs. of simultaneous heat and mass transfer 3 − 1790
- metal, from discharge tube wall, Rozhdestvenskii hook method appl. 3 − 14619
- metal evaporation under powerful optical pulses 3 − 33658
- moisture on small cylindrical bodies in longitudinal flow, heat and mass transfer 3 − 1791
- molecular gas dynamics, boundary conditions, surface shocks, continuum flows, review 3 − 33261
- optical materials, CO_2 laser radiation, pulsating conditions *(Russian)* 3 − 763
- pentane, iso and cyclo evaporation in glycerine-water solns., average heat transfer coeffs. 3 − 24250
- plasma, non-isothermal, chem. evaporation of solids rel. to C transport 3 − 2644
- production of fresh water from sea, present state and trends in development *(German)* 3 − 7947
- re-entrainment of small particles from flat surfaces 3 − 17528
- single drops containing solids, drying characteristics rel. to sprays 3 − 2764

evaporation continued
- spray drying apparatus, boundary temps. and evaporation zone dimensions 3 − 4558
- thermal design of evaporative coolers, calc. method 3 − 112
- thermodynamics of gas/liquid interfaces in a porous medium, condensation/evaporation processes, viscous flow 3 − 26847
- vapour-gas mixture, in a capillary, convective diffusion with evaporation 3 − 26784
- water, adiabatic evap., heat and mass transfer dynamics 3 − 20863
- water, anomalous, enthalpy of evaporation 3 − 1789
- water, condensation coeff. obs. for water evaporated in different gas atmospheres *(Russian)* 3 − 14995
- water, from droplets *(German)* 3 − 17967
- water droplets, heating by optical radiation 3 − 27112
- water drops in Ar and CO_2 atmospheres, rates *(Russian)* 3 − 33660
- water from porous bodies, obs. of simultaneous heat and mass transfer 3 − 1790
- As, exptl and computer-simulated studies, effect of surface morphology 3 − 38665
- As_2S_3 glass, clearing coatings production MgF_2 film deposition by thermal evaporation *(Russian)* 3 − 5904
- Bi-Sb, film, deposition by steady state evaporation 3 − 24787
- $CdSe_xTe_{1-x}$ solid solution, vapour composition determ. and X-ray phase analysis *(Russian)* 3 − 11734
- Cr thin film deposition, in rotary drum evaporator 3 − 37609
- GaAs amorphous films, electron diffraction study of struct., laser induced evaporation *(Russian)* 3 − 8059
- GaP amorphous films, electron diffraction study of struct., laser induced evaporation *(Russian)* 3 − 8059
- Ge, optically pumped, evaporation of metallic exciton droplets 3 − 18106
- HI isolated clouds in interstellar medium, hydrodynamic treatment of phase change 3 − 37481
- He superfluid film, fast evaporation, shock wave generation 3 − 7396
- Hg, evaporation into a vacuum under isothermal conditions 3 − 38663
- Hg evaporation technique for convective mass transfer from stationary and moving surfaces 3 − 20286
- Kcl, crystals subjected to molecular beams, condensation and vaporisation kinetics investigation *(German)* 3 − 7920
- Li_2F_2, Li_3F_3 crystals subjected to molecular beams, condensation and vaporisation kinetics investigation *(German)* 3 − 7920
- NaCl whiskers, surface structure obs. and interpretation of evaporation processes 3 − 1964
- PbS, thin films, photoelectromotive force and thin layer structure depend. on substrate temperature and evaporation speed *(Russian)* 3 − 27323
- W, field evaporation, model and expt. 3 − 27600
- $Zn_xVd_{1-x}Te$ solid solution, vapour composition determ. and X-ray phase analysis *(Russian)* 3 − 11734

Evershed effect *see sunspots*

exchange forces in nucleus *see nuclear forces*

exchange interactions (electron)
- *see also antiferromagnetism; ferromagnetism; superexchange interactions*
- : 3 − 39033
- alloy, ferromag. anomalous Hall effect, cond. electron scatt. on magnons *(Russian)* 3 − 36589
- rel. to bandwidth renormalization 3 − 15337
- diamond:N, e.s.r., exchange broadening of hyperfine components *(Russian)* 3 − 8436
- dielectric crystals, e.p.r. study of exchange interactions of Cu^{2+}-Cu^{2+} *(Polish)* 3 − 24610
- dilute alloy, dynamics of local mag. moments with electron-electron interaction 3 − 34100
- dilute mag. alloys, elec. resist. rel. to localised mag. moment exchanges, RKKY s-d exchange model 3 − 30439
- dilute mag. alloys, thermoelec. power rel. to localised mag. moments interaction, s-d exchange model 3 − 30456
- dilute magnetic alloys, s-d exchange interaction, formal theory 3 − 18304
- electron gas, exchange and correlation 3 − 38766
- electron gas, rel. to energy in quantum strong-mag. field limit 3 − 8077
- electron polarisation, chemically induced, theory 3 − 34723
- electron spin-lattice relaxation, exchange interaction effects 3 − 15404
- e.p.r. spectrum, exchange and dipole-dipole broadening of individual hyperfine components *(Russian)* 3 − 34189
- excited-state exchange interaction, molecular orbital theory 3 − 36718
- Fermi surface, nesting, spin density wave and soft phonon mode 3 − 36524
- ferromagnet, quantum theory of double exchange 3 − 21192
- ferromagnet, spin-wave spectrum, spatial dispersion due to antisymmetric exchange 3 − 18330
- ferromagnetic homogeneous spin system, application of Abrikosov's pseudofermion technique 3 − 38970
- ferromagnetic insulators, nuclear spin interactions, excitation spectrum 3 − 34066
- ferromagnetic insulators, nuclear spin interactions, thermodynamic props. 3 − 30592
- ferromagnetic metal, exchange model and Fermi fluid approach to magnetiz. *(Russian)* 3 − 15377
- ferromagnetic plate, magnetiz. oscillations spectrum *(Russian)* 3 − 30649
- ferromagnetism, exchange interaction model, crit. point props., single-ion anisotropy effects 3 − 38936
- film, biaxial, exchange energy rel. to angle between magnetisation vectors, thickness depend. 3 − 21282
- fluorophosphate phosphors energy transfer between Mn and Sb 3 − 21025
- free electron exchange approximation study by many body perturbation theory for metals 3 − 8085
- free radical complexes with transition metals, e.s.r. and n.m.r. obs. of magnetic interactions and motions 3 − 26696
- haematite-ilmentite solid solution series, Mossbauer spectra 3 − 34819
- Heisenberg ferromagnet, cond. band influence via s-d exchange interaction *(German)* 3 − 5091

exchange interactions (electron) continued
Heisenberg ferromagnet, exchange interaction of surface spins causing surface antiferromagnetism 3—38951
Heisenberg ferromagnet, localised modes due to impurity pairs 3—27366
Heisenberg model two-dimensional ferromagnet, spontaneous magnetiz., exchange interaction effects *(French)* 3—30587
μ-hydroxobis [pentamminechromium (III)] chloride monohydrate, struct. and magnetic susceptibility of the acid rhodo complex 3—18301
inert gas atoms, diamagnetic susceptibility and orbital momentum, free-electron gas exchange correlation calc. 3—38204
influence on pseudopotential calcs. 3—33771
Invar, exchange interaction theory of magnetostriction, anomalous thermal expansion 3—18348
Invar alloys, mag. exchange contrib. to elastic consts., rel. to anomalous elastic props. 3—24597
Jahn-Teller coupling and direct exchange 3—18088
Jahn-Teller impurity ion pair, vibron reduction effects of Coulomb and exchange interactions 3—33813
LEED, depend. of exchange refl. on diffr. conditions 3—23995
magnetic bubble domains, generation through exchange coupling 3—34162
magnetic cluster complexes, exchange striction mechanism 3—15323
magnetic conductors, inhomogeneous ferro-antiferromag. state 3—21223
magnetic exchange interaction between two ions in cubic field *(French)* 3—36702
magnetic semiconductor, rel. to sample boundary and domain wall effects 3—34170
magnetic semiconductors, s-f exchange interactions, review 3—8350
magnetisation curves calc. for magnetostriction exchange model *(French)* 3—30614
magnetism theory, application of random-walk method 3—18288
magnetite, n.m.r. spectrum, spin-echo method, 77-125 K 3—39042
magnetoactive cryst., Mott transition without collectivization of d-electrons 3—2015
metal, k dependent pot., applic. to Ca and Al 3—8086
metal, k dependent pot., theory 3—8085
metals, diagrammatic analysis of dynamics of localised moments 3—34058
metals with paramagnetic impurities, dynamics of u.s. propagation 3—18365
m.i.m. structure, zero bias anomalies, due to paramag. impurities, theory 3—30548
molecular crystals, $s={}^{1}.{}_{2}$, X-irradiated, electron spin lattice relaxation, exchange interactions between radicals 3—12051
one-dimensional system, TANOL radical, l.f. behaviour of spin-correl. functions 3—2454
optically active impurities, indirect interaction caused by plasma oscills. *(Russian)* 3—8123
optimized model pot. for 33 elements including exchange correlation corrections 3—36507
organic nitroxide radicals, exchange intermol. coupling, paramag. susceptibility 3—21211
paramagnet, exchange enhanced, surface effects on static spin susceptibility 3—34090
paramagnetic ion pair, e.s.r., theory allowing for antisymmetrical exchange interaction 3—34204
paramagnetic spin polaron, self-trapped, mobility 3—30433
phase transition in two-dimensional exchange interaction model, numerical evidence 3—34106
phosphate glass, exchange interaction role in energy transfer between Eu^{3+}, Sm^{3+}, Dy^{3+} and UO_2^{2+} *(Russian)* 3—8651
polarons, small, role in metal-insulator transition, antiferromagnetic exchange interactions 3—30420
polynuclear complex salts, exchange reaction consts., from luminesc. spectra *(Russian)* 3—36927
polyphosphoric acid, exchange interaction role in energy transfer between Eu^{3+}, Sm^{3+}, Dy^{3+} and UO_2^{2+} *(Russian)* 3—8651
quantum crystals, multiple exchange processes 3—30310
rare earth alloy, RAl_2, ferromag., n.m.r. obs. of cond. electron exchange polarisation 3—15430
rare earth intermetallic compounds, orbital contributions to transferred mag. hyperfine fields 3—38937
rare earth metals, two-ion anisotropic exchange interaction, effect, on excitation spectra 3—2269
rare earths, heavy, spatial dependence along the c axis 3—30413
RKKY interaction, electron conc., cryst. and magnetic struct. 3—24550
ruby, chronospectroscopy of exchange-coupled Cr^{3+} ion pairs 3—21439
semiconductor, indirect exchange interactions involving photoelectrons, photoexchange integrals 3—21117
semiconductor organic molecular crysts., mag. excitations 3—2230
semiconductors, Coulomb excitons and exchange interaction screening 3—4981
single crystal with arbitrary crystal field and exchange interactions, paramag. susceptibility calc. 3—34089
singlet ground state systems, combined electron nuclear mag. ordering phenomena 3—38969
spinel with mag. ions at B-sites only, mag. props. *(Japanese)* 3—2282
superconductor, rel. to coexistence of superconductivity and magnetism 3—38914
thermodynamics of s-d metal with mag. impurities at low temp., path integral method 3—34101
transferred hyperfine interaction, modal calc. on exchange core polarisation 3—21013
transition metal compound, 3d group, core electron exchange splitting 3—15144
transition metal cpds., core electron exchange splittings of 2s and 3s electrons, hyperfine fields 3—30417
tunnel junction, with mag. impurities, effect of exchange scatt. by mag. moments 3—30547
YIG films, obs. of exchange dominated surface spin wave 3—2400
$\{Cr_3O(CH_3COO)_6(H_2O)_3\}Cl.6H_2O$ Mossbauer study on the magnetism 3—2262
$\{Fe_3O(CH_3COO)_6(H_2O)_3\}Cl.6H_2O$ Mossbauer study on the magnetism 3—2262

exchange interactions (electron) continued
Al:Gd(Dy)(Er), e.s.r. meas. of exchange integral 3—15413
$Al_2O_3:Cr^{3+}$, exchange coupled ionic pairs, e.s.r. study of coupling force *(German)* 3—15418
Au-Yb, negative s-f interaction 3—24561
$Ba_{3-x}Sr_xZn_2Fe_{24}O_{41}$, hexagonal type-Z, rel. to noncollinear struct. *(Russian)* 3—8372
$BiFeO_3$, exchange integral determ. from Mossbauer effect and mol. field approx. 3—27447
$(CH_3NH_3)_2MnCl_4$, magnetic susceptibility meas., a quasi two-dimensional Heisenberg antiferromagnet 3—5098
$Ca_3Fe_2Si_3O_{12}$, andranite garnet, magnetic structure, indirect exchange interaction 3—34137
$CdCr_2S_4$, exchange interactions rel. to e.p.r. and mag. susceptibility 3—21314
$CdCr_2Se_4$, exchange interactions rel. to e.p.r. and mag. susceptibility 3—21314
$Cd(NH_3)_2.Ni(CN)_4.2C_6H_6:Cu^{2+}$, exchange coupled pairs, e.s.r. obs. 3—39018
$Ce_{1-x}R_xAl_3(R=Y,La)$, n.m.r. and mag. susceptibility 3—27434
Co, paramag. f.c.c. phase, electronic structure calc., exchange energy contrib. 3—36515
Co complexes, 2p photoelectron lines, multiplet splitting evidence, exchange splitting in paramagnetic complexes 3—12209
Co(III) complex, hexamminecobalt(III) chlorocuprates(I,II) 10/3 effect in e.p.r. 3—27400
Cr(III) complex, hexamminechromium(III) chlorocuprates(I,II), 10/3 effect in e.p.r. 3—27400
$CsCoCl_3.2H_2O$, neutron diffr. study 3—24568
Cu, band struct. calc. using non-local screened exchange 3—1980
Cu complex, CuNSal, nearest neighbour exchange stregth for spin $^1/_2$ linear chain 3—15355
$Cu(C_6H_5COO)_23H_2O$, linear chain antiferromag. rel. to e.s.r. obs. 3—8426
$Cu(NO_3)_2.2{}^{1}.{}_{2}H_2O$, specific heat and n.m.r. at the high field phase transition, antiferromagnetic exchange interactions 3—27370
$CuWO_4$, short-range interactions, effect on mag. props. 3—34104
$DyCo_{3-x}Ni_x$, intermetallic, mag. ordering rel. to electron conc. 3—21245
$Dy_6(Fe_{1-x}Mn_x)_{23}$, 4f-3d interaction 3—2268
$DyFe_{3-x}Ni_x$, intermetallic, mag. ordering rel. to electron conc. 3—21245
$DyVO_4$, rel. to relax. of Mossbauer spectra, temp. depend. 3—36825
$Er_6(Fe_{1-x}Mn_x)_{23}$, 4f-3d interaction 3—2268
Eu^{3+} and Fe^{3+} ions in $R_2EuMFe_4O_{12}$ (R=Lu or Y, M=Al or Ga) garnet 3—21259
$Eu_xLa_{1-x}\ Al_2$, e.s.r. study, g-shift meas. for Eu^{2+} to obtain exchange integral 3—2358
EuS thin films, from magneto-optical props. 3—2323
Fe, ferromagnetic relaxation of resonance spin waves by s-d exchange 3—21315
Fe-Ni alloy films, exchange parameters 3—2324
β-Ga_2O_3-Fe_2O_3 solid solution, e.p.r. obs. 3—27406
Gd-Y alloys, information from mag. transition temp. variation with hydrostatic pressure 3—2273
GdAu, e.p.r., g_s value, 77-300K, exchange parameter, s-f model 3—2343
$GdCl_3$, exciton spectrum, anisotropic exchange effects 3—38801
$Gd_3Fe(Co)(Ni)$, and Neel metamagnetism theory 3—21232
$Gd_xLa_{1-x}\ Al_2$, e.s.r. study, g-shift meas. for Gd^{3+} to obtain exchange integral 3—2358
$Gd(OH)_3$, exciton spectrum, anisotropic exchange ffects 3—38801
$Gd_xTh_{1-x}PdIn$, evidence for RKKY-type ineraction 3—27364
$Gd_xY_{1-x}PdIn$, evidence for RKKY-type interaction 3—27364
^3He, solid, t-matrix perturbation theory, antiferromag. props. 3—7991
$HoCo_{3-x}Ni_x$, intermetallic, mag. ordering rel. to electron conc. 3—21245
$Ho_6(Fe_{1-x}Mn_x)$, 4f-3d interaction 3—2268
$HoFe_{3-x}Ni_x$, intermetallic, mag. ordering rel. to electron conc. 3—21245
KCl, optically detected e.p.r., n.m.r. and ENDOR with F-centre pairs 3—21310
$KCuF_3$, anisotropic interactions between pairs of Cu^{2+} ions 3—2264
$KMgF_3$:Mn and $KZnF_3$:Mn, bilinear and biquadratic exchange interactions, effect on mag. susceptibility 3—27363
$KMnF_3$, antiferromagnetic resonance frequencies and sublattice magnetiz. for antisymmetric exchange interaction 3—8351
$K_2ZnF_4:Ni^{2+}$, cryst. field and exchange interaction of Ni^{2+}, lattice distortion effects, e.s.r. obs 3—15357
LaAg:Gd, wave vector depend. of exchange interaction, e.s.r. obs. 3—34202
$LaFe_{1}$-$_xCr_xO_3$, antiferromagnetic perovskite, obs. of ferromagnetic interaction by Mossbauer effect 3—39065
Li, Slater type conduction band-core exchange effects of phonon frequencies 3—30219
$Li_{0.5}Fe_{2.5}O_4$, and spin waves, neutron scattering obs. 3—21252
$MgAl_2O_4$, nearest-neighbour interactions between Cr^{3+} ions, e.s.r. obs. 3—2380
$Mn_3Cr_2Ge_3O_{12}$ garnet, intrasublattice rel. to ferrimag. props. *(Russian)* 3—2266
Mn_3Ge_2, and mag. props. in pulsed mag. fields *(Russian)* 3—12015
MnO-MgO solid solns., exchange phenomena between Mn^{2+} ions, e.p.r. and mag. susceptibility *(French)* 3—38964
$Mn(pyrazole)_2Cl_2$, antiferromag. interaction determ. 3—30612
NdN(P)(As)(Sb), rel. to mag. ordering 3—30630
Ni, ferromagnetic, self-consistent calculation of energy bands 3—18073
Ni-Fe film, ferromag. exchange const., spin wave resonance obs. 3—34105
$NiBr_2.2H_2O$, rel. to sp. ht., 1.2-23 K, anomalous behaviour 3—36722
$NiCl_2.4H_2O$, exchange parameter determ. from molecular field model 3—34120
$Ni_{75-x}Fe_xGa_{25}$ giant moment system, ^{57}Fe Mossbauer expt., determ. of hyperfine fields, isomeric structure, quadrupole splitting 3—39074
$Ni(IO_3)_2.2H_2O$, heat capacity maxima, exchange parameter, 1—30 K 3—8360

exchange interactions (electron) continued
- NiO, antiferromagnetic, low energy electron, exchange diffraction by 3d electrons in crystal 3−30156
- Pd, exchange-enhanced generalized susceptibility, tight binding model for d-bands 3−2253
- Pd-Ni, dilute alloy, localised exchange enhancement model rel. to low temp. elec. resist. 3−15170
- PdFe- like alloys, influence of mol. field spatial fluctuations on low temp. props. 3−27365
- Pr-Tb alloy, exchange field at Pr ion rel. to comp. 3−2267
- RbMnF$_3$, antiferromag., Jahn-Teller and exciton-exciton interaction energies 3−11867
- TmNi mag. structure, crystal field effect 3−15375
- V-B-N, of cation anion bonds rel. to antiferromag. Curie temp. meas. *(Russian)* 3−15333
- V(CO)$_6$, solid state mag. behaviour 3−36703
- Y, e.p.r. of Gd, g-shifts, line narrowing, exchange effects, satellite lines 3−2376
- YAg(Cu):Gd, wave vector depend. of exchange interaction, e.s.r. obs. 3−34202
- YAl$_2$, exchange integral between Gd moment and cond. electrons 3−2375
- YFe$_x$Cr$_{1-x}$O$_3$, antiferromag. props., exchange interaction for Fe^{3+} and Cr^{3+} ions 3−5103
- YbNi$_2$, ^{107}Yb Mossbauer obs. 3−30610
- ZnGa$_2$O$_4$, e.p.r. spectra of nearest neighbour Cr^{3+} pairs 3−34199
- ZnGa$_2$O$_4$, nearest-neighbour interactions between Cr^{3+} ions, e.s.r. obs. 3−2380
- ZnS:Mn, concentration narrowing of e.p.r. spectrum and reln. to critical exchange distance *(French)* 3−12056
- Zr-Sc-H alloy system, p.m.r. obs. *(Russian)* 3−36805

exchange models *see peripheral models*

exchanges (chemical) *see chemical exchanges*

excimers *see molecular excitation*

excitation
- *see also atomic excitation; molecular excitation; nuclear excitation; vibration excitation*
- cats anesthetized, middle ear muscle contractions rel. to bone conduction 3−31856
- cross-correlation coeff. of excitation and response meas. 3−3753
- dipole chain, one-dimensional, in external field *(Russian)* 3−33649
- Earth-ionosphere resonator excited by cosmic sources, v.l.f. noise spectrum characts. 3−34931
- e.e.g. frequency sensitivity rel. to photic stimulation, epoch averaging 3−31849
- electronic transitions observed by inelastic electron tunnelling spectroscopy 3−8279
- elementary, in Liouville space, statistics and interactions 3−26156
- ferromagnetic plate, infinite, magnetostatic mode parametric excitation theory 3−8449
- gas discharge, triggering utilizing transverse extension of normal glow discharge *(German)* 3−38508
- H$_{21}$waves in circular waveguide 3−19557
- hot-stage vacuum gauge oscillation, improvement *(German)* 3−146
- hydrogenic ions with infinite Z Coulomb-Born-Oppenheimer cross-sections for electron impact 3−20039
- impact damper, response to stationary random excitation 3−28846
- laser cavity resonator, semiopen cylindrical with dielectric object, soln. *(Russian)* 3−10558
- linear, electromagnetic wave scattering from perfectly conducting rotational bodies of arbitrary form by obliquely incident plane wave or linear antenna 3−19562
- magnetic domain wall, eigenvalue equation for excitation modes 3−15394
- modal spectrum of e.m. field in small cavity 3−10402
- nerve, i.r. spectrophotometry 3−401
- nerve tissue, using magnetic fields 3−16558
- plane impedance waveguide, mode spectrum *(Russian)* 3−26106
- plasma e.m. slow waves, excitation by longitudinal electric fields 3−29953
- relativistic, of cavity modes, calc. 3−10685
- somatosensory evoked responses to tactile tap in man 3−28329
- visual, device 3−25981
- Ar$^+$ cw laser, excitations of laser states 3−4096
- GaAs targets for miniature pulsed laser 3−26237
- He-Ne visible gas laser design, r.f. excited 3−37958

excitons
- absorption light, surface irregularities in semiconductor crystals and polycrystals 3−30806
- alkali halide, exciton bands of D$_{2h}$ model, nearly orthogonal basis 3−33857
- alkali halide-Cu halide, excitonic doublets, test for coherent-potential approximation 3−30436
- alkali halides, absorption spectra in vacuum u.v. due to excitons, ligand field theory calcs. 3−27509
- alkali halides, optical line shape, theory 3−38815
- alkali halides photoinduced evaporation, exciton-phonon decay *(German)* 3−27186
- anthracene, crystn., hole detrapping by singlet excitons or photons, photoenhanced current obs. 3−24470
- anthracene, delayed fluoresc. quenching due to triplet exciton-hole interaction 3−2587
- anthracene, exciton transitions in crysts. with k perpendicular to (010) plane 3−2029
- anthracene, mag. field modulation of prompt electrolum., charge transfer exciton fission 3−24747
- anthracene, singlet exciton fission, 77 K 3−36904
- anthracene, triplet exciton liberation of carriers rel. to photocond. spectrum temp. depend. 3−8228
- anthracene crysts., surface quenching of fluoresc. and photoefffect *(Russian)* 3−8648
- anthracene thin molecular crystal, absorption and fluorescence, plane wave exciton-photon states 3−34373
- antiferromagnet, intensity of exciton-magnon transitions, strong mag. field effects *(Russian)* 3−8558
- antiferromagnetic crystal, magnetic excitons transfer model between antiparallel spin sites 3−11868
- antiresonance in exciton spectrum, phonon contrib. 3−8128

excitons continued
- aromatic hydrocarbons, planewise summation of point dipole-dipole interations, exciton processes 3−18102
- benzene, n-dichloro- and n-dibromo- mixed cryst., electronic spectra at 4 K 3−15505
- benzene and monohalogensubstituted derivatives, exciton effects on Raman spectra *(Russian)* 3−8570
- benzene methyl derivatives, exciton interactions effect on Raman spectra 3−15489
- benzol crystals, exciton-phonon interaction and energy transmission *(Russian)* 3−27534
- benzophenone, radiative and radiationless triplet exciton decay 3−11865
- benzophenone crystals, spin memory during triplet-triplet exciton energy transfer, ODMR obs. *(Russian)* 3−36912
- benzophenone crystals, triplet exciton annihilation influence on quantum efficiency and phosphorescence decay law 3−2031
- benzophenone crystals, triplet excitons migration and annihilation, excitation and array structure effect *(Russian)* 3−36910
- chrysene, crystalline, delayed fluorescence and triplet lifetime 3−21470
- condensation in momentum space, under optical pumping *(Russian)* 3−4978
- coronene molecular crystal, exciton spectrum calc. *(Russian)* 3−11872
- coupled coherent and incoherent motion, mean square displacement 3−21034
- deuterobenzol crystals, exciton-phonon interaction and energy transmission *(Russian)* 3−27534
- diamond exciton energy spectrum *(Russian)* 3−11874
- 1,4-dibromo-naphthalene, e.s.r. of triplet excitons, opt. detection 3−2835
- diffusion and energy transfer to impurity centres 3−33848
- durene crystals, neat and mixed Raman-active librations and torsions, 100 and 25K, exciton explanation 3−18441
- electron-hole liquids in semiconductors 3−21009
- electronic energy transfer in impure solids, two mols. embedded in lattice 3−18097
- energy losses of fast electrons due to exciton creation in strong mag. fields 3−36339
- energy spectra, calc. for diamond and sphalerite type crysts. *(Russian)* 3−8134
- exciton-neutral donor complex, ionic and electronic polarization effects on binding energy of complex *(French)* 3−11866
- exciton-phonon system, ground state calc. 3−38640
- excitonic molecules, binding energy calc. of complex 3−8125
- excitonic mols., stability, bonding mechanism 3−8126
- excitons fluctuations rel. to elec. cond., thermal cond., nuclear spin-lattice relax 3−33859
- ferromagnet, insulating, magnon-exciton bound states, Oguchi method 3−27376
- forbidden interband edge, excitonic transitions 3−33854
- free-deep trapped triplet annihilation, delayed fluorescence wave form 3−12172
- Frenkel, selfinduced transparency and giant polaritons 3−24402
- ground state energy with Coulomb pot. screening, mag. field depend. 3−2034
- Heisenberg alternating linear antiferromagnet, exciton interactions rel. to susceptibility 3−34075
- hexagonal crystals, transverse mag. field and deformation effects on exciton luminescence polarisation 3−2595
- h.f. Franz-Keldysh effect on excitons 3−30435
- Hubbard mag. insulator, exciton spectra, moments and lattice walks rel. to spin configuration 3−15341
- II-VI semiconductors, exciton luminescence and photoconductivity at high densities of excitation *(Russian)* 3−27531
- inert gas, solid, bound states and resonances at valence absorption edge 3−33849
- inert gas liquid lasers employing luminescence of self-localised excitons *(Russian)* 3−35692
- ionic crystals, highly localised excitons in photoabsorption spectra 3−39155
- ionic crysts., luminesc. impurity centres, energy transfer, excitonic mechanisms *(Russian)* 3−27537
- ionic polarisation effects on shallow exciton at finite temp. 3−24399
- laser transitions in highly excited semiconds., review of results 3−750
- light propagation, quantum statistical theory 3−27233
- light refl., surface excitons effects, surface level excitation frequency, radiative transition probability 3−24718
- localized biexciton, hole-nuclear double reson. 3−2428
- magnetic materials, neutron diffr., review 3−24572
- magnetic semiconductors, s-f exchange interactions, review 3−8350
- magnetoactive cryst., Mott transition without collectivization of d-electrons 3−2015
- metal-insulator transition, impurity effects on excitonic phase in strong mag. fields 3−30421
- metals, crystalline electric field, physical aspects 3−30582
- molecular cryst., coherent exciton states, low temp. e.s.r. absorpt. 3−2344
- molecular cryst., optical nucl. polarization in high mag. fields 3−2425
- molecular cryst., substitutionally disordered, phonons and excitons, interacting bands, coherent pot. theory 3−30379
- molecular crystal exciton→exciton transitions, effect on nonlinear optical props. 3−22939
- molecular crystals, calc. and use of retarded and static dipole sums in mol. exciton theory 3−18103
- molecular crystals, incoherent singlet-triplet biexcitons 3−21028
- molecular crystals, oscillator strength of exciton transitions 3−18465
- molecular crystals, rel. to vibr. coupling and bulk photocond. 3−15222
- molecular crystals, temp. dependence of absorption bands intensities of the spectra at Fermi resonance, mass operator and band shape 3−2538
- molecular crysts., entire phonon spectrum by localized exciton side-band method 3−7872
- molecular crysts., exciton diffusion coeff. calc. 3−36549
- molecular solids, excitonic polarons 3−36552

excitons continued
molecular solids, rel. to optical mapping of phonon density of states 3−1735
motion, coupled coherent and incoherent, calc. of moments 3−15165
Mott exciton spectrum in elec. field 3−4979
naphthalene: pyrene, singlet exciton migration and energy transfer 3−24735
naphthalene, entire phonon spectrum by localized exciton sideband method 3−7872
naphthalene, in heavy-atom hosts, wavelength-dependent triplet state population mechanisms, spin aligned exciton bands 3−18793
naphthalene cryst., with heterocyclic impurities, absorpt. spectra, local excitons 3−18476
naphthalene cryst. with impurities depolarization of exciton absorpt. bands 3−15525
naphthalene crystals with indole and thionaphthene impurities, local excitons *(Russian)* 3−36908
nitronaphthalene, luminescence, photoconductivity, triplet excitons lifetime *(Russian)* 3−36909
optical activity and ellipticity due to exciton dispersion 3−27480
organic crystals, singlet and triplet exciton interactions *(Russian)* 3−27229
organic molecular crystal, singlet to triplet non-radiative transition, ordering and spin-orbital effects 3−4968
organic molecular crystals, annihilation of singlet on triplet 3−4969
organic molecule impurities in solid rare gases, extravalence molecular excitations, Wannier impurity states 3−24721
organic semiconductor film, Stark effect and charge-transfer excitons 3−36538
organic single crystals at low guest concentrations and low temps., triplet state energy transfer to host exciton bands, e.p.r. obs. 3−25090
organic solid, doped, exciton diffusion theory of luminesc. emission 3−21471
organic solid, doped, exciton diffusion theory of luminesc. emission 3−21472
organometallic compounds, surface exciton states and luminescence spectra *(Russian)* 3−27535
p-chloroaniline cryst., study of triplet state, Zeeman splitting and excitons 3−8596
perylene type molecular crystals, polarization of singlet-triplet transitions 3−36553
polar crystal, ground state energy of a Wannier exciton 3−8132
polar crystal, ground-state energy of Wannier exciton 3−21039
polar crystals, bound polarons, Wannier excitons, perturbation approach 3−36562
polariton resonant Brillouin scattering, spatial dispersion effects 3−8131
polariton resonant scattering, spatial dispersion effects, additional boundary conditions for polarisation fields 3−8130
polymer, band ellipticity from Frenkel model and fully retarded expression for circular dichroism 3−12109
polymer, helical, with substitutional impurities, exciton transitions 3−1299
prism technique for optical coupling to nonradiative surface waves 3−36646
pyrene, cryst., triplet exciton lifetime 3−27888
pyrene crystals, mag. field effect on delayed fluorescence 3−27565
quinoxaline and quinoxaline-d$_6$, in durene, durene-d$_{14}$, naphthalene and naphthalene-d$_{10}$, mixed crystal electronic polarisation spectra 3−39141
rare gas crystal, epitaxially grown on Nb (100), excitonic transitions in energy loss spectra of LEED 3−11655
self induced transparency, bound exciton-photon states 3−11873
self-localised, recomb. luminesc., magneto-optical effects *(Russian)* 3−27538
semiconducting chalcogenides, intrinsic piezobirefringence obs. 3−12110
semiconductor, biexcitons, electron-hole droplet for motion, radiant recombination, helium temp. *(Polish)* 3−38816
semiconductor, cubic, exciton ground state in mag. field, perturbation theory 3−36555
semiconductor, interband magneto-optical transitions rel. to isotropic excitons 3−11869
semiconductor, light absorpt. by bound excitons 3−4982
semiconductor, role in electronic processes *(German)* 3−15168
semiconductor, two-photon absorpt. indirect exciton transitions, theory 3−16913
semiconductor-metal and mag. phase transitions, Hamiltonian model 3−38806
semiconductors, at high excitation densities, emission spectra theory, exciton mol. role *(Russian)* 3−27539
semiconductors, Coulomb excitons and exchange interaction screening 3−4981
semiconductors, longitudinal and transverse, energies and wavefunctions, photon transition oscillator strengths 3−27231
semiconductors, low-mobility, mol. excitons and charge carrier mobility 3−30514
semiconductors, paraelectric resonance 3−24400
semimetal, transition to excitonic insulator in strong mag. field 3−30423
sodium uranyl acetate, interpretation of Cotton effect 3−30797
spectrum in quantizing magnetic field, adiabatic method of calc. *(Russian)* 3−15164
sphelerite type crystals, exciton energy spectrum *(Russian)* 3−11874
spontaneous and stimulated radiation emission by excitons at high concentrations *(Russian)* 3−27515
superconductivity, high temperature, exciton mechanism, review 3−24532
superconductivity mechanism, semiconductor-metal model 3−18240
superconductors, collective excitations, exciton-like modes 3−18239
TCNQ ion radical salts, Overhauser effect and exciton motion 3−2469
TCNQ salts, triplet excitations at high temps., mag. susceptibility 3−15163
tetracene, singlet exciton fission, 77 K 3−36904
1,3,5-(sym)-triazine, electronic states, absorpt. spectra of pure and mixed crysts. 3−31278

excitons continued
two-photon exciton transitons in semiconductors, phonon-assisted, band models 3−18105
ZnTe, atomic displacement energies, cathodoluminescence edge emission spectroscopy, monoenergetic electron irrad. 3−33556
Ag halides at low temperature 3−27218
AgCl, magnetoabsorption of indirect exciton 3−12143
n-Al$_x$Ga$_{1-x}$As, luminescence, exciton bands *(Russian)* 3−36931
Al$_2$O$_3$, photocond. near intrinsic absorpt. edge, exciton nature of absorpt. band 3−5032
As$_2$S$_3$ layer cryst., edge refl. spectrum, exciton peculiarities 3−2559
BaF$_2$ core band-conduction band excitons, temp. depend., Auger effect 3−2036
BaF$_2$ films spectra of electronic excitations in 8-150 eV range 3−2032
Bi, exciton phase transition in strong mag. field, u.s. absorption obs. 3−27230
CO thin films, transmission and reflection in vacuum u.v., study of intermolecular interactions of excited species 3−2568
CaF$_2$ films spectra of electronic excitations in 8-150 eV range 3−2032
CaF$_2$ of core band-conduction band excitons, temp. depend., Auger effect 3−2036
CdS, exciton gas degeneracy after single photon excitation *(Russian)* 3−11870
CdS, green edge luminesc. rel. to exciton emission, 20.4K *(Russian)* 3−21482
CdS, high carrier and exciton conc., low temp. emission recomb. study *(Russian)* 3−27541
CdS, LA-phonon exciton interaction, luminesc. study *(Russian)* 3−36916
CdS, luminescence spectra obs. for free exciton lifetime 3−8659
CdS, mag. field effect on polarisation of light from free and bound excitons 3−2594
CdS, photoluminesc., exciton-phonon interaction study *(Russian)* 3−27536
CdS, photoluminescence at high exciton densities at 4.2K 3−39184
CdS, refl. phase spectrum in exciton region at 4.2 K 3−15517
CdS, rel. to elec. field induced Raman scatt. 3−21407
CdS, rel. to uniaxial stress depend. of birefrigence 3−15511
CdS, u.v. excited at 4.2K, recomb. processes in stimulated emission 3−15523
CdS:Li(Na)(Ag), furnace doping, rel. to bound exciton spectra 3−12184
CdS:Te, rel. to piezoemission 3−18492
CdS(Se), luminesc. line shape due to elastic collision of anisotropic excitonic molecules 3−24738
CdS(Se), new luminesc. line due to inelastic collision of excitonic molecules 3−24739
CdS$_x$Se$_{1-x}$, peculiarities of reflection spectra in exciton absorption region *(Russian)* 3−34381
CdS; bound exciton form. kinetics 3−8133
CdSe, Bose condensation of excitonic molecules, luminesc. obs. 3−30437
CdTe, recrystallised thin film,s exciton-phonon interaction *(Russian)* 3−11871
CsI, field effect on luminescence 3−33850
CuBr two photon absorption, exciton region 3−10570
CuBr(Cl), magneto-optical spectra due to excitons 3−8556
CuCl, Faraday rotation near absorpt. edge, interband and exciton effects 3−15474
CuCl, fusion of two polaritons to longitudinal excitons 3−18107
CuCl, high carrier and exciton conc., low temp. emission recomb. study *(Russian)* 3−27541
CuCl, two photon absorption, at 4.2K 3−10571
CuGaS$_2$, absorpt. and refl. spectra, low temp. 3−15510
CuGaS$_2$, absorpt. and refl. obs. rel. to excitons and spin orbit splitting 3−18108
Cu$_2$O, excitonic structure from two photon absorption spectrum 3−2567
Cu$_2$O, modulated excitonic absorption in elec. and mag. fields 3−2037
Cu$_2$O, obs. of exciton line splitting in mag. field, diamag. effects 3−12123
Cu$_2$O, optical absorpt. spectra obs. of Mott excitons in elec. field 3−8129
Cu$_2$O, Raman scattering, luminescence, exciton-phonon coupling 3−8581
Cu$_2$O, resonance Raman scattering at the forbidden yellow exciton 3−21408
Fe$_{1-x}$s, semiconducting uniaxial ferroelectric, model 3−8531
GaAs, high-purity, polariton reflectance and photoluminescence 3−39185
GaAs, luminesc. due to exciton-exciton collision 3−30871
GaAs, magnetization bh polarized light 3−4956
GaAs, uniaxial stress effect on free exciton line and photoluminesc. 3−21036
GaAs:Cu, photolum. of excitons bound to Cu complex centres 3−34418
GaAs$_{1-x}$P$_x$, rel. to absorpt. study of indirect Γ_{8v}-X$_{1c}$ band gap 3−21003
GaN, resonant Raman scattering A$_1$ to F$_1$ and E$_2$ optical phonons 3−8584
GaP, at high excitation levels, excitonic luminesc. and photocond. study *(Russian)* 3−27542
GaP, fluoresc. from bound excitons, quenching and enhancement by far i.r. radiation 3−36940
n-GaP, liq.-encapsulated-Czochralski-grown, luminesc. 3−5235
GaP, recombination processes responsible for room-temp. near-band-gap radiation 3−34416
GaP, reson. fluoresc. due to bound excitons, laser excited 3−18484
GaP, stimulated emission from excitons bound at isoelectronic traps 3−24720
GaP:Li, Zn, bonding of excitons by neutral donors and acceptors *(Russian)* 3−36932
GaP:N, bound exciton spectra and radiation kinetics during two-photon excitation 3−18491
GaP:N, isoelectronically doped, radiative recombination 3−24754

excitons continued
  GaP:N, rel. to high energy part of seven line luminesc. spectrum 3 − 34420
  GaP:Te, photocond. due to Auger recomb. of bound excitons 3 − 27283
  GaSe, intense excitation by electron beam 3 − 15563
  GaSe, layer type semicond., thermoreflectance meas. rel. to exciton selection rules 3 − 33855
  p-GaSe, optical orientation of excitons and Hanle effect 3 − 34428
  GaSe, optical transmission in fields up to 93.5 kG, exciton behaviour, effective mass of electrons and holes, g-factors 3 − 30803
  GaSe, photolum. spectra, carrier assisted radiative recomb. of free excitons 3 − 15553
  GaSe, rel. to stimulated emission under intense laser beam excitation 3 − 27517
  GaTe, layer cpd., thermoreflectance spectra in exciton region 3 − 30839
  $GdCl_3$, exciton spectrum, anisotropic exchange effects 3 − 38801
  $Gd(OH)_3$, exciton spectrum, anisotropic exchange effects 3 − 38801
  Ge, biexcitons and exciton concentrations *(Russian)* 3 − 27228
  Ge, electron-hole drop binding energy from luminescence spectrum 3 − 21476
  Ge, free exciton spectra at submillimetre wavelengths *(Russian)* 3 − 5242
  Ge, microwave breakdown 3 − 21033
  Ge, optical absorp. var. with mag. field intensity, determ. of band struct. *(German)* 3 − 34332
  Ge, oscill. of recomb. radiation of electron-hole drops in strong mag. field *(Russian)* 3 − 2030
  Ge, radiative recomb. of biexcitons, photolum. *(Russian)* 3 − 8663
  Ge optically pumped, evaporation of metallic exciton droplets 3 − 18106
  Ge:Sb, direct absorp. edge, exciton plasma resonance obs. *(Russian)* 3 − 5211
  Ge:Sn, Si, luminesc. of indirect excitons, zero phonon radiative annihilation 3 − 21479
  He II, neutral excitations 3 − 18004
  $In_{1-x}Ga_xAs_{1-y}P_y$ alloys, electron zones, cathodoluminesc. struct. study *(Russian)* 3 − 36946
  n-InP, luminescence polarisation of 1.41 eV band due to exciton recombination 3 − 2593
  In_3Te_4, thin films, abs. spectra at fund. obs. edge, rel. to exciton transition *(Russian)* 3 − 30818
  KI, recomb. luminesc. lifetimes rel. to self trapped excitons 3 − 21468
  KI:In, luminescence, energy transfer from excitons to activator *(Russian)* 3 − 12170
  $KI:Tl^+$, exciton diffusion in electron induced sputtering 3 − 21502
  MnO, rel. to absorpt. spectrum fine struct. *(Russian)* 3 − 15522
  $MoS_2(Se_2)(Te_2)$, two dimensional excitons 3 − 12145
  $MoSe_2$, for photon energy 0.5 to 3.8 eV 3 − 12151
  $MoTe_2$, for photon energy 0.5 to 3.8 eV 3 − 12151
  NH_4Br in phases II and III, u.v. reflection spectra 3 − 24711
  NaCl, form. yield of self trapped excitons and F-centres between 10 and 130K 3 − 30432
  $NaCl:Br^-$, rel. to absorpt. and luminesc. of Br^- clusters 3 − 21464
  $PbBr(Cl)_2$, blue and violet luminesc., excitons rel. to energy transport mechanism 3 − 34407
  $PbCl(Br_2)$, photoluminesc., thin film absorpt. rel. to exciton form. 3 − 27561
  $PbF_2(Cl_2)(Br_2)$, rel. to low temp. X-ray luminesc. and photolum. 3 − 30863
  PbI_2, excitons at band edge, electric field effects 3 − 33856
  PbI_2, temp. and press. effects on exciton spectrum 3 − 21436
  PbI_2 splitting, spectral absorption band, dispersion measurements *(Russian)* 3 − 34379
  Pr, magnetic exciton modes dispersion, neutron scatt. obs. 3 − 2302
  RbI, recomb. luminesc. lifetimes rel. to self trapped excitons 3 − 21468
  RbI, rel. to effect of surfaces on light transmission, 5.5-6.3 eV 3 − 36892
  $RbMnF_3$, antiferromag., two-exciton transitions, Jahn-Teller effect in excited ion pair 3 − 11867
  $RbMnF_3$, cubic antiferromag., mag. dipolar line splitting and uniaxial stress effects on exciton absorpt. lines 3 − 30817
  $RbMnF_3$, two exciton transitions, optical absorption, theory 3 − 38814
  Si, biexcitons and exciton concentrations *(Russian)* 3 − 27228
  Si, coefficient of formation, transient absorp. of microwave obs. *(French)* 3 − 30434
  Si, fine structure in optical absorpt. edge, exciton form. and phonon emission 3 − 18082
  Si, optical absorp. var. with mag. field intensity, determ. of band struct. *(German)* 3 − 34332
  Si:As, Zeeman splitting of photoluminescence of excitons 3 − 38809
  SiC, 6H-polytype, exciton complexes, investigation by isotope substitution 3 − 30867
  SiC, hexagonal, luminesc. of exciton-impurity complexes 3 − 34425
  SnO_2 single crystal, exciton magnetoabsorpt., meas. 3 − 39127
  SrF_2 core band-conduction band excitons, temp. depend., Auger effect 3 − 2036
  SrF_2 films spectra of electronic excitations in 8-150 eV range 3 − 2032
  Te, activated, at high excitation levels, excitonic luminesc. and photocond. study *(Russian)* 3 − 27542
  V_2O_3, enhancement effect in cond. band, electron-hole interaction change through metal insulator transition, positron lifetime spectra obs. 3 − 27212
  $WS_2(Se_2)$, two dimensional excitons 3 − 12145
  WSe_2, for photon energy 0.5 to 3.8 eV 3 − 12151
  WSe_2, line shape of electro-reflectance excitonic structure 3 − 2038
  $W_{1-x}Ta_xSe_2$, absorpt. spectra, absorpt. edge excitons energy 3 − 15518
  ZnO, laser emission under electron beam excitation, exciton-exciton interaction in spontaneous emission band 3 − 16881
  ZnO, luminescence in exciton region with two photon excitation *(Russian)* 3 − 8653
  ZnO, refl. phase spectrum in exciton region at 4.2 K 3 − 15517
  ZnO, two quantum absorption by intrinsic excitons *(German)* 3 − 2564

excitons continued
  ZnS, photocond. spectra at 293 K, 77 K and 4.2 K, fine struct. due to excitons 3 − 21115
  ZnS spectra, excited states, uniaxial deformation effects, piezoreflectance, line splitting 3 − 36557
  ZnS: Te, luminesc. of bound excitons 3 − 39180
  ZnTe, interpretation of asymmetric band shapes in terms of bound exciton complexes 3 − 36948
  ZnTe, luminescence and modulation by CO_2 laser radiation exciton annihilation *(Russian)* 3 − 27551
  ZnTe, rel. to resonant Raman scatt. 3 − 5201
  ZnTe single crystal, photoluminesc. and electroreflectance obs. *(Japanese)* 3 − 11605

executive programs *see supervisory and executive programs*

exhibitions
  Geodesy-Geophysics-71, Moscow, Aug. 1971, geodesic instruments *(Russian)* 3 − 9391
  measuring equipment, Siberian Instruments 1971 Exhibition *(Russian)* 3 − 9900

exoelectron emission *see electron emission*

exosphere
  density variations between 200 and 400 km from Aug. 1969 to May 1970, twilight temp. meas. 3 − 25260
  H abundance, diurnal variation rel. to exospheric temperature 3 − 34923
  ion-exosphere kinetic model for plasma sheet electron precip. 3 − 25309
  temperature rel. to empirical models of upper atmosphere in polar regions 3 − 31401

exotic atoms
  see also mesic and muonic atoms
  kaonic atoms and information on nature of nucleus 3 − 11189
  leptonic, effects of neutral intermediate boson 3 − 23027
  production and investigation techniques 3 − 1134
  review, appl. to nuclear studies 3 − 1135
  vacuum polarization potential 3 − 1133

expanding universe *see cosmology*

expansion, thermal *see thermal expansion*

expansion chambers *see cloud chambers*

experimental tests of quantum electrodynamics
  heavy ion-heavy ion scattering, study of electron shells in over-critical external fields 3 − 6604
  positron autoionization in heavy ion collisions 3 − 7087
  scattering, elastic particle-antiparticle, comments on testing QED 3 − 16983
  3^+e^- elastic scattering 1.4-2.4 GeV, agreement with quantum electrodynamical predictions 3 − 4173
  $e^-e^+ \rightarrow \mu^-\mu^+$, meas. of cross-section at 1 GeV, determ. of limit $\Lambda > 3.1$ GeV 3 − 16984
  e^+e^- colliding beams, study of QED processes and hadronic e.m. current 3 − 858
  $e^+e^- \rightarrow \mu^+\mu^-$, determ. of photon propagator behaviour at time-like momentum transfers, Novosibirsk colliding beam expt. 3 − 13873
  $e^+e^- \rightarrow \mu^+\mu^-$ meas. in φ^0 resonance region, interference effect between lowest order diagram of one photon channel and hadronic vacuum polarisation diagram 3 − 13888
  e^+e^- reactions at Adone Storage Ring 3 − 13871
  e^+e^- scattering expts. at Adone storage ring 3 − 13877
  e^+e^- annihilation, 1.4-2.4 GeV, test of QED 3 − 13850

exploding wires
  dwell times of thin wires 3 − 38513
  explosive conductors, influence of geometric dimensions on effective energy transformation *(Russian)* 3 − 23950
  gas discharge zone formation, review *(German)* 3 − 11519
  instabilities of electrically exploded wires 3 − 36217
  laser, AlF, giving 12.5 to 13.5 μ pulses 3 − 19597
  metal atom oxidation lasers, i.r. action 3 − 31247
  plasma column, non-stationary, radial temp. distrib. meas. method *(German)* 3 − 11505
  plasmas, neutron production 3 − 29989
  underwater sound signal source for explosive echo ranging, patent 3 − 19119
  Cu, exploding in strong axial mag. field, discharge damping 3 − 36218
  Li/ND_3 solutions of metallic conductivity, impulse heating in capacitor discharge, neutron emission 3 − 38483
  W, in air, dwell times rel. to voltage 3 − 17696
  W elec. explosion, X-ray prod. 3 − 17695

explosion bubbles *see bubbles*

explosions
  see also accidents; detonation; exploding wires; nuclear explosions; safety; shock waves
  in atmosphere, self similar solns. stability 3 − 34902
  blast wave propagation, analytic methods, review 3 − 33250
  cylindrical shells, containment of explosions 3 − 28894
  elastic materials, chem. reacting mixture, one dimens. shock wave study 3 − 25049
  electrical pulse from pulsations of explosion products vol. 3 − 33252
  galactic nuclei, explosions rel. to origin of cosmic rays 3 − 13086
  gasdynamics, detonation, shock-wave, blast-wave studies, review 3 − 33253
  giant elliptical galaxies, violent explosions in nuclei and bursts of star formation 3 − 28277
  initial stage of chemical explosions with ejection *(Russian)* 3 − 12510
  large underground explosions, seismic results from world-wide sample 3 − 12635
  magnetic flux compression by implosion 3 − 13667
  modelling of explosion process as source of compressional and shear waves 3 − 9110
  n-material gravitating points, explosive disintegration and simultaneous collision 3 − 35004
  point blasts in explosive gas with variable initial density *(Russian)* 3 − 29885
  refraction of underwater explosion shock waves, Sargasso Sea experiments 3 − 33255
  seismic effects, a comparison with falling weights 3 − 18836

explosions continued
- SH waves from underground explosions rel. to expanding spherical cavity and elastic radiation 3—34813
- shaped charge, seismic surface source 3—9361
- shock wave interaction with matrix discontinuities prod. acoustic oscillations and detonation *(German)* 3—29886
- Sino-Soviet area, seismic wave analysis of earthquakes and explosions, 1966 period report 3—21909
- source for underwater transmission on loss obs., principles in choosing 3—3725
- spherical detonation waves, propagation, finite steady-state velocities $<$Chapman-Jouguet value 3—33256
- stellar C and O burning, p-process nuclei prod. 3—28179
- strong underground explosions, final cavity rel. to parameters of surrounding medium *(Russian)* 3—12610
- Sun, exploding granule phenomenon, mechanism rel. to internal motions 3—18935
- supermassive stars. rel. to obs. of explosions in galaxies 3—28178
- supernovae, Fe star, neutrino star and double layer red giant models, relation to pulsars *(Hungarian)* 3—9553
- underground, Earth's short period attenuation, along teleseismic ray path 3—9149
- underground, elastic wave radiation, comparison with earthquakes 3—12582
- underwater, computer program for analysis of test data as cavity explosion *(Russian)* 3—26066
- underwater, refraction of shock waves 3—2960
- waves in biphase medium, amplification due to secondary reactions *(Russian)* 3—14468
- weakly nonideal gas motion under strong point explosion *(Russian)* 3—4593
- AgN_3, elec. breakdown and explosion, high speed photography 3—36838
- LiF ceramic, optical quality, production by method of explosive compression of powdered inorganic compounds *(Russian)* 3—12434
- N_2F_4-H_2, mixture, laser induced 3—12508

exposure meters *see photometers*

extensive air showers *see cosmic ray showers and bursts*

extensometers
- dilatometer, semi-continuous, design and testing 3—10221
- dilatometer up to 22 kbars 3—16385
- interference, as part of meas. standard for temp. coeff. of linear expansion of solids 3—32022
- with Moire grids and photocell, low modulus measurements 3—9838
- rope, using adapted electro-optical tracking system 3—66
- universal extensional rheometer for polymer melts 3—64

external flows
- water, pure, boundary layer, drag reduction by ejecting additive solutions 3—23740

extraordinary ray *see birefringence*

extraterrestrial atmospheres
- *see also comets; planetary atmospheres; stellar atmospheres*
- cometary H atm. model with multiple scattering, Lyman-α line effects 3—28161
- hydrodynamic waves, effects of Coriolis force, dispersion relationship 3—33282
- reson. line radiation scattering in a homogeneous sphere, planetary nebulae appl. *(Russian)* 3—16286
- Titan, a comparison of theory and obs. 3—25410

extraterrestrial radiofrequency radiation *see radiofrequency cosmic radiation*

extremum control *see optimal control*

eye
- aberration, spherical, crystalline lens contribution 3—31870
- absolute threshold, diplopia and convergence 3—25578
- accommodation, continuous objective measuring apparatus, i.r., lag and transfer function 3—37735
- amentropia and voluntary accommodation response meas. using laser speckle 3—37529
- applanation tonometry, applic. of spherical shell/rigid plate contact press. problem 3—19443
- asymmetric convergence, stereoscopic frame of reference, retina point stimulation response 3—3552
- bovine, photosensitive pigments in pigment epithelium 3—31894
- brightness contrast, surface and border, subserving mechanisms 3—39772
- brightness perception, two stage model 3—5663
- California ground squirrel, visual sensitivity 3—5667
- carp retina, bipolar-amacrine transmission 3—31881
- carp retina, membrane resist. changes underlying bipolar cell response 3—31880
- cat, accommodation obs. method 3—31895
- cat, grating resolution and refraction from evoked cerebral pots. 3—31888
- cat, lateral geniculate cells, P- and I-cell responses 3—31906
- cat, receptive fields, corpus geniculatum lateralis 3—5661
- cat, retinal ganglion cell, repetitive firing 3—31878
- cat, saccadic displacements of retinal image 3—9677
- cat, visual cortex, cell structure and formation correlation determ. by fluorescent dyeing 3—22153
- cat's retina, method for projecting pattern, direct visual control 3—28767
- cat retinal ganglion cells, detection of small image displacements 3—5664
- cats, saccadic and disjunctive movements 3—5659
- cerebral dominance in returning eyes to specified target positions in dark, asymmetries 3—9672
- colour blind observers, spectral sensitivity, cone photopigments 3—5670
- cornea, bovine, dynamic rheo-optical behaviour, temp. and frequency dependence 3—35262
- corneal curvature, diurnal constancy 3—31868
- corneal radius measurement, diffraction effects on precision 3—3886
- crayfish, inhibition of visual units 3—39778
- detection threshold, effects of edge sharpness and expsoure duration 3—39780
- dichoptic spatial interactions, sensitization by annular surrounds 3—39790

eye continued
- directionality of retinal receptors, nasal temporal asymmetry and cones as corresponding points 3—3555
- disability glare factor, controlled accommodation conditions 3—25580
- electrical stimulation effects on increment threshold for square-wave gratings 3—31890
- electro-oculogram, linearity of horizontal component 3—19099
- electro-oculography, dry electrodes and holder 3—19098
- electrooculography, computer automated 3—25581
- exposure to Th, from lenses 3—9708
- eye-movement study in target tracking 3—39798
- fish, focal length of eye lens and visual acuity 3—31889
- fish retina, outer plexiform layer, anoxia sensitivity 3—39792
- for peripheral retina, threshold luminance for optimal movement 3—25579
- foveal increment threshold, contrast sensitivity near borders, influence of test stimulus form, size and duration 3—39777
- foveal spectral sensitivity, heterochromatic additivity 3—35263
- frog, early receptor pot., urea effect 3—31897
- frog, green-rod pigment regeneration in isolated retina 3—31903
- frog, on-off retinal ganglion cells, early light and dark adaptation 3—31907
- frog and outer segments, effects of bleaching on width and index of refraction 3—9678
- frog isolated retina, isolated receptor potential 3—5662
- frog retinal rod photoreceptor membranes phagocyted by pigment epithelium cell, ultrastructural study after aldehyde fixations 3—39779
- frog rod, rapid dark adaptation 3—31887
- fusional information processing by human visual system 3—39797
- fusional response, central component, effect of stimulus parameters 3—31899
- glissade, new explanation 3—39788
- goldfish, chromatically-adapted, effect of temp. on psychophysical and electroretinographic spectral sensitivity 3—9670
- goldfish, parameters of optical components 3—9668
- goldfish retina, ganglion cell activity, stochastic nature 3—31883
- Great Horned Owl, visual acuity, anamotical and behavioural correlates 3—31874
- helix pomatia L, dark-adapted, spectral sensitivity 3—5665
- human, aqueous flow rates, Arrhenius plots 3—31869
- human, Mach bands obs., lateral inhibition 3—31872
- human cornea, diurnal thickness variations 3—28356
- human eye movement control modelling 3—39799
- image formation, model using fibre-optical components and optoelectronic conversion principles *(Russian)* 3—25583
- internal plumbing, drainage, review 3—9665
- isolated carp retina, horizontal cell membrane potential, effects of amino acids 3—39791
- isolated rat retinae, effects of rhodopsin decomposition on PIII responses 3—5658
- laser effects 3—28385
- laser optometer using Badal principle for meas. of eye refractive state 3—28590
- laser safety legislation 3—25606
- Limulus, response to light, mediation by lateral, median and ventral eye loci 3—9673
- Macaque monkey, systematically paralyzed, eye movements 3—31896
- marine fish in Gulf of California, vitamins A_1 and A_2 in retinas 3—5666
- medial rectus muscle, spectral analysis 3—25582
- microscopes and eye fatigue 3—37528
- minimally distinct border, chromaticity comparison 3—5671
- model for demonstrating ocular refraction 3—28451
- modulation transfer function measurement, influence of field of analysis 3—9682
- monkey, saccades and quick phase of nystagmus 3—5660
- Monkey cores and rods, time courses of late receptor potentials 3—9674
- monkeys, movements evoked by collicular stimulation 3—3553
- motion after-effects contingent on direction of gaze 3—39787
- movement control model 3—39796
- movement detection, photoelectric method 3—3907
- multisection tomography for location of foreign bodies 3—25591,
- muscle dynamics model 3—28358
- myoids, optical waveguides with cut-off 3—3557
- neural channel for coding real light and equivalent backgrounds 3—31886
- nictitating membrane of rabbit, inhibitory stimulus control 3—39795
- observer with unilateral defective colour vision, spectral response 3—5669
- ocular holograms for optometric instruction 3—9663
- oculomotor control system, predictive tracking mechanism 3—9683
- ophthalmic research, photographic applications 3—5997
- ophthalmology, crystalline lens and accommodation, bioengineering, visual prosthesis 3—13134
- ophthalmology, u.s. diagnosis 3—32235
- optical component depth and interface amplitudes meas. in live primate eye, effects of transducer manipulation 3—9667
- optical modulation transfer function, approximation by analytical functions 3—31898
- owl eye movements 3—39789
- peripheral threshold of perceived contrast 3—19100
- photoelectric matrix method for two-dimens. eye movement recording 3—28766
- photopic luminosity, by critical frequency method 3—5668
- photoretinoscopy, study of vision from a distance 3—6142
- physiological responses to brief flashes, variability of latency 3—39782
- pigeon, photic evoked pot. in optic tectum, rel. to flash intensity and background illumination 3—31877
- pressure-blinding, visual evoked cortical potentials 3—31900
- primate retina, prominal negative response 3—39781
- pupil control system, systems approach and analogue simulation *(Korean)* 3—31873
- rabbit lens, opacification due to fractionated X-ray and proton irradiation 3—35291
- radiographical and photographical examinations, patent 3—10188

eye continued
- rapid eye movement analyser 3−39775
- rapid movement sleep, in brain tumor patient, delta activity obs. 3−37522
- rat retina, isolated, electroretinogram fast components, ionic environment depend. 3−31892
- relation between detection of size, rate, orientation and direction 3 9669
- resolution, aided and unaided, rel. to illumination intensity 3−26216
- resolving power on object relative velocity in viewfinder 3−22320
- retina, cat, relation between refractive error and spread of image 3−39785
- retina, contrast sensitivity 3−16315
- retina, radiant heating by nonuniform light sources, injury threshold temperature 3−9664
- retina, sensitivity adjustment, high contrast neural image, nerve cell interactions 3−25584
- retina, spectral sensitivity and visual pigment absorbance 3−39801
- retina input system modelling, curvilinear images *(Russian)* 3−16319
- retinal cells, characterization of different classes 3−3546
- retinal disparity variations at fixation point, binocular Vernier method of obs. *(French)* 3−9676
- retinal ganglion cells of cat, variation in response latency 3−39783
- retinal image of nocturnal and diurnal lizard, comparison 3−39786
- retinal landmarks, external projections 3−16316
- retinal pigment system of xenopus laevis, metamorphosis 3−39784
- retinal receptors directionality, corresponding points and change of form of horopter 3−3556
- retinas, neural structures, transient processes, modelling *(Russian)* 3−16320
- rod photoreceptors, study by microscope spectrophotometer 3−3912
- saccadic suppression, in structured background 3−31902
- scotopic vision region, threshold characteristics *(Russian)* 3−9666
- Siamese cats, absence of binocular coding in striate cortex units 3−3554
- signal detection in white gaussian noise for humans, comparison to matched filter detector 3−39800
- skate retina, effect of Mg on horizontal cell activity 3−28357
- spectral sensitivity, by const. CFF, chromatic adaptation effect 3−31912
- spectral sensitivity beyond blind spot, dark adapted retina 3−25577
- teleost fish, scotopic spectral sensitivity, daylength effect 3−31876
- teleost fish, visual pigments 3−39793
- turtle photoreceptors, influence of K, Na and Cl ions on intracellular responses 3−22152
- turtle retina, e.r.g. obtained with flickering light 3−9680
- turtle retina, L- and C-type S-potentials, physiological and morphological identification 3−31891
- visibility of structured and unstructured images 3−31865
- visual accommodation system training 3−31911
- visual acuity as function of exposure duration 3−31871
- visual adaptation math. model, axiomatic construction *(Russian)* 3−16318
- visual evoked response using rapid flash rates technique 3−28330
- visual field extent, test target size, illuminance, kinetic testing 3−39773
- visual photoreceptors, anomalous dispersion 3−31901

F-centres
- alkali halide photoluminescence method of varying spatial distrib. of defects and effect *(Russian)* 3−5227
- alkali halides, coloured, kinetics of F-F' transitions 3−33528
- alkali halides, e.s.r. of relaxed excited states of F centres, reviw *(Japanese)* 3−15421
- alkali halides, piezo-hyperfine interaction concept. rel. to ENDOR 3−2466
- alkali halides, spin-lattice relax. in relaxed excited state, e.p.r. optical detection 3−18368
- alkali metal halides, Rabin and Klick diagram 3−33525
- alkali metal halides, reson. secondary glow, polarisation theory *(Russian)* 3−36918
- defect ionic crystals, F_I' centre properties, formation processes 3−36297
- emission, vibronic model appl. to stress-induced polarisation 3−34415
- ENDOR spectra, effects of applied electrostatic fields and hydrostatic press. 3−18393
- F_{2a}^+ centres in alkali halides, low lying states, pseudopotential calcs. 3−33831
- F_2-centre multiphoton absorpt., transition amplitude calc. 3−2575
- ionic cryst., magneto-optical spectra, electron-phonon interaction effects 3−2580
- optical information storage in KCl and KBr crystals, conversion of F and X centres 3−13329
- polar liquids and solids, trapped dielectron, semicontinuum model 3−38813
- rare-earth fluorides, coloration centres, photoluminesc. meas. *(Russian)* 3−36920
- relaxed excited states, nearly degenerate states of bound lattice polaron 3−21040
- sodalite, damage mechanism, ESCA obs. 3−36298
- BaF_2, absorpt. bands in neutron, irrad. cryst. 3−1623
- BeO, F^+-centre, interactions with next-nearest-neighbour Be nuclei, ENDOR obs. 3−39058
- CaF_2:Ce, near u.v. absorpt. spectra obs. 3−12161
- CaO, magnetic circular dichroism of F band 3−21451
- CaO, Stark effect 3−30858
- CaO:Mg, e.p.r. of F^+ centre 3−36791
- CaS phosphors, F^- aggregate centre formation due to S^{2-} vacancies, e.s.r. obs. 3−39028
- CdO-NaCl heterojunction, optical absorpt. *(Russian)* 3−8627
- $Fe_{1-x}S$, annihilation of positrons by cation vacancy capture 3−17871
- KBr, additively coloured, photoemission study 3−2617
- KBr single crystals containing colour centres, thick hologram recording 3−22369
- KBr:OH^-, O_2^-, O^{2-}, anion impurities influence on optical stability of F-centres *(Russian)* 3−8615
- KCl, additively coloured, photoemission study 3−2617
- KCl, additively coloured, photochem. F→M centre conversion *(Russian)* 3−33526

F-centres continued
- KCl, dipolar complexes resulting from 1.5 MeV electron bombardment 3−12096
- KCl, e.p.r. of loose F aggregate centres, opt. detection 3−2392
- KCl, electron irrad., efficiency of formation, 10-80K 3−20733
- KCl, F_2 centres, spin triplet state disappearance mechanism *(French)* 3−38817
- KCl, γ irradiated crystals, thermoluminescence, plastic deformation effect 3−8677
- KCl, luminescence lifetime, band structure 3−21475
- KCl, optically detected e.p.r., n.m.r. and ENDOR with F-centre pairs 3−21310
- KCl, positron capture, ang. correl. of γ-quanta *(Russian)* 3−33524
- KCl, wave function, pseudopot. method calc. 3−33527
- KCl uniaxially strained, X-irradiated, photostimulated exoelectron emission 3−34458
- KCl:Ag, photochemically coloured, deform. luminesc. 3−5231
- KCl:Li, X-irrad., F-centre accumulation kinetics 3−2576
- KCl:$Li^+(Na^+)$, image recording on F_a centres 3−32082
- KCl:Na, decay of F and F_a' bands produced by light flashes, room temp. 3−27521
- KCl:Na, e.s.r. of relaxed excited state of F_a(Na) centres 3−30695
- KCl:Na, storage properties of F_a-centre holograms 3−22370
- KCl:OH^-, formation during bleaching of Y- and Y'-centres 3−18477
- KF(Cl)(Br)(I), e.p.r. optical detect. of F centre pairs, pumping cycle kinetics 3−12061
- KF(Cl)(Br)(I), energy levels in field of negative ion 3−21031
- KI, diffusion of water molecules, F-band absorp. obs. 3−30120
- $KMgF_3$:Mn, colour centre luminescence 3−34403
- LiF, formed on X-ray radiation, annealing kinetics 3−4757
- LiF, γ-ray prod., effect of dose, dose rate, temp., impurities, sample deform. 3−11620
- LiF, thermal mixing of ^{19}F and ^7Li Zeeman reservoir 3−30716
- LiF, thermionic emission from electron traps 3−30919
- LiF:In, form. of F-emission centres on In diffusion 3−24115
- LiF:O^{2-}, form. from oxygen-vacancy complexes, effect on plasticity 3−24114
- LiH, u.v. irrad., e.p.r. of F-centres 3−8443
- MgO, lattice distortion around F^+ centre, ENDOR obs. 3−27441
- NaCl, e.p.r. optical detect. of F centre pairs, pumping cycle kinetics 3−12061
- NaCl, form. yield of self trapped excitons and F-centres between 10 and 130K 3−30432
- NaCl, positron capture, ang. correl. of γ-quanta *(Russian)* 3−33524
- NaCl, temp. depend. of F-centre absorpt. 3−4755
- NaCl, wave function, pseudopot. method calc. 3−33527
- NaCl uniaxially strained, X-irradiated, photostimulated exoelectron emission, association with F centres 3−34458
- NaCl:Mg X-irradiated crystals, Mg centres expt. study 3−38586
- NaCl:O^{2-}, X-irrad., formation *(Russian)* 3−7756
- NaCl:Pb, thermoluminescence after X-ray irradiation 3−12188
- NaF, proton-irrad., F_1- and F_2-centre accumulation *(Russian)* 3−30119
- NaF, wave function, pseudopot. method calc. 3−33527
- NaN_3, wave functions, calc. by point-ion method 3−38587
- RbBr(I), e.p.r. optical detect. of F centre pairs, pumping cycle kinetics 3−12061
- RbCl(:Na, :Ca), e.s.r. investigation, obs. of hyperfine structure 3−27414
- $SrCl_2$, additive and substractive coloration with O^{2-} impurities 3−20736
- $SrCl_2$, form. of F, V_k, V_{ka} centres on X-irradiation 3−17816
- SrF_2, form. of F, V_k, H centres on X-ray irradiation, temp. depend. 3−17815
- SrF_2 absorpt. bands in neutron irrad. cryst. 3−1623
- Xe:A (A=alkali atoms), e.p.r. line broadening, F-centre model for outer electron 3−36792
- ZnO, electron irrad., displacement thresholds 3−20765
- ZnO, electron irrad., O displacement energy, F^+ centre form. 3−4773
- ZnS, elec. cond. meas. and e.p.r. obs. of F-centres 3−21076

F-layer *see F-region*

F-region
- ambient electron heating, by photoelectron energy degradation 3−12811
- auroral and ring current precipitation effects caused by artificial plasma injection 3−25296
- average scintillation, at u.h.f./v.h.f. 3−37240
- coupling between protonosphere and F-region, numerical solutions 3−16067
- day-sector polar F-layer during magnetospheric substorm 3−31438
- diffusion model for electron density distrib. along geomagnetic field in F-region plasma cloud 3−31430
- disturbance, latitudinal variations in subauroral zone *(Russian)* 3−3076
- echoes, assoc. with slant sporadic-E at high latitudes 3−18887
- electron density equatorial anomaly, longitudinal variation 3−9336
- electron density profile during sunrise, plasma scale height profile obs. 3−9328
- electron density profile of F_1-region from rocket experiments 3−34951
- electron drift meas. rel. to geomag. horizontal field variations during March 1970 geomag. storm 3−25291
- electron temp. meas. from cosmic noise obs. 3−9329
- electron-ion gas nonstationary distrib. for pure ambipolar diffusion 3−34948
- e.m. wave reflection coefficients rel. to thickness of E_s-layer 3−25284
- equatorial, effect of vertical drift on plasma distributions 3−25293
- equatorial, thermal structure, theoretical profiles 3−12802
- equatorial anomaly, American and Asian sectors 3−31440
- equatorial anomaly, day-to-day variability in American and Japanese sectors 3−25294
- equatorial anomaly, effect of electrojet current 3−12791
- equatorial anomaly, time-dependent plasma continuity equation 3−31439
- equatorial anomaly in F_2-region from vertical sounding above Pacific Ocean 3−28067
- equatorial F layer, source and identification of heavy ions 3−12807

F-region continued
equatorial scintillation, effect of irregularities 3−9335
equatorial spread F in region of electrostatic turbulence, vertical drift velocities 3−12808
F2 layer, semi annual variation in electron density 3−5520
F2-layer at noon, standard electron density profile 3−31434
F_1 layer, effect of solar activity on geometric parameters *(Russian)* 3−3075
F_1 layer, nonlinear interaction of radiowaves *(Russian)* 3−3072
F_2 layer, spatial and temporal manifestation of seasonal anomaly *(Russian)* 3−3074
F_2 region electron temp., variation with solar activity 3−12799
F_2-layer max. electron density, mag. storm disturbance variation with storm time on noon meridian 3−34949
F_2-layer max. variations during 1962 December mag. storm 3−25280
frequency shifts of h.f. Doppler sounder due to geomagnetic sudden commencements 3−21972
infrasound generated by severe thunderstorms 3−16024
ion composition during sunrise and sunset above Kiruna, mass spectroscopy meas. 3−25292
ionisation irregularities, zonal drifts caused by meridional winds 3−18886
ionospheric modification by high-powered h.f. transmitter, ionosonde observations 3−16028
ionospheric waves, phase velocity dispersion rel. to e.m. waves 3−21968
irregularities over magnetic equator, characteristics determ. from spaced fading records of radio wave echoes 3−34944
irregularity wavenumber spectrum from ionospheric scintillation obs. of the radiosource Cygnus A 3−12803
Isis 1 satellite observations during 3 Feb. 1969 geomagnetic storm 3−12795
loop structuring of F-region ionogram traces 3−31429
lunar variations in f_0F_2 at low latitude 3−31428
magnetic field-aligned irregularities detected by phase interferometry, wavelike struct. 3−9326
magnetically coupled transport of cold plasma in outer ionsophere at low latitudes 3−31477
mid-latitude disturbances rel. to geomagnetic storms 3−31331
mid-latitude F-layer, causes of storm-time increases 3−31425
mid-latitude F-layer electron concentration seasonal var. in magnetic storm effects 3−31433
mid-latitude trough structure, incoherent radar scatter observations 3−31427
midlatitude parameters during geomagnetic storms 3−12806
minor ion concs., theoretical vertical profile calcs. at the Equator 3−18885
neutral temp. during a mag. storm, geomagnetic effect, satellite obs. 3−16025
neutral wind effect on limiting periods of gravity waves 3−18890
north-south electron drift in equatorial ionosphere above Thumba 3−34952
photoelectron escape altitude calc. as function of latitude 3−12801
polar irregularity zone, equatorward shift as function of Kp index 3−16029
radiowave, production and analysis transmission ionograms 3−9320
scattered signal fadings during F_{sp} phenomena *(Russian)* 3−3079
seasonal anomaly below F_2-layer electron density max. rel. to latitude and time 3−28066
south polar region, f_0F_2 contour maps from ISIS-1 satellite observations 3−31426
spread F, Pc 1 micropulsation relationship 3−15923
spread F echoes, new interpretation 3−12809
topside, electron temp., meas. by a.c. Langmuir probe, global morphology 3−3080
tropical nightglow, O I 5577 angstrom line meas. and electron density determ. 3−15988
tropical u.v. airglow intensity, theoretical calculations 3−12804
v.h.f. propagation between Darwin, Australia and Yamagawa, Japan, propagational mode deduction from signal strengths 3−31436
H^+ distrib. in the low-latitude ionosphere 3−18884
He^+ distrib. in the low latitude ionosphere 3−18884
N_2 vibr., temp. determination from O^+ reaction rate constant 3−3100
N_2^+ dominated afterglows, dissociative recomb. at elevated temps. 3−11293
O line, neutral temp. in the dayglow during a mag. storm 3−16025
O^+ reaction rates, effect of excited states on F-region processes 3−25290
$O(^1D)$ quenching rates, night glow intensity enhancements 3−12810
faces (crystal) *see crystal faces*
facsimile
see also video signals
photograph machining by laser light 3−37649
facsimile communication *see facsimile*
facsimile document reproduction *see photocopying*
facsimile equipment
laser recording and scanning, techniques, systems 3−6526
Radio Astronomy Explorer B antenna aspect data processor 3−35218
facsimile signals *see video signals*
facsimile transmission *see facsimile*
faculae *see sun*
fading
see also radiowave propagation
D-region wind meas. from fading of partially reflected radio waves 3−31432
dye, of motion picture film 3−220
E-region drift meas., skewness of correlation functions of fading records 3−25288
ionospheric drift records, errors in correlation analysis 3−28084
ionospheric regular signal fading during sunrise and sunset transitions at middle latitudes in 12.2 to 23.4 kHz range 3−25273
laser beam fade at receiver due to pointing jitter of transmitter 3−19628
r.f. communications from perfectly conducting sinusoidal ocean surface 3−4063
scattered signal fadings during F_{sp} phenomena *(Russian)* 3−3079
failure analysis
see also wear
chrome-magnesia fired bricks, electron microprobe analysis 3−15755
composite structures, fracture control technique 3−21726
corrosion failure of welded joints, residual stress effects 3−21718
elasto-plastic strengthened material, anti-plain strain around notch, mechanical failure *(Russian)* 3−37823
eyebolt, brittle fracture in first turn of thread, exam 3−24205
first passage analysis under stationary random excitation 3−554
low cycle failure mechanisms review 3−21630
materials aging effect on failure 3−21778
nuclear reactors run-to-failure anal. of EBR-II mark IA failed fuel elements 3−26534
steels and graphite, cumulative damage stochastic models, functional gamma distribution 3−7013
structures subjected to steady load operating in creep region, bounds on life 3−28895
fallout
see also air pollution
atmospheric dust in Bucharest, daily variation of natural radioactivity 3−5510
automatic radioactive inventory system 3−28775
dust and rainwater sample analyses for fission products and radionuclides 3−31389
simulated fallout particles, retention by lichens and mosses 3−9735
^{137}Cs fallout as tracer in obs. of lake sediments 3−34898
^{22}Na in food chain, lichen-reindeer-man 3−3634
^{238}Pu stratospheric injection, graphical distrib. meas. 3−25245
^{32}Si prod. rate, vertical profile meas. for South Pacific 3−34861
Faraday effect
alkali halides, U-centres, magneto-refl., Faraday rot., ellipticity 3−15476
current measurement at h.v., optical technique 3−19655
fading rate of beacon satellite transmission across off-zenith transverse point 3−12790
Faraday rotation technique, low field 3−35409
garnet film, bubble detect. by Faraday effect in waveguide fibre optics 3−35442
glass fibre, for current meas. 3−6028
modified magneto-optic hysteresigraph for direct recording of Faraday rotation 3−6034
phenomenological theory of optical props. of crystals 3−34320
plasma focus device, Faraday rotation meas. with a ruby laser beam 3−20640
plasmas subjected to electric field of circularly polarized waves, creation of global magnetization *(French)* 3−11480
rare-earth iron garnet: Bi substituted 3−34330
resonant, use to determ. relative transition probabilities for absorption lines with Voigt profiles in plasma 3−11473
semiconductor, rotation angle with allowance for carrier density elec. field depend. 3−5180
semiconductors, microwave rotation, transport and band parameters 3−15475
three-mirror resonator linked with frequency polariser and Faraday cell, frequency polarisation characteristics *(Russian)* 3−29108
two-photon radiative interaction operators from relativistic theory for Rayleigh scatt. and Faraday rot. 3−38274
$BaFe_{12}O_{19}$, internal domain structure, power patterns and Faraday effect obs. in i.r. 3−38990
$Bi_{12}SiO_{20}$, self-focusing of Ar laser radiation 3−32602
$CoCr_2S_4$, hot pressed, ferrimagnetic semiconducting spinel, refractive Faraday rotation 3−18435
CuBr(Cl), Faraday rotation due to excitons 3−8556
CuCl, near absorpt. edge, interband and exciton effects 3−15474
$ErFeO_3$, intrinsic Faraday rotation temp. depend. 3−21390
Fe garnets, magneto-optic light modulation at 1.064 μm 3−36856
$FeBO_3$ optical properties, strong absorption spectra, optical rotation 3−36893
n-GaAs in range of non-low doping, electronic effective mass *(Russian)* 3−12125
H magnetised arc plasma, electron density distribution by Faraday effect meas. *(German)* 3−38500
$InAa_xP_{1-x}$ solid solutions, compositions, transport properties, electron effective mass 3−33802
InSb, effect of weak, longit. static field on transverse e.m. wave propag. along magnetostatic field 3−2121
n-InSb, of hot electrons, i.r. 3−2523
n-InSb, strongly compensated, rel. to Hall mobility and coeff. meas. 3−15477
n-InSb, strongly compensated, due to hot electrons 3−15478
MgAl thin films, preparation method and properties 3−36987
Mn-Bi thin films, mag. domain patterns in polarization microscope obs. 3−21283
MnBi film, domain pattern obs. 3−21272
MnBi film, hysteresis loop determ. 3−27384
MnF_2, spin flop domains, n.m.r., Faraday rotation, photographs and optical-absorption spectroscopy investigation 3−34113
MnGaGe, sputtered film, ferromag. props., room temp. polar Faraday rotation 3−36861
MnGaGe film, Curie point writing with laser pulse, magnetisation from Faraday rotation 3−36860
$Y_{3-x}Gd_xFe_5O_{12}$ temp. depend. control of Faraday rotation by Gd substitution 3−8557
YIG, optical rotation, i.r. intensity modulator application 3−5985
YIG, relation between magneto-refl. spectra and Faraday effect *(French)* 3−12126
YIG epitaxial film, stripe domain struct. obs. 3−34160
YIG film, obs. of stripe domain orientation 3−27386
YIG:Pb substituted, anomalous rotation 3−34331
farming
electrostatic crop spraying, and expts. with triboelectrogasdynamic generator system 3−656
fast Fourier transforms
algorithm of microwave hologram in antenna aperture, determ. of far field pattern *(Russian)* 3−35421
CAI of Fourier analysis 3−32019
crystallographic, for use with Cooley-Tukey algorithm 3−23959
e.m. scattering from rough surface, Rayleigh-FFT approach 3−37927

fast Fourier transforms continued
  for fitting experimental data with experimental functions 3−22418
  high intensity proton beams applic., two-dimensional computer simulation of transverse behaviour 3−22426
  image enhancement in nuclear medicine 3−313
  longitudinal e.m. propagation in a magnetoplasma 3−16018
  marine magnetic anomalies, filtering operations with fast Fourier transform 3−18903
  microwave hologram, image reconstruction 3−9955
  modal content of sound in annular and circular ducts, Fourier analysis 3−35368
  simulated random processes, normality and accuracy study 3−32293
fastening *see joining processes*
fatigue
  accelerated estimation of fatigue life by prefracture method, influence of exptl. results dispersion *(Russian)* 3−12473
  aging effect on failure properties 3−21778
  aircraft structure analyses under stationary random excitation 3−553
  alloy, fatigue crack growth, effects of loading freq. and nonreactive external media 3−31234
  alloy, high-hot-strength, fatigue strength under nonsteady state loading 3−37106
  alloy, high-strength, fracture toughness role in low-cycle fatigue crack propag. 3−31047
  alloys, low yield strength fatigue crack propagation using plastic strips 3−21766
  alloys for biomedical applics., corrosion fatigue 3−27657
  Armco iron, detection of microcrack initiation 3−18745
  axial vibrations in nonuniformly heated rod, amplitude distrib. 3−31235
  axle shafts, torsional fatigue strength by program loading *(German)* 3−12489
  biaxial cumulative fatigue damage, octahedral shear strain theory 3 31239
  book 3−21714
  brass, metallurgical factors in fretting behaviour 3−37076
  composite materials, fracture 3−2760
  constructional materials and compressor components, fatigue strength under fretting corrosion conditions 3−34605
  corrosion fatigue, crit. corrosion rate considerations 3−27655
  crack growth behaviour under variable amplitude loading 3−21756
  crack growth data analysis 3−25028
  crack growth monitoring, using acoustic emission technique 3−25040
  crack propag. under stress rel. to fatigue life estimation *(Japanese)* 3−25030
  crack propagation rate analysis *(Japanese)* 3−11678
  cracks, growth rate estimation 3−27804
  cracks, production for bending tests, work of rupture 3−27803
  cumulative, expression for lifetimes 3−27058
  cumulative damage rel. to cyclic plastic strain *(Japanese)* 3−12401
  damage accumulation, analysis of models from common viewpoint *(Russian)* 3−11675
  design element, fatigue life determ. on basis of fatigue failure mechanism concepts 3−37108
  dolomite rock 3−31303
  Duralumin, fatigue crack growth 3−18750
  elevated temperature and slowly time varying loads, inelastic stress-strain law 3−25027
  empirical laws for fatigue crack growth rate and theory *(Japanese)* 3−24815
  α-Fe, low-cycle fatigue, grain boundary sliding, 450-700°C 3−34577
  ferritic materials, fatigue crack propag., stress intensity and microstruct. influence 3−21580
  fibre, porosity, dependence of mech. props. *(Polish)* 3−31174
  fibre composite with metallic matrix, fatigue props. above 800°C 3−18696
  fibre composites, matrix fatigue behaviour under repeated tensile loads 3−31154
  filamentary reinforced metals, mech. prop. considerations 3−31155
  fractography, state-of-the-art review 3−30982
  fracture analysis, fatigue striations exam., SEM technique 3−37027
  fracture toughness parameter calc., engineering method 3−34600
  fretting-fatigue mechanism, effect of direction and motion 3−18557
  friction welded high speed steel, annealed steel, testing *(German)* 3−31118
  glass epoxy composite effect of specimen geometry on fatigue strength 3−21770
  graphite, Poco and RC4, dynamic fatigue behaviour and general fatigue design criterion 3−32951
  life prediction, under nonstationary random excitation 3−574
  life under stationary Gaussian random loads 3−555
  load-bearing capacity of specimens with stress concentrators under repeated loading, deform. effects 3−34686
  low cycle failure mechanisms review 3−21630
  low cycle fatigue law, high vacuum effect 3−39423
  low-cycle, of Incoloy 800, influence of hold-time and temperature 3−8890
  mating roller contact, pitting life tests *(Japanese)* 3−27811
  metal, cyclic creep fracture in low cycle fatigue *(Japanese)* 3−25029
  metal, fatigue crack starter defects prod. by pulsed laser 3−21762
  metal, phys. fatigue limit, structural-energetic theory applic. 3−30193
  metal, plastically deformed, fatigue damage detection by exoelectron emission 3−18534
  metal, plasticity effects in crack propag. 3−30195
  metals, fatigue failure, structural-energetic analysis *(Russian)* 3−8841
  metals, microstructure changes *(German)* 3−5295
  metals, single plastic deformation effect *(German)* 3−5319
  metals, thermal fatigue, under mechanical loading in corrosive medium 3−27798
  metals, unit for torsion investigations at room and high temps. 3−35358
  nuclear piping system, stress range and fatigue damage, computation method 3−1072
  nuclear reactor structures, broad band acoustic fatigue theory 3−14256
fatigue continued
  Nylon 6.6, fatigue failure under cyclic loading, fatigue life calc. 3−15787
  piano wires, low-cycle torsional fatigue under const. strain amplitude at elevated temps. *(Japanese)* 3−18771
  plastic, study of torsion specimens *(German)* 3−21785
  plastics, fatigue tests, rational test piece geometry for cyclic tension-compression tests 3−25033
  plastics, mechanical pulsator with capacity for adjusting cyclic and mean loads during tests *(German)* 3−12488
  plastics, Wohler fatigue curve characts. *(Russian)* 3−4791
  PMMA sheets, growth of part-through thickness fatigue cracks 3−21734
  polurethane soling, tearing energy theory 3−31156
  polyethylene, crack propagation, stress depend., surface microscopy 3−31158
  polymer, crack propagation and failure mechanism *(Japanese)* 3−12455
  polymer, stress ratio effect on fatigue crack growth *(Japanese)* 3−18728
  polymers and composites, servo-controlled axial fatigue machine with strain rate feedback 3−25665
  polystyrene, failure in tensile and cyclic deform. 3−21740
  pulsating stress creep rupture, nonlinear damage law proposal 3−31237
  random data analysis, stochastic function plots by computer 3−2776
  reactor component safety evaluation 3−29439
  review of process 3−24961
  rock, damage induced by acoustic waves 3−2913
  rock, fatigue failure as stochastic process under pulsating tensile stress *(Japanese)* 3−21771
  rock beam, failure, exptl. 3−31308
  rock beam, failure, theory 3−31307
  rolling contact fatigue, formation of spherical particles from metal tongues 3−20801
  rolling contact fatigue tests, effects of surface roughness and form factors of carbon steel and grey cast iron rollers 3−21616
  rotating specimens, temp. meas. during fatigue testing 3−18751
  rotor hydropulsators for use with fatigue testing machines, 'floating zero' effect and kinematic distortions *(Russian)* 3−12475
  S/N curve, shape analysis, ultimate tensile strength to cyclic elastic limit 3−31228
  sheet materials, fracture kinetics, effect of order of applying fatigue crack and heat treatment 3−18621
  silicate glasses, abrading effects 3−9001
  steel, 13 CrMoV 58, curing of fatigue cracks by local welding *(German)* 3−27684
  steel, 4340, fatigue crack growth rate, thickness and orientation effect 3−18646
  steel, austenitic, fatigue crack initiation *(Japanese)* 3−12396
  steel, austenitic, performance of inhibitor-protector against corrosion fatigue failure *(Russian)* 3−4929
  steel, austenitic, preliminary thermocycling influence on hot strength 3−31101
  steel, austenitic, thermal fatigue in liquid Na *(Russian)* 3−12376
  steel, carbon *(Japanese)* 3−24870
  steel, carbon specimens in oil, fatigue crack propagation, numerical analysis 3−21614
  steel, carbonitrided, dislocation substructure study 3−18605
  steel, carburized, impact-fatigue strength, effect of structurally-free ferrite in core 3−21691
  steel, case hardened, effect of residual stress on fatigue strength *(Japanese)* 3−12400
  steel, corrosion fatigue, effect of vacuum-diffusion coating *(Russian)* 3−27665
  steel, Cr-Mo-V, cyclic straining influence on creep behaviour 3−12416
  steel, curve discontinuities *(Russian)* 3−12367
  steel, diamond smoothing effect on surface finish and fatigue strength 3−34596
  steel, durability, effect of fretting after thermochem. treatment *(Russian)* 3−27668
  steel, fatigue crack growth, effects of moisture, temp. and neutron irradiation, for reactor applications 3−21596
  steel, fatigue crack propag., microstruct. change at crack tip 3−21579
  steel, fatigue strength increase due to surface deform. 3−27687
  steel, fatigue strength of standard steel specimens with varying percentages of carbon, under reversed bonding loads 3−24888
  steel, fracture toughness in cyclic loading, rel. to fractographic peculiarities 3−34689
  steel, G-X22CrMoV121, CS-22Mo4, 14MoV63, 13CrMo44, strain holding time, temperature effects 3−31035
  steel, He-implanted, annealed and cold-worked Type 316 stainless, fatigue crack growth 3−27706
  steel, high strength, crack tip yielding during fatigue cycling 3−8882
  steel, high-strength, stress-corrosion and corrosion-fatigue crack vels. 3−5324
  steel, high-strength Type 4140, corrosion fatigue behaviour 3−37051
  steel, HY-130, corrosion fatigue crack propag., temp. and freq. effects 3−27660
  steel, influence of electrical discharge treatment 3−24921
  steel, influence of electrostatic field *(Russian)* 3−12368
  steel, influence of sulphur and sulphides *(French)* 3−24911
  steel, load-bearing capacity of specimens with stress concentrators under repeated loading 3−34598
  steel, low carbon containing inclusions, fatigue-fracture surfaces, exam. 3−8815
  steel, low-C, effect of stress amplitude on annealed and cold-rolled specimens *(Japanese)* 3−12405
  steel, low-C, fatigue crack initiation process in notched specimens *(Japanese)* 3−21597
  steel, low-C, metallurgical factors in fretting behaviour 3−37076
  steel, low-cycle fatigue properties, transformation of retained austenite and cracks 3−37060
  steel, maraging, reverted austenite effect on mech. props. and toughness 3−34583
  steel, maraging for use in military bridge, fatigue crack growth and fracture 3−21626

fatigue continued
- steel, medium-C, strength obs. using push-pull testing under high press. *(Japanese)* 3—12486
- steel, method to increase fatigue strength *(Russian)* 3—12372
- steel, mild, fatigue crack growth under crack opening displacement cycling 3—31046
- steel, mild, grain size and stress distrib. effect on fatigue strength of notched specimens 3—8899
- steel, Ni-Co-C, roll-extruded, effect of degrees of rolling reduction 3—31050
- steel, notched, strength under random and programmed loads *(Japanese)* 3—12403
- steel, pearlitic, low cycle fatigue, heat treatment type depend. 3—37070
- steel, prestress effect on low-cycle fatigue failure 3—21758
- steel, rail-grade, hydrogen effects in prod. and service performance 3—5335
- steel, specimens with cappings, corrosion fatigue strength, heat treatment and rolling effects *(Russian)* 3—27667
- steel, stainless, serrations on load-extension curve, effect of martensitic transform. *(Japanese)* 3—31075
- steel, stainless, stabilized, strain rate effect on high strain fatigue props. 3—34564
- steel, stainless, time and cycle dependent failure at elevated temp. 3—31240
- steel, stainless, type 304, hold-time effects on fatigue crack propag. 3—8880
- steel, stainless, type 304, weldments at high temp., fatigue crack growth 3—34676
- steel, stainless, type 403, corrosion fatigue metallography 3—27658
- steel, stainless 304, hold-time effect in high temp. fatigue fracture 3—27707
- steel, stainless austenitic, behaviour under continuous or repeated stress *(French)* 3—24914
- steel, structural, influence of rest periods on fatigue strength 3—21755
- steel, structural, low-cycle fatigue strength, temp. and hold time effects 3—8824
- steel, tool, fatigue limit in compression 3—21690
- steel, tufftrided mild, fatigue strength and microstructure *(Japanese)* 3—30991
- steel, work hardened, impact strength under cyclic loading at low temp. 3—34682
- steel, workability improvement considerations 3—21681
- steel bits, fatigue strength increase by heat treatment 3—18665
- steel components, contact fatigue kinetics obs. using inductive sensor 3—34692
- steel for dies, fatigue resistance 3—18667
- steel machine parts, notch sensitivity under alternating loads, machining methods influence 3—34693
- steel pressure vessels, cumulative fatigue damage tests, cyclic stress, strain and energy variations 3—34677
- steels, fatigue fracture rate study with aid of fracture mechanics *(French)* 3—15686
- steels, ribbed reinforcing, testing by Prot's method, planning and evaluation *(German)* 3—9030
- strength under varying mean stress *(Japanese)* 3—12402
- stress corrosion, adsorption-electrochemical hypothesis *(Russian)* 3—27670
- stress-strain relation, in bending fatigue specimen 3—28475
- stress-strain relations in low-cycle rotating beam bending *(Japanese)* 3—8869
- structural materials, low-cycle fatigue strength determ. under axial and reversed torsional strain cycling 3—5299
- surface fatigue crack morphology 3—31230
- test machines TsDm-10-Pu, features of use and modernization *(Russian)* 3—12479
- testing, apparatus for testing plastics in biaxially stressed condition 3—18756
- testing, low-cycle, on machines with pendulum load measuring devices 3—18755
- testing, metal hardening, recording at elevatd temps. 3—28465
- testing, probability of faults during cyclic loading, estimation method 3—34694
- testing, steel strand, overhead telephone cable support, comparison of UG and EHS strands 3—12492
- testing fixture, elevated temp. torsional 3—5769
- testing machine, pushpull type for high pressure operation *(Japanese)* 3—12486
- testing machine for plastics 3—18757
- testing method *(German)* 3—31229
- testing on wire reinforcement metal *(Russian)* 3—12474
- testing unit, with pulsating load at specified force and deflection 3—18754
- testing using dynamic force measuring equipment, errors due to force transducers *(Hungarian)* 3—13222
- tests at Langley Research Centre 3—21757
- thin plates dynamic testing with sinusoidal pneumatic excitation *(Japanese)* 3—25036
- turbine blade materials, behaviour under asymmetric loading 3—31232
- two-dimensional stress state testing device 3—35357
- welded specimens, programmed fatigue testing 3—37107
- Windscale AGR circulator diffusers, acoustic fatigue, predicted and measured dynamic strain, comparison 3—14253
- Wohlerdiagram development and applic. of extreme-value method 3—9031
- Al, fatigue cracks, substruct. form. and propag. 3—21610
- Al, fatigue damage, visual display by means of exoelectron emission 3—12468
- Al, internal friction peak behaviour and dislocation-point defect interaction *(French)* 3—11685
- Al, pure, microstruct. influence 3—31110
- Al alloy, 7075-T6, vacuum environment effects on fatigue and fracture 3—27678
- Al alloy, fatigue crack closure at positive stresses, plastic deform. in crack wake 3—14922
- 7075-T6 Al alloy, fatigue damage accumulation 3—12470
- Al alloy, low-cycle fatigue under high hydrostatic pressure, obs. *(Japanese)* 3—8861

fatigue continued
- Al alloy, strength obs. using push-pull testing under high press. *(Japanese)* 3—12486
- Al alloy, stresses during vibr. of plates under acoustic loads 3—31236
- Al alloy with metal plating, residual stresses influence on fatigue limit 3—37072
- Al alloys, corrosion fatigue in aqueous solns., fractographic studies 3—27656
- Al alloys, fatigue, at room temp. and 300 F, low-cycle, axial strain 3—21653
- Al alloys for aircraft structures, thermomech. processing effects 3—31048
- Al foil, tensile and fatigue crack growth obs. 3—21761
- Al/B composite, matrix fatigue behaviour under repeated tensile loads 3—31154
- Al-Al_3Ni aligned eutectic alloy, fatigue fracture behaviour 3—21658
- Al-Mg(5 wt.%) alloy, grain size effect 3—34594
- Al-Si, cyclic hardening and microstructure effects on fatigue 3—15708
- Al-Zn-Mg, corrosion fatigue inhibition, crack growth rate meas. 3—39352
- B epoxy composite effect of specimen geometry on fatigue strength 3—21770
- C fibre reinforced polymers, nondestructive testing, fatigue performance 3—31213
- Cu, fatigued, recovery of shear modulus and internal friction 3—7811
- Cu, grain boundary friction with neutron irradiation and fatigue 3—24117
- Cu, vacuum influence on stages of fatigue failure *(Russian)* 3—24874
- Cu alloy, strength obs. using push-pull testing under high press. *(Japanese)* 3—12486
- Cu and Cu-Al(7.9 wt.%) alloys, corrosion fatigue crack initiation 3—27661
- Cu polycrystal surface layers under fatigue, structure *(Russian)* 3—36991
- Cu torsionally fatigued wires, strain amplitude changes effect on stress amplitude and resistivity 3—27054
- Fe, Armco, coarse- and fine-grained, fatigue crack formation and propag. *(Russian)* 3—27671
- Fe, Armco, tested at fatigue limit, dislocation struct. formation *(Russian)* 3—7758
- Fe, high-purity, fatigue deform., cryst. orientation depend. *(Japanese)* 3—18595
- Fe, polycryst., failure mechanism under plane stress conditions at low temps. 3—31096
- Fe, under fatigue loading, plastic deform. of surface and internal layers 3—27056
- Fe alloy, borided, thermal fatigue resist. 3—27694
- Fe single crystal, slip planes and asymmetric slip obs. 3—7834
- Fe single crystals, asymmetric deform. in net zero strain fatigue 3—36347
- Fe-Ni alloy with hardenable electrodeposited coatings, rolling contact fatigue assessment 3—9026
- Ge single crystals, slow loading effects *(Russian)* 3—30181
- Ni, cyclic endurance and dislocation struct. during fatigue tests, annealing effects *(Russian)* 3—5308
- Ni, preliminary extensional fatigue deform., dislocation struct. changes *(Russian)* 3—27664
- Ni alloy, fatigue strength, test temp. influence 3—34687
- Ni and Nichrome, thoria dispersed, l.p. hydrogen gas influence on fatigue crack growth 3—39347
- Ni based superalloy, elevated temp. fatigue behaviour of single crysts., environment effects 3—39365
- Ni-Co, superlattice form. in fatigue specimens 3—8808
- Ni-Cr-Mo martensitic steel, fatigue crack propagation law in water *(Japanese)* 3—18642
- Ti alloys, cleavage cracking mechanism under loading hydrogen embrittlement 3—18653
- Ti alloys, corrosion fatigue in aqueous solns., fractographic studies 3—27656
- Ti alloys, low-cycle fatigue strength 3—21693
- Ti alloys, vacuum annealing influence on operating characts. 3—24939
- Ti-Al-Mn alloys, effect of hydrogen 3—24882
- Ti-Al-V alloy, surface effects during fretting fatigue 3—15814
- Ti-Al-V and Ti-Al-V-Sn alloys, corrosion fatigue crack propag., freq. and wave form effects 3—27659
- Zn, S/N curve variations due to temp. and grain size 3—34575

fatigue failure *see fatigue*

fatigue life *see fatigue*

fault currents
- *see also flashover; leakage currents; short-circuit currents*
- h.v. insulators, arc, obs. *(Hungarian)* 3—30025

fault location
- bearing shells testing, using eddy currents *(Polish)* 3—27844
- scanning electron microscopes, book contribution 3—10126

f.d.m. *see frequency division multiplexing*

feature extraction *see pattern recognition*

feedback
- *see also control systems*
- climate behaviour, qualitative theory construction, based on system theory 3—39544
- distributed feedback lasers on anisotropic substrate, freq. generation scatt. mechanism 3—22892
- Fabry-Perot interferometer, stabilising method utilising feedback 3—16438
- fast reactor feedback, calc. of hydrodynamic effects 3—38175
- laser, solid, spike suppression using passive negative feedback 3—10547
- mass spectrometer, real-time signal enhancement, feedback control 3—22494
- metropolitan storm-sewer system, as standard regulator problem, optimal control law solution 3—28408
- optical waveguide on anisotropic substrate, mode suppression, freq. tuning 3—22891
- plasma-electron beam system, detection of feedback *(Russian)* 3—38464

feedback continued
  Nd:YAlG laser, stabilised mode locked, using electronic feedback, construction, performance 3−6484

Fermi-Dirac statistics *see quantum statistical mechanics*

Fermi gas *see fermion systems*

Fermi level
  amorphous semiconductors, electronic phenomena, tunnelling conduction near Fermi level 3−24415
  dilute alloys umklapp effect on low temp. thermal resistivity 3−1751
  electron gas, bulk modulus calc. using effective mass at Fermi level 3−18050
  electron gas, very low temps., quantum strong-mag. field limit 3−8077
  ion charge states determ. for e.s.r. by Fermi energy variation 3−2374
  metal, rel. to extended absorpt. edge fine struct., expt. test of theory 3−39200
  metal-semiconductor boundary, Imref behaviour, theory 3−30539
  oligoaniline derivatives, linear, photoelectric props., activation energy depend. on Fermi level position 3−24466
  secondary electron emission, Fermi energy depend. Boltzmann eqn. calc. 3−5253
  Au, electric-field-induced change, interpretation of electroreflectance spectra 3−30800
  Au, electron model for thermoelec. props. 3−38781
  Bi, diamagnetism theory 3−8338
  CdS/Cu_2S solar cell, band model 3−4946
  n-CdTe films, position in forbidden band *(French)* 3−27262
  α-Ce, elec. resist. and magnetisation obs. 3−8143
  Er, 4f-electron energy rel. to Fermi level, u.v. photoemission obs. 3−1991
  Eu, 4f-electron energy rel. to Fermi level, u.v. photoemission obs. 3−1991
  n-GaAs, electron irradiated, defect annealing, cluster formation 3−33558
  GaAs:Sn(Si, Zn), electron irrad., 'near-edge' absorption, annealing 3−33846
  n-GaSb, heavily doped density-of-states tails associated with L-minima of conduction band 3−30425
  GaSb:Te, role in low temp. thermal cond. *(French)* 3−4893
  Ge amorphous thin films, absorption and transport study of the pseudo gap 3−33775
  Ge self-interstitials, geometrical config., migration energy 3−33522
  $GeSb_2Te_4$, single cryst. characterisation 3−5279
  HgSe, density of states at Fermi level, magneto-quantum effects, determ. of band struct. 3−2003
  Mo and Mo-rich-Re and Mo-Nb alloys, rel. to Hall effect and resist. 3−38824
  MoS_2, layered, u.v. photoemission obs. 3−5256
  Nb and Nb-rich-Zr alloys, rel. to Hall effect and resist. 3−38824
  $NbSe_2$, layered, u.v. photoemission obs. 3−5256
  Ni, nucl. relax. rate of ^{101}Ru, rel. to virtual bound state 3−2442
  Ni base fcc ferromag. alloys with Co, Fe, Mn and Cr, density of states calc. 3−8328
  Ni:^{101}Ru, impurity states at this level from relaxation rates meas. 3−5147
  PbN_6, pure and doped thin films, effect of photodecomposition and doping 3−25084
  Pd, using augmented-plane-wave method 3−1983
  Pt, Fermi energy determ., two-zone model approx. *(Russian)* 3−30391
  Si, γ-irrad., zone-purified, induced defects, elec. properties 3−33841
  Si, heavily doped 3−24419
  Si, self-interstitials, geometrical config., migration energy 3−33522
  Si amorphous films, electronic transport and state distribution 3−8172
  Si-Ge alloy, e.p.r. of surface, temp. behaviour, Fermi level change rel. to surface states 3−5047
  Sm, 4f-electron energy rel. to Fermi level, u.v. photoemission obs. 3−1991
  Te thin films, obtained by CPD method 3−15130
  TlSe, reduced Fermi level, temp. depend. *(Japanese)* 3−38796
  U clean surfaces, electron binding energies determ. by photoelectron spectroscopy, 5f states density above Fermi energy 3−36977
  V_3Au cpds., ^{51}V spin-lattice relax., rel to density of states at Fermi level 3−2211
  VO, determ. from augmented-plane-wave method calc. 3−2016
  Yb, 4f-electron energy rel. to Fermi level, u.v. photoemission obs. 3−1991

Fermi liquid *see fermion systems*

Fermi surface
  alkali metal, positron annihilation, solid and liquid, thermal smearing, angular correlation 3−30393
  alloys, long period superstruct. and their interpretation 3−14729
  band model, phonons, lattice distortion, metal-insulator phase transition 3−38807
  brass, study using de Haas van Alphen effect 3−15117
  disordered systems, forward scattering approximation 3−20992
  electronic lifetime anisotropy determ., mosaic spread enhancement of dHvA-Dingle temp. 3−11845
  g-anisotropic metal, theory of many-body effects on conduction-e.s.r. 3−2395
  hexagonal metals, anisotropy in phonon scattering resistivity 3−7876
  Knight shift oscillations and spin-lattice relax in crossed fields 3−18382
  metal, k dependent pot., applic. to Ca and Al 3−8086
  metal, OPW model for pressure depend. 3−33788
  metal, phonon capture by electron from Fermi surface *(French)* 3−38780
  metal, review 3−1978
  metal, singularities of sound attenuation on Fermi surface topology change *(Russian)* 3−1700
  metal, topology, effect on thermal expansion and heat capacity *(Russian)* 3−8099
  metal, topology rel. to cyclotron wave dispersion 3−30507
  metal with convex Fermi surface, X-ray and particle scatt. on e.m. waves *(Russian)* 3−24151
  metallic thin film, rel. to galvanomag. transport coeffs. 3−30458

Fermi surface continued
  metals, polyvalent, umklapp electron-phonon scattering in low temp. resistivity 3−8140
  molecular crystals, temp. dependence of absorption bands intensities of the spectra at Fermi resonance, mass operator and band shape 3−2538
  noble metals, h.f. waves and Landau Fermi-liquid effects 3−21104
  phonon dispersion in systems with a planar Fermi surface 3−7890
  positron annihilation long slit angular distributions, analysis 3−30394
  quantum kinetic equation in Hartree-Fock approx. for Fermi surface in mag. field 3−30395
  semiconductor thin film, rel. to galvanomag. transport coeffs. 3−30458
  semiconductors, magnetoresistance, quantum and ultra quantum fields *(French)* 3−38860
  semimetals and narrow gap semiconductors, band struct. and electronic props. 3−33790
  size effect, radio frequency, Cd Fermi surface data *(Russian)* 3−11847
  spin density wave and soft phonon mode from nesting Fermi surface 3−36524
  superconductor, dirty, Fermi surface topology changes rel. to transition temp. 3−2196
  superconductor transition temp., effect of changes in topology of surface 3−18250
  thin conductors, Shubnikov-de Haas effect 3−21054
  type II superconductor with anisotropic Fermi surface, flux-line lattices at $T \sim 0$ 3−27328
  Ag, oscillatory magnetostriction meas. rel. to stress depend. of Fermi surface necks 3−18350
  Ag, stress derivatives, oscillatory magnetostriction 3−33779
  Al, k dependent potential calc. 3−8086
  Al, supercond. energy gap anisotropy, press. depend. 3−8287
  Al, uniaxial compression effects on the third-zone Fermi surface 3−8093
  Au, oscillatory magnetostriction meas. rel. to stress depend. of Fermi surface necks 3−18350
  Au, stress derivatives, oscillatory magnetostriction 3−33779
  Be, influence of non-locality of Shaw's model potential 3−1979
  Bi, Fermi hole surface anomalies, giant quantum oscillations in ultrasonic attenuation 3−18068
  Ca, APW calc. as function of lattice const. 3−18070
  Ca, de Haas-van Alphen effect obs. 3−36522
  Ca, k dependent potential calc. 3−8086
  Cd, dHvA meas. of Fermi surface changes with uniaxial compression 3−20998
  Cd, from l.f. e.m. wave spectra and damping 3−8216
  Cd, mag. field induced pseudo phase transition 3−24376
  Cd, magnetic surface states 3−8243
  Cd de Haas-van Alphen effect 3−30396
  Co, magnetoresistance and open orbit domains 3−18074
  Cs, compressibility from Fermi surface cross section press. depend. 3−33778
  Cs, u.s. attenuation, mag. field depend. 3−8094
  Cu, band profile in Fermi surface neck region of k-space 3−30837
  Cu, local exchange correlation potentials and the Fermi surface 3−8091
  Cu, magnetic field and temperature dependence of induced torque, anisotropy of closed-orbit torque 3−11884
  Cu, magnetoacoustic open-orbit antiresonances, obs. and mechanism 3−27207
  Cu, open orbit resonance, shear-wave attenuation polarisation depend. 3−8092
  Cu, oscillatory magnetostriction meas. rel. to stress depend. of Fermi surface necks 3−18350
  Cu, rel. to phase-shift anal. of impurity scatt. 3−33863
  Cu, stress derivatives, oscillatory magnetostriction 3−33779
  Cu-Au alloy, rel. to effect of press. on phase transition and ordered structs. of CuAu 3−18610
  Cu-Ge(Ni), positron annihilation study 3−15119
  Cu-Ni, positron annihilation study of Fermi surface necks 3−15118
  β'-CuZn, Fermi surface props. by the APW method, agreement with dHvA expts. 3−8097
  Fe, ferromagnetic, energy band calc. 3−38784
  Fe, paramag. and ferromag. states, self-consistent band calc. 3−21205
  FeGe, antiferromagnetic hexagonal, Fermi surface electrical resistivity and magnetic ordering 3−18327
  Ga, Fermi surface under pressure, quantum oscillations in magnetoacoustic absorpt. 3−33789
  Ga acoustic geometric and acoustic cyclotron resonances 3−8096
  GaAs, acoustic parametric processes discontinuities due to electron-phonon scattering near the Fermi surface 3−1750
  H, cubic atomic crysts., electronic struct., Bloch functions, Fermi surfaces, exact Hartree-Fock calcs. 3−33800
  Hg crystal, magnetoacoustic attenuation giant quantum oscills. 3−33784
  In, magnetoacoustic geometrical resons., interpretation 3−4945
  $InAs_xP_{1-x}$ solid solutions, compositions, transport properties, electron effective mass 3−33802
  Ir, de Haas-van Alphen obs. 3−38785
  Ir, press. effect, de Haas van Alphen effect obs. 3−15123
  Ir, variations with crystal potentials, relativistic APW exam. 3−4944
  Li-Mg, alloys optical properties, band structure, optical and soft X-ray spectra, ellipsometry 3−30836
  $LiNbO_3$, polariton-biphonon Fermi reson. *(Russian)* 3−11708
  Mg, Fermi surface pseudopotential calcs. convergence props. 3−33783
  Mg-Li, alloys optical properties, band structure, optical and soft X-ray spectra, ellipsometry 3−30836
  Mo, press. effects, de Haas-van Alphen effect obs. 3−15122
  Mo-Re alloy crystals Hall effect, Mo electron configuration changes due to Re addition 3−8155
  Ni, ferromagnetic, self-consistent calculation of energy bands 3−18073
  NiS, paramag. metal to antiferromag. semimetal transition, density of states at Fermi surface 3−36540
  Os, press. effect, de Haas van Alphen effect obs. 3−15123

Fermi surface continued
Pb, Fermi surface pseudopotential calcs. convergence props. 3 − 33783
Pd, L-centred pocket of Fermi surface existence, magnetoacoustic evidence 3 − 8095
Pd, press. dependence, electron-phonon interactions 3 − 18075
Re, press. effects, de Haas-van Alphen effect obs. 3 − 15122
Ru, press. effect, de Haas van Alphen effect obs. 3 − 15123
Sb, rel. to temp. depend. of magnetocond. coeffs. 3 − 15183
Sb-Sn alloys, de Haas-van Alphen effect study 3 − 36527
Sn, white band-mass calculations, PW and APW formalisms, one electron crystal potential parameters 3 − 30392
γ-U, relativistic energy band structure and props. 3 − 38788
VO_2, calc. using tight-binding interpolation 3 − 24379
VO_2, metallic, rel. to energy band calc. 3 − 36541
W, high field magnetoacoustic investigation 3 − 20995
W, press. effects, de Haas-van Alphen effect obs. 3 − 15122
Zn, dHvA meas. of Fermi surface changes with uniaxial compression 3 − 20998
Zn, pressure effects *(Russian)* 3 − 1974
ZnCd and ZnHg, axial ratio dependence of mag. susceptibility, Fermi surface charge 3 − 27359

fermion systems
see also electron gas; helium gas; liquid helium-3
alkali metals, Landau Fermi liquid parameters anisotropy, electron-phonon interactions 3 − 27203
anisotropic Fermi liquids, simple models 3 − 33770
basic linked cluster theorem, simple proof 3 − 6358
chaotic beams, study of detection and emission processes in wave-packet formalism 3 − 26154
collective modes, restrictive RPA calcs., influence of exchange interaction on plasmon behaviour 3 − 6352
critical exponents, skeleton graph expansion, many body perturbation theory 3 − 16779
current algebra representations for infinite free Bose or Fermi systems at finite temp. 3 − 28973
degenerate charged fermion fluid, mechanical instability 3 − 30380
degenerate Fermi liquid, decay time of perturbations 3 − 6351
electron correlation consideration in the second quantization method *(Russian)* 3 − 1968
excitations, elementary, in Liouville space, statistics and interactions 3 − 26156
extended Fermi-gas model description of nuclear excitation energy 3 − 23240
Fermi liquid, application of ultralow temperature techniques 3 − 35383
Fermi liquids, role of paramagnons in anomalous specific heat 3 − 11772
Fermion fields, covariant T-product and gauge-invariant vacuum polarisation amplitude 3 − 13809
fields, covariant T-product and gauge-invariant vacuum polarisation amplitude 3 − 13809
gas thermodynamic equilibrium states, kinetic eqns. for the Green functions 3 − 22742
Hartree and Thomas-Fermi approximations for soln. in large particle-number limit *(Russian)* 3 − 13647
Heisenberg ferromagnet with spin 1/2, comparison of Pauli operator and drone-fermion calc. methods 3 − 21202
Ising model soln. with pure triplet interactions, free-fermion model 3 − 28978
Landau's Fermi-liquid parameters, calc. for pure neutron matter 3 − 23242
lattice system with quadratic Hamiltonian time evolution 3 − 10385
magnetism, introduction to the theory, monograph 3 − 2224
many body problem, solvable models construction 3 − 35628
many-body problems, book 3 − 20990
many-fermion inhomogeneous system at finite temp., Green's function eqn. of motion 3 − 16744
metals, parametric magnetization instability of electron liq. 3 − 27211
model system with four-fermion interaction, new method for calc. of quasiaverages 3 − 6355
noninteracting systems, one dimensional, quantum path integrals and reduced density matrices 3 − 16747
nuclear ground state energy variations due to pairing correlations in Fermi system model *(Russian)* 3 − 19787
nuclear liquid drop model, effect of change in number of particles 3 − 17176
pairwise-interacting particles ground state energies, set of inequalities 3 − 22741
quantisation rule for constrained classical model 3 − 6310
quantum crystals, phenomenological theory 3 − 24238
quasi-free state thermodynamics, variational formulation 3 − 37898
quasi-particles in mag. field, quantum kinetic equation 3 − 30395
shifted Fermi gas model of nuclear level density, calc. of isomer ratios for ^{108,110}Pd, ^{196}Pt, comparison with expt. 3 − 14124
specific heat, Landau-theory approach, appl. to liquid He-3 at low press. 3 − 15043
spin 1/2 or 1 interacting with external system, pseudofermion representation 3 − 614
superconductivity theory for interacting fermions system with rigid boundaries 3 − 38913
superconductors, collective excitations 3 − 18239
two-component isotropic fluid, e.m. props. *(Russian)* 3 − 21029
wave function in force field 3 − 11770
zero-field free-fermion model, transfer matrix direct diagonalisation 3 − 37900
K cyclotron phase resonance transmission at 116 GHz, Fermi-liquid effects 3 − 20999
n-methyl phenazinium tetracyanoquinodimethan, antiferromag., spin fluctuations with fermion representation 3 − 15432
Na cyclotron phase resonance transmission at 116 GHz, Fermi-liquid effects 3 − 20999

fermions
see also baryons; fermion systems; leptons
C* algebra, gauge transformation of second type, applic. 3 − 19664
correlated fermion state, construction of excitation operator algebra 3 − 10346
creation and annihilation operators in relativistic Fock space 3 − 6543
dual-fermion model, gauge identities 3 − 10600
dyons, dyonium and parastatistics 3 − 35771

fermions continued
pair composites, Bose condensation 3 − 38121
parafermion algebras of order 2, representation theory of SO(2N + 1) 3 − 35737
quarks with integral charge, heuristic model *(French)* 3 − 29178
radiation from Fermi-particles in field of two e.m. waves *(Russian)* 3 − 14017
radiation from Fermi-particles in field of two e.m. waves *(Russian)* 3 − 14018
Sehgal's low-mass fermion for $K_l^0 \to \mu\mu$ decay, evidence against hypothesis 3 − 32649
Thirring model of fermion fields, expansion of C-number operators on the light cone 3 − 13797
vertices and diffractive dissociation 3 − 10769
$K_2^0 \to \mu^+\mu^-$ puzzle, fermion loop model 3 − 829

fermium
No entries

fermium compounds
No entries

ferrimagnetic properties of substances
see also ferrimagnetism; ferrites; garnets
anisotropy, method for separating components 3 − 5115
ferrimagnet, coercivity behaviour nr. compensation temp. 3 − 36750
ferrite spinels, mixed, nonstoichiometry of aging of mag. props. 3 − 21222
garnet, bubble domain motion, crystal defect influence 3 − 36742
garnets, stress birefringence meas. 3 − 21381
magnetic bubble domain material, characterization using X-ray topography 3 − 34156
orthoferrite, bubble and ring domains, magneto-optical obs. of structure 3 − 34159
orthoferrites, interference patterns, at domain boundary, theory 3 − 5116
perovskite, complex, long-range ordering study using mag. meas. 3 − 24579
rare earth $Co_5(Co_{17})$, ferrimag., rare earth contrib. to mag. anisotropy 3 − 34151
remanent state ferrites, magnetic losses characterisation by average permeability tensor 3 − 21271
spinels, Curie points and Weiss molecular field coeffs. 3 − 30623
$Al_2Mn_3(SiO_4)_3$ spessartite type garnet, obs. of rhombohadral mag. structure 3 − 21247
$Ba_2Co_2Fe_{12}O_{22}$, mag. anisotropy, n.m.r. study 3 − 36801
$Ba_3Co_{2-x}Fe_{24}O_{41}$, mag. anisotropy, n.m.r. study 3 − 36801
$Ba_3Co_2Fe_2O_4$ film, arc plasma deposited 3 − 36772
$BaFe_{12}O_{19}$, internal domain structure, power patterns and Faraday effect obs. in i.r. 3 − 38990
$BaFe_{12}O_{19}$ film, arc plasma deposited 3 − 36772
$Ba_2Ni_2Fe_{12}O_{22}$, mag. anisotropy, n.m.r. study 3 − 36801
BaO ferrites, effects of Bi_2O_3, sintering temperature *(Korean)* 3 − 21263
$Ba_{3-x}Sr_xZn_2Fe_{24}O_{41}$, hexagonal type-Z, noncollinear mag. struct. *(Russian)* 3 − 8372
$Ba_2Zn_2Fe_{12}O_{22}$ film, arc plasma deposited 3 − 36772
$Bafe_{12}O_{19}$ substituted ferrite, coercive force measurement 3 − 34165
$Bi_{3-2x}Ca_{2x}Fe_{5-x}V_xO_{12}$ system, porosities hysteresis, resonance linewidths, mag. inhomogeneity effects 3 − 18342
$Ca_3Cr_2(GeO_4)_3$, mag. struct., neutron diffr. obs. 3 − 24569
$Ca_3Fe_2(GeO_4)_3$, mag. struct., neutron diffr. obs. 3 − 24569
$Ca_xNi_{1-x}Fe_2O_4$ system, determination for phase structure analysis 3 − 8379
Cd rare-earth chalcogenide spinels, determ. of Curie-Weiss law behaviour from susceptibility meas., saturation magnetic moments 3 − 7685
$Co_xZn_{1-x}Fe_2O_4$, mag. permeability, freq. and temp. depend. *(Russian)* 3 − 8349
$CrPt_3$, transition from ferrimag. to paramag. type behaviour with cold working 3 − 21237
$Cr_{0.30}Pt_{0.70}$, ordered and disordered, sp. ht., 1.2-4.2K 3 − 24567
Cr_2SSeTe, meas. of molar susceptibility and molar spontaneous magnetisation, 80-600 K, determ. of Curie point *(Russian)* 3 − 12010
Cu based spinel, mag. props. rel. to structure and cooperative Jahn-Teller distortion 3 − 30632
$DyFeO_3$, magnetostriction, low temp. 3 − 34175
$Dy_{1-x}Th_xFe_3$, magnetisation vs. temp., lattice consts. vs. temp. 3 − 34164
p-$EuCr_2Se_4$, doped, hysteresis, magnetization and coercive force 3 − 27385
$EuEr_2Ga_{0.7}Fe_{4.3}O_{12}$ epitaxial film, for bubble domains, variation of magnetiz., Curie temp., and Ga/Fe ratio with growth temp. 3 − 34157
$Eu_{2.2}Gd_{0.8}Al_{0.6}Fe_{4.4}O_{12}$, growth induced uniaxial anisotropy 3 − 2305
$EuWO_4$, ferrimagnetism of single crystal 3 − 30605
Fe-Cr spinel, magnetoresist. anomalies at Curie point 3 − 30462
$Fe_{3-x}Cr_xO_4$, Mossbauer obs. of cation distrib. and mag. structure 3 − 24641
Fe_2GeS_4, cryst. and mag. structs. at 85 K and 4.2 K, mag. transitions *(French)* 3 − 27373
GdFe garnet, anomalous u.s. attenuation near compensation temp. 3 − 2275
$GdFe_x(Co_x)(Ni_x)$, spontaneous magnetiz., susceptibility, Neel model interpret. *(French)* 3 − 27358
$HoFe_3$, powder neutron diffraction obs. of Ferrimag. coupling 3 − 18325
$HoFeO_3$, magnetostriction, low temp. 3 − 34175
$Li_{0.5}Fe_{2.5}O_4$, spin waves and exchange interactions, neutron scattering obs. 3 − 21252
LiO_2-MgO-MnO-Fe_2O_3 ferrite powder, specific saturation magnetisation *(Russian)* 3 − 15386
Mg ferrite, magnetostriction and anisotropy, ferrimag. resonance obs. 3 − 30673
$MgFe_2O_4$, excitation of magnetoelastic waves *(Russian)* 3 − 8411
$Mg_xMn_{1-x}Fe_2O_4$ film, rel. to use as phase diffr. grating 3 − 36862
Mn-Zn ferrite, solid state O_2 content depend. *(German)* 3 − 8344
$Mn_3Al_2(GeO_4)_3$, mag. struct., neutron diffr. obs. 3 − 24569
Mn_2As-Mn_2Sb system neutronographic investigation of magnetic transformations *(Russian)* 3 − 2291
$Mn_3Cr_2Ge_3O_{12}$ garnet, intrasublattice exchange interactions obs. *(Russian)* 3 − 2266

ferrimagnetic properties of substances continued
$NaCa_2Ni(Co)_2V_3O_{12}$, garnet, absorpt. spectra obs. of $Ni^{2+}(Co^{2+})$ ions, crystal field theory 3—21434
Na_2NiFeF_7, mag. structure and transition to paramag. 3—2301
$NiCr_2O_4$, mag. struct., neutron diffr. appl. of representation anal. 3—24571
$NiFe_{2-x}Al_xO_4$, spinel, magnetisation in ferrimag. and paramag. regions rel. to thermal treatment 3—12033
$NiFe_2O_4$ film, arc plasma deposited 3—36772
$Pb(Fe_{2/3}U_{1/3})O_3$, Neel temp. and saturation mag. moment 3—21231
$SnCr_2S_4$, ferrimag., prep. by heating method, Curie temp. and cell dimensions meas. 3—31261
spin wave theories in the linear approximation 3—21251
Sr ferrite, Al substituted, domain structure, demagnetis. effects 3—36747
$Sr_3Cr_2WO_9$, perovskite type, susceptibility meas. *(French)* 3—24080
$Sr(Fe_{2/3}U_{1/3})O_3$, Neel temp. and saturation mag. moment 3—21231
$Y_{3-2x}Ca_{2x}Fe_{5-x}V_xO_{12}$ system, porosities hysteresis, resonance linewidths, mag. inhomogeneity effects 3—18342
$Y_{3-x}Ce_xFe_5O_{12}$, temp. depend. of magnetostriction, ferromag. reson. study *(Russian)* 3—12046
$YFeO_3$, domain wall mobility, nonlinear applied field depend. 3—30661
YIG, magnetization near Curie point 3—38980
YIG, parallel spin-wave pumping, theory and expt. 3—34143
YIG, spin waves excited by parallel pumping, instability threshold, laser radiation effects 3—34141
YIG film, arc plasma deposited 3—36772
YIG:Cu, octahedrally coordinated Cu^{2+} ions contrib. to magnetocryst. anisotropy 3—2304
YIG:Ge substituted, anisotropy and magnetostriction, ferromag. resonance obs. 3—5136
YIG:Si, mag. anisotropy i.r. induced changes 3—30644
YIG:$Si^{4+}(Ge^{4+})(Ca^{2+})$, mag. after-effect, electronic hopping processes 3—24591

ferrimagnetic resonance
amplified echoes in ferrites, phenomenological theory *(Russian)* 3—27418
ferrite, amplified magnetostatic echo 3—15427
ferrite medium modelling in static approx. *(Russian)* 3—24618
ferrite sphere *(Russian)* 3—24617
spin echo amplification in ferrite sphere *(Russian)* 3—39034
$BaIn_xFe_{12-x}O_{19}$ ferrite, mag. struct., reson. fields temp. depend., torque angular depend. 3—21250
Dy theory, spin system time evolution 3—2406
Li-ferrite, magnetostriction constants meas. in ordered and disordered states 3—8406
Mg ferrite, magnetostriction and anisotropy obs. 3—30673
$Ni_xCd_{1-x}Fe_2O_4$, temp. dependence of intensity of resonance field, line width due to resonant damping and g-factors' 20-360°C *(Russian)* 3—12064
Tb theory, spin system time evolution 3—2406
$Y_{3-2x}Ca_{2x}Fe_{5-x}V_xO_{12}$, rel. to mag. inhomogeneity origin 3—18342
YIG, and mag. domains rel. to i.r. obs., effect of crystal imperfections 3—27379

ferrimagnetism
see also ferrimagnetic properties of substances
ferrimagnet, three-sublattice, mag. struct. induced by field *(French)* 3—38972
magnetism, introduction to the theory, monograph 3—2224
Neel type uniaxial Heisenberg ferrimag., spin wave theory, external mag. field effects 3—11995
Neel type uniaxial Heisenberg ferrimag., spin wave theory, mag. props. 3—15325
quantum theory, isotropic two sublattice ferrimagnet, applied magnetic field, Green's functions 3—38941
spinel containing two types of ions, Weiss mol. field coeffs. 3—2229
$Fe_{1-x}S$, semiconducting uniaxial ferroelectric, model 3—8531

ferrite applications
see also ferrite devices
No entries

ferrite devices
see also ferrite applications
core memory stack, for solar probe project, construction 3—3393
magnetic head, from hot pressed Ni-Zn ferrite 3—2756
magnetic heads, cores and microwave elements, hot pressing method *(Polish)* 3—8972
wire chamber ferrite core readout with software decoding 3—323
BaO ferrite magnets, fabrication, effects of Bi_2O_3, sintering temperature *(Korean)* 3—21263

ferrites
see also ferrimagnetic properties of substances; ferrimagnetism; ferrite applications; ferrite devices
amplified echoes, phenomenological theory *(Russian)* 3—27418
amplified magnetostatic echo 3—15427
ceramic permanent magnets, remanence, X-ray determination, technique, applications *(German)* 3—12006
cermets, ferrites, wear resistant hot pressing production methods *(Russian)* 3—27746
coercivity behaviour, nr. compensation temp. 3—36750
cubic spinel compounds, possible antiferroelec. behaviour, rel. to cryst. struct. 3—30773
Curie and compensation points, meas. using differential test device 3—37667
e.m. wave interactions, definitions 3—15353
ferrite-titanate ceramic substrate, composite formation, hot pressing 3—37079
film prep. by oxidation of metal films, electron microscope exam. of microstruct. 3—27196
flux growth of hexagonal single crysts. with Y struct. *(German)* 3—24800
hexagonal ferrite, ferromag. resonance obs. of magnetogyric ratio anisotropy 3—36730
hot pressing, for device appl. *(Polish)* 3—8972
interference patterns, at domain boundary, theory 3—5116
intermediate phase obs. during form. *(Russian)* 3—15736
isotropic, cross section for crit. neutron scatt., calc. 3—34136

ferrites continued
magnetic fluctuations relax. rel. to anisotropic dipole mag. forces above Curie temp. 3—8412
magnetised, construction and applic. of Brillouin diagrams 3—22829
magnetised, e.m. wave propagation, group velocity diagrams 3—22813
magnetoacoustic resonance, magnetoelastic coupling *(Russian)* 3—12062
magnetostrictive ferrite, u.s. wave propagation consts., low temp. depend. 3—36367
melt growth, stoichiometry and perfection 3—12277
modelling of gyrotropic medium in static approx. *(Russian)* 3—24618
orthoferrite, bubble and ring domains, magneto-optical obs. of structure 3—34159
orthoferrite mag. bubble domain material growth and analysis *(German)* 3—5262
orthoferrites, flux grown, induced nonperiodic growth striations, growth program 3—2662
orthoferrites, spin reorientation temp., phase transitions, heat capacity, domain structure and energy 3—39003
oxyfluoride spinels, elec. cond., hopping mechanism *(French)* 3—27251
rare earth orthoferrite, hyperfine interactions and Neel temp. rel. to covalency parameters 3—21191
rare earth orthoferrites, mag. interactions 3—34107
rare earth orthoferrites, magnetisation curves, reversal mechanism 3—38997
rare earth orthoferrites, paramag. susceptibility, room temp. and 77K 3—21213
rare earth orthoferrites, paramag. susceptibility anisotropy, cryst. field parameters 3—34094
rare earth orthoferrites, $R_{1-x}Ca_xFe_{1-x}Sn_xO_3$, magnetially non-equivalent states of atoms 3—34271
rare earth orthoferrites, ring domains, unidirectional dimens. change in cyclic mag. field 3—21277
remanent state, magnetic losses characterisation by average permeability tensor 3—21271
single crystal state of mag. uniaxial ferrite, controlled motion of cylindrical mag. domains 3—36767
sphere, internal magnetic field *(Russian)* 3—24617
spin echo amplification in ferrite sphere *(Russian)* 3—39034
spin wave propag. theory in inhomogeneous static mag. field 3—5112
spinel, coercive force anomalies in compensation temp. region 3—8394
spinel with mag. ions at B-sites only, mag. props. *(Japanese)* 3—2282
spinels, growth using B_2O_3-Bi_2O_3-BaO flux system 3—2663
spinels, mixed, nonstoichiometry of aging of mag. props. 3—21222
structure of hexagonal ferrites, direct lattice imaging for stacking sequence recognition 3—38530
u.s. nondestructive testing, for magnetic memory heads *(Polish)* 3—12491
Ba, preferred orientation during hot pressing *(Russian)* 3—15743
$Ba_2Co_2Fe_{12}O_{22}$, mag. anisotropy, n.m.r. study 3—36801
$Ba_3Co_{2-x}Fe_{24}O_{41}$, mag. anisotropy, n.m.r. study 3—36801
$Ba_3Co_2Fe_2O_4$ film, arc plasma deposited, mag. props. 3—36772
$Ba_3Co_2Fe_{24-x}Sc_xO_{41}$, Sc ions influence on hexaferrite magnetic structure *(Russian)* 3—15372
$BaFe_{12}O_{19}$, internal domain structure, power patterns and Faraday effect obs. in i.r. 3—38990
$BaFe_{12}O_{19}$, magnetoplumbite structure, anisotropy of hopping cond. and thermoelec. power 3—38829
$BaFe_{12}O_{19}$ film, arc plasma deposited, mag. props. 3—36772
$BaFe_{12}O_{19}$ substituted, coercive force measurement 3—34165
$Ba_4Fe_9O_{20}H_6$, hydrothermally synthesized, cryst. struct. 3—17767
$Ba_8Fe_{13}O_{30}H_6$, cryst. struct. and antiferromag. 3—17768
$BaIn_xFe_{12-x}O_{19}$, mag. struct., reson. fields temp. depend., torque angular depend. 3—21250
$Ba_2Ni_2Fe_{12}O_{22}$, mag. anisotropy, n.m.r. study 3—36801
BaO.6 Fe_2O_3, texture and reaction mechanism in the formation 3—5413
$Ba_{3-x}Sr_xZn_2Fe_{24}O_{41}$, hexagonal type-Z, noncollinear mag. struct. *(Russian)* 3—8372
$Ba_2Zn_2Fe_{12}O_{22}$ film, arc plasma deposited, mag. props. 3—36772
$Be_{3-2x}Ca_{2x}Fe_{5-x}V_xO_{12}$ system, porosities hysteresis, resonance linewidths, mag. inhomogeneity effects 3—18342
$Bi_{3-2x}Ca_{2x}Fe_{5-x}V_xO_{12}$, neutron diffraction obs. of structure 3—8369
$BiFeO_3$, internal mag. field obs. by Mossbauer effect 3—27447
CAVBIG, self interaction of finite amplitude magnetoelastic waves 3—39035
$Ca_2Fe_2O_5$, elec. field gradient tensors at two nonequivalent ferric sites 3—24386
$Ca_xN_{1-x}Fe_2O_4$, dielectric losses and dielectric constant 3—15451
$Ca_xNi_{1-x}Fe_2O_4$, mag. props., phase equilib. 3—8379
$CaO_xNiO_{1-x}Fe_2O_3$, dielectric props. *(French)* 3—34284
CaO.FeO.Fe_2O_3, chem. comp. and precip. microstruct. *(French)* 3—8986
$Cd_{1-x}Co_xFe_2O_4$, paramag. region, elec. field gradients, Mossbauer obs. 3—34268
$Cd_{1-x}Ni_xFe_2O_4$, paramag. region, elec. field gradients, Mossbauer obs. 3—34268
$CoCr_2S_4$, vacuum hot pressed, magneto-optic material 3—18435
$Co_xFe_{3-x}O_4$ film prep. by oxidation, electron microscope exam. of microstruct. 3—27196
$Co_xNi_{1-x}Fe_2O_{4\mp y}$, magnetic anisotropy temp. depend. 3—36728
Co_3O_4, low-spin cpd., cryst. struct. 3—20720
$Co_xZn_{1-x}Fe_2O_4$, mag. permeability, freq. and temp. depend. *(Russian)* 3—8349
$CuFe_2O_4$, cubic-tetragonal transform. and induced uniaxial anisotropy *(French)* 3—15382
$Cu_{1-x}Ni_xFe_2O_4$, extraordinary Hall const., resist., 293-550K 3—24459
$DyFeO_3$, magnetostriction, low temp. 3—34175
$ErFeO_3$, spin reorientation, n.m.r. of ^{57}Fe 3—21332
Fe-Cr-Co-Mo alloy precipitation of ferrite and austenite phases, structural and kinetic features 3—8787
Fe-Mn-Zn, internal friction, delta E-effect and stress sensitivity in alternating magnetic field 3—39009

ferrites continued
- Fe-Ni-Cu, internal friction, delta E-effect and stress sensitivity in alternating magnetic field 3–39009
- Fe_2O_3, NiO-ZnO-Fe_2O_3 formation 3–2812
- Fe_3O_4, magnetite, optical props. for band structure at Verwey transition 3–2506
- Fe_3O_4 (magnetite) single crystals, relaxation processes at low temp. rel. to phase transformation and magnetic viscosity *(Russian)* 3–12645
- αFe_3O_4 film prep. by oxidation, electron microscope exam. of microstruct. 3–27196
- Fe_3O_4 magnetite, band theory of pair-localized electrons 3–2012
- $Ga_xMn_yFe_{3-(x\|y)}O_4$, cryst. growth, Bridgmen method and characterization 3–12267
- $Gd_{3-x}Ca_xFe_{5-x}Sn_xO_{12}$ ferrite-garnets, temp. dependence of EMR and FMR linewidths *(Russian)* 3–36795
- $GdFeO_3$, etch patterns on (001) surface 3–8031
- $HoFeO_3$, mag. props., spin reorientation, 50-120 K *(French)* 3–27380
- $HoFeO_3$, magnetostriction, low temp. 3–34175
- Li-Cr ferrite film, LPE growth on MgO, obs. of substrate contamination 3–1928
- Li-ferrite, magnetostriction constants meas. in ordered and disordered states by ferrimag. reson. 3–8406
- $(Li_{1-x}Fe_x)\,[Li_{x-0.5}Fe_{2.5-x-a}Cr_a]O_4$, paramag. props. 3–38958
- $Li_{0.5}Fe_{2.5-t}Al_tO_4$, lowered Fe^{3+} mag. moment in paramag. region 3–21212
- $Li_{0.5-\alpha}Fe_{2.5}O_{4-\alpha/2}$, nonstoichiometric, point defects, X-ray diffr. obs. 3–33520
- $Li_{0.5}Fe_{2.5}O_4$, spin waves and exchange interactions, neutron scattering obs. 3–21252
- $Li_xMn_yFe_{3-(x\|y)}O_4$, cryst. growth, Bridgman method and characterization 3–12267
- LiO_2-MgO-MnO-Fe_2O_3 powder, synthesis and magnetic properties *(Russian)* 3–15386
- Mg, magnetostriction and anisotropy, ferrimag. resonance obs. 3–30673
- Mg-Mn ferrite films, remagnetization rate and mobility of domain boundaries *(Russian)* 3–8398
- $Mg_{1-y}Co_yFe_2O_4+\gamma'$, relaxation of Co^{2+} ions in single crystals with different inversion degrees 3–15379
- $MgFe_{2-x}In_xO_4$, X-ray diffraction and γ-resonance obs. of spinel structure 3–24087
- $MgFe_2O_4$, excitation of magnetoelastic waves *(Russian)* 3–8411
- $MgFe_2O_4$, thin films, electron diffraction superlattice lines 3–38569
- $Mg_{0.9}Fe_{2.1}O_4$ ferrite, cation redistrib. rates, oxidation effects, saturation magnetisation obs. 3–15387
- $Mg_xMn_{1-x}Fe_2O_4$ film, use as phase diffr. grating 3–36862
- $(MgO)_{0.55}(Fe_2O_3)_{0.45}$, anion vacancies in magnetically square hysteresis loop 3–17804
- $(MgO)_{0.30}(MnO)_{0.35}(Fe_2O_3)_{0.35}$, anion vacancies in magnetically square hysteresis loop 3–17804
- Mn, electrical conductivity temp. depend. 10-100K 3–5001
- Mn-Zn, mag. props,, solid state O_2 content depend. *(German)* 3–8344
- Mn-Zn ferrites, low resistivity, resonant modes in ferromagnetic resonance 3–2398
- $Mn(CrFe)O_4$ Mossbauer study, angular spin configurations of ^{57}Fe nuclei, compensation point, magnetic moments 3–36827
- $MnFe_{2-x}In_xO_4$, X-ray diffraction and γ-resonance obs. of spinel structure 3–24087
- $MnFe_2O_4$, permittivity tensor, visible region, magnetooptic study *(Russian)* 3–8551
- $MnFe_2O_4$, sintering in continuous kilns *(French)* 3–34623
- $Mn_{1.9}Fe_{1.1}O_4$, cubic-tetragonal transition, cation valencies, Mossbauer obs. 3–1798
- $Mn_xFe_{3-x}O_4$, elec. resist. and Seebeck coeff., 100-1000K 3–5010
- $Mn_{0.8}Fe_{0.2}[Mn_{0.2}Fe_{1.8}]O_4$, thin films, electron diffraction superlattice lines 3–38569
- $MnGa_xFe_{2-x}O_4$, chem. and X-ray anal. of inhomogeneity *(Russian)* 3–14971
- $Mn_{1.5-x}Me_xFe_{1.5}O_4$ (Me=Ni or Cr), induced mag. anisotropy 3–15381
- $Mn_xMg_{1-x}Fe_2O_4$, chem. and X-ray anal. of inhomogeneity *(Russian)* 3–14971
- MnO-Fe_2O_3-B_2O_3 glassy system, prepn. and mag. props. 3–18726
- $MnZnFe_2O_4$, comp. variations during sintering *(French)* 3–34624
- $Mn_{1-x}Zn_xFeO_4$, Mossbauer spectra, Fe^{3+} ions nonequiv. positions rel. to relax. effects *(Russian)* 3–39061
- $Mn_xZn_{1-x}Fe_2O_4$, chem. and X-ray anal. of inhomogeneity *(Russian)* 3–14971
- NbC, stability in ferrite 3–15706
- $Nd_{0.95}Ca_{0.05}Fe_{0.95}Sn_{0.05}O_3$, reorientation of induced mag. field at diamag. Sn_2 atom 3–34252
- Ni ferrite, contribution of tetrahedral Ni^{2+} ion to magnetocrystalline anisotropy 3–2303
- Ni-Zn, hot pressed, prep. for mag. heads 3–2756
- Ni-Zn-Co, mag. permeab. and losses, freq. and temp. depend. 3–15395
- $Ni_xCd_{1-x}Fe_2O_4$, temp. dependence of intensity of resonance field, line width due to resonant damping and g-factors' 20-360°C *(Russian)* 3–12064
- $NiFe_2O_4$ ferrite, addition of CaO, effect on electrical conductivity *(French)* 3–8362
- $NiFe_2O_4$ film, arc plasma deposited, mag. props. 3–36772
- $NiFe_2O_4$ mixing process, raw material components, solid-state reactivity *(German)* 3–12428
- $NiFe_2O_4$ with CaO additions and $Ca_xNi_{1-x}Fe_2O_4$, Verwey mechanism of electronic cond. and dielec. polarisation *(French)* 3–34286
- $Ni_xFe_{3-x}O_4$ film prep. by oxidation, electron microscope exam. of microstruct. 3–27196
- $Ni_xMn_{1-x}Fe_2O_4$, cryst. growth, Bridgman method and characterization 3–12267
- $Ni_{0.8}Zn_{0.2}Co_xFe_{2-x}O_4$, temp. and freq. depend. of mag. losses and permeab. 3–8348
- $Ni_{1-x}Zn_xFe_2O_4$ powders, arc plasma deposition on ceramic substrates, magnetic properties 3–8378
- $PbFe_{12}O_{19}$, magnetoplumbite structure, anisotropy of hopping cond. and thermoelec. power 3–38829
- $Pb(Fe_{2/3}U_{1/3})O_3$, cryst. struct. and mag. props. 3–21231

ferrites continued
- $Pb(Fe_{2/3}W_{1/3})O_3$, cryst. struct. and mag. props. 3–21231
- Sr, Al substituted, domain structure, demagnetis. effects 3–36747
- $SrFe_{12}O_{19}$, magnetoplumbite structure, anisotropy of hopping cond. and thermoelec. power 3–38829
- $Sr(Fe_{2/3}U_{1/3})O_3$, cryst. struct. and mag. props. 3–21231
- $Tm_3Fe_5O_{12}$, mag. anisotropy, 77-293K 3–34152
- $Y_3Al_xFe_{5-x}O_{12}$, chem. and X-ray anal. of inhomogeneity *(Russian)* 3–14971
- $Y_{3-2x}Ca_{2x}Fe_{5-x}V_xO_{12}$ system, porosities hysteresis, resonance linewidths, mag. inhomogeneity effects 3–18342
- $YFeO_3$, domain wall mobility, nonlinear applied field depend. 3–30661
- $Y_3Fe_5O_{12}$, etching and polishing in orthophospheric acid, rates of action *(Russian)* 3–11820
- $Y_3Ga_xFe_{5-x}O_{12}$, chem. and X-ray anal. of inhomogeneity *(Russian)* 3–14971
- YIG, polycryst. ceramic, reactive hot pressing 3–31123
- YIG, self interaction of finite amplitude magnetoelastic waves 3–39035
- YIG film, arc plasma deposited, mag. props. 3–36772
- $YbFeO_3$, electron beam induced charge storage memory with read-out and erasure 3–35504
- $Zn_xNi_{1-x}Fe_2O_4:Fe^{3+}$, supertransferred hyperfine fields of Fe^{3+}, n.m.r. study 3–2407
- $Zn_xNiFe_{2-x}O_{4-x}F_x$, spinel structure, props. in paramag. domain, molecular field factors *(French)* 3–38962

ferroacoustic resonance
- magnetoelastic instability, ferromagnetics, anisotropy effects 3–39010
- YIG, ferroacoustic interaction with Rayleigh surface waves 3–24596

ferroelasticity
- *see also plastic deformation; solid-state phase transformations*
- coupled ferroelastic crystals and cooperative phenomena 3–30176
- ferroelectrics and ferroelastics having the index of faintness unequal to the cell multiplicity, discussion 3–2499
- ferroic state shift, second order, mech., elec. and coercive forces 3–12101
- materials with memory and internal changes, gradient theory 3–38607
- memory materials, reduction of deformation theories to alternative properties of constitutive functionals 3–17907
- steel, austenitic stainless, partial shape memory effect 3–18677
- β' AgCd alloys, marmem effect 3–30979
- Au-Cd alloy, thermoelastic martensite, lattice softening, ferroelasticity and shape memory effect 3–14907
- $AuCuZn_2$, thermoelastic martensite, lattice softening, ferroelasticity and shape memory effect 3–14907
- Cu-Al-Mn alloy, martensitic transform., β'-phase deform. influence *(Russian)* 3–18560
- Cu-Zn-Si alloys, pseudoelasticity and shape memory effect 3–21702
- $Gd_2(MoO_4)_3$, ferroelastic-ferroelec., antiphase boundaries and their interactions with domain walls 3–24659
- β'NiAl, thermoelastic behaviour of martensitic transformation 3–21573
- Pt complex, $(C_3H_7NH_3)_2PtCl_6$, hydrostatic pressure depend. of phase transition 3–38614
- Sn complex $(C_2H_7NH_3)_2SnCl_6$, hydrostatic pressure depend. of phase transition 3–38614

ferroelectric devices
- film applications, review 3–8543
- memories, reversible domain polarisation by laser beam, triglycine sulphate plate *(French)* 3–22967
- temperature stability of ferroelectric microthermostats *(Russian)* 3–9849

ferroelectric domains *see electric domains*

ferroelectric materials
- *see also antiferroelectric materials; barium titanate; ferroelectric phenomena; Rochelle salt*
- acoustic transducer ceramics, nonlinearities 3–18686
- ammonium hydrogen chlorotartrate and deuterated analogue, phase transition phenomena 3–18418
- anisotropic, birefringence and dichroism at submillimetre wavelengths *(Russian)* 3–12197
- apparatus for investigating the electrical props. of ferroelectrics *(Russian)* 3–6016
- ceramic, phase change induced by hydrosatatic press. *(French)* 3–2497
- ceramic, prepolarized, remanent polarization determ. *(French)* 3–2486
- colemanite, mineral, n.m.r. relax. studies 3–39047
- critical X-ray scattering, lattice struct. depend. 3–30779
- crystal structure obs. using three dimensional vacuum furance for neutron diffraction 3–17720
- crystals, stimulated emission, Raman and polariton scatt., phase transition and domain structure change obs. 3–778
- dicalcium strontium propionate, proton spin-lattice relax. time, anomaly near Curie point 3–39103
- dicalcium strontium propionate, temp. depend. of sound velocity 3–1699
- dielectric relaxation, polydispersive nature 3–39104
- diglycine sulphate, orthorhombic structure 3–17800
- displacement type, dispersion of dielec. nonlinearity 3–34313
- displacement type transition, method of analyzing stability *(Russian)* 3–21366
- domain structure, thermodynamic relations 3–34312
- domain walls, local electron states *(Russian)* 3–8538
- electrical conductivity, temp. dependence at low temps., meas. method overcoming pyrocurrent interference *(Russian)* 3–8497
- ferroelastics and ferroelectrics having the index of faintness unequal to the cell multiplicity, discussion 3–2499
- film, prep., props., and device appl., review 3–8543
- glycine silver nitrate, crystal struct. 3–17798
- guanidinium aluminium sulphite, e.p.r. of Cr^{3+}, satellite lines due to ion pairs 3–2381
- H-bonded, local mode model, quantum mechanical tunnelling, soft mode 3–5169
- H-bonded, soft mode optical phonon interaction dynamics, Raman scatt. 3–5170

ferroelectric materials continued
H-bonded, transverse Ising model dynamics, soft mode heavy damping 3−2502
improper, dielec. anomaly near phase translation temp. 3−15465
impurity vibronic spectra, anomalies 3−30228
lead dicalcium propionate, logarithmic divergence of proton spin lattice relaxation time 3−30766
lithium ammonium tartrate monohydrate, accurate struct. aalysis rel. to ferroelec. phase transition 3−14840
optical properties, digression from phenomenological theory 3−18423
order-disorder type, dynamics 3−30236
PZT 65/35 ferroelec. ceramic, dielec. breakdown under shock loading 3−18416
rare earth molybdates, $Ln_2(MoO_4)_3$, Czochralski growth 3−12302
Rochelle salt, accurate struct. analysis rel. to ferroelec. phase transitions 3−14839
SbSI, near phase transition, effect of light on parameters 3−27479
semiconductors, short-cct. photo-emf and ferroelec. phase transition *(Russian)* 3−8541
stibiotantalite, mineral, domain structure obs. 3−24665
strontium dicalcium propionate, logarithmic divergence of proton spin lattice relaxation time 3−30766
thiourea, dielec. props. and ferroelec. transitions 3−30774
thiourea, elastic props. near IV-V phase transition 3−21371
thiourea, l.f. Raman spectrum, temp. depend. soft mode behaviour *(French)* 3−5182
thiourea single crystal, Raman spectra in para- and ferroelectric phases, intermolecular force consts. *(French)* 3−27498
transparent, energy loss of spirally moving charge *(Russian)* 3−30165
tri-glycine sulphate, ferroelec. domain struct., electron microscope obs. 3−30777
triglycerine fluoroberylate, nuclear relaxation, rotation of NH_3 group 3−30714
triglycine fluoberyllate, dielec. const. and hysteresis loop meas. rel. to ferroelec. transition 3−34310
triglycine fluoroberylate: $Cu^{2+}(Cr^{3+})$, temp. depend of dielec. props., ferroelec. domains 3−39099
triglycine fluoroberylate:Cu^{2+} single crystals, e.p.r., high-pressure influence 3−34191
triglycine fluoroberylate, proton relax., NH_3^+ group rot., phase transition phenomena 3−2452
triglycine fluoroberyllate, γ-irradiation effect on thermal expansion over Curie temp. range 3−24280
triglycine fluoroberyllate, ferroelec. and paraelec. phases, cryst. struct. and phase transition 3−14841
triglycine selenate, deuterated, ferroelec. and pyroelectric props. in phase transition region 3−34319
triglycine selenate, normal and deuterated, ferroelec. props. near Curie point *(Russian)* 3−8537
triglycine selenate, normal and deuterated, single crystals, γ radiation changes of dielectric props. in phase transition region *(Russian)* 3−8533
triglycine selenate, time depend. of specific resist., effect of cryst. growth conditions *(Russian)* 3−21367
triglycine sulphate, accurate struct. analysis rel. to ferroelec. phase transition 3−14838
triglycine sulphate, crit. X-ray scatt., anisotropy in reciprocal lattice space 3−30780
triglycine sulphate, critical region behaviour, annealing depend. 3−15455
triglycine sulphate, effect of X-ray irradiation on ferroelectric props. 3−30148
triglycine sulphate, ferroelec. domains, direct obs. by second harmonic generation by laser 3−24658
triglycine sulphate, nonlinear effects in sound propag., near phase transition 3−34316
triglycine sulphate, pyroelectric crystals growth for i.r. detector applications 3−31985
triglycine sulphate, Raman spectra meas. from 77 to 350 K, temp. depend. of low freq. lines *(Bulgarian)* 3−34344
triglycine sulphate, thermoluminescence spectra 3−18507
triglycine sulphate, thin films 3−39107
triglycine sulphate, time depend. of specific resist., effect of cryst. growth conditions *(Russian)* 3−21367
triglycine sulphate, X-ray topographic observations of lattice defects 3−27026
triglycine sulphate crystals, growth conditions effect on domain structure 3−39100
triglycine sulphate Curie point, two-dimensional pressure effect 3−2500
triglycinsulphate growth, role of surface and volume diffusion 3−20700
tris-sarcosine calcium chloride, e.p.r. obs. of Mn^{2+} complexes 3−8433
$AgNO_2$, growth from acetonitrile soln., domain struct. 3−30932
$AgNaNO_2$, electrostriction, temp. depend., rel. to improper ferroelectricity 3−24655
$AgNa(NO_2)_2$, accurate struct. analysis rel. to ferroelec. phase transition 3−14804
$AgNa(NO_2)_2$, dielec. relax. determ. by step-function method 3−18409
$AgNa(NO_2)_2$, ferroelec. transition, ^{23}Na n.m.r. obs. 3−21370
$BaCaTlNb_5O_{15}$, lattice parameters, permittivity temp. depend. *(French)* 3−38566
$Ba_2NaNb_5O_{15}$ segregation of impurities and striation rel. to growth speed 3−24804
$Ba_xSr_{1-x}Nb_2O_6$, segregation of impurities and striction rel. to growth speed 3−24804
$Ba_{1-x}Sr_xTiO_3$, O_2 diffusion constant meas. 3−17991
$BaSrTlNb_5O_{15}$, lattice parameters, permittivity temp. depend. *(French)* 3−38566
$BaTiO_3$, current-voltage characteristics and capacitance 3−33937
$BaTiO_3$, doped ceramic, grain boundary resistance model *(German)* 3−33938
$BaTiO_3$, electron microscope obs. of ferroelectric domains in low temp. phase 3−30765
$BaTiO_3$, neutron irradiated, dielectric dispersion near phase transition 3−15467

ferroelectric materials continued
$BaTiO_3:Nb_2O_5$, synthesis, dielec. props. 3−39385
$BaTiO_3:Y_2O_3$ depend. on composition, and cation siting structure and electrical props. 3−14813
$BaTiO_3$-$CaTiO_3$ (5 wt.%), large polarisation depend. photovoltages 3−33951
$Bi_2Bi_4Ti_3Fe_2O_{18}$, perovskite layer type ferroelec., ^{57}Fe Mossbauer obs. from 80 to 1150 K 3−27443
$BiFeO_3$ magnetic and structural props. 3−39064
Bi_2O_3-TiO_2-KF-H_2O, crystallisation, form. and props. of $Bi_2Ti_4O_{11}$, $Bi_4Ti_3O_{12}$, $Bi_{12}TiO_{20}$ 3−24048
$Bi_4Ti_3O_{12}$ film, electrooptical quality, epitaxial growth by r.f. sputtering 3−12252
$Bi_4Ti_3O_{12}$ solid solution, solubility limits and structural stability 3−4841
$(CH_3NH_3)AL(SO_4)_2.12H_2O$, electro-optical and thermo-optical props. 3−34328
$CaB_3O_4(OH)_3.H_2O$, colemanite, n.m.r. and diffraction meas. rel. to atomistic mechanism of Ferroelec. behaviour 3−27424
CsH_2AsO_4, order of phase transform. 3−30782
CsH_2AsO_4, partially deuterated samples, ^{75}As n.q.r. study 3−30725
CsH_2AsO_4, soft mode optical phonon interaction dynamics, Raman scatt. 3−5170
CsH_2AsO_4, X-irrad., e.p.r. of defect centres 3−2388
CsH_2AsO_4 and CsD_2AsO_4, ^{75}As spin-lattice relax. and n.q.r., phase transition phenomena 3−30715
$Fe_{1-x}S$, semiconducting uniaxial ferroelectric model 3−8531
$Gd_2(MoO_4)_3$, dielec. anomaly near phase transiton temp. 3−15465
β'-$Gd_2(MoO_4)_3$, dislocation etchants 3−8028
$Gd_2(MoO_4)_3$, ferroelastic-ferroelec., antiphase boundaries and their interactions with domain walls 3−24659
$Gd_2(MoO_4)_3$, phase transition, neutron irrad. effects 3−36847
$Gd_2(MoO_4)_3$, X-ray topographic study of ferroelec. phase transitions and domains 3−15461
HCl, stress free single crystal growth 3−15631
$K_2BiNb_5O_{15}$, crystal growth, dielectric constants anomalies at Curie temp. 3−8535
$KD_2(H_2)AsO_4$, X-irrad., e.p.r. of defect centres 3−2388
$KD_{2x}H_{2(1-x)}PO_4$, Curie temp. deuterium conc. depend. 3−34318
KD_2PO_4, light scattering investigation of soft ferroelectric and acoustic modes 3−39108
KD_2PO_4, phase transitions, domain influence on elec. field gradient and spin-phonon interactions 3−2413
KD_2PO_4, phase transition, Raman scatt. obs. 3−34305
KD_2PO_4, polarisation and phase transition behaviour 3−34290
KD_2PO_4 single crystal, phase transitions, n.m.r. and acoustic n.m.r. study 3−24660
KH_2AsO_4, order of phase transform. 3−30782
KH_2AsO_4, soft mode optical phonon interaction dynamics, Raman scatt. 3−5170
KH_2AsO_4, X-irradiated, evidence for Slater configurations by e.p.r. study 3−2389
KH_2AsO_4 and KD_2AsO_4, ^{75}As spin-lattice relax. and n.q.r., phase transition phenomena 3−30715
KH_2PO_4, anomalous light scatt. at ferroelec. phase transition, coupled harmonic oscillator model 3−30778
KH_2PO_4, dielec. const. and 'hysteresis' loop rel. to γ irrad. 3−34304
KH_2PO_4, KD_2PO_4 phase transitions in ferroelectrics containing hydrogen bonds, proton and phonon interactions, parameters 3−39112
KH_2PO_4, l.f. i.r. spectra in polar and non-polar phases *(French)* 3−12136
KH_2PO_4, phase transition meas. 3−15459
KH_2PO_4, Raman spectra scatt. phonon direction depend. 3−21422
KH_2PO_4, symmetry of atomic vibrs. and phase transitions nature 3−14953
KH_2PO_4, thermal hysteresis of ferroelec. transition 3−21372
KH_2PO_4 and KD_2PO_4, phase transition mechanism, neutron diffr. obs. 3−15458
KH_2PO_4 crystals, ultraviolet refl. and absorpt. for electronic transition studies 3−2562
KH_2PO_4 interdomain and domain defect interactions 3−8529
KH_2PO_4 type ferroelec. phase transition, Kobayashi's theory 3−21369
KH_2PO_4-type, NQR temp. dependence rel. to soft-mode 3−18392
KIO_3, ferroelectric, piezoelec. moduli, electrooptic phase modulation *(German)* 3−39096
KNO_3, coercive field of ferroelectric phase III single crystals 3−27473
KNO_3, phonon dispersion curves 3−20824
$KNbO_3$, n.m.r. of ^{93}Nb, in single domain cryst., phase transition 3−2414
$KNbO_3$, orthorhombic, domain struct. and single domain cryst. characteriz. 3−15463
$KNbO_3$, soft lattice vibr. modes, spontaneous polarisation and Curie constants 3−34303
$KNbO_3$ single cryst., domain struct., optical studies 3−21368
$KNbO_3$-$NaNbO_3$, phenomenological theory of ferro- and antiferroelectricity 3−18421
K_2SeO_4, cryst. struct. and phase transition 3−14805
$KTa_xNb_{1-x}O_3$, x=0.56, ferroelectric, soft modes and struct. 3−11594
$KTaO_3$, stabilisation of paraelectric phase by strong quartic anharmonicity 3−30776
$LiNbO_3$, Brillouin scatt., room temp. obs., elastic consts., elastooptical moduli *(French)* 3−36864
$LiNbO_3$, Czochralski growth conditions rel. to lattice defects and optical quality 3−21539
$LiNbO_3$, optically induced inhomogeneity of refr. index 3−32604
$LiNbO_3$, single crystals, X-ray topographic studies, relation between growth conditions and lattice defects 3−17747
$LiNbO_3$, thermal expansion in range 70-300K 3−5927
$LiNbO_3$ and $LiTaO_3$ film growth by r.f. sputtering 3−18541
$LiTaO_3$, ^7Li quad. coupling const. temp. depend. near Curie pt. 3−2415
$LiTaO_3$, ferroelectric domain reversal 3−8530
$LiTaO_3$, for piezoelec. filter devices, Czochralski growth 3−12297
$LiTaO_3$, optically induced inhomogeneity of refr. index 3−32604
$LiTaO_3$, struct. temp. depend., neutron diffr. obs. 3−30098

ferroelectric materials continued
$LiTaO_3$ single crystals, X-ray topographic studies, relation between growth conditions and lattice defects 3−17747
$(ND_4)DSO_4$, ferroelectric, deuteron spin-lattice relaxation 3−8477
$(NH_4)_2Cd_2(SO_4)_3$, dielec., optical and domain props. 3−24662
$NH_4H_2AsO_4$, X-irradiated, evidence for Slater configurations by e.p.r. study 3−2389
$NH_4H_2PO_4$ four-sublattice theory of phase transitions, ferroelec.-antiferroelec. 3−8534
NH_4HSO_4, cryst. struct., ferroelectric phase and transition 3−8526
$(NH_4)_2SO_4$, elastic anomaly near ferroelectric transition 3−30763
$(NH_4)_2SO_4$, elastic compliance functions, electrostrictive consts., anomalies at ferroelec. transition 3−15453
$(NH_4)_2SO_4$, hydrostatic pressure effect on ferroelec. transition temp. 3−2501
$(NH_4)_2SO_4$, transition, analysis of long wavelength lattice vibrs. 3−27476
$(NH_4)_2SO_4$ elastic compliance and dielec. meas. rel. to ferroelec. transition 3−30781
$NaD_3(SeO_3)_2$, room-temp. struct. detn. by heavy-atom method 3−7704
$NaH_3(SeO_3)_2$, upper phase transition, X-ray diffr. obs. 3−39106
$NaNO_2$, ^{14}N pure quadrupole relax., temp. depend., thermal motion 3−2440
$NaNO_2$, biaxial, second harmonic generation rel. to phase matching direction 3−22940
$NaNO_2$, electrical breakdown 3−5160
$NaNO_2$, electrostriction, temp. depend., rel. to improper ferroelectricity 3−24655
$NaNO_2$, gradient-elastic tensor component measurement, acoustic n.m.r. technique 3−21321
$NaNO_2$, optical second harmonic generation during switching 3−15466
$NaNO_2$, second harmonic generation at room temp. 3−10567
$NaNO_2$, X-ray topographic study of ferroelec. phase transitions and domains 3−15461
$NaNO_2$ single crystal γ-irradiated, dielectric const. and Curie temp. variation 3−27477
$NaNO_2:Mn^{2+}$, e.p.r. obs., allowed and forbidden hyperfine transitions 3−8430
$NaNbO_3$, phenomenological theory of ferro- and antiferroelectricity 3−18421
Na_2SeO_3, $NaHSeO_3$, H_2SeO_3, $NaH_3(SeO_3)_2$, vibr. spectra and hydrogen bonding effects 3−34341
$NdAlO_3$, soft-mode spectroscopy for trigonal-to-cubic phase transition prediction 3−15502
$Ni_3B_7O_{13}I$, crystal growth 3−17746
PB(Zr,Ti)O_3, La substituted, PLZT ceramic, pressure-sintered samples 3−8950
$(Pb,La)(Zr_y,Ti_z)O_3$, PLTZ ceramics, y=0.60 to 1.0, z=0.4 to 0, antiferroelectric-ferroelectric phase boundary, temperature, d.c. field dependence 3−8525
$Pb_5Ge_3O_{11}$, antiparallel 180° domains, X-ray topographic obs. 3−12102
$Pb_5Ge_3O_{11}$, cryst. struct. 3−17764
$Pb_5Ge_3O_{11}$, Curie pt. behaviour, enantiomorphism and optical activity 3−18419
$Pb_5Ge_3O_{11}$, ferroelec. and optical props. 3−18420
$Pb_5Ge_3O_{11}$, prototypic structure determ. 3−33502
$Pb_5Ge_3O_{11}$, second harmonic generation coefficients 3−13752
$Pb_5Ge_2SiO_{11}$, ferroelec. and optical props. 3−18420
$PbMg_{1/3}Nb_{2/3}O_3$, ferroelec. with smeared phase transition, electrooptical effect linearisation and coeffs. 3−24680
$PbMg_{1/3}Nb_{2/3}O_3$, optical absorpt. coeff. anomalous behaviour in broad ferroelec. transition 3−21438
$PbMg_xNb_{1-x}O_3$, longit. electrooptic effect 3−34327
$PbMg_{1/3}Ta_{2/3}O_3$, ferroelec. with smeared phase transition, electrooptical effect linearisation and coeffs. 3−24680
PbO, pyroelec. currents and phase transitions 3−27472
Pb_3O_4, pyroelec. currents and phase transitions 3−27472
$5PbO.3GeO_2$, electro-optic props. 3−18433
$5\ PbO.3GeO_2$, quasi-elastic scatt. in Raman spectrum near ferroelec. phase transition 3−15495
$5PbO.3GeO_2$, Raman spectra of soft phonon mode at ferroelec. phase transition 3−24691
$PbTiO_3$, ferroelec. perovskite, Raman spectra obs. of lattice modes 3−33634
$PbTiO_3$, low temp. structure 3−39068
$PbTiO_3$, polycryst. film with ferroelec. and antiferroelec. props., deposition by electrophoresis 3−39220
$PbTiO_3:Nb_2O_5$ solid solution, incorporation of Nb_2O_5 into the perovskite lattice 3−5381
$PbZn_{1/3}Nb_{2/3}O_3$, ferroelec. with smeared phase transition, electrooptical effect linearisation and coeffs. 3−24680
$Pb(Zn_{1/3}Nb_{2/3})O_3$ and $Pb(Cd_{1/3}Nb_{2/3})O_3$, microdomain behaviour in diffuse phase transition region 3−15462
Pb(Zr, Ti)O_3, pyroelec. props., comp. and phase struct. depend., i.r. detector characteriz. 3−39098
Pb(Zr,Ti)O_3, La_2O_3-modified, temp.-depend. ferroelec. domain alignment 3−5168
$PbZrO_3$, polycryst. film with ferroelec. and antiferroelec. props., deposition by electrophoresis 3−39220
$PbZr_{1-x}Ti_xO_3$ solid solns., press. induced ferroelec.-antiferroelec. transform., depolarization behaviour *(French)* 3−36842
$PbZr_{1-x}Ti_xO_3+0.8\%\ WO_3$, ferroelec. transition temp.—comp. phase diagram *(French)* 3−5167
$(PrBi)Bi_4Ti_3Fe_2O_{18}$, perovskite layer type ferroelec., ^{57}Fe mossbauer obs. from 80 to 1150K 3−27443
$Pr_2Bi_4Ti_3Fe_2O_{18}$, perovskite layer type ferroelec., ^{57}Fe Mossbauer obs. from 80 to 1150K 3−27443
RbD_2AsO_4, ^{75}As spin-lattice relax. and n.q.r., phase transition phenomena 3−30715
$RbD_2(H_2)AsO_4$, X-irrad., e.p.r. of defect centres 3−2388
RbH_2AsO_4, order of phase transform. 3−30782
RbH_2AsO_4, partially deuterated samples, ^{75}As n.q.r. study 3−30725
RbH_2PO_4 in paraelectric and ferroelectric phases, Raman and vibration spectra of $(PO_4)^{3-}$ *(Russian)* 3−5191
Rb_2PO_4, l.f. i.r. spectra in polar and non-polar phases *(French)* 3−12136
SbSI, Barkhausen effect, rel. to state of defects 3−39114

ferroelectric materials continued
SbSI. deep centres and photopolarization 3−24649
SbSI, domain struct. and local states 3−5172
SbSI, electromechanical hysteresis and photo deformation effect 3−34300
SbSI, phase transition entropy from temp. depend. sp. ht. obs. *(Russian)* 3−8542
SbSI, photodomain effect and deformation 3−34311
SbSI, pleochroism associated with domain struct. 3−36852
SbSI multiple domain effect, illumination induced, hysteresis loop 3−34299
SbSI-SbSeI mixed crysts., far-i.r. reflectivity, l.f. ferroelec. mode behaviour 3−39135
$SbSI_xBr_{1-x}$, semicond., nonequilib. carrier density influence on phase boundary form. 3−39113
$SbSI_xBr_{1-x}$ solid soln., photoelectret and ferroelec. polarization, mechanism *(Russian)* 3−8539
SbSeI, deep centres and photopolarization 3−24649
SbSeI, domain struct. and local states 3−5172
$Sb(TaNb)O_4$, intrinsic absorpt. and thermal props. rel. to phase change 3−5171
$Sr_{0.75}Ba_{0.25}Nb_2O_6$ prism, electrooptic light beam deflection 3−2514
$Sr_2Nb_2O_7$ single crystal growth from melt 3−21373
$SrO.TeO_2$, phase transition 3−15457
$Sr_{1-x}Pb_xLi_{0.25}Nb_{0.75}O_3$, permittivity *(Russian)* 3−14810
$SrTiO_3$, 105 K structural phase transition, birefringence study of anisotropic fluctuations and order parameter 3−2510
$SrTiO_3$, dielec. nonlinearity coeff., Devonshire coeffs., near 110 K transition 3−21374
$SrTiO_3$, distortion enhanced optical absorption at the cubic to tetragonal transition 3−12149
$SrTiO_3$, effect of 110K structural phase transition on conduction bands, LCAO prediction 3−11853
$SrTiO_3$, lattice dynamics above structural phase transformations 3−11706
$SrTiO_3$, lattice parameter var., 10 to 130K, neutron backscattering obs. *(German)* 3−30107
$SrTiO_3$, obs. of stress induced ferroelectric phase by second harmonic generation 3−30764
$SrTiO_3$, permittivity depend. on temp., meas. from 1.2 to 0.025K 3−21359
$SrTiO_3$, spin-lattice relax. of ^{87}Sr, struct. phase transition obs. 3−2450
$SrTiO_3$, stabilisation of paraelectric phase by strong quartic anharmonicity 3−30776
$SrTiO_3$ O_2 diffusion constant meas. 3−17991
$SrTiO_3$-$MTiO_3$, (M=Pb, Ba, Ca), phase transitions, u.s. velocity and permittivity studies 3−27478
$Sr_2TlNb_5O_{15}$, lattice parameters, permittivity temp. depend. *(French)* 3−38566
TiO_2, rutile, static dielec. const. and Raman spectra, press. and temp. depend. 3−18456
tris-sarcosine $CaCl:Mn^{2+}$ e.p.r. investigations of phase transition 3−39109
$YMnO_3$ as-grown monocrystalline ferroelectric, surface effects 3−8527

ferroelectric phenomena
see also ferroelectricity
acoustic wave absorption, piezoelectricity in paraelectric phase, temp. depend. 3−36846
Curie point depend. on nonequilib. carrier conc. 3−24664
ferroic state, enantiomorphous phases and thermodynamic determ. 3−30768
ferroic state shift, second order, mech., elec. and coercive forces 3−12101
Pb, La(Zr, Ti)O_3 ceramic, transition, pulse-echo detect. 3−18689
phase transition, e.m. radiation generation 3−21375
phase transition first-order, in thin films 3−24661
phase transition triggered by instability 3−34307
polarized media, paraelec. to ferroelec. transition, homogeneity effects 3−5102
Rochelle salt, phase transitions at high press. 3−21377
semiconductor, spontaneously polarised, anisotropy of elec. cond. 3−39110
short-cct. photo-emf. and ferroelec. phase transition in semicond. *(Russian)* 3−8541
soft mode phase transitions, basic concepts, review 3−27120
surface bound states and resonances of hydrogen bonded ferroelec. tunnelling model 3−15233
thermodynamic correlations between semiconductor props. in solid solns. involving pressure considerations 3−34306
thiourea single crystal, Raman spectra in para- and ferroelectric phases, intermolecular force consts. *(French)* 3−27498
transition, inherent parameters, group theoretical study 3−27475
tri glycine sulphate, temp. depend. of permitt. orthogonal to ferroelec. axis 3−8503
triglycine fluoberyllate, dielec. const. and hysteresis loop meas. rel. to ferroelec. transition 3−34310
triglycine sulphate crystals, growth conditions effect on domain structure 3−39100
u.s. attenuation, structural transitions above T_c 3−34309
u.s. attenuation anomaly of displacive type ferroelec. at transition 3−8536
$BaTiO_3$, u.s. velocities near paraelect. ferroelec. transition 3−30772
$BaTiO_3$-$CaTiO_3$ (5 wt.%), large polarisation depend. photovoltages 3−33951
$Gd_2(MoO_4)_3$, improper ferroelec., thermal expansion at transition temp. 3−12104
KD_2PO_4, light scattering investigation of soft ferroelectric and acoustic modes 3−39108
KH_2PO_4, anomalous light scatt. at ferroelec. phase transition, coupled harmonic oscillator model 3−30778
KH_2PO_4, dielec. const. and 'hysteresis' loop rel. to γ irrad. 3−34304
KH_2PO_4, KD_2PO_4 phase transitions in ferroelectrics containing hydrogen bonds, proton and phonon interactions, parameters 3−39112
$KNbO_3$, soft lattice vibr. modes, spontaneous polarisation and Curie constants 3−34303
$(NH_4)_2SO_4$, elastic anomaly near ferroelectric transition 3−30763

ferroelectric phenomena continued
- $(NH_4)_2SO_4$, transition, analysis of long wavelength lattice vibrs. 3—27476
- $(NH_4)_2SO_4$ elastic compliance and dielec. meas. rel. to ferroelec. transition 3—30781
- 5 $PbO.3GeO_2$, quasi-elastic scatt. in Raman spectrum near ferroelec. phase transition 3—15495
- $5PbO.3GeO_2$, Raman spectra of soft phonon mode at ferroelec. phase transition 3—24691
- $SbSI_xBr_{1-x}$ solid soln., photoelectret and ferroelec. polarization, mechanism *(Russian)* 3—8539
- $SrTiO_3$, dielec. nonlinearity coeff., Devonshire coeffs., near 110 K transition 3—21374
- $SrTiO_3$, obs. of stress induced ferroelectric phase by second harmonic generation 3—30764
- Tl halides, anharmonicity, low frequency dielectric response, ferroelectric behaviour 3—8502

ferroelectric switching
- triglycine sulphate thin films deposited by low temp. spinning technique 3—39107
- $BaTiO_3$, 180° polarization reversal 3—34314
- $BaTiO_3$, α-domain, antiparallel switching 3—21376
- $BaTiO_3$, kinetics of domain wall motion 3—39102
- $BaTiO_3$ light emission, polarisation switching 3—39111
- KH_2PO_4 type ferroelec. phase transition, Kobayashi's theory 3—21369
- KNO_3, ferroelec. paraelect. transform. 3—12219
- $(NH_4)_2Cd_2(SO_4)_3$, switching mechanism 3—24662
- $NaNO_2$, optical second harmonic generation 3—15466

ferroelectricity
- *see also antiferroelectricity; ferroelectric devices; ferroelectric materials; ferroelectric phenomena*
- coupled ferroelastic crystals and cooperative phenomena 3—30176
- displacive ferroelectrics, statistical mechanics of simple model 3—34308
- hydrogen bonded solids, theory of proton transfer 3—11583
- Ising spin system dynamics in fluctuating environment 3—30771
- modified F model, critical exponents 3—36843
- Mott insulator, spin analogue model 3—33821
- order-disorder and displacive types, review of n.m.r. techniques 3—30767
- phase transitions, Landau models for piezoelec., pyroelec. and ferroelec. crystals 3—18404
- phenomenological theory, appl. to $NaNbO_3$ and $KNbO_3$-$NaNbO_3$ 3—18421
- Rochelle salt, dipole-dipole interaction, electronic shielding effect, Mitui theory 3—27474
- semiconductors, localised electron states in domain walls 3—24663
- surface elastopolarization waves at domain boundaries in ferroelectrics *(Russian)* 3—8540
- surface elec. field due to spontaneous polarisation 3—18208
- transition investigations from rotational invariance of higher order optical susceptibilities 3—29125
- KH_2AsO_4 type ferroelectric, order of phase transform. 3—30782

ferromagnetic metals
- anisotropic metallic medium, ferromagnetic resonance field and linewidth 3—34214
- current-carrying states rel. to spin polarization in photoemission 3—18533
- cylindrical specimens under the influence of field strength dependent permeability eddy-current distribution *(German)* 3—18776
- electrical resistance, electron-phonon and electron-magnon scatt. effects *(Russian)* 3—15181
- electron and neutron scattering and fluctuations by coupled magnons *(Russian)* 3—12032
- electron and neutron scattering by coupled spin waves *(Russian)* 3—12031
- film, spin wave dispersion 3—27378
- isotropic ferromagnets, resistive anomalies at the critical point 3—21236
- magnetisation, direct recording of static curves *(French)* 3—19240
- magnetoresistance, negative, due to spin fluctuations, spin Green function calc. 3—15182
- negative Barkhausen jumps in consecutive asymmetrical magnetization reversal 3—38993
- nondestructive testing using magnetic rubber 3—15807
- permalloy film, mag. anisotropy, electrostatic torquemeter obs. 3—256
- Seebeck coeff. at Curie temp., sp. ht. of charge carriers 3—18319
- Seebeck coeff. at Curie temp., sp. ht. of charge carriers 3—18320
- spin wave modes, theory 3—30634
- spin wave spectrum, exchange model, magnetiz. dispersion eqns. *(Russian)* 3—15377
- spin wave theories in the linear approximation 3—21251
- thermal cond. due to spin degrees of freedom, molecular field approx. 3—30447
- transition metals and alloys, modified Zener model and Curie temp. calc. 3—34085
- Co, sublimation, in range including Curie point, 1320-1410K *(Russian)* 3—8365
- Co electrodeposited, effect of I^- ions on mag. props. *(Bulgarian)* 3—30670
- Co film, effect of ang. dispersion of anisotropy on reson. linewidth *(Russian)* 3—8452
- Co film, monocryst., Hall effect, elec. cond., effective magnetiz. *(Russian)* 3—18120
- Co films, perpendicular anisotropy, rot. moments, superparamag. particles *(Russian)* 3—30641
- Co films with different texture perfections about [0001] axis, perpendicular anisotropy 3—36731
- Co single-domain powders with cubic anisotropy, mag. props. *(Russian)* 3—15390
- Fe, high-purity, creep, const. mag. field influence, dislocation-domain wall interaction *(Russian)* 3—36774
- Fe, magnetised with polarised positrons, positron annihilation, investigation of spin and, momentum density 3—18066
- Fe, magnetization, 5-295K, 0-14 kOe 3—2311
- Fe, positron annihilation, band structure calculation of momentum densities 3—18065

ferromagnetic metals continued
- Fe and Ni carbonyl powders, hot pressing method with subsequent annealing for production of permalloy *(Russian)* 3—27723
- Fe base bcc alloys, electronic struct., coherent potl. approx. calc. 3—11999
- Fe film, evaporated at oblique incidence, domain structure obs. 3—1544
- Fe relaxation of resonance spin waves by s-d exchange 3—21315
- Fe single-domain powders with cubic anisotropy, mag. props. *(Russian)* 3—15390
- Fe zone melted crystals under tensile stress, dislocations and magnetic domain walls, X-ray topographic study 3—17828
- Fe-V alloys transition, V^{51} nuclei, n.m.r., local inhomogeneities 3—34232
- Gd, Hall effect of polycrysts., 4.2K, 46 kOe 3—33874
- Mn-Bi thin films, birefringent compounds 3—21283
- Ni, crit. exponent β determ. from ^{57}Fe Mossbauer effect 3—2477
- Ni, ferromag. reson. linewidth depend. on dislocation density *(Russian)* 3—18370
- Ni, flow stress rel. to mag. field, domain wall dislocation interactions 3—5125
- Ni, helicon mode, standing wave reson. study 3—18178
- Ni, magnetization singularities, mag. transform. temp. range *(Russian)* 3—8383
- Ni, pulsed n.m.r. of ^{61}Ni, Bloch wall effects *(French)* 3—30702
- Ni, sound propag., longit. and transverse wave absorpt., 300-1000 K, mag. field effect *(Russian)* 3—18309
- Ni, spontaneous magnetisation anisotropy from band theory, spin-orbit interaction 3—34150
- Ni, susceptibility, melting pt. discontinuity *(French)* 3—21219
- Ni, transcritical epitaxial film, domain structure 3—30666
- Ni film, evaporated at oblique incidence, domain structure obs. 3—1544
- Ni film, mag. hysteresis loops, domain struct., hypercrit. state *(Russian)* 3—15393
- Ni magnetoelastic attenuation at u.s. freqs. due to domain struct. rearrangement 3—21288
- Ni single-domain powders with cubic anisotropy, mag. props. *(Russian)* 3—15390
- Ni-Co layers covering Cu wires, mag. and mech. treatment effect on mag. props. *(Rumanian)* 3—12043
- Ni-Co-Fe mated film (bifilm) plated wire element, effects of process variables 3—12041

ferromagnetic properties of substances
- *see also coercive force; ferromagnetic relaxation; ferromagnetic resonance; ferromagnetism; magnetic domains; magnetisation process; magnetisation state; remanence*
- alloy, anomalous Hall effect, cond. electron scatt. on magnons *(Russian)* 3—36589
- alloy, dilute, phenomenological theory rel. to paramag.-ferromag. transition 3—21233
- alloy, plastically deformed single cryst., mag. anisotropy and dislocation struct. *(Russian)* 3—36729
- Alnico, domain structure variation in partial hysteresis cycles 3—30664
- amorphous ferromagnet, molecular field theory 3—18279
- amorphous magnet, constant coupling approx. for Ising and Heisenberg models 3—11998
- amorphous mixed ferromagnet, Curie temp. and mag suscept., Heisenberg and Ising models 3—27350
- band structure, transport properties 3—38858
- Barkhausen noise, power spectrum in simple materials, spring model 3—5117
- bulk domains by neutron depolarisation in three dimensions 3—39004
- collective spin excitation in narrow d band 3—5092
- Coulomb law of magnetism, equivalent circuit models *(German)* 3—13666
- critical exponent β meas. by ferromagnetic transmission resonance 3—16465
- dielectric plate, instability of magnetoelastic oscillations 3—36777
- dipole-dipole interactions, critical point behaviour 3—30625
- disc shaped ferromagnetic samples, demagnetisation on the surface 3—21264
- disordered alloy, band theory for residual resistivity 3—15340
- eddy current losses in sheets, calc. 3—21262
- electron gas, spin and charge susceptibility 3—15338
- electron gas, spin polarisation due to mag. impurities 3—15339
- ferrofluid, Ni-Fe alloy particles in Hg, coercive force 3—2321
- ferromagnet, pyromagnetic effect, molecular field approx. 3—18125
- ferromagnets with 'easy plane' type magnetic anisotropy, spin relaxation theory *(Russian)* 3—12063
- film, cylindrical, anisotropy dispersion meas. *(French)* 3—25819
- film, cylindrical, anisotropy field meas. *(French)* 3—25818
- film, demagnetising factor, method of rot. moments *(Russian)* 3—21265
- film, domain wall creep in nonuniform fields, intrinsic fields influence *(Russian)* 3—36736
- film, double-layer, magnetostatically-coupled, crit. curves, mag. reversals *(Russian)* 3—30650
- film, effect of ang. dispersion of anisotropy on reson. linewidth *(Russian)* 3—8452
- film, ferromagnetic, magnetoresist. rel. to domains and magnetisation vector angular dispersion 3—21052
- granular material, sample influences on initial susceptibility determ. *(French)* 3—12005
- Green's function method for exchange-coupled uniaxial anisotropic ferromagnets 3—15327
- hardness, external mag. field on temp. effects *(Russian)* 3—34167
- heavy rare earth metals, electrons and spin waves, review 3—8327
- Heisenberg compressible ferromagnet, susceptibility index 3—30595
- Heisenberg ferromagnet, spectral function calcs. 3—8326
- Heisenberg ferromagnet, two-dimensional, critical temp. depend. on anisotropy 3—30590
- Heisenberg ferromagnet with spin 1/2, comparison of Pauli operator and drone-fermion calc. methods 3—21202
- Heisenberg film, finite size and surface effects on critical behaviour 3—15332
- Heisenberg model, Feynman graph expansion for equation of state near crit. point 3—15330

ferromagnetic properties of substances continued
highly anisotropic ferromag., mag. anisotropy and magnetostriction theory 3−24581
Hubbard model, tenfold d-electron degenerate, antiferromag. to paramag. (ferromag.) transitions 3−21207
hydrothermomagnet, elementary theory 3−12039
hyperfine interaction field sign determination by n.m.r. 3−22412
insulating ferromag., magnon-exciton bound states, Oguchi method 3−27376
interatomic correlation effect on paramag. instability against ferromag. state 3−8330
Invar, 'magnetic anomaly', Debye-Waller factor, Mossbauer effect 3−39071
Invar, internal friction features in variable mag. field, magnetoelastic losses 3−30677
Invar, magnetic susceptibility, high field, saturation magnetisation, magnetometer measurements of moment 3−36713
Invar, magnetovolume, effects, Curie temp. press. depend., localised electron model 3−38979
Invar alloys, mag. exchange contrib. to elastic consts., rel. to anomalous elastic props. 3−24597
Ising and Heisenberg ferromag. model nonmag. impurity effect at Curie temp. 3−8323
Ising ferromagnet, crystal field anisotropy effect on Curie temp. 3−8324
itinerant electron ferromagnet, electron-magnon interaction 3−21204
Kondo temp. for ferromag. and antiferromag. impurity pairs 3−21217
Kovar, magnetostriction, mag. field and temp. depend., below 50K 3−5123
magnesium titanomagnetite, (artificial) magnetic properties and self-reversal of thermoremanent magnetization 3−34154
magnetically soft materials, development, basic properties 3−8377
magnetisation, direct recording of static curves *(French)* 3−19240
magnetisation of polyaxial ferromagnet, mag. texture influence on domain walls 3−30665
magnetite, optic spin wave energy at Verwey transition 3−34140
magnetoacoustic resonance, magnetoelastic instability anisotropy effects 3−39010
magnetoelastic theory of soft ferromagnetic elastic solids of multi-domain struct. 3−34155
magnon spectrum and spin wave damping for ferromagnet with uniaxial anisotropy 3−34080
metal, damped spin wave branches of susceptibility 3−8373
metal, Seebeck coeff. at Curie temp., sp. ht. of charge carriers 3−18319
metal, Seebeck coeff. at Curie temp., sp. ht. of charge carriers 3−18320
metal, spin polarization in photoemission and current-carrying states 3−18533
micromagnetic calc. of magnetoelastic effects 3−21284
Mossbauer diffraction by ferromagnet, dynamical theory 3−24633
Mossbauer diffraction by ferromagnet, kinematical theory 3−24632
nickel squarate dihydrate, mag. transitions, 1.2-4 K 3−18310
NiSpan C, Invar range, precip. hardening effect on phys. props. 3−39345
nondegenerate narrow band, interatomic electron correlation effects on ferromag. and paramag. states 3−21206
nonlinear conducting materials, e.m. field distribution, power losses 3−15396
permalloy bar, magnetisation distribs., magnetostatic energy barriers and drive fields for bubble motion 3−21270
permalloy electrodeposited films micron thickness, reversal of magnetisation by domain wall creep 3−38992
permalloy film, domain wall motion, dynamic properties 3−34161
permalloy film, evap. onto rotating substrate, helical anisotropy 3−34149
Permalloy film, interrupted nsec. mag. reversals *(Russian)* 3−8382
permalloy film, mag. parameters rel. to grain size and film thickness 3−8402
Permalloy film, magnetiz. oscillations due to pulsed transverse field excitation *(Russian)* 3−24586
Permalloy film, nonuniformity of nsec. magnetization reversal *(Russian)* 3−8395
Permalloy film, obliquely deposited, mag. reversals, mechanisms *(Russian)* 3−30651
Permalloy film, obliquely deposited hypercritical, mag. props. and microporosity *(Russian)* 3−24588
permalloy film, obs. of triangular hysteresis loops 3−8393
permalloy film, Ritz model for asymmetric domain walls 3−8388
Permalloy film, spin wave spectrum, surface conditions influence *(Russian)* 3−30698
permalloy film, uniaxial mag. anisotropy rl. to annealing 3−18333
Permalloy film, with banded domain struct., mag. reversals *(Russian)* 3−8381
Permalloy films, bubble domains, h.v. electron microscope obs. 3−30660
permanent magnets, physical quantities, manufacturing methods, hard rare earth-Co_5 alloys *(German)* 3−15384
polarized media, paramag. to ferromag. transition, homogeneity effects 3−5102
pseudo-tetrahedral ferrous compounds, quadrupole splitting and magnetic susceptibilities 3−21190
rare earth, fields at Sn impurity atoms 3−21357
rare earth, heavy, hydrostatic pressure effect on spin disorder resistivity 3−2284
rare earth alloy, RAl_2, n.m.r. obs. of mag. anisotropy and exchange polarisation 3−15430
rare earth alloys, hyperfine fields, model 3−15317
rare earth cobalt permanent magnet alloys, magnetisation, anisotropy and coercivity, review 3−24595
rare earth cobaltide hydrides, RCo_5-H (R=La, Pr, Nd, Sm, Gd), rel. to hydrogen sorption 3−27357
rare earth cobaltides, RCo_5, magnetic moment, easy direction, single crystals 3−36715
rare earth compounds RNiAl and RCuAl 3−20725
rare earth orthoferrite plate, optical contrast of inclined boundaries 3−18436
rare earth-Fe compound, Curie temp. pressure depend. 3−36720

ferromagnetic properties of substances continued
remanence of ferromagnetic material slowly rotating in alternating magnetic fields, remanence 3−24583
semiconductor, anomalous Nernst-Ettingshausen theory, electron scatt. by spin waves 3−36629
sound velocity mag. field depend. 3−21290
spin polarisation of electrons tunnelling from Fe(Co)(Ni)(Gd) ferromag. to Al superconducting film 3−15311
spin wave reson. surface modes of antiferromag.-ferromag. surface coupled film 3−39033
spin wave theory of amorphous ferromagnets 3−12030
spin-wave spectrum, linear contribution to spatial dispersion 3−18330
steel, low-density 9G28Yu9MVB type, saturation magnetiz. and permeability 3−21662
steel, transformer, effect of substruct. *(Russian)* 3−5289
Ticonal alloy, high-coercivity, characteriz. after isothermal thermomag. treatment 3−24943
transformer steel, rel. to grain size and form control *(Russian)* 3−12342
transition metals, 3d, relative stability of ferro- and antiferromagnetic state, models 3−36701
3d transition metals, impurity suppression of ferromag. in strong correlation limit 3−8352
transition metals and alloys, modified Zener model and Curie temp. calc. 3−34085
vibration of magnetisation in ferromag. plates 3−30663
Vicalloy, domain structure variation in partial hysteresis cycles 3−30664
Au-Fe alloys, magnetic ordering rel. to Fe concentration 1-22 at.% 3−2287
AuFe, magnetic moment distribution 3−34134
Au_4V alloy, V^{51} n.m.r. study 3−2408
CAVBIG, self interaction of finite amplitude magnetoelastic waves 3−39035
$CdCr_2S_4$, semicond., heat treatment in sulphur atmosphere, variation of Curie constant and temp. 3−30621
$CdCr_2Se_4$, permeability 3−5033
$CdCr_2Se_4$, refl., mag. ordering effect of low freq. i.r.-active phonon 3−15492
$CdCr_2Se_4$, semiconducting, conductivity switching effects 3−33967
$CdCr_2Se_4$, transport props. of non-degenerate ferromagnetic semiconductor below Curie temp. 3−15205
$Cd_{1-x}In_xCr_2Se_4$, semicond., transport props. near Curie temp. 3−33881
$(Co, Fe)_{17}R_2$ [R=rare earth, La, Y], magnetic symmetries and domains 3−18340
Co, electronic structure calcs. for paramag. (ferromag.) states, exchange energy contrib. 3−36515
Co alloy, spin config. and intrinsic coercive field of narrow domain walls 3−8391
Co films with different texture perfections about [0001] axis, perpendicular anisotropy 3−36731
Co-C alloy, h.c.p., disaccommodation, mag. aftereffect study 3−5121
Co-Fe, mag. moments depend. on comp., effect of h.c.p. to double h.c.p. structural transition 3−30607
Co-Fe-Nb semihard mag. alloy development 3−21261
Co-Fe-Nb semihard mag. alloy characteriz. 3−21279
Co-Fe-Nb semihard magnetic alloy, anisotropy *(Japanese)* 3−18334
Co-Ni-P layers, chem. deposited, anisotropy field *(French)* 3−8404
Co-P film, high-coercivity, domain struct. and reversal processes 3−24592
Co-Pd alloys, interdiffusion coeff., Curie temp. phenomena 3−20899
Co-Pt alloy, high coercivity rel. to struct., electron microscope study *(Russian)* 3−8779
Co-Sn, dilute alloy, two current cond. and impurity resist. 3−36719
Co_5-Sm permanent magnet alloy, sintered anisotropy parameters and coercivity 3−5097
$Co_{17}R_2$ [R=rare earth, La, Y], magnetic symmetries and domains 3−18340
Co_7R_2 [R=rare earth, La, Y], magnetic symmetries and domains 3−18340
Co_5X alloy, X=rare earth, domain wall energy, polarized light metallography obs. 3−5118
^{59}Co films, nuclear mag. levels inverted state 3−30628
$CrBr_3{:}^{53}Cr$, low temp. n.m.r. obs. 3−15431
α-Cr_2O_3, formation and interconversion in Cr oxide gel systems 3−5382
Cr_2SSeTe, meas. of molar susceptibility and molar spontaneous magnetisation, 80-600 K, determ. of Curie point *(Russian)* 3−12010
$Cs_2CuCl_4.2H_2O$, Heisenberg b.c.c. ferromagnet, nuclear quadrupole resonance obs. of magnetic interactions 3−27439
$CsNiF_3$, one dimensional Ferromagnet, spin wave meas. 3−30638
Cu-Mn-Sn, ferromag. beta phase, crystal structure and ordering 3−18324
Cu-Ni-Fe alloy, mag. anisotropy and magnetis. reversal 3−36745
$CuCr_2S_{4-x}Se_x$ solid soln., lattice parameter, Curie temp., mag. moment and effective mag. moment 3−21241
$CuCr_2Te_3I$, mag. hyperfine field, Mossbauer effect obs. 3−30735
Dy, hysteresis of ferromag.-antiferromag. transform., elec. resist. and thermal expansion obs. *(Russian)* 3−15363
Dy, obs. of surface domain patterns 3−21274
Dy-Gd alloy, mag. anisotropy, comp. and temp. depend. 3−34153
DyCd, CsCl type compound, field depend. of magnetisation, ferromag. model 3−36758
$DyCl_3.6H_2O$, caloric and mag. props. 3−38976
Er, mag. struct., neutron diffr. obs. 3−24576
$ErCl_3.6H_2O$, caloric and mag. props. 3−38976
$ErFe_2$, coercive force, remanence and hysteresis near mag. compensation point *(Russian)* 3−8380
$ErFeO_3$, spin reorientation, n.m.r. of ^{57}Fe 3−21332
ErGa, Curie temp., magnetization, hysteresis 3−2319
$Er_xY_{1-x}Al_2$, neutron diffraction determ. of ferromagnetic ordering *(German)* 3−12027
Eu chalcogenides, ferromagnetic, semiconducting, band structure 3−38859

ferromagnetic properties of substances continued
EuO, EuS, dipole-dipole interactions, critical point behaviour 3—30625
EuO, mag. order effect on thermal cond. 3—7979
EuO, spin polarization and existence of paramagnetic surface sheet 3—8368
EuO crystal growth parameters relation to stoichiometry, determ. by i.r. and conductivity meas. 3—7641
EuO:Fe film, thermomag. writing, optimum thickness calc. 3—16915
EuS, effect of mag. structure on thermoreflectance spectra 3—27512
EuS, EuSe, ordering rel. to photoluminescence props. *(German)* 3—18495
EuS, EuSe thin films, spin polarized photoelectrons *(German)* 3—18531
$(Fe, Ti, \square)_3O_4$, ferromagnetic-paramagnetic transitions 3—4735
Fe, energy band calc. 3—38784
α-Fe, low temp. mag. relax. rel. to mag. aftereffect, susceptibility meas. 3—34168
Fe (100) single crystal film, magnetisation ripple 3—8399
Fe whisker, magnetisation process with Landau domain struct. 3—36749
Fe whiskers, X-ray topographic obs. of fir-tree branch and rectangular domains 3—30648
α-Fe:H, magnetic after-effect measurements 3—39001
Fe:Si, ferromag. domains parallel to (111) *(French)* 3—27383
Fe:Tm, perturbed angular correlation for localised moments 3—15359
Fe-Al ferromag. clusters in Alnico type alloy, Mossbauer obs. 3—8491
Fe-Al-C alloy, mag. after effects, directional ordering of interstitial atoms 3—12013
Fe-Cr alloys, ferromag. reson., anisotropy const. determ. 3—2403
Fe-Cr-Co alloy containing Si, permanent mag. material 3—36746
Fe-Cu-Mn system, semihard mag. reed switch material, heat treatment effect on mag. props. 3—36757
Fe-Mn-Co alloys, cold rolled, heat treatment effect on mag. props. *(Japanese)* 3—31077
Fe-N system, aftereffect, for irreversible magnetization process in Rayleigh region 3—18344
Fe-NI-Al, b.c.c., Mossbauer obs. of Al impurities effect on Fe and Ni mag. moments 3—15444
Fe-Ni, f.c.c. alloy, pressure effect on Curie temp., rel. to magnetostriction anomalies 3—34126
Fe-Ni (fcc), specific heat at const. pressure meas. in 300-1000K range, obs. of behaviour at Curie temp. *(Japanese)* 3—18312
Fe-Ni alloy film, modulation of mag. noise spectral distrib. *(Russian)* 3—12042
Fe-Ni alloy films, exchange parameters 3—2324
Fe-Ni alloys, heat treatment depend. 3—21275
Fe-Ni alloys, invar-type, Young's modulus, temp. depend., recovery and recrystn. influence *(Russian)* 3—36773
Fe-Ni thin films, crystal structure dependence 3—8376
Fe-Ni-Co-Al-Ti alloys, temp. depend. of mag. moment, superparamag. props. *(Russian)* 3—8342
Fe-Rh (52 at.%) alloy, antiferromag.-ferromag. transition, optical behaviour *(Russian)* 3—18439
Fe-Si, covered by Ni film, mag. susceptibility temp. depend. meas. rel. to ferromag. domains *(Russian)* 3—24562
Fe-Si, internal friction features in variable mag. field, magnetoelastic losses 3—30677
Fe-Si alloy, effect of Ni surface film *(Russian)* 3—12037
Fe-Si alloys, 0-24%Si, effects of furnace cooling and water quenching on magnetic properties 3—36776
Fe-Si alloys, thermomagnetic treatment, effects of inclusions and internal stresses *(Russian)* 3—8385
Fe-Si single crysts., e.m. losses depend. on surface cryst. orientation *(Russian)* 3—15391
Fe-Si steels, manufacturing processes, development, applications to electrical power 3—15173
Fe-Sn, dilute alloy, two current cond. and impurity resist. 3—36719
(Fe-Ni)-P-C amorphous alloy, low temp. resist. and Curie temp. 3—21234
Fe_3Al, annealing effects on compression induced mag. anisotropy 3—30642
Fe_2B, Mossbauer absorpt. obs. of mag. hyperfine field 3—15443
$FeBO_3$, obs. of light-induced anisotropy by acoustic resonance 3—18335
$Fe_{1-x}Cr_x$, bcc alloy, electronic struct., CPA calc. 3—11999
FeF_3, weak ferromag. Raman spectra, phonon and magnon lines 3—5192
$Fe_xMn_{2-x}P$, mag. props. of different phases, Neel and Curie temps. 3—30608
Fe_2O_3, angular depend. of field-induced antiferromag. to weak ferromag. transition 3—21228
Fe_3O_4, initial permeability in region of low temp. phase transition 3—36768
FePt alloy powders, ordered, anisotropy consts., saturation magnetiz., coercivity *(Russian)* 3—30652
$Fe(Pt_cPd_{1-c})_3$ Curie temp. calc. for ferromag. subsystem 3—12018
FeRh, alloys, positron annihilation study of electron structure of ferromagnetic and antiferromagnetic phases 3—7754
Ga:U, alloy systems, phase relationships 3—33654
Gd, elastic and inelastic behaviour in spin reorientation region, pressure effects 3—34116
Gd, neutron mag. form factor calc. using Dirac-Fock equation 3—21244
Gd, second mag. phase transition, molecular field model to explain anomalies in props. 3—15366
Gd-Y alloys, hydrostatic pressure effect on transition temp. at ferromag. to antiferromag. transition 3—2273
$GdAl_2$, transferred mag. induced ^{27}Al quadrupole interaction 3—34244
$GdCl_3$, ferromagnet with long-range interactions, crit. exponents 3—34121
$GdNi_2$, crit. point thermopower anomaly, spin scatt. vs. static entropy model 3—11888
$GdNi_2$, Landau model for critical susceptibility 3—15320
$GdNi_5$, cooperative phase behaviour, ht. capacity obs. 3—12016

ferromagnetic properties of substances continued
GdP, GdAs and GdSb thin films, spin polarized photoelectrons *(German)* 3—18531
$Gd_xTh_{1-x}PdIn$, evidence for RKKY-type ineraction 3—27364
$Gd_{1-x}Y(La)_xAl_2$, study of n.m.r. spin echo spectra lineshape 3—21328
$Gd_xY_{1-x}PdIn$, evidence for RKKY-type interaction 3—27364
^3He solid, quantum crystal, ferromagnetic next-near-neighbour exchange interaction 3—30310
$HfCo_2$, Laves phase, single region, mag. suscept. 3—27360
$HgCr_2Se_4$, magnetoabsorpt. obs., temp. and field depend. at Curie point 3—12122
$HoFe_3$, coercive force, remanence and hysteresis near mag. compensation point *(Russian)* 3—8380
K_2CrCl_4, optical absorpt. spectra 8000 to 25000 cm^{-1}, temp. range 4.2 to 300 K 3—12150
$KCrS_2$, mag. structure, ferromag. sheets with antiferromag. coupling 3—34132
$K_2CuCl_4.2H_2O$ type crysts., n.m.r. obs. of microscopic and macroscopic behaviour 3—2420
K_2CuF_4, mag. two dimensionality, obs. by neutron scatt. 3—15373
K_2CuF_4, two-dimensional ferromagnet, two-magnon excitation 3—30633
$LaAl_2$-$GdAl_2$, mag. ordering, Curie temp. depend. on Gd conc. 3—34122
Mn-Al alloy powders, comp. and defects influence *(Russian)* 3—24587
Mn-Al-B, magnetis. and coercive force, composition depend. 3—36744
Mn-Ga alloy powders, high-anisotropy, mag. reversals, domain boundary displacement *(Russian)* 3—36737
Mn-Ga alloys, plastically deformed, mag. hardness *(Russian)* 3—36735
MnAlGe, nonstoichiometric film, prep., structure, mag., and optical props. 3—36497
MnAlGe film, self-demagnetisation during thermomag. writing 3—24407
MnAs, ferro-paramag. transition, under the influence of light pulses *(Russian)* 3—2274
MnAs, mag. transform. in strong mag. field *(Russian)* 3—8364
MnBi fil, domain patterns, Faraday effect obs. 3—21272
MnBi film, low temp. props. 3—27384
MnBi single crystal platelets formed by vacuum deposition, flux reversal 3—2308
MnBi-Bi eutectic, directionally solidified, magnetis., single domain behaviour 3—36748
$MnCO_3:Fe^{2+}$, spin system and moment exam., reln. to concentration 3—2289
$Mn_3GaC:^{57}Fe$, Mossbauer obs. of ferromag. spectrum 3—12081
MnGaGe, ferromagnet, prep., struct., Curie temp., saturation magnetisation, mag. moments 3—21268
MnGaGe, sputtered film, ferromag. and magneto-optical props. 3—36861
MnGaGe film, Curie point writing with laser pulse, thermal and mag. profiles comparison 3—36860
Mn_5Ge_3 film, ferromag. reson., g-factor, magnetisation, 0-45°C 3—27419
$Mn_{3-x}Ni_xB_4$, spontaneous and saturation magnetization, and transitions *(Russian)* 3—8396
Mo_2MB_2 (M=3d transition metal), magnetic ordering from ^{57}Fe meas. 3—12083
$(NH_4)_2MnF_5$, linear chain antiferromagnet, weak ferromagnetism and anisotropy 3—30643
$NaNiF_3$, phonon and magnon light scattering 3—39148
$NdFe_2Si_2$, antiferromag. structure of Nd(2a) sublattice, ferromag. sheets, neutron diffraction obs. 3—34135
NdN, mag. ordering, neutron diffr. obs. 3—30630
$NdNi_5$, cooperative phase behaviour, ht. capacity obs. 3—12016
$NdZn_2$, ordering and struct., neutron diffr. obs. 3—27372
Ni, electronic density of states model rel. to locally nonmagnetic surface layer 3—33981
Ni, film, electromag. wave dispersion by spin waves 3—11923
Ni, rotational Hall effect, 80-650K 3—36595
Ni, self-consistent calculation of energy bands 3—18073
Ni, self-reversal of magnetization, temp. depend. *(Russian)* 3—27381
Ni, spin wave excitations, 4.2-715K, temp. depend., change in character above Curie point 3—30637
Ni, thermal variation of magnetostriction coeffs. 3—8409
Ni, transcritical epitaxial film, domain structure 3—30666
Ni, with Cr impurity, high field susceptibility 3—21225
Ni (100) single crystal film, magnetisation ripple 3—8399
Ni alloy:^{57}Fe, mag. impurity interactions and hyperfine field, Mossbauer obs. at 4.2K 3—36819
Ni base fcc ferromag. alloys with Co, Fe, Mn and Cr, CPA and H-F approx. calc. 3—8328
Ni solid soln., giant moments near ferromag. to paramag. transition 3—36716
Ni-Al, temp. depend. meas. showing phase transition *(French)* 3—8361
Ni-Co film, electrodeposited, stripe domains *(Russian)* 3—30667
Ni-Co layers covering Cu wires, mag. and mech. treatment effect on mag. props. *(Rumanian)* 3—12043
Ni-Co-Fe-SiO system, bilaminar films, field of interaction *(Russian)* 3—21267
Ni-Co-P film, cylindrical, anisotropy dispersion meas. *(French)* 3—25819
Ni-Cr disordered alloy, thermodynamic analysis near critical concentration *(Russian)* 3—2272
Ni-Cu, neutron diffraction obs. of mag. moments distrib. 3—15374
Ni-Cu alloy, mag. form factor, neutron diffr. obs. 3—24575
Ni-Cu alloy, magnetocryst. anisotropy consts. at 0°K, conc. depend. 3—21258
Ni-Cu alloys, temp. dependence of mag. susceptibility 3—18303
Ni-Fe, dilute ferromag. alloy, spin polarisation disturbances, Mossbauer obs. 3—27377
Ni-Fe (100) single crystal film, magnetisation ripple 3—8399
Ni-Fe alloy film, mag. hysteresis loops, domain struct., hypercrit. state *(Russian)* 3—15393

ferromagnetic properties of substances continued
- Ni-Fe alloy films with additional surface layers, spin wave reson., high field peak *(Russian)* 3—24615
- Ni-Fe electroless film, temp. and soln. pH effects 3—21278
- Ni-Fe film, damped magnetisation oscillations 3—36741
- Ni-Fe film, ferromag. exchange const., spin wave resonance obs. 3—34105
- Ni-Fe film, oblique incidence evap., mag. anisotropy, deuteron irrad. effects 3—34148
- Ni-Fe film, two layers separated by SiO, magnetic coupling, transverse suscept. obs. 3—34174
- Ni-Fe layers separated by SiO intermediate layer, magnetic coupling energy, transverse susceptibility meas. 3—8400
- Ni-Fe-Mn disordered alloy thermodynamic analysis near critical concentration *(Russian)* 3—2272
- Ni-Fe(25 wt.%) films, domain boundary curvature and displacement, mag. field and elastic stresses influence *(Russian)* 3—30654
- Ni-Mn ordered alloy, thermodynamic analysis near critical concentration *(Russian)* 3—2272
- Ni-Pt alloy, high press. and high field props., near crit. conc. for ferromagnetism 3—30622
- Ni-Sm film, saturation magnetization and hysteresis loops *(Russian)* 3—27382
- Ni-Sn, dilute alloy, two current cond. and impurity resist. 3—36719
- $(Ni_{74.5}Al_{25.5})_{100-x}Fe_x$, neutron obs. of giant moments 3—36717
- $Ni_3B_7O_{13}I$, crystal growth 3—17746
- $Ni_{1-x}Cu_xMnSb$, anomalous line shift in n.m.r. 3—30704
- NiFe, distrib. function of forces exerted by defects on domain walls 3—36756
- NiFe, magnetic moment distribution 3—34134
- $Ni_{75-x}Fe_xGa_{25}$ giant moment system, ^{57}Fe Mossbauer expt., determ. of hyperfine fields, isomeric structure, quadrupole splitting 3—39074
- Ni_3Mn, mag. induction, influence of annealing under load *(Russian)* 3—15729
- $NpC_{0.91}$, sp. ht. and derived thermodynamic props. rel. to mag. ordering 3—24566
- Pd-Ag-Gd solid solution, magnetic and crystallographic characteristics 3—8793
- Pd-Co dil. alloys, ^{57}Fe hyperfine field press. depend. up to 180 kbar 3—18306
- Pd-Fe, dilute ferromag. alloy, spin polarisation disturbances, Mossbauer obs. 3—27377
- Pd-Gd, solid solutions, magnetic and crystallographic characteristics 3—8793
- Pd-Mn(Fe)(Co) dilute alloys, ferromag. transition temp., resist. study 3—30624
- PdFe- like alloys, influence of mol. field spatial fluctuations on low temp. props. 3—27365
- PdMn, dilute alloy, magnetoresist. meas. with acoustic and optic mode excitations 3—15184
- $(Pr, Nd, Sm, Tb, Dy, Ho)Pb_3$, low-field susceptibility, magnetisation, 3-300K *(French)* 3—18302
- $(Pr,Sm)Co_5$, intrinsic coercive force rel. to Sm content 3—24585
- Pt-Fe, dilute ferromag. alloy, spin polarisation disturbances, Mossbauer obs. 3—27377
- Pt-Mn-Sn alloys *(Japanese)* 3—8346
- $PuPt_2$ cubic, mag. susceptibility obs. 3—38966
- $Rb_2CuCl_4.2H_2O$, Heisenberg b.c.c. ferromagnet nuclear quadrupole resonance obs. of magnetic interactions 3—27439
- $RbNiF_3$, acoustic birefr. due to magnetoelastic interaction 3—34177
- $SmAl_2$, crystal field effect on susceptibility and Knight shift 3—15322
- $Sm(Co, Cu)_5$, permanent mag. material, coercive force rel. to annealing 3—30658
- $SmCo_5$ powder, coercivity, grinding duration and method influence *(Russian)* 3—27731
- spin wave theories in the linear approximation 3—21251
- Tb, obs. of surface domain patterns 3—21274
- Tb-Fe alloy, amorphous spin-polarization distribution 3—8367
- TbGa, Curie temp., magnetization, hysteresis 3—2319
- TmNi mag. structure, crystal field effect 3—15375
- U:Ga, alloy systems phase relationships 3—33654
- UAsSe, neutron diffraction obs. of uniaxial ferromag. structure 3—12026
- $UAs_{1-x}Se_x$, ferromag. and antiferromag. props. with different x comps. in field up to 80 kOe 3—21227
- USbSe, neutron diffraction obs. of uniaxial ferromag. structure 3—12026
- U_3Se_4, cubic, magnetisation obs. from fields up to 80 kOe and temps. to above T_c 3—15356
- UTe, U_3Te_4, cubic, magnetisation obs. from fields up to 80 kOe and temps. to above T_c 3—15356
- U_7Te_{12}, meas. of magnetization max. 3—12011
- W_2MB_2 (M=3d transition metal), magnetic ordering from ^{57}Fe meas. 3—12083
- YIG, self interaction of finite amplitude magnetoelastic waves 3—39035
- YIG:Yb, ferromag. resonance instability due to transverse resonance relax. 3—27421
- $YbAl(Cu)_2$, $YbIn_3$, ambiguous mag. behaviour, susceptibility meas. 3—30609
- $YbNi_2$ crystalline fields and exchange interactions, Mossbauer obs. 3—30610
- $Zr_{0.80}Mo_{0.20}Fe_2$, heat treatment effects 3—21649
- $Zr_{0.60}Nb_{0.40}Fe_2$, heat treatment effects 3—21649

ferromagnetic relaxation
- *see also ferromagnetic resonance*
- Fe, ferromagnetic, relaxation of resonance spin waves by s-d exchange 3—21315
- YIG, rare-earth doped, wave vector depend. 3—5137

ferromagnetic resonance
- *see also ferroacoustic resonance; ferromagnetic relaxation*
- anisotropic metallic medium, ferromagnetic resonance field and linewidth 3—34214
- conducting ferromagnetic layer, role of magnetic microstructure in ferromagnetic resonance *(Russian)* 3—8448
- ferrite, hexagonal, ferromag. resonance obs. of magnetogyric ratio anisotropy 3—36730

ferromagnetic resonance continued
- ferromagnets with 'easy plane' type magnetic anisotropy, spin relaxation theory *(Russian)* 3—12063
- film, effect of ang. dispersion of anisotropy on reson. linewidth *(Russian)* 3—8452
- film, magnetoelastic interactions effect, application to Ni 3—34216
- film, magnetoelastic interactions effect 3—34215
- film, multilayer, u.h.f. susceptibility *(Russian)* 3—18371
- film, spin distrib. near surface rel. to boundary conditions, reson. spectrum effects 3—21254
- film, spin-spin relax. 3—21320
- isotropic spherical samples, size limitations rel. to g-factor and magnetic half-line width 3—12048
- Kapron-highly dispersed Fe, Co and Ni, ferromag. resonance, chemisorption effect 3—39409
- line-broadning, chemical magnetic inhomogeneities, permeability behaviour 3—34218
- line-width meter *(Russian)* 3—16466
- magnetic critical exponent β meas. by ferromagnetic transmission resonance 3—16465
- magnetometer incorporating thin-film sensor, patent 3—10001
- magnetostatic mode parametric excitation theory in infinite ferromag. plates by parallel pumping 3—8449
- metallic medium, anisotropic exchange cond. effects 3—2404
- metallic thin films, spin wave dispersion 3—27378
- Mossbauer technique applic. 3—2402
- nonlinear magneotacoustic resonance theory 3—8451
- parametric spin-wave nuclear double resonance, review 3—30678
- Permalloy, ferromag. resonance line width obs. on plastic deformation 3—5139
- Permalloy film, spin wave spectrum, surface conditions influence *(Russian)* 3—30698
- polyceproamide-highly dispersed Fe, Co and Ni, ferromag. resonance, chemisorption effect 3—39409
- semiconductors, electron and neutron scattering by coupled spin waves near ferromagnetic resonance *(Russian)* 3—12031
- spin wave reson. surface modes of antiferromag.-ferromag. surface coupled film 3—39033
- spin-wave approx. model of uniaxial ferromagnet in transverse magnetic field, dynamic eqns. 3—30701
- thin film, mixed boundary conditions, spin-wave reson. spectra analysis 3—21319
- YIG films, used to investigate spin-wave spectra 3—2400
- CAVBIG, self interaction of finite amplitude magnetoelastic waves 3—39035
- $CdCr_2S_4$, anomalies in mag. anisotropy and f.m.r. linewidth due to impurities 3—21318
- $CdCr_2Se_4$, temp. depend. 3—5033
- epitaxial film, induced in-plane mag. anisotropy obs. 3—34147
- Fe, ferromag. reson., 300-1090K, relax. parameter, g-factor 3—8450
- Fe, ferromag. resonance line width obs. on plastic deformation 3—5139
- Fe, ferromagnetic relaxation of resonance spin waves by s-d exchange 3—21315
- Fe:Si, anisotropy of f.m.r. line width 3—18372
- Fe-Cr alloys, anisotropy const. determ. 3—2403
- Fe-Ni alloy films, exchange parameters 3—2324
- Fe_3O_4 film, magnetite, low temp. conversion from α-Fe_2O_3, hematite obs. 3—34173
- $Gd_{3-x}Ca_xFe_{5-x}Sn_xO_{12}$ ferrite-garnets temp. dependence of FMR linewidth near Curie point *(Russian)* 3—36795
- $K_2CuCl_4.2H_2O$, temp. depend. calc. of ferromag. resonance linewidth 3—15425
- $Lu_2EuMFe_4O_{12}$ (M=Al or Ga) garnet, growth-induced mag. anisotropy of epitaxial films 3—21259
- Mn-Zn ferrites, low resistivity, resonant modes 3—2398
- Mn_5Ge_3 film, g-factor, magnetisation, 0-45°C 3—27419
- Ni, highly stressed films, resonance at oblique angles 3—21317
- Ni, linewidth depend. on dislocation density *(Russian)* 3—18370
- Ni, temp. depend. calc. of ferromag. resonance linewidth 3—15425
- Ni-Fe alloy films with additional surface layers, spin wave reson., high field peak *(Russian)* 3—24615
- Ni-Fe film, exchange const. obs. 3—34105
- $Y_{3-x}Ce_xFe_5O_{12}$, magnetostriction study *(Russian)* 3—12046
- $Y_2EuMFe_4O_{12}$ (M=Al or Ga) garnet, growth-induced mag. anisotropy of epitaxial films 3—21259
- $Y_3Fe_{5-x}Ga_xO_{12}$, high pressure effect on line width rel. to dislocations 3—5138
- YIG, grown from soln. in PbO-PbF_2, characterization *(Russian)* 3—30942
- YIG, intrinsic e.m. radiation in presence of domain struct. 3—34217
- YIG, line width, temp. depend., near Curie point *(Russian)* 3—8454
- YIG, nonlinear excitation threshold meas. *(Russian)* 3—15426
- YIG, nonlinear reson., domain struct., instability *(Russian)* 3—8453
- YIG epitaxial film, lattice mismatch effects 3—30700
- YIG film, phonon generation 3—36794
- YIG:Ge substituted, anisotropy and magnetostriction obs. 3—5136
- YIG:Pr^{3+}, angular maxima of ΔH splitting under pressure *(Russian)* 3—2399
- YIG:Yb, instability due to transverse resonance relax. 3—27421

ferromagnetism
- *see also coercive force; domain walls; ferromagnetic metals; ferromagnetic properties of substances; ferromagnetic relaxation; ferromagnetic resonance; Heisenberg model; Ising model; magnetic domains; remanence; spin waves*
- alloy, disordered, Went's theory modification using correlation range 3—15315
- antiferromagnetic semiconductor, inhomogeneous ferro-antiferromag. state 3—21223
- atmospheric ferromag. particles, size depend. rel. to ice crystal formation 3—37227
- atmospheric ferromagnetic particles, conc. and size distrib. meas. technique 3—37260
- collective model, spin wave spectrum, RPA approach *(Russian)* 3—36698
- complete, in perfect crystals, nonexistence 3—5085
- crystal with ferromag.-antiferromag. transition, magnetoacoustic waves 3—21289
- cubic magnet, interaction of surface magnetoelastic waves with elastic Rayleigh waves *(Russian)* 3—8410

ferromagnetism continued
- Curie temp. increase by spin-phonon interaction 3−38971
- degenerate band model 3−38953
- dilute alloy, thermodynamic and kinetic props. 3−34109
- dilute system, Curie temp. conc. depend. *(Japanese)* 3−38981
- double-exchange ferromagnet, spin waves, quantum theory 3−21192
- easy plane hexagonal ferromagnets, phenomenological theory of magnetoelastic modes 3−34138
- exchange interaction model, crit. point props., single-ion anisotropy effects 3−38936
- film, honeycomb domain struct. 3−30662
- film, spin distrib. near surface rel. to boundary conditions, reson. spectrum effects 3−21254
- film, weakly amorphous, density of spin wave states, Heisenberg model calc. 3−30636
- film, with rough surface, spin wave spectrum and magnetization 3−18331
- Heisenberg ferromagnet, exchange interaction of surface spins causing surface antiferromagnetism 3−38951
- Heisenberg ferromagnet with hard magnetisation axis, spin waves 3−30635
- Heisenberg model, amorphous, spin-wave spectrum, calc. 3−30593
- Heisenberg model, anisotropic, crit. temp. 3−24553
- Heisenberg model, spin 1/2, perturbation theory 3−15329
- Heisenberg spin system with two-dimensional defects, localized states *(Russian)* 3−8320
- Heisenberg susceptibilities, calcs. using lattice Green's function 3−22752
- Heisenberg-exchange model, self-consistent selection of ferromagnetic representation 3−38950
- highly anisotropic ferromag., mag. anisotropy and magnetostriction theory 3−24581
- Hubbard model, spin waves in ferromag. state of narrow band 3−15343
- Hubbard model 3−21210
- inhomogeneous electron gas, spin effects 3−33773
- Ising model, two-dimensional, surface tension between oppositely magnetised phases 3−38946
- Ising model variational approximation in a magnetic field 3−36696
- Ising spin systems, bounds on correlations and analyticity properties 3−2235
- isotropic ferromagnet, modified Bloch equation 3−27339
- itinerant electron model, spin wave energy at low temps. 3−34082
- magnetic field influence on magnetic mould properties *(Russian)* 3−34167
- magnetic moment, spin waves, uniform oscillation instability 3−34142
- magnetically dilute system, theory *(Japanese)* 3−38952
- magnetism, introduction to the theory, monograph 3−2224
- magnetoelastic wave theory for finite plates *(Russian)* 3−8405
- magnetovolume effect in nearly and weakly ferromagnetic materials 3−18351
- metals, low frequency oscill. and scattering processes *(Russian)* 3−34146
- micromagnetism, Lorentz approx. 3−5083
- multidomain ferromagnet, kinetics of conduction electrons 3−34169
- particles, weakly nonspherical ferromag., mag. struct. 3−34172
- phase transition in two-dimensional exchange interaction model, numerical evidence 3−34106
- planar Heisenberg ferromagnet, low temp. behaviour 3−34071
- plate, magnetiz. oscillations spectrum *(Russian)* 3−30649
- plate, residual magnetization state, thickness effects *(Russian)* 3−8384
- plate, thin, with easy plane type anisotropy, mag. reversals *(Russian)* 3−15388
- plate, travelling wave excitation, steady state elliptical vector mag. field 3−18341
- proximity effect for weak itinerant ferromag. film in contact with paramag. metal 3−34086
- random-walk method application to theory of magnetism 3−18288
- reversal nuclei, energy barrier of formation 3−18277
- s-d interaction, use of Green's function 3−2245
- self-consistent band calculations for Fe, ferromag. state 3−21205
- semi-infinite gyromagnetic media, surface polaritons 3−36726
- semiconductor, elec. resist., sample boundary and domain wall effects 3−34170
- semiconductors, max. resistivity due to carrier scattering by giant moments of mag. clusters 3−18145
- Smoluchowski-type treatment of fluctuations at the critical point of ferromagnets 3−34063
- solid solutions, anomalous microregions, Mossbauer obs. 3−34272
- spin fluctuations rel. to itinerant electron ferromag. 3−27353
- spin operators represent. through generalized Pauli operators for arbitrary spin magnitudes *(Russian)* 3−36692
- spin ordering, rel. between thermoelectric power and thermal cond. 3−34129
- spin system, Heisenberg Hamiltonian with crystal field anisotropy spin 1, diagram technique 3−34064
- spin system with ferromagnetic exchange interaction, application of Abrikosov's pseudofermion technique 3−38970
- spin systems in d dimens., time-depend. fluctuations 3−38947
- spin wave modes in metallic ferromagnets, theory 3−30634
- spin waves, parametric excitation, ferromagnets with magnetic inhomogeneities, diagrammatic technique 3−38986
- spin-1 model of ferromagnetism, high-temp. series expansion 3−38939
- static field calc. in nonlinear ferromagnetic medium *(Russian)* 3−34050
- static magnetic field in ferromagnetic medium, eqn. formulation by variational approach *(Russian)* 3−34049
- stimulated magnon generation, theory 3−34144
- surface magnetism 3−18278
- suspension of dipolar spherical particles in external field, rotary Brownian motion effects on rheology 3−31199
- thermodynamic properties, spin system, ferromagnetic layer structure, Green function method 3−38932
- thermoelastic eqns. for ferromagnetic bodies 3−37912
- thin films magnetisation direction distribution in band model 3−27352
- tilted helix, intermediate magnetic phase 3−34130

ferromagnetism continued
- Tomita-Tanaka approx. validity in limit of spin 112 Ising ferromagnet 3−34067
- two-magnon bound states 3−34139
- uniaxial ferromagnet, in transverse mag. field, free energy, spatial magnetization fluctuation effects 3−18315
- Van Hove singularities and zero-point slopes in mag. crystals 3−30383
- Van Vleck exchange-induced ferromagnets, surface effects 3−34062
- vector model with long-range interactions, crit. exponents and scaling relations 3−2236
- vector spin model, pair correlation functions 3−30594
- XY model, three-dimens., freq. depend. susceptibility, singularity struct. 3−615

ferromagnets *see ferromagnetic properties of substances*

ferrous alloys *see iron alloys*

f.e.t. *see field effect transistors*

few-nucleon systems *see nuclei with* $A \leqslant 5$

Feynman diagrams
- atomic energy levels for state with two electrons (holes) in unfilled (filled) shell 3−20002
- classification problems and elementary topological ideas in high energy phys. 3−816
- computer calculation, using REDUCE package 3−10684
- critical exponents, skeleton graph expansion, many body perturbation theory 3−16779
- current-voltage problem, quantum field theory approach 3−2075
- dual resonance model, Nakanishi decomposition, Feynman-like rules, extension to general loop amplitudes 3−14033
- eikonal approx. for gravit. vertex of infinite sum of gravitons 3−6343
- eikonal approx. validity and eighth order graphs 3−10623
- finite-energy sum rules for five-point amplitudes and duality 3−35812
- functional integrals in quantum mechanics and field theory 3−28954
- gauge field combinatorics, prescription for obtaining Feynman rules in different gauges 3−10601
- heavy nuclei, parity nonconservation and weak interaction Hamiltonian struct. 3−26369
- high-energy behaviour of particles, in quantum electrodynamics 3−13847
- Kahane algorithm for scalar products of γ-matrices, generalisation 3−10589
- Lee-Yang theorem in functional integral and Hori operator formulations 3−6554
- nucleon-nucleon scatt. sixth order Feynman graphs, calc. by Pade approximants 3−19720
- one-loop generalized Feynman integrals, derivation of differential eqns. 3−28830
- renormalisation using complex space-time dimensions in arbitrary Feynman graph 3−16932
- rules for Higgs model 3−32624
- semiclassical solution theory within Feynman path integral formalism 3−28951
- spontaneously broken gauge theories, divergence cancellations 3−35748
- topological properties, in form of matrix relationship 3−26285
- variable integrals, multidimensional quadrature procedure, adaptive 3−10588
- vertex graphs technique 3−35738
- μ decay, higher-order contributions in spontaneously broken gauge model 3−10665
- π electroproduction at N*(1236), isobaric model calc. using Feynman diagrams 3−13930
- π photoproduction, gauge-invariant field-theory model based on Feynman graph model 3−4179
- πd scatt. in Δ(1236) region, calc. of amplitude from Feynman diagrams *(Russian)* 3−19744

fiber optics *see fibre optics*

fibers *see fibres*

fibre optics
- applied to microscopical method of measuring amplitudes of vibration 3−16383
- bubble detect. in garnet film using waveguide fibre optics 3−35442
- cantilever apparatus for breaking stress distributions 3−25666
- channel plates (fibre-optic electron multipliers) as image intensifiers in transmission electron microscope 3−356
- communication system, using laser-glass fibre transmission paths *(German)* 3−29153
- glass fibre, current meas. using Faraday rotation 3−6028
- glass fibre optical waveguide, low loss, scatt. light angular distrib. 3−675
- glass fibres, radially inhomogeneous, wave propagation 3−16797
- glass fibres activated with Nd_2O_3, properties in amplification region *(Russian)* 3−6488
- high-gain light-intensifying device incorporating fibre-optic X-ray intensifying faceplate 3−28741
- image formation, analytical model using fibre-optical components and optoelectronic conversion principles *(Russian)* 3−25583
- image formation, using self imaging techniques 3−32523
- image transfer element, holographic evaluation of characts. 3−5962
- integrated optics applications *(German)* 3−16806
- laser beam applications *(Spanish)* 3−6456
- laser communication systems, review 3−26249
- laser communication systems 3−35718
- light transmission meas. method for information and nonworking flux components 3−16796
- liquid core, intensification of spontaneous Raman spectra 3−13292
- low loss fibres, double reverse scatt. interference, equalizer 3−149
- multimode, pulse broadening 3−13761
- multimode fibres, with graded and ungraded core indexes, bending mode loss 3−150
- oblique incidence meter, photoelastic coating strain applic. 3−9838
- power handling capacity rel. to stimulated Raman and Brillouin scatt. 3−766
- resolution rel. to manufacturing defects 3−25743
- resolving power and optical transfer function meas. for pile of elements 3−22840
- review of work performed at Bell Laboratories 3−691

fibre optics continued
- Selfoc fibres, imaging, focusing props., spherical 3—13715
- solar magnetograph, fibre optic probe geometry rel. to incident image 3—31826
- spectral reflection meas. using fibre optic techniques 3—35408
- waveguides, loss meas. problems 3—168
- wedges, coherent light propagation, interference patterns *(Russian)* 3—6416
- H beta line shape meas. of transient plasma 3—11502

fibres
- *see also asbestos; carbon fibres; composite materials*
- carpets, incident absorption, reverberation room method rel. to impedance tube method, diffraction effects, absorption coefficients 3—105
- ceramic, reinforced composites strength, theories 3—15777
- composite, brittle matrix ductile fibre, fracture mechanics 3—31134
- composite, filamentary reinforced metals, mech. prop. considerations 3—31155
- composite, matrix fatigue behaviour under repeated tensile loads 3—31154
- composite, metal fibre reinforced ceramics, fabrication and fracture toughness 3—18718
- composite, metal matrix/fibre reinforced, solidified, Piobert-Luders band deform. *(French)* 3—39391
- composite, multiple fracture, theory 3—34633
- composite, polymer based, thermal expansion review 3—34632
- composite, reinforced metal matrix, deform. and fracture behaviour *(Japanese)* 3—34634
- composite material, filamentary, elastic wave propag. characts. 3—6272
- composite materials, fracture phenomena 3—37089
- composite materials, tensile strength, review 3—24992
- composite materials elastic wave propagation theory 3—2761
- composite materials fibre-reinforced, Saint-Venant's principle for plane deformation 3—32333
- composite sandwich, C and glass, Izod impact props. 3—31131
- composites, fibre reinforced, nondestructive prediction of engineering props. 3—34672
- cotton, cellulose crystallite orientation, X-ray meas. 3—31166
- cotton, charge measurement, apparatus 3—6012
- cotton, X-ray diffraction study of crystallite orientation, determ. of average spiral angle 3—31157
- creep theory review for fibre composites 3—15774
- elastic deformation of fibre reinforced incompressible isotropic elastic materials, universal solns. by inverse methods 3—28865
- elastic properties of materials reinforced by unidirectional short fibres *(Russian)* 3—24987
- eutectics, fibrous and lamellar, unidirectionally solidified, microstructure *(Japanese)* 3—18592
- fibre-reinforced plates, constant thickness, optimisation 3—22607
- glass, and resins, adhesion testing *(German)* 3—21730
- glass, ion exchange at low temps. and effect on internal friction 3—25064
- glass, multimode, and laser diode, cooupling losses, obs. *(German)* 3—13742
- glass, reinforced epoxy resin hybrid composite, mech. props. *(Japanese)* 3—18708
- glass, reinforced nylon, tensile strength 3—2759
- glass, reinforced polyester laminates, mech. props. *(Japanese)* 3—18707
- glass, reinforcement of brittle matrices 3—31140
- glass, stability and antifriction props., u.v. irrad. effects *(Russian)* 3—27766
- glass, static hysteresis from −78 to 196°C 3—38619
- glass, statistical strength distrib. functions 3—31147
- glass, strength in polyester resin 3—15772
- glass fabric laminate reinforced composite, compressive strength *(Japanese)* 3—18715
- glass fabric laminate reinforced composite, torsional strength and void effects *(Japanese)* 3—18714
- glass fibre composite, fracture surface energy and transverse fracture 3—12443
- glass fibre reinforced composites, crack propag. vel. 3—21727
- glass fibre-resin composites of high strength 3—34638
- glass reinforced cylindrical shells, elastoplastic deform. 3—27761
- glass reinforced plastic cylindrical shell weakened by circular opening, cantilevered, bending 3—31149
- glass reinforced plastic cylindrical shells, creep stability under long-term external press. 3—31144
- glass reinforced plastic plates, rectangular, with low shear strength, bending 3—24985
- glass reinforced plastic plates with central metal layer, elastoplastic stability 3—24984
- glass reinforced plastic rings, temp. deform. 3—27764
- glass reinforced plastic rings, wound, residual stresses determ. 3—24983
- glass reinforced plastic rings, wound, transverse characts. variation over thickness 3—31150
- glass reinforced plastic shell, orthotropic, effect of local load 3—31145
- glass reinforced plastic shells, anisotropy of props. 3—24979
- glass reinforced plastic shells, cylindrical, stability 3—24982
- glass reinforced plastic shells, stability and shear stresses 3—24980
- glass reinforced plastic shells, two-way reinforcing system effect on load-carrying capacity 3—27760
- glass reinforced plastics, oriented, mech. characts. in shear 3—27779
- glass reinforced plastics, residual stresses determ. 3—27763
- glass reinforced plastics, tensile deform. analysis 3—31148
- glass reinforced plastics, wound, resist. to failure by unwinding 3—24981
- glass reinforced plastics in conical shells, stability of strength 3—31146
- graphite, composite, friction and wear 3—39392
- graphite, filamentary growth on metallic impurities 3—18047
- ion thinning, for transmission electron microscopy, sputtering of rough cylinders 3—36248
- magnesia, fibrous, grown via vapour phase *(Japanese)* 3—8728
- man-made, liquid suspension, alignment in magnetic field 3—5347
- materials science and technology treatise 3—2621

fibres continued
- oblique fibre sparsely reinforced matrix, constitutive eqns., impact-deflection 3—24990
- organic/epoxide composite, evaluation 3—31132
- orientation in electrostatic field, statistical minimum angle determination *(Russian)* 3—29003
- oriented plastics, failure mechanism 3—31183
- plastic, reinforced plates, grillages of maximum strnegth and maximum stiffness optimality conditions 3—3935
- plastic reinforced, design problems analysis 3—15790
- poly(ethylene terephthalate), structure, X-ray obs. 3—24033
- polyacrylonitrile, drawn, struct. changes during annealing 3—20236
- polyamide, polystyrene graft, small angle X-ray obs., intrafibrillar amorphous regions *(Russian)* 3—30077
- polycaproamide, creep behaviour during homogeneous cold drawing 3—21739
- polycaprolactam filament, morphology 3—33176
- polyethylene, drawn from single crysts., mol. struct. 3—33177
- polyethylene, linear, supermol. struct. influence on strength and deform. characts. 3—20232
- polyethylene, oriented, conform. transitions associated with elastic tension 3—29810
- polyethylene fibrillar crysts., hydrodynamically induced crystn. from soln., tensile props. 3—21738
- polyethylene film, h.p., supermol. transitions associated with reorientation 3—23653
- polymer, interference microscopy 3—25727
- polymer, melt-crystallized, spherulitic struct. change during uniaxial stretching 3—20238
- polymer, morphology and macrocrack form. on fracture surfaces 3—20241
- polymer, PRD-49, composite reinforcement, aircraft appl. 3—31133
- polymer, wet formed, porosity *(Polish)* 3—34648
- polymeric, textile, review of mech. props. 3—9010
- porosity, dependence of mech. props. *(Polish)* 3—31174
- refractive index meas. using microscope with spectrum projected into plane of object 3—16411
- reinforced composite, analogies, modelling and similarity criteria 3—27758
- reinforced composite, elasticity theory with microstruct. 3—530
- reinforced composite material, elastic stiffness analysis, structural design 3—31130
- reinforced composites, continuum mixture theory of wave propagation including microstructure 3—24975
- reinforced composites, strengthening mechanisms 3—21731
- reinforced metal, bond strength between fibre ad matrix 3—37093
- reinforced metals, tensile testing, rule of mixing applic. *(German)* 3—24991
- reinforced plastic bonded struct., strength *(Japanese)* 3—18712
- reinforced plastics, impact resist. *(Japanese)* 3—18705
- reinforced plastics, lamination effect on flexure behaviour *(Japanese)* 3—18713
- reinforced plastics, strength reliability and design *(Japanese)* 3—18709
- reinforced plastics, visco-plastic-elastic expression for stress/strain diagram under l.f. loads *(Japanese)* 3—18711
- reinforced plates, comment on paper by Lowe and Melchers on optimisation 3—32356
- reinforced plates, constant thickness, optimal layouts 3—24974
- rheology and spinning, conference (Knoxville, USA Oct. 1971) 3—552
- scanning electron microscope applications 3—12459
- sintered glass, viscosity exam. in softening and annealing temp. regions *(Russian)* 3—11549
- steel, stainless, water saturated sintered fibre wicks, effective thermal conductivity meas. 3—15802
- thermoplastic, fibre reinforced, deformation behaviour rel. to fibre length and orientation 3—8996
- trans-1,4-polyisoprene spherulite, deformation, small angle X-ray diffr., thermal differential analysis, density 3—27786
- X-ray diffr., orientation factors by precession method 3—36235
- X-ray diffraction pattern analysis 3—7602
- Young's modulus meas. method using bending oscillations *(German)* 3—25668
- Al_3Ni, in Al matrix, unidirectional fibre composite, elastic consts., u.s. vel. meas. 3—34637
- Al_2O_3 fibres, h.v. electron microscopy 3—1537
- Al_2O_3 reinforced Ti alloy composite, reactivity and interface struct. 3—31136
- B, compatibility with W substrate and Ti matrix *(Russian)* 3—15784
- B, reinforced epoxy composites, discontinuous, impact toughness 3—31137
- B fibre reinforced Al matrix, transverse tensile props. 3—18716
- B fibre/W substrate, diffusion barrier establishment *(French)* 3—12440
- B fibres in polymer matrix for high heat resist. 3—18697
- B filament, gauge length influence on mechanical strength *(Japanese)* 3—18704
- B/Al composite, matrix fatigue behaviour under repeated tensile loads 3—31154
- Cu water saturated sintered fibre wicks, effective thermal conductvity meas. 3—15802
- Cu-W fibre composite, thermal expansion *(Japanese)* 3—18703
- Fe/Cu single-fibre composite, multiple yield phenomena 3—34636
- Mo, annealing temp. effects on props. rel. to composite fabrication *(Czech)* 3—31153
- Nd:glass fibre amplifiers, threshold characteristics of receivers *(Russian)* 3—740
- Ni water saturated sintered fibre wicks, effective thermal conductivity meas. 3—15802
- SC whiskers, h.v. electron microscopy 3—1537
- SiO_2, silica, fibre fabric, influence of heat treatment on props. *(Russian)* 3—15775
- TaC, and nichrome matrix binary eutectic, orientation determ. by etching 3—18701
- Ti/W composites, solid-state interfacial reactions 3—31139
- W, annealing temp. effects on props. rel. to composite fabrication *(Czech)* 3—31153
- W, reinforced composite, Cu matrix, thermal cycling 3—37092
- W wires, role of fibre boundaries during drawing 3—8903

- **fibres** continued
  - W-3Re:$2ThO_2$, use as fibre reinforcement, dispersion hardening rel. to high temp. strength 3—15696
  - ZrO_2 fibres, h.v. electron microscopy 3—1537
- **field, crystal internal** *see crystal internal fields*
- **field effect devices**
  - *see also metal-insulator-semiconductor devices*
  - image sensors, charge-coupled, sensitivity and resolution at low light levels 3—29058
  - ion implantation technology, advantages and application, 3—18556
  - thin films, semiconducting, screening length, electrostatic analysis of field effect 3—36665
- **field effect transistors**
  - charge amplifier application, for high energy physics 3—28684
  - deep ocean pressure effects 3—3267
  - dendritic growth detection circuit 3—6083
  - m.o.s., charge trapping, slow state effects at Si-SiO_2 interface 3—5056
  - m.o.s., n-channel enhancement type, avalanche injection realisation 3—34000
  - m.o.s., photoresponse 3—38902
  - m.o.s.t., elec. props. of anodically grown SiO_2 film 3—24524
  - neutron irrad., limiting design parameters 3—33991
  - Si m.o.s., nonlinear transport and netative diff. mobility in surface inversion layer 3—11952
  - Si oxidised surface, m.o.s. electron surface mobility in inversion layers at room temp. 3—8268
  - Si-SO_2 m.o.s., X-ray irradiated, drain current, transfer characteristics changes during illumination with visible, u.v. light 3—8270
- **field emission, electron** *see electron field emission*
- **field emission microscopes**
  - *see also electron microscopes; ion microscopes*
  - atom-probe field-ion microscope for surface microscopy and analysis 3—28733
  - ion, identification of metal compound ions, effect of electron multiplier afterpulses 3—19339
  - ion, study of Co-Ti alloy 3—27635
  - mapping of surfaces 3—28735
  - open type, in exptal. chamber *(Russian)* 3—10111
  - specimen holder and air lock, for use in high vacuum field ion microscope 3—13461
  - ultra high vacuum field ion microscope, using an ion pump *(French)* 3—10115
  - Ge emitter tip, obs. of epitaxial growth of Ge 3—33750
  - W emitter, etching technique for preparing fine tip *(Japanese)* 3—19327
- **field intensity patterns (antenna)** *see antenna radiation patterns*
- **field ion microscopy**
  - *see also ion microscopes*
  - atom probe, effect of electron multiplier afterpulses, identification of metal compound ions 3—19339
  - atom probe field ion microscope, construction, uses 3—13472
  - atom-probe microscope for surface microscopy and analysis 3—28733
  - incolour, using multiple imaging gases 3—19331
  - energy spectrum of field ionisation at single atomic site 3—35508
  - field emission, bright spot density 3—19330
  - field ionization processes, time depend. perturbation theory image form. mechanism 3—8708
  - field-ion atom probe analysis 3—28778
  - grain boundaries, field-ion microscope anal. of atomic structure 3—30128
  - grain boundary contrast in images, computer image simulation 3—17853
  - grain boundary contrast in images, rel. to tilt and twist 3—17852
  - grain boundary contrast in images 3—17851
  - grain boundary topography 3—384
  - h.v. electron microscopy of field ion specimens prior to ion microscopic examination for defect location 3—385
  - image formation effect of e.s. field asymmetry 3—19661
  - using image intensifier 3—22502
  - imaging theory, quasiclassical site-current formula 3—19334
  - imaging theory, site current variations origin 3—19335
  - lower field strengths, vacuum and image intensification techniques 3—382
  - metals, quenched or irradiated, obs. of point defects 3—24106
  - moire interpretation 3—33721
  - operation at 4.2K, imaging process and field evaporation 3—6107
  - specimen cleaning, in situ, by Ar ion bombardment 3—23963
  - specimen fracture, electron microscope obs. 3—1533
  - state-of-the-art 3—22512
  - steel, ferrous martensite, as-quenched and tempered, fine struct. 3—34540
  - steel microstructural studies, as complement to transmission electron microscopy 3—383
  - surface studies 3—30322
  - surface texture, corrosion, adsorption 3—1864
  - surface-vacuum interface, conference, Enschede, Netherlands, June (1972) 3—30316
  - thin film and surface studies, review 3—27159
  - tip radius determ. to higher accuracy, field calibration 3—28726
  - Al, techniques for surface investigation 3—28734
  - Au, spot struct. obs. and explanation *(German)* 3—27160
  - Au, techniques for surface investigation 3—28734
  - Co-Ti alloy, preliminary study by field ion microscope 3—27635
  - $CoPt_3$, partially ordered, atomic configs. 3—14738
  - Cu, techniques for surface investigation 3—28734
  - Fe-Cu alloy, phase change in microdomain, field ion microscope images 3—18563
  - Ga deposited on Mo substrate, study of Mo_3Ga form. and anisotropic binding force 3—24319
  - Ga deposited on W substrate, study of pseudomorphic and superstructures 3—24318
  - He ion imaging rel. to Ne 3—3875
  - He-Ne mixture, field adsorption and ionisation rel. to imaging process 3—22514
  - Ir specimens, occurrence of field-induced surface vacancies 3—35507
- **field ion microscopy** continued
  - Mo film, on W. Ir and Re, grown from vapour, struct., field in microscope obs. 3—38753
  - Ni_4Mo, ordered, field-ion image interpretation, computer simulation procedure 3—8804
  - Os surface study using He ions 3—20912
  - Si crystal growth by Pt evaporation technique, obs. of atomic positions and diffusion dynamics 3—11789
  - W, corrosion, H promoted, by O_2 in elec. field, surface topography changes 3—30359
  - W, surface diffusion and clustering, interpretation of ion microscopy data 3—36475
  - W, surface diffusion and clustering, interpretation of field ion microscopy data 3—36476
  - W tips, displacements of individual adatoms by elec. field *(French)* 3—24343
- **field measurement, electric** *see electric field measurement*
- **field measurement, magnetic** *see magnetic field measurement*
- **field plotting**
  - *see also field strength measurement*
  - geophysical fields, cartographic representation method 3—25321
  - parallelogram of linear currents, analysis of magnetic field *(French)* 3—4059
  - GaAs, high ohmic, subthreshold, surface potential mapping using scanning electron microscopy *(German)* 3—8263
- **field strength measurement**
  - *see also electric field measurement; magnetic field measurement*
  - loop and dipole antennas, equipment for checking and calibrating *(Russian)* 3—19237
  - thunderstorm distance determ., spectra components ratio of field strength method 3—25336
- **field theories, unified** *see unified field theories*
- **field theory, classical** *see classical field theory*
- **field theory, crystal** *see crystal field theory*
- **field theory, electromagnetic** *see electromagnetic field theory*
- **field theory, meson** *see meson field theory*
- **field theory, quantum** *see quantum field theory*
- **fields, electric** *see electric fields*
- **fields, magnetic** *see magnetic fields*
- **filament lamps**
  - portable underwater lamp, W-halogen lamp, heat treated globe 3—3258
  - spectral radiance comparator for pyrometric standards *(Japanese)* 3—22328
  - temperature calibrated, brightness temp. checking using differential method 3—25687
  - W, with H and halogen gases, equilibrium of gases and chemical transport reactions *(German)* 3—25101
  - W filaments, void formation 3—27636
  - W incandescent, polarization pattern 3—6410
- **file management** *see file organisation*
- **file organisation**
  - *see also data handling*
  - molecular orbital program OPIT, file-handling scheme for data in large applications program 3—29564
- **films**
  - *see also coating techniques; interface phenomena; liquid films; optical films; substrates; thick films; thin films*
  - adhesive, use to obtain primary impressions in electron microscopy 3—18747
  - bearings, fluid film lubrication, fluid mechanics, review 3—33326
  - plastic, deterioration on accelerated aging in u.v. light *(Japanese)* 3—7279
  - Zircaloy-2 corrosion in hot water and steam, oxide film growth 3—37021
- **filtering and prediction theory**
  - *see also information theory; Kalman filters; random processes*
  - averaged evoked brain potentials of hippocampus, component analysis 3—35241
  - linear prediction analysis of speaker recognition and verification 3—3668
  - low bit-rate coding from autocorrelation method of linear prediction 3—3639
  - modified Gaussian second order filter, for interplanetary orbit determination 3—39585
  - optical filtering consideration 3—4072
  - orbits, difference equations for estimation of biases in filtering problem *(Russian)* 3—16098
  - power spectrum anal. of ionospheric data, use of running means to remove i.f. components 3—25338
  - river flows, real time recursive prediction using stochastic models 3—28092
  - seismic prospecting, Kalman filter as prediction error filter 3—9351
  - seismic velocity filters, Wiener theory applic. 3—3171
  - slot-coupled toroidal resonators, scatter calculation by computer *(Russian)* 3—32401
  - speech, nonlinear inverse filtering 3—3417
- **filters**
  - *see also active filters; band-pass filters; crystal filters; digital filters; electromechanical filters; Kalman filters; microwave filters; optical filters*
  - amplifier, for timing experiments 3—25911
  - broadbanding design for scanning nondestructive testing 3—37100
  - electron microscopy, energy filter for Kikuchi diagrams *(French)* 3—388
  - Fabry Perot narrow-band with dielectric reflectors, enhancement of transparency *(Russian)* 3—3815
  - heave filters for gravity meas. on surface ship 3—9155
  - matched, design for scanning nondestructive testing 3—37100
  - of polarization states, total reflexion *(French)* 3—13677
  - processing, for underwater transmission loss obs., principles in choosing 3—3725
  - quadrupole mass filter, dependence of ion transmission on initial RF phase 3—329
  - quadrupole mass filter, reproducibility of pattern coeff. for 6 hydrocarbons *(Japanese)* 3—22548

filters continued
seismic waves, band varying signals, optimum multichannel system 3–9367
sonar, multipath and reverberation effects, optimum design 3–3736
filters, optical *see optical filters*
finite element analysis
acoustic field in irregular rooms, automobile compartment 3–5733
axially symmetric, comparison of first and second order methods 3–22624
axisymmetric circular plates, static, vibration and buckling analysis 3–32310
axisymmetrically loaded orthotropic shell of revolution 3–10273
bending and stability and of beams and plates, lumped finite element technique 3–32385
blood flow turbulence effects study 3–17495
bounds on eigenvalues in vibration and stability problems 3–563
composite shells, optimal design, subject to natural frequency constraints 3–32367
compression of hollow cylinder, theoretical analysis 3–19424
consistent conjugate stresses computation for elastic finite elements 3–26076
constant curvature beam elements, for in-plane vibrations 3–22685
constant strain/constant moment elastic deformation problems, unification of solution methods 3–32322
containment vessel for loss-of-coolant in nucl. reactor, stress anal. 3–11073
convergence in problems with singularities 3–22616
convergence of Timoshenko beam finite elements 3–564
coupled thermoelastoviscoplasticity in crystalline solids 3–38612
creep analysis of transversely isotropic bodies subjected to time-dependent loading 3–39368
creep bending analysis of plates by finite element method 3–16653
cylindrical shell stability study *(German)* 3–551
discretization of continuous media, determ. of constructive eqn. and eqns. of motion 3–28844
dislocation systems, stress fields 3–27027
doubly curved finite elements for analysis of thin shallow shells with large displacements 3–16616
elastic plane stress and strain in structures 3–22628
elastic plastic, of Saint-Venant torsion problem by hybrid stress model 3–514
elastic-plastic plate bending 3–10274
elasto-plastic stress analysis in partly yielded notched bar, assessment of methods 3–26077
elastoplastic medium, void growth 3–24959
field problems in cylindrical coordinates 3–32494
finite sized plates bonded to elastic half space 3–508
flexibility matrix for exact torsion-bending finite element 3–546
flow of water over spillway crest 3–33195
forced vibrs. of axially symmetric shell *(Russian)* 3–10317
freely supported axisymmetric shells, dynamic analysis 3–28911
generalized systems for boundary value problems 3–16601
guided spherical shell, finite element model rel. to dynamic response of flextensional underwater transducer 3–3728
hybrid displacement method for statics, vibr. and stability of thin elastic plates 3–10282
hydrodynamics application *(Japanese)* 3–1337
incompressible two-dimensional flow applic. *(Japanese)* 3–26769
isoparametric stress elements, basis 3–19425
laminated composite materials, three-dimensional method 3–10275
least squares criterion in formulation for mechanics of deformable bodies 3–26072
limit analysis using linear programming for ultimate load determ. 3–6246
linear elasticity problems *(French)* 3–3953
linear elasticity problems solution, computer programs ELAS 3–6205
linear nucleator cavity field calculation 3–32120
local buckling stresses, finite element structural element analysis 3–35566
longitudinal elastic-plastic stress wave propagation 3–28905
Love waves, propag. in a non horizontally layered media 3–21850
mass and stiffness matrices, automated generation and condensation *(German)* 3–19411
mechanical systems, transition conditions for collision processes *(German)* 3–32349
meteorological applic. 3–28024
mixed scheme for plate bending, convergence 3–37803
multilayer sandwich beams and plates, bending and vibrations 3–26075
natural boundary conditions, paradox illustration 3–22651
natural vibration problems, analogue of modified Rayleigh-Ritz method 3–562
Navier-Stokes equation solution 3–7333
non-Newtonian channel flow 3–7322
non-slef-adjoint systems of partial differential equations 3–28852
nonlinear analysis by combined finite element-finite difference methods 3–10269
nonlinear elastic, theoretical and numerical comparison of methods 3–10276
nonlinear elastic problems reduction to discrete ones *(Russian)* 3–6212
one-group neutron transport eqn. for critical half-thickness of bare slab 3–23390
optimal design of plastic structs. in plane stresses 3–16655
parametric stress concentration, comparison with complex stress function method *(German)* 3–22602
peristaltic pumping, wavelengths and wave amplitudes influence on flow field 3–22157
photogrammetry, block adjustment problems 3–31461
plane frames, finite deflection analysis on basis of bending stiffnesses 3–28859
plane stress analysis, computer program with automatic mesh generation *(Japanese)* 3–10270
plasma MHD instabilities, numerical analysis 3–7508
plastic strains in shake-down of structs. subjected to cyclic loads, upper limits 3–16660
plate bending analysis, hybrid elements 3–517
plates and shallow shells, large deflection stress analysis 3–22623
finite element analysis continued
pure moment loading of axisymmetric finite element models 3–22622
quadratic programming approach to impulsive loading analysis of rigid plastic structures 3–16656
Rayleigh wave propag. at a continental boundary 3–21851
Rayleigh waves, propag. in a non horizontally layered media 3–21850
Saint Venant torsion, solution of stress field 3–22621
shear in C^0 and C^1 bending finite elements 3–28861
SHEBA triangular thin shell element with variable curvature 3–509
shell vibration calc. using triangular finite element scheme *(Russian)* 3–10316
shells of revolution, criteria for finite element discretion 3–32324
stability of rectangular plates in supersonic air flow, calc. using modified finite element method *(Russian)* 3–11425
stiffness matrix, influence of Poisson's ratio on spectral condition number 3–22617
strain meas. of materials of low elastic modulus *(Japanese)* 3–16381
stress analysis, computer program ISTRAN/PL *(Japanese)* 3–26078
stresses calc. in bodies with axial symmetry *(German)* 3–32350
tapered beam vibrs. analysis method 3–19455
of thermodynamical process 3–28996
thin shells, deficiencies in displacement finite elements 3–22618
transient heat conduction calc. *(German)* 3–22790
triangular plate bending element for contact problems 3–22620
unbounded field problems, partial differential-equation solution 3–6296
unsteady MHD duct flow 3–26836
vibrating beam, determ. of optimal frequencies by finite element displacement method 3–22684
vibration of cylindrical shells by hybrid finite element method 3–37830
viscous flow through T-junction, soln. of 2D Navier-Stokes eqn. 3–11369
viscous fluids flow analysis by finite-element method 3–38348
viscous incompressible fluid dynamics applic. 3–29833
Finlay-Freundlich red-shift hypothesis *see gravitational red shift*
fires
see also accidents; combustion; flames; safety
No entries
fission, nuclear *see nuclear fission*
fission counters
see also nuclear fission
neutron multiplicity meas. using a Gd-filled liquid scintillator *(French)* 3–10064
track detector, for diffusion of U in polyethylene 3–27141
fission products *see nuclear fission products*
fission reactors *see nuclear reactors*
fissures *see cracks*
flames
see also combustion; fires
acetylene-air, calc. of degree of ionisation of Ca *(Russian)* 3–31264
aerosol system, normal flame velocity 3–27873
air-acetylene, Ca atomic line-widths meas. by piezoelectric scanning Fabry-Perot interferometer 3–28779
air-acetylene and N_2O-acetylene, Ca atoms absorption linewidths meas. using piezoelectric scanning Fabry-Perot interferometer 3–32260
alkaline-earth monoxide or hydroxide visible bands identification method 3–22547
atomic absorpt. spectrometry, mechanisms of interference and releasing action 3–14291
atomic fluorescence spectrometry, wavelength scanning technique 3–37742
atomic fluorescence spectroscopy, light scattering in laminar and turbulent flames 3–13491
atomic-fluorescence photometer characts. *(Russian)* 3–10213
Bunsen burner, flow conditions determ. using spark tracing method 3–460
combustible jets, turbulent diffusion flame, aerodynamic and thermodynamic analysis 3–23799
combustion nuclei production and electrostatic precipitation 3–5391
emission flame, atomic absorpt. meas. of distrib. of ground state atoms 3–14292
free atom distributions of various elements in different zones *(Russian)* 3–12520
n-hexane-air, temp. meas. using spectrum of scatt. laser light *(German)* 3–9868
industrial, meas. techniques, book 3–5817
laser saturated atomic resonance fluorescence theory 3–14297
mean emissivity of luminous flame from spray combustion of liquid fuel 3–2801
methane-F_2, temp. meas. by means of vibration-rotation spectra of HF *(French)* 3–29645
oxyacetylene, electron energy distrib. 3–27872
plasma, different calor-electric effect manifestations 3–23934
plasmas, electrostatic probe theories and meas. 3–23913
premixed burning, large activation energy, asymptotic analysis 3–4526
propane, laminar flame in a discharge, elec. field effects, photography 3–36211
propane-butane-air calc. of degree of ionisation of Ca *(Russian)* 3–31264
refractive index meas. in far IR 3–33390
saturated resonance fluorescence, non quenching collisions influence 3–14298
spectrometry, recent progress in the study of perturbaton mechanisms *(French)* 3–13501
spectrophotometric apparatus *(Russian)* 3–28792
spectroscopy, technique for direct evaporation of sample from microcrucible *(Russian)* 3–26030
temperature meas. by means of fluorescence spectrometry 3–13248
turbulent diffusion, influence of recirculation flows on length 3–21807
turbulent media, chem. prod. rate *(French)* 3–21798

- **flames** continued
  - CO, laminar flame in a discharge, elec. field effects, photography 3—36211
  - CO flame laser, P-branch i.r. transitions in C_2H_2-O_2 flame, optical gain 3—10473
  - $CS_2/O_2/NO_2$, c.w. laser power from vibr. excited CO 3—32534
  - N_2O-acetylene, laser excited atomic fluorescence of some transition elements 3—32263
  - N_2O-acetylene Ca atomic line-widths meas. by piezoelectric scanning Fabry-Perot interferometer 3—28779
- **flare stars** *see stars*
- **flares, solar** *see solar flares*
- **flash lamps**
  - dye lasers, flashlamp pumped, threshold pump intensity fluorescence character of solution *(German)* 3—10544
  - electronic, using thyristor control, patent 3—9986
  - high-temperature, with symmetrical conductors *(Russian)* 3—9946
  - Marx-Bank coaxial driver flashlamp for excitation of organic dye lasers 3—16449
  - pumping lamps for lasers with optomechanical shutter, synchronising circuit for *(Russian)* 3—5989
- **flash photolysis** *see photolysis*
- **flashover**
  - arc discharge on polluted surface having uniform and time-invariant resistivity 3—7571
  - electrostatic precipitator, interelectrode flahshover voltage meas. *(Polish)* 3—10421
  - long air gaps under switching pulses *(Japanese)* 3—14621
  - polluted surface having uniform and time-invariant resistivity 3—7571
  - pre-flashover discharges at different air moistures, propagation and development *(Czech)* 3—38511
  - short airgaps, predischarge phenomena 3—14612
  - spread, statistical determination *(German)* 3—11513
  - ultrahigh vacuum diode, preflashover mass spectroscopy 3—20673
- **flicker noise** *see random noise*
- **flip-chip devices**
  - *see also thin film circuits*
  - No entries
- **flip-flops**
  - counter MH 7490 applications *(Czech)* 3—16525
  - in electric field detector, testing *(Spanish)* 3—28606
  - four-stage synchronous counters *(German)* 3—10073
- **floating zone refining** *see zone melting and refining*
- **flocculation**
  - *see also colloids; sedimentation*
  - No entries
- **flow**
  - *see also boundary layer flow; compressible flow; Couette flow; external flows; flow measurement; flow of gases; flow of liquids; flow through porous media; Knudsen flow; laminar flow; multiphase flow; non-Newtonian flow; rotational flow; supersonic flow; turbulent flow*
  - annular, Couette-Poiseuille-porous, hydrodynamic stability 3—7340
  - arc heated high speed flows, density measurement 3—28797
  - barotropic fluid motion in cylindrical horizontal channel *(French)* 3—4595
  - biaxial extensional, bubble inflation technique for viscoelastic props. obs. 3—453
  - blasius flow, high Prandtl number heat transfer 3—20280
  - Blasius of non-Newtonian fluid 3—7323
  - boundary layer separation, perturbation technique 3—7373
  - cable equilibrium when connected to free floating body placed in fluid stream 3—5498
  - capillary, in packed homogeneous fluidised beds 3—1452
  - conducting viscous fluid, shear flow instability 3—23763
  - configurational stability *(Russian)* 3—1424
  - conjugate transient heat transfer in fluid flow through insulated pipes, integral equations 3—38361
  - convection, laminar free, Gortler-type series for non-isothermal vertical plate 3—4563
  - convective transport of conc. gradient in periodic struct., Lagrangian description *(French)* 3—1359
  - creeping, incompressible viscous fluid, past deforming sphere 3—4545
  - creeping, viscous, through circular tube of nonuniform cross section 3—7338
  - curved pipes, flow-induced in-plane instabilities 3—6279
  - cylinder vibrations, shroud eccentricity effect on suppression 3—38396
  - distributed flow systems, analogue simulation technique 3—33307
  - drag on isolated sphere, derivation of Stokes' law 3—17512
  - duct with constant wall heat flux, slug flow in thermal entrance region *(German)* 3—7331
  - finite element soln. of 3D flow problem and Reynold's eqn. 3—1351
  - fluid flow patterns in breaking bubbles 3—11409
  - fluids, acoustic wave propagation 3—5708
  - granular materials, photoelastic verification of mechanical model 3—1440
  - heat transfer and flow friction characteristics of dense mesh wire screen regenerator matrices at cryogenic temps. 3—9881
  - heat transfer in slotted channels with obstacles 3—4540
  - high Reynolds number flow around a rigid fixed cylinder, meas. of dynamic pressure and lift 3—7315
  - hydrodynamic processes in pneumatic conveyance systems for containerized cargoes 3—4538
  - hypersonic, mass spectroscopy meas. of spacecraft re-entry plasma 3—23928
  - incompressible jet, in fluid control elements 3—11368
  - incompressible two-dimensional, applic. of finite element analysis *(Japanese)* 3—26769
  - inviscid, of Newtonian fluid through sudden contraction, analytical soln. 3—7328
  - jet-flapped airfoil problem, two-dimensional, numerical solution 3—11378
  - Kutta-Joukowski condition in three dimensional flow *(French)* 3—7388
- **flow** continued
  - Lagrangian density for motions of perfect fluid in general relativity 3—26131
  - linear field, hydrodynamic interaction of two small freely-moving spheres 3—7330
  - local flow blockage in fibr., obs. of wake pressure 3—1052
  - mass and heat transfer from cavity in duct, separated flow *(German)* 3—1332
  - mass transfer from sphere at high Prandtl nos., u.s. vibrations effects 3—4534
  - material functions in annular flow, expt. meas. *(Japanese)* 3—4532
  - material functions in annular flow, meas. theory *(Japanese)* 3—4531
  - MHD, between rotating disks, effects of finite wall conductance 3—4604
  - MHD, in rectangular duct with variable conductivity walls *(Russian)* 3—7435
  - MHD, strong transverse magnetic field, variable area ducts with insulating walls 3—4608
  - MHD, unsteady, between porous parallel plates 3—20376
  - MHD flow due to elec. current past sphere immersed in fluid 3—11442
  - MHD induction pump duct characteristics in dimensionless flow *(Russian)* 3—7424
  - molecular flow evaporation apparatus for vapour pressure and heat of sublimation 3—16397
  - Newtonian, in cone, plate, parallel plate systems, perturbation soln. 3—7326
  - nozzle outflow, action of flat plate, calc. of total pressure and discharge coeffs. 3—17496
  - nozzles, reflected, flow at starting process *(Japanese)* 3—23810
  - Orr-Sommerfeld eqn., composite approximations to solns. 3—33192
  - oscillatory, pipe, simulation on analogue computer 3—7334
  - particle motion in crossed e.m. fields with large Reynolds no. in conducting medium *(Russian)* 3—7432
  - peristaltic pumping, finite element analysis 3—22157
  - physiological fluids, peristaltic motion 3—7335
  - pipe, past flat plates, single cylinders and single spheres, forced convection heat transfer 3—11365
  - plane heterogeneous shear, hydromag. stability 3—20378
  - plug flow in channel flow, effects of upstream and downstream boundary conditions on heat or mass transfer with axial diffusion 3—20285
  - polar fluids, dynamics 3—14427
  - pollutant transport, stochastic processes 3—1375
  - polybutadiene, shear modulus and flow rate through capillary *(Russian)* 3—7288
  - polyisoprene, shear modulus and flow rate through capillary *(Russian)* 3—7288
  - polymer melts, errors in pressure-hole meas. 3—10216
  - polymers, molten, composite formation during extrusion, viscoelastic fluids in flow dispersion modes 3—2762
  - pressure fluctuations in separated flow, analysis and correlation of data 3—11395
  - protons, earthward flow in geomagnetic tail at lunar distances 3—12657
  - rate-of-strain-dependent memory function, simple-integral model, appl. to shear flow 3—29829
  - reactor coolant, induced rod vibrs., analytical model 3—1071
  - ribbed flow of viscoelastic fluid from flat channel 3—23678
  - rotor wakes, three dimensional anal. using a constant temp. hot wire anemometer 3—7313
  - separated, past bluff bodies attached to plane wall, free streamline theory 3—7329
  - shear, acoustic transmission, 1/N power law boundary layer 3—5707
  - shear, interaction with large amplitude shallow water waves 3—7404
  - shear, inviscid, simple waves, similarity solutions 3—7405
  - shear, stability of finite amplitude internal wave, appl. to atm. and ocean 3—26781
  - spherically symmetric, radiative transfer equation calcs. appl. to linear and nonlinear stellar pulsations 3—22042
  - stability of flows started from rest 3—4564
  - stationary flow of viscous incompressible fluid around circular cylinder *(French)* 3—33193
  - steady and periodically oscillated two-dimensional potential flow, finite element method analysis *(Japanese)* 3—1337
  - steady MHD channel flow with anisotropic conductivity, second order solns. 3—14487
  - Stokes resistance of spheres in contact in linear shear field 3—4520
  - Stokes three-dimensional steady application of calc. to effect of no-shear zones on shear flow 3—1342
  - Stokesian flow about a sphere, heat transfer and temp. distrib. anal. 3—10408
  - subsonic, random and tubulent, response of cylindrical shell 3—6277
  - suction, kinetic theory 3—14428
  - three-dimensional incompressible trailing edge, flow region obs. *(French)* 3—26849
  - torsional, incompressible Reiner-Rivlin fluids, appl. of orthogonality principle 3—4543
  - transverse alternating pressure gradient effects on flow in passage 3—4537
  - turbines interblade channels, analysis by graphical method *(Russian)* 3—7360
  - uniqueness and Holder continuous dependence for linear micropolar fluid motion 3—23675
  - velocity fluctuation obs. by temperature sensing downstream of hot wire 3—3769
  - viscometric of elastic fluid, stress state data 3—11367
  - viscous fluids flow analysis by finite-element method 3—38348
  - water, in internally heated annulus with rotating outer boundary, heat transfer 3—11375
- **flow birefringence**
  - liquid crystal, smectic A-smectic C transition region obs. *(French)* 3—17733
  - polyethylene, molten, viscoelastic flow in parallel slit entrance region *(Japanese)* 3—4533
  - polymer melts, material functions theoretical determ. *(Japanese)* 3—4492
  - polystyrene solution, oscillating shear field *(Russian)* 3—29820
- **flow charts** *see flowcharting*

flow control
  atmospheric sampling, use of differential flow controllers 3−37746
  chemical vapour deposition instrumentation 3−12250
  conference, Sheffield, England (1972) 3−461
  epitaxial growth, computer control 3−12231
  liquid metals, by induction MHD apparatus *(Russian)* 3−20391
  literature survey 3−450
  rotating vane anemometer, electronic system design 3−464
  source liquid, for semicond. device manufacture 3−30960
flow diagrams *see flowcharting*
flow measurement
  see also flowmeters
  air currents flow rate in mines 3−4587
  air unsteady flow rates in channels, meas. by hot-wire anemometer method 3−32269
  air-cooled heat exchangers, airflow and veloc. distrib. 3−471
  anemometers, electronic, constant current constant temperature, probes, operation, applications, analysis techniques 3−16581
  aortic blood flow meas., pulsed Doppler technique 3−37734
  blood, aortic velocity and acceleration by u.s. device 3−37731
  blood, appl. of const. temp. anemometry 3−9646
  blood, implantable extravascular interferometric ultrasonic technique, FM telemetering 3−397
  blood, using e.m. flowmeter 3−395
  blood velocity measurement, and cardiac output detn., continuous obs. using thermal method 3−25992
  boundary layer meas. by holographic interferometer 3−22375
  brachial artery flow velocity meas. after cardiac surgery 3−39803
  carotid artery diameter and flow, noninvasive technique using Doppler effect 3−37733
  conductance, by dynamical method *(German)* 3−28796
  conductance to free molecular flow measurement by substitution procedures 3−25715
  conference, Sheffield, England (1972) 3−461
  correlator design, time delay measurement 3−465
  electro-optical techniques, conference (Southampton, Eng., Sept. 1972) 3−472
  e.m., of blood in anaesthetized rats 3−3562
  e.m. flowmeter apparatus, patent 3−10227
  fluid and gaseous effluent, continuous meas. by liquid scintillation counting, review *(German)* 3−32277
  fluids, viscous shear sensor 3−463
  gaseous, spark tracing method 3−460
  gases, constant density, elimination of thermodynamic corrections 3−467
  holographic interferometry applied to right circular cone at angle of attack 3−22574
  human myocardial blood flow meas. using ^{133}Xe 3−35269
  hydrodynamic flow visualisation, applications, review 3−32282
  hypersonic He flow, transition and hot wire meas. on sharp cones 3−11417
  jet, turbulence distribution, laser photon correlation spectroscopy, Doppler effect 3−22510
  laser Doppler anemometers 3−19654
  laser Doppler method, frequency shifting by electro-optic techniques 3−337
  laser Doppler system, broadband demodulation of signals using gated zero crossing detector 3−476
  laser Doppler velocimeter, Fourier optical model 3−473
  laser Doppler velocimetry, ambiguity noise level reduction with cross-correlation technique 3−791
  laser flow velocity meter *(French)* 3−32273
  laser flowmeter, light scattering rel. to differential Doppler heterodyning technique 3−792
  laser velocimeter applications to supersonic wind tunnel for meas. of flow velocity 3−477
  linear independent components, scattered light beam method 3−474
  liquid metal, using u.s. Doppler velocimeter 3−26040
  liquids, by cross-correlation of temperature fluctuations 3−10222
  liquids, turbulent shear flow, transverse velocity component and Reynold's stresses measurement using dual-wedge hot-film probe 3−28794
  literature survey 3−450
  longitudinal dispersion of ink in turbulent flow of water, electro-optical measurement 3−1376
  magnetic flowmeters, past and present development 3−19379
  NEL laser velocimeter, new developments and treatment of data 3−342
  nonuniform stream flow, elimination of head losses 3−469
  oceanographic current meter, solid state 3−5543
  oceanographic research velocimeters, calibrations 3−37262
  open channel, effluent and pollution monitoring 3−468
  optical Doppler techniques development 3−475
  phase objects, using shadow bands 3−162
  plain intake, for pipelines flow meas. 3−22576
  pneumatic vortex angular rate sensor analysis 3−13520
  radioactive tracers, small-vol. flow-proportional counter 3−6161
  respiratory flow transducers, characteristics 3−6144
  rheometer, high pressure capillary *(Polish)* 3−32279
  rotating vane anemometer, electronic system design 3−464
  sandy materials, metrological guarantee *(Russian)* 3−6166
  Separan AP30, dil. polymer solution, drag reduction degradation 3−479
  separated flows, probe development 3−13527
  signal convertor and amplifier, for additive flow metering, patent 3−10226
  slit flow converter with rectangular slit and variable section chamber *(Russian)* 3−6167
  solids, using correlation methods 3−341
  spark discharge method of flow meas. using stereoscopic photography 3−1532
  spark tracing method, application to flow meas. in cross-stream air classifier 3−243
  spontaneous heterogeneous character of flowing material 3−466
  standard orifice, pipe flow, plant disturbance elimination, defined disturbance, method, tolerances *(German)* 3−13524
  supersonic turbines, flow in nozzle cascade with angular points, optical investigation 3−23748
  surface water flow studies using radioisotope tracer technique, application to pollution and supply problems 3−22559
flow measurement continued
  turbine type volumetric flowmeter, patent 3−10225
  turbulent flow, laser Doppler-shift velocimeter applications 3−448
  turbulent liquid flow meas. 3−37778
  ultrasonic Doppler sensor for blood flow meas., internal and external 3−37777
  unsteady flow meas. in hydraulic servo systems using laser velocimeter 3−793
  velocity, laser, radioionisation and correlation methods, analysis *(Polish)* 3−26252
  water, by u.s. waves *(German)* 3−16390
  water flow conditions determ. by d.c. hot wire thermoanemometer 3−32272
  Weissenberg rheogoniometer, for flow measurements of non-newtonian fluids 3−28799
  wind speed, by computer-controlled system 3−28751
  ^{133}Xe multibolus fractionation technique for human cerebral blood flow distribution meas. 3−22526
flow of gases
  see also acoustic streaming; aerodynamics; anemometers; effusion
  air, laminar free convection in heated vertical corner 3−4561
  air, resonance conditions for pulsating flow through an orifice in pipes, model 3−23747
  air, shear layer behind circular cylinder, vortex shedding, acoustic field effects 3−29859
  air, vibrations induced in flat plates in rectangular passage 3−16337
  air flow and heat transfer to the atmosphere from the surface of thermal electric power plant cooling ponds 3−29847
  air flow in axial flow inducer, visualisation study 3−26858
  air flow in channel, spark tracing method of obs. 3−460
  air jets, from entry holes of high-intensity combustor-liner, mass flows 3−17494
  air subsonic flow, heat exchange in the critical zone ahead of a cylindrical step *(Russian)* 3−29857
  air through planar nozzles, expt. study 3−1335
  air turbulently flowing in smooth annuli at high temp. heat transfer and friction coeffs. 3−23698
  air unsteady flow rates in channels, meas. by hot-wire anemometer method 3−32269
  air-cooled heat exchangers, airflow and veloc. distrib. 3−471
  arc discharge in turbulent flow, intermittent behaviour 3−7585
  atmospheric pollution, buoyant plumes, vehicular and aircraft wakes 3−33325
  boundary layer at crit. pt. of indestructible body washed by flow of ionized air 3−23737
  boundary value problems, solution *(Russian)* 3−11432
  capillary behaviour, boundary effects 3−14476
  chemically reacting gas turbulent isobaric flow in a heated tube 3−33321
  chemically reactive flows in afterglows, reaction kinetics 3−39438
  compressible, flow calorimeter for heat capacity determ. at high pressures 3−22284
  compressible gases with suction, turbulent boundary layer, calc. method 3−33224
  condensation process in vapour flow inside a vertical cylinder 3−24257
  conductance, by dynamical method *(German)* 3−28796
  conducting, dusty, plane parallel flow, magnetic lines of force fixed relative to plate 3−36128
  conducting dusty gas, plane parallel flow in transverse mag. field 3−20379
  confined-discharge plasma generator with local fluid construction, heat transfer and fluid dynamic effects 3−26904
  conical diffuser, variation in characteristics study as a function of inlet conditions 3−33312
  conical diffusers experiments 3−33313
  Couette flow nonlinear rarefied with heat transfer, gas statistical models with and without internal energy states 3−33259
  critical point of phase equilibrium, possible gas-dynamic effects *(Russian)* 3−29880
  in cylindrical furnace, mathematical simulation of radiant heat transfer using Monte Carlo method 3−623
  diatomic with vibration-relaxation, Knudsen layer, hydrodynamic eqns. *(Russian)* 3−29889
  diffusion around convex obstacle, finite mean free path effect 3−20349
  dust content determ. *(German)* 3−22562
  dust in air, hydraulic resistance meas. during flow 3−4622
  electric arc and gas flow interaction, computation 3−36230
  electrolysis, gas removal process, hydrodynamic transition 3−25073
  electrostatically controlled heat shutter 3−32045
  film of gas flow patterns above NaCl melt 3−11569
  flooding rates determination in regular packings, calc. 3−26841
  flowmeter using vortex refrigeration effect *(Spanish)* 3−16583
  fluidic amplifier jet flow 3−20348
  free molecule flow in a right circular cylinder 3−33260
  freon jet, in cocurrent air stream, dimensions and location of mixing zone 3−4522
  Freon-12, vertically upwards in heated tube, meas. of temp. distrib. at and beyond dryout 3−32934
  gas-liquid mixtures, bubble type supersonic flows 3−33286
  gas-pseudoplastic liquid mixtures, meas. of momentum transfer 3−7450
  Generalised Roche Model (Astrophysical appl), self-similar isothermal flow behind spherical shock waves 3−25360
  generalized numerical solution for subsonic and supersonic flows with heat transfer 3−4586
  gravitational force effect on aerosol motion in curvilinear gas flow 3−23793
  growth and decay of sonic waves in a thermally conducting radiative gas 3−17530
  heat and mass transfer on the surface of glass-graphite materials in high temperature gas stream *(Russian)* 3−26786
  heat exchangers, single phase pressure drop, considering the change of fluid props. along the flow path 3−33213
  heat transfer augmentation in tube flow 3−1344
  heat transfer in a region of accelerated flow when a system of two-dimensional streams is incident on a flat surface normal to it 3−23705

flow of gases continued

- heat transfer of heated plate in sinusoidally oscillating flows, applic. to internal combustion engine 3—1360
- heated thin wire, temp. distribution in gas flow 3—36077
- Helmholtz-Rayleigh instabilities in barotropic atmospheric non-divergent horizontal stream *(German)* 3—12707
- high frequency flare discharge, elastic field effects, dep. air flow rate 3—33405
- high pressure flows with and without heat transfer 3—38389
- high temp. flow, pressure and temp. meas. using calorimetric probe *(Russian)* 3—9870
- at high temperature, gas dynamics *(German)* 3—14430
- highly heated sphere, for small Reynold's number *(Russian)* 3—1409
- hydrodynamic flow visualization, applications, review 3—32282
- hypersonic, over flat plate with sharp leading edge, flow models for non-continuum regimes 3—1411
- inclined and horizontal turbulent flow to produce incipient rolling, sliding and suspension of particles 3—29909
- intensive blowing through a permeable surface, nature of flow 3 -33303
- ionised, wall heat transfer reduction, cylindrical pipe, localised magnetic field, calculations *(Italian)* 3—20277
- ionized in rectangular channels, radiation coefficients *(Russian)* 3—11357
- jet flow rel. to noise, direct correlation 3—7355
- jets, turbulent cocurrent, mixing in ducts with profiled walls, minimum losses determ. 3—33309
- Joule-Thomson effects on thermal entrance region heat transfer in pipes with uniform wall temperature 3—20302
- Karman vortex, from two tubes at various spacings 3—4569
- laminar and turbulent jet mixing flow with boundary layer growth 3 -1354
- laser Doppler anemometer appl. 3—22577
- longitudinal turbulent in cylinder, of air, influence of temperature factor on local skin friction *(Russian)* 3—1407
- mass flowmeters, volumetric measurement 3—470
- measurement, constant density, elimination of thermodynamic corrections 3—467
- measurement and control, rotating vane anemometer, electronic system design 3—464
- MHD, steady transverse plane flows, compatibility eqn. 3—4605
- mixed flow impeller, diffusion losses due to negative velocity gradients in boundary layer 3—4582
- mixing chamber for opposing isothermal annular flows, construction and operation *(Russian)* 3—23750
- mixing in transverse magnetic field *(Russian)* 3—7413
- mixtures, in turbulent flow, hot-wire anemometry 3—22564
- mixtures, laminar, rotational, turbulent, exhaust-jet flows, laser-Doppler velocimeter 3—32281
- molecular gas dynamics, boundary conditions, surface shocks, continuum flows, review 3—33261
- molecular transmission probability in a plane channel, wall roughness influence *(Russian)* 3—7398
- nonisothermal, applic. of methods of design of hydraulic loops 3—4585
- nonstationary flows of general gas, determ. of time-invariant parameters *(Russian)* 3—29878
- nonviscous incandescent gas supersonic stream, radial thermal flux distribution at surface of a sphere *(Russian)* 3—29887
- numerical methods for soln. of gas dynamic problems 3—1416
- one dimensional flow of gas with arbitrary internal rate processes, thermodynamic relaxation *(German)* 3—20346
- packed bed, liquid holdup in gas-liquid countercurrent flow 3—33284
- parallel steam-generating tubes, flow pulsations 3—26842
- plane of gaseous mixtures acted on by magnetic field, stability of combustion *(Russian)* 3—2808
- over plate, noise abatement, STOL aircraft 3—3650
- pressure drop of fibrous filter at reduced ambient press. 3—17511
- pseudo-fluidised bed, transverse nonuniformity in inhomogeneity distrib. 3—20398
- radiating gases, quasi isothermal transonic flow *(French)* 3—26818
- radiative energy transfer at laminar boundary layer 3—23734
- regimes in unsteady rectilinear flow of perfect gas 3—1398
- resonant acoustic oscillations with damping, small rate theory 3—38390
- secondary flows, turbomachinery aerodynamics, review 3—33221
- shear, with const. vortex, of heavy fluid around thin profile *(French)* 3—20343
- shock wave formation in shock tube from interaction of finite amplitude compression waves *(Russian)* 3—11433
- through small diameter packed beds, heat transfer 3—622
- with solid suspensions, through packed beds, pressure drop analysis 3—23790
- spherical and cylindrical gaseous expansions into a vacuum 3—38388
- strongly blown gas past flat body, soln. to Cauchy problem for non-linear eqn. *(Russian)* 3—1410
- subsonic, resonance method meas. of unsteady aerodynamic forces 3—23749
- subsonic jets, plane baffles, stagnation point, free stream turbulence 3—1330
- supersonic gas flow, vibrational temp. meas. 3—36116
- Swirlmeter, electronic totalizer system 3—462
- thrust nozzle optimization, including boundary layer effects, using numerical relaxation scheme 3—1333
- transient molecular flow, influence of adsorption time *(German)* 3—26824
- transonic, around bodies of revolution, approx. calc. methods 3—1412
- transonic airfoils, transonic flow, computational methods, review 3—33247
- turbulent air stream, optical system for concentration fluctuation obs. 3—3786
- turbulent atmosphere, refractive index meas. by laser correlation technique 3—37259
- turbulent motion, near-sonic, outflow function determ. using variational techniques *(Russian)* 3—4560
- two dimensional gas particle flow, anal. of boundary layer 3—7379

flow of gases continued

- two-phase flow, residence time distribution, tracer injections 3—36135
- underexpanded sonic jet, properties on retardation 3—23802
- unidimensional periodic flow in pipe, linearization of eqns. of continuity, motion, energy and state *(Russian)* 3—1348
- unsteady expansion of gas into near vacuum, shock wave generation 3—4590
- u.s. flow, quantitative analysis using mirror shearing interferometer *(Russian)* 3—6173
- variable properties laminr gas flow heat transfer in the entry region of parallel porous plates 3—20298
- viscous, in tube, effect of wall temp. on characteristics *(Russian)* 3—7390
- viscous hypersonic, oscillating slender cone 3—1339
- viscous incompressible turbulent flow in axisymmetric channel under conditions of preliminary swirl in the entry zone 3—33317
- wake flow of a cascade of oscillating airfoils 3—38411
- water vapour, in differential thermal analysis furnace 3—28497
- water vapour cross flow, in optical absorption cell 3—26027
- water vapour through parallel plate channels, surface flow of multilayer adsorbed films 3—29924
- weakly nonideal gas motion under strong point explosion *(Russian)* 3—4593
- Ar, condensation of Cs vapour in flow 3—1345
- Ar, high temp. flow in pipe, heat transfer 3—14408
- CO_2 waveguide laser operated in flowing gas configuration, characteristics 3—727
- He, heat transfer with wall temperature up to 2800K *(Russian)* 3—7389
- KOH vapour, condensation, MHD generator 3—36414

flow of liquids

see also acoustic streaming; flow birefringence; hydrodynamics; superfluidity

- artificial lakes, hydrodynamical props. *(Italian)* 3—34978
- bearings, fluid film lubrication, fluid mechanics, review 3—33326
- boiling drop-form liquid, flow out of a Laval nozzle, accel. meas. 3—36142
- bubbly water, unidimensional flow through nozzle, integration of hydrodynamic eqns. *(Russian)* 3—1443
- buoyancy-induced flows, instability transition and turbulence, review 3—33217
- channel, complex heat transfer calcs. 3—23692
- channel flow turbulence meas. 3—33204
- circulation regimes, evaporator tubes, semireversed flow 3—1331
- in coaxial circular MHD channels, effects of asymmetric magnetic field *(Russian)* 3—7420
- concentration profile in two-dimensional stagnation flow *(French)* 3—36076
- condensate liquid film flow down inclined wall, stability characteristics 3—33233
- confined laminar jet mixing in circular channel, arbitrary entrance vel. distrib. 3—4528
- convective flow regimes in a periodic external force field *(Russian)* 3—29856
- dilute aqueous polymer soln. pipe flows, viscous sublayer and adjacent wall region 3—20278
- dilute polymer solutions, in pipe, response to motion of thin sleeve, stability 3—11364
- double layer system, Taylor diffusion in falling liquid films 3—1962
- drag reducing polymer solutions, early turbulence in pipe flow 3—11387
- dusty viscous liquid in channel and pipe, unsteady flow 3—23673
- dusty viscous liquid through rectangular channel 3—23672
- dynamics of sea currents, exact solns. *(Russian)* 3—2945
- elastico-viscous, normal/shear stresses relationship 3—29836
- elastico-viscous liquids, axially symm. flows 3—11380
- electrostatic charge generated, a.c. meas. method 3—665
- external vortex action of liquid flow in semi-infinite medium *(Russian)* 3—39493
- falling films, liquid viscosity effect on mixing 3—26860
- falling liquid films stagnant band analysis 3—33228
- film flow, entrance effects 3—36107
- flooding rates determination in regular packings, calc. 3—26841
- flow caused by air-lubricated edge moving over viscoelastic liquid 3—22569
- forced, in ducts, boiling, heat transfer crisis 3—14990
- forced convection mass transfer from wetted grooves, liquid flow meas. 3—26800
- Freon-12, vertically upwards in heated tube, meas. of temp. distrib. at and beyond dryout 3—32934
- gas-liquid mixtures, bubble type supersonic flows 3—33286
- generalised Couette flow of an elastico-viscous liquid between two co-axial porous circular cylinders 3—38378
- head loss calc. employing Levi's formula *(Russian)* 3—17509
- heat transfer augmentation in tube flow 3—1344
- heat transfer for transitional longit. flow over tube bundle 3—23712
- heavy liquid jet flow past a curvilinear obstacle, numerical soln. *(Russian)* 3—29930
- hydrodynamic flow visualization, applications, review 3—32282
- hypersonic air streams, multiple-orifice liquid injection 3—38415
- incompressible, viscous liquid, flow near accelerated plate in mag. field 3—23773
- interface of 2 sharply separated liquids, resistance coefficient *(Japanese)* 3—23784
- internal waves and interfacial effects in density stratified flows 3—33276
- irrotational vibrs. of perfect compressible liq. in elastic reservoir, variational approach *(French)* 3—7399
- jet, cylindrical laminar liquid, ejecting into a gas, heat transfer 3—38417
- jet, turbulent liquid, gas absorption *(French)* 3—29922
- laser Doppler anemometer appl. 3—22577
- lava flow, depend. of length on rate of effusion and initial viscosity rel. to 1971 Etna eruption 3—21895
- magnetohydrodynamic channel flow, effects of thermal radiation 3—14493
- MHD, jets in flow wake in longitudinal magnetic field *(Russian)* 3—7434

flow of liquids continued
MHD longitudinal edge effects with flow of liquid in travelling mag. field *(Russian)* 3—7430
MHD shear flow of non-Newtonian liquid with rheological power law *(Russian)* 3—7436
MHD with heat transfer over porous plates *(Russian)* 3—7431
micropolar, asymptotic suction 3—4620
motion in a cracked-porous stratum with nonstationary filtration *(Russian)* 3—29919
multiphase, in presence of phase transitions, hydrothermodynamic eqns. 3—33287
Navier-Stokes equations, numerical treatment 3—36109
Newtonian blob in narrow gap, Hele Shaw flow 3—14422
non-Newtonian behaviour of suspension of liquid drops in tube flow 3—11452
non-Newtonian falling liquid films, gas absorption 3—36108
nonlinear viscous liquids, evaluation of error of approximate solns. *(Russian)* 3—29837
nonuniform stream flow, elimination of head losses 3—469
oil-magnetite mixtures, eff. of mag. field on critical Reynold's number *(Russian)* 3—20315
oil-magnetite mixtures, rheological study for transverse magnetic fields *(Russian)* 3—20271
open-channel flow, longitudinal dispersion, turbulent mixing, review 3—33215
operating below capacity, improvement of anticavitation props. 3—3922
packed bed, liquid holdup in gas-liquid countercurrent flow 3—33284
packed beds, trickle flow 3—7473
polyethylene, molten, viscoelastic flow, rheo-optical studies *(Japanese)* 3—4533
polymer melts, elongational flow 3—7321
polymer melts, plane Couette flow, heat dissipation *(German)* 3—7336
polymer solutions, adsorbed entangled layer in drag reduction 3—29864
pressure filtering through pores in nonhomogeneous layers *(Russian)* 3—33304
pseudoplastic liquid-gas meas. of momentum transfer 3—7450
pulsatile, in rigid tube, momentum integral soln. 3—9645
Reynolds number, var. for jet-splitter system transverse oscillations 3—1334
rigid core surrounded by annular liquid layer through horizontal tube 3—1338
rivers, real time recursive prediction using stochastic models 3—28092
rotating disc in fluid, hydrodynamic and thermal boundary layers, analysis 3—23722
rotating liquid, stability *(Russian)* 3—4575
rotational viscoelastic flow around simple bodies and agitators 3—7363
Separan AP30, dil. polymer solution, drag reduction degradation 3—479
slender fish-like body with finite body thickness, unsteady flow 3—14421
spherical-cap bubbles, wake structure, review 3—33324
over spillway crest, finite element analysis 3—33195
stability of cable in axial stream of viscous incompressible liquid *(Russian)* 3—29838
stability of Hartmann flow in channel with elastic walls *(Russian)* 3—7416
static electrification of liquids in pipes, review 3—2171
streaming potential fluctuation around a cylinder in water 3—33207
streaming solutions, mass transfer hydrodynamics 3—1355
supercavitated flow past profiles, effect of water tunnel wall 3—4600
supercritical water flowing in tubes, heat transfer 3—1370
surface motion, press.- and accel.-induced distortion, computation 3—1391
thermocapillary flow in thin layers, determ. of film profile 3—1349
turbulence intermittency, nonhomogeneous flows 3—33216
turbulence meas. 3—37778
turbulence with circular flow of liquid metal in magnetic field *(Russian)* 3—7415
turbulent, velocity distribution at porous surface 3—4557
turbulent boundary layers, in incompressible fluids with longitudinal pressure gradients 3—4579
turbulent free convection 3—4556
turbulent in tube, distributed grit type roughness effects on spectrum of wall pressure fluctuations 3—4565
turbulent shear flow, transverse velocity component and Reynold's stresses measurement using dual-wedge hot-film probe 3—28794
two layer ocean current, instability with antisymmetric velocity profile in upper layer *(Russian)* 3—2942
two-phase flow, residence time distribution, tracer injections 3—36135
visco-elastic liquid, flow in wake past a 2 dimens. grid 3—7362
viscoelastic liqs., mechanical eqns. of state for simple flow systems *(Dutch)* 3—29808
viscous incompressible, in channel with step, numerical solution 3—4544
vortex systems comprising circular cylinders normal to flat plate 3—20326
water, in pipe, response to motion of thin sleeve, stability 3—11364
water, membrane transport, continuum mechanical approach to flow equations 3—35234
water, shear layer flow regimes and wave instabilities, reattachment lengths downstream 3—7339
water, swirling cavity flow through straight circular pipe 3—36101
water, swirling flow through convergent-divergent nozzle to horizontal tube, annular hydraulic turbulent jumps 3—29927
water, through straight circular pipe, swirling cavity flow 3—36100
water and aqueous surfactants, thinning of oil films, rupture, flow velocity dependence 3—39465
water compressible flow, discharge velocity issuing from nozzles 3—33318
water flow conditions determ. by d.c. hot wire thermoanemometer 3—32272
water in an annulus, friction and heat transfer in the swirl flow 3—20283
water in enclosed rectangular cavity, effect of inversion temp. on convection 3—4562
water in tubes at high pressure, heat transfer *(Japanese)* 3—1353
water laminar free convection flow at 4°C from a vertical plate with variable wall temperature 3—29843
weirs, thin plate, sharp crested rectangular, suppressed and contracted, discharge, theoretical analysis, experimental data 3—7317
H_2O, surface boiling, hydraulic resistance in a tube, arbitrary heat flux distribution 3—36081
He, film flow, superflow speed rel. to chem. gradient driving force, dissipation 3—36450
He I, boiling under forced flow in vertical tube 3—9894
He II film, transitions in flow rates 3—36451
^{4}He, superfluid, u.s. modulated flow through small orifice, attempt to observe a.c. Josephson effect 3—30301
Hg, turbulent flow in annuli, effect of wetting 3—1371
K, boiling, in pipes, heat transfer, effect of nonuniformity of heat supply on critical heat flow 3—14986
$MgSO_4.7H_2O$, cryst. growth resist. expt. using flow system 3—8713

flow process charts *see flowcharting*

flow resistance *see viscosity*

flow through porous media
adsorption in packed bed, three simultaneous resistances *(French)* 3—4624
aerosol penetration through glass fibre filters, probabilistic theory 3—17553
binary diffusion through heterogeneous medium, pore size distribution and capillary effects, bounds using moment and transport constraints 3—29917
boundary layers with suction, velocity distribution calc. by Shvets-Targ method 3—33226
compressible laminar boundary layer flow at a three-dimensional stagnation point with intensive suction or injection 3—33234
convection, combined free and forced, past a porous vertical circular cylinder 3—38355
dispersion tensor in laminar flow through anisotropic porous media, random walk model 3—7472
drying of hygroscopic capillary porous solids, liquid capillary flow, vapour diffusion and heat transfer 3—20409
fibrous filter, gas flow at reduced ambient press. 3—17511
fixed beds, radial dispersion coefficients, annular source *(German)* 3—22561
generalised Couette flow of an elastico-viscous liquid between two co-axial porous circular cylinders 3—38378
heat transfer, application to eccentric annular region 3—23797
heat transfer between fluid and media 3—627
heat transfer by free convection through porous layer heated from below 3—1361
heat transfer for air turbulent flow with suction in a porous tube 3—20295
heat transport bounds in a porous layer 3—26790
horizontal layer, heat transfer by natural convection *(French)* 3—29916
hydrodynamic dispersion, radioactive tracer decay and absorption 3—15857
hydromagnetic flow, universal stability 3—33305
independently rotating disc of variable distance with blowing 3—29860
inhomogeneous media flow theory 3—29918
inhomogeneous medium, generalised Darcy's law, analysis 3—36139
instabilities in two-phase flow through porous media, similarity soln. 3—36138
intensive blowing through a permeable surface, nature of flow 3—33303
interference between body and permeable walls in water tunnel test section, supercavitated flow 3—33271
jets, isothermal turbulent, two-dimensional, at a curved porous wall 3—33311
Knudsen permeability, temp. depend. developed from kinetic theory relations 3—7471
liquid motion in a cracked-porous stratum with nonstationary filtration *(Russian)* 3—29919
liquid pressure filtering through pores in nonhomogeneous layers *(Russian)* 3—33304
mass transfer in free volume of fixed granules bed 3—4626
mixed convection in porous media *(French)* 3—20287
motion of small spheres in gases, diffusion coeff. of porous membranes 3—33258
oil recovery from underground porous sources, fingering reduction using macromolecular solutions 3—3164
oscillatory flow, past an infinite, vertical, porous plate with constant suction, free convection effects 3—33211
oscillatory flow past an infinite, vertical, porous plate with constant suction, free convection effects 3—33212
packed bed, Markov chain model 3—7470
packed beds, prediction of breakthrough curves, single parameter models 3—11456
packed beds, trickle flow 3—7473
packed beds and tube bundles, forced convection heat transfer 3—11365
poly(ethylene terephthalate) molten, through packed beds of glass beads 3—7469
sloping porous layer, natural convection 3—20307
spiral flow in a porous pipe 3—29862
supersonic boundary layer, on permeable plate *(Italian)* 3—23745
thermal conductivity meas., across direction of flow of gas *(German)* 3—23685
thermoconvective flow in inclined homogeneous porous layer *(French)* 3—7348
thermodynamics of gas/liquid interfaces in a porous medium, condensation/evaporation processes, viscous flow 3—26847
transient thermal processes in counterflow equipment employing layered granular beds 3—4628
trickle flow through packed beds, mixing 3—4625
turbulent boundary layer at a permeable surface 3—33225
turbulent flow with wavy permeable boundaries 3—38365

flow through porous media continued
unsteady flow of an incompressible viscous fluid in a porous annulus 3−20408
unsteady laminar boundary layer with suction or blowing 3−33223
variable properties laminar gas flow heat transfer in the entry region of parallel porous plates 3−20298
viscous, model for groundwater movement 3−15856
viscous fluid flow past permeable body at small Reynolds number 3−26846
viscous fluids through spherical shells 3−11379
water, equivalent nonlin. permeability coeff. calc. 3−7474
C, sublimation in flow of inert gas, 2800-3500K 3−26845

flowcharting
see also systems analysis
vibration problems, flowgraph methods comparison 3−22681

flowmeters
see also anemometers; flow measurement; laser velocimeters
automatic volumetric measuring tank for metering solid-water flow in pipelines 3−22573
blood, catheter type, three-electrode probe 3−400
blood, e.m. type 3−395
catheter type, using thermal method, for blood velocity measurement, and cardiac output detn. 3−25992
chemical vapour deposition instrumentation 3−12250
conference, Sheffield, England (1972) 3−461
contactless, with travelling field for channels of arbitrary cross-section, numerical calc. *(Russian)* 3−19381
d.c. hot wire thermoanemometer for determining water flow conditions 3−32272
digital meter for nonstationary flow, Siberian Instruments 1971 Exhibition *(Russian)* 3−9900
Doppler anemometry 3−22577
e.m., for blood flow meas. 3−395
e.m., with rectangular and circular channels, sensitivity *(Russian)* 3−6165
e.m. apparatus, patent 3−10227
e.m. pulsed-field, for blood flow meas., design 3−396
float type, accuracy of calculated scales *(German)* 3−16574
fluid, using optoelectric cells, patent 3−455
fluidic, in on-line process control applic. 3−13521
gas, using vortex refrigeration effect *(Spanish)* 3−16583
high pressure gas, sonic nozzles calibration 3−6164
hot-wire anemometer, sensor resolution, errors occurring due to turbulence, estimation *(Russian)* 3−32274
induction, with axisymmetric mag. field, operational principles and construction *(Russian)* 3−19380
induction flowmeter theory in T-tube of circular cross section 3−22567
laser flow velocity meter *(French)* 3−32273
literature review 3−450
magnetic, past and present development 3−19379
magnetic, using nonhomogeneous magnetic field, patent 3−456
mass, volumetric meas. of gas flows 3−470
noise vapour discharge meas., by means of gauging diaphragms *(Russian)* 3−19382
oceanographic current meter, solid state 3−5543
optical, laser Doppler anemometer method 3−19654
Pitot tube anomalous dynamic press.-meas. in suspensions 3−32278
rotameter, effects of tilting on readings *(Russian)* 3−6169
separated flows, probe development 3−13527
signal convertor and amplifier, for additive flow metering, patent 3−10226
slit flow converter with rectangular slit and variable section chamber *(Russian)* 3−6167
standard differential pressure type 3−10223
standard orifice, pipe flow, plant disturbance elimination, defined disturbance, method, tolerances *(German)* 3−13524
standardized *(German)* 3−13525
Swirlmeter, gases, electronic totalizer system 3−462
turbine, for supercritical He, operation and calibration 3−6175
turbine type volumetric, patent 3−10225
ultrasonic flowmeter, frequency technique 3−10219
u.s., cross-correlation technique 3−37781
vortex, Karman vortices principle 3−1383
water, small pressure differences meas. 3−13526
Weissenberg rheogoniometer, for flow measurements of non-newtonian fluids 3−28799
^{3}He/^{4}He gas flowmeter for use with dilution refrigerator 3−22560
Na, liquid, using crosscorrelation techniques *(Japanese)* 3−10218

fluctuations
see also Brownian motion; current fluctuations; noise; random processes
adiabatically isolated systems, calc. of fluctuations by Gibbs ensembles method *(Russian)* 3−22749
Benard instability and the hydrodynamic eqns., effect of nonlinear terms 3−11361
Brownian motion of spherical particle in a compressible fluid, hydrodynamic fluctuation theory 3−37896
distribution functions fluctuations around steady state, fluctuation dissipation theorem 3−4027
e.m. wave in localized smoothly varying turbulence 3−6400
fluid, diffusion of tagged particles, long time behaviour 3−35631
ionospheric oblique and oblique-backscatter sounding, energy spectra characts. of signal level 3−25269
ionospheric radio wave reflection, depend. of freq. correlation of fluctuations 3−34934
ionospheric vector electric field modes, component of e.l.f. hiss 3−16016
ionospheric vector electric field modes, satellite obs. 3−16015
irreversible processes, linear Rayleigh gas model 3−32449
Ising model, stochastic, fluctuations and response in nonlinear system 3−38948
kinetic eqns. for fluctuations of occupation numbers, stochastic theory derivation *(German)* 3−22737
Langevin equation, fluctuation and stability 3−19537
liquid, density fluctuations, generalized hydrodynamic approach 3−7611
luminescent solns. intermolecular relaxation-fluctuational processes and spectra, review *(Russian)* 3−27524

fluctuations continued
magnetic field, interplanetary, description from cosmic ray propag. theory using kinetic eqn. *(Russian)* 3−12884
nonequilibrium gas with binary collisions, theory of fluctuations 3−22748
nuclear reactor neutron population and γ-ray emission, relaxation effects study using stochastic model 3−23394
nuclear reactor noise analysis, exptl. obs. of fluctuations in neutron population and γ-ray emission, stochastic model analysis 3−23395
phase fluctuations of wave in stochastic medium 3−32450
plasma, anisotropic unstable, mag. fluctuation energy, thermodynamic bounds 3−29936
plasma of combustion products, statistical properties of parameter fluctuations for subsonic flow 3−17591
pressure fluctuations on a membrane in gases of 1 atmosphere 3−17486
semibounded plasma, fluctuation theory, surface oscillations *(Russian)* 3−11464
source fluctuation effects in radiation diagnosis of voided fluidic systems 3−17325
spontaneous, limitation of vacuum meas. 3−144
steady-state system far from equil. entropy changes 3−4039
structural phase transitions, nucl.-relax. study of correls. and fluctuations 3−7932
temp. fluctuations of turbulent fluid flow in circular tube 3−29845
temperature fluctuations in small systems 3−16769
temperature fluctuations of the heated surface at one active nucleation site of bubbles 3−27110
two-dimensional guiding centre plasma, fluctuation phenomena 3−14511
wall pressure fluctuations in turbulent flow in tubes *(Russian)* 3−4567
He-Ne laser, influence of elastic collisions on intensity of natural fluctuations *(Russian)* 3−22888

fluerics *see fluidics*

fluid composition control *see chemical variables control*

fluid composition measurement *see chemical variables measurement*

fluid dynamics
see also aerodynamics; electrohydrodynamics; flow; hydrodynamics; magnetohydrodynamics; Navier-Stokes equations; rarefied fluid dynamics; relativistic fluid dynamics; turbulence
actuator disk theory for incompressible highly rotating flows 3−1381
airflow in fluid amplifier, steady-state pattern and switching mechanism 3−20348
biophysical, model of expiration 3−26854
capillary-gravitational waves of finite amplitude, establishment on surface of fluid over wave-shaped bottom *(Russian)* 3−17541
chemical reactors, residence time and flow cycles, distrib. func. 3−6168
complex fluid waves, exptl. study, comparison with calculated wave profiles 3−17539
conference, Dutch Physical Society, Amsterdam (Feb. 1973) 3−28428
cylindrical waves, actual and mean energies at third order approx., steepness effect 3−17540
diffusion-convection equation, finite element soln. 3−14429
gas-liquid systems, elements of hydrodynamics 3−4616
Helmholtz-Rayleigh instabilities in barotropic atmospheric nondivergent horizontal stream *(German)* 3−12707
hyperbolic partial differential eqns., soln. by periodic method of characteristics 3−26852
laminar jet thrust measurement apparatus 3−3923
levitation technique, for exposing single particle to high temp. gas 3−13528
liquid floating zones in simulated zero gravity 3−11360
movement of liquid on part filled tanks model 3−20365
nonlinear distributed parameter systems, optimal control computation 3−6191
numerical solution, extensions to Eulerian methods 3−20266
oscillating cylinders, Stokes' paradox 3−7409
polar fluids 3−14427
quasilinear hyperbolic differential equations, solution by explicit second order method of characteristics 3−10252
Rayleigh-Taylor instability, growth rate of disturbances 3−1421
shallow submarine volcano model, blast wave expansion of high temp. condensible fluid 3−9181
transport algorithm, flux corrected, for soln. of continuity eqn. 3−23668
turbulence phenomena, eddies at interfaces 3−20316
wakes, from hypersonic cones in free flight, expt. study 3−38416
wakes of circular cylinder, effects of base-bleed and suction on pressure distribution 3−36146

fluid flow *see flow*

fluid mechanics
see also capillarity; cavitation; compressibility of gases; compressibility of liquids; fluid dynamics; hydrostatics; Mach number
annual review, book 3−33191
environmental pollution control, research program *(German)* 3−36147
measurements, literature review 3−450
microelectrode applications *(French)* 3−27875
nonlocal microfluid mechanics, generalisation of Eringen theory 3−20265
oscillating system, delinearization *(Russian)* 3−10309

fluid structure
see also classical theories of fluid structure; liquid structure; quantum theories of fluid structure
No entries

fluid valves *see valves*

fluidic amplifiers
flowmeters, in on-line process control applic. 3−13521
wall attachment type, flow pattern and switching mechanism 3−20348

fluidic devices
accumulator for high frequency ripple absorption in hydraulic system 3−16575
actuators for control and safety of pressure tube reactors 3−26494

fluidic devices continued
- gas mixtures, binary, fluidic-electronic composition analyser 3—6153
- glass fibre probe for local void fraction measurement in Mg-air flow 3—16576
- moment meas. sensor, for leaf springs *(German)* 3—13224
- nuclear reactor failed fuel detection 3—23447

fluidics
- pulling force tester, pneumatic 3—2775
- wall attachment device, particle flow 3—1471
- wall attachment device design for solid particle transportation 3—4618

fluidised beds
- adsorption matter transfer, theoretical soln. of penetration curve *(French)* 3—7463
- aerodynamics of jets discharged into fluidized beds 3—4627
- annular, inner wall transfer rates 3—29910
- bubble chain coalescence 3—7460
- bubble formation at orifice in 2D fluidized bed 3—1477
- bubble particle interactions in gas fluidised bed 3—7443
- bubbles, break-up mechanism in fluidised beds 3—26843
- catalytic reactors, countercurrent backmixing model, applicability to simplified solns. 3—7448
- circulation patterns velocity distributions and heat transfer coeff. variations 3—4610
- coating of thin plates, heat transfer with a moving boundary 3—14501
- compound heat exchange between a high temperature gas fluidized bed and a solid surface 3—20396
- concentration, local dispersion estimation using space correlation function 3—1448
- conical hoppers, cohesionless granular material flow, hour-glass theory applic. 3—23785
- cooling of finely dispersed material 3—2763
- countercurrent three-phase mass transfer investigation 3—29904
- electrically conducting particles, nonlinear relation between specific resist. and current density 3—23783
- fine particles, interaction of gas jets 3—1457
- fixed beds, radial dispersion coefficients, annular source *(German)* 3—22561
- flow through, forced convection heat transfer 3—11365
- fluctuations, correlation theory *(Russian)* 3—14504
- gas, bubble free, of fine fluid cracking catalyst particles, expansion and cavities 3—4612
- gas, delayed bubbling 3—33285
- gas, grid leakage studies 3—23781
- gas, large, solids entrainment obs. 3—1450
- gas fluidisation types, characterised density and particle size 3—1458
- gas transfer from bubbles to the dense phase 3—29905
- gas-solid suspensions above bed, velocity distrib. and friction factor 3—1451
- heat and mass transfer problems 3—1462
- heat transfer, wall-to-bed 3—11445
- heat transfer coefficients *(Russian)* 3—7451
- heat transfer obs. using harmonic anal. 3—1461
- heat transfer to wall, mechanism 3—1460
- inhomogeneous, concentration field, mean porosity determ. 3—1446
- liquid holdup in gas-liquid countercurrent flow 3—33284
- local particle concentration fields obs. 3—1447
- mass transfer in free volume of fixed granules bed 3—4626
- minimum fluidization velocity determ. 3—39418
- moving homogeneous, expansion 3—1454
- moving-bed exchange equations, asymptotic solution, interphase mass transfer 3—29902
- multistage, residence time distribution 3—29906
- packed, homogeneous, capillary flow and porosity functions 3—1452
- packed beds, non isothermal, two-dimensional flow maldistribution 3—36134
- packed beds, pressure drop and transport at intermediate Reynolds numbers 3—33289
- packed beds, forced convection mass transfer at low Reynolds number 3—33[illegible]00
- particle bed in field of vibr., mass flow rate 3—7456
- particle concentration obs. using capacitance transducer 3—458
- particle trajectories about rising bubble, model 3—17552
- particles, pyrolytic C deposition, microstructure, electron microscopy 3—24994
- percolating smooth spherical particle through three-dimensional cluster of stationary spheres, computer determination of path 3—31207
- powder cooling of IC chips, 1.5 to 2.0 watts at room temp. 3—11451
- pseudo-fluidised, transverse nonuniformity in inhomogeneity distrib. 3—20398
- pyrocarbon deposition rate, effect of surface area and hydrocarbon conc. 3—1054
- reactor, design based on mass transfer coeff. and mixing coeffs. 3—459
- reactor simulation and identification, frequency domain approach 3—1466
- reactors, two phase models which allow for bubble size variations 3—7464
- rotating model of particle behaviour in a colloid core reactor 3—7361
- shallow, viscosity obs. 3—1449
- solids, open channel flow behaviour 3—7455
- solids-in-gas suspensions flow, pressure drop analysis 3—23790
- space non-uniformity, design of reactors and gas distributors 3—1445
- spherical particles, flow of non-Newtonian liquid through 3—1455
- spherical particles under 1st and 3rd order boundary conditions' interphase mass and heat transfer 3—1463
- streams, load transport, sandy bottom, experimental investigation *(Italian)* 3—7445
- three phase, phase hold-up characteristics 3—1456
- turbulence, diffusion coeff. calc. by moving interface *(Japanese)* 3—23787
- two and three phase, hold-up and axial mixing characts. 3—23782
- two dissimilar materials, motion and distrib. of large particles 3—7465
- uniform, expansion based on theory of similarity 3—1453
- vibrated, effect of homogenization on heat transfer 3—1465

fluidised beds continued
- vibrated, props. and appls. in chemical technology 3—1464
- void fraction data, correl. 3—11447
- volume changes accompanying bubble splitting 3—36124
- wall-to-bed heat transfer 3—33201
- water-silica sand, moving homogeneous, expansion 3—1454
- (U, Pu)O_2 prod. from nitrides, development of continuous process 3—19949

fluidised powders *see powders*

fluidity *see viscosity*

fluids
- *see also bubbles; discharges (electric); disperse systems; fluid mechanics; fluid structure; gases; gravity waves; liquids; non-Newtonian fluids; plasma; quantum fluids*
- acoustic wave propagation, in fluid layer bound by two solids 3—30333
- classical, critical exponent 3—643
- classical binary collision operator estimate, utility in theory of ransport processes in classical fluids 3—22755
- compressible BKZ fluid, decomposition theorem on scalar potential 3—22798
- dielectric constant of nonpolar fluids 3—22735
- electron mobility in simple fluid near critical point 3—21044
- free convection, variation of fluid properties *(Japanese)* 3—20324
- free energy calc. of fluids near critical point 3—16772
- heat pipe fluids in mag. fields of fusion reactors, props. 3—11092
- light scattering Hamiltonian theory 3—26206
- mean spherical model for 6:12 potential 3—6383
- mixtures, inviscid mechanical theory 3—3942
- multicomponent fluids, Landau-Placzek ratio of ternary systems 3—10418
- nondeforming media, anisotropic transport processes 3—620
- nu fluid, relaxation of stress with decay of homogeneous turbulence 3—14450
- pure dense, formulations of the corresponding states principle for the transport properties 3—19519
- radial distrib. function and thermodynamic props., quantum corrections 3—16775
- radiating, thermal stability, Benard problem 3—38366
- Reiner-Rivlin, incompressible, torsional flow and swelling jets 3—4543
- ribbed flow of viscoelastic fluid from flat channel 3—23678
- rotating stratified fluid, dynamically forced neutral waves 3—14482
- stratified, upwelling in rotating annulus, linear theory 3—11402
- supercritical, laminar forced convective heat transfer, buoyancy effects *(Japanese)* 3—20323
- surface waves, stationary problems in linear theory for heavy fluid layer 3—17543
- three-dimensional boundary layer flow, regular solid surfaces, ducts, review 3—36113
- uniqueness and Holder continuous dependence for linear micropolar fluid motion 3—23675
- viscoelastic, drop breakup in simple shear fields 3—7447

fluorescence
- *see also fluorescent lamps; fluorescent screens; X-ray fluorescence*
- 1,4-dimethoxybenzene, acetonitrile soln., quenching, charge transfer interaction 3—34401
- 2-naphthylamine, deactivation by proton transfer in the excited state 3—12543
- 1,12-benzoperylene trapped in methylcyclopentane, 9K, quasiline fluoresc. spectra *(French)* 3—21815
- acridine dye aggregates, emission maxima, pK depend. *(French)* 3—34399
- air pollution, laser beam resonance fluoresc. obs. *(German)* 3—34895
- air pollution measurement, using i.r. tunable laser, review 3—3187
- alkali dimers in supersonic nozzle beams, internal state distribution, white light and laser-induced fluorescence analysis 3—17477
- alkaline earth sulphates, Eu^{2+} activation, fluorescence and excitation spectra 3—39172
- alkane fluoresc. quenching by CCl_4, nsec. decay time meas. 3—5405
- amino acids and peptides at the picomole level, fluorescent reagent development, application to automated assay 3—35524
- aniline in soln., quantum yields, solvent and conc. effects *(French)* 3—39456
- anthracene, crystals and solution, nonlinear fluorescence quenching at intense excitation *(Russian)* 3—27533
- anthracene, delayed fluoresc. quenching due to triplet exciton-hole interaction 3—2587
- anthracene, fluorescence, polarisation effects *(German)* 3—24742
- anthracene, singlet exciton fission, 77 K 3—36904
- anthracene crysts., surface quenching of fluoresc. and photoefffect *(Russian)* 3—8648
- anthracene derivatives, fluoresc., 423 to 648 K, relax. process, influence on spectral characts. *(Russian)* 3—26687
- meso-anthracene derivatives in n-hexane at 4 K, fluoresc. spectra 3—34413
- anthracene single crysts., with surface disturbed by impurity *(Russian)* 3—8647
- anthracene thin molecular crystal, absorption and fluorescence 3—34373
- anthracene triplet-triplet transfer of electron energy in gaseous phase *(Russian)* 3—36041
- anthraoxadiazole cryst. solns., quasiline fluoresc. spectra *(Russian)* 3—8641
- anthraselenodiazole, fluoresc. spectra at 77K 3—34409
- anthrathiadiazole cryst. solns., quasiline fluoresc. spectrum *(Russian)* 3—8645
- p-9′-anthryl-N,N-dimethylaniline, intramolecular exciplex emission based laser action 3—22893
- aromatic hydrocarbons, fluorescence quenching by stable free radical di-t-butylnitroxide 3—34738
- aromatic hydrocarbons, quenching of excited states by electron donors 3—15840
- atmosphere gaseous constituents, remote mapping laser induced fluorescence obs. 3—3191

fluorescence continued
- atmospheric species, cross sections for electron elastic and inelastic scattering 3−29738
- atom, level crossing, optical double reson. line shape, rel. to pulsed oscills. 3−7052
- atom, radiative decay of multilevel system, neoclassical and q.e.d. theories 3−37946
- atomic fluoresc. spectroscopy, definition of types of transition 3−7050
- atomic fluorescence flame photometer with continuous spectrum source *(Russian)* 3−10211
- atomic resonance interaction, multipole relax. and transfer rates in impact approx. 3−26585
- azulene, photophys. parameters derivation 3−12546
- azulene derivatives, fluorescence and radiationless transitions from the second excited rates 3−11278
- 1,2-benzanthracene, activated intersystem crossing from fluorescent state 3−4457
- benzene, solvent effects on relax. of $^1B_{2u}$ state 3−21826
- benzene and alkylbenzenes, liq., photoioniz. and recomb. fluoresc. 3−25081
- benzophenone low pressure gas, radiative decay 3−29701
- 19-benzoylanthracene derivatives, intersystem crossing and fluoresc. yield 3−31276
- 3,4-benzpyrene and methyl derivatives, quasilinear fluorescence and excitation spectra *(Russian)* 3−30877
- 3,4-benzpyrene in 2-methylpentane, anomalous vibr. relax. of hot S_1^* state 3−21824
- bilirubin excitation spectra in pyridine 3−5401
- biochemical fluorescence spectroscopy, measurements of absolute values, review 3−35522
- biologically important compounds, fluorometric analysis methods 3−35523
- biphenyl, vibrational analysis of spectrum 3−4456
- biphenyl, vibronic coupling mechanism explanation of vibrational features in spectrum 3−4455
- 1, 3-bis(trifluoromethyl) benzene, fluoresc. quantum efficiency and quenching rate parameters meas. 3−39457
- c ZnS, simultaneous photovoltage and fluoresc. meas. 3−5028
- carbazole, direction of the transition moment and dipole moment of the first excited singlet state, absorption and fluorescence spectra *(German)* 3−26652
- carbazole, transition moment direction and dipole moment of excited state determ. from absorption and fluorescence spectra *(German)* 3−17416
- chlorophyll a, in polar and non-polar solvents, fluoresc. excitation spectrum 3−15542
- chlorophylls in soln., fluoresc. polarization 3−1301
- cholesteric mesophases, achiral molecules, circular polarisation, fluorimeter study, circular dichroism measurements *(German)* 3−36938
- chromophores in liquid crystal solvents, detection by means of absorption and fluorescence meas. 3−11231
- chrysene, crystalline, delayed fluorescence and triplet lifetime 3−21470
- chrysene-naphthacene thin layers, sensitized luminesc. 3−15541
- coherence resonances in elec. field induced atomic alignment-orientation coupling 3−11142
- coronene in n-heptane, fluorescence spectrum at 77 K, doublet splitting into single bands *(Russian)* 3−30873
- cyanine dyes, mode-locking, fluoresc. quantum efficiency, lifetimes and triplet-triplet absorpt. 3−27887
- delayed wave form from free-deep trapped exciton annihilation 3−12172
- 1,2,5,6-dibenzanthracene in PVC matrices, O_2 enhanced fluorescence study 3−7220
- 1,8-dichloro 10-methyl anthracene, photochemistry, cryst. struct. and fluorescence *(French)* 3−2830
- 1,8-dichloro 9-methyl anthracene, photochemistry, cryst. struct. and fluorescence *(French)* 3−2830
- 3,3-diethylthiatricarbocyanine dye laser, extinction of generation and shortwave fluorescence *(Russian)* 3−10545
- N,n-dimethyl-p-cyanoaniline molecular interactions in ground and excited states, electronic spectra 3−11243
- p-N,N-dimethylamino-benzonitrile, anomalous fluoresc. interpret. 3−36039
- 2-p-dimethylaminophenyl-5-phenyl-1,3-oxazole-polymethyl methacrylate system, photochem. transforms. 3−25097
- N,N-dimethylaniline, gas phase, absolute fluorescence lifetimes and quantum yields 3−26689
- 1,2-dimethylindole fluoresc. and absorpt. spectra, determ. of dipole moment 3−4429
- diphenyl octatetraene, polarized fluoresc. spectra 3−29700
- diphenylamine, triplet-triplet annihilation and subsequent two-photon ionisation *(Russian)* 3−37135
- dithiin complexes, with trinitrobenzene and tetracyanoethylene, fluoresc. study 3−23593
- dye lasers, flashlamp pumped, threshold pump intensity fluorescence character of solution *(German)* 3−10544
- dye lasers, Raman absorption lines within stimulated fluorescence spectrum 3−22896
- dyes, short fluoresc. quenching times, meas. *(Russian)* 3−27892
- electron beam fluorescence probe measurements, apparatus and techniques 3−35493
- erythrosin molecules, vibrational decay in excited state 3−11283
- ethylene in ethylene-X mixtures (X=inert gas, diatomic mol.), vibr. deactivation, laser induced fluoresc. study 3−17473
- fast ionisation gauge, rarefied gas puff transient behaviour, electron beam fluorescence probe obs. 3−1507
- flame atomic-fluorescence photometer characts. *(Russian)* 3−10213
- flame temp. meas. by means of fluorescence spectrometry 3−13248
- fluorescein dye, ionic forms problem *(Russian)* 3−12179
- fluorescein in water and glycerol, quasimonochromatic characteristics, dependence on bandwidth of exciting and observed light 3−8637
- fluorophores, nonradiative energy transfer rates 3−20174
- formaldehyde, rel. to ozone-induced chemilum. oxidation of acetaldehyde 3−2797

fluorescence continued
- glass:Nd, laser-induced-fluorescence-line-narrowing spectroscopy 3−21474
- glasses:Tb^{3+}, cathodoluminescence for surface fluorescence study 3−2598
- Hanle effect, press. dependence in sensitised fluorescence 3−29494
- N-heterocyclic compounds, fluoresc. and phosphoresc., relative quantum yields in 77 K *(Russian)* 3−27544
- n-hexane:1,12-benzperylene, broadening, profile and shift of phononless lines, 4.2-77K *(Russian)* 3−8661
- hexane matrix, 1, 12-benzperylene and coronene impurities, zero-phonon lines and electron-phonon interactions 3−27567
- hydrocarbons, saturated, fluorescence, effect of molecular structure 3−23590
- I_2 mol. energy transfer research, resonance fluorescence spectrum 3−11304
- indole, fluoresc. and absorpt. spectra, determ. of dipole moment 3−4429
- inorganic ions in glasses and polycrystalline pellets as fluorescence standard reference materials, review 3−35349
- internal conversion from vibrationally excited levels as radiationless decay mechanism 3−26685
- i.r. analytical technique, gas monitoring appl. 3−26028
- isotropic solns., excited by intensity modulated primary light, fluoresc. curves expressions 3−21459
- ketones, cyclic α,β-unsaturated, excited state props. 3−37131
- ketones in cyclohexane soln., singlet-singlet electronic energy transfer, steric effects and rate const. 3−2798
- laser saturated atomic reson. fluoresc., theory 3−1111
- laser saturated atomic resonance fluorescence theory 3−14297
- lifetime meas., using tunable flashlamp pumped dye laser 3−14390
- lifetime meas. with versatile, high intensity, nanosecond light source 3−13295
- liquid crystal, fluoresc. quenching at nematic isotropic phase transition 3−36258
- M82 galaxy, $H\alpha$ fluorescence source in filaments 3−28258
- marine plankton sensing by dye laser induced fluorescence 3−3237
- methane and deuteromethane mixtures, model for vibr.-translation and vibr.-rot. relax. 3−26733
- 9-methyl anthracene molecules, photoassociation study 3−31281
- methyl chloride, laser fluorescence study of vibrational energy transfer in collisions 3−33163
- methyl fluoride, laser induced fluorescence, in rare gas, O_2, N_2, H_2 and D_2 mixtures, vibrational relaxation 3−33162
- methyl fluoride, partial vibration energy transfer map, laser fluorescence study 3−33164
- N-methylaniline, gas phase, absolute fluorescence lifetimes and quantum yields 3−26689
- methylfluoride vibration-vibration energy transfer 3−11310
- microscopy *(German)* 3−25739
- molecular crystals, organic, quenching due to singlet-triplet exciton annihilation 3−4969
- molecular solution, Brownian motion induced depolarization, computer simulation 3−26748
- molecule, overlapping of fluorescent and absorpt. spectra rel. to chem. struct. *(Russian)* 3−1250
- molecules, depolarization by anisotropic rotational diffusion 3−7219
- molecules, with closely spaced energy levels, absorpt.-emission processes, time-depend. Schrodinger eqn. soln. 3−29707
- molecules between mirrors, fluoresc. lifetime, quantum theory calc. 3−36040
- multielement electrodeless discharge lamps for atomic fluorescence analysis 3−37742
- N-methylindole fluoresc. and absorpt. spectra, determ. of dipole moment 3−4429
- naphthalene: pyrene, fluoresc. meas. for host sensitized energy transfer investigation 3−24735
- naphthalene, γ-irradiated crystal, detection of new free radicals *(French)* 3−18791
- naphthalene, entire phonon spectrum by localized exciton sideband method 3−7872
- naphthalene, kinetics of fluorescence in photochemical reactions *(Russian)* 3−25099
- naphthalene, quantum yield, excitation energy depend. 3−26685
- naphthalene, quantum yield of S_2 emission 3−29698
- naphthalene derivative charge transfer complexes with aliphatic amines *(Russian)* 3−12183
- naphthalenes, substituted, polarization of singlet-singlet electronic transitions *(Zekaaq)* 3−12545
- β-naphthol, excited state, acid dissoc., time depend. 3−36049
- 2- naphthol, fluorescence extinction mechanism by pyridine *(Russian)* 3−29709
- β-naphtholate, hydrated electron form. and fluoresc., wavelength and temp. depend. effects 3−12551
- naphthoxadiazole and naphthothiadiazole cryst. solns., quasiline spectra 3−15546
- nitroanilines, isomeric, and N-methylated derivatives, emissive characts. 3−25093
- nitrobenzenes, intermolecular interaction and radiationless transitions *(Russian)* 3−29702
- nuclear resonance, by continuous γ-ray from Pu-Be neutron source 3−3840
- n-octane:perylene, broadening, profile and shift of phononless lines, 4.2-77K *(Russian)* 3−8661
- organic compounds in solid solns., laser excited, effect of fine structure 3−15545
- organic compounds in solution, inorganic ions in glasses, as fluorescent standard reference materials, review 3−35350
- organic dye molecules in aqueous soln. intermolecular reactions study by fluorescence quenching and difference absorption spectrophotometry 3−7806
- organic dyes, two photon absorption enhanced by matrix 3−13751
- organic dyes excited by the He-Ne laser radiation 3−32564
- organic dyes in soln., lifetime meas. using two-photon absorption 3−13759
- particle atm. tracer, possible toxicity hazard 3−39819
- Penning ioniz. opt. spectroscopy, metastable He interaction with diatomic mols. 3−29731
- perilene in n-hexane, hot luminescence at 4.2 K 3−8644

fluorescence continued
- perylene, planar vibr. freqs. calc. and i.r. and fluoresc. spectra interpretation 3—20112
- perylene excimer fluoresc. in cyclohexane 3—21818
- phenanthrene and naphthalene guests in biphenyl host mixed crystals, delayed fluorescence at liquid He temp. 3—25086
- phenanthrene in 4, 6 polyurethane, evidence of ordered arrangement 3—8643
- photochemical generation of stable fluorescent compounds 3—27897
- photochemical reaction kinetics *(Russian)* 3—25099
- phthalimide derivates, two-photon excitation and degree of polarization *(Russian)* 3—12177
- phthalocyanine, near i.r. emission of single crysts. and films 3—21465
- PMMA-benzopyrene solid solution, two-quanta absorption of 632-8 nm line of c.w. He-Ne laser 3—39181
- polar dye solution, excited state quenching, inhomogeneous spectral broadening *(Russian)* 3—34383
- polarisation, effects of fluorescence light emitted by plastic NE 102A *(German)* 3—24742
- polymers, mol. orientation distrib., polarised Raman scatt. and fluoresc. investigation 3—26743
- polyvinyltoluene, fluoresc. degradation under u.v. irrad. 3—30862
- protoporphyrin in n-octane, 4.2 K, reversible transforms. of luminescent impurity centres 3—15547
- pyrene, cryst., triplet exciton lifetime 3—27888
- pyrene, liq., laser induced transient absorpt., long- and short-lived components 3—34737
- pyrene, triplet-triplet transfer of electron energy in gaseous phase *(Russian)* 3—36041
- pyrene cryst., monomer emission, fluoresc., decay times 3—30857
- pyrene crystals, mag. field effect on delayed fluorescence 3—27565
- pyrene vapour, fluoresc. decay, biphotonic excitation and vibr. redistrib. kinetics 3—20173
- quantum beats, pulsed dye laser excitation, determination of relaxation times and splitting factors 3—22968
- quasimonochromatic characteristics, dependence on bandwidth of exciting and observed light 3—8637
- quinoxaline vapour, phosphoresc. and fluoresc. emission spectra 3—11281
- radiationless transitions in condensed media, rate constants *(Russian)* 3—8636
- randomly oriented molecules, polarisation of two photon excited fluorescence 3—20178
- rare earth complexes with aurinitricarboxylic acid and amines, absorpt. and luminesc. 3—15543
- resonance Raman fluorescence, manifestations of press. broadening 3—33154
- retinol, polarized fluoresc. spectra 3—29700
- rhodamine 6G dye, photon quenching model, liquid lasers 3—22899
- rhodamine 6G in water, effect of soap on fluorescent lifetime and quantum yield 3—32562
- rhodamine 6G solutions, calorimetric determ. of fluorescence energy yields using Ar^+ laser *(Russian)* 3—30846
- Rhodamine 6J in ethanol soln., natural impurities effect on generation characts. *(Russian)* 3—6483
- rhodamine dyes in ethanol soln., substitution effects *(Russian)* 3—24683
- ruby, higher energy levels of Cr^{3+} ion pairs, excitation and absorpt. spectra 3—15551
- saturated resonance fluorescence, non quenching collisions influence 3—14298
- short lived decay meas., single photon counting method 3—25733
- Shpolskii systems, hot luminescence 3—8644
- small molecules, intramol. perturbations and quenching 3—26684
- solutions, kinetics in the presence of energy transfer, migration of donor excitation *(Russian)* 3—35693
- solutions, selfdepolarisation of fluorescence, analysis of experimental data 3—18494
- solutions of organic dyes, emission anisotropy depend. on concentration 3—21457
- spectral radiance factor curve, separation into reflected and fluoresced components 3—22345
- spectrofluorimeter-spectrophotometer combination, computer centred 3—28770
- spectrofluorometry, emission standards, spectrometer calibration methods 3—35532
- spectroscopy, for organic analysis of lunar and geological samples 3—32268
- trans-stilbenes, di-para-substituted, multiple transitions in low energy absorpt. band fluoresc. spectral evidence 3—17426
- p-terphenyl with tetracene impurity, vibron. relax., role of delocalized and pseudolocalized vibrs. 3—27090
- tetracene, singlet exciton fission, 77 K 3—36904
- s-tetracyanobenzene, charge transfer fluoresc. by excited electron donor-acceptor complex 3—9090
- tetracyanobenzene-biphenyl complex, delayed charge-transfer fluoresc. in cryst. state 3—21820
- tetraphenyl-butadiene, u.v. fluorescence, fluorescence wavelength convertor 3—18479
- tetraphenylethylene in highly viscous solns., intramol. relax. influence on fluoresc. freq./time behaviour 3—21827
- tissue, formaldehyde vapour induced, holder 3—35525
- Tl^+:oxide glass, energy level assignments 3—12168
- TMPD in aqueous solns., photoioniz., fluorescent yields and decay times 3—2829
- transition elements, laser excited atomic fluorescence in N_2O-acetylene flame 3—32263
- triazolopyrazines, solvent effects on electronic spectra 3—4452
- triazolopyrimidine, solvent effects on electronic spectra 3—4452
- 2, 4, 6-trimethyl pyrylium cation, absorption, fluorescence and phosphorescence spectra 3—4435
- trypaflavine in water and glycerol, quasimonochromatic characteristics, dependence on bandwidth of existing and observed light 3—8637
- universal relation to heat radiation spectra 3—14391
- zinc porphin in n-octane, first excited singlet state, Jahn-Teller instability 3—8599

fluorescence continued
- Ag fluorescence resistograms using an atomic fluorescence photometer *(Russian)* 3—28791
- α-Al_2O_3:Cr^{3+} direct optical excitation into excited states of Cr^{3+} pairs 3—8657
- Ar, K-shell fluoresc. yields 3—26570
- BF, reson. fluoresc., vibronic transition probabilities 3—29699
- BaO fluorescent scattering by sunlight at 106 km, electronic transition moment of the $A^1\Sigma$-$X^1\Sigma$ band system 3—17424
- $BaSb_2O_6$:$Bi^{3+}(Pb^{2+})$, obs. for each excitation band 3—21478
- Bi^{2+}:oxide glass, energy level assignments and decay time meas. 3—12168
- $BiCl_3$ Raman spectra, method for resonance fluorescence effect elimination 3—28542
- CN, B state, fluoresc., time depend. 3—26688
- CO, excited states, elastic cross relax. 3—36042
- CO, produced by CO_2 photodissociation population distribution of triplet vibrational level 3—26683
- CO, shock heated, variation in equilibrium i.r. fluorescence 3—4453
- CO, u.v. photoionisatin cross sections 3—11282
- CO, V-V energy transfer rate from CO(v=2) using tunable parametric oscillator excitation 3—38314
- CO cross-section for, through photodissociation of CO_2 3—20193
- CO + Hg collisions, time-of-flight sensitized fluoresc. vel. depend. of Hg excitation 3—11312
- CO_2, collision with O_2 and N_2 mols., fluorescence of stretching vibration *(Russian)* 3—26736
- CO_2 vibr. deactivation using laser induced fluoresc. in CO_2; $CO_2 + {}^{14}N_2$, $CO_2 + {}^{15}N_2$; $CO_2 + He$ 3—11280
- CO_2^+ spectra, cross-section meas. 3—1249
- $Ca_{2-2x}Na_{1\|x}Eu_xMg_2V_3O_{12}$, Eu^{3+} fluoresc., energy levels, point symmetry *(French)* 3—18480
- $Ca_{2-2x}Na_{1\|x}Eu_xMg_2V_3O_{12}$, of Eu^{3+}, temp. and conc. depend. *(French)* 3—21460
- CaO, r.f. sputtered films, pure and Sm- and Tm-doped, X-ray excited fluoresc. 3—27568
- $CaO.P_2O_5$ glass:Cu^+, comp. and temp. depend. 3—30869
- $CaSb_2O_6$:$Bi^{3+}(Pb^{2+})$, obs. for each excitation band 3—21478
- $CaWO_4$:Am^{3+}, fluoresc. emission props. 3—34405
- Cd atoms, excitation transfers between 5^3D_1, $5D_2$, 5^3D_3 excited levels, cross section detn. *(French)* 3—11143
- CdF_2, cooperative luminesc. of Yb^{3+} and Er^{3+} *(French)* 3—30855
- CdS:Ce^{3+}, Ag, Cu fluorescence spectra, probability of emission calc. *(Russian)* 3—27546
- Cl, K-shell fluoresc. yields 3—26570
- Cr complex, $[Cr(atp)_6]X_3$, atp = antipyrene, X = SO_3F, BF_4, SCN, ClO_4, anion effects *(German)* 3—8679
- Cs, vapour, excited by light of 852.1-894.3 nm reson. lines, fluoresc. spectrum 3—23480
- CsI:Tl fluorescence, polarisation effects *(German)* 3—24742
- Cu complex with octamethylporphins, combinational dispersion spectra *(Russian)* 3—11284
- Cu fluorescence resistograms using an atomic fluorescence photometer *(Russian)* 3—28791
- D_2 vibrational relaxation in ^3He and ^4He mixtures, study by laser-induced vibrational fluorescence technique 3—23628
- DCl, V→T, R and V→V relaxation, by laser fluorescence technique 3—33165
- Er^{3+} doped fluorides, i.r. excited visible luminesc., host lattice effects 3—21469
- Eu^{3+}, primary and secondary solvation spheres, effect on electric quadrupole transitions 3—15536
- Eu^{3+} in D_2O, secondary fluorescence quenching rate constants for ethanol, acetic acid and H_2O 3—34421
- EuS, EuSe and EuTe *(German)* 3—18495
- GE:Sb, high frequency monochromatic phonon spectroscopy 3—1765
- GaP, from bound excitons, quenching and enhancement by far i.r. radiation 3—36940
- GaP, reson. fluoresc. due to bound excitons, laser excited 3—18484
- Gd^{3+} in solution, radiative and radiationless transitions, temp. effects 3—34402
- H_2 electron beam stabilized discharge, superfluorescence due to HF quenching 3—19599
- HBr, V=2 state, vibrational excitation and relaxation 3—11313
- HCl, shock heated, variation in equilibrium i.r. fluorescence 3—4453
- HCl, vibr. excitation and relax. of V=2 state, vibr. fluoresc. obs. 3—11321
- HCl gas, vibration-vibration energy transfer 3—11309
- HF (v=2) deactivation rate, use of direct overtone excitation 3—20172
- HF vibrational deactivation in pure HF and HF-additive mixtures, meas. using laser-excited vibrational fluorescence 3—7250
- He excitation by H atoms, spectroscopic analysis of radiation emitted during decay of products 3—26607
- He flowing afterglow, pumped, excitation transfer, quenching reaction rate coeffs. 3—9056
- He flowing afterglow, pumped, excitation transfer, rate coeff. for rot. relax. of He_2 3—9057
- Hg atom collisions with buffer gases, depolarisation of resonance radiation 3—33060
- ^{202}Hg, forbidden transition 6^2S_0-6^3P_0 in mag. field *(French)* 3—2342
- I_2, $B\ {}^3\Pi(O_4{}^+)$ state, mag. fluorescence quenching, direct inversion 3—38303
- I_2, excited by ionized Ar and Kr lasers, obs. 3—23588
- I_2, intermodulated fluoresc. obs. of hyperfine couplings 3—4454
- I_2, monochromatically excited, energy transfer processes, quenching by I 3—23625
- I_2, nonlinear level crossing in $X^1\Sigma_g{}^+$ state 3—1251
- I_2, selective excitation, reson. fluoresc. 3—29711
- I_2 B-state lifetimes, magnetic field dependence 3—7218
- I_2 vapour, resonance flourescence under off-resonance monochromatic excitation 3—17451
- KCl:Sm^{2+}, fluoresc. spectral meas. of ion-defect pair energies 3—24736
- KI:Tl fluorescence, polarisation effects *(German)* 3—24742
- $LaAlO_3$, higher energy levels of Cr^{3+} ion pairs, excitation and absorpt. spectra 3—15551

fluorescence continued
- $LaBr_3{:}Tb^{3+}$, absorpt. and fluoresc. spectra, 77 K 3–30866
- $LaCl_3{:}Pr^{3+}$, i.r. quantum counter upconversion, laser optical double reson. 3–18487
- $LaF_3{:}Pr^{3+}$, i.r. quantum counter upconversion, laser optical double reson. 3–18487
- N, atomic, produced by photoabsorpt. of extreme u.v. radiation by N_2 3–33029
- N_2, u.v. photoionisation cross sections 3–11282
- N_2 electron beam stabilized discharge, superfluorescence due to HF quenching 3–19599
- NO γ-band system, meas. of vertical distrib. in 60-170 km altitude region 3–3044
- NO_2, in atmosphere, laser induced fluorescence obs. 3–3018
- NO_2 visible band system, partial rot. analysis using laser-induced fluoresc. decay 3–26654
- N_2O, u.v. photoionisation cross sections 3–11282
- Na, $3^2P_{1/2}$-$3^2P_{3/2}$ states, coherence transfer induced by inert gas collisions 3–38229
- Na, fluoresc. quenching by N_2, energy depend. cross sections 3–33030
- Na, high-resolution spectroscopy, using c.w. dye laser 3–37634
- Na, trace amounts detection by fluorescence emission excited by continuous wave organic dye laser 3–28776
- Na-Hg(6^3P_1), atomic collisions, induced sensitized fluorescence, excitation transfer to Na 3–26569
- $NdZrF_4$, of Nd^{3+}, matrix characterization *(French)* 3–18481
- Ne, K-shell yield, Hartree-Fock-Slater model calc. for all multiply ionized states 3–14296
- Ne, laser optically pumped fluoresc. saturation resons. due to mag. mode crossing 3–20026
- Ni complex with octamethylporphins, combinational dispersion spectra *(Russian)* 3–11284
- O_2, u.v. photoionisation cross sections 3–11282
- OH radicals, by tunable dye laser 3–7222
- PN, reson. fluoresc., vibronic transition probabilities 3–29699
- Pb^{2+}:oxide glass, energy level assignments 3–12168
- 1,10-phenanthroline in aq. soln., spectral meas., excited-state dimerisation study 3–23592
- $PrCl_3$, effect of pump laser wavelength, pump power and temperature 3–18471
- Rb, excitation transfer between fine structure components of states, collision study 3–23477
- Rb_2 vapour, nonlinear absorpt. of ruby laser emission *(Russian)* 3–7221
- S, K-shell fluoresc. yields 3–26570
- SF_6, laser induced i.r. fluoresc., thermal heating, mass diffusion and collisional relax. 3–1248
- SF_6-rare gas collisions, i.r. fluoresc. obs. of excited vibr. states of SF_6 3–23631
- SO_2, fluorescence decay from single vibronic states 3–11279
- SO_2, resonance fluorescence excited by Zn^+, vibrational and rotational analysis 3–29697
- SO_2 and hydrocarbon gases, air pollution, remote meas. by u.v laser induced fluorescence 3–37541
- $SrSb_2O_6{:}Bi^{3+}(Pb^{2+})$, obs. for each excitation band 3–21478
- Tm^{3+}, Er^{3+} in borate and phosphate glasses, energy transfer processes, efficiencies, decay times 3–21466
- Xe, quasi-molecular, VUV fluorescence emission quenching 3–29077
- $YAlO_3{:}Er^{3+}$, energy levels, cryst. field components 3–5225
- $Y_3Al_5O_{12}$, non-radiative decay from 5d states of rare earths, fluoresc. meas. 3–34396
- Yb^{3+} doped fluorides, i.r. excited visible luminesc., host lattice effects 3–21469
- ZnS, powdered, X-ray induced a.c. cond., thermostimulation, fluoresc., thermolum. 3–38868
- ZnS:Ag, Cu fluorescence spectra, probability of emission calc. *(Russian)* 3–27546

fluorescent lamps
- Illuminating Engineering Society, Annual conference 3–5930
- life performance testing, IES approved method 3–5906
- photometric testing, IES approved method 3–5907
- $Zn_2SiO_4{:}Mn$, chem. anal. and luminesc. spectra of phosphor 3–30854

fluorescent screens
- *see also display systems; electroluminescence*
- picture tubes screens colour meas. by direct-reading colorimeter 3–25748
- X-ray paper radiography system (instead of film) using u.v. screens 3–28745

fluorimetry *see chemical analysis*

fluorine
- atom, reaction with hydrides, energy partitioning and i.r. chemilum. 3–31254
- atom, reactions with org. cpds., energy partitioning and i.r. chemilum. 3–31253
- atom, vibr. relax. of HF and DF 3–1289
- atomic, dissociatively prod., pulsed laser emission in elec. discharge 3–10520
- collisions with H or D, Monte Carlo calc. of reaction rates and vibrational level populations of products 3–31255
- electron affinity in alkali metal compound 3–1117
- glass melts with high fluoride content, F loss to atmosphere effects *(German)* 3–27161
- hydrous phase coexistence with peralkaline granite in South Greenland 3–34796
- ion fractionation at sea-air interface, enrichment values 3–12691
- ions, collisions with Ar, Kr, Xe at 35.7 MeV, dependence of target X-ray production cross sections on ionic charge state 3–1129
- isotope shifts in trichlorofluoromethane, temp. var. 3–7225
- liquid, sound vel. meas. 3–27071
- methane-F_2 flame temp. meas. by means of vibration-rotation spectra of HF *(French)* 3–29645
- molecule, effect on HF vibr. relax. rate 3–10467
- molecule, electron impact ionization cross section, 15-100 V 3–1284
- molecule, Raman cross section and depolarisation ratio for chem. laser diagnostics 3–36018
- multiconfigurational approximation *(Russian)* 3–23462

fluorine continued
- spectrochemical determination in W, using molecular bands *(Russian)* 3–13515
- $D_2 + F$ reaction, dynamics, on a semiempirical valence-bond potential energy surface, Monte Carlo trajectories 3–25052
- $F\text{-}CH_4$ laser, vibr. rot. state populations, output spectra 3–10479
- $F\text{-}H_2$ laser, vibr. rot. state populations, output spectra 3–10479
- F-HBr laser, vibr. rot. state populations, output spectra 3–10479
- F-HCl laser, vibr. rot. state populations, output spectra 3–10479
- F-HI laser, chem., obs. of laser reaction by equal gain technique 3–10498
- F-HI laser, vibr. rot. state populations, output spectra 3–10479
- $F + H_2(D_2) \rightarrow H(D) + HF(DF)$ temperature parameter for rotational state of product 3–31245
- $F + H^+$ collisions, molecular theory approach 3–29519
- $F + H^+$ collisions, molecular theory, cross sections calc. 3–29520
- F^-, electron detachment by CO and H_2, rate meas. 3–11300
- F^-, in NaBr, potential, calc. 3–36834
- F^-, in NaBr, potential, theory 3–36835
- F_2 mol., loge localization analysis 3–11210
- F_2-H_2, reaction behind shocks 3–11317
- F_2-H_2 laser, emission rel. to H_2 press. 3–10493
- $F_2 + Li \rightarrow LiF + F$, pot. energy surfaces calc. 3–23637
- F^{6+} passed through foil, yield of excited autoionized metastable states 3–20033
- F^{9+} beam collision with Ar at 1 to 2 MeV/amu, charge dependence of K-shell ionisation 3–20067
- FI, $2p^43d$ and $2p^44d$ configs., energy levels calc. 3–17346
- FI spectral lines, Stark broadening and shift 3–7047
- F_2-H_2 laser, excitation by relativistic electron beam, energy characts. *(Russian)* 3–4093
- ^{18}F, short-lived, production by Van de Graaff accelerators 3–270
- ^{19}F, one-electron atoms, oriented nuclei obs. 3–23504
- ^{20}F, uniform high energy gamma tube source using, design 3–13477
- $GaAs{:}F^-$, ion implantation profile, Auger spectroscopy determ. 3–12309
- $H + F_2 \rightarrow HF + F$, determ. of energy distribution among products using arrested relaxation variant of i.r. chemiluminescence technique 3–5377
- $H + F_2 \rightarrow HF + F$ reaction, potential energy surface calc. 3–25053
- H_2-F_2 laser, photochem., submicrosecond pulses, output energy and pulsewidth rel. to gas press. 3–4084
- $H_2 + F_2$ pulsed laser, H_2 pressure effect on stimulated emission 3–6460
- $NaF{:}Li^+$, e.s.r. study of F_3^{2-} molecule ion with Li impurity forming di-interstitial centre 3–2390

fluorine compounds
- fluoride crystal windows, vacuum seals 3–169
- fluoride-to-chlorinity ratio determ. in region south of Greenland 3–39500
- fluorite type crysts., band struct. and optical props. 3–33793
- group IV tetrafluorides, Raman spectra, 20 to 420°C, Coriolis and force const. determ. 3–29662
- group IV tetrafluoro cpds., photoelectron spectra, ionization energies 3–7169
- inorganic pentafluorides, association in saturated vapours, molecular beam mass spectra 3–25924
- $CdF_2{:}Na^+(La^{3+})$, F self diffusion, depend. on doping 3–7972
- Er^{3+} doped fluorides, i.r. excited visible luminesc. 3–21469
- $F^{12}C^{15}N$, Zeeman effect, mag. susceptibility anisotropy, g-value quadrupole moment 3–33135
- F_2CO, vibr. intensities, dipole moment derivatives 3–26640
- F_2CS, vibr. intensities, dipole moment derivatives 3–26641
- FH SCF-MO calculations using basis sets of Gaussian lobe functions 3–4404
- FH_2, potential energy surfaces calc. 3–23635
- F_2O thermal decomposition kinetics 3–9048
- HOF, photoelectron spectrum, valence region orbitals analysis 3–36047
- Yb^{3+} doped fluorides, i.r. excited visible luminesc., host lattice effects 3–21469

flux (magnetic) *see magnetic flux*

flux (neutron) *see neutron flux*

fluxmeters
- *see also magnetic field measurement; magnetic flux*
- exposure meter M4C, semiautomatic positive Mililux *(Czech)* 3–35436
- employing Hall generator, description *(Polish)* 3–258
- restoring torque, electrostatic correction, soln. *(Polish)* 3–259

foams
- *see also bubbles*
- adsubble processes, foam and bubble fractionation 3–12464
- aquatic frontal systems, element enrichment 3–12690
- biliquid, oil lamella type and water lamella type 3–2769
- bubbly water, unidimensional flow through nozzle, integration of hydrodynamic eqns. *(Russian)* 3–1443
- cellular, elastic modulus, porosity influence 3–37098
- ocean foam, microwave emissivity effects on radiral radiometric measurements 3–15945
- polyurethane, compression wave behaviour 3–31205
- polyurethane, rigid, fracture under biaxial stress 3–31206
- solid phase presence rel. to syneresis and stability 3–31195
- surface energy of aqueous solns. of surface active materials 3–5359
- thick liquid films and threads, Gibbs elasticity, thermodynamic theory 3–38708

focused collision sequences *see sputtering*

focusing
- Astron resistor config. for electron focusing 3–16923
- asymmetrized quadrupole lenses, paraxial chromatic aberration 3–13782
- charged particles in combination bihelical system with uniform mag. field 3–13765
- cold-cathode operation at low pressures, formation of gas-focussed electron beam 3–17671
- converging beam holography, aberrations *(Russian)* 3–698
- defocused optical syst. with slit aperture, focusing props. 3–677
- double magnetic prism-e.s. mirror system, optimal characteristics, exptal. determ. *(French)* 3–13452
- E-region radiowave focusing by irregularlities 3–9330

focusing continued
electron beam, intense, production and focusing, expt. obs. 3 — 35724
electron beam, stability regions in axially symmetric periodic focusing mag. field 3 — 26255
electron beams, relativistic, intense, cone focus trajectories, adiabatic envelope conservation 3 — 32616
electron beams relativistic, intense, cone focusing 3 — 32615
electron focusing systems, electrostatic, periodic 3 — 13781
electron high output beams, in mag. fields 3 — 13780
electron lenses, round and cylindrical with field free object space, theory *(German)* 3 — 26256
electron microscopes, detection by scanning 3 — 365
field emission illum. systems, performance estimates, design criteria, aberrations, defocus, stability 3 — 803
filter, axially symmetric, pupil functions, diffr. field, foci 3 — 22316
flying-spot microscope with focus-assist device 3 — 22503
gamma scintillation camera, new method for design optimisation of parallel-hole collimators 3 — 22521
high-current electron beam gas focusing 3 — 17652
hollow cylindrical electron beam, reversible focusing 3 — 13766
image resolution and contrast, effect of lens aberrations for coherent illumination in electron microscope 3 — 10581
injection laser, theory of transient evolution and self-focusing behaviour of lasing filaments 3 — 29103
intensity fluctuations, focus of circular aperture, turbulent medium, amplitude filters 3 — 37939
ion, short duration intense electron beams *(Russian)* 3 — 6533
ion orbits, Nth order aberrations in static magnetic fields 3 — 808
laser, broadening in self-focusing of single ultrashort pulses in glass 3 — 16908
laser bams, elliptical, self-focusing, time independent, beam shape 3 — 29148
laser beam thermal self defocusing, diffr. effects 3 — 22938
laser beams, thermal self-focusing, steady state theory 3 — 22957
laser glasses, self-focusing, damage, subnanosecond pulses, n_2 measurements 3 — 29150
laser operation, under external self-focusing *(Russian)* 3 — 29127
laser radiation, self-focusing in $Bi_{12}SiO_{20}$ crysts. 3 — 32602
laser radiation self-focusing with alkali halide single crystals, focus of damage displacement 3 — 32600
lenses, ground glass, focusing criterion from MFT meas. 3 — 28511
magneto-optic system with linear focusing units for neutrino expts. 3 — 3857
microwave self-focusing in semiconds., nonlinear mechanisms 3 — 35715
optical elements with regularly distributed refractive index, review *(Russian)* 3 — 35430
optimum conditions, parametric gain in birefringent crystals 3 — 781
particle, in circular accelerators, field configurations 3 — 16494
particle beams, device 3 — 10034
photon echoes, radius of curvature expressions 3 — 37984
plasma, e.m. wave focusing in inhomogeneous mag. field 3 — 23823
polar molecule, state selection by alternate gradient focusing 3 — 7265
propagation of cylindrical waves in ducts 3 — 10430
proton accelerator with asymmetric variable-phase focusing particle motion, numerical simulation 3 — 35460
rotating and deflecting a line focus, electron optical props. 3 — 37991
Rowland system with concave holography gratings, stigmatism conditions *(French)* 3 — 35676
screens, incoherent contact edge-imaging, image sharpness, modulation transfer function 3 — 13278
self, stimulated Raman scattering of light *(Russian)* 3 — 775
self focusing in optical glasses, relative contribution of Kerr effect and electrostriction 3 — 29149
self-focusing, short pulses, nonlinear media, focal structure, theoretical analysis 3 — 22959
self-focusing and small scale filaments of laser beams in nonlinear media 3 — 19635
Selfoc fibres, imaging, focusing props., spherical 3 — 13715
semiconductor, elemental, e.m. beam self focusing in inhomogeneous mag. fields 3 — 10568
semiconductor, nonparabolic, a.m. microwave self distortion rel. to self focusing 3 — 32593
semiconductors, of laser beams, damping criteria 3 — 16906
slit aperture, high numerical system with spherical aberration and defocusing, diffr. 3 — 26202
solid liquid compound hydroacoustic lens, low aberrations 3 — 35324
stress waves, in elastic sphere 3 — 32379
uniaxial crystals, with double refr., optimum focusing conditions for parametric gain 3 — 10565
u.s., solid cylindrical plastic lenses 3 — 37554
GaAs, laser focusing, intervalley transfer mechanism 3 — 10552

focusing, particle *see focusing; particle optics*

fog
conductive-radiative model of growth and formation 3 — 28004
droplet vaporisation and fragmentation by 10.6μm laser pulse 3 — 16891
droplets, explosive vaporisation by 10.6 μm laser pulse 3 — 37196
electrical stimulation of warm fog for droplet coalescence *(Polish)* 3 — 25330
formation by steaming of warm-water lagoon used for power station cooling 3 — 39511
jet aircraft wake dissipation effects 3 — 25216
particle size distrib., evaluation of statistical characts. of aerosol microstructure in surface layer *(Russian)* 3 — 28016
SO_2 absorption in polluted areas, formation of sulphate ion 3 — 15970

Fokker-Planck equation *see transport processes*

Foldy-Wouthuysen transformation *see quantum field theory*

food processing industry
pollution, atomic absorption anal. 3 — 5691

forbidden gap *see energy gap*

Forbush decreases *see cosmic ray variations*

force
see also atomic forces; coercive force; force measurement; molecular force constants; nuclear forces
axial, prestressed cylindrical shells with arbitrary boundary conditions, effect on free vibration 3 — 10303

force continued
centrifugal, prestressed cylindrical shells with arbitrary boundary conditions, effect on free vibration 3 — 10303
Chu-Haus-Penfield principle of virtual power, criticism 3 — 28931
function expansion, for two homogeneous spheroids with noncoincident symmetry planes *(Russian)* 3 — 16116
between metal plates arising from contact pot. 3 — 10422
mixture., balance of forces, new definition of partial stress tensor 3 — 32295
Newtonian analogue of force in Kerr metric 3 — 19498
nonholonomic systems, generalized inertia forces, kinetic energy applic. 3 — 19405
penetration of cone into compressible fluid, determ. of pressure and force distrib. *(Russian)* 3 — 29879
ponderomotive forces, electrostatic field effects, heat transfer boiling dielectric fluids 3 — 1801
principle of virtual power of Chu-Haus-Penfield, criticism 3 — 28932
prismatic shells, transmission of concentrated forces perpendicular and parallel to ridge 3 — 16625
random, probability distrib. in stellar gravit. systems 3 — 31741
reactions of mechanical systems to random forces *(Russian)* 3 — 28842

force constants *see lattice dynamics; molecular vibration*

force measurement
see also dynamometers
alternating force registration, amplitude and frequency obs. of harmonic oscillations of mass *(Russian)* 3 — 5767
harmonic forces, new measuring equipment for materials testing applications *(Hungarian)* 3 — 21763
load cells, nonstationary processes *(Hungarian)* 3 — 54
piezoelectric technique for multi-component meas. *(German)* 3 — 253
pulling force tester, pneumatic 3 — 2775
space vehicle bodies, in Mach number range $Ma_\infty = 3$ to 10 *(German)* 3 — 38386
standard instruments, France, units *(French)* 3 — 16378
transducer, low drift, for crayfish stretch receptor obs. 3 — 25985

force meters *see force measurement*

forecasting, technological *see technological forecasting*

form factors
$\pi\pi$ scatt., detn. from current algebra, analycity and unitarity 3 — 19732
A = 12 system, finite-momentum-transfer test of conserved vector current 3 — 23197
analytic triangle, in quantum field theory 3 — 6549
atomic pots., calc. using form-factor techniques 3 — 29540
axial vector nucleon form factor determ. from $\nu d \to \mu^- pp$ 3 — 10682
baryon e.m., calc. using phenomenological mass operator for hadrons 3 — 10693
Bincer, Bjorken limit, application to wave function renormalisation constant 3 — 14100
bound state poles of form factors in eikonal approximation and infinite component wave equations 3 — 13866
composite Fermi model, convergence function and e.m. form factors in time like region 3 — 13852
deuteron, form factors of e.m. current of np system determ. in terms of Jost matrix 3 — 26301
deuteron electromagnetic structure by inclusion of virtual particle effects 3 — 6606
deuteron e.m. form factors, calc. from elastic eD scatt. 3 — 16989
dual currents with cut-off, construction of amplitudes 3 — 17071
dynamic resonance model, with e.m. interaction, calc. of elastic form factor 3 — 14021
dynamic resonance model of form factor for electroproduction on meson target 3 — 13854
elastic, asymptotic behaviour, composite field model 3 — 37992
electroproduction interactions, relationship with scaling function 3 — 16979
e.m., meas. for $S_{11}(1535)$ reson. 3 — 38034
e.m., meromorphic function approach 3 — 840
e.m. interactions, C-violation from $\rho\gamma\gamma$ and $\gamma\gamma\gamma$ vertices in $e^+e^- \to \rho^0\gamma$ and $e^+e^- \to \mu^+\mu^-\gamma$ 3 — 38042
equal-time commutators of charge and current sandwiched between states of unequal momenta 3 — 4150
hadron and photon induced reactions, effects of one-photon-exchange model 3 — 13864
hadron weak form factor, calc. of electromagnetic corrections using gauge invariance *(Russian)* 3 — 10696
hadrons, e.m. struct., review 3 — 6612
influence of electronic exchange and correlation on pseudopotential calcs. 3 — 33771
liquid metal, nearly-free-electron, computer program calc. of form factor and resistivity 3 — 36585
local field theory, derivation of set of integral eqns. 3 — 6544
model of relativistic quantum mechanics of interacting particles with form factors 3 — 13824
neutrino-hadron scatt., elastic and inelastic generalized form factors *(Russian)* 3 — 19684
new particle obs. by Niu group, effect of form factor on decay rate 3 — 32653
nuclear, K-matrix theory 3 — 6798
nucleon, anomalous field dimensions and asymptotic scale invariance 3 — 19688
pion form factor, ambiguity in determ. from electroproduction 3 — 16987
pion mechanical, consistency of ε and S* dominance with unsubtractedness, Ward identities and S-wave pion-pion phonon 3 — 35786
resonance and νW_2 at small ω' in quark model with broken SU(6) 3 — 29201
strangeness-changing current, nonrenormalisation in the chiral symmetry limit 3 — 32635
transfers between heavy ions, microscopic form factors 3 — 14231
triple-Regge scaling and behaviour of form factors for resonance couplings 3 — 35817
two-particle transfer form factors, approximate calc. method 3 — 19831
d, for pd elastic scattering below 1.0 GeV/c 3 — 23130
d, form very soft core N-N potential *(French)* 3 — 19789

form factors continued
d, relationship of form factors with physical S matrix of n p scattering 3−29203
d e.m. form factor, reln. to physical S matrix, relativistic parametrization 3−23060
$ed \to epn$, coincidence meas. of cross sections, determ. of e.m. form factors of n. 3−17055
$e^-e^+ \to K^-K^+$ prod. in colliding beam, 1.2 GeV, meas. of cross-section and e.m. form factors 3−17015
$e^-e^+ \to \pi^+\pi^-$ prod. in colliding beam, 1.2 GeV, meas. of cross-section and e.m. form factors 3−17015
$e^-e^+ \to \pi^\pm +$ hadrons calc. of form factors from sum rules, using Regge residues 3−13899
$e^+e^- \to e^+e^-X \to e^+e^-\gamma\gamma(X=\pi^\circ,\eta$ or $\eta')$ vertices study for one almost real photon and one highly virtual 3−17037
$e^+e^- \to pp$, cross-section meas. at total energy of 2.1 GeV by optical spark-chamber counter 3−29205
eN inelastic scattering, resonance form factors, scaling and Regge behaviour 3−35799
$ep \to e'AB$, parton model, asymptotic limit rel. to form factors 3−13965
ep elastic scatt. at low momentum transfer, meas. of proton form factor and r.m.s. radius 3−17016
ep scatt., inelastic, in region of $\Delta(1236)$ resonance for two values of q^2, coincidence expt. 3−14005
$\gamma N\Delta$, semi-exptl. determ. from resonant multipoles in electroproduction reactions 3−13941
$K \to \mu\nu$, calc. of decay form factors through similarity transform with π_{l2} 3−13831
$K \to \pi\mu(e)\nu$, absolute bounds for form factors 3−35777
$K \to \pi\mu(e)\nu$, and $K\pi$-scatt. phase shift 3−6580
$K \to \pi\mu(e)\nu$, bounds on scalar form factor from low-energy $K\pi$ phase shift 3−26288
$K \to \pi\mu(e)\nu$, calc. of decay form factors through similarity transform with π_{l3} 3−13831
$K \to \pi\mu(e)\nu$, chiral-limit theorems and PCAC corrections for scalar divergence form factor 3−29187
$K \to \pi\mu(e)\nu$, determ. of form factors from hard meson current algebra 3−16974
$K \to \pi\mu(e)\nu$, slope of decay form factor, mechanism based on exact threshold theorem 3−32650
$K \to \pi\mu(e)\nu$ double pole model 3−13858
$K \to \pi\mu(e)\nu$ form factors, chiral symmetry breaking 3−13832
$K^0 \to \pi\mu\nu$, exptl. limits on form factors 3−29188
$K^\pm$ e.m. form factors above φ resonance determ. in Novosibirsk colliding beam expt. 3−13873
$K^\pm \to \pi^+\pi^-e^\pm\nu_e$, form factors of weak hadronic current 3−23031
N, axial, calc. from π electroproduction at threshold 3−38044
N, axial vector, relation to π e.m. form factors 3−10714
N, e.m., based on vector-meson dominated dispersion relations 3−13851
N, elastic and inelastic, rel. to structure functions of deep inelastic electroproduction 3−13865
N, evaluation of e.m. form factors using method of sideways dispersion relations 3−6605
N, vector meson dominance model approach 3−26298
N e.m., effect of uncorrelated three-pion state in iso-scalar part 3−13855
N e.m. form factors, semi-phenomenological fits 3−23058
N elastic e.m. form factor, expressed as density and correlation functions for partons 3−14026
NN interactions, rank-one separable potentials for all partial waves to $L=2$ 3−29247
$NN\pi$, Veneziano representation and the Goldberger-Treiman relation 3−35787
p, elec. form factor from elastic ep scatt. obs. 3−23097
p dipole form factor in analysis of ISR pp diffraction data using Chou-Yang model 3−17100
p e.m. form factor, analytic properties, upper and lower limits for mean square radius 3−23059
p elastic, effect on p polarisation in ep elastic scattering 3−13917
π, anomalous field dimensions and asymptotic scale invariance 3−19688
π, determ. from single π^+ electroproduction at 2 GeV 3−13987
π, e.m., relation to axial vector N form factors 3−10714
π, large charge radius implications 3−6611
π, optimal bounds from analyticity and exptl. data 3−38033
π, upper bounds, rel. to inelastic $e\pi$ scatt. 3−10705
π, vector meson dominance model approach 3−26298
π charge, analyticity derivation of dispersive inequalities 3−13859
π e.m., analyticity constraints at high energy given low-energy theorem 3−4167
π e.m., calc. from electroproduction at threshold 3−38044
π e.m., dispersion sum rules for behaviour in asymptotic domain, heavy ρ-meson existance *(Russian)* 3−23061
π e.m. form factor, analytic properties, upper and lower limits for mean square radius 3−23059
π e.m. form factor, bounds and its derivative 3−23056
π electroproduction, calc. of form factors from electric Born term model with absorpt. effects 3−17061
π factors in Veneziano representation including photon coupling to vector meson 3−13862
π form factor, on-mass-shell asymptotic behaviour rel. to struct. functions in scaling limit 3−13853
π form factors determ. in electroprod. expts., non-uniqueness 3−17051
$\pi^\pm$ e.m. form factors above ρ resonance determ. in Novosibirsk colliding beam expt. 3−13873
$\pi d \to \pi d$, determ. of recoil form factor for double-scattering term using eikonal approximation 3−4210
$\pi^\pm\Delta$ electroproduction in electric Born model 3−14007
$\pi\pi \to NN$, isovector nucleon form factors in ρ region, higher order cut contributions 3−14056
$\rho^0 \to \nu\nu$, calcs. of decay width using ν e.m. form factor and $\gamma\nu\nu$ vertex 3−38023
${}^{114}Cd(e,e){}^{114}Cd$, inelastic $2_1{}^+$, $2_2{}^+$ form factors, phonon model 3−23260
${}^2H_2$ Yamaguchi-type potentials with repulsion in ${}^3S_1$ eigenchannel 3−29318
${}^3H$, exchange magnetic moment form factor 3−32773

form factors continued
${}^3H$, inelastic electron form factors calc. by harmonic polynomial method *(Russian)* 3−10964
${}^3H$, off-shell effects, Faddeev eqns. solved by Pade approximants 3−19753
${}^3He$, exchange magnetic moment form factor 3−32773
${}^3He$, inelastic electron form factors calc. by harmonic polynomial method *(Russian)* 3−10964
${}^3He$ charge form factor and radius 3−29321
${}^4He$, charge form factor and centre-of-mass spuriosity 3−4250
${}^4He$, short-range correlation calcs. 3−26397
${}^6Li$, wave function zeroes of mutual motion of αd and τt from scattering phases and form factors *(Russian)* 3−35871
${}^{106}Pd(e,e){}^{106}Pd$, inelastic $2_1{}^+$, $2_2{}^+$ form factors, phonon model 3−23260
${}^{46}Ti(p, t)$, ang. distrib. of transitions and DWBA calc., $E=19$, 23 and 27 MeV 3−32842
${}^{48}Ti(p, t)$, ang. distrib. of transitions and DWBA calc., $E=19$, 23 and 27 MeV 3−32842
${}^{50}Ti(p, t)$, ang. distrib. of transitions and DWBA calc., $E=19$, 23 and 27 MeV 3−32842
${}^{51}V(e,e)$, meas. using $E_e=183$ and 250 MeV 3−32837

formal logic
abstract quantum logics, vector space models 3−26118

formation, heat of *see heat of formation*

forming processes
see also rolling
composites, secondary fabrication problems 3−12418
diallyl phthalate resin molding, curing quality testing, differential scanning calorimetry applications 3−5797
e.m. forming of metals, X-ray diffraction meas. 3−25959
metal, adsorption effect in drawing with organic lubricants, oxide film form. 3−33604
polycaproamide fibres, creep behaviour during homogeneous cold drawing 3−21739
polyethylene, high and low mol. wt., struct. changes during deform. 3−20239
polymers, molten, composite formation during extrusion, viscoelastic fluids in flow dispersion modes 3−2762
polymethylmethacrylate lenses, injection moulding *(Russian)* 3−5911
polyolefins, cold-drawn, reversibility of deform. 3−25009
polypropylene, hydrostatic extrusion 3−21744
powder body moulding, structural and plastic components *(Russian)* 3−8942
Al, alloys, horizontal strip costing in stationary d.c. moulds, properties 3−12417
Al-Mg work-hardened sheet, forming-limit diagrams in biaxial tension 3−12381
6Al-V(4)-Ti, metal diffusion bonding, fracture surface characteristics 3−15702
α-Al_2O_3, polycryst., sintering and shaping process effects on form, topotaxy and texture *(German)* 3−12424
CdTe high power laser windows for 10.6 μm, hot pressing 3−5983
Co-Fe-Be, mag. and mech. props with annealing and cold drawing *(Japanese)* 3−12398
Nb_3Sn, hydrostatic extrusion effect on comp. and microhardness 3−24955
Ti sheet, mech. deep drawing *(Japanese)* 3−12393
W wires, role of fibre boundaries during drawing 3−8903
W:K, Si, Al, wire, evaporation rate meas. in production using thermogravimetric method 3−18682
Zn-Al sheet, superplastic forming, anisotropy *(German)* 3−2730
Zn-Al superplastic alloy, effect of strain-rate and drawing temp. on drawing force and mechanical properties *(Japanese)* 3−18636
ZnSe high power laser windows for 10.6 μm, hot pressing 3−5983

forward biased p-n light emitters *see light emitting diodes*

Foucault currents *see eddy currents*

fountain effect *see liquid helium-4; superfluidity*

Fourier analysis
see also Fourier transforms; harmonic analysis; waveform analysis
astronomical telescopes resolving power evaluation 3−28302
CAI, application of fast Fourier transforms 3−32019
convective heating with time-depend. heat-transfer coeff. 3−22786
correlation technique combined, for acoustic parameter determ. 3−3698
crystallography, phase relationships determ. 3−14644
electron micrographs, optics 3−375
geological images classification, optical processors applic. 3−9202
geomagnetic tides in declination, a spectral anal. of discrete Fourier transforms 3−18841
human vision, multiple-channel models, bandwidth consideratons 3−35261
image characteristics, transform techniques, truncated triangular wave periodic targets, linear image motion, Fourier transform techniques 3−32525
BL Lacertae, radioastronomical source, periodic component identification in flux density 3−25474
n.m.r. analyser, analogue device 3−28616
noise meas. technique based on digital Fourier analysis 3−263
optical Fourier synthesis for analysis of X-ray diffraction patterns 3−7603
optical model for laser Doppler velocimeter 3−473
physics fundamental axiom 3−35593
Schrodinger equation and Hill's function representation in terms of Fourier expansion coefficients 3−35590
solar flare type IV microwave bursts, pulsation anal. 3−37316
sound envelope/frequency connection 3−25620
spectroscopy, phase errors multiplicative correction procedure 3−19212
turbulence, heated-grid, spectral transfer of scalar and vel. fields 3−38363
wave dispersion direct measurement by a space Fourier analysis 3−19322
wind field objective analysis, Fourier analysis procedure rel. to Cressman's method 3−37255

Fourier series *see series (mathematics)*

Fourier-transform spectroscopy *see Fourier transforms; spectroscopy*

Fourier transforms
see also fast Fourier transforms; Fourier analysis
architectural acoustics, techniques 3−3696
asymptotic estimation by phase oscillation method, ep inelastic scattering, light cone dominance 3−26308
biopolymers, bond angle and internal rot. model determ., ^{13}C Fourier transform n.m.r. 3−36058
Boolean function, symbolic computation 3−486
canonical anticommutation relation, Fourier transformation and Weyl relations 3−28817
incoherent optical data processing 3−6434
complex refractive indices determ. with Fourier-transform interferometry 3−22361
covariant wave eqns. in weak gravitational field, Green's functions forms, scalar D'Alembert eqn. *(German)* 3−35616
2,5-dichloro-p-xylene, oriented in nematic phase, proton magnetic resonance recording by Fourier transform technique 3−23597
driven equilib. Fourier transform NMR technique, expt. study 3−7230
e.m. scattering, transient response, spherical shell of arbitrary thickness 3−671
exponential, study of dynamics of coupled harmonic oscillator chains 3−10348
exterior e.m. boundary value problem of wedge 3−19480
finite strip problems, dynamic stress-intensity factors determ. 3−22626
Fourier spectrometer, monitoring by real time computer, airborne i.r. astronomy 3−3385
Fourier spectrometer, Williams interferometer type, modulation transfer function 3−5960
Fourier transform all-reflection interferometer, design, characts. 3−28566
geomagnetic tides in declination, spectral anal. 3−18841
Griffiths crack in elastic strip, parallel to edge, soln. of equilibrium eqn. 3−13567
interferogram transform calc., interferometer design 3−9952
light coherence, van Cittert-Zernike theorem 3−10444
Michelson type Fourier i.r. spectrometer, construction, props., applications 3−5937
modulated zone plates, computer drawn, Fourier transforming and imaging props. 3−29052
neutron wave propagation, complete-backscattering effects, study using Fourier transform technique 3−29431
NMR, solid state driver 3−35451
NMR, spin-lattice relax. and expt. methods 3−7275
n.m.r. spectroscopy of ^{13}C as technique for mol. struct. studies 3−1262
nuclear mag. reson. free induction decay and cw line shape, conditions for transform relationship 3−8458
optical, of i.r. interferograms 3−29048
optical cavities and filters, spectral response, delta function transform 3−35673
optical filtering consideration 3−4072
optical image reconstruction from finite number of projections, Fourier transform methods 3−22852
optical spectra, inverse Fourier spectroscopy 3−185
optical transforms in teaching 3−6435
parametric excitation problems, applic. 3−26103
Poincare group, non-unitary representations and fourier transform 3−37784
pulsed n.m.r. and Fourier transform n.m.r. spectroscopy, review 3−34180
radiation condition, source in rot. stratified fluid, threefold Fourier transforms anal. 3−36099
response to $\pi/2$ pulse of single nucleus of spin 1/2 interacting with strong rf field 3−4367
shape recognition applic. using coherent optics system *(Russian)* 3−16447
spectral derivation and correl. possibilities in grating spectrometers *(French)* 3−35415
spectral line pressure-broadening theory, density expansion of the memory operator 3−29463
spectrometer, effect of precision of interferograms on form of apparatus function *(Russian)* 3−22355
spectrometer for far i.r. spectroscopy 3−32081
spectroscopy, far i.r., diffraction limitations of lamellar grating interferometer 3−28562
spectroscopy, introductory book 3−9949
spectroscopy, polarisation interferometer 3−22363
spectroscopy, theory, instrumentation and appls., review 3−9944
spectroscopy, undergraduate scanning interferometer and high gain photodiode detector-amplifier 3−9950
spectroscopy from 10^6 samples, vacuum operation and automation *(French)* 3−32078
spectroscopy with PDP 11/20 computer 3−28549
spectrum, far i.r., of matrix isolated $GeBr_2$ 3−18798
spectrum analyzer resolution, Fourier transformations using Moire structures *(Russian)* 3−181
time-varying electrical signals analysis by optical method 3−16804
underwater image transmission, modulation transfer functions, Fourier transform 3−6430
wave eqn., scalar, in stratified media, generalised Fourier transform 3−16780
HCl rotation spectra, He-induced line broadening *(French)* 3−7190
W, meas. of spectral emissivity using Fourier transform spectroscopy 3−28556

fractionation *see distillation*

fracture
see also cracks; mechanical strength
accelerated estimation of fatigue life by prefracture method, influence of exptl. results dispersion *(Russian)* 3−12473
acoustic emission meas. applic. to fracture mechanics 3−34679
alloy, high-strength, fracture toughness role in low-cycle fatigue crack propag. 3−31047
alloy, inter- and transcrystalline, rel. to stress corrosion *(Russian)* 3−8801
alloys, high temp. Ti-, Co-, and steel, cyclic creep-rupture behaviour 3−18650
alloys, metastable, effect of overheating 3−21707
amorphous thermoplastic, craze, electron microscopy 3−34650

fracture continued
atactic polystyrene, solvent nature influence 3−27774
ball bearing surfaces, fracture and formation of spherical particles from metal tongues 3−20801
bi-material plates, collocated interfaced elastic stress intensity factors 3−21724
β-brass, stress corrosion cracking, fractographic obs. 3−31042
α-brass phase change correlation with stress corrosion fracture 3−27648
brittle, near stress concentrations, limiting equilibrium state for infinite plate *(Russian)* 3−28887
brittle, rail specimen resistance assessment in impact machine tests using rolled grid *(Russian)* 3−12476
brittle amorphous materials, curves on fracture surfaces 3−38617
brittle bodies, rupture in surface-active medium, crack growth kinetics *(Russian)* 3−27059
brittle crack initiation at elastic/plastic interface 3−33601
brittle cracks, integral solns. for propagation at constant and accelerating speeds 3−32318
brittle elastic bodies, spallation theory, spall damage rel. to stiffness and thermal cond. 3−17920
brittle material, fracture toughness and specific fracture energy 3−36357
brittle non-metallic material, mech. impact rel. to fracture 3−8995
butadiene-styrene copolymer based filled systems, temp. effect on fracture surfaces 3−25005
cement pastes and mortars, fracture toughness meas. methods 3−27813
ceramics, brittle, fracture energy rel. to strength loss on thermal shock 3−8985
Charpy testpieces, fracture behaviour rel. to notch angle 3−15804
chip formation, mechanism, expt. verification 3−21710
comminution, physical aspects and law formulation 3−39417
composite, brittle matrix ductile fibre, fracture mechanics 3−31134
composite, C fibre reinforced, Ni matrix, elevated temp. stability, morphological and mech. prop. degradation 3−31138
composite, C-fibre-reinforced epoxy resin, impact and fracture props. 3−31142
composite, fibre reinforced metal matrix, deform. and fracture behaviour *(Japanese)* 3−34634
composite, fibrous, multiple fracture, theory 3−34633
composite, fracture mechanism based on change in Poisson's ratio *(Japanese)* 3−18710
composite cylinder, helically wound, burst fracture strength under internal press. *(Japanese)* 3−8998
composite cylinder, helically wound, torsional fracture strength *(Japanese)* 3−5349
composite material, two-component, initial stages of rupture, effect of form of inclusion *(Russian)* 3−27755
composite materials, fracture 3−2760
composite materials, fracture problems and solns. 3−21725
composite structures, fracture control technique 3−21726
continuum mechanics rel. to adhesive fracture 3−7840
controlled failure of hollow rock cylinders in uniaxial compression 3−12625
crack formation at segregation rel. to fracture theory and precipitation thickness *(German)* 3−7837
crack opening displacement and plasticity in shells 3−22666
cracklength, u.s. determ. during fracture toughness testing 3−13231
in creep test extrapolation, model considerations *(French)* 3−25032
deformation bounds for creeping structure approaching rupture, energy principle relation 3−30191
ductile materials, near tip strain concept 3−31052
ductile strain, criteria from theory of plasticity 3−22661
elastoplastic medium, void growth 3−24959
electroslag welded joints, 80 mm thick, fracture toughness, COD approach application 3−21625
epoxy compositions subjected to cyclic loading, relief of fracture surfaces 3−27780
eyebolt, brittle fracture in first turn of thread, exam 3−24205
fatigue life, high vacuum effect on low cycle fatigue law 3−39423
fatigue striations exam., SEM technique 3−37027
f.c.c. cryst., relation between twinning and strain to fracture 3−20808
α-Fe, low-cycle fatigue, grain boundary sliding, 450-700°C 3−34577
fibre composite materials fracture phenomena 3−37089
fibrous composite materials, fracture toughness, tensile strength, review 3−24992
field ion microscopy specimen fracture, electron microscope obs. 3−1533
fractography, state-of-the-art review 3−30982
fracture mechanics, review of work from Griffith to COD 3−13562
fracture-surface energies of rocks, X-ray diffraction studies 3−5444
glass, bending, stress waves 3−33606
glass, due to laser generated stress pulses 3−16896
glass fibre composite, fracture surface energy and transverse fracture 3−12443
glass reinforced plastic rings, wound, residual stresses determ. 3−24983
glass reinforced plastics, tensile deform. analysis 3−31148
glass reinforced plastics, wound, resist. to failure by unwinding 3−24981
graphite electrical resistivity change during compressive tests, fracture mechanism 3−23432
Hastelloy alloy X, elevated temp. ductility min. and associated props. 3−15705
homogeneous material, statistical features of time to break 3−1678
HTR particle coatings, Young's modulus and fracture stress meas. by the brittle ring test 3−18768
Inconel alloy X-750, precip. parameters role upon creep rupture props. 3−37024
kinetic models for structural (service) reliability 3−21764
laminate composites, fracture mechanism transitions 3−31141
linear elastic fracture mechanics compatibility with general yielding fracture mechanics 3−30197
long-running ductile, K_{Ic} measurement 3−25039
materials science and technology treatise 3−2621
measurement method of plane strain fracture toughness, evaluation 3−21765

fracture continued
  mechanics, role of nondestructive testing 3—27829
  mechanics of slit-like cracks in anisotropic elastic media 3—3959
  metal, cyclic creep fracture in low cycle fatigue *(Japanese)* 3—25029
  metal, f.c.c., b.c.c., Peierls stresses and glide systems from normal modes of vibr. 3—17919
  metal, stat. eval. of strength at brittle fracture 3—31097
  metal, thermoelectric method for determ. of specific work fracture, optimal placement of thermocouples *(Russian)* 3—8843
  metal fibre reinforced ceramics, fabrication and fracture toughness 3—18718
  metals. brittle fracture 3—18662
  metals, development of surfaces, unstable cavity expansion 3—38618
  mica crystal, fracture energy and healing effect 3—7839
  noble metals, rupture parameters, anal. *(Russian)* 3—8836
  nonlinear defect model, microscopic, local fracture and residual strain *(Japanese)* 3—20806
  nonlinear defect model of crack propag. in one-dimens. cryst. *(Japanese)* 3—20805
  nonmetallic materials, mech. and strength 3—4794
  nuclear piping systems, fracture mechanics applic. 3—19933
  nuclear reactor components fracture safety 3—6981
  nuclear reactor pressure vessels *(German)* 3—6980
  nuclear reactur fuels, mixed oxide ceramics, cracking behaviour, prediction using basic deformation characteristics 3—6976
  Nylon 6.6, fatigue failure under cyclic loading, fatigue life calc. 3—15787
  orthotropic materials, linear fracture mechanics, calibrated finite element technique, stress intensity factor 3—13563
  phase study, creep damage rules determ. 3—1675
  phenol-formaldehyde polymer, tensile fracture obs. 3—29806
  plane orientation, identification system 3—15675
  plastic material, applic. of dynamic growth of a void 3—3972
  plasticity effects in adhesive fracture 3—3973
  PMMA, complex stress effects, angled crack problem 3—24198
  PMMA, correl. of fracture data 3—20804
  PMMA, fracture toughness, mol. kinetics of fracture 3—14405
  PMMA, morphology of fracture surface layer and fracture mechanism 3—20242
  polyester resin, casts and laminates, fracture toughness, crack propag. 3—12454
  polyethylene, determ. of extensional stress flow patterns and melt fracture in die inlet *(German)* 3—31182
  polyethylene, fatigue crack propagation, stress depend., surface microscopy 3—31158
  polyethylene and polytetrafluoroethylene, tensile stress/strain, 78K, liquid N_2 effect 3—31170
  polyethylene in fabricated parts, mech. props. temp. depend. 3—25003
  polymer, empirical approach 3—7298
  polymer, glassy, tensile strength rel. to stress crazing and brittle fracture *(Japanese)* 3—7280
  polymer, loaded, u.v. radiation effect on submicroscopic crack form. 3—33602
  polymer, morphology and macrocrack form. on fracture surfaces 3—20241
  polymer, oriented, crack density increase rel. to tensile strain 3—31178
  polymer, oriented cryst., morphology influence on submicrocrack form. 3—20240
  polymer, structure/property relationships rel. to engng. material applics. 3—31186
  polymer, survey of theory 3—7297
  polymers, microfracture process, thermodynamics of irreversible processes 3—38616
  polymers under load in low-stress region, u.v. radiation effect on lifetime 3—25011
  polymethyl methacrylate in surface-active medium, longevity dependence on rupture energy and crack size *(Russian)* 3—11677
  polystyrene, failure in tensile and cyclic deform. 3—21740
  polystyrene, injection-moulded, technique for demonstrating flaws at which fracture initiates 3—31164
  polystyrene, morphology of crazes formed in thin films and bulk specimens 3—27770
  polyurethane foam, rigid, fracture under biaxial stress 3—31206
  probability as criterion of crack propagation under cyclic stress *(German)* 3—27060
  α-quartz, synthetic, test meas., 50-545°C, fracture resist., environment effects 3—30182
  replicas, lucite for electron fractography 3—21769
  review of the kinetic nature of strength of solids *(Russian)* 3—1679
  rock, around underground nuclear explosions 3—31304
  rock, at pressures up to 7kbar, implications for earthquake faulting 3—5461
  rupture, stress depend. of activation energy 3—33600
  scanning electron microscopy, appl. to fractography 3—12360
  sheet material, crack line loaded, fracture toughness testing, crack growth resist. curves 3—13219
  sheet material, crack line wedge loaded, fracture toughness testing, crack growth resist. curves 3—13220
  sheet materials, fracture kinetics, effect of order of applying fatigue crack and heat treatment 3—18621
  of solid bodies, kinetic analysis *(Bulgarian)* 3—9011
  under static loading, processes at crack tip, fractographic obs. 3—24200
  steel:carbon, obs. of fracture structure on aging *(Russian)* 3—24899
  steel, ausformed, electron-beam weld props. 3—21645
  steel, austenitic, stress corrosion cracking, fractographic obs. 3—31042
  steel, austenitic stainless, fracture surfaces in stress corrosion cracking *(Japanese)* 3—34561
  steel, bainitic, notch acuity effect on fracture toughness testing 3—25031
  steel, characteriz. for cryogenic technology, stress concentrators influence 3—34603
  steel, Cr-Mn, acoustic emission meas. crack tip plasticity characteriz. 3—34679
  steel, deformed by tension, orientation depend. of carbide cracking 3—34539
  steel, delayed failure mechanism, hypotheses *(French)* 3—5329

fracture continued
  steel, delayed fracture due to hydrogen, industrial consequences *(French)* 3—2735
  steel, dynamic fracture toughness, material props. influence 3—31049
  steel, effective surface energy of fracture and brittle rupture *(Russian)* 3—8842
  steel, fatigue strength increase due to surface deform. 3—27687
  steel, fracture toughness in cyclic loading, rel. to fractographic peculiarities 3—34689
  steel, heavily alloyed, resistance to failure 3—34601
  steel, high strength, fracture toughness enhancement by microstruct. control 3—31051
  steel, high strength, in Cl_2 and hydrogen halide gas environments, slow crack growth 3—18680
  steel, high strength, tensile props. rel. to plane-strain fracture toughness *(Japanese)* 3—8864
  steel, high-strength, crack vel. and fractography, heat treatment effect, stress intensity 3—5332
  steel, high-strength, tensile ductility, gaseous hydrogen influence 3—5323
  steel, hydrogen embrittlement sensitivity, thermal processing depend. *(French)* 3—5328
  steel, hypoeutectoid, ductile fracture, new morphological element of the microsurface *(Russian)* 3—2725
  steel, inclusions rel. to crit. mech. props., metallurgical processing incl. vacuum melting 3—27629
  steel, inclusions rel. to crit. mech. props., vacuum melting effects 3—27630
  steel, influence of sulphur and sulphides *(French)* 3—24911
  steel, inter- and transcrystalline, rel. to stress corrosion *(Russian)* 3—8801
  steel, low carbon containing inclusions, fatigue-fracture surfaces, exam. 3—8815
  steel, low-alloy, fracture toughness of martensitic and martensitic-bainitic microstructs. 3—21641
  steel, low-alloy 18Gps, susceptibility to brittle fracture 3—21663
  steel, low-C alloy, duplex microstruct. rel. to fracture behaviour 3—21646
  steel, maraging, fractographic lines and fracture toughness 3—34573
  steel, maraging, non-metallic inclusions and fracture behaviour 3—21586
  steel, maraging for use in military bridge, fatigue crack growth and fracture 3—21626
  steel, martensite, for machine construction, resist. to brittle fracture 3—24937
  steel, martensite, obs. of anomalous fracture under torsion at high temps. *(Russian)* 3—12410
  steel, mild, effect of up to 1% Sn 3—8846
  steel, mild, stress corrosion cracking, in nitrate solns., effect of C content 3—39354
  steel, MnS inclusions morphology, etched and fractured surfaces examination 3—8788
  steel, near tip strain as ductile fracture criterion 3—31052
  steel, Ni-Co-C, roll-extruded, effect of degrees of rolling reduction 3—31050
  steel, rail-grade, hydrogen effects in prod. and service performance 3—5335
  steel, reactor pressure vessel, deform. and fracture behaviour, acoustic emission meas. 3—34680
  steel, rel. to fatigue curve discontinuities *(Russian)* 3—12367
  steel, soft, time dependence to the resistance to spalling 3—31095
  steel, stainless, time and cycle dependent failure at elevated temp. 3—31240
  steel, stainless 304, hold-time effect in high temp. fatigue fracture 3—27707
  steel, structural, delayed and premature fractures *(French)* 3—5331
  steel, structural, influence of residual stresses on fracture behaviour in K_{Ic} temp. range 3—21624
  steel, tempered carbon, C45, yield stress, temp. and load depend. 3—34681
  steel, type 304(+ 15% Ti), post irrad. creep-rupture and tensile props. 3—17915
  steel, V-notched specimen, delayed fracture *(Japanese)* 3—8867
  steel, work hardened, impact strength under cyclic loading at low temp. 3—34682
  steel balls, crack form. during quenching, effect of technological parameters 3—24951
  steel EBR II control-rod thimble, assessment of postirradiation room-temperature fracture due to bending 3—23441
  steel for dies, effect of double tempering on brittle fracture 3—18672
  steel weld, hydrogen-induced cracking, microstruct. effect 3—34567
  steels, fatigue fracture rate study with aid of fracture mechanics *(French)* 3—15686
  steels showing thickness delamination, fracture toughness and its size dependence 3—21620
  stress intensity factor corrections 3—31219
  stress-corrosion of structures under random loading 3—21627
  tensile bars, notched perfectly plastic, large deform. 3—25037
  tensile panels, fracture due to damage from projectile impact 3—21628
  ternary eutectic composites, mechanical props. and thermal stability *(Japanese)* 3—15701
  tests at Langley Research Centre 3—21757
  thickness effects on toughness obs. on Ti-(6wt.%) Al-(4wt.%)V 3—24881
  time to fracture, various loading regimes, calc. *(Russian)* 3—27672
  toughness of materials, review 3—24206
  toughness parameter calc., engineering method 3—34600
  toughness testing, repeated determ. with one specimen 3—27805
  tube steel welded joints, resistance to hot cracking, Mo additives *(Russian)* 3—5298
  Weibull's statistical theory of mechanical strength, stress density function, fracture probability, ceramic materials *(German)* 3—12429
  weld joints, strength testing *(German)* 3—31231
  work of rupture, production of fatigue cracks for bending tests 3—27803
  Zircaloy, fracture toughness characteriz. 3—8879
  Zircaloy-2, hydrogenated, deformability testing method based on high vel. deform. *(French)* 3—9035

fracture continued
- Zircaloys, acoustic emission during stress corrosion cracking, correl. with fractography of cracking 3—31045
- Al, 1145, microfracture and structural failure under dynamic loading 3—2722
- Al, brittle, change of tensile strength with temp., determ. of critical inflexion temp. 3—21699
- Al, spall fracture, dislocation dynamics approach 3—14923
- Al, time dependence to the resistance to spalling 3—31095
- Al alloy, 7075-T6, vacuum environment effects on fatigue and fracture 3—27678
- Al alloy, near tip strain as ductile fracture criterion 3—31052
- Al alloys, inclusions role in ductile fracture and fracture toughness 3—30984
- Al alloys, tendency to brittle rupture *(Russian)* 3—27669
- Al alloys for aircraft structures, thermomech. processing effects 3—31048
- Al high tensile alloys, fractographic investigation 3—27807
- Al sheet secondary workability obs. *(Japanese)* 3—8863
- Al-Al_3Ni aligned eutectic alloy, fatigue fracture behaviour 3—21658
- 6Al-V(4)-Ti, metal diffusion bonding, fracture surface characteristics 3—15702
- Al_2O_3, alumina ceramics, mirror formation, dimensions dependence Young's modulus, fracture energy, temperature 3—8959
- Al_2O_3:MgO, grain boundary segregation, intergranular fracture surface struct. 3—27739
- B filament, gauge length influence on mechanical strength *(Japanese)* 3—18704
- B_4C, fast-neutron irradiated, study of defect microstructure due to He, Li disposition 3—26528
- B_xC_y fast-reactor irradiated pellets, examination of microstructure 3—26527
- C, istropic pyrolytic, Young's modulus fracture stress, annealing effect, electron microscopy 3—24993
- C, pyrolytic, isotropic, neutron irrad. effect 3—32945
- C fibres, mechanisms 3—15781
- C fibres in epoxy, matrix and interface modification effect on local fractures 3—5348
- Cr, rare earth metal additions effect 3—34604
- Cr 18% stainless steel, secondary workability obs. *(Japanese)* 3—8862
- Cu, continuously cast, fracture surfaces produced by high temp. creep 3—34535
- Cu, continuously cast, high temp. creep cavitation mechanisms 3—34536
- Cu, OFHC, microfracture and structural failure under dynamic loading 3—2722
- Cu, time dependence in the resistance to spalling 3—31095
- Cu alloy, fractography and fatigue obs. using push-pull testing under high press. *(Japanese)* 3—12486
- Cu sheet secondary workability obs. *(Japanese)* 3—8863
- Cu-CuZrSi pseudo-binary eutectic alloys, directionally solidified, tensile props. 3—34565
- Fe, Armco, microfracture and structural failure under dynamic loading 3—2722
- Fe, b.c.c. crack extension by bond rupture, fracture toughness and crystal structure relation 3—15724
- Fe, delayed fracture due to hydrogen, industrial consequences *(French)* 3—2735
- Fe, high-purity, effect of up to 1% Sn 3—8846
- Fe, microcrack form. around inclusions during solidification 3—34537
- Fe, single crystals at 78 and 4K, gliding, twin formation, fracture *(German)* 3—34612
- Fe-C(1.86 wt.%) alloy, martensitic microstruct. and microcracking development 3—34504
- Fe-Co-V(2 wt.%) alloy, ordered, h.p. prestrain effect on fracture stress and yielding 3—37061
- Fe-Ni-Al alloy, microstructure and fracture *(Japanese)* 3—15672
- Fe-Ni-Cr, stress corrosion cracking susceptibility, nuclear reactor water environments 3—39351
- Fe-Ta alloys, Laves phase precip. phenomena 3—37049
- KCl, press forged, charact. for laser window applications 3—5979
- LiF, rupture stress, effect of space charge 3—36325
- $LiNbO_3$, ion irrad., expansion, crazing and exfoliation 3—17880
- Mg-Al alloy, transgranular stress corrosion cracking 3—30983
- Mg-Al spinal crystal, isochronous curves and isotherms of fracture load, rel. to age strengthening kinetics 3—30930
- $MgAl_2O_4$ crystals orientation dependence, fracture topography 3—7836
- MgO, polycryst., microyield and fracture 3—20789
- MgO crystals, orientation dependence, fracture topography 3—7836
- Mo, cast, intercrystalline fracture by grain boundary precip. *(Russian)* 3—24853
- Mo, effect of C and O *(French)* 3—21590
- Mo, fracture energy calc. based on phonon theory of brittle fracture 3—17923
- Mo fracture energy 3—14924
- Ni, number of cycles to fracture, preliminary deform. effects *(Russian)* 3—27664
- Ni, time dependence in the resistance to spalling 3—31095
- Ni, u.s. irrad. and annealed, struct. changes *(Russian)* 3—15718
- Ni based superalloy, elevated temp. fatigue behaviour of single crysts., environment effects 3—39365
- Ni electrode, intergranular cracking at cathodic potentials 3—31266
- Ni-V (18.1 at.%) alloy, scanning electron microscope study of deformation and fracture 3—15703
- Pu-Ga (1 wt.%) cold rolled, annealing, yield strength, strain hardening and ductility meas. by tensile tests 3—12384
- Si, during grinding with sapphire hemisphere *(French)* 3—30194
- SiC, fracture surface energy meas. 3—8983
- SiC, reaction bonded, neutron irradiated, reduction of mechanical properties 3—24968
- Si_3N_4, fracture surface energies meas. 3—15738
- Si_3N_4 ceramics, high temperature strength slow crack propagation 3—8958
- Ti alloys, characteriz. for low temp. applics. 3—31098
- Ti-5Al-2.5Sn, gaseous hydrogen induced cracking, kinetics study 3—15704
- Ti-Al-Mo-V alloy, cleavage cracking in gaseous hydrogen 3—31044

fracture continued
- Ti-Al-V alloy, fracture toughness specimen thickness depend. 3—24881
- Ti-Al-V alloys, susceptibility to brittle fracture of simulated weld seams 3—24942
- Ti-Mo-Zr-Sn, βIII alloy, combined high and low temp. deform. processing effects 3—34578
- UO_2, Si, Al_2O_3, Fe, U, impurities, effect on fracture stress 3—39384
- UO_2 fuel pellets, surface cracking during hydrogen sintering 3—14259
- $UO_{2\|x}$, $0\leqslant x\leqslant 0.25$, porosity, grain size and excess O effect on Young's modulus and fracture strength 3—24967
- V, high-purity, deform. mechanism at low temps. 3—37055
- W, chemical vapour deposited, mech. behaviour, 800-1600°C 3—37085
- W composite cast heat resistant alloys, creep rupture strength 3—24989
- WC/Co, sintered, carbide phase recovery *(Japanese)* 3—31121
- WC-Co, sintered, cemented carbide, fracture behaviour, continuum mechanics analysis 3—14921
- Zn-Al eutectoid base alloy, superplastic deformation, ductile-brittle fracture 3—39362
- ZrC, high-temp. creep characts. 3—37088

francium
- No entries

francium compounds
- No entries

Franck-Condon factors *see luminescence*

Frank-Read sources *see dislocations*

Fraunhofer lines *see solar spectra*

free field rooms *see anechoic chambers*

free radicals
- acetyl, i.r. spectra at 77K 3—20163
- acetyl, selection of geometrical parameters in semiempirical calculations 3—33090
- in adamantane, due to high energy irrad. 3—2823
- in adamantane, due to high energy irrad. 3—2824
- aliphatic bromide, γ-irradiation produced, electronic struct., e.s.r. obs. 3—34733
- alkyl, β-proton isotropic hyperfine coupling const., ang. depend. 3—29593
- 2-n-alkyl radicals from C_4 to C_{16}, chemically activated, decomposition rates, test of the RRKM theory 3—21804
- amino groups, electrostatic interactions 3—29756
- amino radicals, localized mol. orbitals and spin polarisation 3—11199
- anthracene anion radicals, autoionisation in photoelectron emission 3—18528
- p-benzosemiquinone ions electron spin lattice relaxation 3—23605
- benzyl, selection of geometrical parameters in semiempirical calculations 3—33090
- di-t-butylnitroxide stable free radical fluorescence quenching of aromatic hydrocarbons 3—34738
- carbazyl radical, randomly oriented, proton hyperfine tensor, ENDOR obs. 3—5402
- carbonyl compounds, excited triplet, photochemically produced radicals, general theory 3—25083
- chemically induced dynamic nucl. and electron polarization, hydrodynamic theory 3—27865
- chemically induced electron spin polarisation and radical pair re-encounters 3—21821
- 2 chloroethyl radical, halogen bridging 3—17389
- complexes with transition metals, e.s.r. and n.m.r. obs. 3—26696
- cyanoacetohydrazide, X-irradiated, RNHNH radical characterisation 3—31275
- cyclopropenyl cation and radical, stability, geometry, electronic structure 3—29552
- diacyl peroxide decomposition reactions, chem. nucl. polarisation study 3—31258
- m-dibenzoylbenzene radical anion, conformation, ENDOR obs. 3—26700
- diborane, free radicals produced by γ-irradiation, e.s.r. spectra 3—1261
- dilute solns., electron spin echo obs. of spin exchange processes 3—2341
- 2, 5 ditertiary butyl-p-benzosemiquinone ions electron spin lattice relaxation 3—23605
- DNA photolysis, formation of thymine radicals 3—21836
- DPPH, compound struct. influence on p.m.r. spectrum 3—2419
- durosemiquinone ions electron spin lattice relaxation 3—23605
- dynamic polarisation of ^{13}C nuclei in free radical solns. 3—12495
- electron polarisation, chemically induced, theory, Larmor frequency differences between interacting radicals 3—34723
- e.p.r. in solids, review 3—30682
- e.p.r. of mols. undergoing slow tumbling, phase memory times 3—12050
- e.p.r. spectra, saturation and double reson. effects, theory, average ENDOR and ELDOR lines 3—34183
- e.p.r. transitions of radicals produced by γ-irrad. of glycolic acid crysts. 3—2828
- e.s.r. spectra of radicals produced by reduction of pyridine and pyrazine 3—18784
- ethyl, chem. and thermal activation, unimol. reactions theory appl. 3—34724
- ethyl radical, anisotropic proton hyperfine interaction 3—18794
- β- fluoroethyl radicals, INDO and variable temp. ESR study 3—20184
- formyl, selection of geometrical parameters in semiempirical calculations 3—33090
- hydrazine derivatives, i.r. spectra and structure *(Russian)* 3—26677
- hydrazyl, e.s.r. spectrum 3—21813
- hydronium radical obs. by e.p.r. of u.v.-irrad. perchloric acid glass 3—34735
- imidogen, ground state, dissoc. energy ab initio determ. 3—23610
- iminoxy, pairwise prod. from u.v.-irrad. dimethylglyoxime, e.p.r. study 3—30681
- iminoxyl radicals of 3-imidazoline 3-oxide and imidazoline, n.m.r. and long-range hyperfine interactions 3—23607

free radicals continued
i.r. and u.v. spectroscopic studies of free radicals and molecular ions isolated in inert solid matrices, review 3—11251
ketyl, from d-benzophenone in paraffin solvents, emission spectra decay for electron spin-lattice relax. times 3—25063
magnetic field effects on free radical reactions 3—25062
methyl, interaction with methane and ethylene, molecular orbital calc. 3—29574
methyl radical kinetics, relax. vs. H-atom abstraction in flash photolysed mixtures 3—37134
methyl radical reactive scatt. ang. distrib. meas. 3—12502
methyl substituents, role in ELDOR spectra of irrad. organic acid crysts. 3—27396
methylene group, zero-field splitting ang. depend., spin-orbit coupling second-order effect 3—20094
molecular crystals, $s = {}^1{\cdot}_2$, X-irradiated, electron spin lattice relaxation 3—12051
naphthalene, γ-irradiated crystal, fluorescence of new free radicals *(French)* 3—18791
NCO in Δ vibronic state, hyperfine interactions 3—11222
5-nitrouracil, ^{15}N-labelled, X-ray irradiated, free radical 3—1260
nitroxide radicals, exchange intermol. coupling, paramag. susceptibility 3—21211
oxy-radicals, photolytic addition to SF_4, e.p.r. study 3—15838
oxydiodine, in aqueous soln., formation spectra and chem. props. 3—25048
peroxy radical rot. freqs. in polymers 3—12547
phosphoranyl radical, stereochemically non-rigid penta-coordinate, ligand mobility, e.s.r. obs. 3—25080
quartet, randomly oriented, numerical calc. of e.s.r. spectra 3—4459
R_2CCR_2X, R=Hor alkyl, X-Cl, Br, I, PR_2 or AsR_2, e.s.r. data and p-p homoconjugation 3—29713
rotational levels determ. by microwave and radiofrequency spectra, review 3—11273
semiempirical calc. of hyperfine interaction consts., selection of geometrical parameters 3—33090
slow tumbling, e.s.r. spectra, review 3—34190
solution, e.s.r. hyperfine structure rel. to spin exchange 3—12053
Tanol, solid, l.f. behaviour of spin-correl. functions 3—2454
TBP-dodecane-HNO_3 systems, irradiated e.s.r. study, stable radicals detection 3—15837
tetramethyl-2,2,6,6, piperidinol-4, oxyl-1, antiferromag. linear chain, sp. ht. study 3—18314
triatomic, bond angle determ. from e.s.r. 3—20081
1,2,4-triazole crystal, ENDOR study of the radical created by gamma irradiation at room temp., proton hyperfine tensors and spin density distribution 3—21814
trichloromethyl, in irrad. trichloroacetamide crysts. 3—27883
trifluoromethyl radicals, excited, formed during radiolysis, reactivity and electronic structure 3—5411
$AsCl_3^-$ produced by γ-irradiation of $AsCl_3$, determ. of e.s.r. parameters 3—4462
AsF_3^- produced by γ-irradiation of AsF_3, determ. of e.s.r. parameters 3—4462
BF, reson. fluoresc., vibronic transition probabilities 3—29699
BF_2, bond angle determ. from e.s.r. 3—20081
BH_2, pot. energy surfaces, ab initio calc. 3—29605
BrO, μ-wave spectrum, equilib. struct. and dipole moment 3—29694
CCH radical, X-ogen, astronomical 89.190 GHz emission line 3—3278
CCl_3, i.r. spectra at 77K 3—20163
CCl_nF_{3-n}, hyperfine coupling and equilib. geometries, INDO study 3—29606
CH, chemi-ionisation with O atoms, cross section and rate const. calc. 3—14397
CH spin-orbit splitting calc. 3—29635
CH^+, Franck-Condon factors for $A^1\Pi$-$X^1\Sigma^+$ transition, appl. to interstellar models 3—26647
CH^+, interstellar line profile in spectra of Ophiuchi 3—35150
CH^+ molecules, interferometric studies of interstellar 4232 Å line for 28 stars 3—39737
CH_2^+, pot. energy surfaces, ab initio calc. 3—29605
CH_nCl_{3-n}, hyperfine coupling and equilib. geometries, INDO study 3—29606
CH_nF_{3-n}, hyperfine coupling and equilib. geometries, INDO study 3—29606
CH_2O^-, ^{13}C hyperfine const. determ. 3—12538
CN, absorpt. coeff. determ. for 0.4-3 μ at 1000°, 3000° and 5000°K, stellar appl. 3—38259
CN, B state, fluoresc., time depend. 3—26688
CN, excitation emission and cross sections, u.v. spectrum 3—33114
CN, g-tensors calc. 3—29635
CN, location of fundamental rotation-vibration band, stellar appl. 3—36002
CN, produced by HCN + Ar collision, rot. excitation and energy distrib. 3—20128
CN, shock tube determ. of CN ground state dissociation energy and CN violet electronic transition moment 3—20198
CN radical, lifetimes of A $^2\pi$ and B $^2\Sigma$ states 3—7224
CN radical mol., h.f.s. of $A^2\pi$ and $B^2\Sigma^+$ states 3—14382
CNC, NCC unstable intermediates, ab initio calcs. of equilib. bond lengths 3—20095
CO_2, i.r. spectra of 77K 3—20163
CO_2^-, bond angle determ. from e.s.r. 3—20081
ClF_4, e.p.r. spectrum 3—34739
DCO radical, $1_{01} \leftarrow 0_{00}$ transition, hyperfine component frequency meas. 3—19070
D_2S^+ ion radical, rot. anal. of emission spectra, 400 to 500 nm 3—1207
HCO radical, $1_{01} \leftarrow 0_{00}$ transition, hyperfine component frequency meas. 3—19070
H_2S^+ ion radial, rot. anal. of emission spectra, 400 to 500 nm 3—1207
LuO, $^2\Sigma(6_{\beta j}) \rightarrow {}^2\Sigma(6_{\beta s})$ transition, anal. *(French)* 3—33109
N_3^0 and N_3^{2-} anisotropic hyperfine interactions, p spin densities from e.s.r. spectrum 3—38308
NF_2, mass spectroscopic study of ionisation and dissociation processes 3—17460
NH, mol. consts. and transition probabilities 3—29644
NH_2, pot. energy surfaces, ab initio calc. 3—29605

free radicals continued
NNC, NCN, unstable intermediates, ab initio calcs. of equilib. bond lengths 3—20095
NO radicals, ELDOR spectra in soln. 3—2333
^{93}Nb-centred radicals, from $K_2NbOF_5.H_2O$ cryst., e.p.r. study 3—39453
OD, hyperfine Λ-doubling transitions of lower-J states, radioastronomical appl. 3—36037
OH, fluorescence by tunable dye laser 3—7222
OH, potential energy curves, configuration-interaction calc. of electronic energies 3—29583
OH, radiative and predissociative lifetimes of $A^2\Sigma^+$ state 3—23579
OH $^2\Pi_{3/2}$, J=5/2 state obs. in 6 interstellar sources 3—37479
OH based radicals, pulsed electron beam radiolysis, e.p.r. expts. 3—31273
OH cosmic maser sources, analytic approx. for saturation region 3—37483
OH line, lunar occultation of Galactic centre region at 1665, 1667 and 1720 MHz 3—39730
OH vibr. excited radicals, g-factor differences and Λ-doubling calcs. from e.p.r. data 3—11288
Oh $^2\Pi_{3/2}$ J=5/2 interstellar interferometric obs. at 5 cm 3—37493
P_2^+, electronic band system analysis *(French)* 3—29640
P_2^+, rot. analysis of (0,2) band of $C^2\pi$-$X^2\pi$ transition, vibr. scheme *(French)* 3—26656
PN, reson. fluoresc., vibronic transition probabilities 3—29699
S_3^- formed on MgO surface, e.p.r. characteriz. 3—27919
S_2Cl in inert matrix at 4.2K, interpretation of e.s.r. spectrum 3—4461
$S_1H_nF_{3-n}$, hyperfine coupling and equilib. geometries, INDO study 3—29606
SiH_3, SiH_3^+ and SiH_3^- radicals, CI calcs. of low lying electronic states 3—26630

freezing
see also refrigeration
binary liquid local conc. fluctuations, temp. depend. light scatt. obs. *(French)* 3—27101
binary mixture with chemical reaction, freezing curve 3—34710
condensation trail of aircraft, ice crystal formation by droplet freezing 3—25232
droplets of aqueous solution for cryochemical process 3—9872
emulsion, spherical double dispersion model applic. to change of state processes of dispersed phase *(French)* 3—27791
frost formation on air coolers rel. to natural convection conditions for cooled plate 3—1780
frost layer, heat and mass transfer anal. 3—20852
heat transfer with melting or freezing in a wedge shaped enclosure 3—14982
ice compression in freezing of supercooled water in capillaries 3—24247
ice cryst. formation in cloud supercooled region at warm temps. 3—25227
ice cryst. growth in supercooled H_2O droplet clouds by diffusion, numerical simulation 3—25226
ice-forming ability rel. to formation conditions of AgI nuclei, stoichiometric ratio effects 3—25228
monatomic system, molecular dynamic study 3—11726
moving boundary transport problems in finite media, freezing, integral transforms 3—34703
myoglobin single crystals, water/ice III, 2500 atmospheres, lattice order, method 3—38576
plane moving boundary problems, freezing and melting, integral transforms 3—34702
polyethylene, oxide, melting, freezing, supercooling, Gruneisen and Rao consts. 3—18722
saline solutions, salt rejection, absence of free convection 3—34701
spherical crysts. growth by freezing, interface growth stability 3—20701
water, effects of NH_3 on electrification of freezing and splashing drops 3—27106
water drops, supercooled, freely suspended in wind tunnel 3—9280
AgI particles, freezing action on water drops in aerosol *(Bulgarian)* 3—9303
Bi film, melting and freezing, obs. in electron microscope 3—14980
CsCl-NaCl binary system, pressure effect on temperature of eutectic minimum 3—18813
CuS particles on or in surface of supercooled H_2O drops, a comparison of icebuilding activity *(Russian)* 3—21945
H_2O, freezing pot. in liq.-ice transition 3—5156
NaCl, segregation from NaCl aq. solns. during freezing, vibrs. effects 3—12220
NaCl-CsCl binary system, pressure effect on temperature of eutectic minimum 3—18813
NaF-NaCl binary system, pressure effect on temperature of eutectic minimum 3—18813

Frenkel defects
diamond, Si, mech. of defect production 3—33521
excitons, selfinduced transparency and giant polaritons 3—24402
polymer, exciton model circular dichroism determ., fully retarded expression 3—12109
space-charge-limited currents, 'capacitor' model for V-I characts. allowing for Poole-Frenkel effect 3—15196
AgCl single crystal, relaxation obs. 3—27022
Al, deformed, annealing of struct. discontinuities *(Russian)* 3—24854
γ-CuCl, energy of formation, calc. 3—30114
CuCl single crystal, relaxation obs. 3—27022
$Fe_{1-x}S$, nonstoichiometric, energetics of defect formation and interaction 3—4752
Ge, annealing processes after irradiation with 1 MeV electrons at 85K 3—11616
Ge, n- and p-type impurities, electron irrad., annealing, Frenkel pair model, vacancy release 3—33561
LiF, thermal neutron irrad., lattice expansion due to defect production, X-ray diffr. 3—4774
Si, radiation damage in p-type with H impurity and high purity n-type, hole density, annealing 3—33546
Te, electron irrad., recovery steps, isochronal and isothermal annealing expts. 3—33562
TlCl(Br)(I), formation energy calc. 3—27019

frequency changers *see frequency convertors*

- **frequency control**
  - c.w. dye laser, freq. stabilization 3−37634
  - laser multisurfaced reflectors, frequency tunable, general theoretical requirements 3−28578
- **frequency converters** *see frequency convertors*
- **frequency convertors**
  - electro-optical, classification of suitable media 3−19644
  - laser radiation, u.v., cascade freq. conversion in nonlinear crysts. *(Russian)* 3−13749
  - optical parametric oscillator and down converter, i.r. generation, high power, tunable 3−22947
  - optical rangefinders, freq. conversion, double modulation of light 3−22319
  - solar to sidereal time referred frequencies, phase-locked convertor 3−37583
  - tetraphenyl-butadiene, u.v. fluorescence, fluorescence wavelength convertor 3−18479
- **frequency division multiplexing**
  - digital data channel of optical communication link 3−29051
  - wideband optical f.d.m. communications, birefringent branching filters 3−22307
- **frequency-domain analysis**
  - fluidised bed reactor simulation and identification, frequency domain approach 3−1466
  - induced polarisation, geophysical prospecting, comparison of time, frequency phase meas. 3−9355
  - least squares smoothing operators 3−28838
  - mangetic maps, interpretation, freq. domain techniques 3−9371
  - room acoustics linear system approach 3−3697
- **frequency measurement**
  - absolute standard, Mg or Ca atomic beam 3−3747
  - methane-stabilized laser, by i.r. frequency synthesis, techniques, deduction of speed of light 3−153
  - nuclear quadrupole resonator, pulsed radio spectrometer *(Russian)* 3−6044
  - optical comparison of microwave modulation and direct mixing methods 3−13196
  - primary standards, Nat. Phys. Lab. work 3−13194
  - resonance, automatic meas. of difference between two resonators using a differential microwave spectrometer *(French)* 3−9942
  - signal amplitude, phase, and frequency, definitions and their significance for meas. 3−19134
  - technological forecast 3−58
  - TV sync. pulse reception method, accuracy 3−22236
  - ulnar bones 3−32241
  - water vapour laser, Lamb-dip stabilized, 28μ, absolute freq. meas. 3−35688
  - H storage beam, standard, low-Q cavity maser 3−3749
- **frequency meters**
  - digital low freq. meter, Siberian Instruments 1971 Exhibition *(Russian)* 3−9900
- **frequency modulation**
  - cavity freq.-oscillator freq. locking techniques rel. to e.p.r. spectrometer sensitivity 3−264
  - chirped Gaussian pulse, ionospheric distortion 3−39550
  - gas laser, internal, by variation of medium refractive index 3−26225
  - gas laser, intra-cavity electro-optical modulation 3−720
  - laser radiation, detection problems 3−19630
  - telemetric thermometers *(Russian)* 3−5800
  - transmitters for Interkosmos 3 satellite *(Czech)* 3−9390
- **frequency regulation** *see frequency control*
- **frequency response**
  - acoustic emission transducers, frequency response characteristics calibration 3−25671
  - blood pressure catheter system requirements for arterial pressure wave processing 3−28320
  - human vision, multiple-channel models, bandwidth consideratons 3−35261
  - two-dimensional rigid airfoil, meas. using a wind tunnel *(German)* 3−6295
  - SiO_2-Si m.o.s. structures, weakly inverted, surface state admittance 3−8269
- **frequency stability**
  - *see also frequency control*
  - c.w. dye laser, freq. stabilization 3−37634
  - gas lasers, in the visible and i.r. *(Russian)* 3−6467
  - laser, CO_2 or N_2O, stabilization using second laser, rapid sampling method *(French)* 3−32096
  - laser, detection and identification of environmental noise 3−29156
  - laser, Lamb dip stabilization 3−32097
  - laser radiation wavelength using nonlinear absorpt. of separated beams 3−13753
  - ruby laser with freq. selection and tuning, spikeless oscill. 3−22909
  - secondary frequency standards, solid state oscillators coupled to superconducting cavity 3−25804
  - state-of-the-art of very stable frequency generators *(French)* 3−25652
  - Texas A&M cyclotron, freq. stabilization by injection locking 3−13369
  - CO_2 laser, stabilization method 3−22884
  - H maser, rel. to output, mag. polarisation field and relaxation, meas. *(German)* 3−10459
  - He-Ne gas lasers, high stability, freq. stabilisation methods *(Russian)* 3−13725
  - He-Ne laser, simple, single freq. for practical uses 3−32538
  - He-Ne laser, single freq., stabilisation *(Russian)* 3−13726
  - He-Ne lasers, frequency shift of Lamb dip minimum *(Russian)* 3−16824
- **frequency synthesizers**
  - *see also frequency convertors*
  - programmable, digital for high resolution n.m.r. spectrometer 3−32117
- **frequency synthetizers** *see frequency synthesizers*
- **friction**
  - *see also internal friction; lubrication*
  - air turbulently flowing in smooth annuli at high temp. 3−23698
  - atmospheric ablation rates for Barwell meteorite 3−28162

- **friction** continued
  - atmospheric frictional forces over N.Atlantic and Europe during 1962 Hamburg stormy weather situation *(German)* 3−25242
  - brass, against filled polyethylene, wear resist. 3−25013
  - ceramic, wear rel. to structure, deformation and surface chemistry 3−34617
  - classical von Karman friction-factor-Reynolds number correlation for fluidised beds 3−1451
  - composites of solid lubricants and metals, comp. effect 3−15785
  - compressible fluid, heat transfer, turbulent and laminar flow in circular tube 3−36080
  - Coulomb, first law, modification for wooden surfaces 3−28843
  - Coulombic in mechanical systems, stagnation conditions *(Russian)* 3−32298
  - cryotribometer, apparatus for meas. dry friction at low temperatures 3−5755
  - dilute polymer solns., correlation of friction factor for turbulent pipe flow 3−7352
  - eddy friction in atmosphere rel. to hydrodynamical model for long-range forecasting *(Russian)* 3−18857
  - elastic contact with finite friction, eigenvalue problem 3−10283
  - elastic fibre suspension, turbulent dynamics rel. to drag reduction 3−20407
  - elastomer, in glass transition region, temp. and rate depends. on normal press. 3−27790
  - epoxy-novolac block copolymers, cured, wear resist. obs. 3−34649
  - flow, of dense mesh wire screen regenerator matrices at cryogenic temps. 3−9881
  - flow of evaporating two-phase mixtures in smooth tubes, and channels, pressure gradients due to friction 3−20397
  - fluorapatite single crystals, wear and surface failure investigations 3−36363
  - forced vibrations of complex bar system, method of small parameters proportional to friction force *(Russian)* 3−28917
  - fretting-fatigue mechanism, effect of direction and motion 3−18557
  - gas flow, viscous, in tube, effect of wall temp. on characteristics *(Russian)* 3−7390
  - granite, frictional sliding characteristics rel. to earthquake mechanism at faults 3−15895
  - graphite, effects of adsorption of benzol and CCl_4 *(Russian)* 3−11682
  - graphite fibre composite, pin-disk sliding contact method 3−39392
  - graphite layer, organosilicon bonded, effect of thermostabilising additions on antifriction props. *(Russian)* 3−14925
  - Hartmann-Sprenger tube, thermal phenomena, mechanical energy dissipation by friction and irreversibility of shock waves *(French)* 3−20292
  - hollow cylinder, axial compression, analysis of friction effects on elastic-plastic deformation using finite element method 3−19424
  - hydrofoil, lift and drag measurements in polyox dilute solutions 3−17499
  - integranular friction values of certain coal measure rocks affected by weathering 3−5443
  - jet, turbulence influence on flow of a boundary layer, friction stress of flat plate calc. *(Russian)* 3−29931
  - junction deformation models for asperities in sliding interaction, comments 3−4803
  - junction deformation models for asperities in sliding interaction, reply to comments 3−4804
  - liquid crystal, nematic, friction coeff. calc. 3−33447
  - lunar soil friction angle and density var. from boulder tracks 3−39641
  - magnetic Rayleigh problem, variational solution for a non-Newtonian power law conducting fluid, mag. field influence on coefficient of friction 3−20377
  - materials in liquid and alkali metal gas environments, apparatus for high-temperature antifriction characteristics *(Russian)* 3−9827
  - metal, wear due to dry friction, stacking fault energy and elastic modulus effects *(Russian)* 3−7844
  - mixing chamber for opposing isothermal annular flows, calc. of friction coeffs. *(Russian)* 3−23750
  - piston rod gland packings, 50 mm lipped and solid, friction behaviour 3−24208
  - polyacetal, effects of carbon fibre and PTFE powder *(Japanese)* 3−18727
  - polyethylene thin layer, friction coeff. and shear strength at high pressure 3−36359
  - polyformaldehyde as antifriction material 3−25007
  - polymer film, friction coeff. as function of shear strength and press. 3−4797
  - polymer/metal pair in sliding friction, liq. media effect on deform. of surface layers 3−31181
  - polymeric materials operating in vacuum in presence of ionizing radiations, accelerated testing 3−27845
  - polymers, antifriction props., u.v. irrad. effects *(Russian)* 3−27766
  - polymers, factors affecting tribological behaviour 3−11684
  - polymers subjected to external friction, deform. of supermol. struct., method of investig. 3−25006
  - polytetrafluoromethylene, heat treatment, speed and temperature effects 3−36360
  - porous materials, determ. of skin friction by Karman-Pohlhausen method 3−11681
  - pressure drop and friction coeff. meas. of turbulent flow meas. through rough channels 3−1368
  - rare earth metal, friction and wear in air 3−18625
  - reduction of friction by perpendicular oscillation 3−33603
  - rolling contact, pitting, measurement of coefficient of kinetic friction *(Japanese)* 3−27811
  - rubber on ice 3−1683
  - sapphire grinding of Si, friction coeff. decrease *(French)* 3−30194
  - Separan AP30, dil. polymer solution, drag reduction degradation 3−479
  - skin, 2D compressible turbulent boundary layer, theory 3−1392
  - skin, in MHD oscillatory flow along plate with variable suction 3−20392
  - skin, on wall at hypersonic nozzle, measurement 3−1328
  - skin friction coeff., turbulent pipe flow with mass transfer, anal. 3−1374
  - skin in parabolic flow over flat plate with main stream wave disturbance 3−20339

- **friction** continued
  - soil, skin friction, static and dynamic, meas. for wave eqn. analysis 3—21768
  - solid solution, wear due to dry friction, stacking fault energy and elastic modulus effects *(Russian)* 3—7844
  - stability of friction dominated materials and systems 3—16615
  - stagnation point skin friction parameter, var. with altitude for curved surface 3—1393
  - static friction maximum force, teaching approach 3—32004
  - steel, against filled polyethylene, wear resist. 3—25013
  - steel, load carrying capacity rel. to sliding velocity, additive effects of tricresyl phosphate *(German)* 3—4799
  - steel, rel. to hot rolling model 3—8848
  - surface coeffs. at flat plate 3—4578
  - temperature fields produced in a workpiece by repeated applications of a source of heating, numerical calc. 3—24962
  - time dependent, possible mechanism for seismic aftershocks 3—9148
  - turbulent boundary layer at a permeable surface, local friction resistance coefficients calc. 3—33225
  - turbulent flow, accelerated, in pipe, hydraulic friction drag coeff. 3—23710
  - turbulent flow, rel. to pressure gradient effect 3—23682
  - turbulent flow fully developed, in non circular ducts, friction factors and shear stress distribution 3—26791
  - turbulent flow in non-circular channels, friction factors prediction method 3—36083
  - turbulent flow of two-phase solids-in-air system 3—1433
  - water, pure boundary layer, friction meas, drag reduction by ejecting additive solutions 3—23740
  - water in an annulus, friction and heat transfer in the swirl flow 3—20283
  - wave shoaling, effect of friction on linearized Navier-Stokes equations 3—15946
  - welding of high speed steel to annealed steel, testing *(German)* 3—31118
  - white layer formation at rubbing surfaces 3—12406
  - white layer formation at rubbing surfaces 3—24209
  - Al, foil, dislocations due to friction, lubrication and oxide layer effects 3—27063
  - Al-Sn alloys composition and structure changes due to *(Japanese)* 3—8768
  - CaF$_2$, anisotropy in Knoop indentation hardness and friction of diamond cones 3—20788
  - Cu, effects of crystalline structure and single cryst. orientation rel. to working *(Russian)* 3—8873
  - Cu alloys, adsorption-induced loss of strength during selective transfer in boundary friction 3—21706
  - Cu-Sn-Pb alloys, composition and structure changes due to *(Japanese)* 3—8768
  - Fe sintered, unlubricated frictional behaviour 3—27710
  - Fe-Co alloys rel. to Si influence 3—7846
  - MoS$_2$ behaviour in high vacuum 3—14928
  - Ni-based alloys, glazes prod. at high temps. 3—34590
  - Ti-Al-V alloy, surface effects during fretting fatigue 3—15814
- **friction, internal** *see internal friction*
- **frictional electricity** *see triboelectricity*
- **fuel**
  - *see also coal; nuclear reactor fuel; pulverised fuels*
  - liquid hydrogen, handling, transport and storage, experience 3—3774
  - luminous flame, mean emissivity from spray combustion of liquid fuel 3—2801
- **fuel batteries** *see fuel cells*
- **fuel cells**
  - ceramic use in oxygen concentration cells as electrolytes 3—15758
  - electrochemical gas detectors, review 3—35551
  - ionic transport in solids with tunnel and layer structures 3—5018
  - zirconia electrolytes, application to cells 3—15833
  - I to I$_2$, photochemical oxidation 3—15839
- **fugacity**
  - *see also diffusion in gases; kinetic theory of gases*
  - Mount Etna 1971, direct meas. of O$_2$ on S$_2$ fugacities in active vents 3—21898
  - olivine, elec. cond. meas. as function of temp. and O fugacity 3—25114
- **full wave rectification** *see rectification*
- **function approximation**
  - *see also Chebyshev approximation; interpolation*
  - irregular Coulomb wave functions 3—19487
  - iterative methods for laminar flow of rigid viscoplastic incompressible fluid *(French)* 3—14437
  - lattice sums, analytic procedures for evaluation in terms of zeta and related functions 3—28980
  - least-squares approach for e.m. wave scattering 3—13685
  - Lorentz invariant momentum-space integral for particles of equal masses, computer approximation method 3—29182
  - minimax, spectral colour matching 3—3805
  - multipoint Pade approximant to series of Stieltjes on real line, bounding properties 3—28827
  - multipoint Pade approximants to series of Stieltjes, variational approach 3—28828
  - sixth order Feynman graphs, calc. by Pade approximants 3—19720
  - statistical distributions curve fitting, computer subroutine suite OPTIME 3—28966
  - viscoelasticity, boundary problems in linear theory, approximation with rational functions *(Russian)* 3—16650
  - ^{4}He, numerical calc. of 2-nucleon correlation function 3—6733
- **function evaluation**
  - least squares method for determination of experimental function with linear exponents 3—16600
  - matrix exponential e^{hV}, algorithm 3—37783
- **function generators**
  - *see also pulse generators; signal generators*
  - controlled current and controlled potential electroanalytical expts. 3—6151
  - l.f.-h.v., for discharge detection, rel. to power system apparatus 3—17712
  - muscle-pulling system for neural function studies 3—16570
- **functional analysis**
  - *see also harmonic analysis*
  - Anderson model, functional integral approaches, comparison of results in limiting cases 3—15142
  - least squares analysis of complex weighted data, dielectric applications 3—34280
  - Low's problem, investigation using power series expansions 3—10628
  - Newton's method for solving Boltzmann eqn. 3—22760
  - plane sections method for functions of two variables, application to quantum scattering models 3—32289
  - rheological media, constitutive nonlinear functionals, inversion operational method 3—19409
  - variational method for kinetic coefficients calc. *(Russian)* 3—28991
- **functional equations**
  - dual eqns. application to calc. of stress intensity factor for crack in elastic solid 3—32335
- **functionals** *see functional equations*
- **functions**
  - *see also Bessel functions; Boolean functions; Green's function methods; random functions; transfer functions*
  - autocorrelation, lower bound, ergodicity 3—37893
  - bianalytic, conjugation problem, connection with elastoplastic problem *(Russian)* 3—529
  - Dirac delta function and density of states of several systems 3—3741
  - functional integrals in quantum mechanics and field theory 3—28954
  - holomorphic, analytic extension to region outside two circles *(Russian)* 3—19393
  - Neumann's, generalization with extra parameter not dependent on Legendre functions 3—10239
  - normalized Legendre functions and tesseral harmonics of 7th order for calcs. of energy levels of rare earth ions in crystals 3—4953
  - Pade approximation application in nuclear physics *(German)* 3—35867
  - potential, in magnetohydrodynamics *(Italian)* 3—20373
  - product $\delta(x).x^{-\alpha}(\alpha>0$, real), definition and its applications 3—37789
  - sampling, geopotential representation technique 3—34771
  - special functions, high-order iterative formulae for evaluation of zeros *(Dutch)* 3—28834
  - time-dependent correlation functions, rigorous bounds 3—19506
  - variational integrals containing linear operation, application of Noether's theorem 3—28832
- **fundamental constants** *see constants*
- **fundamental law tests**
  - friction, first law, modification for wooden surfaces 3—28843
- **fundamental particles** *see elementary particles*
- **fundamental physics concepts** *see physics fundamentals*
- **fundamentals of physics** *see physics fundamentals*
- **furnaces**
  - *see also electric furnaces; refractories*
  - chill casting in vacuum from 2500°C *(Russian)* 3—13257
  - cylindrical, mathematical simulation of radiant heat transfer 3—623
  - differential thermal analysis furnace, using dynamic flow of water vapour 3—28497
  - graphite tube, for production and excitation of diatomic molecules *(French)* 3—3772
  - microfurnace with large working space at 1600-1700°C *(Russian)* 3—9867
  - miniature for single crystal and powder X-ray obs. 3—4696
  - plasma arc melting system design 3—27714
  - for semiconductor technology, double-ended, gas flow analysis 3—39294
  - temperature profile measurement by thermocouple 3—9866
  - thermal variation apparatus for X-ray diffraction expts. *(French)* 3—3881
  - windowless reflectance furnace, for i.r. studies of corrosive melts 3—22290
  - X-ray diffractometer meas. at high temps, design of furnace for room temp. to 1000K range 3—28736
- **Furry theorem** *see quantum electrodynamics*
- **fusion** *see melting*
- **fusion, nuclear** *see nuclear fusion*
- **fusion reactors**
  - *see also nuclear fusion*
  - advantages and viability prospects *(Swedish)* 3—26544
  - D-T neutron flux in metals, simulation of displacement effects 3—20770
  - development, plasma compression and ignition *(Dutch)* 3—32990
  - direct-conversion collector, computed efficiencies 3—38188
  - as energy source, hydrogen-electric utility system, future trends 3—4346
  - environmental impact of reactors, including radiological hazards 3—19969
  - future developments, discussion 3—32989
  - laser pumping of exhaust plasma 3—19971
  - laser-driven pulses, wetted-wall concept, feasibility for commercial power generation 3—38190
  - magnetic field effects on heat pipe performance 3—11092
  - microfission explosion by laser or relativistic electron-beam high-density compression, reactor prospects 3—32932
  - modelling and optimisation of controlled thermonuclear fusion reactor system 3—38180
  - neutron void swelling and creep 3—17322
  - neutronic anal. of blanket benchmark by discrete ordination 3—19970
  - neutronics of subcritical fast fission blankets 3—4345
  - nuclear science, conference, Miami USA (1972) 3—28622
  - plasma confinement and heating methods, comparison 3—1083
  - plasma heating, intense relativistic electron beams review 3—7547
  - pulsed high beta, design study 3—4343
  - shielding of supercond. magnets 3—11103
  - superconducting coil applications, review 3—7016
  - technological development in UK, review of progress 3—19965
  - technological problems in design 3—23449
  - technological problems in methods and materials, discussion 3—19968
  - thermonuclear, feasibility and future prospects 3—19963
  - thermonuclear, present state and future prospects *(German)* 3—1082

fusion reactors continued
- Tokamaks machines development *(French)* 3−11506
- tokomak, θ-pinch, mirror and laser-pellet reactors, design details 3−19967
- toroidal, at University of Wisconsin, design studies 3−4344
- toroidal, lithium cooled, design 3−4342
- Li, cooling, effect of oxygen on corrosion of Nb and Ta 3−26533
- ^{6}LiD fuelled fusion reactors modified Lawson criterion 3−38189
- ^{7}Li(n,n$'$t)^{4}He, t-prod. meas. for fusion reactor blanket design 3−19865
- Nb, He implantation and re-emission at elevated temps. 3−7014
- T breeding, production measurement 3−26543

g-factor
- *see also gyromagnetic ratio*
- acetylene, mol., sign determ. 3−14357
- alkali halide, e.p.r. obs. of hyperfine and g-components of V_k centres 3−18369
- atom one-electron, g_j and g_I calc. for arbitrary hydrogenic states 3−11137
- bromoacetylene, mol. g-values from Zeeman effect 3−20168
- conduction electron, expression for orbital average as meas. in de Haas-van Alphen effect 3−24369
- conduction electrons in Cu and K, meas. by de Haas-van Alphen effect 3−1977
- crystals, e.s.r., g tensors determ., generalization of methods 3−24603
- electron positron anomalies 3−13860
- formaldehyde, Zeeman effect of transitions, g-tensor diagonal elements determ. *(French)* 3−1234
- g_j-factor meas. for diamagnetic molecules using high-temp. microwave spectrometer *(German)* 3−35411
- II-VI semiconductor, g-shift of S-state ions 3−21016
- isomeric high-spin states, nucleon effective spin and orbital mag. moments determ. 3−14120
- isotropic spherical samples, size limitations 3−12048
- leptons, techniques for meas. anomaly using resonance technique 3−6689
- orbital, in effective hamiltonian for linear molecule 3−1199
- orbital, reln. to E1 sum rule for photoabsorption, effect of exchange currents 3−38118
- organic molecules, mol-Zeeman effect, g-values, magnetic susceptibility anisotropies and mol. quadrupole moments determ. 3−29629
- picryl-N-amino carbazyl, e.s.r. spectral lineshape and g-value 3−1254
- radicals and small molecules, spin-orbit splitting and g-tensors calc. 3−29635
- rare earth compounds, with ziron struct., theory 3−38802
- selenophene, Zeeman effect in rotational spectrum, g-values and magnetic susceptibility anisotropy 3−11271
- semiconductor, group II-VI cpds., g-shift of s-state ions 3−2377
- sodoborate glasses with ZnO, X-irrad., e.p.r. of Zn^{+} centres, g-factor anisotropy *(French)* 3−30684
- $T_z=0$ and mirror nuclei, g-factor variation, multi-shell mixed configuration calc. 3−10848
- zeolites, NaX and NaY type, e.s.r. of Gd^{3+}, nonequivalent position obs. 3−2386
- [Ti(H$_2$O)]$^{3+}$, Jahn-Teller complex ion, paramagnetic resonance and relaxation 3−34197
- BaMg$_2$Y$_2$Ge$_3$O$_{12}$, e.s.r. of Nd^{3+}, highly anisotropic g-factor 3−2384
- Bi:Sn, hole g-factor meas. 3−8089
- Br atoms, excited, gas-phase e.p.r. spectrum of $^{2}P_{1/2}$ state 3−1108
- C, black, e.p.r., localized centres, conduction electrons, 4.2-300K *(French)* 3−24614
- CSe mol., from Zeeman effect meas. 3−23580
- CaF$_2$:Yb^{3+}, rel. to covalency 3−2009
- CdGa$_2$S$_4$:Mn^{2+}, e.p.r. spectra meas. spin Hamiltonian description 3−12059
- CdGa$_2$Se$_4$:Mn^{2+}, e.p.r. spectra meas. spin Hamiltonian description 3−12059
- CdS:Cu^{2+} ang. depend. from e.s.r. spectrum 3−2357
- ^{111}Cd, magnetic shielding, g_I factors meas. by n.m.r. 3−36804
- ^{113}Cd, magnetic shielding, g_I factors meas. by n.m.r. 3−36804
- Ce complex, CDP, g-tensors from e.p.r. 3−15416
- CeO$_2$:Gd^{3+}, S-state, e.p.r. anal. method and g value determ. 3−27401
- ^{55}Co, dipole moment and ground state g-factor meas. by n.m.r. technique 3−23201
- Cr complex, 2[Cr(en)$_3$Cl$_3$].KCl.6H$_2$O, ground state 3−8600
- ^{133}Cs free atoms, g-factor ratios determ. 3−29489
- Cu(II) complex perchlorate tris-octamethylpyrophosphoramide, e.s.r. study, g-value determ. 3−30685
- DyVO$_4$, soft acoustic mode and the strain dependence of the g factor 3−1761
- Er^{3+}, in solids, C_{3h}, D_{2d}, O_h site symmetry, rel. to crystal field parameters 3−2234
- ^{166}Er, 6^{+} rot. state 3−26377
- Eu$_x$La$_{1-x}$ Al$_2$, e.s.r. study, g-shift meas. for Eu^{2+} to obtain exchange integral 3−2358
- ^{151}Eu, g-factors and hyperfine splitting constants from Mossbauer effect meas. *(German)* 3−954
- ^{153}Eu, g-factors and hyperfine splitting constants from Mossbauer effect meas. *(German)* 3−954
- F^{12}C^{15}N, mol. Zeeman effect obs. 3−33135
- Fe, ferromag. reson., 300-1090K, relax. parameter, g-factor 3−8450
- Fe(II) six coordinated compounds, spin $S=1$, low temp. magnetism, Mossbauer effect and electronic struct. 3−34250
- ^{55}Fe, g-factors determ. using ^{52}Cr(α, n) reaction 3−32740
- GaSe, optical transmission in fields up to 93.5 kG, exciton behaviour, effective mass of electrons and holes, g-factors 3−30803
- GdAu, e.p.r., g_s value, 77-300K, exchange parameter, s-f model 3−2343
- Gd$_x$La$_{1-x}$ Al$_2$, e.s.r. study, g-shift meas. for Gd^{3+} to obtain exchange integral 3−2358
- HCN, mol. g-values from Zeeman effect 3−20168
- HCP, mol. g-values from Zeeman effect 3−20168
- ^{177}Hf, magnetic moments of excited states meas., nuclear g-factor determ. 3−38103
- HgS(Se)(Te), g-shift of s-state ions 3−2377
- KBr:Tl, mag. circular dichroism in C-band meas. of g-factors and electron-lattice coupling 3−18430

g-factor continued
- K$_2$C$_2$O$_4$.H$_2$O, γ-irradiated single crystals, e.p.r. study 3−8415
- KCl:Cd^{+}, X-ray irrad., e.s.r., hyperfine coupling const., g-factor, 77-300 K 3−27402
- K$_2$PbCu(NO$_2$)$_6$, rel. to Jahn-Teller effect 3−30687
- K$_2$SO$_4$:Hg^{+}, X-irrad., e.s.r. 3−39026
- (KSO$_3$)$_2$NOH, X-irradiated single crystals, (KSO$_3$)$_2$NO structure, ^{14}N hyperfine coupling constants 3−8424
- Mn$_5$Ge$_3$ film, from ferromag. reson. 3−27419
- NH$_3$, mol. Zeeman effect, inversion transitions 3−20209
- (NH$_4$)$_2$C$_2$O$_4$.H$_2$O, γ-irradiated single crystals, e.p.r. study 3−8415
- Ne, optically pumped, double reson. meas. of Lande factors *(French)* 3−35964
- Ni^{2+} complexes of benzene 1,3- and 1;4-diamines, wavefunctions, Lande and spin-orbit splitting coeffs. 3−8110
- O$_2$ mol., laser mag. reson. using 119 and 78 μm H$_2$O laser lines 3−4464
- OH vibr. excited radicals, g-factor differences and Λ-doubling calcs. from e.p.r. data 3−11288
- ^{a}Os, A=186, 188, 190, 192, recoil implanted in Ni, meas. for first 2^{+} excited states 3−14119
- PbSe, determ. from emission line splitting in mag. field 3−15524
- Pd, e.p.r. of Dy^{3+} analysis 3−2352
- ^{210}Po, 6_1^{+} and 8_1^{+} states, g-factor difference meas. 3−32746
- ^{192}Pt, 316 and 612 keV states, effect of mean lifetime meas. on g-factor analysis 3−23258
- ^{85}Rb, g_I factor derived from Larmor frequency 3−12072
- ^{85}Rb, magnetic shielding, g_I factors meas. by n.m.r. 3−36804
- ^{87}Rb, magnetic shielding, g_I factors meas. by n.m.r. 3−36804
- ^{87}Rb free atoms, g-factor ratios determ. 3−29489
- Si:As, Zeeman splitting of photoluminescence of excitons 3−38809
- Si:B, acceptor ground state, magneto-Raman scatt. study 3−5203
- Si:B, deformation potentials and g-values from Zeeman splitting of Raman spectra 3−38809
- Si:B, rel. to mag. field depend. of u.s. attenuation by neutral acceptors 3−4967
- n-Si:P, spin susceptibility, g-value and e.s.r. linewidth, unified treatment 3−36780
- SiS, g_j value sign determ. *(German)* 3−11230
- ^{152}Sm, magnetic moments of excited states meas., nuclear g-factor determ. 3−38103
- Sm^{3+}(4f^{5}) ion, calc. from energy struct. for intermediate coupling 3−29495
- ^{181}Ta, magnetic moments of excited states meas., nuclear g-factor determ. 3−38103
- ^{204}Tl, 1.118 MeV 7^{+} level, study by ^{204}Hg(d,2n) reaction 3−941
- Y, e.p.r. of Gd, g-shifts, line narrowing, exchange effects, satellite lines 3−2376
- YIG, temp. depend., near Curie point *(Russian)* 3−8454
- Yb^{2+}, in alkaline earth fluorites, g-factor meas., var. with cryst. field strength 3−24682
- ZnHgSe(Te) mixed crysts., e.p.r. of Mn^{2+} 3−2378

G-matrix *see molecular internal mechanics*

gadolinium
- Auger electron spectra, up to 530 eV *(Russian)* 3−15579
- converter for neutron radiography 3−25025
- elastic and inelastic behaviour in spin reorientation region, pressure effects 3−34116
- elastic moduli, hydrostatic press. derivatives, electrostatic model and band struct. contrib. 3−27051
- e.p.r. in Y, g-shifts, line narrowing, exchange effects, satellite lines 3−2376
- e.p.r. in YAl$_2$, 5-70K, conc. and temp. depend., relax. phenomena, spin-flip scatt. 3−2375
- film, obs. of f.c.c. structure and oxidation 3−18042
- Hall effect of polycrysts., 4.2K, 46 kOe 3−33874
- hardness vs. annealing temp. behaviour rel. to O$_2$ content 3−24884
- ionisation loss in inelastic electron refl. from Gd surface 3−5252
- isotopes, X-ray transitions, isotope shifts 3−1107
- liquid scintillator for fission neutron-multiplicity meas. *(French)* 3−10064
- L.P.E. growth of YIG:Ga films, effect of substituting Gd for Y 3−1924
- magnetic critical exponent β meas. by ferromagnetic transmission resonance 3−16465
- magnetic form factor calc. using Dirac-Fock equation 3−21244
- mechanical props. determ. from 78 to 675 K 3−18624
- molecular field model to explain anomalies in props. near 226K, second mag. phase transition 3−15366
- nitrate glass; Eu, Sm, Gd, Tb, Dy absorption, luminescence, excitation spectra *(Russian)* 3−30878
- n.m.r. of ^{155}Gd and ^{157}Gd, isotropic hyperfine field and quadrupole coupling const. 3−24631
- spin polarisation of electrons tunnelling from Gd ferromag. to Al superconducting film 3−15311
- transport props., high temp., electrical resistivity, thermal diffusivity 3−33864
- Al:Gd, e.s.r. meas. of exchange integral 3−15413
- Al:Gd, spin scatt. cross sections 3−18300
- CaF$_2$:Gd, thermal depolarisation spectra before and after O contamination 3−24652
- CdF$_2$:Gd^{3+}, e.p.r., fluorine superhyperfine struct. 3−18363
- CdF$_2$:Gd^{3+}, spin lattice interactions 3−8429
- CdF$_2$:Gd^{3+}. orthorhombic ESR spectra 3−30690
- CeO$_2$:Gd^{3+}, S-state, e.p.r. anal. method and g value determ. 3−27401
- Gd, hydrostatic pressure, effect on spin disorder resistivity 3−2284
- Gd^{3+}, e.p.r. in single crystals of La(NO$_3$)$_3$ phenanthroline complex 3−34194
- Gd^{3+}, ground state splitting, role of relativistic cryst. field 3−30410
- Gd^{3+}, in CeO$_2$(ThO$_2$), zero-field splittings 3−18358
- Gd^{3+} doped Li$_2$O-Al$_2$O$_3$-SiO$_3$ glasses, e.s.r. meas. during crystn. 3−27403
- Gd^{3+} e.p.r. in zirconia-lime system *(French)* 3−18356
- Gd^{3+} e.s.r. in zeolites 3−2386
- Gd^{3+} in solution, radiative and radiationless transitions, temp. effects 3−34402
- La-zn double nitrate:Gd^{3+}, e.s.r. in trigonal crystal field, spin hamiltonian interpretation 3−36789

gadolinium continued
  LaAg:Gd, wave vector depend. of exchange interaction, e.s.r. obs. 3−34202
  $LaRu_2$:Gd, in supercond. state, localised mag. moment e.p.r. obs. 3−24541
  $LiNbO_3:Gd^{3+}$, e.p.r. and zero field resonance obs. of crystal field 3−34203
  $SrO:Gd^{3+}$, spin lattice interactions 3−8429
  YAg(Cu):Gd, wave vector depend. of exchange interaction, e.s.r. obs. 3−34202
  YIG:Gd,Ga uniaxial films, epitaxial growth by r.f. sputtering 3−12237
  $ZrO_2\text{-}CaO:Gd^{3+}$, e.s.r. spectral obs. rel. to structure 3−8432
  $(ZrO_2\text{-}CaO):Gd^{3+}$, e.p.r. in X band 3−39020

gadolinium compounds
  $\{GdCa_2\}[Sn_2](Fe_3)O_{12}$ magnetic fields, induced diamagnetic tin atoms in antiferromagnetic garnets, Mossbauer effect 3−34270
  $\{Gd_3\}\ [Gd_{0.03}Ga_{1.97}](Ga_3)O_{12}$, lattice constants meas. 296-1400 K, Czochralski grown crystal 3−11753
  $CaF_2:GdF_3$, density, rel. to impurity incorporation 3−20759
  G_2O_3 paint to reduce ^{41}Ar activity in reactor exposure volume 3−1088
  $\beta\text{-}Ga_2O_3\text{-}Fe_2O_3$ solid solution, mag. interactions, e.p.r. obs. 3−27406
  GaP, phonon-assisted two-photon exciton transitions, band models and symmetry calc. 3−18105
  Gd complex, $Gd(DMP)_3Cl_3$, (DMP=2,6-dimethyl-4-pyrone), cryst. struct. 3−17776
  Gd-Ca garnet, growth by Czochralski method, perfect cryst. prod. *(German)* 3−5272
  Gd^{3+} compounds, Mossbauer studies at very low temps. 3−2478
  $GdAlO_3$, point defect form. with optical floating zone technique and heat treatment 3−20731
  $GdAlO_3$, spin dynamics near spin flops transition, antiferromag. reson. obs. 3−2401
  $GdAlO_3:Ho^{3+}$, absorpt. and luminesc. spectra obs. rel. to energy levels 3−8655
  $GdAlO_3:Nd^{3+}$ single crystals, preparation, absorption, luminescence and stimulated emission spectra *(Russian)* 3−24731
  $GdAlO_3:Tm^{3+}$, absorpt., luminesc., and stimulated emission spectra obs. 3−12174
  $GdBe_{13}$, ^9Be spin-lattice relax. and mag. moment dynamics 3−2444
  $Gd_{3-x}Ca_xFe_{5-x}Sn_xO_{12}$ ferrite-garnets, temp. dependence of EMR and FMR linewidths *(Russian)* 3−36795
  $GdCl_3$, exciton spectrum, anisotropic exchange effects 3−38801
  $GdCl_3$, ferromagnet with long-range interactions, crit. exponents 3−34121
  $GdCo_2$, ferrimag., spontaneous magnetiz., susceptibility, Neel model interpret. *(French)* 3−27358
  $GdCo_5$-H, ferromag. hydrides, thermodynamic and mag. props. 3−27357
  GdF_3, impurity-conditioned solid-solid transform., rel. to melt growth 3−12274
  GdFe garnet, anomalous u.s. attenuation near compensation temp. 3−2275
  $GdFe_2$, ferrimag., spontaneous magnetiz., susceptibility, Neel model interpret. *(French)* 3−27358
  $GdFe(Co)_{0.4}Si_{1.6}$, isomorphic, paramag. above 4.2K with Fe and Co atoms in high spin state 3−2290
  $GdFeO_3$, equilib. reduction, enthalpy and entropy, O_2 press. *(Russian)* 3−15077
  $GdFeO_3$, etch patterns on (001) surface 3−8031
  $GdFeO_3$, paramag. susceptibility, room temp. and 77K 3−21213
  GdGa garnet, lattice parameters in faceted regions, X-ray double cryst. analysis 3−1609
  GdGa garnet, macroscopic strain in facetted regions 3−33493
  GdGaG, stress birefringence measurement 3−21381
  GdGaG substrate, heteroepitaxial growth of YIG film by hydrothermal synthesis 3−1922
  $Gd_3Ga_5O_{12}$, garnet, ceramic, influence of initial comp. and firing temp. in prep. *(Russian)* 3−15746
  $Gd_3Ga_5O_{12}$, garnet, computer controlled Czochralski growth 3−12290
  $Gd_3Ga_5O_{12}$, substrate material for bubble domain film, lattice parameter thermal exp. 3−34158
  $Gd_3Ga_5O_{12}$ garnet, elastic and thermoelastic constants *(German)* 3−7816
  $Gd_3Ga_5O_{12}$ single cryst. dislocation-free growth 3−36989
  $Gd_{1-x}La_xAl_2$, study of n.m.r. spin echo spectra lineshape 3−21328
  $Gd_2Me_3(NO_3)_{12}.24H_2O$, Me=Mg, Mn, Zn, Co, Ni spectra, substitution on vibration bands of water, Stark splitting of Gd^{3+} *(Russian)* 3−8571
  $Gd_2(MoO_4)_3$, dielec. anomaly near phase transiton temp. 3−15465
  $\beta'\text{-}Gd_2(MoO_4)_3$, dislocation etchants 3−8028
  $Gd_2(MoO_4)_3$, ferroelastic-ferroelec., antiphase boundaries and their interactions with domain walls 3−24659
  $Gd_2(MoO_4)_3$, improper ferroelec., thermal expansion at transition temp. 3−12104
  $Gd_2(MoO_4)_3$, phase transition, neutron irrad. effects 3−36847
  $Gd_2(MoO_4)_3$, X-ray topographic study of ferroelec. phase transitions and domains 3−15461
  GdN, synthesis, vaporization and crystal growth 3−2642
  $GdNi_2$, ferrimag., spontaneous magnetiz., susceptibility, Neel model interpret. *(French)* 3−27358
  GdO, film, structure and defect substructure obs. 3−8067
  Gd_2O_3, elec. cond., high temp. variations, equil. oxygen press. depend. *(French)* 3−38831
  GdOF phase transitions, rhombohedral/cubic, high pressure effects 3−33666
  $Gd(OH)_3$, cooperative transitions rel. to mag. specific heat 3−34117
  $Gd(OH)_3$, exciton spectrum, anisotropic exchange effects 3−38801
  Gd_2O_2S, long wave i.r. spectra *(Russian)* 3−30825
  GdP, GdAs and GdSb thin films, spin polarized photoelectrons *(German)* 3−18531
  $GdPO_4$, mag. susceptibility curves anomalies at high temps., n.m.r. obs. 3−30707
  $Gd_{2.3}Tb_{0.7}Fe_5O_{12}$, refractive index dispersion meas. rel. to film thickness determ. 3−27481
  $Gd_{2.3}Tb_{0.7}Fe_5O_{12}$ garnet, single cryst. growth by grain growth technique 3−21526

gadolinium compounds continued
  GdTbIG, ferrimagnetic, stress birefringence meas. 3−21381
  $Gd_{1\ x}Y_xAl_2$, study of n.m.r. spin echo spectra lineshape 3−21328
  $(GdY)_3(GaFe)_5O_{12}$, liquid phase epitaxial growth on $Gd_3Ga_5O_{12}$ substrate by tipping process 3−12278
  $(GdYYb)_3(GaFe)_5O_{12}$, liquid phase epitaxial growth on $Gd_3Ga_5O_{12}$ substrate by tipping process 3−12278
  $Y_{3-x}Gd_xFe_5O_{12}$ temp. depend. control of Faraday rotation by Gd substitution 3−8557

gain (amplification) *see amplification*

gain control
  see also automatic gain control
  radiotelescope, gain stabilisation by gain modulator *(Spanish)* 3−31815

gain measurement
  HF CW laser, zero power gain meas. using pulsed probe laser 3−32537
  He-Zn hollow cathode laser, single pass gain *(Japanese)* 3−19608

gain regulation *see gain control*

galactic cosmic rays
  heading is late addition, see also cosmic rays
  10-30 MeV/nucleon particles, composition determ. 3−39573
  adiabatic propag. away from galactic mag. field source 3−37272
  atmospheric excess radiation at small heights rel. to galactic cosmic rays 3−25353
  chemical composition rel. to diffuse model 3−31482
  deuterons and ^3He formation and destruction in proton induced spallation of light ($Z \leqslant 8$) nuclei 3−21987
  energy spectrum of nuclei outside modulation energy *(Russian)* 3−12888
  gamma rays from ^7Li nuclear de-excitation rel. to cosmic radiation from galactic centre 3−18905
  high energy cosmic rays in Galactic disk, mean path length 3−28095
  intensity obs. by Pioneer 10 from 1-2 AU heliocentric radial distances 3−12883
  interstellar e^-e^+ flux, contrib. of π production by primary nucleons 3−37279
  light element origin by interaction with interstellar matter 3−31512
  magnetic field effects for cosmic ray propag. above 10^{17} eV 3−25350
  magnetic storms effects on intensity, N-S asymmetry 3−34984
  metagalactic X-ray prod. by relativistic dust grains 3−31487
  modulation of low energy rays at solar max. 3−16083
  nucleus species, phenomenological study of propag. 3−28094
  pulsed galactic nuclei rel. to origin of cosmic rays 3−13086
  rocket and stratospheric meas., electrons and protons *(Russian)* 3−12896
  secondary nuclei/primary nuclei ratio effect at high energies, Galactic disc trapping of particles 3−25351
  secondary prod. of cosmic ray electrons by collision of primary cosmic rays 3−31481
  upper atmosphere capture by ionization loss *(Russian)* 3−12889
  γ-ray line feature from Galactic centre direction 3−28110
  γ-ray production from proton-proton reactions and pion decay in galactic disc 3−12929

galactic radio waves *see radiofrequency cosmic radiation*

galaxies
  see also h i regions; h ii regions; intergalactic matter; nebulae; the galaxy
  1971 Palomar sueprnova search and search of 41 bright ScI galaxies 3−25506
  Abell 194 cluster, low-dispersion spectra, colour-magnitude diagram 3−39736
  Abell 2670, cluster of galaxies, photometric obs. for mass-to-light ratio determ. 3−35173
  Abell clusters, development of correlation in expanding universe 3−31515
  Abell clusters, three-dimensional spatial correlation function estimation method 3−28280
  active galaxies and Seyfert nuclei, models for high i.r. and X-ray luminosity objects 3−22106
  And III, dwarf spheroidal galaxy, M31 companion, high resolution observations 3−22108
  associations with radiosources, observations at 2.7 and 5 GHz 3−25472
  black hole model of galactic nuclei, plasma turbulence effects 3−34996
  3C 273, Seyfert, variability in 10-micron flux 3−13092
  3C 299, identification as radio galaxy with intermediate red shift 3−31752
  3C 84, Seyfert, visibility and structure from 606 MHz transcontinental interferometry 3−31717
  cD-type galaxy in centre of Abell 2670, luminosity function determ. 3−35173
  Centaurus chain, photometric and spectroscopic obs. 3−37455
  central black hole rel. to Newtonian analysis of initial cosmological perturbation 3−13091
  central regions of nearby galaxies, photometric obs. and Hα equiv. width determ. 3−28284
  CGCG 1439+5344, extremely compact, spectral obs. 3−5614
  chain of 6 radio sources near 4C 19.15 radio source, 3100 MHz observations 3−28226
  cluster of, X-ray sources in Uhuru error box 2U2358−29 3−39712
  clusters of, effect of neutrinos of nonzero mass on gravit. dynamics, appl. to Coma cluster 3−35005
  clusters of, redshift lists 3−35177
  clusters of, relic radiation obs. as test of X-ray radiation nature 3−35171
  clusters of galaxies, effect of mass loss to gravit. radiation on stability, N body problem soln. appl. to Virgo cluster 3−28255
  clusters of galaxies, relation of X-ray luminosity to virial mass, Perseus, Virgo and Coma cluster data 3−25491
  clusters of galaxies, stability considerations *(Polish)* 3−25508
  clusters of galaxies, vel. dispersion rel. to Compton X-ray emission 3−37463
  clusters of galaxies rel. to cosmic background light 3−31737
  Coma cluster, extended X-ray source observations from Uhuru 3−19046

galaxies continued
Coma cluster, H I in intergalactic regions, heating mechanism and model 3−37460
Coma Cluster, luminosity functions rel. to magnitudes 3−25493
Coma Cluster, Lyman α emission rel. to models of intracluster gas 3−28278
Coma cluster, Lyman-α obs. for upper limit on intracluster medium 3−37464
Coma cluster, red shift rel. to total magnitude and nuclear region 3−28254
Coma cluster, soft X-ray flux meas. 3−28279
Coma cluster, spectroscopy and redshifts of outlying faint galaxies 3−39719
compact, HI observations and correlation with optical emission spectra 3−28292
core radii of clusters of galaxies at different redshifts rel. to gas-sphere model 3−37449
core-halo config., thermal equilib. states of classical hard-sphere gas with gravit. 3−35643
counts, cosmological implications 3−18923
counts in field surrounding quasars 3−9595
density functions, orbit computational viewpoint 3−3371
diffuse X-radiation from intergalactic gas in clusters of galaxies 3−31511
discrete, quantized outflow velocities by radiation pressure in Seyfert nuclei 3−31670
dynamics of dense stellar systems rel. to galactic nuclei, review 3−39734
elliptical, stellar evolution 3−9523
elliptical companion of NGC 5846, surface photometry 3−39721
ellipticals, stellar evolution model for 12.10^9 years 3−18997
ellipticals, var. in spectral-energy distrib. and absorption-line strengths 3−31738
ellipticals in the 6 cm. radio continuum, survey 3−37461
ellipticals with high surface brightness, tidal origin 3−28260
evolution, condensation of expansion, protostars 3−5605
evolution effect on diameter-redshift relation 3−19059
explosion obs. in active galaxies rel. to supermassive stars 3−28178
faint radio galaxies, spectroscopic observations 3−31771
flat, photometric parameters 3−37474
flat, response of orbit to axisymmetric perturbations 3−31749
formation, turbulence at early epochs in a Friedmann universe 3−16259
formation, universal turbulence hypothesis 3−25496
formation by material flowing out of singularities hypothesis 3−5613
formation from annihilation-generated supersonic turbulence in the baryon-symmetric big-bang cosmology 3−16093
gas content and luminosities, theoretical 3−3367
giant elliptical, variations in q_0 from magnitude-redshift diagram 3−28282
giant elliptical, violent explosions in nuclei and bursts of star formation 3−28277
giant ellipticals, optical polarisation meas. for detection of nonthermal optical emission 3−31757
gravitational clustering, kinetics 3−39716
gravitational radiation, model for peaking using geometrical optics 3−13094
groups, interaction with primordial gravitational waves 3−3373
Hoyle-Narlikar cosmology, magnitude-redshift relation for galaxies 3−28125
Hubble diagram based on photoelectric meas. of cluster galaxies 3−16257
Hubble diagram for radiosources from UBV obs. 3−16258
I Zw 1727+50, confirmation as radio source from optical and radio observations 3−25505
IC 342, aperture synthesis of neutral H 3−28271
IC 3576, spiral, identification with X-ray source in Virgo 3−28281
IC 3576, X-ray source, H I region obs. 3−19062
infall of matter into, gas streaming 3−3375
integrated background light from distant galaxies, information content rel. to cosmology 3−35007
interacting, radio continuum emission at 21 cm 3−19067
IZw187 (lacertid), relationship between optical amplitude and radio spectrum 3−16267
BL Lacertae, nucleus, periodic components in flux-density variations, SHF obs. 3−25474
BL Lacertae, optical obs. during March 1969 to Jan. 1971 period *(French)* 3−39726
BL Lacertae, photoelectric obs. showing short-term variability 3−28283
Large Magellanic Cloud, comparison between Sanduleak and Fehrenbach-Duflot catalogues *(French)* 3−5612
Large Magellanic Cloud, light variations of high luminosity O and B stars 3−5602
Large Magellanic Cloud, objective-prism techniques for faint stars *(French)* 3−16290
Large Magellanic Cloud, obs. in radiocontinuum at 6 cm wavelength, catalouge of sources with brightness contours 3−3347
Large Magellanic Cloud, radiosource obs. at 11 cm wavelength, map of radio brightness 3−3349
Large Magellanic Cloud, variable star survey 3−19063
Large Magellanic Cloud spectra of continuum radiosources, determ. of spectral indices 3−3350
late-type, history of star formation and UBV colours 3−28261
LMC, discovery of nine supernova remnants, combined optical and radio obs. 3−37451
LMC, five colour photometry of supergiants 3−22057
LMC, kinematics of 27 planetary nebulae 3−13083
LMC, photometric standards, stellar population 3−9607
LMC, radio source ejection from supernovae remnants 3−28185
LMC, supergiant stars with strong H lines *(French)* 3−13093
LMC, zone of avoidance in period-amplitude diagram of Cepheids 3−25502
LMC supergiants and foreground stars, UBV and spectro-graphic data 3−37374
Local Supercluster, orientation of galaxies 3−9594
M31, diameters of H II regions, comparison with M33 regions 3−28294
M31, evolutionary model for star formation based on diagrams of spiral structure 3−28257
M31, interstellar absorpt. for Cepheids in NGC 206, dust-to-gas ratio meas. 3−35186
M31, novae discovery in 1963-1970 period 3−37466
M31, radio spectrum at 2695 MHz rel. to spiral arms and nucleus 3−35183
M31, search for hard X-rays in 20-300 keV range 3−28244
M31, spectrum of pointlike nucleus rel. to velocity dispersions and mass 3−37450
M31, stellar motions near nucleus, E-line observations 3−39724
M31, variation of emission-line strengths for H II regions 3−39717
M31 galactic companions, search for free-free emission from ionized gas at 3.8 cm, gas deficiency 3−25492
M33, diameters of H II regions, comparison with M31 regions 3−28294
M33, discovery of 5 novae in galaxy and supernova in field galaxy 3−22070
M33, evolutionary model for star formation based on dynamics of spiral structure 3−28257
M33, H I emission regions at two Holmberg radii 3−28262
M33, HI 21 cm. survey 3−22113
M82, H α fluorescence source in filaments 3−28258
M82, linear polarization of scattered micron radiation 3−37292
M87, circular polarimetry 3−39680
M87, search for hard X-rays in 20-300 keV range 3−28244
M87, UBV photometry of jet, observed magnitude and colour indices 3−39720
M 31, observations of three Hubble-Sandage variables 3−22107
M 33, observations of five Hubble-Sandage variables 3−22107
M 87 (3C 274, Virgo A), nearby radiogalaxy, X-ray emission rel. to inverse Compton effect 3−9574
Maffei 2, aperture synthesis observations at 21 cm. wavelength 3−16261
Maffei 2, optical and near i.r. obs. of nearby spiral galaxy, distance meas. 3−37444
Magellanic clouds, Large and Small, contour diagrams for radio continuum brightness at 11 cm wavelength 3−3348
Markarian, H I 21-cm.line observations of II objects 3−22104
Markarian, spectral obs. exhibiting emission lines *(Russian)* 3−16254
Markarian, UBV obs. of galaxies with a u.v. continuum *(Russian)* 3−16256
Markarian 205, nearby late-type star as suspected radiosource 3−16262
Markarian 205, NGC 4319, Hα emission 3−3366
Markarian 205, no connection with NGC 4319 in Hα photograph, N-type galaxy 3−3365
Markarian 78, spectroscopic observations of mass motions 3−28259
Markarian 8, spectral obs., morphological and dynamical structure *(Russian)* 3−37440
Markarian galaxies, search for radio emission at 9.5-mm wavelength 3−9593
mass to luminosity ratio of spiral and irregular galaxies 3−22103
metal abundances, time variations 3−16268
model binary clusters in galactic gravitational fields, stability 3−9603
motions in spherically symmetric clusters of galaxies rel. to instabilities 3−37473
multiple, bridges and tails as tidal relics of close encounters 3−25490
N galaxies, nature, Hubble diagram and validity of redshifts as distance indicators 3−37448
NCG 5055, photographic magnitudes and light curves of supernova 3−22066
NGC 1068, Seyfert, variability in 10-micron flux 3−13092
NGC 1068 (M77), energy distribution in nonnuclear portions compared to M81 and M51 3−22100
NGC 1068 Seyfert nuclei, rapid variations of Hα intensity 3−35182
NGC 1275, extended X-ray source observations from Uhuru 3−19046
NGC 1275, giant elliptical galaxy, evolution 3−9601
NGC 1566, luminosity distribution in Seyfert galaxy of Dorado group 3−39722
NGC 1614, central region, spectrographic obs. 3−19052
NGC 1889, vel. dispersion meas. using Coude spectra 3−28256
NGC 2403, aperture synthesis study of neutral H, discussion 3−39728
NGC 2403, aperture synthesis study of neutral H, obs. 3−39727
NGC 2992/3 rel. to blue stellar object (Weedman 2) 3−19060
NGC 3031 (M81), energy distribution in nonnuclear portions compared to M77 and M51 3−22100
NGC 3109, irregular-type, distrib. of neutral H and vel. field 3−28268
NGC 3115, vel. dispersion meas. using Coude spectra 3−28256
NGC 3516, Seyfert nucleus, spectral var. rel. to spectroscopic observations 3−22105
NGC 3516 Seyfert nuclei, rapid variations of Hα intensity 3−35182
NGC 4151, gas motions in nucleus of Seyfert galaxy, image-tube spectra 3−39723
NGC 4151, Seyfert, 21 cm neutral H meas. for structure determ. 3−31775
NGC 4151, Seyfert, variability in 10-micron flux 3−13092
NGC 4151, Seyfert galaxies, i.r. variability of dust model 3−13087
NGC 4151 Seyfert nuclei, rapid variations of Hα intensity 3−35182
NGC 4236, aperture synthesis study of neutral H, discussion 3−39728
NGC 4236, aperture synthesis study of neutral H, obs. 3−39727
NGC 4244 (Scd-type), H I 21 cm line study rel. to mass distribution 3−25500
NGC 4258, kinetics of H$_\alpha$ emission of abnormal filament *(French)* 3−9599
NGC 4258, radio emission and possible origin of spiral structure 3−5609
NGC 4319, Markarian 205, N-type galaxy 3−3365
NGC 4473, vel. dispersion meas. using Coude spectra 3−28256
NGC 4486, galaxy assoc. with Virgo A, upper limit to flux variation 3−37412
NGC 4486 (M87) nucleus, linear polarisation in u.v. 3−31758

galaxies continued
NGC 4486 (M87) nucleus, obs. of Virgo A at 3.8 cm between 1971 Feb. and 1972 Aug. 3−31715
NGC 4486 (M 87), Virgo galaxy, mass-to-light ratio determ. 3−35192
NGC 4486 jet, optical brightness variability *(Russian)* 3−16255
NGC 4494, vel. dispersion meas. using Coude spectra 3−28256
NGC 4656/7, interacting galaxies, continuum radio emission at 408 MHz 3−25504
NGC 4676A, radial velocity meas. in tail from obs. of OII 3727 Å emission 3−25507
NGC 5128, giant elliptical galaxy, evolution 3−9601
NGC 5128, peculiar radio galaxy, possible assoc. shred object Fourcade-Figueroa 3−28276
NGC 5128 (Centaurus A), X-ray observations for UHURU 3−37432
NGC 518 (M33), distrib. and kinematics of neutral H 3−28270
NGC 5194 (M51), energy distribution in nonnuclear portions compared to M77 and M51 3−22100
NGC 5194 (M51), neutral H obs., tidal interaction with NGC 5195 3−35187
NGC 5253, jet and nuclear complex rel. to possible violent event 3−37457
NGC 5253, supernova 1972, UBVRIJK photometry and magnitude determinations 3−13052
NGC 5253, supernova (type I), i.r. obs. 3−22071
NGC 5253, supernova SN 1972e rel. to supernova rate 3−19027
NGC 545-547, associated galaxies rel. to PKS0123-01, radiosource 3−3345
NGC 5548, Seyfert, meas. of broad component of Hα emission 3−31756
NGC 5846, surface photometry of tidally truncated elliptical companion 3−39721
NGC 6946, aperture synthesis of neutral H 3−28271
NGC 7331 and Stephan's Quintet, correcting faint nebulous material 3−22109
NGC 7752/3, instability of double system 3−35181
NGC 891, late Sb galaxy, continuum radio emission at 408 MHz 3−25504
nonaxisymmetric kinematics in galaxies with axisymmetric mass distrib. 3−31736
nonlinear global theory of rot. and struct., Vlasov eqn. soln. applic. *(French)* 3−9598
nuclear regions, spectral scan, stellar population synthesis 3−13081
nuclei, mag. dipole radiation from supermassive oblique rotator 3−37282
nuclei, turbulent plasma 'piles' with max. intensity in the i.r. *(Russian)* 3−16269
nuclei of N galaxies and Seyfert galaxies, photographic identification with quasars 3−31723
nuclei of spiral galaxies rel. to radio emission 3−19061
origin of galaxies and clusters of galaxies rel. to blackbody radiation fluctuations 3−37305
peculiar, gaps in red shift distrib. 3−35184
peculiar galactic nuclei, finding list from Hubble Plate Collection 3−37470
Perseus cluster, extended X-ray source observations from Uhuru 3−19046
PKS 1504-16.7, variable source at 408 MHz 3−9580
PKS 1524-13, variable source at 408 MHz 3−9580
polytropes (weakly distorted) under external press., stability against radial perturbations 3−28106
primordial random motions and angular momenta of galaxies and galaxy clusters in expanding universe 3−37447
properties of galaxies with known dynamical parameters, star formation rate 3−28273
protogalaxies, density fluctuations due to turbulence in self-gravitating media 3−34999
pulsed galactic nuclei rel. to origin of cosmic rays 3−13086
radio obs. of normal galaxies at 4.5 and 2.8 cm 3−35176
radio positions and identifications for sources of about 1 flux unit at 408 MHz 3−3346
radio sources, number-flux relation anomaly 3−16235
radiogalaxies, luminosity function at 178 MHz 3−13088
radiosource optical identification of bright galaxies second Bologna Catalogue, radio luminosity function determ. 3−35160
red shift meas. of galaxies near radio source RN 8 (3C 61.1) correlation with blue stellar object 3−31755
red shifts of galaxies near radiosource RN 8 rel. to optical identifications 3−31769
redshifts of quasars 3−9582
relativistic disks at centres of galaxies rel. to gravitational wave production 3−22728
resonant stellar orbits in spiral galaxies 3−37294
rotating, core contraction (gravothermal catastrophe) leading to core-halo system 3−31747
rotating gaseous spheroids, dynamical contraction, formation of stars and galaxies 3−37286
rotating magnetised gaseous disk model, equilib., stability and evolution 3−31746
rotation, methods of observation and analysis 3−25497
rotation and evolution, conference, Bologna, Italy (1971) 3−25356
Sculptor group, H I obs., velocities and distances determ. 3−28274
self-gravitating, non-rotating gas layer with stellar, mag. and cosmic ray components, linear stability anal. 3−28101
Seyfert, i.r. spectra rel. to thermal radiation from surrounding dust envelope 3−37418
Seyfert, short time-constant phenomena, lower limit to e.m. energy pulse duration, appl. to NGC 4151 3−37284
Seyfert, surface brightness gradient rel. to other props. *(Russian)* 3−37443
Seyfert nuclei, discrete quantized outflow velocities of matter by radiation pressure 3−31720
Seyfert nuclei, rapid variations of Hα intensity 3−35182
Seyfert nuclei, UBV observations rel. to optical and radio variabilities 3−37472
Seyfert nuclei, variability of optical radiation *(Russian)* 3−37439
Seyferts, electron scattering effects on emission line profiles 3−16209
Shakhbazian I, cluster of galaxies, radial vel. meas. 3−31759

galaxies continued
SMC, by photometry of Cepheids, instability strip and constant period *(Russian)* 3−13060
SMC, discovery of first supernova remnant 3−22110
SMC, dust content revealed from UBV photometry of 11 stars 3−31773
SMC, kinematic properties of 30 H II regions 3−28263
SMC, photometric standards, stellar population 3−9607
SMC, search for H I remnants of strong tidal disruption with the Galaxy 3−25499
SMC structure *(French)* 3−9600
SN 1972 in NGC 5253, search for h.f. optical pulsar 3−22080
spiral arms, review of Lin-Shu density-wave theory 3−31739
spiral structure, development and application of computer models 3−3376
star formation in the spiral arms, shock wave effects 3−25503
Stephan's Quintet and NGC 7331, correcting faint nebulous material 3−22109
structure, stationary collisionless self-gravitating gas model, freq. function soln. 3−35195
synchrotron radiation, polarization in inverse Compton scattering, optically thin and thick sources studies 3−25359
tidal interaction, anal. using applied celestial mechanics *(Russian)* 3−5615
tidal interaction on close passage, computer simulation *(Russian)* 3−16265
tidal interaction on spiral structure and vel. field of matter falling into galactic plane 3−28269
Ton 534 a and b, Seyfert-like galaxies forming pair, spectrophotometric and red shift meas. 3−31754
2U 0328-52, Uhuru X-ray source, possible identification with cluster of galaxies 3−3363
velocity dispersions in groups of galaxies, interpretations 3−39731
Virgo cluster, radial velocities 3−13089
Westerbork Synthesis Radio Telescope 1415 MHz survey, identification of radio sources 3−28232
X-ray emission from three nearby radiogalaxies rel. to inverse Compton effect 3−9574
VII Zw 8, compact object with ring, interpretation of structure 3−39732
H I region study of galaxies with small ang. dias. 3−25501
HI 21-cm. line study of early type galaxies 3−5610

gallium
acoustic geometric and acoustic cyclotron resonances 3−8096
closed-tube diffusion, controlled surface conc. 3−39258
crystal structure of δ-Ga *(French)* 3−20710
diffusion in Ge substrate during GaAs epitaxial growth *(Russian)* 3−27606
diffusion in Si, effect of SiO$_2$ layer 3−18212
diffusion in SiO$_2$, summary of data 3−21546
diffusion in ZnSe, optical props. 3−24712
elasticity and thermal expansion anisotropy 3−27053
electron-phonon scattering using heat pulse measurements 3−2047
in Fe meteorites, by X-ray fluorescence analysis 3−5451
Fermi surface under pressure, quantum oscillations in magnetoacoustic absorpt. 3−33789
film, size effect parameters rel. to electron transport 3−30448
in finely dispersed state, thermodynamic characts. 3−33686
$K_{\beta 2}$ X-ray emission bands in GaSb *(German)* 3−15569
liquid, diffusion of O, 750-950°C, potentiostatic electrochem. study 3−30278
liquid, elec. resist. to 1000°C, temp. depend. 3−4999
liquid, embrittlement technique applic. to grain boundary precipitate exam. in Al-Fe bicrysts. 3−37025
liquid, nuclear mag. relaxation and quadrupolar coupling 3−21338
liquid, quadrupole and Knight shift relax. of ^{71}Ge, 40-1050°C 3−2434
liquid, supercooled, elastic and inelastic neutron scattering obs. of structure 3−20687
liquid, temp. dependence of surface tension and density *(Russian)* 3−11798
liquid, thermoelectric props., temp. depend., m.p.-1200K 3−24408
liquid structure factor data accuracy evaluation 3−1562
metastable phases in dispersions 3−11740
multiply charged ions, atomic lifetimes of low-lying levels 3−11156
in Mundrabilla meteorite shower, X-ray fluorescence spectrometry 3−5452
plasmon damping, volume, momentum dependency 3−2123
pseudomorphic and superstructures for Ga on W substrate, field ion microscope study 3−24318
quadrupole interaction of Ge nuclei following nuclear reactions 3−34255
specific heat of supercooled liquid and metastable β and γ crystalline phases *(French)* 3−36425
spectral line intensity of a series of elements, effect of In, Ga and Sn *(Russian)* 3−35543
superconductor, type I, anomalous attenuation of longitudinal ultrasound in intermediate state 3−24542
superconductor, type I, supercooling and superheating at transition 3−15295
thermal expansion, temp. depend., 78-293K *(Russian)* 3−7945
n-CdGr$_2$S$_4$(Se$_4$):Ga, cond. min. and magnetoresist. 3−27267
Ga:Sn, in porous glass, ^{119}Sn Mossbauer, phonon spectrum, supercond. critical temp. 3−21355
Ge:As, Ga, indirect semicond., direct transition probability in impurity luminesc. 3−15554
Ge:Ga, distrib. coeffs. for Ga doping during growth in open iodide system *(Russian)* 3−15643
Ge-Si:Ga,Li, temp. depend. of Li solubility *(Russian)* 3−14974
KCl:Ga, absorp. bands and luminesc. of Ga^0 centres 3−27024
LiH:Ga, excitation and luminesc. spectra *(Russian)* 3−21462
Si:Ga, impurity photocond. oscills., 4.2-10K *(Russian)* 3−2134
YIG:Gd,Ga uniaxial films, epitaxial growth by r.f. sputtering 3−12237
ZnO:Ga, shallow bound states, cyclotron reson., Zeeman splitting, 30-100 cm^{-1}, 5-100K 3−2028

gallium alloys
see also gallium compounds
rare earth Ga garnet, Czochralski growth to produce substrate, defect and strain elimination 3−12293

gallium alloys continued
- Ag-Ga, liq., mag. susceptibility *(Japanese)* 3–30600
- $Au_{50}Cu_{50-x}Ga_x$, thin specimens study of AuCu II phase with periodic antiphases and AuCu III phase *(French)* 3–31003
- β-CoGa, low temp. magnetic behaviour 3–34098
- (Cu, Ga)-V, supercond. V_3Ga layers at interface, growth and props. *(German)* 3–8311
- Cu-Ga, liq., mag. susceptibility *(Japanese)* 3–30600
- Fe-Ga-C, f.c.c., interactions between insertion and substitution atoms *(French)* 3–8777
- Ga-As-impurity ternary systems, rapid method for triangulating phase diagrams *(Russian)* 3–12330
- Ga-In, liquid alloy, nuclear quandrupole relax. rate 3–18391
- Ga-Pb, liquid alloy, thermodynamic props. 3–30271
- $Ga_xAl_{1-x}As$ obs. of disorder-activated acoustic phonon mode in Raman spectrum 3–2542
- $Ga_xIn_{1-x}P$:S, band structure from Hall effect and resistivity meas. 3–15215
- Gd-Ga, melt grown garnet, X-ray topographic anal. of dislocations and growth bands 3–30946
- Gd-Ga garnet substrate, chem. etching 3–8029
- Mn-Ga, plastically deformed, mag. hardness *(Russian)* 3–36735
- Mn-Ga powders, high-anisotropy, mag. reversals, domain boundary displacement *(Russian)* 3–36737
- Mn-Ga(32.5 at.%), metastable phase form. *(Russian)* 3–30968
- Mo-Ga system, $MoGa_4$ phase, struct. determ. using direct methods 3–17759
- $MoGa_5$ peritectic in Mo-Ga system at 835°C 3–21566
- Mo_3Ga, form. and anisotropic binding force for Ga deposited on Mo substrate 3–24319
- Ni_3Ga, low temp. elec. resist. and spin density fluctuation theory 3–21046
- Pu-Ga, plastic deformation, mechanical props. influence of homogeneity *(French)* 3–34589
- Pu-Ga (1 wt.%) cold rolled, annealing 3–12384
- U-Ga phase diagrams, magnetic properties 3–33654

gallium arsenide
- acoustoelectric domains, on and off axis, observation by stroboscopic illumination 3–5037
- acoustoelectric domains, piezoelec. potential and carrier distrib., microwave absorpt. and Brillouin scatt. 3–5040
- acoustoelectric domains in epitaxial films 3–24483
- adsorption of Cs on (110) surface, 77-450 K 3–20941
- amorphous, refr. index, dispersion and magnitude 3–36851
- band structure, crit. pt. determ., in 4-9 eV region 3–2005
- band structure, pressure depend., combined pseudopot. calc. 3–27214
- band structure and effective masses, combined pseudopotential-k.p calc. 3–18079
- carrier concentration and mobility, temp. depend., 80-300K *(Russian)* 3–18133
- carrier recombination, carriers generated in vicinity of surface 3–34426
- cathodoluminescence, temp. depend., 27-300K 3–36949
- coated with Ba, photoemission 3–15592
- compensated, effect on luminesc. props. 3–2591
- compensation of high resistivity film, dominant oxygen contrib. 3–15156
- conduction band effective mass anisotropy rel. to uniaxial compression *(Russian)* 3–15137
- crystal growth, vertical gradient freeze method, theory and practice 3–15635
- crystals grown in magnetic field, crystallizing unit *(Russian)* 3–12313
- damage layer eval. using using X-ray anomalous dispersion 3–15056
- damage produced by fast neutrons, model for 3–33567
- defect levels induced by electron irradiation 3–21022
- detector probes, application in nuclear medicine 3–32141
- deuteron irradiated, defect distrib., luminesc. study *(Russian)* 3–1655
- dielectric function, calc. using Penn's model 3–2000
- diffusion, of Zn, vacancies, influence of As vapour pressure, distribution regions, surface treatment 3–33696
- diffusion and solubility of Co, temp. depend., 580 to 1160°C, conc. distrib. 3–33699
- dislocation structure, rel. to thermal conditions in the floating zone growth process 3–33533
- dislocations, obs. by X-ray refl. topography, optimum refl. 3–4760
- doping characts. of flash-evaporated thin films 3–27611
- doping profile measurement, using reverse current characs. of imperfect Schottky barriers 3–39301
- double heterostructure laser short pulse modulation with TRAPATT diodes 3–32569
- electrical characts., laser irrad. effects *(Russian)* 3–27248
- electrical transport props. depend. on heat treatment, thermal conversion rel. to impurities *(Russian)* 3–38832
- electron and neutron irrad., B, C impurities, i.r. local mode abs. 3–34395
- electron backscattering coefficients, and influence of Cs and CsO layers 3–5248
- electron concentration, change on fast neutron irrad. *(Russian)* 3–27041
- electron energy relaxation time, determination from 34 GHz complex conductivity measurements in presence of d.c. field 3–2118
- electron transfer high freq. behaviour, dynamical Monte Carlo study 3–11902
- electron-hole liquids, ground state energy 3–21009
- electron-phonon coupling, LO phonon creation by Frohlich type interaction 3–30224
- electron-phonon interaction and intervalley scattering, pseudopotential calc. 3–5005
- electronic props. of bivalent flaw in n-GaAs, noise meas. 3–18101
- electroreflectance from semiconductor surfaces, Schottky barrier effect, diffusion potential, impurity concentration 3–33982
- ellipsoidal valleys, soln. of Boltzman equation for ⟨100⟩ valleys 3–33883
- e.m. waves in doped GaAs, absolute instability and microwave emission 3–24461

gallium arsenide continued
- epitaxial film, produced by vapour transport reactions, crystallization condits. *(Russian)* 3–8725
- epitaxial films, growth on spinel and characterization 3–39266
- epitaxial growth, effect of surface states on amphoteric behaviour of Sn 3–24393
- epitaxial growth, for Gunn devices, optimisation for high purity layers 3–2686
- epitaxial growth, Ga-$AsCl_3$-H_2 system, Ga:As ratio, chemical thermodynamics calc. *(German)* 3–15095
- epitaxial growth, liquid phase, impurity incorporation, depend. on growth rate and cryst. orientation 3–1638
- epitaxial growth, liquid phase, in silica boat, Si contamination control 3–2684
- epitaxial growth, review 3–27192
- epitaxial growth, small angle shadowing and chem. decoration obs. of growth surface 3–20956
- epitaxial growth and characterisation for microwave devices 3–2685
- epitaxial growth by rotating boat technique 3–34481
- epitaxial growth of Ag on GaAs(110) obs. by LEED 3–15087
- epitaxial growth of $Ga_xIn_{1-x}As$ on GaAs substrate, anisotropic bending 3–15085
- epitaxial growth on Ge, diffusion of Ga and As in substrate *(Russian)* 3–27606
- epitaxial growth substrate, characterisation, disloc., impurity, and precipitate obs. 3–1938
- epitaxial layers, micromorphology and electron distrib., effect of growth time in iodide system *(Russian)* 3–30933
- epitaxial n-GaAs films as high-sensitivity submillimetre receiver *(Russian)* 3–119
- epitaxially grown, electrical props. depend. on $AsCl_3$ temp. 3–8756
- exciton states, free, uniaxial stress effects and photoluminesc. 3–21036
- film, epitaxial, electron mobility, anomalous magnitude and temp. depend. *(Russian)* 3–2091
- film, epitaxial, Ga vacancies and impurity profiles 3–14883
- film, epitaxial, hole diffusion length rel. to heterostruct. 3–36667
- film, linear and nonlinear optics 3–2605
- film, on insulators, vapour phase epitaxy by reactions involving organometallics 3–12251
- film, refl. and transmission secondary emission 3–5246
- film, vapour growth on sapphire substrate in ultrahigh vacuum conditions 3–15619
- films, oxidation process 3–15080
- GaAs:He(N,S,Zn), ion implantation, elec. conduction due to defect centres 3–33906
- Gunn device, i.r. light emission phenomenon 3–18498
- Gunn diode fabrication by mesa-etching technique 3–36990
- Gunn diodes, ohmic contacts by condensation of metallic plasma 3–25798
- Gunn threshold depend. on transverse mag. field for GaAs coplanar epitaxial device 3–21089
- Hall factor, n-type, 77-300K, and p-type, 78K *(Russian)* 3–2110
- Hall field calc. inside non-spherical radiation damage regions 3–38856
- Hall meas. on X_{1c} electrons at low temp., scattering mechanisms and band structure 3–21097
- heavily doped, electron mobility rel. to electron-electron scatt. and nonparabolic energy band shape 3–18139
- high ohmic, subthreshold working, field pattern mapping using scanning electron microscopy *(German)* 3–8263
- high purity, donor species identification, ionization energy determination using optically pumped NH_3 laser 3–2018
- high purity, liquid and vapour phase epitaxy 3–2676
- imperfections, photoluminesc. investigation *(Russian)* 3–36914
- implantation of Kr and Tl, energetic ion collection, saturation effects 3–11646
- implantation of Kr and Tl, ion conc. profile and ion range probability distrib. 3–11647
- impurities, spectral determ. 3–16567
- injection laser, absorpt. coeff. and gain 3–22919
- ion implantation profile of F^-, Auger spectroscopy determ. 3–12309
- ion irradiated, cond. in disordered regions *(Russian)* 3–2072
- i.r. absorpt. of localised longit. optical phonons 3–30232
- i.r. absorption from neutral acceptors 3–21413
- i.r. reflection, damping effects on plasmon-phonon spectrum *(Russian)* 3–8592
- i.r. window, X-ray examination of defects and strains 3–9935
- junction laser, physics and technology, review 3–749
- large diameter ingots, for i.r. window appl., crystal. growth 3–15634
- laser, action on photosensitive materials *(Russian)* 3–16914
- laser, close confinement, threshold current density and beam spread depend. on pot. barrier height 3–26236
- laser, double-heterostructure, with thick waveguide, zero-order transverse mode operation 3–22917
- laser, electron-beam pumped, laser dynamics and wavelength tuning 3–745
- laser, injection, modal power distrib. 3–22916
- laser, junction, solution grown, current limitations and maximum stimulated output as functions of laser length at 77 K 3–29102
- laser, pumping using pulsed elec. discharge in vacuum 3–37971
- laser, student experiments to study electro-optical devices 3–16360
- laser damage, surface, solid lasers, 0.694 and 1.06 μm 3–29120
- laser damage at 1.06 μm 3–35707
- laser diode, pulse position modulation technique for point-point voice communication 3–26209
- laser diodes, neutron damage 3–19619
- laser filaments as optical waveguides 3–4108
- laser focusing, intervalley transfer mechanism 3–10552
- lattice parameter meas. by double diffr. technique 3–36240
- layer, substrate surface orientation effect on growth rate of epitaxial layers 3–33748
- light emitting diodes, near-field intensity variation in Fabry-Perot structure by pulsed electron injection 3–39193
- light pulse transmission, nonlinear absorption *(Russian)* 3–777
- liquid encapsulated zone refining 3–12307
- liquid phase epitaxial growth temp. gradient cell 3–12261
- liquid phase epitaxy from Ga free Sn melts *(German)* 3–4933

gallium arsenide continued
longitudinal optical phonon-plasmon coupling 3—36551
luminescence, heat treatment effects on 0.93, 1.0 and 1.28 eV bands 3—21477
luminescence due to exciton-exciton collision 3—30871
magnetization of charge carriers and excitons by polarized light 3—4956
magnetoresistance of epitaxial films 3—24456
melt growth in space, Skylab programme 3—12287
microhardness rel. to phase transition pressure, hardness temp. depend. 3—7931
microwave emission, with TEM wave round-trip gain 3—12195
mobility, anomalously high at room temp., resist. and Hall meas. 3—18140
molecular beam epitaxy 3—2677
n-type, acoustoelectric gain and lattice attenuation meas. 3—11935
n-type, donor and acceptor conc. determ. from hot electron mobility 3—38812
n-type, elec. cond., mm. wave investigation 3—21084
n-type, electroabsorpt meas., valence sub-band parameters 3—39123
n-type, electrochemical characterization, automatic plotting system 3—30953
n-type, electron scattering processes *(Russian)* 3—2076
n-type, epitaxial, acoustoelec. instability, transverse mag. field effect 3—18195
n-type, epitaxial growth by vapour phase process 3—1937
n-type, evaporated silver contacts, electrical resistance, surface cleaning by ion bombardment, experimental results 3—15250
n-type, galvanomagnetic coeffs., determ. by one-point method 3—24454
n-type, Gunn effect threshold, transverse mag. field effects, Hall field contribution 3—18157
n-type, Gunn oscillations, low field mobility temp. variation effects 3—18146
n-type, homogeneities rel. to doping, optical absorpt. obs. *(French)* 3—34386
n-type, intervalley absorpt., LA and TA phonons contrib. *(French)* 3—24726
n-type, magnetoresistance, transverse, Gunn diodes, 300 to 800 K, carrier mobility, electron transfer between conduction bands 3—36624
n-type, millimeter wave characteristics of hot electrons, experimental study using electrodeless method 3—27263
n-type, millimeter wave freq. response of hot electrons 3—2119
n-type, Nernst-Ettingshausen effects in phonon drag region *(Russian)* 3—8232
n-type, non-low doping, Faraday effect *(Russian)* 3—12125
n-type, optical absorpt. increase with electron irrad. selective bands 3—39164
n-type, optically excited, doping dependence of photon yield as function of excitation energy 3—8638
n-type, phonon drag effect, electron-acoustic phonon interaction by deformation potential 3—11913
n-type, piezoelec., ultrasonic wave attenuation and velocity between 4.2 and 240 K 3—24219
n-type, positron lifetime meas. on deformed GaAs for electric charge on dislocations 3—11863
n-type, shallow donor states, cyclotron reson., Zeeman splitting, cond. electrons effective masses 3—2026
n-type iterative method for hot carrier distrib. calc. 3—18152
n-type LSA diode, purity, evaluation determ. by low field temp. depend. mobility 3—2085
n-type substrates, SiO_2 thin films growth from vapour 3—24785
n-type surface polariton theory with and without external mag. field 3—2039
negative differential conductance, e.m. surface wave growth 3—18150
neutron irrad., electroreflectance obs. of metal-like plasma reson. 3—4973
noncollinear phase matching for generation of far i.r. difference freq. radiation 3—35711
optical cavity, totally internally reflecting 3—752
optical waveguide components for integrated optics 3—25728
oscillation band periodicity, temperature dependence *(Russian)* 3—30408
oxide layer growth by anodisation in aqueous H_2O_2 3—39251
p^+-n photodiodes, electron irrad., defect studies, differential capacity and conductance measurements 3—33845
p-n junction, barrier layer capacity with deep centres *(German)* 3—33987
p-n junction, capacitance relax. determ. of impurity atom parameters 3—15157
p-n junction, light emitting diode, optical absorpt. influence on near-field intensity 3—21490
p-n junction, photo-e.m.f., under action of self-recomb. radiation *(Russian)* 3—27303
p-n junction, rectifier e.m.f. and short-circuit current, neutron flux flow depend. *(Russian)* 3—28643
p-n junction, vapour-grown, defect morphology and electrolum., gas-phase stoichiometry effects 3—11950
p-type, i.r. plasma refl., carrier conc. determ. 3—18454
p-type, luminesc. reduction due to dislocations introduced during polishing 3—27559
p-type, magnetophotocond., 260-350K, and electron irrad. effects 3—18185
p-type, proton bombarded, optical and electrical properties 3—21442
p-type, reflection spectra obs. of temp. depend. of hole effective mass 3—24382
p-type, surface micromorphology, effeft of surface treatment *(Russian)* 3—18009
photocathode, high-sensitivity transmission-mode, struct. and method of construction 3—34457
photoconductivity in mag. field, 2 MeV α-particle irrad. effects at 300K 3—21108
photoelectron energy distrib. spectra, core levels 3—15591
photoemission from (100) and (110) surfaces 3—21520
photoemission valence-band density of states 3—5257
photographic system of high resistivity GaAs 3—32109
photoluminescence, As vacancy related near 8900 A 3—30861
photoluminescence, regions damaged by laser beam 3—27571

gallium arsenide continued
photoluminescence spectra of epitaxial films 3—24741
plastically deformed, dislocations, i.r. cathodolum. study 3—38699
plate alloyed with Te, Zn diffusion, non planar p-n transitions for increasing emissive power of injection laser *(Russian)* 3—29105
point defects, precision lattice parameter measurements after quenching and annealing 3—33523
point defects in single crysts., nature and struct., density and X-ray meas. *(Russian)* 3—7753
polarised luminescence due to optical orientation of electrons *(Russian)* 3—36934
polariton reflectance and photoluminescence in high-purity sample 3—39185
precipitation, of Cu, electron microscope examination 3—36329
preparation and devices, conference, Aachen, Germany, (Oct. 1970) 3—2675
radiation annealing of defects formed by ion bombardment 3—33553
radiation damage study by obs. of shift in reflectance peaks by optical modulation spectroscopy 3—27040
radiative recomb. rel. to press. 3—2590
Rayleigh waves, refl. loss at cleaved edges 3—33726
recombination characteristics, effect of impurities *(Russian)* 3—24392
recombination light, circular polarisation in weak mag. field 3—8660
resistivity meas. with d.c. four point probe with nonpenetrating tip 3—27281
resonant Brillouin scattering, and absorpt. edge modulation by intensely amplified phonon beams 3—5204
Schottky barrier height of metal-GaAs system 3—8264
single crystal growth, bulk and thin-film, methods 3—21548
single crystal growth, review of methods 3—30948
solid solutions with replacement impurities, equil. with gaseous phase *(Russian)* 3—11641
structure factor determ. by reflection profile mwthod using triple-crystal diffractometer 3—23968
structure factor meas. rel to electron distrib. and bonding 3—14784
subsidiary indirect cond. band minima, donor levels, phonon struct. of interband transitions 3—2027
substrate passivation with pyrolytically deposited Si_3N_4 film 3—18555
substrates, surface contaminations, spectrochemical analysis 3—26014
surface centres, radiative recomb. on (110) surface, ruby laser excited *(Russian)* 3—2154
surface contamination during photo etching 3—8757
surface damage induced by 50 keV Zn^+ ions, study by isochronal annealing expts. 3—24168
surface film evaluation by ellipsometry and its effect on Schottky barriers 3—39239
surface photovoltage spectroscopy obs. 3—37714
surface structure, interpretation of scanning HEED meas. 3—36460
targets for miniature pulsed laser 3—26237
thermal expansion, temp. depend., 20-800°C 3—24279
transferred electron device material, carrier mobility 3—24424
tunnel junction, heavily doped, differential conductance 3—33995
vacuum deposited films, electrical properties meas. *(Japanese)* 3—36603
vapour deposition of GaP onto GaAs substrate, influence of liquid Ga 3—2652
vapour epitaxial growth, parameters which influence purity and morphology 3—1918
vapour epitaxial growth of $InAs_{1-x}P_x$ on GaAs substrate, influence of substrate orientation 3—1917
vapour growth of CdS heteroepitaxial layers on GaAs substrate, contamination effect 3—2653
vapour phase epitaxial growth, effect of As vapour pressure on elec. props. 3—27191
vapour phase epitaxial growth, rate of growth and purity of layers 3—34477
vapour phase homoepitaxial growth, transmission electron microscope obs. 3—15096
X-ray diffraction by perfect acentric crystals 3—30049
X-ray K emission bands, one-electron approx. calc. 3—27587
n-$Al_xGa_{1-x}As$, luminescence, exciton bands *(Russian)* 3—36931
$Al_xGa_{1-x}As$ luminescence spectra, radiative transition kinetics, 4.2-77K, influence of temperature 3—34422
$Al_xGa_{1-x}As$:Ge epitaxial film, photolum., 1.1-2 eV *(Russian)* 3—2589
$Al_xGa_{1-x}As$:Mg, molecular beam epitaxy 3—18553
$Al_yGa_{1-y}As$-$Al_xGa_{1-x}As$ double heterostructures, electroabsorpt. 3—39119
$Ga_{1-x}Al_xAs$, local and collective phonon modes, Raman scatt. 3—5200
$Ga_xAl_{1-x}As$ obs. of disorder-activated acoustic phonon mode in Raman spectrum 3—2542
GaAs, GaP, electron and neutron irrad., B, C impurities, i.r. local mode abs. 3—34395
GaAs:Cr, extrinsic photocond., long term effects and quenching *(French)* 3—5027
n-GaAs:Cr, magnetoresist. and recombination instability in mag. field 3—30500
GaAs:Cr, photocond. after 0.8 MeV electron irradiation, induced impurity trap levels 3—36637
GaAs:Cr, semiinsulating, photocond., electric field and thermal quenching *(Russian)* 3—5031
n-GaAs:Cu, 1.26-1.30 eV photolum. band rel. to recombination centres 3—39186
GaAs:Cu, photolum. of excitons bound to Cu complex centres 3—34418
GaAs:Cu, supersaturated solid solution, dislocation decoration on decomp. 3—33542
GaAs:Fe, sensitizing centres, photo Hall effect, photocond. 3—36547
GaAs:Fe(Cu), electron absorpt. obs. rel. to impurity energy levels *(Russian)* 3—15532
p-GaAs:Ge, epitaxial, electron diffusion length, recomb. lifetime 3—18164
p-GaAs:Ge, epitaxial layer, minority carrier diffusion length variation with carrier conc. 3—24449

gallium arsenide continued
GaAs:Ge, solution-grown electron diffusion length 3−21093
GaAs:Mg, molecular beam epitaxy 3−18553
GaAs:Si, epitaxial layers, characterisation of p-n structure, etching, cathodoluminescence 3−39195
GaAs:Si, free carrier conc. rel. to annealing 3−18141
GaAs:Si, photolum. spectra at 77K, origin of 1.4-1.42 eV band 3−18489
GaAs:Si epitaxial layer, Cs-O, CsF-Cs activated, photoemission 3−2620
GaAs:Sn, defect props. rel. to growth conditions, elec., luminesc. and lattice const. meas. 3−36267
n-GaAs:Sn, epitaxial layer, minority carrier diffusion length variation with carrier conc. 3−24449
GaAs:Sn(Si, Zn), electron irrad., 'near-edge' absorption, annealing 3−33846
GaAs:Te, heavily doped, mag. susceptibility, 4.2-300K *(Russian)* 3−2252
GaAs:Te, impurity-defect interaction with Te ions bombard., amorphous layer form. 3−18062
GaAs:Te, ion implantation, influence of implantation temp. and surface protection 3−12310
n-GaAs:Te, photolum., 80 K, surface treatment effects 3−27570
GaAs:Zn, Cd, Si, Ge epitaxial layer, near band-edge photoluminesc. 3−34406
p-GaAs:Zn, mag. field effect on impurity cond. 3−11914
p-GaAs:Zn, optical orientation of electron spins, surface influence determ. *(Russian)* 3−8662
n-GaAs/Ni/Au-Ge ohmic contact, Auger electron spectroscopy and sputter etching 3−4903
GaAs-$\mathrm{Al_xGa_{1-x}As}$, heterojunction, p-n-p-n structure electroluminesc. props. 3−18500
GaAs-AlAs mixed crystals, reson. Raman scatt., 2K 3−34359
GaAs-AlAs solid solution, polarised luminescence due to optical orientation of electrons *(Russian)* 3−36934
GaAs-GaAlAs, profiling of periodic structures by nuclear backscattering 3−39238
GaAs-GaP, energy band calc. by combining empirical pseudopotential method with virtual crystal approximation *(Korean)* 3−27213
GaAs-GaP heterojunction, TEM obs. of misfit dislocations 3−36305
GaAs-GaP solid solution, polarised luminescence due to optical orientation of electrons *(Russian)* 3−36934
GaAs-InAs solid solution, disorder scattering 3−30470
n-GaAs-p-$\mathrm{Al_xGa_{1-x}As}$, photodiode, excess noise rel. to flow of current mechanism 3−38888
GaAs-PbS n-p heterojunctions, near i.r. detection 3−22283
GaAs-ZnSe p-n heterojunction, r.f. sputtered 3−33988
$\mathrm{GaAs_{1-x}P_x}$, chem. vapour deposition, sensors and control elements 3−12250
$\mathrm{GaAs_{1-x}P_x}$, indirect Γ_{8v}-X_{1c} band gap, absorpt. and photolum. studies 3−21003
$\mathrm{GaAs_{1-x}P_x}$:N, laser operation on photopumped $\mathrm{NN_3}$ pair transitions 3−37972
$\mathrm{GaAs_{1-x}P_x}$:N, $\mathrm{N_2}$ isoelectronic trap, luminescence, l.e.d. applications 3−39175
$\mathrm{Ga_{1-x}In_xAs}$ laser, optically pumped, performance 3−4109
heavily doped, neutron displacement damage, i.r. optical reflectiivty studies 3−33568
impurity states of Si, anomalous behaviour, temp. depend. of Hall coeff., centre concentrations 3−33834
$\mathrm{In_{1-x}Ga_xAs_{1-y}P_y}$ alloys, electron zones, luminesc. struct. study *(Russian)* 3−36946
InP, electron energy relax. time as function of elec. field 3−24420
n-type, electron irradiated, defect annealing, cluster formation 3−33558
Ni-GaAs interface and free GaAs surface, Schottky potential barrier height anisotropy 3−30534
p-type, heavily doped, neutron irradiation effects, elec. conductivity, Mott transitions, Hall coeff. 3−33823
Zn implanted, $\mathrm{H^+}$ ion bombardment, channelling expts., annealing behaviour of disorder density 3−33578
n-ZnSe-p-GaAs, light emitting heterojunc., improved generation-recomb. processes *(German)* 3−15558

gallium compounds
see also gallium alloys; gallium arsenide
GaP, electron, neutron irrad., B, C, impurities, i.r. local mode abs. 3−34395
polariton mode lifetime, stimulated Raman effect obs. 3−34351
$\mathrm{\{Ga_3\}[SnSb](Fe_3)O_{12}}$ magnetic fields, induced, diamagnetic tin atoms in antiferromagnetic garnets, Mossbauer effect 3−34270
$\mathrm{BaPO_3F}$-$\mathrm{GaF_3}$-Li(Na)(K)(Zn)(Cd)(Pb)$\mathrm{F_x}$, glass, vitrification and crystallisation capacity *(Russian)* 3−14698
Ga complex, trispyrrolidylcarbodithioate:Fe, Mossbauer spectra 3−24635
p-GaAlAs:Ge, electron diffusion lengths Al content depend. 3−18165
GaAlAs-GaAs, profiling of periodic structures by nuclear backscattering 3−39238
$\mathrm{Ga_{1-x}Al_xAs}$, liq. phase epitaxy, variation of solid comp. with temp. 3−12258
$\mathrm{Ga_{1-x}Al_xAs}$, room temp. thermal cond. meas. 3−24304
n-$\mathrm{Ga_{1-x}Al_xAs}$:Si, catholum. obs. rel. to energy gap meas. 3−30886
$\mathrm{Ga_{1-x}Al_xAs}$:Si, L.P.E. growth, depend. of carrier conc. profiles on growth conditions 3−27190
$\mathrm{Ga_{1-x}Al_xAs}$:Si, liquid phase epitaxy, amphoteric behaviour of Si, effect of As soln. conc. 3−5278
p-$\mathrm{Ga_xAl_{1-x}As}$, spin polarisation of electrons and nuclei under optical pumping 3−2596
Ga(As, P):I highly doped mixed crystals, problems of growth *(German)* 3−8765
GaAs, acoustic parametric processes discontinuities due to electron-phonon scattering near the Fermi surface 3−1750
GaAs, epitaxial growth over wide range of crystallisation conditions, comparison with GaP *(Russian)* 3−8051
GaAs, excess Ga and As in the vapour phase influence on epitaxial growth in (111) direction *(Russian)* 3−8749
GaAs, inhomogeneities in epitaxial layers *(Russian)* 3−8050
n-GaAs, interzone scattering study by specific resistance at high press. meas. *(Russian)* 3−8162

gallium compounds continued
GaAs amorphous films, electron diffraction ivestigation of struct. *(Russian)* 3−8059
GaAs:Sn, selective diffusion of Zn using $\mathrm{SiO_2}$ layer 3−15244
GaAs-GaAlAs superlattice, ultra high vacuum epitaxy system 3−39297
GaAs-GaP system, correlation between miscibility and lattice parameter mismatch 3−11720
$\mathrm{GaAsO_4}$, in plasma oxide film on $\mathrm{GaAs_{1-x}P_x}$, composition and optical props. *(Japanese)* 3−11821
$\mathrm{GaAs_{0.2}P_{0.8}}$, electroluminesc. from controlled splits 3−24746
$\mathrm{GaAs_{1-x}P_x}$, epitaxial growth by pyrolysis of $\mathrm{Ga(CH_3)_3}$, $\mathrm{AsH_3}$ and $\mathrm{PH_3}$ 3−15640
$\mathrm{GaAs_{1-x}P_x}$, growth by pulling from Ga rich soln. using liquid encapsulation 3−24805
$\mathrm{GaAs_{1-x}P_x}$, plasma oxide film growth, composition and optical props. *(Japanese)* 3−11821
$\mathrm{GaAs_{1-x}P_x}$, pyrolytic epitaxial growth, analysis of growth rate 3−1914
$\mathrm{GaAs_{1-x}P_x}$, superlattice, X-ray diffraction obs. of lattice distortion and structure 3−17788
$\mathrm{GaAs_{1-x}P_x}$, tunnel breakdown and photocurrent in reverse-biased p-n junctions 3−24503
$\mathrm{GaAs_{1-x}P_x}$ diode, use as stable pulsed light source 3−5909
$\mathrm{GaAs_{1-x}P_x}$ solid solutions, thermal conductivity, composition 3−33702
$\mathrm{GaAs_{1-x}P_x}$ superlattice, vapour growth, layer spacing uniformity 3−2687
$\mathrm{GaAs_{1-x}P_x}$:N, isoelectronic trap transitions in resonant enhancement region 3−30430
$\mathrm{GaAs_{1-x}P_x}$-GaAs, alternate layers forming superlattice structure, electron microprobe and X-ray obs. of comp. 3−12324
$\mathrm{GaAs_{(1-x)}P_x}$, optically induced paramagnetism 3−2513
$\mathrm{GaAs_xP_{1-x}}$, cathodoluminescence, temp. depend., 27-300K 3−36949
$\mathrm{Ga_xAs_{(1-x)}P}$, epitaxial growth on GaAs, lattice mismatch strain rel. to dislocation equilib. 3−11828
GaAsSb, photoemission, heterojunction barrier model 3−2619
$\mathrm{(Ga_2Br_7)^-}$ vibrational spectra in $\mathrm{KGa_2Br_7^-}$ in solid state *(French)* 3−21404
$\mathrm{(Ga_2Cl_7)^-}$ vibrational spectra reassignments from meas. on $\mathrm{(Ga_2Br_7)^-}$ in $\mathrm{KGa_2Br_7^-}$ in solid state *(French)* 3−21404
$\mathrm{GaF_3}$, partial vapour press., entropy and enthalpy of sublimation 3−30256
$\mathrm{GaF_6^{3-}}$, force constants and Coriolis coupling constants calc. 3−33103
$\mathrm{GaF_6^{3-}}$, force consts., Coriolis coupling consts., mean amplitudes of vibration 3−29622
$\mathrm{GaFeO_3}$ single crystals, magnetoelectric phenomena 3−30496
$\mathrm{Ga_{1-x}In_xAs}$, vapour phase epitaxial growth for i.r. photocathodes 3−2678
$\mathrm{Ga_{1-x}In_xAs}$ film, chem. vapour deposition using organometallics 3−21531
$\mathrm{Ga_xIn_{1-x}As}$ on GaAs substrates, anisotropic bending during epitaxial growth 3−15085
$\mathrm{Ga_xIn_{1-x}Sb}$, vertical freeze grown material characterisation 3−5280
$\mathrm{Ga_xMn_yFe_{3-(x\|y)}O_4}$, cryst. growth, Bridgmen method and characterization 3−12267
GaN, band structure calc. 3−11850
GaN, heteroepitaxial thermal gradient soln. growth 3−12257
GaN, i.r. lattice vibrations and free-electron dispersion 3−18455
GaN, impurity electron binding energy, using dielectric theory *(German)* 3−15159
GaN, resonant Raman scattering $\mathrm{A_1}$ to $\mathrm{F_1}$ and $\mathrm{E_2}$ optical phonons 3−8584
GaN, u.v. d.c. electrolum. generation by forward bias injection 3−15556
GaN thin film waveguides, Raman scatt. 3−39131
GaN:Zn electro-luminesc. diodes, manufacture and characts. *(Russian)* 3−36945
GaN-GaN:Mg light emitting diode, violet luminesc. 3−34432
n-GaN(:Zn) film, vapour phase grown, Hall meas., carrier conc. 3−33884
$\beta\mathrm{Ga_2O_3}$, in plasma oxide film on $\mathrm{GaAs_{1-x}P_x}$, composition and optical props. *(Japanese)* 3−11821
GaP, amorphous, refr. index, dispersion and magnitude 3−36851
GaP, at high excitation levels, excitonic luminesc. and photocond. study *(Russian)* 3−27542
GaP, attenuated total refl. for nonradiation surface phonons 3−2554
GaP, band structure, crit. pt. determ., in 4-9 eV region 3−2005
GaP, birefringence, spatial dispersion induced 3−2512
GaP, cathodoluminescence, temp. depend., 27-300K 3−36949
GaP, constant diameter crystal, liquid encapsulated Czochralski growth 3−12319
GaP, dielec. function, calc. using Penn's model 3−2000
GaP, donor-acceptor radiative recomb. of C-S and Zn-S pairs *(Russian)* 3−8633
GaP, doping homogeneity meas. using laser scanning device 3−5277
GaP, electron effective mass *(Russian)* 3−5008
GaP, energy states of isolated donor-acceptor pairs and influence of polarisation interaction on pair energy 3−33830
GaP, evidence for nonradiative Si,O defect 3−21023
GaP, fluoresc. from bound excitons, quenching and enhancement by far i.r. radiation 3−36940
p-GaP, hole effective mass, cyclotron reson. determ. 3−27215
GaP, hydrostatic pressure effect on second order Raman spectrum 3−30824
GaP, i.r. absorpt. of localised longit. optical phonons 3−30232
GaP, i.r. absorption from netural acceptors 3−21413
GaP, impurity ionisation energies and Bohr radius calc. from recomb. spectrum anal. expression *(Russian)* 3−36897
GaP, impurty electron binding energy, using dielectric theory *(German)* 3−15159
GaP, large crystal, liquid encapsulated Czochralski growth 3−12317
GaP, light emitting diode, device physics, material characterisation 3−39191
n-GaP, liq.-encapsulated-Czochralski-grown, deep hole traps, luminesc. study 3−5235
GaP, liquid encapsulation and growth from Ga rich soln. 3−12320
GaP, local strain fields due to impurities 3−2023

gallium compounds continued
- GaP, localised vibr. modes of interstitial O and O complexes 3–11707
- GaP, melt growth in pressure furnace system with modified Bridgeman technique 3–12318
- GaP, molecular beam epitaxy 3–2677
- GaP, neutron irradiated, optical absorption *(Russian)* 3–30851
- GaP, oxide layer chem. comp. from Rutherford scatt. 3–33744
- GaP, p- and n-type, proton bombarded, optical and electrical properties 3–21443
- GaP, p-n junc., barrier layer capacity with deep centres *(German)* 3–33987
- GaP, p-n junction with deep centres, space charge capacitance 3–33989
- GaP, p-type dopants for green light emitting diodes 3–8734
- GaP, photoionisation of electrons and holes at oxygen donors 3–33950
- GaP, recombination processes responsible for room-temp. near-band-gap radiation 3–34416
- GaP, reson. fluoresc. due to bound excitons, laser excited 3–18484
- GaP, second-order Raman spectra and phonon dispersion 3–21396
- GaP, selective epitaxial growth 3–2683
- GaP, single crystal, liq. encapsulation-Czochralski and vertical gradient freeze techniques 3–39247
- GaP, states with two bound particles, Auger transitions at defects 3–36546
- GaP, stimulated emission from excitons bound at isoelectronic traps 3–24720
- GaP, structure factor meas. rel. to electron distrib. and bonding 3–14784
- GaP, substrate, orientation influence on vapour epitaxial growth on $InAs_{1-x}P_x$ 3–1917
- GaP, surface excitations, expt. obs. using attenuated total reflection 3–24493
- GaP, surface morphology of liquid-phase epitaxial layers 3–38747
- GaP, thin film, physical and electrical properties, molecular beam growth 3–39298
- GaP, two-photon absorpt. indirect exciton transitions, theory 3–16913
- GaP, uniform dia. crystals, liq. encapsulation Czochralski growth, X-ray imaging technique 3–39248
- GaP, vapour deposition onto GaAs substrate, influence of liquid Ga 3–2652
- GaP amorphous film, ohmic, hopping cond. and Poole Frenkel behaviour obs. 3–36604
- GaP amorphous films, electron diffraction investigation of struct. *(Russian)* 3–8059
- GaP ellipsoidal valleys, soln. of Boltzmann equation for ⟨100⟩ valleys 3–33883
- GaP epitaxial growth over wide range of crystallisation conditions, comparison with GaAs *(Russian)* 3–8051
- GaP films, epitaxial growth from liquid- and vapour-phase, lattice defects 3–15091
- GaP red-emitting lamp, O content and electrolum. efficiency 3–30537
- GaP:Be, homogeneous doping in vapour growth, elec. props. *(Russian)* 3–15644
- GaP:Cu, luminesc. bands at 2.179 eV and 1.922 eV due to diffused Cu 3–2592
- GaP:Cu, red pair luminesc. 3–15544
- GaP:Fe^{3+}, deep levels, photocond. obs. 3–18095
- GaP:Li, Zn, bonding of excitons by neutral donors and acceptors *(Russian)* 3–36932
- GaP:N, bound exciton spectra and radiation kinetics during two-photon excitation 3–18491
- GaP:N, isoelectronically doped, radiative recombination 3–24754
- GaP:N, seven line luminesc. spectrum of (Neeh) complex 3–34420
- GaP:N, Te(Zn), LPE layer, minority carrier lifetimes and electrolum. efficiencies 3–30493
- GaP:N diodes, influence of temp. on electroluminescence spectra 3–24750
- GaP:O, donor deep states, optical cross section, energy levels, conc., photocapacitance obs. 3–30427
- GaP:O, donor deep states, capture cross sections, photocapacitance obs. 3–30428
- GaP:O, electrical props. of crystal grown from melt 3–24442
- GaP:O, epitaxial, O conc., nuclear microanalysis 3–39249
- GaP:Te, photocond. due to Auger recomb. of bound excitons 3–27283
- GaP:Te,O, liq. phase epitaxy, Te and O incorporation 3–39234
- GaP:Zn, O, free hole to impurity centre bound electron recomb. at 300K 3–30494
- GaP:Zn,O, Czochralski-grown photoluminesc., minority carrier lifetime, effect of heat treatment 3–39176
- GaP:Zn,O, use of $Zn(PO_3)_2$ glass as doping source 3–8755
- GaP-GaAs, chem. vapour deposition, sensors and control elements 3–12250
- GaP-GaAs, indirect Γ_{8v}-X_{1c} band gap, absorpt. and photolum. studies 3–21003
- GaP-GaAs heterojunction, TEM obs. of misfit dislocations caused by lattice mismatch 3–36305
- GaP-ZnS, absorpt. and photolum. spectra, band gap energy 3–34404
- GaP_1:Zn, O, chem. vapour deposition, form. of Zn-O radiative centre 3–2672
- GaP_2As_{1-x}:N, N_2 isoelectronic trap, luminescence, l.e.d. applications 3–39175
- GaP_xAs_{1-x}, p- and n-type, epitaxial film, solid soln., luminesc. depend. on comp. 3–39187
- GaP_xAs_{1-x}:N, laser operation on photopumped NN_3 pair transitions 3–37972
- $GaP_{1-x}N_x$ crystal growth, solubility and solid-gas distrib. coeff. of N in GaP 3–12259
- $GaPo_4$, in plasma oxide film on $GaAs_{1-x}P_x$, composition and optical props. *(Japanese)* 3–11821
- GaS, layer struct., growth mechanism 3–1580
- GaS-Ag, Schottky barrier, reverse characts. 3–33993
- $GaS_{0.4}Se_{0.6}$, layer struct., growth mechanism 3–1580
- $Ga_2S_{3x}Se_{3(1-x)}$, reflection spectrum obs. 3–8603
- GaSb, birefringence, spatial dispersion induced 3–2512
- GaSb, e.m.f. induction by Q-switched CO_2 laser 3–30520

gallium compounds continued
- n-GaSb, elec. cond., mm. wave investigation 3–21084
- GaSb, electron mobility in Γ_{1c} band, temp. and press. depend. 3–24422
- n-GaSb, heavily doped density-of-states tails associated with L-minima of conduction band 3–30425
- GaSb, Landau transitions at higher energy gaps, spin-orbit splitting 3–33809
- GaSb, ohmic contacts, Au and Ag alloy by vacuum evap. and chemical deposition *(Polish)* 3–30538
- p-GaSb, optical pumping of spin polarised conduction electrons and inelastic scattering by neutral acceptors 3–34398
- GaSb, p-type, u.s. absorpt. at low temps. 3–17938
- p-GaSb, phonon-phonon and phonon-charge carrier interactions *(French)* 3–1706
- GaSb, piezoreflectivity, 1.9-2.6 eV, $\Lambda_1 \rightarrow \Lambda_1$ transitions 3–21426
- GaSb, plasmon-phonon interactions, i.r. refl. obs. 3–21042
- GaSb, reflectivity and photoemission, dielec. func. and core levels obs. *(French)* 3–30831
- GaSb, resonant Raman scatt. 3–5201
- GaSb, structure factor meas. rel. to electron distrib. and bonding 3–14784
- p-GaSb, u.s. longitudinal waves, attenuation due to phonon-hole interactions 3–7858
- GaSb:Te, and undoped p-, acceptor radiative recomb., photoluminesc. spectral comparison *(Russian)* 3–36915
- GaSb:Te, low temp. phonon scatt., two cond. band role, Te doping depend. *(French)* 3–4893
- GaSb-InSb alloyed solid solns., distrib. coeffs. of Te and Zn *(Russian)* 3–11642
- GaSe, anisotropic linear expansion and isothermal compressibility 3–4860
- GaSe, comparison of different growth methods from vapour phase 3–2650
- GaSe, cryst. growth, Bridgman Stockbarger method 3–2671
- GaSe, LEED studies 3–38698
- GaSe, layer struct., growth mechanism 3–1580
- GaSe, layer type semicond., thermoreflectance meas. rel. to exciton selection rules 3–33855
- p-GaSe, light effect on switching props. at 77K 3–21126
- GaSe, luminescence, intense excitation by electron beam 3–15563
- GaSe, needle cryst., growth by sublimation process, struct. 3–2633
- GaSe, nonlinear optical properties *(Russian)* 3–2505
- p-GaSe, optical orientation of excitons and Hanle effect 3–34428
- GaSe, optical transmission in fields up to 93.5 kG, exciton behaviour, effective mass of electrons and holes, g-factors 3–30803
- GaSe, photoelec. props. rel. to minority carrier diffusion length and mobility 3–21112
- GaSe, photolum. spectra, carrier assisted radiative recomb. of free excitons 3–15553
- GaSe, spontaneous and stimulated emission, under intense laser beam excitation 3–27517
- GaSe film, photographic image formation *(Russian)* 3–9092
- GaSe layer compound, band structure calc. using empirical pseudopotential method, charge densities and bonding 3–30404
- GaTe, layer cpd., thermoreflectance spectra in exciton region 3–30839
- GaTe, thermoreflectance meas. near room temp. 3–24713
- GaTe thin films, structure, elec. and photoelec. props. *(Russian)* 3–33755
- GaTe:Ge, high-resistivity, radiative capture of holes by luminescence centres 3–24740
- Ga_2Te_3 and GaTe, Mossbauer effect of ^{129}I *(Russian)* 3–12087
- Ga_2Te_3-Cu_2Te system, phase diagram showing $Cu_2Ga_4Te_7$ phase, band and transport props. 3–38660
- Ga_3Te_4 thin films, crystal microstructure during annealing *(Russian)* 3–33754
- $(Ga_{1-x}Zn_x)Mn_3C$, mag. and crystallographic meas. from 4.2 to 320 K *(French)* 3–30631
- Gd-Ca garnet, growth by Czochralski method, perfect cryst. prod. *(German)* 3–5272
- In-Ga-Sb system, liquidus and solidus data at 500C 3–1775
- $In_{1-x}Ga_xAs_{1-y}P_y$, electron zones, luminesc. struct. study *(Russian)* 3–36946
- $In_{1-y}Ga_yAs_{1-x}P$, Cs_2O-activated, photoemission 3–34456
- $In_{1-x}Ga_xP$:N laser operation, reson. enhancement of recomb. probability associated with isoelectronic trap states 3–18472
- $In_xGa_{1-x}P$ solid solns., epitaxial growth from gas phase *(Russian)* 3–12240
- $(Pr^{-r})Ga$ garnets with R = small rare earths on two crystallographic sites 3–7689
- Si_3N_4-Ga_2O_3-Al_2O_3 solid soln., solubility limits, comp. 3–39378
- V_3Ga, supercond. layers at V-(Cu,Ga) interface, growth and props. *(German)* 3–8311

gallium phosphide light emitting diodes *see light emitting diodes*

galvanomagnetic effects *see magnetoelectric effects*

galvanomagnetism *see electromagnetism*

galvanometers
- long-period, for seismometric applic. 3–28079
- magnetometers using superconducting galvanometers, sensitivity considerations 3–6039
- mirror type, over-damped, parameter meas. 3–35440

galvanothermomagnetic effects
- graphite, low-temp. thermopower in mag. field, phonon drag 3–2107
- Al, thermal magnetoresist., anisotropy determ. 3–24410

game theory
- *see also information theory*
- differential, spacecraft reorientation 3–6188
- minimax risk, determ. of lower bound *(Russian)* 3–16599

gamma fission reaction *see photofission*

gamma radiation *see gamma-rays*

gamma-ray absorption
- *see also Mossbauer effect; nuclear reactions and scattering due to photons*
- airborne gamma-ray mapping of rocks and soils covered by absorbing layer *(Russian)* 3–12612
- astrophysics, photon absorpt. at super-high energies in Universe *(Russian)* 3–37280

gamma-ray absorption continued
- attenuation coeffs. for Al, Cu, Fe, Pb, Zr $E_\gamma = 6\text{-}10$ MeV 3−17329
- buildup factors, approx. by geometric progression 3−11095
- dosimetry, track length distribution 3−9718
- extragalactic γ-rays, interactions with universal radiation, absorption due to hadron production 3−34983
- narrow frequency tunable γ-ray nuclear resonances induced by laser radiation 3−35518
- self-absorption of γ-rays, in disc shaped sources 3−25855
- Al, attenuation coefficients, by scintillation spectrometer 3−25856
- C, attenuation coefficients, by scintillation spectrometer 3−25856
- Cd, in-beam meas. of static quadrupole interaction produced by 247 keV level of ^{111}Cd 3−2476
- Cu, attenuation coefficients, by scintillation spectrometer 3−25856
- $Ni + NiCl_2$ liquid mixtures at 1323 K, density determ. 3−15020
- Pb, attenuation coefficients, by scintillation spectrometer 3−25856
- Sn, attenuation coefficients, by scintillation spectrometer 3−25856

gamma-ray angular distribution
- *see also gamma-ray spectra*
- acoustic vibration detection, angular γ-γ correlation *(Russian)* 3−34273
- applications of perturbed angular correlation meas., review 3−34275
- backscattering from semi-infinite medium simulating soils, Monte Carlo calcs. of distributions 3−19975
- coherent sound vibration, effects on γ-γ ang. correl. 3−34269
- conservation of angular distrib. in γ-cascades from (α,xn) reaction 3−23245
- gamma-gamma directional correlation coeffs. for states of high angular momenta, tables 3−967
- least squares fitting, exact 3−19289
- nuclear quadrupole interactions determ. in metals and insulators by PAC 3−39062
- perturbation of γ-γ ang. correls. by coherent acoustic vibrs. in cryst. lattice 3−2474
- planetary albedo γ-rays, model for scanning-angle distrib. 3−31485
- positron annihilation, diffraction effect 3−20766
- positron annihilation in alkali halides, positron-anion bound state existence, Wigner-Seitz approx., γ-ray angular correlation curve 3−24157
- spatial distrib. of cage-type γ-rad. source *(Japanese)* 3−17201
- time dependent perturbations, e.s.r. transition effects 3−36779
- time differential perturbed angular correlation, imperfect crystal lattices, electric field gradient parameter 3−15440
- β-γ angular correlations, induced tensor interaction 3−10935
- pp collisions at ISR energies, meas. of angular distrib. and momentum spectra 3−10818
- ^{25}Al, energies, lifetimes, decay modes, γ-ray angular distribs. and mixing ratios of levels populated by $^{24}Mg(p,\gamma)$ 3−23314
- $^{27}Al(p,\gamma)^{28}Si$, 1118 keV, angular distrib. meas. of spin and parity of 8413 keV state in ^{28}Si 3−23200
- $^{36}Ar(\alpha,\gamma_0)^{40}Ca$, 6-17 MeV, meas. of γ-ray angular distrib., study of giant dipole resonances 3−26472
- ^{10}B, γ-γ ang. correl. determ. of spin 3−970
- $BaTiO_3$, positron annihilation study 3−36335
- $^{9}Be(^{3}He,\gamma)^{12}C$, 1-6MeV, obs. of transitions to ground and first two excited states, excitation curves and angular distribs. 3−11014
- ^{209}Bi, Coulomb excitation of low-lying levels, absolute γ-ray yields and angular distribs. 3−19808
- $CaF_2:Er^{3+}$, effect of dislocations on perturbed angular correlations in paramagnetics 3−34256
- Cd compounds: $^{117}In(^{111}Cd)$, excited state nucl. quadrupole interactions, PAC obs. 3−12085
- ^{111}Cd 247-keV level excited by (d,p) reaction on ^{110}Cd metal, time-differential perturbed angular distrib. expt. 3−2476
- ^{111}Cd nuclei, time-differential quadrupole interaction with cubic Ag lattice after implant. by (α, 2n) 3−33808
- $^{113}Cd(n,\gamma)^{114}Cd$, 9.04 MeV, investigation of P-odd interaction, meas. of γ-ray angular anisotropy *(Russian)* 3−10992
- ^{115m}Cd, beta decay, spectroscopic investigations *(German)* 3−29367
- ^{140}Ce, directional correlations of coincident γ transitions 3−17199
- $^{50}Cr(p,\gamma)^{51}Mn$, ^{51}Mn excited states, spin states proposal 3−26460
- $^{52}Cr(\alpha, n)^{55}Fe$, nuclear g-factors of ^{55}Fe determ. 3−32740
- ^{134}Cs, decay study by beta-gamma-gamma angular measurements 3−29354
- Cu, angular correl. anisotropy of γ annihilation radiation at 925°C 3−5150
- Cu, annealed single crysts., positron annihilation, ang. correl. meas. 3−27206
- ^{171}Er decay to levels of ^{171}Tm, meas. of angular distrib. of γ-rays determ. of magnetic hyperfine field 3−6757
- $^{19}F(p,\alpha\gamma)^{16}O$, gamma rays relative intensities and angular distributions 3−10990
- Fe, mag. h.f. field at ^{99}Tc, perturbed ang. correl. obs. 3−5154
- Fe alloyed with ^{54}Mn, ^{57}Co, ^{182}Ta, ^{191}Ir, nonalignment effects under mag. saturation at 25 mK 3−24565
- Fe:^{44}Sc, hyperfine field meas. using time differential perturbed angular correlation technique 3−34260
- Fe:Hg, time-differential-perturbed-angular correlation meas. of hyperfine mag. field 3−39067
- ^{53}Fe from $^{50}Cr + \alpha$ reaction, gamma-ray spectroscopic studies of high spin states 3−32769
- Ga, quadrupole interaction of Ge nuclei meas. 3−34255
- ^{154}Gd, multipole mixing ratios determ. from γ-ray angular correlation meas. 3−32800
- Ge, single crystal surface, electronic structure determ. by positron annihilation technique 3−38878
- o-H_2, solid, libron spectrum by small-angle scatt. of nucl. γ-rays 3−21352
- $^{2}H(d,\gamma)^{4}He$, meas of angular distrib. of γ-rays, determ. of differential cross section, E2 transition process 3−19833
- ^{177}Hf, γ-e, γ-γ-correlations of 208-113 keV cascade 3−19811
- $^{131}I \rightarrow ^{131}Xe$ decay, β-γ ang. correls. *(Russian)* 3−23275
- ^{115}In, $\gamma\gamma$-angular correlations *(Russian)* 3−35880
- KCl, positron capture by F-centres, ang. correl. of γ-quanta *(Russian)* 3−33524
- KI positron lifetime measurements 3−33551
- ^{42}K, γ-γ ang. correl. determ. of spin 3−970
- ^{176m}Lu, beta decay, β-γ directional correlation meas. 3−29366
- ^{53}Mn gamma-ray spectroscopic studies of high spin states 3−32769

gamma-ray angular distribution continued
- NaCl, positron capture by F-centres, ang. correl. of γ-quanta *(Russian)* 3−33524
- ^{23}Na, γ-γ ang. correl. determ. of spin 3−970
- $^{147}Nd \rightarrow ^{147}Pm$ decay, β-γ ang. correls. *(Russian)* 3−23275
- Ni:^{187}Re, hyperfine field meas. using time differential perturbed angular correlation technique 3−34260
- $^{64}Ni(^{16}O, 2n)^{78}Kr$, determ. of ^{78}Kr level scheme from γ-ray meas. 3−968
- ^{16}O highly ionized atoms, time-differential meas. of hyperfine structure of 6.13 MeV state 3−32761
- $^{17}O(p, \gamma)^{18}F$, 3−17154
- ^{186}Os, directional correlation meas. on the (631-137) keV γ-γ cascade 3−29337
- $PbHfO_3$, electric quadrupole interaction from $\gamma-\gamma$ ang. correl. and Mossbauer spectroscopy 3−21353
- ^{a}Pb, A = 194, 196, 198, 200, study of levels populated in heavy-ion induced reactions through de-excitation gamma-rays *(French)* 3−23251
- ^{192}Pt, angular correlation test of T-invariance 3−14159
- ^{192}Pt 308→296→316 keV cascade, γ-γ-γ ang. correl. obs. 3−10918
- ^{194}Pt quadrupole moment influence on ang. correl. following Coulomb excitation 3−23204
- $^{106g}Rh \rightarrow ^{106}Pd$, γ-γ directional correlation measurements 3−32817
- ^{a}Sb, A = 126, 127, 128, nuclear orientation study of decays 3−14241
- Se-Te alloy, struct., perturbed ang. γ-γ correl. study 3−14740
- ^{74}Se energy levels and spin following decay of ^{74}Br 3−29350
- $^{75}Se \rightarrow ^{75}As$ decay, $\gamma\gamma$directional correl. perturbation of ^{75}As 3−6784
- $^{30}Si(\alpha, n)^{33}S$, spin and parity assignments from gamma-ray polarization obs. 3−17257
- ^{144}Sm, level scheme study using (γ,γ') reaction 3−32806
- ^{150}Sm quadrupole moment influence on ang. correl. following Coulomb excitation 3−23204
- ^{120}Sn, level scheme study using (γ,γ') reaction 3−32806
- ^{203}Tl, ^{205}Tl, Coulomb excitation of low-lying levels, absolute γ-ray yields and angular distribs. 3−19808
- $^{48}V \rightarrow ^{48}Ti$ decay, β-γ ang. correls. *(Russian)* 3−23275
- Xe isotopes, neutron-rich, radiation transition multipolarities *(Russian)* 3−17188
- ^{168}Yb, from (^{4}He,xn) and (^{12}C,xn) reactions, ground state rotational bands from γ-ray meas. 3−29416
- ^{169}Yb decay to levels of ^{169}Tm, meas. of angular distrib. of γ-rays, determ. of magnetic moments 3−6757
- ^{170}Yb, from (^{4}He,xn) and (^{12}C,xn) reactions, ground state rotational bands from γ-ray meas. 3−29416
- ^{172}Yb, from (^{4}He,xn) and (^{12}C,xn) reactions, ground state rotational bands from γ-ray meas. 3−29416
- ^{175}Yb decay to levels of ^{175}Lu, meas. of angular distrib. of γ-rays, determ. of magnetic moments 3−6757
- Zn, quadrupole interaction of Ge nuclei meas. 3−34255
- ^{66}Zn, level scheme study using (γ,γ') reaction 3−32806

gamma-ray applications
- abdominal aortic aneurysm, radionuclide angiography 3−37732
- aircraft nuclear instrument landing system using frequency-modulated gamma-radiation 3−19346
- backscattering, sea floor prospecting, ocean sediments, chemical composition 3−3170
- brain scanning, with Scinticamera IV 3−16552
- dynamic radiography, imaging technique 3−19350
- irradiated fuel elements, cladding failure detection, automated system 3−17312
- moisture meter, measurement error and optimum parameters 3−37758
- nondestructive thickness and density meas. *(Italian)* 3−35514
- scintigraphy of liver and spleen in children 3−39807
- scintillation camera, new method for design optimisation of parallel hole collimators 3−22521
- soil density gauge, gamma-ray backscatter, Monte-Carlo simulation 3−37724
- subsurface gamma density gauge, Monte Carlo calcs. 3−37725
- surface gamma density gauge, Monte Carlo calcs. 3−2779
- thermometry from 20-400 mK 3−9884
- Cs, 137 and power reactor 134/137 mixtures, current and potential radiation applications 3−19993
- Cs 137, and power reactor 134/137 mixtures, practical considerations in industrial use 3−19994
- Cs-134/137 power reactor mixtures, gamma source market evaluation 3−19995
- $Ni + NiCl_2$ density determ. of liquid mixtures at 1323 K 3−15020

gamma-ray astronomy
- constellation Cygnus, γ-quanta flux meas. for cosmic ray point source determ. *(Russian)* 3−12885
- cosmic gamma rays from ^{7}Li nuclear de-excitation rel. to cosmic radiation from galactic centre 3−18905
- rel. to cosmic rays 3−34982
- Crab Nebula, pulsed gamma-ray obs. between 5 and 25 MeV 3−39742
- Crab Nebula and NP 0532, obs. above 20 MeV 3−37434
- diffuse cosmic gamma ray flux observed at equatorial balloon altitude 3−25349
- Galactic central region, energy spectrum of gamma rays 3−28265
- Galactic centre obs. of $E > 10$ MeV energies 3−39713
- galactic centre region, gamma-ray emission in 0.1-2.5 GeV range 3−37431
- gas-Cherenkov telescope, performance 3−39754
- in high energy astrophysics, current status and results 3−3397
- low energy spectra, 473 keV line, neutron star source 3−19051
- lunar compositional mapping, Apollo orbital measurements 3−31624
- NP0532 (Crab pulsar), gamma-ray detection using baloon-borne telescope 3−37510
- NP 0532, pulsed γ emission 10-100 MeV 3−5607
- old neutron stars, nuclear gamma rays and redshifted positron annihilation radiation 3−28109
- photon absorpt. at super-high energies in Universe *(Russian)* 3−37280
- small astronomy satellite B 3−31813
- solar gamma ray lines during August 1972 solar activity, OSO observations 3−22018
- spark chamber data, analysis procedure 3−316
- by spark chambers, accelerator evaluation 3−37697

gamma-ray astronomy continued
spark chambers, automatic analysis method for gamma-ray events 3−22129
spectral line detection from Galactic centre during lunar occultation of GX 3+1 X-ray source 3−28251
statistical appl. to published results 3−22131
supernovae, Type I, Monte Carlo calcs. of γ-ray line formation, Compton scattering effects 3−28171
supernovae remnants, evolutionary effects on γ-ray galactic background flux 3−25487
telescope, using double Compton process 3−28306
universal cosmic-ray theory for gamma-ray astronomy 3−21988
^{7}Li cosmic ray scattering prod., γ-ray line feature in direction of Galactic centre 3−28110

gamma-ray detection and measurement
see also dosimetry; gamma-ray spectrometers; particle detectors; radioactivity measurement
absorbed dose, absolute measurement, comparison of different calorimeters 3−28390
absorbed dose at exit determ., film technique 3−13167
adsorbed dose assessment with surface dosemeter 3−9726
Anger camera, resolution improvement using signal processing and movable filter plate 3−25858
Anger scintillation camera system, collimation 3−25867
annihilation radiation, spark chamber detector 3−13420
astronomical telescope, using double Compton process 3−28306
automatic analysis of γ radiation spectra 3−25862
camera, count rate loss correction method 3−10174
camera uniformity 3−10178
camera using coaxial Ge(Li) detector, for patient diagnosis 3−402
condensed unbounded medium, detect. from photo-Compton currents 3−36636
depth dose determ. for neutrons and γ-rays, Monte Carlo program and standard man phantom 3−28393
dose field investigation, industrial sources, RK-M1 radiative loop model, construction, operation *(Russian)* 3−26546
dose-field characteristics, industrial cylindrical irradiator *(Russian)* 3−26548
dose-field characteristics, planar industrial irradiators, radiation modification of polymers *(Russian)* 3−26547
dosimetry, by Si surface barrier detectors, temp. influence on sensitivity 3−32166
dosimetry, response of Si avalanche detector 3−404
energy measurement, capability of Ge(Li) spectrometers for precise determ. 3−10920
high energy cosmic rays, celestial distribution showing galactic and extragalactic components, OSO-3 obs. 3−12880
image recording system for γ-camera for vascular obs. 3−418
irradiated fuel elements, nondestructive examination, new gamma scanning system, computer controlled 3−17305
large area, Pb scintillator sandwich with optical spark chambers 3−32161
lithium-drifted germanium detector, evaluation 3−13433
Monte Carlo method for calibration of astronomical detectors 3−13113
multiwire proportional quantameter, energy resolution and props. 3−10049
nondestructive assay of Pu n scrap, calorimetric and γ spectrometric method 3−21783
nuclear reactor noise analysis, exptl. obs. of fluctuations in neutron population and γ-ray emission, stochastic model analysis 3−23395
nuclear reactors, fluctuations in neutron population and γ-ray emission, stochastic model studies 3−23394
precision energy meas. of high energy rays occurring in decays of nuclei, calibration standards 3−3858
prompt γ-rays from interactions of 14.5 MeV neutrons, exptl. set-up 3−35905
radioactive fuel material, photopeak unfolding of pulse-height spectrum meas. by Ge(Li) detector 3−22467
radioactive sources, microcalorimetric measurement of γ-radiation *(French)* 3−28659
scintillator, plastic, lead loaded, detection cross sect. for γ-rays, 10-200 keV, calc. 3−13424
spark chamber gamma camera, computer simulation 3−10173
three-dimensional system tests and calibration 3−25905
time-of-flight resonance, Mossbauer effect meas. applic. 3−35515
CdTe, γ-ray and X-ray detectors, current evaluation and potential application 3−19304
^{252}Cf pellet-to-pellet fuel rod assay system, using delayed γ-ray activity 3−21782
Ge detectors, charge collection times by time pick-off techniques 3−32138
Ge(Li) detectors, absolute efficiency, ^{108}Ag^{m} as calibrating source 3−32164
Ge(Li) detectors, effects of fast neutron damage on energy resolution 3−22466
Ge(Li) detectors, efficiencies for $E_{\gamma}=0.04$ to 11 MeV 3−10052
Ge(Li) planar detector, polarimetric efficiency 3−25861
Ge(Li)-Ge(Li) asymmetric linear sum-peak coincidence spectrometer, use in γ-γ coincidence and directional correlation expts. 3−22489
^{192}Ir γ-rays emergent dose meas. in humans accidentally exposed 3−9721
LiF, thermolum. response of rad. of X-rays and γ-rays 3−28392
LiF, type 7, irrad. with low energy X-rays and γ-rays 3−28391
NaI well-type detectors, calc. of efficiency values, applications to mineralogy 3−22444
NaI(Tl), and solid organic scintillation detectors, comparison rel. to remote sensing of terrestrial gamma rays 3−22445
Si(Li), p-i-n, detector, voltage-capacity charact. *(Russian)* 3−22465
Si(Li) detector, determ. of Fano factor 3−28641
Si(Li) planar detector use as polarimeter, sensitivity determ. 3−25860
Th-U nucl. fuel, nondestructive assay using γ-ray spectroscopy system 3−21781
^{133}Xe multibolus fractionation technique for human cerebral blood flow distribution meas. 3−22526

gamma-ray effects
see also nuclear reactions and scattering due to photons
adamantane, γ-irrad., ENDOR of 2-adamantyl radical 3−12535
adamantane, free radial prod. during high energy irrad. 3−2823

gamma-ray effects continued
adamantane, free radical prod. during high energy irrad. 3−2824
ADP-KDA mixed crysts., X-ray and γ-ray irrad., paramag. centres e.s.r. 3−15422
alkali tellurite glasses, e.p.r. spectra, irrad. effects *(Russian)* 3−21309
alkanes, γ radiolysis, simple exponential distribution for initial electron-positive ion separation distances 3−25077
aniline, gamma irradiation products 3−9093
anthracene single cryst., low temp. irradiation and meas. colour centres 3−132
bacteria dried on glass or plastic surfaces, sterilized by heat or γ-rays, pyrogenic activity 3−13157
1,3-butadiene gaseous, γ-ray radiolysis, decomp. product yields 3−12542
t- butyl cyclohexane, radical formation in solid *(French)* 3−5399
condensed unbounded medium, photo-Compton currents 3−36636
diborane, free radicals produced by γ-irradiation, e.s.r. spectra 3−1261
dogs, acute mortality response 3−3599
dosimetry for monoenergetic photons 3−31948
glass borosilicate, hydrogen-impregnated, e.p.r. study 3−18359
glasses, alkali metal-silicate, γ-irrad. at high pressures, e.p.r. of paramagnetic defects *(Russian)* 3−27417
glasses, electrovacuum, density change meas. and mechanism of radn. damage *(Russian)* 3−11548
latent sub image production in photographic films 3−9976
leukocytes, of swine 3−31940
mammalian intestine, response to ionisation 3−9710
metal film, elec. resist. changes *(Russian)* 3−18231
2-methyltetrahydrofuran glass, γ-irrad., luminescence study in temp. range 77 to 97K 3−12166
m.i. structures, current transfer through dielectric 3−24526
monkey, e.e.g. and behaviour 3−3604
m.o.s. structs., surface props. rel. to γ-irrad. *(Russian)* 3−24517
naphthalene, γ-irradiated crystal, fluorescence detection of free radicals *(French)* 3−18791
particulate matter collection from smokestacks using γ-ray ioniz. 3−17866
polyethylene, crystn., n- and γ-irradiation, effect on kinetics and morphology *(Russian)* 3−7636
polyethylene, low density bulk, gamma-irrad., morphology and tensile strength, SEM obs. 3−36331
polymer, pulsed gamma-neutron irrad. effects on dielec. parameters *(Russian)* 3−20256
polymer modification, planar industrial irradiators, dose-field characteristics *(Russian)* 3−26547
positronium form. probability for γ-irrad. crysts. 3−21812
quartz, γ-irradiated, hypersonic attenuation 3−1707
quartz, fused, irrad., spin diffusion and spin-lattice relax. of H atoms 3−34187
ruby:Cr^{4+}, elimination of Cr^{4+} ions as a source of strong resonant phonon scattering *(French)* 3−1846
ruby, γ-irrad., valence transitions of V ions, e.p.r. obs. *(Russian)* 3−39027
ruby, cross relaxation of Cr^{3+} ions 3−34193
ruby with vandium impurities, γ-irrad., colour centre form. *(Russian)* 3−12156
steel, martensite, irrad., redistrib. of C *(Russian)* 3−5288
trained beagles and miniature pigs, transient performance decrement 3−3597
1,2,4-triazole crystal, ENDOR study of the radical created by gamma irradiation at room temp., proton hyperfine tensors and spin density distribution 3−21814
triglycine fluoroberyllate, effect on thermal expansion over Curie temp. range 3−24280
triglycine selenate, normal and deuterated, single crystals, γ radiation changes of dielectric props. in phase transition region *(Russian)* 3−8533
viscous magnetization, stability before and after γ-irradiation *(Russian)* 3−9216
water vapour, desorption 3−22306
Ag, cold-worked and γ-irrad., modulus defect and internal friction during recrystn. 3−5314
Al-polydimethyl siloxane-Al, capacitance and loss tangent of metal-dielectric-metal assemblies *(Russian)* 3−39083
Al_2O_3, pure and Mg-doped, effect on thermal cond. 3−30293
Al_2O_3:V^{4+} acoustic paramagnetic resonance 3−2347
CO adsorbed on H-Y zeolite, ioniz., CO^{+} radical studies 3−21809
CaF_2:Np^{3+}(:Pu^{3+},:Am^{3+},:Cm^{3+}), effect of γ-irradiation on actinide ions obs. in optical absorption and thermoluminescence meas. 3−5238
Cd, damage produced by 247 keV level of ^{111}Cd excited in (d,p) reaction 3−2476
^{60}Co gamma radiation build-up effects, use of LiF dosimetry *(German)* 3−5681
^{60}Co tangential breast therapy, analysis of skin reactions 3−13150
Cu radiation damage, u.s. attenuation due to dislocation damping 3−17865
Ge, fast surface state conc. and surface potential *(Russian)* 3−24490
n-Ge, high purity, γ-irrad., carrier-conc.-depend. mobility 3−36627
Ge, O-doped, Li-diffused, irrad., carrier conc. and mobility 3−18136
n-Ge:Au piezoresist., influence of deep levels of radiation defects *(Russian)* 3−2074
p-Ge:Ga, gamma irrad., role of Li in annealing processes 3−33844
Ge:group V, defect formation under γ irradiation 3−33545
$H_2N.NH_3Cl_2(Br_2)$, irrad., e.p.r., V-centres and H atom spectra 3−2393
H_3PO_4/H_2O glass, γ-irradiated at 77K, ENDOR spectra of trapped H atom 3−25078
H_2SO_4 vitreous aqueous solution, irrad., spin diffusion and spin-lattice relax. of H atoms 3−34187
H_2SO_4/H_2O glass, γ-irradiated at 77K, ENDOR spectra of trapped H atom 3−25078
InAs, InP, InP_xAs_{1-x} solid soln., neutron and gamma irrad., elec. and optical props. 3−33907
KBr, hardening by heavy gamma irradiation at LNT 3−27035
KCl:Pb, Br, irrad., BrCl^{-} and associated centres, e.p.r. and optical absorpt. 3−39031

gamma-ray effects continued
KCl:Tl, irrad., ionized Tl-pair centre, absorpt. study 3−21445
KH_2PO_4, dielec. const. and 'hysteresis' loop rel. to γ irrad. 3−34304
KH_2PO_4/H_2O matrix, γ-irradiated at 77K, ENDOR spectra of trapped H atom 3−25078
$KHSO_4/H_2O$ matrix, γ-irradiated at 77K, ENDOR spectra of trapped H atom 3−25078
KI, defect clusters, planar dislocation loops produced by electron, γ-irradiation, obs. at 5 K with electron microscope 3−30126
$KMnO_4$, γ-irrad., e.s.r. of radicals 3−27416
$K_2NbOF_5.H_2O$, γ-irrad., ^{93}Nb-centred radicals, e.p.r. obs. 3−39453
LiF, complex defect form., annealing kinetics 3−4757
LiF, F-centre prod., effect of dose dose rate, temp. impurities, sample deform. 3−11620
4-methyl, 2,6-ditertiarybutylphenol, γ irradiated, tunnelling resonances in proton spin-lattice relaxation 3−18389
MgO, hypersonic attenuation, impurity and defects effect 3−1701
MgO, V_{al} and V^- centre prod. 3−24113
NaCl, annealing of γ-irradiation induced hardening 3−36330
NaCl crystals, thermal annealing of radiation damage, positron annihilation techniques 3−33543
$NaNO_2$ single crystal γ-irradiated, dielectric const. and Curie temp. variation 3−27477
NaOH ice, trapped electrons, ELDOR study 3−39454
Pb-polydimethyl siloxane-Pb, capacitance and loss tangent of metal-dielectric-metal assemblies *(Russian)* 3−39083
RbN_3, e.p.r. of N^{4-} defects 3−39032
Si, humidity role in atmospheric oxidation, retardation of surface film growth by γ irradiation *(Russian)* 3−8036
n-Si, irrad., recomb. studies 3−5020
Si, irradiated and annealed, diffusion, role of defects, other semiconductor materials 3−33701
Si, radiation damage in p-type with H impurity and high purity n-type, hole density, annealing 3−33546
Si, radiation effects, obs. using junction-capacitance techniques 3−33926
Si, zone-purified, induced defects, elec. properties 3−33841
SiO_2 films, impurity ion mobility 3−18222
Sn-polydimethyl siloxane-Sn, capacitance and loss tangent of metal-dielectric-metal assemblies *(Russian)* 3−39083
ThO_2, thoria, trapping centres, thermoluminescence 3−8675
ThO_2 crystals, i.r. absorption spectroscopy, gamma-ray irradiation and heat treatment effects 3−27735
V_2O_5:Cr, e.p.r., irrad. influence 3−2382

gamma-ray interactions
see also nuclear reactions and scattering due to photons; photon interactions
$\gamma\, p \to \pi^+ \pi^- p$, 6-18 GeV longitudinal phase analysis 3−850
$\gamma\, p \to \pi^+ \pi^- \pi^+ \pi^- p$, 6-18 GeV, longitudinal phase space analysis 3−850
Al, attenuation coefficients, by scintillation spectrometer 3−25856
C, attenuation coefficients, by scintillation spectrometer 3−25856
Cu, attenuation coefficients, by scintillation spectrometer 3−25856
Pb, attenuation coefficients, by scintillation spectrometer 3−25856
Sn, attenuation coefficients, by scintillation spectrometer 3−25856

gamma-ray internal conversion
see also conversion electron spectra
atomic screening and chem. environment effects for all atomic shells 3−10907
directional correlation of L X-rays and γ-rays 3−10930
K- and L-shell coeffs. for two lowest electric and magnetic multipoles for high-energy transitions 3−19809
low energy transitions, discrepancies in calc. 3−29347
$^{129}Ba \to {}^{129}Cs$ decay, level struct. 3−19766
^{207}Bi decay, directional correlation of L X-rays and γ-rays 3−10930
^{134}Cs, 127.37 keV E3 transition, internal conversion investigations, half-life of isomeric state 3−23244
^{177}Hf, γ-e, γ-γ-correlations of 208-113 keV cascade 3−19811
^{115}In, study by beta and Compton suppressed spectrometer 3−25919
^{191}Os M3 transition, K conversion coefficient near threshold 3−29348
$^{130}Sb \to {}^{130}Te$, 40 min β-decay, energy level struct. of Te from conversion spectra 3−10864
$^{149}Sm(n,\gamma)^{150}Sm$, internal conversion electron spectrum *(Russian)* 3−32795
^{121}Te M4 transitions, N-shell internal conversion *(Russian)* 3−17187
^{123}Te M4 transitions, N-shell internal conversion *(Russian)* 3−17187
^{125}Te M4 transitions, N-shell internal conversion *(Russian)* 3−17187
^{127}Te M4 transitions, N-shell internal conversion *(Russian)* 3−17187
^{129}Te M4 transitions, N-shell internal conversion *(Russian)* 3−17187
^{91}Y internal conversion coeff. and multipolarities of levels populated by ^{91}Sr β-decay 3−29362
$^{174}Yb(\alpha,2n)^{176}Hf$, 18-24 MeV, obs. of γ-rays, determ. of low-K bands in ^{176}Hf 3−23224
^{90}Zr, two-photon decay of 1.76 MeV 0^+ state, meas. 3−17198

gamma-ray production
coupled neutron and secondary γ-ray transport through concrete for incident neutrons 15-75 MeV 3−19899
disc-shaped sources, self-absorption 3−25855
high energy tube source using ^{20}F, design 3−13477
production rates from proton-proton reactions and pion decay in galactic disc 3−12929
quantum source accompanying geomag. field disturbance, e.m. signal characts. 3−25169
source, industrial irradiation simulation, RK-M1 radiative loop model, construction, operation, dose field investigation *(Russian)* 3−26546
thermal neutron-capture γ rays for study of reaction in energy region up to 11 MeV, review 3−35900
^{57}Co high-power Mossbauer sources, study of model parameters *(Russian)* 3−22436
Cs, 137 and power reactor 134/137 mixtures, current and potential radiation applications 3−19993
Cs 134/137 mixtures from power reactors, comparison with ^{60}Co source parameters and dose uniformity ratios 3−19992

gamma-ray production continued
Cs 137, and power reactor 134/137 mixtures, practical considerations in industrial use 3−19994
Cs-134/137 power reactor mixtures, gamma source market evaluation 3−19995
Cs-134/137 power reactor mixtures, feasibility and prospects for private separation and marketing 3−19996
^{137}Cs radiation sources, safety aspects 3−19345
$^{19}F(p,\alpha\gamma)^{16}O$, gamma rays relative intensities and angular distributions 3−10990
^{7}Li cosmic ray scattering prod., γ-ray line feature in direction of Galactic centre 3−28110
PuO_2 fuel heat source in spacecraft operation, radiation fields 3−19991
$^{238}U(\alpha,2n)^{240m}Pu$, determ. of limits on pre-isomeric fission γ-ray photons 3−23375

gamma-ray scattering
see also Compton effect; nuclear reactions and scattering due to photons; photon scattering
backscatter soil density gauge, Monte-Carlo simulation 3−37724
backscattering from semi-infinite medium simulating soils, Monte Carlo calcs. of distributions 3−19975
controlled thermonuclear reactor blanket studies, neutron-photon transport, variational methods 3−38187
radiation field characteristics, calc. in double-scatt. approx. *(Russian)* 3−14019
Rayleigh scatt. by K-shell electrons, Z-depend. of linear polarization 3−26556
reflected energy spectra calc. by Monte Carlo method *(Russian)* 3−24762
resonance scattering techniques, for borehole analysis, comparison 3−37723
semiconductor, under conditions of sound instability *(Russian)* 3−7893
Cu, total γ-ray cross sections, 60-1400 keV 3−29462
Er, incoherent scatt. by K-shell electrons, cross-sect. detn. 3−17337
KCl, Mossbauer obs. of inelastic scatt. at Bragg reflection, multiphonon scatt. contrib. 3−15446
Pb, total γ-ray cross sections, 60-1400 keV 3−29462
W, incoherent scatt. by K-shell electrons, cross-sect. detn. 3−17337
W, total γ-ray cross sections, 60-1400 keV 3−29462

gamma-ray sources *see gamma-ray production*

gamma-ray spectra
see also gamma-ray angular distribution; nuclear decay theory
473 keV line, neutron star source 3−19051
airborne particulate material, neutron activation analysis with computer resolution of gamma ray spectra 3−18871
atmospheric, in 40-1500 GeV range, meas. using Pb-emulsion sandwich detector 3−12899
automatic analysis, applic. to activation analysis 3−431
computer analysis of data from semiconductor detectors *(Japanese)* 3−28752
continuum at fossil-fuel plant site, meas. by Compton recoil spectroscopy 3−19980
cosmic ray gamma quanta, polarisation and energy spectra determ. method *(Russian)* 3−12893
diffuse cosmic gamma ray flux in 100 keV to 8.5 MeV range 3−25349
Doppler shift attenuation method for nucl. lifetime meas. 3−17186
energy measurement, capability of Ge(Li) spectrometers for precise determ. 3−10920
fission products, short-lived, β-decay, meas. of total-absorption γ-spectra, determ of β strength functions 3−29361
Galactic centre region line detection during lunar occultation of GX 3+1 X-ray source 3−28251
heavy nuclei, radiative capture of 10 MeV neutrons 3−26455
meteorite Tillaberi, radioactivity *(French)* 3−18991
non destructive activation analysis of W in steel and low grade wolframites by neutron activation analysis and γ-ray spectrometry 3−13512
nuclear acoustic hypersuperradiance phenomena detection 3−2453
positron transmission and scattering meas. using superposition of annihilation lineshapes, backscatter coeffs. 3−11653
precision energy meas. of high energy rays occurring in decays of nuclei, calibration standards 3−3858
radiative capture of 14.1 MeV neutrons, prompt γ-ray spectra and integrated cross sections 3−26454
radioactive fuel material, photopeak unfolding of pulse-height spectrum meas. by Ge(Li) detector 3−22467
rare earth nuclei, low energy gamma rays from thermal neutron capture 3−23343
reflection, Monte Carlo calc. *(Russian)* 3−24762
seabed mineral deposits off Yorkshire coast, radiometric meas. 3−31310
semiconductor detectors, computer treatment *(French)* 3−6064
solar gamma ray lines during August 1972 solar activity, OSO-7 observations 3−22018
spent fuel elements, gamma spectrometry meas. of decay ratios for determ. of initial props. 3−19989
stabilisation by remotely controlled time-dividing system 3−3862
standard fitting method for photopeak and semiconductor detectors 3−295
(n,γ)-line meas. using high-resolution Dumond-type diffractometer 3−10091
n-p radiative capture, dispersive approach 3−26398
$\nu e^- \to \nu e^- \gamma$, ang. and energy distribs. *(Russian)* 3−4163
ω neutral decays, branching ratio determ. from energy spectrum of γ's 3−4161
pp collisions at ISR energies, meas. of angular distrib. and momentum spectra 3−10818
$^{12}(d,p\gamma)^{13}C$, 0.8-2.1 MeV, angular distrib. of p near resonance obtained by shape studies of γ-ray lines 3−19873
$^{108m}Ag \to {}^{108}Pb$, γ-γ directional correlations and γ-ray spectra, determ. of ^{108}Pb spin parity assignments 3−19759
^{37}Ar, excited states from $^{34}S(\alpha,n\gamma)^{37}Ar$ reaction, spin values proposal 3−26473
^{37}Ar, linear polarization, resolution improvement for NaI Compton polarimeter, analysis 3−14160
$^{209}At \to {}^{209}Po$ decay, excited states of ^{209}Po *(Russian)* 3−23267

gamma-ray spectra continued
^{209}At → ^{209}Po decay scheme, $\gamma\gamma$-coincidence spectra *(Russian)* 3-23268
^{197}Au, pygmy reson. in resonant n-γ spectra 3-17245
^{198}Au, spin and parity of levels from γ-ray spectra from neutron capture in resonances of ^{197}Au *(French)* 3-38131
^{198}Au → ^{198}Hg, beta-(circularly polarized gamma) correlation, detn. as function of β energy 3-23279
^{126}Ba → ^{126}Cs → ^{126}Xe, decay investig. using Ge(Li) detectors 3-26424
^{131}Ba, γ-spectra following electron capture decay 3-14176
^{a}Bi decay, A=202, 200, 198, study of levels in ^{198,200,202}Pb by obs. of γ- and β-rays and γ-γ coincidences *(French)* 3-23252
^{205}Bi β-decay, γ-γ directional correlation meas., determ. of ^{205}Pb energy levels 3-19807
^{208}Bi, γ-decay of particle-hole states meas. in particle-γ coincidence expt. for ^{209}Bi(d,t) reaction 3-32801
^{208}Bi, M1 transition meas. by Doppler shift attenuation method 3-6764
^{209}Bi, Coulomb excitation of low-lying levels, absolute γ-ray yields and angular distribs. 3-19808
^{209}Bi(γ,γ'), photoexcitation using neutron-capture γ-rays, determ. of effective cross section and ground state width 3-23304
^{11}C γ spectra and transitions from ^{9}Be(^{3}He,n)^{11}C 3-26470
^{40}Ca(^{16}O,X), 41 MeV, meas. of γ and positron activities, determ. of isomeric ratios in ^{53}Fe and ^{53}Co 3-32809
^{44}Ca, meas. of E2 transition strength by Coulomb excitation 3-6754
^{46}Ca, meas. of E2 transition strength by Coulomb excitation 3-6754
^{111}Cd(n, γ)^{112}Cd, γ-ray spectra, total capture yields and p-wave resonances 3-29397
^{116}Cd(p,p'γ), deduced levels and comparison to phonon model, $E_p=12$ MeV 3-35904
^{252}Cf, even-odd effects in γ de-excitation of fission fragments 3-6948
^{35}Cl(n, γ)^{36}Cl, relative and absolute γ-ray intensities detn., 1.8-11 MeV 3-10976
^{35}Cl(n,γ)^{36}Cl, thermal neutron capture study 3-17235
^{37}Cl, excited states from ^{34}S(α,pγ)^{37}Cl reaction, spin values determ. 3-26474
^{37}Cl(n,γ)^{38}Cl, thermal neutron capture study 3-17235
^{40}Cl, half-life, consequent γ-rays, β-branching *(French)* 3-10924
Co, neutron capture γ-rays, spectral enhancement 3-5455
^{60}Co γ-ray instrument calibration using collimated photon beam 3-10149
^{51}Cr, photon spectrum meas. from radiative capture 3-6783
^{52}Cr, ^{54}Cr α-induced reactions, meas. of coincidence, yield, angular distrib. and polarization of γ-decay 3-10850
^{52}Cr(α,pγ)^{55}Mn, 10.5, 11.5 MeV, meas. of p-γ coincidences, determ. of e.m. properties of ^{55}Mn levels 3-23256
^{53}Cr(n, γ)^{54}Cr, relative and absolute γ-ray intensities detn., 1.8-11 MeV 3-10976
Cu, angular correl. anisotropy of γ annihilation radiation at 925°C 3-5150
^{64}Cu, meas. of moments, lifetimes and γ-decay of 6^- states 3-10845
^{66}Cu, meas. of moments, lifetimes and γ-decay of 6^- states 3-10845
^{157}Dy, high-spin rotational states populated by (p,3n) and (α,xn) reactions, obs. of γ-ray emission 3-14125
^{158}Dy, ground state rot. band studies 3-14138
^{160}Dy, ground state rot. band studies 3-14138
^{162}Dy, ground state rot. band studies 3-14138
^{163}Dy(n,γ)^{164}Dy, correl. of partial radiation and neutron widths *(Russian)* 3-6841
^{158}Er, mean lifetime of 14^+, 16^+, 18^+ levels using ^{130}Te(^{32}S,4n)^{158}Er 3-26422
^{173}Er → ^{173}Tm, β^- decay, meas. of γ-γ and γ-β coincidences, determ. of levels in ^{173}Tm 3-23266
^{152}Eu beta decay, low energy γ-rays meas. 3-14174
^{154}Eu → ^{154}Gd decay 3-6771
^{155}Eu, half-life re-measured 3-29353
^{19}F(γ,xγ'), photodisintegration, deexcitation spectra 3-17222
^{19}F(p,$\alpha\gamma$)^{16}O, gamma rays relative intensities and angular distributions 3-10990
^{56}Fe, helion-induced reactions, meas. of excitation functions from spectra 3-6860
^{156}Gd, effect of level struct. on intensity of partial radiative transitions in ^{155}Gd(n,γ)^{156}Gd reson. 3-23338
^{157}Gd, thermal neutron capture, conversion electron spectra *(Russian)* 3-10969
Ge(Li) detector γ-ray spectra, computer evaluation 3-37689
^{198}Hg energy scale, comparison with Po-α energy scale 3-10943
Hg(γ,γ'), photoexcitation using neutron-capture γ-rays determ. of effective cross section and ground state width 3-23304
^{162}Ho decay scheme *(Russian)* 3-23273
^{109}In decay, level scheme of ^{109}Cd 3-6773
^{113}In isomeric state, $\gamma\gamma$ decay 3-26416
^{115}In, levels populated in ^{115m}Cd decay, determ. of M1 strengths and half-lives from γ-ray meas. 3-23257
^{115}In(n,γ)^{116}In, meas. of γ-ray spectra and γ-γ coincidences, determ. of ^{116}In level scheme 3-6721
^{116}In ground state decay to ^{116}Sn levels, obs. of γ-ray spectra 3-32805
^{192}Ir → ^{192}Pt, meas. of $\beta\gamma\gamma$ coincidences, determ. of lifetimes of 316 and 612 keV states of ^{192}Pt 3-23258
^{39}K(^{16}O,X), 41 MeV, meas. of γ and positron activities, determ. of isomeric ratios in ^{53}Fe and ^{53}Co 3-32809
^{76}Kr → ^{76}Br, β- and γ-ray spectroscopy, determ. of spin-parity assignments for ^{76}Br states 3-19758
^{77}Kr decay scheme *(Russian)* 3-23274
^{81}Kr, from decay of ^{81}Rb, γ-singles, γ-γ and β-γ coincidence meas., determ. of branching ratios and log ft values 3-23265
^{138}La, decay, gamma-ray intensities meas. 3-29351
^{171}Lu, meas. and calc. of E1 transition probabilities between Nilsson states 3-6763
^{173}Lu, meas. and calc. of E1 transition probabilities between Nilsson states 3-6763
^{176}Lu, half-life meas. 3-10915
^{12}Mg, comparison of Po-α and ^{198}Hg energy scales by meas. of excitation energy and γ-decay 3-10943
^{24}Mg, comparison of Po-α and ^{198}Hg energy scales by meas. of excitation energy and γ-decay 3-10943

gamma-ray spectra continued
^{26}Mg(t,pγ)^{28}Mg, 2.5-3.2 MeV, p-γ coincidence meas. of ^{28}Mg excited states, Doppler shift attenuation meas. of mean lives *(French)* 3-6759
^{54}Mn, photon spectrum meas. from radiative capture 3-6783
^{14}N(n, γ)^{15}N, relative and absolute γ-ray intensities detn., 1.8-11 MeV 3-10976
^{23}Na, neutron-induced gamma-ray production cross sections in energy range 4.85-7.5 MeV 3-19849
^{147}Nd → ^{147}Pm β^- decay 3-6786
^{59}Ni, γ-transitions of levels populated in ^{59}Cu β^+ decay 3-32797
^{64}Ni(n, γ)^{65}Ni, determ. of energy level scheme for ^{65}Ni 3-6839
^{65}Ni, 2.6h, decay investigation, ^{65}Cu spin and parity assignments 3-6772
^{16}O(α,γ)^{20}Ne, 3-7.6 MeV, capture γ-ray meas. on excited $k^\pi=0^+$ bands in ^{20}Ne near 7 MeV 3-6855
Os isotopes, short-lived, halflives *(Russian)* 3-17202
^{186}Os γ-vibrational band populated in decays of ^{186}Ir and ^{186}Re, relative transition probabilities 3-6760
^{31}P(γ,xγ'), photodisintegration, deexcitation spectra 3-17222
^{31}P(p,γ)^{32}S, 300-1130 keV, study of γ-decay scheme of ^{32}S 3-23247
Pb, neutron deficient isotopes, de-excitation γ cascades meas. for low-lying high spin states study 3-26374
^{a}Pb, A=194, 196, 198, 200, study of levels populated in heavy-ion induced reactions through de-excitation gamma-rays *(French)* 3-23251
^{208}Pb, multipole mixing ratios of γ-transitions 3-6762
^{101}Pd (heavy ion, xn) reactions, γ-ray cascade excitation, band struct. evidence 3-32758
^{110}Pd(p,P'γ), deduced levels and comparison to phonon model, $E_p=13$ MeV 3-35904
^{230}Po → ^{230}Th, meas. of γ and electron-singles spectra and γ-γ coincidences, determ. of levels in ^{230}Th 3-23211
^{144}Pr, unconfirmed γ-ray intensities, upper limits using coincidence technique 3-14166
^{232}Pu decay, gamma-ray and alpha spectroscopy, half lives determ. 3-23263
^{233}Pu decay gamma-ray and alpha spectroscopy, half lives determ. 3-23263
^{234}Pu decay, gamma-ray and alpha spectroscopy, half lives determ. 3-23263
^{78}Rb decay to levels in ^{78}Kr 3-968
^{84}Rb, energy-dependent β-γ circular polarization 3-17204
^{85}Rb(n, n'γ)^{85}Rb, determ. of energy levels 3-10984
^{87}Rb(n, n'γ)^{87}Rb, determ. of energy levels 3-10984
^{183}Re, gamma-ray spectra in decay scheme 3-4279
^{184}Re isomers, and conversion electron spectra *(Russian)* 3-23272
^{185}Re, γ transition intensities meas. 3-26415
^{106g}Rh decay, level scheme of ^{106}Pd *(French)* 3-23264
^{35}S, excitation energies γ-ray decay scheme and lifetimes of levels populated by ^{34}S(d,pγ) reaction *(French)* 3-6761
^{28}Si photodisintegration, meas. of de-excitation γ-rays 3-14196
^{79}Sr decay, energies and intensities 3-14154
^{93}Sr → ^{93}Y, β, γ-ray spectra *(German)* 3-14175
^{94}Sr produced by fission, half lives and gamma-ray energies determ. 3-29338
^{95}Sr, produced by fission, half lives and gamma-ray energies determ. 3-29338
^{172}Ta β decay, meas. of energies and relative intensities of γ-rays 3-38143
^{148}Tb → ^{148}Gd decay scheme obs. *(Russian)* 3-23269
^{148}Tb → ^{148}Gd decay scheme, γ-γ coincidence spectra *(Russian)* 3-23270
^{149}Tb decay, conversion electrons *(Russian)* 3-4296
^{150}Tb → ^{150}Gd decay scheme obs. *(Russian)* 3-23269
^{150}Tb → ^{150}Gd decay scheme, γ-γ coincidence spectra *(Russian)* 3-23270
^{155}Tb, γ-decay observations 3-14158
^{99}Tc, γ-γ directional correlation study, spin assignment and mixing ratio 3-10911
^{105}Tc → ^{105}Ru, meas. of singles and coincidence spectra, study of low-lying levels in ^{105}Ru 3-23213
^{48}Ti(α,nγ) ^{51}Cr, determ. of mean lifetimes of ^{51}Cr levels below 4.1 MeV excitation by Doppler shift attenuation method 3-23250
^{51}Ti, high spin states obs. from yield functions and $\gamma\gamma$-coincidence meas. 3-26375
^{194}Tl decay modes *(Russian)* 3-976
^{203}Tl, ^{205}Tl, Coulomb excitation of low-lying levels, absolute γ-ray yields and angular distribs. 3-19808
^{235}U, γ-ray energies and lifetimes from fragments in slow neutron fission 3-6951
^{235}U(n,γ), (n,f) meas. of low-energy γ-ray spectra, 1.5-58 EV, spin assignments 3-26490
^{238}U(n,γ)^{239}U, high-energy regions meas., states of ^{239}U 3-1000
^{236m}U fission isomer decay, search for γ-branch 3-23367
Yb, A=170, 171, 172, 173, 174 and 176, neutron time-of-flight resonance spectroscopy meas. 3-32863
^{166}Yb → ^{166}Tm decay study 3-38139
^{62}Zn β-decay, population of states in odd-odd ^{62}Cu, meas. of γ-ray spectra 3-29312
^{91}Zr(p,nγ)^{91}Nb, 3.25-5.51 MeV, obs. of isobaric analogue resonances in de-excitation gamma-rays, spin-parity assignments 3-23202

gamma-ray spectrometers
see also gamma-ray spectra
24-wire liquid Xe camera, performance 3-28696
activation analysis, high-resolution spectrometer with automated data analysis 3-37743
active sample anticoincidence guarded Ge(Li) spectrometer low level radionuclide analysis 3-28773
active sample coincidence guarded Ge(Li) spectrometer for environmental radionuclide analysis 3-19300
airborne gamma-ray mapping of rocks and soils covered by absorbing layer *(Russian)* 3-12612
collimator, effective area for γ-rays 3-3866
Compton recoil, continuous radiation monitoring in natural environment 3-31949
crystal, pendulum system for bending *(German)* 3-25916
crystal spectrometer, curved and DuMond type, at Fribourg Univ., Switzerland *(German)* 3-25915

gamma-ray spectrometers continued
- diffractometer, high-resolution Dumond-type, for meas. of (n,γ)-lines 3−10091
- displacement generator with constant acceleration for Mossbauer effect 3−28749
- exact determination of energies of ^{57}Fe 122 and 136 keV lines 3−13480
- non-destructive meas. of low enriched uranium types of equipment 3−19344
- nuclear plants effluent monitoring, on-line operation 3−29452
- for nuclear power plant effluent monitoring, using digital computer 3−32229
- on OSO-7 spacecraft, response function for solar rays 3−37504
- probe output, impurities in Nb and NbO_5, neutron activation analysis *(Russian)* 3−10198
- scintillation, thermal stability circuit 3−22476
- scintillation spectrometers, timing characteristics 3−28698
- timing system, digitally stabilized 3−10074
- β-γ coincidence spectrometer, 4π geometry using Si(Li) and NaI(Tl) detectors 3−10078
- β-γ-γ, multidimensional, development and application 3−28692
- CdTe, for nondestructive analysis of nuclear fuels 3−32198
- HPGe, with Al regrowth p^+ contacts 3−35487
- Ge spectrometer, operational characteristics when cooled by closed-cycle cryogenic refrigerator 3−32199
- Ge(Li), capability for precise determ. of γ-ray energies 3−10920
- Ge(Li), energy resolution dependence obs. based on Gaussian response to monoenergetic photon source 3−326
- Ge(Li) bore hole probe, for in situ activation analysis 3−31457
- Ge(Li) detectors gamma-ray spectra computer analysis *(Japanese)* 3−28752
- Ge(Li) diode curved crystal spectrometer as band filter 3−3868
- Ge(Li)-Ge(Li) asymmetric linear sum-peak coincidence spectrometer, use in γ-γ coincidence and directional correlation expts. 3−22489
- ^{116}In source, for undergraduate expts. 3−28443
- NaI Compton polarimeter, γ-ray linear polarization spectra, resolution improvement 3−14160
- NaI(Tl), energy resolution dependence obs. based on Gaussian response to monoenergetic photon source 3−326
- Pb glass Cherenkov X-ray spectrometer, energy resolution for electron beam 3−28701
- Si(Li) energy resolution dependence obs. based on Gaussian response to monoenergetic photon source 3−326

gamma-rays
- angular correlation with charged particles 3−22441
- atmospheric, balloon-borne acoustic spark chamber investigation *(Russian)* 3−12713
- cosmic, from pulsars, origin, calc. 3−12890
- diffuse cosmic gamma ray flux observed at equatorial balloon altitude 3−25349
- dose in cylindrical phantom, Monte Carlo method 3−22178
- self-absorption, in disc shaped sources 3−25855
- shielding, effectiveness of ribbed slab, engineering investig. 3−11099
- shielding, effectiveness of ribbed slabs, experiment and theoretical 3−11098
- visible light gamma ray velocities, experimental comparison 3−35661
- $\gamma \rightarrow e^+e^-$, experiment for students 3−9794

Gamow-Teller transitions *see beta-decay*

garnets
- *see also ferrimagnetic properties of substances*
- almandine-pyrope, elec. cond. meas., earth mantle elec. props. 3−15928
- bubble domain propagation, cct. analysis for bubble domain propagation 3−36752
- bubble domains, epitaxially grown, magnetisation, wallenergy, coercivity, temp. depend. 3−36764
- chemical vapour deposition, chlorination of Y_2O_3 in presence of C 3−8717
- compositional zoning from granulite facies rocks, Austria 3−5427
- Czochralski growth, automatic diameter control using digital computer control algorithm 3−12289
- defects, rel. to bubble domain motion 3−36742
- epitaxial growth, chemical vapour deposition for bubble domain devices 3−36771
- epitaxial mag. films, effect of substrate defects 3−15090
- ferrimagnetic, stress birefringence meas. 3−21381
- film, comp. determ. by radioactive tracer technique 3−26022
- film, control of product phases in chemical vapour deposition 3−12249
- film, epitaxial, method of producing extraordinary bubbles 3−28610
- film, epitaxial growth for substrate facet replication 3−38749
- film, for bubble devices, epitaxial growth 3−12276
- film, mag., growth by liq. phase epitaxy on nonmag. substrate 3−1912
- film, mag. bubble detect. using waveguide fibre optics 3−35442
- liquid phase epitaxy, state-of-the-art 3−12275
- liquid-phase epitaxial, production and applic. to integrated optical components 3−27610
- magnetic bubble domain, stability, effect of thin permalloy film overlay 3−18336
- magnetic bubble domain material, characterization using X-ray topography 3−34156
- melt growth, stoichiometry and perfection 3−12277
- mixed rare earth iron garnet, vapour growth by chem. transport 3−24791
- mixed rare earth iron $RM_2Fe_5O_{12}$ type, growth induced noncubic mag: anisotropy 3−21256
- mixed rare earth iron type, epitaxial film, anisotropy field and domain wall coercivity temp. depend. 3−21257
- mixed rare earth iron type, growth induced noncubic mag. anisotropy 3−21255
- peridotite, basanite magma melting conditions determ. at high temp. and press. 3−21857
- rare earth, appl. of Zeeman effect theory for rare earth ions in D_2 symm. cryst. field 3−18466
- rare earth, liquid phase epitaxy for bubble domain devices 3−36770

garnets continued
- rare earth Fe, epitaxial liquid phase growth, mag. props. and defects obs. 3−2667
- rare earth Ga garnet, Czochralski growth to produce substrate, defect and strain elimination 3−12293
- rare earth Ga garnets, substrate material for bubble domain films, thermal expansion of lattice parameters 3−34158
- rare earth iron garnet, chemical vapour deposition for bubble domain devices 3−24792
- rare-earth iron garnet: Bi substituted, Faraday effect 3−34330
- rare-earth iron garnets, nuclear quadrupole coupling constants 3−2010
- resonant scattering of phonons in garnets doped with trivalent rare-earth ions 3−4837
- spin Hamiltonians for Co^{3+} ions in gargets, $3d^n$ ions in tetrahedral symmetry 3−38934
- substrate prep. by liq. phase homoepitaxy 3−34483
- YIG, rare-earth doped, relax., wave-vector depend. 3−5137
- $\{Ca_2La\}[Zr_2](Ga_3)O_{12}$, lattice constants meas. 296-1400 K 3−11753
- $\{Ca_{2.5}Zr_{2.5}\{[Zr_2](Ga_3)O_{12}$, lattice constants meas., 296-1400 K 3−11753
- $\{Ca_{2.5}Zr_{2.5}\}[Zr_2](Ga_3)O_{12}$, lattice constants meas., 296-1400 K 3−11753
- $\{Ga_3\}[SnSb](Fe_3)O_{12}$ magnetic fields, induced, diamagnetic tin atoms in antiferromagnetic garnets, Mossbauer effect 3−34270
- $\{GdCa_2\}[Sn_2](Fe_3)O_{12}$ magnetic fields, induced, diamagnetic tin atoms in antiferromagnetic garnets, Mossbauer effect 3−34270
- $\{Gd_3\}$ $[Gd_{0.03}Ga_{1.97}](Ga_3)O_{12}$, lattice constants meas. 296-1400 K, Czochralski grown crystal 3−11753
- $\{Na_2Ca\}[Zr_2](Ge_3)O_{12}$ lattice constants meas., 296-1400 K 3−11753
- $\{Y_{1.05}Ca_{1.95}\}Ti_{1.95}$-$Ga_{3.05}O_{12}$, 296-1400 K 3−11753
- $\{Y_3\}[In_{0.6}Ga_{1.4}](Ga_3)O_{12}$, 296-1400 K 3−11753
- $\{Y_3\}[Y_{0.505}Ga_{1.495}](Ga_3)O_{12}$, 296-1400 K, lattice constants meas. 3−11753
- $Al_2Mn_3(SiO_4)_3$ spessartite, obs. of rhombohedral mag. structure 3−21247
- $BaMg_2Y_2Ge_3O_{12}$, e.s.r. of Nd^{3+}, g-factor, mag. ion symmetry 3−2384
- $Be_{3-2x}Ca_{2x}Fe_{5-x}V_xO_{12}$ system, porosities hysteresis, resonance linewidths, mag. inhomogeneity effects 3−18342
- $Bi_{3-2x}Ca_{2x}Fe_{5-x}V_xO_{12}$, neutron diffraction obs. of structure 3−8369
- CAVBIG, self interaction of finite amplitude magnetoelastic waves 3−39035
- $Ca_3Cr_2(GeO_4)_3$, mag. struct., neutron diffr. obs. 3−24569
- $Ca_3Fe_2(GeO_4)_3$, mag. struct., neutron diffr. obs. 3−24569
- $Ca_3Fe_2Si_3O_{12}$, andranite magnetic structure, indirect exchange interaction 3−34137
- $Ca_{2-2x}Na_{1\|x}Eu_xMg_2V_3O_{12}$, Eu^{3+} fluoresc., energy levels, point symmetry *(French)* 3−18480
- $Ca_{2-2x}Na_{1\|x}Eu_xMg_2V_3O_{12}$, fluoresc. of Eu^{3+}, temp. and conc. depend. *(French)* 3−21460
- $Ca_3Sn_3Ga_2O_{12}$, lattice constants meas., 296-1400 K 3−11753
- $Dy_3Ga_5O_{12}$, ceramic, influence of initial comp. and firing temp. in prep. *(Russian)* 3−15746
- Eu-Y-Ga-Fe, dynamics of magnetic bubble domain arrays 3−36765
- $EuEr_2Ga_{0.7}Fe_{4.3}O_{12}$ epitaxial film, for bubble domains, variation of magnetiz., Curie temp., and Ga/Fe ratio with growth temp. 3−34157
- $EuEr_2Ga_xFe_{5-x}O_{12}$, $Eu_xEr_{3-x}Ga_{0.7}Fe_{4.3}O_{12}$ epitaxial films, for bubble domains, thermal expansion of lattice parameters 3−34158
- $Eu_2ErX_{0.7}Fe_{4.3}O_{12}$, (X = Al,Ga), refractive index dispersion meas. rel. to film thickness determ. 3−27481
- $Eu_{2.2}Gd_{0.8}Al_{0.6}Fe_{4.4}O_{12}$, growth induced uniaxial anisotropy 3−2305
- $(EuY)_3(GaFe)_5O_{12}$, liquid phase epitaxial growth by tipping process 3−12278
- $Eu_{1.1}Yb_{1.9}Fe_5O_{12}$, garnet film, LPE growth by isothermal dipping with axial rotation 3−30945
- $(Fe, Mg)_3Al_2(SiO_4)_3$, hyperfine interactions of ^{27}Al and ^{29}Si, quadrupole coupling const., paramag. shift 3−8482
- Fe, equatorial Kerr effect, rare earth sublattice effects *(Russian)* 3−12124
- Fe, magneto-optic light modulation at 1.064 μm 3−36856
- GaGd, lattice parameters in faceted regions, X-ray double cryst. analysis 3−1609
- Gd-Ca garnet, growth by Czochralski method, perfect cryst. prod. *(German)* 3−5272
- Gd-Ga, dislocation spirals mechanism for formation 3−20751
- Gd-Ga, melt grown garnet, X-ray topographic anal. of dislocations and growth bands 3−30946
- Gd-Ga garnet substrate, chem. etching 3−8029
- $Gd_{3-x}Ca_xFe_{5-x}Sn_xO_{12}$ ferrite-garnets, temp. dependence of EMR and FMR linewidths *(Russian)* 3−36795
- GdFe, anomalous u.s. attenuation near compensation temp. 3−2275
- GdGa, macroscopic strain in facetted regions 3−33493
- $Gd_3Ga_5O_{12}$, ceramic, influence of initial comp. and firing temp. in prep. *(Russian)* 3−15746
- $Gd_3Ga_5O_{12}$, computer controlled Czochralski growth 3−12290
- $Gd_3Ga_5O_{12}$, elastic and thermoelastic constants *(German)* 3−7816
- $Gd_3Ga_5O_{12}$ single cryst. dislocation-free growth 3−36989
- $Gd_{2.3}Tb_{0.7}Fe_5O_{12}$, refractive index dispersion meas. rel. to film thickness determ. 3−27481
- $Gd_{2.3}Tb_{0.7}Ge_5O_{12}$ single cryst. growth by grain growth technique 3−21526
- $(GdY)_3(GaFe)_5O_{12}$, liquid phase epitaxial growth by tipping process 3−12278
- $(GdYYb)_3(GaFe)_5O_{12}$, liquid phase epitaxial growth by tipping process 3−12278
- $H_{1.25}Ho_{0.1}Er_{0.55}Tm_{0.5}Yb_{0.6}Al_5O_{12}$ film on $Y_3Al_5O_{12}$, coherent emission 3−736
- Ho:YAG laser, sensitising ions for lamp-pumped rods 3−19616
- $LaGaO_3$, ceramic, influence of initial comp. and firing temp. in prep. *(Russian)* 3−15746
- $Lu_2EuMFe_4O_{1m}$(M = Al or Ga), growth-induced mag. anisotropy of epitaxial films 3−21259
- $Mn_3Al_2(GeO_4)_3$, mag. struct., neutron diffr. obs. 3−24569
- $Mn_3Al_2Ge_3O_{12}$, antiferromag., mag. struct., neutron diffr. obs. *(French)* 3−21248
- $Mn_3Cr_2Ge_3O_{12}$, ferrimagnetic props., intrasublattice exchange interactions obs. *(Russian)* 3−2266

garnets continued
ND:YAG, self driven laser producing 1 nsec bandwidth limited pulses 3−29093
ND:YAlG laser, stabilised mode locked, using electronic feedback, construction, performance 3−6484
$NaCa_2Co_2V_3O_{12}$, mag. and atomic struct., Co spin state *(Russian)* 3−12025
$NaCa_2Co_2V_3O_{12}$, mag. ordering in octahedral lattice *(Russian)* 3−12024
$NaCa_2Ni(Co)_2V_3O_{12}$, absorpt. spectra obs. of $Ni^{2+}(Co^{2+})$ions, crystal field theory 3−21434
$NaCa_2Ni_2V_3O_{12}$ mag. ordering in octahedral lattice *(Russian)* 3−12024
Nd:YALO, oscill. at 0.930 μm at 300K, end pumped with Xe laser 3−6486
Nd^{3+}: YAG laser, plane mirror, self sustaining modes *(Russian)* 3−13738
Nd^{3+}:YAG, high-power laser with explosion-type lamp 3−22911
Nd^{3+}:YAG, laser oscillation, megawatt power at 1.318μ 3−16851
(Pr^{-r})Ga garnets with R=small rare earths on two crystallographic sites 3−7689
TAG, spin-lattice relaxation of ^{27}Al 3−39053
TbAl, Tb^{3+} fundamental multiplet cryst. field splitting 3−27342
TbAl antiferromag. garnet, molecular field approx. of two-singlet model for metamag. transition 3−27341
$Tm_3Ga_5O_{12}$, vibro-electronic Raman effect of Tm^{3+} 3−30809
Y-Al, zero field splitting of ground state 3−36787
Y-Eu, epitaxial film, magnet domain wall velocity 3−36734
YAG, in-grown dislocations, obs. by etching 3−24118
YAG, rare earth activated, recomb. luminesc., thermolum. and photolum. obs. 3−21480
YAG large crystals, laser quality, commercial growth, Czochralski process 3−12288
YAG laser, internal modulation techniques for high data rate communications 3−35695
YAG laser cryst., transient absorpt., detection using combined laser 3−29091
YAG:Ce^{3+} and its solid solutions, cathodolum. 3−30883
YAG:Cr^{3+}, lasing parameters 3−37970
YAG:Nd, Li, laser crystal, absorpt. and luminesc. props. with doping 3−19617
YAG:Nd, obs. of inclusions and dislocations using transmission electron microscopy 3−36319
YAG:Nd, testing of the homogeneity of single crystals by means of cathodoluminescence *(German)* 3−7789
YAG:Nd laser, longitudinal mode selection by intracavity mode selecting resonator 3−4102
YAG:Nd solid state laser, diode pumped, slope efficiency and threshold 3−16852
YAG:Nd^{3+}, growth from flux, site selectivity 3−11560
YAG:Nd^{3+}, Monte Carlo method for solving excitation transfer 3−34412
YAG:Nd^{3+} film, epitaxial growth and lasing props. 3−29094
YAG:Nd^{3+} Q-switched laser, pumping $LiNbO_3$ low Q parametric oscillator 3−754
$Y_3Al_5O_{12}$:Er resonance phonon scattering at average and high temps. 3−1767
$Y_3Al_5O_{12}$-Nd^{3+} electron-phonon interactions, point model of crystal field, Hamiltonians, shift and broadening of phononless lines 3−36384
$Y_{3-2x}Ca_{2x}Fe_{5-x}V_xO_{12}$ system, porosities hysteresis, resonance linewidths, mag. inhomogeneity effects 3−18342
$Y_{3-x}Ce_xFe_5O_{12}$, temp. depend. of magnetostriction, ferromag. reson. study *(Russian)* 3−12046
$Y_{2.4}Eu_{0.6}Ga_{1.2}Fe_{3.8}O_{12}$, epitaxial garnet film, growth-induced mag. anisotropy, annealing effects 3−30640
$Y_2EuMFe_4O_{12}$ (M=Al or Ga), growth-induced mag. anisotropy of epitaxial films 3−21259
$Y_3Fe_4GaO_{12}$, 296-1400 K 3−11753
$Y_3Fe_{5-x}Ga_xO_{12}$, epitaxial garnet film, growth by chemical vapour deposition 3−12248
$Y_3Fe_{5-x}Ga_xO_{12}$, growth of single crysts. from liq. melt soln. *(German)* 3−5273
$Y_3Fe_{5-x}Ga_xO_{12}$, high pressure effect on ferromag. resonance line width rel. to dislocations 3−5138
$Y_3Fe_{5-x}Ga_xO_{12}$ film, growth by liq. phase epitaxy *(German)* 3−5274
$Y_3Fe_5O_{12}$ Cotton-Mouton effect, birefringence, internal stress effects, anisotropy 3−39128
$Y_3(GaFe)_5O_{12}$, liquid phase epitaxial growth by tipping process 3−12278
$Y_3Ga_5O_{12}$, ceramic, influence of initial comp. and firing temp. in prep. *(Russian)* 3−15746
$Y_{3-x}Gd_xFe_5O_{12}$ temp. depend. control of Faraday rotation by Gd substitution 3−8557
YIG, cryst. growth from soln. in PbO-PbF_2 *(Russian)* 3−30942
YIG, Faraday rotation, i.r. intensity modulator application 3−5985
YIG, ferrimag. resonance and i.r. obs. of mag. domains, effect of crystal imperfections 3−27379
YIG, ferroacoustic interaction with Rayleigh surface waves 3−24596
YIG, ferromag. reson. and e.s.r. linewidths and g-factor, temp. depend. *(Russian)* 3−8454
YIG, Ga substituted, nearly compensated, compensation magnetic domain walls 3−36732
YIG, intrinsic e.m. radiation in presence of domain struct. 3−34217
YIG, laser beam interact. with spin and magnetoelastic waves 3−36859
YIG, mag. anisotropy depend. on pressure and temp. 3−5114
YIG, magnetization near Curie point 3−38980
YIG, magneto-optical effects, light modulation and transducer applications *(German)* 3−12121
YIG, nonlinear ferromag. reson., domain struct., instability *(Russian)* 3−8453
YIG, parallel spin-wave pumping, theory and expt. 3−34143
YIG, polycryst. ceramic, reactive hot pressing 3−31123
YIG, relation between magneto-refl. spectra and Faraday effect *(French)* 3−12126
YIG, self interaction of finite amplitude magnetoelastic waves 3−39035

garnets continued
YIG, spin waves excited by parallel pumping, instability threshold, laser radiation effects 3−34141
YIG, top-seeded soln. growth using borate fluxes 3−15637
YIG, vapour growth by chem. transport 3−24791
YIG epitaxial film, ferromag. resonance, lattice mismatch effects 3−30700
YIG film, in in-plane mag. field, orientation of stripe domains 3−27386
YIG film, on grounded dielec. substrate, surface wave group delay time 3−8408
YIG film, phonon generation by ferromag. resonance 3−36794
YIG film on GdGaG substrate, heteroepitaxial growth by hydrothermal synthesis 3−1922
YIG substrate, dielectrically induced surface wave 3−27471
YIG thin films, r.f. sputtering from powder mixture of Fe_2O_3 and Y_2O_3, magnetic properties 3−8401
YIG:Al epitaxial film, chemical vapour deposition for bubble domain devices 3−33746
YIG:Cu, octahedrally coordinated Cu^{2+} ions contrib. to magnetocryst. anisotropy 3−2304
YIG:Ga, L.P.E. growth, effect of substituting Gd(Sm)(La) for Y 3−1924
YIG:Gd,Ga uniaxial films, epitaxial growth by r.f. sputtering 3−12237
YIG:Ge substituted, anisotropy and magnetostriction, ferromag. resonance obs. 3−5136
YIG:Pb substituted, anomalous Faraday rotation 3−34331
YIG:Pr^{3+}, ferromagnetic resonance, angular maxima of ΔH splitting under pressure *(Russian)* 3−2399
YIG:Si, dichroism and torque data, analysis using small polaron theory 3−24398
YIG:Si, mag. anisotropy i.r. induced changes 3−30644
YIG:$Si^{4+}(Ge^{4+})(Ca^{2+})$, mag. after-effect, electronic hopping processes 3−24591
YIG:Yb, ferromag. resonance instability due to transverse resonance relax. 3−27421
YiG:Si,Ca,Sr photoconductivity 3−8229
gas *see gases*
gas analysis *see chemical analysis*
gas breakdown *see electric breakdown of gases*
gas bubbles *see bubbles*
gas discharge lamps *see discharge lamps*
gas-discharge tubes
see also ion sources; thyratrons
Al hollow cathode discharge tube, use with vacuum grating spectrograph in u.v. region *(German)* 3−3779
flash lamp, high temperature with symmetrical conductors *(Russian)* 3−9946
ion laser tube with internal gas return bores, starting technique 3−6471
noise generator loaded with helical coaxial line, theory 3−26902
with turbulent flow, lifetime of plasma fluctuations 3−7527
Ne-Na discharges, transport processes study by Eindhoven AVF cyclotron, Netherlands 3−20668
gas discharges *see discharges (electric)*
gas dynamics *see aerodynamics*
gas ionisation *see ionisation of gases*
gas lasers
airborne dust particle size measurement 3−5537
capillary tubes, moving striations analysis *(Japanese)* 3−35685
characteristics, dependence on parameters of intracavity absorber 3−719
chemical, atom-diatomic mol. reactions suitable for laser action 3−10495
chemical, diagnostics, appl. of F_2, NO, ONF Raman cross sections and depolarisation ratios meas. 3−36018
chemical, mixing layers nonuniform index of refr. effects 3−10515
chemical, multilevel short pulsed, model, diagnostic relations, performance limits 3−10492
chemical, numerical formulation for constant-gain calcs. 3−22877
chemical, pulsed, initiation by laser photolysis 3−10500
chemical, reaction study using microwave resonator 3−26239
chemical, survey of current research 3−29078
chemical, visible wavelength, based on metal oxides and nitrides chemilum. 3−10518
chemical and mol., vibr. energy near reson. energy transfer theory 3−10482
chemical and mol. diatomic mols., energy transfer is vibr. inelastic collisions 3−11318
chemical and molecular, conference, St. Louis, Mo., USA, May (1972) 3−10465
chemical diffusion type, flame sheet anal. of coupled collisional and radiative relaxation 3−10463
chemical laser device bibliography 3−10481
chemical lasers, bibliography 3−19594
chemical lasers, high pressure, kinetics *(Russian)* 3−32557
chemical lasers, nozzle design accounting for viscous effects and chem. nonequilib. 3−9962
cold cathode arrangement, patent 3−6475
coupling with nonlinea absorber 3−19604
c.w. water vapour, 118 μm, gain and freq. characteristics 3−6479
cyanide c.w. laser with CH_4-N_2-He working gas mixture, operating conditions 3−13733
diatomic gasdynamic lasers, vibr. relax. in supersonic expansion, numerical model 3−10504
1.1difluorethylene, submillimeter-band gas laser pumped by CO_2 laser 3−22880
double discharge, high power, TEA device, amplification process anal. 3−728
electro-ionization and pumping of highly compressed gases for generating laser pulses and freq. 3−6464
electro-optical frequency modulation 3−720
emission, J=0 reversible transition to J=1, polarisation props. 3−32545
energy level inversion in gases caused by shock waves *(Italian)* 3−10461
explosive gas or gas mixture, electron beam generator, patent 3−6476

gas lasers continued
frequency stabilization in the visible and infrared *(Russian)* 3−6467
gasdynamic, advances in last 2 years 3−6463
high-powered molecular, review *(French)* 3−37961
high-stability, based on nonlinear absorption, electronic automatic frequency stabilisation system *(Russian)* 3−16448
hollow-waveguide, mode losses, theory 3−10553
internal frequency modulation, by variation of medium refractive index 3−26225
iodine perfluoralky photodissociative, selective pumping effect *(Russian)* 3−10540
ion laser, special cathode design for pulsed and CW operation 3−13338
ion laser tube with internal gas return bores, starting technique 3−6471
i.r. spectrometers, spread function measurement *(Russian)* 3−9945
Lymann transition in u.v. laser *(Russian)* 3−723
metal atom oxidation lasers, i.r. action 3−31247
methane, 3.39 μm molecular transition used in laser stabilisation, accurate freq. 3−22872
methane, 3.39 μm radiation wavelength meas. 3−29076
methane, wavelength of 3.39 μm laser saturated absorpt. line 3−22873
methylamine, submillimeter-band gas laser pumped by CO_2 laser 3−22880
molecular, in far i.r., review 3−10475
molecular, time history of power pulses 3−722
molecular laser-emissions in the i.r., rotational and vibrational-rotational transitions 3−11267
molecular vapours, investigation of electrically pulsed discharges, search for laser media with high quantum efficiency 3−726
operation, weak perturbations effect on laser with uniform working transition line 3−16842
optically pumped, cavity detuning and multimode operation 3−4097
optically pumped, theory 3−22878
passive Q-switching and mode locking, patent 3−32558
photoionization generation of laser plasmas 3−4095
plasma electrons quick heating by ultrashort laser pulses, far vacuum u.v. emission 3−16841
plasma-beam discharge laser 3−32555
pumping, combined action of external ionization source and applied elec. field 3−26229
Q-switching, theoretical aspects *(Rumanian)* 3−22867
rare gas, electron beam excitation mechanism 3−10521
rare gas pulsed ion laser, milti-mode operation *(German)* 3−29073
ring laser, radiation fluctuations, mag. field effect 3−32551
saturated atomic resonance fluorescence theory 3−14297
saturated resonance fluorescence, non quenching collisions influence 3−14298
spatial-angular characteristics of emission, holographic control method *(Russian)* 3−13339
stability condition for intense two-mode region *(French)* 3−37957
stimulated emission at low and i.r. frequencies, intensity fluctuations *(Russian)* 3−10539
theory of interaction between standing wave and gas *(Russian)* 3−10541
third order Lamb theory, corrections and appl. to mode locking 3−16844
threshold behaviour, gas press. depend. 3−37960
transfer chem. laser, review 3−10469
travelling wave amplifier, effect of spontaneous emission on the operation 3−32549
tuning, using intracavity tilted etalon with piezoelec. drive *(German)* 3−32543
Van Vleck-Weisskopf gas, excitation by reson. μ-wave pulse, response calc. 3−14358
velocity distrib. function of fast inelastic collision processes 3−10487
vibrational energy distribs., obs. by equal-gain and zero-gain temp. techniques 3−10468
vinyl cyanide, submillimeter-band gas laser pumped by CO_2 laser 3−22880
water vapour, Lamb-dip stabilized, 28μ, absolute freq. meas. 3−35688
AlF exploding-wire giving 12.5 to 13.5 μ pulses 3−19597
Ar, c.w., pumping Ba_2NaNbO_{15} doubly resonant parametric oscillator 3−755
Ar, effect of laser field on contours of lines amplified by neighbouring transitions *(Russian)* 3−22889
Ar arc, wall-stabilised low-pressure, radial gain profile of 4880 Å ionic laser line and distrib. of charge carriers *(German)* 3−23951
Ar continuous wave, intensity stabilizing circuit 3−9964
Ar ion, output power saturation with discharge current 3−32553
Ar ion laser, pulsed, multistep electron collision excitation mechanism, coherence length *(German)* 3−16839
Ar ion laser modification for gas phase Raman scatt. enhancement 3−5974
Ar neutral, line competition, transition uncertainties 3−4087
Ar-ion study of transitions from obs. of spectral intensities in Ar arc discharge *(Dutch)* 3−30030
Ar-Kr mixed ion, cw, current depend. of spontaneous emission 3−32539
Ar^+, mutual influence of two laser transitions at 4880 and 5145 Å *(German)* 3−37962
Ar^+, with berrylia discharge channel *(Russian)* 3−13727
Ar^+ cw laser, excitations of laser states 3−4096
Ar^+ ion laser discharge at high current 3−16834
Au, impulse lasers, expt. obs. *(Russian)* 3−35690
C, dissociatively prod., pulsed laser emission in elec. discharge 3−10520
C IV, vacuum u.v. laser emission 3−37954
CN violet and red band excitation by metastable Ar and Xe reactions with CN containing cpds. 3−31251
CO, CO_2, electrochemical organic molecule oxidation, directly excited CW 3−16831
CO, CW chem. laser, single line operation 3−10507
CO, c.w. laser emission from flowing gas HCHO near i.r. laser 3−35687
CO, c.w. power from $CS_2/O_2/N_2O$ flames 3−32534
CO, chem., based on a CS-O reaction, characts. 3−10512

gas lasers continued
CO, chem., based on flash initiated reaction O_3-XCN, X=Cl, Br, I, CN 3−10523
CO, chemical, using reaction $O + CSe \rightarrow CO^* + Se$ 3−6457
CO, detection of NO small concentrations by Zeeman effect 3−13308
CO, fast flow, construction, characts. 3−10510
CO, Lamb dip, vibrational-rotational lines 3−16828
CO, meas. of density and collision frequency of electrons in plasma using resonator method 3−16845
CO, model in pulsed and CW operation 3−10494
CO, N_2O detection, amplified absorption 3−29129
CO, operation kinetics calc., vibr. distrib. function 3−10474
CO, output characts. rel. to electronegative gaseous additions 3−10509
CO, P-branch i.r. transitions in C_2H_2-O_2 flame, optical gain 3−10473
CO, pumped, study of CO dissociation by i.r. absorption 3−16899
CO, radiation absorpt. by water vapour 3−19627
CO, supersonic flow, elec. excited, mol. energy transfer processes 3−10511
CO, V-V energy transfer rate from CO(v=2) using tunable parametric oscillator excitation 3−38314
CO, VT relax., meas. by vibr. pumping technique 3−10484
CO, vibr. energy transfer, relax. rates 3−10466
CO, vibr. energy transfer cross sections calc. without Born approx. 3−11323
CO, vibr. excited relative populations in pulse discharged CS_2-O_2-He mixtures 3−10496
CO, vibr. relax. at 85 ± 8 K 3−11319
CO, vibr. relax. in supersonic expansion, numerical model 3−10504
CO, vibrational energy exchange *(Russian)* 3−23632
CO CW, chem., prod. in N_2-O_2-CS_2 fast flow system 3−10472
CO chem., kinetic theory, computer model 3−10491
CO intracavity breakdown threshold calc. 3−10477
CO laser, resonant i.r. absorption of laser light by magnetically tuned NO, pressure broadening of spectral lines 3−14388
CO/N_2 molecular system, energy-transfer processes, modelling 3−4091
CO-CO_2, vibr.-vibr. energy transfer rate, 175-350 K 3−11320
CO-mixing laser, electric discharge, N_2 vibrationally excited, c.w. output 3−711
CO-N_2, radiative gain of CO vibr.-rotation transitions 3−6470
CO_2, 10.6μm at 150W 3−32556
CO_2, 300-J multigigawatt, transverse electric discharge 3−16829
CO_2, 9.33 and 10.18 μm molecular transitions used in laser stabilisation, accurate freqs. 3−22872
CO_2, amplifier, electron beam controlled, performance 3−10478
CO_2, asymmetric stretch mode vibr. temp. rel. to laser action 3−16837
CO_2, c.w. laser emission from flowing gas HCHO near i.r. laser 3−35687
CO_2, chem. laser based on CO-N_2O reaction catalyzed with Na 3−10514
CO_2, double discharge TEA, powerful nanosecond pulses by stable passive mode-locking 3−26219
CO_2, effect of proton beam on generation power *(Russian)* 3−6472
CO_2, efficient elec. laser using preionization by u.v. radiation 3−16826
CO_2, electron beam pumped amplifier, nanosecond pulse amplification 3−26217
CO_2, evaporation of optical materials, pulsating conditions *(Russian)* 3−763
CO_2, freq. stabilization 3−22884
CO_2, glow discharge, vibr. translation rates for $(10^{0}0)$ and $(00^{0}1)$ levels 3−36054
CO_2, helical TEA, performance characts. 3−712
CO_2, helical TEA laser 3−35689
CO_2, high pressure, powered by slow compression heater *(French)* 3−26228
CO_2, high prsss. pulsed chem. transfer laser, props. 3−10470
CO_2, high-power elec. discharge, closed cycle performance 3−715
CO_2, high-press. c.w. waveguide, mode locking 3−714
CO_2, modulation of c.w. He-Ne laser, using ultrafast Kerr effect in CS_2 3−32581
CO_2, optical pumping with blackbody radiation *(Russian)* 3−6468
CO_2, population inversion, role of CO 3−721
CO_2, pulsed, kinetics *(German)* 3−6459
CO_2, radial mode, performance 3−26221
CO_2, relax. rates of lower laser levels 3−37952
CO_2, reliable high efficiency atm. press. laser 3−16843
CO_2, TEA, dynamical processes, giant pulse form. 3−718
CO_2, TEA, high press., gain and power, theory rel. to expt. 3−10476
CO_2, TEA, photoinitiated, photosustained by u.v. irradiation of gases and cathode 3−710
CO_2, TEA, resistive electrode discharge system 3−25781
CO_2, TEA, small signal gain distrib. 3−717
CO_2, TEA, translational temp. and vibr. temp. from gain spectral behaviour 3−19602
CO_2, TEA, triggering characs., output optimisation 3−32541
CO_2, TEA double discharge grid amplifier, performance characs. 3−26220
CO_2, transition freqs., standard deviations 3−10537
CO_2, transversely sustained, photoinitiated, props. rel. to discharge parameters 3−22869
CO_2, unstable confocal resonator modes spatial props. 3−4086
CO_2, vibr.-vibr. energy transfer of ν_3 mode 3−33161
CO_2, volume excited TEA, operational characteristics 3−4092
CO_2, waveguide laser, gain and saturation intensity meas. 3−26222
CO_2, with varying Q-factor, population inversion and radiation density *(Russian)* 3−29081
CO_2 atmospheric pressure pulsed laser with semiconducting plastic electrodes 3−10464
CO_2 chem., based on H-O_3 and OH-CO pumping reactions 3−10525
CO_2 chemical pumping, lasing mechanism, discharge and rapid expansion pumping, high pressure pulsed chemical laser 3−19600
CO_2 discharge, gain correl. with sidelight and plasma impedance props. 3−13729

gas lasers continued

CO_2 electric-discharge convection lasers, unstable resonators 3−16883
CO_2 electron beam controlled, current, voltage, gain meas. 3−10519
CO_2 frequency stabilization using second laser, rapid sampling method *(French)* 3−32096
CO_2 gas laser, vibration relaxation meas. *(Russian)* 3−4515
CO_2 intracavity breakdown threshold calc. 3−10477
CO_2 laser, pulse amplitude modulation in electro-optic thin film waveguide 3−28581
CO_2 laser, pulsed discharge and electron beam controlled, performance comparison 3−35686
CO_2 laser amplifier, cold-cathode electron-beam controlled 3−716
CO_2 laser beam, effect on energy levels of low pressure hydrogen discharge 3−14290
CO_2 laser discharge, vibr.-vibr. energy transfer 3−6458
CO_2 laser Michelson interferometer, phase relations, obs. 3−13318
CO_2 laser oscillator with unstable resonator cavity, performance 3−26218
CO_2 laser pulse shaping with saturable gas absorbers 3−35714
CO_2 lasers, calorimeter for energy output measurement 3−35428
CO_2 lower laser level, relax. of excess populations 3−1247
CO_2 mixing into supersonic N_2, continuous lasing action 3−22882
CO_2 output power rel. to cavity length 3−4085
CO_2 stability and output rel. to nitrogen oxide impurities 3−10499
CO_2 TEA, optically pumped by NH_3 laser, submillimeter laser action 3−13731
CO_2 TEA laser, output-power pulse shape, theory 3−16835
CO_2 transverse discharge pulsed chemical transfer laser 3−32533
CO_2 waveguide laser operated in flowing gas configuration, characteristics 3−727
CO_2 wavelength and velocity of light meas. 3−9923
CO_2:N_2:He c.w. waveguide laser, using B + O capillary tube 3−13732
CO_2-He, similarity law, disturbing electrodes effect 3−13730
CO_2-N_2, model 3−10506
CO_2-N_2, pulse amplifier, idealized rate eqn. analysis 3−10505
CO_2-N_2 mixtures, electrodeless induction high-freq. discharge as pumping source 3−32550
CO_2-N_2-He pumped by electrically heated plasma, laser oscillations 3−19596
CO_2-N_2-He system, amplification rel. to temperature 3−19605
CO_2-N_2(He) (N_2-He) plasmas, stationary state, small signal gain coeffs. for rot.-vibr. transitions *(French)* 3−7223
CO_2-O_3-D_2, 10.6 μ, vibr. energy transfer from OD to CO_2 3−19603
$CO_2{}^+N_2{}^+$He mixture expanding in supersonic jet, light amplification factor 3−19607
COS, photodissociated, lasing due to S_2 *(Russian)* 3−4458
CS_2-O_2 chemical flow laser, CW, operation, flash photolysis 3−10508
$CS_2 + O_2$ chemical laser, reaction mechanisms 3−16836
Ca-Xe system, population inversion calc. using near-reson. charge exchange as pumping mechanism 3−37953
Cd lasing lines and possible appls. 3−22885
Cd-He cataphoresis-laser, determ. of plasma charged-particle densities and electron temp. 3−16846
Cl, dissociatively prod., pulsed laser emission in elec. discharge 3−10520
Cl-HBr, vibr. rot. state populations, output spectra 3−10479
Cl-HI, vibr.-rot. state populations, output spectra 3−10479
ClN_3, chem. laser, excited N_2 source 3−10522
Co_2, vibr. relaxation mechanism 3−19606
Cu, impulse lasers, expt. obs. *(Russian)* 3−35690
Cu vapour, supersonic elec. discharge 3−10462
DF, chem. CW laser, performance in unstable cylindrical confocal oscillators 3−10490
DF, diagnostic techniques, cavity characts. 3−9961
DF, vibr. relax. rates in presence of deactivating gases 3−11316
DF, vibr. relax. times calc. 3−11315
DF-CO_2, chem. transfer, efficiency rel. to gas flow rates and static press. 3−10503
DF-CO_2 pulsed chem. transfer laser, kinetic model, computer simulation, review 3−10471
F, dissociatively prod., pulsed laser emission in elec. discharge 3−10520
F-CH_4, vibr.-rot. state populations, output spectra 3−10479
F-H_2, vibr.-rot. state populations, output spectra 3−10479
F-HBr, vibr.-rot. state populations, output spectra 3−10479
F-HCl, vibr.-rot. state populations, output spectra 3−10479
F-HI, chem. laser, obs. of laser reaction by equal gain technique 3−10498
F-HI, vibr.-rot. state populations, output spectra 3−10479
F_2-H_2 excitation by relativistic electron beam, energy characts. *(Russian)* 3−4093
H halide pulsed lasers, H atom sources, performance optimization 3−10501
H_2, laser power densities for Lyman and Werner bands 3−4082
H_2, ultrashort laser pulses from vibr.-rot. transitions *(Russian)* 3−10536
H_2 electron beam stabilized discharge, superfluorescence due to HF quenching 3−19599
H_2 VUV, four level, electron beam excitation 3−22883
H_2-ClF_3, possible chain-branching chem. -laser, comment on results 3−22875
H_2-ClF_3, possible chain-branching chem. laser, reply to comments on results 3−22876
H_2-F_2, emission rel. to H_2 press. 3−10493
H_2-F_2, photochem., submicrosecond pulses, output energy and pulsewidth rel. to gas press. 3−4084
$H_2 + F_2$ pulsed laser, H_2 pressure effect on stimulated emission 3−6460
HCHO, flowing gas near i.r. laser producing CO(CO_2) c.w. laser emission 3−35687
HCl, vibr. excitation in NH-vinyl chloride reaction, deactivation 3−11324
HCl, vibr.-vibr. energy transfer with tunable opt. parametric oscillator excitation 3−36055
HF, chem., based on F atom reaction with saturated and unsaturated hydrocarbons, energy partitioning 3−10524
HF, chem., based on H_2-SF_6 reaction, chem. efficiency 3−10533

gas lasers continued

HF, chem., based on $NF_3{}^+$ H donor transverse discharge, performance 3−10527
HF, chem., based on O(^{1}D) atom reaction with chlorofluoromethanes 3−10526
HF, chem., CW performance, chain vs. cold reaction 3−10535
HF, chem., formed in H_2-F_2-He mixtures, performance and enhanced initiation 3−10529
HF, chem., laser action above second explosion limit of F_2-H_2(D_2) mixtures 3−10531
HF, chem., pulsed, performance, effect of CO_2 laser irrad. 3−10502
HF, chem., TEM_{00} short pulse oscillator, construction and performance 3−10530
HF, chem. CW laser, performance in unstable cylindrical confocal oscillators 3−10490
HF, chem. laser, based on NF_3-H_2 reaction energy output press. depend. 3−10532
HF, chemical, time sequencing rel. to energy content under different cavity configs. 3−22871
HF, chemical laser, high repetition rate 3−26224
HF, DF, vibr. relax. times, quasiclassical trajectory calcs. 3−38315
HF, diagnostic techniques, cavity characts. 3−9961
HF, electrically initiated SF_6-ethane mixtures, performance 3−26223
HF, optically pumped,laser oscill. and anisotropic gain in $1 \to 0$ vibr. band 3−713
HF, vibr. deactivation in H_2-F_2 chain reaction 3−10485
HF, vibr. energy distrib., formed in methylene methyl fluoride, tandem laser obs. 3−11325
HF, vibr. energy transfer, relax. rates 3−10466
HF, vibr. excitation, formed by elimination from chem. activated ethyl fluorides 3−11326
HF, vibr. relax., meas. at intermediate temps. 3−10483
HF, vibr. relax. rate, 295-730K, effect of SF_6, N_2 and F_2 diluents 3−10467
HF, vibr. relax. rates in presence of deactivating gases 3−11316
HF, vibr. relax. times calc. 3−11315
HF, vibr.-vibr. transfer time, apparent decay time 3−10488
HF (v=2) deactivation rate, use of direct overtone excitation 3−20172
HF action rel. to electrode structs. 3−10480
HF CW laser, diffr. limited performance using edge coupled nonfocal unstable resonator 3−32577
HF CW laser, zero power gain meas. using pulsed probe laser 3−32537
HF chem. laser, 10 J, operating parameters 3−35684
HF chem. pumped by NF_3-H cpd. reaction, model, kinetic transfer rates 3−10528
HF collisional deactivation processes, laser amplifier meas. 3−10513
HF diffusion type chemical laser, numerical study 3−37955
HF gain, relax., spatial and temporal depends. 3−10486
HF gas, prod. of Dicke superradiant pulse with ringing 3−22886
HF laser, pumped by H_2-F_2 chain reaction, cavity chem. mechanism interactions 3−10489
HF product of abstraction reaction between F atoms and org. cpds., energy partitioning and i.r. chemilum. 3−31253
HF product of abstraction reaction between F atoms and hydrides, energy partitioning and i.r. chemilum. 3−31254
HF-DF, CW combustion/mixing laser, construction., props. 3−10534
HF-H_2, vibr. activated HF deactivation in reaction flow tube 3−11322
HI, chem., from $H + I_2$ reactions, vibr. population inversion 3−29074
H_2O, discharge diagnostics by obs. of OH u.v. emission 3−10497
H_2O, gas temp. measurement in pulsed laser discharge, spectroscopic obs. 3−4090
H_2O, output, He addition effect, spectroscopic gas temp. obs. 3−16830
He-^{20}Ne laser with absorption cell, 0.63 μ line shift, line broadening *(Russian)* 3−7026
He-As, c.w. laser oscillation in As^+, charge transfer reaction 3−37959
He-CO_2, absorpt. coeffs. of emission by CO_2, NH_3 and water vapour *(Russian)* 3−6474
He-metal vapour, C.W. systems, hollow cathode device 3−22382
He-Ne, axial mode obs. using Fabry-Perot interferometer 3−190
He-Ne, based on nonlinear absorption, optical system *(Russian)* 3−16823
He-Ne, distance meas. applic. *(Japanese)* 3−213
He-Ne, frequency shift of Lamb dip minimum *(Russian)* 3−16824
He-Ne, high stability, based on nonlinear absorpt. at 0.63 μm, freq. stabilisation methods *(Russian)* 3−13725
He-Ne, influence of elastic collisions on intensity of natural fluctuations *(Russian)* 3−22888
He-Ne, mode selection at 0.63 μm *(Russian)* 3−13724
He-Ne, modulation using ultrafast Kerr effect in CS_2, 10.6 μ 3−32581
He-Ne, nonlinear absorbing cell in resonator for measuring electron concentrations in plasma *(Russian)* 3−7567
He-Ne, operating in TEM_{00} axial mode, optimum lasing conditions *(Russian)* 3−6465
He-Ne, operation of pressed cathodes 3−22389
He-Ne, output power depend. on discharge current, gas pressure and tube radius 3−6461
He-Ne, propagation through atmosphere, beam spread 3−10576
He-Ne, relax. oscillations, range of existence, gas press. effect *(Russian)* 3−4094
He-Ne, saturation parameter depend. on discharge current 3−6462
He-Ne, simple single freq. for practical uses 3−32538
He-Ne, single freq., stabilisation *(Russian)* 3−13726
He-Ne, single-frequency, mode selection using Michelson interferometer, continuous frequency tuning with Doppler line width limits *(Russian)* 3−10556
He-Ne, transition processes at 0.63 μm *(Russian)* 3−10542
He-Ne, wavelength measurement *(French)* 3−9817
He-Ne, with metal internal wall surface, active element *(Russian)* 3−6466
He-Ne c.w., two-quanta absorption of 632.8 nm line by benzopyrene solid solution in PMMA 3−39181

gas lasers continued
He-Ne discharge, 3.39 μm Ne linewidth, mixture composition depend. 3−32546
He-Ne discharge, meas. of Ne 3.39μ transition decay rates using laser Faraday rotation 3−29079
He-Ne single freq., freq. fluctuations rel. to sound press. and freq., external vibrs. 3−4083
He-Ne visible gas laser design, r.f. excited 3−37958
He-Se, self-mode locking 3−22879
He-Se discharge, detection of small laser gains using dye laser assisted oscill. 3−32544
He-Se$^+$, positive column, plasma parameters in gas discharge 3−16833
He-Zn hollow cathode, single pass gain measurement *(Japanese)* 3−19608
He + Ne laser radiation analysis with spectrometer *(Russian)* 3−5942
Hf, H_2-F_2 reaction behind shocks, collisional relax. 3−11317
Hg vapour, characteristics and optimum working conditions *(Russian)* 3−29082
I, $^2P_{1/2}$-$^2P_{3/2}$ hyperfine struct. transition, induced emission spectra 3−32547
I, photodissoc. laser, $^2P_{1/2}$-$^2P_{3/2}$ transition, linewidth 3−32548
I photochemical laser, 1.2 GW 3−19598
I photodissociation laser, luminesc. of $^2P_{1/2}-{}^2P_{3/2}$ transition 3−32554
I_2, 5-ns, gigawatt power, construction and props. 3−10517
I_2, photochem. energy storage and transfer 3−10516
I_2 photodissociation type, emission line press. broadening, energy storage capacity increase 3−22870
K intense spontaneous violet emission due to coherent two photon excitation 3−19601
Kr II, molecular absorp. of three lines by $^{127}I_2$ *(German)* 3−36010
Kr-Hg gas mixture, possible u.v. laser *(German)* 3−725
Mg lasing lines and possible appls. 3−22885
Mn, impulse lasers, expt. obs. *(Russian)* 3−35690
N, dissociatively prod., pulsed laser emission in elec. discharge 3−10520
N_2, chem., ClN_3 source 3−10522
N_2, first positive system (2,0) band, pulsed oscill., new lines obs. 3−32552
N_2, high power, pulsed, for pumping dye laser 3−26226
N_2, pumping dye laser, coherent double freq. system *(Russian)* 3−26230
N_2, pumping dye laser, generation of tunable near i.r. 3−13735
N_2, VT relax., meas. by vibr. pumping technique 3−10484
N_2 design, operation, pump for dye laser 3−19595
N_2 electron beam stabilized discharge, superfluorescence due to HF quenching 3−19599
N_2 laser amplifier, gain measurements 3−6473
N_2 TEA u.v. laser with reduced spectra 3−22881
N_2 vibr. relax. in supersonic expansion, numerical model 3−10504
N_z pulsed, 3371 Angstroms, electric discharge pumping power supply system 3−22887
NCl chem., based on O(^{1}D) atom reaction with chlorofluoromethanes 3−10526
NH_3, optical pumping of CO_2 TEA laser, submillimeter laser action 3−13731
NO, vibr. energy transfer, relax. rates 3−10466
N_2O, optically pumped, laser action at 10.8μ 3−16825
N_2O frequency stabilizaton using second laser *(French)* 3−32096
Ne, with 350 psec pulse duration and subnanosecond jitter at 6143 Å 3−35683
Ne laser action, characteristics of $3s_2 \rightarrow 3p_1$ ($\lambda = 4218$ nm) 3−32536
Ne superradiance pulses, shape and duration *(Russian)* 3−724
Ne-He, spontaneous emission from lower laser level, double reson. 3−26227
Ne(I), optical coherence of 6328 Å laser transition, global dipole 3−13728
^{20}Ne-^{22}Ne, 3.39μm line, spectral contour meas. method 3−16840
O, 8446 Å, interactions among multiple lines 3−10538
O, 8446 Å, selective reabsorpt. leading to multiple oscillations 3−13734
O + CS_2 transverse flow laser, CO vibr. energy distrib., long-range force theory calc. 3−37956
O_2, Z-pinch discharge, laser oscill. of OV obs. 3−32540
OCS-He, i.r. lines due to OCS and C atom 3−4088
Pb, impulse lasers, expt. obs. *(Russian)* 3−35690
Rb, influence of buffer on efficiency of optical pump *(Russian)* 3−16827
S gaseous compounds, i.r. laser emission from discharges 3−22874
SF_6 + H_2 chemical laser, properties 3−29080
SO_2, far i.r. transition excitation mechanism 3−16838
Xe, 3.99 μm transition, 128, 126 and 124 isotope shifts *(French)* 3−6469
Xe, high gain, saturation power determ. 3−16832
Xe, high press., operating in u.v. 3−32542
Xe, ionic assignment of unidentified lines 3−29075
Xe, quasi-molecular, VUV fluorescence emission quenching 3−29077
Xe, TEA, output pulses time behaviour 3−4089
Xe-Ar phase-matched mixture, generation of 1182 Å radiation 3−32535
Xe-ion laser for repetitive pumping of dye laser 3−32560
Zn lasing lines and possible appls. 3−22885

gas permeability *see permeability*

gas technology, natural *see natural gas technology*

gas turbines
see also turbogenerators
cooled by air injection into flow paths 3−1379
cryogenic expansion, appl. to refrigeration plant delivering 10 kW at 25 K 3−5833
mixed flow impeller, diffusion losses due to negative velocity gradients in boundary layer 3−4582
surfaces temperature measurement, using wedge type resistance thermometer *(Russian)* 3−19172

gases
absorption in liquid film falling on sphere, gas absorption 3−4535

gases continued
absorption line and press. broadening coeffs., laser spectroscopy 3−19650
in carbonyl Ni, evolved gas analysis *(Russian)* 3−10197
combustion gases, thermal radiation 3−14419
composition meas. standard 3−22243
compressor, design description 3−28803
condensation, gases with elec. dipole moment, spontaneous polarization 3−20942
distribution function representation for homogeneous gas using maximum entropy principle *(Russian)* 3−26183
electron diffr. studies at high temps., photographic procedure 3−13457
electron self-trapped states, conduction band free-electron-like states 3−38772
flames, turbulent diffusion, influence of recirculation flows on length 3−21807
ideal, molar volume measurement *(French)* 3−9820
mathematical model to meas. gas props. with alpha particle gauges 3−335
mixtures, prep. and certifying, for gas analyser calibration 3−19371
molecular, Lamb dip centre, anomolous shift decrease *(Russian)* 3−14418
nonisothermal medium, total spectral absorptivity, black radiation, heat transfer 3−1325
partially ionized, elec. cond. and Hall coeff. in mag. field, theory *(Czech)* 3−4518
polyatomic, sound absorption, Greenspan rule for many internal degrees of freedom 3−7304
predictive eqns. in adsorption kinetics 3−33735
radiating grey, propag. of periodic disturbances, singular eigenfunction expansions 3−14425
radiative heating applicability of an approximate expression 3−17487
radioisotopic analyser, automatic for control of sulfur in gases *(Russian)* 3−10135
Raman spectra line intensity, influence of internal field effect *(German)* 3−2553
temperature measurement, wedge type thermometer transient behaviour *(Russian)* 3−19172

Gaussian noise *see random noise*

gegenschein *see zodiacal light*

Geiger counters
monitoring β contamination on floor 3−10066
resolving time measurement, using time to amplitude convertor 3−318
window, effective position 3−13422

Geiger Muller counters *see Geiger counters*

gelatin
see also gels
contact energy of gel formation, crit. shear stress 3−39397
gel, struct.-mech. props. rel. to benzene solubilisation and hydrophobic binding 3−34655
growth of alkaline earth orthophosphates in gelatin gel 3−24783
history of gelatin Ag halide emulsions 3−222
raster lenticules, imaging properties *(German)* 3−32105
rate of penetration by developing agents, OH^- and HCHO, dependent on pH, ionic strength and total alkalinity 3−2836
$CuSO_4$ doped gelatin, X-ray coherent emission under laser irrad. 3−24759
$CuSO_4$:gelatin, collimated X-ray emission on laser irrad. 3−13721

gels
butadiene-styrene latex, gelling, condensation structures, rheology, electron microscopy 3−39398
electrodiffusion of divalent ions (Ca^{2+}, Sr^{2+}, Cd^{2+}, SO_4^{2-}) determ. by radiotracers 3−39451
gelatin gels, contact energy of gel formation, crit. shear stress 3−39397
gelatine, struct.-mech. props. rel. to benzene solubilisation and hydrophobic binding 3−34655
natural latex, gelling, condensation structures, rheology, electron microscopy 3−39398
polyarylate F-1, adsorption on macroporous silica gel, chromatographic adsorbents 3−38714
polymer, gel formation, theory 3−38334
silica gel, internal friction peaks due to adsorbed and capillary water 3−21754
silica gel, pore size analysis from multilayer thickness relationship 3−31210
silica gel for growth of Ba(Sr)WO_4 single crystals 3−21527
sol-gel and gel precipitation techniques for preparation of alloy and mixed oxide powders 3−5363
Cr oxide gel systems, formation and interconversion of CrOOH and Cr_2O_3 3−5382
$Fe_2(OH)_3$ amorphous, characterisation and phase transformation 3−5383
H_2O-Na_2CO_3(NaOH)-SiO_2, quartz hydrothermal growth, nature of nonstruct. admixture in heavy phase 3−31197
SiO_2:MgO gels, sorption props., surface area, porosity, hydrothermal treatment effects 3−31196

general purpose computers
seismic profiling system, appl. to signal to noise ratio meas. 3−31462

general relativity
see also cosmology; gravitation; gravitational red shift; Schwarzschild metric; unified field theories
action-at-a-distance Currie-Hill mechanics, nonrelativistic limit 3−10371
anisotropic media, e.m. props., relativistic treatment *(French)* 3−22732
anisotropic universe with torsion, Einstein-Cartan theory 3−22724
antigravitational effects in behaviour of neutral particle in field of charged particle *(Russian)* 3−22727
artificial satellite experiment *(French)* 3−35603
averaged Lagrangian technique for approx. soln. to Einstein's eqn., high-frequency gravitational waves 3−28961
black hole accretion from interstellar gas, fluid mechanical and radiation process effects 3−39586

general relativity continued
black holes, Friedmann model of an expanding universe, propagation of light 3−16112
black holes, Schwarzschild, vector and tensor radiation from relativistic circular geodesics 3−37288
Bondi-Metzner-Sachs group, structure for asymptotically flat space times 3−10362
Brans-Dicke eqn., analogous solns. to Reissner-Nordstrom soln. 3−10372
Brans-Dicke eqns., static solns. 3−13631
Brans-Dicke theory and anisotropic cosmologies, Bianchi types I and IX, solns. 3−39598
charged spinning magnetic particles, stationary solution of Einstein-Maxwell equations 3−606
clocks, behaviour in a non-rotating frame of reference 3−19503
cold (neutron) stars props. determ. using energy variational principle 3−28103
comparative study of Brans-Dicke and general relativistic cosmologies rel. to observationally measurable quantities 3−12943
conformal invariancy of coupled spinor-vector fields 3−22721
conservation laws, Parametrised Post-Newtonian Formalism 3−10375
conservation of particles, topological derivation Christoffel symbols 3−4019
coordinate systems of asymptotically shear-free null congruences 3−16726
cosmological anisotropic model, hydrodynamic motions and vacuum stage 3−35010
De Sitter type cosmological models, consequences of field quantization 3−35006
decomposition identity for class of Riemannian invariants 3−6336
deformation and elastic bodies, interaction with gravitational waves 3−19434
differentiable and causal structures of space-time for freely falling particles and light signals 3−37882
Dirac's principle and variability of fund. consts. 3−6339
Dirac canonical formalism, simplification of constrants 3−6328
Einstein's cosmology, Copernican character 3−22009
Einstein's eqns, model universe soln. consisting of uniformly rotating sphere, third approx. 3−28963
Einstein's equations, time-dependent, numerical integration method 3−32425
Einstein curvature tensor, relation of invariants to Ricci tensor invariants 3−32431
Einstein eqns., new formulation from manifold characterization of gravitational fields 3−26142
Einstein eqns. application of future projective infinity concept for certain space-times 3−26136
Einstein eqns. for fluid sphere in polar Gaussian coords. 3−32429
Einstein equation, general cosmological soln. with time singularity 3−35011
Einstein equations, nature of Sato-Tomimatsu solution 3−22725
Einstein tensor, computation from covariant tensor, FORMAC program 3−10365
Einstein theory generalization using $T^{\nu}_{\mu;\nu}=\lambda R$ 3−22726
Einstein-Cartan eqns., derivation of analogue of Mathisson-Papapetrou eqn. of motion for spinning particle 3−16722
Einstein-like Lagrangians, $SL_{6,c}$ gauge invariance 3−10369
Einstein-Maxwell fields, method for generating Weyl class 3−35611
Einstein-Maxwell stationary field eqns., covariance for Killing vector 3−35606
Einstein-Maxwell-Yukawa fields, time depend. axially symmetric solutions 3−19497
elasticity theory, formulation and application to small motions about stable equilib. configuration 3−16730
electrovacuum horizons, stationary bifurcate, with axial symmetry and topology $S^2\times R^1$ 3−19502
e.m. boundary conditions, covariant derivation 3−13629
equal proper time formalism, effect on three main tests of general relativity 3−594
equation of motion for sources of asymptotically flat spaces 3−19499
equations, rel. to anisotropic cosmology and cosmic structure 3−28131
equations of motion of point with variable rest mass based on Minkowski's procedure 3−16732
external gravitational field of relativistic astrophysical objects *(Polish)* 3−25363
external sources, inhomogeneous Maxwell eqns. 3−597
field equations, imbedding method for finding maximal extensions of solutions 3−28960
force on prestressed body in curved space and design of gravitational wave detector 3−35605
Galilei and Lorentz structures, comparison of geometry and physics 3−22715
generalised variational space, study of trajectories for matter with spin *(French)* 3−16721
geodesic deviation eqn. under arbitrary separation rate assumption 3−16724
gravitation, finite range, possibility 3−22716
gravitation theory, solar system expts. 3−32433
gravitational field of charged mass point in scalar-tensor theory 3−22734
gravitational origin of strong interactions from general relativity rel. to universal creation 3−9457
gravitational theory, Einstein and symmetry groups *(German)* 3−13620
gravitational waves in perfect fluid with axial symmetry initial value problem 3−32430
group structure and field equations in Einstein universe *(German)* 3−28959
gyromagnetic factor of massive body with large space-time curvature 3−35610
Hamiltonian systems in multitemporal formulation 3−4018
higher-order gravitational Lagrangian in Einstein field eqns., effect on gravitational collapse 3−28105
inertial gravitational fields, relative strengths 3−35607
initial-value problem, conformally invariant orthogonal decomposition of symmetric tensors 3−37878

general relativity continued
Kerr field, visual field of non-equatorial observer, numerical calc. by Runge-Kutta method 3−6329
Kerr geometry as complexified Schwarzschild geometry, derivation from Einstein free space field eqn. 3−6332
Kerr-Taub-NUT metric, global analysis 3−37881
Klein-Gordon equation, effect of substitution of Schwarzschild metric 3−26138
Lagrange densities, degenerate, variational derivative 3−10373
Lagrangian density for motions of perfect fluid 3−26131
linear formalism, covariant expression for gravit. energy-momentum 3−6326
linearisation of Einstein's eqns. *(German)* 3−35617
linearity props. of multi-component vectors *(German)* 3−13632
Lorentz manifold, compact, analytic non-Hausdorff extension for which no geodesic bifurcates 3−37880
Lorentz-covariant reference tetrad theories 3−13625
Mach's principle, review 3−35601
magnetoelastic interactions in relativistic continua, constitutive theory 3−22722
matter creation in external nonstationary gravitational field 3−18918
Maxwell's equations new solns. by extension into complex Minkowski space 3−10368
mechanics of continua in Riemannian spaces, intrinsic coordinates and integration of indefinite equations 3−16731
Minkowski relativistic continua with directors, constitutive eqns. detn. 3−10367
Minkowski space time, initial stability *(French)* 3−6322
mixmaster universe, h.f. sound waves to eliminate horizon 3−25388
modern relativity *(German)* 3−35012
negative gravit. energy in two-geometries, physical implications 3−16735
neutrino-gravitational fields with zero energy-momentum tensor 3−601
Newman-Penrose quantities, study of radiation fields in Schwarzschild background 3−6330
Newtonian analogue of force in Kerr metric 3−19498
non-linear Hamiltonian evolution equations, global solutions 3−28826
nonlinear hyperbolic eqns., instability theorem *(French)* 3−22587
Nordtvedt metric expansion for n-body equation, reln. to scalar tensor theories 3−16725
null Killing vectors, conditions on Ricci tensor for existence 3−6335
objectivity principle and transformation equations of kinematic, thermodynamic and e.m. quantities 3−32428
one-kink metric tensor and the inverse square law 3−10366
one-meson loop, invariant regularization in curved space time 3−29170
parity and time reversal in gravitational interaction and existence of massless scalar particle 3−32629
particle model, ether flow through drainhole 3−6333
particle motion in equatorial plane of gravit. monopole-quadrupole field, classifcation 3−35564
perfect fluid static sphere, general metric in canonical coords. 3−19504
perturbation analysis of general relativistic perfectly elastic medium 3−37876
Petrov classification of gravitational fields with directional symmetry for null direction 3−35604
Petrov classification of Riemannian space-times, algebraic representation 3−37879
polytropic differentially rotating fluids, appl. of post-Newtonian eqns. to determ. equilib. config. 3−28104
position operators in (3+1) de Sitter space 3−6331
predictive relativistic dynamics, local solns. *(French)* 3−13627
preferred frame theories, gravimetric, length-of-day and perihelion shift of planets obs. 3−10376
principle of reciprocity, consequences for red-shift test by search for blue-shifted lines in galactic spectra 3−16118
pseudo-Riemannian manifold with non-symmetric connection, calc. of field eqns. *(French)* 3−13626
Ptolemy-Copernicus problem, geocentric and heliocentric world systems *(Russian)* 3−13633
quantisation of nonlinear relativistic field without perturbation theory 3−6342
quantum many-body theory in Riemannian space-time 3−26139
and quantum theory, continuous-discrete and probability-deterministic theory 3−32427
quasar red shift mechanism using scalar gravit. field 3−39704
quaternion formalism, matter-antimatter relationships 3−6334
quotient spaces, canonical formalisms 3−35598
radiowave deflection by Sun, comparison of prediction with 1972 October obs. 3−31530
Rainich conditions for neutrino fields in curved space-time, classification of symmetric second-rank tensors 3−13630
regular model universes, gravitational instability in modified theory of general relativity 3−28129
relativistic astrophysics, hydrodynamical equations and relativistic shock waves *(Polish)* 3−25364
relativistic Coulomb Green function, Sturmian expansions 3−26121
relativistic degeneracy in gravitational collapse, energy release of stars 3−9453
relativistic disks at centres of galaxies rel. to gravitational wave production 3−22728
relativistic electrodynamics of eddy-current brake *(German)* 3−37877
relativistic group of canonical transformations, including Poincare group and dilatations 3−16727
relativistic high-pressure theory of perfectly elastic solid 3−599
relativistic rotating perfect fluids, thermodynamics 3−33306
Riemann curvature tensor, algebra 3−19505
Riemannian manifold, 7 dimensional 3−22580
Ross' muon model, criticism 3−14105
rotating charged bodies and Kerr-Newman solns. of Einstein-Maxwell eqns. 3−35609
rotating incoherent matter, numerical integration 3−26132
rotating relativistic stellar models, anal. of adiabatic radial pulsations 3−28115
scalar curvature, positive, conformally flat spaces 3−22579

general relativity continued
- scalar-tensor gravitation theory, collapse *(Russian)* 3−26134
- secular instability of supermassive stars 3−5596
- SL(2C) invariance of gravit. field eqns., Yang-Mills type theory 3−16723
- slow-motion approximations, field equations decomposition 3−596
- sound propagation speed in high-pressure elastic general-relativistic solid 3−37883
- space-time, Riemannian, conformed energy-momentum tensor for scalar field with quartic self-interaction 3−35608
- space-time singularity, local structure, gravitational collapse 3−34997
- spin 2 fields, stress tensors and conformal properties 3−26258
- spinor fields in general relativity, validity of Rarita-Schwinger theory for high spins *(French)* 3−13611
- stars, nonradial pulsation of general-relativistic models, corrections 3−39662
- static charged dust distribs. with plane symmetry 3−28962
- static charged fluid ball with pressure, e≠m, calc. of interior metric 3−16739
- static plano-symmetrical de Sitter space-time, metrics *(Russian)* 3−26135
- stellar images, gravitational aberrations 3−16220
- synchrotron radiation from relativistic Schwarzschild circular geodesics, polarisation 3−37289
- tidal accel. near black hole, conditions for kinematic magnification 3−6324
- time flow from future to past *(Japanese)* 3−595
- vacuum metrics external to black holes, axisymmetric system stability, Carter's theorem 3−10364
- zero-mass scalar and electrostatic fields with central symmetry 3−13628

generators, acoustic *see acoustic generators*

generators, electric *see electric generators*

geochemistry
- *see also earth structure; geology*
- granulite facies rocks, geochemistry rel. to origin in continental regions 3−21878
- Iceland hot mantle plume, geochemical study of Rejkjanes Ridge 3−37163
- mineralogy and O isotope geochemistry of hydrothermally altered rocks of Ohaki-Broadlands geothermal area, New Zealand 3−34790
- multi-element analysis of samples using instrumental activation analysis 3−22538
- ocean water bubble spray, geochemistry rel. to salts in precipitation 3−12681
- oceanography chemistry, conference (Lerum, Sweden, Aug. 1971) 3−5489
- origin of simple inorganic compounds in the Earth *(Japanese)* 3−5449
- photoactivation analysis, geological samples, 25 MeV betatron 3−18896
- quartz from Pacific pelagic sediments, O isotope abundance 3−12614

geochronology *see earth age*

geodesy
- *see also gravity*
- aerotriangulation, computer solution method SAPGO, in FORTRAN IV 3−5532
- artificial satellite appl. *(German)* 3−34752
- artificial satellites for geodesy, symposium (Washington D.C., 15-7 April 1971) 3−34755
- boundary value problem using known surface of Earth 3−27938
- continental margin of western Africa, free-air gravity map and gravity anomalies 3−15892
- Crimea, linear tidal terrestrial deformations and analysis of results *(Russian)* 3−21903
- critical configurations of fundamental range networks 3−34756
- data acquisition at sea, digital computer systems 3−3176
- density layer models in satellite geodesy, error propagation in computed orbits 3−34769
- diurnal tidal waves in tilts of crust along Sumy-Kherson profile *(Russian)* 3−21907
- earth's crust, global movements *(German)* 3−34830
- Earth gravitational model, computation methods from combination of terrestrial and satellite data 3−34766
- earth potential, influence of tesseral harmonics on motion of artificial satellites *(Russian)* 3−16097
- Earth potential representations by buried masses 3−34770
- Echo 1, physical and optical properties rel. to precise geometric geodesy 3−34781
- European datum, geometrical adjustment with simultaneous laser and photographic obs. 3−34760
- European Datum, relation to geocentric reference system, GEOS satellites meas. 3−27934
- field transformations, Wiener filter application 3−31287
- figure of planet in Clairaut's problem, equation *(Russian)* 3−9486
- Geodetic Reference System 1967, comments *(German)* 3−12600
- geoidal height and deflection of vertical, truncation error furmulas 3−27937
- geological interpretation of gravity data for profile across Pacific Ocean 3−15891
- geophysical profiles, invariant building for higher order moments *(German)* 3−12604
- geopotential coeffs. accuracy, satellite and terrestrial gravity data 3−34775
- geopotential coeffs. determ. using satellite-to-satellite tracking 3−34773
- geopotential expansion, harmonic coeffs. *(Russian)* 3−15873
- geopotential in satellite geodesy, simple layer model 3−34768
- geopotential representation using sampling functions 3−34771
- geopotential zonal harmonics determ. using data from Dial, SAS and Peole 3−34774
- Geos 1 Secor observations in Pacific area (Solution SP 7) 3−34762
- Geos C altimetry experiment, mini-arc orbit determination 3−34763
- gravity anomalies rel. to bathymetry and convection in the earth 3−37150
- gravity field meas. using orbiting rotating gravity gradiometers 3−34780

geodesy continued
- heave filters for gravity meas. on surface ship 3−9155
- horizontal isostasy, preservation of mass and pressure *(German)* 3−12601
- hydrostatic elevation difference meter for mining prospecting 3−25311
- internal geometric accuracy from simultaneous laser range measurements to satellites 3−34757
- isostasy, deformations of gravitational potentials in Earth interior *(German)* 3−12602
- Israel geodetic network survey, evidence of vertical crustal movements 3−25146
- laser ranging to satellites appl., polar motion meas. 3−34779
- lunar retroreflectors, laser ranging meas. of Earth crustal movements 3−34971
- mean sea level rel. to geodetic land levelling around Australia 3−21927
- multilateration, satellite geodetic measurement system 3−31464
- networks, numerical problems *(German)* 3−34968
- Oslo Graben, permian, crustal structure from gravity obs. 3−9191
- Pageos, physical and optical properties rel. to precise geometric geodesy 3−34781
- Parkfield 1966 earthquake, geodetic network deformation predicted by rock dilatancy model 3−21856
- potential and vector gradient fields, differential parameters and curvature perturbations *(German)* 3−12605
- random error propagation model for weakly constrained angular networks 3−27936
- SAO 1969 Standard Earth, error model using satellite tracking data 3−34776
- satellite, gravity anomalies determ. by least squares method 3−34777
- satellite laser tracking to determ. Goddard Space Flight Center latit. var. due to polar motion 3−12628
- satellite network precision, numerical investigation using doppler, laser and photographic obs. *(German)* 3−28080
- satellite orbit determ. 3−37244
- satellite resonance, inclination changes due to longit.-depend. part of geopotential 3−25147
- satellite timing using Loran C, atomic clocks and very-long-baseline interferometry 3−34970
- satellite triangulation, absolute orientation rel. to geograv words, Earth centre of mass 3−34758
- Secor equatorial network, preliminary results 3−34761
- stars ephemerides of Talcott pairs, e.d.p. by Minsk 22 computer *(Russian)* 3−3394
- surface gravity obs. rel. to satellite obs. 3−5420
- survey improvement and calibration analysis for AFETR with Geos C 3−34765
- surveying, network planning and control technique *(German)* 3−25328
- tectonics, global *(German)* 3−27971
- terrestrial biaxial ellipsoid, reln. between coeffs. of spherical and ellipsoidal resoln. of gravitational force, computer soln. *(Russian)* 3−25160
- tidal tilts at Katerinovka, recording errors and calibrations *(Russian)* 3−21906
- tidal variations in gravity, data processing using Venedikov's method *(Russian)* 3−21978
- tilt measurements at Daryevka rel. to block structure of Earth's crust *(Russian)* 3−21905
- tilt measurements in old salt mine rel. to Kiev-Poltava-Artemovsk profile *(Russian)* 3−21904
- tracking-station coordinates from Geos 1 and Geos 2 optical flash data 3−34764
- two colour distance meas. 3−157
- vector separations between antenna sites using interferometry expts. on extragalactic radio sources 3−12627
- worldwide geometric satellite triangulation programme, data reduction and analysis methods 3−34759

geodetics *see geodesy*

geoelectricity *see terrestrial electricity*

geology
- *see also earth crust; rocks*
- Alpine-type ultramafic rocks, origin and emplacement 3−2876
- Andesite Line rel. to global tectonics and advanced petrology 3−9186
- Archaen Basement, uniformitarian evolutionary models 3−37166
- Australo-Antarctica horizontal displacement during Ordovician rel. to Australian geology 3−18826
- Avalon, Newfoundland Late Precambrian volcanic rocks, spilite-keratophyre province 3−37148
- basal Palaeozoic in North America, possible stratotype sequences 3−34788
- basalt and other rocks, stress patterns rel. to spheroidal weathering 3−2880
- boudinage and pressure shadow formation, stress distributions 3−25155
- British Tertiary igneous province, K-Ar ages of dykes and lavas from Mull, Scotland 3−34812
- Canadian granitoid rocks, Li distrib. 3−37149
- Canal Flats region, British Columbia, geomorphology and geochemistry of gypsum karst 3−37145
- Carpathians, plate tectonics rel. to geological structure 3−25153
- continental positions rel. to S. American shear zone before opening of Bay of Biscay 3−25120
- continiental margin off Labrador and E. Newfoundland, morphology and geology 3−9101
- Deccan traps, India, preliminary palaeomagnetic stratigraphy 3−34854
- disclinations in folded structures and geological strata 3−2869
- Dome de Barrot (France), palaeosedimentological implications 3−34826
- Earth-comet collisions rel. to geological periods 3−25145
- Eastern Grand Canyon Precambrian basaltic flows and red beds, palaeomagnetism meas. 3−34833
- Eastern Sudan, Tertiary basalts 3−31316
- electron probe analysis application, quantitative procedures 3−37769
- fibrous calcite beds in Middle Devonian beds rel. to stratigraphy and formation 3−12569

geology continued
  folded metamorphic rocks rel. to single-layer folds in viscous media 3−25154
  galenas from North Australia, ^{204}Pb rel. to ^{206}Pb, ^{207}Pb and ^{208}Pb 3−18830
  glacial cycle and geological records of climatic events 3−39533
  gravity data, geological interpretation for profile across Pacific Ocean 3−15891
  Great Glen and Minch Faults, hypothesis of dextral displacements 3−2877
  Hebrides, geological structure of sea floor rel. to continental drift 3−18825
  hydrogeologic investigations using induced potentials method for finding groundwater 3−25315
  interglacial and postglacial climates rel. to pollen records 3−39532
  Jan Mayen volcanic rocks, Sr comp., comparison with Spitzbergen rocks 3−34803
  Jurassic palaeomagnetism rel. to sedimentological study 3−12664
  Kaipokok Bay, Newfoundland, history compared with S.W. Greenland 3−27940
  kaolin deposit from Tanzfleck/Oberpfalz, geological and petrographic investig. *(German)* 3−12565
  Lake Huron surficial sediments, Hg distrib. 3−37266
  Langjokull Region, Iceland, volcanic history and tectonics 3−37146
  Late Cenozoic evolution of Cape Coast, South Africa 3−9193
  Late Cretaceous Pocos de Caldas alkaline complex, palaeomagnetic meas. 3−25165
  Lewisian gneiss from Outer Hebrides, U-Pb ages rel. to geochronology 3−15887
  lightning hazards to overhead power lines, dependence of frequency on geological and geoelectrical characteristics of ground *(Croatian)* 3−18837
  Limpopo mobile belt in southern Africa, geology and evolutionary aspects 3−21880
  lunar rocks, petrology of Apollo 16 and 14 samples 3−5579
  Magdalen sedimentary basin, gravity and magnetic survey rel. to possible salt deposits 3−12570
  mean annual sediment yield var. rel. to mean annual precipitation 3−39474
  Mount Etna, 1971 eruption, petrography of the lavas 3−21889
  North Sea Cainozoic subsidence, initiation rel. to Mesozoic extensional tectonics 3−34802
  NW Illinois, stratigraphy and origin of paha topography 3−9195
  optical processors applic. in image classification 3−9202
  organic analysis of geological samples by fluorescence spectroscopy 3−32268
  Oslo Graben, permian, crustal structure from gravity obs. 3−9191
  palaeolimnology, use of palaeomagnetic meas. of freshwater sediments 3−31330
  palaeomagnetic field models for 6 geological periods using spherical harmonic anal. 3−25166
  Pangaea welding, rel. to Gondwanan curve, South American Palaeozoic palaeomag. meas. 3−34834
  Peruvian Andes, plate tectonics models 3−2881
  photoactivation analysis, geological samples, 25 MeV betatron 3−18896
  Pine Prairie salt dome, mapping with v.h.f. pulse-radar well-logging system 3−25317
  position, shape, magnetization of source of geomagnetic anomaly in Soest 3−5479
  Precambrian crustal evolution, conference (London, 22-3 March 1972) 3−21872
  Proterozoic gneissic complex of Kola peninsula rel. to magnetic data 3−25139
  quartz from Pacific pelagic sediments, O isotope abundance 3−12614
  Quaternary paleoecology and stratigraphy of sea cliffs, Washington 3−9194
  Rayleigh waves in alluvial valley rel. to irregular geological structures 3−9187
  Sanbagawa metamorphic belt, Shikoku, velocities rel. to geological struct. 3−27962
  sand grains, surface texture rel. to depositional history 3−34821
  Sar e Sang, Afghanistan, kyanite-talc schist and episodes of metamorphism 3−34801
  solid and drift geology mapping, use of seabed mineral deposit radiometry 3−31310
  South Cariboo Region, British Columbia, petrology of Late Tertiary dolerite plugs 3−37147
  spectrophotometry of natural formations from Soyuz-9 manned spacecraft 3−25106
  Spitzbergen volcanic rocks, Sr comp., comparison with Jan Mayen rocks 3−34803
  strain modification of angular density distributions on contoured stereograms 3−25156
  test models with rigid and deformable inclusions, compression and simple shear 3−34829
  Tombstone stock, petrography of Devonian granodiorite intrusions 3−9102
  Troodos Massif, Cyprus, volcanic evidence for ocean floor origin 3−25144
  Troodos Massif rocks, u.s. vel. meas. indicating ocean crust origin 3−39483
  Variscan orogenic belt, geothermal gradients of granite compositions 3−34823
  Worcester Area, Massachusetts, stratigraphy of Pennsylvanian and pre-Pennsylvanian rocks 3−27932
  Yucatan Peninsula-British Honduras area, metamorphic sediments, K-Ar dating 3−34804
  ^{14}C dating of vegetable matter and hard-water error 3−15904
geomagnetic storms *see magnetic storms*
geomagnetic variations
  see also micropulsations
  27-day oscillation of low-latitude magnetic field, evening/forenoon asymmetry 3−25183
  1880 to 1960, spherical harmonic analysis of geomagnetic world charts *(German)* 3−12642
  activity indices, relation to interplanetary plasma parameters 3−2924
  afternoon depression in horizontal component at Trivandrum, seasonal variation and lunar modulation 3−31326
geomagnetic variations continued
  airborne recording system for collecting total field magnetic meas. and flight parameters 3−3174
  archaeological secular inclination var. in USSR, archaeomagnetic maps 3−25177
  bays, negative, production by storm sudden commencements 3−13008
  Canadian Arctic, vertical mag. field rel. to regional tectonics 3−37181
  Caucasus, secular geomagnetic field variations 3−25175
  caused by changes in quiet time solar wind pressure 3−5478
  central Arctic Ocean, statistical analysis *(Russian)* 3−2918
  climatic changes related to magnetic intensity changes in the 1925 to 1970 period 3−25250
  daily var. and magnetotelluric method theory rel. to daily rotation of Earth 3−25179
  directional analysis of e.m. variations, comments *(Russian)* 3−12646
  directional analysis of magneto-telluric observations, further comments *(Russian)* 3−12647
  disturbance field due to solar corpuscular flux, intensity rel. to polar-cap auroras 3−28056
  DP1 and DP2 current systems, oscillations rel. to ionospheric conductivity 3−34939
  drift of main eccentric dipole rel. to geomagnetic data for 1829-1965 period 3−34841
  early Cenozoic, evidence for short polarity intervals from oceanic crust 3−18839
  East-West component effect on currents equivalent to mag. perturbations at high latitudes *(French)* 3−12636
  effect of geomagnetic storms on nighttime E-layer during increasing maximum solar activity *(Bulgarian)* 3−9338
  effect on medium latitude lower ionosphere during geomagnetic disturbances 3−9325
  electron and proton geomagnetic cutoffs, daily var. calculation for Fort Churchill 3−12650
  e.l.f. signal generation rel. to geomagnetic disturbance and solar protons 3−21976
  equational region, lunar partial tides 3−2923
  Europe, short period variations *(German)* 3−12643
  Kamchatka, secular variations between 1965 and 1967, rel. to tectonics and volcanology 3−25170
  latitudinal energy distribution of geomagnetic disturbances 3−34838
  magnetic anomaly in Soest, magnetization of source body 3−5479
  magnetic declination, global distrib. of zero isopors rel. to polar rotation 3−25176
  magnetospheric electric field variations and auroral activity, relationships 3−16047
  magnetospheric magnetic pulsations, review 3−21914
  magnetospheric substorms, magnetic field var., interpretation of ground-based and satellite observations 3−2932
  new form of short-period geomagnetic pulsations in 5-10 sec. range 3−25173
  offshore magnetic survey using optically-pumped ^{87}Rb magnetometer 3−260
  polar cap, interplanetary mag. field 3−12648
  polar cap geomagnetic disturbances, quiet day daily var. and DP-2, comments 3−34852
  polar variations on moderately disturbed days rel. to equatorial electrojet 3−15930
  $S_q{}^p$ var. rel. to magnetotail current system interaction with polar ionosphere 3−31451
  S_q-variations, effect of radial distrib. of Earth's electrical conductivity 3−25174
  sea wave effect mag. field variations *(Russian)* 3−2920
  seasonal var. of solar and lunar daily geomagnetic variations 3−12640
  secular, effect on distribution function of inner-zone protons 3−12840
  secular field var. for epoch 1965-70, observatory and satellite observations 3−34840
  secular var. determ. from total vector absolute value var. distribution 3−34842
  short polarity event obs. by transforming marine mag. profiles to pole 3−9217
  sidereal periodic var. rel. to solar and lunar tides 3−15932
  solar daily variations rel. to deep e.m. sounding of Earth 3−34846
  South Atlantic Magnetic Anomaly, horizontal low latitude vars. 3−12666
  Southern Kazakhstan, investigations of secular variations in seismically active area *(Russian)* 3−2855
  spectral analysis of simultaneous PDP recordings by longitudinal chain of observatories 3−34845
  spherical analyses of main field during 1550-1800 period 3−34843
  Sq variability from hour-to-hour 3−31327
  sudden commencements, effects on F-layer frequency shifts of h.f. Doppler sounder 3−21972
  sudden field anomalies effect on 164 kHz waves rel. to D-region seasonal structure var. 3−25286
  summary of Japanese daily obs. results for Oct. 1969 to Dec. 1971 period 3−39610
  Toolangi, lunar and solar daily variations 3−31336
  total intensity anomalies, magnetic-doublet method of interpretation 3−12667
  twelve-month wave, harmonic anal. of single activity sequences 3−15922
  whistlers, relationship with geomagnetic activity 3−31362
  Z component diurnal, in E-region, rel. to interplanetary field variations *(French)* 3−39551
geomagnetism
  see also geomagnetic variations; magnetic storms
  aa indices, 100-year series, solar activity dependence 3−15926
  activity index Ap, spectral anal. 3−15924
  activity rel. to solar activity and meas. of coronal 5303 Å intensity 3−35026
  aeromagnetic surveys of Ross Island and Taylor glacier quadrangles 3−12669
  anomalies in mag. field produced by stresses due to man-made lakes 3−9221

geomagnetism continued
asynchronous relation of geomagnetic activity to solar activity and solar wind 3−25398
auroral X-rays, balloon obs. at Syowa Station, Antarctica, geomagnetic conjugacy *(Japanese)* 3−31402
autocorrelation functions for geomagnetic data, character of variation 3−25129
Bay of Biscay, remanent magnetization vector direction and statistical properties of magnetic anomalies 3−25168
Brazilian anomaly, enhanced electron precipitation associated with sudden commencement 3−9223
Bullard-Gellman-Lilley dynamo model, nonsteady states 3−21918
conjugate mag. obs. (near $L=4$) 3−12670
cosmic ray cutoff sharpness, calc. with polar coupling coefficients *(Russian)* 3−12908
cyclotron resonance in geomagnetic field, intrinsic bandwidth 3−5523
dike anomalies interpretation 3−12852
dipole coordinate system rel. to transport processes in geomagnetic field 3−27973
dipole moment change, effect on rate of Earth's rotation 3−2857
disturbances following activity of solar equatorial coronal arches 3−16139
DR-currents belt formation rel. to magnetosphere 3−25303
drift shell determ. for noon and midnight meridians 3−34957
dynamo integrals, Adams and Elsasser, props. and evaluation 3−12665
early Cenozoic, evidence for short polarity intervals from oceanic crust 3−18839
eccentric geomagnetic dipole arbitrarily located in sphere, magnetic field considerations 3−22804
eccentric pole parameter determination *(Russian)* 3−2921
electrical conductivity structure, comparison of magnetotelluric and geomagnetic depth sounding methods 3−9388
e.m. core-mantle coupling, shell model 3−21864
e.m. induction in earth at low latitude, mathematical structure 3−31333
e.m. probing for earth's crust, mutual e.m. coupling of loops on two-layer model 3−5432
equatorial electrojet, magnetic field fluctuations 3−16001
exploration geophysics, conference, Paris, France (1972) 3−9347
extension of Alaskan structural trends beneath Bristol Bay, det. from magnetic profiles 3−9170
F-region neutral temp. during a mag. storm, satellite obs. 3−16025
F-region plasma cloud, diffusion model for electron density distrib. along geomagnetic field 3−31430
ferromanganese nodules, remanent magnetisation meas. of freshwater and deep sea samples 3−21912
field component meas. error due to departure from coil system geometry *(Russian)* 3−2922
field disturbance with nonstationary γ-quantum source, e.m. signal characts. 3−25169
field models, scalar and vector potential, induction vector and gradient tensor calculation by computer program 3−21911
field reversal meas. from archaeological studies 3−37183
field transformations, Wiener filter application 3−31287
field-aligned currents in auroral and polar latitudes, satellite meas. 3−25307
geomagnetic tail, equilibrium config. rel. to steady two-dimensional model 3−25298
geomagnetic tail, plasma sheet, force balance requirements 3−12843
geophysical fields, cartographic representation method 3−25321
Greater Antilles long profile analysis using two-dimensional modelling of magnetized bodies 3−5468
H component power spectra, 54-day line detection 3−15927
high latitude variations, interplanetary magnetic field effects 3−16201
horizontal field variation rel. to E_s-q layer, meas. during March 1970 geomag. storm 3−25291
horizontally layered terrains, new magnetotelluric interpretation theory 3−9212
Iceland, tectonic interpretations of geomagnetic anomalies 3−25185
Iceland-Faeroe Ridge, joint interpretation of two-dimensional gravity and magnetic anomalies 3−12589
ilmenite-haematites, thermoremanence decay due to an ionic reordering mechanism 3−25163
interplanetary mag. variations, effect on geomag. activity, Pioneer 8 study 3−18843
inversion process, possible vanishing of field *(Russian)* 3−9214
ionospheric electron content at medium latitude conjugate stations 3−9321
Jurassic palaeomagnetism rel. to sedimentological study 3−12664
Kamchatka, secular variations between 1965 and 1967, rel. to tectonics and volcanology 3−25170
large ocean with island, electric current flows, magnetic field of disturbing currents 3−15931
mag. field research in volcano district Hegau *(German)* 3−5480
Magdalen sedimentary basin, gravity and magnetic survey rel. to possible salt deposits 3−12570
magnetic activity index, freq. and period relationships with Pi2 micropulsations 3−31332
magnetic declination, global distrib. of zero isopors rel. to polar rotation 3−25176
magnetic dipole inclination, calc. of magnetosphere surface 3−31453
magnetic profiles, appl. of Hilbert transforms 3−34837
magneto-telluric sounding and profiling, effect of terrain on measurements 3−25180
magnetometer, three-axis for balloon borne apparatus, with digital readout 3−12851
magnetospheric tail, quantitative model 3−9220
magnetospheric tail self-consistent, under static conditions 3−9344
magnetostatic anomalies of dipping prisms, magnetic profiles 3−5469
magnetotail, mag. field determ. from model, drift pattern construction 3−31455
magnetotelluric method theory rel. to daily rotation of Earth 3−25179
magnetotelluric modelling, finite element method 3−31298

geomagnetism continued
magnetotelluric simplifications for two-dimens. structs. *(French)* 3−34832
magnetotellurics, principle and recording technique 3−9213
mangetic maps, interpretation, freq. domain techniques 3−9371
marine biology rel. to geomagnetism 3−12668
marine magnetic anomalies, filtering operations with fast Fourier transform 3−18903
MHD phenomena in rot. fluids, NATO Advanced Study Institute meeting 3−26838
Nigeria, magnetotelluric variations 3−21917
non-dipole terms, obs. of linear polarization of radio radiation 3−3299
nondipole field, drifting and standing, core motion 3−21919
northern Lake Superior, magnetic data rel. to late Precambrian keweenawan rocks 3−12637
ocean ridge model, effect on geomagnetic variations 3−18840
ocean swell generated magnetic field components, simulation 3−2934
open field lines, boundary and electron polar cap 3−12655
palaeointensity determ. of geomag. field from anhysteretic remanent mag. meas. 3−9389
particles of low-charge low energy geomagnetically forbidden, observation 3−12658
Pc 1 micropulsations, ionospheric spread F relationship 3−15923
Pc 3 and Pc 4 micropulsations, diurnal variation of correlation characteristics with magnetic activity 3−12656
plasma sheet, spatial distrib. of magnetic field, effect of geomagnetic activity at 60 Earth radii 3−12824
polar field obs., interplanetary mag. field variations 3−13005
polar field obs. during sunspot cycles for interplanetary mag. field inference 3−25429
polar magnetic substorms, triggering by storm sudden commencements 3−13008
protons in keV range, earthward flow in geomagnetic tail at lunar distances 3−12657
radio absorption and stratospheric temp. distrib., activity effects 3−18862
radiocarbon content of dated specimens for past mag. field var. *(Russian)* 3−12901
remanent magnetization vector direction and statistical properties of magnetic anomalies 3−25168
representation of mag. field of different geological epochs by field of single central mag. dipole *(Russian)* 3−2919
role in oceanography, review 3−2963
Sea of Japan, Fe_2S in sediment cores, terrestrial heat flow 3−2850
secular climatic changes rel. to variable solar output, gravity and geomagnetism 3−39541
single magnetic profile analysis using statistical models approach 3−34966
South Atlantic, mag. smooth zones 3−2929
spherical $\alpha\omega$-dynamos by variational method rel. to Earth dynamo model 3−37180
sporadic-E layer ionisation at high latitudes rel. to geomag. activity 3−34947
Sq(H), abnormal depression under equatorial electrojet in afternoon 3−21915
sudden impulse, observations of accompanying electron precipitation event 3−16019
surface magnetic field intensity rel. to excitation of magnetospheric resonators 3−34956
survey, appl. of crosscorrelation function in anal. 3−12850
synchrotron radiation in geomagnetic field, registration of cosmic electrons 3−21995
telluric and magnetotelluric prospecting using natural 8 Hz e.m. fields 3−25316
thick plate model, automatic interpretation 3−12638
thin sheet mag. anomalies, appl. to geological subsurface formations 3−34836
tides in declination at Alibag, spectral anal. of discrete Fourier transforms 3−18841
tornado initiation, geo-electromagnetic aspects 3−31381
total intensity anomalies, magnetic-doublet method of interpretation 3−12667
trapped and precipitating protons above 100 keV, ESRO IA/B obs. at high latitudes 3−3136
Venetian hinterland, structural, magnetotelluric surveys 3−9126
He atmospheric budget, ion pumping by solar wind during geomagnetic field reversals 3−12757

geometrical optics
beam, highly focussed, interaction of light rays *(Russian)* 3−6507
in curved space-time, effect of gravity on polarization 3−16717
cylindrical wave focusing in ducts 3−10430
double plane symmetric systems, aberration coeffs. 3−35679
edge diffraction cone detection, obs. 3−4070
flux density, over arbitrary receiver surface, for ray propagation 3−29032
lenses, surfaces of best focus, aberration coeffs. 3−37940
radar cross-sections calc. 3−6409
ray Bundle, infinitely narrow, path through arbitrary surface shape 3−26205
ray tracing, an interactive instruction session 3−37577
scattering by non-Gaussian surfaces, expansion in orthogonal polynomials method 3−22822
Schmidt all-reflecting telescope, improved geometry 3−37500
sphere, specular reflection description and nomenclature 3−29028
thin double-plane-symmetric lenses, third order aberrations 3−32524
wave geometrical optics transition zone, intensity distrib. calc. *(German)* 3−16792

geometry
see also space time configurations
adjustment problems 3−3926
contoured projections of three-dimensional space, projective determination *(German)* 3−35559
coordinate systems of asymptotically shear-free null congruences 3−16726
geodesy, internal geometric accuracy from simultaneous laser range measurements to satellites 3−34757
hyperbola, curve fitting and iteration, instructional paper 3−13183

geometry continued
isoperimetric inequalities, generalised for certain Green's functions 3—35556
multisymplectic formulation of classical field theory, Poisson bracket definition 3—28933
packings of equal spheres in cylindrical vessels, geometrical properties 3—19916
projectivity of conformally-plane spaces created by the hydrodynamic energy-pulse tensor *(Russian)* 3—6327
quantum mechanical 2-state systems with time-independent Hamiltonian geometrical model 3—16709
Riemann metric, conditions for torsion freee connection to be Levi-Civita connection 3—6177
Riemannian space, congruences of curves 3—19389
six-dimensional K-space, C-umbilical hypersurfaces 3—16589
solid angles formed by arbitrary diaphragms, calc. for expt. phys. *(French)* 3—10234
thin-film laser requirements 3—29095
vertical Al cones, calc. of free convective heat transfer 3—10414
Yang-Mills fields and the minimal electromagnetic interaction principle 3—10586

geons *see gravitons*

geophones *see seismometers*

geophysical aspects of cosmic rays
anomalous barometer coeff. of neutron monitor at Mt. Norikura 3—12914
anomalous recurrent diurnal anisotropy in cosmic ray intensity var. rel. to garden hose direction 3—25354
atmospheric excess radiation at small heights rel. to solar cycle var. 3—25353
flux direction changes due to Earth motion through solar wind *(Russian)* 3—12900
geomagnetic cut-off rigidity determ. using ionospheric data 3—25352
geomagnetic cutoff for protons of energy between 1.2 and 39 MeV 3—16080
geomagnetic mechanism for production of 30-140 MHz pulses in EAS 3—12918
isotope comp. meas. using geomag. field 3—9431
latitude effects on sea level muon spectra 3—16088
low momentum integral muon spectrum at sea level near geomagnetic equator 3—31490
magnetic storm effects on intensity N-S asymmetry 3—34984
negative muons stopping rate near sea level 3—12913
particles of low-charge low energy geomagnetically forbidden, observation 3—12658
planetary albedo γ-rays, model for scanning-angle distrib. 3—31485
polar cap ionosphere bombardment by solar particles, D-region effects 3—25295
scintillations of cosmic rays inside magnetosphere, broad-band fluctuations 3—16081
solar flare particle tracks in lunar and meteoritic minerals 3—3317
solar neutrino archaeology by double β-decay effects in old rocks 3—5545
solar neutrons, correlations between intensity changes and sun-spots and mag. storms *(Bulgarian)* 3—34986
solar protuberances, terrestrial effects, literature on obs., review *(Russian)* 3—12954
Swinson sidereal time var. and heliocentric radial gradient in cosmic ray density 3—16084
n latitude distribution 1967-9, relationship to solar activity cycle *(Russian)* 3—12910
^{32}Si prod. rate, vertical profile meas. for South Pacific 3—34861

geophysical equipment
see also geophysical prospecting; seismometers
acoustic radar, atmosphere and meteorological probe 3—9406
acoustic vel. profilometer for sediment cores 3—3260
active semiconductor devices, deep ocean pressure 3—3267
airborne particulate matter examination, photomicrographic technique 3—35312
Aitken nuclei counters, stratospheric particle count errors 3—15971
anchored geophone for continuous velocity logging and seismic well logging 3—9114
atm. i.r. spectral transmittance meas., instrument and technique *(Russian)* 3—21981
atmospheric boundary-layer research, airborne instrument system 3—3181
atmospheric ferromagnetic particles, conc. and size distrib. meas. technique 3—37260
auroral scanner, dual wavelength ground based 3—5538
bathymetric surveying, long range 3—3261
black-and-white film for underwater photography 3—246
centroid and tapered arrays, design and appl. 3—9115
colour film for water penetration photography 3—245
data buoy with hydro-acoustic data transmission channel 3—31474
deep sea vane-shear device for undrained clay strength 3—3250
deep submersible equipment, optimal maintenance policy 3—3239
digital mag. tape data recording and data processing system 3—9402
disposable thermistor strings for subsurface temp. meas. 3—9380
double resonance differential magnetometer, mobile instrument for geological field work 3—9370
E-phase′, airborne-resistivity mapping, prospecting for industrial minerals 3—9210
Earth Resources Technology Satellite expts., a collection of summaries 3—18892
electrical conductivity structure, comparison of magnetotelluric and geomagnetic depth sounding methods 3—9388
electrical equipment in water, insulation 3—3268
e.m. depth sounding systems, topographic effects 3—9378
for e.m. pulse method of exploration 3—9375
equipment size, type, deep ocean mining, environmental planning 3—3169
Ewing heat probe frame, take-down model, design 3—31471
exploration geophysics, conference, Paris, France (1972) 3—9347
field mill for tethered balloons, electric field in lower atm. 3—9403
four channel well logging apparatus, prospecting for solid minerals and water 3—9208
geodesic instruments, Geodesy-Geophysics-71 exhibition Moscow, August 1971 *(Russian)* 3—9391

geophysical equipment continued
geodynamic piezoelectric instrumentation, seismological appl. *(French)* 3—34962
geomagnetic electrokinetograph, cooling water availability for coastal power stations detn. 3—25344
geophone arrays, arrangements 3—12849
geostationary artificial satellite system METEOSAT, ground control system *(German)* 3—3166
global geoid mapping using satellite altimetry in high-inclination orbit 3—34969
gravity gradiometers in orbit for geodetic appl. 3—34780
heave filters for gravity meas. on surface ship 3—9155
high-volume air sampling system using cellulose filters 3—39818
hydrostatic elevation difference meter for mining prospecting 3—25311
Interkosmos 3 satellite with f.m. transmitter *(Czech)* 3—9390
i.r., for environmental disruption measuring systems 3—21977
ITOS spacecraft system modified 3—12856
long baseline optical interferometry for secular earth crusted strain rates meas. 3—194
magnetic coil, effect of geometry on error in meas. of component *(Russian)* 3—2922
magnetometer, three-axis for balloon borne apparatus, with digital readout 3—12851
marine buoy Z-variometer on pendulum suspension, stabilization *(Russian)* 3—3202
marine sediment sampler, remote controlled, in situ meas. device 3—3263
microwave radiometers for remote sensing of Earth resources 3—9384
miniature straddle packer, servo-controlled testing of rock failure mechanisms 3—25329
Mount Etna 1971, direct meas. of O_2 on S_2 fugacities in active vents 3—21898
near-bottom equipment, precise positioning using relay transponder 3—28089
neutron radiation-resonance detector for geophysical research *(Russian)* 3—13419
ocean engineering, conference, New York (1972) 3—3228
oceanographic current meter, solid state 3—5543
oceanographic instrumentation, sonar, TV and remote sensors, review 3—3220
oceanographic research velocimeters, calibrations 3—37262
Puerto Rico International undersea laboratory (PRINUL) 3—5540
radar, as diagnostic tool for lightning 3—12740
radiobuoy telemetric method for remote optical meas. *(Polish)* 3—25340
remotely selective seismic cable variational depth controller, patent 3—39557
rotating contact excited electric field, meas. of soil electrical parameters 3—9207
sea ice measurement 3—9410
sea return, wave spectrum 3—3233
seismic instruments, basic tendencies and developments 3—25324
seismic laboratory simulation of testing at sea 3—12848
seismic profiling system, signal-to-noise ratio meas. 3—31462
soil density gauge, gamma-ray backscatter, Monte-Carlo simulation 3—37724
solid-state switching devices and multiplexing system 3—3266
spacecraft electronic design, instrumentation 3—5530
spacecraft global oceanographic requirements for remote sensing 3—3238
subsurface gamma density gauge, Monte Carlo calcs. 3—37725
surface impact location system, acoustic analysis 3—3269
tethered vehicle for deep ocean viewing, computer aided design 3—3223
two colour distance meas. for geodesy 3—157
two-laser optical distance-measuring instrument with atmospheric refractive index correction 3—16917
undereater propagation path prediction, exptal. digital system 3—37565
unmanned Arctic research submersible, acoustic homing system 3—2961
u.s. scanning systems for testing of marine sediment cores 3—31470
v.h.f. pulse-radar well-logging system for salt dome mapping 3—25317
v.l.f. transmitting facility for magnetospheric research 3—12867
Ag/Zn batteries for high density energy storage in deep submersibles 3—3264
AgZn batteries, oceanograph8c applications, lifetime, Hg contamination, resistance to ground problems 3—3213
$PbCl_2$-$CuCl_2$, electrodes, use in salt water batteries 3—3265
^{87}Rb magnetometer, narrow line, for high accuracy field meas. 3—5531

geophysical prospecting
see also minerals
advanced remote sensing systems, cost-effectiveness 3—3199
computer aided, digital data processing, seismology, Geocom and Sperry Univac, oil 3—21902
computer appls. 3—9124
conducting object detection in lossy environment, comparison of use of electric and magnetic dipole scattering 3—3175
conductive buried masses, electrode arrangement 3—9373
conductors (buried) position determ. by e.m. induction method *(Polish)* 3—22401
continuous activation logging, optimal velocities 3—25325
correlation of beds in sedimentary strata *(Russian)* 3—5442
d.c. resistivity profiling with two-electrode array, field tests 3—25178
deep magnetotelluric sounding in Sakhalin *(Russian)* 3—5472
deep ocean mining, environmental planning, equipment type, equipment size 3—3169
deep sea mining, FeMn deposits, environmental effects 3—3167
dike magnetic anomalies interpretation 3—12852
dry valleys in Antarctica, electrical and depth sounding 3—12630
Earth resources, remote sensing by microwave radiometry 3—9384
Earth Resources Technology Satellite, photographic and sensing systems 3—9386
Earth Resources Technology Satellite expts., a collection of summaries 3—18892

geophysical prospecting continued
Earth satellite applications, review 3−27970
eastern Atlantic continental margin, survey 3−21931
electrical sounding over an inclined interface, interpretation method 3−12853
e.m. anomaly enhancement by conducting overburden 3−9353
e.m. depth sounding systems, topographic effects 3−9378
e.m. mapping, probing of plate conductors near surface formations 3−9374
e.m. probing for earth's crust, mutual e.m. coupling of loops on two-layer model 3−5432
e.m. pulse method, theory and instruments 3−9375
e.m. sounding curves for spherical Earth model *(Russian)* 3−5441
exploration geophysics, conference, Paris, France (1972) 3−9347
fault zone, separating two media of high resistivity, transient e.m. response 3−31459
Finland, digital two-plane rotary field airborne system with magnetic method 3−5528
four channel well logging apparatus, prospecting for solid minerals and water 3−9208
frequency sounding, central and dipole, comparison 3−12854
gamma-spectral prospecting, temp. inversions as interference source *(Russian)* 3−9137
geoelectric dipole arrays, application to deep explorations 3−9372
geothermal reservoirs from ground-noise surveys in 0.5 to 5 Hz range 3−25124
hydrogeologic investigations using induced potentials method for finding groundwater 3−25315
hydrostatic elevation difference meter for mining prospecting 3−25311
inclined bed rock, depth, from surface potential meas. 3−31299
induced polarisation, comparison of time, frequency phase meas. 3−9355
induced polarisation, interpretation theory for time-domain vertical soundings 3−9352
induced polarisation method *(Spanish)* 3−31463
induced polarization field prospecting, interpretation 3−9376
industrial minerals, airborne resistivity with E-phase' 3−9210
INPUT response to single-turn conductive circuit 3−5470
Israel, southern coastal plain, exploration using seismic detonating cord 3−9108
l 3−31460
layered conducting earth, with dipping anisotropy, impedance of plane e.m. wave at surface 3−29013
magnetic induced polarization method, mathematics and results 3−9377
magnetotelluric modelling, finite element method 3−31298
magnetotelluric sounding, computer processing of data *(Russian)* 3−5473
magnetotelluric soundings, processing and interpretation 3−34964
marine seismic exploration, review 3−37153
minerals, comparison of radiative capture and decay γ-ray methods in borehole logging 3−439
ocean resources exploitation, surveying and drilling 3−31472
resistivity pseudosections of buried spherical conductor body, computer calc. 3−9354
resistivity surveying for Sanguine transmitter site selection 3−3173
salt domes boundary surfaces by magnetotelluric method *(German)* 3−18895
salt formations, ECHO-LOG determination of form of leached cavities *(German)* 3−9356
sandstone, kerosene-filled, thermal effects on seismic wave propagation 3−37825
sea floor mining, open cut mining, environmental analysis 3−3168
sea floor prospecting, ocean sediments, chemical composition, γ ray backscattering 3−3170
seismic, imaging and modelling, diffraction technique 3−9106
seismic, Kalman filter as prediction error filter 3−9351
seismic array effectiveness rel. to no. and spacing of sensors 3−31456
seismic exploration, data processing and interpretation, review 3−37154
seismic exploration, for oil and gas, review 3−37152
seismic prospecting, Nippon Geophysical Prospecting Co., Ltd. 3−31302
seismic prospecting by refraction method and fan-shooting for deep bed-rock 3−31301
seismic refraction data study on first arrivals, digital processing 3−9350
seismic velocity depth functions, parameter optimisation 3−9357
seismology, current technology and future trends in petroleum industry 3−39558
sequential analysis, seismic traces *(French)* 3−9348
shallow seismic reflection technique 3−9117
shielded conductor, time domain e.m. response, theory 3−29014
spectrophotometry of natural formations from Soyuz-9 manned spacecraft 3−25106
subterranean cylindrical inhomogeneity excited by line source, e.m. fields determ. 3−32477
superheavy transuranium elements, fission method investigations *(German)* 3−37164
telluric and magnetotelluric prospecting using natural 8 Hz e.m. fields 3−25316
total intensity anomalies, magnetic-doublet method of interpretation 3−12667
transient electromagnetic response, for conducting sphere, theory 3−29012
Turam interpretation by curve matching using line current approximation 3−9349
uranium ores, low grade, from US electron probe analysis 3−39486
v.h.f. pulse-radar well-logging system for salt dome mapping 3−25317
well logging techniques, review 3−37155
well velocity survey, continuous velocity logging and seismic well logging 3−9114
Ge(Li) bore hole probe, for in situ γ-ray spectrometry 3−31457
Mn nodule detection, pattern recognition 3−9381
SnO_2 (cassiterite) ores, electrical properties rel. to e.m. search methods *(Russian)* 3−12613

geophysics
see also geodesy; geology; geomagnetism; geophysical equipment; meteorology; oceanography; radiation belts; rocks; seismology; space research; terrestrial atmosphere; upper atmosphere
Adirondack earthquake, 1971, field study and tectonic stress meas. 3−21854
African orogenic belts delineation by gravity surveys 3−9184
African plate, comments on stationary behaviour 3−39478
alkaline igneous rock lineaments rel. to transform directions in Africa and S. America 3−34800
alluvial streams, origin of meandering and braiding 3−25194
Andesite Line rel. to global tectonics and advanced petrology 3−9186
Antarctic, analog to Mars permafrost terrain 3−12633
Antarctica, local surface energy balance and subsurface temp. 3−9182
Archaean craton of North Atlantic region 3−21882
Archaean crust, plate tectonic model 3−21877
Arctic ice-cap removal rel. to model of general atmospheric circulation 3−15980
artificial lakes, hydrodynamical props. *(Italian)* 3−34978
Australo-Antarctica large-scale horizontal displacement during Ordovician 3−18826
Baffin Basin, seismic refraction studies rel. to tectonic development of ocean basin 3−25126
Bay of Biscay, eocene, deep water sand fan 3−2948
Blueschist metamorphism rel. to press.-temp. regimes in active subduction zones 3−37175
boudinage and pressure shadow formation, stress distributions 3−25155
Bouguer gravity map of Nigeria 3−5462
British Isles, location of proto-Atlantic suture rel. to Scottish faults 3−27964
Canadian Arctic, vertical mag. field rel. to regional tectonics 3−37181
Carpathians, plate tectonics rel. to geological structure 3−25153
cartography, projection routines for displaying geophysical data 3−25318
catalogue of palaeomagnetic directions and poles 3−25184
Caucasus, secular geomagnetic field variations 3−25175
China Basin, tectonic evolution rel. to Mesozoic palaeography of Borneo 3−34806
coastal boundary layers of lake, effect of finite vertical Ekman number 3−27995
Colorado plateau crustal-upper mantle model from Moses Rock dike intrusive breccia 3−18815
computer graphics for geophysical data 3−25314
continental alkaline provinces, mechanism for salic magma bias 3−31315
continental crust, problems concerning evolution, review 3−21873
continental drift, rel. to paleomagnetic data *(Russian)* 3−2919
continental drift rel. to unstable tetrahedral mantle-convection model 3−34827
continental margins, granite cycle triggering mechanisms 3−15909
Corsica-Sardinia microplate rotation date, radiometric age meas. of Apuane Alps metamorphism 3−21866
crest and fracture zone geometry of mid-Atlantic ridge between 10° and 16°N 3−2871
Crimea, linear tidal terrestrial deformations and analysis of results *(Russian)* 3−21903
crustal evolution in Bay of Biscay rel. to Iberian sub-continent 3−15876
Czechoslovakia, geophysical research 3−34753
Danakil depression (Ethiopia), isotopic comp. determ. of water samples 3−25345
data acquisition at sea digital computer system 3−3176
debonding at interface flow of elastic solids under transient wave influence 3−13589
deep-sea cores, method for palaeomagnetic meas. aboard ship *(German)* 3−16052
deformation of rocks, geometric effects of vol. changes during tectonic processes 3−25157
diurnal tidal waves in tilts of crust along Sumy-Kherson profile *(Russian)* 3−21907
Dome de Barrot (France), palaeotectonic and palaeosedimentological implications 3−34826
dynamic uplift of Andean mountains and island arcs 3−31314
early Precambrian crust evolution of southern Africa rel. to greenstone belts 3−21875
early Proterozoic continental margin evolution rel. to coronation geosyncline 3−21885
Earth's crust, contemporary vertical movements *(Russian)* 3−9133
Earth models, var. principle with arbitrary initial static stress field 3−12560
Earth Resources Technology Satellite 3−9385
Earth-comet collisions rel. to geological periods 3−25145
east Pacific, mechanisms of earthquakes and plate motions 3−15882
East Pacific Rise system, compatibility of topographic and magnetic interpretations 3−18822
energy flow obs. in Antarctic 3−12629
environmental science and engineering, conference, New York, USA (1972) 3−34754
Eurasian plate, lines of volcanoes rel. to concentric plume traces 3−21870
evaluation of gravity anomalies directly from satellite observations 3−12590
Exploration Geophysics Institute, development 3−9379
explosive volcanic eruptions, atmospheric trajectories of pyroclasts 3−34811
extension of Alaskan structural trends beneath Bristol Bay, det. from magnetic gravity and seismic profiles 3−9170
fault clay, characteristics and origin 3−27959
fault detection using correlation techniques 3−9120
fields, cartographic representation method 3−25321
fluxgate magnetometer, aeromagnetic geophysical surveying, direct reading, total feedback, solid state design 3−3165
focal mechanisms and plate tectonics of S.W. Pacific 3−9171
fold axes development oblique to regional trend 3−5460
fold morphology and geometrical implications of theories of fold development 3−5458

geophysical prospecting continued
geophysics continued
gaseous mud volcanoes, peculiarities 3−12617
Gediz earthquake, 1970, March 28, seismotectonic aspects 3−25125
geodynamic models and undation theory, book 3−15916
geomagnetic declination, global distrib. of zero isopors rel. to polar rotation 3−25176
geophysical profiles, invariant building for higher order moments *(German)* 3−12604
geostationary environmental satellites, infrared radiometer 3−13121
global reactions and petrology (experimental), conference (Montreal 24 Aug. 1972) 3−37170
global tectonics *(German)* 3−27971
global tectonics as framework for igneous and metamorphic petrology 3−37171
Goodnews Bay, Alaska, mertieite, new Pd mineral 3−27923
Great Basin, Cenozoic volcano-tectonic evolution 3−15877
Great Glen and Minch Faults, hypothesis of dextral displacements 3−2877
Great Valley, Pennsylvania, faulting sequence 3−27931
Green River Formation, Wyoming, K-feldspar and analcime in tuffs 3−27927
Grenville front and rifting of Canadian shield 3−2873
groundwater movement, viscous flow model 3−15856
Hebrides, geological structure of sea floor rel. to continental drift 3−18825
Heimaey volcanic eruption, lava microphotographs 3−21865
Hercynian continental collision rel. to palaeogeography of south west England 3−21871
Hercynian tectonic belt, strain meas. of deformed elliptical quartz grains in slaty rocks 3−25158
holocene late glacial maximum and marine transgression in eastern Canadian Arctic 3−2874
hydraulics, inverse problem, single layer equifer, water table, approximate solution, theoretical model *(Italian)* 3−9097
hydrological systems analysis, treatment as linear, nonlinear systems *(Greek)* 3−31478
Iberia, rotation rel. to Caenozoic palaeomagnetism from Portugal 3−34853
Iberian Peninsula, crust-mantle seismic velocities rel. to tectonics and seismicity 3−12591
Iberian variscan orogen, a geotectonic model showing the crustal evolution 3−15912
Iceland, tectonic interpretations of geomagnetic anomalies 3−25185
Iceland plateau, origin and structure 3−9175
Icelandic geothermal activity and Hg concentrations of Greenland ice-cap 3−25143
igneous and tectonic events in NE Cape Breton Island, Nova Scotia 3−5422
Imperial Valley 1940 earthquake, tectonic stress determ. for testing a source-theory 3−21853
Indian Ocean, mid-plate tectonics rel. to Ceylon-Cocos seismic zone 3−15897
Indian Ocean plate contemporary stress rel. to mechanisms of Australian earthquakes 3−34805
Indian plate tectonics, boundary and motion 3−31295
Indian regional tectonics, comparison with seismicity maps 3−21842
Indian-Antarctic-Pacific plates triple junction 3−15878
Indo-Gangetic Basin, ring structures rel. to continental drift 3−39482
Indonesian island arc tectonics, relation to Pleistocene migrations of pygmy stegodonts 3−18823
information-management service, possibilities and future 3−34782
Insubric Line displacement rel. to Pennine and Southern Alps 3−21869
island arcs and trenches, subduction of aseismic ridges 3−18821
Italy, anticlockwise roatation between Eocene and Miocene from Colli Euganei palaeomagnetism 3−15883
Kamchatka Peninsula, secular geomagnetic variations (1965-1967), rel. to tectonics and volcanology 3−25170
Kilauea volcano, Hawaii, e.m. sounding survey 3−9167
Lac Rouvray anorthosite mass, tectonic evolution 3−31297
Lagrange invariant in MHD geophysical aspects rel. to E-region magnetic parameter *(Russian)* 3−17548
Lake Huron surficial sediments, anal. 3−37267
Lake Ontario, sediment discharge from Canadian Basins 3−37265
lake sediments, Hg pollution due to industry 3−25346
landslide into water basin, calc. of wave propagation *(Italian)* 3−31291
Langjokull Region, Iceland, volcanic history and tectonics 3−37146
late Quaternary vertical movement, evidence of glacio-isostatic rebound, a review 3−25150
Ligurian country, seismic refraction profiles *(French)* 3−31323
Limpopo orogenic belt, southern Africa, structural interpretation of northern margin 3−21881
lithospheric plate motion rel. to mantle plume traces, palaeomagnetism and polar wandering 3−25142
lithospheric plates, displacement of dipping oceanic slabs, flow movements 3−15875
Mach Einstein doctrine, some secular consequences *(German)* 3−12593
magma origin in oceanic and circium-oceanic regions rel. to phase tectonics 3−37172
magmatism and tectonic settings 3−9168
magneto-telluric sounding and profiling, effect of terrain on measurements 3−25180
mantle plume hypothesis, rel. to seismic refl. profile of Reykjanes Ridge 3−25113
marginal fracture ridge off coast of S. Africa, seismic profiling data 3−31309
marine basalts, rock magnetism rel. to sea floor spreading and global tectonics 3−9203
matrix methods of joint interpretation of two-dimensional gravity and magnetic anomalies 3−12589
mean annual sediment yield var. rel. to mean annual precipitation 3−39474
mean gravity anomaly prediction, comparison of two methods 3−27935
Mediterranean island arcs, origin of high potash volcanoes 3−9103
meshed grid system solutions, numerical method and applic. to two dimensional model 3−25326

geophysical prospecting continued
geophysics continued
metamorphic paired and unpaired belts, occurrence rel. to regional tectonics 3−37174
Midway Atoll lavas, palaeomagnetism and northward movement of Pacific plate 3−15917
Minch Fault, dextral movement theory 3−27966
Mineral Bluff formation, natural folds rel. to fold model for quartzite and marble 3−39473
Mohorovicic discontinuity determ. from deep seismic sounding and outer gravity field 3−27939
Monar, Scotland, analysis and interpretation of minor folds in Moine rocks 3−34828
mountainous watershed, effective net radiation 3−3156
New Hebrides, descending lithospheric slab, evidence from seismic waves and earthquakes 3−27963
New Zealand, rate of horizontal fault displacement 3−37162
New Zealand geosyncline rel. to geotectonics 3−18827
North-West Scottish Tertiary volcanic islands, underlying basic and ultrabasic igneous rocks 3−37165
northwestern Caribbean, structure from seismic reflection and gravity profile 3−15880
ocean floor origin, volcanic processes evidence from Troodos Massif, Cyprus 3−25144
ocean ridges, thermal model modifications 3−39480
oceanic crust, age rel. to tectonics and Deep Sea Drilling Project 3−9100
oceanic rifts, analytical and numerical models 3−15910
opening of Labrador Sea 3−9174
ore stratigraphy comparison in continents subjected to drift *(German)* 3−2887
organic geochemistry, effects of lunar C chemistry 3−35088
Outer Hebrides, structure and origin of anomalously low-intensity finite deformation areas in basement gneiss 3−5463
Pacific plate, variable rate of movement rel. to California from deep-sea sediments 3−15908
Palaeozoic oceans, continental collisions and ocean closures 3−9185
paleostrain anal., scale problem 3−5459
Papuan Ultramafic belt, major overthrust of ocean floor, petrology 3−12579
pattern recognition system for geophysical data 3−25322
Peruvian Andes, plate tectonics models rel. to geology 3−2881
petrology, criteria for predicting liquid immiscibility in silicate melts 3−2884
plains streamflow anal., theoretical freq. distrib. 3−37243
plate tectonics, driving mechanism, evolution 3−9147
plate tectonics and lateral velocity gradients for Rayleigh waves 3−25152
polarization phenomena found in geophysical applications *(French)* 3−5418
potential and vector gradient fields, differential parameters and curvature perturbations *(German)* 3−12605
Pre-Ordovician polyphase structure in Burlington Peninsula of Newfoundland Appalachians 3−21868
Precambrian crustal development rel. to oldest Archaean rocks 3−21874
Precambrian crustal evolution, conference (London, 22-3 March 1972) 3−21872
Precambrian of northern West Greenland, recumbent folding and flat-lying structure 3−21884
Proterozoic mobile belts in Greenland, tectonic displacements and thermal activity 3−21883
proto-Gulf of California, Miocene volcano-tectonic rift zone 3−15879
Puget Sound region, seismicity, structure and tectonics determ. and crustal model generation 3−21843
Pyrenean tectonogenesis, rel. to formation of Bay of Biscay 3−25116
pyrolite upper mantle under mid oceanic ridges, stable crusts and island arcs, melting relations 3−37177
regional strain variations in S. Nevada 3−9169
Rhodesian Archaean craton rel. to cratonic evolution and greenstone belts 3−21876
Rincon oil field, South Texas, geoseismic history and development 3−25123
rivers, meadering and braided, effect of grain size on formation 3−21986
Sardinian rotation completion date determ. from palaeomagnetism meas. 3−39488
Scottish Highlands, Alpine-type ultramafic rocks rel. to mountain building 3−31313
S.E. Asia as part of Gondwanaland 3−9189
sea floor spreading and continental drift, book 3−18834
sea-floor spreading, numerical simulation of convection and plate motion 3−15903
S.E.Asia and W.Pacific, plate convergence, transcurrent faults and internal deformation 3−9162
Sedmochislenitsi Mine, Bulgaria, new mineral balkanite, $Cu_9Ag_5HgS_8$ 3−27924
solar activity effects, comparison with biological effects 3−22173
south Greenland, heat flow and surface radioactivity at two sites 3−15900
South Pacific near Easter Island, evidence for two crustal microplates 3−2878
southeastern Africa, possible Precambrian obduction and plate tectonics 3−2879
southern California, crustal spreading 3−9197
spectrophotometry of natural formations from Soyuz-9 manned spacecraft 3−25106
strong underground explosions, final cavity rel. to parameters of surrounding medium *(Russian)* 3−12610
submarine volcanic eruptions, spectral banding in hydroacoustic signals 3−9163
tectonic plate motion rel. to convection process between elastic lithosphere and viscous asthenosphere 3−15896
tectonic strian release by underground nuclear explosions, seismic surface wave anal. 3−27950
tectonics, Afar region in Ethiopia 3−9192
tectonics, model expt. of plate movements 3−39479

geophysical prospecting continued
geophysics continued
tectonics, ridge transform fault spreading pattern in freezing wax 3−25151
tectono-eustatic changes in sea level and seafloor spreading 3−39477
Thomas-Fermi model, shell structure effects on eqn. of state at high press. 3−32435
tidal tilts at Katerinovka, recording errors and calibrations *(Russian)* 3−21906
tidal variations in gravity, data processing using Venedikov's method *(Russian)* 3−21978
tilt measurements at Daryevka rel. to block structure of Earth's crust *(Russian)* 3−21905
tilt measurements in old salt mine rel. to Kiev-Poltava-Artemovsk profile *(Russian)* 3−21904
u.v. obs. from lunar based instruments 3−9623
Venetian hinterland, structural model 3−9126
vertical clustal movements along E. coast of United States, sea level meas. 3−15890
vertical crustal movements between Dead Sea Rift and Mediterranean, geodetic anal. 3−25146
volcanic activity systems, magma chamber depth rel. to gas pressure 3−34787
waves, polarisation properties by three-dimensional covariance matrix 3−12559
West Borneo microplate, age problems 3−27969
western British Isles, evidence for crustal low-velocity seismic zone 3−12592
Whin Sill intrusion, Northern England, prehnite from contact metamorphic aureole 3−27928
world distribution of volcanoes, catalogues, maps and eruption bulletins *(Japanese)* 3−2858
Wright and Victoria dry valleys in Antarctica, analog to Mars 3−12632
O_2 dissolved, and temp. variations in stratified lake 3−25196
geopotential *see geodesy*
geothermal power stations
geothermal energy extraction from dry well, numerical solutions 3−18816
Mexico, energy exploration and utilization *(Spanish)* 3−31479
germanium
absorption coeff. rel. to resist. at 10.6 μm 3−30787
acoustic surface wave, energy flow direction by acoustoelectric probe 3−8005
adsorption, of H and D, cooperative, (111) faces, pulsed time of flight mass spectrometry, exchange reactions, kinetics 3−36485
adsorption and nucleation of Zn on (110) Ge surface 3−11806
adsorption at O_2 and H_2 on (100) face of single crystals *(Russian)* 3−15068
adsorption in gas media, effects on surface electrical characts. *(Russian)* 3−24338
adsorption of Au, disperse struct. growth *(Russian)* 3−20943
amorphous, cohesive energy and density of states 3−36521
amorphous, d.c. cond. and pseudogap struct. 3−38839
amorphous, doped film, temp. depend. of conductivity, spectral depend. of absorption 3−18131
amorphous, electron spectra, effect ov valence angles deform., LCAO calcs. *(Russian)* 3−8084
amorphous, l.f. Raman scatt., freq. depend. coupling const., elastic continuum limit 3−8586
amorphous, reactor irradiation expts., resistivity var. with heat treatment 3−15195
amorphous, refr. index, dispersion and magnitude 3−36851
amorphous, thermoelec. power and low field conduction 3−8174
amorphous film, a.c. cond., contactless meas. in microwave region 3−15189
amorphous film, electronic structure, elec. and optical props. study 3−15116
amorphous film, magnetoresist. in fields up to 25 kG, impurity level effects 3−21095
amorphous film, Poole-Frenkel cond., calc. including hot electron effects 3−5015
amorphous film, Zeeman splitting of localized levels model approach to magnetoresist. 3−15213
amorphous sputtered film, annealing activation energies, elec. cond. study 3−30369
amorphous thin films, absorption and transport study of the pseudo gap 3−33775
amorphous thin films, hopping transport, thickness depend. 3−38838
amorphous thin films, optical props. 3−15575
annealing processes after irradiation with 1 MeV electrons at 85K 3−11616
antireflection coating, prep. and properties 3−3799
Auger electron yield for adsorbed C(N)(O)(P)(S)(Cl) 3−2611
axial yield strengths and phase-transition stresses 3−4807
band structure, crit. pt. determ., in 4-9 eV region 3−2005
Benedicks effect due to heating of nonequilibrium carriers by microwave fields 3−15209
biexcitons and exciton concentrations *(Russian)* 3−27228
birefringence, spatial dispersion induced 3−2512
Borrmann multiple diffraction study of reciprocal space 3−11528
boundary scattering of phonons 3−1840
cathodic deposition, of hydrogen, hydrogen overvoltage mechanism, temperature effects 3−37128
charge carrier capture and reemission by shallow levels, field depend. 3−21091
conduction band effective mass anisotropy rel. to uniaxial compression *(Russian)* 3−15137
cryostats, demountable high-vacuum tight high voltage feedthrough, description *(German)* 3−9912
crystal growth, shaped ribbons, tubes and filaments 3−15629
crystalline and amorphous phases, band struct. and density of states 3−33776
crystals grown in magnetic field, crystallizing unit *(Russian)* 3−12313
current-voltage characts. of single crystal under strong injection mag. field effects 3−24447
detector, γ-ray efficiency 3−28658
germanium continued
detector, efficiency calibration and properties for low energy photons 3−19298
detector, hole traps 3−37693
detectors, charge collection times by time pick-off techniques 3−32138
detectors, collimated beam scanning, radial dependence of depletion layer width 3−28656
detectors, operational characteristics at high temp. 3−28657
diamagnetic specific susceptibility rel. to disorder 3−30599
dielectric function, calc. using Penn's model 3−2000
diffused layers, production methods 3−24810
diffusion, of Li, drift velocity, depth of drift, electric field configuration 3−33697
dislocation relaxation in single crystals, internal friction meas., temp. depend. 3−17847
divacancies and single vacancies, statistical problem 3−15150
donors and acceptors distribution 3−28655
electrical characts., laser irrad. effects *(Russian)* 3−27248
electrical props. of p- and n-type, influence of single dislocations 3−24439
electrodeposition, from fused LiCl-KCl eutectic 3−21808
electron diffr. and mobility 3−15190
electron energy relaxation time, as function of lattice temp. 3−30472
electron radiation and surface roughness 3−27593
electron scatt., crit. voltage effect involving vanishing 3rd order Kikuchi lines 3−24003
electron states under uniaxial stress, pseudopotential calc. 3−33801
electron velocity field characts., negative differential mobility, meas. 3−33913
electron-hole drop binding energy from luminescence spectrum 3−21476
electron-hole drops, oscill. of recomb. radiation in strong mag. field *(Russian)* 3−2030
electron-hole liquids, ground state energy 3−21009
electron-hole plasma, high-field domain formation 3−24444
electron-hole plasma, pinch effect 3−33946
electron-phonon interaction and intervalley scattering, pseudopotential calc. 3−5005
electroreflectance meas. rel. to E_1 transition, two or three dimensions 3−18434
e.m.f. induction by Q-switched CO_2 laser 3−30520
energy band structure from a nonlocal separable potential model 3−33797
epitaxial, polycryst., amorphous, Hall mobility, carrier conc., cond., noise, 100-400 K 3−38855
epitaxial films, on Ge substrate, sputter deposition at low temps. 3−18554
epitaxial growth on Si, interface dislocation struct., transmission electron microscope obs. 3−1941
epitaxial layer, tripyramid growth obs. *(Japanese)* 3−1931
exciton, microwave breakdown 3−21033
excitonic mols., stability, bonding mechanism 3−8126
extended dislocations, work-beam high-resolution micrographs 3−36318
extended X-ray absorption fine struct., meas. of shielding of impurities 3−18511
far i.r. optical consts., room temp. and 1.5 K 3−24669
in Fe meteorites, by X-ray fluorescence analysis 3−5451
field emitters, Au adsorption, metal-semiconductor boundary growth 3−15251
film, amorphous, density, effects of annealing 3−1958
film, amorphous, order-disorder transformation obs. 3−1800
film, amorphous, structure, electron microscope obs. 3−1949
film, amorphous, thermopower, comparison with crystalline film 3−2116
film, electroresist. and resist. rel. to deposition conditions 3−38909
film, emission microscope obs., fine electron beam broadening by multiple scatt. 3−14666
film, epitaxial vacuum-deposited on Si, elastic strains 3−27194
film, impurity effects on structure with different preparation methods 3−20968
film, influence of substrate props. on microwave losses 3−24463
film, obs. of Kikuchi line doubling rel. to block structure 3−24364
film, prep. rel. to detector applic. 3−15641
film, vacuum deposited, cond. and Hall effect obs. *(Russian)* 3−24431
film, vacuum deposition on glass, struct. and elec. conductivity 3−18542
film growth, thermal decomp. kinetics of GeH_4 3−8719
films, obtained by zone melting, nucleation and growth *(Russian)* 3−12303
free exciton spectra at submillimetre wavelengths *(Russian)* 3−5242
galvanomagnetic effects in high electric fields *(Russian)* 3−11910
gamma-ray Compton profiles, band structure test 3−11649
group V dopants, O, Te impurities, electron irrad., E_c-0.2 eV level, defect model 3−33842
group V-doped, defect formation under γ irradiation 3−33545
groups III and V impurities, electron irrad., unusual donors and acceptors 3−33843
growth form and soln. form relation *(German)* 3−9079
Hall field calc. inside non-spherical radiation damage regions 3−38856
heat-pulse propagation in p-type under uniaxial stress 3−20842
heteroepitaxial films, Hall effect and magnetoresistance *(Russian)* 3−11966
high pressure and amorphous phases, struct., electronic and optical props. 3−30095
hole density of states effective mass under stress and strain 3−18081
hole scattering by acoustic and optical phonons in homogeneously deformed sample *(Russian)* 3−24417
hollow cylindrical sample, current-interchange instability in electron-hole plasma *(Russian)* 3−8201
homoepitaxial layers, dislocation struct., effect of crystn. conditions 3−24356
homogeneous, heated by microwave field, Benedick's thermo-e.m.f. *(Russian)* 3−2114
hopping conduction, giant hopping piezoresist. predicted from percolation method 3−15197
hopping conductivity, activationless, in compensated Ge 3−18144

germanium continued
hot-pressing effects on neutron topographs 3−23983
implantation of Kr and Tl, energetic ion collection, saturation effects 3−11646
implantation of Kr and Tl, ion conc. profile and ion range probability distrib. 3−11647
impurity breakdown, origin of S-shaped I-V charact. 3−24443
impurity breakdown and recombination kinetics connected with excited states of shallow donor 3−18166
impurity in Si, electron irrad., selective trapping of vacancies migration of interstitials 3−33925
incoherent precipitate in Al-Ge alloy, vacancies and nucleation influence *(German)* 3−34550
interband transitions and cyclotron resonance of light holes, strong elec. fields *(Russian)* 3−8109
internal friction of deformed crystals from 4.2 to 150 K 3−14936
intervalley scattering of hot electrons, impurity and phonon mechanisms, transition times 3−33919
ion bombarded, H^+, O^+, B^+, divacancy-like optical absorption 3−34394
ion bombarded, relax. of electron emission *(Russian)* 3−8694
laser excited photoluminescence, radiative transition 3−5233
lattice defect obs. using ^{73}Ge, 13.3 keV Mossbauer effect 3−34279
lattice disorder induced by 0.3 MeV D^+ random bombardment, 1.5 MeV D^+ channelling measurements 3−1656
layer, transverse mag. field influence on microwave transmission *(French)* 3−18174
metal-dielec. transition, microwave obs. *(Russian)* 3−11940
microwave Faraday rotation, transport and band parameters 3−15475
m.i.s. structures, photoelectromagnetic effect measurements, impurity levels, recombination centres, other props. *(German)* 3−15259
multiply charged ions, atomic lifetimes of low-lying levels 3−11156
in Mundrabilla meteorite shower, X-ray fluorescence spectrometry 3−5452
muonium as deep donor, hyperfine splitting 3−18099
n- and p-type impurities electron irrad., annealing, Frenkel pair model, vacancy release 3−33561
n-type, amorphous, doped highly compensated cryst. semiconductor model for switching and memory 3−36644
n-type, anisotropy factor rel. to temperature, magnetoplasma wave obs. *(Russian)* 3−24558
n-type, elec. cond. anisotropy, hot electron drift velocity temp. depend *(Russian)* 3−8196
n-type, electron bombardment induced annealing stage 3−38598
n-type, free carrier Voigt magnetoabsorpt. 3−27486
n-type, galvanomagnetic coeffs., determ. by one-point method 3−24454
n-type, helicon propag., effect of quantizing mag. fields *(Russian)* 3−2122
n-type, high purity, γ-irrad., carrier-conc.-depend. mobility 3−36627
n-type, hot electron Hall transport, calc. 3−38848
n-type, impurity ionization 3−8192
n-type, in Voigt config., microwave transmission 3−2522
n-type, microwave photocond. and radiative recomb. under high optical excitation at low temp. 3−38871
n-type, polarisation of photocond. rel. to edge dislocations 3−27287
n-type, recombination centres, properties and nature, τ, majority carrier density 3−33924
n-type, Sb-doped, far i.r. cyclotron reson. 3−15127
n-type, second harmonic generation, efficiency and optimum d.c. bias field 3−30509
n-type, specific resist., effect of multiple deformations of alternating sign *(Russian)* 3−18129
n-type, surface hole mobility and density, scatt. in surface inversion channels, Hall meas. *(Russian)* 3−27299
n-type, symmetry relations between mobility and differential mobility tensor components in hot carrier range 3−8190
n-type, thermoelectromotive force, rel. to electron-phonon mutual entrainment *(Russian)* 3−21101
n-type, transport props., negative differential cond., impurity effects at 20K 3−21085
n-type, transverse magnetoresist. in quantizing mag. fields 3−15214
n-type, Voigt magnetoabsorption at low temp. 3−30802
n-type, warm electron anisotropy 3−2102
neutron induced damage studies using channelling of 1 MeV protons 3−24163
optical transitions between excited states of V impurities, photocond. 3−33826
optically pumped, evaporation of metallic exciton droplets 3−18106
oxidized, crystallographic anisotropy of surface props. *(Russian)* 3−27296
p-n junction, trapping level influence on microplasma bistable state 3−15246
p-n junctions, influence of doping elements *(Russian)* 3−24502
p-n junctions, ionization energy of adhesion levels and thermogeneration centres in a volume of microplasma *(Russian)* 3−4960
p-n junctions, tunnelling electrons effective mass, electron-hole pair prod. energy 3−18213
p-type, anisotropy of magnetothermal conductivity obs. 3−1842
p-type, annealing of radiation induced defects rel. to recovery and defect energy levels 3−15158
p-type, double layer film, Hall coeff., elec. cond., transverse magnetoresistance, thickness effects *(Russian)* 3−8284
p-type, even Hall effect rel. to mag. field at 300 K *(Russian)* 3−8210
p-type, Ga-doped, Li-compensated, gamma irrad., Annealing processes 3−33844
p-type, hot carrier distrib. determ. with uniaxial stress 3−18154
p-type, influence of mag. field on hopping conduction 3−24440
p-type, iterative method for hot carrier distrib. calc. 3−18152
p-type, photon drag anisotropy 3−2140
p-type, photon drag voltage superlinear depend. on incident power density 3−24464
p-type, size effect rel. to elec. cond. and hole cooling length 3−18161
p-type field emitters, breakdown 3−39219
p-type film, transverse magnetoresistance, size anisotropy effects *(Russian)* 3−8283

germanium continued
p-type solid phase epitaxial growth from Al-Ge 3−8759
p-type substrates, transverse magnetoresistance, 80 to 300°K optical phonon scattering 3−8208
paramagnetic surface states 3−24604
phonon-assisted two-photon exciton transitions, band models and symmetry calc. 3−18105
phonon-phonon interaction, mechanism *(Russian)* 3−2117
photoemission valence-band density of states 3−5257
photoepitaxy and surface memory effect of uniaxial texture form 3−8054
photographic effect spectral sensitisation of AgBr films *(Russian)* 3−12554
photon drag effect, Q-switched CO_2 laser obs. 3−2130
photon spectrometer, operational characteristics when cooled by closed-cycle cryogenic refrigerator 3−32199
photovoltaic effect with uniaxial stress 3−18191
piezo-electroreflectance, high resolution and uniaxial, using Ge-Cu_2S heterojunction 3−2520
piezoreflectivity, 1.9-2.6 GeV, $\Lambda_3 \rightarrow \Lambda_1$ transitions 3−21426
piezoresistance mechanism in surface space charge layers 3−2164
plasma, enhanced Bohm-like diffusion across mag. field 3−8215
plastic deformation on slow loading *(Russian)* 3−30181
plasticity, effect of preliminary deform. *(Russian)* 3−4788
polytype, pseudopotential calcs. rel. to band structure and form factor 3−21005
pseudopotential, nonlocal calc. 3−38792
radiation damage, proton, single crystals, shadow effect, defect kinetics, radiation stability of lattice 3−33573
radiation defects due to 45-50 MeV electrons, carrier density and minority carrier lifetime obs. *(Russian)* 3−36332
radiation detector, elec. props. and growth 3−12314
radiation detector, formation of signal *(Russian)* 3−310
radiative recombination at dislocations, influence of electron irradiation and annealing 3−34423
radiative recombination of biexcitons, photolum. *(Russian)* 3−8663
Raman spectrum, second order, Raman tensor 3−30822
recombination characteristics, effect of impurities *(Russian)* 3−24392
reflectivity spectra, 1.8-3.0 eV, Al absorpt. effects 3−39162
resistance thermometer, a.c. and d.c. resistance determinations 3−25691
resistance thermometer, four terminal, using a.c. bridge circuit 3−5808
resistivity and lifetime changes during deform. before fracture 3−27279
resonant Raman scattering, room temp. and 77K 3−5201
self-interstitials, geometrical config., migration energy 3−33522
shallow donor impurities, chem. shift parameters 3−27224
shallow donor impurity near-surface states, theory 3−24494
single crystal discs, transmission electron microscope obs. 3−38705
single crystals, Na^+ induced lattice radiation damage, effects on angular and energy distributions of scattered ions, $E<5$ keV *(Russian)* 3−11663
solubility of Au, Si influence *(Russian)* 3−7783
sputtered amorphous layer, effect of deposition rate on physical props. 3−4934
structure change and elec. resist. step of evaporated Ge film, depend. on substrate temp. 3−30372
structure factor determ. by reflection profile mwthod using triple-crystal diffractometer 3−23968
substrate, Cd film deposition, initial stages 3−18036
substrate, Cd film deposition, nucleation, growth, and evaporation 3−18037
substrate, diffusion of Ga and As during epitaxial growth of GaAs *(Russian)* 3−27606
surface, defects due to lapping with diamond powders *(Russian)* 3−20918
surface, electronic structure determ. by positron annihilation technique 3−38878
surface electron impurity states *(Russian)* 3−8247
surface potential, in electrolyte, change under mechanical deform. 3−21139
surface properties, fast state conc. and surface potential, γ-ray effects *(Russian)* 3−24490
surface state energy spectrum, kinetics of pulse field effect 3−24499
surface states, bound and scattering, theory *(German)* 3−15237
surface states absorpt. spectrum, oxidation effect 3−2163
thermal cond., longitudinal and transverse phonons contrib. in Ziman limit 3−17940
thermal conductivity fluctuation, spectral density *(Russian)* 3−1838
thin film, amorphous-crystal boundary, electron diffraction pattern 3−11839
thin film, temp. distrib. on crystn. by zone melting *(Russian)* 3−34485
third harmonic generation, in strong microwave field *(Russian)* 3−11924
three dimension camera, for positron emitting radioisotopes 3−32197
three-phonon umklapp resistance, upper and lower bounds 3−27089
two electron donor pair system, light absorpt. and mag. susceptibility 3−2579
two-layer dielectric thin films thickness meas. on Ge substrate using ellipsometric method 3−13230
two-phonon deformation potential 3−7883
ultrapure, shallow donor levels, photocond. obs., two-step process 3−4965
vapour growth in open iodide system, efficiency of Ge transport *(Russian)* 3−15615
wafers, cleaning procedures, Auger analysis of residual surface contamination 3−39252
wettability by Au alloys *(Russian)* 3−8006
whisker, elastic props. and torsional strength 3−38759
X-ray diffraction, Borrmann many-wave effect *(Russian)* 3−26951
X-ray monochromator of high definition and intensity using Si(111) or Ge(111) crystals 3−26945
γ-ray spectrometer, with Al regrowth p^+ contacts 3−35487
$Al_xGa_{1-x}As$:Ge epitaxial film, photolum., 1.1-2 eV *(Russian)* 3−2589

germanium continued
As-Se-Ge amorphous films, photo-darkening effect 3−5212
Bi_2Se_3:Ge, lattice defects, reflectivity meas. at plasma resonance 3−33824
$Eu_{1-x}Gd_xO$, refl. in visible and i.r. spectra, effect of Gd^{3+} ions for elec. cond. 3−5214
GE:Sb, high frequency monochromatic phonon spectroscopy 3−1765
p-GaAlAs:Ge, electron diffusion lengths Al content depend. 3−18165
p-GaAs:Ge, epitaxial, electron diffusion length, recomb. lifetime 3−18164
p-GaAs:Ge, epitaxial layer, electron diffusion length variation with hole conc. 3−24449
GaAs:Ge epitaxial layer, near band-edge photoluminesc. 3−34406
p-Ge, autoemission volt ampere characts. with O_2 adsorption rel. to elec. breakdown 3−8709
Ge, growth form and soln. form relation *(German)* 3−9079
Ge, optical absorp. var. with mag. field intensity, determ. of band struct. *(German)* 3−34332
Ge I and II, neutral and singly ionized, absolute transition probabilities 3−33024
Ge:Al, implanted acceptor levels, rel. to carrier generation at room temp. 3−2083
Ge:As, Ga, indirect semicond., direct transition probability in impurity luminesc. 3−15554
Ge:As,Sb, luminesc. spectra due to electron-hole radiative recomb., virtual bound state, 2K 3−8632
Ge:As system, phase separation, X-ray photoemission study 3−36421
N-Ge:Au, hysteresis of I-V characts., and props. of elec. domains *(Russian)* 3−2100
Ge:Au, impact ionisation of deep acceptor impurities 3−33918
n-Ge:Au piezoresist., influence of deep energy levels *(Russian)* 3−2074
p-Ge:Au whiskers, plastic deform., 760°C *(Russian)* 3−27055
Ge:B, excitation spectra, Zeeman effect with linearly polarized light 3−2566
Ge:B, neutron irradiated, X-ray obs. 3−17876
n-Ge:Cu, current fluctuations, 77-200 K *(Russian)* 3−27257
Ge:Cu, effect of impurity on kinetics of annealing of radiation defects 3−24111
Ge:Cu, space charge limited currents rel. to photoelec. amplification 3−15198
Ge:Ga, distrib. coeffs. for Ga doping during growth in open iodide system *(Russian)* 3−15643
Ge:Mn; Sb, recomb. wave current instability rel. to mag. field *(Russian)* 3−8180
n-Ge:Ni, local negative photoconductivity in strong electric fields 3−24479
n-Ge:Ni, surface domains in strong elec. field, 77-300K *(Russian)* 3−8245
Ge:Sb, Cu, kinetics for Cu precipitation, interaction with Sb 3−14979
Ge:Sb, direct absorp. edge, exciton plasma resonance obs. *(Russian)* 3−5211
Ge:Sb, dislocation mobility study, depend. on temp. and loading *(Russian)* 3−24120
Ge:Sb, relaxation processes involving trapping levels in bistable microplasmas 3−24452
Ge:Sb, reson. scatt. of phonons by bound donor electrons 3−30223
Ge:Sb,(:As), phonon conductivity, determ. of density of states effective meas. in 1 to 20 K range 3−8121
Ge:Sn, heavily doped single cryst., Hall mobility, impurity conc. depend. 3−33885
Ge:Sn, Si, luminesc. of indirect excitons, zero phonon radiative annihilation 3−21479
Ge/Al thin film system, surface mass transfer mechanism, diffusion phenomena *(Russian)* 3−11836
Ge-electrolyte interface, current multiplication noise *(Russian)* 3−5051
Ge-metal, non-rectifying point contact, hot hole noise dep. on lattice temp. *(Russian)* 3−33992
n-Ge-Pb Schottky barriers, under press., phonon tunnelling spectroscopy 3−36379
Ge-Si alloy or radiation detector 3−306
Ge-SiO_2, Ge-SiO_2-Si_3N_4 semiconductor-insulator boundaries, surface states, C-V method, low temp., 77K *(German)* 3−15264
Ge^{4+} in MgO crystal, cation diffusion studies using a sectioning technique 3−33694
Ge(Li) coaxial detectors, carrier drift velocity variation with electric field 3−3859
Ge(Li) coaxial detectors, total efficiencies with disc sources 3−304
Ge(Li) detector, coaxial, in γ-ray camera for diagnostics 3−402
Ge(Li) detector, efficiency calibration and properties for low energy photons 3−19298
Ge(Li) detector, Monte Carlo calculation of efficiencies and response functions for thick disc γ-ray sources 3−3853
Ge(Li) detector, using flexible cryostat 3−25704
Ge(Li) detector γ-ray spectra, computer evaluation 3−37689
Ge(Li) detectors, absolute efficiency, $^{108}Ag^m$ as calibrating source 3−32164
Ge(Li) detectors, counting circuit 3−13442
Ge(Li) detectors, effects of fast neutron damage on energy resolution 3−22466
Ge(Li) detectors, efficiency calibration by ^{90m}Y 3−25878
Ge(Li) detectors, efficiency calibration by ^{169}Yb and ^{110m}Ag 3−25880
Ge(Li) detectors, linear adding circuit 3−32196
Ge(Li) detectors, timing system 3−319
Ge(Li) diode curved crystal spectrometer as band filter for γ-rays 3−3868
Ge(Li) planar detector, polarimetric efficiency 3−25861
Ge(Li) planar detector, polarimetric efficiency 3−25865
Ge(Li) planar detectors, influence of magnetic field and temp. on pulse rise time 3−3850
Ge(Li) spectrometer, dead time reduction system *(German)* 3−10087
Ge(Li) thin window detectors, efficiency near absorption edge of Ge 3−25877

germanium continued
Ge(Li) X- and γ-ray spectrometer energy resolution dependence obs. based on Gaussian response to monoenergetic photon source 3−326
GeS semiconductor-insulator boundary, m.i.s. structure, capacity, field emission, measurements *(German)* 3−15263
GeSi film, anomalous photovoltage, detection of X-rays *(Russian)* 3−10045
Li, diffusion into Ge at low temps., technique 3−11645
LiH:Ge, excitation and luminesc. spectra *(Russian)* 3−21462
LiH:Ge, red luminesc., 120 and 293 K *(Russian)* 3−15538
n-type, intervalley instability of current due to nonequilib. carriers 3−15208
Nb-Ti-Ge alloys, superconductivity, effect of Ge addition *(Japanese)* 3−30563
O doped and Li diffused, carrier density and mobility studies, effect of photon irradiation and annealing 3−18136
O_2 covered (100) surface, scattering of metastable molecular beams 3−39204
Sb_2Te_3:Ge, reflectivity meas. with different Ge content 3−8605
Si diffused layers, reproducibility 3−30954
Si:Ge, radioactive tracer meas. of ^{71}Ge diffusion 3−24293
SiO_2-Si_3N_4 combination layers *(German)* 3−30957
in Ti-Nb system, phase equil. *(German)* 3−24837
YIG:Ge substituted, anisotropy and magnetostriction, ferromag. resonance obs. 3−5136
YIG:Ge^{4+}, mag. after-effect, electronic hopping processes 3−24591

germanium compounds
germania glass, atomic ordering 3−14691
germania glasses, diffr. patterns, cryst. ordering study 3−30076
organometallic, conformational equilib. force field calcs. 3−11221
p-n junction on Ge alloy surface, catalytic effect 3−8257
Al-Ge alloys, vacancies influence on nucleation of incoherent Ge precipitates 3−2702
$As_{30}Ge_{10}S_{12}Te_{48}$ amorphous film, switching props. *(German)* 3−15229
CoO-MgO-GeO_2, spinel-olivine and olivine-phenacite transitions, thermodynamic and vol. relations 3−27122
CoO-ZnO-GeO_2, thermodynamic relations among olivine, spinel and phenacite structures 3−27123
Fe-Ge alloys, diffusivity, permeability and solubility of hydrogen 3−1828
n-GaAs/Ni/Au-Ge ohmic contact, Auger electron spectroscopy and sputter etching 3−4903
Ge-As-Te-Si, Ge-As-Te amorphous films, switching and memory effects 3−18198
Ge-Se system, current-voltage characteristics and temp. depend. of low-field conductivity 3−38843
Ge-Si-Sb phase diagram study *(French)* 3−17959
Ge-Te glass quenched, oxygen effect on struct. props. 3−33458
Ge-ZnP_2 system, phase diagram, rel. to $ZnGeP_2$ cryst. growth 3−12271
GeAs-GeP system, phase diagram *(Russian)* 3−14962
$GeBr_2$, matrix isolated, Fourier transform far i.r. spectrum 3−18798
GeF, rot. struct. in $A^2\Sigma^+$, $B^2\Sigma^+$ and $a^4\Sigma^- - X^2\Pi$ transitions 3−23555
GeF_2, weak emission bands in 3250-3700 Å region 3−33110
GeF_4, bond dissoc. energies, ioniz. pots. and electron affinities 3−20191
GeH_4, i.r. and laser Raman gas spectra 3−29661
GeH_4 thermal decomposition, Ge film growth 3−8719
GeH_3Br microwave rational spectra of vibrational states 3−20169
GeI, u.v. spectra, 220 to 250 nm band interpretation 3−29643
Ge(IV) mixed coordination compounds, i.r. spectra *(Russian)* 3−26673
GeO, relative escape depth of Auger and photoelectrons 3−21505
GeO, thermogram at high temps. obs. of endo and exo-effects *(Russian)* 3−12512
GeO_2, hexagonal, lattice parameters, thermal expansion coeff., 36-516°C 3−36280
GeO_2, hyperfine, superhyperfine and quadrupole interactions for V^{4+} 3−34198
GeO_2, interband optical transitions strengths 3−34362
GeO_2, vitreous scattering of low frequency phonons at low temps. 3−1769
GeO_2 thin vitreous surface layer, struct. study by i.r. reflection spectra *(Russian)* 3−36467
GeO_2-CdO-Na_2O-H_2O system, crystallisation under hydrothermal conditions at constant temperature 3−33508
GeP_3, crystal struct. note 3−7694
$(GePbSn)_{0.5}Te_{0.5}$ amorphous film, photocond., temp. and intensity depend. 3−18186
GeS, amorphous, black P struct. model 3−33457
GeS, Ge semiconductor-insulator boundary. m.i.s. structure, capacity, field emission, measurements *(German)* 3−15263
GeS film, i.r. absorpt. spectra during amorphous-polycryst. transition *(Russian)* 3−15109
$GeSb_2Te_4$, crystal growth and semicond. props. 3−5279
GeSe, amorphous, black P struct. model 3−33457
GeSe, cryst. growth, transport rate, growth mechanism and morphology 3−11573
GeSe film, i.r. absorpt. spectra during amorphous-polycryst. transition *(Russian)* 3−15109
$Ge_{0.5}Si_{0.5}$ amorphous film, struct. and Raman scatt. 3−36501
$Ge_{0.5}Sn_{0.5}$ amorphous, l.f. Raman scatt., freq. depend. coupling const., elastic continuum limit 3−8586
GeTe, amorphous, black P struct. model 3−33457
GeTe, amorphous film, switching and memory effects 3−18206
GeTe, crystalline and amorphous, similarities in valence bands, X-ray photoemission determ. 3−33796
GeTe film, amorphous, thermopower, comparison with crystalline film 3−2116
GeTe film, i.r. absorpt. spectra during amorphous-polycryst. transition *(Russian)* 3−15109
GeTe-A^{II}Te solid solution, thermoelectric properties, temperature dependence 3−30502
$Ge_{0.175}Te_{0.825}$, struct. of amorphous and liq. state from neutron scatt. 3−33456
$Ge_{15}Te_{81}S_2As_2$, amorphous, IV characts, hydrostatic press. depend. 3−38830
GeX_4, where X=halogen, n.m.r., ^{73}Ge chemical shift, coord. depend. 3−29715

germanium compounds continued
  Na_2O-CdO-GeO_2-H_2O system, hydrothermal crystallisation *(Russian)* 3—17745
  Na_2S-GeS_2, struct. investigation of sodium thiogermanate with infinite $(GeS_3)^{2n-}{}_n$ chains *(French)* 3—14817
  Ni-Ge (2% Ge), optical constants *(Russian)* 3—15469
  NiO-MgO-GeO_2, spinel-olivine and olivine-phenacite transitions, thermodynamic and vol. relations 3—27122
  NiO-ZnO-GeO_2, thermodynamic relations among olivine, spinel and phenacite structures 3—27123
  $Pb_{1-x}Ge_xTe$ laser, c.w. operation, 4-6μ, and appl. to NO spectroscopy 3—4107
  PbSe-$Ge_{1.5}As_{0.5}Se_3$, pseudobinary system, immiscibility, liquidus temp., electron microscopy 3—20853
  PtGe, single cryst. growth and characterization 3—5268
  $Se_{50}Te_{20}As_{20}Ge_{10}$, amorphous, stress thermally induced by switching 3—27293
  Si-Ge, epitaxial layer grown on Si substrate, crystal defects obs. 3—1920
  Si-Ge, solid soln., anal. of vapour grown homogenous crystals 3—2649
  Si-Ge alloys, oxidation to form m.o.s. capacitors and transistors 3—1902
  n-Si-Ge alloys, Si-rich electron magnetic susceptibility and band structure 3—36530
  Si-Ge:P alloy, electron micro. exam. after annealing at 500°C *(Russian)* 3—12346
  SiGe alloys, radioisotope thermoelectric generator, space vehicle power plant, sublimation mechanisms of alloy 3—5266
  SiGe alloys, thermoelectric props., dopant precipitation, experimental model, long term projections of properties 3—5024
  SiGe alloys as thermoelectric materials, electrical props., dopant precip. 3—5023
  Te-As-Ge-Si film, accumulation effects in switching 3—18200
  Te-As-Ge-Si film, freq. depend. cond., and capacitance 3—2092
  Te-Ge-As alloy film, laser writing and erasing 3—4113

getters
  see also electron tube manufacture; vacuum techniques
  electrostatic getter-ion pump, performance 3—37611
  ion pump, for processing electrostatically focused klystron amplifier 3—19183
  r.f. getter sputtering plant, gas analysis by mass spectrometry 3—22303
  Si, ion-damaged surface layers, gettering rates of fast-diffusing metal impurities 3—5276
  Zr-Al bulk getter, secondary electron emission 3—19182

GeV nuclear reactions and scattering *see high-energy nuclear reactions and scattering*

giant pulsations (earth) *see micropulsations*

Gibbs function *see thermodynamics*

Ginzberg-Landau theory *see superconductivity*

glaciers
  Alpine glacier meltwater and transport of major cations by sorption 3—9099
  Antarctic ice sheet surges rel. to sea level rises and interglacial climates 3—39540
  Arctic ice pack, removal of aircraft altitude var. from laser profiles 3—25343
  Arctic ice-cap removal rel. to model of general atmospheric circulation 3—15980
  Artic ice-water boundary, ambient noise generation in 100 to 1000 Hz. range 3—2950
  Camp Century, Greenland, $^{18}O/^{16}O$ ratio in deep ice cores rel. to glaciation 3—39539
  Carstensz, last major advance, maximum age 3—2866
  eastern Baffin Island, glaciological responses to climate 3—39534
  floating ice plates, deformation and stress 3—3944
  floating ice tongue on Antarctic seawater, stable isotope analysis 3—15854
  flour dissolution Antarctic Circumpolar Current as a silica source 3—21929
  global climate effects of ice sheet growth, dynamics of ocean-cryosphere system 3—39501
  holocene late glacial maximum and marine transgression in eastern Canadian Arctic 3—2874
  interglacial and postglacial climates rel. to pollen records 3—39532
  Langjokull ice sheet, Iceland, volcanic history and tectonics 3—37146
  late Quaternary vertical movements, evidence of glacio-isostatic rebound, a review 3—25150
  Laurentide ice sheet, estimated volumes during Late Wisconsin (Pleistocene) 3—25347
  paleoclimatology, review 3—9291
  polar ice sheets rel. to unstable tetrahedral mantle-convection model 3—34827
  Present Interglacial, conference (Rhode Island, 26-7 January 1972) 3—39570
  Present Interglacial and Future Ice Age, climatic conditions 3—39536
  seismic P-wave velocities rel. to density of firn and ice *(German)* 3—15915
  temperate, compositional variation of gases 3—2842
  under-ice acoustic transmission loss rel. to ice roughness and seawater-ice interface 3—2843

glass
  see also amorphous semiconductor materials; glass industry; glass-metal seals; vitreous state
  activated fibres, properties in amplification region *(Russian)* 3—6488
  activation energy for viscous flow in transformation range 3—33460
  adsorbent, adsorption kinetics of polar polymers 3—36486
  air-glass-air system, verification of Fresnel and Airy equations 3—37
  alkali aluminosilicate and aluminogermanate melts and glasses, isostructural relations *(German)* 3—21735
  alkali borate, density *(Japanese)* 3—21747
  alkali metal-silicate, γ-irrad. at high pressures, e.p.r. of paramagnetic defects *(Russian)* 3—27417
  alkali silicate, u.s. velocity, temp. depend., liq. He temps. 3—36368

glass continued
  alkali silicate glass, e.p.r. spectral linewidth of hole centres *(Russian)* 3—39029
  alkali tellurite, e.p.r. spectra, irrad. effects *(Russian)* 3—21309
  aluminophosphate glass, struct. obs. using ^{57}Fe Mossbauer effect 3—24636
  aluminosilicate, transition metal ion substitution, Mossbauer and i.r. obs. 3—7631
  alumosilicate thin films, electrical inhomogeneity in m.i.m. structures, residual polarisation measurement *(Russian)* 3—11960
  Annual review of materials science vol. 2, 1972 3—24778
  antireflection coatings, high vacuum deposition *(Rumanian)* 3—22337
  in Apollo 15 soils, major element composition 3—5588
  arsenosilicate glass source, As diffusion in Si, through SiO_2 layer 3—39260
  bead compacts, sintering obs. of neck growth and closed pores 3—15749
  bead filled styrene-acrylonitrile copolymer, surface particle protrusion and dewetting 3—34647
  bead/polymer composite, stress-strain behaviour, crazing, permeability 3—24986
  bending, fracture, stress waves 3—33606
  blanks, for minimum rejection of moulded components, optimal dimensions selection 3—25747
  borate:$Tb^{3+}(Gd^{3+})(Eu^{3+})$, cathodoluminescence of $^5D_3$ and $^5D_4$ levels for surface fluorescence study 3—2598
  borate and phosphate, Tm^{3+}, Er^{3+}, fluorescence, energy transfer processes, efficiencies, decay times 3—21466
  borono-silicate, radioactive waste glasses, investigation 3—35939
  borosilicate, abraded and pristine state, static fatigue data 3—9001
  borosilicate, hydrogen-impregnated, e.p.r. study of radiation damage 3—18359
  borosilicate, ion diffusion and influence of two-site mechanism 3—14699
  borosilicate, ion exchange chemical strengthening 3—15789
  borosilicate films, sintered, Vickers microhardness characterisation 3—39377
  borosilicate thin films, electrical inhomogeneity in m.i.m. structures, residual polarisation measurement *(Russian)* 3—11960
  cationic cyanine dye molecules adsorption on glass, ionisation energies 3—27901
  ceramic, transmission electron microscope exam., thin foil prep. technique, microstruct. characteriz. 3—34645
  ceramics, tetrasilicic mica, strength depend. on mica grain size 3—8982
  ceramics, texture development 3—5343
  chalcogenide, electronic conductivity and switching 3—18134
  chalcogenide, low temp. thermal conductivity 3—1848
  chalcogenide, reversible thermal breakdown as a switching mechanism 3—18197
  chalcogenide film, differential thermal anal., structure and switching 3—8061
  chalcogenide glass alloys, thermal and non thermal processes threshold structures 3—8236
  chalcogenide glass thin film bolometers, props. 3—13235
  chalcogenide thin layers, softening point, thickness dependence 3—8064
  chalcogenide threshold switches, thermal and nonthermal relax. processes 3—21127
  colour filter glasses, photolum. props. 3—28555
  composite, effect of specimen geometry on fatigue strength 3—21770
  composite, glass microsphere/epoxy resin, adhesion, hydrolytic stability, thermomechanical props. *(Russian)* 3—31152
  contact with Au or Ni, electrification of metal 3—2168
  cordierite, crystn., oxide additive effects on devitrification characts. 3—34643
  cordierite, crystn., oxide additive effects on devitrification characts. 3—34644
  cordierite, review of anal. methods for crystallisation 3—12453
  coupled conduction-radiation heat transfer, spectral and boundary effects 3—33703
  crystallization effect on spin-lattice relax. time, Mossbauer spectra h.f.s. 3—36826
  crystallization from supercooled melts, statistical thermodynamics 3—30073
  Darwin, possible impact crater 3—2853
  defect form. and crystal growth on electron bombard. 3—7790
  determination of silica by X-ray diffraction *(French)* 3—13497
  diamond drilling, temp. field calc. 3—22780
  dichromated gelatin bonded, holographic display element 3—203
  dielectric films, X-ray induced photoconductivity 3—18184
  dielectric relaxation, high and low frequency and molecular mobility 3—24651
  diffusion interactions from anion conc. discontinuities 3—18723
  diffusion of Na, atmosphere effects 3—1816
  dispersive properties of rough screens in near i.r. region *(Russian)* 3—25740
  dosimeter with fluoride-based radiophotoluminescent glass *(German)* 3—26545
  DTA method for evaluation of glass-forming tendency of melts 3—1575
  dynamic contact angle of liquids on glass, velocity effects 3—8007
  E-glass, absorpt. of water vapour, thermodynamic nature of adsorbate adsorbent interface 3—8016
  electric tank furnaces for melting of Pb containing glass 3—22340
  electron correlation and susceptibility 3—15319
  electron induced emission spectra at low temp., in glass containing adenine 3—30887
  electrovacuum, density change meas. and mechanism of radn. damage due to electrons, neutrons or γ-rays *(Russian)* 3—11548
  epoxy composite plates, post-buckling behaviour 3—27756
  e.p.r. of trapped H atoms and cross relaxation induced by Cu(II) complexes 3—8414
  etched laser filament tracks, self-focusing 3—19642
  europium silicate, Mossbauer effect, recoilless fraction 3—21348
  fabric laminate reinforced composite, compressive strength *(Japanese)* 3—18715
  fabric laminate reinforced composite, torsional strength and void effects *(Japanese)* 3—18714

glass continued
  fabric reinforced plastic shells, anisotropy of props. 3−24979
  fibre, statistical strength distrib. functions 3−31147
  fibre laser communication system components, development *(German)* 3−16919
  fibre laser communication systems *(German)* 3−16918
  fibre optical waveguides for laser communication systems 3−35718
  fibre reinforced composites, crack propag. vel. 3−21727
  fibre reinforced cylindrical shells, elastoplastic deform. 3−27761
  fibre reinforced polyester laminates, mech. props. *(Japanese)* 3−18707
  fibre/C fibre sandwich composite, Izod impact props. 3−31131
  fibres, radially inhomogeneous, wave propagation 3−16797
  fibres, static hysteresis from −78 to 196°C 3−38619
  fracture due to laser generated stress pulses 3−16896
  germania, diffr. patterns, cryst. ordering study 3−30076
  germania 3−14691
  glass:Nd, laser-induced-fluorescence-line-narrowing spectroscopy 3−21474
  glass:Nd Q-switched laser, giant pulse laser action 3−4105
  glass:Yb, Tb(Eu) luminescence, cooperative processes *(Russian)* 3−36907
  glass-ceramic microstructures formation by two stage heat treatment, high nucleation density 3−12439
  glass-ceramics, solid state reactions 3−15786
  glassy state of liq., liq. cryst., cryst. 3−14692
  grain prep. for durability testing, investigation 3−15788
  heat and mass transfer on the surface of glass-graphite materials in high temperature gas stream *(Russian)* 3−26786
  history of glassmaking, book 3−9786
  hopping Hall effect, single phonon contribution 3−27274
  ideal, plastic flow via dislocations 3−17833
  IFS25, IKS27 glass protective coatings for optical filters vacuum deposition *(Russian)* 3−5916
  impact glasses from suevite of Nordlinger Ries crater 3−15888
  inclusions, gaseous, anal. using quadrupole mass spectrometer 3−13504
  induced Mandelstam-Brillouin scatt. power 3−19645
  inorganic, structure, review 3−24032
  inorganic ions in glasses and polycrystalline pellets as fluorescence standard reference materials, review 3−35349
  invisible, coating techniques 3−19190
  ion exchange at low temps. and effect on internal friction 3−25064
  ion exchanged gasses, Rayleigh wave study of ionic diffusion and stress buildup 3−4916
  i.r. spectra at high pressures 3−12134
  kaolinite glasses, pure and Fe-doped, recrystallisation 3−7632
  laminated glass beams in 4-point bending, experimental and theoretical study of strength 3−32354
  laminates, glass reinforced epoxy and polyester, creep mechanism 3−9000
  lanthanide oxide-silicate, preparation and i.r. absorption spectra 3−5187
  laser, Hoya LCG11, laser damage, surface effects, thresholds 3−28591
  laser, self-focusing, 'SELFOC', continuous oscill. and amplification characts. 3−19614
  laser, self-focusing, damage, subnanosecond pulses, n_2 measurements 3−29150
  laser, stable oscillator producing harmonics 3−22380
  laser, surface damage, Owens-Illinois ED2 glass 3−29116
  laser damage, bulk, interaction gradients light scattering, concurrent and stimulated Brillouin 3−29115
  laser irradiated, energy balance and dynamics of damage *(Russian)* 3−6498
  laser rods, change in thermooptical constant 3−19226
  liquid chalcogenide, atomic reorientation rates, n.m.r. in Se and As_2Se_3 3−5143
  lithium disilicate, space-charge limited current 3−8173
  low temp. thermal conductivity in electric and magnetic fields 3−1849
  lunar, Apoloo 17 orange soil 3−37340
  lunar, thermal history 3−3309
  lunar glasses from Luna 20, major element composition 3−12985
  lunar soil glasses, electron probe analysis 3−39646
  Lunar spherules, Luna 16, surface features 3−18986
  materials, review of advances *(Japanese)* 3−18730
  melt, physical solubility, of He, Ne and N_2 *(German)* 3−7906
  melt with high fluoride content, surface convection and fold formation during cooling *(German)* 3−27161
  2-methyltetrahydrofuran glass, γ-irrad., luminescence study in temp. range 77 to 97K 3−12166
  milk type, MS20, light refl., spectral and integral characts. 3−22324
  mixed alkali effect, equations for ionic cond., mobility, diffusion coefft. and transport number 3−11765
  $Na_2O.3SiO_2$, mech. and ionic relaxation meas. and comparison with dielec. relax. 3−18410
  nitrate glass: Eu, Sm, Gd, Tb, Dy absorption, luminescent and excitation spectra *(Russian)* 3−30878
  non-silicate, coating with antireflection and water vapour protecting layers 3−25744
  obsidian from Lipari Island (Italy), fission track dating of obsidian prehistoric artefacts 3−34820
  obsidian glass, fission-track stability rel. to water concentrations, dating 3−18814
  opalescent, technology, light-scattering characteristics *(Russian)* 3−5910
  optical, for athermalized optical systems, with inhomogeneous temp. distrib. 3−5891
  optical, fund. polishing mechanism, ellipsometric obs. *(French)* 3−28534
  optical, glasses, photoluminescence 3−5925
  optical, self-focusing, relative contribution of Kerr effect and electrostriction 3−29149
  optical glass, control of refractive index during annealing *(Polish)* 3−5174
  optical glasses, self-focusing threshold powers 3−13758
  optical glasses, stress-optic coeff. dispersion, 5700-3200 Å, strain polarizability const. 3−2509

glass continued
  optical stress coefficients, dispersion 3−27483
  organic, molecular theory of viscoelastic behaviour 3−24029
  organic compounds in solution, inorganic ions in glasses, as fluorescent standard reference materials, review 3−35350
  oxide glasses with high refractive index, correlation of refractive index and density, Newton-Drude relation 3−5902
  Pb-glass, origin of fission fragment tracks 3−24135
  permeability of He, silica comp. depend. *(German)* 3−30284
  permittivity meas. using TM_{020} mode resonant cavity at 9.34 GHz 3−6026
  phosphate:$Tb^{3+}(Gd^{3+})(Eu^{3+})$, cathodoluminescence of $^5D_3$ and $^5D_4$ levels for surface fluorescence study 3−2598
  phosphate, crystn., compositional effects 3−26974
  phosphate, crystn., refining time effect, viscosity 3−26975
  phosphate, exchange interaction role in energy transfer between Eu^{3+}, Sm^{3+}, Dy^{3+} and UO_2^{2+} *(Russian)* 3−8651
  phosphate, Fe-containing, formation 3−20697
  phosphate, irrad., radiational capture centre, e.p.r. *(Russian)* 3−27415
  phosphate glasses, lanthanide activated, polarization study of luminescent centres *(Russian)* 3−24733
  phosphosilicate, chem. vapour deposition at low substrate temps. from SiH_4, O_2 and $POCl_3$ 3−2632
  phosphosilicate, passivating film, in m.o.s. struct., surface state charge, influence of deposition conditions 3−8266
  phosphosilicate glass layers, analysis by Rutherford backscatt. and channelling meas. 3−38539
  phosphosilicate glass passivation, SiO_2 films on Si, ion bombardment effects 3−39288
  phototropic, TlCl activation 3−27737
  polymer, low temp. equation of state 3−4499
  polynary telluride glasses containing Ag, softening point obs. 3−7630
  polystyrene glass, structure obs. 3−12452
  porous, C-impregnated, thermometric props. at low temps. 3−5807
  porous, hygroscopicity and no dimming phenomena *(Japanese)* 3−20935
  pyrex, d.c. resistance, apparatus for measurement 3−13351
  Pyrex, radiation blackened, restoration to transparency 3−35455
  Pyrex 7740, heat capacity in field to 90 kG 3−30616
  Pyrex glass, carbon fibre reinforced, mechanical props., strength 3−18700
  pyroxene, glass. Eu^{3+}, effect of thermal working on luminescence spectra *(Russian)* 3−30874
  quartz: V_2O_5 (CoO, Al_2O_3)(V_2O_5, Al_2O_3)(Eu_2O_3), spectral obs. coeff., temp. dep. 3−36865
  quartz, pure and alloyed, temperature dependence of velocity of sound 3−27076
  quartz containing metal oxides, degree of darkness *(Russian)* 3−27491
  radioactive high level waste storage, phosphate and borosilicate glasses for, obs. 3−35940
  reactions in vitreous and amorphous solids 3−5389
  refractive index, dispersion and magnitude 3−36851
  reinforced plastic cylindrical shell weakened by circular opening, cantilevered, bending 3−31149
  reinforced plastic cylindrical shells, creep stability under long-term external press. 3−31144
  reinforced plastic plates, rectangular, with low shear strength, bending 3−24985
  reinforced plastic plates with central metal layer, elastoplastic stability 3−24984
  reinforced plastic rings, temp. deform. 3−27764
  reinforced plastic rings, wound, residual stresses determ. 3−24983
  reinforced plastic rings, wound, transverse characts. variation over thickness 3−31150
  reinforced plastic shell, orthotropic, effect of local load 3−31145
  reinforced plastic shells, cylindrical stability 3−24982
  reinforced plastic shells, stability and shear stresses 3−24980
  reinforced plastics, oriented, mech. characts. in shear 3−27779
  reinforced plastics, residual stresses determ. 3−27763
  reinforced plastics, tensile deform. analysis 3−31148
  reinforced plastics, wound, resist. to failure by unwinding 3−24981
  reinforced plastics in conical shells, stability of strength 3−31146
  rubber-glass contact, elec. double-layer force meas. between liquid immersed contact surfaces 3−6020
  self-diffusion processes in different glasses 3−4882
  sensitizing of radiophotoluminescent and Ag activated glasses *(German)* 3−5408
  Silas-balloon filled polystyrene composites, mech. props. *(Japanese)* 3−21728
  silica, atomic ordering 3−14691
  silica, diffr. patterns, cryst. ordering study 3−30076
  silicate, hydrolysis of surface bonds, influence of mechanical stress 3−39469
  silicate, Pr_2O_3 and Nd_2O_3 mixtures combined with NiO effects on transparency curve *(Russian)* 3−12159
  silicate, struct. and props. 3−5355
  silicate glasses, diffusion rates and solubilities of He and Ne as a function of SiO_2 content 3−4883
  sintered optical fibre, viscosity exam. in softening and annealing temp. regions *(Russian)* 3−11549
  soda borosilicate glasses, composition determ. by tie-line plotting 3−10203
  soda-lime, abraded and pristine state, static fatigue data 3−9001
  soda-lime, doped with iron, Mossbauer study 3−18396
  sodium borosilicate, B coordination state rel. to comp., n.m.r. obs. *(Russian)* 3−14694
  sodium borosilicate, metastable phase separation regions, tie line directions determ. 3−7926
  sodoborate glasses with ZnO, X-irrad., e.p.r. of Zn^+ centres, g-factor anisotropy *(French)* 3−30684
  solid state detectors, heavy ions measurement *(German)* 3−35482
  spark chambers, glass sealed, clearing field effects 3−16519
  spectral absorption *(Czech)* 3−35399
  spectral broadening in self-focusing of single ultrashort light pulses 3−16908
  spherical surfaces control by interferometry *(Czech)* 3−35404
  stoichiometric diopside, microscopic study *(Russian)* 3−30074

glass continued
- strength, environmental effects via surface water release 3−24999
- strength behaviour, obs. and theories 3−5356
- substrate, Au film covered, laser damage 3−10560
- substrate, critical temp. for vapour deposition of CaSe, Ca, Se 3−15622
- substrate, thin film adhesion, meas. by direct pull method *(Russian)* 3−31238
- surface flatness change over 10 years 3−13281
- surface properties, review 3−25017
- synthetic Apollo 11 composition glasses, subsolidus reduction and metallic Fe 3−12994
- tektites, halogens and U contents rel. to obsidians and impact glasses 3 16199
- thermal diffusivity at elevated temps. 3−24978
- tie-line plotting determ. by structural methods 3−10203
- titania-silica, optical attenuation, bleaching, H_2 evolution 3−21447
- transition metal oxide, switching delay time measurement 3−18199
- transition metal semiconducting phosphate, transport props. 3−8175
- trapped dielectron at 77K, semicontinuum model 3−38813
- tungstate:$Tb^{3+}(Gd^{3+})(Eu^{3+})$, cathodoluminescence of $^5D_3$ and $^5D_4$ levels for surface fluorescence study 3−2598
- uniaxial strength, porosity effects, working model 3−39383
- u.s. attenuation, low temp., resonant absorpt. 3−7861
- u.s. cleaning *(Czech)* 3−34467
- vapour pressure curves and solubility, temperature dependence *(German)* 3−14985
- vibrational excitations, review 3−1770
- viscosity changes below vitrification temp. *(Russian)* 3−14697
- waveguide, optical Kerr effect 3−32583
- waveguide, small signal Raman gain 3−32582
- As-S-I:Mn^{2+} e.p.r. study 3−30686
- As-Se-Ge film, transmission, refractive index, edge shift, laser irradiation effect 3−19639
- As-Te-I:Mn^{2+} e.p.r. study 3−30686
- $As_{30}Ge_{10}S_{12}Te_{48}$ amorphous film, switching props. *(German)* 3−15229
- As_2O_3-SiO_2, diffusion source for As in Si and SiO_2 3−21545
- As_2O_3-SiO_2 film, diffusion sources, effect of heat-treatment on comp. 3−20963
- As_2S_3 glass, clearing coatings production *(Russian)* 3−5904
- As_2S_3 glass and crystalline phases, magnetic susceptibility 3−8334
- AsSI, AsSeSI, semiconducting, i.r. transmissivity, instability at softening temp. *(Russian)* 3−2552
- $AsSe_x$ glasses, $x=1$-20 electrical conductivity between 300-700K *(Russian)* 3−8160
- As_2Te_3 melt, DTA method for evaluation of glass-forming tendency 3−1575
- Au-glass cermet film, strain sensitivity and t.c.r. 3−5065
- B_2O_3 glass, static and dynamic PVT obs. using acoustic densitometer 3−1774
- B_2O_3-BaO-Fe_2O_3, dielectric constant meas. 77 to 300 K, morphology magnetisation curve 3−12020
- B_2O_3-Li_2O, B_2O_3-BeO-Li_2O, Be_2O_3-BeO-SiO_2 and Be_2O_3-BeO systems, i.r. spectra and structural analysis *(Russian)* 3−27508
- $B_2O_3-Li_2O(Na_2O)(K_2O)$, effect of adding N_2 at different temps. *(German)* 3−7628
- $BaO.P_2O_5$ glass, absorpt. spectra rel. to redox behaviour of Fe 3−24723
- $BaPO_3F$-$Al(Ga)F_3$-$Li(Na)(K)(Zn)(Cd)(Pb)F_x$, vitrification and crystallisation capacity *(Russian)* 3−14698
- BeF_2, ^{19}F, n.m.r. 3−34224
- BeO-Al_2O_3-SiO_2-MgO, thermographic and X-ray study of struct. transforms. *(Russian)* 3−11547
- Bi^{2+}:oxide glass, absorpt., fluoresc., excitation and decay time meas. 3−12168
- CaO-MgO-P_2O_5-SiO_2 glass, effect of fluorine addition on crystallisation 3−20698
- $CaO.P_2O_5$ glass, absorpt. spectra rel. to redox behaviour of Fe 3−24723
- $CaO.P_2O_5$ glass:Cu^+, fluoresc. 3−30869
- $CdAs_2$ melt, DTA method for evaluation of glass-forming tendency 3−1575
- $Co(PO_3)_2$-$CsPO_3$, glasses and melts, effect of water on molar props. *(Russian)* 3−14696
- Cr^{3+} in glass, interference states in absorption spectrum *(Russian)* 3−8620
- Cs_2O-Al_2O_3-SiO_2, areas for glass form. 3−7629
- Cu-As-Se, light-induced memory effect 3−16895
- Cu-As-Se-Au, memory effect rel. to Au content 3−33969
- $x\ CuO(1-y-x)PbO.y\ SiO_2$, infl. of CuO content on conductivity *(Russian)* 3−11889
- Fe phosphonates, X-ray diffraction study of struct. 3−33461
- Ge-Te melts. quenched, oxygen effect on struct. props. 3−33458
- K_2O-SiO_2-Al_2O_3 system, study of crystalline phases by i.r. spectroscopy and X-ray analysis *(Russian)* 3−24031
- K_2O-SiO_2-BeO system glasses and crystn. products, synthesis and characteriz. *(Russian)* 3−11551
- $K_2O.2SiO_2$, homogeneous nucleation rate 3−33459
- La_2O_3-SiO_3, radiation centres investigation by e.p.r., absorption spectra and thermal decolourising *(Russian)* 3−30697
- Li_2O-Al_2O_3-SiO_2, Gd^{3+} doped, e.s.r. during crystn. 3−27403
- Li_2O-K_2O-TiO_2-SiO_2 type, n.m.r. of ^7Li, alkaline ions position determ. 3−2410
- Li_2O-SiO_2, liq. phase separation and crystal nucleation 3−30075
- $Li_2O.Al_2O_3.2SiO_2$, internal friction 3−1693
- $Li_2O.2SiO_2$, homogeneous nucleation rate 3−33459
- MgO-Al_2O_3-SiO_2-TiO_2 glass-ceramic, crystn. and struct. 3−31161
- $MgO.P_2O_5$ glass, absorpt. spectra, rel. to redox behaviour of Fe 3−24723
- MnO-Fe_2O_3-B_2O_3 glassy system, prepn. and mag. props. 3−18726
- Na_2O-B_2O_3, electron irrad., optical absorpt. spectra *(Russian)* 3−18474
- Na_2O-B_2O_3, Na_2O-NaCl-B_2O_3 glasses, u.v. absorption of Bi(III) rel. to stoichiometry of complexes 3−24724
- Na_2O-B_2O_3-SiO_2 glasses, u.s. loss 3−7860
- Na_2O-CaO-SiO_2 system, crystallisation process study by i.r. spectroscopy *(Russian)* 3−30248
- Na_2O-CdO-GeO_2-H_2O system, hydrothermal crystallisation *(Russian)* 3−17745

glass continued
- Na_2O-Cs_2O-SiO_2 glasses, self diffusion and interdiffusion coeffs. of alkali ions 3−11764
- Na_2O-K_2O, Na^+ and K^+ mobilities, 350-500°C *(French)* 3−5013
- Na_2O-La_2O_3-SiO_2, radiation centres investigation by e.p.r., absorption spectra and thermal decolourising *(Russian)* 3−30697
- Na_2O-PbO-SiO_2, absorpt. spectra rel. to redox behaviour of Fe and Cu 3−24722
- Na_2O-SiO_2, i.r. absorp., pressure depend., i.r. vibrations and elastic parameters obs. 3−5186
- Na_2O-TiO_2-SiO_2 glasses, X-ray diffraction studies 3−11550
- NaOH photoexcitation of $Mo(CN)_8^{4-}$, electron formation 3−25087
- $Na_2O.SiO_2$, γ-irradiated, effect of alkaline-earth oxides on optical and e.p.r. spectra *(Russian)* 3−15479
- $x\ NaO.(1-x)SiO_2$, internal friction, heat treatment eff., −200 to 440°C *(Russian)* 3−11686
- $Na_2O.2SiO_2$, homogeneous nucleation rate 3−33459
- $Na_2O.3SiO_2$, electrical relax. and alkali diffusion 3−18411
- $NaPO_3$, containing water, internal friction 3−33607
- Na_2SiO_3:La photochromic, darkening characteristics caused by u.v. emission and colour centres formation *(Russian)* 3−30852
- $Na_2Si_2O_5$-$BaSi_2O_5$, phase equilibrium and crystallisation kinetics 3−24030
- Na_2TeO_3, anal. of e.p.r. spectrum of oxygen vacancies *(Russian)* 3−39030
- Nd glass laser with adjustable pulse duration *(Russian)* 3−22913
- Nd:glass fibre amplifiers, threshold characteristics of receivers *(Russian)* 3−740
- Nd:glass laser, 110 mm square aperture, face pumped, design and props. 3−19613
- Nd:glass laser, ultrashort pulses, nonlinear radiation losses *(Russian)* 3−738
- Nd:glass mode locked laser, interpulse coherence 3−4106
- Nd-doped, amplifier gain, energy transmission, two-photon absorption process 3−767
- Nd^{3+}:glass, time variation of ion luminescence, estimation of electron excitation migration 3−19621
- Nd^{3+}:glass laser, giant-pulse Porro-prism Q-switched, output energy characts. and energy utilization factor study 3−19612
- Nd^{3+}:glass laser, pumping efficiency improvement method 3−6485
- Pb glass Cherenkov X-ray spectrometer, energy resolution for electron beam 3−28701
- Pb silicate film, for solid state electronics, chemical, mech. and electrical properties *(German)* 3−15281
- Pb silicate glasses, radiation induced colouring in Cherenkov counters 3−35476
- Pb^{2+}:oxide glass, absorpt., fluoresc., excitation and decay time meas. 3−12168
- PbO-B_2O_3 system, secondary phase separation rel. to second phase volume fraction 3−9004
- PbO-B_2O_3 type, i.r. refl., band positions, conc. depend. *(Russian)* 3−12139
- PbSe-$Ge_{1.5}As_{0.5}Se_3$, pseudobinary system, immiscibility, liquidus temp., electron microscopy 3−20853
- Se based, photoreceptor, performance and applic. to zerography 3−16455
- Se-As alloys, vacuum deposited thin films, vitreus state, vibrational reflectivity spectra 3−8057
- $Se_{87}Te_{13}$, elec. switching in glass transition range 3−33970
- on Si substrates, discontinuities detection by NaOH anisotropic etch 3−11968
- fused SiO_2, abraded and pristine state, static fatigue data 3−9001
- SiO_2, superstruct., internal struct., morphology, in early crystn. 3−14693
- SiO_2, vitreous, diffusion of Ne, 189-720°C, obs. and models 3−30289
- SiO_2 fused below 1K, nonlinear phonon propag. 3−17952
- SiO_2 surface, plasma-modification effects, reaction kinetics with low pressure discharge *(German)* 3−31286
- SiO_2-Al_2O_3 thin film, splat cooling prepn. for transmission electron microscopy 3−18537
- SiO_2-Al_2O_3-Na_2O, improvement of mech. props. *(Polish)* 3−8989
- SiO_2-Al_2O_3-Na_2O glasses, containing TiO_2 as nucleation agent, props. and struct. *(Polish)* 3−4721
- SiO_2-Na_2O:SnO_2,$TiO_2(ZrO_2)(PbO)$, nuclear spectroscopy study of impurity effects on structure and props. *(Russian)* 3−14973
- $Sn_x(As_2Se_3)_{1-x}$ glass, struct obs. using ^{119}Sn Mossbauer effect 3−24637
- $SrO.P_2O_5$ glass, absorpt. spectra rel. to redox behaviour of Fe 3−24723
- $TINO_3$-$Cd(NO_3)_2$, i.r. spectra,, comp. depend., NO_3^- vibrations 3−21405
- Te chalcogenide, Mossbauer obs.,rel. to switching action *(German)* 3−15230
- Te-As-Ge-Si film, accumulation effects in switching 3−18200
- TiO_2-SiO_2 system, expansion optical materials 3−5890
- Tl^+:oxide glass, absorpt., fluoresc., excitation and decay time meas. 3−12168
- V_2O_5-P_2O_5, d.c. cond. by polarons, 90-520K 3−33886
- V_2O_5-P_2O_5, in m.i.m. struct., elec. characts. *(Russian)* 3−2190
- V_2O_5-P_2O_5 type, absorpt. tail, fund. absortp. edge, band gap, forbidden transitions 3−21444
- V_2O_5-P_2O_5-CaO based m.i.m. structure, elec. characts. *(Russian)* 3−27318
- ZnO-SiO_2, radiational trapping centres, e.p.r. study *(Russian)* 3−18367
- $Zn(PO_3)_2$, use as doping source for GaP:Zn,O 3−8755
- $Zn(PO_3)_2$-MPO_3:Co (M = Na, K, Cs), glasses and melts, molar props., softening temp. and structure *(Russian)* 3−14695

glass fibres *see fibres*

glass industry
- history of glassmaking, book 3−9786

glass-metal seals
- *see also electron tube manufacture*
- solid-state bonding, mechanism 3−8966

glassy state *see vitreous state*

glossaries
- crystallography dictionary, English-German-French-Russian 3−9787

glow discharge lamps *see discharge lamps*
glow discharge microphones *see microphones*
glow discharges
arc discharge transition, measurement using IC device *(Japanese)* 3−20676
cathode sputtering rate depend. on discharge current and gas pressure *(Russian)* 3−7574
circular cathode luminescence *(Russian)* 3−23954
current-voltage characteristic in toroidal discharge in radial magnetic field 3−17682
electron density and temp., r.f. and d.c. probes 3−14615
inert gases, electron energy in Faraday dark space 3−30040
interelectrode glow rel. to spark current growth stage in vac. breakdown at const. voltage *(Russian)* 3−38512
microwave spectrometer 3−25768
negative glow, kinetic theory 3−36221
overdense discharge, energy of positive ions in the hollow cathode *(Russian)* 3−7590
p.i.g. regime, hollow cathode effect 3−17599
plasma column, macroscopic instability and anomalous diffusion *(Polish)* 3−23848
positive column, study of elec. and light phenomena *(Rumanian)* 3−17705
potential distrib. in a space-charge sheath meas. by a nonperturbing probe *(Russian)* 3−6027
radial coherence, stabilisation 3−7583
r.f. diode glow discharge sputtering, positive-ion bombardment of substrates 3−18516
steel, stainless, type 304 and Nitralloy 135M, glow-discharge nitriding 3−8851
transverse extension, utilization for triggering of previously nonconducting discharge section *(German)* 3−38508
uncontracted type of longit. d.c. glow discharge, production at atmospheric pressure 3−33416
weak-current switches, analysis *(German)* 3−30031
Al_2O_3 sintering technique 3−18695
Ar ion, adsorption and desorption on Mo in glow discharge 3−15072
CO_2, vibr. translation rates for (10^00) and (00^01) levels 3−36054
CO_2, vibr.-vibr. energy transfer 3−6458
CaO, r.f. sputtering, glow discharge anal. by spectroscopic method 3−5244
Fe I, emission lines, Van der Waal's broadening induced by neutral He in glow discharge 3−35981
H_2 negative glow, velocity distrib. of plasma electrons 3−1531
He, effect of gas purification method on normal cathode fall of potential 3−38507
He, initial stage of reactance oscillations 3−36225
He negative glow, velocity distrib. of plasma electrons 3−1531
He plasma local transient phenomena induced by microsecond periodic pulse 3−20611
He-Ne, in hollow sectionalised cathodes, cathode pot. step, current distrib. *(Russian)* 3−14629
He-Ne, initial stage of reactance oscillations 3−36225
Hg vapour and foreign gas binary mixtures, 3884 Å band emission from electrodeless glow discharges 3−20674
N_2 exposed Na_2SO_4, visible spectra, green glow phenomena 3−17343
Ne, initial stage of reactance oscillations 3−36225
Ne, potential distrib., falling part of current-voltage charact. *(Russian)* 3−26910
Ne plasma local transient phenomena induced by microsecond periodic pulse 3−20611
O_2, electron energy distrib. functions meas. 3−23929
Si_3N_4 film, deposition by microwave glow discharge 3−30937
gold
adatom diffusion and cluster migration, on alkali halide cleavage planes, rel. to thin film growth 3−1888
adsorption in Ge, disperse struct. growth *(Russian)* 3−20943
adsorption of H_2O, CO_2, CO, surface sensitivity of photoelectron spectroscopy 3−11944
adsorption of S on (111), (100), (110) faces, Auger and LEED obs. *(French)* 3−20940
adsorption on clean Ge field emitters, metal-semiconductor boundary growth 3−15251
atomic lifetimes of isoelectronic sequences 3−17338
Auger electron and charact. energy loss spectra from clean and black surfaces 3−34452
backscattering of H and ^{4}He, ion fraction, 25-150 keV 3−30912
cold-worked, stage II and III recovery, internal friction and modulus defect, trace impurity effects 3−5315
concentration determination in solutions, accuracy and sensitivity of atomic absorpt. anal. 3−16564
conduction band structure study by photoelectron spectrometer 3−28716
crystal field theory, 5d and 4f mixing coeffs. for rare earth ions 3−33810
crystallisation on (111) face of fluorite, condensation conditions *(Russian)* 3−8069
crystallites, Debye-Waller factor rel. to size 3−36247
cylindrical particles, i.r. scatt. and absorpt. calc. *(Russian)* 3−6426
deposition, on Si surface, and redistrib. on thermal treatment 3−39289
deposition on alkali halides, thin film nucleation kinetics 3−38755
deposition on u.h.v. cleaved rocksalt, thin film nucleation kinetics 3−36498
diffusion in CdS, 500-800°C 3−30286
diffusion in Si, determ. from precip. kinetics of Si-Au solid soln. *(Russian)* 3−1779
electrification, in contact with glass or quartz, elec. field and temp. effects 3−2168
electron backscatt., angular distrib. 3−15580
electron channelling, electron microscope obs. 3−24169
electron energy-loss function rel. to transverse and longitudinal e.m. excitation 3−21030
electron irrad., stable interstitial at 300K 3−4748
electron model for thermoelec. props. 3−38781
electron scattering, elastic and inelastic, from solid 3−30151
electron-impurity scatt., anisotropy study using de Haas-van Alphen effect 3−11881
gold continued
electroreflection phenomena interpret. rel. to surface electron density *(French)* 3−18432
electroreflection spectrum, influence of the potential, electrochemical electrodes 3−36855
epitaxial growth, influence of decoration of monatomic surface steps on crystallite mobility *(French)* 3−36495
epitaxial growth of Cu on Au(111) platelet, influence of intermediate amorphous C layer 3−24357
epitaxial growth rel. to dislocation density, X-ray rocking curve obs. 3−11830
equation of state, semiempirical, rel. to mech. props. *(Russian)* 3−27618
evaporated thin film epitaxial growth and condensation on NaCl covered by an amorphous dielectric intermediate layer 3−38746
exoelectrons, intensity and energy, simultaneous meas. after low temp. deform. *(Russian)* 3−21522
Fermi surface stress derivatives, oscillatory magnetostriction 3−33779
field ion microscopy, spot struct. obs. and explanation *(German)* 3−27160
field-ion microscopy, for surface investigation 3−28734
film, (001) oriented, crecrystn. into (111) orientation 3−20973
film, (001) oriented, recrystn. into (111) orientation *(French)* 3−20975
film, elec. resist., γ-irrad. effects *(Russian)* 3−18231
film, electromigration, local variations of current density and temp. influence *(French)* 3−30282
film, electromigration, void and hillock growth 3−36437
film, electron energy loss spectra, surface excitations influence *(French)* 3−33580
film, electron scatt., ang. distrib. of secondary electrons *(German)* 3−18521
film, epitaxial growth on Ag single cryst., effect of amorphous intermediate layers 3−1933
film, epitaxial growth on NaCl, influence of elec. field on orientation *(Russian)* 3−30364
film, epitaxy and recrystn., on mica and NaCl *(French)* 3−15092
film, in contact with Al film, interaction *(Russian)* 3−4871
film, light ion channelling 0.5-2 MeV, scatt. and transmission probabilities, light emission *(French)* 3−20771
film, mean free path determ. for low energy electrons 3−15277
film, noncrystalline, electron diffraction and resistivity study 3−8062
film, on Si, diffuse interface, Auger spectroscopy study 3−38751
film, optical props., influence of grain boundaries and lattice defects, theory 3−36958
film, optical radiation on passage of electrons up to 100 keV 3−24771
film, photoelectron angular distrib. 3−34460
film, piezo-, thermo- and electro-refl., and electro-transmittance 3−12154
film, polycrystalline, dynamical effects in electron scatt. for structure obs. 3−24014
film, self-diffusion along dislocations 3−15032
film, single crystal, transillumination proton diffraction for structure obs. 3−24363
film, sputtered, discontinuous on dielectric, magnetoresistance depend. on morphology 3−2061
film, vacuum deposition, effect of electric field on orientation and particle arrangement 3−1934
film, vapour deposited, growth kinetics obs. 3−1951
film, with island struct., I-V characts. rel. to electrolum. 3−21488
film grown on NaCl, small-angle torsion boundary structure in (001) phase 3−4940
film on glass substrate, laser damage 3−10560
films, recovery process for films vacuum deposited on substrate at liquid He temp. 3−2720
on glass substrate, spectral specular reflectance, standard reference materials, preparation and calibration 3−19143
growth of evaporated particles along steps on NaCl surface 3−15098
Hall effect, temp. dependence in dilute alloys, intermediate field condition 3−21057
h.v. electron microscopy, multi-beam imaging technique 3−23991
impulse lasers, expt. obs. *(Russian)* 3−35690
interface of Au substrate with Pb monolayers, spontaneous alloying 3−36463
ion beam transmission through single cryst., absence of channelling effect 3−1110
island condensates, on NaCl chips, transverse section, electron microscopy 3−18035
kaonic atom X-rays, determ. of K− mass and K− polarisability 3−29542
lattice contraction due to quenching-in vacancies 3−30118
layer on Si substrate, backscatter coefficient, when bombarded with average-speed electrons *(German)* 3−8696
light ions scattering in the weakly screened Coulomb field of Au nuclei 3−11182
magnetostriction meas. rel. to stress depend. of Fermi surface necks 3−18350
mechanical strength, calc. using semiempirical equation of state *(Russian)* 3−8836
moderator, low energy positron emission in backscatt. mode 3−30926
m.o.s. capacitor, Au diffused on Si, capacitance transient response 3−5055
Mossbauer linewidth measurements, search for anomalous narrowing of transition in ^{197}Au 3−34254
negative ion source, bombardment of solid surfaces by positive alkali ions *(Russian)* 3−6061
negative positron work function calc. 3−15151
neutron irrad., damage due to radioactive decay 3−11660
nucleation, on clean W substrate, contact angle meas. rel. to heterogeneous nucleation theory *(Japanese)* 3−20699
nucleation on SiO_2 for surface structural defects obs. 3−8027
optical constants 3−8548
optical electromodulated properties in 1.3-7.3 eV photon energy range 3−30800
painting of surface faults in alkali halides *(French)* 3−15074
phonon viscosity, dislocation drag, and u.s. attenuation 3−38625

gold continued
photoemission from polycryst., ang. anisotropy phenomena 3−5258
photostimulated diffusion in Si 3−33691
positron annihilation for dislocation density estimation in f.c.c cold-worked polycrystal 3−30159
powder particle adhesion, charge contribution 3−5049
pure, deformed, point defect clusters 3−17807
quench-hardened single crysts., yield stress and surface morphology, dislocation-stacking fault interaction 3−36350
radiative heat transfer among surfaces, directional effects 3−26178
refractory, exploding-wire measurement of heat of fusion and electrical conductivity 3−30247
roughness, obs. by diffuse X-ray refl. at grazing incidence *(French)* 3−1863
shock wave propagation, deform. energy and collision velocity determ. *(Russian)* 3−27066
single crystal whiskers, vapour phase growth for electron field-emitter cathodes, electric field effects *(Russian)* 3−12245
solubility in Ge, Si influence *(Russian)* 3−7783
solubility of carbon, impurity effects *(French)* 3−38689
sputtering by bombardment with Ar^+ and Xe^+ ions, 20-50 keV 3−8692
structure of Au(100), (110), (111) surfaces, LEED obs. 3−24314
substrate for Ag film, stress from elastic deformation 3−36494
surface, (110), diffuse LEED pattern, temp. depend. 3−24313
surface, bombardment with N^+, Na^+, Cu^+, Ag^+ and Au^+ ions, electron ejection, positive ion refl. 3−2608
surface structure of Au(100), LEED obs. 3−36462
suspension of Au particles, controlled nucleation for particle size regulation 3−18738
thermotransport of Ag, heat of transport 3−24281
thin film, conduction electron diffusion by surface defects *(French)* 3−36584
thin film, electron probe analysis, substrate, operating voltages and thickness effects 3−37764
thin film, strain effect on electrical conduction 3−33865
thin film activated with BaO, change in work function of isolated centres 3−36658
thin film on glass plate, elec. conductivity rel. to temperature and voltage under vacuum 3−18234
thin film on Si, energy dependence of He^+ and H^+ channelling 3−33581
thin film techniques for N_2 ionisation growth meas., emission phenomena explanation 3−14398
thin film techniques for N_2 ionisation growth meas., emission phenomena revised explanation 3−14399
thin films, Debye-Waller factor, temperature dependence, electron diffraction determination *(Russian)* 3−33637
thin films 3−13350
thin platelets, lattice spacings, electron diffr. study 3−4730
vacancy form. by quenching under press., volume determ. *(French)* 3−21703
valence band, X-ray photoemission study 3−11846
valence band X-ray photoelectron spectra 3−2616
vaporisation as reference substance for transpiration determ. of BeO in water vapour 3−26019
vapour deposition of Au nuclei on NaCl substrates, mobility and coalescence 3−2643
volume decoration of dislocations in CsI 3−18024
wear due to dry friction, stacking fault energy and elastic modulus effects *(Russian)* 3−7844
L X-ray prod. by 0.5 to 30 MeV protons 3−23493
X-ray prod. by electron irrad. 3−16540
adsorption of H_2O and Hg measurement of change in work function by retarding potential method 3−38725
$^{108}Ag^m$, calibrating source for Ge(Li) detectors 3−32164
Al:Au, spin scatt. cross sections 3−18300
$Al-Al_2O_3-Au$ sandwich cathodes, energy ang. distrib. of electrons emitted *(Russian)* 3−30550
$Al-Al_2O_3-Au$ structure, transmission coeff., applied field depend. 3−8280
Au:Fe, temp. dependence of Hall effect, spin component of mag. solute 3−21058
Au/Cu planar couples, mass diffusion of base metal to electroplate surface 3−38685
Au-Cr bimetallic film, Cr diffusion into Au, work function study 3−15030
Au-glass cermet film, strain sensitivity and t.c.r. 3−5065
Au-Ni thin-film thermocouple, transmission electron microscopy, specimen temp. increases 3−24011
$Au-SiO_2$ multilayer structure, characterization as artificial semicond. 3−38790
$Au-SiO_x$ cermet film, structural and electrical changes during heat treatment 3−5064
$Au-SrTiO_3$ boundary, surface barrier energy determ. 3−5052
Au-ZnTe Schottky barrier height determination 3−18215
Au^- dye-laser photodetachment studies 3−29503
Au^+ diffusion over interstitial sites in Si 3−33700
N-Ge:Au, hysteresis of I-V characts., and props. of elec. domains *(Russian)* 3−2100
Ge:Au, impact ionisation of deep acceptor impurities 3−33918
n-Ge:Au piezoresist., influence of deep energy levels *(Russian)* 3−2074
p-Ge:Au whiskers, plastic deform., 760°C *(Russian)* 3−27055
KCl:Au^-, study of absorption bands and related luminescence centres 3−12167
Ni-Au film couple, surface diffusion, electron microscope obs. 3−1878
inSi, gettering by ion-damaged surface layers 3−5276
Si:Au, absorpt., 0.3-1.05 eV, impurity photoionization cross section determ. *(Russian)* 3−5221
Si:Au, high-resistivity, i.r. absorpt., rel. to impurity conc. determ. *(Russian)* 3−2673
Si:Au diode, field independence of thermal emission rate of holes 3−4964
Si-Au diode, pressure sensitivity meas. 3−15255
$Ta-Ta_2O_5-ZnS:Tb^{3+}$-Au film, electrolum., light emission voltage depend. 3−39192
Ti-Pd-Au sputtered multilayer system, use in film IC 3−21163

gold alloys
see also gold compounds
base alloys with B metals, concentration dependence of the lattice constant and its relation to the lattice modulus *(German)* 3−1666
dislocation model for critical flow stress calc., effect of solute atom conc. 3−24189
neutron activation analysis, matrix components, rapid determ. 3−28769
ohmic contacts, for GaSb, by vacuum evap. and chemical deposition *(Polish)* 3−30538
rare earth MAu_2Si_2, crystal structure 3−20713
Ag-Au, shock wave effect on mech. props. *(German)* 3−34608
Au-Ag, liq., thermotransport of Ag 3−24281
Au-Ag, short-range ordering upon quenching and cold-work, calorimetric and resistometric study 3−21713
Au-Cd, thermoelastic martensite, lattice softening, ferroelasticity and shape memory effect 3−14907
Au-Cd-In, double h.c.p., liquisol quenching effect on struct. 3−34559
Au-Cd(47.5 at.%), martensitic pretransformation phenomena 3−18561
Au-Ce, dilute, obs. of Ce impurity by nuclear orientation meas. 3−2257
Au-Co, quasielastic neutron scattering cross section for paramag. impurities 3−5095
Au-Cr, high concentrated alloy, elec. resist. min. at low temp. 3−30449
Au-Cr, paramag.-antiferromag. critical composition, anisotropic diffuse scatt. of neutrons 3−38973
Au-Cu, wear due to dry friction, stacking fault energy and elastic modulus effects *(Russian)* 3−7844
Au-Cu (25-33%Au), fine struct., X-ray diffr. obs. *(French)* 3−14739
Au-Cu alloys electrodepositing from cyanide free acid solution *(French)* 3−9071
Au-Cu binary disordered, size effect and multisite correlations 3−17761
Au-Cu film, order-disorder transformation obs. 3−1800
β-Au-Cu-Zn, phase stability, absolute thermoelec. power, cond. electron mag. susceptibility, comp. depend. 3−33871
β-Au-Cu-Zn alloys, lattice softening, phase stability and elastic anomaly 3−2719
Au-Cu-Zn martensite, cryst. struct., electron diffr. obs. 3−1604
Au-Fe, internal friction due to quenched-in vacancies 3−37040
Au-Fe, magnetoresist. meas. in high fields 3−36592
Au-Fe alloys, magnetic ordering rel. to Fe concentration 1-22 at.% 3−2287
Au-Hg, Hg and H_2O adsorption, measurement of change in work function by retarding potential method 3−38725
Au-Ni and Cu-Ni-Au, mag. hyperfine structure coupling and Mossbauer isomer shift of ^{197}Au 3−34257
Au-Ni-Pt, phase diagrams, thermodynamic calc., expt. obs. 3−34511
Au-Pd, short-range order destruction by cold working 3−39372
Au-Pt electron irrad., recovery during stage II annealing, interstitial rearrangement 3−11618
Au-transition metal, short range order, eledtron microscope and diffr. obs. 3−14734
Au-V, n.m.r. of ^{51}V, relax. times, 1-300 K 3−5146
Au-V, quasielastic neutron scattering cross section for paramag. impurities 3−5095
Au-Yb(Ce)(Gd), negative s-f interaction 3−24561
AuCo dilute alloys, n.m.r. of ^{59}Co 3−34226
AuCr, (3.3, 10.6 at. % Cr), elec. resist., $T^{3/2}$ depend. of impurity resist. 3−36581
$AuCu_3$, surface long range order above bulk transition temp. 3−20913
Au_3Cu, I and II-type superlattice structure 3−8805
Au_3Cu ordered alloys, use of Morse potential function to determ. harmonic props. 3−7868
$Au_{50}Cu_{50-x}Ga_x$, thin specimens study of AuCu II phase with periodic antiphases and AuCu III phase *(French)* 3−31003
$AuCuZn_2$, soft acoustic phonons near martensitic transition 3−14942
$AuCuZn_2$, thermoelastic martensite, lattice softening, ferroelasticity and shape memory effect 3−14907
AuFe, magnetic moment distribution 3−34134
$AuGa_2$, n.m.r., lattice constants and mag. susceptibility of solid and liquid 3−21334
$AuIn_2$, n.m.r., lattice constants and mag. susceptibility of solid and liquid 3−21334
AuMn, localised spin fluctuation and Kondo system, resist. temp. depend. 3−36582
Au_2Mn:^{119}Sn, mag. hyperfine interaction, Mossbauer study *(Russian)* 3−12088
Au_4Mn, micromagnetic to superparamag. transition, effect of atomic ordering 3−21229
$AuPb_3$, formed from spontaneous alloying of Au substrate with Pb monolayers 3−36463
$Au_{0.95}Pd_{0.05}Ga_2$, n.m.r., lattice constants and mag. susceptibility of solid and liquid 3−21334
AuV, localised spin fluctuation and Kondo system, resist. temp. depend. 3−36582
Au_4V, ordered ferromagnetic, V^{51} n.m.r. study 3−2408
β'-AuZn, Hall coeffs. at 77 and 275K 3−38826
AuZn ordered alloys; activation volumes for self-diffusion 3−7973
β'AuZn single crystals, operative slip modes and dislocation mechanism 3−31023
Cu-Au, effect of press. on phase transition and ordered structs. of CuAu 3−18610
Cu-Au, press, depend. of long period of CuAuII 3−20712
Cu-Au and Cu-Au-Al, plastic deform., electron microscope study *(Russian)* 3−5306
$Cu_{1-x}Au_x$-Fe(Cr), mag. field depreciation of Kondo magnetoresist. 3−33872
Cu_3Au, temperature depend. of flow stress in range 4 K to 300 K 3−36351
Cu_3Au, type ordering, short range and long range, energy, second coordination sphere 3−38551
Cu_3Au order-disorder transition temp. 3−36400

gold continued
gold alloys continued
Cu$_3$Au ordered alloys, use of Morse potential function to determ. harmonic props. 3–7868
Dy-Au, alloy system, phase diagram and structure obs. 3–30971
n-GaAs/Ni/Au-Ge ohmic contact, Auger electron spectroscopy and sputter etching 3–4903
Ge wettability by Au alloys *(Russian)* 3–8006
Pb-Au dilute alloys dehancement of Au diffusivity 3–34546
Pb-Au nonsubstitutional solid solns., comp. depend. of supercond. transition temp. 3–24533
Pb-Au solid soln., kinetics and morphology of AuPb$_3$ precip. 3–24843
Si, wettability by Au alloys *(Russian)* 3–8006
Sm-Au, alloy system, phase diagram and structure obs. 3–30971
gold compounds
see also gold alloys
Au complexes, dialkyl sulphide complexes of gold (I and III) halides, vibr. spectra 3–4449
Au-SiO$_x$, cermet film, structure and elec. props. with heat treatment 3–15201
Au-Sn-Te system, phase diagram of AuTe$_2$-SnTe and AuSn-SnTe parts *(French)* 3–2689
AuBe B-X system bands, Franck-Condon factors and r-centroids 3–1177
AuCN, search for anomalous narrowing of Mossbauer transition of ^{197}Au 3–34254
AuH B-X system bands, Franck-Condon factors and r-centroids 3–1177
Au(I) and Au(II) complexes, with 1,5-cyclooctadiene, i.r. and Raman spectra 3–26668
n-Si-Au solid solution, precip. kinetics *(Russian)* 3–1779
goniometers
automatic control system 3–10132
corneal angular apertures, diffraction effects on precision 3–3886
for cryostat orientation determ. 3–25705
i.r., refractive index dispersion measurement, acousto-optical material, Sellmeier coefficients 3–22317
low temperature electron microscope goniometer stage, design 3–22513
single crystal, for e.s.r. spectra 3–28620
u.s. application to nondestructive testing of mechanical props. 3–18767
Weissenberg goniometer, low and high temp. attachments 3–25653
Weissenberg rheogoniometer, for flow measurements of non-newtonian fluids 3–28799
grain boundaries
activity, determ. by Auger spectroscopy 3–7767
alloy, dispersion hardened, recrystallisation rel. to grain boundary form. 3–5311
alloy with b.c.c. lattice, dispersion hardened, recrystallisation rate rel. to grain size 3–31011
alloys, ordered, interfaces study, grain boundaries, twinning, martensitic transformation, thermal antiphase walls *(French)* 3–17855
atomic structure of grain boundaries, field-ion microscope anal. 3–30128
benzene, grooves, solid-liquid interfacial energy measurements 3–36473
brass, f.c.c., grain boundaries and surface tensions meas. by zero creep method 3–34543
camphene, grooves, solid-liquid interfacial energy measurements 3–36473
carbon tetrabromide, grooves, solid-liquid interfacial energy measurements 3–36473
ceramic, grain boundary sliding deform. mechanism 3–8979
coincident site lattices in arbitrary cryst. lattice *(French)* 3–17849
contrast in field ion microscope images, computer image simulation 3–17853
contrast in field ion microscope images, rel. to tilt and twist 3–17852
contrast in field ion microscope images 3–17851
creep deform. at high temp. importance of grain boundary sliding 3–14860
cubic bicrystal, tilt and twist boundaries 3–11622
cubic structure, rel. to general analysis of tilt boundaries 3–7761
dielectric behaviour of ceramic grain boundaries from electron beam scanning obs. 3–36302
diphenyl, grooves, solid-liquid interfacial energy measurements 3–36473
double diffr. electron microscopy *(French)* 3–7605
ethylene dibromide, grooves, solid-liquid interfacial energy measurements 3–36473
f.c.c. polycrystalline metals elastic limit rel. to grain interaction *(French)* 3–33592
α-Fe, low-cycle fatigue, grain boundary sliding, 450-700°C 3–34577
fractography, state-of-the-art review 3–30982
glass ceramics, texture development 3–5343
high angle, applicability of the grain boundary (secondary) dislocation model 3–17848
ice water NaCl system, grooves, solid-liquid interfacial energy measurements 3–36473
Incoloy-800, heat treatment effect on B distribution, carbide precipitation at grain boundaries 3–12386
Inconel alloy X-750, precip. parameters role upon creep rupture props. 3–37024
interface, geometrical theory, mathematical aspects 3–34518
internal friction obs., book 3–20813
ion mobility along grain boundaries 3–4877
magnetic material, birefringent, optical contrast of inclined boundaries 3–18436
metal, influence on mech. props., review 3–37037
metal, polycrystalline, rel. to stress-strain distrib. in grains under elastic deformation 3–5300
metallic film, groups I-IV, rel. to electromigration 3–4879
metallic thin films, effect on optical props., theory 3–36958
metals, large angle, dislocation structure, recrystallisaton 3–38594
migration impeding during secondary recrystallisation, direct obs. 3–18568
Monte Carlo methods for theoretical study, review 3–20916
grain boundaries continued
naphthalene, grooves, solid-liquid interfacial energy measurements 3–36473
Nimonic alloy, notched creep strength, microstruct. effects 3–8932
planar matching model for boundary structure 3–20749
polycrystalline solid, model for grain boundary sliding 3–17840
pore isolated on grain boundary, volume diffusion controlled shrinkage 3–36292
pores interacting with grain boundaries, pore volume changes 3–31126
porous solid, rel. to volume-diffusion-controlled final-stage densification 3–5365
o-pyroxene, exsolution lamellae 3–37157
radiation damage in structural materials 3–29449
sheet metals at high temperatures, examination using sample deformation under emission microscope *(German)* 3–8795
sintering kinetics, significance to grain boundary width and effective surface layer 3–31125
sliding in polycryst. specimens, meas. methods 3–21601
sliding role in superplasticity and creep phenomenological theory 3–33598
solid-liquid interface, morphological stability near grain boundary groove 3–11557
stainless steel, pseudo-subgrain boundaries, electron microscope obs. 3–12357
steel, austenite, boron distrib. between grain boundary and matrix sites 3–37030
steel, austenitic, microstruct. changes during creep deform. at 600°C 3–8921
steel, austenitic, Nb-stabilized, low stress creep behaviour 3–8926
steel, austenitic, stainless, u.s. attenuation coeff. reln. to grain size 3–9034
steel, austenitic stainless, intergranular corrosion, microstruct. and microsegregation effects 3–37032
steel, austenitic stainless, solid soln. decomp. kinetics 3–21603
steel, austenitic stainless, type 316, aged, boron effect on precipitated phases 3–21587
steel, Cr-Ni, secondary creep deform. mechanism, stress and temp. depend. 3–8938
steel, hydrogen trapping sites *(French)* 3–2742
steel, investigation using electron microprobe *(German)* 3–8794
steel, low alloy, containing vanadium carbide, microstruct. effects on creep props. 3–8935
steel, low C, and chem. homogeneity rel. to $\delta \rightleftharpoons \gamma$ transition *(Russian)* 3–8803
steel, low-C, austenite grain size influence on carbon and sulphur diffusion *(Russian)* 3–39331
steel, low-C, precip. on grain boundaries, electron microscope obs. 3–18577
steel, mild, grain size and stress distrib. effect on fatigue strength of notched specimens 3–8899
steel, proeutectoid ferrite transform., manganese partition 3–39320
steel, stainless, ferritic, intergranular corrosion and chromium depletion 3–27653
steel, stainless, Ni ion-bombarded, surface struct. 3–4777
steel, stainless, Type 304, cyclotron-injected helium effect on void form. characts. 3–35934
steel, stainless, type 304, intergranular crack propag., influence of deform. rate 3–21593
steel, stainless, types 304 and 316, grain boundary diffusion of tritium 3–27628
steel, stainless ferritic, intergranular corrosion 3–20946
steel, temper embrittled, segregation of Mn and Sb to grain boundaries 3–39346
steel, Ti stabilised austenite stainless, intergranular corrosion, carbide morphology and composition effect 3–8853
steel austenitizing treatment effect on temper embrittlement, search for Sb segregation at grain boundaries 3–34544
steel creep processes, model conceptions regarding composition 3–31036
stress field accommodation, under heterogeneous shear by initiation of microcracks 3–4792
subgrain boundary misorientation, determ. from split Kikuchi lines 3–24009
succinonitrile, grooves, solid-liquid interfacial energy measurements 3–36473
superplastic metals determ. of deformation mechanism 3–1673
thin crystals vacuum decoration technique, microstructure obs. *(Russian)* 3–38750
tilt boundaries, general analysis in simple cubic struct. 3–7761
topography, by field ion microscopy 3–384
Zircaloy, slowly cooled, zirconium hydride distrib. 3–31001
Zircaloy tubing, annealed, intergranular and intragranular hydride conc. and orientation 3–8819
Zircaloy-2, grain boundary hydride precipitates 3–5297
Zircaloy-2, hydride precip. distrib. 3–8820
Zircaloy-2 corrosion in hot water and steam, weight gain and metallographic examination 3–37021
Ag, grain boundary migration under compression at 500°C 3–37042
Ag, grain boundary sliding and particle effects on rate 3–34532
Ag film, rel. to Pb diffusion, Pb/Ag/Au and Pb/Ag/Pd layered struct. obs. 3–7976
Ag:^{124}Sb, grain boundary electromigration of ^{124}Sb *(French)* 3–8806
Ag-Zn alloys, massive precipitates study by selected area electron channelling 3–21576
Al, annealed and crept, bright and dark field transmission electron microscopy 3–1632
Al, creep-deformed, dislocation struct. of subgrain boundaries 3–24121
Al, intergranular corrosion in pressurized water, hydrogen/grain boundary interactions *(French)* 3–1909
Al, lubricant trapping under cold compression, surface struct. examination *(Japanese)* 3–30990
Al, rolled plate, recrystallisation 3–15664
Al and Al alloys, axisymmetric extrusion, plastic flow, strengthening at grain boundaries 3–39360
Al film, rel. to electromigration, quantitative mass distrib., scanning electron microscope obs. 3–7977
Al wire, neutron irradiated, grain boundary viscosity 3–1668

grain boundaries continued
- Al-Cu oriented bicrysts., intergranular precip. *(French)* 3−27626
- Al-Fe bicrysts., grain boundary precipitate exam. by Ga embrittlement technique 3−37025
- Al-Mg-Si alloy, β' precipitate nucleation at subgrain boundaries *(Japanese)* 3−15699
- Al-Mg-Zn alloy, microstruct. influence on mech. props. and stress corrosion susceptibility 3−39342
- Al-Zn alloys, decomposition, effect of high temp. aging; precip. at grain boundaries 3−37015
- Al-Zn-Mg alloys, grain boundary corrosion and stress corrosion cracking relationship *(Japanese)* 3−31072
- Al-Zn-Mg alloys, stress corrosion cracks, h.v. microscope studies 3−30981
- Al_2O_3:MgO, grain boundary segregation 3−27739
- B_xC_y fast-reactor irradiated pellets, examination of microstructure 3−26527
- $BaTiO_3$ ceramics, current-voltage characteristics and capacitance 3−33937
- $BaTiO_3$ doped, model *(German)* 3−33938
- Bi, grain boundary energy determ. 3−4762
- Cd alloys multicomponent impurities influence on density change during thermocyclic treatment *(Russian)* 3−8844
- Co-W-Ti alloy, second phase precip. phenomena *(Russian)* 3−24846
- Cr_2O_3, grain growth on final sintering 3−8981
- Cu, continuously cast, high temp. creep cavitation mechanisms 3−34536
- Cu, ductility, temp. depend., grain boundary migration *(Russian)* 3−39355
- Cu, grain boundary energy, 1030°C 3−36308
- Cu, influence in creep deform. 3−14880
- Cu, internal friction with neutron irradiation and fatigue 3−24117
- Cu, lubricant trapping under cold compression, surface struct. examination *(Japanese)* 3−30990
- Cu alloys, dil., collective recrystn., excess grain boundary energy determ. *(Russian)* 3−8832
- Cu-Ag-Al solid soln. alloys, isothermal recrystn. kinetics 3−21592
- Cu-Fe alloys, ageing characts., precipitate transform. 3−37075
- Cu-Ni alloys, internal friction peak interpret. *(Russian)* 3−24210
- Cu-Ni alloys, void nucleation and growth in stressed heat-affected-zone 3−21637
- Cu-Zn alloys, γ-phase, grain boundary diffusion, 25°C *(German)* 3−24840
- Cu-Zn alloys, massive precipitates study by selected area electron channelling 3−21576
- Er films, He implanted, dimensional expansion and surface microstructure 3−7994
- ErD films, He implanted, dimensional expansion and surface microstructure 3−7994
- Fe, Armco, hydrogen trapping sites *(French)* 3−2742
- α-Fe, diffusion of sulphur, temp. and grain size depend. *(Russian)* 3−24292
- α-Fe, grain boundary sliding in creep, investigation 3−21612
- Fe, lubricant trapping under cold compression, surface struct. examination *(Japanese)* 3−30990
- Fe, P diffusion, radioactive tracer study, P-rich segregates at grain boundaries *(French)* 3−31002
- Fe, u.s. attenuation coeff. reln. to grain size 3−9034
- Fe-Co-V(2 wt.%) alloy, ordered, h.p. prestrain effect on fracture stress and yielding 3−37061
- Fe-Cr-Co-Mo alloy, precipitation, structural and kinetic features 3−8787
- Fe-Cu(1.7 wt.%) alloy Cu precipitation from α-Fe in pre-peak and peak hardness range of ageing 3−8797
- Fe-Ni-Al alloy, microstructure and fracture *(Japanese)* 3−15672
- Fe-Ni-Cr alloy, grain boundary internal friction spectra, relax. phenomena 3−37028
- Fe-Si (3.25 wt.%) alloy, impurity effects on grain growth in strain-anneal and secondary recrystn. 3−37041
- Fe-Si alloy, surface energy anisotropy meas. from grain boundary dihedral angle 3−20926
- Fe-Ta alloys, Laves phase precip. phenomena 3−37049
- α-HgS, cinnabar, single crystals, Berg-Barrett X-ray topographic study of small angle boundaries 3−38525
- InSb film, rel. to carrier mobility and field effect 3−27260
- KCl, step lines, local struct., X-ray obs. 3−38596
- LiF, strength of small-angle boundaries, influence of space charge 3−36325
- $LiNbO_3$ single crystals, X-ray topographic studies, relation between growth conditions and lattice defects 3−17747
- $LiTaO_3$ single crystals, X-ray topographic studies, relation between growth conditions and lattice defects 3−17747
- Mg-Ce alloy, precipitation on grain boundaries with aging *(Japanese)* 3−12351
- Mg-Y(8.7 wt.%) alloy, elevated temp. precip. stages 3−39340
- MgO, polycryst., microyield and fracture 3−20789
- MgO, polycryst., preferential diffusion of O 3−4873
- MgO:Fe, polycrystalline, viscous grain boundary sliding rel. to transient creep 3−7831
- Mo, cast, intercrystalline fracture by grain boundary precip. *(Russian)* 3−24853
- Mo, precipitation of C and O *(French)* 3−21590
- NaCl crystals, reverse deformation comparison with annealing, polygonisation, dislocations at sub-grain boundaries 3−17903
- Ni, creep, grain boundary pore form. correl. with internal friction *(Russian)* 3−24877
- Ni, torque terms and grain boundary surface energy anisotropy 3−36307
- Ni electrode, intergranular cracking at cathodic potentials 3−31266
- Ni-P film, rel. to oxidation effects on elec. resist. 3−18028
- Ni-W(6 wt.%) solid soln., environment and grain size effect on creep behaviour 3−37057
- P, white, grooves, solid-liquid interfacial energy measurements 3−36473
- Si, high angle grain boundaries in pulled crysts. 3−36323
- Si, polycryst. thin films, resistivity model function of film parameters 3−38836
- Si-metal boundary, rel. to I-V and C-V characts. 3−24507
- Si_3N_4, hot pressed 3−12421

grain boundaries continued
- CrV steel, grain boundary segregation and free enegy of Sn and Sb *(Czech)* 3−31027
- Ti-Mo(15 wt.%) alloys, effect of preceding working and solution treatment on precipitation site of alpha during ageing *(Japanese)* 3−18588
- U, hydrogen contamination effects 3−8908
- UO_2, polycrystalline, deformed, transmission electron microscope examination 3−11050
- UO_2, porosity changes during sintering at 1700 to 2200 °C rel. to grain growth 3−24969
- UO_2, sintering of grain boundary cavities 3−12437
- V, α-irrad., He gas bubble nucleation and distrib. 3−33572
- V, motion at 1400°C, emission electron microscope obs. 3−18574
- W, wires, doped, recrystallisation effect on brittleness, large grains with long boundaries formation *(Japanese)* 3−31065
- W fine wire with thoria dispersion, creep behaviour 3−37086
- W wire, doped temp. gradient effect on bubble growth 3−37087
- Zn, lubricant trapping under cold compression, surface struct. examination *(Japanese)* 3−30990
- Zn, pure and impure, grain boundary migration role during creep 3−34527
- Zn bicrystal, study of boundary motion 3−30127
- Zr-Pd(Ru) dil. alloys, heat treated, microstruct. of martensite plates *(Japanese)* 3−31079
- ZrO_2, CaO stabilised creep, grain boundary sliding 3−27740

grammars
- pattern classification, chromosome images, stochastic syntax analysis 3−3400

gramophones
- No entries

Granato-Lucke theory *see dislocations*

granular structure
- ceramic raw materials, measurement methods, conference 3−15793
- ceramic raw materials and ground minerals *(French)* 3−15796
- grain size, relation with X-ray diffraction line structure *(French)* 3−15798
- material, grain porosity, pore size distribution *(German)* 3−34664
- particle size measurement, review of methods *(French)* 3−15794
- quartz powder, structure determ. by differential thermal anal., grinding effects 3−31208
- superconductor, orientational phase transition 3−8294
- Al_2O_3, surface grain size estimation by optical scatt., application to microelectronics industry 3−4906
- Si, granular phase formed by diffusion of O_2, optical consts. calc. *(Russian)* 3−24673

graph theory
- chromatographic separation, multicomponent samples, graph theory application 3−26007
- Feynman diagram techniques and classification problems 3−816
- two-connected almost-pancyclic graphs 3−32288

graphic equipment, computer *see computer graphic equipment*

graphics, computer *see computer graphics*

graphite
- absorption of ^{3}He and ^{4}He monolayers, structure 3−20910
- adsorption of Ar and Xe, surface microstruct. 3−38712
- adsorption of He, calc. of ground state energy for superlattice states 3−38723
- adsorption of He atoms, study by plane wave method *(Italian)* 3−30531
- adsorption of N_2, Ar, CO, Kr and O_2, on preadsorbed NO 3−38720
- adsorption of NO, isotherms, 77.5 and 90.2 K 3−38720
- artificial generalization of theory of plasticity, stress-strain curves 3−39393
- billets for reentry nose tips, computer aided u.s. test system 3−37099
- bond length and angles meas., diffraction spot anomalies 3−17793
- calorimeter, construction and testing 3−22289
- carbon-graphite materials, crystallite size effect on strength 3−34652
- carrier lifetime anisotropy, Shubnikov de Haas meas. 3−18168
- chemisorption of atomic oxygen on basal faces, photoelectron spectra 3−24347
- coating layer of sintered $MoSi_2$ to protect against high temp. oxidation 3−18616
- colloidal dispersion of graphite, paint-on vacuum system heater 3−28509
- colloidal suspensions, rheological props. 3−31192
- compatibility of Ta with graphite at high temp. 3−35932
- cyclotron resonance, by using circularly polarized radiation, exam., 23 and 69 GHz 3−11849
- cyclotron resonance, theory and determination of the degree of band warping 3−8100
- elastic-plastic single crystals, thermally-induced plane waves 3−3985
- electrical resistivity change during compressive tests 3−23432
- electrical transport props. assuming acoustical phonon scattering 3−11897
- epitaxial growth of Xe, liquid He stage in transmission electron microscope 3−1940
- epoxy composite plates, post-buckling behaviour 3−27756
- evaporation of impurities, determ. by atomic absorption method *(Russian)* 3−11648
- exfoliated, low temp. adsorption of ^{4}He, Ar and N_2 3−36480
- failure modes, cumulative damage stochastic models, functional gamma distribution 3−7013
- fibre composites, friction and wear 3−39392
- filamentary growth on metallic impurities 3−18047
- filaments, development of Ta_2C and Nb_2C coatings 3−15771
- fine-granular ceramic contact development for l.v. apparatus design *(Russian)* 3−27749
- fluidized bed particles, nonlinear relation between specific resist. and current density 3−23783
- friction, effects of adsorption of benzol and CCl_4 *(Russian)* 3−11682
- graphite:Fe, oscillatory magnetoresist., charged impurity selective scatt. 3−11864
- graphite-reflected U metal cylinders and annuli, criticality meas. 3−11065
- heat and mass transfer on the surface of glass-graphite materials in high temperature gas stream *(Russian)* 3−26786

graphite continued
- heat transfer of ablating body in hypersonic radiating air plasma 3–1403
- heatshields filament wounds, stress analysis 3–37091
- impact, damage criterion rel. to temp. 3–5369
- impact data rel. to fracture 3–8995
- impulse loading by subnanosecond laser pulses 3–29109
- in-pile irradiation damage, temp. rel. to flux density *(French)* 3–29443
- interaction with Ti and Zr, kinetics for carbide layer form. and growth *(Russian)* 3–15826
- Landau levels, effect of trigonal warping 3–1996
- laser heated, particle emission mechanism 3–30900
- layers preferred orientations, integrated intensities rel. to uniaxial orientation 3–4734
- mechanical behaviour under biaxial tension, stress strain behaviour 3–33595
- melting, b.p. characts. and nature of liq. carbon, model approach *(Russian)* 3–14981
- microstructure, unusual, obs. in Ni-C alloys 3–31016
- moderators, Poco and RC4, dynamic fatigue behaviour and general fatigue design criterion 3–32951
- neutron distribution, non-exponential decay 3–11061
- neutron slowing down time 3–6970
- neutron spectra, graphite, determ. of thermalization and diffusion parameters, 14 MeV 3–32910
- neutron wave propag., interference phenomena calc. by eigenvalue expansion 3–1041
- nucleation of graphite during first stage graphitization on eutectic solidification of cast irons 3–8817
- optical props., dispersion relations for π-bands 3–30785
- organosilicon bonded graphite layer, effect of thermostabilising additions on antifriction props. *(Russian)* 3–14925
- packing defects, infl. on structures, X-ray diffr. study *(Russian)* 3–7779
- phonon dispersion curves and elastic constants 3–38639
- point defect, elastic interaction with prismatic disloc. loop 3–4747
- polycrystalline, porous effects on electrical and thermal conductivity 3–27796
- pulsed neutron decay data, spectral analysis 3–32915
- pyrolytic, crystal-oriented, directional depend. of thermal conductivity 3–27148
- pyrolytic, heat treatment influence on low temp. heat capacity 3–17980
- pyrolytic, low electron energy loss spectrum and plasmon excitation *(French)* 3–7800
- pyrolytic, mol. beam study, scatt. energy, phase shift 3–5251
- pyrolytic, rate of oxidation of basal and prismatic surfaces in the transition regime 3–33742
- pyrolytic and single cryst., Alfven wave propag. and damping, 35 GHz 3–30510
- quenching of cast iron:Ce, graphite rosette form. rel. to mech. strength *(Russian)* 3–12411
- reaction kinetics with SiO_2 and Al_2O_3 3–18785
- reactor graphite, irradiation behaviour at high temp., review of structural changes, thermal and mech. props. 3–14896
- reactor-grade neutron-irradiated, annealing at 350°C, effect on electrical resistivity and thermal conductivity 3–11060
- resistivity meas. for thin graphite crystals, effect of crystal thickness 3–30469
- rethermalization of neutrons in graphite-Bi system 3–19895
- shock conversion to diamond *(Polish)* 3–24217
- single crystal, pyrolytic, polarised emission of the K-band 3–34438
- specific heat, eval. of meas. at const. press. 3–7941
- spherical particles, surface plasmon excitation by X-rays 3–15232
- spheroidal graphite austenitic cast irons, microstruct. effects on creep-rupture props. 3–8929
- spheroidal graphite form. in cast iron 3–8816
- stress-strain characts. of irradiated and non-irradiated graphite 3–29442
- structural faults, enhanced reactivity microscopic studies 3–11788
- sublimation in flow of inert gas, 2800-3500K 3–26845
- surface, electron irrad., momentum transfer, blow off vapour yield, 300-5000K 3–24765
- surface, growth of n-alkane crysts. 3–20703
- surface thermal expansion 3–15023
- symmetry of LEED patterns and diperiodic space groups for surface structures 3–24315
- thermal diffusivity meas. at high temp. by modulated electron beam technique 3–28495
- thermal neutron scatter matrices assuming isotropic cryst. struct. 3–7012
- thermoelectric power at temps. above 5 K, electron irrad. effects, annealing effects 3–27278
- thermomagnetic effects, low-temp., phonon drag 3–2107
- thin crysts., Hall coeff. and magnetoresist., field and thickness depend. 3–30554
- transformation into diamond under high static pressure 3–33672
- unsteady heat conduction in graphite in combustion region, soln. to 1-D problem *(Russian)* 3–22789
- wettability of metal melts on substrate, catalytic graphitisation 3–11796
- X-ray appearance potential spectroscopy, soft X-rays, plasmons, electronic excitations, degree of disorder 3–27586
- X-ray emission spectra, expt. confirmation of many-electron processes 3–36955
- X-ray plasmon and Compton scattering 3–30144
- X-ray Raman scattering 3–30143
- X-ray technique for crystallography obs. behind shock wave front 3–26930
- C, graphitisation under high press. 3–14999
- C graphitisation of diamond, high pressure and temp., nucleation and planar growth 3–12450
- $C_{27.5}CrO_2Cl_2$ crystal structure, electric conductivity and thermal stability obs. 3–33491
- Cs-Rb-graphite system, mixed sorption models and isotherms at high temps. 3–20927
- MgO-C, composite material, elasticity, effects of shape of dispersed particles 3–2750

graphs
- *see also Bode diagrams; nomograms*
- paper for depicting moment of inertia of high spin nuclear rotational states 3–10228
- seismic source parameters, graphical representation 3–9159

gratings (diffraction) *see diffraction gratings*

gratings (optical) *see diffraction gratings*

gratings (spectra) *see diffraction gratings*

gravimeters
- geodynamic piezoelectric instrumentation *(French)* 3–34962
- hydrostatic elevation difference meter for mining prospecting 3–25311
- laser gravimeter, accuracy better than 10^{-7} *(Russian)* 3–13517
- thermogravimetric meas. of evaporation rate in W wire production 3–18682
- vibrating string, dependence of frequency on amplitude *(Russian)* 3–9382
- vibrating string gravimeter, temperature dependence studies *(Russian)* 3–10215
- volumetric adsorption apparatus 3–13518

gravimetric instruments *see gravimeters*

gravimetry
- *see also density measurement*
- inverse potential field problems, point (dipole) solutions, mass-pressing method 3–19375
- liquids, standard liquids and measurement methods 3–32024
- recording gravimetric rain-gauge, ground level reference instrument 3–21982
- thin films thickness, meas. using quartz oscillator *(French)* 3–35359
- UN samples, sintered, unsintered powder, 1.572 powder, chemical analysis techniques 3–6978

gravitation
- *see also general relativity; gravitational collapse; gravitational red shift; gravitons; quantum theory of gravitation; Schwarzschild metric; unified field theories*
- acceleration measurement, absolute detn. at Khar'kov State Inst. 3–32027
- anomalous interaction of muons with gravitational field, quantum field theory *(Russian)* 3–38003
- antigravitational effects in behaviour of neutral particle in field of charged particle *(Russian)* 3–22727
- attraction of three-dimensional bodies in spherical or ellipsoidal earth, computing method 3–18804
- Brans-Dicke field equation, position-depend. Robertson-Walker solns. 3–22723
- clusters of galaxies and Universe, effect of nonzero mass-neutrinos on gravit. dynamics 3–35005
- comets, nongravitational forces rel. to heliocentric distance, effects on orbits of long period 3–31633
- cosmological neutrino problem, field-particle aspects, role of gravitational field 3–12948
- Earth gravitational model, computation methods from combination of terrestrial and satellite data 3–34766
- Einstein's theory, harmonic frames of reference *(Russian)* 3–13634
- Einstein and symmetry groups in gravitational theory *(German)* 3–13620
- Einstein field eqns., decomposition for slow-motion approximation in general relativity 3–596
- Einstein theory generalization using $T^{\nu}{}_{\mu;\nu}=\lambda R$ 3–22726
- Einstein-Cartan eqns., derivation of analogue of Mathisson-Papapetrou eqn. of motion for spinning particle 3–16722
- Einstein-Cartan equations 3–26143
- Einstein-like Lagrangians, $SL_{6,c}$ gauge invariance 3–10369
- Einstein-Maxwell eqns., solns. for spinning particles at rest, balancing of e.m. and gravitational forces and torques 3–26140
- external gravitational field of relativistic astrophysical objects *(Polish)* 3–25363
- Fermi transport, generalised in generalised gravitat. theories 3–35615
- field characterisation using manifold theory, new formulation of Einstein eqns. 3–26142
- field effect on gas/liquid solutions, partial pressure, conc., equilib. relationships 3–34711
- field of charged mass point in scalar-tensor theory 3–22734
- finite range, possibility 3–22716
- fluid sphere, gravitating, with radiative transfer, equation of motion 3–28184
- galaxy clustering, kinetics using BBGKY hierarchy 3–39716
- generally covariant nonlinear electrodynamics with a tensor potential, analogy with Einstein's gravitation theory *(Russian)* 3–3996
- gravitational origin of strong interactions from general relativity rel. to universal creation 3–9457
- hard-sphere gas, thermal equilib. states of classical system with gravit., astrophysical appl. 3–35643
- Heisenberg's relations used to obtain information about e.m., nuclear and gravitational forces 3–10335
- inertial gravitational fields, relative strengths 3–35607
- Kerr metric as gravit. field of rotating sphere, Florides Synge method 3–16733
- linear relativistic formalism, covariant expression for gravit. energy-momentum 3–6326
- liquid convective flow regimes in a periodic external force field *(Russian)* 3–29856
- Lorentz manifold, compact, analytic non-Hausdorff extension for which no geodesic bifurcates 3–37880
- Mach's principle, review 3–35601
- massive superpropagators depend. on gravitational coupling consts. 3–4139
- massless tensor field, conformal-invariant field equations, dynamic inconsistency 3–10370
- matter creation in external nonstationary gravitational field 3–18918
- Maxwell equations, noninertial coordinate system 3–605
- MHD wave stability, propag. through uniform incompressible viscous gravitating fluid 3–17586
- modelling of Einstein's gravit. field geodesics appl. to solar field 3–16715
- modern relativity *(German)* 3–35012

- **gravitation** continued
  - motion of test particle moving towards a spherically symmetric gravitating body in Schwarzschild metric 3—10363
  - negative gravit. energy in two-geometries, physical implications 3—16735
  - neutrino-gravitational fields with zero energy-momentum tensor 3—601
  - new constants of motion for system of free gravitating particles in Newton's and Einstein's theory 3—22731
  - non-radiative one- and two-shrinking body systems, calc. of gravit. field, Synge's method 3—16714
  - nonlinear growth in expanding gases 3—12937
  - North Atlantic, gravit. modes of free oscill. 3—9261
  - noumenon, a generalization of relativistic events and space-time, basis for gravit. 3—19494
  - Parametrised Post-Newtonian Formalism, perferred frame theories 3—10375
  - Petrov classification of gravitational fields with directional symmetry for null direction 3—35604
  - plasma gravitational instability dispersion relation, effects of collisions and gyroviscosity 3—20490
  - plasma in gravitational field, origin of polarization electric field 3—29935
  - plasma resistive gravitational instabilities in Cartesian geometry, magneto-viscous effects 3—29977
  - Poincare gauge invariance and dynamical role of spin in gravitational theory 3—22730
  - postulational derivation of theory 3—22733
  - precession of locally inertial systems in neighbourhood of rotating sphere *(French)* 3—13622
  - projectivity of conformally-plane spaces created by the hydrodynamic energy-pulse tensor *(Russian)* 3—6327
  - random force in stellar gravit. systems, probability distrib. 3—31741
  - regular model universes, gravitational instability in modified theory of general relativity 3—28129
  - retarded interactions, two-body problem, stability, circular motion *(Russian)* 3—604
  - review of recent results and developments in theoretical mechanics and mathematical physics 3—16584
  - scalar-tensor gravitation theory, collapse *(Russian)* 3—26134
  - scalar-tensor theory and conformal invariance in Jordan theory 3—37887
  - scalar-tensor theory in a Lyra manifold 3—10377
  - scalar-tensor theory of neutron stars, comparison with general relativity 3—18915
  - shift of spectral lines and deflection of light rays, tests of general relativity, equal proper time formalism 3—594
  - SL(2C) invariance of gravit. field eqns., Yang-Mills type theory 3—16723
  - spherically symmetric metrics and field eqns. in four-dimens. space 3—37888
  - spline fitting method for subgrid resolution of field due to mass distrib. 3—26768
  - stability of strongly non-homogeneous self-gravitating equilibria 3—12936
  - stabilized nucleons in theory of generalized gravitational potential 3—13790
  - stars, spherical, non-rotating, exterior field Schwarzschild coordinates 3—3323
  - stars and gas, combined system, energy conservation for gravitational interaction 3—12938
  - stationary vacuum metrics with shearing geodesic eigenrays, general solutions 3—10361
  - stellar images, gravitational aberrations 3—16220
  - synchronous artificial Earth satellite motion using approx. computation method 3—25368
  - T-solutions of Einstein's equations in non-static spherically symmetrical gravitat. field *(Russian)* 3—600
  - terrestrial biaxial ellipsoid, reln. between coeffs. of spherical and ellipsoidal resoln. of gravitational force, computer soln. *(Russian)* 3—25160
  - theory, solar system expts., general relativity 3—32433
  - torque, gravitational between two bodies expressed in terms of external potential fields 3—22595
  - twistor theory, an approach to quantisation of fields and space-time 3—22717
  - uniformly rotating sphere, gravitational field in third approx. 3—28963
  - virtual particles in e.m. field as sources of gravit. field 3—16716
  - weak fields, e.m. radiation from point charges 3—26128
  - Weyl gravitational field, critique of direct singularity concept 3—6337
  - Yilmaz-Tupper theory, cosmological singularity 3—26141
  - e.m. current and charge due to interaction with free e.m. field 3—19500
- **gravitational acceleration** *see gravitation*
- **gravitational collapse**
  - *see also black holes; cosmology*
  - collapsed objects, e.m. structure of magnetized rotating sphere 3—25358
  - electrically charged star collapsing to Reissner-Nordstrom black hole, scalar perturbation method 3—19001
  - endpoints of stellar evolution, astrophysical aspects especially pulsars and X-ray sources 3—3324
  - energy release in stars, relativistic degeneracy 3—9453
  - higher-order gravitational Lagrangian in Einstein field eqns., effect on gravitational collapse 3—28105
  - Kerr-Taub-NUT metric, global analysis for closed inhomogeneous e.m.-gravitational field 3—37881
  - local structure of space-time singularity 3—34997
  - nonsymmetric, of infinite dust-filled cylinder 3—16111
  - partially collapsed spherical matter distrib. analysis based on Yilmaz exponential metric 3—28235
  - rotating galaxies, gravothermal catastrophe leading to core-halo system 3—31747
  - rotating gaseous spheroids, dynamical contraction formation of stars and galaxies 3—37286
  - universe model, using spin and torsion to avert gravitational singularities 3—28128
- **gravitational constant**
  - new method of determination with high sensitivity for measuring very small forces 3—13214
  - variability rel. to variations from A.D. 1663-1972 of rotation of Earth 3—25103
  - variations detection 3—10380
- **gravitational experiments**
  - detection of waves using seismic signal measurements 3—602
  - detectors of gravitational waves, design and calibration 3—22729
  - extraterrestrial gravitational radiation, observations from two gravitational antennas *(Russian)* 3—609
  - force on prestressed body in curved space and design of gravitational wave detector 3—35605
  - inertial-to-gravit. mass ratios for Al, Pt, torsion balance meas. 3—16742
  - Newtonian grav. constant variations detection 3—10380
  - preferred frame theories, gravimetric, length-of-day and perihelion shift of planets obs. 3—10376
  - radiation, review of expts. and theoretical implications 3—610
  - radiowave deflection by Sun during 1972 October, comparison with general relativity prediction 3—31530
  - relativistic gravity testing, gravitational-wave obs., implications 3—37886
- **gravitational radiation** *see gravitational waves*
- **gravitational red shift**
  - *see also cosmology*
  - quasar mechanism using scalar gravit. field 3—39704
  - validity relations establishment *(French)* 3—19496
  - white dwarfs, mass and radius determ. 3—13037
- **gravitational waves**
  - *see also gravitons*
  - absorption by dissipative fluid, eikonal approximation 3—35612
  - astronomical aspects of gravitational waves rel. to Weber's results *(Japanese)* 3—3280
  - black holes, Schwarzschild, gravitational radiation from mass projected inside with nonzero kinetic energy 3—35614
  - black holes, Schwarzschild, vector and tensor radiation from relativistic circular geodesics 3—37288
  - clusters of galaxies, effect of mass loss to gravit. radiation on stability, N-body problem soln. appl. to Virgo cluster 3—28255
  - curvature collineation classification of plane-fronted pure waves 3—16736
  - deformation and elatic bodies, interaction 3—19434
  - detection, thermal noise limitations 3—35613
  - detection by method of light scatt. from elastic waves *(Russian)* 3—37884
  - detection of gravitational waves using seismic signal measurements 3—602
  - detectors, design and calibration 3—22729
  - diadic components of curvature tensor *(Russian)* 3—10374
  - extraterrestrial, observations from two gravitational antennas *(Russian)* 3—609
  - field of rotating radiating source, generalization of Kramer's soln. 3—4020
  - force on prestressed body in curved space and design of gravitational wave detector 3—35605
  - galactic, central disks, relativistic, rel. to gravitational wave production 3—22728
  - Galactic centre, radio pulses at 858 MHz rel. to gravit. radiation 3—28225
  - galactic radiation, model for peaking using geometrical optics 3—13094
  - gravitational-e.m. reson. in ring wave guide, for gravit. wave detection 3—16737
  - high-frequency, approx. solns. to Einstein's eqns. by averaged Lagrangian technique 3—28961
  - interaction of weak waves with gas 3—32434
  - interaction with planetary bodies 3—599
  - liquids, thermal equilib. near crit. point, effects on thermal conductivity 3—36442
  - lunar maximum seismic activity rel. to pulsar CP1133 and gravitational waves 3—3315
  - macroscopic high frequency quantum generator and detector of gravitational radiation 3—16738
  - neutrino-gravitational fields with zero energy-momentum tensor 3—601
  - observational technique and interpretations 3—6340
  - orbiting astrophysical bodies, matter ejection and gravitational radiation 3—25362
  - perfect fluid with axial symmetry, initial value problem in general relativity 3—32430
  - phase fluctuations of wave in stochastic medium 3—32450
  - primordial interaction with groups of galaxies 3—3373
  - propagation speed anomalies 3—37886
  - radiation, review of expts. and theoretical implications 3—610
  - radiation of falling particle in black hole, 4-dimens. Green's function approach 3—37885
  - radiation of spinning test body in field of black hole 3—12947
  - in Schwarzschild background, study of Newman-Penrose quantities 3—6330
  - search for seismic signals from pulsar CP1133 gravitational radiation 3—2868
  - source location of Weber's gravitational events rel. to galactic nucleus 3—16734
  - synchrotron radiation, polarization 3—603
  - terrestrial seismic vibrations caused by pulsar CP1133, possible gravitational waves 3—2867
  - weak, quantisation in closed Fridman model 3—28964
- **gravitons**
  - dispersion relation techniques, mass struct. investigation using gravitons 3—608
  - eikonal approx. for gravit. vertex of infinite sum of gravitons 3—6343
  - higher-order gravitational Lagrangian in Einstein field eqns., effect on gravitational collapse 3—28105
  - mass calculation, from graviton decay into two photons 3—26145
  - mass determ., theory 3—607
  - virtual graviton scattering on hadronic target, light-cone commutators 3—32623

gravitons continued
- f-meson-graviton mixing model, massive superpropagator evaluation 3−6550
- π e.m. self-energy in presence of spin-two gravitons 3−35790
- $\pi^- p \to f^0 n$, reln. of f^0-meson to massive gravitons at high energies 3−14067

gravity
- *see also gravitation*
- algorithm for computing vertical deflections gravimetrically 3−9164
- anomalies, free air, correl. with oceanic age-depth relationship 3−37150
- anomaly, vertical deflections, undulations of geoid 3−9139
- autocorrelation functions for gravimetric data, character of variation 3−25129
- B-type star models with low surface gravity, comparison with HZ 22 primary component 3−28176
- Bouguer gravity map of Nigeria 3−5462
- Burdwood Bank, negative gravity anomaly 3−27991
- conference, 16 to 18 Aug. 1972, earth gravity models 3−18835
- earth, models, conference, 16 to 18 Aug. 1972 3−18835
- earth's field meas. using orbiting rotating gravity gradiometers 3−34780
- Estonia, diurnal variations meas., harmonic anal. compared with meas. in Europe and Central Asia *(Estonian)* 3−25122
- evaluation of gravity anomalies directly from satellite observations 3−12590
- extension of Alaskan structural trends beneath Bristol Bay, det. from gravity profiles 3−9170
- field resolution using satellite-to-satellite Doppler tracking 3−34772
- field transformations, Wiener filter application 3−31287
- finite amplitude convection occurring in a modulated gravity field *(Russian)* 3−26787
- G- and K-type supergiants, line spectra anal. of gravities 3−31667
- geometrical optics in curved space-time 3−16717
- geophysical fields, cartographic representation method 3−25321
- geopotential coeffs. accuracy, satellite and terrestrial gravity data 3−34775
- geopotential coeffs. determ. using satellite-to-satellite tracking 3−34773
- geopotential in satellite geodesy, simple layer model 3−34768
- geopotential model, from satellite Doppler data 3−9140
- geopotential representation using sampling functions 3−34771
- geopotential zonal harmonics determ. using data from Dial, SAS and Peole 3−34774
- gravitational moments computation for Jupiter and Saturn *(Russian)* 3−3301
- Iceland-Faeroe Ridge, joint interpretation of two-dimensional gravity and magnetic anomalies 3−12589
- inverse potential field problems, point (dipole) solutions, mass-pressing method 3−19375
- laser ranging to satellites appl., polar motion meas. 3−34779
- late type stars, rel. of Ca II K_2 and Hα line widths to gravity 3−35135
- lunar, empirically derived field 3−18983
- lunar gravity field determ. from long-period satellite motion 3−39594
- lunar gravity model, truncated spherical harmonic expansion with mascon terms 3−35099
- lunar physical librations due to third and fourth harmonics of lunar gravity potential 3−39639
- Magdalen sedimentary basin, gravity and magnetic survey rel. to possible salt deposits 3−12570
- Mare Serenitatis mascon, mass distrib. from Lunar Orbiter and Apollo 15 gravity data 3−18976
- Mars, cloud obs. compared with radar and gravity field meas. indicating large scale surface structure 3−31579
- Mars' gravity field determ. from Mariner 9 Doppler tracking data 3−31611
- mean gravity anomaly prediction, comparison of two methods 3−27935
- in mines, false anomalies, reduction of meas. *(Russian)* 3−5440
- Mohorovicic discontinuity determ. from deep seismic sounding and outer gravity field 3−27939
- RW Monocerotis, eclipsing binary star, gravity darkening of secondary component 3−13047
- moving fields of Galilean satellites used for Jupiter orbiter trajectories 3−9449
- North-West Scottish Tertiary volcanic islands, underlying basic and ultrabasic igneous rocks, gravity survey 3−37165
- northwestern Caribbean, structure from seismic reflection and gravity profile 3−15880
- ocean ridges, positive free-air gravity anomalies, satellite obs. and surface meas. 3−12588
- Papuan Ultramafic belt, major overthrust of ocean floor 3−12579
- potential deformations in Earth interior, isostasy *(German)* 3−12602
- prospecting methods, high precision, developments 3−9369
- SAO 1969 Standard Earth, error model using satellite tracking data 3−34776
- satellite geodesy, gravity anomalies determ. by least squares method 3−34777
- satellite-determined gravity anomalies, mathematical model 3−34767
- sea meas., accelerations and errors 3−9155
- second derivatives of Newtonian potential, effect of sea swell on determ. *(Russian)* 3−5436
- secular climatic changes rel. to variable solar output, gravity and geomagnetism 3−39541
- superconductor, induced internal elec. fields and effects 3−30581
- surface, U Trianguli, determ. by spectroscopic obs. 3−19023
- surface obs. rel. to satellite obs. 3−5420
- survey, appl. of crosscorrelation function in anal. 3−12850
- surveys to delineate African orogenic belts 3−9184
- terrestrial tidal variations in gravity, data processing using Venedikov's method *(Russian)* 3−21978
- tidal variations rel. to terrestrial deformations in Crimea *(Russian)* 3−21903
- Venetian hinterland, structural model 3−9126
- Venus, gravity anomalies rel. to physical features of interior 3−35078

gravity continued
- Venus, potential contour, radar mapping 3−35076
- vertical gravity gradients for improvement of seismic S/N ratio 3−37246

gravity meters *see gravimeters*

gravity waves
- acoustic wave propagation in an isothermal atm. using a geometrical acoustics approximation 3−15963
- air waves, quasi-static loading of Earth 3−9172
- atmospheric, equivalent gravity mode approx. of solar semidiurnal tide 3−34890
- atmospheric, satellite pictures 3−5501
- atmospheric impulses, propagation tracks *(German)* 3−12705
- atmospheric internal gravity waves, integrated ionospheric response 3−31415
- atmospheric wave generation during solar eclipses, supersonic motion of Moon's shadow and Earth's terminator 3−25249
- capillary in an electrolyte, excitation 3−36132
- diffraction in harbour, SOGREAH method *(Polish)* 3−25199
- free surface gravity flows, dynamics of electromechanical flow structs. 3−29899
- galactic spiral density wave rel. to star migration studies 3−39733
- inertia-gravity waves propag. during geostrophic adjustment, variable Coriolis parameter effects 3−27984
- internal, ducting on stable layer with shear 3−12727
- internal, generated by buoyantly rising fluid in stratified medium, spectrum obs. 3−20361
- internal wave propagation in rotating stratified fluid with random stability freq. 3−33275
- ionosphere lower F-region, phase velocity dispersion rel. to e.m. waves 3−21968
- ionospheric F-region, neutral wind effect on limiting periods of gravity waves 3−18890
- ionospheric spatial resonance rel. to internal gravity wave and natural ionospheric drift 3−31420
- liquid surface wave interaction with capillary waves, surface tension influence *(Russian)* 3−27978
- long, large amplitude, interaction with ambient shear flow 3−7404
- mixed gravity-Rossby waves, stratospheric penetration by equatorial waves 3−31367
- nonlinear, finite element approach 3−28024
- pressure point motion pattern 3−14480
- propagation, anisotropic, inhomogeneities, valve effect 3−36129
- refraction of uniform wave trains and transient wave groups near straight caustic 3−12678
- shallow water, laser velocimeter design 3−22377
- spectra of duration-limited waves, observations at Angus Island tower, Bermuda 3−12679
- sporadic-E ionisation, thunderstorm effect, global characteristics, formation by atmospheric gravity waves 3−31424
- stationary waves, Lagrangian descriptions *(Russian)* 3−1422
- steady state internal in stratified liquid, general method of solution 3−14485
- stratospheric-ionospheric interaction during movement of deep planetary wave 3−3034
- surface waves, nonlinear gravity-capillary, in study varying current, propag. 3−29893
- thermosphere, effect of viscosity, thermal conduction and ion drag on wave propagation 3−16013
- upper atmosphere, gravity waves in high wind shear region rel. to Li vapour trails 3−34921
- water, progressive and standing waves 3−11439

greasing *see lubrication*

Green's function methods
- γ-radiation field characteristics, calc. in double-scatt. approx. *(Russian)* 3−14019
- acoustic field response, acoustic propagation 3−3689
- acoustic propagation, scalar wave functions 3−3690
- alkali metals, liq., determ. of mag. susceptibility 3−30597
- alloys, binary, off-diagonal randomness, theoret. approach comparison 3−30384
- antiferromagnet, anisotropic Green's function theory 3−30584
- antiferromagnetism on Hubbard model, non-existence of selfconsistent solns. 3−5093
- atom, photoioniz. theory 3−20034
- atomic collision cross sections, second Born approx. studies 3−20043
- basic linked cluster theorem, simple proof 3−6358
- benzene, lower excited levels 3−4410
- Bethe-Salpeter and Coulomb Green's functions, f-dimensional nonrelativistic, transformed to algebraic eqn. 3−10595
- Bethe-Salpeter eqn. as relativistic eqn. 3−35733
- boundary layer flow past cylinder, soln. of general heat-transfer problem 3−23688
- composite semi-infinite slab, heat transfer to surface 3−32459
- conductivity of disordered harmonic solids, thermal Bethe-Salpeter equation 3−27149
- covariant wave eqns. in weak gravitational field, Green's functions forms, scalar D'Alembert eqn. *(German)* 3−35616
- covariant wave eqns. in weak gravitational field, Green's functions form, linearisation of Einstein's gravitational eqns. *(German)* 3−35617
- cylindrical shells, prestressed, dynamic response study using Green's tensor technique 3−37835
- direct nucl. reaction, calc. of hole spectral function by shell model and Green's function 3−10889
- elastic field with couple stresses, wave propag. 3−26099
- elasticity, couple stress theory, Green's function matrix integrals in inhomogeneous region 3−26073
- elasticity of composites, stochastic Green functions 3−37794
- electron-electron correlations in metals by numerical methods 3−36511
- electron-phonon interaction, threshold singularity, electron optical phonon coupling spectrum, polarisation interaction 3−36385
- electron-plasmon approx., single particle Green's function 3−20980
- electrostatic problem, Green's function and images 3−22799
- e.m. radiation from point charges in weak gravitational fields 3−26128

Green's function methods continued
e.m. wave scattering from cylindrical boundary of arbitrary shape 3 – 29021
e.m. zero-point energy shift induced by conducting closed surfaces 3 – 19552
even-odd nuclei, theory of moments and transitions 3 – 19755
ferrimagnet, isotropic two sublattice, applied magnetic field, quantum theory 3 – 38941
ferroelectric tunnelling model and induced moment system, solns. for surface bound states 3 – 15233
ferromagnet, s-d interaction 3 – 2245
ferromagnetic crystals with two sublattices, low temp. analysis 3 – 36697
ferromagnetic metals, negative magnetoresistance, due to spin fluctuations, spin Green function calc. 3 – 15182
gas thermodynamic equilibrium states, kinetic eqns. for the Green functions 3 – 22742
grand-canonical ensemble Green functions, rigorous resolution of the hierarchy 3 – 22743
gravitational radiation of falling particle in black hole, 4-dimens. Green's function approach 3 – 37885
heat transfer with melting or freezing in a wedge shaped enclosure 3 – 14982
Heisenberg ferromagnet, impurity spin orientation, calc. 3 – 8322
hot-electron conductivity, Green function approach 3 – 18153
impurity level calculation, network model for monatomic lattice 3 – 20984
impurity level theory, expression for Green's function 3 – 36548
induced moment system containing vacancy impurities, Green's function theory 3 – 34099
integral representations for the Laplace and Helmholtz equations 3 – 16596
Ising model, exact relations for correl. functions 3 – 18290
Ising model cumulant Green functions, general formalism 3 – 36695
isoperimetric inequalities, generalised 3 – 35556
isotropic medium, infinite, shear dislocation loop, displacement field calc. 3 – 7762
jellium, impure, longitudinal sound for small frequency and wavevector, phonon Green's function 3 – 20989
Kondo effect, Green's function relation using pseudofermion representation 3 – 614
lattice function for cubic lattice in terms of Mellin-Barnes type integral 3 – 35630
lattice Green's function for simple cubic and tetragonal lattices at arbitrary points, Heisenberg model calcs. 3 – 22752
lattice vibrs., microscopic theory 3 – 7870
light-cone ordered Green functions, construction, current commutators and sea-gull terms 3 – 23008
liquid metal, electronic density of states determ., tight-binding model 3 – 38773
liquid metals, Van Hove theory application, Green-function diagrammatic method 3 – 38771
liquid surface waves, caused by motion of rigid body *(Polish)* 3 – 23766
magnetic insulators, one-electron Green function of Hubbard model in atomic limit 3 – 15334
magnetic properties of exchange-coupled uniaxial anisotropic ferromagnets 3 – 15327
magnetic systems with various cryst. field level schemes, excitations study and Hamiltonian anal. 3 – 21189
many-body problems, book 3 – 20990
many-body theory appl. to Li atom props. 3 – 26560
many-fermion inhomogeneous system at finite temp., Green's function eqn. of motion 3 – 16744
Martin-Schwinger-Puff many-body theory, diagrammatic approach 3 – 16746
m.i.s. array, depletion layer profile, surface potential, Green's function calc. 3 – 27313
mixed boundary value problems, numerical solution using numerical Green's functions 3 – 22770
model Hamiltonian of BCS theory, determ. of partition function, Green's function method 3 – 27324
molecular impurity centre scattering of lattice waves 3 – 1746
multielectron system, calculation of excitation energy 3 – 20007
noncollinear magnetic sublattice structure, spin-wave energy and mean value of Hamiltonian 3 – 2227
nonstationary diffusion in a semiinfinite isotropically scattering medium *(Russian)* 3 – 12716
nuclear ground state energy variations due to pairing correlations in Fermi system model *(Russian)* 3 – 19787
open-shell SCF eqns. derivation for atoms and mols. 3 – 33002
paramagnetic ions, resonant phonon scattering, coupled mode and perturbation theory approaches comparison 3 – 1766
perturbation series solns. to stochastic 3 – 35560
phonon Green's function for regular polymers, exact computation, semianalytical method 3 – 29765
phonon relaxation in Ising model 3 – 1759
pion model, chiral invariant, coordinate-independent Green's functions 3 – 35752
plasma, truncation technique for real time two-particle Green function 3 – 26861
quantum electrodynamics, electron and muon as eigensolns. under Green function $\delta(x^2+l^2)$, quantization 3 – 35785
quantum field theory, one-dimensional, anomalous dimensions, Green's function behaviour 3 – 26261
quantum optics applications 3 – 10457
quantum statistical mech. thermodynamic limit of boundary conditions 3 – 6354
quantum systems, resonance wave function props. 3 – 32416
relativistic Coulomb Green function, Sturmian expansions 3 – 26121
relativistic three-body problems, treatment with retarded part of two-time Green's function 3 – 32641
second order equations with discontinuous coeffs., difference soln. *(Russian)* 3 – 13539
self-consistent polarization propagator method calc. of electronic particle-hole propagator of H_2 3 – 7112
semiconductor, elec. current passage under conditions of nonhomogeneity of cond. parameters and relax. time *(Russian)* 3 – 2127
semiconductor, light absorpt. by deep traps in quasi-classical random field, calc. *(Russian)* 3 – 34385

Green's function methods continued
simple cubic lattice Green function analytical properties, applications in lattice statistics 3 – 19518
single ion anisotropy, high temp. depend. determ. by Green's function method 3 – 21260
spectral variational principle for Green's functions 3 – 6317
spin system, ferromagnetic layer structure, ferromagnetic layer structure 3 – 38932
spin-orbit coupled system, Green's function form for the dynamic paramagnetic susceptibility 3 – 26635
Suhl magnon instabilities and parallel pumping, theory 3 – 2300
surface electronic states study 3 – 33977
tensor force and collective excitations in nuclear matter 3 – 38129
thermal conductivity of two-layer wall for time-varying heat-transfer coeff. 3 – 22787
Tomita-Tanaka approx. validity in limit of spin 112 Ising ferromagnet 3 – 34067
two-level atoms, frequency shifts in emission and absorption by resonant systems 3 – 33000
water wave in unbounded region bounded internally by circular cylinder, determ. of Green's function 3 – 20354
Al, liq., determ. of mag. susceptibility 3 – 30597
B_2Cl_4, analysis of mol. consts. 3 – 14343
B_2F_4, analysis of mol. consts. 3 – 14343
Fe, ferromagnetic, relaxation of resonance spin waves by s-d exchange evaluation by Green functions 3 – 21315
He, scattering and bound-state props., many-body Green's functions appl. 3 – 11122
^{3}He-^{4}He solid, mass fluctuation waves, impurity effects on magnons, Green's function approach 3 – 36457
HgTe, semimetal mag. moment and suscept., two-point matrix Green func. calc. *(Russian)* 3 – 5099
InSb, spontaneous spin-flip Raman line shape, theory 3 – 36870
KCl surface electron states, two-band crystal model 3 – 38881

grinding
ceramic materials for transmission electron microscopy 3 – 33436
diamond tool, spherical, designing for lens grinding 3 – 25746
machined surface layer strwture and thermal residual stress by grinding 3 – 21708
NC machine, for manufacture of optical aspheric surfaces 3 – 22333
optical blank grinding, tool design 3 – 16425
optical surface loose abrasive grinding, working parameters 3 – 5897
parabolic mirrors, refinement of grinding technique *(Dutch)* 3 – 28536
quartz powder, structure determ. by differential thermal anal., grinding effects 3 – 31208
strain free laser rods, grinding and polishing method 3 – 13285
Al_2O_3, corundum, diamond wheel techniques *(Russian)* 3 – 5912
Si, with sapphire hemisphere, fracture behaviour *(French)* 3 – 30194
Si_3N_4, high density, effects on mechanical strength 3 – 8953
$SmCo_5$ powder, coercivity, grinding duration and method influence *(Russian)* 3 – 27731

grinding mills *see grinding*

ground services, aerospace *see ground support systems*

ground support systems
see also aircraft communication; navigation; telemetering systems
AEROS project, adaptation of German polar ground station 3 – 16065
geostationary artificial satellite system METEOSAT, ground control system *(German)* 3 – 3166
lightning protection, triggering, space vehicle launching, fuelling, wire deployment 3 – 3012
nuclear instrument landing system using frequency-modulated gamma-radiation 3 – 19346
OAO-A2, review 3 – 31817

group theoretical schemes
$(3,3^*)\oplus(3^*,3)$ model of $SU(3)\otimes SU(3)$ symmetry breaking, new estimate of parameter c 3 – 23001
external symmetry group formation from Dirac's eqn. 3 – 23052
non-polynomial field theories as functions of time 3 – 10597
O(2, 1) as SGA of quantum-mechanical problem, new method of quantisation 3 – 13615
Poincare group, unitary representations in octonionic Hilbert space 3 – 32632
SO(6, 1) spectrum generating algebra 3 – 14103
U(6, 6) $\otimes$ O(3, 1) symmetry is parameter-free Reggeized absorption model for meson-baryon scattering 3 – 23111
U(nm) spin down $U(n)\times U(m)$ reduction, application to hadron, atomic and nuclear physics 3 – 37785

group theory
see also Clebsch-Gordan coefficients; crystal symmetry; elementary particle theory; group theoretical schemes; Lie groups; SU_n theory
astrophysical differential equations, reduction 3 – 12942
Bondi-Metzner-Sachs group, structure for asymptotically flat space times 3 – 10362
character system construction method 3 – 28805
complex Lorentz quantum-field group *(Russian)* 3 – 16934
conformal group in Poincare basis, principle discrete series 3 – 6179
conformal invariance on the light core and canonical dimensions 3 – 13818
coset symmetrization operators 3 – 26119
de Sitter group O(4,1), determ. of matrix elements of irreducible representations 3 – 32285
disturbance of coherence through interaction with hydrogen like atoms, group theory treatment of scattering *(German)* 3 – 13716
dynamical invariance groups of Kepler problem and harmonic oscillator 3 – 10644
dynamical symmetries and nonlinear realizations, geometric approach 3 – 10645
dynamical symmetry group for hydrogen atom *(French)* 3 – 16697
eigenvalues of Casimir operators of U(n) and SU(n) for totally symmetric and antisymmetric representations 3 – 32415
equation for the product of semi groups defined by the method of bilinear forms and its application to the Schrodinger equation *(Russian)* 3 – 589
field equations and group structure in Einstein universe *(German)* 3 – 28959
Finsler's geometry, introduction of covariant spinor derivatives *(Russian)* 3 – 28809
free topological groups, universal algebras *(Russian)* 3 – 13531

group theory continued
- Galilei group, calc. of automorphisms 3—6178
- generalised U(3(n-1)) scheme model, matrix element calc. *(Russian)* 3—35850
- generalized Clifford group, use in study of elementary particle phenomenology 3—10643
- gravitational theory, Einstein and symmetry groups *(German)* 3—13620
- H_4.SL(2,C) group, local represents. *(French)* 3—26047
- harmonic analysis orthogonal and Poincare groups application 3—28820
- Heisenberg relations, non-Abelian representation 3—6314
- ideal fluids, group classification of hydrodynamic eqns. *(Russian)* 3—29828
- inhomogeneous Lorentz group, unitary representations *(Hungarian)* 3—26130
- intertwining operators for reduction from infinite- to finite-dimensional representation of Lorentz group 3—16728
- invariance groups in classical and quantum mechanics 3—35599
- irreducible tensor operators for finite groups 3—16588
- kernel G_1 calc: on stationary space-time *(French)* 3—28807
- Litvin's lemma and decomposition of direct products of irreducible representations 3—35555
- Lorentz group, three-dimensional, construction of principal series representations 3—26050
- Lorentz-group expansion of relativistic scattering amplitudes for particles with arbitrary spin 3—23019
- Maxwell group and quantum theory of particles in e.m. field 3—19484
- mixing transformations on metric spaces 3—19390
- multiperipheral dynamics, semi-group approach 3—26337
- non-unitary zero mass induced representation of Poincare group on space of tensor-valued functions 3—10631
- nonlinear representations 3—10232
- nonlinear spinor theory, nonlinear group representation *(Russian)* 3—19674
- nonsingular free solns. of Maxwell's eqns., analytic continuation representation of group 3—32658
- normal sub-groupoids and normal subcategories *(German)* 3—35558
- nuclear spectroscopy, applications *(Polish)* 3—23196
- O(3) shift operators derivation of irreducible representations of groups O(4), O(3,1) and E(3) 3—28811
- O(4) transformation, three-body decays for particles with arbitrary spin 3—23020
- O(5), construction of physical basis, automatic performance of symbolic transformations *(Russian)* 3—10235
- periodic system of elements, geometrical realisation of Aufbau scheme 3—38201
- Poincare group, non-unitary representations and fourier transform 3—37784
- Poincare group spin algebra and Shirokov's method *(French)* 3—16590
- point groups O and D_4, class sum operator approach 3—26049
- polarisation optics, group theory unified formalism 3—29034
- polytopes, algebra *(German)* 3—26052
- projection operators of representations of U_2 on basis of Un, determ. of matrix elements *(Russian)* 3—28816
- quadratic form and essential self-adjointness 3—32409
- quantum harmonic oscillator, radial wave function calc. by noncompact group in $Sp_{6,r}$ 3—10352
- quantum-mechanical models with modified Coulomb potentials, soln. by algebraic method based on SO(4,2) dynamical group 3—22707
- quotient spaces 3—35598
- relativistic group of canonical transformations, including Poincare group and dilatations 3—16727
- renormalisation group techniques for logarithmic corrections in critical and tricritical transitions 3—13663
- Riemann metric, conditions for torsion freee connection to be Levi-Civita connection 3—6177
- rigid molecule model, group theoretical selection rules in inelastic neutron scattering 3—7887
- semiconductor, with famatinite lattice, electron energy spectrum determ. *(Russian)* 3—30397
- semidirect product, generalized for group extensions 3—10231
- semigroups, $A^{n,a}$ ($n=0,1,2,\ldots;\ o \leqslant a < 1$) convergence theorems *(Russian)* 3—13532
- $SL_{2,c}$, transformation function from jm-basis to Z-basis for unitary representation 3—28819
- SL(2C) invariance of gravit. field eqns., Yang-Mills type theory 3—16723
- space group representations for nth symmetrized powers, subgroup formulae 3—16587
- spherical harmonics and second order tensorial multipoles *(French)* 3—26048
- spinor field eqns. construction, in cosmological space *(Russian)* 3—5555
- spinor ladder model of π^0 photoproduction and NN scatt. 3—13898
- symmetric group S_n symmetry adapted to subgroups, N^{th} rank tensor representations double-coset decomposition 3—28814
- thermodynamic dual lattice, classical system of arbitrary spin 3—13637
- trilinear Lorentz invariant forms of SL(2,C), distribution theoretic soln. 3—16586
- U(3), tensor operators characterized by maximal null space, canonical structure 3—16705
- U(3) × U(1) broken gauge invariance theory with calc. of baryon masses 3—26276
- U(3) pattern calculus rules and canonical splitting, tensor operators and unitary groups 3—16704
- vibrating polygon 3—22686
- Yang-Mills fields and the minimal electromagnetic interaction principle 3—10586
- H atom, group-theoretic connection between Stark and free-field wave functions 3—11118
- SO(5) and Sp(4), matrix elements and canonical Wigner coefficients 3—38008
- SO_0(p,1), multiplier representations of supplementary series 3—35557
- SU(4) and Sp(4), irreducible representations in boson calculus by lowering operators 3—38009

Gruneisen coefficient
- alkali halide, optic mode Gruneisen parameters rel. to anharmonic interactions 3—27094
- alkali halides, calc. from ionic Rydberg potential function 3—38549
- elastic constants, relationshp at finite temps., and Gruneisen approx. 3—38606
- elements, V and VI, from thermal expansions, compressibility and Morse functions 3—17983
- Fusion curves of solids at high pressure rel. to Gruneisen coeff. pressure depend. 3—17963
- glasses, press. dependence of i.r. vibration mode frequencies 3—12134
- ionic cryst., Anderson-Gruneisen parameter, comment 3—20878
- parameter Γ meas. from free surface velocity of thermoelastic materials 3—17982
- polyethylene oxide, from bulk modulus press. depend 3—18722
- polymer, determ. rel. to thermoviscoelastic behaviour on shock wave propag. 3—24177
- polymers, calc. from cell model 3—20221
- polymethyl methacrylate calc. and comparison with thermal expansion, heat capacity and compressibility 3—20221
- polystyrene, calc. and comparison with thermal expansion, heat capacity and compressibility 3—20221
- polytetrafluoroethylene, Gruneisen parameter and interchain specific heat, pressure dependences 3—27129
- spinel, rigid ion approx. model calcs. 3—7875
- Al, thermal expansion meas., 3-35 K 3—30273
- Dy, elastic moduli study 3—27051
- Er, elastic moduli study 3—27051
- Gd, elastic moduli study 3—27051
- Ge-Si alloy, determ. from inertial thermoelastic stress meas. 3—24278
- Na_2O-SiO_2 glass, i.r. absorp. spectra pressure dependence obs. 3—5186
- Ne, solid, equation of state to 20 kbar 3—36405
- Ne, solid, sp. ht., 1K to melting line 3—36427
- β-Sn, rel. to Mossbauer effect probability at high press. 3—27457
- SnO_2, Raman active phonons, Gruneisen parameters, 10-500 K, 0-4 kbar 3—33633
- Zr, thermal expansion 3—11752

Gudden-Pohl effect *see electroluminescence*

guided electromagnetic wave propagation
- *see also waveguides*
- PP micropulsations in magnetosphere, *PP* dotting 3—5476
- attenuation in Earth crust waveguide, e.l.f. to v.l.f. 3—34855
- circular waveguide, H_{21} wave excitation 3—19557
- coaxial line, permittivity and dielectric thickness effect *(Japanese)* 3—26107
- coaxial waveguide with lossless reactive guiding surfaces 3—13606
- collisional, multi-ion horizontal duct producing v.l.f. noise bands 3—16014
- cut off wavelengths of TE and TM modes 3—10332
- cylindrical compressible argon-gas plasma, excitation experimental studies of e.m. waves 3—23826
- dielectric slab waveguides with inhomogeneous core, soln. of Maxwell's eqn. 3—10328
- field problems in cylindrical coordinates, finite element solution 3—32494
- free space and planar waveguide, diffraction 3—26196
- glass fibres, radially inhomogeneous 3—16797
- interaction with electron beams in wave guides with resistive walls *(French)* 3—32497
- ionospheric conjugate ducted echoes, Alouette II ionograms 3—5518
- longitudinally nonuniform dielectric *(Russian)* 3—13609
- multi-modal transient excitation effects in infinite parallel-plate wave guide 3—10329
- neutron, thin films 3—17277
- nonlinear dielectric boundary surface waves, dispersion curves and mode patterns 3—32496
- open periodic structure with single iris, dispersion charact. determ. using variable length cavity *(French)* 3—29011
- with past comb of limited length, dispersion *(Russian)* 3—13610
- perforated flat plates, transmission charact. 3—10331
- phase velocity and group velocity in homogeneous media 3—37857
- plane impedance waveguide, mode spectrum *(Russian)* 3—26106
- plasma-filled transversely magnetized rectangular waveguide charact., collision frequency effect 3—1491
- power flow, stored energy, variational expressions 3—13607
- rectangular waveguide, filled with homogeneous lossy anisotropic plasma, dispersion relation 3—23830
- rectangular waveguide dielectric loaded bends, reflection coefficients 3—16690
- rectangular waveguides, filled with lossy warm plasma, characteristics 3—20451
- relativistic electron bundles in circular waveguide with stratified dielectric filling, parametric radiation 3—29161
- scaling method for e.m. fields with applic. to matching problem 3—37858
- scattered fields from round metal post and gap 3—35664
- semiconductor, in rectangular waveguide, strong magnetostatic field effects 3—18175
- semiconductor, with negative differential cond., e.m. surface wave growth 3—18150
- slow wave structure, higher order evanescent modes 3—10330
- spherical waveguide rel. to earth and ionosphere model 3—32403
- stripline, coupled, in multilayer dielectric, freq. dependent propagation characteristics *(German)* 3—19481
- surface wave decay coeff. calc., of cylindrical corrugated metal rod 3—4065
- surface waves along lossless structs., inhomogeneous waves at planar interfaces 3—16686
- u.l.f. wave dipole excitation in earth crust waveguide 3—18819
- voltage-reflection coefficient and VSWR 3—16689
- waveguide, periodic, approximate computation *(Russian)* 3—10431
- waveguide, periodic delay system, dispersion charact., calc. *(Russian)* 3—10435
- waveguide exposure chamber 3—16691
- waveguide junctions scattering, moment method with mixed basis functions 3—37856

Guiner-Preston zones *see crystal microstructure*

Gunn devices
  see also Gunn diodes; transferred electron devices
  computer calculation, using finite difference method for solving partial differential eqns. 3−27268
  i.r. light emission phenomenon 3−18498
  GaAs, carrier mobility determ. 3−24424
Gunn diodes
  coplanar epitaxial device, Gunn threshold depend. on transverse mag. field 3−21089
  multilayer heterostructure type, negative differential cond. 3−15211
  S-type current-voltage characteristics, impact ionisation effects 3−36613
  voltage-current characts., time-averaged, increased width in mag. field, obs. 3−21090
  GaAr planar diodes, ohmic contacts by condensation of metallic plasma 3−25798
  GaAs, fabrication by mesa-etching technique 3−36990
  GaAs, pulse code modulator for GaAs laser 3−37975
  n-GaAs magnetoresistance, transverse, 300 to 800 K, carrier mobility, electron transfer between conduction bands 3−36624
Gunn effect
  see also limited space charge accumulation; negative resistance effects
  computer calculation, using finite difference method for solving partial differential eqns. 3−27268
  coplanar epitaxial device, Gunn threshold depend. on transverse mag. field 3−21089
  domain dynamics, in presence of field-independent trapping 3−18151
  semiconductor, feasibility of suppression of Gunn domains *(Russian)* 3−8199
  GaAs, high freq. behaviour of electron transfer, dynamical Monte Carlo study 3−11902
  n-GaAs, low field mobility temp. variation, threshold elec. field and peak to valley ratio effects 3−18146
  GaAs, n-type, transverse mag. field effects on threshold electric fields 3−18157
  InP, high freq. behaviour of electron transfer, dynamical Monte Carlo study 3−11902
Gunn effect devices *see Gunn devices*
Gunn oscillators
  secondary frequency standards, solid state oscillators coupled to superconducting cavity 3−25804
  GaAs, optimisation of epitaxial growth for high purity layers 3−2686
guns, plasma *see plasma guns*
gyration *see rotation*
gyromagnetic effect
  see also gyromagnetic ratio; magnetic resonance
  magnetic domains steady state motion, force integrals, gyroscopic and dissipative terms 3−18343
gyromagnetic ratio
  see also g-factor; magnetic resonance
  electrons, sixth-order contributions 3−836
  ferrite, hexagonal, ferromag. resonance obs. of magnetogyric ratio anisotropy 3−36730
  massive body with large space-time curvature 3−35610
  muons, sixth-order contributions 3−836
  proton, meas. using magnetically isolated cable solenoid 3−13210
  proton, meas. with NPL weak-field apparatus 3−13209
  proton, precision meas. at NBS 3−13211
  μ anomalous magnetic moment, precise measurement 3−13861
  α-Al_2O_3:Co^{2+}, H^+ e.s.r. spectra and magnetic consts. g and A 3−5131
  ^{157}Gd, meas. of lifetime of second excited state, determ. of magnetic parameters 3−969
  ^2H, n.m.r. determ. in D_2O 3−4251
  ^{172}Hf, magnetic moments and gyromagnetic ratio of excited states determ. 3−38103
  ^{177}Hf, evoluation from perturbed angular correlation meas. 3−19811
  $Ni_xCd_{1-x}Fe_2O_4$, temp. dependence of intensity of resonance field, line width due to resonant damping and g-factors' 20-360°C *(Russian)* 3−12064
  ^aOs, A=186, 188, 190, 192, recoil implanted in Ni, detn. from lifetime meas. 3−14119
  ^{152}Sm, magnetic moments and gyromagnetic ratio of excited states determ. 3−38103
  Ta_3Sn, n.m.r. of ^{181}Ta 3−36798
  ^{181}Ta, magnetic moments and gyromagnetic ratio of excited states determ. 3−38103
gyroscopes
  see also navigation
  eye resolving power on object relative velocity in viewfinder 3−22320
  floating, gimbal errors, taking drift into account *(Russian)* 3−65
  gyrocompass, suitable for undergraduates 3−28448
  gyrostabiliser, three-axis power, precessional eqns. *(Russian)* 3−13557
  gyrostat, with stationary point during precessional motion, conditions for existence *(Russian)* 3−16609
  gyrostat cone of axis of uniform rotation *(Russian)* 3−13549
  gyrostat in central Newtonian force field, regular precsssion *(Russian)* 3−13556
  gyrostat in Newtonian field of force, eqns. of motion *(Russian)* 3−13554
  Kovalevskii, S.V., stability of uniform rotation 3−13550
  Lagrange system of successively combined joints, determ. of regular precessions *(Russian)* 3−13551
  motion in gimbals, influence of small nutational oscillations on speed of precession *(Russian)* 3−19401
  precession of locally inertial systems in neighbourhood of rotating sphere *(French)* 3−13622
  radial elastic field inhomogeneity, of symmetric springs *(Russian)* 3−10319
  relativistic precession, in artificial satellite, rel. to general relativity theory test *(French)* 3−35603
  stability in conditions of resonance for gyroscope on vibrating support *(Russian)* 3−10266
  stability of precessional motion in conditions of resonance *(Russian)* 3−501
gyroscopes continued
  system with partial dissipation, characteristic indices of vanishing solution *(Russian)* 3−19402
  universal suspension, eqns. of motion *(Russian)* 3−13552
  universal suspension, rate of drift of axis of rotor *(Russian)* 3−13553
H centres *see colour centres*
H i regions
  21 cm H line, calibration profiles 3−39751
  compact galaxies, 21 cm obs. and correlation with optical emission spectra 3−28292
  cosmic-ray heating of HI clouds by magnetic stars 3−28291
  Cygnus X-3, neutral H absorpt. spectrum obs. 3−25485
  Cygnus X-3 distance determ. by comparison with 21 c.m. absorption meas. 3−22087
  dark clouds kinematical distrib., obs. of 4830 MHz formaldehyde line 3−31780
  disc stars, abundances of the elements 3−13117
  galactic centre, anomalous velocity H I concentrations, origin and formation mechanism 3−31770
  Galactic structure, existence of gas clouds in interarm regions 3−35174
  galaxies with small ang. dia., neutral H dia. determ. 3−25501
  heating, rel. to galactic cosmic ray phenomena 3−9421
  heating and ionisation by soft X-rays and cosmic rays, props. determ. 3−28293
  high velocity clouds rel. to outer spiral structure of Galaxy 3−19065
  high-velocity clouds in galactic spiral arms, non-circular motions 3−28267
  high-velocity neutral H, effects on spiral arms of tidal interaction of galaxies 3−28269
  IC 342, Scd galaxy, aperture synthesis obs. of neutral H 3−28271
  IC 3576, spiral galaxy, HI to optical luminosity ratio 3−28281
  IC 3576 X-ray source, radio obs. 3−19062
  interacting galaxies, flux determ. 3−19067
  intergalactic, photoionisation by quasar-emitted radiation 3−39715
  intermediate-negative-vel. neutral H at high galactic latitudes 3−35199
  intermediate-negative-velocity gas in l=238°, b=+75° region 3−35200
  interstellar grains, electrostatic potential rel. to H I ans H II regions and circumstellar envelopes 3−39749
  isolated HI clouds, hydrodynamic treatment of phase change 3−37481
  Kh 713, H I feature in unusual dark cloud 3−25517
  local component kinematics rel. to Gould's Belt 3−37488
  low energy diffuse X-rays, galactic latitude dependence 3−12882
  low-velocity gas, large-scale distrib. at high galactic latitudes 3−35198
  M33, H I emission regions at two Holmberg radii 3−28262
  in NGC 2403, aperture synthesis study of neutral H, discussion 3−39728
  in NGC 2403, aperture synthesis study of neutral H, obs. 3−39727
  NGC 3109, irregular galaxy, distrib. parameters of neutral hydrogen 3−28268
  NGC 4151, Seyfert galaxy, 21 cm obs. for structure determ. 3−31775
  in NGC 4236, aperture synthesis study of neutral H, discussion 3−39728
  in NGC 4236, aperture synthesis study of neutral H, obs. 3−39727
  NGC 5194 (M51), spiral arm structure, tidal interaction with NGC 5195 3−35187
  NGC 598 (M33), Sc-type galaxy, distrib. and kinematics of neutral H 3−28270
  NGC 6946, Scd galaxy, aperture synthesis obs. of neutral H 3−28271
  optical depth determ. of 21-cm emission line profiles 3−9608
  physical properties of two clouds with spin temperatures less than 25 K 3−9609
  radiation field, excited atom population, low energy cross sections 3−3378
  recombination radio lines, ionisation source *(Russian)* 3−16280
  Sculptor group of galaxies, velocities and distances determ. 3−28274
  spiral arm tracers, radial vel. distrib. comparison 3−39725
  W51 galactic radio source region, distance meas. 3−35163
H ii regions
  compact, origin of molecules, thermochemical calc. 3−28289
  cyanoacetylene cloud in Sagittarius B2, s.h.f. measurements 3−16276
  density shock waves in H II regions rel. to mechanism for star and cloud formation 3−22121
  diameters of regions in galaxy M31, comparison with M33 regions 3−28294
  DR 15, detection in far i.r. balloon measurements 3−22093
  DR-21, 21-μ i.r. flux and colour temperature determinations 3−13103
  dusty Stromgren spheres, analytic approximations from far i.r. observations 3−13104
  dynamics and effects of u.v. stars 3−39739
  filament formation in fossil H II regions rel. to Gum Nebula 3−13105
  interstellar grains, electrostatic potential rel. to H I ans H II regions and circumstellar envelopes 3−39749
  interstellar scattering and H II region rel. to angular diameters of radio-source OH components 3−25512
  i.r. obs., multicolour photometry giving colour temps., i.r. emission 3−13102
  M17, 21-μ contour map and colour temperature determinations 3−13103
  M17 (NGC 6618), observations of four bright i.r. sources 3−16250
  in M31, variation of emission-line strengths 3−39717
  NGC 1976 (M42), O III and N II profiles and line splitting 3−16281
  NGC 2024, 21-μ i.r. flux and colour temperature determinations 3−13103
  NGC 2236, O III profile and line splitting 3−16281
  NGC 3372 in η Carinae complex, characts. 3−28264
  NGC 6523 (M8), O III profile and line splitting 3−16281
  NGC 6611 (M16), O III profile and line splitting 3−16281
  NGC 6618 (M17), O III profile and line splitting 3−16281

H ii regions continued
  NGC 7635, internal movements and radial velocities *(French)* 3 – 25521
  Orion A, radial velocities from radio recombination lines 3 – 16241
  Orion A, radio brightness distrib. at 4.1 mm 3 – 35162
  Orion Nebula, obs. of D in assoc. molecular cloud 3 – 37486
  radial vel. meas. for determ. of galactic differential rotation 3 – 31750
  RCW 117, detection in far i.r. balloon measurements 3 – 22093
  S101 in Cygnus, 11 and 6 cm obs., excitation parameter of exciting star determ. 3 – 35201
  Sagittarius B2, 21-μ i.r. flux and colour temperature determinations 3 – 13103
  Sagittarius B2, 6 cm emission, formamide obs. 3 – 39698
  Sagittarius B2, thioformaldehyde obs. 3 – 39740
  Sco OB 1 association, stellar kinematics rel. to subgroups and H II distributions *(French)* 3 – 9596
  Sh 138, i.r. photometric obs., surface brightness and colour temp. meas. 3 – 22120
  Sh 152, i.r. photometric obs., surface brightness and colour temp. meas. 3 – 22120
  Sh 270, i.r. photometric obs., surface brightness and colour temp. meas. 3 – 22120
  Sharpless 162, internal movements and radial velocities *(French)* 3 – 25521
  Small Magellanic Cloud, kinematic properties of 30 H II regions 3 – 28263
  spiral arm tracers, radial vel. distrib. comparison 3 – 39725
  stars in H II regions, Mk spectral types, and UBV photoelectric photometry 3 – 35137
  supernova remnants and HII regions, classification from recombination line emission 3 – 3334
  turbulent intercloud medium, temp. determ. 3 – 37489
  W3 (OH), interferometric observations at 2.695 and 8.085 GHz 3 – 22083
  W49, radio obs. of formaldehyde, ^{13}CO, C^{18}O and CS lines 3 – 35197
  W51, radio obs. of formaldehyde, ^{13}CO, C^{18}O and CS lines 3 – 35197
  W$_3$, IR sources, interstellar dust, ionised gas, H_2O maser emission 3 – 3358
  $^{13}C^{16}O/^{12}C^{18}O$ ratios from line emission from nine H II regions 3 – 19072
  H_2, molecules inside neutral globules 3 – 25519

hadron classification schemes
  baryon level structure, analysis using two-body quark potential 3 – 4188
  baryonnc quark states, fractional parentage decomposition 3 – 869
  baryons, in SU(3) Regge scheme 3 – 14036
  broken U(3) × U(3) symmetry gauge model for strong interactions 3 – 35815
  chiral saturation scheme of mesons in SU(4) × O(3), calc. of F and ρ Regge couplings between mesons using FESR 3 – 23107
  chiral U(3) x U(3) symmetry breaking and $X \to \eta\pi\pi$ decay amplitude 3 – 35757
  high-energy physics review for 25 years 3 – 10779
  ladder representations complete set and relativistic generalisations 3 – 26331
  nonchiral SU(2) × SU(2) classification of hadron states, connection with field-current identity and CP violation 3 – 14037
  physical ladders, generalization to relativistic case *(Russian)* 3 – 29233
  SU(3)⊗SU(3) and unified gauge theories of hadrons and leptons 3 – 38002
  three triplet hadron model, broken weak and e.m. interaction symmetry 3 – 17074
  triality selection rule, formal description by means of boson operator 3 – 16956
  U(nm) spin down U(n) × U(m) reduction, application to hadron, atomic and nuclear physics 3 – 37785

hadron current
  see also current algebra
  A = 12 system, finite-momentum-transfer test of conserved vector current 3 – 23197
  deep inelastic structure functions, symmetry principles and constraints 3 – 16955
  dual currents with cut-off, construction of amplitudes 3 – 17071
  dual model, rubber-band field of Virasoro-Shapiro model and complex field 3 – 35813
  dual resonance model, factorisation of pomeron sector and currents 3 – 10728
  e.m. connection between anomalous field dimensions and asymptotic scale invariance 3 – 19688
  equal-time correlations in hadrons 3 – 23007
  exotic, weak, existence of isotensor or isospin 3 – 23012
  field-current identity, CP violation and nonchiral SU(2) × SU(2) classification of hadron states 3 – 14037
  high-energy physics review for 25 years 3 – 10779
  leading light-cone singularities and hadron collisions 3 – 35804
  light-cone asymptotic props. of hadrons of free massless quarks and dual model 3 – 14028
  non-conservation of unitary-singlet axial-vector current, possible role of Fujii boson 3 – 32639
  short distance behaviour 3 – 13816
  strangeness-changing weak hadronic current, pseudo Cabibbo structure in gauge theory of interactions 3 – 38020
  strong and electromagnetic, dynamical Lagrangian theory 3 – 16959
  weak, Cabibbo angle calc. and deformed current algebra 3 – 38013
  weak and electromagnetic currents, connections 3 – 13815
  weak short-range interactions and scale invariance 3 – 16971
  $e^{+}e^{-}$ colliding beams, study of QED processes and hadronic e.m. current 3 – 858
  $K^{\pm} \to \pi^{+}\pi^{-}e^{\pm}\nu_{e}$, form factors of weak hadronic current 3 – 23031

hadron decay
  see also baryon decay; meson decay
  fireball decay, explicit solution of integral equation 3 – 16969
  heavy resonance, effective temp. in statistical bootstrap model 3 – 26322
  nonleptonic decay, broken scale invariance and weak current model 3 – 16971
  Weinberg's algebraic relations 3 – 13788

hadron elastic scattering
  No entries

hadron interactions
  see also baryon interactions; bootstrapping; electromagnetic corrections; meson interactions; Pomeranchuk poles and trajectories; Regge poles and trajectories; Veneziano model
  ab $\to$ c + anything, fragmentation in φ^3-theory ladder model 3 – 23186
  automodelity and dimensional anal. for hadron-hadron collisions 3 – 6647
  average charged-particle multiplicity, energy dependence 3 – 32734
  cascades at high energies, Monte Carlo anal. in 3 dimensions and computer simulation 3 – 10801
  CERN intersecting storage rings, first results 3 – 17097
  coherent hadron-nucleus collisions, inclusive particle spectra, diffraction excitation models 3 – 10819
  coherent nuclear production of multi-body states having broad mass spectrum 3 – 14070
  collisions, illustration of the uncertainty relation 3 – 31984
  collisions with nuclei at high energies, scaling 3 – 10820
  cosmic ray multiple production, review 3 – 22001
  dimension of hadronic matter with harmonic forces in infinite-momentum plane, estimate 3 – 38062
  divergence free dynamical model 3 – 16931
  dominance of e.m. effects in high energy hadron and photon induced reactions 3 – 23062
  dual parton dynamics and distribs. reln. to hadron level struct. 3 – 29220
  dual-resonance amplitudes, connections between smoothed and narrow-resonance discontinuities 3 – 29229
  electromagnetic structure, review 3 – 6612
  e.m. dominance near kinematic limit of hadron spectum 3 – 16985
  e.m. effects of one-pion-exchange in high energy reactions 3 – 13864
  exotic exchange suppression, tests 3 – 32692
  fireball chain decay, integral eqns. from thermodynamic model 3 – 29244
  fragmentation in high energy reactions, discrete structure 3 – 6667
  hadron-hadron, massive μ-pair production in dual-resonance model 3 – 14035
  hadron-hadron multiple production, mean multiplicities of secondaries *(Russian)* 3 – 19745
  hadron-lepton, Weinberg's model, and hadron and lepton struct. 3 – 19679
  high energy, diffraction dissociation model 3 – 876
  high energy collisions, multiplicity distrib. and production mechanisms 3 – 17121
  high energy collisions, Vol. II. Oxford, England (April 1972) 3 – 885
  high energy processes, models review 3 – 6632
  high energy production processes, multiplicity distribs. and integrated momentum distrib. functions 3 – 930
  at high transverse momentum, point-like interaction behaviour 3 – 38092
  high-energy hadron-hadron, charge transfer in fragmentation model 3 – 38070
  high-energy interaction with nuclei, study of fundamental processes 3 – 6657
  high-energy physics review for 25 years 3 – 10779
  high-energy scattering to two particle final states, Durham data bank, analysis and model comparison project 3 – 29256
  Huygens' principle, application at high-energy approx. 3 – 23150
  inclusive, diffraction fragmentation models for one and two particle distribs. 3 – 875
  inclusive, model for two particle distribs. and correlation functions 3 – 878
  inclusive, polarization effects, absorptive mechanism 3 – 934
  inclusive high energy collisions sealing of multiplicity distribs. 3 – 932
  inclusive photon distributions, π^0 and bremsstrahlung contributions 3 – 23189
  inclusive photon-hadron reactions, limiting fragmentation hypothesis and duality, Regge formalism 3 – 13997
  inclusive reactions at large transverse momenta, bound-state model 3 – 918
  inclusive single particle spectra and strong thermodynamic bootstrap soln. 3 – 914
  inclusive spectra, diffractive dissoc. and correls. 3 – 4232
  linear absorption model, A$_2$ exchange calc. in $\pi p \to \pi^0 n$ 3 – 17083
  many-particle inclusive cross-sections and correlations at very high energy, theory 3 – 29285
  mass spectrum, statistical approach starting from S-matrix, Bernstein-Dashen-Ma formalism and bootstrap 3 – 38069
  multi-Veneziano integrand and special unitary groups, connection 3 – 10633
  multiparticle production processes, role of inclusive reaction in asymptotic behaviour 3 – 17127
  multiparticle spectra, dynamic models, cluster decomposition analysis 3 – 10760
  multiparticle spectra, inclusive and exclusive, cluster-decomposition analysis of simple theoretical models 3 – 903
  multiperipheral dynamics, two-particle azimuthal correl. 3 – 4200
  multiperipheral theory at high energies, Bethe-Salpeter eqn. for properties of elastic and inelastic processes *(Russian)* 3 – 23190
  multiple prod., phenomenological anal. using uncorrelated-jet model 3 – 904
  multiplicity prod. at 200 GeV and inverse-square falloff 3 – 6656
  nuclear targets, study of hadron structure in high-energy collisions 3 – 29398
  one-pion exchange reactions, density matrix elements and amplitudes determination 3 – 6684
  partially inclusive reactions, limiting behaviour, test for dynamical basis of scaling 3 – 933
  particle prod. multiplicities, high energy, scaling relation 3 – 23171
  parton and dual model approach, calc. of s-channel helicity 3 – 13960
  peripheral dynamics, off-shell behaviour, inclusive sum rules 3 – 4201
  photon-hadron interactions, reln. to light cone 3 – 19695
  photon-hardon diffractive interactions, vector-meson dominance and coupled Pomeranchukon model 3 – 23095
  quark model, class '(a) relations, helicity amplitudes, test of equal phases assumption in $0^{-}\ {}^{1}.{}_{2}{}^{-}\ {}^{3}/{}_{2}{}^{+}$ 3 – 29218

hadron interactions continued
quark model class (a) relations for reactions $0^- \, {}^1/_2{}^+ \rightarrow 1^- \, {}^3/_2{}^+$, lack of independence 3−29217
scaling model of Feynman, relevance of cosmic ray data above 10^{12} eV 3−31488
semi-classical absorption model for multiplicity moments 3−19710
semi-inclusive, bubble chamber expts., sealing properties of cross-sections 3−931
statistical bootstrap eqn., truncated, for fireballs in two-body interactions 3−32679
thermodynamic single-particle spectra, kinematical cut-off 3−915
total cross sections for γ(hadron)-hadron collisions, leading light-cone singularities 3−35804
two component description for production of hadronic multiparticle final states 3−19712
two-fireball cross section, complex Regge poles and sign of two-Pomeranchukon discontinuity 3−38067
uncorrelated jet model, grand partition function 3−874
weak form factor, calc. of electromagnetic corrections using gauge invariance *(Russian)* 3−10696
π production, multiplicity moments and tranverse momentum distribution 3−17138

hadron lepto-production
see also baryon production; meson production
π^0 electroproduction in second resonance region, expt. 3−14010
Adler inelastic lepton-hadron sum rule saturation in quark-parton model 3−849
charge conjugation state prod. in ee and $\gamma\gamma$ reactions, one photon exchange model 3−13973
coincidence electroproduction and hadronic channels at edge of deep continuum 3−14004
deep-inelastic electroproduction in inclusive channels, final hadron states 3−13938
duality results for p-n electroprod. struct. function difference 3−13870
dynamic resonance model of form factor for electroproduction on meson target 3−13854
electroproduction, (8,8) models of Barnes-Isham type, SU(3) violation and σ terms 3−23133
electroproduction, inelastic, and Compton effect, Regge pole model 3−23071
electroproduction, semi-inclusive, Drell-Yan scaling 3−38053
electroproduction, semi-inclusive deep inelastic cross sections, azimuthal dependence 3−23087
electroproduction, threshold props. and sructure functions 3−29212
electroproduction, two-component framework with dual reson. contribution 3−19700
electroproduction and neutrinoproduction, multiplicities 3−26315
electroproduction at high energy, diffraction-dissociation model 3−38048
electroproduction coincidence cross sections in $\Delta(1232)$ region from coupled multipole eqns. 3−13941
electroproduction in first resonance region 3−13875
electroproduction of π, $\pi^+\Delta$, other pseudoscalar mesons and vector mesons in forward direction, coincidence meas. 3−13937
electroproduction of π, K,p, comparison with inclusive photoproduction data at 3.2 GeV 3−23089
electroproduction of single pion, vector meson dominance model 3−13890
electroproduction on nucleons in deep inelastic region, Regge model 3−13904
electroproductive struct. functions, derivation of sum rules and locality conditions 3−16960
e.m. self-mass of hadrons, finiteness criteria from Bjorken's asymptotic scaling 3−16988
inclusive electroproduction cross-section for π^+ in proton fragmentation region, prediction via factorization 3−17031
inelastic electroproduction, range, light cone dominance and scaling at low Q^2 3−23080
ladder-graph model relating e^+e^- annihil. and electroproduction 3−23093
neutrons prod. by cosmic-ray muons, depth-intensity curve *(Russian)* 3−22002
photon-hardon diffractive interactions, vector-meson dominance and coupled Pomeranchukon model 3−23095
pion form factor, ambiguity in determ. from electroproduction 3−16987
Pomeranchukon residue in Regge asymptotic region 3−23137
$e(\mu)mp \rightarrow e(\mu)cx$(c-stable hadron) triple Regge model 3−13975
$e^- + p \rightarrow e^- + \pi^\pm + X$ inclusive electroproduction reactions, scaling 3−32670
$ed \rightarrow e\pi^\pm\Delta(1236)$, coincidence meas. and nucleon cross-sect. detn. for Δ channels 3−17041
$e^-e^+ \rightarrow K^-K^+$ prod. in colliding beam, 1.2 GeV, meas. of cross-section and e.m. form factors 3−17015
$e^-e^+ \rightarrow \pi^+\pi^-$ prod. in colliding beam, 1.2 GeV, meas. of cross-section and e.m. form factors 3−17015
$e^-e^+ \rightarrow \pi^\pm +$ hadrons Regge pole and scale invariant model and form factors 3−13899
$e^+e^- \rightarrow 2$ hadrons, calc. with frame dependent cut-off in field theory 3−6614
e^+e^- colliding beams, 1.4-2.0 GeV 3−13943
e^+e^- colliding beams, multiplicity in hadron prod. 3−17028
$e^+e^- \rightarrow$ protons + hadrons Regge model satisfying scale-invariance 3−13904
$e^+e^- \rightarrow \sigma\gamma$, current algebra derivation of Ward identity 3−13817
$e^+e^- \rightarrow \sigma\gamma\gamma$, current algebra derivation of Ward identity 3−13817
$e^\pm e \rightarrow n\pi^+ + n\pi^-\gamma$, calc. of amplitude by soft-pion techniques and PCAC 3−13972
eN, electroproduction cross sections, separation of resonant and nonresonant contribs., isotensor currents 3−13983
eN, electroproduction of nucleonic resonances, relativistic quark model 3−13996
$eN \rightarrow eZx$, deep-inelastic semi-inclusive process, test of light-cone bilocal algebra of currents 3−16957
$eN \rightarrow e +$ hadrons, connection with deep inelastic Compton scattering in softened-parton-field model 3−23083
$ep \rightarrow e'AB$, reaction with highly virtual photons, parton model 3−13965

hadron lepto-production continued
$ep \rightarrow e'\pi^+\Delta^0(1236)$, electroproduction, meas. of differential cross section 3−13990
$ep \rightarrow e'p\eta^o$, e.m. form factor meas. for $S_{11}(1535)$ reson., comparison with quark-model calc. 3−38034
$ep \rightarrow en\pi^+$, 2 GeV, analysis using Chew-Low extrapolation and fixed t dispersion relations, determ. of π form factor 3−13987
$ep \rightarrow epM_x$, electroproduction coincidence meas. in deep inelastic region, determ. of cross sections 3−13991
$ep \rightarrow epX^0$, coincidence electroproduction in ρ mass region, meas. of cross sections for 0-1Gev/c^2 missing masses. 3−13956
$ep \rightarrow ep\pi^+\pi^-$, streamer chamber study for $0.3 < Q^2 < 1.5$ GeV^2 and $m_p \leqslant W < 2.8$ GeV, Δ^{++} and ρ^o production 3−38047
$ep \rightarrow ep\pi^\circ$, coincidence meas. of backward production 3−17040
$ep \rightarrow e\pi^+\Delta^0$, vector meson dominance 3−14008
$ep \rightarrow e\pi^+M_y$, electroproduction coincidence meas. in deep inelastic region, determ. of cross sections 3−13991
ep inelastic scatt., twofold diffl. cross-sect. at small scatt. angles detn. 3−17043
ep inelastic scattering, semi-inclusive and inclusive processes, phenomenological model based on statistical assumption 3−26312
ep inelastic scattering amplitudes in resonance region, relativistic quark model 3−14002
$e^-p \rightarrow e^-K^+\Lambda$, coincidence meas., −0.17 to −1.2 GeV^2 3−14011
$e^-p \rightarrow e^-n\pi^+$, determ. of optimal bounds for π e.m. from factor 3−38033
$e^-p \rightarrow e^-pX^\circ$, X° is undetected meson system, coincidence meas. in backward direction 3−17049
$e^-p \rightarrow e^-p\omega$, study of backward meson prod., 1.8 to 2.3 GeV 3−17044
$e^-p \rightarrow e^-p\pi^\circ$, coincidence experiments near first nucleon resonance 3−14009
$e^-p \rightarrow e^-p\rho^\circ$, study of backward meson prod., 1.8 to 2.3 GeV 3−17044
$e^-p \rightarrow e^-\pi +$ anyting, low t theorems and minimal gauge invariant extension of one-pion exchange 3−38049
n production by cosmic-ray muons at 4300 m w.e. 3−22000
$\nu p \rightarrow \mu^-\Delta^{++}$, comparison of various models using spin-density matrix data 3−23045
ω-mesons production as test of $\rho\omega\pi$-vertex and coupling constant 3−17042
$\varphi \rightarrow K^+K^-, K_s{}^0K_l, \pi^-\pi^+\pi^0$, determ. of decay modes in e^+e^- colliding beam 3−16977
π electroproduction, calc. of form factors from electric Born term model with absorpt. effects 3−17061
π electroproduction, light-cone dominance 3−13798
π electroproduction, low-energy, current algebra calc. for physical pions 3−35796
π electroproduction, threshold behaviour of struct. function 3−13853
π electroproduction, vector meson dominance predictions 3−17011
π electroproduction at N*(1236), isobaric model calc. using Feynman diagrams 3−13930
π electroproduction at threshold, implications of gauge invariance 3−10714
π electroproduction at threshold, calc. of axial nucleon and e.m. pion form factors 3−38044
π electroproduction in dual relativistic quark model, U_6 symm. breaking 3−13931
π form factors determ. in electroprod. expts., non-uniqueness 3−17051
π^- electroproduction into bound state of mesoatom *(Russian)* 3−38054
π^0 electroproduction at first resonance, multipole amplitude analysis, determ. of magnetic dipole amplitude 3−13940
π^0 electroproduction on protons in backward direction, determ. of differential cross section 3−13988
π^0 photoproduction, triangle anomaly, second-order radiative corrections 3−23029
π^+ electroproduction in $ep \rightarrow e'\pi^+n$, meas. of differential cross sections 3−13989
$\pi^\pm$, from deuterium, coincidence expts. 3−14012
$\pi^\pm\Delta$ electroproduction in electric Born model 3−14007
$\pi_\nu p \rightarrow \pi^-\Delta^{++}(1236)$ cross sections for electroproduction at 1.9 GeV and $-k^2 = 0.7$ GeV^2 Born and vector-dominance models 3−17001
ρ, from deep inelastic electron scattering, coincidence meas. 3−14001
ρ^0 electroproduction at $0.3 < Q1.5$ GeV^2 and $1.7 < W < 2.8$ GeV, study in $ep\pi^+\pi^-$ final state 3−23086
ρ^0 electroproduction on protons 3−13957

hadron photoproduction
see also baryon photoproduction; meson photoproduction
associated photoproduction, in γN reactions below 3 GeV 3−13874
cross sections and asymmetries, determ. from coupled multipole eqns. 3−13941
dispersion relation techniques for unknown partial wave amplitudes 3−13969
$\gamma d \rightarrow np$ exptl. test of time-reversal invariance 3−13804
$\gamma N \rightarrow O^-N$, s-channel helicity conservation and Regge cuts in t-channel 3−13901
$\gamma_\nu N \rightarrow \omega\Delta$, model without pomeron exchange 3−10699
$\gamma_\nu N \rightarrow \omega N$ forward electroproduction, mass dependence of diffractive production 3−10699
$\gamma p \rightarrow cx$(c-stable hadron), triple Regge model 3−13975
$\gamma p \rightarrow pm^0$, search for boson photoproduction by missing mass technique, meas. of s and t distrib. of hadronic continuum 3−13952
$\gamma p \rightarrow p\pi^+\pi^-$, 2-8 GeV, non-strange boson resonance production 3−10716
$\gamma p \rightarrow p\pi^+\pi^-\pi^\circ$, 4.3-7.5 GeV, non-strange boson resonance production 3−10716
$\gamma p \rightarrow \pi^+\pi^+\pi^-n$, 4.3 7.5 GeV, non-strange boson resonance production 3−10716
γp total cross sections for hadron production, 0.275 to 4.225 GeV 3−13984
π, gauge-invariant field-theory model based on Feynman graph model 3−4179
π^0, 3-7 GeV, recoil proton polarisation 3−10701

hadron production
see also baryon production; hadron lepto-production; hadron photoproduction; meson production
correlation functions, integral equations 3−19718

hadron production continued
high-energy nuclear reactions, structure studies 3−29398
multiparticle prod. models and multiperipheral dominance 3−6646
multiple, role of diffractive excitation mechanism 3−26352
multiple prod., total and π multiplicities calc. 3−6679
pair production by e^+e^- colliding beams, 1.2-2.4 GeV, total cross section meas. 3−38039
pN interactions, cascade calcs. of ang. distrib., empirical formulae 3−19724
e^+e^- collisions, hadron production, existence of new vector meson 3−13994
$e^+e^- \to \pi^+\pi^-$ + anything, multihadron production, 1.2-2.4 GeV 3−26309
$\gamma\gamma$, interactions of extragalactic γ-rays with universal radiation, γ-ray absorption due to hadron production 3−34983
$\gamma\gamma \to$ hadrons, from finite energy sum rules 3−13995

hadron scattering
see also baryon scattering; bootstrapping; hadron elastic scattering; lepton scattering by hadrons; meson scattering; Pomeranchuk poles and trajectories; Regge poles and trajectories
asymptotic, on deuterium, Doppler effect in extraction of total neutron cross sections 3−6674
backward, Regge analyses ambiguities, due to $\sqrt{u}$ dependence of fermion Regge poles 3−38066
boson resonances, intermediate, correspondence to intermediate structures in nuclear reactions 3−4214
charge distrib. of partons and scaling in deep inelastic scatt. 3−10725
covariant dual quark parton model for inclusive deep inelastic scattering 3−866
diffraction dissociation processes at high energies 3−14061
diffractive dissociation processes 3−14062
diffractive excitation model for multiparticle production processes 3−877
diffractive models in nondiffractive regions 3−23120
diffractive scatt. slopes and effective shape of spectral functions 3−10790
dual resonant model, transverse momentum distrib., exponential cutoff 3−14030
elastic differential cross-sections, unitarity bounds 3−23127
electromagnetic structure, review 3−6612
e.m. effects on hadron scatt., violation of Pomeranchuk theorem 3−841
hadron, hadron, multiplicities and reln. to other processes in parton model 3−26315
hadron-hadron, effect of 'Van der Walls force' on scattering amplitudes 3−32697
hadron-hadron high energy elastic, relativistic eikonal approx. and vector meson exchange effect 3−26340
high energy, description of scattering amplitudes as function of s and nz 3−886
high energy, particle and antiparticle, electromagnetic contrib. to difference of total cross sections *(Russian)* 3−912
high energy quasi-pot. scatt., Pade approx. *(Russian)* 3−14042
inclusive, on nuclei at high-energy, momentum loss spectra 3−32851
inelastic, deep, pomeron generated correction terms and light-cone processes 3−6638
inelastic electron scattering at high energies, review of single-arm and coincidence expts. 3−857
inelastic resonance effects, dynamical model 3−23125
lepton-hadron scattering, Han-Nambu partons and internal symm. 3−863
light cone current algebra and Regge couplings 3−6642
line-reversed reaction cross sections, asymptotic equality 3−4196
Linear Absorption Models, fund. constraints 3−10749
Moravcsik's partial wave analyses, applications 3−17082
multiple scattering mechanism, Regge cut rel. to urbaryon line diagrams 3−4197
multiple-scatt. formalism, generalized eikonal approx. at high energies 3−14060
multiplicity processes, high energy, charge correlations 3−23151
neutrino-hadron scatt., elastic and inelastic generalized form factors *(Russian)* 3−19684
off-mass-shell behaviour of scatt. matrix using effective Lagrangian model 3−26361
one-particle exchanges of spin J, strongly absorbed, explicit sum from 1 to ∞ 3−6659
polarised hadron scattering of ν and ν, determ. of cross-section difference using Adler Cabibbo Radicatti sum rules *(Russian)* 3−10678
Regge shrinkage in π exchange 3−6641
relativistic quark model, spin predictions for baryon decuplet production 3−29223
total cross section constancy with Pomeranchuk poles, self-consistent description and reln. to energy *(Russian)* 3−29242
transverse-momentum distributions in high-energy collisions, Gaussian model study 3−23175
unitarity equation and generalized optical theorem, existence and uniqueness 3−10752
unitary symmetry and duality 3−10732
virtual graviton scattering on hadronic target, light-cone commutators 3−32623
Weinberg's algebraic relations 3−13788
μ pair prod. by inelastic hadron-hadron collision, various Regge limits 3−14086
π-hadron threshold theorem 3−4217

hadrons
see also baryon resonances; baryons; hadron classification schemes; hadron current; hadron decay; hadron interactions; hadron scattering; meson resonances; mesons
cosmic ray, discontinuity in burst and differential hadron spectrum 3−28100
cosmology, hadron era for first 100 μ seconds in life of universe 3−28124
dimension of hadronic matter with harmonic forces in infinite-momentum plane, estimate 3−38062
electric dipole polarizabilities, nonrelativistic symmetric quark model using sum rules 3−29200
e.m. form factors, meromorphic function approach 3−840
e.m. mass shift, divergence 3−13856
excitation of hadronic matter, calc. of sound velocity, H-quantum 3−32642

hadrons continued
fermion quark model 3−19719
long-range-potential model 3−23117
parity-violating e.m. interaction 3−32663
polarisability and quark models 3−14022
quantum-field formalism of nucleon-K_a-boson model *(Russian)* 3−13827
size barriers, cosmological aspects 3−35009
$SU(3) \otimes SU(3)$ and unified gauge theories 3−38002
symmetry breaking due to weak interactions 3−35761
three-triplet model, rel. to $U(1) \times SU(2)$ gauge model 3−32644

haemoglobin *see proteins*

hafnium
Auger electron spectra, up to 530 eV *(Russian)* 3−15579
diffusion in Ni, electron microprobe measurement, temperature dependence *(German)* 3−7969
ionisation loss in inelastic electron refl. from HF surface 3−5252
oxidation kinetics in air *(French)* 3−33745
protective coating on Cr alloys 3−18657
thermal, electrical and emissivity properties, 1200-2000K 3−24404
thermophysical props., Moscow State University research *(German)* 3−36579
α-Hf, low temp. deformation, thermal activation parameters 3−31088
Hf-H system, mag. susceptibility and spin-lattice relax. *(Russian)* 3−38965
^{176}Hf-^{176}Lu pair, solar system abundance determ. and use as an s-process nucleochronometer 3−22010
Ni:Hf, lattice-location of implanted impurity in ferromag. host, chanelling obs. 3−18305

hafnium alloys
see also hafnium compounds
omega phase transition, Monte Carlo simulation 3−36418
Hf-W, liquidus curves, m.p., eutectic temps., solubilities 3−30969
$HfCo_2$, Laves phase, single phase region, mag. suscept. 3−27360
$HfCo_2$, occurrence of Laves phases, X-ray, differential and microstruct. analysis *(Russian)* 3−12334
$HfFe_2$, occurrence of Laves phases, X-ray, differential and microstruct. analysis *(Russian)* 3−12334
$HfNi_2$, occurrence of Laves phases, X-ray, differential and microstruct. analysis *(Russian)* 3−12334
Nb-Hf-N, temp. depend. of intl. frict. *(Russian)* 3−1689

hafnium compounds
see also hafnium alloys
carbides, nonstoichiometric, concentration dependence of hardness *(Russian)* 3−12433
tetrahalides, general and orbital valence force field constants calc. 3−29609
Hf-O system, near $HfO_{1/6}$, interstitial superstruct. and order-disorder transform. 3−14847
HfB_2, Knoop hardness anisotropy 3−30198
HfC, superconducting transition temp. 3−8292
HfO_2, axial thermal expansion and phase transform. obs. 3−7944
HfO_2, c.v.d. on Si, structure, optical and elec. characts. obs. 3−2658
HfO_2-Dy_2O_3 system, of cubic solid solutions, phase diagram determ. by X-ray analysis at temps. 1000-1700°C *(Russian)* 3−11715
HfS_2, elec. props. and memory effects 3−30527
HfS_2, octahedral coordination, transmission spectra obs. rel. to band structure 3−12144
$HfS_2(Se_2)$, long wavelength optical modes, Raman scatt. and i.r. studies 3−4833
$HfS_2(Se_2)(Te_2)$, i.r. refl. spectra 3−39146
$HfSe_2$, octahedral coordination, transmission spectra obs. rel. to band structure 3−12144
HfSi thin film growth on Si 3−20958
$HfTe_{2-x}$, $x=0.061$, preparation and X-ray characterization 3−7691
$HfTiO_4$, $Hf_{1.26}Ti_{0.74}O_4$, thermal expansion coeffs., compressibility, polymorphism, X-ray diffr. obs. 3−8976

half adders *see adders*

half-lives (radioactive) *see radioactive decay periods*

half wave rectification *see rectification*

halides
see also alkali metal halides
alkaline earth, luminesc. impurity centres, energy transfer, excitonic mechanisms *(Russian)* 3−27537
group IIIA elements, fund. vibr. energy 3−1190
history of gelatin Ag halide emulsions 3−222
hydrogen halide and Cl_2 gas environments, high strength steel slow crack growth 3−18680
metal, equation of state, one-parameter isothermal eqn. 3−7900
metal halide-NH_4NSC aq. soln., mol. anion addition, luminesc. spectral effects *(Russian)* 3−36922
noble metal ion, ratio of shell charges, electrical and mechanical polarisability 3−1152
Ag halide emulsions, reduction sensitization producing electrostatic charges and Ag centres 3−2837
Pd(II) complexes, mono(ethylenediamine) halides, i.r. and far i.r. spectra, group vibr. assignments 3−21417
Pt(II) complexes, mono(ethylenediamine) halides, i.r. and far i.r. spectra, group vibr. assignments 3−21417
W-halogen-O systems, gas phase composition and chem. transport reactions *(German)* 3−21792

Hall constant *see Hall effect*

Hall effect
alloy, ferromag., anomalous effect, cond. electron scatt. on magnons *(Russian)* 3−36589
alloy, magnetic, dilute, s-d scatt., many body theory 3−8157
p- AlSb, mechanisms of carrier scattering 3−24455
amorphous semiconductors, electronic phenomena, review 3−24415
amorphous semiconductors, hopping Hall effect, single phonon contribution 3−27274
anisotropic metals and semiconductors, meas. of Hall mobility by disc method 3−25791
band gap width meas. method, electron and hole mobility determ. 3−18060
complex semiconductor chalcogenides, physical props. *(Russian)* 3−8168

Hall effect continued
conductivity of system of interacting electrons, quantum effect, application of Wigner representation 3−27234
disordered materials, effective-medium theory 3−33929
electrically conducting rotating fluid, waves, Hall current effects 3−26871
electrolyte solns., Brownian-like liq. struct. effects on d.c. transport 3−2065
electrolytic solns., meas. method *(German)* 3−15832
electron-hole plasma, caused by self-mag. field of current, kinetic theory *(Russian)* 3−2108
equatorial sporadic E layer, cross-field instability due to upward Hall polarisation electric field and horizontal magnetic field 3−25289
ferromagnet, current-carrying states rel. to spin polarization in photoemission 3−18533
GaAs:Zn, H^+ ion bombardment, channelling expts., annealing behaviour of disorder density Hall effect correl. 3−33578
GaAs, n-type, transverse mag. field effects on Gunn effect threshold 3−18157
glass, hopping Hall effect, single phonon contribution 3−27274
graphite thin crysts., Hall coeff. and magnetoresist., field and thickness depend. 3−30554
Hall-angle derivation for a sphere 3−21064
high-ohm samples 3−25797
hopping type charge transport, Hall coeff. sign 3−18169
hydromagnetic flow near an accelerated plate, Hall currents effect 3−29898
impurity level depth, determ. for arbitrary degeneracy *(Russian)* 3−33827
Lagrange invariant in MHD involving the Hall effect *(Russian)* 3−17548
liquid, electronically conducting, ambipolar cond. rel. to Hall mobility temp. depend. 3−21056
liquid semiconductor, migration mechanism determ. 3−33902
magnetic-acoustic phenomena, influence of Hall effect on cylindrical waves *(Italian)* 3−30438
metal, liquid and vapour states, Hall mobility meas. up to 1600°C and 2000 atm. 3−36590
metallic thin films, determ. using Boltzmann equation *(Russian)* 3−30463
metallic thin films, rel. to H_2 and O_2 chemisorption 3−15278
metals, two frequency AC apparatus 3−25811
MHD plasma, stability under Hall currents and friction with neutral atoms 3−4636
mobility calc. 3−8207
partially ionized gas, Hall coeff., theory *(Czech)* 3−4518
plasma, anomalous cond., exactly solvable electrodynamic model 3−36151
plasma, rotating, tearing, tearing mode instabilities with Hall effect 3−20515
plasma heating, anomalous, by Hall current 3−23883
plasma instability, inelastic electron energy losses 3−33356
plasma sheath formation in centre of polytron Hall acceleration 3−20643
polar semiconductors, calc. of coeff. factor 3−11909
polar semiconductors, inclusion of higher order terms for energy distribution function of hot carriers at high temp. 3−8193
probe loop, for nulling induced voltages from a.c. magnetic fields 3−25810
refractory, obs. rel. to admixture effect *(Russian)* 3−8987
semiconductor, coeff. determ. by one-point method 3−24454
semiconductor, periodic impurity distrib., diffusion scatt. theory *(Russian)* 3−8209
semiconductor, strongly compensated, hopping mobility 3−33900
semiconductor, with two types of carrier *(Russian)* 3−2111
semiconductor and semimetal, Hall, magnetoresist., and drift mobilities, Boltzmann equation soln. 3−21098
semiconductor anomalous, field thory approach 3−33928
semiconductor layers, in-depth-inhomogeneous, probe-bar and multiprobe methods of meas. of Hall mobility *(Russian)* 3−6015
semiconductors, polar, non-degenerate, III-VI and III-V 3−21074
small constants meas. *(Russian)* 3−9989
steady MHD channel flow with anisotropic conductivity, second order solns. 3−14487
superconductor, II, dirty, vortex state Hall effect, conductivity tensor 3−34028
TCNQ charge transfer complexes, current carrier effective mass determ. 3−2368
Ag:Mn, temp. dependence, spin component of mag. solute 3−21058
$(Ag_xCu_{1-x})_2Se$, electronic and ionic conductor 3−21123
Ag_2Te, electronic and lattice thermal conductivity 3−1843
-AgZn, Hall coeffs. at 77 and 275K 3−38826
Al film, Hall voltage meas. rel. to size effect parameters 3−30448
AlB_2, carrier conc. determ. 3−11878
n-$Al_xGa_{1-x}As$, temp. depend. of Hall coeff. 3−30478
$Al_xGa_{1-x}As$:Mg, molecular-beam-epitaxially grown 3−18553
Au, temp. dependence in dilute alloys, intermediate field condition 3−21057
Au:Fe, temp. dependence, spin component of mag. solute 3−21058
Au-SiO_x, cermet film, Hall voltage meas. after heat treatment 3−15201
β'-AuZn, Hall coeffs. at 77 and 275K 3−38826
BeTeI film, temp. depend. *(Russian)* 3−21067
Bi and Bi-Sb alloy powder compacts characteriz., 300-77 K 3−36593
Bi film, Hall coeff. anomalous temp. depend. 3−30551
Bi-Sb(30%), 8-300 K *(German)* 3−11916
Bi_2S_3, sintered, variations with temperature *(French)* 3−36406
Bi_2Se_3:Ge, lattice defects, Hall const. meas. 3−33824
$C_5H_6NI.8AgI$, superionic, ionic Hall effect 3−38875
Cd, temp. depend. *(Russian)* 3−8154
Cd_3As_2, resistivity and Hall effect under high press. 3−27272
$Cd_xHg_{1-x}Te$, anomalous temp. dependence of Hall coefficient 3−24458
$Cd_xHg_{1-x}Te$, temp. depend. on annealing 3−8339
$CdIn_{2(1-x)}Cr_{2x}S_4$, meas. as function of temp. 3−2263
$CdIn_2S_4$ single crystal, DC cond., Hall effect and magnetoresist. meas. 3−33894
$CdIn_2Se_{4x}Te_{4(1-x)}$, solid soln., forbidden zone width from absorpt. and Hall coeff. meas. *(Russian)* 3−15126

Hall effect continued
CdO, high temp., from room temp. data and high temp. cond. 3−2080
CdO single crystal, degenerate semicond., carrier conc. and mobility obs. 3−2087
CdS, under thermal equilib. conditions 3−18172
CdS film, evaporated, resist. and Hall mobility rel. to prep. conditions 3−27322
p-CdSb, rel. to technology applic. *(Russian)* 3−24430
n-CdSb, temp. depend. rel. to recombination and photoresistor applic. *(Russian)* 3−24476
CdSe, impact ionisation, breakdown, photoinduced switching, meas. of cond., Hall coeff., mobility, 4.2-300K 3−30487
CdSe electron scattering mechanism, Hall effect measurements 3−30466
CdSe film, In surface doping effects *(Russian)* 3−2192
CdSe:Cu,In and undoped, high temp. defect equilibria 3−7745
$CdSnAs_2$, point defects, heat treatment effects, elec. props. study *(Russian)* 3−14853
CdTe, compensated doped crystals, density of states tails, Hall mobility, conduction band, conductivity 3−33832
CdTe:Fe, study rel. to impurity absorption and energy levels 3−15531
Co film, monocryst., struct. depend. *(Russian)* 3−18120
Cu, temp. dependence in dilute alloys, intermediate field condition 3−21057
Cu thin film coeff. rel. to temperature and magnetic field *(German)* 3−24413
Cu:Fe_2 and Cu:Mn, temp. dependence, spin component of mag. solute 3−21058
$Cu_{1-x}Ni_xFe_2O_4$ ferrite, extraordinary Hall const., resist., 293-550K 3−24459
Cu_2S:S, thermal e.m.f. coeff., conductance, Hall constant meas. 3−36577
$CuSO_4$ electrolyte solution, H^+ ion mobility calc. using two carrier expression 3−11755
Cu_2Te:Te, thermal e.m.f. coeff., conductance, Hall constant meas. 3−36577
EuO, Hall coeff. insulator-metal transition rel. to mag. order 3−2147
Fe, and Nernst-Ettingshausen effect, anomalies near Curie pt. *(Russian)* 3−12014
Fe, Hall effect and magnetoresistance 3−38825
Fe-Co, Hall effect and mangetoresistance 3−38825
Fe-Cr, Hall effect and magnetoresistance 3−38825
$Fe_{1-x}Co_xAl$ solid solns., conc. depend. *(Russian)* 3−30087
$Fe_{1-x}Ni_xAl$ solid solns., temp. depend., 80-300K *(Russian)* 3−18121
FeS_2, pyrite, natural, resist., Hall effect, rel. to energy gap and mobility 3−38837
FeS_2, temp. depend., down to 1.3K 3−21070
$FeSi_2$:Mn, Co, semiconductor-metal transition resist., thermoelec. and Hall effect obs., 300-1400 K 3−33973
Ga film, Hall voltage meas. rel. to size effect parameters 3−30448
GaAs, depend. on heat treatment temp., thermal conversion rel. to impurities *(Russian)* 3−38832
GaAs, field calcs. inside non-spherical radiation damage regions 3−38856
p- GaAs, heavily doped, neutron irradiation, effects, elec. conductivity, Mott transition 3−33823
GaAs, meas. on X_{1c} electrons at low temp., scattering mechanisms and band structure 3−21097
GaAs, mobility, anomalously high at room temp., resist. and Hall meas. 3−18140
GaAs, n-type, 77-300K, and p-type, 78K *(Russian)* 3−2110
GaAs, props. of high purity liquid and vapour phase epitaxial material 3−2676
GaAs ellipsoidal ⟨100⟩ valleys, soln. of Boltzmann equation, Hall and drift mobility 3−33883
GaAs:Fe, sensitizing centres, photo Hall effect, photocond. 3−36547
GaAs:Mg, molecular-beam-epitaxially grown 3−18553
GaA_s:Si impurity states, anomalous behaviour, temp. depend of Hall coeff., centre concentration 3−33834
GaA_s:Te, heavily doped, rel. to mag. susceptibility *(Russian)* 3−2252
$GaAs_{1-x}P_x$, Hall mobility meas. for melt grown crystals 3−24805
$Ga_xIn_{1-x}P$:S, band stricture elucidation 3−15215
$Ga_xIn_{1-x}Sb$, vertical freeze grown material characterisation 3−5280
n-GaN(:Zn) film, vapour phase grown, Hall meas., carrier conc. 3−33884
GaP, thin film, technique for determination of electrical properties 3−39298
GaP ellipsoidal ⟨100⟩ valleys, soln. of Boltzmann equation, Hall and drift mobility 3−33883
n-GaSb, heavily doped, stress-induced changes of Hall mobility, density-of-states tails calc. 3−30425
GaSb, temp. and press. depend. 3−24422
Gd, polycrysts., 4.2K, 46 kOe 3−33874
Ge, epitaxial, polycryst., amorphous, Hall mobility, carrier conc., cond., noise, 100-400 K 3−38855
p-Ge, even Hall effect rel. to mag. field at 300 K *(Russian)* 3−8210
Ge, field calcs. inside non-spherical radiation damage regions 3−38856
p-Ge, galvanomagnetic effects in high electric fields *(Russian)* 3−11910
Ge, heteroepitaxial films, Hall effect and magnetoresistance *(Russian)* 3−11966
n-Ge, high purity, γ-irrad., carrier-conc.-depend. mobility 3−36627
n-Ge, hot electron Hall transport, calc. 3−38848
n-Ge, surface hole mobility and density, scatt. in surface inversion channels, Hall meas. *(Russian)* 3−27299
p-Ge double layer film, Hall coeff., elec. cond., transverse magnetoresistance thickness effects *(Russian)* 3−8284
Ge film, vacuum deposited *(Russian)* 3−24431
Ge:Sn, heavily doped single cryst., mobility depend. on impurity conc. 3−33885
$GeSb_2Te_4$, Hall coeff., single cryst. characterisation 3−5279
HgSe film, amorphous, Hall mobility obs. 3−5009
HgTe, anomalous temp. dependence of Hall coefficient 3−24458

- **Hall effect** continued
  - p-HgTe, doped, hydrostatic pressure effect on Hall coeff. and elec. cond. 3−21099
  - In film, Hall voltage meas. rel. to size effect parameters 3−30448
  - $InAa_xP_{1-x}$ solid solutions, compositions, transport properties, electron effective mass 3−33802
  - InAs, electron irradiation damage studies 3−33555
  - InAs, meas. to 90 kbar rel. to structural transition and band structure 3−21096
  - InAs, temp. depend., electron effective mass determ. *(Russian)* 3−27250
  - n- InAs transport phenomena, heavily doped, Hall coeff. 3−36608
  - $InAs_{1-x}P_x$, vapour phase epitaxial material 3−2680
  - InP, vapour phase epitaxial material 3−2680
  - InP:Ge,Sn,Te, liquid phase epitaxial layer, carrier conc. and mobility 3−1637
  - InSb, anomalous effect, low temp. 3−8205
  - InSb, dependence of Hall voltage and electrical resistance on temperature and magnetic field 3−5021
  - n-InSb, magnetic freeze out, theory 3−30498
  - n-InSb, strongly compensated, Hall coeff. meas. at low temp. 3−15216
  - n-InSb, strongly compensated, Faraday effect rel. to Hall mobility and coeff. meas. 3−15477
  - n-InSb band tailing, hot electron magnetophotocond., cond. and Hall coeff. obs. 3−2138
  - InSb based mixed crystal film, Hall coeff. and mobility meas. 3−36622
  - InSb film, hot wire zone refined, Hall mobility 3−2669
  - InSb films, electrical props. rel. to structure of size quantisation 3−24528
  - p-InSb Hall coeff. mag. field depend. rel. to temp. *(Russian)* 3−8212
  - n-InSb impurity conduction, Hall coefficient, activation energies, impurity concentrations 3−30501
  - K, coeff. determ. by helicon transmission method 3−36594
  - K single crystal, meas. at 4.2 K, high and low-field limits 3−24412
  - Mg_2Ge, melt-grown, characterization 3−12270
  - Mo and Mo-rich-Re and Mo-Nb alloys, 4.2-295 K 3−38824
  - Mo-Re alloy crystals Mo electron configuration changes due to Re addition 3−8155
  - Nb and Nb-rich-Zr alloys, 4.2-295 K 3−38824
  - NbO, resist. and Hall coeff. meas. in high mag. field showing metallic behaviour 3−33888
  - Nd-Sb system alloys, physical props. and correlation with the phase diagram *(Russian)* 3−11882
  - Nd-Y alloy, conc. and temp. depend., 100-800 K *(Russian)* 3−27245
  - Nd-Y alloys, 100 to 800 K, precip. depend. *(Russian)* 3−15683
  - Ni, and Nernst-Ettingshausen effects, anomalies near Curie pt. *(Russian)* 3−12014
  - Ni, rotational Hall effect, 80-650K 3−36595
  - Ni film, thickness depend., 77K and room temp. 3−27244
  - Ni-Ge alloy film, conc. and thickness depend. *(Russian)* 3−18123
  - Pb, Hall effect and magnetoresistance 3−38825
  - $Pb_{1-x}Sn_xSe$, grown from vapour, Hall mobility 3−24438
  - $Pb_{1-x}Sn_xTe$, single-zone annealing, Hall mobility meas. at 77 K 3−24619
  - PbTe, single-zone annealing, Hall mobility meas. at 77K 3−24619
  - Pd, film, artificial ageing effect on resist. and hence Hall effect 3−8159
  - Pt island condensates on NaCl cleavages, Hall and Gauss effects *(Russian)* 3−2060
  - Re, single cryst., and Nernst-Ettingshausen effect 3−18127
  - Sb single crystals Hall coefficient and electrical resistivity 3−36625
  - Sb single crystals low temperature depend., electrical resistivity 3−36625
  - Sb_2Te_3:I, Hall voltage meas., I impurity influence 3−8607
  - Si, epitaxial on Al_2O_3, mobility anisotropy 3−11967
  - Si, field calcs. inside non-spherical radiation damage regions 3−38856
  - p-Si, inversion layer, surface quantization obs. by Hall effect meas. 3−2162
  - Si, ion implanted, sample holder 3−37662
  - Si film, chem. vapour deposited 3−8753
  - Si film, impurity centres, carrier mobility meas. by m.o.s. Hall technique 3−18094
  - Si film on sapphire, accumulation and inversion layer mobilities 3−18218
  - Si on sapphire, thin films surface charge effects, surface depletion 3−2185
  - p-Si:Al, (B), (Ga), electron irrad., annealing, effect of O and acceptor impurities 3−33560
  - Si:B film, epitaxial growth, thermal oxidation treatment, Hall mobility obs. *(German)* 3−18236
  - Si:Li neutron irrad., defect interactions, Hall effect, i.r. absorption studies 3−33570
  - n-(221)Si/(1122)Al_2O_3 film, anisotropy 3−11961
  - SiC, rel. to annealing *(Russian)* 3−8211
  - SiGe alloys as thermoelectric materials, dopant content 3−5023
  - SnSb single cryst., Hall coeff. meas., Sn atom deficiency *(Russian)* 3−30264
  - $SnSe_2$, meas. under pressure rel. to band structure 3−8176
  - SnTe:Mn, growth, transport props. rel. to mag. impurities 3−33882
  - SnTe-PbSe system, comp. and temp. depend. *(Russian)* 3−11918
  - $SrTiO_3$, Hall coeff. meas. rel. to oxygen vacancies as electron traps 3−27225
  - Ta-H system, 77-300K 3−20711
  - Te, electron irrad., recovery steps, isochronal and isothermal annealing expts. 3−33562
  - Te, meas. rel. to carrier mobility anisotropy 3−21111
  - TiC-Nb(Ta)(Mo)(W), cermet *(Russian)* 3−8988
  - Tl film, Hall voltage meas. rel. to size effect parameters 3−30448
  - Tl_xIn_xSe, temp. and comp. depend. 3−17957
  - $(V_{1-x}Cr_x)_2O_3$, ceramic, high pressure Hall meas. through Mott transition 3−27744
  - VO_2, Hall effect near semiconductor-to-metal transition 3−33971
  - Yb, study through f.c.c.-h.c.p. transformation 3−2059
  - Zn, temp. depend. *(Russian)* 3−8154
  - ZnO, ion-implanted, anneal characts. 3−30955
- **Hall effect** continued
  - ZnO:In temp. depend. 5 to 300K *(German)* 3−11899
  - ZnO(:Cu), elec. cond. and Hall effect, 5 to 300 K *(German)* 3−33933
  - p-$ZnSiAs_2$, 77-900 K 3−24425
- **Hall effect devices**
  - applic. in flux meter, improvements *(Polish)* 3−258
  - convertor, in apparatus for induction meas. in steady mag. fields 3−25816
  - gaussmeter for transient magnetic field 3−22410
  - generator, magnetic field measurement 3−13354
  - magnetic field measurement applic. *(German)* 3−13357
  - magnetic fields, three components, evaluation from voltages induced on 3 Hall probes *(French)* 3−3835
  - thermogravimetric balance for chemical analysis 3−3915
  - Bi_2Se_3 magnetometer, for low temp. work 3−35446
  - InSb, n-type pickup, for thermally stable probe of magnetic focusing system 3−25815
- **Hall effect transducers**
  - No entries
- **Hall generators** *see Hall effect devices*
- **halogens**
  - *see also astatine; bromine; chlorine; fluorine; halides; iodine*
  - difluorochlorine (III) cation, ^{19}F n.m.r. study 3−11286
  - gas, H-halogen system with W, gas equilibrium and chemical transport reactions *(German)* 3−25101
  - methyl halide-halogen collisions, energy losses of hot atoms 3−7263
  - molecular Cartesian force consts., computer calc. 3−4423
  - molecule collisions with alkali metal atoms, fragmentation of halogen negative ions 3−26715
  - negative ions, multi-photodetachment rates 3−11153
  - Ni-Cr-ThO_2, Cr diffusion by halogen carrier in Ni-ThO_2 3−8941
- **Hamidashi effect** *see ferroelectric phenomena*
- **hard soldering** *see brazing*
- **hard-sphere gases** *see quantum fluids; statistical mechanics*
- **hardness**
  - *see also abrasion; dispersion hardening; hardness testing; radiation hardening; work hardening*
  - alkali halide, indentation hardness theory rel. to resist. to dislocation motion 3−24203
  - alkali halide, NaCl-type, microhardness rel. to dislocation rosette length 3−17837
  - alloy, dispersion hardened, recrystallisation rel. to grain boundary form. 3−5311
  - alloys precipitation hardening, a strengthening parameter 3−21704
  - austenite formation during hardening of high speed steel tools, grain size formation rel. to annealing 3−18655
  - borosilicate films, sintered, Vickers microhardness characterisation 3−39377
  - compacted metal powders, pressures up to 10 kbar 3−12379
  - composite material strengthening mechanisms 3−21731
  - composites of solid lubricants and metals, comp. effect 3−15785
  - diamond structure crystal, microhardness print mechanism on local phase transition 3−7931
  - kamacite in 119 meteorites, hardness meas. rel. to shock histories 3−18992
  - metal, crystalline, athermal weakening on cold plastic deform., microhardness meas. 3−33599
  - metal, hardness-temperature relationships, stress coeff. 3−34557
  - metal hardening during fatigue testing, recording at elevated temps. 3−28465
  - microhardness of T-111 alloy container material for radioisotopic heat sources 3−18693
  - neutron spectra, conversion to 14 MeV equivalences 3−17274
  - polymer, shock-compressed, physicomech. props. variation with loading 3−30204
  - polymers, microhardness, u.v. irrad. effects *(Russian)* 3−27766
  - PVC, partly plasticized, filler effect 3−31179
  - solid solution hardening, crit. resolved shear stress, conc. depend. 3−24898
  - steel, 110G13L, effects of modifiers on hardening during strain hardening 3−18668
  - steel, 18KhGT, thermomechanical effect on wear resistance 3−24934
  - steel, austenite thermal stabilization characteristic, microhardness meas. 3−24953
  - steel, austenitic, type 304L, hydrogen embrittlement effects 3−2745
  - steel, Cr-Mn-N stainless, var. with grain size 3−8825
  - steel, Cr-Mo-V, carbide hardening and characteriz. 3−21686
  - steel, effect on notch toughness *(German)* 3−27685
  - steel, electron irrad. effects on hardenability 3−24948
  - steel, ferrous martensite, as-quenched and tempered, fine struct. depend. 3−34540
  - steel, high-speed tool, characterization 3−21682
  - steel, maraging, Cr-Ni-Co-Mo, strengthening and precip. phenomena *(Russian)* 3−31060
  - steel, maraging, nitriding, nonbrittle case form. 3−27690
  - steel, Mossbauer obs. of strengthening mechanisms *(Russian)* 3−24875
  - steel, Ni-Cr-Mo, rare earth treated, temper embrittlement response and toughness 3−34584
  - steel, stainless, influence of deoxidation on mechanical properties 3−24919
  - steel, stainless maraging, influence of alloying elements on properties, low temp. study 3−24925
  - steel, structural, temp. effect on physical and mechanical properties 3−24927
  - steel for cryogenic technology 3−24916
  - steel hardened by alloying or heat treatment 3−24947
  - steel plate, diffusion chromizing, effect of alloying elements 3−27689
  - steel U7, thermomech. treatment for mech. prop. improvement 3−21675
  - steels containing Mn, Cr, V, wear resistance and mech. props. 3−24928
  - rel. to ultimate tensile strength, improved eqn. 3−34587
  - Vicker's indentation hardness, effect of load 3−5445
  - Vickers type hardness impressions, photometric meas. technique *(German)* 3−16384

hardness continued
Ag-Au alloy, shock wave effect on mech. props. *(German)* 3–34608
Ag-Be alloys, internal oxidation and hardening 3–21712
Ag-Li alloys, internal oxidation and hardening 3–21712
Ag_5SbS_4, stephanite, in phase transition region *(Russian)* 3–30259
Al and alloys, polycryst., work softening obs. and mechanism 3–37066
Al bronzes, casting and wear props., effect of iron *(Polish)* 3–31033
Al crystals, yield locus curves determ. with the aid of knoop hardness measurements *(German)* 3–2732
Al-(Ni,Cu,Be,Fe,Co) eutectics, directionally solidified, struct. morphology and microhardness *(Russian)* 3–39328
Al-Al_2O_3, following recrystallisation 3–18581
Al-Cu (4 at wt.%) alloy, precipitation study by internal friction, hardness and electron microscopy meas. *(French)* 3–15687
Al-Cu alloys, reversion phenomenon study, hardness and elec. resist. meas. 3–39326
Al-Mg_2Si, microhardness meas. for Fe effect on zone formation 3–8884
Al-Mg-Si alloy, plastic deformation effect on precipitation, hardness meas. *(Japanese)* 3–15699
Al-Mg-Zn alloy, microstruct. influence 3–39342
Al-transition metal, microhardness variation with comp. 3–31087
Al-Zn (ZN 15 at.%) alloy, microhardness and structure transformations in ageing at elevated temp. 3–2714
Al-Zn-Mg-Cu alloy, thermomech. treatment processed, age hardening mechanisms 3–24897
Be single crystals, ageing 3–24932
BiTeI film, effect of substrate temp. *(Russian)* 3–18033
Ca sulphoaluminate and sulphosilicate, hydraulic hardening process *(Russian)* 3–15742
CaF_2, anisotropy in Knoop indentation hardness and friction of diamond cones 3–20788
CaF_2, hardening due to contamination by atmospheric O 3–4806
CdS-CdTe system, microhardness meas. *(Russian)* 3–24273
Co-Fe-Be alloy, age hardening, hardness-controlling additions *(German)* 3–8901
Co-Fe-Nb, semihard mag. alloy characteriz. 3–21279
Cr sputtered deposit, substrate bias and deposition temp. effects 3–4936
Cu, heavily deformed, true-stress/true-strain rel. to hardness and subgrain size 3–12383
Cu, Knoop hardness meas. *(Japanese)* 3–12391
Cu composite coatings with corundum inclusions, microhardness 3–18670
Cu crystals, yield locus curves determ. with the aid of knoop hardness measurements *(German)* 3–2732
Cu neutron irradiation hardening, effect of alloying elements Si and Al 3–18630
Cu-Ag-Al solid soln. alloys, isothermal recrystn. kinetics 3–21592
Cu-Cd, hardening effect, transmission electron microscope examination 3–4805
Cu-Co alloy, precip. hardened, effect of Nb addition 3–8881
Cu-Fe alloys, ageing characts., precipitate transform. 3–37075
Cu-Ni-Be-Si, rel. to aging *(Japanese)* 3–12352
Cu-Ti alloy, effect of boriding *(German)* 3–8902
Cu_5As_2 single crysts., microhardness *(Russian)* 3–12329
Fe, graphitic cast, tensile strength calc. formula *(Spanish)* 3–31111
Fe, grey cast, induction furnace melting, mech. props. 3–24960
Fe alloy D16, aging effect on mech. props. 3–21677
Fe-Cr alloys, nitriding characts. *(Russian)* 3–15719
Fe-Cr-Ni alloy system, microstructural change study using selective etching *(Korean)* 3–5291
Fe-Cr-Ni steel, austenitic, shock wave effect on mech. props. *(German)* 3–34608
Fe-Cu(1.7 wt.%) alloy Cu precipitation from α-Fe in pre-peak and peak hardness range of ageing 3–8797
Fe-Ni alloy, microhardness meas. of austenite start temps. 3–18654
Fe-Ni-Al alloy, subspinodal, hardening obs. and mechanism *(Czech)* 3–31103
Fe-Ni-Sn Invar alloy, precip. hardening by Sn additions, Mossbauer obs. 3–21634
Fe-Ta alloys, Laves phase precip. phenomena 3–37049
Fe-Ti solid solns., temp. and conc. depend. of mech. props. *(French)* 3–31038
Gd, vs. annealing temp. behaviour rel. to O_2 content 3–24884
Hf nonstoichiometric carbides, concentration dependence of hardness *(Russian)* 3–12433
HfB_2, Knoop hardness anisotropy 3–30198
InBi, intermetallic, characterisation by etching and indentation 3–11817
KBr, hardening by heavy gamma irradiation at LNT 3–27035
KBr-$CaCl_2$, solubility of $CaCl_2$ rel. to hardening 3–11719
$KBr_{0.5}I_{0.5}$, heat treatment effects 3–7843
KCl, with centres of colloid type, after annealing *(Russian)* 3–14855
$KCl:Sr^{2+}(Ba^{2+})$, heat treatment effects 3–7843
KCl-KBr, meas. for Czochralski crystal grown in protective atmosphere 3–12292
Mg-Ce, meas. for precipitation process on aging *(Japanese)* 3–12351
Mn-Cr-Ni alloys, Elinvar type, heat treatment and cold working effects *(Japanese)* 3–8858
Mn-Cu-Co nonmag. Elinvar-type alloys characteriz. 3–37074
Mn-Cu-Cr alloys, nonmag. Elinvar-type 3–21291
Mn-Cu-Ni alloys, nonmag. Elinvar-type 3–21292
Mn-Ni nonmagnetic Elinvar type alloys, heat treatment and cold working, mech. props. meas. 3–8894
Mn-Ni-Co elinvar-type alloys, meas. of Young's moduli at −150-400°C and rigidity moduli and hardness at room temp. *(Japanese)* 3–17897
Mn-Ni-Fe alloys, Elinvar type, heat treatment and cold working effects *(Japanese)* 3–8859
Mo alloyed with Hf, Ta, W, Re, Os, Ir, Pt, hardness rel. to electron conc. 3–2721
Mo ingot, Ru and Pt addition effect on hardness *(Japanese)* 3–31073
Mo-Re alloys, effect of C 3–18663
NaBr single crystals, solute strengthened 3–7835

hardness continued
NaCl, annealing of γ-irradiation induced hardening 3–36330
NaCl quenched crystals, influence of impurity distrib., applic. of electron microscopic decoration method and microhardness meas. 3–1676
NaCl quenched crystals, microhardness rel. to quenching temp. and contamination, obs. 3–1677
NaCl single crystals, solute strengthened 3–7835
NaCl-KCl polycrystalline window materials, Czochralski, Bridgman crystals 3–5901
Nb nonstoichiometric carbides, concentration dependence of hardness *(Russian)* 3–12433
Nb-H solid solns., solute interactions role 3–2743
Nb-N-O solid solutions, rel. to nitrogen conc. determ. *(Russian)* 3–39335
Nb_3Sn, hydrostatic extrusion effect on comp. and microhardness 3–24955
Ni, 99.999% pure, hardness max. following annealing after plastic deformation *(German)* 3–27711
Ni, dispersion-hardened with ThO_2, recrystn. 3–21669
Ni, electrodeposited from ethylene glycol electrolyte 3–25071
Ni, u.s. irrad. and annealed, struct. changes *(Russian)* 3–15718
Ni steels, 9%, modified by Mn, Cu, Mo, Nb, thermomech. treatment effects, obs. *(Japanese)* 3–8860
Ni/Al_2O_3 composite, electrodeposited 3–37059
Ni-Be alloy, age hardening, hardness-controlling additions *(German)* 3–8901
Ni-Cr alloys, Sn alloying effect 3–21668
Ni-Cr-Nb heat resistant spring alloy characteriz. 3–24944
Ni-Mo-W corrosion resistant hard alloy development 3–21667
Ni-P coatings on steel, struct. and props. rel. to annealing temp. and time 3–27691
Ni-Ti (Ni rich) alloy, precipitation and its hardening effect *(Japanese)* 3–30992
Ni_4Mo, ordered, domain structs. and hardening 3–37026
NiTi cpds., Ni-rich, quench-hardening and mech. props. 3–37073
Pd-Ag(Ce) alloys, effects of hydrogen 3–2737
Ta nonstoichiometric carbides, concentration dependence of hardness *(Russian)* 3–12433
Te, effect of elec. field and illumination on scratch hardness *(Russian)* 3–14912
Ti, hardening by O_2 3–15725
Ti alloy, meas. to study, reverse structural transform. under external tensile stresses 3–30977
Ti nonstoichiometric carbides, concentration dependence of hardness *(Russian)* 3–12433
Ti/W composites, solid-state interfacial reactions 3–31139
Ti-C-O system crystallographic and metallographic obs. *(French)* 3–7698
Ti-Sn-O ternary system, rel. to phase diagram determ. *(Russian)* 3–14961
TiB_2, Knoop hardness anisotropy 3–30198
TiC, deposited by activated reactive evaporation, effect of substrate temp. on microhardness 3–27631
TiC/Co(Ni) cermets, Vickers hardness under reduced charge, comp. depend. *(French)* 3–24971
W-Ni-Mo, comparison with Fe alloys 3–8783
W-Zr-C alloy, dispersion struct. changes during annealing and recrystalln., electron microscope obs. *(Russian)* 3–8875
WC/Co cermets, Vickers hardness under reduced charge, comp. depend. *(French)* 3–24971
Zr nonstoichiometric carbides, concentration dependence of hardness *(Russian)* 3–12433
Zr-Pd(Ru) dil. alloys, heat treated *(Japanese)* 3–31079
ZrB_2, Knoop hardness anisotropy 3–30198

hardness testing
indenter cone angle and tip radius influence on Rockwell-C hardness meas. 3–5370
microhardness meas. device, at low temps. 3–13226
photometric meas. of Vickers type hardness impressions, diffr. theory analysis *(German)* 3–5933
α-quartz, synthetic, test meas., 50-545°C, fracture resist., environment effects 3–30182
stainless steel, microhardness with different cold work percentages 3–31224
steel, austenite, isothermal decomp. products characts. 3–21673
steel, mild, impact props. of cold-extruded rod 3–21642
steel, tufftrided mild, fatigue strength and microstructure *(Japanese)* 3–30991
Al alloy high temp. aging effect on hardness *(Bulgarian)* 3–15655
KBr single crystals, solute strengthened 3–7835
KCl single crystals, solute strengthened 3–7835
MnSe inclusions in steel, hot hardness 3–34579
Pd-Al alloy 3–24879

harmonic analysis
see also waveform analysis
angular velocity impulse discs, pulse frequency and variable-velocity time function harmonic relationship *(German)* 3–9818
averaged evoked brain potentials of hippocampus, component analysis 3–35241
complex sound signals, loudness conversion model *(Russian)* 3–13132
elasticity of nonuniform isotropic media, harmonic functions applic. *(Russian)* 3–525
fluidised bed heat transfer obs. 3–1461
fundamental frequency tracking algorithm for examination of harmonic structure of speech signals 3–3424
generalised U(3(n-1)) scheme model, matrix element calc. *(Russian)* 3–35850
geomagnetic activity, twelve-month wave detection 3–15922
gravity variations in Estonia, comparison with meas. in Europe and Central Asia *(Estonian)* 3–25122
harmonic solids, modified moments 3–7885
magnetospheric electron density variations, whistler dispersion 3–18891
orthogonal and Poincare groups application 3–28820
palaeomagnetic field models for 6 geological periods using spherical harmonic anal. 3–25166
Peierls stress, dynamic initial slip in a linear chain due to dislocation subjected to shock wave 3–7849

harmonic analysis continued
solar photosphere temp. variations, Legendre polynomials representation 3—28135
stability of steady-state response of certain nonlinear dynamic systems subjected to harmonic excitations 3—19467
structural hardening calc. procedures and thermal strength problems 3—32347

harmonic generation
see also lasers
alkali metal vapour-inert gas mixture, optical third harmonic generation 3—26246
direct acoustically induced optical harmonic generation coefficient calc. 3—16911
lithium formate monohydride, harmonic generation of tunable coherent radiation from 2300-3000 Å 3—32589
magnetised crystals and isotropic bodies, and nonlinear magneto-optical effects 3—37978
microwaves in an inhomogeneous and non-uniformly magnetised plasma 3—14590
nonlinear crystals, influence of linear inhomogeneity of refractive index *(Russian)* 3—773
optical susceptibilities, higher order, rotational invariance 3—29125
phase-matched second harmonic generation with laser beam in TEM$_{mn}$ mode 3—16912
powders, optical second harmonic generation as centre of symmetry test in X-ray crystallography 3—30760
proustite, nonlinear polarisation coeff. 3—22963
resonator element for parameter optimisation of quasi-c.w. Nd:YAG laser 3—22912
rhodamine dyes, two photon cross section dispersion 3—10569
second, in molecular crystals, influence of interband transitions 3—22939
second harmonic conversion of laser radiation generated under free oscillation conditions 3—22961
second harmonic generation phase matching using artificial periodic structs. 3—6504
selection rules in nonlinear optics 3—6508
semiconductor, e.m. waves, optimum slab thickness 3—18512
semiconductor, s.h.g. due to hot electrons, efficiency and optimum d.c. bias field 3—30509
statistical intensity fluctuations of third harmonic *(Russian)* 3—16900
triglycine sulphate, ferroelec. domains, direct obs. by second harmonic generation by laser 3—24658
two pass internal second harmonic generation by internal cavity freq. doubler with prism coupler 3—6505
uniaxial crystals, noncollinear phase matching effects 3—29128
u.v. pulse formation, subpicosecond, by multiple nonlinear conversion 3—19640
AgGaSe$_2$, second harmonic generation, nonlinear optical coeffs. 3—4120
AgInSe$_2$, second harmonic generation, nonlinear optical coeffs. 3—4120
BaTiO$_3$, model of polarizable ions 3—32601
Bi, second generation during anomalous skin effect 3—18179
Bi$_{12}$GeO$_{20}$, acoustic surface waves 3—17932
Cd vapour, phase matching, v.u.v. generation 3—780
inCdGeAs$_2$, phase matching, second and third harmonic generation 3—782
CdTe, nonlinear susceptibility, at 28.0 μ by comparison with Te 3—19637
CuGaSe$_2$, second harmonic generation, nonlinear optical coeffs. 3—4120
GaSe, second harmonic generation and nonlinear optical props. *(Russian)* 3—2505
Ge, third harmonic generation, in strong microwave field *(Russian)* 3—11924
InSb, nonlinear susceptibility, at 28.0 μ by comparison with Te 3—19637
KH$_2$PO$_4$, maximum permissible pulse duration in second harmonic generation 3—22962
KH$_2$PO$_4$, second harmonic generation, temp. depend. of index matching angle 3—10566
KH$_2$PO$_4$ paraelectric, second harmonic generation, temp. dependence of index-matching angle 3—29141
LiIO$_3$, model of polarizable ions 3—32601
LiNbO$_3$, acoustic surface waves 3—17932
LiNbO$_3$, model of polarizable ions 3—32601
LiNbO$_3$, phase matching curve, temp. and angular widths *(Russian)* 3—776
NaNO$_2$, biaxial, second harmonic generation rel. to phase matching direction 3—22940
NaNO$_2$, ferroelec., second harmonic generation at room temp. 3—10567
NaNO$_2$, optical SHG during ferroelectric switching 3—15466
Pb$_5$Ge$_3$O$_{11}$, ferroelectric material 3—13752
PbMoO$_4$ acoustic harmonic generation *(French)* 3—33612
Se, nonlinear susceptibility, at 28.0 μ by comparison with Te 3—19637
SrTiO$_3$, obs. of stress induced ferroelectric phase by second harmonic generation 3—30764
Te, nonlinear polarisation coeff. 3—22963
Te second-harmonic generation nonlinear optical susceptibility at 28.0 μm, meas. 3—19634
Xe-Ar phase-matched mixture, generation of 1182 Å radiation by third harmonic generation 3—32535
ZnS, phonon assisted second harmonic generation 3—779
ZnS noncolinear, second harmonic, phase matching, lamellar structures, model *(French)* 3—22948

harmonics
see also harmonic analysis
bounce harmonic structure in mirror-confined plasmas, stabilization of modified negative mass instability 3—4647
e.l.f. propagation using zonal harmonics 3—3062
f.m. optical radiation 3—19630
magnetic pulsed multipole, correction *(French)* 3—25817
nonlinear v.l.f. wave turbulence in the magnetosphere 3—16035
spherical harmonics and second order tensorial multipoles *(French)* 3—26048
waveguide with limited comb *(Russian)* 3—13610

harmonics continued
BaF$_2$, high-freq. acoustic harmonic generation by Bragg light scatt. 3—7859
CaF$_2$, high-freq. acoustic harmonic generation by Bragg light scatt. 3—7859
CdS, photoconductive, harmonic conversion of acoustoelectrically amplified phonons 3—2141
SrF$_2$, high-freq. acoustic harmonic generation by Bragg light scatt. 3—7859

Hartree-Fock approximation *see Hartree-Fock method*

Hartree-Fock method
see also atomic structure
Anderson model, physical props. from mag. Hartree-Fock soln. 3—36700
antiferromagnet uniform chain, instability, Heisenberg interaction in Hartree Fock approx. 3—38943
antisymmetric wavefunction densities from coherent diffraction data 3—4712
atomic orbital exponents derivation *(French)* 3—23458
Beliaev-Zelevinsky-type expansion about Hartree-Fock minimum 3—32414
chemical dissociation of asymmetric two-centre two-electron system, unrestricted Hartree-Fock theory 3—27870
closed-shell atoms, relativistic Hartree-Fock eqns., local exchange pot. 3—33008
complex atoms, simplified Hartree-Fock method for opacity calculations 3—33003
computer program for multiconfiguration eqn., bound state atoms 3—11113
cusp constraints in extended wavefunctions 3—14283
diamond, crystalline H.F. formalism for ground state computations 3—18052
effective charge, random phase approx. calc. of effective charge 3—10902
electronic excitations in open shell systems 3—1157
Fermi surface in mag. field, quantum kinetic equation in Hartree-Fock approx. 3—30395
generalised H-like radial orbitals application to the normal configuration of Na and Al type atoms *(Russian)* 3—11116
group V elements, spectra from Hartree-Fock calcs., need for LS-depend. parameters 3—7035
Hartree-Fock-Slater model approach to photoelectron and opt. spectral of VCl$_4$ and TiCl$_4$ 3—27489
HFB and BCS methods, reduced density matrix interpret. 3—26400
Hubbard model, narrow half filled band, electrical conductivity and thermodynamics, semiconductor-metal transition investigation 3—11842
hydrocarbons, ^{13}C chemical shifts calc., coupled Hartree-Fock perturbation method, Slater orbital exponents 3—23598
hydrocarbons, alternant, triplet-triplet absorpt. spectra in time-depend. Hartree-Fock approx. 3—21819
hydrocarbons, monocyclic unsaturated, mol. diamag. susceptibility, Hartree-Fock calc. 3—29601
Indeno[1,2,3-cd]-fluoranthene, mol. orbital study by Pariser-Parr-Pople and Hartree-Fock methods 3—11198
ionic soft sphere parameters from Hartree-Fock charge densities 3—26559
iterative sequences, extrapolation method 3—20003
many-body problems, book 3—20990
molecular electron scatt., collision amplitudes and electron distribs. 3—26727
molecular electron scatt., static pot. calc. 3—4480
molecular electronic struct. calcs. 3—1156
multiconfiguration method with non-orthogonal orbitals, generalized version 3—23457
multielectron atom, excitation spectrum calc. 3—20006
neutral atoms, He to Rn configuration energies, ground- and near-ground-states 3—11112
non-local potentials, application of method of equivalent local potentials, distortion effects *(Russian)* 3—35864
nonalternant closed-shell systems, Hartree-Fock eqns. solns., stability conditions 3—29589
nuclear intrinsic wavefunction projection computer method 3—10901
nuclear structure group theoretical investigation of the Hartree-Fock-Bogoliubov state *(German)* 3—35873
nuclei removal, and single particle energies 3—35853
orbital energy crossing, use of unrestricted Hartree-Fock theory 3—14334
particle-hole calcs., importance of H F self-consistency 3—38128
polarisabilities calc. for simple atoms and diatomic mols. 3—29486
potential function, new derivation, adjustable set of unoccupied bound orbitals 3—11123
quantum chemistry, review 3—34715
rare earth metals, 4f^{n}6s^2 config., orbit-orbit interactions *(Russian)* 3—33012
relativistic energies, perturbation analysis of current calc. methods 3—14286
semiconductors, X-ray atomic scattering functions, influence of tetrahedral covalent bonds *(Russian)* 3—11582
simple molecules, electronic charge distributions and chemical bonding 3—4707
Skyrme's interaction, Hartree-Fock calc. for axially deformed nuclei 3—17181
Slater-Condon parameters, semi- and nonempirical values, one-centre electron repulsion parametrization 3—1096
Strutinsky method for extracting shell corrections from Nilsson single particle energies 3—19797
superconducting film, conductivity, nonlinear external field effects 3—8301
superconductors with transition metal impurities, calc. of props. 3—15298
superheavy element calc. by Hartree-Fock and single-particle shell model, review 3—17172
superheavy magic numbers calc. 3—17179
superheavy nuclei, Hartree-Fock method study *(French)* 3—6963
time-dependent theory, variational approxs. 3—23463
transition metals, oscillator strengths for 3d^{n}4s→3d^{n}4p, Hartree-Fock gf-values 3—23470
transition-metal atoms calc. of analytic SCF wave functions by Hartree-Fock-Roothaan method 3—4352

Hartree-Fock method continued
uncoupled variation perturbation methods, first order perturbed orbitals approx. 3−14282
water, ground state calculations 3−7114
Xα statistical exchange pot., transition state, total energy 3−29465
X-ray scattering by Al and Al^+, intensity calc. *(Russian)* 3−11132
Al, localised orbital wave functions, comparison between theory and expt. 3−8082
Ar, localised orbital wave functions, comparison between theory and expt. 3−8082
C, X-ray scattering factors by anal. radial orbitals *(Russian)* 3−33006
^{40}Ca, higher-order corrections to Brueckner-Hartree-Fock calcs. and two-body correlation corrections 3−29299
^{40}Ca, renormalized Brueckner-Hartree-Fock calcs. using different prescriptions for intermediate-state spectrum 3−10903
Ce, A=126, 134, 140, 150, constrained H.F. calcs. of deformation energy curves 3−6750
Ce films, soft X-ray absorption, theory *(Russian)* 3−12192
Ce isotopes, deformation energy curves calc. with constrained Hartree-Fock method 3−29309
ClF, dipole polarity and field gradient deriv. from Hartree Fock functions calc. 3−35998
Cr, even isotopes, HF and HFB spectra, angular momentum states projection 3−17180
Cr isotopes, Hartree-Fock-Bogoliubov projected spectra, intrinsic states calc. 3−32785
Cs, electron impact excitation of autoionizing level 3−35972
Cs autoionising states, energies, wave functions *(Russian)* 3−26580
Cs electron ionisation by impact, 6s and 5p, cross-section, Born approximation, threshold, calculations *(Russian)* 3−26598
^{134}Cs, 127.37 keV E3 transition, internal conversion investigations, Hartree-Fock-Slater atomic model 3−23244
Er^{3+}, soft X-ray absorption by 4d-electrons, theory *(Russian)* 3−11133
Eu, screening ratios, relativistic contributions 3−14287
Fe, even isotopes, HF and HFB spectra, angular momentum states projection 3−17180
Fe isotopes, Hartree-Fock-Bogoliubov projected spectra, intrinsic states, calc. 3−32785
H, cubic atomic crysts., electronic struct., Bloch functions, Fermi surfaces, exact Hartree-Fock calcs. 3−33800
HF magnetic shielding of ^{1}H and ^{19}F, linked cluster many body perturbation theory 3−11214
H_2O molecule in field of Na^+ or K^+, complex structure and energy surfaces calc. 3−25044
He, orbitals derivation from resolvent of hydrogen atom 3−7031
He, perturbative corrections to Hartree-Fock oscillator strengths 3−11126
^{4}He, fully self-consistent Brueckner-Hartree-Fock and renormalized Brueckner-Hartree-Fock calcs. 3−32784
^{4}He, Hartree-Fock and Brueckner theories for binding energies and wound integrals 3−23241
La films, soft X-ray absorption, theory *(Russian)* 3−12192
Li, phonon dispersion curves calc. 3−11704
Li_2^+, Hartree-Fock potential energy curves, spectroscopic consts., 1-electron props. for lowest $^2\Sigma_g^+$ and $^2\Pi_u$ states 3−29642
LiF, Adams-Gilbert local-orbitals equations, choice of localising potentials 3−36537
LiH, energy band calc. 3−30401
LiO vibrational and electronic oscillator strengths calc. 3−35999
Mg atom, Hartree-Fock calculations of principal configurations 3−20023
MgIV, even configurations, reevaluation of parameters 3−33011
$^{24}Mg(\alpha,\alpha')^{24}Mg$, cross-section calc. using Hartree-Fock densities 3−14225
^{23}Na, multishell Hartree-Fock wave function calcs. with NN interact. 3−19799
Ne, third-harmonic coeff. calc. 3−14284
$^{20}Ne(\alpha,\alpha')^{20}Ne$, cross-section calc. using Hartree-Fock densities 3−14225
^{21}Ne, multishell Hartree-Fock wave function calcs. with NN interact. 3−19799
Ni base fcc ferromag. alloys with Co, Fe, Mn and Cr, H-F approx. calc. 3−8328
^{56}Ni, Hartree-Fock and shell model studies of low lying energy levels 3−32755
O_2, excitation to $^1\Delta_g$ state by electron impact, Hartree-Fock wave functions calc. 3−36053
OH, isotropic hyperfine interaction in $^2\Pi$ ground state with linked cluster many-body perturbation theory 3−11214
^{16}O, fully self-consistent Brueckner-Hartree-Fock and renormalized Brueckner-Hartree-Fock calcs. 3−32784
^{16}O, higher-order corrections to Brueckner-Hartree-Fock calcs. and two-body correlation corrections 3−29299
^{16}O, negative parity levels from three body forces *(French)* 3−32754
^{16}O, renormalized Brueckner-Hartree-Fock calcs. using different prescriptions for intermediate-state spectrum 3−10903
^{208}Pb, higher-order corrections to Brueckner-Hartree-Fock calcs. and two-body correlation corrections 3−29299
^{208}Pb, renormalized Brueckner-Hartree-Fock calcs. using different prescriptions for intermediate-state spectrum 3−10903
^{240}Pu, constrained H.F. calcs. of deformation energy curves 3−6749
S, X-ray scattering factors by anal. radial orbitals *(Russian)* 3−33006
S containing radicals, unrestricted H-F spin density calculations, d-orbitals role in π-electron treatment 3−4411
Si, X-ray scattering factors by anal. radial orbitals *(Russian)* 3−33006
Ti, even isotopes, HF and HFB spectra, angular momenum states projection 3−17180
Tm^{3+}, soft X-ray absorption by 4d-electrons, theory *(Russian)* 3−11133
Yb^{3+}, soft X-ray absorption by 4d-electrons, theory *(Russian)* 3−11133
^{170}Yb, constrained H.F. calcs. of deformation energy curves 3−6750
^{104}Zr, constrained h.f. calcs. of deformation energy curves 3−6750

He *see helium*

headphones
see also earphones
No entries

health effects of radiation *see biological effects of radiation*

hearing
see also ear; hearing aids; speech
acoustically evoked potential, recovery cycle 3−25566
acoustics conference, Miami Beach, Fla., USA (1972) 3−3637
action potentials, influence of hair-cell nonnormalcy 3−25 63
age determination in male voice 3−3505
amplitude compression effect on speech intelligibility for normal and pathological hearing groups 3−3487
association cortex potentials, reaction time in auditory discrimination 3−28325
audiometer reference and free field thresholds *(German)* 3−31865
audiometric effects of continuous and impulse noises 3−3514
auditory assessment of partition wall sound insulation efficiency *(Japanese)* 3−5734
auditory displays, multidimensional coding within temporal microstructure 3−35254
auditory evolved potentials, selective attention 3−19095
auditory nerve evoked potential, changes following intense sound stimulation 3−3483
auditory system, simulation of information processing mechanism 3−31862
aural harmonics, nonlinearity and loudness 3−3451
averaged e.e.g. response, effects of stimulus rate and number 3−25568
aviators, as function of flight time and aircraft type, normal and h.f. obs. 3−3509
band limited noise, detection of detection and insertion of tones 3−3534
basilar membrane, computer simulation of nonlinear model, determ. of distortion products 3−3472
basilar membrane motion, nonlinear phenomenological model 3−3471
basilar membrane motion, temporal relationship with initation of nerve impulses in auditory nerve fibres 3−3474
beats of sinusoidally a.m. signal with tone near modulation frequency 3−3461
binaural detection model, varying signal parameters, noise identical at both ears 3−3494
binaural interaction between real tones and cubic distortion product 3−3495
cat, binaural processing, detection of diotic and dichotic tones 3−3499
cat, binaural processing, lateralization 3−3498
channel capacity of ear as function of frequency 3−3484
children, perceptual and memory tasks 3−25570
coal miners, loss of hearing for speech and non-speech signals 3−3512
cochlear injury in chinchilla, whole-nerve action potentials as index of severity 3−3480
cochlear microphonics, electric network effects 3−31857
cochlear partition, comparison of effects of biasing with electrical current and sound stimulation of DIF SP responses 3−3477
cochlear potentials of guinea pig, modelling and simulation 3−25561
cochlear whole-nerve response to acoustic transients, origin of negative deflection N_2 3−3476
complex waveform generation using device with D/A convertor followed by low pass filter 3−28482
connected discourse speech intelligibility 3−25554
conservation, rel. to industrial health 3−37525
consonant intervals, conjunction of musical context 3−5649
critical masking interval measurement 3−5652
cubic difference tones prediction from model of pitch perception 3−3464
damage, industrial noise, code of practice, in UK 3−9657
damage risk criteria and their meas. 3−25574
detectability of complex signals 3−3450
detection of alterations of one component in multiple tone complex 3−3542
dichotic listening, shift of ear superiority to temporally patterned non-verbal stimuli 3−31859
dichotic perception of lexical tone by English and Thai speakers 3−3507
dichotic right ear advantage in male and female children 3−3530
dichotically presented vowels 3−31860
differential reinforcement of high responding rate with changes in sound intensity as reinforcer 3−3452
directional perception, absolute difference limen *(German)* 3−39768
discrimination test for nonspeech signals 3−3511
dolphins, auditory processing of signals related to signature whistles 3−3447
ear advantage rel. to degree of encodedness, ear-monitoring task 3−3527
ear advantage rel. to degree of encodedness, temporal-order judgement task 3−3526
ear protectors, dBA attenuation 3−35257
electroacoustic units using verbo-tonal system for hearing-impaired people 3−3516
English consonants, perceptual structure 3−25634
equal loudness pressure and normal ear 3−3455
forward coarticulation, perceptual effects 3−25571
four dimensional sounds, perceptual confusions 3−35258
frequency discrimination and homophasic and antiphasic tonal signal detection in noise 3−3537
frequency transition detection 3−31858
histological effects of continuous and impulse noise interaction 3−3515
human click action potentials and click loudness, postmasking recovery 3−25556
human directional, theories of, and relation to stereophony *(German, French)* 3−25575
human sound localization response underwater 3−35251
human underwater sound localization response, precision 3−3503
in-ear microphone meas. of ear protective devices, reliability and validity 3−3465
in-ear monitoring of noise exposure 3−3525

hearing continued
insular-temporal lesions in kittens, recovery of function 3—25586
interaural crosscorrelations, for multichannel loudspeaker reproduction 3—9655
interaural time and intensity, discrimination 3—25559
interaural time difference detection in short-duration l.f. tones 3—3497
interaurally alternated speech, intelligibility, shadowing and subjective rating methods 3—3491
Japanese carp, Cyprinis carpio, pure-tone auditory thresholds 3—25564
localization in median plane, effect of pinnae cavity occlusion 3—35252
loudness, measurable dimensions of sound, audio reproduction, compensation 3—9656
loudness adaptation meas. by monaural procedure 3—3456
loudness enhancement with monaural, binaural and dichotic stimulation 3—3500
loudness evaluation of sound from electric clock 3—3453
loudness summation, tones from two loudspeakers 3—3492
macaca mulatta, interaural intensity or phase differences as cues for lateralization responding 3—3523
masker bandwidth effects on function relating detectability to signal duration 3—5653
masking of pure tones by frequency modulated tones 3—3540
masking with ripple noise and spatial frequency anal. 3—3539
mechanism research, potential appl. of engineering science disciplines 3—9658
memory for dichotic pairs, ear report performance disruption by speech-nonspeech distinction 3—3528
middle ear transfer characts., tympanic muscle effects 3—3445
minicomputer psychoacoustic system 3—3460
monaural and binaural free-field speech reception under noise and reverberation 3—3501
monaural chinchilla, direct and indirect obs. of critical bands 3—3535
monaural thresholds, binaural masking by two mutually independent noises 3—28349
monaural unmasking by addition of wide band noise to tone masker 3—5654
monkey, regulation of voice amplitude in presence of noise 3—3544
monosyllabic words, intellegibility, initial and final consonants 3—3490
motor recall, with phonetic interference 3—25567
newborn infants, behavioral responses, acoustic stimulus duration 3—25569
noise and pure tone attenuation of hearing protectors 3—3468
noise effect evaluation, damaging *(German)* 3—16311
noise level, by Stevens Mark VII method 3—35334
noise perception, measured noise levels, comparison 3—13191
noise reduction ear enclosures 3—3467
nonlinear ear protectors, evaluation using constant temporary threshold shift technique 3—3466
normal listeners, threshold adaptation 3—35256
optimal and preferred listening levels in aircraft acoustical environments 3—3488
perception and production of stops in bilinguals and unilinguals 3—5650
perception of auditory patterns, factors affecting 3—3541
perception of rhythm and accent in English words and phrases 3—3427
periodicity pitch, binaurial interaction 3—3493
periodicity pitch perception, jittered pulse trains *(Japanese)* 3—31854
peripheral auditory system, information theory of neural noise 3—25572
permanent loss due to noise *(Dutch)* 3—28348
phonetic responses of hard of hearing and deaf subjects, multidimensional anal. 3—5641
pitch, pattern transformation mode 3—3463
pitch of complex signals, influence of number and phase of harmonics on perceptibility 3—19125
pitch perception, rel. to speech synthesis 3—31970
pitch perception and effects of partial Hamming function modulation of tone bursts 3—3462
pitch scaling and octave judgements, convergence of western and non-western data 3—5651
pitch shift and masking by sinusoids and narrow band noise 3—3538
post-stimulus signal processing, attentional aspects 3—3536
potential response at round window membrane of cat 3—25565
preschool deaf children, evaluation of verbo-tonal method of habilitation 3—3517
proportion correct, response-contingent measure 3—25560
pure tone and speech-evoked response in normal and noise-exposed squirrel monkeys 3—3513
pure tones, attack transient patterns 3—5647
quiet threshold shift, in absence of noise 3—37526
reaction time to clicks in sentences, emergence of linguistic structures with extended processing 3—3485
right ear advantage for speech processing 3—3529
right ear advantage in dichotic listening, effect of memory load 3—3531
scaling perception of aircraft noise 3—35341
self-recording and manual audiometry, systematic effects shown by unpractised subjects 3—19096
single cochlear nerve fibres, response patterns to click stimuli for cat 3—25562
SKAT, automated self-administered preschool auditory screening test 3—3508
sound location in median sagittal plane, influence of timbre 3—3502
sound pressure transformation from free field to eardrum 3—3442
sound signals, complex, loudness conversion model *(Russian)* 3—13132
spatially weighted speech discrimination by hearing-impaired subjects 3—3486
spectral analysis techniques 3—3458
speech, acoustical bases 3—39769
speech perception, categorical and noncategorical modes along voice onset time continuum 3—3532
speech recognition of complex sounds 3—25557
subliminal underwater sound localization 3—3504

hearing continued
suprathreshold masking, rel. to reaction time 3—3449
temporal modulation transfer functions 3—3448
temporal order discrimination, identification and recognition by trained listeners 3—3470
temporal order discrimination, recognition without identification by untrained listeners 3—3469
temporal summation for tones or threshold 3—3454
temporary threshold shift, combined steady state and impulse noise 3—5646
three-tone complexes, second effect of pitch shift 3—31861
thresholds during deep saturation He-O$_2$ dives 3—3510
time and level difference determ. away from median plane 3—3496
time intensity trading ratio, effect of preceding sound 3—5648
timing model for intensity and frequency discrimination functions 3—3457
tonal residues of short duration 3—35259
tone and pitch perception, language processing 3—3506
tunnel of Corti, recording of local potentials using microelectrodes 3—3475
two tone inhibition, interference, nonlinear effects 3—35253
two-tone unmasking, rel. to saturation effects 3—3543
tympanic, submicroscopic vibration, obs. by stroboscopic holography 3—3446
verbal transformation effect, phonetically trained and nonphonetically trained listeners 3—3533
word intelligibility, U.S. navy aircraft radios, nasality, sibilation and voicing 3—3489

hearing aids
amplitude compression and distortionless amplification 3—3459
electroacoustic, conical coupler for measurements *(German)* 3—37594
electrode placement for activation of VIIIth nerve by electrical stimulation in cases of sensorineural hearing loss 3—3482
intracochlear, multimicroelectode for differential electrical stimulation of cochlear nerve in human sensory deafness 3—3481

heat
see also heat transfer; heating; latent heat; specific heat; temperature; terrestrial heat; thermal variables measurement; thermodynamic properties; thermodynamics
relativistic transformation of heat and temp. *(Russian)* 3—644

heat capacity *see specific heat*

heat conduction
see also thermal conductivity
anisotropic media with property variations, nonlinear heat flow and heat generation 3—35642
approximate solution of some nonlinear problems of heat conduction theory 3—22775
boundary-layer film boiling, effect o radiation 3—23733
collisionless plasma in a turbulent mag. field 3—11497
conductor with nonlinear heat source, nonstationary temp. behaviour *(Russian)* 3—32461
coupled system, sinusoidal press. variation influence on contact resist. during vibrs. *(French)* 3—4045
demonstration, quantitative, for students using liquid crystals 3—16370
differential equation boundary value problem, extremum principles and error bounds 3—28988
dispersed liquid metal-gas packed bed heat exchanger 3—39303
eccentric ring, nonstationary thermal conductivity calc. 3—35633
electrically moving temp. fields, simulation method 3—22781
elliptical cylinder, third boundary problem 3—19533
equation, for plane rectangle, solution 3—10407
fluid in rectangular region heated from below, effect of wall conduction on stability 3—26797
fluids, confined exothermically reacting, dynamic stability 3—15823
Fourier theory, modified *(French)* 3—38653
Fourier theory deviations *(French)* 3—38652
gas mixtures, binary, heat cond. between parallel flat plates 3—23658
general theory, transient thermal waves with finite wave speeds 3—6379
Gibbs eqn., generalised, accounting for finite wave speed 3—19534
hollow cone with radiation, integral transform with spherical function kernel 3—37786
ice, pressure melting and regelation by round wires 3—14984
ice, sublimation process 3—38666
infinite media with thermal resistivities being linear functions of temperature, constant line sources 3—37909
laminar boundary layer, radiative transfer, viscous dissipation, convection and heat conduction 3—23734
laminar flow heat transfer from wedge-shaped bodies with limited heat conductivity 3—20284
linearised, quasilinear nonstationary problem, qualitative anal. *(Russian)* 3—6380
liquid crystal, nematic, non-Fourier 3—24301
Newtonian fluids, with axial conduction, unsteady energy equation, transform solution 3—36079
non gray media, simultaneous radiative and conductive heat transfer 3—28986
non-stationary, variational principle application *(German)* 3—3946
nonlinear, approximate calculation method 3—626
nonlinear heat conduction equations solutions by numerical methods 3—19527
nonlinear problem with fourth order boundary conditions, modelling 3—22788
nonstationary, simulation by elec. models 3—22782
null point calorimeters, heat flux, arc heaters 3—131
numerical solution of equations, survey 3—10399
one dimensional eqn., cubic spline technique 3—26175
optimal linearisation application 3—37907
orthotropic plates, butt-joined, heating by sources with heat exchange 3—19532
periodic problem in a hollow infinite cylinder 3—22774
plane gray layer bounded by black wall, transient combined conductive and radiative transfer 3—26179
regions with generation, steady heat conduction, boundary value problem 3—32463

heat conduction continued
rod of variable length drawn from melt with const. vel. 3−26176
semitransparent solids, coupled conduction-radiation heat transfer, spectral and boundary effects 3−33703
slabs, cylindrical and spherical shells, with non-uniform heat generation, steady-state 3−16767
solar wind proton gas, kinetic model 3−16135
synthesis method for cylinder with variable surface heat transfer 3−637
temperature field in presence of continuous heat sources with boundary conditions of second kind in case of an infinite plate 3−16765
time-variable heat exchange coeff. case, exact soln. 3−22779
transient, application of finite element solution technique, cooling of a locked form in V-belt-vulcanisation *(German)* 3−22790
transient, heat transfer coeff., approximate expression, nuclear reactor dynamics 3−7009
transient, one-dimensional problems in cylindrical coordinate system, solution by numerical methods 3−16764
transient nonlinear, with temperature dependent thermal properties, finite difference method of soln. 3−19524
turbulent mixing at boundary of parallel flows 3−29844
unsteady-state with moving boundary, special soln. of eqn. 3−22767
^{4}He liquid energy transfer from a pulsed thermal source 3−30300
Nb-Zr system, solid solutions singularities of the temperature dependences of the heat conduction coefficients *(Russian)* 3−2209
UO_2 composite fuels, assessment of heat conduction effectiveness 3−23443

heat content *see enthalpy*

heat convection *see convection*

heat dissipation *see cooling*

heat engines
Rankine cycle automobile condensers, perforated plate-fin heat transfer surfaces 3−4048

heat exchange *see heat transfer*

heat exchangers
see also cooling towers
air-cooled, airflow and veloc. distrib. 3−471
corrugated plate, design and characteristics 3−110
counter-flow regenerative, temperature fields of nozzle and gases *(Russian)* 3−9848
for dilution refrigerator, phonon passage through thin foils 3−5844
for dilution refrigerators 3−5843
heat transfer coefficients, averaging over length 3−13659
heat transfer thin-walled circular pipe, dynamic response to fluid temp. var. 3−10405
multistage cross flow, heat and mass transfer 3−111
parallel plate, with turbulent flow on one side and laminar flow on the other, calc. of heat transfer parameters 3−22276
refrigerants, NH_3 evaporators, boiling, film flow, heat transfer 3−1438
subsonic diffusers, effect of entrance configuration on local heat transfer coefficients 3−23715
thermoelectric modular type packaging 3−19167
transient thermal processes in counterflow equipment employing layered granular beds 3−4628
tube bundles, turbulent exchange coefficients 3−10224
turbulisators, design, operation and performance 3−126
CO_2 resonator design for gas-cooled nuclear reactor, computer display applic. *(French)* 3−16347
Cu, sintered, use in superfluid He expts. 3−28501
Nb tubes, with Na heat carrying medium, design and characteristics *(Russian)* 3−5814

heat flow *see heat transfer*

heat losses
: 3−34889
enhanced cooling of cryogenic electrical leads rel. to heat losses, comments and critique 3−5822
heat defect of ionizing radiation absorption in tissue equivalent plastic 3−5676
solar corona conductive losses due to solar wind effects 3−31570
stellar magnetised isothermal atm., thermal convective instability 3−39589
superconducting magnet support low heat leak temp. stabilized column type 3−22295

heat measurement *see thermal variables measurement*

heat of adsorption
film, phase transform. rel. to work function and heat of desorption 3−20971
graphite, low temp. adsorption of ^{4}He, Ar and N_2 3−36480
metal atoms on metal surfaces, semi-empirical relation *(German)* 3−38728
mixed beds, interpretation of meas. of heat of adsorption *(French)* 3−27181
solution surface, reversible adsorption, expt. determ. for alcohols 3−38718
solution surfaces, reversible adsorption thermodynamic calc. for nonionic surfactants 3−38717
vapour, nonideal, adsorpt. isotherm calcs. 3−30341
zeolite, Faujasit-type, apparent molar ht. of water, 90-300 K *(German)* 3−27174
η-Al_2O_3 water vapour heat of adsorption *(French)* 3−27187
Ba films on W, Mo (011) face 3−8018
Ni, of H_2, on polycryst. wire, correl. with catalytic reaction kinetics 3−11809
Ni benzene and cyclohexane adsorption 3−27922
Ni polycrystalline surfaces, H_2 adsorption states at different temps. 3−11801
NiO benzene and cyclohexane adsorption 3−27922
W, of H_2, on polycryst. wire, correl. with catalytic reaction kinetics 3−11809

heat of combustion
No entries

heat of crystallisation
No entries

heat of dissociation
Al_4C_3, determ. by atomic absorption method *(Russian)* 3−11648
$As_4(g)=2As_2(g)$, heat of dissociation and formation determ. 3−31256

heat of formation
benzodioxane-1,4 soln. in n-octane, self-association, proton magnetic resonance spectra *(Russian)* 3−34709
1,2-dehydrobenzene, extended basis SCF calcs. 3−20082
diallyl phthalate resin curing, differential scanning calorimetry applications 3−5797
gelatin gels, contact energy of gel formation, crit. shear stress 3−39397
hydrocarbons and N-containing heteromolecules, heats of formation by semi-empirical method 3−31250
nitriles, bond indices and heats of formation 3−31242
$Ag_2Te(c)$, $Ag_{1.9}Te(c)$ and $Ag_{1.64}Te(c)$, enthalpies of formation 3−15828
Al-Zn alloys, α-phase, enthalpies of form. 3−21600
As_2 from $As_4(g)=2As_2(g)$, heat of dissociation and formation determ. 3−31256
$B_3N_3H_6$, and dimeric boronimide 3−7142
Bi_2S_3, dissociation pressure meas. in 806-904K range, determ. of heat of formation from thermodynamic laws *(Russian)* 3−12511
C_3 molecule, and entropy 3−27852
Co_3Nb, phase thermodynamic stability, electrochem. determ. 3−2691
$Cu_2Te(c)$, enthalpy of formation 3−15828
IrO_2, free energy of form. by solid electrolyte galvanic cell method 3−37124
$LaCoO_3$, galvanic cell obs. 3−1797
NaAg molecule, dissociation energies, third law enthalpies, heat of formation 3−29728
NaF-ZrF_4 mixture, calorimetric study of the enthalpies of dissolution of NaF and ZrF_4 at 1030°C *(French)* 3−7907
$PF_3(g)$, enthalpy of formation 3−15827
PbTe, enthalpy of form. *(French)* 3−30242
SnTe, enthalpy of form. *(French)* 3−30242
XeF_2, standard entropy calc. from heat capacity meas. at 5-350K 3−1805
$XeF_6(c)$, $XeF_4(c)$, $XeF_2(c)$ enthalpies of formation 3−15827

heat of fusion
covalent systems, quantum dielectric theory of electronegativity 3−20709
metal in finely dispersed state, 80-320K, characteriz. 3−33686
oxalyl fluoride from 13 K to its boiling point, thermodynamic props. 3−34705
poly(ethylene terephthalate), cryst., annealing during polymerisation 3−31169
Au refractory, exploding-wire measurement of heat of fusion and electrical conductivity 3−30247
Au-Ni-Pt alloys phase diagrams, thermodynamic calc., expt. obs. 3−34511
fused B_2O_3, meas. at high temps. *(Russian)* 3−11722
Ir refractory, exploding-wire measurement of heat of fusion and electrical conductivity 3−30247

heat of mixing
alkali halide binary liq. mixtures, enthalpies of mixing 3−9039
alloy, random cubic binary solns., atomic pots. applic. 3−24814
alloys, binary, symmetrical mixing enthalpy, statistical investigation *(French)* 3−7913
binary liquid systems, determ. by thermometric titration *(German)* 3−22285
continuous determ. method for heats of mixing by quasi-isothermal heat flow calorimetry *(German)* 3−9858
covalent systems, quantum dielectric theory of electronegativity 3−20709
differential calorimeter, polymer monomer interactions 3−37596
ethanol-carbon tetrachloride-benzene, vapour-liquid equilib. data and heats of mixing 3−24251
ethanol-n heptane-n pentanol, vapour-liquid equilib. data and heats of mixing 3−24251
non-ideal solns., vapour liquid equilib. data and heats of mixing from Wilson's eqn. 3−24251
polymer and solvent, entropy of mixing derivation from free volume concept 3−29786
polymer solutions, crosslinked, thermodynamic functions for mixing derived 3−29789
polymer solutions, generalization of Flory-Huggins free enthalpy 3−29787
water + acetic acid, 17 to 50°C *(German)* 3−9047
Bi-Sn liq. system, partial heats of mixing 3−37007
Bi + Se, enthalpy of mixing in liquid state 3−14976
Ni alloys, liq., hydrogen solubility, thermodynamic behaviour 3−5296
NiO-ZnO solid solns., enthalpy of mixing, activity meas. 3−36429
Sb + Se, enthalpy of mixing in liquid state 3−14976
γ-U-Mo solid solns., excess thermodynamic props. 3−32947

heat of reaction
see also heat of combustion; heat of dissociation; heat of formation
explosions gasdynamics, detonation, shock-wave, blast-wave studies, review 3−33253
formaldehyde/Li^+ complexes, ab initio calcs., interaction of ligands with alkali cations 3−34718
magnetite, thermoanalytical method for heat of oxidation meas. 3−15078
periodic heat evolution during temporal chemical oscillations 3−27869
$O + CSe \rightarrow CO^* + Se$, rel. to CO chemical laser operation 3−6457

heat of solution
Cs-Rb alloy system, calculation as a function of alloy composition 3−33481
GaAs solid solns. with replacement impurities, equil. with gaseous phase *(Russian)* 3−11641
K-Rb alloy system, calculation as a function of alloy composition 3−33481
K-Rb(Cs) alloys, Hume-Rothery's 15% rule and pseudo-alloy-atom model 3−24817
$LiF{:}MhF_2$, Debye-Huckel interactions and solubility 3−4881
Na-K(Rb)(Cs) alloys, Hume-Rothery's 15% rule and pseudo-alloy-atom model 3−24817
NaI, in acetonitrile solns., conc. depend. 3−31259
Rb-Cs alloys, Hume-Rothery's 15% rule and pseudo-alloy-atom model 3−24817
Sn, of Dy and Er, calorimetric meas. *(French)* 3−4839

heat of solution continued
Tl-S melt, thermodynamic activity 3−9046
heat of sublimation
organic compounds, by molecular flow evaporation apparatus 3−16397
heat of transformation
cholesteryl n-alkyl carbonates, synthesis and mesomorphic characterization 3−24022
metal, activation energy for melting correl. with binding energy *(Russian)* 3−14983
^{3}He-^{4}He, heat of transition of ^{3}He from ^{3}He enriched phase to ^{4}He enriched phase 3−33714
Pb-Bi alloy, peritectic, heat of nonequilibrium solidification 3−39323
SbSI, ferroelec. phase transition entropy from temp. depend. sp. ht. obs. *(Russian)* 3−8542
heat of vaporisation
critical heat flux for power reactors, compensated distortion model using fluid with lower latent heat than water 3−19905
oxalyl fluoride from 13 K to its boiling point, thermodynamic props. 3−34705
water, anomalous, enthalpy of evaporation 3−1789
Co, third-law heat, 1519-1926 K 3−4851
K$_2$CO$_3$ aq. soln., of H$_2$O 3−24253
heat of wetting *see wetting*
heat pumps
No entries
heat radiation
Apollo 14 fines, thermal radiation properties 3−39637
black radiation, total spectral absorptivity, gases, nonisothermal medium 3−1325
bounded radiation field, autocorrel. 3−638
buoyant plume above horizontal line heat source 3−23696
flux contours on a plane for parallel radiation specularly reflected from a cone, a hemisphere and a paraboloid 3−19526
helical surface, cylindrical cavity, angular coeffs. of radiation 3−35634
magnetohydrodynamic channel flow, thermal effects 3−14493
Map, outgoing thermal radiation rel. to transfer equation, models *(Russian)* 3−35069
partially transparent mats. at high temps., meas. method and automatic unit 3−25694
quasars, nuclei macroscopic parameters determ. 3−37421
radiation energy density and heat flux in small rectangular cavities 3−10402
specular reflection from an arbitrary reflector surface to an arbitrary receiver surface 3−19525
supermassive stars, thermal radiation spectra 3−31647
thermal deformations of a sphere, radiation from a point source 3−37805
twofold spectral-ratio pyrometry, selective radiation, error elimination 3−35370
universal relation to luminesc. spectra 3−14391
Venus, upper (above-cloud) atmosphere outgoing thermal radiation, models *(Russian)* 3−35069
X-ray astronomical sources, thermal radiation spectra 3−31647
CO-water vapour, calc. radiation from two plane isothermal layers 3−36066
H, nonisothermal shock layer, radiative flux, temp. dependent spectral absorption coeff. 3−1327
H$_2$O vapour, calc. radiation of nonisothermal gas 3−36067
H$_2$O vapour-CO$_2$ calc. radiation from two plane isothermal layers 3−36066
MgO, radiation degree of blackness, electric resistance 3−36423
SiO$_2$, radiation degree of blackness, electric resistance 3−36423
heat systems
see also boilers; heating
No entries
heat transfer
see also convection; cooling; heat conduction; heat radiation; radiative transfer; thermal diffusion
during adiabatic saturation of hot gas in wetted-wall tube 3−1321
air flow and heat transfer to the atmosphere from the surface of thermal electric power plant cooling ponds 3−29847
air in small cells, thermal convection 3−7351
air subsonic flow, heat exchange in the critical zone ahead of a cylindrical step *(Russian)* 3−29857
air turbulent flow with suction in a porous tube 3−20295
air turbulently flowing in smooth annuli at high temp. 3−23698
air-sea, BOMEX expts. 3−9253
amorphous semicond., switching effect at discontinuous changes in heat transfer 3−30528
analytic determ. in straight fins with periodic variation of base temp., calc. of fin efficiencies 3−10411
anisotropic media with property variations, nonlinear heat flow and heat generation 3−35642
arc plasma, magnetically confined laser heated, heat propag. 3−7491
Atlantic, tropical, upper 12m, eddy thermal cond., diurnal temp. change depth variation 3−27989
atmosphere, lower layer above sea, structural features, turbulent heat transfer, wind speeds 3−34881
axially varying heat flux effects for turbulent flow of liquid metals 3−11078
benzene, evaporation from porous bodies, obs. of simultaneous heat and mass transfer 3−1790
bibliography, Japanese works 3−632
bibliography 3−633
bibliography 3−22768
bibliography of soviet works 3−22769
binary mixtures, pool nucleate boiling 3−30252
blood circulation, peripheral, rheodynamic model for Fahraeus-Lindquist effect and flow in capillaries 3−17497
blunt conical nosetip, turbulent and transitional transfer rates 3−11416
bodies with moving interfaces, analytical study *(Russian)* 3−35640
boiling, nucleate, at high heat fluxes, forces acting on heated surface 3−30251

heat transfer continued
boiling, refrigerants, film flow, liquid NH$_3$, NH$_3$ evaporators, heat exchangers 3−1438
boiling heat transfer mechanism rel. to growth of vapour bubbles 3−7917
boiling two-phase channel flow, heat transfer in nucleate boiling region 3−29849
boiling two-phase channel flow patterns, and heat transfer 3−29908
boundary layer, stagnation, spatial stability 3−7374
boundary layer at crit. pt. of indestructible body washed by flow of ionized air 3−23737
boundary layer eqns., known temp. gradient at moving flat plate in parabolic flow, solns. 3−7372
boundary layer flow past cylinder, soln. by Tolubinskii integral method 3−23688
bubbles, nonspherical, effect on motion 3−1444
n-butanol, evaporation from porous bodies, obs. of simultaneous heat and mass transfer 3−1790
carbon tetrachloride, evaporation from porous bodies, obs. of simultaneous heat and mass transfer 3−1790
channel with porous wall, turbine cooling appl. 3−23717
chemical vapour deposition, heat transfer and temp. oscills. 3−12253
closely-spaced metal surfaces at low temperature, effect of discrete modes of radiation field 3−10410
composite media, indirect thermal sensing, theoretical calc. 3−35639
composite semi-infinite slab, heat transfer to surface 3−32459
compressible fluid, turbulent and laminar flow in circular tube 3−36080
condensation, steam, steam-gas mixture 3−628
condensation, water vapour, vertical pipes 3−629
conduction, solution by Laplace transformations, special boundary value problems 3−6381
conduction, transient, one-dimensional problems in cylindrical coordinate system, solution by numerical methods 3−16764
confined-discharge plasma generator with local fluid construction, heat transfer and fluid dynamic effects 3−26904
conjugate transient heat transfer in fluid flow through insulated pipes, integral equations 3−38361
convection, rel. to simultaneous mass transfer 3−11388
convection in porous layer heated from below 3−1361
convective, for turbulent flow in tubes *(Russian)* 3−11393
convective, forced, effect of 2-dimens. roughness 3−22765
convective transfer from cavity in duct with separated flow *(German)* 3−1332
convectively cooled pipe, correction on the length of ice-free zone 3−20300
coolant throughflow in a rotating, shrouded, parallel disc system 3−20328
cooling towers, computer code for thermal design 3−17285
correlation for stable natural-convection film boiling 3−11732
Couette flow nonlinear rarefied with heat transfer, gas statistical models with and without internal energy states 3−33259
counter gradient vertical flux, planetary boundary layer meas. and theoretical expression 3−15969
counter-flow regenerative heat exchanger, temperature fields of nozzle and gases *(Russian)* 3−9848
coupled with momentum and moisture transfer in flow of drying particles 3−1467
critical flux in open vertical channels filled with superfluid helium under press. *(French)* 3−11773
critical heat flux for boiling water power reactors, compensated distortion model 3−19905
cryogenic multilayer thermal insulation 3−22293
crystal growth rate from melts and solutions, transfer rate effects 3−1579
curved surface, second order boundary layer solns. 3−1393
cylinder, synthesis method, soln. of heat-conduction problem 3−637
cylinder under homogeneous boundary conditions, semidiscrete-least squares approximation 3−10259
cylinders, infinite, transfer pots., integral eqn. approach 3−35637
cylinders and spheres under internal pressure with steady radial heat flow, reference stresses and temps. 3−28893
cylindrical layer of absorbing medium bounded by nonblack surfaces 3−22778
dense layer with transversely finned cylinders 3−23707
dense mesh wire screen regenerator matrices at cryogenic temps. 3−9881
diffuse highly reflecting material, radiation fields, temp. distrib. 3−621
discharge, temp. distrib. in heterogeneous medium with radiative heat transfer *(Russian)* 3−11515
in discharge chamber of arc gas heater with boundary conditions in wandering speck *(German)* 3−4688
dispersed liquid metal-gas packed bed heat exchanger 3−39303
dispersed system consisting of uniform mixture of coarse- and fine-grained material 3−23792
dispersion relations for relativistic hyperbolic heat eqns. 3−17555
dropwise condensation, drop size distributions and heat transfer 3−20857
drying of hygroscopic capillary porous solids, liquid capillary flow, vapour diffusion and heat transfer 3−20409
drying rate of porous solids rel. to heat and mass transfer 3−2774
duct with constant wall heat flux, slug flow in thermal entrance region *(German)* 3−7331
effects of upstream and downstream boundary conditions on heat or mass transfer with axial diffusion 3−20285
in electrolyte solution, eff. of mag. field *(Russian)* 3−20313
electronic melts, mechanisms 3−24299
electrostatically controlled heat shutter 3−32045
evaporation, porous walls, water, multiphase flow 3−1437
evaporation of moisture on small cylindrical bodies in longitudinal flow 3−1791
film, draining down vertical wall, numerical solns. 3−20290
film boiling, oscillation effects of sphere 3−27115
film boiling of aqueous binary mixture with volatile component, heat transfer coeff. 3−1788
film condensation, vapours, laminar flow, turbulent flow, pressure gradient 3−1347

heat transfer continued
- film evaporation of liquid patches, heat transfer coeff. determ. 3−30254
- flow disturbed by 2-D crack in elastic strip under strain 3−13566
- flow in slotted channels with obstacles 3−4540
- fluidised bed, wall-to-bed transfer 3−11445
- fluidised bed coating of thin plates, heat transfer with a moving boundary 3−14501
- fluidised bed-to-wall, mechanism 3−1460
- fluidised beds, annular, inner wall transfer rates 3−29910
- fluidised beds, coefficients calc. *(Russian)* 3−7451
- fluidised beds, cooling of finely dispersed material 3−2763
- fluidised beds, obs. using harmonic anal. 3−1461
- fluidised beds, vibrating 3−1462
- fluidised beds, wall-to-bed heat transfer 3−33201
- fluidised beds of spherical particles under 1st and 3rd order boundary conditions 3−1463
- forced convection for flow in pipes, past flat plates and for flow in packed beds 3−11365
- forced convection heat transfer from humid air to frost surface 3−1363
- forced convective, supercritical water flowing in tubes 3−1370
- forced laminar fluid flow between parallel plates, effect of magnetic field 3−14431
- fractional vertical condensers, obs. techniques 3−127
- free convection, schlieren TV method for thermal boundary layer obs. 3−124
- free convection boiling, Freons, refrigerator tube material 3−1786
- free convective heat transfer from vertical Al cones 3−10414
- freon 12 and 12, condensation study 3−27111
- Freons, boiling, finned tubes, intertube spacing, fin geometries, shell exchangers 3−117
- frost formation on air coolers rel. to heat transfer coeff. of cooled plate 3−1780
- frost layer, heat and mass transfer anal. 3−20852
- fully developed nucleat boiling, heating surfaces, microgeometry, adhesive properties 3−1787
- gas diffusion to a liquid film flowing down inclined surface, asymptotic eigenvalues for heat or mass transfer 3−26779
- gas flow, heated laminarizing, in square ducts 3−36082
- gas flow, viscous, in tube, effect of wall temp. on characteristics *(Russian)* 3−7390
- gas flow around heated thin wire 3−36077
- gas flow through small diameter packed beds 3−622
- gas high pressure flows with and without heat transfer 3−38389
- gas-liquid systems, internal and external processes 3−639
- gaseous mixtures, variation with concentration of components 3−1320
- gases and liquids flowing in tubes, augmentation 3−1344
- generalised hydrodynamic eqns. 3−14434
- glass-graphite materials in high-temperature gas stream, heat and mass transfer on the surface *(Russian)* 3−26786
- Graetz extended problem, higher eigenvalues determ. 3−10415
- granular beds, radiation effects on temp. distrib. 3−20395
- graphitic body ablating in hypersonic radiating air plasma 3−1403
- growth law of fast moving spherical second phase, heat and mass transfer limitations 3−24245
- heat and mass transfer between two phases, effects of convection *(French)* 3−2840
- heat eqn. soln., polynomial approximations 3−10406
- heat exchanger, averaging over length 3−13659
- heat exchanger, parallel plate, with turbulent flow on one side and laminar flow on the other, calc. of heat transfer parameters 3−22276
- heat exchangers, single phase pressure drop, considering the change of fluid props. along the flow path 3−33213
- heat flux and temp. distribs. in turbulent equilib. boundary layers 3−1388
- heat flux in transient and steady-state nucleate boiling 3−11733
- heated plate in sinusoidally oscillating flows, applic. to internal combustion engine 3−1360
- helical cooling coil in agitated vessel, regression analysis of experimental data 3−23714
- helical cooling coils in agitated vessels, turbulent heat transfer 3−1364
- hemispherical bubble growth in binary mixture at liquid solid interface 3−4611
- high speed flows, three dimensional heat and mass transfer, ablation distances 3−38354
- horizontal annular air layers at low Grashof numbers *(Russian)* 3−7354
- hypersonic turbulent boundary layer, blowing of coolant gas through slit *(Russian)* 3−11405
- hypersonic turbulent flow at wedge compression corner, heat transfer 3−14465
- infinite plate with a circular hole, generalised dynamic problem of thermoelasticity *(Russian)* 3−6207
- influenced by entropy waves generated in a Rijke tube *(Russian)* 3−5712
- integral balance method, generalization for problems of interconnected heat and mass transfer *(Russian)* 3−32460
- interferometric methods of obs. using Mach Zehnder interferometer and motion picture camera 3−123
- ionised gas flow, cylindrical pipe, wall heat transfer reduction, localised magnetic field, calculations *(Italian)* 3−20277
- jet, cylindrical laminar liquid, ejecting into a gas, heat transfer 3−38417
- jets, turbulent and reattached on inclined flat plate, mass transfer 3−17516
- jets, turbulent with adjacent boundaries, flow development and mass transfer 3−17515
- Joule-Thomson effects on thermal entrance region heat transfer in pipes with uniform wall temperature 3−20302
- knife jet dryers, effect of turbulence *(German)* 3−26780
- laminar boundary layer temperature field near two dimensional stagnation point 3−14462
- laminar flow between heated parallel plates 3−14443
- laminar flow with surface reaction, thermal simulation *(French)* 3−20322

heat transfer continued
- laminated shells, heat transfer and temperature fields, calc. 3−26173
- liquid crystals, nematic, review 3−24300
- liquid fluidised bed, heat transfer coeff. variations 3−4610
- liquid in channel, complex heat transfer calcs. 3−23692
- liquid layer heated from below, thermal and rotational instability in hydrodynamics, mathematical equivalence 3−26793
- liquid phase epitaxy, heat and mass transfer in growth process 3−1923
- liquid-filled porous media, thermal effects on wave propagation 3−37825
- liquids, boiling, heat transfer crisis 3−14990
- liquids and eutectic alloys, melting or freezing in wedge shaped enclosure 3−14982
- mass transfer, bibliography 3−634
- mass transfer in turbulent flow, numerical solns. for heat transfer 3−14448
- meas. methods, in ice-water vapour phase transition in vacuum *(Russian)* 3−9860
- measurement, in compressible turbulent boundary layers 3−22273
- measurement using Pt film resistance thermometer 3−22286
- Mediterranean, heat loss in winter to atmosphere 3−27982
- melting, numerical calc. 3−30244
- melting ice with a water jet 3−14420
- metal surfaces in contact, heat transfer mechanism rel. to thermal contact resistance 3−2174
- metal surfaces thermal contact resistance 3−2173
- metals, liquid, turbulent flow through closely spaced rod bundles in nuclear reactors 3−11075
- metals, liquid, turbulent flow through closely spaced rod bundles in nuclear reactors 3−11076
- MHD channel flow 3−1427
- MHD Couette flow 3−29897
- MHD Couette flow between conducting walls 3−4609
- MHD flow and heat transfer between conducting parallel walls, variational approach 3−23775
- MHD flow over porous plates *(Russian)* 3−7431
- MHD non-stationary flow between parallel porous walls with heat transfer *(Russian)* 3−20380
- in mixed convection on vertical plate 3−1319
- Moon, thermal structure rel. to Apollo 15 surface heat flow measurements 3−18975
- motion of small spheres in gas 3−33257
- moulds used for continuous casting of metals, thermal fluxes in walls 3−24891
- moving surfaces stability in fluid systems with heat and mass transfer 3−29865
- multiphase flow, boiling Freons, air coolers, flow turbulization 3−1439
- multiphase fluid in presence of phase transformations, hydrothermodynamic eqns. 3−33287
- multiphase laminar flow between parallel plates, radiative characts. 3−1475
- multistage cross flow heat exchanger 3−111
- Newtonian fluids in circular pipes, motion energy dissipation on heat transfer for laminar flow 3−23708
- non-Newtonian fluids in anchor-agitated vessels at low Reynolds number 3−7325
- nonstationary and stationary conditions, comparison of heat exchange intensity 3−22783
- nonstationary interaction of thermal radiation with pure metal surface, heat transfer localisation 3−33720
- nonviscous incandescent gas supersonic stream, radial thermal flux distribution at surface of a sphere *(Russian)* 3−29887
- nuclear reactor assemblies without grid, multicell calcs. near wall 3−11070
- nucleate boiling heat transfer mechanism rel. to boiling liquid films 3−1785
- numerical solution of transient heat flow, educational example 3−28434
- ocean floor heat flow and circulation of interstitial waters 3−9234
- one-dimensional frictional unsteady compressible flow, numerical procedure for solution 3−11420
- in packed beds, mathematical model 3−6377
- packings, influence of thermal radiation and pressure *(German)* 3−22766
- paramagnetic solutions, infl. of non-uniform mag. field *(Russian)* 3−20314
- pentane, iso and cyclo evaporation in glycerine-water solns., average heat transfer coeffs. 3−24250
- planar air jet striking a concave surface 3−23704
- in plane Couette flow of rarefied gas 3−14471
- plane Couette-Poiseuille flows, application of special form of Galerkin's method 3−23699
- plane moving boundary problems, freezing and melting, integral transforms 3−34702
- plane-parallel duct with artificially roughened walls, heat transfer and hydraulic resist. 3−20311
- plasma systems, magnetically rotated arcs 3−26866
- plate, mutually connected heat and mass transfer by integral balance method *(Russian)* 3−10404
- plate with infinite fluid stream around *(Russian)* 3−7353
- plate-separated two fluid system, thermal flux and temp. distrib. calc. 3−23689
- plume swaying due to free convective heat transfer from horizontal cylinder *(Japanese)* 3−23684
- Poland, heat flow data from four deep bores 3−18828
- pollutant transport, stochastic processes 3−1375
- polymer, molten flowing, temp. profiles, viscous dissipation and Nusselt-Graetz relations 3−31189
- polymer melts, plane Couette flow, heat dissipation *(German)* 3−7336
- pool boiling, binary mixtures, macroscopic correl. account for transfer mechanism 3−1783
- pool boiling, flat heaters, first critical heat flux, contact angle 3−1366
- porous cooled medium, application to eccentric annular region 3−23797
- porous media cooled by fluid 3−627

heat transfer continued
Pt wire, natural convective boiling, heat transfer to binary mixtures *(Japanese)* 3−24274
pulse thermal diffusivity, meas., finite pulse-time and heat loss effects 3−35373
pulsed bubbling columns, heat and mass transfer 3−26782
quartz, fused, thermophysical props. and radiation component of heat transfer 3−1837
quenching bodies of complex shape, cooling time calc. 3−21694
quiescent rarefied gas contained between coaxial cylinders 3−4511
radiant interchange configuration factors within an enclosure, efficient computation 3−10412
Rankine cycle automobile condensers, perforated plate-fin surfaces 3−4048
rates in pool boiling, single component liquids 3−1782
reactor cooling systems, coeff. during rewetting of hot dry patch, anal. 3−1067
reactor core spray cooling after loss of coolant, numerical soln. of Yamanouchi model 3−11074
refractory, obs. rel. to admixture effect *(Russian)* 3−8987
relaxation model for solid-liquid suspension thermal cond. calc. 3−20403
reservoir, statistical mechanical representation using cubic lattices 3−4050
Rivlin-Ericksen fluid containing rotating heated sphere, calc. of thermal boundary layers 3−26812
rotating discs in fluid, thermal boundary layers, analysis 3−23722
roughness meas. of heat transfer surfaces 3−20299
Russian notation, specific terms and concepts 3−625
salt solutions, boiling, heat transfer rate determ. using similarity theory and mol. characts. 3−20864
saturated porous media, thermal field visualisation by Christiansen effect 3−19377
sea-air interaction, model of long-term heat and moisture exchange processes *(Russian)* 3−39495
semi-infinite solids, integral method 3−37911
semi-infinite steel body melting in an Fe-C alloy, heat and mass exchange eqns. 3−24827
shuttle heat transfer problem in refrigeration cycles 3−5839
solar energy collector, linear, heat transfer characts. 3−25529
solar wind, quiet and collisionless, parallel heat flux through collision transition region 3−31527
solid interface, acoustic wave transmission coeff., thermal contact resist. *(French)* 3−38709
solids-gas jet, development of heat-diffusion method for meas. of turbulence intensity on axis *(Russian)* 3−23789
south Greenland, heat flow and surface radioactivity at two sites 3−15900
spectrum, integral, absorpt. coeffs. of medium 3−35636
specular diffuse reflection of radiation at plane layer for combined conductive and radiant transfer 3−4046
stagnation point heat transfer, first Damkohler similarity parameter 3−26821
steam, condensation, drop behaviour and surface temp. fluctuation correspondence 3−20855
steam, heat transfer during condensation at a rotating disc 3−26785
steam flow in vertical tube, condensation and pressure drop 3−17517
steam generator tube plate, convective flow *(Russian)* 3−16768
from stripwise heated surface, natural convection 3−22275
strongly accelerated turbulent boundary layer, expt. obs. 3−38360
subsonic and supersonic flows, numerical solution 3−4586
subsonic diffusers, effect of entrance configuration on local coefficients 3−23715
subsonic jet flow, plane baffles, stagnation point, free stream turbulence 3−1330
sun radiation, effects on the sea 3−21930
superconductors, energy currents, entropy current, quasistatic time dependent order parameter 3−30571
supercritical fluid, rel. to eddy diffusivity for turbulent flow in tubes *(Japanese)* 3−38368
supersonic viscous flow over a yawed circular cone 3−38384
surface film boiling under free convection, eff. of cylinder diameter 3−20869
suspension, gas-solid, in stabilised flow, to channel walls 3−23791
temperature distrib. calcs., boundary extrapolation 3−35638
temperature stresses in thin viscoelastic plates with heat transfer 3−22629
thermal boundary layer growth in the entrance region of an annulus 3−14459
thermal contact conductance, in vacuo, correlations using dimensionless analysis 3−10409
thermal contact resistance under vacuum calc. 3−22776
in thermal entrance region of rectangular channels with partially heated circumference *(German)* 3−23721
thin-walled circular pipe, dynamic response to fluid temp. var. 3−10405
through wavy liquid film in laminar flow 3−7320
total spectral absorptivity, black radiation, gases, nonisothermal medium 3−1325
transient, between metal balls and liq. stream at const. temp. 3−23706
transient, to walls of cylindrical channel filled with liq. 3−19531
transient temp. fields in a plane slab with embedded cylindrical sources, point matching technique 3−37910
transitional longit. flow over tube bundle 3−23712
transpiration cooling, heat and mass transfer equations 3−26168
transpiration cooling, heat transfer phenomenon 3−7918
triangular ducts, with laminar forced convective flow 3−1343
tube bundles, turbulent exchange coefficients 3−10224
tube heated by radiation, calc. at thermal entry section *(Russian)* 3−6378
turbulence, energy dissipation and intensity value, relationship establishment 3−33202
turbulence, heated-grid, spectral transfer of scalar and vel. fields 3−38363
turbulence effects 3−1362
turbulence in transfer calcs. at stagnation pt. of jet interacting with planar obstacle 3−20312
turbulent, from rough surfaces 3−7344

heat transfer continued
turbulent, from wall of jacketed tank 3−624
turbulent boundary layer in adverse press. gradient, effect of transpiration 3−1387
turbulent falling films 3−20301
turbulent flow of macromol. solns., momentum and heat transfer 3−17518
turbulent fluid flow in circular tube, temp. fluctuations 3−29845
turbulent Graetz problem, heat transfer rates for fully developed and entry region of pipe 3−4549
turbulent heat and mass transfer in pipes, channels and boundary layers 3−1367
turbulent isothermal flow of incompressible gas in circular rot. pipe 3−23709
turbulent momentum transfer in rough pipes, statistical props. 3−11390
turbulent transfer in ducts, large Prandtl or Schmidt nos. 3−11389
turbulent tubular flow involving endothermic chemical reaction, calc. of heat transfer coeffs. *(Dutch)* 3−29926
two dimensional temperature fields in rectangular fins *(German)* 3−26180
two-dimensional steady state with constant heat generation, numerical Green's function method of solution 3−22770
two-dimensional streams incident normal to flat surface, heat transfer in region of accelerated flow 3−23705
two-liquid systems with asymmetric stress tensors, model construction *(Russian)* 3−28853
two-phase real conc. particulate systems, high Reynolds number fluid dynamics and transfer processes 3−36136
ultimate heat transfer limit of cylindrical heat pipes, theory 3−14436
unstable film boiling dynamics, process transfer function 3−20865
unsteady conjugated, between semi-infinite surface and incoming compressible flow, analytical solution 3−630
unsteady conjugated, between semi-infinite surface and incoming compressible flow, temp. field determination 3−631
unsteady heat conduction in solids, with moving boundary, soln. to 1-D problem *(Russian)* 3−22789
unsteady heat transfer for Stokes flow about a sphere 3−10408
unsteady laminar boundary layer on a semi-infinite flat plate, heat transfer theory 3−20293
unsteady laminar boundary layer on a semi-infinite plate, experimental results from an oscillating plate 3−20294
unsteady-state, boundary conditions determ. 3−23693
unsteady-state heat transfer during gas cooling in a duct, meas. of coeffs. *(Russian)* 3−20325
vapour condensation, pressure of noncondensing gas, heat and mass transfer 3−36413
vapour deposition in vacuum 3−2631
vapour film boiling around spheres, destabilisation and energy transfer 3−20859
vapour-water stream in helically coiled tubes 3−14499
variable properties laminr gas flow heat transfer in the entry region of parallel porous plates 3−20298
vibrated fluidised beds, effect of homogenization 3−1465
water, adiabatic evap., heat and mass transfer dynamics 3−20863
water, bubble boiling, influence of the thermal props. of the heating surface on the heat transfer *(German)* 3−33661
water, evaporation from porous bodies, obs. of simultaneous heat and mass transfer 3−1790
water, subcooled, pool boiling heat transfer study 3−30253
water, with pseudoboiling 3−14989
water flow in internally heated annulus with rotating outer boundary 3−11375
water flowing in tubes at high pressure *(Japanese)* 3−1353
water in an annulus, friction and heat transfer in the swirl flow 3−20283
water organic solvent binary mixtures condensation heat transfer coeffs. 3−1784
wedge flow with variable props., variational technique application 3−38374
Widder temperature representations 3−22771
between wire and gases with free convection rel. to strong change of gas physical props. 3−23694
yawed cylinders in laminar flow 3−36117
Ar, high temp. flow in pipe, heat transfer during cooling 3−14408
Ar electric arc chamber, heat transfer to a biased wall 3−33417
Ar plasma, experimental and analytical aspects of heat transfer 3−33343
CO_2, supercritical, laminar forced convective heat transfer, buoyancy effects *(Japanese)* 3−20323
CO_2, turbulent flow at supercrit. press., local worsening obs. 3−23691
CO_2, turbulent flow with combined forced and free convection *(Russian)* 3−11392
CO_2 in air, heat and mass transfer obs. using interferometry 3−1319
H_2O, surface boiling, hydraulic resistance in a tube, arbitrary heat flux distribution 3−36081
H_2O in vertical tube, forced and free convection 3−4550
He, solid/vapour, at low temp. 3−9897
He, supercritical liquid, meas. of forced convection 3−9893
He flow, with wall temp. up to 2800K *(Russian)* 3−7389
He I, boiling under forced flow in vertical tube 3−9894
He II, saturated liquid, correlation of vaporisation onset heat flux for cylinders 3−9895
He II in long tubes, saturated and subcooled, critical heat flux 3−9896
He in air, heat and mass transfer obs. using interferometry 3−1319
K, boiling in pipes, effect of nonuniformity of heat supply on critical heat flows 3−14986
K, liquid, convective, during turbulent flow 3−14445
K vapour condensation, in pipe cooled by liquid alkali metal 3−14987
NH_3, plane layer, radiant-conductive heat transfer 3−23711
$N_2O_4 \rightarrow NO_2$, heat transfer *(Russian)* 3−12507
Na-Ar two-phase flow in vertical channel, void fractions and heat transfer coefficients 3−1434
Na-K heat transfer agent, selective surveillance of impurity content by means of reactor plug indictor *(Russian)* 3−14246
NaF, phonon cond., calc. using nonlinear theory of heat transfer 3−27095

heat treatment
see also annealing; heat treatment of alloys; recrystallisation; work hardening
carbons, amorphous nature of spin centres from e.s.r. signal obs. 3-34182
cementite, influence of matrix on Cr contents 3-8790
copper phthalocyanine pigments, α and β forms, adsorption props., optical props., effect of heating 3-38713
electroslag weld metals, properties without high-temperature treatment *(Russian)* 3-8823
ferrite, hot pressing, for device appl. *(Polish)* 3-8972
glass ceramics, texture development 3-5343
glass reinforced plastic rings, wound, residual stresses determ. 3-24983
glass-ceramic microstructures, two stage formation 3-12439
glasses, phototropic, TlCl activation, TlCl crystallite precipitation due to heat treatment 3-27737
graphite, pyrolytic, influence on low temp. heat capacity 3-17980
kaolinite-illite-quartz mixtures, high-temp. refiring and ceramic props. 3-15751
lunar glass, thermal history 3-3309
metal fibre reinforced ceramics, fabrication and fracture toughness 3-18718
metals, quenched, obs. of point defects by field ion microscopy 3-24106
n-p-n transistor, enhanced P emitter diffusion, correlation with elec. props. 3-39291
Ni, quenched, elec. resistivity exam. of point defects *(French)* 3-11611
nylon 6, morphological changes and effect on dynamic mech. props. 3-20243
perspex electrets in nonuniform fields, heat treatment effect on brekdown voltage 3-21362
polymer, hydrodynamic analysis of hot rolling 3-25001
polymethylmethacrylate, tensile strength during thermophoto-aging, effect of alcohols *(Russian)* 3-27768
polytetrafluoroethylene, effect on friction and wear properties 3-36360
quenching bodies of complex shape, cooling time calc. 3-21694
resorcinol polycondensation products, structural conversion *(Russian)* 3-23646
rutile, abraded, electron microscope study of structure before and after annealing 3-15753
salt baths, self-diffusion coeff., numerical computation, eqn. 3-7956
sheet materials, fracture kinetics, effect of order of applying fatigue crack and heat treatment 3-18621
steel, austenite residual percentages prediction from transformation curves during cooling *(French)* 3-24910
steel, KVK-42 (42Kh2NGSM), austenite formation during high speed heating and deform. *(Russian)* 3-8874
steel, martensitic, ferritic, phase transform. after hot working by torsional technique *(Russian)* 3-24906
steel, obs. of retained austenite in α-phase during testing at 1000 deg./sec. *(Russian)* 3-24904
steel, quenched, plastic deformation effect on tempering process *(Russian)* 3-24901
steel, tempered hardened, rapid heating and plastic deform., magnetometric exam. *(Russian)* 3-8876
Al, rolled plate, heated to 488°C, grain structure after recrystallisation 3-15664
Al, sources of flaws during heat treatment, X-ray obs. *(French)* 3-15057
Al alloy as electric conducting wire, effect on conductivity *(Norwegian)* 3-5304
Al foil, X-ray television method for grain growth obs. under heat and stress treatment 3-26936
Al sheet solution, eddy current conductivity meas. near solidus point 3-27830
Al-Zn-Mg-Zr alloy, recrystallisation temp. eff. of heat treatment *(Russian)* 3-2716
Al_2O_3, alumina ceramics, quenching, effects on high temperature impact resistance 3-8960
Al_2O_3, fused to glassy substrate, boundary layer formation *(German)* 3-12425
Al_2O_3, thermally shocked, strength degradation and crack propagation 3-2752
As_2O_3-SiO_2 film, diffusion source, effect on comp. 3-20963
Au, lattice contraction due to quenching-in vacancies 3-30118
Au, vacancy form. by quenching under press., volume determ. *(French)* 3-21703
Au film, (001) oriented, recrystn. into (111) orientation *(French)* 3-20975
Au-Cu alloy film, order-disorder transformation obs. 3-1800
Au-SiO_x, cermet film, structure and elec. props. with heat treatment 3-15201
Au-SiO_x cermet film, structural and electrical changes on heat treatment 3-5064
B filament, gauge length influence on mechanical strength, effect of heat treatment *(Japanese)* 3-18704
Ba ferrite, preferred orientation during hot pressing *(Russian)* 3-15743
δ-$BaCO_3$, metastable phase, props. study 3-4855
BeF_2-KF-MF_2, BeF_2-KF-AlF_3-MF_2, BeF_2-KF-AlF_3-CaF_2-MF_2 (M = Mg, Ca, Sr, Ba), phase compositions *(Russian)* 3-11545
Bi, effect on twinning rate *(Russian)* 3-31057
C, crystallite preferred orientation with heat treatment under high pressure 3-9002
C fibres, examination of structure after oxidation, carbonization or graphitization 3-15778
C fibres, graphitization, X-ray and electron diffr. study 3-15780
$C_{27.5}CrO_2Cl_2$ crystal structure, electric conductivity and thermal stability obs. 3-33491
Cd alloys, multicomponent impurities influence on density change during thermocyclic treatment *(Russian)* 3-8844
$CdCr_2S_4$, ferromag. semicond., in sulphur atmosphere, variation of Curie constant and temp. 3-30621
CdF_3:Er^{3+}, C_{3v} local-site symmetry from correlated e.p.r. and optical obs. 3-21305

heat transfer continued
heat treatment continued
CdS, CdSe, heat treated epitaxial films, structure, composition, photoelec. props. *(Russian)* 3-33948
CdTe, electron and neutron irrad., excess, dissociative Cd pressure, defect behaviour, photoluminescence spectra 3-34431
CdTe, photoluminescence, lattice defect investigation with use of heat treatment, neutron and electron irradiation *(Russian)* 3-27550
Fe, dynamic hot pressing, C diffusion *(Russian)* 3-8945
Fe, hot-rolled, effect of processing variables on preferred orientation 3-8850
Fe-Ni-Al alloy, subspinodal, quenched and tempered, hardening obs. and mechanism *(Czech)* 3-31103
n-GaAs, effects on 0.93, 1.0 and 1.28 eV luminesc. bands 3-21477
GaAs, elec. transport props. depend. on heat treatment, thermal conversion rel. to impurities *(Russian)* 3-38832
GaAs, point defects, precision lattice parameter measurements after quenching and annealing 3-33523
GaAs, surface contamination during photo etching, heat treatment 3-8757
GaP:Zn,O, Czochralski-grown photoluminesc., minority carrier lifetime, effect of heat treatment 3-39176
$GdAlO_3$ rel. to point defect form. 3-20731
Ge, amorphous, prop. var. during reactor irradiation expts. 3-15195
Ge, hot pressing effects on neutron topographs 3-23983
Ge film, amorphous, order-disorder transformation obs. 3-1800
K_2O-SiO_2-Al_2O_3 system of glasses, crystalline phases produced *(Russian)* 3-24031
K_2O-SiO_2-BeO system glasses and crystn. products, synthesis and characteriz. *(Russian)* 3-11551
Li_2O-Al_2O_3-SiO_2 glasses, Gd^{3+} doped, e.s.r. meas. during crystn. 3-27403
Mg/MgO composites, effect of dispersed particles on structural stability 3-39376
$MgAl_2O_4$, transition due to hot-pressing 3-18688
MgO-Al_2O_3-SiO_2-TiO_2 glass-ceramic, crystn. and struct. 3-31161
MnO_2, commercially electrodeposited, heat treatment effect on the semiconductor properties 3-2086
x NaO.$(1-x)SiO_2$ glass, internal friction, −200 to 440°C *(Russian)* 3-11686
$Ni_{1-x}Al$ alloys, ordering of n-type vacancies 3-11614
$NiFe_{2-x}Al_xO_4$, spinel, cation transfer kinetics, during thermal treatment 3-20885
$NiFe_{2-x}Al_xO_4$, spinel, magnetisation in ferrimag. and paramag. regions rel. to thermal treatment 3-12033
Pt, lattice contraction due to quenching-in vacancies 3-30118
Pu, hydrogen impurity conc. determ. by hot vacuum extraction *(French)* 3-2746
PuO_2 fuel for space vehicles, thermophysical and thermomechanical properties 3-19958
PuO_2 fuel form, He migration and release, heat treatment expts. 3-19957
PuO_2 spherical fuel form development for use in space flight, hot pressing technique 3-19955
Si, irradiated, neutron and electron, heat treated, i.r. absorption band, high order vacancy defects, uniaxial stress response 3-34393
Si, redistrib. of Au deposited layers 3-39289
Si, stacking faults and prismatic dislocation loops due to O_2 precipitation, X-ray topography 3-17829
Si, thermal defects, formation, destruction and effect on elec. props. *(Russian)* 3-11890
Si, wafers, high temperature X-ray topography, defect generation during heating and cooling 3-39283
Si plates masked with amorphous SiO_2, in H_2, Si and SiO_2 interaction during heat tretment *(Russian)* 3-11815
Si slices, with and without dislocations, temp. quenching effects 3-4759
Si:Li, neutron irrad., defect interactions, Hall effect, i.r. absorption studies 3-33570
Si-SiO_2 system, low-temp., effect on electrical and recomb. characts. *(Russian)* 3-24519
SiO_2, silica, fibre fabric, influence on props. *(Russian)* 3-15775
Ta_2O_5, anodic, oxidation state after heat treatment 3-8039
ThO_2 crystals, i.r. absorption spectroscopy, gamma-ray irradiation and heat treatment effects 3-27735
Tl, polymorphic transform. mechanism *(Russian)* 3-15714
U, Ni plated, heating effect on bond strength 3-24887
U, polycrystalline, α, β and γ, elastic moduli, texture development by thermal cycling 3-18629
UO_2, UC_2 resin based fuels for HTGRs 3-11048
U_3O_8-UO_2 system, surface area rel. to Y_2O_3 content and calcining temp. 3-9023
W-Zr-C alloy, dispersion struct. changes during annealing and recrystalln., electron microscope obs. *(Russian)* 3-8875
$YAlO_3$, rel. to point defect form. 3-20731
ZnO, thermally shocked, strength rel. to Hasselman theory 3-8978
Zr, hydrided, quenching effect on slow-bend behaviour 3-18631

heat treatment of alloys
(rare earth-misch metal)-copper-cobalt, chill cast, effect on permanent magnet props. *(Japanese)* 3-34562
austenite, kinetics of thermal stabilization process 3-24915
α/β brass, heat treatment, serrated flow 3-31091
Elinvar, Cr type, tempering influence on Young's modulus and its temp. depend. 3-31084
Elinvar, thermal expansion, elastic props., influence of heat treatment and cold working *(German)* 3-34610
Fe alloys, engineering design and production 3-31054
Incoloy-800, heat treatment effect for B distribution 3-12386
Invar, thermal expansion, elastic props., influence of heat treatment and cold working *(German)* 3-34610
magnet, machined, method of corrosion protection 3-24956
manganin type, characteriz. for precision resistors 3-24946
martensite steel containing 12% Cr, tempering, carbide precipitation *(Portuguese)* 3-8892
martensitic cast iron, residual austenite content rel. to tempering time 3-30963
metastable effect of overheating on creep resistance 3-21707
Nimonic, notched creep strength, microstruct. effects 3-8932
quenching, ultrarapid, in piston and 'ski jump' apparatus *(French)* 3-12388

heat treatment of alloys continued
steel, 000N18K9M5T, influence of heating on phase content, structure and mechanical properties 3 – 24831
steel, 110G13L, effects of modifiers on hardening during strain hardening 3 – 18668
steel, 18KhGT, thermomechanical effect on wear resistance 3 – 24934
steel, ausformed, electron-beam weld props. 3 – 21645
steel, austenite, transformation of steel 15KhSND during continuous cooling 3 – 24931
steel, austenite thermal stabilization characteristic, microhardness meas. 3 – 24953
steel, austenitic, microstruct. changes during creep deform. at 600°C 3 – 8921
steel, austenitic, Nb-stabilized, low stress creep behaviour 3 – 8926
steel, austenitic, preliminary thermocycling influence on hot strength 3 – 31101
steel, austenitic, thermomech. hardening effect *(Russian)* 3 – 37045
steel, austenitic Cr-Mn, cold-worked unstable, heating effect on martensitic transforms. *(Russian)* 3 – 30966
steel, austenitizing processes, high-temp. studies 3 – 18661
steel, C, strengthening by thermomechanical working 3 – 24924
steel, carburized, internal oxidation of surface case 3 – 27692
steel, cast heat resistant, with low Ni content, characteriz. 3 – 27696
steel, cold worked, influence of high temp. austenitization on ductility 3 – 24935
steel, complex-alloyed die, decomp. of retained austenite during tempering 3 – 27695
steel, Cr-Mn-N austenitic stainless partial shape memory effect obs., after martensitic transformation and heat treatment 3 – 18677
steel, Cr-Mo-V, carbide hardening and characteriz. 3 – 21686
steel, Cr-Ni type, dislocation distribs. during creep and recovery at 700°C 3 – 8920
steel, durability, effect of fretting after thermochem. treatment *(Russian)* 3 – 27668
steel, durability of superheater tubing at elevated temps 3 – 27701
steel, electron irrad. effects on hardenability 3 – 24948
steel, ferritic stainless, stress corrosion cracking, heat treatment and comp. effects 3 – 31040
steel, heat treatment, application of the diffusion laws *(French)* 3 – 18659
steel, high strength, fracture toughness enhancement by microstruct. control 3 – 31051
steel, high-strength, effect on crack vel. and fractography 3 – 5332
steel, hydrogen embrittlement, temp. depend. *(French)* 3 – 5333
steel, hydrogen embrittlement sensitivity, thermal processing depend. *(French)* 3 – 5328
steel, hypoeutectoid, grain refinement by thermal cycling 3 – 34563
steel, influence on crack form. *(Russian)* 3 – 12370
steel, KhN35VTYuL, influence of method of melting, crystallization conditions 3 – 24929
steel, large forgings, primary heat treatment, shattercrack form. 3 – 24950
steel, low alloy, containing vanadium carbide, microstruct. effects on creep props. 3 – 8935
steel, low-alloy, struct. and phase comp. changes 3 – 21687
steel, low-C, containing tungsten tempering behaviour and carbide form. 3 – 37050
steel, low-C, low-Mn, Nb additions effect on plastic anisotropy 3 – 37054
steel, low-C, melting and dissolution in iron-carbon melts 3 – 37052
steel, low-C, pressurization and quenching effects on yield behaviour 3 – 24867
steel, low-C, recrystn. texture, effect of heating rate 3 – 21695
steel, low-C alloy, duplex microstruct. rel. to fracture behaviour 3 – 21646
steel, low-C austenite, recrystn., 900-1000°C 3 – 8849
steel, maraging, effect on change in dimensions 3 – 21666
steel, maraging, nitriding, nonbrittle case form. 3 – 27690
steel, maraging N18K9M5T, forgings, influence on impact strength 3 – 24926
steel, martensite, effect of cold work on tempering *(Russian)* 3 – 5305
steel, martensite obtained under h.p. and in pulse mag. fields, struct. singularities *(Russian)* 3 – 39330
steel, mechanical properties at low temp. 3 – 24916
steel, metastable austenitic Cr-Mn, warm rolling effect on mech. props. *(Russian)* 3 – 18612
steel, method to increase fatigue strength *(Russian)* 3 – 12372
steel, mild, slack quenching, effect of process parameters on struct. and mech. props. 3 – 8847
steel, Mossbauer obs. of strengthening mechanisms *(Russian)* 3 – 24875
steel, N14Kh5M3TYu, effect on mech. props. 3 – 21665
steel, Ni, influence of austenite deformation on properties 3 – 24920
steel, Ni-Cr-Mo, rare earth treated, temper embrittlement response and toughness 3 – 34584
steel, nickel-free complex-alloyed, struct. recrystn. 3 – 24952
steel, pearlitic, low cycle fatigue, heat treatment type depend. 3 – 37070
steel, pearlitic, tendency to grain growth on remelting 3 – 27698
steel, phase transitions during hot working, obs. of C and SiC segregation *(Russian)* 3 – 12354
steel, quenched, X-ray determ. of retained austenite vol. fraction 3 – 12349
steel, rail-grade, hydrogen-depressing melting operations 3 – 5335
steel, specimens with cappings, effect on corrosion fatigue strength *(Russian)* 3 – 27667
steel, stability of influence of high temp. thermomechanical working on mechanical properties 3 – 24922
steel, stainless, Cr-Ni, Nb-stabilized, steady state creep, temp. depend. 3 – 8922
steel, stainless, martensitic, influence of composition and heat treatment on mechanical props. and struct. *(French)* 3 – 34588
steel, stainless, rel. to magnetostriction characts. 3 – 24954
steel, stainless, type 304, hold-time effects on fatigue crack propag. 3 – 8880
steel, strengthening by directional transform. 3 – 31113
steel, structural, temp. effect on physical and mechanical properties 3 – 24927

heat treatment of alloys continued
steel, tool, fatigue limit in compression 3 – 21690
steel, workability improvement considerations 3 – 21681
steel 1Kh17N2, mech. props. after vacuum heat treatment 3 – 21676
steel and non-ferrous metals, critical impact velocity, mech. props., pretreatment effect *(German)* 3 – 31081
steel balls, crack form. during quenching, effect of technological parameters 3 – 24951
steel bits, fatigue strength increase 3 – 18665
steel for dies, effect on brittle fracture 3 – 18672
steel hardened by alloying or heat treatment, mech. props. 3 – 24947
steel sheet, cold-rolled, annealing-induced changes in texture in cross section *(Russian)* 3 – 30987
steel strip, hot rolling, roll load and torque functions, theory 3 – 8848
steel U7, thermomech. treatment for mech. prop. improvement 3 – 21675
steels, 25Kh5MVFS, 50Kh12MVFS, thermomechanical working influence on quantity of residual austenite 3 – 24923
structural and tool steels, subjected to intense u.s. vibrations, internal friction and heat release 3 – 27705
Superinvar prep. and characteriz. 3 – 24945
Ticonal, high-coercivity, characteriz. after isothermal thermomag. treatment 3 – 24943
two-phase lamellar structs., thermal stability 3 – 37012
Vicalloy 1, phase transforms., order-disorder changes *(Russian)* 3 – 30965
weld heat affected zones, martensite tempering rel. to hydrogen cracking 3 – 8910
Zircaloy, fracture toughness characteriz. 3 – 8879
Al, for machine construction, mechanisms of strengthening 3 – 21685
Al, quenching effects on quadrupolar n.m.r. 3 – 34248
Al, thermomech. processing, improved fracture resist. 3 – 31048
Al-Cu, effect on strain ageing 3 – 31080
Al-Cu alloy, structural and phase changes in welded joints 3 – 24832
Al-Cu-Mg-Ag, struct. of metastable precip. 3 – 15662
Al-Fe, dil., cold-worked, effect on internal friction and Young's modulus 3 – 27703
Al-Li, decomp. of solid soln., resist. obs. 3 – 21606
Al-Mg alloy, Portevin-Le Chatelier effect, vacancies elimination by heat treatment *(French)* 3 – 31092
Al-Mg commercial alloys, stress corrosion cracking and its prevention *(Japanese)* 3 – 18635
Al-Mg-Si;Cu, aging, effects of Mg loss, elec. resistance meas. 3 – 39361
Al-Si, liq. quenching effect on age-hardening 3 – 39371
Al-Zn alloys, decomposition, effect of high temp. aging 3 – 37015
Al-Zn-Mg, alloys, grain boundary corrosion and stress corrosion cracking relationship *(Japanese)* 3 – 31072
Al-Zn-Mg-Cu, thermomech. treatment processed, age hardening mechanisms 3 – 24897
Au-Cd-In, double h.c.p., liquisol quenching effect on struct. 3 – 34559
Cu-Be, eutectoid decomp., ordering with metastable solid soln. form. during quenching *(Russian)* 3 – 37001
Cu-Pt, short-range order and atom displacement parameters *(Russian)* 3 – 39329
Fe, AK6, mech. props. consistency after deform. heat treatment 3 – 21670
Fe, Armco, cold deform. and subsequent heat treatment, effect on mech. props. *(Russian)* 3 – 5307
Fe, borided, thermal fatigue resist. 3 – 27694
Fe, E1437B, ageing/deformation treatments influence on struct. and mech. props. *(Russian)* 3 – 24873
Fe, gray cast, wear resistance improvement by low-temp. liquid cyaniding 3 – 18666
Fe, malleable, Bi-containing, trace element effects on malleabilization kinetics and mech. props. 3 – 39357
Fe, nonmag. spring alloy, paramag. susceptibility as heat treatment check 3 – 21696
Fe alloys, engineering practice, review 3 – 31053
Fe-Co-Ni-Al-Ti-Cu, thermomag. treatment effects *(Russian)* 3 – 8386
Fe-Cu-Mn system, semihard mag. reed switch material, heat treatment effect on mag. props. 3 – 36757
Fe-Fe_2B fibrous eutectic alloy, thermal stability 3 – 8999
Fe-Mn-Co, cold rolled, effect on mag. props. *(Japanese)* 3 – 31077
Fe-Ni and Fe-Ni-Cr, martensitic transform. kinetics, external factors influence *(Russian)* 3 – 37002
Fe-Ni-Cr-Mo, effect on struct. changes, Mossbauer obs. *(Russian)* 3 – 31056
Fe-Si, 0-24%Si, effects of furnace cooling and water quenching on electric and magnetic properties 3 – 36776
Fe-Si alloys, thermomagnetic treatment, effects of inclusions and internal stresses *(Russian)* 3 – 8385
Mn-Cu, martensitic transform., shape memory effect *(Russian)* 3 – 5317
Mn-Cu-Co nonmag. Elinvar-type alloys characteriz. 3 – 37074
Mn-Cu-Cr Elinvar props. 3 – 21291
Mn-Cu-Ni, Elinvar props. 3 – 21292
Mn-Ni nonmagnetic Elinvar type alloys, heat treatment and cold working, mech. props. meas. 3 – 8894
Mn-Ni-Cr, Elinvar type, effects on Young's modulus, rigidity, hardness *(Japanese)* 3 – 8858
Mn-Ni-Fe, Elinvar type, effects on Young's modulus, rigidity, thermal expansion and hardness *(Japanese)* 3 – 8859
Mo alloy, struct. changes, emission electron microscope obs. 3 – 18574
Nb-Mo-Zn-C cast alloys, ductility increase 3 – 18664
NbTi alloys, effect of metallurgical history on superconducting critical current density 3 – 38926
Ni steels, 9%, modified by Mn, Cu, Mo, Nb, effects on low-temp. hardness and tensile strength, obs. *(Japanese)* 3 – 8860
Ni-Al and Ni-Co(Fe)-Al, phase transform. *(Russian)* 3 – 8831
Ni-In aligned eutectics, phase morphology 3 – 39318
Ni-Mo-W corrosion resistant hard alloy development 3 – 21667
Ni-P alloys, resist. decrease during tempering, hydrogen emission *(French)* 3 – 2738
Ni-P alloys tempering changes in resistivity *(French)* 3 – 12359
Ni-P coatings on steel, struct. and props. rel. to annealing temp. and time 3 – 27691

heat treatment of alloys continued
Ni_3Mn, ordering kinetics, influence of previous heat treatment *(Russian)* 3−31061
NiTi cpds., Ni-rich, quench-hardening and mech. props. 3−37073
Pb-Ag(Au) nonsubstitutional solid solns., comp. depend. of supercond. transition temp. 3−24533
Pb-Ca, rel. to appl. as grid materials for Pb-acid batteries 3−21635
$r_{0.80}Mo_{0.20}Fe_2$, effect on crystallographic and mag. props. 3−21649
Ti, low-cycle fatigue strength 3−21693
Ti alloy VT9, heat-induced phases, X-ray diffr. analysis *(Russian)* 3−2717
Ti-Al, with isomorphous β-stabilizing elements, mech. props. characteriz. 3−24940
Ti-Fe(19 wt.%) alloy, precipitation from supersaturated solid soln. on quenching from 1000°C and ageing at 650°C *(Russian)* 3−12344
Ti-Mo-Zr-Sn, B-III titanium, thermomech. treated, struct. and props. 3−34582
Ti-Si(1 wt%), Mo effect on quenched and aged struct. 3−31064
TiAl containing Nb, oxidation resist. at 800 and 1000°C *(Russian)* 3−15716
U-Ni-N ternary system, phase relationships 3−12332
WC-Co, struct. changes, emission electron microscope obs. 3−18574
$Zr_{0.60}Nb_{0.40}Fe_2$, effect on crystallographic and mag. props. 3−21649
heated cathodes *see thermionic cathodes*
heating
see also electric heating; induction heating; plasma heating; refractories
atmosphere, due to local industry *(French)* 3−21956
auroral heating of neutral atmosphere by particles rel. to thermospheric composition 3−34917
autoclave, study of crystal growth and dissolution at high temps. 3−3776
biological tissue, temperature rise during focused u.s. irradiation 3−5678
ceramics, thermal shock resist. rel. to failure 3−8984
chromospheric heating of very hot stars by radiation driven sound waves 3−25435
D-region, by a horizontal terrestrial current carrying wire 3−12813
F-region ambient electron heating by photoelectrons 3−12811
F-region thermal balance, effect of excited states of O ions 3−25290
flat heaters, pool boiling, first critical heat flux, contact angle 3−1366
flow-resistance gas heater 3−19173
global atmosphere, monthly zonal mean radiative heating rates 3−25223
haematite, in air and water vapour, spinel formation 3−2875
intergalactic H I in Coma cluster of galaxies, heating mechanism and model 3−37460
interstellar medium, by Mira variable stars 3−9615
ionospheric electron gas heat flux at heights > 180 km 3−25270
macroscale external heating in atmosphere rel. to hydrodynamical model for long-range forecasting *(Russian)* 3−18857
radiation, of specimen, influence of sealed pyrometric device 3−9865
radioisotopic heat source, metallographic image analysis 3−18693
semi-infinite isotropic elastic medium, soln. to plane strain problem 3−13588
solar chromosphere, heating rel. to absence of flares at 3835 Angstroms 3−18943
solar corona, heating rel. to ion energies in transition zone from high resolution spectra 3−22015
solar u.v. emission line profiles rel. to heating and production of corona 3−18944
solar wind protons 3−12967
stripwise heating of horizontal surface, heat transfer efficiency 3−22275
sulphide minerals, effect of temp. on magnetic susceptibility during continuous heating and cooling, phase change obs. *(Russian)* 3−12009
Sun, empirical models, effect of mechanical waves rel. to heating 3−31553
sunspots, heating and decay rel. to supergranular motion suppression *(Russian)* 3−12970
surfaces, microgeometry, adhesion, fully developed nucleate boiling, heat transfer 3−1787
temperature fields produced in a workpiece by repeated applications of a source of heating, numerical calc. 3−24962
tube, by radiation, heat transfer rates calc. at thermal entry section *(Russian)* 3−6378
turbulent atmosphere of light beam, intensity fluctuations *(Russian)* 3−3019
upper atmospheric during aurorae, estimation of heating and cooling powers 3−34906
Cu-Al alloys, influence of precipitation of γ_2 phase on order-disorder transformation 3−27617
W-Mo, steel, electron bombardment, thermal characteristics *(Russian)* 3−12326
heating elements
see also electric heating
paint-on vacuum system heater, colloidal dispersion of graphite 3−28509
Heaviside layer *see E-region*
heavy water
see also nuclear reactors
density effects on dynamic struct., spin-lattice relax. obs. 3−1566
dioxane D_2O system, u.s. study of molecular association 3−21790
enrichment, Sulzer rectifying plants 3−23439
e.s.r. linewidth variation with temp., comparison with heavy water 3−2365
ice, dispersion relations at 223K from neutron scatt. 3−20829
molecular anharmonic force constants *(Russian)* 3−1191
molecules, formation of H^+ and D^+ by 18-40 eV electron impact 3−4479
neutron moderation, Monte Carlo studies, for time of flight expts. 3−16501
nuclear reactors, prospects for use and potential capacities of CIRENE reactor *(Italian)* 3−23413
production capacity, Canada 3−1081
heavy water continued
production processes 3−19902
radiative decomposition at high temps. and press. 3−18792
Stark splitting of millimetre wave transitions, meas. technique 3−25763
u.s. absorpt. excess, from relax. times and relaxing compressibility 3−4813
vapour, localized excess electrons 3−31241
$CuCl_2.2D_2O$, zero field deuteron mag. reson., quadrupole consts., internal field, fine struct. *(French)* 3−21339
HDO in water-nonelectrolyte mixtures, i.r. intensities 3−8568
H_2O-D_2O mixture, neutron scattering, structure factor 3−1651
height measurement
ionospheric irregularities, height determ. with radio holographic method 3−16069
magnetic disc head flight height measurement technique 3−10577
moon, distrib. for maria, continental region and near side *(Russian)* 3−16185
sea level, vertical crustal movements along E. coast of United States 3−15890
Heisenberg model
algebraic representation for spin operators of Liu and Chow, erroneous results 3−18286
amorphous magnet, constant coupling approx. 3−11998
anisotropic classical ferromagnet, critical behaviour of cubic systems 3−38945
antiferromagnet, alternating, linear, exciton interactions rel. to susceptibility 3−34075
antiferromagnet, dynamical props., comparison of equation of motion and diagrammatic techniques 3−21198
antiferromagnet, model, Van der Waals coupled spin systems with a Heisenberg interaction 3−18289
antiferromagnet, rutile structure CoF_2, two-magnon neutron scattering 3−21197
antiferromagnet, rutile structure MF_2, (M = Ni, Fe, Co), two-magnon light scattering 3−21196
antiferromagnet, two-magnon correlations, equation of motion study 3−21195
antiferromagnet uniform chain, instability, Heisenberg interaction in Hartree Fock approx. 3−38943
antiferromagnets with arbitrary interaction range, zero-point effects 3−15326
chain, anisotropic one-dimensional, eight-vertex model 3−28976
critical behaviour of classical Heisenberg ferromagnet with many degrees of freedom 3−34070
decoration transform. for dilute anisotropic model 3−11997
dilute ferromag. model, nonmag. impurity effect at Curie temp. 3−8323
eight-vertex model in lattice statistics and 1-d anisotropic Heisenberg chain, fundamental eigenvectors 3−26160
eight-vertex model in lattice statistics and Heisenberg chain, eigenvectors of transfer matrix and Hamiltonian 3−26161
exchange model, self-consistent selection of ferromagnetic representation 3−38950
ferrimagnet, Heisenberg uniaxial Neel type, spin wave theory, external mag. field effects 3−11995
ferrimagnet, Heisenberg uniaxial Neel type, spin wave theory, mag. props. 3−15325
ferromagnet, amorphous, mixed, Curie temp. and mag. suscept. 3−27350
ferromagnet, amorphous, spin-wave spectrum, calc. 3−30593
ferromagnet, anisotropic, crit. temp. 3−24553
ferromagnet, classical, Monte Carlo calc. of scaling equation of state 3−34077
ferromagnet, compressible, susceptibility index 3−30595
ferromagnet, cond. band influence via s-d exchange interaction *(German)* 3−5091
ferromagnet, exchange interaction of surface spins causing surface antiferromagnetism 3−38951
ferromagnet, Fermi operator description 3−27351
ferromagnet, Feynman graph expansion for equation of state near crit. point 3−15330
ferromagnet, impurity spin orientation, calc. by Green function method 3−8322
ferromagnet, localised modes due to impurity pairs 3−27366
ferromagnet, spectral function calcs. 3−8326
ferromagnet, spin 1/2, perturbation theory 3−15329
ferromagnet, spin system with two-dimensional defects, localized states *(Russian)* 3−8320
ferromagnet, two-dimensional, critical temp. depend. on anisotropy 3−30590
ferromagnet with hard magnetisation axis, spin waves 3−30635
ferromagnet with spin 1/2, comparison of Pauli operator and drone-fermion calc. methods 3−21202
ferromagnet with uniaxial anisotropy, calc. of magnon spectrum and spin wave damping 3−34080
ferromagnetic crystals with two sublattices, low temp. analysis 3−36697
ferromagnetic film, finite size and surface effects on critical behaviour 3−15332
ferromagnetic film, weakly amorphous, density of spin wave states, calc. 3−30636
ferromagnetic spin system Heisenberg Hamiltonian with crystal field anisotropy, spin 1, diagram technique 3−34064
ferromagnets, Smoluchowski-type treatment of fluctuations at the critical point 3−34063
Heisenberg Hamiltonian, symmetric, eigenvalue solution in spin-wave representation 3−11996
LEED, rel. to depend. of exchange refl. on diffr. conditions 3−23995
linear chain, spin dynamics 3−18292
linear chain (nearly one-dimens.) system, interchain coupling effects on e.p.r. 3−18354
linear chain molecules, and Ising model to describe mag. coupling 3−21203
linear chain of classical spins, spin-wave modes 3−5090
Mossbauer effect forced harmonic oscillator and zero-phonon transition 3−31983
nuclear spin interactions in ferromagnetic insulators, excitation spectrum 3−34066

Heisenberg model continued
nuclear spin interactions in ferromagnetic insulators, thermodynamic props. 3—30592
one-dimensional anisotropic X-Y-Z model, thermodynamics 3—15328
one-dimensional antiferromagnet, determ. of spin-wave spectrum when long-range order is absent 3—27348
one-dimensional system, TANOL radical, l.f. behaviour of spin-correl. functions 3—2454
paramagnet, dynamic properties 3—18285
paramagnet, spin fluctuations, kinetic theory and approx. high temp. soln. 3—34078
planar Heisenberg ferromagnet, low temp. behaviour 3—34071
rare earth metals, collective excitations, Heisenberg ferromag., effect of strong cryst. fields 3—2243
spin system with long range order, critical relaxation 3—27347
spin systems in d dimens., time-depend. fluctuations 3—38947
spinel ferrimagnet containing two types of ions, Weiss mol. field coeffs. 3—2229
susceptibilities for ferro- and antiferromagnets, calcs. using lattice Green's function 3—22752
two-dimensional 3 × 3 square lattice, ferromag. and antiferromag. coupling 3—38944
two-dimensional ferromagnet, spontaneous magnetiz., exchange interaction effects *(French)* 3—30587
two-time spin-pair correlation function of magnet at infinite temp. 3—34069
Co alloy, spin config. and intrinsic coercive field of narrow domain walls 3—8391
Cr^{3+} extra-exchangeable ions in polynuclear complex salts, luminescence, spin-spin interaction in Heisenberg model *(Russian)* 3—36927
K$_2$MnF$_4$ and K$_2$NiF$_4$, specific heat of two-dimensional Heisenberg antiferromagnets 3—34114
Heising modulation *see amplitude modulation*
helicity (elementary particles) *see elementary particle theory*
helicons
see also solid-state plasma
collisionless plasma, helicon turbulence, calc. *(Russian)* 3—7533
semiconductor, effect of quantizing mag. fields *(Russian)* 3—2122
semiconductor, finite, overheating instability of helicons 3—33945
semiconductor, helical instability in strong mag. fields, quasiclassical discussion *(Russian)* 3—8217
semiconductors, microwave transmission by helicons, satellite dimens. resons. 3—21103
K, Hall coeff. determ. by helicon transmission method 3—36594
Ni, ferromagnet, helicon mode, standing wave reson. study 3—18178
heliotron *see plasma devices*
heliports *see airports*
helium
see also helium atoms; helium gas; solid helium
abundance in RR Lyrae stars from pulsational blue edges of instability region 3—19008
adsorbed on graphite calc. of ground state energy for superlattice states 3—38723
afterglow, ambipolar-to-free diffusion, electron and ion temporal behaviour 3—20434
arc plasma, parametric heating with 0.337 mm laser radiation, threshold intensity calc. 3—17631
core-He-burning in massive stars, effects of semiconvection 3—13013
cyclotron-injected into stainless steel, effect on void form. characts. 3—35934
diffusion and solubility of NaCl, desorpt. study 3—33698
discharge, d.c., ion acoustic waves spontaneous excitation in He 3—23879
discharge, high pressure, spectroscopic and plasma characteristics 3—30029
flash, evolution of Population II stars from main sequence 3—28193
flowing afterglow, pumped, excitation transfer, quenching reaction rate coeffs. 3—9056
flowing afterglow, pumped, excitation transfer, rate coeff. for rot. relax. of He$_2$ 3—9057
glow discharges, electron energy in Faraday dark space 3—30040
Grw + 70°8247, white dwarf, He$_2$ bands explained by model atmospheres 3—25452
H I region ionisation by soft X-rays and cosmic rays, comparison H/He ionisation 3—28293
HD 37017, He absorpt. line strength enhancement, binary mass transfer possibilities 3—22050
highly charged He-like ion lines, satellite spectra, solar flares, electron temperature, laboratory plasma spectra 3—3332
injected in proton irrad. steel, effect on void form. 3—11607
interplanetary, ionisation resulting in electromagnetic instabilities 3—13007
ion backscatt. spectra in planar channelling, oscillations stochastic model approach *(French)* 3—27589
ion beam interactions, unidirectional and interpenetrating in an external magnetic field *(Russian)* 3—32618
ion channelling in Fe, oscillating trajectories, backscatt. obs. 3—4778
ion distrib. in the low-latitude ionosphere 3—18884
ion implantation, in polycrystalline Nb, radiation blistering 3—17881
ion scattering from metallic surfaces, cut off of l.f. radiation 3—27588
ion-beam-plasma system, instability wave growth and surface waves propagation 3—23854
ions, fast, impact dissoc. into ions of O$_2$, CO and NO molecules 3—23621
jets, heavy ion recoils, absolute transport efficiency 3—35452
I Lacertae, open cluster, He abundance determ. 3—39718
low temperature nozzle beam source 3—20070
massive stars, secondary nucleosynthesis during core He burning 3—22041
metastable beam, scattering, from O$_2$ covered (100) surface of Ge 3—39204
negative ion source, with K vapour charge exchange 3—13407
NGC 2264, open cluster, He abundance determ. 3—39718
night sky, ionizing radiations, rocket study 3—3051
helium continued
plasma, electronic recomb., He$_3^+$ ions contrib. 3—20435
plasma, ion acoustic nonlinear turbulent fluctuations, ion mass effect 3—23878
plasma, lifetime of charged particles calc. 3—36149
plasma, O$_2$-He-Ar mixture, external high frequency modulation of an electron beam, heating effect of ions *(Russian)* 3—17627
plasma, supersonically streaming beam, injection into mirror machine 3—30001
plasma, weakly ionised isothermal, in magnetic field, stability 3—36179
plasma glow discharge, local transient phenomena induced by microsecond periodic pulse 3—20611
plasma helical microwave source in high density high magnetic field regime, operating props. 3—29993
plasma in Heliotron-D stellarator, confinement studies 3—20596
plasma produced by α-particle irradiation of high pressure gas, meas. of optical line intensities from excited states 3—20552
plasma production and heating by laser beam 3—29991
plasma RF heating in Heliotron D 3—20554
plasma shock waves in an e.m. shock tube, shadow photography obs. 3—29986
positive column, electron temp. and density meas. *(Japanese)* 3—30011
proton-He magnetosphere, propag. of Pcl micropulsations 3—5477
quasi-elastic scattering cross sections in tissue like media 3—3593
red giant variable star models with mass 0.7-10 M$_\odot$, comparison with R Corona Borealis stars 3—28173
refractivity, corrected for impurities 3—24672
II Scorpii, open cluster, He abundance determ. 3—39718
shock waves structured by nonequilibrium ionizing and thermal phenomena 3—29884
silicate glasses, diffusion rates and solubilities as a function of SiO$_2$ content 3—4883
solar wind abundance, velocity and flux dependence 3—16131
solar wind relative abundance variations, dependence on solar activity 3—16137
spark chambers, time characteristics and efficiency 3—22469
stars, Stephenson-Sanduleak 3378, B-type star, UBV obs. 3—25453
stellar spectra of the bright variable α Centauri, model 3—16228
strong He line stars, UBV and UBVr obs. 3—25466
supersonic jets, noise generating disturbances, holographic study 3—5705
weakly ionized plasma, propagation of ion acoustic waves *(German)* 3—14540
^{38}Ar/^{39}Ar ages of chondritic meteorites, determ. of cosmogenic rare gas production rates 3—5428
CO$_2$-He and CO$_2$-N$_2$-He plasmas, small signal gain coeffs. for rot.-vibr. transitions *(French)* 3—7223
Er films, He implanted, dimensional expansion and surface microstructure 3—7994
ErD films, He implanted, dimensional expansion and surface microstructure 3—7994
H/He surface ratio defect on C-star spectra 3—13023
He + H$_2$ spark chambers, time characteristics and efficiency 3—22469
He CO$_2^+$N$_2^+$ mixture expanding in supersonic jet, light amplification factor 3—19607
He I 4471/He II 4541 ratio meas. of O-type stars for effective temp. scale determ. 3—28187
He I 5876 Å line in O-star spectra 3—13028
He I D$_3$ emission line in coronal spectrogram taken at 1970, March 7 eclipse 3—18941
He I lines in O type stars spectra compared to models 3—28186
He II lines in O type stars spectra compared to models 3—28186
He II resonance lines, plasma polarization shift at 304 and 256 Angstroms 3—17355
He-O$_2$-CS$_2$, pulsed discharged mixture, relative populations of vibr. excited CO 3—10496
He-Xe, vapour + solid equilibrium 3—33664
He + Kr, vapour + solid equilibrium 3—33663
He$^+$, energy dependence of channelling in Si overlaid with Au films 3—33581
He$^+$, energy spectrum of field ionisation at single atomic site 3—35508
He$^+$, interplanetary, annual variation in velocity distribution at 1 AU 3—13006
He$^+$ ions, coherent excitation in passage through Ag crystal film 3—24170
He$^+$ ions, excitation by transmission through Au cryst., absence of channelling effect 3—1110
He$^+$ plasma, d.c. electric resistivity perpendicular to mag. surface, meas. 3—11471
He$^+$ scattering in the weakly screened Coulomb field of Au nuclei 3—11182
He^{++} in solar wind, kinetic temp. 3—28139
He$_2$, double-exchange contrib. to first-order interaction energy 3—11329
He$_2$ mol., local orbitals method, overlap approx. 3—33076
He^{2+}, diffusion limited destruction of metastable states 3—11470
He$_2^+$ electronic recombination, afterglow analysis technique 3—17704
He$_2$X$^1\Sigma_g^+$ pot., intra-atomic correl. energy, ab initio calc. 3—23523
^{3}He polarized particle beams, current state of physics and technology for prodn. 3—35727
^{3}He$_2^+$, ^{4}He$_2^+$, electronic-recomb. coeff. 3—33150
^{4}He, backscatt. by Si, Au, Cu, ion fraction, 25-150 keV 3—30912
^{4}He ions, specific energy loss, in Si, amorphous, polycrystalline and single crystal 3—17884
$He^* + H_2 \rightarrow HeH^+ + H + e$, 0.05 to 10 eV, cross-sections 3—9052
MgO:He, ion implanted, photolum. from damage related defect centres 3—21463
Nb, He implantation and re-emission at elevated temps. 3—7014
helium, solid *see solid helium*
helium-3 interactions
see also nuclear reactions and scattering due to helium-3
$\gamma ^3He \rightarrow pd$, disintegration in $\Delta(1236)$ region 3—6617
helium-3 scattering
see also nuclear reactions and scattering due to helium-3
elastic, odd-even absorption and level struct. of ^{6}Be 3—17258

helium atoms
adsorbed monolayers, mobile limit, low-temp. sp. ht. 3−33682
adsorption on graphite, study by plane wave method *(Italian)* 3−30531
afterglow, decay of 2^3S_1 state 3−14620
autoionisation and He^- autodetachment following bombardment by H^+, H_2^+, He^+, He atoms 3−23490
autoionizing states, low energy electron impact, 42-48 eV, 57-65 eV, excitation struct. 3−7065
collisions with CO_2, shock widening and probability of P20 (00°1-100) CO_2 transition *(Russian)* 3−29754
collisions with Hg atoms, depolarisation of Hg resonance radiation 3−33060
collisions with metastable Xe, Xe^+ excitation 3−17380
collisions with N_2, second positive (0, 0) transition, emission cross sections 3−11327
collisions with Tl atoms, excitation transfer between the $6^2D_{3/2}$ and $6^2D_{5/2}$ states 3−14318
Compton scatt. of 25 keV electrons 3−38237
constrained density matrix study of simple basis sets of 1s-type orbitals 3−29469
correlated wavefunctions form calc. 3−20008
correlation energies computation using strong-orthogonal correl. functions 3−7037
Coulomb holes and expectation values, explicitly correlated wavefunctions 3−23464
elastic electron-neutral atom interactions meas. at ultralow energies 3−29525
elastic scattering of positrons, phase shifts 3−17375
electron emission spectra excited by proton impact, $2s(^1S)$ autoionisation state 3−7067
electron excitation of $(1s, nd)^1D$ and $(ns, mp)^1P$ states 3−26591
electron impact, Coulomb effects in final state of ionizing collision 3−26595
electron impact, exchange excitation cross sections, calc. using Ochkur approx. 3−11172
electron impact double ionisation, classical collision theory appl. 3−38234
electron impact excitation of forbidden transition in range 300 to 500 eV 3−38233
electron impact excitation rates for transitions in He I and II 3−38241
electron loss passing through inert gases and molecular H_2, N_2 and O_2 3−11166
electron sactt., variational calcs. 3−4387
electron scatt., elastic, optical pot. model 3−20047
electron scatt., elastic, second order pots. 3−26590
electron scatt., polarization role in intermediate energy range 3−1125
electron scatt. inelastic, generalised oscillator strength and excitation cross-section 3−23495
electron-impact excitation of 2^1P state, differential and integrated cross-sections by distorted-wave approx. 3−23500
electron-impact excitation of p-levels *(German)* 3−1124
excitation by electron impact, alignment relaxation meas., collisions and cascades influence *(German)* 3−14311
excitation by fast protons, charge exchange study 3−38244
excitation by H atoms, spectroscopic analysis of radiation emitted during decay of products 3−26607
excitation energy of 1^1S-2^1S, transition-matrix calc. 3−20006
excitation transfer, 3^3D-4^3D levels, by electron impact 3−23499
excitation transfer cross section, 3^1P state, temp. depend. 3−23502
excited state wavefunctions calc. 3−38205
excited states, Coulomb hole calc. 3−38206
fast, impact dissoc. into ions of O_2, CO and NO molecules 3−23621
fine struct. calc. for 2^3P state 3−33016
fine structure, calc. of ^3P contributions 3−20000
ground state calc. using series soln. of nonrelativistic three-body problem 3−32444
Hartree-Fock orbitals derivation from resolvent of hydrogen atom 3−7031
Hartree-Fock oscillator strengths, perturbative corrections 3−11126
Hartree-Fock polarisabilities calc. 3−29486
He^{2+}, 4686 and 3203 lines, temp. determ. from relative line-to-continuum intensity 3−14303
in high intensity laser field perturbation atomic levels near ionization threshold 3−1114
inert gas-Br_2 systems, energy transfer collisions, trajectory studies of atomic recombination reactions 3−26732
ionization cross section for slow electron ejection by fast charged particles 3−33045
ions, charge-exchange phenomena with Zn, Cd, Hg, Te, spectroscopic study 3−33058
ions, distribution function for electron angular correlation 3−4354
ions, excitation of K X-ray spectra of Al metal, oxide and nitride, chemical effects 3−4365
K-shell photoionisation cross section and threshold energy determ. 3−14300
metastable, excitation of Rb ions in thermal collisions 3−33057
metastable, impact on metal surfaces, flux determination by measurement of secondary electron ejection coefficients 3−19324
metastable, Penning ioniz. reactions with diatomic mols. 3−29731
metastable, photoionisation meas. near threshold 3−38226
metastable $(1s2s{:}^3S)$, hyperfine pressure shift, many body perturbation theory study 3−11186
metastable atom density calc., fine struct. effects *(French)* 3−38198
metastable atoms, collisions with inert gas atoms, Penning ionization spectra 3−11154
metastable atoms in 2^3S and 2^1S states, chemiionisation in collisions with H and H_2 3−38252
metastable atoms in (2^1S) and (2^3S) states, cross sections for chemiionisation with H 3−38253
metastable formation, excitation functions, comment on previous report 3−7080
metastable states, photoionisation above n=2 threshold, determ. of differential cross sections for photoelectric transitions 3−11150
modified effective electron model for interaction energy calc. 3−7088
multiconfiguration wavefunctions, two-by-two rot. method applic. 3−7038

helium atoms continued
multiply charged ions, plasma parameters determ. for plasma-beam discharges 3−23916
odd-parity D state positions, variational calc. 3−4347
photoionisation, cross section calc. above n=2 threshold 3−11151
photoionisation absorption coeffs. in 60−230 eV energy range 3−11152
plasma, low temp., atomic and mol. afterglow 3−23915
polarisability and shielding factors effective field calc. 3−29488
polarisation of the 492.2 nm line (excited by electrons), at energies near 60 eV 3−17376
positron -He scattering length, variational calc. using approximate target wavefunctions 3−14310
proton scatt., total differential cross section 3−33059
quenching of 2^1S_0 metastable state by elec. field 3−29498
scattering and bound-state props., many-body Green's functions appl. 3−11122
scattering from Ag surface, one-phonon contrib. 3−11791
scattering from metal surface, two-phonon terms 3−11792
scattering of zero energy electrons, simplified model 3−14309
solar flare particles, charge states and energy dependent composition 3−35025
solar flare X-ray spectra, He-like lines of Si and S 3−35056
spontaneous emission, forbidden $2^3S_1 \rightarrow 1^1S_0$ line, obs. and transition rate meas. 3−38220
Stark shift in low elec. field 3−11127
stimulated Raman scatt. and two-photon absorpt. on excited atoms in plasma 3−4672
structure 1^1S ground state, expectation values, lower bounds 3−29457
time-dependent studies of vacuum u.v. emissions 3−29530
total cross sections for charge transfer and stripping of Al^+, Cr^+, Er^+, and Er^{2+} in He and N_2 3−11181
Van der Waal's broadening of Fe I emission lines induced by neutral He 3−35981
variational calc. of third harmonic coefficient 3−11121
vibrational relax. of CO 3−23617
X-ray coherent scattering amplitude 3−4377
D_3 filter observations of solar prominences rel. to structure 3−35038
H-He potential determ. from molecular beam expts. 3−11165
H_2-He collisions, classical S-matrix elements for vibrational excitation in three dimensions 3−7251
$H_2^+ + He \rightarrow HeH^+ + H$, 1-25 eV, crossed beam studies 3−39439
He, electron impact, double ioniz. cross sections 3−20045
He D_3-line study of chromosphere during 1968, Sept 22 total aclipse *(Russian)* 3−12972
He I, beam-foil excitation, zero-field oscillations in $3p\ ^3P \rightarrow 2s^3S$ transition 3−29533
He I, off-diagonal matrix elements in Stark-broadening of neutral lines in plasma 3−4358
He I, photoioniz. reson. profile parameters of $3s3p^1P_1$ two-electron excitation 3−33035
He I 10830 Angstroms triplet, near-by lines of water vapour absorption from the atmosphere 3−31387
He I 4026 2^3P-5^3D, 5^3F profile at low electron densities, non-adiabatic ion dynamic contribs. 3−20019
He II, determ. of Rydberg constant from n=3-4 (4686 Å) line complex 3−13205
He II reson. lines, plasma polarization shift 3−33338
He II spectral lines used in determ. of Rydberg const., dependence of line structure on excitation conditions 3−13206
He II underabundance in galactic centre, H and He radio recombination line obs. 3−35194
He-Ar atom pairs, interacting, dipole moment 3−29538
He-As mixture, c.w. laser oscillation in As^+, charge transfer reaction 3−37959
He-D_2 total scatt. cross sections, 760-2600 m/sec 3−1294
He-H_2 thermal opacity in atm. of major planets 3−31576
He-He^+ collisions, 80-1100 keV, cross sections for excitation of 4^1S-, 4^1D- and 3^1P-levels 3−4395
He-Li, (Na), collision-induced absorpt., model pot. calcs. at 300 and 1000 K 3−38230
He-Li^+ collision, inelastic transition mechanism 3−20061
He-Ne discharge, 3.39 μm Ne linewidth, mixture composition depend. 3−32546
He-Ne low energy potential structure in total transfer cross sections 3−26586
He + He collisions, total cross section, energy depend., 0.30 to 3.00 keV 3−29536
He + He ionizing collisions, metastable, rate coeff. 3−29528
He + He scatt., low energy, scaling rule derivation 3−29521
He + LiF, atom-solid elastic scatt., theoretical study 3−34445
He + N_2^+ collisions, 0.5 to 3 keV, elastic scatt. and vibro-rot. dissoc., classical theory 3−38320
He + O^+, low energy collisions, pot. curves and inelastic cross sections 3−35986
He^- ions, detachment cross sections in He, H_2 and Ar gases 3−14312
He^+, low-energy elastic scatt. by Ne, curve crossing 3−20062
He^+, Rydberg constant derivation 3−20022
He^+, $S_{1/2}$-$P_{1/s}$ Lamb shift in n=5 state 3−26566
He^+ 4686 Angstroms line search in solar low chromosphere and studies of He I 4713 Angstroms line 3−31555
He^+ collision with methane mol. rainbow phenomena meas. in differential elastic cross section 3−29535
He^+ collisions with Zn, Cd and Se, charge transfer into excited states 3−14313
He^+ impact on Cu clean surface, light emission 3−18501
He^+ near resonant charge transfer collisions with K, Rb, and Cs, long-range forces effect 3−35976
He^+ prod. in He_2^+-He collisions near threshold 3−38248
He^+-Ne inelastic collisions, uniform WKB theory 3−20069
He^+ + He collisions, direct and exchange excitations, u-g symmetry effect 3−38243
He^+ + Ne, elastic differential scattering expts., investigation of two state molecular system 3−11185
He^+ + Ne, semiclassical collision theory within Feynman path integral formalism 3−28951
He^+ + Ne collisions, differential scatt. cross section for Ne excitation 3−33055

helium atoms continued
- He^{++}, elastic differential scatt. by He, collision energies 4 to 75 eV 3−38249
- $He^{2+}+H$ collisions, electron transfer and excitation, coupled-state calcs. 3−26602
- $He^{2+}+He$ collisions, electron capture and excitation 3−26604
- $He^{(+)}+He$, ioniz. processes in slow collisions 3−26605
- HeH, long-range hyperfine shift computation 3−26611
- ^{3}He, hyperfine structure studies by zero-field quantum beats 3−17357
- $^{3}He/D_2/HCl$ D_2 vibrational relaxation 3−23628
- ^{4}He, fine struct. intervals meas. by level crossing *(French)* 3−38216
- ^{4}He, zero-field level-crossing resons. and weak mag. field meas. 3−7058
- ^{4}He $5^{1}D_2$ state, lifetime and alignment meas. by beam-foil level crossing 3−23483
- ^{4}He fine-structure meas. by zero-field quantum beats 3−11130
- ^{4}He I, fine structs. from intensity modulations in radioactive decays *(French)* 3−17336
- $(^{4}He\ \mu)_{2s}{}^{+}$ ionic system, meas. of Auger effect, contribution to de-excitation of system 3−26613
- $^{4}He/D_2/HCl$ mixtures, D_2 vibrational relaxation 3−23628
- ^{4}He-^{4}He, repulsive pot. up to 0.14 eV, from inversion of total cross-section meas. 3−38254
- $^{4}He+{}^{4}He$ scatt., Ramsauer-Townsend effect 3−20036
- $He(1s^2)$, ionisation by H impact 3−20063
- $Li^{+}+He$ collisions, charge exchange, rot. coupling 3−20059
- N_2 and He mixture, spectral intensities, effect of different parameters, detection method *(Russian)* 3−35541
- Na/He atom pair, avoided crossings among excited states 3−20037

helium compounds
- HeH^{+}, 10 keV, dissociation, collision induced, rotational predissociation of the $X^{1}\Sigma$ state 3−17463
- HeH^{+} isotopes, quasibound states theory, comparison with experiment 3−26714
- $HeH^{+}+H\rightarrow H_2{}^{+}+He$, 1-25 eV, crossed beam studies 3−39439

helium gas
- atmospheric budget, ion pumping by solar wind during geomagnetic field reversal 3−12757
- blowing in air, heat and mass transfer obs. 3−1319
- breakdown at 10.6 micron, loss mechanisms 3−23665
- bubble growth in cyclotron implanted Type 316 stainless steel 3−27043
- bubbles in α-irrad. W 3−18656
- bubbles in irrad. V, nucleation and distrib. 3−33572
- charge changing and electron loss cross section for $C^{4+}(N^{4+})$ ions 3−11178
- dense, electron mobility, model for structurally disordered systems 3−33858
- depolarisation of negative muons *(Russian)* 3−14306
- discharge, electron energy distribution and electrical props. of striations 3−36224
- discharge, positive column, transition from homogeneous to striated state 3−4686
- discharge, pulsed, elec. and opt. meas. *(Russian)* 3−7578
- electron impact, mean energy loss per ion pair and stopping power 3−26592
- fission release from neutron irradiated B_4C 3−26529
- flow, heat transfer with wall temperature up to 2800K *(Russian)* 3−7389
- flow, heated laminarizing, in square ducts 3−36082
- foreign hot dense gas, shift and broadening of resonance lines of Ca, Sr, Ba 3−17345
- glow, negative, velocity distrib. of plasma electrons 3−1531
- glow discharge, effect of gas purification method on normal cathode fall of potential 3−38507
- glow discharge, initial stage of reactance oscillations 3−36225
- h.f. discharge stability at 95-105 MHz rel. to industrial trace gas chromatography *(French)* 3−432
- hot compressed, pressure shift and broadening of resonance lines of alkali and singly ionised alkine earth atoms 3−33033
- ion imaging in field ion microscope rel. to Ne 3−3875
- isotopic composition in solar corpuscular streams for solar history study *(Russian)* 3−12955
- laser, He-Ne, saturation parameter depend. on discharge current 3−6462
- laser, output, temp. obs. 3−16830
- liquefaction and purification 3−5832
- migration and release in PuO_2 fuel forms 3−19957
- mobility of mass-identified U^{+} and Hg^{+} ions 3−7308
- parametric acceleration of ions in alternating magnetic field, simulation of plasma transport processes *(Russian)* 3−13783
- permeability in glass, silica comp. depend. *(German)* 3−30284
- plasma electron temp. determ. from ambipolar elec. field reversal under mag. field 3−4676
- positive column discharge, improved probe curve analysis 3−4684
- resonance line, photoionization of atoms and molecules, electron angular and energy distrib. *(Russian)* 3−10077
- shock waves, generation by fast evaporation of superfluid films 3−7396
- in solids, influence on void form. during irrad. 3−24136
- solubility in glass melt *(German)* 3−7906
- speech translation by segmentation-expansion method 3−39839
- static structure factor, 4.995K, X-ray scatt. 3−36065
- thermal conductivity, column method meas. up to 2100 K 3−38338
- two stage shock tube for MHD power generation expts., gas dynamic characteristics 3−20351
- CH_4-N_2-He, working gas mixture for cyanide c.w. laser, operating conditions 3−13733
- CO_2-He laser, similarity law, disturbing electrodes effect 3−13730
- CO_2-N_2-He system, amplification rel. to temperature 3−19605
- Cd-He cataphoresis-laser, determ. of plasma charged-particle densities and electron temp. 3−16846
- H-He mixture, ionizing shock wave struct. 3−14416
- He, Boltzmann eqn. soln. for Navier-Stokes coeffs. at 1-20K 3−6367
- $He{:}CO_2{:}N_2$ c.w. waveguide laser, using B + O capillary tube 3−13732

helium gas continued
- He/N_2 gas mixture, dense phase gas solid suspension, positive expulsion fluidization tank 3−4619
- He-^{20}Ne laser with absorption cell, 0.63 μ line shift, line broadening *(Russian)* 3−7026
- He-Ar, modified Stefan cell for diffusion measurements 3−32214
- He-CO_2 laser, absorpt. coeffs. of emission by CO_2, NH_3 and water vapour *(Russian)* 3−6474
- He-H_2-D_2 gas mixtures, permeation through Pd tubes, model 3−7305
- He-Hg mixture, weakly ionized, electron distrib. function 3−14604
- He-Kr mixture, hypersonic vel. and absorpt. meas. from Brillouin spectra 3−1322
- He-N_2 modified Stefan cell for diffusion measurements 3−32214
- He-Ne, glow discharge in hollow sectionalised cathodes, cathode pot. step, current distrib. *(Russian)* 3−14629
- He-Ne discharge, meas. of Ne 3.39μ transition decay rates using laser Faraday rotation 3−29079
- He-Ne gas mixture, K^{+} mobility calc. 3−38424
- He-Ne laser, axial mode obs. using Fabry-Perot interferometer 3−190
- He-Ne laser, freq. stabilisation methods *(Russian)* 3−13725
- He-Ne laser, influence of elastic collisions on intensity of natural fluctuations *(Russian)* 3−22888
- He-Ne laser, mode selection at 0.63 μm *(Russian)* 3−13724
- He-Ne laser, modulation using ultrafast Kerr effect in CS_2, 10.6 μ 3−32581
- He-Ne laser, operation of pressed cathodes 3−22389
- He-Ne laser, relax. oscillations, range of existence, gas press. effect *(Russian)* 3−4094
- He-Ne laser, simple, single freq. for practical uses 3−32538
- He-Ne laser, single freq., freq. fluctuations rel. to sound press. and freq., external vibrs. 3−4083
- He-Ne laser, single freq., stabilisation *(Russian)* 3−13726
- He-Ne laser, transition processes at 0.63 μm *(Russian)* 3−10542
- He-Ne laser, with metal internal wall surface, active elements *(Russian)* 3−6466
- He-Ne laser beam, third-order intensity correlation function, meas. 3−13748
- He-Ne laser operating in TEM_{00} axial mode, optimum lasing conditions *(Russian)* 3−6465
- He-Ne laser output power depend. on discharge current, gas pressure and tube radius 3−6461
- He-Ne laser wavelength measurement *(French)* 3−9817
- He-Ne mixture, field adsorption and ionisation rates 3−22514
- He-Ne mixture glow discharge, initial stage of reactance oscillations 3−36225
- He-Ne visible gas laser design, r.f. excited 3−37958
- He-OCS laser, i.r. lines due to OCS and C atom 3−4088
- He-Se discharge, detection of small laser gains using dye laser assisted oscill. 3−32544
- He-Se laser, self-mode locking 3−22879
- He-Se^{+} discharge, for positive-column lasers, electron temp. and density 3−16833
- He-Xe discharge, pulsed laser action mechanism, excitation characteristics with external electrodes 3−33412
- He-Xe mixture, pulsed discharge generation mechanism 3−17701
- He-Zn hollow cathode laser, single pass gain measurement *(Japanese)* 3−19608
- ^{3}He, adsorbed on zeolite, n.m.r., spin-lattice and spin-spin relax. obs. 3−30344
- ^{3}He, density dependence of the diffusion constant and nuclear spin-lattice relaxation time by spin echo meas. 3−26699
- ^{3}He, n.m.r. relax. time, kinetic theory calc. 3−38307
- ^{3}He filled streamer chamber for pion scattering 3−314
- $^{3}He/^{4}He$ gas flowmeter for use with dilution refrigerator 3−22560
- ^{3}He-^{4}He system 5.5 to 240K, thermal diffusion factor in quantum region 3−23662
- ^{4}He, adsorption on exfoliated graphite, adsorption isotherms 3−36480
- ^{4}He, dense gas, electron mobility and localisation 3−38345
- ^{4}He, for cryostat, temp. down to 0.7 K 3−25701
- ^{4}He, PV isotherms at low temps., 2-20K 3−3773
- ^{4}He, viscosity, thermal conductivity self-diffusion coefficient calc. 3−14409
- ^{4}He neutron counter, line shape for energies 1 to 20 MeV 3−28662
- $Xe+He\rightarrow Xe^{+}+He+e$, metastable atom collision with excited ion production *(Russian)* 3−7072

helium nuclei *see nuclei with $A\leqslant 5$; nuclei with $6\leqslant A\leqslant 19$*

Hellman-Feynman theorem *see quantum theory*

hemodynamics
- *see also blood*
- abdominal aortic aneurysm, ultrasonographic and radionuclide angiographic study 3−37732
- aneurysm of circle of Willis, model, qualitative analysis of Austin's differential equation 3−33322
- aorta parameters, determ. using cost function analysis 3−9637
- aortic velocity and acceleration by u.s. device 3−37731
- arterial pressure waves, ventricular ejection, computer-aided analysis 3−28320
- biomechanics, hereditary processes, evolution in terms of difference-differential equations 3−35229
- blood velocity measurement, and cardiac output detn., continuous obs. using thermal method 3−25992
- brachial artery flow velocity meas. after cardiac surgery 3−39803
- brain, e.e.g., interpretation, blood circulation, electric currents and metabolism of the brain *(Swedish)* 3−13486
- canine circulatory response to graded stimulation of carotid chemoreceptors 3−9688
- carotid artery diameter and flow, noninvasive technique using Doppler effect 3−37733
- catheter type flowmeter, three electrode probe 3−400
- catheter-densitometer and thermistor systems, analogue computer correction of sampling distortion 3−25993
- cats, left ventricle rel. to flow and pressure source 3−36141
- cats, normal myocardial function and energetics in volume overload hypertrophy 3−37512
- cerebral, HP Ge detector array 3−28759
- cerebral blood flow, by Anger camera 3−22530
- cerebral regional blood flow, meas. using ^{133}Xe inhalation technique 3−28369

hemodynamics continued

- circulation in lower extremities using blood flow monitor system 8 3−419
- coronary circulation, effect of electric shocks 3−9694
- directional reversible currents of blood flow in spinal cord arteries 3−3404
- e.m. flowmetry in anaesthetized rats 3−3562
- flow rate and transport functions, from tracer expts. in closed circulations, indeterminacy 3−9648
- flowmeter, e.m., and use 3−395
- flowmeter, e.m. pulsed-field, design 3−396
- haemodialysers, flow and mass transfer, influence of non-Newtonian blood flow 3−17525
- hemorheology, flow obs. *(German)* 3−5672
- human portal vein, streamline flow 3−29925
- interactive computers as research aid 3−5627
- intra-arterial flow measurement, appl. of const. temp. anemometry 3−9646
- laminar blood flow through tapered tubes, expts. 3−9647
- mammalian embryo heart rate, prompt effects of X-radiation 3−25605
- n.m.r. transducer, pickup coil space filling coefficient calculation *(Russian)* 3−19248
- patient diagnosis, ultrasonics 3−420
- plasma substitutes and equivalent viscosity in oscillatory flow 3−25588
- polyelectrolyte red cell system, energy flow mediation 3−39765
- pressure and flow transmitter, FM telemetering 3−397
- pressure regulation by sympathetic nerve fibres and adrenal medulla in normotensive and hypertensive rats 3−22135
- pulmonary artery, dia. and pulsatile variation meas. using u.s. device 3−25987
- pulsatile flow in rigid tube, momentum integral soln. 3−9645
- rabbit, early development, red and white muscle 3−28322
- rats, effect of methylprednisolone on renal function and zonal distribution 3−16299
- red cells moving towards orifice, holographic verification of model 3−28760
- renal and plasma renin activity after renal artery constriction 3−22141
- simulated aortic valvular stenosis in pulsatile quasiphysiological flow, loss considerations 3−3901
- thyroid, compartmental analysis by ^{133}Xe clearance method 3−33328
- turbulence, effects on blood flow, finite element analysis 3−17495
- ultrasonic Doppler sensors for internal and external chronic use 3−37777
- Willis circle, functional dynamics 3−23809
- ^{99}Tc, quantitative radioisotope method for in vivo evaluation of cephalic circulation in the rat 3−31932
- ^{133}Xe multibolus fractionation technique for human cerebral blood flow distribution meas. 3−22526

Hertzsprung-Russell diagram *see stellar evolution*

heterodyne detection *see demodulation*

h.f. transmission lines *see high-frequency transmission lines*

high-energy cosmic ray interactions

- aeonic flux, detn. from lunar rocks 3−39576
- chemical and isotopic comp. determ. from balloon flights 3−9438
- galactic cosmic ray secondary electron prod. by collision of primary cosmic rays 3−31481
- hadron, discontinuity in burst and differential hadron spectrum 3−28100
- metagalactic X-ray prod. by relativistic dust grains 3−31487
- multiple prod. law for secondary particles *(French)* 3−25355
- primary energy spectrum break at $\sim 10^{15}$ eV, model based on hadron interaction characteristics and Fermi mechanism 3−9433
- propagation, $Z \geqslant 74$ nuclei, relative abundances as function of leakage time 3−12919
- proton-induced stars in 70 GeV/c interactions with nuclear emulsion *(Russian)* 3−34992
- two-particle correlations in inclusive reactions on light nuclei in emulsion, 50-10^5 GeV 3−34991
- π production by primary nucleons, contrib. to interstlar e^-e^+ flux 3−37279

high-energy nuclear reactions and scattering

- electron scatt. off bound electron, model approach 3−26431
- general survey of $B=0$, $B=1$ and $B=2$ exchange reactions involving light nuclei 3−38147
- hadron inclusive scattering, momentum loss spectra 3−32851
- hadron scattering, inelastic sum rule, influence of N-N correlations 3−29391
- hadron structure study in coherent production processes 3−29398
- heavy ion induced interactions, $E \geqslant 100$ MeV/nucleon, He emission 3−34993
- light nuclei, inelastic and charge exchange scattering of high-energy protons, integral cross section calc. 3−29390
- neutron rich light nuclei prod. in high energy reactions 3−6909
- nucleon-nucleus high-energy collisions, new method for primary energy estimation 3−10994
- optical potentials and eikonal approximations 3−14184
- particle-nucleus collisions test of multiparticle production mechanisms in particle-nucleon collisions at high energies 3−4204
- short range fragment emission from K^- interactions 3−11028
- K^- events on heavy nuclei, 1.5 GeV/c, triton, ^{3}He and hypernuclei prod. 3−26480
- K^- induced fragmentation of light nuclei in emulsion, 1.5 GeV/c 3−26479
- K^- interaction with emulsion nuclei, $_2^8$He nuclei obs. among hammer fragments 3−26481
- p elastic scattering, two coupled channel formalism including spin and isospin effects 3−26449
- p scattering on Be, C, Cu and Pb targets, 19-24 GeV/c, meas. of momentum distribs. 3−32850
- p-nucleus interactions at 24 GeV, asymmetric scattering of secondary pions 3−23323
- p annihilation cross-section, meas. of var. with mass number at 3 GeV/c *(French)* 3−17240
- pp total cross section meas. by Coulomb scattering at CERN ISR, 23 and 31 GeV 3−23155

high-energy nuclear reactions and scattering continued

- π^- production by 600 MeV protons on light nuclei, forward cross section calc. 3−19859
- $\pi^\pm$, model for production from nuclei bombarded by protons 3−14213
- $\pi^\pm$ production cross section from nuclei bombarded by protons 3−14212
- $2\pi^-\pi^+$ coherent generation by π^- on light nuclei 3−17267
- ^{27}Al(γ,2pn)^{24}Na, 1-7 GeV, meas. of yield curve, deduction of cross section 3−6817
- ^{27}Al(γ,π^+)^{27}Mg, 1-7 GeV, meas. of yield curve, deduction of cross section 3−6817
- ^{197}Au, proton and ^{16}O bombardment, fragments with $6 \leqslant Z \leqslant 15$ emission, $E=2.1$ GeV 3−17262
- ^{197}Au(γ,xn), 1-7 GeV, meas. of yield curve, deduction of cross section 3−6817
- ^{9}Be(p,π^+)^{10}Be, 185 MeV, meas. of energy spectra and angular distribs. 3−32855
- ^{9}Be(p,π^+)^{10}C, 185 MeV, meas. of energy spectra and angular distribs. 3−32855
- ^{12}C, elastic and inelastic proton scatt. at 1 GeV, differential cross sections 3−4317
- ^{12}C(γ,n)^{11}C, 1-7 GeV, meas. of yield curve, deduction of cross section 3−6817
- ^{12}C(π^+,πN) reactions at 130 MeV in bubble-chamber, cross-sections, impulse approx. model 3−38171
- ^{4}He, deuteron splitting and stripping reaction at 2 GeV, multiple scatt. model *(Russian)* 3−19838
- ^{4}He(p,2p)^{3}H nucleon ejection probability, short-range correlations 3−6804
- ^{127}I(γ,ypxn), 1-7 GeV, meas. of yield curve, deduction of cross section 3−6817
- K^- events in emulsion, meson hyperfragment obs. 3−26413
- ^{6}Li, elastic proton scatt., 20 GeV, optical model analysis 3−10995
- ^{6}Li, structure determ. from elastic and inelastic proton scattering at 1 GeV 3−23332
- ^{6}Li(e, e′p)^{5}He, 1200 MeV, s-shell and p-shell effects, p ang. distrib. obs. 3−10966
- ^{7}Li, elastic proton scatt., 20 GeV, optical model analysis 3−10995
- ^{a}Ni(A=64,58), proton interactions, isotopic effect in prod. of ^{3}H, ^{3}He at 660 MeV *(Russian)* 3−19867
- ^{a}Sn(A=112,124) proton interactions, isotopic effect in prod. of ^{3}H, ^{3}He at 660 MeV *(Russian)* 3−19867

high field effects

- *see also Poole-Frenkel effect*
- coupled acoustoelectric and thermoelectric instability, theory and expt. *(Russian)* 3−2099
- crystal, current-stimulated emission of e.m. waves, mechanism *(Russian)* 3−8200
- current and electron-phonon interaction in a strong electric field 3−38853
- ferromagnetic semiconductors, non-degenerate, transport properties 3−8194
- n-Ge, impurity ionisation 3−8192
- Gunn diodes, S-type current-voltage characteristics, impact ionisation effects 3−36613
- hot carrier energy relaxation time measurement, elec. field effects *(Russian)* 3−36615
- III-V semiconductors, cond., mm. wave investigation 3−21084
- impact ionization in Zener diode for reverse field breakdown 3−2098
- MBBA, isotropic phase, chem. and electrochem. activity rel. to d.c. conduction 3−15203
- metals, high field magnetocond., coherent state representation 3−24411
- oxide cathodes, elec. cond. through pores and grains, theory and obs. 3−15207
- polyethylene films, d.c. conductivity measurements 1×10^7 to 3×10^7 Vm^{-1}, model, hexane treatment 3−36614
- semiconductor, carrier fluctuations in current saturation region, time depend. *(Russian)* 3−8197
- semiconductor, carrier heating in microwave field, investigation method *(Russian)* 3−8198
- semiconductor, complex low freq. cond., imaginary part *(Russian)* 3−2101
- semiconductor, electron heating in elec. field, effect of finite width of cond. band 3−33921
- semiconductor, impact ionisation of impurity by carriers in magnetoabsorpt. spectra 3−5222
- semiconductor, impact ionization coeff., meas. using Schottky barrier 3−24445
- semiconductor, intervalley population transfer 3−5012
- semiconductor, Monte Carlo simulation of response to periodic elec. field 3−36611
- semiconductor, nonpiezoelec., acoustic wave generation by moving domains *(Russian)* 3−2145
- semiconductor, with negative differential cond., e.m. surface wave growth 3−18150
- semiconductor compound, parabolic bands with phonon scatt., hot electron high field transport 3−27265
- semiconductors, conductivity, arbitrary electron bandwidths and electron-thermostat coupling 3−38851
- semiconductors, influence of adhesions on characteristics of domain recombination *(Russian)* 3−11905
- semiconductors, many-valley, in strong alternating electric fields 3−24446
- solid-state plasma, screening breakdown, strong e.m. wave, h.f. effects 3−33943
- Al_2O_3 thin films, electroforming and dielec. breakdown *(Russian)* 3−30530
- Au-Fe, magnetoresist. meas. in high fields 3−36592
- B, beta-rhombohedral, field effect meas. rel. to transport phenomena 3−18158
- β-B, rhombohedral, Poole-Frenkel effect, current-voltage characteristics 3−36619
- Bi, magnetoresist., under pulse conditions in strong crossed elec. and mag. fields 3−24453
- Bi_2S_3 crystals, thermostimulated electron emission, ionisation energy of trapping centres calc. *(Russian)* 3−12206

high field effects continued
CdCr$_2$Se$_4$, Ferromag. semicond., high-field transport props. above Curie temp. 3−5017
CdCr$_2$Se$_4$, transport props. of non-degenerate ferromagnetic semiconductor below Curie temp. 3−15205
n- CdS, deviations from Ohm's law at 77 K 3−30485
CdS, two step current saturation on application of high voltage pulse and illumination 3−8195
CdS single crystals, effect on optical quenching 3−15223
CdSe, impact ionisation, breakdown, photoinduced switching, meas. of cond., Hall coeff., mobility, 4.2-300K 3−30487
CdTe, electron diffusion, applied field depend., Monte Carlo study 3−18149
CdTe, Monte Carlo calcs. on high field electron transport 3−8191
n-CdTe films, cond., trap and free carrier density, Fermi level position *(French)* 3−27262
Ce autoionising states, excitation by electron impact *(Russian)* 3−26599
Cs electron ionisation by impact, 6s and 5p, cross-section, Born approximation, threshold, Hartree method *(Russian)* 3−26598
GaAs, doped, absolute instability of e.m. waves and microwave emission 3−24461
n-GaAs, millimeter wave freq. response of hot electrons 3−2119
GaP amorphous film, ohmic, hopping cond. and Poole Frenkel behaviour obs. 3−36604
n-Ge, breakdown and recombination kinetics connected with excited states shallow donor 3−18166
Ge, charge carrier capture and reemission by shallow levels, field depend. 3−21091
n-Ge, elec. cond. anisotropy, hot electron drift velocity temp. depend. *(Russian)* 3−8196
Ge, electron velocity field characts., negative differential mobility, meas. 3−33913
Ge, high-field domain in electron-hole plasma 3−24444
n-Ge, hot electron Hall transport, calc. 3−38848
n-Ge, intervalley instability of current due to nonequilib. carriers 3−15208
Ge, third harmonic generation, in strong microwave field *(Russian)* 3−11924
Ge intervalley scattering of hot electrons, impurity and phonon mechanisms, transition times 3−33919
Ge single crystal, current-voltage characts. under strong injection conditions, mag. field effects 3−24447
Ge:Au, impact ionisation of deep acceptor impurities 3−33918
n-Ge:Ni, surface domains in strong elec. field, 77-300K *(Russian)* 3−8245
InAs, impact ionisation and scattering mechanisms rel. to band structure 3−21088
InSb, electron velocity field characts., negative differential mobility, meas. 3−33914
InSb, impact ionisation and scattering mechanisms rel. to band structure 3−21088
n-InSb, microwave props. in d.c. mag. field, hot electron effect, scatt. mechanism, 4-300K 3−21087
InSb film, carrier trapping at slow surface states *(Russian)* 3−30492
n-InSb microwave emission spectrum, avalanche impact ionised plasma, external magnetic field 3−33942
InSb thin films, electrical conduction, breakdown, intercrystalline potential barriers 3−38852
K, Hall coeff. determ. by helicon transmission method 3−36594
Se current saturation rel. to internal potential barrier, 77-290 K 3−30486
Si, Auger recomb., impact ionization, ionizing collisions transition rate rel. to electron energy 3−2103
Si, charge carrier capture and reemission by shallow levels, field depend. 3−21091
n-Si, hot electron energy relaxation time measurement, elec. and microwave field effects *(Russian)* 3−36616
Si p-n junctions, quantum efficiency of internal photoelectric effect and impact ionisation 3−24480
SiC, electron reson. tunnelling through superlattice, I-V characts. obs. in high fields 3−33910
Si$_3$N$_4$ film, Poole-Frenkel conduction mechanism *(German)* 3−15199
Te, electron domain propag. in the temp. range 77°K to 293°K 3−18156
Te-As-Ge-Si films 3−36668
ZnSe, electroluminesc., rel. to improved generation-recomb. processes in light emitting diodes *(German)* 3−15558
high-frequency discharges
beam-produced plasma, hot electron prod. 3−1506
electrodeless induction discharge, CO$_2$-N$_2$ laser pumping mechanism 3−32550
high frequency flare discharge, electric field effects, atomic absorption 3−33405
plasma electron cyclotron frequency, mag. field uniformity degree effect on radiation of harmonics *(Russian)* 3−14568
plasma filament, free, in high freq. field at high press., temp. determ. 3−17661
plasma parameters determ. using thermoanemometer-Langmuir probe method 3−20613
radiation-induced transformation of defects in CaF$_2$, BaF$_2$, and SrF$_2$ *(Russian)* 3−30694
resonantly sustained plasma at plasma reson. or cavity reson. *(French)* 3−38469
stability at 95-105 MHz rel. to industrial trace gas chromatography *(French)* 3−432
structured discharges in 4 MHz r.f. plasmas generated using solenoidal coil configs. 3−38509
Ar, low-power, h.f., optical and probe investigs. at atmos. pressure 3−23905
CO$_2$, excitation at low press. *(Russian)* 3−7593
Cd excited atoms in discharge effective slow electron collision cross sections 3−17699
O$_2$ plasma, mol. dissoc. obs. by e.p.r. *(French)* 3−36046
high-frequency effects
see also helicons; hot carriers; skin effect; solid-state plasma
antiferromagnetic semiconductors and metals, reson. between spin and MHD waves 3−34145
high-frequency effects continued
computer circuits and components, coupling analysis 3−29002
e.m. wave scattering and transformation by fluctuations in nonequilibrium plasma in semiconductor 3−18180
excitation of carrier density oscillations by light 3−15217
Franz-Keldysh effect on excitons 3−30435
metal, compensated, e.m. waves, l.f., spectrum and wave damping 3−8216
metal, h.f. e.m. phenomena *(Danish)* 3−15169
metal, with slightly distorted Fermi surface, cyclotron wave dispersion 3−30507
noble metals, h.f. waves and Landau Fermi-liquid effects 3−21104
semiconductor, e.m. wave propagation in rectangular waveguide, strong magnetostatic field effects 3−18175
semiconductor, helical instability in strong mag. fields, quasiclassical discussion *(Russian)* 3−8217
semiconductor, microwave harmonic generation, optimum slab thickness 3−18512
semiconductor, piezoelec., microwave absorpt. by bunched carriers in acoustoelec. domains 3−30896
semiconductor, two-valley, contact thermalisation effects, importance in high freq. devices 3−30508
semiconductors, low-temp. negative differential microwave conductivity following electron elastic scattering 3−38863
semiconductors, microwave transmission by helicons, satellite dimens. resons. 3−21103
semiconductors microwave Faraday rotation, transport and band parameters 3−15475
solid-state plasma, screening breakdown, high field effect, strong e.m. wave 3−33943
Bi$_{0.9}$Sb$_{0.1}$ crystals, magnetoplasma wave dispersion *(Russian)* 3−11922
GaAs, doped, absolute instability of e.m. waves and microwave emission 3−24461
n-Ge, free carrier Voigt magnetoabsorpt., X-band study 3−27486
Ge, third harmonic generation, in strong microwave field *(Russian)* 3−11924
n-InSb, microwave props. in d.c. mag. field, hot electron effect, scatt. mechanism, 4-300K 3−21087
n-InSb microwave emission spectrum, avalanche impact ionised plasma, external magnetic field 3−33942
K, Hall coeff. determ. by helicon transmission method 3−36594
Ni, ferromag. film, electromag. wave dispersion by spin waves 3−11923
Te-As-Ge-Si, frequency dependence of capacitance and conductance 3−27321
high-frequency heating *see radiofrequency heating*
high-frequency transmission lines
computer circuits and components, coupling analysis 3−29002
high-pressure effects in solids
adamantane, pressure-induced phase transition 3−20872
alkali halide crystal, metal-insulator transition at pressures up to 2000 kbar *(Russian)* 3−38804
alkali halide lattice, stability under hydrostatic pressure 3−7930
basalts, physicomechanical and electrical properties at high pressurs and temp. 3−25134
Birch-Murnaghan equation of states for rocks and minerals under high pressure *(German)* 3−34814
Borelius' equation of state, derivation and appl. to alkali halides 3−20844
carbon tetrachloride, high pressure polymorph at 10 kbar, crystal and molecular structure determ. 3−27016
coesite-quartz direct phase transformation at high press. 3−30258
conference, Bochum, Germany, (Mar. 1972) 3−9901
diamond, direct transform. from graphite under high static pressure 3−33672
diamond, electrical conductivity to metallic state at 1 Mbar 3−18204
electronic transitions and structure, review 3−33814
equations of state for solid phases, appl. to minerals 3−25118
ferroelectric semiconductor solid solutions, physical props. in vicinity of phase transition point 3−34306
Fusion curve nonlinearity rel. to Gruneisen coeff. pressure depend. 3−17963
glass, alkali metal-silicate, γ-irrad. at high pressures, e.p.r. of paramagnetic defects *(Russian)* 3−27417
glasses, i.r. spectra, intertetrahedral Si and Si-O stretching modes 3−12134
granite, water-saturated and under-saturated melting relations determ. 3−25121
lanthanide oxide fluorides, rhombohedral/cubic transitions, up to 40 kbar 3−33666
metal, hydrostatic press. effects at room temp. *(Japanese)* 3−12404
metal powders, compaction at up to 10 kbar, hardness, electrical resistivity 3−12379
metals, verification of Thomas-Fermi model under high pressure 3−20816
nylon 6, crystallisation, obs. 3−18732
phase transitions, pressure influence, review 3−24485
phenol, I-II transition under press. 3−24269
piezoelectricity, hydrostatic pressure effects rel. to cryst. symmetry 3−8522
piezoelectricity, hydrostatic pressure effects rel. to symmetry, zincblende crysts. 3−8521
polyethylene thin layer, friction coeff. and shear strength at high pressure 3−36359
polymer, mech. behaviour 3−31187
polymer, shock-compressed, physicomech. props. variation with loading 3−30204
rare earth alloys, heavy, magnetic properties, effect of hydrostatic pressure 3−36708
rare earth monochalcogenide, pressure-induced semicond.-metal and structural transitions 3−27221
rock fracture at pressures up to 7kbar, implications for earthquake faulting 3−5461
rock specimens, axial compression and destruction under high multilateral pressure 3−25133
steel, on long-term strength, Ar, H, Bi and Li pressure transmitters *(Russian)* 3−12378
transition metals and alloys, high pressure effects on transition temp. *(German)* 3−34026

high-pressure effects in solids continued
- triglycine fluoroberylate:Cu^{2+} single crystals, e.p.r., high-pressure influence 3−34191
- Ag isothermal compression and NaCl phase transform. at 300 kbar 3−36349
- Ag_2HgI_4, pressure depend. of transport and optical props. 3−30471
- AgI(α and β), polymorphism, elec. cond. obs. 3−7686
- Al, uniaxial compression effects on the third-zone Fermi surface 3−8093
- Al alloy, low-cycle fatigue, obs. *(Japanese)* 3−8861
- $AlMgBO_4$, sinhalite, olivine type structure, hydrothermal synthesis at high pressure *(French)* 3−38571
- Al_2O_3, sapphire, pressure effect on dielectric strength 3−27464
- Ba, supercond. transition temp. press. depend. 3−30561
- Ba ferrite, preferred orientation during hot pressing *(Russian)* 3−15743
- $BaTiO_3$, polarized ceramic, piezoelec. props. under uniaxial transverse compression 3−5164
- Bi, semimetal-semicond. transition under press. 3−33822
- BiSn, body centred tetragonal structure, obs. under high pressure 3−4732
- Bi(V), crystal structure 3−11584
- C, crystallite preferred orientation with heat treatment under high pressure 3−9002
- C, graphitisation under high press. 3−14999
- C graphitisation of diamond, high pressure and temp., nucleation and planar growth 3−12450
- Cd_3As_2, resistivity and Hall effect under high press. 3−27272
- CdS, cond. band effective mass anisotropy rel. to uniaxial compression *(Russian)* 3−15137
- Ce, alpha phase, low temp. elec. resist. under pressure 3−30451
- $CeOs_2$ polymorphism, lattice parameters, transition point 3−33488
- Co-Si system, rate of reactive diffusion, high press. eff. *(Russian)* 3−7962
- $CuCr_2O_4$, crystal structure changes, Jahn-Teller effect 3−27118
- EuB_4HP, on Eu^{3+} spectrum *(Russian)* 3−8113
- $EuCl_3.6H_2O$, on Eu^{3+} spectrum *(Russian)* 3−8113
- $Eu_2(SO_4)_3.8H_2O$, on Eu^{3+} spectrum *(Russian)* 3−8113
- Fe-Ni, f.c.c. alloy, pressure effect on Curie temp., rel. to magnetostriction anomalies 3−34126
- Fe-Ni shocked alloys, stability of mag. phase transition 3−36721
- $FeCl_2$, antiferromagnetic resonance, phase transitions 3−18374
- $FeNiBO_4$, dense warwickite type formed by hydrothermal synthesis at high pressure *(French)* 3−38571
- $FeTaO_4$, polymorphic transition from rutile to wolframite type structure under high pressure 3−33670
- Ga, Fermi surface under pressure, quantum oscillations in magnetoacoustic absorpt. 3−33789
- GaAs, band struct., pressure depend., combined pseudopot. calc. 3−27214
- GaAs, cond. band effective mass anisotropy rel. to uniaxial compression *(Russian)* 3−15137
- GaP, hydrostatic pressure effect on second order Raman spectrum 3−30824
- Ge, cond. band effective mass anisotropy rel. to uniaxial compression *(Russian)* 3−15137
- Ge, hot pressing effects on neutron topographs 3−23983
- H solid, low temp. compression using shock waves 3−32049
- H_2, molecular to metallic transition under press. 3−24271
- $HgSe_xTe_{1-x}$ pressure induced phase transitions 3−15011
- InP, electrorefl. spectra rel. to hydrostatic press. *(Russian)* 3−8610
- K complex, $K_2Pt(CN)_4Br_{0.3} \times 2.3H_2O$, elec. cond. at press. to 10^5 atm. 3−15180
- KH_2PO_4, u.s. absorption and phase transition 3−17939
- KNO_2 crystallography and disorder, phases, X-ray diffraction, analysis 3−11595
- La superconductivity, transition temp., pressure dependence, up to 250 kbar 3−38921
- $LaOs_2$ polymorphism, lattice parameters, transition point 3−33488
- $LiAlGeO_4$ phase transformations, zones, PT diagram 3−12607
- Li_2WO_4, phase transforms. at high pressure, structure obs. for III(IV) phases 3−33668
- MnSe modification of crystal structure, NiAs structure type, X-ray diffraction data *(German)* 3−11737
- Mo, mechanical behaviour under high press. at elevated temp. 3−30180
- Ni-Sb system, rate of reactive diffusion, high press. eff. *(Russian)* 3−7962
- $NiCr_2O_4$, crystal structure changes, Jahn-Teller effect 3−27118
- Pb:Ni, Ni interstitial diffusion under pressure up to 50 kbar 3−17996
- PbI_2, exciton spectrum between 1 and 3-5 kbar 3−21436
- PdCo dil. alloys, ^{57}Fe hyperfine field press. depend. up to 180 kbar 3−18306
- Pt complex, $(C_3H_7NH_3)_2PtCl_6$, hydrostatic, ferroelastic phase transition 3−38614
- ReC, synthesis of cubic form 3−24535
- Se, Raman spectra, first order freq., hydrostatic pressure depend. 3−27500
- Si, cond. band effective mass anisotropy rel. to uniaxial compression *(Russian)* 3−15137
- Sn, $\alpha \rightarrow \beta$ transform. under press., Mossbauer study 3−33673
- β-Sn, Mossbauer effect probability at high press. and Gruneisen const. 3−27457
- Sn complex $(C_2H_7NH_3)_2SnCl_6$, hydrostatic, ferroelastic phase transition 3−38614
- Ta, mechanical behaviour under high press. at elevated temp. 3−30180
- Te, Raman spectra, first order freq., hydrostatic pressure depend. 3−27500
- V_2O_3, electronic heat capacity meas. in metallic phase at high pressure 3−33684
- V_3Si, pressure induced elasticity changes 3−24176
- $Y_3Fe_{5-x}Ga_xO_{12}$, effect on ferromag. resonance line width rel. to dislocations 3−5138
- Zn-Al alloy, pressure effect during solidification on structure and tensile strength *(Japanese)* 3−27680
- $ZnGa_2S_4$ phase transformations at high pressures up to 150 kbar, crystal structure 3−11738

high-pressure phenomena and effects
see also high-pressure effects in solids
- alkali metal nitrates, specific conductances up to 12 Kbar *(German)* 3−11901
- p-azoxyanisole, p methoxybenzylidene n butylaniline, on the phase transitions in nematic liquid crystals 3−33453
- deep ocean pressure, effect on active semiconductor devices 3−3267
- diamond, carbonado type, usefulness at high press., 2.5-3 megabar *(Russian)* 3−3778
- gases, thermal cond. meas. 3−35369
- liquid mixture, binary, excess volumes at high pressure 3−27848
- liquids, thermal cond. meas. 3−35369
- moisture-saturated rocks, electrical conductivity at high pressures and temperatures 3−25141
- myoglobin single crystals, freezing, water/ice III, 2500 atmospheres lattice order, method 3−38576
- n-alkanes, rotational transition and melting curves, high pressure DTA apparatus 3−11721
- rock metamorphosis models 3−15914
- Thomas-Fermi model, shell structure effects on eqn. of state of matter at geophysical pressures 3−32435
- u.s. absorption in ethyl acetate at high pressures, sound absorption coeff. meas. *(Russian)* 3−4814
- AgI, ionic conduction under hydrostatic pressure 3−33690
- Ar, molar volume along melting curve up to 10 kbar 3−27105
- Cs, liquid, resist. and thermoelec. power calcs. under 40 kbar pressure 3−36586
- H_2O, radiative decomposition 3−18792
- Ne + Kr, solid-vapour and liquid-vapour equilibrium, to 95 atm 3−14996
- Th rare-earth carbide, superconducting, high pressure formed 3−21187

high-pressure techniques
- absolute high-press. microviscometer based on refr. index 3−6170
- absolute pressure gauge for high-pressure calibration 3−35385
- apparatus operating at 15 kbar in v. high mag. fields 3−28507
- autoclave, study of crystal growth and dissolution at high temps. 3−3776
- calorimeter constant volume heat capacity meas. of ^4He in h.c.p. phase 3−30309
- chemical reaction kinetics, spectrophotometric vessel *(Russian)* 3−9940
- conference, Bochum, Germany, (Mar. 1972) 3−9901
- cyclohexane, self-diffusion measurement, diaphragm cell, theory, results, analysis 3−10100
- device up to 10000 atmospheres, for electrical properties of semiconductor samples *(Slovak)* 3−139
- diamond, carbonado type, usefulness at high press., 2.5-3 megabar *(Russian)* 3−3778
- differential pressure transmitters, span-shift errors with static pressure 3−25709
- dilution refrigerator cryostat for high press. exprts. 3−9885
- droplet combustion, photographic investigation 3−3777
- fatigue testing machine, push-pull type for high pressure operation *(Japanese)* 3−12486
- float-transformer gauge, to meas. liq. surface level, multiposition *(Russian)* 3−19176
- flow calorimeter for heat capacity determ. of compressible fluids at high pressures 3−22284
- high temperature gel growth in pressurized chambers 3−12224
- i.r. absorption by fluids, measuring cells, corrosives, results 3−9920
- i.r. spectroscopy of molecular solids at low temps. *(French)* 3−13310
- liquid-vapour equilibrium at high pressure, apparatus *(Russian)* 3−9906
- meas. of selective refl. of spectral lines of vapours *(French)* 3−9943
- mechanical press., opposed-anvil, low-temp. work, pressure induced superconductor search 3−9902
- multiple-anvil sliding system, guide blocks and compressible pads for operation 3−28506
- multiplicator and superconducting magnet combined system 3−5855
- n-pentane, u.s. parameters, viscosity and density 3−25672
- optical cell, for biochemical reactions 3−28525
- piezometer, phase transformations in solids at high pressures 3−5853
- piston and cylinder apparatus for solid-state studies at 0 to 3 kbar 3−13261
- reaction kinetics, high pressure laser temperature jump apparatus 3−31257
- reaction kinetics in solution, review 3−34727
- reactor pressure vessel, hairline crack discovery by various methods 3−26495
- reverse valve, flat contact surfaces, up to 20 kbar *(Russian)* 3−9904
- specific heat of solids, simultaneous measurements of conductivity and diffusivity 3−9845
- tetrahedral anvil apparatus, optical studies under high hydrostatic pressures 3−13262
- toluene, expt. determ. of thermal conductivity at high pressures 3−22279
- transition metal oxides, oxyfluorides, oxyhydrides, high press. synthesis, struct. characterisation 3−14800
- u.s. velocity obs. in molten metals and fused salts 3−101
- valve, with manual and e.m. drive, operating at 2 kbar *(Russian)* 3−9903
- viscometer for metalworking fluids 3−451
- X-ray diffraction, polychromatic, powder sample, semiconductor detector, diffraction and fluorescence spectra, apparatus 3−11530
- X-ray diffractometer, high pressure unit up to 100 kbar for powder samples 3−13475
- H solid, low temp. compression using shock waves 3−32049
- H_2 purification by diffusion through Pd membranes at high pressure *(Russian)* 3−9905
- $NaMn_7O_{12}$, synthesis at 80 kbar, crystal structure study 3−27007
- O_2, vibrational relaxation times, measured by acoustic absorption 3−5781

high-temperature phenomena and effects
- basalts, physicomechanical and electrical properties at high pressurs and temp. 3−25134

high-temperature phenomena and effects continued
concrete, strengths and elasticity, effect of long time exposure to elevated temperatures *(Japanese)* 3−5352
materials characteriz. for chem. industry 3−8919
materials technology rel. to stress-rupture props. 3−8917
metal, spectral radiating power meas. at high temperatures, analysis 3−22287
moisture-saturated rocks, electrical conductivity at high pressures and temperatures 3−25141
quartz, blackness determ. 3−24666
quartz, fused, thermal conductivity, 350-1100K 3−24302
rocks, thermal parameters meas. for periodites in 300 to 1300 K temp. range 3−25140
solid, n.m.r. motional narrowing, phenomenological equation 3−36810
steel, martensite, anomalous fracture under torsion at temps. up to 1275°C *(Russian)* 3−12410
stellar atm., search for density and press. inversions in high-temp., low gravity models 3−37345
α-Fe, recrystallization dependence on deformation and annealing, following high temp. torsion deformation 3−15707
C, sublimation in flow of inert gas, 2800-3500K 3−26845
C-C composites, high-temp. strength up to 2000°C 3−31135
Fe_2O_3 polycrystalline powder ceramic, stress, high temp., grain size, porosity and O_2 partial pressure effects on creep 3−27738
$FeSi_2$, thermal conductivity meas. of metallic and semiconducting cpd. 3−18117
Gd transport props., electrical resistivity, thermal diffusivity 3−33864
Ge crystal, dislocation relaxation, internal friction meas. 3−17847
H_2O, radiative decomposition 3−18792
$LiAlGeO_4$ phase transformations, zones, PT diagram 3−12607
Mo-Rh alloys, elec. resistivity meas. at high temps. 3−36576
Ni based alloys, glazes prod. by high-temp. wear and friction 3−34590
Rh, elec. resistivity meas. at high temps. 3−36576
Si-SiO_2 semicond.-insulator boundaries, thermal equilibrium state, 1000C, work functions, surface charge calculations *(German)* 3−15248
SiO_2 pyrolytic film on semiconductor substrate, structure defects, transmission electron microscopy *(Russian)* 3−27197

high-temperature techniques
see also refractories
coated materials strength and creep testing apparatus for temps. above 1400°C 3−32047
crystal growth in controlled temperature gradient furnace 3−12232
Czochralski growth, film showing use of vertical thermal-imaging furnace 3−12294
DES-12 spectrometer, attachment for study of Raman spectra *(Russian)* 3−35412
electrothermal analyzer, Shimadzu, meas. of resistivity of Ni, Cu and stainless steel wire *(Japanese)* 3−13253
ferroelectric crystal, three dimensional vacuum furnace for neutron diffraction structure obs. 3−17720
flow-restriction gas-heater concept 3−19173
furnace temperature profile, thermocouple with high temperature shunting errors 3−9866
gel growth in pressurized chambers 3−12224
goniometer, Weissenberg, low and high temp. attachments 3−25653
i.r. absorption by fluids, measuring cells, corrosives, results 3−9920
levitation technique, for exposing single particle to high temp. gas 3−13528
l.f. tension compression loading of sample, low cycle load and holding *(Russian)* 3−9831
low cycle testing with holding at high temperature, programming unit *(Russian)* 3−12478
meas. of selective refl. of spectral lines of vapours *(French)* 3−9943
metal, spectral radiating power meas. at high temperatures, analysis 3−22287
metal hardening during fatigue testing, recording at elevated temps. 3−28465
metallography, accessories for IMASh-5C-65 and IMASH-9-66 instruments *(Russian)* 3−12481
micro differential thermal analysis apparatus, application as macro DTA *(Japanese)* 3−13258
microfurnace with large working space at 1600-1700°C *(Russian)* 3−9867
piston and cylinder apparatus for solid state studies at high pressure and temp. 3−13261
plasma arc spraying technology, book contrib. 3−11511
pyrometer, automatic thermoelec., high temp. differential thermal anal. *(Russian)* 3−9871
radiating power partially transparent mats. at high temps., meas. method 3−25694
radiation heating of specimens influence of sealed pyrometric devices 3−9865
sintering kiln, 1700°C, for nucl. ceramics *(French)* 3−34625
thermal analysis equipment, modifications 3−35380
thermal conductivity measurements of Earth materials at high temperatures using CO_2 laser system 3−18894
thermal expansion measurement, optical microtelescopes, target configurations and fiducial marks, experimental aspects 3−9863
thermal variation apparatus for X-ray diffraction expts. *(French)* 3−3881
thermometry above 1000 K 3−28494
translation balance for mag. susceptibility meas. *(French)* 3−6030
transparent refractory ceramics based on alkali earth oxides, baking process *(Russian)* 3−24972
u.h.v. outgassing meas. up to 2200K 3−38731
u.s. absorption coeff. meas., in solids 3−25673
u.s. velocity obs. in molten metals and fused salts 3−101
windowless reflectance furnace, for i.r. studies of corrosive melts 3−22290
X-ray diffraction, polychromatic, powder sample, semiconductor detector, diffraction and fluorescence spectra, apparatus 3−11530
X-ray diffraction furnace for structure obs. 3−26944
X-ray diffractometer chamber *(Slovak)* 3−22291

high-temperature techniques continued
X-ray diffractometer meas. at high temps, design of furnace for room temp. to 1000K range 3−28736
Al_2O_3, Lucalox, thermal conductivity meas., heat pipe technique 3−16399
Al_2O_3, sapphire, gradient furnace growth method 3−11572
K, saturated vapour press. meas., high b.p. substances 3−35384
Sm_2Co_{17}, Czochralski crystal growth in thermal imaging furnace 3−12295
Ta, spectral emissivity meas. visible region, 1200 to 2400K 3−35378
W, meas. of spectral emissivity using Fourier transform spectroscopy 3−28556
Y_2Co_{17}, Czochralski crystal growth in thermal imaging furnace 3−12295

high-voltage engineering
plasma commutator, d.c. to multiphase a.c. *(Czech)* 3−23924

high-voltage techniques
electrode conditioning, at large gaps in industrial vac. 3−13265
electrostatic power supply design 3−663
ionisation measurement system *(German)* 3−23930
liquid-immersed electrostatic generator for medium power output 3−664
pulse trains, oscillograms, automatic initiation, streak photography 3−252
spark pulse generator for quantitative spectrochemical analysis 3−26023
water droplets used for self-excited high voltage generation 3−16358

history
astronomy, first extraterrestial obs. of deuterium by astronomical techniques 3−28148
astronomy, historical aspects, book 3−34994
climatic influence of human activities since Industrial Revolution *(French)* 3−21956
earthquakes, in Tokyo 3−27955
Electron Microscopy and Analysis Group of the Institute of Physics, early history 3−350
Giordano Bruno (1564-1600), scientist or heretic 3−9782
glassmaking, book 3−9786
instrumentation for invisible information, origins with Galilean telescope 3−28427
Japanese astronomical almanacs, a review *(Japanese)* 3−25532
Nippon Geophysical Prospecting Co., Ltd., seismic prospecting 3−31302
photoconductivity, development, 1873-1972 3−24472
Rankine, W.J.M., 1820-1872, short biography 3−5739
review of standardisation in the horology industry *(French)* 3−3746
velocity of light, three centuries of observations of Jupiter's satellite Io rel. to possible var. 3−32504
weighing scales calibration 3−22254
William Gregor (1761-1817) discoverer of Ti, account of his scientific work 3−19128

hodoscopes *see cosmic ray apparatus; radiation detectors*

hole mobility *see carrier mobility*

hole theory of liquids *see liquid theory*

holes *see charge carriers*

hollow cathodes *see cathodes*

holmium
dispersion relations, curves, h.c.p., modified Sharma-Joshi model 3−30220
elastic constants between 78 and 300 K, u.s. meas. 3−20780
film, obs. of f.c.c. structure and oxidation 3−18042
magnetic susceptibility, temp. depend. near Neel point *(Russian)* 3−12012
magnetic susceptibility measurements, polycrystalline and single crystal, 293-873 K, paramagnetic properties 3−30601
wear and friction in air 3−18625
$GdAlO_3:Ho^{3+}$, absorpt. and luminesc. spectra obs. rel. to energy levels 3−8655
Ho, hydrostatic pressure, effect on spin disorder resistivity 3−2284
Ho^{2+} ENDOR in CaF_2, hyperfine lines, spin Hamiltonian parameters 3−2468
Ho^{3+}, Monte Carlo method for solving excitation transfer 3−34412
Ho^{3+} coherent emission in epitaxial aluminium garnet films 3−736
Ho^{3+} supersensitive transitions in complexes with different numbers of ligands *(Russian)* 3−12180
$^{165}Ho^{2+}$, low temp. relax. in $SrCl_2$, coupled nuclear-electronic spin system 3−18362

holmium compounds
HoF_3 and HoF_3-ErF_3, impurity-conditioned solid-solid transform., rel. to melt growth 3−12274
$HoFeO_3$, 3d density distrib. and intrinsic temp. depend. of Mossbauer isomer shift 3−34262
$HoFeO_3$, equilib. reduction, enthalpy and entropy, O_2 press. *(Russian)* 3−15077
$HoFeO_3$, mag. props., spin reorientation, 50-120 K *(French)* 3−27380
$HoFeO_3$, magnetostriction, low temp. 3−34175
$HoMnO_3$, paramag. Curie temp., mag. susceptibility, 4.2-400 K 3−34103
$HoMn_2O_5$, helimagnetic order of Mn, neutron diffr. obs. *(French)* 3−36723
$HoMn_2O_5$, magnetocrystalline anisotropy, mag. susceptibility meas. 3−36704
HoN, synthesis, vaporization and crystal growth 3−2642

holographic instruments
see also holography
analyzers for microwave spectrum 3−19217
Bragg acousto-optic imaging system, noise reduction 3−22366
coherent optic devices for one-dimens. signal separation determ. *(Russian)* 3−13708
coherent optical filters, increase of dynamic range by modulating gratings 3−19218
coherent optics devices, image generalised spectral analysis, dissociation coeffs. calc. *(Russian)* 3−13707
correlator, ground glass, autocorrelation function, automatic displacement and distortion detection 3−22374
educational low-cost system 3−40

- **holographic instruments** continued
  - for electrical explosion of conductors 3—22368
  - filter, for holographic image deblurring, increasing dynamic range 3—5972
  - gauge for spatial separation of images *(Russian)* 3—3791
  - hologram recording and reproduction apparatus, speckle reduction *(German)* 3—16446
  - holographic microscope system with triangular interferometer, dynamic recording 3—13326
  - interferometer for temperature meas. 3—22375
  - interferometry, demountable specimen support 3 − 35422
  - large telescopes, weak zone plate fabrication and evaluation 3 − 32092
  - movie camera for recording images of objects in motion 3 − 35419
  - recording system, front surface detail from scene moving at high velocities, comments 3 − 35420
  - rotational multiplexing system, for 3 dimens. holograms on 2 dimens. film 3 − 22365
  - visual display application of off-axis, off-bisector refl. type holographic element 3 − 19213
- **holography**
  - *see also acoustic holography; holographic instruments; laser beams; optical storage devices; optical stores*
  - ablative holographic recording, erasable, on thin dielec. layers 3 − 5963
  - aerosol sizing, magnification 3 − 22259
  - air, pulsed interferometric holography of laser-produced breakdown 3 − 33189
  - amplitude holograms, diffraction efficiency calc. 3 − 32522
  - analogue memory by intensity level modulation, feasibility 3 − 22858
  - analysis of process, and applications 3 − 5971
  - aspheric wavefront testing using computer generated holograms 3 − 5899
  - binary, synthetic, prod. and computation method *(German)* 3 − 6444
  - binary Fourier hologram computer synthesis 3 − 16812
  - blood, red cells moving towards orifice, holographic verification of model 3 − 28760
  - camphene, holographic anal. of morphology in dendrite growth 3 − 11564
  - chalcogenide metal photosensitive materials for holographic recording, props. 3 − 28571
  - character recognition, spatial filtering technique 3 − 28574
  - code transformations of u and v signals, image deform. 3 − 16803
  - coherence limitations relax. 3 − 19574
  - coherent optic devices for one-dimens. signal separation determ. *(Russian)* 3 − 13708
  - coherent optics devices, image generalised spectral analysis, dissociation coeffs. calc. *(Russian)* 3 − 13707
  - colour reproduction from multicolour holograms, white light reconstruction 3 − 28567
  - complex optical wavefronts synthesis, coding schemes 3 − 4073
  - and computer generated holograms, book 3 − 19577
  - conductors, electrical explosion investigation 3 − 22368
  - converging beam, focusing properties *(Russian)* 3 − 698
  - c.r.t. testing, impact of steel ball, pulsed holographic study 3 − 5773
  - depth of field, longitudinal multimode laser coherence props. 3 − 29054
  - deterministic diffusers, amplitude equalization 3 − 201
  - dichromated gelatin, bonded on plexiglas, holographic display element 3 − 203
  - diffuse object arrays, optical correlation using single lensless Fresnel hologram 3 − 19214
  - digital information processing experiments 3 − 16799
  - double-exposure holographic interferometry, wavefront tilter 3 − 16444
  - dynamic process, cinehologram production 3 − 6445
  - electrical signals, recording and reconstruction using one dimens. holograms 3 − 28604
  - electron and ion beam technology, conference, Houston, Texas, (1972) 3 − 13473
  - electron microscope for limiting resolution *(Russian)* 3 − 10118
  - electron microscope image improvement by holographic image deblurring deconvolution, contrast inversion removal 3 − 13465
  - electron microscopy, high resolution, image improvement using holographic image-deblurring deconvolution 3 − 25948
  - electron microscopy, holography without fringes 3 − 6108
  - electron microscopy image improvement, holographic image deblurring 3 − 3880
  - fibre optics image transfer element holographic evaluation of characts. 3 − 5962
  - finite fringe interferometry applied to right circular cone at angle of attack 3 − 22574
  - flaw detection by holographic interferometry *(Czech)* 3 − 37645
  - focused images, real-time interferometry 3 − 5958
  - focused optical imaging systems for vibration meas. 3 − 165
  - focusing reflaxicon applications 3 − 202
  - Fourier spectroscopy for microwave spectrum 3 − 19217
  - Fourier transform, storage and retrieval system, patent 3 − 10454
  - Fresnel holograms, spectral line resolution 3 − 13307
  - gaussian beam, one dimens., diffr. by amplitude sinusoidal grating of zero thickness 3 − 10442
  - glass plates, in interferometric homogeneity testing, with holographic compensation *(German)* 3 − 9930
  - high contrast phase holograms by coating technique *(German)* 3 − 22371
  - holo-diagram, application in coherent optics 3 − 3817
  - hologram grating, with modulation, diffraction efficiency 3 − 29030
  - hologram interferometry, time average, of vibr. objects, holographic subtraction 3 − 13709
  - hologram production on photographic film recoverably by white light, positional stability *(Russian)* 3 − 200
  - hologram quality, radiation polarisation effect 3 − 22861
  - holograms, computer generated, coding techniques for recording on computer controlled c.r.t. 3 − 198
  - holograms, writing on $LiNbO_3$ using pulsed lasers 3 − 22364
  - holograms multiplication 3 − 13712
  - holograms with a nonspherical reference wave in an incoherent radiation field *(German)* 3 − 13713
  - holographic interference fringe patterns, interpretation 3 − 26214
- **holography** continued
  - holographic interferogram interpretation, three orthogonal displacements determ. 3 − 16809
  - holographic interferograms, double exposure, multiplexing method 3 − 197
  - holographic interferometry, increased contrast by elimination of background speckle 3 − 22357
  - holographic interferometry, small static deflection meas. of diffusely refl. surfaces 3 − 28461
  - holographic interferometry materials testing technique 3 − 9028
  - holographic interferometry test specification for deform. and fault testing *(German)* 3 − 19154
  - holoseismic reconstruction technique for multiple reflections of seismic waves 3 − 9111
  - image construction, from plane hologram in paraxial region *(Russian)* 3 − 19221
  - image holography through moving fog, scatt. effects 3 − 29053
  - image quality, wavefront aberration evaluation using ray-tracing 3 − 10453
  - images, higher order amplitudes on film with power law 3 − 22855
  - images and their spatial freq. spectra, multiplication method using Fresnel holograms 3 − 16818
  - images of objects in parabolic motion, phase characts. function 3 − 35675
  - images rel. to spectral coherence, Fresnel transform formulation 3 − 697
  - imaging, for nondestructive testing, imaging techniques, conference, Los Angeles, USA (1972) 3 − 19349
  - imaging and aberrations, incorrectly repositioned hologram in system with lenses having aberrations 3 − 37643
  - In-line, magnification and location of images 3 − 16811
  - industrial meas. techniques *(Swedish)* 3 − 32090
  - information storage applications *(Hungarian)* 3 − 26215
  - interference fit fasteners, nondestructive evaluation 3 − 35417
  - interference of equal inclination, from diffused surface, coherence 3 − 9956
  - interferogram prod. with variable sensitivity 3 − 13332
  - interferometer and fringe analyser, supersonic flow obs. 3 − 22571
  - interferometric determ. of isothermal differential diffusion coeffs. *(French)* 3 − 2814
  - interferometry, appl. to acoustic meas. 3 − 212
  - interferometry, dual, two-dimensional density distrib. obs. 3 − 208
  - interferometry, inspection of unpolished surfaces, shape monitoring *(Russian)* 3 − 5917
  - interferometry, polychromatic with recording in three dimensional medium *(Russian)* 3 − 3813
  - interferometry, review 3 − 19222
  - interferometry, using image plane holograms, patent 3 − 9958
  - interferometry, wavefront sampling, image reconstruction 3 − 22860
  - interferometry and basic theory, review *(Czech)* 3 − 10452
  - laser beam applications, review 3 − 29157
  - laser speckle photographs, visualisation of phase objects by spatial filtering 3 − 5969
  - liquid surface holographic u.s. imaging unit for soft tissue structures 3 − 10162
  - local reference beam holography, holograms of objects several metres from plate 3 − 25775
  - lower beam directivity improvement using nonstationary holography 3 − 19629
  - materials for stereoscopic display system 3 − 28576
  - memories, data storage, high capacity, rapid access, feasibility, basic design considerations 3 − 22857
  - memory, planes conception by computer *(French)* 3 − 5967
  - microfilm, recording information density, increasing using holograms *(Russian)* 3 − 16459
  - microscopy, speckle averaging 3 − 19189
  - microwave, antenna far field pattern determ. by machine reconstruction of hologram in aperture *(Russian)* 3 − 35421
  - microwave, double circular scanning 3 − 28575
  - microwave, fast method 3 − 13327
  - microwave, for cross-polarization antenna characteristics 3 − 22367
  - microwave, imaging of objects obscured by dielectric media 3 − 32089
  - microwave, synthetic aperture interferometry 3 − 9957
  - microwave hologram, numerical reconstruction of images 3 − 9955
  - modulated zone plates, computer drawn, Fourier transforming and imaging props. 3 − 29052
  - monobath processing 3 − 28568
  - motion analysis, time average recording and reconstruction, thin phase recording materials 3 − 22372
  - moving object, using mode-locked pulses 3 − 37644
  - moving objects, recording problems, special geometry and exposure conditions 3 − 32084
  - multiple exposure, recording linearity 3 − 13711
  - multiple exposure of object transparencies with binary tone 3 − 13710
  - multiplexed image plane hologram, recording and reconstruction method 3 − 19216
  - noise, intensity quantised hologram, transform analysis 3 − 22859
  - non-optical distributions, improved optical images using multi-level display system 3 − 32088
  - nondestructive testing, data reduction, display systems 3 − 22376
  - nonlinearly recorded holograms, coupled wave theory 3 − 6442
  - ocular holograms for optometric instruction 3 − 9663
  - optical components interferometric testing using circular computer holograms 3 − 3798
  - optical computing 3 − 13704
  - optical heterodyne imaging device, hologram instead of lens 3 − 5973
  - optical information storage in KCl and KBr crystals, conversion of F and X centres 3 − 13329
  - optical inhomogeneities in large fields, investigation using holographic methods 3 − 22847
  - optical material for holographic recording *(Russian)* 3 − 235
  - optical memories, bit-by-bit and holographic image storage 3 − 32608
  - optical memories, point efficiency, signal-to-background ratio 3 − 6441
  - optical seismic data processing, deconvolution method 3 − 9363
  - optimal measuring techniques in industry *(Hungarian)* 3 − 28535
  - particles in moving aerosols, sampling technique 3 − 16445
  - pattern classification, cross-correlation of training patterns with random mask 3 − 692

holography continued
phase hologram reconstruction with He-Cd laser 3−16810
phase holograms, small-size for binary information storage, characts. 3−13331
photographic emulsions, nondeveloped layers, OTF 3−13345
photographic nonlinearity diffraction by thick, periodically stratified gratings with complex dielectric constant 3−19568
photopolymer holographic recording materials, dry packaging technique 3−207
photopolymer recording material 3−5964
photopolymers, holographic recording, phase materials 3−699
photoresist, relief phase hologram recording 3−206
pile-of-holograms, diffracted beam intensification, reln. to intensity reduction factor 3−16808
pinhole imaging 3−19575
plankonvex lens, optical transfer function, holographic meas. of autocorrelation function 3−199
plasma focus, neutron meas., and holographic interferometry 3−20620
plasma Focus machine, neutron fluences, electron density and deuteron temp. meas. by holographic interferometry 3−20637
plasma high beta density profiles holographic interferometry technique at $\lambda=3\mu m$ 3−20634
plastic deformation obs. 3−22660
polarisation holography, review *(German)* 3−32521
polarisation recording of holograms 3−32087
polymethylmethacrylate:p-benzoquinone, light sensitive thermoplastic, hologram recording 3−205
production testing, interferometry, displacement or distortion measurement 3−5966
projected Moire fringes holographic analogues 3−10451
pulsed laser, nondestructive testing applic. 3−34671
pulsed single mode injection semiconductor laser, coherence of radiation *(Russian)* 3−747
radio method for determ. of heights of ionospheric irregularities 3−16069
radiographic data processing, computer-generated holograms 3−22856
read only memory with semiconductor photodetection matrix *(French)* 3−5968
reconstruction efficiency, low intensity reference beam, pre- or postexposure 3−37646
reconstruction efficiency of image recorded on postexposed and preexposed media 3−6440
recording, with electron beam 3−13333
recording of complete closed surface 3−35418
reflected light microscopy of moving objects 3−28573
reflection holograms, high quality bleached, low noise processing, commercial photographic emulsion 3−22373
relief hologram prod. by photoanodic engraving on photocond. surfaces 3−13328
review *(Polish)* 3−3820
review 3−19591
review of laser applications, work performed at Bell Laboratories 3−784
Rowland system with concave holography gratings, stigmatism conditions *(French)* 3−35676
scale reducing methods *(Russian)* 3−32091
in seismology, patent 3−12634
spark discharges produced by nsec. pulses visualisation 3−5970
spatial-angular characteristics of laser emission, holographic control method *(Russian)* 3−13339
spatially incoherent holography, short exposure, with plane wave illumination 3−28569
speckle interferometry of multiple star systems, stellar brightness distrib. reconstruction 3−22126
speckle reduction by partial coherent object illumination simulation 3−19215
spherical surfaces control by interferometry *(Czech)* 3−35404
steam turbine engine and generator design *(German)* 3−37642
stereomodels, topographic mapping, optical considerations 3−6446
steroscopic slide translation on an hologram, white light reproduction *(German)* 3−19220
storage, digital data, principles, techniques, media *(German)* 3−16807
stroboscopic interferometry, triple exposure technique for recording time reduction 3−22360
supersonic jets, noise generating disturbances, holographic study 3−5705
synthesis and restitution of holograms, computer simulation *(Russian)* 3−19576
synthetic holograms with spherical reference waves, adjustment *(German)* 3−6443
thermoplastic reversible recording by increasing surface charge *(German)* 3−32086
three dimensional holograms, high resolution holographic emulsions for, comparison 3−6006
three-dimensional difference extraction between two similar object forms 3−28572
tomosynthesis, holographic method for variable depth display 3−28765
turbine motor vibration analysis by holography 3−19219
tympanic, submicroscopic vibration, obs. by stroboscopic holography 3−3446
velocity meas., of diffusely reflecting objects 3−19578
vibration meas. by vibrating plate hologram 3−28470
vibrations, visualisation, using reference beams phase modulation 3−28570
visualisation of eigenmodes of free-free violin plates 3−5698
volume recording, in extended thickness photographic emulsions 3−13330
X-ray hologram obtained by using synchroton radiation 3−5965
X-ray information, holograms 3−4074
Ag halide, holographic films, MTF determ. by diffraction and phase effects 3−13344
Ar, electron distribution determ. by holographic electron laser microscope 3−4714
$BaCl_2$, holographic storage, efficiency, inscription duration *(French)* 3−35437

holography continued
KBr, KCl storage, diffraction efficiency, coloration methods, room temperature 3−32085
KBr single crystals containing colour centres, thick hologram recording 3−22369
KCl:Na F_a-centre holograms, storage properties 3−22370
KH_2PO_4 state of soln. obs. during the growth of single crystals 3−33475
$LiNbO_3$ holograms, unfixed, self-enhancement 3−16443
$LiNbO_3$:(Fe,Mo), alterable holographic medium, wavelength dependence 3−204

homopolymers *see polymers*

hopping conduction
see also diffusion in solids
amorphous semiconductor film, variable-range hopping cond., theory 3−30476
amorphous semiconductors, hopping Hall effect, single phonon contribution 3−27274
amorphous solids, single-phonon contribution 3−2082
disordered solid, theory of stochastic transport 3−38841
disordered systems, between nearest neighbour centres, temp. depend. 3−30477
disordered systems, thermally assisted hopping transport 3−30483
excitation decay, hopping mechanism of energy transfer 3−33835
ferrite oxyfluoride spinels, elec. cond., hopping mechanism *(French)* 3−27251
glass, hopping Hall effect, single phonon contribution 3−27274
Hall coeff. sign in hopping type charge transport 3−18169
Hubbard model, metal-insulator transition depend. on hopping parameter 3−38765
photon stimulated, in disordered semicondutors *(Russian)* 3−2131
semiconduction, disordered solid impurity conduction by stochastic transport 3−38842
semiconductor, lightly doped, percolation theory and activation energy 3−15197
semiconductor, strongly compensated, theory 3−33900
semiconductor compensation determination from hopping conduction saturation 3−24441
semiconductors amorphous, and glasses, single phonon contribution to low field magnetoresistance 3−36626
transition metal semiconducting phosphate glass, small polaron hopping 3−8175
vitreous ionic conductors, role of long range diffusion process in dielec. relax. 3−30748
AlB_{12} semiconductors, thermoelectric props., thermal and elec. cond., temp. depend. 3−36630
B, at low temp. rel. to local order 3−21075
BC_x semiconductors, thermoelectric properties, thermal and electrical conductivity, temperature dependence 3−36630
$BaFe_{12}O_{19}$, ferrite with magnetoplumbite structure, anisotropy of hopping cond. and thermoelec. power 3−38829
Eu chalcogenides, ferromagnetic, semiconducting 3−38859
GaP amorphous film, ohmic, hopping cond. and Poole Frenkel behaviour obs. 3−36604
Ge, amorphous, d.c. cond. and pseudogap struct. 3−38839
Ge, amorphous, hopping transport, thickness depend. 3−38838
Ge, compensated, activationless conductivity 3−18144
Ge, heteroepitaxial films, Hall effect and magnetoresistance *(Russian)* 3−11966
p-Ge, influence of mag. field 3−24440
Nb/Al_2O_3 cermet film, activation energy *(Russian)* 3−30482
Nb/Al_2O_3 thin cermet films, hopping conduction through localised states 3−11895
NiO, bound-polaron hopping, activation energy 3−5006
$PbFe_{12}O_{19}$, ferrite with magnetoplumbite structure, anisotropy of hopping cond. and thermoelec. power 3−38829
Se liq., charge transport by hopping, hole photogeneration *(Russian)* 3−8179
Si, amorphous and anneal stable state, evidence for Mott model 3−5007
Si amorphous films, electronic transport and state distribution 3−8172
Si_3N_4 film, electronic cond. mechanisms *(German)* 3−15199
$SrFe_{12}O_{19}$, ferrite with magnetoplumbite structure, anisotropy of hopping cond. and thermoelec. power 3−38829
V_2O_5-P_2O_5 glass, d.c. cond. by polarons, 90-520K 3−33886
YIG:$Si^{4+}(Ge^{4+})(Ca^{2+})$, mag. after-effect, electronic hopping processes 3−24591
ZnO:In, elec. cond. and Hall effect obs., 5-300 K *(German)* 3−11899

horology *see time measurement*

hot carriers
see also semiconductors
amorphous dielectric solid, Poole-Frenkel cond., calc. including hot electron effects 3−5015
beam-produced plasma, hot electron prod. 3−1506
conduction phenomena, book contrib. 3−21065
cubic semiconductors in hot carrier range, symmetry relations between mobility and differential mobility-tensor components 3−8190
Ferroelectric, wide band, Curie point depend. on nonequilib. carrier conc. 3−24664
n-Ge, impurity ionisation, hot electron mobility 3−8192
Green function approach to hot electron conductivity 3−18153
III-V compounds, donor and acceptor conc. determ. from hot electron mobility 3−38812
ionic crystal, hot electron effects 3−36601
metal film, hot electron transport, metal base triode obs. 3−5062
metallic discontinuous film, elec. cond., electron emission and electrolum. rel. to hot electrons 3−15171
m.i.m. structure, hot electron emission *(German)* 3−15270
in n-type GaAs, microwave conductivity measurement 3−27263
polar semiconductors, inclusion of higher order terms for energy distribution function of hot carriers at high temp. 3−8193
semiconductor, carrier heating in microwave field, investigation method *(Russian)* 3−8198
semiconductor, energy relaxation time measurement, elec. field effects *(Russian)* 3−36615
semiconductor, fluctuations of hot photoelectrons 3−33956

- **hot carriers** continued
  - semiconductor, homogeneous, space charge induced by hot carrier regime 3 – 36617
  - semiconductor, interband transitions of hot holes, and cyclotron reson. of light holes *(Russian)* 3 – 8109
  - semiconductor, iterative method for hot carrier distrib. calc. 3 – 18152
  - semiconductor, noise temp. and spectral density of hot carrier velocity fluctuations 3 – 15204
  - semiconductor, second harmonic generation, efficiency and optimum d.c. bias field 3 – 30509
  - semiconductor, transport props. in strong mag. field 3 – 27264
  - semiconductor compound, parabolic bands with phonon scatt., hot electron high field transport 3 – 27265
  - semiconductor device, carrier heating and cooling, charge and energy transport theory 3 – 33916
  - semiconductor with non-parabolic dispersion law, in mag. field, high freq. cond. 3 – 2109
  - semiconductors, hot current carriers e.m.f. photogradient meas. technique *(Russian)* 3 – 11931
  - semiconductors, in an external electric field, anisotropy in diffusion-noise temp. and differential mobility 3 – 27269
  - semiconductors, theory of e.m. wave absorption *(Russian)* 3 – 11906
  - semiconductors, transport noise decomposition under space charge conditions, diffusion and hot electron effects 3 – 33915
  - $Cd_xHg_{1-x}Te$, hot electron interaction with phonons rel. to photocond. oscillations 3 – 18159
  - CdS, oxygen photodesorption, influence of nonequilib. minority carriers 3 – 15210
  - n-GaAs, millimeter wave freq. response 3 – 2119
  - Ge, Benedicks effect due to heating of nonequilibrium carriers by microwave fields 3 – 15209
  - Ge, capture and reemission field depend., Poole-Frenkel effect 3 – 21091
  - n-Ge, elec. cond. anisotropy, hot electron drift velocity temp. depend. *(Russian)* 3 – 8196
  - p-Ge, hot carrier distrib. determ. with uniaxial stress 3 – 18154
  - n-Ge, hot electron Hall transport, calc. 3 – 38848
  - Ge, interband transitions of hot holes, and cyclotron reson. of light holes *(Russian)* 3 – 8109
  - Ge, rel. to photon drag effect, Q-switched CO_2 laser obs. 3 – 2130
  - p-Ge, size effect rel. to elec. cond. and hole cooling length 3 – 18161
  - Ge electrons, intervalley scattering, impurities and phonons, transition times 3 – 33919
  - Ge-metal, non-rectifying point contact, hot hole noise dep. on lattice temp. *(Russian)* 3 – 33992
  - n-InAs, i.r. birefringence due to hot electrons, 80K *(Russian)* 3 – 8555
  - n-InSb, Faraday effect of hot electrons, i.r. 3 – 2523
  - n-InSb, hot electron scatt. at 4.2 K 3 – 38850
  - n- InSb, hot electron Shubnikov-de Haas effect 3 – 36623
  - InSb, hot electron-phonon interaction in nonparabolic cond. band., 4.2K 3 – 33912
  - n-InSb, microwave props. in d.c. mag. field, hot electron effect, scatt. mechanism, 4-300K 3 – 21087
  - n-InSb, strong compensated, Faraday effect due to hot electrons 3 – 15478
  - n-InSb band tailing, hot electron magnetophotocond., cond. and Hall coeff. obs. 3 – 2138
  - InSb Monte Carlo calc. of hot electron mobility 3 – 36612
  - n-InSb non ohmic transport and phonon amplification 3 – 8189
  - Si, (111) surface, rel. to spectral oscills. of photocond. 3 – 18015
  - Si, capture and reemission field depend., Poole-Frenkel effect 3 – 21091
  - n-Si, hot electron energy relaxation time measurement, elec. and microwave field effects *(Russian)* 3 – 36616
  - Si surface inversion layer, nonlinear transport and negative diff. mobility, m.o.s.f.e.t. obs. 3 – 11952
- **hot cathode tubes** *see thermionic tubes*
- **hot cathodes** *see thermionic cathodes*
- **hot electrons** *see hot carriers*
- **hot shortness** *see brittleness*
- **hot strength** *see tensile strength*
- **Hubble model** *see cosmology*
- **hue** *see colour*
- **Hugoniot diagrams** *see equations of state*
- **human factors**
  - *see also biocybernetics; man-machine systems*
  - real-time speech recognition system performance 3 – 31852
- **human-machine systems** *see man-machine systems*
- **humidity**
  - *see also atmospheric humidity; hygrometers*
  - absorption, by instrument materials 3 – 28459
  - air at dewpoint, continuous supply *(Japanese)* 3 – 17972
  - atmospheric aerosol particles, extinction coeff. to mass ratio, humidity depend. 3 – 17493
  - dust storms, ground level meas. 3 – 15966
  - fabrics and explosives, electrostatic charge accumulation, relative humidity effects 3 – 658
  - hygroscopicity and no dimming phenomena in porous glass *(Japanese)* 3 – 20935
  - polymethylmethacrylate, effect on tensile strength 3 – 20807
- **humidity measurement**
  - *see also hygrometers*
  - air currents in mines 3 – 4587
  - hygrometers, continuously operating, capacitance, cooled mirror, electrolytic, operation, advantages, applications, use 3 – 16054
  - radiosonde obs. 3 – 9264
  - water droplet content of wet air, thermodynamic method based on throttling calorimeter *(German)* 3 – 25675
- **h.v. engineering** *see high-voltage engineering*
- **hybrid computer methods**
  - *see also hybrid computer programming*
  - many-particle interaction problems, computation by special purpose processors 3 – 28972
  - nonlinear structure earthquake responses, simulation 3 – 12571
  - Poiseuille flow, simulation 3 – 7337
- **hybrid computer programming**
  - nuclear reactor control rod drop time computation 3 – 6999
- **hybrid computers**
  - analog-digital integrator for soln. of partial differential equations in mathematical physics *(Russian)* 3 – 13542
  - multi-channel data-logging system, with multiplexer and A/D convertor 3 – 25964
  - system for detecting and quantifying e.e.g. spike and wave patterns 3 – 3891
- **hybrid integrated circuits**
  - *see also beam-lead devices; flip-chip devices*
  - laser trimming, high-speed, installation 3 – 6528
  - for multiwire proportional counter 3 – 28649
  - resistor trimming, industrial laser system design 3 – 32609
- **hydrated electrons** *see solvated electrons*
- **hydraulic control equipment**
  - *see also hydraulic motors*
  - incompressible jet flow and reattachment effects 3 – 11368
  - microdrive, for remote control of micromanipulation 3 – 16551
- **hydraulic motors**
  - microdrives, for micromanipulators remote control 3 – 16551
- **hydraulic systems**
  - hydrodynamic flow visualization, applications, review 3 – 32282
  - inverse problem, single layer equifer, water table, approximate solution, theoretical model *(Italian)* 3 – 9097
  - loops, nonisothermal, applic. of methods of design of hydraulic loops to nonisothermal gas 3 – 4585
  - optimal regulator for metropolitan storm-sewer system 3 – 28408
  - pressure measurement, dynamic characteristics 3 – 22299
  - tidal channel inertia simulator 3 – 449
  - unsteady flow meas. in hydraulic servo systems using laser velocimeter 3 – 793
  - Mn nodules, hydraulic system for recovery from sea bed at great depths *(German)* 3 – 9407
- **hydraulic turbines**
  - interblade channels flow analysis by graphical method *(Russian)* 3 – 7360
- **hydroacoustics** *see underwater sound*
- **hydrodynamics**
  - *see also flow of liquids; jets; liquid oscillations; liquid waves; magnetohydrodynamics; viscosity of liquids*
  - alluvial streams, origin of meandering and braiding 3 – 25194
  - barycentric averaging, in systems with arbitrary vertical coordinate *(German)* 3 – 17500
  - Benard instability, nonlinear eqns., effect on fluctuations 3 – 11361
  - Bose fluid, quantum hydrodynamics 3 – 38692
  - broken symmetry, nematic liquid crystals 3 – 1574
  - Brownian motion, hydrodynamic models 3 – 6359
  - Brownian motion of spherical particle in a compressible fluid, hydrodynamic fluctuation theory 3 – 37896
  - configurational stability of flows *(Russian)* 3 – 1424
  - cosmological anisotropic model, hydrodynamic motions and vacuum stage 3 – 35010
  - Couette flow of viscoelastic fluids, fluid model, overstability and disturbance form 3 – 11362
  - Czochralski growth method, hydrodynamic stability in forced convection 3 – 11568
  - density fluctuations in simple liquid 3 – 7611
  - diatomic gas with vibration-relaxation, Knudsen layer, hydrodynamic eqns. *(Russian)* 3 – 29889
  - distant turbulent wake parameters, first moments of hydrodynamic fields calc. *(Russian)* 3 – 26850
  - in electrodialysis 3 – 9067
  - electrolysis, hydrodynamic transition 3 – 25073
  - external load effect on underground water filtration *(Bulgarian)* 3 – 14426
  - fast reactor feedback, calc. of hydrodynamic effects 3 – 38175
  - film between mating surfaces, coupled hydrodynamic and elastic equations 3 – 25785
  - finite element method application *(Japanese)* 3 – 1337
  - flow processes in pneumatic conveyance systems for containerized cargoes 3 – 4538
  - flow through porous media, dispersion, radioactive tracer decay and absorption 3 – 15857
  - fluid oscillations in mobile cylindrical cavities, approx. calc. of hydrodynamic coeff. *(Russian)* 3 – 23765
  - fluids, three-dimensional classical, asymptotic props. of autocorrelation functions, Enskog expansion 3 – 28995
  - fuel, multirod bundles, pressure drop correlations 3 – 17288
  - gas-liquid systems 3 – 4616
  - growth system, vapour phase, effect of natural and forced convection 3 – 2647
  - heat transfer theory, generalised hydrodynamic eqns. 3 – 14434
  - Hungarian theoretical meteorological studies of hydrothermodynamics *(German)* 3 – 12704
  - hydraulic resistance for axial flow of bundles of smooth and ribbed rods 3 – 6974
  - hydrofoil, lift and drag measurements in polyox dilute solutions 3 – 17499
  - hydrofoils, ventilation inception on surface piercing foils or struts 3 – 14424
  - ideal fluids, group classification of hydrodynamic eqns. *(Russian)* 3 – 29828
  - internal hydrodynamical problem, wall pressure fluctuations in turbulent flow in tubes *(Russian)* 3 – 4567
  - Irish Sea, density current in Liverpool Bay area rel. to hydrodynamical theory 3 – 34863
  - jet-flapped airfoil problem, two-dimensional, numerical solution 3 – 11378
  - laminar films, vapour flow, momentum transfer, condensation 3 – 1346
  - laser radiation dispersion characteristics of an aqueous medium subject to hydrodynamic disturbance, time variation *(Russian)* 3 – 29113
  - lift of an impulsively started elliptic cylinder at incidence 3 – 11373
  - linearized hydrodynamic modes in statistical physics, binary mixtures 3 – 17501
  - liquid crystal, cholesteric, hydrodynamic instabilities under thermal gradient 3 – 26968

hydrodynamics continued
liquid crystals, nematic, acoustic wave dispersion and absorption, unified hydrodynamic theory 3—24216
liquid crystals, unified theory 3—4718
liquid phase epitaxy, consideration of hydrodynamic factor 3—1923
RR Lyrae type stellar atmospheres, a nonlinear model of shock wave effects 3—25431
mass transfer, from streaming solutions 3—1355
mass transfer to fixed particle in agitated tank, extrapolation problems *(French)* 3—4598
modes damping and scattered light spectrum effects of chemical reactions 3—11358
molecular fluids, translational hydrodynamics and light scatt. 3—4030
multiphase fluid in presence of phase transformations, hydrothermodynamic eqns. 3—33287
Navier-Stokes eqns., invariant solutions calc. *(Russian)* 3—29839
non-Newtonian two-phase flow in pipes 3—33283
photons in inhomogeneous plasma 3—17580
plane wave propagation in dissipative heat-conducting medium, application of averaging method *(Russian)* 3—13603
planetary wave long-range forecasting, hydrodynamic model using meteorological information 3—37222
plasma, nonideal, thermodynamics and shock waves 3—11461
plasma hydrodynamic longitudinal oscillations instability 3—20542
plasma hydrodynamic longitudinal oscillations instability in a non-uniform magnetoactive plasma 3—20489
platelet suspension, optical props. anisotropic changes on hydrodynamic shear field appl. 3—9017
polymer, spherical molecules, in suspension, intrinsic viscosity calc. 3—36063
polytropic differentially rotating fluids, appl. of post-Newtonian eqns. to determ. equilib. config. 3—28104
postive column, acoustic instability, hydrodynamic eqns. 3—29985
pressure fluctuations in separated flow, analysis and correlation of data 3—11395
projectivity of conformally-plane spaces created by the hydrodynamic energy-pulse tensor *(Russian)* 3—6327
relativistic astrophysics, hydrodynamical equations and relativistic shock waves *(Polish)* 3—25364
rheology of sintering, spreading and leveling of fluids 3—4548
rotating gaseous spheroids, dynamical contraction, formation of stars and galaxies 3—37286
rotating star, radiative zone time dependent hydrodynamics of meridional circulation 3—5595
seals, mech. radial-face, hydrodynamic theory 3—26853
single rock joint, hydrodynamic dispersion of contaminant 3—21863
slow motion of plate in rotating fluid at arbitrary angle-of-attack 3—7403
solar wind proton gas, comparison with kinetic model 3—16135
spherically symmetrical accretion flow, stability, polytropes 3—3284
stability, of Couette-Poiseuille-porous annular flow 3—7340
stability of two-dimens. flow, Taylor-Goldstein eqn., Howard's technique 3—23676
Stokes resistance of spheres in contact in linear shear field 3—4520
supermassive star model, explosive features rel. to obs. of active galaxies 3—28178
swirling flows, hydrodynamic and hydromag. stability, semicircle theorems 3—33279
thermal and rotational instability, mathematical equivalence 3—26793
tidal channel inertia simulator 3—449
transport coefficients, mode coupling contributions from drift and dissipative terms 3—10400
turbulence, similarity hypothesis 3—17522
unsteady flow around a slender fish-like body with finite body thickness 3—14421
unsteady forced flow against rotating disk, solutions using Zeytounian's technique 3—7318
vapour-water stream in helically coiled tubes 3—14499
Vlasov transition from nonrelativistic distribution functions to hydrodynamics *(Russian)* 3—11472
water channel, high speed 3—16579
Weber's hydrodynamical equations rel. to action integral, meteorological problems *(German)* 3—12702
wedge entry problem, incompressible fluid, numerical conformal mapping 3—4547
Ar, liq., density fluctuations, generalized hydrodynamic approach 3—24172
Cl_2, liquid, ^{35}Cl nuclear spin lattice relaxation times meas., molecular reorientation, hydrodynamic and cell models 3—24626
HI isolated clouds in interstellar medium, hydrodynamic treatment of phase change 3—37481
He, liq., crit. velocity in rough channels, model 3—36453
hydroelectric power stations
see also dams; hydraulic turbines; tidal power stations
American Power Conference, Chicago, USA (1972) 3—14273
hydraulic mains dynamical charact. *(Russian)* 3—20355
underground positioning, rock property determ. using seismic wave velocities 3—9116
wakes, asymmetric turbulent with zero excess momentum, integral method for mean velocity computation 3—33314
water flow through porous media, equivalent nonlin. permeability coeff. calc. 3—7474
hydrogen
see also deuterium; hydrogen ions; hydrogen neutral atoms; hydrogen neutral molecules; protons; tritium
absorption and desorption on Ta *(French)* 3—1890
absorption by Ta, surface barrier influence *(French)* 3—4921
absorption on Er film, elec. cond. changes 3—30553
adsorbed on Ni thin film, elastic scattering of conduction electrons 3—27301
adsorption, on Si and Ge, cooperative, (111) faces, pulsed time of flight mass spectrometry, exchange reactions, kinetics 3—36485
adsorption on γ-Al_2O_3 and Al powders 3—1889
adsorption on (100) face at Ge single crystals *(Russian)* 3—15068
adsorption on iron in sulphuric acid soln., action of inhibitors *(French)* 3—1911
adsorption on metal/electrolyte interface *(French)* 3—2820

hydrogen continued
adsorption on Ni (100) surface, flash desorpt. obs. 3—30349
adsorption on Ti and alloys during corrosion and cathodic polarization 3—1910
in alkali metals, methods of conc. determ. 3—445
annealing of internally oxidised Cu-$Al_2O_3(MgO)(TiO_2)$ in H_2, brittleness obs. *(Japanese)* 3—12395
in aqueous acid, frozen, e.s.r., forbidden transitions *(Russian)* 3—8420
atmospheric, laser-Raman radar detection, using sampling technique 3—3190
bubble chamber, vapour bubble behaviour, effect of u.s. field 3—25904
bubble chamber, vapour bubble dynamics 3—4614
cathodic deposition, on Ge, hydrogen overvoltage mechanism, temperature effects 3—37128
charging of Armco iron, influence on yield stress and ultimate strength *(French)* 3—5321
charging of austenitic Fe-Cr-Ni alloys *(French)* 3—2747
chemisoroption and electrocatalysis in H evolution reaction 3—38735
chemisorption and catalysis on W and Ni polycryst. wires, ht. of absorption/reaction kinetics correl. 3—11809
chemisorption on metallic thin films, effect on Hall effect 3—15278
chemisorption on Pt, crystal field surface orbital-bond energy bond order model 3—4926
chemisorption on transition metals, review *(French)* 3—1897
chemisorption on W(100), absolute sticking probability, coverage and electron stimulated desorption 3—36490
compressibility at densities 0.5-2 gm/cm^3, 0.4-8 Mbar, metallization, eqns. of state determ. *(Russian)* 3—11713
contamination of Nb following UHV degassing 3—15723
cracking in steel welds, microstruct. effect 3—34567
cryopumping by adsorption on condensed gases 3—9917
cubic atomic crysts., electronic struct., Bloch functions, Fermi surfaces, exact Hartree-Fock calcs. 3—33800
degassing, soft iron alloy, main parameters *(German)* 3—8888
degassing from fused quartz ampoules 3—21742
desorption from dil. Ni-Fe alloys, Mossbauer obs. *(French)* 3—1891
desorption from iron and steel *(French)* 3—1892
diffusion, permeability and solubility in Pd alloys 3—1834
diffusion and solubility in Fe-Si solid solns. *(Russian)* 3—30283
diffusion coefficients determ. in Ta, by X-ray meas. of lattice expansion 3—27145
diffusion in α-Fe, alloying additions influence 3—1829
diffusion in Armco iron, stress effects *(French)* 3—1830
diffusion in Fe, coeff. determ. from permeability meas. *(French)* 3—1827
diffusion in liq. metals and alloys, rel. to metallurgical processes 3—4865
diffusion in metal, uptake detection method using anodic oxidation 3—12522
diffusion in Ni, anomalous mechanism and quantum diffusion *(French)* 3—1822
diffusion in steel, effects on embrittlement 3—5325
diffusion in TiH_{2-x}, γ-phase, model 3—27138
diffusion in transition metal hydrides and their alloys *(French)* 3—4888
diffusion in Zircaloy-yttrium welded sheet 3—26500
diffusion through oxide films on steel 3—21644
diffusivity, permeability and solubility in iron and alloys 3—1828
diffusivity in liq. Ni and Cu 3—36433
diffusivity in metals, low temp., meas. by Gorsky effect 3—36440
discharge, electron energy distribution and electrical props. of striations 3—36224
discharge, pulsed, plasma diagnostics, electron conc. determ. 3—17660
drag, effects on orbit accel. of balloon satellites 3—35222
dry, effect on surface self-diffusion of Ni 3—27179
electrical discharge effects on size of H clusters 3—4661
electromigration in transition metals *(French)* 3—1823
embrittlement and delayed fracture of steel *(French)* 3—2735
embrittlement by aqueous lithia soln. corrosion of polycrystalline Zircaloy-2, hydride orientation *(French)* 3—12385
embrittlement cracking, lattice dilatation, complete elastic soln. 3—39353
embrittlement cracks, subcrit. crack branching 3—4796
embrittlement of austenitic steel 3—2745
embrittlement of austeno-martensitic struct. of Fe-Ni alloys *(French)* 3—5320
embrittlement of Fe-C alloys, and permeability, cathodic charging *(French)* 3—21661
embrittlement of group V transition metals and hydride form. 3—34530
embrittlement of high-strength aluminium alloys 3—5336
embrittlement of high-strength steel 3—5323
embrittlement of iron, low carbon additions influence *(French)* 3—5322
embrittlement of metals 3—2723
embrittlement of pearlitic steel 3—27654
embrittlement of rail-grade steel, effects in service performance 3—5335
embrittlement of stainless steel 3—5330
embrittlement of steel, effect on weld microstructures 3—39364
embrittlement of steel, rel. to stress corrosion cracking 3—21622
embrittlement of steel, stress corrosion cracking 3—8904
embrittlement of steel, temp. depend. *(French)* 3—5333
embrittlement of steel, thermal processing depend. *(French)* 3—5328
embrittlement of steel and crack development *(French)* 3—8905
embrittlement of steel and iron, rel. to hydrogen/dislocation interaction 3—2744
embrittlement of steels, meas. methods *(French)* 3—5327
embrittlement of structural steels *(French)* 3—5331
embrittlement of Ta *(French)* 3—5337
embrittlement of Ti alloy, rel. to stress corrosion cracking *(French)* 3—8907
embrittlement of Ti-Al-Mn alloys and effect on fatigue life 3—24882
embrittlement of titanium alloy *(French)* 3—5334
embrittlement of zirconium 3—8909
embrittlement role in stress corrosion cracking of steel 3—2736

hydrogen continued
emission, 21 cm wavelength, review of work at Argentine Radiostronomy Institute *(Spanish)* 3−31814
fusion reactors, solid H_2-plasma interaction in relation to the refuelling problem 3−19972
gas, CO_2 laser-induced breakdown 3−17689
gas, H-halogen system with W, gas equilibrium and chemical transport reactions *(German)* 3−25101
gas-induced cracking of Ti-5Al-2.5Sn, kinetics study 3−15704
glow, negative, velocity distrib. of plasma electrons 3−1531
o-H_2, solid, damping of librons 3−1578
hollow cylindrical cathode, elec. field distrib. in cathode fall, radial model *(German)* 3−4690
impurities in Ar plasma, local thermodynamic equilib. in stabilised arcs 3−33387
inclusion in carbonyl Ni, evolved gas analysis *(Russian)* 3−10197
intergalactic nongaseous H rel. to missing cosmological mass, critique 3−19054
interplanetary, ionisation resulting in electromagnetic instabilities 3−13007
ionisation energy, white dwarfs and neutron stars 3−13024
jets, planar, natural breakdown, hydrogen bubble technique for flow visualisation 3−23804
laser, VUV, four level, electron beam excitation 3−22883
laser light scattering from marginally stable H plasma 3−4673
liquid, coherent neutron scattering, collective excitation 3−26964
liquid, handling, transport and storage 3−3774
liquid, polyatomicity, acoustic method 3−7613
liquid H particle target with thin mylar side walls 3−6060
liquid target, 3 metres 3−22430
liquid target, conical 3−22429
maser, performance *(German)* 3−19588
mesosphere and lower thermosphere diural variations 3−3038
mesospheric concs. during sunrise 3−18863
in metal, in presence of applied stress field, thermodynamic anal. 3−5292
metallic, phase transitions under press. 3−24271
metallic, random-phase-approx. correl. energy using Hartree-Fock Bloch functions 3−36525
1-naphthol, H-randomization under electron impact 3−11193
in Nb, b.c.c., thermodynamic behaviour *(German)* 3−27616
neutron-inelastic-scatt. data interpretation from large momentum transfer expansions 3−14671
non-equilibrium spin state ratio meas. 3−15816
nova shells, ionization equation for H shells rel. to optical depth 3−5598
nuclear jet target in vacuum 3−22432
nuclear liquid target vessels of Dacron film 3−22433
optically thin plasma, collisional-radiative and population coefficients 3−1481
permeability in metals, stress and elec. field effects 3−1824
permeation and diffusion in Mo and W 3−1833
planetary atmospheres, collision narrowed quadrupole spectral line profiles 3−35070
plasma, electron density distribution meas. with ion temp. deviating from electron temp. *(German)* 3−38500
plasma, heating by relativistic electron beam 3−7541
plasma, hybrid resonance due to two ion species 3−20483
plasma, in constricted discharge, fireball formation plasma potential and electron temp. and velocity meas. 3−26898
plasma, magnetised, 'switch-on' shocks obs. 3−36165
plasma, radiative transfer, comparison of exact and mean beam length technique results 3−17565
plasma, sheath admittance, meas. by floating voltage swept double probe 3−17658
plasma, shock wave propagation in a longitudinal magnetic field 3−23873
plasma, turbulent, Balmer-line anomalies 3−38498
plasma, turbulent, spectroscopy 3−29944
plasma, turbulently heated, microwave radiation 3−20626
plasma electron cyclotron frequency, mag. field uniformity degree effect on radiation of harmonics *(Russian)* 3−14568
plasma electron temp. determ. from ambipolar elec. field reversal under mag. field 3−4676
plasma in ST-Tokamak, time behaviour description 3−38474
plasma ionisation, recombination and population of excited levels 3−29938
plasma N_2^+-H_2^+ mixtures, recombining nozzle flow, electron and electronic temp. comparison, theory 3−36166
plasma N_2^+-H_2^+ mixtures, recombining nozzle flow, electron and electronic temp. comparison, experiment 3−36167
plasma turbulent heating, ion energy distribution meas. 3−26899
plasma weakly ionised, quasistatic Stark broadening, electron contribution 3−33329
plasma-microwave interaction, electric field strength determ. by means of Stark effect 3−30012
polarized particle beams, current state of physics and technology for prodn. 3−35727
precipitation in Nb and resultant embrittlement 3−8818
purification by diffusion through Pd membranes at high pressure *(Russian)* 3−9905
refrigerator for 20 K region with $LaNi_5H_x$ thermal absorption compressor 3−5842
replacement of H by CO_2 on a W surface, mechanism proposal *(Russian)* 3−8021
solid, anisotropic intermolecular interactions in the rotation-vibration Raman spectrum 3−27492
solid, ground state energy, compressibility, press. 3−33479
solid, $H^+(H_2)_n$ cluster production model 3−36965
solid, librational anharmonicity effects 3−38641
solid, low temp. compression using shock waves 3−32049
solid, phonon dispersion relations from inelastic coherent neutron scattering 3−20832
solid, shear strength rel. to pressure variation 3−30201
solid, transition to metallic state in compression wave induced by laser pulse 3−20874
solubility in liq. Ni alloys 3−5296
solubility in liq. silicates 3−4866
solubility in metals and alloys *(French)* 3−2708

hydrogen continued
solubility in Ni-W system rel. to the thermodynamic props. of the system *(German)* 3−27624
solubility in rare earth earth metals, solid soln. form., α-phase studies *(French)* 3−2707
sorption mechanism on KC_{24} *(French)* 3−1880
sorption on stainless steel, effects on work funcion rel. to elec. charge 3−24496
in steel, dislocation role in hydrogen transport *(French)* 3−2741
in steel, low carbon mild type, hydrogen-dislocation interaction *(French)* 3−2706
in steel and Armco iron, hydrogen trapping sites *(French)* 3−2742
stellar evolution, H flash rel. to collapse of interstellar gas and solar nebula 3−35116
superfluorescence in electron beam stabilized discharge, due to HF quenching 3−19599
supergiant stars with strong H lines in Large Magellan Cloud *(French)* 3−13093
surface potential on Ti film 3−33984
thermal diffusion of D_2 and HD at 85°C composition depend. *(German)* 3−14412
track sensitive target in Ne-H cryogenic bubble chamber, physics pictures 3−28639
ultrashort laser pulses from vibr.-rot. transitions *(Russian)* 3−10536
uniformly rotating stars with H- and metallic-line blanketed model atmospheres 3−9516
u.s. bubble chambers, track formation 3−25896
vapour growth of Si_3N_4 layer, effect of H_2 on growth rate *(Russian)* 3−15618
white dwarf envelope, thermal evolution calc. *(Russian)* 3−16203
Ar:H_2, solid, lattice excitation assignment to reson. mode of H_2Ar mol. 3−24237
Ar + H_2 discharge deionisation process 3−30041
in Cu, internal friction, dislocation pinning by hydrogen *(French)* 3−2740
F_2-H_2 laser, excitation by relativistic electron beam, energy characts. *(Russian)* 3−4093
in Fe and Fe-Ni alloys, dislocation-hydrogen interactions 3−4887
Fe:H, zone melted and armco, H effect on elec. resist. at low temps. 3−8807
Ge, H^+, O^+, B^+, ion bombardment, divacancy-like optical absorption 3−34394
H track sensitive target, in Ne-H bubble chamber, operation 3−25847
H x lines in O type stars spectra compared to models 3−28186
H/He surface ratio effect on C-star spectra 3−13023
H-D three metre liquid nuclear target of stabilized density 3−32129
H-deficient stars, Stephenson-Sanduleak 3378, B-type star, UBV obs. 3−25453
H-He mixture, ionizing shock wave struct. 3−14416
H_2, probability of π absorpt. rel. to chem. bonds *(Russian)* 3−11190
o-H_2, solid, libron spectrum by small-angle scatt. of nucl. γ-rays 3−21352
H_2, solid, specific heat, 0.5 to 5K 3−11747
H_2 diffusion in metals, quasielastic neutron scatt. theory considering finite jump times 3−38687
H_2-D_2 solid mixture, specific heat, 0.5 to 5K 3−11747
H_2-D_2-inert gas mixtures, permeation through Pd tubes, model 3−7305
H_2-F laser, vibr. rot. state populations, output spectra 3−10479
H_2-F_2, reaction behind shocks 3−11317
H_2-F_2 laser, emission rel. to H_2 press. 3−10493
H_2-F_2 laser, photochem., submicrosecond pulses, output energy and pulsewidth rel. to gas press. 3−4084
H_2-N_2, positive column, electron energy distribution in striations 3−30039
H_2-N_2F_4, mixture, laser induced explosion 3−12508
HD thermal diffusion in H_2 at 85°C composition depend. *(German)* 3−14412
in KCl:U, trapping of molecules by M-centres 3−20732
in Mg, by vacuum heating method 3−26017
Na contamination by H_2, determ. of content to 0.1 ppm amalgamation method 3−32942
in Nb, solute interactions role in mech. props. 3−2743
Nb:H, quasi-elastic neutron scatt. intensity 3−30230
Ne-H bubble chamber, operation 3−25847
in Ni, interaction with dislocations *(French)* 3−1629
Ni polycrystalline surfaces, H_2 adsorption states at different temps. 3−11801
Ni-Fe:H dilute alloy with high H conc., magnetoresistivity rel. to local mag. moments 3−8158
in Ni-P alloys, rel. to resist. decrease during tempering *(French)* 3−2738
in Pd-Ag(Ce) alloys, hydrogen cycling through α-β transform. 3−2737
in Pu, impurity conc. determ. by hot vacuum extraction *(French)* 3−2746
Si, radiation damage in p-type with H impurity and high purity n-type, hole density, annealing 3−33546
Ta:H, H diffusion activation energy, elec. resist., 77-400K 3−38682
inTi, effect on mech. props. *(French)* 3−8906
inU, contamination effects on tensile props. 3−8908
W-O_2-H_2 system, thermodynamics, gas phase composition, chemical transport reactions *(German)* 3−34712
Zr_3P-H solid solution, crystallographic study 3−11602

hydrogen bonds
see also molecular bonds
acetic acids, halogenated, and dimeric adducts, CNDO/2 calcs. 3−20090
aliphatic alcohols, n.m.r. and association processes 3−27433
amines, primary, hydrogen bonding effect on in-plane deform. vibrs. *(Russian)* 3−7162
arylazonaphthols, crystalline, hydrogen bonds, i.r. spectra obs. 3−11580
1,4,8,11-tetra-azacyclotetradecanes, i.r. spectra and hydrogen bonding study 3−23576
benzoic acid, rel. to elec. dipole moment 3−7174
3-benzoylaminopropionic acid, i.r. spectra study of intramolecular bonding *(Russian)* 3−29684

hydrogen bonds continued
bromoacetic acid, vibr. spectra, cyclic hydrogen bonded dimer evidence 3−36028
t-butanol in electron donating solvents, i.r. spectra phenol, in electron donating solvents, i.r. spectra *(Russian)* 3−23554
carbazole, luminescence quenching mechanism *(Russian)* 3−8652
carboxylic acid single crysts., irrad., proton tunnelling from positive hole through intramol. hydrogen bond 3−5400
carboxylic acids, monomers, dimers, mixed complexes, photoelectron spectra of H-bonded systems 3−7173
cellulose copolymers from cellulose reaction with aromatic epoxypropylamines, i.r. spectra, strong intramolecular H-bonds *(Russian)* 3−31265
cesium hydrogen trifluoroacetate, i.r. and Raman spectral study of O-H-O bonding 3−11261
charge-transfer theory and relation between bonded complexes dipole moment energy and enhancement 3−20207
chloroform, p.m.r. study of hydrogen bonding with N,N-distributed amides and sulphoxides 3−4466
clathrate hydrates, double, monomer conc. in liq. water determ. 3−34343
Cu(II) complex, tetrasodium dicopper-dl-tartrate decahydrate, H-bonds in H_2O mols. from cryst. and mol. struct. anal. 3−7696
cyanoacetic acid, structure from i.r. vibr. spectra 3−15483
diazaphospholane-1,3,2 derivatives NH vibr. valence mode and intermol. bond study *(French)* 3−17442
diazaphosphorinane-1,3,2 derivatives, NH vibr. valence mode and intermol. bond study *(French)* 3−17441
diethylamine, i.r. investigation 3−4431
1,4-dihydroxy 2-methyl and 1,8-dihydroxy 3-methyl anthraquinone, effect on vibr. models 3−11257
2,6-dimethyl-4-oxy-1,2,3,4-tetrahydroquinoline, u.v. and i.r. spectra, intramolecular interaction in isomers, hydrogen bonding *(Russian)* 3−29646
diortho-hydroxybenzoic acid, study of conformers by CNDO/2 method, intramolecular hydrogen bonds 3−17398
DNA base-pairs, competition among biprotonic phototautomerism, excimer formation and proton tunnelling, review 3−11337
ethyl 1-naphthate, in hexane and water, intermolecular hydrogen bonds, proton transfer 3−33108
formaldehyde excited states interacting with water, hydrogen bond energy 3−29584
glycine silver nitrate, ferroelectric, crystal struct. 3−17798
glyoxylic acid, microwave spectrum, conformation, dipole moment, centrifugal distortion, weak intramolecular hydrogen bond 3−14386
guaiacol derivatives, dipole moments, expt. and theoretical, comparison giving intramol. bond information 3−29558
p-hexyloxybenzoic acid liquid crystal, coupling of H bonding to irientational fluctuation modes 3−1571
HF-HCN, hydrogen bonding through lone pair and π system 3−23530
hydrocarbons, halogenated, CH group hydrogen bonding ability n.m.r. meas. method limitations for XH_2 and XH_3 grou 3−20186
ice, hexagonal, mol. orbital calcs. 3−17758
ice IX, nearly proton-ordered structure 3−17786
i.r. stretching bonds depend. on bond form. 3−1170
localized orbital study of inter- and intramol. bonding 3−11204
molecular orbital theoretical study of ROH...OCH_2 dimers (R=H, CH_3, NH_2, OH, F) 3−38262
1-naphthoic acid, in hexane and water, intermolecular hydrogen bonds, proton transfer 3−33108
2- napthol, fluorescence extinction mechanism by pyridine due to complex hydrogen bonds *(Russian)* 3−29709
O...O H bonds in carboxylic acid dimers, calculation of isotopic stretching 3−23539
ortho-hydroxybenzoic acid, study of conformers by CNDO/2 method, intramolecular hydrogen bonds 3−17398
phenol complexes, influence on luminesc. *(Russian)* 3−29703
phenol-pyridine hydrogen bonded complexes, far-i.r. spectra, band assignments 3−7204
phenols, chlorosubstituted, self-assoc., i.r. spectra and OH hydrogen bonding study 3−33130
in polyribonucleic acid 3−31279
polyurethane containing large and small amounts of hydrogen bonds, i.r. spectra, band struct. of first valency vibration overtone of NH group *(Russian)* 3−29776
potassium hydrogen trifluoroacetate, i.r. and Raman spectral study of O-H-O bonding 3−11261
potential energy function refinement 3−7108
1,3propanediol, intramol. hydrogen bonding, ab initio calcs. 3−20089
proton transfer theory in bonded solids 3−11583
pyrazine, luminescence quenching mechanism *(Russian)* 3−8652
pyrroles at −180°C, rel. to i.r. and Raman spectra *(French)* 3−2529
quinones, substituted, intermolecular interaction with aprotic and proton-donating solvents *(Russian)* 3−36882
α-resorcinol, neutron diffr. study 3−24093
rock-forming silicates, valence balance of hydrogen-bonded systems 3−15859
rubidium hydrogen di-tetrachloroacetate, vibrational spectra, normal coordinate analysis, symmetrical hydrogen bonds 3−7196
salicylic acid, neutron diffr. study 3−24093
sodium cyanoacetate, structure from i.r. vibr. spectra 3−15483
tetrachlorohydroquinone hydrogen-bonded cryst., mol. packing 3−14822
transfer of the vibrational energy of the proton 3−36001
trioctylamine complex with halogenoacetic acids, i.r. study of proton transfer and hydrogen bonds 3−29633
triphenylalkylidenephosphoranes, hydrogen bonding ability 3−12516
water, O-H...O hydrogen bond potentials in Monte Carlo calculations 3−33685
water, self-diffusion down to −31°C 3−7953
water molecules, to surface hydroxyls on PuO_2, rel. to adsorption model 3−38719
water molecules in free state and in solid hydrates, ab initio calcs. 3−7118
$[H_2O...Cl]^-$ complex, SCF LCAO MO calcs. 3−29587

hydrogen bonds continued
α-Al_2O_3, $Al(OH)_3$, AlO(OH), $MgAl_2O_4$, struct. effects on chem. shift, X-ray photoelectron spectra 3−30920
B_2O_3, i.r. spectra interpretation 3−1230
$B(OH)_3$, i.r. spectra interpretation 3−1230
$CaHAsO_4.3H_2O$, and cryst. struct. 3−14762
$CaHAsO_4.3H_2O$, three circle diffraction study in crystalline state 3−17756
$CuCs_2(SO_4)_2.6H_2O$, neutron diffraction study 3−17757
$CuK_2(SO_4)_2.6H_2O$, neutron diffraction study 3−17757
$DF_2{}^-$, MO LCAO SCF calcs. 3−1171
HBO_2, i.r. spectra interpretation 3−1230
$H_{3\|x}Co_x{}^{II}Co_{1-x}{}^{III}(CN)_6.yH_2O$, hydrogen bonding and hydronium ion effects *(French)* 3−14806
$HF_2{}^-$, MO LCAO SCF calcs. 3−1171
$HF_2{}^-$, strength from. calc. of enthalpy change of reaction $HF_2{}^- \rightarrow HF + F^-$ 3−1593
$H_{3\|x}Fe_x{}^{II}Fe_{1-x}{}^{III}(CN)_6.\ yH_2O$, hydrogen bonding and hydronium ion effects *(French)* 3−14806
$(H_3N\text{-}H...NH_3)^+$, SCF calc. of hydrogen bonds 3−17400
H_2O, liquid, hydrogen bonded mols., i.r. spectral evidence 3−36031
$H_2O_2.2H_2O$, crystalline, hydrogen bonding types, correlation with O-H stretching modes *(French)* 3−2530
$Li(NH_4)SeO_4$, Raman and i.r. spectra, hydrogen bonding 3−39144
$MgFe_4((OH)_2|(SO_4)_6).20H_2O$, copiapite, crystal structure and H bonding 3−7716
$MgHAsO_4.7H_2O$, Roesslerite, struct. rel. to hydrogen bonding 3−20717
$MgHAsO_4.7H_2O$, rosslerite, and cryst. struct. 3−14762
$MgNH_4AsO_4.6H_2O$, arsenstruvite, bonding in crystal state, structure refinement 3−38558
$MgNH_4AsO_4.6H_2O$, As-struvite, and cryst. struct. 3−14762
NH_4Br, $NH_4{}^+$ libration study by Raman spectroscopy, hydrogen bond breaking process 3−34346
$NH_4H_3(SeO_3)_2$, crystal struct., X-ray obs. 3−27002
$(NH_4)_2SeO_4$, $(ND_4)_2SeO_4$, Raman and i.r. spectra, hydrogen bonding 3−39144
Na_2SeO_3, $NaHSeO_3$, H_2SeO_3, $NaH_3(SeO_3)_2$, vibr. spectral obs. 3−34341
OH groups on surface of oxides, i.r. spectra, struct. of oxides, hydrogen bonding effect 3−34365
$RbH_3(SeO_3)_2$, crystal structure, hydrogen bond lengths 3−33496
$U(BH_4)_4$, i.r. spectrum, nature of hydrogen bridging in vapour phase, relation to solid phase 3−1228

hydrogen compounds
see also deuterium compounds; ice; steam; tritium compounds; water
aqueous acid, frozen, e.s.r. of atomic H, forbidden transitions *(Russian)* 3−8420
halide gas environments, high strength steel slow crack growth 3−18680
halide pulsed lasers, H atom sources, performance optimization 3−10501
halides, absorption cell for study at variable temp. *(French)* 3−13303
ion-hydrates in ionosphere, reaction mechanisms and bonding energies 3−3066
isocyanates, MO SCF calcs. of energies charge densities and bond indices 3−4401
metal/hydrogen systems, conf., Paris, France (May-June 1972) 3−2688
perchloric acid glass, u.v.-irrad., hydronium radical obs. by e.p.r. 3−34735
polyphosphoric acid, exchange interaction role in energy transfer between Eu^{3+}, Sm^{3+}, Dy^{3+} and $UO_2{}^{2+}$ *(Russian)* 3−8651
transition metal-hydrogen solid solns. electronic struct., X-ray emission spectra interpret. 3−2603
transition metal/hydrogen systems, electron-nucl. interactions 3−2439
Ar-HCl rotationally inelastic scattering semi-classical calcs. using computer program implemented algorithm 3−11305
$CL + HI(DI) \rightarrow I + HCl(DCl)$, temperature parameter for rotational state of product 3−31245
$Cl + HI \rightarrow ClH + I$, distribution of reaction products 3−18786
$ClH(v=1,2) + H = HCl + H$, vibr. relax., classical Monte Carlo trajectory study 3−23619
DNO, microwave spectrum, transitions, rot. consts., quadrupole coupling consts., moments 3−1240
HAt sticking coeffs. for on-line anal. of mol. beam with short-lived nuclides 3−10205
HBF_2, thermodynamic props. calc. 3−39426
HBO_2 i.r. spectra in terms of OH absorption and H bonding 3−1230
HBS, rotational spectrum and structure 3−23581
HBr, Penning ioniz. reactions with metastable He, fluoresc., vibr. populations 3−29731
HBr, Raman spectra, lattice modes in molecular crystal 3−5183
HBr, V=2 state, vibrational excitation and relaxation 3−11313
HBr, vibration-to-vibration energy transfer 3−38319
HBr acid, corrosion of Ni-Mo alloy 3−8041
HBr collision with O, collinear H transfer probability calcs. 3−21802
HBr spectra, photoelectron, ionisation energies, predissociation 3−23546
HBr-Cl laser, vibr. rot. state populations, output spectra 3−10479
HBr-F laser, vibr. rot. state populations, output spectra 3−10479
$H^{79}Br$, dipole moment coeffs. calc. 3−11241
HCHO, flowing gas near i.r. laser producing $CO(CO_2)$ c.w. laser emission 3−35687
HCN, high-resolution i.r. spectra of ν_2 and $2\nu_2$ bands 3−29681
HCN, mol. Zeeman effect 3−20168
HCN, phonon dispersion and phase transition 3−7873
HCN collisions with metastable Ar atoms, dissoc. excitation of CN radical 3−20128
HCN in interstellar matter, obs. of Orion molecular cloud 3−37486
HCN isotopes in Ar matrices, i.r. spectra, examination of assumptions of matrix isolation spectroscopy 3−7193
HCN-DCN isotopic pair, inverse vibrational problem, intensity calc. 3−14347
HCN-HNC molecules, isomerism, calculations using minimum basis of Slater orbitals 3−1140
HCN^+, low-energy photoelectron spectra, bond length changes 3−1141

hydrogen compounds continued
- HCNO, photoelectron spectrum, CNDO/2 calcs. 3–33089
- H_2CO, degree of orbital delocalisation, comparison with canonical SCF solns. 3–23531
- $H_{3\|x}CO_x{}^{II}CO_{1-x}{}^{III}(CN)_6.yH_sO$, H-bonding and hydronium ion effects *(French)* 3–14806
- HCP, mol. Zeeman effect 3–20168
- HCP, u.v. spectrum, mag. and elec. field induced perturbations 3–4432
- HCl, Born-Oppenheimer approx., equilib. bond length calc. 3–33085
- HCl, DCl reorientation in liquid tetrachlorides, exptl. angular correlation functions 3–33437
- HCl, dissolved in CCl_4, vibr. and rot. motion, fluctuations from i.r. and Raman spectra theoretical anal. *(French)* 3–38284
- HCl, dissolved in weakly perturbatory solvents, fluctuations influence of rotational and vibrational states on the i.r. and Raman profiles *(French)* 3–26664
- HCl, in-situ monitor, using nondispersive i.r. technique 3–37753
- HCl, inert gas perturbed, induced low temp. absorpt. spectrum *(French)* 3–29637
- HCl, influence on early deposition of GaP on GaAs 3–2652
- HCl, N_2 perturbed, isotropic Raman spectrum, mol. shocks influence *(French)* 3–38287
- HCl, Penning ioniz. reactions with metastable He, fluoresc., vibr. populations 3–29731
- HCl, Raman spectra, lattice modes in molecular crystal 3–5183
- HCl, Si epitaxial deposition, addition of HCl to silane gas stream 3–2655
- HCl, spectra of aqueous soln. compared with spectra of Venus 3–25405
- HCl, stress free single crystal growth 3–15631
- HCl, V→V relaxation by laser fluorescence technique 3–33165
- HCl, vibr. and rot. energy transfer with HF, DF and CO_2 3–26734
- HCl, vibr. excitation and relax. of V=2 state, vibr. fluoresc. obs. 3–11321
- HCl, vibr. excitation in NH-vinyl chloride reaction, deactivation 3–11324
- HCl, vibr.-vibr. energy transfer with tunable opt. parametric oscillator excitation 3–36055
- HCl, vibration-to-vibration energy transfer 3–38319
- HCl dimers trapped in monatomic solids, far-i.r. spectra, orientational motions 3–39139
- HCl gas, vibration-vibration energy transfer 3–11309
- HCl laser, chem., based on $O(^1D)$ atom reaction with chlorofluoromethanes 3–10526
- (HCl) m.o.s. capacitors, oxide stability, surface state density and substrate generation lifetime obs. 3–24513
- HCl rotation spectra, He-induced line broadening, Fourier-transform methods *(French)* 3–7190
- HCl shock heated, variation in equilibrium i.r. fluorescence 3–4453
- HCl vibr. relax. in inert gas collisions 3–26731
- $HCl/D_2/{}^3He$ and $HCl/D_2/{}^4He$ mixtures, D_2 vibrational relaxation 3–23628
- HCl-F laser, vibr. rot. state populations, output spectra 3–10479
- HCl + Ar collisions, semi-classical approach to inelastic cross sections calc. 3–38323
- $HCl(v=1,2)+Cl=Cl+ClH$, vibr. relax., classical Monte Carlo trajectory study 3–23619
- HD, rotational-vibrational dipole transitions 3–17413
- HDCO, microwave transition of vibr. excited state, i.r. microwave double reson. 3–38300
- HF, collisional relax. behind shocks 3–11317
- HF, DF, vibr. relax. times, quasiclassical trajectory calcs. 3–38315
- HF, electric dipole matrix elements computation 3–20124
- HF, electronic spectrum, $B^1\Sigma^+$-$X^1\Sigma^+$ band system 3–26653
- HF, F-atom vibr. relax. rates, Monte Carlo calcs. 3–1289
- HF, H- and D-atom vibr. relax. rates, Monte Carlo calcs. 3–1290
- HF, in liquid SF_6, far i.r. rotational spectrum 3–20151
- HF, in-situ monitor, using nondispersive i.r. technique 3–37753
- HF, laser excited vibr. energy transfer, relax. rates 3–10466
- HF, optically pumped,laser oscill. and anisotropic gain in 1→0 vibr. band 3–713
- HF, perturbed by compressed He, broadening of (0-1) rot. line *(French)* 3–26717
- HF, self-broadened line widths and strengths in second overtone band 3–7252
- HF, vibr. and rot. energy transfer with DF, HCl and CO_2 3–26734
- HF, vibr. deactivation in H_2-F_2 chain reaction 3–10485
- HF, vibr. energy distrib., formed in methylene methyl fluoride, tandem laser obs. 3–11325
- HF, vibr. excitation, formed by elimination from chem. activated ethyl fluorides 3–11326
- HF, vibr. relax., meas. at intermediate temps. 3–10483
- HF, vibr. relax. by Ar, quasiclassical trajectory study 3–38318
- HF, vibr. relax. rate, 295-730K, effect of SF_6, N_2 and F_2 diluents 3–10467
- HF, vibr. relax. rates in presence of deactivating gases 3–11316
- HF, vibr. relax. times calc. 3–11315
- HF, vibr.-vibr. transfer time, apparent decay time 3–10488
- HF, vibration vibration transfer rate meas. from v=3 using optical pumping technique 3–29710
- HF, vibration-rotation spectra for temp. meas. of methane-F_2 flame *(French)* 3–29645
- HF (v=2) deactivation rate, use of direct overtone excitation 3–20172
- HF CW laser, diffr. limited performance using edge coupled nonfocal unstable resonator 3–32577
- HF CW laser, zero power gain meas. using pulsed probe laser 3–32537
- HF chem. laser, 10 J, operating parameters 3–35684
- HF chemical laser, high repetition rate 3–26224
- HF diffusion in ice, X-ray topographical study of dislocations 3–17826
- HF diffusion type chemical laser, numerical study 3–37955
- HF gas, prod. of Dicke superradiant pulse with ringing 3–22886
- HF in ice, X-ray topographical study of dislocations 3–20746
- HF in N_2 electron beam stabilized discharge, quenching effect causing superfluorescence 3–19599
- HF laser, action rel. to electrode structs. 3–10480

hydrogen compounds continued
- HF laser, chem., based on F atom reaction with saturated and unsaturated hydrocarbons, energy partitioning 3–10524
- HF laser, chem., based on $O(^1D)$ atom reaction with chlorofluoromethanes 3–10526
- HF laser, chem., based on NF_3 + H donor transverse discharge, performance 3–10527
- HF laser, chem., based on NF_3-H_2 reaction energy output press. depend. 3–10532
- HF laser, chem., based on H_2-SF_6 reaction, chem. efficiency 3–10533
- HF laser, chem., CW, performance in unstable cylindrical confocal oscillators 3–10490
- HF laser, chem., CW performance, chain vs. cold reaction 3–10535
- HF laser, chem., formed in H_2-F_2-He mixtures, performance and enhanced initiation 3–10529
- HF laser, chem., laser action above second explosion limit of F_2-$H_2(D_2)$ mixtures 3–10531
- HF laser, chem., pulsed, performance, effect of CO_2 laser irrad. 3–10502
- HF laser, chem., TEM_{00} short pulse oscillator, construction and performance 3–10530
- HF laser, chem. pumped by NF_3-H cpd. reaction, modes, kinetic transfer rates 3–10528
- HF laser, chemical, time sequencing rel. to energy content under different cavity configs. 3–22871
- HF laser, diagnostic techniques, cavity characts. 3–9961
- HF laser, electrically initiated SF_6-ethane mixtures, performance 3–26223
- HF laser, gain, relax., spatial and temporal depends. 3–10486
- HF laser, pumped by H_2-F_2 chain reaction, cavity chem. mechanism interactions 3–10489
- HF laser system, collisional deactivation processes, laser amplifier meas. 3–10513
- HF low-density discharge, Stark broadened Balmer lines *(German)* 3–38515
- HF magnetic shielding of ^1H and ^{19}F using many body perturbation theory 3–11214
- HF mol., model pseudopot. calcs. of valence electron props. 3–20091
- HF product of abstraction reaction between F atoms and org. cpds., energy partitioning and i.r. chemilum. 3–31253
- HF product of abstraction reaction between F atoms and hydrides, energy partitioning and i.r. chemilum. 3–31254
- HF solvated electrons, semi-empirical UHF treatment 3–4402
- HF vibrational deactivation in pure HF and HF-additive mixtures, meas. using laser-excited vibrational fluorescence 3–7250
- HF-DF laser, CW combustion/mixing laser, construction., props. 3–10534
- HF-H_2, vibr. activated HF deactivation in reaction flow tube 3–11322
- HF-HCN, hydrogen bonding through lone pair and π system, mol. orbital theory 3–23530
- HF + H, reaction rates and energy distrib., Monte Carlo calcs. 3–37120
- HF_2^-, charge distribution and strength of hydrogen bond 3–1593
- HF_2^-, vibr. struct. and equil. geom., ab initio calcs. 3–1171
- $H_{3\|x}Fe_x{}^{II}Fe_{1-x}{}^{III}(CN)_6$-$yH_2O$, H-bonding and hydronium ion effects *(French)* 3–14806
- HI, chem. laser, from $H+I_2$ reactions, vibr. population inversion 3–29074
- HI, i.r. specrometry study of solvent effects on fundamental and harmonic vibration frequencies *(French)* 3–11255
- HI-Cl laser, vibr. rot. state populations, output spectra 3–10479
- HI-F laser, chem., obs. of laser reaction by equal gain technique 3–10498
- HI-F laser, vibr. rot. state populations, output spectra 3–10479
- HIO_3, alpha-phase, determ. of optical rectification coeffs. 3–26241
- α-HIO_3, Raman scatt. by optical phonons, Fermi reson. 3–21406
- α-HIO_3, Raman scatt. by polaritons 3–34369
- α-HIO_3, spontaneous parametric radiation excited by Ar laser radiation 3–22955
- α-HIO_3 cryst., refr. indices, meas. 3–12107
- $HK_8Rh_3Br_{18}.10H_2O$, cryst. struct. 3–17769
- $HK_8Rh_3Br_{18}.10H_2O$, cryst. and mol. struct. 3–24072
- HNCO and HNCS, far-i.r. matrix isolated spectra, vibr. mode assignment 3–29656
- HNCO molecular force field 3–17405
- HNCS molecular force field 3–17405
- HNO_3 vapour distrib. in stratosphere, i.r. atm. emission meas. 3–25233
- HNO_3 water solns., scatt., nonlinear high-order effects 3–772
- $H_2N.NH_3Cl_2(Br_2)$, γ-irrad., e.p.r., V-centres and H atom spectra 3–2393
- H_2O, collision with electrons, crossed beam and target gas methods for optical excitation function 3–11306
- H_2O_2, polarization functions and geometry optimization in ab initio calc. of rotational barrier 3–7105
- H_2O_2, vibr. spectra and consts. 3–33129
- H_2O_2, volume-regulation of irradiated murine lymphoma cell in vitro 3–28378
- H_2O_2 and D substituted products, internal rot. barriers, conformations and vibr. spectra 3–33074
- H_2O_2 form. by adiabatic expansion of H_2-O_2 gas mixture 3–5372
- H_3O^+, conformational anal. from p-toluenesulphonic acid monohydrate neutron diffr. study 3–17799
- H_3O^+, force constant calc., comparison with exptl. results, effect of crystal environment on geometry *(French)* 3–7152
- HOF, centrifugal distortion analysis of rot. spectrum 3–1237
- HOF, photoelectron spectrum, valence region orbitals analysis 3–36047
- HOF, photoionization with mass analysis 3–26713
- HOF, proton and ^{19}F n.m.r. meas. for low temp. liquid and room temp. gas, determ. of atomic charge 3–4460
- $H_2O_2.2H_2O$, crystalline, i.r. and Raman spectra at 80K, O-H stretching modes *(French)* 3–2530
- H_3PO_4/H_2O glass, γ-irradiated at 77K, ENDOR spectra of trapped H atom 3–25078
- H_2S, ang. distrib. of photoelectron spectra 3–23545

hydrogen compounds continued
H_2S, compound states, study using electron transmission spectroscopy 3–17466
H_2S, electronic states linearity barriers; curvilinear and rectilinear models, comparison 3–23528
H_2S, heterogeneous oxidation below 1000 ppm in N/air mixtures over metal oxide catalysts 3–37198
H_2S, proton affinity, rel. to water 3–25043
H_2S oxidation by O_3 in aqueous solution 3–9292
H_2S-H_3S^+, momentum transfer collision rate consts., temp. depend. 3–17474
H_2S^+, ion radical, rot. anal. of emission spectra, 400-500 nm 3–1207
H_2SO_4 vitreous aqueous solution, spin lattice relax. of H atoms, effects of paramag. ions 3–34186
H_2SO_4 vitreous aqueous solution, spin diffusion and spin-lattice relax. of H atoms 3–34187
H_2SO_4/H_2O glass, γ-irradiated at 77K, ENDOR spectra of trapped H atom 3–25078
H_2SeO_3, Raman and i.r. spectra, vibr. and hydrogen bonding 3–34341
$H_{0.46}WO_3$, hydrogen tungsten bronze, pulsed NMR study of proton mobility 3–34223
Nb-H system, quasi-elastic neutron scatt. 3–1819
Nb-Zr-H, n.m.r. exam. and H self-diffusion *(Russian)* 3–1815
O_2-HCl, thermal oxidation of Si, electrically stable SiO_2:Cl 3–39287
Pd-B-H system, statistical thermodynamics, electron interaction energy *(German)* 3–30240
Si-H-Cl system, thermodynamic evaluation 3–11716
hydrogen ion activity *see pH*
hydrogen ion concentration *see pH*
hydrogen ions
admixtures effect on He^{2+}, 4686 and 3203 lines, temp. determ. from relative line-to-continuum intensity 3–14303
beams, charge changing processes in gases and alkali metal vapours, review 3–35983
D-region, effect on positive ion composition 3–3097
fast, impact dissoc. into ions of O_2, CO and NO molecules 3–23621
hydrogenic ions, highly excited, charged particle excitation 3–38235
ionospheric distrib. at low latitudes 3–18884
kinetic processes, non-stationary *(Russian)* 3–7300
multiphoton ionisation, reson. nature 3–14302
multiply charged ions, plasma parameters determ. for plasma-beam discharges 3–23916
plasma diagnostics in a pulsed discharge in a mixture containing H_2 3–14587
positive, bombardment of Al surface, negative ions energy distrib. 3–15583
proton-atomic H scattering, theoretical study 3–11179
Stark profiles in static elec. field *(French)* 3–1102
BaF_2, calc. of H^- impurity vibr. 3–36390
CaF_2, calc. of H^- impurity vibr. 3–36390
$CaF_2:H^-$ i.r. relectivity study of high concs. of H^- ions 3–4836
H plasma, underdense, Compton scatt. of laser radiation by ions 3–20431
H storage beam, frequency standard, low-Q cavity maser 3–3749
H-D ion mixture, plasma, h.f. heating under ion-ion hybrid resonance conditions *(Russian)* 3–1511
H^-, 1^1S ground state, expectation values, lower bounds 3–29457
H^-, Coulomb holes and expectation values, explicitly correlated wavefunctions 3–23464
H^-, electron detachment, Born-Ochkur approx. 3–35973
H^-, electron impact, double ioniz. cross sections 3–20045
H^-, photoionisation, cross section calc. above $n=2$ threshold 3–11151
H^- injection system for TRIUMF 500 MeV cyclotron, Vancouver, Canada 3–13401
H^- source, h.f., optimal current *(French)* 3–280
H^+, energy dependence of channelling in Si overlaid with Au films 3–33581
H^+, H_2^+, bombardment of helium, He autoionisation and He^- autodetachment study 3–23490
H^+ and H_2^+, two-ion species, hybrid resonance, in plasma 3–23862
H^+ and H^- ion recombination in slow collisions 3–7085
H^+ charge transfer collisions with H atoms, Faddeev approach 3–35977
H^+ collision with HeH^+ isotopes, quasibound states theory, comparison with experiment 3–26714
H^+ collisions with He, time-dependent studies of vacuum u.v. emissions 3–29530
H^+ flux beteen plasmasphere and ionosphere. diurnal variation 3–16040
H^+ impact on Cu clean surface, light emission 3–18501
H^+ scattering in the weakly screened Coulomb field of Au nuclei 3–11182
H^+ thermal ions, in magnetosphere 3–3148
H^+/O^+ transition level during day and night in ionosphere 3–9319
H^+-H^- collisions, charge transfer, atomic wave functions calc. 3–14315
H^+-Kr charge exchange collisions, spin polarisation 3–35978
$H^+ + Ar$, elastic differential scattering expts., investigation of one state molecular system 3–11185
$H^+ + H$ scatt., hydrogenic expansion convergence 3–1128
$H^+ + H_2$ inelastic scatt., differential cross sections, rainbow max., semiclassical treatment 3–33153
$H^+ + Kr$, elastic differential scattering expts., investigation of one state molecular system 3–11185
$H^+{}_2$ like systems, polarisation expansion, using convergence props. of Rayleigh-Schrondinger perturbation expansion 3–14333
H_2^+, Delta function model and perturbation expansions of energy and wavefunction 3–7109
H_2^+, energy level calc. 3–36000
H_2^+, exchange polarisation energy calc. 3–29757
H_2^+, moment functions calc. from dipole oscillator strengths 3–4408
H_2^+, polarisability, quantum mechanical calculations 3–23476
H_2^+, proton-impact dissociation and ionisation study 3–20200
H_2^+, variational approxs. to trial wavefunctions 3–26636
H_2^+ collisions with H_2 from 0.6 to 1.5 MeV, electron emission 3–36050
H_2^+ dipole strengths, calc. using asymptotic techniques 3–11211
hydrogen ions continued
H_2^+ energy spectrum of field ionisation at single atomic site 3–35508
H_2^+ in $1s\sigma_g$ state, collisional dissociation *(German)* 3–38310
H_2^+ photodissoc. by monochromatic light, energy analysis of ejected H^+ ions 3–11289
H_2^+ plane beam, transformation into hollow cylindrical *(French)* 3–276
$H_2^+ + CO_2$ reaction rates meas. by ion cyclotron resonance 3–26721
$H_2^+ + He \rightarrow HeH^+ + H$, 1-25 eV, crossed beam studies 3–39439
$H_2^+ + N_2O$ reacton rates meas. by ion cyclotron resonance 3–26722
$H^{3+} + N_2 \rightarrow N_2H^+ + H_2$, proton transfer reactions in flowing afterglows, kinetics 3–39438
H_4^+ potential surface calc. with wavefunctions based on valence band configuration interaction 3–17397
$H^+(H_2)_n$, $H^+(H_2O)_n$ cluster production on solid H_2 and ice, models 3–36965
HII regions, classification as radio sources using recombination line emission 3–3334
NH_3-H^+ collisions, first order orientation dependent forces 3–4487
SrF_2, calc. of H^- impurity vibr. 3–36390
hydrogen neutral atoms
absorption profile for H I in galactic centre region and measures of radiosources distances 3–25498
adsorption on W(100), through-bond interaction of two H atoms 3–30343
atomic energy levels and multiplet tables 3–29483
atomic mass determ. 3–11107
atomic mass determ. 3–32998
balmer emission lines in coronal spectrogram taken at 1970, March 7 eclipse 3–18941
Balmer line emission from interstellar medium and geocorona 3–28286
Balmer lines from low-density HF discharge, Stark broadening *(German)* 3–38515
Balmer lines H10, H11, H12 identification in spectrum of Herbig-Haro No.1 object 3–28202
beams, charge changing processes in gases and alkali metal vapours, review 3–35983
binding energies for small clusters of $^3\Sigma_u^+$ H and D atoms, calc. 3–17386
bound-bound transitions in strong mag. field, astrophysical appl. 3–26564
charge transfer collisions with H^+, Faddeev approach 3–35977
chemisorption on metal surfaces, charge densities and binding energies calc. 3–33740
collinear atom transfer probability calcs. for reaction $O + HBr \rightarrow OH + Br$ 3–21802
collisions, fast, classical binary encounter approx. approach 3–33054
collisions with e^+, calc. of S-wave phase shift and positronium formation cross section using close-coupling method 3–4384
collisions with electrons at intermediate energies, classical cross sections calc. 3–14308
collisions with F_2, Monte Carlo calc. of reaction rates and vibrational level populations of products 3–31255
collisions with $He(2^1S)$ and $He(2^3S)$ metastable atoms, cross sections for chemiionisation 3–38253
collisions with $He(2^3S)$ and $He(2^1S)$ metastable atoms, chemiionisation 3–38252
collisions with N_2, second positive (0, 0) transition, emission cross sections 3–11327
complex-valued classical trajectories for reactive tunneling in three dimensional collisions of H and H_2 3–25056
Cygnus X-3 radio source, distance meas. from 21 cm obs. 3–35161
damping of Na D-lines by atomic H in solar spectrum and spectra of atmosphere of cool stars 3–9465
dynamical symmetry group *(French)* 3–16697
early type galaxies, HI 21-cm. line study 3–5610
elastic scattering of e^- and p, closed-form Glauber cross sections 3–26597
electron and proton inelastic scatt. at intermediate energies, Eikonal distorted wave theory 3–33050
electron collisional excitation function, threshold behaviour 3–20046
electron impact ioniz. cross section meas. 3–33158
electron S state elastic scattering resonances in absence of degeneracy 3–7077
electron scatt., close coupled calcs. using noniterative integral eqn. technique 3–4382
electron scatt., close coupled calcs. using noniterative integral eqn. technique 3–4383
electron scatt., differential cross sections, off-shell Coulomb T matrix 3–7079
electron scatt., least squares method applic. 3–20042
electron scatt., microscopic optical-model analysis 3–4388
electron scatt., S-state expansion convergence at intermediate energies 3–20048
electron scattering, long-range dipole interactions, threshold law for $n \rightarrow n+1$ transitions 3–7076
electron scattering, singlet s-wave scattering below first excitation threshold 3–38236
electron transmission spectroscopy, resons. in total scatt. cross section 3–7083
electron-H atom system state in an intense e.m. field 3–35953
electron-transfer collisions with protons, second-order Born terms 3–4394
energy transfer collisions, vibr. relax. of HF and DF 3–1290
e.p.r. study, signal time depend. 3–31274
even wave functions evaluation in the Feynmann path-integral formalism 3–26120
exosphere, H abundance, diurnal variation rel. to exospheric temperature 3–34923
fast, impact dissoc. into ions of O_2, CO and NO molecules 3–23621
G195-19 (mag. white dwarf), 21 cm continuum radiation upper unit 3–22065
galactic H I remnants of strong tidal disruption with SMC, search at 21 cm wavelength 3–25499
Gaussian wave functions *(French)* 3–23515
Glauber exchange amplitude, reduction 3–11170

hydrogen neutral atoms continued
grazing collision of high-energy charged particles, bounds on mean excitation energies 3—20038
Grw + 70°8247 (mag. white dwarf), 21 cm continuum radiation upper unit 3—22065
highly excited, effective cross sections of electron collisions *(German)* 3—14307
hydrogenic atoms, highly excited, charged particle excitation 3—38235
hydrogenlike atoms, Bethe-Salpeter eqn., soln. as test of numerical technique accuracy 3—29173
hyperfine pressure shift measurements in Ar buffer gas 3—35982
impact excitation of He 3—26607
impact excitation of He by H atoms, spectroscopic analysis of radiation emitted during decay of products 3—26607
impact ionisation of He($1s^2$) and Li^+($1s^2$) using semiquantal theory 3—20063
inelastic collision of fast charged particles, cross sections 3—20049
interacting system, nonadditive polarizability 3—14294
intergalactic H I in Coma cluster of galaxies, heating mechanism and model 3—37460
K-shell photoionisation cross section and threshold energy determ. 3—14300
long-range interactions, finite-difference approach 3—35985
Lyman α emission from Coma Cluster of galaxies rel. to models of intracluster gas 3—28278
Lyman α high spatial resolution photographs after 1972, July 10 eclipse 3—31556
Lyman-α, Stark broadened profile, unified calc. 3—33019
Lyman-α airglow, spatial and temporal var. rel. to H I distributions 3—31399
Lyman-α line broadening by Stark effect, satellite prod. by proton perturbations 3—29475
Lyman-α observations of aspherical H geocorona at 18 Earth radii 3—16005
Lyman-α radiation in H atm. of comets, model with multiple scattering 3—28161
M33, nearby galaxy, HI 21 cm. survey 3—22113
magnetic h.f. interactions, Schrodinger, Dirac and QED perturbation calcs. 3—33017
Markarian galaxies H I 21-cm. line observations of II objects 3—22104
maser frequency stability rel. to output, mag. polarisation field and relaxation, meas. *(German)* 3—10459
matrix elements off diagonal, continuum wave functions in calc. 3—17339
metastable, collisional quenching by inert gases 3—17382
metastable 2S state, 2 photon spontaneous emission, momentum-translation approximation 3—11110
momentum translation approximation for threshold ionisation by a laser beam 3—38199
multiphoton ionisation, reson. nature 3—14302
multiphoton ionisation by intense e.m. fields, momentum translation method application 3—38223
multiphoton ionisation in intense laser beam 3—38224
multiphoton ioniz., circular versus linear polarisation cross sections 3—33037
multiphoton ionization at 0.53 μ 3—11157
mutliphoton absorpt., in intense e.m. fields, relativistic correction 3—29474
NGC 4244 (Scd-type galaxy), H I 21 cm line study rel. to mass distribution 3—25500
nonisothermal shock layer, radiative flux, temp. dependent spectral absorption coeff. 3—1327
one-electron systems, electron density pointwise bounds and expectation value estimates 3—14274
photo-effect, two-quantum, ang. distrib. 3—38227
photoionisation of ground, 1S and metastable 2S state with phase polarised light of threshold freq. 3—26582
plasma, high optical densities meas., special features of the line absorption method 3—14586
polarization field for transistors 3—29197
positron scatt., inelastic S-wave variational calcs. 3—4389
proton struct. and h.f. splitting 3—6600
proton-atomic H scattering, theoretical study 3—11179
quantum statistical mech., correl. functions, from bounds for thermodynamic Green's functions 3—16748
quantum-mechanical models with modified Coulomb potentials, soln. by algebraic method based on SO(4,2) dynamical group 3—22707
quasi-elastic scattering cross sections in tissue like media 3—3593
quasi-Landau spectrum of hydrogen-like system in strong mag. field 3—33038
quenching of 2S state by inert gas collisions 3—11164
radiation transfer of Lyman-α in pure H nebulae, Monte Carlo techniques 3—37491
Raman photon absorption or emission transition amplitude calc. 3—11128
redshift meas. of Stark-broadened lines, odd Balmer line shifts in Sirius 3—20012
retarded interatomic potential energy of 2 ground state H atoms, Dirac theory 3—20073
scattering of electrons and protons in coupled state approx., impact parameter formulation 3—11176
Scorpius X-1, Hα, Hβ and Hγ equivalent widths and profiles rel. to B magnitude 3—13077
second level populations in a plasma medium 3—23473
self-diffusion in lithium-ammonia and sodium-ammonia solutions, n.m.r. meas. 3—20883
Seyfert galaxies, surface brightness gradient rel. to H-line emission *(Russian)* 3—37443
on silica gel, adsorbed O_2, paramagnetic relaxation 3—37144
solar flare ^{1}H differential energy spectra meas. 3—39601
solar flare of 1972, August 11, photograph in Hα light at Boyden Observatory 3—9466
solar flares, Lyman lines model calculations rel. to column density 3—18967
solar Lyman-α control of 2775 kHz ionospheric absorption 3—31412
solar Lyman-α emission, u.v. meas. by Vertical-1 rocket 3—25394
spectra, seventh series 3—23468

hydrogen neutral atoms continued
spectral lines, Balmer and Lyman, tables of Stark broadening 3—35951
spectral lines used in determ. of Rydberg const., dependence of line structure on excitation conditions 3—13206
spectrum, 14 lowest states spectrum in strong mag. field, 10^6-10^8 G 3—23456
Stark and free-field wave functions, group-theoretic connection 3—11118
Stark effect, first order in low elec. field 3—11127
Stark effect of first excited level and Lyman α line in 3 dimens. stochastic fields 3—17342
structure, in intense magnetic field 3—1093
thermal motion in crystallographic models, riding motion and higher cumulants determ. 3—14664
three-dimensional, as a restricted four dimensional harmonic oscillator 3—37866
wavepacket solution, classical limit 3—28936
zero-field quantum beats of Lyman-α radiation subsequent to beam-foil interaction 3—7062
Ar + H collisons, total differential cross section 3—33059
$D + H_2 = DH + H$, low temp. rate consts. using e.p.r. detection 3—39437
$F + H^+$ collisions, molecular theory, cross sections calc. 3—29520
$F_2 + H \rightarrow HF + F$ reaction, potential energy surface calc. 3—25053
H, atoms in 2S, 2P states, dissociation from photon collisions *(German)* 3—33155
μH, μ transfer to gaseous Xe in collisions 3—20077
H beta/N_2^+ 4709 angstrom intensity ratio meas. in proton-excited aurora 3—15990
H I line, lunar occultation of Galactic centre region at 1420 MHz 3—39730
H I regions, optical depth determ. of 21-cm emission line profiles 3—9608
H/Fe rel. abundance var. in North Galactic Pole K-type giant stars, UBVRI photometry 3—9543
H-e^+ collisions, Faddeev approach investigation 3—23501
H-He potential determ. from molecular beam expts. 3—11165
$H + C_2H_4$ reaction, press., stoichiometry and third body species effects 3—37118
$H + F_2 \rightarrow HF + F$, determ. of energy distribution among products using arrested relaxation variant of i.r. chemiluminescence technique 3—5377
$H + H_2$, exchange reaction probability calc. using quasi-classical trajectory calc. 3—27859
$H + H_2$ collinear isotopic systems, exchange reactions, quantum mech. studies 3—31262
$H + H_2$ collinear reaction, semi-classical, exact quantum and quasi-classical transition probabilities 3—31248
$H + H_2(v = 1,2) = H_2 + H$, vibr. relax., classical Monte Carlo trajectory study 3—23619
$H + H_2 \rightarrow H_2 + H$ collinear exchange reactions, analytical energy surfaces 3—20205
H + HF, reaction rates and energy distrib., Monte Carlo calcs. 3—37120
$H^+ + F$ collisions, molecular theory approach 3—29519
$H^+ + H$ scatt., hydrogenic expansion convergence 3—1128
$H(D) + Cl_2 \rightarrow Cl + HCl(DCl)$ temperature parameter for rotational state of product 3—31245
HI lines in the star X Persei, spectroscopic changes 3—25464
H_3PO_4/H_2O glass, γ-irradiated at 77K, ENDOR spectra of trapped H atom 3—25078
H_2SO_4/H_2O glass, γ-irradiated at 77K, ENDOR spectra of trapped H atom 3—25078
H(2S), H(2P) formation in H collision with planetary atmosphere constituents, Lyman-α emission cross-sections 3—33151
H(2s) cross section meas., prequench losses 3—7060
Hα, Hβ profile meas. for electron temp. determ. of M42 (Orion Nebula) 3—28296
Hα emission broad component in NGC 5548, Seyfert galaxy 3—31756
Hα emission in central regions of nearby galaxies, correl. with blue colour index 3—28284
Hα emission search around companion radiosources of Sco X-1, X-ray source 3—3353
Hα filter observations of solar prominences rel. to structure 3—35038
Hα filtergrams of moving magnetic features near sunspots 3—31559
Hα fluorescence in M82 galaxy, source in filaments 3—28258
Hα intensity in nuclei of Seyfert galaxies, rapid variations 3—35182
Hα line emission from chromospheric surges, dynamics and localisation determ. 3—35048
Hα line width in late type stars, rel. to gravity and effective temp. 3—35135
Hα solar activity rel. to type III radio bursts, 1970 May 22 active region study 3—35029
Hα solar chromospheric spectral investigation, mottles and model of overall structure 3—35034
Hβ intrinsic polarisation in 53 Camelopardalis (mag. Ap star) 3—25454
Hβ line in solar spectra, correlations of fluctuations with Ca II H and K lines and Mg b 3—39629
Hβ solar line oddities on spectrograms of good spatial resolution 3—39616
He + H collisions, total differential cross section 3—33059
$He^{2+} + H$ collisions, electron transfer and excitation, coupled-state calcs. 3—26602
HeH, long-range hyperfine shift computation 3—26611
$HeH^+ + H \rightarrow H_2^+ + He$, 1-25 eV, crossed beam studies 3—39439
^{4}He, backscatt. by Si, Au, Cu, ion fraction, 25-150 keV 3—30912
KH_2PO_4/H_2O matrix, γ-irradiated at 77K, ENDOR spectra of trapped H atom 3—25078
$KHSO_4/H_2O$ matrix, γ-irradiated at 77K, ENDOR spectra of trapped H atom 3—25078
NO-H atom reaction rate constants, phase shift meas. 3—39431
Si, surfaces, H and H_2O adsorption, desorption spectrometric results 3—11805

hydrogen neutral molecules
21-cm line profiles of interstellar medium, statistical analysis 3—25518

hydrogen neutral molecules continued
autoionizing transitions produced by electron impact 3−33156
Cartesian force consts., computer calc. 3−4423
chemisorption on SnO_2 film, var. of electrical conductance *(Japanese)* 3−8024
cluster production, in condensed molecular beam for particle loss compensation in thermonuclear devices 3−4677
coherent X-ray scattering intensity, evaluation of two-centre integrals 3−23514
collision with acetaldehyde rotational line broadening, molecular quadrupole moments 3−23634
collision with F^-, electron detachment rates meas. 3−11300
collision with He^- ions, detachment cross sections 3−14312
collision with He atoms, electron loss 3−11166
collision with O^-, associative detachment 3−20201
collisions with DCl, V→T, R and V→V relaxation, by laser fluorescence technique 3−33165
collisions with He(2^3S) and He(2^1S) metastable atoms, chemiionisation 3−38252
collisions with Hg^+ from 0.6 to 1.5 MeV, electron emission 3−36050
collisions with K atoms, coherence transfer between K $^2P_{1/2}$ and $^2P_{3/2}$ states 3−26606
collisions with laser excited methyl fluoride, vibrational relaxation 3−33162
collisions with methyl chloride, laser fluorescence study of vibrational energy transfer 3−33163
collisions with T, hard sphere reactions, chattering 3−38321
complex-valued classical trajectories for reactive tunneling in three dimensional collisions of H and H_2 3−25056
depolarised Rayleigh lineshape, mol. reorientation rot. depend. 3−4433
differential collision cross section, energy depend. 3−1292
dilute solution in liquid Ar i.r. absorption spectra 3−21412
dissociation and recombination, rotational contribution, master equation 3−29727
dissociative and non-dissociative photoionisation at 304 and 584 Å 3−33149
dissociative excitation by electron impact, metastable fragment form. 3−4481
dissociative photoionization through $1s\sigma_g$ ionic state 3−20196
distorted-atoms in molecules model, spatial electronic wavefunctions 3−38265
electron impact ioniz., Glauber theory 3−29524
electron scatt., polarization role in intermediate energy range 3−1125
electronic particle-hole propagator calc. using self-consistent polarization propagator method 3−7112
energy parameters in Lennard-Jones potential between atoms determ. from second virial coefficients 3−14402
flow in capillaries, boundary effects 3−14476
fundamental state energy using Gaussian wave functions *(French)* 3−23515
ground-state wavefunction by basis sets in quantum mechanical calculations 3−1160
Hartree-Fock polarisabilities calc. 3−29486
Heitler-London approx., and variable orbital exponents 3−7111
intermediate coupling between Hund's cases for 3d Rydberg states 3−11205
interstellar cloud heating by vibrationally excited molecular H 3−31784
interstellar clouds, H_2 detection in 4.4 to 28.2 microns wavelength region 3−25514
interstellar medium, radiative lifetime as function of vibrational quantum number 3−13098
interstellar mol. H bands in u.v. spectrum of δ Scorpii 3−25510
ionisation, inelastic electron impact cross-section 3−1281
ionization function meas., appearance of reson. struct. *(Dutch)* 3−29733
isoteric adsorption enthalpy, of Pd and Pt atomically disposed thin film on C substrate *(German)* 3−27921
laser power densities for Lyman and Werner bands 3−4082
luminescence of Na and K in pulse discharge, H_2-addition effect 3−33413
Lyman-band absorpt. contrib. to u.v. opacity in the Sun and other stars 3−25438
Lymann transition in u.v. laser *(Russian)* 3−723
magnetic susceptibility, calc. by variation of vector potential and induced current *(Russian)* 3−33081
microwave optical magnetic resonance, induced by electrons, line shape and intensity considerations 3−29717
mixtures, ortho and para, viscosity model below 25 K 3−23636
multiphoton ionization at 0.53 μ 3−11157
nuclear liquid foam-insulated target for streamer chambers 3−3841
ortho, fine and hyperfine struct. of vibrational levels by microwave optical magnetic resonance induced by electrons 3−29716
ortho-para mixtures, rotational transitions and thermal diffusion 3−7249
para, generalised hydrodynamic eqns., transport coeffs. calc. 3−32599
Pariser-Parr-Pople method with retention of bonded differential overlap, choice of parameters 3−11197
polarisability and anisotropy in ground state, Rayleigh and Raman cross-sections for photon scatt. 3−20153
pressure-induced H_2 band in spectra of Jupiter at 24 microns, atm. temp. rel. to Neptune 3−28149
pressure-induced H_2 band in spectra of Neptune at 24 microns, atm. temp. rel. to Jupiter 3−28149
proton affinity determ. from $H_2O^+ + H_2 \rightarrow H_3^+ + OH$ reaction 3−2802
Q branch Raman band, J depend. of the depolarization ratio of the rotational components 3−17430
quadrupole lines observed in Jovian spectrum, interpretation 3−31614
Raman scattering cross-section for rotational lines and Q-branch of the vibrational transition 3−20100
scattering of Li^+ on H_2, vibr. quantum transitions, differential cross sections meas. 3−14396
second order intermol. forces, overlap effects 3−7267

hydrogen neutral molecules continued
solid, i.r. spectroscopy at high pressure and low temp. *(French)* 3−13310
sorption, molecular sieve type, on alkali graphite intercalation compounds 3−33732
static polarizability tensor calc. in screened valence bond approx. 3−38266
thermal dissoc. rate, rot. effect 3−2799
total inelastic cross section for collisions with fast charged particles 3−11303
track sensitive target for 500 litre Ne-H_2 chamber 3−10071
u.v. absorption by H_2 in stellar atmospheres rel. to opacity of main sequence A-type stars 3−25433
vibrational relaxation study using Raman excitation in rare gas mixture 3−29735
vibrationally excited, quantitative vacuum u.v. absorption studies 3−11254
$CO_2 + p\text{-}H_2(0\text{-}H_2)$ collisions, simultaneous vibr.-translation, vibr.-rot. and rot.-translation exchanges *(French)* 3−23614
$Cl + H_2 \rightarrow HCl + H$ reversible reaction, rate const. ratio 3−21795
$F + H_2(D_2) \rightarrow H(D) + HF(DF)$ temperature parameter for rotational state of product 3−31245
(H_2, D_2) exchange reaction mechanism potential barrier 3−25054
H II regions, H_2, molecules inside neutral globules 3−25519
$H + H_2$, exchange reaction probability calc. using quasi-classical trajectory calc. 3−27859
$H + H_2$ collinear reaction, semi-classical, exact quantum and quasi-classical transition probabilities 3−31248
$H + H_2 \rightarrow H_2 + H$ collinear exchange reactions, analytical energy surfaces 3−20205
$H^+{}_2$ like systems, polarisation expansion, using convergence props. of Rayleigh-Schrondinger perturbation expansion 3−14333
p-H_2, 1s 4p $^3\Pi_u$, v=0, N=1 level, non-zero mag. field crossing 3−17453
H_2, 2p and 3p $^3\Pi_u$ states, fine and hyperfine struct. calc. 3−17402
H_2, elastic and inelastic photon scatt. as function of kinetic energy *(German)* 3−33155
H_2, H_3, ground states, non-empirical approx. calc. including complete config. interaction 3−11203
0-H_2, in various rot. sublevels, collisions with inert gases, meas. of cross-section *(Dutch)* 3−29737
H_2 and D_2, ionisation shift between energy thresholds, meas. using new mathematical technique 3−29500
H_2 in H_2-inert gas mixture, collision, induced i.r. absorpt. profile anal. and intercollisional interference effect 3−23563
o-H_2 separation process using He gas cryogenerator 3−135
H_2-ClF_3, possible chain-branching chem. -laser, comment on results 3−22875
H_2-ClF_3, possible chain-branching chem. laser, reply to comments on results 3−22876
H_2-HF, vibr. activated HF deactivation in reaction flow tube 3−11322
H_2-He collisions, classical S-matrix elements for vibrational excitation in three dimensions 3−7251
H_2-He thermal opacity in atm. of major planets 3−31576
$H_2 + CO_2^+$ reaction rates meas. by ion cyclotron resonance 3−26721
$H_2 + D = H + DH$, low temp. rate consts. using e.p.r. detection 3−39437
$H_2 + F_2$ pulsed laser, H_2 pressure effect on stimulated emission 3−6460
$H_2 + H$ collinear isotopic systems, exchange reactions, quantum mech. studies 3−31262
$H_2 + H^+$ inelastic scatt., differential cross sections, rainbow max., semiclassical treatment 3−33153
$H_2 + N_2O^+$ reaction rates meas. by ion cyclotron resonance 3−26722
$H_2 + Ne$, excitation and dissociation only observed 3−1274
para-H_2 + para-H_2, crossed beam elastic scatt. meas., intermol. pot. determ. 3−7269
H_2^+, Delta function model and perturbation expansions of energy and wavefunction 3−7109
H_2^+, moment functions calc. from dipole oscillator strengths 3−4408
H_2^+, variational approxs. to trial wavefunctions 3−26636
$H_2^+ + He \rightarrow HeH^+ + H$, 1-25 eV, crossed beam studies 3−39439
H_3, potential energy contour maps of ground and electronically excited states 3−20085
H_3 potential energy surface, calc. using configuration interaction method 3−26625
$H_2(B^1\Sigma^+{}_u$ state), ab initio and Rydberg-Klein-Rees pot. energy curves, comparison 3−17406
HD, $\Delta v=1$ electric dipole transition, amplitude estimate 3−29628
HD, intensities and Faro line shape in i.r. spectrum 3−26659
HD, Raman Q(J) lines, obs. for range of densities 3−20139
HD collisions with T, hard sphere reactions, chattering 3−38321
$H_2(D_2)$-Br(I), reaction mechanism, classical dynamical study 3−37119
He + H_2 spark chambers, time characteristics and efficiency 3−22469
$He^* + H_2 \rightarrow HeH^+ + H + e$, 0.05 to 10 eV, cross-sections 3−9052
$H_2(v=1,2) + H = H + H_2$, vibr. relax., classical Monte Carlo trajectory study 3−23619
$Li + H_2 \rightarrow LiH + H$ collinear exchange reactions, analytical energy surfaces 3−20205
Mo(110) chemisorption of H_2 and N_2 3−11811
N_2-H_2 rarefied mixture, supersonic jet, rotational temp. and concentration around blunt body *(Russian)* 3−29929
$SF_6 + H_2$ chemical laser, properties 3−29080
hydromagnetic waves *see magnetohydrodynamic waves*
hydromagnetics *see magnetohydrodynamics*
hydrometers
see also density measurement
No entries
hydrophones
see also sonar
calibration, multiple interference smoothing 3−5782
line array, l.f. technique for underwater calibration 3−3732
nearfield calibration arrays, theoretical design 3−31468
pressure sensitive, extended range, ocean noise measurement 3−9409
hydrophotometers *see photometers*

hydrostatics
liquid crysts. magnetohydrostatic theory for cryst. lying between two coaxial cylinders 3−26971
magnetohydrostatic equil., stationary, analogy with hydrodynamics *(French)* 3−20374

hygiene
see also medicine
No entries

hygrometers
see also humidity measurement
continuously operating, capacitance, cooled mirror, electrolytic, operation, advantages, applications, use 3−16054
dew point, Brown Boveri Co., ±1°C accuracy *(German)* 3−5811
quartz crystal, using parametric convertor 3−37779

hyperfine field interactions in crystals *see crystal hyperfine field interactions*

hyperfine structure *see atomic spectra; molecular spectra*

hyperfragments *see hypernuclei*

hypernuclei
$A \geqslant 10$, nonmesonic decay and $\Lambda n/\Lambda p$ stimulation ratios 3−26414
binding energies of p- and s-d-shell Λ-hypernuclei 3−4277
double, around $A=10$, binding energy and Λ-Λ interaction parameter 3−17184
excited states, Λ-N interaction spin depend. 3−10906
heavy hyperfragment non-mesic decay, $(\Lambda n/\Lambda p)$ stimulation ratio 3−11026
heavy hyperfragments from K^- captures in emulsion nuclei, lifetime obs. 3−11025
heavy hyperfragments produced in K^--nucleus interactions, short lifetime obs. 3−11024
light $A \leqslant 15$, new determ. of binding energy values 3−19806
meson hyperfragments produced by K^- interaction in emulsion, binding energies 3−26413
production by 1.5 GeV/c K^- events on heavy nuclei 3−26480
spectroscopy, Λ-N interaction consequences and hypernuclear states information 3−963
K^- induced fragmentation of light nuclei in emulsion, 1.5 GeV/c 3−26479
Λ particle binding in nuclear matter for central ΛN potential, reaction-matrix calcs. 3−19803
Λ-d bound states ($J={}^1\!/_2, {}^3\!/_2$), Faddeev formalism for binding energy 3−17145
$\Lambda\Sigma$ conversion effect in hypernuclear matter 3−10905
^{10}Be hyperfragment prod. by K interaction in emulsion 3−26413
^{12}C excited state and excitation energy determ. 3−26413
${}^4H_\Lambda \rightarrow \pi^-\ {}^3$He n decay mode, compilation of exptl. studies, theoretical model 3−17183
${}^3He_\Lambda$, properties and decay branching ratios 3−17185
${}^4He(K^-, \pi\Lambda_0)R_3$, R_3 is residual nucleus, single-channel calc. of final-state interaction 3−35897
${}_\lambda{}^5$He, mesonic decay, final state interaction 3−26412
$({}^6Li_\Lambda)^* \rightarrow p + {}^5He_\Lambda$, observation of event in nuclear emulsion 3−14151

hyperon absorption
see also nuclear reactions and scattering due to hyperons
No entries

hyperon capture
see also nuclear reactions and scattering due to hyperons
Σ^- mean orbital capture time determ. from K^- capture on hydrogen in emulsion 3−26478

hyperon decay
hyperon-antihyperon nonleptonic decays, upper limit on CP violation effects 3−19669
non-leptonic, amplitudes determ. 3−10675
non-leptonic, in quark model 3−10674
non-leptonic P-wave, Lee-Sugawara relation 3−833
nonleptonic, parity-violating, $SU(6)_w$ model 3−23036
nonleptonic, role of final-state interactions in producing $\Delta I=1/2$ rules 3−35779
nonleptonic, s- and p-wave amplitude detn. from quark model 3−19682
semi-leptonic, muonic modes, calc. of asymmetries 3−35776
Λ, polarised, beta decay, correlations in centre-of-mass system and p recoil spectrum 3−23032
$\Lambda \rightarrow p\pi^-\gamma$ radiative decay mode meas. 3−13836
$\pi\Lambda \rightarrow \pi\Sigma$, dispersion sum rules for $\Sigma\Lambda$ transition magnetic moment 3−23138
$\Sigma \rightarrow p+\gamma$, weak current model for asymmetry parameter 3−16971
Σ^+ decay branching ratio determ. from K^- capture on hydrogen in emulsion 3−26478
$\Sigma^+ \rightarrow p\pi^0$, test of $\Delta I=1/2$ rule and Lee-Sugawara relation by meas. of decay proton polarisation 3−16976
$\Sigma^\pm \rightarrow \Lambda e^\pm \nu$, determ. of vector to axial vector coupling const. ratio, branching ratio, axial-magnetism to axial-vector coupling const. ratio 3−4159

hyperon detection and measurement
No entries

hyperon-deuteron interactions
No entries

hyperon-deuteron scattering
No entries

hyperon effects
see also nuclear reactions and scattering due to hyperons
No entries

hyperon interactions
see also hypernuclei; hyperon-deuteron interactions; hyperon-nucleon interactions; kaon-hyperon interactions; nuclear reactions and scattering due to hyperons
quark-model predictions for reaction with hyperon beams 3−29225

hyperon magnetic moment
Λ^0, spin rotation measurement, in pulsed magnetic field *(Russian)* 3−839
Ξ^-, polarization 3−6608

hyperon mass
magnified neutron oscillator, energy term yeti 3−38099
Σ, charged, from K^-p interaction obs. 3−4245
Ξ masses meas. using 2.1 GeV/c K^- exposure 3−13857
$\Xi^*(1530)$ mass, width and mass differences 3−4166

hyperon-nucleon interactions
hypernuclear matter, $\Lambda\Sigma$ conversion effect 3−10905
quark-model predictions for reaction with hyperon beams 3−29225
Λ p, in momentum range 6-21 GeV/c, meas. of total cross-sections 3−928
$\Lambda\varphi$ n, in momentum range 6-21 GeV/c, meas. of total cross-sections 3−928
$\Lambda\varphi$ p, in momentum range 6-21 GeV/c, meas. of total cross-sections 3−928
Λn, in momentum range 6-21 GeV/c, meas. of total cross-sections 3−928
$\Sigma^\pm$n low-energy interaction in K^-d capture at rest, determ. of complex scattering lengths 3−29248

hyperon-nucleon scattering
invariant and helicity amplitudes determ. by reduction of equivalence theorems and Fierz transforms 3−4208
$\Sigma^\pm$p cross-section data, determ. of low-energy scattering parameters using K-matrix formalism 3−4207

hyperon production
by antineutrinos in Gargamelle 3−6594
K^-d interactions at 5.5 GeV/c, to $\Sigma^+\pi^\pm\pi^-(\pi^0)$, $\Sigma^-K^+K^-$, $K^-\pi^-p$ final states in which hyperon is produced 3−29274
K^-p interactions at 4.25 GeV/c, meas. of hyperon polarisation in $\pi^\circ\Lambda$, $\eta\Lambda$ and $\pi\Sigma$ final states 3−17108
Λ, in K^-p interaction of 14.3 GeV/c, determ. of average polarization 3−14068
Λ^0, from p-p collisions, 6.6−28 GeV/c 3−6677
Λ^0, in π p interactions at 20 GeV/c 3−32722
Λ° polarization meas. in π^- p interactions in 3-6 GeV/c range 3−900
Λ^* (1404) in KN radiative capture *(Russian)* 3−32715
$np \rightarrow \Lambda p$, weak production at low energies, $d\sigma/d\Omega$ estimates 3−6652
$\pi^+n \rightarrow K^+\Lambda$, 5.1 GeV/c, Λ differential cross-section and polarization 3−32712
$\pi^+p \rightarrow K^+\Sigma^+$ backward scattering at 3.5 GeV/c, polarisation meas. 3−38082
Σ amplitudes and absorption pattern in two-body scatt. 3−23162
Σ^-/Σ^+ prod. ratio determ. from K^- capture on hydrogen in emulsion 3−26478
Σ^+, in K^-p interaction at 14.3 GeV/c, determ. of average polarization 3−14068
$\Sigma^\pm$, from p-p collisions, 6.6−28 GeV/c 3−6677
$Y_1^*(1385)$, in K^0p interactions, obs. in $\Lambda\pi^+\gamma$ final state 3−883

hyperon resonances
production in K^-n at 4.56 eV/c, sudy of final states with three charged particles and visible Λ 3−35839
quark-model predictions for reaction with hyperon beams 3−29225
$Y_0^*(1405)$, interpretation as bound state of quarks 3−19750
Δ^{++} photoproduction in $\gamma p \rightarrow p\pi^+\pi^-$ at 2.8 and 4.7 GeV determ. of production mechanism 3−13948
Λ^* (1405), production in KN radiative capture *(Russian)* 3−32715
Σ reson. role in interference model applic. to K $n \rightarrow \pi^-\Lambda^0$ 3−10800
Σ^+ (1385), produced in K^-p interaction at 14.3 GeV/c, determ. of density matrix elements 3−14068
$\Xi^*(1530)$ mass, width and mass differences 3−4166
$Y^*(1385)$ polarisation measurements and polarisation domain 3−26362
Y_1^*WU(1385) production in K^0p interactions, obs. in $\Lambda\pi^+\gamma$ final state 3−883

hyperon scattering
see also hyperon-deuteron scattering; hyperon-nucleon scattering; kaon-hyperon scattering; nuclear reactions and scattering due to hyperons; pion-hyperon scattering
No entries

hyperon spin and parity
decay, nonleptonic, parity-violating, $SU(6)_w$ model 3−23036
Λ^0, spin rotation in pulsed magnetic field, mag. moment detn. *(Russian)* 3−839

hyperons
see also hyperon resonances
system without saturation, possibility of conversion of nuclei into collapsons *(Russian)* 3−19800

hypersorption *see sorption*

hypertritons *see hypernuclei; tritons*

hypervirial theorem *see quantum theory*

hypochromism *see light absorption*

hypothetical particles
see also intermediate bosons; magnetic monopoles; quarks; tachyons
dyon formation, model 3−23193
pseudo-Goldstone, approximate symmetries in theories with spontaneously broken and local symmetries 3−6556
new Nagoya model of urbaryons, study of $\Delta S=0$ and $\Delta N'=1$ non-leptonic decay processes 3−26289
new particle obs. by Niu group, effect of form factor on decay rate 3−32653
selection rule of weak processes based on law of configuration conservation, decays of new particles 3−32652
uniton, quantized gravitational charge, determ. from Weyl gauge invariance 3−10379

hysteresis
see also coercive force; dielectric hysteresis; elastic hysteresis; magnetic hysteresis; remanence
carbon tetrachloride boiling hysteresis, electric field effect 3−38664
Josephson junction, suppression by application of a.c. *(Russian)* 3−8310
metal, preliminary plastic strain effect on form of mech. hystersis loop 3−34599
modified magneto-optic hysteresigraph 3−6034
nonlinear ferromagnetic materials, conducting, e.m. field distribution, power losses 3−15396
photographic zenith tube timing device accuracy determ. *(Japanese)* 3−19086
single domain particles in nonmag. matrix, hysteresis, remanence, antihysteresis susceptibility, coherence field 3−30668
steel, structural, hysteretic behaviour under cyclic bending *(Japanese)* 3−39374
wetting hysteresis effect on state of gas trapped by liquid in a capillary 3−20925

hysteresis continued
- Cr, influence of mag. field on thermal hysteresis of mag. struct. *(Russian)* 3−8371
- Fe-Si crystal, rotational hysteresis loss in (001) plane *(Japanese)* 3−24582
- Fe_3O_4 (magnetite) single crystals, relaxation processes at low temp. and tightened hysteresis loops *(Russian)* 3−12645
- ND_4Br, volume-temp. hysteresis loop in transitions calc. 3−38668
- NH_4Br, volume-temp. hysteresis loop in transitions calc. 3−38668
- NH_4Cl, volume-temp. hysteresis loop in transitions calc. 3−38668
- $(NH_4)_3FeF_6$, phase transition hysteresis, Mossbauer obs. 3−7933
- Ni, influence of mechanical stresses in elastic deformation region on hysteresis loop behaviour 3−38991
- Sn, $\alpha \rightarrow \beta$ transform. under press., Mossbauer study 3−33673
- Sn-Pb alloys, off-eutectic, hysteresis in composite-dendrite transition 3−34507
- ZrO_2, martensitic transform., metallographic obs. 3−24267

IC *see integrated circuits*

IC engines *see internal combustion engines*

ice
- *see also glaciers; snow*
- adiabatic and isobaric mixing with humid air *(French)* 3−31379
- adsorption of water on AgI, ice structure, i.r. studies 3−39468
- amorphous, i.r. absorpt. spectrum 3−2541
- Antarctic, natural conc. of Ag and I_2 3−12564
- Antarctic, sheet dynamics 3−12563
- Antarctic ice cap, distrib. meas. from Kosmos 384 *(Russian)* 3−39475
- Antarctica, salinity prod. mechanism for Weddell Sea 3−39489
- Arctic, acoustic transmission, reverberation and noise under ice 3−2962
- Arctic ice pack, removal of aircraft altitude var. from laser profiles 3−25343
- Arctic ice-cap removal rel. to model of general atmospheric circulation 3−15980
- Arctic sea ice, underside mapping, by backscattered sound 3−37190
- Artic ice-water boundary, ambient noise generation in 100 to 1000 Hz. range 3−2950
- break-up in Colville River Delta, Arctic 3−37268
- bulk electrical prop. determ. using microwave radiometric technique 3−9157
- Cabot Strait, shallow water ambient noise effect of floe ice coverage 3−2952
- cavity model, absorpt. spectral peak press. shift at high press. 3−12141
- cloud seeding using Portland cement 3−37229
- in clouds, contents remote meas. from Raman scattering 3−9399
- compression in freezing of supercooled water in capillaries 3−24247
- condensation trail of aircraft, ice budget growth meas., formation by droplet freezing 3−25232
- convectively cooled pipe, correction on the length of ice-free zone 3−20300
- crystal formation at warm temps. in cloud supercooled regions 3−25227
- crystal formation by airborne ferromag. particles 3−37227
- crystal growth in supercooled H_2O droplet clouds by diffusion, numerical simulation 3−25226
- crystal terminal vel. meas. at varying altitude 3−25230
- crystals, dynamical behaviour of dislocations 3−20739
- defect structure, electron microscope obs. 3−7746
- dislocations, X-ray topographical study in pure and HF doped ice 3−20746
- dynamic stiffness computation 3−22696
- e.m. wave backscatter, 26 to 40 GHz 3−37269
- epitaxial growth and substrate elec. props. 3−1927
- erosion by a falling film of water in a short vertical tube 3−11725
- fall patterns and velocities of rimed cryst., relationship to cryst. dimens. 3−25229
- floating ice tongue on Antarctic seawater, stable isotope analysis 3−15854
- floating plates, deformation and stress 3−3944
- floes in Gulf of St. Lawrence, wind stress and turbulence 3−12728
- forced convection heat and mass transfer from humid air to frost surface 3−1363
- formation ability rel. to formation conditions of AgI nuclei, stoichioetric ratio effects 3−25228
- freezing pot. in liq.-ice transition 3−5156
- friction of rubber 3−1683
- growth from melts, morphology of solid-liquid interface, dendritic and planar growth 3−38542
- heavy ice, dispersion relations at 223K from neutron scatt. 3−20829
- hexagonal, mol. orbital studies 3−17758
- impure specimens obtained by solidification of $(NH_4)_2SO_4$, dielec. props. *(French)* 3−36830
- impure specimens obtained by solidification of $(NH_4)_2SO_4$ aqueous solns., complex permittivity model *(French)* 3−27463
- intermolecular vibrs. and diffusion, −5 to 95°C cold neutron scatt. obs. 3−1810
- interstellar dirty ice particles surrounding early type stars, evaporation and size distrib. 3−35202
- Lake Superior icefoots, formation, structure and geomorphic importance 3−28093
- linear compressibility at low hydrostatic pressures, meas. technique 3−16051
- liquid water-ice IV-ice V-ice VI, equilib. curves, vol. change and dielectric obs. 3−1795
- Mars, south polar region 3−16149
- melting heat transfer with a water jet 3−14420
- neutron moderation, variational method 3−4335
- nucleation from adsorbed water molecules on AgI surface 3−24335
- oceanic tidal ice drift, numerical model with floe interaction *(Russian)* 3−39497
- optical constant calc. in 100-2000 Å region *(Russian)* 3−5173
- orientational order, local, Kirkwood theory cluster expansion approach 3−30237
- phase diagram, molecular interpretation by model studies 3−27099
- pressure melting and regulation by round wires 3−14984
- pressure ridge formation in sea ice, kinematic model 3−15855
- proton-ordered structure 3−17786

ice continued
- pure and HF doped, X-ray topographical study of dislocations 3−17826
- sea, measurement, top and bottom surfaces, diving techniques, measurement systems, evaluation 3−941[illegible]
- sea, millimetre wave reflectivity 3−2956
- sea, pressure ridge statistics, spatial aspects based on a probability density function 3−15852
- sea, ridge distributions statistics from theoretical negative exponential functions 3−15853
- sea, stalactites growing beneath the pack ice, observations, laboratory experiments, processes, desalination 3−9098
- sea ice, roughness parameters determ. from wind profiles 3−15851
- sea-ice, conductivity and surface impedance meas., in situ at v.l.f. 3−28091
- seismic P-wave velocities rel. to density of firn and ice *(German)* 3−15915
- seismic wave velocity, deep drill hole in Antarctica 3−9160
- stable growth of single doped crystals *(German)* 3−8739
- sublimation process 3−38666
- sublimation rate at low pressures 3−24264
- thermal properties, conductivity and specific heat, from 4-273 K 3−5815
- thermodielectric effect in vapour-ice transition 3−5156
- thickness meas. using radio echo sounding 3−12562
- trapped dielectron at 77K, semicontinuum model 3−38813
- under-ice acoustic transmission loss rel. to ice roughness and seawater-ice interface 3−2843
- under-ice reverberation modelling using multiple regression techniques 3−2844
- Weddell Sea, polynyas and leads, haline convection 3−9250
- CuS particles on or in surface of supercooled H_2O drops, a comparison of icebuilding activity *(Russian)* 3−21945
- $H^+(H_2O)_n$ cluster production model 3−36965
- Hg concentrations of Greenland icecap and Icelandic geothermal activity 3−25143
- NaOH ice, trapped electrons, ELDOR study 3−39454

identification
- *see also correlation methods; frequency response; modelling; simulation*
- dynamic tracer data, parameter estimation 3−3567
- environmental noise detection and identification by frequency instability 3−29156
- modified Newton-Raphson method for vortex flow parameter identification 3−7391
- radioactivity, behaviour of, terrestrial atmosphere *(French)* 3−32792
- vowels in isolation and h-d context 3−16331

i.g.f.e.t. *see field effect transistors*

ignition
- *see also electric ignition*
- Na, NaO_2, Na_2O_2 mixtures in air and inert atmospheres 3−14257

II-VI semiconductors
- c ZnS, simultaneous photovoltage and fluoresc. meas. 3−5028
- chalcogenides, intrinsic piezobirefringence obs. 3−12110
- crystal growth from gaseous phase, improved process *(Russian)* 3−12239
- crystals activated by transition metal ions, luminescence mechanism *(Russian)* 3−36933
- diffusion processes, anomalous, phenomenological interpretation *(German)* 3−15036
- edge emission rel. to donor-acceptor pair recombination 3−8630
- electron-phonon interaction, far i.r. cyclotron resonance absorption 3−36388
- epitaxial growth from vapour phase by vacuum sublimation *(French)* 3−5265
- exciton luminescence and photoconductivity at high densities of excitation *(Russian)* 3−27531
- film, on amorphous substrate, conditions of formation of stable and metastable structs. *(Russian)* 3−15101
- film, on insulators, vapour phase epitaxy by reactions involving organometallics 3−12251
- g-shift of s-state ions 3−2377
- g-shift of S-state ions \3−21016
- Hall, magnetoresist., and drift mobilities, Boltzmann equation soln. 3−21098
- interface reactions rel. to growth by spontaneous nucleation 3−2645
- intrinsic defects and stability, classical chemical thermodynamics interpretation *(German)* 3−14854
- ion implantation doping, review 3−30166
- luminescence, recomb., and photoconduction study, review *(Russian)* 3−27545
- polar, non-degenerate, low field mobility and Hall effect 3−21074
- reflectance, far u.v., and correl. with Penn-Phillips gap 3−39158
- vacancies, interstitials, Jahn-Teller distortions, molecular orbital models 3−33837
- X-ray atomic scattering, functions, influence of tetrahedral covalent bonds *(Russian)* 3−11582
- zincblende structure crystals, heat of atomisation;, effective charges and lattice dynamics 3−36270
- Ag_2Te, electronic and lattice thermal conductivity 3−1843
- BeO, far u.v. refl., and correl. with Penn-Phillips gap 3−39158
- $Cd_xHg_{1-x}Te$, films, elec. cond. *(Russian)* 3−24433
- $Cd_xHg_{1-x}Te$, refl., comp. and electron density depend., rel. to band struct. *(Russian)* 3−2548
- $Cd_xHg_{1-x}Te$, spin effects on Shubnikov-de Haas oscillations, semimetal-semicond. transition 3−33795
- $Cd_xHg_{1-x}Te$ film, sputtering in Hg vapour plasma 3−8727
- $Cd_xHg_{1-x}Te$ magnetoresistance, Shubnikov-de Haas oscillations, 77-120K 3−36628
- CdO(S)(Se)(Te), far u.v. refl. and correl. with Penn-Phillips gap 3−39158
- CdS, acoustoelec. domains, piezoelec. potential and carrier distrib., microwave absorpt. and Brillouin scatt. 3−5040
- CdS, acoustoelec. gain and lattice attenuation, Brillouin scatt. obs. 3−33961
- CdS, acoustoelec. multi-peak domain propag., Brillouin scatt. study 3−24481

II-VI semiconductors continued
CdS, acoustoelectric effects in homogeneous crystals with trapping centres 3-24482
CdS, angular dispersion effects in acoustoelectric interaction 3-30522
CdS, birefringence, uniaxial stress depend., room temp., 0.1-2.3 eV 3-15511
CdS, Brillouin scatt. by propag. acoustoelec. domains 3-33960
CdS, Brillouin scatt. from acoustoelectrically amplified flux domains, dispersion spectrum 3-34352
CdS, CdS-ZnS mixed crystals, melt growth 3-15630
CdS, current fluctuations under sound amplification conditions *(Russian)* 3-2144
n- CdS, deviations from Ohm's law at 77 K 3-30485
CdS, dielec. relax. time exceeding minority carrier diffusions lifetime, evidence from photocond. meas. 3-30756
CdS, diffusion of noble metals, 300-800°C, u.s. study 3-30286
CdS, dispersion of birefringence *(Russian)* 3-2511
CdS, dispersion of Raman cross section over wide energy range 3-36872
CdS, elec. field induced Raman scattering 3-21407
CdS, electroluminesc. from controlled splits 3-24746
CdS, electron irrad., Cd-displacement threshold at liq. He temp., cathodoluminesc. obs. 3-5247
CdS, electron traps distribution *(Japanese)* 3-18183
CdS, electron-phonon interactions, first principles energy band calcs. 3-36535
CdS, exciton gas degeneracy after single photon excitation *(Russian)* 3-11870
CdS, field emission under pulse conditions, periodicity effect 3-27599
CdS, Hall and thermoelec. effects under thermal equilib. conditions 3-18172
CdS, high carrier and exciton conc., low temp. emission recomb. study *(Russian)* 3-27541
CdS, isoelectronic Ni impurity, absorpt. spectra *(Russian)* 3-8618
CdS, LA-phonon exciton interaction, luminesc. study *(Russian)* 3-36916
CdS, laser pulse duration control, nonlinear absorption *(Russian)* 3-215
CdS, luminesc. excitation spectral obs. for bound exciton form. kinetics 3-8133
CdS, luminescence from impurities and fast neutron radiation defects 3-5224
CdS, nonlinear interaction of Bleustein-Gulyaev waves 3-8004
CdS, oxygen photodesorption, influence of nonequilib. minority carriers 3-15210
CdS, photocond., acoustoelectric aftercurrent obs. 3-2129
CdS, photocond., i.r. quenching, spectral response 3-18189
CdS, photoconductive, current instability due to elastic surface waves 3-34297
CdS, photoelectron spectral response, surface recomb. layer thickness 3-18525
CdS, photoluminesc., exciton-phonon interaction study *(Russian)* 3-27536
CdS, piezoelectric scattering anisotropy *(Russian)* 3-2078
CdS, polarity of bending strength and photoplastic effect 3-1669
CdS, polycryst. film, elec. cond., ambient O_2 depend. 3-8185
CdS, recomb. waves induced by optical quenching 3-38866
CdS, relax. time and cathodolum. efficiency *(Russian)* 3-5237
CdS, subharmonic generation of surface and bulk acoustic waves at high pump amplitudes 3-1869
CdS, thin wafer, shift in steady state contact pot. difference on bending 3-2161
CdS, two-photon interband transitions, joint matrix element 3-34337
CdS, u.s absorpt. and velocity, transport theory *(Russian)* 3-1704
CdS, u.v. excited at 4.2K, recomb. processes in stimulated emission 3-15523
CdS, X-ray atomic scattering factors, electronic structure, correl. atoms, crystal *(Russian)* 3-33625
CdS acoustoelectric platelet oscillators, current saturation rel. to illum. 3-11936
CdS and glass multilayer film, light-intensity modulation 3-12198
CdS coating on $LiNbO_3$ piezoelec. crystal, Rayleigh acoustic surface wave amplification and dispersion, calc. 3-11794
CdS conduction band effective mass anisotropy rel. to uniaxial compression *(Russian)* 3-15137
CdS crystals, d.c. and microwave-biased photoconductive response at 22 GHz 3-15221
CdS film, bulk compensation effect on chemisorption dependent semiconductivity 3-33889
CdS film, cubic forms in surface morphology *(Russian)* 3-30376
CdS film, evaporated, resist. and Hall mobility rel. to prep. conditions 3-27322
CdS film, photocond., effect of cryst. struct. after recrystn. 3-15226
CdS films, photoconductivity *(Russian)* 3-24474
CdS films on Ge, epitaxial growth and struct. 3-36493
CdS needles and platelets, growth mechanism 3-11574
CdS single crystals, effect on optical quenching 3-15223
CdS thin film, acoustoresistance, surface acoustic wave 3-38872
CdS thin films, shallow trapping levels, structure defects, photoconductivity relaxation 3-33833
CdS thin films, textures, oblique, growth electron bombardment evaporation, reflection electron diffraction study 3-38758
CdS:Be, i.r. absorpt. due to localized vibr. mode 3-27523
CdS:Li single crystals, doped and undoped, photoluminescent props. at low temps., effects of doping and heat treatment *(Japanese)* 3-8656
CdS:Li(Na)(Ag), furnace doping, rel. to bound exciton spectra 3-12184
CdS:S system as photoelectret electrophotographic layer, photopolarisation study 3-36833
CdS:Te, piezoemission study 3-18492
CdS-CdTe system, mutual solubility *(Russian)* 3-24273
CdS-Cu contact, elec. and photoelec. props. 3-8265
CdS-$CuGaS_2$ n-p diode, green electrolum. 3-39188
CdS-PVK and CdSe-PVK, internal photoemission of holes 3-18217

II-VI semiconductors continued
CdS(Se) laser, pumping using pulsed elec. discharge in vacuum 3-37971
$CdS_{1-x}Se_x$, electro-absorption reduced effective mass 3-15471
$CdS_{1-x}Se_x$ film, photocond., effect of cryst. struct. after recrystn. 3-15226
CdS_xSe_{1-x}, epitaxial, growth of graded gap crystal layer, luminesc. obs. 3-8053
CdS_xSe_{1-x}, peculiarities of reflection spectra in exciton absorption region *(Russian)* 3-34381
CdSe, Bose condensation of excitonic molecules, luminesc. obs. 3-30437
CdSe, electroluminesc. from controlled splits 3-24746
CdSe, electrophyscial props., influence of growth conditions 3-24428
CdSe, films, structure and electrical resistance, electron microscope examination *(Russian)* 3-38752
CdSe, impact ionisation, breakdown, photoinduced switching, meas. of cond., Hall coeff., mobility, 4.2-300K 3-30487
CdSe, laser pulse duration control, nonlinear absorption *(Russian)* 3-215
CdSe, luminescence from impurities and fast neutron radiation defects 3-5224
CdSe, photocurrent, saturation and acoustoelectric oscillations *(Russian)* 3-11930
n-CdSe, shallow impurity states, cyclotron reson., Zeeman splitting, cond. electrons effective masses 3-2026
CdSe, vapour deposition, critical temp. of glass substrate 3-15622
CdSe, vapour growth on SiO_2 seed plate at 1225°C 3-15614
CdSe, X-irrad., traps, photocond. study 3-30426
CdSe barrier in supercond. tunnel junction, photosensitivity 3-36688
CdSe coating on $LiNbO_3$ piezoelec. crystal, Rayleigh acoustic surface wave amplification and dispersion, calc. 3-11794
CdSe electron scattering mechanism, Hall effect measurements 3-30466
CdSe epitaxial film, electrodispersion and electroabsorpt. spectra obs. 3-30801
CdSe film, acoustoelectric effect as cause of current saturation *(German)* 3-15228
CdSe film, polycryst., elec. props., field effect, capacitance and C-V characts. obs. 3-15279
CdSe film, with Schottky barriers as contacts, photoconductive gain greater than one 3-21107
CdSe layers on Y-Z-$LiNbO_3$ substrate, piezoelec. coupling of Rayleigh acoustic surface waves 3-30761
CdSe single crystals, memory props. 3-24484
CdSe single crystals self-diffusion of Cd and Se investigation 3-33689
CdSe thin film deposition, nucleation conditions, molecular cloud vapour density *(German)* 3-38757
CdSe vapour phase epitaxial growth on sapphire substrate, growth conditions 3-30362
CdSe:Be, i.r. absorpt. due to localized vibr. mode 3-27523
CdSe:Cu,In and undoped, high temp. defect equilibria 3-7745
CdSe-CdTe, solid solns., comp. and elec. charact. depend. on method of deposition 3-33762
CdSe-CdTe, thin films, solid solns., comp. and elec. charact. depend. on method of deposition 3-33762
CdSe-Dy_2O_3 film struct., elec. props. 3-27312
CdSe-Dy_2O_3 thin-film structure, elec. and interface props. 3-15265
CdSe-electrolyte interface, current multiplication noise *(Russian)* 3-5051
CdSe-Si_xO_y film struct., elec. props. 3-27312
CdTe, amorphous, struct. and elec. cond. 3-1942
CdTe, cathodoluminescence from lattice defect centres, quenching mechanism 3-15561
CdTe, defect struct., transmission electron microscope obs. 3-17830
CdTe, edge emission spectra, electron irrad. effects 3-18488
CdTe, elastic consts. and thermal expansion, 4.2-300 K 3-30170
CdTe, electron and neutron irrad., defect behaviour, photoluminescence spectra, excess, dissociative Cd pressure 3-34431
CdTe, electron diffusion, applied field depend., Monte Carlo study 3-18149
CdTe, high power i.r. laser window materials, state-of-the-art review 3-5980
CdTe, hole mobility, Poole-Frenkel effect, 130-430K, 5-50kV/cm 3-21086
CdTe, hot pressing for high power laser windows at 10.6 μm 3-5983
CdTe, impurities, high temp. elec. cond. study *(Russian)* 3-27031
CdTe, investigation of doubly charged acceptors 3-24478
CdTe, modified Bridgman growth for high power laser windows at 10.6 μm, optical properties 3-5984
CdTe, physical vapour deposition for high power laser windows at 10.6 μm 3-9960
n-CdTe, shallow impurity states, cyclotron reson., Zeeman splitting cond. electron effective masses 3-2026
CdTe, sonic casting for high power laser windows at 10.6 μm 3-5982
CdTe, thin films, photovoltaic effect dep. on mech. stress *(Russian)* 3-30518
CdTe compensated doped crystals, density of states tails, conductivity, Hall mobility, conduction band 3-33832
n-CdTe films, cond., trap and free carrier density, Fermi level position *(French)* 3-27262
CdTe films, photoelectric properties *(Russian)* 3-24475
CdTe low resistivity films, d.c. e.m.f. in a.c. fields *(Russian)* 3-11964
CdTe monocrystals, undoped and doped with Na, As, preparation by direct solidification, electrical properties *(Czech)* 3-21061
CdTe p-n junctions, photomagnetic effect, general relationships 3-33990
CdTe recrystallized thin films, exciton-phonon interaction *(Russian)* 3-11871
CdTe valence band structure investigations near gamma point 3-36531
n- CdTe with Au rectifying contacts, elec. props. meas. 3-18216
CdTe:Cd, thin films, electrical conductivity *(Russian)* 3-33891

II-VI semiconductors continued

CdTe:Cd oblique deposited films, rectification effect *(Russian)* 3−33936
CdTe:Cd thin films, V-A characteristics, anisotropy *(Russian)* 3−33892
CdTe:Cu single cryst. prep. and characteriz. 3−15632
CdTe:Fe, Hall effect and photocond. meas. rel. to impurity absorption 3−15531
CdTe:In, absorption band edge of compensated crystals 3−24717
$(CdTe)_{1-x}(AlSb)_x$ solid solutions, absorption edge, coefficient, photoelectric method, band structure 3−34376
p-CuI-n-ZnS:Mn film, low voltage electroluminesc. *(Russian)* 3−24748
GaP, dielec. function, calc. using Penn's model 3−2000
n-$Hg_{1-x}Cd_xTe$, Auger limited band to band and Shockley-Read recomb., photocond. meas. 3−36634
α-HgS, elastic and piezoelectric properties 3−36840
HgSe, band struct., determ. from magneto-quantum effects 3−2003
HgSe, iterated solns. of Boltzmann eqn. with Fermi statistics 3−36598
HgSe film, amorphous, Hall mobility obs. 3−5009
HgTe, anomalous temp. dependence of Hall coefficient 3−24458
HgTe, dielec. function, refl. spectra in far i.r., 8K-300K 3−2565
p-HgTe, doped, hydrostatic pressure effect on Hall coeff. and elec. cond. 3−21099
HgTe, electron mobility anomalous temp. depend. 3−2095
HgTe, impurity diffusion, 200-300°C 3−36441
HgTe, impurity states 3−2022
HgTe, iterated solns. of Boltzmann eqn. with Fermi statistics 3−36598
HgTe-CdTe, narrow band gap semiconductors, zero bandgap transition 3−38800
n-Hgs, cubic, band inversion, optical absorpt. and intra-band refl. rel. to carrier conc. and temp. 3−2002
InAs p-n junction, kinetics of photo-e.m.f. *(Russian)* 3−2177
InSb:Cd, p-n technique 3−34489
MgO, far u.v. refl. and correl. with Penn-Phillips gap 3−39158
PbSe, band inversion under hydrostatic press., elec. resist. and galvanomag. obs. 3−2004
ZnHgSe(Te) mixed crysts., e.p.r. of Mn^{2+}, g-factor 3−2378
$Zn_xHg_{1-x}Se(Te):Mn^{2+}$, e.p.r., rel. to band struct. 3−15409
ZnO, angular dispersion effects in acoustoelectric interaction 3−30522
ZnO, dispersion of Raman cross section over wide energy range 3−36872
ZnO, ion-implanted, anneal characts. 3−30955
ZnO, luminescence in exciton region with two photon excitation *(Russian)* 3−8653
ZnO, macroscopic elec. fields, induced double refr. study *(Russian)* 3−2515
ZnO, photoconductivity from surface electron states on prism surfaces 3−15234
ZnO single crystal surface, surface donor states influence on oxygen chemisorption kinetics, theory 3−33738
ZnO single crystal surface, surface donor states influence on oxygen chemisorption kinetics, experimental results 3−33739
ZnO thin films, photoelectric 3−18182
ZnO:In electron conc. and mobility, temp. depend. 5 to 300 K *(German)* 3−11899
ZnO:Li, thermolum., 4.2-300K, trapping and recomb. processes 3−15566
ZnO:Ni^{2+}, near i.r. absorpt. obs. of crystal field, dynamic Jahn-Teller effect in $^3T_2$ state 3−21446
ZnO(:Cu), elec. cond. and Hall effect, 5 to 300 K *(German)* 3−33933
ZnO(S)(Se)(Te), far u.v. refl., and correl. with Penn-Phillips gap 3−39158
ZnS, elec. cond. meas. and e.p.r. obs. of F-centres 3−21076
ZnS, impurity ionisation energies and Bohr radius calc. from recomb. spectrum anal. expression *(Russian)* 3−36897
ZnS, laser deposited films, expt. technique and data *(French)* 3−36988
ZnS, macroscopic elec. fields, induced double refr. study *(Russian)* 3−2515
ZnS, photocond. spectra at 293 K, 77 K and 4.2 K, fine struct. due to excitons 3−21115
ZnS, powdered, X-ray induced a.c. cond., thermostimulation, fluoresc., thermolum. 3−38868
ZnS, u.v. cathodolum., temp. depend., 80-400K *(Russian)* 3−15560
ZnS polytypes, photoresponse meas. 3−15224
ZnS:Ag, Al, photocond. caused by redistrib. of charge carriers over trapping centres *(Russian)* 3−15220
ZnS:Cu, β-irrad. at 5K, fast light emission 3−24753
ZnS:Cu, Mn, Cl, film, doping in vacuum growth rel. to electrolum. props. 3−15559
ZnS:Cu and ZnS:Cu,Al, electrolum., Gaussian component intensity, alternating voltage freq. depend. *(Russian)* 3−21486
ZnS:Mn, Cl, thermal quenching of luminesc., elec. field effects *(Russian)* 3−27555
ZnS:Mn, low voltage d.c. electroluminescence *(Russian)* 3−24749
ZnS:Mn, phonon induced hyperfine fields, molecular orbital model *(German)* 3−15161
ZnS:Ni^{2+}, near i.r. absorpt. obs. of crystal field, dynamic Jahn-Teller effect in $^3T_2$ state 3−21446
ZnS:Ni^{2+} ion-hole complexes, electron struct., optical absorpt. study *(Russian)* 3−12155
ZnS:Sc^{2+}, e.p.r., 1.3-4.2 K, dynamic Jahn-Teller effect obs. 3−21302
ZnS-Te, alloy thin film preparation, structure and lattice constants, electron microscopy and X-ray diffraction 3−39233
ZnS(Cu, Cl) electroluminophores, shallow traps and deterioration 3−30880
$ZnS_{1-x}Se_x$, meas. of electron transitions and energy bands by optical reflection techniques *(German)* 3−34339
ZnSe, chemical vapour deposition for high power laser windows at 10.6 μm 3−5981
ZnSe, cubic, wavelength depend. of linear electro-optical coeff. *(French)* 3−18463

II-VI semiconductors continued

ZnSe, defect centres, energy levels and effective radii, thermally stimulated current obs. *(German)* 3−15160
ZnSe, dielec. function, calc. using Penn's model 3−2000
ZnSe, electroluminesc., rel. to improved generation-recomb. processes in light emitting diodes *(German)* 3−15558
ZnSe, high power i.r. laser window materials, state-of-the-art review 3−5980
ZnSe, hot pressing for high power laser windows at 10.6 μm 3−5983
ZnSe, impurity ionisation energies and Bohr radius calc. from recomb. spectrum anal. expression *(Russian)* 3−36897
ZnSe, phonon dispersion 3−7869
ZnSe, undoped, p-type cond. 3−36602
ZnSe:Al, Ga and In, optical absorption, diffusion of impurities 3−24712
ZnSe:Mn, e.p.r., defect and macroscopic defect obs. *(German)* 3−15420
ZnSe:Mn, phonon induced hyperfine fields, molecular orbital model *(German)* 3−15161
ZnSe:Mn, photocapacitance meas. of impurity created energy levels 3−15153
ZnSe-CdSe solid solution, identity periods and mean-square displacements of ions *(Russian)* 3−4739
ZnSe-Si, ZnSe-GaAs n-p heterojunctions, r.f. sputtered 3−33988
ZnSe-SnO_2 heterojunction, injection electroluminescence *(Russian)* 3−27575
ZnSe-ZnTe, heterojunctions, influence of laser excitation on photoelectric props. 3−24504
ZnTe, acceptor defect levels, elec. transport 3−18096
ZnTe, amorphous, optical props. 3−2526
ZnTe, amorphous, struct. and elec. cond. 3−1942
ZnTe, atomic displacement energies, cathodoluminescence edge emission spectroscopy, monoenergetic electron irrad. 3−33556
ZnTe, birefringence, spatial dispersion induced 3−2512
ZnTe, electron irradiated, Zn displacement threshold, Zn vacancy luminescence 3−33557
ZnTe, photoluminescence using laser excitation *(Russian)* 3−30879
ZnTe, resonant Raman scatt. 3−5201
ZnTe, shallow donor level, field-assisted detrapping obs. 3−24391
ZnTe amorphous thin films, O_2 chemisorption effect on electrical conductivity 3−27320
ZnTe single crystal, microscopic obs. and optical props. *(Japanese)* 3−11605
ZnTe:Cu, electron-beam excited, visible luminesc. 3−30884
ZnTe:Cu, single crystal, photoluminescence and absorption 3−15552
p-ZnTe:Ga(In), photoelectronic props., electron trap level rel. to Ga(In) impurities 3−36635
ZnTe-Au(Ni)(Ta)(Al) Schottky barrier height determination 3−18215
ZnTe-ZnSe heterojunctions influence of laser excitation on photoelectric props. 3−24504

III-V semiconductors

see also gallium arsenide; indium antimonide
alloy, lattice match in heteroepitaxy 3−4932
p- AlSb, mechanisms of carrier scattering 3−24455
chemical vapour deposition, mass spectrometric and thermodynamic studies 3−2639
donor and acceptor conc. determ. from hot electron mobility 3−38812
effective charge transfer and covalent bonding 3−7656
electron gas, possibility of simulating relativistic plasma *(Russian)* 3−8218
electron phonon coupling influence on energy shift of donor-acceptor pair emission 3−36939
epitaxial growth, comparison of liquid phase and chemical vapour phase methods 3−30363
film, on insulators, vapour phase epitaxy by reactions involving organometallics 3−12251
Hall, magnetoresist., and drift mobilities, Boltzmann equation soln. 3−21098
hopping conduction, giant positive magnetoresist. predicted from percolation theory 3−15197
n- InP, hot electrons diffusion 3−15202
interband absorption of light, drag of electrons by photons *(Russian)* 3−2135
intrinsic defects and stability, classical chemical thermodynamics interpretation *(German)* 3−14854
ion implantation doping, review 3−30166
optoelectronic properties and device applications, book 3−32574
polar, drag of carriers by other carriers, mobility 3−33899
polar, non-degenerate, low field mobility and Hall effect 3−21074
polar semiconductors, inclusion of higher order terms for energy distribution function of hot carriers at high temp. 3−8193
rare-earth chalcogenides, electrical props. from meas. of specific heat, thermal expansion and conductivity 3−15019
solid solution system, phase diagrams rel. to heterojunc. and light emitting diode fabrication 3−2682
solid solutions, disorder scattering 3−30470
spin props. of conduction electrons, small-gap semiconductors 3−38845
spin-orbit splitting, electroreflectance study 3−2013
superlattice of different III-V semicond. layers, light absorpt. rel. to complex band structure 3−15519
surface plasmon excitation, reflectivity obs. *(French)* 3−18438
ternary alloy-Cs_2O photocathode, heterojunction barrier model 3−2619
two photon conductivity obs. with nanosecond and picosecond light pulses 3−2137
vapour phase growth 3−8762
vapour transport equation derivation for vapour growth 3−2651
X-ray atomic scattering, functions, influence of tetrahedral covalent bonds *(Russian)* 3−11582
zincblende structure crystals, heat of atomisation;, effective charges and lattice dynamics 3−36270
AlAs, band struct. and pseudopotential form factors 3−15128
AlAs, impurity electron binding energy, using dielectric theory *(German)* 3−15159
AlAs, Lindemann-Gilvarry melting law and Debye temps. 3−36393

III-V semiconductors continued
AlAs, optical critical point analysis using pseudopotential calculation of band structure 3−36863
$Al_2Ga_{1-x}As$, local and collective phonon modes, Raman scatt. 3−5200
$Al_xGa_{1-x}As$, etching in strong alkaline soln., Al content dependency 3−38740
$Al_xGa_{1-x}As$, molecular beam epitaxy 3−2677
$Al_xGa_{1-x}As$, reson. Raman scatt., 2K 3−34359
$Al_xGa_{1-x}As$, tunnel breakdown and photoconduction in reverse-biased p-n junctions 3−24503
$Al_xGa_{1-x}As$:Ge epitaxial film, photolum., 1.1-2 eV *(Russian)* 3−2589
$Al_yGa_{1-y}As$-$Al_xGa_{1-x}As$ double heterostructures, electroabsorpt. 3−39119
AlN, refl. and luminesc. excitation spectra, 3-40 eV 3−18493
AlP, band struct. and pseudopotential form factors 3−15129
AlP, impurity electron binding energy, using dielectric theory *(German)* 3−15159
AlP, Lindemann-Gilvarry melting law and Debye temps. 3−36393
AlSb, impurity electron binding energy, using dielectric theory *(German)* 3−15159
AlSb, resonant Raman scatt. 3−5201
AlSb, X-ray emission bands of $SbL_{\gamma 4}$ *(German)* 3−15569
AlSb film, X-ray and u.v. photoemission spectra, core levels, valence band electrons plasma freq. 3−15590
$(AlSb)_x(CdTe)_{1-x}$ solid solutions, absorption edge, coefficient, photoelectric method, band structure 3−34376
BP, Lindemann-Gilvarry melting law and Debye temps. 3−36393
CdS type crystal, spontaneously polarised semicond. electrical cond. anisotropy 3−39110
$Ga_{1-x}Al_xAs$, liq. phase epitaxy, variation of solid comp. with temp. 3−12258
n-$Ga_{1-x}Al_xAs$:Si, catholum. obs. rel. to energy gap meas. 3−30886
$Ga_{1-x}Al_xAs$:Si, liquid phase epitaxy, amphoteric behaviour of Si, effect of As soln. conc. 3−5278
$Ga_xAl_{1-x}As$, junction laser, physics and technology, review 3−749
Ga(As, P):I highly doped mixed crystals, problems of growth *(German)* 3−8765
GaAs, epitaxial growth over wide range of crystallisation conditions, comparison with GaP *(Russian)* 3−8051
GaAs, excess Ga and As in the vapour phase influence on epitaxial growth in (111) direction *(Russian)* 3−8749
GaAs, inhomogeneities in epitaxial layers *(Russian)* 3−8050
n-GaAs, interzone scattering study by specific resistance at high press. meas. *(Russian)* 3−8162
p-type GaAs, proton bombarded, optical and electrical properties 3−21442
GaAs, soln. of Boltzmann eqn. for ellipsoidal ⟨100⟩ valleys, Hall and drift mobility 3−33883
GaAs amorphous films, electron diffraction ivestigation of struct. *(Russian)* 3−8059
GaAs and related compounds, conference, Aachen, Germany, (Oct. 1970) 3−2675
GaAs light pulse transmission, nonlinear absorption *(Russian)* 3−777
GaAs:Sn, selective diffusion of Zn using SiO_2 layer 3−15244
GaAs-GaAlAs superlattice, ultra high vacuum epitaxy system 3−39297
GaAs-GaP system, correlation between miscibility and lattice parameter mismatch 3−11720
n-GaAsP-Cr, temp. coeff. of Schottky junction 3−15252
$GaAs_{1-x}P_x$, plasma oxide film growth, composition and optical props. *(Japanese)* 3−11821
$GaAs_{1-x}P_x$, tunnel breakdown of photoconduction in reverse-biased p-n junctions 3−24503
$GaAs_{1-x}P_x$ superlattice, vapour growth, layer spacing uniformity 3−2687
$GaAs_{1-x}P_x$:N, isoelectronic trap transitions in resonant enhancement region 3−30430
$GaAs_{1-x}P_x$:N, laser operation on photopumped NN_3 pair transitions 3−37972
$GaAs_{1-x}P_x$:N, N_2 isoelectronic trap, luminescence, l.e.d. applications 3−39175
$GaAs_{(1-x)}P_x$, optically induced paramag. by distrib. change in cond. electron spins on recombination 3−2513
$Ga_{1-x}In_xAs$, vapour phase epitaxial growth for i.r. photocathodes 3−2678
$Ga_{1-x}In_xAs$ film, chem. vapour deposition using organometallics 3−21531
$Ga_xIn_{1-x}As$ on GaAs substrates, anisotropic bending during epitaxial growth 3−15085
$Ga_xIn_{1-x}P$:S, band structure from Hall effect and resistivity meas. 3−15215
$Ga_xIn_{1-x}Sb$, vertical freeze grown material characterisation 3−5280
GaN, heteroepitaxial thermal gradient soln. growth 3−12257
GaN, i.r. lattice vibrations and free-electron dispersion 3−18455
GaN, impurity electron binding energy, using dielectric theory *(German)* 3−15159
GaN, resonant Raman scattering A_1 to F_1 and E_2 optical phonons 3−8584
GaN, u.v. d.c. electrolum. generation by forward bias injection 3−15556
GaN thin film waveguides, Raman scatt. 3−39131
GaN:Zn electro-luminesc. diodes, manufacture and characts. *(Russian)* 3−36945
GaN-GaN:Mg light emitting diode, violet luminesc. 3−34432
n-GaN(:Zn) film, vapour phase grown, Hall meas., carrier conc. 3−33884
GaP, amorphous, refr. index, dispersion and magnitude 3−36851
GaP, at high excitation levels, excitonic luminesc. and photocond. study *(Russian)* 3−27542
GaP, birefringence, spatial dispersion induced 3−2512
GaP, donor-acceptor radiative recomb. of C-S and Zn-S pairs *(Russian)* 3−8633
GaP, doping homogeneity meas. using laser scanning device 3−5277
GaP, electron effective mass *(Russian)* 3−5008
GaP, energy states of isolated donor-acceptor pairs and influence of polarisation interaction on pair energy 3−33830
GaP, evidence for nonradiative Si,O defect 3−21023

III-V semiconductors continued
GaP, fluoresc. from bound excitons, quenching and enhancement by far i.r. radiation 3−36940
p-GaP, hole effective mass, cyclotron reson. determ. 3−27215
GaP, i.r. absorpt. of localised longit. optical phonons 3−30232
GaP, i.r. absorption from netural acceptors 3−21413
GaP, implantation of Kr and Tl, energetic ion collection, saturation effects 3−11646
GaP, implantation of Kr and Tl, ion conc. profile and ion range probability distrib. 3−11647
GaP, impurity electron binding energy, using dielectric theory *(German)* 3−15159
GaP, impurity ionisation energies and Bohr radius calc. from recomb. spectrum anal. expression *(Russian)* 3−36897
GaP, light emitting diode, device physics, material characterisation 3−39191
n-GaP, liq.-encapsulated-Czochralski-grown, deep hole traps, luminesc. study 3−5235
GaP, local strain fields due to impurities 3−2023
GaP, molecular beam epitaxy 3−2677
GaP, neutron irradiated, optical absorption *(Russian)* 3−30851
GaP, p- and n-type, proton bombarded, optical and electrical properties 3−21443
GaP, p-n junc., barrier layer capacity with deep centres *(German)* 3−33987
GaP, p-type dopants for green light emitting diodes 3−8734
GaP, photoionisation of electrons and holes at oxygen donors 3−33950
GaP, reson. fluoresc. due to bound excitons, laser excited 3−18484
GaP, second-order Raman spectra and phonon dispersion 3−21396
GaP, selective epitaxial growth, liquid phase 3−2683
GaP, single crystal, liq. encapsulation-Czochralski and vertical gradient freeze techniques 3−39247
GaP, soln. of Boltzmann eqn. for ellipsoidal ⟨100⟩ valleys, Hall and drift mobility 3−33883
GaP, states with two bound particles, Auger transitions at defects 3−36546
GaP, stimulated emission from excitons bound at isoelectronic traps 3−24720
GaP, thin film, physical and electrical properties, molecular beam growth 3−39298
GaP, two-photon absorpt. indirect exciton transitions, theory 3−16913
GaP, uniform dia. crystals, liq. encapsulation Czochralski growth, X-ray imaging technique 3−39248
GaP amorphous film, ohmic, hopping cond. and Poole Frenkel behaviour obs. 3−36604
GaP amorphous films, electron diffraction investigation of struct. *(Russian)* 3−8059
GaP epitaxial growth over wide range of crystallisation conditions, comparison with GaAs *(Russian)* 3−8051
GaP red-emitting lamp, O content and electrolum. efficiency 3−30537
GaP:Be, homogeneous doping in vapour growth, elec. props. *(Russian)* 3−15644
GaP:Cu, red pair luminesc. 3−15544
GaP:Fe^{3+}, deep levels, photocond. obs. 3−18095
GaP:Li, Zn, bonding of excitons by neutral donors and acceptors *(Russian)* 3−36932
GaP:N, bound exciton spectra and radiation kinetics during two-photon excitation 3−18491
GaP:N, isoelectronically doped, radiative recombination 3−24754
GaP:N, seven line luminesc. spectrum of (Neeh) complex 3−34420
GaP:N, Te(Zn), LPE layer, minority carrier lifetimes and electrolum. efficiencies 3−30493
GaP:N diodes, influence of temp. on electroluminescence spectra 3−24750
GaP:O, donor deep states, optical cross section, energy levels, conc., photocapacitance obs. 3−30427
GaP:O, donor deep states, capture cross sections, photocapacitance obs. 3−30428
GaP:O, electrical props. of crystal grown from melt 3−24442
GaP:O, epitaxial, O conc., nuclear microanalysis 3−39249
GaP:Te, photocond. due to Auger recomb. of bound excitons 3−27283
GaP:Te,O, liq. phase epitaxy, Te and O incorporation 3−39234
GaP:Zn, O, free hole to impurity centre bound electron recomb. at 300K 3−30494
GaP:Zn,O, Czochralski-grown photoluminesc., minority carrier lifetime, effect of heat treatment 3−39176
GaP:Zn,O, use of $Zn(PO_3)_2$ glass as doping source 3−8755
N-GaP-Au, temp. coeff. of Schottky junction 3−15252
n-GaP-Cr, temp. coeff. of Schottky junction 3−15252
GaP-GaAs, indirect Γ_{8v}-X_{1c} band gap, absorpt. and photolum. studies 3−21003
GaP-GaAs heterojunction, TEM obs. of misfit dislocations caused by lattice mismatch 3−36305
GaP-GaAs solid solution polarised luminescence due to optical orientation of electrons *(Russian)* 3−36934
$GaP_{1-x}N_x$ crystal growth, solubility and solid-gas distrib. coeff. of N in GaP 3−12259
GaP(Sb), structure factor meas. rel. to electron distrib. and bonding 3−14784
GaSb, birefringence, spatial dispersion induced 3−2512
GaSb, diffusion current, rel. to impurity density-of-states tails 3−11844
GaSb, e.m.f. by Q-switched CO_2 laser 3−30520
n-GaSb, elec. cond., mm. wave investigation 3−21084
GaSb, electron mobility in Γ_{1c} band, temp. and press. depend. 3−24422
GaSb, Ga $K_{\beta 2}$ and $SbL_{\gamma 4}$ X-ray emission bands *(German)* 3−15569
n-GaSb, heavily doped density-of-states tails associated with L-minima of conduction band 3−30425
GaSb, Landau transitions at higher energy gaps, spin-orbit splitting 3−33809
GaSb, ohmic contacts, Au and Ag alloy by vacuum evap. and chemical deposition *(Polish)* 3−30538
p-GaSb, optical pumping of spin polarised conduction electrons and inelastic scattering by neutral acceptors 3−34398
GaSb, p-type, u.s. absorpt. at low temps. 3−17938

III-V semiconductors continued
p-GaSb, phonon-phonon and phonon-charge carrier interactions *(French)* 3−1706
GaSb, plasmon-phonon interactions, i.r. refl. obs. 3−21042
GaSb, reflectivity spectra, photoemission, dielec. function and core levels obs. *(French)* 3−30831
GaSb, resonant Raman scatt. 3−5201
p-GaSb, u.s. longitudinal waves, attenutation due to phonon-hole interactions 3−7858
GaSb:Te, and undoped p-, acceptor radiative recomb., photoluminesc. spectral comparison *(Russian)* 3−36915
GaSb:Te, low temp. phonon scatt., two cond. band role, Te doping depend. *(French)* 3−4893
GaSb-InSb alloyed solid solns., distrib. coeffs. of Te and Zn *(Russian)* 3−11642
p-GaSe, light effect on switching props. at 77K 3−21126
GaSe, photoelec. props. rel. to minority carrier diffusion length and mobility 3−21112
n-InAs, absorpt. spectra near fund. absorpt. edge, coeff. rel. to photon energy 3−5217
n-InAs, cond. band nonparabolicity, confirmed by optical absorpt. study *(Russian)* 3−38797
n-InAs, elec. cond., mm. wave investigation 3−21084
InAs, electron irradiation damage studies 3−33555
n-InAs, electroreflectance spectra, line shape, electrolyte method *(Russian)* 3−34371
InAs, energy band struct., refl., modulated refl., dielec. function, pseudopot. calcs. 3−30403
InAs, hall effect meas. to 90 kbar rel. to structural transition and band structure 3−21096
n-InAs, i.r. birefringence due to hot electrons, 80K *(Russian)* 3−8555
InAs, impact ionisation and scattering mechanisms rel. to band structure 3−21088
InAs, InP, InP_xAs_{1-x} solid soln., neutron and gamma irrad., elec. and optical props. 3−33907
n-InAs, intraband absorpt. of light, drag of electrons by photons *(Russian)* 3−2135
InAs, reson. Raman scatt. near E_1 gap, uniaxial stress effects 3−5206
InAs and InAs-CdTe solid solutions, absorption band structure from absorption spectra 3−24383
InAs film, chem. vapour deposition using organometallics 3−21531
InAs p-n junction transitional processes in photodiode mode 3−21147
n- InAs transport phenomena, heavily doped 3−36608
InAs:Se(Te), electron effective mass, determ. from temp. depend. of transport props. *(Russian)* 3−27250
InAs-GaAs solns., Zn and Te impurity effect on crystallisation *(Russian)* 3−7782
InAs-oxide-Pb tunnel junction, conductance characts., effect of accumulation layer 3−38901
$InAs_{1-x}P_x$, vapour phase epitaxial growth and elec. props. 3−2680
$InAs_{1-x}P_x$, vapour-grown epitaxial layers, electron microprobe characterization 3−20955
$InAs_{1-x}P_x$ film, chem. vapour deposition using organometallics 3−21531
$InAs_xP_{1-x}$ solid solutions, compositions, transport properties, electron effective mass 3−33802
$In_xGa_{1-x}As$ laser, optically pumped, performance 3−4109
$In_{1-x}Ga_xAs_{1-y}P_y$, electron zones, luminesc. struct. study *(Russian)* 3−36946
$In_{1-y}Ga_yAs_{1-x}P$, Cs_2O-activated, photoemission 3−34456
$In_{1-x}Ga_xP$, electroluminescence, free electron-bound hole recomb. 3−2597
$In_{1-x}Ga_xP$:N, N_2 isoelectronic trap, luminescence, l.e.d. applications 3−39175
$In_{1-x}Ga_xP$:N laser operation, reson. enhancement of recomb. probability associated with isoelectronic trap states 3−18472
$In_xGa_{1-x}P$ solid solns., epitaxial growth from gas phase *(Russian)* 3−12240
n-InP, absorpt. spectra near fund. absorpt. edge, coeff. rel. to photon energy 3−5217
InP, crystal growth by liquid encapsulation, and elec. props. 3−2679
InP, electron energy relaxation time, determination from 34 GHz complex conductivity measurements in presence of d.c. field 3−2118
InP, electron energy relax. time as function of elec. field 3−24420
InP, electron transfer high freq. behaviour, dynamical Monte Carlo study 3−11902
InP, electron-phonon interaction and intervalley scatt., pseudopotential calc. 3−5005
InP, electrorefl. spectra rel. to hydrostatic press. *(Russian)* 3−8610
InP, facility for growth of crysts. from melt *(German)* 3−8738
InP, n- and p-type, spin orientation by optical pumping 3−2593
n-InP, shallow impurity states, cyclotron reson., Zeeman splitting, cond. electron effective masses 3−2026
InP, subsidiary indirect cond. band minima, donor levels, phonon struct. of interband transitions 3−2027
InP, vapour phase epitaxial growth and elec. props. 3−2680
InP, vapour phase epitaxial growth, photoluminesc. props. 3−2681
n-InP, velocity field characs., microwave obs. 3−30484
n-InP, velocity/field characteristics from dipole domain measurements 3−8186
InP effective electron mass, scattering factor measurement 3−36599
InP epitaxial, carrier concentration profiles 3−24808
InP film, chem. vapour deposition using organometallics 3−21531
InP laser, optically pumped, performance 3−4109
InP layer prod. by Nicoll and Sirt short path transport method *(German)* 3−8729
InP:Ge,Sn,Te, liquid phase epitaxial growth, impurity distribution coeffs. 3−1637
InSb, cond. electrons stimulated spin-flip Raman scatt., theory appl. to magnetically handle i.r. laser 3−6510
n-InSb, phonon-phonon and phonon-charge carrier interactions *(French)* 3−1706
InSb junction lasers operated at low temp., longitudinal mag. field effect on power output 3−37973
InSb:Cd, p-n technique 3−34489
p-InSb:Ge, ion pairing induced by X-rays 3−15152

III-V semiconductors continued
InSb:Te, Se, S, transport phenomena, 77-300K, press. to 15k bar 3−2096
InSb-type, Raman scattering by electronic excitations 3−39153
InSe film, amorphous, crystallisation and decomposition, electron microscope obs. 3−7936
ZnSe, electronic struct. of zinc blende phase and rock salt phase 3−21011

illumination *see lighting*

image amplifiers *see image intensifiers*

image convertors
see also fluorescent screens; image intensifiers
charge-coupled, sensitivity and resolution at low light levels 3−29058
electronic imaging systems, pulsed light sources, high speed photography, high speed cine cameras 3−228
image information content and transfer efficiency, single parameter descrip. 3−32519
image tubes as shutters in high speed photographic system 3−9984
injection lasers, time characteristics study 3−25778
ion-electron image converter for ion microscopes *(Russian)* 3−6116
multi-channel image tube for photoelectron counting in astronomical spectroscopy 3−31836
nonlinear optical, image formation theory *(Russian)* 3−16813
page composer, acousto-optic type, Bragg imaging applic. 3−4132
particle size distrib. by area analysis, Saltykov method modifications and extensions 3−35520
for photometric measurements, criteria *(French)* 3−9936
photometry of image on screen 3−25750
radiography, computer enhancement 3−32233
u.s., allowing diver to see in turbid water 3−80
X-ray, EXICON solid state device 3−19342

image intensifiers
applic. in ultrahigh speed photography *(French)* 3−9973
applications to astronomy, recent developments 3−31832
astronomical applications, established and recently developed devices, review 3−9629
channel plates (fibre-optic electron multipliers) as image intensifiers in transmission electron microscope 3−356
channeltron, used with electron microscope, operation results 3−22506
for compact neutron radiography facility *(German, English)* 3−19284
electron microscopes, transmission and scanning 3−22501
in field-ion microscopy 3−22502
foveal contrast sensitivity, quantum efficiency 3−16313
high-gain light-intensifying device incorporating fibre-optic X-ray intensifying faceplate 3−28741
image integration and display system for guiding on stars beyond visual detection limit 3−31837
interference-shadow marking of three-dimensional models 3−26210
neutron radiography 3−25025
for neutron radiography in nondestructive testing 3−27828
photographic emulsion sensitivity, intensification technique for u.v. spectroscopy 3−9983
radioautography, rapid image generation using microchannel plate electron image amplifiers 3−35526
radiograph image enhancement via video system 3−27835
smoothing dissector, intensifier addition to image dissector 3−31834
TV cameras, Si target vidicon, viewing distance, underwater appls. 3−3216
X-ray, for indirect radiography 3−16548
X-ray, image transfer to subsequent system 3−16547
X-ray image intensifier tube E5703, description 3−32232
for X-ray Moire topography 3−23969
X-ray nondestructive testing 3−27828
X-ray telescopes 3−25527
Na laser amplifier, image amplification 3−6473

image storage tubes
glowing spot removal using laser radiation 3−6529
pyrolectric image tubes 3−13238
Si, for dosimetry, fluoroscopic dose reduction and image manipulation 3−411

images, optical *see optical images*

imaging, acoustic *see acoustic imaging*

imaging, infrared *see infrared imaging*

immittance *see electrical impedance*

impact
see also ballistics
acrylic resin, tensile and impact strength, 4.2-300 K 3−25010
brittle non-metallic material, mech. impact rel. to fracture 3−8995
composite, B fibre reinforced epoxy, discontinuous, impact toughness 3−31137
composite, C-fibre-reinforced epoxy resin, impact and fracture props. 3−31142
crater near Mt. Darwin, Darwin glass examination 3−2853
craters in dense crystalline rocks, empirical formulae and model 3−39649
c.r.t. testing, impact of steel ball, pulsed holographic study 3−5773
cylindrical shells with discontinuous cross-sectional area, longit. impact 3−22692
damage due to liq. drop high speed impacts 3−18622
elastic, rigid cone and elastic half-space, Hertz's theory 3−32297
elastoplastic string, unloading boundary determ. in transverse impact 3−22689
fin, from shipping cask, plastic impact testing, energy absorption characteristics 3−39424
graphite, damage criterion rel. to temp. 3−5369
graphite surface, electron irrad., momentum transfer, blow off vapour yield, 300-5000K 3−24765
hypervelocity microparticle impact on metal surface, plasma production 3−33375
interaction of absolutely solid body with two-mass elastic system *(Russian)* 3−32299
liquid-solid high-speed impact, shock wave velocity 3−36120
materials testing, high speed methods analysis 3−37110
metal, non-ferrous, critical velocity, mech. props., pretreatment effect *(German)* 3−31081

impact continued
- metal-metal high velocity collision, surface phenomena *(Russian)* 3—4911
- metals, shockwave propag., deform. energy and collision velocity determ. *(Russian)* 3—27066
- Moon, transient winds from lunar meteorite impacts, model of gas cloud 3—16180
- oblique fibre sparsely reinforced matrix, constitutive eqns., impact-deflection 3—24990
- ocean surface, acoustic location system 3—3269
- perspex, erosion due to water jet impact, damage threshold vel. prediction 3—1681
- piezoelectric rod, longit, impact and boundary conditions *(Russian)* 3—6273
- polymer, apparatus for investigating effects of high-vel. impact 3—22264
- polyurethane foam, compression wave behaviour 3—31205
- simultaneous impact craters and structure of lunar craters 3—39636
- special impact test specimen *(Russian)* 3—12484
- steel, Cr-Mo-V-Nb, nickel content influence on struct. and high temp. props. 3—8937
- steel, critical velocity, mech. props., pretreatment effect *(German)* 3—31081
- steel, damage criterion rel. to temp. 3—5369
- steel, heavily alloyed, resistance to failure 3—34601
- steel, high-C ferrite-pearlite, struct./prop. relationships 3—21647
- steel, influence of electrical discharge treatment on constructional props. 3—24921
- steel, mild, impact behaviour, effect of up to 1% Sn 3—8846
- steel, mild, impact props. of cold-extruded rod 3—21642
- steel, Ni-Cr-Mo, rare earth treated, temper embrittlement response and toughness 3—34584
- steel, work hardened, impact strength under cyclic loading at low temp. 3—34682
- steel ball on oscillating brass plane, periodic impact 3—26069
- steel hardened by alloying or heat treatment, mech. props. 3—24947
- steel plate, mild, performation by flat-ended cylindrical projectile 3—25026
- straight circular elastic tubes, pulse propag. 3—22693
- supersonic particles on moving body, triboelectric charging 3—660
- surface state of bombarded solids, secondary ion-electron emission 3—36968
- tektites, halogens and U contents rel. to obsidians and impact glasses 3—16199
- tensile panels, fracture due to damage from projectile impact 3—21628
- two masses, along line of centres, analogue computer modelling *(German)* 3—32302
- wave formation in elastic half-space with nonlinear transitional wave process excitation *(Russian)* 3—32378
- Al-Al hypervelocity impacts, metallic plasma, flash spectral line radiation, impurity radiation effects 3—1484
- α-brass, erosion due to water jet impact, damage threshold vel. prediction 3—1681
- C fibre/glass fibre sandwich composite, Izod testing 3—31131
- CaF$_2$ type fluorides, changes in real structure due to compressive impact 3—33503
- Fe, Armco, impact strength, effect of cold deform. and subsequent heat treatment *(Russian)* 3—5307
- Fe, high-purity, impact behaviour, effect of up to 1% Sn 3—8846
- Si surface relief structure after ion bombardment 3—15059
- Ti alloys, impact strength, rel. to low temp. applic. 3—31098

impact avalanche transit-time devices *see IMPATT devices*

impact ionisation *see high field effects*

IMPATT devices
- *see also IMPATT diodes*
- No entries

IMPATT diodes
- oscillator, marginal for e.p.r. simple, for students 3—16361

impedance, acoustic *see acoustic impedance*

impedance, electrical *see electrical impedance*

impedance matching
- lever as mechanical analogue of matching transformer 3—33
- medium with real refractive index with interface with complex input impedance by inhomogeneous layer 3—5709
- mismatch error in microwave amplifier noise meas. 3—25651

impedance measurement, electrical *see electrical impedance measurement*

imperfections, crystal *see crystal defects*

imperfections, semiconductor *see semiconductor defects*

impermeability *see permeability*

impulse generators *see pulse generators*

impulse voltages *see transients*

impulse welding *see resistance welding*

impurities, crystal *see crystal impurities*

impurity electron states and effects
- *see also electron traps*
- acoustic resonance absorption, paraelectric, quadrupole transitions, noncentral impurity ions 3—38624
- activated radiationless processes, orientation relax. of polar mols. 3—2573
- activation energy, estimation from carrier conc. temp. depend. *(Russian)* 3—33828
- alkali halide:Tl$^+$, many-photon excitation of Tl$^+$ impurity centres on laser irradiation 3—5230
- alkali halide, impurity doped, review of Z-centres 3—8624
- alkali halide, In$^+$- or Sn^{2+}-doped, absorpt. spectra, high press. 3—39166
- alkali halide, phonon sidebands in emission spectrum of O$_2^-$ 3—39182
- alkali halide, temp. depend. of half-widths and integral absorpt. of impurity vibration bands 3—21450
- alkali halide as CO$_2$ laser window material, intrinsic and impurity absorpt. at 10.6 micron 3—28580
- alkali halide crystals, laser destruction mechanisms and multiphoton ionization of impurity centres 3—5162

impurity electron states and effects continued
- alkali metal halide:Th, In phosphors, absorption and phosphorescence spectra depend. on lattice parameters and refractive index *(Russian)* 3—30875
- alloy, disordered, substitutional, density of states in impurity band, CPA calcs. 3—24371
- alloys, disordered binary, random transfer integrals and electronic struct., impurities effect 3—36519
- amino acid:Cu^{2+}, ligand hyperfine interaction, e.p.r. spectra 3—24605
- Anderson three dimensional disordered model, localisation degree 3—18056
- anthracene, thermally stimulated current meas. of trapping level depth and frequences 3—18167
- antiferromagnet with substitutional impurities, magnon density of states calc. 3—8331
- carrier scattering by screened surface charges 3—21133
- charge densities in presence of strong attractive impurity potentials 3—38808
- charge density oscillation around resonant scatt. impurities 3—4961
- chrysene, oriented phosphorescent, e.p.r. absorption at mag. fields below 125 G., multiple orientation of chrysene triplets in p-terphenyl single crystals 3—25091
- compensation determination from hopping conduction saturation 3—24441
- copper phthalocyanine:vanadyl phthalocyanine, energetic trap distrib. rel. to impurity 3—38811
- cubic crystal with substitutional impurities, i.r. absorpt. and dielec. susceptibility 3—18478
- diamond: B, dominant acceptor in semiconductor 3—38810
- diamond:Li, implanted, elec. cond., after annealing at 1400°C *(Russian)* 3—2070
- diamond:N, u.v. and i.r. absorption spectra *(Russian)* 3—2578
- diamond, defect energies and states, defect-molecule method, extended Huckel calc. 3—33838
- diamond, luminescence quenching and zero-phonon line broadening associated with defect interaction 3—30860
- diamond, semiconducting, defect calc., LCAO-MO methods, extended Huckel theory 3—33840
- diamond, semiconducting p type, high field magnetoresistance, hole conduction in uncoupled valence bonds 3—11912
- diamond, semiconducting vacancies, electronic levels, defect. molecule model, extended Huckel approx. 3—33839
- diamonds, natural type IIb, resonant scattering 3—1841
- diamonds, type I and IIa, pulse irradiation 3—8673
- donor-acceptor pairs, emissive recomb. spectrum, anal. expression *(Russian)* 3—36897
- electronic energy transfer in impure solids, two mols. embedded in lattice 3—18097
- electronic lifetime anisotropy determ., mosaic spread enhancement of dHvA-Dingle temp. 3—11845
- energy transfer kinetics, crysts. with systems of donor and acceptor impurity atoms 3—34424
- e.p.r. lineshape due to defect random distrib. 3—2379
- excitation decay, hopping mechanism of energy transfer 3—33835
- exciton insulators, deep impurity levels behaviour 3—21027
- excitons diffusion and energy transfer to impurity centres 3—33848
- F_{2a}^+ centres in alkali halides, low lying states, pseudopotential calcs. 3—33831
- ferromagnetic semiconductors, max. resistivity due to carrier scattering by giant moments of mag. clusters 3—18145
- fluorophosphate phosphors energy transfer between Mn and Sb 3—21025
- GaAs:He(N,S,Zn), ion implantation, elec. conduction due to defect centres 3—33906
- garnets doped with trivalent rare-earth ions, resonant scattering of phonons 3—4837
- glass:Nd, laser-induced-fluorescence-line-narrowing spectroscopy 3—21474
- glass:Yb, Tb(Eu), luminescence, cooperative processes *(Russian)* 3—36907
- glasses, phototropic, TlCl activation, optical absorption meas. 3—27737
- graphite:Fe, oscillatory magnetoresist., charged impurity selective scatt. 3—11864
- group V, II-VI semiconductors, alkali halides, vacancies, interstitials, Jahn-Teller distortions, molecular orbital models 3—33837
- Gunn domain dynamics, in presence of field-independent trapping 3—18151
- Hall effect determination of impurity level depth *(Russian)* 3—33827
- n-hexane, carrier mobility rel. to impurities, nanosecond X-ray ionization pulses obs. 3—2084
- II-VI semiconductor, edge emission rel. to donor-acceptor pair recombination 3—8630
- III-V compounds, donor and acceptor conc. determ. from hot electron mobility 3—38812
- III-V semiconductor, impurity electron binding energy, using dielectric theory *(German)* 3—15159
- impurity atom, location exact determ. by means of channelling effect *(Russian)* 3—1660
- inert gas alloys, dil., solid and liq., emission spectra of deep impurity states 3—2581
- inorganic crystals, rare-earth-doped, dominant energy transfer mechanism 3—36936
- inorganic crystals, rare-earth-doped, energy transfer and optical transitions 3—39178
- inorganic crystals, rare-earth-doped, transition probability calc. 3—39177
- inorganic ions in glasses and polycrystalline pellets as fluorescence standard reference materials, review 3—35349
- ionic crysts., defect levels, theory 3—11855
- ionic crysts., luminesc. impurity centres, energy transfer, excitonic mechanisms *(Russian)* 3—27537
- IV-V transition metal carbides, concentration dependence of hardness in terms of impurities *(Russian)* 3—12433
- Jahn-Teller impurity ion pair, vibron reduction effects of Coulomb and exchange interactions 3—33813
- jellium, impure, small frequency and wavevector, longitudinal sound damping 3—20989

impurity electron states and effects continued
Josephson junction, effect of paramagnetic impurities on Josephson current 3—21185
luminescence in solids, sensitized, diffusion of electronic excitation, energy transfer by resonance 3—27566
metal, inhomogeneously strained, with impurities, elec. cond., calc. *(Russian)* 3—30443
metal, Kondo effect, resist. due to 3d impurities, s-d interaction model 3—2042
metal, polyvalent, impurity scatt. and residual resist. 3—18115
metal, rel. to electron-phonon interactions 3—38646
metal with nonmag. impurities, impurity quasilocal vibration rel. to conducting state 3—4986
metal-insulator transition, impurity effects on excitonic phase in strong mag. fields 3—30421
metallic alloys, electron theory treatment of relaxations around lattice of point defects 3—1971
metals, electron-phonon umklapp interaction anisotropy and deviations from Matthiessen's rule 3—38820
1, 1′- methylene-2, 2′-cyanine, anomalous absorption and luminescence spectra 3—27569
m.i.m. systems, dielectric relaxation effect on isothermal electrical characteristics of defect insulators 3—11959
m.i.m. systems, dielectric relaxation effect on thermal electric characteristics, Poole-Frenkel mechanism 3—8276
molecular crystal, impurity and surface states in linear systems *(Russian)* 3—2021
molecular crystals, doped, polarisation luminescence method for struct. determ. *(Russian)* 3—27525
molecular impurity centre scattering of lattice waves 3—1746
molecular solids, photoemission rel. to impurities and defects 3—15588
monatomic lattice with defects, network model 3—20984
Monte Carlo method for solving excitation transfer 3—34412
n-type, impurity ionization 3—8192
naphthalene cryst. with impurities depolarization of exciton absorpt. bands 3—15525
naphthalene crystals with indole and thionaphthene impurities, local excitons *(Russian)* 3—36908
naphthalene guest molecules, low concentrations in diphenyl, triplet state energy transfer at low temp., e.p.r. obs. 3—25090
neutral, impurity density-of-states tails 3—11844
nitrate glass: Eu, Sm, Gd, Tb, Dy absorption, luminescent and excitation spectra *(Russian)* 3—30878
optical phononless lines, electron phonon interaction operator, thermal broadening and shift, adiabatic approximation 3—36900
optical transitions between excited states of V impurities, photocond. 3—33826
optically active impurities, indirect exchange interaction caused by plasma oscills. *(Russian)* 3—8123
organic impurity molecules, asymmetry of tunnel spectrum intensities 3—21142
organic molecule impurities in solid rare gases, extravalence molecular excitations, Wannier impurity states 3—24721
p-n junction, thermally stimulated capacitance for shallow majority carrier traps in edge region 3—36661
n-paraffin matrix, impurity mols., linear spectra and impurity centre theory *(Russian)* 3—36896
phenanthrene guest molecules, low concentrations in diphenyl, triplet state energy transfer at low temp., e.p.r. obs. 3—25090
phonon coupled states with impurity centres, multiplicity of dielectric local modes *(Russian)* 3—36924
phonon free path determination using shallow donors in He-cooled semiconductors 3—14950
phonon thermal resistivity due to spherical inclusions 3—1724
phosphate glass, exchange interaction role in energy transfer between Eu^{3+}, Sm^{3+}, Dy^{3+} and UO_2^{2+} *(Russian)* 3—8651
photoinert organic solids with aromatic impurities, phosphorescence induced by u.v. and X-ray irradiation 3—5234
photoionization of shallow impurity centres, photoelec. effects due to drag phenomena 3—2139
piezoelectric semiconductor, degenerately doped, acoustoelec. gain const., calc. 3—18194
point defects and diffusion, monograph 3—1621
polymers, charge trapping, role of unsaturated groups 3—30468
polyphosphoric acid, exchange interaction role in energy transfer between Eu^{3+}, Sm^{3+}, Dy^{3+} and UO_2^{2+} *(Russian)* 3—8651
protoporphyrin in n-octane, 4.2 K, reversible transforms. of luminescent impurity centres 3—15547
pyroxene, glass. Eu^{3+}, effect of thermal working on luminescence spectra *(Russian)* 3—30874
quartz, γ-irrad., phonon-assisted tunnelling transitions of trapped hole at substitutional impurity 3—1707
rare earth hydroxides, energy levels of Er^{3+}, optical spectra 3—2572
rare-earth ions, resonance phonon scattering at average and high temps. 3—1767
recombination centres and electron traps, kinetics of non-equilibrium carrier density *(Russian)* 3—24450
relativistic treatment of impurity states in Saxon-Hutner model 3—8120
ruby:Cr^{4+}, elimination of Cr^{4+} ions as a source of strong resonant phonon scattering *(French)* 3—1846
ruby, γ-irrad., valence transitions of V ions, e.p.r. obs. *(Russian)* 3—39027
ruby, higher energy levels of Cr^{3+} ion pairs, excitation and absorpt. spectra 3—15551
scattering of electrons from random impurity centres, transport equation 3—11875
semiconduction, disordered solid impurity conduction by stochastic transport 3—38842
semiconductor, compensated, heavily doped, large-scale potential props., microwave absorpt. *(Russian)* 3—8165
semiconductor, deep impurity levels influence on double injection and recombination 3—8203
semiconductor, deep level impurity determination, Schottky barrier capacitance meas. 3—24510
semiconductor, deep traps in quasi-classical random field, light absorpt. *(Russian)* 3—34385
semiconductor, defect deep levels, molecular orbital treatment 3—30429

impurity electron states and effects continued
semiconductor, doped periodically, carrier mobility, elec. cond. anisotropy *(Russian)* 3—8178
semiconductor, effective mass theory 3—15155
semiconductor, e.p.r. obs. *(German)* 3—15419
semiconductor, group II-VI cpds., g-shift of s-state ions 3—2377
semiconductor, highly degenerate, diffusivity-mobility ratio, influence of band tails 3—24423
semiconductor, magnetoabsorpt. spectra, inelastic carrier-impurity interaction 3—5222
semiconductor, multiple energy level defects, continuity and Poisson equations 3—24418
semiconductor, nondegenerate, rel. to mag. field depend. of i.r. cyclotron reson. 3—36533
semiconductor, rel. to light absorpt. in presence of strong e.m. field *(Russian)* 3—8628
semiconductor, shallow acceptor states, effective mass theory, strong spin-orbit coupling limit 3—2025
semiconductor, shallow donor impurities, chem. shift parameters 3—27224
semiconductor, strongly compensated, rel. to hopping mobility 3—33900
semiconductor, tetrahedrally co-ordinated, shallow defect level, electron binding energy *(German)* 3—15138
semiconductor, zero-gap, quasi-discrete acceptor states *(Russian)* 3—8124
semiconductor electron equilib. distrib. instability *(Russian)* 3—8184
semiconductor overheating instabilities, low-temp. impurity breakdown 3—24395
semiconductor with deep traps, injection current theory 3—30488
semiconductor-metal contacts, impurity effects on tunnelling 3—38891
semiconductors, gapless, with HgTe type band struct. 3—2022
semiconductors, heavily doped, temp. dependence of, density-of-states effective meas. in 1 to 20 K range 3—8121
semiconductors, many-valley, Luttinger-Kohn and Slater-Koster methods 3—30431
semiconductors, with deep traps, ambipolar mobility and injection currents 3—27254
semiconductors phonon scattering by electrons and holes 3—1748
shielding of impurities as measured by extended X-ray absorption fine struct. 3—18511
Si, defect energies and states, defect-molecule method, extended Huckel calc. 3—33838
spectral bandshapes, symmetry of quadratic mode absorption and emission band shapes 3—8631
superconductivity in Anderson model perturbational calc. of s-electron Green function 3—5071
superconductors with transition metal impurities, props., Hartree-Fock calcs. 3—15298
TCNQ salts, impurity effects on electrical conductivity and activation energy anisotropy *(German)* 3—30504
tetrahedral impurities, coupling strengths of α_1, ε and τ_2 phonons to A→T optical transitions 3—27522
theory of impurity levels, expression for Green's function 3—36548
rel. to thermoluminescence theory 3—30888
transition metal: ^{181}Ta, 6.2 KeV Mossbauer γ rays, temp. effects 3—30736
transition metal-hydrogen solid solns., X-ray emission spectra interpret. 3—2603
triglycine fluoroberylate:Cu^{2+} single crystals, e.p.r., high-pressure influence 3—34191
AgBr(Cl):Li(Na), absorpt. bands due to impurity localised modes 3—30850
AgCl:Cu^{2+}, blue light irrad., growth and decay of self-trapped holes, e.s.r. obs. 3—39019
Al, mag.-field dependence of microwave absorptivity near energy gap 3—18262
Al valence electron redistrib. and positron trapping at vacancies 3—21026
Al-Mn:Fe, dilute alloy, temp. depend. of impurity resist. 3—21048
Al-Ti(V)(Fe)(Cu)(Zn), dilute alloy, temp. depend. of impurity resist. 3—11876
n-$Al_xGa_{1-x}As$, impurity conc. rel. to elec. transport props. 3—30478
AlN, rel. to refl. and luminesc. excitation spectra 3—18493
Al_2O_3, influence of electric field on parameters of impurity centre 3—36951
Al_2O_3 pyrolytic layer, in m.o.s. capacitor, trap struct. 3—18220
Al_2O_3:Cr^{3+}, electron spin echo for high Cr^{3+} concs. 3—8435
Al_2O_3:Cr^{3+}, electron spin-lattice time by continuous saturation method 3—34201
Al_2O_3:V^{3+}, phonon spectroscopy on the resonant scattering of V^{3+} and other impurities by tuning the 'Bremsspectrum' of a superconducting tunnel junction 3—1768
Al_2O_3:V^{4+}, acoustic paramagnetic resonance 3—2347
As-S-I:Mn^{2+}, e.p.r. study 3—30686
As-Te-I:Mn^{2+} glasses, e.p.r. study 3—30686
As_2S_3 glass and crystalline phases, magnetic susceptibility, paramagnetic contributions due to Fe impurities 3—8334
Au, electron-impurity scatt., anisotropy study using de Haas-van Alphen effect 3—11881
Au film activated with BaO, change in work function of isolated centres 3—36658
AuCr, (3.3, 10.6 at. % Cr), elec. resist., $T^{3/2}$ depend. of impurity resist. 3—36581
BaF_2:$Eu^{2\cdot}$ impurity-induced Raman scatt. 3—39147
$BaSb_2O_6$:Bi^{3+}(Pb^{2+}), fluorescence obs. for each excitation band 3—21478
$BaTiO_3$:Al ceramic, piezo-electric effect 3—21363
$Be_3Al_2Si_6O_{18}$:V^{3+}, beryl, optical and i.r. absorpt. rel. to crystal field parameters 3—34389
n-BiI_3 single crystals, photoconductivity and photoluminescence *(Russian)* 3—11932
Bi_2Se_3:Ge, donor levels, free-carrier concentration determ. by reflectivity meas. at plasma resonance 3—33824
CaF_2:Cd^{3+}, Pr^{3+}, Yb^{3+}, luminescence, energy transfer from Cd^{3+} to Pr^{3+} and Yb^{3+} *(Russian)* 3—36905
CaF_2:Ce,Na, near u.v. absorpt. spectra obs. of defect centres 3—12161

impurity electron states and effects continued
CaF_2:Eu crystals, thermoluminescence and X-ray stimulated luminescence 3 − 27580
CaF_2:Mn(Ce,Mn), cathodoluminescence, trapped hole diffusion 3 − 39197
CaF_2:Sm^{2+}, stimulation of nonradiating transitions by strong light excitation *(Russian)* 3 − 36925
CaF_2:Tm^{2+}, covalency contribution on the values of $g\Gamma_7$ and $g\Gamma_{7'}$ *(Russian)* 3 − 11861
CaF_2:X^{3+}, X=Ce, Pr, Sm, Eu, Tb polarisation storage, optical absorption for 4f-5d transition of rare earth in local crystal field 3 − 18406
CaF_2:Yb^{3+}, covalency, ab initio calc. 3 − 2009
CaO:Bi, Sb, Tl photoluminescence, radical-recombination luminescence of the O atoms *(Russian)* 3 − 30876
$CaO_xNiO_{1-x}Fe_2O_3$, $0 \leqslant x \leqslant 0.7$, variation in Curie temperature and electrical conductivity with conc. *(French)* 3 − 8362
$Ca_{10}(PO_4)_6F_2$:Sn, oxidation and reduction of Sn, luminescence effect of O_2 partial pressure 3 − 39470
CaS:Bi^{3+}, Pd^{2+}, phosphorescence decay characteristics, trap depth calc. 3 − 30856
$CaSO_4$:V, Ln, (Ln=Y, Dy, Sm, Tb), energy transfer by sensitizer-activator pairing 3 − 30868
$CaSb_2O_6$:$Bi^{3+}(Pb^{2+})$, fluorescence obs. for each excitation band 3 − 21478
$CdCr_2S_4$, anomalies in mag. anisotropy and f.m.r. linewidth due to impurities 3 − 21318
n-$CdCr_2S_4(Se_4)$:Ga, cond. min. and negative magnetoresist. 3 − 27267
CdF_2:In, optical absorpt. and elec. cond. meas. 3 − 21448
CdF_2:In^{3+}, semicond., resonance Raman spectra 3 − 36871
CdF_3:Er^{3+}, C_{3v} local-site symmetry from correlated e.p.r. and optical obs. 3 − 21305
Cd_3P_2:Cu, deep levels, effect on optical props. 3 − 30794
CdS, donor states, rel. to stimulated emission 3 − 15523
CdS, isoelectronic Ni impurity, absorpt. spectra *(Russian)* 3 − 8618
CdS, photoluminesc., donor-acceptor pair recomb. 3 − 5224
CdS film, bulk compensation effect on chemisorption dependent semiconductivity 3 − 33889
CdS:Ce^{3+}, Ag, Cu, fluorescence spectra, probability of emission calc. *(Russian)* 3 − 27546
CdS:Ni^{2+} absorpt. spectrum obs. of linear Stark effect 3 − 8625
CdS:Te, piezoemission study 3 − 18492
CdS-Cu_{2-x}S heterojunctions, impurity photoeffect 3 − 27309
CdSe, photoluminesc., donor-acceptor pair recomb. 3 − 5224
n-CdSe, shallow donor states, cyclotron reson., Zeeman splitting, cond. electrons effective masses 3 − 2026
CdSe at low temps., S-type negative resistance due to electron scattering by ionised impurity pairs 3 − 33911
CdSe film, surface elec. props., surface doping effects *(Russian)* 3 − 2192
CdSe:Co, degenerate discrete excited states, absorpt. and photocond. spectra obs. 3 − 2024
CdSe:Ni, degenerate discrete excited states, absorpt. and photocond. spectra obs. 3 − 2024
CdTe, cathodoluminescence from lattice defect centres, quenching mechanism 3 − 15561
CdTe, electron and neutron irrad., excess, dissociative Cd pressure, defect behaviour, photoluminescence spectra 3 − 34431
CdTe, investigation of doubly charged acceptors 3 − 24478
CdTe, ionized impurity scatt. rel. to high field electron transport 3 − 8191
CdTe, rel. to high temp. relax of cond. *(Russian)* 3 − 2071
n-CdTe, shallow impurity states, cyclotron reson., Zeeman splitting, cond. electrons effective masses 3 − 2026
CdTe compensated doped crystals, density of states tails, conductivity, Hall mobility, conduction band 3 − 33832
CdTe:Fe, Hall effect and photocond. meas. rel. to impurity absorption 3 − 15531
CdTe:In, absorption band edge of compensated crystals 3 − 24717
CdTe:Ti, degenerate discrete excited states, absorpt. and photocond. spectra obs. 3 − 2024
CdTe:V, degenerate discrete excited states, absorpt. and photocond. spectra obs. 3 − 2024
Ce, effect of impurities on α-γ transition 3 − 21238
Ce-La alloys, α-γ electronic transition, La impurity effects 3 − 38669
Ce-La alloys, α-γ electronic transition, La impurity effects 3 − 38670
CeF_2, Pr^{3+} absorpt. spectra and energy levels *(Russian)* 3 − 12157
Co:$^{51}V(^{103}Rh)$, information from meas. of relaxation rates 3 − 5147
Cs halide, study of impurity induced first order Raman spectrum 3 − 21411
Cs:Tl fluorescence, polarisation effects *(German)* 3 − 24742
CsF:Tl single crystals, luminescence props. *(Russian)* 3 − 12175
CsI:$Wo^{2-}(MoO^{2-})$, i.r. absorpt. and local symmetry 3 − 8621
Cu, impurity scatt., phase-shift anal. 3 − 33863
Cu alloy, magnetoresist. and dHvA meas. rel. to impurity scatt. of electrons 3 − 21055
Cu-Au(Fe), Kodon effect in dilute magnetic α-phase alloys 3 − 21218
Cu-Fe alloy, dil., impurity-induced gigantic thermo-e.m.f. *(Russian)* 3 − 8152
Cu-Fe dilute alloy, oscill. of cond. electron density near solute atoms, ^{63}Cu n.m.r. obs. 3 − 2462
Cu(Al), impurity scattering anal. in terms of s, p and d partial waves 3 − 8135
Cu(Fe), impurity scattering anal. in terms of s, p and d partial waves 3 − 8135
CuI film, rel. to electrical and luminescent props. *(Russian)* 3 − 24432
Cu(Ni), impurity scattering anal. in terms of s, p and d partial waves 3 − 8135
Cu_2Te, n and p type, electrical props., conduction mechanisms *(Russian)* 3 − 8170
Fe:$^{175}Lu(^{175}Yb)$, ang. correlation meas. of hyperfine fields at impurity nuclei 3 − 15141
Fe:Co, ^{57}Fe c.w. n.m.r. spectra obs. of hyperfine field at impurities 3 − 21326
Fe:Co(Ni)(Sn), temp. depend. of hyperfine fields, c.w. n.m.r. obs. 3 − 21327
Fe-transition metal, dilute alloys, Mossbauer spectra, hyperfine field, isomer shift changes analysis 3 − 30733

impurity electron states and effects continued
FeS_2, rel. to low temp. resist. and Hall effect 3 − 21070
GE:Sb, high frequency monochromatic phonon spectroscopy 3 − 1765
GaAs, effect on recombination characs. *(Russian)* 3 − 24392
GaAs, elec. transport props. depend. on heat treatment, thermal conversion rel. to impurities *(Russian)* 3 − 38832
n-GaAs, electrochemical characterization, automatic plotting system 3 − 30953
n-GaAs, electron irradiated, defect annealing, cluster formation 3 − 33558
GaAs, high purity, donor species identification, ionization energy determination using optically pumped NH_3 laser 3 − 2018
GaAs, high resistivity film, dominant oxygen contrib. to compensation 3 − 15156
n-GaAs, identification of bivalent flaw from noise meas. 3 − 18101
n-GaAs, optically excited, doping dependence of photon yield as function of excitation energy 3 − 8638
GaAs, p^+-n photodiodes, electron irrad., defect studies, differential capacity, conductance measurements 3 − 33845
GaAs, p-n junction, capacitance relax. determ. of impurity atom parameters 3 − 15157
n-GaAs, rel. to temp. depend. of electron mobility *(Russian)* 3 − 2076
n-GaAs, shallow donor states, cyclotron reson., Zeeman splitting, cond. electrons effective masses 3 − 2026
GaAs, thin film, flash-evaporated, doping characts. 3 − 27611
GaAs, V.P.E. growth, effect of As vapour pressure on deep level impurities 3 − 27191
GaAs heavily doped, electron mobility rel. to electron-electron scatt. and nonparabolic energy band shape 3 − 18139
GaAs subsidiary indirect cond. band minima, donor levels, phonon struct. of interband trransitions 3 − 2027
GaAs:Cr, photocond. after 0.8 MeV electron irradiation, induced impurity trap levels 3 − 36637
n-GaAs:Cu, 1.26-1.30 eV photolum. band rel. to recombination centres 3 − 39186
GaAs:Fe, sensitizing centres, photo Hall effect, photocond. 3 − 36547
GaAs:Fe(Cu), electron absorpt. obs. rel. to impurity energy levels *(Russian)* 3 − 15532
n-GaAs:S, Sc, Te, interzone scattering study by specific resistance at high press. meas. *(Russian)* 3 − 8162
GaAs:Si, epitaxial layers, characterisation of p-n structure, etching, cathodoluminescence 3 − 39195
GaAs:Si anomalous behaviour, temp. depend. of Hall coeff., centre concentrations 3 − 33834
GaAs:Sn, epitaxial growth, effect of surface states on amphoteric behaviour of Sn 3 − 24393
GaAs:Sn(Si, Zn), electron irrad., ‘near-edge’ absorption, annealing 3 − 33846
GaAs:Te, heavily doped, mag. susceptibility, 4.2-300K *(Russian)* 3 − 2252
GaAs:Te, impurity-defect interaction with Te ions bombard., amorphous layer form. 3 − 18062
n-GaAs:Te, rel. to surface treatment effects on photolum. 3 − 27570
GaAs:Zn, Cd, Si, Ge epitaxial layer, near band-edge photoluminesc 3 − 34406
p-GaAs:Zn, mag. field effect on impurity cond. 3 − 11914
$GaAs_{1-x}P_x$:N, isoelectronic trap transitions in resonant enhancement region 3 − 30430
$GaAs_{1-x}P_x$:N, N_2 isoelectronic trap, luminescence, l.e.d. applications 3 − 39175
$Ga_xIn_{1-x}P$:S, band structure from Hall effect and resistivity meas. 3 − 15215
GaN-GaN:Mg light emitting diode, rel. to violet luminesc. 3 − 34432
GaP, energy states of isolated donor-acceptor pairs and influence of polarisation interaction on pair energy 3 − 33830
GaP, evidence for nonradiative Si,O defect 3 − 21023
GaP, fluoresc. from bound excitons, quenching and enhancement by far i.r. radiation 3 − 36940
GaP, impurity ionisation energies and Bohr radius calc. from recomb. spectrum anal. expression *(Russian)* 3 − 36897
n-GaP, liq.-encapsulated-Czochralski-grown, deep hole traps, luminesc. study 3 − 5235
GaP, local strain fields due to impurities 3 − 2023
GaP, p-n junction with deep centres, space charge capacitance 3 − 33989
GaP, photoionisation of electrons and holes at oxygen donors 3 − 33950
GaP, recombination processes responsible for room-temp. near-band-gap radiation 3 − 34416
GaP, states with two bound particles, Auger transitions at defects 3 − 36546
GaP red-emitting lamp, O content and electrolum. efficiency 3 − 30537
GaP:Cu, red pair luminesc. 3 − 15544
GaP:Fe^{3+}, deep levels, photocond. obs. 3 − 18095
GaP:Li, Zn, bonding of excitons by neutral donors and acceptors *(Russian)* 3 − 36932
GaP:N, isoelectronically doped, radiative recombination 3 − 24754
GaP:N diodes, influence of temp. on electroluminescence spectra 3 − 24750
GaP:O, donor deep states, optical cross section, energy levels, conc., photocapacitance obs. 3 − 30427
GaP:O, donor deep states, capture cross sections, photocapacitance obs. 3 − 30428
GaP:Zn, O, Zn-O radiative centre form. during chem. vapour deposition 3 − 2672
GaP:Zn,O, Czochralski-grown photoluminesc., minority carrier lifetime, effect of heat treatment 3 − 39176
n-GaSb, heavily doped density-of-states tails associated with L-minima of conduction band 3 − 30425
p-GaSb, phonon-phonon and phonon-charge carrier interactions *(French)* 3 − 1706
GaSb:Te, role in low temp. thermal cond. *(French)* 3 − 4893
GaTe:Ge, high-resistivity, radiative capture of holes by luminescence centres 3 − 24740
$GdAlO_3$:Ho^{3+}, absorpt. and luminesc. spectra obs. rel. to energy levels 3 − 8655

impurity electron states and effects continued
$GdAlO_3:Tm^{3+}$, absorpt., luminesc., and stimulated emission spectra obs. 3–12174
Ge, amorphous film, magnetoresist. in fields up to 25 kG, impurity level effects 3–21095
p-Ge, anisotropy of magnetothermal conductivity 3–1842
n-Ge, breakdown and recombination kinetics connected with excited states shallow donor 3–18166
Ge, Coulomb potential of ionized impurities *(Russian)* 3–24417
Ge, effect on recombination characs. *(Russian)* 3–24392
Ge, H^+, O^+, B^+, ion bombardment, divacancy-like optical absorption 3–34394
Ge, impurity breakdown, origin of S-shaped I-V charact. 3–24443
Ge, muonium as deep donor, hyerfine splitting 3–18099
Ge, n- and p-type impurities, electron irrad., annealing, Frenkel pair model, vacancy release 3–33561
Ge, self-interstitial charge states, assignment of donor and acceptor levels 3–33522
Ge, shallow donor impurity near-surface states, theory 3–24494
Ge, surface electron inpurity states *(Russian)* 3–8247
Ge, two electron donor pair system, eigenvalue problem, Heitler-London method soln. 3–2579
Ge, ultrapure, shallow donor levels, photocond. obs., two-step process 3–4965
Ge film, vacuum deposited, acceptor levels, i.r. obs. rel. to elec. characs. *(Russian)* 3–24431
Ge heteroepitaxial films, Hall effect and magnetoresistance, conduction mechanisms depend. on impurity density *(Russian)* 3–11966
Ge p-n junctions, ionization energy of adhesion levels and thermogeneration centres in a volume of microplasma *(Russian)* 3–4960
n-Ge transport props., negative differential cond., impurity effects at 20K 3–21085
Ge: group V, γ-irrad., donor and acceptor formation 3–33545
Ge: groups III and V, electron irrad., unusual donors and acceptors 3–33843
Ge:Al, implanted acceptor levels, rel. to carrier generation at room temp. 3–2083
Ge:As, Ga, indirect semicond., direct transition probability in impurity luminesc. 3–15554
Ge:Au, impact ionisation of deep acceptor impurities 3–33918
n-Ge:Au piezoresist., influence of deep energy levels *(Russian)* 3–2074
Ge:Cu, effect of impurity on kinetics of annealing of radiation defects 3–24111
Ge:Cu, space charge limited currents rel. to photoelec. amplification 3–15198
p-Ge:Ga, gamma irrad., role of Li in annealing processes 3–33844
p-Ge:N, effect of impurity conc. on magnetoresistance 3–24440
n-Ge:Ni, local negative photoconductivity in strong electric fields 3–24479
$Hg_2F_2(Cl_2)(Br_2)(I_2)$, rel. to excitation and emission spectra 3–30864
HgS(Se)(Te), g-shift of s-state ions 3–2377
In-SiO_2-Si junction, impurity local mode effect on tunnelling conductance 3–15266
$In_{1-x}Ga_xP$:N, N_2 isoelectronic trap, luminescence, l.e.d. applications 3–39175
$In_{1-x}Ga_xP$:N, soln. growth, effect of N-trap states on photoluminesc. and elec. props. 3–24797
$In_{1-x}Ga_xP$:N laser operation, reson. enhancement of recomb. probability associated with isoelectronic trap states 3–18472
n-InP, shallow impurity states, cyclotron reson., Zeeman splitting, cond. electrons effective masses 3–2026
InP, subsidiary indirect cond. band minima, donor levels, phonon struct. of interband transitions 3–2027
InP, vapour phase epitaxial layer, donor conc., photoluminesc. obs. 3–2681
InP:Ge,Sn,Te, liquid phase epitaxial layer, carrier conc. and mobility 3–1637
n-InSb, highly doped, u.s. propag., longitudinal mag. field effects 3–38626
InSb, hydrogenic impurity bands in an external magnetic field 3–33829
n-InSb, magnetoresist. meas., impurity cond. effects 3–38857
n-InSb, phonon-phonon and phonon-charge carrier interactions *(French)* 3–1706
InSb, rel. to anal. of recomb. processes *(Russian)* 3–15212
InSb, rel. to spontaneous spin-flip Raman line shape 3–36870
n-InSb conduction, Hall coefficient, activation energies, impurity concentrations 3–30501
n-InSb donor deionisation, impurity cond., CW laser cyclotron reson., magnetocond., temp. depend. 3–15149
InSb:Fe, elec. and galvanomag. props., impurity levels and hole scatt. mechanisms 3–38844
p-InSb:Ge, ion pairing induced by X-rays 3–15152
n-InSb:Se, Te transmission spectra rel. to Moss-Burstein effect 3–4963
InSb deep impurity levels *(Russian)* 3–4959
$(In_2Te_3)_x-(Hg_3Te_3)_{1-x}$, influence of impurity compensation effect on negative magnetoresistance 3–27277
KBr:MnO_4^-, vibronic spectra obs. 3–8616
KBr:OH^-, O_2^-, O^{2-}, anion impurities influence on optical stability of F-centres *(Russian)* 3–8615
KCl, i.r. absorpt. of aligned H^--Na^+-H^- complex 3–24727
KCl:Ag, photochemically coloured crystals, luminesc. on deformation 3–5231
KCl:Cu, optical props. of complex centres 3–15528
KCl:Eu^{2+} calc. of localised one-electron states, mechanisms of recombinational process *(Russian)* 3–24389
KCl:KOH and KI:KOH, tunnelling levels of hydroxide ion 3–27226
KCl:Li, cond. electron scatt. by tunnelling states of defects 3–33920
KCl:Li^+, structure of potential wells responsible for nonequidistant spectrum 3–34392
KCl:Na, i.r. absorpt. rel. to softening of short range force consts. 3–15527
KCl:Pd, e.s.r. due to trace impurities 3–15412
KCl:Sn, Pb, single crystals, u.v. spectra 3–39154
KCl:Sn phosphor, polarized C radiation and energy level diagram for Sn^{2+} centres *(Russian)* 3–8649
KCl:Tl, γ-irrad., ionized Tl-pair centre, absorpt. study 3–21445

impurity electron states and effects continued
KCl:Tl, optical delocalization of holes from Tl^{2+} centres 3–34390
KCl:Tl, thermal decay of Tl^0 centres rel. to exoelectron emission slow decay 3–30928
KCl:Tl^0, spectral lineshape for $^2P_{1/2}\rightarrow{}^2P_{3/2}$ parity forbidden transition 3–30849
KCl(Br):Eu^{++}(Sm^{++})(Yb^{++}), thermoluminesc. of Z_1 centres 3–8678
KCl.KI-Tl crystal, intracentre luminescence, excitation bands *(Russian)* 3–27562
KI:Pd, e.s.r. due to trace impurities 3–15412
KI:Tl, fluorescence, polarisation effects *(German)* 3–24742
KI:WO^{2-}(MoO^{2-}), i.r. absorpt. obs. of local symmetry 3–8621
KI-Tl^+ phosphors, relax. excited states, linear electron-lattice interaction description *(Russian)* 3–36917
(La, Ce)Al_2 dilute alloy with Ce impurities, superconducting-Kondo system, specific heat 3–5072
$LaAlO_3$, higher energy levels of Cr^{3+} ion pairs, excitation and absorpt. spectra 3–15551
$LaBr_3$:Dy^{3+}, electronically excited ions, radiationless relax., multiquantum scatt. processes 3–24390
$LaBr_3$:Tb^{3+}, absorpt. and fluoresc. spectra, 77 K 3–30866
$LaCl_3$:Nd^{3+}(Dy^{3+}), electronically excited ions, radiationless relax., multi-quantum scatt. processes 3–24390
$LaCl_3$:Sm^{3+} crystal field splitting with inclusion of J mixing 3–18087
LaF_3, excited Nd^{3+} ion metastable state deactivation processes 3–34427
LiH:Ga(Ge)(As), excitation and luminesc. spectra *(Russian)* 3–21462
MgO, hypersonic attenuation, impurity and defects effect 3–1701
MgO, paramagnetic defects at the surface 3–5048
Mg_2TiO_4:Mn^{4+}, Cr^{3+}, phosphors, luminescence *(Russian)* 3–36928
Mo, chemisorpt. of O_2 and CO, adsorbate dependent surface states, optical refl. obs 3–38879
Mo-W dil. alloys, anisotropic point-scatt. lifetimes, Landau-level lifetimes 3–4962
MoO_3, localization of $4d^1$ electrons near protons, e.s.r. 3–2353
NaCl:Br, absorpt. and luminesc. of Br^- clusters 3–21464
NaCl:Ca, impurity induced Raman spectra of annealed and quenched crystals 3–21409
NaCl:KF, obs. of i.r. absorpt. line 3–8622
NaCl:Mg X-irradiated crystals, Mg centres expt. study 3–38586
NaCl:Mn^{2+}, forbidden e.s.r. transitions 3–27407
NaCl:Pb, thermoluminescence after X-ray irradiation 3–12188
NaCl:Pb^{2+}, absorpt., A- and B-band structs. 3–18098
NaF:Eu^{3+}, Eu^{3+} luminesc. centres, spectral anal. 3–5229
Na_2SiO_3:La photochromic glass, darkening characteristics caused by u.v. emission and colour centres formation *(Russian)* 3–30852
α-$NaYF_4$:Yb^{3+}, Er^{3+}, phosphors, visible luminescence during i.r. excitation *(Russian)* 3–36906
Ni, nucl. relax. rate of ^{101}Ru, rel. to virtual bound state 3–2442
Ni:^{101}Ru, information from meas. of relaxation rates 3–5147
Ni:^{175}Lu, ang. correlation meas. of hyperfine fields at impurity nuclei 3–15141
$NiFe_2O_4$ ferrite CaO addition effect on electrical conductivity *(French)* 3–8362
OH groups on surface of oxides, i.r. spectra and struct. of oxides 3–34365
$PbCl_2$:Nd^{3+} and $PbCl_2$:Pr^{3+}, optical absorption spectra and crystal field calcs. 3–15515
PbS-GaAs p-n heterojunction, rel. to near i.r. detection 3–22283
ruby:Cr^{2+}, Cr^{3+}, Cr^{4+} luminescence, quantum losses *(Russian)* 3–36929
SbSI, deep centres and photopolarization 3–24649
SbSeI, deep centres and photopolarization 3–24649
Sb_2Te_3, Mossbauer spectra, verification of two different states of ^{119}Sn atoms 3–36823
n-Si, anisotropy of electron scatt. by charged impurities, absorpt. study *(Russian)* 3–2077
p-Si, anisotropy of magnetothermal conductivity obs. 3–1842
Si, effect on recombination characs. *(Russian)* 3–24392
Si, electron irradiated, charge state dep. of defects 3–33554
Si, electron irradiation, vacancy interaction with Sn impurities 3–18093
Si, electron irradiation at 0.5K, a.c. conductivity changes dopant dependent 3–7794
Si, electron spectra rel. to doping, level bending 3–8690
Si, group V impurity atom-vacancy, binding energy, diffusion 3–33836
Si, γ-irrad., zone-purified, induced defects, elec. properties 3–33841
Si, heavily doped, transport eqns. derived 3–24419
n-Si, impurity core effect on electron mobility 3–11894
Si, muonium as deep donor, hyperfine splitting 3–18099
Si, proton irradiated, recombination centres, photoconductivity measurements 3–33575
Si, radiation effects, obs. using junction-capacitance techniques 3–33926
Si, self-interstitial charge states, assignment of donor and acceptor levels 3–33522
Si, shallow donor form. by proton bombardment and annealing 3–17861
Si, shallow donor impurity near-surface states, theory 3–24494
Si, strongly-doped, optical consts., spectral depend. in region of plasma reson. of charge carriers *(Russian)* 3–30789
Si, surface charge, effect of organic electron donors and acceptors 3–2153
Si, surface negative electron affinity due to Cs and O adsorpt. 3–30536
Si, two electron donor pair system, eigenvalue problem, Heitler-London method soln. 3–2579
Si, with group III or V dopant, impurity photocond. oscills., 4.2-10K *(Russian)* 3–2134
Si electron recombination cross-section at group V donor impurity centres, 1.5-20K 3–27270
Si film, elec. resist., doping conc. depend. 3–21069
Si film, impurity centres, carrier mobility meas. by m.o.s. Hall technique 3–18094

impurity electron states and effects continued
Si heavily-doped, metal-nonmetal transition, ^{29}Si n.m.r. obs. 3−21333
Si irrad., neutrons and electrons, heat treated, i.r. absorpt. band, high order vacancy defects 3−34393
Si ordinary p-n junctions, deep level centres 3−11947
Si:Ag, thermal emission rates and activation energies of electrons, holes at Ag centres 3−8122
Si:As, bulk resist. vs. As doping curves rel. to diffusin temp. 3−21024
Si:As, Zeeman splitting of photoluminescence of excitons 3−38809
Si:Au, absorpt., 0.3-1.05 eV, impurity photoionization cross section determ. *(Russian)* 3−5221
Si:Au diode, field independence of thermal emission rate of holes 3−4964
p-Si:B, cyclotron reson., effect of positively charged acceptor centres 3−36528
Si:B, defect and impurity distribution, radiation damage 3−4766
Si:B, deformation potentials of acceptor ground state, Raman scatt. study 3−5203
Si:B, deformation potentials and g-values from Zeeman splitting of Raman spectra 3−38809
Si:B, ion implantation defect centre studies 3−33587
Si:B, magneto-Raman scatt., g-value determ. for acceptor ground state 3−5203
Si:B, u.s. attenuation by neutral acceptors, mag. field depend. 3−4967
Si:Co, thermal emission rates and activation energies of electrons and holes 3−15154
Si:Mg^{+}, ground state and photoconverted metastable state of donor, e.s.r. 3−30692
Si:Pd, electrical props. 3−24436
Si:Zn, photoionisation cross sections of holes at Zn centres 3−24468
Si:Zn, thermal ionization rates and hole energies at double acceptor centres 3−15193
SiC, hexagonal, spectrum of nonisolated donor-acceptor pairs 3−34425
SiC, ion bombardment, annealing, intrinsic luminescent defects 3−34430
β-SiC:B, low temp. luminesc. due to donor-acceptor pair emission 3−34419
SiC:O, B, enhancement of luminescence brightness by O_2 3−39173
SiO_2 films, ion neutralisation processes, impurity migration effects 3−34450
Sn, residual electrical resistance, impurity effects *(Russian)* 3−8137
SnTe:Mn, growth, transport props. rel. to mag. impurities 3−33882
SrF_2:Eu^{2+}, impurity-induced Raman scatt. 3−39147
SrF_2:Tm^{2+}, crystal field splitting *(Russian)* 3−11860
$SrSb_2O_6$:Bi^{3+}(Pb^{2+}), fluorescence obs. for each excitation band 3−21478
$TbPO_4$:Tb^{3+}, absorpt. spectrum obs. of crystallographic phase transition 3−12019
Te, acceptor states, theory 3−36544
Te, electron irrad., recovery steps, isochronal and isothermal annealing expts. 3−33562
p-Te, magnetoresist., transverse and longit., impurity band like states 0.4-4.2K 3−27275
Te, states near valence band 3−24394
Th-Ce dil. alloys, thermopower, 2-300 K, impurity scatt. contrib. 3−30459
ThO_2 crystals, i.r. absorption spectroscopy, association of bands with impurity content 3−27735
Tl_2Te:Te,In, liquid, thermoelec. props. rel. to compensation of impurity elements 3−33935
V_2O_3, pure and doped, metal-insulator transitions 3−33820
W, thermoelec. props. depend. on impurity conc. below 3 K 3−30455
WO_3, electrical conductivity from −190° to +580°C, variation due impurities 3−27261
$YCl_3.6H_2O$:Yb^{3+}, proton polarisation and relaxation 3−18388
YVO_4:Eu^{3+}, photoluminescence, concentration and temp. characteristics *(Russian)* 3−30872
YiG:Si,Ca,Sr photoconductivity 3−8229
ZnHgSe(Te) mixed crysts., e.p.r. of Mn^{2+}, g-factor 3−2378
ZnO:Ga, shallow bound states, cyclotron reson., Zeeman splitting, 30-100 cm^{-1}, 5-100K 3−2028
ZnO:In, impurity band conduction, expt-obs. 5-300 K *(German)* 3−11899
ZnO:Li, thermolum., 4.2-300K, trapping and recomb. processes 3−15566
ZnO(S):Ni^{2+}, near i.r. absorpt. obs. of crystal field, dynamic Jahn-Teller effect in $^3T_2$ state 3−21446
ZnS, impurity ionisation energies and Bohr radius calc. from recomb. spectrum anal. expression *(Russian)* 3−36897
ZnS phosphors activated by heterovalent impurities, luminescence spectra peculiarities *(Russian)* 3−27549
ZnS: Ag, Cu fluorescence spectra, probability of emission calc. *(Russian)* 3−27546
ZnS:Cl, luminescence spectra *(Russian)* 3−27548
ZnS:Cr^{+}, Cu, C e.p.r. and luminescence studies *(Russian)* 3−27552
ZnS:Cu, β-irrad. at 5K, rel. to fast light emission 3−24753
ZnS:Cu, multiphoton impurity luminescence 3−34384
ZnS:Mn, phonon induced hyperfine fields, molecular orbital model *(German)* 3−15161
ZnS:Ni, Cu crystal, phototransfer of holes from Ni^{2+} to Cu^{+} ions 3−34411
ZnS:Ni^{2+} ion-hole complexes, electron struct., optical absorpt. study *(Russian)* 3−12155
ZnS:Sc^{2+}, e.p.r., 1.3-4.2 K, dynamic Jahn-Teller effect obs. 3−21302
ZnS-CdS phosphors, activation by Cu diffusion at low temperature *(Russian)* 3−36943
ZnSe, energy levels and effective radii, thermally stimulated current obs. *(German)* 3−15160
ZnSe, impurity ionisation energies and Bohr radius calc. from recomb. spectrum anal. expression *(Russian)* 3−36897
ZnSe:Mn, e.p.r. obs. *(German)* 3−15420
ZnSe:Mn, photocapacitance meas. of impurity created energy levels 3−15153

impurity electron states and effects continued
ZnTe, acceptor defect levels, elec. transport 3−18096
ZnTe, shallow donor level, field-assisted detrapping obs. 3−24391
ZnTe, time resolved spectroscopy involving ionisable donor acceptor states 3−36947
ZnTe:Cu, electron-beam excited, rel. to visible luminesc. 3−30884
p-ZnTe:Ga(In), photoelectronic props., electron trap level rel. to Ga(In) impurities 3−36635
$ZrSiO_4$:Eu^{3+}, Eu^{2+} radioluminescence *(Russian)* 3−8672

incandescent lamps *see filament lamps*

inclusive reactions, elementary particle *see elementary particle inclusive reactions*

independent particle model *see nuclear optical model; nuclear shell model*

indeterminancy
energy-time uncertainty relation, time operators and partial stationarity 3−26122
hadron model, determ. of mass operator from uncertainty principle 3−10718
Heisenberg's relations used to obtain information about e.m., nuclear and gravitational forces 3−10335
N-interacting particles in configuration space 3−19678
philosophical aspects of observational errors 3−9785
weak uncertainty relations in quantum theory from weak convergence in Hilbert space 3−13616

indexing
No entries

indicating devices *see indicators*

indicating instruments *see indicators*

indicators
see also alarm systems
charge measurement on cotton fibres, apparatus 3−6012
cryogenic liquid level *(French)* 3−22297
multiwire proportional counters, high spatial resolution using e.m. delay line readouts 3−28647
photographic exposure, patent 3−9987

indium
adhesion to steel ball, contact zones 3−4798
alkali halide phosphor, In-activated, X-irrad., time-lag of photostimulated luminesc. *(Russian)* 3−18483
alkali metal halide:Th, In phosphors, absorption spectra and phosphorescence spectra depend. on lattice parameters and refractive index *(Russian)* 3−30875
alloying element in Cu-Al (1 at wt.%) alloy effect on internal oxidation *(Japanese)* 3−15700
atom, doubly and triply ionized, obs. of forbidden transitions in electrodeless discharge, 340-2440 Å 3−7043
Auger spectra, quasi-atomic fine struct. 3−30907
diffusion in Cu, 760-1070°C *(Russian)* 3−11756
diffusion in HgTe, 200-300°C 3−36441
diffusion in ZnSe, optical props. 3−24712
electron scattering, angular distrib. of secondary electrons *(German)* 3−18521
evaporation from discharge tube wall, Rozhdestvenskii hook method appl. 3−14619
Fermi surface, OPW model for pressure depend. 3−33788
film, for information recording 3−6007
film, size effect parameters rel. to electron transport 3−30448
lattice dynamics 3−20830
lattice dynamics freq. distrib. spectrum heat capacity 3−1730
lattice thermal conductivity of very pure In 3−1725
liquid, diffusion of O, 750-950°C, potentiostatic electrochem. study 3−30278
liquid, struct. microheterogeneities, kinetic viscosity, temp. depend. *(Russian)* 3−17729
liquid, surface tension, temp. depend. 3−38710
liquid, temp. dependence of surface tension and density *(Russian)* 3−11798
liquid, thermoelectric props., temp. depend., m.p.-1200K 3−24408
magnetoacoustic geometrical resons., interpretation 3−4945
normal and supercond., flow stress and yield pt. obs. 3−5076
oxidation, In_2O_3 film growth, ellipsometric obs. 3−1908
small particles in the quantum size regime, magnetic moment 3−18347
specific heat anomaly and disorder *(German)* 3−24276
spectral line intensity of a series of elements, effect of In, Ga and Sn *(Russian)* 3−35543
superconducting, current induced phase transition 3−34029
superconducting film, conversion of electromag. into acoustic energy 3−15305
superconducting films without vortices, effect of mag. field direction on thermal conductivity 3−38928
superconducting thin films, critical thicknesses 3−34011
superconductor, thermal fluctuation induced diamagnetism above transition temp. 3−30575
thermal diffusivity and heat capacity, meas. and apparatus *(Russian)* 3−9864
thermal linear magnetoresist. and lattice cond. using Corbino geometry 3−11880
thermotransport of tracer Ag, saddle-point cooperation effects 3−17999
thin film type I superconductors, current induced intermediate state 3−38917
u.s. absorption, amplitude dependent, temperature influence, normal and superconducting, single crystals 3−38627
u.s. attenuation, amplitude-dependent internal friction, normal and supercond. states 3−36679
Bi-In system, contact melting in mag. field *(Russian)* 3−15698
CdF_2:In, optical absorpt. and elec. cond. meas. 3−21448
CdF_2:In^{3+}, semicond., resonance Raman spectra 3−36871
CdSe:Cu,In and undoped, high temp. defect equilibria 3−7745
CdSe:In film, surface elec. props., surface doping effects *(Russian)* 3−2192
In IV, triply ionized, emission spectrum, configs. identification 3−1099
In-PbTe tunnel junction, elec. props., superconductivity *(French)* 3−24545
In-Si bistable device, low-resist. state, supercond. behaviour 3−8233

- **indium** continued
  - In-SiO_2-Si junction, impurity local mode effect on tunnelling conductance 3–15266
  - In-$SrTiO_3$ boundary, surface barrier energy determ. 3–5052
  - In-TiO_3:Nb, Schottky barrier, electron tunnelling current-voltage characts. 3–33994
  - In^+, in alkali halides, high press. absorption spectra 3–39166
  - KBr:In, thermoluminesc., cryst. light-sum storage 3–32595
  - KCl:In, absorp. bands and luminesc. of In^0 centres 3–27024
  - LiF:In, mechanical and emission characts. with In diffused into compound 3–24115
  - LiH:In, red luminesc., 120 and 293 K *(Russian)* 3–15538
  - Pb:In, type II superconductor, plastic deform. influence on flux line pinning *(German)* 3–18258
  - Si:In, impurity photocond. oscills., 4.2-10K *(Russian)* 3–2134
  - Si:In, ion implantation, damage around ion tracks 3–33588
  - Tl_2Te:Te,In, liquid, thermoelec. props. rel. to compensation of impurity elements 3–33935
- **indium alloys**
  - *see also indium compounds*
  - rare earth intermetallic, $LnIn_3$, mag. props. and ordered struct. *(French)* 3–24563
  - superconducting films without vortices, effect of mag. field direction on thermal conductivity 3–38928
  - umklapp effect on low temp. thermal resistivity 3–1751
  - Au-Cd-In, double h.c.p., liquisol quenching effect on struct. 3–34559
  - Cu-In, form. of aligned composite material by solid state decomposition 3–24976
  - Ga-In, liquid alloy, nuclear quandrupole relax. rate 3–18391
  - $Gd_xTh_{1-x}PdIn$, mag. props., 4.2-300 K, evidence for RKKY-type interaction 3–27364
  - $Gd_xY_{1-x}PdIn$, mag. props., 4.2-300 K, evidence for RKKY-type interaction 3–27364
  - Hg-In, liq., Lorenz number and thermal cond. 3–30453
  - Hg-In alloys, liq., electronic spectra, 0.14 to 4 μm 3–39133
  - In-Bi, liquid, nuclear-spin-lattice relaxation meas. for ^{115}In and ^{209}Bi 3–5145
  - In-Bi supercond. foils, eff. of a.c. mag. fields on flux-flow states *(Japanese)* 3–24547
  - In-Cd, superconductivity and hysteresis 3–34009
  - In-Cd, superconductivity and hysteresis, secondary properties 3–34010
  - In-Mg, ordering behaviour of f.c.c. and b.c.c. phases 3–11585
  - In-Pb system, superconducting energy gap from magnetisation meas. 3–34014
  - In-Sb, liquid, nuclear spin-lattice relaxation meas. for ^{115}In and ^{121}Sb 3–5145
  - In-Sn, superconductor, mixed state, audio-freq. impedance 3–36687
  - In-Tl, soft acoustic phonon mode rel. to martensitic transform. 3–30226
  - In-Tl, supercond., fluctuation induced diamagnetism above transition temp. 3–30575
  - In-Tl liquid alloys, structure and electrical conductivity *(Russian)* 3–33443
  - In-Zn, liquid, thermal diffusion of In *(Russian)* 3–7951
  - InBi, elastic behaviour, u.s. wave velocity meas. 3–27048
  - InBi, intermetallic, chem. etchants for characterisation 3–11817
  - $In_{1-x}Ga_xP$ cryst., liq. phase epitaxial growth by sliding method 3–30944
  - InP_xAs_{1-x} solid soln., absorpt. spectra near fund. absorpt. edge, coeff. rel. to photon energy 3–5217
  - InP_xAs_{1-x} solid soln., i.r. refl. spectra *(Russian)* 3–8589
  - $(In_2Te_3)_x-(Hg_3Tr_3)_{1-x}$, influence of impurity compensation effect on negative magnetoresistance 3–27277
  - Na-In, dil., liq., density and surface tension, 170-400°C, comparison with Na-Cd alloys 3–36994
  - Nb-Ti-Zr superconducting sheets, relation between microstructure and applied magnetic field vs. critical current density characteristics *(Japanese)* 3–18257
  - Ni-In, form. of aligned composite material by solid state decomposition 3–24976
  - Ni-In aligned eutectics, phase morphology 3–39318
  - Pb-In, hard non-ordered, electrical resistivity concentrational dependence *(Russian)* 3–11883
  - Pb-In, type II superconductor, vortex state, microwave surface resistance 3–18261
  - Pb-In system, supercond. sheath state, flux motion dynamics and a.c. losses 3–36677
  - Pb-In-Sn, supercond., flux flow states under mag. and thermal disturbances 3–21175
  - Pb-In(17%), superconductor, complex cond. of surface sheath, mag. field depend. 3–30573
  - Pb-In(4.56 wt.%), supercond., sign change in entropy flux associated with vortex motion *(French)* 3–38925
  - Sb-In, liq., self-diffusion coeffs., conc. depend. *(French)* 3–30275
  - Sb-In, liq., self-diffusion coeffs., temp. depend. at equiatomic comp., ionic salt concept *(French)* 3–30276
  - $YbIn_3$, ambiguous mag. behaviour, susceptibility meas. 3–30609
  - Zn-In-Pb solns., liq., miscibility gap, zinc isoactivity and molar functions 3–38675
- **indium antimonide**
  - amorphous, l.f. Raman scatt., freq. depend. coupling const., elastic continuum limit 3–8586
  - coating on $LiNbO_3$ piezoelec. crystal, Rayleigh acoustic surface wave amplification and dispersion, calc. 3–11794
  - cyclotron resonance, i.r., in pulsed mag. fields up to 1.4 MG 3–30405
  - deep impurity levels *(Russian)* 3–4959
  - degenerate, u.s. attenuation, mag. field influence *(French)* 3–5041
  - doped, thermal e.m.f., 300K *(Russian)* 3–11917
  - eelectron velocity field characts., negative differential mobility, meas. 3–33914
  - elastic moduli, press. depend., up to 5.5 kbar *(Russian)* 3–7812
  - electric-field-induced transient spin-flip Raman laser pulses 3–4116
  - electron-phonon coupling, LO and TO phonons 3–30224
  - e.m.f. induction by Q-switched CO_2 laser 3–30520
- **indium antimonide** continued
  - energy band struct., refl., modulated refl., dielec. function, pseudopot. calc. 3–30403
  - film, carrier mobility and field effect 3–27260
  - film, carrier trapping at slow surface states *(Russian)* 3–30492
  - film, hot wire zone crystallisation, bulk props. 3–2669
  - film, quantum size effect with realistic surface potential 3–18207
  - film, surface depletion by SiO and CaF_2 films 3–18219
  - Hall effect, anomalous, low temp. 3–8205
  - hot electron mobility, Monte Carlo calc. 3–36612
  - hot electron Shubnikov-de Haas effect in n-type 3–36623
  - hot electron-phonon interaction in nonparabolic cond. band., 42.K 3–33912
  - hydrogenic impurity bands in an external magnetic field 3–33829
  - impact ionisation and scattering mechanisms rel. to band structure 3–21088
  - i.r. reflection meas. for surface plasmon dispersion curve 3–2554
  - Landau transitions at higher energy gaps, spin-orbit splitting 3–33809
  - lattice vibrs. from Banerjee-Varshni second neighbour ionic model 3–14951
  - melt growth, thermo-hydrodynamic effects 3–11563
  - n-type, acoustic gain optimum freq. depend. on carrier density 3–8231
  - n-type, a.m. microwave self distortion rel. to self focusing 3–32593
  - n-type, band tailing, hot electron magneto photocond., cond. and Hall coeff. obs. 3–2138
  - n-type, deformation potential parameters calc. 3–8105
  - n-type, donor and acceptor conc. determ. from hot electron mobility 3–38812
  - n-type, donor deionisation, impurity cond., CW laser cyclotron reson., magnetocond., temp. depend. 3–15149
  - n-type, elec. cond., mm. wave investigation 3–21084
  - n-type, e.s.r. saturation conditions, reson. increase in kinetic temp., elastic scatt. effects *(Russian)* 3–8446
  - n-type, Faraday effect of hot electrons, i.r. 3–2523
  - n-type, heavily doped, Kane band model for dispersion law 3–21007
  - n-type, highly doped, u.s. propag., longitudinal mag. field effects 3–38626
  - n-type, hot electron scatt. at 4.2 K 3–38850
  - n-type, impurity conduction, Hall coefficient, activation energies, impurity concentrations 3–30501
  - n-type, lattice absorpt. of sound, 77K, freq. depend. 0.5-3.0 GHz 3–33963
  - n-type, mag. controlled negative resist. and coherent oscills., 77K 3–5011
  - n-type, magnetic freeze out, in strong mag. field, theory 3–30498
  - n-type, magnetoresist. meas., impurity cond. effects 3–38857
  - n-type, microwave emission, sample geometry and surface condition depend. 3–5016
  - n-type, microwave emission spectrum, avalanche impact ionised plasma, external magnetic field 3–33942
  - n-type, microwave props. in d.c. mag. field, hot electron effect, scatt. mechanism, 4-300K 3–21087
  - n-type, non ohmic transport and phonon amplification 3–8189
  - n-type, photo-induced magnet phonon resonance at 4.2K 3–24477
  - n-type, round-trip amplification of u.s. waves, under transverse mag. field 3–5038
  - n-type, strongly compensated, cyclotron resonance meas. 3–11851
  - n-type, tunable far i.r. radiations from hot electrons 3–34442
  - n-type, u.s. amplification anisotropy in mag. field at 77K model 3–18349
  - n-type Hall pickup, for thermally stable probe of magnetic focusing system 3–25815
  - n-type reson. hole-TO and hole-LO phonon coupling magnetooptical study 3–4831
  - n-type surface polariton theory with and without external mag. field 3–2039
  - negative differential conductance, e.m. surface wave growth 3–18150
  - p-type, Hall coeff. mag. field depend. rel. to temp. *(Russian)* 3–8212
  - p-type, negative differential resistivity at 77°K, injected carrier oscillations due to trapping and recombination 3–11908
  - p-type, reflection spectra obs. of temp. depend. of hole effective mass 3–24382
  - p-type thin crystals, current voltage characts., surface cond. effects *(Russian)* 3–2073
  - photoelectron energy distrib. spectra, core levels 3–15591
  - photographic image form. at InSb-active gas interface 3–15841
  - pressure transducers 3–35386
  - quantum oscill. and pump depletion effects in spin-flip laser 3–32571
  - Raman laser, pulsed, Stokes power output time depend. 3–4119
  - Raman scattering, spin-flip, Stokes-anti-Stokes cavity oscillations, conversion efficiency 3–22950
  - recombination processes, anal. using wave function method in two-zone approx. *(Russian)* 3–15212
  - resonance Raman scattering near E_1 gap, uniaxial stress effects 3–5206
  - spontaneous spin-flip Raman line shape, Green's function theory 3–36870
  - stimulated Raman scatt., saturation model, spin saturation and pump depletion 3–4118
  - surface excitations, expt. obs. using line gratings attenuated total reflection 3–24493
  - surface photovoltage and internal photoemission meas. at anodised InSb surface 3–21114
  - surface polaritons, response functions 3–24327
  - thin films, electrical props. rel. to structure of size quantisation 3–24528
  - thin films, high field electrical conduction, breakdown intercrystalline potential barriers 3–38852
  - two-phonon deformation potential 3–7882
  - two-photon absorpt. at 10.6 μm 3–22941
  - ultrasonic attentuation, degenerate crystals, direction of propagation and magnetic field, de Haas-van Alphen oscillations, relaxation time *(French)* 3–27389
  - u.s. wave amplification in Hall and Corbino configs., 77K, 1 GHz *(French)* 3–21118

indium antimonide continued

- valence band degeneracy rel. to freq. depend. of two-quantum transitions near absorpt. edge 3—21435
- work function changes under irradiation, photoemission and contact pot. difference meas. 3—11945
- X-ray emission bands of Sb $L_{\gamma 4}$ *(German)* 3—15569
- GaSb-InSb alloyed solid solns., distrib. coeffs. of Te and Zn *(Russian)* 3—11642
- $InAs_xSb_{1-x}$, film, Hall coeff. and mobility meas. 3—36622
- $In_{1-x}Ga_xSb$, film, Hall coeff. and mobility meas. 3—36622
- InSb, galvanomagnetic effects, dependence on temperature and magnetic field 3—5021
- InSb, resonant Raman scattering in $E_1-E_1+\Delta_1$ region 3—2545
- InSb:Cd, p-n technique 3—34489
- InSb:Fe, elec. and galvanomag. props., impurity levels and hole scatt. mechanisms 3—38844
- p-InSb:Ge ion pairing induced by X-rays 3—15152
- n-InSb:Se, Te transmission spectra rel. to Moss-Burstein effect 3—4963
- InSb:Te, growth from melt, obs. of strain patterns 3—12315
- InSb:Te, Se, S, transport phenomena, 77-300K, press. to 15k bar 3—2096
- InSb:Te,Se, liquid epitaxial growth, solubility and distrib. of Te and Se *(Russian)* 3—15093
- InSb:Zn(Cd)(Ag), acceptor excitation spectra, obs. of Zeeman splitting 3—24728
- InSb-NiSb eutectic alloy, structure by unidirectional solidification *(Japanese)* 3—15673
- n-type, strong compensated, Faraday effect due to hot electrons 3—15478
- n-type, strongly compensated, elec. cond. and Hall coeff. meas. at low temp. 3—15216
- n-type, strongly compensated, photocond. meas. at microwave wavelength 3—15225
- n-type, strongly compensated, Faraday effect rel. to Hall mobility and coeff., meas. 3—15477

indium compounds

- *see also indium alloys; indium antimonide*
- γ-In_2S_3, crystals grown from vapour, X-ray and electron microscope investigation of struct. faults *(German)* 3—7781
- n- InP, hot electrons diffusion 3—15202
- $(CdS)_{3x}$-$(In_xS_3)_{1-x}$, optical and photocond. props. rel. to band structure 3—18085
- $Ga_{1-x}In_xAs$ film, chem. vapour deposition using organometallics 3—21531
- In complex, trispyrrolidylcarbodithioate:Fe, Mossbauer spectra 3—24635
- In-Ga-Sb system, liquidus and solidus data at 500C 3—1775
- n-InAs, absorpt. spectra near fund. absorpt. edge, coeff. rel. to photon energy 3—5217
- InAs, band structure, crit. pt. determ., in 4-9 eV region 3—2005
- n-InAs, cond. band nonparabolicity, confirmed by optical absorpt. study *(Russian)* 3—38797
- n-InAs, elec. cond., mm. wave investigation 3—21084
- InAs, electron irradiation damage studies 3—33555
- n-InAs, electroreflectance spectra, line shape, electrolyte method *(Russian)* 3—34371
- InAs, energy band struct., refl., modulated refl., dielec. function, pseudopot. calc. 3—30403
- InAs, hall effect meas. to 90 kbar rel. to structural transition and band structure 3—21096
- n-InAs, i.r. birefringence due to hot electrons, 80K *(Russian)* 3—8555
- InAs, impact ionisation and scattering mechanisms rel. to band structure 3—21088
- InAs, InP, InP_xAs_{1-x} solid soln., neutron and gamma irrad., elec. and optical props. 3—33907
- n-InAs, intraband absorpt. of light, drag of electrons by photons *(Russian)* 3—2135
- InAs, reson. Raman scatt. near E_1 gap, uniaxial stress effects 3—5206
- InAs, substrate, orientation influence on vapour epitaxial growth of $InAs_{1-x}P_x$ 3—1917
- n-InAs, surface polariton theory with and without external mag. field 3—2039
- InAs and InAs-CdTe solid solutions, absorption band structure from absorption spectra 3—24383
- InAs film, chem. vapour deposition using organometallics 3—21531
- InAs p-n junction, kinetics of photo-e.m.f. *(Russian)* 3—2177
- InAs p-n junction transitional processes in photodiode mode 3—21147
- n- InAs transport phenomena, heavily doped 3—36608
- InAs:Se(Te), electron effective mass, determ. from temp. depend. of transport props. *(Russian)* 3—27250
- InAs-GaAs alloyed solns., Zn and Te impurity effect on crystallisation *(Russian)* 3—7782
- InAs-InP, GaAs-InAs solid solutions, disorder scattering 3—30470
- InAs-oxide-Pb tunnel junction, conductance characts., effect of accumulation layer 3—38901
- InAsP-Cs_2O, photoemission, heterojunction barrier model 3—2619
- $InAs_{1-x}P_x$, $(0.7 \leqslant x \leqslant 1)$, vapour epitaxial growth and characterization 3—1917
- $InAs_{1-x}P_x$, vapour phase epitaxial growth and elec. props. 3—2680
- $InAs_{1-x}P_x$, vapour-grown epitaxial layers, electron microprobe characterization 3—20955
- $InAs_{1-x}P_x$ film, chem. vapour deposition using organometallics 3—21531
- $InAs_xP_{1-x}$ solid solutions, compositions, transport properties, electron effective mass 3—33802
- $InAs_{0.07}Sb_{0.93}$ films, photoelectronic props. 3—33958
- $InAs_xSb_{1-x}$ film, Hall coeff. and mobility meas. 3—36622
- InBi whisker, growth by squeeze technique, morphology 3—1963
- $InCl_6{}^{3-}$, force consts., Coriolis coupling consts., and mean amplitudes of vibration 3—33102
- InF molecule, r.f. spectrum, h.f.s. determ., search for elec. hexadecapole interaction of In nucleus 3—1236
- $In_xGa_{1-x}As$ laser, optically pumped, performance 3—4109
- $In_{1-x}Ga_xAs_{1-y}P_y$, electron zones, luminesc. struct. study *(Russian)* 3—36946
- $In_{1-y}Ga_yAs_{1-x}P$, Cs_2O-activated, photoemission 3—34456

indium compounds continued

- $In_{1\;x}Ga_xP$, electroluminescence, free electron-bound hole recomb. 3—2597
- $In_{1-x}Ga_xP$:N, N_2 isoelectronic trap, luminescence, l.e.d. applications 3—39175
- $In_{1-x}Ga_xP$:N, soln. growth, effect of N-trap states on photoluminesc. and elec. props. 3—24797
- $In_{1-x}Ga_xP$:N laser operation, reson. enhancement of recomb. probability associated with isoelectronic trap states 3—18472
- $In_xGa_{1-x}P$ solid solns., epitaxial growth from gas phase *(Russian)* 3—12240
- $In_{1-x}Ga_xSb$, film, Hall coeff. and mobility meas. 3—36622
- $InNbO_4$, cryst. struct. *(German)* 3—7668
- InO, solar cell coverslide coatings, effect of u.v. and charged particle irradiation 3—5924
- In_2O_3, thermodynamic properties 3—27856
- In_2O_3 film, growth on In, ellipsometric obs. 3—1908
- In_2O_3:Sn film, r.f. sputtered, transparency and elec. cond. 3—12200
- In_2O_3-SnO_2 transparent conducting films, structure obs. by electron diffraction and spectroscopy 3—33763
- InOF, cryst. struct., X-ray determ. *(French)* 3—27001
- $In(OH)_3$, p.m.r. meas. from 4.2 to 400 K 3—27422
- n-InP, absorpt. spectra near fund. absorpt. edge, coeff. rel. to photon energy 3—5217
- InP, Bridgeman and Czochralski growth with liquid encapsulation 3—12321
- InP, carrier concentration profiles 3—24808
- InP, crystal growth by liquid encapsulation, and elec. props. 3—2679
- InP, electron energy relaxation time, determination from 34 GHz complex conductivity measurements in presence of d.c. field 3—2118
- InP, electron energy relax. time as function of elec. field 3—24420
- InP, electron transfer high freq. behaviour, dynamical Monte Carlo study 3—11902
- InP, electron-phonon interaction and intervalley scatt., pseudopotential calc. 3—5005
- InP, electrorefl. spectra rel. to hydrostatic press. *(Russian)* 3—8610
- InP, facility for growth of crysts. from melt *(German)* 3—8738
- InP, InAs, InP_xAs_{1-x} solid soln., neutron and gamma irrad., elec. and optical props. 3—33907
- InP, n- and p-type, spin orientation by optical pumping 3—2593
- n-InP, shallow donor states, cyclotron reson., Zeeman splitting, cond. electrons effective masses 3—2026
- InP, subsidiary indirect cond. band minima, donor levels, phonon struct. of interband transitions 3—2027
- InP, vapour phase epitaxial growth, elec. props. 3—2680
- InP, vapour phase epitaxial growth, photoluminesc. props. 3—2681
- n-InP, velocity field characs., microwave obs. 3—30484
- n-InP, velocity/field characteristics from dipole domain measurements 3—8186
- InP effective electron mass, scattering factor measurement 3—36599
- InP film, chem. vapour deposition using organometallics 3—21531
- InP laser, optically pumped, performance 3—4109
- InP layer prod. by Nicoll and Sirt short path transport method *(German)* 3—8729
- InP:Ge,Sn,Te, liquid phase epitaxial growth, impurity distrib. coeffs. 3—1637
- In_2S_3, dislocations and stacking faults, X-ray topograph and electron microscope obs. *(German)* 3—17834
- β-In_2S_3, phase transforms. and thermal expansion, X-ray diffr. obs., 30-975°C 3—15003
- γ-In_2S_3 growth from melt of As_2S_3 *(German)* 3—8741
- InSb, cond. electrons stimulated spin-flip Raman scatt., theory appl. to magnetically handle i.r. laser 3—6510
- InSb, effect of weak, longit. static field on transverse e.m. wave propag. along magnetostatic field 3—2121
- n-InSb, phonon-phonon and phonon-charge carrier interactions *(French)* 3—1706
- InSb, second harmonic generation, nonlinear susceptibility, at 28.0 μ by comparison with Te 3—19637
- InSb junction lasers operated at low temp., longitudinal mag. field effect on power output 3—37973
- InSb-type semiconductors, Raman scattering by electronic excitations 3—39153
- InSbP-Cs_2O, photoemission, heterojunction barrier model 3—2619
- InSe film, amorphous, crystallisation and decomposition, electron microscope obs. 3—7936
- InSe film, photographic image formation *(Russian)* 3—9092
- InSe-TlSe pseudobinary system, constitutional diagram and elec. props. 3—17957
- $InSe_2$, thermodynamic props. 3—33662
- In_2Se_3-Sb_2Te_3, X-ray obs. of phase diagram, elec. props. depend. on comp. *(Russian)* 3—14964
- In_4Se_3, cryst. struct. *(French)* 3—7680
- $In_xSe(x=1,2)$, luminesc. study, 0.5 to 11 μ waveband, appl. as radiation detectors and lasers *(Russian)* 3—27576
- $In_{2-x}Sn_xO_{3-y}$ film, transparent, highly conductive, prep. by d.c. diode sputtering 3—2193
- $InTaO_4$, cryst. struct. *(German)* 3—7668
- InTe, anisotropy of thermal expansion, electron diffraction obs. 3—4861
- β-In_2Te_3, cryst. growth, struct., and photocond. *(Russian)* 3—8724
- In_2Te_3 and InTe, Mossbauer effect of ^{129}I *(Russian)* 3—12087
- In_2Te_5, photocond. spectra, 500-1400 nm at 290 and 82 K *(Russian)* 3—8225
- In_3Te_4, thin films, abs. spectra at fund. obs. edge, rel. to exciton transition *(Russian)* 3—30818
- $InVO_4$, thermoluminescence *(Russian)* 3—15565
- In(111) complexes, tropolonates, i.r. spectra, electron spin pairing and Jahn Teller distortion effects 3—36026
- $ZnIn_2S_4$, layer struct. cryst., meas. of Raman spectrum 3—15487

INDOR

- *see also Overhauser effect*
- No entries

inductance

- cylindrical sample, conductivity meas. by RF induction method 3—37659
- e.m. coil encircling 2-conductor rod, solution to induction problem 3—27821
- measurement standard, the henry 3—37581

inductance continued
plasma, scalar-pressure toroidal, stability by energy principle with specific inductance 3—38487
inductance measurement
No entries
induction heating
see also electric furnaces
cooled inductor, insertion in high vacuum chamber 3—19168
furnaces, construction, refractory concrete applic. *(German)* 3—15765
laboratory demonstration with linear air track 3—9806
liquid metal elec. cond. meas. apparatus, 1000-2500 K 3—32111
plasma arc melting system design 3—27714
transverse flux technique, R&D, ECRC Capenhurst 3—1521
induction motors
conducting thin plate, current induction *(French)* 3—32488
magnetic field distribution, under load conditions 3—13668
noise reduction, design and testing 3—25637
inductor microphones *see microphones*
inductors
see also coils; transformers
with flat conductive shielding, magnetic field analysis by vector potential method *(Russian)* 3—32476
microwave bimodal X-band spin inductors, e.s.r. spectroscopy 3—35448
teaching-aid demonstration 3—19132
industrial atmospheres *see air pollution*
industrial control
see also process control; production control; quality control
dust emission suppression and control methods in cement industry 3—37537
emission to air reduction in power generation industry, best practicable control means 3—37538
nuclear isotopes production scheduling, linear programming applic. 3—32118
semiconductor industry, Si cryst. growth, computer-controlled 3—12323
industrial economics *see economics*
industrial plants
flicker photometer, automatic synchronised, evaluation and applications *(German)* 3—28538
noise control, criteria and design specifications 3—9749
noise control, use of acoustical absorbents 3—9750
industrial research management *see research and development management*
industrial standards *see standards*
industries
this heading is restricted to those industries which are not covered by other specific headings
see also automobile industry; brick industry; cement industry; ceramic industry; chemical industry; food processing industry; glass industry; metallurgical industries; paper industry; petroleum industry; textile industry
sound level meas. 3—5788
inert gases
see also argon; helium; krypton; neon; radon; xenon
afterglow plasma, electron and positive ion current collection by cylindrical Langmuir probe 3—14584
alkali metal vapour-inert gas mixture, optical third harmonic generation 3—26246
atom, modified effective electron model for interaction energy calc. 3—7088
atom, X-ray scatt., Thomas-Fermi model with quantum corrections 3—29461
atom collisions with Sr^+, $5^2S_{1/2}$ ground state spin depolarisation 3—38251
atom collisions with very slow electrons, pressure shifts of high series spectral lines and scattering cross sections, calc. 3—35975
atom pairs, interacting, dipole moment 3—29538
atom-atom excitation and ioniz. in shock waves 3—33040
atomic collisions with He metastable atoms, Penning ionization spectra 3—11154
atomic scattering of inert gas ions, singularities involving inner shell excitation 3—20064
bubble growth in solids, non uniform size effect 3—7744
closed shell systems, interaction pots., theory 3—26609
collision processes with Ca, broadening and shift in reson. line 3—7090
collision with k^+ and Na^+, intermolecular potentials 3—17383
collision-induced rot. transitions in HCN-inert gas mixtures, μ-wave double reson. study 3—17471
collisional quenching of metastable H atoms 3—17382
collisions with DCl, V→T, R and V→V relaxation, by laser fluorescence technique 3—33165
collisions with Eu atoms with spin polarised 4f shell, relaxation *(German)* 3—35980
collisions with K atoms, coherence transfer between K $^2P_{1/2}$ and $^2P_{3/2}$ states 3—26606
collisions with laser excited methyl fluoride, vibrational relaxation 3—33162
collisions with methyl chloride, laser fluorescence study of vibrational energy transfer 3—33163
collisions with o-H_2 mols., anisotropic cross section meas. *(Dutch)* 3—29737
condensed, self-diffusion coeff., temp. and density depend. 3—7955
cosmogenic production rates in chondritic meteorites 3—5428
crystal impurities in $Ba(Ca)F_2$, form. at interstitial sites 3—17814
dense fluid, soln, of Percus-Yevick integral equation with Kihara potential 3—17484
dense fluid soln. of Percus-Yevick integral equation with Kihara potential 3—17483
diamagnetic susceptibility and orbital momentum, free-electron gas exchange correlation calc. 3—38204
diffusion in cold worked Ag, gas release meas. 3—24287
diffusion mobility in metals *(Russian)* 3—24286
dilute alloys, solid and liq., emission spectra of deep impurity states 3—2581

inert gases continued
discharge, cooled hollow-cathode, elec. and opt. characts. *(Russian)* 3—7577
electron impact double ionisation, cross section calc. 3—11169
electron impact excitation, absolute intensity calibration method for vacuum u.v. spectrometer, 50 to 120 nm 3—37637
electrons, resonance trapping and drift velocity in inert gases 3—23667
epitaxial growth of rare gas crystals 3—1925
fission products, tritiated water vapour monitor for use in presence of inert gases 3—32992
fluidity, general theory 3—7961
interaction potentials between alkali metal and inert gas atoms 3—17385
ion, low energy scatt. in surface struct. meas. 3—30325
ions, backscatt. by Ni surface, energy distrib. rel. to surface struct. 3—30324
ions, bombardment of Si(111) surface, electron emission *(German)* 3—27590
ions, charge transfer rate consts. to difluorobenzene and dichloroethylene 3—33152
ions and atoms, reson. charge exchange and fine struct. of levels *(Russian)* 3—4393
i.r. and u.v. spectroscopic studies of free radicals and molecular ions isolated in inert solid matrices, review 3—11251
laser, electron beam excitation mechanism 3—10521
laser, pulsed, multi-mode operation *(German)* 3—29073
lasers, high press., operating in u.v. 3—32542
leakage of radioactive noble gases into gas blanket of reactor primary circuit *(Russian)* 3—23423
liquid lasers, employing luminescence of self-localised excitons *(Russian)* 3—35692
matrices containing methane mols., i.r. absorpt. theoretical study 3—24685
matrices for benzene, location of E_{2g} state, photoexcitation spectra 3—38292
methane, sorption, molecular sieve type, on alkali graphite intercalation compounds 3—33732
mixtures, absorption coeff. detn. by quantum mech. description of translational motion *(French)* 3—7071
mixtures, crystn., mixed cryst. form., electron diffr. diagrams *(French)* 3—24043
mixtures with HCl, induced low temp. absorpt. spectrum *(French)* 3—29637
molecules, third-order hyperpolarizabilities, quantum calcs. 3—38275
Mossbauer isomer shift, metal atom in inert matrix, covalency versus overlap distortion 3—18398
pair interactions, Morse-6 hybrid potential 3—1132
postive column, acoustic instability, hydrodynamic eqns. 3—29985
proton ionization, meas. of ion pair prod. as function of press. 3—7309
radioactive tracers for transport no. determ. during Ta oxidation 3—38743
repulsive interaction potential in the Fermi-Amaldi model 3—14320
second virial coefficient of Lorentz-Lorentz function meas. using Fabry-Perot interferometer 3—11714
solid, excitonic effects on valence absorption edge 3—33849
solid, organic molecule impurities absorption spectra, extravalence molecular excitations 3—24721
solid, stress tensor depend. on deform. gradient 3—7808
solid mixtures, extreme u.v. spectra, electron energy states 3—21452
solid solutions, cathodoluminescence 3—18504
sublimation, equation of state *(French)* 3—20871
ternary collision translational spectrum simplified model 3—29515
thermal conductivity, comparison between theory and experiment in transport processes *(French)* 3—7302
transport in liquid metals during boiling expts., diffusion model soln. 3—19904
transport props., tables of collision integrals for potentials 3—26739
van der Waals interaction between inert gas atoms in dense classical fluid 3—17384
CO, perturbed by inert gases, determ. of linewidths in 0→2 bands *(French)* 3—7214
H_2-inert gas mixture, collision induced i.r. absorpt., profile anal. and intercollisional interference effect 3—23563
Li-inert gas systems, absolute total scatt. cross sections, pot. parameters 3—1127
Na + inert gas collisions, coherence transfer study 3—38229
SF_6-rare gas collisions, i.r. fluoresc. obs. of excited vibr. states of SF_6 3—23631
inertial navigation
pendant accelerometer with electronic damping and analogue restoring 3—13218
infinite series *see series (mathematics)*
inflammability *see combustion*
information retrieval
see also information storage
diffraction powder patterns, Joint Committee on Powder Diffraction Standards, data collection and search 3—26929
Earth physics information-management service, possibilities and future 3—34782
information retrieval systems
holographic Fourier transform, storage and retrieval system, patent 3—10454
holographic information storage *(Hungarian)* 3—26215
mass spectra, computer identification, highly compressed spectral codes, Aldermaston collection 3—28702
information services
crystallography, structural, system features, review 3—26915
diffraction powder patterns, Joint Committee on Powder Diffraction Standards, data collection and search 3—26929
Earth physics information-management service, possibilities and future 3—34782
prospective research, documentary activity *(Rumanian, English)* 3—13180
information storage
see also information retrieval
holographic, applications *(Hungarian)* 3—26215

information storage continued
  holographic Fourier transform, information retrieval system, patent 3−10454
  human memory, efficiency improvement schemes, models 3−39761
  photographic storage device 3−9982
  powder data collection file and search 3−26929
information storage systems *see information retrieval systems*
information theory
  see also codes; correlation theory; decision theory and analysis; estimation theory; filtering and prediction theory; modulation; signal detection; signal processing; speech intelligibility
  autocorrelations functions for mag. and gravity anomalies, character of variation 3−25129
  entropy of meas. theory *(Polish)* 3−25641
  image device, information content and transfer efficiency, single parameter descrip. 3−32519
  least squares smoothing operators, analysis in frequency domain 3−28838
  nonequilibrium velocity distrib. for ideal gas, information theoretic derivation 3−4034
  optical information transfer by electron beam collective states 3−29050
  peripheral auditory system, neural noise, analysis 3−25572
  planar box, information theory and entropy 3−16352
  pulsed signal detection in presence of nongaussian background noise, optimal method *(Russian)* 3−6431
  radiographic viewboxes, information capacity 3−10159
  receiver operating characteristic curves, evaluation 3−10157
  signal amplitude, phase, and frequency, definitions and their significance for meas. 3−19134
  vernier judgement information content 3−39770
infrared astronomical observations
  Becklin-Neugebauer i.r. point source in Orion Nebula, 2.8-13.5 μ obs. 3−28238
  binary stars, spectral energy distrib. of 6 stars in energy ranges 3300-7300 Å and 0.88-1.53 μ 3−37380
  α Bootis (Arcturus), statistical line blanketing coefficient description 3−39686
  brightness temps. of the planets in the 30-300 μ region 3−18971
  3C 273, Seyfert, variability in 10-micron flux 3−13092
  VY Canis Majoris, circular polarisation meas. at 1.7 μ and 2.2 μ 3−31689
  η Carinae, i.r. and broad-band photometric obs. 3−31705
  η Carinae, i.r. spectrum and angular size 3−25456
  o Ceti (Mira), Ti isotope abundance ratio determ. 3−22060
  circumstellar circular polarization at 0.84 microns in four i.r. stars 3−31695
  Comet Bennett, central coma, 1.1 μ spectrogram 3−13002
  R Coronae Austrinae, nearby young stellar group 3−31740
  R Coronae Borealis, i.r. measurements during 1972 March-June minimum 3−22074
  R Coronae Borealis type variable stars and related objects, i.r. photometry 3−31671
  Crab Nebula, interstellar reddening determ. from S II lines obs. 3−37492
  NML Cygni, circular polarisation meas. at 1.7 μ 3−31689
  Cygnus X-3, search for i.r. candidate at 1 μ 3−31730
  diffuse nebulae, comparison of far i.r., optical, and radiofrequency data 3−31787
  DR 15, H II region, detection in far i.r. balloon measurements 3−22093
  dust emission nebulae around Orion O- and B-type stars in Trapezium, 8-20 micron radiation 3−37370
  dusty Stromgren spheres, analytic approximations from far i.r. observations 3−13104
  early-type emission-line stars and related objects, near i.r. magnitudes and HKL photometry 3−25461
  early-type stars of Orion population, energy distrib., visual variations correlation 3−19011
  earth's surface radiation temp. determ. in 0.8-8 cm. region *(Russian)* 3−39475
  Europa, 10 μ obs. for construction of thermal model 3−31609
  far i.r. and submillimeter background radiation, rocket measurements 3−19029
  G-99-37, magnetic white dwarf, observations of Zeeman effect and circular polarization measurements 3−28210
  Galactic centre region, molecular clouds, CO obs. at 2.6 mm. 3−19068
  Galactic nucleus obs. at 350 μ, optically thin thermal model formation 3−31751
  Galilean satellites, thermal props. determ. from 20 μ obs. of eclipses 3−31608
  Galilean satellites of Jupiter, 1-4 μ obs. 3−31581
  Ganymede, 10 μ obs. for construction of thermal model 3−31609
  H II regions, multicolour photometry giving colour temps., i.r. emission, rocket telescope 3−13102
  HD 50138, spectroscopic observations in photographic i.r. region up to 9500 Å *(French)* 3−28206
  α Herculis, 4000 to 4800 cm^{-1} obs., atomic and mol. absorpt. band features identification 3−28215
  α Herculis, 5700 to 6700 cm^{-1} obs., CO second overtone bands identification 3−28216
  interstellar clouds, H_2 detection in 4.4 to 28.2 microns wavelength region 3−25514
  intraday variability in radio sources, simultaneous optical, i.r. and radio obs. 3−19035
  IO, 10 μ obs. for construction of thermal model 3−31609
  IRC + 10420, comparison of i.r. and photographic spectra with η Carinae 3−25482
  IRC-20385, identification as globular cluster 3−28237
  JHKL photometry of bright i.r. object, possible association with OH 338.5+0.1 radiosource 3−25483
  Jupiter, interpretation of $3v_3$methane R-branch obs. 3−31614
  Jupiter, i.r. maps using new scanning equipment 3−9496
  Jupiter, limb brightening obs. at 7.9 μ 3−31580
  K-giants from IRC catalogue, luminosity functions determ. method 3−39677
  Kleinmann-Low nebula complex near Orion Nebula, 2.8-13.5 μ obs. 3−28238
infrared astronomical observations continued
  late type stars, i.r. excesses resulting in vanishing of H and K line reversals 3−13036
  M17 (NGC 6618), observations of four bright i.r. sources 3−16250
  M, S, and C-type stars, long wavelength spectrometry and photometry 3−9529
  M-type stars, scanner photometry of weak TiO bands in i.r. spectra 3−37371
  Maffei 2, optical and near i.r. obs. of nearby spiral galaxy, distance meas. 3−37444
  Mars, circular polarisation meas. 3−31689
  Mars, CO_2 distrib., absorp. obs. 3−31588
  Mars, H_2O 2.8 to 3.5 microns absorption band obs. during 1971 opposition using airborne Hadamard-Transform Spectrometer 3−35221
  Mars, Mariner 6 and 7 and ground based CO_2 meas. *(Russian)* 3−16168
  Mars, O_2 A band line spectroscopy 3−25411
  Moon as absolute radiometric standard for microwave and i.r. obs. of extended sources 3−39633
  nebulous emission-line stars, association with cometary nebulae 3−19012
  Neptune, temp. meas. at 24 microns 3−28149
  NGC 1068, Seyfert, variability in 10-micron flux 3−13092
  NGC 4151, Seyfert, variability in 10-micron flux 3−13092
  NGC 4151, Seyfert galaxies, i.r. variability of dust model 3−13087
  NGC 5253, supernova 1972, UBVRIJK photometry and magnitude determinations 3−13052
  NGC 5253, supernova (type I), emission features identification 3−22071
  NGC 6231-92, highly reddened star, obs. at 2.2, 3.5 and 10.6 μ 3−28203
  NGC 6523 (M8), obs. of i.r. radiation from Herschel 36 and other objects 3−31786
  NGC 7027, i.r. observations and reddening values 3−39745
  NGC 7027, planetary nebula, spatial distrib. of 11.7 micron radiation 3−37497
  night sky background, 2.7°K blackbody source 3−19037
  α Orionis spectrum, vibration-rotation bands of NH radical 3−13041
  β Persei (Algol), 5-microns emission 3−28213
  photosphere and faculae, CO harmonic line equivalent widths *(Russian)* 3−16140
  protostars in young clusters, 2-20 micron obs. 3−16231
  quasars and Seyfert galaxies, i.r. radiation from surrounding dust envelope 3−37418
  RCW 117, H II region, detection in far i.r. balloon measurements 3−22093
  Saturn, phase dependence of polarisation for disc areas 3−28156
  Saturnian satellites, Iapetus and Rhea, radius, albedo and 20 μ brightness temperature measurements 3−12974
  seeing, model computations of discs 3−39505
  Seyfert galaxies, surface brightness gradient rel. to i.r. emission *(Russian)* 3−37443
  Sh 138, surface brightness and apparent colour temp. meas. 3−22120
  Sh 152, surface brightness and apparent colour temp. meas. 3−22120
  Sh 270, surface brightness and apparent colour temp. meas. 3−22120
  solar quiescent prominence, cavity-like obs. 3−37323
  southern Wolf-Rayet stars, i.r. photometry 3−28194
  Sun, relative umbral intensity of large sunspot 3−31558
  symbiotic object discovery behind Coalsack with combination spectrum 3−25467
  T Tauri stars, energy distrib., visual variations correlation 3−19011
  RV Tauri southern stars, i.r. excess 3−28197
  RVTauri-type stars, [3.6]−[11.3] colour meas. exhibiting large i.r. excesses 3−22049
  terrestrial water vapour absorption spectrum in vicinity of He I 10830 Angstroms triplet 3−31387
  unidentified sources, spectroscopic classification, 2m sky survey 3−9620
  Uranus, temp. meas. at 24 microns 3−28149
  Uranus satellite system, near-i.r. search for satellites using methane filter 3−9497
  Venus clouds, comparison of spectra with laboratory spectra of aqueous HCl soln. 3−25405
  W49, i.r. emission from OH/H_2O sources 3−35170
  young stellar objects, CS envelopes characts. and effects, review 3−28195
  CN red system of lines in sunspots, polarization meas. 3−31557
  D/H ratio determ. for Jupiter from obs. of mono-deuterated methane 3−28148
  H II regions, 21-μ contour maps, i.r. flux meas. and colour temperature determinations 3−13103
  OH emission lines at 1665 MHz and 1667 MHz, association with M type long period variables 3−13075
  Rb I 7800 Angstroms solar resonance line, measure of $^{87}Rb/^{85}Rb$ ratio for Sun 3−18932
  S IV 10.5 μ transition, collision strengths rel. to gaseous nebulae 3−9610
infrared astronomy
  100-micron objects observed at 85 GHz 3−39709
  9558 Angstroms photomultiplier performance improvement, astronomical applications 3−25526
  R Agr, 20 μ flux, from interferometric diameter obs. and model atmosphere 3−9559
  airborne Hadamard-Transform Spectrometer, i.r. obs. of Mars during 1971 opposition 3−35221
  Becklin-Neugebauer i.r. point source in Orion Nebula, 2.8-13.5 μ obs. 3−28238
  α Boo, 20 μ flux, from interferometric diameter obs. and model atmosphere 3−9559
  μ Cep, 20 μ flux, from interferometric diameter obs. and model atmosphere 3−9559
  circumstellar matter, i.r. emission 3−9539
  VY CMa, 20 μ flux, from interferometric diameter obs. and model atmosphere 3−9559
  o^2 CMa, B3Ia, i.r. spectra, equivalent widths and line profiles 3−13055

infrared astronomy continued
RS CVn, eclipsing binary, i.r. excesses, JHKL photometry 3−9557
NML Cyg, 20 μ flux, from interferometric diameter obs. and model atmosphere 3−9559
V1057 Cygni, far i.r. and UVBY photometry 3−9560
NML Cygni, i.r. source, circular polarisation meas. at 1.7 μ 3−31689
Cygnus X-3, search for i.r. candidate at 1 μ 3−31730
detectors at focus of telescope 3−31805
DR 15, H II region, detection in far i.r. balloon measurements 3−22093
early-type stars, i.r. excesses, free-free emission explanation 3−9536
RZ Eri, eclipsing binary, i.r. excesses, JHKL photometry 3−9557
galactic nuclei emission, black hole model including plasma turbulence effects 3−34996
β Gem; 20 μ flux, from interferometric diameter obs. and model atmosphere 3−9559
α Her, 20 μ flux, from interferometric diameter obs. and model atmosphere 3−9559
Z Her, eclipsing binary, i.r. excesses, JHKL photometry 3−9557
hot stars, correlation between i.r. excesses and mass loss 3−25446
interferometer for solar obs. 3−16292
interstellar matter, i.r. line radiation meas. using u.v. line absorpt. 3−37485
interstellar OH mols. pumped by i.r. radiation, optical thickness determ. for s.h.f. lines 3−25516
IR sources, H II region W_3, interstellar dust, ionised gas, H_2O maser emission 3−3358
IRC + 10216 20 μ flux, from interferometric diameter obs. and model atmosphere 3−9559
IRC + 10420, comparison of i.r. and photographic spectra with η Carinae 3−25482
JHKL photometry of bright i.r. object, possible association with OH 338.5 + 0.1 radiosource 3−25483
Kleinmann-Low nebula complex, low-temp. extended source, 2.8-13.5 μ obs. 3−28238
AR Lac, eclipsing binary, i.r. excesses, JHKL photometry 3−9557
R Leo; 20 μ flux, from interferometric diameter obs. and model atmosphere 3−9559
lunar regolith from Mare Foecunditatis, i.r. reflection, emission and transmission spectra 3−31622
M17 (NGC 6618), observations of four bright i.r. sources 3−16250
M1-82, optical obs. 3−9587
models for extragalactic objects with very high i.r. and X-ray luminosity 3−22106
Moon as absolute radiometric standard for microwave and i.r. obs. of extended sources 3−39633
NGC 2264, optical obs. 3−9587
NGC 6523 (M8), obs. of i.r. radiation from Herschel 36 and other objects 3−31786
novae, i.r. emission, possible energy sources and mechanisms *(Russian)* 3−28240
α Ori, 20 μ flux, from interferometric diameter obs. and model atmosphere 3−9559
β Peg, 20 μ flux, from interferometric diameter obs. and model atmosphere 3−9559
LX Per, eclipsing binary, i.r. excesses, JHKL photometry 3−9557
β Persei (Algol), 5-microns emission 3−28213
progress and development of planetary and stellar i.r. emission, popular survey *(French)* 3−22133
SZ Psc eclipsing binary, i.r. excesses, JHKL photometry 3−9557
quasars and Seyfert galaxies, i.r. radiation from surrounding dust envelope 3−37418
R Cr B, photometry during decline 3−13057
RCW 117, H II region, detection in far i.r. balloon measurements 3−22093
α Sco, 20 μ flux, from interferometric diameter obs. and model atmosphere 3−9559
Seyfert galaxies, surface brightness gradient rel. to i.r. emission *(Russian)* 3−37443
supergiants, i.r. excesses as evidence for silicates 3−9537
α Tau, 20μ flux, from interferometric diameter obs. and model atmosphere 3−9559
Venus spherical albedo, pure scattering atm. in continuum in 0.6-1 μ range 3−28157
W49, i.r. emission from OH/H_2O sources 3−35170
H_2O 1.35-cm emission sources, association with i.r. stars and OH emission sources 3−37410
PbS detectors, photoresponse variations without use of Fabrylens 3−31801

infrared communication *see optical communication*

infrared detectors
see also photodetectors
absorption by fluids at high temps. and pressures, measuring cells, corrosives, results 3−9920
applications in science and technology, 5-30 μm *(Polish)* 3−5804
astronomical, at focus of telescope 3−31805
autodyne quantum receiver, sensitivity *(Russian)* 3−10578
chalcogenide glass thin film bolometers, props. 3−13235
environmental disruption measuring systems 3−21977
fundamentals and applications, book 3−13256
heterodyne, microwave bias, pyroelec., 3-25 μm range, review *(Polish)* 3−5803
heterodyne radiometer, applic. to remote sensing of atmospheric pollution 3−3193
moisture measurement 3−9853
photoemission, two-photon surface effect, appl. to i.r. detection 3−39212
photon detectors contamination cause, prevention and remedy 3−32043
pneumatic nondispersive i.r. detector, analytical model 3−22278
pyroelectric, characteristics, applications 3−22282
pyroelectric, gas filled tube, temperature distribution and noise 3−28486
pyroelectric detectors, construction, operation, characts. *(Polish)* 3−5805
quantum and thermal detectors, mechanisms and efficiency *(German)* 3−3768
quantum counters, two-photon, Raman thermal excitation noise rel. to background radiation 3−19583

infrared detectors continued
radiation thermometry, development trends 3−19170
reactor, liquid metal fast breeder, thermal scanning of fuel pin simulators 3−28491
scan radiometer on board geostationary environmental satellite 3−13121
semiconductor detector materials *(Polish)* 3−6067
semiconductor radiation detectors, conference, Warsaw, Poland 7-8 Feb (1972) 3−6066
sensitivity limits for extrinsic and intrinsic detectors 3−28487
thermistor device, theory of operation and derivation of transfer function *(Russian)* 3−9851
$CdF_2:Er^{3+}$, i.r. quantum counter, optical parameters for Er^{3+} sites of $C_{2v}(C_{3v})$ symmetry 3−35397
p-CdSb, exptl. material applic. *(Russian)* 3−24430
PbS-GaAs p-n heterojunctions, near i.r. detection 3−22283
$Pb(Zr, Ti)O_3$, pyroelec. props., comp. and phase struct. depend., i.r. detector characteriz. 3−39098
$Pb_xsN_{1-x}Te$ films, r.f. sputtering, i.r. detector arrays 3−8688

infrared imaging
Bouwers concentric system, Ge corrector lens, image quality 3−22308
C-5 aircraft fail-safe strap panels employing traversing inspection system 3−37599
lenses, transmission meas. 3−3794
metallic plate, normal spectral emission factor using i.r. thermography *(French)* 3−30267
meteorological satellite direct-readout i.r. pictures and quantitative temp. data 3−37257
microscopy using TV camera with i.r. sensitive vidicon 3−25723
for nondestructive testing, imaging techniques, conference, Los Angeles, USA (1972) 3−19349
pyroelectric detector arrays 3−25779
pyroelectric imaging system, thermal spread analysis 3−28485
solar cell array, i.r. testing, using thermovision infrared scanner 3−25684
synthetic aperture optical system applications 3−28483
thermal imaging by i.r. to visible image upconversion 3−5794
upconverter, high resolution and high field of view, multipass matrix pumping scheme 3−5795
Cu_2HgI_4, thermochromic, i.r. recording, image recording sensitivity, refl. vs. temp. phase transition hysteresis 3−108

infrared sources
alkali metal vapours, tunable coherent i.r. source from four wave parametric conversion 3−35712
dye laser, far i.r. generation by self-beating, phase matching method 3−16905
far i.r. background radiation balloon meas. using liquid He-cooled radiometer 3−28239
generator, parametric oscillator and down converter, high power, tunable 3−22947
health lamps, history, development, use, benefits 3−3572
lasers, tuning methods, review 3−743
Cs, high press. lamp 3−5938
OH sources associated with i.r. late-type stars 3−5608

infrared spectra of organic molecules and substances
see also molecular rotation; molecular vibration
1,2-bis(diphenylphosphine)ethane, band assignments, gauche form identification 3−4424
acenaphthylene, polarised i.r. and Raman spectra, crystal structure 3−39134
acetal, perturbation of i.r. vibrs. by free orbitals of neighbouring oxygen atoms *(French)* 3−23564
acetamide, liquid and single-crystal films in polarized light *(Russian)* 3−15499
acetone, fine struct. of $\nu(C=O)$ vibr., low temp. *(French)* 3−38285
acetone and acetone-d_6, Fermi reson. and intermol. forces in ν_{co} absorption *(French)* 3−26660
acetonitrile, i.r. study of reorientational potential barrier 3−36878
N-acetyl glycine, and deuterated compound, vibr. spectra and assignments 3−20142
acetylacetone, electronic structure and absorption spectra *(Russian)* 3−1233
acetylene, rot. struct. of i.r. bands 3−1220
acetylene, vibr.-rot. spectrum in 5μ region 3−1221
acetylene in nitrogen matrix, low temp. absorpt. spectra *(Russian)* 3−4442
acetylenes, i.r. intensities *(German)* 3−14378
acrolein, polar properties of bonds and absolute intensities of i.r. bands 3−20125
adamantanes, 1-substituted, for i.r. spectra, torsional freqs. and internal rot. barriers 3−29680
alcanes, trichloro-1,1,1 halogeno-3, vibr. spectra and rot. isomerism *(French)* 3−20162
alcoholic solutions, A/D conversion for automatic analysis, Perkin Elmer 521, numerical data, circuits *(French)* 3−13503
aldehyde trimers, perturbation of i.r. vibrs. by free orbitals of neighbouring oxygen atoms *(French)* 3−23564
aldoximes, far i.r. group freq., torsional vibr. 3−29651
aliphatic azides, vibration spectra and structure *(Russian)* 3−29683
alkenyl succinic anhydrides, high mol. wt., succinic anhydride group analysis by i.r. spectroscopy *(Russian)* 3−28785
alkenyl succinic anhydrides, hydrolysis study *(Russian)* 3−25067
amides, interaction of H^+ 3−11239
amines, primary, hydrogen bonding effect on in-plane deform. vibrs. *(Russian)* 3−7162
amines, secondary aliphatic, vibr. freqs. 3−17411
amino acids, charact. group freqs. assignments 3−7206
p-aminophenylacetate, preorientation pot. barriers of mols. in cryst., nematic cryst. and isotropic phases 3−21415
ammonium uranyl oxalate crysts., dichroism of i.r. absorpt. *(Russian)* 3−12178
aprotic acids, electron-donating capacity study by i.r. spectroscopy *(Russian)* 3−29685
aromatic nitrocarboxylic acid esters phenol electron donating substituents effect on i.r. spectra *(Russian)* 3−29686
arsine compounds, $(CH_3)_2AsH$, $(CH_3)_2AsD$, i.r. spectra and normal coord. anal. *(German)* 3−17440

infrared spectra of organic molecules and substances continued
arylazonaphthols, crystalline, hydrogen bonding, electronic and vibrational spectra investigation 3−11580
1,4,8,11-tetra-azacyclotetradecanes, i.r. spectra and struct. interpretation 3−23576
1-aziridinyl carboxamide-d_0 and N,N-d_2, i.r. and far i.r. 3−7191
benzene, carbon tectrachloride and carbon disulphide binary mixture, intensities of i.r. bands, dispersion 3−2535
benzene, far-i.r. absorpt. of single crysts., internal vibrs. *(French)* 3−8562
benzene, rare gas matrices location of $^1E_{2g}$ state, photoexcitation spectra 3−38292
benzene and derivatives, magnetic circular dichroism spectra 3−23567
benzene derivatives, i.r. absorpt. bands, broadening on addition of inert solvent *(French)* 3−23586
benzene-benzonitrile mixture, far i.r. absorption spectra of non-polar liquids 3−2537
benzofuran *(French)* 3−17434
benzonitriles, substituted, intramol. interactions quantitive meas. 3−17443
benzothiophene *(French)* 3−17434
3- benzoylaminopropionic acid, i.r. spectra study of intramolecular bonding *(Russian)* 3−29684
benzyl compounds, m-substituted, for i.r. and Raman spectra 3−36029
biphenyl and perdeuterated derivative, gaseous, vibr. spectra *(French)* 3−23565
biphenyl ring, electron delocalization effects *(French)* 3−29652
borine carbonyl, high resolution i.r. absorpt. spectrum, vibr. states, rot. anal. 3−29664
bromoacetic acid, and deuterated analogues, vibr. spectra and assignments 3−36028
bromoacetone, rotational isomerism 3−14375
bromobenzene in soln., i.r. absorpt. band contour form study by method of moments *(Russian)* 3−11266
bromoform and deuterated analogues, i.r. dispersion studies, determ. of band intensities and vibrational polarisations 3−1225
1,3-butadiene, i.r. and Raman spectra, vibr. assignments 3−29679
t-butanol, H-bonding in electron donating solvents, i.r. spectra *(Russian)* 3−23554
p-n-buthylanilines p-methoxy- and p-ethoxybenzilidene, preorientation pot. barriers of mols. in cryst., nematic cryst. and isotropic phases 3−21415
di-T-butyl carbinol, near i.r. heteroassociation study and choice of mol. complex equilib. conc. scale 3−23575
butyne-1, deuterated assignment of stretching vibration, obs. of overtones of angle deformation vibration *(French)* 3−7189
caesium hydrogen trifluoroacetate, thin film spectra determ. of O-H-O bonding 3−11261
carbon disulphide, benzene and carbon tetrachloride binary mixture, intensities of i.r. bands, dispersion 3−2535
carbon tetrachloride, benzene and carbon disulphide binary mixture, intensities of i.r. bands, dispersion 3−2535
carbon tetrachloride isotopic structure, determ. of frequencies for overtones and combinations 3−26690
carboxylate ion, asymmetrically perturbed, ν(CO) freqs. 3−14376
carboxylic acid H-complexes, torsional vibrs., Fermi reson. and isotopic effects 3−11264
carboxylic acids of carbonyl fluoride telomers, assignment of main vibrational modes 3−1258
cell for combined study of i.r. and Raman spectra of adsorbed molecules 3−22346
cellobiose, far i.r. spectra at liquid He temp. 3−4450
cellulose copolymers from cellulose reaction with aromatic epoxypropylamines *(Russian)* 3−31265
chemical bonding detection between sulphonamide azo-dyes and albuminous polyacrylate film *(Russian)* 3−29658
chloroacetamide, N- and N,N-di-, vibr. spectra and force consts. 3−29677
chlorocyclohexane, conformational transitions, activation energies determ. by i.r. spectra 3−14373
chlorodimethylaminotetraphosphonitriles, vibr. spectra and assignments 3−36027
chloroform, liq., dielec. relax. and far i.r. dispersion 3−21398
chloroform and deuterated analogues, i.r. dispersion studies, determ. of band intensities and vibrational polarisations 3−1225
clathrate hydrates, double, monomer conc. in liq. water determ. 3−34343
copper formate tetrahydrate, liquid air and room temp. spectral comparison 3−5199
cyanoacetic acid, vibr. spectra of crystal 3−15483
cyanogen, high resolution spectra up to 4.7 μ *(French)* 3−20166
cycloalkenethiones, valence vibr. of C=S group *(French)* 3−7185
cyclohexane, fine struct. of ν(C=O) vibr., low temp. *(French)* 3−38285
cyclohexane-1,1,4,4,-d_4 and 1,1,2,2,4,4,5,5-d_8, i.r. and Raman spectra, assignment study 3−26669
cyclopropane carboxylic acid, determ. of structure *(French)* 3−1223
cyclopropanecarboxylic acid and cyclopropanecarboxamide 3−29666
cyclopropyl methyl ketone, conformational behaviour and vibrational spectra 3−14372
cytosine, i.r. and laser-Raman spectra, planar vibr. 3−29773
data collection for 223 molecules, from U.S. department of commerce 3−11235
trans-cisdiacetamide, and C- and N-deuterated derivatives, i.r. dichroism and out-of-plane vibr. 3−20165
dialkylethers, phenyl substituted, H bending and ring deform. vibrs. *(German)* 3−17444
dialkylureas in dil. carbon tetrachloride soln., N-H stretching freqs. and conformations 3−17437
dialkylureas in soln., bond stretching freqs. meas. 3−26666
diazaphospholane-1,3,2 derivatives, NH valance vibr. mode and intermol. hydrogen bond study *(French)* 3−17442
diazaphosphorinane-1,3,2 derivatives, NH valence vibr. mode study *(French)* 3−17441
1,4-diazine, σ-electron distribution study by i.r. absorption intensities 3−38289

infrared spectra of organic molecules and substances continued
dibenzene p,p'-diaminobiphenyl, preorientation pot. barriers of mols. in cryst., nematic cryst. and isotropic phases 3−21415
dibenzofuran, in frozen hexane, solns., excited states vibronic spectra at 4K 3−20111
dibenzothiophene, in frozen hexane solns., and single cryst. in polarized light, excited states vibronic spectra at 4K 3−20111
dibenzoxanthones, stretching vib. band obs. 3−26670
dibenzoylmethane, electronic structure and absorption spectra *(Russian)* 3−1233
dibenzyl, crystalline, assignment of characteristic frequencies, determ. of molecular geometry 3−1226
o-dichlorbenzol, vibr. transition polarization, vibr. absorpt. bands obs. *(Russian)* 3−14352
2,6-dichloroaniline Raman spectra of liquid phase and i.r. absorption spectra of solid phase 3−30811
dichlorobenzaldehydes, vibr. assignment 3−7186
dichloroethane, i.r. absorpt. bands, broadening on addition of inert solvent *(French)* 3−23586
cis-dichloroethylene, i.r. absorpt. bands, broadening on addition of inert solvent *(French)* 3−23586
dideuteromethane, ν_3 vibr.-rot. band *(French)* 3−33122
N,N-diethyl acetamide, meas. and calc. of solvent shifts 3−7197
diethylamine, NH stretching vibr. bands, hydrogen bonding and rot. isomerism 3−4431
p-dihalobenzenes and deutero-derivatives, rel. to vibr. spectra interpretation *(Russian)* 3−2531
dihalomethane (halogen=Cl, Br), i.r. absorpt. bands, broadening on addition of inert solvent *(French)* 3−23586
1,4-dihydroxy, 2-methyl and 1,8-dihydroxy 3-methyl anthraquinone, vibr. modes 3−11257
diimide, solid and matrix isolated, i.r. and Raman spectra 3−26663
dimethoxybenzene, meta and para, Raman and i.r. spectra 3−38288
dimethyl esters of dicarboxylic esters, effect of alkyl chain on C=O band *(Russian)* 3−26679
dimethyl sulphoxide solns. in presence of proton donor, νS=0 bands identification *(Russian)* 3−7198
dimethyl zinc, vibrational spectra 3−38295
2,2'-dimethyl-1,1'-binaphthyl anion radical circular dichroism and electronic spectra 3−29639
2,6-dimethyl-4-oxy-1,2,3,4-tetrahydroquinoline, pi bonding of hydroxyl O with aromatic ring *(Russian)* 3−36007
2,6-dimethyl-4-oxy-1,2,3,4-tetrahydroquinoline, u.v. and i.r. spectra, intramolecular interaction in isomers, hydrogen bonding *(Russian)* 3−29646
N,N-dimethylacetamide, normal vibr. analysis 3−11227
dimethylhalosilanes, i.r. and Raman spectral meas., vibr. assignments and torsional barrier heights 3−20146
1,2-dimethylindole fluoresc. and absorpt. spectra, determ. of dipole moment 3−4429
dimethylphosphinous acid methyl ester, i.r. spectra and structure *(Russian)* 3−36035
dimethylsulphoxide-Lewis acid, addition compound study vibr. spectra *(French)* 3−23574
1,4-dioxan, monosubstituted derivatives *(Russian)* 3−26675
1,2,3-dioxaphophorinans, phosphoryl heterocycle conformation *(French)* 3−4399
dioxydinaphthyl film, vibr. spectra, elec. field induced variations 3−23573
dipeptides, charact. group freqs. assignments 3−7206
diphenyl i.r. spectra study of structure *(Russian)* 3−29687
diphenylamine, solid, vibrs. assignment *(French)* 3−20728
diphenyloxide, stretching vib. band obs. 3−26670
dipyridiyl, i.r. spectra study of structure *(Russian)* 3−29687
p-dithian, charge-transfer complexes with I_2, IBr, far i.r. spectra, vibr. and assignments 3−26667
enols, dienols, stereoisomers, conformational study *(French)* 3−17391
ethane, deuterated derivatives, i.r. absorpt. spectra, dipole moment derivatives 3−29682
ethers, stereoisomers, conformational study *(French)* 3−17391
ethyl 1-naphthate, in hexane and water intermolecular hydrogen bonds, proton transfer of ground and lowest excited singlet states 3−33108
ethyl esters of phenylhydrazones of diketobutyric acid and related compounds *(Russian)* 3−26678
ethylene and deuterium derivatives, cryst. films, i.r. spectra, general harmonic force field 3−39142
ethylenediammonium ion, i.r. spectra, rotational isomerism 3−38291
ethylidene norbornene copolymers with ethylene and propylene *(Russian)* 3−22553
ethylmesitylene, vibr. transition polarization, vibr. absorpt. bands obs. *(Russian)* 3−14352
ferrocene-h_{10} and -d_{10} low temp. i.r. spectrum 3−36033
fluorene, in frozen hexane solns., excited states vibronic spectra at 4K 3−20111
fluoroacetone, vibrational assignments and rotational isomerism 3−29665
formaldazine, i.r. and Raman spectra, vibr. assignments 3−29679
formaldehyde, CNDO calc. of dipole moment derivatives and i.r. intensities 3−29630
formaldehyde, in Ar, N_2, matrix conc. and temp. depend. 3−29676
formaldehyde, i.r. microwave double resonance, microwave pumping, i.r. detection 3−1222
free radicals, CO_2, CCl_3 and acetyl, i.r. spectra at 77K 3−20163
free radicals and molecular ions isolated in inert solid matrices, i.r. and u.v. spectroscopic studies, review 3−11251
furfural, Fermi reson. in rot. isomers 3−4421
galactose, far i.r spectra at liquid He temp. 3−20160
glucose, far i.r. spectra at liquid He temp. 3−4450
glutamic acid hydrochlorides, L- and DL-, vibr. spectra and assignments 3−20143
glutaric anhydride, meas. and calc. of solvent shifts 3−7197
glycerol, ν_{oh} stretching vibr. investigation *(French)* 3−30819
l- glycosane, effect of crystal surface of KBr plates on i.r. spectra and struct. *(Russian)* 3−35547
halopropynals (halo=chloro, bromo, iodo), vibr. spectra and force const. calcs. 3−17439
1,2,4,5-hexatetraene, vibr. spectra and mol. struct. 3−17438

infrared spectra of organic molecules and substances continued
hydrazine free radicals and their original hydrazines *(Russian)* 3−26677
hydrogen bonded gaseous complex, ClH...O(CH$_3$)$_2$, i.r. profile analysis 3−11260
hydroquinone charge-transfer complexes 3−36032
hydroxybiphenyl, phase change effects on hydrogen bridges, i.r. absorpt. spectra *(French)* 3−29654
indole, fluoresc. and absorpt. spectra, determ. of dipole moment 3−4429
indole-pyridine systems, association constants by i.r. intensity meas. 3−29730
iso-phthalaldehyde, 250-4000 cm^{-1} 3−7187
isocyanuric acid, di- and tri-substituted *(Russian)* 3−14380
isopropyl compounds, low-frequency vibrations, torsional modes and barriers to internal rotation 3−5188
keontes, valence vibr. perturbation by intermol. forces *(French)* 3−1244
lactose, far i.r. spectra at liquid He temp. 3−20160
liquid crystal, cholesteric, i.r. circular dichroism, mol. vibrs. 3−5184
2,3-lutidine, liquid and vapour i.r. and Raman spectra 3−17429
malononitrile, i.r. study of reorientational potential barrier 3−36878
metal dipicrylaminates, in solution i.r., visible and u.v. absorption spectra *(Russian)* 3−36880
methane, 3.39 μm molecular transition used in laser stabilisation, accurate freq. 3−22872
methane, 7.9 μ limb brightening obs. of Jupiter 3−31580
methane, ν_3-fundamental laboratory obs. rel. to planetary gases at low temps. 3−29650
methane, bideuterated, ground-state rot. consts. 3−36024
methane, $F_1^{(2)}$ line Stark broadening at 3.39 μm, inverted Lamb dip obs. 3−26681
methane, high order spectroscopic constants, analysis of ν_3 3−23569
methane, solid in inert gas matrices, i.r. absorpt. theoretical study 3−24685
methane, wavelength of 3.39 μm laser saturated absorpt. line 3−22873
methane absorption band spectrometry of Jupiters disc *(Russian)* 3−16144
methane absorption bands of Jupiter and Saturns discs *(Russian)* 3−16145
methane in Jovian atm., interpretation of 3$\nu_3$methane R-branch obs. 3−31614
methyl acetylene, structure of CD-stretching vibration of 2 ν, band and accompanying hot bands 3−33096
methyl cyclopropylcarboxylate, conformational behaviour and vibrational spectra 3−14372
methyl esters of aliphatic monocarboxylic acids, effect of alkyl chain on C=O band *(Russian)* 3−26679
3-methyl-1, 2-butadiene, vibr. spectra and struct. 3−1219
methylcarbamate, and N,N-dichloro-, vibr. anal. 3−29678
trans-methyldiazenes, deuterated, vibr. assignments 3−20145
methylene-group containing compounds, vibr. spectra for bending vibr.. anharmonicity and Fermi reson. study *(French)* 3−20156
methylphosphonic acid and its anions 3−29617
methylphosphonic acid and its anions 3−29667
3-methylpyridine in soln., i.r. absorpt. band contour form study by method of moments *(Russian)* 3−11266
methylzinc borohydride, solid, vibr. spectra, force consts. 3−24689
N-methypyrrolidone, internal rot. barrier 3−1178
molecular crystals, three top molecules with C_s symmetry, low frequency modes, methyl torsions and barriers to internal rotation 3−24687
monodeuteromethane, compressed gaseous, rot. diffusion 3−33185
monohalogenodiacetylenes, triple bond stretching modes, reassignment 3−29675
monohydrosilanes, Si-H valency vibration band frequencies and intensities *(Russian)* 3−26676
monomethylisothiazoles, vibrs. assignments *(French)* 3−17428
N-methylindole fluoresc. and absorpt. spectra, determ. of dipole moment 3−4429
naphthalene, far-i.r. absorpt. of single crysts., internal vibrs. *(French)* 3−8562
1-naphthoic acid in hexane and water, intermolecular hydrogen bonds, proton transfer of ground and lowest excited singlet states 3−33108
1,4-naphthoquinone, room temp. vibr. spectra, fund. vibr. assignments 3−20164
nitro-derivatives, 2-thienyl-phenyl-ketone, i.r. and u.v. spectra 3−17445
nonpolar liquids, contribution of induced dipoles 3−2537
α-olefines, molecular dynamics *(Russian)* 3−14406
organic liquids, i.r. absorption band widths, temp. depend. 3−14379
oxalylhalides, vibr. spectra and rot. isomerism *(German)* 3−7207
oximes, far i.r. group freq., torsional vibr. 3−29651
pectin films *(Russian)* 3−26674
pentacene, monoanions and dianions, i.r. absorpt. spectra obs. 3−33132
pentacene in solid soln., low temp. absorpt. spectrum *(French)* 3−8561
cyclopentadienylnickelnitrosyl, cryst., i.r. spectra in polarised light, space group assignments 3−18460
pentafluoroacetophenone with polarisation meas. 3−7183
p-penthoxybenzoic acid, preorientation pot. barriers of mols. in cryst., nematic cryst. and isotropic phases 3−21415
perylene, planar vibr. freqs. calc. and i.r. and fluoresc. spectra interpretation 3−20112
phenanthrene, in frozen hexane solns., excited states vibronic spectra at 4K 3−20111
phenanthrene, polarized spectra, vibr. analysis 3−15486
p-phenetidine, liquid phase, i.r. spectrum, vibrational modes 3−20144
phenol, H-bonding in electron donating solvents, i.r. spectra *(Russian)* 3−23554
phenol-pyridine hydrogen bonded complexes, band assignments 3−7204
phenols, chlorosubstituted, self-assoc., i.r. spectra and OH hydrogen bonding study 3−33130
phosphine compounds, (CH$_3$)$_2$PH, (CF$_3$)$_2$PD, vibr. spectra and normal coord. anal. *(German)* 3−17440

infrared spectra of organic molecules and substances continued
picoline N-oxide i.r. spectrum in various solvents, in the NO group valency vibration range 3−34340
planetary atmospheres, high-resolution i.r. spectroscopy review 3−12982
poly(β-benzyl L-aspartate) films, conformation, mol. wt. effect 3−29766
poly(ethylene glycol) dimethyl ethers, cryst., i.r spectra, absorpt. band assignments 3−36060
polyethylene, B_{2u} lattice mode, far i.r. continuum absorption spectra 3−4822
polyethylene, Gruneisen parameters determ. 3−4504
polyethylene, oriented films, study of microfibrilar struct. *(Russian)* 3−7289
polyisoprenes, 1,2- and 3,4-, linear and cyclized, out-of-plane deform. vibr. study 3−29771
polymer, far i.r. spectrometry, book contrib. 3−11346
polymer, stress distrib. from atomic bonds 3−34367
polymer determ. of molecular ordering by i.r. spectroscopy in solid state *(German)* 3−11552
polymers, far i.r. spectra, modern expt. methods 3−13299
polypeptides in acidic solution, i.r. spectra, helix-coild transitons *(French)* 3−29796
polyvinylformal highly stretched films, polarised spectra, struct. 3−7273
potassium citrate monohydrate, solid 3−21402
potassium hydrogen trifluoroacetate, thin film spectra determ. of O-H-O bonding 3−11261
potassium pyrrolates, C_4H_4NK and C_4D_4NK, vibr. freqs. *(French)* 3−17427
propanal, deuterated derivatives, cis rotamers, complete vibr. assignments 3−4446
propane, deuterated derivatives, i.r. absorpt. spectra, dipole moment derivatives 3−29682
propanes, substituted, vibrational spectra, dipole moments and conformations 3−14370
propanes, substituted, vibrational spectra and conformation 3−14371
propenes, vibr. spectra meas., normal coord. anal. and valence field calc. *(French)* 3−20157
propynal, ν_6 band, i.r. press. broadening 3−11275
pyrazole, anomalous band contours in gas spectrum 3−36022
pyrazole hydrochloride, gaseous, monomer spectrum 3−36023
pyrene charge-transfer complexes 3−36032
pyrrole-pyridine systems, association constants by i.r. intensity meas. 3−29730
pyrroles at −180°C, 4000-30 cm^{-1}, intra- and intermolecular vibrations *(French)* 3−2529
quinones, substituted, intermolecular interaction, with aprotic and proton-donating solvents *(Russian)* 3−36882
quinoxaline, mixed crystal electronic polarisation spectra crystal effects 3−39141
resorcinol polycondensation products, structural conversion during thermal working *(Russian)* 3−23646
ring mols., far i.r. data for ring-puckering vibr. semi-rigid model 3−29612
rubidium hydrogen di-tetrachloroacetate, vibrational spectra, normal coordinate analysis, symmetrical hydrogen bonds 3−7196
saccharose, far i.r. spectra at liquid He and N_2 temps. 3−4450
seleninyl chloride, vibrational assignments, solvent effects on XO bond 3−7194
silacyclopent-3-enes, vibr. analysis 3−11265
sodium cyanoacetate, vibr. spectra of crystal 3−15483
sodium cyclopropane carboxylate, determ. of structure *(French)* 3−1223
sodium furan 2,5-dicarboxylate, vibr. and struct. study *(French)* 3−23577
sodium hydroxylmethyl phosphonate, vibr. spectrum *(French)* 3−1215
sodium oleate, interaction with TiO_2 surface, chemisorption, i.r. studies 3−39410
sorbose, far i.r. spectra at liquid He temp. 3−4450
styrene, vibr. transition polarization, vibr. absorpt. bands obs. *(Russian)* 3−14352
styrene-acrylic nitrile copolymerisation, i.r. spectra *(German)* 3−11341
succinonitrile, i.r. study of reorientational potential barrier 3−36878
tellurolesters, arylic, carbonyl vibr. study *(French)* 3−20158
tetracene, monoanions and dianions, i.r. absorpt. spectra obs. 3−33132
tetrachloroethylene, i.r. absorpt. bands, broadening on addition of inert solvent *(French)* 3−23586
tetrahydrothiophene, charge-transfer complexes with I_2, IBr, far i.r. spectra, vibr. and assignments 3−26667
tetraphenylenediamine charge-transfer complexes 3−36032
thiacyclohexane, charge-transfer complexes with I_2, IBr, far i.r. spectra, vibr. and assignments 3−26667
thieno-(2, 3-b)-thiophene, gaseous, liq. and cryst. phases, vibr. spectra analysis 3−15490
thiobenzoylmethane, electronic structure and absorption spectra *(Russian)* 3−1233
β-thionaphthol, vibrational assignments, effect of substitution on position of Γ_4 vibration of naphthalene *(French)* 3−7153
thionyl chloride, vibrational assignments, solvent effects on XO bond 3−7194
thiophene, four solid modifications, disorder, cryst. struct. 3−27494
2-thiophenecarboxamides, identification of N-H, C=O stretching and N-H deform. bands 3−4445
thiophenes, 2,5-disubstituted, analysis of vibrational spectra over range 200-1700 cm^{-1} *(French)* 3−17433
thiophenes, vibr. assignments *(French)* 3−29653
tri-nuclear phenols, effect of crystal surface of KBr plates on i.r. spectra and struct. *(Russian)* 3−35547
s-triazine, σ-electron distribution study by i.r. absorption intensities 3−38289
sym-triazine derivatives with NH_2, OR, and NHR substituents *(Russian)* 3−26672
triazolopyrazines, solvent effects on electronic spectra 3−4452
triazolopyrimidine, solvent effects on electronic spectra 3−4452

infrared spectra of organic molecules and substances continued
- 1,2,4-trichlorobenzene-d_3, normal coord. anal. of out-of-plane vibrs. 3—4448
- trichloroiodomethane, i.r. and Raman spectra, Urey-Bradley force const. calc. 3—33126
- trifluoro-acetonitrile ν_8 band in the i.r., study 3—38290
- N-trimethylborazines, vibr. spectra analysis *(Russian)* 3—1194
- trimethylchlorosilane, solid and gaseous states, methyl torsional modes, lattice modes 3—1238
- trimethylpyridines, vibr. spectra and fundamental freqs. assignments 3—20159
- trimethylsilanol, vibr. spectra and bond assignments *(French)* 3—20155
- trioctylamine complex with halogenoacetic acids, i.r. study of proton transfer and hydrogen bonds 3—29633
- uranyl thiocyanoacetates, i.r. and luminesc. spectra *(Russian)* 3—20167
- xanthone, stretching vib. band obs. 3—26670
- xylenols, fundamentals and assignments 3—1216
- CH_4 solid, in phase I and II, i.r. spectra and cryst. struct. 3—12128
- CH_3X group containing compounds, vibrs. and Fermi reson. in CH_3 groups 3—4420
- CO_4 solid, in phases I and II, i.r. spectra and cryst. struct. 3—12128
- $^{12}CH_4$, $\nu_1+\nu_4$ band, 4136 to 4288 cm^{-1} *(French)* 3—33131
- Cu complex with octamethylporphins, combinational dispersion spectra *(Russian)* 3—11284
- 2,2-difluoropropyl chloride, vibrational spectra and rotational isomerism 3—29668
- dimethyl cadmium, vibrational spectra 3—38295
- N-ethylacetamide, n.m.r. and i.r. study of conformational struct. 3—29669
- N-isopropylacetamide, n.m.r. and i.r. study of conformational struct. 3—29669
- Ni complex with octamethylporphins, combinational dispersion spectra *(Russian)* 3—11284

infrared telescopes *see telescopes*

infrared transmitters *see infrared sources*

infrasonic waves *see acoustic waves*

initial value problems *see boundary-value problems*

injection lasers *see semiconductor lasers*

injury by radiation *see biological effects of radiation*

inorganic insulators *see insulating materials*

inorganic molecule configurations and dimensions
- bis-dipivaloylmethane mercury *(German)* 3—14807
- Mn(II) complex, ii), bond lengths and angles 3—7104
- sulphurhydroxohalogenoborane, BX_2SH, struct. and mol. force field determ. from vibrational spectra *(French)* 3—14348
- transition metal complexes with N,N′-bis(dithiocarboxy)piperazine, i.r. vis. and u.v. spectra, polymeric chain structure 3—1208
- water, near Hartree-Fock calculations of ground state, bond length and angle 3—7114
- water molecules in free state and solid hydrates, LCAO calcs. of equilibrium geometry 3—7118
- zeolite, decationized, geometrical arrangement and thermal mobility of struct. OH groups *(German)* 3—4470
- $[H_2O...Cl]^-$ complex, SCF LCAO MO calcs. of hydrogen bond 3—29587
- ArF_2, hypothetical, bond length 3—29550
- AsF_3^- free radical, planar-T configuration determ. from e.s.r spectra 3—4462
- BF_2 radical, bond angle determ. from e.s.r. 3—20081
- BH_2 radical, bond lengths and angles, ab initio calcs. 3—29605
- $BaCl_2$, electric dipole moment determ., bond angle 3—23552
- Be complex, bis(cyclopentadienyl), in crystal at −120° and in gas phase 3—23513
- $BeBH_5$ and BeB_2H_8, ab initio calcs. 3—29548
- BeF_2, low lying states, nonempirical LCAO MO SCF studies 3—23529
- BeF_2, nonempirical LCAO MO SCF studies, bonding trends 3—20096
- BrHBr, equilibrium bond distances, bond-energy—bond-order calc. 3—1181
- BrO, radical, μ-wave spectrum, equilib. internucl. dist. 3—29694
- $C_2N_2^+$, low-energy photoelectron spectra, bond length changes 3—1141
- CO, Born-Oppenheimer approx., equilib. bond length calc. 3—33085
- CO_2^- radical, bond angle determ. from e.s.r. 3—20081
- CO(III) complex, $[Co(3,2,3\text{-tet})\times_2]^+$, $x=Cl^-$ and No_2^-, $42NH(CH_2)_3NH_2$ 3—17774
- CaF_2, nonempirical LCAO MO SCF studies, bonding trends 3—20096
- ClHCl, equilibrium bond distances, bond-energy—bond-order calc. 3—1181
- Cl_3PO, microwave spectrum, determ. of rotational consts. and structural parameters 3—1242
- Cu (II) complex, bis-(N,N′-di-n-propyldithiocarbamate), and cryst. struct. 3—24073
- Cu(I), Cu(II) complexes of 2,2′-bipyridine and 1,10-phenanthroline, determ. of structural information from i.r. spectra 3—1227
- Cu(II) complex, copper(II) bis(N,N′-di-n-propyldithiocarbamate) 3—17778
- Cu(II) complex, tetrasodium dicopper-dl-tartrate dehydrate X-ray anal. 3—7696
- Cu(II) complex, di-μ-thiocyanato-bis di(2-aminoethyl)amine copper(II) 3—17779
- p-D_2, solid orientationally disordered structures, analysis 3—38546
- DF_2^-, equil. geom., ab initio calcs. 3—1171
- D_2S^+ ion radical, determ. of bond lengths and angles from emission spectrum 3—1207
- Fe complex, tetrafluoroethylene-tetracarbonyl iron, gas-phase electron diffr. 3—14324
- $Fe(CO)_4.I_2$, pseudoeightfold coordination, Mossbauer obs. 3—1137
- Fe(III) complex, chlorobis-(N-n-propylsalicylaldiminato)iron(III), and cryst. struct. 3—24076
- GeH_4, i.r. and Raman spectra, interatomic distance calc. 3—29661
- HBS, rotational spectrum and structure 3—23581

inorganic molecule configurations and dimensions continued
- HCN^+, low-energy photoelectron spectra, bond length changes 3—1141
- HCl, Born-Oppenheimer approx., equilib. bond length calc. 3—33085
- $H_{3\|x}Co_x{}^{II}Co_{1-x}{}^{III}(CN)_6.yH_2O$, H-bonding and hydronium ion effects *(French)* 3—14806
- HF_2^-, equil. geom., ab initio calcs. 3—1171
- $H_{3\|x}Fe_x{}^{II}Fe_{1-x}{}^{III}(CN)_6.yH_2O$, H-bonding and hydronium ion effects *(French)* 3—14806
- $HK_8Rh_3Br_{18}.10H_2O$, and cryst. struct. 3—24072
- $(H_3N\text{-}H...NH_3)^+$, SCF calc. of hydrogen bonds 3—17400
- H_2O, energy terms, geometrical depend. using floating spherical Gaussian orbital model 3—29568
- H_2O_2, polarization functions and geometry optimization in ab initio calc. of rotational barrier 3—7105
- H_2O_2 and D substituted products, internal rot. barriers, conformations and vibr. spectra 3—33074
- H_2S^+ ion radical, determ. of bond lengths and angles from emission spectrum 3—1207
- IHI, equilibrium bond distances, bond-energy—bond-order calc. 3—1181
- IOF_5, bond angles and lengths 3—14323
- KCN, matrix-isolated, i.r. spectra, isotope shift meas. 3—38294
- $K_2[Ru(NO)Cl_5]$, and cryst. struct. 3—24071
- LiCN, electronic struct., polytopic bond study 3—29594
- LiCl, Born-Oppenheimer approx., equilib. bond length calc. 3—33085
- MgF_2, ab initio estimate of correlation energy, determ. of equilibrium geometry 3—4403
- MgF_2, nonempirical LCAO MO SCF studies, bonding trends 3—20096
- Mo complex, $K_4(CN)_8Mo.2H_2O$, neutron diffr. study 3—14780
- ND_4Br, solid orientationally disordered structures, analysis 3—38546
- NH_2 radical, bond lengths and angles, ab initio calcs. 3—29605
- NSCl, mol. struct. and vibr., electron diffr. study 3—26617
- NaCN, matrix-isolated, i.r. spectra, isotope shift meas. 3—38294
- Na_3P_{11}, phosphide with isolated P_{11}^{3-} groups *(German)* 3—36286
- Ni(II) complex, bis(1-methyl-3-orthochlorophenyl triazene 1-oxide) nickel (II) 3—17777
- Ni(II) complex, bis(2,4-dithiobiuret)nickel(II).glycol 3—14777
- Pb^{2+} oxides, fluorides and oxide fluorides, calcs. of bond lengths and angles 3—33073
- $Pd(CO)_4$, i.r. and Raman spectroscopic data 3—7192
- Pd(II) chloro- and isocyanato-complexes, i.r. spectra, determ. of stretching frequencies, internal vibs. 3—36020
- $Pt(CO)_4$, i.r. and Raman spectroscopic data 3—7192
- Pt(II) chloro- and isocyanato-complexes, i.r. spectra, determ. of stretching frequencies, internal vibs. 3—36020
- $RbH_3(SeO_3)_2$, crystal structure, hydrogen bond lengths 3—33496
- Re(I) complex, μ-[tetraphenylporphyrin]-bis-[tricarbonyl-rhenium(I)] 3—14779
- Ru complex, $(\varphi_3P)_2[(CF_3)_2C_2S_2]$-RuCO, orange and violet isomers 3—14772
- S_{18}, molecular structure determ. 3—36283
- $S_1H_nF_{3-n}$, hyperfine coupling and equilib. geometries, INDO study 3—29606
- SO_3, high resolution i.r. spectrum, mol. struct. 3—14374
- $SPHF_2$, microwave and i.r. spectra and struct. 3—29670
- Sb^{3+} oxides, fluorides and oxide fluorides, calcs. of bond lengths and angles 3—33073
- Si_2Cl_6, molecular struct. determ. *(German)* 3—35989
- Te^{4+} oxides, fluorides and oxide fluorides, calcs. of bond lengths and angles 3—33073
- Tl_3BO_3, stereochem. role of Tl I doublet in cryst. struct. *(French)* 3—20721
- Tl_2MoO_4, gas phase electron-diffr. study 3—29557
- $U(BH_4)_4$ i.r. spectrum, nature of hydrogen bridging in vapour phase, relation to solid phase 3—1228
- $UO_{2(3)}$ matrix-isolated vapour species, i.r. spectra, bond angle 3—29655
- Zn(II) complex, bis(dithiobenzoato)zinc(II), four-membered chelate ring obs. 3—17771

inorganic molecule electronic structure
- covalent mols., distorted-atoms-in molecules model, spatial electronic wavefunctions 3—38265
- diatomic mols., Born-Oppenheimer approx., equilib. bond length calc. 3—33085
- diatomic mols., Born-Oppenheimer approx. breakdown, dipoles moment and nucl. quadrupole coupling const. effect 3—29596
- equations-of-motion method of calc. excited states 3—20092
- group IV cpds., MX_4 type, core binding energies for analogous gaseous cpds. of C, Ge and Si 3—14340
- hydrazine, photoelectron spectra, CNDO/2 and MINDO/2 analysis 3—35993
- I_2 mol., Lamb-dip spectroscopy, hyperfine struct. in electronic spectrum 3—11276
- isocyanates, MO SCF calcs. of energies charge densities and bond indices 3—4401
- metal hydrides, floating type wave functions in molecular pseudopotential calculations 3—38260
- methylphosphine borane, comparison of CNDO/2 calcs. and microwave data 3—7117
- paramagnetic complexes, semiempirical scheme for calculating spin density in organic addends 3—23535
- transition metal complex, effective charge number and config., game-theoretical model 3—35994
- transition metal complex, ML_4, tetragonally distorted tetrahedral, ligand field induced splitting 3—33080
- transition metal coordination compounds, donor-acceptor props. of ligands, X-ray photoelectron spectroscopy 3—17415
- triatomic, from ang. distrib. of photoelectron spectra 3—23545
- $[H_2O...Cl]^-$ complex, SCF LCAO MO calcs. of hydrogen bond 3—29587
- AlH_3 mols., electronic struct. calc. *(Russian)* 3—11213
- AlO, $F^2\Sigma^+-A^2\Pi_i$ electronic transition 3—26658
- B compounds, BCN, BNC, BCC, CBC, BBC, BCB, ab initio electronic struct. calcs., optimum bond lengths determ. 3—20093
- BF_3, pot. barrier to electron passage through electronegative atoms 3—1196

inorganic molecule electronic structure continued
  BF_2OH, CNDO/2 and INDO calcs. of total charges, Wiberg populations of effective chemical bonds and total dipolar moment components *(French)* 3−7127
  $BH_3.NH_3$ and perfluoro derivatives, CNDO/2 calc. *(French)* 3−17403
  $B_3N_3H_6$, boronimide and dimeric boronimide, electronic structures and energies, ab initio calculations 3−7142
  BX_3, X=H, F, Cl, CNDO/2 calcs. of electronic properties, comparison with BX_4^-, valence force field modification 3−7130
  BX_4^-, X=H, F, Cl, CNDO/calcs. of electronic properties, comparison with BX_3, valence force field modification 3−7130
  BaF, molecular constants for green band system 3−33117
  BeH^+, distorted-atoms-in molecules model, spatial electronic wavefunctions 3−38265
  BrF, photoelectron spectra study 3−1161
  BrF_3, photoelectron spectra study 3−1161
  CO, excited state computation using equations-of-motion method 3−20092
  CO, fine struct. and perturbation analysis of $a^3\pi$ state 3−14368
  CO, generalized oscillator strengths for lowest $\Pi \leftarrow \Sigma$ transitions 3−4407
  CO, perturbations in $a^3\pi$ and $A'\pi$ states 3−14342
  CO, potential energy curves for excited states, equations of motion method 3−33084
  $CO(d^3\Delta)_{v=5}$, spin multiplet relax. and radiative lifetimes 3−20177
  ClF, photoelectron spectra study 3−1161
  ClF_3, photoelectron spectra study 3−1161
  CrO_4^{2-} in alkali halides, vibr. and electronic spectra 3−27091
  CrO_8^{3-} ion, nature of metal-ligand bonding in K_3CrO^8 *(French)*. 3−7715
  Cr_2O_3, $K_2Cr_2O_7$, KCr_3O_8 spectra, X-ray photoelectron, electronic structure relations 3−23548
  $E + D_2$ reaction, dynamics, on a semiempirical valence-bond potential energy surface, Monte Carlo trajectories 3−25052
  F_2, loge localization analysis 3−11210
  $F^{12}C^{15}N$, mol. Zeeman effect obs. 3−33135
  Fe complex, Baudisch complex, chem. characteriz. 3−26631
  FeN_2, vibr. spectra and electronic struct. calc. 3−29673
  p-H_2, 1s 4p $^3\Pi_u$, v=0, N=1 level, non-zero mag. field crossing 3−17453
  H_2, electronic particle-hole propagator calc. using self-consistent polarization propagator method 3−7112
  H_2, ground-state wavefunction by basis sets in quantum mechanical calculations 3−1160
  H_2, Heitler-London approx. and variable orbital exponents 3−7111
  H_2, intermediate coupling between Hund's cases for 3d Rydberg states 3−11205
  H_2, static polarizability tensor calc. in screened valence bond approx. 3−38266
  H_2 distorted-atoms-in molecules model, spatial electronic wavefunctions 3−38265
  H_2^+, energy level calc. 3−36000
  H_2^+, moment functions calc. from dipole oscillator strengths 3−4408
  H_2^+, variational approxs. to trial wavefunctions 3−26636
  HCNO, photoelectron spectrum, CNDO/2 calcs. 3−33089
  HF, model pseudopot. calcs. of valence electron props. 3−20091
  HF magnetic shielding of ^1H and ^{19}F, linked cluster many body perturbation theory 3−11214
  HF_2^-, charge distribution and strength of hydrogen bond 3−1593
  H_2O, electronic states linearity barriers, curvilinear and rectilinear models, comparison 3−23528
  H_2O, geometry, energy terms depend. using floating spherical Gaussian orbital model 3−29568
  H_2O, model pseudopot. calcs. of valence electron props. 3−20091
  HOF, photoelectron spectrum, valence region orbitals analysis 3−36047
  H_2S, electronic states linearity barriers, curvilinear and rectilinear models, comparison 3−23528
  Hg halides, spectroscopic studies of potential energy consts., root-mean-square amplitudes and coriolis coupling consts. 3−7182
  I_2 B-state lifetimes, magnetic field dependence 3−7218
  $KClO_3$, Cl X-ray spectra for ClO_3^- struct. determ. 3−29598
  $KClO_4$, Cl X-ray spectra for ClO_4^- struct. determ. 3−29598
  KrF_2, HeII photoelectron spectra, band assignments 3−23542
  Li_2, loge localization analysis 3−11210
  LiCN, polytopic bond study 3−29594
  LiH, distorted-atoms-in molecules model, spatial electronic wavefunctions 3−38265
  LiH, electronic transition moments for Σ and Π states 3−1159
  LiH, electronic wavefunctions for Σ and π states 3−1158
  LiH, Heitler-London approx. and variable orbital exponents 3−7111
  Li_3NbO_4, electronic structure and Nb-Nb band study using INDO type method 3−20084
  Mn complexes, $Mn(CO)_5X$, $(X=H,CH_3,Cl,CN)$, ab initio calcs. 3−29603
  MnH, $^7\Sigma^+$ and $^7\Pi$ electronic states, SCF calcs. 3−26634
  Mn(II) complex, ii) 3−7104
  $Mo(CN)_8^{4-}$ $Mo(CN)_8^{3-}$ electronic structure in terms of SCCC MO method 3−7146
  N_2, electron impact excitation, valence states reson. phenomena 3−38312
  N_2, electron impact excitation, Rydberg states 3−38313
  N_2, excited state computation using equations-of-motion method 3−20092
  N_2, generalized oscillator strengths for lowest $\Pi \leftarrow \Sigma$ transitions 3−4407
  N_2, potential energy curves for excited states, equations of motion method 3−33084
  N_2^- resonance, stabilization calculations 3−23623
  N_2^+, Meinel band system transition probabilities 3−20108
  N_2^+ rotational analysis of first 6 bands 3−20114
  $N_2^+(A^2\Pi_u)$, Meinel band radiative lifetimes meas. 3−20107
  NO^-, resonant states, Rydberg orbitals 3−35996
  NaCl, valence-electron-only calcs., pseudopot. method 3−38261
  Ni complex, 1, 5-diphenylformazan nickel(II) in soln., calc. of u.v. and visible absorption spectra 3−20136
  O_2, ground state fine struct. const. determ. 3−4406

inorganic molecule electronic structure continued
  O_2-N_2 solid binary mixtures, light absorption by O_2, simultaneous electron transitions *(Russian)* 3−34382
  O_2^- excited state calc. with CI variational trial functions 3−11215
  OD, hyperfine Λ-doubling transitions of lower-J states, radioastronomical appl. 3−36037
  OH, isotropic hyperfine interaction in $^2\Pi$ ground state with linked cluster many-body perturbation theory 3−11214
  OH, potential energy curves, configuration-interaction calc. of electronic energies 3−29583
  OH^+ spectra, $A^3\Pi - b^1\Sigma^+$ perturbation, determ. of information on unobserved perturbing state and calc. of Λ doubling parameters 3−11244
  Os complexes, $[OsN_2(NH_3)_5]^{2+}$, vibr. spectra and electronic struct. calc. 3−29673
  PbO, nonrelativistic SCF calcs., spectroscopic consts. prediction 3−38263
  Ru complexes, $[RuN_2(NH_3)_5]^{2+}$, vibr. spectra and electronic struct. calc. 3−29673
  Ru_xN_2 (x=1, 2), vibr. spectra and electronic struct. calc. 3−29673
  S_2^- and S_3^- trapped in KI, stress-induced linear dichroism obs. 3−30848
  S_2Cl π-radical, obs. in e.s.r. spectrum 3−4461
  SF_6, SCF MO LCAO calcs. of optical absorpt. and X-ray emission 3−1151
  SO_2, electronic states linearity barriers, curvilinear and rectilinear models, comparison 3−23528
  Se_2, level shifts on discrete levels of $BO^+{}_u$ state by interaction with repulsive state 3−4413
  SeO, new electronic transition 3−33116
  Se_2^- trapped in KI, stress-induced linear dichroism obs. 3−30848
  SiH_3, SiH_3^+ and SiH_3^- radicals, CI calcs. of low lying electronic states 3−26630
  TiN_2Ti, vibr. spectra and electronic struct. calc. 3−29673
  UO_4^{2-}, impurity in scheelite type crystals, energy structure and spectroscopic characteristics *(Russian)* 3−8619
  XeF_6, MS-Xα calc. of energy level struct. 3−4409
  $XeOF_4$, photoelectron spectra, electronic struct. 3−33088
input-output media (computers) *see computer peripheral equipment*
insolubility *see solubility*
inspection
  see also quality control; reliability; testing
  irradiated nuclear fuel elements, fission product analysis, remote controlled techniques 3−17306
  nuclear reactor pressure sections, acoustic holography applications, evaluation 3−6447
  nuclear reactor pressure vessels, in-service inspection, acoustic emission applications 3−5791
  nuclear reactor pressure vessels, in-service inspection, u.s. techniques, equipment 3−5793
  nuclear reactor pressure vessels, nondestructive testing technique 3−5790
  nuclear reactor pressure vessels, remote inspection, u.s. techniques 3−5792
  physicochemical instruments *(Russian)* 3−6100
  PWR pressure vessels, in-service inspection technique 3−5789
  spot welded joints, non-destructive inspection by thermography *(Russian)* 3−9857
instability *see stability*
installation
  see also commissioning
  monitors for river water quality measurement 3−22192
  nuclear fuel reprocessing plants, decommissioning of Eurochemic installations *(French)* 3−38185
instrumentation
  see also aerospace instrumentation; digital instrumentation; digital readout; nuclear instrumentation; signal generators; signal sources
  computer assisted instruction in a chemical instrumentation course 3−9791
  Coulter orifice fields, pulse shapes from traversing particles 3−10105
  curriculum, interdisciplinary master's degree 3−28429
  fast track following system, PDP-15 directed interactive control 3−25965
  flue gas control system, alkali scrubbing facility 3−25619
  graduate program, University of Arkansas 3−9824
  harmonic force measuring equipment for materials testing applications *(Hungarian)* 3−21763
  high pressure liquid separator 3−6162
  industrial process, metrication effects 3−25644
  Instrument Society of America, 27th conference, New York, U.S.A., Oct. (1972) 3−22249
  laboratory with instruments for rent to small companies in Norway *(Norwegian)* 3−5740
  large orbital space stations, large telescopes development *(German)* 3−35217
  magnetic flyer plate for materials testing 3−25041
  measuring equipment supervision procedure *(Russian)* 3−5743
  physicochemical meas., organising inspection *(Russian)* 3−6100
  science, suggestion of formal teaching 3−9821
  science, suggestion of formal teaching as independent subject 3−9823
  science, teaching of art 3−9822
  scientific, minicomputer applic. 3−16380
  technical level determination *(Russian)* 3−5741
  turbulent liquid flow meas. 3−37778
  unfolding and simulating meas. distrib., interactive graphical computing 3−10140
  X-ray macroprobe, specimen distance effect, automatic traversing device 3−28748
  X-ray spectrometer/computer combination for wide conc. range alloy analysis 3−28747
instruments
  see also individual types of instruments, e.g. astronomical instruments, bridge instruments, optical instruments
  calibration and standards 3−13192
  electromedical, faults due to poor design and maintenance, rectification, international standards 3−10141
  humidity absorption, by instrument materials 3−28459

instruments continued
  inertial plasma instruments with inplatrons for meas. moving parameters *(Russian)* 3−9835
  measuring instruments, catalogue 3−5753
  s.h.f. power meas., USSR standards and instruments *(Russian)* 3−16379
  standard measurement, force and pressure, France, Newton and Pascal *(French)* 3−16378
  standards economic effectiveness 3−37580
insulated gate field effect transistors *see field effect transistors*
insulating coatings
  see also coating techniques; varnish
  oceanographic electrical equipment in water, insulation 3−3268
  polymer, test stand for studying long-term strength 3−18760
  SiO_2 pyrolytic film on semiconductor substrate, structure defects, transmission electron microscopy *(Russian)* 3−27197
insulating materials
  see also asbestos; ceramics; composite insulating materials; dielectric materials; glass; mica; organic insulating materials; thermal insulating materials
  American Vacuum Society, symposium, Chicago, USA (1972) 3−37608
  breakdown mechanism *(French)* 3−30759
  characterisation by thermal analysis techniques 3−39076
  electrical detectors, method 3−24644
  electrochemical conference, Chicago, USA (1973) 3−38760
  epitaxial deposition of Si on insulating substrate, combination of two growth methods 3−2655
  insulator, with trapped space charge, photocurrents transit times and pulse shapes 3−18188
  ion implantation, charge-removal studies using ion-induced characteristic X-rays 3−11669
  i.r. and Raman spectra analysis 3−39140
  isothermal currents, and trap parameter determ., material with arbitrary trap distrib. 3−36620
  liquids, elec. breakdown, photographic techniques 3−13342
  liquids, interfacial parametric electrohydrodynamics 3−7412
  microscopic dielectric constant including self-polarisation correction 3−27466
  for nuclear radiation environment 3−11105
  paramagnetic, single particle density of states in mag. field 3−15113
  partial discharges recording method 3−32112
  photoemission-determined valence band gaps and ionicity parameters, relation 3−24380
  physical properties, at cryotemperatures 3−9996
  roller electrification of belts 3−647
  Saturn 5, in nuclear radiation environment 3−11104
  sheet, permittivity meas. at microwave freq. 3−22232
  thermally stimulated currents, material with arbitrary trap distrib. 3−36621
  Al_2O_3, AlN, SiO_2 semicond.-insulator boundaries in m.i.s. structures, surface charge, hysteresis curve, frequency response, advantages of aluminium compounds *(German)* 3−15261
  Al_2O_3, h.v. insulator for vacuum apparatus, surface charging 3−140
  Al_2O_3, time decay of d.c., modelling using nonlinear regression analysis, comparison with experiment 3−8509
  MgO, time decay of d.c., modelling using nonlinear regression analysis, comparison with experiment 3−8509
  Si cpds., charging-up phenomena in Auger electron spectroscopy 3−30917
  SiO_2, time decay of d.c., modelling using nonlinear regression analysis, comparison with experiment 3−8509
insulating materials, thermal *see thermal insulating materials*
insulating oils
  binary mixture, permittivity and loss factor, expt. confirmation of theory 3−2484
  chlorobiphenyls with dissolved water and air, space charge effects 3−18415
  dielectric relax. at low temps., glass transition and supercooling 3−18408
insulating thin films
  see also insulating coatings
  Auger electron spectroscopy for anal. 3−1946
  barium stearate 'built up' films, d.c. destructive breakdown field, temp. depend. 3−5161
  barium stearate multilayer films, breakdown field temp. depend. 3−27469
  borosilicate, alumosilicate glasses, electrical inhomogeneity in m.i.m. structures, residual polarisation measurement *(Russian)* 3−11960
  borosilicate glass, Vickers microhardness characteriz. 3−39377
  chalcogenide glass, softening point, thickness dependence 3−8064
  characterization by nuclear microanalysis 3−37754
  dielectric, photocurrent pulse shape, inhomogeneous light absorption *(Russian)* 3−27286
  dielectric, thermally assisted tunnelling 3−8278
  disordered, Kronig-Penney-type calculations for electron tunnelling 3−8254
  electronic transport processes 3−18237
  ESCA studies of dielectric films 3−39245
  ferroelectric, prep., props. and device appl., review 3−8543
  glasses on Si substrates, discontinuities detection by NaOH anisotropic etch 3−11968
  graphite thin crystal, residual resist. depend. on crystal thickness 3−30469
  Langmuir thin molecular films, dielec. breakdown thickness depend. 3−39095
  localized electronic breakdown, review 3−5159
  non-crystalline, transport phenomena 3−2093
  organic dielectric films, charge transport 3−38834
  organic monolayer, in m.i.s. struct., CV characts. 3−5059
  organo-silicon polymer, deposition by decomp. of $Si(OC_2H_5)_4$ in r.f. glow discharge 3−21535
  oxide, plasma anodisation, role of plasma negative ions 3−1905
  oxide films on Zr, electrolytic rectification 3−2175
  phosphosilicate glass, passivating in m.o.s. struct., surface state charge, influence of deposition conditions 3−8266
  poly-N-vinylcarbazole complexed with trinitrofluorenone, bulk recomb. of charge carriers 3−30513
insulating thin films continued
  polyamide 66, v.l.f. dielectric relaxation and conductivity meas. at room temp. 3−18413
  polyethylene, d.c. conductivity measurements, 1×10^7 to 3×10^7 Vm^{-1}, model, hexane treatment 3−36614
  polymer, d.c. glow discharge polymerisation and electronic conduction mechanisms *(German)* 3−15282
  polymer, in m.i.s. struct., refractive index and dielectric const. 3−5060
  polymer films, initial behaviour of excess electrons 3−39093
  polymeric, semiconductor device passivation, sputter coating 3−24809
  polymers, influence of preloading on strength in water *(Russian)* 3−12449
  polytetrafluoroethylene, r.f. sputtering system and film characts. *(Russian)* 3−30941
  r.f. sputtered dielectric film, in m.i.s. struct., interface props., CV and Cole-Cole plot obs. 3−8274
  rhodamine 6G-doped polyurethane, distributed-feedback laser, fabrication by ion milling 3−734
  for solid state electronics, chemical, mech. and electrical props. *(German)* 3−15281
  superimposed dielectric layers, effect on elec. cond. of metal film 3−30552
  tetracene, structure of vacuum deposited films 3−15103
  thickness and refractive index meas., nondestructive optical method 3−13286
  thickness measurement, from optical refl. relations 3−15647
  triglycine sulphate, ferroelectric properties 3−39107
  trimethylethyltin-based thin polymer films, electrical conductivity *(Russian)* 3−8187
  X-ray induced photoconductivity 3−18184
  AL_2O_3, alumina, preparation and structure *(German)* 3−15608
  Al-CeF_3-Al thin film capacitor system, stimulated dielectric relaxation currents 3−8277
  Al_2O_3, amorphous, electrical inhomogeneity in m.i.m. structures, residual polarisation measurement *(Russian)* 3−11960
  Al_2O_3, anodic, on Al, breakdown and repair, electron microscope obs. 3−8060
  Al_2O_3, anodic films, branching colony pore structure, electron microscope examination 3−1948
  Al_2O_3, anodised, comparison of step and ramp voltage breakdown 3−8518
  Al_2O_3, electroforming and dielec. breakdown *(Russian)* 3−30530
  Al_2O_3, i.r. transmission spectra, boundary interaction with substrate *(Russian)* 3−15102
  Al_2O_3, in m.i.m. capacitor, inhomogeneities, visualization by liq. cryst. layers 3−15284
  Al_2O_3, made from evaporated sapphire, behaviour in m.i.s. and m.i.m. structs. 3−27317
  Al_2O_3, on Al, thickness meas. 3−36500
  Al_2O_3, on Si, electronic charge trapping, photoinjection-photodepopulation and C-V studies 3−5066
  Al_2O_3, plasma-deposited coating, effective thermal conducting, struct. and temp. effects 3−24359
  Al_2O_3, r.f. sputtered, surface charge density rel. to H_2 annealing 3−2187
  Al_2O_3 anodic film growth on Si 3−39246
  Al_2O_3 on Si, tunnel and epitaxial layer prep. and charact. *(German)* 3−8056
  Al_2O_3 pyrolytic layer, in m.o.s. capacitor, trap struct. 3−18220
  As_2O_3-SiO_2 glass diffusion sources, effect of heat-treatment on comp. 3−20963
  Au-SiO_x, cermet film, structure and elec. props. with heat treatment 3−15201
  $BaTiO_3$, polycryst. film with ferroelec. and antiferroelec. props., deposition by electrophoresis 3−39220
  BeO, cryst. or amorphous, prep. by reactive evaporation of Be *(German)* 3−21534
  Bi_2O_3 high-resistance anodic film formation on Bi 3−8038
  $Bi_4Ti_3O_{12}$ electrooptical quality, epitaxial growth by r.f. sputtering 3−12252
  CaF_2 overlay, surface depletion of InSb film 3−18219
  CaO, r.f. sputtered, pure and Sm- and Tm-doped, X-ray excited fluoresc. 3−27568
  CaO, r.f. sputtering, glow discharge anal. by spectroscopic method 3−5244
  CeF_3, between Al electrodes, isothermal dielec. relax. currents 3−36666
  Dy_2O_3-CdSe film struct., elec. props. 3−27312
  Ge, combination layers of SiO_2-Si_3N_4 *(German)* 3−30957
  GeO_2 thin vitreous surface layer, struct. study by i.r. reflection spectra *(Russian)* 3−36467
  HfSi on Si, growth kinetics and composition 3−20958
  MgF_2, adhesion, scratch test apparatus obs. *(Japanese)* 3−20959
  MgF_2, influence of prep. and measurement conditions on transport props. *(French)* 3−2094
  MgF_2 Malter emission, primary current magnitude effects *(Russian)* 3−12204
  MgO high-porosity layer, secondary-electron conductivity 3−15206
  Na_3AlF_6, adhesion on glass substrates, meas. by direct pull method *(Russian)* 3−31238
  NaCl, deposited onto leading edge on fused SiO_2, struct. 3−20961
  $PbTiO_3$, polycryst. film with ferroelec. and antiferroelec. props., deposition by electrophoresis 3−39220
  $PbZrO_3$, polycryst. film with ferroelec. and antiferroelec. props., deposition by electrophoresis 3−39220
  Si_3N_4, 50-100 Å, conduction mechanism 3−38910
  Si_3N_4, identification of electronic cond. mechanisms *(German)* 3−15199
  Si_3N_4, local conductivity, scanning low energy electron beam obs. *(German)* 3−15283
  Si_3N_4, passivating layer, low temp. prep. *(German)* 3−15609
  Si_3N_4, reactively sputtered, dielectric breakdown 3−34295
  Si_3N_4 layer, in m.n.o.s. struct., cond. mechanism 3−27316
  Si_3N_4 thickness meas. in Ge-SiO_2-Si_3N_4 system using ellipsometric method 3−13230
  SiO, Al and/or Ag electrodes, conductivity, field and temp. depend., switching, memory effect 3−21124
  SiO, in m.i.m. struct., elec. breakdown *(Russian)* 3−15280

insulating thin films continued
SiO, vacuum deposition, props. of evaporated material used in prep. 3−15624
SiO on W, nucleation and growth exam. using field emission microscope 3−15107
SiO overlay, surface depletion of InSb film 3−18219
SiO_2, anodically grown, elec. props., m.o.s. capacitor and m.o.s.t. studies 3−24524
SiO_2, charge injection from reverse-biased junctions 3−34006
SiO_2, deposited on n-Si in r.f. glow discharge, diffusion of B, 1100-1200°C 3−27144
SiO_2, deposition by decomp. of $Si(OC_2H_5)_4$ in r.f. glow discharge 3−21535
SiO_2, electrically stable, growth on Si using Cl_2 and HCl 3−39287
SiO_2, formation on Si by thermal oxidation in dry O_2 at 400°C 3−11823
SiO_2, growth from vapour on n-GaAs substrates 3−24785
SiO_2, growth in plasma microwave discharge 3−15625
SiO_2, growth on Si substrate by thermal decomposition of tetraethoxisilane, flow-through process *(Czech)* 3−21543
SiO_2, HCl- or Cl_2-grown, Auger anal. of Cl 3−38597
SiO_2, high elec. fields produced by corona charging, surface pot. meas. rel. to dielec. breakdown 3−24654
SiO_2, in m.i.s. struct., tunnelling mechanisms *(German)* 3−15258
SiO_2, local conductivity, scanning low energy electron beam obs. *(German)* 3−15283
SiO_2, on Si, effect on Ga diffusion 3−18212
SiO_2, passivation for m.o.s. struct., growth in presence of HCl 3−5061
SiO_2, r.f. sputtered, cone shaped defects 3−18045
SiO_2, r.f. sputtered, Na^+ motion, meas. using thermally stimulated ionic currents 3−33688
SiO_2, silica, film growth, reaction kinetics for silane oxidation 3−24786
SiO_2, silica, ion movement in applied field, diffusion eqn. calc. *(German)* 3−15037
SiO_2, steam-grown, devitrification 3−8752
SiO_2 films, γ-ray radiation sensitivity dependence on impurities 3−18222
SiO_2 films, ion neutralisation processes, impurity migration effects 3−34450
SiO_2 films on Si, phosphosilicate glass passivated, ion bombardment effects 3−39288
SiO_2 layer, in m.n.o.s. struct., cond. mechanism 3−27316
SiO_2 thermally grown on Si, electron trapping levels 3−8262
SiO_2 thickness meas. in Ge-SiO_2-Si_3N_4 system using ellipsometric method 3−13230
SiO_2 transparent, silicon substrates, thickness measurement, optical method, instrument and procedure 3−3790
SiO_2/electrolyte interface, mobile ion transfer from contaminating aqueous solutions 3−39241
SiO_2-Au multilayer structure, characterization as artificial semicond. 3−38790
SiO_2-Si_3N_4 combination layers on Ge *(German)* 3−30957
SiO_n, degree of oxidation, determination using electron microprobe analysis *(German)* 3−8066
SiO_x, stoichiometry, impurity content, correlation with electrical properties, examination using Rutherford scattering of MeV α-particles 3−7788
Si_xO_y-CdSe film struct., elec. props. 3−27312
SiON, from NO-NH_3-SiH_4 reaction, critical assessment 3−39244
Ta_2O_5, anodic, defect photocond. 3−38865
Ta_2O_5, anodic, mechanical props. rel. to microstruct. and electrolytic breakdown, bulge test obs. 3−1684
Ta_2O_5, anodic, oxidation state after heat treatment 3−8039
Ta_2O_5 thermal currents, energy peaks, dipolar polarisation model, dipole moments and density *(French)* 3−38911
TiO, vaccum deposition, props. of evaporated material used in prep. 3−15624
TiO_2 temperature dependence of dark-decay properties *(Japanese)* 3−18171
Y_2O_3, electron beam evaporated film, structure, conduction, permittivity and internal photoemission 3−24320

insulation
see also cable insulation; electric breakdown; insulating materials; insulators
airborne sound insulation between rooms 3−5732
vacuum insulated cryocable installations, thermal and electrical insulation 3−5818
SF_6 gas, electric field calc. of hemispherically capped rod and plane electrodes 3−13672

insulation testing
dielectric loss analyser 3−24644
i.r. spectrography applications, measurement and sampling techniques *(French)* 3−13511
organic insulators, degradation under electric and thermal stresses, gas chromatography applications *(French)* 3−13510
polyethylene, breakdown strength determ. method for small test pieces *(German)* 3−15806

insulator-metal boundaries *see metal-insulator boundaries*

insulator-semiconductor boundaries *see semiconductor-insulator boundaries*

insulators
i.e. insulating devices. For materials see insulating materials
see also insulation
carrier concentrations and electric fields for small p.d. applied to long specimen *(French)* 3−33895
h.v., fault currents due to arc, obs. *(Hungarian)* 3−30025
h.v., for vacuum apparatus, surface charging 3−140
surface charging, highvoltage in vacuum 3−21131

integral equations
see also integro-differential equations
3-dimensional quasistationary e.m. field calculation in homogeneous conducting media *(Russian)* 3−32482
Abel, inversion 3−36209
Abel's eqn., eval. of numerical methods of soln. 3−13543
analog method for diffusion coeffs. determ. 3−22761
Ball-Zachariasen eqn., analyticity of soln. Riemann surface, numerical determ. 3−16593

integral equations continued
bending of rectangular plates with stepped variation of thickness, analysis by Bubnov-Galerkin method *(Russian)* 3−28877
cantilever beams of variable cross-section, non-linear bending, numerical soln. 3−22612
Cauchy problem soln. for conoid *(French)* 3−19392
coupled, reduction of inverse problem for hyperbolic dispersive partial differential eqn. uniqueness 3−28831
coupled Fredholm type in calc. of emergent distribs. for anisotropic slab albedo problem 3−22757
diffraction of plane shear elastic wave by circular rigid disc and penny shaped crack 3−3990
dynamical theory of electron diffraction within a distribution formalism 3−33432
dynamo integrals, Adams and Elsasser, props. and evaluation 3−12665
eddy currents calculation in axially symmetric a.c. current carrying conductors, by computer *(Russian)* 3−32485
eddy currents distribution in thin plates and conducting spherical shells *(Russian)* 3−32473
edge crack, normal to edge of strip, calc. of stress distrib., Fredholm integral eqn. 3−13571
elastic disc edge crack, stress intensity determ. by Mellin transform of dual eqns. 3−13569
elastic layer/half-space receding contact problems 3−22645
elastic problem with boundary conditions on three-dimens. wedge *(Russian)* 3−3961
elasticity problems, plane orthotropic, soln. by integral method 3−6232
elastoplastic deformation of thick-walled cylinder, non-linear integral eqn. for circular strain hardened zone *(Russian)* 3−28898
e.m. induction in infinite plane sheet with circular hole, dual integral eqn. solns. 3−26187
e.m. scattering, nonuniqueness consequences 3−35663
e.m. wave diffraction, dielectric loaded waveguide 3−669
e.m. wave diffraction from N-bodies 3−13687
e.m. wave scattering from ocean-like surfaces 3−32503
first kind, numerical soln. using a priori information of function *(Russian)* 3−10242
first kind, theory and appl. to physics *(Russian)* 3−3927
Fredholm eqn. for radial crack in point loaded disc, determ. of stress intensity factors 3−19429
Fredholm eqn. for stress intensity factor of edge crack in finite rotating elastic disc 3−19428
Fredholm eqn. systems for elastic equil. of anisotropic bodies 3−16639
functional, and Hamiltonian orderings for quantum mechanics and field theory 3−37863
generalized, for radiative heat transfer 3−13656
Green's functions, integral representations for the Laplace and Helmholtz equations 3−16596
Greuling-Goertzel approx. to neutron collision probability method, analytic soln. 3−19894
hadron fireball chain decay, integral eqns. from thermodynamic model 3−29244
for hadronic correlation functions in multiparticle reactions 3−19718
heat flow disturbed by 2-D crack in elastic strip, dual eqn. method 3−13566
Helmholtz scattering integral rel. to sea surface forward scattering 3−3685
hybrid elements, for plate bending problems analysis 3−517
integrands containing spherical harmonics, evaluation by summing Legendre series 3−11108
Kirchhoff integral equation, for e.m. wave propagation 3−10429
Kirchhoff-Huygen's integral and underwater modulation effects 3−3729
magnetic field problem formulation, dipole and current models 3−29004
magnetic field problem formulation, magnetisation vector approach 3−29005
Mellin-Barnes type for lattice Green's function for cubic lattice 3−35630
molecular structure box model, evaluation procedure *(German)* 3−7121
momentum integral eqns., derivation for boundary layer of particulate gas flow 3−7379
N/D method differential method eqns., conditions for existence of solns. 3−26282
near-sonic turbulent gas motion determ. *(Russian)* 3−4560
noniterative technique for close coupled calcs. of atomic electron scatt. 3−4382
noniterative technique for close coupled calcs. of atomic electron scatt. 3−4383
nonlinear Volterra, hereditary processes in biomechanics, evolution in terms of difference-differential equations 3−35229
nonrelativistic four-body problem in S-approx. for two-particle interaction, spin variables *(Russian)* 3−23227
nuclear power plant containment structures subjected to seismic excitations, vertical soil-structure interaction, numerical soln. 3−19918
oscillations of non-linear systems with distributed parameters, application of method of harmonic balance to determ. integral eqns. *(Russian)* 3−19477
particles with identical masses, integrals for relative motion *(Russian)* 3−500
plastic shells, creep stability, modelling 3−26092
potential flow about arbitrary bodies, approximation to linear equations, and numerical solution 3−33196
prolate spheroidal functions, asymptotic expressions and eigenvalues 3−10238
rydberg-Klein-Rees integrals, eval. method 3−1147
Rydberg-Klein-Rees integrals, fast accurate computation 3−1149
Rydberg-Klein-Rees integrals, numerical eval. 3−1148
Saint-Venant torsion problem elastic-plastic analysis, by hybrid stress model 3−514
Salzburg-Kirkwood eqn., soln., influence of boundary conditions on reduced density matrix 3−22745
singular, for electrostatic induction problems *(Russian)* 3−19546
singular Lippmann-Schwinger eqn., comment on direct-matrix soln. 3−13544

integral equations continued
spinning elastic medium damped by conical shell, use of coupled pair of integral eqns. *(Russian)* 3−16649
static fields calculation in piece-wise-homogeneous anisotropic media *(Russian)* 3−32483
static magnetic field calculations in nonlinear ferromagnetic medium *(Russian)* 3−34050
static magnetic field in ferromagnetic medium, eqn. formulation by variational approach *(Russian)* 3−34049
stochastic, mean-square stability of random solution 3−28824
structural analysis, soln. using analogue computers 3−33421
subharmonic resonance of order 1/2 with asymmetrical restoring force 3−22675
three-body system, numerical solution 3−581
three-particle scattering with three-particle interactions 3−35772
Timoshenko beam finite element convergence 3−564
torsion, of rigid circular plates, on inhomogeneous elastic ground *(German)* 3−522
transfer pots., heat and mass, for infinite cylinders, integral eqn. approach 3−35637
transmission of water waves through small apertures, integral equation formulation 3−7402
transport integral eqn. with anisotropic scatt. as linear system computer calc. of matrix elements 3−19522
two-dimensional convolutions, asymptotic solutions and appl. *(Russian)* 3−3928
two-dimensional Neumann problem, higher order numerical solution 3−20344
unbounded field problems, finite-element solution 3−6296
viscoelastic hollow cylinder enclosed in elastic shell, axisymmetric problem 3−22631
Volterra eqns. for coupled lateral-rotational foundation-soil interaction of building structures, soln. of Lamb problem 3−19439
Weber's hydrodynamical equations rel. to action integral, meteorological problems *(German)* 3−12702

integral transforms *see transforms*

integrated circuit production
see also masks
ceramic dielectrics, laser micromachining 3−8954
deposition techniques, photoengraving processes, review 3−8712
diffusion system, computer control 3−34488
electron beam microfabrication, computer-controlled 3−35513
film circuit, use of sputtered conductors 3−21163
hybrid, high speed laser trimming, installation 3−6528
hybrid IC resistor trimming, industrial laser system design 3−32609
ion implantation, beam technology 3−15648
ion implantation technique, survey *(German)* 3−34487
laser beam interferometry applications *(French)* 3−13319
low power switching circuits, electron beam pattern generation and ion implantation 3−15653
Moire techniques for photolithographic mask alignment in IC prod. 3−188
multilayer metal circuits, Al beveling, etching, anodic oxidation 3−38739
negative electron resist exposure, voltage dependent parameters 3−35505
photo-etching techniques *(French)* 3−15075
polyisoprenes, bicyclic for photoresist 3−15847
selective oxidation, of Si through Si_3N_4 mask 3−39292
soft X-ray replication of scanning electron microscope generated patterns 3−13481
sputtler-etching process, spectroscopic monitor 3−37712
thin polymer films, electron beam exposure profiles 3−14903
$BaSO_4$ substrates, thermal decomposition kinetics 3−2804
Si, high press. steam apparatus for accelerated oxid. 3−39250
Si beam-lead devices, vapour deposition of Pt using c.w. laser energy 3−5264
Si mesas, solid-phase epitaxial growth from Al metallization 3−21542
Si wafer, defect. obs. using X-rays 3−19348
Si wafer, lot size optimisation for quality control 3−21549

integrated circuit testing
inspection, gated optical comparator 3−4133
monolithic, laser scanner for, description 3−799
surface defects, counting and sizing, with rastered Gaussian spot 3−6531

integrated circuits
see also digital integrated circuits; hybrid integrated circuits; large scale integration; linear integrated circuits; masks; monolithic integrated circuits; substrates
deep ocean pressure effects 3−3267
electron and ion beam technolgoy, conference, Houston, Texas (1972) 3−13473
heartrate indicator application 3−25994
laboratory, electronics, introductory with operational amplifier 3−9807
light reflective shutter control apparatus, patent 3−9985
optical *(Japanese)* 3−9921
Al_2O_3, surface grain size estimation by optical scatt., application to microelectronics industry 3−4906
W, low-voltage sputtered film as microelectronic cct. conductor 3−24515

integrated data processing *see data processing*

integrated optics
see also laser beam applications
circuit fabrication by electron beam technique 3−35390
component fabrication technique employing ion beam micromachining 3−28531
general introduction *(German)* 3−16806
glass fibre laser communication systems *(German)* 3−16918
injection laser output beamspread reducing device for coupling to integrated optic elements 3−22914
liquid-phase-epitaxy garnets, production and applic. 3−27610
thin film waveguides, etched grating couplers 3−5866
thin-film optical waveguides, scattering of light by acoustic waves colinear acousto-optic interaction 3−28416
waveguide, thin film, anisotropic and gyrotropic, normal mode anal. 3−19567

integrated optics continued
$BaSiO_3$ film, for use in integrated optics ccts., r.f. sputtering prep. 3−36983
GaAs, waveguide components 3−25728

integrating circuits
analog-digital integrator for soln. of partial differential equations in mathematical physics *(Russian)* 3−13542
current, with digital read-out, student apparatus 3−28452

integration
see also large scale integration
analytical soln. of new integral arising in mathematical physics 3−487
atomic electron scatt. exchange integrals, numerical evaluation using anal. basis set 3−26588
atomic fluorescence spectrometry, dual channel synchronous integration measurement system 3−22534
Bessel functions related to Webers second exponential integral 3−485
double integrals of form $x^i\psi(y)$, $y^i\varphi(x)$, approx. cubic formulae *(Russian)* 3−16603
elastodynamics, numerical integration methods, evaluation 3−22604
electron scatt., analytic evaluation of integrals in variational calcs. suitable for computer solns. 3−19486
finite element analogue of modified Rayleigh-Ritz method for natural vibration problems 3−562
Gibbs-Duhem eqn. integration method 3−36993
Hamilton-Jacobi integration method, extension to non-holonomic systems *(Russian)* 3−16602
integrating meters, construction, rating and performance, Indian Standards 3−22237
invariant generalised measures path integral generalisation *(French)* 3−22582
Legendre fn. infinite integral calc. 3−29007
magneto-elastic oscillations of thin shells and plates, soln. by asymptotic integration *(Russian)* 3−28913
mechanics of continua in Riemannian spaces, intrinsic coordinates and integration of indefinite equations 3−16731
motion of a heavy particle near Earth's surface, integration of differential equation system 3−19404
multidimensional quadrature procedure, adaptive 3−10588
non-exchange type integral evaluation in electron-atom scattering theory, program 3−23496
nonlinear transient heat transfer in semi-infinite solid 3−37911
numerical interconversion for creep compliance and relaxation modulus 3−534
numerical simulation of stress effects on f.c.c. metal crysts. *(French)* 3−38609
ordinary differential eqns. numerical integration, multi-step method 3−10262
plasma emission coefficient calc., influence of random errors *(Russian)* 3−7494
plasma physics integrals involving Chebyshev polynomials, soln. by Olver's algorithm 3−19396
resonance integrals in cosmic ray diffusion theory 3−37271
Schrodinger eqn., coupled one-dimensional, direct numerical integration 3−10338
second order equations with discontinuous coeffs., difference soln. *(Russian)* 3−13539
shell equations for stress distribution in corrugated tube or bellows 3−3955
Slater integral coeffs., program 3−35957
stellar clusters, dynamical evolution 3−3325
time dependent equations in reaction kinetics by analogue computer 3−5378
two centre integrals, evaluation using Lowdin's α functions 3−28940
vision, figure and ground perception, integrative mechanisms 3−3549

integro-differential equations
atmospheric dynamic eqns. discretisation and weather prediction scheme construction using integro-interpolative method *(Russian)* 3−28014
boundary layers, Ekman-Hartmann, nonlinear hydrodynamic and hydromag. spin-up 3−23732
elastic half-space contact problems *(Russian)* 3−523
elastic layer mixed boundary value problem, soln. by invariant imbedding 3−512
electron energy distribution in hollow cathode 3−30038
magnetic field generation by thin closed shells, integral eqn. 3−29008
membrane, nonlinear and viscoelastic, axisymmetric deform. due to spinning 3−22640
nonlinear, for finite deflection of thin viscoelastic beams 3−516
nonlinear, for large deflections of viscoelastic plates, soln. by method of successive approxs. 3−37795
plasma theory, nonlinear dynamical problems, computer solution 3−20662
polymers with excluded volume, Born-Green-Yvon treatment, integro-differential eqns. relating density functions 3−29762
radiative transfer, transformation of eqn. for numerical soln. of steep source gradient problems 3−19521
relaxing waves, generalized solns. in terms of Laplace transforms 3−10307
scattering, multichannel process, noniterative integral-eqn. approach 3−38239
scattering functions, time dependent radiative transfer, spherical shell media, transmission 3−3322
second-order Boltzmann eqn. for neutron transport, determ. from invariant imbedding theory 3−23389

intelligibility, speech *see speech intelligibility*
intensification *see amplification*
intensity measurement
see also acoustic intensity measurement
absolute calibration at 26 Å by branching ratios to the visible 3−16545
absolute quantum efficiencies, techniques and instrumentation, review 3−35533
cortical potential in anesthetized guinea pig, evoked by electrical stimulation of VIIIth nerve 3−3412
solar corona, during Sept. 22 1968 eclipse 3−9476

intensity measurement continued
- u.s., calorimetric det. 3—82
- variable emission recording by method of counting single photons *(Russian)* 3—35681
- V.U.V. calibrated detector 3—22310
- X-ray diffraction, semiconductor detector, technique 3—26950

interacting control systems *see multivariable control systems*

interatomic potentials *see atomic forces*

interface phenomena
- *see also adsorption; crystal surface and interface vibrations; films; interface structure; surface phenomena*
- acoustic wave propagation, in fluid layer bound by two solids 3—30333
- acoustic wave transmission coeff., thermal contact resist. *(French)* 3—38709
- adhesive fracture by interfacial debonding 3—7840
- air-water interface, wave effect and eddy diffusivity, small scale turbulent transfer mechanism 3—27996
- aqueous soln. adjacent to charged nonmetallic interface, fluctuation pot. of ion in diffuse region 3—12556
- binary mixtures of miscible vapours, condensation on cooled vertical plates, interfacial suction at vapour-liquid interface 3—20860
- capillarity-controlled entrainment of a liquid by a thin cylindrical filament moving through an interface 3—30334
- contact between rough and flat surface considerations 3—14929
- contact of random surfaces, Whitehouse and Archard theory, Greenwood and Williamson theory 3—18017
- contact real area between rough and flat surface 3—14927
- convection and interface movement effects on heat and mass transfer in crystn. process *(French)* 3—2840
- corrosion at glue metal interfaces 3—8042
- cracks at interface of elastic half-spaces, opening displacement rel. to screw dislocation distrib. 3—24199
- critical angle of acoustic reflection at water-quartz interface, general definition 3—4917
- critical angle of acoustic reflection at water-quartz interface, experimental determination 3—4918
- deformation of contacting rough surfaces, initial contact position estimation 3—5302
- deformation of contacting rough surfaces, new contact theory 3—5303
- deformation of contacting rough surfaces, topography 3—5301
- dislocation pile ups against plane interfaces, anal. 3—17925
- double diffusive convection, transport and profile meas. of diffusive interface 3—20305
- E-glass, adsorpt. of water vapour, thermodynamic nature of adsorbate adsorbent interface 3—8016
- eddies and turbulence 3—20316
- electrode-solution interface, elec. double layer, review 3—31272
- electron kinetic energy flow through an interface 3—28394
- e.m. surface waves along lossless structs., inhomogeneous waves at planar interfaces 3—16686
- energy between crystal and solution by inverted bubble method, morphology prediction 3—14707
- epitaxial growth problem, dislocations at film/substrate interface 3—33747
- epoxy adhesive, glass transition temp. relation to adhesive strength 3—5353
- external field influence on the interface position of two phases near the critical point *(Russian)* 3—26184
- fluid-solid interactions, eqns. for statistical mechanical distrib. functions 3—4024
- gas/liquid interfaces in a porous medium, thermodynamics, condensation/evaporation processes, viscous flow 3—26847
- generalised van der Waals density gradient theory for surface tension and interfacial width 3—27918
- glass/metal, hardness detection of surface stress 3—39377
- graphite interacting with Ti and Zr, kinetics for carbide layer form. and growth *(Russian)* 3—15826
- Great lakes, thermally and wind induced currents 3—31358
- III-V different semicond. layers forming superlattice, light absorpt. rel. to complex band structure 3—15519
- ionic double layer study and adsorption phenomena at electrodes 3—12530
- Kapitza resist. of thin metallic films *(French)* 3—4998
- Kapitza resistance, influence of thin surface-dislocation layer 3—7986
- liquid floating zones in simulated zero gravity 3—11360
- liquid interfaces, critical exponent probing by u.s. refl. meas. 3—5785
- liquid-solid interface, acoustic frequency of least reflection, interpretation at Rayleigh angle 3—4915
- liquids, sharply separated, resistance coefficient at interface *(Japanese)* 3—23784
- metal melts on graphite and glasslike carbon substrates, wettability and catalytic graphitisation 3—11796
- metal-metal oxide system, binary and ternary, eutectic solidification 3—11561
- misfit dislocations during interdiffusion, interaction forces 3—36472
- molecular crysts., polymorphic transition, simple interface model 3—27121
- osseous attachment of non-porous metals by composite bonding 3—2794
- oxides of Al and Ta, growth of dielectric layers *(German)* 3—20951
- planar turbulence free interfacial diffusion layer, condensation nuclei deposition 3—17550
- plane liquid-solid interface, reflected and reradiated u.s. waves 3—4919
- plasma guide, azimuthal electron density variation, backward surface wave propag. 3—17564
- plasma/vacuum, e.m. refl., boundary problem 3—23816
- polydimethylsiloxane monolayers, thermodynamic properties, surface viscosity, at water-air interface 3—39406
- Rayleigh wave propagation at piezoelectric insulator-semiconductor boundary 3—4910
- rubber-glass contact, elec. double-layer force meas. between liquid immersed contact surfaces 3—6020
- seawater vaporization, molecular aspects of aqueous interfacial structures 3—12684

interface phenomena continued
- semiconductor-electrolyte, current multiplication noise *(Russian)* 3—5051
- semiconductor-metal junction, many-body effects, self energy and band structure distortion 3—38890
- slender foil unsteady motion near interface between two different fluids, numerical soln. 3—33272
- solid-liquid interface, morphological stability near grain boundary groove 3—11557
- solution-air interface, effective age calc. rel. to surface tension meas. 3—5759
- solution-air interface, surface tension depend. on effective surface age 3—5760
- spherical crysts. growth by freezing, interface growth stability 3—20701
- spherical shell/rigid plate contact press., applanation tonometry applic. 3—19443
- surface film growth rate-controlling factor, true diffusion current of substrate ions 3—20969
- thermodynamics of irreversible processes in interfacial regions and anisotropic media, general relations *(French)* 3—27853
- thermodynamics of irreversible processes in interfacial regions and anisotropic media, phenomenological relations *(French)* 3—27854
- thin oil films, stability, removal from metallic surfaces by washing, interfacial tension and viscosity dependence 3—39465
- Ag-Au pseudomorphic bi-crystals, stress from elastic deformation 3—36494
- AgBr, contacting 1:1 electrolyte, surface struct. props. 3—12526
- AgCl, contacting 1:1 electrolyte, surface struct. props. 3—12526
- AgCl(Br)(I), surface contacting water, zero charge point temp. depend. 3—8248
- Al_2O_3, anodic, on Al, breakdown and repair, electron microscope obs. 3—8060
- Al_2O_3, fused to glassy substrate, boundary layer formation *(German)* 3—12425
- $BaO.6Fe_2O_3$, texture and reaction mechanism in the formation at the 3 interface 3—5413
- CO_2 absorption into monoethanolamine water mixtures by oscillating jet, interfacial tension meas. 3—11795
- CdS, interface reactions rel. to growth by spontaneous nucleation 3—2645
- CdS(Se), electrolum. from controlled splits 3—24746
- CdSe-electrolyte, current multiplication noise *(Russian)* 3—5051
- Cu-Mg-Ni alloy, monovariant eutectic, unidirectional solidification, aligned microstructs., interface stability criteria 3—12347
- $GaAs_{0.2}P_{0.8}$, electrolum. from controlled splits 3—24746
- Ge/Al thin film system, surface mass transfer mechanism, diffusion phenomena *(Russian)* 3—11836
- Ge-electrolyte, current multiplication noise *(Russian)* 3—5051
- He II-solid interface, Kapitza resist. rel. to thin surface films 3—33704
- $^3He/Ce$, $Mg_3(NO_3)_{12}.12H_2O$ boundary resist., nucl. spin-electron spin dipolar interaction 3—30303
- ^4He-solid interface, Kaptiza resistance reduction through surface dislocation scattering 3—1764
- Pb-Cd eutectic; Sn interface instability 3—39309
- S, metallic, cavity formation at metal-S interface during growth of thick layers of S 3—4753
- Si oxidised surface, m.o.s. electron surface mobility in inversion layers at room temp. 3—8268
- Si:Sl, Czochralski growth, study of impurity striations and interface shapes 3—12322
- Si/SiO_2, surface charge and mech. stress relationships 3—38900
- SiO_2 layer on Si surface, surface props. and interface charge with ion beam irradiation 3—14899
- SiO_2/Si, ion bombardment effects, impurity ion transport, ^{22}Na radiotracer 3—39288
- Ti/W composites, solid-state interfacial reactions 3—31139
- TiO_2 anatase surfaces, model, interpretation of some interface processes 3—5414
- ZnO-NiO solid solution, Ni-Zn ferrite formation 3—2812

interface structure
- n-alkane cryst. growth on graphite and C fibre surfaces 3—20703
- alloys, ordered, interfaces, study, grain boundaries, twinning, martensitic transformation, thermal antiphase walls *(French)* 3—17855
- crystal and grain boundaries, 0-lattice theory 3—34518
- Czochralski process, crystal growth from melt, expts. on the dynamics of the phase limits *(German)* 3—8743
- energetics, kinetics and topography of interfaces 3—1861
- epitaxial growth, closely spaced misfit dislocation 3—15082
- epitaxial mag. garnet films, effect of substrate defects 3—15090
- epitaxy, lattice matching quality, geometrical interpretation *(French)* 3—1930
- ice, grown from melts, morphology of solid-liquid interface, dendritic and planar growth 3—38542
- III-V semiconductor alloy, lattice match in heteroepitaxy 3—4932
- lattice-gas interface structure, Monte Carlo simulation 3—28981
- layered stratified lattice, X-ray diffraction profile showing preferred orientation 3—11783
- Monte Carlo methods for theoretical study, review 3—20916
- rare earth garnet, for bubble domain device, liquid phase epitaxy, lattice mismatch 3—36770
- stress corrosion cracking via surface diffusion, interface morphology development 3—34570
- substrate facet replication by epitaxial garnet film, lattice parameter distrib. 3—38749
- Al_2O_3, growth of amorphous and epitaxial layers on Si *(German)* 3—8056
- Au, substrate with Pb monolayers, spontaneous alloying, LEED and Auger obs. 3—36463
- Au film grown on NaCl, small-angle torsion boundary structure in (001) plane 3—4940
- Cu crystals solid-liquid interface shape determ. method during Czochralski growth 3—8735
- Er_2O_3/Er film, ion microprobe analysis obs. 3—20965
- Ga deposited on Mo substrate, Mo_3Ga alloy form. and anisotropic binding force 3—24319
- Ga deposited on W substrate, pseudomorphic and superstructures, field ion microscope study 3—24318

interface structure continued
GaAs-GaP system, solidus boundary, correlation between miscibility and lattice parameter mismatch 3−11720
GaAs$_{1-x}$P$_x$, superlattice, X-ray diffraction obs. of lattice distortion and structure 3−17788
GaP-GaAs heterojunction, TEM obs. of misfit dislocations caused by lattice mismatch 3−36305
Ge detectors, collimated beam scanning, radial dependence of depletion layer width 3−28656
Ge/Si, dislocation network via mismatch on Ge epitaxy, t.e.m. obs. 3−1941
Si surface reaction with Ni, struct. 3−20911
Si/sapphire, epitaxy, electron microscope exam., sample preparation 3−1939
Si-SiO$_2$, defect struct. and irradiation behaviour of noncrystalline SiO$_2$ 3−4770
Si-SiO$_2$ interface state, negative bias-heat treatment approach 3−15256
SiO$_2$ pyrolytic film on semiconductor substrate, structure defects, transmission electron microscopy *(Russian)* 3−27197
Ti/Al$_2$O$_3$ composites, filament reinforced, reactivity and interface characts. 3−31136
YIG epitaxial film, ferromag. resonance, lattice mismatch effects 3−30700
YIG epitaxial film, lattice mismatch rel. to domain struct. and stress 3−34160

interface tension *see surface tension*

interface vibrations *see crystal surface and interface vibrations*

interfaces, computer *see computer interfaces*

interfacial tension *see surface tension*

interference
see also acoustic wave interference; electromagnetic interference; electromagnetic wave interference
liquid crystals, their educational use for illustration 3−16366
neutron wave propag. in polycryst., calc. by eigenvalue expansion 3−1041
seismic waves distorted by interference, optimal detection algorithm *(Russian)* 3−12611
Fe-Al Kossel patterns evaluation by computer *(German)* 3−4693
Fe-Si, Kossel patterns evaluation by computer *(German)* 3−4693

interference spectrometers
Coude telescope spectrometer systems, polarisation effects on transmission 3−37501
cryogenic, low level emittance and absorptance measurement in laser windows and mirrors 3−28594
Fabry-Perot spectrometer, photoelectric, refractometer 3−28565
Fourier, effect of precision of interferograms on form of apparatus function *(Russian)* 3−22355
Fourier, fast scanning, for 2 to 18 μm range optical design *(Russian)* 3−5961
Fourier spectrometer, monitoring by real time computer, airborne i.r. astronomy 3−3385
Fourier spectrometer, Williams interferometer type, modulation transfer function 3−5960
Fourier spectroscopy, interferometer design 3−9952
Fourier spectroscopy, polarisation interferometer 3−22363
Fourier transform, construction from scanning interferometer and high gain photodiode detector-amplifier 3−9950
Fourier transform, spectral derivation and correl. possibilities *(French)* 3−35415
Fourier transform, undergraduate scanning interferometer and high gain photodiode detector-amplifier 3−9950
Fourier transform all-reflection interferometer, design, characts. 3−28566
Fourier transform spectrometer for far i.r. spectroscopy 3−32081
Fourier transform spectroscopy from 10^6 samples, vacuum operation and automation *(French)* 3−32078
grille spectrometers 3−9953
high-resolution i.r. spectrographs, large plane gratings 3−9954
i.r., scanning Fabry-Perot, 7-25 μ region *(Russian)* 3−25774
lamellar grating interferometer, i.r. diffraction limitations, for Fourier transform spectroscopy 3−28562
laser heterodyne, for low angle quasielastic light scatt. meas. 3−24282
Michelson, automated, for spectral emissivity meas. on W, 1700-2300K, 700-1100 nm. 3−28556
multiple Fabry-Perot, scanning, low resolution 3−35416
SISAM using synchronous detection *(French)* 3−32072
spectroheliograph, multichannel Fabry-Perot configuration 3−25540
vacuum u.v., 50 to 120 nm, absolute intensity calibration method using electron impact excitation 3−37637

interference spectroscopy *see spectroscopy*

interference suppression
coherent optical processing, spatial freq. diversity, noise reduction, multiple filtering 3−22850
holographic recording Bragg acousto-optic imaging system, noise reduction 3−22366
modern measurement techniques in control engineering, noise rejection properties 3−56
n.m.r. signal storage, capacitive device *(Russian)* 3−10002
optical communication link with subcarrier PCM and frequency multiplexing of digital data channels, noise immunity analysis 3−29051
optical fibre double-reverse-scatter interference reduction equaliser 3−149

interferometers
see also acoustic wave interferometers; electromagnetic wave interferometers; interferometry
device for demonstration of electron interference 3−32010
dilatometer, as part of meas. standard for temp. coeff. of linear expansion of solids 3−32022
Fabry-Perot, use as periodic filter in laser Raman scatt. obs. of atmospheric pollutants 3−3192
Fabry-Perot etalon, new design suggestion for dye lasers 3−25777
fringe counting laser interferometer manometer 3−25707
interferograms, automatic processing algorithm *(Russian)* 3−32518
Jamin use for student laser optics expt. 3−16364
Michelson interferometers for high resolution spectrometry 3−13117

interferometer, continued
mirror shearing, u.s. gas flow analysis applications *(Russian)* 3−6173
scanning, with high gain photodiode detector-amplifier for undergraduate Fourier transform spectroscopy lab 3−9950
for small linear displacement meas., improved sensitivity *(Russian)* 3−22262
wavefront tilter, for double-exposure holographic interferometry 3−16444

interferometry
see also acoustic wave interferometry; electromagnetic wave interferometry; interferometers
air, pulsed interferometric holography of laser-produced breakdown 3−33189
apochromatic path-difference compensator for automatic instruments *(Russian)* 3−9951
double-exposure holographic, wavefront tilter 3−16444
dual hologram, two-dimensional density distrib. obs. 3−208
Fabry Perot narrow-band filter, enhancement of transparency *(Russian)* 3−3815
Fabry-Perot, optical probe of continuously propagating surface acoustic waves 3−19112
glass tube interference between reflections from inner and outer surfaces 3−16788
holographic, inspection of unpolished surfaces, shape monitoring *(Russian)* 3−5917
holographic, polychromatic with recording in three dimensional medium *(Russian)* 3−3813
holographic, review 3−19222
holographic, using image plane holograms, patent 3−9958
holographic, with variable sensitivity 3−13332
holographic and fringe analyser, supersonic flow obs. 3−22571
hot dielectrics, noise temperature and noise coefficient of temperature, measurement technique *(Russian)* 3−27459
inert gases, second virial coefficient of Lorentz-Lorentz function meas. using Fabry-Perot interferometer 3−11714
intensity, in spatial domain, for stellar observation 3−31807
interferograms, processing by equidensitometric curve method 3−25773
laser, for distance meas. *(Japanese)* 3−213
lunar topography, global determ. by radar interferometry and delay-Doppler stereoscopy 3−25422
lunar topography, radar-interferometer meas. of the Alphonsus-Ptolemaeus-Arzachel region 3−25423
multilayers, method for measuring dispersive phase shifts *(Russian)* 3−13320
narrow band metallic grid filters, for far i.r. 3−5952
photon properties, det. by interferometric spectroscopy of black body 3−10455
plasma Focus machine, neutron fluences, electron density and deuteron temp. meas. by holographic interferometry 3−20637
plasma high beta density profiles holographic interferometry technique at $\lambda=3\mu$m 3−20634
plasma production by fast rise time laser pulses on solid D$_2$ targets, density meas. by interferometry 3−20562
plastic deformation obs. 3−22660
radii of curvature areas, on small surface areas *(Russian)* 3−22263
radio, extragalactic source obs. for precision geodesy meas. 3−12627
shock-wave, optical fiducial system 3−5771
small phase difference changes in interference devices, review of measurement methods 3−28563
stroboscopic holography, triple exposure technique for recording time reduction 3−22360
turbulent flow meas. using photon correlation spectroscopy 3−32276
^{114}Cd hot cathode spectral lamp, as secondary standard 3−3748
He+Ne laser radiation analysis with spectrometer *(Russian)* 3−5942
^{198}Hg hot cathode spectral lamp, as secondary standard 3−3748
W, meas. of spectral emissivity using Fourier transform spectroscopy 3−28556

intergalactic matter
heading is late addition
see also galaxies
accretion of intergalactic gas onto the Galaxy rel. to soft X-ray background 3−25495
clusters of galaxies, stability criteria rel. to invisible intergalactic matter *(Polish)* 3−25508
Coma Cluster, Lyman α emission rel. to models of intracluster gas 3−28278
Coma cluster of galaxies, H I in intergalactic regions, heating mechanism and model 3−37460
Coma cluster of galaxies, Lyman-α obs. for upper limit on intracluster medium 3−37464
Cygnus A, ram pressure deceleration of radio components 3−13064
diffuse X-radiation from intergalactic gas in clusters of galaxies 3−31511
electric wave propag. in warm plasma, effect of non-zero photon mass 3−25515
filaments, computer simulations, tidal forces 3−3370
galactic bridges and tails as tidal relics of close encounters 3−25490
galactic chromosphere of hot interstellar gas accreted from intergalactic space 3−16266
galaxy evolution rel. to gravitational drag and accretion of intergalactic matter 3−37447
hot intergalactic gas rel. to isotropic X-ray background 3−13082
NGC 5128, peculiar radio galaxy, possible assoc. shred object Fourcade-Figueroa 3−28276
NGC 7331 and Stephan's Quintet, connecting faint nebulous material 3−22109
SMC, search for H I remnants of strong tidal disruption with the Galaxy 3−25499
Stephan's Quintet and NGC 7331, connecting faint nebulous material 3−22109
universes with some intergalactic matter, distance-redshift relations 3−31514

intermediate bosons
fine struct. fermi coupling constants rel. to boson mass 3−14109

intermediate bosons continued
formation in crossed beams, $W_1^\pm$ and $W_0^\pm$, cross-section *(Russian)* 3−29295
Fujii boson, possible role in non-conservation of unitary-singlet axial-vector current 3−32639
mass estimation 3−32646
neutral, eff. on leptonic atoms 3−23027
nonlocal theory of e.m. and weak interactions with W-boson, S-matrix structure 3−26259
resonances, correspondence to intermediate structures in nuclear reactions 3−4214
six-fermion coupling theory calc. of muon spectra in $\nu p\to\nu\mu^+\mu^- p$ 3−32657
three-triplet model, rel. to U(1) × SU(2) gauge model 3−32644
vector, decay muon zenith-angle intensity distrib., comparison with cosmic ray muon distrib. in Mont Blanc tunnel 3−31492
virtual-boson effects in neutrino trident production 3−19680
weak interactions with maximal CP violation, W boson model 3−6575
$\eta\to\pi^0\gamma\gamma$, large branching ratio, possible existence of new intermediate boson state 3−32654
$\nu_\mu Z\to Z\nu_\mu\mu^+\mu^-$, influence of intermediate W-boson on ang. and energy distribs., 200 GeV *(Russian)* 3−19685
W^+, lepton spectra in production in a neutrino beam *(Russian)* 3−834
$W^+\to l^+ + \nu_l$, produced in $\nu_\mu N\to\mu^- W^+ N'$, meas. of angular and energy distrib. of l^+ *(Russian)* 3−10677

intermetallic compounds *see alloys*

intermodulation
distortion produced by centre clipping 3−3638

intermolecular forces
see also Van der Waals forces
σ-σ and π-π interactions in complementary bases 3−29758
acetone and acetone-d_6, Fermi reson. and intermol. forces in ν_{co} absorption *(French)* 3−26660
adenine-thymine base pairs, perturbation energies 3−29758
atom-diatom collisions, semi-classical approach to inelastic cross sections calc. 3−38322
atom-diatom collisions, semi-classical approach to inelastic cross sections calc. 3−38323
benzene, cryst. vibr. calc., refinement of intermol. pots. 3−24228
benzene-halogen complexes, approximate interaction potentials 3−20212
benzol molecules, dispersion interaction energy calc. to π electron approx. *(Russian)* 3−29759
charge overlap effects, second order, represents. 3−7267
chlorinated benzene crysts., intermol. force field, model approach 3−30238
closed-shell mols., double-exchange contrib. to first-order interaction energy 3−11329
4,4′-dimethoxyazoxybenzene, molecular field theory of nematic mesophase 3−11542
electrostatic force theory, ground and excited state molecular shapes 3−33083
electrostatic force theory 3−33082
electrostatic representations of mol. groups. 3−29756
ethylene, deuterated, intermolecular force parameters in the gas phase, calc. from virial coefficient data *(German)* 3−26740
exchange interactions, Rayleigh-Schrodinger perturbation theory applic. 3−7084
guanine-cytosine base pairs, perturbation energies 3−29758
hydrogen-bonded complexes, charge transfer theory and relation between dipole moment energy and enhancement 3−20207
ice, local orientational order, Kirkwood theory cluster expansion approach 3−30237
imidazole model dimer systems, perturbation energies 3−29758
keontes, valence vibr. perturbation by intermol. forces *(French)* 3−1244
Kihara molecules, Percus-Yevick theory for binary mixtures 3−17484
Kihara potential, solution of Percus-Yevick integration for dense fluids (Ar, Kr, Xe) 3−17483
liquid mixtures, molecular model *(German)* 3−12498
liquids, struct. and thermodynamic props., perturbation theories *(Dutch)* 3−30060
methane, methane-d, differences in second virial coeffs. rel. to intermol. pots. *(German)* 3−26738
mice sheets at v. small separation, attraction 3−1296
molecular crys., harmonic vibr. freqs. and anharmonic intermol. pot. *(French)* 3−20822
molecular crystals, lattice sum transformations and potential function expansions in lattice dynamics 3−33621
multipole represents. of mol. potentials, domain of convergence 3−11328
organic molecular crystal, non-radiative transition from singlet to triplet exciton 3−4968
polar gases, calc. of Stockmayer potential function by least-squares analysis of second virial coeffs. 3−1772
polymer soln., dil., binary cluster integrals 3−23649
polymers, struct. from intramol. pot. energy, van der Waals and electrostatic interactions 3−14700
potential energy functions from second virial coefficients, direct determination 3−4486
for protein conformation, review 3−29760
resonance line broadening in the impact limit, resonance transfer contributions intermolecular potentials 3−17475
short-range, determination by scattering of fast particle beams 3−36057
spatially defined fragments of mol. systems, virial relationship, mol. charge distribution 3−17478
thiourea single crystal, Raman spectra in para- and ferroelectric phases, intermolecular force consts. *(French)* 3−27498
three cylinders, model for interaction between 3 conducting molecules 3−1295
three-parameter potential function exam. 3−4485
vandyl acetylacetonate, anisotropic interaction parameter, rel. to temp. and pressure depend. of e.s.r. linewidth 3−23596
Ar, three-parameter pair potential from second virial coeffs. 3−7268
Ar-N_2, intermolecular pot. calc., orientational averaging of rot. transition probabilities 3−17407
CO_2 potential parameters and combination rules, determ. from diffusion data 3−1293
H_2, intermol. pot. energy function shape 3−1292
para-H_2 + para-H_2, crossed beam elastic scatt. meas., intermol. pot. determ. 3−7269
HCl + Ar collisions, semi-classical approach to inelastic cross sections calc. 3−38323
He-D_2 total scatt. cross sections, 760-2600 m/sec 3−1294
He_2, double-exchange contrib. to first-order interaction energy 3−11329
Kr, three-parameter pair potential from second virial coeffs. 3−7268
Kr potential parameters and combination rules, determ. from diffusion data 3−1293
Li clusters, symmetric group and method of diatomics 3−33168
N_2-Ar, intermolecular pot. calc., orientational averaging of rot. transition probabilities 3−17407
NH_3 model dimer systems, perturbation energies 3−29758
NH_3-H^+ collisions, first order orientation dependent forces 3−4487
Na^+-inert gas potentials, molecular beam determination 3−17383
OCS molecular crystal, lattice dynamics, variational formalism and intermolecular forces 3−33620
Xe, three-parameter pair potential from second virial coeffs. 3−7268
$XeOF_4$, ^{19}F magnetic resonance study, molecular interaction in the liq. 3−36813

intermolecular mechanics
see also association; intermolecular forces; liquid structure; liquid theory; Morse potential
activated liquid systems, activator electronic levels relative positions, influence of intermol. relax. and fluctuation processes 3−23639
adenine tautomers, protonated, MO study and their intermol. interactions 3−11200
adenine.HCl single crystals, electronic spectrum study, intermolecular interactions within dipole approximation 3−30828
anthracene, in different solvents, spectroscopic study of intermolecular interactions *(Russian)* 3−30826
benzene solution of PMMA, n.m.r., spin lattice relaxation, molecular interactions 3−39045
binary gas mixtures, intermolecular pair potentials calc. for like and unlike molecules *(German)* 3−33182
9-bromoanthracene, in various solvents, intermolecular effects, spectroscopic studies *(Russian)* 3−36879
chloranhydrides of unsaturated phosphoric acids, intermolecular interactions obs., Raman spectra obs. *(Russian)* 3−15822
clustering in hard parallel squares, mol. dynamics study 3−13662
cycloalkanes and corresponding saturated heterocyclics, intermol. effects and n.m.r. *(French)* 3−26691
dense fluids, Monte Carlo methods *(Portuguese)* 3−26151
diatomic homonuclear liquids molecular-dynamic simulation 3−30061
p-dibromobenzene-p-iodchlorobenzene mixed crystal, Raman spectra, frequencies and linewidths *(Russian)* 3−8575
dioxydinaphthyl film, vibr. spectra, intermol. interaction effect 3−23573
1,8-diphenyl-1,3,5,7,-octatetraene, in different solvents, spectroscopic study of intermolecular interactions *(Russian)* 3−30826
ethers of carbonic acids and their solutions in CCl_4, self-diffusion coeffs., intermolecular hydrodynamic interactions *(Russian)* 3−7957
fluid activated systems, mol. interactions and stimulated emission spectra, relax. and fluctuation processes 3−18473
gas of Lennard-Jones particles, fourth virial coeff. calc. 3−36064
homonuclear, diatom-atom collisions, rotational-vibrational scattering, intermolecular potentials 3−29749
inert gas potentials, tables of collision integrals 3−26739
Lennard-Jones (6,12) pair potential parameters, determ. from equations of state of liquids 3−1565
Lennard-Jones fluid, radial distrib. function, perturbation theory Monte Carlo study 3−23638
liquid cavity radius calc., effect of translatory mol. motion 3−1561
liquid theories, review 3−33438
luminescent solns. intermolecular relaxation-fluctuational processes and spectra, review *(Russian)* 3−27524
Mie (n,6) potential prediction of saturated liquid properties 3−4715
nitrobenzenes, intermolecular interaction and radiationless transitions *(Russian)* 3−29702
phthalocyanine dyes in soln., self-association obs. by electron spectra and e.s.r. 3−31252
quinones, substituted, intermolecular interaction, with aprotic and proton-donating solvents *(Russian)* 3−36882
relaxation and transfer processes, theory *(Russian)* 3−7257
rubber elasticity, intermolecular obstruction theory 3−7278
water structural model based on intermolecular potential function 3−30062
Ar, solid, Raman two-phonon spectra, mol. dynamics 3−34353
CsF + Ar, (Kr), (Xe), integral total cross sections meas., attractive pot. investigation 3−38324
H-He potential determ. from molecular beam expts. 3−11165
H_2, solid, anisotropic intermolecular interactions in the rotation-vibration Raman spectrum 3−27492
H_2^+, exchange polarisation energy calc. 3−29757
Kr solid, Raman two-phonon spectra, mol. dynamics 3−34353
SiF_4 and SiH_4, molecular models for thermal diffusion separation of Si isotopes 3−38197
Xe, solid, Raman two-phonon spectra, mol. dynamics 3−34353

internal combustion engines
exhaust gases, NO catalytic reduction using Fe-containing materials 3−37535
exhaust gases, NO catalytic reduction using oxidized stainless-steel surface 3−37536

internal fields, crystal *see crystal internal fields*

internal friction
see also damping
alloy, ternary b.c.c., anisotropy of substitutional-interstitial internal friction peaks 3−36365
b.c.c. alloys, substitutional-interstitial interactions 3−2704
counterbalanced reed pendulum apparatus for obs. 3−3755
covalent crystals, obs. using regenerative feedback loop and composite oscillator 3−5770

internal friction continued
- of crystal defects, book 3−20813
- cubic lattice, Wert-Marx law generalization and interstitial vibr. freq. *(French)* 3−1688
- drag reduction in rotational viscoelastic boundary layer flow in polymer solutions 3−26810
- foils, electrical resistance, cyrostats 3−251
- glass, ion exchange at low temp. effects 3−25064
- glass fibres, static hysteresis from −78 to 196°C 3−38619
- rel. to impurity atom diffusion along dislocations *(Russian)* 3−1692
- interaction between point defects and dislocations 3−7766
- Invar, internal friction features in variable mag. field, magnetoelastic losses 3−30677
- Invar, props. of internal friction mag. peak at 253K 3−30676
- I.f., measurement instrumentation system 3−28467
- metal, b.c.c., dislocation pinning by impurities *(Russian)* 3−14866
- metal, hydrogen diffusivity meas., low temp., Gorsky effect 3−36440
- metallic rod, optical meas. of strain during torsional oscill. 3−25038
- metals, friction phenomena rel. to point defects 3−24105
- metals and plastics after irradiation at low temperature *(Greek)* 3−9032
- microporous substances, internal friction peaks due to adsorbed and capillary water 3−21754
- polymer, two-component heterogeneous composition, composite specimen method of dynamic props. simulation 3−27784
- rocks, uniaxially compressed *(Russian)* 3−5439
- solid solution hardened alloys, Zener relation *(Russian)* 3−15715
- steel, hydrogen embrittlement and hydrogen/dislocation interaction 3−2744
- steel, low-C, internal friction during strain aging, Snoek peak magnitude *(Russian)* 3−18614
- steel, structural, temp. effect on physical and mechanical properties 3−24927
- strongly outgassed terrestrial analogue of lunar basalt 3−37167
- structural and tool steels, subjected to intense u.s. vibrations 3−27705
- structure of defects in solids, point-defect-pinned dislocations obs. by relaxational internal friction 3−24099
- theory for multiwell potentials in which anelastic strain elements (diffusing particles) redistribute 3−14934
- Ag, cold-worked and γ-irrad., variation during recrystn. 3−5314
- Al, Bordoni relax., secondary features 3−33608
- Al, deformed, neutron irrad. effects *(French)* 3−30207
- Al, fatigued, de Hasigutti peak and dislocation-point defect interaction *(French)* 3−11685
- Al, high velocity dislocation damping at high strain rates 3−36301
- Al, neutron irradiated and deformed at low temp., internal friction and modulus anomaly *(French)* 3−14935
- Al-Cu(4 at wt.%) alloy, precipitation study by internal friction, hardness and electron microscopy meas. *(French)* 3−15687
- Al-Fe, dilute alloy, cold-worked, effect of heat treatment 3−27703
- Au, cold-worked, stage II and III recovery, trace impurity effects 3−5315
- Au-Fe alloy, due to quenched-in vacancies 3−37040
- $BaTiO_3$, influence of domain struct. 3−36845
- Co, internal friction peak at 300°C rel. to lattice defects 3−30208
- Cu, dislocation pinning after neutron irrad. at liq. He temp., internal friction and dynamic modulus obs. 3−38600
- Cu, dislocation pinning by hydrogen *(French)* 3−2740
- Cu, fatigued, recovery 3−7811
- Cu, grain boundary friction with neutron irradiation and fatigue 3−24117
- Cu Bordoni peak, cold worked single crystals and polycrystalline specimens, 20 to 200 K, 10 to 25 kHz 3−36364
- Cu foil, α-irrad. at 78K *(German)* 3−7851
- Cu frequency dependence for technical purity metal *(Russian)* 3−1691
- Cu whisker, anisotropy of dislocation internal friction 3−8071
- Cu whisker, obs. rel. to primary recrystallisation nuclei formation kinetics on torsional straining *(Russian)* 3−12365
- Cu-Ni alloys, peak interpret., grain boundary behaviour *(Russian)* 3−24210
- Cu-Si(5.09 at wt.%) alloy, aged, internal friction meas. 3−18678
- Cu-Zn (30 wt.% Zn), variation with annealing temp. 3−4818
- Fe, hydrogen embrittlement and hydrogen/dislocation interaction 3−2744
- Fe and alloys, hydrogen influence *(French)* 3−2739
- Fe and Fe-Ni alloys, hydrogen-dislocation interactions 3−4887
- Fe frequency dependence for technical purity metal *(Russian)* 3−1691
- Fe-C solid solutions, b.c.c., Snoek peak broadening *(French)* 3−31018
- Fe-Ga-C alloys, f.c.c., interactions between insertion and substitution atoms *(French)* 3−8777
- Fe-Mn-Zn ferrite, measurement in alternating magnetic fields of various frequencies 3−39009
- Fe-Ni alloy, n irrad., Snoek peak and strain-amplit. of intl. frict., meas. 3−17929
- Fe-Ni-C alloys, internal friction meas., Snoek-peak, C interstitials diffusion towards dislocations mechanism 3−34542
- Fe-Ni-Cr alloy, grain boundary internal friction spectra, relax. phenomena 3−37028
- Fe-Ni-Cu ferrite, measurement in alternating magnetic fields of various frequencies 3−39009
- Fe-Si, internal friction features in variable mag. field, magnetoelastic losses 3−30677
- Fe−Co(3.18-42.5 wt%) alloy, Zener relax. 3−24213
- Ge crystal, dislocation relaxation, temp. depend. 3−17847
- Ge crystals, deformed, meas. from 4.2 to 150 K 3−14936
- Ge whisker, effect of dislocations 3−38759
- In, normal and superconducting, amplitude-dependent dislocation, u.s. attenuation 3−36679
- In, normal and superconducting, amplitude depend. 3−38627
- LiF, effect of light before and after irradiation *(Russian)* 3−7850
- $Li_2O.Al_2O_3.2SiO_2$ glass, proton-exchanged 3−1693
- MgO crystal, point defects-dislocation interaction 3−30117
- Mo, dislocation pinning after neutron irrad. at liq. He temp., internal friction and dynamic modulus obs. 3−38600

internal friction continued
- Mo, dislocation-interstitial interactions using dislocation damping obs. 3−36312
- Mo, effect of H on temp. depend. *(Russian)* 3−1690
- Mo frequency dependence for technical purity metal *(Russian)* 3−1691
- Mo single crystal, study using ultrasonic wave decay, dislocation damping *(Russian)* 3−24211
- $x\,NaO.(1-x)SiO_2$ glasses, heat treatment eff., −200 to 440°C *(Russian)* 3−11686
- $NaPO_3$ glass, containing water 3−33607
- Nb, neutron irradiated at low temp., internal friction, relaxation peaks due to dislocation and point defects interaction 3−17875
- Nb frequency dependence for technical purity metal *(Russian)* 3−1691
- Nb-H system, domain boundary effects 3−38620
- Nb-H system, explanation for α-peak 3−27069
- Nb-Hf-N alloys, temp. depend. *(Russian)* 3−1689
- Nb-N-O solid solutions, electrical conductivity, microhardness, lattice dimension and Snoek peak measurement *(Russian)* 3−39335
- Nb-Zr-N alloys, temp. depend. *(Russian)* 3−1689
- Ni, creep, grain boundary pore form. correl. with internal friction *(Russian)* 3−24877
- Ni, rel. to hydrogen-dislocation interaction *(French)* 3−1629
- Ni frequency dependence for technical purity metal *(Russian)* 3−1691
- Re frequency dependence for technical purity metal *(Russian)* 3−1691
- Ta frequency dependence for technical purity metal *(Russian)* 3−1691
- Te single crystals, u.s. attenuation meas. 3−36366
- Ti frequency dependence for technical purity metal *(Russian)* 3−1691
- $UO_{2\|x}$ including U_4O_{9-y}, internal lattice strain 3−11687
- V-C supersaturated solid soln., carbon precip. obs. 3−37036
- W frequency dependence for technical purity metal *(Russian)* 3−1691
- Zr alloys, I.f. meas. using torsion pendulum 3−18779
- Zr frequency dependence for technical purity metal *(Russian)* 3−1691

internal friction of liquids *see viscosity of liquids*

internal mechanics, molecular *see molecular internal mechanics*

internal mechanics of atoms *see atomic structure*

internal stresses
- alloy, ordered, type Ll_2 superstruct., dislocation barriers *(Russian)* 3−30986
- atactic polystyrene, solvent nature influence 3−27774
- chemical stress of vacancy and interstitial supersaturations 3−7751
- circular twist disclination loop moving in 2 phase material, calc. of elastic field 3−14863
- composite, fibrous, multiple fracture, theory 3−34633
- composite solid consisting of two half-planes, distribution of stresses 3−531
- corrugated tube or bellows, application of shell equations to stress distribution 3−3955
- coupled thermoplastic media, properties of modelling eqns. including heat effects *(Russian)* 3−16663
- crack tip, rel. to crack control by means of elastic waves *(Russian)* 3−11680
- cubic crystal, long-range elastic interaction between dislocation and ellipsoidal inclusion 3−36303
- cylinders and spheres under internal pressure with steady radial heat flow, reference stresses and temps. 3−28893
- dislocation arrays, hexagonal, screw, long-range rotational stresses of terminated multipoles 3−30129
- dislocation distributions, equilibrium 3−36314
- dislocation distributions, linear stress-velocity law 3−36313
- dislocation line pair generation of stress components *(Russian)* 3−3997
- dislocation motion, lattice resist. under influence of hydrostatic press. *(Russian)* 3−36299
- dislocation networks and cells, stress distrib. mapping by computer, rot. stress field obs. 3−11626
- dislocations moving in elastic solid, calc. of stress field 3−14862
- distribution near tip of array of screw dislocations piled up against an inclusion 3−1625
- edge dislocations in surface layer, calc. of elastic fields, Peach-Kochler force 3−14861
- elastic interaction of dislocation array with phase boundary 3−38588
- elastic sphere, homogeneous, containing penny-shaped crack, stress distrib. 3−6206
- Elinvar, ageing effect on Young's modulus temp. depend. *(Russian)* 3−31055
- filamentary reinforced metals, mech. prop. considerations 3−31155
- forced vibrations in linear theory of micropolar elasticity, determ. of displacement, rotations and stresses 3−16674
- glass reinforced plastic rings, wound, residual stresses determ. 3−24983
- glass reinforced plastics, residual stresses determ. 3−27763
- grain boundary under heterogeneous shear, stress field accommodation by microcrack initiation 3−4792
- heterophase solid, domain structure caused by internal stresses 3−30266
- hexagonal screw dislocation array, stresses of semiinfinite multipole 3−27029
- ice plates, floating 3−3944
- infinite slab, axisymmetric quasi-static thermal stresses 3−16623
- Kirkendall shifts during neutron irrad. due to stress gradients 3−11767
- Kossel line techniques, tensile testing 3−1548
- lattice sp. ht., dislocation strain field effects, higher order elasticity theory 3−27128
- lunar stress differences as evidence for cold Moon, solid Moon model 3−39640
- machined surface layer strwture and thermal residual stress by grinding 3−21708
- magnetic bubble domain material, X-ray topography obs. 3−34156
- martensite, twinned γ_1' phase, invariant plane strain approach 3−31021

internal stresses continued
martensite, work hardening origins, strength-differential effect 3−37067
mechanical interaction between crack tip and point defect 3−36358
metal, cubic, cleavage in intrinsic dislocation dipoles 3−24204
metal, f.c.c., b.c.c., Peierls stresses and glide systems from normal modes of vibr. 3−17919
metal, plasticity effects in crack propag. 3−30195
metallic springs, irrad. creep in materials testing reactor 3−27809
mixtures, balance of forces, new definition of partial stress tensor 3−32295
non-fissile materials, neutron irradiated, creep theory, internal stresses leading to plastic yielding 3−17293
nonlinear defect model, microscopic, local fracture and residual strain *(Japanese)* 3−20806
nuclear reactor fuel elements, deformation effects on temp. distrib., computer anal. 3−26515
nuclear steam generator shell behaviour under plastic deformation, relations for limiting pressure or thickness 3−23408
paraelectric resonance lineshape, theory 3−27460
plane stress wave reflection in elastic-plastic medium with variable yield limit *(Polish)* 3−19470
polyacrylamide, meas. of capillary wall normal stresses by slit die method 3−29814
polyethylene, determ. of extensional stress flow patterns and melt fracture in die inlet *(German)* 3−31182
polyethylene single crysts. on Cu and NaCl substrates, crit. shear stress for slip 3−33596
polymer, fatigue crack propagation and failure mechanism *(Japanese)* 3−12455
polymer, stress distrib. from atomic bonds, i.r. spectra 3−34367
polymer blocks, transparent, laser induced destruction 3−22936
polymeric cylinder, mech. props. influence on temp. stresses, edge effect 3−26082
polypropylene, oriented, tensile and compressive yield criteria 3−21745
poroelastic bodies in contact, determ. of Bielayev's point 3−22611
PVC tubes, band-deform. on slowly increasing internal press. 3−31163
rate-of-strain-dependent memory function, simple-integral model, appl. to shear flow 3−29829
rock test models with rigid and deformable inclusions, compression and simple shear 3−34829
solid solution hardening, crit. resolved shear stress, conc. depend. 3−24898
steel, carbon *(Japanese)* 3−24870
steel, high-strength, internal stress effects on susceptibility to stress corrosion 3−21692
steel, low carbon specimens, changes of residual stress due to slip band accumulation under fatigue loading 3−21578
steel, low-C, fatigue crack initiation process in notched specimens *(Japanese)* 3−21597
steel, mild, config. of moving crack tip zones 3−30196
steel, rel. to fatigue curve discontinuities *(Russian)* 3−12367
steel, stainless, Cr-Ni, Nb-stabilized, steady state creep, temp. depend. 3−8922
steel, stress field surrounding inclusions, photoelastic analogue 3−21585
steel austenitic, explosive bonded and hot rolled clad flat plates, residual stresses *(German)* 3−27837
steel EBR II control-rod thimble, assessment of postirradiation room-temperature fracture due to bending 3−23441
steels, high-strength, comparison of hydrogen embrittlement and stress corrosion cracking 3−21622
structural and tool steels, subjected to intense u.s. vibrations, internal friction and heat release 3−27705
thermal, excitation of hypersound, by short laser pulses 3−7857
thin oxide film heteroepitaxial stresses, origin, magnitude, config. 3−1944
viscoelastic rod, nonlinear stress wave propag., perturbation method 3−32314
weld heat affected zones, martensite tempering rel. to hydrogen cracking 3−8910
Y_2O_3-ZrO_2, lattice strain of cubic stabilized phase 3−15759
Al, in high temp. creep 3−7832
Al alloy, welded, distortion and residual stresses, rel. to use as struct. material 3−31108
Al alloy with metal plating, residual stresses influence on fatigue limit 3−37072
Al thin film, d.c. sputtered, low resistivity, sputtering bias effects 3−39225
Al-Mg(0.8 wt.%) alloy, rolling textural stability, role of deform. and shear banding 3−21582
BiTeI film, effect of substrate temp. *(Russian)* 3−18033
CaF_2, anisotropy in Knoop indentation hardness and friction of diamond cones 3−20788
Cu, macroscopic yielding of highly perfect crysts. *(Japanese)* 3−30184
Cu whisker, relax. obs. rel. to primary recrystallisation nuclei formation kinetics on torsional straining *(Russian)* 3−12365
Cu-Al solid solns., high temp. steady state creep deform. behaviour *(Japanese)* 3−31076
Fe alloys, strength-differential effect, effective modulus interpret. 3−37063
Fe alloys, strength-differential effect, effective modulus interpret. 3−37064
Fe-Mn-Zn ferrite, sensitivity, measurement in alternating magnetic fields of various frequencies 3−39009
Fe-Ni-Cu ferrite, sensitivity, measurement in alternating magnetic fields of various frequencies 3−39009
Fe-Si alloys, thermomagnetic treatment, effects of inclusions and internal stresses *(Russian)* 3−8385
GaP, local strain fields due to impurities 3−2023
KCl, internal stress relax. by deformation luminesc. obs. 3−5232
Mg hydrostatic extrusion, critical back pressure to prevent central cracking 3−21615
MgO, polycryst., microyield and fracture 3−20789
MgO crystal, dislocation-defects interaction, internal friction obs. 3−30117
$MgO:Cr^{3+}$, strain broadening of e.s.r. absorp. spectrum 3−27412

internal stresses continued
Mo, cast, intercrystalline fracture by grain boundary precip. *(Russian)* 3−24853
Mo, single crystals, shear, pre-macro yielding and orinentation dependence 3−38613
Ni, electrodeposited from ethylene glycol electrolyte 3−25071
Ni films, on Ni substrate, growth effects on stress 3−38754
Ni-base superalloy, Udimet 700 shock wave aging effect on tensile and stress-rupture properties 3−27682
Ni-Fe(25 wt.%) films, domain boundary curvature and displacement, mag. field and elastic stresses influence *(Russian)* 3−30654
Ni-Mo alloy electrolytic deposits, exptl. parameters depend. *(French)* 3−5287
Ni_4Mo, ordered, domain structs. and hardening 3−37026
$Se_{50}Te_{20}As_{20}Ge_{10}$, amorphous, stress thermally induced by switching 3−27293
SiC coatings for particle fuels of HTGR type reactors, mechanical design, neutron exposure and coating stresses 3−23407
SiON, thin insulating film from NO-NH_3-SiH_4 reaction 3−39244
Sn-Pb(15 wt.%) alloy, rheological behaviour in crystn. range 3−34505
Ta with interstitial H, determ. of strain field from meas. of elastic Curie const., 300 to 450 K 3−20812
Te on Ag, stress relief behaviour *(French)* 3−15105
α-Ti, oxygen conc. influence on internal stress and dislocation arrangements 3−34534
$UO_{2||x}$ including U_4O_{9-y}, internal lattice strain 3−11687
W, low-voltage sputtered film on SiO_2-Si substrate, stress depend. on deposition parameters 3−24515
YIG epitaxial film, due to lattice mismatch and thermal exp. 3−34160
α-Zr, cyclic straining, effective and internal stresses variation 3−39369
Zr single crysts., basal slip mechanism, critical resolved shear stress 3−24183
Zr-O alloys, strain aging parameters, dislocation cell struct., irrad. effects 3−27675

internuclear double resonance *see INDOR*

interplanetary magnetic fields
see also interplanetary matter
bow shock obliquity, local field geometry effects 3−12831
cosmic ray diurnal anisotropy, long-term modulation by interplanetary magnetic field 3−31484
cosmic ray modulation, off ecliptic control 3−9429
cosmic ray propag. in mag. field on basis of kinetic eqn. *(Russian)* 3−12884
cosmic ray transport eqn. without particle energy restrictions 3−39571
critical component, geomagnetic var. in polar cap 3−12648
discontinuities, solar wind effects, satellite l.f. obs. 3−12956
early magnetic field rel. to natural remanent magnetizations of carbonaceous chondrites 3−13000
East-West component depend. of diurnal variations of mag. field vertical component in E-region *(French)* 3−39551
East-West component effect on currents equivalent to mag. perturbations at high latitudes *(French)* 3−12636
ecliptic component influence om magnetosphere, asymmetry rel. to Earth-Sun direction *(French)* 3−39553
electron precipitation at high latitudes, effects of interplanetary magnetic field 3−16006
flare-associated solar wind disturbances rel. to interplanetary magnetic field structure 3−12960
fluctuations in solar wind field rel. to lunar elec. conductivity 3−25417
geomagnetic activity rel. to interplanetary mag. irregularities, Pioneer 8 study 3−18843
heliosphere, theory and properties of solar wind and interplanetary magnetic field *(Japanese)* 3−3291
inhomogeneous solar wind, hydrodynamic approximations *(Russian)* 3−3292
origin, turbulent dynamo mechanism 3−31503
particle diffusion, large scale hydromag. turbulence effects, Mariner 4 data 3−25428
plasma parameters, indices of geomagnetic activity 3−2924
polar geomagnetic field obs. during 5 sunspot cycles 3−25429
polar magnetic substorms, triggering by storm sudden commencements 3−13008
polar substorms, excitation by northward interplanetary magnetic field 3−2933
polar-cap electric field distributions, rel. to interplanetary magnetic field direction 3−12829
polarity variations, annual and solar mag. cycle 3−13005
sector structure long term behaviour, geomagnetic field variations at high latitudes 3−16201
solar energetic particles radio tracking obs. for mag. field configs. 3−28098
solar proton intensity structure in magnetosphere during interplanetary anisotropies 3−9346
solar wind electrons, heat conduction 3−11497

interplanetary matter
see also comets; cosmic dust; interplanetary magnetic fields
Apollo 16 soils, extralunar materials rel. to decay rate of extralunar flux 3−12992
charged particle propagation in scattering medium, magnetic focusing *(Russian)* 3−3319
comet tail (type I) model, Kelvin-Helmholtz instability and growth rate of MHD waves 3−28164
cosmic dust astronomy and space research *(German)* 3−22124
cosmic ray density gradients in interplanetary space, for various propag. models *(Russian)* 3−12904
cosmic ray deuteron and ^3He obs. and adiabatic deceleration 3−9432
cosmic ray diffusion coeff., rigidity and heliocentric distance dependence 3−16075
cosmochemistry, space research results, review *(German)* 3−31516
debris, size distributions rel. to telescopic observations of meteor showers *(Japanese)* 3−5593
disperse matter with Tunguska meteorite fall, associated anomalous atmospheric optical phenomena *(Russian)* 3−35106
electron irregularity characteristics from 1967-9 scintillation radio obs. *(Russian)* 3−13009

interplanetary matter continued
Forbush decreases and connection with solar activity and interplanetary medium parameters *(Russian)* 3—12907
hard rock cosmic ray archaeology 3—34981
heliosphere, solar wind, interplanetary glow and interstellar wind *(Japanese)* 3—5561
low temp. plasma meas. using electron beams 3—18893
neutral particle ionisation effects, electromagnetic wave excitation 3—13007
non-stationary processes, phase methods for elimination of derivatives of electron content 3—25339
nonstationary processes meas. using quantum freq. standards 3—34972
orientation of dust grains rel. to polarisation of cometary radiation 3—28300
plasma, e.m. fluctuations in mag. plasma in presence of strong e.m. radiation *(Russian)* 3—3320
plasma parameters, indices of geomagnetic activity 3—2924
radio source scintillation, anal. of non-Gaussian spectra 3—37411
scintillation of 3C 48, obs. of recurrent solar wind streams 3—5565
shock waves, delayed solar particle events, steady-state approximation 3—12961
shock waves in interplanetary medium, velocity determination 3—35109
solar cosmic ray distrib. *(Russian)* 3—12892
solar cosmic ray scattering in interplanetary space, anisotropic propagation *(Russian)* 3—13004
solar light scattered by isolated volume of interplanetary matter, intensity and polarization *(French)* 3—9463
solar wind and interplanetary electron meas. from Apollo 15 subsatellite in low lunar orbit 3—12958
solar wind velocities from orientations of ionic comet tails 3—39652
waves, electric and magnetic 3—3128
zodiacal light model optical props., spatial variation of dust particles 3—31638
zodiacal light photometric model rel. to brightness of zodiacal light and gegenschein 3—18996
He^+ velocity distribution, annual variation at 1 AU 3—13006

interplanetary medium *see interplanetary matter*

interpolation
see also function approximation
atmospheric dynamic eqns. discretisation and weather prediction scheme construction using integro-interpolative method *(Russian)* 3—28014
irregular interval, computer programme use for ephemerides *(Japanese)* 3—19081
optimum techniques, streamline analysis, streamline maps, field parameters 3—3163

interstellar dust *see cosmic dust*

interstellar magnetic fields
see also interstellar matter
galactic fields, cellular or filamentary structure 3—31777
galactic loops as supernova remnants in local galactic mag. field 3—35188
Galactic magnetic field and upper limit of photon rest mass 3—19064
origin, turbulent dynamo mechanism 3—31503
sound vibrations, cosmic ray effects in presence of mag. field *(Russian)* 3—37478
star formation in rotating cloud with mag. field 3—35120

interstellar matter
see also cosmic dust; H I regions; H II regions; interstellar magnetic fields; nebulae
absorption, 1900-1930 research development 3—3381
accretion problem, new steady-state solutions 3—9519
accretion vortices rel. to X-ray sources 3—9590
Alfven waves nonlinear mode-mode coupling 3—14537
B-type stars interaction with dust, radial vel. rel. to apparent magnitude 3—35136
Balmer line emission, galactic component meas. 3—28286
black hole accretion from interstellar gas, emergent radiation spectrum 3—39586
chemical composition of interstellar gas from X-ray attenuation meas. 3—28287
cloud formation, three-dimensional time-dependent model 3—31779
cloud formation mechanism rel. to density shock waves in H II regions 3—22121
cloud heating by vibrationally excited molecular H 3—31784
clouds, mass spectrum, total coalescence, time dependence 3—3377
collapse of interstellar gas rel. to H flash in stellar evolution 3—35116
colliding gas clouds, non-thermal emission source 3—28288
R Coronae Borealis, i.r. measurements rel. to dust clouds surrounding star 3—22074
cosmic dust astronomy and space research *(German)* 3—22124
cosmic maser model with resonance-scattering feedback, appl. to OH and H_2O clouds 3—28290
cosmic ray deuteron and ^{3}He obs. and adiabatic deceleration 3—9432
cosmic ray electron component and isotopic comp. relation 3—9422
cosmic ray sources, accel. of ionised interstellar gas particles by mag. stars 3—39572
Crab Nebula reddening determ. by obs. of S II lines 3—37492
cyanoacetylene cloud in Sagittarius B2, s.h.f. measurements 3—16276
Cygnus OB2 star no. 12, extinction curve and diffuse interstellar bands 3—39688
dark clouds kinematical distrib., obs. of 4830 MHz formaldehyde line 3—31780
diffuse line obs. at 5780 A and 5797 A, prod. by pure electronic transition 3—22048
dirty ice particles surrounding early-type stars, evaporation and size distrib. 3—35202
dust, obs. and astrophys. implications *(Japanese)* 3—9616
early-type stars at high galactic latitude, interstellar reddening determ. 3—35128
electric wave propag. in warm plasma, effect of non-zero photon mass 3—25515
electrostatic potential of grains rel. to H I and H II regions and circumstellar envelopes 3—39749

interstellar matter continued
emission continua of H and D molecules, radiative lifetime studies 3—13098
energy source for driving the interstellar gas 3—19071
evolution due to heavy element depletion on grains 3—37480
evolutionary models, excitation state due to supernova explosions 3—39741
extraterrestrial organic compounds, anal., review 3—35016
formaldehyde 6 cm line obs. near galactic centre 3—35175
formaldehyde in dust clouds, anomalous hyperfine lines 3—22119
formation of diatomic molecules in interstellar clouds 3—19069
fragmentation in collapsing interstellar cloud rel. to resulting stellar mass spectrum 3—25524
galactic centre, anomalous velocity H I concentrations, origin and formation mechanism 3—31770
Galactic centre radiofrequency emission pulse limit due to interstellar medium 3—39702
Galactic centre region, molecular clouds, CO obs. at 2.6 mm. 3—19068
galactic chromosphere of hot interstellar gas accreted from intergalactic space 3—16266
galactic cosmic ray bombardment of interstellar gas, element prod. 3—9418
galactic cosmic ray secondary electron prod. by collision of primary cosmic rays 3—31481
Galactic ridge recombination lines rel. to electron temperature 3—95 9
Galactic structure, existence of gas clouds in interarm regions 3—35174
galactic theoretical gas contents, luminosities 3—3367
globular clusters, search for free-free emission from ionized gas at 3.8 cm, gas deficiency 3—25492
grains injection into interstellar clouds 3—3382
Gum Nebula, high-velocity Ca II interstellar gas from spectra of two stars 3—19073
HD 154368, O-type star, interstellar spectrum obs. 3—31702
heating by Mira variable stars 3—9615
heliosphere, solar wind, interplanetary glow and interstellar wind *(Japanese)* 3—5561
high-velocity clouds, max. H column density rel. to radial velocity 3—35180
interaction of stars with local dust formations, densities and motion *(Russian)* 3—13108
interstellar cloud collisions and statistical theory rel. to evaporation 3—37482
i.r. line radiation determ. using u.v. line absorpt. 3—37485
isocyanic acid, interstellar emission line from Sgr B2 at 1.4 centimeters 3—16274
isocyanic acid interstellar line, detection from Sgr B2 and W51 directions 3—16273
isolated HI clouds, hydrodynamic treatment of phase change 3—37481
light elements in Universe, prod. by interaction with galactic cosmic rays 3—31512
M31, interstellar absorpt. for Cepheids in NGC 206, dust-to-gas ratio meas. 3—35186
M31 galactic companions, search for free-free emission from ionized gas at 3.8 cm, gas deficiency 3—25492
masers, molecular recoil mechanism for intensity variations *(Russian)* 3—16279
methanimine, interstellar emission multiplet in Sagittarius B2 spectrum at 5 GHz 3—25513
methyl alcohol, new interstellar emission line from 5_1-4_0(E_2) transition 3—16271
methyl alcohol interstellar line, detection of 4_1-3_0 (E_2) transition line from Sgr B2 clouds 3—16272
molecular cloud heating by low-energy cosmic rays 3—31782
molecular clouds, galactic, stellar and planetary evolution 3—37487
molecular clouds, review 3—5617
molecular line width differences rel. to collapsing protostars 3—25511
molecule formation by chemical reactions involving negative ions 3—39738
molecules, microwave spectral line radiation 3—16278
molecules detection by microwave and radiofrequency spectra 3—13101
molecules in compact H II regions, thermochemical calc. of origin 3—28289
motion of small spheres in gas, drag and heat transfer 3—33257
neutral component, solar wind interaction effects 3—12962
neutron-rich iron-peak nuclei, formation in supernovae 3—13097
Nova FH Serpentis 1970, diffuse interstellar lines and local reddening 3—39692
nuclear statistical equilibrium, composition changes in adiabatically cooling gas 3—28111
Ophiuchi, interstellar Na I, K I, Ca II and CH^+ line profiles 3—35150
orientation of dust grains rel. to interstellar polarisation 3—28300
plasma, propagation of Whistler mode, use in pulsar detection 3—16248
polytropes (weakly distorted) under external press., stability against radial perturbations 3—28106
pressure equilibrium of finite-size clouds in interstellar medium 3—28285
Puppis region, distribution of dust 3—9602
radio halos around old pulsars, ghost supernova remnants 3—25480
reddening law in u.v. for early-type stars, OAO-2 obs. 3—35121
reddening rel. to distance for early-type stars near six planetary nebulae 3—39744
shock wave structure and spectrum 3—16275
Small Magellanic Cloud, dust content revealed from UBV photometry of 11 stars 3—31773
sound vibrations, cosmic ray effects in presence of mag. field *(Russian)* 3—37478
star formation in rotating cloud with mag. field 3—35120
supernovae remnant shell interaction, a numerical model 3—19003
supernovae remnant shell interaction, radio emission source 3—19004
u.v. stars, evolution and interstellar gas 3—39739

interstellar matter continued
Vela direction absorption determ. by distrib. determ. of O-A0 stars 3−22117
X-ogen, unidentified interstellar microwave line in four new galactic sources 3−37484
CH, formation in ion-molecule reactions 3−13100
CH^+, Franck-Condon factors for $A^1\Pi$-$X^1\Sigma^+$ 3−26647
CH^+ formation in ion-molecule reactions 3−13100
CH^+ molecules, interferometric studies of interstellar 4232 Å line for 28 stars 3−39737
CO rotational cooling in dark clouds 3−31783
^{14}CO in galactic ^{12}CO sources, obs. at 105871.11 MHZ 3−13099
Ca II interstellar K-lines in spectra of γ Pegasi and ι Herculis 3−31675
D, obs. of Orion molecular cloud 3−37486
DCN hyperfine structure obs. in Orion Nebula 3−31781
DCN mols., identification from line emission from M42 (Orion Nebula) 3−31785
DCO radical $1_{01}\leftarrow 0_{00}$ transition, laboratory microwave obs. 3−19070
Fe anionic species in interstellar dust 3−13107
H I 21-cm line profiles of interstellar medium, statistical analysis 3−25518
H mol. bands obs. in u.v. spectrum of δ Scorpii 3−25510
H_2, molecules inside neutral globules imbedded in H II regions 3−25519
H_2, Raman scattering cross-section determ. 3−20100
H_2 detection from interstellar clouds in 4.4 to 28.2 microns wavelength region 3−25514
HCO radical $1_{01}\leftarrow 0_{00}$ transition, laboratory microwave obs. 3−19070
He atoms ionized by solar wind, annual variation of velocity distribution at 1 AU 3−13006
^7Li cosmic ray scattering prod., γ-ray line feature in direction of Galactic centre 3−28110
Mg II, Mg I in direction of Cassiopeia and Orion 3−9614
NaOH, laboratory microwave obs. of rotational transitions in ground vibrational state 3−29688
OD mols. $A^2\Sigma^+$ states, lifetimes and predissociation probabilities for rotational levels 3−22118
OH $^2\Pi_{3/2}$, J=5/2 state obs. in 6 sources 3−37479
OH $^2\Pi_{3/2}$ J=5/2 interferometric obs. at 5 cm 3−37493
OH components of radiosources, angular diameters rel. to interstellar scattering and H II regions 3−25512
OH emission regions, analytic approx. for saturation region 3−37483
OH excitation by collisional dissociation of water 3−31778
OH mols. $A^2\Sigma^+$ states, lifetimes and predissociation probabilities for rotational levels 3−22118
OH mols. pumped by i.r. radiation, optical thickness determ. for s.h.f. lines 3−25516

interstitials
alkali halide, review of interstitial centres 3−4754
alkali halides, Jahn-Teller distortions, molecular orbital models 3−33837
alloy, ternary b.c.c., anisotropy of substitutional-interstitial internal friction peaks 3−36365
b.c.c. alloys, substitutional-interstitial interactions 3−2704
bimetallic strip bending due to interstitial diffusion 3−1825
chemical stress of vacancy and interstitial supersaturations 3−7751
creep, chemical stress by vacancy and interstitial supersaturations 3−17916
crowdion supersonic motion, one-dimens. model with nearest neighbour nonlinear interaction 3−33519
cubic lattice, Wert-Marx law generalization and interstitial vibr. freq. *(French)* 3−1688
diamond, mech. of defect production 3−33521
diamond, neutron irrad., semiconducting interstitials, e.s.r. studies 3−33571
diffusion, light interstitial electromigration and thermomigration, quantum theory 3−30287
electron irradiation defect production rate at temperatures above stage I 3−30158
f.c.c. lattice, interstitial migration, molecular dynamics study 3−7748
f.c.c. Lennard-Jones system, form. energy, volume and entropy calcs. 3−4745
f.c.c. metal, mech. after-effect due to long range dislocation-interstitial interaction *(German)* 3−7823
f.c.c. metals, irradiated, nature of low temp. self-interstitial 3−14849
group IV, II-VI semiconductors, vacancies, interstitials, Jahn-Teller distortions, molecular orbital models 3−33837
impurity atom, location exact determ. by means of channelling effect *(Russian)* 3−1660
irradiation creep due to interstitial loop growth 3−17812
rel. to large prismatic dislocation loop generation at inclusions 3−24122
loops, growth mechanism and that for dislocation spirals 3−20751
mechanical interaction between crack tip and point defect 3−36358
metallic springs, irrad. creep in materials testing reactor 3−27809
metals, neutron irradiated, deformation and void growth under stress, vacancy and interstitial diffusion into sinks 3−31020
metals, role of interstitials and vacancies, role in recovery 3−24104
metals irradiated by 3MeV electron microscope, formation and annihilation 3−14851
nuclear reactor materials, neutron irradiated, diffusion controlled creep process, interstitials and vacancies flux into dislocation 3−24196
point defects behaviour study, stochastic processes application 3−17989
quasistationary reactions between vacancies and interstitials 3−38584
rare earth hydrides, hydrogen mobility mechanism *(French)* 3−1826
rare earth/hydrogen systems, α-phase studies *(French)* 3−2707
refractory metal solid solns. containing C, N, and O, thermodynamics and phase relations 3−34501
refractory metal systems with N, O and C, mechanisms and kinetics of absorption and desorption 3−37035
steel, carbides and nitrides occurrence, review 3−15674
steel, electron irrad. effects on hardenability 3−24948

interstitials continued
steel, ferritic, Mo-containing, comp. and microstruct. effects on creep strength 3−8933
steel, hydrogen trapping sites *(French)* 3−2742
steel, stainless, Type 304, cyclotron-injected helium effect on void form. characts. 3−35934
transition metal alloy, ternary, with interstitial elements, phase equil., composite phase stability *(Russian)* 3−27622
transition metals, b.c.c., group VA, stage III annealing mechanism 3−34592
transition metals, b.c.c., group VA, stage III recovery mechanism 3−34593
void nucleation in materials supersaturated with vacancies and interstitials, effect of insoluble gas mols. 3−27034
void nucleation in solids containing excess vacancies, interstitials and helium atoms 3−24136
water, interstitial model approach to liq. struct. 3−20686
AgBr:Cd, ionic thermocurrents meas. rel. to interstitial-vacancy complex form. 3−33518
AgCl, diffusion mechanism of Mn^{2+} 3−20888
Al, deformed, neutron irrad. effects on anelastic behaviour *(French)* 3−30207
Au, electron irrad., stable interstitial at 300K 3−4748
Au, pure, deformed, point defect clusters 3−17807
BaF_2, vacancies, interstitials and inert gases in fluorite structures 3−17814
C fibres, micromorphology stability and interstitial compounds 3−31172
CaF_2, doped, interstitial anion clusters, formation mechanism 3−30113
CaF_2, vacancies, interstitials and inert gases in fluorite structures 3−17814
CaF_2:R, R=Ce, Pr, Sm, Eu, Tb, ionic thermocurrent obs. of reorientational properties 3−7787
CdF_2, insulator to semicond. transition, F_2 interstitials diffusivity 3−4947
CdSe single crystals self-diffusion of Cd and Se, interstitial and interchance mechanism 3−33689
CdSe:Cu,In and undoped, high temp. defect equilibria 3−7745
CdTe, electron and neutron irrad., excess, dissociative Cd pressure, defect behaviour, photoluminescence spectra 3−34431
Cr, early stage of N precipitation 3−37038
Cu, caused by cyclotron irradiation, compared with Cu_3Au 3−14898
Cu, cold-worked, mech. after-effect caused by dumb-bell interstitials *(German)* 3−1663
Cu, internal friction, dislocation pinning by hydrogen *(French)* 3−2740
Cu, neutron irradiated, X-ray meas. 3−14895
Cu, plastically deformed, angular correlation of positron annihilation 3−17869
Cu foil, α-irrad., rel. to internal friction and Young's modulus *(German)* 3−7851
α-Cu-Zn alloy, electron irrad., short range order, interstitial diffusion 3−11617
Cu_3Au caused by cyclotron irradiation, compared with Cu 3−14898
Fe, Armco, hydrogen trapping sites *(French)* 3−2742
Fe and Fe-Ni alloys, hydrogen-dislocation interactions 3−4887
Fe:H, zone melted and armco, H effect on elec. resist. at low temps. 3−8807
Fe-C solid solutions, b.c.c., Snoek peak broadening due to C interstitials *(French)* 3−31018
Fe-Ga-C alloys, f.c.c., interactions between insertion and substitution atoms *(French)* 3−8777
Fe-N alloys, rapid strain aging, Snoek ordering, conc. depend. 3−24868
Fe-Ni-C alloys, internal friction meas., Snoek-peak, C interstitials diffusion towards dislocations mechanism 3−34542
Fe-Si solid solns., diffusion and solubility of hydrogen, ordering influence *(Russian)* 3−30283
Fe-Ti solid solns., temp. and conc. depend. of mech. props. *(French)* 3−31038
$Fe_{100}N_{23}$, interstitial distrib. at octahedral sites, Mossbauer spectra *(French)* 3−39060
GaAs, Co diffusion mechanism 3−33699
GaAs, GaP, electron and neutron irrad., B, C impurities, i.r. local mode abs. 3−34395
GaAs, point defects, precision lattice parameter measurements after quenching and annealing 3−33523
GaAs, surface damage induced by 50 keV Zn^+ ions, study by isochronal annealing expts. 3−24168
GaP, localised vibr. modes of O and O complexes 3−11707
Ge, prod. via 1.2 MeV β^- recoil of ^{73}Ga on $^{74}Ge(\gamma,p)^{73}Ga$, obs. by ^{73}Ge, 13.3 keV Mossbauer effect 3−34279
Ge, self-interstitials, geometrical config., migration energy 3−33522
Ge: groups III and V, electron irrad., (O_4) interstitial clusters, unusual donors and acceptors 3−33843
Hf-O system, near $HfO_{1/6}$, interstitial superstruct. and order-disorder transform. 3−14847
KI, interstitial migration of water molecules, F-band absorp. obs. 3−30120
MgO:Be^{2+}, tracer diffusion meas. up to 2340°C, interstitial diffusion mechanism 3−20891
Mo, dislocation-interstitial interactions using dislocation damping obs. 3−36312
Mo, interstitial migration on electron irradiation, recovery mechanism 3−11615
Mo, neutron irradiated, stage I defects 3−14850
Mo alloys, deformed, interstitial solid soln. decomp. during recrystn. *(Russian)* 3−37018
Na, rel. to self-diffusion mechanism 3−36439
NaCl, annealing of γ-irradiation induced hardening 3−36330
NaF:Li^+, electron irradiated, e.s.r. study of di-interstitial centre 3−2390
$NaNO_3$, calc. of migration enthalpies of Frenkel defects, application of Mott and Littleton methods 3−24294
Nb, diffusion of nitrogen, activation energy temp. depend. 3−20898
Nb alloy, softening rel. to interstitial interactions and dislocation motion 3−18627

- **interstitials** continued
  - Nb suboxides, superstructure spots appearing in electron diffraction 3−17794
  - Nb-D(2 at.%), location determ. by channelling of deuterons *(German)* 3−27017
  - Nb-H solid solns., solute interactions role 3−2743
  - Nb-H system, internal friction, domain boundary effects 3−38620
  - Nb-N-O, snoek peak height, determ. from internal friction in torsion, impurity conc. *(Russian)* 3−39335
  - Nb-O solid solns., dislocation dynamics 3−36311
  - Nb-S system cpds., nonstoichiometry rel. to elec. props. at thermodynamic equil. *(French)* 3−2113
  - Ni, cold-worked, mech. after-effect caused by dumb-bell interstitials *(German)* 3−1663
  - Ni, hydrogen-dislocation interaction, binding energy *(French)* 3−1629
  - Ni_4N, electron diffraction obs. of N interstitials and structure factors 3−14783
  - Pb:Hg alloys, modified interstitial vacancy-pair model for Hg diffusion 3−20894
  - Pb:Mg alloys, diffusion of Mg and Pb, interstitial-vacancy pair model 3−20893
  - Pb:Ni, pressure effect on Ni interstitial diffusion 3−17996
  - Pb-Ag(Au) nonsubstitutional solid solns., comp. depend. of supercond. transition temp. 3−24533
  - Pb-Au solid soln., kinetics and morphology of $AuPb_3$ precip. 3−24843
  - Pd-B-H system, statistical thermodynamics, electron interaction energy *(German)* 3−30240
  - Pt, electron irrad., recovery during stage II annealing, interstitial rearrangement 3−11618
  - Pt-Au alloy, electron irrad., recovery during stage II annealing, interstitial rearrangement 3−11618
  - Si, diffusion of Cu^+, Ag^+ and Au^+ ions over interstitial oxygen sites 3−33700
  - Si, electron irrad., 130 K annealing stage of divacancy, i.r. transmission spectra 3−33559
  - Si, electron irradiation at 0.5K, a.c. conductivity changes 3−7794
  - Si, irradiated and annealed, diffusion, role of defects, other semiconductor materials 3−33701
  - Si, mech. of defect production 3−33521
  - Si, proton irradiated, defect studies by channelling backscattering measurements 3−33579
  - Si, rel. to diffusion and electrotransport of Mg, 1000-1350°C *(Russian)* 3−7975
  - Si, self-interstitials, geometrical config., migration energy 3−33522
  - Si:Ge(Sn), O electron irrad., selective trapping of vaccancies migration of interstitials 3−33925
  - Si:Li neutron irrad., defect interactions, Hall effect, i.r. absorption studies 3−33570
  - SiC, ion bombardment, annealing, intrinsic luminescent defects 3−34430
  - SiO_2, noncrystalline, defect struct. and irradiation behaviour 3−4770
  - SrF_2:R, R=Ce, Pr, Sm, Eu, Tb, ionic thermocurrent obs. of reorientational properties 3−7787
  - Ta with interstitially dissolved H, meas. of elastic Curie const., 300 to 450 K 3−20812
  - Ti, single crystals, deformation kinetics for {1010} ⟨1120⟩ slip 3−17901
  - α-Ti single crysts., thermal activation parameters of plastic deform. *(Russian)* 3−24184
  - Tu, hydrogen embrittlement mechanism *(French)* 3−5337
  - $(U,Pu)O_{2-x}$ fuel pellets, compressive creep, diffusion of cation vacancies and interstitials 3−6991
  - V, α-irrad., He gas bubble nucleation and distrib. 3−33572
  - V, high-purity, deform. mechanism at low temps. 3−37055
  - V wire, deformation, low temp. relaxation, Snoek peak, dislocation motion 3−30206
  - V-D alloys superstructure determ. by neutron and X-ray diffr. studies and sp. ht. meas. 3−18606
  - V_4O, interstitial superstructure, O long range order 3−30112
  - W, neutron irrad., raft form. mechanism 3−33563
  - W film, r.f. sputtered, elec. resist., rel. to defect struct. 3−27241
  - ZnF_2:LiF, dielec. relax. and polarisation using vacancy and interstitial models 3−24650
  - Zr-O alloys, strain aging parameters, dislocation cell struct., irrad. effects 3−27675
  - Zr-O solid solution, interstitial order-disorder transform., neutron diffr. 3−14848
- **invariance**
  - *see also conservation laws*
  - conformal, of coupled spinor-vector fields in Minkowski space 3−22721
  - conformal, on the light core and canonical dimensions 3−13818
  - covariant wave functions with invariant helicity for massless particles 3−13806
  - Einstein-like Lagrangians, $SL_{6,c}$ gauge invariance 3−10369
  - e.m. quantities under space inversion, time reversal, charge conjugation, transform. props. 3−28998
  - gauge, in Compton scattering 3−35797
  - gauge decomposition of Yang-Mills potentials 3−10594
  - gauge invariance, current conservation and GIAO's 3−23459
  - hypercharge and isotopic-spin conservation constraints in inclusive reactions 3−26356
  - logarithmic scaling and spontaneous breaking 3−6568
  - Poincare-invariant wave eqns., quantisation, invariant scalar products 3−32634
  - reducible scale invariance at short distances, conformal symmetry and canonical scaling 3−38005
  - scale invariance, vector meson dominance approach 3−847
  - tensors, Cartesian, invariant under point group transformations, zero component determ. 3−17751
  - vacuum polarisation, gauge invariance 3−10683
- **iodine**
  - admixture with Ar, of Townsend coeff. *(German)* 3−4682
  - adsorption on Ag(111), site determ. by l.e.e.d. 3−11803
  - atmospheric, remote mapping, tunable laser technique 3−3191
  - atoms, $^2P_{1/2}$-$^2P_{3/2}$ hyperfine struct. transition, induced emission spectra 3−32547
  - atoms, $^2P_{1/2}$-$^2P_{3/2}$ transition, induced emission, linewidth 3−32548
- **iodine** continued
  - chemical transport reaction thermodynamics, Ta transport by I 3−2641
  - complex formation of I_2 with pyridine in cyclohexane soln. effect on positronium I_2 reaction 3−25100
  - complexes, charge-transfer, with saturated cyclic sulphides, far i.r. spectra 3−26667
  - crystal growth of Si-Ge solid son. by sealed tube I transport method 3−2649
  - electron affinity in alkali metal compound 3−1117
  - energy transfer research 3−11304
  - gaseous and particulate samples in marine atmosphere at Oahu, Hawaii 3−12750
  - growth of GaSe crystals by I transport, comparison with other vapour growth methods 3−2650
  - in hydrocarbons, chem. effects of $^{127}I(n,2n)^{126}I$ and $^{130m}I(I.T.)^{130}I$ reactions 3−12541
  - ions, response of Si surface barrier detector 3−13428
  - labelling with ^{131}I or ^{125}I 3−39460
  - Lamb-dip spectroscopy, hyperfine struct. in electronic spectrum 3−11276
  - laser, gas, photochem., energy storage and transfer 3−10516
  - laser, photochemical 1.2 GW 3−19598
  - laser, photodissociation type, emission line press. broadening, energy storage capacity increase 3−22870
  - laser amplifier, 5-ns, gigawatt power, construction and props. 3−10517
  - methanol-I_2 solutions, boiling, stress-corrosion cracking effect on Zircaloy-2 3−24886
  - molecular, absorpt. spectra, 45-160 eV, inner electron excitation in gaseous and solid phase 3−29647
  - molecular, H.F.S. of optical transitions 3−1210
  - molecule, and nucl. quadrupole coupling in Σ and π states 3−4454
  - molecule, B $^3\Pi(O_4{}^+)$ state, mag. fluorescence quenching, direct inversion 3−38303
  - molecule, nonlinear level crossing in $X^1\Sigma_g{}^+$ state 3−1251
  - molecule, pot. function from spectroscopic data obs. regularities 3−26645
  - molecule, selective excitation, reson. fluoresc. 3−29711
  - molecule, visible-i.r. absorpt. spectrum, resolution 3−36008
  - natural content of Antarctic ice 3−12564
  - in nuclear plant atmosphere, removal by sprays, computerized model calcs. 3−7002
  - photodissociation laser, luminesc. of $^2P_{1/2}-{}^2P_{3/2}$ transition 3−32554
  - solid, phonn dispersion and symmetry 3−24236
  - tektites, I concentrations rel. to obsidians and impact glasses 3−16199
  - vapour, excited by ionized Ar and Kr lasers, fluoresc. obs. 3−23588
  - vapour, resonance fluorescence under off-resonance monochromatic excitation 3−17451
  - vapour growth of Ge in open iodide system, efficiency of Ge transport *(Russian)* 3−15615
  - Ga(As, P):I highly doped mixed crystals, problems of growth *(German)* 3−8765
  - I to I_2, photochemical oxidation 3−15839
  - I V to I VIII, spectrograms, broad line features at about 140 Angstroms 3−17368
  - I^- ions, effect on mag. props. of electrodeposited Co films *(Bulgarian)* 3−30670
  - I^- ions, effect on structure of electrodeposited Co *(Bulgarian)* 3−30366
  - I^- reson. in I_3^- aq. solns., exchange study from n.m.r. line broadening obs. 3−25050
  - I_2, gaseous, mol. dissoc. energies 3−20188
  - I_2, monochromatically excited, energy transfer processes, quenching by I 3−23625
  - I_2 B-state lifetimes, magnetic field dependence 3−7218
  - I_2 dissolved in hydroxylic solvents, photolysis, atom charge transfer complex identification 3−34736
  - I_2 in hydrocarbons, chem. effects of (n,γ) reactions 3−12540
  - I_2-Ar interactions, Raman spectra, resonance, laser induced, vibrational frequencies 3−23620
  - I_3^-, i.r. and Raman spectra, determ. of fundamental vibrations and splitting of bands 3−1224
  - $I(Br)-H_2(D_2)$, reaction mechanism, classical dynamical study 3−37119
  - ^{123}I cyclotron production, $^{122}Te(^4He,3n)^{123}Xe \rightarrow {}^{123}I$ 3−37681
  - $^{127}I_2$, molecular absorp. of three Kr II laser lines *(German)* 3−36010
  - ^{129}I implanted ions in semiconductors and alkali halides, Mossbauer study 3−34261
  - ^{131}I treatment of thyroid cancer 3−3584
  - Sb_2Te_3:I, reflectivity obs. rel. to band structure and transport props. 3−8607
- **iodine compounds**
  - group IV tetraiodides, Raman spectra, 20 to 420°C, Coriolis and force const. determ. 3−29662
  - perfluoralkyl photodissociative laser, selective pumping effect *(Russian)* 3−10540
  - IBr, charge-transfer complexes with saturated cyclic sulphides, far i.r. spectra 3−26667
  - IBr, collision with K_2, reactively scatt. K atoms, ang. distrib. meas. 3−29750
  - IBr, vacuum u.v. spectrum, Rydberg transitions in wavelength region 160 to 130 nm 3−1213
  - IBr_2^-, i.r. and Raman spectra, determ. of fundamental vibrations and splitting of bands 3−1224
  - ICN, μ-wave spectra 3−29693
  - ICl reactive collisions with Ba, Sr, Ca, Mg, crossed beams product angular distributions 3−27864
  - ICl_2^-, i.r. and Raman spectra, determ. of fundamental vibrations and splitting of bands 3−1224
  - ICl_4^-, i.r. spectra, force consts. *(French)* 3−1173
  - IHI, computed bond energies and vibr. freq., including isotope effects 3−1181
  - IOF_5, bond angles and lengths 3−14323
- **ion beam effects**
  - coated metal surfaces, probability distributions of emitted electrons *(German)* 3−27591
  - crystalline defect anal., ion beam techniques 3−33577

ion beam effects continued
electron cyclotron drift instability, controlled steady-state experiment 3—14553
figuring miniature aspherics, ion polishing technique 3—28530
Ge, lattice disorder induced by 0.3 MeV D^+ random bombardment, 1.5 MeV D^+ channelling measurements 3—1656
implantation techniques for semiconductor device manufacture and anal. *(Dutch)* 3—30162
integrated optics component fabrication technique employing ion beam micromachining 3—28531
ion cyclotron plasma instability production by fast beam 3—7538
massive deposits produced by high rate vapour deposition process, effects on microstructure 3—27632
metal, polycrystalline, surface, noble metal ion bombardment, electron ejection, positive ion refl. 3—2608
metal foils, ion bombardment induced voids, location by vibratory polishing 3—21772
orientation of single crystals, by shadow effect, improvement using streak-camera *(Russian)* 3—11524
r.f. diode glow discharge sputtering, positive-ion bombardment of substrates 3—18516
secondary electron yields, ion impacts on thin film oxide surfaces, spectrometer 3—28709
semiconductors, ion and electron irrad., clustering of defects 3—33576
Si, lattice disorder induced by 0.3 MeV D^+ random bombardment, 1.5 MeV D^+ channelling measurements 3—1656
solid, emitted neutral atoms and ions energy spectra *(Russian)* 3—15578
solid surface examination, X-ray production by heavy ion bombardment 3—24770
steel, nitriding by ion bombardment of 18-10 stainless steel *(French)* 3—24908
steel, stainless, Ni ion-bombarded, surface struct. 3—4777
thinning apparatus for sample prep. for electron microscopy, applic. to epitaxial Si on sapphire 3—1939
Al film, He ion pre-injected, electron irradiation effect on void form. 3—20967
Al_2O_3, sapphire polishing, surface laser damage threshold 3—29118
Au, sputtering by bombardment with Ar^+ and Xe^+ ions, 20-50 keV 3—8692
Cu, heavy ion bombardment, shadow effect 3—33574
Cu, X-rays from Ne^+ collision with solid target 3—27585
GaAs, irrad., cond. in disordered regions *(Russian)* 3—2072
GaAs, surface damage induced by 50 keV Zn^+ ions, study by isochronal annealing expts. 3—24168
GaAs:Te, impurity-defect interaction with Te ions bombard., amorphous layer form. 3—18062
GaAs:Zn, H^+ ion bombardment, channelling expts., annealing behaviour of disorder density 3—33578
Ge, H^+, O^+, B^+, ion bombardment, divacancy-like optical absorption 3—34394
Ge, N_2^+ and Kr^+ bombarded, relax. of electron emission *(Russian)* 3—8694
Ge single crystals, Na^+ induced lattice damage, effects on angular and energy distributions of scattered ions, $E<5$ keV *(Russian)* 3—11663
He interaction of interpenetrating beams moving unidirectionally in an external magnetic field *(Russian)* 3—32618
$LiNbO_3$, growth of craters during ion etching 3—1859
$LiNbO_3$, irrad., expansion, crazing and exfoliation 3—17880
Mo, irrad., depth of damaged zone *(Russian)* 3—4776
Nb, blister formation due to 0.5 MeV ^4He ion impact, morphology, irradiation temperature and channelling effects 3—1653
Nb_3Sn layer, O ion irradiation effect on superconducting critical current density *(German)* 3—2210
Ni, shapes of irradiation produced voids 3—30111
Ni, void prod. by ion irrad., electron stereomicroscopy analysis 3—11608
Pb, surface machining, metallographic prep. 3—8887
Si, form. and annealing of isolation regions on Si^+ bombard. 3—7798
Si, formation of disordered layers by Ar^+, Ne^+ and B^+ ion bombardment 3—24167
Si, ion beam irrad., VV centre prod., e.s.r. *(Russian)* 3—8444
Si, ion implantation, radiation damage 3—33585
Si, ion implanted, defect formation 3—33586
Si, surface structure rearrangement on bombard. with Ne, Kr and Ar ions 3—1860
Si, X-ray spectra on excitation by O ion beam 3—30894
Si amorphous film, ion-implanted, circular etch pits 3—33752
Si amorphous layers, produced by ion irrad., interdiffusion with Pd film 3—27142
Si irradiated with B and P ions, spatial distrib. of radiation defects 3—24166
Si layers, epitaxial, thinning for transmission electron microscope of cross-sections 3—1552
p-Si single crystal secondary electron emission influence of K^+ and Cs^+ bombardement 3—21506
Si single crystals, Na^+ induced lattice damage, effects on angular and energy distributions of scattered ions, $E<5$ keV *(Russian)* 3—11663
Si surface relief structure after ion bombardment 3—15059
Si:B, ion implantation defect centre studies 3—33587
Si:Ge(Sn), O electron irrad., selective-trapping of vacancies, migration of interstitials 3—33925
Si:In, ion implantation, damage around ion tracks 3—33588
SiC, ion bombardment, annealing, intrinsic luminescent defects 3—34430
SiO_2, vitreous, ion bombardment, threshold energy 3—7797
SiO_2, X-ray spectra on excitation by O ion beam 3—30894
SiO_2 films, ion neutralisation processes, impurity migration effects 3—34450
SiO_2 films on Si, C-V degradation 3—17879
SiO_2 films on Si, phosphosilicate glass passivated, ion bombardment effects 3—39288
SiO_2 layer on Si surface, effect on surface props. and interface charge 3—14899
Si(111) bombarded with 1.5-25 keV inert gas ions, electron emission *(German)* 3—27590
ion beam effects continued
Sn, inhibition of radiation blistering 3—24165
Ta autocathode, structure changes on He ion bombard. *(Russian)* 3—8689
Ti and alloys, nitriding by ion bombardment *(French)* 3—24909
UO_2 thin films, ion beam sputtering preparation technique, annealing, structural investigations 3—33756
W, heavy ion bombardment, shadow effect 3—33574
W surface, nitrided layer formation by ion bombardment 3—4922

ion beams
see also energy loss of particles; ion beam effects; ion optics; mass spectrometers; particle accelerators; sputtering
aberrations, Nth order, for ion orbits in static magnetic fields 3—808
accelerator, 30 kV, for erosion studies 3—10027
ceramic material thinning for transmission electron microscopy 3—33436
ceramics, electron microscope specimens, prep. and ion beam machining 3—24008
chemical accelerator beam instrument for ion-molecule reaction kinetics, 0.1-100eV 3—25923
collective acceleration during neutron prod. in high-current diode 3—3843
conference, Dutch Physical Society, Amsterdam (Feb. 1973) 3—28428
crystal and molecular classification, ion scatt. study *(Dutch)* 3—30082
cyclotron, formation of neutrals 3—28633
cyclotron, isochronous, horizontal motion and phase dilatation of internally injected ion beam 3—25838
cylindrical beam, combined effects of space charge and external fields 3—37989
emittance improvement 3—10036
emittance meas. in low energy ion source 3—32205
energetic, production, apparatus for, design problems 3—6536
energy recovery from charged particles in thermonuclear mirror reactor *(Russian)* 3—23448
excitation of long wave oscillations by the secondary electron stream in a plasma formed by an ion beam *(Russian)* 3—11495
field emission microscopes, characteristics at tip of field-emitter point *(Russian)* 3—10117
focusing of short duration intense electron beams *(Russian)* 3—6533
heating and slowing-down of ion beams in plasma 3—14521
heavy ion acceleration to energies above 200 MeV/nucleon 3—25829
impurity atom, location exact determ. by means of channelling effect *(Russian)* 3—1660
injected into plasma transversely to magnetic field, relax. *(Russian)* 3—14517
insulator surface bombardment, mobilization 3—36972
insulator surface bombardment, neutralization 3—36971
Li, polarized particle beams, current state of physics and technology for prodn. 3—35727
line focusing for accelerators by electrostatic lens 3—25839
magnetic and electrostatic deflectors 3—25840
magnetoactive plasma with transverse ion beam, instability at multiples of ion gyro-frequency 3—17615
mass spectrometer, width by symmetrical analyzer 3—19659
mass spectrometer design and performance using beam transport theory 3—331
microprobe analysis of small particles 3—37766
microprobe mass analyzer, quantitative correction procedure, CARISMA program 3—37768
negative, electron binding energy determ. from charge exchange cross sections 3—38242
nonlinear interaction between fast ion beam and plasma electrons 3—26890
plane, transformation into hollow cylindrical *(French)* 3—276
plasma-beam instability, nonlinear transformation and stabilisation 3—26887
plating, review 3—39228
profile measuring device and focusing aid 3—10034
profiles meas. method 3—25940
range in matter for relativistic heavy ions 3—33583
scattering of H_2, D_2 and rare gases from Ag(111) single crystal, surface roughness effects 3—21507
scattering of ions by atomic chain rel. to atomic surface structure determ. 3—34451
surface composition by analysis of impact radiation 3—36973
surface physics studies, review 3—39208
surface topography, composition and orientation of single cryst. determ. by ion impact studies *(Dutch)* 3—30903
transition metal oxide scales, study of grain structure 3—24859
trochoidal, in deflecting wedge field mass spectrometer 3—32211
ultra-high vacuum system for use with ion accelerator 3—9911
Al target, X-ray emission under O^{+n} bombardment, charge-state depend., dynamic screening 3—24768
Ar penetration profiles in Ta, determ. by (p, γ) reaction 3—26010
Ar^+, bombardment of Al surface, negative ions energy distrib. 3—15583
B ion equilibrium charge distributions after interaction with C foil 3—11662
Be I and II, energy levels and radiative lifetimes, beam foil studies 3—11159
Cl 30 MeV beam, high resolution K X-ray spectrum 3—7049
D^+, neutrals formation in cyclotron 3—28633
H, polarized particle beams, current state of physics and technology for prodn. 3—35727
H^+, bombardment of Al surface, negative ions energy distrib. 3—15583
H^+ scattering in the weakly screened Coulomb field of Au nuclei 3—11182
H_2^+, neutrals formation in cyclotron 3—28633
H_2^+, plane, transformation into hollow cylindrical *(French)* 3—276
^2H, polarized particle beams, current state of physics and technology for prodn. 3—35727
He, backscatt. spectra in planar channelling, oscillations stochastic model approach *(French)* 3—27589
He^+, channelling in Fe, oscillating trajectories, backscatt. obs. 3—4778
He^+, excitation by transmission through Au cryst., absence of channelling effect 3—1110

ion beams continued

He^+ ion-beam-plasma system, instability wave growth and surface waves propagation 3−23854
He^+ scattering in the weakly screened Coulomb field of Au nuclei 3−11182
He^{++}, neutrals formation in cyclotron 3−28633
^3He, polarized particle beams, current state of physics and technology for prodn. 3−35727
Li^+ scattering in the weakly screened Coulomb field of Au nuclei 3−11182
^7Li, ion beam, diffraction at atoms rel. to scatt. undulations 3−14314
N^+_2, Meinel system extension to high vibr. levels of $A^2\Pi_a$ state 3−26655
$N_{14}{}^{7+}$, multicharged, prod. *(French)* 3−281
$O^+ + D_2$ collisions below 4 eV, production of excited OD^+ 3−29747
SiO_2, O_2:HCl grown, residual Cl distrib., He^+ scatt. study 3−30951
Ta ions stripped in gases and solids, with energies 2-15 MeV, equilib. charge-state distributions 3−11183
ThO_2, axial channelling of 6.5-MeV $^3He^{2+}$ ions 3−17883
U ions stripped in gases and solids, with energies 2-15 MeV, equilib. charge-state distributions 3−11183

ion counters *see counters*

ion density

atmospherc density and composition rel. to time varying model aurora 3−34916
atmospheric precipitation, chemical composition meas. using station network, ion concentrations 3−28048
D and E-region, negative ion composition 3−3102
D region profiles during solar cosmic ray bombardment at polar latitudes 3−25295
D- and E-region ion-neutral reactions 3−3104
D-region, dependence of positive ion composition on O and H concentration 3−3097
D-region, negative ion conc. 3−3103
D-region, negative-ion changes during sudden ionospheric disturbances 3−25281
D-region ion density model rel. to diurnal var. of electron density 3−3116
D-region ionization Winter anomaly, meas. of positive ion conductivities 3−3117
daytime D-region, negative ion composition 3−25282
dense plasmas, ionization equilibrium theory 3−14509
Explorer 31, ionospheric satellite, ion flux angular distrib. in wake 3−25276
F region, equator vertical profile calcs. 3−18885
fast MHD waves diffraction by plasma layer of a periodically varying density 3−17588
hypersonic sphere wake meas. 3−11503
ionosphere, large-scale nonuniformities at 600 km altitude 3−31404
ionospheric research, use of VLF radiowaves, whistler mode, ion electron density and temperature studies, review 3−18900
ionospheric rocket borne probe meas. 3−3058
laser plasma injection into a stellarator, plasma densities and confining mag. field strength 3−20567
mesosphere, charged particle concentration and mobility measurements 3−3031
metal-ion concentrations in sea-surface microlayer and marine atmospheric aerosol samples in Hawaii 3−12680
plasma, anodic, spectrometric study of emitted light, electron, ion and atomic densities *(French)* 3−26897
plasma density decay meas. in different field geometries 3−20609
plasma high beta density profiles holographic interferometry technique at $\lambda = 3 \mu m$ 3−20634
plasma in shielded volume *(Russian)* 3−4631
plasma stream movement stability investigation in the mag. field of a divertor, plasma density meas. *(Russian)* 3−14535
plasma theta pinch, instabilities study by microwave scattering, density, fluctuations meas. 3−20522
plasmapause, light-ion trough and main trough 3−16044
Pleiade accelerator, ion current density studies 3−20654
silicate glasses, diffusion rates and solubilities of He and Ne as a function of SiO_2 content 3−4883
weakly ionised gas, analysis of positive ion current in region of highly negative probe, boundary layer approx. 3−20610
Ar, dense plasma production in plug-shaped mag. field by an electron beam, plasma density meas. *(Russian)* 3−17628
Ar ionisation meas. behind shocks with microwaves and a pulsed Langmuir probe *(German)* 3−14594
H^+ thermal ions, in magnetosphere 3−3148
$O^+{}_2/NO^+$ in E-region, photochemical activity 3−3098

ion emission

see also secondary ion emission; thermionic ion emission
electronics and vacuum physics, conference, Kralovopolska, Czechoslovakia, Oct. (1972) 3−15576
field evaporation models, image-lump or image force model, intersection model 3−15599
field ionisation energy spectra, resonance tunnelling, surface plasmon creation 3−34466
field ionization processes, time depend. perturbation theory image form. mechanism 3−8708
Si, ion-electron emission, relax. effect, temp. and current depend. 3−21510

ion engines

see also aerospace propulsion; rockets
Kaufman ion thruster, electrostatic dual-grid beam deflection system 3−11512
rocket engine, discharge characteristics 3−29995
throttled ion thruster, hollow cathode discharge effects 3−38514

ion exchange

borosilicate glass, ion exchange chemical strengthening 3−15789
calcite, cationic distrib. and structural changes of mixed Mg-Ca layers 3−15849
chromatography, lunar fines, contamination problems in search for amino acids 3−35095
chromatography, use in lunar organic anal. 3−32267
glass, low temp. and effect on internal friction 3−25064
interdiffusion coeffs. meas. of alkali ions in Na_2O-Cs_2O-SiO_2 glasses 3−11764

ion exchange continued

on-line radiochemical analysis to recover transplutonium elements 3−18801
oxyhydrate ion-exchange matrices, formation by polymerisation *(Russian)* 3−15824
proteins, sorption by ion exchange resins, kinetics 3−34748
Rayleigh wave study of ionic diffusion and stress buildup in ion exchanged glasses 3−4916
transuranic element recovery, in nuclear fuel reprocessing *(French)* 3−38184
Cu ammine complex, from a cation exchange resin, elution kinetics 3−34704

ion exchanging *see ion exchange*

ion implantation

see also semiconductor doping
beam technology, state of the art review 3−15648
cyclotron applications in mats. science, review 3−20761
dopants change, description of fast method 3−25941
electron and ion beam technology, conference, Houston, Texas, (1972) 3−13473
equipment, 150/300 kV 3−13410
equipment, for semiconductor manufacturing 3−15651
GaAs:He(N,S,Zn), ion implantation, elec. conduction due to defect centres 3−33906
impurity distribution, enhanced diffusion by vacancy mechanism 3−33537
insulators, charge-removal studies using ion-induced characteristic X-rays 3−11669
isotope separator implantation of radioactive ion for hyperfine interaction studies 3−32217
low power switching integrated circuit production 3−15653
metal-semiconductor contacts, preparation, technique conditions, homogeneity, low-resistance *(German)* 3−15646
microelectronics, comparison with diffusion method *(German)* 3−34487
m.o.s. device, threshold voltage increase by P ion implantation 3−33998
m.o.s. devices, advantages and application 3−18556
quartz optical waveguide, single mode and multimode characts. with Ar and Li 3−17889
review of ion implantation doping of compound semiconductors 3−30166
semiconductor, ion and electron irrad., clustering of defects 3−33576
semiconductor device production, dopant concentration control 3−15649
semiconductor manufacture, production machine requirements 3−15650
trapping and gas release apparatus 3−28713
AgBr, of Ag, P and Cd ions, photosensitivity obs. 3−17891
B^+, in Si, depth distrib. of defects and impurities 3−17890
Cs^+, range in Ni rel. to preliminary low-energy bombardment 3−14901
GaAs, of Kr and Tl, energetic ion collection, saturation effects 3−11646
GaAs, of Kr and Tl, ion conc. profile and ion range probability distrib. 3−11647
GaAs:F^-, implantation profile, Auger spectroscopy determ. 3−12309
GaAs:In,Zn diode, fabrication, elec. and optical props. 3−11948
GaAs:Te, influence of implantation temp. and surface protection 3−12310
GaAs:Zn, H^+ ion bombardment, channelling expts., annealing behaviour of disorder density 3−33578
GaP, of Kr and Tl, energetic ion collection, saturation effects 3−11646
GaP, of Kr and Tl, ion conc. profile and ion range probability distrib. 3−11647
Ge, of Kr and Tl, energetic ion collection, saturation effects 3−11646
Ge, of Kr and Tl, ion conc. profile and ion range probability distrib. 3−11647
He ions, in polycrystalline Nb, radiation blistering 3−17881
^{129}I implanted ions in semiconductors and alkali halides, Mossbauer study 3−34261
MgO:He, Ar, Fe, Cr, photolum. from defect related centres 3−21463
Na^+, range in Ni rel. to preliminary low-energy bombardment 3−14901
^aOs, A = 186, 188, 190, 192, recoil implanted in Ni, mag. dipole moments of first 2^+ states 3−14119
Pa:D, obs. of superconducting transitions up to temps. of 11 K following ion implantation at liquid He temps. 3−8297
Pa:H, obs. superconducting transitions up to temps. of 9 K following ion implantation at liquid He temps. 3−8297
Si, amorphous layers formation by Si^+ implantation 3−17888
Si, anodic oxidation, sample holder 3−37662
in Si, concentration profiles 3−15652
Si, defect formation 3−33586
Si, diffusion of B from shallow ion implants 3−7784
Si, high energy C^+ bombarded, damage profiles 3−17887
Si, lateral spread of implanted Kr ions, backscatt. study 3−18551
Si, lattice defects and spatial distribution of deposited energy *(Japanese)* 3−14884
p-Si, N^+_2 ions, lateral photovoltaic effect due to 3−2124
Si, of Kr and Tl, energetic ion collection, saturation effects 3−11646
Si, of Kr and Tl, ion conc. profile and ion range probability distrib. 3−11647
n^+- and p^+-Si, ohmic contacts by Al ion implantation 3−18214
Si, radiation damage 3−33585
Si amorphous film, ion-implanted, circular etch pits 3−33752
Si devices, review *(Polish)* 3−15642
Si technology, advantages over doping by diffusion *(Danish)* 3−8748
Si transistor manufacture 3−8761
Si:Ar, X-ray study of lateral strains 3−38603
Si:B, defect and impurity distribution, radiation damage 3−4766
Si:B, implanted single crystal, X-ray diffraction for defect structure obs. 3−38522
Si:B, implanted through thermal SiO_2 films, resist. 3−24523

- **ion implantation** continued
  - Si:B, ion implantation, defect centre studies 3−33587
  - Si:B, masking using W film 3−30949
  - Si:Tn, damage around ion tracks 3−33588
  - SiC, 6H type, ${}^{11}B^+$ implantation, phosphor prep. 3−30956
  - SiC, ion bombardment, annealing, intrinsic luminescent defects 3−34430
  - SiC, of ${}^{14}N^+$, ${}^{11}B^+$, ${}^{27}Al^+$ ions, effects 3−1633
  - SiC, prep. by Si ion implantation of diamond *(Russian)* 3−8764
  - ZnO, implanted, anneal characts. 3−30955
- **ion lenses** *see lenses*
- **ion microscopes**
  - *see also ion beams; ion optics*
  - autoionic projector, thin films, electron bombardment 3−344
  - field, with time of flight mass analysis 3−381
  - field emission, study of Co-Ti alloy 3−27635
  - image appearance det. by statistics of imaging-gas atoms 3−380
  - ion stream characteristics at tip of field-emitter point *(Russian)* 3−10117
  - ion-electron image converter for ion microscopes *(Russian)* 3−6116
  - microprobe analyser, secondary ion collection system 3−6111
  - specimen holder and air lock, for use in high vacuum field ion microscope 3−13461
  - trace analysis techniques for solids, and instrumentation, review 3−22555
- **ion microscopy**
  - *see also field ion microscopy*
  - optical parameters, microanalysis applications 3−13474
  - scanning heavy ion, feasibility 3−28730
- **ion mobility** *see ion velocity; ionic conduction in solids*
- **ion optics**
  - *see also ion beams; ion microscopes; mass spectrometers*
  - aberrations, Nth order, for ion orbits in static magnetic fields 3−808
  - chopper buncher system to produce short ion bursts for linac 3−10033
  - double focusing mass spectrometer with parallel beams *(Rumanian)* 3−10094
  - double focusing uniform field magnet, with circular poles 3−19278
  - field emission image formation, effect of e.s. field asymmetry 3−19661
  - field emission microscopes, characteristics at tip of field-emitter point *(Russian)* 3−10117
  - image of off-axis point source in cylindrical-mirror electrostatic analyzer *(Russian)* 3−6096
  - ion cluster acceleration, in electron ring device 3−13383
  - ion-electron image converter for ion microscopes *(Russian)* 3−6116
  - Kaufman ion thruster, electrostatic dual-grid beam deflection system 3−11512
  - magnetic and electrostatic deflectors, for beams 3−25840
  - mass spectrometer with trochoidal ion beam instrument, theory 3−13453
  - parametric acceleration of ions in alternating magnetic field, simulation of plasma transport processes *(Russian)* 3−13783
  - probes and microscopes, microanalysis applications 3−13474
  - spectrograph, dependence of design line shape on ion-optical parameters *(Russian)* 3−6097
  - system with ideal magnetic field, positions and widths of image lines, first-order theory 3−19660
  - Uppsala tandem Van de Graaff accelerator, ion beam transport system 3−32123
  - He interaction of interpenetrating beams moving unidirectionally in an external magnetic field *(Russian)* 3−32618
- **ion pumps**
  - electrostatic getter-ion pump, performance 3−37611
  - getter ion pump, for processing electrostatically focused klystron amplifier 3−19183
  - ultra high vacuum for a field ion microscope *(French)* 3−10115
- **ion recombination**
  - cyclohexane, liquid, electron-pulse radiation induced conductivity *(Russian)* 3−5394
  - D-region, theoretical estimate of effective recombination coeff. 3−3082
  - D-region ion chemistry charges during solar flares rel. to ion recombination 3−3109
  - kinetic rate constants in an O afterglow *(French)* 3−11517
  - mass spectrometer, ion-electron recombination cross section meas. *(Japanese)* 3−32206
  - Onsager's recombination theory appl. to liquid alkanes 3−5396
  - triplet state form in spurs, calc. of fractional number 3−1265
  - X-ray satellite spectra formation in solar flares 3−18956
  - Ar plasma, experimental and analytical aspects of heat transfer 3−33343
  - $Ar+H_2$ discharge deionisation process 3−30041
  - $Ar+H_2O$ discharge deionisation process 3−30041
  - H plasma ionisation, recombination and population of excited levels 3−29938
  - H^+ and H^- in slow collisions 3−7085
  - $H_3O^+.(H_2O)_n$ with electrons in D-region 3−3107
  - $H_3O^+.(H_2O)_n$-series ions, electron recomb. meas. 3−14395
  - He^+-$He_2{}^+$, low temp. plasma, atomic and mol. afterglow 3−23915
  - $He_2{}^+$ electronic recombination, afterglow analysis technique 3−17704
  - ${}^3He_2{}^+$, ${}^4He_2{}^+$, electronic-recomb. coeff. 3−33150
  - $N_2{}^+$ dominated afterglows, dissociative recomb. at elevated temps. 3−11293
  - $Ne_2{}^+$, electron temp. dependence of recombination coeff., microwave meas. 3−33389
  - $O_2{}^+$ dominated afterglows, dissociative recomb. at elevated temps. 3−11292
  - SiO_2 films, ion neutralisation processes, impurity migration effects 3−34450
- **ion scattering**
  - atom-heavy ion collisions, vacancy occupation probabilities 3−38245
  - atomic surface structure analysis by multiple ion reflection 3−30323
  - charged particle scattering by a localised mag. field, teaching approach 3−37574
  - inert gas by inert gas atoms, singularities involving inner shell excitation 3−20064
- **ion scattering** continued
  - insulator surface bombardment, mobilization 3−36972
  - insulator surface bombardment, neutralization 3−36971
  - magnetic mirror 2X decay, ion scattering due to Rosenbluth-Post convective loss cone instability 3−20445
  - metallic scattering of He ions, cut off of l.f. radiation 3−27588
  - at strippers, in tandem Van de Graaff accelerators, beam optics calculations 3−16473
  - surface analysis by ion scattering, spectrometry 3−32259
  - surface struct. by low energy noble gas ion scatt., outermost atomic layer struct. 3−30325
  - thick target, equilibrium charge distribution meas. 3−25893
  - Ar, Rb ion collision, quasimolecular state interference 3−20066
  - Cd, inelastic collisions with slow alkali and alkaline earth ions, threshold to 1000 eV 3−20065
  - Cs^+ scattered from surface of W crystal, meas. of fine structure in energy spectra 3−18520
  - GaP, oxide layer chem. comp. from Rutherford scatt. 3−33744
  - Ge single crystals, Na^+ beam induced lattice damage, effects on energy and angular distributions of scattered ions, $E<5$ keV *(Russian)* 3−11663
  - Li^+ by He mechanism of inelastic transitions in collisions 3−20061
  - $N_2{}^+ + He$, 0.5 to 3 keV, elastic scatt. and vibro-rot. dissoc., classical theory 3−38320
  - Ni, backscatt. of noble gas ions, energy distrib. rel. to struct. of surface 3−30324
  - Si single crystals, Na^+ beam induced lattice damage, effects on energy and angular distributions of scattered ions, $E<5$ keV *(Russian)* 3−11663
- **ion sources**
  - *see also ion emission*
  - alkali metal 3−28637
  - automatic ion current control of direct inlet system 3−25842
  - cathode sputtering technique for introduction of solid substances into discharge atmosphere *(Russian)* 3−10042
  - cold-cathode source for heavy ion beams at Texas A and M cyclotron, USA 3−13402
  - combination ion source and surface ionisation 3−32208
  - constricted, fireball formation, plasma potential, electron temp. across sheath, electron drift velocity investigation 3−26898
  - cyclotron, Grenoble, France, axial injection system 3−13399
  - cyclotron injection systems 3−13398
  - duoplasmatron, use of spike cathode to increase cathode life 3−16500
  - duoplasmatron type, for 150/300 kV ion implantation equipment 3−13410
  - electron bombardment, used with time-of-flight mass spectrometer 3−35489
  - emittance improvement 3−10036
  - gun, computer design 3−22523
  - heavy, technology and chemistry 3−32131
  - laser, mass spectroscopy determ. of molecular stoichiometric composition 3−28781
  - laser irradiation of solid surface, highly stripped ion source 3−286
  - laser source of multiply-charged ions, production of ${}^{12}C^{6+}$ and ${}^{27}Al^{12+}$ 3−19283
  - low divergence extraction system, design 3−19285
  - low energy, meas. of beam emittance 3−32205
  - magnetic fields, longitudinal, effects, optical meas. *(Hungarian)* 3−17559
  - mass selected beam source for low energy ion-neutral crossed beam studies 3−16498
  - molecular beam source for mass spectrometer for reactive species 3−25924
  - monoplasmotron ion gun for microtechnology applications, experimental experiences with *(Slovak)* 3−20649
  - negative ions, bombardment of solid surfaces by positive alkali ions *(Russian)* 3−6061
  - Penning, high charge state output, analysis 3−35464
  - pulsed r.f. source, mass and energy of charged particles *(Japanese)* 3−279
  - quasi-neutral heavy ion plasma, magnetic field confinement *(French)* 3−26894
  - surface ionization high temp. ion source for isotope separators 3−13406
  - telefocus ion gun, with variable beam profile 3−13411
  - transistor modulator for ion source of mass-spectrometer *(Russian)* 3−10037
  - twin anode, for specimen thinning equipment in electron microscopy 3−13459
  - d, polarized, for Birmingham cyclotron, England 3−13400
  - As, possible beam sources 3−22428
  - B, possible beam sources 3−22428
  - Cs primary ion source for sputtering mass spectrometer 3−25931
  - D polarized negative beam production 3−22431
  - H^-, h.f., optimal current *(French)* 3−280
  - H^- injection system for TRIUMF 500 MeV cyclotron, Vancouver, Canada 3−13401
  - He negative ions, with K vapour charge exchange 3−13407
  - Li source, Blewett-Jones type, design and props. 3−10038
  - P, possible beam sources 3−22428
  - ${}^{90}Sr$-${}^{90}Y$ β-ray source bonded in Al, for dosimetry 3−32132
  - W-Re (3 at wt %) alloy, mass spectrometer filament lifetimes in presence of O_2 3−25929
- **ion thrustors** *see ion engines*
- **ion velocity**
  - *see also electrolytic ion velocity*
  - activated ion-mol. reactions in strong electric fields, rate calc. from asymptotic velocity distribution expressions 3−11299
  - aqueous soln., protonic, relation to frictional relax. drag 3−27134
  - asymptotic behaviour of the velocity distribution of drifting ions in strong electric fields 3−11298
  - auroral ionosphere distrib. 3−9322
  - distribution in weakly ionized gas in uniform electric field of arbitrary strength 3−4519
  - disturbed ionosphere, ion and electron kinetics at 100 to 200 km height 3−28059
  - gaseous ion motion in electrostatic fields, Monte-Carlo simulation 3−33335
  - insulator surface bombardment, mobilization 3−36972

ion velocity continued
ionospheric plasma flow past semi-infinite cylinder 3−9323
KI/DMSO system, K^+ and I^- mobility determ. from conductivity and transport number meas. by interface diffusion method *(German)* 3−37130
magnetosphere, effect of electric field induced by time-dependent ring current on drift motion 3−9343
migration rate of radioactivity in soil 3−5433
mixed alkali glasses model based on short range electrodynamic interaction concept 3−11765
He, of mass-identified U^+ and Hg^+ ions 3−7308
^3He-^4He solns. in strong elec. fields, charged particle motion *(Russian)* 3−7990
Li diffusion drift velocity in Ge, depth of drift, electric field configuration 3−33697
O^+, in polar wind flow restrictions 3−16022

ionic conduction in solids
see also ionic semiconductors
defect effect on conduction, three types of conduction 3−15026
electrolytes, conductivity rel. to cryst. struct. 3−27282
insulating thin films, electronic transport processes 3−18237
mixed alkali effect in glasses, equations for ionic cond., mobility, diffusion coefft. and transport number 3−11765
piezogalvanic effect, in solid ionic conductor 3−30506
semiconductor, nonstoichiometic oxide, meas. method *(French)* 3−11938
solids with tunnel and layer structures, ionic transport 3−5018
Teltow model generalisation of direct current condution in ionic crystals 3−38678
Teltow theory, generalised, models 3−36436
vitreous, role of long range diffusion process in dielec. relax. 3−30748
AgBr, photographic emulsion grains, ionic cond., dielec. loss, meas. 3−31283
AgBr film, due to interstitial Ag ions 3−8285
AgBr impurity ions and vacancies, interactions 3−27227
AgCl impurity ions and vacancies, interactions 3−27227
AgCl with Frenkel defects 3−27022
AgI, hydrostatic pressure effects 3−33690
β-Al_2O_3, Na- and Mg-content depend. 3−11758
$C_5H_6NI.8AgI$, superionic, ionic Hall effect 3−38875
CaF_2:R, R=Ce, Pr, Sm, Eu, Tb, ionic thermocurrent obs. of reorientational properties 3−7787
CaF_2:YF_3, conc. and mobility of interstitial fluorine ions rel. to intrinsic cond. 3−30489
CsCl:$SrCl_2$, mobility of cation vacancies in f.c.c. phase 3−30480
CuCl with Frenkel defects 3−27022
CuI, film growth by Cu tarnishing in I atmosphere, estimation of ionic cond. 3−38683
KBr:Ba^{2+}, kinetics of conc. decrease of nonequilib. cation vacancies 3−38585
KHF_2, mixed ionic cond., e.m.f. meas. 3−33968
KH_2PO_4 paraelectric, in vicinity of Curie point, effect on refractive index 3−29141
LiF, rel. to space charge influence on rupture stress 3−36325
LiF:MgF_2, Debye-Huckel interactions and solubility 3−4881
NH_4Cl, undoped and divalent cation doped, ionic thermal currents 3−33917
NaCl, electrode behaviour and defect energy detn. 3−38679
NaCl:$SrCl_2$, X-ray and ionic conductivity expts. comparison 3−17857
Na_2O-K_2O glasses, Na^+ and K^+ mobilities, 350-500°C *(French)* 3−5013
$RbAg_4I_5$, thin solid electrolyte film, vacuum-deposited, prep. and electrochem. charact. 3−39223
RbI and RbI:Sr, ionic conductivity Schottky defect, positive-ion and negative-ion vacancy enthalpies and entropies 3−24290
SiO_2 film, r.f. sputtered, Na^+ motion, meas. using thermally stimulated ionic currents 3−33688
SiO_2 films, γ-ray radiation induced impurity ion mobility 3−18222
SrF_2:R, R=Ce, Pr, Sm, Eu, Tb, ionic thermocurrent obs. of reorientational properties 3−7787

ionic conductivity in solids *see ionic conduction in solids*

ionic semiconductors
see also ionic conduction in solids
AgBr, optical absorpt. below fund. edge, Urbachs rule, 50-950K 3−5218
AgCl, optical absorpt. below fund. edge, Urbachs rule, 50-950K 3−5218
β-AgI, pellets, pure and PbI_2 doped, phase stability, elec. cond. 3−14966
CaF_2:YF_3, conc. and mobility of interstitial fluorine ions rel. to intrinsic cond. 3−30489
CsCl:$SrCl_2$, mobility of cation vacancies in f.c.c. phase 3−30480
KHF_2, mixed ionic cond., e.m.f. meas. 3−33968

ionisation
see also autoionisation; electron affinity; electron ionisation; ionisation of atoms; ionisation of gases; ionisation of liquids; ionisation of molecules; ionisation of solids; ionisation potential; photoionisation; surface ionisation
auto, astronomical u.v. obs. of effects, a review 3−19078
autoionisation in electron-capture decay, model 3−19813
clouds in upper atm., artificial ionisation, motion determ. 3−34932
cosmic ray muons, specific ionisation meas. in 5 to 500 GeV/c region using Cosmic Ray Spectrograph 3−12926
Cr, ionisation balance, collisional ionisation, autoionisation, radiative recombination and dielectric recombination 3−11458
current sources calibration, capacitor charging method *(Russian)* 3−9995
energy loss of relativistic heavy nuclei, corrections to Bethe-Bloch formula 3−22439
ion neutralisation spectroscopy for solid surfaces, derivation of band energy 3−2613
ion production for vacuum deposition, high rate system 3−25716
particulate matter collection from smokestacks using γ-ray ioniz. 3−17866
perfluorocyclobutane, ionization by electron impact 3−1282
perfluorocylobutane, dissociative ionization 3−1283

ionisation continued
planetary nebulae, elemental abundances and ionisation distrib. rel. to theoretical models 3−39743
plasma, diffusion approx. of kinetic eqns. for ionization processes *(Russian)* 3−11460
plasma discharge ionisation instability, influence of boundaries 3−36170
plasma instability, inelastic electron energy losses 3−33356
plasma jet, measured by introducing various substances *(Russian)* 3−7566
plasmas, measurement of high d.c. voltage *(German)* 3−23930
radiation effects, probability density function of ionising events 3−22473
radio, for velocity flow measurement, analysis of method *(Polish)* 3−26252
sporadic-E ionisation, thunderstorm effect, global characteristics 3−31424
supersonic wave caused by laser beam in plasma 3−17634
Al, ionisation balance, collisional ionisation, autoionisation, radiative recombination and dielectric recombination 3−11458
Ar, ionisation balance, collisional ionisation, autoionisation, radiative recombination and dielectric recombination 3−11458
Ar plasma, local equilib. in stabilised arcs 3−33387
Au L X-ray prod. by 0.5 to 30 MeV protons 3−23493
CH+O chemi-ionisation, cross section and rate const. calc. 3−14397
Ca, ionisation balance, collisional ionisation, autoionisation, radiative recombination and dielectric recombination 3−11458
Cl, ionisation balance, collisional ionisation, autoionisation, radiative recombination and dielectric recombination 3−11458
Fe, ionisation balance, collisional ionisation, autoionisation, radiative recombination and dielectric recombination 3−11458
K, ionisation balance, collisional ionisation, autoionisation, radiative recombination and dielectric recombination 3−11458
Mn, ionisation balance, collisional ionisation, autoionisation, radiative recombination and dielectric recombination 3−11458
Na, ionisation balance, collisional ionisation, autoionisation, radiative recombination and dielectric recombination 3−11458
Ni, ionisation balance, collisional ionisation, autoionisation, radiative recombination and dielectric recombination 3−11458
O_2^+ as source of ionisation in D-region 3−16026
P, ionisation balance, collisional ionisation, autoionisation, radiative recombination and dielectric recombination 3−11458
Ta ions stripped in gases and solids with energies 2-15 MeV, equilib. charge-state distributions 3−11183
U ions stripped in gases and solids with energies 2-15 MeV, equilib. charge-state distributions 3−11183

ionisation chambers
Campbell method appl. to small signal to noise ratio meas. *(German, English)* 3−10046
cavity, obs. of dose rate from cervical X-ray applicators 3−3626
collection efficiency, for pulsed beams 3−32167
current integral equation, method of solution *(Russian)* 3−19290
current measuring circuit, using MOS FET circuitry 3−32181
for dosimetry 3−35306
incident beam ionisation chamber and charge integration system for X-ray diffr. stabilisation 3−35472
liquid, background current 3−35479
low current generator using chamber, for testing current meas. devices *(French)* 3−10008
neutron, with pneumatic monitoring device 3−28664
neutron flux measurements, by γ-compensated pulsed mode operation chambers 3−32152
paired, for reactor dosimetry, separation of γ and n dose 3−3632
photoionisation, low to high ionisation rate transition, continuum anal. 3−38496
recombination, fast neutron personnel dosimetry studies, review *(Czech)* 3−3620
saturation effects, response to intense pulsed beams 3−303
streamer chamber pictures, computer-controlled measurements 3−19356
thoron meas., ioniz. current calibration *(Japanese)* 3−3011
ultrahigh energy particle separation by transition-radiation method *(Russian)* 3−13421
universal characteristic, theoretical proof for plane geometry 3−19293
u.v., description *(French)* 3−16505
SO_2 concentration meas. in flue gases 3−3860
T, portable monitor in air 3−13431

ionisation gauges
double-pin, use for shock wave detection 3−28802
fast, rarefied gas puff transient behaviour, electron beam fluorescence probe obs. 3−1507
Schulz type, design and characteristics *(Japanese)* 3−22302

ionisation of atoms
alkali atoms, determ. of cross-section by freq. doubling with dye laser *(Dutch)* 3−29492
alkali metals, photoionisation cross sections using Hellmann-like pots. 3−17363
atom, multiphoton ioniz. probability, effect of forced resonant transitions *(Russian)* 3−7069
atom, narrow resonance in nuclear transition from absorpt. saturation of electron transition 3−26573
cathodic sputtering of metallic sample subjected to ion bombardment, delayed formation of ions *(French)* 3−2607
classical binary encounter approx. approach 3−33054
collision rate coeff. meas. for laboratory plasmas 3−17569
Coulomb multiple inner-shell, by heavy, charged particles, simultaneous ejection of K- and L-shell electrons 3−1130
cross sections, ionisation by high energy electron impact, calcs. 3−20053
double-electron ejection, internal and external, direct collision amplitudes 3−26584
electron impact, Born II approx., scatt. amplitude, phase factors 3−26589
electron impact, double ioniz. cross sections, wavefunction 3−20044
electron production mechanisms in ion-atom collisions 3−26601
electron transitions in hydrogen-like particles, generalized oscillator strengths 3−33041
field ionisation, temperature dependences 3−26575

ionisation of atoms continued
gaseous metal atom ionisation energy correl. with solid work function, by electrostatic model 3−4376
high-Z region, Coster-Kronig and fluoresc. yields for L_2 and L_3 subshells 3−26571
highly ionized atoms of fifth period elements, energy levels and classification 3−17368
hydrogenic atoms, differential cross section for ionisation by electron impact 3−7078
inert gases, electron impact double ionisation, cross section calc. 3−11169
inner-shell ionization of medium-heavy atoms by electrons, calc. of cross-section 3−11174
interplanetary particles, electromagnetic instabilities in the solar wind 3−13007
ion-atom collisions, inner-shell vacancy production, review 3−35979
ion-atom collisions, vacancy occupation probabilities 3−38245
ion-atom collisions at moderate nuclear velocities, ionization of inner shells 3−1131
K-shell ioniz. by heavy charged particles, universal cross sections 3−29537
K-shell where projectile is moving faster than orbiting electron 3−38250
lower ionosphere, impact and bremsstrahlung photoionisation due to precipitating electrons 3−34945
many-electron atoms, calc. of energies and widths of autoionizing states 3−4373
on metal surface, rel. to plasma ion temp. investig. 3−33396
multiphoton, effect of const. elec. field *(Russian)* 3−7068
multiphoton, spin-orbit coupling and photoelectron polarisation effect 3−23488
multiphoton absorpt. of laser photons 3−33036
multiphoton processes, bound-free transitions in e.m. field of arbitrary intensity 3−26578
multiphoton transition amplitude for high-order e.m. transitions, momentum translation approx. 3−26579
multiphoton transitions, bound-free transition integrals in compact forms 3−26577
Penning, polarisation mechanism of ejected electrons and ions 3−7066
Penning ionization electron spectra of collisions between rare gas atoms and He metastable atoms 3−11154
Penning reactions of metastable He with diatomic mols. 3−29731
photo-, K-shell cross sections and threshold energies 3−14300
photo-effect, two-quantum, ang. distrib. 3−38227
photoelectric effect above 10 keV, review 3−35968
photoionisation, Green's function theory 3−20034
photoionisation of atomic system, theory of measurements in terms of density matrix 3−7064
photoionization, angular and energy distrib. of electrons *(Russian)* 3−10077
photoionization, low-energy cross sections 3−4374
positron autoionization in heavy ion collisions 3−7087
quasi-Landau spectrum of hydrogen-like system in strong mag. field 3−33038
R-matrix methods in atomic calcs. 3−11171
single, charge density anal. 3−7034
spectral lines determ. in arcs and sparks, degree of ionisation determ. *(Russian)* 3−29482
sputtering, quantum mechanical model 3−27594
stopping power of atomic matter for relativistic ions, mesons, electrons and positrons, Born approx. energy-loss formulas 3−7082
symmetrical charge transfer cross section depend. on pot. 3−20060
universal function for collisional ionization by structureless charged particles 3−17365
X-ray emission cross sections and fluorescence yields for light atoms and molecules by electron impact 3−17468
X-ray prod. by protons, cross sections for Kα and L α X-rays 3−33046
A, equilib. calc. for solar atm. elements 3−18960
Ag, K-shell Coulomb ionization cross-section, impact parameter depend with 0.3-3.0 MeV protons 3−23487
Ag$^-$ beams, photodetachment by Ar-ion-laser beam, electron affinities 3−29502
Ag$^-$ dye-laser photodetachment studies 3−29503
Al, equilib. calc. for solar atm. elements 3−18960
Al, K-shell Coulomb ionisation cross-section, impact parameter depend with 0.3-3.0 MeV protons 3−23487
Al, multiple ioniz. cross sections determ. from high resolution spectra 3−1106
Ar, 3s subshell, photoionisation in threshold region, photoelectron spectroscopy study 3−29508
Ar, autoionizing state detection using mathematical technique 3−29500
Ar, by He metastables, electron energy spectra 3−33053
Ar, electron-impact, energy and angular correlations 3−26600
Ar, electron-impact, in eikonal and Born approxs. 3−38240
Ar, inner-shell ioniz. cross sections by 1.5-5.0 MeV protons 3−33047
Ar, proton-reduced L X-ray spectrum 3−17353
Ar collision with beams of C^{6+}, N^{7+}, O^{8+}, F^{9+} at 1 to 2 MeV/amu, charge dependence of K-shell ionisation 3−20067
Ar ionisation meas. behind shocks with microwaves and a pulsed Langmuir probe *(German)* 3−14594
Ar photoionisation, 60−230 eV, meas. of absorption coeffs. 3−11152
Ar photoionisation cross section, threshold to 50 eV, calc. by many-body perturbation theory 3−29510
Ar proton scatt., total differential cross section 3−33059
$Ar^{(+)}$ + Ar, ioniz. processes in slow collisions 3−26605
Au^- dye-laser photodetachment studies 3−29503
Ba, cross section meas. by energy resolved electrons 3−11173
Be, electron impact, photoioniz. cross sections calc. 3−26594
Be III ionized species, far u.v. absorpt. spectra *(French)* 3−20030
BeI isoelectronic sequences, energy levels and spectra meas. 3−17369
C, effects of multiple ionisation of fluorescence yield 3−4366
C^+-C collision, K-shell ionisation in keV-MeV range, Fano-Lichten theory 3−26603

ionisation of atoms continued
Ca, equilib. calc. for solar atm. elements 3−18960
Ca, K-shell Coulomb ionization cross-section, impact parameter depend with 0.3-3.0 MeV protons 3−23487
Ca ionisation degree calc. in acetylene-air and propane-butne-air flames *(Russian)* 3−31264
Cd I, emission spectra, autoionisation resonances and configuration-mixing 3−7044
Cd(I), autoionising d^9s^2np level, intermediate coupling calcs. 3−7063
Ce autoionising states, excitation by electron impact *(Russian)* 3−26599
Cl, equilib. calc. for solar atm. elements 3−18960
Cr, equilib. calc. for solar atm. elements 3−18960
Cr^{4+} spectra, term values and ionisation energy determ. 3−33026
Cs, electron impact excitation of autoionizing level 3−35972
Cs, photoabsorption 3−20035
Cs 6^2P reson. levels, photoionisation by 488 nm light 3−23486
Cs $8^2P_{1/2}$ ionizing transitions in a low temperature plasma *(Russian)* 3−11160
Cs atomic beam, reson. multiphoton ionisation by Nd-glass laser 3−23489
Cs autoionising states, wave functions, energies, Hartree method *(Russian)* 3−26580
Cs electron ionisation by impact, 6s and 5p, cross-section, Born approximation, threshold, Hartree method *(Russian)* 3−26598
Cu, local thermodynamic equil. of autoionizing levels 3−33393
Cu I, v.u.v. absorption spectrum, autoionized resonances 3−29504
Cu^- beams, photodetachment by Ar-ion-laser beam, electron affinities 3−29502
Er III, level structure, spin orbit parameters 3−29505
F^{6+} passed through foil yield of excited autonised metastable states 3−20033
Ge I and II, neutral and singly ionized, absolute transition probabilities 3−33024
H, atoms and H like ions, multiphoton ionisation, reson. nature 3−14302
H, chemiionization by He(2^1S) and He(2^3S) metastables, cross sections calc. 3−38253
H, electron impact ioniz., Glauber theory 3−29524
H, energy determ. for mag. white dwarfs and neutron stars 3−13024
H, multi-photon ionisation of ground, 1S and metastable 2S state 3−26582
H, multiphotoionisation in intense laser beam 3−38224
H, multiphoton ionisation by intense e.m. fields, momentum translation method application 3−38223
H, multiphoton ioniz., circular versus linear polarisation cross sections 3−33037
H, multiphoton ionization at 0.53 μ 3−11157
H atom momentum translation approximation for threshold ionisation by a laser beam 3−38199
H collisions with He(2^3S) and He(2^1S) metastable atoms, chemiionisation 3−38252
H plasma ionisation, recombination and population of excited levels 3−29938
H-like atoms, multiphoton ionisation by intense linearly polarised light 3−26581
H^-, electron detachment, Born-Ochkur approx. 3−35973
H^-, electron impact, double ioniz. cross sections 3−20045
H^-, photoionisation, cross section calcs. above $n=2$ threshold 3−11151
He, autoionisation and He^- autodetachment following bombardment by H^+, H_2^+, He^+, He atoms 3−23490
He, autoionizing states, low-energy electron impact, 42-48 eV, 57-65 eV, excitation struct. 3−7065
He, differential ioniz. cross section for slow electron ejection by fast charged particles 3−33045
He, electron emission spectra excited by proton impact, 2s(^1S) autoionisation state 3−7067
He, electron excitation of (1s, nd)^1D and (ns, mp)^1P states 3−26591
He, electron impact, Coulomb effects in final state of ionizing collision 3−26595
He, electron impact, double ioniz. cross sections. 3−20045
He, electron impact double ionisation, classical collision theory appl. 3−38234
He, in high intensity laser field perturbation atomic levels near ionization threshold 3−1114
He, metastable atoms, meas. near threshold 3−38226
He, photoionisation, cross section calcs. above $n=2$ threshold 3−11151
He, proton scatt., total differential cross section 3−33059
He electron loss passing through inert gases and molecular H_2, N_2 and O_2 3−11166
He I, photoioniz. reson. profile parameters of $3s3p^1P_1$ two-electron excitation 3−33035
He II reson. lines, plasma polarization shift 3−33338
He metastable states, photoionisation above $n=2$ threshold, determ. of differential cross sections for photoelectric transitions 3−11150
He photoionisation, 60−230 eV, meas. of absorption coeffs. 3−11152
He-Ne mixture, field ionisation and field ion microscopy 3−22514
He + He ionizing collisions, metastable, rate coeff. 3−29528
He^- ions, detachment cross sections in He, H_2 and Ar gases 3−14312
He^+ collisions with Zn, Cd, Se, charge transfer into excited states 3−14313
He^+ prod. in He_2^+-He collisions near threshold 3−38248
$He^{(+)}$ + He, ioniz. processes in slow collisions 3−26605
He($1s^+$), by H impact 3−20063
Hg, ang. distrib. of photoelectrons from 5d-subshell 3−29501
Hg(I), autoionising d^9s^2np level, intermediate coupling calcs. 3−7063
K, equilib. calc. for solar atm. elements 3−18960
K, multiphoton resonance ionization 3−23491
K, two-photon ioniz. with polarized photons 3−20031
K^{2+}, radiative mean lifetimes of levels, beam foil spectra 3−11158
Kr, 4p photoelectron ang. distrib., far u.v., using synchrotron light source 3−29507
Kr, inner-shell ioniz. cross sections by 1.5-5.0 MeV protons 3−33047

ionisation of atoms continued
  Kr, obs. of multiply excited and ionised states during continuous analysis of X-ray absorption using bremsstrahlung 3 − 4364
  Kr, photoionisation cross section, in vicinity of outer d-subshell threshold 3 − 29509
  Kr$^{(+)}$ + Kr, ioniz. processes in slow collisions 3 − 26605
  KrI, ioniz. pot. and 4s4p^{6}nl levels 3 − 26576
  Li, atom, ground state, reduced density matrix and ionisation pot. from Green's function theory 3 − 26560
  Li, two-photon ioniz. with polarized photons 3 − 20031
  Li$^+$, electron impact, double ioniz. cross sections 3 − 20045
  Li$^+$, electron impact double ionisation, classical collision theory appl. 3 − 38234
  Li$^+$, singly ionized by electron impact, lifetime and polarization of 2 ^{3}P term 3 − 29499
  LiI isoelectronic sequences, energy levels and spectra meas. 3 − 17369
  Li + (1s^2), by H impact 3 − 20063
  Mg, electron impact, photoioniz. cross sections calc. 3 − 26594
  Mg, photoioniz. cross section near threshold 3 − 33039
  Mn, equilib. calc. for solar atm. elements 3 − 18960
  N, photoioniz., independent-particle model approach 3 − 29513
  Na, equilib. calc. for solar atm. elements 3 − 18960
  Na, two-photon ioniz. with polarized photons 3 − 20031
  Ne, autoionizing states, low energy electron impact, 42-48 eV, excitaion struct. 3 − 7065
  Ne, electron-impact, in eikonal and Born approxs. 3 − 38240
  Ne, Ne$^+$, Ne^{++}, photoionisation cross sections for isoelectronic sequences 3 − 26583
  Ne, photoionisation, autoionisation states, calc. 3 − 14304
  Ne photoionisation, 60 − 230 eV, meas. of absorption coeffs. 3 − 11152
  Ne$^+$ collisions with Mg charge transfer into excited states 3 − 14313
  Ne$^{(+)}$ + Ne, ioniz. processes in slow collisions 3 − 26605
  Ne$^+$C(Al) collisions, K-shell ionization cross sections 3 − 23503
  Ni, K-shell Coulomb ionization cross-section, impact parameter depend with 0.3-3.0 MeV protons 3 − 23487
  O, electron impact excitation and ioniz., cross sections 3 − 4390
  O, photoioniz., independent-particle model approach 3 − 29513
  O$^-$, autodetachment states 3 − 29511
  O$^-$, photodetachment cross sections, many-body calc. 3 − 4375
  O$^-$ collision with CO, H_2 and O_2 associative detachment 3 − 20201
  O^{5+} passed through foil, yield of excited autoinized metastable states 3 − 20033
  P, equilib. calc. for solar atm. elements 3 − 18960
  P XII and P XIII, e.v.u.v. spectra, energy levels 3 − 29484
  Pb, L- and M-shell X-rays, from 0.5 to 14.0 MeV proton beams 3 − 38228
  ^{147}Pm β decay, inner shell vacancy creation 3 − 4369
  Pt$^-$, dye-laser photodetachment studies 3 − 29503
  Rb total electron impact ionisation cross section from threshold to 250 eV 3 − 38232
  Rb^{2+} radiative mean lifetimes of levels, beam foil spectra 3 − 11158
  Sc Rydberg series and autoionisation resonances in absorption spectrum 3 − 33042
  Sn, characteristic L X-ray spectra from proton, α-particle and ion bombardment 3 − 33044
  ^{50}Sn, inner-shell ionization, calc. of cross-section, relativistic effects 3 − 11174
  ^{99}Tc, β-decay, K-shell internal ionization probability meas. 3 − 14170
  ^{185}W β decay, inner shell vacancy creation 3 − 4369
  Xe, 5p photoelectron ang. distrib., far u.v., using synchrotron light source 3 − 29507
  Xe, by He and Ne metastables, electron energy spectra 3 − 33053
  Xe, inner-shell ioniz. cross sections by 1.5-5.0 MeV protons 3 − 33047
  Xe, photoionisation cross section, in vicinity of outer d-subshell threshold 3 − 29509
  Xe + He → Xe$^+$ + He + e, metastable atom collision with excited ion production *(Russian)* 3 − 7072
  Xe$^+$ excitation in collisions of metastable Xe and He atoms 3 − 17380
  Y, Rydberg series and autoionisation resonances in the absorption spectrum 3 − 33043
  Zn I, emission spectra, autoionisation resonances and configuration-mixing 3 − 7044
  Zn(I), autoionising d^{9}s^{2}np level, intermediate coupling calcs. 3 − 7063

ionisation of gases
  see also atmospheric ionisation; plasma; Townsend discharge
  air, calc. of O formation from electron density behind shock waves 3 − 7397
  air, rate of ionisation behind shock waves, expt. obs. *(Russian)* 3 − 33248
  autoionisation lines, effect on stellar opacities 3 − 39655
  boundary layer at crit. pt. of indestructible body washed by flow of ionized air 3 − 23737
  breakdown initiation mechanism, review 3 − 38346
  dense plasmas, ionization equilibrium theory 3 − 14509
  electro-ionization and pumping of highly compressed gases for generating laser pulses and freq. 3 − 6464
  Galactic latitude distribution, recombination line obs. at 18 c.m. 3 − 19053
  high-energy particle detection in gas counter, transition effect in ionisation losses 3 − 22458
  inert gas ionization by protons, meas. of number of ion pairs produced 3 − 7309
  inert gases, atom-atom excitation and ioniz. in shock waves 3 − 33040
  interstellar matter, excitation state due to supernova explosions, time-depend. models 3 − 39741
  ion velocity distribution in weakly ionised gas in uniform electric field of arbitrary strength 3 − 4519
  ionising shock waves, in a magnetic field, study of adiabatic curves *(Russian)* 3 − 26823
  kinetic processes, non-stationary *(Russian)* 3 − 7300
  Lagrange invariant in MHD rel. to completely and weakly ionised gases *(Russian)* 3 − 17548
  laser-induced gas breakdown with preionisation 3 − 29825
  lower nighttime ionosphere, l.f. absorption *(Russian)* 3 − 3053
  metal atom ionisation energy correl. with solid work function, by electrostatic model 3 − 4376

ionisation of gases continued
  microwave radiation effect on shock-produced electron precursor 3 − 20454
  neutral atoms in dense discharge, excitation and ionisation by electron impact 3 − 23497
  NGC 1614 central region, extension of Hα wing to the blue, gas outflow effects 3 − 19052
  nonlinear generation of ionisation waves 3 − 20492
  proportional counter gas amplification mechanism *(French)* 3 − 32168
  shock waves structured by nonequilibrium ionizing and thermal phenomena 3 − 29884
  solar flare energy prod. by ionisation loss process due to accel. charged particles 3 − 31569
  stellar interiors, pressure ionisation effects on eqn. of state 3 − 31651
  Ar ionization by protons, meas. of Jesse effect as function of press. 3 − 7309
  CO, microwave breakdown 3 − 23666
  Cs Townsend discharge, first ionisation coeff. 3 − 14415
  H-He mixture, ionizing shock wave struct. 3 − 14416
  H_2^+ energy spectrum of field ionisation at single atomic site 3 − 35508
  He$^+$, energy spectrum of field ionisation at single atomic site 3 − 35508
  Kr, ionisation-relaxation time meas. following shock heating *(German)* 3 − 11434
  NO, photoelectron spectra obs. of autoioniz. process *(Russian)* 3 − 7247
  Ne-Ar mixtures, pressure dependence of primary ionisation in Townsend discharge 3 − 17702
  Ne$^+$. energy spectrum of field ionisation at single atomic site 3 − 35508
  O_2 electron transport coeffs., thermal and near-thermal, time-of-flight swarm technique 3 − 1482
  O_2 + CO mixtures, coeff. as CO tends to zero 3 − 14414
  Xe, ionisation relaxation behind a shock-wave front 3 − 36180
  Xe, ionisation-relaxation time meas. following shock heating *(German)* 3 − 11434

ionisation of liquids
  alkanes, γ radiolysis, simple exponential distribution for initial electron-positive ion separation distances 3 − 25077
  alkanes, Onsager's recombination theory 3 − 5396
  aqueous solutions, irradiated, transient conductivity induced using h.v. pulse 3 − 5397
  benzene and alkylbenzenes, photoioniz. and recomb. fluoresc. 3 − 25081
  cyclohexane, capture and recombination reactions of electrons *(Russian)* 3 − 5394
  hydrocarbons, initial ioniz. yield and scavengable electron yield 3 − 5249
  o-pyrocatechuic acid in water and water-methanol mixtures, ionisation consts. and related thermodynamic functions 3 − 18783

ionisation of molecules
  acetylene, photoionisation near threshold 3 − 26711
  acetylene and acetylene-d_2, dissoc. attachment and ioniz. efficiency meas. *(French)* 3 − 7243
  anthracene anion radicals, autoionisation in photoelectron emission 3 − 18528
  benzene, absorpt. cross section, photoionisation efficiencies, in vacuum u.v. 3 − 29648
  cationic cyanine dye molecules adsorption on glass, ionisation energies 3 − 27901
  chloroethylenes, ionisation potentials determ. by photoelectron spectroscopy 3 − 11290
  2-decene. cis and trans, comparison of photon and electron impact ionization 3 − 1268
  dissociative and non-dissociative photoionization of molecules at 304 and 584 Å 3 − 33149
  fragmentation in ion-molecule reactions, ballistic theory 3 − 26719
  Franck-Condon factors for transitions on ionization of diatomic molecules 3 − 23624
  Gelius-Siegbahn model for cross sections calc. from mol. orbitals 3 − 36048
  group IV tetrafluoro cpds., photoelectron spectra, ionization energies 3 − 7169
  group IV tetramethyles, photoelectron spectra, ionization energies 3 − 7169
  halogen collisions with alkali metal atoms, fragmentation of halogen negative ions 3 − 26715
  Huckel mol. orbital parameters, calc. method using ionisation pots. 3 − 29576
  hydrazine, photoelectron spectra, CNDO/2 and MINDO/2 analysis 3 − 35993
  hydrocarbons, photoioniz., ionic fragmentation patterns, Penning ioniz. comparison 3 − 38309
  metal atom + O_2 crossed beams, assoc., reactive and electron transfer ioniz. 3 − 29746
  metallocenes, electron impact ioniz., appearance pots., negative and positive ion form. 3 − 29739
  multiple field ionisation mechanism 3 − 26709
  Penning reactions of metastable He with diatomic mols. 3 − 29731
  photoionization, angular and energy distrib. of electrons *(Russian)* 3 − 10077
  polyatomic, low energy electron attachment, temp. depend. 3 − 26712
  spacecraft re-entry plasma, mass spectroscopy meas. 3 − 23928
  sparks, nanosecond, breakdown and channel production electron impact ionisation 3 − 30037
  styrene, absorpt. cross section, photoionisation efficiencies, in vacuum u.v. 3 − 29648
  thermally excited ions, decomposition, statistical theory of mass spectra 3 − 36975
  X-ray emission cross sections and fluorescence yields for light atoms and molecules by electron impact 3 − 17468
  xylenes, isomers electronic struct. and spectra, ionisation potentials, modified CNDO-CI study 3 − 33093
  B hydrides and derivatives, relative abundances of doubly charged ions in mass spectra 3 − 26707
  CO, dissoc. into ions by impact of fast ions and atoms of H, He, Ne, Ar and Kr 3 − 23621

ionisation of molecules continued
- CO_2 vibr. temp. meas. using $H(2^3S)$ Penning ioniz. technique 3−23618
- CO^+, relative intensities for ionisation of lowest 3 electronic states by electron impact 3−33159
- CO_2, shake up satellite lines, identification by ESCA 3−11294
- CO_2/H_2 system, ion-molecule reactions, ion cyclotron resonance 3−26721
- COS, shake up satellite lines, identification by ESCA 3−11294
- CS, high resolution photoelectron spectrum, ioniz. pots. 3−4427
- CS_2, shake up satellite lines, identification by ESCA 3−11294
- Cl_2, electron impact ionisation cross section, 15-100 V 3−1284
- ClO_4^-, X-ray photoelectron spectrum, line intensities 3−36048
- Cu_2, Cu_2^+ particles, ab initio study 3−11201
- D_2, dissoc. photoioniz. through $1s\sigma_g$ ionic state 3−20196
- D_2, electron ioniz. cross section meas. 3−33158
- F_2, electron impact ionisation cross section, 15-100 V 3−1284
- GeF_4, bond dissoc. energies, ioniz. pots. and electron affinities 3−20191
- H_2, autoionizing transitions produced by electron impact 3−33156
- H_2, dissoc. photoioniz. through $1s\sigma_g$ ionic state 3−20196
- H_2, electron ioniz. cross section meas. 3−33158
- H_2, inelastic electron impact cross-section 3−1281
- H_2, multiphoton ionization at 0.53 μ 3−11157
- H_2, proton affinity determ. from $H_2O^+ + H_2 \rightarrow H_3^+ + OH$ reaction 3−2802
- H_2 and D_2, ionisation shift between energy thresholds, meas. using new mathematical technique 3−29500
- H_2 appearance of reson. struct. in meas. of ionization function *(Dutch)* 3−29733
- H_2 collisions with $He(2^3S)$ and $He(2^1S)$ metastable atoms, chemiionisation 3−38252
- H_2 molecular dissociative and non-dissociative photionization at 304 and 584 Å 3−33149
- H_2^+, proton-impact dissociation and ionisation study 3−20200
- HOF, photoelectron spectrum, valence region orbitals analysis 3−36047
- He + He ionizing collisions, metastable, rate coeff. 3−29528
- I_2, absorpt. spectra, 45-160 eV, inner electron excitation in gaseous and solid phase 3−29647
- N_2, autoionizing transitions produced by electron impact 3−33156
- N_2, electron impact vibr. excitation, cross-section 3−36052
- N_2, inelastic electron impact cross-section 3−1281
- N_2, ionisation growth meas. using thin Au film techniques, secondary electron emission explanation 3−14398
- N_2, ionisation growth meas. using thin Au film techniques, secondary electron emission revised explanation 3−14399
- N_2, Koopmans' theorem breakdown 3−26704
- N_2, photoabsorpt. of extreme u.v. radiation, fluoresc. of atomic nitrogen 3−33029
- N_2, vibr. temp. meas. using $H(2^3S)$ Penning ioniz. technique 3−23618
- N_2 molecular dissociative and non-dissociative photoionization at 304 and 584 Å 3−33149
- NF_2, mass spectroscopic study of ionisation and dissociation processes 3−17460
- N_2F_4 mass spectroscopic study of ionisation and dissociation processes 3−17460
- NO, dissoc. into ions by impact of fast ions and atoms of H, He, Ne, Ar and Kr 3−23621
- NO, photoionisation mass spectrometric study, threshold region vibr. autoionisation fine struct. obs. 3−17462
- N_2O, photoionisation at 73.6 and 58.4 nm, collision induced dissociation at thermal kinetic energies 3−29732
- N_2O ion-molecule reactions with H_2 and CH_4, ion cyclotron resonance 3−26722
- O_2, dissoc. into ions by impact of fast ions and atoms of H, He, Ne, Ar and Kr 3−23621
- O_2, negative molecular ion formation in electron collision $E + O_2 \rightarrow O_2^{-*}$ 3−29741
- O_2 molecular dissociative and non-dissociative photoionization at 304 and 584 Å 3−33149
- O_2^{2+}, mass spectrum detection 3−26708
- XeF_6, MS-Xα calc. of energy level struct. 3−4409

ionisation of solids
- anthracene, photoioniz. and photogeneration of carriers 3−15219
- molecular crystals, solid-state ionisation energies, photoemission 3−8703
- rare earth metal surfaces, ionisation losses in inelastic electron refl. spectra 3−5252
- semiconductor, electromag. field effect on valence band ionisation by cond. electron collision 3−4951
- transparent dielectrics, excitation of cascade ionization by strong alternating e.m. field *(Russian)* 3−8517
- X-ray prod. on thick targets, charact./continuous radiation ratio 3−27583
- Be:Si surface, Auger and ionisation loss spectra meas. before and after oxidation 3−21508
- Cs, electron impact excitation of autoionizing level 3−35972
- n-Si, high field effects 3−5014

ionisation potential
- *see also work function*
- alkanes linear, calculation using exciton theory 3−1272
- aromatic solutes in solid solns., 77K, photoioniz. 3−21828
- atoms, symmetrical charge transfer cross section depend. 3−20060
- carboxylic acids, monomers, dimers, mixed complexes, photoelectron spectra of H-bonded systems, electron mol. orbital ionisation pot. 3−7173
- 2,4-dicarbaheptaborane(7), rel. to ground-state charge distrib. 3−26616
- 4,5-dicarbahexaborane(8), rel. to ground-state charge distrib. 3−26632
- ethylene, planar, orbital calcs. 3−7124
- ferrocene derivatives, photoionisation in Geiger counter 3−33188
- Huckel mol. orbital parameters eval. 3−29576
- hydrocarbons, alternant, ionization potential calc. by simplified IOC-ω technique 3−1267
- metallocenes, electron impact ioniz., appearance pots., negative and positive ion form. 3−29739
- methane, inner-shell ionization energies and ESCA shifts 3−4372

ionisation potential continued
- nitrogen-containing organic compounds, thermal ionisation, positive ions, tungsten and tungsten oxide emitters 3−36974
- perfluorocyclobutane radicals, C−F bond energies, electron affinities, ionization pots. calc. from appearance pots. 3−1283
- QSOs, ionization potential-redshift correlations in absorption line spectra 3−19040
- thiocarbonyl fluoride photoelectron spectrum, obs. of vibrational structure and fluorine substitution shifts 3−7168
- $TiCl_4$, photoelectron spectra, Hartree-Fock-Slater model 3−27489
- 1,3,5-trifluorobenzene, far u.v. and photoelectron spectra, ionisation potential assignments 3−11253
- water, near Hartree-Fock calculations of ground state 3−7114
- BCl_3, ab initio SCF calcs. 3−23609
- BF_3, ab initio SCF calcs. 3−23609
- CS, high resolution photoelectron spectrum obs. 3−4427
- GeF_4, bond dissoc. energies, ioniz. pots. and electron affinities 3−20191
- H-like multielectrons atoms, empirical effective parameters based on ionisation potential and radius 3−29458
- HBr, DBr photoelectron spectra, predissociation 3−23546
- HF mol., model pseudopot. calcs. 3−20091
- H_2O mol., model pseudopot. calcs. 3−20091
- HOF, photoelectron spectrum, valence region orbitals analysis 3−36047
- He, scattering and bound-state props., many-body Green's functions appl. 3−11122
- He^+ near resonant charge transfer collisions with K, Rb and Cs, cross sections determ. from polarisability and ionisation potential 3−35976
- KrI, Ritz formula calcs. and $4s4p^6nl$ levels 3−26576
- Li, inner-shell ionization energies and ESCA shifts 3−4372
- LiO, determ. by electron-impact mass spectrometry 3−5376
- Li_2O, determ. by electron-impact mass spectrometry 3−5376
- N fluorides, molecules and ions, CNDO/2 calculation of atomization energies 3−7245
- N_2, Koopmans' theorem breakdown 3−26704
- P fluorides, molecules and ions, CNDO/2 calculation of atomization energies 3−7245
- SbSe type cpds., gaseous phase *(French)* 3−7240
- U clean surfaces, electron binding energies determ. by soft X-ray appearance-potential spectroscopy 3−36977
- VCl_4, photoelectron spectra, Hartree-Fock-Slater model 3−27489
- W_2Cl_{10} and $W_2Cl_9^{3-}$ dimers, mol. orbital calc., diagonal matrix elements equated with valence-state ionisation pot. 3−35990
- Y(VI), from emission spectrum 3−14288

ionisation time *see ionisation*

ionised gases *see ionisation of gases*

ionogen *see electrolytes*

ionosondes *see ionospheric measuring apparatus*

ionosphere
- *see also D-region; E-region; F-region; ionospheric electromagnetic wave propagation; ionospheric measurement; ionospheric measuring apparatus; sporadic-E layer*
- amplitude scintillations, fading characteristics, cumulative amplitude probability distribution function 3−25277
- artificially ionized clouds, motion determ. 3−34932
- auroral, ion velocity distrib. 3−9322
- auroral, plasma drifts, Ba cloud data 3−3061
- auroral eastward electrojet, closure of a partial ring current 3−16009
- auroral ionosphere, electron intensity rel. to Ba cloud, rocket flight obs. 3−12785
- backscatter spectrum, plasma time enhancement by heating 3−18879
- c-layer formation at dawn, diurnal effects 3−3115
- Cherenkov radiation prod. by electron beam injection 3−28058
- Cherenkov radiation produced by electron beam injection, coherent emission *(French)* 3−39548
- complex refractive index for frequencies less than electron gyrofrequency 3−21961
- current determ. using three-layer model of near-earth space 3−25265
- currents induced by solar wind interaction with planetary atmospheres 3−31421
- daytime equatorial lower ionosphere above Thumba, electron density profiles 3−3069
- disturbances of March 6-10, 1970 rel. to solar activity 3−34930
- double layer formation in homogeneous plasma carrying constant current 3−23759
- DP1 and DP2 current systems, oscillations rel. to ionospheric conductivity 3−34939
- E_s-q layer disappearance during mag. storms, equatorial ionosphere electric field reversal effects 3−25291
- electric and mag. dipoles in dielectric sphere, radiation resistance and reactance meas. 3−34926
- electric field rel. to ionospheric currents 3−25304
- electrodynamics of day/night side variability in cond., potential distrib. determ. 3−25302
- electrojet current, equatorial, effect on drift 3−12791
- electron content at medium latitude geomagnetically 3−9321
- electron density distrib. at mid-latitudes during quiet mag. periods, Ariel 3 obs. 3−18880
- electron density distribution in ionospheric satellite wake 3−18878
- electron density meas. rel. to solar X-ray flare temp. determ. 3−31529
- electron density of lower ionosphere, var. with zenith angle, solar cycle and during eclipses 3−3068
- electron density profiles computation using min. number of parameter 3−34935
- electron density profiles obtained by v.l.f. propagation over long distances *(German)* 3−9337
- electron gas heat flux at heights > 180 km, cooling and heating sources 3−25270
- electron intensity enhancement at 100 km due to interaction between whistlers and energetic electrons 3−25308
- electron temp. meas., comparison of modulation Langmuir probe and incoherent scatter radar techniques 3−25272
- electron temperature anisotropy in topside ionosphere 3−21964
- electrostatic emissions from the high-latitude ionosphere, satellite v.l.f. obs. of electric fields 3−16015

ionosphere continued
e.m. variations near coastline for localized current systems in ionosphere 3−34850
equatorial anomaly, day-to-day variability in American and Japanese sectors 3−25294
equatorial electrojet, electric fields and currents determ. 3−34927
equatorial lower ionosphere, tunnelling transmission of e.l.f. and v.l.f. e.m. waves 3−31414
excess radiation in equatorial region between 200 and 350 km. 3−34910
Explorer 31, ionospheric satellite, ion flux angular distrib. in wake 3−25276
geomagnetic cut-off rigidity and solar cosmic ray spectrum determ. using ionospheric data 3−25352
geomagnetic disturbances, effect on medium latitude lower ionosphere 3−9325
gradient instability in Gaussian sporadic E-layers 3−25283
heating by transverse electric fields, night variations 3−25264
height, apparent, variation with frequency multiple reflection obs. 3−9314
height determ. of ionospheric irregularities with radio holographic method 3−16069
inhomogeneity structure, magnetoionic component scatt. 3−34929
integrated response to internal atmospheric gravity waves 3−31415
ion and electron kinetics in disturbed ionosphere at 100 to 200 km. height 3−28059
ion chemistry in simulated disturbed ionosphere 3−3067
ion density, lapge-scale nonuniformities at 600 km altitude 3−31404
ion density and electron temps., probe meas. 3−3058
ion-cyclotron whistlers, multiple reflection full-wave study 3−18882
ion-hydrates, reaction mechanisms and bonding energies 3−3066
irregularity structure, two beam obs., at Arecibo 3−28064
l.f. equatorial electric field fluctuations, ionospheric turbulence relationship 3−16017
l.f. sounding of lower ionosphere, solid state sounder, multiphase integration 3−3200
longitudinal currents, polar magnetic substorms *(Russian)* 3−3120
low-latitude dynamics, 6300 Å night glow obs. 3−18874
lower, impact and bremsstrahlung photoionisation due to precipitating electrons 3−34945
lower, rel. to atmospheric dynamics 3−3063
lower nighttime, l.f. absorption, ionization processes *(Russian)* 3−3053
magneto-ionic wave coupling, dependence of whistler activity on geomag. latitude 3−12722
magnetoacoustic channel under dome of plasmasphere *(Russian)* 3 -3121
magnetospheric interaction 3−3126
mid-latitude disturbances rel. to geomagnetic storms 3−31331
mid-latitude topside ionosphere during local sunrise, electron density and scale height 3−31408
midlatitude, during winter, electron density distrib. 3−3064
minor neutral constituents, photochemistry and transport 3−3043
models, spatial impulse response functions 3−39549
Monte Carlo simulation of model ionosphere rel. to energy flow and dissipation 3−21965
multistatic incoherent scatter meas. of ionospheric drift velocity 3−28063
nighttime obs., signal phase difference and polarisation plane rotation angle meas. 3−34933
NO, vertical distribution in 60-170 km, altitude region 3−3044
photoelectron heating, modified Monte Carlo method 3−28065
photoelectron interaction with ambient electrons, Coulomb collision effects 3−31422
plasma, characteristics of electric field far and close to a radiating antenna around lower hybrid resonance 3−21962
plasma drift velocities at high mag. latitudes 3−16000
plasma flow past semi-infinite cylinder 3−9323
plasma wave transmission 3−12561
polar cap bombardment by solar cosmic rays, D region effects 3−25295
polar ionosphere interaction with magnetotail current system rel. to S_q-p var. 3−31451
polar wind model, singularities and critical points of equations 3−16022
positive ion composition at low altitudes 3−3065
potential double layers using Langmuir theory and Bohm self-consistency condition 3−25263
potential electric field eqns., iteration method 3−25266
reflection of FM electromagnetic pulses 3−25278
scale height determination from refraction of radiowave satellite signals 3−9319
seasonal anomalies in lower ionosphere radio wave absorption, effect of pressure var. above mesopause 3−12775
seasonal variations of air-earth current density, columnar resistance, ionospheric potential 3−28035
solar corpuscular radiation effect on characts. *(Russian)* 3−3036
solar X-ray spectrum, 1.9 Å line effects on SOLRAD detectors and lower ionosphere 3−31413
southern mid-latitude electron content, June 1965-August 1971 continuous recordings 3−31416
spatial resonance rel. to internal gravity wave and natural ionospheric drift 3−31420
spectral analysis of simultaneous PDP recordings by longitudinal chain of observatories 3−34845
stratospheric-ionospheric interaction during movement of deep planetary wave 3−3034
striations onset in barium clouds 3−9318
sudden commencement absorption, quadruple conjugate pair observations of event on June 17, 1965 3−12794
sudden disturbances, assoc. with solar optical flares and microwave bursts 3−31411
summary of Japanese daily obs. results for Oct. 1969 to Dec. 1971 period 3−39610
symmetric double probe, ionospheric plasma temperature 3−28087
thermospheric wind effects on ionosphere during magnetic disturbances 3−31394
tidal theory of ionospheric intermediate layer rel. to dynamics and ionization 3−21966

ionosphere continued
topside, Isis 1 satellite observations during 3 Feb. 1969 geomagnetic storm 3−12795
topside, magnetic storms and seasonal anomaly rel. to electron distributions 3−25274
topside, spatial and temporal manifestation of seasonal anomaly *(Russian)* 3−3074
topside at high southern latitudes, Aerial 3 observations of electron density 3−31407
topside electron densities and scale heights rel. to shallow solar zenith angle 3−9317
topside electron density variation during 1962 December mag. storm 3−25280
total electron content enhancement in S. auroral zone rel. to magnetospheric substorms 3−31419
total electron content meas. during visible auroras over Macquarie Island 3−31418
transverse ion temperature, ionospheric wind tunnel obs. 3−5536
vector electric fields, electric component of e.l.f. hiss 3−16016
v.l.f. mode conversion at middle latitudes in 12.2 to 23.4 kHz range 3−25273
v.l.f. region, sudden changes in integrated intensity of atmospherics 3−21949
H^+ flux beteen plasmasphere and ionosphere. diurnal variation 3−16040
H_2O cluster ions composition at low altitudes 3−3065
NO^+ composition at low altitudes 3−3065
$O_2{}^+$ composition at low altitudes 3−3065
$O(^1D)$ distribution *(Russian)* 3−3078
OI dayglow emission line meas., excitation mechanism 3−16021
^{222}Rn daughter small ions, mobility distribution meas. 3−15967

ionospheric electromagnetic wave propagation
see also atmospherics
absorption at 2.4 MHz, lunar effects 3−12792
absorption of 1.725 MHz radiowaves, Winter anomaly during sunspot minimum 3−3071
attenuation of radiowaves in 3-100 MHz range 3−28062
auroral-type E_s-layer in winter, reflection meas. from Dixon 3−28068
average velocity, D-region variations, v.l.f. 3−9340
beyond horizon expt., from satellite to mid-latitude station 3−5539
celestial polarisation, electron content meas. 3−3057
characteristic waves through infinite slab of irregularities in magneto-ionic medium 3−25271
chirped Gaussian pulse, distortion 3−39550
complex refractive index for frequencies less than electron gyrofrequency 3−21961
conjugate ducted echoes, Alouette II ionograms 3−5518
conjugate ionospheric absorption observations of electron precipitation event rel. to sudden impulse in geomagnetic field 3−16019
correlation analysis of ionospheric drift records, errors 3−28084
D-region differential-absorption, differential-phase partial-reflection experiments 3−12805
D-region ionization charges and electron densities from partial reflection differential absorption experiment 3−5521
D-region ionization Winter anomaly, meas. using A1 and A3 radiowave absorption techniques 3−3117
D-region lunar variations from long-path 10.2 kHz phase measurements 3−16027
D-region neutral gas winds and A3 radiowave absorption meas., correlation studies 3−3118
D-region wind meas. from fading of partially reflected radio waves 3−31432
E-region, v.h.f. absorption rel. to electron collision frequency from rocket and ground-based measurements 3−25279
E-region drift meas., skewness of correlation functions of fading records 3−25288
E-region irregularities, phase path measurements 3−3081
effect of geomagnetic storms on nighttime E-layer rel. to M.F. absorption at 593 kHz *(Bulgarian)* 3−9338
e.l.f. and v.l.f. tunnelling transmission in equatorial lower ionosphere 3−31414
e.l.f. propagation using zonal harmonics 3−3062
enhanced scintillation, 6300Å nightglow emission obs. 3−5517
F-region, average scintillation, at u.h.f./v.h.f. 3−37240
F-region, v.h.f. propagation between Darwin, Australia and Yamagawa, Japan, propagational mode deduction from signal strengths 3−31436
F-region e.m. wave reflection coefficients rel. to thickness of E_s-layer 3−25284
F-region irregularity wavenumber spectrum from ionospheric scintillation obs. of the radiosource Cygnus A 3−12803
F-region modification by high-powered h.f. transmitter, ionosonde observations 3−16028
fading, between earth and ionosphere, modelling 3−32403
Faraday fading rate of beacon satellite transmissions across off-zenith transverse point 3−12790
FM pulses, reflection 3−25278
f.m.c.w. partial reflection meas. of D-region, preliminary investigation 3−16032
geomagnetic activity variations, spectrum of the index Ap 3−15924
ground-based generation of Pc 1 frequency artificial micropulsations 3−16064
group refractive index involving temp. and ion effects 3−18877
h.f. electric field excitation of ionospheric plasma rel. to heating experiments 3−16020
h.f. signal behaviour at reception point with operating freq. near max. usable freq. 3−28060
homogeneous isotropic media 3−14532
incoherent radar scatter observations, mid-latitude F-region trough structure 3−31427
inhomogeneity structure, magnetoionic component scatt. 3−34929
ion cyclotron whistlers in upper ionosphere 3−31403
ionization by celestial X-ray sources, continuous monitoring 3−3360
ionospheric absorption, Winter anomaly above Kjeller during solar cycle 3−3070
irregularities in E and F regions over magnetic equator characteristics determ. from spaced fading records of radio wave echoes 3−34944
irregularity structure, two beam obs., at Arecibo 3−28064

ionospheric electromagnetic wave propagation continued
- Kosmos-381 signal reception from magnetically conjugate regions 3−25297
- l.f. propagation and d.c. probe techniques for measuring lower ionosphere electron densities from rockets 3−16031
- l.f. radiowave reflection theory in ionosphere near critical coupling frequency 3−21963
- longitudinal, transmitted pulse shape determ. for both circularly polarised waves 3−16018
- low dispersion whistlers, simultaneous obs. at two low latitude stations 3−34940
- lower F-region ionospheric waves, phase velocity dispersion rel. to e.m. waves 3−21968
- lower nighttime, l.f. absorption, ionization processes *(Russian)* 3−3053
- magnetoplasma, Cherenkov radiation 3−21960
- magnetospheric propagation modes of radioelectric whistlers and gyroelectric echoes received at middle latitudes *(French)* 3−31441
- multiple reflections, variation of apparent height with frequency 3−9314
- multistatic incoherent scatter meas. of ionospheric drift velocity 3−28063
- narrow beam radiowaves, nonlinear interactions E and F_1 layers *(Russian)* 3−3072
- nighttime obs., signal phase difference and polarisation plane rotation angle meas. 3−34933
- nonstationary processes meas. using quantum freq. standards 3−34972
- North Atlantic, ship-borne A1 absorption meas. at 2 MHz during winter anomaly 3−31417
- oblique and oblique-backscatter sounding, spectral characts. of signal level fluctuations 3−25269
- parametrically generated elctrostatic waves refraction by e.m. pump 3−33365
- phase and amplitude var. of 40 kHz waves propagating over 7.1 Mm. path 3−25275
- plane stratified ionospheric models, l.f. radiowave propagation 3−34942
- plasma, characteristics of electric field far and close to a radiating antenna in ionosphere around lower hybrid resonance 3−21962
- polar cap absorption events, D region enhancements 3−16030
- polarimetric study of anomalous absorption of cosmic radio waves in midlatitude ionosphere 3−25262
- prediction possibilities of US Navy Navigation Satellite System 3−16068
- pulsar detection by propagation of whistler mode in surrounding and interstellar plasmons 3−16248
- radio emission, from magnetosphere *(Russian)* 3−39554
- radio signal spreading, absorpt. dispersion effects in lower layers 3−34938
- radio wave reflection, depend. of freq. correlation of fluctuations 3−34934
- radiocommunication, equatorial ionosphere effects, review 3−9324
- radiowave absorpt. meas. by vertical sounding (A1 method) 3−34937
- radiowave absorption, measuring method *(Russian)* 3−3056
- radiowave absorption by electrojet absorption 3−18873
- radiowave reflection, obs. of angles of arrival *(Russian)* 3−3055
- radiowaves, parametric excitation of Langmuir oscillations *(Russian)* 3−31406
- radiowaves, reflection from inhomogeneous layers in Fraunhofer zone, fluctuations in angles of arrival *(Russian)* 3−12797
- radiowaves, VLF, use in ionospheric research, review 3−18900
- reflected radio waves, use of Stokes parameters in polarisation anal. 3−25268
- reflection field distrib., verification using quantitative statistical confidence criterion 3−25267
- resonant at $3f_h$, caused by two waves beating 3−12796
- r.f. electron density meas. employing Ariel 4 satellite 3−25337
- scale height determination from refraction of satellite signals 3−9319
- scatter link digital data system with automatic interrogation *(Russian)* 3−3194
- scattered signal fadings during F_{sp} phenomena *(Russian)* 3−3079
- seasonal anomalies in lower ionosphere radio wave absorption, effect of pressure var. above mesopause 3−12775
- short-wave propag. rel. to inhomogeneities of topside ionosphere 3−34928
- sky wave phase informations as function of apparent reflection height, l.f. field strength observations *(German)* 3−9313
- solar activity cycle, winter anomaly variations in absorpt. 3−34936
- solar Lyman-α control of 2775 kHz ionospheric absorption 3−31412
- sporadic-E layers at mid-latitudes, importance of mode coupling 3−25287
- sporadic-E thin layers, mode coupling process rel. to echoes on ionograms 3−25285
- strong radiowave effects on electron density and inhomogeneous structure 3−28061
- sudden field anomalies effect on 164 kHz waves rel. to D-region seasonal structure var. 3−25286
- summary of Japanese daily obs. results for Oct. 1969 to Dec. 1971 period 3−39610
- time delay resolution, along E-W and N-S paths 3−3060
- transequatorial v.l.f. radio waves, anomalous diurnal changes 3−31409
- transmission and reflection of magnetospheric whistlers 3−5519
- transmission ionograms, production and analysis 3−9320
- two-component magnetoplasma, attenuation and phase coefficients 3−9315
- type I equatorial E-layer instability, nonlinear saturation by wave energy transfer to electrons 3−15991
- u.l.f. waves and particles, behaviour in magnetosphere 3−16049
- vector electric field turbulence resulting in radio signal scattering 3−16017
- v.h.f./u.h.f. signals, diffraction statistics 3−37239
- v.l. waves, effect of diurnal variation on TM and TE components *(Russian)* 3−31405
- v.l.f., vertical inhomogeneity, mode conversion program 3−3059
- v.l.f. duct, collisional losses associated with the lower-hybrid resonance freq. 3−16014

ionospheric electromagnetic wave propagation continued
- v.l.f. mode conversion at middle latitudes in 12.2 to 23.4 kHz range 3−25273
- v.l.f. noise spectrum characts. during cosmic excitation of Earth-ionosphere resonator 3−34931
- v.l.f. phase and amplitude meas. during 1972, January 22 solar flare 3−31437
- v.l.f. propagation, effects during ionospheric substorms 3−31410
- wave normal direction of whistler mode signals in ionosphere, rocket-Doppler technique 3−34941
- waveguide, multiple wave numbers of normal waves *(Russian)* 3−3054
- winter absorption anomaly, auroral and magnetic activity influences 3−18862

ionospheric measurement
- *see also electron density; ion density; ionospheric measuring apparatus*
- beyond horizon propag. expt., from satellite to mid-latitude station 3−5539
- calculation errors reduction in meas. of true height using a phase ionosonde 3−9404
- collision frequency of charged particles, use of quadrupole probe on rocket, 0-1000 Hz *(French)* 3−31423
- correlation analysis of ionospheric drift records, errors 3−28084
- D- and E-region, electron density profiles rel. to experimental techniques 3−3111
- D- and E-region ion chemistry, conference (Urbana, USA, July 1971) 3−3083
- D- and E-regions, electron density meas. by incoherent-scatter technique at Millstone Hill 3−3114
- D-region electron density diurnal var. using wave interaction technique 3−3116
- D-region electron density meas., comparison of two ground-based techniques 3−3112
- D-region electron density profiles, comparison of two ground-based techniques 3−3113
- D-region ionization Winter anomaly, meas. using A1 and A3 radiowave absorption techniques 3−3117
- density profiles, manual processing of ionograms *(Russian)* 3−3182
- digital data with automatic interrogation on ionospheric scatter link *(Russian)* 3−3194
- E_s layer structure, space time variations of frequency parameters, spaced soundings *(Russian)* 3−3077
- E-region ion concentration and compos. obs. using incoherent scatter radar 3−3095
- electron content, radiowave technique, celestial polarization 3−3057
- electron densities from rocket meas. using l.f. radio propagation and d.c. probe techniques 3−16031
- F-layer frequency shifts of h.f. Doppler sounder due to geomagnetic sudden commencements 3−21972
- F-region disturbance, latitudinal variations in subauroral zone *(Russian)* 3−3076
- F-region ionogram traces, loop structuring 3−31429
- f.m.c.w. partial reflection meas. of D-region, preliminary investigation 3−16032
- height determ. of ionospheric irregularities with radio holographic method 3−16069
- minicomputer applications, Institut Royal Meteorologique, Belgium *(French)* 3−21980
- minor neutral component distrib., seasonal effects on 3−3046
- modulation Langmuir probe and incoherent scatter radar techniques, comparison rel. to ionospheric electron temp. measurements 3−25272
- non-stationary processes, phase methods for elimination of derivatives of electron content 3−25339
- nonstationary processes meas. using quantum freq. standards 3−34972
- nose extension method for whistlers 3−31448
- oblique and oblique-backscatter sounding, spectral characts. of signal level fluctuations 3−25269
- plasma resonances, slow-wave echoes 3−12793
- plasma-wave particle interactions, Aerial 4 expt. 3−25337
- power spectrum anal. of ionospheric data, use of running means to remove i.f. components 3−25338
- profile determ. from impulse response function meas., feasibility 3−39549
- radar meas. of motion in presence of current induced spectral asymmetries 3−12866
- radiowave absorption *(Russian)* 3−3056
- radiowaves, VLF, use in ionospheric research, review 3−18900
- rocket-borne resonance probe system for meas. of daytime equatorial lower ionosphere 3−3069
- scatter sounder *(French)* 3−25335
- spread F, Pc 1 micropulsation relationship 3−15923
- temp. determ. from plasma wave phenomena 3−16061
- transmission ionograms, production and analysis 3−9320
- vertical sounding (A1 method), radiowave absorpt. meas. 3−34937
- wave normal direction of whistler mode signals in ionosphere, rocket-Doppler technique 3−34941
- whistler nose frequency determ. method and min. group delay when causative spheric unknown 3−31449
- NO concentration during polar cap absorption event 3−3085
- O profiles in lower thermosphere 3−3050
- O_2, mesospheric, determ. of photodissociation rate by solar radiation in 1025-2500Å range 3−3047

ionospheric measuring apparatus
- auroral scanner, dual wavelength ground based 3−5538
- digital ionosonde for automatic electron density profiles 3−12865
- h.f. quadrupole probe, electron density and temp. meas. 3−9316
- l.f. sounder for lower ionosphere, solid state sounder, multiphase integration 3−3200
- phase ionosonde, improved true height reduction technique 3−9404
- quadrupole probe on rocket, 0-1000 Hz, meas. of charged particle collision frequency *(French)* 3−31423
- satellite-borne positive ion mass spectrometer 3−39565
- scatter sounder *(French)* 3−25335
- topside sounder system of ionosphere sounding satellite, computer simulation 3−39566

ionospheric measuring instruments *see ionospheric measuring apparatus*

ionospheric propagation *see ionospheric electromagnetic wave propagation*

ionotophoresis *see electrophoresis*

ions

see also atoms; electrolytic ions; hydrogen ions

- air ion, image interaction with conductive fluid droplet *(Russian)* 3−34893
- alkali halides, ratio of shell charges, electrical and mechanical polarizabilities 3−1152
- Alpine glacier meltwater and transport of major cations by sorption 3−9099
- atmospheric electricity *(Spanish)* 3−5625
- D-region, clustering of gas to alkali metal ions, rate constants 3−3105
- D-region, negative ion chemistry 3−3101
- dissociation of multiply-charged organic ions in field ionisation mass spectrometer 3−26706
- E-region composition meas. during sunrise and sunset above Kiruna 3−25292
- ethylenediammonium ion, i.r. spectra, rotational isomerism 3−38291
- F-region (lower) composition meas. during sunrise and sunset above Kiruna 3−25292
- gaseous, in elec. field, energy partitioning 3−33332
- heavy ion tracks in Lexan for charge and energy information 3−6065
- hydrogenic, infinite Z, Coulomb-Born-Oppenheimer cross-sections for electron impact 3−20039
- inert gases, charge transfer rate consts. to difluorobenzene and dichloroethylene 3−33152
- interstellar molecule formation by chemical reactions involving negative ions 3−39738
- ionosphere, ion-hydrates, reaction mechanisms and bonding energies 3−3066
- i.r. and u.v. spectroscopic studies of free radicals and molecular ions isolated in inert solid matrices, review 3−11251
- magnetosphere, satellite observations during geomagnetic storm of 17 Dec. 1971 3−12659
- molecular, metastable, decay process 5-500 μsec *(German)* 3−7248
- multiphoton transitions, bound-free transition integrals in compact forms 3−26577
- mutual neutralization in positive negative ion collisions *(Russian)* 3−11177
- noble metal halides, ratio of shell charges, electrical and mechanical polarizabilities 3−1152
- paramagnetic, resonant phonon scattering, coupled mode and perturbation theory approaches comparison 3−1766
- production methods improvement and r.f. spectroscopy using optical pumping technique 3−1116
- rare earth metals, Sternheimer shielding-antishielding parameters, calc. 3−30416
- solar flare current layer in accel. by plasma oscill. 3−37326
- three-electron, ^2S and ^2P states, natural anal. 3−29473
- transition series, second, self-consistent-field atomic orbitals calc. 3−35954
- two-electron, singlet-triplet expectation value differences 3−23466
- Ag^+, diffusion in borosilicate glass, influence of two-site mechanism 3−14699
- CO_3^{--} in calcite, Einstein coeff. spectra 3−24696
- ClO_3 in $RbClO_3$ and $CsClO_3$, n.q.r. 3−8481
- ClO_3^-, ClO_4^-, electronic struct. from Cl X-ray spectra meas. in $KClO_3$ and $KClO_4$ 3−29598
- Fe group ions, optical interaction spectra *(Russian)* 3−1104
- H_2O cluster ions, shock layer meas. of decomposition reaction rate 3−3106
- He-like ions, X-ray line emission mapping of solar corona 3−18946
- Li-like, in solar e.u.v. lines, relative intensities 3−18955
- N fluoride cations and anions, CNDO/2 calculation of atomization energies 3−7245
- NH_4^-. chemical anal. of Delhi rainwater in 1964-67 period 3−37228
- NO_3^-, chemical anal. of Delhi rainwater in 1964-67 period 3−37228
- O^-, O^-_2 and O^-_3 clustering rates with H_2O vapour in ionosphere 3−3108
- P fluoride cations and anions, CNDO/2 calculation of atomization energies 3−7245
- SO_4^{2-}, chemical anal. of Delhi rainwater in 1964-67 period 3−37228
- SO_4^{2-} ion symmetry in gypsum 3−1611

i.r. astronomy *see infrared astronomy*

i.r. detectors *see infrared detectors*

IR drop *see electric potential*

i.r. imaging *see infrared imaging*

i.r. sources *see infrared sources*

irasers *see lasers*

iridium

- band struct. and Fermi surface variations with crystal potentials, relativistic APW exam. 3−4944
- electrical conductivity obs. 293-2275 K 3−21045
- Fermi surface, de Haas-van Alphen obs. 3−38785
- Fermi surface, press. effect, de Haas van Alphen effect determ. 3−15123
- field-ion microscope specimens, occurrence of field-induced surface vacancies 3−35507
- malleability and plastic anisotropy study 3−18651
- refractory, exploding-wire measurement of heat of fusion and electrical conductivity 3−30247
- solubility of C, 825-1256°C 3−8812
- superconducting transition temp., electron-phonon mass enhancement theory 3−18246
- temperature conductivity meas., wide temp. range 3−36578
- thermophysical props., Moscow State University research *(German)* 3−36579
- valence band X-ray photoelectron spectra 3−2616
- work function of (110) and (111) surfaces, determ. by field emission retarding potential method 3−21137
- Ni:^{192}Ir, elec. quadrupole interaction on ^{192}Ir, n.m.r. obs. 3−2461

iridium alloys

see also iridium compounds

- Fe-^{191}Ir dilute alloy, hyperfine field nonalignment effects under mag. saturation, meas. at 25 mK 3−24565
- Fe-Rh-Ir, electronic sp. ht. obs. rel. to antiferro-ferromag. transition 3−34128

iridium compounds

see also iridium alloys

- Ir complex, nitrosylpentahalogeno, Raman and i.r. spectra, fund. modes assignments 3−5193
- Ir complex, nitrosylpentahalogeno, i.r. and Raman spectra, fund. modes assignments 3−5194
- Ir coordination compounds, donor-acceptor props. of ligands, X-ray photoelectron spectroscopy 3−17415
- Ir organometallic, π-bonding of butadiene to Ir 3−14825
- IrF_5, association in vapour phase, molecular beam mass spectra 3−25924
- Ir(I) complex, five-coordinated, X-ray photoelectron and Mossbauer spectroscopy 3−21343
- IrO_2, cryst. growth, vapour phase method 3−12256
- IrO_2, free energy of form. by solid electrolyte galvanic cell method 3−37124
- Ir_2S_3, thermodynamic props., 920-1110 K 3−27130
- α-IrW, stacking fault role in martensite phase formation from fcc struct. *(Russian)* 3−2699

iron

- aquatic frontal systems, element enrichment in films and foams 3−12690
- Armco, investigation of microcrack initiation and slip band structure in fatigued specimens 3−18745
- Armco, lower yield stress considerations 3−21659
- asymmetric deformation in net zero strain fatigue 3−36347
- atmospheric spectral absorption bands rel. to iron particle shape and orientation *(Russian)* 3−18860
- Auger electron and charact. energy loss spectra from clean and slow oxidized surfaces 3−34452
- Auger spectra rel. to oxidation 3−30908
- barrier as shield for fast neutrons 3−7022
- b.c.c., temp. effect on crack extension, model approach 3−30199
- carbonyl powders, hot pressing with Ni carbonyl powder with subsequent annealing for production of permalloy *(Russian)* 3−27723
- cast, induction furnace melting, mech. props. 3−24960
- cast iron:Ce, Ce effect on mech. strength with quenching *(Russian)* 3−12411
- cathode, dynamics of precathodic region at various rates of changing current in impulse discharges *(Russian)* 3−30046
- cavitation erosion study using water tunnel system and magnetostriction vibratory unit 3−2785
- channelling of 1.9 MeV He^+ ions, oscillating trajectories, backscatt. obs. 3−4778
- coarse magneto soft powder, sintering effect on coercive force *(Russian)* 3−27718
- coating on Si, effect on thermal oxidation, 692-1003°C 3−11824
- Compton profile and electron distribution, meas. using $K\alpha$ X-rays 3−1982
- contact charge density of 4s electrons, internal conversion expt. 3−15124
- core binding energy in silicate minerals, ESCA technique 3−5431
- corrosion, inhibiting action on hydrogen adsorption in sulphuric acid solns. *(French)* 3−1911
- crack extension by bond rupture 3−15724
- cracklength, u.s. determ. during fracture toughness testing 3−13231
- creep of high-purity specimens, const. mag. field influence, dislocation-domain wall interaction *(Russian)* 3−36774
- Curie temp., pressure variation 3−2276
- deformation restance, temp. and strain rate depend. *(Russian)* 3−31058
- densities of unfilled one-electron levels, X-ray continuum isochromat study 3−36536
- desorption of hydrogen, kinetics *(French)* 3−1892
- Deybe-Waller factor and Debye temperature, general force const. model calc. 3−30234
- diffusion in Al, surface barrier to diffusion, Mossbauer obs. 3−38684
- diffusion in Fe-metal-C system, successive *(Russian)* 3−7963
- diffusion of Ag 3−17990
- diffusion of C in Fe samples with dynamic hot pressing *(Russian)* 3−8945
- diffusion of hydrogen, alloying additions influence 3−1829
- diffusion of hydrogen, coeff. determ. from permeability meas. *(French)* 3−1827
- diffusion of hydrogen and dislocation-hydrogen interactions 3−4887
- diffusion of sulphur, temp. and grain size depend. *(Russian)* 3−24292
- diffusivity, permeability and solubility of hydrogen, conc. and temp. depend. 3−1828
- dislocation description of twin dynamic behaviour 3−20748
- dislocation motion in stretched single crystal foil, high voltage electron microscope obs. 3−11628
- dislocation movement, edge and screw, low temp. obs. using HVEM 3−11631
- dislocation multiplication rate in polycrysts. 3−38611
- electrodeposition on Cu, epitaxy relationships *(French)* 3−24355
- electronic spectra and density of states, cluster calc. 3−36516
- electroplating using Sn, Zn and Ti 3−9073
- embrittlement and delayed fracture due to hydrogen, industrial consequences *(French)* 3−2735
- embrittlement by hydrogen, low carbon additions influence *(French)* 3−5322
- embrittlement by hydrogen and hydrogen/dislocation interaction 3−2744
- energy bands of ferromagnet 3−38784
- epitaxial intergrowth of Fe sheets and thin films, form. of nitride phases *(German)* 3−1926
- epitaxy on Ag substrate platelets 3−20953
- equation of state of alpha and epsilon phases, empirical 3−33652
- failure mechanism under plane stress conditions at low temps., polycryst. specimens 3−31096
- fatigue, in single cryst., slip planes and asymmetric slip obs. 3−7834

iron continued
fatigue, low-cycle, of α-phase specimens, grain boundary sliding, 450-700°C 3 − 34577
ferromagnet, current-carrying states rel. to spin polarization in photoemission 3 − 18533
ferromagnetic, relaxation of resonance spin waves by s-d exchange 3 − 21315
ferromagnetic reson., 300-1090K, relax. parameter, g-factor 3 − 8450
ferromagnetic resonance with plastic deformation 3 − 5139
film, (100) single cryst., magnetisation ripple and dislocations 3 − 8399
film, deposition using laser beam, and Mossbauer spectra *(Russian)* 3 − 30934
film, electron energy loss spectrum 3 − 17885
film, evaporated at oblique incidence domain structures 3 − 1544
film, Hall effect rel. to H_2 and O_2 chemisorption 3 − 15278
film, oxidation mechanism, ferrite film form. 3 − 27196
film, vacuum deposition for Mossbauer study 3 − 34476
films, cylindrical, Procopiu effects study 3 − 36775
films, thin, vacuum deposited on amorphous carbon substrates, effect of oxygen 3 − 8722
garnets, magneto-optic light modulation at 1.06 μm 3 − 36856
glide dislocations, unstable, in α-Fe at elevated temps., elastic anisotropy factors calc. 3 − 31024
grain growth and secondary recrystn. 3 − 21591
graphite:Fe, oscillatory magnetoresist., charged impurity selective scatt. 3 − 11864
gray, hypo-eutectic, eutectic solidification study *(Japanese)* 3 − 27679
grey cast, rolling contact fatigue tests, effect of surface roughness and form factors 3 − 21616
Hall and Nernst-Ettingshausen effect, anomalies near Curie pt. *(Russian)* 3 − 12014
Hall effect and magnetoresistance 3 − 38825
h.c.p. and b.c.c., effect of pressure and low temps. on props., Mossbauer study of mag. ordering 3 − 2285
high purity, quenched, lattice defects, resist. study 3 − 4749
high-purity, density, influence of slip and mech. twinning *(Russian)* 3 − 7826
high-purity, fatigue deform., cryst. orientation depend. *(Japanese)* 3 − 18595
hot-rolled, effect of processing variables on preferred orientation 3 − 8850
hydrogen charging, uptake detection method using anodic oxidation at bipolar electrodes 3 − 12522
hydrogen-induced surface blisters and internal cracks, electron probe obs. 3 − 39349
impact behaviour of high-purity samples, effect of up to 1% Sn 3 − 8846
interaction lengths of energetic pions and protons in, 9.3-18 GeV 3 − 29456
internal friction, freq. depend. for technical purity metal *(Russian)* 3 − 1691
internal friction, hydrogen influence, interaction with dislocations *(French)* 3 − 2739
ionisation balance, calc. for collisional ionisation, autoionisation, radiative recombination and dielectric recombination 3 − 11458
ions, optical interaction spectra *(Russian)* 3 − 1104
kaolinite glasses, pure and Fe-doped, recrystallisation 3 − 7632
line strengths determ. for intermediate coupling, solar Fe abundance 3 − 38208
liquid, electrolytic deoxidation at 1600°C 3 − 5313
liquid, temperature and alloying element effects on evolution of gas 3 − 31034
local losses, in magnetic sheet, thermometric meas. *(Japanese)* 3 − 24599
Lorenz number determ. at high temps. 3 − 18118
lubricant trapping under cold compression *(Japanese)* 3 − 30990
Luders band motion during nonuniform deform. 3 − 17910
magnetic aftereffect, susceptibility meas. of low temp. mag. relax. 3 − 34168
magnetic h.f. field at ^{99}Tc, perturbed ang. correl. obs. 3 − 5154
magnetic susceptibility, high temp. meas. *(French)* 3 − 6030
magnetised with polarised positrons, positron annihilation, investigation of spin and momentum density 3 − 18066
magnetization, 5-295K, 0-14 kOe 3 − 2311
mech. strength of crystal lattice calc. *(Russian)* 3 − 8845
melting relations, temperature of Earth's core 3 − 12581
meteorites, determ. of Ni, Ga and Ge, by X-ray fluorescence analysis 3 − 5451
microcrack form. around inclusions during solidification 3 − 34537
microcrystals, substruct., X-ray obs. 3 − 36505
Mossbauer γ-ray energy shift of ^{57}Fe, anal. 3 − 27451
Mossbauer spectrum anomaly at 0.01K, obs. of ^{57}Fe and ^{119}Sn, Mossbauer thermometer *(Russian)* 3 − 5149
multiple charge states, in CaO, CaF_2, Mossbauer obs. of isomer shift 3 − 27455
neutron multi-group theory, energy-dependent buckling 3 − 1042
neutron removal cross section at 14.1 MeV 3 − 6971
neutron spectra, time-energy study using fast neutrons 3 − 6968
neutron spectra inside cylindrical Fe shield from 14 MeV source 3 − 6972
RS Ophiuchi, nova, Fe II lines formation region 3 − 37389
oxidation, photoelec. work function and Auger spectroscopy study 3 − 38741
oxidation kinetics and morphological development of oxide state at 800°C, O_2 press. depend. 3 − 38742
oxidation mechanism, electron microscope obs. of fine particles 3 − 38744
oxidation of (011) Fe at room temp., LEED obs. 3 − 38745
oxidation of ideal clean surface, kinetics and struct. changes 3 − 8043
particles, oxid., electron microscope obs. of oxide-metal boundary 3 − 15076
passive, passivating film, thickness, complex refr. index and absorpt. coeff. meas. *(German)* 3 − 27163
Peierls-Nabarro barrier and stress of $a/2\langle 111 \rangle$ edge dislocation in α-Fe 3 − 14858
permeability of hydrogen, stress and elec. field effects 3 − 1824
phlogopite mica:Fe^{3+}, e.s.r. of Fe^{3+} centres 3 − 12057

iron continued
plastic deformation of surface and internal layers, under fatigue loading 3 − 27056
polymorphic $\gamma \to \alpha$ transform. in high-purity Fe *(Russian)* 3 − 12340
positron annihilation, band structure calculation of momentum densities 3 − 18065
powder with P additive, sintering conditions effect on shrinkage on magnetic props. *(Russian)* 3 − 27720
powders, particle shape effect on compactability *(Russian)* 3 − 27717
powders with 1% P additives, sintering conditions effect on magnetic and mechanical props. *(Russian)* 3 − 27719
quartz: $Fe^{2+}(Fe^{3+})$, impurity absorpt. near 78μ band 3 − 5216
reactions on exposure to molten Sn 3 − 37078
relaxation, real structure and migration props., magnetic after-effect obs. *(Polish)* 3 − 24212
secondary electron emission from Fe(110) single crystal 3 − 36962
self diffusion coeff. temp. depend. at Curie point *(Russian)* 3 − 11761
self-consistent band calculations, paramag.- and ferromag. states 3 − 21205
sheet, contact thermal conductivity, as fn. of contact pressure *(Russian)* 3 − 9850
shock wave propagation, deform. energy and collision velocity determ. *(Russian)* 3 − 27066
single crystals, tensile test of foil specimens at room and low temp., dislocation motions 3 − 17820
single crystals at 78 and 4K, gliding, twin formation, fracture *(German)* 3 − 34612
single-domain powders with cubic anisotropy, mag. props. *(Russian)* 3 − 15390
sintered, unlubricated frictional behaviour 3 − 27710
slab, bremsstrahlung, transmitted energy spectra of radiation produced in Fe and Au targets 3 − 17328
small crysts., diameter ⩽30 Å, cryst. struct. 3 − 14735
solar flare particles, charge states and energy dependent composition 3 − 35025
solubility of N, calc. 3 − 8786
spectra analysis, matrices for interaction energies of d^3.d and d^7.d electronic configurations *(Spanish)* 3 − 38207
spectral lines determ. in arcs and sparks, degree of ionisation determ. *(Russian)* 3 − 29482
spectral regularities for d-electrons 3 − 38210
spin polarisation of electrons tunnelling from Fe ferromag. to Al superconducting film 3 − 15311
stress exponent of dislocation vel. from strain rate cycling tests *(Japanese)* 3 − 31078
surface, adsorbed O, correl. of proton-excited X-ray and Auger spectroscopy anal. 3 − 1879
surface oxidation, static method secondary ion mass spectrometry obs. 3 − 1906
synthetic Apollo 11 composition glasses, subsolidus reduction and metallic Fe 3 − 12994
thermoelectric power, magnetic field dependence 3 − 11885
u.s. attenuation coeff. reln. to grain size 3 − 9034
vacancies, lattice distortion, interaction energies, discrete lattice model 3 − 30116
wettability of melt on graphite and glasslike carbon substrates, catalytic graphitisation 3 − 11796
whisker, magnetisation process with Landau domain struct. 3 − 36749
whiskers, X-ray topographic obs. of fir-tree branch and rectangular mag. domains 3 − 30648
whiskers production and properties 3 − 24796
X-ray K-absorption spectra *(Russian)* 3 − 18509
X-ray spectra of highly ionized states in 1 to 2 Angstroms region 3 − 17354
yield strength, lower, depend. on grain size and temp., α-Fe specimens 3 − 37053
zone formation in Al-Mg_2Si, effect of Fe 3 − 8884
zone melted crystals under tensile stress, dislocations and magnetic domain walls, X-ray topographic study 3 − 17828
α-Fe, recrystallization dependence on deformation and annealing following high temp. torsion deformation 3 − 15707
Al-Mn:Fe, dilute alloy, temp. depend. of impurity resist. 3 − 21048
^{26}Al formation by 0.6 and 24 GeV proton bombard., captive cross sectio determ., astrophysical appl. 3 − 23315
As_2S_3 glass and crystalline phases, magnetic susceptibility, paramagnetic contributions due to Fe impurities 3 − 8334
in$BaO.P_2O_5$ glass, redox behaviour rel. to absorpt. spectra 3 − 24723
CaO:Co, Fe, Mossbauer study of ^{57}Fe rel. to dynamical Jahn-Teller effect 3 − 24639
in $CaO.P_2O_5$ glass, redox behaviour rel. to absorpt. spectra 3 − 24723
CdF_2:Fe, point defects, Mossbauer and mag. investigation 3 − 39063
CdTe:Fe, Hall effect and photocond. meas. rel. to impurity absorption 3 − 15531
in Cr, impurity lattice dynamics, Mossbauer obs. 3 − 33638
in Cu, solute effect on self-diffusion *(French)* 3 − 24289
Cu-Zn:Fe, Mossbauer effect isomer shift meas. 3 − 15441
EuO:Fe film, thermomag. writing, optimum thickness calc. 3 − 16915
Fe, Armco, microfracture and structural failure under dynamic loading of Armco Fe 3 − 2722
α-Fe, grain boundary sliding in creep, investigation 3 − 21612
Fe, oxide films, X-ray photoelectron spectra 3 − 8701
Fe I, $3d^64s^2$, electronic struct., numerical Hartree-Fock functions 3 − 33009
Fe I, emission lines, Van der Waal's broadening induced by neutral He in glow discharge 3 − 35981
Fe I 5233 and 5250 Å solar lines meas. of small-scale structure of magnetic fields and narrow filaments 3 − 39617
Fe I Fraunhofer lines, saturation effects rel. to solar curve of growth 3 − 22016
Fe I resonance lines (Multiplet 1, 5110 to 5255 angstroms), oscillator strength meas. 3 − 11147
Fe II 6149.2 Å line profile of sunspot umbral dots 3 − 35036
Fe IX to Fe XVI emission lines and isoelectronic lines in laboratory and solar spectra 3 − 18952
Fe XI 3986 Å line in solar corona, luminosity conditions 3 − 39606
Fe XI to Fe XIV multiplet lines in solar spectrum in 200 to 400 Angstroms region, identifications 3 − 18969

iron continued
Fe XIII spectrum excitation in solar corona, statistical equilibrium equations 3—37318
Fe XIV coronal line emission from the Cygnus Loop 3—22122
Fe XV e.u.v. spectrum of solar flare in 200 to 500 Å region, line identifications 3—31522
Fe XVII emission from solar corona in 13-17 Å region 3—37319
Fe XVII lines in solar X-ray spectrum of 13-18 Angstroms range 3—37320
Fe XVIII to Fe XXIV emission lines in solar flare spectra, classification 3—18953
Fe XXIII and XXIV lines in soft X-ray spectra of solar flares 3—39600
Fe: ^{220}Rn, ^{224}Ra, hyperfine interactions of Rn and Ra, alpha decay PAC obs. 3—2270
Fe:^{175}Lu(^{175}Yb), hyperfine fields at impurity nuclei and annealing props. 3—15141
Fe:^{44}Sc, hyperfine field meas. using time differential perturbed angular correlation technique 3—34260
Fe:Co, ^{57}Fe c.w. n.m.r. spectra obs. of hyperfine field at impurities 3—21326
Fe:Co(Ni)(Sn), temp. depend. of hyperfine fields, c.w. n.m.r. obs. 3—21327
Fe:H, zone melted and armco, H effect on elec. resist. at low temps. 3—8807
Fe:Hg, time-differential-perturbed-angular correlation meas. of hyperfine mag. field 3—39067
Fe:$LiNbO_3$, alterable holographic medium, wavelength dependence 3—204
Fe:Si, anisotropy of ferromag. resonance line width 3—18372
Fe:Si, ferromag. domains parallel to (111) *(French)* 3—27383
Fe:Si, Mn, influence of impurities on supercooling *(Russian)* 3—24829
Fe:Si, neutron inelastic scatt. obs. of spin wave intensity 3—15378
Fe:Tm, ferromag., perturbed angular correlation for localised moments 3—15359
Fe:Zr, Ti, Si, Al, supercooling and macrostructure, influence of refractory oxides *(Russian)* 3—24828
Fe/Cu single-fibre composite, multiple yield phenomena 3—34636
Fe/H rel. abundance var. in North Galactic Pole K-type giant stars, UBVRI photometry 3—9543
Fe/S ratio determ. for pyrrhotite-bearing rocks rel. to remanence self-reversal 3—25171
Fe-Mo solid solns., field ion microscopy, bright spot density 3—19330
Fe-mortar shielding material, engineering and economic aspects 3—11097
Fe-Si, internal friction features in variable mag. field, magnetoelastic losses 3—30677
Fe-Si crystal, rotational hysteresis loss in (001) plane *(Japanese)* 3—24582
Fe^{+} in equatorial F layer, source and identification 3—12807
Fe^{2+}, in H_2SO_4 vitreous aq. soln., effect on spin-lattice relax. of H atoms 3—34186
Fe^{2+} in Al_2O_3, detection using spin-lattice relax. of Cr^{3+} and Fe^{3+} 3—2372
Fe^{2+} in ruby, a.p.r. obs. 3—2373
Fe^{3+}, e.p.r. in adamite, co-substituting Cu^{2+} and Fe^{3+} in Zn sites 3—15415
Fe^{3+}, e.p.r. in SiO_2, α-tridimite, vitreous and crystalline struct., crystal field strength, symmetry 3—21298
Fe^{3+}, in As_2Se_3 and $TlAsSe_2$ glasses, e.s.r. *(Russian)* 3—5133
Fe^{3+}, in $CuGaS_2$ chalcopyrite, e.s.r. obs. of magnetically inequivalent metal sites 3—30689
Fe^{3+}, in ferric ammonium citrate, e.p.r. obs. 3—18355
Fe^{3+} faradaic shot noise of charge transfer step in Pt-Fe^{2+}/Fe^{3+} system 3—15835
Fe^{3+} in $Al_2SiO_4F_2$, e.p.r. spectrum, ^{19}F ENDOR study for hyperfine struct. tensors 3—21342
Fe^{3+} in II-VI semiconductors, g-shift 3—2377
Fe^{4+}, possible obs. in Al_2O_3, by thermal cond. studies 3—30293
FeII line identification in spectrum of Herbig-Haro No.1 object 3—28202
^{57}Fe, Mossbauer spectra, curve fitting, fitting by Monte Carlo method 3—34179
^{57}Fe in Ni(Pd)(Pt) alloys, mag. interactions, Mossbauer obs. at 4.2K 3—36819
^{57}Fe^{3+} ENDOR at different sites in SnO_2 3—2467
^{57}Fe^{3+} Mossbauer spectra in diamag. host lattice, hyperfine splitting 3—34253
^{58}Fe, synthesis in supernovae 3—13097
Fe(111) surface structure determination using LEED and Auger spectroscopy 3—15054
GaAs:Fe, electron absorpt. obs. rel. to impurity energy levels *(Russian)* 3—15532
GaAs:Fe, sensitizing centres, photo Hall effect, photocond. 3—36547
GaP:Fe^{3+}, deep levels, photocond. obs. 3—18095
γ-ray attenuation coeffs., $E_\gamma = 6\text{-}10$ MeV 3—17329
InSb:Fe, elec. and galvanomag. props., impurity levels and hole scatt. mechanisms 3—38844
KCl:^{57}Co, ^{57}Fe, Mossbauer obs. of colour centres 3—15447
$LiNbO_3$:Fe, e.p.r. obs. of Fe impurities and n.m.r. obs. of stoichiometry 3—12060
MgO:Fe, e.s.r. and Mossbauer spectroscopy, effect on surface reactivity study 3—15439
MgO:Fe, ion implanted, photolum. from damage related defect centres 3—21463
MgO:Fe, polycrystalline, transient creep rate 3—7831
in $MgO.P_2O_5$ glass, redox behaviour rel. to absorption spectra 3—24723
Mn_3GaC:^{57}Fe, Mossbauer obs. of paramag. and ferromag. spectra 3—12081
$NH_4H_2PO_4$:^{57}Fe^{3+}, antiferroelec. transition, Mossbauer obs. 3—15468
NaCl:^{57}Co, ^{57}Fe, Mossbauer obs. of colour centres 3—15447
NaCl:Mn^{2+}, Fe, bulk crystals, phase transformations 3—4768
in Na_2O-PbO-SiO_2 glass, redox behaviour rel. to absorption spectra 3—24722

iron continued
Ni-Fe layers separated by SiO intermediate layer, magnetic coupling energy 3—8400
P diffusion, radioactive tracer study *(French)* 3—31002
inSi, gettering by ion-damaged surface layers 3—5276
$SmFe_{0.67}Ge_{1.33}$:Sm^{3+} no Fe atoms contrib. to mag. moment 3—2290
in $SrO.P_2O_5$ glass, redox behaviour rel. to absorption spectra 3—24723
TiO_2:Fe^{3+}, e.p.r., Ka band Hamiltonian parameters 3—27405
UO_2, Si, Al_2O_3, Fe, U, impurities, effect on fracture stress 3—39384
V_2O_5:Fe^{3+}, e.s.r. meas. of charge compensation 3—21303
$YCrO_3$:Fe, impurity-host Fe^{3+}-O-Cr^{3+} antiferromag. superexchange, ^{57}Fe hyperfine field meas. 3—30611
ZnS:Fe, e.p.r. obs. of cubic and axial sites 3—15414

iron alloys
see also iron compounds; Permalloy; steel
ageing/deformation treatments influence on struct. and mech. props. *(Russian)* 3—24873
AK6, mech. props. consistency after deform. heat treatment 3—21670
Alnico domain structure variation in partial hysteresis cycles 3—30664
Armco, coarse- and fine-grained, fatigue crack formation and propag. *(Russian)* 3—27671
Armco, cold deform. and subsequent heat treatment, effect on mech. props. *(Russian)* 3—5307
Armco, diffusion of hydrogen, stress effects *(French)* 3—1830
Armco, tested at fatigue limit, dislocation struct. formation *(Russian)* 3—7758
Armco iron, hydrogen charging influence on yield stress and ultimate strength *(French)* 3—5321
Armco iron, hydrogen trapping sites *(French)* 3—2742
austenite, $\delta \rightarrow \gamma$ transform. influence on subsequent transforms. *(French)* 3—8827
austenite, kinetics of thermal stabilization process 3—24915
austenite, supercooled, in steel 75KhSMF, isothermal transformation 3—21570
austenitic, resistance to abrasive wear 3—18669
bcc ferromag. electronic struct., coherent potl. approx. calc. 3—11999
binary substitutional, b.c.c., wire drawing and alloy content effects on work hardening and ductility 3—34572
borided, thermal fatigue resist. 3—27694
cast, containing Cr and Cr-Mo, electrochem. props., rare earth additive effects *(Russian)* 3—27666
cast, high-Mn malleable, isothermal transform. to austenite 3—24834
cast, shear, compressive and tensile characts., comparison 3—27674
cast, wear resistance improvement by low-temp. liquid cyaniding 3—18666
cast iron, deformation of contacting rough surfaces, topography 3—5301
cast iron, eutectic solidification, nucleation of graphite during first-stage graphitization 3—8817
cast iron, internal and external oxidation 3—8047
cast iron, metallographic polishing technique 3—8886
cast iron, spectrochemical analysis, effect of sample structure when using vacuum quantometers *(Russian)* 3—10208
cast iron, spheroidal graphite form. 3—8816
creep strength of synthesized alloys containing Mn, Mo and Cr 3—21640
D16, aging effect on mech. props. 3—21677
dispersion of carbides and nitrides, gas-solid reaction, thermal stability, homogeneous distributions *(French)* 3—34526
Elinvar, ageing effect on Young's modulus temp. depend. *(Russian)* 3—31055
Elinvar, Cr type, tempering influence on Young's modulus and its temp. depend. 3—31084
Elinvar, thermal expansion and elastic props. *(German)* 3—34610
eutectic composite, fibre-reinforced M-M_7C_3, (M = Fe + Co + Cr), $M_7C_3 \rightarrow M_{23}C_6$ transform. 3—31143
fatigue crack propag., stress intensity and microstruct. influence 3—21580
ferritic, solubility of vanadium carbide and nitride *(Japanese)* 3—34528
graphitic cast, tensile strength, calc. method *(Spanish)* 3—31111
heat treatment in engineering design and production 3—31054
heat treatment practice in engineering, review 3—31053
high temperature materials characteriz. for chem. industry 3—8919
high-hot-strength, fatigue strength under nonsteady state loading 3—37106
Incoloy 800, low-cycle fatigue, influence of hold-time and temperature 3—8890
Incoloy-800, heat treatment effect on B distribution 3—12386
Inconel, X-750, precip. parameters role upon creep rupture props. 3—37024
internal friction, hydrogen influence, interaction with dislocations *(French)* 3—2739
Invar, 'magnetic anomaly', Debye-Waller factor, Mossbauer effect 3—39071
Invar, exchange interaction theory of magnetostriction, anomalous thermal expansion 3—18348
Invar, internal friction features in variable mag. field, magnetoelastic losses 3—30677
Invar, mag. exchange contrib. to elastic consts., rel. to anomalous elastic props. 3—24597
Invar, magnetic susceptibility, high field, saturation magnetisation, magnetometer measurements of moment 3—36713
Invar, magnetovolume, effects, Curie temp. press. depend., localised electron model 3—38979
Invar, magnetovolume effect 3—2325
Invar, props. of internal friction mag. peak at 253K 3—30676
Invar, thermal expansion and elastic props. *(German)* 3—34610
Invar alloys, Sn-containing, plastic deform. effect on Mossbauer parameters 3—37003
Invars, dispersion-hardening, Young's modulus anomaly *(Russian)* 3—21631
Kovar, thermal expansion and magnetostriction, below 50K 3—5123
liquid Fe-C alloys, impurities removal and structure control *(German)* 3—2729
magnetic casting mould powder development *(Russian)* 3—27726

iron alloys continued
malleable, Bi-containing, trace element effects on malleabilization kinetics and mech. props. 3−39357
martensite, work hardening origins, strength-differential effect 3−37067
martensite morphology and deform. of cryst. form during athermal transform. *(Russian)* 3−24824
martensitic cast iron, residual austenite content rel. to tempering time 3−30963
Mu-metal, magnetomechanical props. by shear strain meas. technique *(German)* 3−35447
Nimonic, age-hardening, temp. depend. of strengthening characts. *(Russian)* 3−8839
NiSpan C, Invar range, precip. hardening effect on phys. props. 3−39345
nonmagnetic spring alloy, paramag. susceptibility as heat treatment check 3−21696
oxide scales, diffusion and partitioning of elements 3−2696
Permendur, 2V, hot-rolled sheet, order-disorder transform. mechanism *(Japanese)* 3−8865
plasticity and strength characteristics, influence of grain size in presence of Hg *(Russian)* 3−12369
radiation strengthened, residual elements effect 3−18645
rare earth−Fe ternary cubic Laves compounds, spin orientation diagrams and mag. anisotropy 3−38987
rare earth-Fe compound, Curie temp. pressure depend. 3−36720
rare earth-iron compounds, Lu_2Fe_{17} and Y_2Fe_{17}, cryst. struct. 3−17760
relaxation, real structure and migration props., magnetic after-effect obs. *(Polish)* 3−24212
soft, H_2 degassing, main parameters *(German)* 3−8888
solutionized cupro/nickel, stress corrosion resistance in ammoniacal environment, effect of Fe 3−31041
strength differential effect, effective modulus interpretation, reply to comments 3−18679
strength-differential effect, effective modulus interpret. 3−37063
strength-differential effect, effective modulus interpret. 3−37064
Superinvar, thermal expansion, alloying effect, γ-phase stability 3−27699
Superinvar prep. and characteriz. 3−24945
tensile props. at high temp. of alloys containing Mo and Cr 3−21639
Ticonal, high-coercivity, characteriz. after isothermal thermomag. treatment 3−24943
Ticonal alloy, lattice conjugation of metastable tetragonal phases 3−31009
turbine blade materials, behaviour under asymmetric loading 3−31232
ultrasonic inspection of cast iron pipe 3−31223
Vicalloy, domain structure variation in partial hysteresis cycles 3−30664
Vicalloy 1, phase transforms. *(Russian)* 3−30965
Al bronzes mechanical properties, casting properties, effect of iron *(Polish)* 3−31033
Al bronzes transformations, structure and phase, iron effect *(Polish)* 3−30962
Al-Al_3Fe eutectics, directionally solidified, struct. morphology and microhardness *(Russian)* 3−39328
Al-$CuAl_2$-$FeCu_2Al_7$ ternary eutectic composite, mechanical props. and thermal stability *(Japanese)* 3−15701
Al-Fe, dil., cold-worked, internal friction and Young's modulus, heat treatment effects 3−27703
Al-Fe bicrysts., grain boundary precipitate exam. by Ga embrittlement technique 3−37025
Al-Fe(3.6 at.%), supersaturated solid solns., annealing and diffusion kinetics 3−36438
Armco Fe, nitrate solns., stress corrosion cracking, mild steel, effect of C content 3−39354
Au-Fe, internal friction due to quenched-in vacancies 3−37040
Au-Fe, magnetoresist. meas. in high fields 3−36592
Au-Fe alloys, magnetic ordering rel. to Fe concentration 1-22 at.% 3−2287
β-Au-Sn alloys, martensitic transformations 3−8895
AuFe, magnetic moment distribution 3−34134
Ca-Fe enthalpy meas. on the allotropic transformations *(French)* 3−17976
cast, speroidal graphite austenitic, microstruct. effects on creep-rupture props. 3−8929
Co-Elinvar, meas. of thermal expansion and Young's moduli in 150-500°C range, obs. rigidity modulus of polycrystal *(Japanese)* 3−17896
Co-Fe, double h.c.p. structure from X-ray diffraction study, rel. to mag. props. 3−1600
Co-Fe, mag. moments depend. on comp., effect of h.c.p. to double h.c.p. structural transition 3−30607
Co-Fe-Be, age hardening, hardness-controlling additions *(German)* 3−8901
Co-Fe-Be, mag. and mech. props with annealing and cold drawing *(Japanese)* 3−12398
Co-Fe-Nb, semihard mag., anisotropy 3−21261
Co-Fe-Nb, semihard mag., characteriz. 3−21279
Co-Fe-Nb, semihard magnetic, anisotropy *(Japanese)* 3−18334
Co-Fe(Co-rich) alloys, temp. dependence of single crystal elastic constants 3−38605
$CoFe_2$ film, oxidation mechanism, ferrite film form. 3−27196
CoNiFe film, domain wall motion rel. to low freq. creep 3−36738
12%Cr-Fe-C-N, structural diagrams and phase reactions, 1300-700°C 3−8772
7%Cr-Fe-C-N, structural diagrams and solid phase reactions, 1300-700°C 3−8773
Cr-Fe(1%), phonon dispersion relation anomalies, neutron scatt. obs. 3−14948
Cu/Kovar/Cu three-layer band, expansion coeffs. determ. 3−27700
Cu-Fe, ageing characts., mech. props. 3−37075
Cu-Fe, dil., n.m.r. of ^{63}Cu, spin-lattice relax. mechanism 3−2443
Cu-Fe, dil., oscill. of cond. electron density near solute atoms, ^{63}Cu n.m.r. obs. 3−2462
Cu-Fe, dil., resist. and thermo-e.m.f., 4.2-273K *(Russian)* 3−8152
Cu-Fe, dilute, in supercond. sandwich, mag. props from supercond. proximity meas. 3−8341
Cu-Fe, dilute, Kondo temp. conc. depend. 3−21216

iron alloys continued
Cu-Fe, sp. Lt., magnetisation, effect of ordering and precip. 3−34166
Cu-Fe, spin-scatt. anisotropy and exchange coupling energy meas. using de Haas-van Alphen effect 3−33781
Cu-Fe Kondo system, eqn. of state from phenomenological model 3−5096
Cu-Ni-Fe, mag. anisotropy and magnetis. reversal 3−36745
$Cu_{1-x}Au_x$-Fe, mag. field depreciation of Kondo magnetoresist. 3−33872
$DyFe_2$-$DyAl_2$, struct. and mag. studies 3−18323
Er-Fe system, hysteresis of $ErFe_2$, near mag. compensation temp. *(Russian)* 3−8380
Fe, oxidation in air and wet hydrogen at elevated temps. for sealing of soft glass, growth of whiskers *(Japanese)* 3−18590
Fe, Ti-gettered, flow stress components meas., appl. to strength differential effect theory 3−21701
Fe alloyed with ^{54}Mn, ^{57}Co, ^{182}Ta, ^{191}Ir, hyperfine field nonalignment under mag. saturation, meas. at 25 mK 3−24565
Fe:H, zone melted and armco, H effect on elec. resist. at low temps. 3−8807
Fe-3Si tensile loaded plates, mechanics of deep semielliptical surface cracks 3−21621
Fe-Al, superlattice dislocations, fourfold dissociation in DO_3 type order 3−17839
Fe-Al alloys, oxide films, X-ray photoelectron spectra 3−8701
Fe-Al clusters in Alnico type alloy, Mossbauer obs. 3−8491
Fe-Al Kossel interference patterns evaluation by computer *(German)* 3−4693
Fe-Al liquid alloys, specific electrical resistance *(Russian)* 3−8146
Fe-Al powders, cold worked and annealed, magnetisation, temperature and field dependence 3−12040
Fe-Al-C alloy, mag. after effects, directional ordering of interstitial atoms 3−12013
Fe-Al-Mn, splat quenched, decomposition mechanism 3−2712
Fe-Al(40 at%), quenched-in vacancies annealing kinetics 3−37039
Fe-Al(40 at.%), ordered, quenched defect recovery *(French)* 3−24839
Fe-Be (23 at%) alloy, aged above 400°C, Mossbauer study of hyperfine fields 3−34264
Fe-C, elastic consts., composition and temp. depend. 3−17899
Fe-C, permeability and embrittlement by cathodic hydrogen *(French)* 3−21661
Fe-C martensite, carbon multiplet creation during deform. obs. *(French)* 3−8829
Fe-C solid solutions, b.c.c., Snoek peak broadening *(French)* 3−31018
Fe-C(1.86 wt.%), martensitic microstruct. and microcracking development 3−34504
Fe-Co, elastic consts., composition and temp. depend. 3−17899
Fe-Co, Hall effect and magnetoresistance 3−38825
Fe-Co, ordering process, mass spectrometric obs. of secondary ion emission *(Russian)* 3−33490
Fe-Co alloys, Si influence on friction and wear 3−7846
Fe-Co single-domain powders with cubic anisotropy, mag. props. *(Russian)* 3−15390
Fe-Co-Mn, cold worked, strain gauge factor and elec. resist. meas. *(Japanese)* 3−12399
Fe-Co-Ni-Al-Ti-Cu, thermomag. treatment effects *(Russian)* 3−8386
Fe-Co-V, Mossbauer spectra temp. depend., mag. transform. of γ phase *(Russian)* 3−30731
Fe-Co-V, permendur type alloy, long-range order effect on low temp. deform. 3−30189
Fe-Co-V(2 wt.%), ordered, h.p. prestrain effect on fracture stress and yielding 3−37061
Fe-Co(Ni), X-ray K-absorpt. spectra *(Russian)* 3−18509
Fe-Cr, elastic consts., composition and temp. depend. 3−17899
Fe-Cr, ferromag. reson., anisotropy const. determ. 3−2403
Fe-Cr, Hall effect and magnetoresistance 3−38825
Fe-Cr, low C and N content, gamma region *(French)* 3−27620
Fe-Cr, ordering process, mass spectrometric obs. of secondary ion emission *(Russian)* 3−33490
Fe-Cr, sigma phase detection by electron microscopy 3−8811
Fe-Cr, solubility of N, nitriding characts. *(Russian)* 3−15719
Fe-Cr, stress corrosion cracking 3−31039
Fe-Cr platings, electrodeposition *(German)* 3−9072
Fe-Cr spinel, magnetoresist. anomalies at Curie point 3−30462
Fe-Cr-Co containing Si, permanent mag. material, mag. props. 3−36746
Fe-Cr-Co-Mo alloy, precipitation, structural and kinetic features 3−8787
Fe-Cr-Ni, austenitic, hydrogen charging and effects *(French)* 3−2747
Fe-Cr-Ni, embrittled, Mossbauer obs. *(Japanese)* 3−27634
Fe-Cr-Ni alloy system, microstructural change study using selective etching *(Korean)* 3−5291
Fe-Cr-Ni liq. system, thermochem. parameters 3−25045
Fe-Cr(V)(Ni)(Co), deviation from additivity rules, X-ray absorpt. obs. *(Russian)* 3−12337
Fe-Cu, phase change in microdomain, field ion microscope images 3−18563
Fe-Cu-Mn system, semihard mag. reed switch material, heat treatment effect on mag. props. 3−36757
Fe-Cu(1.7 wt.%) alloy Cu precipitation from α-Fe in pre-peak and peak hardness range of ageing 3−8797
Fe-Fe_2B fibrous eutectic alloy, thermal stability 3−8999
Fe-Ga-C, f.c.c., interactions between insertion and substitution atoms *(French)* 3−8777
Fe-Ge, diffusivity, permeability and solubility of hydrogen, conc. and temp. depend. 3−1828
Fe-Ir, elastic consts., composition and temp. depend. 3−17899
Fe-Mn, elastic consts., composition and temp. depend. 3−17899
Fe-Mn, γ-solid solution, self-diffusion and interdiffusion determ. *(Japanese)* 3−30994
Fe-Mn marine and freshwater nodules, thermomagnetic behaviour 3−25182
Fe-Mn-C, structural features of martensitic transform. 3−30976
Fe-Mn-C, thermally cycled, long period stacking order structs. and phase transitions 3−15665

iron alloys continued
- Fe-Mn-C alloys, infl. of mag. transformations on physical props. *(Russian)* 3−2271
- Fe-Mn-Co, cold rolled, heat treatment effect on mag. props. *(Japanese)* 3−31077
- Fe-Mn-Ni, Elinvar type, Young's modulus, thermal expansion, hardness heat treatment and cold working effects *(Japanese)* 3−8859
- Fe-Mn-Ti, Laves phase comp. and struct., χ phase obs. *(French)* 3−39305
- Fe-Mn-X, martensitic transformation, alloying elements X effect on ϵ-Fe stability *(Japanese)* 3−18643
- Fe-Mn-Zn ferrite, internal friction, delta E-effect and stress sensitivity in alternating magnetic field 3−39009
- Fe-Mn(0.05 wt.%), stress exponent of dislocation vel. from strain rate cycling tests *(Japanese)* 3−31078
- Fe-Mo-Ni, continuously cooled carbon-free, transform. kinetics and microstruct. 3−39317
- Fe-N, alloys, cold-drawn, magnetisation anomaly 3−12034
- Fe-N, rapid strain aging, Snoek ordering, conc. depend. 3−24868
- Fe-N system, aftereffect, for irreversible magnetization process in Rayleigh region 3−18344
- Fe-NI-Al, b.c.c., Mossbauer obs. of Al impurities effect on Fe and Ni mag. moments 3−15444
- Fe-Ni, Curie temp., pressure variation 3−2276
- Fe-Ni, elastic consts., composition and temp. depend. 3−17899
- Fe-Ni, f.c.c. alloy, pressure effect on Curie temp., rel. to magnetostriction anomalies 3−34126
- Fe-Ni, Fe-Ni-C, martensite, crystallographic aspects 3−18566
- Fe-Ni, hydrogen embrittlement of austeno-martensitic struct. *(French)* 3−5320
- Fe-Ni, hydrogen-dislocation interactions 3−4887
- Fe-Ni, invar-type, Young's modulus, temp. depend., recovery and recrystn. influence *(Russian)* 3−36773
- Fe-Ni, mag. props., heat treatment depend. 3−21275
- Fe-Ni, mantensite-to-austenite transition, plastic deformation effect 3−18654
- Fe-Ni, martensite-austenite transform., struct. mechanism *(Russian)* 3−24823
- Fe-Ni, martensitic struct., nondestructive testing using u.s. attenuation *(German)* 3−12490
- Fe-Ni, morphology of thin plate-like martensite 3−37043
- Fe-Ni, photostimulated exoelectron emission, temp. depend. 3−30921
- Fe-Ni, spontaneous volume magnetostriction, lattice const., 4.2-1000 K 3−30671
- Fe-Ni (2.86 wt.%), solid solution softening mechanism 3−34545
- Fe-Ni (fcc), specific heat at const. pressure meas. in 300-1000K range, obs. of behaviour at Curie temp. *(Japanese)* 3−18312
- Fe-Ni alloy, n irrad., Snoek peak and strain-amplit. of intl. frict., meas. 3−17929
- Fe-Ni alloy with hardenable electrodeposited coatings, rolling contact fatigue life test 3−9026
- Fe-Ni alloys, temperature dependent property for measurement errors compensation in magnetic devices *(German)* 3−15385
- Fe-Ni and Fe-Ni-Cr, martensitic transform. kinetics, external factors influence *(Russian)* 3−37002
- Fe-Ni film, galvano- and thermomag. effects depend. on phase comp. 3−33873
- Fe-Ni film, modulation of mag. noise spectral distrib. *(Russian)* 3−12042
- Fe-Ni films, exchange parameters 3−2324
- Fe-Ni Invar alloy, Mossbauer obs. of stress effects 3−27445
- Fe-Ni invar alloys, effect of mag. props. on plastic deformation 3−14914
- Fe-Ni invars influence of Mn on some physical props. *(Russian)* 3−8355
- Fe-Ni martensite, deform. twinning 3−34574
- Fe-Ni particles in Hg, ferrofluid, mag. props., thermal growth, effect of inhibitors 3−2321
- Fe-Ni shocked alloys, stability of mag. phase transition 3−36721
- Fe-Ni single-domain powders with cubic anisotropy, mag. props. *(Russian)* 3−15390
- Fe-Ni system, metastable high-pressure equilibrium from phase diagrams 3−30978
- Fe-Ni system, physicochem. props., effect on spectral line intensity in d.c. carbon arc *(Russian)* 3−28772
- Fe-Ni thin films, magnetic properties, dependence on phase structure 3−8376
- Fe-Ni:Al_2O_3, dispersion strengthened composite, alloying additions effect on structural stability 3−15782
- Fe-Ni-Al, microstructure and fracture *(Japanese)* 3−15672
- Fe-Ni-Al, subspinodal, hardening obs. and mechanism *(Czech)* 3−31103
- Fe-Ni-C, reverted austenite, prior deform. effects on strength and annealing behaviour 3−37048
- Fe-Ni-C, strain-induced martensite and thermally transformed martensite morphology 3−21575
- Fe-Ni-C alloys, internal friction meas., Snoek-peak, C interstitials diffusion towards dislocations mechanism 3−34542
- Fe-Ni-Ce, Mossbauer study of Fe mag. moment 3−2471
- Fe-Ni-Co and Fe-Ni-Co-Mo(W), redistrib. of alloying element atoms, effect of Co, Mossbauer obs. *(Russian)* 3−5294
- Fe-Ni-Co mated film (bifilm) plated wire element, effects of process variables 3−12041
- Fe-Ni-Co-Al-Ti, temp. depend. of mag. moment, superparamag. props. *(Russian)* 3−8342
- Fe-Ni-Cr, grain boundary internal friction spectra, relax. phenomena 3−37028
- Fe-Ni-Cr, stress corrosion cracking susceptibility, nuclear reactor water environments 3−39351
- Fe-Ni-Cr-Mo, deform. and heat treatment effect on struct. changes, Mossbauer obs. *(Russian)* 3−31056
- Fe-Ni-Cu ferrite, internal friction, delta E-effect and stress sensitivity in alternating magnetic field 3−39009
- Fe-Ni-Mn, martensite morphology depend. on isothermal transform. temp. *(Russian)* 3−24878
- Fe-Ni-Mo, N24M5, isothermal and athermal martensitic transforms. 3−24835
- Fe-Ni-O, system, activities, thermodynamics, equilib. O_2 press., comp., at 1000°C 3−2793

iron alloys continued
- Fe-Ni-Sn Invar alloy, precip. hardening by Sn additions, Mossbauer obs. 3−21634
- Fe-Ni-Ti, aged, martensitic transforms. *(Russian)* 3−15684
- Fe-Ni-Ti-Al-Nb, ageing in two-phase $(\alpha + \gamma)$ states, effects on props. and struct. *(Russian)* 3−12363
- Fe-Ni(V)(Cr), X-ray absorpt. spectra obs. of polymorphism *(Russian)* 3−12336
- Fe-Ni(29.7 at.%), martensitic pretransformation phenomena 3−18561
- Fe-Ni(3 wt.%), stress exponent of dislocation vel. from strain rate cycling tests *(Japanese)* 3−31078
- Fe-Pd, f.c.c., ave. mag. moment of atoms *(Russian)* 3−8343
- Fe-Pt, elastic consts., composition and temp. depend. 3−17899
- Fe-Pt (32-35 at.%), struct. and mag. props. *(Russian)* 3−15389
- Fe-Re, elastic consts., composition and temp. depend. 3−17899
- Fe-Re-C, defect cluster influence on martensite form. *(Russian)* 3−12353
- Fe-Rh, elastic consts., composition and temp. depend. 3−17899
- Fe-Rh (52 at.%), optical props., mag. transform. behaviour, cond. electron relax. *(Russian)* 3−18439
- Fe-Rh alloy, Fe-Rh-Ir alloy, electronic sp. ht. obs. rel. to antiferro-ferromag. transition 3−34128
- Fe-Ru, elastic consts., composition and temp. depend. 3−17899
- Fe-S-Mn, sulphide form. and brittleness, Mn conc. depend. *(French)* 3−27645
- Fe-S(Si)(Sn), grain boundary activity, determ. by Auger spectroscopy 3−7767
- Fe-Sb polyphase pulverulent, sintering *(French)* 3−21715
- Fe-Si, 0-24%Si, effects of furnace cooling and water quenching on electric and magnetic properties 3−36776
- Fe-Si, (8 to 11 at% Si), Si diffusion 3−15033
- Fe-Si, annealing, 480-680°C, effect of mag. field on softening process *(Russian)* 3−27673
- Fe-Si, covered by Ni film, mag. susceptibility temp. depend. meas. rel. to ferromag. domains *(Russian)* 3−24562
- Fe-Si, cyclically strained, topography, X-ray obs. *(Russian)* 3−8840
- Fe-Si, density, influence of slip and mech. twinning *(Russian)* 3−7826
- Fe-Si, diffusivity, permeability and solubility of hydrogen, conc. and temp. depend. 3−1828
- Fe-Si, effect of Ni surface film on mag. props. *(Russian)* 3−12037
- Fe-Si, long-range order, A_7B types, config. energies 3−38550
- Fe-Si, mag. susceptibility, 1000-1900°C, conc. depend., solid-liq. transition *(Russian)* 3−36707
- Fe-Si, oxidation, photoelec. work function and Auger spectroscopy study 3−38741
- Fe-Si, polygonization, influence of bending orientation during annealing *(Russian)* 3−8834
- Fe-Si, S content study by high resolution scanning electron microscope *(French)* 3−32222
- Fe-Si, single crysts. deformed by tension, −196°C, polygonization by slip 3−34549
- Fe-Si, thermomagnetic treatment, effects of inclusions and internal stresses *(Russian)* 3−8385
- Fe-Si (2.94 wt%), solid solution softening mechanism 3−34545
- Fe-Si (3 at wt.%), Al_2O_3 dispersed, Newtonian viscous creep 3−31094
- Fe-Si (3 at wt.%) single crystals, tensile test of foil specimens at room and low temp., dislocation motions 3−17820
- Fe-Si (3.25 wt.%), impurity effects on grain growth in strain-anneal and secondary recrystn. 3−37041
- Fe-Si alloy, surface energy anisotropy meas. from grain boundary dihedral angle 3−20926
- Fe-Si alloy, X-ray meas., crystal struct. *(German)* 3−8809
- Fe-Si deformed single cryst., texture form. during primary recrystn. *(Russian)* 3−18572
- Fe-Si Kossel interference patterns evaluation by computer *(German)* 3−4693
- Fe-Si single cryst., texture formation during recrystallization, struct. changes during annealing *(Russian)* 3−12341
- Fe-Si single crysts., deformed, substruct. *(Russian)* 3−24847
- Fe-Si single crysts., e.m. losses depend. on surface cryst. orientation *(Russian)* 3−15391
- Fe-Si solid solns., diffusion and solubility of hydrogen, ordering influence *(Russian)* 3−30283
- Fe-Si(12.1 at.%), screw dislocation retardation mechanism *(Russian)* 3−30988
- Fe-Si(3 wt.%) single crysts., deform. twins influence on rolling and recrystn. textures *(Russian)* 3−24848
- Fe-Si(3 wt.%) texture variations at recovery stage with recrystallisation annealing 3−31012
- Fe-Si(3.2 wt.%), normal stress influence on yielding behaviour 3−14908
- Fe-Si(5.3 at.%), deformed, screw dislocations and prismatic loops, annealing effects 3−18632
- Fe-Sn, dilute ferromag., two current cond. and impurity resist. 3−36719
- α-Fe-Sn solid solns., interaction between precip. reactions *(German)* 3−24838
- Fe-Sn system, liq., thermodynamic excess functions, mass spectrometry obs. 3−37011
- Fe-Sn-C system, phase diag., cpd. formation via decarburation *(French)* 3−24830
- Fe-Ta, Laves phase precip. phenomena 3−37049
- Fe-Ti solid solns., temp. and conc. depend. of mech. props. *(French)* 3−31038
- Fe-Ti(Co) systems, TiFe and FeCo phases, X-ray emission study *(Russian)* 3−15572
- Fe-transition metal, dilute alloys, Mossbauer spectra, hyperfine field, isomer shift changes analysis 3−30733
- Fe-V, electron diffraction examination of transformation twins 3−2711
- Fe-V, magnetisation temp. depend., spin-wave stiffness coeff. temp. depend. 3−2312
- Fe-V, ordering process, mass spectrometric obs. of secondary ion emission *(Russian)* 3−33490
- Fe-V ferromagnetic, V^{51} nuclei, n.m.r., local inhomogeneities 3−34232

iron alloys continued
Fe_7W-C, morphology of eutectic 3—18567
Fe-Y-Co, mag. props., moment values at 4.2K 3—2294
Fe-Zn mixed powder compacts formation kinetics *(Japanese)* 3—15731
Fe-Zn supersaturated solid solution, alloying elements influence on the precipitation behaviour. *(German)* 3—2694
(Fe-Ni)-P-C, amorphous, low temp. resist. and Curie temp. 3—21234
FeAl alloys, localised magnetic moment effects on positron annihilation parameters 3—38599
Fe_3Al, annealing effects on compression induced mag. anisotropy 3—30642
Fe_3Al, ordering mechanism and kinetics 3—37013
Fe_3Al type alloy determination of order parameters by Mossbauer spectroscopy methods 3—39070
$Fe_{1-x}Co_x$, bcc alloy, electronic struct., CPA calc. 3—11999
$Fe_{1-x}Co_xAl$ solid solns., lattice parameter, elec. resist., Hall coeff., thermo-e.m.f., mag. susceptibility *(Russian)* 3—30087
FeCr, Mossbauer effect, α-σ transition obs. *(Russian)* 3—2479
$Fe_{1-x}Cr_x$, bcc alloy, electronic struct., CPA calc. 3—11999
FeGe, $Fe_{3.25}Ge$, Fe_3Ge, Fe_2Ge, Fe_4Ge_3, X-ray spectroscopic examination, emission spectra 3—21499
FeGe hexagonal single crystal, electrical resistivity meas. at 411 K 3—21239
$Fe_{1-x}Mn_x$, bcc alloy, electronic struct., CPA calc. 3—11999
Fe_8N, with ultrahigh mag. moment, vapour deposition from nitrogen atmos. *(Japanese)* 3—8403
FeNi, (75 at. % Fe), transformation of fine particles from f.c.c. to b.c.c. structure with temp., mag. hyperfine field at Fe nuclei *(Korean)* 3—30734
FeNi, single crystal, obs. of resonance gamma quanta diffraction 3—24642
FeNi:Mn, n.m.r. of ^{55}Mn, local moments obs. 3—36799
$Fe_{1-x}Ni_x$, bcc alloy, electronic struct., CPA calc. 3—11999
$Fe_{1-x}Ni_xAl$ solid solns., elec. resist., thermo-e.m.f., Hall effect, 80-300K *(Russian)* 3—18121
$Fe_{75}P_{15}C_{10}$, amorphous, crystallite morphology during crystn. 3—21595
FePd, ordered, plastic deform. influence on structural state and coercive force *(Russian)* 3—18338
$FePd_3$ specific heat, low temperature, spin wave contribution 3—27371
FePt, ordered, plastic deform. influence on structural state and coercive force *(Russian)* 3—18338
FePt powders, ordered, anisotropy consts., saturation magnetiz., coercivity *(Russian)* 3—30652
$Fe_{1-x}Pt_x$, $0.25 \leqslant x \leqslant 0.3$, ferromag. Curie temp. rel. to atomic ordering 3—30618
$Fe(Pt_xPd_{1-x})_3$, ordered, mag. transforms. *(Russian)* 3—18308
FeRh Mossbauer meas. of ferromagnetic-antiferromagnetic transitions 0 to 700C *(Hungarian)* 3—8485
FeRh positron annihilation study of electron structure of ferrimagnetic and antiferromagnetic phases 3—7754
$Fe_{1\|\delta}Sb$, obs. of mag. superstructure lines below and above Neel point 3—12022
FeSn, electrical resistivity 4.2-420 K 3—21240
$Fe_{1-x}Ti_{1\|x}$, thermoelec. power anomalies rel. to superparamag. clusters 3—30457
Fe—Co(3.18-42.5 wt%), Zener relax. 3—24213
Gd_3Fe, antiferromag. props. and structure 3—21232
Ge-Fe, liquid state, resistivity, theory 3—8147
$HfFe_2$, occurrence of Laves phases, X-ray, differential and microstruct. analysis *(Russian)* 3—12334
Ho-Fe system, hysteresis of $HoFe_3$, near mag. compensation temp. *(Russian)* 3—8380
$HoFe_3$, powder neutron diffraction obs. of Ferrimag. coupling 3—18325
$Ho(Fe_{1-x}Co_x)_2$, Mossbauer obs. of Laves phases 3—36820
Lu-Fe intermetallic, struct., X-ray and neutron diffr. obs. 3—1602
Mn-Fe, antiferromag., Neel temp. determ., elec. resist. meas. 3—34119
Mn-Fe-Be system, n.m.r. of ^9Be in $Mn_{1-x}Fe_xBe_2$ 3—2436
$NbFe_2$, Laves phase, homogeneity range and defect struct. 3—27637
Ni-(50% wt.)Fe, melting process effect on coercive force *(Korean)* 3—5120
Ni-Co-Fe-SiO system, bilaminar ferromag. films, field of interaction *(Russian)* 3—21267
Ni-Fe, dil., Mossbauer obs. of hydrogen desorption *(French)* 3—1891
Ni-Fe, f.c.c., atomic size-modulus influence on cyclic deform. curve 3—7825
Ni-Fe electroless film, mag. props., temp. and soln. pH effects 3—21278
Ni-Fe film, (100) single cryst., magnetisation ripple and dislocations 3—8399
Ni-Fe film, damped magnetisation oscillations 3—36741
Ni-Fe film, ferromag. exchange const., spin wave resonance obs. 3—34105
Ni-Fe film, mag. hysteresis loops, domain struct., hypercrit. state *(Russian)* 3—15393
Ni-Fe film, oblique incidence evap., mag. anisotropy, deuteron irrad. effects 3—34148
Ni-Fe film, two layers separated by SiO, magnetic coupling, transverse suscept. obs. 3—34174
Ni-Fe films with additional surface layers, spin wave reson., high field peak *(Russian)* 3—24615
Ni-Fe:H dilute alloy with high H conc., magnetoresistivity rel. to local mag. moments 3—8158
Ni-Fe-Al, phase transform. on heating *(Russian)* 3—8831
Ni-Fe-Mn, disordered, mag. props., thermodynamic analysis near critical conc. 3—2272
Ni-Fe(25 wt.%) films, domain boundary curvature and displacement, mag. field and elastic stresses influence *(Russian)* 3—30654
$(Ni_{74.5}Al_{25.5})_{100-x}Fe_x$, ferromag., neutron obs. of giant moments 3—36717
$Ni_3(Fe,V)$, V atom redistrib. obs., Mossbauer spectra *(Russian)* 3—12080
NiFe, distrib. function of forces exerted by defects on domain walls 3—36756

iron alloys continued
NiFe, magnetic moment distribution 3—34134
$NiFe_2$, film, oxidation mechanism, ferrite film form. 3—27196
Ni_3Fe, antiphase slip boundaries and dislocation config. *(Russian)* 3—34522
Ni_3Fe, dislocations, elastic anisotropy effect on dislocations 3—17838
Ni_3Fe, relative bond energies from field ion images 3—36272
Pb-Fe dilute alloys, spin-disorder resistivity meas. as function of temp. in 0-60 kOe 3—2057
Pd-Fe, dil., ferromag. transition temp., resist. study 3—30624
Rh-Fe dilute alloy, Mossbauer meas. of hyperfine field at ^{57}Fe 3—30739
Rh-Fe-Mn, Rh-Mn, Rh-Fe alloys, low temp. meas. and comparisons of elec. resist., magnetoresist. and magnetiz. 3—4990
S content obs. by high resolution scanning electron microscope of α-Fe *(French)* 3—32222
Tb-Fe, amorphous spin-polarization distribution 3—8367
Ti-Fe(19 wt.%), precipitation from supersaturated solid soln. on quenching from 1000°C and ageing at 650°C *(Russian)* 3—12344
TiFe, electronic structure, stability investigation by self-consistent KKR method 3—15335
$Y(Fe_{1-x}Co_x)_2$, Mossbauer obs. of Laves phases 3—36820
$ZrFe_2$, occurrence of Laves phases, X-ray, differential and microstruct. analysis *(Russian)* 3—12334
$Zr_{0.80}Mo_{0.20}Fe_2$, crystallographic and mag. props., heat treatment effects 3—21649
$Zr_{0.60}Nb_{0.40}Fe_2$, crystallographic and mag. props., heat treatment effects 3—21649

iron compounds
see also ferrites; iron alloys
bis(cyclooctatetraene)iron, evidence for dynamic tautomerism 3—24091
boracite, growth by modified Schmid three crucible technique 3—2634
boride coating form. of Fe-plated metals and alloys 3—27693
carbide fibre-reinforced composite, M-M_7C_3 eutectic, $(M = Fe + Co + Cr)$, $M_7C_3 \rightarrow M_{23}C_6$ transform. 3—31143
complex, seven coord., of Fe(III), Mossbauer spectra, paramag. relax. effects 3—27450
$Fe_{1-x}O$, Mossbauer line broadening and diffusion mechanisms 3—4884
ε-Fe_2O_3, mag. props. and Mossbauer spectra 3—27361
garnet, mixed rare earth iron $RM_2Fe_5O_{12}$ type, growth induced noncubic mag. anisotropy 3—21256
garnet mixed rare earth iron type, epitaxial film, anisotropy field and domain wall coercivity temp depend. 3—21257
garnets, equatorial Kerr effect rare earth sublattice effects *(Russian)* 3—12124
garnets, mixed rare earth iron type, growth induced noncubic mag. anisotropy 3—21255
goethite in lunar samples, origin and stability rel. to normal low-temp. processes 3—12993
haematite in lunar samples, origin and stability rel. to normal low-temp. processes 3—12993
interstellar dust, FeO_4^{2-} and FeO_2^- anionic species 3—13107
iron(II) formate anhydride in magnesium-iron(II) formate mixed crystal, Mossbauer obs. of α and β phases *(German)* 3—27458
magnetite, electron exchange interactions, 77-125 K, n.m.r. spectrum, spin-echo method 3—39042
magnetite, multiple mag. ordering rel. to metal insulator transition 3—15369
magnetite, optic spin wave energy at Verwey transition 3—34140
magnetite, thermal expansion meas. over temp. range 20 to 1100°C *(Russian)* 3—15024
magnetite, thermoanalytical method for heat of oxidation meas. 3—15078
magnetite, Verwey transition 3—8117
magnetite in lunar samples, origin and stability rel. to normal low-temp. processes 3—12993
phosphate glass, formation 3—20697
pseudo-tetrahedral ferrous compounds, quadrupole splitting and magnetic susceptibilities 3—21190
pyrrhotite mono crysts., melt growth by modified Bridgman method 3—12262
pyrrhotites $(Fe_{1-x}S)$, stability relations and structures 3—14743
sulphide minerals, effect of temp. on magnetic susceptibility during continuous heating and cooling *(Russian)* 3—12009
$\{Fe_3O(CH_3COO)_6(H_2O)_3\}Cl.6H_2O$ Mossbauer study on the magnetism 3—2262
$Co_xFe_{3-x}O_4$, prep. and characteriz. 3—18741
Cr_2O_3-Fe_2O_3, Mossbauer obs. of mag. structure 3—8490
Cu_2S-FeS liquid quasi-binary mixtures, temp. dependence of density and surface tension 3—30168
$FE(CN)^{3-}$ reduction to $Fe(CN)_6^{4-}$ by electron irradiation, Mossbauer study 3—2822
$(Fe, Mg)_3Al_2(SiO_4)_3$ garnet, hyperfine interactions of ^{27}Al and ^{29}Si, quadrupole coupling const., paramag. shift 3—8482
$(Fe, Ti, \square)_3O_4$, cation deficient, magnetic props. 3—4735
$(Fe,Ti)_3S_4$, cryst. struct. 3—14758
Fe complex, Baudisch complex, chem. characteriz. 3—26631
Fe complex, cis-$H_2Fe[C_6H_5P(OC_2H_5)_2]_4$, cryst. struct. 3—14774
Fe complex, clathrochelate, disorder in cryst. struct. 3—17773
Fe complex, $Ph_3SnFe(\pi$-$C_5H_5)(CO)(\pi$-$C_2Ph_2)$, cryst. struct. 3—14826
Fe complex, tetrafluoroethylene-tetracarbonyl iron, molecular struct., gas-phase electron diffr. 3—14324
Fe complexes, abnormal mag. transitions *(French)* 3—8354
Fe phosphonates, X-ray diffraction study of struct. 3—33461
FeAs, obs. of helimagnetic structure below Neel temp. 77K 3—15370
$FeAsO_4$, type-I, cryst. struct. *(French)* 3—4733
Fe_2B, Mossbauer absorpt. obs. of mag. hyperfine field 3—15443
$FeBO_3$, obs. of light-induced mag. anisotropy by acoustic resonance 3—18335
$FeBO_3$, Raman scatt. from magnons and phonons 3—34358
$FeBO_3$ optical properties, strong absorption spectra, Faraday rotation 3—36893
$Fe_3B_7O_{13}Cl(Br)(I)$, growth by chem. transport reaction, effect of different growth conditions *(Russian)* 3—15606

iron compounds continued
$Fe_3B_7O_{13}I$, crystal, lattice strain *(Japanese)* 3−14845
$FeBr_2$, magnetic susceptibility, uniaxial tension at 4.2°K, metamagnetic properties, antiferromagnetism *(French)* 3−27390
$FeBr_2$, magnetiz. press. depend. meas. *(French)* 3−6032
$FeBr_2$, metamag. transition, magnetiz. variation with temp., press. and mag. field *(French)* 3−30615
$FeBr_2$, metamagnetic phase transition *(French)* 3−27368
FeC melt, C effect on surface energy and wetting of Al_2O_3 *(Russian)* 3−8883
$FeCO_3$, exciton-magnon transitions, effect of strong mag. field on intensity *(Russian)* 3−8558
$FeCO_3$, mag. layer struct., Mossbauer spectra recoilfree factor anisotropy 3−8489
$FeCO_3$, siderite, anomalous temp. depend. of Mossbauer linewidth 3−34266
$FeCO_3$, siderite, Raman scatt., 4.2-300K, freqs. up to 2000 cm^{-1} 3−34366
$Fe(CO)_5$ in rare gas matrices, i.r. spectrum, stretching bands 3−36025
$Fe(CO)_4.I_2$, Mossbauer effect of ^{129}I, config. obs. 3−1137
$(Fe_{1-x}Ca_x)_2SiO_4$, Mossbauer absorpt. meas. rel. to quadrupole splitting 3−34263
$FeCl/H_2O$ frozen soln., glass transitions study by Mossbauer effect and DTA 3−38540
$FeCl_2$, 3d density distrib. and intrinsic temp. depend. of Mossbauer isomer shift 3−34262
$FeCl_2$, antiferromagnetic resonance, high-pressure effects 3−18374
$FeCl_2$, optical abs. spectrum, 0.6-3 eV, 1.2-300K and spin dynamics below Neel temp. 3−8597
$FeCl_2$, thermal conductivity 3−20843
$FeCl_2$ magnetic susceptibility, uniaxial tension at 4.2°K, metamagnetic properties, antiferromagnetism *(French)* 3−27390
$FeCl_3$, 3d density distrib. and intrinsic temp. depend. of Mossbauer isomer shift 3−34262
$FeCl_3$ in conc. aq. soln., Raman 3−15482
$Fe(ClO_4)/H_2O$, frozen soln., glass transitions study by Mossbauer effect and DTA 3−38540
$Fe(ClO_4)_3$, effect of weak mag. fields on paramag. hyperfine struct. of Mossbauer line *(Russian)* 3−8494
$Fe(ClO_4)_3$ frozen aqueous solution, paramag. relax., Mossbauer obs. 3−21346
$FeCl_2.2py$, cryst. phase transition, Mossbauer obs. 3−21344
$FeCl_2.4H_2O$, heat capacity 0.4−5.3K 3−2278
$Fe_{1-x}Co_xS_2$, narrow band ferromag., elec. resist. below Curie point, anomalous temp. depend. 3−4992
$FeCoVO_4$, spinel oxide, Mossbauer obs. 3−39066
$FeCr_2O_4$ 0.25 $FeAl_2O_4$ Apollo 15 basalts, solid soln., subsolidus reduction and compositional characteristics 3−5587
$Fe_{3-x}Cr_xO_4$, ferrimag., Mossbauer obs. of cation distrib. and mag. structure 3−24641
$FeCr_2S_4$, low temp. transition, Mossbauer obs. 3−5151
$FeCr_2S_4$, resist. and magnetoresist., 77-450 K 3−27258
$FeCr_3S_4$ gas transport and characterisation *(German)* 3−8730
$FeCr_2Se_4$, production and properties *(Russian)* 3−14811
FeF_2, 3d density distrib. and intrinsic temp. depend. of Mossbauer isomer shift 3−34262
FeF_2, calc. of pressure and temp. depend. of hyperfine mag. field 3−34059
FeF_2, Heisenberg antiferromagnet, rutile structure, two-magnon light scattering 3−21196
FeF_2, magnetoelastic waves and selection rules for magnon-phonon interaction 3−34131
FeF_3, 3d density distrib. and intrinsic temp. depend. of Mossbauer isomer shift 3−34262
FeF_3, Fe Mossbauer line shift, electron-phonon contribs. 3−18399
FeF_3, phonon Raman spectrum 3−30820
FeF_3, Raman scatt. from magnons and phonons 3−34358
FeF_3, weak ferromag., Raman spectra, phonon and magnon lines 3−5192
FeF_6^{3-}, force constants and Coriolis coupling constants calc. 3−33103
FeF_6^{3-}, force consts., Coriolis coupling consts., mean amplitudes of vibration 3−29622
$FeF_3.H_2O(3H_2O)$, Mossbauer study of mag. props. *(French)* 3−27449
$FeF_2.4H_2O$, Mossbauer study of mag. props. *(French)* 3−27449
$Fe_2F_5.7H_2O$, Mossbauer study of mag. props. *(French)* 3−27449
FeGe, antiferromagnetic hexagonal, Fermi surface electrical resistivity and magnetic ordering 3−18327
FeGe, susceptibility meas. and magnetic ordering 3−18326
FeGe hexagonal single crystals, magnetoresistance between 4.2 K and 30 K 3−18328
$FeGe_2$, anisotropy of thermal cond. and diffusivity 3−36445
$FeGe_2$, elastic consts. temp. depend. rel. to antiferromag. transition 3−5105
Fe_2GeS_4, cryst. and mag. structs. at 85 K and 4.2 K, mag. transitions *(French)* 3−27373
Fe(II) complex, tris[2-(2′-pyridyl)benzimidazole]iron(II), 80-300K, $^5T_2$-$^1A_1$ spin equil. 3−24634
Fe(II) oxalate complex, electrochemical investigation of photographic process *(Russian)* 3−234
Fe(III) complex, chlorobis-(N-n-propylsalicylaldiminato)iron(III), cryst. and mol. struct. 3−24076
Fe(III) complex, $K_3Co_{1-x}Fe_x(CN)_6$, Mossbauer and e.s.r. spectra, interpretation 3−30732
Fe(III) complex of bidentate sulphur chelate, quadrupole splitting origin 3−8484
Fe(III) complexes, tropolonates, i.r. spectra, electron spin pairing and Jahn Teller distortion effects 3−36026
Fe(III) dithiocarbamates, dependence of Mossbauer isomer shift on magnetic moments 3−8486
$Fe(IO_3)_3$, cryst. growth, boiling solvent technique 3−12235
$FeIn_2S_4$, cation distrib., mag. susceptibility temp. depend. 3−34102
FeM_2O_4, (M=Rh, Mn, V, Fe, Cr), interionic metal-oxygen distances, formulae *(Russian)* 3−17784
FeMn deposits deep sea mining, environmental effects 3−3167
$Fe_{3-x}Mn_xO_4$, i.r. spectra and cation distrib. 3−30807
$Fe_{3-x}Mn_xO_4$ solid solution, cation distribution and local distortion 3−30729

iron compounds continued
FeMnP, mag. struct., neutron diffr. obs. 3−30629
$Fe_xMn_{2-x}P$, mag. props. of different phases, Neel and Curie temps. 3−30608
Fe_2MoO_4, spinel, Mossbauer spectra, 90-578 K 3−34251
FeN_2, vibr. spectra and electronic struct. calc. 3−29673
$Fe_{100}N_{23}$, interstitial distrib. at octahedral sites, Mossbauer spectra *(French)* 3−39060
$FeNb_2O_6$, paramag., mag. susceptibility meas. rel. to structure and ionic mag. moments *(Russian)* 3−15346
$FeNiBO_4$, dense warwickite type formed by hydrothermal synthesis at high pressure *(French)* 3−38571
FeO, wustite, formed below 570°C, Mossbauer spectra 3−24638
FeO wustite reduction with H_2 or CO, nucleation of iron phase and its growth *(Japanese)* 3−18637
FeO/(FeO + MgO), in lunar rock 12039 3−5586
FeO_4^{2-} diluted in NaOH, paramag. hyperfine interactions in e_g^2 config. of ^{57}Fe 3−2470
$Fe_{1-x}O$-M′O, (M′=Mg, Ca, Sr, Zn, Al), Neel temp. comp. depend. *(French)* 3−8363
Fe_2O_3, angular depend. of field-induced antiferromag. to weak ferromag. transition 3−21228
Fe_2O_3, electrophoretic mobilities determ. by microelectrophoresis method 3−5393
γ-Fe_2O_3, heating on thermoplastic in magnetic field, transparency change *(Russian)* 3−19231
α-Fe_2O_3, hematite, anisotropy of Fe atom vibrs., Mossbauer obs. 3−33639
α-Fe_2O_3, hematite, equilib. form, from Hartman and Perdock method *(French)* 3−33492
α-Fe_2O_3, hematite, nonlinear susceptibility and anisotropy to Morin temp. 3−2261
α-Fe_2O_3, high field antiferromagnetic resonance, theory and expt. comparison 3−27420
Fe_2O_3, Mossbauer study of quadrupole splitting and isomer shift of ^{57}Fe, and magnetic hyperfine field at the nucleus *(Korean)* 3−27452
α-Fe_2O_3, natural hematite, mech. induced mag. anisotropy, Mossbauer obs. 3−5148
Fe_2O_3 polycrystalline powder ceramic, high temp. deformation 3−27738
Fe_2O_3-Al_2O_3 mixed oxides, conc. depend. of lattice parameters *(French)* 3−7679
Fe_3O_4, initial permeability in region of low temp. phase transition 3−36768
Fe_3O_4, macroscopic strain-coupling induced symmetry change accompanying Verwey transition 3−27222
Fe_3O_4, magnetite, optical props. for band structure at Verwey transition 3−2506
Fe_3O_4, Verwey transition, model 3−4958
Fe_3O_4 film, magnetite, low temp. conversion from α-Fe_2O_3, hematite 3−34173
αFe_3O_4 film prep. by oxidation, electron microscope exam. of microstruct. 3−27196
Fe_3O_4 magnetite, band theory of pair-localized electrons 3−2012
Fe_3O_4 powders, initial susceptibility determ. *(French)* 3−12005
FeOCl, mag. susceptibility, 300-4.2 K, antiferromag. order *(French)* 3−30604
$Fe_2(OH)_3$ amorphous gel, characterisation and phase transformation 3−5383
δ-FeOOH, dynamics group theory analysis, prediction of l.f. Raman line 3−14943
$Fe_2O_3.Eu_2O_3.SrO$ phase in Fe_2O_3-Eu_2O_3-SrO system 3−20849
FeP-MP solid solutions, M=As, Co, Mn, W, Mossbauer studies 3−36818
$Fe_3(PO_4)_2.8H_2O$, Mossbauer obs. of Fe atom vibrations 3−5152
$Fe(Pt_cPd_{1-c})_3$ mag. transforms. anal. by effective field method 3−12018
FeS, electrical conductivities under high pressures *(German)* 3−12594
FeS-EuS, partial phase diagram 10 to 70 mole % EuS 3−20850
FeS_2, elec. resist. and Hall coeff., down to 1.3K 3−21070
FeS_2, Mossbauer obs. of Fe atom vibrations 3−5152
FeS_2, pyrite, natural, resist., Hall effect, rel. to energy gap and mobility 3−38837
FeS_x colloid, ageing 3−2770
$Fe_{1-x}S$, nonstoichiometric, energetics of defect formation and interaction 3−4752
$Fe_{1-x}S$, positron annihilation due to capture by cation vacancies in F-centres 3−17871
$Fe_{1-x}S$, semiconducting uniaxial ferroelectric model 3−8531
Fe_2S in Sea of Japan sediment cores, terrestrial heat flow 3−2850
Fe_3S_4, elec. field induced anisotropy, electron diffr. studies 3−5163
Fe_3S_4, greigite, cryst. growth 3−21525
Fe_3S_4, oriented growth of thin films 3−15089
Fe_9S_8, pentlandite, Ni-free, flash evaporation prep. 3−27608
$FeSO_4$ dosimetry, molar extinction coeff. determ., radiotherapy appls. 3−6138
$FeSO_4$ dosimetry, rel. to ionization dosimetry, for MeV electrons 3−406
$FeSi_2$, new amorphous material, structural, electrical and optical props. 3−36419
$FeSi_2$, thermal conductivity at high and low temps. 3−18117
$FeSi_2$:Mn, Co, semiconductor-metal transition resist., thermoelec. and Hall effect obs., 300-1400 K 3−33973
Fe_3Si, FeSi, $FeSi_2$, electron struct. electron and X-ray spectra obs. *(Russian)* 3−24760
$(Fe_{1-x}T_x)Be_2$, T=V, Cr, Mn, Co, Ni, low temp. sp.ht. and magnetisation, virtual bound states concept 3−39002
$FeTaO_4$, polymorphic transition from rutile to wolframite type structure under high pressure 3−33670
Fe_2Te_3, ^{125}Te Mossbauer obs. of quadrupole splitting 3−21354
$FeTiO_3$, ilmenite, anisotropy of Fe atom vibrs., Mossbaurer obs. 3−33639
$FeTiO_3$, in composite ferrite-titanate substrate, hot pressing 3−37079
$FeTiO_3$ (ilmenite) and Fe_2TiO_4 (ulvospinel) in lunar rocks, Zr partitioning rel. to cooling histories 3−16177
Fe_2TiO_4 Apollo 15 basalts, solid soln., subsolidus reduction and compositional characteristics 3−5587

iron compounds continued
$FeWO_4$-$MnWO_4$, mixed crystal, coexistence of two antiferromag. phases 3–34124
$FeWO_4$-$MnWO_4$, spontaneous magnetisation irregularities, modified effective field model 3–34060
$FeWO_4$-$MnWO_4$, wolframite, mag. phase diagram, molecular field approx. 3–34125
${}^{59}Fe$ solutions, ${}^{60}Co$ contamination in pharmaceutically prepared samples 3–407
Fe(1,10-phenanthroline)$_2F_2.4H_2O$ low temp. magnetism, Mossbauer effect and electronic struct. 3–34250
Fe(1,10-phenanthroline)$_2$malonate.$7H_2O$, low-temp. magnetism, Mossbauer effect and electronic struct. 3–34250
Fe(1,10-phenanthroline)$_2$oxalate.$5H_2O$ low-temp. magnetism, Mossbauer effect and electronic struct. 3–34250
β-Ga_2O_3-Fe_2O_3 solid solution, mag. interactions, e.p.r. obs. 3–27406
$Gd_{3-x}Ca_xFe_{5-x}Sn_xO_{12}$ ferrite-garnets, temp. dependence of EMR and FMR linewidths *(Russian)* 3–36795
$Mg_xTi_yFe_3O_4$ thermoremanence self-reversal rel. to composition and mechanism 3–24589
MnO-Fe_2O_3-B_2O_3 glassy system, prepn. and mag. props. 3–18726
MoO_2-FeO-Fe_3O_4 system, phase equilib. relations 3–17956
Na_2NiFeF_7, mag. structure, separation of ferromag. chains by FeF_6 octahedra 3–2301
$YFe_xCr_{1-x}O_3$, antiferromag. props., exchange interaction for Fe^{3+} and Cr^{3+} ions 3–5103
$Zn_xNi_{1-x}Fe_2O_4$:Fe^{3+}, n.m.r. study of supertransferred hyperfine fields of Fe^{3+} ions 3–2407
$ZrFe_2$, $ZrFe_2H_{0.3}$, effect of H on electron structure of Fe atoms, nucl. γ-reson. method obs. *(Russian)* 3–12079

irradiation effects *see radiation effects*

isentropic flow *see entropy*

Ising lattices
see also Ising model
binary alloys, substitutional, equilibrium solution of Vineyard's equation for the kinetics of long range order 3–34494
cell-site transform. and scaling law, coupling parameters, non-mixing 3–37901
compressible, phase transitions, harmonic lattice vibrations, critical pressure 3–38651
copolymeric Ising chains, disordered, detailed balancing approach 3–23640
correlation length divergence along crit. isotherm 3–32468
decay of order in classical many-body systems, Ising model at low temp. 3–34076
diamond lattice, equivalence of eight-vertex and Ising models 3–11696
ferromagnetic spin systems, bounds on correlations and analyticity properties 3–2235
free-fermion model, soln. of Ising model with pure triplet interactions 3–28978
higher order spin systems and continuum fluids, FKG inequalities 3–616
lattice-gas interface structure, Monte Carlo simulation 3–28981
macromolecule, linear, high ionic strength, competitive cooperative binding 3–38326
partition function per spin, calc. of converging upper and lower bound sequences 3–16760
semi-decorated square, anomalous behaviour in its phase transition, finite specific heat 3–26163

Ising model
see also Ising lattices
(4-ε) dimensional, eqn. of state *(Russian)* 3–5087
algorithm of Yang calcs. using special purpose computing registers 3–28972
alloys, order-disorder transformations in generalised Ising model 3–36401
amorphous magnet, constant coupling approx. 3–11998
anisotropic model, magnetisation, susceptibility, critical temp., crossover experiment, upper bounds 3–21201
antiferromagnet, b.c.c., near critical field, phase transitions, Monte Carlo study 3–5089
antiferromagnetic spin system, equilib. state uniqueness in phase transition region 3–21194
computer simulation of second and first order phase transitions 3–645
correlation functions, exact relations obtained by Green functions method 3–18290
critical behaviour of Ising systems on extremely anisotropic lattices, simple cubic lattice 3–27344
critical exponents, symmetry *(French)* 3–19536
critical parameter $\delta(=5)$, zero momentum fluctuations, atomic length scale independence 3–32454
cumulant Green functions, general formalism 3–36695
d-dimensional system, reduced susceptibility crossover behaviour 3–5088
decay of order in classical many-body systems, Ising model at low temp. 3–34076
decoration transform. for spin-one model 3–11997
dilute ferromag. model, nonmag. impurity effect at Curie temp. 3–8323
with dilute impurities, critical properties 3–27349
disordered state, dynamical susceptibility in transverse mag. field 3–34079
equilibrium correlation functions, calc. from algebraic struc. 3–10395
equilibrium states at low temp., finite range pair pot. 3–8321
f.c.c. and simple cubic models with lattice anisotropy, high temp. r-series for critical behaviour 3–15331
ferroelectrics, H-bonded, soft mode optical phonon interaction dynamics, Ising Hamiltonian 3–5170
ferroelectrics, H-bonded, transverse Ising model dynamics, soft mode heavy damping 3–2502
ferroelectrics, Ising spin system dynamics in fluctuating environment 3–30771
ferromagnet, amorphous, mixed, Curie temp. and mag. suscept. 3–27350

Ising model continued
ferromagnet, connection between amorphous and anisotropic models 3–38942
ferromagnet, correlation functions, rel. to vector spin model 3–30594
ferromagnet, crystal field anisotropy effect on Curie temp. 3–8324
ferromagnetic spin systems, bounds on correlations and analyticity properties 3–2235
finite three-dimensional, statistical mechanics modifications of critical phenomena at second order phase transitions 3–8325
generalised ice-type, equivalence to eight-vertex model 3–28976
ground state of Ising chains with finite range interactions 3–24552
higher order spin systems and continuum fluids, FKG inequalities 3–616
interdimensional scaling laws 3–19542
isotherm, crit., scaling theory test 3–18307
isothermal discontinuity, first order phase transition, book *(German)* 3–13653
Josephson inequality, conditions 3–2241
kinetic, critical properties by Wilson's expansion methods 3–6364
linear, long-range interactions, many-particle correlators 3–2238
linear chain molecules, and Heisenberg model to describe mag. coupling 3–21203
low temp. critical behaviour with $S>{}^{1}._{2}$ spin 3–30591
low temperature expansions, derivation for spin $S>{}^{1}/_{2}$ 3–34065
magnetic susceptibility and local magnetisation fluctuations in Ising ferromagnetic 3–27346
modified F model, critical exponents 3–36843
neutron scattering observation of critical slowing down of Ising system 3–38949
nonequilibrium properties of ferromagnet 3–18291
Onsager-Yang-value of spontaneous magnetisation and relation to free energy 3–30589
partition function for mag. lattice systems, domain of zeros, crit. temp. and mag. field 3–34074
phase transitions in Ising lattice with superexchange 3–24555
phonon relaxation 3–1759
planar model, high temp. correl. functions 3–21200
polymeric chain, dielectric relax. theory, using time depend. model 3–1312
scaling with parameter for thermodynamic functions and pair correl. function 3–2239
second-neighbour chain as model for spin-phonon interactions 3–18284
series analysis, generalised and extended methods, application to Ising model 3–32470
solvable compressible Ising model 3–34072
solvable decorated Ising model with superexchange interaction 3–34073
spin model, exact solution 3–2242
spin-1/2, with anisotropy, scaling with respect to parameter for Gibbs potential and pair correl. 3–24554
spin-phonon interaction, magnetoelastic interactions 3–24598
stochastic model, exactly solvable, crit. slowing down and nonlinear response 3–38948
three-dimensional, exact solution for finite continuous spins and non-zero external field 3–30588
three-dimensional, phase transition within phase boundary 3–1716
three-dimensional, with crit. exponent varying with parameter, universality, susceptibility 3–2240
three-dimensional, with many-body interaction, continuously variable crit. exponents 3–15324
Tomita-Tanaka approx. validity in limit of spin 112 Ising ferromagnet 3–34067
transfer matrices and largest eigenvector, new representation 3–18287
two-dimensional, surface tension between oppositely magnetised phases 3–38946
two-dimensional, with spatially varying nearest neighbour coupling, exact free energy 3–2237
variational approximation in a magnetic field 3–36696
vector model with long-range interactions, crit. exponents and scaling relations 3–2236
weak scaling theory limitations for correlation functions at small distance 3–27345
$CoCl_2.2H_2O$, proton spin lattice relax. by Ising spin excitation 3–21337
$Co_xZn_{1-x}Cs_3Cl_5$, random Ising spin system, calorimetric obs. 3–8359

isobaric analog states *see isobaric analogue states*

isobaric analogue states
see also nuclear excitation
${}^{55}Mn$, anomalies in elastic proton scattering at isobaric analogue states 3–14187
A=25, mass meas. for isobaric multiplets for $T={}^{3}/_{2}$ states 3–32748
collective contribution to escape width of analogue resonance 3–23291
Coulomb energy shifts, width calcs. and fine struct. study 3–17215
e.m. transitions, γ-decay props. for A>40 *(Hungarian)* 3–6755
inelastic scattering of protons to negative-parity levels for even-even N=82 nuclei through isobaric analogue resonances of N=83 nuclei 3–19778
isospin coupling pot. below quasi-elastic (p,n) thresholds 3–4308
review, consequences of Laue potential on bombarding particle and target nuclei *(Hungarian)* 3–6800
three-body model, exactly soluble for thresholds and resonances 3–32823
(p, n) quasielastic excitation of isospin analog states, polarized protons 3–6840
${}^{209}Bi(p,n)$ spectra, widths of analog states 3–10987
${}^{48}Ca(p,n){}^{48}Sc$, neutron decay from ${}^{49}Ca$ ground-state analog in ${}^{49}Sc$ 3–10985
${}^{141}Ce$, ${}^{7}._{2}{}^{-}$ ${}^{5}._{2}{}^{+}$ beta transition, nonunique first-forbidden decay, analysis 3–32813
${}^{33}Cl$, isospin-forbidden resonances and higher $T={}^{3}._{2}$ resonances 3–19757
${}^{35}Cl$ excited level studies using ${}^{34}S(p,\gamma)$ reaction *(French)* 3–947
${}^{56}Co$ possible fragmentation of ground-state isobaric analogue strength on basis of $({}^{3}He,p)$ and (t,p) cross-section data 3–23352
I, reson. obs. from proton reactions on Te *(Russian)* 3–4311

isobaric analogue states continued
- ^{115}In(p,p)^{115}In, analog resonance analysis, 6.6-7.6 MeV 3−14210
- ^{139}La(p,p), (p,p′), ^{140}Ce deduced analog resonances; E_p=9-12 MeV 3−26437
- ^{6}Li isobaric analogue states prod. as mechanism for solar neutrino flux 3−25399
- ^{25}Mg, meas. of T=^{3}.$_{2}$ state using threshold photoneutron technique 3−14189
- Mo isotopes, study of hole-state analogues excited in (p,d), (d,t), (^{3}He,α) reactions 3−23336
- ^{a}Mo(p, np) 1A reaction (A=94, 95, 66) study of (p, n) charge exchange 3−14206
- ^{92}Mo(^{3}He,t)^{92}Tc, 27.5 MeV, determ. of Q-value and excitation energy of isobaric ground state analogue of ^{92}Mo 3−19770
- ^{94}Mo, absence of proton weak coupling states in ^{93}Nb studied through isobaric analogue resonances in ^{94}Mo 3−955
- ^{96}Mo, proton elastic and inelastic scatt., structure of states detn. from resonances 3−17165
- Nb, A=91,93, lowest analogue resons., internal isospin mixing from polarised-proton expts. 3−32742
- ^{91}Nb, levels populated in ^{91}Zr(p,nγ) reaction, obs. of isobaric analogue resonances, spin-parity assignments 3−23202
- ^{142}Nd(p,p′) IA reaction, to meas. level struct., J^{π} 3−19772
- ^{144}Nd(d,p), (d,t), analog resonances obs. 3−26435
- ^{144}Nd(p,p_0), (p,p′) analog resonances obs. 3−26435
- ^{18}O(p,p)^{18}O, 3.4-6.2 MeV, meas. of excitation function, study of resonances using R-matrix theory 3−26458
- ^{208}Pb, proton decay of isobaric analogue state obs. in ^{208}Pb(p,n) reaction, determ. of relative strengths 3−29392
- ^{208}Pb(p,n)^{208}Bi(IAS) reaction, optical model anal., complex form factors 3−10974
- Pb(p,n) spectra, widths of analog states 3−10987
- ^{49}Sc, with Kuo-Brown and PMM forces, e.m. transitions 3−17213
- ^{28}Si from ^{27}Al(p, γ)^{28}Si 3−14190
- ^{145}Sm, partial decay widths from resons. 3−4263
- ^{47}Sr bound level reson. obs. from elastic proton scatt. on ^{86}Sr 3−4314
- ^{46}Ti, high-resolution proton elastic and inelastic scattering, 1.5-3.1 MeV, ^{47}V deduced isobaric analogue resonances 3−19856
- ^{51}Ti, angular-correlation study for ^{50}Ti(p, pγ) 3−14188
- ^{50}V, level study and isobaric analogue states from ^{49}Ti(^{3}He,d), ^{51}V(^{3}He,α), ^{48}Ti(^{3}He,p) and ^{48}Ti(^{3}He,pγ), E=22 MeV 3−32767
- ^{51}V(p,n)^{51}Cr, abs. cross sect. meas. over isobaric analog resonance near 2.34 MeV 3−14211
- ^{87}Y bound level reson. obs. from elastic proton scatt. on ^{86}Sr 3−4314
- ^{89}Y, lowest analogue resons., internal isospin mixing from polarised-proton expts. 3−32742
- ^{90}Zr, lowest analogue resons., internal isospin mixing from polarised-proton expts. 3−32742
- ^{90}Zr(γ,p)^{89}Y, meas. of proton spectra, obs. of isobaric spin mixing in ^{90}Zr analogue states 3−32741
- ^{93}Zr reduced normalization determ. in sub-Coulomb stripping reaction, comparison with analogue resonance results 3−6847

isobars *see atmospheric pressure and density*

isomer shift
- magnesium-iron(II) formate mixed crystal, Mossbauer obs. of α and β phases of iron(II) formate anhydride, isomer shifts *(German)* 3−27458
- Mossabuer, covalency versus overlap distortion 3−18398
- nuclear-charge distrib. rel. to isotope or isomer shift 3−4348
- rare earth chalcogenides, $EuLn_2S_4$ type, mag. interactions and isomer shift rel. to struct., Mossbauer obs. 3−2481
- rare earth orthoferrite, and mag. hyperfine interactions rel. to covalency parameters 3−21191
- rare-earth nuclei, 2^+ isomer shifts 3−26389
- rare-earth nuclei, change of radii due to rotation, calc. of Mossbauer and muonic isomer shifts 3−26368
- transition metals, Mossbauer isomer shifts, systematics 3−21349
- Al:^{57}Fe, electronic density on Fe nuclei 3−36822
- Au-Ni alloys, mag. hyperfine structure coupling and Mossbauer isomer shift of ^{197}Au 3−34257
- $Bi_2Bi_4Ti_3Fe_2O_{18}$, perovskite layer type ferroelec., Mossbauer obs. of anomalous behaviour at Curie 3−27443
- CaF, Fe multiple charge states, Mossbauer obs. 3−27455
- CaO, Fe multiple charge states, Mossbauer obs. 3−27455
- Cu-Ni-Au alloys, mag. hyperfine structure coupling and Mossbauer isomer shift of ^{197}Au 3−34257
- Cu-Zn:Fe, Mossbauer effect isomer shift meas. 3−15441
- EuM_2Si_2, (M=Mn, Fe, Co, Ni, Cu, Ag), Mossbauer spectral obs. rel. to valency 3−14785
- Fe, rel. to Mossbauer γ-ray energy shift of ^{57}Fe 3−27451
- Fe compounds, 3d density distrib. and intrinsic temp. depend. of Mossbauer isomer shift 3−34262
- Fe_2B, discontinuity at ferromag. transition, Mossbauer obs. 3−15443
- $Fe(CO)_4.I_2$, Mossbauer effect of ^{129}I, config. obs. 3−1137
- $FeCoVO_4$, spinel oxide, Mossbauer obs. 3−39066
- FeF_3, Fe Mossbauer line shift, electron-phonon contribs. 3−18399
- Fe(III) dithiocarbamates, dependence of Mossbauer isomer shift on magnetic moments 3−8486
- Fe_2O_3, Mossbauer study of quadrupole splitting and isomer shift of ^{57}Fe, and magnetic hyperfine field at the nucleus *(Korean)* 3−27452
- $Ho(Fe_{1-x}Co_x)_2$, Laves phases, mag. hyperfine field and isomer shift, Mossbauer obs. 3−36820
- $KMgF_3$, ^{57}Fe n.m.r., isomer shift calibrations using multivalent states 3−18400
- Ni, hyperfine interactions of ^{181}Ta 3−18397
- ^{108}Pb, shifted Fermi gas model of nuclear level density, comparison with exptl. isomer ratios 3−14124
- ^{110}Pd, shifted Fermi gas model of nuclear level density, comparison with exptl. isomer ratios 3−14124
- $(PrBi)Bi_4Ti_3Fe_2O_{18}$, perovskite layer type ferroelec., Mossbauer obs. of anomalous behaviour at Curie point 3−27443
- $Pr_2Bi_4Ti_3Fe_2O_{18}$, perovskite layer type ferroelec., Mossbauer obs. of anomalous behaviour near Curie point 3−27443
- ^{196}Pt, shifted Fermi gas model of nuclear level density, comparison with exptl. isomer ratios 3−14124
- $SbCl_5$ quick-frozen non-aqueous solutions, solvent effects on Mossbauer parameters, isomer-shift values 3−12082
- Sb_2Te_3, verification of two different states of ^{119}Sn atoms 3−36823

isomer shift continued
- $SnCl_4$ quick-frozen non-aqueous solutions, solvent effects on Mossbauer parameters, isomer-shift values 3−12082
- SnI_4 quick-frozen non-aqueous solution, solvent effects on Mossbauer parameters, isomer-shift values 3−12082
- Sn(II) compounds, electronic structure determ. by nuclear gamma resonance from isomeric shift *(Russian)* 3−1168
- $Y(Fe_{1-x}Co_x)_2$, Laves phases, mag. hyperfine field and isomer shift, Mossbauer obs. 3−36820
- $ZrFe_2$, $ZrFe_2H_{0.3}$, nucl. γ-reson. method obs. *(Russian)* 3−12079

isomerisation *see isomerism*

isomerism
- *see also nuclear isomerism*
- alcanes, trichloro-1,1,1 halogeno-3, vibr. spectra and rot. isomerism *(French)* 3−20162
- bromoacetone, rotational isomerism 3−14375
- butene-2, SO_2 photosensitized cis-trans isomerization, quenching effects of O_2 and NO 3−5407
- chalcones and heterocyclic analogues, trans configurations 3−20187
- chlorodimethylaminotetraphosphonitriles i.r. spectra, isomer differentiation from stretching modes 3−36027
- cyclopropanecarboxylic acid and cyclopropanecarboxamide, rotational conformers 3−29666
- cis- and trans-1,2-dichloroethylene, Coriolis coupling constants and inertia defects 3−7154
- meso and dl 2,5-dichlorohexanes, coupling constants and chemical shifts rotational isomerism 3−26697
- divinyl ether flash photolysis into vinyl and vinoxy radicals 3−25085
- enols, dienols, stereoisomers, conformational study, vibr. spectra *(French)* 3−17391
- ethers, stereoisomers, conformational study, vibr. spectra *(French)* 3−17391
- ethylene glycol, energy difference between rot. isomers, Raman spectra obs. 3−11263
- ethylenediammonium ion, i.r. spectra, rotational isomerism 3−38291
- ethylenic oximes, electronic absorption spectra, determ. of isomer structure *(French)* 3−1198
- fluoroacetone, rotational, vibrational assignments 3−29665
- formaldoxime, electronic structure calc. of rotational isomers *(French)* 3−29597
- guaiacol derivatives, dipole moments and geometrical isomerism 3−29558
- i.r. spectrum, linear structure and force constants 3−7188
- macromolecular structure, high-resolution n.m.r. 3−38328
- mesityl oxide oxime isomers, structure determ. using dipole moments meas. *(French)* 3−7177
- methyl isocyanide isomerization, nonempirical SCF calcs. for points on potential surface 3−1138
- methylcyclopropane, activated, isomerisation effect on ketene photolysis 3−18797
- oxalylhalides, vibr. spectra and rot. isomerism *(German)* 3−7207
- 1-phenyl-1-propene, photochemical cis-trans isomerism 3−39458
- piperylenes, photosensitised isomerisation, magnetic field effect 3−21825
- polyethylene fibre, oriented, conform. transitions associated with elastic tension 3−29810
- polymer conformational statistics, charact. function of rot.-isomeric model 3−23643
- polymer conformational statistics, probability distrib. 3−23642
- pyridines, monosubstituted, CNDO/2 calcs. on tautomerism 3−33071
- pyrimidines, monosubstituted, CNDO/2 calcs. on tautomerism 3−33071
- stilbenes, photosensitised isomerisation, magnetic field effect 3−21825
- 2,2-difluoropropyl chloride, vibrational spectra and rotational isomerism 3−29668
- HCN-HNC molecules, calculations using minimum basis of Slater orbitals 3−1140
- H_2O_2, trans rotational barrier and geometry optimization 3−7105

isomorphism
- monatomic solid regularities, semi-theoretical models 3−14723
- solid solution crystals, isomorphic interchangeability *(Russian)* 3−11578
- FeP-MP solid solutions, M=As, Co, Mn, W, Mossbauer studies 3−36818

isotope detection
- *see also mass spectra; radioactivity*
- cosmic ray isotope analysis with cryogenic magnet 3−6075
- cosmic ray isotope analysis with nucl. emulsions 3−6082
- cosmic ray isotope comp. meas. using geomag. field 3−9431
- cosmic ray nuclei isotope comp. meas. using counters 3−6074
- cosmic ray nuclei isotope determ. by tracks in plastics 3−6081
- mass spectra low resolution, computer calc. of ionic formulae and monoisotopic spectrum 3−7024
- nuclear reactor fuel, irradiated, adjustment of burn-up code for chemical and isotopic analysis 3−19936
- radioisotopic analyser, automatic for control of sulfur in gases *(Russian)* 3−10135
- secondary ion mass spectrometry with ion microprobe techniques 3−13489
- ^{133}Xe multibolus fractionation technique for human cerebral blood flow distribution meas. 3−22526

isotope effects
- *see also isotope shifts*
- atomic spectra, study by optical spectroscopy *(Rumanian)* 3−11129
- benzenes, ^{14}C-substituted, meas. of tracer-diffusion coeffs., isotope effects 3−24285
- carbon tetrachloride isotopic structure in i.r. spectrum 3−26690
- carboxylic acid dimers, calculation of isotopic stretching of O...O H bonds 3−23539
- carboxylic acid H-complexes, torsional vibrs., Fermi reson. and isotopic effects in i.r. spectra 3−11264
- chemisorption of H_2 and D_2 on W(100) 3−36490
- diffusion of light interstitials, electromigration and thermomigration, quantum theory 3−30287

isotope effects continued
dimethyl sulphoxide and dimethylsulphoxide-d_6, vapour pressure 3−14994
divacancy formation and migration, self-diffusion in b.c.c. metals, correlation factor 3−30288
ethylene, deuterated, intermolecular force parameters in the gas phase, calc. from virial coefficient data *(German)* 3−26740
ethylene, deuterated, isotope effects in the second virial coefficients *(German)* 3−26763
methane, methane-d, differences in second virial coeffs. rel. to intermol. pots. *(German)* 3−26738
molecular force constants calc. from mean amplitudes of vibration, isotope effect 3−33098
naphthalene, deuterium effect on triplet radiative decay rate 3−21823
paramagnetic solns., deuteron relax. study, isotope effect on internal rot. 3−21336
toluene, deuterium effect on triplet radiative decay rate 3−21823
triglycine selenate, ferroelec. props. near Curie point, deuteration effects *(Russian)* 3−8537
triplet excited mols., isotope effect in photodissoc. processes *(Russian)* 3−9087
water, natural and heavy, e.s.r. linewidth variation with temp. 3−2365
BrHBr, computed bond energies and vibr. freq., including isotope effects 3−1181
ClHCl, computed bond energies and vibr. freq., including isotope effects 3−1181
CoBr visible emission spectrum, Br isotope effects in E and G systems 3−20130
Cu, diffusion of Co 3−7965
Eu^{3+} in D_2O, secondary fluorescence quenching by H_2O 3−34421
IHI, computed bond energies and vibr. freq., including isotope effects 3−1181
KH_2PO_4 and KD_2PO_4, ferroelec. phase transition mechanism, neutron diffr. obs. 3−15458
KH_2PO_4-KD_2PO_4 system, on protons and deuterons orientation distrib. in short O-O bonds 3−1614
Li:Na(Ag), comparison for ^{22}Na, ^{24}Na(^{105}Ag, ^{110m}Ag) diffusion 3−38688
N_2^+, isotope effects in predissoc. of $C^2\Sigma_u^+$ state 3−33148
^{a}Ni(A=64,58), proton interactions, isotopic effect in prod. of ^{3}H, ^{3}He at 660 MeV *(Russian)* 3−19867
β-PdH(D)$_n$ isotope mixtures, diffusion isotopes effects of D and t 3−27136
SiC, 6H-polytype, exciton complexes, investigation by isotope substitution 3−30867
SiS rotational spectrum, Born-Oppenheimer approx. breakdown corrections *(German)* 3−11230
Sn, nuclear charge distribution 3−14278
^{a}Sn(A=112,124), proton interactions, isotopic effect in prod. of ^{3}H, ^{3}He at 660 MeV *(Russian)* 3−19867
γ- U alloys, isotope effect in superconducting transition 3−38919
$UO_2(NO_3)_2$ hydrates, effect of D_2O substitution on luminesc. spectra *(Russian)* 3−21485

isotope exchanges
carboxylic acids and hydrogen, deuterium isotope exchange 3−27861
Danakil depression (Ethiopia), ^{18}O enrichment of hot springs water 3−25345
W hot filament, interaction with O_2, isotopic mixing obs. *(Japanese)* 3−20932

isotope relative abundance
see also element relative abundance
cosmic ray electron component and isotopic comp. relation 3−9422
cosmic ray isotope analysis with nucl. emulsions 3−6082
cosmic ray isotopic comp. determ. from balloon flights 3−9438
cosmic rays, HEAO satellite proposal on chem. and isotopic comp. 3−9439
Danakil depression (Ethiopia), isotopic comp. determ. of water samples 3−25345
double focusing, double collecting mass spectrometer for light stable isotope radio analysis 3−25928
lunar biogenic elements, origin and distrib. 3−35090
primary cosmic ray comp., conf., Lyngby, Denmark (Mar. 1971) 3−9414
s-process in stellar interiors, effect of convective region neutron exchange rate 3−28182
Ag isotopes in low-level radioactive bars on world Ag market 3−14152
Be comp. in cosmic rays 3−9419
CO emission at 2.6 mm. from molecular clouds in the Galactic centre region 3−19068
CO in atmosphere 3−2973
^{12}C/^{13}C, determ. of origin of lunar carbon 3−35085
^{12}C/^{13}C meas. in extragalactic sources and solar neighbourhood rel. to element origin 3−25385
^{13}C^{16}O/^{12}C^{18}O ratios from line emission from nine H II regions 3−19072
D, Galactic obs., relevance to stellar nucleo-synthesis 3−22043
D/H in interstellar matter, obs. of Orion molecular cloud 3−37486
D/H ratio determ. for Jupiter from obs. of mono-deuterated methane 3−28148
D/H values for sepentine in ultramafic rocks 3−34789
^{151}Eu/^{153}Eu ratio and abundance from high resolution spectra of solar photosphere 3−39614
He, in solar corpuscular streams for solar history study *(Russian)* 3−12955
^{3}He/^{4}He ratio, determ. from solar flare differential energy spectra 3−39601
O abundance in quartz from Pacific pelagic sediments 3−12614
^{18}O/^{16}O ratio in deep ice cores at Camp Century, Greenland rel. to glaciation 3−39539
^{18}O/^{16}O ratio of deep-sea cores rel. to Quaternary hypsithermals 3−39542
^{18}O/^{16}O ratio of hydrothermally altered rocks of Ohaki-Broadlands geothermal area, New Zealand 3−34790
^{18}O/^{16}O values for sepentine in ultrafic rocks 3−34789
^{204}Pb rel. to ^{206}Pb, ^{207}Pb and ^{208}Pb in galena from Mountain Pass carbonatite 3−18829

isotope relative abundance continued
^{204}Pb rel. to ^{206}Pb, ^{207}Pb and ^{208}Pb in galenas from North Australia 3−18830
^{206}Pb/^{204}Pb ratio for Luna 20 and Apollo 16 lunar highland soil samples 3−12990
^{207}Pb/^{206}Pb ratio for Luna 20 and Apollo 16 lunar highland soil samples 3−12990
^{210}Pb, deep sea disequilibrium due to fast scavenging 3−25189
^{222}Ra profiles for the E. Equatorial Pacific, vertical diffusion-advection model 3−25190
^{87}Rb/^{85}Rb ratio in Sun from Rb I 7800 Angstroms resonance line 3−18932
^{32}Si, vertical profiles for South Pacific 3−34861
^{87}Sr solar content from Sr I photospheric lines 3−18933
^{87}Sr/^{86}Sr in Mid-Indian Oceanic Ridge basalts 3−34797
^{87}Sr/^{86}Sr meas. in volcanic rocks from Jan Mayen and Spitzbergen 3−34803
Ti isotopes in *o* Ceti (Mira) 3−22060
Xe isotope abundances in carbonaceous chondrite meteorites 3−9514
Xe isotopic composition and abundances in solar system 3−35013
^{129}Xe, lunar breccias, prod. from ^{244}Pu fission and ^{129}I decay, Apollo 14 abundance meas. 3−22038

isotope separation
see also isotope exchanges; radiochemistry
far unstable nuclei, determ. of decay energies using ISOLDE facility at CERN 3−10934
ion source for isotope separators 3−13406
rare earth metals, method 3−1092
Cs 137, and power reactor 134/137 mixtures, practical considerations in industrial use 3−19994
Cs-134/137 power reactor mixtures, feasibility and prospects for private separation and marketing 3−19996
D_2 analysis with automatic mass spectrometer in dynamical regime 3−32212
^2H_2O, enrichment, Sulzer rectifying plants 3−23439
He, distillation 3−5841
^{15}N from ^{14}N by photodissociation of NH_3 using laser 3−38196
Si, by thermal diffusion of SiF_4 and SiH_4 3−38197
U enrichment, ultracentrifuge development in Netherlands, review *(Dutch)* 3−19901
$^{235}UF_6$ flow, stochastic fluctuation in uranium-enriching cascade 3−19947

isotope shifts
see also atomic spectra
ethanol, normal and ^{18}O-labelled, Raman spectra, C-O stretching vibr., comparison with sodium ethoxide meas. 3−36034
force constants calc. from heavy-atom isotopic-substitution data 3−20103
isopropyl compounds, isotopic shift with deuteration, assignment of lattice frequencies to vibrational and translational motions 3−5188
isovector, effect of α-particle clustering in nuclear surface involving isovector monopole vibration 3−38127
mass shifts, relativistic corrections to atomic spectra 3−1098
molecule, isotopic freq. shifts as direct constraints in force field calcs. 3−11224
nuclear-charge distrib. rel. to isotope or isomer shift 3−4348
quinoxaline, mixed crystal electronic polarisation spectra, crystal effects 3−39141
rare earth netals, isotope shifts of X-ray transitions 3−1107
sodium ethoxide, normal and ^{18}O-labelled, Raman spectra, C-O stretching vibr., comparison with ethanol meas. 3−36034
toluene, protonated and deuterated, mol. motion, ^{13}C, ^{2}D relaxation times 3−36815
trichlorofluoromethane, F isotope shift, temp. var. 3−7225
$X^{II}ZO_4$ scheelite-type compounds (Z=Mo,W), new Raman data and assignments 3−4419
Bi IV, application of Slater-Condon theory with configuration interaction to various odd configurations 3−4360
BrCl, Raman spectra, vibrational hot bands 3−20140
^{13}C frequency shifts, ethylene and deuterium derivatives, cryst. films, i.r. spectra, general harmonic force field 3−39142
^{13}C-enriched NaCN and KCN, i.r. spectra 3−38294
Cl_2, Raman spectra, vibrational hot bands 3−20140
He-Ne laser, fundamental line broadening process *(Russian)* 3−7026
HgI, application of Slater-Condon theory with configuration interaction to various odd configurations 3−4360
^{183}Hg, ^{185}Hg anomalous isotope shift, search for rotational fine structure 3−29368
Li_2O(x=1,2), from matrix deposition of Li and N_2O in spectra 3−17431
MgO:Cr^{3+}, isotope effect in e.p.r. 3−21301
^{92}Mo, ^{100}Mo in $(NH_4)_3MoO_2S_2$, Raman spectra, force consts. determ. *(German)* 3−4451
^{15}N-enriched NaCN and KCN i.r. spectra 3−38294
$Na_2Fe(CN)_5NO.2H_2O$, single cryst. and polycryst. complexes containing ^{15}NO, ^{14}NO, combination bands polarised i.r. spectra *(French)* 3−21418
Ne I, odd-even isotope shift in 6096 and 6074 Å lines, h.f.s. coupling consts. 3−33020
^{20}Ne-^{22}Ne, 3.39μm line, spectral contour meas. method 3−16840
^{20}Ne-^{22}Ne isotope shift in i.r. spectrum 3−26565
NiD, absorption spectra between 290 and 700 nm behind reflected shock waves, electronic isotope shift 3−14365
Pb III, application of Slater-Condon theory with configuration interaction to various odd configurations 3−4360
Pb isotope shifts of X-ray transitions 3−1107
^{204}Pb, ^{206}Pb, ^{207}Pb, ^{208}Pb, radial moment analysis to muonic atoms and meas. of isotope shifts 3−33068
Sn, isotope shift and hyperfine struct. in atomic spectrum 3−14277
$SnCl_4$, i.r. spectra, vibrational frequency calc., isotope shift *(German)* 3−1231
$SnCl_4$, solid, Raman spectrum in temp. range 4 to 160 K, Cl_2 isotope and cryst. splittings 3−2528
Tl II, application of Slater-Condon theory with configuration interaction to various odd configurations 3−4360
Xe laser, 3.99 μm transition, 128, 126 and 124 isotope shifts *(French)* 3−6469

isotopes
see also radioisotopes
accelerator production, Brookhaven LINAC Isotope Producer, remote target positioning mechanism 3–16476
cosmic ray particles isotopic comp. *(German)* 3–9413
far unstable nuclei, determ. of decay energies using ISOLDE facility at CERN 3–10934
fission gas prod. reactor loop development 3–7006
heavy fragment cumulative yields in fast neutron fission of ^{238}U 3–17269
luminous flux, sonoluminescence, radioluminescence, radioactivity, acoustic cavitation, standardization 3–298
nuclear, production scheduling using linear programming 3–32118
radioiodine labelling of elemental I 3–39460
radioisotope production, application of binomial statistics 3–22419
radioisotope production facility at LAMPF 3–19260
radioisotopes, Pb shielding for transport 3–11096
radioisotopes, production and research, Australian Atomic Energy Commission, 20th Annual Report (1971-72) 3–14242
^{11}C, short-lived, production by Van de Graaff accelerators 3–270
^{14}C, natural, uses in science, review 3–17334
Cs, 137 and power reactor 134/137 mixtures, current and potential radiation applications 3–19993
Cs 134/137 mixtures from power reactors, comparison with ^{60}Co source parameters and dose uniformity ratios 3–19992
Cs-134/137 power reactor mixtures, gamma source market evaluation 3–19995
^{137}Cs γ-radiation sources, safety aspects 3–19345
^{18}F, short-lived, production by Van de Graaff accelerators 3–270
^{123}I cyclotron production, ^{122}Te(^{4}He,3n)^{123}Xe$\rightarrow^{123}$I 3–37681
^{13}N, short-lived, production by Van de Graaff accelerators 3–270
^{15}O, short-lived, production by Van de Graaff accelerators 3–270
^{170}Os, new isotope found 3–6961
^{171}Os, new isotope found 3–6961
U enrichment methods *(German)* 3–6965
U-Pb isotope method as age indicator using apatite 3–25111

isotopic generators *see radioactive sources*

iteration methods *see iterative methods*

iterative methods
see also predictor-corrector methods
axisymmetric buckling of uniformly loaded spherical caps undergoing plastic deformation, numerical soln. 3–37820
cantilever beams of variable cross-section, non-linear bending, numerical soln. 3–22612
celestial mechanics, special satellite orbit points prediction, analytical iterative algorithm, Brouwer theory 3–39583
coordinate relaxation method for iterative calc. of eigenvalues and eigenvectors of very large symmetric matrices 3–23465
deconvolution, spectroscopic data containing random noise 3–32070
for difference eqns. 3–3957
elastic cylinder, dislocations, boundary value problem, iterational method of soln. 3–26087
elastoplastic analysis soln. by matrix displacement or finite element method 3–22652
electromagnetic wave inverse problem of scattering by smooth convex-shaped conductors for high frequency, system-synthesis approach 3–22833
extrapolation method, applic. to Hartree-Fock SCF sequences 3–20003
fast reactors, optimal fuel enrichment distrib. soln. using automatic double iteration search procedure 3–19941
function minimization, non-differentiable *(French)* 3–14437
generalized axially symmetric potential theory, soln. of boundary problems *(Russian)* 3–13540
geomagnetic thin sheet anomalies, vertical profile anal. 3–34836
hermitic matrix, approx. diagonalization by units, successive Van Vleck transforms. *(French)* 3–16698
induction motors, magnetic field distribution under load 3–13668
inverse vibrational problem, computational method based on common solns. of vibrational eqns. of two isotopic species 3–14346
isochronous cyclotron of Michigan State Univ. USA, field trimming computer program 3–13395
Newton's method applic. to elastic stability problem 3–19476
non-uniform elastic circular region, iterative soln., convergence *(Russian)* 3–28867
nonlinear problems, extended Kantorovich method applic. 3–19406
nuclear power plant containment structures subjected to seismic excitations, vertical soil-structure interaction, numerical soln. 3–19918
plasma probes, spherical electrostatic, Runge solution of the continuum equations 3–38493
plastic design problems for plane frame, computer applic. 3–541
radiation damage function unfolding procedure, error estimation 3–23454
radiative transfer eqn. iterative method for direct soln., application to Rayleigh and Mie atmospheres 3–16761
shock waves, real gas equilibrium state calc. 3–7392
skin effect of wire of arbitrary cross-section 3–15218
spacecraft double impulse rendezvous manoeuvres calc. using coasting trajectories 3–31509
special functions, high-order iterative formulae for evaluation of zeros *(Dutch)* 3–28834
suspensions, radiative transfer of turbulent flow in circular tube 3–38357
unsteady state diffusion equation, quasilinearization technique for numerical soln. 3–19523
variable-phase eqn., variation-iteration soln. 3–19515
vibrating beam, determ. of optimal frequencies using finite element displacement method 3–22684
vortex by modified Newton-Raphson methods 3–7391
wire of arbitrary cross-section, skin effect 3–15218

itinerant model of magnetism *see band model of magnetism*

Jahn-Teller effect
alkali metal halides, luminesc. centres, reson. secondary glow, polarisation theory *(Russian)* 3–36918
canonical transform. approach to intermediate coupling T-t dynamical Jahn-Teller problem 3–33811
diamond, semiconducting vacancies, electronic levels, defect. molecule model, extended Huckel approx. 3–33839
direct exchange between two Jahn-Teller ions 3–18088

Jahn-Teller effect continued
DyVO$_4$ thermal conductivity at low temps. 3–1847
group V, II-VI semiconductors, alkali halides, vacancies, interstitials, Jahn-Teller distortions, molecular orbital models 3–33837
impurity ion pair, vibron reduction effects of Coulomb and exchange interactions 3–33813
ionic cryst., magneto-optical spectra of colour centres, electron-phonon interaction effects 3–2580
ions, (3d)^4, acoustic paramagnetic resonance at high magnetic fields 3–2346
metal tropolonate complexes, i.r. spectra, electron spin pairing and Jahn Teller distortion effects 3–36026
methane, electron impact spectra, oscillator strengths 3–23543
nπ* singlet state, reinterpretation of non-fluorescent properties, effect of pseudo Jahn-Teller distortion 3–7216
nonlinear canonical transforms, in coupling between degenerate low and high energy excitations 3–4014
orbital mag. and struct. phase transitions in crysts. with Jahn-Teller ions 3–34053
paraelastic resonance of Jahn-Teller and off-centre ions 3–24387
paramagnetic ion, coupling of E$_g$ orbitals to cluster, harmonic approx. 3–8115
rare earth compounds, with zircon struct., theory 3–38802
reduction factors of Jahn-Teller systems 3–36539
scattering by Jahn-Teller defects in cubic crystals 3–1755
structural phase transitions induced by pseudo Jahn-Teller effect 3–18089
tetrafluoromethane, electron impact spectra, oscillator strengths 3–23543
zinc porphin in n-octane, optical and Zeeman studies of first excited singlet state 3–8599
[Ti(H$_2$O)]$^{3+}$, Jahn-Teller complex ion, paramagnetic resonance and relaxation 3–34197
Al$_2$O$_3$:Cr^{2+}, Jahn-Teller effect of ^{5}E ground state 3–30688
Al$_2$O$_3$:Ni, thermal conductivity at low temps. *(French)* 3–1845
Al$_2$O$_3$:V^{4+}, acoustic paramagnetic resonance 3–2347
CaF$_2$ distortion of Ag^{2+} ions, alternate interpret. of e.p.r. data using O$^-$ ion 3–2356
CaO:Co, Fe, study from ^{54}Fe Mossbauer obs. 3–24639
Ca(OD)$_2$:Cu^{++}, trigonal Jahn-Teller effects in e.p.r. 3–39024
CdIn$_2$S$_4$:Fe^{2+}, optical absorption spectrum 3–21455
Co$_x$Mn$_{2.9-x}$Fe$_{0.1}$O$_4$, Mossbauer obs. of Jahn-Teller distortion 3–8492
Cu based spinel, mag. props. rel. to structure and cooperative Jahn-Teller distortion 3–30632
Cu^{2+} octahedrally coordinated, low temperature ligand field reflectance spectra *(German)* 3–36877
CuCr$_2$O$_4$, rel. to structure changes under high pressure 3–27118
CuFe$_2$O$_4$, cubic-tetragonal transform. and induced uniaxial anisotropy *(French)* 3–15382
DySb, elastic const. softening rel. to Jahn-Teller strain coupling at phase transition 3–33591
DyVO$_4$, elastic anomalies near cooperative Jahn-Teller transitions 3–2014
DyVO$_4$, soft acoustic mode and the strain dependence of the g factor 3–1761
DyVO$_4$, structural transition, due to spontaneous Jahn-Teller distortions 3–24266
Fe-Cr spinel, Jahn-Teller lattice distortions rel. to magnetoresist. anomalies at Curie point 3–30462
FeCr$_2$S$_4$, low temp. transition, Mossbauer obs. 3–5151
Fe$_3$O$_4$, macroscopic strain-coupling induced symmetry change accompanying Verwey transition 3–27222
p-Ge, anisotropy of magnetothermal conductivity 3–1842
KBr:Tl, mag. circular dichroism in C-band, singular behaviour of spectra 3–18430
KCl:Tl, stress induced dichroism and energy shifts in A, B and C absorption bands 3–21454
KI-Tl$^+$ phosphors, relax. excited states, linear electron-lattice interaction description *(Russian)* 3–36917
K$_2$PbCu(NO$_2$)$_6$, e.p.r. study 3–30687
Li$_{0.5}$Ga$_{2.5}$O$_4$:Cu^{2+}, e.p.r. spectrum 3–21300
Mn^{2+} ion, effect on Zeeman patterns in octahedral or tetrahedral crystal field 3–2011
NH$_3$, electron spectra, vibr. struct. and Jahn-Teller effects 3–38280
NiCr$_2$O$_4$, elastic props. and cooperative Jahn-Teller phase transition 3–24181
NiCr$_2$O$_4$, rel. to structure changes under high pressure 3–27118
Ni$_x$Zn$_{1-x}$Cr$_2$O$_4$ elastic anomalies near cooperative Jahn-Teller transitions 3–2014
Np complex, ((C$_2$H$_5$)$_4$N)$_2$NpCl$_6$, absorpt. spectra of inequivalent sites of Np^{4+} 3–2557
RbMnF$_3$, antiferromag., two-exciton transitions, Jahn-Teller effect in excited ion pair 3–11867
p-Si, anisotropy of magnetothermal conductivity obs. 3–1842
SrCl$_2$:Y^{2+}(Sc^{2+}), e.p.r. obs. of dynamic Jahn-Teller effect 3–33807
SrF$_2$, distortion of Ag^{2+} ions, alternate interpret. of e.p.r. data using O$^-$ion 3–2356
TbAsO$_4$, Jahn-Teller induced phase transition, optical absorpt. study 3–2560
TbVO$_4$, Jahn Teller distortion rel. to specific heat anomaly 3–11748
TbVO$_4$, struct. transition, due to spontaneous Jahn-Teller distortions 3–24266
TmVO$_4$ thermal conductivity at low temps. 3–1847
XeF (x=2,4), gaseous and solid far u.v. spectra, dynamic Jahn-Teller effect 3–17423
ZnO(S):Ni^{2+}, near i.r. absorpt. obs. of crystal field, dynamic Jahn-Teller effect in ^{3}T$_2$ state 3–21446
ZnS:Sc^{2+}, e.p.r., 1.3-4.2 K, dynamic Jahn-Teller effect obs. 3–21302

jellies *see gels*

jet stream *see atmospheric movements*

jets
see also plasma jets; sprays
acoustic field of hot jet, computation from turbulence parameters, crossed beam technique 3–3636
aerodynamics of jets discharged into fluidized beds 3–4627
air, escape into dead end tube 3–4523

jets continued
  air, from entry holes of high-intensity combustor-liner, mass flows 3—17494
  air, subsonic, for noise field 3—3652
  axial press. profiles in non-Newtonian flow, viscometric flow and relax. phenomena anal. 3—11371
  axisymmetric, interacting with planar obstacle, turbulence in heat transfer calcs. at stagnation pt. 3—20312
  bistable fluid device, solid particle flows 3—1471
  buoyancy, thermal, in round, laminar vertical jets 3—23800
  buoyancy-induced flows, instability, transition and turbulence, review 3—33217
  capillary break-up of non-Newtonian liquid, yield stress effect 3—4521
  rel. to charge generation during washing of tanks with water sprays 3—655
  circular free, impinging on flat plate, mass transfer 3—1336
  coaxial, Prandtl eddy viscosity model 3—38412
  coaxial streams, turbulent, recirculation patterns in initial region 3—23719
  combusitible, turbulent diffusion flame, aerodynamic and thermodynamic analysis 3—23799
  conducting liquid, in flow wake in longitudinal magnetic field *(Russian)* 3—7434
  confined, nonseparated mixing, theoretical model 3—1373
  confined laminar mixing in circular channel, arbitrary entrance vel. distrib. 3—4528
  curved two-dimension, vel. profiles, similarity soln. 3—20412
  cylindrical laminar liquid jet ejecting into a gas, heat transfer 3—38417
  eddy structure of convected vortices 3—36098
  exhaust flow, refraction of acoustic duct waveguide modes 3—33244
  falling under gravity from horizontal slot at large Froude number 3—38420
  flow measurement, turbulence distribution, laser photon correlation spectroscopy, Doppler effect 3—22570
  flow rel. to noise, direct correlation 3—7355
  fluid dilatations rel. to flow noise 3—1378
  fluidic amplifier jet flow 3—20348
  fluidic anemometer employing axisymmetrical free submerged jet 3—16582
  formation by explosives with lined trumpet cavities 3—11427
  free, radiometer for i.r. probing *(French)* 3—25695
  freon, in cocurrent air stream, dimensions and location of mixing zone 3—4522
  gas, interaction with fluidised beds of fine particles 3—1457
  gas jet transportation system, for fission products 3—25828
  generalized Helmholtz resonator, jet flow model 3—31972
  Hartmann-Sprenger tube, thermal phenomena, strong flow oscillations induced by cold gas jet *(French)* 3—20292
  heavy liquid flow past a curvilinear obstacle, numerical soln. *(Russian)* 3—29930
  hypersonic, base pressure distribution meas. of cone 3—38413
  hypersonic air streams, multiple-orifice liquid injection 3—38415
  impulse water jets at high press., study by cinephotography *(Russian)* 3—454
  incompressible flow and reattachment effects in fluid control elements 3—11368
  injection into moist two-phase flow, undecayed portion 3—14498
  isothermal turbulent, two-dimensional, at a curved porous wall 3—33311
  jet tone, in pipe, sinusoidal sound wave in continuous flow, excitation of subharmonics 3—39825
  knife jet dryess, effect of turbulence on heat and mass transfer *(German)* 3—26780
  laminar, elliptical 3-dimensional orifice, viscous energy transfer, numerical analysis 3—4527
  laminar, general soln. of linearized problems 3—33323
  laminar, viscous, stability, initial disturbance level influence 3—7311
  laminar and turbulent jet mixing flow with boundary layer growth 3—1354
  laminar jet mixing with and without free stream, numerical soln. 3—26848
  laminar thrust measurement apparatus 3—3923
  laminar viscous, stability, ambient gas influence 3—20411
  laser anemometry, meas. of mean velocity and turbulence in free jets 3—478
  low-speed water jet fed into liquid surface, take-up of air *(German)* 3—7314
  mixing in longitudinal magnetic field *(Russian)* 3—14490
  noise, moving source problem 3—9746
  noise abatement, upper surface blowing lift augmentation system 3—3649
  noise reduction, interaction with lift augmenting flaps 3—3648
  non-Newtonian pseudoplastic fluid, laminar two-dimens. free jet 3—23728
  oscillations, transverse, in jet-splitter system 3—1334
  planar, external excitation, vortex growth 3—20331
  planar, natural breakdown, vortex formation 3—23804
  planar air jet striking a concave surface, heat transfer 3—23704
  plane, flapping frequency 3—29928
  plane turbulent wall jet, flow development and mass transfer 3—17515
  over plate, noise abatement, flow of fluid over plate, STOL aircraft 3—3650
  plumes, forced, scale diagrams 3—36144
  power spectrum of axisymmetric choked jet, noise spectrum in jet segments *(Russian)* 3—4566
  pulsed excitation of turbulent boundary layer 3—1395
  radiating gas, optically thin, analysis by quasi-one-dimensional flow method, radiative effects 3—23811
  semiconstrained turbulent submerged, integral method 3—33310
  slow viscous flow down inclinded plane, similarity soln. 3—38350
  solids-gas jet, development of heat-diffusion method for meas. of turbulence intensity on axis *(Russian)* 3—23789
  spark induced cavitation bubble collapse, photographic study, high speed microjet formation 3—26831
  spray, particle size distrib. 3—23794

jets continued
  spreading of jet of uni-polarly charged particles in hydrodynamic flow, numerical soln. *(Russian)* 3—29901
  stability of curved gas/liquid interface 3—20410
  steam, penetration characteristics of submerged jet in subcooled liquid water bath 3—7312
  submerged laminar liquid, vel. profiles in exit region 3—4534
  subsonic jets, plane baffles, heat transfer, stagnation point, free stream turbulence 3—1330
  supersonic, blunt body in rarefied N_2 and N_2-H_2 mixtures *(Russian)* 3—29929
  supersonic detached flow between two bodies, turbulent jet theory application 3—33316
  supersonic free, dimer conc. 3—1401
  supersonic jets, noise generating disturbances, holographic study 3—5705
  swelling, incompressible Reiner-Rivlin fluids, appl. of orthogonality principle 3—4543
  swirling turbulent jet 3—26857
  three dimensional turbulent boundary layer on the confining wall of an impinging jet, momentum integral solution 3—26813
  thrust nozzle optimisation, including boundary-layer effects, using numerical relaxation scheme 3—1333
  triple jet system for liquid extensional viscosity measurement 3—19383
  turbulence influence on flow of a boundary layer *(Russian)* 3—29931
  turbulent, diffusion and vortex models 3—33315
  turbulent cocurrent, mixing in ducts with profiled walls, minimum losses determ. 3—33309
  turbulent flow and mass transfer, when reattached on inclined flat plate 3—17516
  turbulent jet joise, determ. of intensity and directivity *(Russian)* 3—26859
  turbulent liquid, gas absorption *(French)* 3—29922
  turbulent nearfield pressure data for predicting farfield acoustic radiation 3—5716
  turbulent open and confined flow experiments 3—33203
  turbulent wall jets, opposing plane, interaction produced by collision in still air 3—38419
  turbulent wall jets, three-dimens. nature 3—20303
  two-dimensional heated laminar jet, temp. distribution 3—36145
  underexpanded sonic, properties or retardation 3—23802
  undersaturated, affected by obstacle, law of central shock displacement 3—23803
  unsteady viscous flow into stationary surroundings, numerical calc. 3—33308
  upstream facing wall jet interaction with supersonic stream 3—36140
  vertical buoyant, radial spreading as free surface layer 3—4525
  vibrating, surface aging 3—29923
  viscous incompressible turbulent flow in axisymmetric channel under conditions of preliminary swirl in the entry zone 3—33317
  vortex core jet near pt. of generation, vel. field analysis 3—1415
  wall, deflected exhaust, near field acoustic environment, VTOL jets 3—3651
  wall, potential vortex, extension of Gurevich's soln. 3—4573
  water, ice melting heat transfer 3—14420
  Ar-air high-temp. jets with Ti dispersive particles, electroconductivity *(Russian)* 3—11455
  CO_2+N_2+He mixture expanding supersonically, light amplification factor 3—19607
  He, heavy ion recoils, absolute transport efficiency 3—35452
  Hg, in metallic conduits under non-wetting and amalgamating conditions 3—1372
  O_2, subsonic, mass transfer to liq. Ag 3—39304
jitter *see vibrations*
jogs *see dislocations*
Johnsen-Rahbek effect *see adhesion; electrostatics*
Johnson noise *see thermal noise*
joining processes
  see also brazing; cable jointing; soldering; welding
  composites, secondary fabrication problems 3—12418
  electroslag welded joints, 80 mm thick, fracture toughness, COD approach application 3—21625
  laser beam welding of butt joints between dissimilar metals *(Russian)* 3—4130
  laser beam welding of winding conductors in their insulation *(Russian)* 3—6523
  vacuum tight gluing, plastic to stainless steel *(Russian)* 3—9907
jointing, cable *see cable jointing*
jointing (electric connectors) *see electric connectors*
Jordan-Thiry field *see cosmology; general relativity*
Josephson junctions
  see also tunnelling
  2e/h determ. comparison of point-contact and thin film Josephson junctions 3—13199
  2e/h determination, at NPL 3—22248
  2e/h measurements at NBS using D.C. Josephson effect, implications for fine structure constant 3—13202
  2e/h measurements at NPL using a.c. Josephson effect, monitoring of voltage standard 3—13201
  2e/h measurements at PTB using point contact junctions 3—13200
  a.c., monitoring of NSL standard e.m.f. 3—3750
  current through S-N-S junction, containing paramag. impurities with local states within gap 3—30578
  d.c. Josephson effect, effect of noise 3—21182
  effect of a.c. on steady-state characts. *(Russian)* 3—8310
  effects at high current densities 3—36690
  e.m. radiation emission, freq. pulling 3—5080
  externally shunted, inductance effects 3—18272
  granular superconductor, orientational phase transition 3—8294
  oxide barrier Josephson junction, quasiparticle pair interf. rel. to current voltage characts. 3—34021
  parametric capacitance 3—21183
  SNS junctions, effect of paramagnetic impurities on Josephson current 3—21185
  SNS type, Josephson effect theory 3—30577
  stability problems in nonlinear sine-Gordon eqn. 3—26058

Josephson junctions continued
transitions from zero-voltage to voltage state, inductances, in subnanosecond range 3—18267
tunnel effect in superconducting alloys with local states within the gap 3—21184
type-II, penetration depth as upper size limit 3—34046
video detection of microwaves and millimetre waves, sensitivity 3—16461
voltage-frequency reln., flux conservation implications 3—18271
vortex propagation 3—18274
weak link, shunted junction and mechanical models 3—5079
Al-Formvar-Pb, logarithmic derivative curves and trap-assisted current transport 3—24544
Pb-Pb oxide-Pb tunnel junctions, mag. field depend. of Josephson plasma reson. freq. 3—2218
Pb-Pb_xO_y-Pb, thermal effect on voltage current characts. 3—11986
in Sn ring, multiple-quantum-state, behaviour and stability of states 3—2220
Sn-I-Sn tunnel junction, quasiparticle relax. and phonon emission 3—27338
Sn-Sn_xO_y-Sn, thermal effect on voltage-current characts. 3—11986
Sn-SnO-Sn junction, r.f. induced current voltage characts. 3—11985
Joshi effect *see glow discharges*
Joule-Thomson effect
fluids and fluid mixtures, prediction of thermodynamic props., applications 3—34699
refrigerator for obs. in 30 K region, based on Linde principle 3—5830
thermal entrance region heat transfer in pipes with uniform wall temperature 3—20302
junction field effect transistors *see field effect transistors*
junction lasers *see semiconductor lasers*
junctions, waveguide *see waveguide couplers*
Jupiter
astrolable obs. between 1965 and 1967, a comparison of ephemerides *(French)* 3—22031
atmospheric dynamics, review 3—35074
atmospheric Jupiter 8-13 μm spectrum, ν_2 band of NH_3 3—5578
atmospheric scale height, measurement discrepancies 3—9491
brightness temp. obs. in far i.r. 3—18971
clouds, entry probe mission, remote sensing, communications link, flyby mission, Grand Tour, interplanetary bus 3—3296
cometary group, original orbits determ. using Tisserand's constants 3—35002
Danjon astrolabe observations in 1965-7 period rel. to ephemeride positions *(French)* 3—28151
decametre radiation rel. to solar radiation 3—9495
decametric radio emission, new high-energy component 3—35061
decametric radio emission at 18.3 MHz *(French)* 3—31606
decametric radio emission source, Io phase asymmetry 3—31604
decametric rotation period 3—9485
electron streams in Jovian magnetosphere rel. to intense decametric radiation 3—25406
Galilean satellites obs. at 1-4 μ 3—31581
gravitational field, use for escape of space vehicles from ecliptic plane along heliocentric orbit 3—25369
gravitational moments computation *(Russian)* 3—3301
Io-modulated decametric radio emissions, asymmetry of satellite ephemeris positions 3—12975
i.r. maps of Jupiter using new scanning equipment 3—9496
limb brightening obs. at 7.9 μ 3—31580
magnetic fields, non-dipole terms, obs. of linear polarization of radio radiation 3—3299
methane absorption band spectrometry of Jupiters disc *(Russian)* 3—16144
methane and NH_3 absorption bands of Jupiters disc *(Russian)* 3—16145
occultation of beta Scorpii, emersion and immersion curves 3—9489
orbiter trajectory based on gravitational field of Galilean satellites 3—9449
radiation belts, solar wind source of electrons 3—31605
radiation polarisation rel. to P, T invariance 3—28155
radio bursts, fine structure obs., effect of Io's position 3—22036
radio bursts recording using automatic dynamic spectrum analyser 3—39750
radio emission beaming, non Io related 3—3298
radio flux density and polarisation meas. at 13 cm during 1969 to 1971 period 3—31603
rotation, solar activity, superposition analysis 3—3294
rotational profiles (for 1970 and 1971) 3—9492
satellite mutual eclipses and occultations (1973-74) 3—31621
β Scorpii occultation, radius determ. 3—22030
tidal effects on sunspots 3—3293
u.v. absorpt. in continuous spectrum, 3300 to 4800 Å obs. 3—35064
D/H ratio and mono-deuterated methane abundance determ. from i.r. obs. 3—28148
H_2 quadrupole and methane obs., radiative props. of visible clouds 3—31614
K-capture *see nuclear electron capture*
K mesons *see kaons*
K-N interactions *see kaon-nucleon interactions*
Kalman filters
nuclear reactors, for non-measurable variables 3—32923
seismic prospecting, prediction error filter 3—9351
kaon-baryon interactions
see also kaon-hyperon interactions; kaon-nucleon interactions
No entries
kaon-baryon scattering
see also kaon-hyperon scattering; kaon-nucleon scattering
No entries
kaon decay
see also kaon hadronic decay; kaon leptonic decay
CPT invariance test 3—19668
gauge models, physical constraints imposed by Higgs particle exchange and higher-order effects 3—26286
nonleptonic, strong isotopic-spin breaking 3—19681
$K\to\pi\mu(e)\nu$, absolute bounds for form factors 3—35777
$K\to\pi\mu(e)\nu$, bounds on scalar form factor from low-energy $K\pi$ phase shift 3—26288

kaon decay continued
$K\to\pi\mu(e)\nu$, calc. of decay form factors through similarity transform with π_{l3} 3—13831
$K\to\pi\mu(e)\nu$, chiral-limit theorems and PCAC corrections for scalar divergence form factor 3—29187
$K\to\pi\mu(e)\nu$, determ. of form factors from hard meson current algebra 3—16974
$K\to\pi\mu(e)\nu$, modified soft-pion theorem 3—820
$K\to\pi\mu(e)\nu$, relativistic quark model 3—32678
$K\to\pi\mu(e)\nu$, slope of decay form factor, mechanism based on exact threshold theorem 3—32650
$K\to\pi\mu(e)\nu$, spin-0 phenomenology in K*-pole model 3—23030
$K\to\pi\mu(e)\nu$, theoretical study using current algebra, light cone algebra and related techniques 3—10671
$K\to\pi\mu(e)\nu$, value of ξ parameter from pion-gauge condition 3—16975
$K\to\pi\mu(e)\nu$ double pole model of form factor 3—13858
$K\to\pi\mu(e)\nu$ form factors, chiral symmetry breaking 3—13832
$K\to\pi\mu(e)\nu$, symmetry breaking in chiral SU(3) × SU(3) 3—10637
$K^-\to\mu\nu$ Lee-Prentki-Zumino model calcs. involving charged Higgs-Kibble scalars 3—16973
K^0 mesons, decay recording installation 3—28678
$K^0\to\pi^-\mu^-\nu$ Lee-Prentki-Zumino model calcs. involving charged Higgs-Kibble scalars 3—16973
$K^0\to\pi\mu(e)\nu$, produced in 1.2-1.7 GeV/c K^+p interactions, study of $\Delta S=\Delta Q$ selection rule 3—13833
$K^0\to\pi\mu\nu$, CP-violating charge asymmetry 3—10670
$K^0\to\pi\mu\nu$, exptl. limits on form factors 3—29188
$K^0_l\to\mu^+\mu^-$, boson pair model unification with CP nonconservation and excess μ anomaly 3—16951
$K^+\to\pi^+e^+e^-$, determ. of lower bound on magnitude of decay rate 3—29190
$K^\pm\to\pi^+\pi^-e^\pm\nu_e$, form factors of weak hadronic current and π-π phase shift 3—23031
$K^\pm\to\pi^\pm\pi^0\gamma$, test of CP invariance 3—26290
$K_l^0\to\pi^\pm\mu^\mp\nu$, meas. of charge asymmetry 3—830
$K_l^0\to\pi\mu\nu$, study of charge asymmetry 3—29189
$(K_l^0\to\pi\mu\nu)/(K_l^0\to\pi e\nu)$, $(K_l^0\to\pi^+\pi^-\pi^0)/(K_l^0\to$ all charged) branching ratios detn. 3—23033
$K_{s,l}\to\gamma\gamma$, CP violation 3—16992
$K_s^0\to\gamma\gamma$, unitarity relations for two-pion intermediate states 3—32666
$K^{*+}(890)$ coherent production on nuclei, determ. of upper limit for radiative decay width $K^{*+}\to K^+\gamma$ 3—19741
K^+K^-, produced in $\pi^-p\to nK^+K^-$, 3.1-3.6 GeV/c, meas. of decay angular distribs. 3—6669
$\kappa\to\pi\mu(e)\nu$ form factors and $K\pi$-scatt. phase shift 3—6580
kaon hadronic decay
CP preserving phenomenology 3—10673
phase difference between $\eta_{00}=A(K_l\to\pi^0\pi^0)/A(K_s\to\pi^0\pi^0)$ and $(K_s\to\pi^+p-)$ 3—35775
$K\to\pi\pi$, current algebra and soft-pion limit 3—13834
$K\to\pi\pi$, $\Delta I={}^3/_2$, ${}^5/_2$ contributions to decay amplitudes and $(\delta_0$-$\delta_2)$S-wave π-π phase shifts 3—35778
$K\to\pi\pi$, nonlinear chiral Lagrangians and $\Delta I={}^1/_2$ rule 3—6581
$K\to\pi\pi$, role of final-state interactions in producing $\Delta I=1/2$ rules 3—35779
$K^0\to2\pi$, self-contained determ. of phase of CP-invariant parameter η_{+-} 3—4162
K^0 CP-violating decay, nonlocality and unitary transformation 3—38024
$K^0\to\pi^+\pi^-$, precise meas. of opening angle, use for identification of events in $K^-p\to K^0n$ 3—17116
$K^+\to\pi^+\pi^0\pi^0$, exptl. study of matrix element by two independent analyses 3—4160
$K_l^0\to\pi^+\pi^-$, branching ratio meas. 3—38025
$K^0\to\pi^+\pi^-$, meas. of K^0_s mean life in hydrogen bubble chamber 3—6582
$K^\circ\to\pi^+\pi^-\pi^\circ$, exptl. study and $\eta_{+-0}=K^\circ_s/K_l$ reln. detn. 3—6583
$K^*\to K\pi\pi$, quark-model $^1F_3$ state, singlet boson trajectory 3—6584
$Q^+\to K^{*0}(890)\pi^+\to K^+\pi^-\pi^+$, Berman-Jacob two-step analysis, spin-parity assignments, Monte-Carlo technique tests 3—23034
kaon-hyperon interactions
No entries
kaon-hyperon scattering
No entries
kaon interactions
see also kaon-baryon interactions
K^-d, 5.5 GeV/c, to $\Sigma^\pm\pi^\pm\pi^-(\pi^0)$, $\Sigma^-K^+K^-$, $K^-\pi^-p$ final states in which hyperon is produced 3—29274
K^-d, to $K^-\pi^+\pi^-d$ and $K^-\pi^+\pi^-n$ final states, 3.4 GeV/c, cross sections and resonance production 3—32719
$K^-d\to p\pi^-\Lambda$, polarization, matrix elements, double scattering terms 3—38074
$K^-d\to\pi^\pm\Sigma^\pm n$ at rest, study of low-energy $\Sigma^\pm n$ interaction 3—29248
$K^+d\to K^0\pi^+d$, coherent reaction at 2 GeV/c, determ. of cross section and parameters of ω trajectory 3—23166
KK distribs. in pionization region 3—6678
$K^-p\to K^\circ n$, differential cross sections for high energy K° production 3—898
$K^+p\to K^0X^{++}$ inclusive reaction, 5.0 and 8.2 GeV/c, behaviour in terms of angular variables 3—6676
$K^+p\to K^0\pi^+X^+$ inclusive reaction, 5.0 and 8.2 GeV/c, behaviour in terms of angular variables 3—6676
$K^+p\to K^\circ N^{*++}$, differential cross sections for high energy K° productions 3—898
$K\pi$, dispersion relation analysis for s- and p-waves to 1 GeV *(Russian)* 3—19733
πK distribs. in pionization region 3—6678
kaon leptonic decay
CP preserving phenomenology 3—10673
muonic atom data, limitations *(Russian)* 3—828
$K\to ll\gamma$, CP nonconservation 3—4158
$K\to\mu\nu$, calc. of decay form factors through similarity transform with π_{l2} 3—13831
K^0, nonlinear theory, time reversal and combined inversion *(Russian)* 3—38007
$K_2^0\to\mu^+\mu^-$ puzzle, fermion loop model 3—829
$K_l\to2\mu$, formulation of quantum theory without superposition principle *(Russian)* 3—10356

kaon leptonic decay continued
$K_l \to 2\mu$, possibility of production of new particles in yet unobserved decay channels 3−4156
$K_l \to \mu^+\mu^-$, contrib. of massive axial photon or Weinberg's Z meson 3−32648
$K_l \to \mu^+\mu^-$, models and reln. to CP invariance, review 3−32647
$K_l \to \mu^+\mu^-$, neutral current contrib. 3−10669
$K_l \to \mu^+\mu^-$, review of exptl. data in relation to proposed solutions of problem 3−10667
$K_l \to \mu^+\mu^-$ amplitude, effects of possible CPT violation 3−38022
$K_l \to \mu\mu$, reln. to unified gauge theories of weak and e.m. interactions 3−32643
$K_l^0 \to \mu^- e^+$, parity violation by neutral lepton currents 3−4155
$K_l^0 \to \mu^+\mu^-$ branching ratio, lower bound considerations 3−13830
$K_l^0 \to \mu\mu$ anomalously low rate evidence against Sehgal's low-mass fermion 3−32649
$K_{s,l} \to \mu\mu$, CPT constraints 3−4157
$K_s \to \mu^+\mu^-$, search, branching ratio prediction 3−38021
$K_s \to \mu^+\mu^-$ branching ratio for T, CP and CPT invariances 3−10664
$K_{s(l)} \to 2\mu$, W boson model approach 3−6575
$K^0_l \to \mu^+\mu^-$, validity of assumptions on which theoretical lower bound for process is based 3−10668

kaon-nucleon interactions
charge- and hypercharge exchange above 36 GeV/c, phenomenological characteristics of absorption 3−26348
coherent production on nuclei by K, experiments 3−14090
hypercharge-exchange, application of Ringland-Roberts-Roy-Tran Thanh Van Reggeized absorption model 3−10795
K^- interactions on nuclei with $A \sim 20$, coherent production of multimeson final states, 5.5-12.7 GeV 3−23159
modified phase-shift analysis of $I=0$, K-N system, existence of exotic baryon resonances 3−35826
total cross-sections, comparison with γN interactions in quark model *(Russian)* 3−19697
K^- meson absorpt. by protons in propane, determ. of probability 3−14052
K^- p collisions at 10 GeV/c, results on many-body processes 3−911
$K_p^+ \to K^*\Delta$, helicity amplitudes, reln. to double resonance prodn. and equal-phase hypothesis 3−29260
$K^*(1760)$ observation in the $K\pi$ system 3−32723
$K^+A \to K^0\pi^+A$, A=C, Al, Ti, Ag, Pb at 10, 13, 16 GeV/c, obs. of coherent production of $K^{*+}(890)$ 3−19741
K^-d, total cross-sections, 15-65 GeV/c with Glauber correction *(Russian)* 3−26360
$KN \to K\pi N$, isospin conservation and choice of B_5 amplitudes 3−901
$KN \to NX$, inclusive finite mass sum rules and duality study of meson resonance production cross sections 3−32735
$KN \to Y + \gamma$ $(Y=\Lambda, \Sigma)$, radiative capture, production of Λ^* (1405) *(Russian)* 3−32715
K^-n 4.5 GeV/c, study of final states with three charged particles and visible Λ 3−35839
$K^-n \to \pi^-\Lambda^0$, role of Σ resons. in interference model applic. 3−10800
$K^-n \to \Sigma^+\pi^-\pi^-$, helicity for malism, isobar models and symmetrization effects 3−23145
K^+N coherent interactions, 10 GeV/c. $K^+\pi^+\pi^-$ system analysis 3−4225
$K^+n \to K^0p$ complex-Regge-pole model consistent with dual absorption 3−19727
$k^+n \to K^+\pi^-p$, absorptive effects, single pion exchange absorption model 3−4227
$K^+n \to K^+\pi^-p$ at 9 GeV/c, obs. of S-wave structure in $K\pi$ spectrum 3−32721
$K^\pm n$, Regge pole SU(3) model approach to total cross sections 3−10821
$K^\pm N$ charge-exchange, search for Q^0 and Q^{++} production 3−35830
Kp, inclusive longit. momentum spectra of pions, thermodynamical model calc. 3−916
K^-p, 10 GeV/c, production of Y* (1385) resonance, meas. of complete spin density matrix, quark model predictions 3−10802
K^-p, 14.3 GeV/c, differential and total cross sections for N K^0, $\Lambda\pi^0$, $\Sigma^+\pi^-$, $\Sigma^+(1385)\pi^-$ final states 3−14068
K^-p, 4.25 GeV/c, meas. of total and differential cross sections for K^0n, $\pi^0\Lambda$, $\eta\Lambda$, $\eta'\Lambda$, $\pi^-\Sigma$, $\pi^+\Sigma^-$, $K^+\Xi^-$ final states 3−17108
K^-p, at c.m. energies 1580-1720MeV in bubble chamber, study of neutral final states 3−35831
K^-p, charged particle multiplicity in annihilation and non-annihil. interact., 8.25 GeV/c 3−23142
K^-p, inclusive reaction, two-body, cross-sect. and correlation function, detn. at 9 GeV/c 3−23187
K^-p, mass determ. for charged Σ hyperons 3−4245
K^-p, total cross-sections, 15-65 GeV/c with Glauber correction *(Russian)* 3−26360
$K^-p \to k^-\pi + n$, absorptive effects, single pion exchange absorption model 3−4227
$K^-p \to K^-\pi^+n(K^0\pi^-p)$, 5.5 GeV/c, study of s-wave $K\pi$ resonance at 1360 MeV 3−23164
$K^-p \to K^0X$, 14.3 GeV/c, triple Regge analysis 3−29292
$K^-p \to K^0n$, meas. of charge-exchange cross sections at 25 and 35 GeV/c 3−17116
$K^-p \to K^0n$ complex-Regge-pole model consistent with dual absorption 3−19727
$K^-p \to K^0\pi^-p$, 8.25 GeV/c, cross sections and effective mass distribution 3−38087
$K^-p \to K^{*-}p$, 8.25 GeV/c, behaviour of differential cross sections and density matrix elements 3−38087
$K^-p \to K^{*0}n$ amplitude as test of smoothed veneziano model 3−17072
K^-p low-energy, Coulomb and mass difference corrections in K-matrix treatment 3−32699
$K^-p \to \Lambda X$, 14.3 GeV/c, triple Regge analysis 3−29292
$K^-p \to \Lambda\pi^+\pi^-$, analysis for 300-470 MeV/c near $\Lambda(1520)$ 3−19730
$K^-p \to nK^0$, $\Lambda\pi^0$, $\Sigma^+\pi^-$ and $\Sigma^+(1385)\pi^-$, two-body inelastic reactions, 14.3 GeV/c 3−35829
$K^-p \to \pi^-\Sigma^+$ amplitudes and absorption pattern 3−23162
$K^-p \to \pi^+\Sigma^-$, calc. of finite-energy sum rules, deviations from pure Regge pole behaviour 3−10792
$K^-p \to \pi^+\pi^-X$, applications of Mueller theory 3−35846
$K^0p \to Y\pi^+x^0$, search for $\Lambda\pi^+\gamma$ final state consistent with $Y_1^*(1385)$ production, determ. of branching ratio 3−883
K^+p, correls. in multiparticle prod. 3−10822

kaon-nucleon interactions continued
K^+p, elastic scattering and single-pion production at 4.27 GeV/c, resonance production 3−29262
K^+p inclusive one-particle distrib. in wee-x region, diffractive-excitation model, blackbody radiation 3−38097
$K^+p \to K^0p\pi^+$, 1.2-1.7 GeV/c, study of selection rule $\Delta S = \Delta Q$ in K^0_{e3} and $K^0_{\mu3}$ decays 3−13833
$K^+p \to K^0p\pi^+\pi^+\pi^-\pi^0$, four-pion resonance at ~1630 MeV 3−17124
$K^+p \to K^+pKK$, 10 GeV/c, cross sections for φ and f' production, determ. of resonance parameters 3−10805
$K^+p \to K^+pP^+\pi^-$, 10 GeV/c, study of $I=1/2$ $p\pi^+\pi^-$ system 3−38086
$K^+p \to K^+p\pi^+\pi^-$, 5 GeV/c, with K*(1892) and N*(1236) production, spin density matrix elements 3−29273
$K^+p \to KN\pi$, final states cross-sect. and energy dependence at 7.3 GeV/c 3−29272
$K^+p \to KN\pi\pi\pi$, 5GeV/c, study of resonance production 3−14077
$K^+p \to K^{*0}\pi^+p$, spin and parity of double Regge amplitude in Q region 3−29266
$K^+p \to \pi^-\pi^-X$, applications of Mueller theory 3−35846
$K^+p \to \pi^+ + X$, comparison with $\gamma p \to \pi^- + X$, cross-section meas. 3−17050
$K^+p \to Q^+p$, study of Q-region of $K\pi\pi$ mass from 2.5 to 12.7 GeV/c, determ. of differential cross section and spin-parity 3−6671
K^+p six-prong interactions at 12.7 GeV/c, obs. of π angular correlations 3−29275
$K^\pm p$, Regge pole SU(3) model approach to total cross sections 3−10821
$K^\pm p \to K^+(890)$, cross section energy depend. 3−4221
$K^\pm p \to \Lambda +$ anything, 13 GeV/c, role of diffractive processes 3−17136
$K^+p \to K^{*+}(890)X$, single particle spectra, pion pole effect in fragmentation region 3−26354

kaon-nucleon scattering
σ-term and BBS-coupling constants 3−23141
σ-term estimate from off-mass-shell Veneziano amplitude with Adler-Weisberger sum rule 3−32700
diffractive dissociation of K on nucleons and nuclei, comparison with elastic scattering 3−14069
diffractive scatt. slopes and effective shape of spectral functions 3−10790
dispersion relations, rel. to nucleon coupling of ω and φ mesons 3−10761
low-energy parameters, scattering lengths and magnitude of σ-commutator 3−23143
normalized differential scattering sections at various energies, comparison with theory *(Russian)* 3−38072
resonant state below $\Lambda(1520)$, direct channel production 3−23139
sum rules, finite-energy, based on ρ and ω exchange 3−23018
total cross-sections, base current-quark masses and light-cone algebra 3−29224
$\varepsilon\kappa\kappa$ coupling const. determ., importance of $\varepsilon(700)$ meson in SU(3) symmetry scheme 3−10826
K-p, elastic at 25 and 40 GeV/c, determ. of cross-sections 3−893
$K^\pm$ p elastic differential cross-sections, 3-6 GeV/c, comparison of particle-antiparticle cross-sections 3−895
K^+d, extraction of stable neutron scattering cross sections from deuteron expts. 3−26343
$KN \to \Lambda\pi$, exchange structure of N, Δ backward peaks, polarisation expts. 3−10793
KN scatt. at 1.0-2.0 GeV/c, s-channel helicity partial wave, function of impact parameter 3−23178
KN t-channel helicity-flip amplitude in charge and hypercharge-exchange reactions, fixed poles 3−14049
K^+n, extraction of stable neutron scattering cross sections from deuteron expts. 3−26343
K^-p, azimuthal correlations, protostatistical model analysis 3−14082
K^-p, double diffraction dissociation and n-particle cross sections 3−14044
K^-p, duality model of exotic peaks and exotic cross-section fall off 3−17105
K^-p elastic amplitude, model-independent test for Adler-Weisberger sum rule for kaons 3−23013
$K^-p \to \Xi^-K^+$, comparison with backward K^+p scattering 3−23163
K^+p, below 2 GeV/c, dispersion-relation analysis 3−35825
K^+p, total cross sect. meas., 0.57-1.16 GeV/c 3−19731
K^+p elastic polarisations, transient phenomena at intermediate energies 3−23140
K^+p elastic scatt., accelerated-convergence-expansion-partial-wave analysis, criticism 3−23144
K^+p elastic scatt. at 1.3-2.5 GeV/c, data anal. in Veneziano model with single Regge-pole pomeron 3−19739
K^+p inelastic reactions, 1.37-2.17 GeV/c, cross section for single-pion and two-pion final states 3−4228
$K^\pm p$, calc. of σ term using off-mass-shell dispersion relations, determ. of coupling constants 3−29252
$K^\pm p$, elastic, meas. of differential cross section, 3-6 GeV/c, comparison of particle-antiparticle normalization 3−888
$K^\pm p$, energy depend. of elastic scatt., 3-30GeV 3−10785
$K^\pm p$ elastic, 20-5000 GeV, impact picture 3−32707
$K_l^0p \to pK_s^0$ backward scattering from 1.0 to 7.5 GeV/c 3−17110

kaon production
photoproduction, meas. of inclusive cross sections at 3.2 GeV, comparison with electroproduction 3−23089
suppression, dynamical pomeron coupling model 3−10737
transverse momentum distrib. of 5 GeV/c secondaries produced in 53 GeV collisions 3−10813
$e^+e^- \to K^-K^+$ prod. in colliding beam, 1.2 GeV, meas. of cross-section and e.m. form factors 3−17015
$e^-p \to e^-K^+\Lambda$, coincidence meas., −0.17 to −1.2 GeV^2 3−14011
$\gamma p \to K^\pm X$ from H_2, cross-section meas. at 18 GeV, forward angles 3−17056
K/π inclusive production ratio in central region, generalized f,f′-coupled Pomeron model 3−23183
K^0 photoproduction from Al nuclei at 10° to γ-beams, cross section determ. 3−32673
K^+ photoproduction, exchange of trajectory at pomeron cuts, Regge-pole dominance 3−13968

kaon production continued
- K^+ photoproduction, polarisation predictions from pion data and duality, Reggeized absorption model 3−26305
- $K^\pm$, in pp inclusive reactions at 14.2, 19.2, 24.0 GeV/c, meas. of cross-sections 3−921
- $K^\pm$ e.m. form factors above φ resonance determ. in Novosibirsk colliding beam expt. 3−13873
- K_5, effect on particle-production ratios of e.m. and weak decays, importance as π source 3−38093
- $K_l{}^0$, from electrons on Be above 10 GeV, meas. of yield and absorption cross section on Pb 3−29214
- K°, differential cross sections for production in high energy π^-p, $K^\pm p$ interactions 3−898
- K*(1760) observation in the $K\pi$ system 3−32723
- $K^{*+}(890)$, production cross sections and parameters in K^+p interactions at 4.27 GeV/c 3−29262
- $K^{*+}(890)$ coherent production on nuclei, determ. of upper limit for radiative decay width $K^{*+} \rightarrow K^+\gamma$ 3−19741
- KK effect in $\pi\pi$ scattering, δ_{00} phase shift, coupled-channels model 3−38075
- $K^+n \rightarrow K^+\pi^-p$ at 9 GeV/c, obs. of S-wave structure in $K\pi$ spectrum 3−32721
- $np \rightarrow Kp$, weak production at low energies, $d\sigma/d\Omega$ estimates 3−6652
- pp annihilations into $\pi^+\pi^-$, K^+K^-, $\pi^+\pi^-\pi^0$, $\pi^+\pi^-$ + neutrals, 2150-2240 MeV 3−29261
- pp collisions, longitudinal momentum spectra of K^+, π^+ and inelastic protons, 22-5 GeV/c 3−14093
- $\pi N \rightarrow \Delta\pi\pi$, effects of KK threshold on π ang. distrib. 3−17094
- π^-p interactions, 20 GeV/c 3−35832
- $\pi^-p \rightarrow NKK^-$ reactions in generalised Veneziano model 3−19743
- $\pi + p \rightarrow K^+\Sigma^+$ backward scattering at 3.5 GeV/c, polarisation meas. 3−38082

kaon resonances *see meson resonances*

kaon scattering
- *see also kaon-baryon scattering*
- elastic differential cross sections in 0.9 to 1.9 GeV/C region 3−884
- K^+d, total cross sect. meas., 0.57-1.16 GeV/c 3−19731
- $K\Delta$ scattering, sum rules, finite-energy, based on ρ and ω exchange 3−23018
- KK, bootstrap calc. of φ and f′ using effective-potential method 3−32680
- Kp, possible new 1930 MeV Y* resonance 3−10786
- K^+p, hypercharge and isotopic-spin conservation constraints 3−26356
- $K\pi$, harmonic moments and amplitude zero interplay, resolution of anomalies 3−17096
- $K\pi$ amplitudes, crossing symmetric integral relations 3−10799
- $K\pi$ low-energy phase shift, determ. of bounds on $K \rightarrow \pi\mu(e)\nu$ scalar form factor 3−26288
- $K\pi$ phase shift and K_{l3} form factors 3−6580
- $K\pi$ scatt. and vacuum SU(3) symmetry 3−6563
- πK, phenomenological investigation, $\pi\pi$-KK partial waves 3−38076

kaons
- Adler-Weisberger sum rule, model-independent test 3−23013
- soft-k mass difference calc. in Weinberg model 3−26300
- K^- mass and polarisability determ. from kaonic atomic X-rays 3−29542
- K^0, nonlinear theory, time reversal and combined inversion *(Russian)* 3−38007
- $K^\pm$-K^0 3−32662
- K* and K_a, gauge model of vector-meson masses with broken U(3) × U(3) symmetry 3−35815

KDP *see potassium compounds*

Kennelly-Heaviside layer *see E-region; ionosphere*

keratin *see proteins*

Kerr electro-optical effect
- alkali halide, due to paraelec. defects, in stress-free crysts. 3−21386
- alkali halide, due to paraelec. defects, stress effects 3−21387
- benzene, liquid, Kerr consts. meas. 3−39121
- carbon tetrachloride, liquid, Kerr consts. meas. 3−39121
- freons, CF_2Br_2, CF_2Cl_2 and $CFCl_3$, temp. depend., sign change *(French)* 3−39120
- glass waveguide 3−32583
- h.v. meas. by laser and Kerr cell 3−3787
- liquids, interaction of vibr. enhancement and orientational Kerr effect 3−32590
- pentachlorodiphenyl, liq., relax. of elec. birefringence, temp. depend. *(French)* 3−24674
- polymer stiff-chain molecules in solution 3−21383
- self-focusing in optical glasses, relative contribution of Kerr effect and electrostriction 3−29149
- voltage meas. by interference band displacement in birefringent wedge *(Czech)* 3−3829
- CS_2, liquid, Kerr consts. meas. 3−39121
- CS_2, ultrafast Kerr effect, 10.6 μ, appl. to laser beam modulation 3−32581
- $KBr:OH^-$, due to paraelec. defects, in stress-free crysts. 3−21386
- $KCl:OH^-$, due to paraelec. defects, in stress-free crysts. 3−21386
- $KCl:OH^-$, due to paraelec. defects, stress effects 3−21387

Kerr magneto-optical effect
- film, early stage of high speed switching obs. 3−36740
- microanalyzer, for magnetic parameters 3−25814
- modified magneto-optic hysteresigraph 3−6034
- optical interferometry investigation 3−28559
- transverse, maximization 3−5178
- $CoCr_2S_4$, hot pressed, magneto-optic props., digital memory application 3−36858
- Fe garnets, equatorial Kerr effect rare earth sublattice effects *(Russian)* 3−12124

kicksorters *see counting circuits*

Kikuchi lines *see electron diffraction crystallography*

kinematic viscosity *see viscosity*

kinematics
- *see also acceleration; ballistics*
- air track relative motion car, demonstrations 3−28440
- anomalous thresholds, kinematical interpretation 3−17210
- 3C 279 radiosource components, relative angular velocity and kinematical analysis 3−28222

kinematics continued
- classical transmission angle problem of Alt, for four-bar linkages 3−35565
- comets, type I ion tail axes rel. to kinematics and irregularities observed from photographs 3−28159
- droplet growth kinetics by condensation with adiabatic expansion of air *(Russian)* 3−14507
- elastic-plastic finite strains 3−35574
- Eulerian dynamics of rotating rigid body, construction in Hilbert space, reln. to time-independent Schrodinger eqn. 3−19489
- galactic structure, coincidences in spiral arm tracers 3−39725
- galaxies, nonaxisymmetric kinematics with axisymmetric mass distrib. 3−31736
- Large Magellanic Cloud, kinematics of 27 planetary nebulae 3−13083
- Markarian 78, galaxy with u.v. excess, spectroscopic observations of mass motions 3−28259
- NGC 3109, irregular galaxy, distrib. of neutral H and vel. field determ. 3−28268
- NGC 598 (M33), props. of neutral H, 21 cm obs. 3−28270
- optical tracking systems, analysis of pointing and tracking, null image motion 3−37623
- sea ice pressure ridge formation, kinematic model 3−15855
- Small Magellanic Cloud, kinematic properties of 30 H II regions 3−28263
- Thomas precession, physical explanation 3−14
- two-level system with diffusion-modulated interaction 3−6373
- $pp \rightarrow cX$ ($c = p, p, \pi\pm, K^\pm$), single particle production spectra, scaling predictions sum rules and kinematics 3−29265
- H I regions, kinematics of local component rel. to Gould's Belt 3−37488

kinematography *see cinematography*

kinescope *see television picture tubes*

kinetic theory
- *see also Boltzmann equation; collision processes; intermolecular mechanics; kinetic theory of gases*
- atomic kinetic energy evaluation from neutron scatt. expts. 3−38527
- binary mixtures, Thorne's modified eqn., transport coefficients 3−28983
- classical systems, exact kinetic eqn. 3−22763
- dissipative system, in presence of mag. field, first integral of kinetic equation 3−33333
- electron density fluctuations in a magnetised, collision-dominated plasma in an electric field 3−15996
- equation for hard sphere correlation functions 3−26148
- finitely extendible dumbbells, dilute suspensions 3−6345
- fluctuations of occupation numbers, kinetic eqns. *(German)* 3−22737
- ions, in elec. field, energy partitioning 3−33332
- Lennard-Jones liquid near triple point, computer expt. on 864 particles 3−38657
- linearized Balescu-Lenard operator, spectral properties 3−7480
- liquids, u.s. propag., effect of anomalies of kinetic coeffs. near crit. points 3−33610
- magnetoactive plasma, electromagnetic wave reflection on boundary 3−23829
- memory functions involving projection operators, integral eqns. 3−13638
- mixture of gas and small spherical solid particles, flow, Boltzmann eqn. calc. 3−33290
- molecular chaos and Boltzmann eqn. *(French)* 3−32436
- negative glow, kinetic theory 3−36221
- one particle distribution function, kinetic eqn. *(Russian)* 3−10384
- particle density in μ space, new kinetic eqn. determ. from Boltzmann eqn. 3−32457
- plasma, classical non-ideal, rel. to kinetic equations 3−33334
- plasma, gravitational, polarisation electric field origin, kinetic theory derivation 3−29935
- plasma drift kinetic equation recursive derivation 3−14513
- plasma electron angular distribution, kinetic equation with retarding potential *(Russian)* 3−7482
- plasma ion scattering by resonant symmetric charge exchange near an electrode, ion distribution function 3−23815
- plasma Langmuir wave dispersion, kinetic eqns. *(Russian)* 3−29987
- plasma probe, spherical, characteristics for a collisional plasma calc. from kinetic theory and two-side distribution function 3−30016
- plasmas, dense, light scattering theory 3−38422
- radial-limited plasma-electron stream system with preset plasma radial-heterogeneous configuration, space in stability *(Russian)* 3−11463
- self-diffusion, fully renormalized kinetic theory 3−10383
- semibounded plasma, fluctuation theory, surface oscillations *(Russian)* 3−11464
- solid in stationary temp. gradient, kinetic equations and brownian motion 3−1817
- spatially homogeneous gravitating medium, kinetic theory of small perturbations 3−37311
- stability theory of stationary states, kinetic model *(German)* 3−612
- stochastic dynamic systems, power transfer among modes of oscillation 3−16743
- time correlation functions and structure of kinetic equation 3−26149
- time-dependent spin correlations in anisotropic systems, solution of the high temp. kinetic eqns. in the presence of a crystal field 3−18281
- time-dependent spin-correlation functions in anisotropic systems, infinite temp. kinetic eqns. in the presence of a crystal field 3−18280
- variational method for kinetic coefficients calc. *(Russian)* 3−28991
- velocity autocorrelation, fully renormalized kinetic theory 3−13639
- He liquid, atomic kinetic energy evaluation from neutron scatt. expts. 3−38527

kinetic theory of gases
- *see also association of gases; Brownian motion; collision processes; diffusion in gases; equations of state; intermolecular mechanics; Joule-Thomson effect*
- accommodation coeffs. in viscous interaction region of hypersonic slip-flow boundary layer 3−23755
- binary mixture, Bhatnagar-Gross-Krook model, appl. 3−38336
- Boltzmann eqn., collision duration correction, quantum mech. derivation 3−6369

kinetic theory of gases continued
- Boltzmann eqn., long-lived collisions, effects 3−6368
- Boltzmann eqn. for reaction gas mixture, approx. soln. *(Russian)* 3−7299
- Boltzmann equation for monatomic gas, derivation with adiabatic switching-off of interactions 3−4043
- Carnahan-Starling eqn., real gas, crit. parameters effect 3−37916
- Chapman-Enskog kinetic theory of gas diffusivity, anomalous B diffusion in Si, effect of inert gas 3−39257
- dense gas, phase-space density correlation function 3−37892
- equilibrium tendency and linear approx. *(French)* 3−14407
- Fokker Planck eqn., stochastic effects of plasma electron cyclotron resonance heating 3−17637
- heat cond. for mixtures of dilute gases of linear diamag. mols. in mag. field 3−4510
- irreversible processes, linear Rayleigh gas model 3−32449
- Knudsen permeability, temp. depend. developed from kinetic theory relations 3−7471
- Maxwell theory, rigidity of gas, application to simple shear problem 3−38337
- mixed oxide fuel pins, elimination of CO_2 and H_2O as O_2 transport species, kinetic calculations 3−17323
- molecular gas dynamics, boundary conditions, surface shocks, continuum flows, review 3−33261
- molecular transmission probability in a plane channel, wall roughness influence *(Russian)* 3−7398
- partially ionized, rel. to theory of elec. cond. and Hall coeff. in mag. field, theory *(Czech)* 3−4518
- photons and particles joint diffusion in a semi-infinite vacuum, excited atoms distribution kinetic eqn. *(Russian)* 3−23478
- plasma, two-dimensional, magnetised, Balescu-Lenard limit 3−20420
- plasma, two-dimensional, magnetised, limit of a very large magnetic field 3−20421
- plasma collisional transport theory for a two dimensional guiding centre plasma 3−20436
- polyatomic gas mixtures, kinetic equations of vibrational energy relaxation *(Russian)* 3−29755
- polyatomic gases and molecular mixtures, relax. and transfer processes *(Russian)* 3−7257
- polyatomic transport processes in inhomogeneous electric and magnetic fields, kinetic theory calc. 3−26764
- rarefied gas, kinetic equation deriv. Liouville equation 3−34721
- relativistic dissipative media, sound dispersion and absorpt. 3−33184
- small spheres motion in gases, theory 3−14477
- small spheres motion in gases, thermo-phoresis, diffusio-phoresis and related phenomena 3−14478
- solar wind proton gas, comparison with hydrodynamic model 3−16135
- thermodynamic equilibrium states, kinetic eqns. for the Green functions 3−22742
- wetting hysteresis effect on equations of state of a gas trapped by liquid in a capillary, kinetic eqns. 3−20925
- ^{3}He, n.m.r. relax. time, kinetic theory calc. 3−38307

kinetic theory of liquids *see kinetic theory; liquid theory*

kinetics *see kinematics*

kinetics of chemical reactions *see reaction kinetics*

kink bands *see dislocations*

Kirchhoff adders *see adders*

Kirkendall effect *see diffusion in solids*

klystrons
- *see also reflex klystrons*
- electrostatically focused, processing by non-evaporable getter-ion pump 3−19183
- multi-stage bunching, kinematic theory 3−13772

Knight shift
- alkali binary liq. alloys, Knight shifts, Pauli susceptibilities, from contact density in pseudopotential 3−34234
- alkali metal, press. effect, calc. by KKR method 3−36806
- alkali metals, Knight shifts, Pauli susceptibilities, from contact density in pseudopotential 3−34234
- cubic crystal, Knight shift anisotropy and spin orbit coupling 3−15434
- liquid metal, temp. depend. calc. rel. to Debye-Waller correction to theoretical interference function 3−24016
- multiple-pulse techniques, application 3−8466
- n.m.r., sweeped multiple pulse sequence technique for shift meas. in solids 3−2332
- oscillations in crossed fields 3−18382
- rare earth beryllium intermetallics, ^{9}Be relax. and mag. moment dynamics 3−2444
- transition metal/hydrogen systems, electron-nucl. interactions 3−2439
- Al-Cr(Mn) dil. alloys, n.m.r. spectra, satellite struct. interpret. 3−2431
- $AuGa_2$, $Au_{0.95}Pb_{0.05}Ga_3$ and $AuIn_2$, solid and liquid meas. 3−21334
- Be, value of diamagnetic Knight shift and its anisotropy 3−18380
- Bi-Sn alloys, liq., n.m.r. linewidths, conc. depend. 3−2412
- Cd-Hg(Mg) alloys, ^{113}Cd n.m.r., alloying depend. 3−2433
- Cd-Hg(Mg) alloys, of ^{113}Cd, Knight shifts, alloying depend. 3−2433
- $Ce_{1-x}R_xAl_3$(R=Y,La), n.m.r. and mag. susceptibility 3−27434
- Cr_2Al_{11}, temperature dependence measurements, magnetic susceptibility 3−36807
- Ga liquid, quadrupole and Knight shift relax. of ^{71}Ge, 40-1050°C 3−2434
- γ-$Li_{1\|x}V_3O_{8\|\lambda}$, ^{7}Li magnetic resonance study, Knight shift and second moment determ. 3−39044
- $Mn_{1-x}Fe_xBe_2$, of ^{9}Be 3−2436
- Na, liquid and solid, temp. depend. in nearly free electron approx. 3−8468
- NbAl alloys, obs. and rigid-band model approach 3−18381
- $Pb_{1-x}Sn_xTe$, meas. for characterisation of single zone annealed sample 3−24619
- PbTe, meas. for characterisation of single zone annealed sample 3−24619
- Si, heavily-doped, metal-nonmetal transition study 3−21333
- $SmAl_2$, ferromag., crystal field effect 3−15322
- $SmSn_3$, antiferromag., crystal field effect 3−15322

Knight shift continued
- $V_3(Ge_{1-y}Ga_y)$, $V_3(Ge_{1-y}Al_y)$, and supercond. T_c conc. depend. *(Russian)* 3−8288
- VO_2, metallic phase, n.m.r. spectrum interpret. 3−2432
- VS, V_3S_4-V_2S_3 and V_5S_8, correl. with states of d-electrons 3−27355
- $V_3Si_xGe_{1-x}$, supercond., conc. depend. *(Russian)* 3−18242
- Zr-Sc-H alloy system, p.m.r. obs., exchange interactions *(Russian)* 3−36805

Knudsen flow
- Boltzmann eqn. at large Knudsen no., asymptotic theory 3−14472
- diffusionphoresis of volatile aerosol particles in slip conditions, depend. on Knudsen number 3−34663
- gas permeability through porous medium, temp. depend. developed from kinetic theory relations 3−7471
- molecular gas dynamics, boundary conditions, surface shocks, continuum flows, review 3−33261
- polyatomic gas layer, BGKM method, parietal temp. discontinuities *(French)* 3−29888
- rarefied gas thermal in a circular tube 3−38395
- rectangular duct of finite length *(Russian)* 3−14475

Knudsen number *see Knudsen flow*

Kohn effect *see lattice dynamics*

Kondo effect
- alloy with Ce and Yb impurities, rel. to cryst. field 3−2256
- Anderson model of superconductivity, perturbational calc. of s-electron Green function 3−5071
- charge density oscillation around resonant scatt. impurities 3−4961
- conduction electron Green's function, use of pseudo-fermion representation 3−614
- dilute alloys, temperature variation with nature and concentration of solute metal 3−36710
- dilute alloys polarised neutron scattering by impurities, Kondo effect, spin fluctuations, inelastic phenomena, survey 3−21224
- dilute mag. alloys, elec. resist. rel. to localised mag. moment exchanges, RKKY s-d exchange model 3−30439
- dilute magnetic alloys, homogeneous dynamical susceptibilities 3−12004
- divergence in the RKKY interaction 3−18299
- local spin fluctuation systems, long range correlations 3−15352
- magnetism, introduction to the theory, monograph 3−2224
- metal, resist. due to 3d impurities, s-d interaction model 3−2042
- numerically solvable Kondo model 3−36712
- rare earth alloys, role of crystal field 3−30446
- scattering from mag. impurity pair, Kondo temp. for ferromag. and antiferromag. pairs 3−21217
- superconductor with mag. impurities, behaviour near T_c 3−5073
- thermodynamics of s-d metal with mag. impurities at low temp. path integral method 3−34101
- two impurity Kondo effect theory with impurity impurity exchange interaction 3−15350
- type II superconductors containing magnetic impurities 3−11973
- Au-Co, quasielastic neutron scattering cross section for paramag. impurities 3−5095
- Au-V, quasielastic neutron scattering cross section for paramag. impurities 3−5095
- Au-Yb, negative s-f interaction 3−24561
- AuMn(V), localised spin fluctuation and Kondo system, resist. temp. depend. 3−36582
- Cu-Au(Fe), specific heats of dilute magnetic α-phase alloys 3−21218
- Cu-Fe alloy, dil. temp. depend. of resist. *(Russian)* 3−8152
- Cu-Fe alloy, dilute, Kondo temp. conc. depend. 3−21216
- Cu-Fe dil. system, eqn. of state from phenomenological model 3−5096
- Cu-Fe dil. system, far-i.r. surface resist. 3−5046
- $Cu_{1-x}Au_x$-Fe(Cr), mag. field depreciation of Kondo magnetoresist. 3−33872
- (La, Ce)Al_2 dilute alloy with Ce impurities, superconducting-Kondo system, specific heat 3−5072
- La:Ce, cubic crystalline field effect on magnetic susceptibility rel. to Kondo effect 3−24560
- $La_{3-x}Ce_xAl$, specific heat jump of superconducting-Kondo system 3−30558
- $Ni_{41}Pd_{41}B_{18}$:Cr, amorphous, elec. resist. meas. showing Kondo effect 3−33869
- PdCr, interimpurity interaction effects below spin fluctuation temp., elec. resist. meas. 3−15348

Kramers-Kronig relations *see dielectric properties of substances; optical constants*

Kramers systems *see determinants*

Kromayer lamps *see mercury vapour lamps*

krypton
- adsorption on graphite with preadsorbed NO, 77.5 K 3−38720
- atom, collisions, with Fl ions at 35.7 MeV, dependence of X-ray production cross sections on ionic charge state 3−1129
- atom, excited state, quadrupole moment calc. 3−29487
- atom, inner-shell ioniz. cross sections by 1.5-5.0 MeV protons 3−33047
- atom, polarisability and shielding factors, effective-field calc. 3−29488
- atom, X-ray absorption spectrum, 8-0.8 keV, determ. of mass-attenuation coeffs. by continuous analysis 3−4364
- atom charge exchange collisions with H^+, spin polarisation 3−35978
- atom electron-impact excitation of p-levels *(German)* 3−1124
- Auger spectra, high resolution, $L_{2,3}MM$ and $M_{4,5}NN$ 3−17364
- charge changing and electron loss cross section for C^{4+} (N^{4+}) ions in Kr gas 3−11178
- collisions with He atoms, electron loss 3−11166
- collisions with Hg atoms, depolarisation of Hg resonance radiation 3−33060
- crystal, epitaxially grown on Nb (100), inelastic scatt. and energy loss spectra 3−11655
- crystal, epitaxially grown on Nb (100), LEED and absorpt. 3−11654
- crystals, force constants and phonon dispersion, theoretical parameters 3−38645
- fast atoms and ions, impact dissoc. into ions of O_2, CO and NO molecules 3−23621
- glow discharges, electron energy in Faraday dark space 3−30040

krypton continued
implantation in Si, Ge, GaAs and GaP, ion conc. profile and ion range probability distrib. 3−11647
ion, implanted in Si, Ge, GaP and GaAs, ion collection, saturation effects 3−11646
ionisation-relaxation time meas. following shock heating *(German)* 3−11434
ions, multiply charged, plasma parameters determ. for plasma-beam discharges 3−23916
isotopic composition in terrestrial materials 3−5429
isotopic thermal diffusion factors from column meas. 3−23663
labelled, adsorption study of powder surfaces, differential standard entropies and isotherm shape determ. *(French)* 3−27175
laser, pulsed, multi-mode operation *(German)* 3−29073
muonium hyperfine interval, precision meas. 3−33067
pair potential from second virial coeffs. 3−7268
Percus-Yevick integral equation for dense fluid, soln. with Kihara potential 3−17483
4p photoelectron angular distribution, far u.v., using synchrotron light source 3−29507
photoionisation cross section, in vicinity of outer d-subshell threshold 3−29509
plasma, continuous, sustained by focused high-power CO_2 laser 3−36187
plasma-beam discharge laser 3−32555
potential parameters and combination rules, determ. from diffusion data 3−1293
quadrupole relax. mechanism of ^{83}Kr 3−1115
radiative lifetime meas. for neutral atoms and ions by beam foil spectroscopy at low initial ion energies 3−17348
reactor fuel element reprocessing, off gas treatment and krypton disposal 3−32967
reactor fuel reprocessing, krypton removal by selective absorption 3−32970
resonance transitions, self broadened absorption linewidths 3−29491
self diffusion coefficient, density depend. 3−17489
self-diffusion at intermediate density 3−14410
solid, elastic consts. from neutron diffr. by acoustic phonons, 77 K 3−27049
solid, excitonic effects on valence absorption edge 3−33849
solid, luminesc. spectra *(Russian)* 3−5236
solid, Raman two-phonon spectra, mol. dynamics 3−34353
Ar:Kr, far. i.r. absorpt. spectra at 2K 3−2574
Ar-Kr coagulator, basics 3−32245
Ar-Kr mixed ion cw laser, current depend. of spontaneous emission 3−32539
CO_2-Kr mixtures, relaxation of bending vibration 3−23537
$H^+ + Kr$, elastic differential scattering expts., investigation of one state molecular system 3−11185
He-Kr gas mixture, hypersonic vel. and absorpt. meas. from Brillouin spectra 3−1322
He + Kr, vapour + solid equilibrium 3−33663
Kr I, meas. of lifetimes of levels excited by short electron pulse using delayed coincidence technique 3−4361
Kr II, laser, molecular absorp. of three lines by $^{127}I_2$ *(German)* 3−36010
Kr II, meas. of lifetimes of levels excited by short electron pulse using delayed coincidence technique 3−4361
Kr-Ar liquid mixtures, shear viscosity calcs. 3−38677
Kr-Hg gas mixture, possible u.v. laser *(German)* 3−725
Kr-methane solid phase diagram, X-ray determ. 3−24244
Kr-Ne(Ar) mixtures, thermal diffusion, temp. and comp. depend. 3−36070
Kr-Xe, Kr-Ar solid solutions, cathodoluminescence 3−18504
$Kr + CO^+ \rightarrow CO + Kr^+$, 0.04-3 eV 3−20058
Kr + CsF, integral total cross sections meas., attractive pot. investigation 3−38324
Kr^+-Kr collision, 50-200 keV, X-ray production 3−29526
$Kr^+ + CO \rightarrow Kr + CO^+$, 0.04-3 eV 3−20058
$Kr^+ + Kr \rightarrow Kr + Kr^+$, 0.04-3 eV 3−20058
$Kr^{(+)} + Kr$, ioniz. processes in slow collisions 3−26605
KrI, ioniz. pot. and $4s4p^6nl$ levels 3−26576
^{85}Kr atmospheric dosimetry 3−5683
Ne + Kr, solid-vapour and liquid-vapour equilibrium 3−14996
O_2-Kr mixture, viscosity meas. 3−38342

krypton compounds
KrF_2, HeII photoelectron spectra, band assignments 3−23542
KrF_2 crystal structure, X-ray diffraction meas. at −80°C 3−36289

Kuhn-Thomas sum rule *see molecular electronic structure*

Kurie plots *see beta-decay theory*

Kyropoulous method *see crystal growth*

laboratories
see also acoustical laboratories
Bell Laboratories' work on optical communication 3−691
Bell Laboratories' work on optics, TV and vision 3−3545
clinical laboratory data transmission using PDP-15 and PDP-8/E computers 3−26005
electronics education and training at physics research laboratory for untrained personnel 3−28627
electronics project-type undergraduate lab using op-amps 3−9795
instrument laboratory for rent to small Norwegian companies *(Norwegian)* 3−5740
lunar, at Sheffield Univ., for anal. of rock and soil samples 3−5585
practical physics preliminary course, using programmed instruction 3−9792
program suitable for a course in physics for nonscience majors 3−16357

laboratory apparatus and technique
see also high-pressure techniques; high-temperature techniques; low-temperature techniques; optical design techniques; optical workshop techniques; vacuum techniques; X-ray apparatus
absorption and desorption isotherm meas., fully automatic apparatus *(German)* 3−16531
aerodynamic body surface, pressure distribution meas. using special interrogator 3−32270
air-glass-air system, verification of Fresnel and Airy equations 3−37
apparatus for investigating the electrical props. of ferroelectrics *(Russian)* 3−6016

laboratory apparatus and technique continued
astronomical, Earth orbital and rotational motion 3−3743
chemostat, fementor usable as continuous culture apparatus 3−3873
clinical chemical analysis, automation *(German)* 3−10204
cloud chamber, diffusion, design and construction for demonstration purposes 3−28680
Compton scatt. expt., teaching apparatus 3−45
cooling vessel for low-pressure discharge tube with liquid N_2 *(Czech)* 3−25934
correlation micro-pickup for meas. of pressure fluctuations in turbulent boundary layer 3−32271
cryostat low-cost instrument, construction and operation 3−9808
crystal growth, manual 3−9815
crystalliser, well stirred isothermal, stability analysis 3−34717
current integrator with digital read-out, circuit description 3−28452
differential thermal analysis apparatus, simple design *(Japanese)* 3−13249
ebulliometric system for measuring liquid vapour pressures *(Spanish)* 3−28505
edge error correction in lineal analysis, reply to comment 3−28729
edge error correction in lineal analysis, using TV for solid structure examination 3−28728
electrochemical electrode processes and adsorption study, special techniques, review 3−12533
flameless mounting of crystals in capillaries 3−17715
fluidity meas. in metal casting 3−12487
focal length of diverging lens, simple method of meas. 3−43
Gedanken experiment, action and reaction in relativistic system 3−36
Genap III, random binary digit generator 3−37727
hydrogen uptake detection method using anodic oxidation at bipolar electrodes 3−12522
instrument displacement controls, viscous drive device 3−37584
integrated circuit operational amplifier in introductory course 3−9807
leaf electrometer with charge polarity discrimination 3−44
light, vel. meas. 3−32012
linear air track, double spark source 3−39
magnetic properties investigation of thin weak magnetic films *(Russian)* 3−25820
metallographic polishing, simplified technique 3−21655
MHD slow-mode shock waves, launching method, expt. and model 3−33353
micro differential thermal analysis and evolved gas detection, simultaneous meas. apparatus *(Japanese)* 3−13251
micro thermal analyzer, Shimadzu, sample sealer and crimper *(Japanese)* 3−13250
micro thermobalance, Shimadzu TGA-20B, applications *(Japanese)* 3−13519
paddle device for removal of temp. gradients in n.m.r. spinning tubes 3−6046
permeation device for preparation of trace gas mixtures 3−13523
polystyrene monodisperse aerosols production with a spinning disc 3−28800
small pulse-operated X-ray apparatus for schools and laboratories *(German)* 3−37726
solid state track detector for ^{235}U content in natural U determ., undergraduate expt. 3−9814
sorption apparatus for diffusion studies with molten polymers 3−32215
sound level meter 3−48
specimen holder and air lock, for use in high vacuum field ion microscope 3−13461
spectroscopy of laboratory plasmas rel. to astrophysics, review 3−18917
splat-cooling apparatus for non crystalline solids preparation 3−9005
steel research, X-ray analysis, computerised *(Japanese)* 3−28740
tensile testing, machine 3−51
thermal expansion corrections when ΔT is not small 3−9844
thermomechanical analyzer, Shimadzu TMA-20B, application *(Japanese)* 3−13252
thermometer clamp, for low temperature thermal conductivity 3−5810
tritium removal from laboratory air 3−39821
uniform microsphere production 3−28710
u.s. appl. in medical laboratory practice 3−25973
Si, ion implanted, anodic oxidation, sample holder 3−37662

labryrinth speakers *see loudspeakers*

Lamb shift *see atomic spectra*

lambda point *see liquid helium-4; superfluidity*

laminar flow
anisotropic porous media, analysis of dispersion tensor using random walk model 3−7472
around small cylindrical bodies, evaporation of moisture, heat and mass transfer 3−1791
asymmetrically developing flow in ducts, press. drop anal. 3−1352
bearings, fluid film lubrication, fluid mechanics, review 3−33326
Bingham plastic, transient free convection on vertical flat plate 3−26796
blood, through tapered tubes, expts. 3−9647
blood circulation, peripheral, rheodynamic model for Fahraeus-Lindquist effect and flow in capillaries 3−17497
boundary layer, along concave wall, laminar flow instability, development of turbulence *(German)* 3−26815
boundary layer, disturbance propagation 3−38382
boundary layer, natural instabilities, rel. to wall deform. *(French)* 3−7367
boundary layer, over oblating surfaces, nonsimilar soln. 3−1341
boundary layer, perturbation response and propagation of disturbances 3−38381
boundary layer at crit. pt. of indestructible body washed by flow of ionized air 3−23737
boundary layer development, rear stagnation point on cylinder 3−4581
boundary layer eqns., approx. solns. in presence of blowing 3−23736
boundary layer flow over small hump on flat plate 3−29872
boundary layer in laminar inlet flow, velocity profiles 3−11374

laminar flow continued
boundary layer two dimensional flow with applied pressure gradient, asymptotic analysis 3—14451
boundary layers with suction, velocity distribution calc. by Shvets-Targ method 3—33226
boundary-layer separation from moving boundaries 3—33236
boundary-layer theory, two dimensional steady flow, incompressible fluid medium, review 3—33235
buoyancy-induced flows, instability, transition and turbulence, review 3—33217
circular pipe orifice, numerical study of fluid motion 3—33197
circular vortex ring with density difference under gravity, flow patterns 3—20330
closed streamlines associated with channel flow over cavity 3—7332
compressible boundary layer flow on moving continuous surfaces, parametric study 3—26805
compressible conducting fluid, MHD laminar source flow between two parallel discs 3—26832
compressible fluid, heat transfer, hydrodynamic resistance, turbulent and laminar flow in circular tube 3—36080
compressible laminar boundary layer flow at a three-dimensional stagnation point with intensive suction or injection 3—33234
condensate film flow down a vertical wall, stability 3—14433
condensate liquid film flow down inclined wall, stability characteristics 3—33233
confined jet mixing in circular channel, arbitrary entrance vel. distrib. 3—4528
convection, natural, around plane plate in incompressible fluid *(French)* 3—26776
convection, unsteady, in uniformly heated vertical pipes 3—20308
convection between two parallel vertical walls, stability 3—36075
convective, combined free and forced, in inclined tubes, numerical soln. 3—23681
convectively cooled pipe, correction on the length of ice-free zone 3—20300
coolant throughflow in a rotating, shrouded, parallel disc system 3—20328
critical Reynold's number of Orr-Sommerfeld eqn. 3—23679
cylinder moving in stratified fluid, flow field ahead 3—4572
cylinder with square cross-section, stagnation and reattachment line determ. 3—26773
cylinders, rotating, numerical solutions 3—11376
detachment forces for particles submerged in laminar layer 3—33294
dilute aqueous polymer solns., laminar natural convection heat transfer 3—4542
duct, acoustically induced vibrations of rods 3—35339
dynamic behaviour of tubes subjected to internal and external axial fluid flow 3—17514
elliptical flows of elastic fluids 3—17513
entrance region flows, inelastic fluids loss coeffs., prediction method 3—17506
falling liquid films stagnant band analysis 3—33228
film condensation, vapours, turbulent flow, heat transfer coefficient, pressure gradient 3—1347
film condensation due to rotating disc 3—14439
film condensation with suction 3—11414
fluid in pipe, energy dissipation due to sudden enlargements and contractions, head loss, interpolar formulae *(Italian)* 3—7350
fluids, three-dimensional boundary layer flow, regular solid surfaces, ducts, review 3—36113
forced, between parallel plates, heat transfer, effect of magnetic field 3—14431
forced turbulent convection in circular tubes, reverse transition from turbulent to laminar flow 3—38359
free convection, from rotating radial plate 3—23718
free convection, in closed spherical containers 3—23716
free convective over isothermal nonconducting plate in transverse magnetic field 3—38403
gas, conductance, by dynamical method *(German)* 3—28796
gas flow, heated laminarizing, in square ducts 3—36082
gas mixtures, laminar, rotational, turbulent and exhaust jet flows, laser-Doppler velocimeter, review 3—32281
generalised Couette flow of an elastico-viscous liquid between two co-axial porous circular cylinders 3—38378
gravitational ideal incompressible fluid about fine profile limited to free line *(French)* 3—29830
gravitational ideal incompressible fluid about fine profile limited to free line *(French)* 3—29831
Hartmann flow, stability *(Russian)* 3—1423
Hartmann flow stability *(Russian)* 3—26833
heat exchanger, parallel plate, with turbulent flow on one side and laminar flow on the other, calc. of heat transfer parameters 3—22276
heat transfer, extended Graetz problem, higher eigenvalues determ. 3—10415
heat transfer in periodic boundary layer near 2 dimensional stagnation point 3—14462
high speed flows heat transfer steady state disturbances in compressible laminar and turbulent boundary layers 3—38354
horizontal tubes in transition regime, interaction of free and forced convection 3—23700
human portal vein, streamline flow 3—29925
hypersonic boundary layers, displacement interaction and surface curvature effects 3—38372
ideal fluid, flow past body with reverse stream 3—33198
incompressible, fast paraboloid of revolution, numerical solns. 3—1340
incompressible conducting laminar flow along a vertical wall, transverse mag. field effect 3—17546
incompressible liquid between rotating discs *(Russian)* 3—14432
incompressible viscous fluid in entrance of converging channel 3—26770
instability, force field theory 3—36072
isobaric laminar boundary layer flow, vectored injection 3—26814
isothermal, Newtonian fluids, through abrupt contraction 3—7319
jet, cylindrical laminar liquid, ejecting into a gas, heat transfer 3—38417
jet, elliptical 3-dimensional orifice, viscous energy transfer, numerical analysis 3—4527
jet, submerged laminar, vel. profiles in exit region 3—4534

laminar flow continued
jet, viscous, stability, ambient gas influence 3—20411
jets, thrust measurement apparatus 3—3923
jets, unsteady viscous flow into stationary surroundings, numerical calc. 3—33308
Joule-Thomson effects on thermal entrance region heat transfer in pipes with uniform wall temperature 3—20302
laminar forced convective flow and heat transfer in triangular ducts 3—1343
laminar free convection stagnation heat transfer, isothermal cylinder with internal sources/sink 3—26774
laminar jet mixing with and without free stream, numerical soln. 3—26848
laminar-turbulent transition as Sturm-Liouville eigenvalue problem 3—33199
linear flow model, residence time distrib. anal. for parameter estimation 3—17507
liquid film, wavy, heat transfer through 3—7320
liquid film falling on sphere, gas absorption 3—4535
liquid in channel, complex heat transfer calcs. 3—23692
magnetic boundary layer theory 3—38377
Magnus effect, influence of boundary-layer stability 3—36102
mass transfer in co-current laminar gas flow in wetted-wall tower *(Japanese)* 3—23680
mass transfer in drag reducing fluid systems 3—11384
mass transfer in sublimation by laminar free convection *(German)* 3—26801
MHD, in plane duct, effect of travelling magnetic field *(Russian)* 3—7422
MHD channel flow of electrically conducting Prandtl-Eyring fluid in magnetic and electric field *(German)* 3—38400
MHD free convection laminar flow of an elastico-viscous fluid along an infinite porous wall 3—20375
MHD geometry 3—7411
mixed convection problems 3—1356
modulated plane Poiseuille flow, energy balance 3—4546
multiphase, between parallel plates, heat transfer 3—1475
natural convection, influence of various surface roughness 3—20297
natural convection boundary layer flow over horizontal and slightly inclined surfaces 3—38379
natural convection in vertical cells of rectangular cross section, expt. study 3—14447
Navier-Stokes eqns., invariant solutions calc. *(Russian)* 3—29839
Navier-Stokes eqns. for viscous incompressible flow through orifice, mathematical analysis 3—20268
Navier-Stokes eqns. in inlet regions, numerical solns. for two-dimens. flow 3—20273
Newtonian fluids in circular pipes, motion energy dissipation on heat transfer 3—23708
Newtonian in open channels, surface tension effects 3—23674
non-Newtonian, momentum transfer coeffs. use 3—38349
non-Newtonian behaviour in ducts of unusual cross section 3—7327
non-Newtonian fluids, laminar pulsed flow 3—33265
non-Newtonian liquids, laminar pulsed flow 3—33266
non-Newtonian two-phase flow in pipes, hydrodynamics 3—33283
non-viscometric, with proportional stretch histories 3—38330
nozzle flows, design 3—23807
ocean, past island, application to Bermuda 3—5483
oil pipe line, influence of volume tank on oil hammer and transients response 3—17505
oil pipeline, studies on oil hammer and transient response 3—17504
open-channel flow, longitudinal dispersion, turbulent mixing, review 3—33215
Poiseuille, plane, subcritical bifurcation 3—38351
Poiseuille flow and thermal conductivity of phonons in dielectric films 3—1722
Poiseuille flow simulation 3—7337
Poissonian type, pot. created and vel. induced by uniform source distrib. on polygon *(French)* 3—4529
polarizable liq., induced viscosity changes theory 3—14441
polymer, hydrodynamic analysis of hot rolling 3—25001
polymer solutions, frictional resistance of rotating disc 3—17503
potential, about arbitrary three-dimensional bodies, direct integral equation method of analysis 3—33196
power law fluids, inertia effects in laminar radial flow 3—29832
power-law fluids flow behaviour in entrance region of annuli 3—36106
rarefied gas between parallel plates, Poiseuille flow and thermal creep 3—38394
relativistic Navier-Stokes eqn., plane solns. for laminar incompressible and compressible flows 3—17556
secondary, in curved tube 3—20270
seepage flow, transition zone between laminar and turbulent flow *(Japanese)* 3—38367
shear flow, breakdown mechanism, kinematic wave theory 3—14454
shear layer transition and excitation by sound excitation, turbulent breakdown 3—14453
shockless axisymmetric with heat addition, analysis 3—38353
single rock joint, hydrodynamic dispersion of contaminant 3—21863
slender-wing aircraft, nonlinear lateral oscillations investigation 3—11377
slot injection into a supersonic laminar boundary layer 3—14463
slow viscous flow down inclinded plane, similarity soln. 3—38350
spherical-cap bubbles, wake structure, review 3—33324
over spillway crest, finite element analysis 3—33195
spiral flow in a porous pipe 3—29862
stability and transition turbulence 3—4539
stability of two-dimens. flow, Taylor-Goldstein eqn., Howard's technique 3—23676
stationary, of perfect fluid, variational inequality *(French)* 3—20269
steady above horizontal line heat source, numerical solution *(Japanese)* 3—23684
steam, in vertical tube, heat transfer, condensation and pressure drop 3—17517
streaming solutions, mass transfer hydrodynamics 3—1355
subsonic incompressible flow, computer simulation methods 3—23727

laminar flow continued
suddenly started laminar flow of power-law fluids in the entrance region of a straight channel 3—20335
supercritical, in divergent channel 3—20359
supersonic viscous flow over a yawed circular cone 3—38384
with surface reaction, thermal simulation *(French)* 3—20322
three dimensional body, singularities near edge or corner 3—20267
three-dimensional, on highly swept hypersonic wings, nonequilibrium boundary layer 3—23730
transient free-convection horizontal laminar flow between heated parallel plates, heat transfer 3—14443
transition region from laminar to turbulent flow of dilute polymer solutions 3—7345
transition to turbulent flow in boundary layer at plate 3—4577
tubular flow involving endothermic chemical reaction, calc. of heat transfer coeffs. *(Dutch)* 3—29926
turbulence, in tubes, origin and development, expt. obs. 3—33205
turbulent shear flows, low Reynolds number phenomena, two-equation model 3—38356
two dimensional viscous MHD, in coaxial channels *(Russian)* 3—7419
two-dimensional heated laminar jet, temp. distribution 3—36145
two-dimensional laminar compressible flows with embedded shock waves, Navier Stokes eqns. numerical soln. 3—26822
two-stream plug flow processes, optimal control 3—4541
ultimate heat transfer limit of cylindrical heat pipes, theory 3—14436
unsteady boundary layer flow along flat plate, similarity solution 3 -11413
unsteady convective diffusion with interphase mass transfer, miscible dispersion theory 3—33292
unsteady laminar boundary layer with suction or blowing 3—33223
vapour flow, film condensation, momentum transfer, hydrodynamics 3—1346
variable properties laminr gas flow heat transfer in the entry region of parallel porous plates 3—20298
viscoplastic rigid incompressible fluid, iterative methods *(French)* 3—14437
viscoplastic substances, characterisation and laminar flow 3—36073
viscous, incompressible, Stokes problems for suspensions of particles 3—23669
viscous, nonadiabatic, through supersonic nozzle 3—26856
viscous, numerical solution of Navier-Stokes equation by finite element method 3—7333
viscous, past group of circular cylinders, 2-dimens. laminar wakes 3—26851
viscous, slow-moving, two dimens. bubbles, behaviour 3—36137
viscous, through porous media, model for groundwater movement 3—15856
viscous flow, two-dimensional, through T-junction, finite difference method 3—11369
viscous flow around cylinders, convergence criteria for relaxation solutions 3—36096
viscous flows satisfying mixed no-slip and no-shear conditions 3—11381
viscous fluid, eqns. of motion continuum theory 3—7385
viscous fluid, steady plane flow in symmetrical channel with slowly curving walls 3—20272
viscous fluid between rot. cylinders, stability 3—38352
viscous fluids around and through porous bodies 3—11379
viscous incompressible, finite element solution 3—29833
viscous incompressible liquid in channel with step, numerical solution 3—4544
viscous incompressible unsteady flow through circular tube, velocity and temp. distrib. 3—7324
viscous liquid, flow through pipe, arbitrarily changing flow rate 3—36074
viscous magnetohydrodynamic, in channel, effects of thermal radiation 3—14493
water and aqueous surfactants, thinning of oil films, rupture, flow velocity dependence 3—39465
water laminar free convection flow at 4°C from a vertical plate with variable wall temperature 3—29843
wedge-shaped bodies with limited heat conductivity, laminar flow heat transfer 3—20284
yaw angle influence in circular cylinder pressure drag and wake characteristics 3—23805
yawed cylinders, heat transfer calc. 3—36117
CO_2, supercritical, laminar forced convective heat transfer, buoyancy effects *(Japanese)* 3—20323
H_2O sheet, fan-shaped, absorption of CO_2 3—4536
Hg, in metallic conduits under non-wetting and amalgamating conditions 3—1372

laminations
No entries

lamps
see also discharge lamps; filament lamps; light sources
explosion type, operation of high-power Nd:YAG laser 3—22911
health, u.v., i.r., history, development, use, benefits 3—3572

Lande g-factor *see g-factor*

Lande splitting factor *see g-factor*

landing fields *see airports*

Langmuir probes
see also plasma diagnostics
afterglow plasma, diffusion coeff. across mag. field, Langmuir probe curves 3—17566
bakeable hollow cathode device 3—7564
boundary value problem in dense plasma 3—14592
cylindrical and spherical, under collisionless conditions orbital limited current-voltage characteristics, non-Maxwellian electron energy distributions effect 3—14577
electron and positive ion current collection under orbital limited conditions 3—14584
electron velocity distribution meas. in an electron cyclotron resonance plasma 3—14589
glow discharge meas., electron density and temp. 3—14615
ion saturation currents in collision dominated flowing plasma 3—14583
in magnetized plasma, current voltage characteristics 3—7562

Langmuir probes continued
modulation Langmuir probe and incoherent scatter radar techniques, comparison rel. to ionospheric electron temp. measurements 3—25272
nonequilibrium low-density plasma, meas. density of charged particles 3—36196
plasma boundary layer, meas. *(Japanese)* 3—23922
positive column, improved probe curve analysis 3—4684
resonance behaviour of ion sheath capacitance near plasma ion freq. 3—23909
rocket-borne resonance probe system for meas. of daytime equatorial lower ionosphere 3—3069
spherical, admittance in warm electron-ion plasma calc. 3—30005
thermoanemometer-Langmuir probe method for plasma parameters determ. 3—20613
topside, electron temp., meas. by a.c. Langmuir probe, global morphology 3—3080
Ar ionisation meas. behind shocks with microwaves and a pulsed Langmuir probe *(German)* 3—14594
O_2 glow discharge, electron energy distrib. functions, meas. using probe technique 3—23929

language translation and linguistics
tone intonation and segmental duration in Serbo Croatian, model 3—3430

lanthanum
Auger electron spectra, up to 530 eV *(Russian)* 3—15579
ionisation loss in inelastic electron refl. from La surface 3—5252
liquid, spectral emissivity obs. 3—27126
L.P.E. growth of YIG:Ga films, effect of substituting La for Y 3—1924
protective coating on Cr alloys 3—18657
soft X-ray absorption, theory *(Russian)* 3—12192
superconducting energy gap from far-i.r. absorpt. 3—5069
superconductivity, transition temp., pressure dependence, up to 250 kbar 3—38921
surface, energy loss spectra of reflected electrons *(Russian)* 3—12205
thermoelectric power, room temp. to m.p. 3—2062
thermoelectric power meas. near melting point 3—18128
wear and friction in air 3—18625
$CdF_2:Na^+(La^{3+})$, F self diffusion, depend. on doping 3—7972
inCo alloy, X-ray emission spectra rel. to oxidation 3—36491
Cr alloy:La, zone refining rel. to low temp. ductility *(Russian)* 3—12305
La:Ce, cubic crystalline field effect on magnetic susceptibility rel. to Kondo effect 3—24560
Na_2SiO_3:La photochromic glass, darkening characteristics caused by u.v. emission and colour centres formation *(Russian)* 3—30852

lanthanum alloys
see also lanthanum compounds
$(La, Ce)Al_2$ dilute alloy with Ce impurities, superconducting-Kondo system, specific heat 3—5072
La-Cd, phase diagram 3—21567
La-Gd giant susceptibilities 3—8340
La-Pu, mag. susceptibility, obs. of mag. decoupling at Pu 3—2255
LaAg:Gd, wave vector depend. of exchange interaction, e.s.r. obs. 3—34202
$LaAl_2$-$GdAl_2$, mag. ordering, Curie temp. depend. on Gd conc. 3—34122
$LaAl_2$-$GdAl_2$, specific heat jump at supercond. transition 3—34022
$LaOs_2$ lattice parameters, $MgCu_2$ type, polymorphic transition point, high pressure effects 3—33488
Pd-La, lattice spacing and mag. susceptibility meas. 3—18298
Th-La, sp. ht. and superconductivity 3—21168

lanthanum compounds
see also lanthanum alloys
fergusonite type cryst. containing Pr^{3+}, line broadening and vibr. spectra study 3—15526
$3CsCl.LaCl_3.3H_2O:Nd^{3+}$, absorption spectra *(Russian)* 3—24730
$Ba_2LaLiNa_2Nb_{10}O_{30}$, cryst. growth from melt, and characterization 3—12268
La complex, $[La(DMP)_8](ClO_4)_8$, (DMP=2,6-dimethyl-4-pyrone), cryst. struct. 3—17776
La-zn double nitrate:Gd^{3+}, e.s.r. in trigonal crystal field, spin hamiltonian interpretation 3—36789
$LaAlO_3$ higher energy levels of Cr^{3+} ion pairs, excitation and absorpt. spectra 3—15551
$LaAlO_3:Pr^{3+}$, probabilities for radiative and non-radiative decay 3—36937
LaB_6 cathodes in electron optical instruments 3—805
LaB_6 field emission cathodes, for electron probes 3—13474
$LaBe_{13}$, ^9Be spin-lattice relax. and mag. moment dynamics 3—2444
$LaBr_3:Dy^{3+}$, electronically excited ions, radiationless relax., multi-quantum scatt. processes 3—24390
$LaBr_3:Tb^{3+}$, absorpt. and fluoresc. spectra, 77 K 3—30866
LaC_2-UC_2 solid solutions, composition dependence of cubic→tetragonal phase transformations 3—11739
$La_{3-x}Ce_xAl$, specific heat jump of superconducting-Kondo system 3—30558
$La_{1-x}Ce_xF_3$, u.v. transmission spectra, variable band width filter 3—15503
$LaCl_3:Dy^{3+}(Nd^{3+})$, electronically excited ions, radiationless relax., multi-quantum scatt. processes 3—24390
$LaCl_3:Pr^{3+}$, i.r. quantum counter upconversion, laser optical double reson. 3—18487
$LaCl_3:Sm^{3+}$ crystal field splitting with inclusion of J mixing 3—18087
$LaCo_5$-H, ferromag. hydrides, thermodynamic and mag. props. 3—27357
$LaCoO_3$, phase change and free energy of formation, galvanic cell obs. 3—1797
LaF_3, crystalline, vacuum u.v. reflectivity meas. 3—34374
LaF_3, excited Nd^{3+} ion metastable state deactivation processes 3—34427
LaF_3, symmetry, struct., screening consts. 3—7662
$LaF_3:Er^{3+}$, electronically excited ions, radiationless relax., multi-quantum scatt. processes 3—24390
$LaF_3:Nd^{3+}$, electron-phonon interaction, stimulated emission study *(Russian)* 3—6487

lanthanum compounds continued
$LaF_3:Nd^{3+}$, excitation spectra for 1.06 micron luminesc. 3−24734
$LaF_3:Pr^{3+}$, i.r. quantum counter upconversion, laser optical double reson. 3−18487
LaF_3-$SrF_2:Nd^{3+}$, stimulated emission in $^4F_{3/2} \rightarrow {}^4I_{13/2}$ transition 3−27516
LaF_6, thermal vibrs. of atoms, 300-1000 K *(Russian)* 3−27078
$LaFe_{1-x}Cr_xO_3$, antiferromagnetic perovskite, obs. of ferromagnetic interaction by Mossbauer effect 3−39065
$La_2F_6(g)$, stabilities rel. to dimerization 3−27851
$LaGaO_3$, garnet, ceramic, influence of initial comp. and firing temp. in prep. *(Russian)* 3−15746
$La_{10/3}Ga_6S_{14}$, sulphurized compound family of melilite type *(French)* 3−30102
$(LaGd)Al_2$, superconducting, nuclear spin-relaxation and pair breaking 3−18264
La_2GeS_5, crystal structure obs. *(French)* 3−38557
LaH_2, low temp. specific heats 3−11744
$LaLiNb_4O_{12}$, cryst. growth from melt, and characterization 3−12268
$LaLiNb_4O_{12}$, structure rel. to tungsten bronze 3−38572
$La_3Li_3Nb_8Zr_2O_{30}$, cryst. growth from melt, and characterization 3−12268
$La_3Li_3Nb_8Zr_2O_{30}$, structure rel. to tungsten bronze 3−38572
$La_2Me_3(NO_3)_{12}.24H_2O$, Me=Mg, Mn, Zn, Co, Ni spectra, substitution on vibration bands of water, Stark splitting of La^{3+} *(Russian)* 3−8571
$La_2Mg_3(NO_3)_{12}.24H_2O$, thermal expansion coefficients between 10K and 300K 3−17986
$La_2Mg_3(NO_3)_{12}.24H_2O:Nd^{3+}$, meas. of temp. and angular depend. of proton relax. 3−34230
$La_2Mn_3(NO_3)_{12}.24H_2O$ paramagnetic saturation investigation 3−18297
$LaMnO_3$, doped, quantum theory of double exchange 3−21192
$La(NO_3)_3$ complex with phenanthroline, e.p.r. of Gd^{3+} in single crystals 3−34194
$LaNbO_4$, spin-lattice relax. of Mo^{5+}, 1.5-250 K, Debye temp., Raman process probability 3−34207
$La_{0.4}Nd_{1.6}O_3$, single crystal, paramag. susceptibility anisotropy meas. *(French)* 3−38961
$LaNi_5$-hydride, thermal absorption compressor for H refrigerator *(German)* 3−28503
$LaNi_5H_x$ thermal absorption compressor for H_2 refrigerator for 20 K region 3−5842
$La_2O_3:Bi^{3+}$, photoluminescence props. *(Russian)* 3−36930
LaOF phase transitions, rhombohedral/cubic, high pressure effects 3−33666
$La(OH)_3$, growth from two component nutrient La_2O_3 and Al_2O_3 system below 425°C 3−12281
La_2O_2S, Czochralski growth 3−12298
La_2O_2S, long wave i.r. spectra *(Russian)* 3−30825
La_2O_2S, rare-earth activated thin films, cathodolum. 3−8671
$LaPO_4$, enthalpy and heat capacity, temp. depend. *(Russian)* 3−11745
$LaRu_2:Gd$, in supercond. state, localised mag. moment e.p.r. obs. 3−24541
LaS, La_2S_3 and La_2S_3/La_3S_4, dielec. consts., i.r. obs., ionic and covalent behaviour *(Russian)* 3−8595
LaSe, dissociation energies, mass spectroscopic obs. 3−29729
$La_2Ti_2O_7$, for light modulation 3−27602
$LaVO_4$, thermoluminescence *(Russian)* 3−15565
$Pb_{1-kx}La_xTiO_{3\|x(1.5-k)}$, with A-site and B-site vacancies, X-ray struct. study 3−17792
$Pb_xLa_{1-x}(Zr, Ti)O_3$ powder, cold pressing and low temperature sintering 3−27734
$Pb(Zr,Ti)O_3$, La_2O_3-modified, temp.-depend. ferroelec. domain alignment 3−5168
$Pr^{3+}:LaAlO_3$, laser induced two photon decay 3−29135

Laplace transforms
acoustical Green's function, right parallelepiped, perfectly reflecting walls, boundary conditions, acoustic potential 3−3687
exterior e.m. boundary value problem of wedge 3−19480
moving phase boundary, determ. of solute distribution using Laplace transform methods 3−4848
numerical inversion for percentage labelled mitoses experiments 3−25547
semi-infinite steel body melting in an Fe-C alloy, heat and mass exchange eqns. derivation by integral Laplace transform 3−24827
spherical wave propagation, applic. to soln. of one boundary value problem *(Russian)* 3−37836
suspension of solid particles in gas, relaxation effects on supersonic flow around wedge, Laplace transform. soln. *(German)* 3−23796

large scale integration
see also integrated circuit production
No entries

laser accessories
acousto-optic light deflector as optical isolator 3−32093
acousto-optical modulator for beam deflection from interior of laser resonator 3−22383
acoustooptic Bragg cell for wavelength tuning of a dye laser, angular dispersion 3−22378
alkali halide as CO_2 laser window material, intrinsic and impurity absorpt. at 10.6 micron 3−28580
atmospheric windows for use in 2.7-3.2 μ range, computer study 3−5977
beam diverging lens system 3−9959
Brewster window, electrostatic sealing technique 3−32067
chemical lasers, nozzle design accounting for viscous effects and chem. nonequilib. 3−9962
constant deviation tuning device 3−35425
diffraction grating for tuning dye lasers, angular dispersion 3−22379
dye lasers, vessel-cavity and Fabry-Perot etalon, new design suggestion 3−25777
electrically conductive laser beam reflector cooling, patent 3−35431
electro-optic shutter *(Russian)* 3−5986
electro-optical modulators, anisotropic crystals, simulation of electric fields *(Russian)* 3−32102
electrooptic laser beam deflection system, multiple-pass using KH_2PO_4 crystals with quadrupole electrode arrangement *(Russian)* 3−9967

laser accessories continued
electrostatic spatial filter for high powered pulsed laser, patent 3−32101
Fabry-Perot laser, angle-selecting aperture addition, anal. 3−32576
focusing lenses with one aspherical surface used in lasers, analysis and calc. 3−22321
focusing optical elements with regularly distributed refractive index, laser light transmission *(Russian)* 3−35430
frequency stabilization of CO_2 or N_2O using second laser, rapid sampling method *(French)* 3−32096
frequency stabilization using Lamb dip *(Russian)* 3−13042
gas, based on nonlinear absorption, electronic automatic frequency stabilisation system *(Russian)* 3−16448
gas laser travelling wave amplifier, effect of spontaneous emission on the operation 3−32549
glass, Hoya LCG11, laser damage, surface effects, thresholds 3−28591
high power window materials, for use at 10.6 μm, optical characterisation 3−5978
high-resolution scanning photometer 3−35429
hollow cathode device for C.W. He-metal vapour systems 3−22382
image convertor, for time characteristics of injection lasers 3−25778
image recorder 3−5975
integrated ten element linear electro-optic modulator array 3−9966
ion laser, special cathode design for pulsed and CW operation 3−13338
i.r. intensity modulator, using Faraday rotation in YIG 3−5985
i.r. laser window materials, state-of-the-art review 3−5980
laser microprobes, analysis of biological specimens *(German)* 3−28762
laser Raman spectrometers, double and triple monochromators *(French)* 3−25780
liquid chemical injector, for arc-driven gas dynamic and chemical lasers 3−28589
Marx-Bank coaxial driver flashlamp for excitation of organic dye lasers 3−16449
m.i.m. point contact diodes for direct freq. meas. of laser radiation 3−32094
mirror, with adjustable radius of curvature 3−32100
mirror, with variable focal length 3−32099
mirrors, dielectric, intermediate reflectances, optical thickness of terminal layer, design method 3−22384
mode locking using electro-opto-optical modulator 3−28584
multisurfaced reflectors, frequency tunable, general theoretical requirements 3−28578
optical element strongly anisotropic, nonlinear cooling, approximation calculation method 3−22868
optical periodic coupler, leaky wave analysis 3−28583
optico-acoustic beam modulator *(Russian)* 3−9963
optometer using Badal principle for meas. of eye refractive state 3−28590
passive shutter of periodic ruby laser, effect of thermal distortion *(Russian)* 3−35696
Pockels cell with all surfaces at Brewsters angle, design 3−28579
prefocused objective pinhole unit, beam expanding, spatial filtering 3−28577
pressed cathodes, operation in He-Ne lasers 3−22389
protection filters, for $\lambda=633$, 694 and 1060 nm 3−5990
proustite upconverter, parametric background signals 3−5991
pulse train external shaping by nonlinear optical systems external to cavity 3−28585
pyroelectric detector arrays, characts. of high power lasers 3−25779
Quasimodo, for suspending solid particles at focus of laser 3−35427
reflectors, cylindrical 3−22386
resistive electrode discharge system, for TEA CO_2 laser 3−25781
scanning laser recording system, image quality, system evaluation 3−227
semiconductor diode as gas laser modulator 3−22387
semiconductor laser windows, thermal runaway, critical power 3−5976
spatial energy distrib. sensing using microencapsulated cholesteric films 3−35426
spatial filter 3−35429
stabilization of frequency and power by Lamb dip method 3−32097
step recovery diode for optical modulation in double heterostructure at 2.3G bit/s *(Germany)* 3−37647
strain free laser rods, grinding and polishing method 3−13285
switching system, 60 kV, for pulsed excitation 3−5988
synchronising circuit for pumping lamp firing, optomechanically shuttered system *(Russian)* 3−5989
TEA laser, improved uniform-field electrode profiles 3−32098
tuning, using intracavity tilted etalon with piezoelec. drive *(German)* 3−32543
TV-rate raster scanner with Bragg cell 3−28587
vacuum photodiodes in systems for laser energy and power meas., limitations 3−35423
variable length pulse generation, using Michelson interferometer 3−9965
waveguide, electro-optic thin-film, for pulse amplitude modulation of CO_2 laser 3−28581
window materials, high power lasers, absorption mechanisms, thermal damage 3−28592
windows, coated, formulas for absorpt., transmission and reflectivity 3−35424
windows, high power i.r., failure, absorption, recent developments 3−28593
windows, optical distortion rel. to press. 3−16452
windows and mirrors, low level emittance and absorptance measurement, interferometric spectrometer 3−28594
Ar ion laser modification for gas phase Raman scatt. enhancement 3−5974
CO_2 laser, nonlinear absorpt. cell for freq. stabilisation 3−22884
CO_2 lasers, calorimeter for energy output measurement 3−35428
CS_2, crossed polariser system for base-line noise reduction in laser pulse trains 3−28582
CdTe windows, modified Bridgman growth for 10.6 μm, optical properties 3−5984
CdTe windows for 10.6 μm, sonic casting from solidifying melt 3−5982
CdTe windows for 10.6 μm, hot pressing 3−5983

laser accessories continued
CdTe windows for 10.6 μm, physical vapour deposition 3−9960
GaAs double heterostructure laser, short pulse modulation with TRAPATT diodes 3−32569
KBr windows, press forged, mechanical, microstructural properties 3−5979
KCl windows, press forged, mechanical, microstructural properties 3−5979
KCl-KBr mixed crystal CO_2 laser window material, Czochralski growth, i.r. transmissivity 3−16453
N_2 power supply system, gas laser, pulsed, 3371 Angstroms, electric discharge pumping 3−22887
TeO_2 TV-rate raster scanner 3−28588
ZnSe windows for 10.6 μm, chemical vapour deposition 3−5981
ZnSe windows for 10.6 μm, hot pressing 3−5983

laser beam applications
see also integrated optics
absolute quantum efficiencies, techniques and instrumentation, review 3−35533
absorption coefficient measurement, for liquid, photomixing obs. with He-Ne laser 3−32059
acoustic surface wave propagation loss measurement 3−5778
air pollution, remote detection and analysis, laser-Raman radar, review 3−3189
air pollution detection improvement using laser Raman backscattering technique 3−28399
air pollution measurement, Mie scattering techniques, review 3−3188
air pollution measurement, using i.r. tunable laser, review 3−3187
air pollution measurement *(German)* 3−34895
air pollution monitoring by dye laser meas. of differential absorpt. of elastic backscatt. 3−37248
airborne dust particle size measurement 3−5537
alignment 3−6521
anemometers, EUROMECH 36 report 3−3925
anemometers, literature review 3−450
astronomical instrumentation, conference (Tucson, Arizona March 1972) 3−31816
atmosphere composition, laser-Raman radar detection, using sampling technique 3−3190
atmosphere composition, remote mapping of specific gaseous constituents, tunable laser techniques 3−3191
atmospheric aerosol content, as function of relative humidity, lidar obs. 3−3017
atmospheric aerosol meas. from optical radar total scatt.-backscatt. ratio 3−9263
atmospheric laser Doppler velocimeter analysis, comments 3−9392
atmospheric laser Doppler velocimeter analysis, reply to comments 3−12857
atmospheric NO_2 determination, laser induced fluorescence obs. 3−3018
atmospheric pollutants, Raman scatt. obs. using Fabry-Perot periodic filter 3−3192
atmospheric pollution remote sensing, using i.r. heterodyne radiometer 3−3193
atmospheric scintillation meas., at high altitudes 3−31374
atomic and molecular spectroscopy, saturation, level-crossing and double-resonance 3−1105
atomic Na layer, obs. in the upper atm. 3−18872
atoms, optical separation of isomeric nuclei by laser radiation 3−29506
autodyne i.r. quantum receiver, sensitivity *(Russian)* 3−10578
automatic workpiece shaping, patent 3−6530
Bragg-diffraction imaging, application to nondestructive testing 3−21786
ceramic dielectrics, micromachining for microelectronic packaging 3−8954
ceramics, machining techniques, review 3−31128
chalcogenide films amorphous, crystallization kinetics and amorphising energy 3−22930
chemical reaction probing using chem. lasers 3−10196
clouds, plane-stratified, optical sounding, statistical estimation of light pulse deform. *(Russian)* 3−29041
CO_2, TV transmission *(German)* 3−13763
communication engineering *(German)* 3−19653
communication system, using glass fibre channels *(German)* 3−29153
communications in lower atmosphere, noise problem 3−19656
commutation switch, injection semiconductor laser *(Russian)* 3−789
compact laser radar for remote atmospheric probing 3−12861
computer output to microform, laser recording system, patent 3−13764
controlled thermonuclear fusion in the USSR 3−17680
controlled thermonuclear fusion research in the USA 3−17679
controlled thermonuclear reactions, single pulse tailoring 3−29112
conventionally plotted curves, analysis, coherent optical processing 3−6437
correlation, using diffuse objects 3−6438
cutting, of stainless steel sheet, using c.w. CO_2 laser 3−4131
data transmission systems, equipment availability, reliability, capacity analysis 3−797
depolarisation rel. to atmospheric turbulence *(Russian)* 3−28018
deposition rate meas., in matrix isolation spectroscopy 3−13302
digital scanning edge detection microscope *(German)* 3−32064
diphenylpolyenes, nonuniform resonance Raman effect, laser excitation of 1600 cm^{-1} ring vibrations 3−17481
distance meas. *(Japanese)* 3−213
distance measurement, He-Ne laser interferometer *(Czech)* 3−16440
distance measurement 3−6519
distance measurement through atmosphere 3−6518
distance measuring system, patent 3−790
Doppler anemometry, fluid measurement 3−22577
Doppler effect classroom demonstration *(Russian)* 3−52
Doppler spectroscopy, operational limits, polydispersity effects, aerosol meas. appl. 3−16429
Doppler spectroscopy for aerosol particle size meas., theory and expt. techniques 3−16428
Doppler spectroscopy of polyelectrolyte solns. for colloid stability determ. 3−34661

laser beam applications continued
Doppler turbulence meter and velocimeter, Siberian Instruments 1971 Exhibition *(Russian)* 3−9900
droplet growth rate in air-H_2O medium using laser scatt. meas. 3−18736
dynamic deformation of coals due to sorption processes *(Russian)* 3−13223
edge diffraction cone detection, obs. 3−4070
electron, addressable memory, description 3−786
electron micrographs analysis using high power laser diffractometer 3−378
electron microscopy, tensile test pieces, microwelding techniques 3−20684
electron microscopy image improvement, holographic image deblurring 3−3880
electronic battlefield surveillance, airborne system *(German)* 3−19657
energy crisis, role of lasers in fusion 3−38191
energy transfer studies, bibliography 3−6527
energy transfer systems 3−4135
environmental noise detection and identification by frequency instability 3−29156
eye, ametropia and voluntary accommodation response meas. using laser speckle 3−37529
Fabry-Perot acoustic surface vibr. detector, application to acoustic holography 3−32083
Fabry-Perot laser interferometer, refractive index and thickness meas. of transparent materials 3−22336
facsimile transmission systems, recording and scanning, techniques 3−6526
far i.r. freqency meas. and two-laser mixing, part I of NPL programme for determ. of speed of light 3−13322
far i.r. plasma reflectometry, instability detection, cyanide laser obs. 3−4671
fatigue crack starter defects prod. by pulsed laser in metals 3−21762
fibre-optical systems *(Spanish)* 3−6456
film deposition method, appl. to Fe *(Russian)* 3−30934
flame temperature measurement, n-hexane-air system *(German)* 3−9868
flames, refractive index meas. in far IR 3−33390
flow measurement, jet, turbulence distribution, laser photon correlation spectroscopy, Doppler effect 3−22570
fluid flow measurement, Doppler anemometers 3−19654
frequency meas. in far i.r., techniques for high-accuracy, part-II of NPL programme for speed of light determ. 3−13323
fringe counting laser interferometer manometer 3−25707
fusion, laser-driven pulses, wetted-wall concept, feasibility for commercial power generation 3−38190
gas, absorpt. line and press. broadening coeffs., laser spectroscopy 3−19650
geodesy, internal geometric accuracy from simultaneous laser range measurements to satellites 3−34757
geodesy, satellite ranging for polar motion and interstation distance meas. 3−34779
glass fibre communication system components, development *(German)* 3−16919
glass fibre laser communication systems *(German)* 3−16918
high resolution Raman spectroscopy, CH_4 3−38293
holes formation, workpiece material thermophysical properties *(Russian)* 3−10579
holographic interferometer for temp. meas. 3−22375
holographic technique for sampling particles in moving aerosol 3−16445
h.v. meas. by electrooptic method using laser and Kerr cell for h.v. meas. 3−3787
h.v. power transmission lines, current measurement, optical technique based on Faraday effect 3−19655
hybrid IC resistor trimming, industrial laser system design 3−32609
hybrid integrated cct. resistor trimming, installation 3−6528
I_2 mol. energy transfer research, optical lasers excitation sources 3−11304
IC, surface defects, counting and sizing, with rastered Gaussian spot 3−6531
IC fabrication, vapour deposition of Pt using c.w. laser energy 3−5264
IC testing, laser scanner for, description 3−799
image plane detection using laser speckle patterns 3−35677
image recording, KCl:Li(Na)$^+$, on F_a centres 3−32082
image tube, removal of glowing spot 3−6529
inferferometric vibration obs., homodyne and heterodyne techniques 3−196
inside and outside dimensions, laser interferometer *(German)* 3−32030
interferometer, meas. of particle sizes, number density and veloc. 3−5892
interferometer system, for meas. of high velocity of reflecting surface 3−3872
interferometers, measurement applics. *(Russian)* 3−16437
interferometry application to masking systems for microelectronics *(French)* 3−13319
interferometry for students with Jamin interferometer 3−16364
ionization of alkali atoms, determ. of cross-section by freq. doubling with dye laser *(Dutch)* 3−29492
i.r. spectrometers, spread function measurement using gas lasers *(Russian)* 3−9945
i.r. spectroscopy, laser applications, intermolecular forces determ., nonlinear absorption techniques, review 3−32076
Kerr consts. meas. using multimode He-Ne laser 3−39121
laser beam welding of butt joints between dissimilar metals *(Russian)* 3−4130
laser beam welding of winding conductors in their insulation *(Russian)* 3−6523
laser Doppler anemometer, velocity and turbulence meas. of turbulent swirling flow in water 3−794
laser gravimeter, accuracy better than 10^{-7} *(Russian)* 3−13517
laser Raman spectrometers, double and triple monochromators *(French)* 3−25780
laser scan system for object scanning and image recording *(German)* 3−16457

laser beam applications continued
- lead measurement of leadscrews, laser interferometer method 3−22252
- length meas., He-Ne laser interferometer *(Spanish)* 3−19211
- lifetime meas., using tunable flashlamp pumped dye laser 3−14390
- light source using plasma emission of laser irrad. Al plate 3−13301
- light velocity determ. by direct meas. of frequency and wavelength of methane-stabilized laser 3−153
- light velocity meas. 3−6517
- lighting, image forming techniques for theatre and TV studio scenic effects *(German)* 3−29155
- liquid core fibre optic intensification of spontaneous Raman spectra 3−13292
- liquid crystal display, experimental system, development 3−6524
- longitudinal dispersion of ink in turbulent flow of water, electro-optical measurement 3−1376
- Luna 21 reflector on Moon, laser echoes analysis *(French)* 3−39634
- lunar libration meas. using laser Moon-ranging *(French)* 3−28158
- lunar ranging, effect of astronomical ephemeride errors *(French)* 3−31505
- lunar retroreflectors, laser ranging meas. of Earth crustal movements 3−34971
- macromolecular solutions, Rayleigh scatt., biochemical applications 3−28312
- magnetic disc head flight height measurement technique 3−10577
- marine plankton sensing by dye laser induced fluorescence 3−3237
- materials working, telecommunications, holography, medicine, review 3−29157
- measurement of Na hyperfine structure using c.w. dye laser and atomic beam 3−37963
- measurement techniques in industry *(Swedish)* 3−32090
- memories, ferroelectric, reversible domain polarisation in triglycine sulphate plate *(French)* 3−22967
- metals, surface topography monitoring during surface tension meas. 3−39325
- microcircuit pattern inspection, gated optical comparator 3−4133
- microprobe, analysis of biological specimens *(German)* 3−28762
- microspectral analysis 3−26251
- mode-locking laser, picosecond phenomena, meas. and appls. 3−796
- Model OC2-2 optical communication link, pulse position modulation transmission 3−798
- modulators and deflectors 3−6516
- molecular transition identification in visible and i.r. region using resonant interaction of monochromatic fields 3−4434
- multilateration, satellite geodetic measurement system 3−31464
- multimode fibres pulse broadening 3−13761
- narrow frequency tunable γ-ray nuclear resonances induced by laser radiation 3−35518
- naval gun projectile, initial velocity measurement, laser Doppler velocimeter 3−32611
- nondestructive testing, of plastic materials *(German)* 3−15811
- nonlinear spectroscopy, resolution increase up to natural width 3−13309
- nuclear fusion reactors, advantages and viability prospects *(Swedish)* 3−26544
- optical characteristics of aqueous media determ. by pulse sounding method *(Russian)* 3−25741
- optical communication, future development 3−13705
- optical communication, review *(German)* 3−29154
- optical communication systems, present state, overview *(German)* 3−13762
- optical communication using glass fibre optical waveguides 3−35718
- optical communications, bandwidth capacity, review 3−26249
- optical information processing modulation system *(Russian)* 3−19573
- optical materials, surface roughness meas., light scattering method 3−13287
- optical memories, bit-by-bit and holographic image storage, laser-addressed 3−32608
- optical sound spectrographs, recording techniques 3−3767
- opto-electronic micro-machining *(French)* 3−788
- optometer using Badal principle for meas. of eye refractive state 3−28590
- organic molecules, molar triplet excitation coeffs., c.w. laser excitation 3−28550
- page composer, acousto-optic type, description 3−4132
- parabolic mirror, off axis, alignment by laser surface refl. obs. 3−19649
- particle size, continuous measurement by diffraction of beam *(French)* 3−15800
- particle size, number density and velocity meas. using laser interferometry 3−4129
- particle track diameter by Fraunhofer diffraction method 3−19308
- pattern recognition, invariant *(Russian)* 3−6429
- p.c.m. trunk transmission systems using optical fibre waveguides, design considerations 3−751
- photograph machining 3−37649
- photon-sail spacecraft propulsion 3−22966
- plasma, anomalous ion heating 3−14565
- plasma and gaseous diagnostics, using tuned GaAs laser diode 3−4670
- plasma compression and ignition *(Dutch)* 3−32990
- plasma density and electron temp. meas. in shock heated megavolt theta pinch 3−17644
- plasma prod., conditions for fusion, expt. work and prospects, review 3−1512
- plasma prod., flux, temp. and ionisation equilib. meas. 3−17638
- plasma production, expansion 3−20619
- plasma production by fast rise time laser pulses 3−20562
- plasma sheath formation in centre of polytron, thickness meas. by current meas. and laser scattering 3−20643
- plasmas, X-ray emission, conversion ratio calc. 3−20563
- plasmas and controlled thermonuclear fusion 3−17641
- pollution monitoring of water, particle detection and shape discrimination 3−35308
- poly-γ-ethyl-glutamate, cholesteric, mag. alignment meas., diffraction expt. 3−11544

laser beam applications continued
- printed circuits, integral solid circuits installing 3−32606
- pulsed, transparent substrates, thin films, thickness measurement, interference microscopes 3−191
- pulsed laser/holography applic. to nondestructive testing 3−34671
- Raman spectra, pulse characteristics rel. to Stokes component *(Russian)* 3−25772
- reaction kinetics, high pressure laser temperature jump apparatus 3−31257
- refractive index meas. in turbulent air flow 3−37259
- refractory oxide growth by floating zone melting method using a CO_2 laser *(German)* 3−5275
- relativistic acceleration of charged particles by superintense laser beams 3−22970
- review *(Polish)* 3−3820
- review *(Italian)* 3−6525
- review 3−19591
- review of laser applications, work performed at Bell Laboratories 3−784
- review of laser applications to physical science research, work performed at Bell Laboratories 3−785
- rocket pitch and yaw meas. by laser-optical lever system 3−32055
- satellite power supplies, photovoltaic cell activation by Earth-based laser, feasibility 3−4136
- saturated absorpt. spectroscopy of mol. I_2 3−1210
- scanning device, for doping homogeneity meas. in GaP 3−5277
- seam welding, Br.B2 bronze sheet contact components 3−19651
- shape recognition, by modulating spectral analysis of interference patterns in Fourier plane *(Russian)* 3−16447
- sinusoidal vibr. displacement amplitude meas., laser homodyne technique 3−28460
- small calibre cartridge cases, surface flaw inspection system 3−4134
- solid surface irradiation, highly stripped ion source 3−286
- sorption properties of surfaces, laser-probe method 3−26250
- source of multiply-charged ions, prduction of $^{12}C^{6+}$ and $^{27}Al^{12+}$ 3−19283
- space telescope, large, interferometric alignment sensor 3−31822
- speckle photographs, visualisation of phase objects by spatial filtering 3−5969
- spectroscopy, high resolution, with lasers, review 3−35410
- spectroscopy, high-resolution, using c.w. dye laser 3−37634
- spectroscopy role of and possibility of tunability 3−5945
- stack plume SO_2 content, laser-Raman radar obs. 3−787
- steam turbine-gnerator alignment, advantages 3−29152
- supersonic flow velocity, laser Doppler meas. 3−4588
- thermal conductivity measurements of Earth materials at high temperatures using CO_2 laser system 3−18894
- thermomagnetic writing, optimum film thickness, theory 3−16915
- thermonuclear fusion *(French)* 3−20550
- thick film resistors trimming *(German)* 3−32607
- thickness, distance and velocity measurement, piezoelectric laser beam deflector, triangulation method *(German)* 3−19225
- thickness, width, contour, wires and fibres meas. 3−6520
- thin film deposition method, appl. to SiO, ZnS, and MgF_2 *(French)* 3−36988
- thin films, thermal cond. meas. by injection pulsed laser 3−22915
- thin uniform target prep. for trace elemental analysis by laser evaporation 3−16916
- thin-film optical waveguides, scattering of light by acoustic waves colinear acousto-optic interaction 3−28416
- time resolved picosecond spectroscopy, light gate method 3−28545
- torque meter coupling *(Italian)* 3−22251
- transverse vibration meas., interferometry with diffuse laser light 3−5772
- triglycine sulphate, ferroelec. domains, direct obs. by second harmonic generation by laser 3−24658
- turbulent flow, velocity correlations using single laser Doppler-shift velocimeter, analysis 3−448
- turbulent flow meas. using photon correlation spectroscopy 3−32276
- two-laser optical distance-measuring instrument with atmospheric refractive index correction 3−16917
- velocity flow measurement, analysis of method *(Polish)* 3−26252
- velocity meas. employs Doppler velocimeter systems 3−22965
- velocity of light, from CO_2 laser wavelength and freq. 3−9923
- velocity of working surfaces, Doppler meter *(Russian)* 3−22390
- visible laser frequency meas. by up-conversion of CO_2 laser radiation, part III of NPL programme for speed of light determ. 3−13324
- water pollution, concentration monitoring, depolarization of scattered laser light 3−34977
- wave optics., simple demonstration using He-Ne laser *(Russian)* 3−13184
- welding, electron tube anode-cathode assemblies, high melting point metals, technique, advantages 3−19652
- welding, of lap joints with gap *(Russian)* 3−13760
- wind induced ripple on water surface, laser detecting instrument 3−37261
- workshop inspection, minute changes detection in size and shapes 3−19193
- α-Al_2O_3:Cr^{3+} direct optical excitation into excited states of Cr^{3+} pairs 3−8657
- Ar discharge by CO_2 laser, electron density growth dependence on magnetic field 3−7310
- C arc plasma, interferometry, electron density determination 3−11504
- CO_2 laser, use as surgical instrument in experimental urology 3−29151
- CO_2 laser use in welding and cutting 3−22969
- Cr steel, atomic absorption spectra in vapour cloud formed by laser irradiation 3−26021
- D-T targets, laser-driven implosion yielding thermonuclear burn conditions 3−14564
- GaAs, high purity, donor species identification, ionization energy determination using optically pumped NH_3 laser 3−2018
- GaAs laser diode, pulse position modulation technique for point-point voice communication 3−26209
- HF (v=2) deactivation rate, use of direct overtone excitation 3−20172

laser beam applications continued
He arc plasma, parametric heating with 0.337 mm laser radiation, threshold intenstity calc. 3 − 17631
He-Cd laser, phase hologram reconstruction 3 − 16810
He-Ne, propagation through atmoshpere 3 − 10576
He-Ne stabilised by saturated absorption in methane, for frequency generator standards *(French)* 3 − 25652
LiNbO$_4$, surface acoustic waves, laser optical probe, with high relution interferometry 3 − 19112
MnAlGe film, self-demagnetisation during thermomag. writing 3 − 24407
MnGaGe film, Curie point writing with laser pulse, thermal and mag. profiles comparison 3 − 36860
NO detection, using Zeeman effect and CO laser 3 − 13308
^{15}N separation from ^{14}N by photodissociation of NH$_3$ using laser 3 − 38196
NaCl, single crystal, u.s. diffraction, laser beam optical probing 3 − 32036
Nd:YAG laser pumping, using GaAs laser diode 3 − 4103
^{20}Ne-^{22}Ne isotope shift in i.r. spectrum, laser spectroscopy meas. 3 − 26565
OH radicals, fluorescence 3 − 7222
SO$_2$ and hydrocarbon gases, air pollution, remote meas. by u.v laser induced fluorescence 3 − 37541
Se amorphous film, optical memory laser induced, voltage bias effects 3 − 32610
Yb excitation of atomic levels, pulsed dye laser, fluorescence, determination of relaxation times and splitting factors 3 − 22968
ZnSiP$_2$ luminescence excitation spectra at 2K 3 − 8654

laser beam effects
absorption in low loss media, thermally induced index changes, thermooptic meas. method 3 − 16404
absorption of picosecond light pulses by solid targets 3 − 20565
air, breakdown and plasma mirror formation in CO$_2$ laser cavity *(Russian)* 3 − 1527
air, pulsed interferometric holography of laser-produced breakdown 3 − 33189
alkali dimers in supersonic nozzle beams, internal state distribution, white light and laser-induced fluorescence 3 − 17477
alkali halide:Tl$^+$, many-photon excitation of Tl$^+$ impurity centres 3 − 5230
alkali halide crystal, electron avalanche breakdown induced by ruby laser light 3 − 30757
alkali halide crystals, laser destruction mechanisms and multiphoton ionization of impurity centres 3 − 5162
alkali halides, laser induced bulk damage due to electron avalanche breakdown 3 − 35705
anomalous heating of plasma by interaction with solid D$_2$, correlation of neutron yield to anomalous effects 3 − 4662
anthracene luminescence at intense excitation by N$_2$ laser *(Russian)* 3 − 27532
benzene, liquid, l.f. Raman lines, picosecond laser excitation 3 − 22951
breakdown in gases, u.v. radiation, threshold intensity, focal volume dependence 3 − 23940
bulk viscosity effects on amplification function of Stokes signal interacting with laser beam in fluid 3 − 32588
chalcogenide film, laser writing and erasing 3 − 4113
chalcogenide films amorphous, crystallization kinetics and amorphising energy 3 − 22930
comparison of laser, pseudothermal and thermal radiation effects with photographic film 3 − 32106
crystal, absorpt. coeff. for linearly polarised light with intense laser bias 3 − 21395
damage, bulk, alkali halides, self-focusing elimination 3 − 29147
damage, Hoya LCG 11 laser glass, surface effects, thresholds 3 − 28591
damage, inhomogeneous thin films and multilayers, thresholds, structural dependence 3 − 29124
damage, metal and dielectric coated mirrors, mechanisms, results 3 − 28595
damage, multiple layer dielectric mirrors, thresholds, nanosecond and picosecond pulses 3 − 29122
damage, thin film coatings, damage thresholds, film scattering 3 − 29123
damage, thin films and substrate surfaces, time resolved study 3 − 29121
damage, totally internally reflecting surfaces 3 − 13747
damage in optical solids, bulk interaction gradients, light scattering, concurrent and Brillouin 3 − 29115
damage mechanisms in laser glasses, self-focusing subnanosecond pulses, n$_2$ measurements 3 − 29150
damage probability, surface, 1.06 and 0.69 μm 3 − 29119
dense plasma focus, laser beam scattering meas. of ion energy, neutron emission 3 − 20638
diatomic heteronuclear molecule, multiphoton dissociation by intense i.r. radiation 3 − 26705
9,10-dichloroanthracene, α and β, ruby laser induced photoconduction 3 − 11928
dielectric, transparent, energy balance and dynamics of damage *(Russian)* 3 − 6498
dielectric mirror, laser damage rel. to pulse duration and beam radii 3 − 35703
dye-laser photodetachment studies 3 − 29503
energy level shift in low pressure hydrogen discharge on CO$_2$ laser beam irradiation 3 − 14290
ethylene, chem. reactions during CO$_2$ laser irrad. 3 − 39430
eye, and its protection 3 − 28385
films and multilayers, laser damage rel. to struct., comp. and stress 3 − 35702
fluorescence, organic compounds in solid solns., effect of fine structure 3 − 15545
fog droplet vaporisation and fragmentation by 10.6μm laser pulse 3 − 16891
fog droplets, explosive vaporisation by 10.6 μm laser pulse 3 − 37196
free liquid surface, radiation pressure, using focused pulsed laser light 3 − 13754
gas, narrow resonance of γ-ray absorption and emission 3 − 17414
gas breakdown, focal spot size depend. arising from particulate ionization 3 − 38465

laser beam effects continued
gas breakdown by short laser pulse 3 − 33409
gas breakdown in presence of preionisation 3 − 29825
gas breakdown initiated by u.v. photoionisation in presence of spark 3 − 17492
gas mixtures, laminar, rotational, turbulent, exhaust-jet flows, laser-Doppler velocimeter 3 − 32281
glass:Nd, laser-induced-fluorescence-line-narrowing spectroscopy 3 − 21474
glass, etched laser filament tracks, self-focusing 3 − 19642
glass, fracture due to laser generated stress pulses 3 − 16896
glass surfaces, damage, Owens-Illinois ED2 laser glass 3 − 29116
graphite laser heated, particle emission mechanism 3 − 30900
heating of turbulent atmosphere by light beam, intensity fluctuations *(Russian)* 3 − 3019
human damage by picosecond impacts of high-output systems 3 − 31937
II-VI semiconductors, exciton luminescence and photoconductivity at high densities of excitation *(Russian)* 3 − 27531
impulse loading of targets by subnanosecond laser pulses 3 − 29109
Kapitza-Dirac effect at high laser intensities 3 − 35721
kinetic cooling, in the atmosphere, interferometric obs. 3 − 39503
laser induced damage in optical materials, Boulder, Colo., USA, June, (1972) 3 − 29114
laser spark in fluid, fluid parameters determ. 3 − 20548
laser-excited broadside acoustic array at modulation frequency 3 − 9751
lateral expansion of a laser-supported detonation wave in a gas 3 − 38466
longitudinal hypersonic waves, excitation in solid bodies 3 − 7857
metal, fatigue crack starter defects prod. by pulsed laser 3 − 21762
metal, irrad., stress-pulse propag., dispersion 3 − 7847
metal evaporation under powerful optical pulses 3 − 33658
metals enhanced with liquid layers, interaction of TEA-CO$_2$ pulses 3 − 18518
methyl chloride, laser fluorescence study of vibrational energy transfer in collisions 3 − 33163
methyl fluoride, laser excited, in rare gas, O$_2$, N$_2$, H$_2$ and D$_2$ mixtures, vibrational relaxation 3 − 33162
methyl fluoride, partial vibration energy transfer map, laser fluorescence study 3 − 33164
methyl fluoride, thermal lensing obs. of vibr. relax., translational cooling 3 − 4472
microfission explosion by laser or relativistic electron-beam high-density compression, reactor prospects 3 − 32932
molecular crystals, stoichiometric composition determ. using mass spectrometer with a laser ion source 3 − 28781
monopulse development in micro-inhomogeneous active media 3 − 22932
multiphonon summation i.r. absorption, exponential frequency dependence in NaCl and CaF$_2$ struct. crystals 3 − 4827
nonhomogeneous plasma, conductivity-type laser heating, spherical or cylindrical waves 3 − 36183
nonlinear interaction of spontaneous radiation field with active medium of laser *(Russian)* 3 − 768
optical elements laser induced damage, status report 3 − 35699
optical material, transparent dielectric, laser induced damage rel. to cracks, pores, absorbing inclusions 3 − 35701
optical materials, surface damage probability at 1.06 μm and 0.69 μm 3 − 35704
optical materials, transparent dielectrics, laser induced surface damage 3 − 35700
optically transparent dielectrics, study of laser induced surface damage, obs. of microstructure 3 − 16898
organic dyes excited by He-Ne laser radiation, fluorescence 3 − 32564
pasma heating, one-photon inverse bremsstrahlung process *(Japanese)* 3 − 1504
phonon damping with optical pumping induced by intense laser light 3 − 14945
picosecond light pulses absorption by solid targets 3 − 20553
plasma, continuous, sustained by focused high-power CO$_2$ laser 3 − 36187
plasma, dense, laser light absorption obs. 3 − 33347
plasma, dense spherically symmetric, dynamics and neutron production 3 − 26893
plasma, heating of theta-pinch by pulsed CO$_2$ laser 3 − 23885
plasma, inhomogeneous, enhanced laser light absorption by optical resonance 3 − 33381
plasma, laser produced, spherical expansion, early-time model 3 − 38444
plasma, laser-produced, self-generated fields, press. depend. 3 − 33394
plasma, turbulent heating by ultrashort pulses, possible mechanisms *(Russian)* 3 − 14566
plasma density fluctuations in presence of optical mixing of light beams 3 − 4653
plasma focus device, Faraday rotation meas. with a ruby laser beam 3 − 20640
plasma heating, averaged props. of wave solns. for hypersonic thermal wave 3 − 20544
plasma heating, energy relax. by electron-ion collisions *(Japanese)* 3 − 1505
plasma heating, formulation without subsidiary condition *(Japanese)* 3 − 1503
plasma heating, fund. formulation *(Japanese)* 3 − 1502
plasma heating, nonrelativistic, diffusion coefficients, rates, review 3 − 23892
plasma heating, polarisation of reflected radiation, plasma magnetic field measurement 3 − 23921
plasma heating, radiative thermal wave propagation in moving plasma 3 − 29983
plasma heating and containment in crossed laser beams 3 − 33377
plasma heating by beating of laser beams 3 − 33379
plasma heating by multiphoton inverse Bremmstrahlung in a laser beam 3 − 29994
plasma in magnetic field, scatt. cross-section resonances *(French)* 3 − 23903
plasma injection into a magnetic trap 3 − 30004
plasma injection into a stellarator 3 − 20567

laser beam effects continued
plasma interaction, heating, stimulated Compton effect, inverse bremsstrahlung 3—23887
plasma prod., review 3—23890
plasma production, adiabatic expansion 3—20564
plasma production, damage to laser glasses, plasma heating, Thomson scattering, diagnostics 3—23894
plasma production, experimental and theoretical studies of Institut fur Plasmaphysik Garching, survey 3—23893
plasma production, experimental study of X-ray and neutron radiation, gas dynamic and magnetic cumulations 3—20636
plasma production, harmonic generation and parametric excitation of waves 3—33364
plasma production, self-generated magnetic fields investigation 3—20566
plasma production by ultrashort laser pulse irrad. of solid target 3—17630
plasmas, laser irradiated, nonlinear behaviour of stimulated Brillouin and Raman scattering 3—36159
polymer, etched laser filament tracks, self-focusing 3—19642
polymer blocks, transparent, mech. damage 3—22936
polystyrene, sound speeds from stimulated Brillouin scatt., annealing effects, laser induced damage 3—1307
quartz, laser produced damage, cumulative effects of microstructure damage 3—765
radiation damage in transparent solids 3—765
reflecting dielectric coatings, vacuum deposited, damage due to ruby laser radiation *(Russian)* 3—5919
refractive index damage, electrooptic crystals, mechanisms, susceptibility reduction 3—29146
ruby, damage threshold rel. to impurities *(Russian)* 3—13750
ruby laser single pulse radiation, effect on Hg lamp plasma 3—23917
saturated atomic reson. fluoresc., theory 3—1111
second harmonic generation, refractive index of nonlinear crystals *(Russian)* 3—773
self-focusing and self-trapping of laser light 3—783
semiconductor laser windows, thermal runaway, critical power 3—5976
semiconductor surface, laser induced reflectivity changes 3—39115
semiconductors, e.m.f. induction by Q-switched CO_2 laser 3—30520
sharp-line self-induced transparency, obs. with HgII laser intersecting Rb atomic beam 3—4114
spark generation in air, mode locked laser pulses, single pulse mechanism 3—23939
steel in water, u.s. reflection and transmission 3—22198
temperature distrib. in laser irradiated thermally conducting translucent medium 3—32586
transition elements, laser excited atomic fluorescence in N_2O-acetylene flame 3—32263
transparent dielectric, optical strength reduction on laser radiation due to macroscopic defects 3—5175
transparent dielectric surface, laser damage, morphological asymmetry 3—757
transparent medium, laser induced surface and bulk damage 3—22931
transparent solids, laser produced damage 3—765
two-photon excitation fluorescence of phthalimide derivatives *(Russian)* 3—12177
water, laser induced stresses, calc. 3—16894
water drop vaporization, by i.r. laser 3—6496
water droplets, evaporation regimes 3—27112
Ag^- photodetachment by Ar-beam, electron affinities 3—29502
AgCl colloidal particles in water, scattered light power spectra, Lorentzian shifted from zero frequency due to heating 3—180
Al, laser-induced stress-wave and impulse augmentation 3—756
Al films, irrad., microstruct. and electromigration 3—20974
Al_2O_3, sapphire damage, surface, plasma formation 3—29117
Al_2O_3, sapphire damage, surface threshold, ion beam polishing 3—29118
Ar, effect of c.w. laser on pulsed gas breakdown threshold 3—17491
Ar plasma, laser Rayleigh scattering determm. of radial gas density and temp. distributions 3—30009
As-Se-Ge amorphous films, photo-darkening effect 3—5212
As-Se-Ge glass film, refractive index, optical transmission, irradiation power depend. 3—19639
Au film on glass substrate, laser damage 3—10560
Be film, SEM obs. of laser damage 3—35708
Be plasma production, in stellarator 3—33374
$Bi_{12}GeO_{20}$, a self-focusing of A laser radiation by Raman scattering 3—4128
C, pyrolytic rods, formation in hydrocarbon atmos. heated by focused laser beam 3—2807
CO_2, discharge current change due to CO_2 laser beam, mechanism 3—26914
CO_2 collision with O_2 and N_2 mols., fluorescence of stretching vibration, excited by Q-switched CO_2 laser *(Russian)* 3—26736
CO_2 vibr. deactivation using laser induced fluoresc. in CO_2; $CO_2+{}^{14}N_2$, $CO_2+{}^{15}N_2$; CO_2+He 3—11280
$CaF_2:Sm^{2+}$, stimulation of nonradiating transitions by strong light excitation *(Russian)* 3—36925
Cs, reson. multiphoton ionisation by Nd-glass laser 3—23489
Cs vapour, efficient parametric conversion 3—16903
Cu-As-Se glass, light-induced memory effect 3—16895
Cu-Pt alloy, atomic motion under action of laser pulse, X-ray obs. *(Russian)* 3—29111
Cu^- beams, photodetachment by Ar-laser beam, electron affinities 3—29502
Cu_2O, Raman scattering, luminescence, exciton-phonon coupling 3—8581
$CuSO_4$ doped gelatin, X-ray coherent emission under laser irrad. 3—24759
$CuSO_4$:gelatin, collimated X-ray emission on laser irrad. 3—13721
D-T plasma, concentric conduction type laser heating 3—36184
D-T two temperature plasma, laser concentric conduction heating 3—36185
DCl, V→T, R and V→V relaxation, by laser fluorescence technique 3—33165
GaAs, damage at 1.06 μm 3—35707
GaAs, electrical characts., laser irrad. effects *(Russian)* 3—27248
GaAs, photolum., regions damaged by laser beam 3—27571

laser beam effects continued
GaAs amorphous films, electron diffraction study of struct., laser induced evaporation *(Russian)* 3—8059
GaAs damage, surface, solid lasers, 0.694 and 1.06 μm 3—29120
GaP, reson. fluoresc. due to bound excitons, laser excited 3—18484
GaP amorphous films, electron diffraction study of struct., laser induced evaporation *(Russian)* 3—8059
GaSe, spontaneous and stimulated emission, under intense laser beam excitation 3—27517
Ge, electrical characts., laser irrad. effects *(Russian)* 3—27248
H atoms and mols. multiphoton ionization at 0.53 μ 3—11157
H-like atoms, multiphoton ionisation by intense linearly polarised light 3—26581
H_2, CO_2 laser-induced breakdown 3—17689
H_2, solid, transition to metallic state in compression wave induced by laser pulse 3—20874
H_2-N_2F_4, mixture, laser induced explosion 3—12508
H_2^+ photodissoc. by monochromatic light, energy analysis of ejected H^+ ions 3—11289
HBr, V=2 state, excitation by pulsed HBr chemical laser, vibrational fluoroscence 3—11313
HF laser, chem., pulsed, performance, effect of CO_2 laser irrad. 3—10502
α-HIO_3, spontaneous parametric radiation excited by Ar laser radiation 3—22955
He, heating of laser-induced plasma 3—29991
He atom, in high intensity laser field perturbation atomic levels near ionization threshold 3—1114
He-Xe discharge, pulsed laser action mechanism, excitation characteristics with external electrodes 3—33412
n-InSb donor deionisation, impurity cond., CW laser cyclotron reson., magnetocond., temp. depend. 3—15149
K atoms, laser-excited, field splitting of violet lines *(Russian)* 3—7061
$KCl:Li^+(Na^+)$, image recording on F_a centres 3—32082
$LaCl_3:Pr^{3+}$, i.r. quantum counter upconversion, laser optical double reson. 3—18487
$LaF_3:Pr^{3+}$, i.r. quantum counter upconversion, laser optical double reson. 3—18487
Li exploded wire plasma, obs. of core by laser light reflection 3—23910
LiH and LiD, ion expansion energy spectra related to laser plasma parameters 3—38468
$LiNbO_3$, laser-induced damage, internal electric field 3—29142
$LiNbO_3$, $LiTaO_3$ damage, surface, solid laser free oscillation and giant pulse conditions, threshold, mechanisms 3—22937
$LiNbO_3$, optically induced inhomogeneity of refr. index 3—32604
$LiTaO_3$, optically induced inhomogeneity of refr. index 3—32604
NH_3, pyrolysis by CO_2 laser radiation 3—12509
NO, pressure broadening of magnetically tuned i.r. absorption spectrum, using CO laser 3—14388
Na, trace amounts detection by fluorescence emission excited by continuous wave organic dye laser 3—28776
Pd surface, rate of CO desorption *(German)* 3—11807
$Pr^{3+}:LaAlO_3$, laser induced two photon decay 3—29135
Si, electrical characts., laser irrad. effects *(Russian)* 3—27248
Si solar cells under laser irradiation, determ. of damage depth 3—32578
Te, fast photoelectromagnetic effect, induced by 10.6μ laser radiation 3—27288
Te, highly-excited state, elec. conductivity calc. 3—8221
Te based chalcogenide film as memory material, crystallisation after short laser pulse 3—30524
U laser produced plasma, u.v. emission 3—30006
YIG, interaction with spin and magnetoelastic waves 3—36859
YIG, spin waves excited by parallel pumping, effect on instability threshold 3—34141
ZnSe-ZnTe heterojunctions, influence of laser excitation on photoelectric props. 3—24504
ZnTe, damage at 1.06 μm 3—35707
ZnTe, luminescence and modulation by CO_2 laser radiation *(Russian)* 3—27551
ZnTe, photoluminescence using laser excitation *(Russian)* 3—30879

laser beams
see also holography
absorbing atm., propagation of collimated, pulsed beam 3—21947
absorbing fluid medium, laser beam thermally induced nonlinear propagation 3—35710
angular divergence and refraction, ground layer of atmosphere *(Russian)* 3—3020
atmospheric propag. in long high path, deflection and spread 3—21933
atmospheric propagation, effect of finite transmitter apertures on scintillations 3—21946
atmospheric transmission, beam spreading 3—18852
beamspread reducing device for injection laser output 3—22914
clouds, plane-stratified, optical sounding, statistical estimation of light pulse deform. *(Russian)* 3—29041
coherent optical pulse propag. in inhomogeneously broadened medium, conservation laws 3—4071
coherent radiation scattered from a rough surface, longitudinal correlation props. 3—16897
coherent submillimetre pulse prod. by heterodyne method *(French)* 3—16893
coupled oscills., phase difference determ. 3—22934
defocusing media, aberrations and extreme divergences *(Russian)* 3—6512
diffraction field of beam from circular aperture *(German)* 3—22838
directivity improvement using nonstationary holography 3—19629
dye laser system, simultaneous two frequency oscillation 3—29089
electrooptic deflection system, multiple pass, uses KH_2PO_4 crystals with quadrupole electrode arrangement *(Russian)* 3—9967
electrovacuum instrument, fine-structure of pulse *(Russian)* 3—5987
energy measurement, 1% accuracy level attainment 3—16450
fade at receiver due to pointing jitter of transmitter 3—19628
filament formation mechanism *(Russian)* 3—6513
flash from strong shock wave of laser spark, mag. field effect 3—19631
f.m. radiation detection problems 3—19630

laser beams continued
- focusing, thermal self-focusing, steady state theory 3–22957
- focusing in semiconds., damping criteria 3–16906
- focussed, elec. field components, integral expansions 3–13745
- gas, coupling with nonlinear absorber 3–19604
- Gaussian, beam formulas from Huygens principle and diffr. theory 3–35706
- gaussian beam, one dimens., diffr. by amplitude sinusoidal grating of zero thickness 3–10442
- gaussian beam near focus, field anomalies 3–32579
- Gaussian beam propag. in planar and cylindrical inhomogeneous media, vector theory 3–760
- glass rods, change in thermooptical constant 3–19226
- Goos-Hanchen shift amplification by interposition of thin films *(French)* 3–6503
- high energy system alignment control 3–5992
- high power lasers, mode-locking by intensity and time dependent Q-switching 3–28584
- h.v. nanosecond pulse generator, triggering *(Russian)* 3–10554
- integrated pulse, circuit for display of peak value 3–214
- laterally confined beam undergoing total refl., lateral shift calc. *(French)* 3–16902
- lidar and nephelometric scatt. by power law aerosols, Mie theory calcs. 3–6422
- light polarization effect on miltiphoton scattering processes 3–10564
- light scattering experiments 3–6522
- mode-matching of beams *(Japanese)* 3–37976
- modulation, 10.6 μ, using ultrafast Kerr effect 3–32581
- modulation with optico-acoustic device *(Russian)* 3–9963
- multiple scattering of laser pulses transmitted through clouds 3–22844
- non-Gaussian scattered light, scaled photocount correlation 3–16892
- nonlinear absorpt. of separated beams by Doppler broadened transition 3–13753
- nonlinear medium, beam-breakup and self collapse, elimination *(Russian)* 3–4123
- Pellin-Broca prism mounting method for laser work 3–13275
- phase-matched second harmonic generation with laser beam in TEM$_{mn}$ mode 3–16912
- photon counting statistics in inhomogeneous random medium 3–687
- photon counting statistics in turbulent atmosphere on Gaussian medium 3–688
- photon echo on homogeneously broadened spectral line 3–35716
- picosecond spectroscopy using picosecond continuum 3–19197
- plasma scattering, electron temp. and diffusion 3–17581
- polarising emission power interaction with isotropic resonating medium *(Russian)* 3–10563
- power and energy meas., calorimetric method 3–13337
- power reduction and fluctuations caused by motion 3–22929
- pulse formation using electro-optical shutter *(Russian)* 3–5986
- pulse shaping with saturable gas absorbers 3–35714
- pulse train external shaping by nonlinear optical systems external to cavity 3–28585
- pulsed, atmospheric propagation, perturbative treatment of thermal blooming 3–764
- pulsed focused Gaussian beam, thermal blooming in gas 3–19625
- pulsed lidar reflectance from clouds, comments 3–25207
- pulsed lidar reflectance from clouds, discrepancy between meas. and calcs. 3–21934
- pulses through linear amplifying and absorbing media, regular propag. study *(Russian)* 3–19632
- radiance volume density concept 3–22807
- radiation dispersion characteristics of an aqueous medium subject to hydrodynamic disturbance, time variation *(Russian)* 3–29113
- Rayleigh scattering, N noninteracting particles, intensity correlation fns. 3–10561
- reduction of ruby laser beam in surface layer of atmosphere due to temperature changes in wavelength *(Russian)* 3–28053
- resonant medium, external radiation interaction, correl. approx. *(Russian)* 3–6497
- ruby laser, ultrashort pulse prod. and meas. by two photon fluoresc. obs. 3–29092
- seawater, transmission of finite cross section beams 3–18844
- second harmonic conversion of laser radiation generated under free oscillation conditions 3–22961
- self-focusing, time independent elliptical beam, beam shape 3–29148
- self-focusing and small scale filaments of laser beams in nonlinear media 3–19635
- self-induced beam distortion, irradiance profiles, bending, lab. simulation, 10.6 μ 3–19626
- single pulse 100J with stabilized spectrum and radiation alignment *(Russian)* 3–26234
- spatial distrib., homogeneity improvement *(Russian)* 3–762
- spatial-distribution, heterojunction injection laser, Fabry-Perot resonators, waveguide models 3–32573
- spectral line width, influence of field inhomogeneity *(Russian)* 3–29110
- stochastic Gaussian beam, propagation in strongly focussing medium with random deviations 3–6495
- thermal Rayleigh scattering, forward stimulated 3–19638
- thermal self defocusing, diffr. effects 3–22938
- thermally self defocused, interference 3–32580
- thin lenses, achromatic triplets, Gaussian optics *(German)* 3–6449
- third and higher order intensity correlation in laser light 3–10562
- turbulent medium, focused laser irradiance fluctuations, fourth moment 3–22845
- 2Nπ ultrashort light pulses, analytical expressions 3–13756
- ultrashort pulse formation, using mode-locked laser and two-component medium *(Russian)* 3–758
- ultrashort pulse generation, review *(Russian)* 3–761
- ultrashort pulse measurements 3–6494
- u.s. wave production in absorbing liquid from interacting beams 3–22933
- u.v., cascade freq. conversion in nonlinear crysts. *(Russian)* 3–13749
- water vapour, CO laser radiation absorpt. 3–19627
- H plasma, underdense, Compton scatt. of laser radiation by ions 3–20431
- He-Ne, third-order intensity correlation function, meas. 3–13748

laser beams continued
- Kr II, molecular absorp. of three lines by $^{127}I_2$ *(German)* 3–36010
- Nd:glass, emission spectrum 3–16909
- Nd:glass emission spectra, polyhedral-resonator, long pulse pumping 3–22910
- Nd:glass laser, dye mode locked, interpulse coherence, picosecond pulses, interferometric measurements 3–22908
- Nd^{3+} laser, with nonlinear absorber, picosecond pulse structure, electron optical image converter obs. *(Russian)* 3–759
- Ne, nonlinear, interference effects, influence of laser field polarization 3–32603
- Rb$_2$ vapour, deform. of ruby laser pulses 3–22935

laser cavity resonators
- *see also ring lasers*
- amplification with resonator frequencies displaced relative to amplification contour of active medium *(Russian)* 3–22928
- antiresonant ring interferometer, appl., output coupling, mode locking, cavity dumping 3–16885
- beam deflection from interior by acousto-optical modulator 3–22383
- circular lasers generation in the capture region *(Russian)* 3–29107
- compound, effect on radiation spectrum of GaAs laser 3–16887
- confocal unstable, beam steering, mirror misalignment effects 3–16884
- cylindrical configuration 3–19623
- diffraction losses, calc. *(Russian)* 3–10557
- double cavity dye laser, emission spectrum, 2 nsec pulses 3–29085
- dye lasers, vessel-cavity and Fabry-Perot etalon, new design suggestion 3–25777
- excitation, semiopen cylindrical resonator with dielectric object, soln. *(Russian)* 3–10558
- Fabry-Perot resonator, spectral width *(Russian)* 3–10559
- flat mirror ring, modes and losses 3–4112
- flat-mirror, spectrum of stimulated radiation *(Russian)* 3–4111
- fluorescene-Na, under lamp pumping, induced reversible absorpt. 3–22954
- folded spherical, excitation using HCN laser 3–22925
- gas laser, internal frequency modulation, by variation of medium refractive index 3–26225
- hollow-waveguide lasers, mode losses, theory 3–10553
- internal lens, end pumped, dye laser, c.w., passively mode locked, picosecond pulses 3–22897
- internal-reflection laser, based on reflection coeff. between media of greater than one *(Russian)* 3–706
- intracavity absorber, gas laser characteristic dependence 3–719
- intracavity absorption cell, N$_2$O detection, amplified absorption, CO$_2$ laser 3–29129
- intracavity modulator alignment 3–19224
- laser beam pulse generation, triggering of h.v. nanosecond generator *(Russian)* 3–10554
- laser diodes, Fabry-Perot cavity, radiation trapping 3–19622
- Michelson interferometer, variable length pulse generation 3–9965
- mirror resonator, quasi 90° roof type, low loss modes and resonances 3–13743
- mode locked, acousto-optic dumping 3–16886
- mode locking concept 3–6492
- mode selection, lowest-order, anal. 3–32576
- nonlinear absorbing cell in resonator for measuring electron concentrations in plasma *(Russian)* 3–7567
- passive mode locking, effects of saturable absorber transmission and optical pumping 3–26238
- passive negative coupling mechanism *(Russian)* 3–29143
- Pockels cell Q-switch for single longit. mode selection 3–10555
- rapid frequency tuning, by electromechanical technique 3–3819
- Rhodamine 6G, under lamp pumping, induced reversible absorpt. 3–22954
- ring, contraction of capture zone by external noise *(Russian)* 3–26240
- ring laser, mode locking rel. to retardational plates motion 3–13744
- ring laser, self-pulsing, generalized model 3–29106
- ring resonator, unstable, ang. selector, effect on selective props. 3–16888
- rotating circular resonator, natural polarisation conditions *(Russian)* 3–35698
- ruby, luminescent line widths in an optical resonator *(Russian)* 3–29099
- ruby laser, emission parameters study in resonator, elastic deformation effect on threshold characteristics *(Russian)* 3–29101
- ruby laser, emission wavelength control with a dispersion resonator *(Russian)* 3–29096
- ruby laser, generation spectra with frequency scanning *(Russian)* 3–10548
- semiconductor laser, pulsation analysis 3–26235
- single quasimode laser operation 3–37951
- stimulated Mandelshtam-Brillouin emission in optical resonator 3–22956
- stimulated Raman radiation and Mandel'stam-Brillouin radiation 3–22945
- sweep frequency laser, He-Ne laser mode selection using Michelson interferometer, automatic frequency control system *(Russian)* 3–10556
- telescopic, radiation control by external signal, free oscillation conditions 3–22927
- three-mirror resonator with anisotropic elements, frequency polarisation characteristics *(Russian)* 3–29108
- travelling-wave, polarisation properties, calc. of anisotropic resonator and nonlinear interaction 3–16889
- travelling-wave laser of three- and four-mirrors, effect of resonator parameters on performance 3–16890
- unstable, variable reflectivity, effect of mode selection and mirror misalignment 3–4110
- waveguide structure, semiconductor laserm electron beam pumped, laser threshold 3–22926
- CO$_2$, unstable confocal resonator modes spatial props. 3–4086
- CO$_2$ electric-discharge convection lasers, unstable resonators 3–16883
- CO$_2$ laser, with varying Q-factor, population inversion and radiation density *(Russian)* 3–29081
- CO$_2$ laser oscillator with unstable resonator cavity, performance 3–26218

laser cavity resonators continued
 CO_2 mixing into supersonic N_2, continuous lasing action 3−22882
 DF laser, chem., CW, performance in unstable cylindrical confocal oscillators 3−10490
 GaAs double heterostruct., single mode laser radiation using composite cavity 3−16879
 GaAs thin film optical cavity, totally internally reflecting 3−752
 HF, action rel. to electrode struct. 3−10480
 HF, chemical, time sequencing rel. to energy content under different cavity configs. 3−22871
 HF, optically pumped, laser oscill. and anisotropic gain in 1→0 vibr. band 3−713
 HF CW laser, diffr. limited performance using edge coupled nonfocal unstable resonator 3−32577
 HF laser, chem., CW, performance in unstable cylindrical confocal oscillators 3−10490
 He-Ne, based on nonlinear absorption, optical system *(Russian)* 3−16823
 He-Se, self-mode locking 3−22879
 Nd:YAG laser, parameter optimisation with nonlinear element in resonator 3−22912
 Nd-liquid column, combined with Nd:glass rod in cavity, spiking behaviour 3−22894
 YAG laser, internal modulation techniques for high data rate communications 3−35695
laser modes
 antiresonant ring interferometer, appl., output coupling, mode locking, cavity dumping 3−16885
 dielectric modulation by acoustic wave of single-mode laser 3−4080
 eigenfunction anal. of mode-locking process 3−35682
 flat mirror ring resonator 3−4112
 gas, optically pumped, cavity detuning and multimode operation 3−4097
 generated in channels at lower levels, interaction phenomena *(Russian)* 3−6499
 He-Ne laser, single frequency, mode selection using Michelson interferometer, sweep frequency laser system *(Russian)* 3−10556
 high power lasers, mode-locking by intensity and time dependent Q-switching 3−28584
 hollow-waveguide lasers, mode losses, theory 3−10553
 injection lasers, single-mode generation 3−22918
 intensity fluctuations of lasers in intensity coupled two-mode operation 3−32532
 locking concepts 3−6492
 mirror resonator, quasi 90° roof type, low loss modes and resonances 3−13743
 m.i.s. structs., as pulsed laser, theoretical analysis of feasibility, allowable modes 3−16875
 mode-matching of beams *(Japanese)* 3−37976
 one-mode laser, spiking operation *(Russian)* 3−4081
 optical waveguide on anisotropic substrate, mode suppression, freq. tuning 3−22891
 passive mode locking, effects of saturable absorber transmission and optical pumping 3−26238
 radiation field structure, under synchronization of transverse modes *(Russian)* 3−32531
 resonator, variable reflectivity, unstable, effect of mode selection and mirror misalignment 3−4110
 ring laser, mode locking rel. to retardational plates motion 3−13744
 ruby laser, active quality modulation by extra-generative amplification *(Russian)* 3−13737
 ruby laser, longitudinal mode selection by intracavity mode selecting resonator 3−4102
 ruby laser, Q-switched, frequency stability 3−32567
 semiconductor, second-order mode locking, Paoli-Ripper model 3−16865
 semiconductor, transverse mode control, fundamental mode of oscill. 3−16863
 semiconductor injection laser, transverse mode selection mechanism 3−32570
 single longit. mode selection using Pockels cell Q-switch 3−10555
 single-mode conduction modulation 3−37948
 solid, generation dynamics, self sustaining modes, compensating phase modulation *(Russian)* 3−13738
 third order Lamb theory, corrections and appl. to mode locking 3−16844
 CO_2, asymmetric stretch mode vibr. temp. rel. to laser action 3−16837
 CO_2, unstable confocal resonator modes spatial props. 3−4086
 CO_2 high-pressure c.w. waveguide laser, mode locking 3−714
 CO_2 pulsed, high pressure chemical pumping, discharge and rapid expansion pumping 3−19600
 GaAs homostruct. and double heterostruct., spontaneous emission, current depend. at laser modes onset 3−16857
 GaAs homostruct. laser, dielec. waveguide propag. modes, TE and TM modes displacement 3−16859
 He-Ne, axial mode obs. using Fabry-Perot interferometer 3−190
 He-Ne, mode selection at 0.63 μm *(Russian)* 3−13724
 He-Se, self-mode locking 3−22879
 Nd:YAG laser, longitudinal mode selection by intracavity mode selecting resonator 3−4102
 Nd^{3+}:YAG, higher order mode-locking and mode locked state separation, rel. to optical p.c.m. link 3−737
laser radar *see optical radar*
laser theory
 see also laser transitions; population inversion
 active modulation, transition process, pulse generation theory *(Russian)* 3−13720
 chemical, atom-diatomic mol. reactions suitable for laser action 3−10495
 chemical, mixing layers nonuniform index of refr. effects 3−10515
 chemical, multilevel short pulsed, model, diagnostic relations, performance limits 3−10492
 chemical and mol., vibr. energy near reson. energy transfer theory 3−10482
 chemical laser, numerical formulation for constant-gain calcs. 3−22877
 circular lasers generation in the capture region *(Russian)* 3−29107
 diatomic gasdynamic lasers, vibr. relax. in supersonic expansion, numerical model 3−10504
laser theory continued
 diffusion type chemical lasers, flame sheet anal. 3−10463
 dye amplifier, flash pumped, amplification gain eqn. 3−29084
 energy level inversion following shock waves *(Italian)* 3−10461
 flat-mirror resonator, spectrum of stimulated radiation *(Russian)* 3−4111
 fluctuations in amplitude, polarisation, quasiclassical theory, review *(Russian)* 3−708
 gas laser, theory of interaction between standing wave and gas *(Russian)* 3−10541
 gas laser stimulated emission at low and i.r. frequencies, intensity fluctuations *(Russian)* 3−10539
 gaussian beam near focus, field anomalies 3−32579
 injection laser, theory of transient evolution and self-focusing behaviour of lasing filaments 3−29103
 m.i.s. structs., as pulsed laser, theoretical analysis of feasibility 3−16875
 mode locking concept 3−6492
 one-mode laser, spiking operation *(Russian)* 3−4081
 optically pumped gas laser 3−22878
 partial differential eqn. with polynomial coeffs. soln. of associated moment eqns. 3−28829
 quantum frequency converter, condition for continuous periodic energy exchange, theorem 3−19592
 quantum monomode laser, nonstationary behaviour 3−16822
 radiation field structure, under synchronization of transverse modes *(Russian)* 3−32531
 semiconductor, resonance effects, rate eqns., transient phenomena, review 3−32572
 semiconductor, second-order mode locking, Paoli-Ripper model 3−16865
 semiconductors, intraband edge absorpt. of light, theory 3−15506
 single quasimode laser operation 3−37951
 single-mode conduction modulation 3−37948
 third and higher order intensity correlation in laser light 3−10562
 two mode laser, intensity fluctuations in intensity coupled two-mode operation 3−32532
 Van der Pol oscillator model, exact photocount statistics 3−19587
 X-ray and u.v. lasing, tests for occurrence 3−37950
 CO, model in pulsed and CW operation 3−10494
 CO, operation kinetics calc., vibr. distrib. function 3−10474
 CO chem., kinetic theory, computer model 3−10491
 CO_2, TEA, high press., gain and power, theory rel. to expt. 3−10476
 CO_2 gas, lasing mechanism, chemical pumping, discharge and rapid expansion pumping, high pressure pulsed chemical laser 3−19600
 CO_2 laser, with varying Q-factor, population inversion and radiation density *(Russian)* 3−29081
 CO_2-N_2, pulse amplifier, idealized rate eqn. analysis 3−10505
 CO_2-N_2 gas dynamic laser, model 3−10506
 DF-CO_2 laser, pulsed chem. transfer, kinetic model, computer simulation, review 3−10471
 H_2, laser power densities for Lyman and Werner bands 3−4082
 HF, chem., CW performance, chain vs. cold reaction 3−10535
 HF, optically pumped, laser oscill. and anisotropic gain in 1→0 vibr. band 3−713
 HF chem. pumped by NF_3-H cpd. reaction, model, kinetic transfer rates 3−10528
 He-Ne gas laser, saturation parameter depend. on discharge current 3−6462
 He-Ne gas laser output power depend. on discharge current, gas pressure and tube radius 3−6461
 Nd^{3+}:YAG, nonadditive phonon induced line broadening, elastic ion lattice interaction 3−22907
 Ne laser action, characteristics of $3s_2 \to 3p_1$ ($\lambda = 4218$ nm) 3−32536
 Ne(I), optical coherence of 6328 Å laser transition, global dipole 3−13728
laser transitions
 active modulation, transition process, pulse generation theory *(Russian)* 3−13720
 chemical and mol., vibr. energy near reson. energy transfer theory 3−10482
 gas laser emission, J=0 reversible transition to J=1, polarisation props. 3−32545
 Lymann transition in u.v. laser *(Russian)* 3−723
 methane, 3.39 μm molecular transition used in laser stabilisation, accurate freq. 3−22872
 methane, wavelength of 3.39 μm laser saturated absorpt. line 3−22873
 molecular laser-emissions in the i.r., rotational and vibrational-rotational transitions 3−11267
 naphthalene crystals, mechanism of multiple quanta transitions 3−32587
 polyacenes, possibility of a laser effect *(French)* 3−27886
 rhodamine 6G ethylene glycol c.w. dye laser, diffusion independent triplet quenching 3−32561
 ruby laser, emission wavelength control with a dispersion resonator *(Russian)* 3−29096
 semiconductor, heavily doped, band transitions, optical gain, analysis 3−22924
 semiconductors, highly excited, review of results 3−750
 single-mode model, nonequilibrium phase transition 3−707
 Ar, effect of laser field on contours of lines amplified by neighbouring transitions *(Russian)* 3−22889
 Ar neutral laser, transition uncertainties, line competition 3−4087
 Ar^+, mutual influence of two transitions at 4880 and 5145 Å *(German)* 3−37962
 As^+ c.w. laser oscillation in He-As mixture, charge transfer reaction 3−37959
 C, dissociatively prod., pulsed laser emission in elec. discharge 3−10520
 CO, laser excited vibr. energy transfer, relax. rates 3−10466
 CO flame laser, P-branch i.r. transitions in C_2H_2-O_2 flame, optical gain 3−10473
 CO_2, 9.33 and 10.18 μm molecular transitions used in laser stabilisation, accurate freqs. 3−22872
 CO_2, transition freqs., standard deviations 3−10537
 CO_2 lower laser level, relax. of excess populations 3−1247
 Cl, dissociatively prod., pulsed laser emission in elec. discharge 3−10520

laser transitions continued

- F, dissociatively prod., pulsed laser emission in elec. discharge 3 – 10520
- GaAs, pump light conversion to laser radiation at room temp. 3 – 16861
- H_2 laser, ultrashort laser pulses from vibr.-rot. transitions *(Russian)* 3 – 10536
- HF, laser excited vibr. energy transfer, relax. rates 3 – 10466
- HF, vibr. relax. rate, 295-730K, effect of SF_6, N_2 and f_2 diluents 3 – 10467
- HF, vibr.-vibr. transfer time, apparent decay time 3 – 10488
- He-Ne gas laser output power depend. on discharge current, gas pressure and tube radius 3 – 6461
- I, $^2P_{1/2}$-$^2P_{3/2}$ hyperfine struct. transition, induced emission spectra 3 – 32547
- I, photodissoc. laser, $^2P_{1/2}$-$^2P_{3/2}$ transition, linewidth 3 – 32548
- I photodissociation laser, luminesc. of $^2P_{1/2}-{}^2P_{3/2}$ transition 3 – 32554
- K vapour, intense spontaneous violet emission due to coherent two photon excitation 3 – 19601
- N, dissociatively prod., pulsed laser emission in elec. discharge 3 - 10520
- N_2, first positive system (2,0) band, pulsed oscill., new lines obs. 3 – 32552
- NO, laser excited vibr. energy transfer, relax. rates 3 – 10466
- Ne, spontaneous emission from lower laser level, double reson. 3 – 26227
- Ne(I), optical coherence of 6328 Å laser transition, global dipole 3 – 13728
- OV, in Z-pinch discharges 3 – 32540
- S_2 lasing due to $^1\Sigma^+{}_g \rightarrow {}^3\Sigma^-{}_g$ transition in photodissociated COS *(Russian)* 3 – 4458
- SO_2, far i.r. transition excitation mechanism 3 – 16838
- Xe, 3.99 μm transition, 128, 126 and 124 isotope shifts *(French)* 3 – 6469

laser velocimeters

- 3-dimensional, for studying gravity waves in shallow water, design consideration 3 – 22377
- anemometer, broadening of meas. freq. spectrum due to interference plane gradients 3 – 13529
- anemometers, EUROMECH 36 report 3 – 3925
- atmospheric, analysis, comments 3 – 9392
- atmospheric, analysis, reply to comments 3 – 12857
- differential Doppler laser velocity measuring instrument using a Fabry-Perot interferometer 3 – 16454
- Doppler, anal. of simulators and tracking systems 3 – 340
- Doppler, broadband demodulation of signals using gated zero crossing detector 3 – 476
- Doppler, dual beam, geometric anal. of probe volume 3 – 336
- Doppler, flow felocity obs. 3 – 475
- Doppler, Fourier optical model 3 – 473
- Doppler, frequency shifting by electro-optic techniques 3 – 337
- Doppler, turbulent transport obs. 3 – 338
- Doppler and interference types, comparison 3 – 22385
- Doppler effect, evaluation of systematic error by computer simulation *(Russian)* 3 – 16573
- Doppler effect type, applications to gas and liquid streams *(Russian)* 3 – 13334
- Doppler effect type, reduction of const. component and noise in output signal *(Russian)* 3 – 13335
- Doppler laser anemometer *(French)* 3 – 16577
- Doppler Meter for working surfaces, laser technique *(Russian)* 3 – 22390
- Doppler speedometer, Siberian Instruments 1971 Exhibition *(Russian)* 3 – 9900
- Doppler velocimeter signal for turbulent flow, spectral anal. 3 – 35553
- flow velocity meters *(French)* 3 – 32273
- fluid flow, signal generator for testing 3 – 3924
- frequency-shifted laser interferometer obs. of small dynamic motions 3 – 28561
- gas mixtures, laminar, rotational, turbulent and exhaust jet flows, laser-Doppler velocimeter, review 3 – 32281
- interferometer system, for meas. of high velocity of reflecting surface 3 – 3872
- laser anemometry, meas. of mean velocity and turbulence in wind tunnel 3 – 478
- laser Doppler anemometry of electric arcs, fluid velocity meas. 3 – 795
- laser Doppler velocimetry, ambiguity noise level reduction with cross-correlation technique 3 – 791
- light scattering in laser flowmeter rel. to differential Doppler heterodyning technique 3 – 792
- literature review 3 – 450
- naval gun projectile, initial velocity measurement 3 – 32611
- NEL laser velocimeter, new developments and treatment of data 3 – 342
- optical-anemometry signals, light source and geometrical requirements for optimisation 3 – 163
- piezoelectric laser beam deflector *(German)* 3 – 19225
- sampling demodulator circuit, f.m. wideband 3 – 6103
- signal-to-noise ratio of photocurrent 3 – 32095
- supersonic wind tunnel applications for meas. of flow velocity 3 – 477
- suspensions, Doppler signal correl. time rel. to conc. *(Russian)* 3 – 13336
- turbulence spectra meas. by laser velocimeter, Doppler ambiguity effect 3 – 22558
- turbulent flow, velocity correlations 3 – 448
- unsteady flow meas. in hydraulic servo systems using laser velocimeter 3 – 793
- wind speed, remote meas. using laser Doppler systems 3 – 31465
- Ar, spatial coherence in water 3 – 339
- CO_2 laser anemometer for long range wind velocity determination 3 – 3196

lasers

- *see also gas lasers; laser beams; liquid lasers; ring lasers; semiconductor lasers; solid lasers*
- cross-field, divergence reduction, device description 3 – 753
- development in Poland *(Polish)* 3 – 37949

lasers continued

- direct pumping of lasers by exhaust plasma in fusion reactors 3 – 19971
- energy measurement, 1% accuracy level attainment 3 – 16450
- frequency stabilization using Lamb dip *(Russian)* 3 – 13723
- high-power pulse emission frequency increasing method 3 – 29132
- infrared light sources, tuning methods, review 3 – 743
- internal-efelection, based on reflection coeff. between media of greater than one *(Russian)* 3 – 706
- i.r., tunable, applic. to air pollution measurement, review 3 – 3187
- irreversible quantum statistical thermodynamics, laser applications 3 – 19508
- irreversible quantum statistical thermodynamics of operation 3 – 19590
- parameters, external high freq. modulation *(Russian)* 3 – 19593
- picosecond pulse lasers, investigation of ultra-fast transient phenomena 3 – 1105
- principles, review 3 – 19591
- pumping techniques for advanced lasers 3 – 705
- Q-switching, theoretical aspects *(Rumanian)* 3 – 22867
- quantum theory of interaction of atoms and mols. with e.m. fields, review 3 – 19699
- quasicontinuous, mode locking, ultrashort pulse generation 3 – 13722
- Raman, pulsed, Stokes power output time depend. 3 – 4119
- safety legislation 3 – 25606
- spatial-angular characteristics of emission, holographic control method *(Russian)* 3 – 13339
- stabilization of frequency and power by Lamb dip method 3 – 32097
- temperature field measurement of laser with high anisotropy in parallelepiped form *(Russian)* 3 – 9859
- X-ray and vacuum u.v. spectra possibility *(Russian)* 3 – 709

latent heat

- *see also heat of fusion; heat of sublimation; heat of vaporisation*
- heat transfer with melting or freezing in a wedge shaped enclosure 3 – 14982

latent heat of adsorption *see heat of adsorption*

latent heat of combustion *see heat of combustion*

latent heat of crystallisation *see heat of crystallisation*

latent heat of dissociation *see heat of dissociation*

latent heat of formation *see heat of formation*

latent heat of fusion *see heat of fusion*

latent heat of mixing *see heat of mixing*

latent heat of reaction *see heat of reaction*

latent heat of sublimation *see heat of sublimation*

latent heat of transformation *see heat of transformation*

latent heat of vaporisation *see heat of vaporisation*

latent image *see photographic process*

lattice constants

- Am alloys, Laves phases 3 – 4731
- anthracene-acridine binary system 3 – 11718
- ferroelectrics and ferroelastics having the index of faintness unequal to the cell multiplicity, discussion 3 – 2499
- hydroxyapatite, hydrothermal growth method, comparison with natural apatite 3 – 12282
- Kossel patterns, lattice parameter computation 3 – 1547
- martensite:C, polycrystals, determ. from martensite line components 3 – 31010
- monomer-dimer mixtures, boundary effects evaluation for simple cubic lattice by lattice constants method 3 – 38711
- orthogonal cryst., unit cell lattice parameters calc., program 3 – 30080
- perfect monocrystals, X-ray spectrometry, by comparison with standards *(Russian)* 3 – 11525
- spacing meas. using new X-ray interferometry techniques, determ. of Avogadro's number 3 – 13212
- substrate facet replication by epitaxial garnet film, lattice parameter distrib. 3 – 38749
- surface, by LEED 3 – 30329
- TCNQ salt, NMP type, non-mag. semicond. phase obs. 3 – 2066
- unit cell dimens. meas. from X-ray diffr. lines pairs 3 – 36239
- X-ray double diffraction meas. technique 3 – 36240
- Ag base alloys with B metals, concentration dependence of the lattice constant and its relation to the elastic modulus *(German)* 3 – 1666
- Ar, compressed solid, X-ray diffr. technique and lattice parameter meas. 3 – 20678
- Au base alloys with B metals, concentration dependence of the lattice constant and its relation to the elastic modulus *(German)* 3 – 1666
- $AuGa_2$ and $AuIn_2$, anomalous behaviour below 100K 3 – 21334
- Ca, electronic structure as function of lattice const., APW calc. 3 – 18070
- $CaAl_2(NH_2)_8.NH_3$, monoclinic *(French)* 3 – 1607
- $Ca_2Nb_2O_7$, orthorhombic *(French)* 3 – 1606
- $Cd(PO_3)_2$, orthorhombic *(French)* 3 – 11591
- Cr, lattice parameter variation in thin films 3 – 26992
- Cu base alloys with B metals, concentration dependence of the lattice constant and its relation to the elastic modulus *(German)* 3 – 1666
- Cu_2SnSe_3, variation of lattice parameter with temp. and thermal expansion 3 – 14815
- $Dy_{1-x}Th_xFe_3$, magnetisation vs. temp., lattice consts. vs. temp. 3 – 34164
- Er, antiferromag. sinusoidal, magnetostrictive calc. of periodic variation *(French)* 3 – 27388
- Fe-Al Kossel interference pattern computation *(German)* 3 – 4693
- Fe-Ni alloy lattice const., spontaneous volume magnetostriction, 4.2-1000 K 3 – 30671
- Fe-Si Kossel interference pattern computation *(German)* 3 – 4693
- $FeAsO_4$, type-I *(French)* 3 – 4733
- Fe_2O_3-Al_2O_3 mixed oxides, conc. depend. of parameters *(French)* 3 – 7679
- GaAs, point defects, precision lattice parameter measurements after quenching and annealing 3 – 33523
- GaAs:Sn, defect props. rel. to growth conditions, elec., luminesc. and lattice const. meas. 3 – 36267
- GaAs-GaP system, correlation between miscibility and lattice parameter mismatch 3 – 11720
- $Gd_2(MoO_4)_3$ improper ferroelec., temp. depend. at transition temp. 3 – 12104
- GeO_2, hexagonal, 36-516°C 3 – 36280

lattice constants continued
- In_2Se_3-Sb_2Te_3, X-ray obs. of phase diagram, hexagonal lattice parameters depend. on comp. *(Russian)* 3—14964
- KBr(Cl)-TlBr(Cl), depend. on comp. 3—7912
- MgO powder, strain atmosphere effects, crystallite size 3—33509
- $Mn_xFe_{3-x}O_4$, i.r. spectra and cation distrib. 3—30807
- MnTe, 300-700 K, expansivity 3—15365
- Ni-Cu alloy, lattice const., spontaneous volume magnetostriction, 4.2-1000 K 3—30671
- NiS_2, non-stoichiometry influence at insulator-metal transition 3—2017
- Np alloys Laves phases 3—4731
- Pb-Bi system, structure of metastable phase 3—18569
- Si-Ge, solid soln., meas. for comp. of vapour grown homogeneous crystals 3—2649
- $Sn_xZr_{1-x}S_2$, layer compound, vapour growth conditions and structure parameters 3—38543
- $SrTiO_3$, lattice parameter var., 10 to 130K, neutron backscattering obs. *(German)* 3—30107
- Ta, diffusion of H_2, coefficients determ. by X-ray meas. of lattice expansion 3—27145
- Tm, antiferromag. sinusoidal, magnetostrictive calc. of periodic variation *(French)* 3—27388
- V, lattice parameter variation in thin films 3—26992
- $Y_{2.4}Eu_{0.6}Ga_{1.2}Fe_{3.8}O_{12}$, garnet film, annealing effects on mag. anisotropy and lattice consts. 3—30640
- YIG:Ga, L.P.E. growth, controlled lattice const. mismatch by substituting Gd(Sm)(La) for Y 3—1924
- YSeF polytypes *(French)* 3—1605
- ZnS-Te, variation of lattice parameters with composition 3—30402

lattice defects *see crystal defects*

lattice dynamics
- *see also crystal surface and interface vibrations; Gruneisen coefficient; lattice localised modes; lattice phonons; non-polar crystal lattice vibrations; polar crystal lattice vibrations; vibrational states in disordered systems*
- acoustic vibrations, generated by acoustoelectric effect, dynamical X-ray diffr. analysis 3—27088
- alkali halides, Anderson-Gruneisen parameter 3—1714
- alkali halides, anharmonicities and reststrahlen frequencies 3—38631
- anharmonic character of vibrations, study using high temp. X-ray diffractometer, furnace design 3—28736
- anharmonic cryst. self-consistent theory *(Hungarian)* 3—7879
- anharmonic crystal lattice with vacancies, stability, dense lattice gas model 3—20835
- anharmonic crystals, evaluation of free energy 3—38649
- anharmonic crystals, linear chain model properties, self-consistent theory in pseudoharmonic approx. *(Hungarian)* 3—20820
- anharmonic crystals, path integral theory 3—36374
- anharmonic crysts., statistico-thermodynamic approach *(Russian)* 3—36371
- anthracene, single cryst. and powder, Raman spectral meas. 200 to 1700 and 2900 to 3100 cm^{-1}, lattice vibr. obs. 3—21419
- meso-anthracene derivatives in n-hexane at 4 K, solvent cryst. vibr. with electronic and vibronic transitions 3—34413
- b.c.c. metals, model for lattice dynamics 3—4826
- charge density analysis, effect of models for thermal motion and two-centre scatt. 3—14654
- chlorinated benzene crysts., intermol. force field, model approach 3—30238
- chrysene, lattice dynamics and thermal diffuse scatt. of X-rays 3—24226
- classical, and localized potential method 3—30216
- coherent acoustic vibrs. detection by γ-γ ang. correls. 3—2474
- crystal defect, atomic vibrational behaviour, time averaged atom arrangement, computer simulation 3—33512
- Debye-Waller temp. factors, atomic mass depend. 3—14938
- diaquobismethoxyacetato Co(II), polarised absorp. spectra vibronic interact. and mag. dipole effects 3—27501
- diazines, laser Raman polarisation spectra, lattice vibr. study 3—36873
- dielectric crystals, thermal conductivity and anharmonic forces 3—31990
- p-dihalobenzenes and deutero-derivatives, vibr. spectra, calc. *(Russian)* 3—2531
- dilute alloys, effect of umklapp on low temp. thermal resistivity 3—1751
- dipole coupled anisotropic cryst., optical props., sum rules 3—27080
- rel. to dislocation motion in lattice 3—20742
- dissipative lattice, perturbation soln. for shock waves 3—38622
- effective harmonic system, vibr. props., atomic mean square velocity bounds 3—33616
- elastic wave attenuation in crysts. with linear defects, anharmonicity *(Russian)* 3—14932
- external modes of molecular crystals, symmetry properties computation, adaptation to computer program 3—11702
- f.c.c. metal, model including ion-ion and electron-ion interactions 3—17945
- ferroelectric crystals, phase transition and domain structure change obs. 3—778
- ferroelectrics and antiferroelectrics, order-disorder type 3—30236
- ferroelectrics and ferroelastics having the index of faintness unequal to the cell multiplicity, discussion 3—2499
- force fields, review 3—33104
- glasses, vibrational excitations, review 3—1770
- glycerol, ν_{oh} stretching vibr. investigation using Raman and i.r. spectroscopy *(French)* 3—30819
- graphite, pyrolytic, rel. to heat treatment influence on low temp. heat capacity 3—17980
- harmonic approx. reln. to linear theories of elasticity and piezoelectricity, review 3—33615
- harmonic isotopically disordered high conc. mixed crysts., lattice thermal conductivity 3—30235
- harmonic lattice, entropy of binding between vacancies and solute atoms, lattice vibr. 3—33515
- harmonic solids, modified moments 3—7885
- h.c.p. lattice, vibr. consts. 3—24233
- h.c.p. metals, noncentral force model 3—33617
- impurities in solids, effects on emission and absorption spectra 3—2577

lattice dynamics continued
- intermetallic compounds with linear chains, theoretical model for large critical superconducting temps., lattice instabilities 3—2203
- introduction, monograph 3—1728
- invariant finite strain meas. 3—32329
- i.r. and Raman selection rules for molecular and lattice vibrations, correlation method, book 3—7209
- Ising lattices, compressible, harmonic lattice vibrations, critical pressure, phase transitions 3—38651
- isopropyl compounds, low-frequency vibrations, torsional modes and barriers to internal rotation determ. from i.r. spectra 3—5188
- lattice sp. ht., dislocation strain field effects, higher order elasticity theory 3—27128
- lattice with random substitutional impurities 3—14946
- Lindemann law of melting for ideal solids, lattice dynamical study 3—24246
- Louck's method extension for calc. normal modes for finite lattices 3—17941
- metal, cubic, anharmonic thermal scatt. of X-rays 3—38524
- metal, elec. resist. rel. to umklapp electron electron scatt. 3—30440
- metal with nonmag. impurities, impurity quasilocal vibration rel. to conducting state 3—4986
- metallic hexaborides, thermal vibrs. of atoms, 300-1000 K *(Russian)* 3—27078
- metallic lattices, Lennard-Jones type potentials, lattice vibrational frequency calc. 3—38630
- metals, f.c.c. and h.c.p., atomic scattering factors, h.v. electron diffraction 3—38528
- metals, h.c.p., lattice dynamics using modified Bhatia model 3—36373
- metals, polyvalent, umklapp electron-phonon scattering in low temp. resistivity 3—8140
- metals, umklapp interaction anisotropy and deviations from Matthiessen's rule 3—38820
- molecular crystals, lattice sum transformations and potential function expansions 3—33621
- monoclinic crystal, i.r. dichroism of lattice vibrations of the B_u species 3—2539
- Mossbauer effect applics., book *(French)* 3—34276
- noncentral interaction in crystals and molecules, valence bond model, Slater wave functions 3—36383
- perovskite, critical dynamics at structural transition 3—15014
- plasmon dispersion in metals, long wavelength, electron correlation effects on density 3—4972
- point defects and diffusion, monograph 3—1621
- polar media, nonradiative transitions, processes with mixing of quantum and classical degrees of freedom 3—7865
- polar media, nonradiative transitions, processes without mixing of quantum and classical degrees of freedom 3—1717
- polyethylene, single-crystal textured, l.f. Raman spectra, librational modes 3—36867
- polytetrafluoroethylene 3—20218
- quantum crystal point transformation theory, zero-temp. self-consistent phonons 3—36378
- quartz, crit. force const. of struct. phase transition 3—17953
- quasiharmonic system, vibr. props., atomic mean square velocity bounds 3—33616
- Raman scatt. in solids, review *(Japanese)* 3—2525
- rare earth borates, vibr. spectra, struct. 3—2555
- rare earth hydrides, struct., dynamics, H diffusion, slow neutron scatt. obs. 3—1615
- rigid-body vibrations tensors, least-squares determination, unit weight matrices 3—38628
- scattering of channelled ions in crystals 3—17886
- second moment expression for solids containing reorienting nuclear spins 3—24231
- sheet silicates, optical vibr. 3—34348
- shell model, sensitivity to high frequency dielectric constant 3—1737
- shock compression of solid second sound at high temp. 3—38623
- SiO_2, minerals, seismic wave velocity rel. to lattice structure *(Japanese)* 3—5447
- soft mode phase transitions, basic concepts, review 3—27120
- solids, temp. depend. of n.q.r. frequencies and external modes approximation for lattice dynamics 3—30721
- spinel in the rigid ion approximation lattice dynamics at zero wavevector and elastic constants 3—7875
- stimulated phonon-electron-photon scatt. theory 3—1738
- stimulated photon-photon-polariton scatt. theory 3—1738
- structural phase transition, inelastic neutron scatt., broad neutron groups and anomalous anisotropy of dispersion 3—27087
- superconductors, type II, flux lattice dislocation motion in mixed state 3—24539
- surface of crystal, thermal expansion 3—20919
- symmetry groups for lattice vibrations 3—14717
- rel. to thermal diffuse scattering in electron diffraction 3—23994
- thermal motion anal. of non-rigid body, X-ray diffraction obs. 3—14941
- thermal motion coupling of atoms in crystal from acoustic spectrum of thermal diffuse scatt. 3—11695
- thermal motion in crystallographic models, riding motion and higher cumulants determ. 3—14664
- transition metal, thermal expansion, anal. in quasiharmonic approx. 3—33642
- trimethylchlorosilane, lattice modes in far-i.r. spectra 3—1238
- uniaxial crystals, directional depend. of extraordinary i.r. oscillator parameters 3—18453
- velocity density systematics, Debye theory, ionic size 3—7863
- vibrations, microscopic theory 3—7870
- zincblende structure crystals, effective charges obtained from bulk moduli and Lippincott function 3—36270
- AgCl(Br), covalency and deformability of Ag^+ ions 3—1733
- $AgNO_3$, totally symmetric N-O stretching mode, asymmetric shape, obs. in laser Raman spectra 3—2532
- Ar, Monte Carlo calc. 3—38650
- Au_3Cu, ordered alloy, Morse pot. function applic. 3—7868
- BaF_2:Sm^{2+} shell model, sensitivity to high frequency dielectric constant 3—1737
- $BaTiO_3$, cubic phase, wave vectors, dispersion relation *(French)* 3—20826

lattice dynamics continued
CDS, Debye charact. temp., rel. to lattice oscillation spectra *(Russian)* 3−24221
CaF_2 containing heavy metal impurities, i.r. absorption and thermal conductivity 3−36898
Cd, 80K, X-ray diffuse scatt. study 3−1731
$CdBr_2$, lattice vibrations, i.r. and Raman spectra 3−30813
$CdCl_2$, lattice vibrations, i.r. and Raman spectra 3−30813
$CoCl_2$, lattice vibrations, i.r. and Raman spectra 3−30813
Cr, mean square displacements for volume atoms 3−30218
Cu, modified Bhatia's model 3−38635
Cu-Ni alloys, third and fourth order anharmonic coeffs., X-ray determ. *(Russian)* 3−33619
Cu_3Au, ordered alloy, Morse pot. function applic. 3−7868
Cu_2Te, electrical props. carrier scattering at 10K by thermal lattice vibrations *(Russian)* 3−8170
D_2, solid, librational anharmonicity effects 3−38641
$FeCO_3$, siderite, Raman scatt., 4.2-300K, freqs. up to 2000 cm^{-1} 3−34366
Ge, thermal cond. fluctuation, Debye approx. *(Russian)* 3−1838
$Ge_{0.5}Si_{0.5}$ amorphous film, struct. and Raman scatt. 3−36501
H_2, solid, librational anharmonicity effects 3−38641
HCN, dispersive curves and phase transition 3−7873
^4He, umklapp phonon thermal resistivity anisotropy 3−1856
In, thermal linear magnetoresist. and lattice cond. using Corbino geometry 3−11880
K, thermal resistivity between 1.5 and 15 K, umklapp processes 3−20841
KD_2PO_4, light scattering investigation of soft ferroelectric and acoustic modes 3−39108
$KTa_xNb_{1-x}O_3$, $x=0.56$, ferroelectric, soft modes and struct. 3−11594
Mg_2SiO_4, i.r. reflectivity and Raman scattering obs. of lattice vibrations 3−21410
$MnCl_2$, lattice vibrations, i.r. and Raman spectra 3−30813
N_2 emission spectrum vibron- and phonon-induced dipole radiation, study of cooperative effects 3−2568
$NaCl:CN^{-1}$, mol. lattice relax. of CN^-, dynamic heat capacity meas., 0.3−4 K 3−7867
NbS_2Cl_2, vibrational modes of $|Nb(S\text{-}S)_2Nb|$ octahedral cage *(French)* 3−27082
OCS molecular crystal, lattice dynamics, variational formalism and intermolecular forces 3−33620
Pb, anharmonic lattice vibration contrib. to heat capacity 3−7940
Pb grains, rel. to sp. ht. below 5 K 3−27329
RbF microcrystals, density of phonon states and i.r. absorpt., calc. 3−36380
$Rb_2UO_2Cl_4.2H_2O$ crystals force consts. and normal vibrations of $[UO_2Cl_4.2H_2O]^{2-}$ anion *(Russian)* 3−36386
$RbUO_2(NO_3)_3$ crystals, polarised luminescence spectra, triplets, due to low-frequency vibrations *(Russian)* 3−36942
Se, trigonal, valence-force-field model 3−24223
Si, anharmonicity, rel. to struct. factor 3−24064
Si, thermal cond. fluctuation, Debye approx. *(Russian)* 3−1838
β-Sn, rel. to transition under press. 3−27457
$SrF_2:Sm^{2+}$ shell model, sensitivity to high frequency dielectric constant 3−1737
Ti, and elastic consts. rel. to anisotropic thermal expansion 3−17987
$TlNO_3$, totally symmetric N-O stretching mode, asymmetric shape, obs. in laser Raman spectra 3−2532
U_3O_8, i.r. spectra, U-O lattice vibr. calc. 3−36874
ZnS(Te), neutron diffraction study of crystal structure, anharmonic thermal vibration of ions 3−11697
Zr, two- and three-body interactions, Gruneisen functions and thermal expansion 3−11752

lattice energy
see also binding energy
alkali metal hydrofluorides, electrostatic energies, Madelung parameters 3−1593
binary alloys, f.c.c. and b.c.c., electrostatic energy expressions rel. to ordering, applic. to In-Mg, Li-Mg, Al-Zn 3−11585
calcite, cationic distrib. and structural changes of mixed Mg-Ca layers 3−15849
Coulomb energies, rapid-convergence algorithm 3−1594
ionic cryst., finite, equil. ion spacing and ion-pair electrostatic energy, point-ion model 3−7654
Madelung constant calc. method 3−33484
metal carbide (nitride) (oxide), electron config. influence on wetting props. *(German)* 3−8766
potential energy calcs. rel. to mol. packing determ. 3−24061
pyrochlore structures, electrostatic potential and energy, calc. by Bertaut's method *(French)* 3−26988
Ar, solid, thermodynamic props. 3−20838
$BaPdF_4$, preparation, madelung part of lattice energy *(German)* 3−14814
$CaPdF_4$, preparation, madelung part of lattice energy *(German)* 3−14814
KCl-RbCl solid solutions, Debye temp. and lattice energy calcs. *(Russian)* 3−7862
KHF_2, calc. of electrostatic lattice energies, effect of fractional changes and cooperative movement of protons 3−7655
KI-KBr solid solutions, Debye temp. and lattice energy calcs. *(Russian)* 3−7862
Kr, solid thermodynamic props. 3−20838
$MgZn_2$ Madelung constant and energy, in terms of parameters of crystal type, calculation *(German)* 3−1598
NaBr, potential of F^-, calc. 3−36834
NaBr, potential of F^-, theory 3−36835
$PbPdF_4$, preparation, madelung part of lattice energy *(German)* 3−14814
$SrPdF_4$, preparation, madelung part of lattice energy *(German)* 3−14814

lattice gas *see lattice theory and statistics*

lattice localised modes
cubic lattice, Wert-Marx law generalization and interstitial vibr. freq. *(French)* 3−1688
diamond:N, u.v. and i.r. absorption spectra *(Russian)* 3−2578
dislocation resonance, dislocation-phonon scatt. 3−1745
elastic wave attenuation in crysts. with linear defects, anharmonicity *(Russian)* 3−14932

lattice localised modes continued
ferroelectric, impurity vibronic spectra, anomalies 3−30228
ferroelectrics, H-bonded, local mode model, quantum mechanical tunnelling, soft mode 3−5169
ferroelectrics, H-bonded, soft mode optical phonon interaction dynamics, Ising Hamiltonian 3−5170
ferroelectrics, H-bonded, transverse Ising model dynamics, soft mode heavy damping 3−2502
garnets doped with trivalent rare-earth ions, resonant scattering of phonons 3−4837
glass, low temp. thermal conductivity in electric and magnetic fields 3−1849
harmonic lattice, rel. to displacement amplitude of atoms 3−33515
host lattice point defect system, local or gap mode freqs. 3−38647
ionic crystals, symmetry-dependent effective force const. changes around impurities 3−36391
Jahn-Teller impurity ion pair, vibron reduction effects of Coulomb and exchange interactions 3−33813
light absorb., temp. dependence of integrated intensity 3−27514
molecular crystals, $s=\frac{1}{2}$, X-irradiated, electron spin lattice relaxation, local mode effects 3−12051
molecular impurity centre scattering of lattice waves 3−1746
molecule in dense medium, vibr. relax. 3−30229
nonmetallic crystals, absolute magnitude and temp. dependence of the thermal conductivity 3−1720
paramagnetic ions, resonant phonon scattering, coupled mode and perturbation theory approaches comparison 3−1766
phonon coupled states with impurity centres, multiplicity of dielectric local modes *(Russian)* 3−36924
phonon thermal resistivity due to spherical inclusions 3−1724
rare-earth ions, resonance phonon scattering at average and high temps. 3−1767
ruby, vibr. spectra of Cr^{3+}, rel. to pair spectra anal. 3−15551
scattering by Jahn-Teller defects in cubic crystals 3−1755
semiconductor, polar, i.r. absorpt. of localised longit. optical phonons 3−30232
spin phonon spectrometer 3−1754
p-terphenyl with tetracene impurity, vibron. relax., role of delocalized and pseudolocalized vibrs. 3−27090
topologically disordered chain, localisation of vibrational modes 3−11709
vibration localised basis functions 3−30231
Al, Mossbauer study of ^{57}Fe impurities, 4-1000 K 3−4835
$Al_xGa_{1-x}As$, Raman scatt. 3−5200
$Al_xGa_{1-x}As$, reson. Raman scatt., 2K 3−34359
$Al_2O_3:Ni$, thermal conductivity at low temps. *(French)* 3−1845
$Al_2O_3:V^{3+}$ phonon spectroscopy on the resonant scattering of V^{3+} and other impurities by tuning the 'Bremsspectrum' of a superconducting tunnel junction 3−1768
$Ar:H_2$, lattice excitation assignment 3−24237
BaF_2, calc. of H^- impurity vibr. 3−36390
$BaF_2:H^-$, impurity induced far i.r. absorpt. 3−34387
CaF_2, calc. of H^- impurity vibr. 3−36390
$CaF_2:H^-$, impurity induced far i.r. absorpt. 3−34387
$CaF_2:H^-$ i.r. relectivity study of high concs. of H^- ions 3−4836
$CdF_2:In^{3+}$, semicond., rel. to resonance Raman spectra 3−36871
CdS:Be, i.r. absorpt. 3−27523
CdSe:Be, i.r. absorpt. 3−27523
Cr, Mossbauer effect of ^{57}Fe, impurity lattice dynamics 3−33638
CrO_4^{2-} in alkali halides, vibr. and electronic spectra 3−27091
$CsI:WO^{2-}(MoO^{2-})$, i.r. absorpt. obs. of local symmetry 3−8621
$(Cu_xZn_{1-x})M_2(SO_4)_2.6H_2O$, electron spin-lattice relax. processes 3−2362
α-Fe_2O_3, hematite, anisotropy of Fe atom vibrs., Mossbauer obs. 3−33639
$FeTiO_3$, ilmenite, anisotropy of Fe atom vibrs., Mossbauer obs. 3−33639
GE:Sb, high frequency monochromatic phonon spectroscopy 3−1765
GaP, vibr. modes of interstitial O and O complexes 3−11707
Ge-Si, local and resonance modes from Raman scattering 3−24702
GeO_2, vitreous scattering of low frequency phonons at low temps. 3−1769
K halides, quantum mechanical calcs. of i.r. props of H^- ions 3−21453
$KBr:MnO_4^-$, vibronic spectra obs. 3−8616
$KBr:NCO^-$, matrix i.r. spectra and anharmonic force field vibrational features 3−27519
$KCl:NCO^-$, matrix i.r. spectra and anharmonic force field vibrational features 3−27519
KCl-KI, light absorpt. by second harmonics of U-centre oscill., calc. *(Russian)* 3−15533
$KI:WO^{2-}(MoO^{2-})$, i.r. absorpt. obs. of local symmetry 3−8621
$K_2SO_4:CrO_4^{2-}$, vibr. freqs., optical and i.r. absorpt. studies 3−14954
$LaAlO_3$, vibr. spectra of Cr^{3+}, rel. to pair spectra anal. 3−15551
LiF, zero-phonon lines in M-band region of irrad. crystal 3−1622
LiH(D), second order Raman spectrum, phonon modes *(French)* 3−39136
$LiNbO_3$, polariton-biphonon Fermi reson. *(Russian)* 3−11708
MgO, hypersonic attenuation, impurity and defects effect 3−1701
MgO, neutron irrad., thermal cond., 0.4-80 K, quasilocalized modes, defect centre prod. 3−30295
MgO:Ni(Fe)(Cr), paramagnetic impurities, thermal conductivity 3−1844
Mo, Mossbauer study of ^{57}Fe impurities, 4-1000 K 3−4835
$(NH_4)_2SO_4:CrO_4^{2-}$, vibr. freqs., optical and i.r. absorpt. studies 3−14954
$Na_2SO_4:CrO_4^{2-}$, vibr. freqs., optical and i.r. absorpt. studies 3−14954
Nb:H, quasi-elastic neutron scatt. intensity 3−30230
Pb-Sn system, supercond. dynamics of Sn impurity oscills., Mossbauer and u.s. velocity studies *(Russian)* 3−7894
Pd, Mossbauer study of ^{57}Fe impurities, 4-1000 K 3−4835
Rh, Mossbauer study of ^{57}Fe impurities, 4-1000 K 3−4835
Si:C, i.r. absorpt. spectra, local vibr. modes and defect vibr. modes 3−18475
SiC, 6H-polytype, rel. to photolum. spectra 3−30867
SiC, ion implanted, persistent defect, luminesc. obs. 3−30227
SrF_2, calc. of H^- impurity vibr. 3−36390

lattice localised modes continued
SrF$_2$:H , impurity induced far i.r. absorpt. 3−34387
V, Mossbauer study of ^{57}Fe impurities, 4-1000 K 3−4835
VD$_5$, vibrational and diffusional motions of deuterium in α and β phases 3−1820
lattice mechanics *see lattice dynamics*
lattice phonons
adatom interacting pair, phonon contrib. to free energy 3−38724
Ag films, rough decay of nonradiative surface plasmons into light 3−15534
alkali halide, optic mode Gruneisen parameters rel. to anharmonic interactions 3−27094
alkali halide, phonon sidebands in emission spectrum of O_2^- 3−39182
alkali halides photoinduced evaporation, exciton-phonon decay *(German)* 3−27186
alkali metals, axially symmetric model for lattice dynamics, effect of conduction electrons 3−7881
alkali metals, Landau Fermi liquid parameters anisotropy, electron-phonon interactions 3−27203
p- AlSb, mechanisms of carrier scattering 3−24455
ammonium halides, in disordered phases, low frequency Raman spectra, lattice dynamical calc. 3−34347
anharmonic crystals, interference in neutron scattering, one phonon inelastic cross-section 3−38644
anisotropic crysts., i.r. refl. from longit. modes 3−39138
aromatic hydrocarbons, planewise summation of point dipole-dipole interactions, exciton-phonon coupling 3−18102
band model, phonons, lattice distortion, metal-insulator phase transition 3−38807
benzene, cryst., dispersion relations and freq. distrib. calc. 3−24229
benzene, cryst. vibr. calc. 3−24228
benzene, hexamethylbenzene molecular crystals, frequency calculations using atomic interaction potentials *(French)* 3−33626
benzene mixed crystal, Raman spectra, phonon delocalization and trap depths 3−21403
benzol crystals, exciton-phonon interaction and energy transmission *(Russian)* 3−27534
bound polaron, variational estimate of energy spectrum 3−27232
chrysene, lattice dynamics and thermal diffuse scatt. of X-rays 3−24226
coherent sound vibration, effects on γ-γ ang. correl. 3−34269
correlation function calc. in diffraction of particle by solid *(French)* 3−24234
coupled spin-phonon system, resonant phonon scatt. rel. to lattice thermal cond. 3−33636
coupled superconducting tunnel junctions, transfer characts. 3−36689
crystal surface, phonon induced desorption of adatoms, computations for model system 3−18023
crystal surface, theory of phonon induced desorption of adatoms 3−18022
crystals of D^7_{4h} symmetry, two-phonon processes, group-theoretical investigation 3−15491
cubic crystals, exchange-quadrupole forces and dispersion 3−33631
defect crystal lattices, phonon-radiation force 3−7888
deuterobenzol crystals, exciton-phonon interaction and energy transmission *(Russian)* 3−27534
diamond, luminescence quenching and zero-phonon line broadening associated with defect interactions 3−30860
diamond structure, quadrupole interaction 3−30217
dielectric, rel. to thermo-absorpt. and nonlinear absorpt. of sound in hydrodynamic region 3−33613
dielectric materials electron scattering by optical surface phonons 3−8003
rel. to dipole-dipole relaxation of paraelectric impurities 3−8513
dislocation, uniformly moving, generating acoustic signal, lattice normal mode expansion 3−36304
dislocation dynamics, interaction with lattice phonons and electrons 3−14857
dislocation interaction, stress pulse obs., review 3−11625
disordered solids, at low temp., thermal phonon scattering 3−20815
dispersion in systems with a planar Fermi surface 3−7890
durene crystals, neat and mixed Raman-active librations and torsions, 100 and 25K, exciton explanation 3−18441
easy plane hexagonal ferromagnets, phenomenological theory of magnetoelastic modes 3−34138
elastic constants, relationship at finite temps., and Gruneisen approx. 3−38606
electronic energy transfer in impure solids, two mols. embedded in lattice 3−18097
even-even nuclei, microscopic theory of two-phonon states 3−26403
excitation, rel. to complex continuum potential for channelling 3−20772
exciton-phonon system, ground state calc. 3−38640
externally deformed crystals, low temp., deformation description 3−36348
Fermi surface, nesting, spin density wave and soft phonon mode 3−36524
ferroelectrics, H-bonded, local mode model, quantum mechanical tunnelling, soft mode 3−5169
ferroelectrics, H-bonded, soft mode optical phonon interaction dynamics, Ising Hamiltonian 3−5170
free energy alteration of phonon system accounting for surface effects *(Russian)* 3−33725
free path determination using shallow donors in He-cooled semiconductors 3−14950
n-Ge impurity ionisation, pure emission of acoustical phonons 3−8192
generation, rel. to coupled acoustoelec. and thermoelec. instability *(Russian)* 3−2099
graphite, electrical transport props. assuming acoustical phonon scattering 3−11897
graphite, phonon dispersion curves and elastic constants 3−38639
graphite, phonon freq. spectrum at 1800 K, rel. to sp.ht. 3−7941
harmonic crystals, f.c.c. Lennard-Jones, phonon spectra, calc. of thermodynamic averages 3−27079
h.c.p. metals, phonon dispersion, determ. of electron-ion part of dynamical matrix 3−7880
heat propag. in solids, modified Fourier theory *(French)* 3−38653
lattice phonons continued
heavy ice, dispersion relations at 223K from neutron scatt. 3−20829
hexagonal metals, anisotropy in phonon scattering resistivity 3−7876
hexane matrix, 1, 12-benzphenylene and coronene impurities, fluorescence spectra 3−27567
host lattice point defect system, local or gap mode freqs. 3−38647
hydrogen bonded solids, theory of proton transfer 3−11583
imperfect crystal, normal modes allowing for pair and n-tuple effects 3−7884
interacting with high frequency sound, kinetic and hydrodynamic equations 3−27075
interface phonons, theory 3−24330
intersection of phonon spectrum branches in simple crystal lattice 3−24235
intrinsic width, scattering of light in absorbing materials 3−15488
ionic crystal, unified perturbation treatment 3−27086
ionic crystals, rel. to closed formula for nuclear quadrupole relax. 3−18390
ions in a crystal, vibrating struct. of luminescence spectra *(Russian)* 3−36913
i.r. absorption by surface phonons and plasmons in small crysts., continuum model 3−24705
jellium, impure, longitudinal sound for small frequency and wavevector, phonon Green's function 3−20989
Kapitza resist. of thin metallic films *(French)* 3−4998
$LiNbO_3$ optical phonon modes assignment 3−8582
linear chain material, softening mechanism of high q-phonons 3−33635
magnon-phonon selection rules, inelastic neutron scattering 3−34131
metal, calc. of phonon damping due to electron-phonon coupling 3−38638
metal, f.c.c., b.c.c., Peierls stresses and glide systems from normal modes of vibr. 3−17919
metal, optimized model pot. for calc. of phonon spectra 3−36508
metal, simple, dispersion, pseudopotential method 3−27208
metal point contacts, phonon generation 3−18209
metal surface, long wavelength phonon generation by e.m. waves 3−27167
metal surface, scattering of He atoms, two-phonon terms 3−11792
metal surfaces, inelastic scattering of neutral atoms 3−36967
metallic covalent crystal, unified perturbation treatment 3−27086
metals, h.c.p., anisotropic lattice dynamics 3−36377
molecular cryst., libron-phonon interaction, relax. processes, effect on thermal cond. 3−33624
molecular cryst., substitutionally disordered, phonons and excitons, interacting bands, coherent pot. theory 3−30379
molecular crystals, temp. dependence of absorption bands intensities of the spectra at Fermi resonance, mass operator and band shape 3−2538
molecular crysts., entire phonon spectrum by localized exciton sideband method 3−7872
molecular solids, optical mapping of phonon density of states 3−1735
monatomic system with isotropic shell-core coupling, shell model of lattice dynamics 3−17944
Mossbauer effect forced harmonic oscillator and zero-phonon transition 3−31983
multiphonon summation i.r. absorption, exponential frequency dependence in NaCl and CaF_2 struct. crystals 3−4827
naphthalene, entire phonon spectrum by localized exciton sideband method 3−7872
non-metallic crystals heat conductivity, phonon interactions and effect of lattice imperfections 3−33643
noncrystalline systems, freq. spectrum and low-temp. sp. ht. 3−7895
n.q.r. freq. in solids, T^4 depend. rel. to acoustic phonons 3−34246
nylon and polyethylene, phonon freq. distrib. rel. to low temp. thermal props. 3−24303
optical, effects of longitudinal vibrations on electronic excitations of solids 3−20833
paraelastic resonance of Jahn-Teller and off-centre ions 3−24387
paramagnetic ions, cross relaxation obs. by optical absorption method 3−34196
paramagnetic relaxation of resonant phonons at low temp. 3−11705
phase transition dynamics, neutron scatt. 3−14940
phase transition dynamics studies *(French)* 3−4834
phonons, scatt., variational treatment 3−24227
photoemission, electron energy loss rel. to plasmon and phonon excitation 3−21517
photon, phonon and plasmon interactions in solids 3−36550
polar crystal, ground-state energy of Wannier exciton 3−21039
polar crystal, surface effects on optical phonons and phonon-plasmon modes 3−24326
polar semiconductor surface magnetoplasmon-optical phonon interaction 3−24328
polymers, conformational defects, phonon Green's function treatment 3−29764
polymers, regular, phonon Green's function, exact computation, semianalytical method 3−29765
quantum cryst., vacancy wave excitations props. 3−33715
quantum crystal point transformation theory, zero-temp. self-consistent phonons 3−36378
quantum crysts., optimized Jastrow factor and consistent phonons 3−14949
quartz, rel. to crit. force const. of struct. phase transition 3−17953
Raman scatt., second order, under phonon-plasmon Fermi reson. 3−21423
Raman scattering, by optical phonons in crossed elec. and mag. fields 3−5205
Rb, phonon frequencies calc. by optimized model potential method 3−7877
relaxation, xy model, spin-phonon interaction, damping, frequency shift *(Russian)* 3−27084
resonance absorption of phonons into vibrational modes, mass defect influence 3−17950
rigid molecule model, group theoretical selection rules in inelastic neutron scattering 3−7887
ruby, cross relaxation of Cr^{3+} ions, resonant phonon scattering 3−34193
sapphire, dispersion of acoustic phonons 3−27085
sapphire, lattice thermal cond. from 0.4 to 4K 3−7980

lattice phonons continued
scattering, boundary, variational treatment 3−24227
scattering by paramagnetic ions, freq. depend. 3−38636
second-neighbour Ising chain as model for spin-phonon interactions 3−18284
self consistent phonon theory, review 3−36375
semiconductor, group-IV, phonon spectra 3−4825
semiconductor, ionic lattice, rel. to weak turbulence of coupled longitudinal waves 3−33879
semiconductor, low freq. e.m. wave propag., under inelastic carrier-phonon scatt. conditions *(Russian)* 3−8166
semiconductor, nondegenerate, crossed field acoustic amplification in strong mag. fields, relaxation time for acoustic-phonon scattering 3−11937
semiconductor, phonon contrib. to optical electron transitions, impurity absorpt. 3−34391
semiconductor, piezoelectric, hexagonal, anisotropy of phonon generation 3−17951
semiconductor, polar, i.r. absorpt. of localised longit. optical phonons 3−30232
semiconductor, rel. to hard photon and slow neutron scatt., sound instability conditions *(Russian)* 3−7893
semiconductor, theory of phonon electroreflectance 3−27503
semiconductor overheating instabilities, low-temp. impurity breakdown 3−24395
semiconductor quantised thin films, optical absorption by indirect interband transitions *(Russian)* 3−36957
semiconductors, longitudinal mixed waves due to optical phonons and plasma longitudinal oscillations interaction *(Russian)* 3−11926
and spectral band shapes, symmetry of quadratic mode absorpt. and emission profiles in impure solids 3−8631
spectral props. of solids, numerical calcs. by integration over Brillouin zone 3−20983
spin waves, parametric excitation by magnetoelastic interaction with phonon pumping 3−27375
spin-lattice relax., soft optical phonon scatt. mechanism, relax. probability *(Russian)* 3−2334
spin-lattice relaxation, phonon bottleneck theory in Orbach process 3−18353
spin-phonon interaction in Ising model 3−24598
stimulated phonon-photon-polariton scatt. theory 3−1783
surface, exptl. obs. using attenuated total reflection 3−24493
surface phonon h.f. generation rel. to surface defects, emission into dielec. substrates 3−15064
surface specific heat of crystal lattice at low temp., calc. 3−30233
surfaces, reconstructed, optical phonons 3−20920
tetrahedral impurities, coupling strengths of α_1, ε and τ_2 phonons to A→T optical transitions 3−27522
tetrahedrally bonded solids, phonon spectra 3−4825
rel. to thermal conductivity, scattering-induced dispersion effects 3−36396
thermal motions of atoms in a solid influence on neutron scattering 3−20837
thin film, infinite, submerged in an infinite medium heat diffusion bosonic nature of phonons *(Spanish)* 3−28989
thin films, Brillouin spectra structure 3−12135
thin films, density of states 3−27295
thiourea, l.f. Raman spectrum, temp. depend. soft mode behaviour *(French)* 3−5182
TiO_2 uniaxial crystal, surface optical phonons 3−20827
transition metal semiconducting phosphate glasses, transport props., phonon dispersion 3−8175
transport crystals, multiphonon absorption of i.r. due to higher-order electric moments 3−18452
transport relaxation time for phonon-impurity scatt., rel. to thermal cond. 3−1836
two-photon exciton transitons in semiconductors, phonon-assisted, band models 3−18105
uniaxial crystals, electromagnetic waves, plasma oscillations, interactions, spectra 3−33941
Van Hove singularities and zero point slopes in crystals 3−30382
Van Hove singularities and zero-point slopes in mag. crystals 3−30383
X-ray Brillouin scattering when Bragg condition nearly satisfied 3−30146
Ag, phonon viscosity, dislocation drag, and u.s. attenuation 3−38625
Ag halides, low frequency dielectric response, low frequency anharmonic self energy for transverse optic mode 3−8502
Ag surface, scattering of He atoms, one-phonon contrib. 3−11791
AgCl, thermal cond., role of phonon phase and group vels. 3−20839
AgCl(Br), investigation using shell model with deformable ions 3−1733
Al, dielectric screening and phonon dispersion 3−38633
$Al_xGa_{1-x}As$, collective phonon modes, Raman scatt. 3−5200
$Al_xGa_{1-x}As$, reson. Raman scatt., 2K 3−34359
Al_2O_3, pure and Mg-doped, rel. to thermal cond., 1.3-100 K 3−30293
AlSb, rel. to resonant Raman scatt. 3−5201
Ar, solid, Raman two-phonon spectra, mol. dynamics 3−34353
Ar, solid, thermodynamic props. 3−20838
Ar crystals, force constants and phonon dispersion theoretical parameters 3−38645
As_2S_3, laminar semicond., Raman scatt., absorption spectrum, vibr. levels splitting *(Russian)* 3−21425
$As_2(S_xSe_{1-x})_3$ amorphous film, i.r. spectra study 3−36382
$As_2(S_xTe_{1-x})_3$ amorphous film, i.r. spectra study 3−36382
$As_2(Se_xTe_{1-x})_3$ amorphous film, i.r. spectra study 3−36382
Au, phonon viscosity, dislocation drag, and u.s. attenuation 3−38625
$AuCuZn_2$, soft acoustic phonons near martensitic transition 3−14942
$BaMoO_4$, $BaWO_4$, coupled vibrations, i.r. reflection and Raman spectra obs. 3−30815
$Ba(NO_3)_2$, i.r. and Raman study 3−27504
BaO optical phonons at centre of Brillouin zone at 300 and 17K *(French)* 3−8567
$BaTiO_3$, A_1 modes, temp. depend., Raman scatt. study 3−30221
Be, dispersion curves for noncentral force model 3−33617
Be h.c.p., modified Sharma-Joshi model, curves 3−30220

lattice phonons continued
Bi, freq. spectrum, five neighbours Born-von Karman model 3−20821
Bi, lattice dynamics , phonon dispersion, freq. spectra, sp. ht. 3−30215
Bi, sound propag. in strong mag. field, phonon spectra singularities 3−30672
BiOBr, i.r. transmission, two phonon absorpt. processes 3−21424
BiOCl, i.r. transmission, two phonon absorpt. processes 3−21424
BiOCl(Br)(I), two-phonon processes 3−15491
BiOI, i.r. transmission, two phonon absorpt. processes 3−21424
$Bi_{12}SiO_{20}$, light scatt. by optical phonons *(Russian)* 3−8591
Br_2, solid, phonon dispersion and symmetry 3−24236
$CaCO_3$, i.r. refl. from longit. modes 3−39138
$CaCO_3$, trigonal, densities, dispersion curves of external and internal modes 3−33630
CaF_2, anharmonic lattice vibr., calc. and neutron diffr. obs. 3−24222
$Ca(NO_3)_2$, i.r. and Raman study 3−27504
CaO optical phonons at centre of Brillouin zone at 300 and 17K *(French)* 3−8567
Cd, phonon dispersion curves, 80K, X-ray diffuse scatt. study 3−1731
Cd, thermal resistivity anisotropy calc. using Mannari-Ziman-Baym theory 3−20840
$CdCr_2Se_4$, refl., mag. ordering effect of low freq. i.r.-active phonon 3−15492
CdF_2:In^{3+}, semicond., rel. to resonance Raman spectra 3−36871
CdS, rel. to dispersion of Raman cross section over wide energy range 3−36872
CdS, rel. to elec. field induced Raman scatt. 3−21407
CdS, rel. to stimulated emission 3−15523
CdTe, recrystallised thin film,s exciton-phonon interaction *(Russian)* 3−11871
CdTe, X-ray diffuse scatt. to observe dispersion curves of phonons *(Russian)* 3−7892
$Ce_2Mg_2(NO_3)_{12}$, rel. to thermal cond., 0.2-1.5 K 3−36444
$Ce(NO_3)_2$, phonon induction effects at e.s.r. saturation 3−8417,
Co Tutton salts, direct and Raman spin-lattice relaxation, effect of phonon bottleneck 3−27410
Cr-Fe(1%) alloy, phonon dispersion relation anomalies, neutron scatt. obs. 3−14948
Cs, liquid, phonon freq. and elec. resist. calcs. using optimised model potential 3−20828
CsCl(Br)(I), phonon dispersion, modified-rigid-ion model calc. 3−36381
CsI, phonon dispersion curves from neutron scatt. *(Russian)* 3−20836
Cu, phonon dispersion and third order elastic consts. calc. 3−17898
Cu, phonon freqs., modified Bhatia's model 3−38635
Cu, phonon freqs. at 80 K from neutron diffr., Deby temp. 0-300 K 3−33632
Cu, phonon viscosity, dislocation drag, and u.s. attenuation 3−38625
$CuGaS_2$, dielec. dispersion, phonon freqs., i.r. refl. spectrum 3−8585
Cu_2O, Raman scattering, luminescence, exciton-phonon coupling 3−8581
Cu_2O, resonance Raman scattering at the forbidden yellow exciton, phonon assisted absorption threshold 3−21408
D, phonon dispersion relations from inelastic coherent neutron scattering 3−20832
DBr, Raman spectra, lattice modes in molecular crystal 3−5183
DCl, Raman spectra, lattice modes in molecular crystal 3−5183
EuTe, Raman scatt. by coupled plasmon-LO phonon mode, 2K 3−5209
$FeBO_3$, Raman scatt. from magnons and phonons 3−34358
$FeCl_2$, thermal conductivity 3−20843
FeF_3, Raman scatt. 3−30820
FeF_3, Raman scatt. from magnons and phonons 3−34358
Ga:Sn, in porous glass, ^{119}Sn Mossbauer, phonon spectrum, supercond. critical temp. 3−21355
$Ga_xAl_{1-x}As$ alloy system, obs. of disorder-activated acoustic phonon mode in Raman spectrum 3−2542
GaAs, i.r. refl., damping effects on plasmon-phonon spectrum *(Russian)* 3−8592
n-GaAs, intervalley absorpt., LA and TA phonons contrib. *(French)* 3−24726
GaAs, longitudinal optical phonon-plasmon coupling 3−36551
GaAs, reson. Brillouin scatt. and absorpt. edge modulation by intensely amplified phonon beams 3−5204
GaN, free-electron and intrinsic lattice dispersion 3−18455
GaP, hydrostatic pressure effect on TA(TO)(LO) phonon peaks in Raman spectrum 3−30824
GaP, second-order Raman spectra and phonon dispersion 3−21396
p-GaSb, optical pumping of spin polarised conduction electrons, emission of optical phonons 3−34398
GaSb, plasmon-phonon interactions, i.r. refl. obs. 3−21042
p-Ge, heat pulse propagation under uniaxial stress 3−20842
Ge, longitudinal and transverse phonons contrib. to thermal cond. in Ziman limit 3−17940
Ge, rel. to radiative recomb. of biexcitons *(Russian)* 3−8663
Ge, two-phonon deformation potential 3−7883
Ge, upper and lower bounds on the three-phonon umklapp resistances 3−27089
Ge hole scattering by acoustic and optical phonons in homogeneously deformed sample *(Russian)* 3−24417
n-Ge-Pb Schottky barriers, under press., phonon tunnelling spectroscopy 3−36379
H, phonon dispersion relations from inelastic coherent neutron scattering 3−20832
HBr, Raman spectra, lattice modes in molecular crystal 3−5183
HCl, Raman spectra, lattice modes in molecular crystal 3−5183
α-HIO_3, Raman scatt. by optical phonons, Fermi reson. 3−21406
^3He b.c.c., umklapp region thermal cond. 3−36455
^4He, solid, neutron scattering at large momentum transfer, velocity spectrum determ. 3−7992
$HfS_2(Se_2)$, Raman scatt. and i.r. studies 3−4833
α-HgS, vibr. spectrum assignments 3−8583
Ho h.c.p., modified Sharma-Johsi model, curves 3−30220

lattice phonons continued
I_2, solid, phonon dispersion and symmetry 3−24236
In, freq. distrib. spectrum, heat capacity 3−1730
In-Tl, soft acoustic phonon mode rel. to martensitic transform. 3−30226
n-InSb, non ohmic transport and phonon amplification 3−8189
n-InSb, reson. hole-TO and hole-LO phonon coupling, magnetooptical study 3−4831
InSb, two-phonon deformation potential 3−7882
$KBrO_3$, Raman scatt. and i.r. refl. studies 3−2543
KCl, Mossbauer obs. of inelastic scatt. at Bragg reflection, multiphonon scatt. contrib. 3−15446
KCl:KOH and KI:KOH, tunnelling levels of hydroxide ion 3−27226
$KClO_3$, rel. to indirect transitions, fundamental absorp. obs. 3−30832
$KCoF_3$, first order phonon and magnon Raman scattering 3−27499
KH_2PO_4, ferroelec. cryst., Raman spectra scatt. phonon direction depend. 3−21422
KH_2PO_4-structure ferroelectrics, NQR temp. dependence rel. to soft-mode 3−18392
$KMnF_3$, rel. to phase transition dynamics, crit. neutron scatt. obs. 3−1799
KNO_3, ferroelectric, phonon dispersion curves 3−20824
$KNbO_3$, soft lattice vibr. modes, spontaneous polarisation and Curie constants 3−34303
$KTaO_3$, stabilisation of paraelectric phase by strong quartic anharmonicity 3−30776
Kr, solid, Raman two-phonon spectra, mol. dynamics 3−34353
Kr, solid, thermodynamic props. 3−20838
Kr crystals, force constants and phonon dispersion theoretical parameters 3−38645
Kr solid, elastic consts. from neutron diffr. by acoustic phonons, 77 K 3−27049
Li, phonon dispersion curves calc. using Hartree-Fock and pseudopotential methods 3−11704
Li, phonon freqs., local model pseudopotential calc. 3−1734
Li propagation, atomic wavefunction, Slater exchange 3−30219
LiF, small crystals, i.r. absorpt. rel. to particle size, mode absorpt. bands 3−39150
$LiIO_3$, assignment of vibrs. from i.r., Raman and n.q.r. data 3−38637
Mg, dispersion curves for noncentral force model 3−33617
Mg, lattice dynamics, phonon dispersion, freq. spectra, sp. ht. 3−30215
Mg h.c.p., modified Sharma-Joshi model, curves 3−30220
MgF_2 uniaxial crystal, surface optical phonons 3−20827
$MgSO_4.7H_2O$ biaxial crystals, angular dispersion of polar phonons, Raman scatt. study 3−1732
MnO, optical absorpt. spectrum, role of magnons and phonons *(Russian)* 3−15522
MnTe, antiferromag. semicond., optical phonon spectrum obs. over Neel temp. 3−5104
Mo, fracture energy calc. based on phonon theory of brittle fracture 3−17923
MoS_2, laser excited Raman spectra, active long wavelength phonon freqs. 3−21420
$MoSe_2$, laser excited Raman spectra, active long wavelength phonon freqs. 3−21420
$MoTe_2$, laser excited Raman spectra, active long wavelength phonon freqs. 3−21420
ND_4Br and ND_4Cl, inelastic neutron scattering in orientationally disordered mol. crystals 3−20726
NH_4Cl, order-disorder transform., Raman scatt., T_λ region, lattice and internal modes 3−24688
NH_4I, Raman spectra, one-phonon density-of-states and spatial correl. 3−39137
$(NH_4)_2SO_4$, ferroelectric transition, analysis of long wavelength lattice vibrs. 3−27476
N_2O, cryst., i.r. intensities of external modes 3−21397
Na chemically motivated pseudopotential 3−20708
$NaBrO_3$, $NaIO_3$, rel. to indirect transitions, fundamental absorp. obs. 3−30833
NaCl, band struct., optic phonon deform. effects, APW calcs. 3−15135
$NaClO_3$, rel. to indirect transitions, fundamental absorp. obs. 3−30832
$NaCoF_3$, i.r. refl. spectra, vibr. spectra, optical consts. dispersion 3−39149
NaF, lattice thermal cond., phonon contribs., point defect scatt. effects 3−33644
NaF, phonon cond., calc. using nonlinear theory of heat transfer 3−27095
NaI crystalline powder, one-phonon far i.r. absorp. 3−27502
$NaNO_2$, dipole-lattice relax. time near Neel temp. 3−15454
$NaNO_2$, libration mode temp. depend. rel. to dielec. relax. 3−38642
$NaNbO_3$, diffuse X-ray scatt. and phase transition phenomena 3−15001
$NaNbO_3$, soft modes and superlattice struct. 3−39105
$NaNiF_3$, i.r. refl. spectra, vibr. spectra, optical consts. dispersion 3−39149
$NaNiF_3$, phonon and magnon light scattering 3−39148
Nb, superconducting, anomalous u.s. attenuation 3−38929
Nb, superconducting, effect of dislocations on lattice thermal conductivity 3−11634
Nb-Ti alloy, phonon spectrum, Kohn anomaly, in normal state, 2-9 K 3−33623
Nb-W alloy, phonon spectrum, Kohn anomaly, in normal state, 2-9 K 3−33623
Nb_3Sn, phonon linewidths, influence of the superconducting energy gap 3−17948
Nd^{3+}:YAG, nonadditive phonon induced line broadening, elastic ion lattice interaction 3−22907
$NdAlO_3$, soft-mode spectroscopy for trigonal-to-cubic phase transition prediction 3−15502
Ne, interatomic pot. calcs. 3−20071
Ne, solid, inelastic neutron scattering obs. of phonon dispersion 3−7889
Ne crystals, force constants and phonon dispersion theoretical parameters 3−38645
NiO, small crystals, i.r. absorpt. rel. to particle size, mode absorpt. bands 3−39150
Pb, phonon dispersion calcs. using local model pseudopotential 3−17946
Pb, phonon dispersion using Ashcroft model pseudopotential 3−17947
$Pb(NO_3)_2$, i.r. and Raman study 3−27504
$5PbO.3GeO_2$, Raman spectra of soft phonon mode at ferroelec. phase transition 3−24691
$PbTiO_3$, ferroelec. perovskite, Raman spectra obs. of lattice modes 3−33634
Pd, dispersion of lattice waves 3−17942
Pt at 90K, cryst. dynamics from inelastic neutron scatt. meas. 3−11699
Rb, lattice vibr. dispersion curves, inelastic neutron scatt. meas. 3−33618
$RbClO_3$, Raman spectra obs. of props. of normal and oblique optical phonons 3−17949
RbF microcrystals, density of phonon states and i.r. absorpt., calc. 3−36380
SbSI-SbSeI mixed crysts., far-i.r. reflectivity, l.f. ferroelec. mode behaviour 3−39135
SbSi cryst., mid-i.r. absorpt. and indirect transitions, phonon energy and energy gap calc. 3−24697
Sc, phonon dispersion and elastic consts. 3−30225
Sc, phonon dispersion calc. 3−33627
Se, resonant Raman scatt. 3−5202
Se, trigonal, dispersion curves, valence force field model 3−27081
Se-Te, Raman spectra obs. rel. to lattice modes 3−8578
Si, fine structure in optical absorpt. edge, exciton form. and phonon emission 3−18082
p-Si, heat pulse propagation under uniaxial stress 3−20842
Si, lattice thermal cond., three phonon relax. rate, 2-1400 K 3−33645
Si, multiphonon Raman spectrum 3−39145
SiC, 15R polytype, single-phonon absorpt. rel. to reststrahlen band structure 3−15497
SiC, i.r. refl., damping effects on plasmon-phonon spectrum *(Russian)* 3−8592
SiC polytypes, i.r. latice absorpt. bands 3−36875
SiF_4, cryst., one- and two-phonon absorpt., i.r. and Raman spectra 3−27495
SiO_2 fused below 1K, nonlinear phonon propag. 3−17952
Sn-I-Sn superconducting tunnel junction, quasiparticle relax. and phonon emission 3−27338
SnO_2, Raman active phonons, Gruneisen parameters, 10-500 K, 0-4 kbar 3−33633
$(Sr_{1-x}Ba_x)TiO_3$ mixed cryst. system, phase transitions obs. 3−15456
$SrMoO_4$, $SrWO_4$, coupled vibrations, i.r. reflection and Raman spectra obs. 3−30815
$Sr(NO_3)_2$, i.r. and Raman study 3−27504
SrO optical phonons at centre of Brillouin zone at 300 and 17K *(French)* 3−8567
$SrTiO_3$, rel. to phase transition dynamics, crit. neutron scatt. obs. 3−1799
$SrTiO_3$, stabilisation of paraelectric phase by strong quartic anharmonicity 3−30776
p-Te, anisotropic phonon coupling in magnetophonon resonance 3−7874
Te, resonant Raman scatt. 3−5202
Ti, dispersion and sp. ht., calc. by electron gas model 3−1729
TiO_2, rutile, static dielec. const. and Raman spectra, press. and temp. depend. 3−18456
$TiS_2(Se_2)$, Raman scatt. and i.r. studies 3−4833
Tl, dispersion curves for noncentral force model 3−33617
Tl h.c.p., modified Sharma-Joshi model, curves 3−30220
Tl halides low frequency dielectric response, low frequency anharmonic self energy for transverse optic mode 3−8502
TlCl, band edge temp. dependence, two-photon absorption and multiphonon processes 3−12148
TlI, mol. struct., anharmonicity, i.r. and Raman investigations 3−20825
V_3Si, mag. field influence on soft mode behaviour near martensitic transition temp. *(French)* 3−4854
Xe, solid, Raman two-phonon spectra, mol. dynamics 3−34353
YIG film, phonon generation by ferromag. resonance 3−36794
YZn alloy, phonon dispersion curves determ. by inelastic neutron scattering 3−7886
Zn, dispersion relations, calc. by pseudo-pot. method 3−4824
Zn, h.c.p., phonon dispersion rel. to dielec. screening, pseudopotential approach 3−36376
Zn, lattice dynamics, phonon dispersion, freq. spectra, sp. ht. 3−30215
Zn, thermal resistivity anisotropy calc. using Mannari-Ziman-Baym theory 3−20840
ZnO, rel. to dispersion of Raman cross section over wide energy range 3−36872
ZnS, cubic, i.r. active 2-phonon processes 3−39130
ZnS:Mn, phonon induced hyperfine fields, molecular orbital model *(German)* 3−15161
ZnSe, dispersion 3−7869
ZnSe:Mn, phonon induced hyperfine fields, molecular orbital model *(German)* 3−15161
$ZnSiP_2$, luminescence excitation spectra at 2K, sharp emission lines identification as phonon replicas 3−8654
$ZnSiP_2$, opt. vibrs. freqs., phonon lifetime *(Russian)* 3−8572
ZnTe, rel. to resonant Raman scatt. 3−5201
$ZrS_2(Se_2)$, Raman scatt. and i.r. studies 3−4833
lattice structure, crystals *see crystal atomic structure*
lattice theory and statistics
see also Ising lattices
anharmonic crystals, linear chain model properties, self-consistent theory in pseudoharmonic approx. *(Hungarian)* 3−20820
antiferromagnetic Husimi-Temperley model, distrib. of zeros of partition function above and below critical temp. 3−5084
atom assembly, thermodynamic and mech. stability rel. to crystal growth mechanism 3−1586
Bogolyubov eqns. for equilibrium crystal with three-particle interaction, thermodynamic props. 3−26167

lattice theory and statistics continued

- cell materials, perturbation expansions for random heterogeneous materials, effective elec., thermal and magnetic props. 3−39077
- chain, propagation of localized impulse 3−9793
- chain of interacting harmonic oscillators, propagation of disturbances 3−10394
- classical rotators on a linear lattice, thermodynamic properties calc. 3−32451
- critical exponent expansion in inverse powers of spin dimensionality 3−26164
- critical exponent relation validity restriction to four dimensions 3−32453
- critical exponents, expansion in inverse power of spin dimensionality 3−13650
- cubic lattice, simple, self-avoiding walks, average span 3−16759
- diamond lattice, eight-vertex three dimensional model 3−11696
- dimensionality dependence in spherical model for various critical point parameters 3−35629
- disordered linear chain with nearest neighbour correlations, calc. of energy spectrum 3−32455
- dynamical systems with few degrees of freedom, numerical expts. 3−26147
- eight-vertex model, equivalence to generalized ice-type lattice model 3−28976
- eight-vertex model in lattice statistics and 1-d anisotropic Heisenberg chain, fundamental eigenvectors 3−26160
- eight-vertex model in lattice statistics and Heisenberg chain, eigenvectors of transfer matrix and Hamiltonian 3−26161
- electrostatic potential of point charge in dielectric solid, shell model 3−18407
- equivalent criteria for modularity of lattice of all physical decision effects 3−28835
- Fermi lattice system, quasi-free state thermodynamics, variational formulation 3−37898
- films, thin, long-range order absence and reln. to broken symmetry 3−11838
- gas model, crit. points in less than two dimens. 3−28992
- Green's function for simple cubic and tetragonal lattices at arbitrary points, Heisenberg model calcs. 3−22752
- heat reservoir, statistical mechanical representation using cubic lattices 3−4050
- Heisenberg Hamiltonian, symmetric, eigenvalue solution in spin-wave representation 3−11996
- integral, Mellin-Barnes type for lattice Green's function for cubic lattice 3−35630
- interacting linear chains, electron network model description 3−26162
- Langevin eqn. for general harmonic heat bath 3−26165
- lattice sums, analytic procedures for evaluation in terms of zeta and related functions 3−28980
- lattice-gas model with particle-hole symm. and singular coexistence-curve dias. 3−13652
- limiting ring closure probability index for self avoiding random walk problem 3−28979
- limiting ring closure probability on square lattice, calc. by Monte Carlo technique 3−4040
- linear chain spectra, study using Kodaira's type theory for ordinary linear second order difference operators 3−13651
- linear harmonic oscillator chain dynamics 3−6363
- metals statistical mechanics of phase diagrams, a simple cell model 3−24241
- metastable crystal, quantum formation of nucleation centres 3−36392
- model for solid-solid and solid-fluid phase transitions 3−38655
- n-fold occupation of linear array of m sites 3−6362
- occupation statistics of parallel dimers on m × n lattice 3−22754
- one dimensional anharmonic lattice, wave modulation 3−4041
- phase transition in 2-dimensional lattice gas with long range attractions 3−37902
- phase transitions of first order in lattice-gas models, chemical systems of equivalent particles with pairwise interaction, book *(German)* 3−13653
- polymer chain, lattice model for adsorption 3−29779
- quantum crystals, Fermi-type, phenomenological theory 3−24238
- quantum lattice system, time evolution in automorphism of quasi-local algebra 3−28977
- random walks on 2-D lattice with traps, determ. of propag. function 3−26166
- response to an applied external force by semi-infinte lattice 3−22751
- self-avoiding walks, counting theorems 3−32452
- self-avoiding walks in f.c.c. and triangular lattices, end-to-end length distrib. 3−22753
- simple cubic lattice Green function analytical properties, applications in lattice statistics 3−19518
- solitons and energy transport in nonlinear lattices 3−26146
- spin-1/2 lattice system, group structure and duality transformation generalization 3−10396
- spin-$^{1}\cdot_{2}$ lattice system, duality transformation and correlation functions 3−37899
- thermodynamic dual lattice, classical system of arbitrary spin 3−13637
- two-dimensional systems, ordering, metastability and phase transitions 3−36398
- walks, off-lattice self-avoiding, mean square endpoint separation calc. 3−19517
- XY model, three-dimens., freq. depend. susceptibility, singularity struct. 3−615
- zero-field free-fermion model, transfer matrix direct diagonalization 3−37900
- ^{3}He-^{4}He liquid mixture, quantum lattice gas model 3−38696

lattice vibrations *see lattice dynamics*

Laves phases *see alloys*

lawrencium

- No entries

lawrencium compounds

- No entries

LCAO calculations

- alkaline earth difluorides, nonempirical MO SCF studies, bonding trends 3−20096
- aniline, electronic charges calc. by variable electronegativity π-electron SCF-MO method 3−7123
- approximate MO LCAO calcs. by extended Huckel method on SK_{β} X-ray emission of $K_2S_2O_5$ and KHSO 3−30891
- benzene, electronic spectrum 3−17420
- bond order 3−7126
- computer program for nonempirical SCF LCAO calculations 3−33078
- coronene molecular crystal, exciton spectrum calc. *(Russian)* 3−11872
- cyclopropenyl cation and radical, stability, geometry, electronic structure, LCAO-MO-SCF calc. 3−29552
- DNA periodic models, charge carrier mobility calcs. from cryst. orbitals 3−8171
- Huckel LCAO-MO study of binding energy of crystals 3−1592
- hydrogen bond study of $ROH.OCH_2$ dimers (R = H, CH_3, NH_2, OH, F) 3−38262
- hyperfine structure consts. between molecules and their radicals, linear relationship *(Russian)* 3−7140
- imidazobenzimidazoles, electronic structure, p.m.r. and reactivity 3−20098
- LCAO-MO-SCF electronic charge densities, evaluation of force constants of diatomic mols. 3−20109
- molecules, linear triatomic, spin-orbit coupling consts., non-empirical calc. 3−23532
- Pariser-Parr-Pople method with retention of bonded differential overlap, choice of parameters 3−11197
- periodic systems, band struct. calc. *(French)* 3−1965
- phenol, electronic charges calc. by variable electronegativity π-electron SCF-MO method 3−7123
- polymer energy band local derivatives *(French)* 3−1966
- polymers, generalization of LCAO MO methods *(Hungarian)* 3−7276
- pteridines, amino-substituted, protonation site determ. from SCF-LCAO-MO-CI calcs. 3−29590
- SCF wavefunctions for complex mols., approx. of partial retention of diatomic differential overlap 3−23518
- SCF-MO calcs. of MgF_2 ground state, determ. of equilibrium geometry 3−4403
- surface states on three-dimensional mixed crystals, study by band-edge LCAO method *(Russian)* 3−5044
- symmetrical molecule, orbital structure, topology *(German)* 3−33075
- thioaldehyde, u.v. and visible absorption spectra, MO-LCAO calc. *(German)* 3−11249
- thiocarbonyl compounds, absorption behaviour *(German)* 3−11248
- thioketone, u.v. and visible absorption spectra, MO-LCAO calc. *(German)* 3−11249
- toluene, electronic charges calc. by variable electronegative π-electron SCF-MO method 3−7123
- p, m, o- toluidine, quantum mechanical calc. *(Russian)* 3−11202
- tricyclic heteroaromatic systems, electronic structure rel. to p.m.r. and reactivity 3−20098
- water molecules in free state and solid hydrates, hydrogen bond studies, ab initio calcs. 3−7118
- $[H_2O...Cl]^-$ complex, SCF LCAO MO calcs. of hydrogen bond 3−29587
- AlLi, LCAO-MO-SCF calc. using Gaussian basis functions, configuration interaction calc. 3−23524
- B compounds, BCN, BNC, BCC, CBC, BBC, BCB, ab initio electronic struct. calcs., optimum bond lengths determ. 3−20093
- BeF_2, nonempirical MO SCF studies of low lying states 3−23529
- BeH, configuration interaction LCAO-MO calc. of the $X^2\Sigma^+$ and $A^2\pi$ states 3−26624
- CNC, NCC unstable intermediates, ab initio calcs. of equilib. bond lengths 3−20095
- Co complex, acetylacetonate cobalt (III), u.v. and visible absorption spectra calc. 3−20137
- Cr complex, acetylacetonate chromium (III), u.v. and visible absorption spectra calc. 3−20137
- Cu_2, Cu_2^+ particles, ab initio study 3−11201
- Ge amorphous, electron spectra, effect of valence angles deform., LCAO calcs. *(Russian)* 3−8084
- HF-HCN, hydrogen bonding through lone pair and π system 3−23530
- K, interband optical cond. calc. in range 1 to 10 eV 3−24375
- $KNiF_3$, cubic field splitting parameter, MO-LCAO calc. *(Russian)* 3−11859
- MnO_4^-, SCF LCAO MO ground state calc. 3−11196
- NNC, NCN, unstable intermediates, ab initio calcs. of equilib. bond lengths 3−20095
- Ni complex, 1, 5-diphenylformazan nickel(II), calculation of u.v. and visible absorption spectra 3−20136
- SF_6, SCF MO LCAO calcs. of optical absorpt. and X-ray emission 3−1151
- Ti complex, acetylacetonate titanium (III) u.v. and visible absorption spectra calc. 3−20137

lead

- absorption cross section for 450-1000 MeV photons 3−11163
- adhesion to steel ball, contact zones 3−4798
- anharmonic thermal scattering of X-rays 3−38524
- aquatic frontal systems, element enrichment in films and foams 3−12690
- atom, muonic, screening correction to binding energy 3−11188
- atoms, sticking coefficient on SiO effect of water vapour 3−38734
- cyclotron reson. at high freq., electron-phonon interaction 3−38787
- dating of Onverwacht Series, South Africa; U-Th-Pb systematics 3−2852
- deformation in torsion at high strain rates 3−7828
- dendrite, electrodeposited, habit and morphology rel. to growth parameters 3−33767
- dendrites, grown by electrolysis, crystallographic features 3−4942
- diffusion, in Ag film, Pb/Ag/Au and Pb/Ag/Pd layered struct. obs. 3−7976
- electrical and thermal cond. determ. from 80 to 400 K 3−24405
- embrittlement of steel, comp. depend. 3−21648
- epitaxial films growth on PbTe 3−18238

- **lead** continued
  - equation of state, semiempirical, rel. to mech. props. *(Russian)* 3−27618
  - Fermi surface, OPW model for pressure depend. 3−33788
  - Fermi surface pseudopotential calcs. convergence props. 3−33783
  - film, reflectance meas. in vacuum u.v. rel. to optical constants 3−21379
  - film, supercond., elec. resist., crit. temp., annealing effect *(Russian)* 3−18251
  - flame fluorescence detection with freq. doubled dye laser as excitation source 3−28777
  - gamma-ray scatt., total cross sections, 60-1400 keV 3−29462
  - grains, sp. ht. below 5 K 3−27329
  - Hall effect and magnetoresistance 3−38825
  - heat capacity, anharmonic lattice vibration contrib. 3−7940
  - impregnated porous glass, delineation of Pb morphology 3−8315
  - impulse lasers, expt. obs. *(Russian)* 3−35690
  - interface of Au substrate with Pb monolayers, spontaneous alloying 3−36463
  - ion beam, relativistic, heavy, meas. of range in Pb 3−33583
  - isotopes, X-ray transitions, isotope shifts 3−1107
  - Knight shift anisotropy calc. 3−15434
  - lattice dynamics using local model pseudopotential 3−17946
  - liquid, diffusion and solubility of O_2, electrochem. obs. 3−27133
  - liquid, struct. microheterogeneities, kinetic viscosity, temp. depend. *(Russian)* 3−17729
  - liquid, thermoelectric props., temp. depend., m.p.-1200K 3−24408
  - loaded, plastic scintillator detection cross-sect. for γ-rad., calc. considering ang. depend. of rad., calc. 3−13424
  - melting curve, up to 60 kbar 3−27103
  - metallographic preparation by ion beam machining 3−8887
  - molecular beam, determ. of diatomic:atomic ratio from ESCA 3−29745
  - muonic, elec. quadrupole X-ray transitions 3−7095
  - neutron diffraction, rel. to quasicryst. model for diffr. effects in alloys 3−27640
  - neutron spectra, time-energy study using fast neutrons 3−6968
  - normal and supercond., flow stress and yield pt. obs. 3−5076
  - oxidation of surface, ESCA obs. of polymorphic PbO 3−33741
  - phonon damping due to electron-phonon coupling, calcs. 3−38638
  - phonon dispersion using Ashcroft model pseudopotential 3−17947
  - powder, microimpurities, spectral determ. 3−16568
  - radiation mech. effect, fine strength change on electron irradiation 3−33552
  - shielding for transport of common radioisotopes 3−11096
  - shock wave propagation, deform. energy and collision velocity determ. *(Russian)* 3−27066
  - specific heat anomaly and disorder *(German)* 3−24276
  - superconducting, Landau domain struct. growth 3−15297
  - superconducting and normal states, plastic flow behaviour 3−30183
  - superconducting film, temp. and thickness depend. of crit. mag. fields 3−34018
  - superconducting thin films, critical thicknesses 3−34011
  - superconducting thin films, intermediate quantum resistance states in parallel mag. field, obs. 3−34032
  - superconducting thin films, intermediate state, magnetic structure in perpendicular magnetic fields 3−11990
  - superconducting thin films with Bi impurities, surface impedance *(German)* 3−21165
  - superconducting transition, mag. field induced, volume change 3−36672
  - superconducting transition, plastic deform. kinetics 3−8293
  - superconductor, residual microwave surface resist. 3−27325
  - superconductor, thermal fluctuation induced diamagnetism above transition temp. 3−30575
  - superconductor, thermo-electrostatic effects 3−38916
  - thermal resistivity at high temps. 3−33861
  - thermoreflection, Bragg band-band transition range *(Russian)* 3−8590
  - thin film type I superconductors, current induced intermediate state 3−38917
  - twinning, mech., relation to strain to fracture 3−20808
  - vibrational spectrum, lattice heat capacities 3−30214
  - X-ray prod., L- and M-shell, from 0.5 to 14.0 MeV proton beam interactions 3−38228
  - X-ray scattering, anharmonic thermal diffuse, one- and two-phonon interaction 3−11703
  - X-ray total attenuation coefficients of 25.8 keV photons, meas. 3−39198
  - $Al-Al_xO_y-Pb$, junction, ellipsometrical determ. of tunnelling barrier thickness 3−34004
  - CsCl(Br)(I):Pb, optical absorpt., elec. cond. and dielec. loss studies of Pb-centres 3−24725
  - n-Ge-Pb Schottky barriers, under press., phonon tunnelling spectroscopy 3−36379
  - γ-ray attenuation coeffs., $E_\gamma=6-10$ MeV 3−17329
  - InAs-oxide-Pb tunnel junction, conductance characts., effect of accumulation layer 3−38901
  - in KCl, luminesc., polarisation patterns, wavelength and temp. depend. *(Russian)* 3−36919
  - KCl dopant, microdistribution inhomogeneity, electron microscopic obs. 3−1636
  - KCl:Cd, Pb, reorientation of $Cd^{2+}(Pb^{2+})$-vacancy complex rel. to dielec. relax. 3−34293
  - KCl:Pb, Br, X- or γ-irrad., $BrCl^-$ and associated centres, e.s.r. and optical absorpt. 3−39031
  - KCl:Sn, Pb, single crystals, u.v. spectra 3−39154
  - NaCl:Pb, thermoluminescence after X-ray irradiation 3−12188
  - $NaCl:Pb^{2+}$, absorpt., A- and B-band structs. 3−18098
  - Pb III, application of Slater-Condon theory with configuration interaction to various odd configurations 3−4360
  - Pb:In, type II superconductor, plastic deform. influence on flux line pinning *(German)* 3−18258
  - Pb:Ni, pressure effect on Ni interstitial diffusion 3−17996
  - $Pb/Zn-ZnO_2-Pb$, tunnelling obs. of bound states 3−18270
  - Pb-Cu S-N sandwich, electron interference effects, tunnelling study 3−18269
  - Pb-dielectric cermet film, refr. indices, ellipsometric meas. rel. to Maxwell Garnet theory 3−8544
  - Pb-Formvar-Al junction, logarithmic derivative curves and trap-assisted current transport 3−24544
  - Pb-Pb oxide-Pb tunnel junctions, mag. field depend. of Josephson plasma reson. freq. 3−2218
  - $Pb-Pb_xO_y-Pb$, large Josephson junction, thermal effect on voltage-current characts. 3−11986
  - Pb-polydimethyl siloxane-Pb, metal-dielectric-metal assemblies, γ-ray effects on capacitance and loss tangent *(Russian)* 3−39083
  - Pb-U systematics in lunar basalts rel. to early lunar evolution, critique 3−16176
  - Pb-U-Th systematics of Luna 20 and Apollo 16 lunar highland soil samples 3−12990
  - Pb-Zn-oxide-Pb junctions, tunnelling study of supercond. proximity effect for one atomic layer of Zn 3−2219
  - Pb^{2+} in MSb_2O_6, (M=Ca, Sr, Ba), fluorescence obs. for each excitation band 3−21478
  - Pb^{2+}:oxide glass, absorpt., fluoresc., excitation and decay time meas. 3−12168
  - ^{204}Pb rel. to ^{206}Pb, ^{207}Pb and ^{208}Pb in galena from Mountain Pass carbonatite 3−18829
  - ^{204}Pb rel. to ^{206}Pb, ^{207}Pb and ^{208}Pb in galenas from North Australia 3−18830
  - ^{205}Pb, extinct natural radioactivity determ. from Th anomalies in chondrites and lunar soil 3−5583
  - ^{208}Pb atomic spectrum, lifetimes, oscillator strengths and coherence narrowing 3−20021
  - ^{210}Pb abundance in N. Atlantic and N. Pacific 3−25189
  - U-Pb chronology of chrondritic meteorites 3−2882
  - U-Pb isotope method as age indicator using apatite 3−25111
  - YIG:Pb substituted, anomalous Faraday rotation 3−34331
- **lead alloys**
  - *see also lead compounds*
  - dilute, metal impurities, additional electrical resistivity, experimental results, Ashcroft pseudopotential theory *(Russian)* 3−30452
  - superconducting flux flow resistance minimum, mag. field dependence 3−5077
  - thermopower, Nielsen-Taylor effect in dilute alloys 3−21059
  - Ag-Pd, dilute, test of virtual-level, Friedel-Anderson model 3−38786
  - $AsSe_{1.5}Pb_{0.13}$ glassy alloys, consecutive crystallisation of PbSe and As_2Se phases, meas. of density of quenched patterns *(Russian)* 3−7634
  - $AuPb_3$, formed from spontaneous alloying of Au substrate with Pb monolayers 3−36463
  - Cd-Pb, zone refining, breakdown of regular laminations during growth *(Russian)* 3−24807
  - Cd-Pb dil. solns., equil. distrib. coeff. 3−21557
  - Ga-Pb, liquid alloy, thermodynamic props. 3−30271
  - Pb:Hg alloys, modified interstitial vacancy-pair model for Hg diffusion 3−20894
  - Pb:Mg alloys, diffusion of Mg and Pb, interstitial-vacancy pair model 3−20893
  - Pb-2%Sb, spheres plastic flow during hot-pressing 3−39381
  - Pb-Ag (0.25-2.5%), molten, temp. depend. of internal adsorption *(Russian)* 3−11541
  - Pb-Ag(Au) nonsubstitutional solid solns., comp. depend. of supercond. transition temp. 3−24533
  - Pb-As phase diagram, Pb rich portion 3−21568
  - Pb-Au dilute alloys dehancement of Au diffusivity 3−34546
  - Pb-Au solid soln., kinetics and morphology of $AuPb_3$ precip. 3−24843
  - Pb-Bi, peritectic, heat of non-equilibrium solidification 3−39323
  - Pb-Bi, single crystals, plasticity in superconducting and normal states at 4.2 K 3−36353
  - Pb-Bi film, inhomogeneous, supercond., critical currents and pinning effect 3−15306
  - Pb-Bi liquid solns., self-interaction parameters, limiting activity coeffs. temp. depend. 3−21793
  - Pb-Bi system, structure of metastable phase 3−18569
  - Pb-Ca, controlled solidification, rel. to appl. as grid materials for Pb-acid batteries 3−21635
  - Pb-Cd, single crystals, plasticity in superconducting and normal states at 4.2 K 3−36353
  - Pb-Cd eutectic; Sn interface instability 3−39309
  - Pb-Cu-Sn, changes in composition and structure due to friction and wear *(Japanese)* 3−8768
  - Pb-Fe dilute alloys, spin-disorder resistivity meas. as function of temp. in 0-60 kOe 3−2057
  - Pb-In, hard non-ordered, electrical resistivity concentrational dependence *(Russian)* 3−11883
  - Pb-In, type II superconductor, vortex state, microwave surface resistance 3−18261
  - Pb-In system, supercond. sheath state, flux motion dynamics and a.c. losses 3−36677
  - Pb-In system, superconducting energy gap from magnetization meas. 3−34014
  - Pb-In-Sn, supercond., flux flow states under mag. and thermal disturbances 3−21175
  - Pb-In(17%), superconductor, complex cond. of surface sheath, mag. field depend. 3−30573
  - Pb-In(4.56 wt.%), supercond., sign change in entropy flux associated with vortex motion *(French)* 3−38925
  - Pb-Sb-Sn-As alloys, grain growth and microstructure 3−8785
  - Pb-Sn, hard non-ordered, electrical resistivity concentrational dependence *(Russian)* 3−11883
  - Pb-Sn, liq., u.s. velocity obs. and determ. of thermophysical props. 3−24215
  - Pb-Sn, liquid, viscosity by oscillating crucible method 3−30280
  - Pb-Sn, liquid, viscosity obs., oscillating crucible method, liquidus temp. to 800°C *(Japanese)* 3−7960
  - Pb-Sn, Pb-Sb-Sn, columnar crystals, dendrite spacing *(Japanese)* 3−8792
  - Pb-Sn, pipe form. in solid-liquid region 3−39321
  - Pb-Sn, single crystals, superconducting and normal states at 4.2 K 3−36353
  - Pb-Sn, superplastic, const. stress creep and const. true strain-rate tensile tests 3−21650
  - Pb-Sn, zone refining, breakdown of regular laminations during growth *(Russian)* 3−24807

- **lead alloys** continued
  - Pb-Sn alloys, composition test, using inversely scattered β-radiation 3-26016
  - Pb-Sn lamellar eutectic, fine struct. studies in Pb-rich phase *(French)* 3-24818
  - Pb-Sn liquid alloy, temp. dependence of resistivity 3-30454
  - Pb-Sn superplastic alloys, scanning electron microscope deformation studies 3-1549
  - Pb-Sn system, physicochem. props., effect on spectral line intensity in d.c. carbon arc *(Russian)* 3-28772
  - Pb-Sn system, supercond. dynamics of Sn impurity oscills., Mossbauer and u.s. velocity studies *(Russian)* 3-7894
  - Pb-Sn-Cd, eutectic, anomalous structures 3-37005
  - Pb-Sn(40 wt.%), strain-rate sensitivity origin 3-37056
  - Pb-Tl, single crystals, plasticity in superconducting and normal states at 4.2 K 3-36353
  - Pb-Tl, supercond., fluctuation induced diamagnetism above transition temp. 3-30575
  - Pb-Tl, type II superconductor, intermediate mixed state magnetization meas. 3-2201
  - Pb-Tl 50/50 single crysts., activation area and strain-rate sensitivity, 78 K 3-24895
  - $Pb_{0.9}Bi_{0.1}$, superconducting thermodynamic props. 3-34015
  - $Pb_{1-x}Sn_xTe$ alloys, calc. of band parameters based on two valence band model for Seebeck coeff. *(French)* 3-11854
  - $Pb_{1-x}Sn_xTe$ layers on Si and Ge substrates, i.r. refractive index 3-30783
  - p-$Pb_{1-x}Sn_xTe$ solid soln., i.r. absorpt. spectra due to free carriers, valence bands energy gap *(Russian)* 3-8626
  - $Pb_xSn_{1-x}Te$ alloys, Mossbauer spectra *(Russian)* 3-15438
  - $Pb(Ti,Zr)O_3-Pb(Li_{1/4}Sb_{1/4}Mo_{1/2})O_3$, photochromic solid soln. 3-30784
  - $Pb_{75}Tl_{25}$, supercond. critical current rel. to a.c. fields and a.c. currents 3-8305
  - PdCr, interimpurity interaction effects below spin fluctuation temp., elec. resist. meas. 3-15348
  - PdMn, dilute, ferromag., magnetoresist. meas. with acoustic and optic mode excitations 3-15184
  - Rh-Pb system, phase diagram *(German)* 3-5286
  - Sn-Pb, controlled solidification in melt growth 3-11562
  - Sn-Pb, off-eutectic, hysteresis in composite-dendrite transition 3-34507
  - Sn-Pb eutectic prestrain effect on flow stress 3-18676
  - Sn-Pb system, conc. depend. of pseudopots., atom scatt. cross section, electrotransport *(Russian)* 3-30277
  - Sn-Pb-Sn_4As_3 pseudoternary system, thermalanalysis, metallographic and X-ray methods 3-34497
  - Sn-Pb(15 wt.%) rheological behaviour in crystn. range 3-34505
  - Zn-In-Pb solns., liq., miscibility gap, zinc isoactivity and molar functions 3-38675
- **lead compounds**
  - *see also lead alloys*
  - oxides, thermal expansion coeffs. determ. by X-ray diffraction, layer structure and bonds *(French)* 3-17984
  - Pb, La(Zr, Ti)O_3 ceramic, ferroelectric transition, pulse-echo detect. 3-18689
  - Pb-glass, origin of fission fragment tracks 3-24135
  - scheelite type cryst. containing Pr^{3+}, line broadening and vibr. spectra study 3-15526
  - tetrahalides, general and orbital valence force field constants calc. 3-29609
  - $(GePbSn)_{0.5}Te_{0.5}$ amorphous film, photocond., temp. and intensity depend. 3-18186
  - KCl:$PbCl_2$, flow stresses and relax. of stresses rel. to doping and temp. 3-20797
  - $(Pb,La)(Ti,Zr)O_3$ ceramics, A-site and B-site vacancies distrib. 3-1618
  - $(Pb,La)(Zr_y,Ti_z)O_3$, PLTZ ceramics, y=0.60 to 1.0, z=0.4 to 0, antiferroelectric-ferroelectric phase boundary, temperature, d.c. field dependence 3-8525
  - Pb, La(Tz, Ti)O_3 ceramic, elastic and piezoelectric props., La dependence 3-18691
  - Pb phosphates, i.r., X-ray and chem. anal. of apatite structure and comp. *(German)* 3-33497
  - Pb-Sb-S, semicond., diamag. and paramag. terms in mag. susceptibility 3-8335
  - Pb-SnSe, luminesc. study, 0.5 to 11 μ waveband, appl. as radiation detectors and lasers *(Russian)* 3-27576
  - Pb-SnTe, luminesc. study, 0.5 to 11 μ waveband, appl. as radiation detectors and lasers *(Russian)* 3-27576
  - Pb^{2+} oxides, fluorides and oxide fluorides, calcs. of bond lengths and angles 3-33073
  - $Pb_{26}Ag_9Cu_{24}Cl_{62}(OH)_{48}$, boleite mineral, crystal structure and Ag atom clusters 3-27009
  - PbBr, blue and violet luminesc., excitons rel. to energy transport mechanism 3-34407
  - $PbBr_2$, photoluminesc., thin film absorpt. rel. to exciton form. 3-27561
  - $PbBr_2$ single crystals luminescence and e.p.r. of u.v. irradiated crystals 3-8640
  - PbCl, blue and violet luminesc., excitons rel. to energy transport mechanism 3-34407
  - $PbCl_2$, photoluminesc., thin film absorpt. rel. to exciton form. 3-27561
  - $PbCl_2$ molten binary mixtures with KCl, RbCl, $CdCl_2$, and $SnCl_2$, minima of absorption edge frequencies 3-2558
  - $PbCl_2$ single crystals, luminescence and e.p.r. of u.v. irradiated crystals 3-8640
  - $PbCl_2:Nd^{3+}$ and $PbCl_2:Pr^{3+}$, optical absorption spectra and crystal field calcs. 3-15515
  - $PbCl_2$-$CuCl_2$, electrodes, use in salt water batteries 3-3265
  - $PbF_2(Cl_2)(Br_2)$, low temp. X-ray luminesc. and photolum. 3-30863
  - $PbFe_{12}O_{17}$, free energy, entropy, of parallel plate domain struct. 3-2314
  - $PbFe_{12}O_{19}$, ferrite with magnetoplumbite structure, anisotropy of hopping cond. and thermoelec. power 3-38829
  - $Pb(Fe_{2/3}U_{1/3})O_3$, cryst. struct. and mag. props. 3-21231
  - $Pb(Fe_{2/3}W_{1/3})O_3$, cryst. struct. and mag. props. 3-21231
  - $Pb_5Ge_3O_{11}$, cryst. struct. 3-17764
- **lead compounds** continued
  - $Pb_5Ge_3O_{11}$, ferroelec., antiparallel 180° domains, X-ray topographic obs. 3-12102
  - $Pb_5Ge_3O_{11}$, ferroelec., prototypic structure determ. 3-33502
  - $Pb_5Ge_3O_{11}$, ferroelec. and optical props. 3-18420
  - $Pb_5Ge_3O_{11}$, ferroelec. behaviour, enantiomorphism and optical activity 3-18419
  - $Pb_5Ge_3O_{11}$, ferroelectric material, second harmonic generation coeffs. 3-13752
  - $Pb_5Ge_2SiO_{11}$, ferroelec. and optical props. 3-18420
  - $Pb_{1-x}Ge_xTe$ laser, c.w. operation, 4-6μ, and appl. to NO spectroscopy 3-4107
  - $Pb(H_2PO_2)_2$, radiocrystallographic and i.r. spectroscopic obs. *(French)* 3-7700
  - $PbHfO_3$ from γ-γ ang. correl. and Mossbauer spectroscopy 3-21353
  - PbI_2, cryst. growth in silicon gels, habit and kinetics 3-12223
  - PbI_2, excitons at band edge, electric field effects 3-33856
  - PbI_2, temp. and press. effects on exciton spectrum 3-21436
  - PbI_2 doped β-AgI pellets, elec. cond., phase stability 3-14966
  - PbI_2 refractive index dispersion, thin layers, 360-650 nm range, absorption *(Russian)* 3-34380
  - PbI_2 spectral absorption band, exciton splitting, dispersion measurements *(Russian)* 3-34379
  - Pb(II) complex, thiourea coordination compounds, cryst. struct. 3-14775
  - $Pb_{1-kx}La_xTiO_{3\|x(1.5-k)}$, with A-site and B-site vacancies, X-ray struct. study 3-17792
  - $Pb_xLa_{1-x}(Zr, Ti)O_3$ powder, cold pressing and low temperature sintering 3-27734
  - $Pb_\alpha(MO)_\beta MO_3$, (M=Ta, W and Nb, W) new phases, struct. *(French)* 3-7697
  - $Pb_8M_2(PO_4)_6$, (M=Na, K, Rb, Tl), i.r. spectra and X-ray obs. *(German)* 3-34350
  - $PbMg_{1/3}Nb_{2/3}O_3$, ferroelec. with smeared phase transition, electrooptical effect linearisation and coeffs. 3-24680
  - $PbMg_{1/3}Nb_{2/3}O_3$, optical absorpt. coeff. anomalous behaviour in broad ferroelec. transition 3-21438
  - $PbMg_xNb_{1-x}O_3$, longit. electrooptic effect 3-34327
  - $PbMg_{1/3}Ta_{2/3}O_3$, ferroelec. with smeared phase transition, electrooptical effect linearisation and coeffs. 3-24680
  - p- $Pb_{1-x}Mn_xTe$ solid solutions, energy band scheme from spectra 3-24716
  - $PbMoO_4$ acoustic harmonic generation *(French)* 3-33612
  - $PbMoO_4$ acousto-optical dispersion of refractive index, measurement, i.r. goniometer, Sellmeier coefficients 3-22317
  - $PbMoO_4$ crystal growth, appl. in acoustooptic light deflector 3-27609
  - $PbMoO_4$ standing u.s. Bragg cell, appl. to multiplexing and demultiplexing 3-16408
  - $PbMoO_4$:Cu, Czochralski growth and site occupancy 3-12301
  - $PbMoO_4:Mn^{2+}$, electric field effect in paramagnetic resonance 3-34195
  - $PbMoO_4:Nd^{3+}$, crystal field parameters, calc. using MO LCAO method *(Russian)* 3-8112
  - $PbMoO_4:Yb^{3+}$, crystal field parameters, calc. using MO LCAO method *(Russian)* 3-8112
  - $PbMo_2O_4$, magnetic, electric, dielectric props. and space group detn. *(Russian)* 3-8397
  - PbN_6, pure and doped thin films, photodecomposition, optical absorpt. and cond. meas. 3-25084
  - $Pb(NO_3)_2$, elastic consts., 4-300K, u.s. meas. thermoelastic behaviour 3-17894
  - $Pb(NO_3)_2$, single cryst., i.r. and Raman study at 300 and 80K 3-27504
  - $PbNb_4O_{11}$, $Pb_5Nb_4O_{15}$, $Pb_2Nb_2O_7$, crystallographic unit cells, X-ray diffr. obs. *(French)* 3-4736
  - PbO, between Pt electrodes, memory effect *(Russian)* 3-30525
  - PbO, crystallochemical peculiarities and shape of absorpt. edge 3-8606
  - PbO, nonrelativistic SCF calcs., spectroscopic consts. prediction 3-38263
  - PbO, polycrystalline ceramics, pyroelectric current obs. 3-5166
  - PbO, polymorphic, current inversion study of photoelectret state dark depolarisation 3-21113
  - PbO, pyroelec. currents and phase transitions 3-27472
  - PbO, vapour grown film, obs. of fracture edge, surface structure and higher oxides 3-15628
  - PbO glasses, refractive index >1.75, correlation of refractive index and density, Newton-Drude relation 3-5902
  - PbO monolayer, on Pb surface, ESCA obs. 3-33741
  - (α-)PbO spectra, absorption and luminescence, single crystals 3-34378
  - PbO-B_2O_3 glass system, secondary phase separation rel. to second phase volume fraction 3-9004
  - PbO-B_2O_3 glasses, i.r. refl., band positions, conc. depend. *(Russian)* 3-12139
  - PbO-SiO_2 melts, activity meas. by TIE method 3-36998
  - β-PbO_2, band struct., band gap, Kohn-Korringa-Rostoker method calcs. 3-8107
  - Pb_3O_4, phase transition, X-ray and neutron diffr. and DTA studies *(French)* 3-15009
  - Pb_3O_4, pyroelec. currents and phase transitions 3-27472
  - $mPbO.2UO_3.(4-2m)H_2O$, $0 \leqslant m < 2$ indexing of X-ray powder patterns *(French)* 3-30091
  - $5PbO.3GeO_2$, electro-optic props. 3-18433
  - 5 $PbO.3GeO_2$, quasi-elastic scatt. in Raman spectrum near ferroelec. phase transition 3-15495
  - $5PbO.3GeO_2$, Raman spectra of soft phonon mode at ferroelec. phase transition 3-24691
  - $Pb(PO_3)_2$-$Cu(PO_3)_2$ system, phase diagram *(French)* 3-7901
  - $Pb_2P_2O_7$, Czochralski growth, crystal structure and dielec. props. 3-33470
  - $Pb_5P_4O_{15}$, Czochralski technique growth and dielec. props. 3-1727
  - $Pb_{10}(PO_4)_6O$, i.r. spectra and X-ray obs. *(German)* 3-34350
  - $Pb_{10}(PO_4)_6(OH)_2$, i.r. spectra and X-ray obs. *(German)* 3-34350
  - $PbPdF_4$, preparation, madelung part of lattice energy *(German)* 3-14814
  - PbPo, electron and hole effective masses, calc. 3-30400
  - PbS, eptaxial quasi-static growth, and h.f. props. 3-2674

lead compounds continued
  PbS, mean amplitude of vibration and Debye temp. at room temp., X-ray determ. 3−27077
  PbS, photodiode fabrication, polishing procedure 3−30952
  PbS, thermoabsorpt. spectrum, temp. depend., 18-300 K 3−21429
  PbS, thin films, photoelectromotive force and thin layer structure depend. on substrate temperature and evaporation speed *(Russian)* 3−27323
  PbS epitaxially grown on KCl, Pb form. 3−8052
  PbS evaporated thin film epitaxial growth and condensation on NaCl covered by an amorphous dielectric intermediate layer 3−38746
  PbS film, photographic image formation by internal electrolysis *(Russian)* 3−9091
  PbS film for photodetector, oxidant effects in chem. deposition, structure and chem. props. 3−24360
  PbS films, growth on cleavage surf of NaCl cry. containing macrodefects *(Russian)* 3−8068
  $PbS-Bi_2S_3$ system phases, cryst. struct. 3−15858
  PbS-CdS system, obs. of phase equilibrium diagram *(French)* 3−20851
  PbS-GaAs p-n heterojunctions, near i.r. detection 3−22283
  PbS-PbSe(Te) alloy film, struct., X-ray obs. *(Russian)* 3−18034
  $PbS_{1-x}Se_x$, photodiode fabrication, polishing procedure 3−30952
  PbS(Te), Lorenz number, 77K and lower, calc. 3−33877
  PbSe, band inversion under hydrostatic press., elec. resist. and galvanomag. obs. 3−2004
  PbSe, band struct., k.P perturbation treatment 3−1997
  PbSe, carrier mobility, carrier conc. and temp. depend., 0.3 to 800K 3−27252
  n-PbSe, electron relax. time, i.r. refl. and magnetorefl. study 3−5207
  PbSe, mag. field effect on spontaneous and stimulated emission from p-n junction 3−15524
  PbSe films, vapour phase deposits epitaxially grown 3−30360
  $PbSe-Ge_{1.5}As_{0.5}Se_3$, pseudobinary system, immiscibility, liquidus temp., electron microscopy 3−20853
  PbSe-PbTe alloy film, struct., X-ray obs. *(Russian)* 3−18034
  $Pb_{1-x}Sn_xSe$, $0 \leqslant x \leqslant 0.3$, band inversion under hydrostatic press., elec. resist. and galvanomag. 3−2004
  $Pb_{1-x}Sn_xSe$, grown from vapour, resistivity and Hall mobility 3−24438
  $Pb_{1-x}Sn_xTe$, n.m.r. meas. for characterisation of single zone annealed sample 3−24619
  $Pb_{1-x}Sn_xTe$, vertical epitaxial system for growth from vapour 3−2654
  $(Pb_{1-x}Sn_x)_{1-y}Te_y$, Czochralski-grown, compositional striations 3−39242
  $PbTa_2O_6$, low freq. linear electro-optical effect meas. 3−12115
  PbTe, enthalpy of form. *(French)* 3−30242
  PbTe, epitaxial growth of Pb films 3−18238
  n-PbTe, magnetophonon resonance, electron intravalley scatt. with phonon absorpt. 3−33931
  PbTe, n.m.r. meas. for characterisation of single zone annealed sample 3−24619
  p-PbTe, n.m.r. of ^{207}Pb, high vacancy conc. effects *(Russian)* 3−2409
  PbTe layers, epitaxial growth on CdTe *(French)* 3−8048
  PbTe thin film, photocond., rel. to barrier lowering model 3−30515
  PbTe with excess Pb, supercond. above 7.2K *(French)* 3−38915
  PbTe-In tunnel junction, elec. props., superconductivity *(French)* 3−24545
  PbTe-MgTe alloy system, physical props. 3−7904
  PbTe-SnTe, absorpt. coeff. calc. in nonparabolic region using two-band model 3−15520
  PbTe-SnTe, narrow bandgap semiconductor, zero bandgap transition 3−38800
  PbTe-TlTe system, phase diagrams and electrical props. *(Russian)* 3−8169
  $PbTiO_3$, ^{181}Ta and ^{178}Hf static electric quadrupole interaction meas. using differential PAC and Mossbauer effect 3−12090
  $PbTiO_3$, ferroelec. perovskite, Raman spectra obs. of lattice modes 3−33634
  $PbTiO_3$, ferroelectric, low temp. structure 3−39068
  $PbTiO_3$, polycryst. film with ferroelec. and antiferroelec. props., deposition by electrophoresis 3−39220
  $PbTiO_3$ ceramic, piezoelectric props., effect of additives *(Japanese)* 3−2495
  $PbTiO_3:Nb_2O_5$ solid solution, incorporation of Nb_2O_5 into the perovskite lattice 3−5381
  $Pb_2V_2O_7$, synthetic chervetite, crystal structure, full matrix least squares refinement, bonds, interatomic distances 3−30093
  $PbZn_{1/3}Nb_{2/3}O_3$, ferroelec. with smeared phase transition, electrooptical effect linearisation and coeffs. 3−24680
  $Pb(Zn_{1/3}Nb_{2/3})O_3$ and $Pb(Cd_{1/3}Nb_{2/3})O_3$, microdomain behaviour in diffuse phase transition region 3−15462
  $Pb(Zn_{1/3}Nb_{2/3})O_3-PbTiO_3$, quadratic electro-optic effect, g coeffs. 3−39122
  $Pb_{2-x}Zn_yNb_{2-z}O_{7-x\|y-2,\,5z}$, crystallographic unit cells, X-ray diffr. obs. *(French)* 3−4736
  $Pb(Zr, Ti)O_3$, comp. and phase struct. depend., i.r. detector characteriz. 3−39098
  $Pb(Zr,Ti)O_3$, La substituted, PLZT ceramic, isothermal grain growth, dielectric and ferroelectric properties 3−8950
  $Pb(Zr,Ti)O_3$, La_2O_3-modified, temp.-depend. ferroelec. domain alignment 3−5168
  $Pb(Zr,Ti)O_3$ ceramic pyroelectric detector transient thermal analysis 3−8523
  $PbZrO_3$, polycryst. film with ferroelec. and antiferroelec. props., deposition by electrophoresis 3−39220
  $Pb(ZrTi)O_3$ piezoelectric ceramics, stabilization effects by addition of Mn, Cr or U oxides 3−8507
  $PbZr_{1-x}Ti_xO_3$ solid solns., press. induced ferroelec.-antiferroelec. transform., depolarization behaviour *(French)* 3−36842
  $PbZr_{1-x}Ti_xO_3 + 0.8\%\ WO_3$, ferroelec. transition temp. − comp. phase diagram *(French)* 3−5167
  $Pb_xsN_{1-x}Te$ films, r.f. sputtering, i.r. detector arrays 3−8688
  Pd_2Si contact on Si, specific contact resist. 3−27311
  $SiO_2-Na_2O:SnO_2,PbO$, glass, nuclear spectroscopy study of impurity effects on structure and props. *(Russian)* 3−14973
  SnTe-PbSe system, phase diagram and phys. props. *(Russian)* 3−11918
  $(SnTe)_{1-x}(PbSe)_x$, $(SnTe)_{1-x}(PbTe)_x$ thin layers, structure depend. on phase composition and prep. conditions 3−33761
  $Sr_{1-x}Pb_xTiO_3$, phase transitions, u.s. velocity and permittivity studies 3−27478

leak detection
  airtightness control, practical techniques for industrial use *(French, English)* 3−37672
  container with leak in pre-vacuum stage, temporal press. behaviour 3−13260

leakage, magnetic *see magnetic leakage*

leakage currents
  decaying process from differentiation of surface potential decay curve *(Japanese)* 3−19234

learning systems
  see also adaptive systems
  for invariant pattern recognition by methods of coherent and incoherent optics *(Russian)* 3−6429

least squares approximations
  complex weighted data, dielectric applications 3−34280
  computer instructional programming appl. 3−22228
  crystal geometry shape from X-ray silhouette photos, least squares determ. 3−4703
  data smoothing, analysis in frequency domain 3−28838
  eclipsing binary stars, elements from light curves using generalized method of least squares *(Russian)* 3−13062
  e.m. wave scattering 3−13685
  experimental function with linear exponents determ. 3−16600
  filtering technique, in parameter estimation 3−10249
  finite element formulation of mechanics of deformable bodies 3−26072
  flow model, linear, residence time distrib. anal. 3−17507
  gravity anomalies determ. by satellite geodesy 3−34777
  isolated axisymmetric particles in Stokes flow, drag force 3−36133
  $KH_2PO_4-KD_2PO_4$ system, structural studies and bonding 3−1614
  kinetic data analysis, renal ^{133}Xe washout in dogs and man applic. 3−35273
  linear, computational photogrammetry applic. 3−6000
  liquid crystal, nematic, deformation in elec. field 3−14681
  magnesium picolinate dihydrate, crystal structure, anisotropic full matrix refinement *(French)* 3−38577
  molecular beam differential cross section data, linear least squares fitting using spline functions 3−23633
  molecular empirical parameter evaluation from spectroscopic data by least squares method 3−14353
  Mossbauer thick-absorber single line spectra 3−25954
  optical consts. and polarization rate determ. method *(French)* 3−681
  physics emitter radial distribution calc. 3−36209
  quadratic matrix eqns., soln. by least-squares method 3−6190
  radiation spectra, determ. of peak positions for least-squares fitting method *(Czech)* 3−23065
  rigid body refinement procedure as applied to struct. of α-chitin 3−7096
  rigid-body vibration tensors, unit weight matrices 3−38628
  semidiscrete, for parabolic boundary value heat transfer problem 3−10259
  solubility of O_2 in liquid Na 3−14251
  spectroscopic binaries, mass ratio determ. using modification of Wilson's method 3−28190
  stress relaxation data based on the Johnston-Gilman equation, computer analysis 3−34595
  structure refinement of molecules with librating side groups, use of constraints on thermal motion 3−20079
  structure refinement of molecules with librating side groups, use of constraints, applic. to durene 3−20080
  variational method applic. to scatt. problems 3−20042
  X-ray crystallography, least-squares refinement and weighted difference synthesis 3−26952
  X-ray crystallography, structure refinement program using diffr. from polycryst. aggregate 3−33427
  X-ray powder pattern indexing of $mXO.2UO_3.(4-2m)H_2O$ ($X=Ca$, Ba, Sc, Ba, $0 \leqslant m < 2$) *(French)* 3−30091
  γ-ray angular distributions 3−19289
  Ag, intermediate stage sintering, correlation of grain size and density, least squares plot 3−27713
  Cs_2CuCl_4, struct., crystal forces and charge distribution determ. 3−17785
  $Cu(OH_2)_6^{++}$ complex in aqueous perchloric media, Gaussian absorption curves, least squares fit *(French)* 3−8434
  $CuVO_3(I)$, distorted ilmenite type derivative, cryst. struct. determ. 3−7695
  H_2AsO_4, arsenic acid and its anions, Raman spectra and vibrational analysis, using damped least squares procedure 3−29671
  MgV_2O_6, cryst. struct., e.s.r. of Mn^{2+}, spin hamiltonian parameters 3−11589
  $\beta-VPO_5$, crystal struct. 3−7693

leather *see materials*

Lecher wires *see high-frequency transmission lines*

Lee model
  Bronzan-Lee model, scattering processes in U and V sectors 3−6546
  indefinite metric in state space *(German)* 3−35751
  scattering, unstable particles, LSZ study 3−35735
  two-particle coupled states in Lee model with Fermi commutation relations replaced by Bose relations *(Russian)* 3−10610
  $V \leftrightharpoons N + \theta$, renormalization problems in an indefinite metric 3−6542

LEED *see low energy electron diffraction*

legislation
  air pollution control, Ringelmann Chart 3−25615
  Plowshare project, legal problems with regard to environmental policy 3−19890

length measurement
  see also micrometry
  autocollimating apparatus for tapering rod parallelism meas. 3−22338
  ball and cylinder, diameter comparison, by interferometer 3−37586
  contact deformation nonlinearity errors *(Russian)* 3−19151

length measurement continued
by dilatometer up to 22 kbars 3−16385
droplet size *(German)* 3−22255
electronic system for simultaneous length and temp. meas. 3−19153
Fabry-Perot interferometer, small length modification meas., sensitivities, mag. field, errors *(German)* 3−5955
interferometric meas., error due to mirror rot. movement, multipass corner cube arrangement 3−35354
large diam. meas., with calibrated roller instruments, errors *(Russian)* 3−19150
Mars diameter by optical means 3−16158
optical contacting by interference line with measuring microscopes 3−28468
photoelectric microscope, optimal operating conditions for scanning device 3−19187
semiconductor growth, automated, monitoring lateral dimensions 3−12312
small displacements, improved sensitivity interferometer *(Russian)* 3−22262
He-Ne laser interferometer *(Spanish)* 3−19211
He-Ne laser wavelength *(French)* 3−9817

length standards *see measurement standards*

Lennard-Jones and Devonshire theory *see liquid theory*

Lennard-Jones potential *see intermolecular mechanics*

lenses
see also aspherical lenses; electron lenses; electrostatic lenses; focusing; magnetic lenses; photographic lenses
1X copy, m.t.f. design data 3−172
acoustic, design and construction for imaging system 3−79
automatic design, modified gradient method *(German)* 3−16420
automatic lensometer for meas. of vertex refraction of nonastigmatic lenses *(Russian)* 3−5908
axicon, alignment meas. of optical systems 3−174
birefringent, spatial filtering applications 3−3796
cylindrical, optical testing 3−22341
design, maximum depth of focus 3−173
design, surfaces of best focus, aberration coeffs. 3−37940
electrostatic spatial filter for high powered pulsed laser, patent 3−32101
evolution and the single lens 3−32066
field correctors, paraboloid mirrors, astronomical telescopes, image spread, transmission 3−3391
field curvature correction using single second order aspheric surface *(Russian)* 3−154
focusing optical elements with regularly distributed refractive index, review *(Russian)* 3−35430
frequency-contrast characteristics meas. of film projectors, data processing method by electronic calculators *(Russian)* 3−9933
Fresnel, double, beam splitting and beam recomb. *(German)* 3−5877
gas, e.m. wave propagation, laminar flow 3−37926
glass blanks, for minimum rejection of moulded components optimal dimensions selection 3−25747
ground glass focused lenses, focusing criterion from MTF meas. 3−28511
helical gas lenses, modes, optical beam guiding 3−3784
ion, optical properties and practical realization, review 3−35722
i.r., transmission meas. 3−3794
kinoform, synthesisation by optical means 3−9931
measuring microscope 8K 70/50. new 100x objective 3−28469
objective in 'Grand Schmidt' telescope, use for stellar obs. *(French)* 3−31802
ophthalmic lenses, spherical, testing by automatic vertometer 3−167
photographic objectives, spectral transmittance evaluation *(Czech)* 3−22395
plankonvex lens, optical transfer function, holographic meas. of autocorrelation function 3−199
polymethylmethacrylate, injection moulding experiences *(Russian)* 3−5911
solid liquid compound hydroacoustic lens, low aberrations 3−35324
stigmatic, structure of e.m. field near focus 3−19580
teaching chart for object and image distances, magnification, focal length determ. 3−9797
thin, achromatic triplets, Gaussian optics *(German)* 3−6449
thin, heterogeneous characteristics of stationary generation of 3-dimensional light beams *(Russian)* 3−28528
transmitting axicon, focal depth 3−32058
Yerkes 40-inch refractor, effect on thermal condition of lens on plate scale, Vasilovskis theory 3−28301
zoom lenses for amateur movie cameras, design problems 3−22399
Th containing, eye exposure 3−9708

lepton interactions
see also hadron lepto-production
external symmetry group formation 3−23052
hadron-lepton, Weinberg's model, and hadron and lepton struct. 3−19679
high energy and higher order weak processes 3−6578
high energy diagonalization over particle helicity *(Russian)* 3−10717
high energy processes, models review 3−6632
lepton era of Hot Big Bang model 3−9460
single-particle exchange model of weak lepton interactions *(Russian)* 3−29186
universal weak interactions, theory 3−6577
Weinberg's lepton model, compact version, construction of gauge fields as bound states of spinor fields 3−4154
ll colliding beams at 10^3 GeV, calc. of elastic scatt. cross-section 3−16980

lepton scattering
see also electron scattering; lepton scattering by hadrons; neutrino scattering
deep inelastic, SU(4) light-cone analysis based on four quark schemes 3−23091
high energies, V-A theory, evaluation of higher order terms 3−825
inelastic, deep, structure functions, light cone approach to positivity bounds 3−6621
inelastic lepton-nucleon scattering, relativistic quark parton model 3−13907

lepton scattering continued
lepton-nucleon, inelastic, bare current-quark masses and light cone algebra 3−29224
$ll \rightarrow ll\nu\nu$, $l = e^{\pm}, \mu^{\pm}$, cross sections for inelastic weak processes at high energy *(Russian)* 3−38030

lepton scattering by hadrons
see also electron-proton scattering
Adler inelastic sum rule for neutrino processes, analysis 3−6586
deep inelastic lepton-nucleon scatt. kinematics 3−6625
deep inelastic scattering on nucleons 3−809
inelastic, review of single-arm and coincidence expts. 3−857
inelastic high-energy collisions, scaling and dual amplitudes 3−853
inelastic inclusive reactions, polarization effects 3−6630
lepton-hadron, deep inelastic, core structure of nucleons in framework of quark-parton model 3−26313
lepton-nucleon, deep inelastic scatt., light-cone algebra and field-current identity 3−38052
lepton-nucleon deep inelastic, in quark parton model, consequences of νN and $\bar{\nu}$N total cross section meas. 3−29193
lepton-nucleon inelastic processes, scaling behaviour of cutoff vector-gluon model 3−35802
lepton-nucleon scattering, light cone constraints and asymptotic domains 3−32672
light cone analysis, reln. to fixed mass limits of current amplitudes 3−32640
one particle inclusive reactions, applications of quark parton model in deep inelastic region, sum rules 3−17025
semi-inclusive reactions induced by polarised leptons on unpolarised and spin 1/2 polarised targets 3−10711
semileptonic deep inelastic scattering, quark-hadron amplitudes and structure function behaviour 3−23092
strange particle electroproduction on nucleons, Born approx. *(Russian)* 3−4183
symmetry, sum rule derivation 3−10650
eN elastic scatt., departure from scaling laws, anal. by broken-symmetry 3−17010
eN inelastic, resonance form factors, scaling and Regge behaviour 3−35799
μN, test of scaling at small four-momentum transfers 3−10708
μp, use in testing weak-interaction models, effect of neutral currents in scaling model 3−10712

leptonic decays
see also baryon leptonic decay; meson leptonic decay; muon decay
$e^+e^- \rightarrow l^+l^-$, heavy lepton prod., calc. of decay correlations 3−13895
K^- capture in emulsion, hypernuclei nonmesonic decay and $\Lambda n/\Lambda p$ stimulation ratios 3−26414

leptons
see also electrons; muons; neutrinos; positrons
atoms, effect of neutral intermed. boson 3−23027
charge conservation, milliweak and superweak violation, astronomical consequences 3−6561
charge conservation law, possible effects of violation, Gribov-Pontekorov model *(Russian)* 3−38006
composite lepton states induced by neutrinos 3−29185
conservation and exotic muon capture in nuclei 3−4305
g-factor anomaly meas. technique using resonance technique 3−6689
Green's application of parastatistics, representation theory of parafermion algebras 3−35737
heavy, branching ratios and production cross sections in spontaneously broken gauge theories of weak interactions 3−32645
heavy quasistable, search in pN collisions 3−4235
mass spectrum determ. from discrete scale transformations, partial soln. to muon puzzle 3−14106
model based on discrete scale transformations, prediction of heavy leptons 3−4249
particles of mass between the electron and muon, search *(French)* 3−6688
SU(3)⊗SU(3) and unified gauge theories 3−38002
symmetry, sum rule derivation 3−10650
U(3) nonet scheme with 6 heavy leptons 3−23026
unified model of elementary particles based on leptons 3−16966
Weinberg model of weak and e.m. interactions, triplet representation of leptons 3−13828
$e^+e^- \rightarrow l^+l^-$, heavy lepton prod., calc. of decay correlations 3−13895
$\pi N \rightarrow Bll$, calc. of amplitudes for high energies, small momenta *(Russian)* 3−4213

level control
liquid N level control in dewars, automatic device 3−5821

level crossing (energy) *see energy level crossing*

level measurement
cryogenic liquid level indicator design *(French)* 3−22297
liquid level meter, for blind persons 3−28474
literature review 3−450
metrological gauarantee of instruments *(Russian)* 3−6166
CdTe nucleonic system, for fuel gauging 3−32143

level meters
see also power measurement
cryogenic liquid level indicator design *(French)* 3−22297
cryostat for optical obs., 1.5 to 4.2 K *(Czech)* 3−32048
impulse sound meas. *(German)* 3−13234
liquid level meter, for blind persons 3−28474

levels, energy *see energy levels*

LIDAR *see optical radar*

Lie groups
see also elementary particle symmetry
algebras, infinite-dimensional, subideal struct. and nilpotency considerations 3−16591
book, Lie groups and Lie algebras 3−10236
cobordal deformations of real Lie algebras *(French)* 3−10229
complex algebras, semi-simple, H-diagonal represents. *(French)* 3−28808
derivatives of functions of non-commutating variables, reformation of classical mechanics 3−13612
gauge theories without anomalies, classification corresponding to simple Lie groups 3−35749
general relativity quaternion formalism, matter-antimatter relationships 3−6334

Lie groups continued
- groups of motions of space-times admitting a parallel null vector field 3−28806
- groupuscle determ. from completely standardized algebra *(French)* 3−19388
- infinitely divisible projective representations of Lie algebras 3−6181
- infinitesimal automorphism of contact struct., subalgebras *(French)* 3−482
- infinitesimal automorphisms, algebra derivations *(French)* 3−19385
- infinitesimal automorphisms of contact struct. *(French)* 3−6176
- local Lie-Banach group struct., existence *(French)* 3−19386
- maximal simple Lie algebras from two pairs of Fermi operators, calc. of complete list *(Russian)* 3−28810
- Nagel-Moshinsky operators for $U(p, 1) \supset U(p)$ 3−26051
- nuclear structure, group theoretical investigation of the Hartree-Fock-Bogoliubov state and Valatin-transformation *(German)* 3−35873
- realization of Lie algebra of unitary symplectic group in terms of boson operators 3−28812
- Schrodinger eqn. maximal kinematical invariance group 3−10344
- Schrodinger equation, algebraic solution for velocity-dependent potentials 3−22709
- unimodular infinitesimal automorphisms *(French)* 3−19387

ligand field theory *see crystal field theory; molecular bonds; molecular orbitals*

light
- *see also airglow; optics; sunlight; zodiacal light*
- nature of, electromagnetic and corpuscular, tutorial 3−32505
- neutrino theory, re-examination 3−4069
- radiance volume density concept 3−22807
- retardation in electric field in CS$_2$ and toluene polarization interferometric determ. *(Russian)* 3−24678
- stellar images, gravitational aberrations 3−16220
- T-solutions of Einstein's equations in non-static spherically symmetrical gravitat. field *(Russian)* 3−600

light absorption
- *see also atmospheric optics; densitometry; light transmission; optical constants; optical films; optical filters; pleochroism*
- (dimethyl)amino groups in oxonium and carbonium ions, protonation, u.v. absorpt. spectra 3−36012
- absorption and emission spectra universal relation to combining electron states 3−23551
- adenine.HCl single crystals, electronic spectrum study 3−30828
- air pollution, laser beam resonance absorpt. obs. *(German)* 3−34895
- air pollution measurement, using i.r. tunable laser, review 3−3187
- alkali halide, impurity doped, review of Z-centre absorpt. 3−8624
- alkali halide, In$^+$- or Sn^{2+}-doped, absorpt. spectra, high press. 3−39166
- alkali halide, temp. depend. of half-widths and integral absorpt. of impurity vibration bands 3−21450
- alkali halide as CO$_2$ laser window material, intrinsic and impurity absorpt. at 10.6 micron 3−28580
- alkali halide crystal, far i.r. absorpt. theory 3−18444
- alkali halide-Cu halide, excitonic doublets, test for coherent-potential approximation 3−30436
- alkali halides, absorption spectra in vacuum u.v. due to excitons, ligand field theory calcs. 3−27509
- alkali halides, bound Frohlich polarons, induced i.r. absorption 3−36886
- alkali halides, electronic polaron resonance, optical absorption 3−36570
- alkali halides, exciton optical line shape, theory 3−38815
- alkali metals, optical absorpt., phonon-assisted processes, direct interband absorpt., Drude absorpt. 3−34335
- anthracene, crystn., hole detrapping by singlet excitons or photons, photoenhanced current obs. 3−24470
- anthracene single cryst., low temp. irradiation and meas. colour centres 3−132
- anthracene thin molecular crystal, absorption and fluorescence 3−34373
- anthraquinones, hydroxy- and amino-, absorpt. spectra electronic transitions 3−23561
- antiferromagnet, intensity of exciton-magnon transitions, strong mag. field effects *(Russian)* 3−8558
- atmosphere, i.r., and light polarization by mist haze, distinction from haze *(Russian)* 3−3008
- atmosphere gaseous constituents, remote mapping, differential absorp. and scatt., tuned laser obs. 3−3191
- atmospheric aerosols, optical absorpt. 3−37197
- atmospheric haze spectral attenuation, characteristics in visible and i.r. *(Russian)* 3−15961
- atom, multiphoton absorpt. of laser photons 3−33036
- atomic absorpt. spectrometry, mechanisms of interference and releasing action 3−14291
- azulene trapped in n-pentane, 77K, highly resolved struct. of $S_1 \leftarrow S_0$ electronic transition 3−27518
- benzene, absorpt. cross section, photoionisation efficiencies, in vacuum u.v. 3−29648
- benzene, n-dichloro- and n-dibromo- mixed cryst., electronic spectra at 4 K 3−15505
- benzene, solid, vacuum u.v. absorpt. spectra, π electrons electronic state 3−30834
- benzene and methylated derivatives, triplet-triplet absorpt., CNDO/S calcs. 3−23526
- benzene films, solid, assignment of vibr. bands of $^1B_{1u}$-$^1A_{1g}$ transition 3−12550
- benzodioxane 1.4 solution in CCl$_4$, i.r. absorption rel. to temperature *(Russian)* 3−23571
- borine carbonyl, high resolution i.r. absorpt. spectrum, vibr. states, rot. anal. 3−29664
- bound states of electron and phonon, in mag. field, calc. *(Russian)* 3−8560
- calcite, vacuum u.v refl. spectra, dielec. consts. determ., dichroic absorpt. band 3−27510
- chloranhydrides of unsaturated phosphoric acid, u.v. absorpt. rel. to intramol. interaction *(Russian)* 3−38278
- chloropyrazine vapour, $n\pi^*$ u.v. absorption spectra 3−17421

light absorption continued
- coarse weakly absorbing particles, energy distribution *(Russian)* 3−35672
- colloidal solns., absorpt. band intensities, effect of particle shapes 3−18739
- colloids, small metallic particles, quantum microscopic approach to electric-dipole absorption 3−26207
- complex mols., universal correl. between absorpt. and luminesc. spectra *(Russian)* 3−20179
- continuum polaron theory, equation of motion approach appl. to dynamical props. 3−36566
- crystal, absorpt. coeff. for linearly polarised light with intense laser bias 3−21395
- crystals, absorpt. spectra, stimulated antiresonance 3−21394
- crystals of D^7_{4h} symmetry, two-phonon processes 3−15491
- cubic crystal with substitutional impurities, i.r. absorpt. and dielec. susceptibility 3−18478
- cyclohexane, solid, vacuum u.v. absorpt. spectra, π electrons electronic state 3−30834
- cyclopropylcarbonium ions, (di)arylalkyl- and (di)aryl-, electronic absorpt. spectra, spectral shifts obs. 3−36011
- diamond:N, u.v. and i.r. absorption spectra *(Russian)* 3−2578
- diamond, intermediate type, defect associated with B1 absorpt. bands *(Russian)* 3−5220
- diamond crystals, absorption and luminescence spectra, red region, neutron irradiation effects 3−36901
- diamonds, type I and IIa, pulse irradiation 3−8673
- diaquobismethoxyacetato Co(II), polarised absorp. spectra vibronic interact. and mag. dipole effects 3−27501
- dilute solution of H$_2$ in liquid Ar, i.r. absorption spectra 3−21412
- 2-p-dimethylaminophenyl-5-phenyl-1,3-oxazole-polymethyl methacrylate system, photochem. transforms., absorpt. spectra 3−25097
- dipolar solvents, ionic field effect on i.r. absorption band parameters *(Russian)* 3−36881
- disordered semiconductors in external electric field, determ. of coeffs. of absorption *(Russian)* 3−24681
- disperse medium, statistical particle layer model *(German)* 3−26208
- dye aggregates from polyene type monomers, coupled oscillation and electron gas model 3−37132
- emission flame, atomic absorpt. meas. of distrib. of ground state atoms 3−14292
- epitaxially grown, i.r. absorpt. obs. of optical bandgap 3−11831
- equivalence relationships between diffuse radiation fields for finite slabs bounded by a perfect specular reflector and a perfect absorber 3−22759
- Er$_2$O$_2$S:Er^{3+} crystal field effects on electronic ion structure detn. *(French)* 3−30411
- ethane, detuerated derivatives, i.r. absorpt. spectra, dipole moment derivatives 3−29682
- exciton, surface irregularities in semiconductor crystals and polycrystals 3−30806
- exciton spectrum and effect of elec. field 3−4979
- extinction coeff. meas., slope method 3−28533
- F$_2$-centre multiphoton absorpt., transition amplitude calc. 3−2575
- film, highly absorbing, determ. method 3−9924
- film, resonant intraband absorp., rel. to applic. of quantum size effects 3−2040
- film substrate reflection polarizer, effect of film absorption 3−28519
- film waveguide light attenuation, meas. apparatus 3−35403
- finite anisotropic crystalline array of polarisable dipoles, normal excitation modes 3−18104
- fluorescene-Na, under lamp pumping, induced reversible absorpt. 3−22954
- formaldehyde, u.v. absorpt. spectra determ., Einstein coeffs. calc. 3−33113
- four-photon nonstationary forced diffusion in resonating media *(Russian)* 3−6514
- free polarons optical absorpt. coeff., two phonon sidebands 3−30805
- Frohlich polarons, internal structure determined by optical absorption, cyclotron resonance 3−36561
- gas, absorpt. line and press. broadening coeffs., laser spectroscopy 3−19650
- glass, La-silicate, radiation centres investigation by e.p.r., absorption spectra and thermal decolourising *(Russian)* 3−30697
- glass, spectral absorption *(Czech)* 3−35399
- glasses, phototropic, TlCl activation, optical absorption meas. 3−27737
- glutamic acid hydrochlorides, L- and DL-, Raman and i.r. absorpt. spectra and assignments 3−20143
- group II elements, two-photon absorpt. spectra, intercombination transitions cross sections calc. 3−22953
- halide film, electron beam damage effects 3−34479
- 1, 3, 5-hexatriene, cis- and trans-, lowest energy allowed singlet-singlet transition, u.v. absorpt. spectra 3−38327
- h.f. Franz-Keldysh effect on excitons 3−30435
- high optical densities meas., special features of the line absorption method 3−14586
- hydrogen bonded solids, theory of proton transfer, photon-bond interaction 3−11583
- hydroxybiphenyl, phase change effects on hydrogen bridges, i.r. absorpt. spectra *(French)* 3−29654
- III-V different semicond. layers forming Superlattice, absorpt. rel. to complex band structure 3−15519
- indigo dyes, configuration and conformation of electron donor and acceptor groups *(German)* 3−36291
- insulator, defect absorpt. strength, f-sum rule, Smakulas eqn. effective fields, review 3−12160
- interband absorption, in field of intense acoustic flux, theory *(Russian)* 3−27488
- ionic crystal film, due to bulk vibr. modes, calc. 3−24699
- ionic crystals, effect on optical absorption, electron-phonon interaction 3−36885
- ionic crystals, highly localised excitons in photoabsorption spectra 3−39155
- i.r., fluids at high temps. and pressures, measuring cells, corrosives, results 3−9920
- i.r. absorpt. lines, interpretation procedure using universal absorpt. contour 3−178
- i.r. absorpt. lines, neighbouring, mutual intrusion conditions 3−179

light absorption continued
- i.r. dispersion properties of absorbing films of lampblack and Sb *(Russian)* 3 − 15500
- irradiance attenuation rel. to conc. of suspended matter in sea, least squares method soln. 3 − 25187
- ketones, aromatic, and carbonium ions in soln., u.v. absorpt. spectra 3 − 36012
- l 3 − 34404
- laser, Rhodamine 6G in ethanol, gain curve and triplet-triplet absorpt. study 3 − 13736
- laser cavity resonator, non linear absorption processes *(Russian)* 3 − 29143
- laser light absorption in dense plasma 3 − 33347
- laser pulse duration control, nonlinear absorption in semiconductors *(Russian)* 3 − 215
- laser window materials, high power lasers, absorption mechanisms, thermal damage 3 − 28592
- laser windows, coated, formulas for absorpt., transmission and reflectivity 3 − 35424
- lattice localised mode, temp. dependence of integrated intensity absorption 3 − 27514
- liquid, absorp. coeff., photomixing obs. with He-Ne laser 3 − 32059
- liquid absorbance standards for u.v. and visible spectrophotometry 3 − 25647
- liquid metal, absorpt. and Ziman theory 3 − 21430
- luminescence attenuation, decreasing instrumental errors by statistical method *(Russian)* 3 − 22330
- macromolecules, optical absorption curve calc. using Franck-Condon factors 3 − 26746
- magneto-optical device, low-temp. meas. 3 − 9998
- measurements, liquid He cryostat 3 − 13277
- methane, solid in inert gas matrices, i.r. absorpt. theoretical study 3 − 24685
- methoxyl groups in oxonium and carbonium ions, protonation, u.v. absorpt. spectra 3 − 36012
- 1, 1′- methylene-2, 2′-cyanine, anomalous absorption and luminescence spectra 3 − 27569
- molar absorptivities, accurate measurement 3 − 26018
- molecular crystals, temp. dependence of absorption bands intensities of the spectra at Fermi resonance, mass operator and band shape 3 − 2538
- molecule, linear, two-photon $n \rightarrow \pi^*$ transitions, theory 3 − 29588
- molecule, overlapping pf fluorescent and absorpt. spectra, rel. to chem. struct. *(Russian)* 3 − 1250
- molecules, with closely spaced energy levels, absorpt.-emission processes, time-depend. Schrodinger eqn. soln. 3 − 29707
- monochromatic radiation pulse, two level absorbing medium, theoretical analysis 3 − 22958
- multialkali photocathode, 4000-11000 Å 3 − 30835
- multilayer systems, weakly absorbing, properties in terms of potential transmittance 3 − 16793
- multiphonon summation i.r. absorption, exponential frequency dependence 3 − 4827
- naphthalene cryst., with heterocyclic impurities, absorpt. spectra, local excitons 3 − 18476
- naphthalene cryst. with impurities depolarization of exciton absorpt. bands 3 − 15525
- naphthalene crystals, meas. of triplet level populations based on paramagnetic properties 3 − 32587
- nitrate glasses, far-i.r. spectra, press. effects, quasilattice dynamical interpret. 3 − 21399
- nonlinear, separated beams in Doppler-broadened transition, strong field 3 − 23585
- nonspherical stellar atm. and envelopes, polarisation variations 3 − 28201
- ocean water, light propag., multiple scatt. calcs., effective attenuation coeffs. 3 − 25186
- optical absorpt. spectra of half filled narrow band, Hubbard model, metal insulator transition region 3 − 30804
- optical multimode fibres, with graded and ungraded core indexes, bending mode loss 3 − 150
- organic dye molecules in aqueous soln. intermolecular reactions study by fluorescence quenching and difference absorption spectrophotometry 3 − 2806
- organic molecules, molar triplet excitation coeffs., c.w. laser excitation 3 − 28550
- oxydiodine radicals in aqueous soln., formation spectra and chem. props. 3 − 25048
- particles, cylindrical, extinction coeffs., calc. 3 − 13698
- pentacene, monoanions and dianions, i.r. absorpt. spectra obs. 3 − 33132
- pentacene in solid soln., low temp. absorpt. spectrum *(French)* 3 − 8561
- pentacene in solid soln. in p-terphenyl, compression effect on absorpt. spectra *(French)* 3 − 21816
- petroleum fractions, optical props. rel. to use in liquid lasers *(Bulgarian)* 3 − 34400
- phonon system with disordered force consts., Raman scatt., optical absorpt. 3 − 34349
- photoionization of shallow impurity centres, photoelec. effects due to drag phenomena 3 − 2139
- photon echo on homogeneously broadened spectral line 3 − 35716
- photoresistivity method for weak modulation of radiation meas. 3 − 18470
- phthalimide solutions, excitation power effect on luminescent and absorption characteristics *(Russian)* 3 − 30845
- phytochrome chromophore, optical props. models in π-electron approx. 3 − 29769
- plasma, cylindrically confined, radiation absorption 3 − 20427
- plasma, inhomogeneous, enhanced laser light absorption by optical resonance 3 − 33381
- plasma flare, absorpt. of laser beam 3 − 17634
- plasma layer, oblique incidence absorpt. 3 − 17562
- plastic scintillators, light attenuation quenching method 3 − 16514
- polar crystals, bound polarons, Wannier excitons, perturbation approach 3 − 36562
- polar liquids and solids, trapped dielectron, semicontinuum model 3 − 38813
- polarons plasma-phonon interactions, magnetic field effects 3 − 36572

light absorption continued
- poly(ethylene glycol) dimethyl ethers, cryst., i.r spectra, absorpt. band assignments 3 − 36060
- polyanilines, linear, band struct. and limiting behaviour 3 − 33792
- polyethylene, high density, i.r. absorpt. intensity rel. to elec. field 3 − 34324
- polyisoprenes, 1,2- and 3,4-, linear and cyclized, i.r. study, absorpt. band extinction coeffs. determ. 3 − 29771
- polymer, spectroscopic method for local stress meas. at stress raisers 3 − 28472
- polymers, rel. to charge trapping and carrier mobility 3 − 30468
- powdered samples with unknown refr. index and size distrib., absorpt. coeff. determ. method 3 − 28512
- propane, deuterated derivatives, i.r. absorpt. spectra, dipole moment derivatives 3 − 29682
- pyrene, absorpt. spectrum of first excited singlet state by modulation excitation spectrophotometry 3 − 21817
- pyrene, liq., laser induced transient absorpt., long- and short-lived components 3 − 34737
- quartz: $Fe^{2+}(Fe^{3+})(Co^{2+})$, impurity absorpt. near 78μ band 3 − 5216
- quartz, blackness determ. 3 − 24666
- quartz and fused silica, i.r. absorption at high temperatures *(German)* 3 − 37638
- quartz glass: V_2O_5 (CoO, Al_2O_3)(V_2O_5, Al_2O_3) (Eu_2O_3), spectral obs. coeff., temp. dep. 3 − 36865
- quartz glasses containing metal oxides *(Russian)* 3 − 27491
- rare earth complexes with aurinitricarboxylic acid and amines, absorpt. and luminesc. 3 − 15543
- rare earth films, 2000-8000 Å 3 − 12153
- rare earth hydroxides, energy levels of Er^{3+} 3 − 2572
- rare gas mixtures, absorption coeff. detn. by quantum mech. description of translational motion *(French)* 3 − 7071
- reflection nebulae, strong 4430 Angstroms interstellar absorption in backscattered light 3 − 28295
- resonant medium, intense monochromatic wave 3 − 19648
- Rhodamine 6G, under lamp pumping, induced reversible absorpt. 3 − 22954
- riboflavin solutions, electronic energy transfer frequency, conformity of universal correl. between obs. and luminescence spectra *(Russian)* 3 − 34408
- ruby:Cr^{4+}, elimination of Cr^{4+} ions as a source of strong resonant phonon scattering *(French)* 3 − 1846
- ruby amplifier rod, laser light strong resonance absorption 3 − 32565
- ruby with vandium impurities, γ-irrad., colour centre form. *(Russian)* 3 − 12156
- semiconducting transition metal oxides small polaron concept, d.c. and optical props. 3 − 36568
- semiconductor, absorpt. by bound excitons 3 − 4982
- semiconductor, absorpt. coeff. meas. using Schottky barrier method 3 − 15521
- semiconductor, artificial, formed by alternating thin films of Au and SiO_2, characterization 3 − 38790
- semiconductor, deep traps in quasi-classical random field *(Russian)* 3 − 34385
- semiconductor, disordered, absorpt. coeff. calc. for indirect transition, phonon influence 3 − 21433
- semiconductor, doped, in presence of strong e.m. field *(Russian)* 3 − 8628
- semiconductor, impurity absorpt. in strong elec. field below absorpt. edge 3 − 34391
- semiconductor, indirect magnetooptical transitions due to inelastic carrier-impurity interaction 3 − 5222
- semiconductor, interband absorpt. mechanism with Landau selection rules violation 3 − 21389
- semiconductor, polar, free polaron optical absorpt. const., velocity depend. 3 − 27505
- semiconductor, polar, i.r. absorpt. of localised longit. optical phonons 3 − 30232
- semiconductor, two-photon interband transitions, joint matrix element 3 − 34337
- semiconductor film, electrodispersion and electroabsorpt. spectra obs. 3 − 30801
- semiconductor quantised thin films, optical absorption by indirect interband transitions *(Russian)* 3 − 36957
- semiconductor with Kane-type band struct., internal quantum efficiency, spectral depend. 3 − 34338
- semiconductors, amorphous, glassy, electroabsorption 3 − 34325
- semiconductors, intraband edge absorpt., theory 3 − 15506
- semiconductors, polar, resonant electron-optic mode coupling, magnetic fields 3 − 36564
- semitransparent solids, coupled conduction-radiation heat transfer, spectral and boundary effects 3 − 33703
- sheet silicates, optical vibr. 3 − 34348
- silicate glasses, Pr_2O_3 and Nd_2O_3 mixtures combined with NiO effects on transparency curve *(Russian)* 3 − 12159
- silicon phthalocyanine dimer u.v. absorption spectrum, vibronic interpration 3 − 20134
- solar radiation attenuation through lowest 100 m. of urban atmosphere rel. to pollution 3 − 15973
- solid, two-photon absorpt. coeff. in uniform elec. field 3 − 15480
- solids, effect of absorption on optical props. *(French)* 3 − 16794
- spectra, molecular vibration, dimer, two-phonon region, electron excitation *(Russian)* 3 − 33105
- spectral attenuation coefficients, deep ocean optical meas. 3 − 3257
- spectral line breadth, scattering and absorption compared *(Russian)* 3 − 2551
- spectrophotometer, for deformed solids 3 − 22343
- spectrum, integral, absorpt. coeffs. of medium 3 − 35636
- stannic-phthalocyanine, absorpt. band study for charge-transfer like structures 3 − 2583
- stratified media, total refl. phenomena, total refl. attenuator 3 − 676
- styrene, absorpt. cross section, photoionisation efficiencies, in vacuum u.v. 3 − 29648
- by surface phonons and plasmons in small crysts. i.r. absorpt., continuum model 3 − 24705
- by surface phonons in small crysts., i.r. absorpt, 3 − 24326
- tetracene, monoanions and dianions, i.r. absorpt. spectra obs. 3 − 33132

light absorption continued
s-tetracyanobenzene, excited singlet-singlet absorpt. spectra of electron donor-acceptor complex 3−9090
tetrahedral impurities, coupling strengths of α_1, ε and τ_2 phonons to A→T optical transitions 3−27522
thin films, solid, sorption and porosity, i.r. absorption spectroscopy quantitative property determination 3−36478
thin layers, computation of absorpt. index from refl. and transmission spectra 3−683
thulium perrhenate tetrahydrate, absorpt. spectra and energy levels *(Russian)* 3−20171
titania-silica glass, optical attenuation, bleaching, H_2 evolution 3−21447
transition metal thin films, apparatus for ultra high vac. obs. *(French)* 3−35402
transport crystals, multiphonon absorption of i.r. due to higher-order electric moments 3−18452
trinitrofluorenone-poly-n-vinylcarbazole mixture, amorphous film, complexing study 3−18038
two-photon, Raman effect, spectroscopy, physical background, experimental problems 3−32584
two-photon radiative interaction operators from relativistic theory for Rayleigh scatt. and Faraday rot. 3−38274
water, Lambert absorption coeffs. in far i.r. 3−2508
water droplets, evaporation regimes, heating by optical radiation 3−27112
water films in mica, i.r. spectra *(Russian)* 3−27496
water vapour, CO laser radiation absorpt. 3−19627
windowless reflectance furnace, for i.r. studies of corrosive melts 3−22290
ZnO, two quantum absorption spectrum and depend. on polarization *(German)* 3−2563
Ag film, aggregated, inter-island dielec. const. rel. to optical plasma reson. absorpt. 3−8684
Ag film, partially disordered, anomalous absorpt. prior to annealing 3−36888
Ag halide emulsions, fine absorption struct. and meas. aspects 3−34742
Ag halide emulsions, fine struct. of absorption spectra 3−34743
Ag halides, bound Frohlich polarons, induced i.r. absorption 3−36886
AgBr, optical absorpt. below fund. edge, Urbachs rule, 50-950K 3−5218
AgBr crystals, habit influence on absorption spectra of adsorbed sensitising dyes 3−27902
AgBr long-wavelength, emulsion 3−34377
AgBr(Cl):Li(Na), absorpt. bands due to impurity localised modes 3−30850
AgCl, magnetoabsorption of indirect exciton 3−12143
AgCl, optical absorpt. below fund. edge, Urbachs rule, 50-950K 3−5218
Ag_2IBr, crystals, habit influence on absorption spectra of adsorbed sensitising dyes 3−27902
$Ag_xNa_{1-x}NO_2$, influence of light scatt. on i.r. absorpt. *(Russian)* 3−18440
AlN film, optical band gap, optical absorpt. 3−21004
Al_2O_3, photocond. near intrinsic absorpt. edge, exciton nature of absorpt. band 3−5032
$(AlSb)_x(CdTe)_{1-x}$ solid solutions, absorption edge coefficient, photoelectric method, band structure 3−34376
Ar, photoabsorption cross section, 180-700 Å 3−20014
Ar:Kr, far. i.r. absorpt. spectra at 2K 3−2574
Ar:Ne, far. i.r. absorpt. spectra at 2K 3−2574
As-Se-Ge amorphous films, photo-darkening effect 3−5212
As_2O_3-SiO_2 glass diffusion sources, effect of heat treatment on comp., i.r. absorption study 3−20963
As_2S_3, laminar semicond., Raman scatt., absorption spectrum, vibr. levels splitting *(Russian)* 3−21425
$As_2(S_xSe_{1-x})_3$ amorphous film, lattice phonons, i.r. spectra study 3−36382
$As_2(S_xTe_{1-x})_3$ amorphous film, lattice phonons, i.r. spectra study 3−36382
As_2Se_3, vitreous, chaotic potential field, optical absorption edge shift, deformation potentials 3−20993
As_2Se_3 glassy, optical absorpt. rel. to press. *(Russian)* 3−8608
As_2Se_3 glassy, photocond. spectra rel. to optical absorpt. spectra *(Russian)* 3−8224
$As_2(Se_xTe_{1-x})_3$ amorphous film, lattice phonons, i.r. spectra study 3−36382
Au particles, cylindrical, of i.r. radiation *(Russian)* 3−6426
Au-Cu alloy film, order-disorder transformation on heat treatment obs. 3−1800
BI, u.v. absorpt. spectrum, 265 to 280 nm 3−36013
BS_2, visible and i.r. absorpt. spectra at 4K 3−33128
BaF_2, radiation-induced transform. of defects, obs. *(Russian)* 3−30694
BaF_2:H^-, far infrared impurity induced 3−34387
$Ba_{1-y}Sr_yFeO_{3-x}$ and $Ba_{1-y}Sr_yFe_{1-z}M_zO_{2.5}$ (M = Ga or In) i.r. absorpt. and dielec. props. *(French)* 3−36831
Be, 0.12-4.5 eV 3−36869
$Be_3Al_2Si_6O_{18}$:V^{3+}, beryl, optical and i.r. absorpt. rel. to crystal field parameters 3−34389
BeO, for use as window in v.u.v. 3−28520
BeO film, prep. by reactive evaporation of Be, absence of absorpt. in visible *(German)* 3−21534
Bi^{2+}:oxide glass, energy level assignments 3−12168
$Bi_{12}GeO_{20}$, nonlinear absorpt. of A laser radiation 3−4128
BiOBr, i.r. transmission, two phonon absorpt. processes 3−21424
BiOBr, long wavelength fund. absorpt. edge rel. to press. and elec. field *(Russian)* 3−8609
BiOCl, i.r. transmission, two phonon absorpt. processes 3−21424
BiOCl(Br)(I), two-phonon processes 3−15491
BiOI, i.r. transmission, two phonon absorpt. processes 3−21424
BiOI, long wavelength fund. absorpt. edge rel. to press. and elec. field *(Russian)* 3−8609
C stars, total to selective absorpt. ratio determ. using UBV photoelectric scans 3−28200
CN absorpt. coeff. determ. for 0.4-3 μ at 1000°, 3000° and 5000°K, stellar appl. 3−38259
C_2N_2, Raman and far i.r. spectra 3−33125

light absorption continued
CO_2, continuous absorpt. exponential decrease beyond 4.3μ band head due to far wings contour 3−29734
CO_2, i.r. general absorptance, polynomial representation 3−36015
CO_2, in Martian atmosphere, distribution by i.r. absor. obs. 3−31588
CaF_2, M^+ centre obs. 3−27023
CaF_2, radiation-induced transform. of defects, obs. *(Russian)* 3−30694
CaF_2:Ce,Na, near u.v. absorpt. spectra obs. of defect centres 3−12161
CaF_2:H^-, far infrared impurity induced 3−34387
CaF_2:Mn, thermal and u.v. bleaching of absorpt. bands 3−7755
CaF_2:Sm, absorpt. and thermolum. excitation spectra 3−24758
CaO, multiphonon i.r. absorpt. spectra, lattice vibrs. i.r. active sum modes 3−24693
CaO, zero-phonon line of F^+ centre, elec. field effect 3−30858
$Ca_{10}(PO_4)_6F_2$, strong u.v. absorption 3−8623
$CaWO_4$, temp. broadening of Nd^{3+} energy levels *(Russian)* 3−8617
β- carotene films, amorphous, refractive and absorption indices *(Russian)* 3−36895
$CdCl_2$ molten binary mixtures, minima of absorption edge frequencies 3−2558
CdF_2:$^{169}YbF_3$, Stockbarger technique growth, optical props. of radioactive and nonradioactive samples 3−2664
CdF_2:Er^{3+}, C_{3v} local-site symmetry from correlated e.p.r. and optical obs. 3−21305
CdF_2:In, semicond., absorpt. and elec. cond. meas. 3−21448
$Cd_xHg_{1-x}Te$ monocrysts., comp. distrib. from absorpt. spectrum *(Russian)* 3−12158
CdI_2, far i.r. lattice vibr. spectrum 3−2544
$CdIn_2S_4$:Fe^{2+}, effect of weak Jahn-Teller coupling 3−21455
$CdIn_2Se_{4x}Te_{4(1-x)}$, solid soln., forbidden zone width from absorpt. and Hall coeff. meas. *(Russian)* 3−15126
CdO-NaCl heterojunction, colour centres *(Russian)* 3−8627
Cd_3P_2:Cu, deep impurity level effects 3−30794
CdS, isoelectronic Ni impurity, absorpt. spectra *(Russian)* 3−8618
CdS, photosensitive, modulation of absorption by field effect 3−24679
CdS, recomb. waves induced by optical quenching 3−38866
CdS:Be, i.r. absorpt. due to localized vibr. mode 3−27523
CdS:Ni^{2+} absorpt. spectrum obs. of linear Stark effect 3−8625
CdS-$Cu_{2-x}S$ heterojunctions, impurity photoeffect 3−27309
$(CdS)_{3x}$-$(In_2S_3)_{1-x}$, rel. to band structure 3−18085
CdSe:Be, i.r. absorpt. due to localized vibr. mode 3−27523
CdSe:Co, degenerate discrete excited states, absorpt. and photocond. spectra obs. 3−2024
CdSe:Ni, degenerate discrete excited states, absorpt. and photocond. spectra obs. 3−2024
$CdSiP_2$, absorpt. coeff. meas. *(Japanese)* 3−12146
$CdSiP_2$, pure and doped crystal, long wavelength fund. absorpt. edge 3−39163
CdTe, amorphous, i.r. spectra analysis 3−2526
CdTe, electron-phonon interaction, far i.r. cyclotron resonance absorption 3−36388
CdTe:Fe, Hall effect and photocond. meas. rel. to impurity absorption 3−15531
CdTe:In, absorption band edge of compensated crystals 3−24717
CdTe:N, degenerate discrete excited states, absorpt. and photocond. spectra obs. 3−2024
CdTe:Ti, degenerate discrete excited states, absorpt. and photocond. spectra obs. 3−2024
$(CdTe)_{1-x}(AlSb)_x$ solid solutions, absorption edge, coefficient, photoelectric method, band structure 3−34376
CeF_2, Pr^{3+} absorpt. spectra and energy levels *(Russian)* 3−12157
$CfCl_3$ thin films, absorption spectrum in range 6000-46000 cm^{-1} 3−27497
Cl_2, atmospheric pressure, vacuum u.v. absorption 105 to 550 nm *(Russian)* 3−7181
ClO, vacuum u.v. absorpt. spectrum 3−33119
$CoCr_2S_4$, hot pressed, absorption coeff., 1500-800 cm^{-1} 3−18435
$Co(PO_3)_2$-$CsPO_3$, glasses and melts, effect of water on molar absorption *(Russian)* 3−14696
$CrCl_3$, specific magnetic rotation and optical absorption in crystal field bands 3−5179
Cs, photoabsorption 3−20035
Cs halides, far i.r. absorpt. due to U-centres, defect model 3−15529
CsCl(Br)(I), Pb-centres, obs. 3−24725
$CsCuCl_3$, absorpt. spectra obs. rel. to crystal field levels 3−21414
CsI:Wo^{2-}(MoO^{2-}), i.r. absorpt. and local symmetry 3−8621
Cu films, far-u.v. transmission, N_2 press. influence *(French)* 3−12199
Cu I, v.u.v., autoionized resonances 3−29504
Cu-Al, anomalous shift in interconduction band optical absorption, values for band gaps 3−30837
CuBr(Cl), magneto-optical spectra in exciton absorpt. region 3−8556
CuCl, absorpt. spectra 3−13301
CuCl, two-photon absorpt., confirmation of polariton fusion theory 3−18107
$CuCl_2$, in. aq. and organic soln., energy bands and levels, cryst. field parameter determ. 3−5215
$CuGaS_2$, low temp. spectra 3−15510
$CuGaS_2$, rel. to excitons and spin orbit splitting 3−18108
Cu_2O, modulated excitonic absorption in elec. and mag. fields 3−2037
Cu_2O, optical absorpt. spectra obs. of Mott excitons in elec. field 3−8129
Cu_2O, two photon absorption spectrum 3−2567
Cu_2S, chalcosite thin crysts., unusual form, 0.5-1.1μ 3−24701
D_2O vapour, localised excess electrons, i.r. absorption spectra 3−31241
$DyVO_4$, i.r. absorpt. obs. at low temp. rel. to crystal field splitting 3−18443
EuS, EuSe and EuTe, rel. to photoluminescence *(German)* 3−18495
Fe, passive, passivating film, thickness, complex refr. index and absorpt. coeff. meas. *(German)* 3−27163
Fe-Rh (52 at.%) alloy, mag. transform. behaviour, dispersion laws *(Russian)* 3−18439
$FeBO_3$ strong absorption region spectra, Faraday rotation 3−36893
$FeSi_2$, amorphous material crude band model 3−36419

light absorption continued
GaAs, absorpt. edge modulation by intensely amplified phonon beams 3−5204
n-GaAs, absorpt. increase with electron irrad., selective bands 3−39164
p-type GaAs, after proton bombardment and subsequent annealing 3−21442
GaAs, damage produced by fast neutrons 3−33567
n-GaAs, electroabsorpt. meas. for transitions from spin orbit split to cond. band 3−39123
n-GaAs, electron irradiated, defect annealing, cluster formation 3−33558
n-GaAs, homogeneities rel. to doping, optical absorpt. obs. *(French)* 3−34386
n-GaAs, intervalley absorpt., LA and TA phonons contrib. *(French)* 3−24726
GaAs, nonlinear interaction *(Russian)* 3−777
GaAs, obs. of phonon struct. of interband transitions 3−2027
GaAs injection laser, absorpt. coeff. and gain 3−22919
GaAs:Fe(Cu), electron absorpt. obs. rel. to impurity energy levels *(Russian)* 3−15532
GaAs:Sn(Si, Zn), electron irrad., 'near-edge' absorption, annealing 3−33846
$GaAs_{1-x}P_x$ indirect $\Gamma_{8v}-X_{1c}$ band gap determ. 3−21003
GaN, i.r. absorpt. meas. rel. to lattice vibrations and free-electron dispersion 3−18455
GaP, doping homogeneity, using laser scanning meas. of i.r. absorpt. 3−5277
GaP, neutron irradiated, optical absorption *(Russian)* 3−30851
GaP, p- and n-type, after proton bombardment 3−21443
GaSe, absorp. coeff. in transparency region rel. to nonlinear optical props. *(Russian)* 3−2505
GaSe layer compound, polarization dependence of absorption, band structure calc. 3−30404
$GdAlO_3:Ho^{3+}$, absorpt. and luminesc. spectra obs. rel. to energy levels 3−8655
$GdAlO_3:Tm^{3+}$, absorpt. spectra obs. rel. to energy levels 3−12174
Ge, amorphous, doped layer, spectral depend. of absorption 3−18131
Ge, amorphous sputtered layer, effect of deposition 3−4934
n-Ge, free carrier Voigt magnetoabsorpt. 3−27486
Ge, H^+, O^+, B^+, ion bombardment, divacancy-like optical absorption 3−34394
Ge, high press. phases, comparison with amorphous Ge 3−30095
Ge, indirect absorpt. edge meas. rel. to electron states under uniaxial stress 3−33801
Ge, shallow donor impurity near-surface states, theory 3−24494
Ge, surface states absorpt. spectrum, oxidation effect 3−2163
Ge, two electron donor pair system, eigenvalue problem, Heitler-London method soln. 3−2579
Ge absorption coeff. rel. to resist. at 10.6 μm 3−30787
Ge amorphous thin films, absorption and transport study of the pseudo gap 3−33775
Ge amorphous thin films, optical props. 3−15575
Ge antireflection coating, i.r. 3−3799
Ge film, amorphous, order-disorder transformation on heat treatment obs. 3−1800
Ge film, vacuum deposited, near i.r. absorp., acceptor levels obs. *(Russian)* 3−24431
Ge:Sb, direct absorp. edge, exciton plasma resonance obs. *(Russian)* 3−5211
GeI, u.v. spectra, 220 to 250 nm band interpretation 3−29643
GeS film, i.r. absorpt. spectra during amorphous-polycryst. transitions *(Russian)* 3−15109
GeSbSe amorphous film, optical band gap determ. 3−21080
GeSe amorphous film, optical band gap determ. 3−21080
GeSe film, i.r. absorpt. spectra during amorphous-polycryst. transitions *(Russian)* 3−15109
GeTe film, i.r. absorpt. spectra during amorphous-polycryst. transitions *(Russian)* 3−15109
HCl, inert gas perturbed, induced low temp. absorpt. spectrum *(French)* 3−29637
He excited atoms in plasma, two-photon absorpt. as plasma diagnostic technique 3−4672
$HgCr_2Se_4$, magnetoabsorpt. obs., temp. and field depend. at Curie point 3−12122
n-Hgs, cubic, band inversion, optical absorpt. and intra-band refl. rel. to carrier conc. and temp. 3−2002
I_2, absorpt. spectra, 45-160 eV, inner electron excitation in gaseous and solid phase 3−29647
I_2, H.F.S. of optical transitions 3−1210
I_2, visible-i.r. absorpt. spectrum, resolution 3−36008
$^{127}I_2$, molecular absorp. of three Kr II laser lines *(German)* 3−36010
n-InAs, absorpt. spectra near fund. absorpt. edge, coeff. rel. to photon energy 3−5217
n-InAs, confirmation of cond. band nonparabolicity *(Russian)* 3−38797
InAs, InP, InP_xAs_{1-x} solid soln., neutron and gamma irrad., elec. and optical props. 3−33907
InAs and InAs-CdTe solid solutions, absorption band structure from absorption spectra 3−24383
n-InP, absorpt. spectra near fund. absorpt. edge, coeff. rel. to photon energy 3−5217
InP, obs. of phonon struct. of interband transitions 3−2027
InP_xAs_{1-x} solid soln., absorpt. spectra near fund. absorpt. edge, coeff. rel. to photon energy 3−5217
InSb, freq. depend. of two-quantum transitions near absorpt. edge, peak due to valence band degeneracy 3−21435
n-InSb, in mag. field, reson. hole-TO and hole-LO phonon coupling 3−4831
InSb two-photon absorpt. at 10.6 μm 3−22941
InSb:Zn(Cd)(Ag), acceptor excitation spectra, obs. of Zeeman splitting 3−24728
In_3Te_4, thin films, abs. spectra at fund. obs. edge, rel. to exciton transition *(Russian)* 3−30818
KBr, additively coloured, F-, M- and R-centres 3−2617
KBr cryst. with PO_2^- mol. centre, low temp. luminesc., absorpt. and excitation spectra 3−15549
KBr slab, anharmonic effects on surface mode absorpt. 3−18014
$KBr:BO_3^-$ i.r. absorpt. rel. to vibration spectrum 3−18445

light absorption continued
$KBr:MnO_4^-$, vibronic spectra obs. 3−8616
$KBr:OH^-$, O_2^-, O^{2-}, anion impurities influence on optical stability of F-centres *(Russian)* 3−8615
KCl, additively coloured, F-, M- and R-centres 3−2617
KCl, additively coloured, photochem. F→M centre conversion *(Russian)* 3−33526
KCl, i.r. absorpt. of aligned H^--Na^+-H^- complex 3−24727
KCl cryst. with PO_2^- mol. centre, low temp. luminesc., absorpt. and excitation spectra 3−15549
KCl:Cu, complex centres 3−15528
$KCl:Fe(CN)^{3-}$, electronic and vibrational spectra from i.r. absorpt. meas. 3−18446
KCl:Li, X-irrad., F-centre accumulation kinetics 3−2576
$KCl:Li^+(Na^+)$, image recording on F_a centres 3−32082
KCl:Na, decay of F and F_a' bands produced by light flashes, room temp. 3−27521
KCl:Na, i.r. absorpt. rel. to softening of short range force consts. 3−15527
$KCl:Na^+$, additively coloured, transient absorpt. in F-band, flash-light excitation induced, 600-1100 nm 3−15530
$KCl:OH^-$, u.v. irrad., Y- and Y′-centres, absorpt. 3−18477
KCl:Pb, Br, X- or γ-irrad., $BrCl^-$ and associated centres 3−39031
KCl:Sr, Z centres, photoionisation, absorpt. spectra 3−34741
KCl:Tl, Ga, In, absorp. bands of Tl^0, Ga^0, and In^0 centres 3−27024
KCl:Tl, γ-irrad., ionized Tl-pair centre 3−21445
KCl:Tl, optical delocalization of holes from Tl^{2+} centres 3−34390
KCl:Tl, stress induced dichroism and energy shifts in A, B and C absorption bands 3−21454
KCl-KBr, meas. for Czochralski crystal grown in protective atmosphere 3−12292
KCl-KI, by second harmonics of U-centre oscill., calc. *(Russian)* 3−15533
KCl-KI:Ag, X-irrad. 3−8445
KCl-NaCl solid soln., Cl^--$L_{II,III}$ absorpt., 200-235 eV, at 77K 3−27511
KCl-RbCl solid soln., Cl^--$L_{II,III}$ absorpt., 200-235 eV, at 77K 3−27511
$KClO_3$, fundamental absorp., indirect transitions obs. 3−30832
K_2CrCl_4, optical absorpt. spectra 8000 to 25000 cm^{-1}, temp. range 4.2 to 300 K 3−12150
KI, F-band, rel. to diffusion of water molecules 3−30120
KI, optical reorientation of V_k centres 3−17817
KI polarised, spectra, M-centres, anisotropies 3−27520
KI with trapped S_2^-, S_3^- and Se_2^- mols., stress-induced linear dichroism 3−30848
$KI:WO^{2-}(MoO^{2-})$, i.r. absorpt. obs. of local symmetry 3−8621
KNO_3, influence of light scatt. on i.r. absorpt. *(Russian)* 3−18440
$KNiPO_4$, spectral obs. rel. to local environment of Ni^{2+} ions 3−24719
$K_2SO_4:CrO_4^{2-}$, vibr. freqs., optical and i.r. absorpt. studies 3−14954
K_3Sb, extinction coeff., determ. from transmittance spectra, 0.5 to 6.2 eV 3−39160
Kr, resonance transition, self broadened linewidths 3−29491
La, d-h.c.p., supercond. energy gap from far-i.r. absorpt. 3−5069
$LaBr_3:Tb^{3+}$, absorpt. and fluoresc. spectra, 77 K 3−30866
LaF_3, excited Nd^{3+} ion metastable state deactivation processes 3−34427
$LiBaF_3$, growth by Czochralski and Bridgman methods, doped and pure, absorpt. spectra *(German)* 3−2661
LiF, energies of formation of single, double and triple holes in valence band *(Russian)* 3−8611
LiF, small crystals, i.r. absorpt. rel. to particle size, mode absorpt. bands 3−39150
LiH, thermal discolouring and colour centres *(Russian)* 3−12190
$LiIO_3$, assignment of lattice vibrs. from i.r. absorpt. 3−38637
$LiNbO_3$, ion irrad., expansion, crazing and exfoliation, obs. 3−17880
$LiNbO_3$, stretching vibr. band of OH^- defects, 2.87 μ 3−24729
MgF_2 u.v., optical constants, anisotropy, reflectance measurements, excitations 3−27482
MgO, multiphonon i.r. absorpt. spectra, lattice vibrs. i.r. active sum modes 3−24693
$MgO:Cr^{3+}$, absorpt. meas. rel. to tetragonal field splitting of levels 3−15513
$MgO:Cr^{3+}$, obs. of optical absorpt. strengths for transition lines 3−15512
Mn u.v. absorption linewidths and lineshifts, pressure broadening and foreign gases effect *(French)* 3−17344
Mn vapour, determination of absolute conc. of atoms by atomic absorption *(Russian)* 3−23474
MnF_2, spin flop domains, n.m.r., Faraday rotation, photographs, and optical-absorption spectroscopy investigation 3−34113
MnO, fine struct., role of magnons and phonons *(Russian)* 3−15522
$NH_4Cl:Co^{2+}$, Ni^{2+}, Cu^{2+}, by impurity centres, cryst. field parameters 3−21456
$(NH_4)_2SO_4:CrO_4^{2-}$, vibr. freqs., optical and i.r. absorpt. studies 3−14954
NO, pressure broadening of magnetically tuned i.r. absorption spectrum, using CO laser 3−14388
N_2O, cryst., i.r. intensities of external modes 3−21397
N_2O detection, amplified absorption, CO_2 laser 3−29129
Na, hyperfine struct. meas. using c.w. dye laser and atomic beam 3−37963
Na atoms, photoabsorpt. in vacuum u.v. 3−7046
$NaBrO_3$, $NaIO_3$, fundamental absorp., indirect transitions obs. 3−30833
$NaCa_2Ni(Co)_2V_3O_{12}$, garnet, absorpt. spectra obs. of $Ni^{2+}(Co^{2+})$ ions, crystal field theory 3−21434
NaCl, temp. depend. of F-centre absorpt. 3−4755
NaCl slab, anharmonic effects on surface mode absorpt. 3−18014
NaCl:Br, absorpt. and luminesc. of Br^- clusters 3−21464
$NaCl:Fe(CN)^{3-}$, electronic and vibrational spectra from i.r. absorpt. meas. 3−18446
NaCl:KF, obs. of i.r. absorpt. line 3−8622
NaCl:Mg, X-irradiated crystals, Mg centres expt. obs. 3−38586
$NaCl:Pb^{2+}$, A- and B-band structs. 3−18098
$NaClO_3$, fundamental absorp. indirect transitions obs. 3−30832

- **light absorption** continued
  - $NaClO_3$, phonon-assisted electronic transitions, 50-368K 3−21431
  - NaI crystalline powder, one-phonon far i.r. absorp. 3−27502
  - Na_2KSb, extinction coeff., determ. from transmittance spectra, 0.5 to 6.2 eV 3−39160
  - $NaNO_2$, influence of light scatt. on i.r. absorpt. *(Russian)* 3−18440
  - Na_2O-B_2O_3 glass, electron irrad. *(Russian)* 3−18474
  - Na_2O-SiO_2 glass, i.r. spectra, pressure depend., i.r. vibrations and elastic parameters obs. 3−5186
  - Na_2SO_4:CrO_4^{2-}, vibr. freqs., optical and i.r. absorpt. studies 3−14954
  - Na_3Sb, extinction coeff., determ. from transmittance spectra, 0.5 to 6.2 eV 3−39160
  - Nb, absorpt. or refl. meas. from 0.1 to 36.4 eV, interband effects 3−39159
  - Nb_3Sn, i.r. absorptivity calc. rel. to electronic density of states 3−34360
  - $NdAlO_3$, energy levels and crystal field theory, Raman scatt. and optical absorpt. meas. 3−34357
  - Ne^-, continuous absorpt. coeff. rel. to stellar atmospheres 3−35117
  - NiO, localized electronic excitations, rel. to absorp., 4-7 eV 3−27219
  - NiO, small crystals, i.r. absorpt. rel. to particle size, mode absorpt. bands 3−39150
  - O_2 solid, antiferromag. and light absorpt. due to mol. interaction 3−24549
  - O_2-N_2 solid binary mixtures, light absorption by O_2, simultaneous electron transitions *(Russian)* 3−34382
  - Pb^{2+}:oxide glass, energy level assignments 3−12168
  - $PbCl_2$ molten binary mixtures, minima of absorption edge frequencies 3−2558
  - $PbCl_2$:Nd^{3+} and $PbCl_2$:Pr^{3+}, optical spectra, Stark splitting 3−15515
  - $PbCl(Br_2)$, photoluminesc., thin film absorpt. rel. to exciton form. 3−27561
  - PbI_2 exciton splitting, spectral absorption band, dispersion measurements *(Russian)* 3−34379
  - $PbMg_{1/3}Nb_{2/3}O_3$, optical absorpt. coeff. anomalous behaviour in broad ferroelec. transition 3−21438
  - PbN_6, pure and doped thin films, photodecomposition, optical absorpt. and cond. meas. 3−25084
  - PbO, crystallochemical peculiarities and shape of absorpt. edge 3−8606
  - (α-)-PbO spectra, luminescence spectra, single crystals 3−34378
  - p-$Pb_{1-x}Sn_xTe$ solid soln., i.r. absorpt. spectra due to free carriers, valence bands energy gap *(Russian)* 3−8626
  - PbTe-SnTe, absorpt. coeff. calc. in nonparabolic region using two-band model 3−15520
  - Rb_2 vapour, nonlinear absorpt. of ruby laser emission, fluoresc. *(Russian)* 3−7221
  - RbF microcrystals, density of phonon states and i.r. absorpt., calc. 3−36380
  - RbI, light transmission, 5.5-6.3 eV, effect of surfaces 3−36892
  - $RbMnF_3$, antiferrodielectric, anisotropic, mag. ion Mn^{2+} transitions 3−30838
  - $RbMnF_3$, cubic antiferromag., mag. dipolar line splitting and uniaxial stress effects on exciton absorpt. lines 3−30817
  - $RbMnF_3$, two exciton transitions, theory 3−38814
  - SF_6, narrow reson. in absorpt. saturation by CO_2 laser emission 3−23587
  - SF_6, SCF MO LCAO calcs., electronic props. 3−1151
  - SbI_3, magnetooscillatory effect *(Russian)* 3−34329
  - SbSI, absorpt. edge shift rel. to elec. polarization 3−15507
  - SbSi cryst., mid-i.r. absorpt. and indirect transitions 3−24697
  - $Sb(TaNb)O_4$, intrinsic absorpt. obs. of forbidden band width at ferroelec. transition 3−5171
  - Sc_2O_3 film, transparency, long wavelength absorpt. edge, refr. index, annealing effects 3−24763
  - Se, in CS_2 soln., 2.2-3.0ev, conc. depend. 3−36890
  - SeO_2, 3200 Å absorpt. system analysis 3−14363
  - n-Si, 10.6 μ, anisotropy of electron scatt. by charged impurities *(Russian)* 3−2077
  - Si, core electron spectra, $L_{III,II}$ electron loss spectra and optical absorpt., comparison 3−34449
  - Si, epitaxial deposition, optical absorpt. rel. to quality of films grown by different methods 3−2655
  - Si, i.r. absorpt. meas. after neutron irradiation and annealing 3−15496
  - Si, indirect absorpt. edge meas. rel. to electron states under uniaxial stress 3−33801
  - Si, optical absorpt. near indirect band gap, fine structure 3−18082
  - Si, shallow donor impurity near-surface states, theory 3−24494
  - Si, strongly-doped, spectral depend. in region of plasma reson. of charge carriers *(Russian)* 3−30789
  - Si, surface states absorpt. spectrum, oxidation effect 3−2163
  - Si, two electron donor pair system, eigenvalue problem, Heitler-London method soln. 3−2579
  - Si:Au, 0.3-1.05 eV, impurity photoionization cross section determ. *(Russian)* 3−5221
  - Si:Au, high-resistivity, i.r., rel. to impurity conc. determ. *(Russian)* 3−2673
  - Si:C, i.r. absorpt. spectra, local vibr. modes and defect vibr. modes 3−18475
  - SiAs single crystal, optical consts. and energy gap, absorpt. meas. 3−36850
  - SiC, 15R polytype, single-phonon absorpt. rel. to reststrahlen band structure 3−15497
  - SiC, 4H polytype, far i.r. 3−36876
  - n-6H-SiC, i.r., influence of additional u.v. illum. *(Russian)* 3−2549
  - 6H SiC photoelectric effects, absorption coeff., surface barrier diode 3−34375
  - SiC polytypes, i.r. latice absorpt. bands 3−36875
  - SiC-6H, polished single crystals, mechanical breaking effect on absorption in near i.r. spectral region *(Russian)* 3−30827
  - αSiC(6H), photoionisation spectra of impurity centres at high temp. 3−36902
  - SiGe alloy divacancylike absorption following neutron or proton irradiation 3−21441
  - SiH_4, far-i.r. spectrum, dipole and octople moments 3−36017
  - SiI, u.v. spectra, 220 to 250 nm band interpretation 3−29643
- **light absorption** continued
  - Si_3N_4, spectral depend. 3−30829
  - SiO_2-Al_2O_3-Na_2O glasses, containing TiO_2 as nucleation agent, props. and struct. *(Polish)* 3−4721
  - Si antireflection coating, i.r. 3−3799
  - Sm chalcogenide film, absorpt. spectra, mag. circular dichroism 3−2606
  - $SnCl_4$, vacuum u.v. absorpt. spectra 3−29649
  - SnO_2 single crystal, exciton magnetoabsorpt., meas. 3−39127
  - $SrCl_2$:Yb^{2+}, strong field assignment on $4f^{13}5d$ levels 3−34388
  - SrF_2, radiation-induced transform. of defects, obs. *(Russian)* 3−30694
  - SrF_2:H^-, far infrared impurity induced 3−34387
  - $SrTiO_3$, distortion enhanced optical absorption at the cubic to tetragonal transition 3−12149
  - $SrTiO_3$, electroabsorpt. and band struct. 3−36891
  - $SrTiO_3$, meas. rel. to oxygen vacancies as electron traps 3−27225
  - $TlNO_3$-$Cd(NO_3)_2$ glass, i.r. spectra, comp. depend., NO_3^- vibrations 3−21405
  - $TbAsO_4$, temp. and mag. field depend., rel. to phase transitions 3−2560
  - $TbPO_4$:Tb^{3+}, absorpt. spectrum obs. of crystallographic phase transition 3−12019
  - Te, defect induced absorpt. spectra obs. near electronic band edge 3−21449
  - Te, electron-phonon interaction, for i.r. cyclotron resonance absorption 3−36388
  - Te, intervalence band transitions, absorpt. spectra calcs. 3−21006
  - Te film, 2.5-15 μ, 300 and 90K *(Russian)* 3−2550
  - $TiCl_4$, vacuum u.v. absorpt. spectra 3−29649
  - Tl^+:oxide glass, energy level assignments 3−12168
  - TlBr indirect absorpt. edge in luminesc. excitation spectra 3−2584
  - $TlSbSe_2$ film, characterization *(Russian)* 3−18235
  - VCl_4, vacuum u.v. absorpt. spectra 3−29649
  - V_2O_5-P_2O_5 glass absorpt. tail, fund. absorpt. edge, band gap, forbidden transitions 3−21444
  - WO_3 thin films, optical and photoelectric props. and colour centres 3−36899
  - $W_{1-x}Ta_xSe_2$, absorpt. spectra, absorpt. edge excitons energy 3−15518
  - Xe, continuous spectrum, absorption coefficients calc. *(Russian)* 3−35961
  - Y single crystals, 4.2 K, 0.15-4.4 eV 3−39161
  - YAG laser cryst., transient absorpt., detection using combined laser 3−29091
  - YAG:Nd, Li, laser crystal, absorpt. and luminesc. props. with doping 3−19617
  - $YAlO_3$:Er^{3+}, energy levels, cryst. field components 3−5225
  - YIG:Ge substituted, rel. to ferromag. resonance 3−5136
  - $ZnGeP_2$, absorpt. coeff. meas. *(Japanese)* 3−12146
  - ZnO, two quantum absorption by intrinsic excitons *(German)* 3−2564
  - ZnO(S):Ni^{2+}, near i.r. absorpt. obs. of crystal field, dynamic Jahn-Teller effect in $^3T_2$ state 3−21446
  - $Zn(PO_3)_2$-MPO_3:Co (M=Na, K, Cs) glasses and melts, molar absorption *(Russian)* 3−14695
  - ZnS polytypes, wavelength dependence of photovoltage 3−15224
  - ZnS:Ni^{2+}, ion-hole complexes, electron struct., determ. *(Russian)* 3−12155
  - ZnSe:Al, Ga and In, optical absorption, diffusion of impurities 3−24712
  - $ZnSiP_2$, opt. vibrs. freqs., phonon lifetime *(Russian)* 3−8572
  - ZnTe, amorphous, i.r. spectra analysis 3−2526
  - ZnTe:Cu, single crystal, rel. to photoluminescence 3−15552
- **light amplifiers** *see image intensifiers*
- **light attentuation** *see light absorption*
- **light coherence**
  - *see also laser beams; lasers*
  - atom interaction with radiation field, destruction of coherence 3−29064
  - coherence interferometer, astronomical applications 3−13112
  - coherent optic devices for one-dimens. signal separation determ. *(Russian)* 3−13708
  - coherent optical processing, spatial freq. diversity, noise reduction, multiple filtering 3−22850
  - coherent optics devices, image generalised spectral analysis, dissociation coeffs. calc. *(Russian)* 3−13707
  - coherent states, math. anal., complex variable method *(Russian)* 3−13717
  - diffraction, interference propagation and meas. of degree of coherence 3−6417
  - dispersive media, coherent nonlinear waves 3−28949
  - disturbance of coherence through interaction with hydrogen like atoms, group theory treatment of scattering *(German)* 3−13716
  - filter, for holographic image deblurring, increasing dynamic range 3−5972
  - Gaussian beam propagation, classroom demonstration 3−28449
  - holographic depth of field, longitudinal multimode laser coherence props. 3−29054
  - holographic images rel. to spectral coherence, Fresnel transform formulation 3−697
  - holographic interference of equal inclination, from diffused surface 3−9956
  - holography, spatial and temporal coherence limitations relax. 3−19574
  - interpulse, Nd:glass mode locked laser 3−4106
  - laser beam, spatial coherence in water 3−339
  - laser interference teaching demonstration 3−32002
  - liquids, props. of light scattered from density fluctuations 3−20685
  - lithium formate monohydride, harmonic generation of tunable coherent radiation from 2300-3000 Å 3−32589
  - longitudinal correlation props. of coherent radiation scattered from a rough surface 3−16897
  - Michelson stellar interferometer, monochromator coherence length rel. to visibility drop 3−31808
  - minimum variance of estimators 3−13692
  - optical cavity field, coherence props. transfer by electron beams 3−29050
  - optical coherence functions zeros and spectroscopic appl. 3−13695
  - optical field, spatial coherence fn., variances of estimation 3−29033

light coherence continued
- partially coherent periodic phase objects in ordinary microscopy, minimum path difference detection 3—28517
- partially polarized Gaussian beam, average form of polarization 3—32509
- pulse propag. in inhomogeneously broadened medium, conservation laws 3—4071
- pulsed single mode injection semiconductor laser, coherence of radiation *(Russian)* 3—747
- pump wave, intense coherent, propag. in reson. media 3—32598
- random scenes correlation length, coherent optical meas. method, comments 3—13700
- random scenes correlation length, coherent optical meas. method, reply to comments 3—13701
- real and assoc. complex fields, statistical representation relations 3—10440
- source reconstruction, from modulus of correlation function 3—29029
- spatial along cross section of beam, interferometric analysis 3—22356
- spectrum of optical pulse 3—29036
- van Cittert-Zernike theorem 3—10444
- Nd:glass laser, dye mode locked, interpulse coherence, picosecond pulses, interferometric measurements 3—22908
- Ne(I), optical coherence of 6328 Å laser transition, global dipole 3—13728

light communication *see optical communication*

light diffraction
- *see also holography*
- amplitude holograms, diffraction efficiency calc. 3—32522
- in anharmonic crystals, Raman-Nath diffraction by u.s. 3—29140
- anomalies, echelette grating 3—3795
- astronomical occulting body diameter determ. from single observation using Fresnel diffraction 3—9625
- boundary diffr. waves due ot general point source, circular and ellipsoidal apertures 3—682
- Bragg diffraction for real-time u.s. imaging 3—71
- Bragg-diffraction imaging, application to nondestructive testing 3—21786
- circular aperture, centrally illuminated, Lommel's development approx. formulae *(German)* 3—6415
- circular aperture, exp. and numerical results *(German)* 3—22838
- circular aperture, near and far field diffr., effect of turbulent media 3—10445
- circular aperture, of square beam 3—29027
- by circular apertures, far field, turbulence degraded 3—5513
- coarse weakly absorbing particles, energy distribution *(Russian)* 3—35672
- coherent radiation scattered from a rough surface, longitudinal correlation props. 3—16897
- controllable layer structures, diffr. modulation of optical radiation *(Russian)* 3—13691
- corneal radius measurement, diffraction effects on precision 3—3886
- corrugated structures, asymmetry and blazing effects 3—32507
- filter, axially symmetric, pupil functions, diffr. field, foci 3—22316
- Fresnel, for circular aperture illuminated by partially coherent light 3—16795
- Fresnel, functional analytic formulation 3—32510
- Fresnel, partially coherent, by slit aperture, theoretical analysis 3—29035
- gaussian beam, one dimens., diffr. by amplitude sinusoidal grating of zero thickness 3—10442
- granularity produced by scatterer illuminated in partially coherent light *(French)* 3—6423
- grating, thick, periodically stratified, with complex dielectric 3—19568
- gratings, ghost lines 3—5872
- image characteristics, Fourier transform techniques, truncated triangular wave periodic targets, linear image motion 3—32525
- intensity modulation in multiple images of source produced by two parallel gratings *(French)* 3—26201
- large telescopes, weak zone plate fabrication and evaluation 3—32092
- laser beam applied to continuous measurement of particle size *(French)* 3—15800
- laser Gaussian beam formulas from Huygens principle and diffr. theory 3—35706
- layered electrooptical structures, diffr. modulation of optical radiation *(Russian)* 3—25725
- linear systems with ideally rough objects, diffr. field speckling *(German)* 3—678
- liquid crystal nematic, transverse field electro-optical effects 3—24676
- of Lorentz microscope images 3—377
- mapping of u.s. fields 3—87
- modified Luneburg apodization problem 3—701
- opaque bodies and randomly arranged particles, demonstration usng He-Ne laser *(Russian)* 3—13184
- optical wave fields, spatial distrib. of magnitude and phase 3—37934
- partially coherent, in presence of transverse sinusoidal vibrations 3—22835
- partially coherent 3—6417
- partially coherent periodic phase objects in ordinary microscopy, minimum path difference detection 3—28517
- pattern sampling for real time pattern recognition 3—695
- patterns, random multiple aperture, teaching laboratory obs. technique 3—31998
- periodic objects, quadratic image motion blur 3—22836
- photometric meas. of Vickers type hardness impressions, diffr. theory analysis *(German)* 3—5933
- piezoelectric semicond., by acoustic and electron waves 3—39117
- pile-of-holograms, diffracted beam intensification, reln. to intensity reduction factor 3—16808
- prism, wave functions detn. 3—6414
- by progressive supersonic waves, oblique incidence, exact solution of Raman-Nath equations 3—6428
- S-polarization anomalies in gratings with sinusoidal and triangular profiles 3—680

light diffraction continued
- by semiinfinite plane, for field diffraction, perpendicular polarization 3—32508
- simulation of electron diffraction patterns of metallurgical structures by optical transforms 3—1550
- slit aperture, high numerical system with spherical aberration and defocusing 3—26202
- sound fields, two superposed acoustic waves, partially coherent light, Huygen's principle, general formula 3—37935
- space telescope, large, diffraction limited, image quality criteria 3—31820
- speckling in Fourier transform plane, analysis of mech. oscills. 3—5754
- spherulitic polymers, scattering of linearly polarised light *(Bulgarian)* 3—29782
- thin-screen, by u.s., modulation 3—29031
- transmitting axicon, focal depth 3—32058
- by u.s. beams, parallel adjacent, symmetry properties of diffraction pattern 3—32511
- by u.s. waves, energy meas. 3—85
- using u.s. waves, symmetry of diffraction pattern 3—29026
- vibrating diffraction grating, through slit and circular apertures 3—19565
- Wiener apodization problem 3—702
- zone plate, optically made, diffr. theory 3—22841

light diffusion
- *see also light scattering*
- deterministic diffusers, holographic applications 3—201
- diffusing screens for photolithographic camera illum. systems 3—217
- diffusion problems in spherical-shell media probabilistic model for the resolvent kernel 3—22758
- liquid crystal, cholesteric, rel. to electrohydrodynamic effect *(French)* 3—30072
- quasi-monochromatic weakly dispersed beams in anisotropic dielec. medium, diffusion study *(Russian)* 3—19569
- optical processing method using a random diffuser 3—9922

light dispersion *see optical dispersion*

light emitting devices
- *see also light emitting diodes; light sources; luminescent devices*
- semiconductors, direct and indirect gap, and their appl. to electroluminescent devices 3—18499

light emitting diodes
- *see also semiconductor lasers*
- aging kinetics, electroluminescent diodes and injection lasers 3—29104
- degradation mechanisms under ionising irradiation *(German)* 3—37974
- III-V crystalline solid solution, phase diagram rel. to fabrication 3—2682
- photoemission diode standards for meas. monochromatic u.v. light intensity 3—35406
- physical basis, review *(German)* 3—13703
- solid state, apparatus for velocity of light determ. in air and transparent media 3—3800
- CuGaS$_2$-CdS p-n diode, green electrolum. 3—39188
- GaAs, near-field intensity variation in Fabry-Perot structure by pulsed electron injection 3—39193
- GaAs laser diodes, neutron damage 3—19619
- GaAs p-n junction, optical absorpt. influence on near-field intensity 3—21490
- GaAs p-n junction, vapour-grown, electrolum. gas-phase stoichiometry effects 3—11950
- GaAs:Si, epitaxial layers, characterisation of p-n structure, etching, cathodoluminescence 3—39195
- GaAs:Si, injection diode, electrolum. line shift *(Russian)* 3—8669
- GaAs$_{1-x}$P$_x$, use as stable pulsed light source 3—5909
- GaAs$_{1-x}$P$_x$:N, photopumped thin films, luminescence, variable energy bandstructure, l.e.d. applications 3—39175
- GaN:Zn electro-luminesc. diodes, manufacture and characts. *(Russian)* 3—36945
- GaN-GaN:Mg, violet luminesc. 3—34432
- GaP, green-emitting, use of p-type dopants 3—8734
- GaP, light emitting diode, device physics, material characterisation 3—39191
- GaP red-emitting lamp, O content and electrolum. efficiency 3—30537
- GaP:N diodes, influence of temp. on electroluminescence spectra 3—24750
- In$_{1-x}$Ga$_x$P p-n junction, electroluminescence 3—2597
- In$_{1-x}$Ga$_x$P:N, photopumped thin film, luminescence, variable energy band structure, l.e.d. applications 3—39175
- β-SiC, electroluminescence spectra at ambient and nitrogen temperatures *(Russian)* 3—30881
- β-SiC:B diffused p-n junction, V-I and C-V characts. and electrolum. response, 293 to 800 K *(Russian)* 3—18211
- n-ZnSe-p-GaAs heterojunction, improved generation-recomb. processes *(German)* 3—15558
- ZnTe—CdS heterojunction, electroluminescence 3—2659

light filters *see optical filters*

light guides *see optical instruments; optical waveguides*

light intensifiers *see image intensifiers*

light interference
- *see also light interferometers; light interferometry*
- atomic absorpt. spectrometry, mechanisms of interference and releasing action 3—14291
- beams modulated in anti-phase, double slit expt. 3—32512
- deposition rate meas., in matrix isolation spectroscopy, using small laser 3—13302
- in fibre optic wedges, interference patterns *(Russian)* 3—6416
- Fresnel biprism, demonstration using He-Ne laser *(Russian)* 3—13184
- fringes, alteration by phase object, reduced sensitivity, Moire analysis 3—19566
- grid application by rolling method for meas. involving use of moire patterns *(Russian)* 3—12477
- holography, speckle reduction by partial coherent object illumination simulation 3—19215
- intensity modulation in multiple images of source produced by two parallel gratings *(French)* 3—26201

light interference continued
interference microscopy, polymer fibres 3−25727
interference-shadow marking of three-dimensional models 3−26210
laser anemometer, broadening of meas. freq. spectrum 3−13529
laser beam, thermally self defocused, time depend. ray geometrical treatment 3−32580
laser coherence teaching demonstration 3−32002
laterally loaded plate, moire fringe technique for analysis of moments and deflexions 3−3760
low intensity optical expts., interpretation 3−13694
microscope thickness measurement, thin films, transparent substrate pulsed laser 3−191
Moire fringes, use of irregular rasters in structure deform. eval. 3−37589
moire method of anal. of two dimensional dynamic strain distributions 3−6268
moire pattern due to overlapping zone plates 3−10441
optical cavities and filters, spectral response, delta function transform 3−35673
optical fibres, low loss, double reverse scatt. interference, equalizer 3−149
optical wave fields, spatial distrib. of magnitude and phase 3−37934
orthoferrites, interference patterns, at domain boundary, theory 3−5116
partially coherent 3−6417
polarised light, double-slit expt., demonstration 3−28442
projected Moire fringes holographic analogues 3−10451
quantum mechanical model 3−22864
refractive index meas. of fibres using microscope and wedge interference filter 3−16411
schlieren microscope 3−16410
shadow bands accompanying total solar eclipses 3−35017
sound fields, two superposed acoustic waves, partially coherent light, Huygen's principle, general formula 3−37935
speckling in Fourier transform plane, analysis of mech. oscills. 3−5754
spectrum analyzer resolution, Fourier transformations using Moire structures *(Russian)* 3−181
spherulitic polymers, scattering of linearly polarised light *(Bulgarian)* 3−29782
transparent materials, thermally-induced interference and lensing theory 3−29138
wedge shaped interferometer, Fizeau interference fringes intensity distrib. *(German)* 3−679
wedgeshaped interferometer, multiple-beam Fizeau interference fringes, intensity distribs. *(German)* 3−13317
wide angle narrow band interference filter photography 3−35432
Young's interference pattern, simplified exact formula 3−22834
Cr steel, retained austenite detection using vapour phase deposited interference layers 3−8810
Ne, nonlinear interference effects, influence of laser field polarization 3−32603

light interferometers
see also light interferometry
antiresonant ring for coupled laser cavities 3−16885
apochromatic path difference compensator with wedge shaped plates 3−16442
for ball and cylinder, diameter comparison 3−37586
coherence interferometer, astronomical applications 3−13112
constant beam width type, sensitivity, optical mechanism analysis *(Russian)* 3−13313
displacement detector housing, patent 3−22362
displacement type, band contrast rel. to space coherence *(Russian)* 3−13312
double beam, modified, interferogram equivalent Moire pattern 3−19208
double beam type, modified, using Moire method 3−189
double pass Savart plate, construct. 3−5954
etalons, use as narrow band interference filters 3−28564
Fabry-Perot, as differential Doppler laser velocity measuring instrument 3−16454
Fabry-Perot, optically contacted filter for middle u.v. 3−13315
Fabry-Perot, rapid scan, alignment and mounting procedures 3−13316
Fabry-Perot, scanning spherical mirror, e.m. driven 3−190
Fabry-Perot, small length modification meas., sensitivities, mag. field, errors *(German)* 3−5955
Fabry-Perot, spherical, block defocused with quasi confocal resonator 3−22356
Fabry-Perot, stabilising method utilising feedback 3−16438
Fabry-Perot, ultrastable multiple pass plane mirror instrument 3−5959
Fabry-Perot etalons, solid fused silica spacers, narrow band interference filter, fabrication and performance, Lyot type 3−37641
Fabry-Perot laser, angle-selecting aperture addition, anal. 3−32576
Fabry-Perot piezoelectric scanning, Ca atomic line widths meas. in N_2O-acetylene and air-acetylene flames 3−28779
Fizeau interferometers, meas. of thermal expansion coefficients between 10K and 300K of $La_2Mg_3(NO_3)_{12}.24H_2O$ and O 3−17986
focused optical imaging systems for vibration meas. 3−165
Fourier spectroscopy, interferometer design 3−9952
Fourier transform spectroscopy, far i.r., diffraction limitations of lamellar grating interferometer 3−28562
frequency-shifted laser interferometer obs. of small dynamic motions 3−28561
fringe follower, high speed, construction, basic principles, props. 3−5951
He-Ne laser, distance measurement *(Czech)* 3−16440
heterodyne, real-time optical surface figure meas. 3−5922
holographic, for temp. meas. 3−22375
holographic microscope system with triangular interferometer, dynamic recording 3−13326
Interferoscope, examination of spherical and aspherical surfaces 3−192
laser, for measurement of inside and outside dimensions *(German)* 3−32030
laser, meas. of particle sizes, number density and veloc. 3−5892
laser measurement applics. *(Russian)* 3−16437

light interferometers continued
Mach Zehnder based, velocity obs. 3−195
Michelson, laser, variable length pulse generation 3−9965
Michelson, obs. of nonthermalized spectral features in nightglow 3−16058
Michelson, wedge thin films, fringe refinement, fringe enumeration *(French)* 3−37640
Michelson interferometer He-Ne laser mode selection using, automatic frequency control system *(Russian)* 3−10556
Michelson interferometer used on Mariner 9 3−3384
Michelson stellar interferometer, monochromator coherence length rel. to visibility drop 3−31808
piezoelectric scanning Fabry-Perot interferometer, Ca linewidths in flames meas. 3−32260
reflection plate interferometer, operating characts. 3−35413
shearing, based on Talbot effect, for radial and lateral derivatives 3−3812
space telescope, large, laser interferometric alignment sensor 3−31822
for spherical surfaces control *(Czech)* 3−35404
for star tracking 3−9636
surface measurement, irregularity, radius of curvature, design, application 3−9932
two beam, beam splitters, functions and figures of merit, Jones matrices *(German)* 3−5956
Twyman-Green, performance optimization 3−5953
wedge shaped, Fizeau interference fringes intensity distrib. *(German)* 3−679
wedgeshaped, multiple-beam Fizeau interference fringes, intensity distribs. *(German)* 3−13317
CO_2 laser, Michelson type, phase relations, obs. 3−13318
He-Ne laser, for length meas. *(Spanish)* 3−19211

light interferometry
applications, with emphasis on microelectronics *(French)* 3−13319
aspherical surface decentering meas. by interferometric method 3−13290
Babinet compensator for anomalous dispersion meas. in birefringent media 3−13314
birefringent wedge, band displacement method of electro-optical voltage meas. *(Czech)* 3−3829
brightness temp. distribs. defined by measured intensity interferograms, radio and optical astron. sources 3−28305
computer analysis of asymmetric interferograms 3−28549
deformation meas. by moire technique 3−35355
dielectric layer thickness determ. *(Czech)* 3−22359
Fabry-Perot, refractive index and thickness meas. of tranparent materials 3−22336
film, grown near source axis in evaporation system, thickness uniformity meas. by multiple beam interferometry 3−36984
film, thickness meas. by microdensitometric interoferogram method 3−13229
focused images, real-time holography 3−5958
Fourier transformation of i.r. interferogram 3−29048
Fourier-transform. interferometry determ. of complex refractive indices 3−22361
fringe parameter estimation, limitations at low light levels 3−32506
fringe patterns new interpretation based on simultaneous presence of isochromatic and isopatic half-tones 3−28557
glass plates, in interferometric homogeneity testing, with holographic compensation *(German)* 3−9930
hologram interferometry, time average, of vibr. objects, holographic subtraction 3−13709
holograohic, finite fringe, applied to right circular cone at angle of attack 3−22574
holographic, appl. to acoustic meas. 3−212
holographic, demountable specimen support 3−35422
holographic, production testing, displacement on distortion measurement 3−5966
holographic, wavefront sampling, image reconstruction 3−22860
holographic flaw detection *(Czech)* 3−37645
holographic interference fringe patterns, interpretation 3−26214
holographic interferogram interpretation, three orthogonal displacements determ. 3−16809
holographic interferograms, double exposure, multiplexing method 3−197
holographic interferometry, increased contrast by elimination of background speckle 3−22357
holographic interferometry, small static deflection meas. of diffusely refl. surfaces 3−28461
holographic interferometry and holography, basic theory *(Czech)* 3−10452
holographic interferometry materials testing technique 3−9028
holographic interferometry test specification for deform. and fault testing *(German)* 3−19154
interferometer, double beam, modified, interferogram equivalent Moire pattern 3−19208
interferometric test data analysis, computer program 3−5896
Kerr magneto-optic effect investigation 3−28559
kinetic cooling time constant, water vapour conc. depend., interferometric obs. 3−39503
large optics, fabrication, automatic metrology 3−175
laser, dye, spectral radiation control, meas. using wedge shaped Fabry-Perot interferometer *(Russian)* 3−19611
laser, lead measurement of leadscrews 3−22252
laser in workshop inspection, minute changes detection in size and shapes 3−19193
length meas., error due to mirror rot. movement, multipass corner cube arrangement 3−35354
liquid, direct method for refr. index temp. depend. determ. 3−28558
long baseline, for secular earth crusted strain rates meas. 3−194
Loschmidt diffusion experiment, interferometric method 3−32077
Michelson, meas. of refractive index of water change with temperature 3−30792
micrometer with anlge mirror, performance *(Russian)* 3−28466
Miller Nordland interference method for coeffs. relative signs determ. 3−16418
modulation method for optical delay *(French)* 3−26199
Moire method for deformation meas. of spatial complicated elements *(German)* 3−19210

light interferometry continued
Moire techniques for photolithographic mask alignment in IC prod. 3—188
moire topography of full size living bodies 3—35414
optical components interferometric testing using circular computer holograms 3—3798
particle size, number density and velocity meas. using laser interferometry 3—4129
photographic fringe recordings, conversion to cylindrical microlenticular rasters *(German)* 3—32105
retardation of light waves in electric field, polarization interferometric determ. *(Russian)* 3—24678
Rozhdestvenskii's hook method applied to a system including a Michelson interferometer 3—32080
speckle, multiple star system holography for reconstruction of stellar brightness distrib. 3—22126
spectral radiance comparator for pyrometric standards *(Japanese)* 3—22328
spherical surfaces control *(Czech)* 3—35404
surface roughness, meas. using white light speckle 3—5898
surfaces, spherical and aspherical, examination using interferoscope 3—192
technique for filter function recording 3—4072
thin film optical constants, reflection and transmission determ. *(German)* 3—32079
thin film thickness meas. *(Czech)* 3—32218
thin films, wedge, Michelson interferometer, fringe refinement, fringe enumeration *(French)* 3—37640
transverse vibration meas., with diffused laser light 3—5772
turbine motor vibration analysis by holography 3—19219
two beam, beam splitters, functions and figures of merit, Jones matrices *(German)* 3—5956
two-beam interferometers, white light fringes, finding and imaging method 3—19207
u.s. surface wave detection 3—35363
white light, path difference much larger than coherence length *(French)* 3—28560
Cr-Ni alloys, corroded, obs. using combined microprobe/opt. interferometry technique 3—39350
Nd:glass laser, dye mode locked, interpulse coherence, picosecond pulses, interferometric measurements 3—22908
Si epitaxial layers, thickness meas. using Michelson interferometer 3—30361
light meters *see photometers*
light modulation *see optical modulation*
light polarisation
see also birefringence; optical rotation; photoelasticity; polarimeters
VY Canis Majoris, circular polarisation meas at 1.7 μ and 2.2 μ 3—31689
acenaphthylene, polarised i.r. and Raman spectra, crystal structure 3—39134
alkali metal halides, luminesc. centres, reson. secondary glow, polarisation theory *(Russian)* 3—36918
ammonium halides, in disordered phases, low frequency Raman spectra, polarisation selection rules 3—34347
anthracene, fluorescence, polarisation effects *(German)* 3—24742
artificial fog, propagation laws of space-limited radiation flux in scattering medium *(Russian)* 3—37938
astronomical objects, circular polarisation meas. 3—39680
by atmospheric mist haze, aerosol attenuation in i.r., distinction from haze *(Russian)* 3—3008
birefringent wedge, interference band displacement method of electro-optical voltage meas. *(Czech)* 3—3829
53 Camelopardalis, mag. Ap star, intrinsic polarisation of $H\beta$ and continuum radiation 3—25454
cholesteric mesophases, achiral molecules, circular, fluorescence *(German)* 3—36938
circular polarizers for Cs doublet lines 3—16430
circumstellar circular polarization at 0.84 microns in four i.r. stars 3—31695
circumstellar material, review 3—9538
conducting medium, optical excitation of plane-polarised waves 3—35662
cool stellar photospheres, Monte Carlo radiative transfer solns. for polarisation prod. by Rayleigh scatt. 3—31641
Coude telescope spectrometer systems, polarisation effects on transmission 3—37501
crystal microstructure component orientation and optic axis orientation determ. 3—24858
NML Cygni, i.r. stellar source, circular polarisation meas. at 1.7 μ 3—31689
day light polarisation in 1.25-2.42 μ region, clear sky obs. *(Russian)* 3—21944
day sky light polarisation angle altitude depend., meas. in O 1.27 micron emission band *(Russian)* 3—39519
depolarisation rel. to atmospheric turbulence *(Russian)* 3—28018
far field diffraction, by semiinfinite plane 3—32508
film substrate reflection polarizer, effect of film absorption 3—28519
film-substrate reflection polarisers, wavelength bandwidth, design aspects 3—28513
fluorescence, polarisation effects of light emitted by plastic NE 102A *(German)* 3—24742
gas laser emission, $J=0$ reversible transition to $J=1$, polarisation props. 3—32545
giant elliptical galaxies, detection of nonthermal optical emission 3—31757
Goos-Hanchen shift amplification by interposition of thin films *(French)* 3—6503
grating spectrographs, elliptic polarisation by metallic grating 3—13298
gravity effect on geometrical optics in curved space-time 3—16717
HD215441, mag. Ap star, intrinsic polarisation of $H\beta$ and continuum radiation 3—25454
hexagonal crystals, transverse mag. field and deformation effects on exciton luminescence polarisation 3—2595
holograms, polarisation recording 3—32087
holographic, review *(German)* 3—32521
homogeneous anisotropic media, evolution of ellipse of polarisation 3—35669
light polarisation continued
injection laser, polarisation current depend. 3—35697
interplanetary polarisation rel. to orientation of dust grains 3—28300
interstellar polarisation rel. to orientation of dust grains 3—28300
laser light polarization effect on multiphoton scattering processes 3—10564
laser pulse train, base-line noise reduction using crossed polariser system 3—28582
laser radiation reflected from laser heated plasma, magnetic field measurement 3—23921
linear polarization of light scattered in absorbing semi-infinite medium 3—37292
liquid crystal, cholesteric, evolution of ellipse of polarisation 3—35669
M82 galaxy, $H\alpha$ polarisation, prod. in filaments 3—28258
magnetic stars, wavelength depend., Zeeman effect 3—37381
malachite green acetate, rel. transition moment orientations, polarised azimuthal fluorescence 3—36043
Mars, linear polarisation meas. in i.r. region 3—31689
microscope, correction of extinction effects, using thin film coatings *(French)* 3—13289
microscope, for low temp. obs. of magnetic structure 3—35444
microscope polarisers and analysers, standard transmission directions 3—16412
microscopy, for C fibre structure obs. 3—3793
molecular crystals, doped, polarisation luminescence method for struct. determ. *(Russian)* 3—27525
molecular fluids in vertical-vertical geometry, polarised light scatt. 3—39129
monochromators in far u.v., partially polarized light polarisation rate, least squares method *(French)* 3—681
Muller matrix 3—13693
multiple scatt. by atmospheric aerosol, polarisation, Monte Carlo calcs. 3—6421
multiple scatt. by homogeneous cloud layers, polarization, Monte Carlo calcs. 3—6420
NGC 4486 (M87) elliptical galaxy, linear polarisation in u.v. radiation from nucleus 3—31758
nonmonochromatic light, effect of birefringent plate 3—22842
nonspherical stellar atm. and envelopes, appl. to red giants and mag. and X-ray stars, polarisation by anisotropic mols. and dust particles 3—28201
numerical method for measuring the degree of polarisation *(Russian)* 3—22329
optical system, invariant-azimuth and invariant ellipticity polarisation states loci 3—13274
oscillating stress-plate polarization modulator for magnetic circular dichroism meas. 3—151
partially polarized Gaussian beam, average form of polarization 3—32509
X Persei, possible X-ray star, measures of optical circular polarisation 3—19026
α-phenylethylamine, Raman scatt., intensity of right and left circular polarizations 3—34345
planetary and lunar radiation polarisation rel. to P, T invariance 3—28155
polarisation optics, group theory unified formalism 3—29034
proustite, nonlinear polarisation coeff. 3—22963
quinoxaline, mixed crystal electronic polarisation spectra polarised phosphorescence, crystal effects 3—39141
radiation emerging from spherical shell atmospheres, backward Monte Carlo calcs. 3—685
Raman scattered radiation, polarisation characteristics as a function of angle between incident and scattered beams 3—23568
randomly oriented molecules, polarisation of two photon excited fluorescence 3—20178
reflection images of small hemispherical isotropic crystals in polarising microscope 3—28515
resonant medium, intense monochromatic wave 3—19648
rotating circular resonator, natural polarisation conditions *(Russian)* 3—35698
S-polarization anomalies in gratings with sinusoidal and triangular profiles 3—680
Saturn, circular polarization of scattered light from planet during 1971, November 3—16143
Saturn's disc areas, phase depend. meas. in i.r. and u.v. 3—28156
scattered by elastic waves in cubic crystal 3—18448
scattering in earth's atm., radiative transfer theory 3—31372
Scorpius X-1, X-ray source, circular polarisation in red spectral region *(Russian)* 3—37430
secondary radiation from gas system, polarization characts. 3—23484
selfdepolarisation of fluorescence of solutions, analysis of experimental data 3—18494
Seyfert galaxies, nuclei sources of synchrotron radiation *(Russian)* 3—37439
signal flow graph utilisation in polarisation optical studies 3—37625
solar corona, meas. during 1970 March 7 total eclipse 3—25404
solar corona, vel. effects of scatt. electrons 3—35047
solar far i.r. 3—31528
solar light scattered by isolated volume of interplanetary matter *(French)* 3—9463
solar magnetographic meas., instrum. polarisation effects 3—39758
solar radiation compared with pulsar radiation 3—35119
solar radioburst of 1972, Aug. 7, circular polarisation variations 3—35052
solar spectra, electrograph for predicting electric fields during pre-flare energy build-up 3—37317
solutions, isotropic influence of self-quenching on concentration depolarisation of photoluminescence 3—34397
solutions of anisotropic mols. in simple liquids, depolarised light scattering *(Russian)* 3—32516
stellar, white dwarfs and late type stars with circumstellar shells, broadband circular 3—37396
stellar, X Persei, 5 Persei, 55 Cygni and 30 Pegasi, circular polarisation 3—37397
stellar radial velocity measurement, polarimetric method 3—13118
Stokes parameters, Lorentz transformation properties 3—9627
stratified media, total refl. phenomena, total refl. polarizer 3—676
stress-induced, F-centre emission, appl. of vibronic model 3—34415

light polarisation continued
subsurface region light field, ang. and polarisation characts. *(Russian)* 3−10446
suspension of polystyrene spheres, propagation laws of space-limited radiation flux in scattering medium *(Russian)* 3−37938
tetramethylparaphenylenediamine, rel. transition moment orientations, polarised azimuthal fluorescence 3−36043
three-mirror resonator with anisotropic elements, frequency polarisation characteristics *(Russian)* 3−29108
travelling-wave laser, polarisation properties, calc. of anisotropic resonator and nonlinear interaction 3−16889
travelling-wave laser of three- and four-mirrors, effect of resonator parameters on performance 3−16890
two-photon absorption coefficient in cubic semiconductors, dependence on light polarisation 3−22944
uniaxial optically active crystal, polarisation of transmitted light 3−24668
vector orientation, holographic interference pattern visibility depend. 3−22861
water pollution, concentration monitoring, depolarization of scattered laser light 3−34977
white dwarf star, G99-47 (GR 289), meas. of circular polarisation 3−19019
X-ray stars, polarization of optical radiation and magnetic field 3−25486
Ar dense gas, depolarised light scattering 3−33190
CN red system of lines in sunspots, polarization meas. 3−31557
Ca I 4227 Å line polarization at Sun's limb, theoretical study 3−35031
CaF_2:Na crysts., coloration centres, photoluminesc. and polarisation meas. *(Russian)* 3−36920
CdS, transverse mag. field effect on light emitted from free and bound excitons 3−2594
CsI:Tl fluorescence, polarisation effects *(German)* 3−24742
F_2, Raman cross section and depolarisation ratio for chem. laser diagnostics 3−36018
GaAs, circular polarization of recombination light in weak mag. field 3−8660
GaAs, polarised luminescence due to optical orientation of electrons *(Russian)* 3−36934
GaAs laser, emission threshold current and polarisation rel. to uniaxial stress 3−16868
GaAs-AlAs solid solution, polarised luminescence due to optical orientation of electrons *(Russian)* 3−36934
GaAs-GaP solid solution, polarised luminescence due to optical orientation of electrons *(Russian)* 3−36934
p-GaSe, optical orientation of excitons and Hanle effect 3−34428
He excited by electrons, polarisation of the 492.2 nm line at energies near 60 eV 3−17376
Hg atom collisions with buffer gases, depolarisation of resonance radiation 3−33060
KCl-Pb luminesc., polarisation patterns, wavelength and temp. depend. *(Russian)* 3−36919
KI:Tl, fluorescence, polarisation effects *(German)* 3−24742
α-$LiAlSi_2O_6$:Mn^{2+}, single crystal, polarised cathodoluminescence emission 3−39194
Mn-Bi film, birefringent, mag. domain patterns, polarisation microscope obs. 3−21283
NO, Raman cross section and depolarisation ratio for chem. laser diagnostics 3−36018
Ne, nonlinear interference effects, influence of laser field polarization 3−32603
ONF, Raman cross section and depolarisation ratio for chem. laser diagnostics 3−36018
$RbUO_2(NO_3)_3$ crystals at liquid He temp., polarised luminescence spectra *(Russian)* 3−36942
Si p-n junctions, effects of polarised light on electroabsorption 3−34326
SrF_2:Na crysts., coloration centres, photoluminesc. and polarisation meas. *(Russian)* 3−36920
Te, nonlinear polarisation coeff. 3−22963
W lamp, incandescent, polarisation pattern 3−6410

light reflection
see also optical films
adenine.HCl single crystals, electronic spectrum study 3−30828
alkali halides, reflection spectra in far u.v., interband transitions 3−21437
anodic film on Pt electrode, ellipsometric and refl. obs. 3−5243
As-Se thin films vacuum deposited, vibrational reflectivity spectra, vitreous state 3−8057
attenuated total reflection for adsorbed CO_2 detection 3−25714
attenuated total reflection for observing surface excitations 3−24493
trans-azobenzene, polarized specular refl. spectrum, transitions in low energy band 3−2556
calcite, vacuum u.v refl. spectra, dielec. consts. determ., dichroic absorpt. band 3−27510
cholesteric mixtures with organic solutes, selective reflection of visible light 3−12147
colour metameric spectral reflectance functions numerical calcs. 3−5929
crystals, quasi-one- and quasi-two-dimens., freq. ang. depend., calc. 3−34336
from dense colloidal suspensions of spherical particles 3−29045
dielectric mirror, in obliquely incident light, theory 3−32513
diffuse reflection by isotropic, non-coherent, scattering homogeneous sphere, Combined-Operations method 3−26198
equivalence relationships between diffuse radiation fields for finite slabs bounded by a perfect specular reflector and a perfect absorber 3−22759
extinction coeff. meas., slope method 3−28533
fibre optic technique for obtaining spectral reflection 3−35408
film substrate reflection polarizer, effect of film absorption 3−28519
fluorescence, reflected and fluoresc. components in spectral radiance factor curve, separation 3−22345
flux density, arbitrary curved surface, arbitrary receiver surface, exact analytical formula 3−37936
focusing reflaxicon applications to holography 3−202
Fresnel refl. eqns., determ. of optical consts., inversion restrictions 3−6412

light reflection continued
fruit, coloured, i.r. refl. rel. to ripening 3−9702
glass, milk type, MS20, light refl., spectral and integral characts. 3−22324
glass and quartz of different roughness, near i.r. dispersive props. *(Russian)* 3−25740
Goos-Hanchen shift amplification by interposition of thin films *(French)* 3−6503
holographic filters, compact coherent processing systems 3−3818
images of small hemispherical isotropic crystals in polarising microscope 3−28515
Lambert scatt. by elliptic cylinder, diffuse refl., shadowing effects 3−6411
laser windows, coated, formulas for absorpt., transmission and reflectivity 3−35424
laterally confined beam undergoing total refl., lateral shift calc. *(French)* 3−16902
liquid crystal, distorted cholesteric, reflection props. 3−30842
liquid crystal nematic, transverse field electro-optical effects 3−24676
lunar retroreflectors, laser ranging meas. of Earth crustal movements 3−34971
metal film deposited at oblique angles, optical anisotropy calc. *(Russian)* 3−8686
from mirror, moving, forward refl. 3−29025
mirror, silvered, i.r. refl. rel. to protective coatings 3−13273
multialkali photocathode, 4000-11000 Å 3−30835
multiple, attachment for spectrophotometers for thin polymer coatings exam. in high vacuum infrared 3−182
optical consts. from reflectance ratio meas., computational method 3−170
parabolic mirror, off axis, alignment by laser surface refl. obs. 3−19649
relative reflectance spectra, Kramers-Kronig analysis, optical consts. determ. 3−18426
semiconductor cleaved surface roughness obs. 3−36470
semitransparent solids, coupled conduction-radiation heat transfer, spectral and boundary effects 3−33703
sphere, specular reflection description and nomenclature 3−29028
stratfied media, total refl. phenomena, general recurrence relations 3−676
super-reflectors, reflectance, scatter, basic concepts 3−22837
surface excitons effects, surface level excitation frequency, radiative transition probability 3−24718
thin film optical constants determ. *(German)* 3−32079
thin film optical properties, apparatus achieving 10^{-9} torr and 5-300 K *(French)* 3−35389
transition metal dichalcogenides, layered cpds., polarised light normal incidence refl., optical anisotropy, 78 K and 300 K 3−24707
turbid medium, dispersion and centre of gravity determ. from refl. and transmission meas. *(Russian)* 3−37206
windowless reflectance furnace, for i.r. studies of corrosive melts 3−22290
AlN, 30-40 eV 3−18493
AlN, epitaxially, i.r. reflection obs. of optical bandgap 3−11831
AlN film, i.r. specular refl., optical absorpt., optical band gap 3−21004
As_2S_3 layer cryst., edge refl. spectrum, exciton peculiarities 3−2559
Ba_2Te_3, refl. spectrum structs. due to optical consts. critical transitions 3−21432
Be_2SiO_4, anharmonicity of i.r. vibr. modes, refl. study, 300-1500 K 3−14947
$CdGa_2S(Se)_4$, refl. spectra obs. in polarized light 3−8604
$Cd_xHg_{1-x}Te$, comp. and electron density depend., rel. to band struct. *(Russian)* 3−2548
CdS, refl. phase spectrum in exciton region at 4.2 K 3−15517
$(CdS)_{3x}$-$(In_2S_3)_{1-x}$, rel. to band structure 3−18085
CdS_xSe_{1-x}, peculiarities of reflection spectra in exciton absorption region *(Russian)* 3−34381
Cr, reflection spectra, optical characteristics calc. using Kramers-Kronig relations 3−34372
Cr^{3+} thenoyl tri-fluoro acetonate, diffuse reflectance spectrum 3−18469
Cu, i.r. reflection studies of oxidation in air and inhibition by benzotriazole *(Japanese)* 3−18639
$CuGaS_2$, dielec. dispersion, phonon freqs., i.r. refl. spectrum 3−8585
$CuGaS_2$, low temp. spectra 3−15510
$CuGaS_2$, rel. to excitons and spin orbit splitting 3−18108
p-Cu_2S, carrier effective mass from refl. spectra 3−36534
p-Cu_2Te, carrier effective mass from refl. spectra 3−36534
$Eu_{1-x}Gd_xO$, refl. coeff. of visible and i.r. spectra rel. to elec. cond. 3−5214
GaAs, i.r., damping effects on plasmon-phonon spectrum *(Russian)* 3−8592
p-GaAs, i.r. plasma refl., carrier conc. determ. 3−18454
p-GaAs, reflection spectra obs. of temp. depend. of hole effective mass 3−24382
GaN, i.r. refl. meas. rel. to lattice vibrations and free-eldctron dispersion 3−18455
$Ga_2S_{3x}Se_{3(1-x)}$, reflection spectrum obs. 3−8603
GaSb, 1.7-70 eV, optical and dielectric constants detn. *(French)* 3−30831
GaSb, plasmon-phonon interactions, i.r. refl. obs. 3−21042
Ge, reflectivity spectra, 1.8-3.0 eV, Al absorpt. effects 3−39162
GeO_2 thin vitreous surface layer, struct. study by i.r. reflection spectra *(Russian)* 3−36467
HgTe, dielec. function, refl. spectra in far i.r., 8K-300K 3−2565
n-Hgs, cubic, band inversion, optical absorpt. and intra-band refl. rel. to carrier conc. and temp. 3−2002
InAs, energy band struct., refl., modulated refl., dielec. function, pseudopot. calc. 3−30403
InP_xAs_{1-x} solid soln., i.r. refl. spectra *(Russian)* 3−8589
InSb, energy band struct., refl., modulated refl., dielec. function, pseudopot. calc. 3−30403
InSb, i.r., cyclotron resonance obs. 3−30405
p-InSb, reflection spectra obs. of temp. depend. of hole effective mass 3−24382
$KBrO_3$, i.r., 300 and 4.2K 3−2543

light reflection continued
  KH_2PO_4 crystals, in ultraviolet region for electronic transition studies 3−2562
  LaF_3, crystalline, vacuum u.v. reflectivity meas. 3−34374
  LaS, La_2S_3 and La_2S_3/La_3S_4, dielec. consts., i.r. obs., ionic and covalent behaviour *(Russian)* 3−8595
  Mg film, vacuum deposited mirror coating, i.r. reflectivity 3−35395
  Mg_6MnO_8, mag. susceptibility meas. and optical reflectance spectra 3−34091
  Mg_2SiO_4, i.r. reflectivity and Raman scattering obs. of lattice vibrations 3−21410
  MnTe, antiferromag. semicond., optical-phonon spectrum, far i.r. 3−5104
  Mo, chemisorpt. of O_2 and CO, adsorbate dependent surface states, optical refl. obs 3−38879
  Mo, reflection spectra, optical characteristics calc. using Kramers-Kronig relations 3−34372
  MoS_2, 1-12.5 eV, rel. to band struct. *(Russian)* 3−5213
  NH_4Br in phases II and III, u.v. reflection spectra 3−24711
  $NH_4H_2PO_4$ crystals, in ultraviolet region for electronic transition studies 3−2562
  $NaCoF_3$, i.r. refl. spectra, vibr. spectra, optical consts. dispersion 3−39149
  $NaNiF_3$, i.r. refl. spectra, vibr. spectra, optical consts. dispersion 3−39149
  Nb, absorpt. or refl. meas. from 0.1 to 36.4 eV, interband effects 3−39159
  Pb film, meas. in vacuum u.v. rel. to optical consts. 3−21379
  $PbO-B_2O_3$ glasses, i.r. refl., band positions, conc. depend. *(Russian)* 3−12139
  PrF_3, crystalline, vacuum u.v. reflectivity meas. 3−34374
  Sb_2Te_3:Ge, reflectivity meas. with different Ge content 3−8605
  Sb_2Te_3:I, reflectivity obs. rel. to band structure and transport props. 3−8607
  Si, carrier relax. time temp. depend., i.r. refl. spectra obs. *(Russian)* 3−8182
  Si, optically inhomogeneous, surface free carrier reflectivity 3−5210
  p-Si, refl. spectrum near $L_{2,3}$ edge 3−15504
  SiC, i.r., damping effects on plasmon-phonon spectrum *(Russian)* 3−8592
  Sm_2S_3 and Sm_2S_3/Sm_3S_4, dielec. consts., i.r. obs., ionic and covalent behaviour *(Russian)* 3−8595
  SnTe, i.r. refl. spectra, carrier effective mass. relax. time and density *(Russian)* 3−8588
  Te film, 2.5-15 μ, 300 and 90K *(Russian)* 3−2550
  W, reflection spectra, optical characteristics calc. using Kramers-Kronig relations 3−34372
  Xe solid, reflectivity, Kramers-Kronig analysis 3−30788
  YIG, relation between magneto-refl. spectra and Faraday effect *(French)* 3−12126
  ZnO, refl. phase spectrum in exciton region at 4.2 K 3−15517
  $ZnSiP_2$, opt. vibrs. freqs., phonon lifetime *(Russian)* 3−8572
light refraction
  see also birefringence
  astronomical refraction, introduction to practical computation 3−28304
  astronomical refraction near horizon, seasonal variation 3−39512
  atmosphere, theory 3−5496
  eye, human, accommodation, continuous objective measuring apparatus, i.r., lag and transfer function 3−37735
  flux density, arbitrary curved surface, arbitrary receiver surface, exact analytical formula 3−37936
  gradient-index media, rays in separable systems 3−19570
  by hot gases, meas. of spatial temp. distrib., by variation of refractive index 3−13242
  laser beams, ground layer of atmosphere *(Russian)* 3−3020
  quartz, blackness determ. 3−24666
  ray Bundle, infinitely narrow, path through arbitrary surface shape 3−26205
  spherical wavefronts, by stacks of plane parallel inclined layers with wedge substrates 3−10443
  two-laser optical distance-measuring instrument with atmospheric refractive index correction 3−16917
light scattering
  see also Brillouin spectra; light diffusion; opalescence; Raman spectra; Rayleigh scattering
  absorbing liquids, diffractive scattering of picosecond light pulses 3−4127
  acetylcellulose in diethylene ethyl ether, metastable solution, separation of new disperse phases 3−39402
  on acoustic waves, experiment for advanced student laboratory 3−22222
  aerosol, rel. to Mie scatt. theory 3−13696
  applications 3−6522
  aqueous media, determ. by pulse sounding method *(Russian)* 3−25741
  artificial fog, propagation laws of space-limited radiation flux *(Russian)* 3−37938
  atmosphere gaseous constituents, remote mapping, differential absorp. and scatt., tuned laser obs. 3−3191
  atmospheric aerosol meas. from optical radar total scatt.-backscatt. ratio 3−9263
  atmospheric surface layer, scattering matrix and aureol part of phase function, complex measurements *(Russian)* 3−15960
  atomic fluorescence spectroscopy, scattering in turbulent and laminar flames 3−13491
  binary liquid local conc. fluctuations, temp. depend. *(French)* 3−27101
  bubble nucleus spectrum, influence on cavitation inception, scattered light counting method investigation 3−26046
  butadiene-styrene thermoelastoplastics, block struct. and comp. nonhomogeneity *(Russian)* 3−20255
  chemical reaction effects on spectra 3−11358
  fromchemical reactions, coupled nonlinear, for steady states far from equilibrium 3−2803
  circular discs, binary array, optical correl. analysis 3−686
  clouds, plane-stratified, optical sounding, statistical estimation of light pulse deform. *(Russian)* 3−29041

light scattering continued
  cometary H atm. model with multiple scattering, Lyman-α line effects 3−28161
  corrugated structures, asymmetry and blazing effects 3−32507
  critical unmixing pt. of solns., precision thermostat design 3−22280
  cylinder situated in interference pattern, fringe anemometry and particle sizing 3−22566
  cylindrical lens, numerical result from rigorous theory 3−19579
  from dense colloidal suspensions of spherical particles 3−29045
  depolarization in atomic fluids 3−11138
  dielectric cylindrical particles, attenuation factors calc. for i.r. radiation scatt. 3−24698
  disperse medium, statistical particle layer model *(German)* 3−26208
  by elastic waves in cubic crystal 3−18448
  elementary particle scattering, similarities and differences *(Dutch)* 3−824
  equivalence relationships between diffuse radiation fields for finite slabs bounded by a perfect specular reflector and a perfect absorber 3−22759
  ferromagnet, light scatt. by magnons, two-magnon scatt. 3−39126
  ferromagnetic insulators, two-magnon one phonon process 3−2540
  fluid, light scatt. from turbulent fluctuations 3−35671
  fluids, spectral anal. 3−32446
  from fluids and polymers, quantum mechanical derivation 3−26206
  four-density correlation function of fluid near critical point calc. from scatt. vertices 3−16770
  glass fibre optical waveguide, low loss, scatt. light angular distrib. 3−675
  granularity produced by scatterer illuminated in partially coherent light *(French)* 3−6423
  gravitational wave detection by method of light scatt. from elastic waves *(Russian)* 3−37884
  Heisenberg antiferromagnet, rutile structure MF_2, (M=Ni, Fe, Co), two-magnon light scattering 3−21196
  Heisenberg antiferromagnet, two-magnon correlations for light and neutron scattering 3−21195
  image holography through moving fog, scatt. effects 3−29053
  inhomogeneous media, diffraction theory and fringe waves theory comparison 3−32517
  insulator, light scatt., two-magnon one phonon process 3−2540
  intensity fluctuations, focus of circular aperture, turbulent medium, amplitude filters 3−37939
  ionic nonlinear noncentrosymmetric crystal, parametric scatt. by polaritons, theory *(Russian)* 3−8594
  isotropic, non-coherent, scattering homogeneous sphere, Combined-Operations method for diffuse reflection 3−26198
  L-methionine and S ethyl-L-cysteine random copolymers coil transition studies using optical expts. 3−29763
  Lake Ontario surface albedo, dependence on solar zenith angle 3−2845
  Lambert scatt. by elliptic cylinder, diffuse refl., shadowing effects 3−6411
  laser, concurrent and stimulated Brillouin, optical solids, bulk laser damage, interaction gradients 3−29115
  laser Doppler velocimeter signal for turbulent flow, spectral anal. 3−35553
  laser flowmeter, light scattering rel. to differential Doppler heterodyning technique 3−792
  laser light polarization effect on multiphoton scattering processes 3−10564
  laser light scattering from marginally stable H plasma 3−4673
  laser pulses transmitted through clouds, effects of multiple scattering 3−22844
  laser-induced plasma in air, determ. of parameters by obs. of scattered light spectrum 3−17663
  lidar and nephelometric scatt. by power law aerosols, Mie theory calcs. 3−6422
  linear polarization of light scattered in absorbing semi-infinite medium 3−37292
  liquid cryst., smectic and cholesteric, by plane texture deform. 3−12111
  liquid crystal, cholesteric, driven modes in oscillating mag. fields, feasibility of light scatt. obs. 3−24024
  liquid crystal, cholesteric, voltage effect 3−15472
  liquid crystal, nematic, negative film, secondary dynamic scatt. 3−36257
  liquid crystal, smectic A, edge dislocations effects on inelastic scatt. *(French)* 3−30065
  liquid crystals, electro-optical properties *(Russian)* 3−30799
  liquids, coherent props. after scattering from density fluctuations 3−20685
  low frequency depolarised, from fluids 3−27490
  lycopodium suspension, flux fluctuations, depend. on optical thickness and diameter of receiver aperture *(Russian)* 3−37937
  mean particle size determ., in polydisperse suspensions *(German)* 3−16530
  meas. of scattering in sea water, large and small angles 3−3256
  metal cylindrical particles, attenuation factors calc. for i.r. radiation scatt. 3−24698
  methylmethacrylate random copolymers in acetone, light scatt. and viscosity, coil dimensions 3−29794
  Mie scatt. props. of aerosols., size distribs., Los Angeles Basin 3−2967
  milk solution, flux fluctuations, depend. on optical thickness and diameter of receiver aperture *(Russian)* 3−37937
  molecular fluids, density fluctuations calc. 3−4030
  molecular fluids in vertical-vertical geometry, polarised light scatt. 3−39129
  monatomic gases, collision-induced light scattering, kinetic theory 3−11296
  monodispersed spherical particles, Mie scatt. intensities rel. to wavelength 3−35670
  multiple light scatt. from fluctuating system, doppler broadening effects on spectroscopy 3−22347
  multiple scatt. by homogeneous cloud layers, polarization, Monte Carlo calcs. 3−6420
  non-Gaussian, scaled photocount correlation 3−16892
  nonlinear backward, parametric amplification and oscillation 3−16901

light scattering continued
ocean water, light propag., multiple scatt. calcs., effective attenuation coeffs. 3−25186
optical fibres, low loss, double reverse scatt. interference, equalizer 3−149
optical materials, surface roughness meas. 3−13287
optical systems, effects of mould overgrowth *(Russian)* 3−5882
p-azoxyphenetole, nematic liquid crystal, inelastic spectrum, hydrodynamic fluctuations 3−36887
particle collections, lognormally distrib., extinction information content, size distrib. determ. 3−6419
particle size from low angle light scatt., refr. index effects 3−31190
particles, cylindrical, extinction coeffs., calc. 3−13698
particles of various diameters, spherical and non-absorbing *(Czech)* 3−13697
particles suspended in ocean, refractive index determ. 3−31469
α-phenylethylisocyanate, differential Raman scattering of circularly polarized light 3−20152
photon echoes, focusing, radius of curvature expressions 3−37984
planetary atm. spherical albedo determ. appl. to Venus 3−28157
plasma, high temp., high scatt. by electrons 3−17568
plasma scattering of laser beam, electron temp. and diffusion 3−17581
from plasmas, dense, theory 3−38422
poly(2,6-dimmethyl-1,4-phenylene oxide) toluene mixtures, light scatt. at melting point, determ. of thermodynamic parameters 3−29798
poly(ethylene terephthalate), crystn. kinetics, influence of temp., mol. wt. and additives 3−33179
polydisperse polymer solns., light scatt. spectrum, analysis methods 3−34660
polyethyl methacrylate glass samples, obs. at temps. around and below glass transition temp. 3−1311
polyethylene crystn. from xylene, conc. influence, crit. turbidity 3−33178
polymer, elongation ratio of deformed spherulites, small-angle light scatt. 3−20229
polymer, light scatt., Smoluchowski-Einstein-Zernike theory used to determ. free enthalpy 3−29797
polymer, method for crystn. kinetics of spherulites determ. 3−32060
polymer molecules with partial chain segment of arbitrary length, light ang. distribution 3−11332
polymer solution, influence of molecular weight, chain structure, conditions of preparation 3−29792
polymer stiff chains, light scatt. angular distrib. 3−29761
polymers, interspherulite interference in small-angle scattering of linearly polarised light *(Bulgarian)* 3−29782
polyoxyethylene thin films *(Russian)* 3−29781
polypeptide films, determ. of superstructure 3−1947
polypeptide homopolymers, helix-random coil transition studied by optical dispersion, scatt., viscometry and spectrophotometry 3−29763
quantum cryst., by vacancy wave excitation 3−33715
by quantum harmonic oscillator with single photon emission 3−29071
quasielastic, from large macromolecules, probe of internal motions of polymers in dilute solutions 3−4491
racemic solution, light scattering by fluctuating optical activity 3−18424
radiation field determ. in optically dense medium having strong anisotropic scattering 3−29038
radiation scatt. from slab of atoms, with partial redistribution effects, Monte Carlo calc. 3−6370
radiative transfer, symmetry relations and flux conservation for multiple scattering in inhomogeneous atmospheres using matrix operator theory 3−19530
rainbows, glories, explanation using scalar field approach, limitations 3−18856
random scenes correlation length, coherent optical meas. method, comments 3−13700
random scenes correlation length, coherent optical meas. method, reply to comments 3−13701
randomly rough surface, calc. of ellipsometric parameters using Stratton-Chu-Silver integral 3−29037
reciprocity theorem application, effect of bulk and surface defects *(French)* 3−26200
reflection nebulae, strong 4430 Angstroms interstellar absorption in backscattered light 3−28295
relativistic electrons, differential scattering cross section and plasma diagnostics 3−7560
resonance, quasar clouds, radiation pressure effects 3−16244
resonance scatt. by isolated atom, nonstationary phenomena 3−14276
Rozenberg theory for media with soft scattering particles of small size 3−6425
Saturn's ring system, optical scattering properties rel. to model 3−35059
scattering phase function for restoration of particle size distribution by statistical regularization *(Russian)* 3−16798
self-aligning reference beam method for obs. of linear independent components of flow velocity 3−474
semiconductor cylindrical particles, attenuation factors calc. for i.r. radiation scatt. 3−24698
similarities and differences between particle and light scattering *(Dutch)* 3−10658
sky radiation, multiple scatt., verification of approx. method 3−2968
from solutions, elastic general theory 3−16791
solutions of anisotropic mols. in simple liquids, depolarised light scattering *(Russian)* 3−32516
spectral line breadth, comparison with absorption and emission *(Russian)* 3−2551
spherical particle coated with oriented molecular layer, scattering and extinction cross sections 3−29044
spray jet, particle size distrib. 3−23794
stellar extinction due to aerosol light scatt., blue moon phenomena 3−18850
stimulated Brillouin effect, gases, gain and line widths *(Russian)* 3−1326
stimulated photon-photon-polariton scatt. theory 3−1738

light scattering continued
stimulated Raman effect, self focusing *(Russian)* 3−775
stratospheric 'sulphate layer' 3−3021
super-reflectors, reflectance, scatter coefficients, basic concepts 3−22837
suspension, polystyrene spheres in distilled water, statistical characts. of transmitted radiation *(Russian)* 3−29042
suspension of polystyrene spheres, propagation laws of space-limited radiation flux *(Russian)* 3−37938
suspensions, laser velocimeter obs., Doppler signal correl. time rel. to conc. *(Russian)* 3−13336
tartaric acid, supersaturated soln., crystal dispersity, effect of u.s., latent period of mass crystn. 3−39404
Thomson scattering in magnetic field, quantum treatment 3−15
turbid medium, dispersion and centre of gravity determ. from refl. and transmission meas. *(Russian)* 3−37206
turbulent media, light beam spectra, outer scale effects 3−6424
volume scattering function, deep ocean optical meas. 3−3257
weather classification rel. to light scatt. matrix *(Russian)* 3−39520
$Ag_xNa_{1-x}NO_2$, influence on i.r. absorpt. *(Russian)* 3−18440
Al_2O_3, surface grain size estimation by optical scatt., application to microelectronics industry 3−4906
Ar dense gas, depolarised light scattering 3−33190
Au particles, cylindrical, of i.r. radiation *(Russian)* 3−6426
BaF_2, high-freq. acoustic harmonic generation by Bragg light scatt. 3−7859
$Bi_{12}SiO_{20}$, by optical phonons *(Russian)* 3−8591
CaF_2, high-freq. acoustic harmonic generation by Bragg light scatt. 3−7859
Ge:Sn, heavily doped single cryst., impurity conc. obs. rel. to electron mobility 3−33885
He, superfluid, by thermal surface waves, 1.29-2.14 K 3−7984
He liquid, quantum mechanical formulation 3−11771
^{3}He, liq., freq. power spectrum of density fluctuations 3−11779
^{4}He, liquid, scatt. from first and second sound near λ transition 3−24308
^{4}He liq., near gas-liq. critical point, critical exponents and correl. length 3−1854
KCl, precip. of solid solns. of Sr and Cd 3−33541
KCl, precip. of supersaturated solid soln. of Ba 3−33540
KD_2PO_4, light scattering investigation of soft ferroelectric and acoustic modes 3−39108
KNO_3, influence on i.r. absorpt. *(Russian)* 3−18440
Na D_1-reson. radiation, forward scatt. by Na vapours in mag. field 3−38215
NaCl:divalent cation, scatt. orientation effect 3−15493
NaF, light scatt. by second sound, thermo-optic and elastooptic parameters 3−34323
$NaNO_2$, influence on i.r. absorpt. *(Russian)* 3−18440
$NaNiF_3$, phonon and magnon light scattering 3−39148
$NdAlO_3$ inelastic scatt. meas. of optical phonon freqs., linewidths and cross-sections 3−15502
RbI, rel. to effect of surfaces on light transmission, 5.5-6.3 eV 3−36892
SrF_2, high-freq. acoustic harmonic generation by Bragg light scatt. 3−7859
Xe, spectral linewidth of quasi-elastically scattered light along coexistence curve 3−30246

light sources
see also infrared sources; light emitting devices; photometric light sources; spectroscopic light sources
black radiation, new development 3−22288
colour conversion filter, design *(Czech)* 3−37622
diffusing screens for photolithographic camera illum. systems 3−217
flash lamp, high temperature with symmetrical conductors *(Russian)* 3−9946
optical-anemometry signals, light source and geometrical requirements for optimisation 3−163
photoemission diode standards for meas. monochromatic u.v. light intensity 3−35406
photopolymerisation using light sources of high energy, illumination techniques 3−12552
portable underwater lamp, W-halogen lamp, heat treated globe 3−3258
printing of black and white films *(Russian)* 3−3825
pulsed, using light-emitting diodes 3−5909
pulsed light sources, high speed photography, electronic imaging systems, high speed cine cameras 3−228
in sea water, energy and spectral characteristics of light field, applic. of transport approximation *(Russian)* 3−690
spectral radiance comparator for pyrometric standards *(Japanese)* 3−22328
standard illuminant D65, quantitative assessment fitting method 3−22331
thermal arc plasmas as radiation sources for light intensity calibration in astrophysics 3−4681
thyristor rectifier for film projector light source *(Russian)* 3−9981
u.v., i.r., health lamps, history, development, use, benefits 3−3572
^{114}Cd hot cathode spectral lamp, as secondary standard, for interferometry 3−3748
^{198}Hg hot cathode spectral lamp, as secondary standard, for interferometry 3−3748
I-quartz lamps, photographic props. films during microfilming *(Russian)* 3−3826

light transmission
see also light absorption; optical filters
aerosol, particle size distribution determ. *(Russian)* 3−39411
air-glass-air system, verification of Fresnel and Airy equations 3−37
atmospheric laser beam spreading 3−18852
Coude telescope spectrometer systems, polarisation effects on transmission 3−37501
cylindrical guide, transmitted light angular distrib. 3−16790
disperse medium, statistical particle layer model *(German)* 3−26208
equivalence relationships between diffuse radiation fields for finite slabs bounded by a perfect specular reflector and a perfect absorber 3−22759
extinction coeff. calc. for white light irrad., particle size determ. *(German)* 3−9020

light transmission continued
- Fabry Perot narrow-band filter, enhancement of transparency *(Russian)* 3 − 3815
- fibre-optical element information and nonworking flux components meas. method 3 − 16796
- filters, transparent, integrated transmittance, spectral mask meas. method 3 − 16421
- flexible light bundles quality criteria *(German)* 3 − 9928
- fluid, light scatt. from turbulent fluctuations 3 − 35671
- gradient-index media, rays in separable systems 3 − 19570
- inhomogeneous medium, intensity fluctuations by beam diffusion equation *(Russian)* 3 − 29040
- i.r. transmission through the diffusion, sheet resistance and junction depth meas. 3 − 39286
- laser atmospheric windows, computer study of transmittance, 2.7-3.2 μ 3 − 5977
- laser windows, coated, formulas for absorpt., transmission and reflectivity 3 − 35424
- leucosapphire, grown by Czochralski method, u.v. transmission spectra 3 − 22326
- linear transmission systems, systematic terminology 3 − 35667
- liquid crystal nematic, transverse field electro-optical effects 3 − 24676
- liquid crysts., nematic, optical transmission threshold and capacitance threshold for alignment in mag. field 3 − 20695
- monochromatic radiation pulse, two level absorbing medium, theoretical analysis 3 − 22958
- multialkali photocathode, 4000-11000 Å 3 − 30835
- multilayer systems, weakly absorbing, properties in terms of potential transmittance 3 − 16793
- ocean water, light propag., multiple scatt. calcs., effective attenuation coeffs. 3 − 25186
- optical systems, effects of mould overgrowth *(Russian)* 3 − 5882
- optical transmission function, measurement *(German)* 3 − 22334
- optical transmission of prints of rough surfaces *(Czech)* 3 − 5995
- photocounting of radiation passed through a random medium, description 3 − 37945
- photographic objectives, spectral transmittance evaluation *(Czech)* 3 − 22395
- poly(ethylene terephthalate), crystn. kinetics, influence of temp., mol. wt. and additives 3 − 33179
- quartz, blackness determ. 3 − 24666
- quartz and fused silica, i.r. transmittance at high temperatures *(German)* 3 − 37638
- random scenes correlation length, coherent optical meas. method, comments 3 − 13700
- random scenes correlation length, coherent optical meas. method, reply to comments 3 − 13701
- sapphire, synthetic cryst., vacuum u.v. transmission props. rel. to chem. purity and polishing 3 − 22322
- solids, effect of absorption on optical props. *(French)* 3 − 16794
- solids and liquid, accurate spectrophotometer for measuring transmittance 3 − 25761
- spectrophotometry, high accuracy, physical parameters 3 − 25762
- square non polar lattice, light reflection and transmission 3 − 26203
- stellar opacity, contact binary stars, rotation, Lucy theory, zero age 3 − 3331
- stratfied media, total refl. phenomena, general recurrence relations 3 − 676
- thin film optical constants determ. *(German)* 3 − 32079
- thin film optical properties, apparatus achieving 10^{-9} torr and 5-300 K *(French)* 3 − 35389
- transmitter aperture effects on scintillation, expts. 3 − 21946
- turbid medium, dispersion and centre of gravity determ. from refl. and transmission meas. *(Russian)* 3 − 37206
- turbulent media, effect of outer scale on beam spread 3 − 19571
- turbulent media, light beam spectra, outer scale effects 3 − 6424
- As-Se-Ge glass film, edge shift, laser irradiation effect 3 − 19639
- As_2S_3, amorphous film, kinetics of photo-induced edge shift 3 − 24714
- AsSI, AsSeSI semiconducting glasses, i.r. transmissivity, instability at softening temp. *(Russian)* 3 − 2552
- BiOBr, i.r. transmission, two phonon absorpt. processes 3 − 21424
- BiOCl, i.r. transmission, two phonon absorpt. processes 3 − 21424
- BiOI, i.r. transmission, two phonon absorpt. processes 3 − 21424
- CO_2, i.r. general absorptance, polynomial representation 3 − 36015
- Cu (100) single crystal film, on (100) NaCl, oxidation obs. 3 − 1907
- Cu-Fe Kondo system, far.i.r. surface resist. 3 − 5046
- Cu_xS, electrical resistivity and optical transmission as function of composition 3 − 33904
- GaSe, optical transmission in fields up to 93.5 kG, exciton behaviour, effective mass of electrons and holes, g-factors 3 − 30803
- $GuGa_{1-x}In_xS_2$, band gap comp. depend. from transmission wavelength modulation 3 − 38789
- $HfS_2(Se_2)$, octahedral coordination, spectra obs. rel. to band structure 3 − 12144
- n-InSb:Se, Te transmission spectra rel. to Moss-Burstein effect 3 − 4963
- K thin films, transmission in polarised light at oblique incidence *(French)* 3 − 30899
- KCl-KBr mixed crystal CO_2 laser window material, Czochralski growth, i.r. transmissivity 3 − 16453
- K_3Sb, 0.5 to 6.2 eV 3 − 39160
- $La_{1-x}Ce_xF_3$, u.v. transmission spectra, variable band width filter 3 − 15503
- MgAl thin films, preparation method and properties 3 − 36987
- $MoS_2(Se_2)(Te_2)$, trigonal prismatic coordination, spectra obs. rel. to band structure 3 − 12145
- $NH_4Cl_{1-x}Br_x$, solid soln. system, meas. for determ. of phase diagram 3 − 33656
- Na_2KSb, 0.5 to 6.2 eV 3 − 39160
- Na_3Sb, 0.5 to 6.2 eV 3 − 39160
- Nd-doped laser glass, nonlinear loss, two-photon absorption process 3 − 767
- RbI, 5.5-6.3 eV, effect of surfaces 3 − 36892
- Sc_2O_3 film, transparency, long wavelength absorpt. edge. refr. index, annealing effects 3 − 24763
- $TiS_2(Se_2)$, octahedral coordination, spectra obs. rel. to band structure 3 − 12144
- Tl_3AsS_4, Stockbarger-grown, characterization 3 − 12266

light transmission continued
- $WS_2(Se_2)$, trigonal prismatic coordination, spectra obs. rel. to band structure 3 − 12145
- Y_2O_3 film, transparency, long wavelength absorpt. edge, refr. index, annealing effects 3 − 24763
- $ZrS_2(Se_2)$, octahedral coordination, spectra obs. rel. to band structure 3 − 12144

light velocity
- in air and transparent media 3 − 3800
- constancy, prospects for unified standardization of time, frequency and length 3 − 13196
- constancy of light velocity in vacuum 3 − 32424
- Muller matrix 3 − 13693
- student experimental equipment for determ. 3 − 16367
- superluminal source motion in vacuum, Vasilov-Cerenkov effect and Doppler effect 3 − 29216
- three centuries of observations of Jupiter's satellite Io rel. to possible var. 3 − 32504
- visible and gamma ray velocities, experimental comparison 3 − 35661

light velocity measurement
- closed-path interferometric experiments on speed of light from moving sources, rel. to Einstein second postulate 3 − 6320
- far i.r. frequency meas. and two-laser mixing, part I of NPL programme 3 − 13322
- frequency and wavelength direct meas. of methane-stabilized laser, deduction of speed of light 3 − 153
- frequency meas. in far i.r., techniques for high-accuracy, part-II of NPL programme 3 − 13323
- interference of mm waves using two-beam interferometer, in vacuo meas. 3 − 13325
- i.r. laser emission, meas. of freq. and wavelength to 1 in 10^8 accuracy at NPL, programme 3 − 13321
- Khar'kov State Inst. 3 − 32026
- laser beam appl. 3 − 6517
- light, demonstration apparatus 3 − 32012
- Lloyd mirror interferometer experiments on speed of light from moving source, rel. to Einstein postulate 3 − 6319
- optical frequency, comparison of microwave modulation and direct mixing methods 3 − 13196
- twin superheterodyne principle, meas. of velocity along Niinisalo-Pihnari baseline 3 − 25738
- visible laser frequency meas. by up-conversion of CO_2 laser radiation, part III of NPL programme 3 − 13324
- CO_2 laser wavelengths and frequencies 3 − 9923

light water *see water*

lighting
- ambient light illumination for low light level TV, underwater applications 3 − 3255
- automatic photometry system for development, manufacture and quality control in lighting industry 3 − 9937
- background illumination of celestial and biological origin, deep ocean optical meas. 3 − 3257
- colour characteristics of new discharge lamps for TV and film lighting 3 − 9979
- discomfort glare responses, individual and group differences 3 − 28353
- illumination for, television cameras, for underwater applications 3 − 3216
- illumination optics, conference, Boulder, Colo., USA, Sept. (1972) 3 − 19191
- illumination vector measurement, instruments, review *(German)* 3 − 5932
- laser image forming techniques for theatre and TV studio scenic effects *(German)* 3 − 29155
- physiology of vision, applic. to illumination engineering *(Japanese)* 3 − 16314
- scalar and vector units 3 − 19135
- source in sea water, energy and spectral characteristics of light field, applic. of transport approximation *(Russian)* 3 − 690
- telescope magnifiers with large magnification coeffs., prod. possibility *(Russian)* 3 − 9926

lightning
- atmospheric noise, models based on thunderstorms distribution and propagation conditions 3 − 12769
- ball, analysis of Jennings photograph and critique 3 − 3016
- ball, antiparticle annihilation theory 3 − 29163
- ball, incident description 3 − 12731
- ball, review of current theories 3 − 21954
- cloud-ground flashes, acoustic observation of thunder 3 − 12744
- electric field variations before and after, oscillographic measurement 3 − 21936
- electric fish communication, background noise source 3 − 31851
- flashes, photoelectric observations of emitted light 3 − 25239
- geoelectric effects of lightning hazards from Austrian survey of strikes *(German)* 3 − 12644
- ground flash location using all sky camera bearings 3 − 18861
- hazards to overhead power lines, dependence on geological and geoelectrical characteristics of ground *(Croatian)* 3 − 18837
- induced voltages, using CIGRE antenna 3 − 31388
- locating technique at close ranges 3 − 12759
- Mt. San Salvatore, 1963-1971, current of field strength of upward strokes *(German)* 3 − 9265
- multiple return stroke, time variation of surge current 3 − 3005
- photography in daylight, narrow passband filter centred near H alpha 3 − 16062
- radar as diagnostic tool 3 − 12740
- return-stroke current calc. for cloud-to-ground discharge 3 − 9268
- stepped leaders, effect of pause time distributions on v.l.f. spectra radiation 3 − 12730
- thunderstorms, West Bengal, India, 1968-70 survey 3 − 9269
- transformers and circuit breakers damage *(German)* 3 − 15979

lightning conductors *see lightning protection*

lightning protection
- overhead power lines, hazards dependence of frequency on geological and geoelectrical characteristics of ground *(Croatian)* 3 − 18837
- space vehicles, fuelling, wire deployment, triggering 3 − 3012

lightning rods *see lightning protection*

limit, elastic *see elastic limit*

limited space charge accumulation
see also Gunn effect; negative resistance effects; space-charge limited devices
n-GaAs LSA diode, purity, evaluation determ. by low field temp. depend. mobility 3−2085

linear accelerators
4MV standing wave, X-ray beam, radiation field flatness obs. 3−272
8 MV, diode-scanner-recorder system for monitoring operating parameters 3−271
beam chopper buncher system for short ion bursts, small energy spread 3−10033
Brookhaven LINAC Isotope Producer, remote target positioning mechanism 3−16476
cavity field calculation, by finite element method 3−32120
clinical, fast neutron contamination from 25 MV X-ray beam 3−13147
cryogenic systems for supercon. LINCAS 3−9882
diode scanner recorder system for operating parameters monitoring 3−25894
electron, development at Moscow Engng.-Phys. Inst. *(Russian)* 3−19253
electron, injector, bunching and performance 3−10026
electron diode gun, production of beam single shots and pulse trains by pulse position modulation 3−10035
electron injectors, bunching and performance 3−10026
electron linac with side-coupled struct., design, performance 3−28629
heavy ion acceleration, alternates to cyclotron 3−10013
high current, phase energy eqns., synthesis of accelerating waveguide structure *(Russian)* 3−13387
induction, parameters for conducting wall of accelerator tube 3−16474
interdigital linac structure, characteristics *(French)* 3−25831
Japan Atomic Energy Research Institute, design characteristics of new linac *(Japanese)* 3−32122
Karlsruhe, superconducting, proton, acceleration tests 3−19258
KEK, high gradient drift tube quadrupole magnets 3−19257
LINAC at Ghent, study of isomeric nuclear states via photonuclear reactions *(Dutch)* 3−38109
liquid gas target system for medium energy electron scatt. facility 3−3842
Los Angeles Meson Physics Facility, design and applics. 3−37676
Mainz 300 MeV, electron scattering apparatus *(German)* 3−10009
medical, for patient treatment, X-ray and electron beam characteristics 3−3575
medical, trip-out circuit for arcing or free-running trigger pulses 3−10176
monitoring accelerator waveguide, with variable driving freq. *(Russian)* 3−13385
National Accelerator Laboratory medical programme 3−409
neutron radiography appls. 3−6136
tandem Van de Graaff, simulation of heavy ion scattering at strippers 3−16473
tandem Van de Graaff, Uppsala, ion beam transport system 3−32123
vacuum transients following puncture in evacuated pipe 3−32124
Van de Graaff, combination with split pole cyclotron, for heavy ions 3−10015
Van de Graaff, for short-lived isotope production 3−32871
Van de Graaff, production of short-lived isotopes 3−270
variable frequency, for heavy ion injection for separated sector cyclotron 3−13393

linear algebra
see also determinants; eigenvalues and eigenfunctions; matrix algebra; tensors; vectors
rapid-convergence algorithm for quantum mech. cryst. binding energies 3−1594

linear combination of atomic orbitals calculations *see LCAO calculations*

linear differential equations
boundary-value problems with second-order equations, regularization method 3−16597
Cauchy problem with singular data, asymptotic waves *(French)* 3−22585
computerized model treatment of iodine removal by sprays in nuclear plant atmosphere 3−7002
Hamiltonian systems normalization for eqns. with periodic coeffs., algorithm construct. *(Russian)* 3−497
partial, non-separable solutions 3−32287
second order degenerate soln. using state variables, teaching appl. 3−31996
shallow-water-type equations, barotropic model of forecast of katabatic winds *(Russian)* 3−12714
subsonic and supersonic flows, numerical solution 3−4586

linear expansion *see thermal expansion*

linear integrated circuits
impedance convertor, for biomedical meas. apparatus 3−37741

linear motors
induction in conducting thin plate *(French)* 3−32488
micropositioner, for electrodes positioning in cell membrane 3−22528

linear programming
finite element limit analysis for ultimate load determ. 3−6246
inelastic analysis of reinforced concrete beams 3−16658
nuclear isotopes production scheduling, applic. 3−32118
nuclear many-body problem soln. 3−26399
plastic design problem for plane frame, computer applic. 3−541

linear rectification *see rectification*

linear systems
hydrological systems, analysis *(Greek)* 3−31478
transient response of discrete linear systems to forcing functions rel. to optimal control 3−3662

linear vibrations *see vibrations*

linearisation techniques
nonlinear heat conduction problems, approximate calculation method 3−626
unidimensional periodic flow of gas in pipe, linearization of eqns. of continuity, motion, energy and state *(Russian)* 3−1348

lines (telephone) *see telephone lines*

linewidths (spectral) *see spectral line breadth*

linguistics, language *see language translation and linguistics*

linkages (electric connectors) *see electric connectors*

linking *see joining processes*

Liouville equation *see statistical mechanics*

lip microphones *see microphones*

liquefaction of gases
see also low-temperature production
Hampson type single stage miniature liquefiers, operating parameters 3−25697
molecular gas dynamics, boundary conditions, surface shocks, continuum flows, review 3−33261
pressure cell design for studying condensed gases in electron microscope 3−359
H_2, handling, transport and storage 3−3774
He, refrigeration cycle and liquefaction line, purification 3−5832

liquid alloys
see also liquid metals
alkali binary alloys, Knight shifts, Pauli susceptibilities, from contact density in pseudopotential 3−34234
binary, immiscibility gap of group IB metals 3−18583
binary, local atom distrib. analysis *(French)* 3−27625
binary, nucl. spin relax. and ionic motion 3−2441
binary, solute-solute interactions rel. to enthalpy coeff. *(French)* 3−5283
binary, thermodynamic props. of dil. solutions of oxygen 3−27850
binary alloys of Li, Na and K, miscibility gap 3−18584
cluster model, conc. fluctuations calc. 3−36255
diffusion of hydrogen, rel. to metallurgical processes 3−4865
dilute quaternary, oxygen activity coeffs. prediction using binary data 3−39314
electronic correlation functions, long wavelength 3−30386
eutectic, struct. 3−14675
Gibbs-Duhem eqn. integration method 3−36993
partial structure factors, and conc. flucuations in conformal solns. 3−30063
random cubic binary solns., atomic pots. applic. to heat of mixing, lattice parameter and compressibility 3−24814
reactive diffusion and electron transfer, multipoint semiautomatic unit *(Russian)* 3−9909
steel, inclusions growth and elimination, math. model 3−39338
supercooling, cooling rate effect on bulk samples 3−21561
thermal conductivity, cell theory, temp. depend., data correl. 3−36587
viscosity meas. at high temps. by vibration method 3−4868
Ag-Ga, mag. susceptibility, diamag. peak, temp. and comp. depend. *(Japanese)* 3−30600
Al-Si, cluster existence, rel. to hypo- and hyper-eutectic behaviour 3−34498
Al-Zn, thermodynamic props. 3−21556
Au-Ag, thermotransport of Ag 3−24281
Bi-Cd, temp. and conc. dependence of mag. susceptibility 3−27362
Bi-Sn, n.m.r. linewidths, conc. depend. 3−2412
Bi-Sn system, partial heats of mixing 3−37007
Bi-Zn, volumetric mass determ. *(French)* 3−27855
Cu-Ga(Ge)(Bi), mag. susceptibility, diamag. peak, temp. and comp. depend. *(Japanese)* 3−30600
Cu-Sb, struct. from combined neutron and X-ray diffr. 3−14676
Cu-Sb-Sn, Sn solvent activity equations, by stirred H-cell e.m.f. meas. 3−31269
Fe-Al liquid alloys, specific electrical resistance *(Russian)* 3−8146
Fe-C liquid alloys, impurities removal and structure control *(German)* 3−2729
Fe-Cr-Ni system, thermochem. parameters 3−25045
Fe-Si, mag. susceptibility, 1000-1900°C, conc. depend., solid-liq. transition *(Russian)* 3−36707
Fe-Sn system, thermodynamic excess functions, mass spectrometry obs. 3−37011
Ga-In, nuclear quandrupole relax. rate 3−18391
Ga-Pb, thermodynamic props. 3−30271
Ge-Co, Ge-Fe, electrical resistivity, theory 3−8147
Hg-In, electronic spectra, 0.14 to 4 μm 3−39133
Hg-In, Lorenz number and thermal cond. 3−30453
In-Tl liquid alloys, structure and electrical conductivity *(Russian)* 3−33443
In-Zn, thermal diff. of Zn, conc. depend. *(Russian)* 3−7951
K-Hg, partial struct. factors, model of conformal solns. 3−30063
K-Sn, thermodynamic props., conc. cell e.m.f. 3−31243
K-Sn system, thermodynamic props., conc. cell e.m.f. 3−31243
K-Tl liquid alloys, thermodynamic props. 3−34706
Li_xNa_{1-x}, phase separation theory 3−39322
Na-Cd dilute alloys, state of Cd impurities, temp. dep. of elec. resistivity 3−33868
Na-In, dil., density and surface tension, 170-400°C, comparison with Na-Cd alloys 3−36994
Na-K, electronic correlation functions, long wavelength 3−30386
Na-K, electrotransport, drag coeff. 3−24284
Na-K, interphase surface tension, 20-160°C 3−20924
Na-K, partial struct. factors, model of conformal solns. 3−30063
Ni, solubility, of hydrogen, thermodynamic behaviour 3−5296
Ni-Ti, high temp. thermodynamic props. 3−37010
Pb-Sn, temp. dependence of resistivity 3−30454
Pb-Sn, u.s. velocity obs. and determ. of thermophysical props. 3−24215
Pb-Sn, viscosity, determ. by oscillating crucible method 3−30280
Pb-Sn, viscosity obs., oscillating crucible method, liquidus temp. to 800°C *(Japanese)* 3−7960
Pr-Zn, thermodynamic props. 3−36993
Sb-In, self-diffusion coeffs., conc. depend. *(French)* 3−30275
Sb-In, self-diffusion coeffs., temp. depend. at equiatomic comp., ionic salt concept *(French)* 3−30276
Sn-Bi, mag. susceptibility conc. depend. analysis *(Russian)* 3−8347
Sn-Pb system, conc. depend. of pseudopots., atom scatt. cross section, electrotransport *(Russian)* 3−30277
Sn-Tl, thermal diff. of Tl, conc. depend. *(Russian)* 3−7951
Sn-Zn, dil., Ag effect on Zn activity coeff., 803 K 3−36995
Te-Se liquid alloys, band spectrum from thermal conductivity meas. 3−36632

liquid alloys continued
- Tl-S melt, thermodynamic activity 3−9046
- Tl-Te, molten, electrotransport and density of states *(Russian)* 3−24370
- Zn-In-Pb solns., miscibility gap, zinc isoactivity and molar functions 3−38675

liquid crystal devices
- *heading is late addition, see also display equipment; optoelectronic devices*
- display system, influence of contacts on scattering props. 3−14686
- h.f. acoustic hologram display system 3−19165
- MBBA filled displays, degradation mechanism 3−21796
- optical waveguide modulation using nematic crystals 3−39118
- programmable graticules in optical systems 3−35398
- room temperature, using positive dielec. anisotropy 3−27484
- segmented master character for electronic display device, patent 3−33455

liquid crystals
- N-(p-methyoxybenzylidene-p-n-butylaniline, role of electrode reactions in dynamic scatt. 3−12113
- 4-alkoxybenzal-4′-ethylanilines, isotropic, nematic and smectic A phases, X-ray diffraction obs. 3−36262
- 4-alkoxybenzylidene-2′-alkoxy-5′-aminopyridines, effect of heterocyclic N on mesomorphic behaviour 3−17738
- p-aminophenylacetate, preorientation pot. barriers of mols. in cryst., nematic cryst. and isotropic phases 3−21415
- n-anisal aminocinnamic acid ether, struct. exam. by X-ray and optical methods *(Russian)* 3−7626
- n-anisalaminocinnamic acid, smectic mesophase study by optical analogy method *(Russian)* 3−38534
- anisotropic system, reorientation 3−5127
- anisylidene para aminophenyl acetate nematic liquid crystal, proton magnetic resonance obs. 3−27436
- p-azoxyanisole, nematic mesophase, dielec. dispersion, l.f. region, retardation factor 3−34291
- p-azoxyanisole, p methoxybenzylidene n butylaniline, nematic, pressure effects on the phase transitions 3−33453
- p-azoxyanisole, solid-nematic transition, pretransitional effects, neutron diffr. 3−26973
- p-azoxyanisole, X-ray diffr. obs. under simultaneous action of electric and mag. fields 3−33454
- p,p'- azoxyphenetole, and eutectic mixtures, chromatographic and thermo-optical study of phase transitions 3−24025
- broken symmetry hydrodynamics 3−1574
- p-n-buthylanilines, p-methoxy- and p-ethoxybenzilidene, preorientation pot. barriers of mols. in cryst., nematic cryst. and isotropic phases 3−21415
- 4-n-butyloxybenzylidene-4′-acetoaniline, nematic and smectic A mesophases, molecular organization 3−17739
- CBAOB, smectic-A-phase order-parameter fluctuations near second-order phase transition 3−33451
- cholesteric, Cherenkov struct. radiation 3−1639
- cholesteric, circular dichroism and rotatory dispersion near i.r. absorption bands 3−30830
- cholesteric, compensated, birefringence, temp. depend. 3−30796
- cholesteric, driven modes in oscillating mag. fields 3−24024
- cholesteric, electrohydrodynamic effects and light diffusion *(French)* 3−30072
- cholesteric, evolution of polarised light 3−35669
- cholesteric, hydrodynamic instabilities under thermal gradient 3−26968
- cholesteric, i.r. circular dichroism, mol. vibrs. 3−5184
- cholesteric, shear effects on colour intensity and reflectance wavelengths 3−24709
- cholesteric, spin model 3−30067
- cholesteric, voltage effect on light scattering 3−15472
- cholesteric and nematic solutions of Raman spectra 3−24694
- cholesteric glass, acoustic rotatory power *(French)* 3−7854
- cholesteric mesophase, thickness effect on layer structure of sheared Grandjean texture 3−7616
- cholesteric mixtures with organic solutes, selective reflection of visible light 3−12147
- cholesteric planar texture, imperfectly aligned, elec. field induced blue shift 3−15508
- cholesteric struct. of liq. cry. and interface potential maxima 3−20688
- cholesteric-nematic mixture, optical storage effect 3−4115
- cholesteric-nematic transition, elec. field induced, rel. to dielec. anisotropy 3−4717
- cholesteric-nematic transition, transition feed strength charact. obs., applic. of mag. susceptibility meas. *(French)* 3−14682
- cholesterol branched-chain esters, diastereomeric pair, helical twisting power 3−24018
- cholesteryl ω-phenylalkanoates, synthesis and mesomorphic characterization 3−24023
- cholesteryl n-alkyl carbonates, synthesis and mesomorphic characterization 3−24022
- cholesteryl oleyl carbonate, non-Newtonian viscosity, 15-45°C 3−17737
- 4,4'-di(n-alkoxy)azoxybenzene, n=1 to 6, nematic liquid crystals, splay and bend elastic consts. 3−36264
- dibenzene p,p′-diaminobiphenyl, preorientation pot. barriers of mols. in cryst., nematic cryst. and isotropic phases 3−21415
- dielectric hysteresis, study of spontaneous polarisation and coercive field 3−24026
- diethyl 4,4′-azoxydibenzoate, smectic, Raman spectra at phase transitions, frequency shifts 3−36866
- 4,4′-dimethoxyazoxybenzene, molecular field theory of nematic mesophase 3−11542
- p-dimethylamino-p'-nitrostilbene, fluorimeter study of surface fluorescence, circular dichroism measurements *(German)* 3−36938
- display system, influence of contacts on scattering props. 3−14686
- display system, laser beam applic., development 3−6524
- display system for visualisation of u.s. waves 3−77
- educational use to illustrate interference, dispersion, birefringence and optical rotation 3−16366
- electro-optic of properties, dynamic light scattering *(Russian)* 3−30799
- in electro-optics *(German)* 3−11543

liquid crystals continued
- encapsulated, for obs. of temp. increase due to stresses in piezoceramic bodies 3−67
- e.p.r. lineshapes in slow-motional region 3−39015
- e.s.r. spectra, review 3−34190
- p-p-ethoxyphenylazo-phenyl undecylenate, Raman depolarization ratio and short range order 3−17734
- ethyl p-anisalaminocinnmmate, optical modelling and disorder parameter of molecules, calc. *(Russian)* 3−7625
- ethylene carbonate and thiocarbonate, partially oriented in nematic phase, NMR study 3−7229
- glassy crystalline state 3−14692
- heat capacity, anomalous calc. on basis of de Gennes' theory 3−4856
- p-hexyloxybenzoic acid liquid crystal, coupling of H bonding to orientational fluctuation modes 3−1571
- h.f. acoustic holography, display using liquid crystals 3−19165
- hydrodynamic theory, unified, for crysts., liq. crysts. and isotropic fluids 3−4718
- lamellar, proton, n.m.r. line shapes 3−18375
- l.f. mode, neutron scattering 3−20689
- light scatt. by deform. of plane texture of smectic and cholesteric liquid cryst. 3−12111
- lyotropic, deuteron relax. obs. of D_2O motions at soap-water interface 3−27173
- magnetohydrostatic theory for cryst. lying between two coaxial cylinders 3−26971
- MBBA, chem. and electrochem. stability, rel. to display device degradation 3−21796
- MBBA, isotropic phase, short-range order fluctuations, correl. range 3−33448
- MBBA, nematic, domain formation threshold variation under d.c. dynamic scatt. 3−18422
- MBBA, nematic, surface disclination lines 3−30071
- MBBA, nematic-isotropic phase transition, u.s. obs. 3−26966
- MBBA menatic film, statics of Freederick's transition in mag. field 3−7617
- MBBA-COC, shear induced struct. changes, mechanism 3−36259
- membranes (biological), mol. model for lipid ordering determ. 3−22144
- mesomorphic benzylideneanilines, phase transitions 3−24021
- mesomorphic phase transitions characterized by order parameter arising from violation of rotational invariance 3−26965
- mesophase study by optical analogy to detn. location of diffraction maxima, modelling possibilities 3−7624
- p-methoxybenzilidene p-butylaniline, electrochemical props. *(French)* 3−36261
- p-methoxybenzilidene p-butylaniline, stability to hydrolysis and ionic conductivities *(French)* 3−36260
- p-methoxybenzylidene, p-n-butylaniline with cholesterol benzoate or Canada balsam, exam. of mesomorphic state *(French)* 3−7618
- β-methyl butyl p[(p-methoxy benzylidine)amino] cinnamate, Brillouin scattering 3−34354
- from β-methylbutylaniline, low temp. chiral nematic cryst., synthesis and phys. props. 3−17735
- methylmercuric halides in isotropic and nematic liquid solutions, proton magnetic resonance 3−24622
- microencapsulated cholesteric films, transient surface temperature response to rapid heating 3−35426
- mixed, cholesteric-nematic transition, a.c. elec. field induced 3−17736
- molecular packing in different structures, appls. 3−1573
- nematic, acoustic wave dispersion and absorption 3−24216
- nematic, anomalous u.s. absorpt. and dispersion above clearing pt., dynamic heat capacity 3−36369
- nematic, appl. to optical waveguide modulation 3−39118
- nematic, carbonate Schiff base, synthesis and electro-optic properties 3−1570
- nematic, collective modes, molecular theory 3−17742
- nematic, decay time reduction when driven by d.c. pulse 3−24677
- nematic, deformation in elec. field 3−14681
- nematic, diamag. susceptibility and anisotropy, temp. depend. *(French)* 3−38955
- nematic, dipole relax. behaviour, mol. ordering depend. 3−18412
- nematic, domain wall behaviour above Freedericks transition 3−4719
- nematic, doped negative film, secondary dynamic scatt. 3−36257
- nematic, elec. controlled birefringence, field alignment rel. to pulsed voltage *(French)* 3−8553
- nematic, existence of even indexed disclinations 3−20693
- nematic, friction coeff. calc. 3−33447
- nematic, friction coeff. for moving disinclination 3−17740
- nematic, heat convection 3−36443
- nematic, interaction between disclinations and rubbed surface 3−33452
- nematic, interaction between disinclinations 3−17741
- nematic, molecular motion, neutron scatt. obs. 3−1812
- nematic, molecular theory of collective modes 3−38538
- nematic, neutron diffr. pattern calc. 3−26969
- nematic, new compounds for display devices 3−30066
- nematic, non-Fourier heat conduction 3−24301
- nematic, optical transmission threshold and capacitance threshold for alignment in mag. field 3−20695
- nematic, order parameter from n.m.r. dipolar splittings 3−14684
- nematic, orientation by suitable boundary surfaces 3−1572
- nematic, orienting action of sound 3−7620
- nematic, polarizable, induced viscosity changes theory 3−14441
- nematic, propagating plane disclination surfaces 3−20690
- nematic, self-diffusion in isotropic phase near nematic-isotropic transition 3−33446
- nematic, thermal transport, review 3−24300
- nematic, transverse field electro-optical effects 3−24676
- nematic, with positive dielec. anisotropy, electro-optic props. obs. 3−27484
- nematic and isotropic phases, molecular dynamics, p.m.r. obs. *(French)* 3−33449
- nematic birefringence, ultization in acoustic image detection 3−35362
- nematic electrolyte solns., electric props., influence of sample geometry *(German)* 3−37129
- nematic Frank elastic constants theory 3−20778

liquid crystals continued
- nematic homologous series, clearing temp., alkyl chain length depend. 3−26972
- nematic layer, appl. to visualization of thin film Al-Al$_2$O$_3$-Al capacitor defects 3−15284
- nematic liquid crystal in mag. field, dynamic behaviour 3−26967
- nematic mesophase, MHD effects, n.m.r. obs. 3−36797
- nematic mesophase, solute-solvent interactions 3−24020
- nematic mixtures, with positive dielec. anisotropy, room temp. 3−30068
- nematic p-azoxyphenetole, elec. cond., temp. depend. 3−21071
- nematic phase, thermal conductivity anisotropy 3−27147
- nematic phase of smectic C materials, elec. cond. temp. depend., short range order effects 3−14683
- nematic rotational viscosity coefficient and shear alignment angle meas. 3−20884
- nematic singular lines and points, disclinations 3−21246
- nematic threads, calc. of molecular alignment and elastic deformation energy 3−38537
- nematic to smectic A transition, pretransitional anomaly in elastic bend const. 3−30069
- nematic twisted crystals, electric field induced domains 3−26970
- nematic-isotropic phase transition, fluoresc. quenching 3−36258
- nematic-smectic A transition entropies in homologous series 3−30070
- nematic/isotropic interface, interfacial tension calc. 3−27168
- nematics, Parodi's relation, implications for wave propagation 3−17743
- n.m.r., high resolution, of solutions at room temperature *(German)* 3−24625
- n.m.r. in rot. frame 3−2418
- nondeforming media, anisotropic transport processes 3−620
- p-n-nonyloxybenzoic acid, mol. alignment, elec. and high mag. field effects 3−38535
- n-nonyloxybenzoic acid, smectic mesophase study by optical analogy method *(Russian)* 3−38534
- optical analogy method for structure determ., smectic mesophases *(Russian)* 3−38534
- oriented smectic, anisotropic u.s. properties 3−1703
- p-azoxyanisole, nematic, Raman spectra at phase transitions, frequency shifts 3−36866
- p-azoxyphenetole, nematic, inelastic light scattering spectrum, hydrodynamic fluctuations 3−36887
- on p-n and Schottky junctions, nematic, technique for obs. of electric fields 3−38887
- p-n-octyloxybenzylidene-p'-toluidine, smectic A-phase order parameter fluctuations in nematic phase 3−38536
- PAA nematic liquid crystal, coherent neutron scattering 3−7623
- p-penthoxybenzoic acid, preorientation pot. barriers of mols. in cryst., nematic cryst. and isotropic phases 3−21415
- phase diagrams of binary nematic mesophase systems 3−36263
- phase transitions, crit., biaxial particle fluid model 3−38671
- physical principles, types, digital display devices *(German)* 3−7622
- poly-γ-benzyl-L-glutamate, n.m.r. in static elec. field, solvent mols. orientation 3−30708
- poly-γ-ethyl-glutamate, cholesteric, mag. alignment, laser beam diffraction obs. 3−11544
- polypeptide films, superstructure determ. from small angle light scattering 3−1947
- polypeptide solid film morphology, memories of liquid crystal behaviour 3−29807
- for programmable graticules in optical systems 3−35398
- proton spin thermometry at low fields in solid phase 3−2456
- reflection props. of distorted cholesteric liquid crystals 3−30842
- review of current research and appls. 3−20692
- right-rotatory cholesteric, derivatives of $\Delta^{8(14)}$-cholestanol, synthesis and optical rotation 3−24017
- segmented master character for electronic display apparatus, patent 3−33455
- self-diffusion, meas. by nultiple-pulse n.m.r. method 3−30712
- smectic, supercooled, Mossbauer recoil free fraction rel. to that of solid state 3−20694
- smectic, X-ray scattering 3−7619
- smectic A, B and C, microscopic obs. of mol. arrangements 3−20691
- smectic A, edge dislocations, elastic peak, inelastic light scatt. *(French)* 3−30065
- smectic A, layer vibrs. extent *(French)* 3−1568
- smectic A, Rayleigh scattering induced by static bends of layers 3−18461
- smectic A, self-diffusion const. meas. 3−1813
- smectic A film, possible mag. transitions, critical field 3−4720
- smectic A mesophases, BHPM, EPAB, TLST, X-ray diffraction obs. 3−33444
- smectic A-smectic C transition region obs. by flow birefringence and sound attenuation *(French)* 3−17733
- smectic B modification of mesomorphic cpd., linear local order 3−14678
- smectic C phase, mol. rearrangement under large mag. fields, n.m.r. study 3−33450
- smectic crystals, low freq. Raman mode near phase transition 3−24703
- steroids, influence of Δ^7-double bond on mesophase type and formation 3−24019
- stilbenes, methyl substituted, nematic clearing pt. temps. rel. to mol. geometry 3−14680
- structure, from X-ray analysis and statistical functions of distrib. 3−14679
- tape, ambient light effects on colour/temp. response 3−24710
- temperature measurement applic. for crack detection in aerospace industry 3−31222
- thermal expansion above the clearing point calc. on basis of de Gennes' theory 3−4856
- thickness meas. of nematic liquid crystal layers 3−7621
- thin film, appl. to threshold switching studies in thin film chalcogenide devices 3−27294
- thin layer production, by centrifugal spreading of drop 3−14685
- thin layers, orientation by surface coupling agents 3−38533
- three types, nematic, statistical theory 3−1569

liquid crystals continued
- triterpenes, influence of Δ^7-double bond on mesophase type and formation 3−24019
- twisted nematic layer, mag. field induced motion of disclinations 3−33445
- u.s. velocity, absorption, transmission and reflection obs. 3−1696

liquid drop model (nuclear) *see nuclear liquid drop model*

liquid films
- *see also adsorbed layers; superfluidity; surface tension*
- absorption of CO_2 in rapid laminar fan-shaped water sheet 3−4536
- aquatic frontal systems, element enrichment 3−12690
- capillarity-controlled entrainment of a liquid by a thin cylindrical filament moving through an interface 3−30334
- complex shear modulus, meas. 3−27045
- condensate, stability characteristics 3−33233
- condensate film flow down a vertical wall, stability 3−14433
- condensation on a surface with uniform heat flux and body force convection 3−29850
- dye films, free flowing, for CW dye lasers 3−4099
- evaporation, of liquid patches, heat transfer coeff. determ. 3−30254
- evaporation into turbulent gas flow, mass transfer model 3−29842
- falling, liquid viscosity effect on mixing 3−26860
- falling, stagnant band analysis 3−33228
- falling, Taylor diffusion 3−1962
- falling on sphere, gas absorption 3−4535
- film flow, boiling heat transfer, refrigerants, liquid NH_3, evaporators 3−1438
- flow, entrance effects 3−36107
- gas diffusion to a liquid film flowing down inclined surface, asymptotic eigenvalues for heat or mass transfer 3−26779
- Gibbs elasticity, thermodynamic theory 3−38708
- heat transfer for film, draining down vertical wall, numerical solns. 3−20290
- hydrodynamic and elastic equations, coupled, of film between mating surfaces 3−25785
- internal surface of horizontal capillary, thickness determ. *(Russian)* 3−30337
- Kelvin-Helmholtz wave growth on thin liquid sheets 3−29892
- laminar flow boiling on inclined isothermal flat plates 3−36411
- liquid film, Gibbs elasticity meas. technique and apparatus 3−28464
- on metals, enhancement of TEA-CO_2 laser pulse interaction 3−18518
- microencapsulated cholesteric, crystal, transient surface temperature response to rapid heating 3−35426
- non-Newtonian falling liquid films, gas absorption 3−36108
- nucleate boiling heat transfer mechanism rel. to boiling liquid films 3−1785
- oil, apparatus description of thickness measurement *(Russian)* 3−9829
- oil films at high contact pressures, rheology rel. to lubrication 3−11683
- powder-liquid film method for particle size meas. 3−34665
- printing ink, adhesion to steel and tin plate, effect of film formation 3−39405
- solidification rate of water in a short vertical tube 3−11725
- stability, nonlinear, film adjacent to supersonic gas stream 3−36110
- steam flow in vertical tube, condensate film thickness and heat transfer 3−17517
- thin oil films, stability, removal from metallic surfaces by washing, laminar liquid stream 3−39465
- viscous thin layers, gas stream effect on wave flow 3−20363
- water, bulk and film, struct., X-ray diffr. obs. 3−14673
- water, in mica, i.r. spectra *(Russian)* 3−27496
- water, unstable film boiling dynamics, process transfer function 3−20865
- wavy, flowing, heat transfer through 3−7320
- He, film flow, superflow speed rel. to chem. gradient driving force, dissipation 3−36450
- He, lifshitz theory of Van der Waals forces, verification 3−20214
- He II, sp. ht., surface contrib. 3−30297
- He II accommodation coeff., 1.15-4K, on surface of levitated Nb superconducting sphere 3−27155
- He II film, transitions in flow rates 3−36451
- N, boiling in tubes, disperse regimes 3−9891
- N film boiling crises and transient boiling 3−9892

liquid flow *see flow of liquids*

liquid flow coaxial cables *see coaxial cables*

liquid helium
- *see also liquid helium-3; liquid helium-4; liquid helium sound propagation; superfluidity; vortices*
- a.c. Josephson effect 3−4897
- atomic kinetic energy evaluation from neutron scatt. expts. 3−38527
- boiling transition, cryostatic stabilization 3−8313
- cryogenic ultrahigh vacuum pump with low liquid He consumption 3−35388
- cryostat, 0.3 to 3 K *(German)* 3−28504
- cryostat, for diffractometer 3−25700
- cryostat, for optical absorption measurements 3−13277
- dielectric breakdown rel. to He pressure and gas bubble formation 3−7987
- film, Lifshitz theory of Van der Waals forces, verification 3−20214
- impurity motion, microscopic theory 3−36447
- large-scale refrigerator-liquefier system 3−25703
- level indicator with continuous reading utilizing carbon resistors 3−37601
- level indicator with superconducting filament *(Czech)* 3−9873
- light scattering, quantum mechanical formulation 3−11771
- quantum fluid, struct., pair correl. function determ. procedure 3−35621
- rotating, system of vortices, equil. state 3−20908
- roton dynamics 3−24306
- scanning electron microscope stage 3−348
- solid-liquid boundary, phonon transmission, microscopic theory 3−1763
- supercritical, meas. of forced convection heat transfer 3−9893
- supercritical, turbine flowmeters 3−6175

liquid helium continued
T-matrix theory for many-particle system, inclusion of two-body correlation effects 3−18003
temperature meas. employing CROG thermometer 3−35381
liquid helium-3
see also fermion systems
collisionless sound propag. in normal and extraordinary phases below 3 mK 3−38694
cooling by adiabatic solidification 3−25699
degenerate films, pulsed nucl. reson. obs. of susceptibility and mag. interaction 3−4901
diffusion into ^{4}He near λ-line 3−24310
dilution refrigerator for precooling Pomeranchuk cell, design and construction 3−25698
dilution refrigerator with condensation pump 3−5819
e.m. radiation scatt., freq. power spectrum of density fluctuations 3−11779
ground state energy from sound propag. data 3−20909
heat capacity along melting curve between 1.8 and 4.2 mK, second order phase transition 3−27156
Kapitza thermal boundary resistance between ^{3}He and Cu, meas. from 10-160 mK 3−33712
n.m.r. and solidification curve, hypothetical superfluid phase *(French)* 3−20907
n.m.r. at very low temp., ordered phase obs. *(French)* 3−20905
n.m.r. in hypothetical superfluid phase *(French)* 3−20906
sound propagation, density and viscosity 3−11778
sp. ht. in sintered Cu below 3 mK 3−38695
specific heat at low press., appl. from normal Fermi liquid Landau-theory approach 3−15043
specific heat discontinuity, obs. of second-order phase transition and P-T phase diagram 3−18006
specific heat jump at 2.65×10^{-3}K *(Russian)* 3−15047
structure factor meas. 3−33713
superfluid anisotropic phase, n.m.r. phenomena 3−24309
superfluid condensation, temp. effects on props. 3−18005
surface state calc., liquid helium 3-4 mixture, Andreev's model 3−27158
thermal anomalies, interpretation using BCS pairing in mag. field 3−15048
thermal contact with CeMg nitrate at low temp. 3−36459
zero sound attenuation near low-temperature transitions 3−30304
He I boiling in vertical annular channel *(Russian)* 3−20902
^{3}He/Ce, $Mg_3(NO_3)_{12}.12H_2O$ boundary resist., nucl. spin-electron spin dipolar interaction 3−30303
liquid helium 3-4 mixtures
charged particle motion, in strong elec. fields *(Russian)* 3−7990
diffusion of ^{3}He near λ-line 3−24310
dilute, liq. struct. function 3−11781
dilute, superfluid film form., surface separation 3−4902
dilution refrigeration cryostat, pressure induced semiconducting material search, equipment 3−9902
dilution refrigeration cryostat system, for nuclear orientation studies 3−37605
dynamical behaviour near tricritical pt. 3−7989
heat of transition of ^{3}He from ^{3}He enriched phase to ^{4}He enriched phase 3−33714
Ising generalised model, same free energy as amorphous ferromagnet 3−38942
isotopes distillation 3−5841
isotropic mixtures, ^{3}He diffusion, 3 to 0.4K 3−11780
nuclear relaxation anomaly near T_λ 3−30306
quantum lattice gas model with Bose and Fermi statistics 3−38696
specific heat near junction of λ and phase-separation curves 3−15049
spin diffusion coeff. of ^{3}He 3−30305
superfluid density near superfluid transition point, from second sound velocity 3−30307
thermal resistance of three ^{3}He-^{4}He mixtures 3−7988
tricritical point 3−17960
tricritical points, critical exponents notation 3−13664
^{3}He quasiparticle-roton interaction, scatt. cross-section and diffusion constant calc. 3−24311
^{3}He surface state calc. in Andreev's model 3−27158
^{3}He-He II, new sound mode in superfluid 3−27157
liquid helium-4
see also boson systems; superfluidity
λ-transition, thermodynamic analysis 3−30302
Bose gases, charged and neutral, calc. of critical exponents above λ-transition points 3−1851
cavitation stability due to electron bubbles 3−33710
collective excitations in phonon gas below λ point in addition to second sound 3−20903
critical flux in open vertical channels filled with superfluid helium under press. *(French)* 3−11773
critical phenomena, PVT surface 3−11777
diffusion of ^{3}He near λ-line 3−24310
energy transfer from a pulsed thermal source 3−30300
field emission and field ionisation, press. up to 25 atm. 3−30299
field-theoretic model for crit. behaviour above T_λ 3−4895
film flow, superflow speed rel. to chem. gradient driving force, dissipation 3−36450
first sound absrop. coeff. near T=0 *(Russian)* 3−1853
fluctuations near lambda transition, Guyon-Maki model 3−30296
ground state, correl. function in Bijl-Dingle-Jastrow description at absolute zero 3−20904
ground state energy calc. viscosity, thermal conductivity self-diffusion coefficient calc. 3−14409
ground state energy from sound propag. data 3−20909
ground state wavefunction calc. 3−11774
ground-state, zero-momentum condensate fraction 3−11776
Kapitza resistance, influence of thin surface-dislocation layer 3−7986
light scatt. from first and second sound near λ transition 3−24308
neutron scattering, 1.2 K, press. of 0.7 at 24 atm. 3−30298
phonon radiation from heated NaF crystal face into liquid ^{4}He, meas. of angular distrib. 3−1855
sound velocity temp. depend., 0.07-0.7K, 12-105 MMz 3−33705
supercritical, for cooling superconducting devices *(Japanese)* 3−15038
liquid helium-4 continued
superfluid, accelerated isothermal flow, dissipation mechanism 3−38693
superfluid, cooling by convective heat transport 3−27152
superfluid, in experiments with sintered Cu heat exchangers 3−28501
superfluid, ion-vortex ring formation, models 3−33709
superfluid, light scatt. by thermal surface waves, 1.29-2.14 K 3−7984
superfluid, mean-field theory for interacting rotons 3−4900
superfluid, phonon excitation spectra, self consistent calcs. 3−4896
superfluid, roton-roton interactions, calc. of temp. variation of roton self energy 3−27154
superfluid, search for Bose-Einstein condensation using neutron inelastic scattering 3−4898
superfluid, theory, phenomenological Hamiltonian 3−15044
superfluid, u.s. modulated flow through small orifice, attempt to observe a.c. Josephson effect 3−30301
superfluid critical velocity in rough channels, hydrodynamic model 3−36453
superfluid density under pressure near λ point 3−36452
superfluid film, fast evaporation, generation of He shock waves 3−7396
surface oscillations, model approach *(French)* 3−7983
three-particle variational wave function for ground state 3−4035
two fluid model, density matrix calc. 3−4894
vortices, parallel line, nonlinear behaviour 3−33708
He I, boiling under forced flow in vertical tube 3−9894
He II, as type of second sound wave 3−27151
He II, dispersion of thermal waves with normal component damping *(Russian)* 3−15046
He II, free boundary and Feynmann wave functions 3−33706
He II, negatively charged vortex rings, electron escape from electronic bubble 3−7985
He II, neutral excitations 3−18004
He II, saturated liquid, correlation of vaporisation onset heat flux for cylinders 3−9895
He II, supercrit. counter-flow influence on vel. of second sound *(French)* 3−1852
He II, temp. dependence of phonon velocity and roton minimum 3−36454
He II, two-roton model 3−24307
He II film, accommodation coeff., 1.15-4K, on surface of levitated Nb superconducting sphere 3−27155
He II film, sp. ht., surface contrib. 3−30297
He II film, transitions in flow rates 3−36451
He II in long tubes, saturated and subcooled, critical heat flux 3−9896
He II isothermal flow through plane slits 3−4899
He II layer, strongly attenuated symmetrical waves existence 3−33707
He II quantised vortex vibrs. in long wavelength limit 3−24305
He II surface of discontinuity, jump conditions, from two fluid model 3−27150
He II thermal counterflow and critical heat currents, scaling parameter 3−11775
He II-solid interface, Kapitza resist. rel. to thin surface films 3−33704
He(II), 0.3<T<4.2K, luminesc. prod. by weak α-particle sources 3−15045
^{4}He, light scatt. near gas-liq. critical point, critical exponents and correl. length 3−1854
^{4}He-solid interface, Kaptiza resistance reduction through surface dislocation scattering 3−1764
liquid helium sound propagation
see also second sound; zero sound
collective excitations in phonon gas below λ point in addition to second sound 3−20903
u.s. cavitation in liquid He *(Japanese)* 3−7407
He II layer, strongly attenuated symmetrical waves existence 3−33707
He II layers, wave modes, dispersion relations 3−33711
^{3}He, below 3mK, collisionless sound propag. in normal and extraordinary phases 3−38694
^{3}He, deduced values of density and viscosity 3−11778
^{3}He, ground state energy determ. 3−20909
^{3}He-He II, new sound mode in superfluid 3−27157
^{4}He, ground state energy determ. 3−20909
^{4}He, superfluid, first sound absorp. coeff. near T=0 *(Russian)* 3−1853
liquid lasers
acoustooptic Bragg cell for wavelength tuning of a dye laser, angular dispersion 3−22378
trans-1-(4-)biphenyl-2-(1-)naphthyl-ethylene, laser action 3700-5000 Å *(French)* 3−29087
coumarin dye c.w. laser emission in blue and green 3−29088
c.w. dye laser, description and appl. to meas. of Na hyperfine struct. 3−37963
c.w. dye lasers, rotational relaxation and triplet state processes 3−731
cyanine dyes, mode-locking, fluoresc. quantum efficiency, lifetimes and triplet-triplet absorpt. 3−27887
diffraction grating for tuning dye lasers, angular dispersion 3−22379
distributed feedback lasers on anisotropic substrate, freq. generation scatt. mechanism 3−22892
distributed lasers, periodic layered waveguide structs., evaluation, feedback and scatt. losses 3−16880
double cavity dye laser, emission spectrum, 2 nsec pulses 3−29085
dye, 3,3-diethylthiatricarbocyanine, extinction of generation and short-wave fluorescence *(Russian)* 3−10545
dye, broadly tunable with narrow linewidth, operating in near i.r. 3−29086
dye, continuous, loss analysis, output improvement 3−16848
dye, coupled mode, shock tube excited, near i.r. emission *(French)* 3−19609
dye, c.w., dynamic losses 3−19610
dye, c.w., freq. stabilization and appl. to high-resolution spectroscopy 3−37634
dye, intensity stabilization of radiation by saturated amplification 3−37964

- **liquid lasers** continued
  - dye, laser action props. rel. to struct. and electronic transitions polarisation characts. 3−33143
  - dye, operation, developments and appls. in fund. research 3−732
  - dye, optical pumping using high power pulsed N_2 laser 3−26226
  - dye, pumped by N_2 laser, coherent double freq. output system *(Russian)* 3−26230
  - dye, pumped by N_2 laser, generation of tunable near i.r. 3−13735
  - dye, rapid frequency tuning, by electromechanical technique 3−3819
  - dye, rapid transverse tuning using an acoustooptic technique 3−6478
  - dye, repetitive pumping using Xe-ion laser 3−32560
  - dye, review 3−6477
  - dye, rhodamine 6 G, pulsed, radiation first order coherence, energy and conc. depend. 3−32559
  - dye, rhodamine 6G in methanol, emission rel. to elec. field 3−6480
  - dye, with wide tuning range, using Avco C950 N_2 laser 3−4101
  - dye amplifier, flash pumped, amplification gain eqn. 3−29084
  - dye laser, 1 watt, repetitively pumped, tuned, props. 3−16847
  - dye laser, electronically tuned by acoustooptic filter, transient analysis, computer simulation 3−4098
  - dye laser, far i.r. generation by self-beating, phase matching method 3−16905
  - dye laser, N_2 laser pump 3−19595
  - dye laser system, simultaneous two frequency oscillation 3−29089
  - dye lasers, CW, utilizing unconfined flowing films 3−4099
  - dye lasers, flashlamp pumped, threshold pump intensity fluorescence character of solution *(German)* 3−10544
  - dye lasers, Raman absorption lines within stimulated fluorescence spectrum 3−22896
  - dye lasers, vessel-cavity and Fabry-Perot etalon, new design suggestion 3−25777
  - dye lasers based on spiral pumping lamp *(Russian)* 3−6481
  - dye ring laser, flash-lamp pumped, tunable, extremely narrow bandwidth 3−16849
  - dye superradiant waveguide laser, characts. 3−35691
  - frequency shift, mode-selected dye laser, Fabry Perot wavelength selectors, shift mechanisms 3−22898
  - inert gas liquid lasers employing luminescence of self-localised excitons *(Russian)* 3−35692
  - intramolecular exciplex emission based laser action 3−22893
  - leaky corrugated optical waveguides, laser oscill. 3−22890
  - Marx-Bank coaxial driver flashlamp for excitation of organic dye lasers 3−16449
  - 4-methylumbelliferone dye, temp. tuning 3−37965
  - 2-(1-)naphthyl-5-phenyl, laser action, 3700-5000 Å *(French)* 3−29087
  - optical waveguide on anisotropic substrate, mode suppression, freq. tuning 3−22891
  - organic dye pulsed tunable laser 3−25776
  - organic laser dyes, pH rel. to photobleaching quantum efficiency 3−4100
  - 1,3,4, oxadiazole, laser action, 3700-5000 Å *(French)* 3−29087
  - perylene dissolved in benzene, laser action excited by Q switched ruby laser, 4730 Å, emission characteristics *(French)* 3−22900
  - petroleum fractions, photoluminescence and absorptive props. for use in lasers *(Bulgarian)* 3−34400
  - Rhodamin 6G organic dye laser, effect of concentration on laser threshold 3−22904
  - Rhodamin B organic dye laser, effect of concentration on laser threshold 3−22904
  - Rhodamine, nonsubstituted, luminophor, stimulated emission under anthracene compound addition, energy var. 3−22902
  - Rhodamine 6G, discharge emission, kinetics, spectra and specific radiation loss *(Russian)* 3−22905
  - Rhodamine 6G, luminesc. spectra, two photon excitation 3−32563
  - Rhodamine 6G, spectral radiation control *(Russian)* 3−19611
  - rhodamine 6G, time dependence of gain of optically pumped soln. 3−22903
  - rhodamine 6G dye, c.w., passively mode locked, end pumped internal lens cavity, picosecond pulses 3−22897
  - rhodamine 6G dye, fluorescence quenching by photons, model 3−22899
  - rhodamine 6G dye, pumping using 60 kV switching system 3−5988
  - rhodamine 6G dye laser, superradiant travelling-wave, new emission band 3−22895
  - rhodamine 6G dyes, metachromic effect, effect of copolymer composition luminescence study *(Russian)* 3−35694
  - rhodamine 6G ethylene glycol c.w. dye laser, diffusion independent triplet quenching 3−32561
  - Rhodamine 6G in ethanol, gain curve and triplet-triplet absorpt. study 3−13736
  - rhodamine 6G in ethyl alcohol, excitation by coaxial flash lamp to produce 110-J pulsed laser 3−16850
  - rhodamine 6G in water, effect of soap on fluorescent lifetime and quantum yield 3−32562
  - rhodamine 6G in water-glycerine mixture, kinetics of fluorescence, migration of donor excitation *(Russian)* 3−35693
  - rhodamine 6G solutions, calorimetric determ. of fluorescence energy yields using Ar^+ laser *(Russian)* 3−30846
  - Rhodamine 6J in ethanol soln., natural impurities effect on generation characts. *(Russian)* 3−6483
  - rhodamine 6J with noncongruent pumping, effect of thermooptical distortion on spectra *(Russian)* 3−26232
  - rhodamine dyes, two photon cross section dispersion 3−10569
  - rhodamine-6G, internal-reflection laser *(Russian)* 3−706
  - rhodamine-6G, pinched discharge pumped, divergence time dependence *(Russian)* 3−729
  - Rhodol, luminophor, stimulated emission under anthracene compound addition, energy var. 3−22902
  - single model flashlamp-pumped dye laser 3−29083
  - 1,1,4,4, tetraphenyl-butadiene, laser action 3700-5000 Å *(French)* 3−29087
  - 1,3,6,8 tetraphenyl-pyrene laser action, 3700-5000 Å *(French)* 3−29087
  - thin-film organic dye lasers, waveguide props. and pumping efficiency *(German)* 3−10543
  - tunable flashlamp pumped dye laser, lifetime meas. 3−14390
  - xanthene dyes, quenching of triplet state by polyacenes in flashlamp pumped lasers 3−730
  - HNO_3, stimulated emission, use in thermal laser freq. var. 3−2569

- **liquid lasers** continued
  - H_2O, stimulated emission, use in thermal laser freq. var. 3−2569
  - H_3PO_4, stimulated emission, use in thermal laser freq. var. 3−2569
  - H_2SO_4, stimulated emission, use in thermal laser freq. var. 3−2569
  - Na-fluorescein, luminophor, stimulated emission under anthracene compound addition energy var. 3−22902
  - Nd Q-switching, self, thermal mechanism, theory 3−22901
  - $Nd:POCl_3$, high average power, Q-switched 3−26231
  - $Nd:POCl_3:ZrCl_4$, pumping Nd:glass laser mode locked pulses, effect of freq. shift on power gain 3−13746
  - Nd-liquid column, combined with Nd:glass rod in cavity, spiking behaviour 3−22894
  - $POCl_3:AM^{3+}$ spectral properties, search for laser phenomena 3−6482

- **liquid metals**
  - *see also liquid alloys*
  - acoustic wave velocity, new meas. technique using e.m. detection 3−11688
  - alkali metal, electronic density of states calc. and comparison with free electron model 3−18054
  - alkali metal, pseudopotential form factor rel. to elec. resist. and thermoelec. power 3−21051
  - alkali metal, thermal smearing Fermi surface, angular correlation 3−30393
  - alkali metals, application of significant liquid structure theory to critical properties 3−20862
  - alkali metals, ion-ion interaction calc. 3−33441
  - alkali metals, mag. susceptibility, Green's function calc. 3−30597
  - ambipolar cond. rel. to Hall mobility temp. depend. 3−21056
  - boiling, influence of velocity on wall superheating due to turbulence in boundary layer 3−17970
  - closed circuit, conduction MHD pump, transition processes study *(Russian)* 3−20388
  - cooling power of quenching liquid, general definition *(French)* 3−15720
  - Debye-Waller correction to theoretical interference function 3−24016
  - diffusion, small fluctuation theories 3−36432
  - diffusion model soln. for inert gas transport in liquid metals during boiling expts. 3−19904
  - diffusion of hydrogen, rel. to metallurgical processes 3−4865
  - dispersed liquid metal-gas packed bed heat exchanger, heat transfer processes 3−39303
  - drops, study of liquid-gas interface at different temps. *(Russian)* 3−24260
  - electric properties including conductivity at temps. and pressures above critical, review 3−30385
  - electrical conductivity, theory *(Russian)* 3−8150
  - electrical conductivity of solid and liquid metals at selected temperatures, nomograph 3−27816
  - electrolytic deoxidation at 1600°C 3−5313
  - electron state development in disordered scattering determ. by consideration of resistivity 3−1971
  - electronic structure, short-range order effects 3−38774
  - equilibrium thermodynamic state determ. at high temps. and pressure 3−5854
  - fast breeder reactor, sodium test loop, 300 kW *(French)* 3−32936
  - flow, turbulent, axially varying heat flux effects 3−11078
  - flow control by induction MHD apparatus *(Russian)* 3−20391
  - flow measurement, using u.s. Doppler velocimeter 3−26040
  - flowing turbulently through closely spaced rod bundles, nuclear reactor applic. and heat transfer 3−11075
  - flowing turbulently through closely spaced rod bundles, uniform heat flux at inner surface 3−11076
  - Hall mobility meas. up to 1600°C and 2000 atm. in metallic liquids and vapours 3−36590
  - heat pipes, performance in mag. fields of fusion reactors 3−11092
  - impurity diamagnetism 3−38963
  - induction condenser, optimum relations *(Russian)* 3−7429
  - kinetic eqn. for electrons, elec. and heat cond., Ziman formula *(Russian)* 3−15177
  - MHD convertor working medium, thermodynamics of cycle with separation of one component liquid metal working agent ahead of generator 3−14489
  - MHD generator, hydraulic characteristics *(Russian)* 3−20389
  - molten, effective interionic pot. and props. *(Japanese)* 3−11539
  - molten, paracryst. struct. 3−4716
  - nearly-free-electron computer program calc. of form factor and electrical resistivity 3−36585
  - nucleation during solidification *(German)* 3−2700
  - optical absorpt. and Ziman theory 3−21430
  - optimized model pot. for calcs. of liquid resist. 3−36508
  - pure, liquid-vapour surface tension estimation by means of the cohesive energy *(French)* 3−27169
  - refractories, thermophysical props., Moscow State University research *(German)* 3−36579
  - supercooling, cooling rate effect on bulk samples 3−21561
  - surface tension for estimation of the solid-vapour and solid-liquid interfacial tension *(French)* 3−27170
  - thermal conductivity, cell theory, temp. depend., data correl. 3−36587
  - thermoelectric props., temp. depend., m.p.-1200K 3−24408
  - tight-binding model of electronic structure 3−38773
  - transition metals, electrical resistivity at high temp. 3−36588
  - turbulence with circular flow in magnetic field *(Russian)* 3−7415
  - u.s. velocity obs. at high temps. and pressures 3−101
  - vacuum arc melting, temp. field computation 3−24890
  - Van Hove theory application to disordered systems 3−38771
  - Ag, mass transfer from oxygen jet 3−39304
  - Al, dielectric screening and resistivity 3−5000
  - Al mag. susceptibility, Green's function calc. 3−30597
  - Al molten foil, electron diffr. short term persistence of diffuse remnants of reflections 3−38532
  - Au, thermotransport of Ag 3−24281
  - Be, electronic density of states calc. 3−38776
  - Bi, struct. microheterogeneities, kinetic viscosity, temp. depend. *(Russian)* 3−17729
  - Cd, struct. microheterogeneities, kinetic viscosity, temp. depend. *(Russian)* 3−17729
  - Cd, surface tension, temp. depend. 3−38710

liquid metals continued
Ce, spectral emissivity obs. 3 − 27126
Cs, phonon freq. and elec. resist. calcs. using optimised model potential 3 − 20828
Cs, resist. and thermoelec. power calcs. under 40 kbar pressure 3 − 36586
Cu, diffusivity of hydrogen 3 − 36433
Cu, surface tension, 1100-1500°C, temp. coeff. *(French)* 3 − 1872
Ga, diffusion of O, 750-950°C, potentiostatic electrochem. study 3 − 30278
Ga, elec. resist. to 1000°C, temp. depend. 3 − 4999
Ga, nuclear mag. relaxation and quadrupolar coupling 3 − 21338
Ga, quadrupole and Knight shift relax. of ^{71}Ge, 40-1050°C 3 − 2434
Ga embrittlement technique applic. to grain boundary precipitate exam. in Al-Fe bicrysts. 3 − 37025
Hg, embrittlement of Al, role of solute additions 3 − 34566
Hg, photoemission meas. of density of states rel. to pseudogap 3 − 34463
Hg, X-ray diffr. detn. of atomic distrib. at 15°C 3 − 7615
In, diffusion of O, 750-950°C, potentiostatic electrochem. study 3 − 30278
In, struct. microheterogeneities, kinetic viscosity, temp. depend. *(Russian)* 3 − 17729
In, surface tension, temp. depend. 3 − 38710
K, accurate resistivity and thermoelectric power calculations 3 − 8149
K, convective heat transfer, during turbulent flow 3 − 14445
K, surface tension, 70-160°C 3 − 20924
K liquid, 2-parameter Brovman potential study 3 − 2052
La, spectral emissivity obs. 3 − 27126
Na, accurate resistivity and thermoelectric power calculations 3 − 8149
Na, frequency moments and viscosities 3 − 36254
Na, Knight shift in nearly free electron approx. 3 − 8468
Na, liquid, 2-parameter Brovman potential study 3 − 2052
Na, solubility of O_2 in, general equation 3 − 14251
Na, surface tension, 100-180°C 3 − 20924
Na cooled fast breeder reactor core cooling system, abnormal changes, local effects *(French)* 3 − 32919
Ni, diffusivity of hydrogen 3 − 36433
Pb, diffusion and solubility of O_2, electrochem. obs. 3 − 27133
Pb, struct. microheterogeneities, kinetic viscosity, temp. depend. *(Russian)* 3 − 17729
Pb-Ag (0.25-2.5%), temp. depend. of internal adsorption *(Russian)* 3 − 11541
Pr, spectral emissivity obs. 3 − 27126
Rb, elec. resistivity calc. by optimized model potential method 3 − 7877
Rb, pair potential from pair correlation theory 3 − 26963
Rb neutron scatt. spectra, 4-8 Å^{-1} momentum transfer, ion mean square force determ. 3 − 11538
Sb-Cu decanning of fast breeder nuclear fuel elements *(French)* 3 − 11054
Sn, dissolution of solid Cu, alloy layer growth 3 − 21709
Sn, elec. cond. meas. apparatus, 1000-2500 K 3 − 32111
Sn, molten, soldering reactions with solid iron 3 − 37078
Sn, struct. microheterogeneities, kinetic viscosity, temp. depend. *(Russian)* 3 − 17729
Ta-Na, effect of O on compatibility 3 − 18558

liquid oscillations
see also liquid waves
artificial lake seiches, numerical soln. of Chrystal's eqn. *(Italian)* 3 − 34978
in cavity between two parallel cylinders, determ. of frequencies and combined masses *(Russian)* 3 − 29895
Couette flow, stability investigation using linear theory *(German)* 3 − 11383
Couette flow, stability investigation using nonlinear anal. 3 − 11382
current velocity vector, horizontal gradient effect, comparison with Indian and Atlantic ocean meas. *(Russian)* 3 − 21924
in cylindrical cavities, soln. of boundary problem by Bubnov-Galerkin method *(Russian)* 3 − 14486
cylindrical shell in duct filled with ideal fluid, vibrs. 3 − 3982
cylindrically confined inviscid incompressible two-component liq., inertial wave freq. spectrum 3 − 14503
dichlorethane, motion through water contaminated with surface-active agent, freq. meas. 3 − 1474
drop in viscous field 3 − 7461
elastic longitudinal pulses, vel. meas. for students 3 − 22229
elastico-viscous fluid flow in a circular tube under pressure gradients varying with time 3 − 33264
free oscillations in a stratified compressible ocean of constant depth *(Russian)* 3 − 12674
heated fluid layers, natural oscill. 3 − 26828
hydraulic mains dynamical charact. *(Russian)* 3 − 20355
hydrodynamic coeffs. for fluid oscillations in mobile cylindrical cavities, approx. calc. *(Russian)* 3 − 23765
induced mass of catamarans, effect of frequency of oscillations and depth of water 3 − 33273
irrotational vibrs. of perfect compressible liq. in elastic reservoir, variational approach *(French)* 3 − 7399
jet transverse oscillations in jet-splitter system 3 − 1334
Marangoni instability, influence of Gibbs adsorption 3 − 11435
MHD oscillatory flow along infinite flat plate with variable suction 3 − 20392
motion in cavities, delinearization *(Russian)* 3 − 10309
natural fluctuations in axisymmetric tank with surface forces *(Russian)* 3 − 14481
non-Newtonian fluids, laminar pulsed flow 3 − 33265
non-Newtonian liquids, laminar pulsed flow 3 − 33266
North Atlantic, gravit. modes of free oscill. 3 − 9261
rotating stratified fluid, containing oscillatory point source, radiation condition 3 − 36099
sloshing frequencies of incompressible inviscid fluid in half-space, eigenvalue determ. 3 − 23771
spherical particle movement in a vertically oscillating liquid 3 − 23764
supercritical flow in divergent channel 3 − 20359
surging motion between vertical pipe and reservoir 3 − 20372
viscous liquid, nonlinear oscillations analysis *(Russian)* 3 − 17537

liquid oscillations continued
He, superfluid, surface oscillations, model approach *(French)* 3 − 7983

liquid permeability *see permeability*

liquid semiconductors
ambipolar cond. rel. to Hall mobility temp. depend. 3 − 21056
chalcogenides, thermopower and cond. activation energy differences 3 − 21100
electronic melts, heat-transfer mechanisms 3 − 24299
n-hexane, carrier mobility rel. to impurities, nanosecond X-ray ionization pulses obs. 3 − 2084
melts, thermal cond. rel. to elec. cond. *(Russian)* 3 − 8181
methane, liquid, excess electron and positive charge carrier drift velocities 3 − 36609
migration mechanism and Hall effect 3 − 33902
thermodiffusion, bipolar, conductivity, Wiedemann-Franz ratio, Mott model 3 − 36600
Bi_2Te_3-Sb_2S_3, specific resist. and thermal e.m.f. meas. *(Russian)* 3 − 15192
CuGa(In)Te_2, elec. and thermal cond. meas. *(Russian)* 3 − 15191
Se, low-conductance switching effect, delay time and conductivity expiration 3 − 30526
Se, reversible switching effect above 720°C 3 − 36645
Se drift velocity, hole photogeneration, quantum efficiency *(Russian)* 3 − 8179
Tl-S melt, thermodynamic activity 3 − 9046
Tl_2Te:Te,In, liquid, thermoelec. props. rel. to compensation of impurity elements 3 − 33935

liquid-solid transformations *see solid-liquid transformations*

liquid structure
alkali metal, pseudopotential form factor rel. to elec. resist. and thermoelec. power 3 − 21051
alkali metals, application of significant liquid structure theory to critical properties 3 − 20862
alkali metals ion-ion interaction calc. 3 − 33441
alkanes, binary solutions and pure liquid, study of molecular orientation correlations by depolarized Rayleigh scattering *(French)* 3 − 8566
alloy, binary, conc. fluctuations calc. using cluster model 3 − 36255
alloy, eutectic, X-ray obs. 3 − 14675
alloy, struct. factors, long wavelength limit 3 − 30386
alloys, conc. fluctuations in conformal solns. and partial struct. factors 3 − 30063
Ashcroft-Leckner hard sphere model generalisation for structure factor 3 − 26960
benzene, binary solutions and pure liquid, study of molecular orientation correlations by depolarized Rayleigh scattering *(French)* 3 − 8566
cavity radius calc., effect of translatory mol. motion 3 − 1561
chloroform, mol. motions, dielec. relax. and far i.r. dispersion 3 − 21398
chloroform, press. depend. of reorientational correl. function, Raman spectra 3 − 21400
correlation function from coherent properties of light scattered from density fluctuations 3 − 20685
cyclohexane, packing, rel. to hypersound velocity *(Russian)* 3 − 14937
density fluctuations in simple liquid generalized hydrodynamic approach 3 − 7611
distribution function using first-order perturbation theory 3 − 7612
effective pair pots., density depend. 3 − 1560
ethanol, stimulated Raman scatt., decay route of methyl vibrs. 3 − 8577
factor, assessing accuracy of data 3 − 1562
fluorocarbon, acoustic velocity obs. 3 − 1697
glassy crystalline state 3 − 14692
glycerin, structural relaxation of shear and bulk viscosity meas. *(Russian)* 3 − 4870
halobenzenes, Significant Structure Theory giving Helmholtz free energy 3 − 11540
Henderson's partition function, compressibility and heat capacity computation 3 − 30268
n-heptane, packing, rel., to hypersound velocity *(Russian)* 3 − 14937
n-hexane, packing, rel. to hypersound velocity *(Russian)* 3 − 14937
incoherent neutron scatt. for large momentum transfer quantum effects and appl. 3 − 14671
latex particles, order-disorder theory of fusing *(Japanese)* 3 − 27104
Lennard-Jones (6,12) pair potential parameters, determ. from equations of state of liquids 3 − 1565
Lennard-Jones liquid near triple point, computer expt. on 864 particles 3 − 38657
metal, molten, effective interionic pot. calc. *(Japanese)* 3 − 11539
metal, molten, paracryst. struct. 3 − 4716
methylamines, mol. reorientation mechanisms, n.m.r. obs. 3 − 18386
molecular, use of method of ideal peaks 3 − 33439
n-octane, packing, rel. to hypersound velocity *(Russian)* 3 − 14937
review 3 − 7609
Rochelle salt aqueous soln., struct. determ., rel. to conc. 3 − 14674
saturated liquid properties from Mie (n,6) potential and Barker-Henderson perturbation theory 3 − 4715
silicas, molten, X-ray obs. 3 − 14677
solutions, diffusion and solvation 3 − 36253
system with repulsive pair potential, melting-curve maximum 3 − 24248
toluene, protonated and deuterated, mol. motion, ^{13}C, ^{2}D relaxation times 3 − 36815
trichlorofluoromethane, rot. diffusion, nucl. relax. data interpret. 3 − 30274
water, bulk and film, struct., X-ray diffr. obs. 3 − 14673
water, effect of dissolved $NaNO_3$ and KNO_3, u.s. velocity meas. 3 − 38621
water, Monte Carlo calculations 3 − 33685
water, rot. correl. motion from i.r. spectral study 3 − 17730
water, scaled particle quasilattice model 3 − 36256
water, X-ray diffr. and interstitial model, radial distrib. function 3 − 20686
water structural model based on intermolecular potential function 3 − 30062

liquid structure continued
Al molten foil, electron diffr. short term persistence of diffuse remnants of reflections 3 − 38532
Al_2O_3, molten alumina, radial distrib. function anal. at 2200°C 3 − 26962
Ar, classical liquids, self motion response function and incoherent scattering function 3 − 11537
Ar, Monte Carlo calc. 3 − 38650
Ar, pair pot. from neutron diffr. at low density 3 − 7614
Ar, rel. to density fluctuations 3 − 24172
Ar, triplet correlations 3 − 14670
Bi, struct. microheterogeneities, kinetic viscosity, temp. depend. *(Russian)* 3 − 17729
Cd, struct. microheterogeneities, kinetic viscosity, temp. depend. *(Russian)* 3 − 17729
Cl_2, liquid, ^{35}Cl nuclear spin lattice relaxation times meas., molecular reorientation, hydrodynamic and cell models 3 − 24626
Cu-Sb alloy, liq., struct. from combined neutron and X-ray diffr. 3 − 14676
D_2O, density effects on dynamic struct., spin-lattice relax. obs. 3 − 1566
Ga, structure factor data accuracy evaluation 3 − 1562
Ga, supercooled, elastic and inelastic neutron scattering obs. 3 − 20687
$Ge_{0.175}Te_{0.825}$, struct. of amorphous and liq. state from neutron scatt. 3 − 33456
H, coherent neutron scattering, collective excitation 3 − 26964
HDO, i.r. study and OD stretching vibr. meas. 3 − 29672
HDO in water-nonelectrolyte mixtures, micro-heterogeneous structure from i.r. data 3 − 8568
H_2O, coherent neutron scattering 3 − 1651
H_2O-D_2O mixture, coherent neutron scattering 3 − 1651
^3He, structure factor meas. 3 − 33713
Hg, X-ray diffr. detn. of atomic distrib. at 15°C 3 − 7615
Hg:Tl, amalgams thermodynamic functions, enthalpies of formation 257-583K *(French)* 3 − 33442
In, struct. microheterogeneities, kinetic viscosity, temp. depend. *(Russian)* 3 − 17729
In-Tl liquid alloys, structure and electrical conductivity *(Russian)* 3 − 33443
LiCl aq. soln., struct. and mol. orientation, neutron and X-ray diffr. obs. 3 − 14672
Na, pressure dependence of structure, calc. of pair potentials using Born-Green eqn. *(Japanese)* 3 − 17728
Na-Ar two-phase flow in vertical channel, void fractions and heat transfer coefficients 3 − 1434
Ne, neutron scattering theory 3 − 30064
Ne, pressure dependence of structure calc. of pair potentials using Born-Green eqn. *(Japanese)* 3 − 17728
Ne, structure factor data accuracy evaluation 3 − 1562
Pb, struct. microheterogeneities, kinetic viscosity, temp. depend. *(Russian)* 3 − 17729
Pb-Ag (0.25-2.5%) alloy, temp. depend. of internal adsorption *(Russian)* 3 − 11541
Rb liquid, pair potential from pair correlation function 3 − 26963
Rb neutron scatt. spectra, 4-8 $Å^{-1}$ momentum transfer, ion mean square force determ. 3 − 11538
Rb systems of 250 and 686 atoms, molecular-dynamics calcs. near melting temperature, liquid structure study *(German)* 3 − 4849
Se, atomic struct. 3 − 17732
Sn, struct. microheterogeneities, kinetic viscosity, temp. depend. *(Russian)* 3 − 17729
Sn-Pb system, conc. depend. of pseudopots., atom scatt. cross section, electrotransport *(Russian)* 3 − 30277
Tl:Hg, amalgams thermodynamic functions, enthalpies of formation 257-583K *(French)* 3 − 33442

liquid surface waves
see also oceanography
acoustic wave scattering, capacitive wavestaff for water surface wave measurements 3 − 2966
agitation of liq. system in strong external elec. fields, instability condition 3 − 20362
air-liquid flow, roll waves entrainment 3 − 33263
Antarctic waters, surface dynamic topography showing sea surface slopes and Rossby waves 3 − 15943
causing oil slick movement 3 − 9247
de Saint Venant's eqn. for free surface flow, limits of integration 3 − 33230
diffraction in harbour, SOGREAH method *(Polish)* 3 − 25199
EHO surface waves in conducting fluid, propagation 3 − 38399
e.m. wave scattering, integral equation determination by numerical methods 3 − 32503
energy loss in spectra due to data windowing 3 − 2938
excitation, nonlinear, by moveable charged electrode, anal. 3 − 33262
flow separation at free surface 3 − 20358
gravity wave and capillary wave interactions, effect of surface tension, appl. to oceanography *(Russian)* 3 − 27978
gravity-capillary nonlinear waves in slowly varying current, propag. 3 − 29893
harmonic generation of shallow water waves over topography 3 − 9243
horizontal forces due to waves acting on large vertical cylinders in deep water 3 − 23768
inertia-inertia waves in variable depth fluid 3 − 11438
instantaneous velocities of characteristic waves of water medium under wind air stream action *(Russian)* 3 − 12673
laser velocimeter 3-dimensional, for studying gravity waves in shallow water, design consideration 3 − 22377
motion of rigid body, Greens functions *(Polish)* 3 − 23766
ocean, survey expts. on boat in coastal waters 3 − 2958
ocean wave and tide recording system using cosmic rays 3 − 16074
oceanic turbulence generated by surface waves *(Russian)* 3 − 34869
phase speed, ocean circulation 3 − 9244
scattering of light, viscous liquid, heterodyne spectroscopy, very l.f., spectral width measurement 3 − 26826
sea wind waves interaction with long period waves *(Russian)* 3 − 2947
shallow water, long, large amplitude, interaction with ambient shear flow 3 − 7404
shallow water, nonlinear interactions 3 − 4596

liquid surface waves continued
shallow water plane ripple problem *(French)* 3 − 7400
short wavelength, generation, Miles mechanism 3 − 29894
solitary waves interactions in nonlinear systems, perturbation analysis 3 − 28839
standing waves, normal mode analysers 3 − 22568
stationary waves, Lagrangian descriptions *(Russian)* 3 − 1422
steady shape and finite amplitude waves on surface of infinitely deep liquid 3 − 17542
three-dimensional radiation from cylinder, perturbation method 3 − 14484
time periodic, radiation and scattering by partially immersed objects 3 − 4601
tsunami type waves, deformation in basin of continuously varying depth *(Russian)* 3 − 2946
water, acoustically driven, in reson. tube 3 − 23762
wind, statistical characteristics, Gulf of Gdansk and Baltic Sea *(Polish)* 3 − 25200
wind induced ripple on water surface, laser detecting instrument 3 − 37261
wind-generated waves, intermittency effect in the equilibrium range *(Russian)* 3 − 12676
He, superfluid, light scatt. by thermal surface waves, 1.29-2.14 K 3 − 7984

liquid theory
see also equations of state of liquids
alcohol, ultrasonic absorpt, depend. on pressure, effect of hole volume 3 − 11691
binary liquid mixtures close to Lennard-Jones soln., average potential parameter 3 − 26961
binary-liquid phase transition, decoupled-mode theory of critical diffusion and viscosity 3 − 4843
Bloch equations, with diffusional terms for rotatory motion *(Russian)* 3 − 26959
computer simulation studies of liquid state 3 − 26958
conference, Dutch Physical Society, Amsterdam (Feb. 1973) 3 − 28428
critical point, long-range three-particle correlations 3 − 22794
density fluctuations in simple liquid generalized hydrodynamic approach 3 − 7611
diatomic homonuclear liquids molecular-dynamic simulation 3 − 30061
equilibrium model treatment of liquid mixtures *(German)* 3 − 12498
extended M- and J-diffusion model for symmetric top mols. in liqs. 3 − 7610
fluctuon production in solns. *(Russian)* 3 − 33440
Henderson's partition function, compressibility and heat capacity computation 3 − 30268
hexane, ultrasonic absorpt. and viscosity, press depend., hole theory 3 − 11692
intermolecular forces, role in determ. of struct. and thermodynamic props. *(Dutch)* 3 − 30060
Lennard-Jones fluid, calc. of triplet correlation function by Monte Carlo method 3 − 4025
molecular reorientation in liquids, exptl. angular correlation functions 3 − 33437
organic liquid, ^{14}N nuclear mag. relaxation near critical soln. temp. 3 − 30706
orientational relax., unified theory 3 − 1563
polar, Boltzmann factor for interacting pair of mols., partition function 3 − 1564
radial distrib. function and thermodynamic props., quantum corrections 3 − 16775
self motion in classical liquids 3 − 30059
solutions, average-pot.-model theory, statistical mech. interpretation 3 − 38531
statistical mechanical distrib. functions of molecular fluid interacting with solid boundary 3 − 4024
theories, review 3 − 33438
thermodynamic properties using perturbation theory 3 − 1807
toluene, ultrasonic absorpt. and viscosity, press. depend., hole theory 3 − 11692
transport properties, test of Davis-Rice-Sengers square-well theory using Yvon-Born-Green pair correlation functions 3 − 4862
Ar, classical liquids, self motion response function and incoherent scattering function 3 − 11537
Ar transport properties, test of Davis-Rice-Sengers square-well theory using Yvon-Born-Green pair correlation functions 3 − 4862
Na, atomic dynamics at high freq. for determ. of scatt. and spectral functions 3 − 17731
Na, frequency moments and viscosities 3 − 36254
Ne, neutron scattering theory 3 − 30064

liquid-vapour transformations
see also condensation; liquefaction of gases; vaporisation
alkali metals, application of significant liquid structure theory 3 − 20862
Bose liquid, calc. of thermodynamical functions 3 − 36448
Bose liquid, determ. of excitation energy and Landau f-functions 3 − 15040
condensed Bose liquid, scaling laws and critical exponents 3 − 36449
droplet model and metastable states 3 − 17969
electron mobility in simple fluid near critical point 3 − 21044
equilibrium study at high pressures, apparatus *(Russian)* 3 − 9906
ethanol-carbon tetrachloride-benzene, equilib. data and heats of mixing 3 − 24251
ethanol-n heptane-n pentanol, equilib. data and heats of mixing 3 − 24251
fluid without hole particle symmetry, critical-point thermodynamics 3 − 16773
fluids and fluid mixtures, prediction of thermodynamic props., applications 3 − 34699
fluids and fluid mixtures, thermodynamic props., critical and azeotropic states 3 − 34700
n- hexane, superheated absolute thermodynamic stability in perturbing elec. field, nucleation induction 3 − 20866
lattice-gas model with particle-hole symm. and singular coexistence-curve dias. 3 − 13652
Lebowitz-Penrose limit, determ. from superstability of interaction potential 3 − 16771

- **liquid-vapour transformations** continued
  - liquid metal drops, study of liquid-gas interface at different temps. *(Russian)* 3—24260
  - model fluids, crit. points in less than two dimens. 3—28992
  - non-ideal solns., equilib. data and heats of mixing, determ. from Wilson's eqn. 3—24251
  - power law for the correlation length close to the gas-liquid critical point 3—16777
  - saturation line, calcs. of derivs. of thermal and caloric quantities 3—36412
  - tricritical points, critical exponents notation 3—13664
  - Wilson parameters, binary systems, non-linear regression 3—37115
  - $BiCl_3$ molten salts, supercritical temp. range, continuous density transition, electrical conductance, experimental 3—11728
  - Hg, determ. of transport coeffs. in linear irreversible thermodynamic rate equations 3—11729
  - N_2-Ar-O_2 equilibria, equation of state 3—30249
  - Ne, meas. of viscosity along liquid-vapour saturation line under pressure 3—24263
  - SF_6 spectrum and intensity of scattered light along coexistence wave 3—30245
  - Xe, spectral linewidth of quasi-elastically scattered light along coexistence curve 3—30246
  - Xe ultrasonic attenuation and disperson near critical point, meas. using pulsed acoustic interferometer 3—4852
- **liquid waves**
  - *see also liquid surface waves*
  - Adriatic sea, computer simulation, forecasting of floods in Venice 3—27975
  - capillary waves, optical method of detecton *(Russian)* 3—22575
  - continental slope of ocean, array meas. of internal wave field 3—27976
  - convection, natural, in shallow pools, free-surface deformations 3—26792
  - cylindrical shell in duct filled with ideal fluid, vibrs. 3—3982
  - cylindrically confined inviscid incompressible two-component liq., inertial wave freq. spectrum 3—14503
  - deep sea monochromatic waves rel. to turbulent layer thickness *(Russian)* 3—39492
  - gas/liquid stream, wave characts. of interphase boundary 3—20399
  - Kelvin wave diffr. by changes in depth 3—25195
  - Kelvin-Helmholtz wave growth on thin liquid sheets 3—29892
  - long waves generated by wavemakers in non-linear dispersive systems, mathematical model 3—20366
  - MHD Rossby waves excited by travelling forcing effects 3—23774
  - nonlinear, slightly unstable systems 3—36125
  - oceanic, short period, time-dep. spectra anal. *(Russian)* 3—21923
  - oceanic internal wave characts., laws of probability distribs. *(Russian)* 3—39496
  - oceanic internal wave characts. for given Vaisala freq. profile *(Russian)* 3—39499
  - oceanic internal waves and meso-scale turbulence, comparison using temp. flucutation data *(Russian)* 3—34868
  - oceanic mixing by internal wave shearing 3—34856
  - Poincare wave scatt. by irregular coastline 3—20357
  - propagation in viscous compressible liquids, dispersion reln. soln. using method of eigenvalleys 3—23760
  - reflected, lateral and surface waves, acoustic propagation in a semi-infinite liquid 3—3689
  - rotating deep annulus convection, thermal fields in high amplitude wave regime 3—26802
  - rotating stratified fluid, with laterally varying random inhomogeneities, propagation and stability 3—17544
  - seawater, mag. field variation induced by shallow waves *(Russian)* 3—2920
  - small amplitude, generation by obstacle on bottom of running stream 3—20356
  - solitary irrot. wave motion considering surface tension 3—26827
  - solitary wave moving into deeper water, development 3—11437
  - thermal shear, light scattering spectra 3—30821
  - transmission of water waves through small apertures, integral equation formulation 3—7402
  - turbulence intermittency, turbulent and wave phenomena coupling 3—33216
  - viscous thin layers, gas stream effect on wave flow 3—20363
  - water wave diffraction, theory 3—20811
  - water wave force on infinitely long cylinder in oblique sea 3—23761
  - water wave in unbounded region bounded internally by circular cylinder, determ. of Green's function 3—20354
  - H_2O with surface-active contamination, influence on initiation of wind waves 3—11436
- **liquids**
  - *see also liquid structure; liquid theory; solutions*
  - absorbance standards for u.v. and visible spectrophotometry 3—25647
  - absorption coefficient measurement, photomixing obs. with He-Ne laser 3—32059
  - boiling dielectric fluids, electrostatic fields, heat transfer, ponderomotive forces 3—1801
  - complex permittivity measurement, coaxial line cell, design and construction 3—3832
  - compressible, expansion of spherical cavity 3—4603
  - cream, interrelationship of optical coeffs. *(Russian)* 3—2504
  - cryogenic, level indicator design *(French)* 3—22297
  - electron self-trapped states, conduction band free-electron-like states 3—38772
  - high pressure liquid separator 3—6162
  - latex, interrelationship of optical coeffs. *(Russian)* 3—2504
  - milk, interrelationship of optical coeffs. *(Russian)* 3—2504
  - Newtonian liquid drops falling through viscoelastic liquid, tailing phenomena 3—1441
  - n.m.r., collective nature of heat motion and magnetic relaxation *(Russian)* 3—30720
  - polar, dielectric relaxation 3—5158
  - quantitative meas. of amount of water in liquids by far i.r. spectroscopy *(Russian)* 3—28788
  - Raman spectra, devices for low temp. and high pressure study *(German)* 3—28547
  - Raman spectra, second-order, intensities of combination frequency lines *(Russian)* 3—8574
- **liquids** continued
  - Raman spectra line intensity, influence of internal field effect *(German)* 3—2553
  - spread on surface, in zero gravity *(Russian)* 3—11799
  - surface stability in electric field 3—4607
  - temperature and vapour pressure relns. 3—33651
  - tensile strength, review 3—24173
  - ternary mixtures, u.s. study, free volume 3—7853
  - thermodynamic significance of internal pressure and its role in transport processes 3—18782
  - two-liquid systems with asymmetric stress tensors, model construction *(Russian)* 3—28853
  - u.s. absorption meas., reverberation techniques 3—16389
  - vibrational acoustic relaxation in polyatomic liquids, molecular excitation and deactivation *(Russian)* 3—4477
  - Ar, non-linearity parameter, temp. depend. 3—4857
- **literature reviews** *see reviews*
- **lithium**
  - adsorption of Li on W(112) face 3—20938
  - atom, 2s wavefunction calc. by Messmer method 3—7029
  - atom, ^2S ground state, natural spin orbitals and geminals 3—7030
  - atom, and isoelectronic series, valence electrons, descriptive function *(French)* 3—29468
  - atom, electron excitation cross sections using Born approx. 3—1122
  - atom, Fermi-contact h.f.s., MC SCF wavefunctions 3—33010
  - atom, Gaussian-based model pots. and Gaussian basis functions for valence electron studies 3—1095
  - atom, ground state, reduced density matrix and ionisation pot. from Green's function theory 3—26560
  - atom, h.f.s. of 2^2P, 3^2P and 4^2P states, SCF and HF calcs. 3—33007
  - atom, I and II doubly excited states, transitions, 100 to 2000 Å, classification 3—29481
  - atom, multiconfig. Hartree-Fock method 3—23457
  - atom, two-photon ioniz. with polarized photons 3—20031
  - atomic beams for plasma heating in closed mag. traps *(Russian)* 3—1510
  - atomic Stark shift in low elec. field 3—11127
  - atoms, beyond the ionisation threshold, excitation functions 3—17373
  - Auger spectra, high energy satellites 3—18519
  - Auger spectra 3—36969
  - Canadian granitoid rocks, Li distrib. 3—37149
  - clusters, symmetric group and method of diatomics 3—33168
  - collision reactions with alkali halide molecular beams, beam kinetics 3—25058
  - Compton profile compared with RPA approx. for conduction electron interactions 3—20762
  - diamagnetic susceptibility 3—34096
  - diamond:Li, implanted, elec. cond., after annealing at 1400°C *(Russian)* 3—2070
  - diffusion, in Ge, drift velocity, depth of drift, electric field configuration 3—33697
  - elastic constants, second and third order, calc. 3—27050
  - exchange core polarisation in transferred hyperfine interaction of Li^+ with O^-, model calc. 3—21013
  - film and bulk, struct. model for abnormal optical props. verification *(French)* 3—30365
  - Hartree-Fock polarisabilities calc. 3—29486
  - inner-shell ionization energies and ESCA shifts 3—4372
  - ion source, Blewett-Jones type, design and props. 3—10038
  - ions, ^2S and ^2P states, natural anal. 3—29473
  - ions in $ZnWO_4$, interaction with Cr^{3+} e.p.r. centres 3—2379
  - isoelectronic sequence, spin density of ns^2S states 3—32999
  - Knight shift, press. effect, calc. by KKR method 3—36806
  - liquid, electronic density of states calc. differs from free electron model 3—18054
  - phonon damping due to electron-phonon coupling, calcs. 3—38638
  - phonon dispersion curves calc. using Hartree-Fock and pseudopotential methods 3—11704
  - phonon frequencies, lcal model pseudopotential calc. 3—1734
  - phonon propagation, atomic wavefunction, Slater exchange 3—30219
  - plasma, exploded Li wire, obs. of core by laser light reflection 3—23910
  - plasma, high-current discharge struct. 3—33404
  - plasma, spectral line broadening *(Russian)* 3—30015
  - polarized particle beams, current state of physics and technology for prodn. 3—35727
  - pressure shift and broadening of resonance lines in hot compressed Ar and He 3—33033
  - quasi-elastic scattering cross sections in tissue like media 3—3593
  - radial, bounds for energies 3—10357
  - self-diffusion in lithium ammonia solutions, n.m.r. meas. 3—20883
  - soft X-ray absorpt. edges calcs. 3—30895
  - spherical particles, cond. electron spin echo 3—2396
  - Stark effect in hyperfine struct. 3—14293
  - steel corrosion *(Russian)* 3—12377
  - TSEE activator in BeO, dosimeter characteristics 3—28671
  - upper atmosphere vapour trails in morning twilight, wave structure and turbulence rel. to high shear region 3—34921
  - vacancy diffusion, activation energy proportional to latent heat of melting *(Russian)* 3—24295
  - vapour trail photography for upper atm. wind meas. 3—18876
  - AgBr(Cl):Li, absorpt. bands due to impurity localised modes 3—30850
  - atom, ^2S state, natural orbital config. interaction expansions 3—26561
  - CdS doping, effect on low temp. photoluminescent props. of single crystals *(Japanese)* 3—8656
  - CdS:Li, furnace doping, rel. to bound exciton spectra 3—12184
  - GaP:Li, Zn, bonding of excitons by neutral donors and acceptors *(Russian)* 3—36932
  - Ge, Li diffusion into at low temps., technique 3—11645
  - p-Ge:Ga, gamma irrad., role of Li in annealing processes 3—33844
  - Ge-Si:Ga,Li, temp. depend. of Li solubility *(Russian)* 3—14974
  - Ge(Li) detector, coaxial, in γ-ray camera for diagnostics 3—402
  - KCl:Li, cond. electron scatt. by tunnelling states of defects 3—33920
  - KCl:Li, X-irrad., F-centre accumulation kinetics 3—2576
  - KCl:Li^+, structure of potential wells responsible for nonequidistant spectrum 3—34392

lithium continued
- KCl:Li$^+$(Na$^+$), image recording on F$_a$ centres 3−32082
- Li II (III), lifetimes of excited states by beam-foil technique 3−1109
- Li:Na(Ag), isotope effect comparison for ^{22}Na, ^{24}Na(^{105}Ag, ^{110m}Ag) diffusion 3−38688
- Li/ND$_3$ solutions of metallic conductivity, electrical explosion, obs. of neutron emission 3−38483
- Li-He, (Ne), collision-induced absorpt., model pot. calcs. at 300 and 1000 K 3−38230
- Li-inert gas systems, absolute total scatt. cross sections, pot. parameters 3−1127
- Li-like ions, energy levels in solar and laboratory X-ray satellite spectra 3−23475
- Li-ND$_3$ solns., velocity of 10 MHz compressional waves, metal conc. and temp. depend. 3−1695
- Li + F$_2$→LiF + F, pot. energy surfaces calc. 3−23637
- Li + H$_2$→LiH + H collinear exchange reactions, analytical energy surfaces 3−20205
- Li$^+$, 1^{1}S ground state, expectation values, lower bounds 3−29457
- Li$^+$, electron impact, double ioniz. cross sections 3−20045
- Li$^+$, electron impact double ionisation, classical collision theory appl. 3−38234
- Li$^+$, in KCl, ion-lattice relax. and nuclear spin-lattice relax. 3−36817
- Li$^+$, in KCl, paraelectric resonance lineshape, rel. to theory 3−27460
- Li$^+$, scatt. on H$_2$, vibr. quantum transitions, differential cross sections meas. 3−14396
- Li$^+$, singly ionized by electron impact, lifetime and polarization of 2 ^{3}P term 3−29499
- Li$^+$ Coulomb holes and expectation values, explicitly correlated wave functions 3−23464
- Li$^+$ in KCl, paraelec. reson., relax. behaviour at high dipole conc. 3−2492
- Li$^+$ interaction with amides 3−11239
- Li$^+$ ion bombardment of coated metal surfaces, probability distributions of emitted electrons *(German)* 3−27591
- Li$^+$ scattering by He, inelastic transition mechanism 3−20061
- Li$^+$ scattering in the weakly screened Coulomb field of Au nuclei 3−11182
- Li$^+$-Li$^+$, K$^+$-Li$^+$, repulsive potential calc. from particle beam scattering data 3−33062
- Li$^+$ + He collisions, charge exchange, rot. coupling 3−20059
- Li$_2$ mol., loge localization analysis 3−11210
- Li$_2$ molecule, spectra, A-X band system, molecular consts. *(Spanish)* 3−17436
- Li$_2{}^+$, Gaussian-based model pots. and Gaussian basis functions for valence electron studies 3−1144
- Li$_2{}^+$, Hartree-Fock potential energy curves, spectroscopic consts., 1-electron props. for lowest $^2\Sigma_g{}^+$ and $^2\Pi_u$ states 3−29642
- LiI isoelectronic sequences, energy levels and spectra meas. 3−17369
- ^{6}Li, ^{7}Li isotope exchange reactions in quadruple cell, thermodynamic props. 3−9074
- ^{7}Li, ion beam, diffraction at atoms rel. to scatt. undulations 3−14314
- ^{7}Li cosmic ray deexcitation prod. γ-ray line feature towards Galactic centre 3−28110
- ^{7}Li(d, n) target design, neutron teletherapy 3−13149
- ^{6,7}Li II, 1snp ^{3}P terms, hyperfine struct. 3−38222
- Li$^+$(1s^2), ionisation by H impact 3−20063
- MnF$_2$:Li, cryst. growth, modified Bridgman method 3−12273
- NaF:Li$^+$, e.s.r. study of F$_3{}^{2-}$ molecule ion with Li impurity forming di-interstitial centre 3−2390
- Nb, corrosion in liq. Li, effect of O$_2$ addition at 600°C 3−26533
- NiO:Li electrode, potential distrib. between space charge region and electrolyte Helmholtz layer 3−31268
- Si:Li, photoemission meas. for Li adsorption and segregation to surface 3−24297
- Si(Li), p-i-n, detector, voltage capacity charact. *(Russian)* 3−22465
- Ta, corrosion in liq. Li, effect of O$_2$ addition at 600°C 3−26533
- YAG:Nd, Li, laser crystal, absorpt. and luminesc. props. with doping 3−19617
- ZnO:Li, thermolum., 4.2-300K, trapping and recomb. processes 3−15566

lithium alloys
- *see also lithium compounds*
- Ag-Li, internal oxidation study 3−21712
- Al-Cu-Li, resist. obs. of Al$_2$CuLi precip. 3−21660
- Al-Cu-Li, T$_1$(Al$_2$CuLi) precip. 3−8798
- Al-Li, decomp. of solid soln., resist. obs. 3−21606
- Li-Mg, ordering behaviour of f.c.c. and b.c.c. phases 3−11585
- Li-Mg optical properties, band structure, Fermi surface, optical and soft X-ray spectra, ellipsometry 3−30836
- Li$_x$Na$_{1-x}$, liquid, phase separation theory 3−39322

lithium compounds
- *see also lithium alloys*
- crystal chem. of Li in octahedrally coord. structures, K$_x$Li$_x$Ti$_{4-x/2}$O$_8$ near structure type 3−38573
- disilicate glass, space-charge limited current 3−8173
- dosimetry, irrad. with low energy X-rays and γ-rays 3−28391
- formate monohydrate, p.m.r. study 3−27425
- halides, soft X-ray absorpt., polaron effects 3−5239
- i.r. spectrum, linear structure and force constants 3−7188
- LiF dosimeter, thermoluminescent, mailed, obs. of absorbed dose rel. to dose distrib. of X-rays 3−405
- LiH, (100) surface, ab initio Gaussian orbital calc. 3−11943
- LiNbO$_3$ optical phonon modes assignment 3−8582
- lithium acetate dihydrate, single crystals, proton magnetic resonance study, crystal structure 3−7728
- lithium ammonia solutions, n.m.r. meas. of self diffusion 3−20883
- lithium ammonium tartrate monohydrate, crystal structure, solution using symbolic addition method, three dimensional X-ray intensity data 3−7729
- lithium formate monohydrate, crystal structure obs. 3−38579
- TCNQ salt, Li$^+$TCNQ$^-$, paramag. spin susceptibility meas., symmetry-split band theory 3−34084
- LaLiNb$_4$O$_{12}$, cryst. growth from melt, and characterization 3−12268
- La$_3$Li$_3$Nb$_8$Zr$_2$O$_{30}$, cryst. growth from melt, and characterization 3−12268

lithium compounds continued
- Li-Cr ferrite film, LPE growth on MgO, Mossbauer obs. of substrate contamination 3−1928
- Li-ferrite, magnetostriction constants meas. in ordered and disordered states by ferrimag. reson. 3−8406
- Li-S system, phase diagram determ. using vapour transport technique 3−7902
- Li-S system, phase diagram determ. 3−7903
- Li-Te system, phase diag. 3−38659
- LiAlGeO$_4$ phase transformations, zones, PT diagram, high pressures and temps. 3−12607
- LiAlSiO$_4$, β-eucryptite, average struct. 3−7717
- LiAlSiO$_4$, β-eucryptite, superstruct. 3−7718
- α-LiAlSi$_2$O$_6$:Mn^{2+}, single crystal, polarised cathodoluminescence emission 3−39194
- LiBO$_2$, monoclinic characterisation *(French)* 3−14818
- Li$_2$B$_4$O$_7$:Mn thermoluminescent dosimeter, response to β-rays 0.43-3.54 MeV and γ-rays 8 keV-1.25 MeV 3−311
- Li$_6$B$_4$O$_9$ characterisation *(French)* 3−14818
- LiBaF$_3$, growth by Czochralski and Bridgman methods, doped and pure, absorpt. spectra *(German)* 3−2661
- LiBr, pressure and temp. depend. of elastic constants 3−24175
- LiBr concentrated water solution, n.m.r. study of relaxation times and structural transitions *(Russian)* 3−12517
- LiCN, electronic struct., polytopic bond study 3−29594
- LiCl, Born-Oppenheimer approx., equilib. bond length calc. 3−33085
- LiCl, effect on crystallization of amorphous silica powder 3−18740
- LiCl, pressure and temp. depend. of elastic constants 3−24175
- LiCl aq. soln., struct. and mol. orientation, neutron and X-ray diffr. obs. 3−14672
- LiCl conc. effect, Ti-butylalcohol suspension, particle interaction, frequency effect of elec. field 3−39403
- LiCl concentrated water solution, n.m.r. study of relaxation times and structural transitions *(Russian)* 3−12517
- LiCl solution in Appalachian petroleum reservoir rocks, ^{1}H n.m.r. relaxation 3−34824
- LiCl:Ni^{2+}, visible and near i.r. absorption spectra, bands of d-d transition 3−2570
- LiCl-AlCl$_3$ melt, Raman spectra study of influence of species formation on stability 3−36868
- LiCl(Br):SCN$^-$ aqueous solutions, Raman spectra *(Russian)* 3−15498
- LiClO$_3$:LiNO$_3$, Raman spectra, cooperative effect of internal modes 3−18442
- LiCl.H$_2$O, cryst. struct. *(German)* 3−7672
- Li$_4$CoO$_4$, new oxocobaltate (IV), crystal structure determ. *(German)* 3−36287
- LiCuCl$_3$.2H$_2$O, magnetic transition rounding and Pippard's relations 3−30619
- LiD, second order Raman spectrum, phonon modes *(French)* 3−39136
- LiD, study of second-order Raman and phonon spectra 3−2546
- LiF, Adams-Gilbert local orbitals equations, choice of localising potentials 3−36537
- LiF, annealing kinetics of radiation defects 3−4757
- LiF, blocking effect observation by (n,t) reaction 3−37684
- LiF, cold-worked, recovery of u.s. props. during annealing, dislocation behaviour 3−11624
- LiF, coupling of two nuclear Zeeman reservoirs by electronic spin spin reservoir 3−30716
- LiF, Debye temp. calc. from elastic moduli 3−36394
- LiF, dipole-dipole interactions role in acoustic saturation of n.m.r. 3−2423
- LiF, dislocation density rel. to thermal treatment *(French)* 3−36306
- LiF, elastically stressed, dislocation density rel. to u.s. vibrs. 3−20752
- LiF, electromechanical effect 3−34298
- LiF, electromechanical props., effect of light *(Russian)* 3−7850
- LiF, electron excitations resulting from photoionisation *(Russian)* 3−8611
- LiF, F-centres, γ-ray prod., effect of dose, dose rate, temp., impurities, sample deform. 3−11620
- LiF, generation of harmonics of transverse elastic waves 3−33962
- LiF, integrated intensities of Laue and Bragg reflections, extinction and structure factor determ. 3−23955
- LiF, interaction between dislocations and thermal phonons 3−1745
- LiF, interionic potentials, force const. models 3−26987
- LiF, LEED intensity profile for (100) surface, and bulk energy bands, calc. 3−36466
- LiF, photoelectron spectra and zone structure 3−34464
- LiF, pure and Mg doped, steady state deform. dislocation struct., etch pit studies 3−36322
- LiF, role of entropy in thermally activated deformation 3−7822
- LiF, Schottky defects, formation energy, effect of short-range three-body potential 3−27021
- LiF, self-consistent energy bands 3−21010
- LiF, slip band dislocation struct., influence of dislocation forest *(Russian)* 3−7770
- LiF, small crystals, i.r. absorpt. rel. to particle size, mode absorpt. bands 3−39150
- LiF, solid, He atom elastic scatt., theoretical study 3−34445
- LiF, static dielec. consts., press. and temp. depend., 15-295 K 3−39078
- LiF, strength of small-angle boundaries, influence of space charge 3−36325
- LiF, surface Debye temp., H atom beam scatt. obs. 3−8010
- LiF, surface faults, painting with Au *(French)* 3−15074
- LiF, thermal conductivity in the boundary scattering region 3−1723
- LiF, thermal etching and effect on atomic beam scatt. 3−1900
- LiF, thermal neutron irrad., lattice expansion, X-ray diffr. study 3−4774
- LiF, thermionic emission from electron traps 3−30919
- LiF, thermolum. response of rad. of X-rays and γ-rays 3−28392
- LiF, thin films. thermal conductivity and Poiseuille flow of phonons 3−1722
- LiF, X-ray technique for crystallography obs. behind shock wave front 3−26930
- LiF, yield stress minima and apparent isoelectric temp. relationship 3−20792

lithium compounds continued
LiF, zero-phonon lines in M-band region of irrad. crystal 3−1622
LiF ceramic, optical quality, production by method of explosive compression of powdered inorganic compounds *(Russian)* 3−12434
LiF crystal, creep deform. and dislocation structure of pure and Mg-doped crystal 3−17846
LiF detector, relative energy efficiency 3−28661
LiF dosimeter, thermoluminescent, response to β-rays 0.43-3.54 and γ-rays 8 keV to 1.25 MeV 3−311
LiF dosimetry, use in meas. of build-up effect of ^{60}Co gamma radiation *(German)* 3−5681
LiF film, epitaxially grown on NaCl, electron microscope obs. of annealed structures 3−1929
LiF films, refr. index dispersion meas. *(Russian)* 3−8685
LiF glow peak growth due to annealing 3−291
LiF target, picosecond light pulses absorption 3−20553
LiF:In, mechanical and emission characts. with In diffused into compound 3−24115
LiF:Mg, electron trap depth and supralinear thermolum. response 3−24756
LiF:Mg^{2+}, neutron irrad., annealing of radiation defects *(Russian)* 3−11656
LiF:Mg^{2+}, thermolum. rel. to Mg^{2+} vacancy pairs 3−12189
LiF:MhF$_2$, Debye-Huckel interactions and solubility 3−4881
LiF:Ni^{2+}, Co^{2+}, yield limit concentrational dependences *(Russian)* 3−1672
LiF:O^{2-}, F-centre form. and plasticity 3−24114
LiF:U^{6+}, e.s.r. obs. of charge compensation effects 3−2383
Li_2F_2 crystals subjected to molecular beams, condensation and vaporisation kinetics investigation *(German)* 3−7920
Li_3F_3, crystals subjected to molecular beams, condensation and vaporisation kinetics investigation *(German)* 3−7920
$(Li_{1-x}Fe_x)[Li_{x-0.5}Fe_{2.5-x-a}Cr_a]O_4$, ferrite, paramag. props. 3−38958
$Li_{0.5}Fe_{2.5-t}Al_tO_4$, lowered Fe^{3+} mag. moment in paramag. region 3−21212
$Li_{0.5-\alpha}Fe_{2.5}O_{4-\alpha/2}$, nonstoichiometric, point defects, X-ray diffr. obs. 3−33520
$Li_{0.5}Fe_{2.5}O_4$, spin waves and exchange interactions, neutron scattering obs. 3−21252
$Li_{0.5}Ga_{2.5}O_4$:Cu^{2+}, Jahn-Teller effect 3−21300
$LiGd(MoO_4)_2$:Nd^{3+} c.w. laser, spectroscopic and lasing characts. 3−19615
Li_3GeO_3, 90° phase matchable nonlinear material 3−8613
LiH, Compton profile 3−11650
LiH, distorted-atoms-in molecules model spatial electronic wavefunction 3−38265
LiH, energy bands in Hartree Fock approximation 3−30401
LiH, exchange process, H transport, press. depend. 3−38681
LiH, Gaussian-based model pots. and Gaussian basis functions for valence electron studies 3−1144
LiH, Heitler-London approx. and variable orbital exponents 3−7111
LiH, high temperature luminescence and capture sites *(Russian)* 3−12190
LiH, pot. curves and wavefunctions for Σ and π states 3−1158
LiH, second order Raman spectrum, phonon modes *(French)* 3−39136
LiH, transition moments and rot.-vibr. wavefunctions for Σ and Π states 3−1159
LiH, u.v. irrad., e.p.r. of F-centres 3−8443
LiH, X-ray transition radiation *(Russian)* 3−36953
LiH and LiD, ion expansion energy spectra related to laser plasma parameters 3−38468
LiH Hartree-Fock polarisabilities calc. 3−29486
LiH SCF-MO calculations using basis sets of Gaussian lobe functions 3−4404
LiH:Ga(Ge)(As), excitation and luminesc. spectra *(Russian)* 3−21462
LiH:Mg(Ge)(In)(Tl), red luminesc., 120 and 293 K *(Russian)* 3−15538
$Li(H_2O)^+_n$ extended Huckel method study of complex 3−18780
$LiIO_3$, assignment of vibrs. from i.r., Raman and n.q.r. data 3−38637
$LiIO_3$, growth from acid solns., and i.r. transparency 3−12234
$LiIO_3$, nonlinear optical props., model of polarizable ions 3−32601
$LiIO_3$, nonstationary stimulated Raman scattering by polaritons 3−37983
β-$LiIO_3$, refr. indices, 0.4-2.2 μm 3−30795
$LiIO_3$, u.s. absorpt., temp. depend. 3−33964
$LiIO_3$ crystal in doubly resonant oscillator tuning range 0.415 to 2.1 μ 3−19633
$LiIO_3$ optical rectification, crystals 3−37986
$LiIO_3$ thermoanalytical study of polymorphism 3−1796
$LiLnMo_2O_8$, epitaxial growth on Ln_2GeMoO_8 single cryst. substrate from $LiO_2.2MoO_3$ soln. 3−1913
$LiMg_xV_{2-x}O_4$ mixed oxides, phase comp., lattice parameters, spinel phases 3−38563
$Li_xMn_yFe_{3-(x+y)}O_4$, cryst. growth, Bridgman method and characteriza tion 3−12267
Li_2MoO_4 as flux in $BaMoO_4$ crystal growth by flux pulling method 3−12283
$Li_2Mo_4O_{13}$, $Li_4Mo_5O_{17}$, Czochralski growth from Li_2MoO_4-MoO_3 system 3−2666
$Li(NH_4)SeO_4$, Raman and i.r. spectra hydrogen bonding, ion distortion 3−39144
$LiNO_3$, in $LiClO_3$, Raman spectra, cooperative effect of internal modes 3−18442
$LiNO_3$ concentrated water solution, n.m.r. study of relaxation times and structural transitions *(Russian)* 3−12517
$LiNO_3 + AgNO_3$ melt, interdiffusion coefficients determ. *(German)* 3−36434
$LiNbO_3$, acoustic surface waves, harmonic generation 3−17932
$LiNbO_3$, Brillouin scatt., room temp. obs., elastic consts., elastooptical moduli *(French)* 3−36864
$LiNbO_3$, Czochralski growth conditions rel. to lattice defects and optical quality 3−21539
$LiNbO_3$, Czochralski grown, cryst. perfection, obs. of Pendellosung fringes 3−36279
$LiNbO_3$, dispersion branches of extraordinary polaritons in different wave vector directions 3−21037

lithium compounds continued
$LiNbO_3$, elastic waves collinear interaction with light waves 3−21384
$LiNbO_3$, generation of harmonics of transverse elastic waves 3−33962
$LiNbO_3$, growth of craters during ion etching 3−1859
$LiNbO_3$, holographic materials for stereoscopic display systems 3−28576
$LiNbO_3$, ion irrad., expansion, crazing and exfoliation 3−17880
$LiNbO_3$, laser-induced damage, internal electric field 3−29142
$LiNbO_3$, $LiTaO_3$ laser damage, surface, free oscillation and giant pulse conditions, threshold, mechanisms 3−22937
$LiNbO_3$, luminesc., comments on proposed optical index damage phenomena 3−18485
$LiNbO_3$, luminesc., reply to comments on optical index damage 3−18486
$LiNbO_3$, mixing cryst. for far i.r. generation by self-beating of dye laser light 3−16905
$LiNbO_3$, nonlinear optical props., model of polarizable ions 3−32601
$LiNbO_3$, optically induced inhomogeneity of refr. index 3−32604
$LiNbO_3$, p and d 140 keV irradiation, absorption band 3−2571
$LiNbO_3$, parametric luminescence, line profile *(Russian)* 3−739
$LiNbO_3$, parametric oscillator, pumped with 1.06 μ radiation, optimum focusing conditions 3−10565
$LiNbO_3$, phase matching curve, temp. and angular widths *(Russian)* 3−776
$LiNbO_3$, polariton-biphonon Fermi reson. *(Russian)* 3−11708
$LiNbO_3$, positive refr. index optical waveguiding layers 3−36848
$LiNbO_3$, stoichiometry variations from Raman powder spectroscopy 3−2536
$LiNbO_3$, stretching vibr. band of OH$^-$ defects, 2.87 μ 3−24729
$LiNbO_3$, surface waves, appl. to meas. of surface mobility of adjacent Si 3−38828
$LiNbO_3$, thermal expansion in range 70-300K 3−5927
$LiNbO_3$, transverse polaritons, Raman spectra *(Russian)* 3−8593
$LiNbO_3$, X-ray K-absorpt. edge of Nb 3−27584
$LiNbO_3$, z-cut, strain depend. of piezoelec. polarisation 3−30762
$LiNbO_3$ coated with CdSe, CdS, InSb, Rayleigh acoustic surface wave amplification and dispersion, calc. 3−11794
$LiNbO_3$ crystal, off-resonance excitation to produce high acoustic frequencies for meas. of hypersonic absorption *(Russian)* 3−4815
$LiNbO_3$ crystal, upper dispersion branch of ordinary polaritons 3−38819
$LiNbO_3$ electro-optic prism deflector, appl. to optical multiplexing and demultiplexing 3−16407
$LiNbO_3$ Fermi resonance of polariton, biphonon state 3−36556
$LiNbO_3$ film growth by r.p. sputtering 3−18541
$LiNbO_3$ holograms, unfixed, self-enhancement 3−16443
$LiNbO_3$ low Q parametric oscillator, pumped by Q-switched Nd^{3+}:YAG laser 3−754
$LiNbO_3$ plates, guided elastic waves *(Russian)* 3−14933
$LiNbO_3$ single crystals, X-ray topographic studies, relation between growth conditions and lattice defects 3−17747
$LiNbO_3$ substrate, piezoelec. coupling of Rayleigh acoustic surface waves in evaporated CdSe layer 3−30761
$LiNbO_3$:(Fe,Mo), alterable holographic medium, wavelength dependence 3−204
$LiNbO_3$:Fe, e.p.r. obs. of Fe impurities and n.m.r. obs. of stoichiometry 3−12060
$LiNbO_3$:Gd^{3+}, e.p.r. and zero field resonance obs. of crystal field 3−34203
$LiNbO_3$/Si layered struct., longit. and transverse acoustoelec. effect 3−36641
$LiNbO_4$, surface acoustic waves, laser optical probe, with high relution interferometry 3−19112
$LiNbO_4$ oblique cut crystals, optical beam control *(Russian)* 3−693
$LiNb_3O_8$, Czochralski growth method rel. to optimal props. 3−24803
Li_3NbO_4, electronic structure and Nb-Nb band study using INDO type method 3−20084
LiO, vibrational and electronic oscillator strengths calc. 3−35999
LiO system molecular species, study by electron-impact mass spectrometry 3−5376
LiO_2, Raman spectra, Ar matrix, bonding in $M^+O_2^-$ mols., ionic model 3−30812
LiO_2-MgO-MnO-Fe_2O_3 powder ferrite, synthesis and magnetic properties *(Russian)* 3−15386
Li_2O, Auger spectra 3−36969
Li_2O silicate melt, solubility of He, Ne and N_2 *(German)* 3−7906
Li_2O-Al_2O_3-SiO_2 glasses, Gd^{3+} doped, e.s.r. meas. during crystn. 3−27403
Li_2O-K_2O-SiO_2-Al_2O_3:Sr^{2+} photopyrocerams, dislocation struct. and dielec. props. 3−27753
Li_2O-K_2O-TiO_2-SiO_2 type glasses, n.m.r. of ^{7}Li, alkaline ions position determ. 3−2410
Li_2O-Pd-O_2 system, synthesis, structure and stability of phases 3−33676
Li_2O-SiO_2 glass, liq. phase separation and crystal nucleation 3−30075
Li_xO-TeO_2 glass, e.p.r. spectra., irrad. effects *(Russian)* 3−21309
$Li_2O.Al_2O_3.2SiO_2$, internal friction 3−1693
$Li_2O.SiO_2$ glass, u.s. velocity, temp. depend., liq. He temps. 3−36368
$Li_2O.2SiO_2$ glass, homogeneous nucleation rate 3−33459
$Li_2O(x=1,2)$, from matrix deposition of Li and N_2O in spectra 3−17431
Li_2SO_4, crystal structure 3−20719
$Li_2SO_4.H_2O$, n.m.r. study, second moments method, rotational oscillations of H_2O mol. *(French)* 3−27429
$LiScO_2$:^{57}Fe^{3+}, diamag. host lattice, hyperfine splitting of Mossbauer spectra 3−34253
$LiTaO_3$, ^{7}Li quad. coupling const. temp. depend. near Curie pt. 3−2415
$LiTaO_3$, ferroelectric domain reversal 3−8530
$LiTaO_3$, for piezoelec. filter devices, Czochralski growth 3−12297
$LiTaO_3$, optically induced inhomogeneity of refr. index 3−32604
$LiTaO_3$, positive refr. index optical waveguiding layers 3−36848
$LiTaO_3$, pyroelectric detectors, with low, NEP, construction, props. 3−16400

lithium compounds continued
- $LiTaO_3$, stoichiometry variations from Raman powder spectroscopy 3−2536
- $LiTaO_3$, structure, temp. depend. of ferroelec. phase and paraelectric phase at 940 K, neutron diffr. obs. 3−30098
- $LiTaO_3$ crystal, precision machining for electro-optic elements 3−171
- $LiTaO_3$ film growth by r.p. sputtering 3−18541
- $LiTaO_3$ plates, guided elastic waves *(Russian)* 3−14933
- $LiTaO_3$ single crystals, X-ray topographic studies, relation between growth conditions and lattice defects 3−17747
- $LiTaO_2F_2$, crystal structure anal. 3−30103
- $Li_4Te_2O_7$, lattice parameters *(French)* 3−38564
- $LiVO_3$, atomic structure, least squares refinement, bond lengths and strength 3−30094
- γ-$Li_{1\|x}V_3O_{8\|\lambda}$, ^{7}Li magnetic resonance study, Knight shift and second moment determ. 3−39044
- Li_2WO_4, phase transforms. at high pressure, structure obs. for III(IV) phases 3−33668
- $LiZn_xV_{2-x}O_4$ mixed oxides, phase comp., lattice parameters, spinel phases 3−38563
- ^{6}LiD fuelled fusion reactors modified Lawson criterion 3−38189
- ^{7}LiH(D), elastic consts., 298K, u.s. determ. 3−20782
- MgO-$LiAlO_2$ system, solid soln. studies 3−31160
- ZnF_2:LiF, dielec. relax. and polarisation using vacancy and interstitial models 3−24650

lithospace *see earth crust*

lithosphere *see earth crust*

living systems
- *see also biology; biomedical phenomena; biophysics; brain*
- animals, chronic and asymmetrical cortical foci rel. to bilateral synchrony of epileptic discharge 3−28333
- atmospheric ions effects, obs. *(Spanish)* 3−5625
- caloric vestibular stimulation by u.h.f. microwave irradiation 3−25602
- cat, olfactory pathway, efferent evoked responses 3−28331
- cat, polysensory responses and sensory interaction in pulvinar and related posterolateral thalmic nuclei 3−39774
- cats, brain states 3−31848
- cats, left ventricle rel. to flow and pressure source 3−36141
- cats, normal myocardial function and energetics in volume overload hypertrophy 3−37512
- cats, simultaneous d.c. and multiple unit responses from lateral geniculate 3−37729
- cats anesthetized, middle ear muscle contractions rel. to bone conduction 3−31856
- causality and anticipation, reference to phenomena of life 3−9784
- cell as microcybernetic polymaser *(Spanish)* 3−25548
- chronic animals, intracellular recording in cerebral cortex 3−35521
- dog, sympathetic nerve stimulation on pulmonary vascular resistance 3−37517
- dog common carotid artery, transport of ^{14}C-4-cholesterol between serum and wall 3−37513
- dogs, aortic-wall thickness meas. 3−16557
- frog muscle contractile behaviour under magnetic field *(Russian)* 3−16310
- human electro-oculogram, linearity of horizontal component 3−19099
- humans, evoked cortical potentials 3−31847
- layered tissues, temperature distribution calc. 3−25587
- man, extracellular firing patterns of deep temporal lobe structures 3−39766
- marine plankton sensing by dye laser induced fluorescence 3−3237
- preterm newborn infants, visual and somatosensory evoked responses 3−37523
- siliceous algal and bacterial stromatolites, growth in geyser effluents 3−13124
- space travellers, radiation effects *(German)* 3−35293

lobes (distribution) *see antenna radiation patterns*

local moments in dilute alloys
- Anderson model and renormalizable random phase approx. 3−8329
- coupled local moment-conduction electron Bloch equation, e.s.r. obs. 3−34213
- dilute mag. alloys, elec. resist. rel. to localised mag. moment exchanges, RKKY s-d exchange model 3−30439
- dilute mag. alloys, thermoelec. power rel. to localised mag. moments interaction, s-d exchange model 3−30456
- dynamics of local mag. moments with electron-electron interaction 3−34100
- spin-orbit interactions, induced spin anisotropy effect on elec. resist. 3−36711
- Au-Fe, rel. to magnetoresist. meas. in high fields 3−36592
- AuMn(V), localised spin fluctuation and Kondo system, resist. temp. depend. 3−36582
- CoNi:Mn, n.m.r. of ^{55}Mn obs. 3−36799
- Cr-Mn alloy, equiatomic paramagnetic scatt. of neutrons, rel. to localized moment model 3−2254
- Cu-Cr, mag. depairing energy from supercond. proximity obs. 3−8341
- Cu-Fe mag. depairing energy from supercond. proximity obs. 3−8341
- Cu-Mn, mag. depairing energy from supercond. proximity obs. 3−8341
- FeAl alloys, effects on positron annihilation parameters 3−38599
- FeNi:Mn, n.m.r. of ^{55}Mn obs. 3−36799
- Ni-Fe:H dilute alloy with high H conc., magnetoresistivity rel. to local mag. moments 3−8158
- Pd-rare earth, paramag., anal. using crystal field theory and semiempirical formula 3−15349
- Ru alloy with CsCl structure, Pauli susceptibility with localised moments contrib. 3−34097
- Y, e.p.r. of Gd, g-shifts, line narrowing, exchange effects, satellite lines 3−2376
- YAl_2, exchange integral between Gd moment and cond. electrons 3−2375

localised electron states
- alloy, binary, local order effect on electronic states 3−20994
- alloy, disordered binary, electronic struct. 3−11856

localised electron states continued
- amorphous insulator, u.s. absorpt. by localized two-level systems 3−7861
- amorphous semicond. with chain or layered structure, fluctuation levels 3−15115
- amorphous semiconductor, e.s.r. study 3−18058
- amorphous semiconductors, electronic phenomena, review 3−24415
- Anderson model, functional integral approaches, comparison of results in limiting cases 3−15142
- Anderson three dimensional disordered model, localisation degree 3−18056
- anthracene single crysts., with surface disturbed by impurity, fluoresc. *(Russian)* 3−8647
- band narrowing and tT-matrix pole 3−8075
- bifluctuons, theoretical study *(Russian)* 3−15145
- bond perturbation effect on Stark ladders in crystals 3−27217
- α-1brass, disordered binary, electronic struct. 3−11856
- classical lattice dynamics and localized potential method 3−30216
- coherent potential approximation and Anderson's model of cellular disorder 3−36510
- disordered alloys, localization criteria, single site coherent potential approximation 3−2019
- disordered one-dimens. system, localisation distance, m.f.p., backward scatt. 3−24385
- effective charges and ionicity, empirical correl. 3−36271
- electron self-trapped states, conduction band free-electron-like states 3−38772
- electronic transitions and structure, review 3−33814
- energy levels and line strengths of rare earth ions in crystals, normalized Legendre functions and tesseral harmonics of 7th order 3−4953
- ferroelectric, domain walls, electron localization mechanism *(Russian)* 3−8538
- ferroelectric semiconductors, localised states in domain walls 3−24663
- free-deep trapped triplet exciton annihilation, delayed fluorescence wave form 3−12172
- hole-nuclear double reson. in localized biexciton 3−2428
- insulating thin films, electronic transport processes 3−18237
- Jahn-Teller impurity ion pair, vibron reduction effects of Coulomb and exchange interactions 3−33813
- Josephson current through S-N-S junction, containing paramag. impurities with local states within gap 3−30578
- linear systems, extension of eigenvalue spectra theorems of one-dimens. systems 3−4954
- metal, energy spectra of electronic transition, edge singularity in tight binding approx. 3−18510
- metals, diagrammatic analysis of dynamics of localised moments 3−34058
- metals, V and Fe-Zn, unfilled one-electron levels, X-ray continuum isochromat study 3−36536
- molecular crystal in contact with metal, charge transfer states 3−8252
- molecular solids, exponential carrier trap distributions 3−33825
- molecular solids, photoemission rel. to impurities and defects 3−15588
- nonlinear canonical transforms, in coupling between degenerate low and high energy excitations 3−4014
- one-dimens. Weaire-Thorpe tight binding model, states near E=0 3−8114
- one-dimensional disordered systems, electronic wave functions 3−8083
- paraffin, Compton profiles 3−33806
- polyethylene, photoelectron spectrum comparison with cryst. orbital calcs. 3−27597
- rare earth alloys, cryst. field splitting, rel. to Kondo effect 3−30446
- resonance interaction effect on line profile, Schrodinger equation soln. 3−4955
- role in electron diffraction 3−24312
- semiconductor-metal and mag. phase transitions, Hamiltonian model 3−38806
- solid r.f. spark mass spectra, valence relationships 3−17698
- superconductivity, effect of d and f states 3−8286
- superconductors with transition metal impurities, localised states in energy gap 3−15298
- surface electronic structure determ. by core level excitation techniques 3−38768
- Teflon, Compton profiles 3−33806
- transitions, optical, between degenerate localised levels, theory of moments 3−15535
- X-ray inelastic scattering 3−30142
- YIG films, surface spin wave in parallel resonance config. 3−2400
- Ag halides at low temperature 3−27218
- Al-Pd alloy, electronic struct., soft X-ray band spectra 3−15573
- As_2S_3 glasses, magnetic susceptibility 3−8334
- $AsTe_2Si$ chalcogenide film, thermally stimulated depolariz. current obs. 3−2020
- Ba, localised d states for pseudopotential calcs. 3−8116
- BiI_3, bielectron and bihole energy levels, doublet fine struct. 3−21020
- Ca localised d states for pseudopotential calcs. 3−8116
- Cr, core electron binding energies of surface and bulk atoms, comparison 3−39210
- Cr_2Al_{11}, Anderson model rel. to n.m.r. and susceptibility obs. 3−36807
- $CrCl_3$, specific magnetic rotation in crystal field bands 3−5179
- CrO_4^{2-} in alkali halides, vibr. and electronic spectra 3−27091
- Cu, indirect nuclear interaction coupling constants 3−27216
- $Er_2O_2S:Er^{3+}$, crystal field effects on electronic ion struct., optical absorpt. obs. *(French)* 3−30411
- EuB_4HP, spectrum of Eu^{3+} pressure effects, crystal field theory *(Russian)* 3−8113
- $EuCl_3.6H_2O$, pressure effects on spectrum of Eu^{3+}, crystal field theory *(Russian)* 3−8113
- EuO, press. induced electronic collapse and semicond.-metal transition 3−7929
- $Eu_2(SO_4)_3.8H_2O$, pressure effects on spectrum of Eu^{3+}, crystal field theory *(Russian)* 3−8113
- Fe_3O_4 magnetite, band theory of pair-localized electrons 3−2012
- Fe_3Si, FeSi, $FeSi_2$, electron and X-ray spectra obs. *(Russian)* 3−24760

- **localised electron states** continued
  - GaAs, defect levels induced by electron irradiation 3-21022
  - GaSb, Landau transitions at higher energy gaps, spin-orbit splitting 3-33809
  - Ge film, amorphous, Zeeman splitting of localized levels model approach to magnetoresist. 3-15213
  - GeO_2, interband optical transition strengths, valence orbital delocalisation effects 3-34362
  - ice cavity model hydrated electron absorpt. spectral peak press. shift at high press. 3-12141
  - InSb, Landau transitions at higher energy gaps, spin-orbit splitting 3-33809
  - $KCl:Eu^{2+}$ calc. of localised one-electron states, mechanisms of recombinational process *(Russian)* 3-24389
  - $KMgF_3$, ^{57}Fe n.m.r., isomer shift calibrations using multivalent states 3-18400
  - LiF, Adams-Gilbert local-orbitals equations, choice of localising potentials 3-36537
  - Nb/Al_2O_3 cermet films, rel. to superconductivity and normal state elec. props. *(Russian)* 3-30482
  - Nb/Al_2O_3 thin cermet films, hopping conduction through localised states 3-11895
  - Ni, core electron binding energies of surface and bulk atoms, comparison 3-39210
  - Ni, d-band wave functions *(Russian)* 3-30390
  - Ni, nucl. relax. rate of ^{101}Ru, rel. to virtual bound state 3-2442
  - $NiCr_3$, alloy K-states, X-ray absorption spectra study *(Russian)* 3-34441
  - NiO, valence-electron ionization and optical excitation energies 3-27219
  - SbSI, semiconductor-ferroelectric, domain structure rel. to local states 3-5172
  - SbSeI, semiconductor-ferroelectric, domain structure rel. to local states 3-5172
  - Se-As semiconductors, glassy photoelectric properties, structure and composition 3-33812
  - Si, electron irradiation, vacancy interaction with Sn impurities 3-18093
  - Si amorphous films, electronic transport and state distribution 3-8172
  - Si K_β X-ray spectra prod. by α-particle excitation, local electronic struct. effects 3-21012
  - $Si-SiO_2$, interface band struct., O and Si vacancies energy levels 3-18228
  - SiO_2, interband optical transition strengths, valence orbital delocalisation effects 3-34362
  - SiO_2 fused below 1K, nonlinear phonon propag., resonant scattering by two level localised 'tunnelling states' 3-17952
  - SiO_2 K_β X-ray spectra prod. by α-particle excitation, local electronic struct. effects 3-21012
  - SiO_2 thermally grown on Si, electron trapping levels 3-8262
  - SnO_2, interband optical transition strengths, valence orbital delocalisation effects 3-34362
  - Sr, localised d states for pseudopotential calcs. 3-8116
  - Ti, core electron binding energies of surface and bulk atoms, comparison 3-39210
  - TiO_2, interband optical transition strengths, valence orbital delocalisation effects 3-34362
  - VO, VO_2, V_2O_3 and V_2O_5, localised electron states from Compton profile meas. 3-30139
  - VO_2, parametrized bands, method of obtaining 3-24384
  - VO_x, defects distribution 3-4751
  - $ZrFe_2$, $ZrFe_2H_{0.3}$, effect of H on electronic struct. of Fe atoms, nucl. γ-reson. obs. *(Russian)* 3-12079
- **localised modes in crystals** *see lattice localised modes*
- **localised states, electron** *see localised electron states*
- **loggers** *see data loggers; recorders*
- **logging (recording)** *see recording*
- **logic, formal** *see formal logic*
- **logic circuits**
  - *see also flip-flops; formal logic; NAND circuits; sequential circuits; transistor-transistor logic*
  - digitally controlled, counter applications 3-28685
  - Ge(Li) detectors, counting circuit 3-13442
- **long tailed pair** *see differential amplifiers*
- **loop antennas**
  - 10 GHz design for e.m. field distribution meas. 3-10423
  - e.m. coupling at h.f. over inhomogeneous ground, earth depth depend. 3-32478
  - field strength meters, equipment for checking and calibrating *(Russian)* 3-19237
  - t.w. circular loop, radiation props. in compressible electron plasma 3-36156
- **Lorentz-Lorenz relation** *see permittivity; refractive index*
- **Lorentz transformation**
  - Cherenkov radiation by tachyons, Lorentz-invariant formulation 3-10829
  - Chu-Haus-Penfield principle of virtual power, criticism 3-28931
  - contraction based on the Ampere experiment, elementary derivation for students 3-32003
  - covariant reference tetrad theories 3-13625
  - elementary systems, Lorentz-invariant localization from general transformations 3-35596
  - generalized, in four dimensions, superluminal objects, physical implications 3-28956
  - geometric covariant treatment for anal. of dynamic problems 3-21
  - group, three-dimensional, construction of principal series representations 3-26050
  - inhomogeneous Lorentz group, unitary representations *(Hungarian)* 3-26130
  - intertwining operators for reduction from infinite- to finite-dimensional representation of Lorentz group 3-16728
  - invariant simultaneity 3-592
  - Lorentz-Dirac equations of motion, for charged particles in const. e.m. field 3-29196
  - n-dimensional space-time, structure 3-593
  - plasma e.m. wave dispersion, covariant formulation 3-14530
  - quantum electrodynamics, matrix elements calc. based on Lorentz group transformation *(Russian)* 3-38032
- **Lorentz transformation** continued
  - Riemann curvature tensor, algebra 3-19505
  - Stokes parameters, Lorentz transformation properties 3-9627
  - superluminal inertial frames, determ. of Lorentz transforms 3-26129
  - thought expt. discussion, teaching technique 3-9799
  - trilinear invariant forms of SL(2,C), distribution theoretic soln. 3-16586
  - two port chain, reproduction *(German)* 3-13623
  - of work done by uniform pressure, reversible compression 3-16720
- **Lorenz number** *see electrical conductivity of solids; thermal conductivity of solids*
- **Loschmidt number** *see constants*
- **loss angle**
  - *see also dielectric losses*
  - liquid dielectric mixture, calc. 3-2484
  - lunar soil, frequency temp. and moisture dependence 3-3306
  - polydimethyl siloxane film, between metal electrodes, γ-ray effects *(Russian)* 3-39083
  - trimethylethyltin-based polymer thin films *(Russian)* 3-8187
  - KBr, additively coloured, temp. and freq. depend. 3-39092
  - $Li_2O-K_2O-SiO_2-Al_2O_3:Sr^{2+}$ photopyrocerams, dislocation struct. and dielec. props. 3-27753
- **loss-angle measurement**
  - dielectric materials, C-, L-, S- and X-bands, precision equipment *(Polish)* 3-6014
  - oscillatory method, instrument for 0.1-100 MHz range 3-19239
- **loss measurement**
  - a.c. loss of Nb-Ti-Zr ternary alloys with different compositions 3-11982
  - a.c. losses in Nb and $Ta_{92}Nb_8$ alloy, field of first penetration rel. to lower critical field 3-11981
  - acoustic surface wave, laser beam applic. 3-5778
  - collisional, multi-ion horizontal duct producing v.l.f. noise bands 3-16014
  - magnetisation meas. of twisted superconducting composite conductors 3-11987
  - optical fibres, overview 3-168
  - superconductor losses in pulsing magnetic field, review 3-15300
  - underwater sound, surface duct propagation 3-3717
- **losses**
  - *see also dielectric losses; eddy current losses; heat losses; loss angle; magnetic leakage*
  - acoustic, underwater, layered oceanic microstructure 3-34870
  - acoustic dampers, energy dissipation mechanism 3-31958
  - c.w. dye lasers, for various wavelengths 3-19610
  - e.m. wave diffraction, optical resonator with cylindrical mirrors, calc. *(Russian)* 3-10557
  - ferromagnetic materials, nonlinear, conducting, e.m. field distributions 3-15396
  - flat mirror ring resonator 3-4112
  - iron in magnetic sheet, thermometric meas. *(Japanese)* 3-24599
  - laser diode and multimode glass fibre coupling, obs. *(German)* 3-13742
  - magnetoplasmadynamic arcs, anode losses, influence of magnetic fields 3-36203
  - MHD, lithium cooled toroidal fusion reactor, limitations 3-4342
  - multichannel delayed coincidence spectrometer, dead time counting losses 3-37636
  - optical multimode fibres, with graded and ungraded core indexes, bending mode loss 3-150
  - power transmission, rel. to corona *(Russian)* 3-11516
  - proton, around JINR synchrophasotron in beam extraction mode 3-25832
  - u.s. long delay devices, optimization 3-16392
  - $GaAs-Al_xGa_{1-x}As$ laser, double heterostruct., characts. rel. to doping, loss mechanism 3-16858
  - SiON film, optical waveguide 3-2604
  - Sn-SnO-Sn supercond. tunnel junction, geometric resons., temp. depend. losses 3-24543
- **loudness**
  - *see also acoustic intensity measurement*
  - adaptation meas. by nonaural procedure 3-3456
  - click and human click action potentials, postmasking recovery 3-25556
  - computer program for calculation from third-octave band levels or from critical band levels *(German)* 3-16329
  - electric clock sound 3-3453
  - hearing, enhancement with monaural, binaural and dichotic stimulation 3-3500
  - hearing, measurable dimensions of sound, audio reproduction, compensation 3-9656
  - hearing, summation of tones from two loudspeakers 3-3492
  - masking of one pure tone by two other pure tones *(French)* 3-16330
- **loudspeakers**
  - acoustic radiation field visualisation with photographic device *(Russian)* 3-3766
- **Love waves**
  - nonhorizontally layered media propag., amplitude and phase determ. by a finite element technique 3-21850
  - phase velocities and amplitudes in low velocity zone 3-2905
  - propagation in electrostrictive dielectric media 3-13596
  - propagation in non-homogeneous isotropic layer of finite depth on infinite non-isotropic layer 3-31321
- **low energy electron diffraction**
  - adsorbed gas on solid, structure from LEED and Auger emission spectroscopy 3-24341
  - alkali metal overlayers on W(100), quantitative study 3-38704
  - apparatus for simultaneous LEED and photoelectric work function measurements 3-28712
  - apparatus for thermal studies 10K-300K 3-28731
  - Auger electron spectroscopy, using 2-grid LEED system, and photoelectron multiplier *(Japanese)* 3-35492
  - classification using scatt. theory *(Czech)* 3-11784
  - crystal surface structure determination 3-18008
  - display type, work for change meas. 3-35494
  - elastic scattering, rel. to evaluation of LEED intensities 3-27037
  - exchange reflection, dependence on diffr. conditions, Bethe's dynamical theory 3-23995
  - graphite, surface thermal expansion determination 3-15023

low energy electron diffraction continued
group VIA metals, faceting in dilute O_2 atm., l.e.e.d. and r.h.e.e.d. studies 3−11818
image potential role in electron surface studies 3−21130
inelastic scatt. theory for low energy electrons in multiphonon process 3−17874
intensity calc. in momentum representation 3−27038
intensity profiles, effect of steps in surface 3−38703
metal surface, intrinsic quasi-stationary states and effect on LEED profiles 3−2157
multiple scattering method for intensity calc. 3−30152
optical transforms for simulation of diffraction patterns of surface structure 3−7998
plasmon scattering, surface and bulk coupling 3−11785
plasmon thresholds in the secondary electron yield, expt. 3−4976
rare gas crystal, epitaxially grown on Nb (100), and desorption 3−11654
rare gas crystal, epitaxially grown on Nb (100), inelastic scatt. and energy loss spectra 3−11655
reflected intensities, efficient calc. method 3−30155
S-wave multiple scattering treatment 3−30154
secondary electron yield measurements technique 3−35496
selected area LEED in the emission microscope 3−13469
SEM collection of secondary electrons using small aperture probes 3−35512
semiconductor cleaved surface roughness obs. 3−36470
substrate surface, structure obs. during sputtering and vapour deposition 3−24324
surface, diffr. of very low energy electrons, 0-10 eV 3−15063
surface crystallography, kinematic intensities from intensity data 3−30319
surface electron states, chem. behaviour implications, review 3−8241
surface lattice constants 3−30329
surface plasmon dispersion relation via analysis of inelastic LEED 3−20914
surface potential barriers 3−27182
surface structure determ. 3−1862
surface structure investigation, installation description 3−27162
surface structures and LEED intensity measurement, dynamical approach 3−30312
surface-vacuum interface, conference, Enschede, Netherlands, June (1972) 3−30316
symmetry of LEED patterns and diperiodic space groups for surface structures 3−24315
t-matrix formalism of LEED for clean and overlayer systems 3−24322
Ag epitaxial growth on GaAs(110) 3−15087
Ag-Pd alloys, study of CO adsorption 3−1885
Ag(111), adsorption of I, site determ. 3−11803
Ag(111), thermal diffuse scattering, at low temp. 3−38702
Al, (100) surface, elastic and inelastic LEED, absolute intensity meas. 3−36464
Al, (110) and (111) surfaces, calc. and expt. 3−36465
Al surface structure, LEED intensity evaluation 3−24323
Al(110) surface, influence of surface morphology 3−20915
Al(111) films, inelastic LEED, surface plasmon dispersion determ. 3−38701
Au, (110) surface, diffuse LEED pattern, temp. depend. 3−24313
Au, substrate with Pb monolayers, spontaneous alloying, LEED and Auger obs. 3−36463
Au (100), (110), (111) surfaces, structure obs. 3−24314
Au(100), anomalous surface structure, LEED obs. 3−36462
Au(111), (100), (110), faces, LEED and Auger obs. of S adsorption *(French)* 3−20940
Cu, chemisorpt. of Bi on (100) surface LEED obs. of layer struct. 3−30355
Cu, chemisorption of Bi on (111), LEED obs. of layer struct. 3−30356
Fe (011) oxidation at room temp., obs. 3−38745
Fe(111) surface structure determination 3−15054
GaSe, LEED studies 3−38698
KCl, (100) plane, influence of surface potential on LEED diffraction patterns *(Russian)* 3−27165
LiF, LEED intensity profile for (100) surface, and bulk energy bands, calc. 3−36466
MgO(100), obs. of contour maps for reciprocal lattice points 3−24316
Ni, (110), investigation of chemisorption of CO 3−38721
Ni, (110) surfaces, CO interaction, struct. investigation 3−38716
Ni, LEED at 20K, test of theory 3−4904
Ni/chemisorbed Na system, LEED intensity meas. 3−30312
NiO, exchange diffraction by 3d electrons in crystal 3−30156
P_2 adsorption and desorption kinetics on Si(111) surface, LEED obs. 3−1883
Pt, (100) surface, chemisorption of unsaturated mols., Auger spectroscopic and LEED study 3−11808
Pt, reactivity of low index and stepped single cryst. surfaces 3−11787
Pt, study of S adsorption *(French)* 3−36483
Pt(100), anomalous surface structure, LEED obs. 3−36462
Si, structure of (111) surface, LEED obs. 3−30314
Si, surface, LEED and Auger spectroscopy examination methods 3−15061
Si surface, rel. to electron beam-adsorbate interactions 3−20939
Si surface reaction with Ni, struct. 3−20911
W(001), spin polarisation effects 3−27164
W(112), meas. rel. to Li adsorption 3−20938
Xe, adsorbed layer on Cu and Ag at 77K, struct., LEED obs. 3−30345
Xe, thermal diffuse scatt. of low energy electrons, one phonon contrib. 3−17873
ZnO, calc. of intensities 3−30153

low induction loss *see loss angle*

low-temperature phenomena
see also Joule-Thomson effect; solid helium; superconductivity; superfluidity
a.c. behaviour of Nb crystal, relation to resistivity, Hall coeffs., flux pinning and screening current 3−11983

low-temperature phenomena continued
a.c. losses in Nb and $Ta_{92}Nb_8$ alloy, field of first penetration rel. to lower critical field 3−11981
α-brass powder, cold-worked and stored at liquid N temp., increase in particle size 3−27642
calcite cathodoluminescence, Mn emission 3−18502
epoxy resin/powder composites, thermal conductivity meas. 3−9887
externally deformed crystals, deformation description 3−36348
hematoporphyrin and its metal complexes, low-temp. optical absorption spectra 3−38282
Kapitza resistance, heat transfer calc. between solids 3−18255
Kapitza thermal boundary resistance between ^{3}He and Cu, meas. from 10-160 mK 3−33712
liquid crystal, proton spin thermometry at low fields in solid phase 3−2456
materials potted in epoxy resins, thermal resistance meas. 3−9888
metal, pure, low-temperature resistance *(Russian)* 3−2046
methane, ν_3-fundamental laboratory obs. rel. to planetary gases at low temps. 3−29650
mixed crystal electronic polarisation spectra at 4 K, quinoxaline, crystal effects 3−39141
pulsed n.m.r. thermometer for temperature and spin-lattice relaxation time meas. in millikelvin region 3−28498
radiation heat transfer between closely-spaced metal surfaces 3−10410
semiconductor, biexcitons, electron-hole droplet for motion, radiant recombination, helium temp. *(Polish)* 3−38816
Ag halides local and non-local electron states 3−27218
Al, thermal expansion, 3-35 K 3−30273
BS_2, visible and i.r. absorpt. spectra at 4K 3−33128
Ce Mg nitrate, thermal contact with liquid ^{3}He at low temp. 3−36459
Fe alloyed with ^{54}Mn, ^{57}Co, ^{182}Ta, ^{191}Ir, hyperfine field nonalignment under mag. saturation, meas. at 25 mK 3−24565
$FeSi_2$, thermal conductivity meas. of metallic and semiconducting cpd. 3−18117
GaSb, p-type, u.s. obs. meas. using the pulse echo method 3−17938
$GeSiO_2$, Ge-SiO_2-Si_3N_4 semiconductor-insulator boundaries, 77K, surface states, C-V method *(German)* 3−15264
He, supercritical liquid, meas. of forced convection heat transfer 3−9893
He at low temperatures, dielectric breakdown rel. to He pressure 3−7987
He I, boiling under forced flow in vertical tube 3−9894
^{3}He, sp. ht. in sintered Cu below 3 mK 3−38695
^{3}He solid-liquid mixture, bulk nucl. polarization, below 5 mK 3−30308
^{3}He/Ce, $Mg_3(NO_3)_{12}.12H_2O$ boundary resist., nucl. spin-electron spin dipolar interaction 3−30303
N film boiling crises and transient boiling 3−9892
N film boiling in tubes, disperse regimes 3−9891
$SrCl_2$:$^{165}Ho^{2+}$, coupled nuclear-electronic spin system, low temp. relax. 3−18362
Ti-Sn alloys, strength and plasticity, effect of Sn, low temp. behaviour 3−34602

low-temperature physics *see cryogenics*

low-temperature production
see also Joule-Thomson effect; liquefaction of gases
cryocooler, self-operated, Gifford McMahon cycle, development and operation 3−133
large-scale He refrigerator-liquefier system 3−25703
review of dilution refrigeration, Pomeranchuk cooling, nuclear demagnetization and applications 3−35383
^{3}He cooling by adiabatic solidification 3−25699

low-temperature techniques
see also cryostats; refrigeration
304 stainless steel, low temp. stability, prediction from room temp. deformation test 3−9839
apparatus for short-term indications at 77K 3−269
bolometer, a.c. capacitance 3−5798
closed-cycle cryogenic refrigerator, for Ge γ-ray spectrometer 3−32199
composite method for thermophys. characts. meas., 4.2-400 K 3−19169
cool-down phenomena in v. long duct with length/diameter ratio of 10^4 3−9890
cryobiology, tissue freezing and banking, cryosurgery 3−6146
cryopumping, appls. and developments, review 3−5828
crystal study, low temp. equipment for automatic four circle diffractometer 3−25674
dewar, finger, for e.p.r. meas. 3−22296
electrogasdynamic refrigeration 3−136
electron microscope goniometer stage, for 20 K-room temp., design 3−22513
e.p.r. resonator for 8 mm band with specimen interchangeability at liquid He temps. 3−6043
goniometer, Weissenberg, low and high temp. attachments 3−25653
heat contact expts. at mk temp. 3−9886
high pressure multiplicator and superconducting magnet combined system 3−5855
high resistivity materials, thermally stimulated currents, meas. 3−28601
hysteresis measurement, Ballistic method, apparatus design 3−9997
i.r. spectroscopy of molecular solids, at high pressure *(French)* 3−13310
LEED, thermal diffuse scatt. on Ag(111) at low temps. 3−38702
liquid helium level indicator with continuous reading utilizing carbon resistors 3−37601
low-temperature vacuum tight electrical leads *(Russian)* 3−9876
magnetic structure obs., high resolution polarizing microscope 3−35444
magneto-optical device, absorption spectra of solids 3−9998
and materials research applic., book contrib. 3−9880
measurement *(German)* 3−9877
metals, electronic density of states and low temp. specific heats, 1-20K 3−1806
metals, u.s. attenuation meas., at low temps. 3−28480
n.m.r. detection using SQUID magnetometer 3−2328
organic fluid thermal cond. meas. apparatus 3−22298
probe meas. in discharge column in Ne at 77K *(Czech)* 3−9874
protein crystallography, low temp. device 3−36236

- **low-temperature techniques** continued
  - review of dilution refrigeration, Pomeranchuk cooling, nuclear demagnetization and applications 3–35383
  - sealing, for variable temperature and pressure applications 3–141
  - space simulation chambers 3–3782
  - specific heat measurement, calorimetric technique 3–5849
  - specific heat measurement apparatus, between 0.3 and 3K *(French)* 3–13247
  - thermocouple reference tables (0 to 280 K) 3–9862
  - thermometric detection of n.m.r., 1-4 K 3–30680
  - u.v. absorption cell, for double beam spectroscopy *(German)* 3–16427
  - Al, spontaneous magnetisation when immersed in liquid nitrogen 3–36762
  - C resistance thermometers, use of Teledeltos paper 3–37603
  - Ce, alpha phase, low temp. elec. resist. under pressure 3–30451
  - H solid, low temp. compression using shock waves 3–32049
  - o-H_2 separation process using He gas cryogenerator 3–135
  - He, continuous liquid level indicator with superconducting filament *(Czech)* 3–9873
  - He II, saturated liquid, correlation of vaporisation onset heat flux for cylinders 3–9895
  - He liquid stage for scanning electron microscope 3–348
  - He solid/vapour heat transfer 3–9897
  - Xe epitactic growth on graphite, liquid He stage in transmission electron microscope 3–1940
- **LS coupling** *see Russell-Saunders coupling*
- **LSA** *see limited space charge accumulation*
- **LSI** *see large scale integration*
- **lubrication**
  - *see also friction*
  - bearings, fluid film lubrication, fluid mechanics, review 3–33326
  - cavitation phenomena in lubricated bearings, solns. of Reynolds eqn. 3–17538
  - composites of solid lubricants and metals, comp. effect on tribological props. 3–15785
  - elastohydrodynamics, Grubin's theory 3–1682
  - film described by Reynold's eqn., finite element soln. 3–1351
  - lubricant boundary layers, elec. props. and domain struct. 3–4509
  - magnetogasdynamic externally pressurized bearing with converging film 3–17549
  - metal, adsorption effect in drawing with organic lubricants, oxide film form. 3–33604
  - microviscometer based on refr. index, used for lubricant point contact 3–6170
  - oil films at high contact pressures, rheology rel. to lubrication 3–11683
  - polyethylene, filled, wear resist. of steel and brass in friction 3–25013
  - polyformaldehyde as antifriction material 3–25007
  - polymer compositions based on silicone adhesives, antifriction and mech. props. 3–25012
  - polymer/metal pair in sliding friction, liq. media effect on deform. of surface layers 3–31181
  - rheostatic lubrication tensor eqns. in a curvilinear coordinates *(German)* 3–28854
  - roller bearing, motion of magnetised fluid in lubrication layer *(Russian)* 3–20810
  - seals, mech. radial-face, hydrodynamic theory 3–26853
  - steel, carbon specimens in oil, fatigue crack propagation, numerical analysis 3–21614
  - steel, load carrying capacity rel. to sliding velocity, additive effects of tricresyl phosphate *(German)* 3–4799
  - surface thin metal layer, lubricant boundary conditions influence on microdeform. 3–33605
  - theory for micropolar fluids 3–7845
  - thermoelastohydrodynamic, in sliding and rolling contacts, review 3–27061
  - wear in metals, in lubricating oil containing solid particles expt. 3–24207
  - Al, foil, dislocations due to friction, lubrication and oxide layer effects 3–27063
  - Al, lubricant trapping under cold compression *(Japanese)* 3–30990
  - Cu, lubricant trapping under cold compression *(Japanese)* 3–30990
  - Cu alloys, adsorption-induced loss of strength during selective transfer in boundary friction 3–21706
  - Fe, lubricant trapping under cold compression *(Japanese)* 3–30990
  - MoS_2, lubricating power determ. *(German)* 3–27841
  - Zn, lubricant trapping under cold compression *(Japanese)* 3–30990
- **Ludwig-Soret effect** *see diffusion in solids*
- **luminescence**
  - *see also cathodoluminescence; chemiluminescence; electroluminescence; fluorescence; fluorescent screens; luminescence of gases; luminescence of liquids and solutions; luminescence of solids; luminescent devices; phosphorescence; phosphors; photoluminescence; sonoluminescence; thermoluminescence; triboluminescence*
  - absolute quantum efficiencies, techniques and instrumentation, review 3–35533
  - Achromobacter s.p., luminesc. thermal variations 3–22136
  - amplified spontaneous emission narrowing and rebroadening in high gain laser media 3–32596
  - attenuation measurement, decreasing instrumental errors by statistical method *(Russian)* 3–22330
  - bacterial luminescence, transient suppression by H_2O_2, mechanism 3–16300
  - carbonyl compounds, O quenching rate constants 3–21833
  - complex organic mols. intramolecular relaxation and luminescence *(Russian)* 3–26686
  - damping time meas. by amplitude phase method *(Russian)* 3–32075
  - Dicke model of superradiance, phase transition calc. 3–29067
  - emission and absorpt. spectra universal relation to combining electron states 3–23551
  - excited atom in periodic structure, spontaneous emission *(Russian)* 3–8635
  - filter fluorimeter, meas. of weak luminescent signals 3–3921
  - non-faradaic electrolysis, galvanoluminescence, co-liberation 3–39450
  - phenol complexes, influence of H-bond, calc. *(Russian)* 3–29703
  - photon echo on homogeneously broadened spectral line 3–35716
- **luminescence** continued
  - polyatomic mols., spectral and integrated relationships between absorpt. and emission for electronic state diagrams 3–14355
  - scintillation system, radioisotopes, luminous flux, radioactivity, acoustic cavitation, standardization, efficiency 3–298
  - small molecules, intramol. perturbations and quenching 3–26684
  - spontaneous emission and rotating-wave approx., freq. shift terms addition 3–29070
  - temperature quenching, broad-band and narrow-line emissions, unified model 3–39169
  - variable emission recording by method of counting single photons *(Russian)* 3–35681
  - AgBr(I) in photographic emulsions, luminescence spectrum dependence on emulsification conditions *(Russian)* 3–2838
  - He, spontaneous emission, forbidden $2^3S_1 \rightarrow 1^1S_0$ line, obs. and transition rate meas. 3–38220
  - I, $^2P_{1/2}-{}^2P_{3/2}$ laser transition 3–32554
  - $Sm^{3+}(4f^5)$ ion, energy struct. calc. for intermediate coupling 3–29495
- **luminescence chambers** *see scintillation chambers*
- **luminescence of gases**
  - anthracene derivatives, fluoresc., 423 to 648 K, relax. process, influence on spectral characts. *(Russian)* 3–26687
  - complex mols., universal correl. between absorpt. and luminesc. spectra *(Russian)* 3–20179
  - ethylene, $O(^3P)$ addition, flash photolysis reson. fluoresc. study 3–25088
  - nonviscous incandescent gas supersonic stream, radial thermal flux distribution at surface of a sphere *(Russian)* 3–29887
  - phosphorescence, microwave induced modulation of molecular excited states, optically detected electron spin echoes and free precession 3–18800
  - secondary radiation from gas system, polarization characts. 3–23484
  - Ar-Kr mixed ion cw laser, current depend. of spontaneous emission 3–32539
  - CN, B state, fluoresc., time depend. 3–26688
  - CO, excited states, elastic cross relax. 3–36042
  - CO, vibrationally excited, reaction of O atoms with acetylene, methylacetylene and methane 3–39432
  - Cs, vapour, excited by light of 852.1-894.3 nm reson. lines, fluoresc. spectrum 3–23480
  - I_2, excited by ionized Ar and Kr lasers, fluoresc. obs. 3–23588
  - K, luminesc. in pulse discharge, H_2-addition effect 3–33413
  - Na, luminesc. in pulse discharge, H_2-addition effect 3–33413
  - Ne, spectral lines, $2p^55s^1P_1$, $^3P_{0,1,2}$ upper levels, optical excitation functions 3–26572
  - Rb_2 vapour, nonlinear absorpt. of ruby laser emission, fluoresc. *(Russian)* 3–7221
- **luminescence of inorganic solids**
  - alkali halide:Tl^+, many-photon excitation of luminesc. on laser irradiation 3–5230
  - alkali halide, phonon sidebands in emission spectrum of O_2^- 3–39182
  - alkali halide, photolum., analogue computer modelling *(Russian)* 3–21461
  - alkali halide phosphors, photolum., 10-40 eV 3–27558
  - alkali halide phosphors, X-irrad., time-lag of photostimulated luminesc. *(Russian)* 3–18483
  - alkali halides, F-centre spin-lattice relax. in relaxed excited state, e.p.r. optical detection 3–18368
  - alkali halides with dissolved O_2^-, S_2^-, Se_2^- and SeS^- mols., zero-phonon transitions 3–27556
  - alkali metal halide:Th, In phosphors, absorption spectra and phosphorescence spectra depend. on lattice parameters and refractive index *(Russian)* 3–30875
  - alkali metal halides, reson. secondary glow, polarisation theory *(Russian)* 3–36918
  - alkaline earth sulphates, Eu^{2+} activation, fluorescence and excitation spectra 3–39172
  - alkaline earth sulphides, luminescence spectra *(Russian)* 3–27553
  - c ZnS, simultaneous photovoltage and fluoresc. meas. 3–5028
  - calcium fluorophosphate, e.p.r. study of luminescent and colour centre defects 3–34212
  - cuprous halides, luminesc. during laser excitation, H band emission, electron and hole effective masses 3–27557
  - diamond, low-symmetry impurity centres, rel. to e.p.r. *(Russian)* 3–12058
  - diamond, luminescence quenching and zero-phonon line broadening associated with defect interactions 3–30860
  - diamond, semiconducting, thermolum. excited by elec. field 3–21494
  - diamond crystals, absorption and luminescence spectra, red region, neutron irradiation effects 3–36901
  - F-centre emission, stress-induced polarisation, appl. of vibronic model 3–34415
  - fluorite-type crystals, activation of electron excitations by Er^{3+} ions, Stark splitting 3–36941
  - glass:Nd, laser-induced-fluorescence-line-narrowing spectroscopy 3–21474
  - glass:Yb, Tb(Eu) luminescence, cooperative processes *(Russian)* 3–36907
  - glass, borate and phosphate, Tm^{3+}, Er^{3+}, fluorescence energy transfer processes, efficiencies, decay times 3–21466
  - glass, colour filter photolum. props. 3–28555
  - II-VI semiconductor, edge emission rel. to donor-acceptor pair recombination 3–8630
  - II-VI semiconductors, exciton luminescence and photoconductivity at high densities of excitation *(Russian)* 3–27531
  - II-VI semiconductors, recomb. luminesc. and photoconduction, review *(Russian)* 3–27545
  - impurity luminescent centres, Monte Carlo method for solving excitation transfer 3–34412
  - inert gas alloys, dil., deep impurity excited states obs. 3–2581
  - ionic crysts., luminesc. impurity centres, energy transfer, excitonic mechanisms *(Russian)* 3–27537
  - Mn(II) complex, bis(tetraphenyldithioimidodiphosphinato)manganese (II) 3–7104
  - nitrate glass: Eu, Sm, Gd, Tb, Dy absorption, luminescent and excitation spectra *(Russian)* 3–30878

luminescence of inorganic solids continued
phosphate glass, exchange interaction role in energy transfer between Eu^{3+}, Sm^{3+}, Dy^{3+} and UO_2^{2+} *(Russian)* 3−8651
phosphate glasses, lanthanide activated, polarization study of luminescent centres *(Russian)* 3−24733
potassium halide crysts., T-centres, photoluminesc. meas. *(Russian)* 3−36919
pyroxene, glass. Eu^{3+}, effect of thermal working on luminescence spectra *(Russian)* 3−30874
rare earth ions, in solid state, probability of energy transfer in cooperative transitions *(Russian)* 3−27530
rare earth metal ions, energy degradation mechanism *(Russian)* 3−27543
rare earth oxychloride phosphors, i.r. stimulable, prepn. by sintering 3−2503
rare-earth fluorides, coloration centres, photoluminesc. meas. *(Russian)* 3−36920
rare-earth ions, electron-phonon interaction, spectral effects *(Russian)* 3−36372
rare-earth-doped, dominant energy transfer mechanism 3−36936
rare-earth-doped, energy transfer and optical transitions 3−39178
rare-earth-doped, transition probability calc. 3−39177
ruby, higher energy levels of Cr^{3+} ion pairs, excitation and absorpt. spectra 3−15551
ruby, luminescent line widths in an optical resonator *(Russian)* 3−29099
ruby, photon echo decay mechanism *(Russian)* 3−8634
ruby, superhyperfine interactions on photon echo behaviour 3−34417
semiconducting crystals, I-III-VI$_2$, formation, stoichiometry and props. 3−5269
semiconductor $A_{II}B_{VI}$ crystals activated by transition metal ions, luminescence mechanism *(Russian)* 3−36933
semiconductors, at high excitation densities, emission spectra theory *(Russian)* 3−27539
semiconductors, electroluminesc. and photoluminesc. study, 0.5 to 11 μ waveband *(Russian)* 3−27576
sodium uranyl acetate, electron vibr. spectra 3−23591
transition metal ions, electron-phonon interaction, spectral effects *(Russian)* 3−36372
transition metal ions, energy degradation mechanism *(Russian)* 3−27543
uranyl complex, luminesc. temp. broadening and shift 3−21481
Ag$^+$ salts, luminesc., coloration appearance study *(Russian)* 3−37137
$AgInSe_2$, electronic structure from electroreflectance and photoluminescence meas. 3−39183
n-$Al_xGa_{1-x}As$, luminescence, exciton bands *(Russian)* 3−36931
$Al_xGa_{1-x}As$, p- and n-type, epitaxial film, solid soln., luminesc. depend. on comp. 3−39187
$Al_xGa_{1-x}As$ semiconductor, spectra, radiative transition kinetics, 4.2-77 K, temperature influence 3−34422
$Al_xGa_{1-x}As$:Ge epitaxial film, photolum., 1.1-2 eV *(Russian)* 3−2589
AlN, O centres, luminesc. study *(Russian)* 3−36921
AlN, refl. and luminesc. excitation spectra, 3-40 eV 3−18493
Al_2O_3, influence of electric field on parameters of impurity centre 3−36951
Al_2O_3, thermolum. after X-ray and u.v. irrad., activation energies 3−34435
α-Al_2O_3:Cr^{3+} direct optical excitation into excited states of Cr^{3+} pairs 3−8657
Ar, spectra *(Russian)* 3−5236
As_2Se_3, amorphous, radiative recomb. 3−24737
Au film, with island struct., I-V characts. rel. to electrolum. 3−21488
BaF_2, temp. effect on X-ray luminesc. spectra, Eu^{2+} impurity effect *(Russian)* 3−8650
$BaGa_2S_4$:Ce,Na, cathodolum., rel. to fyling spot scanner appl. 3−12186
$BaSO_4$:Eu(Mn), radiational defects, thermoluminesc. study *(Russian)* 3−27581
$BaTiO_3$, light emission, solid state phase transitions, polarisation switching 3−39111
BiI_3, bielectron and bi hole luminesc. radiation, 1.6-10K 3−18490
BiOBr, spectra, energy levels *(Russian)* 3−8108
BiOCl, spectra, energy levels *(Russian)* 3−8108
BiOI, spectra, energy levels *(Russian)* 3−8108
$CaCO_3$ calcite (synthetic), cathodothermoluminescence, low-temp. effects 3−18502
$CaCO_3$ crystals, containing ions of d^9 config., e.p.r. and luminescence studies 3−36790
CaF_2, temp. effect on X-ray luminesc. spectra, Eu^{2+} impurity effect *(Russian)* 3−8650
CaF_2:Cd^{3+}, Pr^{3+}, Yb^{3+}, luminescence, energy transfer from Cd^{3+} to Pr^{3+} and Yb^{3+} *(Russian)* 3−36905
CaF_2:Er^{3+}, two-photon excitation by dye laser *(Russian)* 3−12181
CaF_2:Eu crystals, thermoluminescence and X-ray stimulated luminescence 3−27580
CaF_2:Mn(Ce,Mn), cathodoluminescence, trapped hole diffusion 3−39197
CaF_2:Sm, X-ray or u.v. excited, thermolum 3−24758
CaF_2:Sm^{2+}, nonradiative transition stimulation by intense optical excitation effects *(Russian)* 3−15539
CaF_2:Sm^{2+}, stimulation of nonradiating transitions by strong light excitation *(Russian)* 3−36925
$CaGa_2S_4$:Ce,Na, cathodolum., rel. to flying spot scanner appl. 3−12186
$Ca_{2-2x}Na_{1\|x}Eu_xMg_2V_3O_{12}$, Eu^{3+} fluoresc., energy levels, point symmetry *(French)* 3−18480
$Ca_{2-2x}Na_{1\|x}Eu_xMg_2V_3O_{12}$, fluoresc. of Eu^{3+}, temp. and conc. depend. *(French)* 3−21460
CaO, F-centre Stark effect 3−30858
CaO, r.f. sputtered films, pure and Sm- and Tm-doped, X-ray excited fluoresc. 3−27568
CaO:Bi, Sb, Te phosphors, photoluminescence, radical-recombination luminescence of the O atoms *(Russian)* 3−30876
$CaO.P_2O_5$ glass:Cu$^+$, comp. and temp. depend. 3−30869
$Ca_{10}(PO_4)_6F_2$:Sn, effect of oxidation state of Sn 3−39470

luminescence of inorganic solids continued
$Ca_{10}(PO_4)_6F_2$:Sn, luminescence, electronic transitions, substitutional sites 3−39174
CaS phosphors, F$^-$ aggregate centre formation due to S^{2-} vacancies, e.s.r. obs. 3−39028
CaS:Bi^{3+}, Pd^{2+} phosphorescence decay characteristics 3−30856
$CaSO_4$:Eu(Mn), radiational defects, thermoluminesc. study *(Russian)* 3−27581
$CaSO_4$:V, Ln, (Ln=Y, Dy, Sm, Tb), energy transfer by sensitizer-activator pairing 3−30868
$CaSO_4$-Mn phosphor, thermoluminesc., excitation by low- and middle-energy protons 3−24757
$CaWO_4$:Am^{3+}, fluoresc. emission props. 3−34405
$CaZrO_3$:Dy^{3+} spectra at 27 K and 300 K, energies and relative intensities of transitions *(Russian)* 3−39171
$CdCrS_4$:In photoluminescence, emission and excitation, single crystals 3−36935
CdF_2, cooperative luminesc. of Yb^{3+} and Er^{3+} *(French)* 3−30855
CdF_2:$^{169}YbF_3$, Stockbarger technique growth, optical props. of radioactive and nonradioactive samples 3−2664
CdF_2:Pr^{3+}. line structure obs. in cathodoluminescence spectrum 3−30885
n- and p-CdP_2, impurity photolum. *(Russian)* 3−8658
Cd_2PO_4F:Mn, Mn activated luminescence 3−2586
CdS, antistokes exciton luminesc. study *(Russian)* 3−27536
CdS, exciton luminesc. spectra obs. for free exciton lifetime 3−8659
CdS, green edge luminesc. rel. to exciton emission, 20.4K *(Russian)* 3−21482
CdS, high carrier and exciton conc., low temp. emission recomb. study *(Russian)* 3−27541
CdS, LA-phonon exciton interaction, luminesc. study *(Russian)* 3−36916
CdS, luminesc. excitation spectral obs. for bound exciton form. kinetics 3−8133
CdS, photoluminescence at high exciton densities at 4.2K 3−39184
CdS, polarisation of light emitted from free and bound excitons 3−2594
CdS, study under intense electron beam excitation 3−8223
CdS:Ce^{3+}, Ag, Cu, fluorescence spectra, probability of emission calc. *(Russian)* 3−27546
CdS:Li(Na)(Ag), furnace doping, rel. to bound exciton spectra 3−12184
CdS(Se), electrolum. from controlled splits 3−24746
CdS(Se), luminesc. line shape due to elastic collision of anisotropic excitonic molecules 3−24738
CdS(Se), new luminesc. line due to inelastic collision of excitonic molecules 3−24739
CdS_xSe_{1-x}, graded gap crystal layer, luminesc. obs. by electron beam excitation 3−8053
CdSe, Bose condensation of excitonic molecules, luminesc. obs. 3−30437
CdTe, edge emission spectra, electron irrad. effects 3−18488
CdTe, photoluminescence, lattice defect investigation with use of heat treatment, neutron and electron irradiation *(Russian)* 3−27550
ClO_2-salts, luminesc., coloration appearance study *(Russian)* 3−37137
Cr complex, $[Cr(atp)_6]X_3$, atp=antipyrene, X=SO_3F, BF_4, SCN, ClO_4, anion effects *(German)* 3−8679
Cr^{3+} extra-exchangeable ions in polynuclear complex salts, luminescence *(Russian)* 3−36927
Cr(111) complex, $(Cr_3O(CH_3COO)_6(H_2O)_3)Cl.6H_2O$, spectroscopic study, ground state parameter determ. 3−12165
CsF:Tl single crystals, luminescence props. *(Russian)* 3−12175
CuCl, high carrier and exciton conc., low temp. emission recomb. study *(Russian)* 3−27541
$CuGaS_2$, grown by I_2 transport, p-type cond. and green photolum. 3−30474
$CuGaS_2$-CdS p-n diode, green electrolum. 3−39188
$CuInSe_2$, electronic structure from electroreflectance and photoluminescence meas. 3−39183
Cu_2O, photoluminescence, existence of excitonic molecules 3−5228
Cu_2O, Raman scattering, luminescence, exciton-phonon coupling 3−8581
Er^{3+} doped fluorides, i.r. excited visible luminesc., host lattice effects 3−21469
Eu complex, tetrakis(benzoylacetonate)europium, laser compound 3−21440
Eu dibenzoylmethane complexes, ion-ion interaction effect on luminescence 3−27527
Eu^{3+}, luminescence spectra in presence of charge transfer *(Russian)* 3−36926
n-$Ga_{1-x}Al_xAs$:Si, catholum. obs. rel. to energy gap meas. 3−30886
GaAs, circular polarisation of recombination light in weak mag. field 3−8660
GaAs, deuteron irrad., defect distrib. determ. *(Russian)* 3−1655
GaAs, double heterostruct. laser, radiative recomb. rel. to press. 3−2590
GaAs, $GaAs_xP_{1-x}$, cathodoluminescence, temp. depend., 27-300K 3−36949
n-GaAs, heat treatment effects on 0.93, 1.0 and 1.28 eV luminesc. bands 3−21477
GaAs, high-purity, polariton reflectance and photoluminescence 3−39185
GaAs, imperfections, photoluminesc. investigation *(Russian)* 3−36914
GaAs, luminesc. due to exciton-exciton collision 3−30871
GaAs, photolum., regions damaged by laser beam 3−27571
GaAs, plastically deformed, dislocations, i.r. cathodolum. study 3−38699
GaAs, polarised luminescence due to optical orientation of electrons *(Russian)* 3−36934
GaAs, recomb. radiation, carriers generated in vicinity of surface 3−34426
GaAs, rel. to compensation 3−2591
p-GaAs luminesc. reduction due to dislocations introduced during polishing 3−27559
GaAs p-n junction, photo-e.m.f., under action of self-recomb. radiation *(Russian)* 3−27303
n-GaAs:Cu, 1.26-1.30 eV photolum. band rel. to recombination centres 3−39186

luminescence of inorganic solids continued
GaAs:Cu, photolum. of excitons bound to Cu complex centres 3−34418
GaAs:Si, epitaxial layers, characterisation of p-n structure, etching, cathodoluminescence 3−39195
GaAs:Sn, defect props. rel. to growth conditions, elec., luminesc. and lattice const. meas. 3−36267
GaAs:Te, implanted, influence of implantation temp. and surface protection 3−12310
n-GaAs:Te, photolum., 80 K, surface treatment effects 3−27570
p-GaAs:Zn, optical orientation of electron spins, surface influence determ. *(Russian)* 3−8662
GaAs-AlAs solid solution, polarised luminescence due to optical orientation of electrons *(Russian)* 3−36934
GaAs-GaP solid solution, polarised luminescence due to optical orientation of electrons *(Russian)* 3−36934
GaAs$_{0.2}$P$_{0.8}$, electrolum. from controlled splits 3−24746
GaAs$_{1-x}$P$_x$, rel. indirect Γ_{8v}-X_{1c} band gap 3−21003
GaAs$_{1-x}$P$_x$:N, photoluminescence meas. rel. to isoelectronic trap transitions in resonant enhancement region 3−30430
GaAs$_{1-x}$P$_x$:N, rel. to laser operation on photopumped NN$_3$ pair transitions 3−37972
GaN, u.v. d.c. electrolum. generation by forward bias injection 3−15556
GaN:Zn electro-luminesc. diodes, manufacture and characts. *(Russian)* 3−36945
GaN-GaN:Mg light emitting diode, violet luminesc. 3−34432
GaP, at high excitation levels, excitonic luminesc. and photocond. study *(Russian)* 3−27542
GaP, donor-acceptor radiative recomb. of C-S and Zn-S pairs *(Russian)* 3−8633
GaP, evidence for nonradiative Si,O defect 3−21023
GaP, fluoresc. from bound excitons, quenching and enhancement by far i.r. radiation 3−36940
GaP, GaAs$_x$P$_{1-x}$, cathodoluminescence, temp. depend., 27-300K 3−36949
n-GaP, liq.- encapsulated-Czochralski-grown, deep hole traps 3−5235
GaP, recombination processes responsible for room-temp. near-band-gap radiation 3−34416
GaP, reson. fluoresc. due to bound excitons, laser excited 3−18484
GaP bands at 2-179 eV and 1.922 eV due to diffused Cu 3−2592
GaP red-emitting lamp, O content and electrolum. efficiency 3−30537
GaP:Cu, red pair luminesc. 3−15544
GaP:Li, Zn, bonding of excitons by neutral donors and acceptors *(Russian)* 3−36932
GaP:N, bound exciton spectra and radiation kinetics during two-photon excitation 3−18491
GaP:N, seven line luminesc. spectrum of (Neeh) complex 3−34420
GaP:N, Te(Zn), LPE layer, minority carrier lifetimes and electrolum. efficiencies 3−30493
GaP:Zn, O, vapour phase epitaxial, form. of Zn-O radiation centre 3−2672
GaP:Zn,O, Czochralski-grown photoluminesc., minority carrier lifetime, effect of heat treatment 3−39176
GaP$_x$As$_{1-x}$, p- and n-type, epitaxial film, solid soln., luminesc. depend. on comp. 3−39187
p-GaSb, optical pumping of spin polarised conduction electrons, photoluminescence 3−34398
GaSb:Te, and undoped p-, acceptor radiative recomb., photoluminesc. spectral comparison *(Russian)* 3−36915
GaSe, intense excitation by electron beam 3−15563
p-GaSe, optical orientation of excitons and Hanle effect 3−34428
GaSe, photolum. spectra, carrier assisted radiative recomb. of free excitons 3−15553
GaSe, spontaneous and stimulated emission, under intense laser beam excitation 3−27517
GdAlO$_2$:Tm^{3+}, luminesc. spectra obs. rel. to energy levels 3−12174
GdAlO$_3$:Ho^{3+}, absorpt. and luminesc. spectra obs. rel. to energy levels 3−8655
GdAlO$_3$:Nd^{3+} single crystals *(Russian)* 3−24731
Ge, laser excited, radiative transition 3−5233
n-Ge, microwave photocond. and radiative recomb. under high optical excitation at low temp. 3−38871
Ge, radiative recomb. of biexcitons, photolum. *(Russian)* 3−8663
Ge:As, Ga, indirect semicond., direct transition probability in impurity luminesc. 3−15554
Ge:As,Sb, luminesc. spectra due to electron-hole radiative recomb., virtual bound state, 2K 3−8632
Ge:Sn, Si, luminesc. of indirect excitons, zero phonon radiative annihilation 3−21479
Hg$_2$F$_2$(Cl$_2$)(Br$_2$)(I$_2$), excitation and emission spectra, 77 K and room temp. 3−30864
I, monochromatically excited, fluoresc. spectra, energy transfer processes, quenching by I 3−23625
In$_{1-x}$Ga$_x$As$_{1-y}$P$_y$ alloys, electron zones, cathodoluminesc. struct. study *(Russian)* 3−36946
In$_{1-x}$Ga$_x$P:N, reson. enhancement of recomb. probability associated with isoelectronic trap states 3−18472
In$_{1-x}$Ga$_x$P:N, soln. growth, photoluminesc. meas. rel. to band gap and N-trap states 3−24797
KBr:Tl(In), thermoluminesc., cryst. light-sum storage study 3−32595
KCl, e.p.r. of loose F aggregate centres, opt. detection 3−2392
KCl, γ irradiated crystals, thermoluminescence, plastic deformation effect 3−8677
KCl, luminesc. flashes on unloading deformed crystal rel. to dislocation motion 3−5232
KCl:Ag, photochemically coloured crystals, luminesc. on deformation 3−5231
KCl:Au$^-$, study of absorption bands and related luminescence centres 3−12167
KCl:Cu, complex centres, emission spectra 3−15528
KCl:Sm^{2+}, fluoresc. spectral meas. of ion-defect pair energies 3−24736
KCl:Sn phosphor, polarized C radiation and energy level diagram for Sn^{2+} centres *(Russian)* 3−8649
KCl:Tl, optical delocalization of holes from Tl^{2+} centres 3−34390

luminescence of inorganic solids continued
KCl:Tl, temp. dependence of efficiency of hole capture by activator *(Russian)* 3−12171
KCl:Tl(Eu), thermoluminesc., cryst. light-sum storage study 3−32595
KCl.KI-Tl crystal, intracentre luminescence, excitation bands *(Russian)* 3−27562
KI, recomb. luminesc. lifetimes rel. to self trapped excitons 3−21468
KI:In, energy transfer from excitons to activator *(Russian)* 3−12170
KI-Tl compound-centres, crystal, A-absorption band excitation, emission and excitation spectra, pulse decay time *(Russian)* 3−27563
KI-Tl$^+$ phosphors, relax. excited states, linear electron-lattice interaction description *(Russian)* 3−36917
KI(Tl), scintillation response to channelled ions 3−34434
KMgF$_3$, impurity and defect centres, thermoluminesc. 3−34436
KMgF$_3$:Mn, colour centre luminescence 3−34403
Kr, spectra *(Russian)* 3−5236
LaAlO$_3$, higher energy levels of Cr^{3+} ion pairs, excitation and absorpt. spectra 3−15551
LaAlO$_3$:Pr^{3+}, probabilities for radiative and non-radiative decay 3−36937
LaBr$_3$:Tb^{3+}, absorpt. and fluoresc. spectra, 77 K 3−30866
LaCl$_3$:Pr^{3+}, i.r. quantum counter upconversion, laser optical double reson. 3−18487
LaF$_3$, excited Nd^{3+} ion metastable state deactivation processes 3−34427
LaF$_3$:Nd^{3+}, excitation spectra for 1.06 micron luminesc. 3−24734
LaF$_3$:Pr^{3+}, i.r. quantum counter upconversion, laser optical double reson. 3−18487
La$_2$O$_3$:Bi^{3+}, photoluminescence props. *(Russian)* 3−36930
La$_2$O$_2$S, rare-earth activated thin films, cathodolum. 3−8671
α-LiAlSi$_2$O$_6$:Mn^{2+}, single crystal, polarised cathodoluminescence emission 3−39194
LiF, thermolum. response of rad. of X-rays and γ-rays 3−28392
LiF:Mg, electron trap depth and supralinear thermolum. response 3−24756
LiF:Mg^{2+}, thermolum. rel. to Mg^{2+} vacancy pairs 3−12189
LiF:U^{6+}, charge compensation effects 3−2383
LiH:Ga(Ge)(As), excitation and luminesc. spectra *(Russian)* 3−21462
LiH:Mg(Ge)(In)(Tl), red luminesc., 120 and 293 K *(Russian)* 3−15538
LiNbO$_3$, comments on proposed optical index damage phenomena 3−18485
LiNbO$_3$, parametric luminescence, line profile *(Russian)* 3−739
LiNbO$_3$ reply to comments on optical index damage 3−18486
MgF$_2$, electron and proton irrad., thermolum. *(Russian)* 3−18505
MgO, thermolum. after X-ray and u.v. irrad., activation energies 3−34435
MgO:He, Ar, Fe, Cr, ion implanted, photolum. from damage related defect centres 3−21463
MgO-Al$_2$O$_3$ synthetic spinel, spectra of Cr and Mn impurities, comp. depend. 3−34429
Mg$_2$TiO$_4$:Mn^{4+}, Cr^{3+}, phosphors, luminescence *(Russian)* 3−36928
NO$_2$-salts, luminesc., coloration apperance study *(Russian)* 3−37137
NaBaVO$_4$, NaCaVO$_4$, NaCdVO$_4$, spectra, temp. and competition effects *(Russian)* 3−39170
NaCl:Br, absorpt. and luminesc. of Br$^-$ clusters 3−21464
NaCl:Mg, X-irradiated crystals, Mg centres expt. obs. 3−38586
NaCl:Tl deformed thermoluminescence 3−15568
NaF:Eu^{3+}, Eu^{3+} luminesc. centres, spectral anal. 3−5229
NaI(Tl), scintillation response to channelled ions 3−34434
NaLnF$_4$:Yb^{3+}, Er^{3+}, (Ln=Y,Gd,La), efficient green-emitting i.r. excited phosphor, prep. 3−8639
NaMVO$_4$, (M=Ca, Cd, Ba), temp. depend. *(Russian)* 3−15537
α-NaYF$_4$:Yb^{3+}, Er^{3+}, phosphors, visible luminescence during i.r. excitation *(Russian)* 3−36906
NdZrF$_4$, fluoresc. of Nd^{3+}, matrix characterization *(French)* 3−18481
Ne, fine struct. splitting *(Russian)* 3−5236
PbBr$_2$ single crystals, luminescence and e.p.r. of u.v. irradiated crystals 3−8640
PbBr(Cl)$_2$, blue and violet luminesc., excitons rel. to energy transport mechanism 3−34407
PbCl$_2$ single crystals, luminescence and e.p.r. of u.v. irradiated crystals 3−8640
PbCl(Br)$_2$, emission spectra obs., thin film absorpt. rel. to exciton form. 3−27561
PbF$_2$(Cl$_2$)(Br$_2$), low temp. X-ray luminesc. and photolum. 3−30863
PrCl$_3$, fluoresc., effect of pump laser wavelength, pump power and temperature 3−18471
RbI, recomb. luminesc. lifetimes rel. to self trapped excitons 3−21468
RbUO$_2$(NO$_3$)$_3$ crystals at liquid He temp., polarised luminescence spectra *(Russian)* 3−36942
ruby:Cr^{2+}, Cr^{3+}, Cr^{4+} luminescence, quantum losses *(Russian)* 3−36929
ScYO$_3$, Nd^{3+} level structs. *(Russian)* 3−12182
Si:As, Zeeman splitting of photoluminescence of excitons 3−38809
SiC, 6H type, prep. by ^{11}B$^+$ implantation 3−30956
SiC, 6H-polytype, exciton complexes, investigation by isotope substitution 3−30867
SiC, hexagonal, spectrum of nonisolated donor-acceptor pairs 3−34425
β-SiC, with radiation defects, cathodolum. mechanism and efficiency *(Russian)* 3−2599
β-SiC:B, low temp. luminesc. due to donor-acceptor pair emission 3−34419
SiC:O, B, enhancement of luminescence brightness by O$_2$ 3−39173
Sm complexes, with tenoyltrifluoroacetone and 1, 10-phenanthroline, luminesc. extinction by impurity lanthanide ions *(Russian)* 3−21483
SrGa$_2$S$_4$:Ce,Na, cathodulum., rel. to flying spot scanner appl. 3−12186
SrS:Bi, activator conc. depend. of characts. 3−27564
SrSO$_4$:Eu(Mn), radiational defects, thermoluminesc. study *(Russian)* 3−27581

luminescence of inorganic solids continued
- $SrSb_2O_6:Bi^{3+}$, photoluminescence props. *(Russian)* 3−36930
- Ta_2O_5 powder, incorporated in polymer, electrolum. *(Russian)* 3−18497
- TbF_3, ZnS-TbF_3, cathodoluminescence, ($^5D_3 \rightarrow {}^7F_j$) transition obs. *(French)* 3−18503
- Te, activated, at high excitation levels, excitonic luminesc. and photocond. study *(Russian)* 3−27542
- TlBr indirect edge in luminesc. excitation spectra confirming indirect band gap 3−2584
- $UO_2(NO_3)_2$ hydrates, effect of D_2O substitution on luminesc. spectra *(Russian)* 3−21485
- Xe, spectra *(Russian)* 3−5236
- YAG, rare earth activated, recomb. luminesc., thermolum. and photolum. obs. 3−21480
- YAG:Ce^{3+} and its solid solutions, cathodolum. 3−30883
- YAG:Nd, Li, laser crystal, luminesc. props. with doping 3−19617
- $YAlO_3:Er^{3+}$, energy levels, cryst. field components 3−5225
- YF_3: Yb, Er phosphor, i.r. to visible conversion, determ. of host parameters 3−39179
- YVO_4, self-excited luminesc. of $^{147}Pm^{3+}$, i.r. emission and laser effect *(French)* 3−8629
- YVO_4 phosphors, extinction of luminesc. of one lanthanide ion by another, quantitative expression *(Russian)* 3−24743
- $YVO_4:Eu^{3+}$, photoluminescence, concentration and temp. characteristics *(Russian)* 3−30872
- Yb^{3+} doped fluorides, i.r. excited visible luminesc., host lattice effects 3−21469
- (Zm,Cd)S-Cu, short wave emission spectra rel. to CdS conc., -150°-70°C 3−21458
- (Zn, Cd)S-Cu phosphors, long wave photolum. rel. to CdS conc. and temp., −150°C to 200°C 3−27526
- ZnCdS pellets, electroluminesc. and stimulated conductivity study *(Russian)* 3−21492
- $Zn_2GeO_4:Mn^{2+}$, luminesc. rel. to free carriers prod. by sub-band-gap excitation, trapping effects 3−21467
- ZnO, i.r. photolum. emission band 3−27560
- ZnO, luminescence in exciton region with two photon excitation *(Russian)* 3−8653
- ZnO spectral investigation of luminescence centres *(Russian)* 3−27547
- ZnS, depend upon O content *(Russian)* 3−21484
- ZnS, electroluminesc. intensity, origin of first peak *(Russian)* 3−21493
- ZnS, powdered, X-ray induced a.c. cond., thermostimulation, fluoresc., thermolum. 3−38868
- ZnS, u.v. cathodolum., temp. depend., 80-400K *(Russian)* 3−15560
- ZnS phosphors activated by heterovalent impurities, luminescence spectra peculiarities *(Russian)* 3−27549
- ZnS powdered phosphor display systems, d.c. electroluminescence 3−24752
- ZnS spectral investigation of luminescence centres *(Russian)* 3−27547
- ZnS: Te, of bound excitons 3−39180
- ZnS:Ag, Cu, fluorescence spectra, probability of emission calc. *(Russian)* 3−27546
- ZnS:Cl, e.p.r. signal and self-activated luminesc. from A-centre, Zn vacancy-Cd donor pair 3−33529
- ZnS:Cl, luminescence spectra *(Russian)* 3−27548
- ZnS:Cl photoluminescence, effect of trapezoidal electric field *(Russian)* 3−36944
- ZnS:Cr^+, Cu, C, e.p.r. and luminescence studies *(Russian)* 3−27552
- ZnS:Cr^{2+}, excitation spectra interpretation by fitting eigenvalues of Tanabe-Sugano matrices 3−2588
- ZnS:Cu, β-irrad. at 5K, fast light emission 3−24753
- ZnS:Cu, multiphoton impurity luminescence 3−34384
- ZnS:Cu and ZnS:Cu,Al, electrolum., Gaussian component intensity, alternating voltage freq. depend. *(Russian)* 3−21486
- ZnS:Mn, Cl, thermal quenching of luminesc., elec. field effects *(Russian)* 3−27555
- ZnS:Mn film, d.c. electrolum. 3−30882
- ZnS:Ni, Cu crystal, phototransfer of holes from Ni^{2+} to Cu^+ ions 3−34411
- ZnS-CdS phosphors, activation by Cu diffusion at low temperature *(Russian)* 3−36943
- ZnS-Cu powder cells, electrolum. decay rel. to trapped electrons 3−21487
- ZnS-GaP, absorpt. and photolum. spectra, band gap energy 3−34404
- ZnS-TbF_3, ZnS:Tb^{3+}, cathodoluminescence, ($^5D_3 \rightarrow {}^7F_j$) transition obs. *(French)* 3−18503
- ZnSe layers, heteroepitaxy, luminescence centres 3−18546
- ZnSe-SnO_2 heterojunction, injection electroluminescence *(Russian)* 3−27575
- Zn_2SiO_4 film, growth on Si substrate, electrolum. props., monolithic display device applications 3−21491
- Zn_2SiO_4:Mn powder, quantitative chem. anal. and luminesc. spectra 3−30854
- $ZnSiP_2$ luminescence excitation spectra at 2K 3−8654
- ZnTe, cathodoluminescence of the donor-double-acceptor pairs *(Russian)* 3−27577
- ZnTe, interpretation of asymmetric band shapes in terms of bound exciton complexes 3−36948
- ZnTe, luminescence and modulation by CO_2 laser radiation *(Russian)* 3−27551
- ZnTe, photoluminescence using laser excitation *(Russian)* 3−30879
- ZnTe, time resolved spectroscopy involving ionisable donor acceptor states 3−36947
- ZnTe:Cu, electron-beam excited, visible luminesc. 3−30884
- $ZrSiO_4:Eu^{3+}$, Eu^{2+}, radioluminescence *(Russian)* 3−8672

luminescence of liquids and solutions
- acridine dye aggregates, emission maxima, pK depend. *(French)* 3−34399
- alkane fluoresc. quenching by CCl_4, nsec. decay time meas. 3−5405
- aniline in soln., quantum yields, solvent and conc. effects *(French)* 3−39456
- anthracene, crystals and solution, nonlinear fluorescence quenching at intense excitation *(Russian)* 3−2 533

luminescence of liquids and solutions continued
- anthracene in n-hexadecane and n-hexane solns., diffusion coefficient of triplet state *(Russian)* 3−37136
- aromatic liquid solns., radioluminescence, scintillations decay law *(French)* 3−39196
- benzene and alkylbenzenes, photoioniz. and recomb. fluoresc. 3−25081
- chlorophyll a, in polar and non-polar solvents, fluoresc. excitation spectrum 3−15542
- chrysene-naphthacene thin layers, sensitized luminesc. 3−15541
- complexes with differnt numbers of ligands, supersensitive transitions of Nd^{3+}, Ho^{3+} and Er^{3+} *(Russian)* 3−12180
- dipole relax. processes, orientational, effect on spontaneous luminesc. and generation spectra 3−15550
- dithiin complexes, with trinitrobenzene and tetracyanoethylene, fluoresc. study 3−23593
- dye lasers, flashlamp pumped, threshold pump intensity fluorescence character of solution *(German)* 3−10544
- dyes, short fluoresc. quenching times, meas. *(Russian)* 3−27892
- fluorescein dye, ionic forms problem *(Russian)* 3−12179
- fluorescein in water and glycerol, quasimonochromatic characteristics, dependence on bandwidth of exciting and observed light 3−8637
- fluorescence of solutions, selfdepolarisation, analysis of experimental data 3−18494
- inert gas alloys, dil., deep impurity excited states obs. 3−2581
- inert gas liquid lasers employing luminescence of self-localised excitons *(Russian)* 3−35692
- intermolecular relaxation-fluctuational processes and spectra of solns., review *(Russian)* 3−27524
- isotropic solns., excited by intensity modulated primary light, fluoresc. curves expressions 3−21459
- kinetics in the presence of energy transfer, migration of donor excitation *(Russian)* 3−35693
- lanthanide ions and uranyl, intercomplex energy transfer in solutions and glasses *(Russian)* 3−24744
- metal halide-NH_4NSC aq. soln., mol. anion addition, luminesc. spectral effects *(Russian)* 3−36922
- 9-methyl anthracene, photoassociation study 3−31281
- 1, 1′- methylene-2, 2′-cyanine, anomalous absorption and luminescence spectra 3−27569
- N,N-dimethyl-p-cyanoaniline, molecular interactions in ground and excited states, absorption and luminescence spectra 3−11243
- naphthalene derivative charge transfer complexes with aliphatic amines, fluoresc. *(Russian)* 3−12183
- organic and inorganic compounds in solutions energy transfer of electron excitation *(Russian)* 3−36911
- organic dyes in soln., fluorescence lifetime meas. using two-photon absorption 3−13759
- perilene in n-hexane, hot luminescence at 4.2°K 3−8644
- phthalimide solutions, excitation power effect on luminescent and absorption characteristics *(Russian)* 3−30845
- polarised liquids, relaxation and fluctuation processes *(Russian)* 3−36923
- polyphosphoric acid, exchange interaction role in energy transfer between eu^{3+}, Sm^{3+}, Dy^{3+} and UO_2^{2+} *(Russian)* 3−8651
- Rhodamine, nonsubstituted, luminophor, stimulated emission under anthracene compound addition, energy var. 3−22902
- Rhodamine 6G, luminesc. spectra, two photon excitation 3−32563
- rhodamine 6G dyes, metachromic effect, effect of copolymer composition luminescence study *(Russian)* 3−35694
- Rhodol, luminophor, stimulated emission under anthracene compound addition, energy var. 3−22902
- riboflavin solutions, electronic energy transfer frequency, conformity of universal correl. between obs. and luminescence spectra *(Russian)* 3−34408
- rigid solution, conc. depolarization of photolum. and intermolecular energy transfer, theory 3−15540
- Shpolskii systems, hot luminescence 3−8644
- sodium fluorescein soln. in glycerine-H_2O, photoluminescence, concentration quenching and depolarisation 3−15555
- solutions, isotropic influence of self-quenching on concentration depolarisation of photoluminescence 3−34397
- tetramethyl-p-benzoquinone, luminesc. spectrum at −180°C 3−17452
- trypaflavine in water and glycerol, quasimonochromatic characteristics, dependence on bandwidth of exciting and observed light 3−8637
- uranyl salt solutions, excitation energy transfer from mixtures of U(IV) and lanthanide elements *(Russian)* 3−24745
- viscous solns., complex mols. in polar medium, obtained with electronic spectra broadening 3−17450
- Eu complexes, with tenoyltrifluoroacetone and 1, 10-phenanthroline, luminesc. extinction by impurity lanthanide ions *(Russian)* 3−21483
- Eu^{3+} in D_2O, secondary fluorescence quenching rate constants for ethanol, acetic acid and H_2O 3−34421
- $EuCl_3$, primary and secondary solvation spheres of Eu^{3+}, effect on electric quadrupole transitions 3−15536
- Gd^{3+} in solution, radiative and radiationless transitions, temp. effects 3−34402
- He(II), $0.3<T<4.2K$, luminesc. prod. by weak α-particle sources 3−15045
- Mn(IV) complexes, $MnW_5O_{20}^{6-}$, $MnMo_9O_{32}^{6-}$, excitation and emission spectra 3−12164
- Na-fluorescein, luminophor, stimulated emission under anthracene compound addition, energy var. 3−22902
- 1,10-phenanthroline, fluoresc. spectral meas., excited-state dimerisation study 3−23592

luminescence of organic solids
- acridine absorbed on silica gel, extinction of luminescence by O_2 and activator distrib. *(Russian)* 3−27574
- aminobenzoic acids, thermolum., trap depths and density 3−15567
- ammonium uranyl oxalate crysts., polarization of photolum. spectra *(Russian)* 3−12178
- anthracene, breakdown electrolum. characts. *(Russian)* 3−12185
- anthracene, crystals and solution, nonlinear fluorescence quenching at intense excitation *(Russian)* 3−27533
- anthracene, delayed fluoresc. quenching due to triplet exciton-hole interaction 3−2587

luminescence of organic solids continued
- anthracene, mag. field modulation of prompt electrolum., charge transfer exciton fission 3−24747
- anthracene, singlet exciton fission, 77 K 3−36904
- anthracene crystals, electroluminescence caused by field-induced minority carriers at moderate temps. 3−39189
- anthracene crysts., surface quenching of fluoresc. and photoefffect *(Russian)* 3−8648
- meso-anthracene derivatives in n-hexane at 4 K, fluoresc. spectra 3−34413
- anthracene in heptane at 77 K, O quenching of luminesc. 3−25098
- anthracene luminescence at intense excitation by N_2 laser *(Russian)* 3−27532
- anthracene single crystals with tetracene impurity, electroluminescence *(Russian)* 3−24751
- anthracene single crysts., with surface disturbed by impurity, fluoresc. *(Russian)* 3−8647
- anthracene thin molecular crystal, absorption and fluorescence 3−34373
- anthraoxadiazole cryst. solns., quasiline fluoresc. spectra *(Russian)* 3−8641
- anthraselenodiazole, fluoresc. spectra at 77K 3−34409
- anthrathiadiazole cryst. solns., quasiline fluoresc. spectrum *(Russian)* 3−8645
- aromatic hydrocarbons in frozen paraffin matrices, phosphorescence, study of rise and decay processes 3−21835
- benzene derivatives in solid org. solns., quasiline phosphoresc. spectra *(Russian)* 3−8646
- benzol crystals, exciton-phonon interaction and luminescence spectra *(Russian)* 3−27534
- benzophenone, phosphoresc. detection of e.p.r. of triplet excitons 3−11865
- benzophenone crystals, spin memory during triplet-triplet exciton energy transfer, ODMR obs. *(Russian)* 3−36912
- benzophenone crystals, triplet excitons migration and annihilation, excitation and array structure effect *(Russian)* 3−36910
- benzophenone in toluene at 4.2 K, quasi-line phosphoresc. emission spectrum 3−34414
- 3,4-benzpyrene and methyl derivatives, quasilinear fluorescence and excitation spectra *(Russian)* 3−30877
- carbazole, quenching mechanism due to hydrogen bonding *(Russian)* 3−8652
- chrysene, oriented phosphorescent, e.p.r. absorption at mag. fields below 125 G., multiple orientation of chrysene triplets in p-terphenyl single crystals 3−25091
- chrysene-naphthacene thin layers, sensitized luminesc. 3−15541
- deuterobenzol crystals, exciton-phonon interaction and luminescence spectra *(Russian)* 3−27534
- 2,3-dichloroquinoxaline, kinetics of the triplet state from microwave-induced phosphorescence transients 3−21834
- halobiphenyls, phosphoresc. lifetime meas., heavy atom effect 3−29708
- N-heterocyclic compounds, fluoresc. and phosphoresc., relative quantum yields in 77 K *(Russian)* 3−27544
- n-hexane:1,12-benzperylene, fluoresc., broadening, profile and shift of phononless lines, 4.2-77K *(Russian)* 3−8661
- hydroxybenzoic acids, thermolum., trap depths and density 3−15567
- ketone, α, β-unsaturated, singlet-triplet transitions investigation by phosphorescence excitation spectroscopy 3−25092
- lithium phosphides, chemiluminescence, molecular structure depend. 3−30853
- methylammonium chloride Tl-activated, excitation and emission spectra *(Russian)* 3−12176
- methylene anthrone, impurity phosphoresc. 3−37138
- 2-methyltetrahydrofuran glass, X-irrad., study in temp. range 77 to 97K 3−12166
- molecular crystals, doped, polarisation luminescence method for struct. determ. *(Russian)* 3−27525
- naphthalene: pyrene, fluoresc. meas. for host sensitized energy transfer investigation 3−24735
- naphthalene, entire phonon spectrum by localized exciton sideband method 3−7872
- naphthalene, in heavy atom hosts, wavelength-dependent triplet state population mechanisms, optically detected mag. resonance expts. 3−18793
- naphthalene, in n-heptane, phosphoresc. growth and decay processes 3−25096
- naphthalene crystals with indole and thionaphthene impurities, local excitons *(Russian)* 3−36908
- naphthalene derivative charge transfer complexes with aliphatic amines, fluoresc. *(Russian)* 3−12183
- naphthoxadiazole and naphthothiadiazole cryst. solns., quasiline spectra 3−15546
- nitronaphthalene, luminescence, photoconductivity, triplet excitons lifetime *(Russian)* 3−36909
- n-octane:perylene, fluoresc., broadening, profile and shift of phononless lines, 4.2-77K *(Russian)* 3−8661
- organometallic compounds, surface exciton states and luminescence spectra *(Russian)* 3−27535
- n- paraffin frozen solns., mol. distrib. among radiating centres *(Russian)* 3−5226
- n-paraffin matrix, impurity mols., linear spectra and impurity centre theory *(Russian)* 3−36896
- phenanthrene crystals, triplet excitation spectrum 3−12173
- phenanthrene in 4, 6 polyurethane, evidence of ordered arrangement 3−8643
- phthalocyanine, near i.r. emission of single crysts. and films 3−21465
- polyadenylic acid, triplet energy transfer, Mn^{2+} phosphoresc. quenching, temp. depend. 3−31279
- polymers, mol. orientation distrib., polarised Raman scatt. and fluoresc. investigation 3−26743
- polymers, thermoluminescence and thermally stimulated cond. meas. 3−30889
- polypropylene, γ-irradiated samples at 77K, thermoluminesc. study 3−30890
- polyvinyltoluene, fluoresc. degradation under u.v. irrad. 3−30862
- protoporphyrin in n-octane, 4.2 K, reversible transforms. of luminescent impurity centres 3−15547
- pyrazine, quenching mechanism due to hydrogen bonding *(Russian)* 3−8652
- pyrene, cryst., triplet exciton lifetime 3−27888
- pyrene cryst., monomer emission, fluoresc., decay times 3−30857
- pyrene crystals, mag. field effect on delayed fluorescence 3−27565
- rare earth complexes with aurinitricarboxylic acid and amines, absorpt. and luminesc. 3−15543
- riboflavin, luminesc. spectra, depend. on exciting photon freq. 3−34410
- riboflavin, luminescence spectrum lineshape variation as function of frequency of exciting light *(Russian)* 3−12169
- stannic-phthalocyanine, infrared luminescence splitting for charge transfer like structure of states 3−2583
- p-terphenyl with tetracene impurity, vibron. relax., role of delocalized and pseudolocalized vibrs. 3−27090
- tetracene, singlet exciton fission, 77 K 3−36904
- tetracyanobenzene-biphenyl complex, delayed charge-transfer fluoresc. in cryst. state 3−21820
- tetraphenyl-butadiene, u.v. fluorescence, fluorescence wavelength convertor 3−18479
- tissue, formaldehyde vapour induced fluoresc., holder 3−35525
- trypaflavine absorbed on silica gel, extinction of luminescence by O_2 and activator distrib. *(Russian)* 3−27574
- uranyl propionates, electron vibr. spectra 3−23591
- uranyl thiocyanoacetates, i.r. and luminesc. spectra, vibr. freqs. determ. *(Russian)* 3−20167
- n-InP, luminescence polarisation of 1.41 eV band due to exciton recombination 3−2593

luminescence of solids
- *see also luminescence of inorganic solids; luminescence of organic solids*
- camera-cryostat installation 3−25756
- cooperative processes, review *(Russian)* 3−27529
- crystal interzonal spectrum, peculiarities under action of intense laser radiation *(Russian)* 3−27540
- decay of nonradiative surface plasmons into light 3−15534
- diamonds, type I and IIa, pulse irradiation 3−8673
- diazaphenanthrene, electronic struct. and luminesc. *(German)* 3−26682
- energy transfer kinetics, crysts. with systems of donor and acceptor impurity atoms 3−34424
- ethylene glycol/water glass, recomb. and photo-induced cond. meas., trapped electron optical excitation study 3−12162
- excitation decay, hopping mechanism of energy transfer 3−33835
- exciton luminescence, low temp., effect of Raman scatt. *(Russian)* 3−27554
- hexagonal crystals, transverse mag. field and deformation effects on exciton luminescence polarisation 3−2595
- ions in a crystal, vibrating struct. of luminescence spectra *(Russian)* 3−36913
- migration theory of electron excitation energy in a crystal *(Russian)* 3−36903
- phonon coupled states with impurity centres, multiplicity of dielectric local modes *(Russian)* 3−36924
- porous article density distrib. determ. method *(Russian)* 3−27797
- recombinational luminescence decay, calc. from initial distrib. of recomb. partners 3−12163
- ruby with reson. excitation, efficiency meas. method 3−15548
- semiconductor, photoinjected electrons interaction rel. to radiative emission spectrum 3−30870
- semiconductor, role of excitons *(German)* 3−15168
- sensitized, and energy transfer, review of new investigations *(Russian)* 3−27528
- sensitized, diffusion of electronic excitation energy transfer by resonance, impurity states 3−27566
- Spol'ski's method for spectral luminescence analysis of mixtures by fast crystallisation *(Russian)* 3−28786
- thermoluminescence, theory 3−30888
- transitions, optical, between degenerate localised levels, theory of moments 3−15535
- tunnel luminescence, theory 3−30859
- CaF_2, M^+ centre obs. 3−27023
- CaF_2:XF_3 (X=Pr,Tb,Nd), gamma-induced luminescence of X^{3+} centres 3−24732
- CdF_2:Er^{3+}, C_{3v} local-site symmetry from correlated e.p.r. and optical obs. 3−21305
- CsI, excitonic, field effect 3−33850
- CuI film, acceptor levels obs. *(Russian)* 3−24432
- p-CuI-n-ZnS:Mn film, electroluminesc., low voltage operation *(Russian)* 3−24748
- Eu chalcogenides, optical electrical and magnetic props., review 3−11848
- GaAs:Si, photolum. spectra at 77K, origin of 1.4-1.42 eV band 3−18489
- GaAs:Zn, Cd, Si, Ge epitaxial layer, near band-edge photoluminesc. 3−34406
- KBr cryst. with PO_2^- mol. centre, low temp. emission 3−15549
- KCl cryst. with PO_2^- mol. centre, low temp. emission 3−15549
- KCl:Tl, Ga, In, from Tl^0, Ga^0, and In^0 centres 3−27024
- KF(Cl)(Br)(I), F centre luminesc., e.p.r. optical obs. 3−12061
- NaCl, F centre luminesc., e.p.r. optical obs. 3−12061
- Rb(Br)(I), F centre luminesc., e.p.r. optical obs. 3−12061
- SiC, ion bombardment, annealing, intrinsic luminescent defects 3−34430
- SiC, ion implanted, localised vibrational modes of persistent defect obs. 3−30227
- YAG:Nd, testing of the homogeneity of single crystals by means of cathodoluminescence *(German)* 3−7789

luminescent devices
- *see also fluorescent screens; phosphors; scintillation counters*
- electroluminescent diodes, red and green, visibility to colour blind observers 3−3558
- Gunn device, i.r. light emission phenomenon 3−18498
- X-ray image convertor, EXICON solid state device 3−19342
- p-CuI-n-ZnS:Mn film, low voltage electroluminesc. *(Russian)* 3−24748
- GaAs:Si, injection diode, electrolum. line shift *(Russian)* 3−8669
- GaAs-$Al_xGa_{1-x}As$, heterojunction, p-n-p-n structure electroluminesc. props. 3−18500

luminescent devices continued
Si, diffused p-n junction, avalanche breakdown luminesc. 3–15557
T_2O_5 powder luminescent cell, prep. and performance *(Russian)* 3–18497
Ta-Ta_2O_5-ZnS:Tb^{3+}-Au film, electrolum., light emission voltage depend. 3–39192
ZnS powdered phosphor display systems, d.c. electroluminescence 3–24752
ZnS:Mn film, electroluminesc. d.c. light source *(Russian)* 3–24749
ZnS:TbF_3 thin film cells, d.c. electroluminescence 3–8667
Zn_2SiO_4 film, growth on Si substrate, electrolum. props., monolithic display device applications 3–21491

luminophors *see luminescence*

luminors *see luminescence*

lumped parameter networks
transmission line simulating e.m. wave propagation in plasma 3–11481

lunar seismology
aseismicity implications, lunar temp. model 3–3312
flares, degassing effects 3–12983
maximum seismic activity rel. to pulsar CP1133 and gravitational waves 3–3315
seismic wave velocity rel. to deep layer of fine rock powder 3–16182

lunar structure
see also moon
Apollo 11, regolith fires, photometric meas. of packing state 3–16183
Apollo 14 samples instrumental activation analysis 3–22538
Apollo 15 basalts, solid soln., subsolidus reduction and compositional characteristics 3–5587
Apollo 15 soils, major element composition of glasses 3–5588
Apollo 16 samples, petrographic and chem. description 3–31628
Apollo 17 age determ. using ^{40}Ar-^{39}Ar and ^{34}Ar-^{37}Ar dating methods 3–37334
basalt internal isochron determ. of Apollo 15 samples by Rb-Sr meas. 3–25416
boulder tracks rel. to friction angle and density var. of lunar soil 3–39641
breccias, Apollo 16 samples, petrographic study 3–31631
breccias, vapour-phase crystallization, microprobe analysis 3–39648
breccias (Apollo 14 samples), Xe prod. from ^{244}Pu and ^{129}I, abundance meas. 3–22038
breccias and vapour deposited crystals formed in their cavities 3–16171
chemistry of the Moon, review 3–35097
composition and origin, thermal props. assuming Ca-Al deep interior model 3–35082
composition of highlands, modal and normative plagioclase contents in anorthositic lithic fragments and glass 3–3304
compositional mapping, Apollo orbital measurements 3–31624
crater counts and meas. for the Hyginus Rille region 3–18988
crater structure rel. to simultaneous impact craters 3–39636
craters with concentric walls, statistical anal. 3–25424
crystalline rock from Apollo 16, Rb-Sr age 3–3308
dating of mechanical events by deformation induced erasure of particle tracks 3–9505
Descartes, Apollo 16 exploration, geologic summary 3–31629
dust and mineral grain radiation damage due to solar particles, electron microscope applics. 3–37333
electron probe analysis of glasses in lunar soils 3–39646
geology 3–16175
hypsometric properties of near side, with respect to moon's centre of mass *(Russian)* 3–16185
impact craters in dense crystalline rocks, empirical formulae and model 3–39649
inter-area chemical characteristics of lunar surface materials 3–9498
interior viscosity after mascon formation 3–39638
internal friction obs. in a strongly outgassed terrestrial analogue of lunar basalt 3–37167
internal thermal states, model of hot interior with cool lithosphere 3–37338
Luna 20 glasses, major element composition 3–12985
Luna 20 site, general features and geology of area 3–12984
lunar gravity model, truncated spherical harmonic expansion with mascon terms 3–35099
mag. fields, volcanic ash particle flow ionisation 3–12995
magma genesis model derived from chemical anal. of Apollo 15 mare basalts 3–35081
Mare Serenitatis mascon, mass distrib. from Lunar Orbiter and Apollo 15 gravity data 3–18976
maria albedo distrib. at 0.62 μ rel. to maria origin 3–37339
mineralogy, conference, Montreal, Canada (1972) 3–2859
object designation system based on spherical coordinates *(Russian)* 3–16186
orange soil, chemical comp. and origin 3–37335
plagioclases, An-rich, two-phase struct. phenomena 3–18974
pyroxenes, intracrystalline variations of major and minor elements, electron probe analysis 3–39647
pyroxenes in Apollo 16 samples, plutonic and metamorphic equilibration hypothesis 3–31626
research results and problems *(German)* 3–35096
rock 12039, mineralogy, petrology and chemistry 3–5586
rock 12053, cation order, domain struct. and exsoln. in pigeonite and augite 3–16170
rocks, metastable growth patterns 3–3310
seismic wave velocity rel. to deep layer of fine rock powder 3–16182
soil, volatile-rich, cometary impact, possible evidence 3–31630
solar flare particle tracks in lunar and meteoritic minerals 3–3317
spinal troctolite and anorthosite in Apollo 16 samples 3–31632
stability relations of ilmenite and ulvospinel in Fe-Ti-O system, applic. to lunar mineral assemblages 3–3307
stress differences as evidence for cold Moon, solid Moon model 3–39640
surface, photometric and polarimetric study 3–18982
surface, photometric obs. 3–18978
surface, radar images, at long wavelengths 3–18913

lunar structure continued
surface composition, spectroscopic remote sensing 3–18980
surface layer, formation, struct., props. 3–25421
thermal radiation properties of Apollo 14 fines 3–39637
thermal structure rel. to Apollo 15 surface heat flow measurements 3–18975
tidal mechanism rel. to origin of magnetism 3–37336
topography, global determ. by radar interferometry and delay-Doppler stereoscopy 3–25422
topography, radar-interferometer meas. of the Alphonsus-Ptolemaeus-Arzachel region 3–25423
volatilisation mass loss determ. by meas. on terrestrial basalt 3–27965
volcanic degassing, detection by an orbiting mass spectometer 3–16179
volcanic domes, identification, structure and distribution 3–39635

lutetium
Fe:^{175}Lu, hyperfine fields at impurity nuclei and annealing props. 3–15141
^{176}Lu-^{176}Hf pair, solar system abundance determ. and use as an s-process nucleochronometer 3–22010
Ni:^{175}Lu, hyperfine fields at impurity nuclei and annealing props. 3–15141

lutetium compounds
$Lu_3Al_5O_{12}$:Nd^{3+} c.w. laser, spectroscopic and lasing characts. 3–19615
$LuAsO_4$, zircon type structure, confirmed by X-ray analysis *(German)* 3–17783
$Lu_2EuMFe_4O_{12}$ (M=Al or Ga), growth-induced mag. anisotropy of epitaxial films 3–21259
$LuMn_2O_5$, helimagnetic order of Mn, neutron diffr. obs. *(French)* 3–36723
$LuMn_2O_5$, magnetocrystalline anisotropy, mag. susceptibility meas. 3–36704
$LuPO_4$, zircon type structure, confirmed by X-ray analysis *(German)* 3–17783

Luxemburg effect *see ionospheric electromagnetic wave propagation*

Lyapunov methods
displacement-energy bound for elastic structures 3–6233
energy-like functionals for stability analysis of linear elastic system on Hilbert space 3–32341
functions, conditions for boundedness and global existence of solns. of differential eqns. 3–22583

M-centres *see colour centres*

M-regions *see sun*

Mach number
see also acoustic wave velocity; shock waves
circular aerofoils with asymptotic critical Mach number, numerical results in relation to transonic similarity rule 3–17533
density-step excited ion acoustic solitons, Mach number increase with initial step ratio 3–20496
embedded ion shock, limiting Mach number 3–33359
hypersonic nozzle, initial development of mixing layer, turbulent mixing, profile data at Mach number of 19.5 3–33327
hypersonic wakes behind wedges at angle of attack at Mach number 6, expt. obs. 3–38410
Mach reflection of strong shock waves in shock tube, pressure measurement 3–33254
MHD shock struct. in strong transverse mag. fields, shock widths for very high Mach numbers 3–29959
plasma, magnetised, 'switch-on' shocks obs., shock front variation with Mach number 3–36165
plasma ion acoustic instability of Hall current during anomalous heat in accelerators, electron temp. and Mach number estimation 3–23883
plasma stable, high Mach number collisionless electrostatic shocks, obs. 3–38462
pseudo-viscous methods for steady supersonic flow past waisted body 3–1405
shock strengthening in conical convergent channel, wave vel. investigation 3–11431
shock waves in earth's rotating atmosphere, variation of Mach number and shock velocity using Whitham's rule 3–21938
two dimensional supersonic sails in high-Mach number airstreams, centred compressions 3–20345
variable properties laminar gas flow heat transfer in the entry region of parallel porous plates, Mach and Reynolds number for main channel flow 3–20298

Mach principle *see cosmology; space-time configurations*

machine bearings
fluid film lubrication, fluid mechanics, review 3–33326
magnetogasdynamic, externally pressurised with converging film 3–1428
oil films at high contact pressures, rheology rel. to lubrication 3–11683
roller, motion of magnetised fluid in lubrication layer *(Russian)* 3–20810
shells, eddy current testing *(Polish)* 3–27844
Fe-Ni alloy with hardenable electrodeposited coatings, rolling contact fatigue assessment 3–9026

machine testing
turbogenerator, efficiency, field performance, calorimetric method *(Japanese)* 3–5796

machine theory
eddy-current brake, relativistic electrodynamics *(German)* 3–37877

machine tools
see also numerical control
lead measurement of leadscrews, laser interferometer method 3–22252
NC grinding machine, for manufacture of optical aspheric surfaces 3–22333
vertical gear-hobbing machine, stiffness meas. 3–19152

machines, electric *see electric machines*

machining
see also cutting; electrolytic machining; electrolytic polishing; grinding; metalworking; spark machining
ceramic dielectrics for microelectronic packaging, laser beam applications 3–8954
chip formation, mechanism, expt. verification 3–21710

machining continued
- chip-breaker-grooved tools, effect of wear 3−25034
- composites, secondary fabrication problems 3−12418
- glass-ceramic thin foil prep. technique for transmission electron microscopy 3−34645
- laser processing apparatus for automatic workpiece shaping, patent 3−6530
- metal machining chips, microscopic plastic instabilities 3−34580
- micro-machining, opto-electronic system using laser beam *(French)* 3−788
- photograph machining by laser light 3−37649
- steel machine parts, notch sensitivity under alternating loads, machining methods influence 3−34693
- u.s. drilling, machining rate, brittle and hard materials, ratio of tool cross-section 3−5783
- $LiTaO_3$ electro-optic element, precision machining 3−171
- Si_3N_4, high density, effects on mechanical strength 3−8953

macromolecular bulk properties
- biological active macromolecules in aqueous solutions, dielectric permeability meas., modified Nernst's bridge 3−32234
- butadiene-styrene latex, gelling, condensation structures, rheology, electron microscopy 3−39398
- butadiene-styrene thermoelastoplastics, block struct. and comp. nonhomogeneity *(Russian)* 3−20255
- copolymer, tensor characts., anisotropy, comp. depend. *(Russian)* 3−20254
- critical slowing down and correl. of conc. fluctuations of soln. near crit. mixing pt. 3−2792
- drag-reducing channel flow, near-wall region flow visualization 3−11410
- gelatin gels, contact energy of gel formation, crit. shear stress 3−39397
- natural latex, gelling, condensation structures, rheology, electron microscopy 3−39398
- α-olefines, molecular dynamics, i.r. spectra and Rayleigh scatt. study *(Russian)* 3−14406
- poly-(m-phenylene isophthalamide), effect of struct. ordering on mech. props. *(Russian)* 3−7291
- polyanilines, linear, band struct. and limiting behaviour 3−33792
- cis-1,4-polybutadiene, evidence for $t^{-a}(a\sim 1/2)$ dependence of chain fluctuations, n.m.r. obs. 3−23650
- polymer, helix-random coil transition, cooperativity parameter determ. from hydrodynamic data 3−23641
- polymer morphology, conf., Prague, Czechoslovakia (Aug.-Sep. 1971) 3−20222
- polymeric chain, dielec. relax. theory, time dependent Ising model 3−1312
- polymers, crystalline linear, negative thermal expansion theory 3−38332
- polymers with long unbranched side chains, surface tension meas. 3−30338
- trans-polypentenamer, strain-induced crystn., kinetics study 3−29801
- polysiloxanes, ladder structure, molecular conformations, hydrodynamics, optical and elec. props. *(Russian)* 3−29767
- polystyrene, u.v. irradiated, change in mechanical properties as fn. of molecular weight *(Polish)* 3−11342
- polytetrafluoroethylene, Gruneisen parameter and interchain specific heat, pressure dependences 3−27129
- viscoelastic behaviour in turbulent pipe flow 3−17518

macromolecular configurations and dimensions
- acetylcholine, ab initio calc., molecular fragment method 3−33169
- amino acids and peptides at the picomole level, fluorescent reagent development, application to automated assay 3−35524
- biopolymers, side chains, internal rot. models and C-C-H bond angles determ. method 3−36058
- butadiene/styrene radial teleblock copolymers, structural effects on adhesive props. 3−5354
- cellulose copolymers from cellulose reaction with aromatic epoxypropylamines, i.r. spectra *(Russian)* 3−31265
- condensed polymer systems, structural model *(Polish)* 3−11334
- conformational analysis of molecular structure relating to the biological function, computer program 3−22138
- excluded volume effect for partial chain segment with arbitrary length in polymer molecules 3−11332
- Ising chains, disordered copolymeric, detailed balancing approach 3−23640
- L-methionine and S ethyl-L-cysteine random copolymers coil transition studies using optical expts. 3−29763
- long chain mols. in soln., config. rel. to chain length 3−14403
- methylmethacrylate random copolymers in acetone, light scatt. and viscosity, coil dimensions 3−29794
- modelling, interactive display system, electron density maps 3−26741
- n.m.r., high-resolution, applic. 3−38328
- poly(β-benzyl L-aspartate) films, conformation, mol. wt. effect 3−29766
- poly(ethylene terephthalate) film, molecular orientation, n.m.r. second moment anisotropy, X-ray obs. 3−33170
- poly(L-alanine), apparent helix-coil transition, n.m.r. 3−38329
- poly-L-alanine, development of secondary structural properties in the NH-group valency vibration region *(Russian)* 3−29775
- polydimethylsiloxane thin films, i.r. spectra and structure *(Russian)* 3−29777
- polyelectrolytes, mol. struct. rigidity rel. to physicochem. props. 3−11345
- polyethylene fibre, oriented, conform. transitions associated with elastic tension 3−29810
- polyethylene glycols, theoretical analysis of i.r. spectra, effects of chain length and conformation *(Russian)* 3−29774
- polyformaldazine, i.r. and Raman spectra, polymerisation mechanism and struct. study 3−29679
- polymer, A-B block, contacts between blocks the function of excluded volume parameter 3−29793
- polymer, helix-random coil transition, cooperativity parameter determ. from hydrodynamic data 3−23641
- polymer, high-resolution n.m.r. obs. 3−11347
- polymer, size distrib. due to formation of crosslinks with scission 3−38334

macromolecular configurations and dimensions continued
- polymer conformational statistics, charact. function of rot.-isomeric model 3−23643
- polymer conformational statistics, modified Gaussian models of stiff chains 3−23644
- polymer conformational statistics, probability distrib. 3−23642
- polymer stiff chains, light scatt. angular distrib. 3−29761
- polymers, charge trapping, role of unsaturated groups 3−30468
- polymers, conformational defects, phonon Green's function treatment 3−29764
- polymers, discussion 3−5357
- polypeptide copolymers, chain conformations 3−1298
- polypeptide homopolymers, helix-random coil transition studied by optical dispersion, scatt., viscometry and spectrophotometry 3−29763
- polypeptides in acidic solution, i.r. spectra, helix-coild transitons *(French)* 3−29796
- polypropylene sulphide, ^{13}C n.m.r. study of configuration obs. of structural defects of main chain *(French)* 3−7271
- polysiloxanes, ladder structure, molecular conformations, hydrodynamics, optical and elec. props. *(Russian)* 3−29767
- polyvinyl acetate, dielec. props. in soln., transition phenomena obs. 3−38333
- polyvinylformal highly stretched films, polarised i.r. spectra, struct. 3−7273
- protein, contraction mechanism on excitation, quantum theory 3−26744
- protein conformation and the theory of intermolecular forces 3−29760
- protein struct. determ. by optically detected mag. struct. 3−1303
- protein structure and function, review 3−33171
- protein three-dimensional structures, comparison using computer program 3−4488
- proteins, folding process simulation, pseudo free energy, interactive computer graphics 3−26742
- resorcinol polycondensation products, structural conversion during thermal working *(Russian)* 3−23646
- Schiff base binding of retinal in visual pigment 3−11333
- self-avoiding walks, counting theorems 3−32452
- simulation, Monte Carlo methods *(Portuguese)* 3−26151
- water polymers formed in molecular beam sources, structure determ. by molecular beam electric deflection studies 3−4490

macromolecular dynamics
- β-cyanoethyl ethers and esters, β-chloroethyl esters, adsorption kinetics, on glass, CdS, channel black 3−36486
- Kirkwood theory applic. to rigid assemblies of beads 3−26747
- polyamides, aromatic, broad-line n.m.r. study, 140 to 530K 3−29772
- cis-1,4-polybutadiene, evidence for $t^{-a}(a\sim 1/2)$ dependence of chain fluctuations, n.m.r. obs. 3−23650
- polydispersivity analysis in intensity correl. spectroscopy 3−1304
- polymer, high-resolution n.m.r. obs. 3−11347
- polymer, supercoiled linear mols., hydrodynamic props. 3−33173
- polymer chain, effects of finite velocity correlation 3−29778
- polymer dil. soln. behaviour 3−23648
- polymers, crystalline linear, negative thermal expansion theory, chain torsional motion 3−38332
- polysiloxanes, ladder structure, molecular conformations, hydrodynamics, optical and elec. props. *(Russian)* 3−29767
- polystyrene chain polymers, internal motion 3−36061
- polytetrafluoroethylene, lattice dynamics 3−20218
- quasielastic light scattering as probe of internal motions of polymers in dilute solutions 3−4491
- rodlike macromolecules dilute suspensions with Brownian motion, stress tensor for arbitrary flows 3−33172
- solution, Rayleigh scatt., biochemical applications 3−28312

macromolecular spectra
- amino acids, laser Raman spectra investigation, determ. of force constants 3−29768
- biological macromolecules, inelastic light scattering and the Raman effect 3−33133
- cellulose copolymers from cellulose reaction with aromatic epoxypropylamines, i.r. spectra *(Russian)* 3−31265
- chlorophylls in soln., π-electron struct. and absorpt. spectra 3−1301
- cytosine, i.r. and laser-Raman spectra, planar vibr. 3−29773
- diphenylpolyenes, nonuniform resonance Raman effect, laser excitation of 1600 cm^{-1} ring vibrations 3−17481
- 1, 3, 5-hexatriene, cis- and trans-, lowest energy allowed singlet-singlet transition, u.v. absorpt. spectra 3−38327
- high-resolution n.m.r. for structure investigation 3−38328
- α-olefines, molecular dynamics, i.r. spectra and Rayleigh scatt. study *(Russian)* 3−14406
- optical absorption curve calc. using Franck-Condon factors 3−26746
- peptides laser Raman spectra investigation, determ. of force constants 3−29768
- poly(ethylene glycol) dimethyl ethers, cryst., i.r spectra, absorpt. band assignments 3−36060
- poly-L-alanine, development of secondary structural properties in the NH-group valency vibration region *(Russian)* 3−29775
- poly-p-xylylene, Raman and i.r. spectra 3−29770
- polyadenylic acid, triplet energy transfer, Mn^{2+} phosphoresc. quenching, temp. depend. 3−31279
- polydimethylsiloxane thin films, i.r. spectra and structure *(Russian)* 3−29777
- polydispersivity analysis in intensity correl. spectroscopy 3−1304
- polyenes, struct. and electron spectra relation *(German)* 3−14404
- polyethylene glycols, theoretical analysis of i.r. spectra, effects of chain length and conformation *(Russian)* 3−29774
- polyformaldazine, i.r. and Raman spectra, polymerisation mechanism and struct. study 3−29679
- polyisoprenes, 1,2- and 3,4-, linear and cyclized, out-of-plane deform. vibr., i.r. study 3−29771
- polymer, linear, electronic absorpt. spectra, generalized susceptibility 3−7274
- polymer, mol. movements investigation by spectroscopic methods *(German)* 3−20216
- polymer, molecular reorientation, obs. by photon correlation spectroscopy 3−23645
- polypeptide homopolymers, helix-random coil transition studied by spectrophotometry 3−29763

macromolecular spectra continued
- polypeptides in acidic solution, i.r. spectra, helix-coild transitons *(French)* 3−29796
- polystyrene, analysis of vibrational spectra *(Russian)* 3−23647
- polyurethane i.r. spectra, band struct. of first valency vibration overtone of the NH group *(Russian)* 3−29776
- proton relaxation enhancement probes 3−1302
- quasielastic light scattering as probe of internal motions of polymers in dilute solutions 3−4491
- resorcinol polycondensation products, structural conversion during thermal working *(Russian)* 3−23646
- riboflavin, luminesc. spectra, depend. on exciting photon freq. 3−34410
- solution, Laser Rayleigh scatt. 3−28312

macromolecules
- *see also polymers; proteins*
- acetylcholine, electronic structure and geometry, ab initio calc., molecular fragment method 3−33169
- biophysical composite protostructures, organization at the macroscopic level 3−29799
- cellulose, crystallite orientation in cotton fibres, X-ray meas. 3−31166
- composite protostructures, organization at the macroscopic level 3−29799
- L- ethyl-(N-acryloyl)-pyroglutamate, optically active, homo and copolymerization, reactivities *(Japanese)* 3−17482
- L- ethyl-(N-methacryloyl)-pyroglutamate, optically active, homo and copolymerization, reactivities *(Japanese)* 3−17482
- light scattering appl. 3−6522
- linear Ising lattice, high ionic strength, competitive cooperative binding 3−38326
- millidyne film balance for intermol. energy meas. 3−10142
- oil recovery from underground porous sources, fingering reduction using macromolecular solutions 3−3164
- pepsin, heavy-atom parameters determ. by X-ray study 3−7277
- riboflavin, luminesc. spectra, depend. on exciting photon freq. 3−34410
- RNA synthesis by temp. sensitive mutants of VS virus 3−9642
- solution, fluoresc. depolarization due to Brownian motion, computer simulation 3−26748

Madelung constant *see lattice energy*

magamps *see magnetic amplifiers*

Magellanic Clouds *see galaxies*

Maggi-Righi-Leduc effect *see magnetothermal effects*

magnesium
- addition to Al-Zn (6.8 at wt.%) alloy, effect on solvus temp. of G.P. zones *(Japanese)* 3−18591
- anisotropy in phonon scattering resistivity 3−7876
- atom, electron excitation cross sections using Born approx. 3−1122
- atom, Hartree-Fock calculations of principal configurations 3−20023
- atom, photoioniz. cross section near threshold 3−33039
- atom, photoioniz. cross sections calc. 3−26594
- atomic beam, absolute frequency standard 3−3747
- Auger and photoelectron spectra of partially oxidised surface, abnormal chem. shift 3−30909
- Auger spectra, high energy satellites 3−18519
- Auger spectra rel. to oxidation 3−30908
- b, and b_2 solar line oddities on spectrograms of good spatial resolution 3−39616
- Bardeen-Herring source obs., climbing dislocations in quenched Mg *(French)* 3−20747
- central cracking during cold-extrusion, prevention by hydrostatic back pressure 3−24869
- collisions with Ne^+, charge transfer into excited states 3−14313
- core binding energy in silicate minerals, ESCA technique 3−5431
- diffusion, electrotransport and solubility in Si, 1000-1350°C *(Russian)* 3−7975
- dislocation creep 3−8871
- dislocation struct. changes during basal slip of single crysts. *(Russian)* 3−24185
- dispersion relations, curves, h.c.p., modified Sharma-Joshi model 3−30220
- Fermi surface, OPW model for pressure depend. 3−33788
- Fermi surface pseudopotential calcs. convergence props. 3−33783
- film, refl., substrate roughness effects 3−12152
- film, vacuum deposited mirror coating, i.r. reflectivity 3−35395
- flame fluorescence detection with freq. doubled dye laser as excitation source 3−28777
- hydrostatic extrusion, critical back pressure to prevent central cracking 3−21615
- K-shell photoionisation cross section and threshold energy determ. 3−14300
- lattice dynamics, phonon dispersion freq. spectra, sp. ht. 3−30215
- lattice dynamics using modified Bhatia model 3−36373
- loss from Al-Mg-Si alloys during aging, effect of Cu addition, elec. resistance meas. 3−39361
- nuclear quadrupole interaction, electronic and lattice contribs. to EFG, cryst. field $l=2$ component 3−21018
- particles, oxid., electron microscope obs. of oxide-metal boundary 3−15076
- phonon damping due to electron-phonon coupling, calcs. 3−38638
- phonon dispersion curves for noncentral force model 3−33617
- plasmon thresholds in the secondary electron yield, expt. 3−4976
- positron annihilation in oriented single crysts., core electron obs. 3−1973
- reaction with Cl_2 and Br, crossed beams chemistry 3−21803
- reactive collisions with ICl, crossed beams product angular distributions of MgCl and MgI 3−27864
- resonance series in vacuum u.v. absorption spectra of dense plasmas 3−17351
- skate retina, effect of Mg on horizontal cell activity 3−28357
- soft X-ray absorpt. edges calcs. 3−30895
- solid solubility of rare earth metals, electron probe determ. for systems with large Z correction 3−37044
- in sporadic E-layer, ionic reactions associated with formation and removal 3−34943
- stacking fault energy calc., loop annealing kinetics using physical electrostatic analogue 3−20755

magnesium continued
- Sun, Mg II doublet profiles of chromospheric inhomogeneities at centre of solar disc 3−28137
- thin film, electron conc. and spectral line width from asymmetric self-reversed spectral lines 3−23941
- titanomagnetite impurities, spinel structure 3−9142
- ultramicrotomed thin slices, plastic deformation 3−17902
- vacancy diffusion, activation energy proportional to latent heat of melting *(Russian)* 3−24295
- $Al_xGa_{1-x}As$:Mg, molecular beam epitaxy 3−18553
- inβ-Al_2O_3, effect on ionic cond. 3−11758
- Al_2O_3:Mg, thermal cond., 1.3-100 K, possible obs. of Fe^{4+} 3−30293
- CaO:Mg, e.p.r. of colour centres 3−36791
- GaAs:Mg, molecular beam epitaxy 3−18553
- GaN-GaN:Mg light emitting diode, violet luminesc. 3−34432
- in GaP, rel. to green light emitting diode appl. 3−8734
- H_2 content, by vacuum heating method 3−26017
- LiF:Mg, electron trap depth and supralinear thermolum. response 3−24756
- LiF:Mg^{2+}, thermolum. rel. to Mg^{2+} vacancy pairs 3−12189
- LiH:Mg, red luminesc., 120 and 293 K *(Russian)* 3−15538
- Mg b line in solar spectra, correlations of fluctuation with Ca II H and K lines and Hβ 3−39629
- Mg I, atomic lifetime meas. by the beam-foil technique 3−20013
- Mg I 4571 A line obs. on solar disk for temp. distrib. determ. 3−35055
- Mg II, atomic lifetime meas. by the beam-foil technique 3−20013
- Mg II, Mg I, interstellar lines in direction of Cassiopeia and Orion 3−9614
- Mg II 2800 Å doublet meas. by balloon-borne u.v. stellar spectrometer telescope 3−35220
- Mg II (2800 Å) emission, from cool stars, OAO obs. 3−22046
- Mg II resonance lines in stellar u.v. spectra, Utrecht orbiting spectrophotometer obs. 3−31673
- Mg II spectrum in B and O stars 3−39654
- Mg IV, ionic spectra, $2p^43d$ and $2p^44d$ configs., energy levels calc. 3−17346
- Mg lasing lines and possible appls. 3−22885
- Mg:Er, dilute mag. alloy, coupled local moment-cond. electron Bloch equation 3−34213
- Mg/MgO composites, effect of dispersed particles on structural stability 3−39376
- Mg-Ca mixed layers on calcite, cationic distrib. and structural changes 3−15849
- Mg-MgO-Mg tunnel junctions, zero bias resist. anomalies 3−34002
- Mg^+, Mg collisions with Cd^+ ions, excitation of resonance levels 3−17377
- Mg^+, oscillator strengths and ground state photoionisation cross sections 3−11146
- Mg^{2+}, spectra, ground term combinations 3−33027
- Mg^{2+} in K(Na)Cl, study of Mg electron centre 3−20737
- Mg^{3+}, extended analysis of spectrum 3−17349
- MgIV, even configurations, reevaluation of parameters 3−33011
- NaCl:Mg X-irradiated crystals, Mg centres expt. study 3−38586
- Ni:Al_2O_3, Mg, effect of Mg additions on high temp. mech. props and microstructure 3−15711
- Si:Mg^+, e.p.r. of ground state and photoconverted state, liq. He temps. 3−2359
- Si:Mg^+, ground state and photoconverted metastable state of donor, e.s.r. 3−30692

magnesium alloys
- *see also magnesium compounds*
- Friauf-Laves phases, struct. relation between stacking variants 3−14732
- high-strength, subcrit. crack branching implications 3−4796
- Ag-Mg, dil., inernally oxidized, strengthening mechanisms 3−24842
- Ag-Mg, dil., partially internally oxidized, deform. and substruct. characts. 3−24841
- Agl-Mg commercial alloys, stress corrosion cracking and its prevention *(Japanese)* 3−18635
- Al-Cu-Mg directionally solidified eutectics, ageing response 3−34581
- Al-Cu-Mg-Ag, heat treatment, struct. of metastable precip. 3−15662
- Al-Mg, dil., neutron irrad. at 4.6K, resist. study 3−27042
- Al-Mg, dilute alloy, recovery after neutron irradiation at 4.6K, elec. resist. obs. 3−11658
- Al-Mg, effect of addition of Bi on stress-corrosion cracking *(Japanese)* 3−18634
- Al-Mg, Guinier-Preston zones, electron diffraction effects *(French)* 3−18604
- Al-Mg, Portevin-Le Chatelier phenomena *(French)* 3−31092
- Al-Mg (1 wt.%), work softening, polycryst. 3−37066
- Al-Mg dilute solid solution, plasma energy loss rel. to band models of alloying 3−7803
- Al-Mg-Si, plastic deformation effect on precipitation *(Japanese)* 3−15699
- Al-Mg-Si, quench-aged, step-wise yielding and unlocking serrations 3−31093
- Al-Mg-Si:Cu, aging, effects of Mg loss, elec. resistance meas. 3−39361
- Al-Mg-Ti-Zr-Mo, AL8 cast alloy, alloying additions influence on Failure under tensile stresses 3−31085
- Al-Mg-Zn, microstruct. influence on mech. props. and stress corrosion susceptibility 3−39342
- Al-Mg(0.13 wt.%) prismatic dislocation loop rotation and self-climb phenomena 3−36317
- Al-Mg(0.8 wt.%), rolling textural stability role of deform. and shear banding 3−21582
- Al-Mg(5 wt.%), grain size effect on fatigue 3−34594
- Al-Si-Mg, Mg effect on Sn and Pb distrib. 3−21572
- Al-Zn-Mg, axisymmetric extrusion, plastic flow, substructure exam. 3−39360
- Al-Zn-Mg, corrosion fatigue inhibition, crack growth rate meas. 3−39352
- Al-Zn-Mg, extrusion load calc., temp. rise meas. 3−37046
- Al-Zn-Mg, grain boundary corrosion and stress corrosion cracking relationship *(Japanese)* 3−31072

magnesium alloys continued
Al-Zn-Mg, mech. props. and fine struct. changes on alloying and ageing 3−21671
Al-Zn-Mg, SCC, soln. chem. influence on repassivation kinetics, alloying effect 3−27652
Al-Zn-Mg, stress corrosion cracks, h.v. microscope studies 3−30981
Al-Zn-Mg-Cu, thermomech. treatment processed, age hardening mechanisms 3−24897
Al-Zn-Mg-Zr, recryst. temp., effect of heat treatment *(Russian)* 3−2716
AlMg5, diffusion coeff. during plastic deform. *(German)* 3−21611
Cd-Mg, n.m.r. of ^{113}Cd, Knight shifts, alloying depend. 3−2433
Cd-Mg, superconducting transition temp. determ. 3−34020
Cu-Ni-Mg, monovariant eutectic alloy, microstructure obs. in unidirectional solidification 3−21589
Mg-Al, MgMn-Al alloys, horizontal strip costing in stationary d.c. moulds, properties 3−12417
Mg-Al, soft X-ray absorpt. edges calcs. 3−30895
Mg-Al alloy, transgranular stress corrosion cracking 3−30983
Mg-Al stress-corrosion resistance, improvement by Bi additions 3−12382
Mg-Al work-hardened sheet, forming-limit diagrams in biaxial tension 3−12381
Mg-Bi, liquid, conc. fluctuations calc. using cluster model 3−36255
Mg-Cd, temp. and concentration depend. of electrical resistivity, phase diagrams *(German)* 3−34551
Mg-Ce, precipitation process on aging *(Japanese)* 3−12351
Mg-In and Mg-Li, ordering behaviour of f.c.c and b.c.c. phases 3−11585
Mg-Li optical properties, band structure, Fermi surface, optical and soft X-ray spectra, ellipsometry 3−30836
Mg-Mn ferrite films, remagnetization rate and mobility of domain boundaries *(Russian)* 3−8398
Mg-Nd, dilute alloy, precip. and structure of equilib. and non-equilib. phases 3−18580
Mg-Ni-Cu, monovariant eutectic, unidirectional solidification, aligned microstructs., interface stability criteria 3−12347
Mg-R system, with large Z correction, R=Gd, Tb, Dy, Ho, Er, Yb, electron probe analysis 3−37044
Mg-Th and Mg-Th-Zr systems, precip. sequences 3−21583
Mg-Y(8.7 wt.%), elevated temp. precip. stages 3−39340
Mg-Zn, Zn distribution, dendrite non-homogeneity, electron microprobe examination 3−8796
Mg-Zn-Zr spherical crysts. growth by freezing, interface growth stability 3−20701
Mg-Zr (0.5 at wt.%), metallography of ZrH_2 precipitation 3−18585
MgAl thin films, for optical storage, preparation method and characterization 3−36987
Mg_3Cd, stoichiometric, thermodynamic description of ordering process 3−21574
Mg_2Si:Al alloy, dissolution and growth of precipitates β', electron micro. obs. 3−8814
Mg_2Sn, logarithmic derivative refl. spectra, 1.3-3.2 eV 3−2561
$MgZn_2$, dislocation mobility, depend. on chemical composition and temperature 3−27028
$MgZn_2$ Madelung constant and energy, in terms of parameters of crystal type, calculation *(German)* 3−1598
Ru-Mg system, intermetallic compounds, X-ray obs. 3−34495

magnesium compounds
see also magnesium alloys
chrome-magnesia fired bricks, electron microprobe analysis of failure 3−15755
cordierite glass, crystn., oxide additive effects on devitrification characts. 3−34643
cordierite glass, crystn., oxide additive effects on devitrification characts. 3−34644
enstatite, high-temp. cryst. chem. 3−15864
ferrite, magnetostriction and anisotropy, ferrimag. resonance obs. 3−30673
magnesia, fibrous, grown via vapour phase *(Japanese)* 3−8728
magnesium aluminate spinel, heteroepitaxial semiconductor film growth of GaAs 3−39266
magnesium picolinate dihydrate, crystal structure obs. *(French)* 3−38577
magnesium-iron(II) formate mixed crystal, Mossbauer obs. of α and β phases of iron(II) formate anhydride, isomer shifts *(German)* 3−27458
omphacite, cryst. struct. 3−15868
silicophosphates, preparation and characterization *(Russian)* 3−11597
talc, preparation for tritium-labelling 3−27916
Al-Mg_2Si, effect of Fe on nucleation and zone formation 3−8884
Al_2O_3:MgO, grain boundary segregation 3−27739
As_2S_3 glass, clearing coatings production MgF_2 film deposition by thermal evaporation *(Russian)* 3−5904
BeO-Al_2O_3-SiO_2-MgO glass, thermographic and X-ray study of struct. transforms. *(Russian)* 3−11547
$Ce_2Mg_3(NO_3)_{12}$, thermal cond., 0.2-1.5 K 3−36444
$Ce_2Mg_3(NO_3)_{12}.12H_2O/^3He$ boundary resist., nucl. spin-electron spin dipolar interaction 3−30303
$Ce_2Mg_3(NO_3)_{12}.24H_2O$, e.p.r. saturation of Ce^{3+}, light scatt. obs. of nonequil. phonon system 3−2370
$Ce_2Mg_3(NO_3)_{12}.24H_2O$, mag. field depend. of spin-spin relax. 3−8478
$Ce_2Mg_3(NO_3)_{12}.24H_2O$, phonon system under Ce^{3+} e.p.r. saturation conditions, Mandelshtam-Brillouin study *(Russian)* 3−8438
$Ce_2Mg_3(NO_3)_{12}.24H_2O$ temperature scale, implications of new data on W specific heat 3−28457
$Co_{0.5}Mg_{0.5}O$ powder, X-ray diffr. line integrated intensity changes, effective Debye parameter rel. to lattice strain 3−33424
CoO-MgO-GeO_2, spinel-olivine and olivine-phenacite transitions, thermodynamic and vol. relations 3−27122
Cu-MgO, internally oxidised, brittleness during annealing in H_2 *(Japanese)* 3−12395
$KMgF_3$, impurity and defect centres, thermoluminesc. 3−34436
Mg/MgO composites, effect of dispersed particles on structural stability 3−39376
Mg-Al spinel crystal, age strengthening kinetics 3−30930
Mg-Ln_2-S_4, ternary sulphides, prep., elec. and opt. props. 3−39243

magnesium compounds continued
$MgAl_2O_4$, etch rate and deterioration in H_2, rel. to appl. as substrate for epitaxial Si 3−11816
$MgAl_2O_4$, fracture as function of orientation, fracture topography 3−7836
$MgAl_2O_4$, nearest-neighbour interactions between Cr^{3+} ions, e.s.r. obs. 3−2380
$MgAl_2O_4$, nearly stoichiometric single cryst. growth, gradient furnace technique 3−5267
$MgAl_2O_4$, spinel stoichiometric single crysts., stacking faults and dislocations, X-ray topographic obs. 3−17854
$MgAl_2O_4$, spinel struct., i.r. spectra interpretation 3−5198
$MgAl_2O_4$, transition due to hot-pressing 3−18688
$MgAl_2O_4$ ceramics, synthesis by thermal decomposition of hydrated nitrate mixtures 3−8968
$MgAl_2O_4$ single crystals, self-diff. coeff. of oxygen detn. 3−7978
$MgAl_2O_4$ spinel, Raman vibrational spectra 3−12133
$MgAl_2O_4$:$^{57}Fe^{3+}$, diamag. host lattice, hyperfine splitting of Mossbauer spectra 3−34253
$Mg_{8.5}As_3O_{16}$, structure analysis rel. to comp. 3−24082
$Mg_3B_{11}O_{15}(OH)_9$, n.m.r. lineshape, quadrupole interaction tensor 3−2411
$Mg_7B_4O_{13}.7H_2O$, i.r. spectra interpretation *(Russian)* 3−36883
MgC-Al_2O_3, stoichiometric spinel, floating zone growth method in arc-image furnace 3−15639
$MgCO_3$, refractory, thermal shock resist. determ. at high temp. 3−15741
Mg_3Cd and MgCd, Young's modulus, temp. changes proportional to long-range order *(Russian)* 3−7809
$MgCl_2$-UCl_3-$CaCl_2$ fusibility, differential thermographic study *(Russian)* 3−24042
$MgCl_2$-UCl_4-$CaCl_2$, fusibility, differential thermographic study *(Russian)* 3−24042
$MgCl_2.6H_2O$, powder proton n.m.r. shift 3−12071
$Mg_{1-y}Co_yFe_2O_4+\gamma'$, relaxation of Co^{2+} ions in ferrite single crystals with different inversion degrees 3−15379
MgF_2, ^{19}F chem. shift tensor and nonionic bonding 3−12070
MgF_2, ab initio estimate of correlation energy, determ. of equilibrium geometry 3−4403
MgF_2, directional depend. of extraordinary i.r. oscillator parameters 3−18453
MgF_2, electron, colour centre prod. mechanism 3−34479
MgF_2, electron and proton irrad., thermolum. *(Russian)* 3−18505
MgF_2, hot pressed, low temp. thermal conductivity 3−1848
MgF_2, laser deposited films, expt. technique and data *(French)* 3−36988
MgF_2, nonempirical LCAO MO SCF studies, bonding trends 3−20096
MgF_2 film, adhesion, scratch test apparatus obs. *(Japanese)* 3−20959
MgF_2 film, influence of prep. and measurement conditions on transport props. *(French)* 3−2094
MgF_2 film, Malter emission, primary current magnitude effects *(Russian)* 3−12204
MgF_2 films, refr. index dispersion meas. *(Russian)* 3−8685
MgF_2 in LiF, Debye-Huckel interactions and solubility 3−4881
MgF_2 optical constants, anisotropy, u.v. absorption region, reflectance measurements, excitations 3−27482
MgF_2 uniaxial crystal, surface optical phonons 3−20827
MgF_2/ZnS evaporated multilayer Fabry-Perot filter, optical thickness changes, determ. from peak shifts 3−9925
$MgFe_{2-x}In_xO_4$, X-ray diffraction and γ-resonance obs. of spinel structure 3−24087
$MgFe_2O_4$, excitation of magnetoelastic waves *(Russian)* 3−8411
$MgFe_2O_4$, thin films, electron diffraction superlattice lines 3−38569
$Mg_{0.9}Fe_{2.1}O_4$ ferrite, cation redistrib. rates, oxidation effects, saturation magnetisation obs. 3−15387
$MgFe_4((OH)_2|(SO_4)_6).20\ H_2O$, copiapite, crystal structure and H bonding 3−7716
Mg_2Ge, cryst. growth, modified Bridgman method 3−12270
$MgHAsO_4.7H_2O$, Roesslerite, struct. rel. to hydrogen bonding 3−20717
$MgHAsO_4.7H_2O$, rosslerite, cryst. struct. and hydrogen bonding 3−14762
MgI emission in night sky spectra 3−9290
$MgIn_2O_4$, X-ray diffraction and γ-resonance obs. of spinel structure 3−24087
MgM_2O_4, (M=Rh, Mn, V, Fe, Cr), interionic metal-oxygen distances, formulae *(Russian)* 3−17784
$Mg_xMn_{1-x}Fe_2O_4$ film, use as phase diffr. grating 3−36862
Mg_6MnO_8, paramag. structure with weak antiferromag. interaction, susceptibility and optical reflectance meas. 3−34091
$MgNH_4AsO_4.6H_2O$, arsenstruvite, structure refinement, hydrogen bonding 3−38558
$MgNH_4AsO_4.6H_2O$, As-struvite, cryst. struct. and hydrogen bonding 3−14762
$Mg(NH_4)PO_4.6H_2O$, cryst. growth in gelatin gels 3−15610
$MgNH_4PO_4.6H_2O$, growth in gelatin gel 3−24783
MgO, calcined, surface area, pore size, water vapour effects 3−31211
MgO, creep-deformed, dislocation structures, transmission electron microscopy 3−38593
MgO, defect formation by 20 MeV protons 3−36337
MgO, dislocation damping in single crysts. 3−36324
MgO, dislocation dipole termination mechanisms 3−1628
MgO, dissociation energies 3−20190
MgO, e.p.r. of Fe group impurities, thermal detection 3−18360
MgO, effect of Li and F ions on press. sintering 3−15770
MgO, electric arc-fusion growth method to produce clear crystals 3−12265
MgO, erosion by fast moving particles, dislocations, obs. by thin film electron microscopy 3−27065
MgO, evidence for intra-ionic anharmonicity in Raman spectra 3−34361
MgO, far u.v. refl. and correl. with Penn-Phillips gap 3−39158
MgO, fracture as function of orientation, fracture topography 3−7836
MgO, growth of high quality crysts. by chem. vapour transport techniques 3−24789

magnesium compounds continued
MgO, hot-pressed, polycrystalline, elastic props., ultrasonic meas. and distorted Kroner theory 3−36341
MgO, hydroxylated, S_3^- form. and characteriz. 3−27919
MgO, hypersonic attenuation, impurity and defects effect 3−1701
MgO, in Mg tunnel junctions, zero bias resist. anomalies 3−34002
MgO, interionic potentials, force const. models 3−26987
MgO, lattice distortion around F^+ centre, ENDOR obs. 3−27441
MgO, multiphonon i.r. absorpt. spectra, lattice vibrs. i.r. active sum modes 3−24693
MgO, neutron irrad., thermal cond., 0.4-80 K, quasilocalized modes, defect centre prod. 3−30295
MgO, neutron irradiated, isotropic e.s.r. line of V^- centre at room temp. 3−34209
MgO, paramagnetic defects at the surface 3−5048
MgO, polycryst., microyield and fracture 3−20789
MgO, polycryst., preferential O diffusion along grain boundaries 3−4873
MgO, polycrystalline, thermoelectric force meas. between 1200 to 1650°C *(German)* 3−15740
MgO, radiation degree of blackness, electric resistance 3−36423
MgO, second order Raman scatt. calc. 3−30823
MgO, secondary creep props., depend. on stress 3−14918
MgO, static dielec. consts., press. and temp. depend., 15-295 K 3−39078
MgO, strength, dehydration of $Mg(OH)_2$ 3−39420
MgO, thermal vibr. and dissociation at 2100°C 3−24225
MgO, time decay of d.c., modelling using nonlinear regression analysis, comparison with experiment 3−8509
MgO, trapped-hole centre displaying orthorhombic symmetry, ESR spectra 3−8440
MgO, V_{al} and V^- centres 3−24113
MgO, X-ray and u.v. irrad., activation energies 3−34435
MgO, X-ray diffraction meas. of Debye-Waller factors 3−14939
MgO, X-ray integrated intensities, primary extinction effects 3−24068
MgO cables, radiation tolerance for instrumentation systems in LMFBR 3−26512
MgO ceramic, polycrystalline function representing planar distribution of grain size 3−24970
MgO containing Mn^{2+}, Cr^{3+} and Fe^{3+} impurities, ^{17}O transferred hyperfine interactions 3−30727
MgO crystal, point defects-dislocation interaction, internal friction obs. 3−30117
MgO foil, stability of edge dislocation loops, effect of surface forces, electron microscope obs. 3−18011
MgO high-porosity layer, secondary-electron conductivity 3−15206
MgO single crystal, cation diffusion studies using a sectioning technique 3−33694
MgO single crystals, creep, dependence on dislocation substructure 3−7829
MgO smoke, mean inner potential, electron interference microscopy 3−24060
MgO substrate, contamination in LPE growth of Li-Cr ferrite film 3−1928
MgO TSEE activator in BeO, dosimetric characteristics 3−28671
MgO: He, Ar, Fe, Cr, ion implanted, photolum. from damage related defect centres 3−21463
$MgO:Be^{2+}$, tracer diffusion meas. up to 2340°C 3−20891
$MgO:Cr^{2+}$, acoustic paramagnetic resonance at high magnetic fields 3−2346
$MgO:Cr^{3+}$, absorpt. meas. rel. to tetragonal field splitting of levels 3−15513
$MgO:Cr^{3+}$, e.s.r. absorp. spectrum, strain broadening 3−27412
$MgO:Cr^{3+}$, isotope effect in e.p.r. 3−21301
$MgO:Cr^{3+}$, obs. of optical absorpt. strengths for transition lines 3−15512
MgO:Fe, polycrystalline, transient creep rate 3−7831
MgO:Fe, valence states detn. by e.s.r. and Mossbauer spectroscopy, effect on surface reactivity 3−15439
MgO:Fe ultrasonic spin echo obs. 3−15407
$MgO:Mn^{2+}$, temp. depend. of hyperfine structure splitting 3−15143
MgO:Ni(Fe)(Cr), paramagnetic impurities, thermal conductivity 3−1844
$MgO:Sr^{2+}$ diffusion of Sr^{2+} 3−17993
MgO-Al_2O_3 synthetic spinel, spectra, luminesc. of Cr and Mn in impurities, comp. depend. 3−34429
MgO-Al_2O_3-SiO_2-TiO_2 glass-ceramic, crystn. and struct. 3−31161
MgO-based, insulating fire-proof concrete, elec. cond., erosion and heat resistance in plasma jet 3−36206
MgO-C, composite material, elasticity, effects of shape of dispersed particles 3−2750
MgO-$LiAlO_2$ system, solid soln. studies 3−31160
MgO-SnO_2, ceramics, firing, binding props. and compressive strength *(Russian)* 3−15745
MgO-ZnO, short-range order in atomic structure 3−4740
$(MgO)_{0.55}(Fe_2O_3)_{0.45}$, anion vacancies in magnetically square hysteresis loop 3−17804
$Mg(OH)_2$, disperse porous structure, strength, influence of dehydration 3−39420
$(MgO)_{0.30}(MnO)_{0.35}(Fe_2O_3)_{0.35}$, anion vacancies in magnetically square hysteresis loop 3−17804
$MgO-MgAl_2O_4$, controlled ceramic microstructures by solidification from melts 3−5344
MgO(100), LEED obs. of contour maps for reciprocal lattice points 3−24316
$MgO.P_2O_5$ glass, absorpt. spectra, rel. to redox behaviour of Fe 3−24723
$Mg_2(PO_4)Cl$, cryst. struct. 3−24069
$MgSO_3.6H_2O$, crystal structure obs. of slightly distorted CsCl arrangement *(French)* 3−38553
$MgSO_4.7H_2O$, polar modes, Raman and i.r. spectra *(French)* 3−2527
$MgSO_4.7H_2O$, resist. to growth using flow system 3−8713
$MgSO_4.7H_2O$ biaxial crystals, angular dispersion of polar phonons, Raman scatt. study 3−1732
$MgSO_4.7H_2O:Mn^{2+}$, zero-field splitting of Mn^{2+} ion S-state, spin-hamiltonian parameters 3−38935

magnesium compounds continued
Mg_2SiO_4, i.r. reflectivity and Raman scattering obs. of lattice vibrations 3−21410
Mg_2SiO_4 fibres dispersed in Newtonian alkyd resin, rheological props. *(German)* 3−6220
Mg_2SiO_4(Tb), optical and thermal effects on thermoluminescence response 3−290
Mg_2Sn, structure obs. in polymorphic phases at high pressure and temp. 3−24270
Mg_2Sn, valence band electron density of states determ. by Auger and photoemission spectroscopy 3−24381
$MgSn(OH)_6$, p.m.r. meas. from 4.2 to 400 K 3−27422
Mg_3TeO_6, vibrational spectrum 3−8569
$Mg_xTi_yFe_3O_4$ thermoremanence self-reversal rel. to composition and mechanism 3−24589
$Mg_2TiO_4:Mn^{4+}$, Cr^{3+}, phosphors, luminescence *(Russian)* 3−36928
MgV_2O_6, cryst. struct. and e.s.r. of Mn^{2+} 3−11589
β-MgV_3O_8, lattice parameters, space group *(French)* 3−38567
Mn_3NiN, magnetization 180-266K, Mn mag. moment rotation in (111) plane *(French)* 3−2283
MnO-MgO solid solns., exchange phenomena between Mn^{2+} ions, e.p.r. and mag. susceptibility *(French)* 3−38964
Mn_nSi_{2n-m}, obs. of metallic MnSi precipitates in diamag. matrix, mag. behaviour 3−27356
$Nd_2Mg_3(NO_3)_{12}.24H_2O$, mag. field depend. of spin-spin relax. 3−8478
$Nd_2Mg_3(NO_3)_{12}.24H_2O$, sp. ht. meas., 2 to 19 K 3−33681
NiO-MgO-GeO_2, spinel-olivine and olivine-phenacite transitions, thermodynamic and volume relations 3−27122
$SiO_2:MgO$ gels, sorption props., surface area, porosity, hydrothermal treatment effects 3−31196

magnetic aftereffect
heading is late addition, see also magnetic properties of substances
irreversible magnetization process in Rayleigh region, theory 3−18344
relaxation, real structure and migrational props. obs. *(Polish)* 3−24212
α-Fe, susceptibility meas. of low temp. mag. relax. 3−34168
α-Fe:H, study of mobile self-defects and impurity atoms 3−39001
$YIG:Si^{4+}(Ge^{4+})(Ca^{2+})$, electronic hopping processes 3−24591

magnetic amplifiers
No entries

magnetic anisotropy
alloy, ferromag., plastically deformed single cryst., rel. to dislocation struct. *(Russian)* 3−36729
antiferromagnet, anisotropic Green's function theory 3−30584
antiferromagnet, low temp. consts. 3−38988
apparatus for investigation of magnetic properties of thin weak magnetic films *(Russian)* 3−25820
bubble domain material, X-ray topography obs. 3−34156
chloroform, p.m.r. study of hydrogen bonding with N-N-distributed amides and sulphoxides, S=O, C=O, P=O group mag. anisotropy 3−4466
dilute alloy, spin-orbit interactions, induced spin anisotropy effect on elec. resist. 3−36711
elliptical mag. bubbles, dynamics, domain wall anisotropy effects 3−36759
ferrimagnetic, method for separating anisotropy components 3−5115
ferrite, hexagonal, ferromag. resonance obs. of magnetogyric ratio anisotropy 3−36730
ferromagnetic film, effect of ang. dispersion of anisotropy on reson. linewidth *(Russian)* 3−8452
ferromagnetic plate, magnetiz. oscillations spectrum *(Russian)* 3−30649
ferromagnetic plate, rel. to thickness effects on residual magnetization *(Russian)* 3−8384
ferromagnetic spin system Heisenberg Hamiltonian with crystal field anisotropy, spin 1, diagram technique 3−34064
ferromagnetic thin film, cylindrical, anisotropy dispersion meas. *(French)* 3−25819
ferromagnetic thin film, cylindrical, anisotropy field meas. *(French)* 3−25818
ferromagnetic thin plate with easy plane type anisotropy, mag. reversals *(Russian)* 3−15388
ferromagnetism, exchange interaction model, crit. point props., single-ion anisotropy effects 3−38936
ferromagnets with 'easy plane' type magnetic anisotropy, spin relaxation theory *(Russian)* 3−12063
garnet, effect of growth conditions in epitaxial liquid phase growth 3−2667
garnet, mixed rare earth iron $RM_2Fe_5O_{12}$ type, growth induced noncubic mag. anisotropy 3−21256
garnet, mixed rare earth iron type, growth induced noncubic mag. anisotropy 3−21255
garnet mixed rare earth iron type, epitaxial film, anisotropy field and domain wall coercivity temp depend. 3−21257
Heisenberg ferromagnet, two-dimensional, critical temp. depend. on anisotropy 3−30590
highly anisotropic ferromag., mag. anisotropy and magnetostriction theory 3−24581
Ising ferromagnet, connection between amorphous and anisotropic models 3−38942
Ising model with lattice anisotropy, high temp. R-series for critical behaviour 3−15331
liquid crystal, nematic, diamag. anisotropy, temp. depend. *(French)* 3−38955
magnetic susceptibility anisotropy meas. in diamagnetic molecules with high temp. microwave spectrometer *(German)* 3−35411
magnetization dynamics, controlled by magnetocryst. anisotropy 3−30659
magnetoacoustic resonance, magnetoelastic instability, ferromagnetics, anisotropy effects 3−39010
magnetostrictive film, anisotropy skew, theory 3−5122
metals, crystalline electric field, physical aspects 3−30582
organic molecules, mol-Zeeman effect, g-values, magnetic susceptibility anisotropies and mol. quadrupole moments determ. 3−29629
permalloy film, electrostatic torquemeter obs. 3−256
permalloy film, evap. onto rotating substrate, helical anisotropy 3−34149

magnetic anisotropy continued
Permalloy film, obliquely deposited, hypercritical, micropore form. effect *(Russian)* 3−24588
permalloy film, uniaxial mag. anisotropy rl. to annealing 3−18333
permalloy single cryst. film, uniaxial mag. anisotropy rel. to annealing *(Russian)* 3−15383
plated wire, angular anisotropic dispersion meas., pulse method *(Polish)* 3−30669
poly-γ-ethyl-glutamate, cholesteric, mag. alignment, laser beam diffraction obs. 3−11544
polypeptide films, anisotropic superstructure determ. from small angle light scattering 3−1947
rare earth−Fe ternary cubic Laves compounds, spin orientation diagrams and mag. anisotropy 3−38987
rare earth alloy, RAl_2, ferromag., n.m.r. obs. of easy direction for magnetisation 3−15430
rare earth $Co_5(Co_{17})$, ferrimag., rare earth contrib. to mag. anisotropy 3−34151
rare earth cobalt permanent magnet alloys, magnetisation, anisotropy and coercivity, review 3−24595
rare earth cobaltides, RCo_5, easy direction, magnetic moment, single crystals 3−36715
rare earth manganites, magnetocrystalline anisotropy, mag. susceptibility meas. 3−36704
rare earth orthoferrites, paramag. susceptibility study. 3−21213
rare earth orthoferrites, second-order anisotropy of iron sublattice 3−34107
single ion anisotropy, high temp. depend. determ. by Green's function method 3−21260
solid solutions, nonrandom, deformation, magnetic anisotropy calc. 3−34548
spin waves, surface, energy detn. and consideration of surface anistropy *(French)* 3−12029
thin films, magnetization curves in the difficult direction in the presence of amplitude dispersion anisotropy *(Russian)* 3−8375
$Ba_2Co_2Fe_{12}O_{22}$, n.m.r. study 3−36801
$Ba_3Co_{2-x}Fe_{24}O_{41}$, n.m.r. study 3−36801
$BaFe_{12}O_{19}$ substituted ferrite, rel. to coercivity 3−34165
$Ba_2Ni_2Fe_{12}O_{22}$, n.m.r. study 3−36801
$CdCr_2S_4$, anomalies in mag. anisotropy and f.m.r. linewidth due to impurities 3−21318
Co films, perpendicular anisotropy, rot. moments, superparamag. particles *(Russian)* 3−30641
Co films with different texture perfections about [0001] axis, perpendicular anisotropy 3−36731
Co-Fe-Nb semihard mag. alloy development 3−21261
Co-Fe-Nb semihard magnetic alloy *(Japanese)* 3−18334
Co-Ni-P layers, chem. deposited, anisotropy field *(French)* 3−8404
Co-Pt alloy, tetragonal phase, rel. to microstruct. effects on coercivity *(Russian)* 3−8779
$Co_xNi_{1-x}Fe_2O_{4\mp y}$, magnetic anisotropy temp. depend. 3−36728
Co_5Sm permanent magnet alloy, sintered 3−5097
$Co_xZn_{1-x}Fe_2O_4$, rel. to freq. and temp. depend. of permeability *(Russian)* 3−8349
Cu-Ni-Fe alloy, rel. to magnetis. reversal process 3−36745
$CuFe_2O_4$, cubic-tetragonal transform. and induced uniaxial anisotropy *(French)* 3−15382
Dy-Gd alloy, comp. and temp. depend. 3−34153
Er^{3+}, in solids, C_{3h}, D_{2d}, O_h site symmetry, rel. to cryst. field parameters 3−2234
$ErFe_2$, and magnetisation, 77-300K 3−5113
p-$EuCr_2Se_4$, doped, hysteresis study 3−27385
$Eu_{2.2}Gd_{0.8}Al_{0.6}Fe_{4.4}O_{12}$, garnet, growth induced uniaxial anisotropy 3−2305
$(Fe, Ti, \square)_3O_4$, cation deficient, magnetic props. 3−4735
Fe, cylindrical films, Procopiu effects study, anisotropy depend. 3−36775
Fe-Cr alloys, ferromag. reson., anisotropy const. determ. 3−2403
Fe-N, alloys, cold-drawn, magnetisation anomaly 3−12034
Fe-Si crystal, rotational hysteresis loss in (001) plane *(Japanese)* 3−24582
Fe_3Al, annealing effects on compression induced mag. anisotropy 3−30642
$FeBO_3$, light-induced, obs. by acoustic resonance 3−18335
α-Fe_2O_3, hematite, nonlinear susceptibility and anisotropy to Morin temp. 3−2261
α-Fe_2O_3, mechanically induced, Mossbauer obs. 3−5148
FePt alloy powders, ordered, anisotropy consts., saturation magnetiz., coercivity *(Russian)* 3−30652
Gd-Lu alloys, determ. of magnetocrystalline anis. consts. 3−2306
Ge, n-type, rel. to temperature magnetoplasma wave obs. *(Russian)* 3−24558
$HoFeO_3$, spin reorientation, 50-120 K *(French)* 3−27380
K_2CuF_4, rel. to temp. depend. of n.m.r. freqs. 3−24623
$K_2ZnF_4{:}Mn^{2+}$, electronic overlap contrib. to uniaxial anisotropy of Mn^{2+}, spin hamiltonian 3−34108
$La_{0.4}Nd_{1.6}O_3$, single crystal, paramag. susceptibility anisotropy meas. *(French)* 3−38961
$Lu_2EuMFe_4O_{12}$ (M = Al or Ga) garnet, growth-induced mag. anisotropy of epitaxial films 3−21259
Mg ferrite, ferrimag. resonance obs. 3−30673
$Mn_{1.5-x}Me_xFe_{1.5}O_4$ (Me = Ni or Cr), relaxation phenomena at low temps. 3−15381
$(NH_4)_2MnF_5$, linear chain antiferromagnet, weak ferromagnetism and anisotropy 3−30643
Nd_2O_3, single crystal, paramag. susceptibility anisotropy meas. *(French)* 3−38961
Ni, spontaneous magnetisation anisotropy from band theory, spin-orbit interaction 3−34150
Ni ferrite, contribution of tetrahedral Ni^{2+} ion 3−2303
Ni-Cu alloy, magnetocryst. anisotropy consts. at 0°K, conc. depend. 3−21258
Ni-Fe film, oblique incidence evap., deuteron irrad. effects 3−34148
$NiBr_2.2H_2O$, rel. to sp. ht., 1.2-23 K, anomalous behaviour 3−36722
α-$RbMnCl_3.2H_2O$, anisotropy fields, antiferromag. reson. study 3−36796

magnetic anisotropy continued
Si, n-type, rel. to temperature magnetoplasma wave obs. *(Russian)* 3−24558
$Sm_{0.5}Pr_{0.5}Co_5$ strongly textured magnet prep. from magnetically anisotropic powders *(Russian)* 3−39375
$Tm_3Fe_5O_{12}$, 77-293K 3−34152
$Y_{2.4}Eu_{0.6}Ga_{1.2}Fe_{3.8}O_{12}$, epitaxial garnet film, growth-induced mag. anisotropy, annealing effects 3−30640
$Y_2EuMFe_4O_{12}$ (M = Al or Ga) garnet, growth-induced mag. anisotropy of epitaxial films 3−21259
YIG, depend. on pressure and temp. 3−5114
YIG epitaxial film, induced in-plane mag. anisotropy, ferromagnetic resonance obs. 3−34147
YIG epitaxial film, rel. to domain struct. and stress 3−34160
YIG:Al epitaxial film, chemical vapour deposited for bubble domain devices 3−33746
YIG:Cu, octahedrally coordinated Cu^{2+} ions contrib. to magnetocryst. anisotropy 3−2304
YIG:Ge substituted, ferromag. resonance obs. 3−5136
YIG:Si, i.r. induced changes 3−30644

magnetic bays *see geomagnetic variations*

magnetic bottles
see also magnetic mirrors
No entries

magnetic bubbles
heading is late addition, see also magnetic domains
domain collapse, micromagnetics theory 3−36766
domain generation through exchange coupling 3−34162
domain wall mobility, determ. by bubble collapse method, anal. 3−38995
domain walls in bubble films, static props. of film thicker than wall width 3−36761
domain walls in bubble films, theory of static props. 3−36760
dynamics of elliptical mag. bubbles, domain wall anisotropy effects 3−36759
epitaxial garnet films, effect of substrate defects on transport 3−15090
extraordinary, formation by cutting strip domains 3−36763
extraordinary, wall energy, statics 3−34163
ferromagnetic film, honeycomb domain struct. 3−30662
garnet, bubble domain motion, crystal defect influence 3−36742
garnet, chemical vapour deposition for bubble domain devices 3−36771
garnet, epitaxial film, method of producing extraordinary bubbles 3−28610
garnet film, bubble detect. using waveguide fibre optics 3−35442
hard ferromag. bubbles, translational mobility 3−8390
in magnetic oxides, uniaxial, new computer information carriers, review *(German)* 3−21280
material evaluation, orthoferrite crystal slices and epitaxially grown films, magnetisation, wall energy, coercivity, temp. depend. 3−36764
materials, thermal expansion and lattice parameters 3−34158
orthoferrite, domain struct., magneto-optical obs. 3−34159
Permalloy films, h.v. electron microscope obs. 3−30660
permalloy layer effect on bubble-domain stability 3−18336
permalloy overlay structures, preparation technique 3−13355
propagation, permalloy cct. analysis 3−36752
propagation and sensing, interaction with magnetic environment 3−15397
rare earth garnet, liquid phase epitaxial growth 3−36770
rare earth iron garnet, chemical vapour deposition for bubble domain devices 3−24792
single-wall domain propag., conductor arrangement, patent 3−18346
susceptibility of bubble materials 3−38999
uniaxial magnetic material, zero temp. sensitivity of bubble diameter 3−18339
Eu-Y-Ga-Fe garnet, dynamics of magnetic bubble domain arrays 3−36765
$EuEr_2Ga_{0.7}Fe_{4.3}O_{12}$ film, variation of magnetiz., Curie temp., and Ga/Fe ratio with epitaxial growth temp. 3−34157
YIG:Al epitaxial film, chemical vapour deposition for bubble domain devices 3−33746

magnetic circuits
Coulomb law of magnetism, ferromagnetic material, equivalent circuit models *(German)* 3−13666
nonconducting with homogeneous or inhomogeneous permeability, effect on a.c. field of coil *(Russian)* 3−32482

magnetic cooling
Kapitza thermal boundary resistance between ^{3}HE and Cu, meas. from 10-160 mK 3−33712
^{3}He, by adiabatic solidification 3−25699
^{3}He solid-liquid mixture, bulk nucl. polarization, below 5 mK 3−30308
$PrCu_6$, nuclear adiabatic demagnetisation, 2.7-40 mK, transition 3−36709

magnetic core stores
ferrite, memory stack, for solar probe project, construction 3−3393

magnetic cores
ferrite, hot pressing method *(Polish)* 3−8972
inductor core, teaching-aid demonstration 3−19132

magnetic devices
see also ferrite devices; magnetic amplifiers; magnetic lenses; magnetic storage devices; magnetic thin film devices; magnetostrictive devices
e.m. field vehicle guidance system, patent 3−10426
e.m. levitation system rel. to magnet design and technology 3−6036
flowmeters, past and present development 3−19379
flowmeters, using nonhomogeneous magnetic field, patent 3−456
flux compression experiments, analysis 3−3833
magnetics conference, Kyoto, Japan, 10-13 April (1972) 3−34048
measurement errors compensation using Fe-Ni alloys having temperature dependent magnetization and permeability *(German)* 3−15385
probe, three coil, computer optimisation 3−6029
repulsive magnetic suspensions for suspended trains, technical assessment 3−6035
superconducting magnetic flux compressor, with mechanical linkage 3−37666
temperature measurement, magneto-thermal effect *(German)* 3−255

magnetic devices continued
  translation balance for mag. susceptibility meas. at high temp. *(French)* 3 – 6030

magnetic dipoles *see magnetic moments*

magnetic disc storage
  head flight height measurement technique 3 – 10577

magnetic disc stores *see magnetic disc storage*

magnetic domains
  see also domain walls; magnetic bubbles
  Alnico, domain structure variation in partial hysteresis cycles 3 – 30664
  antiparallel domains obs. in ferromag. specimen using improved Lorentz electron microscopy method 3 – 13471
  Barkhausen noise, power spectrum in simple materials, spring model 3 – 5117
  birefringent mag. material, optical contrast of inclined boundaries 3 – 18436
  boundary movement, model verification *(Russian)* 3 – 21266
  bubble, effect of thin permalloy film on stability 3 – 18336
  bubble, generation through exchange coupling 3 – 34162
  bubble, hard ferromag., translational mobility 3 – 8390
  bubble, propagation, conductor arrangement, patent 3 – 18346
  bubble, propagation, permalloy cct. analysis 3 – 36752
  bubble collapse method, for wall mobility meas., anal. 3 – 38995
  bubble domain lattices, elastic consts. and elastic waves, domain wall damping 3 – 21269
  bubble domain material, characterization using X-ray topography 3 – 34156
  bubble domains radial susceptibility 3 – 38999
  bubble film domain walls, static props. of film thicker than wall width 3 – 36761
  bubble film domain walls, theory of static props. 3 – 36760
  bubble-domain collapse, micromagnetics theory 3 – 36766
  bubbles, extraordinary, formation method by cutting strip domains 3 – 36763
  bubbles, extraordinary, wall energy, statics 3 – 34163
  bubbles, in uniaxial mag. oxides, new computer information carriers, review *(German)* 3 – 21280
  bubbles, orthoferrite crystal slices and epitaxially grown films, magnetisation, wallenergy, coercivity, temp. depend. 3 – 36764
  bubbles, propagation and sensing, interaction with magnetic environment 3 – 15397
  circular, wall energies, exchange and anisotropy contribs., numerical soln. 3 – 12036
  creep of domain boundaries with transverse constrictions, model approach *(Russian)* 3 – 18337
  cubic materials, ferromagnetic, contrast in scanning electron microscope 3 – 38998
  elliptical mag. bubbles, dynamics, domain wall anisotropy effects 3 – 36759
  excitation spectrum for mag. domain walls, eigenvalues 3 – 15394
  ferrite, magnetically uniaxial, single crystal plate, controlled motion of cylindrical mag. domains 3 – 36767
  ferromagnet, multidomain, kinetics of conduction electrons 3 – 34169
  ferromagnet, polyaxial, mag. texture influence on magnetisation, domain wall energy 3 – 30665
  ferromagnetic bulk domains by neutron depolarisation in three dimensions 3 – 39004
  ferromagnetic film, domain wall creep in nonuniform fields, intrinsic fields influence *(Russian)* 3 – 36736
  ferromagnetic film, domain wall width determ. *(French)* 3 – 8392
  ferromagnetic film, honeycomb domain struct. 3 – 30662
  ferromagnetic thin film, cylindrical, single domain theory, rel. to anisotropy field meas. *(French)* 3 – 25818
  film, dynamic behaviour, variational calculation 3 – 36739
  film, ferromagnetic, magnetoresist. rel. to domains and magnetisation vector angular dispersion 3 – 21052
  film, hypercritical, mag. field influence on ground state *(Russian)* 3 – 36699
  film, subharmonic oscillations of magnetic and crit. curves *(Russian)* 3 – 15392
  film and platelet, theory of domain wall motion 3 – 36754
  garnet, bubble domain motion, crystal defect influence 3 – 36742
  garnet, chemical vapour deposition for bubble domain devices 3 – 36771
  garnet, epitaxial film, method of producing extraordinary bubbles 3 – 28610
  garnet, mixed rare earth iron type, epitaxial film, domain wall coercivity temp. depend. 3 – 21257
  garnet film, mag. bubble detect. using waveguide fibre optics 3 – 35442
  rel. to magnetic aftereffect, for irreversible magnetization process in Rayleigh region, theory 3 – 18344
  orthoferrite, bubble and ring domains, magneto-optical obs. of structure 3 – 34159
  orthoferrites, interference patterns, at domain boundary, theory 3 – 5116
  orthoferrites, spin reorientation temp., phase transitions, heat capacity, domain structure and energy 3 – 39003
  permalloy bar, cylindrical domain propag. due to stray fields 3 – 30657
  permalloy bar, magnetisation distribs., magnetostatic energy barriers and drive fields for bubble motion 3 – 21270
  Permalloy film, l.f. oscillating movement *(Russian)* 3 – 24586
  Permalloy film, obliquely deposited hypercritical, domain width depend. on angle of incidence *(Russian)* 3 – 24588
  permalloy film, Ritz model for asymmetric domain walls 3 – 8388
  permalloy film, transit time limited nonlinear domain wall motion 3 – 36733
  permalloy film, wall motion, dynamic properties 3 – 34161
  Permalloy film, with banded domain struct., mag. reversals *(Russian)* 3 – 8381
  Permalloy films, bubble domains, h.v. electron microscope obs. 3 – 30660
  permalloy thin films, influence of pulse magnetic reversals on domain boundary drift *(Russian)* 3 – 2322
  polarized media, inhomogeneity near ferromag. to paramag. transition rel. to domain structure 3 – 5102
  rare earth cpds., ferromagnetic, thin wall coercivity 3 – 2317

magnetic domains continued
  rare earth garnet, bubble domain material, liquid phase epitaxy 3 – 36770
  rare earth iron garnet, chemical vapour deposition for bubble domain devices 3 – 24792
  rare earth orthoferrites, ring domains, unidirectional dimens. change in cyclic mag. field 3 – 21277
  scanning electron microscopy, Kossel lines, contrast interpretation 3 – 2320
  semiconductor, domain wall effects on elec. resist. 3 – 34170
  steady state motion 3 – 18343
  structure of electrodeposited over-critical films 3 – 39000
  two-dimensional domain wall structures, Lorentz microscopy anal. 3 – 24590
  unaxial crystal, perfect, magnetic domain wall nucleation 3 – 36751
  uniaxial magnetic materials, zero temp. sensitivity of bubble diameter 3 – 18339
  uniaxial platelet, props. of thick-walled cylindrical mag. domains 3 – 36755
  Vicalloy, domain structure variation in partial hysteresis cycles 3 – 30664
  wall energy, pressure due to variations 3 – 5119
  wall motion, eddy current limited, bowing and merging, segmented model 3 – 12035
  $BaFe_{12}O_{19}$, internal domain structure, power patterns and Faraday effect obs. in i.r. 3 – 38990
  $BaFe_{12}O_{19}$ substituted ferrite, onset of single domain behaviour rel. to coercivity 3 – 34165
  $(Co, Fe)_{17}R_2$ [R = rare earth, La, Y], magnetic symmetries and domains 3 – 18340
  Co-P film, high-coercivity, domain struct. and reversal processes 3 – 24592
  CoNiFe film, wall motion rel. to low freq. creep 3 – 36738
  $Co_{17}R_2$ [R = rare earth, La, Y], magnetic symmetries and domains 3 – 18340
  Co_7R_2 [R = rare earth, La, Y], magnetic symmetries and domains 3 – 18340
  Co_5X alloy, X = rare earth, domain wall energy, polarized light metallography obs. 3 – 5118
  Cr, obs. of antiferromagnetic domains by X-ray and neutron topography 3 – 30647
  $Cs_2CuCl_4.2H_2O$, Heisenberg b.c.c. ferromagnet, nuclear quadrupole resonance obs. of magnetic interactions, spontaneous magnetisation within Weiss domains 3 – 27439
  $Cu_{2\|x}MnAl_{1-x}$, Heusler alloy, annealing effects on domain structure, Lorentz microscopy 3 – 1545
  Dy, obs. of surface domain patterns 3 – 21274
  $DyAl_2$-$DyFe_2(Co_2)$, rel. to complex mag. behaviour 3 – 18323
  DyNi intermetallic, mag. struct., neutron diffr. and magnetisation obs. 3 – 15376
  Eu-Y-Ga-Fe garnet, bubble, dynamics of a close-packed hexagonal array 3 – 36765
  $EuEr_2Ga_xFe_{5-x}$, $Eu_xEr_{3-x}Ga_{0.7}Fe_{4.3}O_{12}$ bubble domain films, thermal expansion of lattice parameters 3 – 34158
  $EuEr_2Ga_{0.7}Fe_{4.3}O_{12}$ bubble domain film, variation of magnetiz., Curie temp., and Ga/Fe ratio with epitaxial growth temp. 3 – 34157
  Fe, high-purity, creep, const. mag. field influence, dislocation-domain wall interaction *(Russian)* 3 – 36774
  Fe film evaporated at oblique incidence domain structures 3 – 1544
  Fe whisker, magnetis. process with Landau domain struct. 3 – 36749
  Fe zone melted crystals under tensile stress, dislocations and magnetic domain walls, X-ray topographic study 3 – 17828
  Fe:Si, ferromag. domains parallel to (111) *(French)* 3 – 27383
  Fe-Si, covered by Ni film, mag. susceptibility temp. depend. meas. rel. to ferromag. domains *(Russian)* 3 – 24562
  Fe-Si single crysts., e.m. losses depend. on surface cryst. orientation *(Russian)* 3 – 15391
  FePt alloy powders, ordered, anisotropy consts., saturation magnetiz., coercivity *(Russian)* 3 – 30652
  Mg-Mn ferrite films, remagnetization rate and mobility of domain boundaries *(Russian)* 3 – 8398
  $Mg_xMn_{1-x}Fe_2O_4$ film, rel. to use as phase diffr. grating 3 – 36862
  Mn-Bi thin films, domain patterns from polarization microscopy 3 – 21283
  Mn-Ga alloy powders, high-anisotropy, mag. reversals, domain boundary displacement *(Russian)* 3 – 36737
  Mn-Ga alloys, plastically deformed, mag. hardness *(Russian)* 3 – 36735
  MnBi, study using Kerr effect 3 – 2308
  MnBi film, Faraday effect obs. 3 – 21272
  MnBi-Bi eutectic, directionally solidified, single domain behaviour 3 – 36748
  MnF_2, spin flop domains, n.m.r., Faraday rotation, photographs and optical-absorption spectroscopy investigation 3 – 34113
  Ni, pulsed n.m.r. of ^{61}Ni, Bloch wall effects *(French)* 3 – 30702
  Ni, transcritical epitaxial film, magnetisation distrib. in domain structure 3 – 30666
  Ni, two-dimens. domain wall struct., Lorentz microscopy anal. 3 – 24590
  Ni film, hypercrit. state, hysteresis loops, domain struct. *(Russian)* 3 – 15393
  Ni film evaporated at oblique incidence domain structures 3 – 1544
  Ni magnetoelastic attenuation at u.s. freqs. due to domain struct. rearrangement 3 – 21288
  Ni-Co film, electrodeposited, stripe domains *(Russian)* 3 – 30667
  Ni-Fe alloy film, hypercrit. state, hysteresis loops, domain struct. *(Russian)* 3 – 15393
  Ni-Fe(25 wt.%) films, domain boundary curvature and displacement, mag. field and elastic stresses influence *(Russian)* 3 – 30654
  NiFe, distrib. function of forces exerted by defects on domain walls 3 – 36756
  NiO, antiferromagnetic, crystal structure determined by X-ray topography 3 – 30646
  $PbFe_{12}O_{17}$, free energy, entropy, of parallel plate domain struct. 3 – 2314
  $Rb_2CuCl_4.2H_2O$, Heisenberg b.c.c. ferromagnet, nuclear quadrupole resonance obs. of magnetic interactions, spontaneous magnetisation within Weiss domains 3 – 27439
  Sr ferrite, Al substituted, domain structure, demagnetis. effects 3 – 36747

magnetic domains continued
- Tb, obs. of surface domain patterns 3−21274
- Y-Eu garnet, epitaxial film, magnet domain wall velocity 3−36734
- YFeO$_3$, domain wall mobility, nonlinear applied field depend. 3−30661
- YIG, Ferrimag. resonance i.r. obs., effect of crystal imperfections 3−27379
- YIG, Ga substituted, nearly compensated, compensation magnetic domain walls 3−36732
- YIG, intrinsic e.m. radiation in presence of domain struct. 3−34217
- YIG, nonlinear ferromag. reson., domain struct., instability *(Russian)* 3−8453
- YIG epitaxial film, stripe domain struct. Faraday effect obs. 3−34160
- YIG film, heteroepitaxial growth, obs. of regular band shaped domains 3−1922
- YIG film, in in-plane mag. field, orientation of stripe domains 3−27386
- YIG:Al epitaxial film, chemical vapour deposited, serpentine and circular domains 3−33746
- YIG:Ga, L.P.E. growth, effect of substituting Gd(Sm)(La) for Y 3−1924

magnetic double refraction *see magneto-optical effects*

magnetic field effects
- acoustic wave 3−28479
- alkali halides, magnetically quenchable positron state 3−36545
- antiferromagnet with impurities, mag. field depend. of magnon density of states 3−8331
- arc displacement in transverse mag. field, calc. and expt. *(German)* 3−23947
- asbestos fibre alignment 3−18737
- axial antiparallel bias, influence on energy transfer in high beta diffuse pinch 3−17643
- azimuthal relativistic beam, in magnetic field, instabilities with thermal velocity spread 3−13775
- p-azoxyanisole, X-ray diffr. obs. under simultaneous action of electric and mag. fields 3−33454
- bound electron and phonon states, in strong mag. field due to nonlinear interactions 3−24401
- bound electron-phonon state spectrum in quantizing mag. field 3−4980
- Brownian motion of electrons and diffusion in time-dependent magnetic fields in plasma 3−11469
- bubble domains, interaction with magnetic environment, propagation and sensing 3−15397
- cathode spot, directional motion due to asymmetrical conditions at its boundaries *(Russian)* 3−1529
- charged particle motion, in axially symmetric magnetic field 3−13767
- charged particle motion in time varying axially symmetric mag. field 3−29934
- chemical reactions including free radicals 3−25062
- colloidal solution, ferrite particles, osmotic press. 3−27792
- conducting thin plate, current induction *(French)* 3−32488
- cosmic ray diffusion in static random magnetic field 3−37271
- deflection of radiating electron traversing inhomogeneous magnetic field 3−35585
- disconnection vacuum arc characteristics in magnetic field, effect on arc direction 3−17708
- Earth, overall electrical conductivity distrib. rel. to external magnetic fields 3−34851
- electrets in carnauba wax, produced under simultaneous effects of magnetic and electric fields, orientation phenomena *(German)* 3−8506
- electron cyclotron drift instability, controlled steady-state experiment 3−14553
- exciton, mag. field depend. of ground state energy with Coulomb pot. screening 3−2034
- exciton creation in strong mag. fields due to energy losses of fast electrons 3−36339
- ferrimagnet, Heisenberg uniaxial Neel type, spin wave theory, external mag. field effects 3−11995
- ferrimagnet, three-sublattice, mag. struct. induced by field *(French)* 3−38972
- ferrites, spin wave propag. theory in inhomogeneous static mag. field 3−5112
- ferromagnetic material slowly rotating in alternating magnetic fields, magnetic remanence 3−24583
- field-aligned irregularities detected by phase interferometry, wavelike struct. 3−9326
- formol molecular beam, l.f., Stark effect due to motion in d.c. magnetic field *(French)* 3−33166
- frog muscle contractile behaviour *(Russian)* 3−16310
- Frohlich polarons, internal structure determined by optical absorption, cyclotron resonance 3−36561
- fusion reactors performance of heat pipes 3−11092
- GaAs, n-type, Gunn effect threshold variation Hall contribution 3−18157
- galactic mag. field effects on cosmic rays above 10^{17} eV 3−25350
- gas ring laser, radiation fluctuations 3−32551
- glass, low temp. thermal conductivity in electric and magnetic fields 3−1849
- Gunn diode, increased width of time-averaged voltage-current characts. 3−21090
- heat and mass exchange in paramagnetic solutions *(Russian)* 3−20314
- heat and mass transfer in electrolyte solution *(Russian)* 3−20313
- heat conduction in a plasma, solar wind 3−11497
- hexagonal crystals, wurtzite type, polarisation of exciton luminesc. 3−2595
- III-V semiconductors, small gap, spin props. of conduction electrons, small-gap semiconductors 3−38845
- Ising model of disordered state, dynamical susceptibility in transverse mag. field 3−34079
- Knight shift oscillations and spin-lattice relax in crossed fields 3−18382
- laminar jet of viscous elec. conducting liquid, longitudinal field eff. *(Russian)* 3−20390
- light flash from strong shock wave of laser spark 3−19631
- lipid bilayer spheres, deform. and birefr. 3−37515

magnetic field effects continued
- liquid crystal, nematic, in mag. field, dynamic behaviour 3−26967
- liquid crysts., nematic, optical transmission threshold and capacitance threshold for alignment in mag. field 3−20695
- liquid crysts. magnetohydrostatic theory for cryst. lying between two coaxial cylinders 3−26971
- longitudinal, on type II superconducting rods *(Japanese)* 3−24546
- Lorentz-Dirac eqn. for particle in uniform field, relativistic motion 3−35719
- magnetic film, movement of magnetic moments *(Russian)* 3−38996
- magnetic polytropes, Kelvin, pulsation and unstable mode effects 3−31498
- magnetoelastic theory of soft ferromagnetic elastic solids of multidomain struct. 3−34155
- magnetoplasma heating by magnetic perturbations 3−33378
- MBBA menatic film, statics of Freederick's transition in mag. field 3−7617
- metal-insulator transition, impurity effects on excitonic phase in strong mag. fields 3−30421
- MHD convective instability in changing magnetic field *(Russian)* 3−20386
- multiple scattering of charged particles, in medium, with axisymmetric magnetic field, with energy loss 3−13415
- nerve tissue stimulation 3−16558
- neumatic crystal, wave propagation rel. to Parodi's relation 3−17743
- neutron refraction by shaped mag. fields 3−37988
- p-n-nonyloxybenzoic acid, liquid cryst., mol. alignment, elec. and high mag. field effects 3−38535
- oil-magnetite mixture flow, rheological study for transverse fields *(Russian)* 3−20271
- oil-magnetite mixture flow and eff. of critical Reynold's number *(Russian)* 3−20315
- paramagnetic solid, r.f. mag. field effect on transverse relax. time in saturated spin system 3−15405
- particle beams, magnetic moment, electromagnetic forces, neutron acceleration 3−35726
- permalloy thin films, influence of pulse magnetic reversals on domain boundary drift *(Russian)* 3−2322
- photomultipliers, use of external mag. field for recording weak light fluxes *(Russian)* 3−25753
- piezoelectric semiconductors, parametric amplification of u.s. in strong mag. fields 3−21120
- plamon resonances, Bernstein modes, quantum mag. fields effects, quasiclassical model 3−5025
- plasma, anomalous cond., exactly solvable electrodynamic model 3−36151
- plasma, diffusion in Tokamaks, effect of mag. field modulation 3−14597
- plasma, dilute clouds, high altitude expts. and interaction 3−3042
- plasma, e.m. wave focusing in inhomogeneous mag. field 3−23823
- plasma, high freq. hydrogen discharge, longitudinal field effects *(Hungarian)* 3−17559
- plasma, spatial density distributions in h.f. discharge with superimposed static magnetic field 3−7505
- plasma acceleration in crossed electric and magnetic fields 3−29947
- plasma electron temp. determ. from ambipolar elec. field reversal under mag. field 3−4676
- plasma motion in corrugated mag. field, gas-dynamic description 3−14573
- plasma neoclassical diffusion arising from magnetic-field ripples in Tokamaks 3−38486
- plasma-filled transversely magnetized rectangular waveguide charact., collision frequency effect 3−1491
- polaron energy levels, electron-phonon interactions, magnetic and Coulomb field effects 3−36563
- polarons, electron-phonon interactions, ionic crystals, polar semiconductors, conf., Antwerp, Belgium (Aug. 1971) 3−36558
- polarons, plasma-phonon interactions 3−36572
- pyrene crystals, mag. field effect on delayed fluorescence 3−27565
- quasi-particles in mag. field, quantum kinetic equation 3−30395
- resonance flip of neutron polarization in space periodic magnetic fields 3−6685
- semiconductor, elemental, e.m. beam self focusing in inhomogeneous mag. fields 3−10568
- semiconductor, e.m. wave propagation in rectangular waveguide, strong magnetostatic field effects 3−18175
- semiconductor, helical instability in strong mag. fields, quasiclassical discussion *(Russian)* 3−8217
- semiconductor, indirect magnetooptical transition theory 3−5222
- semiconductor, recent developments in research, book 3−38798
- semiconductor, surface electron states, longitudinal magnetoresistance 3−33983
- semiconductor, surface polariton theory with and without external mag. field 3−2039
- semiconductors, polar, surface plasmons and phonons interaction in d.c. mag. field 3−2160
- sheared magnetic field effect on stability of plasma longitudinal current 3−38427
- smectic C phase, mol. rearrangement under large mag. fields, n.m.r. study 3−33450
- solid state plasma, e.m. excitations in quantising mag. field 3−21105
- stabilisation by a rotating magnetic field *(French)* 3−30033
- stellar absorption lines, effect of random magnetic field on profiles and polarization *(Russian)* 3−13033
- third adiabatic invariant conservation of motion of charged particle in axisymmetric fields 3−29158
- toroidal mag. field, E-layer compression 3−7549
- toroidal plasma in Tuman-2 device, fast radial displacement by transverse magnetic field 3−17653
- two-liquid systems with asymmetric stress tensors, model construction *(Russian)* 3−28853
- vibrating beam plate in magnetic field 3−10314
- X-ray scintillation detectors, mag. effects 3−3847
- $e^-\gamma \to e^-\nu\nu$, photoneutrino energy losses, computation for 10^{13} G mag. field 3−35805
- Al, superconducting, microwave absorptivity near energy gap 3−18262

magnetic field effects continued
- Al, thermal cond. in mag. fields to 50 kOe, 6K-57K *(Russian)* 3—4989
- Al, thermoelectric power in strong field at low temp. 3—24409
- Bi, exciton phase transition in strong mag. field, u.s. absorption obs. 3—27230
- Bi, thin layer, transition from amorphous to crystalline state under mag. field *(Russian)* 3—15015
- Bi-Sb:Te,Se, calc. of thermoelec. figure of merit in mag. field 3—15176
- C and man-made fibres, alignment in liquid suspension 3—5347
- CH spectrum in magnetic white dwarf G99-37, circular polarization caused by magnetic fields 3—26651
- Cd, magnetic surface states, microwave surface impedance obs. 3—8243
- $CdCr_2Se_4$, ferromag. semicond., influence on transport props. 3—5017
- CdS, polarisation of light emitted from free and bound excitons 3—2594
- Cr u.s. attenuation due to polarisation domain relaxation processes in transverse spin density wave phase 3—30675
- Cu, exploding wire in strong axial mag. field, discharge damping 3—36218
- Cu thin film Hall coeff. rel. to magnetic field *(German)* 3—24413
- $Cu_{1-x}Au_x$-Fe(Cr), mag. field depreciation of Kondo magnetoresist. 3—33872
- Cu_2O, modulated excitonic absorption in elec. and mag. fields 3—2037
- DyVO, thermal conductivity at low temps. and in magnetic fields 3—1847
- Fe, cylindrical films, Procopiu effects study 3—36775
- Fe, magnetic field dependence of thermoelectric power 3—11885
- Fe-Co-Ni-Al-Ti-Cu, thermomag. treatment effects *(Russian)* 3—8386
- Fe-Si, annealing, 480-680°C, effect of mag. field on softening process *(Russian)* 3—27673
- Fe-Si alloys, thermomagnetic treatment, effects of inclusions and internal stresses *(Russian)* 3—8385
- n-GaAs:Cr, magnetoresist. and recombination instability in mag. field 3—30500
- p-GaAs:Zn, resist. and magnetoresist. meas. rel. to impurity cond. 3—11914
- Ge, electron-drops, oscill. of recomb. radiation in strong mag. field *(Russian)* 3—2030
- p-Ge, influence on hopping conduction 3—24440
- Ge single crystal, current-voltage characts. under strong injection conditions 3—24447
- Ge:Mn; Sb, recomb. wave current instability rel. to mag. field *(Russian)* 3—8180
- H, 24 lowest states spectrum in strong mag. field, 10^6-10^8 G 3—23456
- H atom, structure, in intense magnetic field 3—1093
- H atom bound-bound transitions in field of 10^7-10^8 gauss, astrophysical appl. 3—26564
- He ion beam interactions unidirectional and interpenetrating in an external field *(Russian)* 3—32618
- ^{3}He solid, effect of magnetic field on melting curve 3—11782
- Hg arc plasma, VI characts. and power relation in transverse mag. field 3—36212
- In and In alloys, superconducting films, thermal conductivity 3—38928
- In-Bi supercond. foils, eff. of a.c. mag. fields on flux-flow states *(Japanese)* 3—24547
- InSb junction lasers operated at low temp., longitudinal mag. field effect on power output 3—37973
- NbO, resist. and Hall coeff. meas. in high mag. field showing metallic behaviour 3—33888
- Nd, mag. struct. mag. field depend. 3—2293
- Ni, dislocation motion in alternating mag. field, oscill. domain wall interactions 3—30674
- Ni, flow stress rel. to mag. field, domain wall dislocation interactions 3—5125
- Ni-Co alloy, flow stress rel. to mag. field, domain wall dislocation interactions 3—5125
- Ni-Cu alloy, dislocation motion in alternating mag. field, oscill. domain wall interactions 3—30674
- Pb alloys, superconducting flux flow resistance minimum, mag. field dependence 3—5077
- PbSe, on spontaneous and stimulated emission from p-n junction 3—15524
- Si, piezoresistance coeff., strain gauge obs. 3—5002
- Te-TeO_2-Pb junction, electron tunnelling at liq. helium temps., phonon and mag. field effects 3—30546
- $TmVO_4$ thermal conductivity at low temps. and in magnetic fields 3—1847
- Yb, thin layer, transition from amorphous to crystalline state under mag. field *(Russian)* 3—15015
- Zn, energy level struct. in mag. field, using single-band effective Hamiltonian 3—36526

magnetic field measurement
- *see also field plotting; fluxmeters; magnetometers*
- betatrons *(Russian)* 3—19262
- Cygnus A, ram pressure deceleration by an intergalactic medium 3—13064
- deep-sea cores, method for palaeomagnetic meas. aboard ship *(German)* 3—16052
- electrical methods, Hall generator, atomic resonance and superconductivity *(German)* 3—13357
- ferromagnetic materials, classification of leakage field methods of defect detection 3—18766
- fluxgate magnetometer, aeromagnetic geophysical surveying, direct reading, total feedback, solid state design 3—3165
- fluxmeter, employing Hall generator, description *(Polish)* 3—258
- fluxmeter, restoring torque correction, soln. *(Polish)* 3—259
- geophysical meas. error due to departure from coil system geometry *(Russian)* 3—2922
- gradient magnets in proton synchrotron, measuring system for slowly varying low field 3—35443
- gradiometer based on superconducting quantum interference device, construction 3—28499

magnetic field measurement continued
- Greater Antilles long profile analysis using two-dimensional modelling of magnetized bodies 3—5468
- Hall generator, magnetically controlled 3—13354
- magnetisation meas. of twisted superconducting composite conductors 3—11987
- nonuniformity of magnets with small gaps, paramagnetic microwave resonance device 3—6045
- palaeointensity determ. of geomag. field from anhysteretic remanent mag. meas. 3—9389
- probes for diagnostics of pulse plasma 3—14581
- pulsed Hall gaussmeter 3—22410
- review of various methods 3—257
- survey of methods, electrical and digital *(German)* 3—13356
- techniques and applic. *(German)* 3—22805
- three components, evaluation from voltages induced on 3 Hall probes *(French)* 3—3835
- weak field meas. using zero-field level-crossing resons. in optically pumped ^{4}He 3—7058
- Li plasma, high-current discharge struct. 3—33404

magnetic field variations, earth *see geomagnetic variations*

magnetic fields
- *see also crystal internal fields; electromagnetic fields; geomagnetism; interplanetary magnetic fields; interstellar magnetic fields; magnetic field effects; magnetic field measurement; solar magnetism*
- 2n-pole symmetrical, sector windings, design calc. *(German)* 3—35453
- a.c. field of coil in presence of nonconducting magnetic circuit and conducting objects *(Russian)* 3—32482
- annihilation at neutral sheets in presence of conducting plasma 3—28071
- attenuation, in presence of non-ideally conducting earth, Airy func. and attenuation func. calc., Algol 60 subroutine *(Polish)* 3—29000
- coils, circular and rectangular *(French)* 3—32487
- constrictions, penetration by intense relativistic electron beams 3—801
- cosmic-rays in random magnetic field, breakdown of quasilinear derivation of kinetic equation 3—31480
- Crab Nebula, time evolution of magnetic field strength rel. to energetic particles 3—25522
- cylindrical coil with flat conductive shielding, analysis by vector potential method *(Russian)* 3—32476
- diffusion of charged particles in random magnetic field 3—31495
- dipole coordinate system rel. to transport processes in geomagnetic field 3—27973
- dipole source, inverse scatt. from perfectly cond. prolate spheroid, in quasi-static domain 3—22819
- eccentric dipole arbitrarily located in sphere 3—22804
- eddy currents calculation in axially symmetric a.c. current carrying conductors, by computer *(Russian)* 3—32485
- electron motion in uniform magnetic field and field of plane e.m. wave, influence of radiation friction *(Russian)* 3—10324
- e.m. induction in infinite plane sheet with circular hole, varying mag. field 3—26187
- energy bounds of charged particle moving in alternating axisymmetric magnetic field *(Russian)* 3—6300
- equation of motion for particle in mag. field, numerical soln. 3—26253
- external, of cylinder with tangential boundary conditions *(Russian)* 3—10325
- far scattered field of conducting cylinder of arbitrary cross-section, convergence of numerical solution 3—22831
- field induction follow up, spin generator, first proton signal sideband 3—261
- generated by conductor of elliptic cross-section *(Polish)* 3—29001
- generation by ocean swell, simulation 3—2934
- generation by thin closed shells, integral eqn. 3—29008
- group of circular coils, calc. *(Czech)* 3—4054
- guided missile cell-like structures, computer-aided analysis 3—32491
- high, pulsed, generated in single turn solenoids 3—4058
- horizontal dipole buried in 2-layer earth 3—22803
- in Indiana isochronous cyclotron 3—10016
- induction motors, field distribution under load conditions 3—13668
- instability changes of Nb-Ti composite wires due to Cu-cladding 3—11989
- integral equation formulation, dipole and current models 3—29004
- integral equation formulation, magnetisation vector approach 3—29005
- Jupiter, non-dipole terms, obs. of linear polarization of radio radiation 3—3299
- Kittel structure and magnetic thin film, magnetisation and demagnetisation fields, computer calc. *(Polish)* 3—24584
- line currents, modified form of Biot-Savart law 3—37921
- lunar, volcanic ash particle flow ionisation 3—12995
- magnetic bodies of arbitrary shape, static field calculation 3—13675
- magnetodynamic compression, motion of cylindrical conducting shell *(Russian)* 3—6395
- magnetosphere, field energy rel. to neutral currents at boundary 3—25301
- magnetospheric observations, review 3—3142
- moon, criticism of lunar dynamo suggestion 3—9509
- motion of charged particles in homogeneous alternating magnetic fields *(Russian)* 3—6299
- near-earth space, three-layer model of small scale motions with allowance for horizontal mag. field component 3—25265
- nonhomogeneous, in magnetic flowmeters 3—456
- noon-midnight meridional plane, ionospheric wave electric field mode fluctuations 3—16016
- origin as Coriolis force from Thomas rotation 3—37853
- origin in the early Universe 3—18926
- parallelogram of linear currents, analysis of magnetic field *(French)* 3—4059
- plasma, laser-produced, self-generated fields, press. depend. 3—33394
- pulsar mag. field generation mechanisms, rotation effects *(Russian)* 3—37422
- quadrupole, magnetic centre determ. 3—16463
- reconnection rate of two oppositely directed fields rel. to solar flares 3—31496

magnetic fields continued

- rotating magnetic field control for bubble-domain experiments 3−6033
- rotating magnetised gaseous disk, quasar and galactic nucleus model 3−31746
- Saturn, explanation of long wavelength radiation 3−31602
- shear stabilization of drift cyclotron instability in a magnetically confined plasma 3−4643
- solar wind spiral, interaction between solar wind and interstellar gas neutral component 3−12962
- spline fitting method for subgrid resolution of field due to charge distrib. 3−26768
- static, calculations in nonlinear ferromagnetic medium *(Russian)* 3−34050
- static, in ferromagnetic medium, eqn. formulation by variational methods *(Russian)* 3−34049
- static field of magnetic head with rounded split-edges, conformal analysis *(German)* 3−29006
- static fields calculation in piece-wise-homogeneous anisotropic media *(Russian)* 3−32483
- superconducting flux exclusion tube, mag. field distribs. 3−19276
- superconductive shells uniform magnetic field, analysis *(Russian)* 3−32479
- thin film testing, patent 3−10427
- turbulent dynamo, functional approach 3−23713
- wedge, in mass spectrometer 3−13449
- white dwarfs, lower limit set by individual line corrections 3−13037

magnetic film stores

- *see also plated wire stores*
- MnAlGe film, self-demagnetisation during thermomag. writing 3−24407

magnetic films *see magnetic thin films*

magnetic flux

- *see also fluxmeters*
- accretion onto a rotating magnetic monopole, sub-Alfven flow 3−12930
- coils, circular and rectangular *(French)* 3−32487
- compression experiments, analysis 3−3833
- compression experiments 3−13667
- compression expts., dynamics of imploding liners 3−32481
- field lines of a centred rectangle of rectilinear and equal currents *(French)* 3−32489
- flux compression experiments analysis 3−10420
- solar photosphere obs., energy spectra of small-scale mag. fields 3−31519
- solar surface eruptions, random nature hypothesis 3−31572
- superconductors, type II, vortex interaction, behaviour near H_{c1} at arbitrary temp. 3−30568
- variation in plasma when subjected to electric field of circularly polarized waves *(French)* 3−11480

magnetic hardness *see ferromagnetic properties of substances*

magnetic hysteresis

- (rare earth-misch metal)-copper-cobalt alloys, heat treatment effect on permanent magnet props. *(Japanese)* 3−34562
- alloys, high-coercive, temp. hysteresis of residual induction *(Russian)* 3−8387
- Alnico, domain structure variation in partial hysteresis cycles 3−30664
- Barkhausen noise, power spectrum in simple materials, spring model 3−5117
- ferromagnetic plate, travelling wave excitation, steady state elliptical vector mag. field 3−18341
- low loss of filament superconducting composite for use in pulsed magnets 3−11992
- low temperature measurement using Ballistic method, apparatus design 3−9997
- permalloy film, evap. onto rotating substrate, coercive force obs. rel. to helical anisotropy 3−34149
- Permalloy film, obliquely deposited, mag. reversals, mechanisms *(Russian)* 3−30651
- permalloy film, obs. of triangular hysteresis loops 3−8393
- steel plates with nonlin. magnetisation characteristics, losses, calc. 3−2313
- superconductor, hysteretic, magnetisation for complete field penetration, crit. state model 3−36669
- superconductor, type-II, irreversibility and mag. hysteresis 3−8300
- Vicalloy, domain structure variation in partial hysteresis cycles 3−30664
- $Ca_xN_{1-x}Fe_2O_4$, phase structure determination, phase equilibrium 3−8379
- Co single-domain powders with cubic anisotropy *(Russian)* 3−15390
- Co-Fe-Nb semihard mag. alloy development 3−21261
- Cr, antiferromagnetic, fields to 20 kOe, 77-450K 3−2310
- Cu-Ni-Fe alloy, squareness ratio and coercivity 3−36745
- Dy, of ferromag.-antiferromag. transform., elec. resist. and thermal expansion obs. *(Russian)* 3−15363
- $ErFe_2$, near mag. compensation temp. *(Russian)* 3−8380
- ErGa, ferromag. props. 3−2319
- p-$EuCr_2Se_4$, doped, fields up to 0.1 Vs/m^2 3−27385
- Fe single-domain powders with cubic anisotropy *(Russian)* 3−15390
- Fe-Co(Ni) single-domain powders with cubic anisotropy *(Russian)* 3−15390
- Fe-Cr-Co alloy containing Si, permanent mag. material, energy product 3−36746
- Fe-Cu-Mn system, semihard mag. reed switch material, heat treatment and cold drawing effects 3−36757
- Fe-Mn-Co alloys, cold rolled, heat treatment effect on mag. props. *(Japanese)* 3−31077
- Fe-Mn-Zn ferrite, internal friction, delta E-effect and stress sensitivity in alternating magnetic fields 3−39009
- Fe-Ni-Cu ferrite, internal friction, delta E-effect and stress sensitivity in alternating magnetic fields 3−39009
- Fe-Si alloys, thermomagnetic treatment, effects of inclusions and internal stresses *(Russian)* 3−8385
- $HoFe_3$, near mag. compensation temp. *(Russian)* 3−8380
- In-Cd alloys, superconductivity and hysteresis 3−34009

magnetic hysteresis continued

- In-Cd alloys, superconductivity and hysteresis, secondary properties 3−34010
- $(MgO)_{0.55}(Fe_2O_3)_{0.45}$, anion vacancies in magnetically square hysteresis loop 3−17804
- $(MgO)_{0.30}(MnO)_{0.35}(Fe_2O_3)_{0.35}$, anion vacancies in magnetically square hysteresis loop 3−17804
- Mn-Ga alloys, plastically deformed, mag. hardness *(Russian)* 3−36735
- Mn-Zn ferrite, hysteresis coeff., solid state O_2 content depend. *(German)* 3−8344
- MnBi film, Faraday effect obs. 3−27384
- MnBi-Bi eutectic, directionally solidified, stepped loop 3−36748
- Ni film, hypercrit. state, hysteresis loops, domain struct. *(Russian)* 3−15393
- Ni single-domain powders with cubic anisotropy *(Russian)* 3−15390
- Ni-Co film, electrodeposited, stripe domain obs. *(Russian)* 3−30667
- Ni-Co-Fe-SiO system, bilaminar films, hysteresis of rotatory moment *(Russian)* 3−21267
- Ni-Fe alloy film, hypercrit. state, hysteresis loops, domain struct. *(Russian)* 3−15393
- Ni-Fe electroless film, temp. and soln. pH effects 3−21278
- Ni-Sm film *(Russian)* 3−27382
- $Ni_3B_7O_{13}I$, crystal growth, ferroelectric and ferromagnetic props. 3−17746
- TbGa, ferromag. props. 3−2319
- Ti-V beta stabilised superconducting alloy, phase precipitation effect on magnetic hysteresis 3−18249
- $Y_{3-2x}Ca_{2x}Fe_{5-x}V_xO_{12}$ garnet system, porosities, resonance linewidths, inhomogeneity effects 3−18342

magnetic impurity interactions

- antiferromagnet with two different impurities, localized spin wave spectrum 3−30639
- chemical inhomogeneities, ferromagnetic resonance line broadening, permeability behaviour 3−34218
- dielectric, paramag. defect spin-orbit interaction rel. to spin-lattice relax. 3−5135
- dilute alloys polarised neutron scattering by impurities, Kondo effect, spin fluctuations, inelastic phenomena, survey 3−21224
- ferromagnet, rel. to stimulated magnon generation, theory 3−34144
- ferromagnetic dilute alloy, rel. to thermodynamic and kinetic props. 3−34109
- ferromagnetic electron gas, spin polarisation due to mag. impurities 3−15339
- Heisenberg ferromagnet, impurity spin orientation, calc. 3−8322
- Heisenberg ferromagnet, localised modes due to impurity pairs 3−27366
- induced moment system containing vacancy impurities, Green's function theory 3−34099
- Ising and Heisenberg ferromag. model nonmag. impurity effect at Curie temp. 3−8323
- Ising model with dilute impurities, critical properties 3−27349
- Josephson current through S-N-S junction, containing paramag. impurities with local states within gap 3−30578
- Kondo effect theory with exchange interaction between two impurities 3−15350
- Kondo temp. for ferromag. and antiferromag. impurity pairs 3−21217
- linear chain model, temp. depend. of localized magnons 3−15380
- liquid metal, impurity diamagnetism 3−38963
- m.i.m. structure, zero bias anomalies, due to paramag. impurities, theory 3−30548
- noble or transition metal alloys, transition impurities, pair description, band structure, magnetic properties 3−30596
- nonmagnetic material, electron distrib. around mag. impurity, Friedel Anderson model 3−15351
- thermodynamics of s-d metal with mag. impurities at low temp. path integral method 3−34101
- tunnel junction, with mag. impurities, effect of exchange scatt. by mag. moments 3−30547
- Al:Ag(Au)(Gd), spin scatt. cross sections 3−18300
- Au_2Mn:^{119}Sn, Mossbauer study *(Russian)* 3−12088
- α-Ce, elec. resist. meas., temp. depend. rel. to mag. impurities 3−33862
- Co-Sn, dilute ferromag. alloy, two current cond. and impurity resist. 3−36719
- Cu:M dil. alloy, M=transition metal, pair description 3−30596
- Eu chalcogenides, ferromagnetic, semiconducting band structure 3−38859
- Fe alloyed with ^{54}Mn, ^{57}Co, ^{182}Ta, ^{191}Ir, hyperfine field nonalignment effects meas. at 25 mK 3−24565
- Fe:Tm, perturbed angular correlation for localised moments 3−15359
- Fe-Al-C alloy, mag. after effects, directional ordering of interstitial atoms 3−12013
- Fe-NI-Al, b.c.c., Mossbauer obs. of Al impurities effect on Fe and Ni mag. moments 3−15444
- Fe-Sn, dilute ferromag. alloy, two current cond. and impurity resist. 3−36719
- K_2ZnF_4:Mn^{2+}, electronic overlap contrib. to uniaxial anisotropy of Mn^{2+}, spin hamiltonian 3−34108
- MgO containing Mn^{2+}, Cr^{3+} and Fe^{3+} impurities, ^{17}O transferred hyperfine interactions 3−30727
- Mn_nSi_{2n-m}, obs. of metallic MnSi precipitates in diamag. matrix, mag. behaviour 3−27356
- Ni, with Cr impurity, high field susceptibility 3−21225
- Ni alloy:^{57}Fe, and hyperfine field, Mossbauer obs. at 4.2K 3−36819
- Ni:Hf, lattice-location of implanted impurity in ferromag. host, chanelling obs. 3−18305
- Ni-Sn, dilute ferromag. alloy, two current cond. and impurity resist. 3−36719
- Pd alloy:^{57}Fe, and hyperfine field, Mossbauer obs. at 4.2K 3−36819
- Pd-Co dil. alloys, ^{57}Fe hyperfine field press. depend. up to 180 kbar 3−18306
- PdCr, interimpurity interaction effects below spin fluctuation temp., elec. resist. meas. 3−15348

magnetic impurity interactions continued
- PdFe- like alloys, influence of mol. field spatial fluctuations on low temp. props. 3−27365
- PdMn, dilute, ferromag., antiferromag. coupling with interimpurity Mn-Mn interaction 3−15184
- Pt alloy:^{57}Fe, and hyperfine field, Mossbauer obs. at 4.2K 3−36819
- SnTe:Mn, e.p.r., localised mag. impurity interaction with free electrons 3−34192
- $YCrO_3$:Fe, impurity-host Fe^{3+}-O-Cr^{3+} antiferromag. superexchange, ^{57}Fe hyperfine field meas. 3−30611

magnetic inks *see character recognition*

magnetic leakage
- remanent state ferrites, characterisation of losses by average permeability tensor 3−21271
- static field of magnetic head with rounded split-edges, conformal analysis *(German)* 3−29006
- superconductor losses in pulsing magnetic field, review 3−15300
- Fe-Si single crysts., e.m. losses depend. on surface cryst. orientation *(Russian)* 3−15391
- Nb superconductor, power frequency losses, effects of cold working, impurities and surface roughness 3−11980
- Nb-Ti and Nb-Zr non-ideal type II superconductors a.c. losses under parallel configurations of currents and magnetic fields 3−11991
- Ni-Zn-Co ferrites, permeab. and losses, freq. and temp. depend. 3−15395
- $Ni_{0.8}Zn_{0.2}Co_xFe_{2-x}O_4$, temp. and freq. depend. of mag. losses 3−8348

magnetic lenses
- achromatic system with minimum electric fields 3−361
- asymmetrized quadrupole lenses, paraxial chromatic aberration 3−13782
- electron, electron microscopes and probe forming systems, developments 3−1538
- electron lenses, round and cylindrical with field free object space, theory *(German)* 3−26256
- numerical calcs., finite difference eqns. for two-dimens. nonlinear Poisson eqn. *(French)* 3−22974
- probe forming, low aberration for s.e.m., design 3−360
- quadrupole, in achromatic deflection system with adjustable nonisochronism for particles with different momenta 3−28636
- quadrupole, potential for given axial gradient 3−13455
- quadrupole system, paraxial electron optical imaging, wave mechanical basis *(German)* 3−35720
- superconducting, optical characts., saturation of iron influence *(French)* 3−22975
- toroidal magnetic multipole, motion of plasmoids 3−14578

magnetic lines of force *see magnetic flux*

magnetic losses *see magnetic leakage*

magnetic materials
- *see also ferrites; ferromagnetic metals; garnets*
- ferrofluid, Ni-Fe alloy particles in Hg, coercive force 3−2321
- magnetics conference, Kyoto, Japan, 10-13 April (1972) 3−34048
- permanent, coercivity *(Dutch)* 3−21276
- semiconducting crystals, electron ground-state, coherent states 3−38799
- semiconductors, s-f exchange interactions, review 3−8350
- semiconductors, valence bond approach, conceptual phase diagrams 3−38803
- uniaxial, zero temp. sensitivity of bubble diameter 3−18339
- uniaxial mag. crystal, surface electromag. wave propag. along various crystal cuts 3−24486
- $NiFe_{2(1-c)}Cr_{2c}O_4$, depend. on comp. and cation lattice point distrib. *(Russian)* 3−38568
- $SmCo_5$ permanent magnet materials *(French)* 3−36753

magnetic memories *see magnetic storage systems*

magnetic mirrors
- 2X decay, ion scattering 3−20445
- ambipolar potential, space structure 3−20600
- bouncing particles high latitude electron fluxes during substorms 3−12649
- charged particle energy carried away at mag. mirrors in fusion reactor, numerical simulation 3−38188
- collinear plasma structures, force-free 3−1517
- confinement of D_2 plasma in magnetic mirror well 3−17656
- cyclotron radiation study of the angular diffusion of a mirror confined to hot electron plasma 3−20443
- DECA II B magnetic well, relaxation of the ion distribution function 3−20598
- electron, confined, ang. distrib. of bremsstrahlung 3−20050
- electron cyclotron heating in magnetic mirrors, stochastic character 3−23895
- electron cyclotron resonance heating in a magnetic mirror, long time and stochastic effects 3−17637
- electron cyclotron resonance heating in magnetic mirror, short time and adiabatic effects 3−4666
- evolution of the angular distribution function of a mirror confined hot ion plasma 3−20599
- Fokker-Planck calculations and fusion energy balance in mirror traps 3−20444
- high current electron beam injection, generation of field-reversing rings of relativistic electrons 3−20661
- inverse ambipolar potential calc. 3−38492
- laser-produced, injection into a magnetic trap 3−30004
- multiple-mirror plasma confinement 3−4663
- open systems, controlled thermonuclear fusion in the USSR 3−17680
- open systems, controlled thermonuclear fusion research in the USA 3−17679
- Penning discharge in a strongly inhomogeneous magnetic mirror field, collective phenomena 3−20642
- pinches, theta, high energy, electron temperatures and thermal conduction, end losses and magnetic mirror ratios 3−33340
- plasma, hot electron, confined in magnetic mirror, synchrotron radiation meas. 3−33392
- plasma, hot electron, production using gun and washer stack source, comparison in a magnetic mirror compression experiment 3−33380
- plasma beam reflection by HF supplemented magnetic mirror near electron cyclotron resonance, energy balance 3−20608

magnetic mirrors continued
- plasma charged particle trapping in a time varying magnetic mirror field 3−26895
- plasma containment in corrugated mag. field 3−38484
- plasma ion heating in mirror confinement by mixing of e.m. waves near electron cyclotron resonance 3−20580
- plasma mirror machine, injection of streaming beam 3−30001
- plasmoids collision at centre, expt. study of force-free collinear structs. 3−29999
- Pleiade accelerator, mirror device, optical meas. for determ. of ion current and acceleration 3−20645
- PR-6 mirror machine, unstable decay of collisional plasma 3−20597
- reflection of charged particles by magnetic mirror at electron cyclotron resonance 3−20607
- 'sloped' diaphragms system, energy recovery from charged particles study, theory 3−20601
- spatial ion wave echoes, collisional damping increased by mag. mirror 3−23858
- toroidally linked mirror systems anisotropic plasma confinement 3−20605
- 'Sloped' diaphragms system, energy recovery from charged particle study, experiment 3−20602

magnetic moments
- *see also atomic magnetic moment; hyperon magnetic moment; local moments in dilute alloys; meson magnetic moment; molecular moments; nuclear magnetic moment; proton magnetic moment*
- classical notion of spin 1/2 particles with zero anomalous magnetic moment 3−37851
- Compton effect, non-Abelian second order, and generalized magnetic-moment radius theorem 3−23066
- deuteron, meson exchange effects 3−6610
- diaquobismethoxyacetato Co(II), polarised absorp. spectra vibronic interact. and mag. dipole effects 3−27501
- dilute system, neutron diffr. obs. of comp. depend. 3−15358
- dipole radiation from supermassive oblique rotator, astrophysical appl. 3−37282
- dipole scattering from perfectly conducting sphere in homogeneous lossy medium 3−3175
- distribution of paleomagnetic poles in Upper Triassic diabase from S.E. Pennsylvania 3−9219
- divergence for mag. moments interacting with conduction electrons 3−18299
- drift of main eccentric geomagnetic dipole rel. to geomagnetic data for 1829-1965 period 3−34841
- dual pion model, e.m. problems and general formula 3−19703
- electron, computation by vertex graphs technique 3−35738
- ferromagnet, spin waves, uniform oscillation instability 3−34142
- ferromagnetic semiconductors, max. resistivity due to carrier scattering by giant moments of mag. clusters 3−18145
- film, hypercritical, mag. field influence on grand state *(Russian)* 3−36699
- horizontal magnetic dipole buried in 2-layer earth 3−22803
- Hubbard mag. insulator, exciton spectra, moments and lattice walks rel. to spin configuration 3−15341
- Invar, magnetometer measurements, high field susceptibility 3−36713
- Ising model, scaling with parameter for thermodynamic functions and pair correl. function 3−2239
- Ising model with lattice anisotropy, high temp. R-series for second moment 3−15331
- magnetic film, movement under field normal to preferred axis *(Russian)* 3−38996
- magnetic semiconductors, band structure, transport properties 3−38858
- metals, crystalline electric field, physical aspects 3−30582
- n.m.r. determination in solution 3−39013
- paramagnetic moment meas. by n.m.r. micro technique 3−3834
- particles, weakly nonspherical ferromag., Brown theorem 3−34172
- Permalloy film, obliquely deposited hypercritical, micropore form. effect on macroscopic moment at grain boundaries *(Russian)* 3−24588
- plasmas subjected to electric field of circularly polarized waves, creation of global magnetization *(French)* 3−11480
- quark model calc. of baryon mag. moments. 3−14025
- rare earth cobaltides, RCo_5, easy direction, single crystals 3−36715
- rare earth ions in hexagonal field, calc. from modified Hamiltonian 3−27343
- rare earth metals, contribution of 5d electrons to saturation moments 3−24564
- rare earth orthoferrites, noncollinear coupling of sublattice moments 3−34107
- rare earth orthoferrites, paramag. susceptibility study 3−21213
- semimetal film, carrier conc. and mag. moment behaviour in semimetal semicond. transition region *(Russian)* 3−18064
- solid or liquid, equilib. correlation functions in linear response to electromag. field 3−24388
- synchrotron radiation of charged point particle with dipole moment in connection with pulsar theory *(Russian)* 3−25366
- transition metal monosilicides, long range order 3−18296
- e, anomalous, calc. and reln. to infinite momentum frame 3−14107
- μ anomalous magnetic moment, precise measurement 3−13861
- μ magnetic moment in Weinberg's model, renormalizable gauge calc. of weak corrections 3−23057
- $[Co(NH_3)_4](ReO_4)_2$, molecular susceptibility *(German)* 3−30099
- Al, Al-3d, transition metal alloys, line broadening; quadrupolar n.m.r. 3−34248
- AuFe, magnetic moment distribution 3−34134
- Cd rare-earth chalcogenide spinels, determ. of Curie-Weiss law behaviour from susceptibility meas., saturation magnetic moments 3−7685
- $Ce_2Mg_3(NO_3)_{12}.24H_2O$, magnetothermodynamics, heat capacity, entropy, magnetic moment, 0.5-4.2K, 90 kG 3−30616
- Co-Fe, depend. on comp., effect of h.c.p. to double h.c.p. structural transition 3−30607
- β-CoAl alloys, low temp. magnetic behaviour 3−34098
- β-CoGa alloys, low temp. magnetic behaviour 3−34098
- $CuCr_2S_{4-x}Se_x$ solid soln., lattice parameter, Curie temp., mag. moment and effective mag. moment 3−21241
- Fe:^{44}Sc, meas. for 68 keV state using angular correlation technique 3−34260

magnetic moments continued
  Fe-NI-Al, b.c.c., Mossbauer obs. of Al impurities effect on Fe and Ni mag. moments 3−15444
  Fe-Ni-Ce, Mossbauer study of Fe mag. moment 3−2471
  Fe-Ni-Co-Al-Ti alloys, temp. depend., superparamag. props. *(Russian)* 3−8342
  Fe(II) six coordinated compounds, spin $S=1$, low temp. magnetism, Mossbauer effect and electronic struct. 3−34250
  Fe(III) dithiocarbamates, dependence of Mossbauer isomer shift on magnetic moments 3−8486
  Fe$_8$N, with ultrahigh mag. moment, vapour deposition from nitrogen atmos. *(Japanese)* 3−8403
  FeNb$_2$O$_6$, paramag., mag. susceptibility meas. rel. to structure and ionic mag. moments *(Russian)* 3−15346
  ^{3}He, hyperfine structure studies by zero-field quantum beats, magnetic dipole hyperfine interaction consts. 3−17357
  HgTe, semimetal, field and temp. depend., two-point matrix Green function calc. *(Russian)* 3−5099
  HoCo$_2$, hyperfine specific heat meas., mag. moment determ. 3−34123
  In small particles in the quantum size regime, magnetic moment 3−18347
  KNiPO$_4$, effective moment *(Russian)* 3−11603
  LaRu$_2$:Gd, in supercond. state, localised mag. moment e.p.r. obs. 3−24541
  Li$_{0.5}$Fe$_{2.5-t}$Al$_t$O$_4$, lowered Fe^{3+} mag. moment in paramag. region 3−21212
  Mg$_6$MnO$_8$, meas. consistent with paramag. structure with weak antiferromag. interaction 3−34091
  MnBi and MnBi$_{0.9}$Sb$_{0.1}$, neutron diffr. obs. 3−24573
  Mn(CrFe)O$_4$ ferrite, Mossbauer study, angular spin configurations of ^{57}Fe nuclei, compensation point 3−36827
  MnGaGe, ferromagnet, prep., struct., Curie temp., saturation magnetisation, mag. moments 3−21268
  Mn$_3$NiN, magnetization 180-266K, Mn mag. moment rotation in (111) plane *(French)* 3−2283
  MnSb, distrib. of unpaired electrons, neutron diffr. obs. 3−24574
  Na$_2$NiFeF$_7$, direction and magnitude in ordered state 3−2301
  NdAs, ordered mag. moments, neutron scatt. obs. 3−2298
  NdP, ordered mag. moments, neutron scatt. obs. 3−2298
  NdSb, ordered mag. moments, neutron scatt. obs. 3−2298
  Ni solid soln., giant moments near ferromag. to paramag. transition 3−36716
  Ni:^{187}Re, meas. for 206 keV state using angular correlation technique 3−34260
  Ni-Co-Fe-SiO system, bilaminar films, rotatory moment curves *(Russian)* 3−21267
  Ni-Cu, ferromag., neutron diffraction obs. of mag. moments distrib. 3−15374
  Ni-Cu alloys, mag. moment in pulsed fields, Pauli susceptibility *(Russian)* 3−30606
  (Ni$_{74.5}$Al$_{25.5}$)$_{100-x}$Fe$_x$, ferromag., giant moments, neutron study 3−36717
  NiFe, magnetic moment distribution 3−34134
  Pb(Fe$_{2/3}$U$_{1/3}$)O$_3$, Neel temp. and saturation moment 3−21231
  Pb(Fe$_{2/3}$W$_{1/3}$)O$_3$, Neel temp. and saturation moment 3−21231
  Pt-Mn-Sn alloys *(Japanese)* 3−8346
  RbFeCl$_3$, per Fe^{2+} ion at 0K from ferromagnetic chain approach 3−18282
  SmFe$_{0.67}$Ge$_{1.33}$:Sm^{3+} no Fe atoms contrib. to mag. moment 3−2290
  Sm^{3+}(4f^5) ion, calc. from energy struct. for intermediate coupling 3−29495
  Sr(Fe$_{2/3}$U$_{1/3}$)O$_3$, Neel temp. and saturation moment 3−21231
  Th$_3$P$_4$-U$_3$P$_4$ solid solution, effective moment of U 3−5022
  TmSb, polarised neutron obs. of induced mag. moment 3−34133
  U$_3$Se$_4$, cubic, from magnetisation obs. in fields up to 80 kOe and temps. to above T_c 3−15356
  UTe, U$_3$Te$_4$, cubic, from magnetisation obs. in fields up to 80 kOe and temps. to above T_c 3−15356
  U$_3$X$_4$, Th$_3$P$_4$ type struct., mag. props., mag. moments, Curie point, remnance magnetization 3−2318
  Y-Co-Ni, pseudobinary, mag. props., moment values at 4.2K 3−2294
  Y-Fe-Co, pseudobinary, mag. props., moment values at 4.2K 3−2294

magnetic monopoles
  attractive potential between electron and fixed monopole, rel. to dyon formation 3−23193
  dyons, dyonium and parastatistics 3−35771
  quantum electrodynamics and Cabibbo-Ferrari two-potentials formalism 3−23053

magnetic permeability
  ferromagnetic resonance line broadening, chemical magnetic inhomogeneities 3−34218
  generalised conductivity of a heterogeneous system from the structure and phase composition 3−36574
  round cylinder in terms of scattered field *(Russian)* 3−19548
  steel, low-density 9G28Yu9MVB type, phase comp. and props. 3−21662
  superconductors, type-II 3−11977
  Ba$_3$Co$_2$Fe$_{24-x}$Sc$_x$O$_{41}$, meas. rel. to Sc ions influence on hexaferrite magnetic structure *(Russian)* 3−15372
  CdCr$_2$Se$_4$, light irrad. effects 3−5033
  Co$_x$Zn$_{1-x}$Fe$_2$O$_4$, freq. and temp. depend. *(Russian)* 3−8349
  Fe-Co-Ni-Al-Ti-Cu, thermomag. treatment effects *(Russian)* 3−8386
  Fe-Ni alloys, heat treatment depend. 3−21275
  Fe-Ni alloys, temperature dependent property for measurement errors compensation in magnetic devices *(German)* 3−15385
  Fe-Si alloy, effect of Ni surface film *(Russian)* 3−12037
  Fe$_3$O$_4$, initial permeability in region of low temp. phase transition 3−36768
  Mn-Zn ferrite, solid state O$_2$ content depend. *(German)* 3−8344
  Ni-Zn-Co ferrites, permeab. and losses, freq. and temp. depend. 3−15395
  Ni$_{0.8}$Zn$_{0.3}$Co$_x$Fe$_{2-x}$O$_4$, temp. and freq. depend. of high resist. samples 3−8348

magnetic permeability measurement
  paramagnetic moment meas. by n.m.r. micro technique 3−3834

magnetic pinch *see pinch effect*
magnetic properties of dilute alloys *see magnetic properties of dilute systems*
magnetic properties of dilute systems
  see also local moments in dilute alloys; magnetic impurity interactions
  Anderson model for dilute alloys, heuristic treatment for one-electron properties 3−2246
  critical conc. rel. to long range mag. order, neutron diffr. obs. 3−15358
  ferromagnet, Curie temp. conc. depend. *(Japanese)* 3−38981
  ferromagnet, magnetically dilute system, theory *(Japanese)* 3−38952
  ferromagnetic alloy, thermodynamic and kinetic props. 3−34109
  Hall effect, s-d scatt., many body theory 3−8157
  Heisenberg spin system with two-dimensional defects, localized states *(Russian)* 3−8320
  homogeneous dynamical susceptibilities 3−12004
  kinetic equation for cond. electron scatt. in dilute non-mag. alloy 3−30603
  Kondo temperature variation with nature and concentration of solute metal 3−36710
  local spin fluctuation systems, long range correlations 3−15352
  magnetic alloys, homogeneous dynamical susceptibilities 3−12004
  molecular crystals, mechanism of spin-lattice relaxation of radicals caused by delocalization of unpaired electron *(Russian)* 3−8439
  noble or transition metal alloys, transition impurity interactions, pair description, band structure 3−30596
  phonon-spin interactions of a dilute system 3−1752
  s-d exchange interaction, formal theory 3−18304
  single domain particles in nonmag. matrix, hysteresis, remanence, antihysteresis susceptibility, coherence field 3−30668
  3d transition metals, impurity effects, Hubbard's model 3−8352
  type II superconductors containing magnetic impurities 3−11973
  Ag-Ce alloy, dilute, obs. of Ce impurity by nuclear orientation meas. 3−2257
  Au-Ce alloy, dilute, obs. of Ce impurity by nuclear orientation meas. 3−2257
  Co-Fe alloy, double h.c.p. structure from X-ray diffraction study, rel. to mag. props. 3−1600
  Cr-Pd alloys, susceptibility, Neel temp., solute effects 3−34111
  Cu:M, M=transition metal, pair description 3−30596
  Cu-Au(Fe), Kodon effect in dilute magnetic α-phase alloys 3−21218
  Cu-Cr alloy, dilute, in supercond. sandwich, mag. props. from supercond. proximity meas. 3−8341
  Cu-Cr(Fe)(Mn) alloys, ^{63}Cu n.m.r., impurity magnetiz. 3−2443
  Cu-Fe alloy, dilute, in supercond. sandwich, mag. props. from supercond. proximity meas. 3−8341
  Cu-Mn alloy, dilute, in supercond. sandwich, mag. props. from supercond. proximity meas. 3−8341
  DyCl$_3$.6H$_2$O, Y-diluted, heat capacity 3−38976
  ErCl$_3$.6H$_2$O, Y-diluted, heat capacity 3−38976
  Ge, mag. susceptibility of two electron donor pair system, eigenvalue problem, Heitler-London method soln. 3−2579
  K$_2$ZnF$_4$:Ni^{2+}, cryst. field and exchange interaction of Ni^{2+}, lattice distortion effects, e.s.r. obs 3−15357
  La-Gd alloy, giant susceptibilities 3−8340
  La-Pu alloy, mag. susceptibility, obs. of mag. decoupling at Pu 3−2255
  Pb-Fe, spin-disorder resistivity meas., temp. depend., 0-60 kOe fields 3−2057
  Pd-Mn(Fe)(Co) dilute alloys, ferromag. transition temp., resist. study 3−30624
  Rh-Fe-Mn, Rh-Mn, Rh-Fe alloys, low temp. meas. and comparisons of elec. resist., magnetoresist. and magnetiz. 3−4990
  Sc-Pu alloy, mag. susceptibility, obs. of mag. decoupling at Pu 3−2255
  Si, mag. susceptibility of two electron donor pair system, eigenvalue problem, Heitler-London method soln. 3−2579
  Y-Np alloy, mag. susceptibility, obs. of mag. decoupling at Np 3−2255
magnetic properties of fine particles
  catalysers, finely divided, ferromag., granulometry and metallic mass. from magnetisation/mag. field curve *(French)* 3−34171
  suspensions, colloidal, of single-domain ferromag. particles, magnetoviscosity theoretical description 3−23788
  weakly nonspherical ferromag. particles, mag. struct., Brown theorem, magnetiz. reversal 3−34172
  Ni, aerosol particles, coercive force and saturation magnetisation from 4.2 to 300 K 3−39006
magnetic properties of substances
  see also antiferromagnetic properties of substances; demagnetisation; diamagnetic properties of substances; ferrimagnetic properties of substances; ferromagnetic properties of substances; magnetic aftereffect; magnetic hysteresis; magnetic permeability; magnetic properties of dilute systems; magnetic properties of fine particles; magnetic structure; magnetic susceptibility; magnetic transitions of substances; magnetisation; paramagnetic properties of substances
  actinides, review 3−2259
  Allende meteorite, natural remanent magnetization and thermomagnetic properties 3−16198
  Annual review of materials science vol. 2, 1972 3−24778
  ASTM standards, Pt.8, annual book (1972) 3−35353
  effective, of cell materials, perturbation expansions for random heterogeneous materials 3−39077
  experimental techniques in neutron scattering survey 3−20680
  magnetics conference, Kyoto, Japan, 10-13 April (1972) 3−34048
  perturbed ang. correl. method applic. 3−25857
  rare earth metals, light, review of mag. props., work done in Denmark 3−2258
  rare earth metals, review 3−2225
  rare earth solids, book 3−11523
  rare earths and actinides, conference, Durham, England, July (1971) 3−2223
  superconductor, type II, magnetic props. using boson characteristic function 3−11974
  transition metal monosilicides, localized moments, long range order 3−18296
  AgCrSe$_2$, susceptibility, Neel pt. *(Japanese)* 3−38968
  Cu complex ((CH$_3$)$_2$NH) CuCl$_3$.2H$_2$O, low temps. 3−1613

magnetic properties of substances continued
- $CuCrSe_2$, susceptibility, Neel pt. *(Japanese)* 3−38968
- $Dy(Co_{2-x}Ni_x)$, $0\leqslant x\leqslant 2$, mag. props. anomalous behaviour in pulsed and static fields 3−2316
- Fe, local losses, in magnetic sheet, thermometric meas. *(Japanese)* 3−24599
- Fe powder with P additive, sintering conditions effect on shrinkage on magnetic props. *(Russian)* 3−27720
- Fe powders with 1% P additives, sintering conditions effect on magnetic and mechanical props. *(Russian)* 3−27719
- MnO-Fe_2O_3-B_2O_3 glassy system 3−18726
- α'-$Mn_{0.85}Ti_{0.15}Bi$ film, magn. and magneto-optic props. 3−2521
- Ni-Cu alloys, mag. moment in pulsed fields, Pauli susceptibility *(Russian)* 3−30606
- $PbMo_2O_4$, mag. transit. and phase reversal *(Russian)* 3−8397
- Pr, magnetic resistivity meas., 4K-ice point, effects of crystalline field 3−8356
- Pr-Tb alloy, rel. to comp. 3−2267
- U monopnictides and monochalcogenides, review of electronic and mag. props. 3−2260
- Y-Co-Ni, pseudobinary, mag. props., moment values at 4.2K 3−2294
- Y-Fe-Co, pseudobinary, mag. props., moment values at 4.2K 3−2294

magnetic recording
- *see also tape recorders*
- e.e.g. application 3−25967
- ferrite head, from hot pressed Ni-Zn ferrite 3−2756
- isocon TV camera/mag. tape recorder system for fast oscilloscope trace analysis 3−3856

magnetic relaxation
- *see also ferromagnetic relaxation; magnetic resonance; spin-lattice relaxation; spin-spin relaxation*
- coupled spin systems, selective nuclear Overhauser effect study of relaxation processes 3−34220
- magnetic fluctuations relax. rel. to anisotropic dipole mag. forces above Curie temp. 3−8412
- methaemoglobin water sorbed cryst., relax. times, temp. and regain depend. 3−12075
- multi-level spin system, kinetic equations *(Russian)* 3−30679
- n.m.r. relaxation times meas. by adiabatic half passage technique 3−27392
- nuclear relaxation of polarization with inhomogeneous e.p.r. broadening 3−8416
- nuclei, spin 3/2, chem. exchange effect 3−7232
- pulsed n.m.r. and Fourier transform n.m.r. spectroscopy, review 3−34180
- spin density matrix, relax. consts., general inequalities 3−2327
- superparamagnetic relaxation time for particles with cubic anisotropy 3−21281
- temperature in spin systems 3−24600
- $Co{:}^{51}V(^{103}Rh)$, meas. of relaxation rates rel. to impurity band structure 3−5147
- Fe-Al-C alloy, relax. rel. to directional ordering of interstitial atoms 3−12013
- $FeCO_3$, siderite, Mossbauer linewidth anomalous temp. depend., obs. and mechanism 3−34277
- Fe_3O_4 (magnetite) single crystals, relaxation processes at low temp. rel. to phase transformation and magnetic viscosity *(Russian)* 3−12645
- He quantum magnetometer, relaxation processes *(German)* 3−10000
- MnF_2 high frequency acoustic waves attenuation on low-temp. side of Neel point, magnetic relaxation theory 3−34112
- Mn(II) complexes in acetonitrile, e.p.r. spectra 3−8425
- $Mn_{1.5-x}Me_xFe_{1.5}O_4$ (Me=Ni or Cr), relaxation phenomena at low temps. 3−15381
- NH_4Cl, orientational quadrupole relax., deuterium nuclei longit. relax. time 3−8483
- $Ni{:}^{101}Ru$, meas. of relaxation rates rel. to impurity band structure 3−5147

magnetic resonance
- *see also acoustic magnetic resonance; antiferromagnetic resonance; cyclotron resonance; ENDOR; ferrimagnetic resonance; ferromagnetic resonance; magnetic relaxation; paramagnetic resonance*
- dipolar coupled rigid lattice, sixth and eighth moments of mag. resonance lines 3−34178
- double resonance, review 3−30678
- Lamb dip appl. to laser frequency and intensity stabilization 3−32097
- neutron polarization resonance flip in space periodic magnetic fields 3−6685
- oscillating r.f. field, semi-classical model 3−20028
- paraelastic resonance of Jahn-Teller and off-centre ions 3−24387
- polar semiconductor, magnetophonon resonance in quantising parallel mag. field 3−27276
- Provotorov equations with field modulation 3−39012
- rigid dipolar coupled lattice of infinite nuclear spins, free induction decay shapes 3−15402
- rotating field misalignment effects 3−20027
- He quantum magnetometer, relaxation processes *(German)* 3−10000
- Hg^+, hyperfine struct. Zeeman splitting 3−23482
- n-InSb, photo-induced magnetophonon resonance at 4.2K 3−24477
- Ne, spontaneous emission from lower laser level, double reson. 3−26227
- O_2 mol., laser mag. reson. using 119 and 78 μm H_2O laser lines 3−4464

magnetic resonance spectrometers
- autodyne n.m.r. signal pickup with controllable high selectivity 3−19242
- cylindrical resonator, for e.s.r. gaskinetic measurements up to 1000 K *(German)* 3−37670
- withdigital data processing, supercond. mag., used in range 1.5-300K 3−6040
- digital frequency synthesizer, programmable 3−32117
- dispersion in weak steady and strong h.f. fields, Bloch theory 3−2331
- ELDOR, for nitroxide radical studies 3−2333

magnetic resonance spectrometers continued
- ENDOR, microwave cavity 3−37668
- e.p.r., sensitivity and design, noise meas. technique 3−263
- e.p.r., sensitivity and design, noise spectral meas. 3−264
- e.p.r., using maser techniques, sensitivity determ. 3−266
- e.p.r. spectrometer, sample holder for applying uniaxial stress and elec. field 3−25821
- e.s.r., flash photolysis, rapid scan apparatus 3−28619
- ferromagnetic resonance, line-width meter *(Russian)* 3−16466
- flowing-liquid n.m.r., minimum width of nutation signal in inhomogeneous mag. field *(Russian)* 3−13359
- Fourier analyser, analogue device 3−28616
- image formation by induced local interactions, zeugmatography 3−28617
- K-band reflection, broad c.e.s.r. line detection 3−265
- linear bidirectional r.f. transmission gate for pulsed n.m.r. 3−37669
- modifications of JEOL-4H-100 spectrometer, n.m.r. relaxation times meas. by adiabatic half passage technique 3−27392
- n.m.r., nonbreakable sample container for radioactive materials 3−6041
- n.m.r. blood flow measurement, pickup coil space filling coefficient calculation *(Russian)* 3−19248
- NMR modulated absorpt. lines, error correction for large amplitudes 3−6042
- n.m.r. pulsed, computer control 3−267
- n.q.r., 150-1000 MHz 3−16467
- nuclear quadrupole resonance spectrometer for phase-shift spin-echo methods 3−19241
- paramagnetic, saturation effect detection 3−28618
- proton stabilizers, autodyne spin generator, n.m.r. spectrometer, sideband operation 3−262
- stopped-flow n.m.r., spectrometer and rapid mixing cell construction 3−10004

magnetic screening *see magnetic shielding*

magnetic shielding
- conductive shells, thin, shielding characts., e.m. induction study 3−22802
- nuclear diamag. shielding tensor, individual elements from atom dipole method 3−7227
- Cd isotopes g_I factors meas. by n.m.r. 3−36804
- Rb isotopes, g_I factors meas. by n.m.r. 3−36804

magnetic storage devices
- heads, u.s. nondestructive testing of dense ferrite *(Polish)* 3−12491
- rare earth memory elements 3−2307
- toroidal solenoid, optimum shape 3−36207
- $CoCr_2S_4$, hot pressed, magneto-optic props., digital memory application 3−36858

magnetic storage systems
- *see also magnetic core stores; magnetic disc storage; magnetic film stores*
- bubbles, mag., in uniaxial mag. oxides, new computer information carriers, review *(German)* 3−21280
- $YbFeO_3$, electron beam induced charge storage memory with read-out and erasure 3−35504

magnetic stores *see magnetic storage systems*

magnetic storms
- *see also micropulsations*
- 30 March, 3-4 April 1971 events *(Russian)* 3−12875
- 1962, December 17-21, topside ionosphere and F_2-layer variations 3−25280
- 1963 September, main phase, growth and decay 3−21916
- 1965, April 17, magnetospheric models rel. to storm observations 3−12844
- 1967, May 24-7 storm, latitudinal energy distribution 3−34838
- 1967, May 25-27, satellite study of mid-latitude electron density trough and v.l.f. 3−21975
- 1968, March-April, space time dynamics of auroral electron spectrum 3−25255
- 1969, February 3, ionospheric observations by Isis 1 satellite 3−12795
- 1969, Jan. 21 and Feb 3, bremsstrahlung X-rays rel. to auroral glow and shape 3−34887
- 1970, March, E_s-q layer meas. at Huancayo 3−25291
- auroral substorms, behaviour of midday auroras 3−34924
- cosmic ray intensity increase before mag. storms, N-S asymmetry 3−34984
- coupling of low altitude energetic protons to outer radiation belt protons 3−9312
- Earth electrical conductivity structure, comparison of magnetotelluric and geomagnetic depth sounding methods 3−9388
- effect of geomagnetic storms on nighttime E-layer during increasing maximum solar activity *(Bulgarian)* 3−9338
- effect on equatorial electrojet current 3−12791
- effect on meas. of ionospheric motion, presence of current-induced spectral asymmetries 3−12866
- electron influx meas. assoc. with a type A aurora, rocket meas. 3−12787
- energetic electron precipitation as source of night-time D-region ionization during magnetic storms 3−31431
- F_2-layer max. electron density, disturbance variation with storm time on noon meridian 3−34949
- F-region midlatitude parameters during geomagnetic storms 3−12806
- F-region neutral temp., in the dayglow, polar region variation 3−16025
- growth phase, magnetospheric configuration changes 3−12817
- growth phase of magnetospheric storms, onset time determination difficulties 3−16041
- high latitude electron fluxes, pitch angle distributions 3−12649
- inner zone electron repopulation, radial diffusion 3−12820
- ionospheric disturbances at mid-latitudes rel. to geomagnetic storms 3−31331
- ionospheric observations by Isis 1 satellite during 3 Feb. 1969 geomagnetic storm 3−12795
- ionospheric substorms, effects on v.l.f. propagation 3−31410
- ions, energetic heavy, satellite observations during geomagnetic storm of 17 Dec. 1971 3−12659
- magnetosphere substorms, neutral sheets theory 3−3144

magnetic storms continued
magnetospheric, pre-midnight asymmetry in 40 keV electron flux profiles 3—3137
magnetospheric models, comparison with Explorer 26 obs. 3—12844
magnetospheric storms and role of electric field 3—25304
magnetospheric substorm, motions of day-sector polar F-layer 3—31438
magnetospheric substorm development, coordinated observations 3—12826
magnetospheric substorms, inertial magnetic field reconnection 3—34959
magnetospheric substorms, longitudinal extension of electron precipitation 3—15983
magnetospheric substorms, magnetic field var., interpretation of ground-based and satellite observations 3—2932
magnetospheric substorms, relation between ground and distant magnetotail events 3—39556
magnetospheric substorms onset, balloon X-ray and electric-field measurements 3—12651
magnetospheric substorms rel. to ionospheric total electron content enhancement in Southern auroral zone 3—31419
magnetospheric substorms rel. to solar wind/ magnetosphere interaction, review 3—2931
mid-latitude F-layer, causes of storm-time increases 3—31425
mid-latitude F-layer electron concentration seasonal var. in magnetic storm effects 3—31433
Pc 1, 2 interaction with Pc 5 micropulsations during magnetic storms 3—12653
Pc 1 micropulsations rel. to ring current and geomagnetic storms 3—18838
PC 5 storm-associated micropulsations, statistical study and occurrence distrib. 3—12654
plasma leakage from magnetotail to magnetosheath rel. to substorms 3—16042
plasma sheet, inner boundary dynamics during substorms 3—28072
plasma sheet substorm behaviour, Vela satellite measurements 3—3154
polar substorm, longitudinal currents *(Russian)* 3—3120
polar substorms, electron and proton acceleration in outer regions of magnetosphere 3—34954
polar substorms, excitation by northward interplanetary magnetic field 3—2933
polar substorms, VLF-LF auroral hiss 3—39547
precipitating electrons during sudden commencement, latitude and time distributions 3—2930
radiation belt slot region, v.l.f. whistler mode wave obs. 3—16034
substorms, in outer magnetosphere, quiet time and disturbed time config. changes 3—12833
sudden commencement absorption, quadruple conjugate pair observations of event on June 17, 1965 3—12794
thermospheric wind effects on ionosphere during magnetic disturbances 3—31394
topside ionosphere, magnetic storms and seasonal anomaly rel. to electron distributions 3—25274

magnetic structure
antiferromagnetic model for two coinciding lattices with interaction 3—15314
conducting ferromagnetic layer, role of magnetic microstructure in ferromagnetic resonance *(Russian)* 3—8448
ferrimagnet, three-sublattice, mag. struct. induced by field *(French)* 3—38972
ferromagnetic spin systems, singular lines and points, disclinations 3—21246
Heesch groups, derivation from aspect groups 3—38982
Ising model, exact solution 3—2242
low temp. obs., high resolution polarizing microscope 3—35444
magnetic order nonexistence in one and two dimens. 3—8318
Mossbauer effect applics., book *(French)* 3—34276
neutron diffraction, review 3—24572
noncollinear sublattice, spin-wave energy and mean value of Hamiltonian 3—2227
particles, weakly nonspherical ferromag., Brown theorem 3—34172
perovskite, complex, ferrimag., long-range ordering study using mag. meas. 3—24579
rare earth chalcogenides, $EuLn_2S_4$ type, mag. interactions and isomer shift rel. to struct., Mossbauer obs. 3—2481
rare earth compounds, magnetic structures, spin hamiltonians and magnetic interactions, review 3—21242
rare earth intermetallics, $LnIn_3$ and $LnSn_3$, neutron diffr. obs. *(French)* 3—24563
rare earth orthoferrites, $R_{1-x}Ca_xFe_{1-x}Sn_xO_3$, magnetially non-equivalent states of atoms 3—34271
rare earths, neutron scatt. obs. 3—2292
rare earths and actinides, conference, Durham, England, July (1971) 3—2223
RKKY interaction, electron conc., cryst. and magnetic struct. 3—24550
spin densities, magnetic neutron scattering expt. methods 3—5109
$Al_2Mn_3(SiO_4)_3$ spessartite type garnet, obs. of rhombohadral mag. structure 3—21247
Au-Cr alloy, paramag.-antiferromag. critical composition, anisotropic diffuse scatt. of neutrons 3—38973
Au-Fe alloys, magnetic ordering rel. to Fe concentration 1-22 at.% 3—2287
$Ba_3Co_2Fe_{24-x}Sc_xO_{41}$, Sc ions influence on hexaferrite magnetic structure *(Russian)* 3—15372
$Ba_8Fe_{13}O_{30}H_6$, cryst. struct. and antiferromag. 3—17768
$BaIn_xFe_{12-x}O_{19}$ ferrite, and reson. fields temp. depend., torque angular depend. 3—21250
$BaMnF_4$, two-dimensional mag. ordering in isotropic Heisenberg antiferromagnet 3—36725
$Ba_{3-x}Sr_xZn_2Fe_{24}O_{41}$, hexagonal type-Z, noncollinear struct., neutron diffr. *(Russian)* 3—8372
$BaTbO_3$, neutron powder diffraction patterns, G-type antiferromagnetic 3—7677
$Bi_{3-2x}Ca_{2x}Fe_{5-x}V_xO_{12}$, neutron diffraction obs. 3—8369
$Bi_2Fe_4O_9$, Mossbauer obs. 3—36724
$Ca_3Cr_2(GeO_4)_3$, neutron diffr. obs. 3—24569
$Ca_2Fe_{2-x}Al_xO_5$, charge in space groups with charge in phase 3—12023

magnetic structure continued
$Ca_3Fe_2(GeO_4)_3$, neutron diffr. obs. 3—24569
$Ca_3Fe_2Si_3O_{12}$, andranite garnet, indirect exchange interaction 3—34137
CaO, long-range magnetic order from neutron scattering meas. and theory comparison 3—2288
CeSb, antiferromag. phase mag. struct., 4.2 K—16 K 3—2297
$CeZn_2$, 2-300 K 3—2299
$CoBr_2.6H_2O$, anomalous behaviour rel. to isotope effects in p.m.r. 3—2421
$CoCO_3$, magnetisation density and magnetic structure at 4.2 K 3—38984
$CoNb_2O_6$, neutron diffr. obs. *(German)* 3—21249
^{59}Co films, nuclear mag. levels inverted state 3—30628
Cr, influence of mag. field on thermal hysteresis of mag. struct. *(Russian)* 3—8371
$CrAs_{0.5}Sb_{0.5}$, crystal distortion at Neel temp., antiferromag. NiAs to helimag. MnP structure 3—33671
Cr_2O_3-Fe_2O_3, Mossbauer obs. 3—8490
$CsCoCl_3.2H_2O$, neutron diffr. study 3—24568
$Cs_{0.4}Mn_{0.4}Fe_{1.6}F_6$, magnetic struct. 3—5108
$Cs_{0.4}Ni_{0.4}Fe_{1.5}F_6$, magnetic struct. 3—5108
Cu based spinel, mag. props. rel. to structure and cooperative Jahn-Teller distortion 3—30632
Cu complex, α-bis-(N-methylsalicylaldiminato)-Cu(II), spin-$^{1}._{2}$ linear chain system, X-ray and e.p.r. exam. 3—2286
Cu-Mn-Sn, ferromag. beta phase, crystal structure and ordering 3—18324
$Cu_2P_2O_7$, mag. struct. using neutron diffr. method 3—18322
Dy helical phase, spin wave energy 3—5110
$DyCo_{3-x}Ni_x$, intermetallic, mag. ordering rel. to electron conc, 3—21245
$DyFe_{3-x}Ni_x$, intermetallic, mag. ordering rel. to electron conc. 3—21245
DyNi intermetallic, mag. struct., neutron diffr. and magnetisation obs. 3—15376
Er, neutron diffr. obs. 3—24576
$ErAl_3$, of cubic and hexagonal phases 3—2296
ErGa, neutron diffr. obs, ferromag. props. 3—2319
$ErMn_2O_5$, helimagnetic order of Mn, neutron diffr. obs. *(French)* 3—36723
$Er_xY_{1-x}Al_2$, neutron diffraction determ. of ferromagnetic ordering *(German)* 3—12027
EuO, Hall coeff. insulator-metal transition rel. to mag. order 3—2147
EuS, EuSe and EuTe, ordering rel. to photoluminescence props. *(German)* 3—18495
Fe, h.c.p. and b.c.c., effect of pressure and low temps. on props., Mossbauer study 3—2285
FeAs, obs. of helimagnetic structure below Neel temp. 77K 3—15370
$FeCO_3$, layer struct., Mossbauer spectra recoilfree factor anisotropy 3—8489
$FeCl_2$, spin dynamics below Neel temp. 3—8597
$Fe_{3-x}Cr_xO_4$, ferrimag., Mossbauer obs. 3—24641
Fe_2GeS_4, cryst. and mag. structs. at 85 K and 4.2 K, mag. transitions *(French)* 3—27373
FeMnP, neutron diffr. obs. 3—30629
$FeNb_2O_6$, paramag., mag. susceptibility meas. rel. to structure and ionic mag. moments *(Russian)* 3—15346
$Fe(Pt_xPd_{1-x})_3$ alloy, ordered, temp. effect, neutron diffr. obs. *(Russian)* 3—18308
$Fe_{1\|6}Sb$, obs. of mag. superstructure lines below and above Neel point 3—12022
$FeWO_4$-$MnWO_4$, mixed crystal, coexistence of two antiferromag. phases 3—34124
$(Ga_{1-x}Zn_x)Mn_3C$, obs. from 4.2 to 320 K with first and second order mag. transitions *(French)* 3—30631
Gd, neutron mag. form factor calc. using Dirac-Fock equation 3—21244
$HoCo_{3-x}Ni_x$, intermetallic, mag. ordering rel. to electron conc. 3—21245
$HoFe_3$, powder neutron diffraction obs. of Ferrimag. coupling 3—18325
$HoFe_{3-x}Ni_x$, intermetallic, mag. ordering rel. to electron conc. 3—21245
$HoMn_2O_5$, helimagnetic order of Mn, neutron diffr. obs. *(French)* 3—36723
$KCrS_2$, ferromag. sheets antiferromagnetically coupled 3—34132
K_2CuF_4, mag. two dimensionality, obs. by neutron scatt. 3—15373
K_2MnF_4, neutron diffr. obs. of two-dimens. mag. behaviour 3—15371
$LuMn_2O_5$, helimagnetic order of Mn, neutron diffr. obs. *(French)* 3—36723
Mg_6MnO_8, paramag. structure with weak antiferromag. interaction, susceptibility and optical reflectance meas. 3—34091
$Mn_3Al_2(GeO_4)_3$, neutron diffr. obs. 3—24569
$Mn_3Al_2Ge_3O_{12}$ garnet, antiferromag., neutron diffr. obs. *(French)* 3—21248
Mn_2As-Mn_2Sb system, neutronographic investigation of magnetic transformations *(Russian)* 3—2291
MnBi and $MnBi_{0.9}Sb_{0.1}$, neutron diffr. obs. 3—24573
$MnCO_3:Fe^{2+}$, spin system and moment exam., reln. to concentration 3—2289
$Mn(CrFe)O_4$ ferrite, Mossbauer study, angular spin configurations of ^{57}Fe nuclei, compensation point 3—36827
Mn_2Hg_5 neutron diffraction obs. of antiferromag. coupling 3—18329
$Mn_2P_2O_7$, mag. struct. using neutron diffr. method 3—18322
MnSb, distrib. of unpaired electrons, neutron diffr. obs. 3—24574
$MnTa_2O_6$, neutron diffr. obs. *(German)* 3—21249
$(NH_4)_2MnF_5$, linear chain antiferromagnet, weak ferromagnetism, spin config. 3—30643
$NaCa_2Co_2V_3O_{12}$, mag. and atomic struct., Co spin state *(Russian)* 3—12025
$NaCa_2Co_2V_3O_{12}$ garnet, mag. ordering in octahedral lattice *(Russian)* 3—12024
$NaCa_2Ni_2V_3O_{12}$ garnet, mag. ordering in octahedral lattice *(Russian)* 3—12024
Nd, mag. field depend. 3—2293
NdAs, neutron scatt. obs. 3—2298

magnetic structure continued
$NdFe_2Si_2$, antiferromag. structure of Nd(2a) sublattice, ferromag. sheets, neutron diffraction obs. 3-34135
$NdFe_2Si_2$, neutron diffr. obs. 3-24570
$NdMn_2O_5$, helimagnetic order of Mn, neutron diffr. obs. *(French)* 3-36723
NdN(P)(As)(Sb), neutron diffr. obs. 3-30630
NdP, neutron scatt. obs. 3-2298
NdS antiferromagnetism, spin configuration, neutron diffraction study 3-27374
NdSb, neutron scatt. obs. 3-2298
$NdZn_2$, neutron diffr. obs. 3-27372
Ni-Cu alloy, form factor, neutron diffr. obs. 3-24575
$NiCl_2$, spin arrangement rel. to temp. depend. of antiferromag. reson. 3-21316
$NiCr_2O_4$, neutron diffr., appl. of representation anal. 3-24571
Ni_3Mn, order-disorder phase transition dynamics study, neutron scatt. meas. 3-38949
γ-O_2, paramag., mag. structure factor calc. 3-34093
γ-o_2, paramag. cubic phase, crystal structure and mag. form factor 3-34092
Pb superconducting thin films, intermediate state 3-11990
$RbFeF_4$, mag. layer struct., Mossbauer spectra recoilfree factor anisotropy 3-8489
Sm, neutron diffr. obs., moments ordering, form factor 3-5107
Sm, neutron diffr. study 3-24577
Sn superconducting thin films, intermediate state 3-11990
Tb_8-$La(Pr)_2$, Sm type structure, neutron diffraction obs. of mag. ordering and transitions 3-18321
TbGa, neutron diffr. obs., ferromag. props. 3-2319
$TbMn_2O_5$, helimagnetic order of Mn, neutron diffr. obs. *(French)* 3-36723
$TbZn_2$, 2-300 K 3-2299
$TlCoF_3$, neutron diffr., antiferromag. config. *(French)* 3-38983
TmNi, crystal field effect 3-15375
U monochalcogenides, mag. ordering, neutron diffr. obs. 3-2295
UAsSe, neutron diffraction obs. of uniaxial ferromag. structure 3-12026
$UAs_{2-x}Se_x$, solid solution, neutron diffraction investigations 3-38985
USbSe, neutron diffraction obs. of uniaxial ferromag. structure 3-12026
U_3Se_4, structure isomorphic to Th_3P_4, no mag. ordering at 77 K, neutron diffr. obs. 3-38959
V_nO_{2n-1}, ordering, electronic ht. capacity obs. at low temps. 3-15368
YMn_2O_5, helimagnetic order of Mn, neutron diffr. obs. *(French)* 3-36723

magnetic susceptibility
alkali binary liq. alloys, Knight shifts, Pauli susceptibilities, from contact density in pseudopotential 3-34234
alkali metals, Knight shifts, Pauli susceptibilities, from contact density in pseudopotential 3-34234
alkali metals, liq., Green's function calc. 3-30597
alkali metals, paramag. spin susceptibility, local pseudopot. calc. 3-8337
Anderson model, symmetric, perturbation calc. of susceptibility 3-24551
Apollo 11 fines, methane and carbide distrib. 3-18989
apparatus for investigation of magnetic properties of thin weak magnetic films *(Russian)* 3-25820
aromatic compounds, theory of anisotropic diamagnetic susceptibility caused by ring currents, allowance for π-electron interaction *(Russian)* 3-7139
bromoacetylene mol., anisotropy from Zeeman effect 3-20168
bubble domains radial susceptibility 3-38999
cholesteric-nematic transition, transition feed strength charact. obs., applic. of mag. susceptibility meas. *(French)* 3-14682
critical behaviour of Ising systems on extremely anisotropic lattices, simple cubic lattice 3-27344
diamagnetic, depend. on surface pot. for confined electron system 3-38957
dilute alloy, local mag. moments, transverse dynamic susceptibility with electron-electron interaction 3-34100
dilute magnetic alloys, homogeneous dynamical susceptibilities 3-12004
electron gas, diamagnetic and paramagnetic susceptibilities 3-27200
electron gas, spin and charge susceptibility 3-15338
electrons, interacting, in solid, wave vector and freq. depend. orbital susceptibility 3-2244
Evans method, solvent density var. with temp., effect on mag. meas. 3-28613
ferromagnet, amorphous, mixed, Heisenberg and Ising models 3-27350
ferromagnetic electron gas, spin susceptibility calc. with mag. impurities 3-15339
ferromagnetic resonance, dynamic eqns., susceptibility calcs. 3-30701
ferromagnets, metallic, rel. to complex spin waves 3-30634
film, field depend. during quasi-static reversals in alternating field *(Russian)* 3-30653
film, hypercritical, mag. field influence on ground state *(Russian)* 3-36699
glasses, electron correl. and susceptibility 3-15319
granular ferromag. material, sample influences on initial susceptibility determ. *(French)* 3-12005
Heisenberg alternating linear antiferromagnet, exciton interactions rel. to susceptibility 3-34075
Heisenberg compressible ferromagnet, susceptibility index 3-30595
Heisenberg ferromag. film, finite size and surface effects on critical behaviour 3-15332
Heisenberg model of ferro- and antiferromagnets, calc. using lattice Green's function 3-22752
hemin, low-temp. susceptibility and zero-field splitting 3-30583
hydrocarbons, monocyclic unsaturated, mol. diamag. susceptibility, Hartree-Fock calc. 3-29601
μ- hydroxobis[pentaamminechromium(III)] chloride monohydrate, struct. and magnetic susceptibility of the acid rhodo complex 3-18301

magnetic susceptibility continued
inert gases, diamag. susceptibility, free-electron gas exchange correlation calc. 3-38204
insulators, one-electron Green function of Hubbard model in atomic limit 3-15334
Invar, high field, saturation magnetisation, magnetometer measurements of moment 3-36713
Ising and Heisenberg ferromag. model nonmag. impurity effect at Curie temp. 3-8323
Ising anisotropic model, magnetisation, susceptibility, critical temp., crossover exponent, upper bounds 3-21201
Ising ferromagnet, high temp. susceptibility expansion for crystal field anisotropy effect 3-8324
Ising ferromagnet, magnetic susceptibility and local magnetisation fluctuations 3-27346
Ising model, d-dimensional system, reduced susceptibility crossover behaviour 3-5088
Ising model, $S=1/2$, series, anal. 3-24554
Ising model, scaling with parameter for thermodynamic functions and pair correl. function 3-2239
Ising model of disordered state, dynamical susceptibility in transverse mag. field 3-34079
Ising model with lattice anisotropy, high temp. R-series for susceptibility 3-15331
Landau diamagnetism, role of field induced surface currents 3-38956
liquid crystal, nematic, diamag. susceptibility, temp. depend. *(French)* 3-38955
magnetic susceptibility anisotropy meas. in diamagnetic molecules with high temp. microwave spectrometer *(German)* 3-35411
measurement method involving specimens in sealed ampoules *(French)* 3-6031
measurement with commercially available milli-oerstedmeters 3-25813
measuring, in rock, phase resonant circuit, design and testing *(Russian)* 3-3158
metal, h.f. paramag. susceptibility and e.s.r. line profile of localized spins 3-34205
metal, small particles, calc. 3-36517
metal film, electron gas, calc. using screened potential 3-8090
metal-molten salt systems, theoretical interpretation 3-1970
metallic electrons, internal energy and susceptibility under de Haas-van Alphen conditions 3-24374
metallic ferromagnet, damped spin wave branches of susceptibility 3-8373
metals, crystalline electric field, physical aspects 3-30582
1-methylcyclopropene, Zeeman parameters quadrupole moments, magnetic susceptibilities calc. 3-29631
molecules, diamag. susceptibility ab initio calc. 3-29567
narrow band electrons, correlation effects on spin susceptibility 3-12000
nickel squarate dihydrate, mag. transitions, 1.2-4 K 3-18310
organic molecules, mol-Zeeman effect, g-values, magnetic susceptibility anisotropies and mol. quadrupole moments determ. 3-29629
organic nitroxide radicals, exchange intermol. coupling 3-21211
paramagnet, exchange enhanced, surface effects on static spin susceptibility 3-34090
paramagnetic, of itinerant antiferromagnetism above Neel temp. 3-12001
paramagnetic phase of narrow energy bands, dynamical spin susceptibility *(German)* 3-5094
pseudo-tetrahedral ferrous compounds, quadrupole splitting and magnetic susceptibilities 3-21190
quantum crystals, Fermi-type, phenomenological theory 3-24238
rare earth alloys, heavy, effect of hydrostatic pressure 3-36708
rare earth beryllium intermetallics, ^9Be relax. and mag. moment dynamics 3-2444
rare earth manganites, magnetocrystalline anisotropy, mag. susceptibility meas. 3-36704
rare earth orthoferrites, paramag. susceptibility, room temp. and 77K 3-21213
rare earth orthoferrites, paramag. susceptibility anisotropy, cryst. field parameters 3-34094
ruby, increase of parallel paramagnetic susceptibility by resonant pumping 3-39021
semiconductor, of electron gas *(Russian)* 3-8336
semiconductors, Van Vleck paramagnetism and bonding parameters 3-2251
single crystal with arbitrary crystal field and exchange interactions, paramag. susceptibility calc. 3-34089
single domain particles in nonmag. matrix, hysteresis, remanence, antihysteresis susceptibility, coherence field 3-30668
spin-orbit coupled system, Green's function form for the dynamic paramagnetic susceptibility 3-26635
sulphide minerals, effect of temp. on susceptibility during continuous heating and cooling, phase change obs. *(Russian)* 3-12009
superconducting dirty films, diamag. susceptibility rel. to fluctuating Cooper pairs 3-21170
TCNQ complexes, temp. depend., 0.1-400 K *(Russian)* 3-8332
TCNQ salt, Li^+TCNQ^-, paramag. spin susceptibility meas., symmetry-split band theory 3-34084
TCNQ salts, triplet excitations at high temps. 3-15163
ten-electron system, perturbation theory calc. of diamagnetic susceptibility 3-23534
tetrakis (dialkylamino) titanium, rot. obs. of central TiN_4 group *(French)* 3-12120
transition metal carbides, paramag. behaviour *(Russian)* 3-15347
transition metal-hydrogen systems, temp. depend., 100-450K, conc. depend. *(Russian)* 3-38965
transition metal/hydrogen systems, electron-nucl. interactions 3-2439
translation balance for high temp. meas. *(French)* 3-6030
transverse nuclear spin relaxation, mol. diffusion through locally inhomogeneous mag. fields 3-36814
$[Co(NH_3)_4](ReO_4)_2$, molecular susceptibility *(German)* 3-30099
$\{Cr_3O(CH_3COO)_6(H_2O)_3\}Cl.6H_2O$ Mossbauer study on the magnetism 3-2262
$\{Fe_3O(CH_3COO)_6(H_2O)_3\}Cl.6H_2O$ Mossbauer study on the magnetism 3-2262

magnetic susceptibility continued
β-Ag-Cu-Zn, phase stability, absolute thermoelec. power cond. electron mag. susceptibility, comp. depend. 3−33871
Ag-Ga alloy, liq., diamag. peak, temp. and comp. depend. *(Japanese)* 3−30600
$AgCrSe_2$, 0-300°C *(Japanese)* 3−38968
Ag_5SbS_4, stephanite, in phase transition region *(Russian)* 3−30259
Al, liq., Green's function calc. 3−30597
Al-Cu alloy, in various metallurgical states, 10-300K *(French)* 3−24559
As_2S_3 glass and crystalline phases, magnetic susceptibility 3−8334
β-Au-Cu-Zn, phase stability, absolute thermoelec. power cond. electron mag. susceptibility, comp. depend. 3−33871
Au-Fe alloys, meas. to determine mag. ordering rel. to Fe conc. 1-22 at.% 3−2287
$AuGa_2$, $Au_{0.95}Pb_{0.05}Ga_3$ and $AuIn_2$, solid and liquid meas. 3−21334
β-B, rhombohedral, diamag. susceptibility, temp. depend. 3−38960
$BaMnF_4$, two-dimensional mag. ordering in isotropic Heisenberg antiferromagnet 3−36725
Ba_2NiF_6 antiferromagnet, single crystals, low temp. measurements 3−36714
Bi, diamagnetism theory 3−8338
Bi-Cd, temp. and conc. dependence of mag. susceptibility 3−27362
$(CH_3NH_3)_2MnCl_4$, magnetic susceptibility meas., a quasi two-dimensional Heisenberg antiferromagnet 3−5098
CSe mol., from Zeeman effect meas. 3−23580
Cd rare-earth chalcogenide spinels, determ. of Curie-Weiss law behaviour from susceptibility meas., saturation magnetic moments 3−7685
$CdCr_2S_4$, exchange interactions rel. to e.p.r. and mag. susceptibility 3−21314
$CdCr_2Se_4$, exchange interactions rel. to e.p.r. and mag. susceptibility 3−21314
CdF_2:Fe, point defects, Mossbauer and mag. investigation 3−39063
$Cd_xHg_{1-x}Te$, lattice, complex lattice defects and electron gas susceptibilities 3−8339
$CdIn_{2(1-x)}Cr_{2x}S_4$, meas. shows antiferromag. behaviour and gives Curie Weiss const. value 3−2263
Ce hydrides, temp. dependent electronic transition, resistivity and mag. susceptibility meas. 3−8237
$CeMg_3(NO_3)_{12}$, powdered, adiabatic susceptibility tensor, mag. field depend. 3−12003
$Ce_2Mg_3(NO_3)_{12}.24H_2O$, mag. field depend. of spin-spin relax. 3−8478
$Ce_{1-x}R_xAl_3(R=Y,La)$, n.m.r. and mag. susceptibility 3−27434
β-CoAl, low temp. magnetic behaviour 3−34098
$CoBr_2.6H_2O$, magnetic susceptibility meas. 3−38977
$CoCl_2.2H_2O$, AC susceptibility meas., mag. phase diagram and relax. times at antiferromag.-ferrimag. transition 3−30626
$CoCl_2.6H_2O$, magnetic susceptibility and antiferromagnetic, spin flop and paramagnetic transitions 3−18313
β-CoGa, low temp. magnetic behaviour 3−34098
$CoIn_2S_4$, cation distrib., mag. susceptibility temp. depend. 3−34102
$Co_xZn_{1-x}Cs_3Cl_5$, random ising spin system 3−8359
Cr-Pd dil. alloys, solute effects 3−34111
Cr-Re alloys, meas. for 10 solid solns. *(Russian)* 3−8358
Cr_2Al_{11}, temperature dependence measurements, Knight shift 3−36807
α-Cr_2O_3, formation and interconversion in Cr oxide gel systems 3−5382
Cr_2SSeTe, meas. of molar susceptibility and molar spontaneous magnetisation, 80-600 K, determ. of Curie point *(Russian)* 3−12010
$CsFeCl_3$, temp. depend., 2 to 250K, interpretation using antiferromag. linear-chain model 3−21220
Cu complex, CuNSal, meas. for spin $^1/_2$ linear chain 3−15355
Cu complex, Schiff base derivatives of iminoxy radicals copper (II) 3−21214
Cu complex $((CU_3)_3NH)$ $CuCl_3.2H_2O$, low temps. 3−1613
Cu:M, dil. alloy, M=transition metal, pair description 3−30596
Cu-Fe Kondo system, eqn. of state from phenomenological model 3−5096
Cu-Ga(Ge)(Bi) alloys, liq., diamag. peak, temp. and comp. depend. *(Japanese)* 3−30600
$CuCr_2S(Se)(Te)_4$, paramagnetic susceptibility temp. depend. 380-650K *(Russian)* 3−15345
$CuCrSe_2$, 0-300°C *(Japanese)* 3−38968
$CuWO_4$, 4.2-300 K, short-range order effects 3−34104
$DyCl_3.6H_2O$, caloric and mag. props. 3−38976
$DyPO_4$, mag. susceptibility curves anomalies at high temps., n.m.r. obs. 3−30707
Er^{3+}, in solids, C_{3h}, D_{2d}, O_h site symmetry, paramag. susceptibility rel. to cryst. field parameters 3−2234
$ErCl_3.6H_2O$, caloric and mag. props. 3−38976
$Er_2O_2S:Er^{3+}$, rel. to crystal field effects on electronic ion structure *(French)* 3−30411
$EuWO_4$, ferrimagnetism of single crystal 3−30605
$F^{12}C^{15}N$, mol. Zeeman effect obs. 3−33135
Fe, high temp. meas. *(French)* 3−6030
α-Fe, low temp. mag. relax. rel. to mag. aftereffect, susceptibility meas. 3−34168
Fe alloy, nonmag., paramag. susceptibility as heat treatment check 3−21696
Fe complex, Baudisch complex, chem. characteriz. 3−26631
Fe-Si, covered by Ni film, temp. depend. meas. rel. to ferromag. domains *(Russian)* 3−24562
Fe-Si alloys, 1000-1900°C, conc. depend., solid-liq. transition *(Russian)* 3−36707
FeAs, measurements obey Curie-Weiss law between 300 and 650K 3−15370
$FeBr_2$, $FeCl_2$ metamagnetic properties, uniaxial tension at 4.2°K, antiferromagnetism *(French)* 3−27390
$Fe_{1-x}Co_xAl$ solid solns., conc. depend. and temp. depend. *(Russian)* 3−30087
FeGe, susceptibility meas. and magnetic ordering 3−18326
Fe(II) complex, tris[2-(2′-pyridyl)benzimidazole]iron(II), 80-300K, $^5T_2$-$^1A_1$ spin equil. 3−24634
Fe(II) six coordinated compounds, spin S=1, low temp. magnetism, Mossbauer effect and electronic struct. 3−34250
$FeIn_2S_4$, cation distrib., mag. susceptibility temp. depend. 3−34102

magnetic susceptibility continued
$Fe_xMn_{2-x}P$, mag. props. of different phases, Neel and Curie temps. 3−30608
$FeNb_2O_6$, paramag., mag. susceptibility meas. rel. to structure and ionic mag. moments *(Russian)* 3−15346
α-Fe_2O_3, hematite, nonlinear susceptibility and anisotropy to Morin temp. 3−2261
ϵ-Fe_3O_3, temp. depend. 3−27361
FeOCl, 300-4.2 K, antiferromag. order *(French)* 3−30604
GaAs:Te, heavily doped, 4.2-300K *(Russian)* 3−2252
$GdFe_x(Co_x)(Ni_x)$, temp. depend., Neel model interpret. *(French)* 3−27358
$GdNi_2$, ferromag., Landau model for critical susceptibility 3−15320
$GdPO_4$, mag. susceptibility curves anomalies at high temps., n.m.r. obs. 3−30707
$Gd_xTh_{1-x}PdIn$, 4.2-300 K 3−27364
$Gd_xTh_{1-x}PdIn$, 4.2300 K 3−27364
Ge, diamag. specific susceptibility rel. to disorder 3−30599
Ge, two electron donor pair system, eigenvalue problem, Heitler-London method soln. 3−2579
H_2, calc. of mag. susceptibility by variation of vector potential and induced current *(Russian)* 3−33081
HCN, mol., anisotropy from Zeeman effect 3−20168
HCP mol., anisotropy from Zeeman effect 3−20168
^3He, nuclear magnetic susceptibility obs. 3−38697
^3He degenerate films, pulsed nucl. reson. obs. of susceptibility and mag. interaction 3−4901
^4He in ^3He dil. mixture, nuclear magnetic susceptibility obs. 3−38697
$HfCo_2$, Laves phase, single phase region 3−27360
HgTe, semimetal, field and temp. depend., two-point matrix Green function calc. *(Russian)* 3−5099
Ho, temp. depend. near Neel point *(Russian)* 3−12012
Ho measurements, polycrystalline and single crystal, 293-873 K, paramagentic properties 3−30601
$HoMnO_3$, paramag. Curie temp., mag. susceptibility, 4.2-400 K 3−34103
$KMgF_3$:Mn and $KZnF_3$:Mn, bilinear and biquadratic exchange interactions, effect on mag. susceptibility 3−27363
$KNiPO_4$, temp. depend. *(Russian)* 3−11603
La:Ce, cubic crystalline field effect on magnetic susceptibility rel. to Kondo effect 3−24560
La-Gd alloy, giant susceptibilities 3−8340
La-Pu alloy, obs. of mag. decoupling 3−2255
$La_{0.4}Nd_{1.6}O_3$, single crystal, paramag. susceptibility anisotropy meas. *(French)* 3−38961
Li, diamagnetic susceptibility 3−34096
$(Li_{1-x}Fe_x)[Li_{x-0.5}Fe_{2.5-x-a}Cr_a]O_4$, ferrite, susceptibility temp. depend in paramag. region 3−38958
Mg_6MnO_8, paramag. structure with weak antiferromag. interaction, susceptibility and optical reflectance meas. 3−34091
α-Mn, paramag., susceptibility maximum phenomena 3−21215
γ-Mn, paramagnetic, d electron, Hamiltonian band structure model, instability criterion 3−30602
α-Mn dilute alloys, paramag., susceptibility maximum phenomena 3−21215
$MnCO_3:Fe^{2+}$, spin system and moment exam., reln. to concentration 3−2289
MnF_2, mag. susceptibility near T_n and Fisher's relation 3−38967
$MnIn_2S_4$, cation distrib., mag. susceptibility temp. depend. 3−34102
MnO-MgO solid solns., temp. depend., exchange phenomena between Mn^{2+} ions *(French)* 3−38964
β-MnSe, prep., Curie-Weiss relationship above 110K 3−30598
MnTe, 300-700 K 3−15365
$Mn(pyrazole)_2Cl_2$, low-temp. susceptibility meas. rel. to antiferromag. interaction 3−30612
NH_4FeCl_3, temp. depend., 2 to 250K, interpretation using antiferromag. linear-chain model 3−21220
Na_2NiFeF_7, meas. to determine mag. structure 3−2301
$Nb_3Al_{0.75}Ge_{0.25}$ alloy, 19-300K 3−18245
Nd-Sb system alloys, physical props. and correlation with the phase diagram *(Russian)* 3−11882
Nd-Y alloys, 100 to 800 K, precip. depend. *(Russian)* 3−15683
$Nd_2Mg_3(NO_3)_{12}.24H_2O$, mag. field depend. of spin-spin relax. 3−8478
Nd_2O_3, single crystal, paramag. susceptibility anisotropy meas. *(French)* 3−38961
Ni, melting pt. discontinuity *(French)* 3−21219
Ni, with Cr impurity, high field susceptibility 3−21225
Ni complex, $Ni(pyrazole)_4$ Cl_2, Br_2, paramagnetic susceptibility from 2 to 80 K 3−8366
Ni-Cu alloys, mag. moment in pulsed fields, Pauli susceptibility *(Russian)* 3−30606
Ni-Cu alloys, temp. dependence rel. to spin wave theory 3−18303
Ni-Fe film, two layers separated by SiO, magnetic coupling, transverse suscept. obs. 3−34174
Ni-Fe layers separated by SiO intermediate layer, magnetic coupling energy, transverse susceptibility meas. 3−8400
Ni_xB, (x=1,2,3), temp. depend., 100-1100K *(Russian)* 3−8333
$NiCl_2.4H_2O$, meas. at antiferromag.-paramag. transition, molecular field model 3−34120
$NiIn_2S_4$, cation distrib., mag. susceptibility temp. depend. 3−34102
NiS, meas. at antiferromag. semimetal to paramag. metal transition 3−36540
NiS_2, non-stoichiometry influence at insulator-metal transition 3−2017
Pb-Sb-S, semicond., diamag. and paramag. terms 3−8335
PbTe with excess Pb, supercond. above 7.2K *(French)* 3−38915
Pd, exchange-enhanced generalized susceptibility, tight binding model for d-bands 3−2253
Pd:M, alloys structures, (M=Gd, Ho, Dy) *(German)* 3−34095
Pd-Ag-Ad solid solution, magnetic and crystallographic characteristics 3−8793
Pd-La(Ce)(Pr), field independent susceptibility depend. on temp. 3−18298
Pd-rare earth, paramag. dilute alloy, temp. depend. meas. and Curie Weiss law 3−15349
PdH_n, equilibrium isotherms 3−30241
$(Pr, Nd, Sm, Tb, Dy, Ho)Pb_3$, low-field susceptibility, magnetisation, 3-300K *(French)* 3−18302

magnetic susceptibility continued
(Pr ʳ)Ga garnets with R=small rare earths on two crystallographic sites, magnetic susceptibility meas. 3−7689
$PrNI_5$, thermal, magnetic and electrical props. 3−8357
Pt-Mn-Sn alloys, Curie-Weiss behaviour above Curie pt. *(Japanese)* 3−8346
α-Pu, mechanism to explain exptl. results *(French)* 3−8345
PuX_n, (X=Ru, Rh, Ir, Pt, n=2 and X=Rh, Pd, Pt, n=3) and elec. resistivity 3−38966
$RbFeCl_3$, temp. depend., 2 to 250K, interpretation using antiferromag. linear-chain model 3−21220
Ru alloy with CsCl structure, Pauli susceptibility with localised moments contrib. 3−34097
Ru^{4+} in single cubic crystals, effect of config. interaction on mag. props. 3−30585
Sc-Pu alloy, obs. of mag. decoupling at Pu 3−2255
Se, diamag. specific susceptibility rel. to disorder 3−30599
Si, two electron donor pair system, eigenvalue problem, Heitler-London method soln. 3−2579
n-Si-Ge alloys, Si-rich electron, computation from total susceptibility 3−36530
Sm, neutron diffr. studies, rel. to susceptibility anomaly 3−24577
Sm and Sm_2O_3, temp. depend., 0-1500K *(French)* 3−8353
$SmAl_2$, ferromag., crystal field effect 3−15322
$SmSn_3$, antiferromag., crystal field effect 3−15322
Sn-Bi liquid system, concentration dependence analysis *(Russian)* 3−8347
$SnMn_3C$, first order mag. transition at 292 K *(French)* 3−15362
$Sr_3Cr_2WO_9$, perovskite type, temp. depend. *(French)* 3−24080
$Sr_yM_{1-y}FeO_{2.5}$-$Sr_yM_{1-y}FeO_{3-x}$,(M=Ba,Ca), meas. to characterise perovskite phases *(French)* 3−27098
$TbPO_4$, mag. susceptibility curves anomalies at high temps., n.m.r. obs. 3−30707
TiO-NiO, TiO-CoO, 100-1000 K, composition and temp. depend. *(Russian)* 3−12008
$TlFeCl_3$, temp. depend., 2 to 250K, interpretation using antiferromag. linear-chain model 3−21220
$Tm_x Y_{1-x}Al_2$, cryst. elect. field transitions, susceptibility, inelastic neutron scatt. 3−18283
UTe_2, temp. depend., value explained assuming singlet ground state 3−12011
U_7Te_{12}, temp. depend., value explained assuming singlet ground state 3−12011
$(U_xTh_{1-x})S$, electronic props., models, mag. susceptibility, sp. ht. and elec. resist. obs. 3−2249
V-B-N, meas. rel. to bond structure *(Russian)* 3−15333
$V(CO)_6$, solid state behaviour, paramag. 3−36703
$V_3(Ge_{1-y}Ga_y)$, $V_3(Ge_{1-y}Al_y)$, and supercond. T_c conc. depend. *(Russian)* 3−8288
$V_xMn_{1-x}O$, depend. on VO conc., 100-1000K *(Russian)* 3−12007
$V_{1-x}Mo_xO_2$, at metal-insulator, monoclinic-tetragonal transition 3−30424
VO-NiO, 100-1000 K, composition and temp. depend. *(Russian)* 3−12008
VO_2, metallic, rel. to Coulomb interactions 3−24556
V_nO_{2n-1} shear struct. cpds., metal-insulator transition 3−18090
VS, V_3S_4-V_2S_3 and V_5S_8, 4-1000K 3−27355
$V_{1-x}W_xO_2$, semicond.-metal transition study, 80-400K 3−18205
Y-Np alloys, obs. of mag. decoupling at Np 3−2255
$YCo_2(Ni_2)$, Pauli behaviour *(French)* 3−1803
YIG, rel. to parallel spin-wave pumping 3−34143
YIG, temp. depend. near Curie point 3−38980
$YMnO_3$, paramag. Curie temp., mag. susceptibility, 4.2-400 K 3−34103
$YbAl(Cu)_2$, $YbIn_3$, ambiguous mag. behaviour, susceptibility meas. 3−30609
$YbMnO_3$, paramag. Curie temp., mag. susceptibility, 4.2-400 K 3−34103
ZnCd and ZnHg, axial ratio dependence of mag. susceptibility, Fermi surface charge 3−27359
Zr-Sc-H alloy system, paramag. susceptibility, p.m.r. *(Russian)* 3−36805

magnetic switching
No entries

magnetic tape recorders *see tape recorders*

magnetic thin film devices
bubble devices, preparation technique 3−13355
rare earth iron garnet, chemical vapour deposition for bubble domain devices 3−24792

magnetic thin film stores *see magnetic film stores*

magnetic thin films
: 3−39033
apparatus for investigation of magnetic properties of thin weak magnetic films *(Russian)* 3−25820
biaxial, exchange energy rel. to angle between magnetisation vectors, thickness depend. 3−21282
Bloch wall films, wall contraction 3−30656
bonded domain, recording of radiation field of pulsed Nd laser *(Russian)* 3−32110
bubble domain material, characterization using X-ray topography 3−34156
bubble domains, epitaxially grown, magnetisation, wallenergy, coercivity, temp. depend. 3−36764
bubble film domain walls, static props. of film thicker than wall width 3−36761
bubble film domain walls, theory of static props. 3−36760
conducting ferromagnetic layer, role of magnetic microstructure in ferromagnetic resonance *(Russian)* 3−8448
domain wall motion in mag. films and platelets, theory 3−36754
domain walls, dynamic behaviour, variational calculation 3−36739
double-layer ferromag., magnetostatically-coupled, crit. curves, mag. reversals *(Russian)* 3−30650
epitaxial garnet films, effect of substrate defects 3−15090
ferromagnet, effect of ang. dispersion of anisotropy on reson. linewidth *(Russian)* 3−8452
ferromagnet, honeycomb domain struct. 3−30662
ferromagnet, weakly amorphous, density of spin wave states, Heisenberg model calc. 3−30636

magnetic thin films continued
ferromagnet, with rough surface, spin wave spectrum and magnetization 3−18331
ferromagnet weak itinerant film-paramag. proximity sample, Hubbard model calc. of Curie temp. 3−34086
ferromagnetic, cylindrical, anisotropy dispersion meas. *(French)* 3−25819
ferromagnetic, cylindrical, anisotropy field meas. *(French)* 3−25818
ferromagnetic, demagnetising factor, method of rot. moments *(Russian)* 3−21265
ferromagnetic, domain wall creep in nonuniform fields, intrinsic fields influence *(Russian)* 3−36736
ferromagnetic, magnetoresist. rel. to domains and magnetisation vector angular dispersion 3−21052
ferromagnetic, mixed boundary conditions, spin-wave reson. spectra analysis 3−21319
ferromagnetic, spin distrib. near surface rel. to boundary conditions, reson. spectrum effects 3−21254
ferromagnetic, spin-spin relax. 3−21320
ferromagnetic double layered film, magnetostatic coupling energy due to peripheral charge 3−39007
ferromagnetic film, domain wall width determ. *(French)* 3−8392
ferromagnetic metal, spin wave dispersion 3−27378
ferromagnetic plate, magnetiz. oscillations spectrum *(Russian)* 3−30649
ferromagnetic resonance, magnetoelastic interactions effect, application to Ni 3−34216
ferromagnetic resonance, magnetoelastic interactions effect 3−34215
field distribution, computer aided determination *(Polish)* 3−24584
garnet, chemical vapour growth for bubble domain devices 3−36771
garnet, epitaxial film, method of producing extraordinary bubbles 3−28610
garnet, epitaxial growth for substrate facet replication 3−38749
garnet, for bubble devices, epitaxial growth 3−12276
garnet, mag. bubble detect. using waveguide fibre optics 3−35442
garnet film, comp. determ. by radioactive tracer technique 3−26022
garnet film, control of product phases in chemical vapour deposition 3−12249
garnet mixed rare earth iron type, epitaxial film, anisotropy field and domain wall coercivity temp depend. 3−21257
Heisenberg ferromag. film, finite size and surface effects on critical behaviour 3−15332
high speed switching, early stage, magneto-optical obs. 3−36740
hypercritical, mag. field influence on ground state *(Russian)* 3−36699
Kerr magneto-optic effect obs. by optical interferometry 3−28559
magnetic critical exponent β meas. by ferromagnetic transmission resonance, microwave power meas. through thin Gd film 3−16465
magnetic moment movement under field normal to preferred axis *(Russian)* 3−38996
magnetisation direction distribution in band model 3−27352
magnetization, subharmonic oscillations and crit. curves *(Russian)* 3−15392
magnetization curves in the difficult direction in the presence of amplitude dispersion anisotropy *(Russian)* 3−8375
magnetoresistance method of measuring H_k and H_c by a four-point resistance probe 3−32114
magnetostrictive, anisotropy skew, theory 3−5122
multilayer, ferromag. reson., u.h.f. susceptibility *(Russian)* 3−18371
optical radiation detectors under nonadiabatic exposure conditions, sensitivity 3−19228
oxide, heteroepitaxial stresses, origin, magnitude, config. 3−1944
permalloy, anisotropy, electrostatic torquemeter obs. 3−256
permalloy, Bloch line motion, behaviour at inhomogeneities, Lorentz electron microscope study 3−12038
Permalloy, bubble domains, h.v. electron microscope obs. 3−30660
permalloy, cct. analysis for bubble domain propagation 3−36752
permalloy, domain wall dynamic properties 3−34161
permalloy, evap. onto rotating substrate, helical anisotropy 3−34149
permalloy, ferromag., mag. parameters rel. to grain size and film thickness 3−8402
Permalloy, interrupted nsec. mag. reversals *(Russian)* 3−8382
Permalloy, magnetiz. oscillations due to pulsed transverse field excitation *(Russian)* 3−24586
Permalloy, nonuniformity of nsec. magnetization reversal *(Russian)* 3−8395
Permalloy, obliquely deposited, mag. reversals, mechanisms *(Russian)* 3−30651
Permalloy, obliquely deposited hypercritical, mag. props. and microporosity *(Russian)* 3−24588
permalloy, obs. of triangular hysteresis loops 3−8393
permalloy, quantitative chemical analysis, X-ray fluorescence spectroscopy *(German)* 3−27387
permalloy, Ritz model for asymmetric domain walls 3−8388
Permalloy, spin wave spectrum, surface conditions influence *(Russian)* 3−30698
permalloy, transit time limited nonlinear domain wall motion 3−36733
permalloy, uniaxial mag. anisotropy rel. to annealing *(Russian)* 3−15383
Permalloy, with banded domain struct., mag. reversals *(Russian)* 3−8381
permalloy electrodeposited films micron thickness, reversal of magnetisation by domain wall creep 3−38992
permalloy film, uniaxial mag. anisotropy rl. to annealing 3−18333
permalloy on bubble-domain material, effect on domain stability 3−18336
permalloy overlay structures for magnetic bubble devices, technique 3−13355
permalloy thin films, influence of pulse magnetic reversals on domain boundary drift *(Russian)* 3−2322
plated wire, angular anisotropic dispersion meas., pulse method *(Polish)* 3−30669
rare earth garnet, liquid phase epitaxy for bubble domain devices 3−36770
rare earth transition metal alloy amorphous films, magneto-optic props., applications 3−36857

magnetic thin films continued
spin polarisation of electrons tunnelling from Fe(Co)(Ni)(Gd) ferromag. to Al superconducting film 3−15311
susceptibility during quasi-static reversals in alternating field *(Russian)* 3−30653
testing, system, patent 3−10427
thermomagnetic writing, optimum film thickness, theory 3−16915
thin to over-critical transition, electrodeposited, domain structure 3−39000
YIG, obs. of exchange dominated surface spin wave 3−2400
$Ba_3Co_2Fe_2O_4$, ferrite, arc plasma deposited, mag. props. 3−36772
$BaFe_{12}O_{19}$, ferrite, arc plasma deposited, mag. props. 3−36772
$Ba_2Zn_2Fe_{12}O_{22}$, ferrite, arc plasma deposited, mag. props. 3−36772
C, amorphous, antiferromag. transition, e.s.r. obs. 3−18317
Co, perpendicular anisotropy, rot. moments, superparamag. particles *(Russian)* 3−30641
Co, with different texture perfections about [0001] axis, perpendicular anisotropy 3−36731
Co electrodeposited, effect of I^- ions on mag. props. *(Bulgarian)* 3−30670
Co-Ni-P layers, chem. deposited, anisotropy field *(French)* 3−8404
Co-P, high-coercivity, domain struct. and reversal processes 3−24592
CoNiFe, domain wall motion rel. to low freq. creep 3−36738
^{59}Co films, nuclear mag. levels inverted state 3−30628
$EuEr_2Ga_{0.7}Fe_{4.3}O_{12}$, epitaxial for bubble domains, variation of magnetiz., Curie temp., and Ga/Fe ratio with growth temp. 3−34157
$EuEr_2Ga_xFe_{5-x}O_{12}$, $Eu_xEr_{3-x}Ga_{0.7}Fe_{4.3}O_{12}$, for bubble domains, thermal expansion of lattice parameters 3−34158
EuO:Fe, thermomag. writing, optimum thickness calc. 3−16915
EuS, EuSe and EuTe spin polarized photoelectrons *(German)* 3−18531
EuS, EuSe and EuTe thin films, spin polarized photoelectrons *(German)* 3−18531
EuS, magneto-optical props., study of spin-orbit coupling and exchange field 3−2323
$(EuY)_3(GaFe)_5O_{12}$, liquid phase epitaxial growth by tipping process 3−12278
$Eu_{1.1}Yb_{1.9}Fe_5O_{12}$, garnet film, LPE growth by isothermal dipping with axial rotation 3−30945
Fe, cylindrical, Procopiu effects study 3−36775
Fe, evaporated at oblique incidence domain structures 3−1544
Fe (100) single crystal, dislocations and magnetic structure 3−8399
Fe-Ni alloy, modulation of mag. noise spectral distrib. *(Russian)* 3−12042
Fe-Ni alloys, exchange parameters 3−2324
Fe-Ni alloys, magnetic properties, crystal structure dependence 3−8376
Fe-Ni film, galvano- and thermomag. effects depend. on phase comp. 3−33873
Fe_8N, vapour deposition from nitrogen atmos., ultrahigh mag. moment *(Japanese)* 3−8403
Fe_3O_4, magnetite, low temp. conversion from α-Fe_2O_3, hematite 3−34173
GdP, GdAs and GdSb spin polarized photoelectrons *(German)* 3−18531
GdP, GdAs and GdSb thin films, spin polarized photoelectrons *(German)* 3−18531
$(GdY)_3(GaFe)_5O_{12}$, liquid phase epitaxial growth by tipping process 3−12278
$(GdYYb)_3(GaFe)_5O_{12}$, liquid phase epitaxial growth by tipping process 3−12278
Li-Cr ferrite, LPE growth on MgO, Mossbauer obs. of substrate contamination 3−1928
$Lu_2EuMFe_4O_{12}$ (M=Al or Ga), growth-induced mag. anisotropy of epitaxial films 3−21259
Mg-Mn ferrite films, remagnetization rate and mobility of domain boundaries *(Russian)* 3−8398
$MgFe_2O_4$, thin films, electron diffraction superlattice lines 3−38569
$Mg_xMn_{1-x}Fe_2O_4$, use as phase diffr. grating 3−36862
Mn-Bi system, birefringent compounds 3−21283
MnAlGe, nonstoichiometric film, prep., structure, mag., and optical props. 3−36497
MnAlGe, self-demagnetisation during theromag. writing 3−24407
MnBi, domain patterns, Faraday effect obs. 3−21272
MnBi, low temp. mag. props. 3−27384
$Mn_{0.8}Fe_{0.2}[Mn_{0.2}Fe_{1.8}]O_4$, thin films, electron diffraction superlattice lines 3−38569
MnGaGe, sputtered film, ferromag. and magneto-optical props. 3−36861
MnGaGe film, Curie point writing with laser pulse, thermal and mag. profiles comparison 3−36860
Mn_5Ge_3, ferromag. reson., g-factor, magnetisation, 0-45°C 3−27419
α'-$Mn_{0.85}Ti_{0.15}Bi$ mag. and magneto-optic props. 3−2521
Ni, evaporated at oblique incidence domain structures 3−1544
Ni, ferromag. film, electromag. wave dispersion by spin waves 3−11923
Ni, high stressed films, ferromagnetic resonance at oblique angles 3−21317
Ni, hypercrit. state, hysteresis loops, domain struct. *(Russian)* 3−15393
Ni, transcritical epitaxial film, domain structure 3−30666
Ni (100) single crystal, dislocations and magnetic structure 3−8399
Ni film on Fe-Si, mag. susceptibility temp. depend. meas. rel. to ferromag. domains *(Russian)* 3−24562
Ni film on Fe-Si alloy surface, effect on mag. props. *(Russian)* 3−12037
Ni-Co, electrodeposited, stripe domains *(Russian)* 3−30667
Ni-Co layers covering Cu wires, mag. and mech. treatment effect on mag. props. *(Rumanian)* 3−12043
Ni-Co-Fe mated film (bifilm) plated wire element, effects of process variables 3−12041
Ni-Co-Fe-SiO system, bilaminar ferromag. films, field of interaction *(Russian)* 3−21267
Ni-Fe, damped magnetisation oscillations 3−36741
Ni-Fe, electroless, mag. props., temp. and soln. pH effects 3−21278
Ni-Fe, ferromag. exchange const., spin wave resonance obs. 3−34105

magnetic thin films continued
Ni-Fe, oblique incidence evap., mag. anisotropy, deuteron irrad. effects 3−34148
Ni-Fe, permalloy, electrodeposition, Watts type bath technique 3−12044
Ni-Fe, two layers separated by SiO, magnetic coupling, transverse suscept. obs. 3−34174
Ni-Fe (100) single crystal, dislocations and magnetic structure 3−8399
Ni-Fe alloy, hypercrit. state, hysteresis loops, domain struct. *(Russian)* 3−15393
Ni-Fe alloy with additional surface layers, spin wave reson., high field peak *(Russian)* 3−24615
Ni-Fe layers separated by SiO intermediate layer, magnetic coupling energy 3−8400
Ni-Fe(25 wt.%), domain boundary curvature and displacement, mag. field and elastic stresses influence *(Russian)* 3−30654
Ni-Ge alloy, Hall and Thomson effects *(Russian)* 3−18123
Ni-Sm, saturation magnetization and hysteresis loops *(Russian)* 3−27382
$NiFe_2O_4$, ferrite, arc plasma deposited, mag. props. 3−36772
Y-Eu garnet, epitaxial film, magnet domain wall velocity 3−36734
$Y_{2.4}Eu_{0.6}Ga_{1.2}Fe_{3.8}O_{12}$, epitaxial garnet film, growth-induced mag. anisotropy, annealing effects 3−30640
$Y_2EuMFe_4O_{12}$ (M=Al or Ga), growth-induced mag. anisotropy of epitaxial films 3−21259
$Y_3Fe_{5-x}Ga_xO_{12}$, epitaxial garnet film, growth by chemical vapour deposition 3−12248
$Y_3Fe_{5-x}Ga_xO_{12}$ garnet, growth by liq. phase epitaxy *(German)* 3−5274
$Y_3(GaFe)_5O_{12}$, liquid phase epitaxial growth by tipping process 3−12278
YIG, epitaxial, ferromag. resonance, lattice mismatch effects 3−30700
YIG, epitaxial, induced in-plane mag. anisotropy, ferromagnetic resonance obs. 3−34147
YIG, ferrite, arc plasma deposited, mag. props. 3−36772
YIG, heteroepitaxial growth on GdGaG substrate by hydrothermal synthesis 3−1922
YIG, in in-plane mag. field, orientation of stripe domains 3−27386
YIG, phonon generation by ferromag. resonance 3−36794
YIG, r.f. sputtering from powder mixture of Fe_2O_3 and Y_2O_3, magnetic properties 3−8401
YIG epitaxial, domain struct. and stress 3−34160
YIG on grounded dielec. substrate, surface wave group delay time 3−8408
YIG:Al, epitaxial, chemical vapour desposition for bubble domain devices 3−33746
YIG:Ga, L.P.E. growth, effect of substituting Gd(Sm)(La) for Y 3−1924
YIG:Gd,Ga, epitaxial growth by r.f. sputtering 3−12237

magnetic transition temperature *see magnetic transitions of substances*

magnetic transitions of substances
see also Curie temperature; Neel temperature
alkali metal iron fluoride, M_xFeF_3, (M=K, Rb, Cs), Mossbauer effect study *(French)* 3−8488
antiferromagnet, crit. neutron scatt. near second order transition 3−34136
antiferromagnetic Husimi-Temperley model, distrib. of zeros of partition function above and below critical temp. 3−5084
antiferromagnetic two-singlet system, molecular field approx. for phase diagram and metamag. transition 3−27340
antiferromagnetism, itinerant, thermodynamic props., first order phase transition 3−5101
$Co_xNi_{(1-x)}O$, single crystals, thermal diffusivity in the region of continuous phase transition 3−4892
critical behaviour of Ising systems on extremely anisotropic lattices, simple cubic lattice 3−27344
critical phenomena and neutron scattering 3−21226
critical phenomena and neutron scattering 3−30613
demonstration for students using Monte Carlo computer program 3−22227
dipolar systems, mag. ordering in molecular field approximation 3−18318
ferrimagnet, three-sublattice, mag. struct. induced by field *(French)* 3−38972
ferrimagnetic, crit. field for collinear to canted transition rel. to anisotropy parameters 3−5115
ferrite, isotropic, crit. neutron scatt. near second order transition 3−34136
ferromagnetic-antiferromagnetic, in ordering alloys with b.c.c. lattice *(Russian)* 3−34127
ferromagnetism, exchange interaction model, crit. point props., single-ion anisotropy effects 3−38936
ferromagnets, Smoluchowski-type treatment of fluctuations at the critical point 3−34063
film, double-layer ferromag., magnetostatically-coupled, crit. curves, mag. reversals *(Russian)* 3−30650
film, hypercritical, mag. field influence on ground state *(Russian)* 3−36699
first order, magnetisation curves calc. *(French)* 3−30614
Heisenberg ferromag. film, finite size and surface effects on critical behaviour 3−15332
Heisenberg ferromagnet, critical behaviour of anisotropic cubic systems 3−38945
Heisenberg ferromagnet, Feynman graph expansion for equation of state near crit. point 3−15330
Heisenberg ferromagnet, two-dimensional, critical temp. depend. on anisotropy 3−30590
Heisenberg model, dilute anisotropic, decoration transform. 3−11997
Ising antiferromagnet, b.c.c., near critical field, phase transitions, Monte Carlo study 3−5089
Ising lattice with superexchange, phase transitions 3−24555
Ising model with dilute impurities, critical properties 3−27349
linear chain cpd. behaviour 3−15361
magnetite, multiple mag. ordering rel. to metal insulator transition 3−15369
magnetite; optic spin wave energy at Verwey transition 3−34140

magnetic transitions of substances continued
- multipolar phase transitions, molecular field approx. 3−30620
- neutron scatt. studies of crit. fluctuations 3−15360
- nickel squarate dihydrate, 1.2-4 K 3−18310
- orthoferrites, spin reorientation temp., phase transitions, heat capacity, domain structure and energy 3−39003
- paramagnetic instability in orbitally nondegenerate narrow band, interatomic correlation effect 3−8330
- partition function for mag. lattice systems, domain of zeros, crit. temp. and mag. field 3−34074
- polarized media, paramag. to ferromag. transition, homogeneity effects 3−5102
- pressure influence on phase transitions, review 3−24485
- quadrupolar ordering, uniaxial and biaxial, molecular field theory 3−15321
- rare earth alloys, binary, transition temps., theoretical expression 3−18311
- rare earth nickelides, $LnNi_5$, thermal props. over range of ordering, entropy and spin-disorder resistivity 3−12016
- rare-earth chalcogenides, determination from specific heat, thermal expansion and conductivity data 3−15019
- scaling law equation of state at critical point free energy and magnetic field-temperature paths 3−27369
- semiconductor-metal and mag. phase transitions, Hamiltonian model 3−38806
- smectic A film, possible mag. transitions, critical field 3−4720
- spin-1 model of ferromagnetism, high-temp. series expansion 3−38939
- spin-1 models dipole and quadrupole phase transitions 3−38938
- spin-phonon interaction effect on neutron scattering from lattice vibrations 3−1758
- tetramethyl-2,2,6,6,piperidinol-4, oxyl-1 free radical, low temp. sp.ht. study 3−18314
- tricritical points, critical exponents notation 3−13664
- two-dimensional exchange interaction model, numerical evidence for phase transition 3−34106
- uniaxial ferromagnet, in transverse mag. field, free energy, spatial magnetization fluctuation effects 3−18315
- α--Fe diffusion of Ag, effect on ferromagnetic to paramagnetic transition 3−17990
- Au-Cr alloy, paramag.-antiferromag. critical composition, anisotropic diffuse scatt. of neutrons 3−38973
- Au_4Mn, micromagnetic to superparamag. transition, effect of atomic ordering 3−21229
- B_2O_3-BaO-Fe_2O_3 glass, magnetic, displacement of magnetisation curve 3−12020
- C film, amorphous, antiferromag. transition, e.s.r. obs. 3−18317
- Ce, effect of impurities on α-γ transition 3−21238
- $CoBr_2.6H_2O$, antiferromagnetic, spin-flop and paramagnetic phases, mag. susceptibility meas. 3−38977
- $CoCl_2.2H_2O$, AC susceptibility meas., mag. phase diagram and relax. times at antiferromag.-ferrimag. transition 3−30626
- $CoCl_2.6H_2O$, magnetic susceptibility and antiferromagnetic, spin flop and paramagnetic transitions 3−18313
- $CoCl_2.6H_2O$, magnetic transition rounding and Pippard's relations 3−30619
- $CoS_{2-x}Se_x$, pyromagnetic obs. of magnetic phase transition 3−34110
- $CrCl_3$, antiferromagnetic to ferromagnetic, specific heat meas. from 4.5 to 20 K 3−38974
- $CrPt_3$, transition from ferrimag. to paramag. type behaviour with cold working 3−21237
- $Cr_{0.30}Pt_{0.70}$, ordered and disordered, sp. ht., 1.2-4.2K 3−24567
- Cr_2S_3, rhombohedral single crystal, paramagnetic Curie temp. 3−12021
- $CsMnCl_3.2D_2O$ magnetic phase diagram, 2-20K, zero-field Neel temp. 3−5100
- $CsNiCl_3$, antiferromag., specific heat anomalies near 4.5 K 3−30617
- $CsNiCl_3$, antiferromagnetic-paramagnetic transitions 3−34115
- $Cu_3(CO_3)(OH)_2$, magnetic transition rounding and Pippard's relations 3−30619
- $CuCr_2S(Se)(Te)_4$, temp. interval from magnetisation meas. in weak fields *(Russian)* 3−15345
- $Cu(NO_3)_2.2^1._2H_2O$, specific heat and n.m.r. at the high-field phase transition 3−27370
- Dy, hysteresis of ferromag.-antiferromag. transform., elec. resist. and thermal expansion obs. *(Russian)* 3−15363
- $DyAsO_4$, paramag. to antiferromag. transition, cryst. phase transition 3−2281
- $DyPO_4$, mag. susceptibility curves anomalies at high temps., n.m.r. obs. 3−30707
- DySb, shear elastic const. meas. near mag. and structural phase transition 3−33591
- $DyVO_4$, elastic anomalies near cooperative Jahn-Teller transitions 3−2014
- $DyVO_4$, molecular field approx. 3−2277
- $DyVO_4$, paramag. to antiferromag. transition, cryst. phase transition 3−2281
- $ErFe_2$, coercive force, remanence and hysteresis near mag. compensation point *(Russian)* 3−8380
- $ErZn_{12}$, antiferromag., spin disorder resist., crit. effects and deviations from Matthiessen's rule 3−30450
- EuS, effect of mag. structure on thermoreflectance spectra 3−27512
- $(Fe, Ti, \square)_3O_4$, ferromagnetic-paramagnetic transitions 3−4735
- Fe complexes with abnormal mag. behaviour *(French)* 3−8354
- Fe-Co-V, Mossbauer spectra temp. depend., mag. transform. of γ phase *(Russian)* 3−30731
- Fe-Mn-C alloys, infl. of mag. transformations on physical props. *(Russian)* 3−2271
- Fe-Ni invars influence of Mn on some physical props. *(Russian)* 3−8355
- Fe-Ni shocked alloys, stability of mag. phase transition 3−36721
- Fe-Rh (52 at.%) alloy, optical behaviour at antiferromag.-ferromag. transform. *(Russian)* 3−18439
- Fe-Rh alloy, Fe-Rh-Ir alloy, antiferro-ferro, electronic sp. ht. obs. 3−34128
- Fe_3Al cluster in Alnico type alloy, ferromag. to superparamag. transition 3−8491
- $FeBr_2$, metamag. transition, magnetiz. variation with temp., press. and mag. field *(French)* 3−30615

magnetic transitions of substances continued
- $FeBr_2$, metamagnetic phase transition *(French)* 3−27368
- $FeCl_2$, antiferromagnetic resonance, high-pressure effects 3−18374
- $FeCl_2$.2py, 10.5K, Mossbauer obs. of ordering 3−21344
- $FeGe_2$, elastic consts. temp. depend. rel. to antiferromag. transition 3−5105
- Fe_2GeS_4, cryst. and mag. structs. at 85 K and 4.2 K, mag. transitions *(French)* 3−27373
- Fe_2O_3, angular depend. of field-induced antiferromag. to weak ferromag. transition 3−21228
- $Fe(Pt_xPd_{1-x})_3$ alloy, ordered, temp. effect, neutron diffr. obs. *(Russian)* 3−18308
- FeRh alloys, Mossbauer meas. of ferromagnetic-antiferromagnetic transition 0 to 700C *(Hungarian)* 3−8485
- $FeWO_4$-$MnWO_4$, mixed crystal, coexistence of two antiferromag. phases 3−34124
- $(Ga_{1-x}Zn_x)Mn_3C$, first and second order transitions as function of comp. *(French)* 3−30631
- Gd, second mag. phase transition, molecular field model to explain anomalies in props. 3−15366
- Gd-Y alloys, hydrostatic pressure effect on mag. transition temp. 3−2273
- $GdAlO_3$, spin dynamics near spin flops transition, antiferromag. reson. obs. 3−2401
- $GdCl_3$, ferromagnet with long-range interactions, crit. exponents 3−34121
- GdFe garnet, anomalous u.s. attenuation near compensation temp. 3−2275
- $Gd(OH)_3$, cooperative transitions rel. to mag. specific heat 3−34117
- $GdPO_4$, mag. susceptibility curves anomalies at high temps., n.m.r. obs. 3−30707
- $HoCo_2$, hyperfine specific heat meas., mag. moment determ. 3−34123
- $HoFe_3$, coercive force, remanence and hysteresis near mag. compensation point *(Russian)* 3−8380
- $LiCuCl_3.2H_2O$, magnetic transition rounding and Pippard's relations 3−30619
- Mn-Cu-Co nonmag. Elinvar-type alloys characteriz. 3−37074
- MnAs, ferro-paramag. transition, under the influence of light pulses *(Russian)* 3−2274
- MnAs, in strong mag. field *(Russian)* 3−8364
- Mn_2As-Mn_2Sb system, neutronographic investigation of magnetic transformations *(Russian)* 3−2291
- $MnCO_3$:Fe^{2+}, weak ferro-to antiferromag. transition at 2%Fe. 3−2289
- $MnCl_2.4H_2O$, crit. exponents α and α', high-resolution specific-heat meas., reanalysis of data 3−2279
- MnF_2, magnetic transition rounding and Pippard's relations 3−30619
- MnF_2, spin flop domains, n.m.r., Faraday rotation, photographs and optical-absorption spectroscopy investigation 3−34113
- Mn_3Ge_2, metamagnetism and mag. props. in pulsed mag. fields *(Russian)* 3−12015
- $Mn_{3-x}Ni_xB_4$, spontaneous and saturation magnetization, and transitions *(Russian)* 3−8396
- MnTe, antiferromagnetic transition 3−15365
- $MnWO_4$-$FeWO_4$, wolframite, mag. phase diagram, molecular field approx. 3−34125
- $(NH_4)_xFeF_3$ Mossbauer effect study *(French)* 3−8488
- Na_2NiFeF_7, paramag. to ferrimag. transition 3−2301
- Ni, crit. exponent β determ. from ^{57}Fe Mossbauer effect 3−2477
- Ni alloys, conc., elec. resist. meas. rel. to crit. cones for mag. transitions 3−4993
- Ni solid soln., giant moments near ferromag. to paramag. transition 3−36716
- Ni-Al, mag., thermal and elec. props. showing phase transition *(French)* 3−8361
- Ni-Pt alloy, high press. and high field props., near crit. conc. for ferromagnetism 3−30622
- $NiCl_2.6H_2O$, magnetic transition rounding and Pippard's relations 3−30619
- $NiCr_2O_4$, elastic props. and cooperative Jahn-Teller phase transition 3−24181
- $Ni(IO_3)_2.2H_2O$, heat capacity maxima, exchange parameter, 1−30 K 3−8360
- NiS, antiferromag. semimetal to paramag. metal transition 3−36540
- NiS_2, non-stoichiometry influence on elec. and mag. props. 3−2017
- $Ni_xZn_{1-x}Cr_2O_4$, elastic anomalies near cooperative Jahn-Teller transitions 3−2014
- $NpC_{0.91}$, sp. ht. and derived thermodynamic props. rel. to mag. ordering 3−24566
- $PbMo_2O_4$, 63K *(Russian)* 3−8397
- Pr, antiferromag.-paramag. transition effect on mag. resistivity 3−8356
- Pr, high field magnetisation, first order transition, nonmagnetic to metamagnetic phase due to crossing of crystal field levels 3−21221
- $PrCu_6$, nuclear adiabatic demagnetisation, 2.7-40 mK, transition 3−36709
- Sm, neutron diffr. study 3−24577
- Sm and Sm_2O_3, susceptibility temp. depend., 0-1500K *(French)* 3−8353
- $SmFe_{0.67}Ge_{1.33}$:Sm^{3+}, paramag. to antiferromag. transitions 3−2290
- $SnMn_3C$, first order mag. transition at 292 K *(French)* 3−15362
- TbAl antiferromag. garnet, molecular field approx. of two-singlet model for metamag. transition 3−27341
- $TbAsO_4$, paramag.-antiferromag., optical absorpt. study 3−2560
- $TbAsO_4$, paramag.-antiferromag., sp. ht. study 3−18316
- $TbPO_4$, mag. susceptibility curves anomalies at high temps., n.m.r. obs. 3−30707
- $TbVO_4$, molecular field approx. 3−2277
- $TmVO_4$, molecular field approx. 3−2277
- $UAs_{0.75}Se_{0.25}$, metamagnetic transition 3−38975
- UAsY (Y=S, Se, Te), electrical resistivity rel. to ordering 3−15175
- $(V_{1-x}Cr_x)_2O_3$, ceramic, paramag. insulator to antiferromag. insulator to metal transition 3−27744
- VO_2, doped, monoclinic-tetragonal transition behaviour, mag. phenomena 3−15000
- V_2O_3, metal/antiferromagnetic insulator transition effect of non-stoichiometry and Ti-, Cr- and Fe- doping 3−18091
- V_2O_3:Cr, Hubbard model, phase stability 3−15344
- V_nO_{2n-1} shear struct. cpds., metal-insulator transition 3−18090

magnetic transitions of substances continued
  $V_{1-x}W_xO_2$, susceptibility, 80-400K, rel. to semicond.-metal transition 3−18205
  Yb, Hall effect study through f.c.c.-h.c.p. transformation 3−2059
  $Zr_{0.90}Mo_{0.20}Fe$, heat treatment effects 3−21649
  $Zr_{0.60}Nb_{0.40}Fe_2$, heat treatment effects 3−21649

magnetic traps
  see also magnetic bottles
  adiabatic motion in charged particle trap 3−14580
  Astron-like systems, relativistic electron beam driven plasma instabilities 3−20530
  axially symmetric, effect of elec. field on transfer processes 3−23902
  collinear plasma structures, force-free 3−1517
  combined spiral magnetic systems for plasma confinement *(Russian)* 3−17645
  configurations with shear and minimum mean magnetic field strength for plasma confinement *(Russian)* 3−14569
  helically symmetric l=2 and l=3 equilibria, plasma stability 3−20593
  hybrid stellarator fields with several values of l 3−38485
  injecting plasma methods into closed magnetic traps, review *(Russian)* 3−14570
  injection of low-energy electrons, laboratory model of earth's radiation belts 3−18901
  plasma, laser-produced, injection into a magnetic trap. 3−30004
  plasma (RF) decay in different field geometries 3−20609
  plasma confinement, design and modelling on toroidal surfaces of various types of spiral windings *(Russian)* 3−17646
  plasma confinement in the Poloidal Heliotron magnetic field 3−23901
  plasma electrical conductivity in strong electric fields, depend. on nature of trap 3−29940
  plasma electron cyclotron frequency, mag. field uniformity degree effect on radiation of harmonics *(Russian)* 3−14568
  plasma MHD wave traps in magnetic traps 3−20479
  poloidal, high β, Tokamak equilibria 3−20472
  poloidal and toroidal mag. fields in Doublet II 3−20588
  polytron, sheath formation at centre 3−20643
  spatially and sinusoidally modulated magnetic field, charged particle non adiabatic motion 3−20417
  spherical multipole, particle loss 3−20606
  stellarators, magnetic well depth determinaton 3−36195
  symmetric toroidal systems, particle diffusion due to fluctuations 3−38488
  theta pinch, initial plasma rel. to multipole cusp field 3−29998
  toroidal, for plasma confinement 3−36191
  toroidal plasma, MHD equilibrium equation, exact solutions 3−38491
  'Uragan' stellarator, development and fabrication of the magnetic system, mag. surfaces with high shear investigation *(Russian)* 3−14595
  weakly corrugated magnetic field, plasma expansion 3−20446
  well formation by plasmoid collision expt. study of force-free collinear structs. 3−29999

magnetic variables control
  rotating magnetic field control for bubble-domain experiments 3−6033

magnetic variables measurement
  see also fluxmeters; magnetic field measurement; magnetic permeability measurement; magnetometers
  ferrite, small size, Curie and compensation temp., using differential test device 3−37667
  ferromagnetic thin film, cylindrical, anisotropy dispersion meas. *(French)* 3−25819
  ferromagnetic thin film, cylindrical, anisotropy field meas. *(French)* 3−25818
  at high pressures and low temps., high pressure multiplicator and superconducting magnet combined system 3−5855
  hysteresis measurement at low temperatures, Ballistic method, apparatus design 3−9997
  induction, in steady magnetic field, apparatus with Hall convertors and automatic compensation 3−25816
  l.f., using r.f. biased pont contact superconducting device 3−9999
  magnetization pressure depend. meas. device *(French)* 3−6032
  plated wire store, angular anisotropic dispersion meas., pulse method *(Polish)* 3−30669
  small Hall constants *(Russian)* 3−9989
  susceptibility, Evans method, solvent density var. with temp., effect on mag. meas. 3−28613
  susceptibility, method involving specimens in sealed ampoules *(French)* 3−6031
  susceptibility in rock, phase resonant circuit, design and testing *(Russian)* 3−3158
  susceptibility meas. with commercially available milli-oerstedmeters 3−25813

magnetic wells *see magnetic traps*

magnetically ordered materials *see magnetic materials*

magnetisation
  see also demagnetisation; magnetisation process; magnetisation state
  Allende meteorite, natural remanent magnetization and thermomagnetic properties 3−16198
  bubble domains, orthoferrite crystal slices and epitaxially grown films, temp. depend. 3−36764
  carbonaceous chondrite meteorites, natural remanent magnetizations rel. to early magnetic field of solar system 3−13000
  catalysers, finely divided, ferromag., granulometry and metallic mass. from magnetisation/mag. field curve *(French)* 3−34171
  disc shaped ferromagnetic samples, demagnetisation on the surface 3−21264
  domain wall creep rate under unipolar field action along axis of hand magnetisation 3−38994
  ferrimagnet, coercivity behaviour nr. compensation temp. 3−36750
  ferromagnet, micromagnetism, Lorentz approx. 3−5083
  ferromagnetic material, direct recording of static curves *(French)* 3−19240
  ferromagnetic metal, exchange model and Fermi fluid approach *(Russian)* 3−15377

magnetisation continued
  Ferromagnetic plate, volume, surface spin and magnetostatic vibrations of magnetisation 3−30663
  ferromagnetic thin plate with easy plane type anisotropy, mag. reversals *(Russian)* 3−15388
  film, ferromagnetic, magnetoresist. rel. to domains and magnetisation vector angular dispersion 3−21052
  film, rel. to high speed switching, magneto-optical obs. 3−36740
  first order magnetic transitions, calc. of magnetisation curves *(French)* 3−30614
  Heisenberg model two-dimensional ferromagnet, spontaneous magnetiz., exchange interaction effects *(French)* 3−30587
  Ising anisotropic model, magnetisation, susceptibility, critical temp., crossover exponent, upper bounds 3−21201
  Ising model, finite three-dimensional, modifications of critical phenomena at second order phase transitions 3−8325
  Kittel structure and magnetic thin film, computer aided field distrib. calc. *(Polish)* 3−24584
  liquid crystal, proton spin thermometry at low fields in solid phase 3−2456
  lunar soils, remanent magnetisation 3−9510
  magnetic domains steady state motion 3−18343
  metals, parametric magnetization instability 3−27211
  permalloy electrodeposited films micron thickness, reversal of magnetisation by domain wall creep 3−38992
  pillow basalt from Juan de Fuca ridge, demagnetisation by sea floor weathering 3−15925
  Preisach distribution density model *(German)* 3−36769
  pressure depend. meas. device *(French)* 3−6032
  random XY model, one-dimensional, magnetic properties 3−34068
  rare earth cobalt permanent magnet alloys, magnetisation, anisotropy and coercivity, review 3−24595
  rare earth metals, high-field magnetisation 3−21221
  remanent magnetization vector direction and statistical properties of magnetic anomalies 3−25168
  scaling law equation of state at critical point free energy and magnetic field-temperature paths 3−27369
  steel, low-C, containing tungsten, thermomag. analysis of tempering behaviour 3−37050
  steel, low-density 9G28Yu9MVB type, phase comp. and props. 3−21662
  stochastic spherical model, critical behaviour 3−28993
  superconductor, hysteretic, magnetisation for complete field penetration, crit. state model 3−36669
  superconductor, magnetisation in dirty limit at T_c 3−15307
  superconductor, nonideal type-II, in field near H_{c2} *(Japanese)* 3−38931
  two-dimensional modelling with inhomogeneously magnetized bodies 3−5468
  water, static proton susceptibility change on n.m.r. saturation 3−2330
  Al, spontaneous magnetisation at cryogenic temp. 3−36762
  $Ba_3Co_2Fe_2O_4$ film, arc plasma deposited, sat. magnetis. obs. 3−36772
  $BaFe_{12}O_{19}$ film, arc plasma deposited, sat. magnetis. obs. 3−36772
  $Ba_2Zn_2Fe_{12}O_{22}$ film, arc plasma deposited, sat. magnetis. obs. 3−36772
  α-Ce, magnetisation, 1.7-80 K, elec. resist., 1.4−25 K 3−8143
  Co film, monocryst., struct. depend. *(Russian)* 3−18120
  Co single-domain powders with cubic anisotropy *(Russian)* 3−15390
  Co-Fe-Nb, semihard mag. alloy characteriz. 3−21279
  Co-Fe-Nb semihard mag. alloy development 3−21261
  Co_5Sm permanent magnet alloy, sintered 3−5097
  Cr_2SSeTe, meas. of molar susceptibility and molar spontaneous magnetisation, 80-600 K, determ. of Curie point *(Russian)* 3−12010
  Cu-Cr(Fe)(Mn) dil. alloys, ^{63}Cu n.m.r., impurity magnetiz. 3−2443
  Cu-Fe alloy, sp. Lt., magnetisation, effect of ordering and precip. 3−34166
  $DyAl_2$-$DyFe_2(Co_2)$, cryogenic temps. 3−18323
  DyCd, CsCl type compound, field depend. of magnetisation, ferromag. model 3−36758
  $Dy(Co_{2-x}Ni_x)$, $0\leqslant x\leqslant 2$, mag. props. anomalous behaviour in pulsed and static fields 3−2316
  DyNi intermetallic, mag. struct., neutron diffr. and magnetisation obs. 3−15376
  $Dy_{1-x}Th_xFe_3$, magnetisation vs. temp., lattice consts. vs. temp. 3−34164
  $ErFe_2$, and mag. anisotropy, 77-300K 3−5113
  ErGa, ferromag. props. 3−2319
  $EuEr_2Ga_{0.7}Fe_{4.3}O_{12}$ epitaxial film, for bubble domains, variation with growth temp. 3−34157
  EuS, EuSe and EuTe rel. to photoluminescence props. *(German)* 3−18495
  $Eu_xYb_{1-x}Sn_3$, Mossbauer effect and magnetisation meas. *(German)* 3−24594
  Fe, 5-295K, 0-14 kOe 3−2311
  Fe (100) single crystal film, ripple due to dislocation strain field 3−8399
  Fe single-domain powders with cubic anisotropy *(Russian)* 3−15390
  Fe-Al alloy powders, cold worked and annealed, temperature and field dependence 3−12040
  Fe-Co(Ni) alloy single-domain powders with cubic anisotropy *(Russian)* 3−15390
  Fe-Ni alloys, temperature dependent property for measurement errors compensation in magnetic devices *(German)* 3−15385
  Fe-Si alloys, 0-24%Si, effects of furnace cooling and water quenching 3−36776
  Fe-v alloy, temp. depend., spin-wave stiffness coeff. temp. depend. 3−2312
  FeGe, susceptibility, magnetisation meas. and magnetic ordering 3−18326
  α-Fe_2O_3, natural hematite rel. to mech. induced mag. anisotropy, Mossbauer obs. 3−5148
  $Fe_2(OH)_3$ amorphous gel, characterisation and phase transformation 3−5383
  $(Fe_{1-x}T_x)Be_2$, T = V, Cr, Mn, Co, Ni, low temp. sp.ht. and magnetisation, virtual bound states concept 3−39002

magnetisation continued
$K_2CuCl_4.2H_2O$ type crysts., n.m.r. obs. of microscopic and macroscopic behaviour 3−2420
$La_2Mn_3(NO_3)_{12}.24H_2O$ paramagnetic saturation investigation 3−18297
$Mg_{0.9}Fe_{2.1}O_4$ ferrite, cation redistrib. rates, oxidation effects, saturation magnetisation obs. 3−15387
$Mg_xTi_yFe_3O_4$ thermoremanence self-reversal rel. to composition and mechanism 3−24589
Mn-Al-B alloy, composition depend. 3−36744
MnBi-Bi eutectic, directionally solidified 3−36748
MnGaGe, ferromagnet, prep., struct., Curie temp., saturation magnetisation, mag. moments 3−21268
Mn_5Ge_3 film, from ferromag. reson. 3−27419
Mn_3NiN, mag. moment rotation of Mn in (111) plane, 180-266K *(French)* 3−2283
NH_4ClO_4, proton spin-lattice relax., second moment and magnetisation study, 1.5 to 100K 3−18384
$(NH_4)_2MnF_5$, linear chain antiferromagnet, weak ferromagnetism and anisotropy 3−30643
Ni, aerosol particles, coercive force and saturation magnetisation from 4.2 to 300 K 3−39006
Ni (100) single crystal film, ripple due to dislocation strain field 3−8399
Ni single-domain powders with cubic anisotropy *(Russian)* 3−15390
Ni-Co layers covering Cu wires, mag. and mech. treatment effect on mag. props. *(Rumanian)* 3−12043
Ni-Fe (100) single crystal film, ripple due to dislocation strain field 3−8399
Ni-Fe film, damped oscillations 3−36741
Ni-Fe film, two layers separated by SiO, magnetic coupling, transverse suscept. obs. 3−34174
$NiFe_{2-x}Al_xO_4$, spinel, in ferrimag. and paramag. regions rel. to thermal treatment 3−12033
$NiFe_2O_4$ film, arc plasma deposited, sat. magnetis. obs. 3−36772
Pd-Gd solid solutions, magnetic and crystallographic characteristics 3−8793
(Pr, Nd, Sm, Tb, Dy, Ho)Pb_3, low-field susceptibility, magnetisation, 3-300K *(French)* 3−18302
$PrNI_5$, thermal, magnetic and electrical props. 3−8357
$Rb_2CuCl_4.2H_2O$, Heisenberg b.c.c. ferromagnet nuclear quadrupole resonance obs. of magnetic interactions 3−27439
$Sm_{0.5}Pr_{0.5}Co_5$ strongly textured magnet prep. from magnetically anisotropic powders *(Russian)* 3−39375
TbGa, ferromag. props. 3−2319
YIG film, arc plasma deposited, sat. magnetis. obs. 3−36772

magnetisation process
see also Barkhausen effect; coercive force; remanence
anisotropic cylinder, magnetis. reversal, micromagnetics 3−36743
dynamics, controlled by magnetocryst. anisotropy 3−30659
ferromagnet, polyaxial, mag. texture influence on magnetisation, domain wall energy 3−30665
Kapiti phonolite of Kenya, palaeomagnetism 3−2916
magnetic aftereffect, for irreversible magnetization process in Rayleigh region, theory 3−18344
metal systems, real structure and migrational props., magnetic aftereffect obs. *(Polish)* 3−24212
paramagnet, uniaxial, longitudinal magnetization by transverse high freq. mag. field 3−34061
rare earth orthoferrites, magnetisation curves, reversal mechanism 3−38997
salt pseudomorph beds of Middle Cambrian age, West Pakistan, palaeomagnetism 3−2914
semiconductors, optically induced, birefringence 3−24593
South-Western Iceland, thickness of magnetic crustal layer 3−2854
thermoremanent magnetisation curves, thermoluminescence theory application 3−38989
Upper Miocene−Pliocene section in New Zealand 3−2915
B_2O_3-BaO-Fe_2O_3 glass, magnetisation curve displacement associated with magnet phase transformation 3−12020
Co-P film, high-coercivity, domain struct. and reversal processes 3−24592
Cu-Ni-Fe alloy, magnetis. reversal 3−36745
Fe cylindrical films, crossed alternating and steady mag. fields 3−36775
Fe whisker, with Landau domain struct. 3−36749
Fe-Ni invar alloys, effect on plastic deformation 3−14914
Mg-Mn ferrite films, remagnetization rate and mobility of domain boundaries *(Russian)* 3−8398
Ni, self-reversal of magnetization, temp. depend. *(Russian)* 3−27381
Pt-Mn-Sn alloys, saturation magnetization *(Japanese)* 3−8346
Sr ferrite, Al substituted, domain structure, demagnetis. effects 3−36747
U_3Se_4, cubic, obs. in fields up to 80 kOe and temps. to above T_c 3−15356
UTe, U_3Te_4, cubic, obs. in fields up to 80 kOe and temps. to above T_c 3−15356

magnetisation state
see also magnetic anisotropy; magnetic domains
cyclic steel plates, hysteresis, loss calc. 3−2313
ferrimagnet, isotropic two sublattice, applied magnetic field, quantum theory 3−38941
ferromagnet, cubic, interaction of surface magnetoelastic waves with elastic Rayleigh waves *(Russian)* 3−8410
at ferromagnetic crit. pts., dipolar interactions 3−30625
ferromagnetic film, domain wall creep in nonuniform fields, intrinsic fields influence *(Russian)* 3−36736
ferromagnetic film, with rough surface, spin wave spectrum and magnetization 3−18331
ferromagnetic metal, electron energy depend. on magnetiz. *(Russian)* 3−15181
ferromagnetic plate, magnetiz. oscillations spectrum *(Russian)* 3−30649
ferromagnetic plate, residual magnetization state, thickness effects *(Russian)* 3−8384
film, double-layer ferromag., magnetostatically-coupled, crit. curves, mag. reversals *(Russian)* 3−30650

magnetisation state continued
film, hypercritical, mag. field influence on ground state *(Russian)* 3−36699
film, subharmonic oscillations of magnetic and crit. curves *(Russian)* 3−15392
film, susceptibility during quasi-static reversals in alternating field *(Russian)* 3−30653
Heisenberg antiferromagnets with arbitrary interaction range, sublattice magnetisation at absolute zero 3−15326
Heisenberg classical ferromagnet, Monte Carlo calc. of scaling equation of state 3−34077
Ising ferromagnet, magnetic susceptibility and local magnetisation fluctuations 3−27346
magnesium titanomagnetite, (artificial) magnetic properties and self-reversal of thermoremanent magnetization 3−34154
Onsager-Yang-value of spontaneous magnetisation and relation to free energy 3−30589
particles, weakly nonspherical ferromag., Brown theorem 3−34172
Permalloy film, interrupted nsec. mag. reversals *(Russian)* 3−8382
Permalloy film, magnetiz. oscillations due to pulsed transverse field excitation *(Russian)* 3−24586
Permalloy film, nonuniformity of nsec. magnetization reversal *(Russian)* 3−8395
Permalloy film, obliquely deposited, mag. reversals, mechanisms *(Russian)* 3−30651
Permalloy film, spin wave spectrum, surface conditions influence *(Russian)* 3−30698
Permalloy film, with banded domani struct., mag. reversals *(Russian)* 3−8381
rare earth alloys, ferromagnetic, rel. to hyperfine fields 3−15317
rare earth cobaltide hydrides, RCo_5-H (R=La, Pr, Nd, Sm, Gd), rel. to hydrogen sorption 3−27357
spin waves, surface, energy detn. and consideration of surface anistropy *(French)* 3−12029
surface effects near ordering temp. 3−34118
TCNQ complexes, up to 70 kOe, 0.1-4K *(Russian)* 3−8332
thin films magnetisation direction distribution in band model 3−27352
uniaxial ferromagnet, in transverse mag. field, free energy, spatial magnetization fluctuation effects 3−18315
$Bi_{3-2x}Ca_{2x}Fe_{5-x}V_xO_{12}$ garnet system, porosities, hysteresis, resonance linewidths, inhomogeneity effects 3−18342
$Ca_xNi_{1-x}Fe_2O_4$ system, measurement for phase structure determination 3−8379
Co films with different texture perfections about [0001] axis, residual/saturation magnetiz. ratio 3−36731
$CoCO_3$, magnetisation density and magnetic structure at 4.2 K 3−38984
Cr complex, quadri-nuclear, mag. spec. ht. and magnetization, analysis *(Japanese)* 3−18345
Cr_2S_3, rhombohedral single crystal, sublattice magnetisation 3−12021
$CsCoCl_3.2H_2O$, neutron diffr. study 3−24568
Cu-Fe alloys, ageing characts., precipitate transform. 3−37075
p-$EuCr_2Se_4$, doped, temp. depend. 3−27385
Fe-Ni alloys, cold-drawn, magnetisation anomaly 3−12034
Fe-Ni alloys, invar-type, Young's modulus, temp. depend., recovery and recrystn. influence *(Russian)* 3−36773
Fe-Ni thin films, saturation magnetisation, crystal structure, phase dependence 3−8376
Fe-Pt (32-35 at.%) alloys, saturation magnetiz., isothermal annealing depend. *(Russian)* 3−15389
$FeBr_2$, metamag. transition, magnetiz. variation with temp., press. and mag. field *(French)* 3−30615
$FeBr_2$, press. depend. meas. *(French)* 3−6032
FePt alloy powders, ordered, anisotropy consts., saturation magnetiz., coercivity *(Russian)* 3−30652
Gd, Hall effect of polycrysts., 4.2K, 46 kOe 3−33874
$GdCl_3$, ferromagnet with long-range interactions, magnetisation meas. of crit. exponents 3−34121
$GdFe_x(Co_x)(Ni_x)$, spontaneous magnetiz., susceptibility, Neel model interpret. *(French)* 3−27358
$Gd_xTh_{1-x}PdIn$, 4.2-300 K 3−27364
$Gd_xTh_{1-x}PdIn$, 4.2300 K 3−27364
$HoFeO_3$, spin reorientation, 50-120 K *(French)* 3−27380
$KMnF_3$, antiferromagnetic resonance frequencies and sublattice magnetiz. for antisymmetric exchange interaction 3−8351
LiO_2-MgO-MnO-Fe_2O_3 ferrite powder, specific saturation *(Russian)* 3−15386
MgAl thin film, prep. and charact. for optical storage 3−36987
Mn-Al alloy powders, comp. and defects influence *(Russian)* 3−24587
Mn-Ga alloy powders, high-anisotropy, mag. reversals, domain boundary displacement *(Russian)* 3−36737
Mn-Ga alloys, plastically deformed, mag. hardness *(Russian)* 3−36735
MnBi film, high and low temp. phases, residual magnetization, temp. depend. 3−27384
$MnCO_3:Fe^{2+}$, spin system and moment exam., reln. to concentration 3−2289
MnGaGe, sputtered film, ferromag. and magneto-optical props. 3−36861
$Mn_{3-x}Ni_xB_4$, spontaneous and saturation magnetization, and transitions *(Russian)* 3−8396
$MnWO_4$-$FeWO_4$, spontaneous magnetisation irregularities, modified effective field model 3−34060
Nb, magnetic props. of type II supercond. at T=0 K 3−2222
Nb-based superconducting alloys, deformed, mag. microstruct. obs. 3−27331
Ni, crit. exponent β determ. from ^{57}Fe Mossbauer effect 3−2477
Ni, singularities, mag. transform. temp. range *(Russian)* 3−8383
Ni base fcc ferromag. alloys with Co, Fe, Mn and Cr, CPA and H-F approx. calc. 3−8328
Ni-Co film, electrodeposited, stripe domains *(Russian)* 3−30667
Ni-Ge alloy film, saturation magnetization, thickness depend. *(Russian)* 3−18123
Ni-Pt alloy, high press. and high field props., near crit. conc. for ferromagnetism 3−30622
Ni-Sm film, saturation magnetization *(Russian)* 3−27382
$PbMo_2O_4$, anomaly in magnetiz. curve *(Russian)* 3−8397

magnetisation state continued
  PdFe like alloys, influence of mol. field spatial fluctuations on low temp. props. 3−27365
  Rh-Fe-Mn, Rh-Mn, Rh-Fe alloys, low temp. meas. and comparisons 3−4990
  $SmCo_5$ powder, coercivity, grinding duration and method influence *(Russian)* 3−27731
  Tm_6Fe_{23}, meas. from 4.2 to 700K 3−21273
  V, magnetic props. of type II supercond. at T=0 K 3−2222
  $Y_{3-2x}Ca_{2x}Fe_{5-x}V_xO_{12}$ garnet system, porosities, hysteresis, resonance line width, inhomogeneity effects 3−18342
  YIG, temp. depend. near Curie point 3−38980
  $Zr_{0.80}Mo_{0.20}Fe_2$, heat treatment effects 3−21649
  $Zr_{0.60}Nb_{0.40}Fe_2$, heat treatment effects 3−21649

magnetism
  see also antiferromagnetism; band model of magnetism; diamagnetism; electromagnetism; ferrimagnetism; ferromagnetism; geomagnetism; Heisenberg model; Ising model; magnetic moments; magnetic monopoles; metamagnetism; paramagnetism; stellar magnetism; superparamagnetism
  coexistence of superconductivity and magnetism 3−38914
  cooperative phenomena, application of ultralow temperature techniques 3−35383
  lunar electric conductivity rel. to magnetic fluctuations in solar wind 3−25417
  magnetic electron gas, spin correlation and density response function 3−30586
  origin as Coriolis force from Thomas rotation 3−37853
  random XY model, one-dimensional, magnetic properties 3−34068
  surface activity centres revealed by electrical, magnetic and thermal diffusion decoration 3−15052
  symmetry props. of transport coeffs. of mag. crystals 3−34051

magnetization *see magnetisation*

magneto-optical effects
  see also Faraday effect; Kerr magneto-optical effect; magnetoreflectance; optical constants
  absorption and luminescence, anal. using mag. field depend. of exciton ground state energy 3−2034
  aliphatic amino acids, mag. circular dichroism, pH depend. *(French)* 3−12494
  alkali halide, impurity doped, review for Z-centres 3−8624
  aniline, gauge-invariant calculations in random-phase approximation 3−7119
  antiferromagnet, intensity of exciton-magnon transitions, strong mag. field effects *(Russian)* 3−8558
  benzene and derivatives, magnetic circular dichroism spectra 3−23567
  benzonitrile, gauge-invariant calculations in random-phase approximation 3−7119
  birefringent mag. material, optical contrast of inclined boundaries 3−18436
  bubble domain recording, orthoferrite crystal slices and epitaxially grown films, magnetisation, wallenergy, coercivity, temp. depend. 3−36764
  excitons, self-localised, recomb. luminesc. *(Russian)* 3−27538
  ferromagnet, light scatt. by magnons, two-magnon scatt. 3−39126
  ionic cryst., spectra of colour centres, electron-phonon interaction effects 3−2580
  light absorption by bound states of electron and phonon, in mag. field, calc. *(Russian)* 3−8560
  liquid crystal, cholesteric, driven modes in oscillating mag. fields, feasibility of light scatt. obs. 3−24024
  low temp.investigation of absorption spectra of solids 3−9998
  nonlinear theory in magnetised crystals and isotropic bodies 3−37978
  orthoferrite, struct. of bubble and ring domains obs. 3−34159
  orthoferrites, interference patterns, at domain boundary, theory 3−5116
  phase shifters, elect. controlled dispersive, theory 3−16910
  phenol, gauge-invariant calculations in random-phase approximation 3−7119
  L-phenylalanine, mag. circular dichroism, pH depend. *(French)* 3−29638
  polaron energy levels, electron-phonon interactions, magnetic and Coulomb field effects 3−36563
  positronium-spin conversion in solids 3−24396
  rare earth pnictides, optical electrical and magnetic props., review 3−11848
  rare earth-transition metal alloy amorphous films, magneto-optic props., applications 3−36857
  rotation, measurement apparatus 3−25734
  semiconductor, appl. of reson. electron-phonon interaction theory 3−4832
  semiconductor, interband magneto-optical transitions rel. to isotropic excitons 3−11869
  semiconductor, magnetoabsorpt. spectra, inelastic carrier-impurity interaction 3−5222
  semiconductors, optomagnetic waves, theory *(Russian)* 3−8559
  semiconductors, polar, resonant electron-optic mode coupling, magnetic fields 3−36564
  semimetals, optomagnetic waves, theory *(Russian)* 3−8559
  tetrakis (dialkylamino) titanium, rot. obs. of central TiN_4 group *(French)* 3−12120
  thermomagnetic writing, optimum film thickness, theory 3−16915
  tryptophan, mag. circular dichroism, pH depend. *(French)* 3−17419
  tyrosine, mag. circular dichroism, pH depend. *(French)* 3−17419
  AgCl, magnetoabsorption of indirect exciton 3−12143
  $BaF_2{:}Yb^{2+}$, f-d transitions, investigation 3−24682
  $CaF_2{:}Yb^{2+}$, f-d transitions, investigation 3−24682
  CaO, magnetic circular dichroism of F band 3−21451
  $CoCr_2S_4$, hot pressed, magneto-optic props., digital memory application 3−36858
  Cr complex, $2[Cr(en)_3Cl_3].KCl.6H_2O$, magnetic circular dichroism of first spin-forbidden transition 3−8600
  $CrCl_3$, specific magnetic rotation in crystal field bands 3−5179
  Cu_2O, obs. of exciton line splitting in mag. field, diamag. effects 3−12123
  Eu chalcogenides, ferromagnetic, semiconducting, band structure 3−38859

magneto-optical effects continued
  Eu chalcogenides, optical electrical and magnetic props., review 3−11848
  EuO:Fe film, thermomag. writing, optimum thickness calc 3−16915
  EuO(S, Se, Te), magneto-Raman scatt. 3−5208
  EuS thin films, study of spin-orbit coupling and exchange field 3−2323
  Fe garnets, magneto-optic light modulation at 1.064 μm 3−36856
  GaAs, circular polarisation of recombination light in weak mag. field 3−8660
  GaAs, magnetization of charge carriers and excitons by polarized light 3−4956
  GaSe, optical transmission in fields up to 93.5 kG, exciton behaviour, effective mass of electrons and holes, g-factors 3−30803
  n-Ge, free carrier Voigt magnetoabsorpt. 3−27486
  n-Ge, in Voigt config., microwave transmission 3−2522
  Ge, optical absorp. var. with mag. field intensity, determ. of band struct. *(German)* 3−34332
  n-Ge, Voigt magnetoabsorption at low temp. 3−30802
  $HgCr_2Se_4$, magnetoabsorpt. obs., temp. and field depend. at Curie point 3−12122
  n-InSb, reson. hole-TO and hole-LO phonon coupling, magnetooptical study 3−4831
  K excited vapour, in presence of strong electric field, electro-magneto-optical effects 3−17347
  $K_3Ni_2F_7$, two magnon scatt. at 35K 3−12119
  $Mg_xMn_{1-x}Fe_2O_4$ film, use as phase diffr. grating 3−36862
  MnAs, ferro-paramag. transition, under the influence of light pulses *(Russian)* 3−2274
  $MnBr_4^{2-}$, magnetic circular dichroism studies on d-d transitions 3−26662
  $MnCl_4^{2-}$, magnetic circular dichroism studies on d-d transitions 3−26662
  $MnFe_2O_4$, permittivity tensor, visible region, magnetooptic study *(Russian)* 3−8551
  MnGaGe, sputtered film, ferromag. and magneto-optical props. 3−36861
  MnGaGe film, Curie point writing with laser pulse, thermal and mag. profiles comparison 3−36860
  α'-$Mn_{0.85}Ti_{0.15}Bi$ film, props. 3−2521
  Na, magnetooptical meas. of equivalent width of D_2-line as function of magnetic field and optical depth *(German)* 3−4362
  $RbMnF_3$, antiferrodielectric, anisotropic light absorption, mag. ion Mn^{2+} transitions 3−30838
  $RbMnF_3$, cubic antiferromag., mag. dipolar splitting of exciton absorpt. line 3−30817
  SbI_3, absorpt., magnetooscillatory effect *(Russian)* 3−34329
  n-Si, anisotropic Voigt effect 3−18437
  Si, optical absorp. var. with mag. field intensity, determ. of band struct. *(German)* 3−34332
  SiC, 6H, interpretation of Dean and Hartman's (1972) data 3−21391
  Sm chalcogenide film, absorpt. spectra, mag. circular dichroism 3−2606
  SnO_2 single crystal, exciton magnetoabsorpt., meas. 3−39127
  $SrF_2{:}Yb^{2+}$, f-d transitions, investigation 3−24682
  $Y_3Fe_{5-x}Ga_xO_{12}$ garnet film, rel. to growth conditions *(German)* 3−5274
  $Y_3Fe_5O_{12}$, garnet Cotton-Mouton effect, internal stress effects, anisotropy 3−39128
  YIG, laser beam interact. with spin and magnetoelastic waves 3−36859
  YIG, light modulation applications, transducer applications *(German)* 3−12121

magnetoacoustic effects
  antiferromagnet, sound velocity mag. field depend. 3−21290
  antiferromagnetic phase of cryst. with ferromag.-antiferromag. transition, magnetoacoustic waves 3−21289
  antiferromagnets, parametric excitation of hypersound 3−34176
  cylindrical plasma oscills. near magnetoacoustic reson., transient behaviour *(German)* 3−7506
  cylindrical waves in magnetic-acoustic phenomena, influence of Hall effect *(Italian)* 3−30438
  Fermi fluid, two-component isotropic, e.m. props. *(Russian)* 3−21029
  ferromagnet, sound velocity mag. field depend. 3−21290
  ferromagnets, nonlinear magnetoacoustic resonance theory 3−8451
  numerical analysis application 3−32492
  paramagnetic crystal, spin $1/2$ system, acoustic wave rotation due to spin-phonon interaction 3−21286
  resonance, magnetoelastic instability, ferromagnetics, anisotropy effects 3−39010
  semiconductor, nondegenerate, crossed field acoustic amplification in strong mag. fields 3−11937
  semimetal, elec. cond. for ultrasound propagating parallel to d.c. mag. field., calc. 3−33927
  semimetal, u.s. absorpt. in external mag. field 3−21287
  solar wind plasma wave instabilities due to periodic electron motion 3−28134
  Bi, sound propag. in strong mag. field, phonon spectra singularities 3−30672
  Cr u.s. attenuation, field dependence, transverse spin density wave phase, polarisation domain relaxation processes 3−30675
  Cs, u.s. attenuation, mag. field depend. 3−8094
  Cu, open-orbit antiresonances, obs. and mechanism 3−27207
  Cu, polarisation dependence of shear-wave attenuation by open-orbit electrons 3−8092
  Ga, Fermi surface under pressure, quantum oscillations in magnetoacoustic absorpt. 3−33789
  Ga acoustic geometric and acoustic cyclotron resonances 3−8096
  Hg crystal, magnetoacoustic attenuation giant quantum oscills. 3−33784
  In geometrical resons., interpretation 3−4945
  n-InSb, highly doped, u.s. propag., longitudinal mag. field effects 3−38626
  InSb, u.s. attenuation rel. to mag. field *(French)* 3−27389
  n- InSb u.s. amplification anisotropy in mag. field at 77K model 3−18349
  Ni magnetoelastic attenuation at u.s. freqs. due to domain struct. rearrangement 3−21288

magnetoacoustic effects continued
- Pd, L-centred pocket of Fermi surface existence, magnetoacoustic evidence 3–8095
- TmFeO$_3$, magnetoacoustic echo in n.m.r. spectra, spin reorientation region 3–27391
- W, Fermi surface, high field magnetoacoustic investigation 3–20995
- YIG, ferroacoustic interaction with Rayleigh surface waves 3–24596

magnetocaloric effects *see magnetothermal effects*

magnetocrystalline anisotropy *see magnetic anisotropy*

magnetoelastic effects *see magnetomechanical effects*

magnetoelastic waves
- compression waves, propagation in weakly conducting magnetoelastic medium *(Russian)* 3–13601
- current-carrying rod inside cylindrical tube, longit. and flexural vibr. *(Russian)* 3–6274
- easy plane hexagonal ferromagnets, phenomenological theory of magnetoelastic modes 3–34138
- electro-conductive thin shells and plates, soln. by asymptotic integration *(Russian)* 3–28913
- ferrite, magnetoelastic coupling in presence of magnetoacoustic resonance *(Russian)* 3–12062
- ferroacoustic resonance, magnetoelastic instability, ferromagnetics, anisotropy effects 3–39010
- ferromagnet, cubic interaction of surface magnetoelastic waves with elastic Rayleigh waves *(Russian)* 3–8410
- ferromagnetic dielec. plate, instability of magnetoelastic oscillations 3–36777
- ferromagnetic plates, theory *(Russian)* 3–8405
- film, magnetoelastic interactions effect, on ferromag. resonance, application to Ni 3–34216
- film, magnetoelastic interactions effect on ferromagnetic resonance 3–34215
- magnetoelastodynamics, difference method for plane problem 3–6282
- magnon-phonon interactions 3–1757
- magnon-phonon selection rules, inelastic neutron scattering 3–34131
- in stressed conducting layer 3–10313
- CAVBIG, self-interaction of finite-amplitude waves 3–39035
- Dy, study of bulk and surface waves 3–21285
- MgFe$_2$O$_4$, excitation *(Russian)* 3–8411
- MnCO$_3$, interaction of hypersonic waves and spin waves in antiferromagnet 3–39008
- Tb, study of bulk and surface waves 3–21285
- YIG, interact. with laser beam 3–36859
- YIG, self-interaction of finite-amplitude waves 3–39035
- YIG film, phonon generation by ferromag. resonance 3–36794

magnetoelectric effects
- *see also galvanothermomagnetic effects; Hall effect; magnetoresistance*
- galvanomagnetic recombination effect in alternating electric and magnetic fields *(Russian)* 3–30499
- galvanomagnetic surface waves of short wavelength, nonlinear excitation theory 3–21060
- magnetophonon effect, oscillatory structure, resolvent analysis of longitudinal configuration 3–30497
- magnetophonon effect meas. in 15 kbar apparatus in v. high mag. fields 3–28507
- Matteucci effect, spontaneous, thermal stability expt. study 3–15185
- metallic thin film, mag. field and thickness depend., theory 3–30458
- metals, influence of magnetic breakdown on l.f. conductivity and weak damping electromagnetic waves 3–11887
- in quantizing wire, transverse galvanomag. phenomena *(Russian)* 3–8153
- semiconductor, coeff. determ. by one-point method 3–24454
- semiconductor, negative resist. due to trapping increase of deep centres with magneto-depletion 3–30490
- semiconductor thin film, mag. field and thickness depend., theory 3–30458
- semiconductor with non-parabolic dispersion law, in mag. field, high freq. cond. of hot carriers 3–2109
- semiconductors, degenerate, in large magnetic field diffusivity-mobility ratio, temp. dependence 3–27273
- semiconductors in h.f. electromagnetic and const. magnetic fields *(Russian)* 3–11911
- semimetal, elec. cond. for ultrasound propagating parallel to d.c. mag. field., calc. 3–33927
- thin slabs, self-contained derivation 3–11915
- Al, low temp. magnetothermoelectric power 3–2058
- BaCoF$_4$, low freq. resonances 3–18170
- Fe, cylindrical films, Procopiu effects study 3–36775
- Fe-Ni film, galvano- and thermomag. effects depend. on phase comp. 3–33873
- n-GaAs, temperature dependence, phonon drag effect, electron-acoustic phonon interaction 3–11913
- GaFeO$_3$ single crystals, magnetoelectric phenomena 3–30496
- InSb, galvanomagnetic effects, dependence on temperature and magnetic field 3–5021
- InSb:Fe, elec. and galvanomag. props., impurity levels and hole scatt. mechanisms 3–38844
- Te, electron irrad., lattice defects, galvanomagnetic props. 3–33934

magnetofluidynamics *see magnetohydrodynamics*

magnetogasdynamics *see magnetohydrodynamics*

magnetohydrodynamic conversion
- thermodynamics, with separation of one component liquid metal working agent ahead of generator 3–14489
- Ar, ionized, supersonic flow induced by shock wave *(French)* 3–29957

magnetohydrodynamic convertors
- conduction MHD pump, transition processes in closed liquid metal circuit *(Russian)* 3–20388
- critical cathode potential drop and current density at the arc transition 3–26903
- disc channel, plasma flow assuming nonuniform ionisation and recombination *(Russian)* 3–26874
- insulating and electrode materials, electrical cond. erosion and heat resistance in plasma jet 3–36206

magnetohydrodynamic convertors continued
- liquid metal MHD generator, hydraulic characteristics *(Russian)* 3–20389
- magnetised viscous conducting fluid motion between two plane electrodes in a transverse magnetic field, generator characteristics *(Russian)* 3–26834
- magnetoplasmadynamic arc used as plasma source, pressure and current effects on thermal efficiency 3–36204
- magnetoplasmadynamic arcs, anode losses, influence of magnetic fields 3–36203
- MHD generators, line-reversal temp. meas., temp distrib. effects 3–7558
- multichannel device, edge effects estimate *(Russian)* 3–20387
- optimum conditions for energy conversion in Faraday type channel *(Russian)* 3–7414
- plasma conductivity determ. 3–23906
- for student laboratory, easy to build 3–16359
- He two stage tube for MHD power generation expts., gas dynamic characteristics 3–20351
- K-seeded Ar plasma in nonequilibrium ionization state, determ. of characts. 3–33388
- KOH vapour, condensation, MHD generator 3–36414

magnetohydrodynamic generators *see magnetohydrodynamic convertors*

magnetohydrodynamic waves
- Alfven cyclotron resonance instability in mirror machines, collisional distribution 3–4644
- Alfven waves, Rankine-Hugoniot relations for thermal anisotropy calc. 3–12965
- Alfven waves in pulsars, instability *(Russian)* 3–16246
- antiferromagnetic semiconductors and metals, reson. between spin and MHD waves 3–34145
- boundary layer of elec. conducting fluid along flat plate, stability *(German)* 3–11444
- comet tail (type I) model, Kelvin-Helmholtz instability and growth rate of MHD waves 3–28164
- compressional Alfven, electrostatic sound and RF wave coupling in ionospheric plasma, characteristics of electric field from radiating antenna 3–21962
- Coriolis force in rotating magnetic astronomical bodies, dispersion relationship 3–33282
- diffraction of fast MHD waves, by plasma layer of a periodically varying density 3–17588
- dissipation of waves rel. to outer corona transition from collisional to collisionless protons 3–39602
- dissipation rel. to outer solar corona, collisionless protons and collisional electrons 3–31520
- dissipation rel. to outer solar corona, transition from collisional to collisionless electrons 3–31521
- dynamic stabilization with standing wave mag. fields in toroidal screw pinch 3–17657
- electrically conducting rotating fluid, Hall current effects 3–26871
- exact helical wave soln. in ideally conducting medium 3–14538
- gas, non-equilib., ionized, steady flow around sharp corners in crossed mag. field 3–11484
- graphite, pyrolytic and single cryst., Alfven wave propag. and damping, 35 GHz 3–30510
- high beta toroidal experiment, diffusing pinch configurations, MHD stability 3–17654
- interaction, accel. in shock tube driver unsteady expansion 3–38398
- interplanetary and magnetospheric Alfven waves 3–3128
- interstellar medium, nonlinear mode-mode coupling of Alfven waves 3–14537
- Landau damping in plasma, heating and acceleration 3–4657
- magnetoplasma, magneto-sound wave excitation 3–23836
- magnetoplasma, self-focussing of transverse waves 3–36158
- magnetosonic wave, large amplitude, interaction with plasma 3–20470
- magnetospheric tail wave penetration of polar cap, Pc2 pulsations 3–34844
- mode coupling, dynamic stabilization in toroidal screw pinch 3–17594
- model plasmasphere, asymmetric eigenmodes with non-uniform Alfven speed 3–34960
- non linear dynamics for coupled three plasmon processes 3–14539
- nonhomogeneous plasma, conductivity-type laser heating, spherical or cylindrical waves 3–36183
- nonlinear, solar wind electron plasma freq. fluctuations detection, Ogo 5 obs. 3–16132
- nonlinear modulation of waves in cold magnetized plasma, perturbation method exam. 3–11488
- oblique shock waves in high β plasma, MHD fluctuations 3–23876
- plasma, astrophysical, damping of MHD waves 3–3281
- plasma, collisionless, with isothermal electron press., nonlinear waves across mag. field 3–36164
- plasma, dense with nonequilibrium ions, stability to MHD waves 3–26878
- plasma, drift instability stabilisation 3–38446
- plasma, excitation by probe in hot magnetised plasma, sheath effect 3–38443
- plasma, fast, excitation, turbulent heating at lower hybrid resonance 3–36190
- plasma, interaction of T-layers with mag. field 3–26877
- plasma, magnetised, ‘switch-on’ shocks obs. 3–36165
- plasma, small amplitude waves, generalised polytrope law 3–29960
- plasma Alfven waves, effects of collisions and gyroviscosity on gravitational instability in a two component plasma 3–20490
- plasma cylindrically symmetric waves in the MHD approximation 3–20469
- plasma drift instabilities distorting the magnetic surfaces of Tokamak-type toroidal systems 3–38440
- plasma MHD anomalous absorption, heating effects 3–38470
- plasma MHD shock struct. in strong transverse mag., fields 3–29959
- plasma MHD wave traps in magnetic traps 3–20479
- plasma screw pinch, MHD mode coupling in dynamic stabilisation 3–20477
- plasma shock waves, structure and heating 3–17622
- plasma turbulent heating by MHD waves 3–20582
- plasma waves, effect of high frequency collisions 3–36168

magnetohydrodynamic waves continued
  plasmasphere, magnetoacoustic channel under dome *(Russian)* 3−3121
  polarisation properties by three-dimensional covariance matrix 3−12559
  propagation, anisotropic, inhomogeneities, valve effect 3−36129
  radial magneto acoustic oscillations of a plasma current discharge column, excitation, dynamic stabilisation 3−20478
  relativistic shock waves in fluid, Taub adiabat, astrophysical appl. 3−29920
  Rossby waves excited by travelling forcing effects 3−23774
  rotating plasma, relativistic MHD, propag. of Alfven and longitudinal sound waves 3−17589
  shock wave struct. in conducting gas in mag. field 3−7410
  shock waves, slow-mode, launching method, laboratory expt. and model 3−33353
  solar atmosphere Alfvenic motions, wave energy flux and bulk velocities 3−37313
  solar envelope, nonthermal turbulent heating by MHD pulses 3−31518
  solar flare-produced coronal MHD wavefronts rel. to Moreton's wave phenomenon 3−35050
  solar quiescent prominence, mag. instability propag. with phase vel. of MHD compressive waves 3−37323
  solar wind He^{+}, kinetic temp. and MHD wave dissipation effects 3−28139
  stability, propag. through uniform incompressible viscous gravitating fluid 3−17586
  sunspot oscillations and waves 3−31539
  transverse propagation in horizontal mag. field and vertical temp. gradient for Hg 3−11440
  Ar plasma, non-axisymmetric Alfven wave propagation 3−38445
magnetohydrodynamics
  see also electrohydrodynamics; magnetohydrodynamic waves
  accretion onto a rotating magnetic monopole, sub-Alfven flow 3−12930
  anisotropic turbulent flow in longitudinal field *(Russian)* 3−20385
  astrophysical magnetic field origin, turbulent dynamo mechanism 3−31503
  belt pinch, equilibrium and stability calc. 3−20592
  boundary layer, incompressible, separation parameter, dimension theory determ. 3−26806
  boundary layers, Ekman-Hartmann, nonlinear hydrodynamic and hydromag. spin-up 3−23732
  breeze, polytropic subsonic stellar winds, MHD flow 3−3328
  channel, convective heat loss and elec. cond. calc. 3−36131
  channel flow, effects of thermal radiation 3−14493
  channel flow, heat transfer 3−1427
  channel flow of electrically conducting Prandtl-Eyring fluid in magnetic and electric field *(German)* 3−38400
  closed cycle, specialist meeting at Eindhoven, The Netherlands (1971) 3−20394
  comet tail (type I) model, Kelvin-Helmholtz instability and growth rate of MHD waves 3−28164
  compressible conducting fluid, MHD laminar source flow between two parallel discs 3−26832
  conducting dusty gas, plane parallel flow in transverse mag. field 3−20379
  conducting gas in tube in strong axisymmetric mag. field *(Russian)* 3−14492
  conducting viscous fluid, shear flow instability 3−23763
  convective instability in changing magnetic field *(Russian)* 3−20386
  cosmic-rays in random magnetic field, breakdown of quasilinear derivation of kinetic equation 3−31480
  Couette flow between conducting walls with heat transfer 3−4609
  cylindrical blast waves in magnetogasdynamics, similarity solutions 3−33281
  cylindrical plasma oscills. near magnetoacoustic reson., transient behaviour *(German)* 3−7506
  diffusion of charged particles in random magnetic field 3−31495
  duct flows, fully insulated, variable-area rectangular ducts with small divergences, strong transverse mag. fields 3−11441
  duct flows, strong transverse magnetic field, variable area ducts with insulating walls 3−4608
  Earth's bow shock, interaction of interplanetary double-shock ensemble, MHD theory 3−12821
  Ekman-Hartmann, boundary layers, steady nonlinear 3−7441
  elastico-viscous fluid MHD free convection laminar flow along an infinite porous wall 3−20375
  electrical conductivity of Hg metal mixture in bubbly and slug flow regions 3−32941
  electrically conducting fluid, rot. action in rot. mag. field *(French)* 3−38402
  e.m. forces and power in secondary, circuit of induction pumps with lateral conductors *(Russian)* 3−7426
  energy loss in MHD channels due to partial shorting of Hall e.m.f. *(Russian)* 3−7438
  externally pressurized bearing, with converging film 3−1428
  flow, oscillatory, along infinite flat plate with variable suction 3−20392
  flow, plane heterogeneous shear, hydromag. stability 3−20378
  flow between rotating discs, effects of finite wall conductance 3−4604
  flow between two rotating disks 3−17547
  flow due to elec. current past sphere immersed in fluid 3−11442
  flow geometry 3−7411
  flow in a porous medium, universal stability 3−33305
  flow in coaxial circular MHD channels, effects of asymmetric magnetic field *(Russian)* 3−7420
  flow in rectangular duct with variable conductivity walls *(Russian)* 3−7435
  flow of conducting dusty gas, plane parallel, magnetic lines of force fixed relative to plate 3−36128
  flow with heat transfer over porous plates *(Russian)* 3−7431
  flowmeters with rectangular and circular channels, sensitivity *(Russian)* 3−6165
  free convective flow in vertical channel, stability analysis 3−38401
  fusion and plasma physics Vol.II (conference, Grenoble, France, Aug. 1972) 3−20413
magnetohydrodynamics continued
  gas stream mixing in transverse magnetic field *(Russian)* 3−7413
  gaseous mixtures acted on by magnetic field, stability of combustion *(Russian)* 3−2808
  gravitating fluid layer stability with mag. field perpendicular to boundary, astrophysical appl. 3−33357
  Hall currents effect on hydromagnetic flow near an accelerated plate 3−29898
  Hartmann flow, stability *(Russian)* 3−1423
  Hartmann flow stability *(Russian)* 3−26833
  heat transfer in Couette flow 3−29897
  helically symmetric equilibrium field, soln. 3−17587
  helically symmetric plasma equilibria, class 3−20591
  hydromagnetic stability of plane vortex sheet in finitely conducting fluid with coplanar magnetic field 3−33220
  hydromagnetic stability of spiral flows with density stratification 3−26835
  hydrothermomagnet, elementary theory 3−12039
  ideal magnetofluid, compressibility effect on vortex sheet stability 3−14494
  incompressible conducting laminar flow along a vertical wall, transverse mag. field effect 3−17546
  induction machine, estimate of influence of velocity profile *(Russian)* 3−7427
  induction pump, cylindrical, with cooled internal magnet core *(Russian)* 3−7439
  induction pump duct characteristics in dimensionless flow *(Russian)* 3−7424
  induction pump efficiencies *(Russian)* 3−7423
  inhomogeneous solar wind, interplanetary magnetic field *(Russian)* 3−3292
  instability of hydromagnetic perpendicular shock in inhomogeneous fluid 3−36130
  instability of toroidal system at high temperature 3−1518
  interstellar gas, cosmic ray effects on sound vibrations in presence of mag. field *(Russian)* 3−37478
  ion beam, injected into plasma transversely to magnetic field, relax. *(Russian)* 3−14517
  ionising shock waves, in a magnetic field, study of adiabatic curves *(Russian)* 3−26823
  isotropic plasma flow near rotating magnetised spheres, appl. to planets 3−23835
  jet mixing in longitudinal magnetic field *(Russian)* 3−14490
  jets in flow wake in longitudinal magnetic field *(Russian)* 3−7434
  Lagrange invariant in MHD involving the Hall effect *(Russian)* 3−17548
  laminar flow in plane duct, effect of travelling magnetic field *(Russian)* 3−7422
  laminar free convective flow over isothermal nonconducting plate in transverse magnetic field 3−38403
  laminar jet of viscous elec. conducting liquid, longitudinal mag. field effect *(Russian)* 3−20390
  laser plasma expansion, early-time model 3−38444
  linearized flows, finite conductivity effects 3−38404
  liquid, incompressible, viscous, flow near accelerated plate in mag. field 3−23773
  liquid crystal, nematic mesophase, MHD effects, n.m.r. obs. 3−36797
  liquid metal flow control by induction MHD apparatus *(Russian)* 3−20391
  liquid metal flow measurement, u.s. Doppler velocimeter 3−26040
  longitudinal edge effects with flow of liquid in travelling mag. field *(Russian)* 3−7430
  losses, in lithium cooled toroidal fusion reactor, limitations 3−4342
  lunar magnetic field generation 3−9509
  magnetic boundary layer theory 3−38377
  magnetic dipole emission in plasma with finite conductivity 3−26873
  magnetic neutral sheet system surrounded by cold, collisionless plasma 3−28071
  magnetic polytropes, hydromag. oscills. and stability determ. using variational method 3−31498
  magnetic Rayleigh problem, variational solution for a non-Newtonian power law conducting fluid 3−20377
  magnetic stars, rotating magnetosphere, simple relativistic model 3−31725
  magnetically rotated arcs, heat transfer in plasma systems 3−26866
  magnetised viscous conducting fluid motion between two plane electrodes in a transverse magnetic field *(Russian)* 3−26834
  magnetogasdynamic externally pressurized bearing with converging film 3−17549
  magnetogasdynamics, self-similar flows behind blast waves 3−26875
  magnetohydrostatic equil. analogy *(French)* 3−20374
  magnetospheric substorms, inertial magnetic field reconnection 3−34959
  magnetotail plasma flow meas., spin modulation in proton fluxes 3−12834
  multichannel conduction apparatus, edge eff. study near magnetic Reynold's number *(Russian)* 3−20387
  non-monatomic distribution of velocity in ducts with rectangular cross section *(Russian)* 3−7437
  non-stationary flow between parallel porous walls with heat transfer *(Russian)* 3−20380
  nonlinear distributed parameter systems, optimal control computation 3−6191
  nonlinear hydromagnetic dynamo problem, magnetic fields generation by convection 3−26837
  nonlinear thermal convection, in conducting Boussinesq fluid 3−7442
  nonstationary flow of viscoplastic media in plane channels *(Russian)* 3−20382
  nonstationary flow of viscoplastic media in plane channels at constant flowrate *(Russian)* 3−20383
  nonstationary flow of viscoplastic medium in plane channels *(Russian)* 3−20381
  nuclear fusion and plasma physics, research activities, overview 3−7015
  numerical simulation of equilibrium in Tokamak devices using eqns. of ideal MHD 3−20475

magnetohydrodynamics continued
opposed plasma streams, linear magnetic octupole, polarization interaction *(Russian)* 3—14579
optimum relations in induction liquid metal condenser *(Russian)* 3—7429
particle diffusion across a mag. field, large scale hydromag. turbulence effects, appl. to interplanetary mag. field 3—25428
particle motion in crossed e.m. fields with large Reynolds no. in conducting medium *(Russian)* 3—7432
pipe flow extremum principles, determ. of bounds for flow-rate 3—23776
plasma, collision dominated, turbulent magnetic fields evolution 3—29961
plasma, cylindrical with elliptical cross section conditions for stability of kink modes 3—20512
plasma, growth rates and spectra of axially symmetric MHD equil. 3—23837
plasma, inviscid perfect magnetized, variational principle 3—7507
plasma, ion viscosity and thermal conductivity, effect on drift velocity, MHD description 3—14547
plasma, rotating, tearing, tearing mode instabilities with Hall effect 3—20515
plasma, stability of two-dimens. equil. 3—23838
plasma, toroidal MHD equilibrium equation, exact solutions 3—38491
plasma belt pinch experiment, three fluid MHD code for dynamic phase 3—20665
plasma between electrodes, hydromagnetic energy principle application 3—38438
plasma current multipole with free boundary 3—23900
plasma focus device, Faraday rotation meas. with a ruby laser beam, comparison with MHD numerical code 3—20640
plasma high beta toroidal experiment, heating studies of Z, theta and screw pinches, comparison with third fluid MHD code 3—20560
plasma inhomogeneity in E×H fields *(Russian)* 3—11483
plasma instabilities, numerical analysis by finite element method 3—7508
plasma magnetic tearing, energy release, nonlinear limit 3—33354
plasma MHD computer code for influence of an axial antiparallel bias mag. field on energy transfer on high beta diffuse pinch 3—20559
plasma MHD source flows 3—38442
plasma on nonconducting walls of MHD channel *(Russian)* 3—14536
plasma pulsed acceleration, MHD model 3—33355
plasma resistive pinch, linear and nonlinear perturbation theory 3—20476
plasma screw instability 3—36178
plasma stability analysis in toroidal Z-pinch ZT-1 3—17593
plasma stability in Tokamaks, toroidal effects 3—20513
plasma stability of force-free fields with constant α 3—20474
plasma stability of helically symmetric l=2 and l=3 equilibria 3—20593
plasma tearing instability due to thermal effects 3—20514
polytrope with toroidal mag. field, non-radial oscill. and convective instability 3—37285
potential functions for incompressible viscous indefinite and electrically conductive fluid *(Italian)* 3—20373
pulsar theory, rotating magnetospheres, 3D solution 3—37428
pump with cross shaped active zone, motion of liquid *(Russian)* 3—7428
quasi-neutral heavy ion plasma, magnetic field confinement *(French)* 3—26894
quasistationary MPD thruster performance, theory and expt. *(Italian)* 3—36205
resistance coeff. of tube with change in cross-section in magnetic field *(Russian)* 3—7421
review of recent results and developments in theoretical mechanics and mathematical physics 3—16584
rotating fluids, MHD phenomena, NATO Advanced Study Institute meeting 3—26838
rotating fluids, review, applications to dynamics of Earth's core 3—20393
rotating magnetic stars, effects on stability and convective motions origin 3—35112
rotating plasma, relativistic MHD 3—17589
rotation of liquid in rotating symmetrical e.m. field *(Russian)* 3—7425
rotation of paraboloid in conducting fluid, exact soln. 3—23772
rotational discontinuities in anisotropic plasma, appl. to solar wind 3—29942
self-gravitating, non-rotating gas layer with stellar, mag. and cosmic ray components, linear stability anal. 3—28101
shear flow of non-Newtonian liquid with rheological power law *(Russian)* 3—7436
shocks, unified geometric and analytical treatment 3—38405
solar convection zone, dynamo action of the global convection 3—22014
solar convective zone hydrodynamics *(Russian)* 3—16130
solar wind, azimuthal structure near equatorial plane, MHD equations 3—25396
solar wind torque effects on rotation of Earth, upper limits 3—12558
spherical $\alpha\omega$-dynamos by variational method rel. to Earth dynamo model 3—37180
spheroids extracted along rotation axis by toroidal mag. field, astron. appl. *(Russian)* 3—36126
stability of Hartmann flow in channel with elastic walls *(Russian)* 3—7416
stability of semi-infinite plasma under Hall currents and friction with neutral atoms 3—4636
steady MHD channel flow with anisotropic conductivity, second order solns. 3—14487
steady rotation of MHD fluid within a cylindrical annulus 3—17545
steady transverse plane flows, compatibility eqn. 3—4605
stellar adiabatic stability for toroidal field 3—37376
streaming flow past a sphere at low Hartmann numbers 3—33280
sunspot cooling mechanism rel. to Carnot cycle and hydromagnetic interactions 3—39619
swirling flows, hydrodynamic and hydromag. stability, semicircle theorems 3—33279
thermal convection, magnetic inhibition 3—14442

magnetohydrodynamics continued
theta pinch devices, investigations of end losses, MHD code for calc. decay of plasma 3—20657
three-dimensional hydromagnetic disturbances generated by magnetic dipole in anisotropic plasma 3—26872
Tokamak equilibria with high β poloidal 3—20472
ST-Tokamak low freq. oscills., rot. and struct. 3—38461
Tokamaks with non circular cross section, numerical studies of MHD equilibrium and stability 3—20473
Tokamaks with non circular cross-section, stability and MHD equilibrium numerical studies 3—17592
toroidal belt-pinch, MHD simulation 3—38441
toroidal configs. with screw mag. axis, mag. line of force coord. reson. increase 3—7548
transient effects in bounded electrolytes 3—36132
turbulence with circular flow of liquid metal *(Russian)* 3—7415
turbulent Hartmann flow *(Russian)* 3—20384
turbulent pulsations in free boundary layers with equilibrium MHD flow in square tube *(Russian)* 3—7433
two dimensional turbulent flow in circular cylinder *(Russian)* 3—7417
two dimensional turbulent flow in rectangular prismatic tube with non-uniformly conducting walls *(Russian)* 3—7418
two dimensional viscous MHD, flow in coaxial channels *(Russian)* 3—7419
two-dimensional steady magneto-fluid-dynamic flows with orthogonal magnetic and velocity field distributions 3—33278
type I solar radio burst chains, prod. by collisionless shock waves in strong mag. field 3—28146
universe, model, filled with magnetofluid 3—39590
unsteady duct flow, finite element analysis 3—26836
unsteady flow between porous parallel plates 3—20376
variational approach, flow and heat transfer between conducting parallel walls 3—23775
viscoelastic fluid layer in mag. field, oscillatory convection 3—14479
viscous flow induced by an oscillating disc 3—26839
viscous incompressible fluid motion about plane plate in case of orthogonal field *(Italian)* 3—29896
viscous plasma, hydrodynamic instability of boundary in mag. field *(Russian)* 3—11494
D_2 arc, explosively driven, as energy source, hydromagnetic model, transport processes 3—36186

magnetomechanical effects
see also gyromagnetic effect; magnetoelastic waves; magnetostriction
Elinvar, Cr type, tempering influence on temp. depend. of Young's modulus 3—31084
Elinvar, Young's modulus temp. depend., ageing effect *(Russian)* 3—31055
ferromagnet, cubic interaction of surface magnetoelastic waves with elastic Rayleigh waves *(Russian)* 3—8410
film, magnetoelastic interactions effect, on ferromag. resonance, application to Ni 3—34216
film, magnetoelastic interactions effect on ferromagnetic resonance 3—34215
Invar, internal friction features in variable mag. field, magnetoelastic losses 3—30677
Invar, magnetovolume, effects, Curie temp. press. depend., localised electron model 3—38979
Invar, magnetovolume effect 3—2325
Invar, props. of internal friction mag. peak at 253K 3—30676
Invar alloys, mag. exchange contrib. to elastic consts., rel. to anomalous elastic props. 3—24597
magneto-elastic torsional vibrations of an orthotropic cylinder and cylindrical shell 3—19461
magnetoelastic interactions, application to Ising model, spin-phonon interaction 3—24598
magnetoelastic interactions in relativistic continua, constitutive theory 3—22722
magnetoelastic theory of soft ferromagnetic elastic solids of multidomain struct. 3—34155
Matteucci effect, spontaneous, thermal stability expt. study 3—15185
metal systems, real structure and migrational props., magnetic aftereffect obs. *(Polish)* 3—24212
Mu-metal, magnetomechanical props. by shear strain meas. technique *(German)* 3—35447
nonlinear magnetoelasticity, boundary problem *(Russian)* 3—3963
polarized elastic materials with electronic spin, relativistic approach to constitutive eqns. 3—12045
rare earth metal, rotationally invariant theory for magnetoelastic interactions effect on elastic constants 3—15401
spin waves, parametric excitation by magnetoelastic interaction with phonon pumping 3—27375
Co-Elinvar, meas. of thermal expansion and Young's moduli in 150-500°C range, obs. rigidity modulus of polycrystal *(Japanese)* 3—17896
$CsMnF_3$, antiferromag., magnetoelastic coupling and sound velocity 3—15400
Fe, cylindrical films, Procopiu effects study 3—36775
α-Fe, low temp. mag. relax. rel. to mag. aftereffect, susceptibility meas. 3—34168
Fe-Ni alloys, invar-type, Young's modulus, temp. depend., recovery and recrystn. influence *(Russian)* 3—36773
Fe-Ni thin films, crystal structure, phase dependence 3—8376
Fe-Ni-Cu ferrite, internal friction, delta E-effect and stress sensitivity in alternating magnetic field 3—39009
Fe-Si, internal friction features in variable mag. field, magnetoelastic losses 3—30677
$FeBr_2$, $FeCl_2$ tension, uniaxial, 4.2°K, metamagnetic properties, susceptibility, antiferromagnetism *(French)* 3—27390
Gd, elastic and inelastic behaviour in spin reorientation region, pressure effects 3—34116
Mn-Cu-Co nonmag. Elinvar-type alloys characteriz. 3—37074
Mn-Cu-Cr alloys, Elinvar props. 3—21291
Mn-Cu-Ni alloys, Elinvar props. 3—21292
Mn-Ni-Co elinvar-type alloys, meas. of Young's moduli at −150-400°C and rigidity moduli and hardness at room temp. *(Japanese)* 3—17897

magnetomechanical effects continued
Ni, dislocation motion in alternating mag. field, oscill. domain wall interactions 3—30674
Ni, flow stress rel. to mag. field, domain wall dislocation interactions 3—5125
Ni, influence of mechanical stresses in elastic deformation region on Barkhausen effect 3—38991
Ni, polycryst., magnetoplastic effect rel. to const. mag. field *(Russian)* 3—15399
Ni-Co alloy, flow stress rel. to mag. field, domain wall dislocation interactions 3—5125
Ni-Cu alloy, dislocation motion in alternating mag. field, oscill. domain wall interactions 3—30674
Ni-Fe(25 wt.%) films, domain boundary curvature and displacement, mag. field and elastic stresses influence *(Russian)* 3—30654
$RbMnF_3$, magnetoelastic mechanism of degeneracy lift in exciton absorpt. spectrum 3—30817
$RbNiF_3$, acoustic birefr. due to magnetoelastic interaction 3—34177

magnetometers
see also magnetic field measurement
autocompensated, superconducting and using current sheet technique 3—28607
direct recording, for static magnetisation curves of ferromagnetic materials *(French)* 3—19240
double resonance differential system, mobile instrument for geological field work 3—9370
electrostatic torquemeter, for mag. film measurement 3—256
ferromagnetic resonance, incorporating thin-film sensor, patent 3—10001
fluxgate. low level, sensor noise, comment 3—28609
magnetic resonance self-oscillating, for construction by student 3—16365
nuclear, E11-2, sensitivity 3—25906
ring core fluxgate sensor, theoretical output 3—28608
SQUID, applic. to n.m.r. detection at low temps. 3—2328
superconducting galvanometers for magnetometers, sensitivity considerations 3—6039
three-axis for balloon borne apparatus, with digital readout 3—12851
Bi_2Se_3 Hall effect magnetometer, for low temp. work 3—35446
Cs vapour, self oscillating, shift in output freq. 3—28612
He, with a.f.c., modulation waveform *(Russian)* 3—16464
He quantum, relaxation processes *(German)* 3—10000
^{87}Rb, narrow line, for high accuracy field meas. 3—5531
^{87}Rb, optically pumped, use for offshore magnetic surveys 3—260

magnetooptics *see magneto-optical effects*

magnetoplasma *see plasma*

magnetoplasmadynamics *see magnetohydrodynamics*

magnetoreflectance
alkali halides, U-centres, magneto-refl., Faraday rot., ellipticity 3—15476
n-PbSe, electron relax. time determ. 3—5207
Te, electron mag. levels from electric field modulated magnetoreflectance 3—2524
ZnO, interband, band struct. parameters detn. 3—27513

magnetoreflection *see magneto-optical effects*

magnetoresistance
see also Corbino effect
antiferromagnetic metal, magnetoresist. due to electron-spin scattering by s-d interaction 3—11886
diamond, semiconducting, high field magnetoresistance 3—11912
ferromagnetic metal, electron-phonon and electron-magnon scatt. effects *(Russian)* 3—15181
ferromagnets, isotropic, resistive anomalies at the critical point 3—21236
film, ferromagnetic, magnetoresist. rel. to domains and magnetisation vector angular dispersion 3—21052
graphite:Fe, oscillatory magnetoresist., charged impurity selective scatt. 3—11864
graphite, Shubnikov de Haas meas. rel. to carrier lifetime anisotropy 3—18168
graphite thin crysts., Hall coeff. and magnetoresist., field and thickness depend. 3—30554
III-V semiconductor, giant positive magnetoresist. in hopping conduction region 3—15197
magnetic semiconductors, band structure, transport properties 3—38858
magnetic thin films, magnetoresistance method of measuring H_k and H_c by a four-point resistance probe 3—32114
metal, transverse magnetoresist., interaction of conduction electrons with adsorbed atoms 3—15186
metallic thin films, determ. using Boltzmann equation *(Russian)* 3—30463
metals, high field magnetocond., coherent state representation 3—24411
negative, of ferromagnetic metals, due to spin fluctuations, spin Green function calc. 3—15182
oscillations, differentiating amplifier for measurement 3—18126
polar semiconductor, low field transport props. in quantising parallel mag. field 3—27276
porous glass, C-impregnated, thermometric props. at low temps. 3—5807
rare earth alloys, Kondo effect, role of crystal field 3—30446
semiconductor, doped, quadratic negative, simple model 3—33930
semiconductor, magnetoresistance, quantum and ultra quantum fields *(French)* 3—38860
semiconductor, periodic impurity distrib., diffusion scatt. theory *(Russian)* 3—8209
semiconductor, surface electron states, longitudinal magnetoresistance 3—33983
semiconductor, with two types of carrier *(Russian)* 3—2111
semiconductor and semimetal, Hall, magnetoresist., and drift mobilities, Boltzmann equation soln. 3—21098
semiconductor films, two-layer, quasisize effect 3—24457
semiconductors amorphous, and glasses, hopping, low field, single phonon contribution 3—36626
theory. electron motion wavefunction description *(German)* 3—33876
thin conductors, Shubnikov-de Haas effect 3—21054

magnetoresistance continued
Al, longitudinal magnetoresist., temp. and weak deform. effects 3—2056
Al, thermal magnetoresist., anisotropy determ. 3—24410
Al film, vacancy influence on transversal magnetoresist. at 4.21 K 3—30460
Au film, discontinuous on dielectric, depend. on sputtered film morphology 3—2061
Au-Cd(47.5 at.%) alloy, martensitic pretransformation phenomena obs. 3—18561
Bi, meas. at digital nitrogen temp. and high pressures rel. to polymorphic transitions 3—18122
Bi, semimetal-semicond. transition under press. 3—33822
Bi, thin films, longitudinal magnetoresistance meas. *(Korean)* 3—27246
Bi, under pulse conditions in strong crossed elec. and mag. fields 3—24453
Bi and Bi-Sb alloy powder compacts characteriz., 300-77 K 3—36593
Bi single crystal film, oscill. in longitudinal magnetoresistance 3—33875
Bi-Sb alloy, magnetoresist. oscillations 3—8206
Bi-Sb(30%), 8-300 K *(German)* 3—11916
$Bi_{1-x}Sb$, gapless state, magnetoresist., semicond.-semimetal-semicond. transition 3—33791
Cd at 78K, 200 to 300 kG, comparison with new theoretical predictions *(German)* 3—33876
n-$CdCr_2S_4(Se_4)$, negative magnetoresist. in Ga-doped samples 3—27267
n-$CdGeAs_2$, temp. and mag. field depend. *(Russian)* 3—2112
$Cd_xHg_{1-x}Te$, spin effects on Shubnikov-de Haas oscillations, semimetal-semicond. transition 3—33795
$Cd_xHg_{1-x}Te$ Shubnikov-de Haas oscillations, 77-120K 3—36628
$Cd_{1-x}In_xCr_2Se_4$, ferromag. semicond., negative effect at Curie temp. 3—33881
$CdIn_2S_4$ single crystal, DC cond., Hall effect and magnetoresist. meas. 3—33894
Co, open orbits domain and Fermi surface 3—18074
$CoCr_2S_4$, temp. depend., 77-450 K 3—27258
Cu, magnetic field and temperature dependence of induced torque, anisotropy of closed-orbit torque 3—11884
Cu alloy, meas. rel. to impurity scatt. of electrons 3—21055
Cu-Cr alloy, dilute, h.f. magnetoresist., 1.6-4.2K mag. field depend. 3—8156
Cu-Fe alloy, meas. from 0.4 to 20 K in high fields 3—36592
$Cu_{1-x}Au_x$-Fe(Cr), mag. field depreciation of Kondo magnetoresist. 3—33872
Eu chalcogenides, ferromagnetic, semiconducting 3—38859
Fe, Hall effect and magnetoresistance 3—38825
Fe-Co, Hall effect and magnetoresistance 3—38825
Fe-Cr, Hall effect and magnetoresistance 3—38825
Fe-Cr spinel, magnetoresist. anomalies at Curie point 3—30462
Fe-Ni(29.7 at.%) alloy, martensitic pretransformation phenomena obs. 3—18561
$FeCr_2S_4$, temp. depend., 77-450 K 3—27258
FeGe, antiferromagnetic hexagonal, Fermi surface electrical resistivity and magnetic ordering 3—18327
FeGe hexagonal single crystals, magnetoresistance between 4.2 K and 30 K 3—18328
n-GaAs, epitaxial films 3—24456
n-GaAs transverse, Gunn diodes, 300 to 800 K, carrier mobility, electron transfer between conduction bands 3—36624
n-GaAs:Cr, magnetoresist. and recombination instability in mag. field 3—30500
p-GaAs:Zn, magnetoresist. meas. rel. to impurity cond. 3—11914
n-GaSb, heavily doped, stress-induced changes of Shubnikov-de Haas amplitude, density-of-states tails calc. 3—30425
Gd, transverse magnetoresist., polycrysts., 46 kOe, 4.2K 3—33874
Ge, amorphous film, 78-450 K in fields up to 25 kG, impurity level effects 3—21095
p-Ge, galvanomagnetic effects in high electric fields *(Russian)* 3—11910
Ge, heteroepitaxial films, Hall effect and magnetoresistance *(Russian)* 3—11966
n-Ge, transverse magnetoresist. in quantizing mag. fields 3—15214
p-Ge double layer film, Hall coeff., elec. cond., transverse magnetoresistance thickness effects *(Russian)* 3—8284
p-Ge film, transverse magnetoresistance, size anisotropy effects *(Russian)* 3—8283
Ge films, amorphous, Zeeman splitting of localised levels model approach 3—15213
Ge layer, transverse mag. field influence on microwave transmission *(French)* 3—18174
p-Ge substrates, transverse, 80 to 300°K 3—8208
p-Ge:N, effect of impurity conc. 3—24440
In, electronic component of linear magnetoresist. in thermal cond., Corbino geometry study 3—11880
n- InSb, hot electron Shubnikov-de Haas effect 3—36623
n-InSb. meas. from 0.5 to 10K in mag. fields up to 5000 Oe. impurity cond. effects 3—38857
n-InSb donor deionisation, impurity cond., CW laser cyclotron reson., magnetocond., temp. depend. 3—15149
$(In_2Te_3)_x-(Hg_3Tr_3)_{1-x}$, influence of impurity compensation effect on negative magnetoresistance 3—27277
MoS_2 sputtered films 3—8282
Ni-Fe:H dilute alloy with high H conc., magnetoresistivity rel. to local mag. moments 3—8158
Pb, Hall effect and magnetoresistance 3—38825
Pb-Fe dilute alloys, spin-disorder resistivity meas. as function of temp. in 0-60 kOe 3—2057
n-PbTe, magnetophonon resonance, electron intravalley scatt. with phonon absorpt. 3—33931
PdMn, dilute ferromag. alloy, with acoustic and optic mode excitations 3—15184
PdRhNi, meas. from 1.5 to 4.2 K 3—21053
Pr, magnetic resistivity meas., 4K-ice point, effects of crystalline field 3—8356
Pt film. discontinuous on dielectric, depend. on sputtered film morphology 3—2061

magnetoresistance continued
- Pt island condensates on NaCl cleavages, Hall and Gauss effects *(Russian)* 3—2060
- Rh-Fe-Mn, Rh-Mn, Rh-Fe alloys, low temp. meas. and comparisons 3—4990
- Sb, magnetocond. tensor coeffs., temp. depend., 4.2-30K 3—15183
- Sn, thermal magnetoresist. and thermoelec. e.m.f., quantum oscillations 3—36591
- p-Te, rel. to anisotropic phonon coupling in magnetophonon resonance 3—7874
- p-Te, transverse and longit., impurity band like states, 0.4-4.2K 3—27275

magnetoresistivity *see magnetoresistance*

magnetosphere
- *see also radiation belts*
- 1968 March-April substorms, space-time dynamics of auroral electron spectrum 3—25255
- aa indices of magnetic activity, solar activity dependence 3—15926
- acceleration mechanisms rel. to auroral u.v. intensity height profiles and rocket spectrograph sensitivity 3—31447
- angular particle distrib., mag. drift shells for noon and midnight meridians 3—34957
- auroral arc electron acceleration between source plasmas, electron intensity meas. 3—25259
- auroral arcs, electron intensities 3—3040
- auroral electron precipitation, angular distributions 3—3139
- auroral particle precipitation patterns 3—3039
- auroral particles, photoelectric meas. 3—3141
- Balmer line emission from geocorona, nongalactic component meas. 3—28286
- bow shock, cyclotron drift instability 3—12835
- bow shock, interaction of interplanetary double-shock ensemble, MHD theory 3—12821
- bow shock crossing of Pioneer 6, reinterpretation 3—12838
- bow shock obliquity, binary index for assessing local character 3—12831
- bow shock wave, structure 3—12837
- Bullard-Gellman-Lilley dynamo model, nonsteady states 3—21918
- charged particles trajectory determ. in DR-currents belt formation 3—25303
- Cherenkov radiation prod. by electron beam injection into ionosphere 3—28058
- Cherenkov radiation produced by electron beam injection, coherent emission *(French)* 3—39548
- collisionless drift waves obs. 3—34958
- configuration changes, substorm growth phase, shift of nightside auroral oval 3—12817
- convection, auroral particle precipitation, Fermi acceleration 3—12777
- convection rel. to ring current 3—3127
- cosmic ray variations of magnetospheric origin, polar coupling coefficients *(Russian)* 3—12908
- current determ. using three-layer model of near-earth space 3—25265
- cyclotron resonance in geomagnetic field, intrinsic bandwidth 3—5523
- day-sector polar F-layer during magnetospheric substorm 3—31438
- dayside region, e.l.f. noise bands, auroral electron precip. 3—12778
- ducted propag. of *PP* micropulsations, *PP* dotting 3—5476
- dynamics and Pc5 geomagnetic pulsations *(Russian)* 3—3122
- East-West interplanetary mag. field component effect on currents equivalent to mag. perturbations *(French)* 3—12636
- electric and mag. dipoles in dielectric sphere, radiation resistance and reactance meas. 3—34926
- electric field measurements, critical review 3—3145
- electric field rel. to magnetospheric storms and charged-particle distrib. 3—25304
- electric field variations, relationship with auroroal activity and geomagnetic perturbations 3—16047
- electric fields and plasma convection, INJUN 5 obs. 3—3146
- electron and proton geomagnetic cutoffs, daily var. calculation for Fort Churchill using mathematical model for magnetosphere 3—12650
- electron intensity enhancement at 100 km due to interaction between whistlers propag. through plasmasphere and electrons 3—25308
- electron precipitation phenomena dynamics 3—28070
- electron precipitation spectra, pitch angles in outer zone 3—3138
- electrostatic electron cyclotron harmonic waves, turbulence, v.l.f. satellite obs. 3—16035
- electrostatic wave dispersion relation meas. technique 3—17604
- electrostatic waves interaction with local plasma particles, OGO 5 measurements 3—3152
- energetic plasma sheet electrons, spatial distribution at 24 Earth radii 3—12823
- equational region, lunar partial tides 3—2923
- equatorial current sheet 3—12841
- excitation of magnetospheric resonators rel. to surface magnetic field intensity 3—34956
- extended geomagnetic tail, simultaneous solar-wind plasma and magnetic-field meas. 3—12822
- field fluctuations and penetration of solar protons to low geomag. latitude 3—5527
- field-aligned currents in auroral and polar latitudes, satellite meas. 3—25307
- geocorona u.v. obs. from lunar based instruments 3—9623
- geomagnetic tail, equilibrium config. rel. to steady two-dimensional model 3—25298
- geomagnetic tail, mag. field determ. from model, drift pattern construction 3—31455
- geomagnetic tail, plasma sheet, force balance requirements 3—12843
- geomagnetic tail, quatitative model 3—9220
- geomagnetic tail, self-consistent, under static conditions 3—9344
- geomagnetic tail reconnection rate, solar particle obs. 3—16037
- geomagnetic wake, nonlinear waves arising from finite oscillation amplitudes 3—16048
- growth phase of magnetospheric storms, onset time determination difficulties 3—16041
- high energy solar protons, geomagnetic tail, access mechanisms 3—12816
- high latitude energetic particle phenomena, coordinate system 3—16036

magnetosphere continued
- high-energy charged particles rel. to v.l.f. radiation, Interkosmos 3 meas. 3—31444
- inner, electron density variations meas. by whistler dispersion obs. 3—18891
- inner radiation belt, high energy proton model 3—3149
- interplanetary mag. field influence, asymmetry rel. to Earth-Sun direction *(French)* 3—39553
- ions, energetic heavy, satellite observations during geomagnetic storm of 17 Dec. 1971 3—12659
- Kosmos-381 signal reception from magnetically conjugate regions 3—25297
- low temp. plasma meas. using electron beams 3—18893
- lunar photoelectron layer rel. to earth's geomagnetic tail and solar photons 3—16181
- lunar transient phenomena rel. to Earth-shine and bow shock of Earth's magnetosphere 3—39644
- magnetic and electric waves in space 3—3128
- magnetic field energy, rel. to neutral currents at boundary 3—25301
- magnetic field line motion, nonuniqueness 3—12846
- magnetic field observations, review 3—3142
- magnetic field var. during substorms, interpretation of ground-based and satellite observations 3—2932
- magnetic field variations, micropulsation frequencies 3—3150
- magnetic neutral sheet system surrounded by cold, collisionless plasma 3—28071
- magnetic pulsations within magnetosphere, review 3—21914
- magnetoacoustic channel under dome of plasmasphere *(Russian)* 3—3121
- magnetopause, diffuse boundary existence characterised by low proton fluxes 3—12832
- magnetoplasma, cold multicomponent, v.l.f.-e.l.f. radiation characteristics of 90°-phased crossed-dipole array 3—12842
- magnetosheath flow, bow shock, satellite plasma observations 3—12815
- magnetosheath plasma at low altitudes in dayside magnetospheric cusps 3—3130
- magnetospheric substorms onset, balloon X-ray and electric-field measurements 3—12651
- magnetotail boundary, low energy solar proton anisotropy changes 3—16046
- magnetotail current system, pressure and magnetic field considerations 3—12827
- magnetotail current system interaction with polar ionosphere rel. to S_q^p var. 3—31451
- magnetotail plasma flow meas., spin modulation in proton fluxes 3—12834
- magnetotail structure, substorm expansive phase 3—12649
- magnetotelluric model rel. to micropulsation field obs. 3—2927
- MHD exact helical wave soln., application to magnetosphere studies 3—14538
- mid-latitude electron density trough and v.l.f. radio emission during 25-27 May 1967 magnetic storm 3—21975
- model current sheet, stability rel. to finite transverse field and finite flow velocity 3—25299
- model plasmasphere, asymmetric eigenmodes with non-uniform Alfven speed 3—34960
- models, comparison with storm observations from Explorer 26 3—12844
- morphology of auroral-zone X-ray events, early morning electron precipitation 3—31445
- morphology of auroral-zone X-ray events, electron precipitation in midnight-morning sector 3—31446
- neutral sheets theory, substorms 3—3144
- non-stationary processes, phase methods for elimination of derivatives of electron content 3—25339
- nonstationary processes meas. using quantum freq. standards 3—34972
- outer, quiet-time and disturbed time config. near midnight 3—12833
- outer regions, electron and proton acceleration during polar substorms 3—34954
- parallel whistler mode instability unified picture 3—37242
- particle arrival at polar caps 3—3134
- particle drift motion, effect of electric field induced by time-dependent ring current 3—9343
- particle populations 3—3129
- particle precipitation and associated auroral emissions 3—15993
- particle precipitation over the auroral zones, a local-time survey 3—15994
- PC1 course, analytical study of wave normal *(French)* 3—25161
- Pc 1 waves, cyclotron amplification 3—9341
- Pc 4 and 5 micropulsation activity at the polar cusp, latitude dependence 3—12652
- pinch effect development in magnetosphere rel. to auroral breakup 3—34955
- pitch angle scattering into loss cone by cyclotron resonance, whistler modes-electron interactions 3—25306
- plasma convection, at geosynchronous orbit altitudes 3—3147
- plasma leakage from magnetotail to magnetosheath rel. to substorms 3—16042
- plasma processes 3—3126
- plasma sheet, balance of stresses rel. to structure and dynamics 3—12825
- plasma sheet, inner boundary dynamics during substorms 3—28072
- plasma sheet, spatial distrib. of magnetic field, diamagnetic effects at 60 Earth radii 3—12824
- plasma sheet electron precip., kinetic ion-exosphere model 3—25309
- plasma sheet structure and solar wind dependence at lunar distances 3—16038
- plasma sheet substorm behaviour, Vela satellite measurements 3—3154
- plasma transport process predicted by drift velocity meas. 3—16000
- plasma waves at conjugate points during December solstice, morphology 3—16045
- plasmapause, light-ion trough and main trough 3—16044
- plasmapause, OGO-V satellite obs., correl. with Pc 1 micropulsations, ground based obs. 3—31442
- plasmasphere, morphology and dynamics, satellite obs. 3—25310
- polar cap absorption events, intensity rel. to solar microwave bursts 3—34961

- **magnetosphere** continued
  - polar cusps, strong pitch angle diffusion 3−3123
  - polar substorm, longitudinal currents *(Russian)* 3−3120
  - polar substorms, excitation by northward interplanetary magnetic field 3−2933
  - polar-cap electric field distributions, rel. to interplanetary magnetic field direction 3−12829
  - polar-cusp region, auroral electron emission of Cherenkov radiation 3−15995
  - potential distrib. when cond. of ionosphere is longit. depend. 3−25302
  - potential electric field eqns., iteration method 3−25266
  - precipitating electrons, magnetic local time dependence, spectral index 3−12818
  - precipitating electrons during sudden commencement, latitude and time distributions 3−2930
  - propagation modes of radioelectric whistlers and gyroelectric echoes received at middle latitudes *(French)* 3−31441
  - proton density determ. from Pc 3 type geomag. pulsations *(French)* 3−39552
  - proton injection mechanisms 3−3131
  - proton pitch angle distribution, by position sensitive detectors 3−39555
  - proton-He, propag. of Pcl micropulsations 3−5477
  - quasi-stationary pinch effect rel. to structure of magnetosphere 3−25305
  - radiation belt slot region, pitch angle diffusion meas. 3−16033
  - radio emission *(Russian)* 3−39554
  - radiowaves, VLF, use in ionospheric research, review 3−18900
  - relativistic electron precipitation events, energy spectra 3−9342
  - ring current, self-consistent model rel. to dipole field and magnetopause 3−25300
  - ring current protons, instability beyond plasmapause during injection 3−12845
  - scintillations of cosmic rays inside magnetosphere, broad-band fluctuations 3−16081
  - shadowing of electron azimuthal-drift motions near noon magnetopause 3−3124
  - solar particle access 3−34953
  - solar particle injection at $25<E<250$ MeV 3−3132
  - solar proton entry at very high latitudes *(French)* 3−28069
  - solar proton entry into tail 3−3133
  - solar proton illumination of polar caps, N-S asymmetry 3−12830
  - solar proton intensity structure in magnetosphere during interplanetary anisotropies 3−9346
  - solar wind discontinuity interaction, effect of low shock and magnetosheath 3−31454
  - solar wind interaction, quiet time pressure changes causing geomag. field variations 3−5478
  - solar wind torque effects on rotation of Earth, upper limits 3−12558
  - structure, summary of 1969-1971 results 3−3125
  - structure and processes, conference, Cortina, Italy (1971) 3−3197
  - substorm development, coordinated observations 3−12826
  - substorms, inertial magnetic field reconnection 3−34959
  - substorms, longitudinal extension of electron precipitation 3−15983
  - substorms, pre-midnight asymmetry in 40 keV electron flux profiles 3−3137
  - substorms, relation between ground and distant magnetotail events 3−39556
  - substorms rel. to ionospheric total electron content enhancement in Southern auroral zone 3−31419
  - substorms rel. to solar wind/magnetosphere interaction, review 3−2931
  - sudden commencement absorption, quadruple conjugate pair observations of event on June 17, 1965 3−12794
  - surface determ. for inclination of Earth's mag. dipole 3−31453
  - tail, self consistent theory, stability 3−3143
  - tail hydromagnetic wave penetration of polar cap, Pc2 pulsations at pole 3−34844
  - trapped and precipitating protons above 100 keV, ESRO IA/B obs. at high latitudes 3−3136
  - trapped electrons, poleward boundary 3−3140
  - u.l.f. waves and particles, behaviour in magnetosphere 3−16049
  - v.l.f. phenomena rel. to wave-particle interactions 3−3153
  - v.l.f. signal amplification by Cherenkov resonance interaction 3−9345
  - v.l.f. transmitting facility for magnetospheric research 3−12867
  - v.l.f. waves, nonlinear hydrodynamic scattering in magnetosphere 3−31452
  - v.l.f. waves propagating through magnetosphere in non-ducted mode 3−21974
  - vortex sheet stability between magnetosphere-solar wind boundary 3−37324
  - wave-particle interactions, particle distrib. function changes rel. to gyroresonant interactions 3−3151
  - whistler side-band growth, non thermal electron population effects 3−15986
  - whistlers, transmission and reflection in ionosphere and lower exosphere at high latitudes 3−5519
  - whistlers obs. in plasmasphere 3−31450
  - X-ray substorms, high resolution energy meas. and temporal variations 3−3155
  - H^+ flux beteen plasmasphere and ionosphere. diurnal variation 3−16040
  - H^+ thermal ions, plasmasphere 3−3148
- **magnetostatic waves**
  - ferromagnetic plate, infinite, magnetostatic mode parametric excitation theory 3−8449
  - Ferromagnetic plate, volume, surface spin and magnetostatic vibrations of magnetisation 3−30663
  - YIG film, on grounded dielec. substrate, surface wave group delay time 3−8408
- **magnetostriction**
  - ferromagnet, amorphous, piezomagnetic effect possibility from spin wave studies 3−12030
  - ferromagnet, micromagnetic calc. of magnetoelastic effects 3−21284
  - film, anisotropy skew, theory 3−5122
  - highly anisotropic ferromag., mag. anisotropy and magnetostriction theory 3−24581
- **magnetostriction** continued
  - Invar, exchange interaction theory of magnetostriction, anomalous thermal expansion 3−18348
  - Invar, low thermal expansion due to large spontaneous magnetostriction *(German)* 3−34610
  - Kovar, mag. field and temp. depend., below 50K 3−5123
  - magnetisation curves calc. for magnetostriction exchange model *(French)* 3−30614
  - magnetostrictive ferrite, u.s. wave propagation consts., low temp. depend. 3−36367
  - Mu-metal, Joule magnetostriction meas. by shear strain meas. technique *(German)* 3−35447
  - paramagnetic and nearly ferromagnetic materials, magnetovolume effect 3−18351
  - steel, stainless, heat treatment depend. of characts. 3−24954
  - weakly ferromagnetic materials, magnetovolume effect 3−18351
  - Ag, Fermi surface stress derivative determ. 3−33779
  - Ag, oscillatory magnetostriction meas. rel. to stress depend. of Fermi surface necks 3−18350
  - Au, Fermi surface stress derivatives determ. 3−33779
  - Au, oscillatory magnetostriction meas. rel. to stress depend. of Fermi surface necks 3−18350
  - Cd, rel. to mag. field induced pseudo phase transition 3−24376
  - $Cs_2CuCl_4.2H_2O$, Heisenberg b.c.c. ferromagnet, nuclear quadrupole resonance obs. of magnetic interactions 3−27439
  - Cu, Fermi surface stress derivative determ. 3−33779
  - Cu, oscillatory magnetostriction meas. rel. to stress depend. of Fermi surface necks 3−18350
  - Cu-Ni alloy, forced, 77 K to Curie temp., 12-20 kOe 3−15398
  - Dy, rel. to coupling between lattice and spin waves 3−21285
  - Dy-Gd alloy, heavy rare earth metals behaviour *(Russian)* 3−5124
  - $DyFeO_3$, field depend., low temp. 3−34175
  - Er, antiferromag. sinusoidal, rel. to periodic variation of lattice parameter *(French)* 3−27388
  - Fe-Ni, f.c.c. alloy, pressure effect on Curie temp., rel. to magnetostriction anomalies 3−34126
  - Fe-Ni alloy spontaneous volume magnetostriction, lattice const., 4.2-1000 K 3−30671
  - Fe-Ni invars influence of Mn on some physical props. *(Russian)* 3−8355
  - Fe-Si alloy, effect of Ni surface film *(Russian)* 3−12037
  - Fe-Si alloys, 0-24%Si, effects of furnace cooling and water quenching 3−36776
  - $HoFeO_3$, field depend., low temp. 3−34175
  - $K_2CuCl_4.2H_2O$ type crysts., n.m.r. obs. of microscopic and macroscopic behaviour 3−2420
  - Li-ferrite, constants meas. in ordered and disordered states by ferrimag. reson. 3−8406
  - $Lu_2EuMFe_4O_{12}$ (M=Al or Ga) garnet, temp. dependence 3−21259
  - Mg ferrite, ferrimag. resonance obs. 3−30673
  - Mo, anisotropy and reln. to anisotropic strain dependence of orbital paramagnetism 3−8407
  - Ni, thermal variation of magnetostriction coeffs. 3−8409
  - Ni-Cu alloy spontaneous volume magnetostriction, lattice const., 4.2-1000 K 3−30671
  - NiO, antiferromagnetic, lattice distortion obs. by X-ray topography 3−30646
  - $Rb_2CuCl_4.2H_2O$, Heisenberg b.c.c. ferromagnet nuclear quadrupole resonance obs. of magnetic interactions 3−27439
  - Tb, rel. to coupling between lattice and spin waves 3−21285
  - Tm, antiferromag. sinusoidal, rel. to periodic variation of lattice parameter *(French)* 3−27388
  - Tm_6Fe_{23}, meas. with strain pickups 3−21273
  - V, anisotropy and reln. to anisotropic strain dependence of orbital paramagnetism 3−8407
  - W, anisotropy and reln. to anisotropic strain dependence of orbital paramagnetism 3−8407
  - $Y_{3-x}Ce_xFe_5O_{12}$, temp. depend., ferromag. reson. study *(Russian)* 3−12046
  - $Y_2EuMFe_4O_{12}$ (M=Al or Ga) garent, temp. dependence 3−21259
  - YIG:Ge substituted, ferromagnetic resonance obs. 3−5136
- **magnetostrictive devices**
  - CAMAC magnetostrictive readout, with Schottky memories, for use with spark chambers 3−28676
- **magnetostrictive microphones** *see microphones*
- **magnetostrictive transducers** *see magnetostrictive devices; transducers*
- **magnetothermal effects**
  - *see also galvanothermomagnetic effects*
  - ferromagnet, pyromagnetic effect, molecular field approx. 3−18125
  - ferromagnetic minerals from pumice fall deposit of Ontake Volcano, thermomagnetism 3−2928
  - ferromagnetic semicond., anomalous Nernst-Ettingshausen theory, electron scatt. by spin waves 3−36629
  - graphite, low-temp. Nernst-Ettingshausen coeff. due to phonon drag 3−2107
  - metal, field excitation by heat flow *(Russian)* 3−2207
  - plasma in inhomogeneous magnetic field under microwave fields 3−26888
  - superconductor, type-II, Righi-Leduc effect in mixed state 3−30570
  - temperature measurement applications *(German)* 3−255
  - thermoremanent magnetisation curves, thermoluminescence theory application 3−38989
  - Al, low temp. magnetothermoelectric power 3−2058
  - Bi-Sb(30%) Nernst-Ettingshausen effect 8-300 K *(German)* 3−11916
  - Cd, Nernst-Ettinghausen effect temp. depend. *(Russian)* 3−8154
  - $Co_2Mg_3(NO_3)_{12}.24H_2O$, magnetothermodynamics, heat capacity, entropy, magnetic moment, 0.5-4.2K, 90kG 3−30616
  - $CoS_{2-x}Se_x$, pyromagnetic obs. of magnetic phase transition 3−34110
  - $Cu(NO_3)_2.2^{1}._{2}H_2O$, specific heat, n.m.r. and magnetothermal expts. at the high-field phase transition 3−27370
  - $DyCl_3.6H_2O$, caloric and mag. props. 3−38976
  - $ErCl_3.6H_2O$, caloric and mag. props. 3−38976
  - Fe, Nernst-Ettingshausen effect, anomalies near Curie pt. *(Russian)* 3−12014
  - Fe-Ni alloys, invar-type, Young's modulus, temp. depend., recovery and recrystn. influence *(Russian)* 3−36773

magnetothermal effects continued
Fe-Ni film, galvano- and thermomag. effects depend. on phase comp. 3−33873
n-GaAs, temperature dependence, phonon drag effect, electron-acoustic phonon interaction 3−11913
n-GaAs Nernst-Ettingshausen effects in phonon drag region *(Russian)* 3−8232
p-Ge, anisotropy of magnetothermal conductivity 3−1842
$GeSb_2Te_4$, Nernest-Ettingshausen coeff., single cryst. characterisation 3−5279
H magnetised arc plasma, electron density distribution meas., Nernst effect *(German)* 3−38500
$InAa_xP_{1-x}$ solid solutions, compositions, transport properties, electron effective mass 3−33802
n-InAs transport phenomena, heavily doped, magnetothermoelectric power, Nernst-Ettinghausen coeff. 3−36608
InAs:Se(Te), transverse Nernst-Ettingshausen effect, temp. depend., electron effective mass determ. *(Russian)* 3−27250
InSb:Te, Se, S, transport phenomena, 77−300K, press. to 15 kbar 3−2096
MnAlGe film, self-demagnetisation during thermomag. writing 3−24407
Nb, sp. ht. field depend., entropy prod. and mixed state behaviour 3−8291
Ni, Hall and Nernst-Ettingshausen effects, anomalies near Curie pt. *(Russian)* 3−12014
Re, single cryst., and Hall effect 3−18127
Sb, Nernst coeff., 2-100K, phonon drag region 3−33932
p-Si, anisotropy of magnetothermal conductivity obs. 3−1842
Zn, Nernst-Ettinghausen effect temp. depend. *(Russian)* 3−8154

magnetrons
Gabor, kinetic plasma instabilities, expt. obs. 3−26892
multicavity, electron trajectories allowing for space charge 3−13769
plasma helical microwave source in high density high magnetic field regime, operating props. 3−29993

magnets
see also electromagnets; permanent magnets; superconducting magnets
double focusing uniform field magnet, with circular poles 3−19278
drift tube quadrupole, high gradient, for KEK linac 3−19257
hydrothermomagnet, elementary theory 3−12039
machined, method of corrosion protection during heat treatment 3−24956
magnet, improvements to increase energy from 19 to 22 MeV 3−16481
BaO ferrites, fabrication, effects of Bi_2O_3, sintering temperature *(Korean)* 3−21263

magnons
see also spin waves
alloy, ferromag. anomalous Hall effect, cond. electron scatt. on magnons *(Russian)* 3−36589
antiferromagnet, intensity of exciton-magnon transitions, strong mag. field effects *(Russian)* 3−8558
antiferromagnetic metal, magnon thermal cond. depend. of temp. and mag. field 3−36727
antiferromagnetic semiconductors, effect of magnon drag 3−38858
antiferromagnetic with substitutional impurities, magnon density of states calc. 3−8331
antiferromagnets, possibility of inverse Suhl instability processes by optical pumping zone boundary magnons excitation 3−24616
easy plane hexagonal ferromagnets, phenomenological theory of magnetoelastic modes 3−34138
Fermi liquids, role of paramagnons in anomalous specific heat 3−11772
ferromagnet, insulating, magnon-exciton bound states, Oguchi method 3−27376
ferromagnet, light scatt. by magnons, two-magnon scatt. 3−39126
ferromagnet, stimulated magnon generation, theory 3−34144
ferromagnet, two-magnon bound states 3−34139
ferromagnet with uniaxial anisotropy, calc. of magnon spectrum and spin wave damping 3−34080
ferromagnetic metal, electron-magnon scatt. effect on elec. resist. *(Russian)* 3−15181
ferromagnetic metals and semiconductors, fluctuations and scattering of electrons and neutrons by coupled magnons *(Russian)* 3−12032
ferromagnetic resonance, dynamic eqns., susceptibility calcs. 3−30701
Heisenberg antiferromagnet, rutile structure CoF_2, two-magnon neutron scattering 3−21197
Heisenberg antiferromagnet, rutile structure MF_2, (M=Ni, Fe, Co), two-magnon light scattering 3−21196
Heisenberg antiferromagnet, two magnon correlation, equation of motion and diagrammatic techniques 3−21198
Heisenberg antiferromagnet, two-magnon correlations, equation of motion study 3−21195
interacting magnon systems, finite temp. theory of parametric effects 3−5111
itinerant electron ferromagnet, electron-magnon interaction 3−21204
linear chain model, temp. depend. of localized magnons 3−15380
magnon-phonon interaction selection rule, inelastic neutron scattering 3−34131
magnon-phonon interactions 3−1757
metal, nearly ferromag., transport coeffs., electron-paramagnon scatt. contrib., temp. depend. 3−27235
microwave ultrasonic interactions, book contrib. 3−20819
neutron diffraction, review 3−24572
optical transitions, formulation of spin-depend. elec. dipole moment 3−21392
phonon scattering in solids, conference, Saclay, France (July 1972). 3−1739
semi-infinite gyromagnetic media, surface polaritons 3−36726
spectral props. of solids, numerical calcs. by integration over Brillouin zone 3−20983
Suhl magnon instabilities and parallel pumping, Green's function theory applic. 3−2300
thin films, density of states 3−27295
Van Hove singularities and zero-point slopes in mag. crystals 3−30383
Cr_2O_3, energies temp. depend., Bloch and Nagai methods calcs. 3−12028

magnons continued
EuO, magnons as dominant heat carriers in thermal cond. 3−7979
(Fe-Ni)-P-C amorphous alloy, electron-magnon interaction, rel. to resist. anomaly and Curie temp. 3−21234
$FeBO_3$, Raman scatt. from magnons and phonons 3−34358
FeF_3, Raman scatt. from magnons and phonons 3−34358
FeF_3, Raman spectra, phonon and magnon lines 3−5192
^3He-^4He solid, mass fluctuation waves, impurity effects on magnons, Green's function approach 3−36457
$KCoF_3$, first order phonon and magnon Raman scattering 3−27499
K_2CuF_4, rel. to temp. depend. of n.m.r. freqs. 3−24623
K_2CuF_4, two-dimensional ferromagnet, two-magnon excitation 3−30633
$K_3Ni_2F_7$, two magnon scatt. at 35K 3−12119
$MnCl_2.4H_2O$, antiferromagnetic, temp. dependence of proton spin-lattice relaxation time 3−39054
MnO, optical absorpt. spectrum, role of magnons and phonons *(Russian)* 3−15522
$NaNiF_3$, phonon and magnon light scattering 3−39148
α-O_2, crystalline, far i.r. absorption bands at 1.3 K, magnon and photon excitation lines 3−18449
Pr, magnetic exciton modes dispersion, neutron scatt. obs. 3−2302

Magnus effect *see fluid dynamics*
maintenance *see maintenance engineering*

maintenance engineering
deep submersible equipment, optimal maintenance policy 3−3239
Hot Fuel Examination Facility-North, Ill., USA, remote controlled repair facilities 3−17316
magnetic disc head flight height measurement technique 3−10577

Majorana forces *see nuclear forces*
majority algebra *see algebra*
Malter effect *see secondary electron emission*

man-machine systems
analysis of spectra *(Russian)* 3−22354
cloud tracking, digital picture processing 3−3198
man-computer graphic interaction, IBM 2250 c.r.t. as interface for interrogating oceanographic data files 3−3209
neurophysiology, -computer interface 3−16524

management
see also administrative data processing; research and development management
nuclear wastes, long term planning 3−35936
plutonium inventory control, nondestructive assay methods of material balance 3−19951
radioactive aqueous wastes, US Atomic Energy Commission's experience 3−35935
radioactive waste, from fuel reprocessing 3−19944
radioactive waste disposal, administrative and legal control 3−32961
radioactive waste disposal, environment, adverse effects *(French)* 3−32956
radioactive waste disposal, high level, in United Kingdom 3−32972
radioactive waste disposal, in France, experiences *(French)* 3−32960
radioactive waste disposal, in Germany 3−32971
radioactive waste disposal, information meeting proceedings, Paris (1972) 3−32953
radioactive waste disposal, planning 3−32974
radioactive waste disposal, progress 3−32959
radioactive waste disposal, symposium, Paris (1972) 3−32964
radioactive waste disposal, transport and handling systems 3−35948
radioactive waste disposal *(French)* 3−32954
radioactive waste disposal 3−32965
radioactive waste disposal control, aquatic environment critical path analysis applic. 3−32957
radioactive wastes, Japanese activities 3−32976
radioactive wastes, United States Atomic Energy Commission plans 3−32975
radioactive wastes, US Atomic Energy Commission's geological survey 3−32981
radioactive wastes from fuel reprocessing, current practices and future trends 3−32977
scanning electron microscope, book contribution 3−10128
water quality, OR applic. 3−35307

Mandelstam representation
bounds on s-wave scattering length and amplitude in terms of d-wave scattering length 3−4147
crossing-unitarity eqn., reformulation in terms of partial waves 3−10757
double spectral representation for invariant amplitude of binary collision process, box diagram amplitude 3−22996
dual amplitude with Mandelstam analyticity, high-energy and Regge asymptotic behaviour 3−4191
dual amplitudes with Mandelstam analyticity, dynamical representation, large angle and Regge behaviour 3−29231
gauge-independent electrically and magnetically charged Mandelstam field, construction of monopole theory with potentials 3−10615
parametric dispersion representation with three-channel symmetry, derivation of sum rules 3−10651
pion-Pomeranchukon cut model based on Mandelstam diagram 3−35816
pionic nucleon capture, angular-momentum analysis in terms of Mandelstam model 3−10970
Pomeron in dual models with Mandelstam analyticity 3−38060
reggeon-particle Mandelstam graph, eikonal approximation 3−17075
two-particle strong-interaction amplitudes, double-discontinuity 3−10625
π-Pomeranchon Regge cut calc. from Mandelstam diagram using Gribov's approach 3−10748
$\pi^0\pi^0$ scatt., optimal set of constraints between s and d waves 3−16961

manganese
alkaline earth sulphates, Mn-doped, radiational defects, thermolumimesc. study *(Russian)* 3−27581
atom in crystal, electronic config. from X-ray spectral obs. of Mn-Al system *(Russian)* 3−2602
diffusion and reaction profiles in pore waters of marine sediments 3−2940
diffusion in HgTe, 200-300°C 3−36441
diffusion in Zr 3−26507

manganese continued

- impulse lasers, expt. obs. *(Russian)* 3—35690
- ionisation balance, calc. for collisional ionisation, autoionisation, radiative recombination and dielectric recombination 3—11458
- ionisation equilib. calc. for solar atm. ions 3—18960
- nodule detection, pattern recognition 3—9381
- nodules on Timor, cretaceous, deep-sea, tectonic and olistostrome implications 3—9188
- paramagnetic, γ, generalised susceptibility, d electron, Hamiltonian band structure model, instability criterion 3—30602
- particles, oxid., electron microscope obs. of oxide-metal boundary 3—15076
- segregation in steel, influence on austenite transform. kinetics *(Russian)* 3—15682
- solar Mn abundance from theoretical line profiles 3—39615
- tris-sarcosine calcium chloride:Mn^{2+}, e.p.r. obs. of Mn^{2+} complexes 3—8433
- TSEE activator in BeO, dosimeter characteristics 3—28671
- u.v. absorption linewidths and lineshifts, pressure broadening and foreign gases effect *(French)* 3—17344
- vapour, determination of absolute conc. of atoms by atomic absorption *(Russian)* 3—23474
- X-ray K-absorption spectra *(Russian)* 3—18509
- AgCl;Mn^{2+}, thermoelec. power and heat transport meas. 3—18173
- Al_2O_3:Mn^{2+}, e.p.r., angular variation, forbidden transitions, spin Hamiltonians *(French)* 3—27404
- Al_2O_3:Mn^{3+}, acoustic e.p.r. spectra obs. 3—8427
- Al_2O_3:Mn^{3+}, elec. field effect on acoustic e.p.r. spectra 3—8428
- As-S-I:Mn^{2+} glasses, e.p.r. study 3—30686
- As-Te-I:Mn^{2+} glasses, e.p.r. study 3—30686
- $BaTiO_3$:Nb, Mn ceramic, semiconducting application as positive temp. coeff. thermistor 3—2152
- in $CaCO_3$, calcite cathodoluminescence, low-temp. effects 3—18502
- CaF_2:Mn, cathode ray coloration, alpha and beta centre form. 3—30121
- CaF_2:Mn, thermal and u.v. bleaching characts. of colour centres 3—7755
- CaF_2:Mn(Ce,Mn), cathodoluminescence, trapped hole diffusion 3—39197
- $CaSO_4$-Mn phosphor, thermoluminesc., excitation by low- and middle-energy protons 3—24757
- CdF_2:Mn^{2+}, ligand ENDOR obs. for F and Cd lattice nuclei 3—18394
- Cd_2PO_4F:Mn, Mn activated luminescence 3—2586
- $Co(NH_4)_2(SO_4)_2.6H_2O$:Mn^{2+}, e.p.r. study 3—15406
- CoNi:Mn, FeNi:Mn, local moments, n.m.r. of ^{55}Mn obs. 3—36799
- Cs_2SO_4:Mn^{2+}, e.s.r. spectrum, temp. depend. *(Russian)* 3—8437
- Cu:Mn, dilute mag. alloy, coupled local moment-conduction electron Bloch equation 3—34213
- Fe:Si, Mn, influence of impurities on supercooling *(Russian)* 3—24829
- Fe-Ni invars influence of Mn on some physical props. *(Russian)* 3—8355
- Fe-Zn supersaturated solid solution, influence on the precipitation behaviour *(German)* 3—2694
- $FeSi_2$:Mn, Co, semiconductor-metal transition resist., thermoelec. and Hall effect obs., 300-1400 K 3—33973
- Ge:Mn; Sb, recomb. wave current instability rel. to mag. field *(Russian)* 3—8180
- KCl:Mn^{2+}, off centre position of Mn^{2+}, e.s.r. obs., 4.2-77K 3—21307
- K_2ZnF_4:Mn^{2+}, electronic overlap contrib. to uniaxial anisotropy of Mn^{2+}, spin hamiltonian 3—34108
- MgO:Mn^{2+}, temp. depend. of hyperfine structure splitting 3—15143
- MgO-Al_2O_3 synthetic spinel, spectra, luminesc. of Cr and Mn in impurities, comp. depend. 3—34429
- Mg_2TiO_4:Mn^{4+}, Cr^{3+}, phosphors, luminescence *(Russian)* 3—36928
- γ-Mn, antiferromagnetic, n.m.r., of ^{55}Mn at 4.2 K in zero external field 3—15428
- α-Mn, paramag., susceptibility maximum phenomena 3—21215
- Mn nodules, hydraulic system for recovery from sea bed at great depths *(German)* 3—9407
- Mn/SiO cermet film, elec. resist. and struct. 3—27754
- Mn^{2+}, e.p.r. in Zn_2GeO_4 3—21297
- Mn^{2+}, in H_2SO_4 vitreous aq. soln., effect on spin-lattice relax. of H atoms 3—34186
- Mn^{2+}, in Rb_2MgCl_4, $Rb_2MgCl_2Br_2$ and Rb_2MgCl_3Br, e.p.r. study of struct. 3—27413
- Mn^{2+}, lifting of degeneracy of $^4E_{1g}$ level in antiferromag. insulator *(Russian)* 3—11994
- Mn^{2+}, phosphoresc. quenching of polyadenylic acid, temp. depend. 3—31279
- Mn^{2+}, substitutional and interstitial diffusion in AgCl 3—20888
- Mn^{2+} activated α-$LiAlSi_2O_6$, single crystal, polarised cathodoluminescence emission 3—39194
- Mn^{2+} e.p.r. in ZnHgSe(Te) mixed crysts. 3—2378
- Mn^{2+} in calcite, e.p.r. study of forbidden hyperfine transitions 3—2355
- Mn^{2+} in $CdGa_2Se_4$ and $CdGa_2S_4$, e.p.r. spectra meas. spin Hamiltonian description, g-values hyperfine constants, covalent bonding effect 3—12059
- Mn^{2+} ion, Zeeman pattern calcs. in octahedral or tetrahedral crystal field 3—2011
- Mn^{3+} in II-VI semiconductors, g-shift 3—2377
- MnBi films, apparatus for co-deposition 3—15607
- ^{54}Mn prod. by nuclear collisions of cosmic-ray Fe on interstellar H 3—39575
- NaCl:Mn, e.p.r. study of Mn centres 3—8441
- NaCl:Mn^{2+}, Fe, bulk crystals, phase transformations 3—4768
- NaCl:Mn^{2+}, forbidden e.s.r. transitions 3—27407
- NaCl:Mn^{2+}, meas. of charge acquired by dislocations and vacancy sweep-up 3—17843
- $NaNO_2$:Mn^{2+}, ferroelec., e.p.r. obs., allowed and forbidden hyperfine transitions 3—8430
- $NiK_2(SO_4)_2.6H_2O$:Mn^{2+}, electron paramagnetic resonance obs. 3—36788
- $Ni(NH_4)_2(SO_4)_2.6H_2O$:Mn^{2+}, electron paramagentic resonance obs. 3—36788

manganese continued

- $PbMoO_4$:Mn^{2+}, electric field effect in paramagnetic resonance 3—34195
- $RbMnF_3$, antiferrodielectric, anisotropic, mag. ion Mn^{2+} transitions 3—30838
- SnTe:Mn, e.p.r., localised mag. impurity interaction with free electrons 3—34192
- SnTe:Mn, growth transport props. rel. to mag. impurities 3—33882
- tris-sarcosine CaCl:Mn^{2+} e.p.r. investigations of ferroelectric phase transition 3—39109
- $ZnAl_2O_4$:Mn^{2+}, e.p.r. *(French)* 3—24611
- Zn_2GeO_4:Mn^{2+}, luminesc. rel. to free carriers prod. by sub-band-gap excitation, trapping effects 3—21467
- $Zn_xHg_{1-x}Se(Te)$:Mn^{2+}, e.p.r., rel. to band struct. 3—15409
- ZnS:Cu, Mn, Cl, film, doping in vacuum growth rel. to electrolum props. 3—15559
- ZnS:Mn, Cl, thermal quenching of luminesc., elec. field effects *(Russian)* 3—27555
- ZnS:Mn, e.p.r. obs. of cubic and axial sites 3—15414
- ZnS:Mn, ZnSe:Mn, phonon induced hyperfine fields, molecular orbital model *(German)* 3—15161
- ZnS:Mn^{++}, spin lattice coupling coeffs. of $3d^5$ ion in trigonal symmetry 3—39025
- ZnS:Mn^{2+}, wurtzite, optical and paramag. spectra, impurity site, cryst. field 3—21306
- ZnSe:Mn, e.p.r., defect and macroscopic defect obs. *(German)* 3—15420
- Zn_2SiO_4:Mn powder, quantitative electron microprobe anal. 3—30854

manganese alloys

- *see also manganese compounds*
- manganin type, characteriz. for precision resistors 3—24946
- Mn-Cu-Cr, Elinvar props. 3—21291
- AgMn:^{55}Mn, relaxation of local-moment nuclei 3—2437
- Al Zn Mg Cu alloy, fibrous struct. and susceptibility to contact corrosion *(German, English)* 3—24354
- Al-Mn, dil., n.m.r. spectra, satellite struct. interpret. 3—2431
- Al-Mn, supersaturated solid solns., annealing and diffusion kinetics 3—36438
- Al-Mn:Fe, dilute alloy, temp. depend. of impurity resist. 3—21048
- AuMn, localised spin fluctuation and Kondo system, resist. temp. depend. 3—36582
- Au_4Mn, micromagnetic to superparamag. transition, effect of atomic ordering 3—21229
- Cr-Mn, melt growth using directional solidification in ZrO_2 crucible 3—12291
- Cr-Mn alloy, equiatomic, paramagnetic scattering of neutrons 3—2254
- Cr-Mn-N austenitic stainess steel partial shape memory effect obs. 3—18677
- CrMnNiN austenitic steel, planar slip during plastic deformation *(German, English)* 3—24132
- Cu-Al-Mn, martensitic alloy, X-ray obs. of twin structure *(Russian)* 3—24130
- Cu-Al-Mn, martensitic transform., β'-phase deform. influence *(Russian)* 3—18560
- Cu-Mn, dil., n.m.r. of ^{63}Cu, spin-lattice relax. mechanism 3—2443
- Cu-Mn, dilute, in supercond. sandwich, mag. props. from supercond. proximity meas. 3—8341
- Cu-Mn dilute alloy single crystals, strain rate and temp. depend. of the flow stress 3—8898
- Cu-Mn-Sn, ferromag. beta phase, crystal structure and ordering 3—18324
- Cu-Mn(0.5 at wt.%), vacancy-impurity complexes study by positron annihilation 3—17868
- Cu-Ni(15 wt.%)-Al(3.5 wt.%)-Cr(2 wt.%)-Mn(3 wt.%), age-hardened, microstruct. characts. rel. to elastic limit and yield pts. *(Russian)* 3—15668
- Cu-Ni(20 wt.%)-Mn(20 wt.%), age-hardened, microstruct. characts. rel. to elastic limit and yield pts. *(Russian)* 3—15668
- CuMn:^{63}Cu, spin-lattice relax., nuclear spin diffusion 3—36800
- Cu_2MnAl Heusler alloy, β phase form. *(French)* 3—30964
- Cu_2MnAl Heusler alloy, order-disorder transform., crit. temps. determ. *(French)* 3—39306
- $Cu_{2\|x}MnAl_{1-x}$, mag. props. obs. by Lorentz microscopy 3—1545
- Fe-^{54}Mn, dilute alloy, hyperfine field nonalignment under mag. saturation, meas. at 25 mK 3—24565
- Fe-Co-Mn, cold worked, strain gauge factor and elec. resist. meas. *(Japanese)* 3—12399
- Fe-Cu-Mn system, semihard mag. reed switch material, heat treatment effect on mag. props. 3—36757
- Fe-Mn, γ-solid solution, self-diffusion and interdiffusion determ. *(Japanese)* 3—30994
- Fe-Mn-C, structural features of martensitic transform. 3—30976
- Fe-Mn-C, thermally cycled, long period stacking order structs. and phase transitions 3—15665
- Fe-Mn-C alloys, infl. of mag. transformations on physical props. *(Russian)* 3—2271
- Fe-Mn-Co, cold rolled, heat treatment effect on mag. props. *(Japanese)* 3—31077
- Fe-Mn-Ti, Laves phase comp. and struct., χ phase obs. *(French)* 3—39305
- Fe-Mn-X, martensitic transformation, alloying elements X effect on ε-Fe stability *(Japanese)* 3—18643
- Fe-Mn-Zn ferrite, internal friction, delta E-effect and stress sensitivity in alternating magnetic field 3—39009
- Fe-Mn(1 wt.%), creep strength 3—21640
- Fe-Ni-Mn, martensite morphology depend. on isothermal transform. temp. *(Russian)* 3—24878
- Fe-S-Mn, sulphide form. and brittleness, Mn conc. depend. *(French)* 3—27645
- $Fe_{1-x}Mn_x$, bcc alloy, electronic struct., CPA calc. 3—11999
- Mg-Mn ferrite films, remagnetization rate and mobility of domain boundaries *(Russian)* 3—8398
- α-Mn dilute alloys, paramag., susceptibility maximum phenomena 3—21215
- δMn-Al, disordered structure elucidation using X-ray intensity equation 3—14875
- Mn-Al binary system, shape and energy position of $K\alpha$ and $K\beta$ bands *(Russian)* 3—2602

manganese alloys continued
Mn-Al powders, comp. and defects influence on mag. props. *(Russian)* 3−24587
Mn-Al-B, magnetis. and coercive force, composition depend. 3−36744
Mn-Al(44 at.%), metastable phase form. *(Russian)* 3−30968
Mn-Cr, antiferromag., Neel temp. determ., elec. resist. meas. 3−34119
Mn-Cu, martensitic transform., shape memory effect *(Russian)* 3−5317
Mn-Cu-Co nonmag. Elinvar-type alloys characteriz. 3−37074
Mn-Cu-Ni, Elinvar props. 3−21292
Mn-Fe, antiferromag., Neel temp. determ., elec. resist. meas. 3−34119
Mn-Fe marine and freshwater nodules, thermomagnetic behaviour 3−25182
Mn-Fe-Al, splat quenched, decomposition mechanism 3−2712
Mn-Fe-Be system, n.m.r. of ^9Be in $Mn_{1-x}Fe_xBe_2$ 3−2436
Mn-Ga, plastically deformed, mag. hardness *(Russian)* 3−36735
Mn-Ga powders, high-anisotropy, mag. reversals, domain boundary displacement *(Russian)* 3−36737
Mn-Ga(32.5 at.%), metastable phase form. *(Russian)* 3−30968
Mn-Ni, multiphase structure form. on annealing 3−18594
Mn-Ni nonmagnetic Elinvar type alloys, heat treatment and cold working, mech. props. meas. 3−8894
Mn-Ni-Co elinvar-type alloys, meas. of Young's moduli at −150-400°C and rigidity moduli and hardness at room temp. *(Japanese)* 3−17897
Mn-Ni-Cr, Elinvar type alloys, Young's modulus, thermal expansion, hardness, heat treatments, cold working effects *(Japanese)* 3−8858
Mn-Ni-Fe, Elinvar type, Young's modulus, thermal expansion, hardness heat treatment and cold working effects *(Japanese)* 3−8859
Mn-Ru, antiferromag., Neel temp. determ., elec. resist. meas. 3−34119
Mn-Sn intermetallic cpd., crit. resolved shear stress, temp. depend. 3−34586
Mn-Sn-Pt, crystal structures, magnetic properties *(Japanese)* 3−8346
Mn-V, antiferromag., Neel temp. determ., elec. resist. meas. 3−34119
MnAl, superconducting critical fields, effect of Mn concentration 3−11972
Mn_2As-Mn_2Sb system, neutronographic investigation of magnetic transformations *(Russian)* 3−2291
MnBi, study using Kerr effect 3−2308
MnBi and $MnBi_{0.9}Sb_{0.1}$, mag. struct., neutron diffr. study 3−24573
MnBi fil, domain patterns, Faraday effect obs. 3−21272
MnBi film, low temp. mag. props. 3−27384
MnBi thin film formation study by elec. resistivity and X-ray diffraction *(Japanese)* 3−34005
MnBi-Bi eutectic, directionally solidified, mag. props. 3−36748
Mn_3Ge_2, metamagnetism and mag. props. in pulsed mag. fields *(Russian)* 3−12015
Mn_5Ge_3 film, ferromag. reson., g-factor, magnetisation, 0-45°C 3−27419
Mn_2Hg_5 neutron diffraction obs. of antiferromag. coupling 3−18329
MnMg-Al alloys, horizontal strip costing in stationary d.c. moulds, properties 3−12417
MnSb, and related compounds, electronic struct., zero-field n.m.r. obs. 3−27440
MnSb, distrib. of unpaired electrons, neutron diffr. obs. 3−24574
$MnSn_2$, antiferromag., effective mag. fields at diamag. Sn atoms 3−5153
Ni steels, 9%, modified, thermomech. treatment effects on low-temp. hardness and tensile strength, obs. *(Japanese)* 3−8860
Ni-Fe-Mn, disordered, mag. props. thermodynamic analysis near critical conc. *(Russian)* 3−2272
Ni-Mn ordered, mag. props., thermodynamic analysis near critical conc. *(Russian)* 3−2272
Ni_3Al, relative bond energies from field ion images 3−36272
$Ni_{1-x}Cu_xMnSb$, ferromag., anomalous line shift in n.m.r. 3−30704
Ni_3Mn, influence of annealing under load on struct. and props. *(Russian)* 3−15729
Ni_3Mn, order-disorder phase transition dynamics study, neutron scatt. meas. 3−38949
Ni_3Mn, ordering kinetics, influence of previous heat treatment *(Russian)* 3−31061
Ni_3Mn, X-ray K-absorpt. spectra *(Russian)* 3−18509
Ni_3Mn-based, ternary alloys, atomic distrib., rel. to electronic struct. *(Russian)* 3−26990
Pd-Mn, dil., ferromag. transition temp., resist. study 3−30624
PdMn, dilute, ferromag., magnetoresist. meas. with acoustic and optic mode excitations 3−15184
Rh-Fe-Mn, Rh-Mn, Rh-Fe alloys, low temp. meas. and comparisons of elec. resist., magnetoresist. and magnetiz. 3−4990
Ti-Al-Mn alloys, effect of hydrogen on fatigue behaviour and low strain rate embrittlement 3−24882
VMn, electronic structure, stability investigation by self-consistent KKR method 3−15335
Zn-Mn quench condensed films, supercond. transition temp. depression 3−34027

manganese compounds
see also manganese alloys
ferrites, electrical conductivity temp. depend. 10-100K 3−5001
Mn(II) complex,
ii), mol. and electronic struct. 3−7104
steel, MnS inclusions morphology 3−8788
steel, plastic deformation of MnS inclusions 3−8852
tetrabutylammonium tetrabromomanganate fused salts, phosphorescence in molten state 3−2582
tetrabutylammonium tetrachloromanganate fused salts, phosphorescence in molten state 3−2582
tetrabutylammonium tetraiodomanganate fused salts, phosphorescence in molten state 3−2582
$(CH_3NH_3)_2MnCl_4$, magnetic susceptibility meas., a quasi two-dimensional Heisenberg antiferromagnet 3−5098
FeMn deposits deep sea mining, environmental effects 3−3167
$Ga_xMn_yFe_{3-(x\|y)}O_4$, cryst. growth, Bridgmen method and characterization 3−12267
$KBr{:}MnO_4^-$, vibronic spectra obs. 3−8616

manganese compounds continued
$Li_xMn_yFe_{3-(x\|y)}O_4$, cryst. growth, Bridgman method and characterization 3−12267
$Mg_xMn_{1-x}Fe_2O_4$ film, use as phase diffr. grating 3−36862
Mn and Ti oxide mixtures, solar cell coverslide coatings, effect of u.v. charged particle irradiation 3−5924
Mn complex, methyl-, ethyl- and N-propyl-ammonium-tetrachloromanganate, two-dimens. paramag. behaviour 3−2369
Mn complexes, $Mn(CO)_5X$, ($X=H,CH_3,Cl,CN$), electronic struct. ab initio calcs. 3−29603
Mn-Zn ferrite, mag. props., solid state O_2 content depend. *(German)* 3−8344
Mn-Zn ferrites, low resistivity, resonant modes in ferromagnetic resonance 3−2398
MnAlGe, nonstoichiometric film, prep., structure, mag., and optical props. 3−36497
$Mn_3Al_2(GeO_4)_3$, mag. struct., neutron diffr. obs. 3−24569
$Mn_3Al_2Ge_3O_{12}$ garnet, antiferromag., mag. struct., neutron diffr. obs. *(French)* 3−21248
MnAs, ferro-paramag. transition, under the influence of light pulses *(Russian)* 3−2274
MnAs, mag. transform. in strong mag. field *(Russian)* 3−8364
$MnBr_4^{2-}$, magnetic circular dichroism studies on d-d transitions 3−26662
$MnBr_2.4H_2O$, heat capacity meas. near Neel temp., effect of chem. impurities 3−15367
$MnCO_3$, antiferromag., spin echo on ^{53}Mn, freq. and temp. depend. of line position 3−2457
$MnCO_3$, interaction of hypersonic waves and spin waves in antiferromagnet 3−39008
$MnCO_3{:}Fe^{2+}$, spin system and moment exam., reln. to concentration 3−2289
$MnCl_2$, lattice vibrations, i.r. and Raman spectra 3−30813
$MnCl_2$ in NaCl, kinetics of clustering 3−4750
$MnCl_4^{2-}$ magnetic circular dichroism studies on d-d transitions 3−26662
$MnCl_2.4H_2O$, antiferromagnetic, temp. dependence of proton spin-lattice relaxation time 3−39054
$MnCl_2.4H_2O$, high-resolution specific-heat meas., reanalysis of data 3−2279
$MnCo(CO)_9$, i.r. and Raman spectra meas. in CO stretching region, stretching modes, force consts. 3−36019
$Mn(CrFe)O_4$ ferrite, Mossbauer study, angular spin configurations of ^{57}Fe nuclei, compensation point, magnetic moments 3−36827
$Mn_3Cr_2Ge_3O_{12}$ garnet, ferrimagnetic props., intrasublattice exchange interactions obs. *(Russian)* 3−2266
MnF_2, conditions for formation and existence of α-PbO_2 type phase *(Russian)* 3−7935
MnF_2, excited-state exchange interaction, molecular orbital theory 3−36718
MnF_2, mag. susceptibility near T_n and Fisher's relation 3−38967
MnF_2, magnetic transition rounding and Pippard's relations 3−30619
MnF_2, photoemission, new multiplet struct. 3−36979
MnF_2, pure and LiF-doped, cryst. growth, modified Bridgman method 3−12273
MnF_2, spin flop domains, n.m.r., Faraday rotation, photographs and optical-absorption spectroscopy investigation 3−34113
MnF_2, temp. dependence of antiferromagnetic resonance linewidth 3−18373
MnF_2 high frequency acoustic waves attenuation on low-temp. side of Neel point 3−34112
$MnFe_{2-x}In_xO_4$, X-ray diffraction and γ-resonance obs. of spinel structure 3−24087
$MnFe_2O_4$, permittivity tensor, visible region, magnetooptic study *(Russian)* 3−8551
$MnFe_2O_4$, sintering in continuous kilns *(French)* 3−34623
$Mn_{1.9}Fe_{1.1}O_4$, cubic-tetragonal transition, cation valencies, Mossbauer obs. 3−1798
$Mn_xFe_{3-x}O_4$, i.r. spectra and cation distrib. 3−30807
$Mn_xFe_{3-x}O_4$ solid solution, cation distribution and local distortion 3−30729
$Mn_xFe_{3-x}O_4$, elec. resist. and Seebeck coeff., 100-1000K 3−5010
$Mn_xFe_{3-x}O_{4\|y}$, spinel, miscibility gap, annealing and X-ray diffr. obs. 3−30265
$Mn_{0.8}Fe_{0.2}[Mn_{0.2}Fe_{1.8}]O_4$, thin films, electron diffraction superlattice lines 3−38569
$Mn_3GaC{:}^{57}Fe$, Mossbauer obs. of paramag. and ferromag. spectra 3−12081
$MnGa_xFe_{2-x}O_4$, chem. and X-ray anal. of inhomogeneity *(Russian)* 3−14971
MnGaGe, ferromagnet, prep., struct., Curie temp., saturation magnetisation, mag. moments 3−21268
MnGaGe, sputtered film, ferromag. and magneto-optical props. 3−36861
MnGaGe film, Curie point writing with laser pulse, thermal and mag. profiles comparison 3−36860
$MnGeN_2$, position parameters of Mn and N atoms, mag. struct., moments orientation *(French)* 3−8370
MnH, $^7\Sigma^+$ and $^7\Pi$ electronic states, SCF calcs. 3−26634
Mn(II) complexes in acetonitrile, e.p.r. spectra 3−8425
$Mn(IO_3)_2$, cryst. growth, boiling solvent technique 3−12235
Mn(IV) complexes, $MnW_5O_{20}^{6-}$, $MnMo_{32}^{6-}$, excitation and emission luminesc. spectra 3−12164
$MnIn_2O_4$, X-ray diffraction and γ-resonance obs. of spinel structure 3−24087
$MnIn_2S_4$, cation distrib., mag. susceptibility temp. depend. 3−34102
MnM_2O_4, ($M=Rh$, Mn, V, Fe, Cr), interionic metal-oxygen distances, formulae *(Russian)* 3−17784
$Mn_{1.5-x}Me_xFe_{1.5}O_4$ ($Me=Ni$ or Cr), induced mag. anisotropy 3−15381
$Mn_xMg_{1-x}Fe_2O_4$, chem. and X-ray anal. of inhomogeneity *(Russian)* 3−14971
$Mn_{3-x}Ni_xB_4$, mag. props. in strong mag. fields *(Russian)* 3−8396
MnO, electron diffraction study of the nature of the chemical bond *(Russian)* 3−4728
MnO, exchange splitting of core electrons 3−15144
MnO, inelastic neutron scattering obs. of antiferromag. spin waves 3−24580
MnO, magnetisation curves calc. for first order magnetic transitions *(French)* 3−30614

manganese compounds continued
MnO, optical absorpt. spectrum, role of magnons and phonons *(Russian)* 3 − 15522
MnO, zero-point effects from theory of Heisenberg antiferromagnets with arbitrary interaction range 3 − 15326
MnO deposits from north of Indian-Antarctic Ridge, morphology and composition 3 − 37195
MnO-Fe_2O_3-B_2O_3 glassy system, prepn. and mag. props. 3 − 18726
MnO-M′O, (M′ = Mg, Ca, Sr, An, Al), Neel temp. comp. depend. *(French)* 3 − 8363
MnO-MgO solid solns., exchange phenomena between Mn^{2+} ions, e.p.r. and mag. susceptibility *(French)* 3 − 38964
MnO_2, commercially electrodeposited, heat treatment effect on the semiconductor properties 3 − 2086
γ-MnO_2, desorption of water, energetics 3 − 38729
MnO_4^-, SCF LCAO MO ground state calc. 3 − 11196
MnP-FeP solid solutions, Mossbauer studies 3 − 36818
$Mn_2P_2O_7$, mag. struct. using neutron diffr. method 3 − 18322
$Mn_2P_2O_7$ single crysts., antiferromag. reson., 1.2 to 14K 3 − 8447
$MnPt_3$ specific heat, low temperature, spin wave contribution 3 − 27371
MnSe, MnTe, high pressure modification of crystal structure, miscibility, NiAs type structure *(German)* 3 − 11737
β-MnSe, prep., paramag. susceptibility 3 − 30598
MnSe inclusions in steel, hot hardness 3 − 34579
$MnSiO_3$, pyroxmangite, cryst. struct. 3 − 17770
$MnTa_2O_6$, mag. struct., neutron diffr. obs. *(German)* 3 − 21249
MnTe, antiferromag. semicond., optical phonon spectrum obs. over Neel temp. 3 − 5104
MnTe, magnetic susceptibility, antiferromagnetic transition, lattice consts., ht. capacity 300-700 K 3 − 15365
α'-$Mn_{0.85}Ti_{0.15}Bi$ film, mag. and magneto-optic props. 3 − 2521
$Mn_{1-x}Ti_xBi$ films, $(0 \leqslant x \leqslant 0.2)$, kinetics of isothermal transformations of high temperature to low temperature phase 3 − 11742
$MnWO_4$-$FeWO_4$, mixed crystal, coexistence of two antiferromag. phases 3 − 34124
$MnWO_4$-$FeWO_4$, spontaneous magnetisation irregularities, modified effective field model 3 − 34060
$MnWO_4$-$FeWO_4$, wolframite, mag. phase diagram, molecular field approx. 3 − 34125
$MnZnFe_2O_4$, comp. variations during sintering *(French)* 3 − 34624
$Mn_{1-x}Zn_xFeO_4$, Mossbauer spectra, Fe^{3+} ions nonequiv. positions rel. to relax. effects *(Russian)* 3 − 39061
$Mn_xZn_{1-x}Fe_2O_4$, chem. and X-ray anal. of inhomogeneity *(Russian)* 3 − 14971
$Mn(pic)_2.2H_2O{:}Zn(pic)_2.4H_2O$, e.p.r. spectrum transitions 3 − 2348
$Mn(pyrazole)_2Cl_2$, antiferromag. interaction determ. 3 − 30612
$Ni_xMn_{1-x}Fe_2O_2$, cryst. growth, Bridgman method and characterization 3 − 12267
ZnS:Mn film, d.c. electrolum. 3 − 30882

manometers
see also pressure measurement
compression, elimination of error associated with evacuating action of Hg vapour jet 3 − 19178
extensometric, with Si strain gauges, up to 40 at. *(Polish)* 3 − 16402
fringe counting laser interferometer to measure differential height 3 − 25707
installation, for pressure pulsation meas. *(Polish)* 3 − 22300
membrane capacitor, temp. effects 3 − 35387
micromanometer for implantation in ventricles of dogs 3 − 3902
micromanometers, top-loading balance applic. 3 − 3775
quartz-fibre, ultra-high vacuum gauge, improvement of excitation of oscillation *(German)* 3 − 146
reference, correlation with dead-weight piston gauge type 3 − 57
transducers, absolute calibration by comparison with compression manometer in cryostated installation 3 − 19177
Hg, high-pressure, standard for calibration of differential pressure transmitters, span-shift errors with static pressure 3 − 25709

manufacture
see also electron device manufacture; steel manufacture
cable making machinery, noise abatement by design analysis 3 − 35343
nuclear components, in Germany, overview 3 − 19912
optical aspheric surfaces, NC grinding machine and testing apparatus 3 − 22333
radioactive isotopes, in Switzerland *(German)* 3 − 1036
semiconductor radiation detectors 3 − 19292

manufacturing processes
see also forming processes; joining processes; manufacture
carbides, sintered, techniques and equipment 3 − 8971
carbides sintered 3 − 8970
ceramics for electronic applications, economics, quality, properties, developments and trends 3 − 18687
nondestructive testing automation *(German)* 3 − 15809
oxides, glass and nitrides production for semiconductor components and IC *(German)* 3 − 21552
permanent magnets, hard rare earth-Co_5 alloys *(German)* 3 − 15384
plant noise reduction and control by equipment design 3 − 28420
sintered carbides, review 3 − 5339

many-body problems
see also BCS theory; quantum statistical mechanics
α-particle nuclei, calc. of matrix elements of three particle operators 3 − 6748
adsorption on solid surfaces 3 − 36479
Beliaev-Zelivinsky boson expansion and particle-vibration coupling methods, exactly soluble model 3 − 10388
Boltmann density matrix, improved classical path matrix 3 − 22756
book 3 − 20990
centre of mass motion and ground-state wave function 3 − 29297
collisional narrowing and foreign gas broadening of spectral line shapes, calc. using propagator technique of many body theory 3 − 11161
Coulomb t matrix, Sturmian expansions 3 − 28952
DWBA validity and soln. of three-body rearrangement reactions 3 − 29370
effective interaction in nuclei, perturbation theory 3 − 32771
exact bound states of N-body systems with two- and three-body forces 3 − 26114

many-body problems continued
exact one-dimensional statistical model for thermodynamic behaviour of gas of identical particles 3 − 16776
Faddeev eqns. in configuration space for three-particle bound state, analysis of ^3H 3 − 29320
few-particle scattering and analogous equations 3 − 10655
finite nuclei in many body theory, exact soln. of Goldstone eqn. for reaction matrix 3 − 19793
functional integral theory, adiabatic approxs. 3 − 4026
g-anisotropic metal, theory of many-body effects on conduction-e.s.r. 3 − 2395
grand-canonical ensemble Green functions, rigorous resolution of the hierarchy 3 − 22743
ground state energies, set of inequalities 3 − 22741
Huang formulation, four-body problem, perturbation region *(Polish)* 3 − 25382
Ideal Resonance Problem, soln. using parallel perturbations method 3 − 37792
many boson theory, application of the Brillouin-Wigner perturbation method *(Dhfakx)* 3 − 22739
Martin-Schwinger-Puff theory, diagrammatic approach by perturbation expansion 3 − 16746
metal/semiconductor interface, many body effects on semiconductor band structure 3 − 2183
multiple scattering theory, three-body treatment of binding effects 3 − 38148
multiple scattering with linearized propagator 3 − 6540
multiproduction final state with resonances, approx. to mass distribs. 3 − 10804
N-body, direct numerical integration 3 − 22116
N-body problem, clusters of galaxies, effect of mass loss to gravit. radiation on stability 3 − 28255
N-body problem of planetary system stability 3 − 37296
n-particle inclusive distribs. in dual reson. model, cluster decomposition 3 − 14029
N-particle Yukawa Hamiltonian, nonnegativity relation 3 − 10390
neutrino-pair emission from neutron stars and white dwarfs 3 − 39659
non-null boundary conditions, influence on reduced density matrix, soln. of Salzburg-Kirkwood eqn. 3 − 22745
nonrelativistic four-body problem in S-approx. for two-particle interaction, spin variables in integral eqns. *(Russian)* 3 − 23227
nonrelativistic quantum mech. three-body problem, series solns. 3 − 32444
Nordtvedt metric expansion for n-body equation, reln. to scalar tensor theories 3 − 16725
nuclear, boson expansion for odd-particle system 3 − 32775
nuclear multiple scatt. theory, three body treatment of binding effects 3 − 6794
nuclear reaction three-body model, exactly soluble for thresholds and resonances 3 − 32823
nuclear struct., soln. with linear programming 3 − 26399
off-shell 3-body scattering amplitude in eikonal approx., cancellation in Watson multiple-scattering series 3 − 4006
off-shell two body t-matrix, sensitivity of low-energy three-body properties 3 − 29323
relativistic quantum many-body theory in Riemannian space-time 3 − 26139
relativistic three-body problem, treatment with retarded part of two-time Green's function 3 − 32641
repulsive N-body problem, completeness of wave operators 3 − 28946
restricted problem of 3 bodies, periodic orbits around L_4 libration point 3 − 37297
restricted three-body problem, comparison of Encke and Cowell integration methods 3 − 39596
scattering from correlated systems, basis states and symmetric unperturbed Hamiltonian calc. 3 − 32841
Schrodinger eqn., coupled one-dimensional, direct numerical integration 3 − 10338
shell model, lower-bound, saturation for non-local two-body interactions 3 − 32439
solvable models construction 3 − 35628
T-matrix theory for many-particle system, inclusion of two-body correlation effects 3 − 18003
three cylinders, model for interaction between 3 conducting molecules 3 − 1295
three interacting particles, ground state solns. 3 − 10353
three-body, restricted, global stability 3 − 18922
three-body break-up reactions parity conservation rel. to polarization effects 3 − 10953
three-body classical relativistic problem, exact nonplanar solutions 3 − 37889
three-body D function parametrization 3 − 10876
three-body nonrelativistic scattering amplitudes, unitary variational approximations 3 − 37869
three-body problem, application of physical basis of O(5) and SU(3) group representations *(Russian)* 3 − 10235
three-body problem, Lorentz covariant, construction in three-dimensional quantum field theory 3 − 29184
three-body problem, singular cores 3 − 35863
three-body problem, sufficient conditions for return of ejected particle 3 − 16109
three-body problem in multichannel scatt. 3 − 17168
three-body problem of commensurable motion in asteroid belt 3 − 31634
three-body problem of near-orbiting satellites, relative motion determ. 3 − 39592
three-body problems in nucleon physics, DWBA model for (d,p) reactions *(Hungarian)* 3 − 6727
three-body reactions, determ. of differential cross section in terms of Biedenharn's triple correlation functions 3 − 14183
three-body scatt. above break-up threshold, complex co-ordinate method 3 − 10351
three-body system, numerical study 3 − 581
three-body system, scattering theory soln. of Faddeev eqn., S-matrix unitary form. 3 − 29369
three-nucleon systems, off-shell effects for two potentials 3 − 14142
three-particle nonrelativistic scattering, connected-kernel Heitler equations 3 − 23024
three-particle resonance, asymptotics of wave function, Fadeev equation *(Russian)* 3 − 22714

many-body problems continued
  tunnelling, molecular impurity assisted, many body theory 3−2176
  two finite body problem. first order perturbations 3−3937
  two-body problem, comparison of recurrence relations with Runge-Kutta integration 3−37301
  two-body problem, elliptic to hyperbolic orbit by slow loss of mass 3−16108
  two-body problem with corpuscular radiation, effects of particle trajectory curvatures 3−28119
  two-body relative state operators between many-body oscillator states, calc. of diagonal matrix elements 3−6742
  vacuum correlation projection operator nonunique realisation in Balescu's projection operator formulation 3−22736
  ρ-ω mixing with three-body mixing formalism, conditions set by unitarity and time-reversal invariance 3−16950
  Ag, frequency dependence in conduction e.s.r., interpretation as new many-body effect in metals with g anisotropy 3−2394
  Al, frequency dependence in conduction e.s.r., interpretation as new many-body effect in metals with g anisotropy 3−2394
  Be, $(1s^22s2p^3p)$ excited state, magnetic hyperfine interaction many-body perturbation theory 3−35952
  Cu, frequency dependence in conduction e.s.r., interpretation as new many-bodied effect in metals with g anisotropy 3−2394
many-particle systems *see statistical mechanics*
manybody problems *see many-body problems*
marine systems
  see also ships
  buoy location using Omega Navigation System 3−3205
  data buoy systems, methodology for developing operational requirements 3−3204
  digital signal processor for use in sonar, seismic and underwater telemetry systems 3−3178
  electronic aids to oil exploration and exploitation *(French)* 3−3201
  hydrographic engineering/marine environment training program 3−12
  ocean engineering, conference, New York (1972) 3−3228
  ocean floor navigation, acoustic systems, temperature fluctuations, transponder installation 3−3739
  on-board data processing system MLCB, design considerations 3−3243
  pressure compensated cables for deep submergence search vehicle 3−3206
  technology rel. to human needs, conference (Washington USA, Sep 1972) 3−3203
marketing
  nuclear fuel industry planning in Australia 3−23425
  Cs-134/137 power reactor mixtures, gamma source market evaluation 3−19995
  Cs-134/137 power reactor mixtures, feasibility and prospects for private separation and marketing 3−19996
Markov chains *see Markov processes*
Markov processes
  chemical reactions, multidimens. pot. surfaces props., model 3−31260
  chemical reactions, reversible first-order 3−39442
  dynamical semi-groups induced by Markov processes on topolgical groups 3−28974
  failure analysis, first passage analysis under stationary random excitation 3−554
  finite systems, random matrix theory and master eqn. 3−4475
  harmonic oscillator with stochastic frequency, Brownian motion 3−37897
  homogeneous Markov chains, multidimensional central limit theorem, speed of convergence *(Russian)* 3−13537
  linear stationary non-Gaussian, existence 3−6187
  multi-dimensional, average time of first approach of boundary 3−22591
  packed bed, Markov chain model 3−7470
  particle distribution in space, stochastic model, Poisson process, probability laws 3−32291
  Schrodinger eqns., boundary conditions, strong Markovian processes 3−26108
  statistical distribution of strong field fluctuations in acoustic wave propagation *(Russian)* 3−5713
Mars
  air glow, study by Mariner 9 u.v. spectrometer 3−16154
  albedo variations, Mariner 9 television results 3−16150
  analog. obs. in Wright and Victoria dry valleys in Antarctica 3−12632
  astronomical observations, from earth, 1965-69, review 3−31585
  atmosphere, Mariner 9 television experiment 3−16151
  atmosphere, origin and evolution, comparison with Earth's atmosphere 3−22037
  atmosphere, study by Mariner 9 radio occultation 3−16157
  atmosphere, thermal structure by radiative-convective model 3−16161
  atmosphere, upper, structure study by Mariner 9 u.v. spectrometer 3−16155
  atmosphere, upper, u.v. emissions 3−16156
  atmosphere, vertical thermal struct., modification by motion 3−31596
  atomic O conc. in atm., Mariner 6 and 7 obs. 3−16163
  brightness temp. obs. in far i.r. 3−18971
  centre of mass-centre of figure offset, topography from radar and u.v. obs. 3−31615
  crater structure rel. to simultaneous impact craters 3−39636
  diameter, optical measurements 3−16158
  dust storms, review 3−31594
  dust-storms, occurrence frequency 3−12980
  frost formation, new equator and slope angle 3−31599
  gravity field determ. from Mariner 9 Doppler tracking data 3−31611
  ground surface, telescopic and space probe observations *(French)* 3−18970
  large scale surface structure, cloud obs. compared with radar and gravity field meas. 3−31579
  limbside diffuse radiation intensity determ. 3−35068
  linear polarisation meas. in i.r. region 3−31689
  Mariner 6 and 7 occultation expts., error analysis 3−31620
Mars continued
  Mariner 9, image processing and products 3−31806
  Mariner 9, mission profile and project history 3−31591
  Mariner 9, star photography Mars picture information decalibration 3−25531
  Mariner 9 mission objectives, communications and control systems *(Spanish)* 3−35214
  Mariner 9 orbital probe, information review, internal heat of planet, surface erosion 3−25415
  Mariner 9 photographs of surface *(German)* 3−9490
  Mars, surface and lower atmosphere study by Mars-3 3−16152
  north polar cap size, optical measurement 3−31598
  outgoing thermal radiation rel. to transfer equation, models *(Russian)* 3−35069
  ozone observations, Mariner 9 u.v. spectrometer obs. 3−31592
  permafrost terrain, Antarctic analog 3−12633
  Phobos and Deimos, lander, lander/orbiter or return missions 3−9487
  photometric observations, by remote sensing 3−31597
  photometry and topography, by Mariner 9 u.v. spectrometer experiment 3−12977
  probe, Soviet 3−25542
  shape, by Mariner 9 radio occultations 3−12978
  shape, satellites orbit precision discrepancy, implications 3−31593
  solar halos at limb and terminator 3−37330
  solar plasma interaction 3−31590
  solar wind interaction region obs., ion energy spectra meas. by Mars-3 3−31584
  solar wind plasma electrons, Mars-2 and Mars-3 orbiter obs. 3−31589
  south polar region, geological units 3−16149
  spacecraft descending into Martian atmosphere, optimal control of final velocity 3−25373
  subsurface, microwave spectrum 3−12979
  surface and atmosphere, by i.r. spectroscopy on Mariner 9 3−16153
  surface and lower atmosphere study by Mars-3 3−16152
  surface geology, Marina 9 report 3−16148
  surface optical parameters, laboratory obs. of simulated planets 3−35066
  temperature, by microwave interferometric observations 3−16160
  temperature measurement by microwave radiometry from Mars 2 and 3 3−16159
  topographical variations computed from radar and CO_2 meas. *(Russian)* 3−16168
  topography and radar scattering properties, high resolution obs. during 1971 opposition 3−31587
  topography and surface properties, radar obs. during 1971 opposition 3−31586
  troposphere (upper), radiative cooling of buoyant thermals by long-wave radiation 3−25222
  Viking mission, implementation of Lander cameras 3−31830
  violet clouds, photometric obs., albedo and Junge parameter determ. 3−35063
  violet haze problem, 1969 blue clearing 3−31600
  violet haze problem, a literative survey 3−25413
  volcanism, water, wind and dust, Mariner 9 obs. 3−35075
  water vapour, exchange between atmosphere and surface 3−31595
  CO_2, electron energy deposition rel. to Mariner u.v. data for Mars 3−12981
  CO_2 distribution, i.r. absorption obs. 3−31588
  CO_2 extinction coefficients, temperature and pressure dependence 3−16164
  CO_2 stability in Martian atmosphere and under radiolysis 3−22034
  H_2O 2.8 to 3.5 microns absorption band obs. during 1971 opposition using airborne Hadamard-Transform Spectrometer 3−35221
  O_2 spectroscopy and aeronomy, effective air mass factor determ. from model 3−25411
maser clocks *see atomic clocks*
masers
  astronomical maser radiosources, 0.0002 sec. resolution obs. of nebulae W3, W49 and Orion Nebula *(Russian)* 3−13069
  astrophysical, props. of polarised radiation 3−28102
  cosmic maser model with resonance-scattering feedback, appl. to OH and H_2O clouds 3−28290
  cosmic OH emission sources analytic approx. for saturation region 3−37483
  cosmic sources, protoplanet formation in protostars 3−25445
  e.p.r. spectrometer using maser techniques, sensitivity determ. 3−266
  high speed tunable for radar and communication receivers, patent 3−10460
  interstellar, molecular recoil mechanism for intensity variations *(Russian)* 3−16279
  molecular beam, principles and review of advances 3−32530
  molecular beam maser spectrometer with very high resolution *(Dutch)* 3−28552
  molecular beam oscillator, freq. noise *(French)* 3−37947
  molecule, dressed, transient coherent emission 3−29072
  single quasimode laser operation 3−37951
  sorting of molecules by four-pass winding system 3−19589
  superradiant phase transition for molecs. in quantized radiation field, Dicke maser model 3−32529
  W49 (radio source), cloud accel. rel. to maser pumping 3−25473
  H, frequency stability rel. to output, mag. polarisation field and relaxation, meas. *(German)* 3−10459
  H, low-Q cavity, frequency standard 3−3749
  H, relaxation time meas. 3−22866
  H_2 performance *(German)* 3−19588
  OH in interstellar medium, excitation by collisional dissociation of water 3−31778
  Rb, instability meas. 3−13719
  Rb, relaxation time meas. 3−22866
  ^{87}Rb, buffer gas mixture effect 3−13718
masks
  see also integrated circuit production; semiconductor device manufacture
  cleaning, by u.s. 3−25670
  high speed computer controlled mask making techniques for optical diffractometer studies of disorder 3−16549

masks continued
IC production, soft X-ray replication of scanning electron microscope generated patterns 3—13481
interferometric applications using coherent light *(French)* 3—13319
photolithographic alignment by Moire techniques 3—188
physical development photographic process applic. 3—27905
polymer film, electron beam exposure profile 3—14903
GaAs, surface contamination due to Cu atoms in resist film stripper during photo-etching 3—8757
GaP selective epitaxial growth, SiO_2 and Si_2N_4 masks 3—2683
Si_3N_4, for selective oxid. of Si in device manufacture 3—39292
Si_3N_4 pyrolytically deposited film passivation of GaAs and Si substrates 3—18555
SiO_2/Si, interactions during heat treatment in hydrogen *(Russian)* 3—11815
W film, ion implantation mask for Si:B 3—30949

masonry dams *see dams*

mass
see also atomic mass; hyperon mass; meson mass; molecular weight
B-type star models with low mass, comparison with HZ 22 primary component 3—28176
Earth, centre of mass from satellite triangulation, absolute orientation rel. to geograv words 3—34758
Earth-Moon mass ratio from Mariner 9 radio tracking data 3—22035
graviton mass calc. from decay into photons 3—26145
inertial-to-gravit. mass ratios for Al, Pt, torsion balance meas. 3—16742
Mars, centre of mass-centre of figure offset, topography from radar and u.v. obs. 3—31615
modified negative mass instabilities in finite mirror-confined plasmas 3—4647
neutrinos of nonzero mass, effect on gravit. dynamics of clusters of galaxies and Universe 3—35005
neutron star formation lower limit rel. to binding energy 3—28180
NGC 4486 (M 87), Virgo galaxy, mass-to-light ratio determ. 3—35192
photon rest mass, upper limit rel. to conventional Doppler shift departures 3—861
quasars, determ. from thermal component of continuum 3—37421
ratios, binary systems, particle trajectories 3—3330
spectrum, interstellar clouds, total coalescence, time dependence 3—3377
white dwarfs, Hamada-Salpeter mass-radius relation using red shift 3—13037

mass differences
see also elementary particle theory
atomic, determ. with new mass spectrometer using second-order focusing theory 3—10096
baryon, in gauge model of strong and e.m. interactions 3—26276
elementary particle mass formulas in renormalizable theories based on spontaneously broken gauge symmetry 3—10642
e.m., cancellation of logarithmically divergent contributions 3—13795
e.m., expression in measurable quantities using dispersion relations 3—6609
e.m. self-mass of hadrons, finiteness criteria from Bjorken's asymptotic scaling 3—16988
hadron e.m. mass shift, divergence 3—13856
hadronic e.m., new calc. method. application to π and K 3—32662
red giant stars mass loss estimation using Ca II K line width 3—35135
spontaneously-broken gauge theory of strongly-interacting bosons based on SU(2) × SU(2) group, chiral invariance and e.m. mass difference 3—17085
SU(2) mass splitting in vector mixing model 3—6564
two-nucleon pot., e.m. mass splitting effect of I=1 mesons 3—16986
Weinberg model of weak and e.m. interactions, calc. of soft-π and soft-k mass differences 3—26300
$ep \rightarrow epX^0$, coincidence electroproduction in ρ mass region, meas. of cross sections for 0-1Gev/c^2 missing masses. 3—13956
$\gamma\gamma \rightarrow \pi\pi$, cross-section determ. from dispersion relations and mass difference *(Russian)* 3—4174
$\gamma p \rightarrow pMM^0$, photoproduction of ρ and ω, 3.0-4.7 GeV, study by missing mass technique 3—13953
$\gamma p \rightarrow pm^0$, search for boson photoproduction by missing mass technique, meas. of s and t distrib. of hadronic continuum 3—13952
$K_1{}^0$ and $K_2{}^0$ meson mass difference calc. *(Russian)* 3—19716
K^-p interactions, low-energy, Coulomb and mass difference corrections in K-matrix treatment 3—32699
n-p, calc. in semirealistic gauge model of weak and e.m. interactions 3—35789
n-p, finite, in spontaneously broken gauge theories 3—35788
p-n, calc. of inelastic and elastic contrib. using Cottingham formula 3—10694
p-n, in unified gauge model of leptons and hadrons 3—26299
p-n, possibility of finite evolution by accounting for Bjorken law violation in eN scatterng 3—29202
p-n, subtraction piece in Cottingham formula 3—6607
p-n, subtraction piece in Cottingham formula 3—10695
p-n mass difference, Compton amplitude representation, scale-invariance of A_2 meson 3—13863
π^+-π^0, calc. to lowest order in model field theory with spin-two gravitons 3—35790
$\pi^-p \rightarrow X^-p(X^on)$, missing mass expt., search for $\delta^-(962)$ meson at energies near production threshold 3—10776
Ξ masses meas. using 2.1 GeV/c K^- exposure 3—13857
$\Xi^*(1530)$ mass, width and mass differences 3—4166
^{35}Cl, ^{37}Cl, meas. of doublet mass differences using peak-matching techniques 3—11107
^{1}H, ^{2}H, meas. of doublet mass differences using peak-matching techniques 3—11107

mass spectra
see also mass spectrometers; mass spectroscopic chemical analysis; mass spectroscopy
atomic mass determ. A=45-58, with highly accurate control measurements 3—10838
atomic mass differences, from peak-matching by computer 3—25922
2-decene. cis and trans, comparison of photon and electron impact ionization 3—1268

mass spectra continued
electron multipliers discrimination for atomic ions, comparison of yields for 61 atoms 3—26555
far unstable light nuclei produced in high energy nuclear reactions, on-line mass spectroscopic analysis 3—10837
heavy fragment cumulative yields in fast neutron fission of ^{238}U 3—17269
hydrocarbons, photoioniz., ionic fragmentation patterns, Penning ioniz. comparison 3—38309
hydrocarbons, reproducibility of pattern coeff. for 6 hydrocarbons *(Japanese)* 3—22548
hydrocarbons, resonance form. theory prod. from mass spectrometric fragmentation processes 3—1269
inorganic pentafluorides, association in saturated vapours 3—25924
ion-molecule thermal energy reactions, study using mass spectrometric sampling of stationary afterglow plasmas 3—1287
low resolution, computer calc. of ionic formulae and monoisotopic spectrum 3—7024
1-naphthol, H-randomization under electron impact 3—11193
organic compounds, ionisation potentials determ., multiple field ionisation mechanism 3—26709
organic molecules, simulated mass spectra generation by computerised pattern recognition technique 3—28703
perfluorocyclobutane, negative ion spectrum 3—1282
polar crysts., absolute configuration assignment by ion refl. mass spectrometry 3—33476
quartz ampoules, fused, hydrogen evolution 3—21742
radioactive isotopes, short half-life, feasibility study of mass meas. 3—10836
solid r.f. spark, valence relationships 3—17698
A_2 production in $\pi^\pm p \rightarrow pX^\pm$, 4 BeV/c, mass spectrum 3—10796
B hydrides and derivatives, relative abundances of doubly charged ions 3—26707
^{35}Cl, ^{37}Cl atomic mass, meas. of doublet mass differences using peak-matching techniques 3—11107
CsCl, vibrational-rotational excitation effects *(Russian)* 3—11220
D atomic mass, meas. of doublet mass differences using peak-matching techniques 3—11107
Fe-Sn system, liq., thermodynamic excess functions determ. 3—37011
H atomic mass, meas. of doublet mass differences using peak-matching techniques 3—11107
HOF, photoionization with mass analysis 3—26713
LiO system molecular species, study by electron-impact mass spectrometry 3—5376
^{11}Li produced in high energy nuclear reactions, on-line mass spectroscopic analysis 3—10837
$N_2{}^+$ collision-broadened absorption line in ion cyclotron resonance mass spectrometer *(Japanese)* 3—28705
$N_2{}^+ + N_2 \rightarrow N_3{}^+ + N$, ion cyclotron mass spectrometric study, rates of formation 3—26724
NO, photoionisation mass spectrometric study, threshold region 3—17462
N_2O, photoionisation at 73.6 and 58.4 nm, collision induced dissociation at thermal kinetic energies 3—29732
^{a}Na, A=27-31, produced in high energy nuclear reactions, on-line mass spectroscopic analysis 3—10837
Nb, and oxides, multiplet lines *(Russian)* 3—6092
$O_2{}^{2+}$, mass spectrum detection 3—26708
SbSe type cpds., gaseous phase, ioniz. pots. and dissoc. energies *(French)* 3—7240
SiH_4 bimol. reactions with $NH_2{}^+$, $C_2H_3{}^+$, $C_2H_6{}^+$ and $C_3H_8{}^+$, form. of $SiH_5{}^+$, proton affinity 3—39433
^{232}Th, mass spectrometric meas. of mass doublets using peak matching techniques 3—10836
^{235}U, ^{238}U, mass spectrometric meas. of mass doublets using peak matching techniques 3—10836

mass spectrometer accessories
see also ion sources
capacitive integration system for isotope ratios 3—19319
channel electron multipliers, used as detectors in organic mass spectrometry 3—13450
digital recording system *(Japanese)* 3—32207
electron bombardment ion gun, used with time-of-flight mass spectrometer 3—35489
electron multiplier, meas. of yields for mass-analysed ions, test of discrimination 3—6087
field anode, for field desorption obs., high temp. activation *(German)* 3—37709
image of off-axis point source in cylindrical-mirror electrostatic analyzer *(Russian)* 3—6096
Knudsen cell for MSKh-3A mass spectrometer *(Russian)* 3—10092
metallurgical industry, chemical analysis *(French)* 3—19362
MI 1305, secondary electron multiplier, sensitivity 3—333
peak-matching by computer, for precise atomic mass differences 3—25922
quadrupole ion store, as source 3—28704
secondary ion collection system for ion microprobe analyser 3—6111
transistor modulator for ion source of mass-spectrometer *(Russian)* 3—10037

mass spectrometer applications
see also isotope separation; mass spectroscopic chemical analysis
α-particle tracks in mica backed by ^{241}Am source 3—25895
acrylonitrile process, analyser system 3—22556
adsorption, binding state of CO_2 on Ti film detn. *(Japanese)* 3—20930
adsorption, on metal surface, replacement of chemisorbed gas obs. *(Japanese)* 3—20928
atmospheric ion chemistry study 3—444
electron stimulated desorption of ions from crystal surfaces, meas. apparatus 3—334
field desorption, field anode high temp. activation *(German)* 3—37709
flashover in ultra high vacuum diode, preflashover mass spectroscopy 3—20673
lunar volcanism, orbital search 3—16179
metal surface oxidation, static method secondary ion mass spectrometry obs. 3—1906
negative ion source, bombardment of solid surfaces by positive alkali ions *(Russian)* 3—6061

mass spectrometer applications continued

- nitrogen-containing organic compounds, thermal ionisation, positive ions, tungsten and tungsten oxide emitters 3−36974
- plasma diagnostic set with quadrupole mass spectrometer *(Russian)* 3−7565
- secondary ion imaging mass spectrometry for surface layers meas. 3−30328
- secondary ion mass spectrometry for surface layers meas. 3−30328
- secondary ion mass spectrometry statistical method for surface investigations 3−30327
- static secondary ion mass spectrometry for surface layers meas. 3−30328
- thermally excited ions, decomposition, statistical theory of mass spectra 3−36975
- thin and surface layers study *(French)* 3−25933
- AlAu$_x$ (x=0.5,2), heats of atomisation, high temp. Knudsen cell mass spectrometric determ. 3−15821
- Al$_2$O$_3$ film, on Al, thickness determ. 3−36500
- BaSrTiO$_3$, O$_2$ diffusion const. meas. 3−17991
- Kcl, crystals subjected to molecular beams, condensation and vaporisation kinetics investigation *(German)* 3−7920
- Li$_2$F$_2$, crystals subjected to molecular beams, condensation and vaporisation kinetics investigation *(German)* 3−7920
- O measurements by rocket-borne mass spectrometers in upper atmosphere 3−16063
- Si film, structure, sputter-ion source mass spectrometry obs. 3−1950
- SrTiO$_3$, O$_2$ diffusion const. meas. 3−17991

mass spectrometers

see also ion optics; mass spectra; mass spectroscopy

- AEI/GEC MS9 for electron impact/chemical ionization studies, modifications 3−32249
- apparatus for ion-electron recombination cross section meas. *(Japanese)* 3−32206
- atomic mass difference determ. with new mass spectrometer using second-order focusing theory 3−10096
- automatic, for D$_2$ analysis in dynamical regime 3−32212
- beam transport theory applications to design, beam emittance effects 3−331
- Bennett radio-frequency, negative background current 3−327
- charged particle analysers, optimum transport 3−3867
- chemical accelerator beam instrument for ion-molecule reaction kinetics, 0.1-100eV 3−25923
- deflecting wedge field, with trochoidal ion beam 3−32211
- double focusing, double collecting mass spectrometer for light stable isotope radio analysis 3−25928
- double focusing, with parallel beams, ion optics *(Rumanian)* 3−10094
- double focussing, influence of fringing fields on image aberrations 3−13454
- double magnetic prism-e.s. mirror system, optimal characteristics, exptal. determ. *(French)* 3−13452
- field ionization, use of conditioned razor blades for organic and analytic applications 3−330
- field ionization mass spectroscopy using scintillation detector 3−328
- fourfold monopole instrument 3−25925
- heavy ion recoils, absolute transport efficiency, with He jet systems 3−35452
- homogeneous mag. field 90° sector type, performance *(Rumanian)* 3−10095
- ion, for chemical and isotope analysis, description and applic. *(Russian)* 3−10093
- ion beam width by symmetrical analyzer 3−19659
- ion cyclotron resonance, for determ. of rate consts. for ion-molecule reactions in ammonia 3−1273
- ion cyclotron resonance mass spectrometer construction *(Japanese)* 3−28705
- ion microprobe mass analyzer, quantitative correction procedure, CARISMA program 3−37768
- low background secondary ion mass spectrometer with quadrupole analyser 3−26011
- luminosity improved spectrometer description 3−19320
- with magnetic wedge field 3−13449
- MI-1305, calibration, meas. of water vapour pressure 3−25930
- modulated molecular beam type for gas-solid reaction investigations 3−26020
- molecular beam mass spectrometer for studying reactive fluorides 3−25924
- monopole mass analyser, optimum dimensions 3−3869
- multiple monopole, electrode arrangements *(German)* 3−25927
- nuclear fission fragment separation, in elec. and mag. fields, instrument design *(Russian)* 3−3870
- on-line monitoring, simultaneous multiple component 3−10192
- parabola spectrometer for fast on-line analysis of fission and heavy ion reaction products 3−10097
- potential distrib. approximation in electrostatic mass spectrometer *(Russian)* 3−6088
- pulsed quadrupole mass spectrometer, theory and design principles *(Russian)* 3−6094
- quadrupole, charged particle oscillations calc. 3−35491
- quadrupole, for glass gaseous inclusions anal. 3−13504
- quadrupole, residual gas analysis and performance limits 3−3871
- quadrupole mass filter, dependence of ion transmission on initial RF phase 3−329
- quadrupole mass filter, reproducibility in pattern coeff. of spectra for 6 hydrocarbons *(Japanese)* 3−22548
- quadrupole residual gas analyzer, performance and capabilities 3−19321
- resolving power of correlation mass spectrometer *(Russian)* 3−6090
- r.f. quadrupole mass filter, detection of large water clusters 3−32210
- r.f. single-pole, for layer-by-layer analysis of solids 3−19318
- r.f. spark source, digital electrode controller 3−25932
- satellite-borne positive ion mass spectrometer 3−39565
- scintillation, ionic emission, discharge current *(French)* 3−25926
- secondary ion mass spectrometry with ion microprobe techniques for isotopic detection 3−13489
- secondary ion spectrometer 3−35490

mass spectrometers continued

- signal enhancement, real-time, online computer feedback control 3−22494
- signal recording in correlation mass spectrometer *(Russian)* 3−6089
- spectrograph, dependence of design line shape on ion-optical parameters *(Russian)* 3−6097
- sputtering mass spectrometer with Cs primary ion source 3−25931
- symmetric prism mass spectrometer, theoretical studies of electron-optics *(Russian)* 3−6095
- three- and four-stage r.f. spectrometer, design and performance characteristics 3−32209
- three-stage, for high abundance sensitivity meas. 3−332
- time of flight mass analysis combined with field-ion microscope 3−381
- time resolved display, offset raster unit 3−13448
- time-of-flight, for field-ion microscopy 3−28733
- time-of-flight spectrometer for heavy nuclei 3−6093
- toroidal e.s. analysers, characteristics determ. *(French)* 3−13451
- transients in switching in mass spectrometric gauge *(Russian)* 3−6091
- trochoidal ion beam instrument, theory 3−13453

mass spectrometry *see mass spectroscopy*

mass spectroscopic chemical analysis

see also isotope separation; mass spectra

- accessories, metallurgical applications *(French)* 3−19362
- acrylonitrile process, analyser system 3−22556
- AEI/GEC MS9 for electron impact/chemical ionization studies, modifications 3−32249
- automatic methods and measuring equipment *(Hungarian)* 3−19368
- 2-decene. cis and trans, comparison of photon and electron impact ionization 3−1268
- drift tube mass spectrometer, meas. of rate-coefficients of o 3−20202
- elemental analysis using combined multiple ion detector-peak matcher device *(Japanese)* 3−13514
- field ionization, use of conditioned razor blades for organic and analytic applications 3−330
- fuel burn-up degree determ. from isotopic comp. change during irrad. *(Czech)* 3−1060
- gas chromatography-mass spectrometry system, capability evaluation 3−434
- gas-solid reactions, by modulated molecular beam mass spectrometry 3−26020
- glass gaseous inclusions 3−13504
- III-V semiconductor, chemical vapour deposition study 3−2639
- ion microprobe analyser, for solid surfaces *(German)* 3−19369
- ion microprobe mass analyzer, quantitative correction procedure, CARISMA program 3−37768
- laser microprobes, analysis of biological specimens *(German)* 3−28762
- lunar fines, contamination problems in search for amino acids 3−35095
- metal ceramic vacuum tubes, analysis, u.h.v. opening technique 3−37614
- metastable peaks, explanation of fine structure 3−435
- molecular crystals, stoichiometric composition determ. using mass spectrometer with a laser ion source 3−28781
- polymer analysis, applications of gas chromatography/mass spectrometry 3−37752
- residual gas composition measurement, spectrometer selection criteria *(Hungarian)* 3−26009
- r.f. getter sputtering plant, gas analysis by mass spectrometry 3−22303
- secondary ion mass spectrometry with ion microprobe techniques 3−13489
- spark source photoplates, computer determination of ion intensities 3−13492
- surface composition analysis 3−22550
- trace analysis techniques for solids, and instrumentation, review 3−22555
- trace analysis with low background secondary ion mass spectrometer with quadrupole analyser 3−26011
- Ba, ultrapure single crystals, preparation by ultrahigh vacuum reactive distillation, spark mass spectrographic analyses of impurities *(German)* 3−8733
- Ca, ultrapure single crystals, preparation by ultrahigh vacuum reactive distillation, spark mass spectrographic analyses of impurities *(German)* 3−8733
- CdSe$_x$Te$_{1-x}$ solid solution, evaporation, vapour composition determ. and X-ray phase analysis *(Russian)* 3−11734
- GaAs amorphous films, electron diffraction study of struct., mass spectrometer study of vapour composition formed by laser induced evaporation *(Russian)* 3−8059
- GaP amorphous films, electron diffraction study of struct., mass spectrometer study of vapour composition formed by laser induced evaporation *(Russian)* 3−8059
- GdN, synthesis, vaporization and crystal growth 3−2642
- Ge alloy surface of p-n junction, obs. of catalytic effect 3−8257
- H$_2$O$_2$ form. by adiabatic expansion of H$_2$-O$_2$ gas mixture 3−5372
- HoN, synthesis, vaporization and crystal growth 3−2642
- NF$_2$ ionisation and dissociation processes study 3−17460
- N$_2$F$_4$ ionisation and dissociation processes study 3−17460
- Ni-based alloys, glazes prod. by high-temp. wear and friction 3−34590
- Si, surface reaction with O$_2$, secondary ion mass spectroscopy statical method obs. 3−24353
- Sr, ultrapure single crystals, preparation by ultrahigh vacuum reactive distillation, spark mass spectrographic analyses of impurities *(German)* 3−8733
- Ta, sputtered thin film, surface and in-depth analysis by secondary ion mass spectra 3−37767
- U, isotopic analysis using new three-stage mass spectrometer with high abundance sensitivity 3−332
- Zn$_x$Cd$_{1-x}$Te solid solution, evaporation, vapour composition determ. and X-ray phase analysis *(Russian)* 3−11734

mass spectroscopy

see also mass spectra; mass spectrometers

- atomic mass difference determ. with new mass spectrometer using second-order focusing theory 3−10096

mass spectroscopy continued
computer identification, highly compressed spectral codes, Aldermaston collection 3−28702
electric field effects on precision meas. with r.f. spectrometer 3−14112
field ionization, dissociation of multiply charged organic ions 3−26706
ion composition meas. in E-region and F-region above Kiruna during sunrise and sunset 3−25292
lifetime of mass spectrometric fragmentation process 3−26710
peak matching, new technique for partially resolved doublets 3−10836
scintillation, ionic emission, discharge current *(French)* 3−25926
spacecraft re-entry plasma, dissoc. and ionisation meas. 3−23928
thin and surface layers study *(French)* 3−25933
UF$_6$, U isotope ratio *(Japanese)* 3−10201
mass standards *see measurement standards*
mass transfer
see also gravity waves
during adiabatic saturation of hot gas in wetted-wall tube 3−1321
air jets, from entry holes of high-intensity combustor-liner, mass flows 3−17494
air-sea interface, chemical mass transport rel. to seawater structure and hydrophobic hydration 3−12686
Algol like binaries, generation of gaseous rings 3−16221
benzene, evaporation from porous bodies, obs. of simultaneous heat and mass transfer 3−1790
bibliography of soviet works 3−22769
binary stars nonthermal radio emission, mass exchange between components 3−31711
book on mass transport phenomena 3−11359
boundary layer on moving circular cylinder, transfer eqns. 3−29867
bubbles, nonspherical, effect on motion 3−1444
n-butanol, evaporation from porous bodies, obs. of simultaneous heat and mass transfer 3−1790
carbon tetrachloride, evaporation from porous bodies, obs. of simultaneous heat and mass transfer 3−1790
in co-current laminar gas flow in wetted-wall tower *(Japanese)* 3−23680
compact astrophysical objects, discrete quantized outflow velocities of matter by radiation pressure 3−31720
complex heterogeneous reactions, mass transfer effect determ. by transitional analysis 3−27868
condensate film flow down a vertical wall, stability 3−14433
conductive heat and mass transfer in a dynamic two-phase layer meas. 3−26783
convection, natural, adjacent to horizontal plates 3−36088
convection, rel. to simultaneous heat transfer 3−11388
convective, from single sphere *(Japanese)* 3−22764
convective mass transfer from stationary and moving surfaces using a Hg evaporation technique 3−20286
convective transfer from cavity in duct with separated flow *(German)* 3−1332
cooling towers, computer code for thermal design 3−17285
crystal growth, and thermal convection in chem. vapour transport process 3−24793
crystal growth rate from melts and solutions, transfer rate effects 3−1579
cylinders, infinite, transfer pots., integral eqn. approach 3−35637
diffusional transport, enhancement by u.s. 3−29851
disperse material, convective drying, in agitated layer in cross flow of coolants 3−25022
dispersed solid material, flow in pipeline under piston conditions of mass transfer *(Russian)* 3−38406
drag reducing fluid systems 3−11384
drying rate of porous solids rel. to heat and mass transfer 3−2774
effects of upstream and downstream boundary conditions on heat or mass transfer with axial diffusion 3−20285
effects on higher-order boundary layer solns., the leading edge of a swept cylinder 3−14460
in electrolyte solution, eff. of mag. field *(Russian)* 3−20313
evaporation, porous walls, water, multiphase flow 3−1437
evaporation of moisture on small cylindrical bodies in longitudinal flow 3−1791
to fixed particle in agitated tank, extrapolarion problems *(French)* 3−4598
flowing fluid, two-dimensional stagnation *(French)* 3−36076
fluidised bed, countercurrent three-phase, mass transfer investigation 3−29904
fluidised beds, annular, inner wall transfer rates 3−29910
fluidised beds, vibrating 3−1462
fluidised beds of spherical particles under 1st and 3rd order boundary conditions 3−1463
forced convection mass transfer from humid air to frost surface 3−1363
forced convection mass transfer from wetted grooves 3−26800
fractional vertical condensers, obs. techniques 3−127
infree volume of fixed granular bed 3−4626
frost formation on air coolers rel. to mass transfer coeff. of cooled plate 3−1780
frost layer, heat and mass transfer anal. 3−20852
gas diffusion to a liquid film flowing down inclined surface, asymptotic eigenvalues for heat or mass transfer 3−26779
gas-liquid dispersions with mass transfer meas. of liquid solute concentrations 3−32275
gas-liquid systems, internal and external processes 3−639
gaseous mixtures, variation with concentration of components 3−1320
Gibbs adsorption effects on Marangoni instability in penetration mass transfer 3−7342
glass melts with high fluoride content, F loss to atmosphere effects *(German)* 3−27161
glass-graphite materials in high-temperature gas stream, heat and mass transfer on the surface *(Russian)* 3−26786
graphite ablation, during hypersonic flow of radiating air plasma 3−1403
growth law of fast moving spherical second phase, heat and mass transfer limitations 3−24245
haemodialysers, flow and mass transfer, influence of non-Newtonian blood flow 3−17525
mass transfer continued
heat and mass transfer between two phases, effects of convection *(French)* 3−2840
heat transfer, bibliography 3−634
high speed flows, three dimensional heat and mass transfer, ablation distances 3−38354
high speed mass ejection from blue and super giants, kinetic energy of process 3−19071
homogenized fluid and sphere with finite interfacial transport coeffs., comment on transient mass transport 3−20405
hot stars, correlation between i.r. excesses and mass loss 3−25446
hot stars, mass loss, plasma perturbation mechanism 3−39669
hydrodynamics from streaming solutions 3−1355
impact craters in dense crystalline rocks, empirical formulae and model 3−39649
integral balance method, generalization for problems of interconnected heat and mass transfer *(Russian)* 3−32460
isobaric laminar boundary layer flow, vectored injection, mass transfer rate 3−26814
jet impinging on flat plate 3−1336
jets, turbulent and reattached on inclined flat plate, heat transfer 3−17516
jets, turbulent cocurrent, mixing in ducts with profiled walls, minimum losses determ. 3−33309
jets, turbulent with adjacent boundaries, flow development 3−17515
knife jet dryers, effect of turbulence *(German)* 3−26780
laminar free convection in sublimation *(German)* 3−26801
lean liquid-liquid dispersions, population balance model for mass transfer, droplet breakage processes 3−33293
liquid film evaporation into turbulent gas flow, mass transfer model 3−29842
liquid viscosity effect on mixing in falling films, mass transfer coefficients calc. 3−26860
in mixed convection on vertical plate 3−1319
moving surfaces stability in fluid systems with heat and mass transfer 3−29865
moving-bed exchange equations, asymptotic solution, interphase mass transfer 3−29902
multicomponent, in turbulent flow 3−7341
multicomponent systems, balance equations *(German)* 3−6372
multistage cross flow heat exchanger 3−111
naphthalene circular discs, forced convective mass transfer meas. 3−33214
nondeforming fluid media, anisotropic processes 3−620
oceanic western boundary currents, baroclinic and bottom topography effects on transport 3−34865
paramagnetic solutions, infl. of non-uniform mag. field *(Russian)* 3−20314
parked beds, forced convection mass transfer at low Reynolds numbers 3−33200
plane moving boundary problems, freezing and melting, integral transforms 3−34702
plasma, electrodynamically accelerated, influence on integral characts. 3−20428
plate, mutually connected heat and mass transfer by integral balance method *(Russian)* 3−10404
plate with infinite fluid stream around *(Russian)* 3−7353
pollutant transport, stochastic processes 3−1375
porous materials, determ. of skin friction by Karman-Pohlhausen method 3−11681
pulsed bubbling columns, heat and mass transfer 3−26782
saline soln., Polyox WSR 301 addition, mass transfer to rot. cone in fluid, expt. and theoretical results 3−36087
saturated vapour-gas mixtures, heat and mass exchange in cooling 3−23656
sea-air interface flux, prediction equations 3−15938
semi-infinite steel body melting in an Fe-C alloy, heat and mass exchange eqns. 3−24827
fromsphere at high Prandtl nos., effects of u.s. vibrations 3−4524
spherical capped gas bubbles rising in aqueous media, mass transfer coefficients calc. 3−29921
stainless steel corrosion products, mass transport in liquid Na PFR coolant 3−14252
star, B-type stars, rapidly rotating, mass loss 3−31658
stellar, Type I supernova model 3−3341
stellar contact binary systems, appl. to W Ursae Majoris systems 3−39663
stellar mass loss by sporadic ejection and effect on angular momentum 3−9533
stellar mass loss effects in diffuse nebulae, approx. similarity solns. 3−28298
suspension, spark discharge method for mass transfer acceleration 3−25021
total mass transfer function for north Atlantic *(Russian)* 3−12675
transpiration cooling, heat and mass transfer equations 3−26168
transport equations for multiphase systems 3−29903
turbulence effects 3−1362
turbulent, from rough surfaces 3−7344
turbulent flow 3−14448
turbulent heat and mass transfer in pipes, channels and boundary layers 3−1367
turbulent momentum transfer in rough pipes, statistical props. 3−11390
turbulent pipe flow, anal. 3−1374
two-body problem, elliptic to hyperbolic orbit by slow loss of mass 3−16108
two-phase real conc. particulate systems, high Reynolds number fluid dynamics and transfer processes 3−36136
unsteady convective diffusion with interphase mass transfer, miscible dispersion theory 3−33292
vapour condensation, pressure of noncondensing gas, heat and mass transfer 3−36413
vapour-gas mixture, in a capillary, convective diffusion with evaporation 3−26784
viscous sublayer in a channel flow, 3 dimensional study by mass transfer meas. *(French)* 3−14435
water, adiabatic evap., heat and mass transfer dynamics 3−20863
water, evaporation from porous bodies, obs. of simultaneous heat and mass transfer 3−1790

mass transfer continued
  water drop, surface temp. during vaporization, interfacial tension during mass transfer 3−1875
  water-organic solvent binary mixtures condensation 3−1784
  CO_2 in air, heat and mass transfer obs. using interferometry 3−1319
  Fe, liq., rel. to diffusion coefficients 3−31034
  He in air, heat and mass transfer obs. using interferometry 3−1319
  KOH vapour, condensation, MHD generator 3−36414
  $MgSO_4.7H_2O$, resist. to growth using flow system 3−8713
  O_2 jet mass transfer to liq. Ag 3−39304
  SF_6, laser induced i.r. fluoresc., thermal heating, mass diffusion and collisional relax. 3−1248
  Ta oxidation, transport nos.of metal and O_2, obs. using noble gas tracers 3−38743

master equation *see transport processes*

materials
  see also individual materials, e.g. ceramics
  bone and muscle, mass energy absorption coeffs. meas. 3−5674
  cement paste, hardened, capillary porosity 3−34668
  granular, equilibrium water content at different temps. 3−5362
  Linus Pauling, his contribution to materials science 3−9783
  mineralized tissues, high resolution surface scanning electron microscopy 3−3910
  nonlocally reacting noise control materials, for air conditioning, acoustic impedance 3−3704
  osseous attachment of non-porous metals by composite bonding 3−2794
  plasterboard walls, transmission loss, studs and cavity absorption effects 3−3701
  Portland cement, use in ice nucleation 3−37229
  standardisation, metrological aspects 3−21773
  stereology, geometrial probability basis, random division of space 3−34515
  technology, conf., Rio de Janeiro, Brazil (Aug. 1972) 3−30931
  tissue equivalent plastic, heat defect in absorption of low energy X-rays 3−5676

materials handling
  see also conveyors; grinding; transportation
  Berkeley Nuclear Laboratories, England, remote handling facilities 3−17320
  Brookhaven circular accelerator, low budget remote handling techniques 3−16477
  coated-fuel particles, micro-handling cell design and construction 3−7019
  conical hoppers, cohesionless granular flow, mass flow rate and stress distribution equations 3−23785
  finely divided powders, automated dispensing device 3−1472
  fuel tanker, filling, estimation of electrostatic hazards 3−659
  Hot Fuel Examination Facility for disassembly of EBR-II ruptured fuel elements 3−17301
  Hot Fuel Examination Facility-North, Ill., USA, remote controlled repair facilities 3−17316
  irradiated fuel elements from LMFBR, remote Na-removal system 3−17310
  irradiated nuclear fuels, computer controlled positioning for Hot Fuel Examination Facility 3−17313
  irradiated reactor fuel elements, bottom loading transfer casks for Fast Flux Test Facility 3−17321
  liqud methane storage tank, airtightness control using NH_3 tracer gas *(French, English)* 3−37672
  liquid hydrogen, handling, transport and storage, experience 3−3774
  nuclear fuel elements, high-burnup, remote metallography facility, sample preparation 3−17315
  nuclear fuel elements for LMFBR, remote system 3−17298
  powders, flow and storage, conference, Chicago, Ill., USA (1972) 3−1468
  powders, tripper surge bin feeder screen system 3−1473
  radioactive materials, alpha and neutron active, water-shielded facilities 3−17331
  radioactive materials, remote hot cell transfer, contamination control equipment 3−17333
  radioactive sources, containers, development *(German)* 3−1047
  remote systems technology, conference, Idaho Falls USA (1972) 3−17296
  ruptured fuel elements, remote system for EBR-II 3−17300
  semiconductor wafer processing, touchless handling 3−39299
  Al, 1145, microfracture and structural failure under dynamic loading 3−2722
  Cu, OFHC, microfracture and structural failure under dynamic loading 3−2722
  Fe, Armco, microfracture and structural failure under dynamic loading 3−2722

materials properties
  this heading is restricted to those properties which are not covered by other specific headings
  see also dielectric properties of substances; electrical properties of substances; mechanical properties of substances; optical properties of substances; thermodynamic properties
  design of specific microstructures using powder metallurgy 3−15677
  hole formation by laser beam, workpiece material thermophysical properties *(Russian)* 3−10579

materials testing
  see also acoustic applications; electron beam applications; insulation testing; laser beam applications; mechanical testing; nondestructive testing; semiconductor materials testing; ultrasonic applications
  accelerated estimation of fatigue life by prefracture method, influence of exptl. results dispersion *(Russian)* 3−12473
  accelerated life test comparisons, stat. precedence theory and tables 3−2777
  acoustic attenuation meas., solid specimen, pulse-echo AB method without reverberations 3−32038
  acoustic emission technique for prediction of material failure *(Japanese)* 3−27843
  acoustic holography applications 3−25042
  adhesion between glass fibres and resins *(German)* 3−21730
  aging effect on failure properties 3−21778

materials testing continued
  alloy, fatigue crack growth, effects of loading freq. and nonreactive external media 3−31234
  alloy, high-hot-strength, fatigue strength under nonsteady state loading 3−37106
  alloys, low yield strength fatigue crack propagation using plastic strips 3−21766
  alloys, stress corrosion test methods 3−9025
  angle probes for u.s. testing, resolution of flaw depth *(German)* 3−18777
  asphalt, elastic modulus and loss factor meas. 3−32028
  ASTM standards, Pt.8, annual book (1972) 3−35353
  austenitic stainless steel sheet metal, spot welds, shear testing, micrographic investigation *(German)* 3−2784
  bearing shells, using eddy currents *(Polish)* 3−27844
  bending tests on discs supported around periphery, for strength determ. 3−34685
  borosilicate films, sintered, Vickers microhardness characterisation 3−39377
  brittle materials, edge effect during heating of cylinder applic. to heat resist. determ. 3−37109
  C-5 aircraft fail-safe strap panels employing traversing i.r. inspection system 3−37599
  cement pastes and mortars, fracture toughness meas. methods 3−27813
  ceramic, creep, evaluation method, computer appl. *(German)* 3−31214
  ceramic nuclear fuel pellets, porosity measurement by image analysis 3−26511
  ceramic-metal soldered joints, mechanical stability research 3−28496
  cermets, measurement methods and instruments 3−27745
  cermets, thermal conductivity *(Russian)* 3−4987
  Charpy testpieces, fracture behaviour rel. to notch angle 3−15804
  chrome-magnesia fired bricks, electron microprobe analysis of failure 3−15755
  composites, effect of specimen geometry on fatigue strength meas. 3−21770
  composites, rate of mixing in tensile testing *(German)* 3−24991
  concrete load deflection characteristics of rectangular reinforced slabs 3−27814
  concrete prestressed reactor pressure vessel 3−35929
  corrosion, loaded spring in corrosive fluid 3−34670
  crack length, u.s. determ. during fracture toughness testing 3−13231
  creep strain data analysis, numerical methods 3−34695
  cryogenic techniques, book contrib. 3−9880
  cyclic elasto-plastic notch stresses, graphical procedure, application to Al alloy 3−12469
  cyclotron applications, conference, Vancouver, Canada (1972) 3−10010
  cyclotron applications 3−20761
  cylindrical specimens under tension, plasticity characts. rel. to geometrical dimens. 3−34683
  drill stress analysis by three-dimensional photoelasticity 3−15812
  ductile materials, fracture toughness meas. 3−31052
  eddy current meas. of conductivity to determ. solidus point 3−27830
  eddy current meas. with coil encircling 2- conductor rod 3−27821
  elastoviscoplastic media, max. shear stress meas., errors using laminated plastometers 3−21774
  electron microscopy, tensile test pieces, microwelding techniques 3−20684
  elevated temperature and slowly time varying loads, inelastic stress-strain law 3−25027
  end closure welds on Fast Flux Test Facility reactor fuel pin, acoustic emission monitoring 3−27834
  energy dissipation determ. from log. decrement of torsional oscillations of compound rod 3−37111
  evaporated thin films, tensile testing machine 3−5368
  failure theory, classical approach rel. to damage accumulation 3−37105
  fatigue crack growth behaviour under variable amplitude loading 3−21756
  fatigue crack morphology 3−31230
  fatigue damage accumulation, analysis of models from common viewpoint *(Russian)* 3−11675
  fatigue damage monitoring by u.s. attenuation meas. 3−13232
  fatigue S/N curve, shape analysis 3−31228
  fatigue strength under random and programmed loads *(Japanese)* 3−12403
  fatigue test machines TsDM-10-Pu, features of use and modernization *(Russian)* 3−12479
  fatigue testing machine, push-pull type for high pressure operation *(Japanese)* 3−12486
  fatigue testing using dynamic force measuring equipment, errors due to force transducers *(Hungarian)* 3−13222
  fatigue tests on wire reinforcement metal *(Russian)* 3−12474
  α-Fe, low-cycle fatigue, grain boundary sliding, 450-700°C 3−34577
  ferromagnetic cylindrical specimens under the influence of field strength dependent permeability eddy-current distribution *(German)* 3−18776
  ferromagnetic materials, classification of leakage field methods of defect detection 3−18766
  fin, from shipping cask, plastic impact testing, energy absorption characteristics 3−39424
  flow analysis by u.s. field meas. 3−2790
  fluidity meas. in metal casting 3−12487
  foam-light refractories, strength testing apparatus *(Russian)* 3−27812
  fracture plane orientation, identification system 3−15675
  graphite billets for reentry nose tips, computer aided u.s. test system 3−37099
  grid application by rolling method for meas. involving use of moire patterns *(Russian)* 3−12477
  harmonic forces measurement, new measuring equipment *(Hungarian)* 3−21763
  high-speed methods analysis 3−37110
  holographic interferometry materials testing technique 3−9028
  holographic interferometry test specification for deform. and fault testing *(German)* 3−19154

materials testing continued
hot adhesive joining of heterogeneous materials, device for stress determ. *(Russian)* 3–12482
IMASH-5S-65 machine, improvements for testing superplasticity in metals *(Russian)* 3–12480
Instrument Society of America, 27th conference, New York, U.S.A., Oct. (1972) 3–22249
lifetime distribution rel. to thermal oscillations *(German)* 3–27839
long-running ductile, fracture, K_{Ic} measurement 3–25039
low cycle load and holding, at high temps. *(Russian)* 3–9831
low cycle testing with holding at high temperature, programming unit *(Russian)* 3–12478
magnetic flyer plate facility 3–25041
magnetic powder crack test with two alternating fields out of phase *(German)* 3–15810
magnetic thin film, patent 3–10427
metal, plastically deformed, fatigue damage detection by exoelectron emission 3–18534
metal, solid and liquid, nomograph of elec. conductivity at selected temps. 3–27816
metal, stress relaxation expts., dislocation behaviour 3–37104
metal foils, ion bombardment induced voids, location by vibratory polishing 3–21772
metal hardening during fatigue testing, recording at elevated temps. 3–28465
metal hoses, failure resist. under low cycle loading 3–34684
metallic springs in materials testing reactor, irrad. creep 3–27809
metrological aspects rel. material standardisation 3–21773
micromechanical testing, microimpression method 3–18753
microstructure, nondestructive investigation, use of surface prints 3–18746
mild steel plates cladded by submerged arc welding, thermal, residual welding stresses *(German)* 3–2783
NDT methods for hydride and alpha-case in Ti alloys, comparison 3–27836
n.m.r., high-resolution technique *(German)* 3–18773
nondestructive, survey of the frontiers 3–18764
nondestructive testing automation in manufacturing processes *(German)* 3–15809
nondestructive testing equipment with multi-channel signals, use of pattern recognition 3–18765
nonmetallic materials, thermal testing apparatus 3–27802
nuclear containment vessel, using strain gauges 3–23422
nuclear fuels, in-reactor creep study at high fission rates using instrumented capsule 3–19945
nuclear reactor, reactor fuel, fission products 3–1063
nuclear reactor fuels, remote hot cell creep testing 3–17309
nuclear reactor materials surveillance programme for components in primary-system sodium 3–26530
nuclear techniques 3–19822
orthotropic materials, transverse strain coeffs. determ. from bending tests 3–27846
plane strain fracture toughness, meas. method, evaluation 3–21765
plastic, electroplated, stress/strain anal. 3–37095
plastic, reinforced, testing apparatus, nonuniform heating 3–32033
plastics, fatigue testing in biaxially stressed condition, apparatus 3–18756
plastics, fatigue testing machine 3–18757
plastics, fatigue tests, rational test piece geometry for cyclic tension-compression tests 3–25033
plastics, mechanical pulsator with capacity for adjusting cyclic and mean loads during tests *(German)* 3–12488
plastics, n.d.t., laser beam applic. *(German)* 3–15811
point load strength test for rock materials, size and shape effects, anisotropy meas. 3–5366
polyethylene, dielec. breakdown strength determ. method for small test pieces *(German)* 3–15806
polymer, programmed static testing machine 3–22265
polymer coatings, test stand for studying long-term strength 3–18760
polymeric materials operating in vacuum in presence of ionizing radiations, accelerated testing 3–27845
polymers, apparatus for dynamic characts. meas. 3–18761
polymers, device for adhesion strength determ. by tangential shear method 3–18762
polystyrene, injection-moulded, technique for demonstrating flaws at which fracture initiates 3–31164
Portevin-Le Chatelier effect in alloys and metals 3–17912
pressure vessels, cyclic plasticity analysis, numerical method 3–32925
pulling force tester, pneumatic 3–2775
quartz, hydrothermal recrystallisation and characterisation for radioelectrical applications 3–34480
α-quartz, synthetic, test meas., 50-545°C, fracture resist., environment effects 3–30182
rail specimen plasticity assessment in impact machine tests using rolled grid *(Russian)* 3–12476
reactor materials and components subjected to time-dependent loading, creep analysis 3–39368
refractory grain porosity, water displacement meas. method 3–28463
rolling contact fatigue tests, effects of surface roughness and form factors of carbon steel and grey cast iron rollers 3–21616
rotor hydropulsators for use with fatigue testing machines, 'floating zero' effect and kinematic distortions *(Russian)* 3–12475
sheet material, crack line loaded, fracture toughness testing, crack growth resist. curves 3–13219
sheet material, crack line wedge loaded, fracture toughness testing, crack growth resist. curves 3–13220
sheet materials, device for compression testing 3–18759
shock testing, impact strength, electronic circuitry for high speed photographic recording *(German)* 3–15803
short period loading, piezoelectric transducer *(German)* 3–9024
shrinkage in stomatology 3–25972
sintering, initial-stage, non-isothermal techniques, study 3–15750
slow crack growth eval. technique 3–31217
soils, granular, membrane effect in triaxial testing 3–34674
solid surface impact viscosity 3–39422
solids, pulsed u.s. visualization using stroboscopic photoelasticity 3–21777

materials testing continued
special impact test specimen *(Russian)* 3–12484
stainless steel, microhardness with different cold work percentages 3–31224
static proneness, appl. of charge and resist. meas. 3–2787
steel, acoustic emission detection of flaws, test 3–27824
steel, annealed, postulate of isotropy consequence test 3–34690
steel, fracture toughness in cyclic loading, rel. to fractographic peculiarities 3–34689
steel, high speed friction welded to annealed steel *(German)* 3–31118
steel, high-strength Type 4140, corrosion fatigue behaviour 3–37051
steel, load-bearing capacity of specimens with stress concentrators under repeated loading 3–34598
steel, low-cycle fatigue properties, transformation of retained austenite and cracks 3–37060
steel, maraging for use in military bridge, fatigue crack growth and fracture 3–21626
steel, mild, fatigue crack growth under crack opening displacement cycling 3–31046
steel, mild, tempered carbon, C45, fracture, yield stress, temp. and load depend. 3–34681
steel, pearlitic, low cycle fatigue, heat treatment type depend. 3–37070
steel, prestress effect on low-cycle fatigue failure 3–21758
steel, reactor pressure vessel, deform. and fracture behaviour, acoustic emission meas. 3–34680
steel, St 35, work hardening and aging behaviour, tensile tests *(German)* 3–27683
steel, stainless, stabilized, strain rate effect on high strain fatigue props. 3–34564
steel, stainless, time and cycle dependent failure at elevated temp. 3–31240
steel, structural, hysteretic behaviour under cyclic bending *(Japanese)* 3–39374
steel, structural, influence of residual stresses on fracture behaviour in K_{Ic} temp. range 3–21624
steel, structural, influence of rest periods on fatigue strength 3–21755
steel, TRIP, subcritical crack growth in air under static loads 3–21629
steel, work hardened, impact strength under cyclic loading at low temp. 3–34682
steel austenitic, explosive bonded and hot rolled clad flat plates, residual stresses *(German)* 3–27837
steel components, contact fatigue kinetics obs. using inductive sensor 3–34692
steel in water, laser effect on u.s. reflection and transmission 3–22198
steel plate, mild, performation by flat-ended cylindrical projectile 3–25026
steel pressure vessels, cumulative fatigue damage tests, cyclic stress, strain and energy variations 3–34677
steels, fatigue fracture rate study with aid of fracture mechanics *(French)* 3–15686
steels, ribbed reinforcing, fatigue testing, planning and evaluation *(German)* 3–9030
steels showing thickness delamination, fracture toughness and its size dependence 3–21620
stress corrosion cracking, acoustic emission applic. 3–31216
stress determ. by X-ray diffraction, on-line 3–27825
stress relaxation technique applic. to superplastic materials 3–37101
stress/strain test data analytical evaluation 3–25024
structural (service) reliability, kinetic fracture models 3–21764
surface analysis by ion microprobe 3–13516
techniques for metals research, book 3–9825
tensile test, international standardisation *(German)* 3–27838
tension grips used on testing machines GSM-50, GRM-1, GRM-2 for thin-walled tubes 3–12485
testing tubes attachment for thin walled tubular specimens *(Russian)* 3–9899
thermal stress resistance determination, brittle materials *(Russian)* 3–2778
thick metal sections, imaging flaws by acoustic holographic scanning 3–21788
tubes for heat exchangers, eddy current testing by using an internal coil system *(German)* 3–18775
turbine blade materials, behaviour under asymmetric loading 3–31232
two-dimensional stress state testing device 3–35357
uniaxial compression tests on brittle porous rock to examine time-dependent behaviour 3–5367
u.s. nondestructive, of dense ferrite for magnetic memory heads *(Polish)* 3–12491
wear measurement with aid of scintillation suppression 3–35360
weld joints, fracture strength testing *(German)* 3–31231
welded specimens, device for testing for long-term bending using cantilever method *(Russian)* 3–12483
welded specimens, programmed fatigue testing 3–37107
welds, studies for promoting ultrasonic testing standard *(Japanese)* 3–27808
Wohlerdiagram development and applic. of extreme-value method 3–9031
Zircaloys, acoustic emission during stress corrosion cracking, correl. with fractography of cracking 3–31045
Al, cracks in space vehicle cabin wall panels, detection by u.s. techniques 3–31227
Al, creep under intermittent loading 3–37103
Al, dynamic stress/strain behaviour in torsion 3–21779
Al alloy, artificial slow crack growth under const. stress, R-curve concept in plane stress 3–31218
7075-T6 Al alloy, fatigue damage accumulation 3–12470
Al alloy, long-term strength, deform. criterion 3–31233
Al alloy, stresses during vibr. of plates under acoustic loads 3–31236
Al alloys, creep rupture testing 3–21652
Al high tensile alloys, fractographic investigation 3–27807
Al matrix composites, survey of fabrication methods 3–8997
C fibre reinforced polymers, fatigue performance 3–31213
C fibres, type II, Kaiser effect in stress wave emission testing 3–15783

materials testing continued
- C single filaments, tensile strength and modulus of elasticity 3−18752
- Cr-Mo-Zr alloyed structural steel, crack restraining properties of weld joints *(German)* 3−2782
- Cu, annealability testing 3−34675
- Fe, cast, pipe, ultrasonic inspection 3−31223
- Fe, deform. resist., temp. and strain rate depend. *(Russian)* 3−31058
- Fe, polycryst., failure mechanism under plane stress conditions at low temps. 3−31096
- Fe-Ni alloy with hardenable electrodeposited coatings, rolling contact fatigue assessment 3−9026
- MnSe inclusions in steel, hot hardness 3−34579
- MoS$_2$, lubricating power determ. *(German)* 3−27841
- Ni alloy, fatigue strength, test temp. influence 3−34687
- Ni based superalloy, elevated temp. fatigue behaviour of single crysts., environment effects 3−39365
- Ti alloys, creep characts. under varying loads 3−37068
- Ti honeycomb structure, presence of Al braze alloy determ. by eddy current testing 3−21767
- W, chemical vapour deposited, mech. behaviour, 800-1600°C 3−37085
- Zn-Al (22 wt.%), superplastic, creep behaviour under bending and plane conditions 3−34678

mathematical analysis
- *see also approximation theory; Bessel functions; calculus; eigenvalues and eigenfunctions; Fourier analysis; integral equations; numerical analysis; series (mathematics); transforms*
- Adelphic integrals, applic. to non- and partially-degenerate dynamic systems, using Hamiltonian functions 3−22581
- astrophysical differential equations, reduction 3−12942
- dense sums of uniformly bounded sequence, existence of weak limits 3−13533
- diffraction of plane wave by infinite array of parallel strips, residue calculus method 3−19561
- dimensional analysis, rel. to streaming currents and decay of apparent cond. 3−650
- infinitesimal transformation for hyperspherical functions and Moshinsky coefficients 3−26365
- Liapunov functions, for boundedness and global existence of solutions of differential eqns. 3−22583
- minimax risk, determ. of lower bound *(Russian)* 3−16599
- non-holonomic systems, linear integrals of eqns. of motion *(Russian)* 3−19394
- non-standard anal., appl. to Schrodinger eqn. and interacting scalar field 3−19662
- nonstandard anal. appl. to $\lambda{:}\varphi_2{}^4(x)$ quantum field model 3−19663
- nonstandard analysis, introduction for physicists 3−26059
- real roots of algebraic eqn., method for determination *(Italian)* 3−28823
- simple cubic lattice Green function analytical properties, applications in lattice statistics 3−19518
- spectral line profile, Fabry Perot profile analysis, Voigt type spectral profiles, determination methods *(French)* 3−23584
- truncating functions, props. and appls. 3−26054

mathematical logic *see formal logic*

mathematical programming
- *see also dynamic programming; linear programming; nonlinear programming*
- composite shells, optimal design subject to natural frequency constraints 3−32367

mathematics
- *see also algebra; combinatorial mathematics; convergence; duality (mathematics); equations; formal logic; functions; geometry; mathematical analysis; number theory; probability; statistics; topology*
- canonical form representations for symmetric functions of 3-vectors 3−33477
- commutator of n noncommuting variables, reln. to Poisson bracket 3−16702
- cosine seminvariants FORTRAN program suite 3−26920
- exponential growth and decay without calculus, teaching paper 3−22214
- interactive computer studies 3−3933
- linear systems study of partial derivative equations 3−10237
- mathematical astronomy for amateurs, book 3−31493
- mathematical structure of physical theories 3−16585
- model for physical theories 3−19397
- rheological appls. 3−6266

matrices *see matrix algebra*

matrix algebra
- beta-decay matrix element extraction in 1st-forbidden decay, comparison of two methods 3−10925
- bounds in eigenvalues in vibration and stability problems, by finite element displacement method 3−563
- coherent potential approximation, matrix formulation 3−8074
- coordinate relaxation method for iterative calc. of eigenvalues and eigenvectors of very large symmetric matrices 3−23465
- correlated fermion state, construction of excitation operator algebra in large number limit 3−10346
- cylindrical shell, stability analysis by finite elements method *(German)* 3−551
- de Sitter group O(4,1), determ. of matrix elements of irreducible representations 3−32285
- error matrices in gas-phase electron diffraction 3−29549
- Euler eqns. of rigid body motion, simple matrix formulation 3−29
- evaluation of matrix exponential e^{hV}, algorithm 3−37783
- fast reactor crit. mass calc. method *(Rumanian)* 3−11080
- finite element analogue of modified Rayleigh-Ritz method for natural vibration problems 3−562
- finite element stiffness matrix, influence of Poisson's ratio on spectral condition number for nearly incompressible solid 3−22617
- free vibration analysis of structures, solution of quadratic matrix equations 3−28906
- generalised U(3(n-1)) scheme model, matrix element calc. *(Russian)* 3−35850
- Greuling-Goertzel approx. to neutron collision probability method, analytic soln. 3−19894

matrix algebra continued
- ground and one-excited U(3(n-1)) states, orbital fractional parentage coeff., nuclei $n \leqslant 16$ *(Russian)* 3−35849
- hybrid elements, for plate bending problems analysis 3−517
- ill-conditioned eqns., physical applications of solutions 3−10230
- K-matrix, monotonous dependence on potential in Kohn variational method *(Russian)* 3−38150
- K-matrix theory of nuclear form factors 3−6798
- level crossing and the space of operators commuting with the Hamiltonian 3−16711
- local instability analysis in plates, stiffened panels and columns 3−515
- Lyapunov matrix eqn., calc. of functionals without preliminary soln. *(Russian)* 3−26053
- mass and stiffness matrices, automated generation and condensation for finite element analysis *(German)* 3−19411
- molecular dynamics, numerical soln. for eigenvalues of infinite matrices 3−11219
- Muller matrix accounting finite speed of light 3−13693
- neutron scattering moments for monatomic gases, integral formulation 3−19898
- off-shell two-body t and K matrices at positive energies, separable approximations 3−6316
- orthogonal transformations of multidimensional angular harmonics for particle permutation operators *(Russian)* 3−19391
- photoelectrons asymmetry parameter β, calc. in terms of matrix elements of relativistic wave functions 3−20032
- point groups, singular matrix representation, comment 3−24052
- projection operators of representations of U$_2$ on basis of Un, determ. of matrix elements *(Russian)* 3−28816
- quadratic matrix eqns., soln. by least-squares method 3−6190
- quantum electrodynamics renormalization of matrix elements, parametrised by number of dimensions 3−4164
- quantum harmonic oscillator, radial wave function calc. by noncompact group in Sp$_{6,r}$ 3−10352
- R-matrix methods for atomic collision processes, computer programs 3−11171
- random-matrix theory, applications to nuclear physics, review 3−29325
- rigid-body vibration tensors least-squares determination, unit weight matrices 3−38628
- spatial linkages, matrix method of acceleration analysis 3−22601
- superfluid thermodynamic equilibrium props., calc. from density matrices in irreducible representation 3−16745
- superpropagators, integral representation 3−26260
- symplectic mappings, stability theory *(Japanese)* 3−18919
- synthetic seismograms at oblique incidence, total inversion algorithm *(French)* 3−3157
- t matrix, convergence of seperable expansions 3−28813
- t-matrix perturbation theory for ground state of solid helium 3−7991
- transformation matrix, U$_n$ group, unitary and orthogonal subgroups *(Russian)* 3−35848
- transport integral eqn. with anisotropic scatt. as linear system computer calc. of matrix elements 3−19522
- two-nucleon reaction matrix depend. of off-shell elements on on-shell elements 3−23285
- vector space theory of matter, introductory course 3−28444
- $YX^1(XX^1)^{-1}$, max. probability matrix, approx. evaluation *(Russian)* 3−16598

Matteucci effect *see magnetoelectric effects; magnetomechanical effects*

maximum principle
- *see also dynamic programming*
- fundamental frequency limits of column carrying conc. mass *(Russian)* 3−28921
- nuclear fast reactors, optimal fuel enrichment distrib. for minimising fuel cycle costs 3−19941
- Pontryagin's, for optimal vibration damping in pin-jointed structure 3−22680
- Pontryagin's for rigid-plastic circular plates, minimum weight design 3−32358
- spacecraft descending into Martian atmosphere, optimal control of final velocity 3−25373
- transfer of spacecraft from hyperbolic to closed orbit round planet by atmospheric drag 3−25377

maxmin technique *see optimisation*

Maxwell-Boltzmann distribution *see statistical mechanics*

Maxwell effect *see flow birefringence*

Maxwell equations *see electromagnetism*

mean free path, carrier *see carrier mean free path*

measurement
- *see also specific measurements, e.g. frequency measurement*
- *see also instruments; recording; units (measurement)*
- Eindhoven A.V.F. cyclotron, automatic control, measurements 3−13380
- electronic, conference, Ilmenau, Germany, 16-21 Oct. (1972) 3−15645
- equipment supervision procedure *(Russian)* 3−5743
- fundamental metrology, International Committee of Weights and Measures address 3−3744
- Instrument Society of America, 27th conference, New York, U.S.A., Oct. (1972) 3−22249
- laser interferometers applic. *(Russian)* 3−16437
- medical metrology 3−22246
- metals physical properties 3−122
- role and value 3−3752
- system for controlling uniformity *(Russian)* 3−5742

measurement errors
- a.c. voltage, using semiconductor diode square law detector 3−19238
- accuracy as a function of number of measurements *(Bulgarian)* 3−53
- block structure kinetics, by microbeam method, error estimation 3−24007
- cloud cover meas., sources of errors in satellite and surface estimates *(German)* 3−9287
- colorimetric analysis, automated, optimum working range, calibration curve, error distribution 3−28783

measurement errors continued
conductometric granulometer, temp. compensation and concentration errors 3-37665
contact deformation nonlinearity errors *(Russian)* 3-19151
Dicke type microwave radiometers *(German)* 3-22274
dielectric, reduction in errors for oscillatory obs. in 0.1-100 MHz range 3-19239
dislocation structure, electron micrography, statistical analysis 3-34519
dynamic, in force meas., using load cells *(Hungarian)* 3-54
dynamic instrumental errors due to inertia, correction *(Polish)* 3-25642
Earth satellite motion parameters, accuracy of estimates using astronomical meas. with correlated errors 3-25371
elastoviscoplastic media, max. shear stress meas., errors using laminated plastometers 3-21774
electron diffraction determ. of molec. struct. in gas phase, error matrices, systematic errors 3-29549
fatigue testing using dynamic force measuring equipment, errors due to force transducers *(Hungarian)* 3-13222
gamma-ray moisture meter, evaluation 3-37758
geoidal height and deflection of vertical, truncation error furmulas 3-27937
gray body temperature measurement using black-body-calibrated radiometer, emissivity errors *(Russian)* 3-5813
group delay using microwave measuring system 3-16374
hot-wire anemometer, sensor resolution, errors occurring due to turbulence, estimation *(Russian)* 3-32274
impulse transmitter for angular velocity measurement, harmonic analysis *(German)* 3-9818
large diam. meas., with calibrated roller instruments *(Russian)* 3-19150
length interferometric meas. 3-35354
luminescence attenuation, decreasing instrumental errors by statistical method *(Russian)* 3-22330
magnetic devices, compensation by using Fe-Ni alloys having temperature dependent magnetization and permeability *(German)* 3-15385
means of measurement instruments, distribution law *(Russian)* 3-19133
median algorithm for data processing of parallel measurements having differing accuracy *(Russian)* 3-13188
microwave amplifiers, standard 3-25651
multiple bounce reflectometer, systematic error reduction 3-5894
noise signal, analysis of accuracy of mean-square value by squaring device based on f.e.t. 3-25640
philosophical aspects 3-9785
polymer melt flow, errors in pressure-hole meas. 3-10216
random signals, time-accuracy tradeoffs in analysis 3-35342
reflection coefficient, analysis 3-22233
rotameter, effects of tilting on readings *(Russian)* 3-6169
sensor error is meas. of solid heated under quasisteady conditions 3-113
spectrochemical analysis, spectrophotometric accurate measurement of molar absorptivities 3-26018
statistical evaluation of test methods 3-13189
systematic, stationary and nonstationary random errors reduction *(Russian)* 3-5744
systems' design principles *(Polish)* 3-55
temperature difference, using resistance thermometers in automatic bridge instruments 3-25686
tidal tilts at Katerinovka, recording errors and calibrations *(Russian)* 3-21906
wind field objective analysis, Fourier analysis procedure rel. to Cressman's method 3-37255

measurement standards
see also temperature scales
1 kg balance, NBS 3-37775
2e/h measurements at NPL using a.c. Josephson effect, monitoring of voltage standard 3-13201
absolute quantum efficiencies, techniques and instrumentation, review 3-35533
absolute radiometer for total irradiance scale 3-9861
aerial mapping lenses, optical transfer function meas. standards 3-226
alpha source standard, checking 3-22459
ASTM Standards, Pt.8, annual book (1972) 3-35353
beta source standard, checking 3-22459
biochemical fluorescence spectroscopy, measurements of absolute values, review 3-35522
and calibration of instruments 3-13192
capacitance, circular four electrode capacitors 3-22240
capacitance, in COMECON-countries 3-22241
d.c. voltage, with Zener diodes 3-5748
e.m.f., monitoring using a.c. Josephson effect 3-3750
far i.r. freqency meas. and two-laser mixing, part I of NPL programme for determ. of speed of light 3-13322
field standard weights, used by weights and measures officials 3-19144
frequency, atomic H storage beam, low-Q cavity maser 3-3749
frequency, state-of-the-art report *(French)* 3-25652
frequency and length unification by meas. of velocity of light using i.r. laser emission 3-13321
frequency and time, technological forecast 3-58
frequency meas. in far i.r., techniques for high-accuracy, part-II of NPL programme for speed of light determ. 3-13323
gas composition meas. 3-22243
inductance, the henry 3-37581
inorganic ions in glasses and polycrystalline pellets as fluorescence standard reference materials, review 3-35349
instruments, economic effectiveness 3-37580
instruments, force and pressure, France, units, Newton and Pascal *(French)* 3-16378
integrating meters, construction, rating and performance, Indian Standards 3-22237
intercomparison of micrometer, nanometer and picometer wavelengths 3-13195
ionizing radiations 3-22242
irradiance, NBS scale 3-35347

measurement standards continued
light velocity constancy, prospects for unified standardization of time, frequency and length 3-13196
liquid absorbance, for u.v. and visible spectrophotometry 3-25647
liquid density, standard liquids and measurement methods 3-32024
Moon as absolute radiometric standard, quiet Sun mm. spectrum meas. 3-35042
Moon as absolute radiometric standard for microwave and i.r. obs. of extended sources 3-39633
neutron flux, source and detector 3-32021
NPL Division of Quantum Metrology, annual report (1971) 3-28458
organic compounds in solution, inorganic ions in glasses, as fluorescent standard reference materials, review 3-35350
pH scale of aqueous solutions 3-22244
photoemission diode standards for meas. monochromatic u.v. light intensity 3-35406
photometric standard sequences for stars in Southern Milky Way areas 3-9525
plane angle, the radian, primary state reference standard 3-19141
pressure, dead-weight piston gauge, gas fluid 3-57
pressure, the pascal, primary state reference standard 3-19140
primary standards, Nat. Phys. Lab. work 3-13194
PTB calibration standard, for adjusting magnification of optical instruments *(German)* 3-32061
radial velocity stars, obs. of 21 9th magnitude IAU stars 3-25450
radiation quantities and units 3-11102
reference air capacitor, high freq. detn. 3-19142
secondary, stable ozone source, atmospheric monitor calibration 3-3186
secondary frequency standards, solid state oscillators coupled to superconducting cavity 3-25804
s.h.f. power, USSR standards and instruments *(Russian)* 3-16379
solar to sidereal time referred frequencies, phase-locked convertor 3-37583
spectral specular reflectance, standard reference materials, preparation and calibration 3-19143
spectrofluorometry, emission standards, spectrometer calibration methods 3-35532
spectrophotometric, role in clinical chemistry laboratory 3-25649
spectrophotometric 3-25650
spectrophotometry and luminescence meas. accuracy (conf. Gaithersburg, USA, Mar. 1972) 3-25759
spherical standard sound source, internal impedance *(Japanese)* 3-28481
standard specimens, metrological experience 3-37582
stars, four-colour photometry of standards and secondary standards 3-31660
surface plates, flatness, cost, precision 3-5763
surface roughness, characteristics of Cali-Block 3-37587
tables of standard data for spectroscopists 3-11111
temperature coefficient of linear expansion, of solids 3-32022
temperature reference, microwave radiometer calibration, target design, technique 3-19139
thermal arc plasmas as radiation standard for light intensity calibration in astrophysics 3-4681
thermal neutron flux density, USSR primary standard *(Russian)* 3-5750
time and frequency, accuracy of TV sync. pulse reception method 3-22236
time and length rel. to atom 3-22239
u.h.f. noise standard, for high temp. plasma meas. 3-33391
USSR, standard of radian, pascal, kelvin and farad *(Russian)* 3-5749
visible laser frequency meas. by up-conversion of CO_2 laser radiation, part III of NPL programme for speed of light determ. 3-13324
wavelength, secondary, sources and measurement methods 3-32023
α-particle absolute energies 3-10940
γ-ray intensities, $^{14}N(n, \gamma)^{15}N$, $^{35}Cl(n, \gamma)^{36}Cl$ and $^{53}Cr(n, \gamma)^{54}Cr$ reactions 3-10976
^{114}Cd interferometric hot cathode spectral lamp 3-3748
^{57}Fe exact determ. of energies of 122 and 136 keV lines 3-13480
^{198}Hg interferometric hot cathode spectral lamp 3-3748
^{85}Rb, Larmor frequency n.m.r., meas., atomic reference scale for liquid and solid state 3-12072

measurement systems
astronomical objects, relative coordinates, scanning measurement system, superorthicon TV camera, deflection circuits *(German)* 3-9631
atomic fluorescence spectrometry, dual channel synchronous integration measurement system 3-22534
computer aided, for X-ray films of vocal tract 3-426
computer-aided data analysis *(Croatian)* 3-25961
Curie and compensation points in small size ferrites 3-37667
design principles *(Polish)* 3-55
distance measurement 3-6519
earth's crust, global movements *(German)* 3-34830
gas composition, standard 3-22243
group delay at microwave, errors 3-16374
lead measurement of leadscrews, laser interferometer method 3-22252
opticoelectron, for displacement meas., contactless method *(Russian)* 3-5768
particle size distribution in air 3-28400
rel. to product quality 3-22247
relaxation time in H and Rb masers 3-22866
sea ice geometry, top and bottom surfaces, diving techniques evaluation 3-9410
for thickness measurement of nuclear wire *(German)* 3-16382
X-ray diffraction deformation rate meas., during e.m. forming of metals 3-25959

measurement theory
accuracy as a function of number of measurements *(Bulgarian)* 3-53
active circuits, voltage waves, current waves and power waves concept 3-5745
control engineering, modern measurement techniques, noise rejection properties 3-56
entropy, information theory applic. *(Polish)* 3-25641
film thickness, criteria 3-22234
and observability theory, real dynamical systems 3-16373

measurement theory continued
- optimisation of observational data of a random quantity input to a recording instrument *(Russian)* 3 − 12878
- quantum, modification of von Neumann's theory 3 − 32406
- radiometry, partially coherent sources, generalisation of basic laws 3 − 22815
- sheet material, permittivity at microwave freq. 3 − 22232
- signal amplitude, phase, and frequency, definitions and their significance for meas. 3 − 19134
- systems' design principles *(Polish)* 3 − 55
- for thickness measurement of nuclear wire *(German)* 3 − 16382

mechanical birefringence
- *see also photoelasticity*
- cornea, bovine, dynamic rheo-optical behaviour, temp. and frequency dependence 3 − 35262
- cyclolinear polyphenylsilsesquioxane films, mol. and supermol. nature of photoelastic effect *(Russian)* 3 − 20253
- ferrimagnetic garnets, stress birefringence meas. 3 − 21381
- optical glasses, stress-optic coeff. dispersion, 5700-3200 Å, strain polarizability const. 3 − 2509
- sheets, stress wave propag. obs. by dynamic polariscope 3 − 32054
- solids, pulsed u.s. visualization using stroboscopic photoelasticity 3 − 21777
- thin-walled cylindrical shell models, from optically active materials, centrifugal casting 3 − 25658
- Tresca-type plastic dielectric in simple shear, optical constitutive eqns. 3 − 32352
- CdS, stress birefringence, room temp. 0.1 to 2.3 eV 3 − 15511

mechanical engineering
- discs, hollow and solid, with loadings having rotational symmetry, computer program *(German)* 3 − 32349
- elasto-plastic stress analysis in partly yielded notched bar, assessment of finite element methods 3 − 26077
- multiple degree of freedom mechanical systems, steady-state forced vibration amplitude determination 3 − 22678
- pitting, mating roller measurement of frictional heating temperature and coefficient of kinetic friction *(Japanese)* 3 − 27811
- SI units, relation with mechanical engineering *(German)* 3 − 19137

mechanical impact *see impact*

mechanical organs *see artificial organs*

mechanical oscillations
- *see also vibrations*
- acoustic oscillations generated in a Rijke tube, production of excitation regions *(Russian)* 3 − 5712
- acoustical system, study by reciprocity theorem 3 − 19123
- analysis by speckling in Fourier transform plane 3 − 5754
- automobile front suspension relative to body, conditions for shimmy occurrence *(Russian)* 3 − 502
- cantilever, vibr. lateral restraint, axial load, influence on eigenfrequencies 3 − 559
- cantilever beams, pre-twisted and tapered, natural vib. freq. by collocation method 3 − 561
- cantilever on rotating disc, elastic oscillations *(Russian)* 3 − 19472
- coupled Duffing eqns., analytic soln. for forced oscillations, Kryloff-Bogoliuboff technique 3 − 26068
- cylinders in fluid, Stokes' paradox 3 − 7409
- cylindrical shell in acoustic medium, dynamic stability 3 − 6276
- cylindrical tank filled with elastic medium, oscillations of elastic tap and bottom *(Russian)* 3 − 28916
- damping by pulsed dynamic dampers 3 − 32394
- dielectric elastic hollow sphere, large amplitude controllable states 3 − 556
- disc in rot. second order fluid, nontorsional oscills. 3 − 7408
- drops, forced oscillations in a viscous medium 3 − 29890
- dynamical system, study by reciprocity theorem 3 − 19123
- elastic plate-fluid system, spectrum of natural freq. 3 − 4599
- film boiling, oscillation effects of sphere 3 − 27115
- fundamental frequency limits of column carrying conc. mass, use of Pontryagin's max. principle *(Russian)* 3 − 28921
- harmonic, of mass, registration of force produced *(Russian)* 3 − 5767
- indenter, response of elastic half-plane to motion and harmonic oscillation 3 − 28909
- mechanico-acoustical system, study by reciprocity theorem 3 − 19123
- metallic rod, torsional oscill., optical meas. of very small strains 3 − 25038
- non-linear springs connecting unequal masses, calc. of free vibrs. by perturbation method 3 − 19399
- non-linear two degree of freedom dissipative system, calc. of forced vibrs., and stable regions 3 − 19400
- railway wagons computer investigation of nonlinear horizontal oscillations *(Russian)* 3 − 492
- reactions of mechanical systems to random forces *(Russian)* 3 − 28842
- resonant acoustic oscillations with damping, small rate theory 3 − 38390
- resonant phenomena during nonlinear oscillations of solid bodies *(Russian)* 3 − 22688
- rod, longit. oscillations, optimal solns. *(Russian)* 3 − 566
- satellite nutational oscillations, damping with internal flywheel 3 − 25375
- semiconductor devices, resonance charact. 3 − 13602
- slender foil unsteady motion near interface between two different fluids, numerical soln. 3 − 33272
- slender-wing aircraft, nonlinear lateral oscillations investigation 3 − 11377
- solar photosphere, 300-second oscillations on large solar surfaces, Na D_1-line and continuum obs. 3 − 35033
- spacecraft, nonstationary motion during atmospheric re-entry at supersonic velocity *(Russian)* 3 − 22599
- spacecraft oscillations with two-position attitude-control system 3 − 25376
- stellar clusters, spherically-symmetric system, resonance damping of oscill. *(Russian)* 3 − 37441
- testing, digital incremental oscillator analyser systems, inherent limitations 3 − 5762
- thermo-acoustic oscillations in forced convection heat transfer to supercritical pressure water 3 − 20282
- thick-walled elastic shells under external press., determ. of oscill. and stability 3 − 557

mechanical oscillations continued
- thin elastic nonuniform plate, nonlinear oscills., numerical soln. 3 − 558
- thin-walled open-section circular rings, free oscillations and eigenfrequencies 3 − 3664
- torsional, of rigid spherical inclusion in elastic stratum 3 − 32392
- trapped modes of rotating viscous fluids in spherical shells, numerical simulation 3 − 20329
- Van der Pol oscillator, quenching of limit cycles 3 − 13598
- viscous fluid, stability of oscillatory Stokes layers, energy theory approach 3 − 20367
- wake flow of a cascade of oscillating airfoils 3 − 38411
- Young's modulus meas. method using fibre bending oscillations *(German)* 3 − 25668

mechanical permeability
- *see also diffusion in solids*
- adsorbed films, permeab. to air determ. using bubble shape theory 3 − 8015
- glass, with high silica content, of He *(German)* 3 − 30284
- polymer films, meas. for corrosive liquids 3 − 25661
- steel, gas diffusivity and solubility meas. and calc. method *(French)* 3 − 1832
- steel, hydrogen penetration and embrittlement, effect of electrolytic charging conditions 3 − 5326
- Al_2O_3, cakes, formed by slip casting, compression permeability 3 − 8974
- Cu, of hydrogen, stress and elec. field effects 3 − 1824
- Fe, hydrogen diffusion coeff. determ. from permeability meas. *(French)* 3 − 1827
- Fe and alloys, of hydrogen, conc. and temp. depend. 3 − 1828
- Fe-C alloys, permeability and embrittlement by cathodic hydrogen *(French)* 3 − 21661
- Fe-Si solid solns., of hydrogen, ordering influence *(Russian)* 3 − 30283
- Ge, of hydrogen, stress and elec. field effects 3 − 1824
- Mo, of hydrogen, 400-1200°C 3 − 1833
- Ni, of hydrogen, stress and elec. field effects 3 − 1824
- Pd alloys, of hydrogen, 300-900°C 3 − 1834
- Pd-Ag(Ce) alloys, hydrogen permeability 3 − 2737
- W, of hydrogen, 400-1200°C 3 − 1833

mechanical properties of liquids
- No entries

mechanical properties of solids *see mechanical properties of substances*

mechanical properties of substances
- *see also anelasticity; bending; brittleness; deformation; elastic constants; elastic relaxation; elasticity; elasto-optical effects; fatigue; fracture; hardness; internal stresses; mechanical permeability; mechanical properties of liquids; mechanical strength; photoelasticity; photoplasticity; piezo-optical effects; plasticity; slip; stress / strain relations; tribology*
- AISI type 304 stainless steel pipe, eff. of exposure to liquid sodium 3 − 20949
- alkali halide, i.r. irrad., photomech. effect and dislocation motion *(Russian)* 3 − 38595
- Annual review of materials science vol. 2, 1972 3 − 24778
- basalts, physicomechanical and electrical properties at high pressurs and temp. 3 − 25134
- ceramics, new, material texture depend. 3 − 5341
- Chordae tendineae of human heart, histomechanics *(German)* 3 − 3754
- concrete and hardened cement paste 3 − 5350
- cubic anisotropic solid, concentrated force, single integral soln. 3 − 16627
- epoxy adhesive, at low temp. *(Japanese)* 3 − 12446
- fibre, polymeric, textile, review 3 − 9010
- film, ion sputter deposited, polygonization patterns, illumination effect on mech. stability 3 − 15106
- glasses, silicate 3 − 5355
- insulating thin films, for solid state electronics *(German)* 3 − 15281
- i.r. laser window materials, state-of-the-art review 3 − 5980
- materials with microstructure, equations of motion using first law of thermodynamics 3 − 14931
- metal, grain boundaries influence on mech. props., review 3 − 37037
- oxides, survey of deformation and physical props *(French)* 3 − 11672
- plastics, review 3 − 9009
- poly-(m-phenylene isophthalamide), effect of struct. ordering on mech. props. *(Russian)* 3 − 7291
- polyester-styrene, plasticized highly crosslinked unsaturated system, mol. parameters and mech. props. correl. 3 − 1316
- polyethylene, branching index, effect on struct. and props. 3 − 11339
- polymeric solids, mechanical properties, review 3 − 25016
- refractories, mechanical properties and defects 3 − 31129
- refractory metals, conference, Atlanta, USA (May 1971) 3 − 34493
- rock specimens, axial compression and destruction under high multilateral pressure 3 − 25133
- roughness of course surface *(Russian)* 3 − 5764
- stainless steel, austenitic, new reactor material *(Czech)* 3 − 1062
- steel, low carbon, after room temp. rolling causing recrystallisation *(French)* 3 − 24912
- steel, stability of influence of high temp. thermomechanical working on mechanical properties 3 − 24922
- steel, stainless, martensitic, influence of composition and heat treatment on mechanical props. and struct. *(French)* 3 − 34588
- steel, type 304(+15% Ti), post irrad. creep-rupture and tensile props. 3 − 17915
- steel and alloy characteriz. for elements of machines and instruments 3 − 21684
- Al matrix composites, review 3 − 15776
- Al-Cu alloy, structural transformations 3 − 12413
- $(Al_2O_3)_3$ $(SiO_2)_2$, mullite, ceramic powder, stoichiometric, synthesis and mechanical props. 3 − 27736
- $B(C_xN_{1-x})$ refractory, physical, mechanical and chemical props. *(Russian)* 3 − 31124
- Cr wire, optimum props. rel. to alloying additions and diam. reduction *(Russian)* 3 − 8878
- Fe powders with 1% P additives, sintering conditions effect on magnetic and mechanical props. *(Russian)* 3 − 27719
- Fe whiskers, production and properties 3 − 24796

- **mechanical properties of substances** continued
  - $(NH_4)_2SO_4$, elastic anomaly near ferroelectric transition 3 − 30763
  - Ni based heat resistant alloys, anisotropy of mechanical properties 3 − 18671
  - Pu-Ga, plastic deformation, mechanical props. influence of homogeneity *(French)* 3 − 34589
  - Ta_2O_5 film, anodic, rel. to microstruct. and electrolytic breakdown 3 − 1684
  - W, chemical vap. deposited, rel. to deposition and annealing 3 − 1960
- **mechanical strength**
  - *see also compressive strength; shear strength; tensile strength*
  - alloy steels, ausformed by extrusion 3 − 34614
  - borosilicate glass, ion exchange chemical strengthening 3 − 15789
  - brittle materials, containing second phase dispersions 3 − 7841
  - brittle strength in surface-active medium, time depend. *(Russian)* 3 − 27059
  - carbon-graphite materials, crystallite size effect 3 − 34652
  - ceramic materials, Rumpf's physical fracture theory, Griffith and critical crack length, cell size, experimental *(German)* 3 − 12430
  - ceramics, brittle, strength loss with thermal shock 3 − 8985
  - ceramics, fibre reinforced composites, theories 3 − 15777
  - ceramics, microstructure dependence, measurement and analysis techniques 3 − 12422
  - ceramics, review 3 − 5340
  - ceramics, thermal shock resist. on heating rel. to failure 3 − 8984
  - ceramics, uniaxial strength, porosity effects, working model 3 − 39383
  - coated materials strength and creep testing apparatus for temps. above 1400°C 3 − 32047
  - composite cylinder, helically wound, burst fracture strength under internal press. *(Japanese)* 3 − 8998
  - composite materials, fracture 3 − 2760
  - ductile materials, near tip strain as ductile fracture criterion 3 − 31052
  - electroslag welded joints, 80 mm thick, fracture toughness, COD approach application 3 − 21625
  - epoxy adhesive, glass transition temp. relation to adhesive strength 3 - 5353
  - fibre reinforced metal, bond strength between fibre and matrix 3 − 37093
  - fracture toughness of materials, review 3 − 24206
  - glass, environmental effects via surface water release 3 − 24999
  - glass, obs. and theories 3 − 5356
  - glass ceramics based on tetrasilicic mica, strength depend. on mica grain size 3 − 8982
  - glass fibre strand, var. with polyester resin wetting props. 3 − 15772
  - glass reinforced plastics, wound, resist. to failure by unwinding 3 − 24981
  - large-grain alloys, resistance to capture 3 − 31062
  - long-term, time to fracture calc. *(Russian)* 3 − 27672
  - long-time strength test results, extrapolation method 3 − 34688
  - manganin type alloy characteriz. for precision resistors 3 − 24946
  - material failure theory, classical approach rel. to damage accumulation 3 − 37105
  - materials science and technology treatise 3 − 2621
  - metal, dispersion strengthened, review of high temp. strength and creep mechanisms 3 − 15695
  - metal, stat. eval. of strength at brittle fracture 3 − 31097
  - metal hoses, failure resist. under low cycle loading 3 − 34684
  - metallic materials, struct. strength concepts and methods of determ. 3 − 21679
  - metals in contact with liquid metals, drilling examination 3 − 21705
  - metals in liquid media, apparatus for long-term strength testing *(Russian)* 3 − 9826
  - noble metals, calc. using semiempirical equation of state *(Russian)* 3 − 8836
  - nonmetallic materials, fracture mech. 3 − 4794
  - parallel plate shaped coherent precipitates arrangement, influence of strain energy 3 − 18607
  - polyethylene filled with glass fibre and plasticized with rubrax, chemical stability in HCl and H_2SO_4 *(Russian)* 3 − 12441
  - polyvinyl alcohol film, u.v. irrad., effect of active dyes *(Russian)* 3 − 27769
  - programed loading and testing machine 3 − 32032
  - reactor weld metals, radiation and temper embrittlement processes 3 − 8889
  - of solid bodies, kinetic analysis *(Bulgarian)* 3 − 9011
  - steel, 000N18K9M5T, influence of heating on phase content, structure and mechanical properties 3 − 24831
  - steel, A-533-B, effects of crack size on gross-strain crack tolerance 3 − 8891
  - steel, austenitic, thermomech. hardening effect *(Russian)* 3 − 37045
  - steel, austenitic Cr-Mn, cold-worked unstable, enhancement due to heating and loading *(Russian)* 3 − 30966
  - steel, diamond smoothing effect on surface finish and fatigue strength 3 − 34596
  - steel, heavily alloyed, resistance to failure 3 − 34601
  - steel, high strength, fracture toughness enhancement by microstruct. control 3 − 31051
  - steel, high-speed tool, characterization 3 − 21682
  - steel, hydrogen influence, crack development *(French)* 3 − 8905
  - steel, KH18N10T, influence of hydrostatic pressure on long-term strength *(Russian)* 3 − 12378
  - steel, KhN35VTYuL, influence of method of melting, crystallization conditions and heat treatment 3 − 24929
  - steel, long-term strength increase due to boron microadditions 3 − 21607
  - steel, low-C non-alloy type, grain size and temp. effects *(German)* 3 − 34606
  - steel, maraging, Cr-Ni-Co-Mo, strengthening and precip. phenomena *(Russian)* 3 − 31060
  - steel, maraging, treatment methods influence on impact strength of forgings 3 − 24926
  - steel, metastable austenitic Cr-Mn, warm rolling effect *(Russian)* 3 − 18612
  - steel, quenched U8, effect of various surface active media on the changes taking place in the strength *(Russian)* 3 − 2726
  - steel, specimens with cappings, corrosion fatigue strength, heat treatment and rolling effects *(Russian)* 3 − 27667
  - steel, structural, temp. effect on physical and mechanical properties 3 − 24927
- **mechanical strength** continued
  - steel, structural strength, rel. to machine part operating characts. 3 − 27686
  - steel, workability improvement considerations 3 − 21681
  - Superinvar alloy prep. and characteriz. 3 − 24945
  - testing machine for plastics 3 − 18757
  - thermoplastics, long term strength, crazing in non-crystalline plastics 3 − 9007
  - tubes, testing stand for strength and creep 3 − 27800
  - uniaxial strength, porosity effects, working model 3 − 39383
  - Weibull's statistical theory, stress density function, fracture probability, ceramic materials *(German)* 3 − 12429
  - whiskers, book 3 − 8073
  - Y_2O_3-ZrO_2, lattice strain of cubic stabilized phase 3 − 15759
  - zircon, phosphate-bonded, production as refractories 3 − 15757
  - Ag-Au alloy, shock wave effect on mech. props. *(German)* 3 − 34608
  - Agl-Mg commercial alloys, stress corrosion cracking and its prevention *(Japanese)* 3 − 18635
  - Al bronzes, casting and wear props., effect of iron *(Polish)* 3 − 31033
  - Al-Zn-Mg alloys, changes on alloying and ageing 3 − 21671
  - Al_2O_3, thermally shocked, strength degradation and crack propagation 3 − 2752
  - Ca sulphoaluminate and sulphosilicate, hydraulic hardening process *(Russian)* 3 − 15742
  - Co alloy, dispersion hardened 3 − 8782
  - Cr alloy, dispersion hardened, high-temp. stability of refractory metal borides 3 − 18626
  - Cr alloys, carbide and boride strengthened, stress rupture props. 3 − 34568
  - Cu alloys, adsorption-induced loss of strength during selective transfer in boundary friction 3 − 21706
  - Cu crysts., plastic constraint as mechanism for film strengthening 3 − 21613
  - Fe, Armco, impact strength, effect of cold deform. and subsequent heat treatment *(Russian)* 3 − 5307
  - Fe, b.c.c. crack extension by bond rupture, fracture toughness and crystal structure relation 3 − 15724
  - Fe, cast, containing Cr and Cr-Mo, rare earth additive effects *(Russian)* 3 − 27666
  - Fe, mech. strength of crystal lattice calc. *(Russian)* 3 − 8845
  - Fe alloy, E1437B, ageing/deformation treatments influence on struct. and mech. props. *(Russian)* 3 − 24873
  - Fe alloys, strength differential effect, effective modulus interpretation, reply to comments 3 − 18679
  - Fe-Cr-Ni steel, austenitic, shock wave effect on mech. props. *(German)* 3 − 34608
  - Fe-Ni-Al alloy, subspinodal, hardening obs. and mechanism *(Czech)* 3 − 31103
  - Fe-Ni-Ti-Al-Nb alloys, ageing in two-phase $(\alpha + \gamma)$ states, effects on props. and struct. *(Russian)* 3 − 12363
  - Ge whisker, elastic props. and torsional strength 3 − 38759
  - KBr, press forged, for laser window applications 3 − 5979
  - KCl, press forged, for laser window applications 3 − 5979
  - KCl-KBr mixed crystal CO_2 laser window material, Czochralski growth, increase by C 3 − 16453
  - LiF:In, mechanical and emission characts. with In diffused into compound 3 − 24115
  - Mg-Al spinel crystal, age strengthening kinetics 3 − 30930
  - $Mg(OH)_2$, disperse porous structure, strength, influence of dehydration 3 − 39420
  - Mo, mech. strength of crystal lattice calc. *(Russian)* 3 − 8845
  - Ni chips, effect of plastic deform. in high-speed cutting *(Russian)* 3 − 18617
  - Ni:ThO_2, dispersion strengthened, high temp. strength mechanisms study using explosion techniques 3 − 18615
  - Ni-base superalloy coherent particle strengthening, stress coarsening effect 3 − 18648
  - Ni-Cr alloys, Sn alloying effect 3 − 21668
  - Ni-Cr base alloy, weldable, stress rupture and ductility props., for use above 100°C 3 − 31063
  - Ni-Cr-ThO_2, dispersion hardened, mech. props. at high temps. 3 − 8941
  - Ni-ThO_2, dispersion strengthened, mech. props. at high temps. *(French)* 3 − 8940
  - Si_3N_4, high density, diamond grinding effects 3 − 8953
  - SiO_2-Al_2O_3-Na_2O glass, strengthening, influence of struct. *(Polish)* 3 − 8989
  - Ti, strengthening by O_2 3 − 15725
  - Ti alloys, impact strength, rel. to low temp. applic. 3 − 31098
  - W, mech. strength of crystal lattice calc. *(Russian)* 3 − 8845
  - ZnSe laser windows formed by chemical vapour deposition 3 − 5981
- **mechanical testing**
  - *see also dynamic testing; hardness testing; mechanical variables measurement*
  - 304 stainless steel, low temp. stability, prediction from room temp. deformation test 3 − 9839
  - adhesion between glass fibres and resins *(German)* 3 − 21730
  - adhesion strength of polymers, device for determ. by tangential shear method 3 − 18762
  - anisotropic metals, re-interpretation of tension and bulge test data 3 − 4784
  - beam specimen, double cantilever, face grooved and contoured, compliance calibrations 3 − 15805
  - bending, fracture probability, stress density function, Weibull's statistical theory of mechanical strength, ceramics *(German)* 3 − 12429
  - bending tests on discs supported around periphery, for strength determ. 3 − 34685
  - ceramic coatings, thermal shock resistance 3 − 22256
  - chip-breaker-grooved tools, effect of wear 3 − 25034
  - coated materials strength and creep testing apparatus for temps. above 1400°C 3 − 32047
  - composites, rate of mixing in tensile testing *(German)* 3 − 24991
  - compression testing, device for sheet materials 3 − 18759
  - concrete load deflection characteristics of rectangular reinforced slabs 3 − 27814
  - concrete specimens, in biaxial and triaxial stressed states 3 − 25656
  - concrete tensile failure under water pore pressure 3 − 27815
  - concrete testing model rel. to physical characteristics of coupled shear wall *(Japanese)* 3 − 3943

mechanical testing continued
- cracking stability and quasielastic concept 3—21759
- creep rupture testing machine with electronic temp. control *(German)* 3—9834
- c.r.t., impact of steel ball, pulsed holographic study 3—5773
- cryostat and straining assembly, mechanical testing of materials, in liquid He 3—5775
- ductile materials, fracture toughness meas. 3—31052
- electrolytic coatings, brittleness testing 3—25657
- fatigue and fracture tests at Langley Research Centre 3—21757
- foam-light refractories, strength testing apparatus *(Russian)* 3—27812
- forming bar stock, stepped loading effect on yield stress 3—34691
- fracture test procedure for crack opening displacement determ. 3—30197
- goniometer, u.s., application 3—18767
- graphite electrical resistivity change during compressive tests 3—23432
- HTR particle coatings, Young's modulus and fracture stress meas. by the brittle ring test 3—18768
- IMASH-5S-65 machine, improvements for testing superplasticity in metals *(Russian)* 3—12480
- international standardisation of the tensile test *(German)* 3—27838
- large-grain, resistance to rupture 3—31062
- long-time strength test results, extrapolation method 3—34688
- low C steel, plastic strain kinetics 3—25654
- low cycle load and holding, at high temps. *(Russian)* 3—9831
- mechanical-acoustic nondestructive testing, review 3—13225
- metallic materials, struct. strength concepts and methods of determ. 3—21679
- microimpression method of micromechanical testing 3—18753
- nuclear fuel element assembly, external meas. of mechanical integrity by accelerometer 3—11072
- nuclear fuels, in-reactor creep study at high fission rates using instrumented capsule 3—19945
- nuclear reactor components, broad band acoustic fatigue, theory 3—14256
- nuclear reactor materials surveillance programme for components in primary-system sodium 3—26530
- orthotropic materials, transverse strain coeffs. determ. from bending tests 3—27846
- plane strain fracture toughness, meas. method, evaluation 3—21765
- plastic, reinforced, testing apparatus, nonuniform heating 3—32033
- polyethylene, optico-deformational absorption meas. *(Russian)* 3—5756
- polymer, programmed static testing machine 3—22265
- polymer coatings, test stand for studying long-term strength 3—18760
- polymeric materials operating in vacuum in presence of ionizing radiations, accelerated testing 3—27845
- pulling force tester, pneumatic 3—2775
- rolling contact fatigue tests, effects of surface roughness and form factors of steel and cast iron rollers 3—21616
- sheet material, crack line loaded, fracture toughness testing, crack growth resist. curves 3—13219
- sheet material, crack line wedge loaded, fracture toughness testing, crack growth resist. curves 3—13220
- small bending deformations of plane samples, recording device 3—18758
- static endurance of testpieces under nonstationary stress, comparative assessment 3—18749
- steel, hydrogen embrittlement meas. methods *(French)* 3—5327
- steel, rail-grade, hydrogen effects in prod. and service performance 3—5335
- steel, St 35, work hardening and aging behaviour, tensile tests *(German)* 3—27683
- steel, structural, influence of residual stresses on fracture behaviour in K_{Ic} temp. range 3—21624
- steel, TRIP, subcritical crack growth in air under static loads 3—21629
- steels showing thickness delamination, fracture toughness and its size dependence 3—21620
- stress intensity factor corrections 3—31219
- structural polymers, elastic characteristics and damping properties 3—25655
- tensile, eccentricity of loading 3—9029
- tensile bars, notched perfectly plastic, large deform. 3—25037
- tension testing without local necking 3—18770
- thin-walled cylindrical shell models, from optically active materials, centrifugal casting 3—25658
- torsion pendulum for l.f. internal friction meas. 3—18779
- tubes, testing stand for strength and creep 3—27800
- tubing, steel clad, effect of small cracks on creep rupture props. 3—31221
- universal extensional rheometer for polymer melts 3—64
- wear measurement with aid of scintillation suppression 3—35360
- welded specimens, device for testing for long-term bending using cantilever method *(Russian)* 3—12483
- wire rope, load, elongation and torque obs. 3—66
- Zircaloy-2, hydrogenated, deformability testing method based on high vel. deform. *(French)* 3—9035
- Al alloy, artificial slow crack growth under const. stress, R-curve concept in plane stress 3—31218
- Al alloys, endurance testing 3—22257
- Cu, annealability testing 3—34675
- Fe, polycryst., failure mechanism under plane stress conditions at low temps. 3—31096
- Fe alloys, AK6, mech. props. consistency after deform. heat treatment 3—21670

mechanical variables control
- *this heading is restricted to those variables which are not covered by other specific headings. See also, for example, force control; thickness control; velocity control; vibration control*
- stabilisation of stationary motion by controlling part of variables *(Russian)* 3—16612

mechanical variables measurement
- *this heading is restricted to those variables which are not covered by other specific headings. See also, for example, force measurement; thickness measurement; velocity measurement; vibration measurement*
- counterbalanced reed pendulum apparatus for obs. of internal friction 3—3755
- cryotribometer, apparatus for meas. dry friction at low temperatures 3—5755
- fluidic sensor for leaf spring moment meas. *(German)* 3—13224
- gimbal errors of floating gyroscope, taking drift into account *(Russian)* 3—65
- horizontal pendulums, effect of energy dissipation on angular drift *(Russian)* 3—503
- impedance, low frequency real time measurement 3—35361
- impedance, transient measurement, data analysis and instrumentation 3—9840
- laser aligning principles 3—6521
- laterally loaded plate, moire fringe technique for analysis of moments and deflexions 3—3760
- linearity, reciprocal method 3—37591
- liquid film, Gibbs elasticity meas. technique and apparatus 3—28464
- load cell, low profile, high precision 3—5774
- Moire method, use of irregular rasters 3—37589
- nuclear containment vessel, using strain gauges 3—23422
- nuclear reactor pressure vessels, in-service inspection, acoustic emission applications 3—5791
- plastic, reinforced, testing apparatus, nonuniform heating 3—32033
- programed loading and testing machine 3—32032
- rods and pipes, e.m. generation elastic waves 3—576
- shape deviation of internal cone, instrument 3—37590
- shock-wave, optical fiducial system 3—5771
- small bending deformations of plane samples, recording device 3—18758
- stiffness, of vertical gear-hobbing machine 3—19152
- swellometer, rapid response for photographic emulsion swelling 3—13346
- tensile strength of C single filaments 3—18752
- thermomechanical analyzer, Shimadzu TMA-20B, application *(Japanese)* 3—13252
- torsional and tensile creep, apparatus 3—22258
- vibrations, digital incremental oscillator analyser systems, inherent limitations 3—5762
- C yarns, wettability meas., wicking method 3—39394
- NaCl quenched crystals, influence of impurity distrib., applic. of electron microscopic decoration method and microhardness meas. 3—1676
- Si sensors for meas. mechanical variables, based on piezoresistance *(Norwegian)* 3—19162

mechanical waves *see elastic waves*

mechanics
- *see also bending; celestial mechanics; classical mechanics; damping; density; dynamics; fluid mechanics; intermolecular mechanics; kinematics; molecular internal mechanics; momentum; statics; statistical mechanics*
- Bohr-Sommerfeld orbits and quantizable symplectic manifolds 3—37868
- conference on theoretical and applied mechanics, Udine, Italy (June 1971) 3—16605
- discs, contact stress distrib. and tangential ultimate bearing capacity, models and numerical calcs. 3—3940
- dual spin bodies with unbalancing mass, stability 3—491
- Duffin bracket for nonconservative systems, algebraic nature 3—28818
- flowgraph methods comparison for mechanical vibration problems 3—22681
- Galilei and Lorentz structures on space-time, comparison 3—22715
- generalised, quantisation and superfluous coordinates 3—37864
- generalised, quantisation scheme, modification of commutation relations 3—37865
- hybrid processing of empirical functions 3—6199
- leading of uniformly loaded clamped sector plate 3—507
- momental ellipsoids and kinetic energy, teaching paper 3—16355
- Noether's theorem, extension to Lagrangian density with higher order derivatives 3—22588
- noumenon, a generalization of relativistic events and space-time 3—19494
- predictive, relativistic approx. solns. for e.m. interactions 3—37873
- reactions of mechanical systems to random forces *(Russian)* 3—28842
- relativistic, transformation eqns. and objectivity principle 3—32428
- role in contemporary knowledge of world *(Russian)* 3—22208
- three-body classical relativistic problem, exact nonplanar solutions 3—37889

mechanics of fluids *see fluid mechanics*

medical effects of radiation *see biological effects of radiation*

medical electronics *see biomedical electronics*

medical information processing
- in book on clinical laboratory electronics 3—10184
- e.c.g., R-R intervals and R wave widths, analogue preprocessor for digital computer measurement 3—25991
- fatigue measurement, computerized data processing system 3—32246
- hospital-based digital computer system, for research and clinical appl. 3—9690
- oxyhaemoglobin dissociation curves, computer-aided data reduction 3—2[illegible]360
- radiographic data processing, computer-generated holograms 3—22856

medical sciences *see medicine*

medicine
- *see also biomedical engineering; cardiology; patient diagnosis; patient monitoring; patient treatment; physiology*
- asbestos fibres aligned by magnetic field, microscope obs. 3—18737
- betatrons, neutron meas., track etch technique 3—16561
- breast cancer, treatment by electron beam from betatron 3—16560
- cancer, preoperational irradiation therapy, from 25 MeV betatron *(Russian)* 3—25598

medicine continued
clinical chemical analysis, automation *(German)* 3–10204
clinical laboratory data transmission using PDP-15 and PDP-8/E computers 3–26005
conference on medical instrumentation, Washington (1973) 3–39802
cyclotron, 19 MeV for X-ray therapy 3–16480
cyclotron, TRIUMF, medical uses 3–22164
cyclotron applications, conference, Vancouver, Canada (1972) 3–10010
cyclotron applications for neutron therapy 3–19251
cyclotron of Argonne cancer research hospital, USA, radionuclide production 3–22161
cyclotron of Harvard university, USA, medical uses 3–22158
cyclotron size for medical applications 3–22165
dose rate control, for betatrons 3–22172
electronic instrumentation in clinical laboratory, book 3–10184
fractionated high energy radiation therapy, optimum treatment schedules 3–22170
health physics, multipurpose radiation monitoring system, ionization chamber and air monitoring, book 3–31921
health physics, nuclear reactors, weapons and accelerators, book 3–35267
health physics training, decontamination and radiation, book exposure 3–31922
laser beam applications, review 3–29157
lung tumours, betatron therapy, clinical considerations 3–22171
muscle contraction effects of Ca ionophore, X-537A 3–35266
National Accelerator Laboratory medical programme 3–409
neutron therapy 3–22166
neutron therapy facility for 30-inch cyclotron 3–22162
nuclear, book on advances 3–3563
nuclear, computer-based scanning system 3–35275
nuclear, computerized image improvement using selected frequency band enhancement 3–416
nuclear, image processing, review 3–35276
nuclear, imaging and image improvement 3–417
nuclear, radioisotope imaging, effect of in-patient scattering 3–35277
Nuclear diagnostic, book 3–11101
nuclear science conference, Miami USA (1972) 3–28622
particle accelerators, medical applications, review 3–31924
peristaltic pumping, finite element analysis 3–22157
pharmaceutical tablet auto-analysers, off-line FOCAL-12 program 3–394
physics, conference (Edmonton, Canada, June 1972) 3–9699
radiosotope scintigraphy 3–35285
radiotherapy clinic using 200 MeV protons in Sweden 3–22160
research, interactive computer use 3–5627
semiconductor detectors, in nuclear medicine and radiobiology, review 3–32140
short-lived isotopes, production using charged particle accelerators, for medical applications 3–32870
sodium urate, nucleation, rel. to gouty arthritis 3–13140
speech pathology, applic. of computer-aided acoustic analysis 3–9654
stomach cancer, results of preoperational irradiation from 25 MeV betatron *(Russian)* 3–25597
technology, interaction between two 3–35225
therapy, adaptation of 30 MeV IAP betatron 3–16483
tracer data, dynamic statistical analysis, parameter estimation 3–3567
transplantation, tissue typing methods 3–28761
transuranium elements, props. and applications *(French, English)* 3–31933
AgI cloud seeding, possible effects on human health 3–37532
^{7}Be, retention and metabolism in mammals 3–35274
Ca mass determination in body by neutron activation analysis using cyclotron 3–22163

Meissner effect *see superconductivity*

melting
see also melting point; zone melting and refining
p-azoxyanisole, solid-nematic transition, pretransitional effects, neutron diffr. 3–26973
basanite magma, high temp. and press. meas. of garnet peridotite 3–21857
defect melting model for three-dimensional crystal 3–17964
diamond, h.p. characts. and nature of liq. carbon, model approach *(Russian)* 3–14981
DNA, inverse problem, melting curves rel. information recorded *(Russian)* 3–1313
electric tank furnaces for melting of Pb containing glass 3–22340
granite, high pressure determ. of water-saturated and under-saturated melting relations 3–25121
graphite, h.p. characts. and nature of liq. carbon, model approach *(Russian)* 3–14981
Gruneisen parameter pressure depend. rel. to Fusion curve of solids at high pressure 3–17963
heat transfer numerical calc. 3–30244
heat transfer with a water jet 3–14420
heat transfer with melting or freezing in a wedge shaped enclosure 3–14982
ice, pressure melting and regelation by round wires 3–14984
Lindemann law for ideal solids, lattice dynamical study 3–24246
metal, activation energy for melting correl. with binding energy *(Russian)* 3–14983
metal, activation energy for vacancy diffusion proportional to latent heat of melting *(Russian)* 3–24295
metal, temp. field in vacuum arc melting 3–24890
metal in finely dispersed state, 80-320K, characteriz. 3–33686
microcrystals in two dimensions, molecular dynamics simulation 3–27102
molecular dynamics studies, dislocation density and pair distribution function 3–36410
n-alkanes, rotational transition and melting curves, high pressure DTA apparatus 3–11721
order-disorder theory of latex particle fusing *(Japanese)* 3–27104
partial fusion in seismic low vel. zone of upper mantle changes in electrical conductivity of basalt 3–5446
pelitic rocks, partial melting and phase equilibria in high-grade metamorphism 3–39472

melting continued
plane moving boundary problems, freezing and melting, integral transforms 3–34702
plasma arc melting system design 3–27714
polyethylene, oxide, melting, freezing, supercooling, Gruneisen and Rao consts. 3–18722
polyethylene, single-textured, morphology 3–20234
polymer, bulk-crystallized, morphological changes during melting 3–20237
polyoxymethylenes, dielec. absorpt. and melting behaviour 3–30754
pyrolite upper mantle under mid oceanic ridges, stable crusts and island arcs, melting relations 3–37177
semi-infinite steel body melting in an Fe-C alloy, heat and mass exchange eqns. 3–24827
solid, spherical and cylindrical, boundary and initial value problems 3–6384
solidification rate of water at its fusion temp. in falling-film flow in a vertical tube 3–11725
steel, low-C, melting and dissolution in iron-carbon melts 3–37052
system with repulsive pair potential, melting-curve maximum 3–24248
temperatures of Earth's core 3–12581
vacuum metallurgy, conf., Pittsburgh, USA, (June 1972) 3–27615
AlAs, Lindemann-Gilvarry melting law and Debye temps. 3–36393
AlP, Lindemann-Gilvarry melting law and Debye temps. 3–36393
Ar, molar volume along melting curve up to 10 kbar 3–27105
Bi film, melting and freezing, obs. in electron microscope 3–14980
Bi-In(Sn)(Cd) systems, contact melting in mag. field *(Russian)* 3–15698
Bp, Lindemann-Gilvarry melting law and Debye temp. 3–36393
$Co(PO_3)_2$-$CsPO_3$, glasses and melts, effects of water on molar props. *(Russian)* 3–14696
Fe, gray, hypo-eutectic, eutectic solidification, metallographic struct. and melting conditions *(Japanese)* 3–27679
Fe, grey cast, induction furnace treatment, mech. props. 3–24960
^{3}He, meas. along the melting curve at millikelvin temps. 3–18007
^{3}He solid, effect of magnetic field on melting curve 3–11782
^{4}He film on graphite, melting anomalies rel. to short range order 3–36458
$KY(MoO_4)_2$, thermal decomposition of the melt *(Russian)* 3–2809
$Ln_2(WO_4)_3$-M_2WO_4 reactions in the melt, where Ln=Nd, Er and M=Rb, Cs *(Russian)* 3–15825
Ni-(50% wt.)Fe, melting process effect on coercive force *(Korean)* 3–5120
Pb, melting curve up to 60 kbar 3–27103
PuO_2, separation of Mo for fuel recovery 3–17291
PuO_2-UO_2, nucl. fuel, linear heat rating for incipient fuel melting, effect of cladding gap size 3–26537
Sb-Se alloys, composition region Sb to Sb_2Se_3, new melting diagram determ. by differential thermal analysis *(Russian)* 3–11723
$XeOF_4$, ^{19}F magnetic resonance study, phase transition, scalar coupling to relaxing quadrupolar nucleus ^{131}Xe 3–36813
Zn, melting curve up to 60 kbar 3–27103
$Zn(PO_3)_2$-MPO_3:Co (M=Na, K, Cs), glasses and melts, molar props., softening temp. and structure *(Russian)* 3–14695

melting point
adsorbed layers, phase transitions 3–36474
complex semiconductor chalcogenides, physical props. *(Russian)* 3–8168
Hf-W alloy, liquidus curves, m.p., eutectic temps., solubilities 3–30969
lunar interior temp. determ. from elec. cond. meas. of olivine and pyroxene 3–25420
metal in finely dispersed state, 80-320K, characteriz. 3–33686
poly(2,6-dimehtyl-1,4 phenylene oxide) toluene mixtures, light scatt. at melting point, determ. of thermodynamic parameters 3–29798
polymer, and glass transition and struct. 3–7293
polymer solns., liq.-liq. phase separation 3–20228
Al, anomalous sp. ht. and disorder *(German)* 3–24276
$Ba_4^{2+}La_6(SiO_4)_4(PO_4)_2O_2$, silicophosphate, preparation and characterization *(Russian)* 3–11597
$Ca_4^{2+}La_6(SiO_4)_4(PO_4)_2O_2$, silicophosphate, preparation and characterization *(Russian)* 3–11597
In, anomalous sp. ht. and disorder *(German)* 3–24276
KCl, rel. to thermal vibrs. of atoms 3–24224
$Mg_4^{2+}La_6(SiO_4)_4(PO_4)_2O_2$, silicophosphate, preparation and characterization *(Russian)* 3–11597
NaCl, rel. to thermal vibrs. of atoms 3–24224
$Na_2S-Na_2S_n-S$ system, three phase equilibria, thermal analysis and quenching obs. 3–27097
NdSb, analysed from Nd-Sb alloy phase diagram, melting temp. meas. of 2075°C *(Russian)* 3–12338
Pb, anomalous sp. ht. and disorder *(German)* 3–24276
PbTe-MgTe alloy system, physical props. 3–7904
Sb, anomalous sp. ht. and disorder *(German)* 3–24276
Sn, anomalous sp. ht. and disorder *(German)* 3–24276
$Sr_4^{2+}La_6(SiO_4)_4(PO_4)_2O_2$, silicophosphate, preparation and characterization *(Russian)* 3–11597
Th-Ta alloy, liquidus curves, m.p., eutectic temps., solubilities 3–30969
Th-W alloy, liquidus curves, m.p., eutectic temps., solubilities 3–30969
Ti-Al-Co system, Ti rich region, annealing, structure 3–24836
TiC_xO_y and TiN_xO_y, correl. with thermal expansion coeff. *(Russian)* 3–11751
$YTaO_4$, formation in Y_2O_3-Ta_2O_5 system *(Russian)* 3–12497
YTa_3O_0, formation in Y_2O_3-Ta_2O_5 system *(Russian)* 3–12497
Zn, anomalous sp. ht. and disorder *(German)* 3–24276
Zr-W alloy, liquidus curves, m.p., eutectic temps., solubilities 3–30969

membranes
see also osmosis
atria, guinea pig, effects of electrical stimulation on membrane potentials during hypothermia 3–22140
basilar, computer simulation of nonlinear model, determ. of distortion products 3–3472
basilar, motion, temporal relationship with initiation of nerve impulses in auditory nerve fibres 3–3474
basilar membrane motion, nonlinear phenomenological model 3–3471

membranes continued
- biological, progress 3−9638
- biological cell membrane, physical forces for adhesion 3−9640
- biomembrane phase transitions theory 3−22142
- biomembranes, cooperativity in *(German)* 3−37516
- biophysics, book 3−28321
- biotransport, continuum mechanical approach to flow equations 3−35234
- biotransport, physiochemical model of permeability 3−35233
- carp retina, bipolar-amacrine transmission 3−31881
- carp retina, membrane resist. changes underlying bipolar cell response 3−31880
- cell transport, irreversible thermodynamics kinetic approach 3−16307
- cholesterol-hexadecyltrimethylammonium bilayer, capacitance rel. to voltage 3−3403
- colloidal solution, ferrite particles, osmotic press., mag. field gradient 3−27792
- counterdiffusion, supersaturation, bubble formation, isobaric inert gas urticaria and vertigo 3−35232
- diffusion layer electrode, polographic analytical instruments *(German)* 3−16563
- elastic, finite axisymmetric deform. due to edge tractions and internal press. 3−535
- electrically excitable, generalised model, systems theoretical approach 3−35240
- electrochemical processes at biological interfaces 3−25550
- electrodiffusion equations, time dependent, numerical solution 3−25549
- erythrocytes, light beating spectrum, active transport mechanism 3−19089
- gating currents assoc. with Na channels 3−35244
- guinea pig taenia coli membrane potential rel. to extracellularly applied ATP and related nucleotides *(Japanese)* 3−37514
- muscle, smooth, contraction and excitation *(Japanese)* 3−35228
- myosin location in physarum polycephalum and role in cytoplasmic streaming 3−16306
- natural membranes with protein in lipid bilayer 3−13128
- nerve impulses, Na ion movement rel. to temp. 3−35230
- nictitating membrane of rabbit, inhibitory stimulus control 3−39795
- nonlinear vibrations, study using modified perturbation method based on Linstedt-Poincare technique 3−22700
- nonlinear viscoelastic, axisymmetric deform. due to spinning 3−22640
- permeable, non-porous, thermo-osmosis of refrigerant gases 3−7307
- phase transitions in biological membranes, mol. model for lipid ordering determ. 3−22144
- pressure fluctuations in gases of 1 atmosphere 3−17486
- production of semipermeable membranes and use in reverse osmosis and ultrafiltration plants *(German)* 3−7948
- radiant heat receivers, characteristics calculation 3−5801
- skeletal muscle excitation-contraction coupling rel. to voltage depend. charge movement 3−31845
- snap-buckling of curved membranes, phase-plane anal. of stability conditions 3−22662
- soils, granular, membrane effect in triaxial testing 3−34674
- star-shaped membrane, Rayleigh's method for frequencies 3−32398
- superconcentration in membrane filtration, without precipitation at surface *(German)* 3−7949
- vesicles bounded by single phospholipid bilayers and loaded with acetylcholine , preparation in suspension 3−13127
- vibrations by const. deflection contours method 3−37845
- yielding of pressurized closed membrane 3−540
- AgBr in aqueous solns., elec. cond. by ion transport 3−2841
- H_2 purification by diffusion through Pd membranes at high pressure *(Russian)* 3−9905
- H_2O structure variations with temp., hyperfiltration streaming pot. meas. 3−35231
- Pd-Ce alloy applic. as diffusion membrane 3−2737

memories *see digital storage*

memory devices *see storage devices*

mendelevium
- No entries

mendelevium compounds
- No entries

mercury (metal)
- adsorbed on Au, surface sensitivity of ESCA for sub-monolayer quantities 3−24334
- adsorbed on Ni(100), orbital energy spectra 3−39206
- adsorption phenomena at electrodes, ionic double layer study 3−12530
- airborne Hg fall-out on snow surrounding Swedish chlor-alkali plants 3−37200
- ambient for deformed metal prop. obs. rel. to grain size *(Russian)* 3−12369
- aquatic frontal systems, element enrichment in films and foams 3−12690
- arc, steady-state, low pressure, velocity of neutral atoms emanating from cathode 3−23935
- arc discharge, current limitation 3−14617
- arc plasma, VI characts. and power relation in transverse mag. field 3−36212
- atom, $6^1S_0 \rightarrow 6^1P_1$,$(7^1S_0)$,$(7^1P_1)$ transitions, generalised oscillator strengths 3−35971
- atom, ang. distrib. of photoelectrons from 5d-subshell 3−29501
- atom, electron impact excited, near-threshold polarization of 6^1S_0-$6^3\mathbf{P}_1$ line 3−7059
- atom, in collision with H_2, D_2, N_2, NO, and CH_4, de-excitation of metastable state, electronic to vibronic energy conversion 3−20057
- atom, light atomic projectiles, differential scatt. cross sections, ang. distribs. 3−29529
- atom, low energy electron scatt. amplitudes, free-electron-gas exchange approx. validity 3−33051
- atom collisions with buffer gases, collisional depolarisation of resonances radiation 3−33060
- atomic lifetimes of isoelectronic sequences 3−17338
- atoms, charge-exchange phenomena with He ions, spectroscopic study 3−33058

mercury (metal) continued
- atoms, optimization of low energy electron scattering for producing beam of spin-polarized electrons 3−11175
- atoms and Hg^+ ions, atomic transition probabilities determ. 3−29479
- contact on Si, for nondestructive C-V meas. 3−2182
- contamination, AgZn batteries 3−3213
- crystal, magnetoacoustic attenuation giant quantum oscills. 3−33784
- discharge, pulsed, low press., vapour press. variations under pulsed arc conditions 3−1523
- discharge, pulsed high-current, characteristics 3−36223
- drop pumping by travelling electric potential wave 3−10098
- embrittlement of age-hardened Cu-1.9 wt pct Co and Cu-3.6 wt pct Ti at room temp. 3−18647
- embrittlement of Al, role of solute additions 3−34566
- evaporation into a vacuum under isothermal conditions 3−38663
- evaporation technique for convective mass transfer from stationary and moving surfaces 3−20286
- ferrofluid containing Ni-Fe alloy particles, mag. props., thermal growth, effect of inhibitors 3−2321
- in finely dispersed state, thermodynamic characts. 3−33686
- flow in metallic conduits under non-wetting and amalgamating conditions 3−1372
- Greenland icecap concentrations and Icelandic geothermal activity 3−25143
- hollow cathode discharge, thrust meas. 3−11522
- Irish sea, dissolved Hg distrib. rel. to pollution sources 3−25197
- Lake Huron surficial sediments, Hg distrib. 3−37266
- laser, characteristics and optimum working conditions *(Russian)* 3−29082
- liquid, disordered material inhomogeneous transport regime 3−33893
- liquid, electronic density of states calc. has depression near Fermi energy 3−18054
- liquid and solid, photoemission meas. of density of states rel. to pseudogap 3−34463
- liquid and vapour states, Hall mobility meas. up to 1600°C and 2000 atm. 3−36590
- liquid-vapour phase change, determ. of transport coeffs. in linear irreversible thermodynamics rate equations 3−11729
- low pressure, high current discharge, anode region phenomena *(Russian)* 3−14624
- magnetohydrodynamic waves transverse propagation in horizontal mag. field and vertical temp. gradient for Hg 3−11440
- manometer, high-pressure, standard for calibration of differential pressure transmitters, span-shift errors with static pressure 3−25709
- particles, cylindrical, attenuation factors calc. for i.r. radiation scatt. 3−24698
- photoemission, two-photon high-probability, from metals in electrolyte solutions 3−39214
- photographic effect spectral sensitisation of AgBr films *(Russian)* 3−12554
- plasma, in thyratron, dielectric const. as function of freq. 3−17686
- plasma, weakly ionised, negative absorpt. of r.f. waves 3−11476
- positron lifetime, temp. depend., −135 to 20°C 3−36334
- thermal cond. meas., three layer thermal diffusivity problem 3−18119
- thermoelectric power in transcritical state, obs. 500-3500 atm., up to 2100°C *(Russian)* 3−2055
- trace element profiles from Apollo 15 deep drill core 3−3303
- turbulent flow in annuli, effect of wetting 3−1371
- vapour, 1 to 20 Torr press., positive discharge column study 3−17700
- vapour, 3884 Å band emission from electrodeless glow discharges, foreign gases effect 3−20674
- vapour at high temp. and press., selective reflection studies of spectral lines *(French)* 3−9943
- water pollution, lake sediments meas. 3−25346
- X-ray diffr. detn. of atomic distrib. at 15°C 3−7615
- Zeeman effect, normal and anomalous, laboratory conditions for obs. 3−22218
- Zeeman effect for student obs. 3−16371
- adsorption on Au and Au-Hg alloy change in work function measurements by retarding potential method 3−38725
- CO + Hg collisions, time-of-flight sensitized fluoresc. vel. depend. of Hg excitation 3−11312
- Fe:Hg, time-differential-perturbed-angular correlation meas. of hyperfine mag. field 3−39067
- He-Hg mixture, weakly ionized, electron distrib. function 3−14604
- Hg, $6s6p^1P_1$ state, electron-impact excitation, spin polarisation and differential cross section 3−20054
- Hg I absorpt. spectrum meas. between 370 and 900 angstroms 3−35958
- Hg lamp plasma, effect of single pulse ruby laser radiation 3−23917
- Hg-H_2O two-phase mixture, meas. of elec. conductivity in bubbly and slug flow area 3−32941
- Hg-N_2 collisions, determ of cross section for 6^3P_1-6^3P_0 excitation transfer by method of delayed coincidences 3−4380
- Hg^+, hyperfine struct. Zeeman splitting 3−23482
- Hg^+ mobility in He 3−7308
- HgI, application of Slater-Condon theory with configuration interaction to various odd configurations 3−4360
- Hg(I), autoionising d^9s^2np level, intermediate coupling calcs. 3−7063
- HgII laser beam intersecting Rb atomic beam, sharp line self-induced transparency 3−4114
- ^{198}Hg hot cathode spectral lamp, as secondary standard, for interferometry 3−3748
- ^{202}Hg, forbidden transition 6^2S_0-6^3P_0 in mag. field *(French)* 3−23472
- KCl:OH^-, Hg, study of Hg diffusion, effect of OH^- impurity 3−20892
- K_2SO_4:Hg^+, X-irrad., e.s.r. 3−39026
- Kr-Hg gas mixture, possible u.v. laser *(German)* 3−725
- Mg-air flow, local void fraction measurement by optical fibre glass probe 3−16576
- Na-Hg(6^3P_1), atomic collisions, induced sensitized fluorescence, excitation transfer to Na 3−26569
- Xe-He d.c. discharge, complex ion formation 3−17691

Mercury (planet)
black drop phenomenon during 1970, May 9 transit, stray light corrections 3−18937
orbital eccentricity, origin and dynamic capture of Moon 3−9508
resonance rotation of celestial bodies and Cassini's laws rel. to Moon and Mercury 3−16110
surface composition from reflection spectrum 3−25414
thermal elastic deformations with period of 176 days 3−16165
tidal effects on sunspots 3−3293
Ar u.v. dayglow lines in atmosphere, models and predicted intensities 3−31616

mercury alloys
see also mercury compounds
Au-Hg, H_2O and Hg adsorption, measurement of change in work function by retarding potential method 3−38725
Cd-Hg, n.m.r. of ^{113}Cd, Knight shifts, alloying depend. 3−2433
Hg:Tl, amalgams thermodynamic functions, enthalpies of formation 257-583K, structure *(French)* 3−33442
Hg-In, liq., Lorenz number and thermal cond. 3−30453
Hg-In alloys, liq., electronic spectra, 0.14 to 4 μm 3−39133
$Hg_{1-x}Cd_xTe$, band structure and charge density calcs. using representative k points 3−18080
$(Hg_3Te_3)_x-(In_2T_3)_{1-x}$, influence of impurity compensation effect on negative magnetoresistance 3−27277
K-Hg, liq. partial struct. factors, model of conformal solns. 3−30063
Mn_2Hg_5 neutron diffraction obs. of antiferromag. coupling 3−18329
Pb:Hg alloys, modified interstitial vacancy-pair model for Hg diffusion 3−20894
Pb:Mg alloys, diffusion of Mg and Pb, interstitial-vacancy pair model 3−20893

mercury compounds
see also mercury alloys
bis-dipivaloymethane mercury, struct. *(German)* 3−14807
diethyldithiophosphate, cryst. struct. 3−14831
ethylxanthate, cryst. struct. 3−14831
halides, electrical pulsed-discharges in vapour, model for population inversion 3−726
halides, spectroscopic studies of potential energy consts., root-mean-square amplitudes and coriolis coupling consts. 3−7182
mercury, N,N′-diethylthiocarbamate, cryst. and molecular struct. 3−14827
$Cd_xHg_{1-x}Te$, refl., comp. and electron density depend., rel. to band struct. *(Russian)* 3−2548
$Cd_xHg_{1-x}Te$, spin effects on Shubnikov-de Haas oscillations, semimetal-semicond. transition 3−33795
$Cd_xHg_{1-x}Te$ film, sputtering in Hg vapour plasma 3−8727
$Cd_xHg_{1-x}Te$ magnetoresistance, Shubnikov-de Haas oscillations, 77-120K 3−36628
$Cd_xHg_{1-x}Te$ monocrysts., comp. distrib. from absorpt. spectrum *(Russian)* 3−12158
$Hg(CH_3CONH)_2$, derivative of DF trypsin, determ. of heavy atom coordinates 3−24098
$Hg_{1-x}Cd_x(SCN)_2$, gel growth 3−15611
n-$Hg_{1-x}Cd_xTe$, Auger limited band to band and Shockley-Read recomb., photocond. meas. 3−36634
$HgCr_2S_4$, critical broadening of e.p.r. line near Curie point 3−21294
$HgCr_2Se_4$, critical broadening of e.p.r. line near Curie point 3−21294
$HgCr_2Se_4$, magnetoabsorpt. obs., temp. and field depend. at Curie point 3−12122
HgF_2, ^{19}F chem. shift tensor and nonionic bonding 3−12070
$Hg_2F_2(Cl_2)(Br_2)(I_2)$, excitation and emission spectra, 77 K and room temp. 3−30864
HgH(D), fine struct. and perturbations in electronic spectra 3−14354
HgI_2 detector, γ-ray efficiency 3−28658
$HgMoO_4$, crystal structure obs. 3−38560
$Hg(OH)NO_3$, cryst. struct. 3−14755
α-HgS, cinnabar, single crystals, Berg-Barrett X-ray topographic study of small angle boundaries 3−38525
α-HgS, elastic and piezoelectric properties 3−36840
α-HgS, vibr. spectrum assignments 3−8583
HgS trigonal small crystals, study of natural absorption region from diffusion reflection spectrum *(Russian)* 3−8612
HgS(Se)(Te), g-shift of s-state ions 3−2377
HgSe, band struct., determ. from magneto-quantum effects 3−2003
HgSe, iterated solns of Boltzmann eqn. with Fermi statistics 3−36598
HgSe film, amorphous, Hall mobility obs. 3−5009
$HgSe_xTe_{1-x}$ pressure induced phase transitions 3−15011
HgTe, anomalous temp. dependence of Hall coefficient 3−24458
HgTe, crit. pt. determ. of band structure, thermoreflectance study 3−2005
HgTe, dielec. function, refl. spectra in far i.r., 8K-300K 3−2565
p-HgTe, doped, hydrostatic pressure effect on Hall coeff. and elec. cond. 3−21099
HgTe, impurity diffusion, 200-300°C 3−36441
HgTe, impurity states 3−2022
HgTe, iterated solns. of Boltzmann eqn. with Fermi statistics 3−36598
HgTe, semimetal, mag. moment and suscept. two-point matrix Green function calc. *(Russian)* 3−5099
HgTe-CdTe, narrow bandgap semiconductor, zero bandgap transition 3−38800
α-$Hg_2V_2O_7$, cryst. struct., X-ray determ. *(French)* 3−26997
$Hg_{1-x}Zn_x(SCN)_2$, gel growth 3−15611
n-Hgs, cubic, band inversion, optical absorpt. and intra-band refl. rel. to carrier conc. and temp. 3−2002
MgTe, electron mobility anomalous temp. depend. 3−2095
NaXHg zeolite, supercond. of Hg in zeolite channels 3−5067
ZnHgSe(Te) mixed crysts., e.p.r. of Mn^{2+}, g-factor 3−2378
$Zn_xHg_{1-x}Se(Te){:}Mn^{2+}$, e.p.r., rel. to band struct. 3−15409

mercury lamps *see mercury vapour lamps*

mercury vapour lamps
O_3 calibration source for analysers and inlet-sample air systems 3−32252

mesic and muonic atoms
see also mesic and muonic molecules; muonium
exotic, description and appl. to nuclear studies 3−1135

mesic and muonic atoms continued
exotic atoms, production and investigation techniques 3−1134
hadronic, particle physics aspects 3−7093
kaonic, K^--nucleus optical potential, calc. X-ray level shifts and relative transitions 3−33069
kaonic, reality of inner state 3−14321
kaonic, strong interaction effects and nucl. matter distrib. shape 3−7092
kaonic atomic X-rays from Au and Ba, determ. of K^- mass and K^- polarisability 3−29542
kaonic atoms and information on nature of nucleus 3−11189
leptonic, effect of neutral intermed. boson 3−23027
muonic atom data, rel. to kaon leptonic decay *(Russian)* 3−828
muonic atoms, nuclear magnetism distribution and electric quadrupole moment 3−33063
muonic atoms, nuclear polarization effects 3−33064
muonic atoms $\alpha(Z\alpha)^2$ vacuum-polarisation correction 3−35987
muonic h.f.s and nucl. excitation by bound muon 3−6724
rel. to negative muon depolarization in solids 3−23508
nonlinear electrodynamics, limiting fields, lower bound calc. 3−29199
nuclear fission barrier penetrability for muonic atoms 3−17270
nuclear motion effect on energy eigenvalues in muonic atoms 3−17387
O, screening correction to binding energy 3−11188
pionic, pion-nucleus optical potential description 3−11187
pionic 2p-1s transitions in very light atoms 3−7091
rare-earth nuclei, change of radii due to rotation, calc. of Mossbauer and muonic isomer shifts 3−26368
rotational nuclei, recalc. of hfs constants in cranking model 3−38113
vacuum polarization in exotic atoms 3−1133
He-like exotic atoms, energies of circular orbits 3−4398
K^--nucleus optical potential 3−20075
μ depolarisation in molecular condensed matter 3−17388
μ-mesic energy levels for nuclear polarisation in adiabatic approximation 3−23507
μ-mesoatoms, nuclear reactions and radiationless transitions *(Russian)* 3−23284
π^- electroproduction into bound state of mesoatom *(Russian)* 3−38054
Ba, screening correction to binding energy 3−11188
Bi, muonic, elec. quadrupole X-ray transitions 3−7095
^{209}Bi, reson. effects, e.m. props. 3−6703
μD, μ transfer to gaseous Xe in collisions 3−20077
μH, μ transfer to gaseous Xe in collisions 3−20077
$(^4He\ \mu)_{2s}^+$ ionic system, meas. of Auger effect, contribution to deexcitation of system 3−26613
^{190}Os, muonic, mag. h.f. splitting of $2^+ \rightarrow 0^+$ transition 3−6767
^{192}Os, muonic, mag. h.f. splitting of $2^+ \rightarrow 0^+$ transition 3−6767
Pb, muonic, elec. quadrupole X-ray transitions 3−7095
Pb, screening corrections to binding energy 3−11188
^{204}Pb, ^{206}Pb, ^{207}Pb, ^{208}Pb, radial moment analysis and meas. of isotope shifts 3−33068
Tl, muonic, elec. quadrupole X-ray transitions 3−7095
Tl, screening correction to binding energy 3−11188
Tl isotopes, reson. effects, e.m. props. 3−6703

mesic and muonic molecules
see also mesic and muonic atoms
H_2, probability of π absorpt. rel. to chem. bonds *(Russian)* 3−11190

mesomorphic state *see liquid crystals*

meson absorption
see also nuclear reactions and scattering due to mesons
No entries

meson-baryon interactions
see also kaon-baryon interactions; pion-baryon interactions
backward, study of SU_3 symmetry of baryon Regge residues by comparison of angular distribs. 3−4198
total cross-sections for πp, πd, Kp and Kd interactions up to 65 GeV/c by hodoscope method *(Russian)* 3−10814
f^o absorption cross sections against nucleons at 3 GeV, Glauber multiple scattering theory 3−10781
ρ^o absorption cross sections against nucleons at 3 GeV, Glauber multiple scattering theory 3−10781

meson-baryon scattering
see also kaon-baryon scattering; pion-baryon scattering
(8,8) model of chiral-symmetry breaking, SU(3) violations and σ terms 3−23133
canonical algebra approach 3−4205
duality, exact, spectroscopic consequences 3−23105
e.m. effects in polarization at high energies, small t *(Russian)* 3−4168
inclusive reactions, extended bootstrap model to include quantum numbers 3−38098
meson-nucleon, inelastic, bare current-quark masses and light cone algebra 3−29224
meson-nucleon σ-term and BBS-coupling constants 3−23141
meson-nucleon σ-term and BBS coupling consts. 3−10764
meson-nucleon scattering, light cone constraints and asymptotic domains 3−32672
parameter-free Reggeized absorption model 3−23111
pseudoscalar, amplitude analysis of charge-exchange and strangeness-exchange processes using dual absorptive model 3−4223
quark model for high-energy scattering 3−13891
t-channel helicity-flip amplitude in charge and hypercharge-exchange reactions, fixed poles 3−14049
urbaryon rearrangement and breaking of line reversal relations 3−35807
N-meson elastic scatt. at high energies, quasipotential approach to spin effects 3−32710
ωN scatt. phase, determ. from $\omega\gamma$ coupling constant 3−13971
ρN forward scatt. amplitude, e^-e^+ photoproduction at 4 GeV 3−17009
$\rho^0 N \rightarrow \pi N$, invariant amplitudes for vector meson dominance model 3−6663

meson capture
see also nuclear reactions and scattering due to mesons
heavy hyperfragment non-mesic decay, $(\Lambda n/\Lambda p)$ stimulation ratio 3−11026

ABSTRACTS AND CURRENT PAPERS JOURNALS

Three main subject areas are covered by INSPEC abstracts and current papers journals: physics, electrical and electronics engineering, and computer and control engineering. For each field an abstracts journal and a companion titles journal are published. The abstracts journals are intended as library tools for retrospective information retrieval, whereas the companion titles journals, which omit the abstracts and associated indexes, are intended as low-cost current-awareness tools for the individual.

SUBSCRIPTION PRICES

ABSTRACTS JOURNALS	Annual subscription Paper or microfiche	Annual subscription Combined paper and microfiche
Physics Abstracts (PA) Published every two weeks in conjunction with the American Institute of Physics, New York, and the Institute of Physics, London	£130	£195
Electrical & Electronics Abstracts (EEA) Published monthly jointly with the Institute of Electrical & Electronics Engineers Inc., New York	£105	£157
Computer & Control Abstracts (CCA) Published monthly jointly with the Institute of Electrical & Electronics Engineers Inc., New York	£55	£82
Combined Subscription to Electrical & Electronics Abstracts and Computer & Control Abstracts (EEA/CCA)	£135	£202

CURRENT PAPERS JOURNALS	Annual subscription IEE, AIP, IEEE, IOP, IERE members	Annual subscription Non-members
Current Papers in Physics (CPP) Published every two weeks in conjunction with the American Institute of Physics, New York, and the Institute of Physics, London	£7	£14
Current Papers in Electrical & Electronics Engineering (CPE) Published monthly jointly with the Institute of Electrical & Electronics Engineers Inc., New York	£7	£14
Current Papers on Computers & Control (CPC) Published monthly jointly with the Institute of Electrical & Electronics Engineers Inc., New York	£6	£12

CUMULATIVE INDEXES

Cumulative indexes are available for *Physics Abstracts, Electrical & Electronics Abstracts*, and *Computer & Control Abstracts*, for both authors and subjects. These cumulations generally cover a period of four years, with the exception of *Computer & Control Abstracts* where the initial volume covered the period 1966–68. The table below shows the prices and periods for the two types of cumulative index.

	Physics Abstracts		Electrical & Electronics Abstracts		Computer & Control Abstracts	
	Subject	Author	Subject	Author	Subject	Author
1955–59	£20	£20	£15	£20	—	—
1960–64	£40	£17	£20	£12	—	—
1965–68	£60	—	£35	£20	—	—
1966–68	—	—	—	—	£15 (combined)	

ORDERING PROCEDURE

AMERICAN SUBSCRIPTIONS
Physics Abstracts
Current Papers in Physics

For AIP members, wherever they reside, and from the public in the Americas, to the Subscription Department, American Institute of Physics, 335 East 45th Street, New York, NY 10017, USA. Please allow six weeks' notice for change of address, send both old and new addresses and include an address label from a recent issue.

Electrical & Electronics Abstracts
Computer & Control Abstracts and associated current papers journals in these fields

For IEEE members wherever they reside, and from the public in the Americas, to the Fulfillment Manager, Institute of Electrical & Electronics Engineers Inc., 345 East 47th Street, New York, NY 10017, USA.

REMAINDER OF THE WORLD
Abstracts Journals
Current Papers
Cumulative Indexes

For all remaining subscriptions, and for all cumulative indexes, to IEE, Savoy Place, London WC2R 0BL, England. Telephone 01-240 1871, Telex 261176, Telegrams Voltampere London WC2.

OTHER INSPEC SERVICES

SDI

(Selective Dissemination of Information.) This is a service individually tailored to the requirements and interests of the engineer or research worker. Details of information relevant to the interest profile of the individual subscriber are selected from the data being processed for the INSPEC database. Information is dispatched weekly on 150 mm × 100 mm (6″ × 4″) cards.

TOPICS

This is an SDI service based on standard profiles. There are 72 subjects covering high-activity areas of research and development. This is an inexpensive card service designed to alert engineers and researchers to the availability of literature within their subject area.

MAGNETIC TAPES

These are produced, containing all the information included in the INSPEC publications. They enable the larger research and development organisations to produce their own internal information and current-awareness services.

For more details of any of these services please write to:
INSPEC Marketing Department, The Institution of Electrical Engineers, Savoy Place, London WC2R 0BL, England

Cables Voltampere London WC2
Grams Voltampere London Telex

Telephone 01-240 1871
Telex 261176

inspec
The Institution of Electrical Engineers

New
Cumulative Indexes
1969–1972

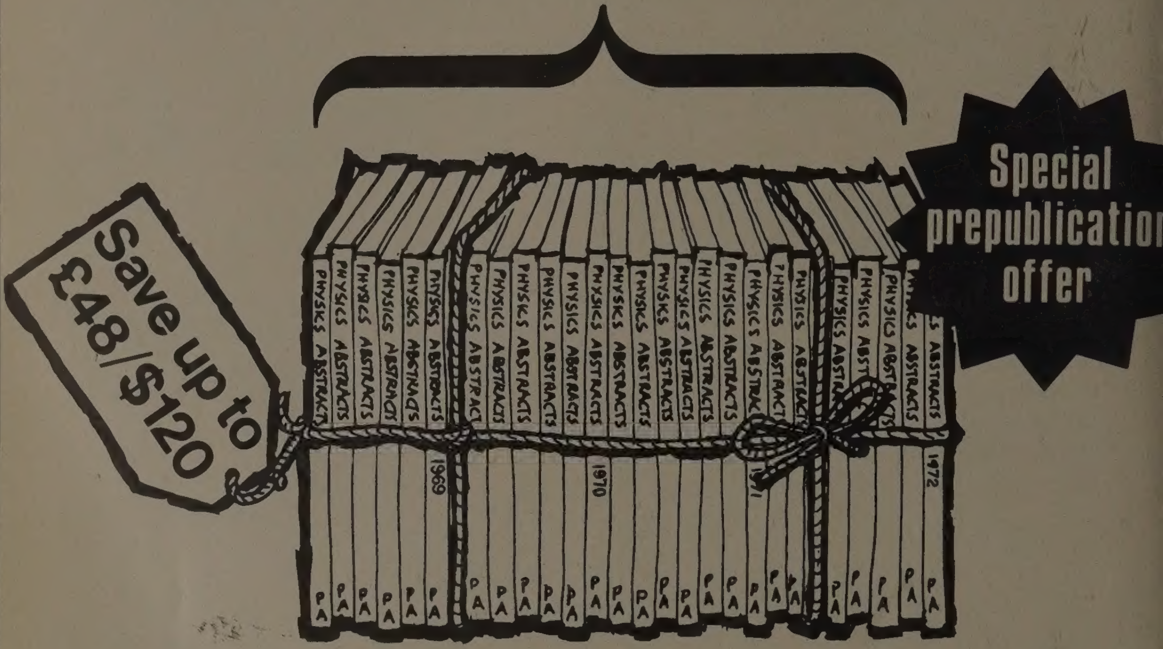

This offer can be worth up to £48/$120 to you and bring you the most comprehensive information-retrieval tool in the English-language in the fields of Physics, Electrical & Electronics Engineering, Computers & Control. For it entitles you to obtain the new four-year Cumulative Author and Subject Indexes to *Science Abstracts* at special prepublication prices.

Prices range from £30 ($78) to £222 ($545). But you can, between now and the 31st December 1973, order any of these Indexes at the special prepublication prices.

Deliveries will start in January 1974 and will be completed for all issues by March 1974.

INSPEC
The Institution of Electrical Engineers

For further details write to one of the addresses below

UK, Europe and Rest of World
INSPEC Marketing Department
The Institution of Electrical Engineers
Savoy Place
London WC2R 0BL
England

USA, Canada and South America
Subscription Department
American Institute of Physics
335 East 45 Street
New York NY 10017 USA

OR
Fulfilment Manager
Institute of Electrical &
Electronics Engineering I
345 East 47 Street
New York NY 10017 US